Ali F. AbuRahma • Dennis F. Bandyk
Editors

Patrick A. Stone • Henrik Sillesen
Associate Editors

# Noninvasive Vascular Diagnosis

## A Practical Guide to Therapy

Third Edition

Springer

*Editors*
Prof. Ali F. AbuRahma, M.D., RVT, RPVI
Department of Surgery
Robert C. Byrd Health Science Center
West Virginia University
Charleston, WV
USA

Charleston Area Medical Center
Charleston, WV
USA

Dennis F. Bandyk, M.D.
Vascular and Endovascular Surgery
University of California, San Diego
La Jolla, CA
USA

*Associate Editors*
Patrick A. Stone, M.D., RVT, RPVI
Robert C. Byrd Health Sciences Center
West Virginia University,
Charleston Area Medical Center
Charleston, WV
USA

Henrik Sillesen, M.D., DMSc
University of Copenhagen
Denmark

ISBN 978-1-4471-4004-7 ISBN 978-1-4471-4005-4 (eBook)
DOI 10.1007/978-1-4471-4005-4
Springer Dordrecht Heidelberg New York London

Library of Congress Control Number: 2012945528



Printed on acid-free paper

Springer is part of Springer Science+Business Media (www.springer.com)

*To my late Chairman, Dr. James Boland, who was our Chairman for 35 years, a mentor, great educator, exceptional surgeon, and my hero.*

*Ali F. AbuRahma*

*And to Dr. John Bergan, co-editor of the two previous editions of this textbook, who is a mentor, vascular surgery pioneer, and world renowned leader in vascular surgery.*

*Ali F. AbuRahma*
*Dennis F. Bandyk*

# Foreword

The evolution of vascular surgery over the past several years has been truly remarkable. Technologic advances have provided an unprecedented variety of therapeutic options available for the care of the vascular patient. The contemporary vascular specialist today must provide the entire spectrum of care for the patient with circulatory disease, including conventional open surgery, minimally invasive endovascular therapy, and medical management. Fundamental to achieving the optimal outcome for the vascular patient is accurate diagnosis, selection of the most appropriate therapy, and long-term surveillance of the natural history of the disease as well as the outcomes of therapeutic interventions. Crucial to this mission is the vascular noninvasive laboratory. Indeed, not only has the vascular noninvasive laboratory benefitted from recent technologic refinement, but at no time in its history has it played a more critical role in the management of the patient with vascular disease.

The first vascular noninvasive laboratory was established by surgeons at the Massachusetts General Hospital in 1946, and the evolution of noninvasive vascular laboratory technology over the last six decades has been pioneered by vascular surgical pioneers such as Bergan, Yao, Cranley, Strandness, and Kempczinski. Dr. AbuRahma, who has been a prolific clinical investigator and author in the field of vascular noninvasive diagnosis, joined the company of these leaders with publication of the first edition of *Noninvasive Diagnosis: A Practical Guide* in 2000. The third edition of this book is an encyclopedic treatise on noninvasive vascular diagnosis, is without question the "gold standard" text in the field, and is a must have volume for any serious practitioner interested in the care of the patient with circulatory disease.

This book provides truly comprehensive coverage of the entire spectrum of noninvasive vascular testing, ranging from conventional noninvasive technology to the latest state-of-the-art advances. The list of part editors and authors of these chapters reads as a "who's who" of leaders in the field who have combined their unique individual expertise and perspectives with the latest published information in clearly written, beautifully illustrated, and extensively referenced chapters. The totality of vascular noninvasive diagnosis topics are covered, even including regulatory issues which will become an increasingly important issue in our evolving health care system.

For example, today there are more than 10,000 noninvasive vascular laboratories in the United States but less than 25% are actually accredited. The initial part of the book directly addresses the issues of laboratory quality and credentialing. The second part, on vascular hemodynamics, sets the foundation for the clinical parts which follow.

The part on cerebrovascular disease includes 14 chapters which cover not only basic noninvasive testing issues, pre-, and post-intervention, but leading edge topics such as transcranial Doppler, intima media thickness, and plaque characterization. These latter modalities will play an increasingly important role in selecting the most appropriate candidates with asymptomatic carotid stenoses for intervention, an issue of growing controversy in contemporary practice and in the future. The comprehensive nature of the part is reflected in the inclusion of a chapter on CT and MRA of the carotid arteries.

Likewise, the parts on peripheral arterial disease and venous disease include the entire spectrum of noninvasive testing from traditional physiologic modalities to the expanding role of Duplex examination in diverse clinical scenarios. The respective roles and the relative

advantages and disadvantages of each of the available testing modalities are clearly highlighted for the reader. Whereas mesenteric vascular disease has historically been a diagnosis of exclusion, often established after an extensive work-up pursuing other potential diagnoses, today Duplex ultrasound has become the initial diagnostic modality of choice. Its role in evaluating the patient with suspected mesenteric as well as renovascular disease, and in follow-up after intervention, is presented authoritatively.

In an era of increasing pressure for health care cost containment, vascular noninvasive testing will play an increasingly important, cost effective, and expanding role in the evaluation of patients with circulatory disease and in many cases will continue to supplant more invasive conventional angiography and expensive radiographic imaging studies. In addition to covering the entire spectrum of conventional noninvasive laboratory examination throughout the body, this text also provides for the reader the most recent information on evolving diagnostic modalities such as intravascular ultrasound, three-dimensional imaging, and contrast-enhanced ultrasound.

*Noninvasive Vascular Diagnosis*: *A Practical Guide to Therapy* should be required reading and in fact part of the curriculum of every vascular surgery resident, as well as interventional cardiology and interventional radiology trainees with an interest in vascular disease. It will be equally valuable to the experienced practicing health care provider who cares for patients with vascular disease. For the busy clinician, each part of the book concludes with a summary chapter on the clinical applications of the information provided in that part. The book even includes a practical chapter on vascular laboratory coding and reimbursement. This book is a truly unique contribution – I know of no other publication in the field that provides such a comprehensive, well organized, and easily readable presentation of state-of-the-art noninvasive vascular testing.

Bruce A. Perler, MD, MBA
Julius H. Jacobson, II Professor of Surgery
The Johns Hopkins University School of Medicine
Chief, Division of Vascular Surgery & Endovascular Therapy
Director of the Vascular Noninvasive Laboratory
The Johns Hopkins Hospital

# Preface

The purpose of the third edition of this popular textbook on noninvasive vascular diagnostics is to highlight recent advances in the investigation of vascular diseases. This new edition is designed to assist physicians and other clinicians in determining the most applicable and practical methods for managing patients with vascular disease in the most cost-effective and efficient manner.

The rapid expansion of this field over the past two decades, and the addition of new diagnostic modalities and new applications, justify this third edition. After three decades of maturation of vascular laboratories, from the days of the early pioneers that were influenced by the late Dr. Gene Strandness and other prominent vascular surgeons, a broader group of physicians, including radiologists, neurologists, cardiologists, and internists have become involved in this technology. With this in mind, this new edition is designed to be comprehensive enough to address the needs of all clinicians who are involved in the care of patients with vascular disease.

This new edition has been divided into parts that have been edited by several nationally and internationally prominent experts in the field of noninvasive vascular diagnostics. This is reflected, not only by the addition of a new editor, Dr. Dennis Bandyk, but also by the addition of associate editors, Dr. Henrik Sillesen and Dr. Patrick Stone. With the new level of maturity and technological advances in the field of noninvasive vascular testing, 15 new chapters have been added and the remaining chapters have been extensively revised, many of which have new authors.

The first part on vascular laboratory operations includes a new chapter on quality assurance, which is essential today; while the second part includes a new chapter on vascular hemodynamics by Dr. Henrik Sillesen. The third part on cerebrovascular diagnosis has several new chapters, including the role of duplex ultrasound in carotid screening, computed tomography angiography and magnetic resonance angiography of the carotids, intraoperative ultrasound assessment of carotid endarterectomy and stent angioplasty, intima media thickness measurement, and errors and artifacts of carotid ultrasound evaluation.

Part IV, edited by Dr. Dennis Bandyk, also has several new chapters, including duplex utilization of radial artery imaging, protocol and mapping techniques prior to hemodialysis access planning, and noninvasive vascular testing in the trauma patient.

The noninvasive diagnosis of venous disorders, Part V, is edited by a new associate editor, Dr. Patrick Stone. Several of these chapters were extensively revised and two new chapters were added on venous duplex ultrasound of the upper extremities and the role of the noninvasive vascular laboratory in thoracic outlet syndromes.

One new chapter on duplex evaluation after renal intervention was added to Part VI, and Part VII includes new chapters on coding and reimbursement for vascular lab testing and the clinical application of ultrasound guidance in arterial and venous access.

Several modalities are described in this new edition by new authors who were selected based on their extensive knowledge and expertise in these fields.

To the contributors, previous authors, and their staff, we, the editors, wish to express our most sincere appreciation. We hope the readers will enjoy this update.

Ali F. AbuRahma, M.D., RVT, RPVI
Dennis F. Bandyk, M.D.

# Acknowledgments

This new edition owes much to our colleagues, who have contributed a great deal, and without their expertise and guidance, this volume would not have become a reality. The editors would like to thank our technical staff for their support, particularly Mona Lett in Charleston, West Virginia, for transcribing and revising the various versions of the chapters and for maintaining contact with contributing authors regarding guidelines and deadlines. We would also like to thank Maynard Chapman in Charleston, West Virginia, for producing some of the illustrations. We also appreciate the efforts of some of my vascular laboratory technicians, including Linda Keffer, Cristyn Coleman, Candace Key, and Kim Riner for their assistance in providing some of the illustrations. Finally, the editors would like to specifically thank Michael D. Sova, Developmental Editor; Grant Weston, Senior Editor, Medicine; and the entire Springer Science + Business Media team for their invaluable support and guidance. Without the support of these people and many others, this new edition would not have seen the light of day.

Ali F. AbuRahma, M.D., RVT, RPVI
Dennis F. Bandyk, M.D.

# Contents

# Contributors

**Shadi Abu-Halimah, M.D.** Department of Vascular Surgery, UNC Hospitals, Chapel Hill, NC, USA

**Ali F. AbuRahma, M.D., RVT, RPVI** Department of Surgery, Robert C. Byrd Health Sciences Center, West Virginia University, Charleston, WV, USA

Charleston Area Medical Center, Charleston, WV, USA

**Andrei V. Alexandrov, M.D.** Department of Neurology, Comprehensive Stroke Center, University of Alabama at Birmingham Hospital, Birmingham, AL, USA

**Jose I. Almeida, M.D, FACS, RPVI, RVT** Department of Vascular Surgery, Miami Vein Center, Miami, FL, USA

**Javier E. Anaya-Ayala, M.D.** Department of Cardiovascular Surgery, Methodist DeBakey Heart & Vascular Center, Houston, TX, USA

**Clifford T. Araki, Ph.D., RVT** Department of Medical Imaging Sciences, School of Health Related Professions, University of Medicine and Dentistry of New Jersey, Newark, NJ, USA

**Paul A. Armstrong, D.O.** Division of Vascular and Endovascular Surgery, University of South Florida, College of Medicine, Tampa, FL, USA

**Enrico Ascher, M.D.** Department of Surgery, Mount Sinai School of Medicine, New York, NY, USA

The Vascular Institute of New York, Brooklyn, NY, USA

**Faisal Aziz, M.D., RVT, RPVI** Jobst Vascular Institute, The Toledo Hospital, Hershey, PA, USA

Section of Vascular Surgery, Department of Surgery, Penn State Hershey College of Medicine, Hershey, PA, USA

**Martin R. Back, M.D., RPVI, RVT** Division of Vascular and Endovascular Surgery, University of South Florida, College of Medicine, Tampa, FL, USA

**J. Dennis Baker, M.D.** Department of Surgery, David Geffen School of Medicine at UCLA, Los Angeles, CA, USA

**Jeffrey L. Ballard, M.D.** Department of Vascular Surgery, St. Joseph Hospital, Orange, CA, USA

**Dennis F. Bandyk, M.D.** Department of Vascular and Endovascular Surgery, UC San Diego, La Jolla, CA, USA

**Donald T. Baril, M.D.** Division of Vascular and Endovascular Surgery, Department of Surgery, University of Massachusetts Medical School, Worcester, MA, USA

**Kristian Barlinn, M.D.** Department of Neurology, Dresden University Stroke Center, University of Technology Dresden, Dresden, Saxony, Germany

Department of Neurology, Comprehensive Stroke Center, University of Alabama at Birmingham Hospital, Dresden, Saxony, Germany

**Hisham Bassiouny, M.D., FACS** Section of Vascular Surgery and Endovascular Therapy, The University of Chicago, Chicago, IL, USA

**Mark C. Bates, M.D., FACC, FSCAI** Department of Surgery, Robert C. Byrd Health Sciences Center, West Virginia University, Charleston Area Medical Center, Charleston, WV, USA

**Phillip J. Bendick, Ph.D.** Division of Vascular Surgery, William Beaumont Hospital, Royal Oak, MI, USA

**Carol B. Benson, M.D.** Department of Radiology, Harvard Medical School, Boston, MA, USA

Department of Radiology, Brigham and Women's Hospital, Boston, MA, USA

**Giorgio M. Biasi, M.D.** Department of Surgical Sciences, University of Milano Bicocca, Monza, Italy

Vascular Surgery Unit, San Gerardo Teaching Hospital, Monza, Italy

**John Blebea, M.D.** Department of Surgery, University Hospitals of Cleveland, Case Western Reserve University School of Medicine, Cleveland, OH, USA

**Diana Call, BS, RVT** Division of Vascular Surgery and Endovascular Therapy, John Hopkins Hospital, Baltimore, MD, USA

**Keith D. Calligaro, M.D.** Section of Vascular Surgery, Pennsylvania Hospital, Philadelphia, PA, USA

**John E. Campbell, M.D.** Department of Surgery, Robert C. Byrd Health Sciences Center, West Virginia University, Charleston Area Medical Center, Charleston, WV, USA

**James R. Campbell II, M.D.** Department of Surgery and Medicine, Robert C. Byrd Health Sciences Center, West Virginia University, Charleston Area Medical Center, Charleston, WV, USA

**Rabih Chaer, M.D.** Division of Vascular Surgery, PUH, Pittsburgh, PA, USA

**Benjamin B. Chang, M.D.** Department of Vascular Surgery, Albany Medical Center Hospital, Albany, NY, USA

**Anthony J. Comerota, M.D., RVT, FACS, FACC** Section of Vascular Surgery, University of Michigan, Toledo, OH, USA

Jobst Vascular Institute, The Toledo Hospital, Toledo, OH, USA

**R. Clement Darling III, M.D.** Department of Vascular Surgery, Albany Medical Center Hospital; Albany Medical College, Albany, NY, USA

The Vascular Group, Albany Medical College, Albany, NY, USA

**Mark G. Davies, M.D., Ph.D., M.B.A.** Department of Surgery, Weill Medical College at Cornell University, Houston, TX, USA

Department of Cardiovascular Surgery, Methodist DeBakey Heart & Vascular Center, Houston, TX, USA

Department of Research and Education, Methodist DeBakey Heart & Vascular Center, Houston, TX, USA

**Edward B. Diethrich, M.D.** Arizona Heart Hospital & Foundation, Phoenix, AZ, USA

**Kevin J. Doerr, BS, RVT** Department of Vascular Surgery, Pennsylvania Hospital, Philadelphia, PA, USA

**Matthew J. Dougherty, M.D.** Section of Vascular Surgery, Pennsylvania Hospital, Philadelphia, PA, USA

**Bryan T. Fisher Sr M.D.** Department of Vascular Surgery, Vanderbilt University Medical Center, Nashville, TN, USA

**Shawn H. Fleming, M.D.** Department of Vascular and Endovascular Surgery, Wake Forest Baptist Medical Center, Winston-Salem, NC, USA

**William R. Flinn, M.D.** Division of Vascular Surgery, University of Maryland School of Medicine, Baltimore, MD, USA

**Mary C. Frates, M.D.** Department of Radiology, Harvard Medical School, Boston, MA, USA

Department of Radiology, Brigham and Women's Hospital, Boston, MA, USA

**Julie Ann Freischlag, M.D.** Department of Surgery, John Hopkins Hospital, Baltimore, MD, USA

**Alberto Froio, M.D.** Department of Surgical Sciences, San Gerardo Teaching Hospital, University of Milano Bicocca, Monza, Italy

**Holly L. Grunebach, MMS, MSPH** Department of Surgery, Johns Hopkins Hospital, Baltimore, MD, USA

**Kimberley J. Hansen, M.D.** Department of Vascular and Endovascular Surgery, Wake Forest Baptist Medical Center, Winston-Salem, NC, USA

**Stephen M. Hass, M.D.** Department of Surgery, Robert C. Byrd Health Sciences Center, West Virginia University, Charleston Area Medical Center, Charleston, WV, USA

**Anil P. Hingorani, M.D.** Division of Vascular Surgery, Maimonides Medical Center, Brooklyn, NY, USA

**Marge Hutchisson, RVT, RDCS** Intersocietal Commission for the Accreditation of Vascular Laboratories (ICAVL), Intersocietal Accreditation Commission, Ellicott City, MD, USA

**Akhilesh K. Jain, M.D.** Section of Vascular Surgery, Yale University, New Haven, CT, USA

**K. Wayne Johnston, M.D., FRCS(C)** Department of Vascular Surgery, University of Toronto, Toronto General Hospital, Toronto, ON, Canada

**Anne M. Jones, RN, BSN, RVT, RDMS, FSVU, FSDMS** Department of Neurology and Neurosciences, Medical University of South Carolina (MUSC), Charleston, SC, USA

**Dimitrios Karakitsos, M.D., Ph.D., MRCP** Intensive Care Unit, General State Hospital of Athens, Athens, Greece

**Jessica Kepplinger, M.D.** Department of Neurology, Dresden University Stroke Center, University of Technology Dresden, Dresden, Saxony, Germany

**Stephen Kolakowski, M.D.** Section of Vascular Surgery, Pennsylvania Hospital, Philadelphia, PA, USA

**Paul B. Kreienberg, M.D.** Department of Vascular Surgery, Albany Medical Center Hospital, Albany, NY, USA

**Nicos Labropoulos, Ph.D.** Division of Vascular Surgery, Department of Surgery, Stony Brook University Medical Center, Stony Brook, NY, USA

**Brajesh K. Lal, M.D., FACS** Department of Vascular Surgery, Baltimore VA Medical Center, Baltimore, MD, USA

Center for Vascular Diagnostics, University of Maryland Medical Center, Baltimore, MD, USA

Department of Surgery, University of Maryland Medical center, Baltimore, MD, USA

**Peter F. Lawrence, M.D.** Department of Surgery, Ronald Reagan UCLA Medical Center, Los Angeles, CA, USA

**Joann M. Lohr, M.D., FACS, RVT** Department of Vascular Surgery, Good Samaritan Outpatient Center, Cincinnati, OH, USA

Good Samaritan Hospital, Cincinnati, OH, USA

**Alan B. Lumsden, M.D.** Department of Surgery, Weill Medical College at Cornell University, Houston, TX, USA

Department of Cardiovascular Surgery, Methodist DeBakey Heart & Vascular Center, Houston, TX, USA

**Robyn A. Macsata, M.D.** Department of Surgery, Washington DC VA Medical Center, Washington, DC, USA

**Michel S. Makaroun, M.D.** Department of Vascular Surgery, University of Pittsburgh Medical Center, Pittsburgh, PA, USA

**M. Ashraf Mansour, M.D., RVT, FACS** Spectrum Health, Grand Rapids, MI, USA

Department of Cardiovascular Surgery, Michigan State University, Grand Rapids, MI, USA

**Natalie Marks, M.D.** Brooklyn, NY, USA

**Luke K. Marone, M.D.** Division of Vascular Surgery, Department of Surgery, University of Pittsburgh Medical Center, Pittsburgh, PA, USA

**William A. Marston, M.D.** Vascular Surgery Division, Department of Surgery, UNC Hospitals, Chapel Hill, NC, USA

**Sandra C. McAffe-Benett, BS, RVT** Department of Vascular Surgery, Pennsylvania Hospital, Philadelphia, PA, USA

**Manish Mehta, M.D., MPH** Department of Vascular Surgery, Albany Medical Center Hospital, Albany, NY, USA

**George H. Meier III, M.D., RVT, FACS** Division of Vascular Surgery, Department of Surgery, University Hospital, Cincinnati, OH, USA

**Frank R. Miele, MSEE** Pegasus Lectures, Inc., Forney, TX, USA

**Gregory L. Moneta, M.D.** Department of Vascular Surgery, Oregon Health and Science University, Portland, OR, USA

**John Moos, M.D.** Division of Vascular Surgery, Department of Surgery, Keck School of Medicine at the University of Southern California, Los Angeles, CA, USA

**Albeir Y. Mousa, M.D.** Department of Surgery, Robert C. Byrd Health Sciences Center, West Virginia University, Charleston Area Medical Center, Charleston, WV, USA

**Kathryn Mueller, BS, RVT** Department of Vascular Surgery, Pennsylvania Hospital, Philadelphia, PA, USA

**Aravinda Nanjundappa, M.D., RVT, FACC, FSCAI** Department of Surgery, Robert C. Byrd Health Sciences Center, West Virginia University, Charleston Area Medical Center, Charleston, WV, USA

**Thomas C. Naslund, M.D.** Department of Vascular Surgery, Vanderbilt University Medical Center, Nashville, TN, USA

**Peter Neglén, M.D., Ph.D.** Department of Vascular Surgery, Trimiklini, Limassol, Cyprus

**David G. Neschis, M.D.** Department of Surgery, The Maryland Vascular Center, Baltimore Washington Medical Center, University of Maryland School of Medicine, Baltimore, MD, USA

**Marsha M. Neumyer, BS, RVT** Vascular Diagnostic Educational Services, Vascular Resource Associates, Harrisburg, PA, USA

**Kathleen J. Ozsvath, M.D.** Department of Vascular Surgery, Albany Medical Center Hospital, Albany, NY, USA

**Federico E. Parodi, M.D.** Division of Vascular and Endovascular Surgery, University of South Florida, College of Medicine, Tampa General Hospital, Tampa, FL, USA

**Savino Pasquadibisceglie, M.D.** Department of Surgical Sciences, San Gerardo Teaching Hospital, University of Milano Bicocca, Monza, Italy

**Philip S. K. Paty, M.D.** Department of Vascular Surgery, Albany Medical Center Hospital, Albany, NY, USA

**Alexis Powell, M.D.** Department of Surgery, University of South Florida, School of Medicine, Tampa, FL, USA

**Jeffrey K. Raines, MME, Ph.D.** Department of Surgery, University of Miami Hospital and Clinics, Homestead, FL, USA

**Donald B. Reid, M.D., FRCS** Department of Vascular and Endovascular Surgery, Wishaw Hospital, Scotland, UK

**Jorge Rey, M.D.** Department of Vascular Surgery, Albany Medical Center Hospital, Albany, NY, USA

**Tracey A. Richardson, AS, RDMS, RVT** Department of Vascular Surgery, University of Pittsburgh Medical Center, Pittsburgh, PA, USA

**Gianluca Rigatelli, M.D., Ph.D.** Department of Cardiovascular Diagnosis and Endoluminal Interventions, Rovigo General Hospital, Rovigo, Italy

**Sean P. Roddy, M.D.** Department of Vascular Surgery, Albany Medical Center Hospital, Albany, NY, USA

**Luca Rossi, M.D.** Department of Surgical Sciences, San Gerardo Teaching Hospital, University of Milano Bicocca, Monza, Italy

**Vincent L. Rowe, M.D., FACS** Division of Vascular Surgery, Department of Surgery, Keck School of Medicine at the University of Southern California, Los Angeles, CA, USA

Healthcare Consultation Center II, Los Angeles, CA, USA

**Robert B. Rutherford, M.D.** Department of Surgery, University of Colorado Medical Center, Corpus Christi, TX, USA

**Leon Salem, M.D.** Department of Vascular Surgery, Albany Medical Center Hospital, Albany, NY, USA

**Sergio X. Salles-Cunha, Ph.D., RVT, FSVU** Department of Imagenology, Itanhaém, São Paulo, SP, Brazil

**Robert P. Scissons, RVT, FSVU** Jobst Vascular Laboratory, Jobst Vascular Institute, The Toledo Hospital, Toledo, OH, USA

**Jennifer A. Sexton, M.D.** Georgetown University Hospital, Washington Hospital Center, Washington, DC, USA

**Dhiraj M. Shah, MD** Department of Vascular Surgery, Albany Medical Center Hospital, Albany, NY, USA

**Melissa D. Shah, M.D.** Department of Vascular Surgery, Albany Medical Center Hospital, Albany, NY, USA

**Anton N. Sidawy, M.D., MPH** Department of Surgery, George Washington University Hospital, Washington, DC, USA

**Henrik Sillesen, M.D., DMSc** Department of Vascular Surgery, Rigshospitalet, University of Copenhagen, Copenhagen, Denmark

**Mohit Srivastava, M.D.** Department of Surgery, Robert C. Byrd Health Sciences Center, West Virginia University, Charleston Area Medical Center, Charleston, WV, USA

**Shaun M. Stickley, M.D.** Division of Vascular Surgery, Department of Surgery, University Hospital, Cincinnati, OH, USA

**Patrick A. Stone, M.D., RVT, RPVI** Department of Surgery, Robert C. Byrd Health Sciences Center, West Virginia University, Charleston Area Medical Center, Charleston, WV, USA

**Pierre-Jean Touboul, M.D.** INSERM U698, Neurology and Stroke Center, Bichat University Hospital and Medical School, Paris, France

**Daynene Vykoukal, Ph.D.** Department of Cardiovascular Surgery, Methodist DeBakey Heart & Vascular Center, Houston, TX, USA

**Fred A. Weaver, M.D., FACS, MMM** Division of Vascular Surgery, Department of Surgery, Keck Medical Center of USC, Los Angeles, CA, USA

**Cindy Weiland, RVT** Department of Quality Assurance, Intersocietal Accreditation Commission, Ellicott City, MD, USA

**Robert M. Zwolak, M.D., Ph.D.** Section of Vascular Surgery, Dartmouth-Hitchcock Medical Center, Lebanon, NH, USA

# Part I

# Vascular Laboratory Operations

Ali F. AbuRahma

# Improving Quality in Noninvasive Testing by Certification and Accreditation

1

J. Dennis Baker and Anne M. Jones

**Abstract**

Over the last half century, noninvasive vascular testing has evolved from a research laboratory curiosity to a well-established clinical component in the management of patients with vascular disease. As with any new field, the search for high-quality work is a critical challenge. An important early step was developing appropriate education for the physicians and the technical staff who would ultimately be examining patients. But providing educational opportunities was only the first step in ensuring a quality operation. It was necessary to define prerequisite knowledge and experience, together with a determination of entry-level knowledge. This step was achieved in 1983 by establishing a certifying examination for vascular technologists. The second quality initiative was to define benchmarks for establishing and running of an examining facility. Relevant issues included quality of equipment, ongoing supervision, examination protocols, standardized diagnostic criteria, reporting standards, and validation studies. In 1991, a formal laboratory accreditation was established to provide a structured approach to this side of improved quality. Over the years, the combination of individual certification and laboratory accreditation has led in the effort to improve the quality of noninvasive testing.

**Keywords**

Noninvasive testing • Vascular laboratory • Credentialing • Accreditation

Noninvasive testing had its roots in early research laboratories more than half a century ago. The first facility in this country was established at the Massachusetts General Hospital in 1946, and others appeared over the following years. The work focused on research efforts with little thought about providing routine clinical testing. By the 1960s, arterial reconstructive procedures became increasingly frequent, and there was a surge in interest in the clinical investigation of blood flow. The ability of the early measurement methods to provide objective noninvasive determination of vascular parameters attracted the interest of vascular surgeons, and by the 1970s, there was regular clinical use of a number of tests. What had been quiet (and often esoteric) research laboratories expanded, providing an increasing volume of routine examinations directed toward patient management. By the late 1970s, the majority of hospital-based facilities were dedicated to routine clinical service rather than to research. At the same time, physicians took the testing modalities into the office, thus increasing the availability of these tests.

J.D. Baker, M.D. (✉)
Department of Surgery,
David Geffen School of Medicine at UCLA,
200 UCLA Medical Plaza Room 510,
Los Angeles, CA 90095, USA
e-mail: jbaker@mednet.ucla.edu

A.M. Jones, RN, BSN, RVT, RDMS, FSVU, FSDMS
Department of Neurology and Neurosciences,
Medical University of South Carolina (MUSC),
Charleston, SC, USA

A.F. AbuRahma, D.F. Bandyk (eds.), *Noninvasive Vascular Diagnosis*,
DOI 10.1007/978-1-4471-4005-4_1, 

## Education and Training

### Physician

The testing in the early laboratories was supervised by the physicians who worked on developing and validating the techniques. These researchers were committed to critical evaluation of the tests being developed and careful work preceded widespread clinical application. Once the value of vascular testing was promulgated, increasing numbers of physicians became interested in the field. The majority of physicians who ran clinical laboratories in the late 1970s and early 1980s lacked the research background and the experience of the original investigators. The newcomers relied on learning what they could from the few published articles and from visits to observe the work done in established laboratories. Over time, there has been an increase in the quality and availability of courses and teaching materials available. Some specialties (including vascular surgery and vascular medicine) require training in vascular testing as part of the core curriculum of residencies. Many programs include didactic presentations, direct participation in examinations, and experience in test interpretation. As the result of these programs, many doctors now complete training much better prepared for vascular testing.

### Technologist

With the expansion of vascular testing into the clinical arena and the increasing demand for services came a need for additional personnel and the training of the providers of vascular testing. The most important change was adding personnel whose job was to perform the different testing protocols. People from a variety of technical backgrounds were recruited, including nurses, radiology technicians, and catheterization laboratory specialists. With time, this hybrid group evolved into vascular technologists. Adequate training and supervision became an obvious problem. Initially, the providers of vascular testing were taught the basics by the supervising physician, who might or might not have an adequate background. In general, most technologists learned how to perform the examinations through "on-the-job" training because of the limited availability of formal education. When a knowledgeable physician supervised the experience, a reasonable level of expertise could result, but often trainees were on their own, learning by rote without understanding what was being done. In the past two decades, noninvasive testing has become more complex both in terms of equipment and procedures. Understanding vascular disease and the instrumentation used has become increasingly important.

Dedicated vascular technology educational programs have continued to evolve over the past decade. Their measured development can be attributed partly to inadequate funding and partly to the classification of vascular technology within the allied health specialty of "cardiovascular technology" (CVT). The CVT specialty was formally recognized by the Committee on Allied Health Education and Accreditation of the American Medical Association in 1981. Essentials and Guidelines of an Accredited Educational Program for Cardiovascular Technology were completed in 1983 and adopted by 12 allied health organizations [including the Society of Vascular Ultrasound (SVU)]. While this step gave credibility to the cardiovascular technology profession and established *Standards and Guidelines*, it failed to recognize the practical specialty of vascular technology. In theory, CVT includes invasive and noninvasive cardiovascular technology as well as peripheral vascular testing. As a result, educational programs in CVT often included very limited didactic or clinical exposure to peripheral vascular testing. However, because vascular testing has continued to grow in clinical, new educational opportunities have developed for vascular technologists and vascular sonographers. Since 1985, the Joint Review Committee on Education in Cardiovascular Technology (JRC-CVT) has reviewed programs seeking accreditation in cardiovascular technology. Currently, 13 Commission on Accreditation of Allied Health Education Program (CAAHEP)–accredited programs in Cardiovascular Technology offer concentrations in Noninvasive Vascular Study. Accredited programs offer certificate, associate, baccalaureate, and master's degrees or credentials. For detailed information about JRC-CVT-accredited programs, visit www.caahep.org or www.jrccvt.org.

A second pathway for education in noninvasive vascular testing is through the Joint Review Committee on Education in Diagnostic Medical Sonography (JRC-DMS), also accredited by CAAHEP. Fifty-four accredited Diagnostic Medical Sonography programs offer concentrations in vascular testing. Three programs offer dedicated vascular education: Nova Southeastern University and Rush University are baccalaureate programs and Long Island University is a certificate program. Students who graduate from accredited CVT and DMS programs are eligible to sit for certification examinations.

The emergence of "distance" or "Internet" educational programs is also impacting the educational choices of vascular technologists. Although several "online" vascular ultrasound educational programs are currently available, the first bachelor's degree program in vascular technology was developed in 1992 by the Oregon Institute of Technology (OIT). The program offers a course of studies for a student entering the profession of vascular technology as well as a completion degree pathway for registered vascular technologists. The program currently enrolls 30–40 students on-campus and up to 100 students in the off-campus each year. The Degree Completion Program integrates basic medical science

and vascular diagnostic courses with a general college education, allowing students to complete a Bachelor of Science Degree in Vascular Technology. The distance program was developed for vascular technologists desiring a degree without leaving their present employment. The program is available to technologists who lack a bachelor's degree, and credits are awarded for achieving certification as a Registered Vascular Technologist (RVT). Details of the program are available at the school's website.

## Certification

From the early days of vascular testing, there was concern about the level of knowledge, experience, and competence of the individual technologist. In 1979, the national association of vascular technologists, the Society of Noninvasive Vascular Technologists (SNIVT, which later became the SVU), recognized that validation of the specialty required documentation of competence through certification. The American Registry of Diagnostic Medical Sonographers (ARDMS) was selected to provide the certification examination. Since 1975, the ARDMS developed and administered practice-based examinations in distinct ultrasound specialty areas. The ARDMS has certified more than 70,000 individuals in seven specialty areas for sonographers/vascular technologists and one specialty interpretation examination for physicians. It is recognized and accredited by the International Standards Organization (ISO), the American National Standards Institute (ANSI), and the National Commission of Credentialing Agencies (NCCA) and has become a recognized standard for diagnostic medical ultrasound credentialing worldwide. The ARDMS has well-defined educational and clinical prerequisites for candidates preparing to sit for ultrasound certification examinations.

These requirements are available on the website (www.ARDMS.org). Once the prerequisites are met, applicants seeking the RDMS, RDCS, or RVT credentials are required to pass two comprehensive examinations to earn a credential: (1) a sonography principles and instrumentation examination (SPI) and (2) a specialty examination. After acquiring a credential, continuing competency is documented through continuing medical education (CME). Evidence of ongoing CME is submitted to the ARDMS upon request through an audit process. In 2012, the ARDMS will launch a Recertification Assessment Program to meet a required standard of the International Standards Organization (ISO) and the American National Standards Institute (ANSI). These accrediting bodies stipulate that the ARDMS must have a measurable way to assure registrant competence and knowledge of current day practice. The recertification examinations will be web-based and available online for all active ARDMS registrants to take during the last 3 years of a 10-year recertification assessment period. Recertification assessment will be required in all specialty areas maintained by registrants; separate physics and instrumentation recertification will not be required.

The first vascular technology examination was administered by ARDMS in 1983; since that time, over 21,000 RVT credentials have been awarded. Over 1,600 RVTs are also MDs. An important component of maintaining information on registrants is the ongoing documentation of the profession of vascular technology through periodic task analysis surveys. These surveys, completed by active RVTs, reflect changes occurring within the practice of vascular technology and assist with examination validation by documenting the tasks routinely performed by vascular technologists in the clinical setting. As new ultrasound technology emerges, and older methods are discarded, the task survey documents the changing clinical practice. The information is used to update examination content so that candidates are assured that the examination reflects technological advances within the profession. The surveys are also required to maintain accreditation by the three accrediting bodies.

Survey results are also used to provide historical data about trends within the specialty. For instance, in 1982, over 75% of practicing vascular technologists were nurses; this number decreased to only 18% by 1994. Similarly, in early surveys, most vascular technologists acquired their training in vascular technology on the job; by 1995, 40% of the respondents had graduated from a technical program in vascular technology, while 37% had a bachelor's or master's degree. Because of the availability of accredited educational programs in vascular technology and sonography, the "on-the-job training" or OJT prerequisite pathway has been discontinued by the ARDMS for candidates seeking certification. Increasingly, the individual seeking the RVT credential may be "cross-trained" in other areas of ultrasound. Recent data collected by the ARDMS shows that only 27% of vascular technologists are "RVT-only," as compared to 55% a decade ago. Additionally, 47% are RVT/RDMS (general sonographers), 10% are RVT/RDCS (cardiac sonographers), and 14% are RDMS, RDCS, and RVT.

A second pathway to certification is through Cardiovascular Credentialing International (CCI). Established in 1988, CCI is a not-for-profit corporation founded for the purpose of administering credentialing examinations. CCI is accredited by the American National Standards Institute (ANSI). The CCI Corporation of today is the result of corporate mergers of the testing components of the National Alliance of Cardiovascular Technologists (NACT), the American Cardiology Technologists Association (ACTA), and the National Board of Cardiovascular Testing (NBCVT). Eight CCI registry examinations are offered in three specialty areas: invasive/cardiac catheterization, noninvasive echocardiography, and vascular technology/ultrasound. The Registered Vascular Specialist (RVS) credential is awarded to candidates who successfully complete a one part, comprehensive examination in vascular technology.

The Registered Phlebology Sonographer (RPhS) credential, established in 2010, is also a comprehensive exam focusing on the subspecialty of phlebography, the noninvasive evaluation of venous disease. As with the ARDMS process, the only mechanism for obtaining the CCI credential is through examination. Candidates for the RVS credential may qualify through four prerequisite pathways, and RPhS candidates may qualify through five potential pathways. Both prerequisite pathways include a 2-year clinical experience or "on-the-job training" option. Although a limited number of physicians have taken the certification examinations, physicians who seek CCI credentials have three possible prerequisite pathways. All prerequisite options are listed on the CCI website (www.cci-online.org). There are currently 1,900 active CCI registrants with the RVS credential; 100 individuals have acquired the RPhS credential. Not surprisingly, Registered Vascular Sonographers are frequently employed by cardiologists, although a growing number are being hired in radiology departments. Ongoing documentation of continuing medical education is required to maintain active status and document continuing competence.

In an effort to demonstrate competence in vascular technology, many vascular surgeons acquired the RVT credential. The majority of MD/RVTs are vascular surgeons. There has been concern expressed that the RVT credential, designed to evaluate the knowledge and competence of the vascular technologist, is not the appropriate vehicle for a physician. To address these concerns, in 2003, the Society for Vascular Surgery submitted a formal request to the ARDMS to explore the interest in a voluntary credential for physicians in vascular ultrasound interpretation. A market analysis was conducted, and based on the favorable response, a physician interpretation examination was developed. This examination is designed to target physicians in many medical specialties who practice vascular ultrasound. The Registered Physician in Vascular Interpretation (RPVI) examination was developed in 2005 by a six-member development task force representing all major medical specialties practicing vascular technology and one registered vascular technologist. A detailed survey of the tasks and expertise relevant to the practice of vascular interpretation was distributed to 6,000 physicians, and the results were used to develop the foundation of the RPVI examination. Prerequisite guidelines and examination format were also developed. By the end of 2006, 277 certificates had been issued; in 2010, the number had risen to 1,107. Examination prerequisites and applications are available on the ARDMS website.

## Accreditation

An important concern in the late 1980s was the lack of any standards or guidelines for establishing and running a vascular laboratory. For the neophyte, there were no benchmarks to be met regarding entry-level education and experience for physicians and technologists, what constituted a complete examination, extent of ongoing supervision, quality of equipment, reporting practices, or validation studies. The great escalation in vascular testing that came in the early 1980s was accompanied by a wide range of quality of the work being done. The problem with the accuracy of the diagnostic examinations came in part as the result of the common practice of a laboratory simply buying equipment and following protocols described in articles or recommended by manufacturers. Likewise, diagnostic criteria were accepted as published, presuming that the accuracies of tests in the newly established laboratory would be similar to those reported by the experts. Internal validation of the work of an individual laboratory was rarely obtained. It became clear that high accuracy of testing is dependent on both (1) technical considerations of protocols and procedures and (2) the knowledge and clinical experience of the technologist performing the examinations. In addition, there was a growing concern among the leaders in noninvasive testing about the calls from the medical insurance companies for regulation of all testing and for elimination of payment for vascular tests. Isolated cases of fraudulent operations were well publicized and caught the attention of many payers. Leaders in the field voiced the need for better self-policing but had no way to bring this about. There was also concern that some state or specialty organizations might take the initiative to create standards for vascular laboratories. Often when regulation comes from government or from a single specialty group, there is limited or unbalanced input from the other professionals to be regulated. In some cases, the regulation is skewed in favor of one or more special interest groups.

### Intersocietal Commission for the Accreditation of Vascular Laboratories

In 1989, an informal meeting of leaders in the field of noninvasive testing proposed the possibility of establishing a voluntary accreditation process. This initial group included vascular surgeons, radiologists, and vascular technologists. They concluded that there was no suitable existing accreditation option and that they needed to study the feasibility of creating an accrediting organization. Support and financial sponsorship were sought from a variety of professional societies whose members were involved in noninvasive vascular testing. The initial goals were (1) to have a broad base of support across different specialty lines and (2) to have an independent entity that was not specifically allied with any one specialty or society. From the very beginning, the emphasis was on an intersocietal approach. The American Academy of Neurology, American College of Radiology, American Institute of Ultrasound in Medicine, International Society for Cardiovascular Surgery (North American Chapter), Society

for Vascular Surgery, Society for Vascular Medicine and Biology, Society of Diagnostic Medical Sonographers, and Society of Vascular Technology committed to sponsor the initial efforts, and a work group was formed with two representatives from each society.

The initial meetings were dedicated to defining the scope of vascular laboratory accreditation and the minimum guidelines necessary for the assurance of quality. The overall objective was "To ensure high quality patient care by providing a mechanism that recognizes laboratories providing quality vascular diagnostic techniques through a process of voluntary Accreditation." This goal was to be achieved by establishing an accreditation process, issuing certificates of accreditation, and maintaining a registry of accredited laboratories. An important principle established early was that the accreditation should be as inclusive as possible, something that could be achieved by even the smallest laboratory that was doing quality work. Another important principle adopted was that accreditation would not require specific medical specialty training but would evaluate the particular education and experience of the doctors and the technologists in each laboratory. Standards for the overall laboratory organization addressed the qualifications of the medical and technical personnel, the layout of the laboratory, the support personnel, reports, record keeping, patient safety, and equipment maintenance. Additional standards were developed for specific testing areas (cerebrovascular, peripheral arterial, peripheral venous, and abdominal vascular). Attention was also given to indications, testing protocols, diagnostic criteria, and quality assurance. Not all components of the standards carried equal weight; some aspects were mandatory or required while others were recommended. It was decided that the accreditation would be limited to 3 years, requiring an application for renewal after that time. In March 1990, the group adopted the constitution and bylaws for the Intersocietal Commission for the Accreditation of Vascular Laboratories (ICAVL), and in November 1990, it was incorporated as a nonprofit corporation in Maryland. The members of the ad hoc work group became the original Board of Directors, and Brian Thiele, M.D., who had chaired the work group, was elected the first president. In January 1991, Sandra Katanick, RN, RVT, was selected as the executive director and charged with creating the administrative structure for the commission.

The accreditation process starts with submission of a detailed application form, which includes documentation of all aspects of the facility. (In the past year, the application has been converted to a web-based form to simplify data entry and to save information for future reaccreditation applications.) The sample cases and their reports are the most important part of the application, for the greatest weight in the evaluation process is on the quality of the testing itself. The final part of each testing section is the laboratory's documentation of validation or quality assurance (see Chap. 3). The Board of Directors reviews applications and decides on granting accreditation. Some applications have noted deficiencies, and in these cases the decision is delayed. Commonly a laboratory is accredited in some areas while having a postponed decision in others. Once the additional material is received completing the application or documenting the correction of a problem, the final review is made. If a laboratory is not considered to be in substantial compliance with the essentials and standards, a required conference call is made in a further attempt to obtain more complete information and to identify possible remedial action. The conference call involves ICAVL personnel and both the medical and technical directors of the laboratory. Only if remaining problems cannot be resolved by the conference call is a mandatory site visit required.

Accreditation is granted for 3 years. Reaccreditation requires an abbreviated application. New personnel complete an information and background section, but for prior staff only an updated listing of CME is required. As with the original accreditation, the most important aspect of the application is the quality of the studies performed. A new set of case studies is required along with copies of the current protocols and diagnostic criteria. The other critical part of the reaccreditation is the adequate documentation of correction of the deficiencies or weaknesses identified in the previous accreditation. The review process is the same as described above, except that special attention is given to evaluating improvement in problem areas.

From its inception, the commission operated on the principle that vascular testing is an advancing field and that the Essentials and Standards needed regular review and consideration for revision. The revisions to the standards give examples of the commission's response to changes in vascular testing. In 1994, the Venous Testing Standard was changed to make duplex scanning the only primary modality, so that laboratories performing only physiologic tests would no longer qualify for accreditation in venous testing. Later, additional testing areas were created for intracranial cerebrovascular and visceral vascular testing. A more recent policy change concerned the minimum volume required for a laboratory to apply for accreditation. The initial philosophy was that some minimum number was required to maintain competence and proficiency in the procedures. The requirement was set at 100 tests per year for each primary test. Ultimately, the Board of Directors went back to its primary philosophy: the most important factor in granting accreditation should be the quality of the work being done. In the experience of the members of the board, low volume laboratories often have trouble producing good quality studies; therefore, the solution adopted was to increase the level of scrutiny for these applications. In 1997, the policy was revised so that laboratories with less than 100 studies per year could apply but would be required to submit a higher number of sample cases, some randomly selected by the ICAVL.

Through the years, the ICAVL board has been concerned about the validity of the review process. Initially site visits were used only when serious concerns were identified in the application. For several years, consideration was given to instituting a process for random site visits to validate applications, the quality of which did not trigger additional scrutiny. In 1998, a policy was established for random site visits of some laboratories to be carried out in conjunction with either initial or repeat accreditation. The findings and recommendations of the site visit team are compared with the recommendations resulting from the regular review of the applications. To date, there have been few differences found in the two reviews. In 2010, a change in this validation process was made, primarily in response to requirements by the Centers for Medicare & Medicaid Services (CMS). At some point during the 3-year accreditation cycle, each laboratory is required to have either a random audit (submission of current facility information and samples of reports) or a random site visit. These processes are intended to substantiate ongoing compliance with the standards.

The commission was created as an independent, self-funded organization, so it was critical to generate sufficient interest in accreditation to be able to cover the entire cost of the operation. At first there were low numbers of applicants, but there has been a continuing steady growth in the number of accredited laboratories, currently totaling 1,687. It was encouraging that most laboratories chose to reapply for accreditation after the first 3 years. One of the leading goals set by ICAVL was to help improve the quality of testing through the education resulting from completing the application process. Probably the most important evidence of impact of accreditation is the fact that most laboratories applying for reaccreditation show improvement over what was found the first time around. Another indicator of success was the fact that ICAVL was used as the basis for the creation of similar accreditation organizations for echocardiography, nuclear medicine, magnetic resonance, computed tomography, and carotid stenting facilities.

## American College of Radiology

Even though the American College of Radiology (ACR) was one of the original sponsors of ICAVL, its leadership decided to create its own ultrasound accreditation. A major reason put forth for this change was the interest by radiologists in having a single accreditation for all the areas of diagnostic ultrasound. This move certainly came in response to the success of ICAVL. In 1997, the new accreditation was offered to radiology-based laboratories. The vascular component directly paralleled that of ICAVL, but the requirements were less stringent and the application therefore was easier to complete. A number of radiology laboratories have stopped renewing their ICAVL accreditation in favor of that offered by ACR. In 2010, 2,164 facilities have this vascular accreditation (compared to 2,329 sites for ICAVL).

## Accomplishments and Impact

Over the years since the introduction of certification and later accreditation, there has been growth in both these areas. The number of RVT certificates issued was low in the early years but has shown a subsequent increase. In general, laboratory directors have found that people who have obtained the RVT are better prepared and ultimately show better potential for improvement of skills. Many institution-based laboratories use the RVT as a lever to place the technologist at a higher pay level than the average hospital technicians. ICAVL has always recommended that all technical personnel be credentialed, and in year 2003, a mandate was introduced requiring that all technical directors hold an approved credential. Starting in 2017 all technologists will have to be credentialed. The growing appreciation of technologist credentialing was also reflected by the creation by CCI of a parallel process.

When ICAVL was incorporated in 1991, there were no standards or guidelines for the evaluation of noninvasive laboratories. One of the original expectations of the founding members of the Board of Directors was that the accreditation would gain recognition and come to be used as an index of quality of vascular testing. Once the commission succeeded in becoming established and surviving as an independent organization, there was growing interest in this type of accreditation. The standards stood the test of time and became the basis for similar efforts by other national groups. In 1996, the American Institute of Ultrasound in Medicine established an accreditation for the areas of general and obstetrical ultrasound and followed the next year by the creation of the ACR ultrasound accreditation. The ICAVL staff participated in the creation of standards for accreditation in other diagnostic areas.

In the early years of noninvasive testing, the insurance companies paying for the work had little to no interest in the quality of testing provided to patients. As one company officer stated, “We assume that anyone billing us for a test is providing a quality examination.” This attitude is changing, and in recent years different insurance programs, including Medicare, have developed an interest in the quality of work done in vascular laboratories. There has been a growing recognition of technologist certification and laboratory accreditation as predictors of higher quality. An important step occurred in March 1998 when the Medicare carrier for Virginia implemented a regulation requiring ICAVL accreditation as a prerequisite for reimbursement. Additional carriers have addressed the quality issue, requiring either

laboratory accreditation or that credentialed technologists perform (or supervise) all tests. (An updated list of Medicare requirements by state can be found in the reimbursement section of the ICAVL web page.) It is encouraging to see that groups outside of Medicare are beginning to look at similar mandates. The Coalition for Quality in Ultrasound (CQU), a group of professional organizations participating in diagnostic ultrasound studies, is conducting an active campaign to increase the mandates for certification and accreditation across the country. The ideal would be to achieve these regulations on a national basis. This will fulfill the goal of wide-reaching improvement in the quality of vascular testing and hopefully the elimination of poor operations, which have been the bane of the specialty throughout the years.

## Appendix

### Education

www.oit.edu/programs/klamath-falls/medical-imaging-technology/vascular-technology/overview (Oregon Institute of Technology)

www.CAAHEP.org (education info)
www.svunet.org

### Credentialing

www.ARDMS.org
www.CCI-online.org

### Accreditation

www.icavl.org
www.acr.org

# Physician Qualifications in the Clinical Diagnostic Vascular Laboratory

2

M. Ashraf Mansour

**Abstract**

The Diagnostic Vascular Laboratory plays a central role in vascular practice. In the evaluation of patients with vascular disease, the first step is a history and physical examination. The next step to investigate vascular disease is often a noninvasive vascular test performed in the Diagnostic Vascular Laboratory. Therefore, it is essential that testing be performed using the highest standards to ensure an accurate diagnosis. To achieve a high degree of accuracy and consistency, the vascular laboratory personnel, including technologists, supervisors, and interpreting physicians, have to be highly qualified. This chapter describes the necessary qualifications for physicians providing interpretation in accredited vascular laboratories.

**Keywords**

Vascular laboratory • Accreditation • Qualifications

## Introduction

The clinical vascular laboratory is an integral part of any busy vascular clinical practice. Vascular clinicians have come to rely on the Diagnostic Vascular Laboratory (DVL) as an extension to the physical examination and comprehensive evaluation of the patient with a vascular disorder. The origins of the DVL go back to the middle of the last century when the specialty of vascular surgery was still in its infancy. Vascular surgeons had to rely on diagnostic angiography to plan revascularization [1]. Noninvasive tests were initially rudimentary and employed only in research and physiology laboratories [2]. It was the pioneering work of Strandness and Sumner at the University of Washington in the 1960s elucidating vascular hemodynamics and the collaborative work with engineers that ultimately led to the development of more sophisticated instruments to detect and measure blood flow [1–3]. Subsequently, the development of ultrasound technology led to noninvasive imaging, now ubiquitous in offices and hospitals around the world. The portability of equipment and the relative ease of running the diagnostic machines have led to the proliferation of testing sites and commercial enterprises that perform vascular testing or screening for profit, and sometimes without regard for quality or accuracy. The purpose of this chapter is to describe the clinical qualifications of the physician interpreting noninvasive studies in the DVL.

M.A. Mansour, M.D., RVT, FACS
Academic Chair of Surgical Specialties Spectrum,
Health Medical Group, Michigan State University,
Grand Rapids, Michigan, USA

Department of Cardiovascular Surgery,
Michigan State University,
4100 Lake Drive SE, Suite 300,
Grand Rapids, MI 49546-8816, USA
e-mail: ashraf.mansour@spectrumhealth.org

## Vascular Laboratory Accreditation

Physicians rely on the vascular laboratory for the diagnosis, management, and long-term follow-up of patients with vascular disorders. Therefore, it is imperative that the quality of the studies performed, and indeed the proper interpretation of these studies, be accurate and reliable. The origin of the

A.F. AbuRahma, D.F. Bandyk (eds.), *Noninvasive Vascular Diagnosis*,
DOI 10.1007/978-1-4471-4005-4_2, 

Intersocietal Commission for the Accreditation of Vascular Laboratories (ICAVL) is traced back to 1990 when several professional societies recognized the need to standardize vascular testing and implement a process for verification [4, 5]. While other organizations have established different standards for accreditation of vascular labs, for example, the American College of Radiology (ACR), it is clear that ICAVL accreditation is more rigorous and sought after. Testing procedures, standards for interpretation, and qualifications of vascular technologists and physician readers and directors are outlined in careful detail on the ICAVL website www.ICAVL.org (ICAVL Standards) [4, 5]. After initial accreditation, each DVL has to go through a reaccreditation process in 3-year cycles. Random on-site visits by trained evaluators are done, and in some cases mandatory visits can be triggered to ensure that testing procedures and protocols are in fact being followed. The process of accreditation is fairly laborious and anxiety provoking for lab personnel but is viewed by most professionals who participate as fair (see Chap. 1). ICAVL is now Intersocietal Accreditation Commission (IAC).

Why should we care if the DVL is accredited and the physician doing the interpretation is qualified? Quite simply, if a patient is sent to the vascular lab and receives a false-positive test, this may expose the patient to additional unnecessary testing or procedures with potential complications. On the other hand, a patient receiving a false-negative test may have a false sense of security, delay in diagnosis, and potentially an adverse clinical event. Unfortunately, this happens too frequently in current clinical practice. A typical example is that of a patient with an asymptomatic cervical bruit referred for a carotid duplex scan. A false-positive scan may lead to another more invasive test, such as a CT or cerebral angiogram. It is less likely, but possible, that this patient could be subjected to an unnecessary carotid endarterectomy based on this erroneous initial test. On the other hand, if the test is a false negative, and the patient has a critical stenosis, watchful waiting may lead to cerebrovascular symptoms, even a stroke.

With the proliferation of vascular labs and mobile units, many payers have begun to require that testing facilities be accredited. According to the ICAVL website, the Centers for Medicare & Medicaid Services (CMS) requirements in most states stipulate that the lab and/or the technologist performing the test needs to be credentialed in order to receive reimbursement. Clearly, this is an important first step to ensure that vascular testing is done properly. The substandard testing in some unaccredited labs should be considered fraud and abuse and invariably leads to repeat testing in an accredited lab [6]. In response to the perceived overuse of diagnostic imaging, the US Congress mandated major payment cuts for all diagnostic modalities in the Deficit Reduction Act of 2006. Thus, reimbursement for many tests performed in the DVL was reduced by up to 40% [7].

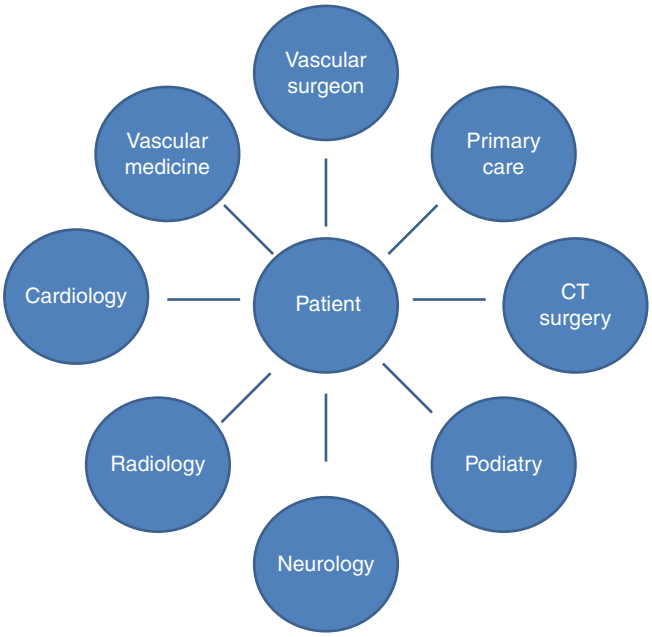


**Fig. 2.1** Medical and surgical specialties interacting with the vascular patient

## Educational Background

Patients with vascular disorders will frequently be touched by multiple specialists from varying backgrounds (Fig. 2.1). Postgraduate education in vascular surgery and vascular medicine are two well-defined pathways to achieve board certification in a vascular specialty. Successful completion of an accredited vascular surgery training program is a requisite to sit for the American Board of Surgery Vascular Certificate. Similarly, training in an accredited Vascular Medicine program will lead to eligibility to sit for the Vascular Medicine Certificate of the American Board of Internal Medicine. The structured curricula in the latter specialties build on the essential elements listed in Table 2.1 [8–10]. Other specialties, such as neurology and radiology, receive more focused instruction and training in their respective areas. Interventional radiologists have broad training in invasive procedures, including angiography and other diagnostic modalities. Therefore, physicians from various backgrounds and training (e.g., neurology, radiology, vascular medicine, vascular surgery) may become qualified to interpret carotid duplex scans or transcranial Dopplers based on their training and area of expertise.

## Physician Qualifications

The ICAVL explicitly states that a DVL is a "unit performing noninvasive vascular diagnostic testing under the overall direction of a medical director" [4]. The intent is to place the

**Table 2.1** Suggested curriculum for physicians interpreting in the vascular laboratory

| |
|---|
| Pathophysiology of vascular disease including arterial (atherosclerotic and nonatherosclerotic), venous, and lymphatic |
| Ultrasound physics, Doppler instruments, transducer technology |
| Basis of physiologic testing (ABI, PPG, APG) |
| Duplex imaging of arteries, veins, vascular conduits, and soft tissue |
| Ultrasound and duplex diagnosis of: |
| Aortic aneurysms and other aortoiliac disease |
| Imaging for aortic stent grafts |
| Renal and mesenteric arteries and veins |
| Renal and liver transplants |
| Portal venous system |
| Carotid arteries and structures in the neck |
| Lower extremity occlusive and aneurismal disease |
| Bypass grafts |
| Venous reflux testing |
| Arteriovenous access for dialysis |
| Statistical methods and understanding of false positive, negative, and accuracy |
| Advantages and limitations of vascular diagnostic modalities |

Adapted from Refs. [8, 10]
*ABI* ankle-brachial index, *PPG* photoplethysmography, *APG* air plethysmography

**Table 2.2** Common pathways leading to RPVI

| |
|---|
| Doctorate in Medicine |
| Valid license to practice medicine (MD or DO) |
| Previous RVT certification (ARDMS) |
| Satisfactory completion of ACGME-approved postgraduate training program |
| Documentation of supervised interpretation of 500 vascular studies in the following areas: |
| Carotid duplex |
| Transcranial Doppler |
| Peripheral arterial physiologic testing |
| Venous duplex ultrasound |
| Visceral duplex ultrasound |
| Satisfactory completion of CME in noninvasive diagnosis |

From: http://www.ardms.org/ Physicians' Vascular Interpretation (PVI) Examination *General App Book*

overall responsibility for a VDL in the hands of a qualified physician who can then ensure that the lab is complying with accepted standards. The medical director should be (1) legally qualified physician and (2) have achieved one or more of the following: (a) completion of a formal residency or fellowship (e.g., vascular surgery fellowship or residency, vascular medicine, radiology, or cardiology with dedicated vascular laboratory rotation during fellowship) that includes appropriate clinical and didactic vascular laboratory experience with a defined number of studies interpreted (this would be the ideal qualification for both a medical director or interpreting physician), (b)self-study training through formal accredited postgraduate education and supervised vascular laboratory experience (preferably in accredited vascular laboratory under formally trained medical director) with interpretation of a defined number of cases, and (c) previous work in a vascular laboratory (preferably in accredited vascular laboratory under formally trained medical director) with interpretation of a defined number of cases [4]. The latter criteria also apply to the interpreting physician.

The general qualifications of physicians interpreting in the DVL and eligible to sit for the RPVI examination are outlined in Table 2.2. Besides the basic requirement of a medical degree and formal training in the field, the following qualifications are essential [10]:

- License to practice medicine in the state
- Board certification
- Thorough understanding of instrumentation, limitations of tests
- Troubleshooting
- Knowledge of vascular disorders
- Knowledge of statistics (false positive, accuracy)
- Continuing Medical Education (CME)
- Knowledge of techs ability and limitations
- Objectivity (no bias or conflict of interest)

Much of the experience gained in formal training programs by attending regular clinics, conferences, and quality assurance meetings in the vascular lab leads to thorough understanding of the tests, their utility, and limitations. Discussions with vascular technologists and other physicians lead to a better understanding of a missed diagnosis, challenges with special anatomic variants, or specific patient conditions. Some diagnostic studies are typically more challenging, such as renal or mesenteric duplex, and it is always helpful to get the most experienced techs and readers to share their knowledge and expertise with colleagues. There is emphasis on a minimum number of tests reviewed to highlight the value of a broad experience.

It is unfortunate that in recent times, there has been a proliferation of weekend courses claiming to deliver sufficient information so that a minimally trained physician can become a certified reader after 20 hours of instruction.

## Credentialing

In the early days of the vascular lab, technologists came from various backgrounds of nursing or other allied health professions. Recently, ICAVL has instituted more rigorous education and training requirements for vascular technologists. The American Registry for Diagnostic Medical Sonography (ARDMS) administers the Registered Vascular Technologist (RVT) test which has two components, ultrasound physics and vascular technology. Individuals enrolled in approved programs in fact can sit for the RVT exam after completing

**Table 2.3** Major content areas on RPVI examination

| |
|---|
| 1. Instrumentation and ultrasound physics |
| 2. Extracranial cerebrovascular |
| 3. Intracranial cerebrovascular |
| 4. Peripheral venous |
| 5. Peripheral arterial |
| 6. Visceral vascular |
| 7. Special testing |
| 8. Quality assurance and ultrasound safety |

From: http://www.ardms.org/ Physicians' Vascular Interpretation (PVI) Examination

their course work. This would enable the graduate to seek employment in an accredited vascular lab immediately upon graduation. The ICAVL has very specific requirements for supervision and oversight in the vascular lab, both by a lead technologist and physician director. This oversight is important to ensure quality studies, procedures, and reporting.

The physician in the DVL needs to be knowledgeable and competent in three main areas: performance of tests, interpretation and reporting, and quality assurance. While the physician does not necessarily have to perform the test, it is important to have a physical presence for supervision and guidance of the technologists [11]. The preliminary and final reports issued by the DVL need to conform to standards and provide accurate and useful information to referring physicians. Finally, maintaining quality and excellence in the DVL, through constant review, training, and completion of CME by attending conferences and courses, keeps the lab personnel and physicians up to date and knowledgeable in this area.

The vascular surgical and medical societies have developed guidelines for hospital privileging [12]. Furthermore, thought leaders from multiple disciplines have published a consensus statement outlining specific recommendations for physicians in the DVL. These recommendations encompass core knowledge, cognitive skills, and training requirements [8, 9]. Clearly, a consensus has emerged that physicians who are in a position to interpret noninvasive vascular studies need to demonstrate that they have mastered certain competencies. The RPVI test, which was developed in 2006, was designed to test such knowledge and competency [5] (Table 2.3). Recently, the American Board of Surgery declared that vascular surgeons seeking certification after fellowship and recertification in vascular surgery after 2014 will need to have the RPVI. It should be noted, however, that having passed the RPVI exam without the proper training as described previously should be discouraged.

Although most DVLs were started and directed by vascular surgeons, the last two decades have seen a gradual shift to other specialties, particularly cardiology, running labs. Data from ICAVL show that in 1993, 76% of DVL directors were vascular surgeons compared to 51% in 2011 (see Fig. 2.2).

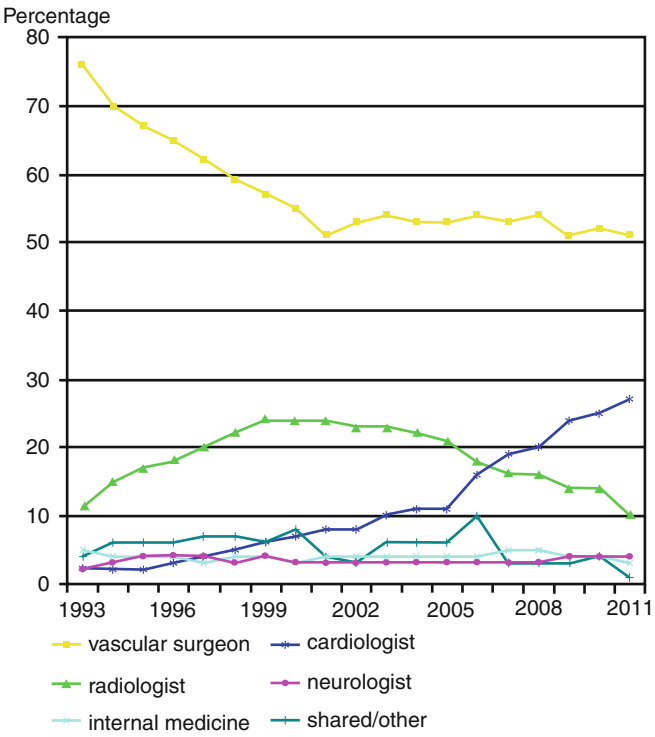


**Fig. 2.2** Medical specialty of the medical director in accredited vascular laboratories (Courtesy of S. Katanick, ICAVL Executive Director, 2011)

While the proportion of DVL directed by radiologists has declined since ICAVL started keeping track, the last decade has seen a significant rise in the number of labs directed by cardiologists. The specialty of physician directors in the DVL is probably irrelevant, as long as good leadership and maintenance of high standards are enforced.

## References

1. Strandness DE. Historical aspects. In: Strandness DE, editor. Duplex scanning in vascular disorders. New York: Raven Press; 1993. p. 1–26.
2. Winsor T. Simplified determination of arterial insufficiency: plethysmographic observation of reactive hyperemia following fifteen minute arterial occlusion at the ankle. Circulation. 1951;3:830–6.
3. Strandness DE, Sumner DS. Measurement of blood flow. In: Strandness DE, Sumner DS, editors. Hemodynamics for surgeons. New York, San Francisco, London: Grune & Stratton; 1975. p. 31–46.
4. Akbari CM, Stone L. Accreditation and credentialing in the vascular laboratory. Semin Vasc Surg. 2002;15:178–81.
5. Zierler RE. Credentialing and accreditation. In: Zierler RE, editor. Duplex scanning in vascular disorders. 4th ed. Philadelphia: Wolters Kluwer; 2010. p. 31–7.
6. Brown OW, Bendick PJ, Bove PG, Long GW, Cornelius P, Zelenock GB, Shanley CJ. Reliability of extracranial carotid artery duplex ultrasound: value of vascular laboratory accreditation. J Vasc Surg. 2004;39:366–71.
7. Mansour MA, Zwolak RM. Office-based vascular lab: is it worth the effort? Perspect Vasc Surg Endovasc Ther. 2009;21:5–8.

8. Creager MA, Goldstone J, Hirshfeld JH, Kazmers A, Kent KC, et al. ACC/ACP/SCAI/SVMB/SVS clinical competence statement on vascular medicine and catheter-based peripheral vascular interventions. JACC. 2004;44:941–57.
9. Creager MA, Cooke JP, Olin JW, White CJ. Task force 11: training in vascular medicine and peripheral vascular catheter-based interventions. JACC. 2008;51:398–404.
10. Ricci MA, Rutherford RB. Qualifications of the physician in the vascular diagnostic laboratory. In: Abu Rahma AF, Bergan JJ, editors. Noninvasive diagnosis. London: Springer; 2007. p. 7–10.
11. Rutherford RB. Qualification of the physician in charge of the vascular diagnostic laboratory. J Vasc Surg. 1988;8:732–5.
12. Calligaro KD, Toursarkissian B, Clagett GP, Towne J, Hodgson K, Moneta G, et al. Guidelines for hospital privileges in vascular and endovascular surgery: recommendations of the Society for Vascular Surgery. J Vasc Surg. 2008;47:1–5.

# Quality Assurance of the Vascular Laboratory

3

Cindy Weiland and Marge Hutchisson

**Abstract**

Documenting the quality of care provided in the vascular laboratory has always been of the utmost importance. However, identifying the weaknesses and strengths associated with the laboratory services has taken an elevated significance in the current health-care environment. Assuring that the expectations of health-care providers, patients, insurers, and other stakeholders are met requires that all aspects of the laboratory are consistently evaluated. Maintaining records that demonstrate efforts to improve laboratory performance, accuracy, and patient management is essential. Developing or enhancing the quality assurance program can be accomplished through good planning, appropriate data collection, and consistent follow-up. The quality initiatives and statistics do not need to be complicated in order to gain valuable information that can positively impact the overall laboratory functions and patient outcomes. Taking the time to document quality measures is critical in assuring the continued success and value of services provided through noninvasive vascular testing.

**Keywords**

QA • Correlation • Validation

## Introduction

The words health care and quality have become increasingly integrated over the past decade. In times of economic difficulty within the vascular laboratory, staff is expected to accomplish more with less, yet demonstrate the utmost dedication to serving its patient population in an efficient manner with exemplary results. The constant improvement and innovations available in medical technology coupled with the increased education and credentialing of sonographers aid in achieving these lofty goals. However, without documenting ongoing quality initiatives, it may be impossible to convince government regulators, insurance payers, accrediting bodies, patients, and other key stakeholders that the services provided in a vascular laboratory are accurate, cost-effective, and more invaluable than ever. Maintaining a quality improvement plan is no longer an option in striving for superior patient care but necessary to ensure the overall success and viability of the vascular laboratory.

## What Is Quality Improvement?

Quality assurance (QA) is defined as "a program for the systematic monitoring and evaluation of the various aspects of a project, service, or facility to ensure that standards of quality are being met" [1]. Quality control (QC), quality assurance (QA), and continuous quality improvement (CQI) are all necessary components of a plan that will be effective in

C. Weiland, RVT
Department of Quality Assurance,
Intersocietal Accreditation Commission,
Ellicott City, MD, USA

M. Hutchisson, RVT, RDCS (✉)
Intersocietal Accreditation Commission - Vascular Testing,
6021 University Blvd, Suite 500,
Ellicott City, MD 21043, USA
e-mail: hutchisson@intersocietal.org

A.F. AbuRahma, D.F. Bandyk (eds.), *Noninvasive Vascular Diagnosis*,
DOI 10.1007/978-1-4471-4005-4_3, © Springer-Verlag London 2013

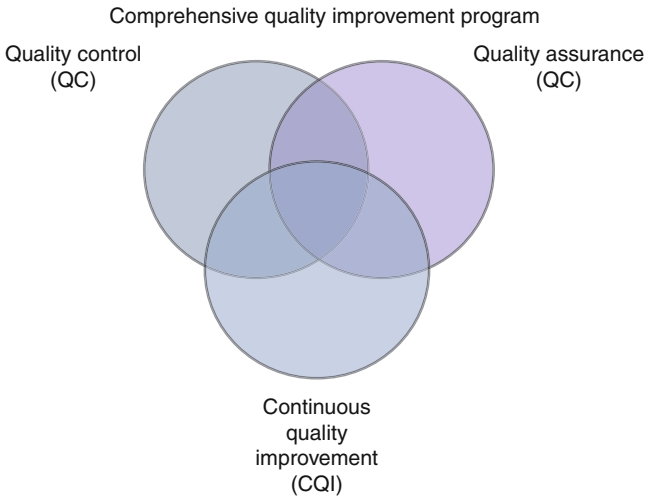


**Fig. 3.1** The three components of a continuous quality improvement program

ensuring safety, enhancement of services, and the advancement of patient management (Fig. 3.1) [2]. Prior to developing or updating the laboratory's quality improvement program, it is important to understand each component:

*Quality assurance* (*QA*) – documents outcomes and accuracy as well as assessing adherence to policies, procedures, and other standards. Examples of QA include comparison of noninvasive examination findings to other diagnostic tests or procedures and peer review.

*Quality control* (*QC*) – the calibration and maintenance of equipment. This is generally achieved through following manufacturer recommendations for routine maintenance, electrical checks, and software updates. Any QC must be documented and accessible in the event equipment performance is called into question.

*Continuous quality improvement* (*CQI*) – the process of becoming a more successful laboratory overall by building upon traditional quality assurance methods and emphasizing the organization and systems.

## How Is a Quality Improvement Program Developed?

Developing the laboratory's quality improvement (QI) plan is probably the easiest part of a successful program. Following a few simple steps prior to implementation will help to avoid possible loopholes and frustrations in the future (Fig. 3.2).

### Allocate Responsibility

When developing and implementing a quality improvement program, it is very important to identify key staff to share in the responsibility of supervising and maintaining it. To ensure the success of the program, all levels of management must truly support the initiative and be willing to provide ample time and resources to carry out the duties associated with sustaining an ongoing plan. Integrating the QI responsibility as part of one or more staff members' written job descriptions helps to clearly define the role of the individual and provides a level of accountability. Depending upon its size and the volume of testing performed in the laboratory, it may be very helpful to establish a QI/QA committee to assist in developing the policies and procedures associated with implementation and continued monitoring of the program. Having multiple people involved in the program helps to provide continuity in the event a staff member holding a key role leaves the establishment.

### Identify Quality Initiatives

When thinking of QA from a laboratory's perspective, it is often limited to the correlation of noninvasive examination results to other diagnostic tests or procedures. Test validation and quality control must be included in the quality improvement program; however, there are additional ways to assess the overall functioning and reliability of the laboratory. Evaluating other areas within the laboratory such as patient satisfaction, appropriateness of testing, safety, report content, report turnaround time, and adherence to testing protocols further strengthens the quality program. The options that may be monitored in the laboratory are endless and integral in enhancing overall laboratory quality.

### Set Thresholds

After determining what quality initiatives will be monitored, the laboratory must establish thresholds that will be met for each item. A threshold is essentially an agreed upon percentage of time that positive or negative outcomes are acceptable. For instance, how often is it satisfactory that examination results do not correlate with another diagnostic procedure or patient outcome? Generally the thought is that it is never acceptable; however, there are very few diagnostic tests in medicine that are correct 100% of the time. Thresholds should be achievable, yet not diluted to the point that they are of no value in identifying problems and inconsistencies. When setting thresholds, it is important to take into consideration current industry standards and expectations. Because of the potential differences between laboratories, it is difficult to set firm universal thresholds, and, consequently, there are no standardized thresholds at this time. Meeting positive thresholds of 80% or greater is generally accepted and may be modified after data has been collected over a period of time. Thresholds are set as a baseline for improvement and

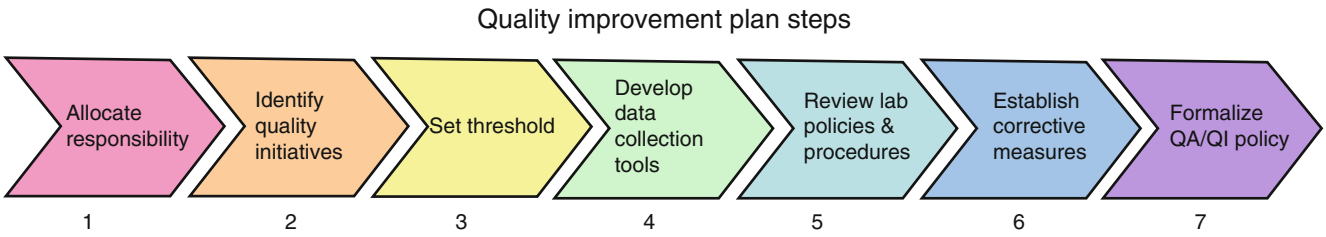


**Fig. 3.2** Seven steps involved developing a quality improvement plan

| | | | Vascular ultrasound results | | | | | | Angiography results | | | | | |
|---|---|---|---|---|---|---|---|---|---|---|---|---|---|---|
| | | | Level1 | Level2 | Level3 | Level4 | Level5 | Level6 | Level1 | Level2 | Level3 | Level4 | Level5 | Level6 |
| | Pt ID | Scan date | Normal | 1–15% | 16–49% | 50–79% | 80–99% | Occluded | Normal | 1–15% | 16–49% | 50–79% | 80–99% | Occluded |
| 1 | MB | 4/10/11 | | | X | | | | | | | X | | |
| 2 | PT | 4/10/11 | | | X | | | | | | X | | | |
| 3 | JC | 4/10/11 | | | | X | | | | | | X | | |
| 4 | MH | 4/13/11 | | X | | | | | | X | | | | |
| 5 | JM | 4/13/11 | | | | | X | | | | | X | | |
| 6 | TM | 4/13/11 | | X | | | | | | | | | X | |
| 7 | CW | 4/13/11 | X | | | | | | X | | | | | |
| 8 | CS | 4/16/11 | X | | | | | | X | | | | | |
| 9 | RM | 4/16/11 | | | X | | | | | X | | | | |
| 10 | KA | 4/16/11 | | | | | X | | | | X | | | |
| 11 | BG | 4/16/11 | | | | | X | | | | | | X | |
| 12 | MM | 4/21/11 | | | | | | X | | | | | | X |
| 13 | MF | 4/21/11 | | X | | | | | | X | | | | |
| 14 | TR | 4/22/11 | | X | | | | | X | | | | | |
| 15 | JI | 4/22/11 | | X | | | | | | | X | | | |
| 16 | SD | 4/22/11 | | | | | | | | | | | | X |
| 17 | LA | 4/22/11 | | | | | X | | | | | | | X |
| 18 | MH | 4/23/11 | | | X | | | | | | X | | | |
| 19 | SK | 4/23/11 | | | | | X | | | | | | X | |
| 20 | PC | 4/23/11 | | | | | | | | | | | | X |
| 21 | | | | | | | | | | | | | | |
| 22 | | | | | | | | | | | | | | |
| 23 | | | | | | | | | | | | | | |
| 24 | | | | | | | | | | | | | | |
| 25 | | | | | | | | | | | | | | |
| 26 | | | | | | | | | | | | | | |
| 27 | | | | | | | | | | | | | | |
| 28 | | | | | | | | | | | | | | |
| 29 | | | | | | | | | | | | | | |
| 30 | | | | | | | | | | | | | | |

**Fig. 3.3** Sample correlation data collection worksheet

should be assessed and adjusted. When success rates fall below a minimum or continually exceed expectations, a departmental review should be performed to determine the causes and implement changes to procedures or adjustment to the thresholds if necessary [3].

## Develop Data Collection Tools

Once you have identified who will gather the data, what will be collected, and set desired outcomes, the next step is to identify data collection methods. Establishing guidelines for how often information is collected, in what format it will be recorded, and how often it is shared with staff members must be established. There are many ways in which the data can be documented; however, the more complicated the process is, the less likely it is to occur (Fig. 3.3). Identifying very specific information and having simple streamlined forms in which to enter the data lead to a more successful quality improvement program.

Documenting patient examination findings that may be used in obtaining correlation to other tests or procedures may be accomplished through something as simple as a notebook. The notebook can be kept in the testing rooms to catalog patients with positive results that may lead to medical follow-up, another correlative procedure, or potential surgical candidates. As well, there are many software programs that have been developed to assist in tracking QA information. Prior to purchasing additional data collection tools, be diligent in assuring that they meet the needs of your laboratory.

**Table 3.1** Partial example of a checklist that can be used in review of the laboratory's procedures and protocols

| Procedure and protocol review checklist | | | |
|---|---|---|---|
| Protocol/procedure title: carotid duplex | | | |
| Date reviewed: April 17, 2011 | | | |
| Reviewer: C. Weiland | | | |
| Components of protocol | Present | Absent | Current |
| Equipment used | | | |
| Patient positioning | | | |
| B-mode image documentation: | | | |
| RCCA | | | |
| R bulb | | | |
| RICA proximal to mid | | | |
| LCCA | | | |
| L bulb | | | |
| LICA proximal to mid | | | |
| Other abnormal findings | | | |

## Review Laboratory Policies and Procedures

For the purposes of monitoring examination accuracy and safety, all laboratory policies and procedures should be reviewed annually to assure that they are up to date and include all components necessary for complete documentation and accurate interpretation. Using a checklist in the review of procedures will help to assure all necessary steps are included (Table 3.1). The procedures should be easily accessible to all staff, and steps must be made to guarantee that everyone follows the current procedures.

Regardless of the number of sonographers in the laboratory, technical protocols should at a minimum include the following components:

- Equipment used
- Patient preparation and positioning
- Examination techniques
- Minimum image/Doppler acquisition
- Additional documentation of abnormal and/or incidental findings
- Appropriate annotation

In that examinations are performed consistently in accordance with the written protocols, it is as imperative to have standardized diagnostic criteria used in the interpretation of each type of testing performed in the laboratory. Criteria must be applied in the same consistent manner by all interpreting physicians. Most laboratories choose to utilize criteria that have been previously validated and published. If the published criteria are modified to better suit the laboratory processes, equipment, or outcomes, it is important that these amended criteria be internally validated to assure its accurateness.

Routine monitoring of these two vital components of the laboratory processes will help ensure a systematic approach to services rendered by the laboratory and generally result in improved standardization, consistent results, and appropriate patient management.

## Establish How Negative Findings Will Be Addressed

If upon analysis of the information collected, weaknesses exist or established thresholds are not being met, there must be a routine method in which problems are addressed. It may be found that deficiencies exist due to procedures or individuals. Regardless of the cause of the inconsistencies or inaccuracies establishing a consistent process of acknowledging problems, establishing a plan for improvement and time frame in which reevaluation will occur is essential.

Later in this chapter we will discuss how using corrective action plans is one method that is useful in identifying and establishing follow-up for virtually any undesirable outcome identified through the QI program.

## Formalize the QA/QI Policy

After the previous steps have been completed, a policy and procedure must be written and communicated to all staff members. The policy should include all of the decisions made in steps 1 through 6 so that everyone involved with the laboratory understands the expectations and importance of the quality program.

# What Should the Laboratory Assess and How?

In addition to examination validation, included below are areas the laboratory could monitor and how that particular data can be documented and evaluated. Keep in mind the goal is to gain useful information that assists in identifying the strengths and weaknesses within the laboratory as a whole and is useful in making suggestions as to how goals will be achieved.

## Patient Satisfaction

It is easy to get caught up in the busy and sometimes impersonal environment that today's health care breeds. Institutions that have recognized that this pace is negatively impacting the patient's experience have taken steps to focus on the person. With the many choices patients and primary care providers have when deciding where to receive their diagnostic imaging, assuring a positive patient experience has become paramount in the continued success of the laboratory regardless

**Fig. 3.4** Sample patient satisfaction survey

**Medical Imaging Specialists**
Patient satisfaction survey

We would like to know how you feel about the services we provide so we can make sure we are meeting your needs. Your responses will help us to improve the quality of care we provide. All reponses will be kept confidential and anonymous. Thank you for your time.

| Please circle how well you think we are doing in the following areas: | Great 5 | Good 4 | OK 3 | Fair 2 | Poor 1 |
|---|---|---|---|---|---|
| **Facility and convenience:** | | | | | |
| Hours of operation | 5 | 4 | 3 | 2 | 1 |
| Convenience of the facility location | 5 | 4 | 3 | 2 | 1 |
| Cleanlines of the facility | 5 | 4 | 3 | 2 | 1 |
| Waiting time in the reception area | 5 | 4 | 3 | 2 | 1 |
| Comfort while waiting | 5 | 4 | 3 | 2 | 1 |
| **Staff:** | | | | | |
| Explanation of the procedure | 5 | 4 | 3 | 2 | 1 |
| Questions answered | 5 | 4 | 3 | 2 | 1 |
| Friendly and helpful to you | 5 | 4 | 3 | 2 | 1 |
| Knowledgeable and professional | 5 | 4 | 3 | 2 | 1 |
| Modesty respected | 5 | 4 | 3 | 2 | 1 |
| Confidentiality respected (HIPPA) | 5 | 4 | 3 | 2 | 1 |
| **Overall satisfaction:** | | | | | |
| Overall impression of visit | 5 | 4 | 3 | 2 | 1 |
| Willingness to return | 5 | 4 | 3 | 2 | 1 |
| Likelihood of referring to others | 5 | 4 | 3 | 2 | 1 |

What did you like best about our facility?

What did you like least about our facility?

Suggestion for improvement?

**Some information about you:**

Gender:
Male _____
Female _____

Age:
Under18 _____
18-30 _____
31-40 _____
41-50 _____
51-60 _____
61-70 _____
Over 70 _____

Are you:
First time patient _____
Returning patient _____

of its setting. Utilizing simple patient satisfaction surveys will provide valuable information in a simple format (Fig. 3.4). The survey may be provided either at the time of departure, via mail or email after the appointment. By simply documenting, the percentage of patients who measured any part of their experience less than the desired outcome is easily tracked in a spreadsheet and identified problem areas addressed through staff education.

## Appropriate Use and Indications

Though it has always been critical to quality care and treatment plans that the appropriate examination be performed, there has been an acute peak in the necessity to assure that the proper procedure be performed for the correct indication or patient symptom. Though at this time the published literature regarding appropriateness criteria in noninvasive vascular testing is somewhat limited, it has become prevalent in other imaging modalities such as echocardiography and nuclear medicine. Basically, "appropriateness criteria" define "when to do" and "how often to do" a given procedure in the context of scientific evidence, the health-care environment, the patient's profile, and a physician's judgment [4]. In addition to good patient care, reimbursement of services often hinges on performing the most suitable test. According to requirements set forth by the Centers for Medicare and Medicaid Services (CMS), "Noninvasive vascular studies are medically necessary only if the outcome will potentially impact the clinical management of the patient. Services are

deemed medically necessary when all of the following conditions are met:

1. Signs/symptoms of ischemia or altered blood flow are present;
2. The information is necessary for appropriate medical and/or surgical management;
3. The test is not redundant of other diagnostic procedures that must be performed. Although, in some circumstances, non-invasive vascular tests are complimentary, such as MRA and duplex, where the latter may confirm an indeterminate finding or demonstrate the physiologic significance of an anatomic stenosis (especially in the carotids and lower extremity arterial system).

In general, noninvasive studies of the arterial system are utilized when invasive correction is contemplated and to follow medical treatment regimens" [5].

Assessing the appropriateness of the examinations performed in the laboratory can be achieved by auditing the indications included on the physician's order, comparing those indications to the patient symptoms, and identifying if all information was correct and suitable. If trends identify inappropriate testing, lack of reimbursement, or negative patient outcome, efforts should be made to notify and educate referring physicians and staff members. Providing the laboratory staff with mechanisms to correct inappropriate orders prior to completing an examination is imperative in assuring the best outcome for the patient.

## Examination Quality and Completeness (Peer Review)

Another means that may be used in assessing the quality and completeness of examinations and interpretations can be accomplished through audit processes or peer reviews. Utilizing these tools helps to provide regular feedback to laboratory staff that assists in improving or maintaining the consistency in the laboratory. Audits and peer reviews must occur for all medical and technical staff members. A defined number of random cases are selected for each staff member at specific time intervals included in the laboratory policy (i.e., monthly, quarterly). Whenever possible, the reviews should remain anonymous. The technical and interpretive reviews will be evaluated for adherence to procedures, overall quality and accuracy. A scoring system should be defined where discrepancies may be minor or major. Any discrepancy trends should be tracked and areas of noncompliance forwarded to the appropriate personnel and when appropriate discussed at the laboratory QA meeting.

In assessing physician interpretation and report content, a review of the reported findings and comparison to the final report by another member of the medical staff may provide insight into the overall consistency of interpretations performed by multiple staff members identifying interobserver and intraobserver variability. Interobserver variability is the degree to which two independent observers are in agreement. Intraobserver variability is how often the same reader makes a differing conclusion. Both inter- and intraobserver variability becomes very important in the follow-up of patients. If the patient were to have the same examination repeated, would the results be the same regardless of what physician is reading the study?

Inconsistencies between the test findings and the final report should be documented. The questions that should be included in the report review/audit include:

1. Did the report include the appropriate header information, description of the test performed, examination findings, and a final impression?
2. Were the diagnostic criteria adhered to?
3. If available, were previous examination results included?
4. When applicable, were incidental findings documented?
5. Was appropriate follow-up included?
6. Was the report available within a timely manner as established by the laboratory policy?

The technical peer review may be completed by the technical director or other qualified designated staff and should focus on whether the documentation follows the laboratory protocol and the quality of the documentation. A complete technical review should address the following questions:

1. Are the image and Doppler waveform documentation complete according to the written protocol?
2. Were the appropriate techniques applied to assure optimum image visualization?
3. Was the Doppler angle correction appropriately aligned?
4. Were Doppler angles 60° or less?
5. When abnormalities were encountered, was additional documentation of those areas provided?
6. If technical limitations were encountered, were they conveyed in the notes to the interpreting physician?

## Correlation and Validation

Whenever possible, examinations performed in the laboratory should be correlated to other imaging modalities such as digital subtraction angiography (DSA), magnetic resonance angiography (MRA), and computed tomography angiography (CTA). However, with the improved technology of duplex ultrasound equipment and increased confidence in the ultrasound findings, patients are often treated and managed based upon the noninvasive examination results thereby eliminating the need for other tests. This increased assurance in ultrasound findings does not negate the need to monitor the accuracy of the noninvasive examination findings in the absence of imaging modalities. Conversely, it becomes imperative to regularly assess the quality of the vascular laboratory examinations through other measures.

$$\text{PPV} = \frac{\text{Number of true positives}}{\text{Number of true positives+Number of false positives}}$$

**Fig. 3.5** Calculating positive predictive value

$$\text{NPV} = \frac{\text{Number of true positives}}{\text{Number of true negatives+Number of false positives}}$$

**Fig. 3.6** Calculating negative predictive value

$$\text{Accuracy} = \frac{\text{Number of true positives+True negatives}}{\text{Number of True Positives + False Positives + False Negatives + True Negatives}}$$

**Fig. 3.7** Calculating overall accuracy

One method of correlating the noninvasive findings is to compare them with interventional procedure findings and outcomes. This can be achieved by reviewing the procedure/surgical report and identifying whether the *severity* of a lesion was found to be consistent with the noninvasive test findings. As well, the *location* of the lesion or abnormality may be confirmed.

As discussed previously, documenting interobserver variability is quite valuable not only in the reporting of the examination but in the test documentation itself. This variability can be assessed by performing a blinded repeat of the examination by a second sonographer. To avoid the possibility of a change in disease state, the repeat examination should be performed at the same setting. The second sonographer should not be provided with any results from the first examination. Documentation from both examinations is then evaluated for adherence to protocol and consistency of results.

When it is not possible to obtain a second test or the patient does not undergo other interventional procedures, clinical correlation may provide some additional information. Clinical correlation refers to reviewing the treatment plan prescribed for the patient based on the noninvasive test results and if at the time of follow-up, whether the symptoms leading to the initial evaluation have diminished or resolved.

If gold standard correlation data is limited, using some type of alternate correlation is the next best way to establish the accuracy and consistency within the laboratory. Documenting these additional measures helps ensure that the laboratory is taking all necessary and available steps to guarantee best practices and quality care.

## Analyzing Correlative Data

Most vascular laboratories do not have access to statisticians. In general, the laboratory staff tasked with the QA data collection are more focused on the health and technology aspects of their profession and may find data analysis a bit intimidating. However, for the purposes of improving patient care and laboratory functions, the methods used to obtain the necessary information to calculate overall examination accuracy are relatively simple. There are a few key terms that should be understood when measuring the accuracy of examinations:

- Sensitivity (true positive) – the probability a test will be positive when disease is present
- Specificity (true negative) – the probability a test will be negative when disease is absent
- Positive predictive value (PPV) – the proportion of patients with positive test results who are correctly diagnosed (Fig. 3.5)
- Negative predictive value (NPV) – the proportion of patients with negative test results who are correctly diagnosed (Fig. 3.6)
- Accuracy – the number of correct findings regardless of whether disease is present or absent (Fig. 3.7)

All of the above values are expressed in percentages and play an integral part in determining the source of a low overall accuracy.

Calculating the overall accuracy can be accomplished by utilizing a simple matrix. The matrix also helps to easily identify outliers and upon completion quickly depicts the number of exams that have undercalled or overcalled disease (Table 3.2).

The matrix includes both vertical columns known as the *Y*-axis and horizontal rows known as the *X*-axis. Categories used for reporting disease from the noninvasive vascular test findings are used for both the X- and *Y*-axes. “The category reported for the noninvasive findings is located on the vertical column at the far left of the matrix (*Y*-axis), and the correlative examination categories are located across the top (*X*-axis). Using the duplex findings, locate the appropriate category on *Y*-axis and place the mark under the category located in the *X*-axis representing the correlative procedure

findings (Table 3.3). Keep in mind that the correlative findings may not utilize identical criteria when interpreting the examination, so these should be placed in the category within which the percent stenosis falls. When the two findings correlate, they will fall on the diagonal axis within the grid, while outliers will be found on either side of the diagonal axis. Those located to the left of the diagonal axis are those in which the ultrasound findings overestimated the amount of disease in comparison to the correlative results. In turn, the outliers falling to the right of the diagonal axis represent vessels where the ultrasound findings underestimated the amount of disease present when compared to the correlative examination (Table 3.2)" [6].

**Table 3.2** Matrix example identifying where positive correlation and noncorrelating findings will be located

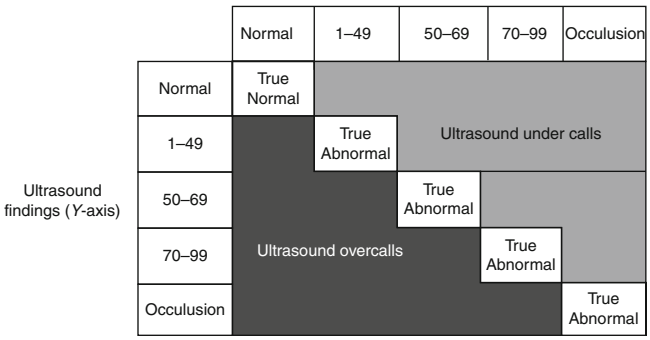


Adapted from Zierler [6]. With permission from Lippincott Williams & Wilkins

In cases when the information obtained from an examination is not quantifiable but identifies only the absence or presence of disease, a modified matrix may be used. Use of this simplified format will identify the true-negative, false-negative, true-positive, and false-positive examinations. This information can be used to further measure the specificity, sensitivity, and overall accuracy of these examinations (Table 3.4).

## What Happens Once the Data Is Collected?

A quality improvement plan with no follow-through is of no use at all. Once data is documented and analyzed, there is no value in it unless it is shared and used to evaluate the laboratory procedures and individual performance. Making time to hold regularly scheduled meetings to discuss the QA findings is imperative to the success of the program. Whenever possible, the meetings should include all medical, technical, and ancillary staff members and should occur at least quarterly to ensure effective follow-up.

A method of documenting identified weaknesses and errors can be achieved through corrective action plans. An effective corrective action plan will fit onto a single page. The longer and more complicated the form, the less receptive staff will be to using it [7]. The following components should be included in the corrective action plan:

- Description/summary of noncompliance (*What is the problem*?)
- Root cause analysis (*What caused the problem*?)
- Date corrective measures begin

**Table 3.3** Example of matrix entry placement

Angiography findings

| Carotid duplex findings | Normal | 1–49% | 50–69% | 70–99% | Occlusion |
|---|---|---|---|---|---|
| Normal | | RICA | | | |
| 1–49% | | | | | |
| 50–69% | | | LICA | | |
| 70–99% | | | | | |
| Occlusion | | | | | |

Adapted from Zierler [6]. With permission from Lippincott Williams & Wilkins
Carotid duplex findings: RICA = Normal + Angiography findings: RICA = 25% stenosis (does not correlate)
Carotid duplex findings: LICA = 50–69% + Angiography findings: LICA = 60% stenosis (correlates)

**Table 3.4** Example of modified matrix for use when quantifiable correlative information is not available

| | | Correlative standard | |
|---|---|---|---|
| | | No DVT | DVT |
| Ultrasound findings | No DVT | True negative | False negative |
| | DVT | False positive | True positive |

Adapted from Zierler [6]. With permission from Lippincott Williams & Wilkins

- Personnel responsible
- Corrective measures (*How are you going to correct the problem*?)
- Documentation of activity
- Assessment (*How will you prevent the same problem from happening again*?)
- Evidence of improvement (*How improvement will be tracked and what are acceptable thresholds*?)

## Example Corrective Action Plan

*Summary of noncompliance*: Forty percent of the venous duplex examinations for the quarter were performed for inappropriate indications.

*Root cause*: All examinations are performed for referring physicians regardless of the indication.

*Corrective measures/assessment*: Inappropriately ordered venous duplex examinations will be identified through preliminary assessment of patient symptoms upon arrival to the exam room. If it is established the test is not indicated, the laboratory medical staff will contact the referring physician to establish the appropriate procedure or course of treatment for the patient. In addition, a letter will be written to referring physicians establishing appropriate indications for examinations.

*Responsible staff*: All technical staff performing venous duplex examinations and all medical staff will be involved in corrective measures.

*Corrective measures begin*: April 25, 2011, and tracked daily as applicable.

*Documentation of activity*: Copies of the following documentation are to be kept in the Venous Duplex Corrective Action folder: examination order, symptom assessment worksheet, laboratory medical staff follow-up results, and notification to referring physician.

*Evidence of improvement*: Reassessment of the venous duplex volume and appropriateness will be performed in 6 months with the expected outcome of decreasing the inappropriately performed examinations to at least 20%.

## Further Demonstrating Your Laboratory's Commitment to Quality

For over 20 years, the Intersocietal Accreditation Commission – Vascular Testing (ICAVL) has provided a mechanism for laboratories to evaluate and demonstrate the level of patient care they provide. Laboratories applying for accreditation through the IAC are required to maintain an ongoing quality assurance program and must provide documentation substantiating adherence to the standards. The current IAC standards require at a minimum formal QA meetings twice each year, a specific number of examination correlations to other imaging modalities and/or surgical procedures with a documented overall accuracy of 70% or greater for each area of testing.

Implementing your laboratory's quality program prior to applying for accreditation will help to ensure successful achievement of accreditation.

### Conclusion

The primary objective of a QA program in the laboratory setting is the enhancement of patient care with the main emphasis of the program on the human factors that can lead to variations in quality care. Acknowledging the potential weaknesses in the laboratory must be seen as a strength that will provide an opportunity to grow and survive and ensure a continued place for the vascular laboratory in an ever-changing health-care environment.

## References

1. Merriam-Webster's Online Dictionary. http://www.merriam-webster.com/dictionary/qualityassurance. Accessed 22 June 2011.
2. Christian PE, Waterstram-Rich KM, editors. Nuclear medicine and PET/CT technologies and techniques. 6th ed. St. Louis: Mosby; 2007. p. 253–65.
3. Burke DR, et al. Quality improvement guidelines for percutaneous transhepatic cholangiography and biliary drainage. JVIR. 1997;8:677–81.
4. Douglas PS, Garcia MJ, Haines DE, ACCF/ASE/AHA/ASNC/HFSA/HRS/SCAI/SCCM/SCCT/SCMR, et al. Appropriate use criteria for echocardiography. J Am Coll Cardiol. 2011. doi:10.1016/j.jacc.2010.11.002.
5. Centers for Medicare and Medicaid Services. Noninvasive vascular testing (N.I.V.T.) (L28586); 2010.
6. Zierler RE, editor. Strandness's Duplex scanning in vascular disorders. 4th ed. Philadelphia: Lippincott Williams & Wilkins; 2010. p. 33–43.
7. Cochran C. The continual improvement process: from strategy to the bottom line. Chico: Paton Press LLC; 2003.

# Part II

# Vascular Hemodynamics and Basic Vascular Physics

Henrik Sillesen

# Principles of Vascular Ultrasound Physics

4

Frank R. Miele

**Abstract**

This chapter describes physics and instrumentation as directly applies to vascular imaging and interpretation. Foundational principles are discussed while describing image acquisition, image optimization, visualization of signals with low contrast such as thrombus and masses, and spatial and temporal resolution. The more advanced topics of harmonic imaging and compound imaging are discussed as well as the underlying principles necessary to understand IMT measurements. The spectral Doppler section explains Doppler basics, angular error, angle correction, spectral broadening artifact, and the appropriate frequency for spectral Doppler data acquisition. Color Doppler includes a discussion on the topics of color scales (PRF), color wall filters, aliasing, appropriate color gain, color priority, and the methodology for achieving maximum color sensitivity.

**Keywords**

Spatial resolution • Axial resolution • Harmonic imaging • Compound imaging • Doppler angle correction • Doppler error • Spectral broadening artifact • Color wall filters • Pulse repetition frequency (PRF) • Color PRF • Contrast resolution • Doppler equation

## Introduction

Understanding ultrasound physics and instrumentation is foundational to vascular interpretation. Acquiring reliable, accurate vascular ultrasound studies requires extensive knowledge of basic physics and instrumentation principles as well as an in-depth understanding of newer, more advanced technologies. Good vascular interpretation can only occur when the studies acquired accurately represent the patient's condition. Since multiple ultrasound modalities are used to acquire vascular studies, and since each modality has strengths and weaknesses, the interpreter must be well versed in the foundational physics and newer technologies as well. This chapter is not intended to serve as a comprehensive physics review but rather as a means of creating a practical foundation to improve vascular interpretation and to focus on targeted physics and instrumentation concepts required to better comprehend the vascular concepts and techniques discussed within this book.

This physics section is organized into four subsections. The first subsection covers general imaging principles including some basics of sound waves, basic image generation, and the concept of compression for gray scale image display. The second subsection discusses more advanced and complex methods of image generation including harmonic imaging, compound imaging, and a specific treatment of parameters associated with appropriate IMT measurements. The third subsection covers spectral Doppler including basics, Doppler sensitivity, angle correction and angular error, and the artifact of spectral broadening. The fourth subsection discusses color Doppler including basic color image generation, appropriate transmit frequency selection, color priority, color gain, appropriate color scales and associated color wall filters, and color frame rate and temporal resolution. It is fully intended

F.R. Miele, MSEE
Pegasus Lectures, Inc.,
109 Dalview Drive, Forney, TX 75126, USA
e-mail: pegasuslectures@aol.com

A.F. AbuRahma, D.F. Bandyk (eds.), *Noninvasive Vascular Diagnosis*,
DOI 10.1007/978-1-4471-4005-4_4, 

that this physics section will serve as a practical foundation for a more comprehensive understanding of the material covered in later chapters.

## Ultrasound Imaging General Principles

In order to better appreciate the challenges of ultrasound image generation and associated impact on interpretation, it is first important to briefly discuss how basic B-mode (2-D) images are generated. From this basic description, it will become much easier to understand spatial, contrast, and temporal limitations, which can directly impact the accuracy and validity of interpretation.

## Image Generation

Ultrasound images are generated by sequentially transmitting a series of pulses from a piezoelectric transducer over time. Each transmitted pulsed sound wave corresponds to an acoustic beam which propagates into the patient. Because sound is a mechanical wave, each transmitted pulsed wave interacts with the medium such that the body modulates the transmitted pulse, returning echoes back toward the transducer. Once the echoes have returned from the greatest depth of interest (determined by the image depth setting on the system), another pulse is transmitted in a nearby location, and the process is repeated until an image (or frame) is produced (see Fig. 4.1). The lateral dimension of the image determines how many beams (often referred to as lines) comprise an image and is set by the user. A narrower image results in the ability to produce more frames per second (a higher frame rate) with a better ability to detect quick changes in time (temporal resolution). However, the improved temporal resolution is achieved at the expense of having a smaller field of view.

## Absorption

To further understand the ultrasound image, it is important to discuss the mechanical interaction between the sound wave and the medium (body) and how these interactions relate to how images are presented. As the sound waves propagate through the tissue, some of the wave energy is lost as heat through absorption. Absorption rates within the tissue types are important for two reasons. First, all of the energy that is absorbed results in less signal to reflect back, decreasing sensitivity. Second, absorption leads to tissue heating which can cause metabolic breakdown resulting in tissue damage (referred to as a thermal bioeffect). It is valuable to know that absorption increases nonlinearly with increasing frequency and depth, implying that higher frequencies are generally not very useful for deeper imaging.

## Reflection

Reflectivity is based on the wavelength of the sound wave relative to the structure geometry as well as the heterogeneity of the acoustic properties of the tissues. When structures are large with respect to the wavelength, a very angle-dependent type of reflection occurs called specular reflection. As the surface appears "rough" with respect to the wavelength, a less angle-dependent type of reflection occurs referred to as backscattering (or sometimes just scattering). When wavelengths are large with respect to the structure, a weak reflective mechanism of Rayleigh scattering occurs. The wavelength is given as

$$\lambda = \frac{c}{f},$$

where

$c$ = speed of the sound,
$f$ = operating (transmit) frequency.

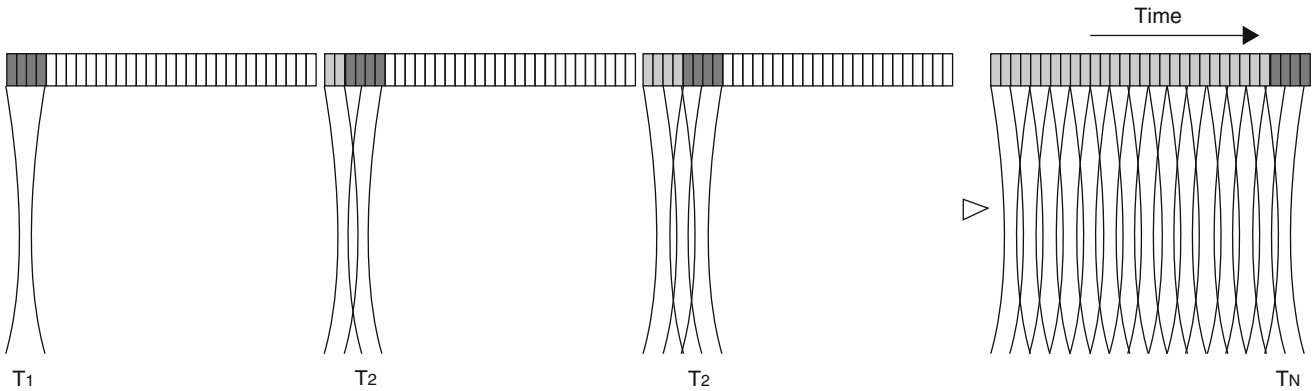


**Fig. 4.1** Sequential image generation (Reprinted from Miele 2008. ©2008 Miele Enterprises, LLC. With permission)

From this equation, we see that shorter wavelengths result from:

- Higher operating frequency (chosen by the person scanning but generally restricted by the required imaging depth)
- Lower propagation velocities (determined by the properties of the medium)

When the transmitted pulse encounters a large change in the acoustic properties of the tissue (referred to as the acoustic impedance), a large reflection results. Similarly, when only a small change in acoustic impedance exists, a small reflection occurs. The varying reflecting echoes return to the transducer and are converted into electrical signals which are then interpreted by the system and converted to color scale (usually gray scale) to produce an image. Large reflections are generally mapped to brighter shades of white, whereas weaker reflections are presented as various shades of gray. No reflection detected either because of medium homogeneity or inadequate sensitivity is presented as black. When differing tissues have very similar acoustic impedances, the contrast between the tissues will be low, and the possibility exists that the two different tissue types will not be differentiable in the image. Such situations can occur when a mass has acoustic properties similar to the surrounding tissue or in cases of a lipid-rich plaque with a thin cap. The ability to differentiate tissues based on brightness is referred to as contrast resolution.

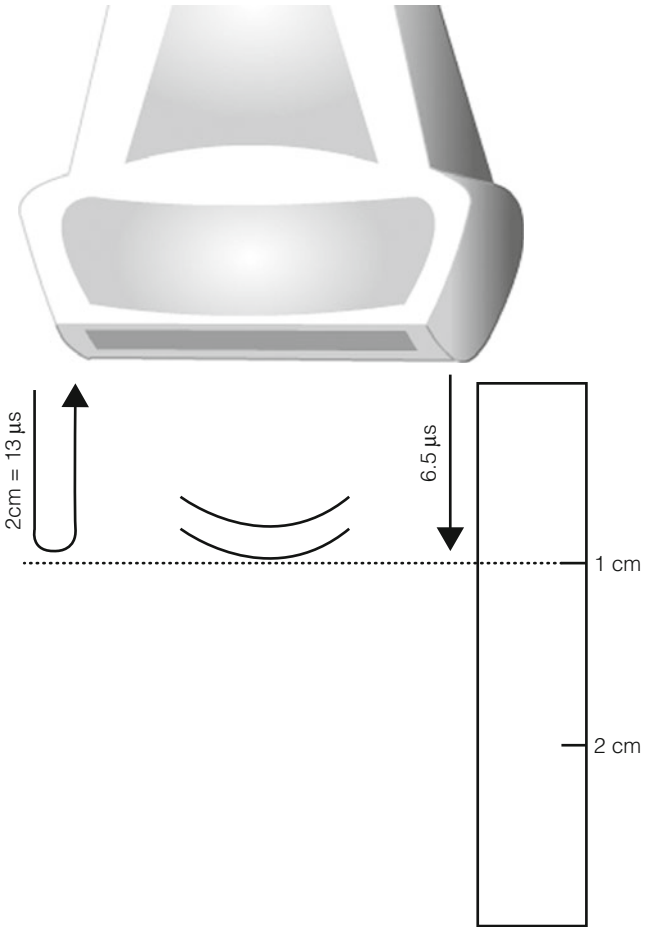


**Fig. 4.2** Speed of sound in tissue (Reprinted from Miele 2008. ©2008 Miele Enterprises, LLC. With permission)

## Depth and Speed of Sound

Mapping the returning echoes to a depth location in the image is a simple matter of applying the distance equation, based on the assumption that sound travels approximately 1,540 m/s in soft tissue. The assumed speed of 1,540 m/s is equivalent to 6.5 µs/cm of travel or equivalent to 13 µs/cm of imaging depth because of the round-trip effect (Fig. 4.2). Of course, when the true speed of sound within the body varies from the assumed speed of sound, echoes are mapped either too shallow (higher than the assumed 1,540 m/s) or too deep (lower than the assumed 1,540 m/s).

## Spatial Resolution

The ability to resolve changes in time (temporal resolution) and the ability to distinguish between tissues based on differences in brightness (contrast resolution) have already been mentioned. The ability to spatially resolve structures within an image is subdivided into three dimensions: axial (depth or longitudinal) resolution, lateral resolution, and elevation resolution. In essence, the best spatial resolution is obtained with a short pulse (axial resolution) and a narrow beam (lateral and elevation resolution). Shorter spatial pulse lengths result in better axial resolution with a greater ability to differentiate structures separated along the axis of the beam. Additionally, shorter pulses result in more accurate measurements in the axial direction. This concept is of course important when measurement accuracy matters such as when making intima-media thickness (IMT) measurements. Narrower beams result in better lateral and elevation resolution. For conventional 1-D array transducers, the lateral beam dimension can be changed by varying the depth of the focus (or foci when multiple foci are activated). When the focal depth is changed, more or fewer elements of the transducer are activated, and the timing of the transmit pulses varied to each element to achieve a deeper or a shallower focus. However, for 1-D arrays, there is only one element in the elevation plane (which corresponds to the "slice thickness" plane), and, hence, the focus cannot be varied in elevation (fixed elevation focus). In the elevation plane, most 1-D arrays have an acoustic lens built into the surface of the

transducer that fixes the focus at a specific "optimal" depth for the application for which the transducer was designed. In general, transducers intended primarily for shallow imaging will have a shallower elevation focus by design since the transducer is not intended for deeper imaging applications.

The ability to differentiate a specific tissue from surrounding tissue is related to the acoustic impedance mismatch between the two tissues. In many cases, the acoustic properties of the two tissues may be only slightly dissimilar, resulting in poor or no differentiation. This problem exists frequently with masses such as liver and kidney lesions and with fresh thrombus which has acoustic properties only slightly different than the surrounding blood. In these cases, even low-level noise can obscure the small contrast that does exist. This problem is exacerbated by the fact that the range of signal amplitudes reflecting from the body well exceeds the range of signals perceptible to the human eye. In many instances, the ratio of the largest to smallest signals reflecting from the body (the dynamic range) exceeds 80 dB (10,000 levels), whereas the human eye can perceive simultaneously less than 36 dB (fewer than 64 shades of gray). As a result, the imaging system must compress the signal dynamic range to better map into the dynamic range of the human eye. Of course, the process of compression implies that differences become smaller, potentially mapping small signal differences to the same gray scale appearance.

## Video Compression

Ultrasound systems allow the user to change the video compression applied to an image (different systems use different terminologies for this control such as gray scale, compression, dynamic range, and postprocessing). By having multiple compression maps with varying slopes, the expectation is that when one map fails to display certain signals, a different map will succeed. This expectation of course can only be realized if the person scanning actively changes the compression settings to determine if any signals are being missed. The two images in Fig. 4.3 are identical except for the applied compression map. Note that the image on the right gives evidence of a thrombus which is not evident in the image on the left.

In addition to gray scale (compression maps), there are many system parameters that should be optimized to decrease the chances of not visualizing weak signals from the surrounding tissue.

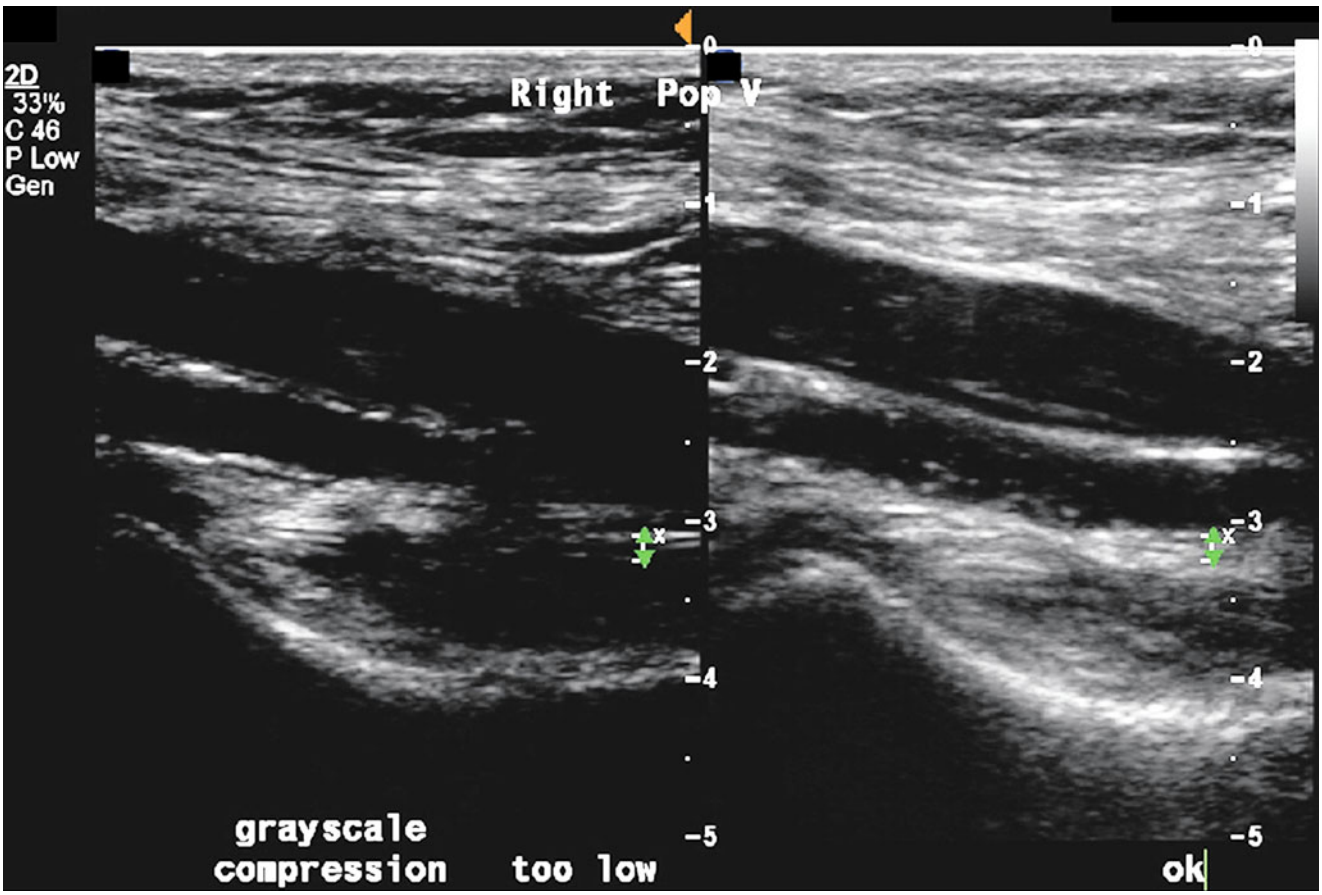


**Fig. 4.3** Compression settings can affect interpretation (Reprinted from Miele 2006. ©2006 Miele Enterprises, LLC. With permission)

The list includes:

- Using the correct transmit frequency (adequate penetration and best possible resolution)
- Using adequate transmit power
- Using harmonics (unless too deep)
- Using compound imaging
- Varying compression maps to improve contrast resolution

Some of the advanced techniques will be discussed in the upcoming section.

## Advanced Imaging Technologies

In addition to improvements in electronics and transducers, there are many advanced techniques which have significantly improved the quality of ultrasound images over the last 10 years. An exhaustive treatment of imaging technologies is beyond the scope of this chapter, but two of the most important techniques are covered in the upcoming section.

## Harmonic Imaging

The principles of second-harmonic imaging are simple. For harmonic imaging, the system transmits at a lower frequency, referred to as the fundamental, and then receives and processes signals at twice the fundamental signal, referred to as the second harmonic. Of course the complexity comes in understanding how fundamental signals are converted into harmonic signals and, more importantly, in understanding the benefits and limitations of harmonic imaging.

There is a nonlinear response of tissue to the compression and rarefaction of sound waves. During compression, the density of the tissue molecules increases, resulting in a slight increase in propagation speed, whereas during rarefaction, the density decreases such that there is a slight decrease in the propagation velocity. The result is that the wave becomes distorted (Fig. 4.4) as it propagates through the tissue, introducing harmonic energy into the wave. The harmonics are not limited to second harmonics, but as of now, ultrasound systems are not processing higher-order harmonics as each higher harmonic signal becomes weaker and is currently too weak for adequate image generation. The generation of harmonic energy is very nonlinear with the beam intensity (related to the parameter called the mechanical index (MI)). In essence, a slightly lower intensity (lower MI) can result in significantly less harmonic signal generation. For this reason, harmonic imaging is very sensitive to where the beam focus is placed as well as to the overall transmit power used.

Making use of the harmonic signals generated by nonlinear propagation requires transducers with enough bandwidth (range of frequencies over which the transducer can operate)

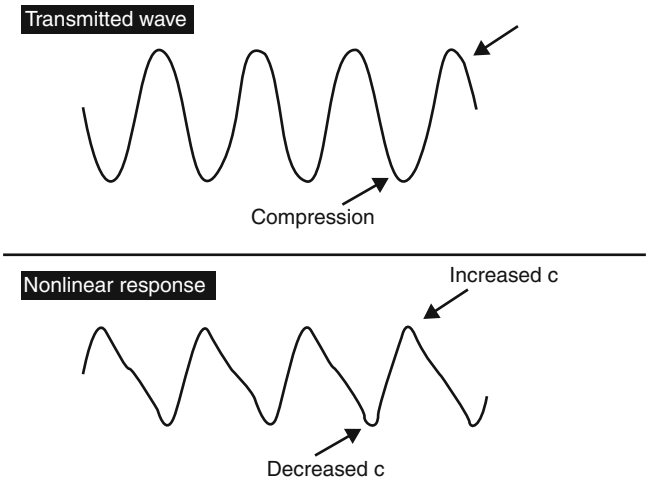


**Fig. 4.4** Distortion of wave producing harmonic energy (Reprinted from Miele 2006. ©2006 Miele Enterprises, LLC. With permission)

so that the transducer can transmit at the fundamental frequency and receive signals at twice the fundamental frequency (the second-harmonic signal). Modern transducers capable of such large dynamic range are commonly referred to as ultra-wide bandwidth transducers. When the system processes the returning echoes, a filter is applied to look at just the second-harmonic bandwidth, explicitly attempting to not overlap with the transmit bandwidth. Any overlap between the fundamental and harmonic bandwidths allows for the clutter from the fundamental to degrade the image quality of the harmonic signal. In order to reduce the overlap between fundamental and harmonic bandwidth, longer transmit pulses are commonly used which result in a narrower bandwidth fundamental. As discussed earlier, a longer transmit pulse (spatial pulse length) results in degraded axial resolution. For this reason, conventional harmonics generally have worse axial resolution and is generally not ideal for axial measurements (measurements made in depth) such as IMT measurements. Some systems now offer novel techniques to get around the narrowbanding issue such as pulse inversion and pulse-modulated harmonics. In essence, these techniques allow for the separation of the fundamental and harmonic bandwidths without using a longer transmit pulse that results in degraded axial resolution.

The benefit of harmonic imaging is primarily a reduction of clutter artifacts. Since harmonic beams are inherently narrower than the fundamental beams, lateral resolution is improved. Additionally, since the beam intensity is generally low in the near field before the beam has converged to the focus, harmonic generation is generally low in the near field. Since most imaging artifacts result from strong reflectors in the near field (clutter signals), lower-level harmonic signals in the near field result in fewer imaging artifacts, improving image quality (Fig. 4.5a–d). Again since harmonic generation drops precipitously with lower beam intensities (lower MI),

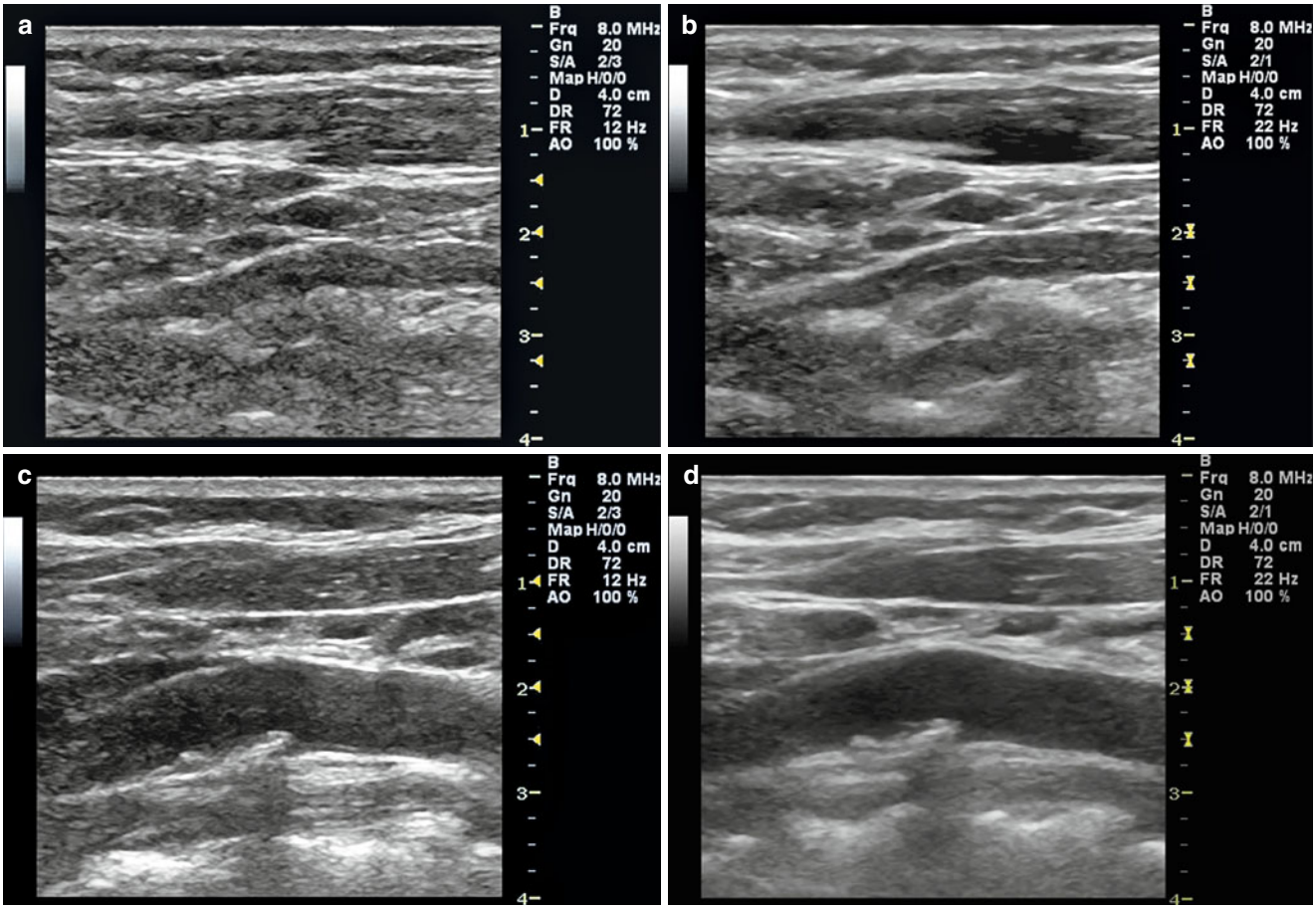


**Fig. 4.5** (**a**) Fundamental. (**b**) Harmonic imaging. (**c**) Fundamental. (**d**) Harmonic imaging

using harmonics when trying to image very deep in a large patient is not recommended as the harmonic signal will offer inadequate sensitivity. In these deep cases, using fundamental imaging is the correct approach.

## Compound Imaging

Compound imaging (known as multiangle imaging, SonoCT or Crossbeam technology by some manufacturers) is a frame-averaging technique which can significantly improve image quality through increased signal-to-noise ratio and by decreasing the presence of artifacts. The angle dependency of ultrasound reflection is reduced by imaging the same region from different directions and "compounding" the resulting multiple frames into one image. Like all averaging techniques, the signal-to-noise ratio is improved when the desired signal does not change from frame to frame, or changes slowly from frame to frame relative to the rate of frame acquisition. In cases where the signal is changing slowly, the signal in each of the frames has the same phase such that adding the frames together results in the signal amplitude increasing by a factor equal to the number of samples. For example, adding four signals with an amplitude of 3 V each would result in a combined signal with an amplitude of 12 V. In contrast, the noise which exists within the image is random from frame to frame, implying that although the noise amplitude also grows with averaging, it grows at a slower rate than the signal. In fact, the noise generally grows by the rate of the square root of the number of frames used in the average. Using the same example, imagine that the noise level is 1 mV, averaging four frames together would result in the noise becoming bigger by the square root of four, or $2 \times 1$ mV equal to 2 mV. Therefore, the signal grew four times larger, whereas the noise grew only twice as large, implying that the signal-to-noise ratio increased by a factor of 4 divided by 2, or two times. In other words, averaging improves the signal-to-noise ratio by the square root of the number of samples in the average.

In addition to averaging, compound image varies the image steering from frame to frame. Recall that specular reflection is very angle dependent. Combining this fact with the fact that most imaging artifacts are caused by specular reflection, it should be clear that compound imaging results in artifacts tending to "average out." The net result is that

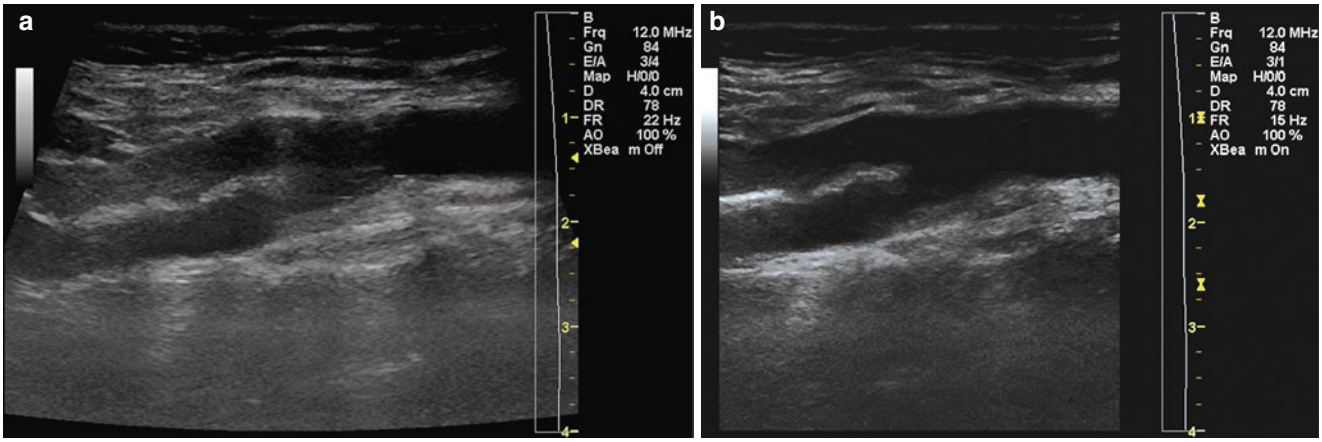


**Fig. 4.6** (**a**) Conventional imaging. (**b**) Compound imaging

compound imaging generally results in images with better signal-to-noise ratio (improved sensitivity) and fewer artifacts, as seen in Fig. 4.6.

Also, because of the angle dependency of ultrasound reflection, by imaging from several angles, the circumference of arteries in cross section becomes more visible with compound imaging compared to single-angle imaging (conventional ultrasound imaging technique).

## Image Optimization

Image optimization requires a comprehensive knowledge of the many system controls discussed above. There are no set rules which always govern when one technology should be applied or another disabled other than understanding the trade-offs as well as the underlying principles of each technology and control relative to the imaging situation. In general, the starting point for good image quality is to ensure adequate signal strength by appropriate transducer frequency selection, focal/foci depth, and imaging window. With respect to identification of artifacts, it is important to vary the incident angle (by electronically steering the image or physically angling the transducer) while looking for changes within the image. When the relative locations of structures vary with varying angles, imaging artifacts are present. Once the appropriate signal strength (signal-to-noise ratio) is achieved, the receiver-gain and time-gain compensation (TGC) should be adjusted so that the full range of existing signals is visible relative to the ambient light and so that similar tissues at differing depths are displayed with similar brightness. Periodically, the compression should be adjusted to vary the contrast resolution so as to make certain that no signals such as fresh thrombus or masses are not being obscured by inappropriate contrast. Newer technologies such as harmonics and compound imaging often provide significant improvement, but are at times inappropriate based on the trade-offs of the technologies. Finally, many systems now offer adaptive processing which attempts to perform image optimization based on internal algorithms. There are times when these adaptive processes will generate better image quality than even the most seasoned sonographer. However, there are other times when a talented sonographer will produce significantly better images than the adaptive processes. For this reason, the best use of these adaptive processes is to first optimize the image by hand, activate the adaptive process, and then compare. It is then useful to optimize again by hand starting with the settings chosen by the adaptive processing technique. If the image only degrades by further manipulation, then reactivating the adaptive process will return the image to the "optimal" quality. By employing this approach, the sonographer can be pretty certain that he or she achieves optimal image quality.

## IMT Measurements

In recent years, carotid intima-media thickness (IMT) measurements have been used as an indicator for atherosclerotic disease with the intent of predicting likelihood of myocardial infarction and stroke. The ability to both accurately and repeatedly measure a vessel's wall thickness is highly dependent on technique and ultrasound system settings. This section outlines those parameters which should be considered when performing IMT measurements. Realizing that equipment from different manufacturers will have different ideal settings, the purpose of this section is to make the reader aware of the potential issues, not to create a standard for measurement. Measurement standards require significant research and potentially may need to vary for different equipment design.

The fundamental difficulty with accurate IMT measurements is related to axial resolution. Even for a single excitation

pulse, the resonance of a transducer results in more than one cycle in the acoustic pulse generated by the transducer. The effect is similar to ringing a bell with a single strike of the clapper. Even with a very short duration single stroke of the clapper, the bell proceeds to ring at its resonant frequency for a period of time. As discussed previously, the more cycles which exist within a pulse, the longer the spatial pulse length, and the worse the axial resolution. For this reason, ultrasound transducers are designed with a backing material to dampen the impulse response, thereby shortening the spatial pulse length, improving the axial resolution. No matter how much damping takes place, practically speaking, every pulse will have a "tail" which tends to exaggerate the axial dimension of a measured structure. The degree to which this tail exists is a function of the transducer operating frequency, the transducer crystal's impulse response, and the backing material used.

There are other parameters which can also affect the axial resolution. As mentioned in the harmonic imaging section, the need to decrease the overlap between the fundamental and receive bandwidths often results in degradation of the axial resolution for conventional harmonic imaging. This fact alone indicates that concern should exist if using conventional harmonic imaging when performing IMT measurements. More advanced harmonic techniques such as pulse inversion and pulse-modulated (chirp Z) harmonics are intended to produce the advantages of harmonics without the corresponding degradation in axial resolution. The degree to which harmonics affect IMT measurements is clearly affected by the specific methodology used by the manufacturers of the specific equipment being used.

For many years, the suggestion has been to make the IMT measurements from the posterior and not the anterior vessel wall. The rationale for this approach is of course rooted in the physics of axial resolution. When assessing the anterior wall of a vessel, the "tail" of the pulse continues to image the wall while the main burst of the pulse has reached the vessel lumen. Although the energy in the pulse tail is weaker than the energy in the main burst, the reflection from the blood is weak (Rayleigh) such that the reflected signal from the lumen is very small. Therefore, the weak signal from the pulse tail potentially overlaps a region that should be displayed as lumen, increasing the apparent thickness of the vessel intima. In contrast, when imaging the posterior vessel wall, the echo from the tail coincides with vessel lumen when the main burst reaches the vessel wall so that there is no impact on the perceived intima thickness. For this reason, the posterior wall became a standard location for IMT measurements.

Other parameters which can clearly impact the perception of intima thickness include the receiver-gain (amplification) transmit power, use of compound imaging, incident angle, and of course video compression. Many systems offer automated measurements which also attempt to reduce variability by making multiple measurements within a specific region and then averaging the multiple measurements.

In reality, there are two different issues that must be considered with respect to IMT measurement accuracy. The first is that serial measurements to assess changes over time should be made holding as many of the system parameters as constant as possible. If the system parameters are changed, it is conceivable that the difference in IMT measurement is attributable to system changes and not to atherosclerotic progression. The second issue is more challenging in that IMT measurements are compared against standards, for which threshold values exist based on age and gender. Here, the problem is that even very repeatable measurements could have a potential skew relative to the method by which the standards were developed. Finally, changes over time may be obscured by the fact that wall thickening/atherosclerosis does not develop uniformly along the circumference of the vessel wall. Given the thin "slice" of the artery in a focused image, scanning the artery from a slightly different angle may reveal another IMT value!

## Spectral Doppler Basics

In B-mode imaging, data is presented based on the amplitude of the reflected echoes. The amplitude is representative of the acoustic properties of the tissue in the region of the body that was scanned. Unlike B-mode imaging, spectral Doppler is a nonscanned modality in which the data is acquired by transmitting repeatedly in the same location. In lieu of spatial information, velocity information is displayed. Therefore, the signal strength is still represented by gray scale, but the horizontal access of the display now represents elapsed time, and the vertical axis represents velocity toward and away from the steered beam (line) from the transducer.

The velocity information is obtained using a Doppler technique. The Doppler effect is essentially a perceived change in frequency as the result of a compression or decompression of the wavelength of a wave as the result of motion of the wave source relative to an observer. When the relative movement results in the source and observer becoming closer together, the wavelength is decreased giving the perception of a higher frequency. When the relative movement results in the source and observer becoming farther apart, the wavelength is increased giving the perception of a lower frequency (as expressed by the wavelength equation). Most people have practically witnessed the Doppler shift in situations such as a very fast moving train, an ambulance, or at the racetrack. In each case, the observer hears a change in pitch (from higher frequency to lower frequency) as the sound source approaches and then moves past. The detected shift in frequencies, referred to as the Doppler shift ($f_{\text{Doppler}}$), is a function of the parameters which affect the relative motion (velocity and

angle) and the parameters which determine the wavelength (operating frequency and propagation velocity), as given in the Doppler equation:

$$f_{\text{Doppler}} = \frac{2 f_o \times v \times \cos(\theta)}{c}$$

where

$f_o$ = operating (transmit) frequency,

$v$ = velocity of blood,

$\theta$ = Doppler angle,

$c$ = speed of sound.

There are two principal forms of spectral Doppler: continuous wave (CW) and pulsed wave (PW) Doppler. With CW, a transmitter continuously fires simultaneously while a receiver continuously listens for echoes. Since the receive and transmit are continuous, echoes returning from all depths are heard simultaneously such that there is no inherent depth discrimination. In essence, unless there is a reference image which indicates the source of specific flow velocity ranges, CW yields no information relative to the source of the detected Doppler signals. In contrast, with PW Doppler, the transmitter and receiver are alternately turned on and off at a rate referred to as the pulse repetition frequency (PRF) such that signals returning at a specific time are received. Through the distance equation, the time for the echo to return is associated with a specific depth. Therefore, PW yields fairly good range resolution. However, since the PW receivers are alternately turned on and off at a rate of the PRF, it is possible that some signals changing very quickly (higher Doppler frequency shifts) will not be detected, resulting in an inability to determine the true peak velocity. This effect is referred to as aliasing as specified by the Nyquist criterion. With PW Doppler, aliasing occurs when the maximum Doppler shift exceeds half of the PRF.

## Understanding Angle Correction

Perhaps the most misunderstood aspect of spectral PW Doppler is angle correction. The Doppler equation illustrates that the detected Doppler shift is dependent on the cosine of the Doppler angle (the angle formed between the steered Doppler beam and the flow direction) with maximal Doppler shifts detected at 0° and 180°. Unlike cardiac Doppler in which the maximum Doppler shifts are often obtained because alignment to flow is usually possible from one of the many cardiac imaging views, vascular Doppler rarely affords detection of the maximum Doppler shift. As a result, angle correction is necessary to compensate for the partial frequency shift detection.

Before explaining angle correction, we must first assess how the Doppler angle affects the Doppler measurement. The system transmits a signal at a known radio frequency (typically from 1.6 MHz to as high as 10 or 12 MHz depending on the system and transducer). The system then detects the frequency of the returning echoes from which the transmit frequency is essentially "subtracted" leaving the Doppler frequency shift. When the Doppler angle is less than 90°, the returning frequency is higher than the transmitted frequency and a positive Doppler shift is detected. Similarly, if the Doppler angle is greater than 90°, the returning frequency is lower than the transmitted frequency and a negative Doppler shift is detected. The important thing to realize is that unless the Doppler angle is 0° or 180°, the system does not detect the full Doppler shift. As the Doppler angle approaches 90°, the Doppler shift converges to 0.

**Table 4.1** Effects of angle on detected Doppler shift and angle correction

| $\theta$ | $f_{\text{Doppler}}$ measured, Hz | Velocity (uncorrected), m/s | Cos($\theta$) | Velocity (angle corrected), m/s |
|---|---|---|---|---|
| 0 | 3,896 | 1 | 1 | 1 |
| 30 | 3,374 | 0.9 | 0.866 | 1 |
| 45 | 2,755 | 0.7 | 0.7071 | 1 |
| 60 | 1,948 | 0.5 | 0.5 | 1 |
| 90 | 0 | 0 | 0 | 0 |
| 120 | −1,948 | −0.5 | −0.5 | −1 |
| 135 | −2,755 | −0.7 | −0.7071 | −1 |
| 150 | −3,374 | −0.9 | −0.866 | −1 |
| 180 | −3,896 | −1 | −1 | −1 |

Note that the negative velocity implies that the flow is presented below the spectral Doppler baseline, representing flow "away" from the transducer

For the times when the full Doppler shift is not detected, as with most vascular applications, the ultrasound system allows for angle correction. Practically speaking, the angle correction is applied by the system user. The user specifies the Doppler angle by aligning a Doppler flow indicator with the perceived direction of the flow. Using basic geometry, the system can then determine the Doppler angle, calculate the cosine of the Doppler angle, and correct the partially detected Doppler frequency shift. Since Doppler yields velocity information, the correction is essentially applied by manipulating the Doppler equation to be expressed in terms of velocity as

$$v = \frac{c \times f_{\text{Doppler}}}{2 f_o \times \cos(\theta)}.$$

Table 4.1 illustrates how the Doppler angle affects the measured Doppler frequency shift and how angle correction works. Assume that the transmit frequency of 3.0 MHz is used and that the true blood velocity is 1 m/s. The first two columns illustrate the Doppler shift that would be detected for a range of specified Doppler angles. Note that for the same flow velocity, different Doppler shifts are detected as the result of the varying Doppler angles. The third column shows the calculated velocity that would result from the

Doppler equation if angle correction is not applied (clearly incorrect at all angles other than 0° and 180°). The fourth column shows the cosine of the angle used for the velocity correction. The fifth column shows that theoretically, the angle-corrected velocity values are now all correct except at 90° at which point no Doppler shift is detected and correction is not possible.

## Why Does Doppler Angle Matter?

Theoretically using any angle other than an angle close to 90° should not make a difference since angle correction is applied. However, the theoretical assessment ignores nonlinear error sources that make the Doppler angle very important. When the flow direction is specified by a user, there is no way of guaranteeing that the flow direction is specified accurately. Since blood flow direction in an artery may be nonaxial, i.e., rotational within the artery, or simply not parallel to the vessel wall at bifurcations or around asymmetrical atherosclerotic lesions, angle correction by assuming vessel direction as flow direction can be erroneous. In addition to angular misalignment in the plane displayed on the ultrasound system screen, there is also the potential for angular misalignment in the elevation plane (corresponding to the image slice thickness). If the flow direction is specified incorrectly, in essence, the wrong "angle correction" is applied, and error is introduced into the velocity measurement.

Hypothetically assume that the flow indicator is misaligned with the flow by 5°. Because of the very nonlinear behavior of the cosine, a 5° error relative to performing Doppler at an angle of 70° results in significantly more error in the measured velocity than the same 5° error relative to performing Doppler at 50°. As the Doppler angle gets larger (closer to 90°), the error increases at increasingly faster rates.

In addition to nonlinear angular error, the artifact of spectral broadening also becomes worse at larger Doppler angles. Spectral broadening is the result of the spread of angles that results from the Doppler sound beam coming from more than one element, resulting in an increase in the measured peak velocity as well as a decrease in the spectral window (when a spectral window would exist). As shown in Fig. 4.7, angle correction is applied based on the angle formed from the center of the beam to the flow. However, note that some of the elements (labeled "L") result in angles larger than the center element, while other elements (labeled "R") result in angles less than the center element. Again since the same cosine correction is applied to the signal from all elements, some signals are overcorrected (resulting in an artificially higher peak velocity), while other signals are underestimated (resulting in a decrease in the spectral window when a window would be otherwise present).

## Standardized Doppler Measurements

For many years, there has been an attempt within vascular labs to standardize Doppler measurements at a Doppler angle of 60°. Certainly, using larger Doppler angles should be avoided if possible since the errors in velocity underestimation and (more frequently) overestimation can become quite significant. It is important to note that 60° does not represent the best Doppler measurements, but rather an angle that was considered to be acceptable since it is relatively repeatable from patient to patient and from measurement to measurement within a patient. Many labs have adopted a range of Doppler angles from 45 to 60 as the standard. With this standard, measurements made at angles less than 60° have the benefit of reducing some degree of the known error sources which are worse with larger angles. As always, standardization and internal validation should be considered within each vascular laboratory.

## Correct Operating Frequency

Reflectivity from blood is based on Rayleigh scattering. Rayleigh scattering is a very weak reflective mechanism, which makes Doppler techniques (both spectral and color Doppler) prone to errors because of inadequate sensitivity. Interestingly, the amount of backscattering increases with increasing frequency. This increase in reflectivity is the result of the size "increase" of the red blood cells relative to the decreasing wavelength. Based on this increase in reflectivity, the conclusion that higher frequencies should create stronger Doppler signals would seem logical but paradoxically is not true. This paradox results because not only does reflectivity increase with increasing frequency but attenuation through absorption also increases with increasing frequency. In fact, since the absorption rate increases exponentially with increasing frequency, the increased attenuation using higher transmit frequencies well exceeds the increase in reflectivity, thereby resulting in weaker Doppler signals. For this reason, with the exception of very superficial Doppler, Doppler should always be performed at the lowest frequency possible. Practically speaking, superficial imaging implies a depth of approximately 1–2 cm or shallower. Figure 4.8 indicates the ideal operating frequency based on Doppler depth. Note that the assumption was made that the lowest frequency Doppler available is about 2 MHz.

When an incorrectly high Doppler frequency is used, the Doppler signal becomes weaker and quite often leads to underestimation of the true peak velocity. In general, there are some relatively easily recognized spectral indicators of Doppler operation at or near the sensitivity limit. When Doppler sensitivity is marginal, the returning signals are so weak that more receiver gain must be applied to visualize the

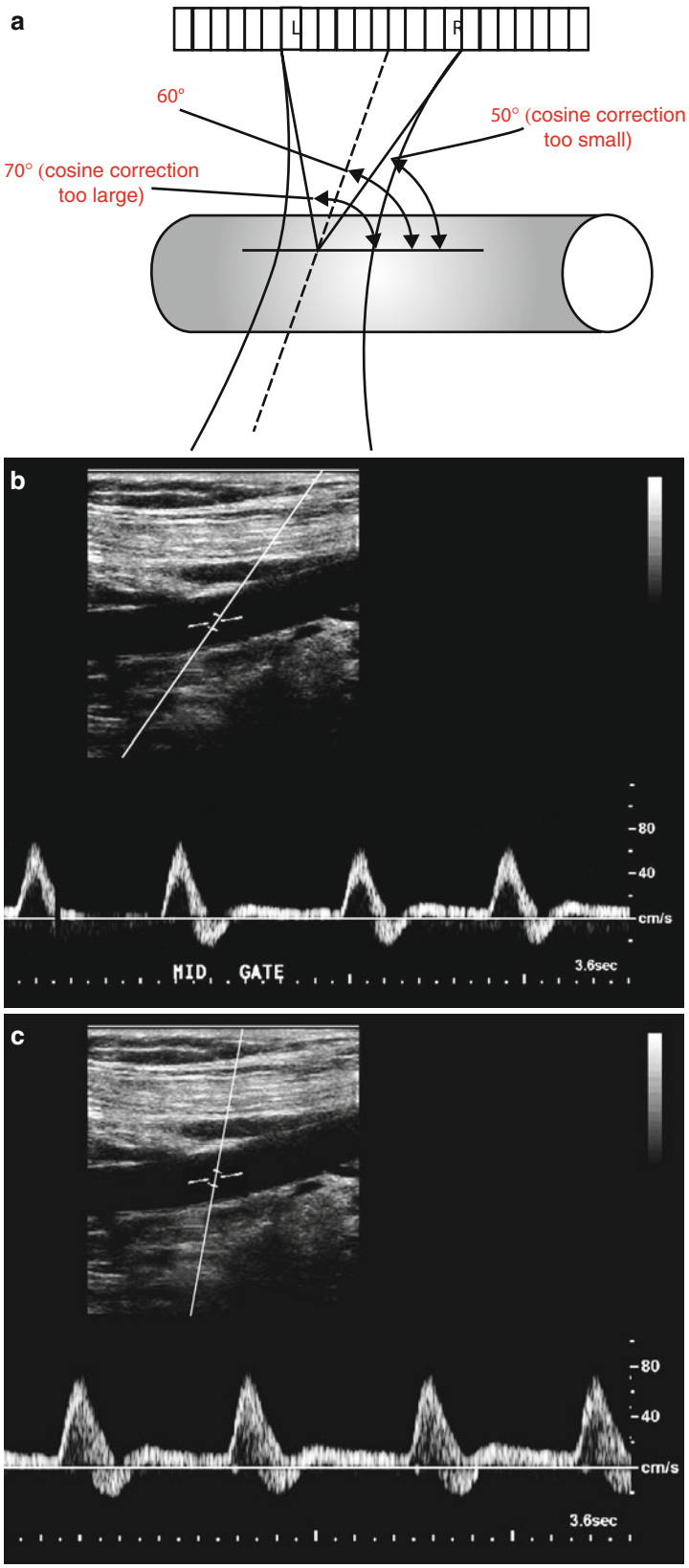


**Fig. 4.7** (**a**) Cause of spectral broadening artifact. (**b**) Spectrum without artifact. (**c**) Spectrum with broadening artifact (Reprinted from Miele 2006. ©2006 Miele Enterprises, LLC. With permission)

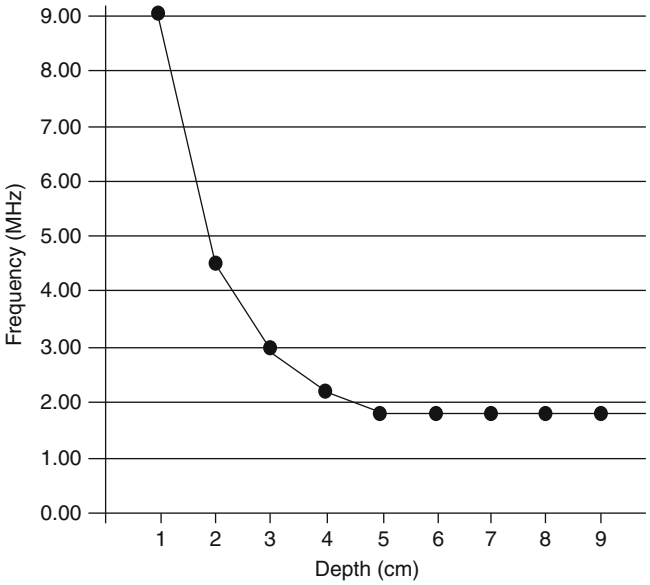


**Fig. 4.8** Ideal Doppler operating frequency based on depth (Reprinted from Miele 2006. ©2006 Miele Enterprises, LLC. With permission)

Doppler spectrum. As the Doppler gain is increased, the noise floor (random white speckle associated with the electronic noise of the Doppler system) becomes apparent within the Doppler spectrum. Therefore, whenever the transmit power is set to maximum (or 100%) and there is evident random white speckle throughout the entirety of the Doppler spectral display, especially if the Doppler spectrum itself is still not that bright, there is a strong indication that a lower Doppler frequency should be used if possible.

## Color Doppler

Color Doppler is similar to B-mode imaging in that spatial dimensions are portrayed. Color Doppler is similar to spectral Doppler in that velocity information is displayed. However, color Doppler is different from both spectral Doppler and B-mode imaging since amplitude information is not displayed.

Color Doppler presents an estimate of the mean velocity at each point within the color box of the scan region. Note that to achieve a mean estimate, a color display line cannot be generated from a single acoustic line (a single transmit pulse) since multiple samples are required to generate a mean. Unlike the simplest case of B-mode imaging described in the first subsection, to generate color images, an entire packet of lines must be transmitted in the same direction, a correlation performed, and then a single "line" of color displayed. Since color is created by transmitting entire packets to generate a single color line, the time required to create a frame increases dramatically, resulting in generally degraded temporal resolution. Since the temporal resolution with color Doppler is generally so poor, scanning techniques such as narrowing the color box width, cropping the color box depth, and potentially decreasing color packet size of color line density to optimize frame rate become very important parameters to control.

## Color Priority and Color Gain

Since color Doppler does not directly display signal amplitude, there are indirect methods of determining whether or not the color receiver gain is adequately set. To understand these techniques, it is important to realize that color Doppler displays color signals based on color signal thresholds. When the color signal amplitude exceeds a specific threshold, color is displayed. If the signal is weaker than the specific amplitude threshold, no color is displayed so that gray scale values are presented. Since an individual pixel cannot represent both tissue and flow, if both flow and gray scale values simultaneously exist, the threshold determines when color is displayed versus when the gray scale value is presented. Most systems provide a user control to specify the color priority which determines at what level the tissue signal must be below to allow color to be displayed. A high color priority implies that color is generally given priority unless the gray scale amplitude is very high (Fig. 4.9a). A low color priority implies that color is given a lower priority so that even moderate-level gray scale values will take priority over displaying color (Fig. 4.9b).

Given that color is a threshold-based technique, receiver gain set too low results in color dropout in regions where flow exists. Since the lack of flow is easily recognized, sonographers generally recognize the problem and take the corrective step of turning up the color gain. The problem of overgaining is more complex to determine. In fact, overgaining in the near field is recognized by a different technique than recognizing overgaining at deeper depths or when color sensitivity becomes an issue. With more superficial imaging and adequate signal, color overgaining results in color bleed over regions of tissue at the flow boundary (Fig. 4.10). When viewing a vessel, the color bleed occurs more commonly and more excessively with the posterior wall. This phenomenon is the result of limited axial resolution sometimes referred to as the color tail (analogous to the situation described in the IMT description).

Setting the gain appropriately for deeper color imaging or when close to penetration limits requires skill. Since imaging deep requires optimal sensitivity, setting the gain too low can result in inadequate color filling, as the lower-level echoes often drop below the amplitude threshold required to display color. The technique for setting the color gain is to increase the color gain until color speckle (noise) appears within the

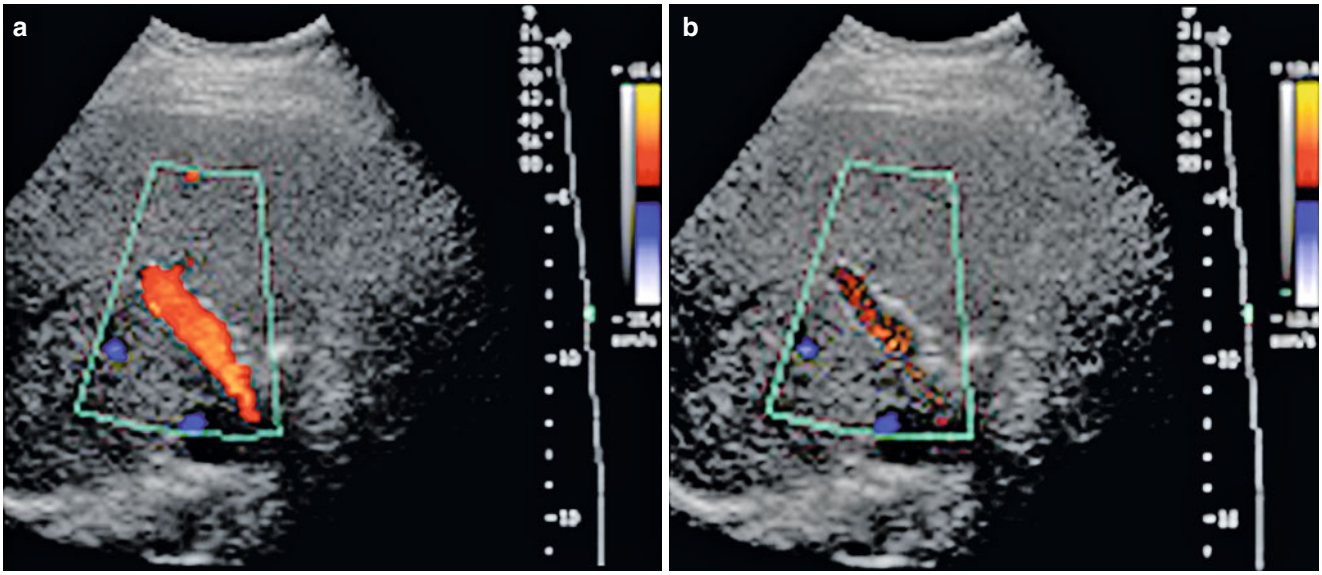


**Fig. 4.9** (**a**) Higher color priority. (**b**) Lower color priority (Reprinted from Miele 2008. ©2008 Miele Enterprises, LLC. With permission)

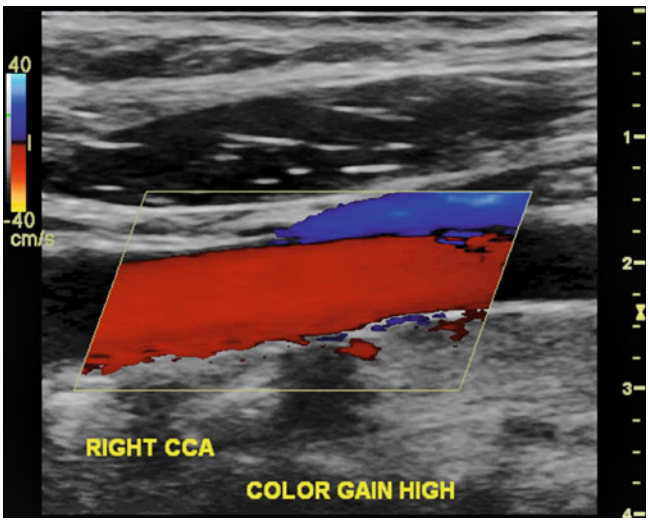


**Fig. 4.10** Color bleed from excessive color gain

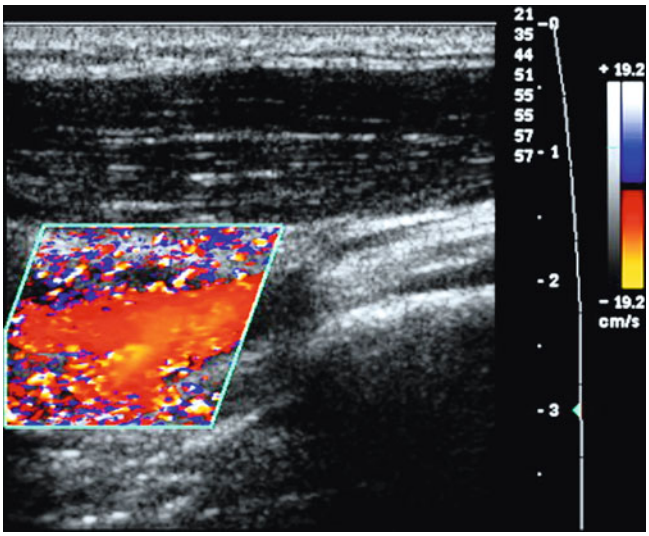


**Fig. 4.11** Color speckle from excessive color gain

color box in regions where flow does not exist (Fig. 4.11). Then, the color gain should be decreased until the color speckle just disappears from the nonflow regions. At this setting, the color gain is set for optimal sensitivity. When color speckle is apparent within the image (in regions where flow does not exist), the color gain is set incorrectly too high.

## Correct Operating Frequency

As with spectral Doppler, color Doppler is very sensitive to the operating frequency. Perhaps even more common than with spectral Doppler, color Doppler is often performed using a transmit frequency higher than appropriate. Since, as discussed in the color gain section above, color Doppler is a threshold-based technique, when an inappropriately high operating frequency is used, color dropout occurs. This problem is particularly disconcerting when the dropout occurs when attempting to determine whether or not flow exists. Figure 4.12a, b shows how even with normal flow situations using a higher operating frequency can result in less appreciated flow.

## Color Scales and Wall Filters

The color pulse repetition frequency (PRF) is also commonly referred to as the color scales. The PRF is simply the reciprocal of the pulse repetition period (PRP). As already discussed

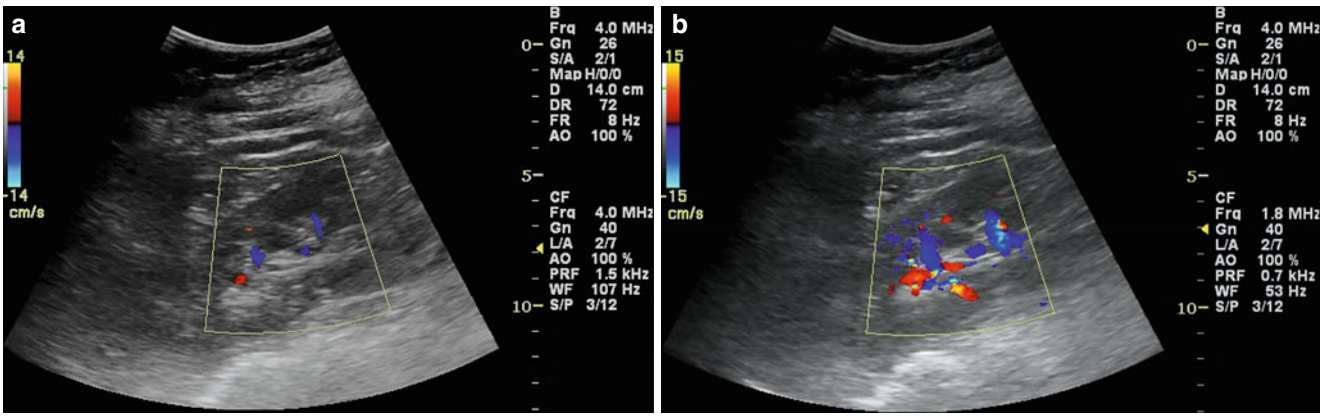


**Fig. 4.12** (**a**) 4.0 MHz: inadequate color. (**b**) 1.8 MHz: appropriate color

in the earlier section on how basic images are produced, the speed of sound is assumed to be 1,540 m/s which requires 13 μs for each cm of imaging depth (6.5 μs for each cm of tissue through which the sound must travel). For a given depth, the minimum PRP is calculated simply as the imaging depth in cm multiplied by the assumed 13 μs/cm travel time. For example, with an imaging depth of 8 cm, the PRP and the PRF are calculated as follows:

$$PRP = 8\frac{cm}{line} * \frac{13\,\text{msec}}{cmf_o} = 104\frac{\text{msec}}{line} \gg 0.100\frac{m\,\text{sec}}{line}$$

$$PRF = \frac{1}{PRP} = \frac{1\,line}{0.100\,m\,\text{sec}} = 10,000\frac{lines}{\text{sec}} = 10\,kHz$$

This calculation shows that for an imaging depth of 8 cm, the ultrasound system can transmit and receive approximately 10,000 beams (lines) per second or 10,000 samples per second. Recalling the Nyquist criterion, the maximum detectable frequency is half of the sample rate. Therefore, at a depth of 8 cm, the highest detectable mean Doppler shift is 5 kHz. If the mean frequency shift exceeds half of the PRF, color aliasing occurs. By employing the Doppler equation, the mean frequency shifts can be presented as mean velocities. Looking at the color bar given in Fig. 4.13, note that the color scales (PRF) are set to ±65 cm/s. For Doppler angles less than 90°, flow with mean velocities below 65 cm/s will be presented as hues of red through orange. If the mean velocity exceeds 65 cm/s, aliasing occurs which implies that the color will wrap first to hues of aqua followed by shades of darker blue. Flow with mean velocities lower than 65 cm/s at angles between 90° and 180° will present as dark blue through aqua. When the mean velocity exceeds 65 cm/s, the color wraps first to shades of orange followed by shades of red.

Imagine that for a specific imaging situation the maximum detectable mean velocity is 65 cm/s, and the mean flow

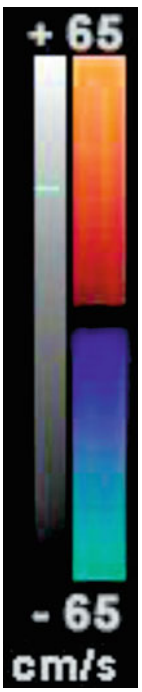


**Fig. 4.13** Color bar

velocity is only 5 cm/s. Clearly, you would want to lower the color scales to better appreciate flow velocity gradients about this low mean. When imaging at the maximum color PRF, the PRF is the reciprocal of the minimum PRP (based on the depth) as exemplified in the calculation above. One method of lowering the PRF would be to increase the imaging depth (color box depth), increasing the PRP. However, this approach makes very little sense as the color box would now be displaying color in regions deeper than the region of interest. The system is designed to use a better approach. For a given depth, lowering the color scales essentially means artificially increasing the PRP to a time greater than needed for the sound to travel to and back from the maximum imaging depth. With lower than the maximum scales (PRF), the system transmits the pulse, waits the required time for the pulse

to reach and return from the maximum imaging depth, and then simply does nothing for a period of time ("dead time") before repeating the process. The added "dead time" increases the PRP, hence decreasing the PRF.

Note that in the center of the color bar is a black band (Fig. 4.13). The center of the band represents the baseline and the span of the black band above and below the center represents the color wall filters. With both spectral and color Doppler, wall filters are necessary to reduce the very large clutter signals from slowly moving structures such as vessel walls and transducer movement so that the lower amplitude signals from the blood are not obscured. The baseline corresponds to no Doppler shift detected. No detected shift can be the result of no flow, poor angle to flow, poor sensitivity, or artifacts which obscure the color signal such as shadowing as occurs with the spiny process when looking at the vertebral arteries. For some systems, the width of the black band represents the extent to which the color wall filters eliminate low mean velocity color signals.

It is important to note that with all ultrasound systems, when the color PRF is changed, the wall filters also change. In essence, the color wall filters are a percentage of the PRF. Therefore, when the color scales are increased, the color wall filters also increase. Similarly, when the color scales are decreased, the color wall filters also decrease. This implies that when trying to detect very low velocity flow, the color scales must be lowered so as to lower the color wall filters. If the color scales are set too high, the corresponding high wall filters can potentially eliminate the signals from the low velocity flows, resulting in no low velocity flow presented in the image. Note that for all ultrasound systems, changing the color scales automatically changes the color wall filters.

A further complexity with color wall filters exists. In addition to the color wall filters changing with the color scales, many ultrasound systems allow the user to set how aggressively the wall filters attenuate the lower mean velocity flow signals. When the wall filters are set to "high," the percentage of the color scales to which the wall filters attenuate increases. With wall filters set less aggressively, the percentage to which the wall filters attenuate decreases. With respect to interpretation, for many systems there is a visual clue given on the color bar (the width of the black band), as shown in Fig. 4.14a, b. In Fig. 4.14a, note that the band is narrower since the wall filter was set to low, whereas in Fig. 4.14b, note that the black band is wider (the wall filter was set to high). For those systems that do not vary the width of the black band, you must look on the screen for the description of the wall filter setting (usually as low, medium, and high).

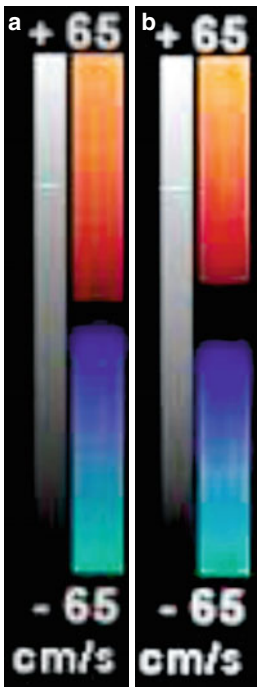


**Fig. 4.14** (**a**) Low wall filters. (**b**) High wall filters

**Conclusion**

For many people, physics is a very challenging topic, especially when presented without a clear connection to specific applications. For this reason, many people mistakenly conclude that physics knowledge is not important for good interpretation skills. Although there are significantly more topics that could be discussed, it is hoped that the approach taken here is deemed more useful than a more expansive physics lecture. It is further hoped that by seeing the physics and instrumentation discussed relative to the direct vascular application, the reader will be less inclined in the future to shy away from physics and instrumentation concepts which form the basis of advancements in vascular medicine.

## Bibliography

Miele FR. Ultrasound physics and instrumentation. 4th ed. Forney: Miele Enterprises, LLC; 2006.

Miele FR. Essentials of ultrasound physics: the board review book. Forney: Miele Enterprises, LLC; 2008.

# Vascular Hemodynamics

5

Henrik Sillesen

**Abstract**

This chapter describes arterial and venous hemodynamics especially relevant for noninvasive assessment by ultrasound imaging and Doppler in addition for peripheral pressure measurement.

Understanding the fundamentals of hemodynamics is crucial for the investigator in order to draw the right conclusions from vascular testing. Using noninvasive methods, diagnosis of most vascular conditions can be made with great accuracy. Also, many invasive interventions can be made based on these tests without the need of invasive diagnostic methods or methods using radiation; however, the most important aspect of noninvasive testing of hemodynamics is that they offer unique information not easily obtainable by other tests plus the fact that noninvasive tests can be repeated whenever needed without endangering the patient.

**Keywords**

Venous and arterial hemodynamics • Vascular resistance • Flow profile • Turbulence • Blood pressure • Pressure gradient • Reflux

## Introduction

Understanding vascular hemodynamics is essential in order to understand, perform, and interpret vascular tests. Normal and pathological hemodynamic criteria constitute the basis for most of the diagnostic criteria used in noninvasive methods that we have in the vascular laboratory. Whereas pathological hemodynamic findings are associated with signs/symptoms of ischemia in the target organ, they most often originate from vessels at some distance, i.e., in patients with large vessel stroke, i.e., in the left hemisphere, the responsible atherosclerotic lesion may be located in the left carotid artery. In fact, atherosclerosis, being killer number one in the Western world, in addition to being responsible for most cases of invalidity and being the most costly disease, is associated with pathological hemodynamics somewhere proximal in the circulation, especially of interest in vessels responsible for the stroke, heart attack, or whatever event/organ that is in focus. Interestingly, atherosclerosis develops slowly over, i.e., four to six decades before symptoms most often develop and is therefore present in many asymptomatic persons, opening the opportunity to screen selected populations where preventive treatment may exist.

This chapter will describe normal and abnormal hemodynamic findings in the peripheral circulation. Focus will be on findings in large- and middle-sized vessels since these are the main targets for noninvasive testing.

## Blood Flow in the Normal Arterial Circulation

Blood is pumped around the human body by the heart, flowing through large- to middle- and small-sized arteries to finally be delivered at the arterioles, which control blood through the

H. Sillesen, M.D., DMSc
Department of Vascular Surgery,
Rigshospitalet, University of Copenhagen,
Blegdamsvej 9, DK2100 Copenhagen, Denmark
e-mail: sillesen@mac.com

A.F. AbuRahma, D.F. Bandyk (eds.), *Noninvasive Vascular Diagnosis*,
DOI 10.1007/978-1-4471-4005-4_5, 

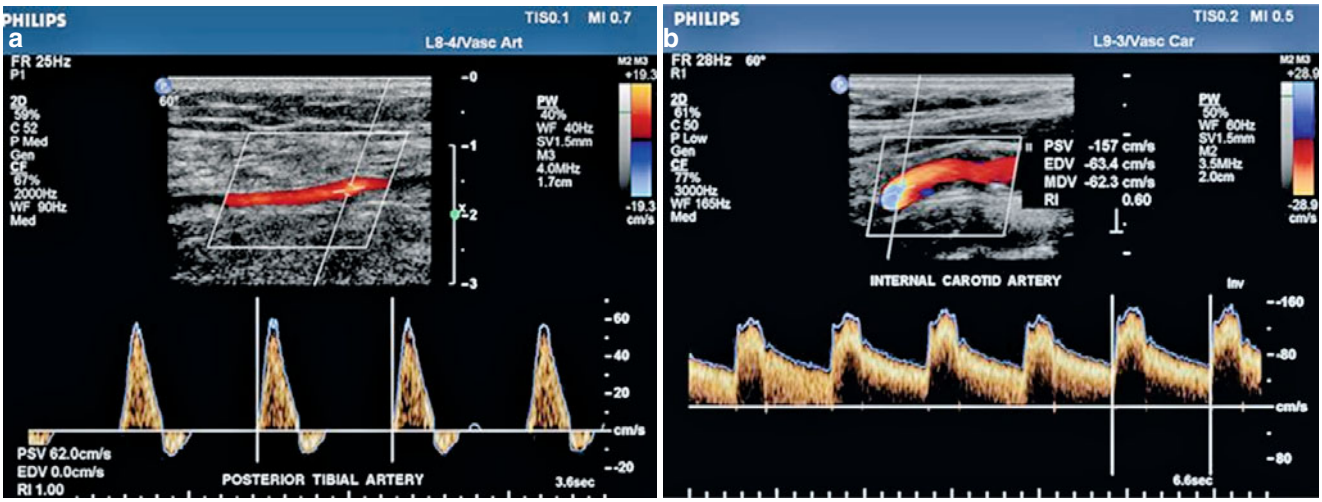


**Fig. 5.1** (**a**) Velocity curve (Doppler spectrum) from posterior tibial artery at rest illustrating how flow velocity is high during systole but low or zero during diastole. Note the steep acceleration and deceleration phase, short negative flow in early diastole – high resistance flow. (**b**) Velocity curve from internal carotid artery. Note the less steep acceleration and deceleration phases and continuous forward flow throughout the cardiac cycle

capillaries where most exchange of oxygen, carbon dioxide, and other particles related to metabolism takes place.

Blood flow is pulsatile due to the heartbeat, being driven forward during all of the cardiac cycle due to the positive pressure even in diastole (because of closure of the aortic valve and resistance in the arterial circulation). However, due to differences in resistance, blood flow is regulated to certain organs by the muscular tone of the arterioles. That is, blood flow to the extremities is low during rest since muscular metabolism is low; thus, the arterioles contract resulting in high resistance in order to limit circulation to the needs. When exercising, the metabolic needs increase, the arterioles dilate, the resistance is reduced, and the blood flow increases. Other organs, i.e., the brain, have more or less constant, high blood demand; thus, the resistance in the arteries supplying the brain is low (Fig. 5.1). For these reasons, blood flow profiles may differ depending on which artery and which state the artery/vascular bed supplied is in. Blood flow to the gut varies with state of "nutrition": When fasting, blood flow is low and resistance high, whereas blood flow increases substantially shortly after eating revealing low resistance pattern. Table 5.1 lists different arteries and their flow properties.

**Table 5.1** Vascular beds and resistance patterns

| | Low resistance | High resistance |
|---|---|---|
| Internal carotid | + | |
| External carotid | | + |
| Vertebral artery | + | |
| Renal artery | + | |
| Superior mesenteric artery | +[a] | +[a] |
| Brachial artery | | +[b] |
| Femoral artery | | +[b] |

[a]When fasting, resistance is high; postprandial vasodilation results in lowering of resistance

[b]High resistance when resting. During muscular exercise, vasodilation takes place, and resistance is reduced

## Flow Profiles

Because arteries are not always straight tubes, but often are curved or bifurcate, blood flow velocity across the vessel may differ. That is, blood flow in the left carotid artery is parabolic in the section between the aortic arch and the carotid bifurcation (parabolic flow: low flow velocities near the vessel walls but high flow in the rest of the artery). However, in the bulb, just before branching into the internal and external carotid arteries (ICA and ECA), blood flow velocities become skewed toward the internal because most flow will be directed to the ICA (Fig. 5.2). Furthermore, flow profiles may vary during the cardiac cycle. As is seen in the flow profile from the ICA, flow is forward during systole in most of the vessel, but opposite the flow divider it is shortly retrograde during systole, whereas in diastole, flow is continuously forward (Fig. 5.3).

## Velocity Profiles

Velocity profiles may differ according to vascular bed being supplied. The CCA bifurcates into the ICA and ECA, the ICA supplying the brain having an almost constant, high blood flow due to a high oxygen demand. Therefore, resistance is

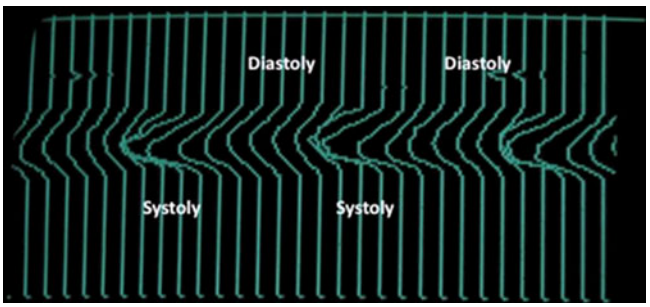


**Fig. 5.2** Flow profile (pulsed multigated Doppler) from the common carotid artery just before bifurcating into the ICA and ECA. Each vertical line represents velocity as a function of depth, with forward illustrated to the left and backward flow to the right. A new line is generated every 80 ms

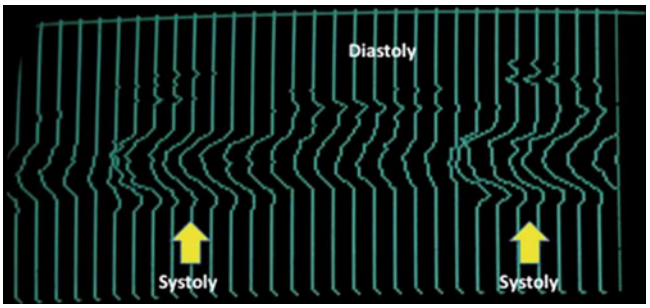


**Fig. 5.3** Flow profile (pulsed multigated Doppler) from carotid bifurcation showing flow separation (*arrows*) during systole. Note flow is retrograde (right shift) along the far wall of the artery during systole

low resulting in high flow throughout the cardiac cycle. The ECA supplies mainly structures outside the skull and reveals a more or less constant high resistance with only low forward flow in diastole.

As mentioned, also physiological states in vascular beds affect velocity profiles. In the resting limb, the velocity profile is triphasic: steep acceleration and deceleration phase during systole, a short period of retrograde flow, and then slow forward flow in diastole. Almost similar, the velocity profile in the superior mesenteric artery reveals only little diastolic flow when fasting, but shortly after a meal, resistance is lowered, and flow is high both in systole and diastole.

The *pulse wave* moves forward from the heart after contraction of the ventricle. The speed depends on stiffness of the arteries it travels through; i.e., it may become faster with age with gradual stiffening of the arteries. Watching an electrocardiogram (ECG) and palpating the radial artery pulse at the same time will reveal that pulse is felt sometime after the t-notch and not during the QRS complex when left ventricle contraction takes place. When the pulse wave moves, the artery due to its elastic properties dilates and recoils, thereby promoting forward blood flow since the aortic valve inhibits backward flow. The dilatation is typically 2–3% but may be up to 10% depending on which artery: the carotid bulb dilates up to 10% and other large arteries a 2–5%. Aortic aneurysms may dilate up to 10% more during systole. If reliable measurements for comparison over time, i.e., of aortic diameter, are to be made, first of all, measurements have to be taken at a defined stage in the cardiac cycle, i.e., during systole or diastole. In order to do accurate repeated measurements in the same patient during the same investigation, ECG triggering may be used to identify exactly the same stage of the cardiac cycle.

The *effect of gravity* is important to have in mind when performing and evaluating vascular testing. For blood pressure measurement, in order to get an estimate of central cardiac blood pressure, the cuff should be at approximately the same level as the heart. Placing it on the upper arm with the patient sitting relaxed with the arm at the side of the chest, or lying down with his arms by the side, the blood pressure will be quite representative. Since the mid-brachium will be at the same level as the heart, both sitting and lying blood pressure measurement should reflect central blood pressure. However, care should be taken when estimating peripheral blood pressure, being it on the antebrachium or at the ankle. Here, it is imminent to evaluate if the location of the blood pressure cuff is at the level of the heart. A difference of, i.e., 10–15 centimeter (cm) will result in a difference in blood pressure of 7–11 mmHg; 15 cm difference equals to 150 mm water which is the same as 11 mmHg (150/13.6). Ankle pressure standing is therefore very high: the central cardiac systolic pressure plus the distance from the heart to the ankle translated into mmHg. For an average person 180 cm in height, the distance from the heart to the ankle may be 140 cm; thus, the ankle pressure standing would be approximately 240 mmHg if the "normal" central pressure is 120/80 mmHg.

Evaluating arterial flow patterns, i.e., with ultrasound Doppler, is best performed with the patient lying; thus, most arteries will be at heart level. Gravity obviously has much greater impact when investigating the venous circulation, which will be discussed later.

## Blood Flow in Diseased Arteries

The far most common arterial disease seen in the western world is atherosclerosis which is an inflammatory process that develops over decades. Atherosclerosis results from thickening of the vessel wall due to lipid accumulation and inflammation in the intima and subsequent plaque develops. Because of the slow buildup of plaque and arterial remodeling, hemodynamic changes do not take place for years. Therefore, early stages of atherosclerosis are not detected by tests that evaluate hemodynamic parameters rather imaging methods should be used. Not before the arterial lumen is reduced by 15–20% may local effects of atherosclerotic plaque/stenoses be detected. Eventually, atherosclerotic

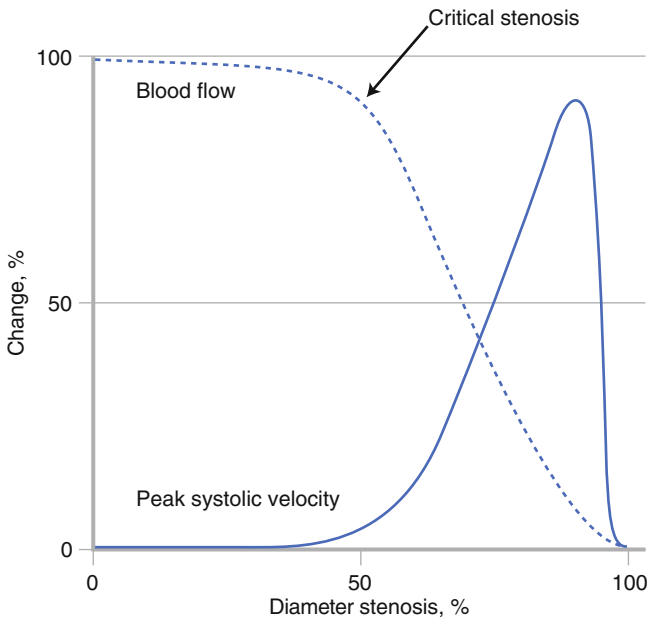


**Fig. 5.4** Diagram showing the relationship between volume flow, degree of stenosis, and pressure. The term "critical stenosis" is typically used when a stenosis exceeds the degree where volume flow decreases

lesions grow and gradually reduce the lumen more and more, and in some cases, acute thrombosis occurs resulting in sudden occlusion at the site of stenosis or dislodgement of thrombotic material (embolism). Other conditions that may result in pathological hemodynamics are trauma, dissection, aneurysms, etc.

Arterial stenosis, from whatever cause, results in a number of flow-related changes of which three are essential to understand when interpreting noninvasive vascular tests: changes in *peak flow velocity*, development of *turbulence*, and *changes in flow profile*.

## Critical Stenosis

Critical stenosis (or significant stenosis) is a term commonly used to describe a lesion severe enough to reduce flow through the artery. In general terms, and with the hemodynamics in the human circulation, we speak about a critical stenosis when the lumen (cross-sectional area) is reduced by 75%, as may be seen in Fig. 5.4. Seventy-five percent luminal reduction corresponds to a 50% reduction in diameter if seen on an arteriogram or longitudinal ultrasound B-mode image (assuming a round artery).

Since blood flow in arteries varies from artery to artery and in different physiological states, it is clear that the same degree of stenosis may not be critical in two different anatomical locations. That is, 75% luminal reduction in a carotid artery may result in reduced volume flow through that artery, but a similar stenosis in the iliac artery may not cause any

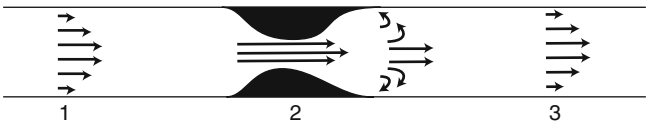


**Fig. 5.5** Drawing of stenosis with velocity vectors within and distal to lesion

symptoms or measurable hemodynamic changes in the lower limb at rest. However, following exercise when blood flow increases dramatically (may increase as much as five- to ten-fold), blood flow reduction and pressure drop may develop, and the patient may complain of pain in the ipsilateral limb (claudication).

## Peak Velocity

Development of stenosis results in compensatory increased flow velocity. Consider watering in a garden holding the water hose in the hand. In order to water those flowers 15–20 ft away, the thumb may be placed at the end of the water hose resulting in a longer jet. In fact, the length of the jet may be regulated by changing the residual lumen at the end of the hose: the smaller, the lumen the longer the jet. Increasing degrees of stenosis has the same effect on blood flow velocity; thus, increases in peak velocity are the most commonly used parameter for diagnosing moderate to severe arterial stenosis.

Peak velocity in an artery is highest within or just distal to the stenosis and gradually returns to "normal" (or lower) with increasing distance from the stenosis (Fig. 5.5). Generally, it can be expected that velocity has normalized 6–8 normal arterial diameters from the stenosis. In a normal sized ICA, the peak velocity most often will have returned to the prestenotic value (or lower) just below the jaw bone unless the bifurcation is very high. In case of severe stenosis with major flow reduction, peak velocity may be lower than prestenotic, depending on whether the prestenotic vessel also delivered blood to other vascular beds, i.e., the ECA.

In arteries with constant flow, such as the ICA, absolute assessment of velocity is useful. Since blood flow to the brain is fairly constant and since the relationship of the carotid arteries to volume flow is reasonably similar from person to person, a peak velocity around 120–130 cm/s has been identified as the maximum in unstenosed arteries (or in arteries with less than 50% diameter reduction = 75% luminal reduction).

In arteries with varying flow, i.e., in the lower limb or the mesenteric artery, it may be difficult to use criteria with an absolute velocity number. Therefore, the ratio of peak velocity in the stenosis and distal to the stenosis may be useful. The assumption necessary for such criteria is that there are no branches between measurement sites in the artery in question (same volume flow where measurements are taken). Another clinical example relates to monitoring of in situ vein bypass

grafts. Since such a graft quite often develops stenoses, either at the anastomoses or somewhere along the graft (i.e., at sites of cut valves), ultrasound Doppler surveillance is used by many. Since there are no branches, velocity ratios are useful – peak velocity within the stenosis compared to peak velocity distally. A ratio >2–3 is indicative of a critical stenosis.

## Turbulence

When blood passes through areas with increased flow velocity due to narrowing of the vessel (stenosis), immediately distally, blood flow in the center stream will seek laterally creating a more "disturbed" flow pattern or so-called turbulence. Development of turbulence is a function of diameter of the artery, mean flow velocity, density, and viscosity of blood. Turbulence can be detected by ultrasound Doppler in lesions only reducing the diameter by 15% or more. Figure 5.6 illustrates how flow is almost uniformly parabolic in a normal vessel and how slight turbulence is detected just distal to a 60% stenosis. In clinical practice, turbulence is the most sensitive hemodynamic sign for identification of atherosclerotic lesions; imaging methods, i.e., ultrasound B-mode, may detect lesions even smaller – see Chap. 7.

## Changes in Velocity Profile

Severe occlusive lesions may induce changes in the velocity profile. In general, what elicits the change is lowering of peripheral resistance due to the pressure drop across the stenosis. Two conditions need to be met in order for a stenosis to result in a pressure drop: First, the degree of luminal narrowing has to exceed 75% (or in case of slightly lesser stenosis, flow has to be very high) and, second, collateral blood supply must be insufficient to compensate for the blood flow reduction. (Collateral blood supply may arise from existing vessels (circle of Willis in the brain, Riolan's artery in the mesentery), or it may be new vessels that develop in response to ischemia.)

Due to the lower peripheral resistance caused by a reduction in blood pressure across the stenosis, a "dampening" of the velocity profile occurs. Where the velocity profile proximal to the stenosis displays a steep acceleration and deceleration phase, distal to the stenosis, the acceleration in systole is less, and similarly, deceleration phase in diastole appears less steep. There is an increase in diastolic flow, and the so-called "triphasic" shape of the velocity profile is replaced by a monophasic (Fig. 5.7).

## Autoregulation

Blood flow to organs/extremities is regulated in order to keep flow more or less constant (when needed constant) and independent of blood pressure. When blood pressure increases, resistance vessels contract and vice versa when pressure drops (autoregulation). The brain can hereby ensure constant blood flow, except when blood pressure becomes very low. Below, i.e., <60–70 mmHg systolic pressure, cerebral blood flow declines. When arterial stenosis, i.e., carotid,

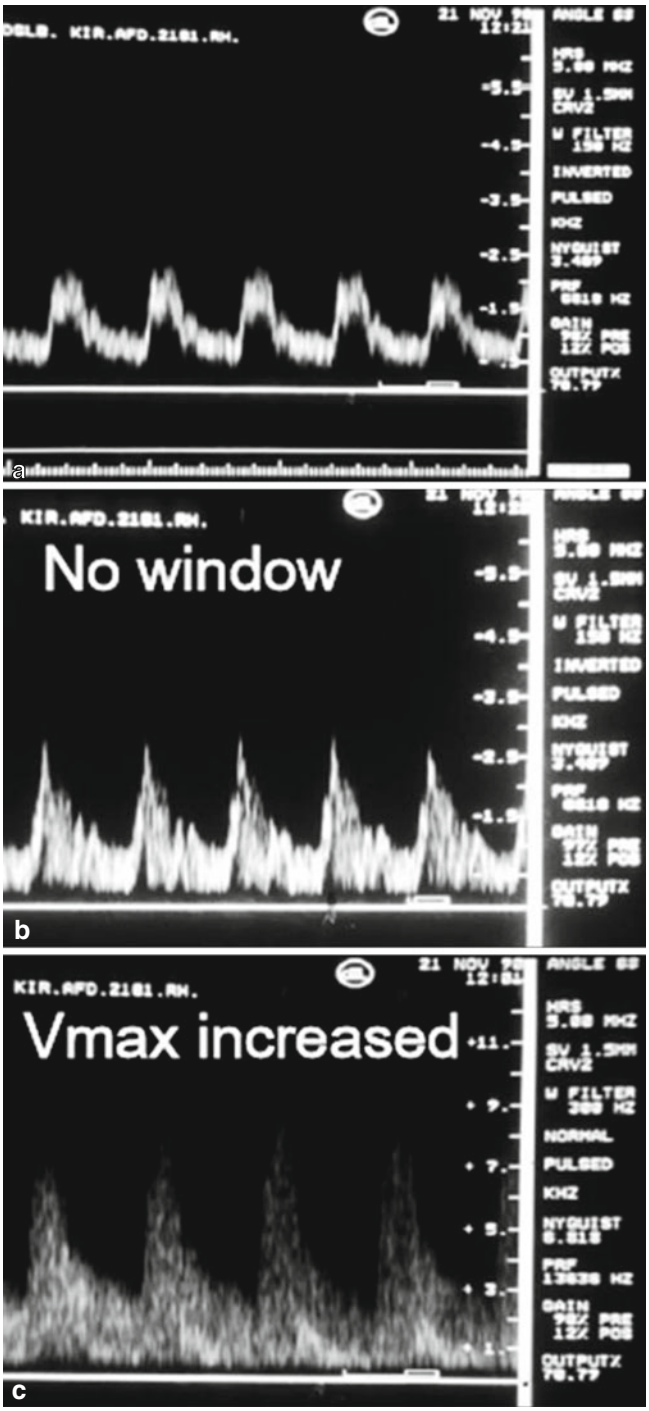


**Fig. 5.6** (**a**) Doppler spectrum from a normal artery, (**b**) Doppler spectrum from artery <50% stenosis, (**c**) Doppler spectrum from artery with >50% stenosis

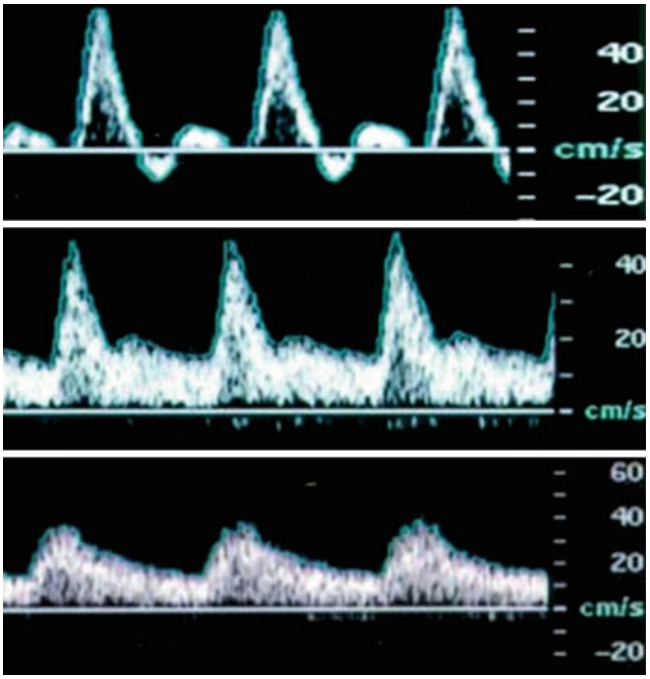


**Fig. 5.7** Duplex scan of mid-thigh superficial femoral artery stenosis in a patient with calf claudication. At rest, a triphasic waveform was recorded proximal and a focal stenosis with a PSV of 441 cm/s was identified (criteria indicating a >50% diameter reducing stenosis). Treadmill exercise (12% grade at 1.5 mph) results in a decrease in ankle pressure from 132 mmHg at rest (ABI=0.8) to 50 mmHg after walking for 2 min. The patient underwent percutaneous transluminal balloon angioplasty of the lesion with restoration of normal limb hemodynamics (ABI > 1.0)

causes chronic pressure reduction across the stenosis, autoregulation ensures cerebral blood flow to a certain extent. In case carotid endarterectomy is performed, and the stenosis is removed, thereby normalizing blood flow through this artery, autoregulation may not be functioning for some time postoperatively (weeks). In this period, blood flow will be pressure dependent, and there may be risk of cerebral hyperfusion and subsequent cerebral hemorrhage. Similarly, in a limb with chronic critical arterial insufficiency, i.e., a patient with rest pain or nonhealing ulcers, operated with a bypass to restore perfusion, autoregulation may be nonfunctioning postoperatively, and the foot will appear very warm and red, and flow profiles in the graft and distal vessels will reveal low resistance at rest. The pressure level at which autoregulation still functions in the lower limb is lower than for the brain, i.e., 20–30 mmHg.

## Vascular "Steal" Phenomena

Direction of flow in an artery is driven by blood pressure and vascular resistance. When major blood pressure drop occurs due to vascular obstruction, flow direction may change. The classical example is the so-called "vertebral steal." In this case, flow is backward in the left vertebral artery due to occlusion (or severe stenosis) of the subclavian artery at its origin from the aortic arch. In this manner, the blood supply to the left arm originates from the vertebral artery, which has reverse flow. In the classic syndrome, the patient experiences episodes of dizziness and other nonfocal neurological symptoms when exercising the left arm, indicating "steal" of blood from the brain to the arm. The syndrome is easy to demonstrate using ultrasound Doppler: with the vertebral artery insonated, flow direction is noted. A blood pressure cuff on the relevant upper arm is inflated above the systolic blood pressure to induce ischemia (1–2 min). When the cuff is deflated, flow will increase if steal is present – as a result of postischemic hyperemia. However, most cases of vertebral steal syndrome are asymptomatic, i.e., either found accidentally or symptoms are unrelated to use of the left arm.

Performing thoracic aortic stent grafting, i.e., to treat dissection, the left subclavian artery may be "overstented," meaning that the left subclavian artery intentionally is covered by the stent graft resulting in occlusion. In these cases, if not treated with a bypass or transposition, vertebral artery steal may occur.

## Blood Flow in the Normal Venous Circulation

Return of blood from the capillaries to the heart takes place through veins. The anatomy is much more variable than that of the arterial circulation; however, some general concepts are important. Veins have thinner walls than arteries and are equipped with valves, preventing retrograde flow (Fig. 5.8). To secure return of blood to the heart, the venous system also serves as "blood reservoir" or capacitance vessels, in addition to acting as part of hemostatic system.

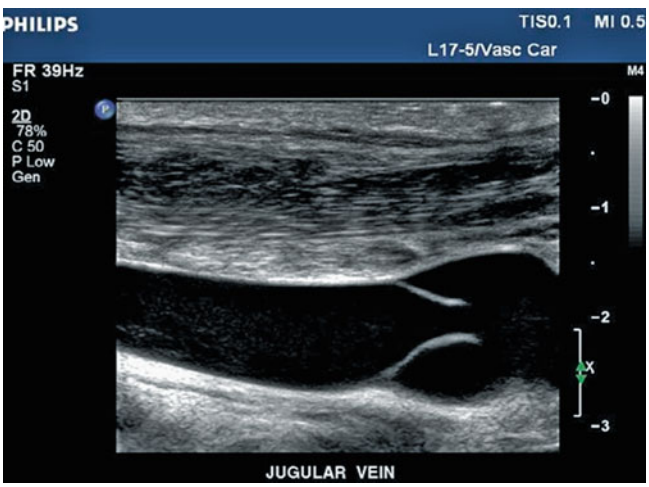


**Fig. 5.8** Ultrasound image of normal jugular vein with valve

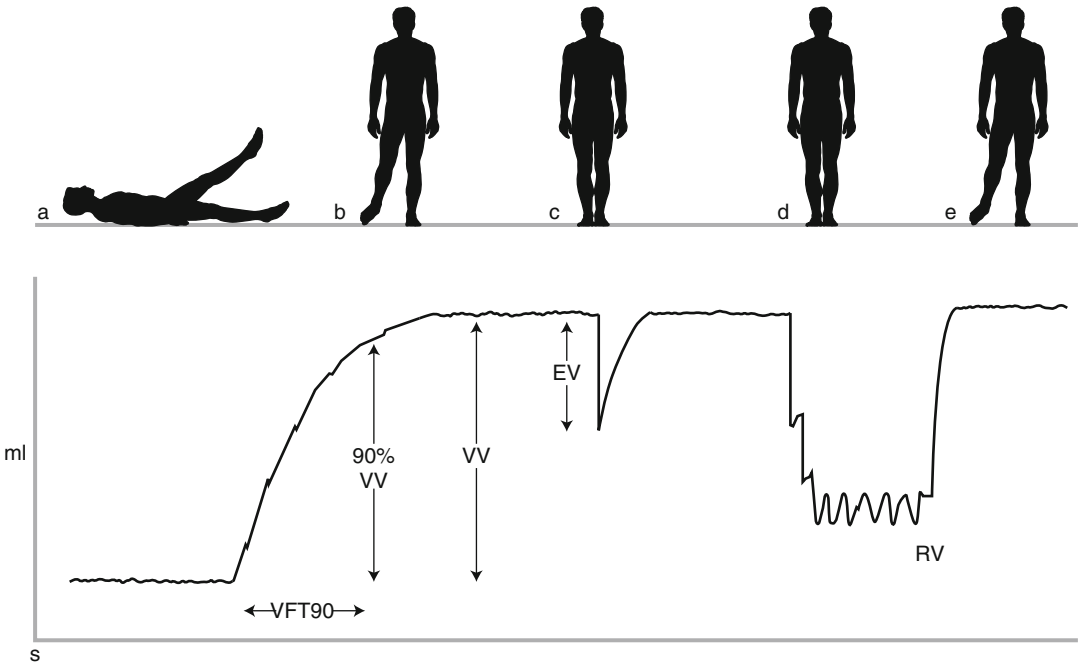


**Fig. 5.9** Relationship between venous volume and activity of the muscle pump. (**a**) Venous volume is low when leg is elevated. (**b**) Standing increases venous volume, and (**c**, **d**) exercise reduces it when the deep valves are intact. (**e**) When standing, veins get filled again

Superficial veins are located above (outside) muscle fascia, whereas deep veins are located within muscle fascia. When muscles contract, they exert pressure on the veins inside the fascia, and since venous valves prohibit retrograde flow, blood is expelled forward toward the heart (muscle pump, Fig. 5.9). Venous valves are located everywhere in the venous system but most abundant in the lower extremity where the effect of gravity is greatest.

Perforating veins (perforators) connect the superficial and deep system with valves directing blood flow inward – from the superficial to the deep venous system. From a pathophysiological perspective, perforators are most important in the lower limb due to hydrostatic pressure and therefore abundance of people/patients with lower limb venous diseases/conditions. The most important perforator locations are sapheno-femoral junction in the groin, sapheno-popliteal junction in the popliteal fossa, and perforators at the medial side of the lower limb connecting the superficial veins with the deep veins.

Blood flow in veins is in the supine position driven by pressure gradients and in the standing position by the "muscle pump." In supine position, blood pressure at the venous end of the capillary is 12–18 mmHg in contrast to 4–7 mmHg in the right atrium. Therefore, blood moves passively along this pressure gradient.

Breathing has an impact on venous flow. During inspiration, when diaphragm moves downward and increases the intra-abdominal pressure, the large veins are compressed, and blood is forwarded toward the heart. The intrathoracic pressure becomes negative also facilitating veins blood flow to the heart. Therefore, especially in the supine position, venous flow will be synchronous with respiration.

When using the muscle pump, the blood pressure may reach 200 mmHg at maximal contraction. The pump is most efficient in the calf muscles where up to 65% of blood is emptied during contraction; in the thigh, only 15% of blood is emptied upon muscle contraction. Consequently, the volume of the calf decreases slightly when exercising.

Venous blood pressure is low in the supine position. However, when standing still, blood pressure in a foot vein increases up to around 80–100 mmHg depending on height (distance from the heart to the foot). When using the muscle pump (i.e., walking), venous blood pressure rapidly declines to 5–15 mmHg, and when standing still again, it increases to 80–100 mmHg again (Fig. 5.10). If valves are incompetent, obviously, this pressure reduction is less or almost abolished, i.e., in severe postthrombotic syndrome.

Supra-aortic veins, on the other hand, will have similar hemodynamics to other veins except when in the upright position. Since blood pressure in the heart (right atrium) is low (4–7 mmHg), it may become negative when standing; because blood pressure in the jugular vein becomes negative when standing, special care should be taken not to have open intravenous access lines in the jugular vein since air will suck into the vein.

Palpating veins will reveal the pressure relationship with gravity: in the upright position, veins are dilated on the extremities and do have some pressure. When supine, veins either collapse or become much thinner and disappear at the lightest touch. Similarly, examining veins with an ultrasound scanner, in supine position veins are easily compressible. In fact, care should be taken not to compress veins simply by pressure from the transducer – obviously depending on depth

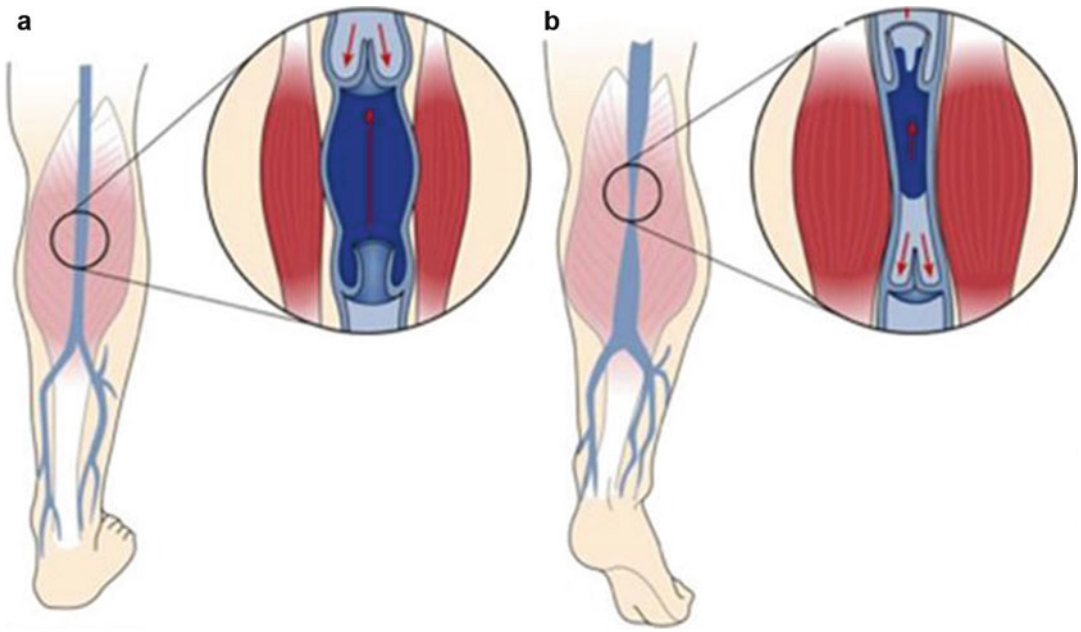


**Fig. 5.10** Venous "muscle pump". (**a**) Relaxed calf musculature with open vein and open valves distal to the muscle. (**b**) Compressed calf muscle and closed valves distally but open central valves so the blood from the compressed vein can flow toward the heart

of the vein. Also venous diameter will change as a function of gravity: examining the jugular vein in supine position will reveal a large structure of variable shape, i.e., triangular, oval, etc.; however, scanning in upright position, the vein will either just be much smaller or have collapsed.

## Blood Flow in Diseased Veins

The main clinical conditions in veins are deep vein thrombosis and superficial thrombophlebitis (thrombosis in one or several venous segments) and development of venous reflux due to valve insufficiency, which can result in either superficial venous insufficiency (varicose veins) or deep venous insufficiency, which is much more complex and may be invalidating.

Superficial thrombophlebitis most often occurs at sites of intravenous lines, either during their use or after removal. This is a benign condition and does not warrant testing. Superficial thrombophlebitis may also develop spontaneously which can be seen in patients with varicose veins but may also be related to other conditions.

Deep venous thrombosis is often related to coagulation disorders, of which the heterozygote form of Factor V Leiden is the most common, but may also occur in people with normal coagulation system. However, in most cases, irrespective of status of the coagulation system, there is a relationship to trauma, surgery, other disease, or condition that has resulted in inactivity. When thrombosis occurs, there is an immediate occlusion of the affected vein. Later, after a few weeks/months, spontaneous lysis may result in opening of the affected vein, however, often with damage to the valves located in the affected venous segment. These patients develop venous hypertension when standing and walking (exercising) because the muscle pump will not be as effective due to insufficient venous valves directed venous flow in both directions upon contraction of the muscle. In other cases, occlusion may become chronic, and if not compensated by development of venous collaterals, venous hypertension may develop and also pain related to walking/exercising, so-called venous claudication. In both cases, due to venous hypertension, valves between the deep and superficial system may become insufficient and result in reverse blood flow through the perforators (from the deep to the superficial veins) and cause development of secondary varicose veins.

Venous reflux is a condition that results in venous hypertension due to gravity. Therefore, almost only the lower limb becomes affected by varicose vein development, except in cases of venous obstruction, which can result in varicosities anywhere. Since the condition, reflux, mainly exists in the horizontal position, testing is also done with the patients standing. As will be described in Chap. 41, older tests using rubber bands and clinical assessment have been abandoned with the development of ultrasound duplex scanning systems using adequate scanning protocols. With the patient standing, the veins can be examined for reflux: standing on the contralateral leg with the examined leg resting, the vein in question (i.e., great saphenous vein) is insonated and flow evaluated by Doppler. Upon compression of the calf muscle, venous flow will increase immediately, and when releasing compression, flow will stop, and in a normal vein, there will

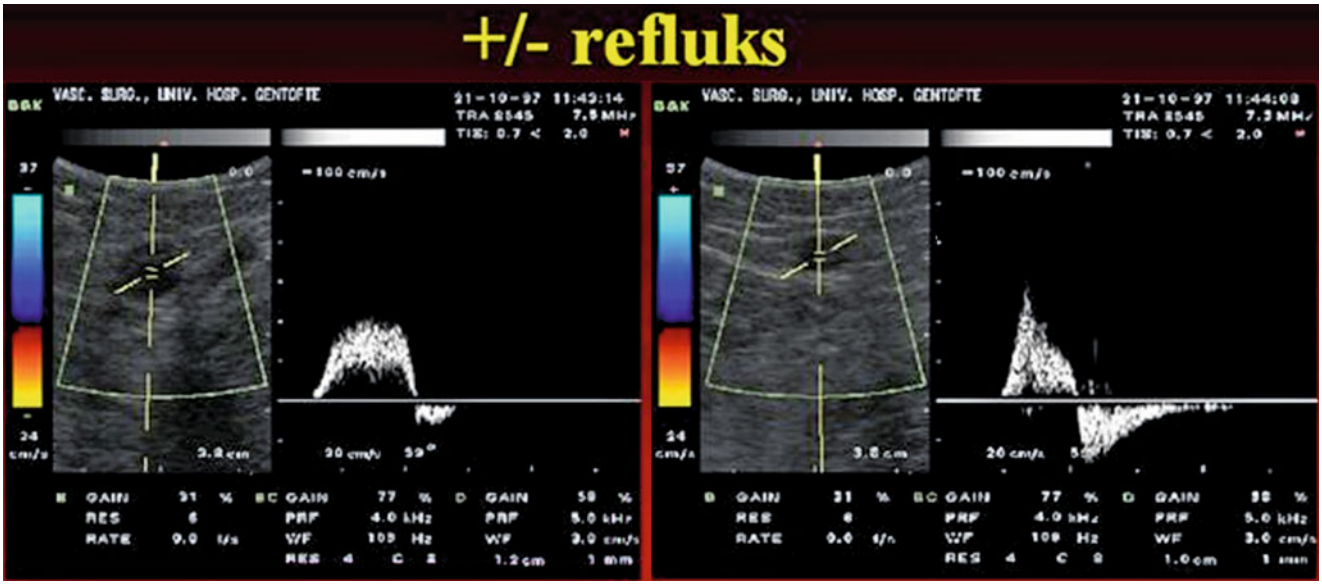


**Fig. 5.11** Doppler spectrum from vein with competent valves and Doppler spectrum from vein with incompetent valves

be a short, small retrograde flow segment in the flow curve followed by no flow or only slight forward flow. Examining an incompetent vein, after the flow increases due to compression, blood flow will be reversed when compression is released (Fig. 5.11). Another way of testing for venous valve function is to ask the patient to perform Valsalva's maneuver while insonating the vein in question.

Finally, hemodynamics in venous obstruction reflects the effects of venous hypertension. First of all, there may not be any signs of venous congestion at rest, i.e., flow appears normal and does increase on peripheral compression. In case of common iliac vein occlusion, venous outflow may be sufficient during rest, and the femoral/external iliac vein may serve as capacitance vessels allowing accumulation of venous blood when peripheral compression test is performed and appears normal. However, when exercising, and drainage increases by a factor V or more, venous collaterals may become insufficient and congestion occurs.

# Part III

# Cerebrovascular Diagnosis

Ali F. AbuRahma

# Overview of Cerebrovascular Disease

6

Ali F. AbuRahma

**Abstract**

Stroke is the third leading cause of death in industrialized nations, with an annual incidence of about 700,000 stroke events. Ischemic strokes constitute 80–86% of all strokes. It has been estimated that ≥50% carotid stenosis may be responsible for up to 25% of all ischemic strokes. This chapter highlights the basic anatomy and pathophysiology of the extracranial carotid system. The common carotid bifurcation and the proximal internal carotid artery account for 50% of the lesions. The most common cause of cerebral ischemic events is embolic phenomena, primarily arterial in origin (carotid) and secondary to cardiac sources. The work-up of patients presenting with asymptomatic carotid bruits or TIAs should include initial carotid duplex scanning. Duplex scanning of the carotid bifurcation provides a highly accurate method of identifying significant lesions of the internal carotid artery as well as of separating lesions into general pathologic categories. Carotid CTA/MRA may be added to the work-up of these patients, particularly if the carotid duplex ultrasound is inadequate, and conventional arteriography is usually reserved for use prior to CAS. Management of these patients includes medical treatment alone or CEA/CAS with medical treatment.

**Keywords**

Cerebrovascular • Disease • Overview

## Introduction

Stroke is the third leading cause of death in industrialized nations (behind heart disease and cancer). It is also a leading cause of long-term disability [1] with an annual incidence of about 700,000 stroke events, of which about 200,000 are recurrent and 500,000 are new strokes [2]. It is the cause of death in approximately 150,000–200,000 Americans annually. The morbidity of those who survive a stroke has a significant socioeconomic impact on our society. It is estimated that strokes account for the disability of two million Americans. The cost of medical bills, hospitalization, and rehabilitation was estimated to be around $69 billion in 2009.

Ischemic strokes constitute 80–86% of all strokes, and the remaining 14–20% are caused by cerebral hemorrhage [3]. It has been estimated that ≥50% carotid stenosis may be responsible for up to 25% of all ischemic strokes. Large population studies using carotid ultrasound estimate the prevalence of ≥50% carotid artery stenosis to be 3–7%. Ideally, patients who are at high risk for stroke could be identified and treated prior to permanent neurological deficit. Unfortunately, only 15% of stroke victims have warning transient ischemic attacks (TIA) prior to stroke, and waiting until symptoms occur is not ideal [4]. This emphasizes the importance of early detection for stroke prevention.

A.F. AbuRahma, M.D., RVT, RPVI
Department of Surgery,
Robert C. Byrd Health Sciences Center,
West Virginia University, 3110 MacCorkle Ave SE,
Charleston, WV 25304, USA

Charleston Area Medical Center,
Charleston, WV, USA
e-mail: ali.aburahma@camc.org

A.F. AbuRahma, D.F. Bandyk (eds.), *Noninvasive Vascular Diagnosis*,
DOI 10.1007/978-1-4471-4005-4_6, 

Significant changes in our thinking and treatment of this disease have occurred over the past 50 years, but this has been a topic fraught with controversy since the first carotid endarterectomy (CEA) was reported. Eastcott et al. [5] performed a carotid resection with reanastomosis of a diseased vessel in a patient who suffered a transient ischemic attack. This was published in 1954, but DeBakey [6] reported a successful performance of this procedure earlier.

Today, CEA is the most commonly performed vascular surgical procedure; however, it is still controversial. The debate over medical versus surgical treatment for carotid artery disease has been extensively analyzed in the medical literature over the past 20 years. The CASANOVA, Asymptomatic Carotid Atherosclerosis Study (ACAS), Veterans Administration (VA) Cooperative Study, and Asymptomatic Carotid Surgery Trial (ACST) looked at medical versus surgical therapy in asymptomatic carotid stenosis [7–10]. Meanwhile, the VA Cooperative Study, the North American Symptomatic Carotid Endarterectomy Trial (NASCET) Collaborators Study, and the European Carotid Surgery Trialists' (ECST) Collaborative Group looked at symptomatic carotid disease [11–13].

Recently, carotid angioplasty/stenting (CAS) has been recommended as an alternative to CEA. Several randomized and nonrandomized prospective trials have been conducted over the past several years to evaluate the efficacy of CAS, in comparison to CEA, for the prevention of stroke for both symptomatic and asymptomatic patients [14–18]. Regardless of which criteria are used to determine whether operative intervention is warranted, a surgeon must stay within the accepted perioperative stroke rate of 3–7% (depending on indication) as recommended by the Ad Hoc Committee of the Stroke Council of the American Heart Association. What is generally agreed upon, however, is that early and accurate detection of stroke-prone patients remains one of the most important problems in medicine, since stroke has an immediate mortality of 20–25% within 30 days. Of the survivors of a first stroke, 25–50% will have an additional stroke.

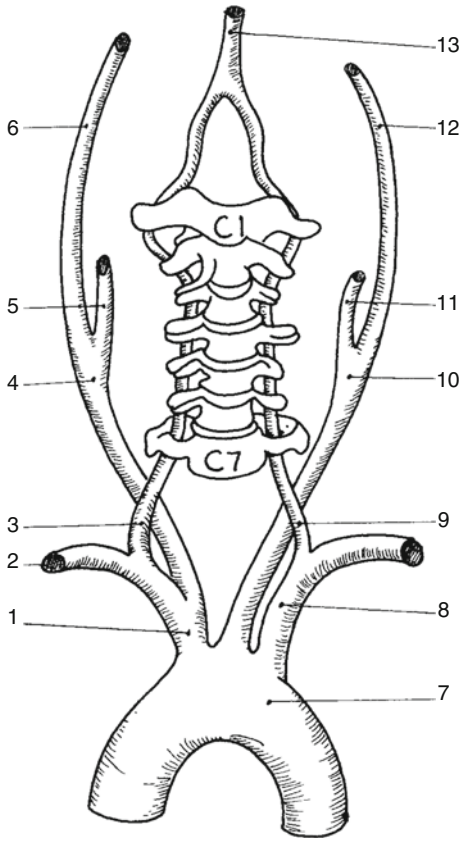


**Fig. 6.1** An illustration showing the aortic arch and its branches: (*1*) brachiocephalic trunk, (*2*) right subclavian artery, (*3*) right vertebral artery, (*4*) right common carotid artery, (*5*) right external carotid artery, (*6*) right internal carotid artery, (*7*) aortic arch, (*8*) left subclavian artery, (*9*) left vertebral artery, (*10*) left common carotid artery, (*11*) left external carotid artery, (*12*) left internal carotid artery, (*13*) the basilar artery

## Anatomy

The aortic arch gives off, from right to left, the innominate (brachiocephalic trunk), the left common carotid, and the subclavian arteries (Fig. 6.1). The innominate artery passes beneath the left innominate vein before it branches into the right subclavian and the right common carotid arteries. The vertebral arteries branch off the subclavian arteries 2 or 3 cm from the arch, but many variations may occur (Fig. 6.1). Overall, there are three types of aortic arch morphologies which are distinguished based on the relationship of the innominate artery to the aortic arch. A type I aortic arch is characterized by the origin of all three major arteries (innominate, left common carotid, left subclavian) in the horizontal plane defined by the outer curvature of the arch. A type II arch has the innominate artery originating between the horizontal planes of the outer and inner curvature of the aortic arch. In a type III aortic arch, the innominate originates below the horizontal plane of the inner curvature of the aortic arch. The left common carotid artery may share a common origin with the innominate, which is frequently called a bovine aortic arch (16%). However, this anatomy is not usually found in cattle; therefore, the term bovine arch is a misnomer [19]. The left common carotid artery may also arise from the innominate artery without having a common origin. The left vertebral artery may arise directly from the aortic arch instead of from the left subclavian arteries (Fig. 6.2). The right vertebral artery may arise as part of a trifurcation of the brachiocephalic trunk into subclavian, common carotid, and vertebral arteries (Fig. 6.3). Occasionally, both subclavian

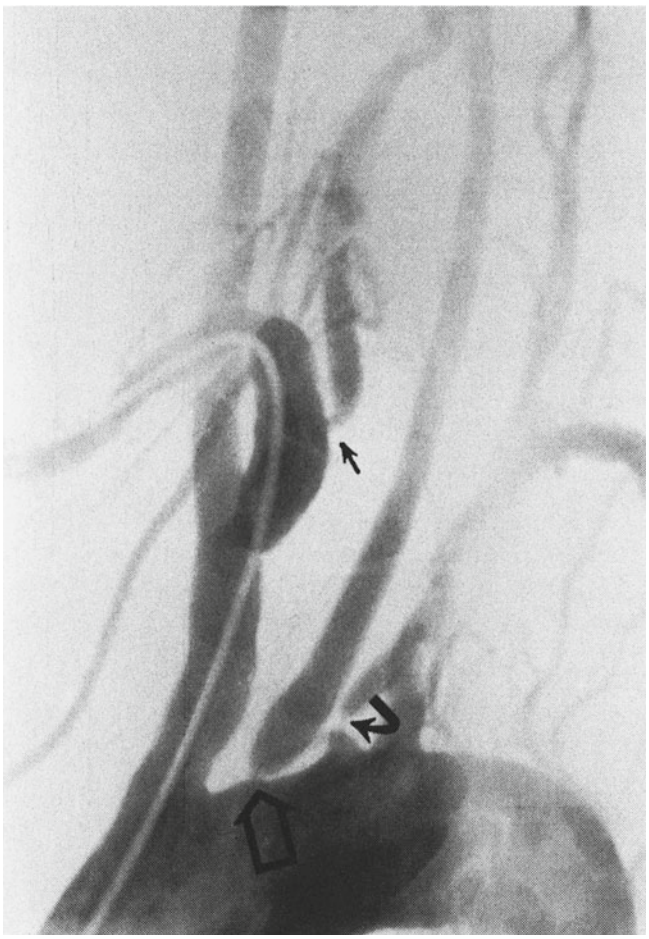

**Fig. 6.2** Arch aortogram showing left vertebral artery originating from the arch of the aorta with tight stenosis at its origin (*curved arrow*) and the right vertebral artery (coming off the right subclavian artery) with a tight stenosis at its origin (*straight arrow*)

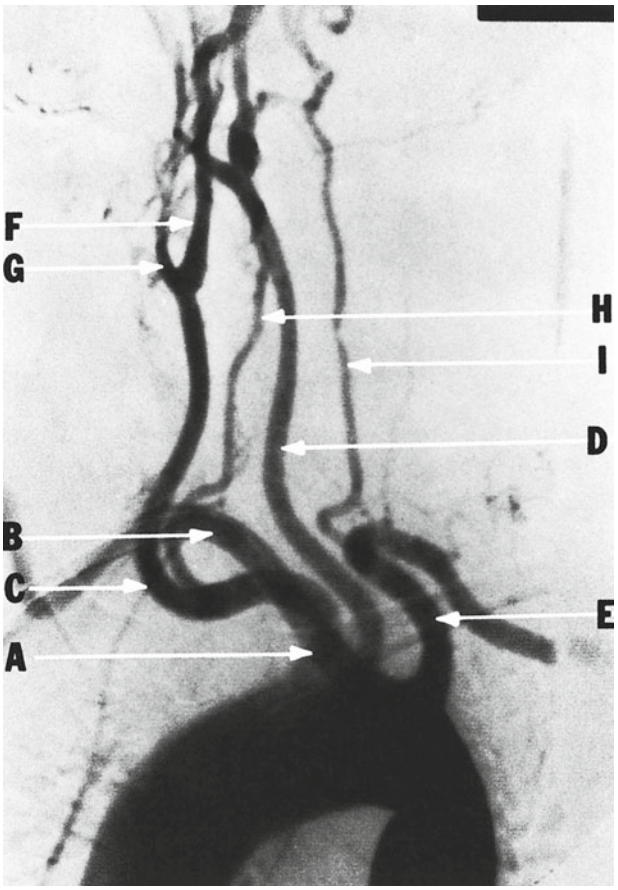


**Fig. 6.3** Abnormal origin of the vertebral artery (*H*) from the right common carotid artery (*C*) in a patient with retroesophageal right subclavian artery (*B*). (*A*) innominate artery; (*B*) right subclavian artery; (*C*) right common carotid artery; (*D*) left common carotid artery; (*E*) left subclavian artery; (*F*) right internal carotid artery; (*G*) right external carotid artery; (*H*) right vertebral artery; (*I*) left vertebral artery (Courtesy of Springer-Verlag. Berguer and Kieffer [20])

arteries originate together as a single trunk off of the arch, or the right subclavian may arise distal to the left subclavian artery and cross to the right side [21].

The common carotid arteries on each side travel in the carotid sheath up to the neck before branching into internal and external carotid arteries just below the level of the mandible. The external carotid artery supplies the face. Important branches of the external carotid artery include the superior thyroid, which can actually arise from the common carotid artery and is important in that it accompanies the external branch of the superior laryngeal nerve and the ascending pharyngeal, lingual, and occipital arteries that have a close association with the hypoglossal nerve (Fig. 6.4). No branches of the internal carotid artery are located in the neck.

The carotid sinus, a baroreceptor, is located in the crotch of the bifurcation of the internal and external carotid arteries. It is innervated by the nerve of Hering, which branches from the glossopharyngeal nerve. The carotid body is a very small structure that also lies in the crotch of the bifurcation and functions as a chemoreceptor, responding to low oxygen

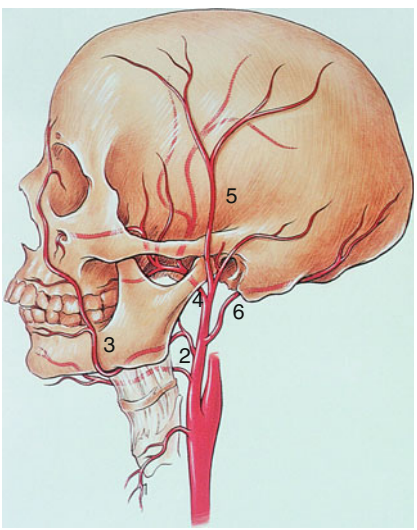


**Fig. 6.4** Main branches of the external carotid artery: (*1*) superior thyroid artery, (*2*) lingual artery, (*3*) facial artery, (*4*) internal maxillary artery, (*5*) superficial temporal artery, and (*6*) occipital artery (Courtesy of Springer-Verlag. Berguer and Kieffer [20])

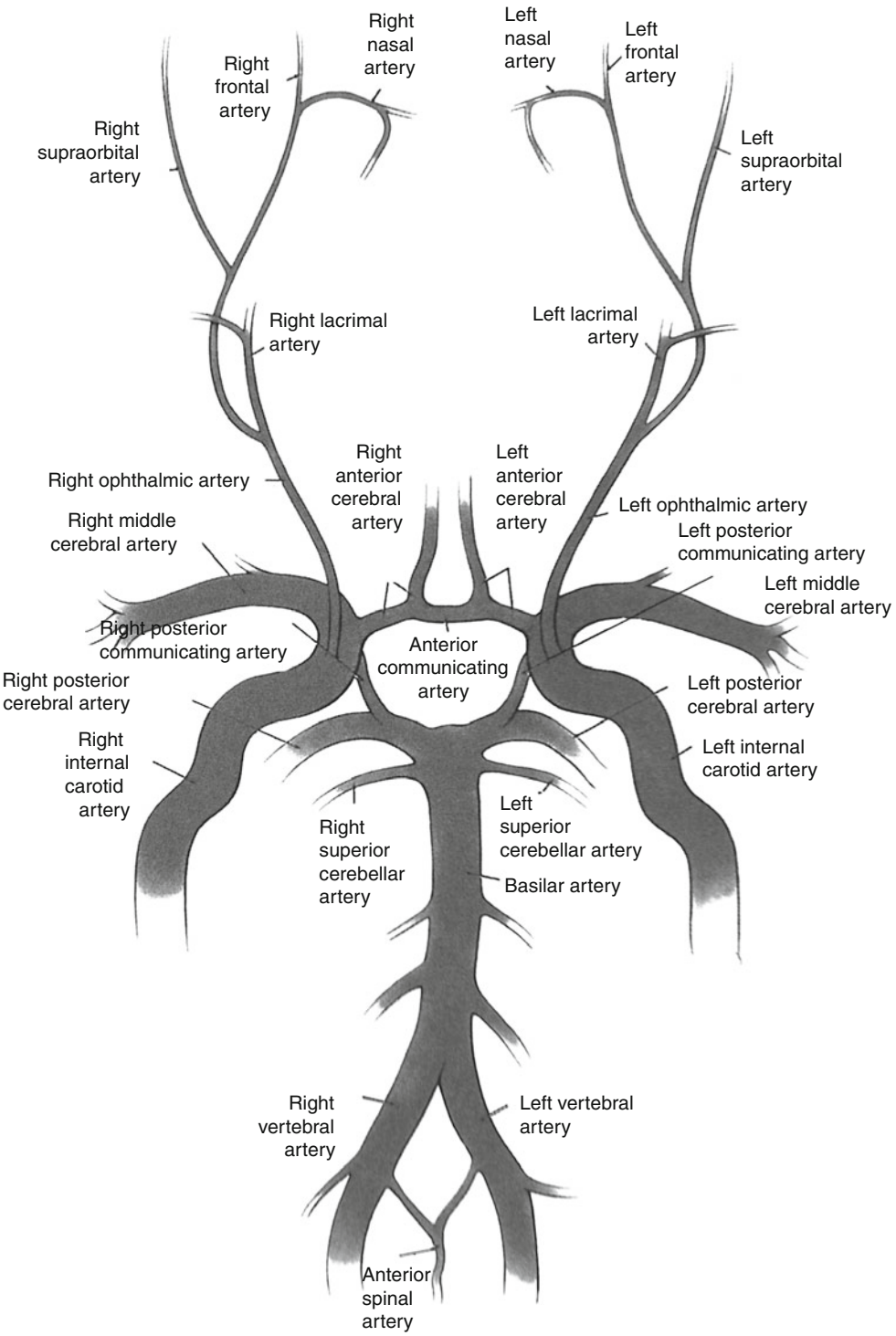


**Fig. 6.5** Major branches of the internal carotid artery (i.e., middle cerebral, anterior cerebral, posterior communicating, and ophthalmic arteries) and vertebrobasilar arteries

or high carbon dioxide levels in the blood. It is also innervated by the glossopharyngeal nerve via the nerve of Hering.

The corticotympanic artery and the artery to the pterygoid canal are branches of the internal carotid artery in its petrous portion. The cavernous, hypophyseal, semilunar, anterior meningeal, and ophthalmic arteries are branches of the cavernous portion of the internal carotid artery. The ophthalmic artery is clinically important since it communicates with the external carotid system, which is the basis of the periorbital Doppler study. The remaining branches of the internal carotid artery arise from the cerebral portion, i.e., the anterior and middle cerebral, posterior communicating, and choroidal branches (Fig. 6.5).

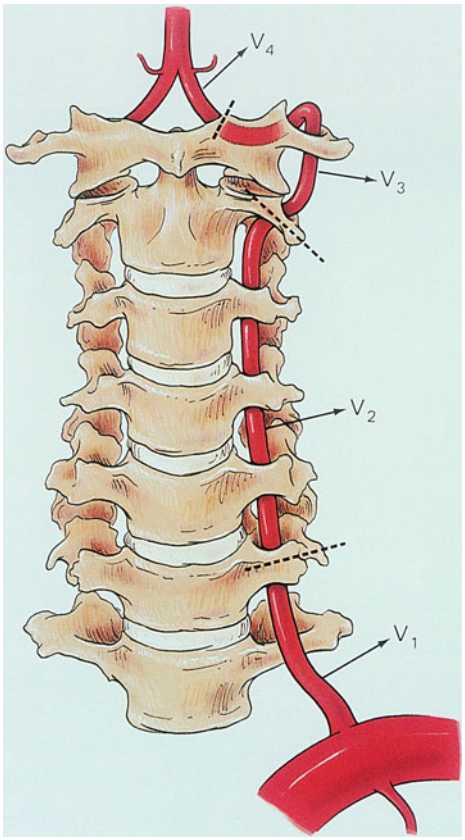


**Fig. 6.6** Relation of the vertebral artery and cervical spine. The dotted line indicates the level at which the vertebral artery becomes intradural. As noted, the vertebral artery is divided into four portions ($V_1$, $V_2$, $V_3$, and $V_4$). $V_1$ is the segment between its origin and the level where it enters the transverse process of the sixth cervical vertebra. $V_2$ is the segment of the artery through the foramina of the transverse processes of the cervical spines until the *dotted line*. $V_3$ is the segment between $C_2$ and $C_1$. $V_4$ is the segment prior to joining the other vertebral artery to form the basilar artery

The vertebral artery leaves the subclavian artery and pushes upward through the foramina of the transverse processes of the cervical vertebrae into the cranium through the foramen magnum (Fig. 6.6). The neck spinal branches enter the vertebral canal through the intervertebral foramen, and muscular branches are given off to the deep muscles of the neck. These latter branches anastomose with branches of the external carotid artery.

Intracranially, the vertebral arteries give off the posterior inferior cerebellar and spinal arteries before they are united at the pontomedullary junction to form the basilar artery. The basilar artery terminates as the posterior cerebral artery after giving off the anterior inferior cerebellar, superior cerebellar, pontine, and internal auditory arteries.

Blood flows through each internal carotid artery at about 350 ml/min, accounting for approximately 85% of the blood supply to the brain, and the vertebral arteries account for about 15% of the total blood supply to the brain [22]. Therefore, the carotid arteries, both from the standpoint of accessibility and functioning, become the system of importance for noninvasive testing.

## Morphologic Variations of the Internal Carotid Artery

Tortuosity of the internal carotid artery (or loop) is generally defined as an S- or C-shaped elongation or curving in the course of the artery (Fig. 6.7a). Coiling is a term used to describe an exaggerated, redundant S-shaped curve, or a complete circle, in the longitudinal axis of the artery (Fig. 6.7b). Tortuosity and coiling are thought to be congenital developmental abnormalities that may become exaggerated with aging. They usually do not produce clinical symptoms.

Kinking is a sharp angulation with stenosis of segments of the internal carotid artery (Fig. 6.7c) and appears to be somewhat different than tortuosity and coiling. Kinking is less frequently bilateral and usually affects a few centimeters or more above the carotid bifurcation.

Poststenotic dilatation may be present. Frequently, an atherosclerotic plaque on the concave side of the kink further narrows the lumen.

Unlike tortuosity and coiling, kinking is thought to be an acquired abnormality, occurring mostly in older people in whom arteriosclerotic disease and hypertension are important factors. Changes in head and neck positions may produce cerebral ischemia in patients with carotid kinking, whereas tortuosity and coiling are usually asymptomatic.

## Cerebral Collateral Pathways

Single stenotic lesions may or may not produce carotid territory symptoms (hemispheric) or vertebrobasilar territory symptoms (nonhemispheric). The collateral system comes into play when resistance in the stenotic major artery is greater than the resistance in the smaller circulative collateral channel. As stenosis becomes more severe and the collateral channel arteries dilate in response to increased flow, the collateral channels will increase flow up to the point of capacity. It can then be seen that the more proximal the obstruction, the greater the potential for collateral pathways to exist. Proximal occlusion of the arteries arising from the aortic arch is, therefore, rarely associated with the stroke syndrome because of this collateral flow. Branches of each subclavian artery may anastomose with collaterals of the opposite subclavian artery and the branches of the external carotid system.

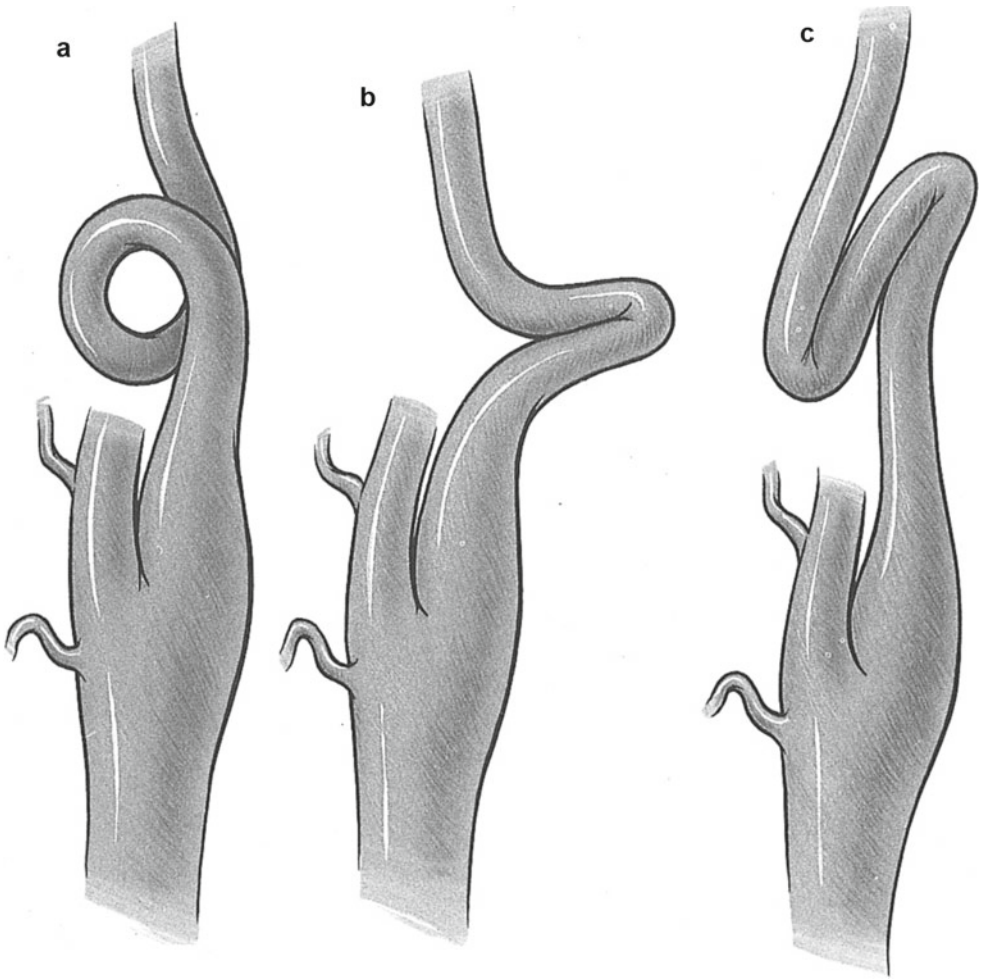


**Fig. 6.7** Three types of redundancy of the internal carotid artery. (**a**) Coil. (**b**) Kink. (**c**) Loop (Courtesy of Springer-Verlag. Berguer and Kieffer [20])

The subclavian steal syndrome [23] occurs with proximal subclavian occlusion and retrograde flow down the vertebral artery (Figs. 6.8 and 6.9a). In innominate artery obstruction, the retrograde flow may be down to the carotid artery (Fig. 6.9b). Therefore, vascular surgeons may use the mechanism of collateral flow in a constructive manner; a patient who has both a carotid stenosis and subclavian steal syndrome may be completely relieved of steal symptoms by CEA.

An interesting collateral pathway is the retrograde flow that may occur in the external carotid system by proximal occlusion of the common carotid artery (Fig. 6.9c). Collateral flow to the internal carotid artery occurs by way of the ophthalmic artery or the circle of Willis. Patients with a proximal internal carotid occlusion might have blood flow up the external carotid artery and retrograde through the supraorbital and frontal arteries into the ophthalmic artery and, finally, antegrade in the distal internal carotid artery and the circle of Willis. This important pathway is the basis of the supraorbital Doppler cerebrovascular examination. Patients with proximal internal carotid occlusion and external carotid stenosis may be relieved of symptoms with correction of the external carotid occlusion, which alleviates symptoms of hypoperfusion [24]. Finally, emboli may course via the external carotid artery to the eye, producing amaurosis fugax in patients with a functional collateral pathway [25].

The major collateral pathway, of course, is the circle of Willis (Figs. 6.10 and 6.11). This unique circle provides the major pathway between the internal carotid, the external carotid, and the vertebrobasilar systems. The circle of Willis is anatomically complete in only one-third of patients, but it is physiologically adequate in around two-thirds of patients (Fig. 6.12). Collateral arteries between the occipital branches of the external carotid arteries may bypass stenosis of the origin of both vertebral arteries and the muscular branches of the vertebral arteries (Figs. 6.13, 6.14, and 6.15), or between the cervical branches of the thyrocervical trunk and vertebral arteries. Figures 6.16, 6.17, and 6.18 summarize the important collateral pathways in patients with an occluded internal carotid artery.

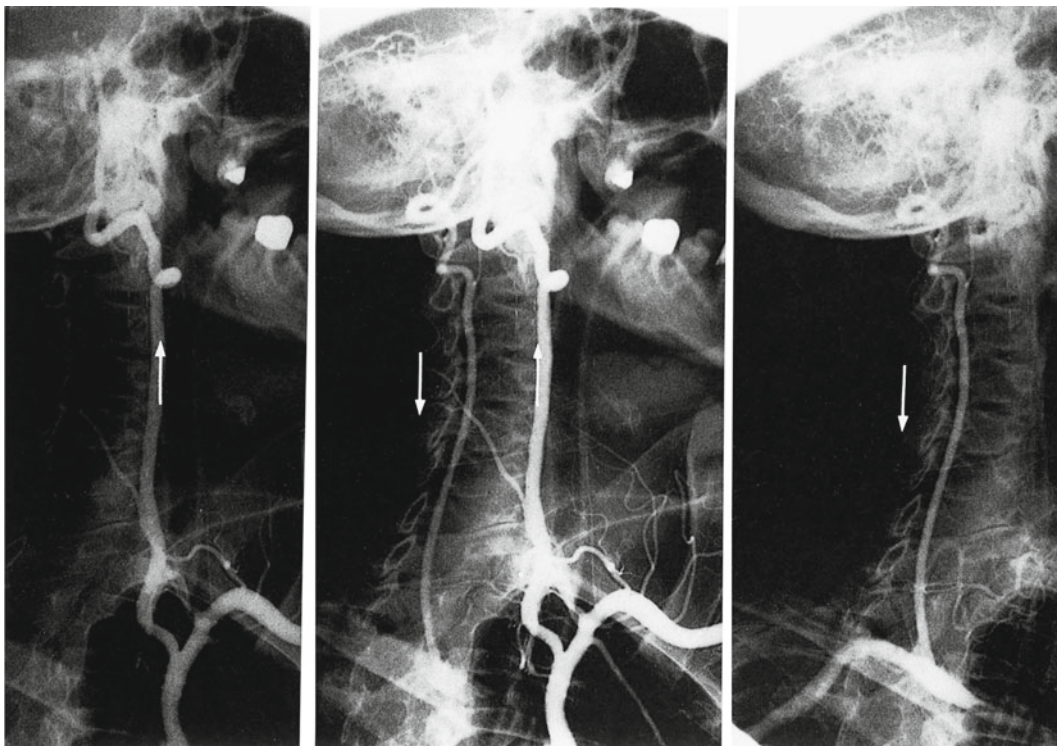

**Fig. 6.8** Right subclavian steal secondary to occlusion of the first segment of this artery. The left vertebral artery is filling from the left subclavian artery as seen on the left side of this figure (*arrow*). In the middle of this figure, flow is seen retrograde in the right vertebral artery (*arrow*), and as seen on the right side of this figure, the right subclavian artery is filling retrograde via the left vertebral artery (*arrow*) (Courtesy of Springer-Verlag. Berguer and Kieffer [20])

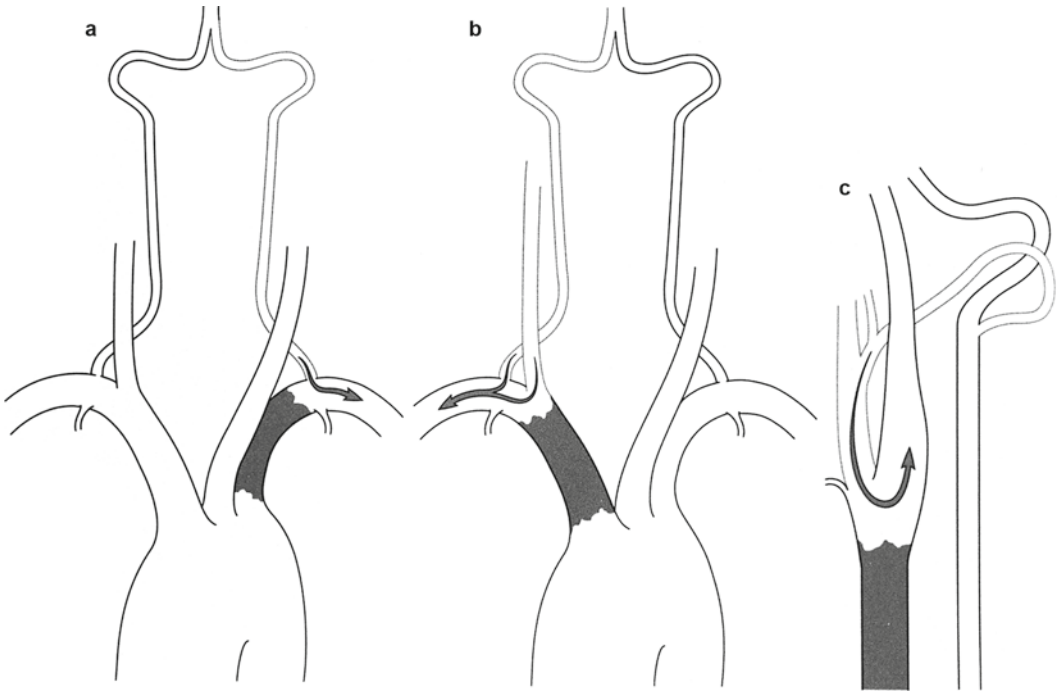


**Fig. 6.9** Three patterns of flow reversal. (**a**) Subclavian steal distal to an occluded left subclavian artery. (**b**) Reversal of flow in the carotid and vertebral arteries distal to an occluded innominate artery (innominate steal). (**c**) Reversal of flow in the occipital artery and proximal external carotid distal to an occluded common carotid artery (carotid steal) (Courtesy of Springer-Verlag. Berguer and Kieffer [20])

## Pathology

Numerous theories exist as to the mechanism by which atherosclerosis develops in the carotid arteries, but whether you prescribe to the mechanical, sheer stress, chemical injury, or infectious theory [26], the basic lesion is essentially the same. Atherosclerosis accounts for approximately 90% of extracranial cerebrovascular disease, with the remaining 10% being attributed to such disease processes as fibromuscular dysplasia, traumatic or spontaneous dissection, aneurysms, and arteritis, including Takayasu's arteritis.

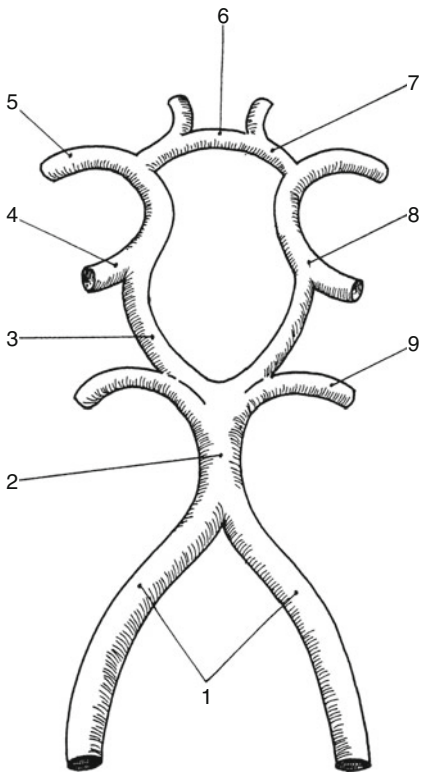


**Fig. 6.10** The circle of Willis: (*1*) right and left vertebral arteries, (*2*) basilar artery, (*3*) right posterior communicating artery, (*4*) right internal carotid artery, (*5*) right middle cerebral artery, (*6*) anterior communicating artery, (*7*) left anterior cerebral artery, (*8*) left internal carotid artery, (*9*) left posterior cerebral artery

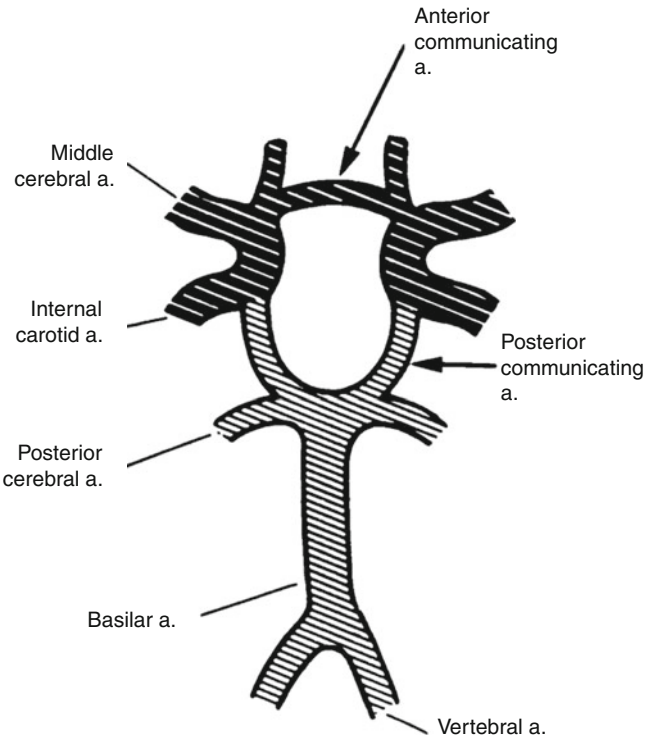


**Fig. 6.11** Circle of Willis showing the anterior cerebral circulation (*shaded black*) and the posterior circulation (*shaded gray*). *a* artery

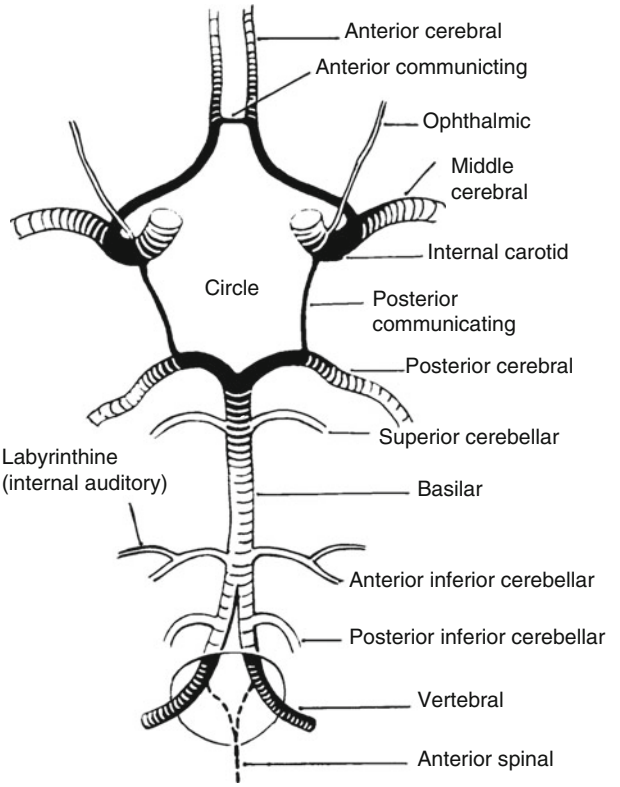


**Fig. 6.12** The circle of Willis demonstrating rudimentary posterior communicating branches

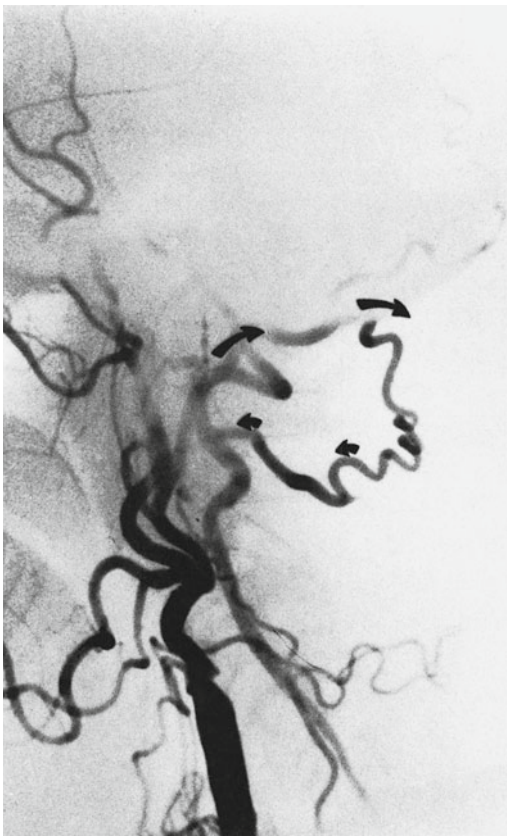

**Fig. 6.13** Occipital connection of the vertebral artery. In this patient with an occluded internal carotid artery, the collaterals (*arrow*) from the occipital artery fill the vertebral artery anterogradely toward the basilar artery and retrogradely toward the base of the neck, where the vertebral artery is occluded

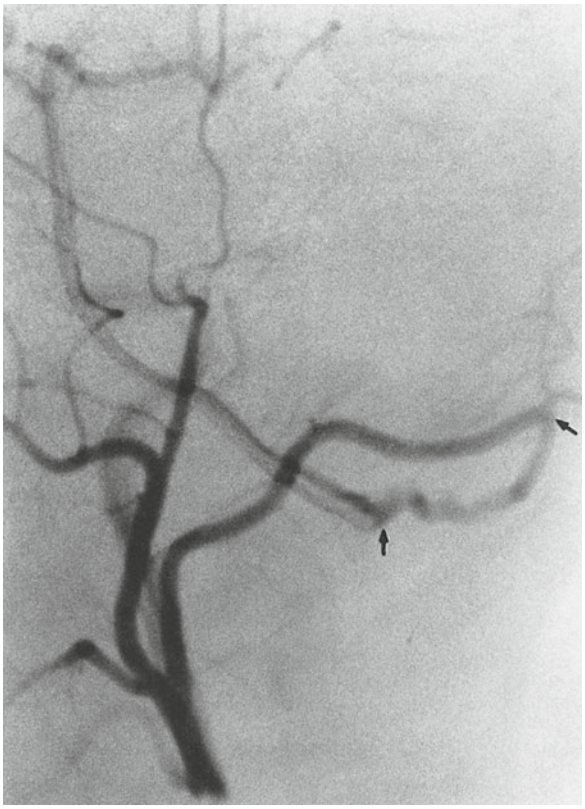

**Fig. 6.14** Occipital collateral may enter the vertebral artery at the level of C1, (*arrow*) as seen in this selective external carotid injection

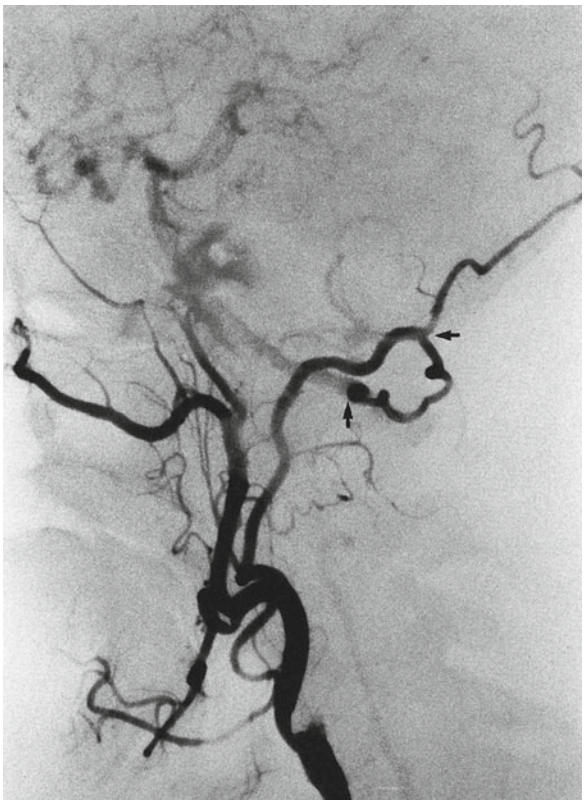

**Fig. 6.15** The importance of the occipital collateral is seen in this patient with an occluded internal carotid (*arrows*)

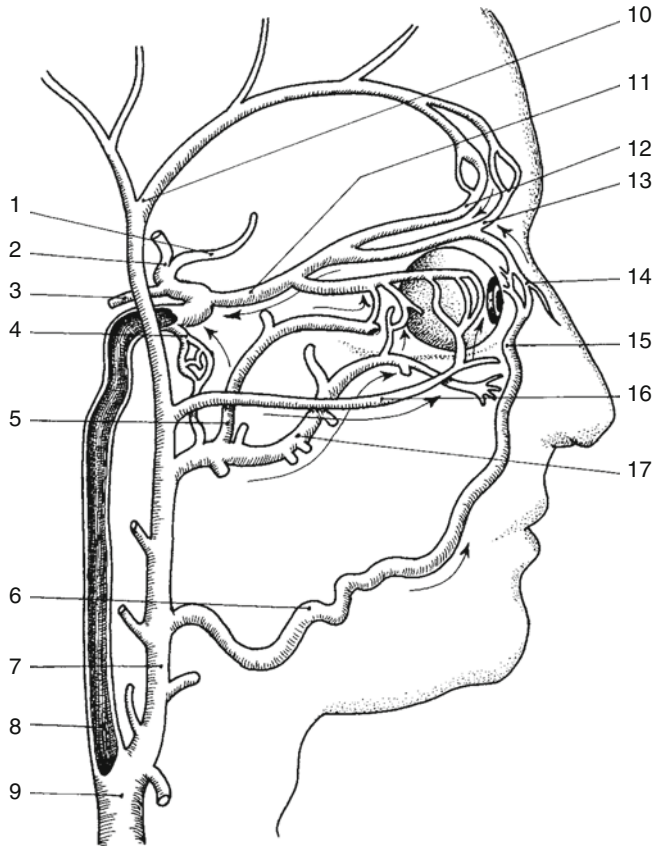


**Fig. 6.16** A patient with an occluded internal carotid artery with a reversal of flow through the ophthalmic artery via periorbital branches of the external carotid artery. (*1*) Anterior cerebral artery, (*2*) middle cerebral artery, (*3*) posterior communicating artery, (*4*) caroticotympanic branch of the internal carotid artery, (*5*) middle meningeal artery, (*6*) fascial artery, (*7*) external carotid artery, (*8*) occluded internal carotid artery, (*9*) common carotid artery, (*10*) superficial temporal artery, (*11*) ophthalmic artery, (*12*) supraorbital artery, (*13*) supratrochlear artery, (*14*) dorsal nasal artery, (*15*) angular artery, (*16*) transverse fascial artery, (*17*) internal maxillary artery

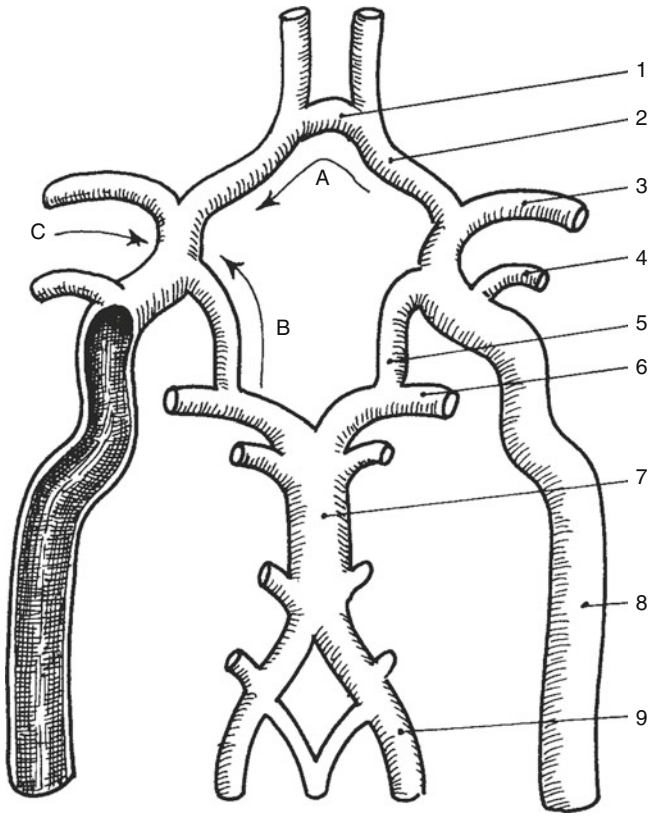


**Fig. 6.17** This illustration is a patient with an internal carotid artery occlusion. The flow to the corresponding cerebral hemisphere is maintained by flow from the opposite internal carotid artery (*A*), the vertebral basilar system (*B*), and the ophthalmic artery via the periorbital branches of the external carotid artery of the same side (*C*). (*1*) Anterior communicating artery, (*2*) anterior cerebral artery, (*3*) middle cerebral artery, (4) ophthalmic artery, (*5*) posterior communicating artery, (*6*) posterior cerebral artery, (*7*) basilar artery, (*8*) internal carotid artery, (*9*) vertebral artery

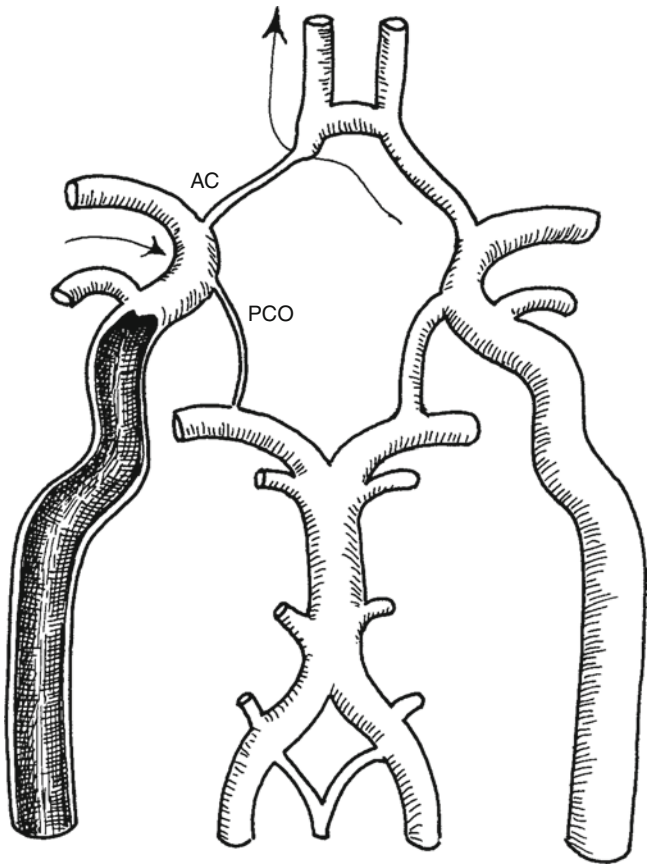


**Fig. 6.18** A patient with an internal carotid artery occlusion where the collateral flow may be reduced by the incomplete circle of Willis (rudimentary right posterior communicating artery [*PCO*] and anterior cerebral artery [*AC*])

The pathology of carotid and vertebral artery atherosclerosis is similar to the process of atherosclerosis affecting coronaries and other arteries. The early stage of the lesion is initiated by intimal accumulation of lipoprotein particles which will undergo oxidative modification and elaborate cytokines that cause expression of adhesion molecules and chemoattractants; this will facilitate the uptake and migration of monocytes into the arterial wall. These monocytes become lipid-laden macrophages (foam cells) as a consequence of accumulation of modified lipoproteins and subsequently release additional cytokines, matrix metalloproteinases, and oxidants. This is followed by smooth muscle cell migration from the media to the intima. These will proliferate and elaborate extracellular matrix as extracellular lipid accumulates in a central core surrounded by a layer of connective tissue, which is called the fibrous cap, which in many advanced plaques becomes calcified. The atherosclerotic lesion initially grows in an outward direction; however, once advanced, it will grow inward and encroach on the lumen, causing stenosis.

These plaques occur preferentially at areas of vessel bifurcations, and the process is similar to that seen with coronary artery disease. It can begin in the bulbous portion of the internal carotid artery on its posterior lateral wall. The atherosclerosis appears as a fatty strip subintimally with a collection of fat cells that progresses to a fibrous plaque in the subendothelial layer, causing gradually decreasing flow. These plaques can enlarge in several ways. They may just continue to slowly enlarge from an accumulation of cholesterol and fibroblasts, leading to a central necrosis and rupture of the intimal lining of the vessel. This will lead to discharge of atheromatous debris into the lumen of the vessel, which can embolize. The exposed necrotic core of the lesion can then become a nidus for platelet deposition and further embolization to the brain. Progressive accumulation of the arteriosclerotic process, often with thrombotic debris, may result in stenosis or total occlusion in the carotid artery, with subsequent thrombosis of the internal carotid artery distal to the lesion (Fig. 6.19). Another mechanism by which there may be sudden plaque enlargement is intraplaque hemorrhage [27], which may produce acute narrowing of the lumen.

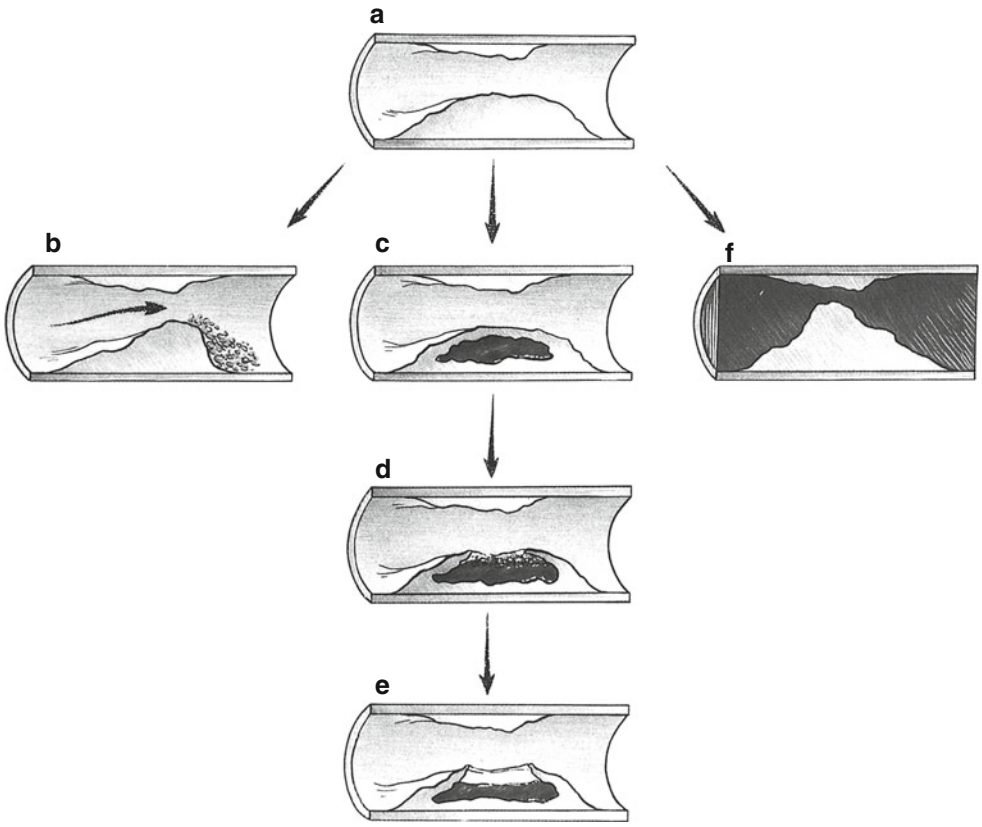


**Fig. 6.19** (**a**) Development of pathologic features in a plaque. (**b**) Partial obstruction created by a plaque may result in accumulation of a fibrin-platelet thrombus downstream from the obstruction. (**c**) The plaque may "soften" in its core. (**d**) This softening may break through to the surface, exposing the contents of the soft core to the bloodstream. (**e**) An ulceration may become covered by a fibrin deposit and even heal. (**f**) The increased size of the obstruction created by the plaque may result in thrombosis of the vessel lumen (Courtesy of Springer-Verlag. Berguer and Kieffer [20])

If the intima overlying the site of the plaque hemorrhage ulcerates, the necrotic contents of the atheromas escape into the lumen and cause cerebral embolization with transient ischemic attacks (TIA) or cerebral infarcts. Nonulcerated lesions may alter flow and produce mural thrombi, which may fragment, causing embolization (Fig. 6.20). The friability of these lesions is often not appreciated until seen by the vascular surgeon (Fig. 6.21).

Blaisdell et al. [28] and Hass et al. [29] studied the distribution of the atherosclerotic lesions involved in cerebrovascular disease and found that approximately one-third of responsible lesions that were surgically inaccessible occurred in the intracranial distribution. The remaining two-thirds of the lesions were in extracranial locations.

The common carotid bifurcation and the proximal internal carotid artery account for 50% of the lesions. Vertebral artery lesions account for 20%, left subclavian arterial lesions account for 10–15%, and lesions of the innominate and right subclavian arteries account for 15%; and more than one lesion may be present (Fig. 6.22).

Generally, the most common cause of cerebral ischemic events is embolic phenomena, primarily arterial in origin (carotid) and secondary to cardiac sources. The irregular plaque surface produces turbulence, which will act as a stimulus for platelet aggregation. If the platelet aggregates become large enough and embolize to an important vessel in the brain, symptoms will occur. If the platelet aggregates break up quickly from mechanical forces or from the effect of arterial prostacyclin, the symptoms will be transient, i.e., TIAs. If the embolic fragment persists, however, it can lead to focal infarction (Fig. 6.23). As noted in Fig. 6.24, the end result of the atherosclerotic plaque might be an internal carotid artery thrombosis. When an arteriosclerotic plaque expands to produce a critical reduction in blood flow, the vessel will ultimately undergo thrombosis. In the case of the internal carotid artery, this column of thrombus stops at the ophthalmic artery and remains stable, and if there is sufficient collateral circulation via the circle of Willis, the thrombotic event may be entirely asymptomatic (Fig. 6.24). However, if small thrombi rather than a thrombotic column form and are subsequently carried to the intracranial vessels by continuous blood flow, then the patient will experience cerebral symptoms that can vary from transient amaurosis fugax or hemispheric events to a profound hemiplegia, depending upon the extent of the propagated thrombus or embolus (Fig. 6.25). In addition, if the collateral circulation to the circle of Willis is inadequate, the sudden loss of blood flow through a diseased internal carotid artery may induce a sudden drop in flow to the cerebral hemisphere, resulting in ischemic infarction as a consequence of inadequate proximal blood flow.

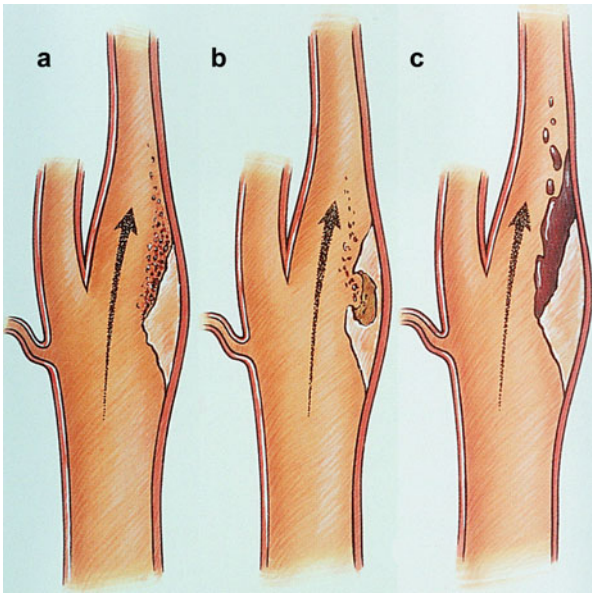


**Fig. 6.20** (**a**–**c**) Three mechanisms for thromboembolization from an internal carotid plaque. (**a**) Fibrin-platelet aggregates associated with an obstructing plaque. (**b**) Atheromatous contents. (**c**) Thrombus forming on the surface (Courtesy of Springer-Verlag. Berguer and Kieffer [20])

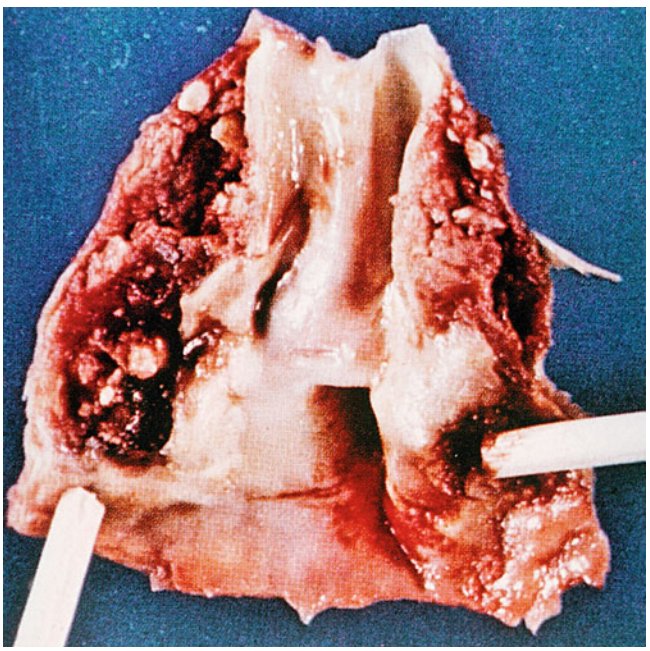

**Fig. 6.21** Carotid endarterectomy plaque

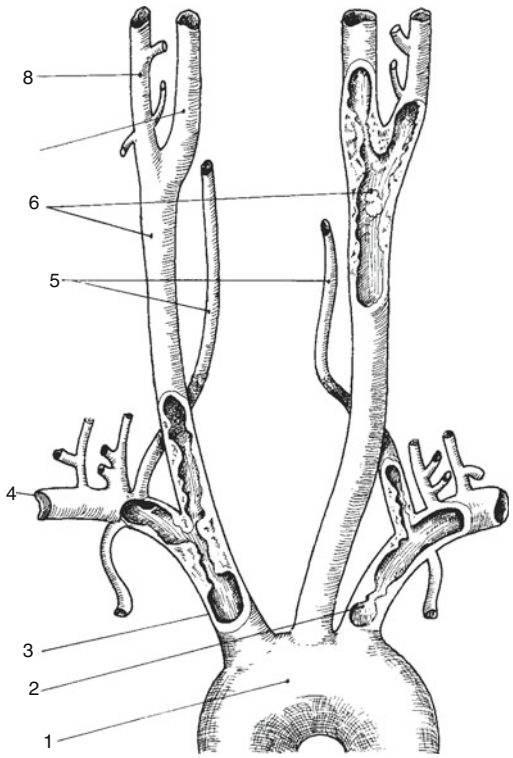


**Fig. 6.22** Sites of atherosclerosis of brachiocephalic vessels. (*1*) Aortic arch, (*2*) left subclavian artery, (*3*) innominate artery, (*4*) right subclavian artery, (*5*) right and left vertebral arteries, (*6*) right and left common carotid arteries, (*7*) right internal carotid artery, (*8*) right external carotid artery (note atherosclerosis at left subclavian, left vertebral, innominate with proximal right common carotid and subclavian arteries and left carotid bifurcation)

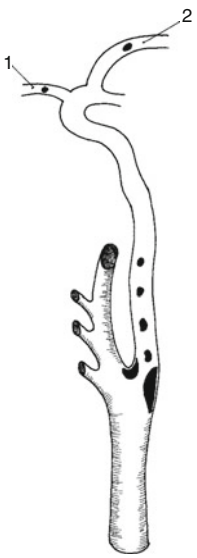


**Fig. 6.23** Embolization from internal carotid artery stenotic lesion to ophthalmic artery (*1*) and middle cerebral artery (*2*)

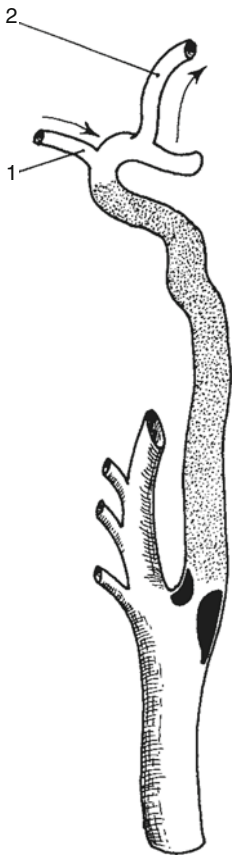


**Fig. 6.24** Internal carotid artery thrombosis with retrograde flow via ophthalmic artery (*1*) to terminal internal carotid artery and middle cerebral artery (*2*)

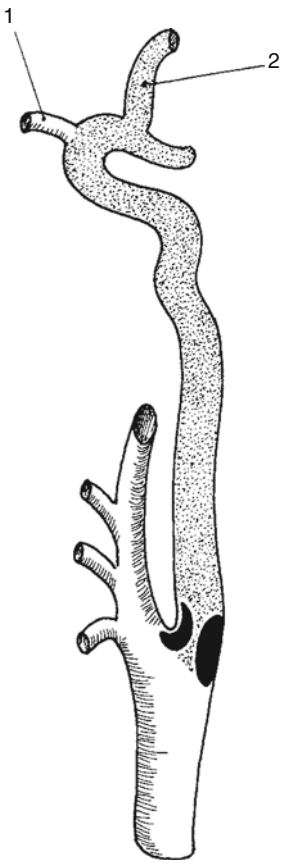


**Fig. 6.25** Internal carotid artery thrombosis which extends to ophthalmic artery (*1*) and terminal internal carotid artery and middle cerebral artery (*2*)

A less common cause of cerebrovascular ischemia is fibromuscular dysplasia (FMD), which is usually more distally located in the internal carotid artery. The most common form of this disease is characterized by hyperplasia of the media producing alternating bands of thinned areas, leading to a beady appearance on angiography. Often, the internal carotid artery is involved at long lengths. Always look for evidence of fibromuscular dysplasia elsewhere. It will involve both internal carotid arteries in 65% of patients [30].

## Pathophysiology

It has been stated that a 70–80% reduction of the cross-sectional area of the arterial lumen must be present to produce a hemodynamically significant drop in the usual flow rate in the cerebrovascular system [31]. However, this may not always be the case. Important mechanisms of collateral flow and hemodynamic events that decrease cardiac output or systemic blood pressure, such as postural hypotension and cardiac arrhythmia, may produce transient episodes of ischemia. Embolization has been a documented cause of TIAs by proven ophthalmologic examination. Intraluminal particles of platelet fibrin aggregates, cholesterol fragments, and small clots have been noted. Most TIAs are probably caused by this mechanism. There is a permanent neurologic deficit as a result of permanently disrupted flow. A pale infarct occurs with focal cell necrosis and cerebral softening. The blood vessels lose integrity at the periphery of the infarct at a relatively ischemic spot. However, where neural death has not occurred, neurologic function may be altered and blood flow, while slow, may still be present.

## Clinical Syndromes

The following well-defined syndromes of cerebrovascular ischemia have emerged:

- TIAs are focal neurologic symptoms or deficits that usually clear completely within 2 h. Some last for only a few moments, and others last for a few hours, but no longer than 24 h.

- Reversible ischemic neurologic deficits (RIND) are focal findings that clear over a period of days.
- Minor stroke, which is defined as a neurologic deficit that clears completely in less than a week.
- Major stroke, which is defined as a major neurologic deficit that lasts longer than a week.
- Stroke in evolution or progressing stroke.
- Complete stroke is a stroke with a significant return of function.
- Diffuse cerebral ischemia or "low-flow" syndrome.

Each of these syndromes requires a thorough history and physical and neurologic evaluation with close attention to the severity of associated cardiovascular disease, hypertension, diabetes, neurologic aid, and diagnostic testing.

The mechanism by which TIAs occur is usually an embolic process. The source for these emboli can be from a number of sources—intracranial lesions, extracranial carotid lesions, extracranial arch vessel lesions, primary cardiac thrombus, or even paradoxical emboli. The majority of TIAs will come from carotid bifurcation lesions, and this must be the site that is worked up first in these patients. When taking a history from patients who present with TIAs, it is important to obtain information as to previous episodes. Patients with a carotid source for their TIA will generally report having identical previous neurologic deficits, in contrast to cardiac TIAs that may vary; this is based on the principles of laminar flow within the carotid vessels that send the embolus to the same area each time.

It is critical in evaluating patients with carotid artery stenosis to determine if these patients are classified as asymptomatic or symptomatic. Most TIAs involve the distribution of the internal carotid arteries, while some may affect the vertebrobasilar system. Typical carotid TIA symptoms include contralateral weakness of the face, arm, and/or leg; contralateral sensory deficit or paresthesia of the face, arm, and/or leg; or transient ipsilateral blindness (amaurosis fugax). If the right cerebral hemisphere is involved, other manifestations may be noted, e.g., agnosognosia, asomatognosia, neglect, and visual or sensory extinction. In contrast, if the left hemisphere is involved, patients may show manifestations of aphasia, alexia, anomia, and agraphesthesia.

The patient with amaurosis fugax will describe these episodes as someone pulling a shade over one of his or her eyes, which quickly resolves. A funduscopic inspection of these patients may reveal Hollenhorst plaques, bright yellow spots on the retina that represent cholesterol crystals. These may be present in asymptomatic patients with atherosclerotic disease as well.

Meanwhile, patients with vertebrobasilar TIAs may have a combination of the following symptoms: vertigo, ataxia, diplopia, visual disturbances, dysarthria, nausea, vomiting, decreased consciousness, and weakness, which may include quadriparesis.

These symptoms may be related to an embolic event from primary atherosclerotic lesions involving the vertebrobasilar system, resulting in an ischemic event to the posterior brain or brain stem. Another mechanism for this may be a significantly diminished blood flow to the brain, or diffuse cerebral ischemia. To have this situation, the patient must have severe stenoses involving the majority of the extracranial vessels, incomplete circle of Willis, or an altered flow state, i.e., subclavian steal syndrome.

Other clinical syndromes include reversible ischemic neurologic deficit (RIND). RIND is a focal neurologic deficit that takes several days to completely resolve. The mechanism by which RIND occurs is poorly understood. It is generally felt that these patients actually suffer focal cerebral infarctions, but these areas are very small and surrounding tissue compensates for the loss. Another syndrome is crescendo TIAs. These are hemispheric deficits that resolve within minutes, but occur with increasing frequency. Stroke in evolution is where initial neurologic symptoms may not completely resolve and subsequent neurologic events are progressive.

A completed stroke is a neurologic deficit that occurs and does not have a complete resolution of symptoms. This may be the result of a large embolus, a small embolus to an end vessel with surrounding vessel thrombosis, or thrombosis of the internal carotid artery.

Casually, patients will present with headache and vague neurologic symptoms and have cerebral imaging, i.e., MRI or CT scans, that shows recent cerebral infarcts, which may be the result of carotid pathology.

Silent cerebral infarcts on brain imaging may be present in patients with asymptomatic carotid stenosis. These infarcts can be large and found particularly in the frontal lobes or the nondominant temporal lobe, or more commonly symmetrical lacunar infarcts, implying small vessel disease. However, they may also be asymmetrical, which tend to point toward carotid stenosis on that side. These can be secondary to blood flow changes distal to carotid occlusion, which may increase the risk of lacunar infarcts in those with small vessel disease. In these patients, even if they do not have classical carotid TIA symptoms, they may be considered clinically relevant. Overall, if these infarcts are old, the patients would be considered asymptomatic. However, Kakkos et al. [32] reported a higher stroke rate in patients with >60–79% asymptomatic stenosis with an annual TIA/stroke rate of 1.3% if there was no silent infarct versus 4.4% if a silent infarct was present.

## Physical Examination

With a good history and thorough physical examination, it is possible to diagnose the nature and location of the vascular lesions with reasonable certainty, and the diagnosis can usually be confirmed by the noninvasive techniques to be

described. The physical examination includes examining or checking the pulses of the superficial temporal artery; the carotid artery, both high and low in the neck; the subclavian artery above the midportion of the clavicle; and the radial artery. One side of the body should be compared with the other. Physical examination may show signs of stroke: facial/eyelid drooping, motor or sensory deficits, and speech disturbances. Ocular examinations can occasionally identify Hollenhorst plaques. Palpation of the carotid artery provides limited data unless there is asymmetry in the pulsation between the two carotids. Neck auscultation may elicit a carotid bruit. The blood pressures in each arm should be compared, and a 15–20 mmHg difference in blood pressure may indicate a significant lesion of the subclavian or innominate arteries. Bruits in the neck, indicating turbulence in stenotic arteries, should be carefully evaluated. Listening for a bruit is also important. Remember that a near or total occlusion of the internal carotid artery has no bruit at all. A good pulsation may be felt under the mandible when a totally occluded internal carotid artery is present due to the palpation of the common carotid artery and the external carotid artery. These cannot be differentiated on a physical examination. It is sometimes difficult to palpate the subclavian arteries in obese or heavy-set individuals, and it is necessary to determine that cervical bruits are not really aortic ejection murmurs. A carotid bruit, heard louder at the level of the mandible than in the lower part of the neck, would probably indicate a stenosis of the internal carotid artery. This could also represent a stenosis of the innominate artery. Moderate stenosis may result in a systolic bruit, whereas more severe stenosis results in a systolic bruit that ends in diastole. A complete neurologic examination should be done.

## Investigations

The work-up of patients presenting with asymptomatic carotid bruits or TIAs should include initial carotid duplex scanning, and based on the findings of this study, the patient can take one of several routes. First, the patient may have no significant disease by duplex. These patients with classical hemispheric TIAs will require a cardiac work-up and/or neurological work-up and, if negative, a systemic disease work-up, or possibly another imaging modality. Second, the patient may have a severe or tight stenosis. In this situation, depending on the patient's operative risk, the surgeon's skill, the accuracy of the duplex, and angiography complication rates, this patient could undergo CTA or magnetic resonance angiography or conventional arteriography (if CAS is anticipated), or surgery, without further work-up. Third, in patients with hemispheric TIAs and only mild to moderate disease by duplex, other sources should be explored as well as CTA or carotid magnetic resonance angiography or arteriography. Again, many factors must be considered when working up patients for TIAs, and each patient must be individualized. A practical approach is described in Chap. 19.

## Overview of Various Noninvasive Cerebrovascular Techniques

Contrast cerebrovascular arteriography has been the definitive diagnostic technique for evaluation of cerebrovascular disease; however, its limitations and complications played a great role in the drive to develop accurate, reliable, and noninvasive diagnostic procedures. Although arteriography serves to define anatomic lesions and is indispensable for most vascular surgeries, it provides little objective data regarding physiologic disability, nor is it without risk.

Most complications of cerebral arteriography can be assigned to technical error, embolic events, or neurotoxic effects of the contrast material. Catheter-related injuries at the puncture site are near 0.2%, with mortality estimated at 0.02% [33]. Allergic reactions to the contrast medium occur in about 2% of cases, while the overall incidence of neurologic deficits is around 1% if the transfemoral approach is used (the figure is slightly higher with the transaxillary route). Both the North American Symptomatic Carotid Endarterectomy Trial (NASCET) Collaborators and the Asymptomatic Carotid Atherosclerosis Study (ACAS) Group reported stroke rates of around 1% [8, 12].

A technical shortcoming of cerebral arteriography is its failure to delineate shallow, superficially ulcerating lesions. Because of this, a potential source of cerebral emboli could be overlooked. If we add to these risks the disadvantages of patient discomfort, the need for hospitalization, and expense, there is little wonder that many physicians are reluctant to subject their patients to cerebral arteriography. These make noninvasive vascular diagnostic techniques highly desirable and cost-effective alternatives.

## Historical Perspectives

Over the past 30 years, extensive research has been done in the field of cerebrovascular diagnosis, resulting in the development of a broad range of noninvasive diagnostic tools, extending to the use of radioactive isotope scanning. While these nuclear studies have been useful in detecting intracranial lesions, they have not been as effective as noninvasive techniques in localizing extracranial disease, the main site of pathology in the carotid tree.

Ultrasound was first applied to the study of carotid circulation as early as 1954 [34], but it was not until 1967 that its clinical application in velocity detection was reported [35].

Brockenbrough, in 1970, further refined the technique and popularized the flowmeter [36].

In 1971, D. E. Hokanson, working in Eugene Strandness' laboratory at the University of Washington in Seattle, was able to piece together all the elements necessary to provide the first noninvasive visualization of an arterial segment using pulsed Doppler methods [37]. The concept was quite simple. If one knew the size and location of the Doppler transducer, the position of the pulsed Doppler sample volume, and could transfer this to a cathode-ray tube, it should be possible to paint a picture containing all points within an arterial segment where flow was occurring. This led to the development of ultrasonic arteriography, which was successfully applied to the study of carotid artery disease. Although this method worked, there were significant limitations: (1) it was time-consuming, (2) an experienced technologist was required, (3) the image was distorted by the patient's movement, (4) arterial wall calcification blocked the transmission of the ultrasound, and (5) the arterial wall and plaque were not visualized. Because of these limitations, Strandness and colleagues began exploring the use of B-mode ultrasound to visualize the arterial wall. Very early in their application of this method, they studied a patient whose internal carotid artery appeared patent by ultrasonic imaging but was found to be occluded by arteriography. This led to the obvious conclusion that thrombus may have acoustic properties similar to flowing blood and, thus, would be missed by imaging alone. The solution appeared to be the addition of a Doppler probe to the ultrasonic imaging to permit assessment of the presence or absence of flow. It was this combination of imaging plus Doppler that led to the term "ultrasonic duplex scanner" [38]. When real-time fast Fourier transform (FFT) spectrum analysis was added, the basic components of the systems that are in widespread use today became available.

Another breakthrough came in 1974 when Gee et al. [39] introduced the use of the oculopneumoplethysmograph for carotid disease screening. From a historical perspective, oculopneumoplethysmography (OPG-Gee) detects the ophthalmic artery pressure by suction ophthalmodynamometry. The main indication for OPG-Gee is the identification of carotid artery stenosis [39–41]; however, it can also be used in measuring ophthalmic artery pressure during external compression of the common carotid artery, reflecting the collateral pressure of the ipsilateral internal carotid artery. It may also be helpful in determining the safety of ligating or resecting the carotid artery.

Another indirect test that was used in the past is the periorbital Doppler examination (ophthalmosonometry), the principle of which is based on evaluating the Doppler velocity flow pattern in the accessible branches of the ophthalmic artery and assessing the response to compression of the branches of the external carotid. The identification of advanced internal carotid stenosis by examination of the periorbital flow patterns with the Doppler detector was first described by Brockenbrough in 1969 [36]. The original technique described by Brockenbrough used a nondirectional velocity detector to examine the signal obtained from the supraorbital artery and the response to the compression of the superficial temporal artery [36]. Further refinement became possible with the development of the directional Doppler detector, which permitted the documentation of reverse flow in the branches of the ophthalmic artery [42, 43].

Duplex with color flow imaging systems using pulsed wave Doppler signals are now the most common direct methods for carotid evaluation; indirect methods such as continuous wave Doppler technique, periorbital Doppler [36], and oculopneumoplethysmography [39–41] are outdated and are no longer used in the modern vascular laboratory for the diagnosis of carotid artery disease.

## Carotid Duplex Scanning

Carotid duplex scanning, originally developed at the University of Washington, combines real-time, B-mode ultrasound imaging with a pulsed Doppler detector. As mentioned previously, although calcified plaques can readily be identified on a B-mode scan due to the high acoustic reflectivity, noncalcified plaques and thrombi have approximately the same acoustic impedance as flowing blood. Therefore, a completely thrombosed vessel may not be distinguished from a patent one based on the B-mode image alone. By using Doppler flow investigation of the vessels that can be imaged, this difficulty can be overcome.

In the initial model of the duplex scanner, the same transducer housed both pulsed echo and pulsed Doppler functions, as well as the multigated pulsed Doppler flow detector. However, after clinical trials, it was apparent that separate transducers were advisable due to the conflicting transducer alignment requirements for the pulsed echo and the pulsed Doppler functions.

The next generation of duplex scanners utilized separate echo and Doppler transducers that alternated pulse transmission in a time-sharing fashion. The scanner also contained a movable, single-gated pulsed Doppler detector. By using the B-mode image as a guide for precise placement of the pulsed Doppler range gate, the characteristics of flow at various points in the carotid arteries could be determined. This duplex scan also had the capability of spectral sound analysis of the Doppler signals. This helped to differentiate high-grade stenosis from occlusion in the carotid arteries accurately as well as aided in the detection of many lesions that were not severe enough to reduce pressure or flow. The strength of an echo is indicated by its brightness on an oscilloscope screen, a double display term "brightness modulation,"

or B-mode. B-scan refers to the imaging technique that utilizes brightness modulation and a moving transducer. The primary difference between the pulsed Doppler and pulsed echo systems is the type of electronic signal processing used to detect the Doppler shift. In the conventional continuous wave Doppler instrument, separate transmitting and receiving transducers are used that operate constantly to detect flow at any point along the sound beam. The duplex scan generally employs a 5-MHz pulsed Doppler instrument with a single transducer that acts as both transmitter and receiver. The transducer emits short pulses of ultrasound, and then by varying the time interval before it operates as a receiver, flow at different depths in tissue can be detected. This technique is referred to as a range gating.

Duplex scanning of the carotid bifurcation provides a highly accurate method of identifying significant lesions of the internal carotid artery as well as of separating lesions into general pathologic categories. It also has the advantage of real-time visualization so that a satisfactory scan does not depend on the patient. This system and its clinical applications are described in detail in Chap. 7. Its major disadvantages are the relative high cost of the equipment and the extensive operator training required. Duplex scanning of the carotid arteries has become the method of choice for noninvasive assessment of extracranial carotid artery disease. The addition of color-coded flow mapping facilitates the examination and allows more accurate frequency and/or velocity measurement. Accuracies of equal to or more than 90% have been reported by several investigators in the past several years [44–57].

## Carotid Color Duplex Scanning

In addition to the technology described for duplex ultrasound, the color duplex carotid scanner utilizes a large number of sampling sites to determine the backscattered frequency and visually depicts this information as a real-time flow image. This development has occurred because of advances in computer technology that enable the rapid processing of large amounts of information. The instrument simultaneously analyzes Doppler information obtained from over 300 small sampling sites in the zone of insonation. This frequency information is subprocessed and displayed in a color-coded format rather than a gray-scale format. The color depiction of the frequencies facilitates identification of focal areas of abnormal flow patterns. This technique is performed in a manner similar to that described for duplex ultrasound with the addition of a hard copy of the real-time color flow image.

Color flow imaging is an alternative to spectral waveform analysis for displaying the pulsed Doppler information obtained by duplex scanning. In contrast to spectral analysis, which evaluates the entire frequency and amplitude content of the signal at a single sample site, color flow imaging provides an estimate of Doppler-shifted frequency or flow velocity for each site within the B-mode image. The color assignments are based on flow direction and a single mean or average frequency estimate for each site in the B-mode image plane. Accordingly, the peak Doppler frequency shifts or velocities shown by spectral waveforms are generally higher than the frequencies or velocities indicated by color flow imaging. In color flow imaging, shades of two or more distinct colors, usually red and blue, indicate the directional flow relative to the ultrasound scan lines. Variations in the Doppler-shifted frequency or flow velocity are then indicated by changes in color, with lighter shades typically representing high-flow velocities. A single sample volume-pulsed Doppler and spectrum analyzer are always available for a detailed evaluation of the flow patterns at specific arterial locations. One of the main advantages of color flow imaging is that it presents simultaneous flow information on the entire image. Although color flow imaging may be helpful in identifying flow disturbances, some high-velocity jets may not be clear on the color flow imaging because the colors are based on mean Doppler frequency estimates rather than peak systolic frequency. Color flow imaging has been especially helpful in identifying unusual anatomic features such as kinking or tortuosity, which can be difficult to recognize with conventional duplex scanning. Color flow imaging is also valuable for documenting internal carotid artery occlusion [49].

This technology generally is user-friendly because it provides real-time anatomic and flow imaging of the vessels being examined. Although this information can be obtained fairly rapidly initially, additional time is required for determining the optimal location of the sample volume for discrete spectra. The major drawback of this technique is its high cost and the fact that a detailed knowledge of Doppler technology is essential for meaningful interpretation of the color images [58]. This technology will be described in more detail in Chap. 7.

## Transcranial Doppler

Transcranial Doppler (TCD) is capable of detecting intracranial stenoses and occlusions. It can also evaluate the collateral circulation in patients with severe carotid artery stenosis or occlusion. One of the most important applications of TCD is its ability to evaluate the onset, severity, and time course of vasoconstriction caused by subarachnoid hemorrhage. Other applications include evaluation of intracranial arteriovenous malformations and assessment of patients with suspected brain death. TCD also allows for the identification of flow abnormalities during many

cerebrovascular and cardiovascular procedures, such as carotid endarterectomy and cardiopulmonary bypass. A significant decrease in the middle cerebral artery flow velocities during the cross clamping of carotid endarterectomy may signal the need for carotid shunting [59]. Auditory signals related to microemboli may also lead the surgeon to alter the operative technique. TCD is usually done using 2-MHz pulsed Doppler with a spectrum analyzer with an assumed angle of insonation of 0°. Three acoustic windows provide access to the intracranial circulation: transtemporal, transorbital, and transforaminal. The transtemporal approach allows for three windows: anterior, middle, and posterior. Accurate vessel identification requires appropriate sample volume size and depth, knowledge of the direction and velocity of the blood flow, the relationship of the various flow patterns to one another, and common carotid artery compression and oscillation maneuvers. This technology will be described in detail in Chap. 10.

## Carotid CTA/MRA/Conventional Arteriography

Carotid CTA/MRA will be covered in depth in Chaps. 15 and 19.

*Conventional Carotid Arteriography*: Intra-arterial injection is usually performed according to the Seldinger technique. The most commonly used artery is the common femoral artery and, to a lesser extent, the axillary or brachial arteries. Digital subtraction angiography (DSA) uses real-time digital video processing to detect the small amount of contrast medium that has been injected into the artery (Figs. 6.26, 6.27, 6.28, and 6.29).

## Interpretation of Stenosis

There are several methods of estimating stenoses. One of the most common methods is the one used by the NASCET trial [12], where the percentage of stenosis is calculated as a diameter reduction. The percentage of stenosis is determined by comparing the least transverse diameter at the stenosis to the diameter of the distal uninvolved internal carotid artery where the arterial walls become parallel (Fig. 6.30). The percentage may then be expressed as the function of either the diameter or the cross-sectional area as follows:

*Percentage of Stenosis Calculation—Diameter Reduction*

Percentage of stenosis equals 1, minus *A,* divided by *B*, and multiplied by 100, i.e.,

$$[1-(A/B)]\times 100$$

*Percentage of Stenosis Calculation—Area Reduction*

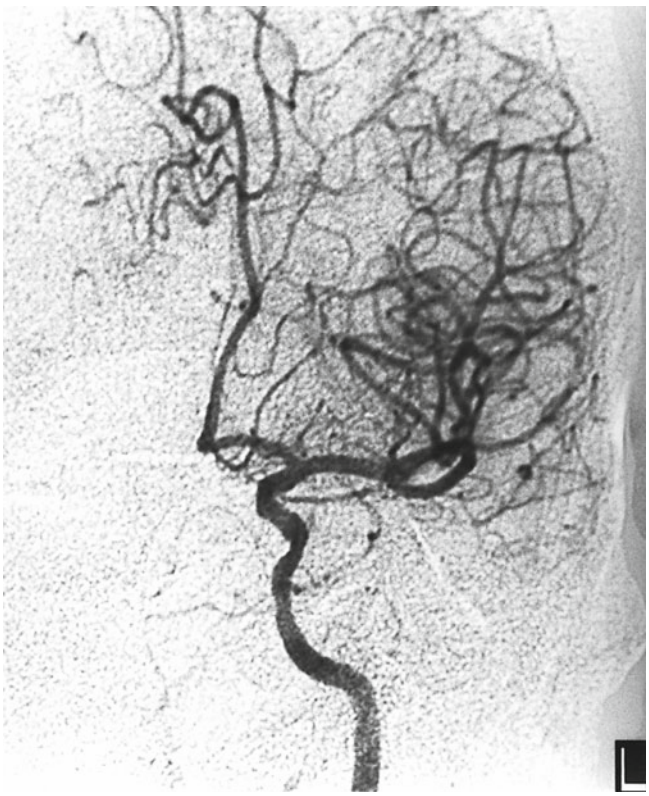

**Fig. 6.26** Carotid arteriogram showing normal distal internal carotid artery and its two major branches: anterior and middle cerebral arteries

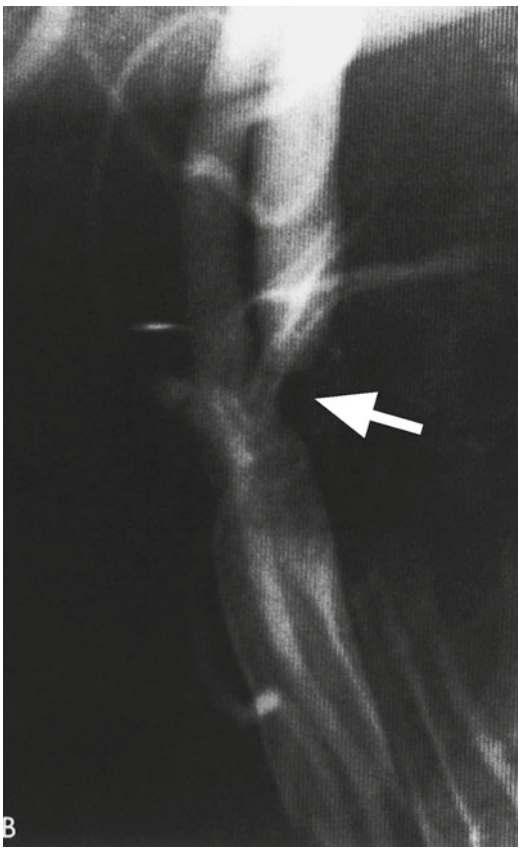

**Fig. 6.27** Carotid arteriogram showing tight stenosis of proximal internal carotid artery (*white arrow*)

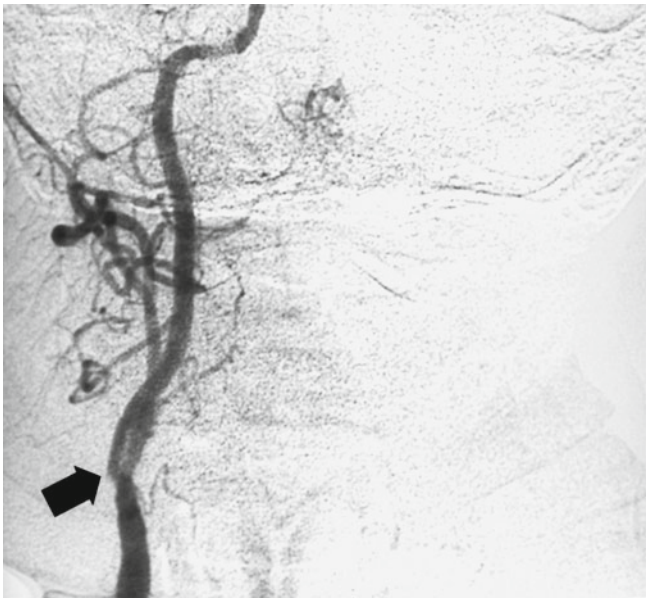

**Fig. 6.28** Carotid arteriogram showing severe stenosis of carotid bifurcation and proximal internal carotid artery (*black arrow*)

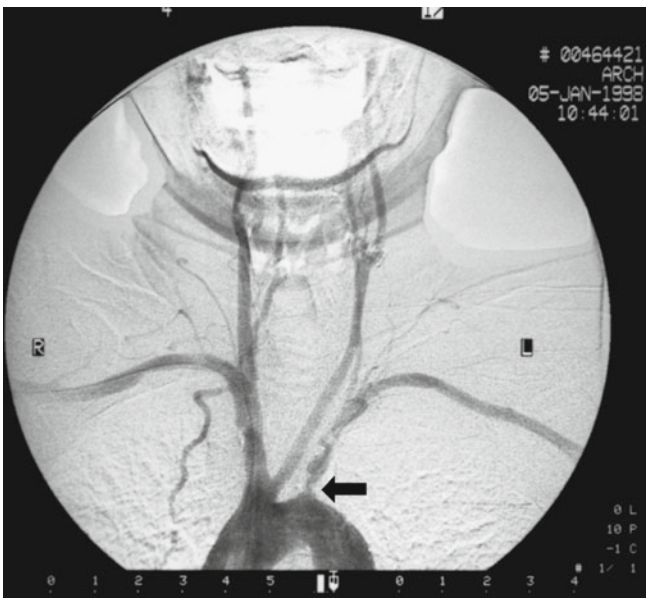


**Fig. 6.29** Four-vessel arch aortogram showing severe stenosis of proximal left subclavian artery (*black arrow*)

To calculate the percentage of stenosis on the basis of the vessel cross-sectional area and assuming the lesion is symmetrical, as seen in Fig. 6.30, the percentage of stenosis (area reduction) will equal to 1 minus $A2$ divided by $B2$ multiplied by 100, i.e.,

$$[1-(A2/B2)]\times 100$$

The third method of calculating the percentage of stenosis is to divide the area of residual lumen ($A$) by the area of the true lumen at the level of the stenosis ($C$), as adapted by the ECST, i.e.,

$$\frac{C-A}{C}\times 100$$

This calculation will require a transverse view of the vessel in question.

Generally speaking, a stenosis that reduces the vessel diameter by 50% (which is equal to 75% area reduction) is considered hemodynamically significant.


**Fig. 6.30** Information required for calculating the percentage of internal carotid artery stenosis (see text for details)

## Treatment

Medical therapy generally includes control of risk factors, e.g., weight, a low-cholesterol diet that may enhance a normal endothelial cell metabolism, antihypertensive drugs for hypertensive patients to decrease shear forces on the endothelialized cells, and cessation of smoking. Specific medical therapy includes antiplatelet agents, such as aspirin, dipyridamole (Persantine, Boehringer), or combined aspirin and extended-release dipyridamole (25/200 mg capsule, Aggrenox, Boehringer), or clopidogrel (Plavix, Sanofi-Synthelabo), and statin therapy.

Surgical intervention, a carotid endarterectomy, is indicated in patients with significant carotid artery stenosis (at least 50%) associated with TIA symptoms or strokes with a good recovery, as recommended by the NASCET study [12]. The NASCET study concluded, after analyzing 659 patients with TIAs or nondisabling strokes occurring within 6 months

preceding presentations and with ipsilateral carotid stenosis of 70–99%, that the cumulative risk of an ipsilateral stroke occurring by the 18-month follow-up was 26% for 331 patients who were treated medically and 9% for 328 patients who were treated surgically. This yielded an absolute risk reduction of 17% ($p<0.001$). The corresponding incidence of major or fatal ipsilateral stroke was 13% and 3% for medically and surgically treated groups, respectively. This translates into an absolute risk reduction of 11% or a greater than 5 to 1 benefit in favor of operation ($p<0.001$). The NASCET investigators concluded that carotid endarterectomy was highly beneficial for patients with recent hemispheric or retinal TIAs or those with nondisabling stroke in the presence of ipsilateral high-grade carotid stenoses. The NASCET study also concluded that carotid endarterectomy was highly beneficial for symptomatic patients with 50% to <70% carotid artery stenosis [60].

Patients with >60% asymptomatic carotid artery stenosis can be candidates for carotid endarterectomy if they are good-risk patients [9]. The ACAS study also concluded that carotid endarterectomy was superior to medical therapy in good-risk patients, and it reduced stroke by 55% over a 5-year period when surgical therapy was compared to medical therapy (5% vs. 11%). Recently, the ACST Collaborative Group reported on the results of carotid endarterectomy in the prevention of stroke for ≥70% asymptomatic stenosis. Their conclusions were somewhat similar to the American study (the ACAS): in asymptomatic patients younger than 75 years of age with a carotid diameter reduction of 70%, immediate carotid endarterectomy decreased the net 5-year stroke risk by one-half, from 12% to 6% (including the 3% perioperative hazard) [10].

Despite the findings of these trials, the management of patients with asymptomatic carotid stenosis has been controversial over the past decade, since most of the landmark studies comparing the best medical therapy with CEA used only aspirin as the antiplatelet agent and occurred prior to the widespread use of statins. Because of which, a significant number of authorities recommend intervention only in good-risk patients with ≥80% asymptomatic stenosis or even optimal medical therapy alone.

Recently, carotid angioplasty/stenting (CAS) has been recommended as an alternative to carotid endarterectomy. Several randomized and nonrandomized prospective trials have been conducted over the past several years to evaluate the efficacy of CAS in the prevention of strokes for both symptomatic and asymptomatic patients. One of these, the SAPPHIRE study, just reported their early results comparing CAS to carotid endarterectomy in high-risk patients. The SAPPHIRE study was a randomized trial that compared carotid stenting using the AngioGuard embolic protection device to carotid endarterectomy in patients at increased risk for carotid surgery. Symptomatic patients with ≥50% stenosis and asymptomatic patients with ≥80% stenosis by ultrasound (constitutes most of the patients), who had one or more of the comorbidity criteria that placed them at increased risk for surgery, were included. The primary endpoints were death, stroke, and myocardial infarction at 30 days post procedure, and ipsilateral stroke and death at 1 year. The composite endpoint of death, stroke, and myocardial infarction at 30 days was 5.8% for the stent group and 12.6% for the surgery group ($p=0.047$).The trial concluded that carotid stenting in high-risk patients was comparable or somewhat favorable to carotid endarterectomy when combined death, stroke, and myocardial infarction were considered [18].

The SPACE trial was designed to test the hypothesis that CAS would not be inferior to CEA in symptomatic patients with ≥70% carotid stenosis [17]. This study compared 584 CEAs with 599 CAS procedures. The primary endpoint was a composite of ipsilateral stroke or death within 30 days of the procedure. Surgeons were required to have performed at least 25 CEA procedures with an acceptable rate of morbidity and mortality in a prior year, and CAS operators were required to have performed at least 25 successful angioplasty or stent procedures. The use of shunting during CEA and embolic protection devices during CAS was optional. The primary endpoint for CEA was 6.3% versus 6.8% for CAS, and all strokes was 6.2% for CEA versus 7.5% for CAS with a disabling stroke rate of 2.9% for CEA versus 4% for CAS.

The EVA-3S trial (Endarterectomy versus Angioplasty in Patients with Symptomatic Severe Carotid Stenosis Trial) randomized patients within 120 days of TIA or complete stroke with >60% ipsilateral carotid stenosis based on duplex ultrasound and angiography [16]. The primary outcome was the composite of stroke or death within 30 days of the procedure. Surgeons were required to have performed at least 25 CEA procedures during the previous year, and CAS interventionalists were required to have performed at least 12 CAS procedures or 35 stenting procedures in other vessels. The use of embolic protection devices was limited. Among the 259 patients randomized for CEA and the 261 patients randomized for CAS, the combined composite endpoint was 3.9% for CEA versus 9.6% for CAS (an odds ratio of 0.38, with $p=0.0133$). The incidence of all strokes was 3.5% for CEA versus 9.2% for CAS (odds ratio of 0.36, $p=0.0108$), with a disabling stroke rate of 0.4% for CEA versus 2.7% for CAS (odds ratio of 0.14, $p=0.0682$). Similarly, the ICSS (International Carotid Stenting Study) is a randomized study comparing CEA versus CAS in symptomatic patients with >50% carotid stenosis [15]. The primary endpoint is the 3-year rate of fatal or disabling stroke. Among 1,713 randomized patients, the 120-day composite rate of stroke, death, or MI was 8.5% in the CAS group versus 5.2% in the CEA group (odds ratio of 1.69). The CREST Trial (Carotid Revascularization Endarterectomy vs. Stent Trial) was a randomized multicenter trial comparing CAS to CEA in both

symptomatic and asymptomatic patients [14]. In this trial and among 2,502 patients followed for a mean of two and a half years, there was no significant difference in the primary events between the two methods of revascularization (combined stroke, death, and MI, 7.2% for CAS versus 6.8% for CEA, odds ratio of 1.11). There were differences in the rates of the component periprocedural events; specifically stroke was significantly more frequent with CAS (4.1% vs. 2.3%, $p=0.01$) and myocardial infarction was more likely after CEA (2.3% vs. 1.1%, $p=0.03$). In a recent systemic review and meta-analysis of randomized trials of CEA versus stenting [61], 13 randomized carotid trials enrolling 7,484 patients, of which 80% had symptomatic disease, showed that compared with CEA, stenting was associated with an increased risk of any stroke (RR = 1.45; 95% confidence interval 1.06–1.99), decreased risk of perioperative myocardial infarction (RR = 0.43; 95% confidence interval 0.26–0.71), and a nonsignificant increase in mortality (RR = 1.40; 95% confidence interval 0.85–2.33). The authors concluded that compared with CEA, CAS significantly increased the risk of any stroke and decreased the risk of myocardial infarction.

## References


1. Centers for Disease Control and Prevention (CDC). Prevalence of disabilities and associated health conditions among adults—United States, 1999. MMWR Morb Mortal Wkly Rep. 2001;50:120–5.
2. Broderick J, Brott T, Kothari R, et al. The greater Cincinnati/Northern Kentucky stroke study: preliminary first-ever and total incidence rates of stroke among blacks. Stroke. 1998;29:415–21.
3. Rosamond W, Flegal K, Furie K, et al. Heart disease and stroke statistics – 2008 update: a report from the American Heart Association Statistics Committee and Stroke Statistics Subcommittee. Circulation. 2008;117:e25–146.
4. Hankey GJ. Impact of treatment of people with transient ischemic attacks on stroke incidence and public health. Cerebrovasc Dis. 1996;6:26–33.
5. Eastcott HHG, Pickering GW, Robb CG. Reconstruction of internal carotid artery in a patient with intermittent attacks of hemiplegia. Lancet. 1954;2:994–6.
6. DeBakey ME. Successful carotid endarterectomy for cerebrovascular insufficiency. Nineteen-year follow-up. JAMA. 1975;233:1083–5.
7. The CASSANOVA Study Group. Carotid surgery vs. medical therapy in asymptomatic carotid stenosis. Stroke. 1991;22:1229–35.
8. Asymptomatic Carotid Atherosclerosis Study Group. Study design for randomized prospective trial of carotid endarterectomy for asymptomatic atherosclerosis. Stroke. 1989;20:844–9.
9. Hobson II RW. Management of symptomatic and asymptomatic carotid stenosis: results of current randomized clinical trials. In: Bernstein EF, editor. Vascular diagnosis. 4th ed. St Louis: Mosby; 1993. p. 446–51.
10. MRC, Asymptomatic Carotid Surgery Trial (ACST) Collaborative Group. Prevention of disabling and fatal stroke by successful carotid endarterectomy in patients without recent neurological symptoms: randomized controlled trial. Lancet. 2004;363:1491–500.
11. Mayberg MR, Wilson SE, Yatsu F. For the veterans affairs cooperative study program 309 trialist group. Carotid endarterectomy and prevention of cerebral ischemia in symptomatic carotid stenosis. JAMA. 1991;266:3289–94.
12. North American Symptomatic Carotid Endarterectomy Trial Collaborators. Beneficial effect of carotid endarterectomy in symptomatic patients with high-grade carotid stenosis. N Engl J Med. 1991;325:445–53.
13. European Carotid Surgery Trialists' Collaborative Group. MRC European carotid surgery trial. Interim results for symptomatic patients with severe (70–99 %) or with mild (0–29 %) carotid stenosis. Lancet. 1991;337:1235–43.
14. Brott TG, Hobson 2nd RW, Howard G, Roubin GS, Clark WM, Brooks W, et al. Stenting versus endarterectomy for treatment of carotid artery stenosis. N Engl J Med. 2010;363:11–23.
15. International Carotid Stenting Study Investigators, Ederle J, Dobson J, Featherstone FL, Bonati LH, van der Worp HB, et al. Carotid artery stenting compared with endarterectomy in patients with symptomatic carotid stenosis (International Carotid Stenting Study): an interim analysis of a randomized controlled trial. Lancet. 2010;375:985–97.
16. Mas JL, Chatellier G, Beyssen B, EVA-3S Investigators. Carotid angioplasty and stenting with and without cerebral protection: clinical alert from the endarterectomy versus angioplasty in patients with symptomatic severe carotid stenosis (EVA-3 S) trial. Stroke. 2004;35:e18–20.
17. SPACE Collaborative Group, Ringleb PA, Allenberg J, Bruckmann H, Eckstein HH, Fraedrick G, et al. 30 day results from the SPACE trial of stent-protected angioplasty versus carotid endarterectomy in symptomatic patients: a randomized non-inferiority trial. Lancet. 2006;368:1239–47. Erratum appears in Lancet 2006;368:1238.
18. Yadav JS, Wholey MH, Kuntz RE, Fayad P, Katzen BT, Mishkel GJ, et al. Protected carotid artery stenting versus endarterectomy in high-risk patients. N Engl J Med. 2004;351:1493–501.
19. Layton KF, Kallmes DF, Cloft HJ, Lindell EP, Cox VS. Bovine aortic arch variant in humans: clarification of a common misnomer. AJNR Am J Neuroradiol. 2006;27:1541–2.
20. Berguer R, Kieffer E, editors. Surgery of the arteries to the head. Heidelberg: Springer; 1992.
21. Anson BJ, McVay CB. Surgical anatomy, vol. 1. Philadelphia: WB Saunders Co; 1971. p. 3–6.
22. Larson Jr CP. Anesthesia and control of the cerebral circulation. In: Wylie EJ, Ehrenfeld WK, editors. Extracranial cerebrovascular disease: diagnosis and management. Philadelphia: WB Saunders Co; 1970. p. 152–83.
23. Reivich M, Hooling HE, Roberts B, et al. Reversal of blood flow through the vertebral artery and its effect on cerebral circulation. N Engl J Med. 1961;265:878–85.
24. Connolly JE, Stemmer EA. Endarterectomy of the external carotid artery: its importance in the surgical management of extracranial cerebrovascular occlusive disease. Arch Surg. 1973;106:799–802.
25. Ehrenfeld WK, Lord RSA. Transient monocular blindness through collateral pathways. Surgery. 1969;65:911–5.
26. Cook PJ, Honeybourne D, LIP GY, et al. Chlamydia pneumonia antibody titers are significantly associated with stroke and transient cerebral ischemia: the West Birmingham stroke project. Stroke. 1998;29(2):404–10.
27. Sillesen H, Nielsen T. Clinical significance of intraplaque hemorrhage in carotid artery disease. J Neuroimaging. 1998;8(1):15–9.
28. Blaisdell FW, Hall AD, Thomas AN, et al. Cerebrovascular occlusive disease. Experience with panarteriography in 300 consecutive cases. Calif Med. 1965;103:321–9.
29. Hass Wk, Field WS, North RR, et al. Joint study of extracranial arterial occlusion. II. Arteriography, techniques, sites, and complications. JAMA. 1968;203:961–8.
30. AbuRahma AF. Overview of cerebrovascular disease. In: AbuRahma AF, Diethrich EB, editors. Current noninvasive vascular diagnosis. Littleton: PSG Publishing; 1988. p. 1–7.
31. Strandness DEJ, Sumner DS. Hemodynamics for surgeons. New York: Grune & Stratton, Inc; 1975. p. 512–24.

32. Kakkos SK, Sabetai M, Tegos T, Stevens J, Thomas D, Griffin M, Geroulakos G, Nicolaides AN. Asymptomatic carotid stenosis and risk of stroke (ACSRS) study group. J Vasc Surg. 2009;49:902–9.
33. Hessel SJ, Adams DF, Abrams HL. Complications of angiography. Radiology. 1981;138:273–81.
34. Miyazaki M, Kato K. Measurement of cerebral blood flow by ultrasonic Doppler technique: hemodynamic comparison of right and left carotid artery in patients with hemiplegia. Jpn Circ J. 1954; 29:383.
35. Goldberg RD. Doppler physics and preliminary report for a test for carotid insufficiency. In: Goldberg RD, Saris LV, editors. Ultrasonics in ophthalmology: diagnostic and therapeutic applications. Philadelphia: WB Saunders; 1967. p. 199.
36. Brockenbrough EC. Screening for prevention of stroke: use of a Doppler flow meter. Seattle: Seattle Parks Electronics; 1970.
37. Mozersky BJ, Hokanson DE, Sumner DS, et al. Ultrasonic visualization of the arterial lumen. Surgery. 1972;72:253–9.
38. Barber FE, Baker DW, Strandness Jr DE, et al. Duplex scanner. II. For simultaneous imaging of artery tissues and flow. Ultrasonic symposium. Proc IEEE. 1974;74:CHO8961SU.
39. Gee W, Smith CA, Hinson CE, et al. Ocular pneumoplethysmography and carotid artery disease. Med Instrum. 1974;8:244–8.
40. AbuRahma AF, Diethrich EB. Diagnosis of carotid arterial occlusive disease. Vasc Surg. 1980;14:23–9.
41. AbuRahma AF, Osborne L. Comparison of the pneumoculoplethysmography (GEE) and the digitalized pulse timing oculoplethysmography (ZIRA). Am Surg. 1983;49:548–50.
42. Muller HR. The diagnosis of internal carotid artery occlusion by the directional Doppler sonography of the ophthalmic artery. Neurology. 1972;22:816–32.
43. Burger R, Barnes RW. Choice of ophthalmic artery branch for Doppler cerebrovascular examination: advantages of the frontal artery. Angiology. 1977;28:421–6.
44. Polak JF, Dobkin GR, O'Leary DH, et al. Internal carotid artery stenosis: accuracy and reproducibility of color Doppler assisted duplex imaging. Radiology. 1989;173:793–8.
45. Spadone DP, Barkmeier LD, Hodgson KJ, et al. Contralateral internal carotid artery stenosis or occlusion: pitfall of correct ipsilateral classification. A study performed with color-flow imaging. J Vasc Surg. 1990;11:642–9.
46. Londrey GL, Spadone DP, Hodgson KJ, et al. Does color-flow imaging improve the accuracy of duplex carotid evaluation? J Vasc Surg. 1991;13:359–63.
47. Mattow MA, Hodgson KJ, Ramsey DE, et al. Identifying total carotid occlusion with color-flow duplex scanning. Eur J Vasc Surg. 1992;6:204–10.
48. AbuRahma AF, Robinson PA, Khan S, et al. Effect of contralateral severe stenosis or carotid occlusion on duplex criteria of ipsilateral stenoses: comparative study of various duplex parameters. J Vasc Surg. 1995;22:751–62.
49. AbuRahma AF, Pollack JA, Robinson Pa, et al. The reliability of color duplex ultrasound in diagnosing total carotid artery occlusion. Am J Surg. 1997;174:185–7.
50. AbuRahma AF, Robinson PA, Stickler DL, et al. Proposed new duplex classification for threshold stenoses used in various symptomatic and asymptomatic carotid endarterectomy trials. Ann Vasc Surg. 1998;12:349–58.
51. Lovelace TD, Moneta GL, Abou-Zamzam AH, Edwards JM, Yeager RA, Landry GJ, Taylor LM, Porter JM. Optimizing duplex follow-up in patients with an asymptomatic internal carotid artery stenosis of less than 60 %. J Vasc Surg. 2001;33:56–61.
52. Nederkoorn PJ, Mali WPTM, Eikelboom BC, Elgersma OEH, Buskens E, Hunink MGM, Kappell LJ, Buijs PC, Wust AFJ, van der Lugt A, van der Graaf Y. Preoperative diagnosis of carotid artery stenosis: accuracy of noninvasive testing. Stroke. 2002;33:2003–8.
53. Ricco JB, Camiade C, Roumy J, Neau JP. Modalities of surveillance after carotid endarterectomy: impact of surgical technique. Ann Vasc Surg. 2003;17:386–92.
54. Moore WS. For severe carotid stenosis found on ultrasound, further arterial evaluation is unnecessary. Stroke. 2003;34:1816–7.
55. Rothwell PM. For severe carotid stenosis found on ultrasound, further arterial evaluation prior to carotid endarterectomy is unnecessary: the argument against. Stroke. 2003;34:1817–9.
56. Nederkoorn PJ, van der Graaf Y, Hunink Y. Duplex ultrasound and magnetic resonance angiography compares with digital subtraction angiography in carotid artery stenosis. Stroke. 2003;34:1324–32.
57. Kern R, Szabo K, Hennerici M, Meairs S. Characterization of carotid artery plaques using real-time compound B-mode ultrasound. Stroke. 2004;35:870–5.
58. Sumner DS. Use of color-flow imaging technique in carotid artery disease. Surg Clin North Am. 1990;70:201–11.
59. Ackerstaff RGA, Moons KGM, van de Vlasakker CJW, Moll FL, Vermeulen FEE, Algra A, Spencer MP. Association of intraoperative transcranial Doppler monitoring variables with stroke from carotid endarterectomy. Stroke. 2000;31:1817–23.
60. Barnett HJM, Taylor DW, Eliasziw MA, et al. For the NASCET collaborators: benefits of carotid endarterectomy in patients with symptomatic, moderate, or severe stenosis. N Engl J Med. 1998;339:1415–25.
61. Murad MH, Shahrour A, Shah ND, Montori VM, Ricotta JJ. A systematic review and meta-analysis of randomized trials of carotid endarterectomy vs stenting. J Vasc Surg. 2011;53:792–7.

# Duplex Scanning of the Extracranial Carotid Arteries

7

Ali F. AbuRahma

**Abstract**

A complete extracranial carotid duplex examination should include the following data: the peak systolic and end-diastolic velocities of common carotid, internal carotid, and external carotid arteries, right and left subclavian arteries, and vertebral arteries; the internal carotid artery to common carotid artery peak systolic velocity ratio; flow direction of the vertebral artery (antegrade or retrograde); analysis of the Doppler spectral waveform of the examined vessels; and the presence or absence of plaque and description of its morphology.

A carotid duplex ultrasound examination should be termed "inconclusive" if the findings are uncertain, and it cannot be ensured that the carotid artery does not have significant carotid artery disease. Calcification and shadowing, high bifurcation, short neck, or any other circumstances that prevent adequate interrogation of the carotid artery can result in an inconclusive examination. In this scenario, other diagnostic modalities must be recommended to delineate the proper pathology.

The accuracy of duplex scanning in the examination of the carotid artery bifurcation has resulted in its use for detecting significant carotid stenosis in symptomatic patients, the evaluation of patients with neck bruits, postoperative imaging of endarterectomized vessels, and the sequential examination of asymptomatic patients to document progression of disease. Other clinical implications include carotid endarterectomy based on duplex ultrasound without angiography, intraoperative assessment of carotid endarterectomy, long-term follow-up after carotid endarterectomy, plaque morphology and outcome, and carotid duplex scanning following trauma.

**Keywords**

Noninvasive vascular testing • Duplex • Diagnosis • Carotid arteries

## Historical Perspectives and the Duplex Concept

Over the past 30 years, there has been a significant evolution in the application of noninvasive technology for the diagnosis of extracranial vascular disease with more widespread utilization of duplex ultrasound techniques. An appreciation of why this technology has enjoyed such acceptance is best obtained by understanding the evolution of the concept of using combined imaging and velocity detection techniques.

A.F. AbuRahma, M.D., RVT, RPVI
Department of Surgery,
Robert C. Byrd Health Sciences Center,
West Virginia University,
3110 MacCorkle Ave SE,
Charleston, WV 25304, USA

Charleston Area Medical Center,
Charleston, WV, USA
e-mail: ali.aburahma@camc.org

A.F. AbuRahma, D.F. Bandyk (eds.), N*on*invasive Vascular Diagnosis,
DOI 10.1007/978-1-4471-4005-4_7, 

When Kossoff [1] applied gray-scale techniques to imaging, he paved the way for identifying vessels with ultrasound. In 1969, Olinger [2] reported on the use of ultrasound echo techniques to identify the carotid arteries and was active in the development of high-resolution imaging technology. In these studies, the walls of vessels were identified as echo-dense parallel structures, while the lumen was an echo-free zone contained between the walls. Atherosclerotic lesions would theoretically be identified as projections into the lumen, and thus, it appeared that this technique alone would be suitable for identifying all degrees of occlusive disease. Early experimental application, however, encountered three major problems, which, in retrospect, seem obvious. The first of these related to the complex acoustic density of atherosclerotic plaques, particularly as the lesions became more severe with zones of hemorrhage and calcification. The areas of hemorrhage were relatively echo-free and appeared as defects within the substance of the plaque, rendering accurate delineation of the plaque surface difficult. The presence of calcification served as an acoustic barrier to deeper penetration of the ultrasound beam, resulting in the production of an acoustic window with subsequent loss of resolution of deeper structures [3]. While a pure imaging technique might accurately identify the surface characteristics if a plaque is homogeneous, the presence of so-called complicated plaques introduced a source of significant error. Finally, because thrombus and flowing blood had similar acoustic densities, it was difficult to differentiate between occluded and non-occluded arteries.

To overcome this problem, a Doppler device was added to the imaging system, and its initial application was reported by Barber et al. in 1974 [4]. It soon became apparent that changes in the flow patterns detected by the Doppler velocity apparatus correlated closely with the severity of stenosis as judged by arteriography [5]. The emphasis in instrument development, therefore, shifted from imaging to Doppler detection of velocity changes. Thus, the duplex concept of combining B-mode imaging and pulsed Doppler flow detection for direct evaluation of arterial disease led to the creation of the first duplex scanning instruments. Using duplex ultrasonography, anatomical and physiological information can be obtained directly from the sites of vascular disease. This is based on the concept that arterial lesions produce disturbances in blood flow patterns that can be characterized by Doppler flow signal analyses. B-mode imaging is used as a guide for placement of a pulsed Doppler sample volume within the artery of interest, and the local flow pattern is evaluated by spectral wave analysis. Duplex scanning permits evaluation of the arterial flow pattern at a discrete site within the B-mode image, using pulsed Doppler. The sample volume of the pulsed Doppler is the region in which flow is actually detected. Adjusting the position and size of the sample volume aids in allowing the center stream pattern to be evaluated without interference from flow disturbances near the arterial wall or in adjacent blood vessels. B-mode imaging is useful in identifying anatomical variants and arterial wall pathology, including thickening or calcifications; however, the classification of arterial disease severity is based primarily on an analysis of the pulsed Doppler spectral waveforms.

## Duplex Ultrasound Components

### Real-Time B-Mode Imaging

B-mode ultrasound imaging has been used extensively for visualizing soft tissue structures. Carotid arteries, however, could not be seen properly until the advent of real-time techniques that have overcome the problem of visualization. With B-mode imaging alone, variations in the acoustic properties of different tissues reflect ultrasound waves and generate an image of the tissues being examined. These variations in acoustic reflectance are represented visually by shades of gray on the image, which facilitates identification of different tissues. The vessel wall, because of its high reflectivity, may thus be visualized. Yet it is this tissue interaction with ultrasound that has imposed severe limitations on techniques that use this method for visualizing atherosclerotic plaques and occluded arteries.

Unfortunately, methods currently used for processing the reflected ultrasound waves are often incapable of differentiating flowing blood, thrombus, and noncalcified plaques. Thus, vessels that are completely occluded may appear patent. Likewise, noncalcified plaques may be entirely missed or, at best, only partly visualized. In addition, when atherosclerotic disease at the carotid bifurcation exists, calcium is a common component of the plaque and prevents the passage of ultrasound waves through this area. Thus, if there is a calcified plaque on the anterior wall of the vessel, a very dense acoustic signal will be registered, but there will be no information concerning the lumen beneath the calcified segment. This is commonly referred to as acoustic shadowing (Fig. 7.1). These limitations are largely overcome by combining B-mode imaging with flow detection techniques using Doppler, such as spectral waveform analysis and color flow imaging. Experience with B-mode imaging techniques for the classification of carotid artery disease has generally shown that interpretation of the image is most accurate for lesions of a minimal to moderate degree of stenosis and least accurate for high-grade stenoses or occlusions. It is often difficult to estimate the size of the arterial lumen from a B-mode image because the interface between the arterial wall and flowing blood is not clearly seen. Calcified atherosclerotic plaque, which is extremely echogenic, results in bright echoes with acoustic shadows (Fig. 7.1).

The ultrasonic carotid plaque morphology may correlate qualitatively with its histological composition; however, the clinical relevance of this information is somewhat controversial [6–9]. The B-mode characteristic of the carotid plaque that appears to correlate most closely with the clinical outcome is heterogeneity. This is generally defined as a plaque that has a mixture of hyperechoic, hypoechoic, and isoechoic plaques, a feature that may be attributed to the presence of

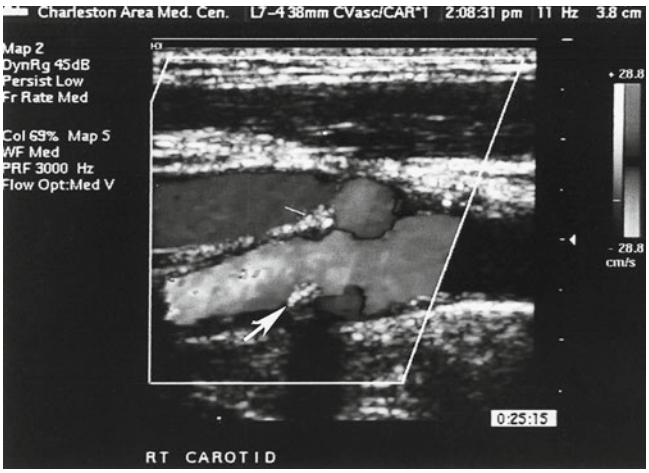


**Fig. 7.1** Color duplex ultrasound image of an internal carotid artery showing calcified plaque where a very dense acoustic signal is registered (*arrow*) with acoustic shadowing (*underneath the arrow*)

intraplaque hemorrhage. This feature has been noted more frequently in patients with neurological events than in asymptomatic carotid stenoses.

## Doppler Spectral Waveform Analysis

A valuable adjunct to B-mode imaging is the use of spectral analysis to analyze the backscattered Doppler signal. Spectral analysis, as applied to Doppler ultrasound, is merely a method of determining the frequency content of the backscattered signal and the relative strengths or amplitude of these component frequencies. The original technique was utilized off-line and employed a Kay sonograph, which although providing more information than was previously available with analog displays, was time-consuming and did not depict forward and reverse flow. Real-time spectral analysis was introduced using fast Fourier transform analysis (FFT). The FFT method makes it possible to display the individual frequencies that make up the return signal. Information related to the intensity of the spectrum is also possible: for example, a narrow well-defined spectrum is displayed when a limited number of frequencies are evident in a laminar flow. Spectral broadening represents a variety of frequencies and is often associated with turbulent flow. The velocity profile shows various frequency shifts on the vertical axis and time on the horizontal axis. The FFT has the advantages of saving time and detecting both forward and reverse flow. This method of signal processing was particularly suitable because pulsed Doppler beams were being utilized in the echo component. Other techniques of spectral analysis, including multiple band-pass filter analysis and time compression analysis, have been used, but have not achieved widespread acceptance.

The availability of the pulsed Doppler technique made it possible to obtain velocity information from a known location and, depending on the sample volume size, from a finite volume of the flow stream. The continuous-wave (CW)

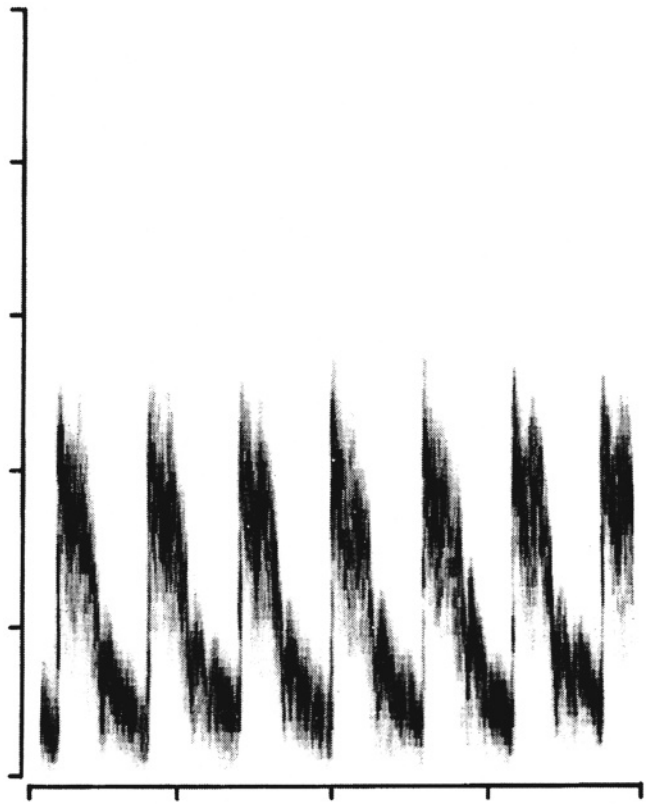

**Fig. 7.2** A normal internal carotid artery Doppler spectra

instruments utilized widely at that time for the detection of disease in the lower extremity were known to have a large sample volume that traversed the whole width of the vessel being insonated, and were really most suitable for determining the mean velocity in the forward or reverse direction. Also, the data analyzed by CW instruments were obtained not only from the vessel of interest but also from other vessels in close proximity. With the pulsed instrument, the examiner could be certain that the data were being obtained from the vessel of interest. It was also possible, because of the finite sample volume, to interrogate a segment of the velocity profile and, perhaps, to detect changes that would not otherwise be apparent with a CW device.

A series of animal studies were conducted to determine the relationship between varying degrees of stenosis and spectral changes as identified by pulsed Doppler and fast Fourier spectrum analysis [10].

The Doppler spectral waveform analysis is a signal-processing technique that displays the complete frequency and amplitude content of the Doppler signal. This Doppler-shifted frequency is directly proportional to blood cell velocity, and the amplitude of the Doppler signal depends on the number of cells moving through the pulsed Doppler sample volume. The signal amplitude becomes stronger as the number of cells producing Doppler frequency shift increases. This spectral information is usually presented graphically with time on the horizontal axis and frequency or velocity on the vertical axis, and amplitude is indicated by shades of gray (Fig. 7.2).

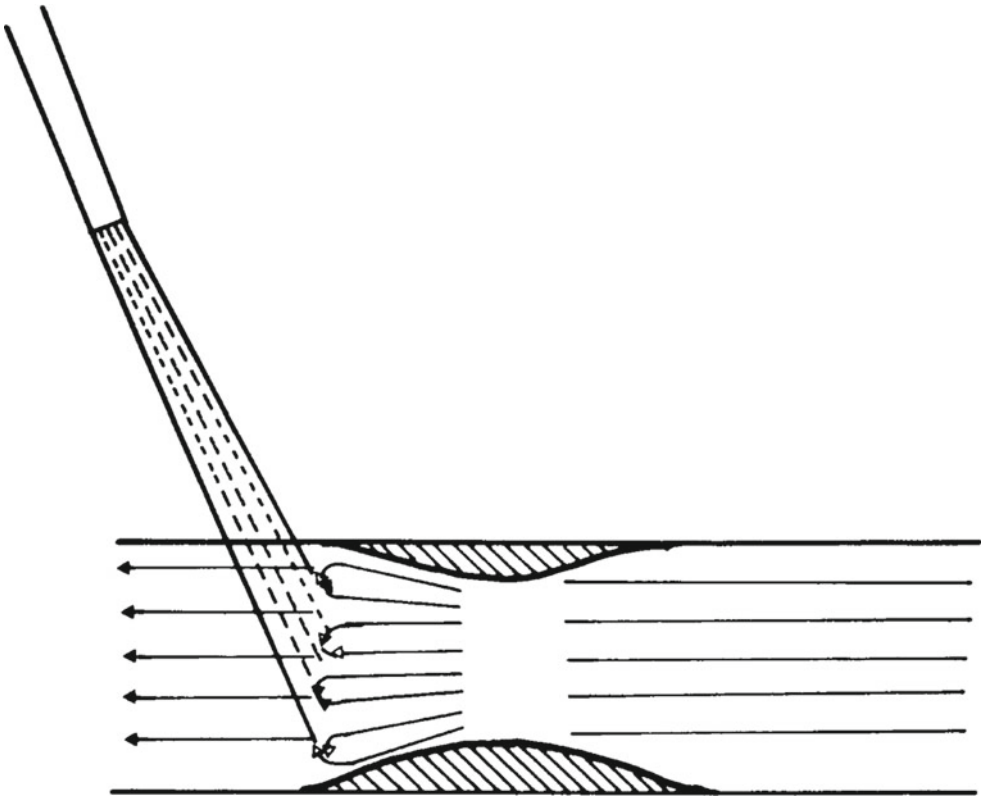

**Fig. 7.3** Schematic representation of minor flow disturbance generated by nonhemodynamically significant stenosis with production of vortical shedding immediately beyond the area of the stenosis with resumption of a normal laminar flow pattern further downstream

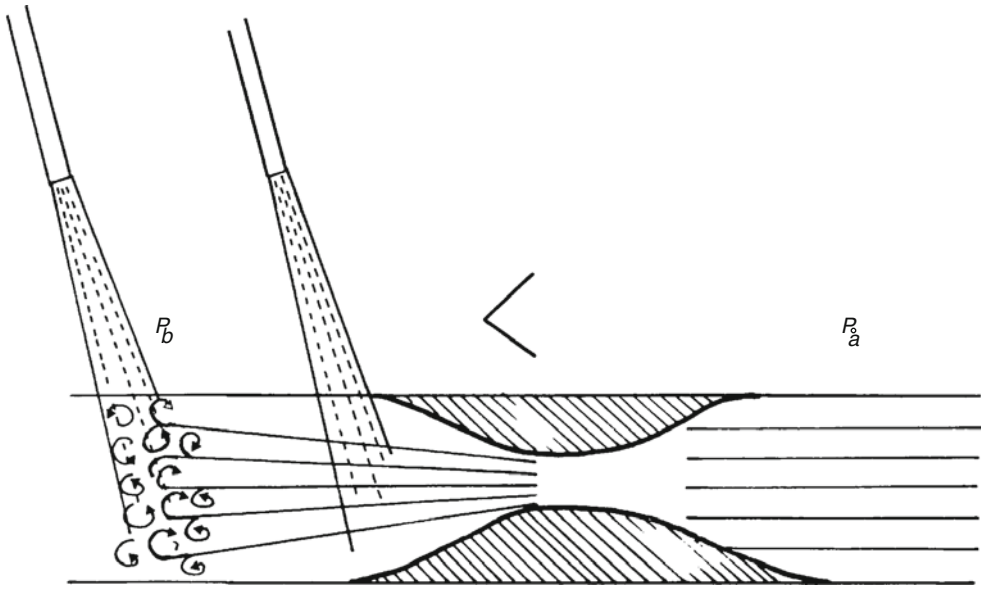


**Fig. 7.4** Schematic representation of major flow disturbance produced by hemodynamically significant stenosis with both increases in peak velocity in and immediately beyond the stenosis with decay of laminar flow to turbulent flow occurring at a maximum two diameters distal to the stenosis

The following is an explanation of these findings as it applies to the flow patterns within vessels. The center stream flow pattern in a normal artery is uniform or laminar, and a spectral waveform taken with the pulsed Doppler sample volume in the center of the lumen shows a relatively narrow band of frequency. It appears that even relatively mild degrees of stenosis are capable of producing deviations from laminar flow (as zones of vortical shedding) in the area distal to the stenosis (Fig. 7.3), with the magnitude of these disturbances being depicted by the magnitude of change in spectral width (spectral broadening). With hemodynamically significant stenoses, not only is spectral broadening present, which is produced by a major decay in the laminar flow pattern, but there is also a marked elevation in peak frequency or peak velocity at systole as a result of the high-speed jet of blood passing through and immediately beyond the stenosis (Fig. 7.4). High-grade

stenoses can therefore be recognized by the presence of both elevations in peak frequency at systole and diffuse spectral broadening [5].

The end-diastolic frequency or velocity is also increased in very severe stenoses. The Doppler spectral waveform criteria for classifying severity of carotid artery stenosis will be described in detail later.

The current application of duplex scanning in the detection of carotid artery disease utilizes this principle of identification of flow disturbance patterns by Doppler velocity detection instrumentation, with the emphasis in later years being on technical improvements in instrument design. A variety of duplex scanning instruments are available, the major differences among them being in the Doppler component. These are of two types: those utilizing CW Doppler and those utilizing pulsed Doppler beams. The outline below applies to the instrumentation available that currently uses pulsed Doppler beams for velocity detection and image generation.

## Instrumentation

The most significant changes in duplex instrumentation have occurred in scan head design. The shape of the pulsed Doppler beam, and therefore its sample volume, has been modified using either medium-focus or short-focus scan heads. The medium-focus scan head, operating at 5 mHz, has a 40-mm focal point, while the short-focus scan head, at a transmitting frequency of 5 mHz, has a 20-mm focal point. The beam width of the medium-focus scan head is most narrow at 35–45-mm depth, whereas that of the short-focus scan head is most narrow at 20–30 mm. The medium-focus scan head is therefore more appropriate for evaluating blood flow in vessels deeper than 30 mm, while the short-focus scan head is ideal for evaluating flow in vessels located close to the surface, 2–3 cm from the skin. Because the carotid arteries lie within 30 mm of the skin surface in the majority of human subjects, the short-focus scan head, at least theoretically, is ideal for evaluating these vessels.

These features are not only important in consideration of the depths of the vessels studied but also in understanding the effects of the sample volume size on the velocity profile being evaluated. If a large sample volume size is used in the evaluation of small-diameter vessels, a wide range of velocities will be detected under normal circumstances, which on spectral analysis will appear as spectral broadening. In these circumstances, this finding is normal and is similar to the spectra generated by CW instruments. Conversely, if a small sample volume is used in a large vessel, particularly if flow is axisymmetric, the velocities in the sample volume are likely to be similar and, on spectral analysis, will not display spectral broadening. At a range of 25 mm, the beam widths for the medium- and short-focus scan heads are 5.5 and 2 mm, respectively, at the 20 dB level. At this range, the sample volumes have been calculated at 3 and 24 $mm^3$ for the short- and medium-focus scan heads, respectively. If spectral broadening therefore is an important feature in the evaluation, it is apparent that a short-focus scan head should be more sensitive than a medium-focus scan head.

An additional feature of the current instruments is the dedicated use of the pulsed signal to the Doppler component, which avoids the problem of aliasing encountered in the original prototypes. In the latter, the signal was shared between the echo and Doppler components and resulted in a limited peak frequency detection capability that could be exceeded when severe disease was present. With the pulsed echo component nonoperative, the usual pulse repetition frequency available to the Doppler component is doubled, increasing the frequency response of the 5-mHz instrument at 60° to 9.5 kHz, which is more than adequate to detect the frequencies associated with severe disease.

The quadrature outputs of the pulsed Doppler signal are then analyzed using an online fast Fourier transform spectral analyzer, providing a full-scale frequency display of 10 kHz, with 7 kHz usually being used for forward frequencies and 3 kHz for reverse frequencies. The amplitude of the component frequencies in the signal is depicted in gray-scale format on the oscilloscope screen.

To improve the signal-to-noise ratio on the spectral display, the signal in many instruments is "normalized," a principle that increases the highest amplitude of each analysis in the spectrum to a particular reference level with the subsequent same scaling factor being applied to all other amplitudes. Following this normalizing process, a variable amount of signal is then displayed depending on the dynamic range used with the Doppler signal. The use of a wide dynamic range enhances the likelihood that, in addition to the Doppler backscattered signal, noise will also be displayed. Narrow dynamic range is ideal for evaluating the Doppler signal only.

The addition of high-definition imaging (HDI) technology revolutionized the front end of the ultrasound image formation process. The extended signal processing, or ESP technology (Advanced Technology Laboratories/Phillips System), extends the momentum into the area of signal processing. The result is a substantial reduction in speckle noise, allowing a higher level of clarity and detail than has ever been seen in ultrasound images. Tissue differentiation and resolution of fine anatomical detail, already hallmarks of HDI images, are enhanced even further through the addition of ESP technology.

The technology developments that make HDI and extended signal processing possible are many and complex. Perhaps the most appropriate place to begin is with the acoustic information that is returned to the ultrasound system from the body.

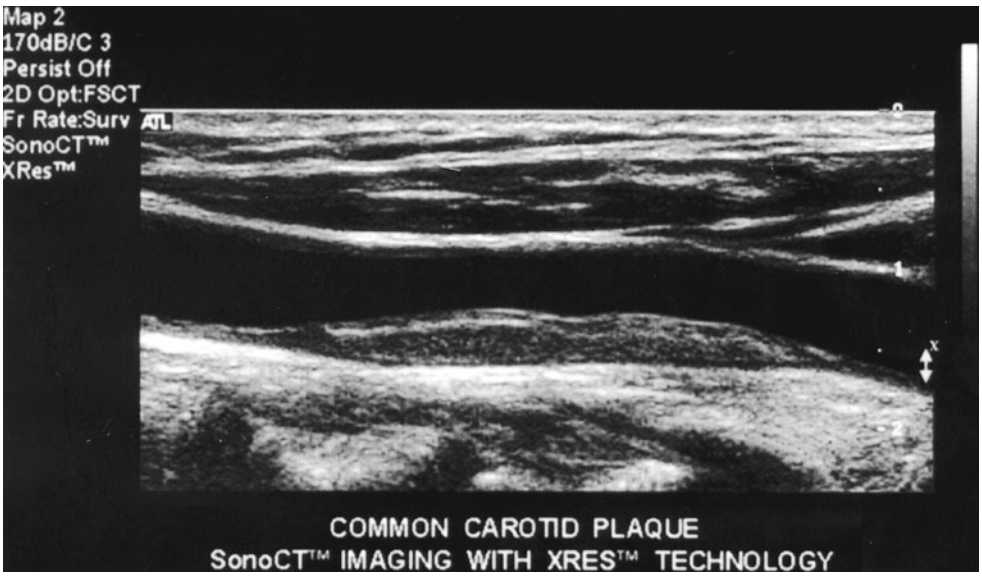


**Fig. 7.5** A SonoCT image showing tissue texture, borders, and margins

Each tissue within the body responds to ultrasound energy of different frequencies in a characteristic way, which is often referred to as the tissue signature. The tissue signature information is carried within the spectrum of ultrasound frequencies returning from the tissue. This band of frequencies is referred to as the frequency spectrum bandwidth, or simply, bandwidth.

HDI preserves the quantity and quality of tissue signature through the capture and preservation of the entire bandwidth. This results in more sonographic information with better detail and definition.

The ultrasound beam former, together with the scan head, determines the ultimate contrast resolution, spatial resolution, penetration, and consistency of the image. If the acoustic information containing the tissue signature is reduced in quantity, or distorted in the beam former, there is no way of recovering it. Beam formation is accomplished by pulsing the transducer elements in the scan head to insonify the target. Sound waves reflected by the target return to the elements of the transducer, generating signals that are essentially separated in time. The beam former delays these signals so when all the channels are summed together, the time variations in the signals are compensated for and the exact tissue definition is obtained. The critical design requirements of the beam former are to preserve the entire bandwidth, which contains all of the acoustic information, and to prevent distortion of the signal during delay.

More recently, SonoCT real-time compound imaging was incorporated into duplex technology. Using up to nine "lines of sight," SonoCT imaging dramatically enhances image quality by providing up to nine times more information than conventional two-dimensional imaging. The resulting real-time image is a more realistic representation of actual tissue.

The clinical benefits of SonoCT real-time compound imaging include improved visualization of plaque border delineation, better assessment of plaque morphology, reduction of clutter artifacts seen in difficult-to-image patients, and reduction of posterior plaque shadowing to reveal the full extent of vascular disease. An example of this system is the Model iU22 xMATRIX (Philips Healthcare, Bothell, WA) which has a breakthrough processing technology that optimizes image quality down to the pixel level. It displays a SonoCT image with unprecedented visualization of tissue texture, borders, and margins, almost free of image-degrading artifacts (Fig. 7.5).

## Carotid Examination Technique

The technician can use any duplex ultrasound imaging system, which includes high-resolution B-mode imaging, pulsed Doppler, and a frequency spectrum analyzer. The carotid examination can be done using several scan heads, e.g., mechanical sector, phased array, or linear array. A linear array scan head is generally used for the mid/distal common carotid artery and carotid bifurcation where these vessels are usually parallel to the skin surface. Meanwhile, the sector-type imaging of a curved array or the smaller footprint phase array may be needed in an examination of the distal internal carotid artery and the vessels in the supraclavicular area.

The examination is conducted with the patient supine and the head slightly extended and turned slightly away from the side being examined and supported to eliminate lateral movement. Copious quantities of water-soluble acoustic gel are applied along the anterior border of the sternomastoid muscle, and the scan head is applied to the skin surface. A 7.5- or 5-mHz transducer is usually used. Presently, we are using the iU22 xMATRIX system (Philips Healthcare, Bothell, WA)

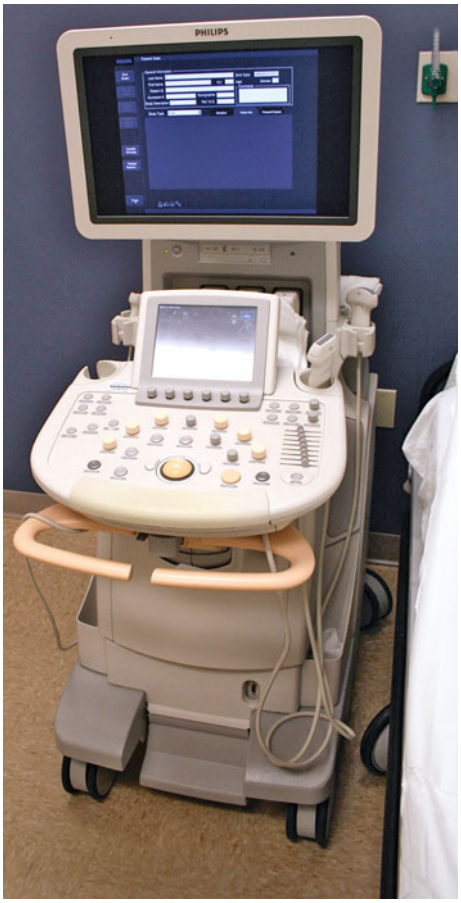


**Fig. 7.6** A duplex ultrasound machine: Model iU22 xMATRIX, Philips Healthcare, Bothell, WA

(Fig. 7.6). If color flow imaging is used, Doppler information is displayed on the image after it is evaluated for its phase (i.e., direction toward or away from the transducer) and its frequency content (i.e., a hue or shade of color). The sample volume of the pulsed Doppler should be kept as small as possible and placed in the center of the vessel or the flow channel. A Doppler angle of 45–60° should be maintained to obtain consistent results in velocity measurements. The vessels are examined both in longitudinal (Fig. 7.7) and transverse views (Fig. 7.8) and followed from the clavicle to the mandible with anterior oblique, lateral, and posterior oblique projections to identify and evaluate any carotid plaques or pathology.

Most of the carotid duplex examination is done using the longitudinal view since it allows the most favorable Doppler angle for recording the velocity data and for color Doppler imaging. Neither the color Doppler image nor the B-mode image will reliably pinpoint the area of maximum velocities and/or flow disturbances, i.e., B-mode imaging and color Doppler are generally helpful for localizing a specific area of interest, which needs to have extra or specific interrogation with pulsed Doppler sampling. Therefore, the gray-

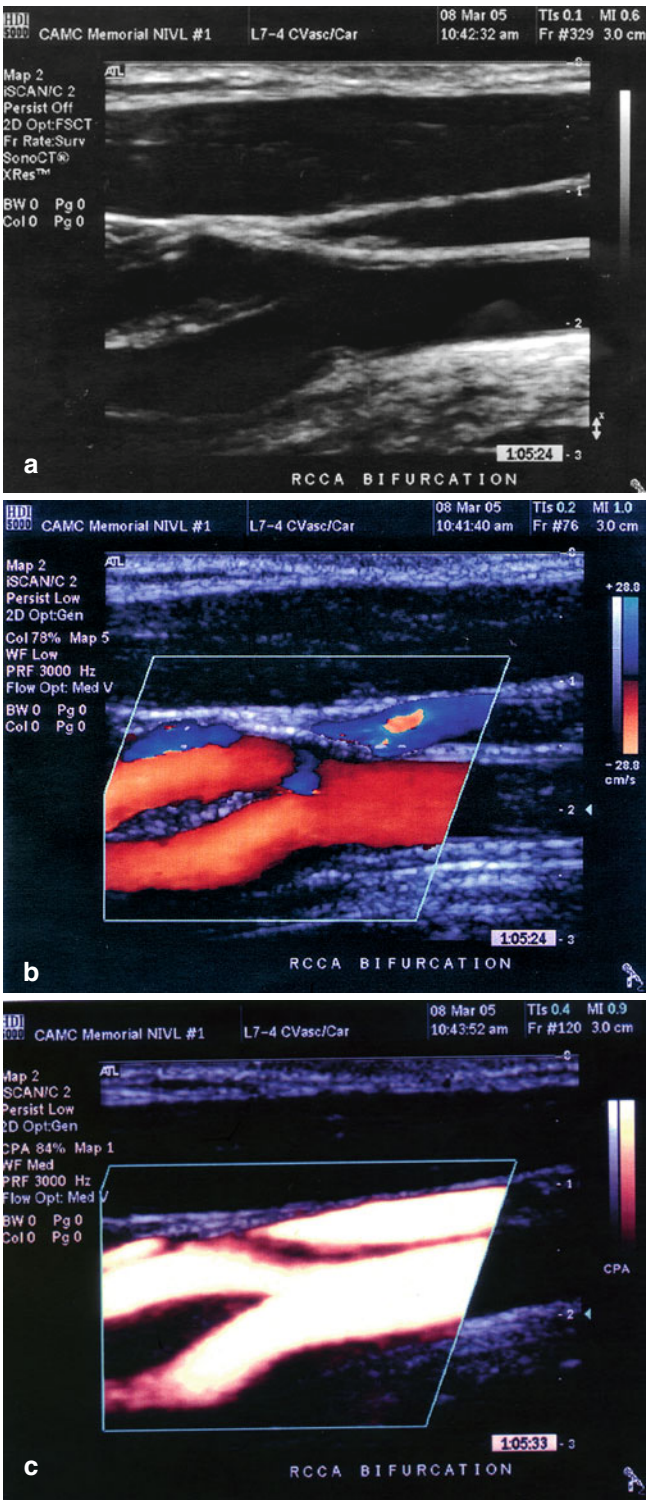


**Fig. 7.7** (**a**) Gray scale of right common carotid artery bifurcation in longitudinal view. (**b**) Color duplex ultrasound of right common carotid artery bifurcation in longitudinal view. (**c**) Power Doppler image of right common carotid artery bifurcation in longitudinal view

scale and color Doppler imaging alerts the technician to the presence of pathology/plaque in the arterial wall that may preclude penetration of the vessel by the pulsed Doppler. It

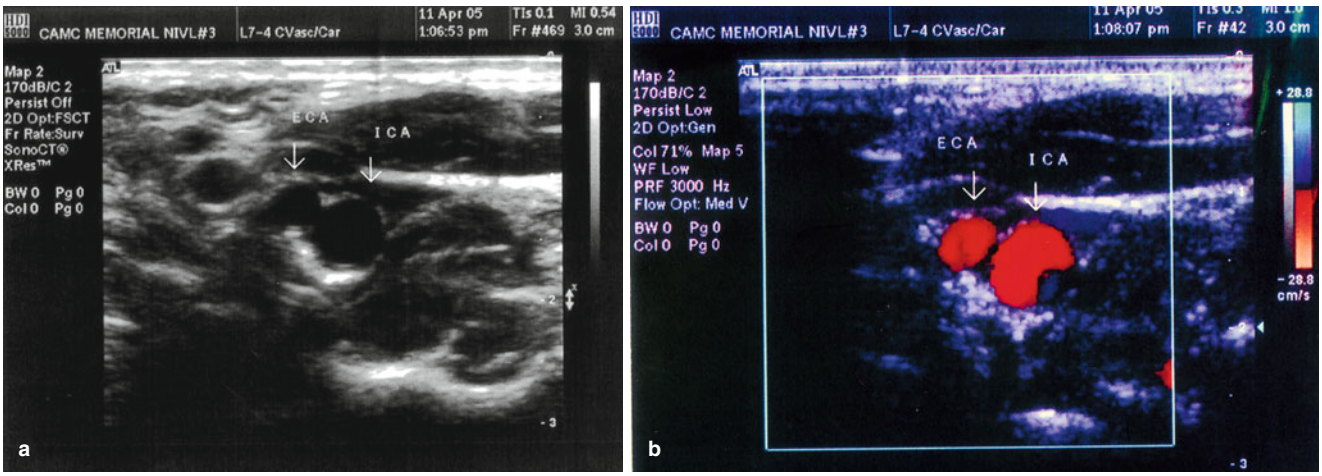


**Fig. 7.8** (**a**) Common carotid artery bifurcation in transverse view (*gray scale*). (**b**) Common carotid artery bifurcation in transverse view (color flow)

should also be noted that velocity waveforms should not be obtained from a transverse view since the Doppler angle in such a view is either unknown or close to being perpendicular to the flow direction, which will result in useless Doppler velocity measurements. Similarly, color Doppler imaging in cross section can be misleading for the same reasons. It should also be noted that ultrasound beam angles for optimal B-mode imaging are different from those required for obtaining Doppler spectral waveforms. As noted in the ultrasound physics chapter, the maximum ultrasound reflection is obtained when the ultrasound beam is perpendicular to the imaged surface. The optimal B-mode imaging angle is therefore 90° to the surface of the artery. The angle that yields the highest Doppler frequency shift is zero degrees or parallel to the direction of flow. However, since it is difficult to achieve Doppler angle parallel to the flow in the carotid arteries in the neck, an angle of up to 60° between these vessels and the Doppler beam is acceptable. Angles greater than 60° will produce erroneous higher velocities, while angles much lower than 60° may reduce aliasing. The technician may observe changes in the hue of the color flow pattern or bleeding of the color outside of the vessel wall (color bruit, Fig. 7.9), which suggests the presence of stenosis.

The scan head is then moved cephalad with the B-mode imaging display activated and with frequent sampling of the center stream velocity signal. Audible interpretation alone is usually used during this phase of the examination. The region of the carotid bifurcation is identified by the presence of two vessels and visualization of the superior thyroid artery branch of the external carotid artery. This may be confirmed by sampling in the center stream just distal to the origin of these vessels and identifying the characteristic differences between the two arteries.

It is recommended that the dynamic range be set to 40–50 dB to optimize the gray-scale image and the time gain compensation (TGC) as needed in regard to the depth of the carotid and vertebral arteries examined.

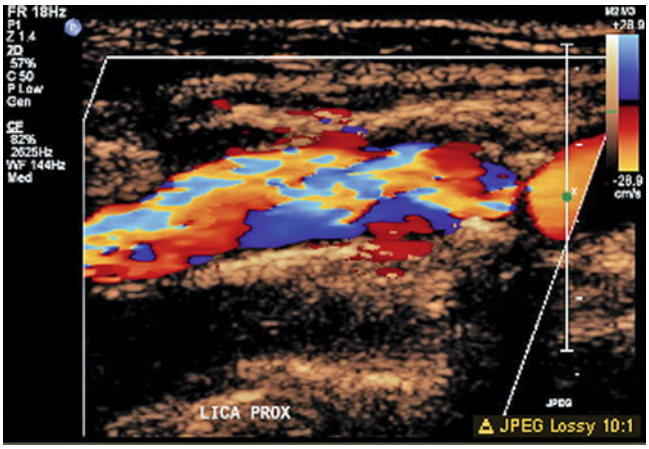


**Fig. 7.9** Color duplex ultrasound of the internal carotid artery: color bruit

The external carotid signal is recognized by the presence of flow reversal, while the internal carotid signal is identified by the absence of flow reversal and the presence of forward flow during diastole. The scan head is moved further cephalad to insonate the proximal few centimeters of the internal carotid artery, which is the common site of disease. Abnormalities in the velocity spectra displayed on the screen are noted for subsequent reference. Once the general anatomy has been outlined, a detailed examination is performed. The initial quick scanning of the vessels provides a reference for determining whether disease is present and, if so, its severity. It is likely that these areas will require more detailed interrogation than areas that are normal.

Following the preliminary scan, the scan head is returned to the base of the neck over the anterior border of the sternomastoid muscle, and the common carotid artery is again visualized. Note is taken of the presence or absence of calcification in the wall represented by dense acoustic shadows and a deeper acoustic window. Representative spectra

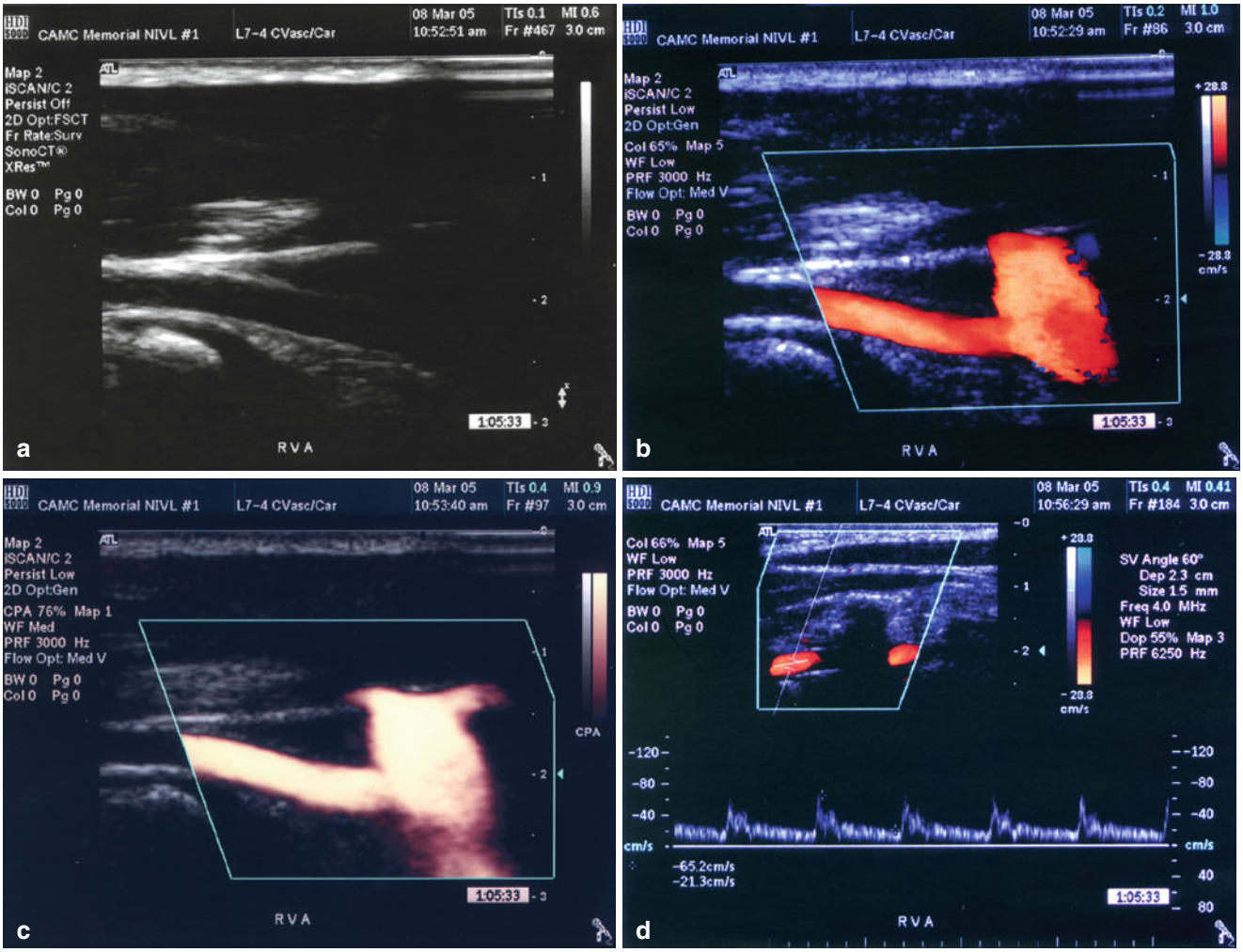


**Fig. 7.10** (**a**) Origin of right vertebral artery in gray scale. (**b**) Origin of right vertebral artery using color duplex ultrasound. (**c**) Origin of right vertebral artery using power Doppler. (**d**) Mid right vertebral artery (series of H appearance)

are then obtained from the center stream with the Doppler beam axis at 60° and the signals recorded for subsequent analysis. During this part of the examination, the peak velocity should be noted and whether the velocity is always in the forward direction throughout the whole of the cycle.

Low peak systolic velocities suggest occlusions of the internal or external carotid arteries, while frequencies approaching zero are suggestive of either high-grade stenosis or occlusion of the internal carotid artery. Other variations in the waveform may occur as a result of significant aortic disease.

The scan head is again moved cephalad with a second center stream sample being obtained just proximal to the region of the bulb. With rapid shifting from B-mode to Doppler mode imaging, the evaluation is continued through and into the proximal internal carotid artery, looking for abnormal spectral displays. Care must always be taken during sampling to ensure that the sample volume cursor is located in the center stream of the vessel and the incident angle of the Doppler beam to the long axis of the vessel is as close as possible to 60°. The presence of disease is suspected by echogenic shadows impinging on the lumen of the vessel associated with either changes in spectral broadening or fluctuations in peak systolic and diastolic velocities. It is frequently necessary to obtain multiple spectra along the center stream axis of the internal carotid artery to determine the location at which the most abnormal spectra occur. These should be recorded for future reference.

Attention is then directed to the subclavian artery in the posterior triangle of the neck, and the vessel is visualized. Scanning proceeds proximally with identification of the origin of the vertebral artery and subsequent sampling with the Doppler component of the orifice in the proximal centimeter of the first portion of this vessel, as this is the usual site of stenotic disease.

With a clear view of the common carotid artery, the probe is slowly angled more posterolaterally to identify the vertebral artery. This artery will have vertical shadows running through it from the spinous processes of the vertebrae, giving it the appearance of a series of Hs (Fig. 7.10). Vertebral flow

is documented, either antegrade or retrograde. Major elevations in peak velocities are characteristic of high-grade orifice stenosis. The contralateral side of the neck is then evaluated in a similar manner, and representative recordings from the common carotid, external carotid, and internal carotid arteries are obtained.

The following considerations are generally helpful in optimizing color flow setup and value. The appropriate color pulse repetition frequency (PRF) must be chosen by setting the color velocity scale for the expected velocities in the examined vessel. The scale should be adjusted to avoid systolic aliasing (low PRF) or diastolic flow gaps (high PRF) in normal vessels. Every effort should be made to avoid using large wider color boxes, which may slow down frame rates and resolution of the imaged vessel. It is recommended that color boxes that cover the entire vessel diameter and are approximately 1–2 cm of its length be used. The color, power, and gain should be optimized so that flow signals are recorded throughout the lumen of the examined vessel with no bleeding of color into the adjacent tissues.

The zero baseline of color bar (PRF) is set at approximately two-thirds of the range with the majority of frequencies allowed in the red direction for flow toward the brain, which will display higher arterial mean frequency shifts without aliasing artifacts. The color PRF and zero baseline may also need to be readjusted throughout the examination to allow for changes in velocity that may occur if carotid tortuosity or stenosis is present. Adjustments in the PRF are generally needed in the examination of the carotid bulb where the color differentiation scale should be set to visualize the slower flow in the boundary separation zone (Fig. 7.11). The PRF range is generally adjusted higher to detect increased velocity in the region adjacent to the flow divider. Similarly, the color PRF should be increased to display higher velocities detected in the presence of carotid stenosis and to avoid aliasing. In the post-stenotic zone, the color PRF should be decreased to observe the lower velocities and flow direction changes in the region of turbulent flow just distal to the stenosis. Color PRF should also be decreased when occlusion is suspected to detect the preocclusive, low-velocity, high-resistance signal associated with tight stenosis or carotid occlusion and to confirm absence of flow at the site of the occlusion. The color PRF should also be decreased in the presence of a carotid bruit to detect the lower frequencies associated with a bruit.

Color sensitivity (ensemble length) should be around 12 in systems where there is an adjustable control. The ensemble length can be increased in regions where more sensitive color representation is needed. Keep in mind that the frame rate will decrease when the ensemble length is increased. The color wall filter should also be set as low as possible, and you may need to decrease the wall filter manually when decreasing the color PRF. The color wall filter may automatically increase as the PRF is increased.

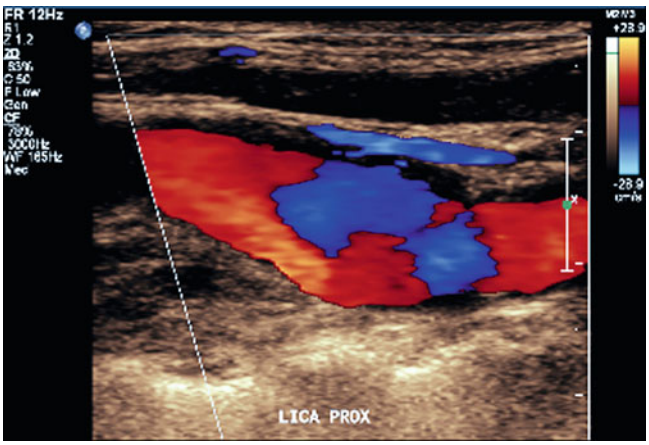


**Fig. 7.11** Color duplex ultrasound of the internal carotid artery: notice boundary separation zone (*blue color*)

The angle of the color box should also be changed to obtain the most accurate Doppler angle between the scan lines and the direction of the blood flow. This will yield a better color display, secondary to better Doppler angle. The color box should be kept to a size that is adequate for visualizing the area of interest, and should be kept small enough to keep the frame rate at a reasonable number. The color gain should be adjusted throughout the examination to detect the changing signal strength. If this is not properly adjusted, too much color may be displaced or some color information may be lost, which may result in seeing color in areas where there is no flow. In patients with very low flow or questionable carotid occlusion, an overgained level may be advantageous to show any flow that may be present.

The desaturation of the color from darker to lighter hues on the color bar indicates increasing velocities. The colors are darkest close to the zero baseline, and as the velocities increase, the colors become lighter. Color should be selected so that the highest frequency shifts in each direction are of high contrast to each other so that you can easily detect aliasing, e.g., the color selection can be set so that low to high velocities are seen as dark blue to light green to aqua in one direction and red to orange to yellow in the opposite direction. Aliasing in these circumstances would appear as aqua, adjacent to yellow.

Since the frame rate is affected by the PRF, ensemble length, depth, and width of the color box, it should be kept as high as possible to capture the rapid change in flow dynamics that occurs with carotid stenosis, particularly in the carotid bulb region. The frame rate decreases with decreasing PRF, and increasing the color ensemble length will also decrease the frame rate. Increased color box width and deep insonation will also decrease the frame rate.

## Limitations of Duplex Technology

Duplex technology of the carotid arteries may be adversely affected by the following: acoustic shadowings from calcification, soft tissue edema or hematoma, the depth or course of the vessel, the size of the neck, and the presence of sutures or skin staples.

Duplex ultrasonography may also overestimate or underestimate the degree of stenoses or plaquing. Underestimation of disease can be noted if it fails to appreciate very-low-level echoes of soft plaque, or the examiner does not carefully interrogate the vessel and misses accelerated flow; or in patients with long, smooth plaque formation, which does not have the accelerated, turbulent flow pattern usually associated with the hemodynamically significant stenoses, or if an inappropriate Doppler angle is used (e.g., above 60°). Stenoses can also be overestimated when an artifact is mistaken for a carotid plaque, if accelerated flow is mistakenly attributed to stenosis, if there is vessel tortuosity or kinking, and in the presence of significant stenoses or occlusion on the contralateral side.

Due to the varying filling phases of the cardiac cycle, cardiac arrhythmia makes it more difficult to evaluate the flow spectra. Also, the flow velocity will be lower in a wider vessel and higher in a narrower vessel at the same flow intensity. Therefore, the flow in a wide carotid sinus can easily be disturbed and may incorrectly suggest pathological findings.

## Interpretation and Determination of Severity of Carotid Stenosis

A complete extracranial carotid duplex examination should include the following data:

1. The peak systolic and end-diastolic velocities of common carotid, internal carotid, and external carotid arteries, right and left subclavian arteries, and vertebral arteries
2. The internal carotid artery to common carotid artery peak systolic velocity ratio
3. Flow direction of the vertebral artery (antegrade or retrograde)
4. Analysis of the Doppler spectral waveform of the examined vessels
5. The presence or absence of plaque and description of its morphology

### B-Mode Imaging Interpretation

An echoic area should be evident between the walls of the vessel, indicating the absence of pathology, i.e., plaquing, whose density usually differs from that of the blood. An echoic line indicating the endothelium may be evident at the vessel lumen. The following abnormalities can be noted on B-mode imaging:

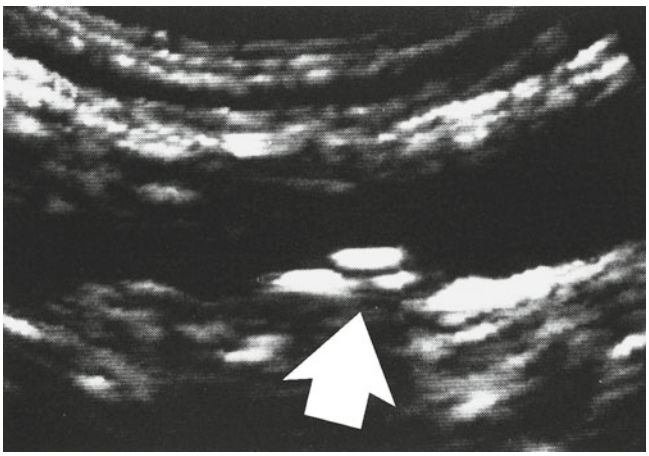

**Fig. 7.12** Duplex ultrasound image of the carotid artery showing homogeneous plaque (*arrow*)

1. Fatty streaks: low-level echoes of similar appearance (homogeneous) can be detected.
2. Fibrous soft plaque (homogeneous): low- to medium-level echoes of similar appearance (Fig. 7.12).
3. Complex plaque (heterogeneous): low-, medium-, and high-level echoes indicating soft and dense areas (Fig. 7.13). This plaque is a mixture of isoechoic, hyperechoic, or hypoechoic plaque.
4. Calcification: very bright, highly reflected echoes are noted. The acoustic shadowing from calcifications prevents a thorough evaluation of the vessel and may result in the calculation of an erroneous percentage of stenosis (Fig. 7.14).
5. Vessel thrombosis: fresh carotid thrombosis may not be detected without using Doppler flow sampling since fresh thrombus has the same echogenicity of flowing blood.

Carotid plaque morphology is generally characterized into smooth (Fig. 7.15) or irregular plaques (Fig. 7.16) according to surface, and homogeneous (Fig. 7.12) versus heterogeneous (Fig. 7.13) according to plaque structure. An ulcerative plaque is usually an irregular plaque with a cleft within the plaque that can be seen on B-mode imaging (Fig. 7.17). Further details of carotid plaque morphology will be described in Chap. 11.

#### Estimation of Stenosis Based on B-Mode Imaging

Ideally, carotid plaque should be visible from at least two of the longitudinal, or sagittal, projections and in the transverse view to give a rough estimate of stenosis. Percent diameter stenosis equals the ratio of the residual diameter to vessel lumen diameter minus 1 multiplied by 100. Percentage of

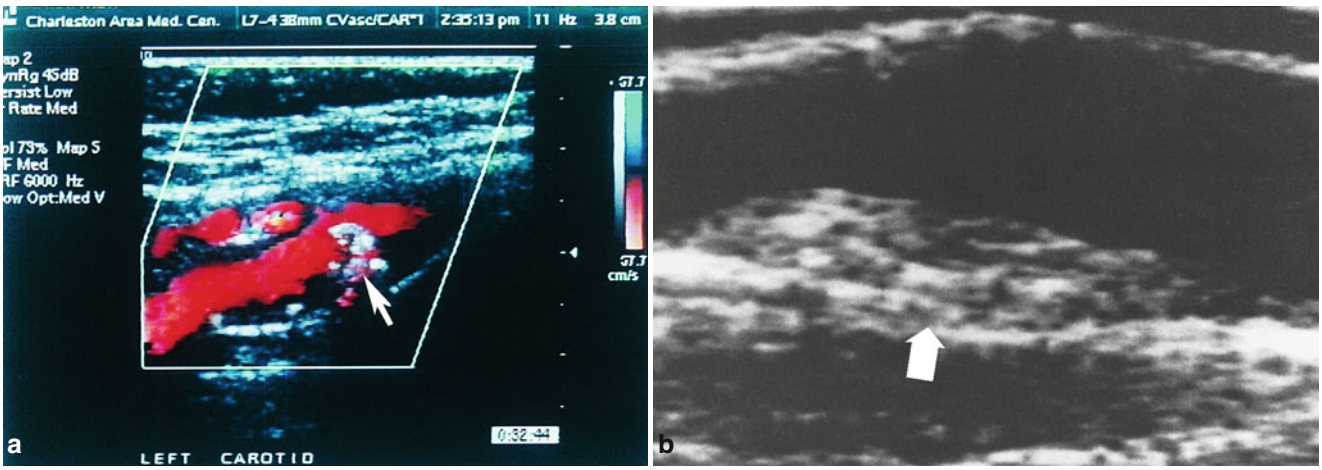


**Fig. 7.13** (**a**) Color duplex ultrasound image of the carotid bifurcation showing a complex heterogeneous plaque at the origin of the internal carotid artery (*arrow*). (**b**) A duplex ultrasound image of the carotid artery showing a heterogeneous plaque (*arrow*)

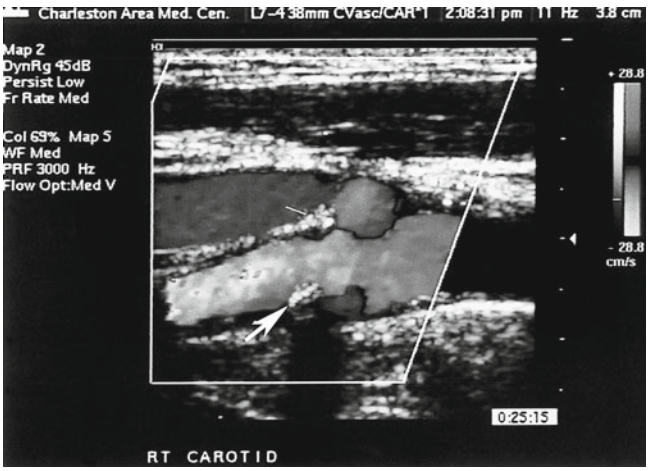


**Fig. 7.14** A color duplex ultrasound image of the carotid artery showing a calcified plaque (*arrow*) with acoustic shadowing underneath (*under the arrow*)

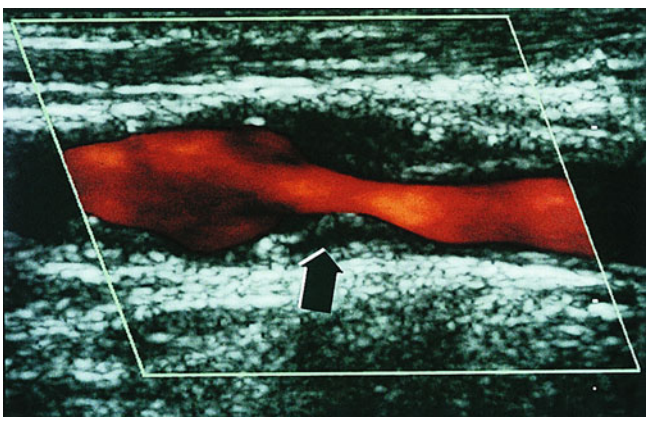

**Fig. 7.15** A color duplex ultrasound image of the carotid artery showing a smooth heterogeneous plaque (*arrow*). The dark center of the plaque may represent intraplaque hemorrhage

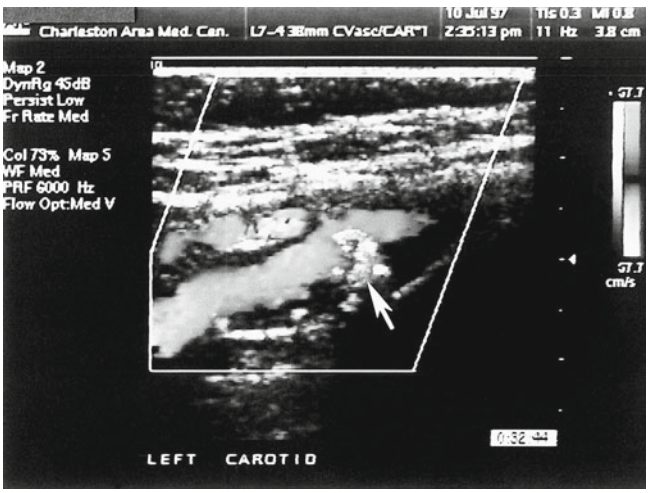


**Fig. 7.16** A carotid color duplex ultrasound image showing an irregular plaque of the proximal internal carotid artery (*arrow*)

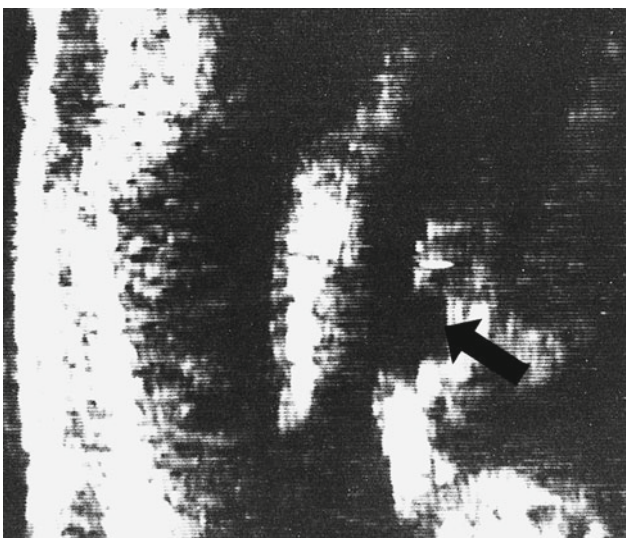

**Fig. 7.17** A duplex ultrasound image of the carotid bifurcation showing an ulcerative lesion of the proximal internal carotid artery (*arrow*)

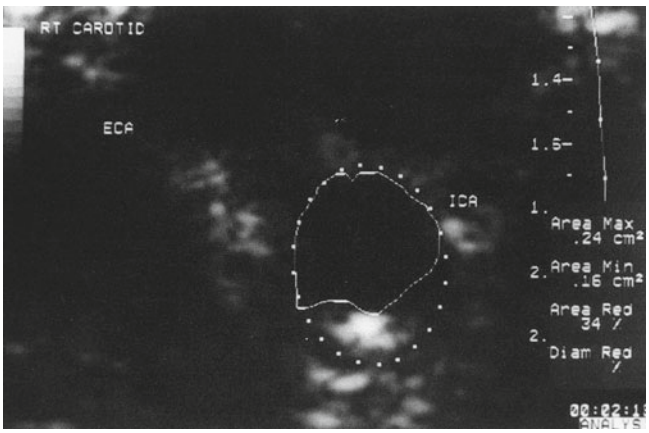


**Fig. 7.18** Calculation of area reduction percent stenosis. This image reflects the greatest stenosis in transverse diameter. An elliptical measurement of the arterial lumen is taken. Then an elliptical trace of the residual lumen is made. The percent area reduction is calculated by the duplex machine. To calculate the diameter reduction percent stenosis, a similar calculation is performed with the vessel in longitudinal view

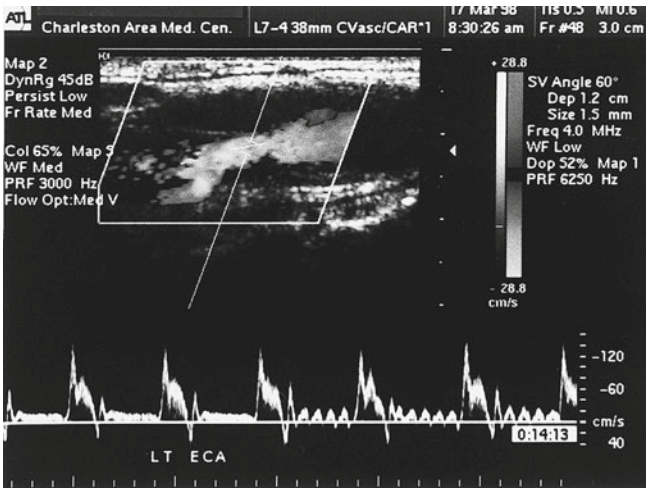


**Fig. 7.19** Color duplex ultrasound image of an external carotid artery. Note that the external carotid artery has a rapid upstroke and downstroke with a very low diastolic component. The diastolic notch is clearly seen, and tapping of the superficial temporal artery causes oscillations in the waveform (*bottom right*)

**Table 7.1** % Diameter stenosis versus % area stenosis[a]

| % Stenosis by: | |
|---|---|
| Diameter stenosis | Area reduction |
| 0 | 0 |
| 10 | 19 |
| 11 | 36 |
| 30 | 51 |
| 40 | 64 |
| 50 | 75 |
| 60 | 84 |
| 70 | 91 |
| 80 | 96 |
| 90 | 99 |
| 100 | 100 |

$$\%\text{Diameter stenosis } (\%\text{Ds}) = 100 \times \left[1 - (\text{inner diameter/outer diameter})\right]$$

$$\%\text{Area stenosis } (\%\text{As}) = 100 \times \left[1 - (\text{inner area / outer area})\right]$$

$$\%\text{As} = 100 - 100 \times (1 - \%\text{DS}/100)^2$$

[a]Assuming concentric circle

area of stenosis is calculated similarly, except you substitute the area for the diameter. The vessel lumen diameter (in longitudinal view) or area (in transverse view) is measured from intima to intima. Then the residual lumen diameter, or area, is measured (Fig. 7.18). The percent reduction is calculated using the above formula. The approximate relationship between diameter and area of stenosis is shown in Table 7.1. These values are applicable to circular geometry.

A chronic arterial occlusion may be diagnosed using B-mode imaging, although Doppler interrogation is essential to this diagnosis. Depending on the type of occlusive process, the artery may be filled with highly echogenic material or be anechoic.

## Interpretation of Doppler Spectral Analysis

### Normal Findings

The external carotid artery supplies blood to the vascular bed that has high peripheral resistance. Therefore, its signal is more pulsatile and very similar to the signal from peripheral arteries, such as the common femoral artery. As shown in Fig. 7.19, the external carotid artery has a rapid upstroke and downstroke with a very low diastolic component. The diastolic notch is clearly seen, and tapping the superficial temporal artery causes oscillations in the waveform (Fig. 7.19).

The internal carotid artery signal is slightly more high pitched and continuous than the signal from the external carotid artery. The blood flow in the internal carotid artery is less pulsatile since the brain is a low-resistance vascular bed, with increased flow during diastole. As shown in Fig. 7.20, the waveform of the internal carotid artery has a rapid upstroke and downstroke with a high diastolic component. A diastolic notch may not be evident. The common carotid artery, meanwhile, has a flow characteristic of both the internal and external carotid arteries (Fig. 7.21). Since most of the flow of the common carotid artery (close to 80%) enters the internal carotid artery, which has low-resistance flow, the flow in the common carotid artery usually shows a low-resistance pattern with a rapid systolic upstroke and forward flow through diastole.

Spectral waveforms must be obtained from the proximal (bulb), mid, and distal cervical internal carotid artery segments. The normal proximal ICA (the bulb), which is generally larger than the mid/distal ICA, will have characteristic

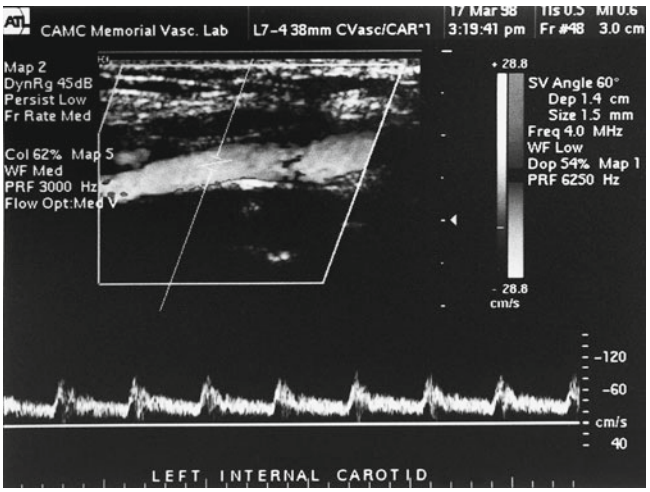


**Fig. 7.20** Color duplex ultrasound image of the internal carotid artery. Note that the waveform of the internal carotid artery has a rapid upstroke and downstroke with a high diastolic component. The diastolic notch may not be evident

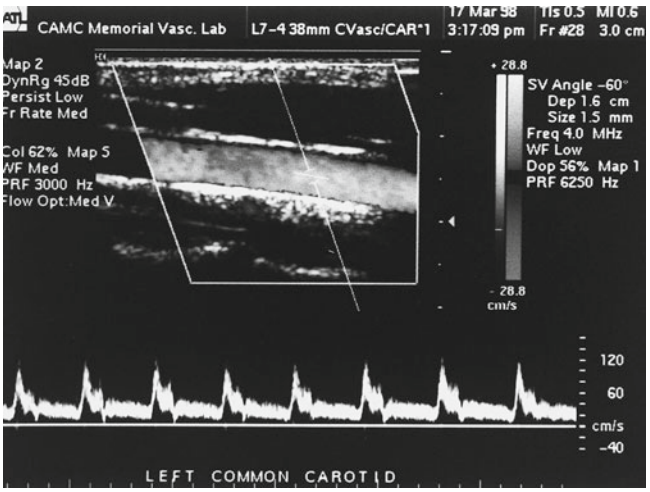


**Fig. 7.21** A color duplex ultrasound image of the common carotid artery. The common carotid artery signal has a flow characteristic of both the internal and external carotid arteries

flow. Unidirectional flow patterns are normally found in the carotid bulb, along the flow divider of the carotid bifurcation, and because there is transient reversal of flow at peak systole near the center stream and at the outer wall opposite to the flow divider, this area of reverse flow is often seen in color Doppler and commonly called an area of boundary layer separation or flow separation. Flow velocities along the outer wall and the separation zone may drop to zero at the end of the diastole. This normal flow pattern is used in conjunction with the absence of visible plaque on B-mode imaging to indicate a normal carotid bulb.

In a pulsed Doppler tracing, and because the sample volume would be more precisely placed in a center stream, the

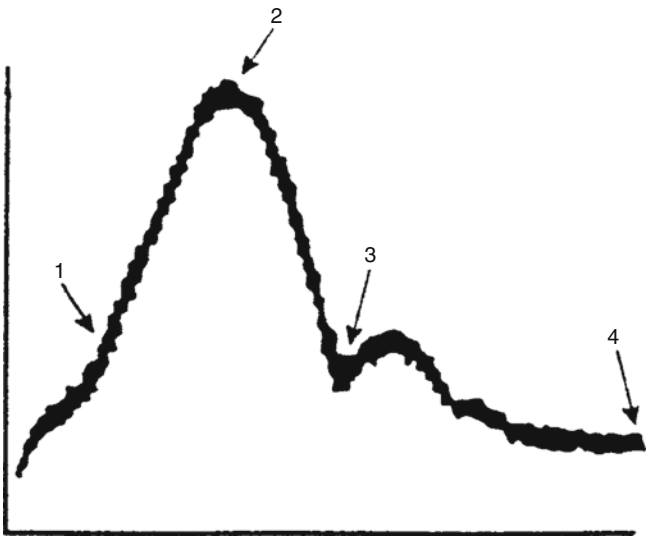


**Fig. 7.22** Spectral analysis of pulsed Doppler waveform: *1* spectral envelope, *2* peak systole, *3* dicrotic notch, *4* diastole

signals will have a narrow band of frequencies in systole with a blank area under that narrow band. The narrow band is called the spectral envelope; the blank area is called the frequency window or spectral window. The presence of these features is generally seen in laminar flow (Fig. 7.22). In contrast, in continuous-wave Doppler, because of the inability to regulate sample size or depth, a frequency window is not clear (Fig. 7.23).

## Abnormal Findings

The auditory signal from a stenotic vessel is characterized by a higher than normal pitch, with a very high-pitched hissing or squealing type of signal evident at significant stenosis. The waveform from a stenotic vessel has a higher than normal amplitude because of the accelerated flow through the stenosis (Fig. 7.24). The very high-pitched hissing signal that is evident at a significant stenosis has a higher than normal amplitude in systole and diastole. In a spectral analysis, the band evident along the top of the waveform during systole may fill in the spectral window to create the spectral broadening that is consistent with turbulent flow (Fig. 7.24). As seen in Fig. 7.24, the more significant the stenosis, the greater the increase in systolic and diastolic frequencies. In severe stenoses, there will be complete loss of the window. Distal to a stenosis, disturbed flow patterns are evident, i.e., dampened monophasic flow (turbulence). Immediately proximal to severe stenosis, the spectral waveform is dampened, and velocities are usually decreased with increased velocities within the stenosis and remain elevated with turbulent flow, which is reflected as spectral broadening just distal to the stenosis. It should be noted that an absent signal may suggest

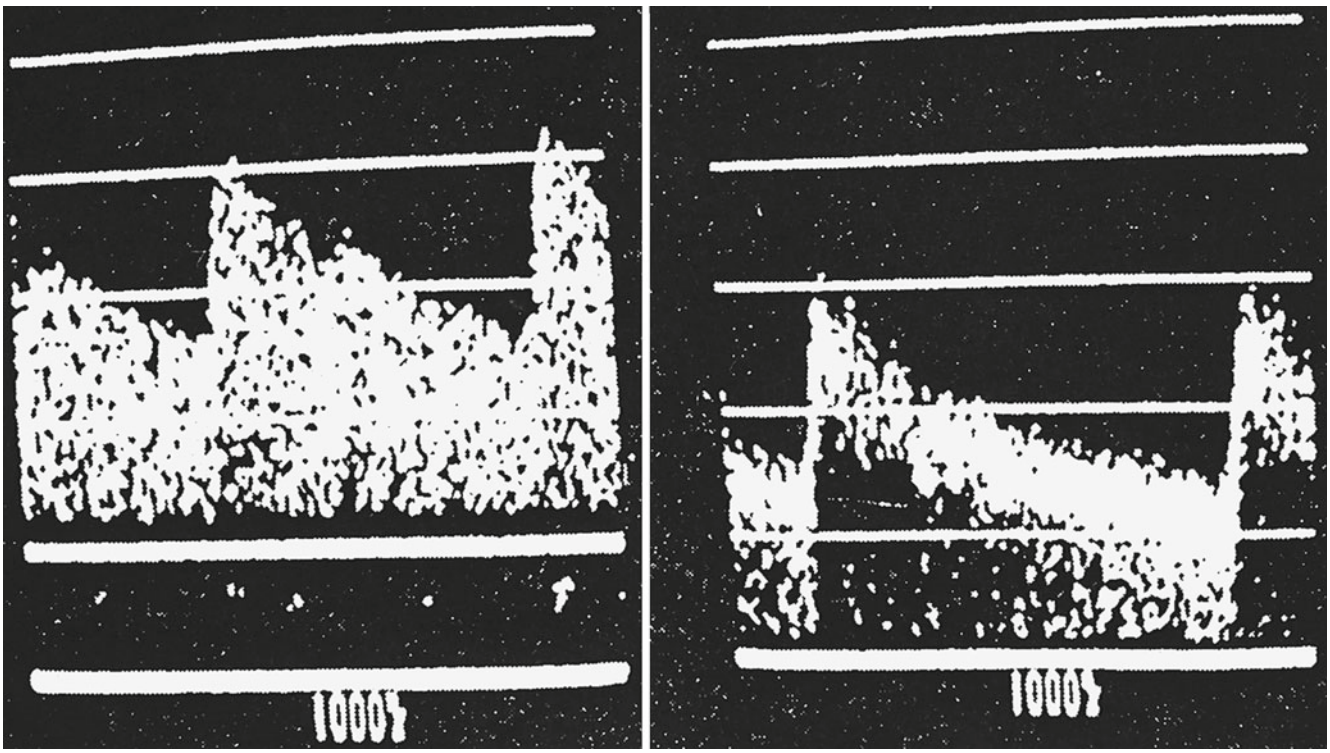

**Fig. 7.23** *Left*: continuous-wave Doppler signal. Note the absence of a frequency window. *Right*: in contrast the pulsed wave Doppler signal has a frequency window

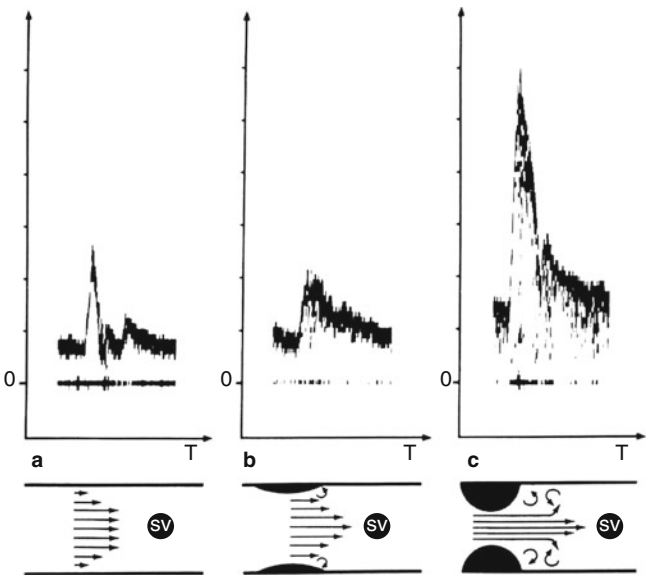


**Fig. 7.24** Waveforms from a normal vessel (**a**) in contrast to a mildly stenotic vessel (**b**) and a severely stenotic vessel (**c**). See text for a more detailed description

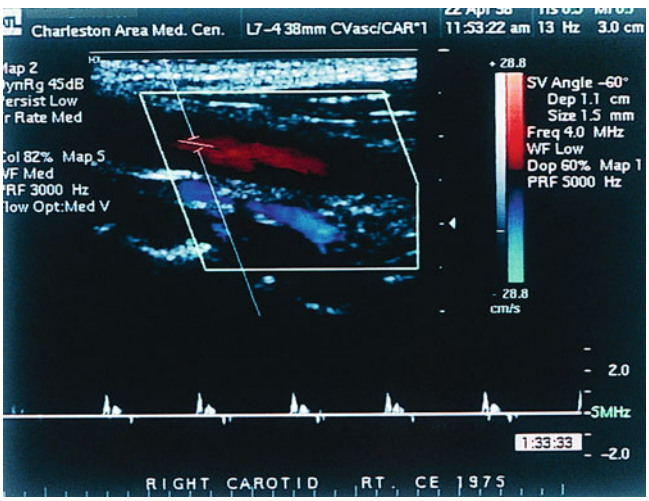


**Fig. 7.25** A color duplex ultrasound image of a patient with occlusion of the internal carotid artery, which is usually associated with a loss of the diastolic component in the ipsilateral common carotid artery (*bottom*)

occlusion; however, a tight stenosis cannot be ruled out since blood flow may be difficult to detect with velocities of less than 6 cm/s.

Occlusion of the internal carotid artery (Fig. 7.25) is usually associated with a loss of the diastolic component in the ipsilateral common carotid artery. If the contralateral common carotid and internal carotid arteries are serving as collateral pathways, increased systolic and diastolic velocities

**Table 7.2** Strandness criteria

| Stenosis/occlusion | |
|---|---|
| Normal | PSV < 125 cm/s |
| | No spectral broadening |
| 1–15% Stenosis | PSV < 125 cm/s |
| | Minimal spectral broadening |
| 16–49% Stenosis | PSV < 125 cm/s |
| | Marked spectral broadening |
| 50–79% Stenosis | PSV ≥ 125 cm/s |
| | EDV < 140 cm/s |
| | Marked spectral broadening |
| 80–99% Stenosis | PSV ≥ 125 cm/s |
| | EDV ≥ 140 cm/s |
| | Post-stenotic turbulence |
| Occlusion | No flow |

may be evident in these arteries. If a carotid siphon stenosis is present, high-resistance flow patterns may be evident in the extracranial internal carotid artery. Flow characteristics from one side must be compared with those on the other as well as those in proximal to distal segments of the ipsilateral carotid system. Generally, this test is somewhat limited in patients with poor cardiac output or stroke volume, which may result in bilaterally diminished common carotid artery velocities. Unilateral reduction of velocities may suggest proximal disease, such as innominate or common carotid artery stenoses.

## Determination of Disease Severity Using Doppler Spectral Analysis

Identification of disease in the carotid system uses both qualitative and quantitative data. Careful attention to unusual echoes on the image serves as a qualitative guide to the presence of disease at sites where careful scrutiny with a Doppler component should be performed. The changes in spectra obtained from the common, internal, and external carotid arteries provide quantitative information for the determination of the severity of disease in these locations. This is probably best considered by describing the normal and abnormal spectra generated in various anatomical locations by disease of varying severity, according to the University of Washington criteria [11]. These original criteria by the University of Washington are described in the following sections (Table 7.2) since they are still commonly used in the United States and they have been the foundation for interpretation of carotid artery stenosis. However, later in this chapter, you will find that other authorities modified these criteria to be compatible with the indication for carotid endarterectomy as proposed by the North American Symptomatic Carotid Endarterectomy Trial (NASCET) and Asymptomatic Carotid Atherosclerosis Study (ACAS) trials.

### Normal Internal Carotid Spectra or Minimal Disease (0–15% Stenosis)

The characteristic features of normal internal carotid artery spectra are shown in Fig. 7.2. The peak systolic velocity is <125 cm/s with minimal degrees of spectral broadening during the initial deceleration phase of systole, followed by mild spectral broadening during diastole. The velocities are always in the forward direction, and, therefore, the frequencies depicted on the scale are always above the zero line. The velocity envelope during systole is relatively narrow and displays a large clear window area under the systolic curve. Correlation with arteriographic findings has supported the view that this type of waveform may also be generated with minimal disease up to 15–20% diameter reduction, and, therefore, identification of this type of waveform confirms the presence of either a normal vessel or one in which only minimal disease is present. Figure 7.26 is a color duplex imaging of a normal common carotid artery, an internal carotid artery, and an external carotid artery.

### Mild Stenosis (16–<50%)

As noted in the discussion regarding findings with animal studies, it is over the range of mild stenosis that spectral broadening changes in both magnitude and timing, and it is the presence of spectral broadening in systole, particularly during the deceleration phase, which is characteristic of the spectra generated by the presence of mild disease. As shown in Fig. 7.27, the peak systolic velocity of <125 cm/s and spectral broadening is also present during diastole, although it may be of greater magnitude than seen in the normal. Again, velocity is always in the forward direction, and therefore, the frequencies, even during diastole, are above the zero frequency line.

### Moderate to Severe Disease (50–<80% Stenosis)

As the lesion becomes progressively more occlusive (50–<80% diameter reduction), the velocity of the red blood cells traversing the stenosis increases, producing an increase in peak velocity at systole (Fig. 7.28). A peak systolic velocity of >125 cm/s and an end-diastolic velocity of <125 cm/s are characteristic of this stenosis.

### Tight Stenosis (80–99%)

With the development of high-grade lesions in excess of 80% diameter reduction, the end-diastolic velocity increases (a peak systolic velocity of ≥125 cm/s and an end-diastolic velocity of ≥125 cm/s) so that the ratio between peak frequency at systole and peak frequency at diastole falls, providing an accurate method of identifying these high-grade lesions. Diffuse spectral broadening is also present during

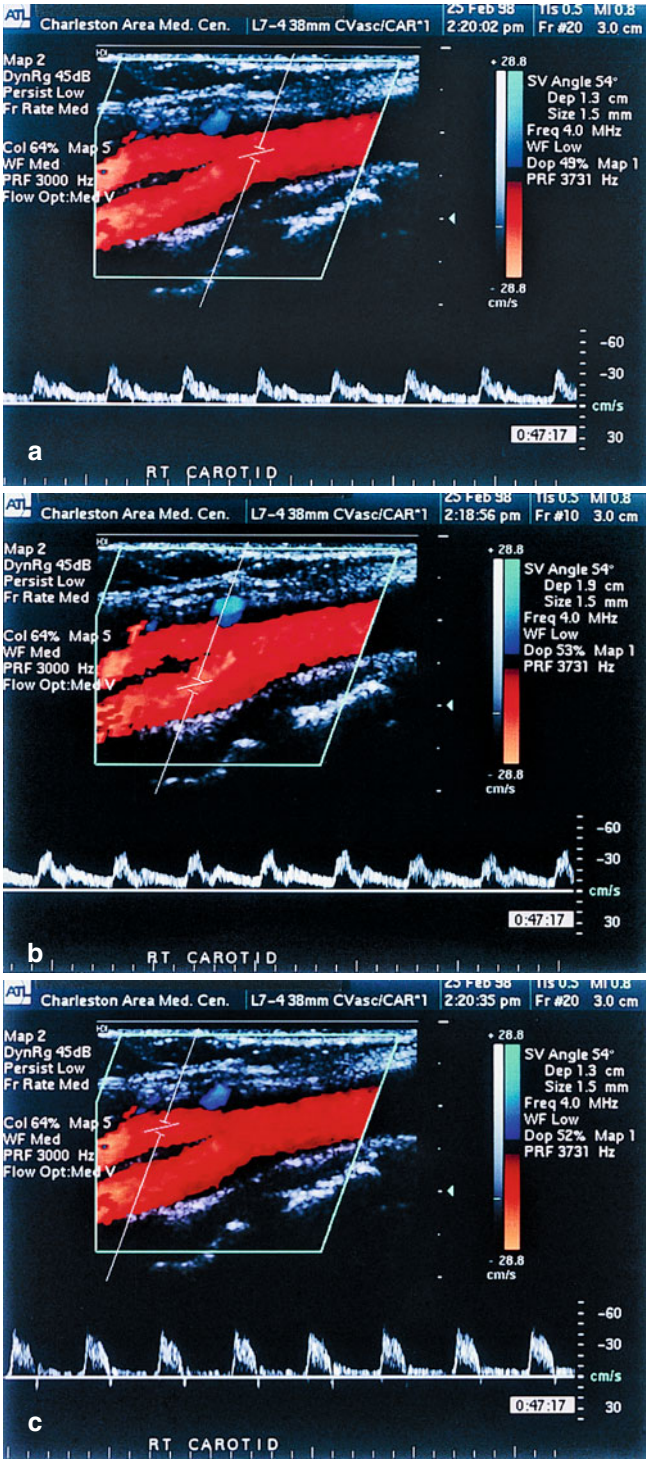


**Fig. 7.26** (**a**) A color duplex ultrasound image showing a normal common carotid artery with a normal Doppler spectra (*bottom of figure*). (**b**) A color duplex ultrasound image of the carotid bifurcation showing a normal internal carotid artery with a normal Doppler spectra (*bottom of figure*). (**c**) A color duplex ultrasound image of the carotid bifurcation showing a normal external carotid artery with a normal Doppler spectra (*bottom of figure*)

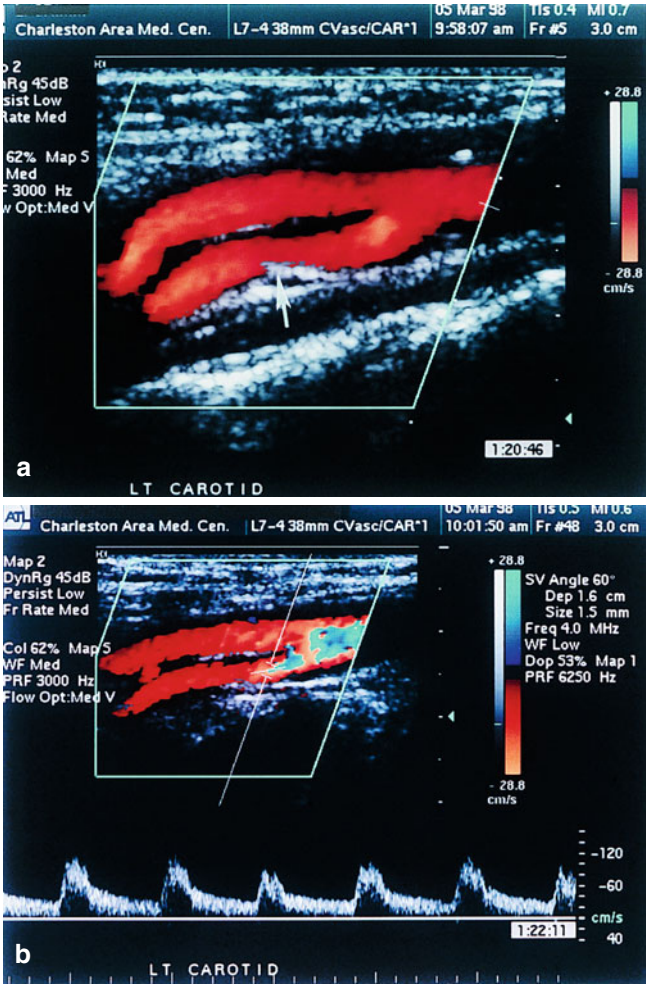


**Fig. 7.27** (**a**) A color duplex ultrasound image showing mild plaquing (15–<50% stenosis) of the internal carotid artery (*arrow*). (**b**) The same patient in (**a**) showing internal carotid artery Doppler spectra associated with mild stenosis

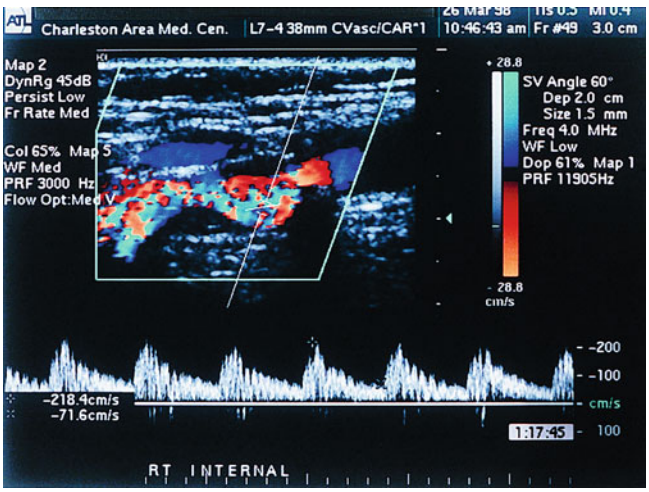


**Fig. 7.28** A color duplex ultrasound image of an internal carotid artery showing Doppler spectra of severe stenosis (50–<80%). The peak systolic velocity on this patient was 218.4 cm/s with an end-diastolic velocity of 71.6 cm/s

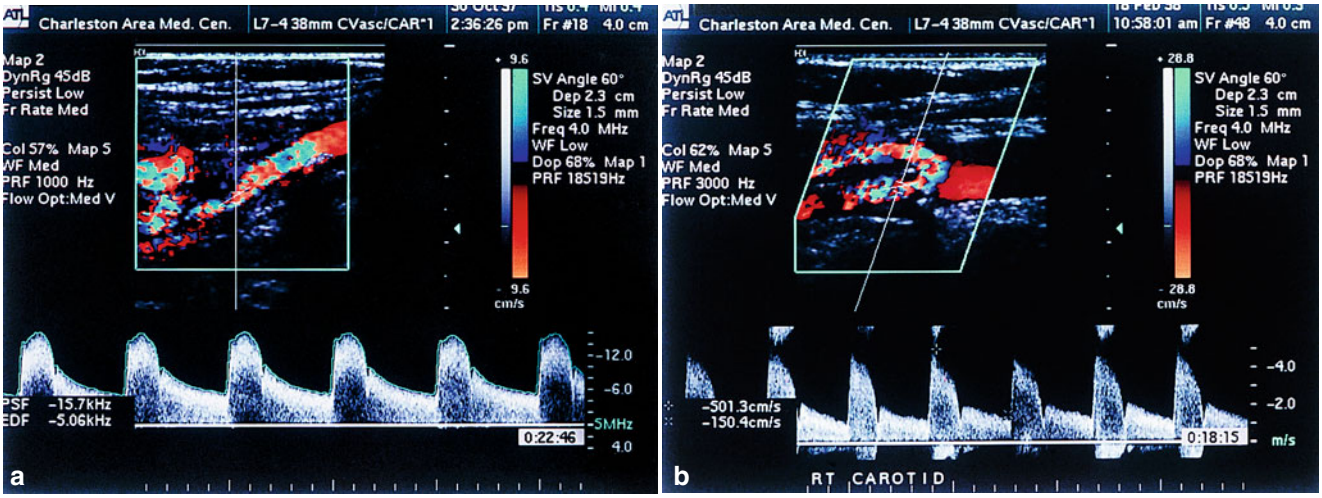


**Fig. 7.29** (**a**) A color duplex ultrasound image of the internal carotid artery showing Doppler spectra of tight stenosis (80–99%). The peak systolic frequency was 15.7 kHz with an end-diastolic frequency of 5.06 kHz. (**b**) A color duplex ultrasound image of an internal carotid artery showing Doppler spectra of tight stenosis (80–99%). The peak systolic velocity was 501.3 cm/s with an end-diastolic velocity of 150.4 cm/s

the whole of the cycle, and with these lesions, the diastolic velocity at the lower frequencies approaches zero (Fig. 7.29).

## Internal Carotid Occlusion

Occlusion of the internal carotid artery (Fig. 7.30) is recognized by imaging a vessel in the characteristic anatomical location of the internal carotid artery with no detectable Doppler signal. It is important to ensure that the internal carotid artery is being examined, and as part of this evaluation, visualization of the external carotid artery is mandatory. The differentiation between the internal and external carotid arteries is made by visualization of the superior thyroid artery branch. Changes in the real-time spectra produced by compression of the superficial temporal artery that increases the outflow resistance usually result in a decrease in peak systolic frequency. Other feature characteristic of occlusion is the presence of frequencies to the zero baseline, or even negative frequencies, indicative of flow reversal obtained from the common carotid artery low in the neck [12]. When the internal carotid artery is occluded, the ipsilateral common carotid artery assumes a velocity pattern similar to that of the external carotid artery, and the external carotid artery may assume flow characteristics of the internal carotid artery, i.e., high diastolic component.

Common carotid artery occlusion can also be diagnosed by color duplex ultrasound. Figure 7.31 shows retrograde flow of the external carotid artery and antegrade flow of the internal carotid artery.

Occlusions are periodically missed due to changes in physiologic parameters attendant upon the presence of internal carotid artery occlusions. Figure 7.32 shows the arteriogram and spectra obtained from a patient in whom internal carotid occlusion was missed because the external carotid artery was a major source of collateral blood flow to the middle cerebral artery and, as such, developed the spectral changes characteristic of a high-grade internal carotid stenosis. Errors such as this can be avoided by careful evaluation of the image for the presence of branches originating from the vessel being examined and the change in the velocity profile induced by superficial temporal artery compression.

## The Role of Power Doppler and Carotid Artery Occlusion

Power Doppler ultrasound displays an estimate of the entire power contained in that part of the received radio frequency ultrasound signal for which a phase shift corresponding to motion of the target is detected; in contrast, conventional color Doppler imaging displays Doppler frequency shift information. In a recent study by us [13], five out of six patients (83%) who were felt to have total carotid occlusion by conventional color duplex were confirmed to have subtotal occlusion by adding power Doppler imaging (Fig. 7.33).

Other clinicians, primarily radiology colleagues, use Zwiebel criteria [14], which are summarized in Table 7.3.

## External Carotid Artery Disease (High-Grade Stenosis)

Lesions producing a greater than 50% diameter reduction of the external carotid artery are identified by the presence of peak frequencies in excess of 4.5 kHz (>125 cm/s) associated with diffuse spectral broadening (Fig. 7.34). The overall shape of the waveform with frequencies in the negative range remains normal.

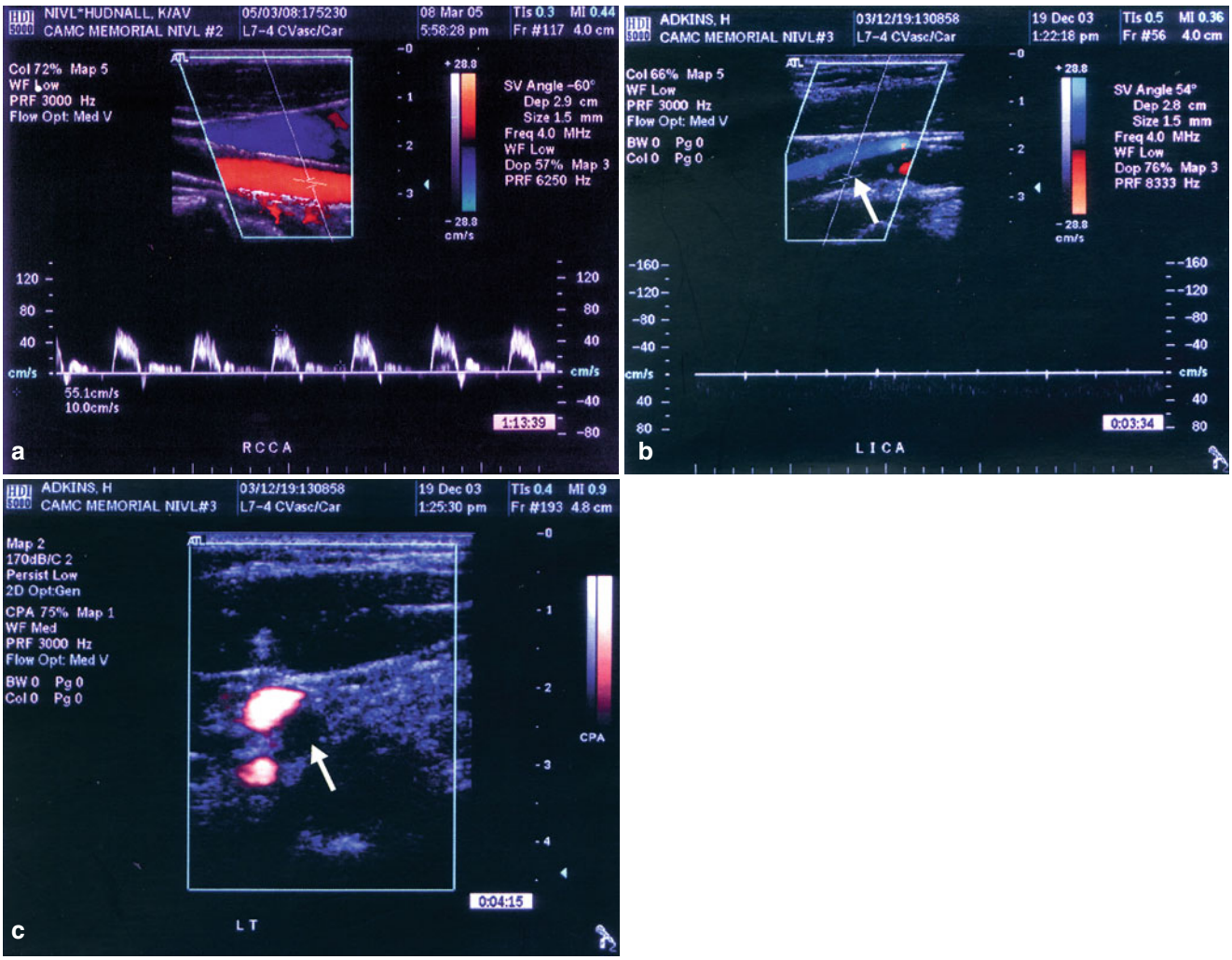


**Fig. 7.30** (**a**) A common carotid artery Doppler spectra produced by occlusion of the ipsilateral internal carotid artery. Peak frequency is not abnormally high, but the characteristic feature is the presence of reverse flow in diastole. (**b**) Internal carotid artery occlusion in longitudinal view (no color flow). (**c**) Internal carotid artery occlusion in transverse (no color flow in power Doppler [*arrow*]; color flow is seen in external carotid artery)

## Duplex Classification for Threshold Stenoses Used in Various Symptomatic and Asymptomatic Carotid Endarterectomy Trials [15]

Based on the duplex criteria, many laboratories, including our own, classified internal carotid artery stenosis into categories patterned after those used at the University of Washington [11]: normal, 1–15% stenosis, 16–49% stenosis, 50–79% stenosis, 80–99% stenosis, and total occlusion. While these classifications have been useful clinically in the past, they do not correlate with threshold stenoses utilized in the recent trials investigating symptomatic (NASCET) [16] and asymptomatic (ACAS) [17] carotid artery diseases. With the publication of the NASCET findings showing conclusive benefit of carotid endarterectomy for symptomatic patients with 70–99% stenosis and also for those with ≥50–<70% stenosis, several recent studies have attempted to develop duplex criteria to identify patients with ≥50% and ≥70% carotid stenosis [18–21]. With the subsequent report from the ACAS group [22] showing significant benefit of carotid endarterectomy in asymptomatic patients with ≥60% stenosis, others [23–26] reported optimal duplex criteria for detecting ≥60% stenosis.

It should be noted that the 5-year absolute risk reduction rate for ipsilateral stroke in the ACAS study was only 5.8%. Therefore, the duplex criteria for screening ≥60% internal carotid artery stenosis should have a high positive predictive value since these patients are likely to undergo invasive carotid angiography and/or carotid endarterectomy. This, along with increasing reports advocating carotid endarterectomy based on carotid duplex results alone,

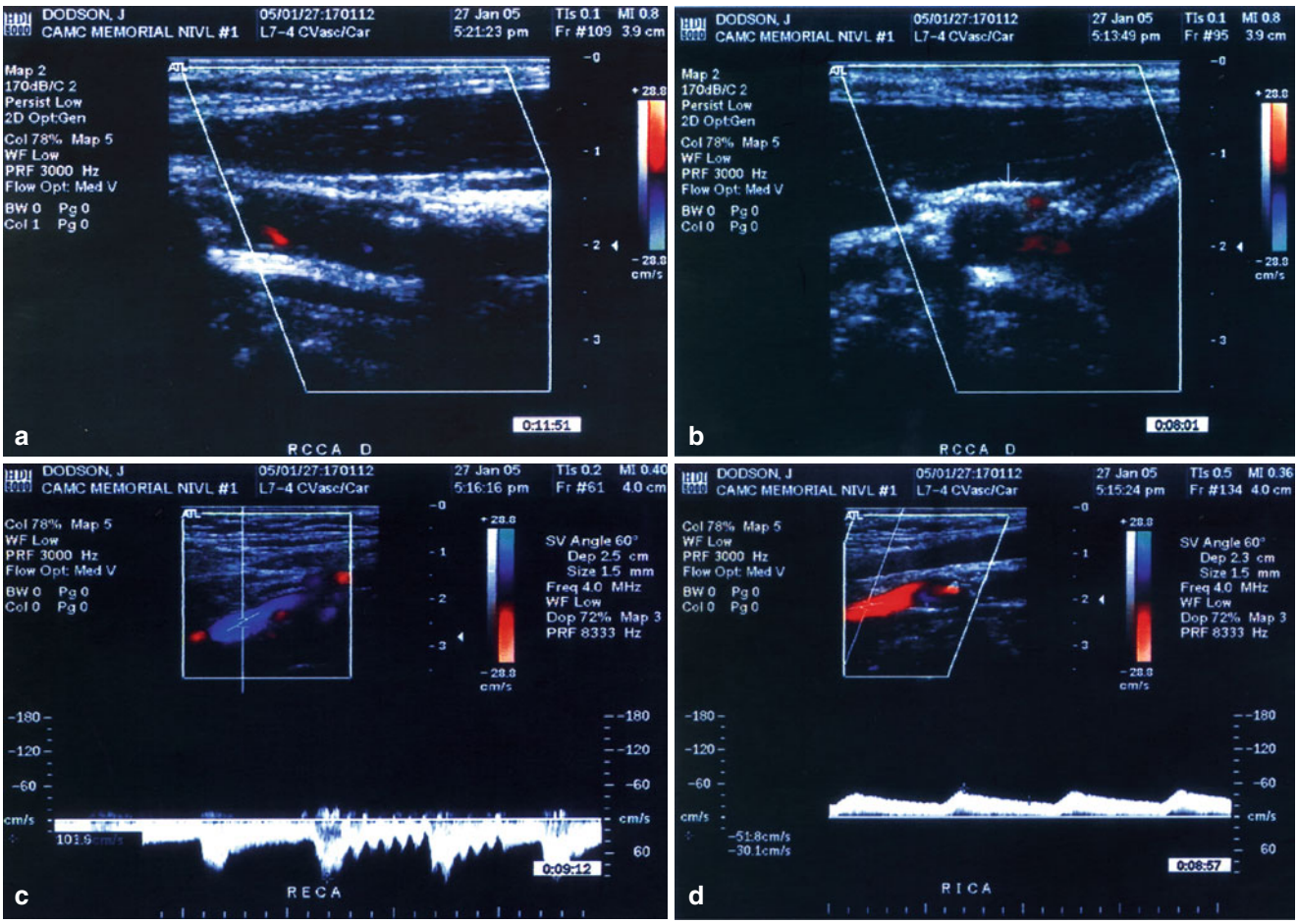


**Fig. 7.31** (**a**) Right common carotid artery occlusion in longitudinal view. (**b**) Right common carotid artery occlusion in transverse view. (**c**) Retrograde flow in external carotid artery. (**d**) Antegrade flow in internal carotid artery

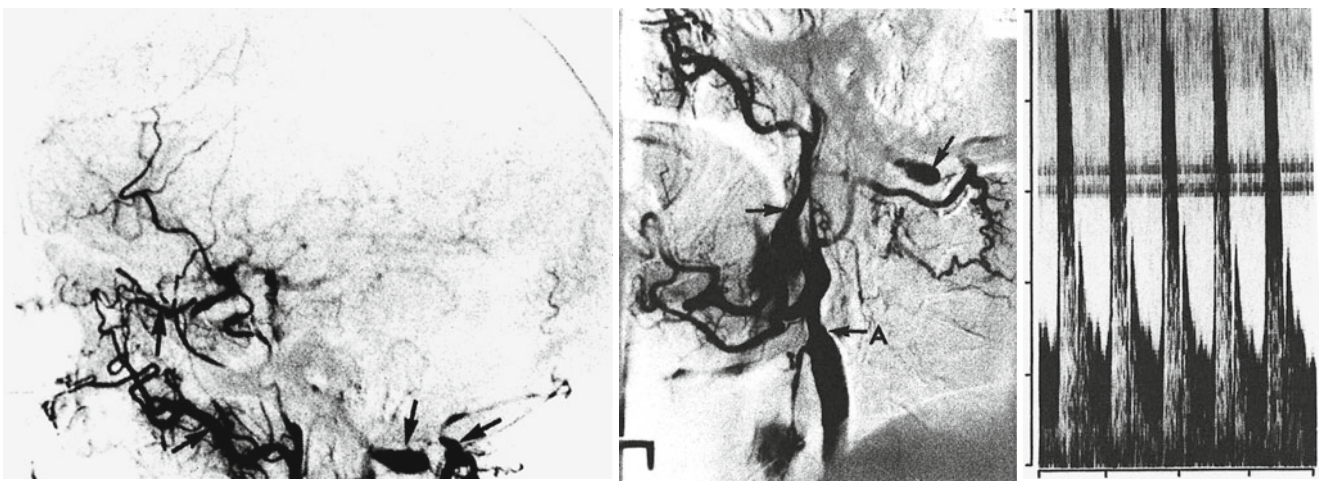


**Fig. 7.32** Arteriogram (*left*) and Doppler spectra (*right*) obtained from a missed internal carotid occlusion showing the external carotid artery functioning as a major collateral to the middle cerebral vessels. The spectra show peak frequencies in excess of 4.5 kHz in association with spectral broadening and no flow reversal. This appearance is produced by the low-resistance outflow bed of the external carotid into the middle cerebral artery

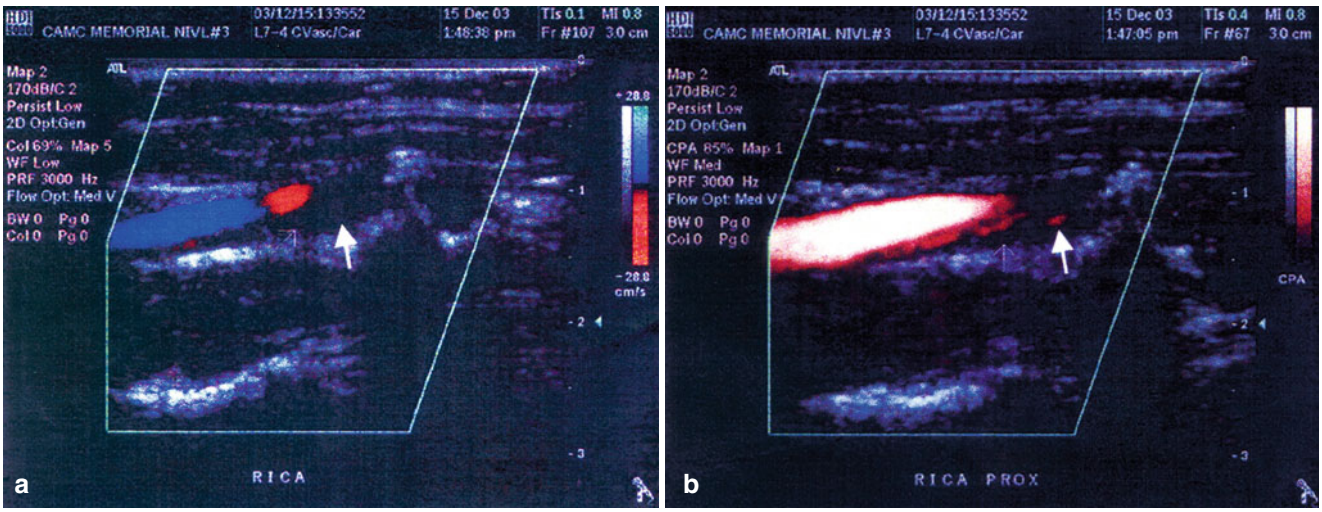


**Fig. 7.33** (**a**) Color duplex imaging of a right internal carotid artery suggesting total occlusion (*arrow*). (**b**) Power Doppler image of same artery showing string sign (*arrow*), i.e., subtotal occlusion

**Table 7.3** Zwiebel criteria for carotid stenosis

| | |
|---|---|
| 0 | ICA PSV < 110 cm/s |
| | EDV < 40 cm/s |
| | PSV ICA/CCA < 1.8 |
| | Spectral broadening < 30 cm/s |
| 1–39% Stenosis | PSV < 110 cm/s |
| | EDV < 40 cm/s |
| | Ratio < 1.8 |
| | Spectral broadening < 40 cm/s |
| 40–59% Stenosis | PSV < 130 cm/s |
| | EDV < 40 cm/s |
| | Ratio < 1.8 |
| 60–79% Stenosis | PSV > 130 cm/s |
| | EDV > 40 cm/s |
| | Ratio > 1.8 |
| 80–99% Stenosis | PSV > 250 cm/s |
| | EDV > 100 cm/s |
| | Ratio > 3.7 |
| Occlusion | No flow |

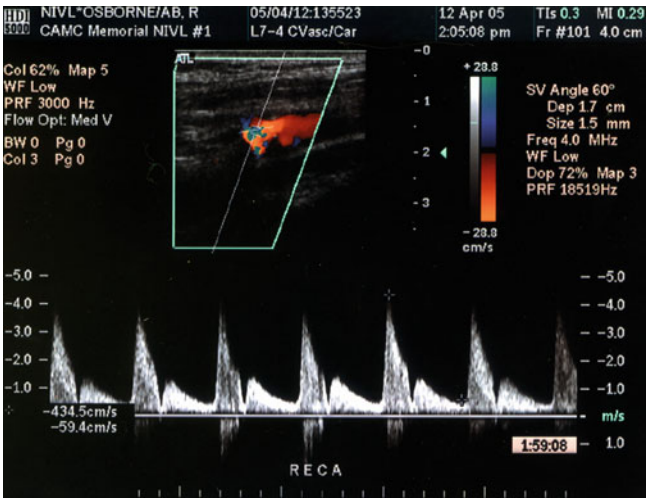


**Fig. 7.34** Doppler spectra produced by high-grade stenosis of external carotid arteries. This patient has a peak systolic velocity of 434.5 cm/s. Flow in diastole reaches the zero baseline

without preoperative arteriography [27, 28], prompted us to identify and evaluate new duplex velocity criteria for threshold stenoses used in various symptomatic and asymptomatic carotid endarterectomy trials (NASCET, ACAS, and VA studies). In addition, we identified the best duplex criteria that yielded a high positive predictive value (≥95%) for the threshold level of asymptomatic internal carotid artery stenosis of ≥60%, therefore minimizing unnecessary arteriography with its associated risk of stroke. We also identified the best duplex criteria that provided a high negative predictive value for the threshold level of symptomatic internal carotid artery stenosis of ≥70% to minimize missing patients who would benefit the most from a carotid endarterectomy. We analyzed 231 patients (462 arteries) who underwent both carotid color duplex scanning and arteriography from January 1992 to December 1994 [26].

Data derived from receiver operator curves were used to calculate the sensitivity, specificity, positive predictive value, negative predictive value, and overall accuracy of selected internal carotid artery peak systolic velocities, internal carotid artery end-diastolic velocities, and ratio of the peak systolic velocity of the internal carotid artery to the peak systolic velocity of the common carotid artery in detecting ≥30%, ≥50%, ≥60%, and ≥70–99% angiographic internal carotid artery stenosis.

**Table 7.4** Accuracy of color duplex ultrasound based on the new criteria

| Duplex criteria (% stenosis) | Sensitivity (%) | Specificity (%) | PPV (%) | NPV (%) | Overall accuracy (%) |
|---|---|---|---|---|---|
| ICA PSV > 120 cm/s (<30% vs. ≥30% stenosis) | 93 | 67 | 90 | 77 | 87 |
| ICA PSV ≥ 140 cm/s (<50% vs. ≥50% stenosis) | 92 | 95 | 97 | 89 | 93 |
| ICA PSV > 150 and EDV ≥ 65 cm/s (<60% vs. ≥60% stenosis) | 82 | 97 | 96 | 86 | 90 |
| ICA PSV > 150 and EDV ≥ 90 cm/s (<70% vs. ≥70% stenosis) | 85 | 95 | 91 | 92 | 92 |

**Table 7.5** Selected optimal criteria with best PPV (≥95%) and overall accuracy in detecting ≥60–99% and 70–99% stenosis

| | PPV (%) | Overall accuracy (%) | Sensitivity (%) | Specificity (%) | NPV (%) |
|---|---|---|---|---|---|
| *Best PPV for 60% ICA stenosis* | | | | | |
| ICA PSV ≥220 cm/s | 96 | 82 | 64 | 98 | 76 |
| ICA EDV ≥ 80 cm/s | 96 | 87 | 79 | 97 | 84 |
| ICA/CCA PSV ratio ≥ 4.25 | 96 | 71 | 41 | 99 | 65 |
| ICA PSV and EDV 150, 65[a] | 96 | 90 | 82 | 97 | 86 |
| *Best PPV for 70% ICA stenosis* | | | | | |
| ICA PSV ≥ 300 cm/s | 97 | 80 | 48 | 99 | 76 |
| ICA EDV ≥ 110 cm/s[a] | 100 | 91 | 75 | 100 | 87 |
| ICA/CCA PSV ≥ none | – | – | – | – | – |
| ICA PSV and EDV 150, 110[a] | 100 | 91 | 75 | 100 | 87 |

[a]These values have the best PPV and overall accuracy

**Table 7.6** Selected optimal criteria with best NPV ≥95% and overall accuracy in detecting ≥60–99% and 70–99% stenosis

| | NPV (%) | Overall accuracy (%) | Sensitivity (%) | Specificity (%) | PPV (%) |
|---|---|---|---|---|---|
| *Best NPV for 60% stenosis* | | | | | |
| ICA PSV ≥ 135 cm/s[a] | 99 | 80 | 99 | 64 | 71 |
| ICA EDV – none | – | – | – | – | – |
| ICA/CCA PSV ratio ≥ 1.62 | 95 | 71 | 97 | 47 | 62 |
| ICA PSV and EDV – none | – | – | – | – | – |
| *Best NPV for 70% ICA stenosis* | | | | | |
| ICA PSV ≥ 150 cm/s[a] | 99 | 80 | 99 | 69 | 65 |
| ICA EDV ≥ 60 cm/s | 96 | 83 | 94 | 77 | 71 |
| ICA/CCA PSV ≥ none | – | – | | – | – |
| ICA PSV and EDV – none | – | – | – | – | – |

[a]These values have the best NPV and overall accuracy

Table 7.4 correlates the results obtained with the new proposed criteria to the percentage of angiographic stenoses in 404 carotid arteries.

The optimal duplex values that provide the best positive predictive value (≥95%) and have a good overall accuracy in detecting ≥60–99% and ≥70–99% internal carotid artery stenoses are listed in Table 7.5, and the optimal duplex values that provide the best negative predictive value (≥95%) and a good overall accuracy in detecting ≥60–99% and ≥70–99% internal carotid artery stenoses are shown in Table 7.6.

In choosing our criteria for peak systolic velocity and end-diastolic velocity, we chose the values that gave the highest overall accuracy. Which criteria to use is therefore dependent on the "outcome" desired by the clinician. Although some surgeons have advocated carotid endarterectomy based on duplex criteria alone [27, 28], the decision to proceed with an arteriogram is based on the duplex findings in the majority of patients. The mortality and morbidity of arteriography vary from institution to institution, but can be significant [22, 29]. We propose that vascular laboratories at institutions with significant morbidity in relation to carotid arteriography use duplex criteria with a ≥95% positive predictive value and the best overall accuracy in order to minimize the number of patients undergoing unnecessary arteriography (Table 7.5). These criteria can also be utilized when carotid endarterectomy is performed without preoperative arteriography. In those institutions where arteriography does not significantly add to the morbidity of the overall treatment of carotid

**Table 7.7** Comparison of several studies correlating angiographic 50–69%, 60–99%, and 70–99% ICA stenosis with duplex scanning

| Duplex scanning | | | | | | | |
|---|---|---|---|---|---|---|---|
| Criteria (reference) | Number of ICAs | Ultrasound system | Accuracy (%) | Sensitivity (%) | Specificity (%) | PPV (%) | NPV (%) |
| *30–49% stenosis* | | | | | | | |
| PSV ≥ 120 cm/s [14] | 462 | ATL, UM9 (HDI) | 87 | 93 | 67 | 90 | 77 |
| *50–69% stenosis* | | | | | | | |
| PSV > 140 cm/s [14] | 462 | ATL, UM9 (HDI) | 93 | 92 | 95 | 97 | 89 |
| PSV ≥ 130 cm/s and EDV ≤100 cm/s [18] | 120 | Acuson 128 | 97 | 92 | 97 | 93 | 99 |
| *60–99% stenosis* | | | | | | | |
| PSV ≥ 150 cm/s and EDV ≥ 65 cm/s [14] | 462 | ATL, UM9 (HDI) | 90 | 82 | 97 | 96 | 86 |
| PSV ≥ 130 cm/s and EDV ≥ 40 cm/s [19] | 120 | Acuson 128 | 80 | 97 | 72 | 62 | 98 |
| PSV ≥ 260 cm/s and EDV ≥ 70 cm/s [23] | 352 | Acuson 128, ATL, UM9 | 90 | 84 | 94 | 92 | 88 |
| PSV ≥ 290 cm/s and EDV ≥ 80 cm/s [23] | | | 88 | 78 | 96 | 95 | 84 |
| *70–99% stenosis* | | | | | | | |
| PSV ≥ 150 cm/s and EDV ≥ 90 cm/s [14] | 462 | ATL, UM9 (HDI) | 92 | 85 | 93 | 91 | 92 |
| PSV ≥ 130 cm/s and EDV ≥ 100 cm/s [18] | 770 | QAD 1, QAD 2000 | 95 | 81 | 98 | 89 | 96 |
| PSV ≥ 270 cm/s and EDV ≥ 110 cm/s [19] | 120 | Acuson 128 | 93 | 96 | 91 | – | – |
| PSV ≥ 325 cm/s [20] | 184 | Acuson 128 | 88 | 83 | 91 | 80 | 92 |
| ICA/CCA PSV ratio ≥ 4.0 [20] | | | 88 | 91 | 87 | 76 | 96 |
| PSV ≥ 130 cm/s and EDV ≥ 100 cm/s[a] [21] | 914 | QAD 2000 | 95 | 87 | 97 | 89 | 96 |
| | | Phillips P700 | | | | | |
| PSV ≥ 130 cm/s and EDV ≥ 100 cm/s[b] [21] | | | 93 | 78 | 97 | 88 | 94 |

*Abbreviations*: *PPV* positive predictive value, *NPV* negative predictive value, *PSV* peak systolic velocity, *ICA* internal carotid artery, *CCA* common carotid artery, *EDV* end-diastolic velocity

[a]Prospective validation of criteria developed in Faught et al. [18] including ICA occlusions

[b]Analysis of criteria developed in Faught et al. [18] excluding ICA occlusion

disease, we suggest using the criteria described in Table 7.6. These criteria have the highest negative predictive value to ensure that only a minimum number of patients with ≥60% or ≥70% stenoses are missed.

This duplex classification would fit into the existing trials (NASCET, ACAS, and VA). By reporting results using these criteria, the clinician will be better able to make decisions regarding the need for carotid endarterectomy or arteriogram based on the risks and benefits for individual patients. With the added risks of arteriography, decisions to operate would be better based on duplex findings alone. Having positive predictive values ranging from 90% to 97% and accuracies of 87–93% can eliminate many unnecessary arteriograms or other invasive imaging.

It is important to note that the data obtained by individual vascular laboratories will vary across the country. Differences in equipment, abilities and consistencies of vascular technicians, and reader interpretations will cause variabilities from laboratory to laboratory [30]. Therefore, each laboratory must adapt a method that employs the equipment it uses and has validated its method when using proposed new duplex criteria.

Other studies have sought to reconcile these trials (NASCET, European Carotid Surgery Trial [ECST], and ACAS) with duplex criteria [18–21, 24, 26]. A summary of these studies can be found in Table 7.7. As noted in this table, different overall accuracies were reported according to each technique and according to specific duplex criteria. This can be partially explained by the differences in scanning techniques, technologists' experience, angle of insonation, or different ultrasound systems. It has been shown that linear array transducers may overestimate peak systolic velocity in a flow phantom [31].

## Accuracy of Duplex Scanning in the Detection of Carotid Stenosis and Severity

Various clinical studies have reported an overall accuracy of 80–97% in diagnosing carotid artery stenosis [15, 18–21, 32–39]. Tables 7.7 and 7.8 summarize some of these studies.

The UK Health Technology Assessment (HTA) published a meta-analysis in 2006 of studies evaluating the accuracy of

**Table 7.8** Accuracy of carotid duplex ultrasound compared to arteriography in recent series

| Author (year) | Carotids/patients | Stenosis (%) | Sensitivity (%) | Specificity (%) |
|---|---|---|---|---|
| Serfaty et al. (2000) [40] | 46/169 | Occlusion | 100 | 90 |
| Hood et al. (1996) [21] | 457/170 | | 100 | 99 |
| White et al. (1994) [41] | 120/171 | | 80 | 100 |
| Turnipseed et al. (1993) [42] | 34/172 | | 100 | 100 |
| Riles et al. (1992) [43] | 75/173 | | 100 | 100 |
| Riles et al. (1992) [43] | 75/173 | ≥80 | 85 | 80 |
| UK Health (2006) [50] | Meta-analysis | ≥70 | 89 | 84 |
| Nederkoorn et al. (2002) [38] | 313/313 | | 88 | |
| MacKenzie et al. (2002) [39] | 375/192 | | 81 | 89 |
| Johnson et al. (2000) [44] | 76/174 | | 65 | 95 |
| Serfaty et al. (2000) [40] | 46/169 | | 64 | 97 |
| Anderson et al. (2000) [35] | 80/40 | | 82 | 71 |
| Back et al. (2000) [36] | 74/40 | | 90 | 74 |
| AbuRahma et al. (1998) [7] | 462/231 | | 85 | 95 |
| Huston et al. (1998) [33] | 100/50 | | 97 | 75 |
| Link et al. (1997) [45] | 56/176 | | 87 | 98 |
| Hood et al. (1996) [21] | 457/457 | | 87 | 97 |
| Patel et al. (1995) [32] | 176/88 | | 94 | 83 |
| Bray et al. (1995) [46] | 128/177 | | 85 | 96–97 |
| Patel et al. (1995) [32] | 171/178 | | 94 | 83 |
| Turnipseed et al. (1993) [42] | 34/172 | | 94 | 89 |
| Bluth et al. (2000) [47] | 40/179 | ≥60 | 62 | 100 |
| Jackson et al. (1998) [48] | 99/180 | | 89 | 92 |
| White et al. (1994) [41] | 120/171 | | 73 | 88 |
| Walters et al. (1993) [49] | 102/181 | | 88 | 88 |
| Johnston et al. (2001) [37] | 452 | ≥50 | 87 | |
| Back et al. (2000) [36] | 74/40 | | 100 | 72 |
| Anderson et al. (2000) [35] | 80/40 | | 35 | 87 |
| Serfaty et al. (2000) [40] | 46/169 | | 94 | 83 |
| Hood et al. (1996) [21] | 457/170 | | 99.5 | 89 |
| Bray et al. (1995) [46] | 128/177 | | 87–95 | 96 |
| Riles et al. (1992) [43] | 75/173 | | 98 | 69 |
| Technology assessment (2006) [50] | | | 36 | 91 |
| Belsky et al. (2000) [34] | 92/46 | 0–100 | 79 | 96 |

noninvasive imaging and concluded that although contrast-enhanced magnetic resonance angiography was the most accurate imaging modality overall, it was limited by unavailability, inaccessibility, and delays. Therefore, they concluded that color duplex ultrasound remained the preferred imaging modality for identifying patients with 70–99% stenosis [50].

This recommendation was based on several factors, including low cost, a much higher number of strokes likely to be prevented in the long term by the rapid availability of carotid duplex ultrasound in contrast to other imaging, and the good sensitivity of imaging in detecting significant stenosis. However, the HTA highlighted the concern about the accuracy of duplex ultrasound in diagnosing 50–69%, which carries a sensitivity of only 36%, with a specificity of 91% [50]. Because of which, other combined imaging was recommended for this category of stenosis.

## Carotid Duplex Consensus Criteria for Grading Carotid Artery Stenosis

Accreditation of noninvasive vascular laboratories, in general, has resulted in an increased degree of standardization of carotid duplex ultrasound examinations; however, a wide range of practice patterns still exist. Clinicians have relied on published institutional experience for interpreting carotid duplex ultrasounds at their institutions. Because of this, a panel of experts from several medical specialties convened in October 2002 in San Francisco, California, under the auspices of the Society of Radiologists in Ultrasound to arrive at a consensus regarding the performance of Doppler ultrasound to aid in the diagnosis of internal carotid artery (ICA) stenosis. This panel of experts recommended a cutoff ICA PSV of ≥125 and ≥230 cm/s for predicting angiographic >50% stenosis and >70% ICA stenosis, respectively [51]. It should be noted that the recommended criteria in the Society

**Table 7.9** Ultrasound consensus criteria for carotid stenosis

| Stenosis range | ICA PSV | ICA EDV | ICA/CCA PSV ratio | Plaque |
|---|---|---|---|---|
| Normal | <125 cm/s | <40 cm/s | <2.0 | None |
| <50% | <125 cm/s | <40 cm/s | <2.0 | <50% diameter reduction |
| 50–69% | 125–230 cm/s | 40–100 cm/s | 2.0–4.0 | ≥50% diameter reduction |
| 70 – near occlusion | >230 cm/s | >100 cm/s | >4.0 | ≥50% diameter reduction |
| Near occlusion | May be low or undetectable | Variable | Variable | Significant, detectable lumen |
| Occlusion | Undetectable | Not applicable | Not applicable | Significant, no detectable lumen |

**Table 7.10** Validation of consensus criteria: duplex ultrasound versus angiographic stenosis

| | Sensitivity | Specificity | PPV | NPV | Overall accuracy |
|---|---|---|---|---|---|
| Consensus normal stenosis | 100 (100, 100) | 100 (100, 100) | 100 (100, 100) | 100 (100, 100) | 100 (100, 100) |
| Consensus < 50% stenosis | 88 (83.6, 91.7) | 99 (95.6, 100) | 100 (98.7, 100) | 68 (58.8, 77.3) | 90 (84, 95.9) |
| Consensus 50–69% stenosis | 93 (89.3, 96.1) | 68 (58.5, 76.9) | 86 (82, 90.8) | 81 (72.2, 89.2) | 85 (77.2, 92.6) |
| Consensus ≥70% stenosis | 99 (97.7, 100) | 86 (80, 92.8) | 93 (89.9, 96.5) | 98 (95.1, 100) | 95 (90.2, 99.1) |

**Table 7.11** Pearson correlation of the consensus criteria

| Duplex variable | Overall correlation (CI) | Correlation to ≥70–99% stenosis (CI) |
|---|---|---|
| Peak systolic velocity | 0.81 (0.77, 0.85) | 0.833 (0.8, 0.86) |
| End-diastolic velocity | 0.7 (0.64, 0.75) | 0.755 (0.71, 0.80) |
| Systolic ratio | 0.57 (0.49, 0.63) | 0.601 (0.53, 0.66) |
| Diastolic ratio | 0.54 (0.46, 0.61) | 0.60 (0.53, 0.66) |

of Radiologists in Ultrasound report are based on an analysis of several published studies and the experience of the panelists and they are not validated criteria. These criteria are summarized in Table 7.9.

These criteria were to be used for new laboratories requesting applicable criteria for prospective validation. It was also recommended for established laboratories, which had previously developed their own criteria that were outdated.

Validation of ultrasound criteria can be difficult since different scanners are used in various laboratories. Therefore, it is important for each laboratory to validate its own criteria and use these accordingly.

## Validation of the Carotid Duplex Consensus Criteria for Grading Carotid Artery Stenosis

Recently, we conducted a study to validate the carotid duplex consensus criteria by analyzing 376 carotid arteries which had both carotid duplex ultrasound and angiography. Receiver operator characteristic curves were used to compare peak systolic velocities (PSV), end-diastolic velocities (EDV) of the internal carotid artery (ICA), and ICA/common carotid artery (CCA) ratios in detecting <50%, 50–69% (ICA PSV of 125–230 cm/s), and 70–99% (PSV of ≥230 cm/s) stenosis according to the consensus criteria.

The consensus criteria use a PSV of 125–230 cm/s for detecting angiographic stenosis of 50–69% stenosis, which has a sensitivity (sens.) of 93%, specificity (spec.) of 68%, and overall accuracy (OA) of 85%. A PSV of ≥230 cm/s for ≥70% stenosis had a sens. of 99%, spec. of 86%, and OA of 95%. Receiver operator curves showed that the ICA PSV was significantly better (area under the curve [AUC] = 0.97) than EDV (AUC = 0.94) or ICA/CCA ratio (AUC = 0.84) ($p = 0.036$) in detecting ≥70% stenosis and ≥50% stenosis. Using Pearson correlations, a statistical difference was found between the correlation of PSV with angiography (0.833, confidence interval [C.I.] 0.8–0.86), EDV with angiography (0.755, C.I. 0.71–0.80), and ICA/CCA systolic ratio with angiography (0.601, C.I. 0.53–0.66) ($p < 0.0001$) in detecting 70–99% stenosis. There was no improvement in accuracy by adding the EDV values and/or the ratios to the PSV values.

The consensus criteria for diagnosing 50–69% stenosis can be significantly improved by using an ICA PSV of 140–230 cm/s with a sens. of 94%, spec. of 92%, and OA of 92%. The results are summarized in Tables 7.10, 7.11, 7.12, 7.13, and 7.14 and Figs. 7.35, 7.36, and 7.37.

We concluded that the consensus criteria can be accurately used for diagnosing ≥70% stenosis; however, the accuracy can be improved for detecting 50–69% stenosis if the ICA PSV is changed to 140–<230 cm/s [52].

## Effect of Contralateral Stenosis or Occlusion on Ipsilateral Carotid Stenosis Duplex Criteria

A number of studies in the recent literature have reported decreased accuracy of duplex scanning in predicting the degree of ipsilateral internal carotid stenosis in the presence

**Table 7.12** Summary of various velocities and ratios for detecting ≥70–99% stenosis

| | Sensitivity | Specificity | PPV | NPV | Overall accuracy |
|---|---|---|---|---|---|
| PSV > 230 | 99 (97, 100) | 86 (79.8, 92.7) | 93 (89.9, 96.5) | 97 (93.5, 100) | 94 (89.7, 98.9) |
| PSV > 240 | 97 (95, 99.4) | 87 (80.2, 93.2) | 94 (90.5, 96.9) | 94 (89.0, 98.6) | 94 (88.9, 98.5) |
| *PSV > 280* | *95 (92.3, 97.9)* | *93 (88.4, 98.5)* | *97 (95.1, 99.4)* | *89 (82.4, 95)* | *95 (90.2, 99.1)* |
| Systolic ratio > 2.75 | 87 (82.8, 91.3) | 85 (76.6, 92.6) | 95 (91.6, 97.6) | 68 (58.8, 77.3) | 86 (79.7, 93.3) |
| Systolic ratio > 3 | 86 (81.3, 90) | 91 (84.2, 97.9) | 97 (95.1, 99.4) | 63 (53.3, 72.5) | 87 (80.1, 93.5) |
| Diastolic ratio > 3 | 87 (82.6, 91.2) | 80 (71.9, 89.1) | 93 (89.3, 96.2) | 68 (58.8, 77.3) | 85 (78.2, 92.3) |
| Diastolic ratio > 3.5 | 86 (81.9, 90.5) | 89 (81.4, 96.1) | 96 (93.9, 98.8) | 65 (55.5, 74.4) | 87 (80.1, 93.5) |
| PSV > 230 and EDV > 50 | 97 (95.0, 99.4) | 88 (82.2, 94.6) | 95 (91.6, 97.6) | 94 (89, 98.6) | 94 (89.7, 98.9) |
| PSV > 230 and/or EDV > 90 | 99 (97, 100) | 86 (79.8, 92.7) | 93 (89.9, 96.5) | 97 (93.5, 100) | 94 (89.7, 98.9) |
| PSV > 220 and diastolic ratio > 2.5 | 88 (84.2, 92.4) | 87 (80, 94.7) | 95 (92.7, 98.2) | 71 (62.1, 80.2) | 88 (81.6, 94.5) |
| PSV > 230 and/or diastolic ratio > 5.5 | 99 (97, 100) | 86 (79.8, 92.7) | 93 (89.9, 96.5) | 97 (93.5, 100) | 94 (89.7, 98.9) |
| PSV > 220 and systolic ratio > 2.5 | 89 (84.8, 92.8) | 91 (84.5, 97.3) | 97 (94.5, 99.1) | 72 (63.3, 81.1) | 89 (83.2, 95.5) |
| PSV > 230 and/or systolic ratio > 4.5 | 99 (96.9, 100) | 85 (78.9, 92) | 93 (89.3, 96.2) | 97 (93.5, 100) | 94 (89.3, 98.7) |
| EDV > 50 and systolic ratio > 2.5 | 88 (84.3, 92.4) | 88 (81.4, 95.6) | 96 (93.3, 98.5) | 71 (62.1, 80.2) | 88 (82, 94.8) |
| EDV > 70 and/or systolic ratio > 4 | 97 (94.2, 99.1) | 83 (76.3, 90.4) | 92 (88.3, 95.5) | 93 (87.6, 97.9) | 92 (86.8, 97.5) |
| *EDV > 100 and/or systolic ratio > 4* | *91 (87.6, 94.8)* | *96 (92, 100)* | *99 (97, 100)* | *78 (70, 86.6)* | *92 (87.2, 97.7)* |
| *PSV > 230 (EDV > 100 or systolic ratio > 4)* | *91 (87.7, 94.8)* | *97(93.9, 100)* | *99 (97.9, 100)* | *78 (70.2, 86.6)* | *93 (87.6, 97.9)* |
| Systolic ratio > 2 and diastolic ratio > 3.5 | 86 (81.6, 90.3) | 90 (82.7, 97) | 97 (94.5, 99.1) | 64 (54.4, 73.5) | 87 (80.1, 93.5) |
| Systolic ratio > 3.5 and/or diastolic ratio > 3 | 87 (83.2, 91.7) | 78 (69.5, 86.8) | 91 (87.7, 95.1) | 70 (61, 79.2) | 85 (77.8, 92) |

**Table 7.13** Sensitivity, specificity, and overall accuracy for velocity cutoffs for the diagnosis of ≥50% and 70–99% stenosis

| | Sensitivity | Specificity | PPV | NPV | Overall accuracy |
|---|---|---|---|---|---|
| *50% stenosis* | | | | | |
| PSV > 140 | 94 (89.7, 98) | 91 (87.5, 95.5) | 88 (83.1, 93.8) | 96 (92.5, 98.6) | 92 (88.6, 96.3) |
| PSV > 150 | 85 (79.7, 91) | 94 (90.5, 97.6) | 93 (88.4, 97.1) | 88 (83, 92.6) | 90 (85.5, 94.3) |
| *****PSV > 137* | *96 (92.6, 99.4)* | *91 (86.6, 94.8)* | *87 (81.3, 92.6)* | *97 (94.8, 99.6)* | *93 (89, 96.6)* |
| *70–99% stenosis* | | | | | |
| PSV > 230 | 99 (97, 100) | 86 (79.8, 92.7) | 93 (89.9, 96.5) | 98 (93.5, 100) | 94 (89.7, 98.9) |
| PSV > 240 | 97 (95, 99.4) | 87 (80.2, 93.2) | 94 (90.5, 96.9) | 94 (89, 98.6) | 94 (88.9, 98.5) |
| *****PSV > 252* | *97 (95.1, 99.4)* | *91 (85.4, 96.6)* | *96 (93.3, 98.5)* | *94 (89, 98.6)* | *95 (91.1, 99.5)* |
| PSV > 280 | 95 (92.3, 97.9) | 93 (88.4, 98.5) | 97 (95.1, 99.4) | 89 (82.4, 95) | 95 (90.2, 99.1) |
| EDV > 70 | 96 (93.1, 98.5) | 85 (77.7, 91.6) | 93 (89.3, 96.2) | 91 (85, 96.5) | 92 (86.8, 97.5) |
| *****EDV > 87* | *93 (89.9, 96.4)* | *95 (90.8, 99.8)* | *98 (96.4, 100)* | *84 (76.1, 90.9)* | *94 (88.9, 98.5)* |

[***]Values with the best overall accuracy

**Table 7.14** Sensitivity, specificity, and overall accuracy validation of our present standard criteria

| | Sensitivity | Specificity | PPV | NPV | Overall accuracy |
|---|---|---|---|---|---|
| Standard normal stenosis | 100 (100, 100) | 100 (100, 100) | 100 (100, 100) | 100 (100, 100) | 100 (100, 100) |
| Standard < 50% stenosis | 93 (89.8, 96.4) | 94 (89.2, 99.1) | 98 (95.8, 99.7) | 84 (76.1, 90.9) | 93 (88.4, 98.3) |
| Standard 50–69% stenosis | 96 (94.0, 98.9) | 82 (73.6, 89.5) | 93 (89.4, 96.1) | 90 (84, 96.7) | 92 (86.3, 97.9) |
| Standard > 70% stenosis | 99 (97.1, 100) | 96 (91.9, 99.8) | 98 (96.4, 100) | 97 (93.4, 100) | 98 (94.9, 100) |

of contralateral high-grade stenosis or carotid occlusion [53–59]. When conventional standard criteria [11] were applied in this circumstance, the result was an overestimation of the degree of ipsilateral stenosis (up to 48%) [58], often resulting in incorrect assignment to a higher category of disease and thus creating a false-positive interpretation [53–59]. It has been proposed that this phenomenon occurs because of a compensatory increase in flow velocity in the ipsilateral carotid system to maintain a stable cerebral circulation via the circle of Willis [55].

Fujitani et al. [58] were the first to recommend modification of the standard duplex criteria in patients with contralateral

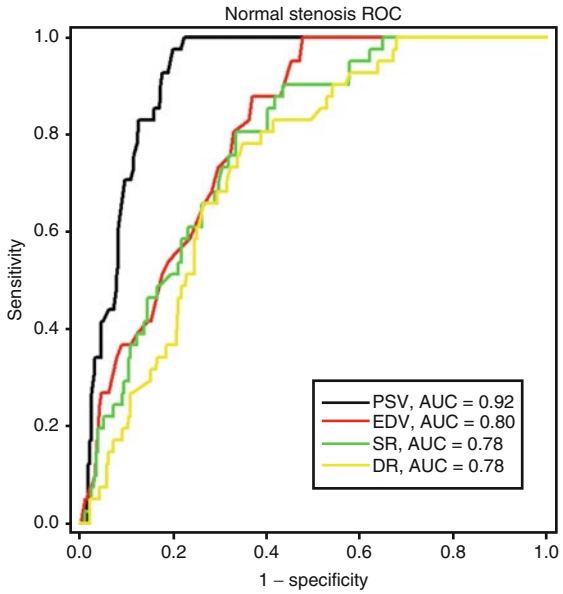


PSV vs. EDV – $p < 0.0001$, PSV vs. SR – $p < 0.0001$, PSV vs. DR – $p < 0.0001$

**Fig. 7.35** Sensitivity versus specificity ROC comparing PSV, EDV, and ratios for normal carotids (Reprinted from AbuRahma et al. [52]. With permission from Elsevier)

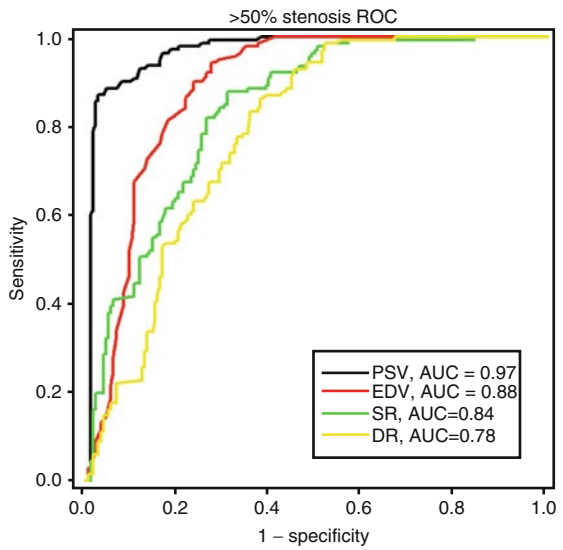


PSV vs. EDV – $p < 0.0001$, PSV vs. SR – $p < 0.0001$, PSV vs. DR – $p < 0.0001$

**Fig. 7.36** Sensitivity versus specificity ROC comparing PSV, EDV, and ratios for ≥50% stenosis (Reprinted from AbuRahma et al. [52]. With permission from Elsevier)

internal carotid occlusion. However, in this study, only the effect of the contralateral total carotid occlusion was studied. Patients with less than total occlusion of the contralateral artery were excluded from the study population.

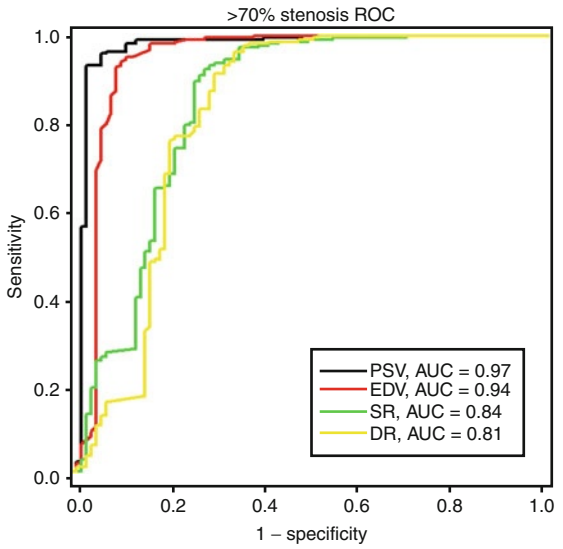


PSV vs. EDV – $p = 0.0363$, PSV vs. SR – $p < 0.0001$, PSV vs. DR – $p < 0.0001$

**Fig. 7.37** Sensitivity versus specificity ROC comparing PSV, EDV, and ratios for ≥70–99% stenosis (Reprinted from AbuRahma et al. [52]. With permission from Elsevier)

The recognition of this phenomenon as consistent and clinically significant led us to undertake a retrospective study to compare the accuracy of various existing duplex criteria (standard [11], Fujitani [58], internal carotid artery/common carotid artery ratio [ICA/CCA] [60]) used in grading ipsilateral carotid stenosis in patients with contralateral high-grade stenosis or occlusion. In addition, we propose new modified duplex criteria that we believe to be superior to the existing criteria in terms of overall accuracy. These criteria are summarized in Table 7.15.

These criteria were developed because of our dissatisfaction with the results of the standard method in grading ipsilateral stenosis in the presence of severe contralateral disease.

One hundred and seventy-eight patients (356 arteries) were identified as having significant (>50%) internal carotid artery stenosis by carotid duplex ultrasonography, and they subsequently underwent carotid arteriography within 6 weeks [61].

Criteria for duplex ultrasonography classification of the degree of stenosis are shown in Table 7.15. Four different sets of criteria for each patient were analyzed: (1) the standard criteria (University of Washington) [11], (2) Fujitani criteria [58], (3) ICA/CCA ratio criteria [60], and (4) the new revised criteria that we are proposing [61]. These criteria were used to assign each artery to one of five categories: 1–15% stenosis, 16–49% stenosis, 50–79% stenosis, 80–99% stenosis, and total occlusion.

The standard method overestimated 56 (16%) of 356 stenoses in contrast to 3% for the new method ($p < 0.001$), and this effect was most evident in the 50–<80% stenosis category (30%). The Fujitani method underestimated 97 (27%) of 356

**Table 7.15** Doppler velocity criteria for carotid artery stenosis

| Arteriographic lesion | Spectral criteria |
|---|---|
| *Standard method* | |
| 1–15% diameter reduction | PSV < 125 cm/s |
| 16–49% diameter reduction | PSV < 125 cm/s |
| 50–79% diameter reduction | PSV ≥ 125 cm/s |
| | EDV < 140 cm/s |
| 80–99% diameter reduction | PSV > 125 cm/s |
| | EDV > 140 cm/s |
| Occlusion | No internal carotid flow signal |
| | Low or reversed diastolic component in common carotid artery |
| *New method (AbuRahma) similar to standard method except for the following* | |
| 16–49% diameter reduction | PSV < 140 cm/s |
| | EDV < 140 cm/s |
| 50–79% diameter reduction | PSV ≥ 140 cm/s |
| | EDV < 140 cm/s |
| 80–99% diameter reduction | PSV > 140 cm/s |
| | EDV > 140 cm/s |
| *Fujitani method – same as standard method except for the following* | |
| 16–49% diameter reduction | PSV > 125 cm/s |
| | EDV < 155 cm/s |
| 50–79% diameter reduction | PSV > 140 cm/s |
| | EDV < 155 cm/s |
| 80–99% diameter reduction | PSV > 140 cm/s |
| | EDV > 155 cm/s |
| *ICA/CCA ratio method* | |
| 1–49% diameter reduction | SVR < 1.5 |
| 50–79% diameter reduction | SVR ≥ 1.5, PEDV < 100 cm/s |
| 80–99% diameter reduction | SVR ≥ 1.8, PEDV > 100 cm/s |
| Occlusion | No internal carotid artery flow signal |

stenoses, and the ICA/CCA ratio overestimated stenoses in 77 (22%) of 356. The overall exact correlation was 94, 82, 70, and 75% for the new, standard, Fujitani, and ICA/CCA ratio, respectively. The $x^2$ statistic and corresponding confidence intervals for the new method ($x^2 = 0.923$, ±0.016) are significantly higher ($p < 0.001$) than those for the standard method ($x^2 = 0.760$, ±0.027), the Fujitani method ($x^2 = 0.608$, ±0.031), and the ICA/CCA ratio method ($x^2 = 0.642$, ±0.051). The overall accuracy in diagnosing ≥50% ipsilateral stenosis in the whole series was 85% for the standard method, 97% for the new method, 95% for the Fujitani method, and 81% for the ICA/CCA ratio. The new method was superior to the standard and ICA/CCA ratio methods ($p < 0.001$) and the Fujitani method ($p = 0.024$).

Tables 7.16, 7.17, and 7.18 summarize the results of the study. The proposed criteria fared very well in the analysis, with only 3% overall overestimation of the disease and 3% overall underestimation of the disease. The overall exact correlation between duplex and arteriographic grading was 94% and was superior to the other criteria in each case ($p < 0.001$).

The proposed criteria yielded sensitivity, specificity, positive and negative predictive values, and overall accuracy values superior to those of the other three criteria in predicting ≥50% ipsilateral stenosis, when all patients with 0–100% contralateral stenosis were included ($p < 0.001$) in each case. When divided into 50–<80% contralateral stenosis and 80–99% contralateral stenosis or total occlusion, the new criteria proved once again to be superior to the standard and ICA/CCA ratio criteria ($p < 0.001$). The differences between the new criteria and Fujitani criteria in these patients did not reach statistical significance. This finding is not surprising because the Fujitani criteria were developed from a study in which the contralateral artery was totally occluded and were designed to be used in such cases rather than to be applied to all vessels studied, as they were in this series.

Some clinicians believe that the most important clinical issue is accuracy in detecting stenoses of greater than or less than 80%, contralateral to a tight stenosis or occlusion. The standard method results were very comparable to the new method and somewhat comparable to the ICA/CCA ratio method in all parameters examined, including overall accuracy. This finding is not surprising because both the standard and new methods require an end-diastolic frequency of the internal carotid artery of >140 cm/s for the diagnosis of ≥80% stenosis. However, the Fujitani method had a poorer sensitivity and an overall accuracy of only 85% in contrast to an overall accuracy of 98% for the new and standard methods in this group of patients (80–99% contralateral stenosis). This finding can be explained by the requirement of an end-diastolic frequency of the internal carotid artery of >5 kHz for the diagnosis of ≥80% stenosis for the Fujitani method. Similar observations were noted in patients with a total contralateral occlusion. Our results were comparable to data previously reported by others [54–59].

Table 7.19 summarizes the duplex accuracy of various criteria in the presence of contralateral stenosis or occlusion.

## Clinical Use of Carotid Duplex Scanning

Overall, the indications for carotid duplex sonography include [62, 63]:

- Cervical bruit in an asymptomatic patient
- Amaurosis fugax
- Hemispheric TIA
- Hemispheric stroke
- Follow-up of known asymptomatic carotid stenosis
- Vascular assessment in a patient with multiple risk factors for atherosclerosis or stroke risk assessment in a patient with coronary or PAD
- Intraoperative assessment during CEA or stenting
- Follow-up after a carotid intervention

**Table 7.16** Comparison of duplex methods versus arteriography for sensitivity/specificity in diagnosis of ≥50% ipsilateral stenosis in patients with arteries of 50–<80% stenosis on contralateral side

| | Carotid arteriogram | | | | | | | |
|---|---|---|---|---|---|---|---|---|
| | <50% stenosis (%) | >50% stenosis (%) | Total | Sen. (%) | Spec. (%) | PPV (%) | NPV (%) | Overall accuracy (%) |
| *Standard method* | | | | | | | | |
| <50% stenosis | 24 (100) | 0 | 24 | 100 | 56 | 78 | 100 | 83 |
| ≥50% stenosis | 19 (22) | 68 (78) | 87 | | | | | |
| *New method* | | | | | | | | |
| <50% stenosis | 42 (95) | 2 (5) | 44 | 97 | 98 | 99 | 95 | 97 |
| ≥50% stenosis | 1 (1) | 66 (99) | 67 | | | | | |
| *Fujitani method* | | | | | | | | |
| <50% stenosis | 42 (91) | 4 (9) | 46 | 94 | 98 | 98 | 91 | 96 |
| ≥50% stenosis | 1 (1) | 64 (99) | 65 | | | | | |
| *ICA/CCA ratio method* | | | | | | | | |
| <50% stenosis | 19 (86) | 3 (14) | 22 | 96 | 44 | 73 | 86 | 76 |
| ≥50% stenosis | 24 (27) | 65 (73) | 89 | | | | | |
| Total | 43 | 68 | 111 | | | | | |

New method versus standard method, $p < 0.001$ ($Z$ statistics for proportion)
New method versus Fujitani method, $p > 0.05$ ($Z$ statistics for proportion)
New method versus ICA/CCA ratio method, $p < 0.001$ ($Z$ statistics for proportion)
*PPV* positive predictive value, *NPV* negative predictive value

**Table 7.17** Comparison of duplex methods versus arteriography for sensitivity/specificity in diagnosis of >50% ipsilateral stenosis in patients with arteries with 80–99% stenosis of the contralateral side

| | Carotid arteriogram | | | | | | | |
|---|---|---|---|---|---|---|---|---|
| | <50% stenosis (%) | >50% stenosis (%) | Total | Sen. (%) | Spec. (%) | PPV (%) | NPV (%) | Overall accuracy (%) |
| *Standard method* | | | | | | | | |
| <50% stenosis | 26 (100) | 0 | 26 | 100 | 53 | 68 | 100 | 76 |
| ≥50% stenosis | 23 (32) | 48 (68) | 71 | | | | | |
| *New method* | | | | | | | | |
| <50% stenosis | 45 (100) | 0 | 45 | 100 | 92 | 92 | 100 | 96 |
| ≥50% stenosis | 4 (8) | 48 (92) | 52 | | | | | |
| *Fujitani method* | | | | | | | | |
| <50% stenosis | 45 (96) | 2 (4) | 47 | 96 | 92 | 92 | 96 | 94 |
| ≥50% stenosis | 4 (8) | 46 (92) | 50 | | | | | |
| *ICA/CCA ratio method* | | | | | | | | |
| <50% stenosis | 23 (92) | 2 (8) | 25 | 96 | 47 | 64 | 92 | 71 |
| ≥50% stenosis | 26 (36) | 46 (64) | 72 | | | | | |

New method versus standard method, $p < 0.001$ ($Z$ statistics for proportion)
New method versus Fujitani method, not significant ($Z$ statistics for proportion)
New method versus ICA/CCA ratio method, $p < 0.001$ ($Z$ statistics for proportion)
*PPV* positive predictive value, *NPV* negative predictive value

Carotid duplex ultrasound reports routinely include flow velocities and the degree of stenoses. However, several carotid reports, particularly those from non-accredited vascular laboratories, have several inconsistencies that can be extremely critical in clinical decision making. A carotid duplex ultrasound examination should be termed "inconclusive" if the findings are uncertain and it cannot be ensured that the carotid artery does not have significant carotid artery disease [64, 65]. Calcification and shadowing, high bifurcation, short neck, or any other circumstances that prevent adequate interrogation of the carotid artery can result in an inconclusive examination. In this scenario, other diagnostic modalities must be recommended to delineate the proper pathology. Inconsistent carotid examination is used when the imaging and velocity determination of the color duplex ultrasound are not consistent with each other, and additional tests are also required in these circumstances. Significant carotid artery stenosis may be present without associated increased flow velocities. This can be partially explained by complex or calcified lesions or dampened flow by an extremely high-grade lesion.

**Table 7.18** Comparison of duplex methods versus arteriography for sensitivity/specificity in diagnosis of ≥50% stenosis in patients with total occlusion on contralateral side

| | Carotid arteriogram | | | | | | | |
|---|---|---|---|---|---|---|---|---|
| | <50% stenosis (%) | >50% stenosis (%) | Total | Sen. (%) | Spec. (%) | PPV (%) | NPV (%) | Overall accuracy (%) |
| *Standard method* | | | | | | | | |
| <50% stenosis | 5 (100) | 0 | 5 | 100 | 33 | 71 | 100 | 74 |
| ≥50% stenosis | 10 (29) | 24 (71) | 34 | | | | | |
| *New method* | | | | | | | | |
| <50% stenosis | 15 (94) | 1 (6) | 16 | 96 | 100 | 100 | 94 | 97 |
| ≥50% stenosis | 0 | 23 (100) | 23 | | | | | |
| *Fujitani method* | | | | | | | | |
| <50% stenosis | 15 (83) | 3 (17) | 18 | 88 | 100 | 100 | 83 | 92 |
| ≥50% stenosis | 0 | 21 (100) | 21 | | | | | |
| *ICA/CCA ratio method* | | | | | | | | |
| <50% stenosis | 6 (100) | 0 | 6 | 100 | 40 | 73 | 100 | 77 |
| ≥50% stenosis | 9 (27) | 24 (73) | 33 | | | | | |

New method versus standard method, $p < 0.01$ ($Z$ statistics for proportion)
New method versus Fujitani method, $p = 0.15$ ($Z$ statistics for proportion)
New method versus ICA/CCA ratio method, $p < 0.01$ ($Z$ statistics for proportion)
*PPV* positive predictive value, *NPV* negative predictive value

**Table 7.19** Accuracy of duplex criteria with contralateral severe stenosis or occlusion

| Criteria and reference | Accuracy (%) | Sensitivity (%) | Specificity (%) | PPV (%) | NPV (%) |
|---|---|---|---|---|---|
| *>50% stenosis* | | | | | |
| Fujitani [55] | 74 | 97 | 57 | 62 | 96 |
| AbuRahma [53] | | | | | |
| Fujitani | 92 | 88 | 100 | 100 | 83 |
| Standard | 74 | 100 | 33 | 71 | 100 |
| AbuRahma | 97 | 96 | 100 | 100 | 94 |
| Ratios | 77 | 100 | 40 | 73 | 100 |
| *50–79% stenosis* | | | | | |
| Fujitani: PSV > 140 cm/s, EDV < 155 cm/s [55] | 71 | 84 | 70 | 28 | 97 |
| AbuRahma [53]: | | | | | |
| Fujitani: PSV > 140 cm/s, EDV < 155 cm/s | 97 | 99 | 98 | 98 | 95 |
| Standard: PSV > 125 cm/s, EDV < 140 cm/s | 83 | 100 | 56 | 78 | 100 |
| AbuRahma: PSV ≥ 140 cm/s, EDV < 140 cm/s | 97 | 97 | 98 | 99 | 95 |
| Ratios: ICA/CCA ratio ≥ 1.5, EDV < 100 cm/s | 76 | 96 | 44 | 73 | 86 |
| *80–99% stenosis* | | | | | |
| Fujitani: PSV > 140 cm/s, EDV > 155 cm/s [55] | 96 | 91 | 97 | 89 | 98 |
| AbuRahma [53]: | | | | | |
| Fujitani: PSV > 140 cm/s, EDV > 155 cm/s | 94 | 96 | 92 | 92 | 96 |
| Standard: PSV > 125 cm/s, EDV > 140 cm/s | 76 | 100 | 53 | 68 | 100 |
| AbuRahma: PSV > 140 cm/s, EDV > 140 cm/s | 96 | 100 | 92 | 92 | 100 |
| Ratios: ICA/CCA ratio ≥ 1.8, EDV > 100 cm/s | 71 | 96 | 47 | 64 | 92 |

The accuracy of duplex scanning in the examination of the carotid artery bifurcation has resulted in its use in symptomatic patients for the detection of disease, the evaluation of patients with neck bruits, postoperative studies of endarterectomized vessels, and the sequential examination of asymptomatic patients to document progression of disease [66]. Other clinical implications include carotid endarterectomy without angiography, intraoperative assessment of carotid endarterectomy, long-term follow-up after carotid endarterectomy, plaque morphology and outcome, and carotid duplex scanning following trauma. The clinical implications of duplex ultrasound technology will be discussed in detail in Chap. 19.

## References

1. Kossoff G. Gray scale echography in obstetrics and gynecology. Report no. 60. Sydney: Commonwealth Acoustic Laboratories; 1973.
2. Olinger CP. Ultrasonic carotid echoarteriography. Am J Roentgenol. 1969;106:282–95.

3. Hartley DJ, Strandness Jr DE. The effects of atherosclerosis on the transmission of ultrasound. J Surg Res. 1969;9:575–82.
4. Barber FE, Baker DW, Nation AWC, et al. Ultrasonic duplex echo-Doppler scanner. IEEE Trans Biomed Eng. 1974;81:109–13.
5. Blackshear WM, Phillips DJ, Chikos RM, et al. Carotid artery velocity patterns in normal and stenotic vessels. Stroke. 1980;11:67–71.
6. Reilly LM. Importance of carotid plaque morphology. In: Bernstein EF, editor. Vascular diagnosis. 4th ed. St. Louis: Mosby-Year Book; 1993. p. 333–40.
7. AbuRahma AF, Kyer PR, Robinson P, et al. The correlation of ultrasonic carotid plaque morphology and carotid plaque hemorrhage: clinical implications. Surgery. 1998;124:721–6.
8. AbuRahma AF, Thiele S, Wulu J. Prospective controlled study of the natural history of asymptomatic 60% to 69% carotid stenosis according to ultrasonic plaque morphology. J Vasc Surg. 2002;36:437–42.
9. Gronholdt M, Nordestgaard B, Schroeder T, et al. Ultrasonic echolucent carotid plaques predict future strokes. Circulation. 2001;104:68–73.
10. Thiele BL, Hutchison KJ, Green RM, et al. Pulsed Doppler waveform patterns produced by smooth stenosis in the dog thoracic aorta. In: Taylor DEM, editor. Blood flow theory and practice. New York: Academic Press; 1983. p. 85–104.
11. Zierler RE, Strandness Jr DE. Noninvasive dynamic and real-time assessment of extracranial cerebrovasculature. In: Wood JH, editor. Cerebral blood flow: physiologic and clinical aspects. New York: McGraw-Hill; 1987. p. 311–23.
12. Bodily KC, Phillips DJ, Thiele BL, et al. Noninvasive detection of internal carotid artery occlusion. Angiology. 1981;32:517–21.
13. AbuRahma AF, Jarrett K, Hayes JD. Clinical implications of power Doppler three-dimensional ultrasonography. Vascular. 2004; 12:293–300.
14. Zwiebel WJ. New Doppler parameters for carotid stenosis. Semin Ultrasound CT MR. 1997;18:66–71.
15. AbuRahma AF, Robinson PA, Stickler DL, et al. Proposed new duplex classification for threshold stenoses used in various symptomatic and asymptomatic carotid endarterectomy trials. Ann Vasc Surg. 1998;12:349–58.
16. North American Symptomatic Carotid Endarterectomy Trial Collaborators. Beneficial effect of carotid endarterectomy in symptomatic patients with high-grade carotid stenosis. N Engl J Med. 1991;325:445–53.
17. Asymptomatic Carotid Atherosclerosis Study Group. Study design for randomized prospective trial of carotid endarterectomy for asymptomatic atherosclerosis. Stroke. 1989;20:844–9.
18. Faught WE, Mattos MA, van Bemmelen PS, et al. Color-flow duplex scanning of carotid arteries: new velocity criteria based on receiver operator characteristic analysis for threshold stenoses used in the symptomatic and asymptomatic carotid trials. J Vasc Surg. 1994;19:818–28.
19. Neale ML, Chambers JL, Kelly AT, et al. Reappraisal of duplex criteria to assess significant carotid stenosis with special reference to reports from the North American symptomatic carotid endarterectomy trial and the European carotid surgery trial. J Vasc Surg. 1994;20:642–9.
20. Moneta GL, Edwards JM, Chitwood RW, et al. Correlation of North American symptomatic carotid endarterectomy trial (NASCET) angiographic definition of 70% to 99% internal carotid artery stenosis with duplex scanning. J Vasc Surg. 1993;17:152–9.
21. Hood DB, Mattos MA, Mansour A, et al. Prospective evaluation of new duplex criteria to identify 70% internal carotid artery stenosis. J Vasc Surg. 1996;23:254–62.
22. Executive Committee for the Asymptomatic Carotid Atherosclerosis Study. Endarterectomy for asymptomatic carotid artery stenosis. JAMA. 1995;273:1421–8.
23. Moneta GL, Edwards JM, Papanicolaou G, et al. Screening for asymptomatic internal carotid artery stenosis: duplex criteria for discriminating 60% to 99% stenosis. J Vasc Surg. 1995;21:989–94.
24. Carpenter JP, Lexa FJ, Davis JT. Determination of sixty percent or greater carotid artery stenosis by duplex Doppler ultrasonography. J Vasc Surg. 1995;22:697–705.
25. Burnham CB, Liguish Jr J, Burnham SJ. Velocity criteria redefined for the 60% carotid stenosis. J Vasc Technol. 1996;20(1):5–11.
26. AbuRahma AF, Pollack JA, Robinson PA, et al. New duplex criteria for threshold stenoses used in the asymptomatic carotid atherosclerosis study (ACAS). Vasc Surg. 1999;33:23–32.
27. Marshall Jr WG, Kouchoukos NT, Murphy SF, et al. Carotid endarterectomy based on duplex scanning without preoperative arteriography. Circulation. 1988;78(Suppl I):I1–5.
28. Geuder JW, Lamparello PJ, Riles TS, et al. Is duplex scanning sufficient evaluation before carotid endarterectomy? J Vasc Surg. 1989;9:193–201.
29. AbuRahma AF, Robinson PA, Boland JP, et al. Complications of arteriography in a recent series of 707 cases: factors affecting outcome. Ann Vasc Surg. 1993;7:122–9.
30. Haynes B, Thorpe K, Raylor W, et al. Poor performance of ultrasound in detecting high-grade carotid stenosis (abstract). Can J Surg. 1992;35:446.
31. Daigle RJ, Stavros AT, Lee RM. Overestimation of velocity and frequency values by multi-element linear array Dopplers. J Vasc Technol. 1990;14:206–13.
32. Patel MR, Kuntz KM, Klufas RA, et al. Preoperative assessment of the carotid bifurcation: can magnetic resonance angiography and duplex ultrasonography replace contrast arteriography? Stroke. 1995;26:1753–8.
33. Huston J, Nichols DA, Luetmer PH, et al. MR angiographic and sonographic indications for endarterectomy. AJNR Am J Neuroradiol. 1998;19:309–15.
34. Belsky M, Gaitini D, Goldsher D, et al. Color-coded duplex ultrasound compared to CT angiography for detection and quantification of carotid artery stenosis. Eur J Ultrasound. 2000;12:49–60.
35. Anderson GB, Ashforth R, Steinke DE, et al. CT angiography for the detection and characterization of carotid artery bifurcation disease. Stroke. 2000;31:2168–74.
36. Back MR, Wilson JS, Rushing G, et al. Magnetic resonance angiography is an accurate imaging adjunct to duplex ultrasound scan in patient selection for carotid endarterectomy. J Vasc Surg. 2000;32:429–40.
37. Johnston DC, Goldstein LB. Clinical carotid endarterectomy decision-making. Neurology. 2001;56:1009–15.
38. Nederkoorn PJ, Mali WP, Eikelboom BC, et al. Preoperative diagnosis of carotid artery stenosis: accuracy of noninvasive testing. Stroke. 2002;33:2003–8.
39. MacKenzie KS, French-Sherry E, Burns K, et al. B-mode ultrasound measurement of carotid bifurcation stenoses: is it reliable? Vasc Endovasc Surg. 2002;36:123–35.
40. Serfaty JM, Chirossel P, Chevallier JM, Ecochard R, Froment JC, Douek PC. Accuracy of three-dimensional gadolinium-enhanced MR angiography in the assessment of extracranial carotid artery disease. AJR Am J Roentgenol. 2000;175:455–63.
41. White JE, Russell WL, Grer MS, Whittle MT. Efficacy of screening MR angiography and Doppler ultrasonography in the evaluation of carotid artery stenosis. Am Surg. 1994;60:340–8.
42. Turnipseed WD, Kennell TW, Turski PA, Acher CW, Hock JR. Combined use of duplex imaging and magnetic resonance angiography for evaluation of patients with symptomatic ipsilateral high-grade carotid stenosis. J Vasc Surg. 1993;17:832–9.
43. Riles TS, Eidelman EM, Litt AW, Pinto RS, Oldford F, Schwartzenberg GW. Comparison of magnetic resonance angiography, conventional angiography, and duplex scanning. Stroke. 1992;23:341–6.
44. Johnson MB, Wilkinson ID, Wattam J, Venables GS, Griffiths PD. Comparison of Doppler ultrasound, magnetic resonance angiographic techniques and catheter angiography in evaluation of carotid stenosis. Clin Radiol. 2000;55:912–20.

45. Link J, Brossmann J, Penselin V, Gluer CC, Heller M. Common carotid artery bifurcation: preliminary results of CT angiography and color-coded duplex sonography compared with digital subtraction angiography. AJR Am J Roentgenol. 1997;168:361–5.
46. Bray JM, Galland F, Lhoste P. Colour Doppler and duplex sonography and angiography of the carotid artery bifurcations. Prospective, double-blind study. Neuroradiology. 1995;37:219–24.
47. Bluth EI, Sunshinte JH, Lyons JB, et al. Power Doppler imaging: initial evaluation as a screening examination for carotid artery stenosis. Radiology. 2000;215:791–800.
48. Jackson MR, Chang AS, Robles HA, et al. Determination of 60% or greater carotid stenosis: a prospective comparison of magnetic resonance angiography and duplex ultrasound with conventional angiography. Ann Vasc Surg. 1998;12:236–43.
49. Walters GK, Jones CE, Meyd CJ, Cavaluzzi JA, Chachich BM. The role of carotid duplex ultrasonography in the therapeutic algorithm of extracranial carotid disease. J Vasc Technol. 1993;17:177–82.
50. Wardlaw JM, Chappell FM, Stevenson M, et al. Accurate, practical and cost-effective assessment of carotid stenosis in the UK. Health Technol Assess. 2006;10:iii–iv, ix–x, 1–182, Review.
51. Grant EG, Benson CB, Moneta GL, Alexandrov AV, Baker JD, Bluth EI, Carroll BA, Eliasziw M, Gocke J, Hertzberg BS, Katarick S, Needleman L, Pellerito J, Polak JF, Rholl KS, Wooster DL, Zierler E. Carotid artery stenosis: grayscale and Doppler ultrasound diagnosis – society of radiologists in ultrasound consensus conference. Ultrasound Q. 2003;19:190–8.
52. AbuRahma AF, Srivastava M, Stone PA, Mousa AY, Jain A, Dean LS, Keiffer T, Emmett M. Critical appraisal of the carotid duplex consensus criteria in the diagnosis of carotid artery stenosis. J Vasc Surg. 2011;53:53–60.
53. AbuRahma AF, Richmond BK, Robinson PA, et al. Effect of contralateral severe stenosis or carotid occlusion on duplex criteria of ipsilateral stenoses: comparative study of various duplex parameters. J Vasc Surg. 1995;22:751–62.
54. Spadone DP, Barkmeier LD, Hodgson KJ, et al. Contralateral internal carotid artery stenosis or occlusion: pitfall of correct ipsilateral classification. A study performed with color flow imaging. J Vasc Surg. 1990;11:642–9.
55. Forconi S, Johnston KW. Effect of contralateral internal carotid stenosis on the accuracy of continuous wave Doppler spectral analysis results. J Cardiovasc Surg. 1987;28:715–8.
56. Hayes AC, Johnston KW, Baker WH, et al. The effect of contralateral disease on carotid Doppler frequency. Surgery. 1988;103:19–23.
57. Beckett Jr WW, Davis PC, Hoffman Jr JC. Duplex Doppler sonography of the carotid artery: false positive results in an artery contralateral to an artery with marked stenosis. AJR Am J Roentgenol. 1990;155:1091–5.
58. Fujitani RM, Mills JL, Wang LM, et al. The effect of unilateral internal carotid arterial occlusion upon contralateral duplex study: criteria for accurate interpretation. J Vasc Surg. 1992;16:459–68.
59. Fisher M, Alexander K. Influence of contralateral obstructions on Doppler-frequency spectral analysis of ipsilateral stenoses of the carotid arteries. Stroke. 1985;16:846–8.
60. Bluth EI, Stavros AT, Marich KW, et al. Carotid duplex sonography: a multicenter recommendation for standardized imaging and Doppler criteria. Radiographics. 1988;8:487–506.
61. AbuRahma AF, Richmond BK, Robinson PA, Khan S, Pollack JA, Alberts S. Effect of contralateral severe stenosis or carotid occlusion on duplex criteria of ipsilateral stenoses: comparative study of various duplex parameters. J Vasc Surg. 1995;22:751–61.
62. Wyman RA, Mays ME, McBride PE, Stein JH. Ultrasound-detected carotid plaque as a predictor of cardiovascular events. Vasc Med. 2006;11:123–30.
63. Culebras A, Kase CS, Masdeu JC, et al. Practice guidelines for the use of imaging in transient ischemic attacks and acute stroke. A report of the Stroke Council, American Heart Association. Stroke. 1997;28:1480–97.
64. Lovelace TD, Moneta GL, Abou-Zamzam Jr AM, Edwards JM, Yeager RA, Landry GJ, Taylor Jr LM, Porter JM. Optimizing duplex follow-up in patients with an asymptomatic internal carotid artery stenosis of less than 60%. J Vasc Surg. 2001;33:56–61.
65. Lavensen GS. The carotid artery ultrasound reports: considerations in evaluation and management. J Vasc Ultrasound. 2004;28:15–9.
66. Roederer GO, Langlois MD, Jager MD, et al. The natural history of carotid arterial disease in asymptomatic patients with cervical bruits. Stroke. 1984;15:605–13.

# The Role of Color Duplex Scanning in Diagnosing Diseases of the Aortic Arch Branches and Carotid Arteries

8

Aravinda Nanjundappa, Gianluca Rigatelli, Clifford T. Araki, and Ali F. AbuRahma

**Abstract**

Duplex ultrasound plays an important role in the diagnosis of arterial and venous diseases in peripheral vasculature. However, the role of duplex ultrasound in the diagnosis of diseases of the aortic arch vessels and proximal carotid arteries is limited. Nevertheless, duplex ultrasound can provide direct and indirect clues to the diagnosis of ostial disease of the aortic arch vessels. The characteristics of the waveforms, direction of flow, and velocity can assist in the diagnosis of occlusive disease of the distal carotid arteries. We aim to describe the anatomy, essentials of duplex imaging, and diagnosis of aortic arch vessels in this chapter.

**Keywords**

Duplex ultrasound • Carotid artery • Innominate artery • Subclavian artery • Velocity Spectral broadening

## Introduction

Extracranial cerebrovascular disease is most commonly diagnosed at the carotid bifurcation/proximal internal carotid artery. While ultrasound is excellent at detecting the bifurcation lesion, it has been limited in its application to diseases in other cerebrovascular segments.

Atherosclerotic diseases in the truncal branches of the aortic arch typically occur at the origin of the branch vessels. The clinical consequences of these lesions include hypoperfusion and thromboembolic events that can impact the anterior or posterior cerebrovascular circulation and circulation to the upper extremities. Their potential for atheroembolic strokes in the anterior circulation and subclavian steal from the posterior circulation is sufficient for surgeons to consider intervention when significant lesions are detected [1].

The incidence of atherosclerotic disease in the branches of the arch is much lower than it is for the carotid bifurcation, but the incidence is not well documented. Studies performed in the 1960s–1970s estimated disease in the arch branches to account for no more than 17% of symptomatic extracranial cerebrovascular diseases [2–4]. In 1968, Hass et al. [5] reported a severe lesion in one or more of the aortic arch branches in one third of patients examined by cerebrovascular arteriography. In 101 autopsy patients, a similar percentage was ascribed to ulcerative disease in the arch branches, second only to the carotid sinus [6].

The incidence of arch lesions has not been systematically evaluated by arteriography, and ultrasound has not been considered sufficient to evaluate the arch and its branches. The lack of an adequate assessment has made the natural history of these lesions unclear, and indications for repair have not been well established. With endovascular surgery poised to

A. Nanjundappa, M.D., RVT, FACC, FSCAI (✉) • A.F. AbuRahma
Department of Surgery, Robert C. Byrd Health Sciences Center, West Virginia University, Charleston Area Medical Center, Charleston, WV, USA
e-mail: dappamd@yahoo.com

G. Rigatelli, M.D., Ph.D.
Department of Cardiovascular Diagnosis and Endoluminal Interventions, Rovigo General Hospital, Rovigo, Italy

C.T. Araki, Ph.D., RVT
Department of Medical Imaging Sciences, School of Health Related Professions, University of Medicine and Dentistry of New Jersey, Newark, NJ, USA

A.F. AbuRahma, D.F. Bandyk (eds.), *Noninvasive Vascular Diagnosis*,
DOI 10.1007/978-1-4471-4005-4_8, 

treat these once difficult lesions, the availability of a reliable noninvasive assessment of the arch lesion now becomes clinically significant.

There are no data available to indicate how many arch lesions are missed in a typical carotid ultrasound exam, and yet the perceived limitations of ultrasound testing may be due to technique more than hardware. New ultrasonic approaches to this poorly assessed structure should be made to extend the characterization of the extracranial cerebrovascular examination for the potential benefit of this subset of patients.

## Anatomy of the Aortic Arch and Brachiocephalic Veins

### Aortic Arch

To ultrasonically evaluate the arch and its branches, the orientation of the arch has to be recognized as it projects from the left ventricle to the descending aorta. The aorta ascends to the right of midline as it leaves the left ventricle. The pericardium attaches to the ascending aorta and pulmonary artery as they leave the heart, just beyond their origination. The arch itself becomes an extrapericardial structure. The aorta ascends from the heart to the right of the pulmonary artery. It arches around and above the right branch of the pulmonary artery, anterior to the trachea, and then forms an oblique trajectory from the right anterior mediastinum to the left posterior mediastinum. It forms the descending thoracic aorta to the left of the trachea and esophagus. As the descending aorta, it continues its course along the posterior wall of the chest, toward the left side of the vertebral column.

The aortic arch is approximately 4.5 cm in length. At 2.5–3 cm, it has a slightly larger diameter than the abdominal aorta that we are accustomed to seeing. Three truncal branches arise from the arch: the innominate artery (brachiocephalic trunk), the left common carotid artery, and the left subclavian artery (Fig. 8.1). All arise perpendicular to the flow axis of the arch and ascend through the mediastinum to carry blood to the upper extremities and head.

The innominate artery is the first and largest arch branch. It arises near midline, anterior to the trachea, and courses gently to the right. Just below the base of the right neck, it bifurcates to form the right subclavian and right common carotid arteries.

The left common carotid artery is typically the second branch from the aortic arch. Arising immediately after the innominate artery, it also originates in front of the trachea and curves gently toward the left side of the neck. Both the innominate and left common carotid arteries start near midline, and then curve gently laterally. The common carotid arteries course to the right and left of midline, where both right and left common carotid arteries approach the carotid bifurcation in a posterior position on either side of the trachea.

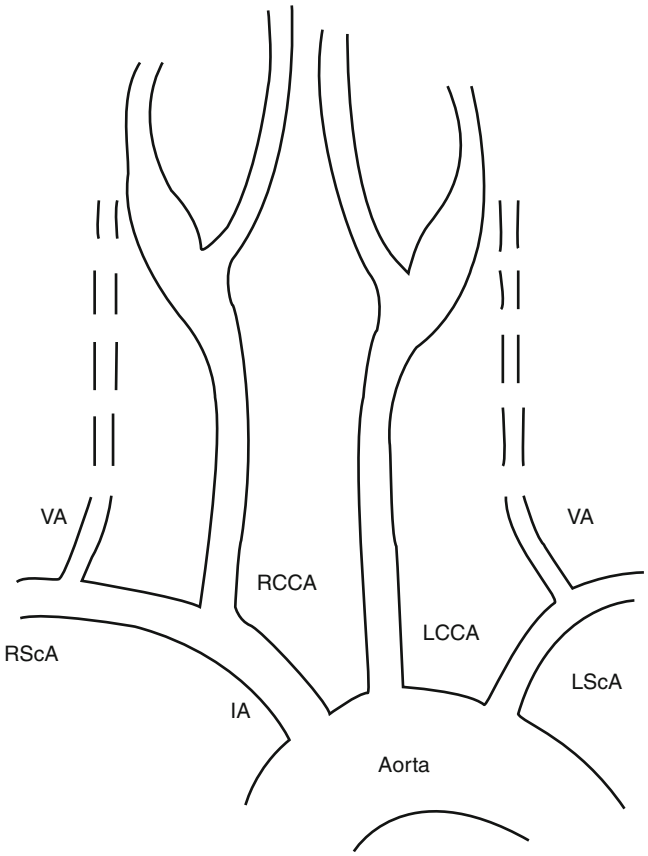


**Fig. 8.1** Aortic arch and its branches. *IA* innominate artery, *RScA* right subclavian artery, *VA* vertebral artery, *RCCA* right common carotid artery, *LCCA* left common carotid artery, *LScA* left subclavian artery

The left subclavian artery is the third arch branch, ascending toward the neck but bending laterally to course through the thoracic outlet. In some, the right subclavian artery may originate from the innominate slightly higher in the chest to take a more downward projection to enter the thoracic outlet.

The arch rises in the superior mediastinum fairly high in the chest, but lies protected by the sternum. The truncal branches also arise behind the sternum and sternoclavicular joints at about the level of the third and fourth thoracic vertebrae. This protected position makes a direct transthoracic ultrasonic approach to the arch impossible.

The basic branch anatomy is shared by two thirds (65%) of the population [7], and the remaining one third has a variant anatomy. The most frequent variant lies in a common origin shared by the innominate and left common carotid arteries, the so-called brachiocephalic branch or bovine configuration, which occurs in 27% of the population. Much less frequently, the vertebral artery originates from the aorta between the left common carotid and the left subclavian arteries (2–6% of cases). Rarely (less than 1%), the right

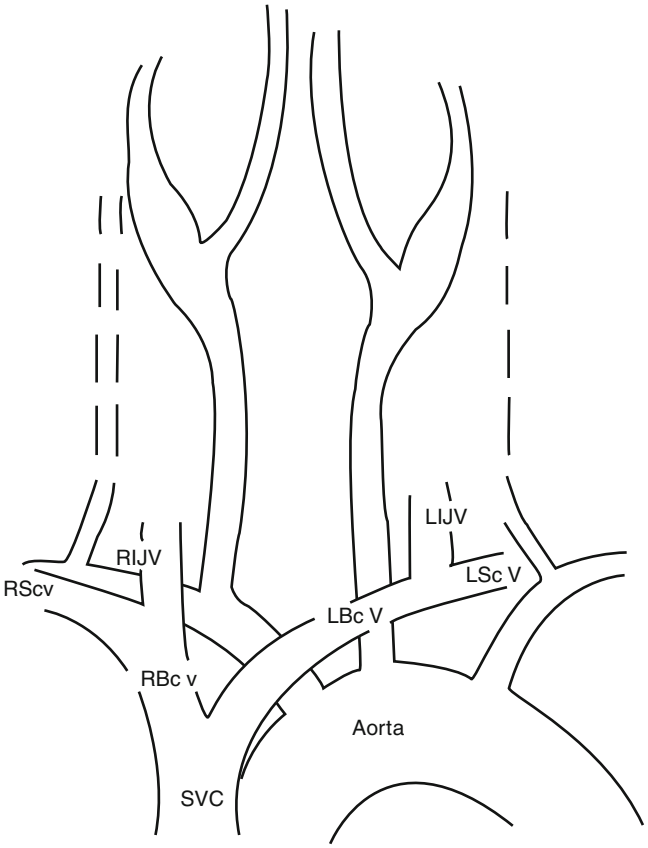


**Fig. 8.2** Brachiocephalic veins and superior vena cava. *RScV* right subclavian vein, *RIJV* right internal jugular vein, *RBcV* right brachiocephalic vein, *LBcV* left brachiocephalic vein, *LScV* left subclavian vein, *LIJV* left internal jugular vein, *SVC* superior vena cava

subclavian artery originates from the arch distal to the left subclavian, or the right vertebral originates from the right common carotid artery or the arch.

## Brachiocephalic Veins

The central veins demonstrate greater symmetry than the supra-aortic arteries (Fig. 8.2). The internal jugular veins of the neck and subclavian veins from the upper extremities are confluent, forming the right and left brachiocephalic veins. The external jugular veins also drain into the subclavian veins bilaterally, near the originations of the brachiocephalic veins. The right and left brachiocephalic veins converge to form the superior vena cava (SVC) at about the level of the aortic arch. The SVC lies to the right of the arch, causing a bit of asymmetry. The right brachiocephalic vein descends directly into the SVC as a short venous segment, but the left brachiocephalic vein is longer and sharply angulated because of the position of the SVC. The left brachiocephalic vein courses obliquely from the left internal jugular (IJ) vein to the right chest, lying anterior to the branch arteries of the arch. Both brachiocephalic veins converge to form the superior vena cava. Approximately 7 cm in length, the SVC is in contact with the pleura of the right lung, the trachea, and aorta. There are no valves in the brachiocephalic trunks or SVC.

## Imaging the Aortic Arch and Brachiocephalic Veins

The arch and branches are a neglected area that is seldom imaged with ultrasound because of dense ultrasound reflections produced by bone and lung air. It is, however, described as part of a standard echocardiographic assessment made through a suprasternal approach [8].

The suprasternal notch is the midline depression that lies at the base of the neck, between the sternum and larynx. Echocardiography uses the notch to visualize the ascending aorta, arch, and descending thoracic aorta as a means for evaluating the aorta for valvular insufficiency, dissection, aneurysm, or coarctation [9]. Though it is described as a standard echo approach, the image is often less than satisfactory and is seldom used in adult echo.

The echocardiographer uses a 2–5 MHz transducer to visualize the ascending aorta, arch, and descending aorta. The transducer produces a small footprint for the more superficial arch branches and is less suited for branch vessel assessment. For the neck, vascular sonographers use high-frequency (5–10 MHz) linear probes to image the extracranial cerebrovascular branches at the carotid bifurcation. The examination approaches the cervical carotid arteries from the lateral neck, alongside the sternocleidomastoid muscle. The scan typically ends centrally at the right common carotid origin and left common carotid artery at the neck base.

As a compromise, the midline, suprasternal approach should be our approach to the supra-aortic vessels, using a low-frequency curvilinear probe rather than the small footprint echo or the high-frequency linear probe. The obvious drawbacks to imaging the arch and its branches from this angle include the following: (1) Interference from the sternum and claviculae which severely limits access. The ultrasound beam is projected downward through a narrow acoustic window which limits the anterior-posterior projection by the sternum and neck. (2) The truncal arteries project directly toward the probe, and veins project directly away from the probe. The resulting B-mode echoes are weakly reflective and poorly illuminate the walls of the central branches. (3) Color Doppler compensates for the weak B-mode image, but the number of large vessel flows and color artifacts picked up from the bright echoreflective surfaces of the mediastinum and pleura produce a confusing image with large swaths of color.

To overcome these problems, recognizing the anatomy of the arch and brachiocephalic veins is important to scanning the central vessels. It is also important to maintain an orientation

that is based upon the known ultrasonic anatomy. The examination can be performed by first placing the curvilinear transducer above the sternum and positioning the probe to produce a panoramic view of both common carotid arteries and internal jugular veins at the base of the neck (Fig. 8.3). With this view as the reference point, the scan can be extended centrally by gray scale and color. The right common carotid artery will be seen to rapidly converge with the subclavian artery to become the innominate artery. On the left, the common carotid artery will be seen to simultaneously continue uninterrupted toward the arch. As the probe is projected centrally, both the innominate and left common carotid arteries will approach one another. The larger innominate artery will approach midline from the patient's right, and the left common carotid artery will course obliquely from the left. From further left, the left subclavian artery will course toward the arch from the clavicle.

The arteries and veins of interest lie in front of the trachea. Because the arch projects obliquely from right to left and anterior to posterior, the probe positioned for a transverse view of the innominate and left common carotid arteries will also capture the aorta in near transverse. The aorta will be seen in gray scale as a 2–3-cm pulsatile mass. By color, flow in the aorta will be notably disturbed. Flow in the innominate and left common carotid will be much more uniform and easily traced as tracks of color flow directed toward the probe. Both arteries can be interrogated by spectral Doppler as they approach the aorta.

Once the relative positions of the arteries are identified, the innominate artery (Fig. 8.4) and left common carotid artery (Fig. 8.5) may be imaged individually in the longitudinal view by rotating the ultrasound probe on the neck base to the left of midline.

The left subclavian artery may be the most difficult to follow. To visualize the subclavian, the transducer probe will be positioned above the clavicle, projecting the heel of the probe toward the left posterior aspect of the notch (Fig. 8.6). Ultrasound reflections will capture bright reflections from the pleura and left lung. Artifactual duplication of the left subclavian artery by B-mode and color could then result from mirror imaging reverberation (Fig. 8.6).

The subclavian artery should be identified as the color flow pattern that lies superficial to any color artifact. To avoid further confusion, the left subclavian artery could be followed from the axillary artery, below the clavicle, through the thoracic outlet to the subclavian artery.

Difficulties in imaging may be associated with configuration of the arch. The arch has been described in coiled and uncoiled configurations with the supra-aortic trunks originating from different points of the arch [10]. The better configuration positions the innominate on the right edge of the apex, and the left subclavian on the left edge. The take-off points, located on the superior wall of the arch, are optimally positioned for ultrasound imaging and endovascular cannulation. The more difficult imaging configuration occurs when the innominate artery arises from the aorta, before the apex, and its origin lies

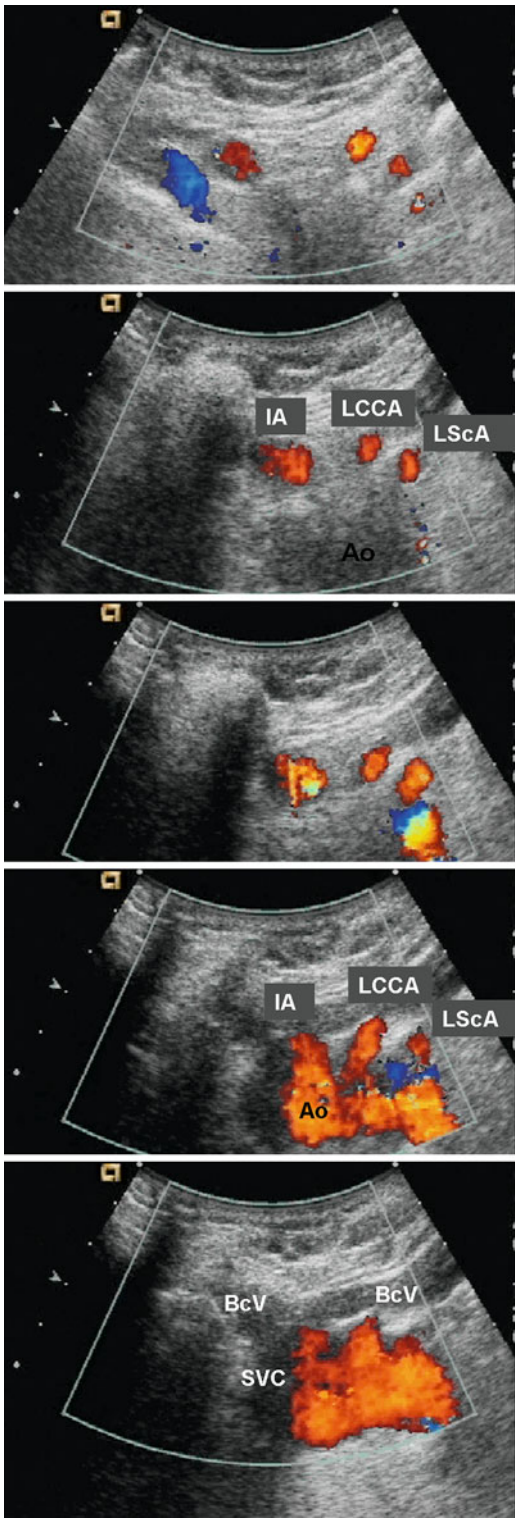


**Fig. 8.3** Imaging the aortic arch and its branches. Branches of the arch from the neck base (*top*) to aorta (*bottom*) are scanned with a 4-MHz curvilinear probe placed horizontally above the suprasternal notch. The innominate artery (*IA*), left common carotid artery (*LCCA*), and left subclavian artery (*LScA*) are shown in oblique slices. Scanning centrally, the supra-aortic branches enter the aorta (*Ao*). With greater probe angulation (*bottom*), the convergence of the right and left brachiocephalic veins (*BcV*) can be imaged to form the superior vena cava (*SVC*). The right sternoclavicular joint produces an acoustic shadow alongside the SVC

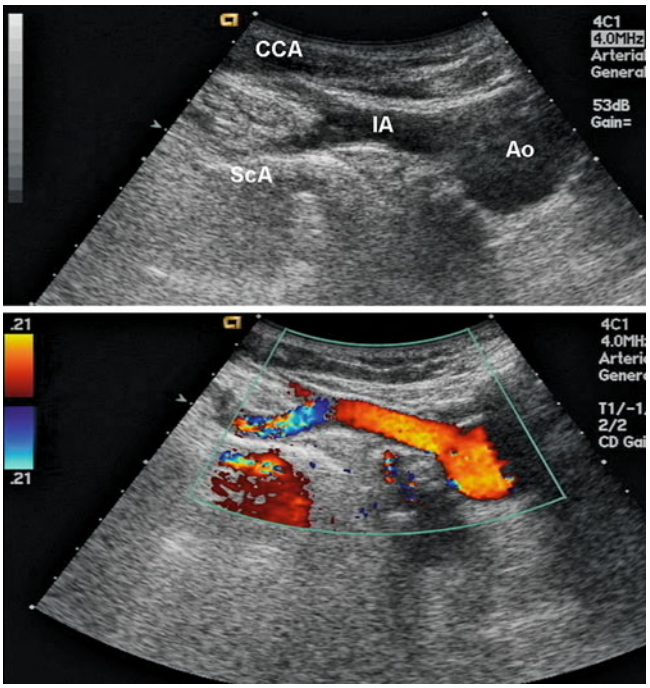


**Fig. 8.4** Longitudinal view of the innominate artery from the aorta (*Ao*) to the innominate artery (*IA*), right common carotid artery (*CCA*), and right subclavian artery (*ScA*), using a 4-MHz curvilinear probe. The probe is placed toward the left of midline. A shadow is cast from the left clavicle at the sternoclavicular joint. A mirror imaging reverberation artifact can be noted below the bright reflector and right subclavian artery

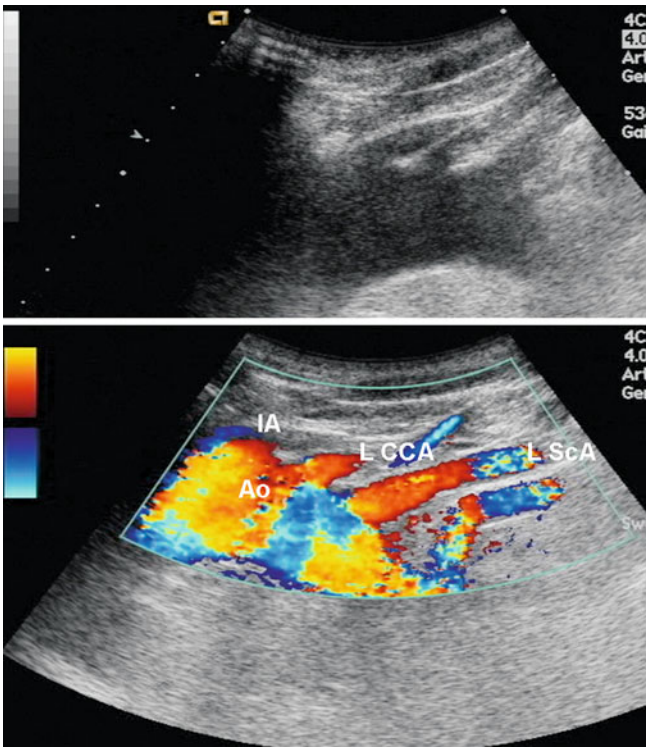


**Fig. 8.6** Longitudinal view of left subclavian artery (*LScA*) and originations of left common carotid artery (*LCCA*) and innominate artery (*IA*) from the aorta (*Ao*). A mirror imaging reverberation artifact can be noted below the bright reflector and left subclavian artery

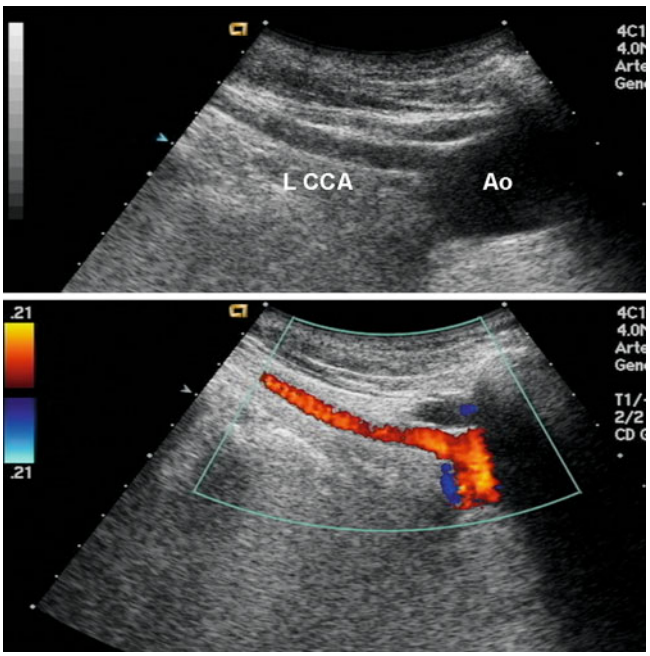


**Fig. 8.5** Longitudinal view of left common carotid artery (*LCCA*) and aorta (*Ao*) scanned with a 4-MHz curvilinear probe, demonstrating origin of the left common carotid artery, internal jugular vein, and shadowing from the sternoclavicular joint

below the level of the apex. In this "uncoiled" position, the left common carotid and subclavian arteries may be similarly displaced to the right. The deeper take-off of the innominate may prevent adequate ultrasonic visualization as well as increase the difficulty of endovascular cannulation.

Difficulties caused by anomalous anatomy, inaccessible origination of any arch branch due to coiling, or confusing color artifacts may be overcome by continually backtracking the scan to familiar territory at the neck base. Retracing the path of each branch should then allow normal anatomy to be separated from variants and artifacts. The lack of branches central to the innominate, left common carotid, and left subclavian should allow indirect spectral Doppler evidence of a hemodynamically significant stenosis or occlusion when the orificial lesion is not accessible.

## Brachiocephalic Veins

Imaging the brachiocephalic veins follows the same reference points as the arterial scan, with a view of the internal jugular veins bilaterally at the base of the neck. From that point, both veins can be followed to their confluence with the subclavian veins and traced to the superior vena cava

(Figs. 8.3 and 8.7). The left brachiocephalic vein lies anterior to the left common carotid and innominate arteries as it approaches the SVC. Visualization requires a greater anterior angulation and may be more difficult than visualizing the truncal arterial branches.

The superior vena cava (SVC) lies to the right of the aorta. This causes some dissymmetry between the right and left brachiocephalic veins that join to form the SVC. The right brachiocephalic vein is short and descends vertically to the SVC. The left brachiocephalic vein will be seen to curve from the patient's left to right as it descends centrally. It is approximately 6 cm in length and will be seen coursing anterior to the branch arteries of the arch. Because the right brachiocephalic vein and superior vena cava are in contact with the pleura of the right lung, there may be substantial color artifact that must be sorted out to identify the confluence.

## Using Color Flow to Assess the Central Vessels

B-mode imaging does not provide an optimal view of the great vessels, and color imaging is important for confirming the relevant structures and guiding the spectral Doppler interrogation. Advantages and limitations of color flow imaging are worth discussing.

Color Doppler technology is the main form of color flow imaging used in commercial instrumentation. Activation of the color Doppler mode displays flow-related color within the borders of a box that is superimposed on the B-mode image. Color Doppler slows the frame rate. While B-mode information can be acquired from single pulses, color Doppler information for a scan line requires multiple insonation pulses. The number of pulses required to collect the Doppler information is called a pulse train or packet [11]. More pulses in a packet provide a better estimate of flow velocities but require more time. Hence, turning the color on decreases the frame rate.

The frame rate also decreases because the color is written within a large number of color gates that are present in the color box. While spectral Doppler uses one gate in one scan line to sample the Doppler shifted frequencies, color Doppler packs the color box with multiple gates in multiple scan lines to display colorized flow anywhere within the box. The vertical dimension of the box determines the number of sample gates along each scan line, and the lateral dimension determines the number of scan lines [12]. The frame rate decreases because the same calculation is made for all gates in the box, whether color is applied to the pixel or not. The operator is able to select the color box size and, to a certain extent, the number of gates in a scan line and the number of scan lines. This affects the size of the color pixel and allows the operator to trade off color resolution for frame rate [13].

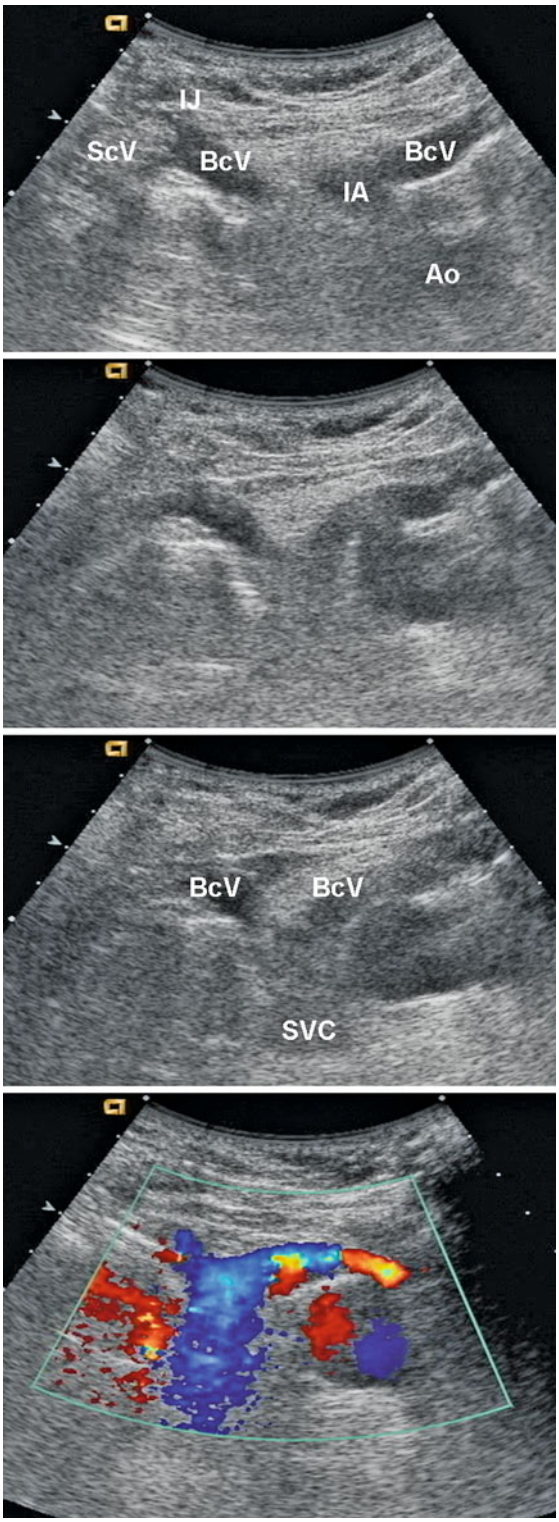


**Fig. 8.7** Imaging the brachiocephalic veins and superior vena cava. From the neck base (*top*), the right subclavian vein (*ScV*) and right internal jugular vein (*IJ*) can be seen to enter the right brachiocephalic vein (*BcV*). The left brachiocephalic vein crosses from left to right anterior to the innominate artery (*IA*), above the aorta (*Ao*). When scanning centrally (*bottom*), the confluence of both brachiocephalic veins (*BcV*) can be seen to form the superior vena cava (*SVC*)

## Color Doppler

Color adds an obvious advantage to standard B-mode/spectral Doppler duplex if it rapidly identifies blood flow and guides the placement of the spectral Doppler. Limitations in color may hinder diagnosis and extend the examination time if it is used as a crutch rather than an aid. Color may:

- Overwhelm subtle grayscale shadings of the B-mode image that may be more important than the color information.
- Slow frame rate to below real-time imaging. Scan times will improve if most of the scan is performed in B-mode, and color is activated only when necessary.
- Mislead the inexperienced sonographer. Color sensitivity adjustments are subjective, experience-based, and instrument-specific. Color registration may be difficult to achieve.
- Have difficulty demonstrating the presence of flow. Echoes received from moving red blood cells are much weaker than the reflections returned for the B-mode image. A relatively good B-mode image of an artery may not be matched by a good velocity signal by color or spectral Doppler simply because of a lack of adequate signal strength. Overreliance on the presence or absence of color may be misleading.
- Overflow the edge of the vessel. The size of a color pixel is variable and can be much larger than the grayscale pixel. Color overflowing the vessel edge may misrepresent the tightness of a stenosis.
- Demonstrate flow where there is none. A mirror image reverberation artifact can occur when a bright reflector lies below the insonated vessel. The result is a false duplication of flow by spectral and color Doppler below the bright interface. A reverberation color artifact may also occur within bright stationary reflectors with the vibration of stiff calcified surfaces.

To the inexperienced sonographer who does not recognize the potential pitfalls and necessary adjustments for optimization, color can be a major frustration. This is particularly true when the dependence on color has limited the person's recognition of grayscale morphology and spectral Doppler waveform characteristics. However, once the limits are recognized, there is a distinct advantage to using color to guide the examination. Among the benefits are as follows:

- Setting the pulse repetition frequency (PRF) at about the expected average velocity will provide good luminal color fill.
- Higher-velocity flows produce color aliasing, which displays a mixture of hues in adjacent pixels. Within the area of aliasing, color mixing occurs over the top of the color bar scale. There is a scattering of color progressions from light red to light blue that occurs through the unsaturated hues, passing through white. Aliasing can be distinguished from physiologic flow reversals, which cause the color to change in adjacent pixels from uniformly saturated reds to saturated blues, passing through black rather than white.
- Turbulence can produce a color bruit. Flow turbulence produces a high-frequency vibration in the vessel wall. This vibration is transmitted to the skin surface as an audible bruit or palpable thrill and is picked up by the color Doppler as an intense speckling of color that spills over the wall of the vessel around the point of greatest turbulence.
- If a stenosis is suspected, possibly with color aliasing or bruit, the point of highest velocity can be located by increasing the PRF. With a tight stenosis or arteriovenous fistula, it is not unusual to find a color hot spot in a tight stenosis or arteriovenous fistula that is continuously lit, indicating continuous forward flow across the stenosis. This is presumably the result of a pressure drop that is maintained throughout the cardiac cycle, indicating that the pressure distal to the stenosis remains lower than diastolic pressure.
- Color is helpful for distinguishing ulcerations from hypoechoic plaque. For this purpose, it would be worth increasing spatial resolution over frame rate to increase the number of sample gates and decrease the size of the color pixel. It is also advisable to decrease the PRF, increase the filter, and increase persistence. The latter adjustments will detect the slower flows filling the ulcerations and smooth the color fill throughout the cardiac cycle.

Through these characteristics, color flow imaging provides an excellent adjunctive modality for assessing the central vessels of the chest. The relatively simple branch anatomy of the large vessels, the lack of potential small branch collaterals, and the assessment made distal to an arterial stenosis or occlusion make the evaluation more straightforward.

## Clinical Role of Color Duplex Ultrasound in Diagnosing Arch Vessels

Despite the limitations of duplex ultrasound in imaging the aortic arch vessels, it can assist in diagnosing ostial lesions [14]. These include ostial lesions of the innominate artery, left common carotid artery, and left subclavian artery. Ultrasound evaluation of the arch vessels should include both gray scale and Doppler-derived velocity waveforms. The grayscale images can illustrate the presence of plaque, calcification, and thrombus. The changes and density of the mosaic pattern of color flow and spectral waveforms can be indicative of hemodynamically significant stenosis [15].

The limited roles of duplex ultrasound in the evaluation of the arch vessels include:

- Ostial involvement of the arch vessels seen in patients with vasculitis such as Takayasu's arteritis.
- Occlusions and stenosis of the ostial lesions in arch vessels in patients with atherosclerosis.
- Acute type A aortic dissection of the aorta, which may involve the arch vessels.

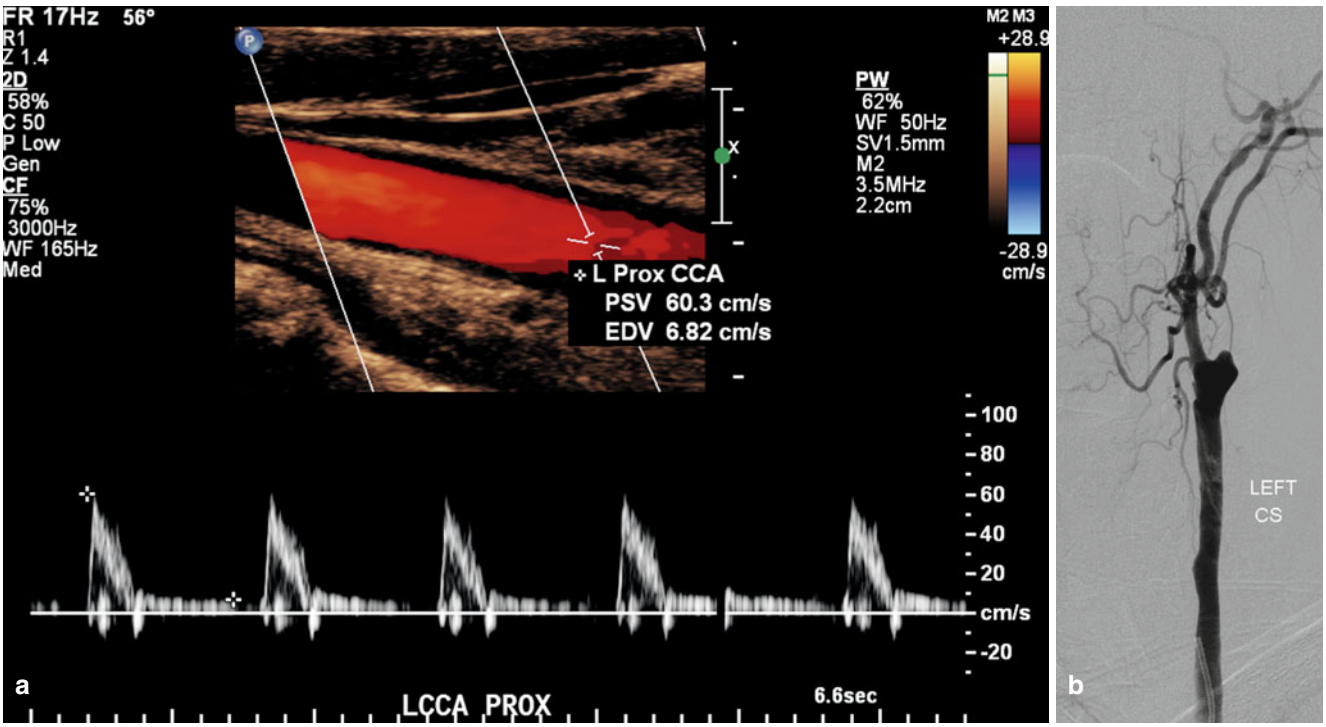


**Fig. 8.8** (**a**) The left common carotid artery duplex showing the pattern of the external carotid artery. This patient has an occluded left internal carotid artery and a patent left external carotid artery. (**b**) Angiogram showing left internal carotid artery total occlusion and a patent left external carotid artery

- Brachiocephalic vein stenosis, which may be associated with patients with multiple sclerosis. Color duplex ultrasound in these patients may aid in diagnosing ostial brachiocephalic and jugular vein stenosis.

It is always imperative to image arch vessels bilaterally to study the flow characteristics. The flow dynamics of one arch artery may be influenced by the status of the contralateral artery. Occlusion or severe stenosis of the common carotid artery of one side can result in compensatory increased flow in the contralateral vessel [15]. The resistive index of such severely diseased common carotid arteries may decrease and aid in diagnosis [16]. Such a compensatory mechanism leads to overestimation of the carotid artery stenosis on the patent side. Thus imaging with the classic intra-arterial angiogram remains the gold standard technique for confirming the severity of stenosis in these patients. The images in this section will be accompanied by confirmatory angiograms.

## Ostial and Proximal Common Carotid Artery Lesions

Traditionally, Doppler images are focused at prelesion, lesion, and postlesion to determine severity. However, in the ostial location, prestenotic and stenotic areas are difficult to image, but the poststenotic images are helpful. A normal common carotid artery waveform should demonstrate a low-resistance flow pattern and an end-diastolic velocity above 0 cm/s. The spectral flow pattern of the common carotid artery is usually a mixture of both internal carotid artery and external carotid artery characteristics. A normal waveform will be of a triphasic nature, a moderate lesion will show a biphasic waveform, and a severe stenosis will show a monophasic pattern. Imaging of the common carotid artery with duplex ultrasound can give indirect clues to an occluded internal carotid artery. The common carotid artery flow pattern will follow the attributes of the internal carotid artery or external carotid artery (high-resistance or low-resistance pattern), depending on the patent vessel (Fig. 8.8a, b).

There are no clear guideline-based criteria to define the severity of common carotid artery stenosis. A peak systolic velocity of >125 cm/s is suggestive of >50% stenosis in the common carotid artery (Fig. 8.9a, b) [17]. A focal-increased velocity in the common carotid artery with poststenotic turbulence is probably indicative of severe ostial stenosis. B-mode imaging may show plaque and/or calcification with spectral broadening. A significant lesion of the common carotid artery will result in an elevated velocity on the contralateral side and elevation of the end-diastolic velocity. Such a common carotid artery lesion will reduce the flow and velocity in the internal carotid artery and underestimates the severity of stenosis. Unilateral stenosis is usually caused by atherosclerosis, and when bilateral ostial common carotid artery lesions are seen, the differential diagnosis should include Takayasu's arteritis. Bilateral common carotid arteries

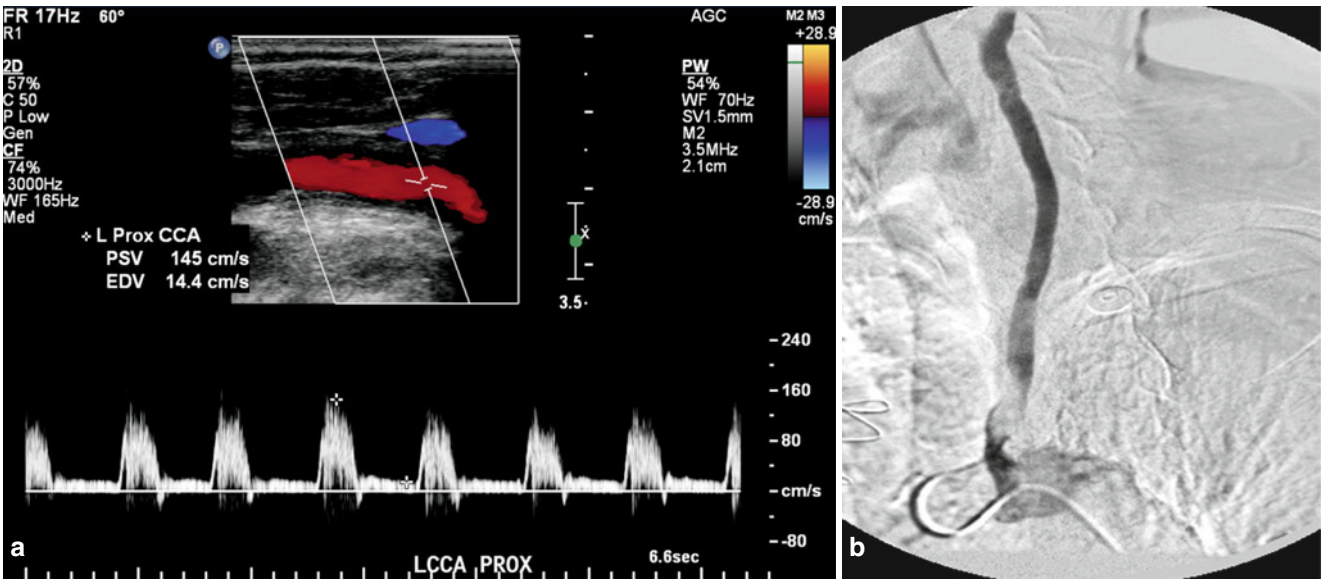


**Fig. 8.9** (**a**) Elevated velocity in the left common carotid artery. (**b**) Confirmatory angiogram shows ostial stenosis of the left common carotid artery

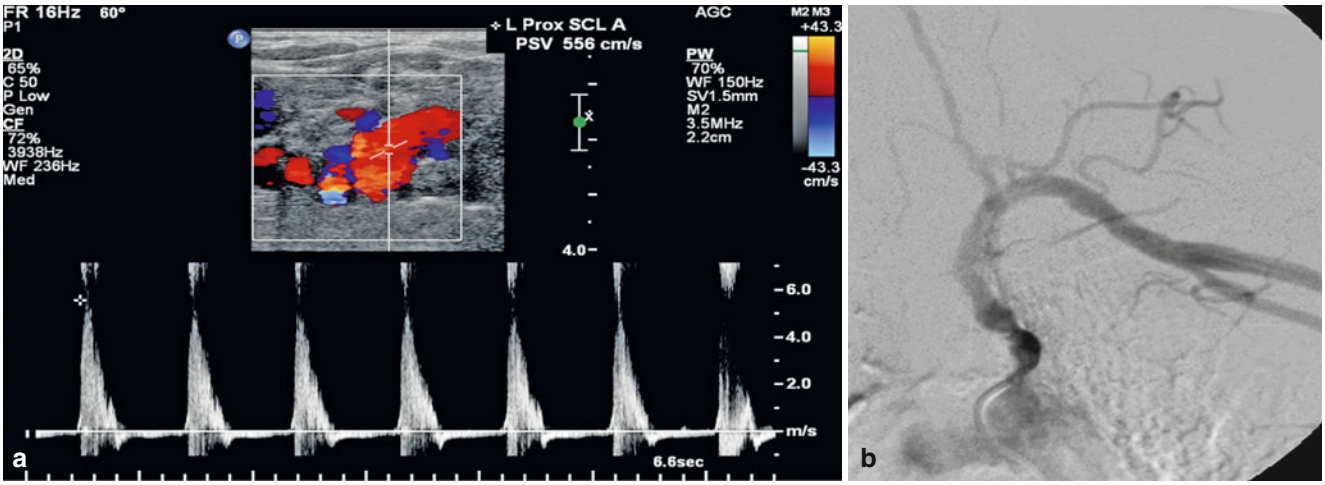


**Fig. 8.10** (**a**) Left subclavian artery in proximal segment shows increased velocity with aliasing. (**b**) Angiogram showing severe stenosis of the ostial left subclavian artery

showing a low flow signal may indicate severe aortic stenosis or a low myocardial function state.

## Occluded Common Carotid Artery

An occluded common carotid artery lesion will result in a dampened monophasic waveform with low velocity in the proximal common carotid artery and a slow rise to peak systole. This is associated with poststenotic dilatation and poststenotic turbulence in color flow. Confirmation of such an ostial occlusion can be seen by imaging the internal carotid artery. The internal carotid artery duplex may show no flow, minimal diastolic flow, or reversal of flow in ipsilateral common carotid arteries [18].

## Ostial Left Subclavian Artery Stenosis and Occlusion

A >50% stenosis of the ostial left subclavian artery is considered to be hemodynamically significant stenosis. Such stenosis will demonstrate increased velocity, biphasic or monophasic waveforms, and poststenotic turbulence (Fig. 8.10a, b). An ostial occlusion may demonstrate a low-velocity dampened monophasic waveform. The poststenotic occlusion is also accompanied by turbulence, and an additional gray scale may show thrombus. Further imaging of the vertebral artery in patients with severe left subclavian artery stenosis includes reversal of flow in the vertebral artery [19].

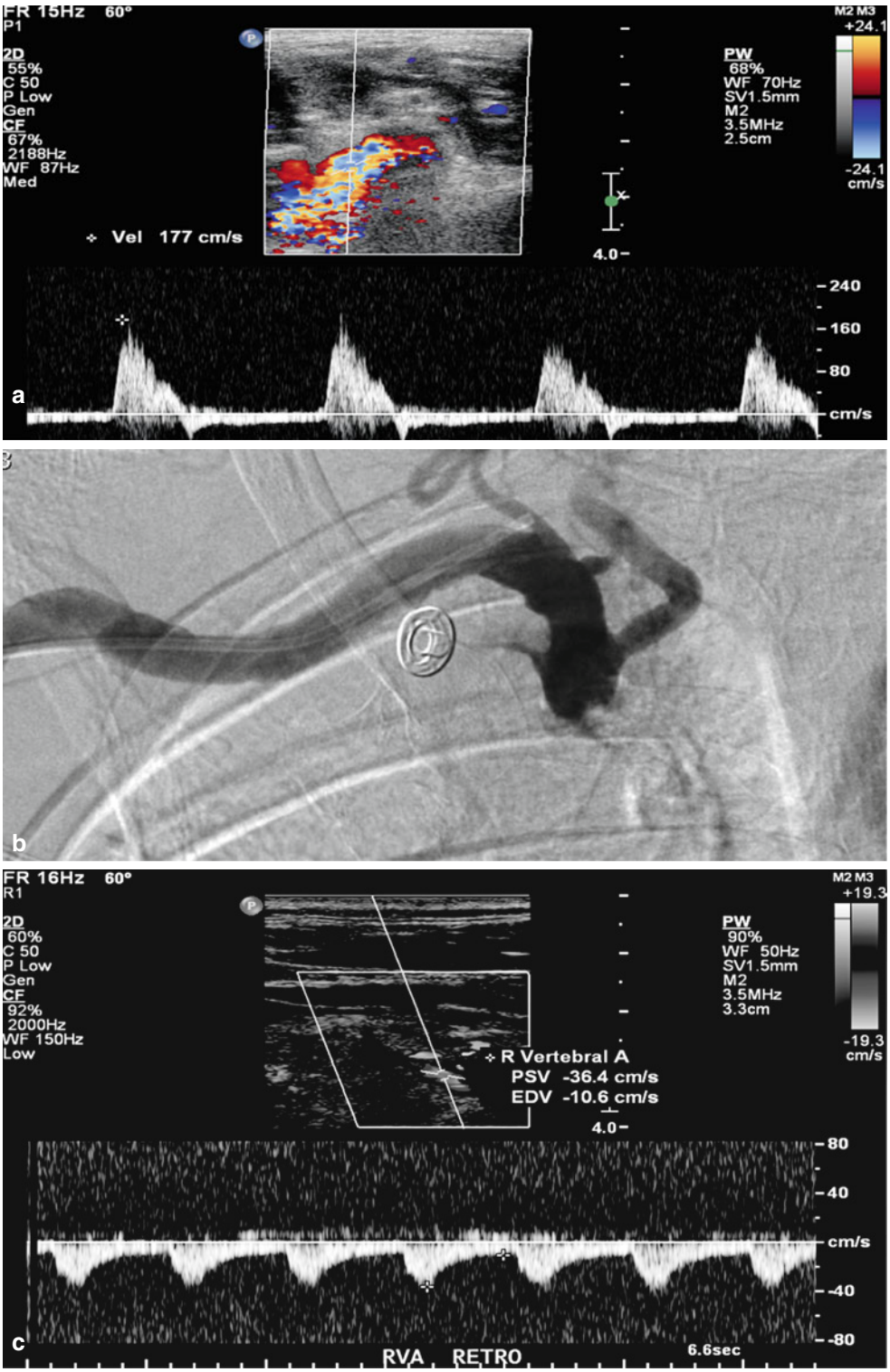


**Fig. 8.11** (**a**) Right subclavian artery showing mosaic flow pattern and biphasic wave pattern in a patient with severe innominate artery stenosis/occlusion. (**b**) Angiogram showing occluded right innominate artery. (**c**) Right vertebral artery showing reversal of flow

## Innominate Artery Stenosis or Occlusion

Ostial innominate lesions are difficult to image; however, indirect clues from duplex ultrasound are helpful. Severe innominate artery stenosis will result in low velocity and a dampened monophasic or a biphasic pattern in the subclavian artery and common carotid artery (Fig. 8.11a–c). The right vertebral artery also will show reversal of flow.

## Type A Dissection of the Aorta Involving the Ostium of the Arch Vessels

Acute aortic dissection can propagate to involve the ostium of the arch vessels, resulting in cerebral ischemia. CT and MR angiograms that are done to diagnose arch vessel involvement carry a very high specificity and sensitivity. However, color duplex ultrasonography may have a limited role in diagnosis

at bedside, especially in the emergency room. The color duplex ultrasound can show narrowing of the true lumen and dual flow separation. Additional findings may include reduced flow, dissection flap, and possible thrombus.

### Conclusions

The prevalence and clinical significance of arch branch disease will only be recognized through routine evaluation. Unfortunately, suprasternal ultrasonic imaging of the aortic arch and brachiocephalic veins will probably not be a routine part of the standard carotid evaluation. The use of color duplex ultrasonography in the diagnosis of aortic arch vessels may be limited. However, combination of data from gray scale, duplex velocity, and spectral characteristics can aid in the diagnosis of ostial lesions and stenosis of the arch vessels. It can also be useful in identifying an arch lesion that is suggested by flow disturbances in the common carotid artery, flow reversals in the vertebral artery, or asymmetrical brachial pressures. Identifying these lesions at the time of a cerebrovascular ultrasound examination can be especially important now that catheter-based intervention may be an easy next step.

Suprasternal imaging of the brachiocephalic veins may also be a valuable tool for an upper extremity venous examination, which tends to be limiting above the clavicle. Ultrasonic imaging may even be useful in determining the placement of central venous catheters.

Used correctly, color Doppler is capable of greatly improving the scan time for a cerebrovascular examination and can be critical for the examination of the aortic arch branches and the quality of a difficult examination. It is still an adjunctive component of the examination, and for the typical patient, color flow imaging may not add to the final outcome.

## References


1. Berguer R. Reconstruction of the supraaortic trunks and vertebrobasilar system. In: Moore WS, editor. Vascular surgery: a comprehensive review. 6th ed. Philadelphia: W.B. Saunders Co; 2002. p. 627–42.
2. Tyras DH, Barner HB. Coronary-subclavian steal. Arch Surg. 1977;112:1125–7.
3. Fields WS, Lemak NA. Joint study of extracranial arterial occlusion. Subclavian steal – a review of 168 cases. JAMA. 1972;222:1139–43.
4. Hadjipetrou P, Cox S, Piemonte T, Eisenhauer A. Percutaneous revascularization of atherosclerotic obstruction of aortic arch vessels. J Am Coll Cardiol. 1999;33:1238–45.
5. Hass WK, Fields WS, North RR, et al. Joint study of extracranial arterial occlusion-II: arteriography, techniques, sites, and complications. JAMA. 1968;203:159–64.
6. Khatibzadeh M, Sheikhzadeh A, Gromoll B, Stierle U. Topographic pattern of advanced atherosclerotic lesions in carotid arteries. Cardiology. 1998;89:235–40.
7. Uflacker R. Thoracic aorta and arteries of the trunk. In: Uflacker R, editor. Atlas of vascular anatomy: an angiographic approach. Baltimore: Williams & Wilkins; 1997. p. 143–88.
8. Allen MN. The transthoracic exam. In: Allen MN, editor. Echocardiography. 2nd ed. London: Lippincott, Williams & Wilkins; 1999. p. 181–206.
9. Peters PJ. Echocardiographic evaluation of the aorta in echocardiography. In: Allen MN, editor. Echocardiography. 2nd ed. London: Lippincott, Williams & Wilkins; 1999. p. 599–614.
10. Eisenhauer AC. Subclavian and innominate revascularization: surgical therapy versus catheter-based intervention. Curr Interv Cardiol Rep. 2000;2:101–10.
11. Zagzebski JA. Color Doppler and color flow imaging. In: Essentials of ultrasound physics. St Louis: Mosby; 1996. p. 109–22.
12. Hedrick WR, Hykes DL, Starchman DE. Chapter7, Color-flow imaging in ultrasound physics and instrumentation. 3rd ed. St. Louis: Mosby; 1995. p. 162–77.
13. Miele FR. Doppler. In: Miele FR, editor. Ultrasound physics and instrumentation, vol 2. Miele Enterprises, Lakeland, FL LLC; Forney, TX; 2003. p. 7–28.
14. Gorican K, Chochola M, Varejka P, Bartůněk P. Value of duplex ultrasound examination of the proximal part of the common carotid artery. Cas Lek Cesk. 2005;144 Suppl 1:27–9.
15. Mitchell EL, Moneta GL. Chapter 9, Ultrasound assessment of carotid stenosis. In: Introduction to vascular ultrasonography. 5th ed. Philadelphia: Elsevier Saunders; 2004. p. 172–87.
16. Fugitani RM, Mills JL, Wang LM, Taylor SM. The effect of unilateral internal carotid arterial occlusion upon contra lateral duplex study: criteria for accurate interpretation. J Vasc Surg. 1992;16:459–67; discussion 467–8.
17. Shakeri AB, Zarrintan S, Shakeri-Bavil M. The diagnostic value of the resistivity index of the common carotid arteries in severe internal carotid artery stenosis. Folia Morphol (Warsz). 2008;67(3):175–8.
18. Roederer GO, Langlois YE, Jager KA, et al. A simple spectral parameter for accurate classification of severe carotid artery disease. Bruit. 1989;3:174–8.
19. Talbot SR, Zwibel WJ. Chapter16, Assessment of upper extremity arterial occlusive disease. In: Introduction to vascular ultrasonography. 5th ed. Philadelphia: Elsevier Saunders; 2004. p. 297–323.

# Vertebral Artery Ultrasonography

9

Jessica Kepplinger, Kristian Barlinn,
and Andrei V. Alexandrov

**Abstract**

Our ability to diagnose and understand the mechanisms of the vertebrobasilar ischemia is less developed compared to the anterior circulation vessels. Fewer validation studies are available for diagnostic criteria of lesions in the posterior circulation, and generally the accuracy parameters for vertebral ultrasound are less specific than those of carotid examinations. An ultrasound examination of the extracranial portions of the vertebral artery constitutes an inexpensive and widely available screening method (being a mandatory part of a carotid duplex examination) to diagnose atherosclerotic disease and a variety of other findings and to further identify candidates for more expensive or invasive diagnostic evaluations. Furthermore, vertebral ultrasonography can help determine the pathogenic mechanism of an ischemic stroke in the emergency room and can lead to an early initiation of a mechanism-specific stroke treatment or prevention. Extracranial vertebral duplex examination should be performed in conjunction with transcranial Doppler examination in patients with stroke and transient ischemic attacks. The aim of this chapter is to describe the methods of vertebral ultrasonography, practical criteria for interpretation, and relevance of these findings to patient management.

**Keywords**

Vertebral artery ultrasonography • Acute stroke • Cerebral ischemia • Noninvasive vascular imaging

J. Kepplinger, M.D.
Department of Neurology, Dresden University Stroke Center,
University of Technology Dresden,
Dresden, Saxony, Germany

K. Barlinn, M.D
Department of Neurology, Dresden University Stroke Center,
University of Technology Dresden,
Dresden, Saxony, Germany

Department of Neurology, Comprehensive Stroke Center,
University of Alabama at Birmingham Hospital,
RWUH M226, 619 19th Street South,
Birmingham, AL 35249-3280, USA

A.V. Alexandrov, M.D. (✉)
Department of Neurology, Comprehensive Stroke Center,
University of Alabama at Birmingham Hospital,
RWUH M226, 619 19th Street South,
Birmingham, AL 35249-3280, USA
e-mail: avalexandrov@att.net

## Introduction

The vertebrobasilar arterial system provides approximately 20% of the total cerebral blood flow, and after the carotid circulation, it is a common location of acute ischemic strokes [1]. Our ability to diagnose and understand the mechanisms of the vertebrobasilar ischemia is less developed compared to the anterior circulation vessels. Fewer validation studies are available for diagnostic criteria of lesions in the posterior circulation, and generally the accuracy parameters for vertebral ultrasound are less specific than those of carotid examinations [2–18]. Nevertheless, examination of the precerebral vertebral arteries (VA) is a required component of what is commonly referred to as carotid duplex examination, while insonation of the terminal vertebral arteries and the basilar artery is an integral part of a complete transcranial Doppler (TCD) testing (see Chap. 10).

A.F. AbuRahma, D.F. Bandyk (eds.), *Noninvasive Vascular Diagnosis*,
DOI 10.1007/978-1-4471-4005-4_9, 

An ultrasound examination of the extracranial portions of the VA constitutes an inexpensive and widely available screening method to diagnose atherosclerotic disease and a variety of other findings and to further identify candidates for more expensive or invasive diagnostic evaluations. Extracranial ultrasound can differentiate normal from diseased arteries, identify all categories of the stenosis, localize the disease process including occlusions, detect progression of the disease, identify the likely source of cerebral embolism, and assess collateral circulation to maintain cerebral blood flow. Furthermore, vertebral ultrasonography can help determine the pathogenic mechanism of an ischemic stroke in the emergency room and can lead to an early initiation of a mechanism-specific stroke treatment or prevention.

Vertebral ultrasonography allows segmental assessment of the VA often obscured by transverse processes of the vertebrae and deep location of the VA's origin. Mastering cerebrovascular ultrasound requires knowledge of anatomy, physiology of cardiovascular and nervous systems, fluid dynamics, and pathological changes in a variety of cerebrovascular disorders as well as basic ultrasound physics and instrumentation.

The aim of this chapter is to describe the methods of vertebral ultrasonography, practical criteria for interpretation, and relevance of these findings to patient management. Rapid bedside evaluation by a skilled sonographer with a portable ultrasound unit is an excellent screening test that can provide an immediate impact on patient management at a lower cost and no time delays compared to other imaging methods.

## Anatomy of the Vertebrobasilar Arterial System

For interpretation of a vascular ultrasound examination, it is necessary to think in three dimensions in terms of the vessel being investigated with respect to transducer position. It is helpful to imagine how this arterial segment would look on an angiogram [19]. Therefore, we strongly encourage those learning and interpreting ultrasound to be familiar with cerebral angiograms since angiography is the gold standard for assessment of accuracy of ultrasound testing.

The VA is divided into four segments, of which segments V0–V3 represent the extracranial portions, whereas V4 forms the intracranial portion. Interestingly, approximately 75% of the population have asymmetric vertebral arteries with one dominant VA, whereas in about 15% of the population, one of the vertebral arteries is less than 2 mm in diameter (hypoplastic VA) [20]. The V0 segment constitutes the origin of the VA, which usually takes off at right angles from both subclavian arteries (right VA may arise from the brachiocephalic trunk). The V1 segment passes the pre-vertebrae tissue and enters the bony canal at the fifth or sixth cervical vertebrae. The V2 segment courses cranially through the transverse foramina of the cervical vertebrae and ends where the VA exits the axis (usually at the C1 level). From that point, the V3 segment extends to the entry into the spinal canal, from where the V4 segments run intracranially and join together to form the basilar artery. The basilar artery courses for about 3 cm or more before terminating in the posterior cerebral arteries, which make up the posterior portion of the circle of Willis (Fig. 9.1).

## Extracranial Duplex Ultrasound Examination Technique and Scanning Protocol

The extracranial duplex examination allows assessment of the VA mid-cervical portion (V2), the proximal VA and its origin (V0/V1), and the most distal portion accessible on the neck (V3). A linear transducer with 4–7-MHz frequency range is commonly used. To optimize the gray scale image on B-mode, set the dynamic range to 40–50 dB, and the time-gain compensation (TGC) as appropriate to the depth of the vertebral arteries. The B-mode image helps with the assessment of the diameter of the VA (which is usually about 3–4 mm). It may also detect atherosclerotic plaque, intraluminal clots, or even a double lumen in case of an arterial dissection. However, these findings are less prevalent than in patients with carotid artery disease.

## Imaging in the Longitudinal Plane

Patients should be placed in a supine position with the neck extended. To find the VA, first visualize the common carotid artery in a longitudinal projection on B-mode with transducer position anterior to the sternocleidomastoid muscle. Slide the probe posteriorly to image one or more levels of the V2 segment of the VA as it courses through the transverse processes of the vertebrae ("acoustic shadows") (Fig. 9.1). Confirm that the direction of flow in the VA is the same as the common carotid artery. Then trace the V2 segment proximally and "heel-toe" the probe above the clavicle to image the pre-vertebrae portion and the origin of the VA as it arises from the SA. It is important to examine this part as V0/V1 is the most common site of atherosclerotic disease [21]. Finally, follow the V2 segment of the VA more distally trying to visualize the V3 segment as it surrounds the axis. However, direct assessment of the V3 segment may be technically difficult, and the diagnosis of vertebral obstruction at this level is based on color-flow and Doppler findings proximal or distal to this

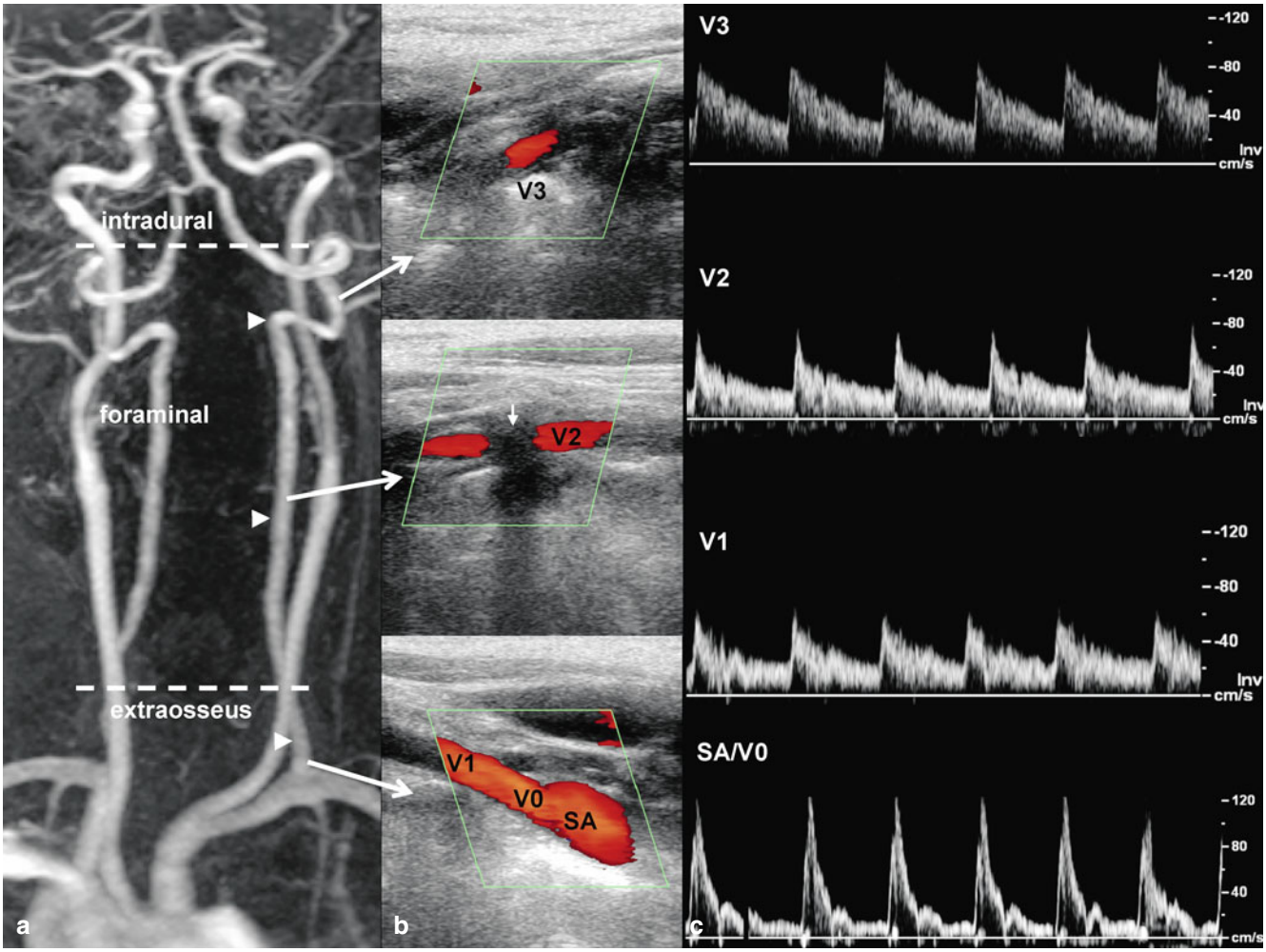


**Fig. 9.1** (**a**) Rotated contrast-enhanced 3D MR angiogram of cervical arteries. The *arrowheads* indicate the right VA. (**b**) Longitudinal plane of the VA (V0 through V3 segments) with superimposed color flow. Note the acoustic shadow of the transverse process between the V2 segments (*small arrow*). (**c**) Doppler spectra depict characteristic waveforms for each VA segment. Note the higher resistance and pulsatility in the VA origin due to proximity to the subclavian artery (*SA*) as opposed to the low-resistance waveforms in more distal VA segments

segment (Figs. 9.1 and 9.2). If color or power flow images are difficult to obtain, spectral interrogation of areas with typical B-mode appearance of surrounding bony structures should still be performed.

## Color-Flow Ultrasound Evaluation of Flow Dynamics

Choose the appropriate color pulse repetition frequency (PRF) by setting the color velocity scale for the expected velocities in the vessel. For normal adult arteries, the peak systolic velocity range is usually between 40 and 50 cm/s. The zero baseline of the color bar is set at approximately two-thirds of the range with the majority of frequencies allowed in the red direction (for flow toward the brain). Adjust the scale further to avoid systolic aliasing (low PRF) or diastolic flow gaps (high PRF or filtering) in normal vessels.

Initially the color or power mode gain should be adjusted to an optimized level, with color displayed throughout the lumen of the vessel and no "bleeding" of color into the surrounding tissue. This is the level at which all color images should be assessed. In situations where there is very low flow, or questionable occlusion, an "over-gained" level may be advantageous to show any flow that might be present, e.g., total occlusion versus a near-occlusion or critical stenosis.

The size of the color box should cover the entire vessel diameter and at least 1–2 cm of its length. Large or wide color boxes will slow down frame rates and resolution of the imaging system. Align the box, i.e., select an appropriate color-flow angle correction, according to the vessel geometry and course.

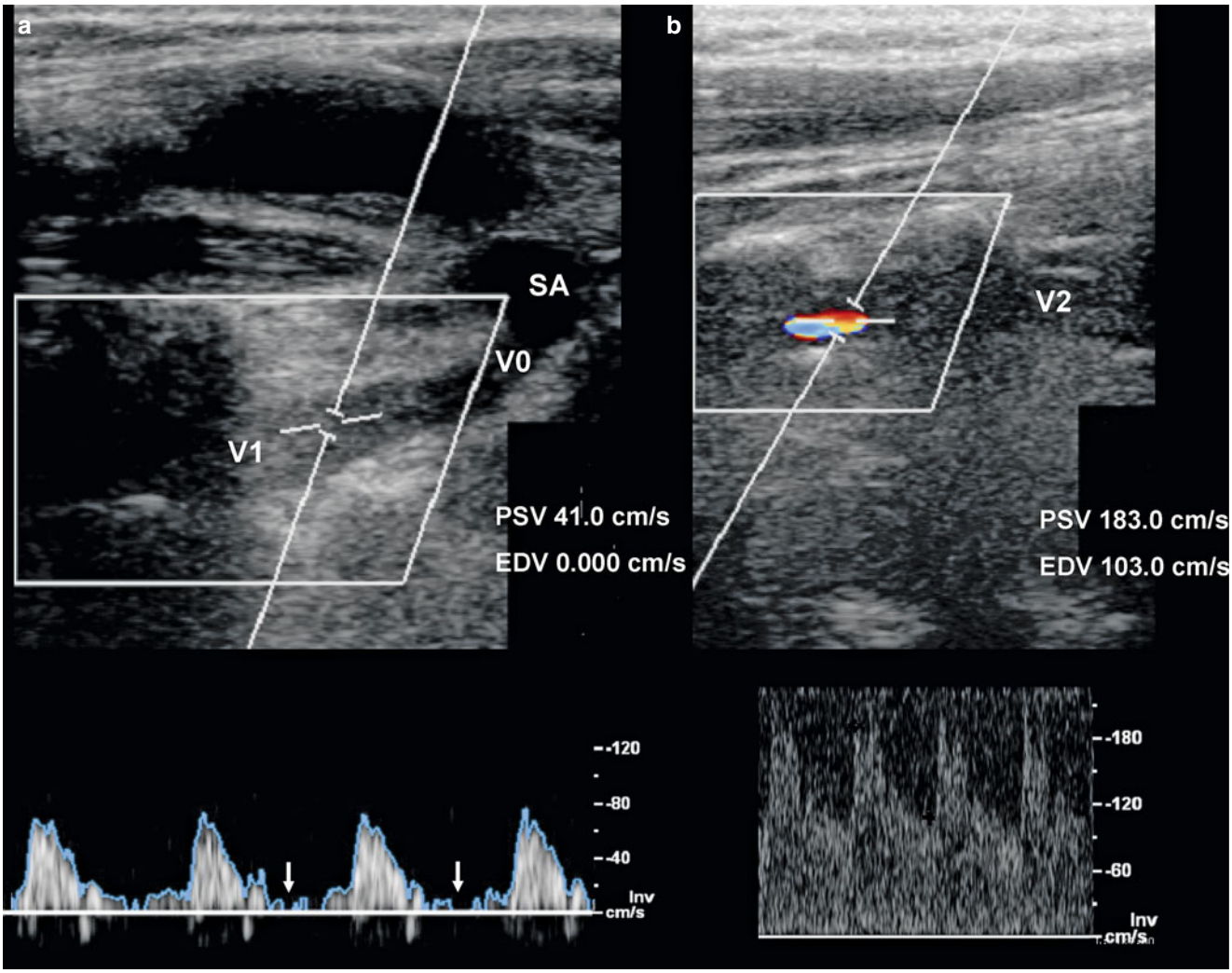


**Fig. 9.2** Two case examples. (**a**) A high-resistance flow in the proximal VA indicates a severe obstruction distally in a patient with an atherosclerotic VA occlusion. Note that there is no end-diastolic flow on Doppler spectra (*arrows*). (**b**) Increased focal flow velocity with a severe stenosis due to angiographically confirmed arterial dissection of the mid-cervical VA at C4 and C5 level. Note aliasing artifact on color-flow image

## Doppler Spectral Evaluation of Flow Dynamics

Display the longitudinal image of the VA. Use color-flow image as a guide for Doppler examination. Begin the examination using a Doppler sample volume size of 1.5 mm positioned in the middle of the vessel. The insonation angle should be parallel to the color blood flow and lower than or equal to 60° in every segment. Adjust the Doppler spectral power and gain to optimize the quality of the signal return. Slowly sweep the sample volume throughout the different inter-vertebrae visualized segments. Identify regions of flow disturbance or absence. Additionally, include Doppler spectral waveforms proximal, within, and distal to all areas where flow abnormalities were observed. Locate the origin or proximal segment of the VA. Record flow patterns paying careful attention to flow direction. Follow accessible cervical segments of the VA. Change angulations of the color box and Doppler sample along with the course of the artery.

## Following Data Should be Provided

1. Highest peak systolic velocity in each VA segment
2. Highest end-diastolic velocity in each VA segment
3. Flow direction of each VA segment
4. Documentation of the Doppler spectral waveform pattern from each VA segment
5. Views demonstrating the presence and location of abnormalities

## Tips to Improve Accuracy

1. Consistently follow a standardized scanning protocol.
2. Always perform a complete examination of each VA segment.
3. Sample velocity signals throughout all arterial segments accessible.

**Table 9.1** Diagnostic criteria for VA ultrasonography

| Diagnostic criteria | B-mode image | Color-flow image | Doppler spectral display |
|---|---|---|---|
| ≥50% stenosis | Structural lesions (e.g., vessel wall thickening/plaque) when able to directly visualize | Diastolic flow signal void proximal to the lesion | Focal significant PSV increase (usually ≥100 cm/s) with PSR ≥2 |
| | | Flow lumen narrowing when able to visualize | Bruit (turbulences), spectral narrowing (when traceable) |
| | | Aliasing artifacts (with proper PRF settings) | Indirect pre- and post-stenotic signs (abnormal pulsatility/waveforms) |
| Occlusion | Hypoechoic vessel lumen (acute/subacute occlusion) | Flow signal void at occlusion site | Absent or minimal (including systolic/dicrotic notch small spikes) Doppler signals at occlusion site |
| | Hyperechoic vessel lumen (chronic occlusion) | Diastolic flow signal void proximal to the lesion | Indirect pre- and post-stenotic signs (abnormal pulsatility/waveforms) |
| Segmental occlusion | Hypoechoic vessel lumen (acute/subacute occlusion) | Flow signal void at occlusion site | Antegrade low-resistance flow pre- and post-lesion |
| | Hyperechoic vessel lumen (chronic occlusion) | Diastolic flow void gap proximal to the lesion | Delayed systolic upstroke distal to the lesion |
| | | Patent distal VA segment | |
| Nondominant VA | Decreased vessel diameter | Undisturbed flow signals corresponding to a relatively diminished lumen | Velocity lower than contralateral side by 20% or more[a] |
| | | | Normal pulsatility (PI 0.6–1.1)[a] |
| Hypoplastic VA | Decreased vessel diameter relative to the other side. | Undisturbed flow signals corresponding to a relatively diminished lumen | Low velocity (PSV < 40 cm/s)[a] |
| | | | High pulsatility (PI ≥ 1.2)[a] |
| Arterial dissection | Vessel wall irregularities (when directly visualized) | Flow signal void (with complete obstruction) | Absent or minimal (including systolic/dicrotic notch small spikes) Doppler signal at occlusion site |
| | Intimal flap (when directly visualized) | Bidirectional flow within the vessel (double lumen) | Low-velocity/high-resistance flow signal along the true lumen with extensive dissection and some residual flow |
| | Double lumen/intramural hematoma (when directly visualized) | Diastolic flow gap proximal to the lesion (with hemodynamically significant obstruction) | Focal significant PSV increase (usually ≥100 cm/s) with PSR ≥ 2 |
| | Pseudoaneurysm (when directly visualized) | | Bruits (turbulence), spectral narrowing at lesion site (if found) |
| | | | Indirect pre- and post-stenotic signs (abnormal pulsatility/waveforms) |
| Subclavian steal | Normal appearance | Normal color-flow signal | Normal antegrade flow |
| | | Alternating color-flow signal | Decreased velocity but no reversed flow |
| | | Reversed color-flow signal | Systolic flow reversal and antegrade flow during diastole (alternating flow) |
| | | | Complete steal with flow reversal during the entire cardiac cycle |

[a]These criteria are arbitrarily used at our own vascular laboratory (not published)

4. Use multiple scan planes.
5. Take time to optimize the B-mode, color, and spectral Doppler information.
6. Videotape or create a digital file of the entire study including sound recordings.
7. Always use the highest imaging frequencies to achieve higher resolution.
8. Account for any clinical conditions or medications that might affect velocity.
9. Integrate data from the right and left VA.
10. Do not hesitate to admit uncertainty and list all causes for limited examinations.
11. Expand Doppler examination to intracranial vessels when possible (see Chap. 10).

## Clinical Indications and Diagnostic Criteria of Vertebral Artery Ultrasonography

In the following, we describe established clinical indications for VA ultrasonography in routine clinical practice, and specific diagnostic criteria derived from previous studies and our own experience (Table 9.1).

### Atherosclerotic Disease

Atherosclerotic disease of the extracranial vertebral arteries is increasingly recognized a cause of posterior circulation ischemia, and it occurs more often in the proximal than in the

mid-cervical or distal segments. Compared with the carotid system, less well-established criteria for grading various degrees of atherosclerotic disease in the extracranial VA exist [2–18].

A normal peak systolic velocity is approximately between 40 and 50 cm/s. However, because of relatively frequent anatomic variations in the vertebral arteries, a wide range of velocities exist which can mislead to an incorrect interpretation of the findings. For example, a peak systolic velocity can be lower than 10 cm/s with both a nondominant/hypoplastic VA and a near-occlusive or post-stenoocclusive VA. Abnormal pulsatility and waveforms may provide a clue to the underlying mechanisms (e.g., increased flow pulsatility in an hypoplastic VA or proximal to a near-occlusion, and decreased flow pulsatility in a post-stenotic VA). A focal (1–2 cm) significant peak systolic velocity increase (usually ≥100 cm/s) in the mid-cervical VA can be considered as a direct sign of a significant stenosis with ≥50% diameter reduction (Fig. 9.2). However, the increased velocity should at least double the velocities found in other segments of the same VA (ratio between pre- or post-stenotic and stenotic segments of 1:≥2). In addition, a harmonic phenomenon indicating a severe stenosis or turbulent flow is the musical murmur simulating a "seagull cry."

Vertebral duplex provides not only information about the portion insonated directly but also indirect information about the proximal and distal vessel segments. A stenosis proximal to the site of insonation can be detected by a "tardus" or "parvus et tardus" Doppler signal seen distal to the stenosis. Parvus indicates a low amplitude, whereas tardus refers to a slow systolic acceleration. If no flow in a VA can be visualized, differentiation from a hypoplastic segment may be challenging. A high-resistance waveform without end-diastolic flow can usually be found with distal VA occlusions (Fig. 9.2). VA occlusions could be complete, elongated, or segmental. With the latter, VA flow with good systolic acceleration and positive diastolic velocities can be found distal to the occlusion arising from muscular collaterals and further masking the VA lesion. Further diagnostic criteria for VA occlusion are presented in Table 9.1.

## Arterial Dissection

Arterial dissections are a frequent cause of stroke in the young, with a lower incidence for vertebral than for carotid arteries. The ultrasonographic findings vary from vessel wall irregularities on B-mode (rarely an intimal flap can be seen) to increased peak systolic velocities suggestive of severe stenoses or occlusions due to significant intramural hematoma (Fig. 9.2). Since the most frequent location is the V3 segment, which is difficult to insonate, one has to look for indirect signs as pre-occlusive flow (high-resistance pulsatile flow without end-diastolic flow proximal to hemodynamically significant dissections). Furthermore, TCD can help confirm the diagnosis through detecting post-stenoocclusive flow patterns or intracranial emboli, which can be often found distal to the dissection. Further consideration should be given to whether the dissection is spontaneous or trauma-related [6, 12, 14, 16, 18].

## Subclavian Steal

Subclavian steal is a hemodynamic phenomenon of reversed flow in one VA caused by a significant stenosis or occlusion in the unilateral subclavian artery (SA) proximal to the origin of the VA [22–26]. It indicates atherosclerotic disease, but hardly ever leads to cerebrovascular events. If symptoms suggestive of posterior circulation ischemia are present, the phenomenon is called "subclavian steal syndrome." Several waveforms have been described indicating different grades of subclavian steal (Fig. 9.3): Latent steal can be demonstrated by the so-called bunny rabbit waveform (corresponding approximately to ≥50% SA stenosis) showing two systolic peaks with a sharp deceleration after the first peak and a more rounded second peak. A bidirectional waveform with initial retrograde systolic flow toward the arm and subsequent diastolic antegrade flow toward the brain (alternating flow signal) may indicate a hemodynamic significant lesion in the SA. A reversed waveform or *complete* retrograde flow is caused by an occlusion or near-occlusion of the SA. Of note, another main finding besides the above-described Doppler flow abnormalities indicating steal is a difference in blood pressure between both arms of ≥20 mmHg.

If the steal waveforms are not present at *rest*, flow reversal can be augmented by the hyperemia cuff test: Inflate a blood pressure cuff over the systolic pressure value on the ipsilateral arm and let the patient open and close the fist (maintain arterial compression for about 1–1.5 min). Then, deflate the cuff rapidly, which will cause hyperemia in the arm and unmask latent steal for a short period of time in the recipient VA, visualizing the above-described Doppler waveforms.

## Indications to Expand the Extracranial Exam to TCD at Our Laboratory

1. Complete TCD examination of the anterior and posterior intracranial arterial segments is performed at our laboratory routinely as part of vascular imaging work-up in all patients with stroke and TIA.

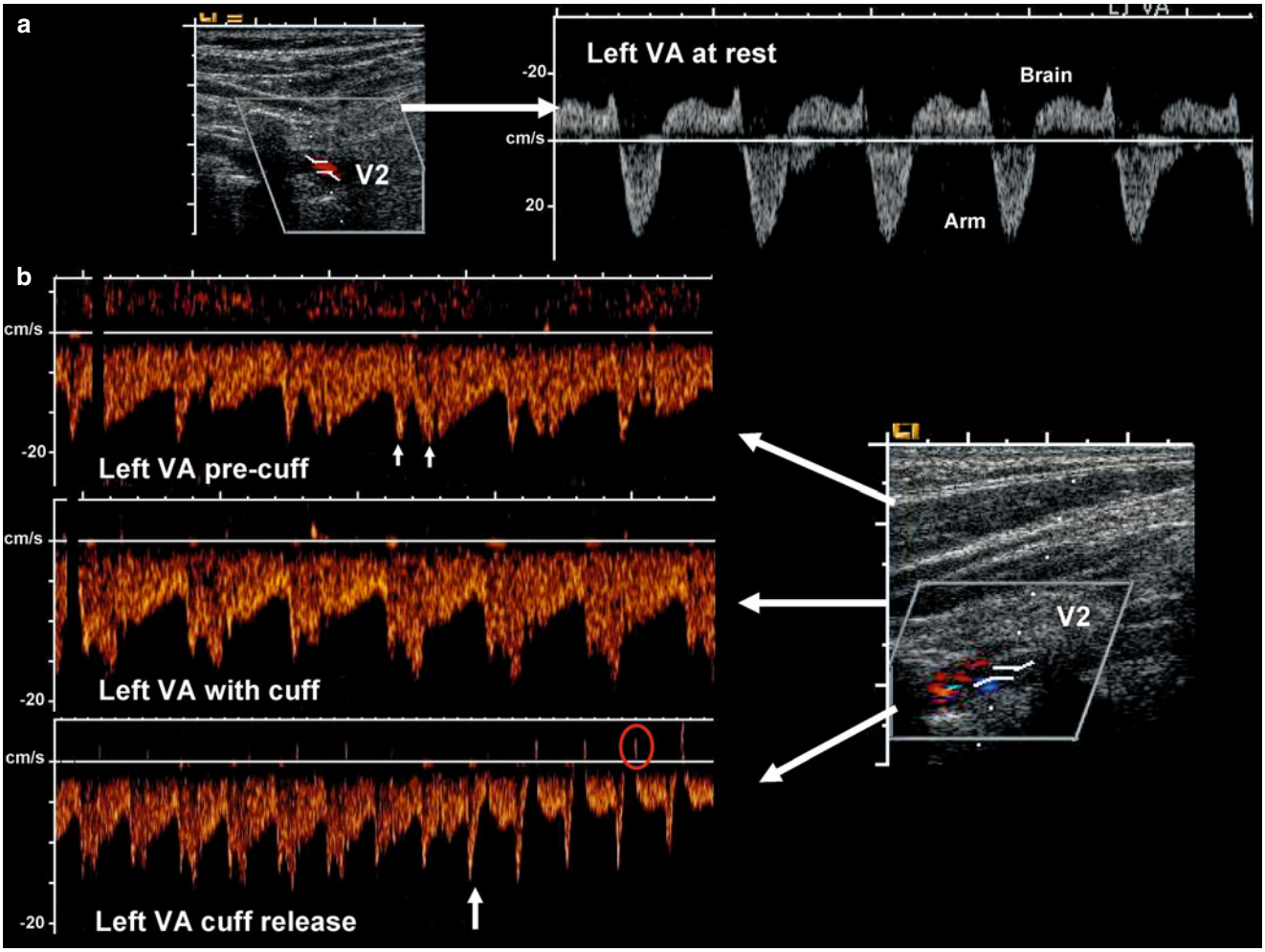


**Fig. 9.3** Examples of subclavian steal waveforms in the mid-cervical VA. (**a**) Alternating flow signal at rest with systolic flow reversal (toward the arm) and remaining diastolic flow toward the brain. (**b**) Hyperemia test with blood pressure cuff inflation unmasks latent subclavian steal. Left VA shows two systolic peaks with a sharp deceleration after the first peak and a more rounded second peak ("bunny rabbit" waveform, *small arrows*). Inflating the blood pressure cuff (*big arrow*) alters the systolic complexes in the left VA (note improved shape of the waveform). Releasing the blood pressure cuff augments steal inducing systolic flow reversal (*red circle*)

2. In patients with posterior circulation symptoms, TCD should particularly be performed to rule out intracranial vertebrobasilar stenoses.
3. If a dissection is suspected, its possible extension to intracranial circulation should be assessed with TCD and other appropriate angiographic testing.
4. Intracranial monitoring to detect microembolic signals distal to a VA stenosis or dissection should be performed particularly in patients with recurrent or fluctuating symptoms.
5. Intracranial assessment of collateral flow distal to a hemodynamic significant VA stenosis or occlusion. The basilar artery usually does not show flow abnormalities with unilateral VA lesions, but this may occur with bilateral VA lesions or a contralateral hypoplastic VA and a complete steal present at rest.
6. High-pulsatility flow (with absent diastolic flow) in one of the extracranial vertebral arteries suggestive of a critical stenosis or occlusion in the intracranial vertebrobasilar circulation.
7. Quantification of vertebrobasilar vasomotor reactivity with a significant extracranial VA stenosis (breath-holding index values are not yet validated for the posterior circulation).

## Conclusion

We summarize broad and specific clinical indications and expected outcomes of VA ultrasonography that should aid referring physicians, sonographers, interpreting physicians, and third-party payers to understand the clinical value and potential impact of VA testing on diagnosis and management decision making (Table 9.2).

**Table 9.2** Clinical indications for and expected outcomes of VA ultrasonography

| Broad indication | Specific indications | Expected outcomes |
|---|---|---|
| Ischemic stroke or TIA | Patients with acute and subacute ischemic symptoms who had cranial CT or MRI | VA ultrasonography (performed as part of required vascular imaging work-up along with carotid duplex and TCD) can identify patients with arterial obstructions in the extracranial portion of the VA explaining the vascular origin of patient symptoms particularly in cases of negative CT and MRI, identifying patients amenable to reperfusion therapies and establishing pathogenesis of an acute event (atheromatous disease vs. dissection, etc.). Even in patients with clear anterior circulation symptoms, VA ultrasonography can reveal such findings as subclavian steal phenomenon and VA atheromatous stenosis that point to polyvascular atheromatous disease and can further aid patient management |
| Ischemic stroke or TIA | Patients with acute and subacute ischemic symptoms in the posterior circulation who had cranial CT or MRI | VA ultrasonography helps determine stroke pathogenic mechanism (vertebrobasilar atheromatous stenosis, thrombosis, or dissection) that in turn determines a specific secondary stroke prevention treatment |
| Symptoms consistent with either vertebrobasilar insufficiency, syncopal episodes, or inner ear problems | Patients with unsteadiness, diziness, falls, incoordination, disorientation, etc.: those who need vascular assessment as part of their work-up to differentiate between vertebrobasilar TIAs, cardiac/systemic hemodynamics, and inner ear problems | VA ultrasonography can identify patients with different grades of subclavian steal (at rest, latent, complete) or hemodynamically significant stenoses in the vertebrobasilar system. Normal VA ultrasonography findings will help support other etiologies of these symptoms |
| Ischemic stroke or TIA | Follow-up | VA ultrasonography is an inexpensive noninvasive follow-up tool that can detect progression or regression in the severity of extracranial stenoses through direct velocity measurements. This information could be helpful in further adjustments of prevention therapies or selecting patients for interventions in case of ineffective medical management |

## References


1. Savitz SI, Caplan LR. Vertebrobasilar disease. N Engl J Med. 2005;352:2618–26.
2. Ringelstein EB, Zeumer H, Hündgen R, Meya U. Angiologic and prognostic evaluation of brain stem injuries. Clinical, dopplersonographic and neuroradiological findings. Dtsch Med Wochenschr. 1983;108(43):1625–31.
3. Davis PC, Nilsen B, Braun IF, Hoffman Jr JC. A prospective comparison of duplex sonography vs angiography of the vertebral arteries. AJNR Am J Neuroradiol. 1986;7(6):1059–64.
4. Touboul PJ, Bousser MG, LaPlane D, Castaigne P. Duplex scanning of normal vertebral arteries. Stroke. 1986;17(5):921–3.
5. Winter R, Biedert S, Staudacher T, Betz H, Reuther R. Vertebral artery Doppler sonography. Eur Arch Psychiatry Neurol Sci. 1987;237(1):21–8.
6. Touboul PJ, Mas JL, Bousser MG, Laplane D. Duplex scanning in extracranial vertebral artery dissection. Stroke. 1988;19(1):116–21.
7. De Bray JM, Blard JM, Tachot C, Ledemeney M, Davinroy M. Transcranial Doppler ultrasonic examination in vertebro-basilar circulatory pathology. J Mal Vasc. 1989;14(3):202–5.
8. Delcker A, Diener HC. The value of color duplex for sonography of the vertebral artery. Vasa Suppl. 1991;33:204–5.
9. Bartels E. Duplex sonography of the vertebral arteries. 2. Clinical application. Ultraschall Med. 1991;12(2):63–9.
10. Schneider PA, Rossman ME, Bernstein EF, et al. Noninvasive evaluation of vertebrobasilar insufficiency. J Ultrasound Med. 1991;10(7):373–9.
11. Bartels E, Fuchs HH, Flügel KA. Duplex ultrasonography of vertebral arteries: examination, technique, normal values, and clinical applications. Angiology. 1992;43(3 Pt 1):169–80.
12. Sturzenegger M, Mattle HP, Rivoir A, Rihs F, Schmid C. Ultrasound findings in spontaneous extracranial vertebral artery dissection. Stroke. 1993;24(12):1910–21.
13. Delcker A, Diener HC, Timmann D, Faustmann P. The role of vertebral and internal carotid artery disease in the pathogenesis of vertebrobasilar transient ischemic attacks. Eur Arch Psychiatry Clin Neurosci. 1993;242(4):179–83.
14. Bartels E, Flügel KA. Evaluation of extracranial vertebral artery dissection with duplex color-flow imaging. Stroke. 1996;27(2):290–5.
15. de Bray JM, Missoum A, Dubas F, Emile J, Lhoste P. Detection of vertebrobasilar intracranial stenoses: transcranial Doppler sonography versus angiography. J Ultrasound Med. 1997;16(3):213–8.
16. de Bray JM, Penisson-Besnier I, Dubas F, Emile J. Extracranial and intracranial vertebrobasilar dissections: diagnosis and prognosis. J Neurol Neurosurg Psychiatry. 1997;63(1):46–51.
17. de Bray JM, Pasco A, Tranquart F, et al. Accuracy of color-Doppler in the quantification of proximal vertebral artery stenoses. Cerebrovasc Dis. 2001;11(4):335–40.
18. Droste DW, Junker K, Stögbauer F, et al. Clinically silent circulating microemboli in 20 patients with carotid or vertebral artery dissection. Cerebrovasc Dis. 2001;12(3):181–5.
19. Krayenbuehl H, Yasargil MG. Cerebral angiography. 2nd ed. Stuttgart: Thieme; 1982.
20. Cloud GC, Markus HS. Diagnosis and management of vertebral artery stenosis. QJM. 2003;96(1):27–54.
21. Bartels E. Color-coded duplex ultrasonography of the cerebral arteries: atlas and manual. Stuttgart: Schattauer; 1999.

22. Grossman BL, Brisman R, Wood EH. Ultrasound and the subclavian steal syndrome. Radiology. 1970;94(1):1–6.
23. von Reutern GM, Büdingen HJ. Doppler sonographic study of the vertebral artery in subclavian steal syndrome. Dtsch Med Wochenschr. 1977;102(4):140–1.
24. Reutern GM, Büdingen HJ, Freund HJ. The diagnosis of obstructions of the vertebral and subclavian arteries by means of directional Doppler sonography. Arch Psychiatr Nervenkr. 1976;222(2–3): 209–22.
25. Klingelhöfer J, Conrad B, Benecke R, Frank B. Transcranial Doppler ultrasonography of carotid-basilar collateral circulation in subclavian steal. Stroke. 1988;19(8):1036–42.
26. Walker DW, Acker JD, Cole CA. Subclavian steal syndrome detected with duplex pulsed Doppler sonography. AJNR Am J Neuroradiol. 1982;3(6):615–8.

# Transcranial Doppler Sonography

10

Kristian Barlinn and Andrei V. Alexandrov

**Abstract**

Transcranial Doppler (TCD) sonography provides a noninvasive and inexpensive vascular imaging modality that can be used in various clinical situations to provide real-time physiological information that is often unobtainable with other testing without increasing patient risks and associated costs. TCD also provides diagnostic and prognostic information that determines patient management decisions across multiple cerebrovascular conditions and periprocedural or surgical monitoring. In this chapter, we describe complete diagnostic TCD performance standards as well as established clinical indications, specific diagnostic criteria, and expected outcomes of TCD testing for patients with cerebrovascular diseases.

**Keywords**

Noninvasive vascular imaging • Transcranial Doppler • Acute stroke • Cerebral ischemia Subarachnoid hemorrhage

## The Principles of Transcranial Doppler

Transcranial Doppler (TCD) was first introduced by Rune Aaslid and colleagues in 1982 to noninvasively measure blood flow velocities in the major branches of the Circle of Willis through the intact skull [1]. A 2-MHz frequency pulse wave ultrasonic beam penetrates the skull and allows returned echo signals to be detected. The frequency shift of the returned echoes is calculated using the Doppler equation $f_D = 2 f_o v \cos\theta / (c - \cos\theta)$, where $f_D$ is Doppler shift, $f_o$ is the emitting frequency, $v$ is the scatterer speed, $\theta$ is the Doppler angle, and $c$ is the sound propagation speed. The average speed of sound in soft tissues is 1.540 m/s, and the Doppler angle for TCD examination is assumed to be 0° for all arteries ($\cos 0° = 1$). Therefore, the Doppler equation is rearranged to calculate the velocity of moving blood in basal cerebral arteries: $v$ (cm/s) = 77 $f_D$ (kHz)/$f_o$ (MHz), where the 77 coefficient is valid for the frequency and velocity units shown in parentheses.

Transcranial Doppler allows the depth and the direction of flow relative to the transducer position and the ultrasonic beam direction to be located. The depth of insonation is manually adjusted: the deeper the vessel location, the slower is the pulse repetition frequency. The direction of flow depends on the angle at which the ultrasonic beam intercepts an artery. The flow moving toward the transducer (i.e., the angle of interception is less than 90°) will increase the frequency of the returned signal compared to the emitted frequency. The flow intercepted at 90° will produce no detectable Doppler shift. And if the arterial flow is directed away from the probe (i.e., the angle >90°), the frequency of the returned signal will be less than the emitted one. Therefore, the Doppler

K. Barlinn, M.D.
Department of Neurology, Dresden University Stroke Center,
University of Technology Dresden,
Dresden, Saxony, Germany

Department of Neurology, Comprehensive Stroke Center,
University of Alabama at Birmingham Hospital,
RWUH M226, 619 19th Street South,
Birmingham, AL 35249-3280, USA

A.V. Alexandrov, M.D. (✉)
Department of Neurology, Comprehensive Stroke Center,
University of Alabama at Birmingham Hospital,
RWUH M226, 619 19th Street South,
Birmingham, AL 35249-3280, USA
e-mail: avalexandrov@att.net

A.F. AbuRahma, D.F. Bandyk (eds.), *Noninvasive Vascular Diagnosis*,
DOI 10.1007/978-1-4471-4005-4_10, © Springer-Verlag London 2013

shifts are coded as positive or negative and the direction of flow is determined accordingly.

## Power Motion (M-Mode) Doppler

As a recent technological improvement in TCD, power motion (M-mode) Doppler (PMD-TCD) utilizes 33 overlapping Doppler samples to display signal intensities in an M-mode format, i.e., color-coded directionality and intensity, simultaneously detectable over 6 cm of intracranial space at a given position of the transducer [2]. The brighter PMD colors reflect stronger intensities, and this "road map" can serve as a guide for more complete spectral analysis. This technology allows easier window finding, better vessel/emboli tracking, and as such can facilitate learning diagnostic TCD and understanding how to target relevant proximal arterial segments that could contain acute occlusions. Furthermore, PMD flow patterns, or signatures, may have their own diagnostic significance, and these flow changes can be observed over large segments of intracranial vasculature in real time.

## Transcranial Color Duplex

Transcranial color-coded duplex (TCCD) is performed with a phased array transducer using a carrier frequency of 2–3.5 MHz and imaging frequency of 4 MHz. It offers a two-dimensional B-mode image that is able to visualize anatomic landmarks in the brain, and the spatial relationship of the vessels can be used for identification of the arteries in the cerebral vasculature [3–7]. TCCD is particularly useful in the detection of distal arterial lesions and tracing the course of tortuous vessels. For example, arterial branches can be identified, the terminal vertebral arteries can be differentiated (left and right), and the basilar artery (BA) can be better identified. Using color flow imaging, regions of disturbed flow, suggestive of focal stenoses or occlusions, and occasionally, arteriovenous malformations [8] or large aneurysms can be detected. At bedside, B-mode imaging is able to demonstrate the midline shift with the malignant middle cerebral artery (MCA) infarctions [9] or hematoma growth with intracerebral hemorrhages.

However, fewer diagnostic criteria are available for the detection and grading of intracranial disease with TCCD, and although TCCD provides several ultrasound techniques, a single-channel spectral Doppler interrogation without angle correction (zero degree angles is also recommended for TCCD) remains the mainstay of diagnosis.

## Examination Techniques

There are four "windows" for insonation: temporal, orbital, foraminal, and submandibular (Figs. 10.1 and 10.2) [10]. The transtemporal approach allows insonation of the MCA, anterior cerebral (ACA), posterior cerebral (PCA), and communicating arteries. The transorbital approach is used to insonate the ophthalmic artery (OA) and internal carotid artery (ICA) siphon [1, 2, 10–12]. The transforaminal approach allows the distal vertebral artery (VA) and BA to be insonated through the foramen magnum. The submandibular approach is used to obtain ICA velocities as they enter the skull. To shorten the time necessary to find the window and different arterial segments, the examination should begin with the maximum power and gate settings (i.e., power 100%, gate 15 mm; if using PMD-TCD, use the smallest gate 3 mm). Identify and store the highest velocity signals and any abnormal or unusual waveforms.

### Transtemporal Insonation Steps

1. Set the depth at 50 mm (midpoint of the M1 MCA). Place the probe above the zygomatic arch and aim it slightly upward and anterior to the contralateral ear/window. Find any flow signal and avoid too anterior and too posterior angulations. Find a flow signal directed toward the probe that resembles MCA flow (low-resistance waveform). Store the highest velocity at this depth.
2. Follow the flow signal until it disappears at shallow (30–40 mm) depths (M2 MCA branches). Store any abnormal signal (avoid sampling meningeal arteries at these depths). Return to the midpoint of the M1 MCA.
3. Follow the M1 MCA stem to its origin at 60–70 mm (insonation of the terminal ICA is possible at this depth). Find the ICA bifurcation at approximately 65 mm and obtain both proximal M1 MCA and A1 ACA (away from the probe) signals. Store a bidirectional signal of the bifurcation.
4. Follow the A1 ACA signal to 70–75 mm depths. Store the distal A1 ACA signal at 70 mm.
5. Find the terminal ICA signal just inferior and sometimes slightly posterior to the bifurcation at 60–65 mm. Store any abnormal signal.
6. Return to the ICA bifurcation and slowly turn the transducer posterior by 10–30° (usually there is a flow gap between the bifurcation and PCA signals). Find PCA signals directed toward (P1) and away (P2) from the probe at a depth range of 55–75 mm. Store the PCA signals with the highest velocity.

### Transorbital Insonation Steps

1. Decrease power to the minimum (17 mW) or 10%. Set the depth at 50–52 mm and place the transducer over the eyelid and angle it slightly medially. Determine flow pulsatility and direction in the distal OA (high pulsatility flow toward the probe). Store the OA signals.
2. Set the depth at 60–64 mm and find the ICA siphon flow signals (usually located medially in the orbital window). Store bidirectional or unidirectional signals directed

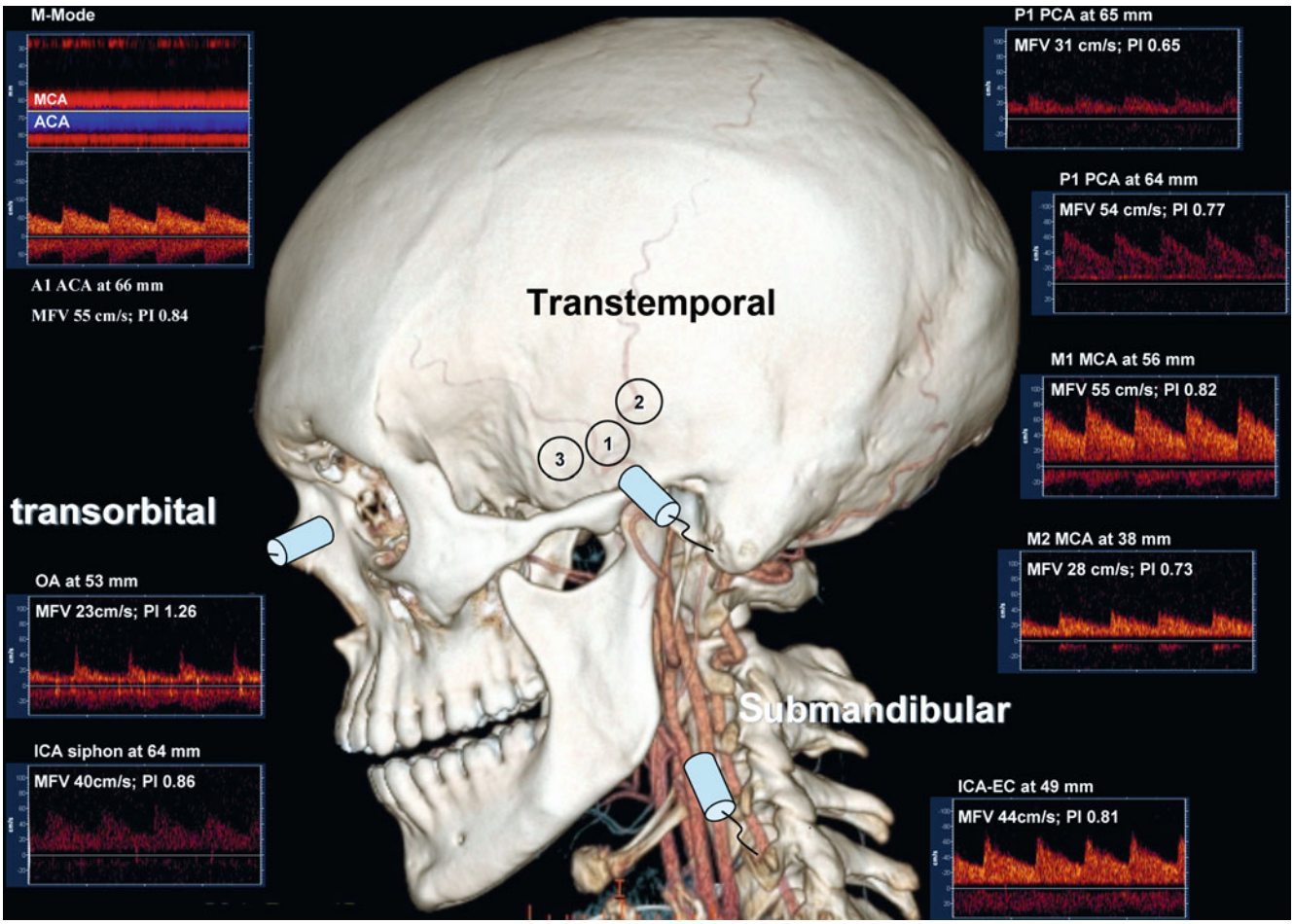


**Fig. 10.1** Three-dimensional CT angiogram shows locations of the acoustic windows for transcranial Doppler examination except transforaminal approach. The transtemporal window for insonation may be found above the zygomatic arch at the (*1*) middle, (*2*) posterior, and (*3*) anterior probe positions. Normal spectral Doppler waveforms obtained through these acoustic windows are shown

toward (lower limb of the siphon) and/or away (upper limb of the siphon) from the probe.

## Transforaminal Insonation Steps

1. Use full power and set the depth at 75 mm (distal VA/proximal BA). Place the transducer at midline 1 in. below the edge of the skull and aim it at the bridge of the nose. Identify a flow signal directed away from the probe (i.e., find the window).
2. Increasing the depth, follow the flow directed away from the probe. Store the proximal BA signal arbitrarily assigned to the depth of 80 mm (mid-BA to 90 mm, distal BA to >100 mm). Bidirectional signals may be found at various depths resembling cerebellar arteries. Store the highest velocity signal obtained at the most distal BA.
3. Set the depth at 60 mm and place the transducer about 1 in. laterally to the midline and aim toward the bridge of the nose or slightly toward the contralateral eye. Find the VA flow signal directed away from the probe and follow its intracranial course from 40 to 80 mm. Store the VA signal at 60 mm (or at the depth with the highest velocity). Repeat the examination on the contralateral side.

## Submandibular Insonation Steps

1. Set the depth at 50–60 mm, place the probe laterally under the jaw, and aim it upward and slightly medially. Find a low-resistance flow directed away from the probe. Store the distal ICA signal at the depth that shows the highest velocity. This approach is reserved for patients with subarachnoid hemorrhage (SAH) when vasospasm grading requires calculation of the Lindegaard index.

The TCD interpretation consists of the assessment of:

1. Mean flow velocity changes (focal or global)
2. Asymmetry of flow parameters (side-to-side, segmental)
3. Pulsatility (high or low resistance)
4. Waveform/sound pattern recognition of flow changes

A normal TCD examination may reveal a wide range of depths of insonation, velocity values, and waveforms.

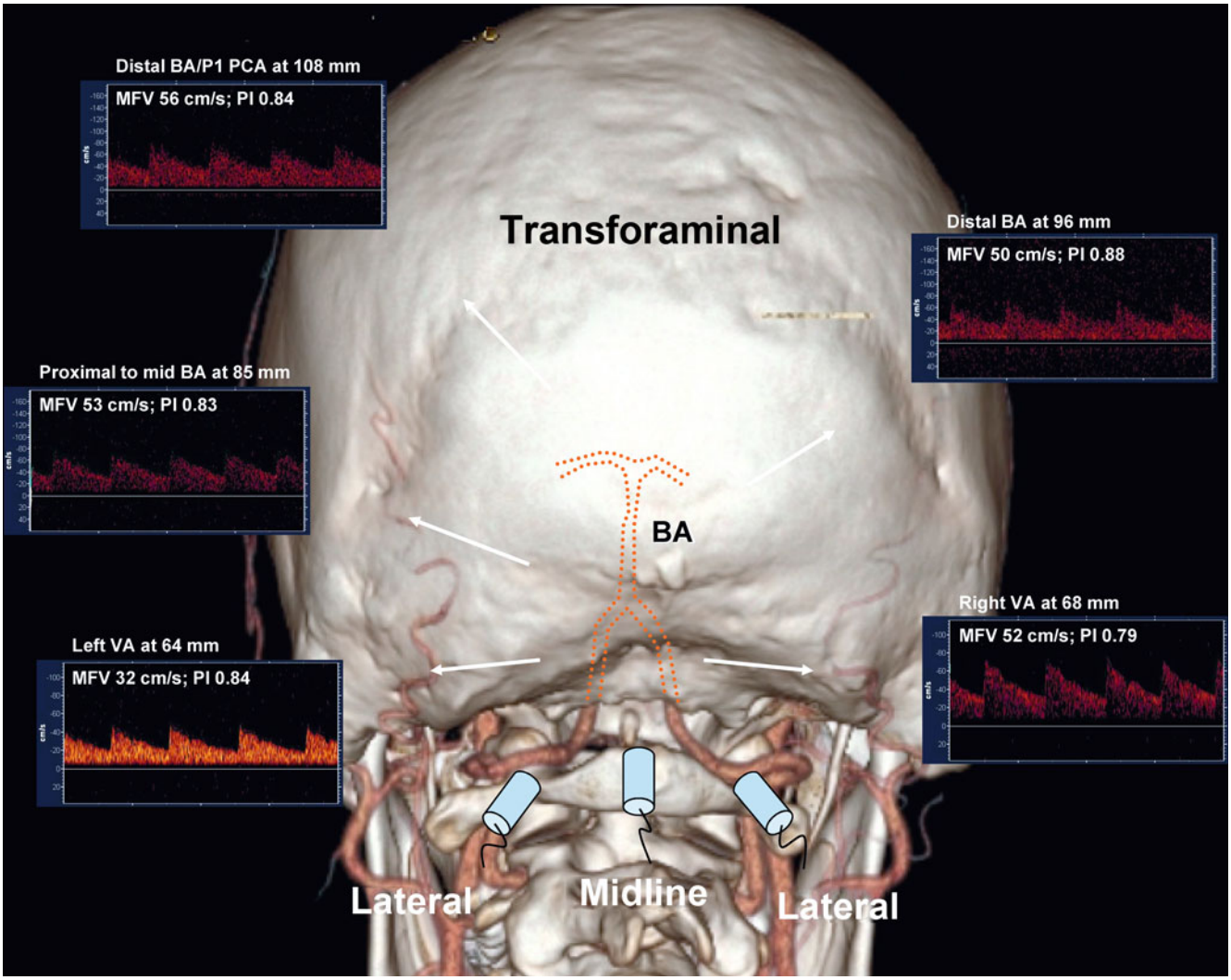


**Fig. 10.2** Transforaminal window is shown relative to a three-dimensional CT angiogram with *dotted lines* identifying terminal vertebral and basilar arteries course. Transducer positions (*midline* and *lateral*) are shown relative to the vessels that could be insonated through these approaches. Normal spectral Doppler waveforms obtained from the terminal vertebral and basilar arteries are shown

## Criteria for Normal TCD Findings

1. Good windows of insonation, all proximal arterial segments found.
2. Directions of flow and depths of insonation are given in Table 10.1.
3. The differences between flow velocities and pulsatility indices in the homologous arterial segments are usually less than 30%: 15% is attributable to the difference in angle of insonation and another 15% to breathing cycles. Normal variations of up to 100% in flow velocities between homologous segments such as PCA or VA can be attributed to a tortuous vessel course, anatomic variants of the circle of Willis, and subdominance/hypoplasia.
4. A normal MCA mean flow velocity (MFV) is in the range of 80–100 cm/s in adults free of anemia and does not exceed 170 cm/s in children with sickle cell disease.
5. A normal velocity ratio: MCA ≥ ACA ≥ siphon ≥ PCA ≥ BA ≥ VA.
6. A positive end-diastolic flow velocity (EDV) of 25–50% of the peak systolic velocity (PSV) values and a low-resistance pulsatility index (PI) of 0.6–1.1 are present in all intracranial arteries while breathing room air. A normal high resistance flow pattern (PI ≥1.2) is seen in the OAs only.
7. Abnormal high-resistance flow patterns can be seen in patent cerebral arteries with aging, chronic hypertension, increased cardiac output, and during hyperventilation.

**Table 10.1** Normal depth, direction, and mean flow velocities at assumed 0° angle of insonation for the arteries of the circle of Willis

| Artery | Depth (mm, adults) | Direction | Children[a] | Adults |
|---|---|---|---|---|
| M2 MCA | 30–45 | Bidirectional | <170 cm/s | <80 cm/s |
| M1 MCA | 45–65 | Toward | <170 cm/s | <80 cm/s |
| A1 ACA | 62–75 | Away | <150 cm/s | <80 cm/s |
| A2 ACA | 45–65 | Toward | N/A | <80 cm/s |
| ICA siphon | 60–65 | Bidirectional | <130 cm/s | <70 cm/s |
| OA | 40–60 | Toward | Variable | Variable |
| PCA | 55–70 | Bidirectional | <100 cm/s | <60 cm/s |
| BA | 80–100+ | Away | <100 cm/s | <60 cm/s |
| VA | 45–80 | Away | <80 cm/s | <50 cm/s |

[a]MFVs are given for children with sickle cell disease

## Cerebrovascular Resistance and Hemodynamic Indices

Cerebrovascular resistance (CVR) is determined by several factors that impede cerebral blood flow (CBF) and thus determine MFV: the vessel radius, length, and blood viscosity. The Hagen-Poiseuille law is often used to describe the impact of resistance on blood flow. It states that the flow of a fluid through a tube is directly proportional to the pressure difference that exists between two ends of a tube and to the fourth power of the vessel radius, and inversely proportional to the length of the tube and fluid viscosity. Thus, the diameter of a blood vessel, which is mostly accomplished by arterial-arteriolar constriction and dilatation, is the most significant contributor of all to the rate of blood flow. Under normal conditions, the brain is a low-resistance arterial system, and the ICA branches have considerably greater end-diastolic flow than the external carotid artery branches. The resistance to flow is described by the pulsatility and the resistance index (RI):

$$\text{PI (Gosling-King)} = \text{PSV} - \text{EDV/MFV (normal values in the range of 0.6–1.1).}$$

$$\text{RI (Pourcelot)} = \text{PSV} - \text{EDV/PSV (normal values are in the range of 0.49–0.63) [13].}$$

These indices quantitatively reflect CVR and depend largely on the strength of the signal recorded as well as the envelope and time averaging software. Therefore, "weak signals," "poor" windows, incomplete examination, and individual variations may produce substantial drawbacks. Additional information can be gained by visual flow pattern recognition. Pathologically increased pulsatility indices (≥1.2) are seen with increased ICP and decreased cerebral perfusion pressure due to decreased EDV. Further increased PIs can be detected proximal to a severe arterial obstruction, in patients with chronic hypertension and during episodes of hypocapnia. Pathologically low pulsatility indices (≤0.5) are mainly seen in the arteries feeding arteriovenous malformations since direct shunting of blood into the venous system results in abnormally low CVR [14]. Low PIs may also be seen distal to a severe extra- or intracranial stenosis indicating compensatory vasodilation and during hypoventilation. Although these indices per se may not be sufficient to diagnose extra- or intracranial cerebrovascular diseases, they should be used in a battery of TCD parameters allowing integrated assessment of intracranial circulation.

The hemispheric index (also known as the Lindegaard ratio) compares MCA MFV to the ipsilateral ICA and may help to differentiate an MCA MFV increase due to vasospasm and/or hyperperfusion [15]. The M1 MCA vasospasm after SAH is usually associated with a Lindegaard ratio ≥3, while a severe M1 MCA vasospasm has been shown to correlate with values ≥6.

Other factors that affect CBF and CVR include age, gender, cardiac function, hematocrit, fibrinogen, and vasodilatory or constricting medications [13].

TCD measurement of flow velocities, however, does not allow calculation of CBF in ml/min because of the variable and unknown arterial diameter and peripheral resistance [16]. However, the area under the waveform envelope, intensity of the signal, and relative change in the mean flow velocities determined with the same angle of insonation are usually proportional to regional CBF changes [17]. For example, MFV changes due to vasomotor reactivity with different vasodilatory stimuli reflect CBF changes assuming that the perfused territory remains constant during investigation [18]. The use of TCD for monitoring physiological responses to vasodilatory substances is based on the concept of cerebral vasomotor reactivity (VMR) in order to identify patients at a particular risk for cerebral ischemic events.

## Specific Clinical Indications and Diagnostic Criteria

The specific established clinical indications for TCD in routine clinical practice include sickle cell disease, cerebral ischemia (stroke, transient ischemic attack; TIA), carotid

artery stenosis and occlusions, arterial vasospasm after SAH, cerebral circulatory arrest, and periprocedural or surgical monitoring. In the following, we provide a summary of various diagnostic criteria previously published by other investigators and generated by our vascular laboratory.

## Sickle Cell Disease

TCD can identify children with the highest risk of first-ever stroke and those in need of blood transfusion [19, 20]. In a pivotal trial [20], TCD detection of time-averaged maximum MFV of 200 cm/s on two separate examinations was used to determine the need for blood transfusion that resulted in 90% relative risk reduction of first-ever stroke. This trial demonstrated that TCD can select patients for the most effective primary stroke prevention intervention to date that had profound implications on management of children with sickle cell disease. Further observations confirmed that children initially selected by TCD for blood transfusion should stay on transfusion schedule to sustain the benefit in stroke risk reduction [21]. Moreover, recent data including long-term follow-up and final results from the Stroke Prevention Trial in Sickle Cell Anemia (STOP) indicated that persistent elevation in TCD velocities indicates ongoing stroke risk [22]. The skill of TCD testing in children with sickle cell anemia is taught through standard tutorials with sonographers receiving specialized certificates, and diagnostic criteria for interpreting physicians are well defined [22, 23].

## Subarachnoid Hemorrhage

Arterial vasospasm following SAH becomes symptomatic in more than 25% of patients leading to a delayed ischemic deficit (DID) [24]. DID usually occurs when vasospasm results in a severe (≤1 mm) intracranial arterial narrowing producing flow depletion with extremely high velocities [25]. It may affect the proximal stem and distal branches of intracranial arteries with the most common locations being:

1. MCA/TICA ± ACA
2. Bilateral ACAs
3. BA ± terminal VA
4. Distal branches [26]

Numerous studies have shown the effectiveness of TCD in diagnosing cerebral arterial vasospasm both in anterior and posterior circulation following SAH [27–35]. More specifically, TCD can detect the development of vasospasm on days 2–5 following SAH, i.e., before it can become clinically apparent, and this information can be used by intensivists to step up with hemodynamic management of these patients [36]. In addition, TCD can detect progression to the severe phase of vasospasm when development of the DID due to perfusion failure through the residual lumen is the greatest. The maximal sensitivity of TCD for detecting severe cerebral vasospasm is at day 8 after SAH onset, while its sensitivity for diagnosing DID is lower [36].

Although quantitative criteria have been studied extensively, grading arterial vasospasm severity remains difficult, and the interpretation of TCD findings should be individualized. Daily TCD examinations may detect considerable flow velocity and pulsatility changes that may be attributed to early development of vasospasm and progression to a severe stage. However, TCD findings should be related to the patient clinical condition, medications, blood pressure, and time after day 0 (usually the onset of the worst headache of patient's life) and ICP findings:

1. Proximal vasospasm in any intracranial artery results in a focal (or present along one or two branching segments) elevation of mean flow velocities without a parallel velocity increase in the feeding extracranial arteries (intracranial/extracranial vessel ratio ≥3).
2. Distal vasospasm in any intracranial artery may produce a focal pulsatile flow (PI ≥ 1.2) indicating increased resistance distal to the site of insonation. No MFV increase may be found since vasospasm is located distal to the site of insonation. Additional findings may include daily changes in velocities, ratios, and PIs during the first 2 weeks but are particularly pronounced during the critical days 3–7 after the onset of SAH.

MCA vasospasm-specific criteria are shown in Table 10.2. The differential diagnosis includes hyperemia, combination of vasospasm and hyperemia in the same vessel (since most SAH patients routinely receive some part of hypertension-hemodilution-hypervolemia therapy; HHH), residual vasospasm, and hyperemia. Arterial vasospasm may also coexist with hydrocephalus, edema, and infarction.

Prognostically unfavorable signs include an early appearance of MCA MFV ≥180 cm/s, a rapid (>20% or >65 cm/s) daily MFV increase during critical days 3–7, an MCA/ICA ratio ≥6, and the abrupt appearance of high-resistance PI ≥ 1.2 of flow in two or more arteries indicating increased ICP and/or distal vasospasm [24].

Grading vasospasm severity in the arteries other than MCA is difficult. Sloan and colleagues showed that TCD is highly specific (100%) for VA and BA vasospasm when mean flow velocities are ≥80 and ≥95 cm/s, respectively, and suggested reporting vasospasm in these arteries as possible, probable, and definite (Table 10.3) [25, 35]. The key indicator of a significant vasospasm is a focal, asymmetric, and disproportionate velocity increase that may occur in an artery distant from the aneurysm site or blood clot collection on computed tomography. The differential diagnosis includes hyperemia and its combination with vasospasm in these arteries.

Soustiel et al. have shown that the ratio between the BA and the extracranial VA (termed Soustiel's ratio) may

**Table 10.2** TCD criteria for grading vasospasm in the proximal MCA

| Mean flow velocity (cm/s) | MCA/ICA MFV ratio | Interpretation |
|---|---|---|
| <120 | ≤3 | Hyperemia |
| ≥120 | 3–4 | Development of mild spasm + hyperemia |
| ≥120 | 4–5 | Moderate spasm + hyperemia |
| ≥120 | 5–6 | Moderate spasm |
| ≥180 | 6 | Moderate-to-severe spasm |
| ≥200 | ≥6 | Severe spasm |
| >200 | 4–6 | Moderate spasm + hyperemia |
| >200 | 3–4 | Hyperemia + mild (often residual) spasm |
| >200 | <3 | Hyperemia |

**Table 10.3** Sloan's optimized criteria for grading vasospasm (VSP) in intracranial arteries

| Artery/MFV | Possible VSP | Probable VSP | Definite VSP |
|---|---|---|---|
| ICA | >80 | >110 | >130 |
| ACA | >90 | >110 | >120 |
| PCA | >60 | >80 | >90 |
| BA | >70 | >90 | >100 |
| VA | >60 | >80 | >90 |

Modified from Alexandrov and Neumyer [37]. With permission from John Wiley & Sons, Inc.

contribute to an improved discrimination between BA vasospasm and vertebrobasilar hyperemia and enhance the accuracy and reliability of TCD in the diagnosis of BA vasospasm [31]. Sviri and colleagues independently validated the accuracy of Soustiel's ratio, and, after showing that this ratio improved the sensitivity and specificity of TCD detection of BA vasospasm, they introduced new TCD grading criteria for BA vasospasm [32, 33].

An ongoing individual correlation of angiography with same-day TCD findings may improve the accuracy of TCD to detect vasospasm onset. A focal and disproportionate to therapy increase in flow velocities indicates the development of vasospasm. For example, an MCA MFV increase by 50 cm/s may indicate a 20% diameter reduction of the vessel, and since flow velocity is inversely proportionate to the vessel radius, a 50% diameter reduction usually doubles the velocity on TCD [38]. Therefore, TCD may be more sensitive to changes in intracranial artery diameter than angiography particularly at the early phases of vasospasm development. Since TCD is a screening tool, the criteria should be adjusted to a higher sensitivity to detect any degree of vasospasm in order to institute components of the HHH therapy. At the same time, a higher specificity threshold should be used for severe vasospasm to minimize the number of false-negative angiograms, particularly if TCD is used to select patients for angioplasty.

Hyperemia is suspected with elevated velocities in the intracranial and often in the feeding extracranial vasculature. Hyperemia changes on TCD are common in patients with SAH receiving components of HHH therapy. The use of Lindegaard ratio [15] and new flow and area indices [39] may help to minimize false-positive TCD results and predict better the diameter of the residual lumen on angiography.

Other hyperperfusion syndromes may occur after carotid endarterectomy (CEA) or angioplasty (post-revascularization hyperemia) usually characterized by a ≥30% increase in MCA MFV unilateral to the reconstructed carotid artery and low-pulsatility waveforms compared with the contralateral side, indicating decreased capacity of distal vasculature to regulate the reestablished flow [40–42]. Hyperemic reperfusion may also develop with systemic thrombolytic therapy and intra-arterial revascularization procedures for acute ischemic stroke [43].

## Acute Cerebral Ischemia

An indication "ischemic stroke" or "transient ischemic attack" may necessitate not only a complete diagnostic TCD examination [44] in order to detect the presence of stenoocclusive disease and collaterals. It can be also extended to include VMR assessment, emboli detection, cardiac right-to-left shunting (RLS) testing, as well as continuous real-time intracranial vessel monitoring. The reasons to perform TCD in patients with suspected or confirmed cerebral ischemia are multiple. First, carotid duplex alone can detect a significant (>50%) carotid stenosis or occlusion in only 15–20% of consecutive patients with stroke or TIA. Thus, the stroke mechanism remains unexplained in the majority of these patients if only carotid duplex is performed for vascular imaging. Second, magnetic resonance angiography (MRA) of the head and neck is often performed, but it is prone to artifacts, often prompting additional contrast angiography or TCD testing.

Complete TCD examination evaluates up to 16 proximal intracranial arterial segments with the goal of detecting normal, stenosed, or occluded intracranial vessels [44]. The assessment of vessel patency has prognostic significance as patients with persisting occlusions have worse outcomes if reperfusion therapy is not instituted timely or is ineffective [45]. This information is also helpful to select patients for catheter angiography, intra-arterial rescue procedures, and potentially hemicraniectomy.

TCD evaluation also has diagnostic significance to identify stroke pathogenic mechanisms, i.e., large-vessel stenosis, or artery-to-artery embolism as opposed to a cardiac or paradoxical embolism source. Patients with intracranial disease are at high (10–15% annually) risk of stroke recurrence.

The same TCD examination can detect collateral flow and the hemodynamic significance of extracranial or intracranial steno-occlusive lesions [46–54]. This information is helpful to identify a proximal arterial obstruction and to clarify carotid duplex or noninvasive angiographic findings including MRA and CT angiography (CTA). Carotid duplex and MRA are known to produce falsely elevated estimates of the degree of carotid stenosis, and TCD, via collateral and downstream hemodynamic effects, can help clarify false-negative and false-positive diagnosis of severe ICA stenosis. A severe ICA stenosis should produce downstream flow changes directly detectable by TCD, and if no delay in systolic flow acceleration is seen or no collaterals are detected, these TCD findings likely indicate moderate proximal ICA stenosis [43, 46, 51]. On the other hand, if extracranial duplex scanning does not reveal a severe ICA lesion (e.g., high carotid bifurcation), the presence of unilaterally delayed systolic flow acceleration or intracranial collaterals would suggest the presence of a severe proximal ICA lesion. It is recommended to perform TCD studies always in conjunction with ultrasound examination of the extracranial brain supplying arteries in patients with stroke or TIA [12].

For intracranial steno-occlusive lesions, intracranial MRA often shows flow gaps due to turbulence or reversal of flow direction, thus overestimating the degree of stenosis. TCD findings of focal elevated velocities confirm the presence of an intracranial stenosis or collaterals when applicable, and validated diagnostic criteria are available [43, 55].

## Intracranial Atherosclerotic Disease

Intracranial atherosclerotic disease is now recognized as a serious risk factor with severe and multiple lesions carrying the highest risk of stroke recurrence. Recent emphasis on identification of ≥50% and ≥70% stenoses prompted reevaluation of the current criteria and development of new ones.

## Middle Cerebral Artery Stenosis

Primary findings for any significant ≥50% MCA stenosis include a focal significant MFV or PSV increase (≥100 or ≥140 cm/s, respectively) or interhemispheric MFV difference of 1:2 in adults free of cerebrovascular disease [48, 51, 56–64]. A ≥70% MCA stenosis could produce higher velocities, and in our laboratory, we use a MFV cutoff >120 cm/s [65]. This velocity increase should be further associated with a ratio to a homologous segment of 1:3 or higher. If anemia, congestive heart failure, and other circulatory conditions associated with elevated or decreased velocities, a focal MFV difference ≥30% between neighboring or homologous arterial segments should be applied to see if the velocity increase reaches any significance. Adult patients with anemia or hyperthyroidism often have increased MCA mean flow velocities. In children with sickle cell disease, MCA MFV ≥170 cm/s is considered abnormal [19].

Additional findings may include turbulence (occasionally a low-frequency noise produced by nonharmonic co-vibrations of the vessel wall and musical murmurs due to harmonic co-vibrations producing pure tones can be heard) or disturbed flow distal to the stenosis or presence of characteristic flow voids on PMD-TCD indicating a low-frequency bidirectional turbulent flow during systole; an increased unilateral ACA MFV may indicate compensatory flow diversion or A1 ACA or ICA bifurcation stenosis, and microembolic signals (MES) found in the distal MCA.

If MFVs are increased throughout the M1 MCA, the differential diagnosis includes MCA stenosis, terminal ICA or siphon stenosis, hyperemia or compensatory flow increase in the presence of contralateral ICA stenosis, ACA occlusion, and incorrect vessel identification.

A critical stenosis or obstruction with near-occlusive thrombus or embolus can either produce a focal velocity increase or a blunted MCA waveform with slow or delayed systolic acceleration, slow systolic flow deceleration, low velocities, and lower MFVs in the MCA than ACA or any other intracranial artery [48, 51, 53]. Decreased or minimal flow velocities with slow systolic acceleration can be found due to a tight elongated MCA stenosis or thrombus causing near-occlusion. These focal lesions should be differentiated from a proximal ICA obstruction that can also produce delayed systolic flow acceleration in the MCA [30, 46–54].

To confirm the presence of a flow-limiting lesion, arterial branches need to be evaluated. Note that an M1–M2 MCA near-occlusion is usually accompanied by flow diversion to the ACA and/or compensatory flow increase in the PCA, indicating transcortical collateralization [53, 66].

## Anterior Cerebral Artery Stenosis

Primary findings for any significant ACA stenosis include a focal significant mean flow velocity increase (ACA > MCA) and/or a ≥30% difference between the proximal and distal ACA segments and/or interhemispheric ACA MFV difference of ≥30% (these are the original criteria, but in reality ACA MFV velocity should at least double the velocity of the reference vessel) [51, 63, 66]. Collateralization via the anterior communicating artery (AComA) can be excluded by a normal contralateral ACA flow direction. Usually an ACA stenosis can be detected at depth of 60–75 mm. The differential diagnosis includes anterior cross-filling due to a contralateral proximal carotid artery obstruction [46–49].

Additional findings may include turbulence and a flow diversion into the MCA and/or compensatory flow increase

in the contralateral ACA. Decreased or minimal flow velocities at the A1 ACA origin may indicate a suboptimal angle of insonation from the unilateral temporal window, an atretic or tortuous A1 ACA segment, or A1 ACA near-occlusion. Since the A2 ACA segment cannot be assessed directly by TCD, its obstruction can be suspected only if a high-resistance flow is found in the distal dominant A1 ACA segment.

Common errors include incorrect vessel identification (terminal ICA versus ACA), velocity underestimation (suboptimal angle of insonation, poor window, weak signals) and inability to differentiate a collateral flow from the stenosis.

## Terminal Internal Carotid Artery and Siphon Stenosis

A terminal ICA (traceable through the temporal window) and ICA siphon (traceable through the transorbital window) stenosis produces a focal significant MFV increase (ICA > MCA, and/or an ICA MFV ≥70 cm/s, and/or ≥30% difference between arterial segments) [43, 51, 63, 67].

The differential diagnosis includes moderate proximal ICA stenosis and/or compensatory flow increase with contralateral significant ICA obstruction. Additional findings in the presence of an ICA stenosis may include turbulence, blunted unilateral MCA, OA MFV increase, and/or flow reversal with low pulsatility. The ICA siphon MFV may decrease due to siphon near-occlusion (a blunted siphon signal) or distal obstruction (i.e., MCA occlusion or increased ICP).

Common errors include incorrect vessel identification such as MCA versus TICA via transtemporal approach or ACA versus ICA with deep transorbital insonation and consequently collateralization of flow via the anterior cross-filling misinterpreted as an arterial stenosis. In the absence of temporal windows, these findings may be the only yet confusing indicators of a significant carotid artery lesion.

## Posterior Cerebral Artery Stenosis

A focally significant PCA stenosis results in an MFV increase PCA > ACA or ICA and/or a PCA MFV ≥50 cm/s in adults [54, 63, 68–70]. Additional findings may include turbulence and a compensatory flow increase in the MCA.

The differential diagnosis includes collateral flow via the posterior communicating artery (PComA) either toward the posterior circulation in case of BA occlusion or toward the anterior circulation in case of MCA, TICA, or tandem extracranial ICA/MCA occlusions and siphon obstruction. Of note, PComA is a tortuous vessel, and its flow direction on TCD does not necessarily indicate where the lesion is that requires collateralization. Using TCCD, it may be possible to differentiate PCA stenosis from collateralization of flow using PSV [71].

Common sources of error include unreliable vessel identification and a top-of-the-basilar stenosis.

## Basilar Artery Stenosis

Primary findings in the presence of a BA stenosis include a focal significant MFV increase BA > MCA or ACA or ICA, and/or an MFV BA ≥60 cm/s in adults, and/or a ≥30% difference between arterial segments [43, 54, 63]. The findings of a recent study indicate that a BA stenosis of ≥50% can be more reliably identified when BA MFV exceeds 80 cm/s [53, 64]. To detect ≥70% intracranial vertebrobasilar stenosis, we use MFV increase >110 cm/s and a stenotic/pre-stenotic ratio ≥3 [65].

The differential diagnosis includes a terminal VA stenosis if elevated velocities are found proximally, i.e., at a depth of 70–80 mm. If elevated velocities are found throughout the entire BA course, the differential diagnosis includes a compensatory flow velocity increase, i.e., in case of a carotid artery obstruction. With the latter velocities are increased in at least one of the VAs.

Basilar artery near-occlusion produces a focal MFV decrease (≤30% difference between neighboring arterial segments and/or BA < VA) resulting in a blunted waveform [54]. The differential diagnosis includes a fusiform (dolichoectatic) BA with or without thrombus since an enlarged vessel diameter may reduce flow velocities. If the end-diastolic flow is absent, the differential diagnosis includes BA occlusion or tortuosity with branch insonation at a suboptimal angle.

Additional findings may include turbulence and disturbed flow signals distal to the stenosis, compensatory flow increase in VAs and posterior cerebellar inferior arteries indicating cerebellar collateralization, and a collateral supply via PComA to PCA with a reversed flow in the distal BA.

Common sources of error include a tortuous basilar ("not found" does not always mean obstructed), elongated BA obstruction, and distal BA lesions that were not reached by TCD or identified due to flow presence to the superior cerebellar arteries producing false-negative results. Application of ultrasound contrast and TCCD may help the detection of the distal BA segment, tortuosity, and distal branches [43, 54, 72, 73]. A collateral flow from the posterior to the anterior circulation in the presence of carotid lesions may increase flow velocity changes associated with mild stenosis and/or tortuosity. In the case of flow collateralization, the dominant VA velocities are also increased [74]. Reversed flow in the BA (low-resistance flow toward the probe) is characteristic for a proximal BA occlusion with retrograde filling of the distal BA through the PComA [54, 75]. The origin of the collateral flow in the anterior circulation can be confirmed with carotid artery tapping that can be transmitted to the reversed flow.

## Intracranial Vertebral Artery Stenosis

Primary findings of an intracranial VA stenosis include a focal MFV increase VA > BA, and/or MFV VA ≥50 cm/s in adults, and/or a ≥30% difference between VAs or its neighboring segments [43, 63, 76]. Recent findings have indicated that a ≥50% VA stenosis can be more reliably identified when VA MFV exceeds 80 cm/s and when the stenotic-to-normal MFV ratio is ≥2 [53, 64]. A ≥70% VA stenosis could produce higher velocities, and in our laboratory, we use a MFV cutoff >110 cm/s and a stenotic-to-normal MFV ratio of ≥3 [65].

The differential diagnosis includes proximal BA or contralateral terminal VA stenoses and a compensatory flow increase in the presence of a contralateral VA occlusion or carotid lesion.

Additional findings may include turbulence or disturbed flow signal distal to the stenosis; a compensatory elevated velocity in the contralateral VA, posterior cerebellar inferior arteries, or other cerebellar arteries (cerebellar collaterals); low BA flow velocities (hemodynamically significant lesion, hypoplastic contralateral VA) and low-resistance flow distal to stenoses (compensatory vasodilation); and the presence of distal MES in the BA or cerebellar collaterals.

Common sources of error include a compensatory flow increase due to hypoplastic contralateral VA, low velocities in both VAs due to a suboptimal angle of insonation, extracranial VA stenosis or occlusion with well-developed muscular collaterals, elongated VA stenosis/hypoplasia, and incorrect vessel identification, i.e., posterior cerebellar inferior artery (PICA).

## Arterial Occlusion

The diagnosis of an acute intracranial arterial occlusion with TCD is difficult. The operator must be experienced and the best results are usually obtained for M1 MCA, terminal ICA/siphon, and BA. The main requirement for confidence in TCD findings is a good window of insonation (or the ability to use imaging or contrast agents) whereby other patent arteries should be identified through the same approach. To achieve better sensitivity to slow and weak flow, a single-gate spectral TCD system should be set at the maximum allowed power and a large sample volume (12–15 mm). A PMD-TCD system should be set at a depth range of presumed arterial occlusion and a small spectral TCD sample volume (3 mm) as it allows a higher power output compared with a large sample volume.

An acute lesion may represent a complete occlusion, subtotal stenosis or partial, yet hemodynamically significant flow obstruction or near-wall thrombus with the only signs being marginal elevation of velocities and occasional distal microemboli. Instead of relying on velocity measurements in detectable segments, the TCD examiner should pay attention to waveform patterns and signs of flow diversion, collateralization, and embolization. Waveform morphology discloses more information about clot location, hemodynamic significance of obstruction, and resistance in the distal vasculature than velocity difference by itself. This approach leads to a greater yield of abnormal TCD findings that are highly predictive of the presence of a thrombus at invasive angiography [77–79]. For example, if the affected MCA MFV is ≤30% compared with the non-affected side and the waveform shows delayed systolic flow acceleration, this could point to a proximal ICA obstruction and not necessarily an isolated MCA lesion. Further waveform analysis of the MCA is required to establish the presence of an additional lesion in the MCA. If diastolic flow disappears at any depth along the MCA, this strongly suggests the presence of a tandem occlusion. The presence of a diastolic flow at 45–65 mm could imply patency of small perforating arteries arising from the M1 MCA. Demchuk et al. developed the Thrombolysis in Brain Ischemia (TIBI) flow grading system to predict success of intracranial clot lysis and short-term improvement after ischemic stroke (Fig. 10.3) [79]. Based on previous studies and our own correlations with invasive angiography, our group described detailed criteria for intracranial occlusions on TCD [57, 68, 78–83].

## MCA Occlusion

For the diagnosis of an MCA occlusion, an abnormal waveform (TIBI flow grades 0–3) has to be found at a depth of 30–65 mm via the transtemporal approach. The presence of positive end-diastolic flow (TIBI flow grades 2–3) implies flow to the nearest branching vessels to the depth at which these were located such as perforators, anterior temporal artery, or M2 MCA.

Additional findings are a flow diversion and/or a compensatory velocity increase in the unilateral ACA and/or PCA, no flow signals in the ACA and ICA with PCA flow identified (possible "T"-type terminal ICA occlusion), and a diastolic flow and overall velocity decrease from the TICA to the distal MCA.

## Intracranial Internal Carotid Artery Occlusion

With an intracranial or TICA occlusion, TCD findings are dependent on collateralization and the extent of occlusion into the MCA such as "T" or "L" types. If an extension into the MCA is present, TIBI flow grades 0–2 are usually found with MCA velocities below 20 cm/s [84]. Additionally, there is either partial or complete anterior cross-filling with A1 ACA reversal and retrograde filling of the siphon. Besides abnormal TIBI waveforms at 60–70 mm and recruitment of

## TIBI flow grade definitions

For credentialing purposes, interpret flow singals above the baseline. supporting flow information may be gained from the entire image. For interpretation, assume all images are optimized (i.e. appropriate gain, power window, angle, sample volume, depth).

**0. Absent**

Absent flow singnals are defined by the lack of regular pulsatile flow signals depite varying degree of background noise

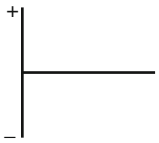


**1. Minimal**

A-systolic spikes of variable velocity and duration

B-absent diastolic flow during all cardiac cycles based on visual interpretation of periods of no flow during end diastoli (ED). Reverberating flow is a type of minimal flow.

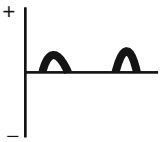


**Caution:** Despite absent ED flow by visual interpretation, TCD equipment may erroneously report end diastolic velocity figures due to noise artifacts. Do not rely on machine ED velocity mesurements to determine the presence or absence of end diastolic flow.

**2. Blunted**

A- flattened or delayed systolic flow acceleration of variable duration compared to control

B- positive end diastolic velocity

C- a pulsatility index (PI) < 1.2.

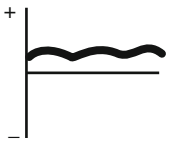


**Caution:** Flow velocities are usually >20% lower than those in the comparison side.

**Caution:** With low velocities, blunted versus minimal signals may hard differentiate. Blunted is distinuished by the visual presence of end-diastolic flow.

**3. Dampened**

A- normal systolic flow acceleration

B- positive end diastolic velocity

C- decreased mean velocities by ≥30% compared to control (plese calculate if close).

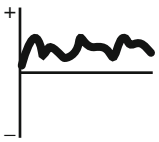


**Caution:**With subtle velocity/PI difference, look for dampened waveforms to have a more pulsatile shape

**Caution:** Dampened versus blunted signals can be differentiated by dampened having a clear peak systolic complex (initially sharp systolic upstroke without flattening).

**Caution:** Dampened versus normal signals can be distinguished by dampened having a more abrupt down-slope of late systoli and early diastoli and other signs of obstruction, i.e. flow diversion (flow velocity ACA > MCA – where flow velocities below the baseline are greater than those above the baseline).

**4. Stenotic**

A-mean flow velocities of ≥80 cm/s AND velocity difference of ≥30% compared to the control side (please calcuate if close); if velocity difference is less than 30% look for additional sighs of stenosis, i.e. turbulence, spectral narrowing

OR

B-if both affected and comparison sides have MFV <80 cm/s due to low end-diastolic velocities, mean flow velocities ≥30% compared to the control side (please calculate if close) AND signs of turbulence.

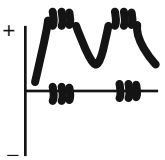


**5. Normal**

A-<30% mean velocity difference compared to control (please calculate if close)

B-similar waveform shapes compared to control

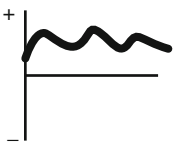


**Caution:** Hypertensive individuals may have symmetric, high resistance signals with PI ≥ 1.2 and low end-diastolic velocities.

**Caution:** Normal versus blunted signals can be differentiated by normal waveforms having initial sharp systolic upstrokes even if the rest of the waveform shows slow deceleration (note slower heart rate).

**Fig. 10.3** Detailed TIBI flow grades definitions (With permission from the Health Outcomes Institute, Inc.)

collaterals and contralateral compensatory velocity increases, ICA occlusions above the origin of the OA can also produce a high resistance or dampened ICA siphon signal transorbitally and velocity reduction and pulsatility increase in the proximal ICA on carotid duplex examination. The hallmark of an isolated distal ICA occlusion is the presence of patent proximal ICA on duplex and traceable MCA signals (often blunted) throughout MCA stem and the presence of collateralization of flow indicating a hemodynamically significant lesion in the ICA.

With a proximal ICA occlusion, the most common findings include a blunted MCA signal and reversed OA or absent orbital signals from the OA and ICA siphon. TCD cannot differentiate complete ICA occlusion from hemodynamically significant proximal high-grade stenosis, and direct carotid examination should be used to answer this question.

Additional findings may include collateral flow in the PComA and/or anterior cross-filling via AComA, compensatory velocity increase in the contralateral ICA, blunted MCA waveform, and MES in the unilateral TICA/MCA.

## Basilar Artery Occlusion

Abnormal waveforms suggestive of a BA occlusion can be found either at the distal end of the dominant VA or at 80–100+ mm via the transforaminal approach. Additional findings may include a flow velocity increase in one or both VAs or PICAs, indicating collateral flow in the cerebellar arteries; a high-resistance flow signal in one or both VAs, indicating proximal BA occlusion; a high-resistance flow signal at the origin of the BA, indicating distal BA occlusion; retrograde (low-resistance, increased velocity) flow toward the probe at the top of the BA (proximal BA occlusion collateralized via anterior circulation); functional PComA with flow directed away from the probe via the transtemporal approach; and decreased velocities in the distal BA or an absent end-diastolic flow indicating distal BA occlusion [43, 54].

## Intracranial Vertebral Artery Occlusion

The most accurate diagnosis with TCD can be made for a terminal VA occlusion [76]. However, the sensitivity of abnormal flow findings is low [84], and a normal intracranial TCD examination cannot completely rule out the presence of a VA occlusion.

An occlusion of the intracranial VA may produce a high-resistance (PI ≥ 1.2) flow in one of the VAs proximal to the obstruction and/or a blunted or minimal flow signal including signals with a reverberating or oscillating pattern. However, the diagnosis of an intracranial VA occlusion is difficult to establish using TCD alone, since it has to be differentiated from an atretic terminal VA segment that could be present distal to PICA origin, may present as a short and collateralized occluded segment, and an extracranial segmental VA occlusion may also be present.

Additional findings may include normal flow signals directed toward the probe on the side of occlusion indicating collateralization of flow from the other side and filling of PICA as well as distal embolization in the PICA [54].

## Intracranial Collateral Pathways

The intracranial collateral channels are "dormant" under normal circulatory conditions. A collateral channel opens when a pressure gradient develops between the two anastomosing arterial systems. TCD can directly detect collateral pathways via AComA (anterior cross-filling), PComA, reversed OA, and reversed BA [43, 51, 54, 85–88].

Collateral flow is directed from the donor to the recipient vessels. When present, a collateral flow rarely implies an anatomic variant. Mostly, detection of a collateral channel implies the presence of a flow-limiting lesion or an anatomic variant proximal to the recipient arterial system and the origin of the collateral channel.

The direction of flow determines which arterial system is the donor (the source of flow) and which is the recipient (the collateral flow destination). TCD can provide information on whether any collateral channel is functioning and in which direction it is working. This information can be used to estimate the level of the arterial obstruction and to refine the extracranial duplex ultrasound or MRA findings. For example, an extracranial hemodynamically significant ICA lesion can be accompanied by abnormal TCD findings. A battery of TCD parameters may be used to decide on the severity of ICA lesions, particularly when multiple lesions are found or the applicability of other tests is limited due to the presence of a distal ICA lesion [46–50].

## Reversed Flow in the Ophthalmic Artery

A reversed flow through the OA via the transorbital approach is primarily directed away from the probe and accompanied by a low PI (transorbital at 40–60 mm depth). The differential diagnosis includes siphon flow and/or low velocity OA flow signals.

Additional findings may include no substantial difference in MFVs detected in OA and siphon; high velocities in the ICA siphon, suggesting either a high-grade proximal ICA and/or siphon stenosis; and no flow signals at depths ≥60 mm, suggesting a proximal ICA occlusion.

If the reversed OA is the only abnormal finding, this indicates possible proximal ICA occlusion or severe stenosis.

Occasionally, this may be the only sign of an ICA dissection. If the reversed OA is found with a delayed systolic flow acceleration in the ipsilateral MCA, there is a probable proximal ICA occlusion or severe stenosis and collateralization capacities through the circle of Willis are likely suboptimal (i.e., atretic A1 ACA or absent PComA). If a reversed OA is found with at least one other collateral channel (i.e., partial anterior cross-filling or PComA), there is a definite proximal ICA occlusion or a high-grade stenosis.

Common sources of error include shallow or deep OA insonation, vessel identification problems (vein, branching and anastomosing arteries in the orbit), ICA dissection with considerable residual flow, terminal ICA occlusion distal to the OA origin, and retrograde filling of the ICA siphon with a normal OA direction. Furthermore, a normal OA direction does not rule out a proximal ICA stenosis.

## Anterior Communicating Artery and Anterior Cross-Filling

The collateral flow through AComA cannot be reliably distinguished from the neighboring A1 and A2 ACA segments due to the smaller AComA length and diameter compared with a large sample volume with which TCD intercepts this area. Therefore, we report findings consistent with the anterior cross-filling via AComA as opposed to the velocity and direction of flow in AComA itself. Sometimes, a high-velocity jet with bruit can be found at midline depth, highly suggestive of flow interception through AComA. Even under these circumstances, other flow findings pointing to collateralization of flow should be found since focal velocity elevations can also be present with an arterial stenosis.

Anterior cross-filling may include elevated A1 ACA MFVs on the donor side presenting as ACA > MCA and/or donor ACA MFVs ≥1.2 times greater than contralateral ACA, possible stenotic-like flow at depths 72–78 mm directed away from the donor side, and a normal or low MFV in A1 ACA of the recipient side with or without A1 flow reversal.

The differential diagnosis includes distal A1 ACA stenosis and compensatory flow increase if one A1 segment is atretic. With the latter, the donor A1 segment supplies both A2 segments (may be present in normal individuals due to anatomic variations of the circle of Willis and also in patients with ICA or MCA obstructive lesions). If an elevated donor ACA velocity is found with stenotic flow at midline depths, the differential includes distal A1 stenosis, ICA siphon stenosis, and anterior cross-filling via AComA. If an elevated donor ACA MFV is found with a reversed contralateral A1, this indicates probable proximal ICA stenosis. If an elevated donor ACA MFV is found with stenotic-like flow at midline depths and a reversed contralateral A1 ACA, there is a definite proximal ICA stenosis or occlusion. The identification of a reversed A1 segment depends on the skills of the operator. With retrograde filling of the ICA siphon, the terminal ICA can have bidirectional flow. Thus, the flow away from the probe (i.e., toward the siphon) may be mistaken for a normal A1 ACA flow direction. A clue to differential diagnosis is that flow velocities tend to be higher, the closer one insonates to the donor site.

## Posterior Communicating Artery

PComA connects the posterior and anterior cerebral arterial systems and can be detected by TCD since it usually has a considerable length of >5 mm and a favorable angle of insonation. When functioning, it may be detected as a flow signal consistently present at varying depths from 55 to 70 mm via the transtemporal approach. Under normal conditions, this area has no detectable flow when the sonographer switches from the ICA bifurcation posteriorly to locate the PCA. The direction of flow in PComA corresponds to collateralization: anterior to posterior collateral flow is directed away from the probe, whereas the posterior to anterior collateral flow is directed toward the probe. Flow direction, however, can be misleading due to the tortuosity of PComA. Without imaging, vessel identification is difficult since the PComA and PCA are prone to anatomic variations.

The velocity range is similar to or higher than those detected in M1 MCA and ICA bifurcation (anterior to posterior collateral flow) or BA (posterior to anterior collateral flow). A possible stenotic-like flow may be present. Elevated velocities can also be found all the way to the top of the basilar and in the P2 PCA segment. The differential diagnosis includes terminal ICA or PCA stenosis.

Of note, collateralization of flow via PComA carries the systolic flow acceleration signature from the donor site. The posterior to anterior circulation flow could have a slight delay in systolic acceleration similar to that seen in the VAs, whereas anterior to posterior collaterals often have more vertical upstroke similar to that in the ICAs.

## Reversed Flow in the Basilar Artery

With advantages in transcranial imaging and also PMD-TCD, it became possible to perform more detailed bedside studies of the distal BA in patients with acute posterior circulation strokes. The finding of a reversed BA arises from either functional PComA or cerebellar collaterals and could explain less devastating symptoms and better prognosis in some patients with a proximal BA occlusion [54, 75].

A reversed flow in the BA may be present with a low-pulsatility flow toward the probe (i.e., reversed basilar flow

at 80–100 mm), an absent antegrade flow signal in the BA via suboccipital insonation, and an anterior circulation flow origin at the top of the BA demonstrated by vertical systolic flow acceleration similar to that in the ICA and also a response to the common carotid tapping (perform carotid tapping only after a significant stenosis or hypoechoic plaque has been excluded by extracranial duplex examination).

## Vasomotor Reactivity

Transcranial Doppler can include assessment of VMR. During this noninvasive test, voluntary breath holding increases the arterial level of carbon dioxide, and TCD is used to measure velocity response to this natural vasodilatory stimulus [89]. Vasomotor reactivity is represented by the breath-holding index (BHI), which is the ratio of the percent MFV increase during hypercapnia over the time of breath holding. Baseline mean flow velocities are obtained (most reliably and reproducibly at the M1 MCA) during inhalation of room air followed by 30 s of breath holding. Subsequently, MFVs are recorded during a 4-s period.

The BHI has been validated against MRI and studied in patients with symptomatic and asymptomatic extracranial carotid artery disease [90–94]. TCD VMR testing can identify high-risk patients for first-ever or recurrent stroke in the setting of extracranial internal carotid artery stenoses or occlusions [90–94]. Interestingly, in patients with asymptomatic or symptomatic carotid artery occlusions and impaired VMR in the absence of collateral pathways, the annual risk of ipsilateral stroke was shown to be 32.7% compared to 0% in carotid artery occlusion patients with normal VMR and normal collaterals [91]. In addition, Silverstrini et al. reported that in patients with severe asymptomatic carotid artery stenosis, the annual ipsilateral ischemic event risk was 4.1% in patients with normal and 13.9% in those with impaired VMR (defined as a breath-holding index of ≤0.69) [90]. This information is not available from carotid duplex ultrasound examination and may require additional contrast studies with CT perfusion, MR perfusion, or single-photon emission CT (SPECT) with acetazolamide (Diamox) that are costly and may lead to complications related to vasoactive acetazolamide effects that last longer than a brief hypercapnia with breath holding.

Findings of a diminished or exhausted vasomotor reactivity were established as a risk factor for stroke [95] and can prompt the consideration of carotid endarterectomy (CEA) or stenting in patients with asymptomatic carotid stenosis or consideration of extra-intracranial bypass surgery in patients with recurrent hemodynamic strokes or TIAs that fail medical therapy. In addition, a recent study showed that a decrease in cerebrovascular reactivity may be responsible for reduction in some cognitive abilities involving the function of the hemisphere ipsilateral to carotid stenosis [96]. Such findings may be of interest for providing a more comprehensive indication to surgical treatment in subgroups of subjects with asymptomatic carotid stenosis.

## Cerebral Embolization

Patients with ischemic strokes, TIAs, or asymptomatic high-grade ICA stenosis can undergo TCD monitoring to detect, localize, and quantify cerebral embolization [97–100]. This information is helpful to establish the diagnosis and change management strategy, if emboli are found pointing to artery-to-artery embolization or continuing embolization despite treatment both in patients with symptomatic and asymptomatic extracranial or intracranial large artery disease [101]. The presence of emboli on TCD distal to a high-grade asymptomatic ICA stenosis identifies patients at higher risk of first-ever stroke that could justify carotid revascularization [100–102]. It can also be used to monitor carotid and cardiac surgery, angioplasty/stenting, and intra-arterial rescue procedures in acute stroke. Occasionally, the presence of emboli on TCD can be the only sign of a proximal arterial dissection, partially occlusive thrombus, or unrecognized cardiac or paradoxical source of embolism [66].

Most microemboli signals (MES) detected by TCD are asymptomatic since the size of the particles producing them is usually comparable to or even smaller than the diameter of the brain capillaries [99]. However, the MES cumulative count is related to the incidence of neuropsychological deficit after cardiopulmonary bypass, stroke after CEA, and the significance of MES as a risk factor for stroke is emerging [97, 98, 103, 104].

Strict standards should be followed when an examiner documents and reports MES on TCD [105]. The gold standard for MES identification still remains the on-line interpretation of real-time, video-taped, or digitally stored flow signals. The spectral recording should be obtained with minimal gain at a fixed angle of insonation with a small (<10 mm) sample volume. The probe should be maintained with a fixation device during at least 30 min of monitoring. The use of a two-channel simultaneous registration and a prolonged monitoring period may improve the yield of the procedure. Multi-gated or multiranged registration at different insonation depths may improve differentiation of embolic signals from artifacts.

According to the International Cerebral Hemodynamics Society definition [106], MES have the following characteristics (Fig. 10.4):

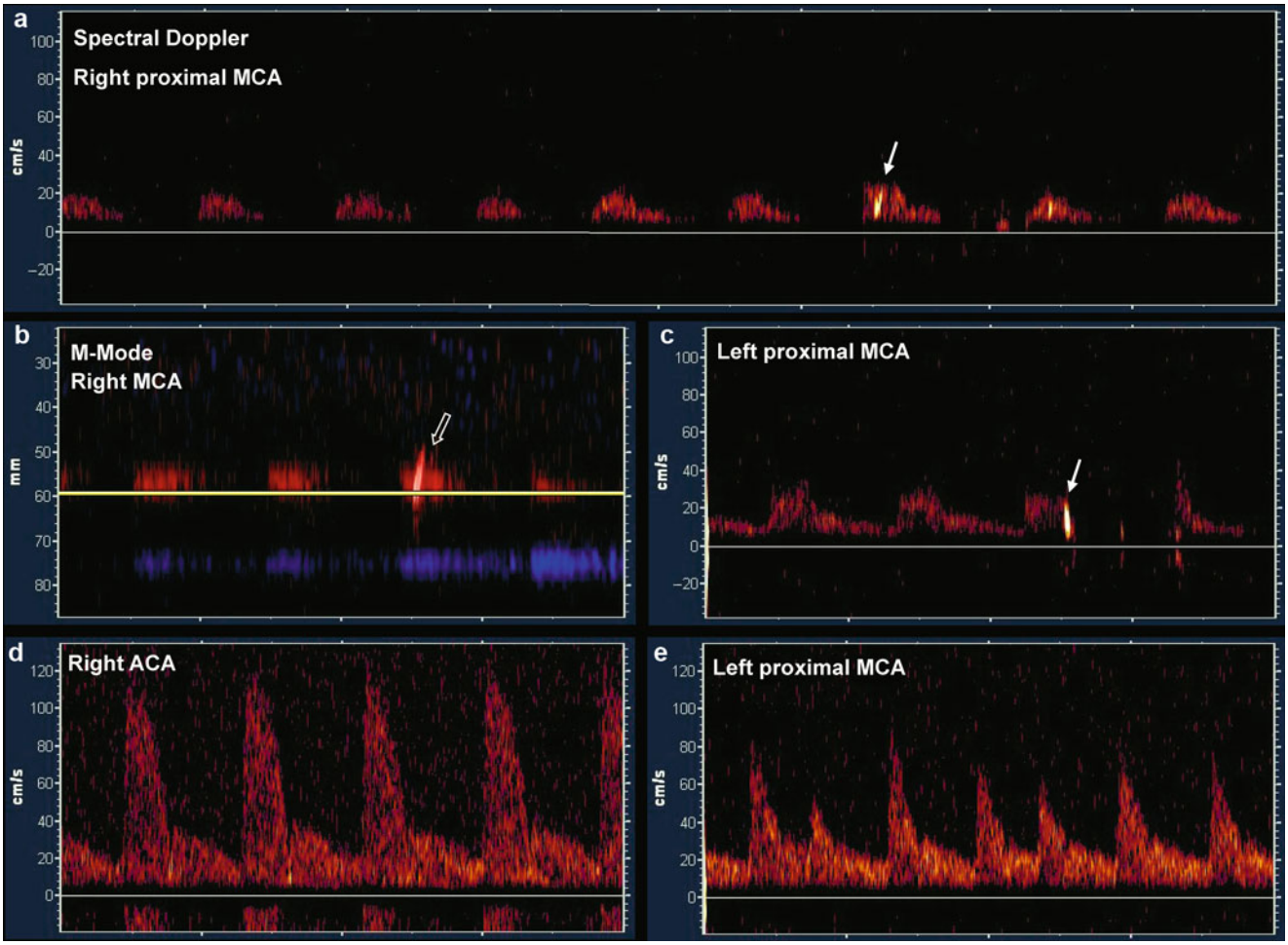


**Fig. 10.4** Pretreatment minimal flow signal (**a** – TIBI flow grade I) and microemboli (**a**–**c**; *arrows* on Doppler spectra, *block arrow* on M-Mode) in a patient with a right middle cerebral artery (*MCA*) occlusion, atrial fibrillation (note microembolic signals in both *MCAs*), and an NIHSS score of 14 points. Right anterior cerebral artery (*ACA*) has flow diversion (**d**) and complete recanalization of the right MCA 24 h after intravenous thrombolysis (**e**)

1. Random occurrence during the cardiac cycle
2. Brief duration (usually <0.1 s)
3. High intensity (>3 dB over background)
4. Primarily unidirectional signals
5. Audible component (chirp, pop)

There is an agreement that no current system of automated embolus detection has the required sensitivity and specificity for clinical use. Therefore, the interpreting physician has to review every stored signal, listen to the sound characteristics, determine the difference between the signal and background (dB), and attempt to determine the source of microemboli.

## Detection of Cardiac Right-to-Left Shunt

Patients with ischemic stroke and TIA and suspected paradoxical embolism can undergo TCD "bubble" test to detect cardiac RLS [107]. TCD detection of RLS is less expensive than echocardiography and has been shown equivalent or even superior to both transthoracic (TTE) and transesophageal (TEE) echocardiography [108–114]. Criteria have been developed and validated to quantify the degree of RLS using MES counts on spectral or PMD-TCD display [112]. Spencer et al. compared the diagnostic yield of single-channel TCD to PMD-TCD for the detection of RLS. They documented significantly more microemboli detectable on PMD than on single-gate TCD (for Spencer's logarithmic scale, see Table 10.4) [112]. Moreover, the diagnostic capabilities of PMD and TEE for detecting PFO were comparable and corresponded to the anatomical findings determined during cardiac catheterization.

The key advantage that TCD offers is that patients can do calibrated Valsalva maneuver, and the test can be repeated with different body positions [112, 114]. TCD has particular value to be performed in younger stroke and TIA patients

**Table 10.4** Spencer's logarithmic scale for the grading of cardiac right-to-left shunt during bilateral middle cerebral artery monitoring

| Grade | No. of embolic tracks[a] |
|---|---|
| 0 | 0 |
| I | 1–10 |
| II | 11–30 |
| III | 31–100 |
| IV | 100–300 |
| V | >300 |

Modified from Alexandrov and Neumyer [37]. With permission from John Wiley & Sons, Inc.
[a]Originally performed on PMD-TCD during bilateral MCA monitoring

with negative echocardiographic studies. Moreover, a recent report demonstrated the utility of TCD in diagnosing residual or secondary RLS following balloon occlusion of patent foramen ovale (prevalence 20%) [115].

## Increased Intracranial Pressure

The brain constitutes a low-resistance vascular system, and with normal or low ICP, this is reflected by a normal waveform on TCD. When ICP increases up to the diastolic pressure in the resistance vessels, EDV is being affected first as it decreases and flow deceleration occurs more rapidly. These changes on TCD are often noted with ICP values of 20 mmHg or higher [116–121]. When ICP becomes greater than diastolic blood pressure, but less than systolic pressure, the result is either a triphasic waveform as seen in the peripheral arteries or a sharply peaked systolic signal and an absent end-diastolic component. A further increase in ICP may lead to cerebral circulatory arrest.

An increasing ICP usually presents on TCD as end-diastolic velocity decrease, PI increase (≥1.2; for previously normotensive young patients), RI increase, shortening of the trans-systolic time, decrease in PSVs and MFVs, abolishment of the end-diastolic flow, appearance of reverberating or oscillating flow signals, and disappearance of detectable blood flow signals.

The following algorithm may help to differentiate among the mechanisms of increased resistance to flow.

If PI ≥ 1.2 and a positive end-diastolic flow are present in:

1. All arteries: hyperventilation, increased cardiac output, hypertension, increased ICP
2. Unilateral: compartmental ICP increase, stenosis distal to the site of insonation
3. One artery: distal obstruction (spasm, stenosis, edema)

If PI ≥ 2.0 and end-diastolic flow are absent in:

1. All arteries: distal arterial occlusion, extremely high ICP, possible cerebral circulatory arrest
2. Unilateral: compartmental ICP increase, distal occlusion
3. One artery: distal obstruction (severe spasm, occlusion, edema)

## Cerebral Circulatory Arrest

Progressive elevation of ICP due to brain edema or mass effect can lead to stepwise compression of small and large intracranial arteries, eventually resulting in cerebral circulatory arrest. A prolonged absence of brain perfusion can be detected using a reverberating (oscillating) flow pattern, systolic spike, or absent flow signals, and this process will lead to brain death [122–130].

TCD is a reliable tool to confirm cerebral circulatory arrest with accuracy parameters close to 100% at experienced centers [122–129]. Based on previous published studies, reviews, and criteria [122–129], and our own clinical experience, we developed the following scanning protocol and algorithm if cerebral circulatory arrest is suspected:

1. Document arterial blood pressure at the time of TCD examination
2. Assess both MCAs and BA
3. If positive MCA or BA end-diastolic flow is found = no cerebral circulatory arrest
4. Absent end-diastolic flow = uncertain cerebral circulatory arrest (too early or too late)
5. Reversed minimal end-diastolic flow = possible cerebral circulatory arrest (continue monitoring, document diastolic blood pressure ≥50 mmHg)
6. Reverberating flow = probable cerebral circulatory arrest (confirm in both MCAs at depths of 50–60 mm and BA at 80–90 mm, then monitor arrest for 30 min if TCD is used as a sole confirmatory test)

TCD cannot be used to diagnose brain death since this is a clinical diagnosis [114]. It can be used to confirm cerebral circulatory arrest in adults and children except in infants younger than 6 months old [105–113]. TCD can be used to monitor progressive flow toward cerebral circulatory arrest. Once a reverberating flow signal is found, it should be monitored for at least 30 min in both MCAs and BA to avoid false-positive findings. Also, avoid insonation of bifurcations, i.e., MCA/ACA, since bidirectional reverberating signals may overlap, creating an illusion of positive EDV.

A transient cerebral circulatory arrest can occur in patients with SAH and head trauma due to A-waves of ICP or in other critically ill patients who cannot sustain their cardiac function and diastolic blood pressure drops below 50 mmHg. The

latter could lead to absent diastolic flow or reverberating flow signals that would be rapidly replaced by low-resistance flow once blood pressure rises.

## Subclavian Steal

The findings of a subclavian steal indicate the presence of a hemodynamically significant obstructive lesion (mostly atherosclerotic) in the subclavian artery [131–135]. Occasionally, this steal phenomenon can produce symptoms related to transient hypoperfusion in the posterior circulation territory (then it is called subclavian steal syndrome). Latent subclavian steal can be demonstrated by showing two systolic peaks with a sharp deceleration after the first peak and a more rounded second peak ("bunny rabbit" waveform, likely indicating ≥50% subclavian artery stenosis). Reactive hyperemia provoked by a blood pressure cuff (hyperemia-cuff test) can provoke a systolic flow reversal in patients with latent subclavian steal. A blood pressure cuff is inflated in the ipsilateral arm to supra-systolic values, and the patient is asked to perform physical exercise of that arm to increase metabolic demand and vasodilation. Upon sudden cuff release, a systolic flow reversal (toward the arm) with low diastolic antegrade flow (toward the brain) can be seen (alternating flow signal). A complete reversal of flow at rest is caused by a total occlusion or near-occlusion of the subclavian artery (for more details, see also the Chap. 9).

## Reversed Robin Hood Syndrome

Early neurological deterioration is a relatively frequent unfavorable course after ischemic stroke and can result in worse functional outcome [136–138]. The underlying causes are mostly neurological including arterial reocclusion, edema progression, and significant hemorrhagic transformation. However, these long-recognized mechanisms do not account for all cases of neurological deterioration or symptom recurrence.

Another potential pathophysiologic mechanism that may have serious short-term and long-term consequences for patients with acute stroke could be $CO_2$ or other vasodilatory stimuli-induced intracranial arterial blood flow steal [139, 140]. More specifically, cerebral VMR is closely interrelated to the arterial level of carbon dioxide, and cerebral blood flow changes have been documented on TCD during episodes of voluntary breath holding or inhalation of $CO_2$ [89, 141]. Under ischemic conditions, the affected vessels are less responsive to vasodilatory stimuli like $CO_2$ since they are already maximally or nearly maximally dilated to compensate for an arterial occlusion or are affected by acidosis [142]. Their vasomotor capacity is also less if compared to non-affected vessels that dilate more and change pressure gradients unfavorably for the ischemic tissues. Thus, blood flow diversion into non-affected brain tissue (along the path of least resistance) is expected to occur and may facilitate further hypoperfusion through the ischemic penumbra.

Our group has recently shown that intracranial blood flow steal is common in acute stroke patients with an acute proximal arterial occlusion and excessive daytime sleepiness (pointing to a possible association with sleep-disordered breathing) and may lead to neurological deterioration during hospitalization and a higher risk of recurrent stroke in the same arterial territory [139, 143].

Intracranial blood flow steal can be noninvasively detected in real time and quantified by TCD as paradoxical MFV reduction in the affected MCA during hypercapnia-induced and time corresponding MFV increase in the non-affected MCA with spontaneous or voluntary breath holding [139].

The steal magnitude (SM, %) is quantified as the maximum negative percentage velocity reduction during breath holding: $SM = [(MFV_m - MFV_b)/MFV_b] \times 100$, where $MFV_m$ = minimum and $MFV_b$ = baseline MFVs.

Arterial blood flow steal is considered present when SM is negative, i.e., SM < 0 in the affected vessel. After steal is documented on TCD, reversed Robin Hood syndrome (RRHS) is suspected if new or recurrent neurological worsening by ≥2 National Institutes of Health Stroke Scale (NIHSS) points is observed without concurrent changes in blood pressure or arterial patency.

In future, we hope to investigate this intracranial arterial steal phenomenon as the pathogenic link between sleep-disordered breathing and adverse short- and long-term outcome in acute ischemic stroke patients and test noninvasive ventilatory correction as potential treatment to reverse this steal and augment brain perfusion [140, 144].

### Conclusion

In summary, TCD provides a noninvasive and inexpensive (relative to angiography) noninvasive vascular test that can be used in a variety of clinical situations to provide real-time physiological information that is often unobtainable with other testing without increased patient risks (repeated radiation doses, contrast injections) and associated costs.

TCD also provides diagnostic and prognostic information that determines patient management decisions across multiple cerebrovascular conditions and periprocedural/surgical monitoring. Established broad and specific clinical indications for, and expected outcomes of, TCD are summarized in Table 10.5. For the most general homodynamic model, see the Spencer's curve (Fig. 10.5).

**Table 10.5** Established clinical indications for, and expected outcomes of, TCD testing

| Broad indication | Specific indications | Expected outcomes |
|---|---|---|
| Sickle cell anemia | Children | Robust first-ever stroke risk reduction based on TCD criteria for the need of blood transfusion and continuing use of blood transfusions |
| Ischemic stroke or TIA | Patients with acute ischemic symptoms who had cranial CT or MRI | TCD can identify patients with proximal arterial obstructions in the anterior and posterior circulation, identifying patients amenable to reperfusion therapies (intravenous thrombolysis or rescue intra-arterial therapies) |
| Ischemic stroke or TIA | Patients with subacute ischemic symptoms who had cranial CT or MRI | TCD helps determine stroke pathogenic mechanism that in turn determines secondary stroke prevention treatment. TCD also helps to localize and grade intracranial atheromatous disease process, (anterior vs. posterior vessels, diffuse vs. local disease, ≥70% stenoses that indicate high risk of stroke recurrence) |
| Ischemic stroke or TIA | Symptomatic patient at any time window who underwent carotid duplex scanning | Carotid duplex ultrasound may explain only 15–25% of all ischemic events since the prevalence of ≥50% proximal ICA stenosis is low. TCD has the ability to further refine stroke mechanism detection by determining the presence of intracranial steno-occlusive disease, embolization, shunting, and impaired vasomotor reactivity |
| Ischemic stroke or TIA | Patients with undetermined stroke mechanism, recurrent TIAs, artery to artery versus cardiac source of embolism, suspected arterial dissections | TCD is the gold standard test to detect, localize, and quantify cerebral embolism in real time. No other modality offers spatial and time resolution to detect microembolic activity, localize its source (artery vs. heart), and confirm vascular etiology of patient symptoms |
| Ischemic stroke or TIA | Patients with suspected paradoxical embolism with negative echocardiography | TCD is equal or superior in its sensitivity to the presence of any right-to-left shunt compared to echocardiography (Valsalva maneuver is best accomplished during TCD, extracardiac shunting can be detected with TCD but not TEE) |
| Ischemic stroke or TIA | Follow-up | TCD is an inexpensive noninvasive follow-up tool that can detect progression or regression in the severity of extra- and intracranial stenoses through direct velocity measurements, collaterals, and vasomotor reactivity assessment |
| Asymptomatic or symptomatic carotid artery stenosis or Occlusion | Patients who have the ICA stenosis or occlusion on carotid duplex or angiography | TCD can help identify patients at highest risk of first-ever or recurrent stroke in the setting of an ICA stenosis of variable degree or complete occlusion. TCD findings of artery-to-artery embolization and impaired vasomotor reactivity indicate 3–4-fold higher risk of stroke compared to patients with similar degree of ICA stenosis and normal TCD findings |
| Subarachnoid hemorrhage | Day 2–5 | TCD can detect the development of vasospasm days before it can become clinically apparent, and this information can be used by intensivists to step up with hemodynamic management of these patients |
| | Day 5–12 | TCD can detect progression to the severe phase of spasm when development of the delayed ischemic deficit due to perfusion failure through the residual lumen is the greatest. This information can help planning interventions |
| | Day 12 – end of ICU stay | TCD can document spasm resolution after treatment or intervention, sustainability of vessel patency, and infrequent cases of late or rebound vasospasm development at the end of the second or into the third week after subarachnoid hemorrhage |
| Suspected brain death | Increased intracranial pressure | TCD can rule out cerebral circulatory arrest if positive diastolic flow is detected at any ICP values. TCD can confirm clinical diagnosis of brain death by demonstrating complete cerebral circulatory arrest in anterior and posterior circulation. TCD offers serial noninvasive assessments and can minimize the number of nuclear flow studies needed to confirm the arrest of cerebral circulation |
| Periprocedural or surgical monitoring | Carotid endarterectomy or stenting | TCD can detect all major causes of perioperative complications, i.e., embolism, thrombosis, hypoperfusion, and hyperperfusion. TCD detects real-time flow changes that precede the development of neurological deficits or changes on electroencephalography |
| Cardiovascular surgical monitoring | CABG, repairs of ascending aorta | TCD can detect cerebral embolization and hypoperfusion. TCD can help guide perfusion pump settings as well as cannulation and body positioning TCD can identify unsuspected causes of massive air embolization and guide surgeons to explore sites of possible arterial puncture |

Adapted from Alexandrov et al. [12]. With permission from John Wiley & Sons, Inc.

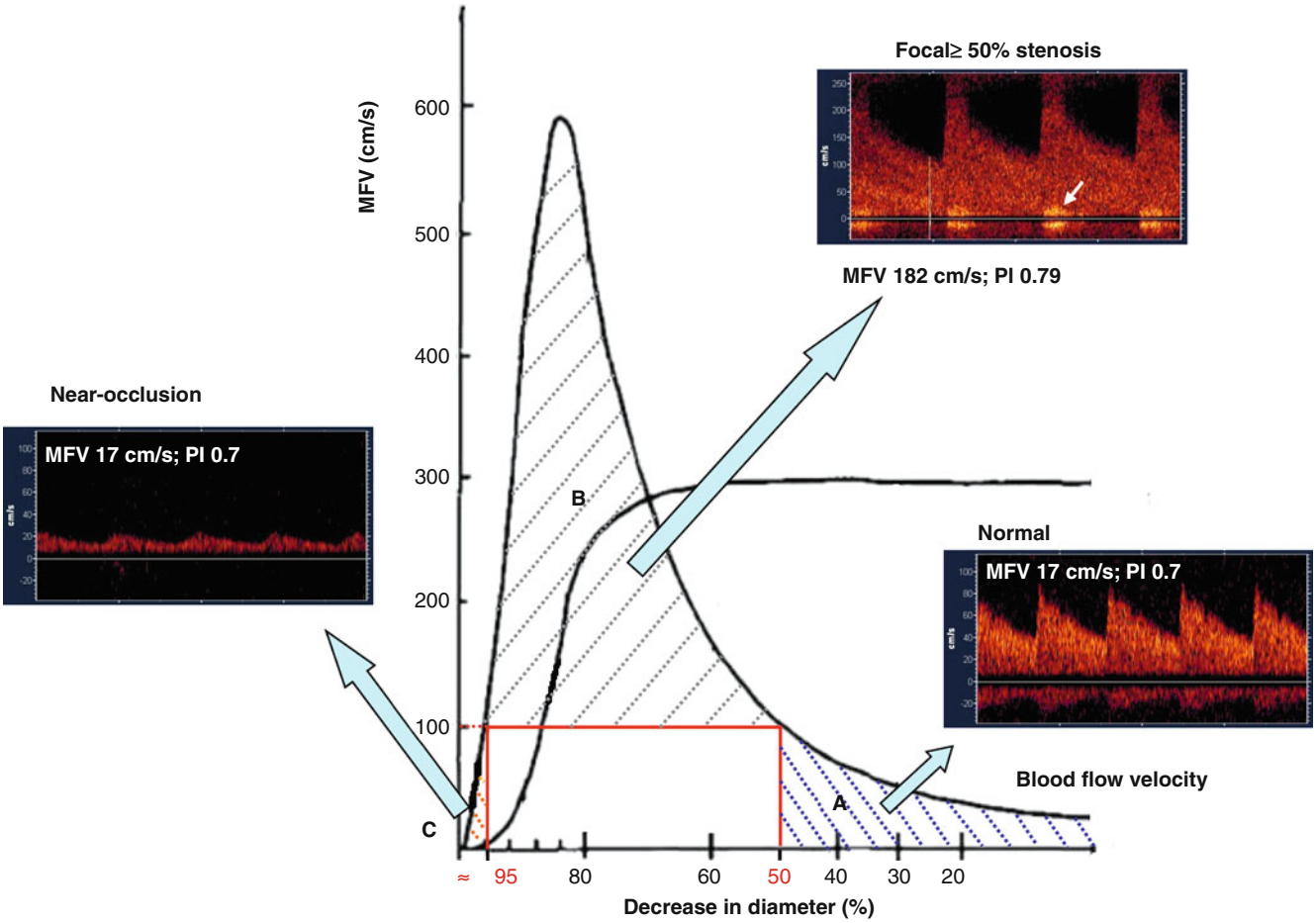


**Fig. 10.5** The Spencer's curve: This hemodynamic model is frequently used to interpret velocity findings in a variety of arterial lesions and circulatory conditions [145]. Stenotic ranges from normal/mild to moderate/severe and near-occlusive states (*A*–*B*) are shown with corresponding velocity and waveform findings. (*A*) With normal vessels or lesions less than 50% stenoses, normal waveforms and normal velocity ranges are expected as well as normal ranges of applicable ratios, i.e., target vessel to feeding vessel. (*B*) With moderate ≥50% stenoses and severe lesions, focal velocity increases are expected with applicable ratios exceeding 2 or greater values. If abnormally high velocity is detected with hyperperfusion/hyperemia, this can be differentiated from a focal stenosis by a low ratio. Bruit (*white arrow*) can be present, but these do not necessarily identify stenoses versus hyperemia. (*C*) With near-occlusive lesions, the velocity paradoxically drops ("the other side of the Spencer's curve"). These lesions can be differentiated from normal vessels and mild disease by the presence of abnormal waveforms or disproportionately abnormal ratios (Adapted from Tsivgoulis et al. [145]. With permission from Lippincott Williams & Wilkins)

## References


1. Aaslid R, Markwalder TM, Nornes H. Noninvasive transcranial Doppler ultrasound recording of flow velocity in basal cerebral arteries. J Neurosurg. 1982;57:769–74.
2. Moehring MA, Spencer MP. Power M-mode transcranial Doppler ultrasound and simultaneous single gate spectrogram. Ultrasound Med Biol. 2002;28:49–57.
3. Schöning M, Walter J. Evaluation of the vertebrobasilar-posterior system by transcranial color duplex sonography in adults. Stroke. 1992;23(9):1280–6.
4. Schöning M, Buchholz R, Walter J. Comparative study of transcranial color duplex sonography and transcranial Doppler sonography in adults. J Neurosurg. 1993;78(5):776–84.
5. Bartels E, Flugel KA. Quantitative measurements of blood flow velocity in basal cerebral arteries with transcranial duplex colorflow imaging. A comparative study with conventional transcranial Doppler sonography. J Neuroimaging. 1994;4:77–81.
6. Bartels E, Fuchs HH, Flügel KA. Color Doppler imaging of basal cerebral arteries: normal reference values and clinical applications. Angiology. 1995;46(10):877–84.
7. Nedelmann M, Stolz E, Gerriets T, Baumgartner RW, Malferrari G, Seidel G, Kaps M, TCCS Consensus Group. Consensus recommendations for transcranial color-coded duplex sonography for the assessment of intracranial arteries in clinical trials on acute stroke. Stroke. 2009;40(10):3238–44.
8. Bartels E, Knauth M. Transcranial color-coded duplex ultrasonography of arteriovenous malformations. Rofo. 2006;178(1):64–70.
9. Gerriets T, Stolz E, Modrau B, Fiss I, Seidel G, Kaps M. Sonographic monitoring of midline shift in hemispheric infarctions. Neurology. 1999;52:45–9.
10. Otis SM, Ringelstein EB. The transcranial Doppler examination: principles and applications of transcranial Doppler sonography. In: Tegeler CH, Babikian VL, Gomez CR, editors. Neurosonology. St. Louis: Mosby; 1996. p. 140–55.
11. Hennerici M, Rautenberg W, Sitzer G, Schwartz A. Transcranial Doppler ultrasound for the assessment of intracranial arterial flow

velocity – part 1. Examination technique and normal values. Surg Neurol. 1987;27(5):439–48.
12. Alexandrov AV, Sloan MA, Tegeler CH, for the American Society of Neuroimaging Practice Guidelines Committee, et al. Practice standards for transcranial Doppler (TCD) ultrasound. Part II. Clinical indications and expected outcomes. J Neuroimaging. 2010. Doi: 10.1111/j.1552–6569.2010.00523.x.
13. Bragoni M, Feldmann E. Transcranial Doppler indices of intracranial hemodynamics. In: Tegeler CH, Babikian VL, Gomez CR, editors. Neurosonology. St. Louis: Mosby; 1996. p. 129–39.
14. Lindegaard KF, Gromilund P, Aaslid R, et al. Evaluation of cerebral AVMs using transcranial Doppler ultrasound. J Neurosurg. 1986;65:335–44.
15. Lindegaard KF, Nornes H, Bakke SJ, et al. Cerebral vasospasm diagnosis by means of angiography and blood velocity measurements. Acta Neurochir (Wien). 1987;100:12–24.
16. Kontos HA. Validity of cerebral arterial blood flow calculations from velocity measurements. Stroke. 1989;20:1–3.
17. Giller CA, Bowman G, Dyer H, Mootz L, Krippner W. Cerebral arterial diameters during changes in blood pressure and carbon dioxide during craniotomy. Neurosurgery. 1993;32:737–42.
18. Aaslid R, Lindegaard KF, Sorteberg W, Nornes H. Cerebral autoregulation dynamics in humans. Stroke. 1989;20:45.
19. Adams R, McKie V, Nichols F, et al. The use of transcranial ultrasonography to predict stroke in sickle cell disease. N Engl J Med. 1992;326:605–10.
20. Adams RJ, McKie VC, Hsu L, et al. Prevention of a first stroke by transfusions in children with sickle cell anemia and abnormal results on transcranial Doppler ultrasonography. N Engl J Med. 1998;339:5–11.
21. Adams RJ, Brambilla D. Optimizing Primary Stroke Prevention in Sickle Cell Anemia (STOP 2) Trial Investigators. Discontinuing prophylactic transfusions used to prevent stroke in sickle cell disease. N Engl J Med. 2005;353:2769–78.
22. Lee MT, Piomelli S, Granger S, STOP Study Investigators, et al. Stroke prevention trial in sickle cell anemia (STOP): extended follow-up and final results. Blood. 2006;108:847–52.
23. Nichols FT, Jones AM, Adams RJ. Stroke prevention in sickle cell disease (STOP) study guidelines for transcranial Doppler testing. J Neuroimaging. 2001;11:354–62.
24. Sloan MA. Transcranial Doppler monitoring of vasospasm after subarachnoid hemorrhage. In: Tegeler CH, Babikian VL, Gomez CR, editors. Neurosonology. St. Louis: Mosby; 1996. p. 156–71.
25. Lindegaard KF, Nornes H, Bakke SJ, Sorteberg W, Nakstad P. Cerebral vasospasm after subarachnoid haemorrhage investigated by means of transcranial Doppler ultrasound. Acta Neurochir Suppl (Wien). 1988;42:81–4.
26. Newell DW, Grady MS, Eskridge JM, et al. Distribution of angiographic vasospasm after subarachnoid hemorrhage: implications for diagnosis by TCD. Neurosurgery. 1990;27:574–7.
27. Sloan MA, Haley Jr EC, Kassell NF, et al. Sensitivity and specificity of transcranial Doppler ultrasonography in the diagnosis of vasospasm following subarachnoid hemorrhage. Neurology. 1989;39:1514–8.
28. Burch CM, Wozniak MA, Sloan MA, et al. Detection of intracranial internal carotid artery and middle cerebral artery vasospasm following subarachnoid hemorrhage. J Neuroimaging. 1996;6:8–15.
29. Wozniak MA, Sloan MA, Rothman MI, et al. Detection of vasospasm by transcranial Doppler sonography the challenges of the anterior and posterior cerebral arteries. J Neuroimaging. 1996;6:87–93.
30. Lindegaard KF, Bakke SJ, Grolimund P, et al. Assessment of intracranial hemodynamics in carotid artery disease by transcranial Doppler ultrasound. J Neurosurg. 1985;63:890–8.
31. Soustiel JF, Shik V, Shreiber R, Tavor Y, Goldsher D. Basilar vasospasm diagnosis: investigation of a modified "Lindegaard Index" based on imaging studies and blood velocity measurements of the basilar artery. Stroke. 2002;33(1):72–7.
32. Sviri GE, Lewis DH, Correa R, et al. Basilar artery vasospasm and delayed posterior circulation ischemia after aneurismal subarachnoid hemorrhage. Stroke. 2004;35:1867–72.
33. Sviri GE, Ghodke B, Britz GW, et al. Transcranial Doppler grading criteria for basilar artery vasospasm. Neurosurgery. 2006;59:360–6.
34. Kincaid MS, Souter MJ, Treggiari MM, et al. Accuracy of transcranial Doppler ultrasonography and single-photon emission computed tomography in the diagnosis of angiographically demonstrated cerebral vasospasm. J Neurosurg. 2009;110:67–72.
35. Sloan MA, Burch CM, Wozniak MA, et al. Transcranial Doppler detection of vertebrobasilar vasospasm following subarachnoid hemorrhage. Stroke. 1994;25:2187–97.
36. Sloan MA, Alexandrov AV, Tegeler CH, Therapeutics and Technology Assessment Subcommittee of the American Academy of Neurology, et al. Assessment: transcranial Doppler ultrasonography: report of the Therapeutics and Technology Assessment Subcommittee of the American Academy of Neurology. Neurology. 2004;62:1468–81.
37. Alexandrov AV, Neumyer MM. Diagnostic criteria for cerebrovascular ultrasound. In: Alexandrov AV, editor. Cerebrovascular ultrasound in stroke prevention and treatment. Elmsford, New York: Blackwell Publishing; 2008. p. 79–129.
38. Piepgras A, Hagen T, Schmiadek P. Reliable prediction of grade of angiographic vasospasm by transcranial Doppler sonography. Stroke. 1994;25:260.
39. Giller CA, Hatab MR, Giller AM. Estimation of vessel flow and diameter during cerebral vasospasm using transcranial Doppler indices. Neurosurgery. 1998;42(5):1076–81.
40. Reigel MM, Hollier LH, Sundt Jr TM, Piepgras DG, Sharbrough FW, Cherry KJ. Cerebral hyperperfusion syndrome: a cause of neurologic dysfunction after carotid endarterectomy. J Vasc Surg. 1987;5:628–34.
41. Powers AD, Smith RR. Hyperperfusion syndrome after carotid endarterectomy: a transcranial Doppler evaluation. Neurosurgery. 1990;26:56–9.
42. Schoser BG, Heesen C, Eckert B, Thie A. Cerebral hyperperfusion injury after percutaneous transluminal angioplasty of extracranial arteries. J Neurol. 1997;244:101–4.
43. Tsivgoulis G, Alexandrov AV, Sloan MA. Advances in transcranial Doppler ultrasonography. Curr Neurol Neurosci Rep. 2009;9:46–54.
44. Alexandrov AV, Sloan MA, Wong LK, American Society of Neuroimaging Practice Guidelines Committee, et al. Practice standards for transcranial Doppler ultrasound: part I – test performance. J Neuroimaging. 2007;17:11–8.
45. Rha JH, Saver JL. The impact of recanalization on ischemic stroke outcome: a meta- analysis. Stroke. 2007;38:967–73.
46. Wilterdink JL, Feldmann E, Furie KL, et al. Transcranial Doppler ultrasound battery reliably identifies severe internal carotid artery stenosis. Stroke. 1997;28:133–6.
47. Christou I, Felberg RA, Demchuk AM, et al. Accuracy parameters of a broad diagnostic battery for bedside transcranial Doppler to detect flow changes with internal carotid artery stenosis or occlusion. J Neuroimaging. 2001;11:236–42.
48. Schneider PA, Rossman ME, Bernstein EF, Torem S, Ringelstein EB, Otis SM. Effect of internal carotid artery occlusion on intracranial hemodynamics. Transcranial Doppler evaluation and clinical correlation. Stroke. 1988;19:589–93.
49. Anzola GP, Gasparotti R, Magoni M, et al. Transcranial Doppler sonography and magnetic resonance angiography in the assessment

of collateral hemispheric flow in patients with carotid artery disease. Stroke. 1995;26:214–7.
50. Akopov S, Whitman GT. Hemodynamic studies in early ischemic stroke: serial transcranial Doppler and magnetic resonance angiography evaluation. Stroke. 2002;33:1274–9.
51. Tsivgoulis G, Sharma VK, Lao AY, et al. Validation of transcranial Doppler with computed tomography angiography in acute cerebral ischemia. Stroke. 2007;38:1245–9.
52. Brunser AM, Lavados PM, Hoppe A, et al. Accuracy of transcranial Doppler compared with CT angiography in diagnosing arterial obstructions in acute ischemic strokes. Stroke. 2009;40:2037–41.
53. Alexandrov AV, Demchuk A, Wein T, et al. The yield of transcranial Doppler in acute cerebral ischemia. Stroke. 1999;30:1605–9.
54. Tsivgoulis G, Sharma VK, Hoover SL, et al. Applications and advantages of power motion-mode Doppler in acute posterior circulation cerebral ischemia. Stroke. 2008;39:1197–204.
55. Latchaw RE, Alberts MJ, Lev MH, American Heart Association Council on Cardiovascular Radiology and Intervention, Stroke Council, and the Interdisciplinary Council on Peripheral Vascular Disease, et al. Recommendations for imaging of acute ischemic stroke: a scientific statement from the American Heart Association. Stroke. 2009;40:3646–78.
56. Navarro JC, Lao AY, Sharma VK, Tsivgoulis G, Alexandrov AV. The accuracy of transcranial Doppler in the diagnosis of middle cerebral artery stenosis. Cerebrovasc Dis. 2007;23:325–30.
57. Lindegaard KF, Bakke SJ, Aaslid R, Nornes H. Doppler diagnosis of intracranial artery occlusive disorders. J Neurol Neurosurg Psychiatry. 1986;49:510–8.
58. de Bray JM, Joseph PA, Jeanvoine H, Maugin D, Dauzat M, Plassard F. Transcranial Doppler evaluation of middle cerebral artery stenosis. J Ultrasound Med. 1988;7:611–6.
59. Ley-Pozo J, Ringelstein EB. Noninvasive detection of occlusive disease of the carotid siphon and middle cerebral artery. Ann Neurol. 1990;28:640–7.
60. Mattle H, Grolimund P, Huber P, Sturzenegger M, Zurbrügg HR. Transcranial Doppler sonographic findings in middle cerebral artery disease. Arch Neurol. 1988;45:289–95.
61. Brass LM, Duterte DL, Mohr JP. Anterior cerebral artery velocity changes in disease of the middle cerebral artery stem. Stroke. 1989;20:1737–40.
62. Schwarze JJ, Babikian V, DeWitt LD, Sloan MA, Wechsler LR, Gomez CR, Pochay V, Baker E. Longitudinal monitoring of intracranial arterial stenoses with transcranial Doppler ultrasonography. J Neuroimaging. 1994;4:182–7.
63. Babikian V, Sloan MA, Tegeler CH, et al. Transcranial Doppler validation pilot study. J Neuroimaging. 1993;3:242–9.
64. Feldmann E, Wilterdink JL, Kosinski A, Stroke Outcomes and Neuroimaging of Intracranial Atherosclerosis (SONIA) Trial Investigators, et al. The stroke outcomes and neuroimaging of intracranial atherosclerosis (SONIA) trial. Neurology. 2007;68: 2099–106.
65. Zhao L, Barlinn K, Sharma VK, Tsivgoulis G, Cava LF, Vasdekis SN, Teoh HL, Triantafyllou N, Chan BPL, Sharma A, Voumvourakis K, Stamboulis E, Saqqur M, Harrigan MR, Albright KC, Alexandrov AV. Velocity criteria for intracranial stenosis revisited: an international multicenter study of transcranial Doppler (TCD) and digital subtraction angiography (DSA). Stroke. 2011;42:3429–34.
66. Alexandrov AV, Demchuk AM, Felberg RA, Grotta JC, Krieger DW. Intracranial clot dissolution is associated with embolic signals on transcranial Doppler. J Neuroimaging. 2000;10:27–32.
67. Hennerici M, Rautenberg W, Schwartz A. Transcranial Doppler ultrasound for the assessment of intracranial arterial flow velocity – part 2. Evaluation of intracranial arterial disease. Surg Neurol. 1987;27:523–32.
68. Demchuk AM, Christou I, Wein TH, Felberg RA, Malkoff M, Grotta JC, Alexandrov AV. Specific transcranial Doppler flow findings related to the presence and site of arterial occlusion. Stroke. 2000;31:140–6.
69. Kimura K, Minematsu K, Yasaka M, Wada K, Yamaguchi T. Evaluation of posterior cerebral artery flow velocity by transcranial color-coded real-time sonography. Ultrasound Med Biol. 2000;26:195–9.
70. Steinke W, Mangold J, Schwartz A, Hennerici M. Mechanisms of infarction in the superficial posterior cerebral artery territory. J Neurol. 1997;244:571–8.
71. Ringelstein EB. Ultrasonic diagnosis of the vertebrobasilar system. II. Transnuchal diagnosis of intracranial vertebrobasilar stenoses using a novel pulsed Doppler system. Ultraschall Med. 1985; 6:60–7.
72. Droste DW, Nabavi DG, Kemény V, et al. Echocontrast enhanced transcranial colour-coded duplex offers improved visualization of the vertebrobasilar system. Acta Neurol Scand. 1998;98:193–9.
73. Postert T, Federlein J, Przuntek H, Büttner T. Power-based versus conventional transcranial color-coded duplex sonography in the assessment of the vertebrobasilar-posterior system. J Stroke Cerebrovasc Dis. 1997;6:398–404.
74. Nicolau C, Gilabert R, García A, Blasco J, Chamorro A, Brú C. Effect of internal carotid artery occlusion on vertebral artery blood flow: a duplex ultrasonographic evaluation. J Ultrasound Med. 2001;20: 105–11.
75. Ribo M, Garami Z, Uchino K, Song J, Molina CA, Alexandrov AV. Detection of reversed basilar flow with power-motion Doppler after acute occlusion predicts favorable outcome. Stroke. 2004;35:79–82.
76. de Bray JM, Missoum A, Dubas F, Emile J, Lhoste P. Detection of vertebrobasilar intracranial stenoses: transcranial Doppler sonography versus angiography. J Ultrasound Med. 1997;16:213–8.
77. Chernyshev OY, Garami Z, Calleja S, et al. Yield and accuracy of urgent combined carotid/transcranial ultrasound testing in acute cerebral ischemia. Stroke. 2005;36:32–7.
78. Burgin WS, Malkoff M, Felberg RA, et al. Transcranial Doppler ultrasound criteria for recanalization after thrombolysis for middle cerebral artery stroke. Stroke. 2000;31:1128–32.
79. Demchuk AM, Burgin WS, Christou I, et al. Thrombolysis in brain ischemia (TIBI) transcranial Doppler flow grades predict clinical severity, early recovery, and mortality in patients treated with intravenous tissue plasminogen activator. Stroke. 2001;32:89–93.
80. Grolimund P, Seiler RW, Aaslid R, Huber P, Zurbruegg H. Evaluation of cerebrovascular disease by combined extracranial and transcranial Doppler sonography. Experience in 1,039 patients. Stroke. 1987;18:1018–24.
81. Zanette EM, Fieschi C, Bozzao L, et al. Comparison of cerebral angiography and transcranial Doppler sonography in acute stroke. Stroke. 1989;20:899–903.
82. Kaps M, Damian MS, Teschendorf U, Dorndorf W. Transcranial Doppler ultrasound findings in middle cerebral artery occlusion. Stroke. 1990;21:532–7.
83. Camerlingo M, Casto L, Censori B, Ferraro B, Gazzaniga GC, Mamoli A. Transcranial Doppler in acute ischemic stroke of the middle cerebral artery territories. Acta Neurol Scand. 1993;88: 108–11.
84. El-Mitwalli A, Saad M, Christou I, Malkoff M, Alexandrov AV. Clinical and sonographic patterns of tandem internal carotid artery/middle cerebral artery occlusion in tissue plasminogen activator-treated patients. Stroke. 2002;33:99–102.
85. Padayachee TS, Kirkham FJ, Lewis RR, Gillard J, Hutchinson MC, Gosling RG. Transcranial measurement of blood velocities in the basal cerebral arteries using pulsed Doppler ultrasound: a method of assessing the circle of Willis. Ultrasound Med Biol. 1986;12:5–14.
86. Bass A, Krupski WC, Dilley RB, Bernstein EF, Otis SM. Comparison of transcranial and cervical continuous-wave Doppler in the evaluation of intracranial collateral circulation. Stroke. 1990;21:1584–8.

87. Schneider PA, Rossman ME, Bernstein EF, Ringelstein EB, Otis SM. Noninvasive assessment of cerebral collateral blood supply through the ophthalmic artery. Stroke. 1991;22:31–6.
88. Rutgers DR, Klijn CJ, Kappelle LJ, van Huffelen AC, van der Grond J. A longitudinal study of collateral flow patterns in the circle of Willis and the ophthalmic artery in patients with a symptomatic internal carotid artery occlusion. Stroke. 2000;31:1913–20.
89. Markus HS, Harrison MJ. Estimation of cerebrovascular reactivity using transcranial Doppler, including the use of breath-holding as the vasodilatory stimulus. Stroke. 1992;23:668–73.
90. Silverstrini M, Vernieri F, Pasqualetti P, et al. Impaired vasomotor reactivity and risk of stroke in patients with asymptomatic carotid artery stenosis. JAMA. 2000;283:2122–7.
91. Vernieri F, Pasqualetti P, Matheis M, et al. Effect of collateral flow and cerebral vasomotor reactivity on the outcome of carotid artery occlusion. Stroke. 2001;32:1552–8.
92. Apruzzese A, Silvestrini M, Floris R, et al. Cerebral hemodynamics in asymptomatic patients with internal carotid artery occlusion: a dynamic susceptibility contrast MR and transcranial Doppler study. AJNR Am J Neuroradiol. 2001;22:1062–7.
93. Vernieri F, Pasqualetti P, Diomedi M, et al. Cerebral hemodynamics in patients with carotid artery occlusion and contralateral moderate or severe internal carotid artery stenosis. J Neurosurg. 2001;94:559–64.
94. Mueller M, Voges M, Piepgras U, et al. Assessment of cerebral vasomotor reactivity by transcranial Doppler ultrasound and breath-holding. A comparison with acetazolamide as vasodilatory stimulus. Stroke. 1995;26:96–100.
95. Diehl RR. Cerebral autoregulation studies in clinical practice. Eur J Ultrasound. 2002;16:31–6.
96. Silvestrini M, Paolino I, Vernieri F, et al. Cerebral hemodynamics and cognitive performance in patients with asymptomatic carotid stenosis. Neurology. 2009;72:1062–8.
97. Deverall PB, Padayachee TS, Parsons S, et al. Ultrasound detection of micro-emboli in the middle cerebral artery during cardiopulmonary bypass surgery. Eur J Cardiothorac Surg. 1988;2:256–60.
98. Spencer MP, Thomas GI, Nicholls SC, et al. Detection of middle cerebral artery emboli during carotid endarterectomy using transcranial Doppler ultrasonography. Stroke. 1990;21:415–23.
99. Russell D. The detection of cerebral emboli using Doppler ultrasound. In: Newell DW, Aaslid R, editors. Transcranial Doppler. New York: Revwn; 1992. p. 52–8.
100. Ritter MA, Dittrich R, Thoenissen N, et al. Prevalence and prognostic impact of microembolic signals in arterial sources of embolism. A systematic review of the literature. J Neurol. 2008;255:953–61.
101. King A, Markus HS. Doppler embolic signals in cerebrovascular disease and prediction of stroke risk: a systematic review and meta-analysis. Stroke. 2009;40:3711–7.
102. Markus HS, King A, Shipley M, et al. Asymptomatic embolisation for prediction of stroke in the asymptomatic carotid emboli study (ACES): a prospective observational study. Lancet Neurol. 2010;70:120–4.
103. Clark RE, Brillman J, Davis DA, Lovell MR, Price TR, Magovern GJ. Microemboli during coronary artery bypass grafting genesis and effect on outcome. J Thorac Cardiovasc Surg. 1995;109:249–57.
104. Diegeler A, Hirsch R, Schneider F, et al. Neuromonitoring and neurocognitive outcome in off-pump versus conventional coronary bypass operation. Ann Thorac Surg. 2000;69:1162–6.
105. Ringelstein EB, Droste DW, Babikian VL, et al. Consensus on microembolus detection by TCD. International Consensus Group on Microembolus Detection. Stroke. 1998;29:725–9.
106. International Cerebral Hemodynamics Society. The international Cerebral Hemodynamics Society Consensus Statement. Stroke. 1995;26:1123.
107. Babikian VL, Feldmann E, Wechsler LR, et al. Transcranial Doppler ultrasonography: year 2000 update. J Neuroimaging. 2000;10:101–15.
108. Droste DW, Silling K, Stypmann J, et al. Contrast transcranial Doppler ultrasound in the detection of right-to-left shunts: time window and threshold in microbubble numbers. Stroke. 2000;31:1640–5.
109. Nyguen AT, Jogestrand T. Detection of patent foramen ovale by transcranial Doppler and carotid duplex ultrasonography: a comparison with transesophageal echocardiography. Clin Physiol. 1998;18:327–33.
110. Jauss M, Kaps M, Keberle M, et al. A comparison of transesophageal echocardiography and transcranial Doppler sonography with contrast medium for detection of patent foramen ovale. Stroke. 1994;25:1265–7.
111. Jauss M, Zanette E. Detection of right-to-left shunt with ultrasound contrast agent and transcranial Doppler sonography. Cerebrovasc Dis. 2000;10:490–6.
112. Spencer MP, Moehring MA, Jesurum J, et al. Power m-mode transcranial Doppler for diagnosis of patent foramen ovale and assessing transcatheter closure. J Neuroimaging. 2004;14:342–9.
113. Lao AY, Sharma VK, Tsivgoulis G, et al. Detection of right-to-left shunts: comparison between the international consensus and Spencer logarithmic scale criteria. J Neuroimaging. 2008;18:402–6.
114. Lao AY, Sharma VK, Tsivgoulis G, et al. Effect of body positioning during transcranial Doppler detection of right-to-left shunts. Eur J Neurol. 2007;14:1035–9.
115. Jesurum JT, Fuller CJ, Renz J, et al. Diagnosis of secondary source of right-to-left shunt with balloon occlusion of patent foramen ovale and power M-mode transcranial Doppler. JACC Cardiovasc Interv. 2009;2:561–7.
116. Nornes H, Angelsen B, Lindegaard KF. Precerebral arterial blood flow pattern in intracranial hypertension with cerebral blood flow arrest. Acta Neurochir (Wien). 1977;38:187–94.
117. Homburg AM, Jakobsen M, Enevoldsen E. Transcranial Doppler recordings in raised intracranial pressure. Acta Neurol Scand. 1993;87:488–93.
118. Mayer SA, Thomas CE, Diamond BE. Asymmetry of intracranial hemodynamics as an indicator of mass effect in acute intracerebral hemorrhage. A transcranial Doppler study. Stroke. 1996;27:1788–92.
119. Richards HK, Czosnyka M, Whitehouse H, Pickard JD. Increase in transcranial Doppler pulsatility index does not indicate the lower limit of cerebral autoregulation. Acta Neurochir Suppl. 1998;71:229–32.
120. Treib J, Becker SC, Grauer M, Haass A. Transcranial Doppler monitoring of intracranial pressure therapy with mannitol, sorbitol and glycerol in patients with acute stroke. Eur Neurol. 1998;40:212–9.
121. Rainov NG, Weise JB, Burkert W. Transcranial Doppler sonography in adult hydrocephalic patients. Neurosurg Rev. 2000;23:34–8.
122. Kirkham FJ, Levin SD, Padayachee TS, Kyme MC, Neville BG, Gosling RG. Transcranial pulsed Doppler ultrasound findings in brain stem death. J Neurol Neurosurg Psychiatry. 1987;50:1504–13.
123. Ropper AH, Kehne SM, Wechsler L. Transcranial Doppler in brain death. Neurology. 1987;37(11):1733–5.
124. Hassler W, Steinmetz H, Pirschel J. Transcranial Doppler study of intracranial circulatory arrest. J Neurosurg. 1989;71:195–201.
125. Bode H, Sauer M, Pringsheim W. Diagnosis of brain death by transcranial Doppler sonography. Arch Dis Child. 1988;63:1474–8.
126. Newell DW, Grady MS, Sirotta P, Winn HR. Evaluation of brain death using transcranial Doppler. Neurosurgery. 1989;24:509–13.

127. Petty GW, Mohr JP, Pedley TA, Tatemichi TK, Lennihan L, Duterte DI, Sacco RL. The role of transcranial Doppler in confirming brain death: sensitivity, specificity, and suggestions for performance and interpretation. Neurology. 1990;40:300–3.
128. Ducrocq X, Hassler W, Moritake K, Newell DW, von Reutern GM, Shiogai T, Smith RR. Consensus opinion on diagnosis of cerebral circulatory arrest using Doppler-sonography: Task Force Group on cerebral death of the Neurosonology Research Group of the World Federation of Neurology. J Neurol Sci. 1998;159:145–50.
129. de Freitas GR, André C. Sensitivity of transcranial Doppler for confirming brain death: a prospective study of 270 cases. Acta Neurol Scand. 2006;113:426–32.
130. Wijdicks EF. The diagnosis of brain death. N Engl J Med. 2001;344:1215–21.
131. Grossman BL, Brisman R, Wood EH. Ultrasound and the subclavian steal syndrome. Radiology. 1970;94:1–6.
132. von Reutern GM, Büdingen HJ. Doppler sonographic study of the vertebral artery in subclavian steal syndrome. Dtsch Med Wochenschr. 1977;102:140–1.
133. Reutern GM, Büdingen HJ, Freund HJ. The diagnosis of obstructions of the vertebral and subclavian arteries by means of directional Doppler sonography. Arch Psychiatr Nervenkr. 1976;222:209–22.
134. Klingelhöfer J, Conrad B, Benecke R, Frank B. Transcranial Doppler ultrasonography of carotid-basilar collateral circulation in subclavian steal. Stroke. 1988;19:1036–42.
135. Walker DW, Acker JD, Cole CA. Subclavian steal syndrome detected with duplex pulsed Doppler sonography. AJNR Am J Neuroradiol. 1982;3:615–8.
136. Grotta JC, Welch KM, Fagan SC, et al. Clinical deterioration following improvement in the NINDS rt-PA stroke trial. Stroke. 2001;32:661–8.
137. Dàvalos A, Toni D, Iweins F, Lesaffre E, Bastianello S, Castillo J. Neurological deterioration in acute ischemic stroke: potential predictors and associated factors in the European Cooperative Acute Stroke Study (ECASS) I. Stroke. 1999;30:2631–6.
138. Alexandrov AV, Grotta JC. Arterial re-occlusion in stroke patients treated with intravenous tissue plasminogen activator. Neurology. 2002;59:862–7.
139. Alexandrov AV, Nguyen HT, Rubiera M, et al. Prevalence and risk factors associated with reversed Robin Hood syndrome in acute ischemic stroke. Stroke. 2009;40:2738–42.
140. Barlinn K, Alexandrov AV. Sleep-disordered breathing and arterial blood flow steal represent linked therapeutic targets in cerebral ischaemia. Int J Stroke. 2011;6:40–1.
141. Ringelstein EB, Sievers C, Ecker S, Schneider PA, Otis SM. Noninvasive assessment of CO2-induced cerebral vasomotor response in normal individuals and patients with internal carotid artery occlusions. Stroke. 1988;19:963–9.
142. Silvestrini M, Vernieri F, Pasqualetti P, Matteis M, Passarelli F, Troisi E, Caltagirone C. Impaired cerebral vasoreactivity and risk of stroke in patients with asymptomatic carotid artery stenosis. JAMA. 2000;283:2122–7.
143. Palazzo P, Balucani C, Barlinn K, et al. Association of reversed Robin Hood syndrome with risk of stroke recurrence. Neurology. 2010;75:2003–8.
144. Tsivgoulis G, Zhang Y, Alexandrov AW, et al. Safety and tolerability of early noninvasive ventilatory correction using bilevel positive airway pressure in acute ischemic stroke. Stroke. 2011;42:1030–4.
145. Alexandrov AV. The Spencer's curve: clinical implications of a classic hemodynamic model. J Neuroimaging. 2007;17:6–10.

# Ultrasonic Characterization of Carotid Plaques and Its Clinical Implications

11

Alberto Froio, Luca Rossi, Savino Pasquadibisceglie, and Giorgio M. Biasi

**Abstract**

In the last years, the concepts of plaque vulnerability, composition of the plaque, and cerebrovascular events have been vastly studied. The gray scale median (GSM) score has been proposed with the intent of identifying asymptomatic patients at high risk of stroke.

Several studies demonstrated the relationship between carotid plaque echolucency evaluated by GSM, hs-CRP, carotid plaque infiltration by macrophage, neovascularization, plaque rupture, embolic load to the brain, and eventually risk of stroke.

The GSM analysis has been included in the current guidelines for treatment of patients with carotid stenoses, both with endovascular and surgical approach.

**Keywords**

Indication to treatment • Echolucency • Gray scale median • Endarterectomy • Stenting Stroke

## Ultrasonic Characterization of Carotid Plaques

In the last years, the concepts of plaque vulnerability, composition of the plaque, and cerebrovascular events have been vastly studied. It is now clear that plaque morphology is one of the most important parameter to assess in order to forecast the behavior of a carotid atherosclerotic lesion [1].

Ultrasonic characteristics of the plaque, divided in plaque echogenicity or echolucency, reflect plaque histology and therefore allow us to categorize different aspects of the plaque at higher risk of neurologic events, such as the presence of a hemorrhagic core, lipid content, and a thin fibrous cap, and how these findings are distributed within the plaque [2–5].

The main problem associated with carotid duplex scanning has always been its wide subjectivity: efforts have been pushed toward the creation of a standardized index that was effective and with high reproducibility so that different centers around the world would be able to detect the same plaque features [6]. The gray scale median (GSM) score has been proposed with the clear intent of identifying asymptomatic patients at high risk of stroke. In order to overcome the wide subjectivity of duplex scanning, B-mode image normalization has been introduced [7].

Several classifications of plaques have been proposed. The Geroulakos classification has been adapted to incorporate the evolution made by the GSM index and therefore provide a visual and computerized classification of different plaques. Carotid plaque echolucency, where most of the pixels of the plaque have a GSM value lower than 25 (which means black), is associated with plaque vulnerability and a greater number of neurologic events [8–10]. The assessment of plaque echolucency after image normalization is one of

A. Froio, M.D. • L. Rossi, M.D. • S. Pasquadibisceglie, M.D.
Department of Surgical Sciences, University of Milano Bicocca,
Vascular Surgery Unit, San Gerardo Teaching Hospital,
Via Pergolesi, 33, Monza 20900, Italy
e-mail: alberto.froio@unimib.it

G.M. Biasi, M.D. (✉)
Department of Surgical Sciences, University of Milano Bicocca,
Via Pergolesi, 33, Monza 20900, Italy

Vascular Surgery Unit, San Gerardo Teaching Hospital,
Via Pergolesi, 33, Monza 20900, Italy
e-mail: giorgio.biasi@unimib.it

A.F. AbuRahma, D.F. Bandyk (eds.), *Noninvasive Vascular Diagnosis*,
DOI 10.1007/978-1-4471-4005-4_11, 

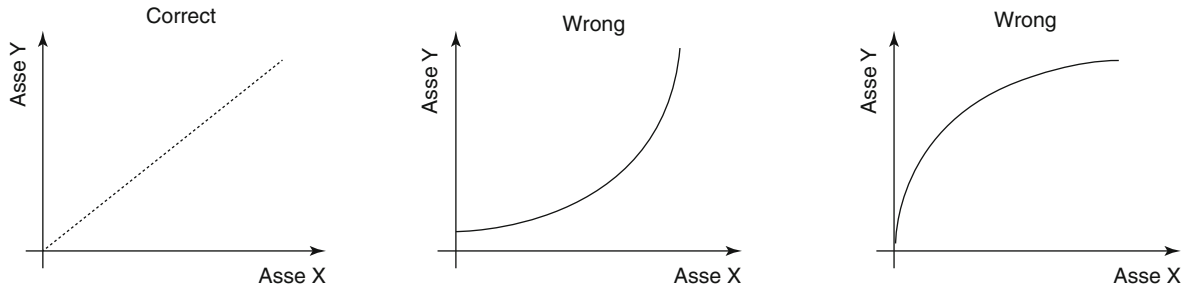


**Fig. 11.1** Postprocessing curves for GSM analysis

the best parameters in order to detect asymptomatic patients at higher risk of stroke during an endovascular or surgical intervention, with the potential to identify the best tailored therapeutic strategy for each asymptomatic patient [1].

## GSM Analysis at the Vascular Surgery Unit, San Gerardo Hospital, University of Milano-Bicocca

GSM calculation requires three steps: (1) setup of the duplex scanner and image recording, (2) image normalization, and (3) image analysis [11].

1. Training is required for ultrasonographers from the participating centers on how to set up the duplex scanner for the collection of the images.

   Every duplex scanner allows the collection of images with the characteristics required for the computer-assisted analysis of echogenicity. For GSM calculation, there are no unsuitable duplex scanners.

   A 7-MHz linear array single- or multifrequency transducer should be used.

   The dynamic range is the range in acoustic power (in decibels) between the faintest and the strongest signals that can be displayed on the screen. The decrease of the dynamic range increases the apparent contrast in the image. For GSM calculation, the maximum dynamic range should be used in order to have the greatest possible display of gray scale values (grayer and flatter image).

   The frame rate, which means the number of scanning that the probe does to produce the images, must be positioned at the maximum level, ensuring good temporal resolution.

   The persistence is the number of frames which are mathematically added to produce each image. Higher persistence tends to suppress noise, but it is always done at the expense of time resolution, and it may blur real targets. The persistence is displayed on the screen device as a series of numbers from 1 to 5, and the correct persistence should be 2 or 3 (medium to low level).

   A linear postprocessing curve is used because image normalization is achieved with linear scaling (Fig. 11.1).

   The overall gain should be increased until the plaque can be easily recognized, and noise appears within the lumen. It should then be decreased to obtain a lumen free of noise (black).

   The time gain compensation (TGC) curve is adjusted (gently sloping) with the aim of obtaining images where the far and near walls of the artery produce the same echogenicity (Fig. 11.2). At the level of the arterial lumen, no gains of the TGC curve must be done. This is essential for normalization of carotid plaques with anterior and posterior components. The consequence of this is that the ultrasound beam should be at 90° to the arterial wall, with a horizontal adventitia (Fig. 11.3).

   The patient should be in a supine position. The carotid vessels are analyzed using different longitudinal views (medial, lateral, and posterolateral). The minimum depth should be used, so that the plaque occupies a large part of the image. Excessive magnification is not required.

   In case of acoustic shadow, the image can be analyzed only if >50% of the area depicts acoustic information. The GSM cannot be calculated in plaques without any ultrasound information due to acoustic shadowing. The bigger the section of plaque that can be visualized, more accurate is the information provided by GSM.

   Before image recording, the following criteria should be fulfilled:

   (a) Blood: a noiseless vessel lumen in the vicinity of the plaque.
   (b) Adventitia: in the proximity of the plaque, it should be bright, thick, and horizontal (Fig. 11.4).
   (c) Plaque: well-defined and with the maximum thickness.

   The following images (in longitudinal projections) should be recorded:

   (a) The B-mode (gray scale) image.
   (b) The color image: it may help in the delineation of the luminal margin of the plaque (especially with hypoechoic dark plaques).

   Attention should be paid in order to have B-mode and color image in the same plane.

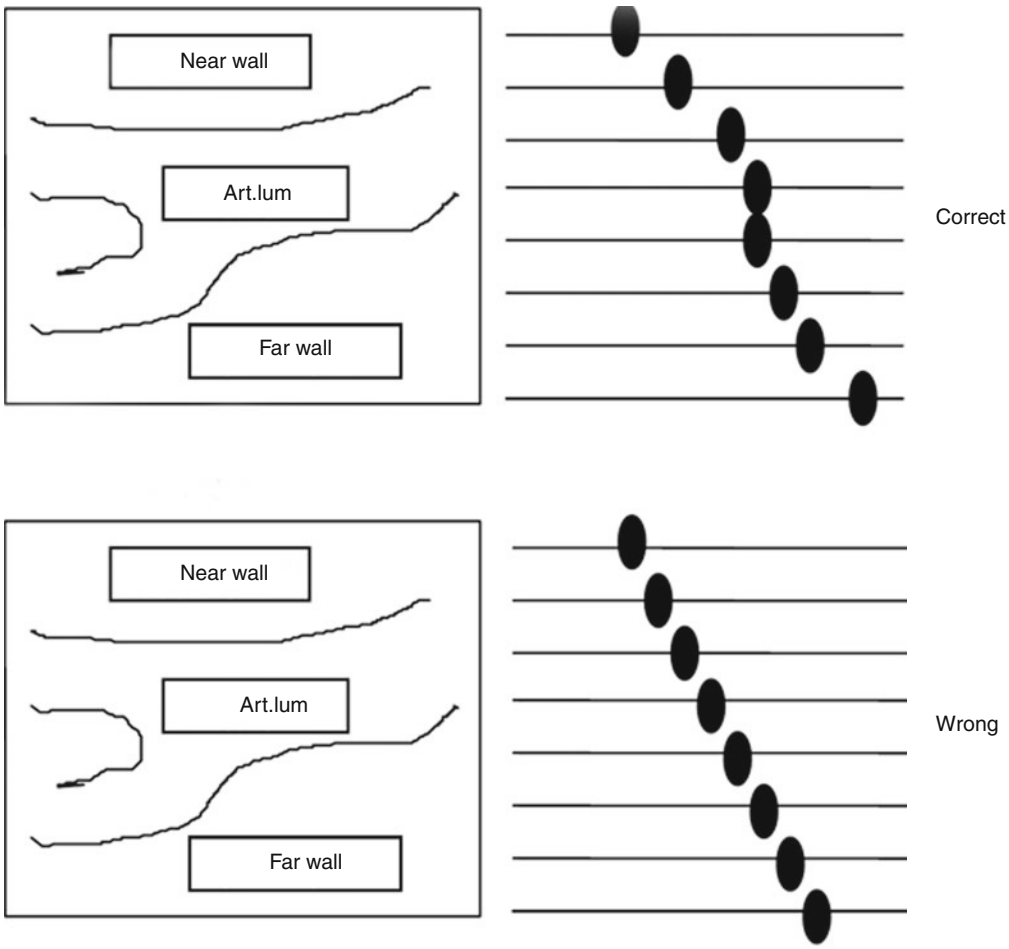


**Fig. 11.2** GSM analysis. The setup of the time gain compensation curve

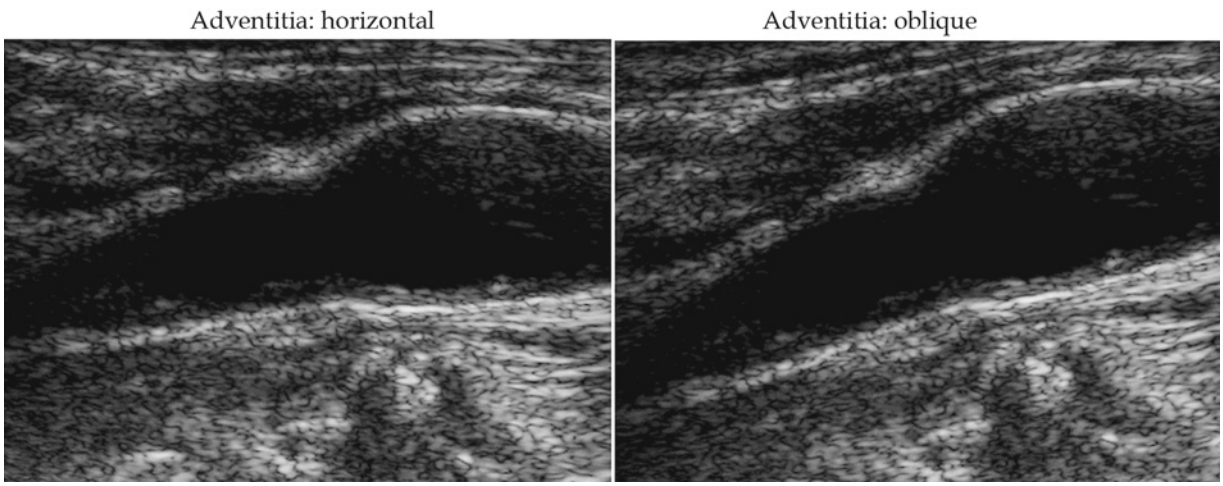


**Fig. 11.3** GSM analysis. The orientation of the adventitia in the common carotid artery

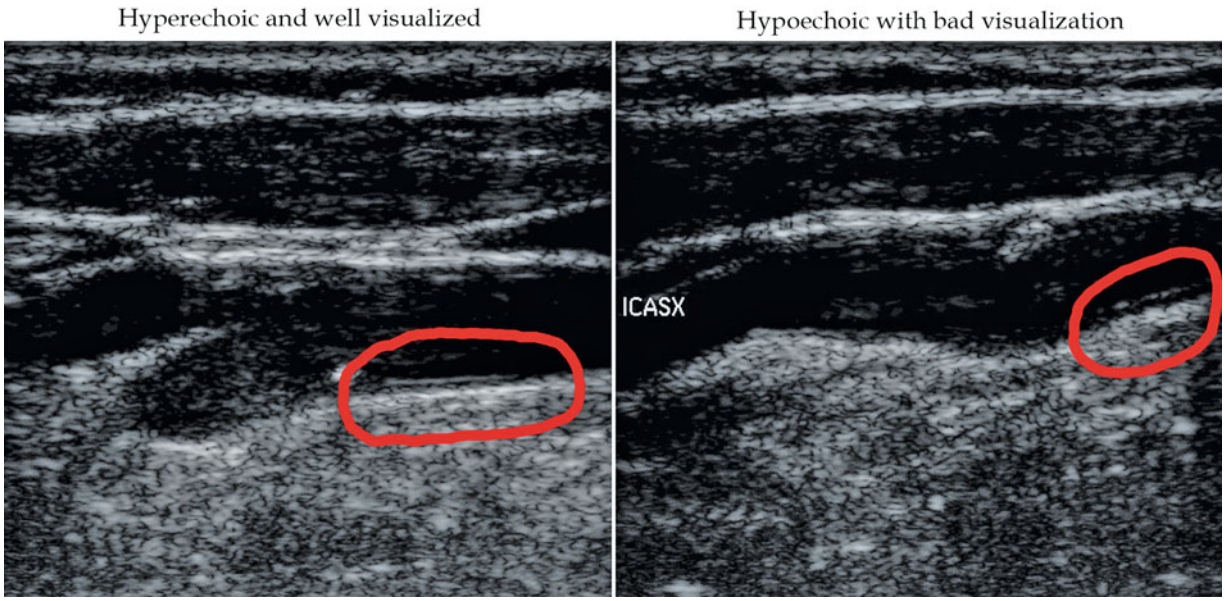


**Fig. 11.4** GSM analysis. The identification of the adventitia suitable for image normalization. *Left red circle*: good visualization of adventitia. *Right red circle*: bad visualization of adventitia

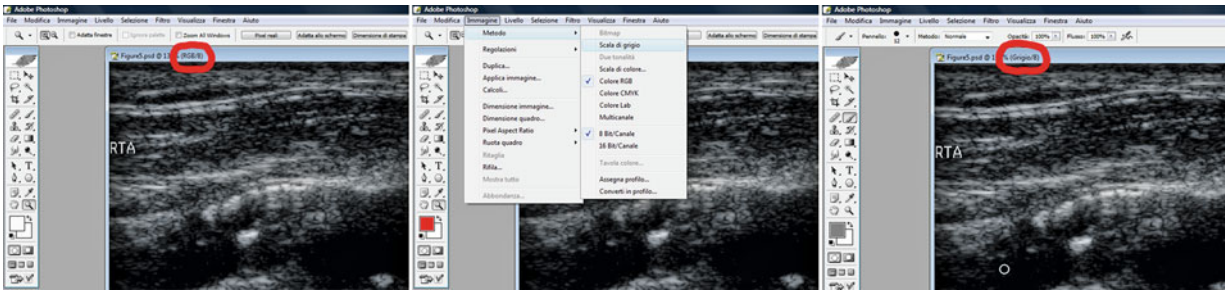


**Fig. 11.5** GSM analysis. The color information should be discharged. *Left red circle*: RGB image; this kind of image should be discarded. *Right red circle*: grey scale image; this is the optimal image for GSM analysis

Digital storage media (magneto-optical disk and compact disk) are preferred to analogical video tape requiring video grabber card.

2. Image normalization is performed using Adobe Photoshop. In Adobe Photoshop, both the B-mode and the color image should be open. In the B-mode image, the color information should be discarded: from the "Image" menu, click on "Mode," then "Gray scale" (Fig. 11.5).

   Using the "Lasso" tool, drag the pointer to outline the plaque. Then, click on "Histogram" in the "Image" menu. The "median" value shown in the panel is the GSM.

   Hypoechoic dark (echolucent) regions are associated with a GSM that tended to approach 0, whereas hyperechoic bright (echogenic) regions are associated with a GSM that tended to approach 255.

   The GSM calculated in this manner is not standardized, and, consequently, the GSM is influenced by duplex scanner settings. The lack of reproducibility of non-standardized GSM has been demonstrated by our group and by others: the GSM cutoff point for the identification of carotid plaques at increased risk of stroke was 50 in Milan and 32 in London.

   Normalization (standardization) allows to compare images from different scanners by different ultrasonographers. Thanks to normalization, GSM is highly reproducible index of echogenicity.

   Image normalization is a gray scale transformation using linear scaling: gray scale values of all pixels in image are adjusted according to two reference points, blood and adventitia. Blood and adventitia were selected because they are easily recognizable near the plaque and constitute the two distinct ends of gray scale (blood = dark, adventitia = bright). The process modifies the image such that in the resultant image the GSM of the blood is 0 and the GSM of the adventitia 190.

   Several steps are required for image normalization.

   Using the "Lasso" tool, drag the pointer to select an area in the blood that should be free of noise. To check this, in the "Image" menu, click on "Histogram." The "median"

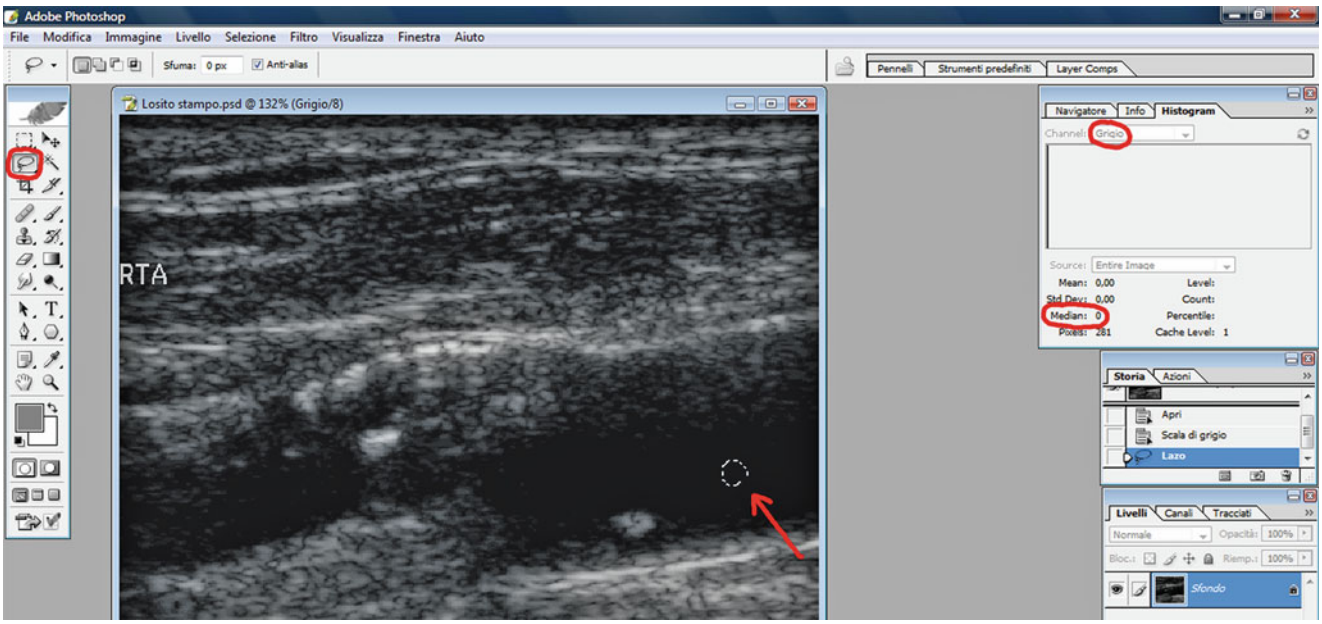


**Fig. 11.6** GSM analysis. The GSM calculation of the blood. *red arrow*: selection of a blood sample with the "lasso" tool

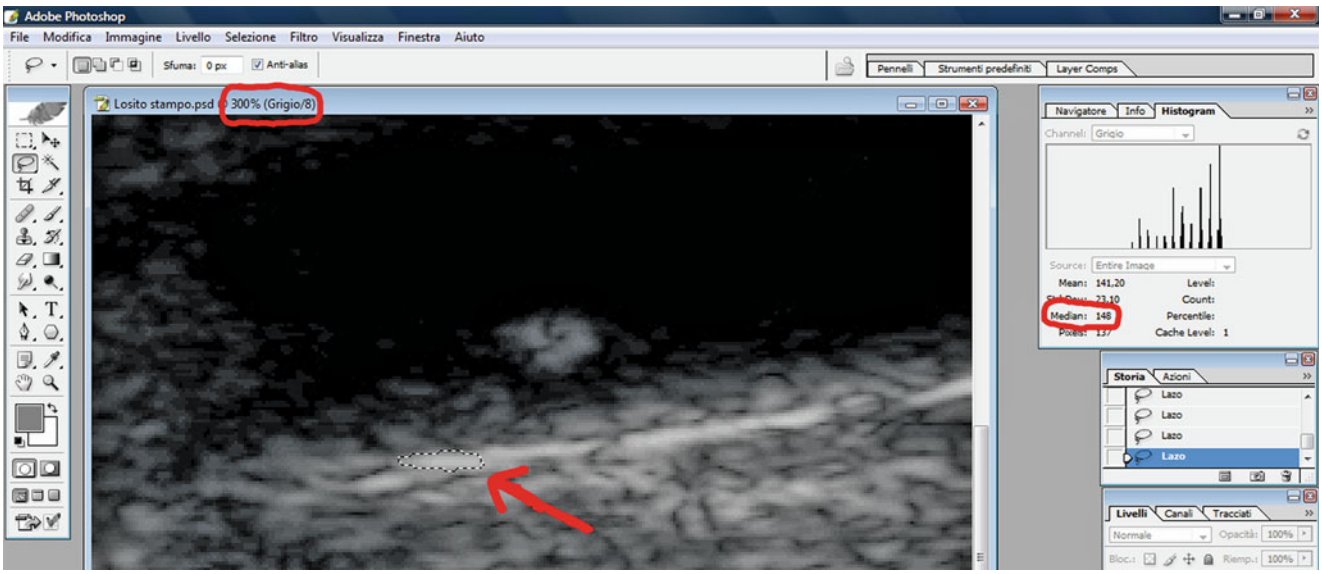


**Fig. 11.7** GSM analysis. The GSM calculation of the adventitia. *red arrow*: selection of a sample of adventitia with the "lasso" tool

value shown in the panel is the GSM. The GSM of the selected area in the blood should be 0 (Fig. 11.6). If not, the gain of duplex scanner is not set properly (see above).

Similarly, using the "Lasso" tool, the brightest part of the adventitia on the same arterial wall of the plaque should be selected (Fig. 11.7). It is important to note that:

- Image magnification should be performed before adventitia outlining.
- The selected area should not be too small (area, not a point!).
- The selected area should be horizontal.

The GSM of adventitia should then be obtained using the "Histogram" function (the GSM of the adventitia in Fig. 11.7 is 148). Unlike the GSM of blood, every GSM value measured in the adventitia is accepted.

To normalize the image, click on "Image" menu, then "Adjustments," and finally "Curves" (Fig. 11.8). The straight line shown in the panel represents the relationship between the gray scale of the input ($x$-axis) image and that

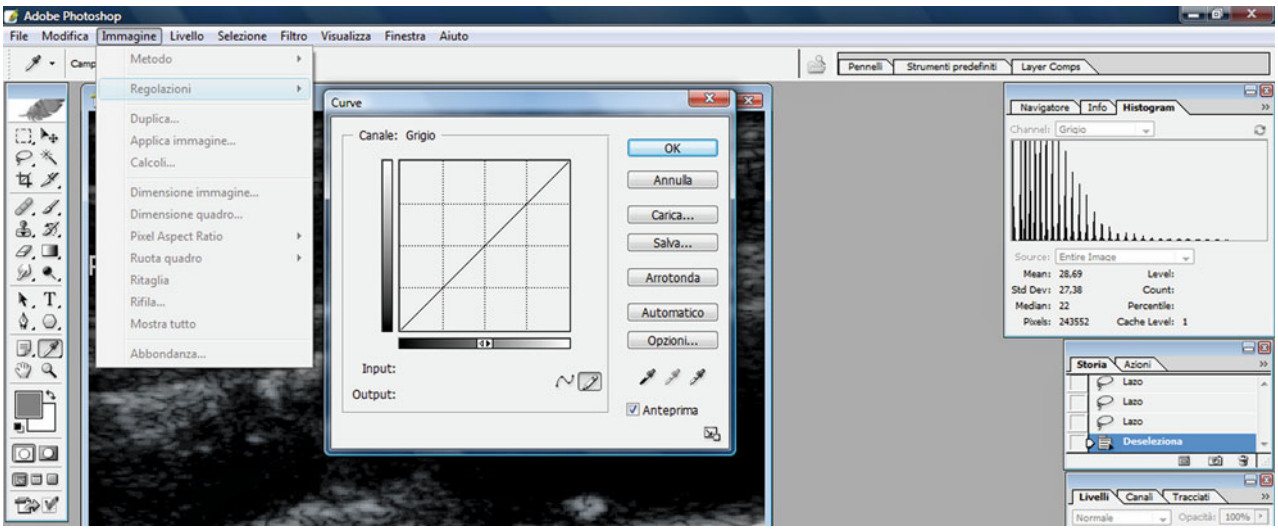


**Fig. 11.8** GSM analysis. The "curve function" in Adobe Photoshop used for image normalization

of the output (*y*-axis). Each axis has a black and a white edge: this is the gray scale, ranging from 0 (completely black) to 255 (completely white).

The aim of normalization is to modify the subjectivity related to the echographic examination. This purpose can be achieved using the brightest (adventitia) and the faintest (blood) areas of the image: in particular conditions (the duplex scanner settings described above), these areas are independent of the type of duplex scanner and the ultrasonographer. Normalizing the image, the faintest point remains unchanged with a GSM value of 0 before and 0 after standardization (a proper gain adjustment is essential for this purpose). On the other hand, the GSM value of the brightest area (adventitia) drives all the normalization process: the adventitial GSM value measured before (input value) is converted arbitrarily to a GSM value of 190 (output value). In the normalized image, the GSM value of blood and adventitia is 0 and 190, respectively, independent of the type of duplex scanner and the ultrasonographer.

In Adobe Photoshop, the straight line shown in the panel should be modified so that the new line crosses a new point with the input value corresponding to measured adventitial GSM value and the output value corresponding to 190 (Fig. 11.9). The image is now standardized (Fig. 11.10).

3. In Adobe Photoshop, using the "Lasso" tool, the plaque should be outlined. In the "Histogram" panel, the following measurements are obtained:
   (a) GSM, defined as the median of overall gray values of the pixels in the plaque (Fig. 11.11).
   (b) Standard deviation (SD). SD is a measure of dispersal, or variation, in a group of numbers. SD tells how tightly a set of values is clustered around the average of those same values.

If you need help to measure the GSM, please feel free to contact us at alberto.froio@unimib.it

## Clinical Trials on Carotid Plaque Echolucency and Clinical Endpoints

With the Imaging in Carotid Angioplasty and Risk of Stroke (ICAROS) study, an international multicenter registry that collected 418 CAS cases from 11 centers, we evaluated the relationship between the echogenicity of carotid plaque, as measured by GSM, and the risk of stroke during CAS in order to obtain a better selection of candidates for CAS [11, 12]. An echographic evaluation of carotid plaque with GSM measurement was made pre-procedurally. The onset of neurological deficits during the procedure and the post-procedural period (30 days) was recorded. The GSM value in complicated patients was significantly lower than in uncomplicated cases, both in the stroke ($p<0.005$) and the stroke plus TIA ($p<0.005$) subsets. A receiver operating characteristic curve was used to choose the best GSM cutoff value: the most successful threshold was 25. The prevalence of a GSM value <25 (echolucent plaques) was high: 37% (155 of 418 patients). Eleven (7.1%) of the 155 patients with GSM ≤ 25 had a stroke compared to 4 (1.5%) of 263 patients with GSM > 25 ($p=0.005$) [11].

The Asymptomatic Carotid Stenosis and Risk of Stroke study (ACSRS) was an international multicenter study whose aim was to detect groups of patients with asymptomatic carotid stenosis associated with greater or lower risk of a

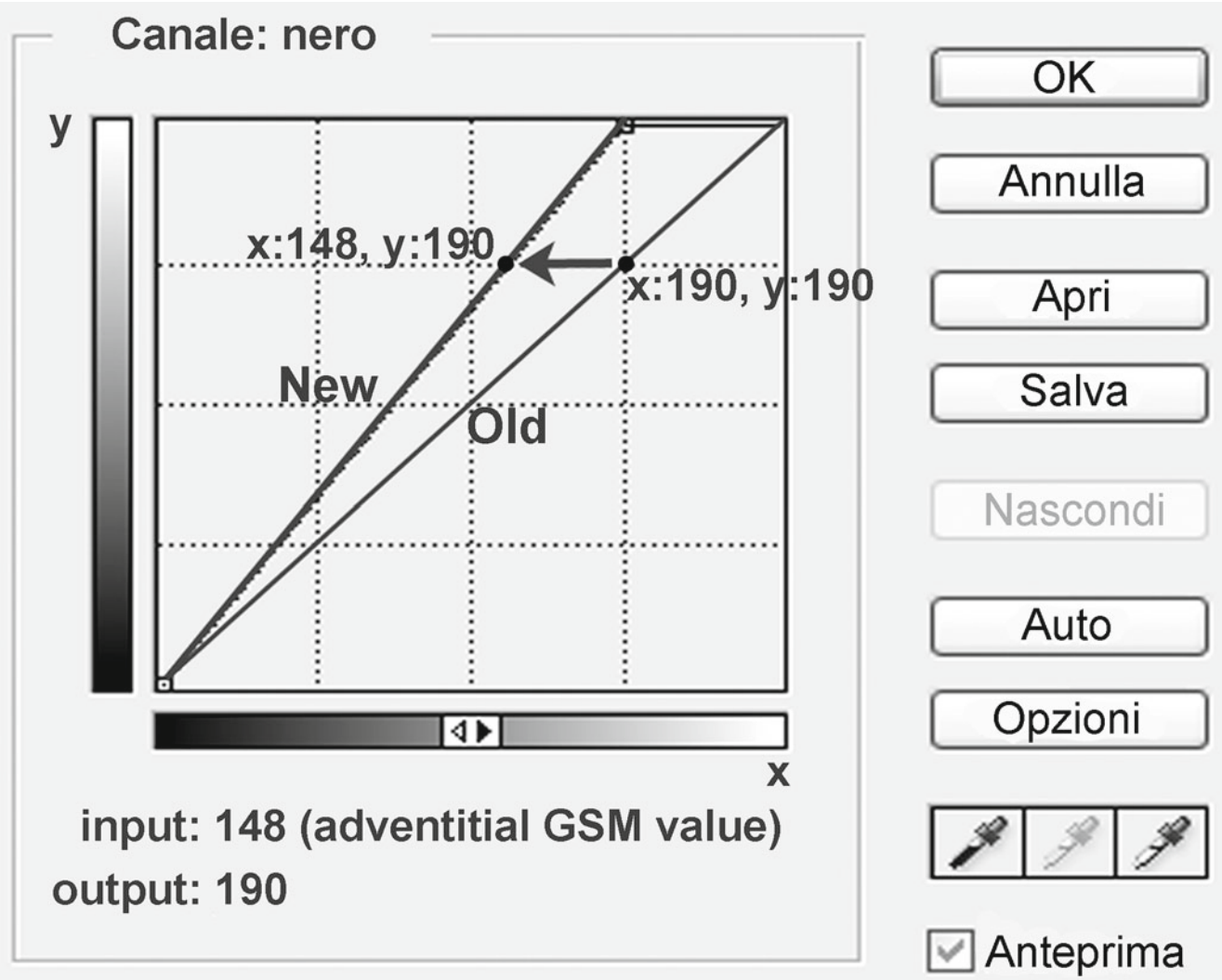


**Fig. 11.9** GSM analysis. The shift of the curve for image normalization

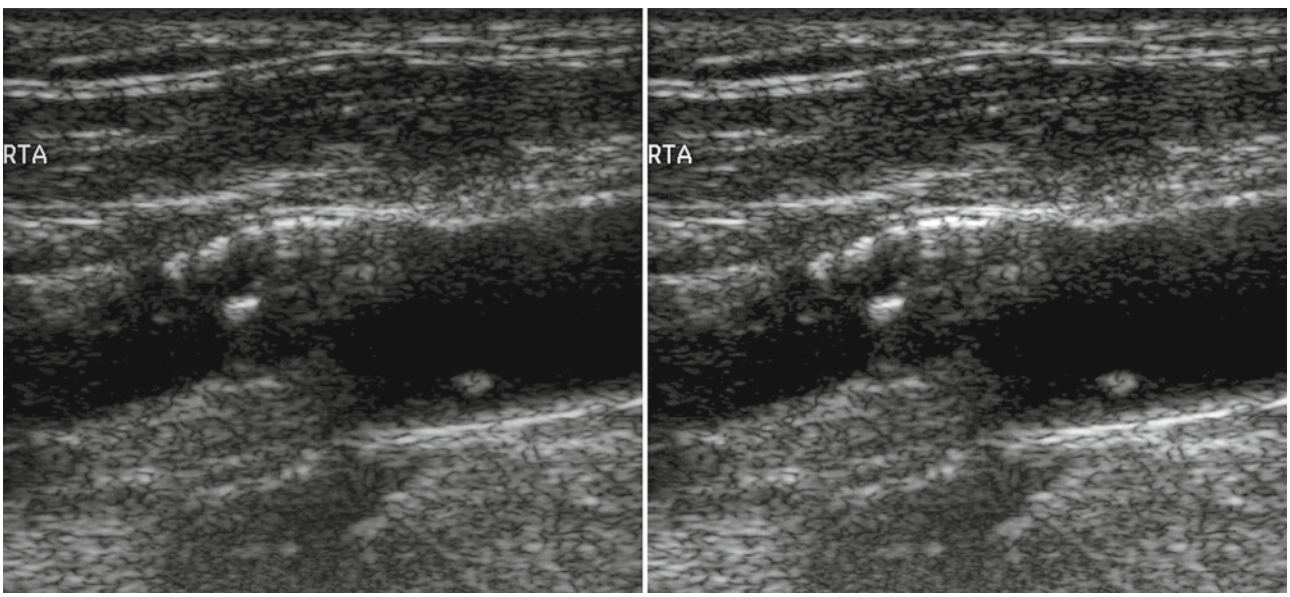


**Fig. 11.10** *Left side*: carotid plaque before image normalization. *Right side*: carotid plaque after normalization

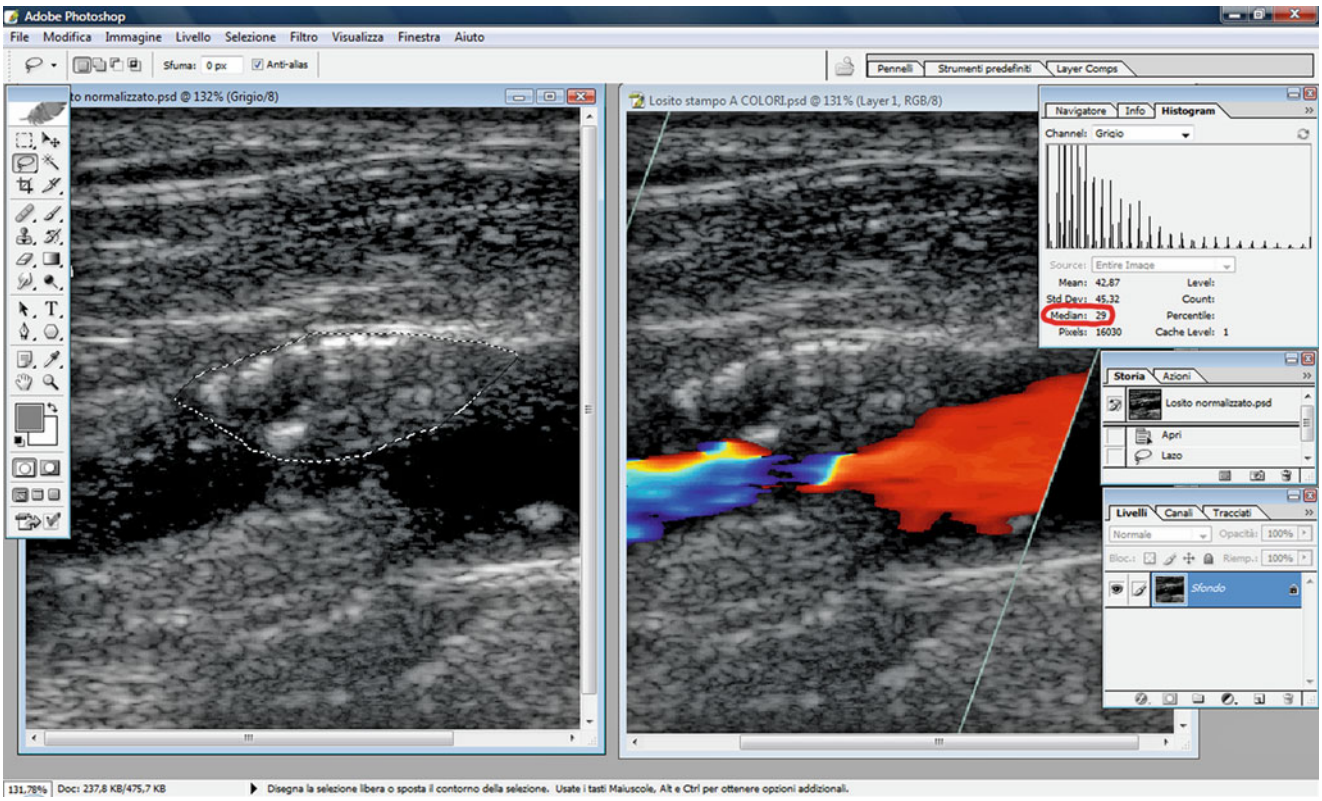


**Fig. 11.11** GSM calculation in the normalized image

natural neurological event [13]. A total of 1,121 patients with 50–99% asymptomatic ICA stenosis in relation to the bulb (European Carotid Surgery Trial [ECST] method) were followed up for 6–96 months (mean, 48). Severity of stenosis; age; systolic blood pressure; increased serum creatinine; smoking history of more than 10 pack-years; history of contralateral transient ischemic attacks (TIAs) or stroke; low gray scale median (GSM); increased plaque area; plaque types 1, 2, and 3; and the presence of discrete white areas (DWAs) without acoustic shadowing were associated with increased risk. Carotid stenosis, history of contralateral TIAs or stroke, GSM, plaque area, and DWAs were independent predictors of ipsilateral events. Combinations of these could stratify patients into different levels of risk for ipsilateral events: in the 923 patients with >70% stenosis, the predicted cumulative 5-year stroke rate was <5% in 495, 5–9.9% in 202, 10–19.9% in 142, and >20% in 84 patients.

The prospective, observational, international multicenter Asymptomatic Carotid Emboli Study recruited subjects with severe asymptomatic carotid stenosis (≥70%), analyzing carotid plaque features and embolic signals (ES) [14]. A total of 164 (37.7%) plaques were graded as echolucent. Plaque echolucency at baseline was associated with an increased risk of ipsilateral stroke alone (HR 6.43, 95% CI 1.36–30.44, $p = 0.019$). A combined variable of plaque echolucency and ES positivity at baseline was associated with a markedly increased risk of ipsilateral stroke alone (HR 10.61, 95% CI 2.98–37.82, $p = 0.0003$). This association remained significant after controlling for risk factors, degree of carotid stenosis, and antiplatelet medication. The combination of ES detection and plaque morphology allows a greater prediction than either measure alone and identifies a high-risk group with an annual stroke risk of 8% and a low-risk group with a risk of <1% per annum.

Ishizu compared carotid ultrasonic imaging with biomarkers such as high-sensitivity C-reactive protein (hs-CRP) and oxidized low-density lipoprotein (LDL) stratifying cardiovascular risk [15]. Carotid plaque echolucency was quantified by measuring GSM. Univariate Cox regression analysis showed CRP and several ultrasonic parameters to be significant determinants for cardiovascular events. Multivariate Cox analysis determined CRP and plaque echolucency to be independent variables predicting cardiovascular events after adjustment for classic CAD risk factors. In Kaplan–Meier plots, patients with both high CRP (≥1.0 mg/L) and echolucent plaque (GSM ≤ 65) showed higher event rates than did patients with high CRP but without echolucent plaque.

The Health Insurance Portability and Accountability Act–compliant study correlated echogenicity and severity of atherosclerotic carotid artery lesions at standard ultrasound with the degree of intraplaque neovascularization at contrast

material–enhanced (CE) ultrasound [16]. Echogenicity was inversely correlated with grade of intraplaque neovascularization ($p<0.001$). More echolucent lesions had a higher degree of neovascularization compared with more echogenic ones ($p<0.001$). The degree of stenosis was significantly correlated with grade of intraplaque neovascularization ($p=0.003$). Intraplaque neovascularization in the carotid arteries detected with CE ultrasound was more pronounced in symptomatic patients with a history of cerebrovascular or cardiac events [17, 18].

At the University of Copenhagen, the association between carotid plaque ultrasound echogenicity and the presence of inflammation depicted with positron emission tomography (PET) of plaques with the use of [18F]-fluorodeoxyglucose (FDG) was evaluated [19]. There was a negative correlation between GSM and FDG maximum standardized uptake values (SUV). Whereas echo-rich plaques tended to show low FDG uptake, echolucent plaques ranged from high to low inflammatory activity, as depicted with PET. There was a positive correlation between CD68 expression and FDG uptake. Choi demonstrated that serum hs-CRP levels were found to be correlated with F-18 FDG target-to-background ratio (TBR) values of carotid arteries [20]. The higher the amount of inflammation in carotid plaques, the higher the risk of stroke: dense plaque inflammation (especially infiltration with macrophages) was the feature most strongly associated with both cap rupture and time since stroke ($p=0.001$) [21].

These studies demonstrated the relationship between carotid plaque echolucency evaluated by GSM, hs-CRP, carotid plaque infiltration by macrophage, neovascularization, plaque rupture, embolic load to the brain, and eventually risk of stroke.

## Clinical Implications of Carotid Plaque Analysis

A 58-year-old man was referred by a cardiologist to the San Gerardo Vascular Surgery Department for the evaluation of a right internal carotid plaque, diagnosed 4 months earlier with a 60% degree of stenosis. The medical history was the following:

- Hypertension
- Type 2 diabetes
- Obesity
- Dyslipidemia
- Smoker
- Myocardial infarction (1997), PTCA on right coronary artery
- Atrial fibrillation on amiodarone (1999)
- Acute pancreatitis treated by papillosphincterotomy (2003)
- Hospital admission for uncontrolled glycemia (2004), successful therapy with glimepiride and metformin
- Anxious state + depression on trifluoperazine + clomipramine
- Gastric ulcer with bleeding, pantoprazole + aspirin (contraindication to warfarin)
- Unstable angina, coronarography, trivessel disease without surgical/endovascular indication (Jan 2007)
- Coronary bypass (July 2009)
- Acute heart failure with atrial fibrillation and pericarditis (Sep 2009), therapy with ramipril, amlodipine, furosemide, and nebivolol

What can we suggest to reduce the cardiovascular risk?

A. Weight loss program
B. Smoking cessation advice
C. Psychotherapy
D. Physical activity program
E. Hypocholesterolemic diet

The patient refused any diet, smoking-cessation, and psychotherapeutic program.

How often should a high-risk patient with a carotid degree of stenosis of 60% be evaluated by ultrasound?

A. Every month
B. Every 3–4 months
C. Every 9 months
D. Every 12 months
E. Every 18 months

The screening program should be very tight in patients with a severe cardiopathy refusing the cessation of smoking and a hypoglycemic and hypocholesterolemic program.

The ultrasound demonstrated an echolucent right internal carotid plaque, with increase of peak systolic velocity and a stenosis of 80–85% (Fig. 11.12)

The patient was asymptomatic for ischemic neurological deficit.

How should the patient be managed?

A. Medical therapy, increasing statin treatment in order to decrease LDL (<70 mg/dL), and a more aggressive antihypertensive and hypoglycemic approach.
B. Medical therapy plus additional imaging (angioCT/angioRM) of vasculature (aortic arch, carotid anatomy, and circle of Willis) and cerebral parenchyma in order to proceed with surgical/endovascular treatment.

The angioCT demonstrated an 85% stenosis of the right internal carotid artery, the lack of abnormalities/diseases of the circle of Willis, a type I aortic arch without atherosclerotic lesions, the lack of tortuosity of the common carotid artery, and the absence of ischemic lesions in the cerebral parenchyma (Fig. 11.13).

Which is the role of carotid plaque morphology at this point?

A. It does not influence the choice to medical vs. invasive treatment.

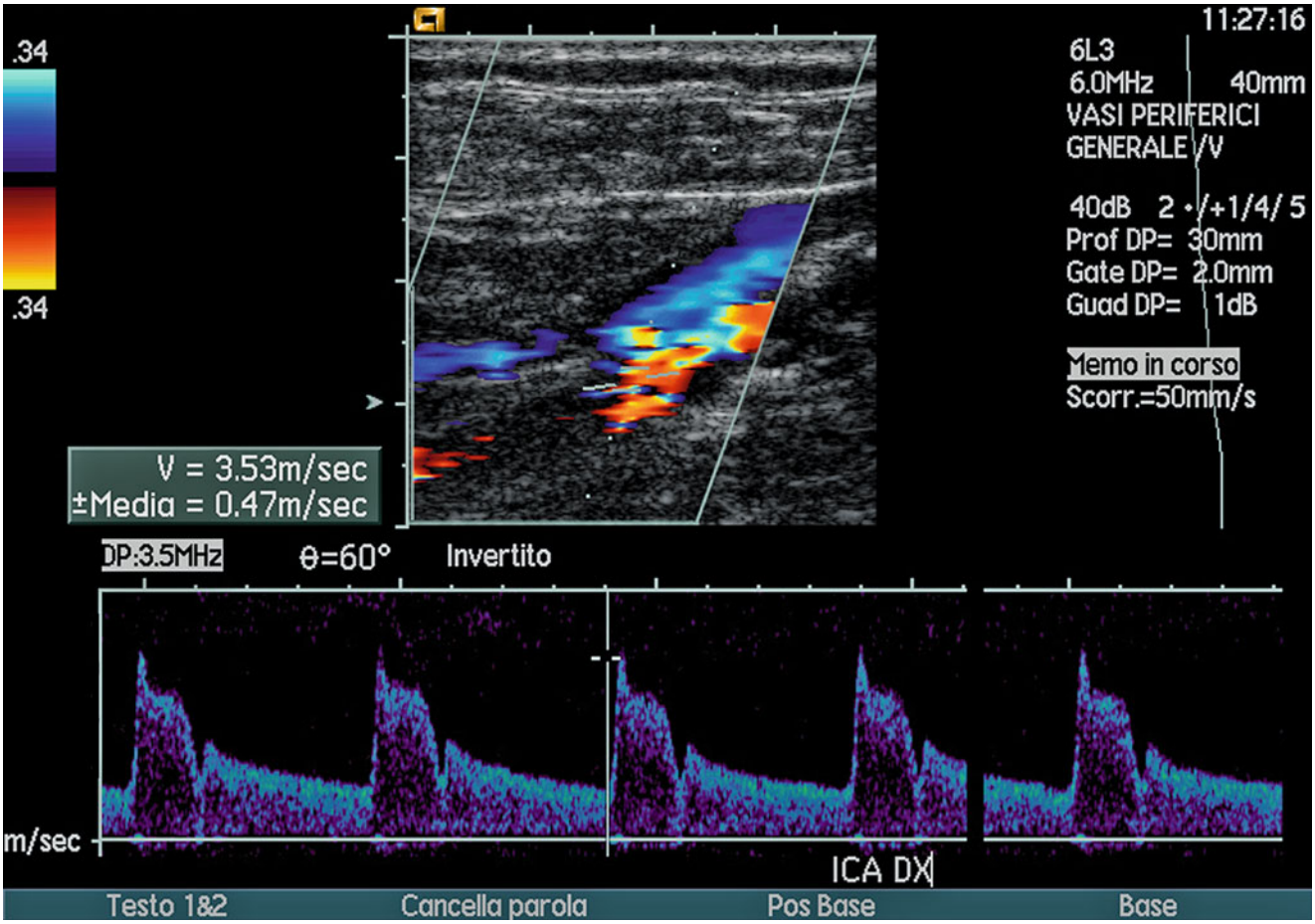


**Fig. 11.12** Carotid duplex scan showing a severe carotid stenosis

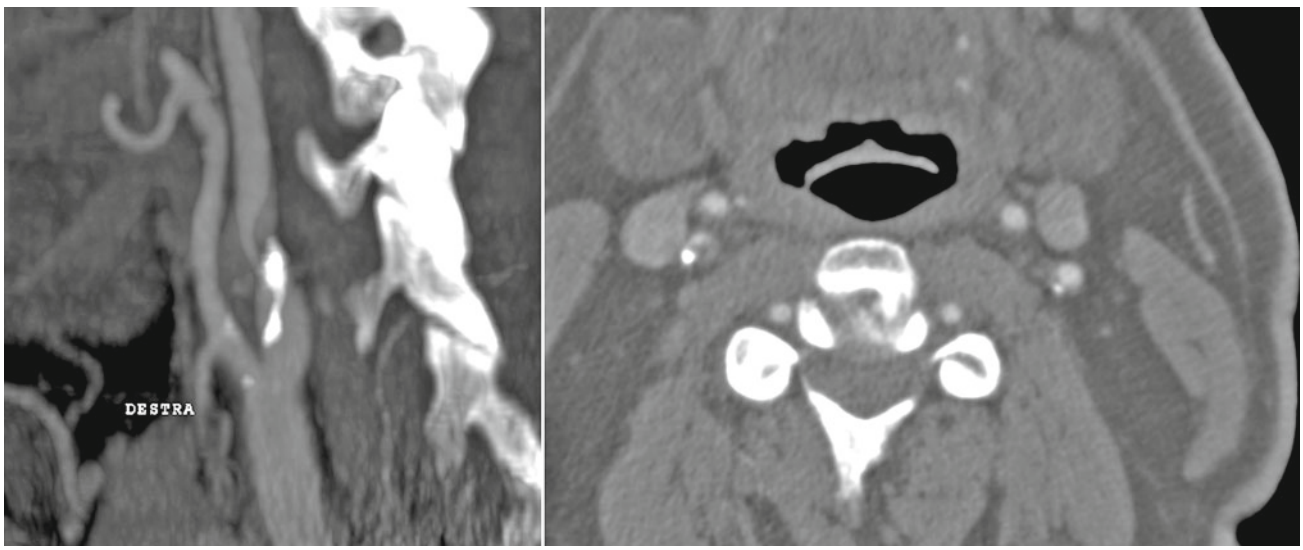


**Fig. 11.13** AngioCT of the neck showing a stenosis of the right internal carotid artery with a mild calcification

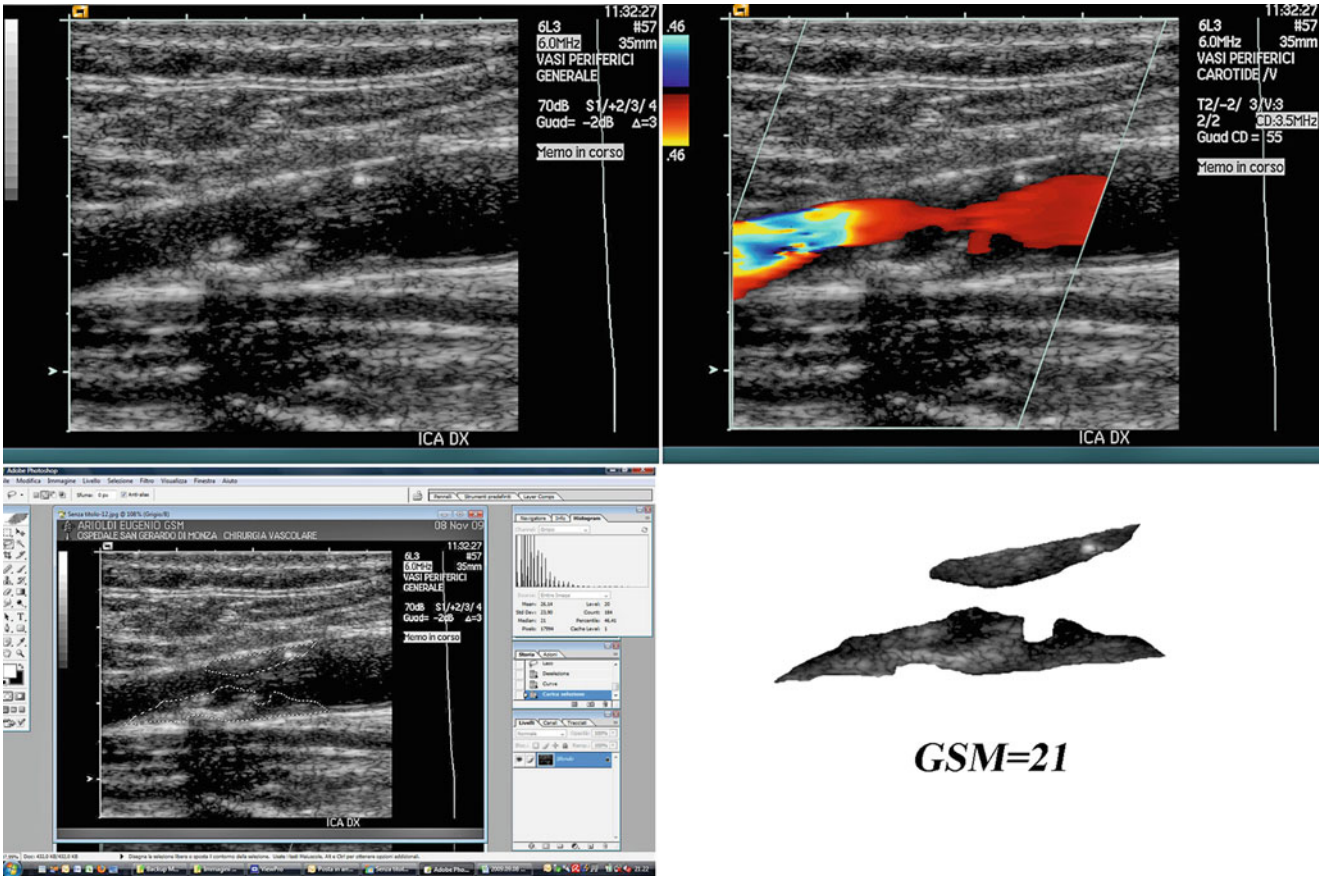


**Fig. 11.14** GSM analysis of the carotid plaque, showing an echolucent lesion

B. It does not influence the choice between endovascular and surgical treatment.

C. It is a parameter that should be always evaluated before any carotid revascularization.

The angioCT demonstrated very accurately that the plaque was only mildly calcified, with the potential to be treated with both surgical and endovascular approaches. The duplex scan demonstrated that the plaque was echolucent, an echographic feature related to an increased risk of stroke in case of medical therapy only. Moreover, the gray scale median (GSM) of the plaque, that is, a computer-assisted index of carotid plaque echogenicity, was 21, confirming an unstable plaque prone to embolize (Fig. 11.14).

According to the presence of multiple uncontrolled risk factors for atherosclerotic disease, the rapid growth of carotid stenosis, and the vulnerable morphology of the plaque, the decision was to treat the patient.

Which factors should be included in the indication to surgical vs. endovascular treatment?

A. Neurological status

B. Degree of stenosis

C. Medical comorbidities

D. Vascular and local anatomical features

E. Carotid plaque morphology

F. All the previous answers are correct

The final situation was:

- A neurologically asymptomatic patient without cerebral ischemic lesions
- A non-subocclusive disease
- A severe ischemic heart disease treated by coronary bypass complicated by a recent acute heart failure without controlling cardiovascular risk factors
- Diabetes and dyslipidemia without optimal control of serum glycemia and cholesterol
- No excessive tortuosity/calcification of aortic arch and common carotid, no tandem lesions, and presence of a very short neck in an obese patient
- An echolucent carotid plaque, prone to embolize, with a limited amount of calcification

The overall evaluation of these features indicated carotid stenting instead of endarterectomy.

One of the most important issues during carotid stenting is embolization to the brain, due to different reasons: crossing of the lesion, angioplasty and stenting with the squeezing of the atherosclerotic core, and protrusion of the plaque through the stent struts.

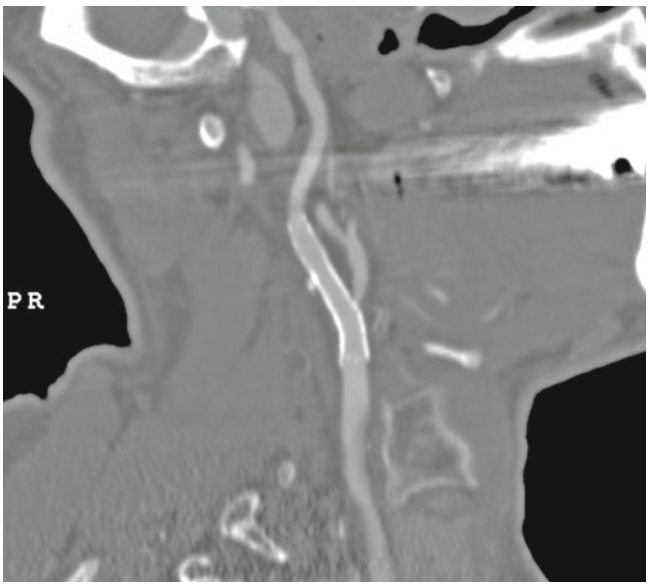


**Fig. 11.15** AngioCT 3 months after carotid stenting

Concerning squeezing of the atherosclerotic core and protrusion of the plaque through the stent struts: Do you think that specific carotid plaque morphology (echolucent vs. echogenic) should be considered for the choice of a specific stent design (open- vs. closed-cell design)?

A. I don't think that carotid plaque echogenicity is useful for the choice of the type of stent.
B. Carotid plaque echogenicity is useful for the choice of the stent: in case of echolucent plaques, stents with closed-cell design should be used.

In order to increase the coverage of an echolucent plaque, a stent with a closed-cell design was used. Actually the stent used in the patient was the self-expanding nitinol 7–10 × 40 mm Cristallo Ideale (Invatec), offering a hybrid solution with open cells in the distal and proximal parts to enhance flexibility and a closed-cell design in the middle to provide the appropriate scaffolding and to prevent plaque prolapse.

Concerning c\rossing of the lesion: Do you think that specific carotid plaque morphology (echolucent vs. echogenic) should be considered for the choice of a specific brain protection device (BPD) (proximal vs. distal)?

A. I don't think that carotid plaque echogenicity is useful for the choice of the type of BPD.
B. Carotid plaque echogenicity is useful for the choice of the BPD: in case of echolucent plaques, proximal BPD with closed-cell design should be used.

Considering that carotid echolucent plaques have an increased risk of stroke during carotid stenting in case of crossing of a distal filter through a soft carotid atheroma, a proximal brain protection device (MoMa, Invatec, with the 8 Fr configuration) was selected.

The procedure was performed without any complication. The patient was discharged 2 days after the procedure. Figure 11.15 shows the postoperative angioCT, performed 3 months following the procedure.

## Discussion

Carotid artery stenting is an alternative method to treat carotid stenosis and to prevent stroke.

Two recent randomized clinical trials comparing carotid artery stenting (CAS) vs. carotid endarterectomy (CEA) in symptomatic patients have been published. The EVA3S trial demonstrated that CAS has higher rates of death and stroke at 1 and 6 months compared to CEA (9.6% vs. 3.9% at 1 month, 11.7% vs. 6.1% at 6 months, respectively) [22]. The SPACE study failed to prove non-inferiority of CAS compared with CEA for the periprocedural (30 days) complication rate (6.84% vs. 6.34%) [23].

The results of these studies are different from those of the SAPPHIRE [24], which demonstrated that CAS with the use of an embolic protection device is not inferior to carotid endarterectomy. The SAPPHIRE included both asymptomatic and symptomatic patients, at high risk due to medical or anatomical factors. EVA3S and SPACE included only symptomatics.

What factor can explain such a big difference between the European and the US studies? In the SAPPHIRE, 27% of patients had received a previous CEA and 29% a previous angioplasty: recurrent stenosis may bias results in favor of stenting because redo endarterectomy is associated with an increased risk of nerve lesions and stroke, while CAS is less risky with restenotic lesions due to the presence of intimal hyperplasia, which is associated to a lower embolic load to the brain. On the other side, the EVA3S and SPACE trials excluded restenoses. This is a huge difference, considering that carotid plaque morphology and echogenicity of restenoses (fibrotic tissue) is completely different from those of primary lesions (lipidic and hemorrhagic tissue). Carotid plaque morphology could be one of the factors explaining the different results of the above-mentioned studies.

The ICAROS study analyzed the role of carotid plaque morphology (evaluated by GSM) as a predictor of stroke following CAS [11]. The GSM is a computer-assisted grading of the echogenicity of carotid plaques. It is a measure of the overall plaque echogenicity, which is a quantitative index of the echoes registered from the plaque. The GSM has two main advantages: it is easily and readily comparable and is calculated using a computer. The ICAROS study demonstrated that the clinical impact of GSM relies on the ability to identify a wide number of patients (the prevalence of a GSM value less than 25 was 37% [155/418 Pts]) at higher risk of

stroke during CAS (7.1% vs. 1.5%, $p<0.005$; OR 7.11) and to distinguish subsets of patients (with restenosis or with protected procedure) in which the rate of neurological complications is different from the overall population. The logistic regression model confirmed the role of GSM as a predictor of stroke in both NASCET/ACAS-eligible and -ineligible patients. As a consequence of this, the effectiveness of GSM can be evaluated both in low- (such as in CREST) and high-risk (such as in SAPPHIRE, ARCHER) patients.

CAS is associated with new areas of cerebral ischemia, as detected by using diffusion-weighted MR imaging (DW-MRI). Not all DW-MRI lesions showed after few days following the procedure are irreversible ischemic lesions, around 40% of early DW-MRI lesions are definite brain infarction on follow-up MRI. Moreover, there is a correlation between the number of lesions in DWI as well as the volume of the lesions and the occurrence of brain infarction on follow-up MRI [25]. The impact of these silent lesions was demonstrated in several studies. The most impressive finding is that the presence of silent brain infarcts at baseline more than doubled the risk of dementia [26]. Brain protection devices (BPDs) significantly reduced the death and stroke rates, as demonstrated in a review including 2,536 CAS procedures. The limitation of BPDs is that they do not protect from silent cerebral ischemia; the rate of DW-MRI lesions in neuroprotected CAS ranges from 23% to 43% [27, 28]. As there is a significant correlation between microembolic signal count measured by transcranial Doppler and new DWI lesions after carotid treatment, the reduction of embolic load to the brain during the CAS procedure is essential to reduce silent cerebral ischemia after the procedure. Once again, low GSM value plaques generated a higher number of embolic particles during CAS [11, 29]. The selection of patients with low embolic potential to the brain may reduce the incidence of cognitive function.

The European Society for Vascular Surgery published the guidelines for indications and techniques for invasive treatment of carotid disease [30]. There are five criteria that should be evaluated prior to any surgical and endovascular treatment:

1. Neurological symptomatology
2. Degree of carotid stenosis
3. Medical comorbidities
4. Vascular and local anatomical features
5. Carotid plaque morphology

The last two parameters deserve particular attention. Complex bifurcation disease with long, multifocal lesions or an angulated internal carotid artery (ICA); extensive aortic or brachiocephalic trunk plaque; severe tortuosity or calcification of the aortic arch vessel; or ring-like, heavy calcifications of the carotid bifurcation are considered contraindications to CAS. On the other hand, CAS is justified in patients with contralateral laryngeal nerve palsy and previous radical neck dissection or cervical irradiation and with prior CEA (restenosis) because the rate of cranial nerve injuries following surgery is higher in this subset. Moreover, CAS can be offered to patients with high bifurcation or intracranial extension of a carotid lesion, where surgical access could be difficult or in patients at high risk of cerebral ischemia during carotid clamping (occlusion of the contralateral internal carotid artery and anomalies of the circle of Willis).

The Cardiovascular Health Study, the Tromso study, Liapis, and Gronholdt demonstrated in nearly 6,000 patients that carotid echolucent plaques were related to the development of future neurologic events [8, 9, 31, 32]. In addition to the role of the GSM in the identification of patients at increased risk of stroke during CAS (ICAROS) and in natural history studies, several papers showed that echolucent carotid plaques with low GSM values have a higher risk of future coronary events in natural history studies [33, 34], a higher risk of restenosis development [35], a higher incidence of a positive brain computed tomography for ischemic lesions, a condition related to neurological dysfunction and dementia [26], and more rapid plaque progression [36]. According to these factors, we decided to treat the patient of the case report.

The stroke rate could not be influenced by carotid plaque morphology if there is huge experience in carotid stenting (several hundreds of cases) or if proximal brain protection device is used that does not require the crossing of the lesion; however, the correct selection of a brain protection device may depend on GSM [37, 38]. Cremonesi enrolled only soft echolucent (GSM lower than 25) carotid lesions in a study of stenting under cerebral protection achieved by a proximal endovascular clamping device, avoiding to cross an emboligenic plaque. The 30-day all death and stroke rate was 2.4%. In 66.7% of patients, visible debris was collected during the procedure. This study demonstrated that the higher risk of stroke observed in the ICAROS study was the consequence of the crossing of an emboligenic carotid plaque with endovascular devices (including a distal BPD). In conclusion, carotid plaque echolucency predicts the risk of stroke in carotid stenting according to the type of brain protection device and the learning curve [39].

Carotid stent design has the potential to influence neurological outcome. The use of closed- vs. open-cell stents is related to different carotid anatomies, neurological symptoms, and types of carotid plaque. A multicenter study analyzing 3,179 consecutive patients showed that the late-event rates varied from 1.2% to 3.4% for free cell areas <2.5 and >7.5 $mm^2$, respectively, being the difference highly pronounced among symptomatic patients [40, 41]. The SPACE trial demonstrated a lower rate of stroke in symptomatic patients treated with a closed-cell stent than in those who received an open-cell stent [42].

In our case report, the choice of a proximal brain protection device and a hybrid stent with a closed-cell design was made to reduce the risk of stroke during and after carotid stenting.

In conclusion, only an appropriate indication to treatment will optimize the treatment for patients with carotid stenoses [1]. The inclusion of carotid plaque morphology with the GSM calculation has the potential to reduce the risk of stroke during CAS and that of neurocognitive dysfunction months or years following the endovascular procedure.

## References


1. Biasi GM, Froio A, Deleo G, Lavitrano M. Indication for carotid endarterectomy versus carotid stenting for the prevention of brain embolization from carotid artery plaques: in search of consensus. J Endovasc Ther. 2006;13:578–91.
2. Tegos TJ, Kalodiki E, Nicolaides AN, Sabetai MM, Stevens JM, Thomas DJ. Brain CT infarction in patients with carotid atheroma. Does it predict a future event? Int Angiol. 2001;20:110–7.
3. Gronholdt ML, Nordestgaard BG, Bentzon J, Wiebe BM, Zhou J, Falk E, Sillesen H. Macrophages are associated with lipid-rich carotid artery plaques, echolucency on B-mode imaging, and elevated plasma lipid levels. J Vasc Surg. 2002;35:137–45.
4. Gronholdt ML, Wiebe BM, Laursen H, Nielsen TG, Schroeder TV, Sillesen H. Lipid-rich carotid artery plaques appear echolucent on ultrasound B-mode images and may be associated with intraplaque hemorrhage. Eur J Vasc Endovasc Surg. 1997;14:439–45.
5. Tegos TJ, Sohail M, Sabetai MM, Robless P, Akbar N, Pare G, Stansby G, Nicolaides AN. Echomorphologic and histopathologic characteristics of unstable carotid plaques. AJNR Am J Neuroradiol. 2000;21:1937–44.
6. Biasi GM, Deleo G, Froio A, Cremonesi A, Inglese L, Lavitrano M, Setacci C. Rationale and design of a multidisciplinary national real-world registry on carotid stenting: the Italian Registry for Carotid Stenting (RISC). J Endovasc Ther. 2006;13:214–20.
7. Sabetai MM, Tegos TJ, Nicolaides AN, Dhanjil S, Pare GJ, Stevens JM. Reproducibility of computer-quantified carotid plaque echogenicity: can we overcome the subjectivity? Stroke. 2000;31:2189–96.
8. Mathiesen EB, Bonaa KH, Joakimsen O. Echolucent plaques are associated with high risk of ischemic cerebrovascular events in carotid stenosis: the tromso study. Circulation. 2001;103:2171–5.
9. Gronholdt ML, Nordestgaard BG, Schroeder TV, Vorstrup S, Sillesen H. Ultrasonic echolucent carotid plaques predict future strokes. Circulation. 2001;104:68–73.
10. Nicolaides AN, Kakkos SK, Griffin M, Sabetai M, Dhanjil S, Thomas DJ, Geroulakos G, Georgiou N, Francis S, Ioannidou E, Dore CJ. Effect of image normalization on carotid plaque classification and the risk of ipsilateral hemispheric ischemic events: results from the asymptomatic carotid stenosis and risk of stroke study. Vascular. 2005;13:211–21.
11. Biasi GM, Froio A, Diethrich EB, Deleo G, Galimberti S, Mingazzini P, Nicolaides AN, Griffin M, Raithel D, Reid DB, Valsecchi MG. Carotid plaque echolucency increases the risk of stroke in carotid stenting: the Imaging in Carotid Angioplasty and Risk of Stroke (ICAROS) study. Circulation. 2004;110:756–62.
12. Biasi GM, Froio A, Deleo G, Piazzoni C, Camesasca V. What have we learned from the Imaging in Carotid Angioplasty and Risk of Stroke (ICAROS) study? Vascular. 2004;12:62–8.
13. Nicolaides AN, Kakkos SK, Kyriacou E, Griffin M, Sabetai M, Thomas DJ, Tegos T, Geroulakos G, Labropoulos N, Doré CJ, Morris TP, Naylor R, Abbott AL, ACSRS Study Group. Asymptomatic internal carotid artery stenosis and cerebrovascular risk stratification. J Vasc Surg. 2010;52:1486–1496.e1–5.
14. Topakian R, King A, Kwon SU, Schaafsma A, Shipley M, Markus HS, ACES Investigators. Ultrasonic plaque echolucency and emboli signals predict stroke in asymptomatic carotid stenosis. Neurology. 2011;77:751–8.
15. Ishizu T, Seo Y, Machino T, Kawamura R, Kimura T, Murakoshi N, Sato A, Takeyasu N, Watanabe S, Aonuma K. Prognostic impact of plaque echolucency in combination with inflammatory biomarkers on cardiovascular outcomes of coronary artery disease patients receiving optimal medical therapy. Atherosclerosis. 2011;216:120–4.
16. Staub D, Partovi S, Schinkel AF, Coll B, Uthoff H, Aschwanden M, Jaeger KA, Feinstein SB. Correlation of carotid artery atherosclerotic lesion echogenicity and severity at standard US with intraplaque neovascularization detected at contrast-enhanced US. Radiology. 2011;258:618–26.
17. Staub D, Patel MB, Tibrewala A, Ludden D, Johnson M, Espinosa P, Coll B, Jaeger KA, Feinstein SB. Vasa vasorum and plaque neovascularization on contrast-enhanced carotid ultrasound imaging correlates with cardiovascular disease and past cardiovascular events. Stroke. 2010;41:41–7.
18. Giannoni MF, Vicenzini E, Citone M, Ricciardi MC, Irace L, Laurito A, Scucchi LF, Di Piero V, Gossetti B, Mauriello A, Spagnoli LG, Lenzi GL, Valentini FB. Contrast carotid ultrasound for the detection of unstable plaques with neoangiogenesis: a pilot study. Eur J Vasc Endovasc Surg. 2009;37:722–7.
19. Graebe M, Pedersen SF, Højgaard L, Kjaer A, Sillesen H. 18FDG PET and ultrasound echolucency in carotid artery plaques. JACC Cardiovasc Imaging. 2010;3:289–95.
20. Choi YS, Youn HJ, Chung WB, Hwang HJ, Lee DH, Park CS, Lee JB, Kim PJ, Chung WS, Lee MY, Seung KB, Chung YA. Uptake of F-18 FDG and ultrasound analysis of carotid plaque. J Nucl Cardiol. 2011;18:267–72.
21. Redgrave JN, Lovett JK, Gallagher PJ, Rothwell PM. Histological assessment of 526 symptomatic carotid plaques in relation to the nature and timing of ischemic symptoms: the Oxford plaque study. Circulation. 2006;113:2320–8.
22. Mas JL, Chatellier G, Beyssen B, Branchereau A, Moulin T, Becquemin JP, Larrue V, Lievre M, Leys D, Bonneville JF, Watelet J, Pruvo JP, Albucher JF, Viguier A, Piquet P, Garnier P, Viader F, Touze E, Giroud M, Hosseini H, Pillet JC, Favrole P, Neau JP, Ducrocq X. Endarterectomy versus stenting in patients with symptomatic severe carotid stenosis. N Engl J Med. 2006;355:1660–71.
23. Ringleb PA, Allenberg J, Bruckmann H, Eckstein HH, Fraedrich G, Hartmann M, Hennerici M, Jansen O, Klein G, Kunze A, Marx P, Niederkorn K, Schmiedt W, Solymosi L, Stingele R, Zeumer H, Hacke W. 30 day results from the SPACE trial of stent-protected angioplasty versus carotid endarterectomy in symptomatic patients: a randomized non-inferiority trial. Lancet. 2006;368:1239–47.
24. Yadav JS, Wholey MH, Kuntz RE, Fayad P, Katzen BT, Mishkel GJ, Bajwa TK, Whitlow P, Strickman NE, Jaff MR, Popma JJ, Snead DB, Cutlip DE, Firth BG, Ouriel K. Protected carotid-artery stenting versus endarterectomy in high-risk patients. N Engl J Med. 2004;351:1493–501.
25. Muller M, Reiche W, Langenscheidt P, Hassfeld J, Hagen T. Ischemia after carotid endarterectomy: comparison between transcranial Doppler sonography and diffusion-weighted MR imaging. AJNR Am J Neuroradiol. 2000;21:47–54.

26. Vermeer SE, Prins ND, den Heijer T, Hofman A, Koudstaal PJ, Breteler MM. Silent brain infarcts and the risk of dementia and cognitive decline. N Engl J Med. 2003;348:1215–22.
27. Flach HZ, Ouhlous M, Hendriks JM, Van Sambeek MR, Veenland JF, Koudstaal PJ, Van Dijk LC, Van Der Lugt A. Cerebral ischemia after carotid intervention. J Endovasc Ther. 2004;11:251–7.
28. Schluter M, Tubler T, Steffens JC, Mathey DG, Schofer J. Focal ischemia of the brain after neuroprotected carotid artery stenting. J Am Coll Cardiol. 2003;42:1007–13.
29. Ohki T, Marin ML, Lyon RT, Berdejo GL, Soundararajan K, Ohki M, Yuan JG, Faries PL, Wain RA, Sanchez LA, Suggs WD, Veith FJ. Ex vivo human carotid artery bifurcation stenting: correlation of lesion characteristics with embolic potential. J Vasc Surg. 1998;27:463–71.
30. Liapis CD, Bell PRF, Mikhailidis D, Sivenius J, Nicolaides A, Fernandes JFE, Biasi G, Norgren L, ESVS Guidelines Collaborators. Invasive treatment for carotid stenosis: indications, techniques. Eur J Vasc Endovasc Surg. 2009;37:S1–19.
31. Polak JF, Shemanski L, O'Leary DH, Lefkowitz D, Price TR, Savage PJ, Brant WE, Reid C. Hypoechoic plaque at US of the carotid artery: an independent risk factor for incident stroke in adults aged 65 years or older. Cardiovascular Health Study. Radiology. 1998;208:649–54.
32. Liapis CD, Kakisis JD, Kostakis AG. Carotid stenosis: factors affecting symptomatology. Stroke. 2001;32:2782–6.
33. Watanabe K, Sugiyama S, Kugiyama K, Honda O, Fukushima H, Koga H, Horibata Y, Hirai T, Sakamoto T, Yoshimura M, Yamashita Y, Ogawa H. Stabilization of carotid atheroma assessed by quantitative ultrasound analysis in nonhypercholesterolemic patients with coronary artery disease. J Am Coll Cardiol. 2005;46:2022–30.
34. Seo Y, Watanabe S, Ishizu T, Moriyama N, Takeyasu N, Maeda H, Ishimitsu T, Aonuma K, Yamaguchi I. Echolucent carotid plaques as a feature in patients with acute coronary syndrome. Circ J. 2006;70:1629–34.
35. Setacci C, de Donato G, Setacci F, Pieraccini M, Cappelli A, Trovato RA, Benevento D. In-stent restenosis after carotid angioplasty and stenting: a challenge for the vascular surgeon. Eur J Vasc Endovasc Surg. 2005;29:601–7.
36. Johnsen SH, Mathiesen EB, Fosse E, Joakimsen O, Stensland-Bugge E, Njolstad I, Arnesen E. Elevated high-density lipoprotein cholesterol levels are protective against plaque progression: a follow-up study of, persons with carotid atherosclerosis the Tromso study. Circulation. 1952;2005(112):498–504.
37. Cremonesi A, Manetti R, Liso A, Ricci E, Bianchi P, Castriota F. Endovascular treatment of soft carotid plaques: a single-center carotid stent experience. J Endovasc Ther. 2006;13:190–5.
38. Reiter M, Bucek RA, Effenberger I, Boltuch J, Lang W, Ahmadi R, Minar E, Schillinger M. Plaque echolucency is not associated with the risk of stroke in carotid stenting. Stroke. 2006;37:2378–80.
39. Froio A, Biasi GM. Carotid plaque echolucency predicts the risk of stroke in carotid stenting according to the type of brain protection device and the learning curve. Stroke. 2007;38:E67–7.
40. Bosiers M, de Donato G, Deloose K, Verbist J, Peeters P, Castriota F, Cremonesi A, Setacci C. Does free cell area influence the outcome in carotid artery stenting? Eur J Vasc Endovasc Surg. 2007;33:135–41.
41. Hart JP, Peeters P, Verbist J, Deloose K, Bosiers M. Do device characteristics impact outcome in carotid artery stenting? J Vasc Surg. 2006;44:725–30.
42. Jansen O, Fiehler J, Hartmann M, Bruckmann H. Protection or nonprotection in carotid stent angioplasty the influence of interventional techniques on outcome data from the SPACE trial. Stroke. 2009;40:841–6.

# Role of Duplex Ultrasound in Carotid Screening

12

Faisal Aziz, Robert P. Scissons, and Anthony J. Comerota

**Abstract**

Screening programs designed to identify disease in the general public have proliferated in recent years, and increased stroke awareness has resulted in both free and for-profit screening programs for carotid disease being offered to the public. This chapter evaluates the effectiveness of screening for carotid artery disease, which by definition means identifying patients with asymptomatic internal carotid disease. A literature review of the history of carotid screening for both general and high-risk populations was undertaken, and the cost-effectiveness of screening programs analyzed. Despite the increased interest related to patients with asymptomatic carotid artery stenosis, screening for carotid artery disease is difficult to justify as the prevalence of asymptomatic carotid artery stenosis and risk of subsequent ipsilateral stroke are low in the general public. Moreover, the number of patients needed to screen in order to prevent one stroke is excessive. At present, there are no data supporting screening for asymptomatic carotid disease in individuals appropriately treated for cardiovascular risk reduction. It is unlikely that screening for carotid artery disease will improve patient care or be cost-effective.

**Keywords**

Asymptomatic carotid artery disease • Doppler ultrasonography • Screening cost-effectiveness • Stroke prevention

F. Aziz, M.D., RVT, RPVI
Department of Surgery, Section of Vascular Surgery,
Penn State Hershey College of Medicine,
Hershey, PA, USA

Jobst Vascular Institute, The Toledo Hospital,
2109 Hughes Dr, Suite 400,
Toledo, OH 43606, USA

R.P. Scissons, RVT, FSVU
Jobst Vascular Laboratory, Jobst Vascular Institute,
The Toledo Hospital,
Toledo, OH, USA

A.J. Comerota, M.D., RVT, FACS, FACC (✉)
Department of Surgery, Section of Vascular Surgery,
University of Michigan,
Ann Arbor, MI, USA

Jobst Vascular Institute, The Toledo Hospital,
2109 Hughes Dr, Suite 400,
Toledo, OH 43606, USA
e-mail: marilyn.gravett@promedica.org

## Introduction

The Asymptomatic Carotid Atherosclerosis Study (ACAS) [1] was the first randomized controlled trial to show that surgical treatment offered to asymptomatic patients with high-grade carotid artery stenosis reduces the risk of subsequent stroke. Other randomized trials subsequently confirmed those findings. Although surgery for symptomatic carotid artery stenosis has become standard treatment for appropriate lesions, enthusiasm for the surgical management of asymptomatic carotid artery stenosis has also increased. This enthusiasm has resulted in a significant increase in the number of asymptomatic patients undergoing carotid revascularization procedures. According to a survey, carotid endarterectomy (CEA) for asymptomatic stenosis accounts for more than 90% of all carotid artery surgeries. The purpose of this chapter is to evaluate the effectiveness of screening for

A.F. AbuRahma, D.F. Bandyk (eds.), *Noninvasive Vascular Diagnosis*,
DOI 10.1007/978-1-4471-4005-4_12, 

carotid artery disease, which by definition means identifying patients with asymptomatic carotid bifurcation disease.

Stroke is associated with serious morbidity and mortality. Eighty percent of strokes are ischemic, and 20% of these are due to large-artery stenosis [2]. Carotid artery duplex is highly sensitive and specific to diagnose internal carotid artery stenosis. The threshold of peak systolic velocity of >130 cm/s is associated with sensitivity of 98% and specificity of 88% in identification of angiographic stenosis of >50%. For diagnosis of angiographic stenosis of >70%, a peak systolic velocity >200 cm/s has a sensitivity of 90% and a specificity of 94% [3]. Carotid artery duplex is the tool for screening asymptomatic people to detect internal carotid stenosis, but to justify its use, one should show that the identification and treatment of an asymptomatic carotid lesion reduces the incidence of stroke. Therefore, it is important to evaluate whether the prevalence, natural history, and current treatment options for asymptomatic carotid artery stenosis support a generalized screening program for the public. There have been no randomized controlled trials to answer this question. Consequently, one needs to determine how many asymptomatic people have to be screened and treated specifically for the lesion found in order to avoid one stroke.

We reviewed the literature on carotid screening for general and high-risk populations and the cost-effectiveness of screening programs. This discussion has become more relevant due to increased public awareness, often resulting from free blood pressure and cholesterol checks offered by pharmacies around the country. Moreover, several agencies are offering screening duplex ultrasounds for detecting peripheral arterial disease, carotid artery stenosis, and abdominal aortic aneurysms. Most people who have these tests are older, and many are unaware of the importance of these tests and their findings. Therefore, it is crucial to determine if such screening programs are necessary and, if so, should be offered by accredited vascular laboratories, which can educate the patients about the results and the importance of their findings.

## Potential Burden of Stroke Resulting from Carotid Artery Stenosis

Stroke is the third leading cause of death and the most common cause of long-term disability in the United States [4]. Each year, about 700,000 people suffer a new or a recurrent stroke on average; every 45 s, someone in the United States has a stroke, and every 3 min, someone dies of a stroke. Stroke accounted for about 1 of every 15 deaths in the United States in 2003. Men's stroke incidence rates are 1.25 times greater than women's. Because women live longer than men, more women than men die of stroke every year. Women accounted for 61% of stroke deaths in the United States [4].

Stroke is a life-changing event. Kelly-Hayes et al. [5] reviewed outcomes from the Framingham Study and found that 12% of those who survive a first stroke or TIA have another within the first year. Twenty-two percent of men and 25% of women who have a stroke die within a year. This percentage is higher for patients who are 65 and older. Approximately 50–70% of stroke survivors regain functional independence, but 15–30% are permanently disabled and 20% require institutionalized care at 3 months after onset. The same data show that among patients who were at least 65 years old, 50% had residual hemiparesis and 26% were institutionalized 6 months after their stroke. Therefore, in light of the devastating consequences of stroke, prevention is desirable by health care professionals, organizations, and society in general. One approach is to offer appropriate screening tests, assuming the causative lesion can be identified and subsequently treated.

## Natural History of Asymptomatic Carotid Artery Stenosis

The occurrence of stroke and death resulting from asymptomatic carotid artery stenosis is proportional to the prevalence and prognosis of untreated disease. Population-based studies using duplex scanning have shown that the prevalence of ≥50% carotid stenosis ranges between 2% and 8%, and those with asymptomatic carotid artery stenosis of 80% or more is between 1% and 2% [6–10]. The cost-effectiveness of carotid screening depends upon the natural history of the asymptomatic carotid lesion.

The low incidence of asymptomatic carotid artery stenosis has implications for carotid artery screening programs. Positive predictive value of any screening modality will change with the prevalence of disease in the tested population [11]. Assuming that duplex scanning for asymptomatic carotid artery stenosis has sensitivity and specificity of 95%, positive predictive value of duplex scanning for a carotid artery stenosis of more than 50% would be approximately 50%, and the positive predictive value of duplex scanning for a carotid stenosis of more than 80% or greater would be 16% [12]. However, the actual sensitivity and specificity of carotid duplex is less than 95%, therefore resulting in lower positive predictive values, even when evaluated in a highly selected patient population [13]. Therefore, with low prevalence in general population, the positive predictive value of a screening study like carotid duplex is severely diminished.

Norris et al. [14] performed a natural history study of 696 patients and demonstrated that the annual risk of ipsilateral stroke was 2.5% for patients with asymptomatic carotid artery stenosis of more than 75%. Lesser degrees of stenosis were associated with a lower annual stroke rate (1.3%).

The European Carotid Surgery Trial (ECST) [15] showed that for patients with asymptomatic carotid artery stenosis of 70% or more, the 3-year risk of ipsilateral stroke was 5.7% (annual risk of stroke 1.9%). For lesser degrees of asymptomatic carotid artery stenosis, the 3-year risk of stroke was 2.1% (annual risk of stroke 0.7%).

The ACAS study found that patients with an asymptomatic carotid artery stenosis ≥60% who were treated medically had an annual rate of 2.12% [1]. In the medical arm of the Veterans Administration trial [16], the ipsilateral stroke rate was 9.4% at 47.9 months for patients with asymptomatic carotid artery stenosis of more than 50% (annual risk of stroke = 2.36%).

To summarize, the average annual risk of stroke from asymptomatic carotid artery stenosis of 50% or greater is approximately 2–3% per year. Taking into account the low prevalence of asymptomatic carotid artery stenosis in the general public, an individual would have less than 0.16% risk per year of stroke or death from undetected asymptomatic carotid artery stenosis of 50% or greater, and a 0.06% risk from asymptomatic carotid artery stenosis of 80% or greater [17].

Sleight et al. [18] reviewed the long-term outcomes for patients enrolled in the medical management cohort of ECST. They excluded symptomatic patients and short-listed 219 patients who have had serial carotid duplex ultrasounds. They stratified patients based on their baseline carotid stenosis into three groups: 15–49% ($n = 2$), 50–79% ($n = 110$), and 80–99% ($n = 107$). At the end of 4-year follow-up, 31 patients regressed to a lower group, 148 remained in the same group, and 37 patients progressed by one group and 3 patients by two categories. These data showed that for patients undergoing medical management for asymptomatic carotid artery stenosis, the mean carotid stenosis does not change over 4 years.

Nehler et al. [19] identified 263 patients with 434 asymptomatic <60% internal carotid artery stenoses, observed them for 20 months, and performed duplex ultrasound every 6 months. At the end of follow-up, 6.5% of patients (4% of carotid arteries) progressed without symptoms to >60%. None of the patients became symptomatic. Clinical risk factors associated with progression to >60% stenosis included elevated systolic blood pressure and decreased ankle-brachial index ($p = 0.05$). The life table-determined rate of freedom from progression to >60% stenosis was 94% at 4 years for asymptomatic internal carotid artery lesions that had initial peak systolic velocity less than 175 cm/s compared to 14% at 3 years for lesions that had initial peak systolic velocities >175 cm/s. This study shows that patients who are at greatest risk of early progression of carotid atherosclerosis are those who have systolic velocities higher than 175 cm/s.

Rockman et al. [20] retrospectively reviewed the records of 282 asymptomatic internal carotid arteries with moderate stenosis (50–79%). Seventeen percent of internal carotid arteries demonstrated progression over 5 years. Estimated cumulative rates for progression of stenosis at 1, 3, and 5 years were 4.9%, 16.7%, and 26.5%, respectively. New ipsilateral strokes occurred in 3.8% and new ipsilateral transient ischemic attacks in 5.9% of patients. Arteries that progressed to >80% stenosis were more likely to have caused strokes than those that remained between 50% and 70% (10.4% vs. 2.1%, $p < 0.02$). Arteries that were unchanged, or stable, in the degree of stenosis were more likely to remain asymptomatic than those that progressed (92.7% vs. 62.5%, $p < 0.001$). The authors concluded that the only factor that appeared to predict increased risk for future stroke is progression of stenosis.

Mansour et al. [21] reviewed outcomes in 344 patients (458 internal carotid arteries) with moderate carotid artery stenosis (50–79%). Life table analysis showed that the annual rate of ipsilateral neurologic events was 8.1% and the annual risk of stroke was 2.1%. Disease progression to 80–99% stenosis or occlusion occurred in 15.5% of arteries. The internal carotid arteries that showed evidence of disease progression had a significantly higher initial peak systolic velocity (251 vs. 190 cm/s, $p < 0.0001$) and end-diastolic velocity (74 vs. 52 cm/s, $p < 0.0001$). A greater amount of disease at baseline predicted progression.

Muluk et al. [22] followed 1,701 carotid arteries in 1,004 patients for a mean follow-up of 28 months and found that the risk of progression of internal carotid artery stenosis increased steadily over time. The four most important variables that affected the progression were baseline ipsilateral internal carotid artery (ICA) stenosis of >50% (RR 3.34), baseline ipsilateral external carotid artery stenosis of >50% (RR 1.51), baseline contralateral ICA stenosis of >50% (RR 1.41), and systolic blood pressure >160 mmHg (RR 1.37). Ipsilateral neurologic ischemic events (strokes/TIAs) occurred in association with 14% of carotid arteries.

Garvey et al. [23] performed prospective serial duplex scan surveillance of 1,470 carotid arteries in 905 asymptomatic patients during a 10-year period, with an average follow-up interval of 29 months. They identified six significant predictors of progression: age, sex, systolic blood pressure, pulse pressure, total cholesterol, and HDL. Multivariate analysis showed that only pulse pressure and HDL remained as significant independent predictors of stenosis progression. The risk ratio of 10 mmHg rise in pulse pressure was 1.12, and the risk ratio of 10 mg/dl decrease in HDL was 1.20.

Shanik et al. [24] reported stenosis progression in 259 carotids over 96 months, with a mean follow-up of 48 months. Thirty-five of 96 (36%) arteries with mild stenosis showed progression, 21 developed 50–79% stenosis, 12 progressed to greater than 80% stenosis, and two progressed to carotid occlusion. Only two of these patients had a stroke.

Ellis et al. [25] reported overall progression of 3.4% in 1,034 arteries with less than 50% stenosis at mean follow-up of 20 months.

All of the studies mentioned in this section were performed 10–22 years ago, which raises the question as to whether their observations are valid today, as the medical management of patients with atherosclerosis has changed dramatically. Proper platelet inhibition, more aggressive control of blood pressure, and the use of statins have substantially reduced neurologic events in both symptomatic and asymptomatic patients.

A number of important observations need to be recognized. The first is that 97% of carotid etiology strokes occur in patients with symptomatic carotid disease [26]. If one can ensure that all individuals with a 60–99% asymptomatic carotid stenosis can be identified and treated with either CEA or carotid angioplasty and stenting with a procedural risk of 2.3% (ACAS procedure risk), it will do little to reduce the overall burden of stroke [26].

An important question to address when evaluating the issue of screening for carotid artery disease is whether the risk of stroke from asymptomatic disease is changing. The seminal studies (ACAS, ACST) reported results of medical treatment of patients nearly 20 years ago. Is it appropriate to equate present-day cardiovascular risk to observations made 20 or more years ago? The answer is a decisive "no."

Even in the ACAS and ACST studies, there was no relationship of the degree of asymptomatic carotid stenosis to subsequent stroke, and there was no benefit to women who underwent CEA versus medical treatment. An important issue that needs to be addressed when carotid screening is being considered is: Has the risk of stroke from carotid artery disease decreased in the last 15–20 years? McPhee et al. [27] reported that of 135,701 procedures performed to treat carotid artery disease, 92% were performed for asymptomatic disease. If one can assume the low procedure risk of 2.3% stroke/death observed in ACAS, and the same risk of stroke in the medically treated patients, 115,730 unnecessary procedures were performed, and the cost to prevent one stroke in 5 years would be $369,685. Bunch and Kresowik [28] performed a US multicenter audit of CEA for asymptomatic disease and showed that the true risk of stroke and death from CEA in the USA was 3.8%; therefore, the cost of preventing one stroke or death over 5 years (in 2005 dollars) would be $428,510. This estimate is based upon the medical risk patients faced over 20 years ago.

There are robust data demonstrating that the medical treatment of asymptomatic carotid disease has improved and that the risk of stroke for an asymptomatic carotid lesion has progressively diminished. Although there are no data reported for changes of medical care during ACAS, there are considerable data showing changes in medical care in ACST, which appear to have altered stroke risk for the asymptomatic carotid lesion during the study. At the initiation of ACST (1996), only 17% of patients were treated with statins. By the year 2000, 58% were on statins, and by 2008, 90% were on statins. The 5-year risk of ipsilateral stroke dropped from 5.3% in the first 5 years of ACST to 3.6% in years 6–10.

It has been reported that diabetics treated with statins had a 46% relative risk reduction (RRR) of stroke [29], and patients with high cardiovascular risk had a 25% RRR of stroke if treated with a statin [30]. The SPARCL investigators [31] showed that in patients with stroke and TIAs randomized to statins, there was a 16% RRR of any stroke ($p = 0.03$) and a 35% risk reduction of a major cardiovascular event ($p < 0.001$). This study demonstrated that in the highest risk symptomatic patients, improved medical management reduces stroke.

The more contemporary Oxford Vascular Study [32] and the SMART study [33] reported annualized risks of ipsilateral stroke from >50% asymptomatic carotid stenosis of 0.34% and 0.7%, respectively. Therefore, with current therapy, it will be difficult to justify operative intervention for most patients with asymptomatic carotid disease. Since most screening programs are designed to identify candidates with disease who would be considered for CEA or angioplasty and stenting, if the proposed intervention would no longer be considered appropriate, the screening program could not be justified.

## Rationale of Stroke Prevention Screening

The majority of strokes are ischemic strokes with sudden deprivation of blood flow to an area of the brain. ICA atherosclerosis, the leading cause of ischemic stroke, can cause a stroke by either reducing the blood flow to the brain or by embolizing atherosclerotic plaque or thrombus. Therefore, the best strategy seems to focus on prevention of stroke. In 1994, the National Stroke Association (NSA) recommended screening all persons over 50 years of age for carotid artery disease, atrial fibrillation, and hypertension. While this was an important statement, the recommended screening protocol included using a stethoscope to find cervical bruits for detection of carotid artery disease, palpating the pulse at the wrist to check for an irregular rhythm, and using a standard blood pressure reading for diagnosing hypertension [34].

## Risk Factors for Stroke

If risk factors for stroke can be defined, we can offer carotid screening only to those people who are at a higher risk of developing stroke. Review of the literature suggests the following factors to be associated with a higher risk for developing stroke:

1. *Transient Ischemic Attack* (*TIA*)

   TIAs are associated with substantially high risk of stroke and death. Johnson et al. followed 1,707 patients who

presented to emergency rooms with TIAs and found that 10% developed stroke within 90 days of their TIA and 5% died within 2 days. They identified any TIA persisting longer than 10 min to be a predictor of stroke [35].

2. *Smoking*
   The relative risk of stroke in heavy smokers (>40 cigarettes a day) is twice that of light smokers (<10 cigarettes a day). Stroke risk decreases significantly after 2 years' cessation of smoking and is at the level of nonsmokers by 5 years after cessation [36].
3. *Blood pressure*
   People with blood pressure less than 120/80 mmHg have about half the lifetime risk of stroke compared to those with hypertension [37].
4. *Physical activity*
   A physicians' health study showed that men who performed vigorous exercise had a lower stroke rate [38]. Harvard alumni study showed similar findings in males [39]. A nurses' health study confirmed these findings for females [40].
5. *Postmenopausal women*
   The Women's Health Initiative, a primary prevention clinical trial of 16,608 females, showed that combination of estrogen and progestin increased ischemic stroke risk by 44%, with no effect on hemorrhagic stroke rate [41].

## How Can We Improve Positive Predictive Value of a Screening Test?

We can improve the positive predictive value of a screening test by performing the test on the subset of population that is statistically more likely to harbor the disease. Review of literature shows that the following three groups of patients may be at a higher risk for developing future strokes:

### Role of Carotid Duplex in Patients Undergoing Coronary Artery Surgery

Atherosclerosis is a systemic disease and involves coronary, carotid, and lower extremity arteries. D' Agostino et al. [42] collected data prospectively for 1,835 patients undergoing coronary artery surgery. Of these patients, 1,279 underwent screening carotid duplex examinations preoperatively. 2.5% of all patients developed an operative stroke. Multivariate analysis identified the following clinical predictors for postoperative stroke: advanced age, female sex, prior stroke or transient ischemic attack, atherosclerotic disease involving ascending aorta, peripheral vascular disease, prior vascular operation, and smoking. The study suggested that preoperative carotid duplex should be considered for patients with a history of neurologic events or peripheral vascular disease; however, the majority of strokes in their study were caused by embolic phenomenon from an atherosclerotic aorta or from the heart. Reed et al. [43] noted that patients with a previous stroke are at a sixfold increased risk of post coronary artery bypass grafting (CABG) stroke. Li et al. [44] retrospectively reviewed 4,325 patients who underwent CABG and/or valve replacement. Clinically definite postoperative stroke incidence was 1.8%. Among stroke patients, only 5.3% of strokes were attributed to ICA stenosis. Interestingly, for patients who had >70% ICA stenosis, the postoperative stroke rate was 15% if they underwent both CABG and CEA, while it was 0% if no CEA was done. This large study demonstrates that (1) the postoperative stroke rate for CABG patients is extremely low; and (2) in patients diagnosed preoperatively with a high-grade ICA stenosis, combined treatment (CABG plus CEA) is actually more harmful than not treating the ICA stenosis at all.

### Role of Routine Carotid Duplex Screening in Patients with Lower Extremity Arterial Occlusive Disease

The real question is whether a high-prevalence population can be reliably identified. Marek et al. [45] performed screening carotid duplex in 188 patients who presented with intermittent claudication and no cerebrovascular symptoms. Twenty percent were found to have a stenosis of 50–79%, 1.6% had stenosis of 80–99%, and 2.7% had evidence of carotid occlusion. The study concluded that the subset of patients aged >65 years, presence of carotid bruit, and ABI of <0.7 had a 45% incidence of >50% ICA stenosis (OR = 5.42).

Turnipseed et al. [46] performed preoperative carotid duplex imaging in 330 patients who underwent coronary artery bypass (170) and peripheral vascular surgery (160). Patients with peripheral arterial disease had a higher incidence of carotid bruits compared to those with coronary artery disease (44% vs. 16%). In those patients who had a carotid bruit, there was 54% incidence of significant carotid artery disease. Patients with PAD had a 52% incidence of significant carotid disease compared with 11.7% of patients who underwent coronary artery bypass. This was not a true screening study as 43% of the patients with PAD had symptoms suggestive of cerebrovascular disease.

Barnes et al. [47] prospectively screened 449 asymptomatic patients with carotid duplex before coronary or peripheral arterial reconstruction. They noted that the prevalence of carotid artery disease was significantly higher in patients who had PAD (28%) than in those patients who had coronary artery heart disease (15%). Additionally, patients who had asymptomatic carotid artery disease had an increased risk of neurologic events (15%) compared with patients without carotid artery disease (0.8%) during a 2-year follow-up.

Moreover, there was an increased risk of perioperative and late death (10.6% and 9.2%, respectively) in patients who had asymptomatic carotid disease compared with patients who did not (0.3% and 0.8%, respectively, $p < 0.001$).

Ahn et al. [48] reviewed the duplex scans of 78 patients who underwent carotid screening solely because of PAD and found that 14% had stenosis >50%, although they did not correlate the severity of the PAD to the presence of carotid stenoses. Their analysis showed that the risk factors of male sex, age > 68 years, hypertension, and previous cardiovascular surgery strongly correlated with carotid stenosis. They concluded that routine carotid duplex screening is indicated in older patients (age > 68 years) who have peripheral vascular disease.

Fowl et al. [49] screened two patient groups in a Veterans Hospital setting for the presence of asymptomatic carotid stenosis. The first group had 152 patients without any history of PAD, and the second group consisted of 116 patients with PAD. Duplex screening revealed a 6.5% incidence of >50% carotid stenosis in the first group compared with 12% for the patients in the second group ($p = 0.058$). They recommended carotid surveillance in asymptomatic patients who have multiple atherosclerotic risk factors.

Gentile et al. [50] reviewed retrospective data on 225 patients who underwent infrainguinal revascularization procedures with no previous carotid surgery and found that the presence of carotid bruit and the presence of rest pain were associated with >50% carotid stenosis. Among the subset of patients who had carotid bruit, 58% were found to have asymptomatic carotid stenosis of more than 50%.

Virgilio et al. [51] prospectively screened patients with lower extremity atherosclerosis and found that 20% of asymptomatic male patients had a carotid stenosis of more than 50%.

Hennerici et al. [52] screened 2,009 asymptomatic patients and divided them into three groups. The first group consisted of 375 patients who were examined before major vascular surgery (on aorta, iliac, or infrainguinal arteries), the second group had 264 patients with severe coronary artery disease, and the third group had 1,370 patients who had risk factors for atherosclerosis. The prevalence of asymptomatic carotid stenosis was 32.8% in the first group, 6.8% in the second group, and 5.9% in the third group ($p < 0.001$). These data suggest that patients undergoing major vascular surgery are at a much higher risk for harboring asymptomatic carotid artery stenosis as compared to those with coronary artery disease and those with risk factors for atherosclerosis.

## Role of Ultrasound Follow-up for the Non-operated Carotid Artery After CEA

The rationale behind postoperative carotid imaging is twofold. First, recurrent stenosis may be identified, and, second, disease progression in the non-operated ICA may be monitored regularly. Naylor et al. [53] followed 219 patients after carotid endarterectomy and specifically monitored their contralateral (non-operated, asymptomatic) ICA. 151 patients had regular duplex ultrasounds in the postoperative period. Cumulative freedom from stroke in the non-operated hemisphere was 99%, 96%, and 86% at 1, 5, and 10 years, respectively, giving a mean incidence of stroke of 1% per annum. Only one stroke was preceded by a transient ischemic event, and no stroke was associated with >70% stenosis of ICA. Ten patients (7%) with initially mild or moderate disease of the non-operated ICA progressed to severe stenosis during follow-up; only three became symptomatic and, in each case, the onset of symptoms preceded recognition of disease progression. The long-term risk of stroke in the non-operated ICA territory was small. The authors concluded that none of the observed strokes could have been prevented by postoperative surveillance following CEA.

AbuRahma [54] performed a similar study evaluating arteries contralateral to a CEA in 534 patients. Serial duplex ultrasound was performed at 1 month postoperatively and thereafter every 6 months. Overall, carotid artery stenosis progressed in 36% of patients at mean follow-up of 41 months. Progression of stenosis was noted in 3% of patients with baseline normal carotid arteries. Carotid artery stenosis progressed in 36% of patients with less than 50% stenosis versus 47% of patients with 50–79% ICA stenosis. Late neurologic events referable to carotid artery stenosis were infrequent (6.7% in the entire series), including 2.4% strokes and 4.3% TIAs. Contralateral CEA was performed in 15% of patients. They concluded that duplex ultrasound should be performed every 6–12 months, if the stenosis is between 50% and 69%, and every 12–24 months if stenosis is less than 50%.

Ballotta [55] followed asymptomatic contralateral ICAs of 599 patients who had undergone CEA for severe carotid disease. They performed duplex at 1 month and then every 6 months for a mean follow-up of 4.1 years. Disease progressed in 34% of patients with mild stenosis (30–49%) versus 47.9% of patients with moderate stenosis (50–69%). The median time to progression was 29.8 months for mild and 18.5 months for moderate stenosis. The rate of late neurologic events referable to contralateral ICA was 3.2% for the entire series and 4.8% for patients with a 30% of greater ICA stenosis. The study suggested duplex surveillance every 6 months in patients with >50% stenosis.

## Cost-Effectiveness of Screening for Carotid Stenosis in Asymptomatic Patients

Lee et al. [56] applied the cost-effectiveness analysis methods to the data from ACAS to determine cost-effectiveness of carotid screening. They assumed that the survival

advantage offered by carotid endarterectomy for a 65-year-old man would last for 30 years, an assumption which is not justified according to insurance company life tables. The lifetime marginal cost-effectiveness of screening relative to no screening was $120,000 per quality-adjusted life year, which would double if life expectancy was targeted at a more realistic 15 years. Sensitivity analysis showed that marginal cost-effectiveness decreased to $50,000 or less per quality-adjusted life year only if a free screening instrument with perfect test characteristics was used in a population in which there was 40% prevalence of carotid stenosis. Therefore, a program to identify candidates for endarterectomy by screening asymptomatic populations for carotid stenosis costs more per quality-adjusted life year than is usually considered acceptable.

Derdeyn et al. [57] developed a computer model to simulate the cost-effectiveness of screening a cohort of 1,000 men during a 20-year time period. Probabilities of stroke and death with surgical and medical management were obtained from published clinical trials. They showed that a one-time screening program of a population with a high prevalence (20%) of >60% stenosis costs $35,130 per incremental quality of life gained. Annual screening costs $457,773 per year of quality life gained. They concluded that the cost-effectiveness of a one-time screening program for an asymptomatic population with a high prevalence of carotid stenosis may be cost-effective, but annual screening is detrimental.

Obuchowski et al. [58] constructed a model of the natural history of carotid artery disease using literature-based estimates of prevalence and incidence of carotid artery stenosis and associated morbidity and mortality. They found that carotid screening is effective only if rate of stenosis progression is >6% per year. However, if this rate is below 6%, screening is effective only if the prevalence rate in population is >20%, and if the rate of progression is below 1%, screening is effective only if the prevalence of disease in the population is more than 30%.

Yin et al. [59] performed a cost-effectiveness analysis with a Markov model with data from ACAS and other trials. They found that for 60-year-old patients with a 5% prevalence of 60–99% asymptomatic stenosis, duplex ultrasound screening increased average quality-adjusted life years (QALY; 11.485 vs. 11.473) and lifetime cost of care ($5,500 vs. $5,012). Screening was cost-effective with the following conditions: disease prevalence was 4.5% or more, specificity of the duplex was 91% or more, stroke rate of patients who were medically treated was 3.3% or more, the relative risk reduction of surgery was 37% or more, the stroke rate associated with surgery was 160% or less than that of North American Symptomatic Carotid Endarterectomy Trial or ACAS perioperative complication rates, and the cost of ultrasound screening was $300 or less.

According to ACAS data, 5-year absolute risk reduction for stroke for asymptomatic patients was 5.8%. Hill et al. [17] calculated that 17 patients in ACAS would require carotid endarterectomy to prevent one stroke (number needed to treat). Given the prevalence of disease in population, the resulting number of patients required to screen to prevent one stroke from ipsilateral asymptomatic carotid stenosis of ≥80% would range from 850 to 1,700 (this figure may be as high as 8,500 if one considers the positive predictive value of duplex scanning used to demonstrate the prevalence of ACAS). The cost efficacy of such an approach would be difficult to justify.

## Scoring System to Identify High-Risk Patients

Qureshi et al. [60] developed and validated a simple scoring system based on routinely available information to identify persons at high risk for asymptomatic carotid artery stenosis using data collected during a community health screening program at various sites in western New York. They studied 1,331 volunteers without previous stroke, transient ischemic attack, or carotid artery surgery. Their evaluation included personal interviews and duplex ultrasound. The main outcome was carotid stenosis of more than 60% by duplex criteria. They identified four variables which were significantly associated with asymptomatic carotid artery stenosis of more than 60%: age > 65 years (odds ratio: 4.1), current smoking (odds ratio: 2), coronary artery disease (odds ratio: 2.4), and hypercholesterolemia (odds ratio: 1.9). They developed three risk groups (low, intermediate, and high) on the basis of total risk score assigned on the basis of strength association. The stratified scheme was validated. The posttest probability for the high-risk group was 35%, for those at intermediate risk 20%, and 7% for the low-risk group.

### Conclusions

Despite the increased interest related to patients with asymptomatic carotid artery stenosis, screening for carotid artery disease is difficult to justify. The prevalence of asymptomatic carotid artery stenosis in the general public and the risk of subsequent ipsilateral stroke are low. The number of patients needed to screen in order to prevent one stroke is excessive. Focused screening in patients at high risk due to peripheral vascular disease, coronary artery disease, or contralateral CEA improves yield; however, there are no data demonstrating that such an approach reduces stroke. At present, there are no data supporting screening for asymptomatic carotid disease in individuals appropriately treated for cardiovascular risk reduction. It is unlikely that screening for carotid artery disease will improve patient care or be cost-effective.

## References


1. Executive Committee for the Asymptomatic Carotid Atherosclerosis Study. Endarterectomy for asymptomatic carotid artery stenosis. JAMA. 1995;273(18):1421–8.
2. Barnett HJ, Gunton RW, Eliasziw M, Fleming L, Sharpe B, Gates P, et al. Causes and severity of ischemic stroke in patients with internal carotid artery stenosis. JAMA. 2000;283(11):1429–36.
3. Jahromi AS, Cina CS, Liu Y, Clase CM. Sensitivity and specificity of color duplex ultrasound measurement in the estimation of internal carotid artery stenosis: a systematic review and meta-analysis. J Vasc Surg. 2005;41(6):962–72.
4. American Heart Association. Heart disease and stroke statistics. 2011. Available at: http://www.heart.org/HEARTORG/General/Heart-and-Stroke-Association-Statistics_UCM_319064_SubHomePage.jsp. Accessed 13 June 2011.
5. Kelly-Hayes M, Beiser A, Kase CS, Scaramucci A, D'Agostino RB, Wolf PA. The influence of gender and age on disability following ischemic stroke: the Framingham study. J Stroke Cerebrovasc Dis. 2003;12(3):119–26.
6. Colgan MP, Strode GR, Sommer JD, Gibbs JL, Sumner DS. Prevalence of asymptomatic carotid disease: results of duplex scanning in 348 unselected volunteers. J Vasc Surg. 1988;8(6):674–8.
7. Ricci S, Flamini FO, Marini M, Antonini D, Bartolini S, Celani MG, et al. The prevalence of stenosis of the internal carotid in subjects over 49: a population study. Epidemiol Prev. 1991;13(48–49):173–6.
8. Warlow C. Endarterectomy for asymptomatic carotid stenosis? Lancet. 1995;345(8960):1254–5.
9. Bots ML, Breslau PJ, Briet E, de Bruyn AM, van Vliet HH, van den Ouweland FA, et al. Cardiovascular determinants of carotid artery disease. The Rotterdam Elderly study. Hypertension. 1992;19(6 Pt 2):717–20.
10. Fine-Edelstein JS, Wolf PA, O'Leary DH, Poehlman H, Belanger AJ, Kase CS, et al. Precursors of extracranial carotid atherosclerosis in the Framingham study. Neurology. 1994;44(6):1046–50.
11. Vecchio TJ. Predictive value of a single diagnostic test in unselected populations. N Engl J Med. 1966;274(21):1171–3.
12. Sackett DL, Haynes RB, Guyatt GH, Tugwell P. Clinical epidemiology: a basic science for clinical medicine. 2nd ed. Boston: Little, Brown and Co; 1991.
13. Faught WE, Mattos MA, Van Bemmelen PS, Hodgson KJ, Barkmeier LD, Ramsey DE, et al. Color-flow duplex scanning of carotid arteries: new velocity criteria based on receiver operator characteristic analysis for threshold stenoses used in the symptomatic and asymptomatic carotid trials. J Vasc Surg. 1994;19(5):818–27.
14. Norris JW, Zhu CZ, Bornstein NM, Chambers BR. Vascular risks of asymptomatic carotid stenosis. Stroke. 1991;22(12):1485–90.
15. European Carotid Surgery Trialists' Collaborative Group. Randomised trial of endarterectomy for recently symptomatic carotid stenosis: final results of the MRC European Carotid Surgery Trial (ECST). Lancet. 1998;351(9113):1379–87.
16. Hobson RW, Weiss DG, Fields WS, Goldstone J, Moore WS, Towne JB, et al. Efficacy of carotid endarterectomy for asymptomatic carotid stenosis. The Veterans Affairs Cooperative Study Group. N Engl J Med. 1993;328(4):221–7.
17. Hill AB. Should patients be screened for asymptomatic carotid artery stenosis? Can J Surg. 1998;41(3):208–13.
18. Sleight SP, Poloniecki J, Halliday AW. Asymptomatic carotid stenosis in patients on medical treatment alone. Eur J Vasc Endovasc Surg. 2002;23(6):519–23.
19. Nehler MR, Moneta GL, Lee RW, Edwards JM, Taylor Jr LM, Porter JM. Improving selection of patients with less than 60% asymptomatic internal carotid artery stenosis for follow-up carotid artery duplex scanning. J Vasc Surg. 1996;24(4):580–5.
20. Rockman CB, Riles TS, Lamparello PJ, Giangola G, Adelman MA, Stone D, et al. Natural history and management of the asymptomatic, moderately stenotic internal carotid artery. J Vasc Surg. 1997;25(3):423–31.
21. Mansour MA, Littooy FN, Watson WC, Blumofe KA, Heilizer TJ, Steffen GF, et al. Outcome of moderate carotid artery stenosis in patients who are asymptomatic. J Vasc Surg. 1999;29(2):217–25.
22. Muluk SC, Muluk VS, Sugimoto H, Rhee RY, Trachtenberg J, Steed DL, et al. Progression of asymptomatic carotid stenosis: a natural history study in 1004 patients. J Vasc Surg. 1999;29(2):208–14.
23. Garvey L, Makaroun MS, Muluk VS, Webster MW, Muluk SC. Etiologic factors in progression of carotid stenosis: a 10-year study in 905 patients. J Vasc Surg. 2000;31(1 Pt 1):31–8.
24. Shanik DG, Moore DJ, Leahy A, Grouden MC, Colgan M-P. Asymptomatic carotid stenosis: a benign lesion? Eur J Vasc Surg. 1992;6(1):10–5.
25. Ellis MR, Franks PJ, Cuming R, Powell JT, Greenhalgh RM. Prevalence, progression and natural history of asymptomatic carotid stenosis: is there a place for carotid endarterectomy? Eur J Vasc Surg. 1992;6(2):172–7.
26. Naylor AR. Delay may reduce procedural risk, but at what price to the patient? Eur J Vasc Endovasc Surg. 2008;35(4):383–91.
27. McPhee JT, Schanzer A, Messina LM, Eslami MH. Carotid artery stenting has increased rates of postprocedure stroke, death, and resource utilization than does carotid endarterectomy in the United States, 2005. J Vasc Surg. 2008;48(6):1442–50.
28. Bunch CT, Kresowik TF. Can randomized trial outcomes for carotid endarterectomy be achieved in community-wide practice? Semin Vasc Surg. 2004;17(3):209–13.
29. Colhoun HM, Betteridge DJ, Durrington PN, Hitman GA, Neil HA, Livingstone SJ, et al. Primary prevention of cardiovascular disease with atorvastatin in type 2 diabetes in the Collaborative Atorvastatin Diabetes Study (CARDS): multicentre randomised placebo-controlled trial. Lancet. 2004;364(9435):685–96.
30. Heart Protection Study Collaborative Group. MRC/BHF Heart Protection Study of cholesterol lowering with simvastatin in 20,536 high-risk individuals: a randomised placebo-controlled trial. Lancet. 2002;360(9326):7–22.
31. Amarenco P, Bogousslavsky J, Callahan III A, Goldstein LB, Hennerici M, Rudolph AE, et al. High-dose atorvastatin after stroke or transient ischemic attack. N Engl J Med. 2006;355(6):549–59.
32. Marquardt L, Geraghty OC, Mehta Z, Rothwell PM. Low risk of ipsilateral stroke in patients with asymptomatic carotid stenosis on best medical treatment: a prospective, population-based study. Stroke. 2010;41(1):e11–7.
33. Goessens BM, Visseren FL, Kappelle LJ, Algra A, van Der GY. Asymptomatic carotid artery stenosis and the risk of new vascular events in patients with manifest arterial disease: the SMART study. Stroke. 2007;38(5):1470–5.
34. Lavenson GS. Stroke prevention screening: rationale, method, and implementation. Vasc Ultrasound Today. 2003;8(1):1–24.
35. Johnston SC, Gress DR, Browner WS, Sidney S. Short-term prognosis after emergency department diagnosis of TIA. JAMA. 2000;284(22):2901–6.
36. Wolf PA, D'Agostino RB, Kannel WB, Bonita R, Belanger AJ. Cigarette smoking as a risk factor for stroke. The Framingham study. JAMA. 1988;259(7):1025–9.
37. Seshadri S, Beiser A, Kelly-Hayes M, Kase CS, Au R, Kannel WB, et al. The lifetime risk of stroke: estimates from the Framingham study. Stroke. 2006;37(2):345–50.
38. Lee IM, Hennekens CH, Berger K, Buring JE, Manson JE. Exercise and risk of stroke in male physicians. Stroke. 1999;30(1):1–6.
39. Lee IM, Paffenbarger Jr RS. Physical activity and stroke incidence: the Harvard Alumni Health Study. Stroke. 1998;29(10):2049–54.
40. Hu FB, Stampfer MJ, Colditz GA, Ascherio A, Rexrode KM, Willett WC, et al. Physical activity and risk of stroke in women. JAMA. 2000;283(22):2961–7.
41. Wassertheil-Smoller S, Hendrix SL, Limacher M, Heiss G, Kooperberg C, Baird A, et al. Effect of estrogen plus progestin on stroke in postmenopausal women: the Women's Health Initiative: a randomized trial. JAMA. 2003;289(20):2673–84.

42. D'Agostino RS, Svensson LG, Neumann DJ, Balkhy HH, Williamson WA, Shahian DM. Screening carotid ultrasonography and risk factors for stroke in coronary artery surgery patients. Ann Thorac Surg. 1996;62(6):1714–23.
43. Reed III GL, Singer DE, Picard EH, DeSanctis RW. Stroke following coronary-artery bypass surgery. A case-control estimate of the risk from carotid bruits. N Engl J Med. 1988;319(19):1246–50.
44. Li Y, Walicki D, Mathiesen C, Jenny D, Li Q, Isayev Y, et al. Strokes after cardiac surgery and relationship to carotid stenosis. Arch Neurol. 2009;66(9):1091–6.
45. Marek J, Mills JL, Harvich J, Cui H, Fujitani RM. Utility of routine carotid duplex screening in patients who have claudication. J Vasc Surg. 1996;24(4):572–7.
46. Turnipseed WD, Berkoff HA, Belzer FO. Postoperative stroke in cardiac and peripheral vascular disease. Ann Surg. 1980;192(3):365–8.
47. Barnes RW, Liebman PR, Marszalek PB, Kirk CL, Goldman MH. The natural history of asymptomatic carotid disease in patients undergoing cardiovascular surgery. Surgery. 1981;90(6):1075–83.
48. Ahn SS, Baker JD, Walden K, Moore WS. Which asymptomatic patients should undergo routine screening carotid duplex scan? Am J Surg. 1991;162(2):180–3.
49. Fowl RJ, Marsch JG, Love M, Patterson RB, Shukla R, Kempczinski RF. Prevalence of hemodynamically significant stenosis of the carotid artery in an asymptomatic veteran population. Surg Gynecol Obstet. 1991;172(1):13–6.
50. Gentile AT, Taylor Jr LM, Moneta GL, Porter JM. Prevalence of asymptomatic carotid stenosis in patients undergoing infrainguinal bypass surgery. Arch Surg. 1995;130(8):900–4.
51. de Virgiolio C, Toosie K, Arnell T, Lewis RJ, Donayre CE, Baker JD, et al. Asymptomatic carotid artery stenosis screening in patients with lower extremity atherosclerosis: a prospective study. Ann Vasc Surg. 1997;11(4):374–7.
52. Hennerici M, Aulich A, Sandmann W, Freund HJ. Incidence of asymptomatic extracranial arterial disease. Stroke. 1981;12(6):750–8.
53. Naylor AR, John T, Howlett J, Gillespie I, Allan P, Ruckley CV. Fate of the non-operated carotid artery after contralateral endarterectomy. Br J Surg. 1995;82(1):44–8.
54. AbuRahma AF, Cook CC, Metz MJ, Wulu Jr JT, Bartolucci A. Natural history of carotid artery stenosis contralateral to endarterectomy: results from two randomized prospective trials. J Vasc Surg. 2003;38(6):1154–61.
55. Ballotta E, Da GG, Meneghetti G, Barbon B, Militello C, Baracchini C. Progression of atherosclerosis in asymptomatic carotid arteries after contralateral endarterectomy: a 10-year prospective study. J Vasc Surg. 2007;45(3):516–22.
56. Lee TT, Solomon NA, Heidenreich PA, Oehlert J, Garber AM. Cost-effectiveness of screening for carotid stenosis in asymptomatic persons. Ann Intern Med. 1997;126(5):337–46.
57. Derdeyn CP, Powers WJ. Cost-effectiveness of screening for asymptomatic carotid atherosclerotic disease. Stroke. 1996;27(11):1944–50.
58. Obuchowski NA, Modic MT, Magdinec M, Masaryk TJ. Assessment of the efficacy of noninvasive screening for patients with asymptomatic neck bruits. Stroke. 1997;28(7):1330–9.
59. Yin D, Carpenter JP. Cost-effectiveness of screening for asymptomatic carotid stenosis. J Vasc Surg. 1998;27(2):245–55.
60. Qureshi AI, Janardhan V, Bennett SE, Luft AR, Hopkins LN, Guterman LR. Who should be screened for asymptomatic carotid artery stenosis? Experience from the Western New York Stroke Screening Program. J Neuroimaging. 2001;11(2):105–11.

# Duplex Ultrasound Velocity Criteria in Carotid Artery Stenting Patients

13

Brajesh K. Lal

**Abstract**

Carotid artery stenting (CAS) has recently emerged as a less invasive alternative to carotid endarterectomy (CEA). Carotid stenting has been demonstrated to be technically feasible and safe in high-risk patients. It has been approved as an acceptable method for revascularization in circumstances where CEA yields suboptimal results. While the final role of CAS in carotid revascularization is still in evolution, it is clear that stenting will continue to be performed in an increasing number of patients with carotid stenosis. Therefore, it is anticipated that there will be a corresponding increase in the number of in-stent restenosis cases. Considerable controversy exists regarding the clinical significance and appropriate diagnostic criteria for recurrent carotid stenosis after CAS. Placing a stent in the carotid artery alters its biomechanical properties and renders it less complaint. This in turn leads to elevations in velocities that do not necessarily reflect a stenosis. If the thresholds to define normal arteries are revised upward, then duplex ultrasonography has been found to be a very effective method of post-CAS surveillance. This chapter analyzes current information on this important clinical problem and presents evidence-based recommendations for the diagnosis of recurrent carotid stenosis after CAS.

**Keywords**

Restenosis • Velocity criteria • Intimal hyperplasia • Morphology • Carotid stenting

## Introduction

Carotid restenosis is attributed to neointimal hyperplasia during the early postoperative period (within 24 months) after carotid artery revascularization or recurrent atherosclerosis thereafter [1–3]. The exact mechanisms involved in the development of neointimal hyperplastic lesions have yet to be defined completely. Late restenosis lesions are indistinguishable from primary atherosclerosis.

B.K. Lal, M.D., FACS
Department of Vascular Surgery, Baltimore VA Medical Center, Baltimore, MD, USA

Department of Surgery and Center for Vascular Diagnostics, University of Maryland Medical School and Vascular Service Baltimore VA Medical Center, 22 South Greene Street, S100, B00, Baltimore, MD 21201, USA
e-mail: blal@smail.umaryland.edu

## Incidence

### Carotid Endarterectomy

Over 150,000 carotid endarterectomies (CEA) are performed annually in the United States [4]. The Asymptomatic Carotid Atherosclerosis Study (ACAS) follow-up data demonstrated that carotid restenosis (CR) 3–18 months after operation, defined as Doppler-determined diameter reductions of ≥60%, occurred in 7.6% of patients [5]. This early development of CR is probably secondary to myointimal hyperplasia. The

A.F. AbuRahma, D.F. Bandyk (eds.), *Noninvasive Vascular Diagnosis*,
DOI 10.1007/978-1-4471-4005-4_13, © Springer-Verlag London 2013

incidence of CR 18–60 months after operation was 1.9%, potentially related to progression of atherosclerotic disease. With life table methods, the probability of developing CR (≥50%) 7 years after CEA was 32% [6, 7].

### Carotid Artery Stenting

Coronary stenting has been associated with lower rates of angiographic and clinical restenosis than angioplasty alone [8]. This salutary effect may be due to the stent's ability to provide larger arterial lumens. Neointimal hyperplasia accompanies virtually every stent placement in the coronary, iliac, or carotid system [8]. Intimal hyperplastic recurrence has been observed after coronary stenting in 16–59% of cases and after iliac stenting in 13–39% [9]. We used life table analysis to provide specific information on in-stent restenosis (ISR) after CAS [10] (Fig. 13.1). Over a follow-up period of 1–74 months (mean 18.8 ± 10), 22/122 patients demonstrated ISR ≥ 40%. All 22 ISR patients were asymptomatic on presentation and were diagnosed by duplex ultrasonography during routine follow-up. Although restenotic lesions ranged from 40% to 99%, only five patients demonstrated high-grade ISR (≥80%), while the remaining fell in the lower ranges: 40–59%, $n = 11$, and 60–79%, $n = 6$. The projected 5-year recurrence rate for ISR ≥ 80% was 6.4%. Cumulative 4-year rate of ISR ≥ 60% was 16.4% and of ISR ≥ 40% was 42.7%. These observations were subsequently confirmed by others [11]. While ISR does not appear to occur at the high rates associated with bare metal stenting of the coronary arteries, a substantial number of patients can be anticipated to progress to moderate- and high-grade ISR.

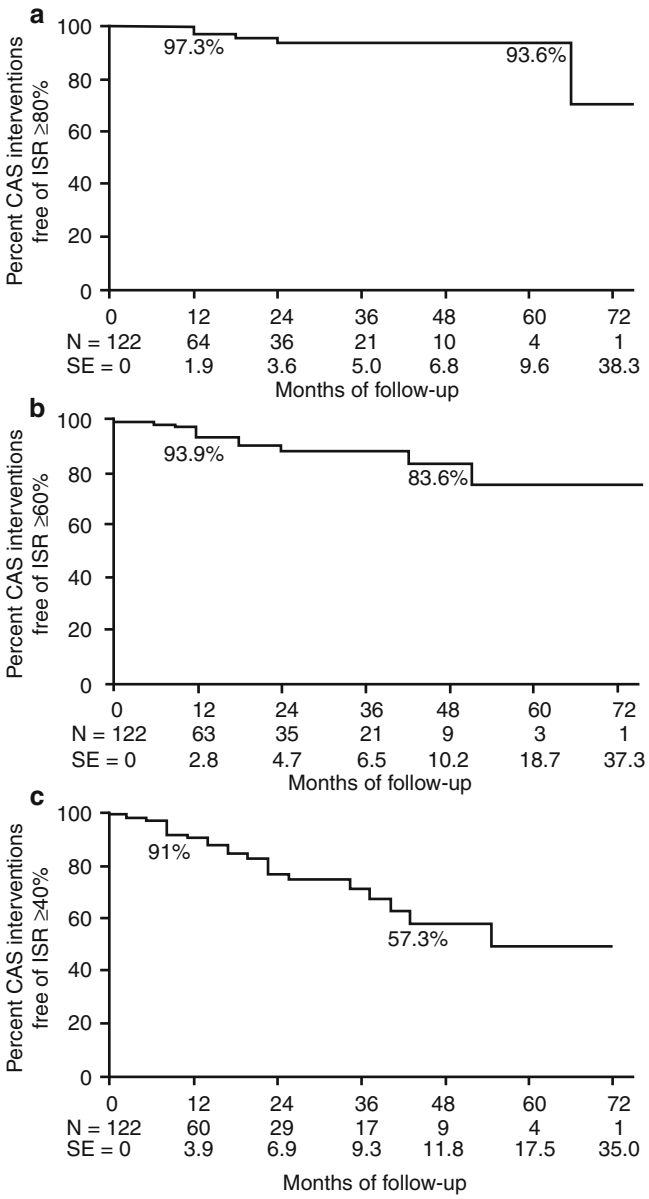


**Fig. 13.1** Incidence of in-stent restenosis after carotid artery stenting (CAS). (**a**) Kaplan-Meier cumulative event rates for clinically significant ISR ≥ 80% after CAS. (**b**) Kaplan-Meier cumulative event rates for ISR ≥ 60% after CAS. (**c**) Kaplan-Meier cumulative event rates for ISR ≥ 40% after CAS. *Number of patients at the beginning of each time interval and standard error are indicated below the X-axis of each graph. N* number at risk, *SE* standard error (Adapted from Lal et al. [10]. With permission from Elsevier)

## Natural History

### Carotid Endarterectomy

The clinical significance of CR after CEA is still debated. Symptomatic CR clearly benefits from repeat revascularization. However, the risk of stroke or progression to total occlusion [2, 7] is known to be low in patients with asymptomatic CR. Therefore, some clinicians have proposed careful surveillance alone for asymptomatic patients [12]. Conversely, most surgeons elect to reintervene on high-grade (≥70%) asymptomatic lesions. The rationale for such an approach is that it is extremely difficult to predict which preocclusive lesions will remain asymptomatic [13, 14]. We also subscribe to this view with respect to restenosis after CEA [15].

### Carotid Artery Stenting

There is limited information on what factors constitute risks for in-stent restenosis (ISR) after CAS. We therefore developed a novel protocol to assess and classify the morphologic patterns of ISR after CAS [16] into types I (focal ≤ 10 mm, end-stent lesions), II (focal ≤ 10 mm, intrastent), III (diffuse > 10 mm, intrastent), IV (diffuse > 10 mm, proliferative, extending outside the stent), and V (total occlusion) (Fig. 13.2). Eighty-five ISR lesions developed after 255 CAS procedures. Their percent distributions were 40, 25.9, 12.9, 20, and 1.2 (types I through V, respectively). The accuracy of our US classification was confirmed by angiography

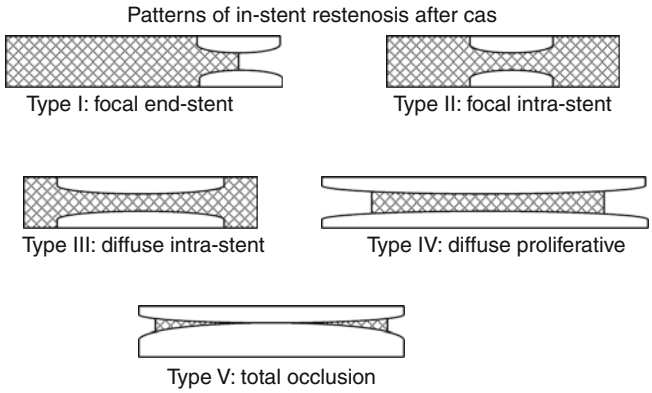


**Fig. 13.2** Classification of the morphologic patterns of carotid in-stent restenosis. The classification is based on the length and geographic location of the neointimal hyperplastic lesion with respect to the stent. The *shaded area* represents the stent (Adapted from Lal et al. [16]. With permission from Elsevier)

($r^2 = 0.82$). Thirteen lesions were ≥80% diameter reducing and required endovascular reintervention. On multivariate analysis, only the type of ISR (odds ratio, 5.1) and a history of diabetes (OR, 9.7) were independent predictors of high-grade recurrent ISR and reintervention [16]. Furthermore, there was a significant increase in reintervention in association with increasing levels of ISR classification (0%, 0%, 27.3%, and 58.8% for types I–IV, respectively; $\chi^2$ trend = 29.4, $p = 0.001$). Follow-up duplex US evaluations after CAS must therefore include an assessment of the morphologic pattern of ISR. While additional prospective data is required to confirm these findings, it is likely that patients with type IV lesions will benefit from a more intensive duplex surveillance program (perhaps every 6 months for life).

## DUS Velocity Criteria

### Carotid Endarterectomy

Duplex ultrasonography (DUS) is the standard technique to follow carotid stenosis patients treated with CEA or medical therapy alone. Duplex ultrasonography offers several advantages in the follow-up of patients treated with carotid revascularization. It is noninvasive, safe, free of complications, readily available in vascular laboratories around the country, and is associated with a large experience with primary and recurrent carotid stenosis of the native carotid artery. The utility of DUS scanning in the detection of native carotid artery disease is well documented and has led to the use of peak-systolic velocities (PSV), end-diastolic velocities (EDV) and PSV/EDV ratio, or internal carotid/common carotid artery PSV ratios (ICA/CCA ratios), alone or in combination, to define normal and increasingly stenosed ICAs. Ultrasound velocities correlate with angiographic percent stenosis in the native carotid artery, and the appropriate threshold velocities signifying different degrees of stenoses have been intensively analyzed and identified [17–19].

### Carotid Artery Stenting

Duplex ultrasound velocity criteria had not been well established for patients undergoing CAS until very recently. Two studies initially reported altered blood flow velocities after carotid stent placement. The authors proposed that these variations in velocity measurements adversely affected the accuracy of duplex ultrasonography (DUS) in CAS patients. They concluded that DUS velocity measurements as an index of stenosis were not reliable after carotid stent placement [20, 21].

#### Carotid Stenting Alters Compliance

In 2004, we reported that the placement of a stent altered the biomechanical properties of the carotid territory such that compliance was reduced [22] (Fig. 13.3). Compliance is a material property measured by the relationship between strain (fractional deformation of wall) and stress (force per unit area of wall). In an artery, compliance is described by the change in volume of a segment of artery in relation to pulsatile change in blood pressure. Assuming a cylindrical conformation for the arterial segment, the volume may be calculated as $\pi r^2 l$ ($r$ = radius; $l$ = length). Since length is usually constant, the relative diameter change per unit pressure has been used as an index of changes in compliance. We also found that the enhanced stiffness of the stent-arterial wall complex rendered the flow-pressure relationship of the carotid artery closer to that observed in a rigid tube [23] so that the energy normally applied to dilate the artery resulted in an increased velocity.

#### Stenting Increases Velocity Measurements

In this first report, we compared post-CAS ultrasound velocities with angiographically measured residual in-stent stenosis after 90 CAS procedures. Mean angiographic residual stenosis after CAS was 5.4%, while corresponding PSV on DUS was 120.4 cm/s; EDV, 41.4 cm/s; PSV/EDV ratio, 3.3; and ICA/CCA ratio, 1.6. Receiver operating characteristic (ROC) analysis demonstrated that a combined threshold PSV ≥ 150 cm/s and ICA/CCA ratio ≥2.16 were optimal for detecting residual stenosis ≥20%. Based on these observations, we concluded that DUS was useful and accurate in identifying stenotic lesions in stented carotid arteries. However, revised velocity criteria would need to be developed to identify higher grades of ISR in this situation.

#### Velocity Thresholds for Restenosis

These observations were followed by at least four studies that addressed this hypothesis. Peterson et al. [24] analyzed DUS velocity and angiographic measurements of stenosis in three patients with high-grade ISR and proposed new criteria

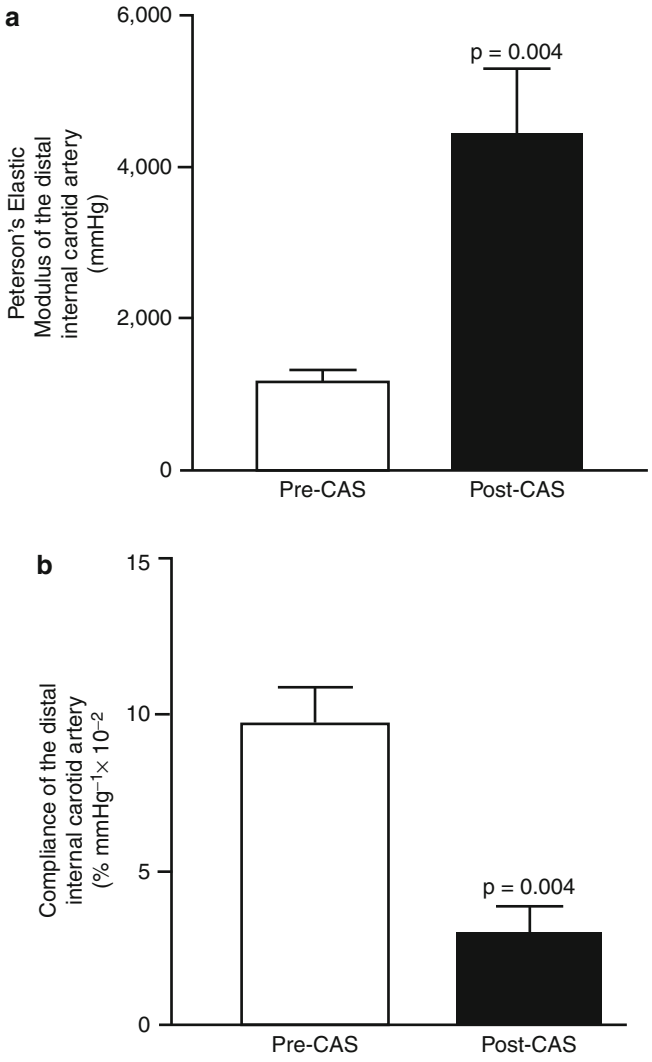


**Fig. 13.3** Carotid artery stenting alters the biomechanical properties of the stent-arterial complex. Measurement of elastic modulus (**a**) and compliance (**b**) of the native internal carotid artery versus stented internal carotid artery (Adapted from Lal et al. [22]. With permission from Elsevier)

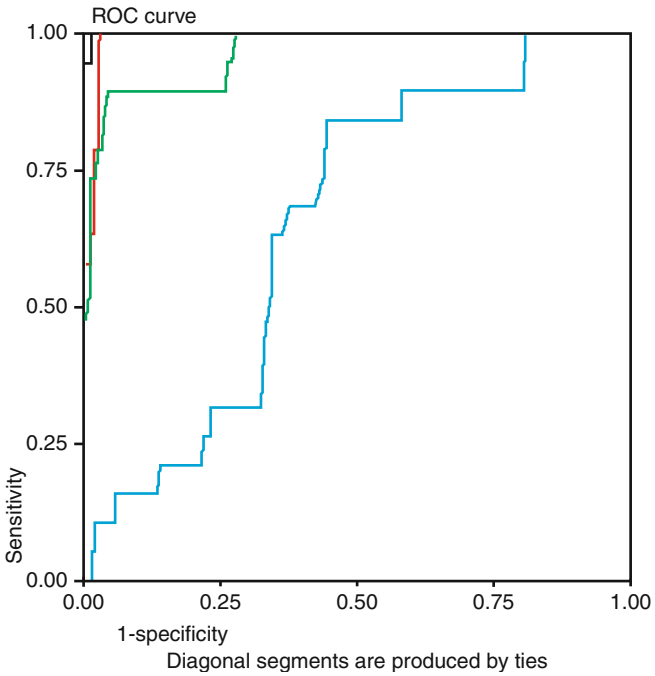


**Fig. 13.4** Receiver operating characteristic (*ROC*) analysis to determine accuracy parameters of threshold velocities appropriate for the identification of high-grade in-stent restenosis (ISR) ≥80%. ROC curves were developed for PSV, ICA/CCA ratios, EDV, and PSV/EDV ratios for each threshold stenosis (Adapted from Lal et al. [28]. With permission from Elsevier)

defining ISR ≥ 70% (PSV > 170, EDV > 120, and velocity increase >50% over baseline). Stanziale et al. [25] analyzed velocity/angiography observations obtained primarily from procedural angiography and selected angiography performed in patients with suspected high-grade ISR during follow-up. They proposed new criteria defining ISR ≥ 70% (PSV ≥350 and ICA/CCA ratio ≥ 4.75) and ISR ≥ 50% (PSV > 225 and ICA/CCA ratio ≥ 2.5). Chi et al. [26] analyzed 13 pairs of DUS and angiogram observations in CAS patients with suspected high-grade ISR. They offered alternate criteria to define ISR ≥ 70% (PSV ≥ 450, or ICA/CCA ratio ≥ 4.3) and ISR ≥ 50% (PSV ≥ 240 or ICA/CCA ratio ≥ 2.45). Chahwan et al. [27] analyzed six pairs of observations from patients with high-grade ISR on follow-up along with procedural angiograms ($n=71$). They concluded that a normal DUS after CAS is reliable in identifying a normal artery, but larger studies would be required to determine appropriate threshold criteria. These studies indicated that higher grades of restenosis were also overestimated in the stented artery when velocity criteria for native arteries were utilized. However, procedural risks precluded routine angiographic follow-up, and comparisons could not be performed across the full spectrum of degrees of restenosis. This explained the wide variation in proposed threshold velocity criteria.

Our group [28] later compared DUS velocity measurements with luminal stenosis measured by either angiography or CT angiography (CTA) during follow-up of all our CAS patients ($n=310$ observations). Patients were followed with annual DUS and CTA at their most recent follow-up visit. Patients with suspected high-grade ISR on US underwent diagnostic carotid angiography. The DUS protocol included peak-systolic (PSV) and end-diastolic velocity (EDV) measurements in the native common carotid artery (CCA), proximal stent, mid stent, distal stent, and distal internal carotid artery (ICA). The accuracy of CTA versus CA was confirmed ($r^2=0.88$). Post-CAS PSV ($r^2=0.85$) and ICA/CCA ratios ($r^2=0.76$) correlated most with the degree of restenosis. Receiver operator characteristic (ROC) analysis demonstrated the following optimal threshold criteria: residual stenosis ≥20% (PSV ≥ 150 cm/s and ICA/CCA ratio ≥ 2.15), ISR ≥ 50% (PSV ≥ 220 cm/s and ICA/CCA ratio ≥ 2.7), and ISR ≥ 80% (PSV ≥ 340 cm/s and ICA/CCA ratio ≥ 4.15) (Fig. 13.4).

**Table 13.1** Suggested velocity criteria defining stenoses in the stented carotid artery compared to criteria for the native carotid artery utilized at our institution

| | |
|---|---|
| *Stented carotid artery* | |
| 0–19% | PSV < 150 cm/s and ICA/CCA ratio < 2.15 |
| 20–49% | PSV 150–219 cm/s |
| 50–79% | PSV 220–339 cm/s and ICA/CCA ratio ≥ 2.7 |
| 80–99% | PSV ≥ 340 cm/s and ICA/CCA ratio ≥ 4.15 |
| *Native carotid artery* | |
| 0–19% | PSV < 130 cm/s |
| 20–49% | PSV 130–189 cm/s |
| 50–79% | PSV 190–249 cm/s and EDV < 120 cm/s |
| 80–99% | PSV ≥ 250 cm/s and EDV ≥ 120 cm/s, or ICA/CCA ratio ≥ 3.2 |

Adapted from Lal et al. [28]. With permission from Elsevier
*PSV* peak-systolic velocity, *EDV* end-diastolic velocity, *ICA* internal carotid artery, *CCA* common carotid artery, *PSV* and *EDV* measurements for stented carotid arteries are performed within the stented segments

We therefore proposed revised velocity criteria [28] for identifying restenosis in stented carotid arteries (Table 13.1). While our results can be used as guidelines, individual laboratories must develop threshold criteria that are accurate for their own environment. These proposed criteria can form the basis for additional prospective validation studies.

## Surveillance Frequency

### Carotid Endarterectomy

The ACAS data on recurrent stenosis [5] emphasize the value of serial noninvasive testing after CEA, particularly during the first few years postoperatively. However, the recommended frequency of noninvasive testing after CEA remains controversial [7, 29]. We generally recommend noninvasive duplex ultrasonography testing of patients at 6-month to 12-month intervals during the first 3 years after CEA. Thereafter, follow-up testing should be based on the development of cervical bruits and neurological symptoms, rather than routine screening. Importantly though, the heterogeneity of published results on restenosis and operative complications [29] suggests that much better data are needed if we are to arrive at reliable recommendations on follow-up frequency.

### Carotid Artery Stenting

We recommend that all patients undergoing CAS must be placed in a regular follow-up protocol. The majority of

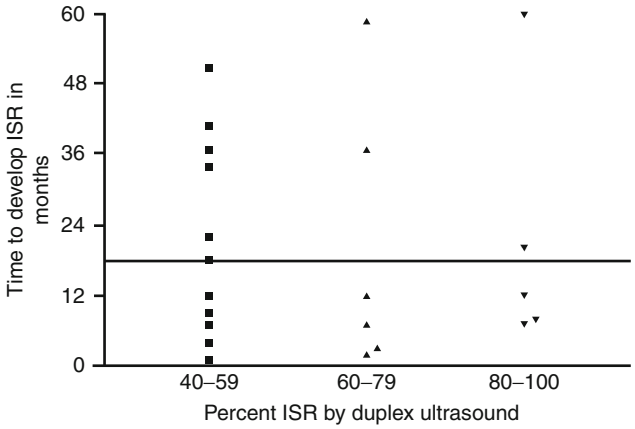


**Fig. 13.5** Distribution of in-stent restenosis cases based on time of diagnosis from initial carotid artery stenting (CAS) procedure. Note that the majority of restenoses occurred within 18 months of the initial CAS procedure. The *dotted line* identifies the 18-month postprocedure mark. *ISR* in-stent restenosis (Adapted from Lal et al. [10]. With permission from Elsevier)

restenoses ≥40% in our series of CAS procedures occurred within 18 months (13/22, 60%), and the majority of high-grade restenoses ≥80% occurred within 15 months (3/5, 60%) of their intervention [10] (Fig. 13.5). We therefore recommend more frequent follow-up duplex ultrasound evaluations early after CAS. In our own practice, we evaluate patients every 6 months for the first 2 years and annually thereafter. We also recommend early registration of baseline velocity measurements after CAS, preferably during the same admission, against which future results can be compared. B-mode imaging of the arterial lumen and spectral waveform analysis must be used to supplement and enhance the accuracy of velocity criteria. Elevations in PSV and/or ICA/CCA ratios are indicative of developing ISR which must then undergo angiographic evaluation when appropriate thresholds are reached.

## DUS Testing Protocol After CAS

The technique of DUS testing after CAS is similar to that used for the diagnosis of native carotid occlusive disease with additional emphasis on B-mode imaging. Bilateral examination using a high-resolution linear array transducer should be performed in cross-sectional and longitudinal scan planes starting at the CCA, through the stented CCA/ICA and bifurcation, and into the distal native ICA. Ultrasound imaging of the native CCA should yield results similar to prestent findings. The stent may traverse the origin of the external carotid artery (ECA), but most often, patency and flow through the stent interstices into the ECA are maintained. The stent is usually placed from the CCA into the proximal ICA. It should be imaged in multiple planes. Note should be made of apposition to surrounding plaque, expansion

of the lumen, and luminal encroachment of neointimal hyperplasia. The morphology of any hyperplastic lesion should be mapped according to the classification mentioned previously. The luminal diameter should be measured at multiple locations. Color flow and power Doppler modes are useful adjuncts for this purpose. The maximum PSV within the stent should be measured as well as the ratio of this value to the native CCA PSV.

## Summary

We recommend the following approach to surveillance after CAS:

1. Patients should have a routine surveillance DUS at baseline and every 6 months for 2 years and then annually thereafter. The first follow-up DUS must occur as soon after the procedure as possible, preferably during the same admission.
2. Stented patients with diabetes, aggressive patterns of ISR (type IV), prior treatment for ISR, or prior cervical radiation or heavy calcification should undergo DU surveillance every 6 months.
3. The DUS protocol should include at least the following assessments:
   (a) Doppler measurement of peak-systolic and end-diastolic velocities in the native CCA; in the proximal, mid, and distal stent; and in the distal native ICA. Modified threshold velocity criteria should be used to interpret the significance of these velocity measurements.
   (b) B-mode imaging and spectral waveform analysis to supplement and enhance the accuracy of velocity criteria to estimate and confirm luminal narrowing.
   (c) B-mode imaging to assess the morphologic pattern of ISR so that patients with type IV lesions can be placed on a more intensive monitoring program.
   (d) B-mode imaging to assess stent apposition to the carotid wall. Areas of poor apposition or underlying calcium may identify future locations for ISR and must be followed.

## References


1. Sterpetti AV, Schultz RD, et al. Natural history of recurrent carotid artery disease. Surg Gynecol Obstet. 1989;168(3):217–23.
2. Lattimer CR, Burnand KG. Recurrent carotid stenosis after carotid endarterectomy. Br J Surg. 1997;84(9):1206–19.
3. Bartlett FF, Rapp JH, et al. Recurrent carotid stenosis: operative strategy and late results. J Vasc Surg. 1987;5(3):452–6.
4. Cronenwett JL, Birkmeyer JD. Carotid artery disease. In: The Dartmouth atlas of vascular health care. Chicago: AHA Press, Div. of Health Forum Inc.; 2001. p. 41–64.
5. Moore WS, Kempczinski RF, et al. Recurrent carotid stenosis: results of the asymptomatic carotid atherosclerosis study. Stroke. 1998;29(10):2018–25.
6. DeGroote RD, Lynch TG, et al. Carotid restenosis: long-term noninvasive follow-up after carotid endarterectomy. Stroke. 1987; 18(6):1031–6.
7. Healy DA, Zierler RE, et al. Long-term follow-up and clinical outcome of carotid restenosis. J Vasc Surg. 1989;10(6):662–8; discussion 668–9.
8. Tepe G, Schmehl J, et al. Drug coated stents for carotid intervention. J Cardiovasc Surg (Torino). 2005;46(3):249–59.
9. Chakhtoura EY, Hobson 2nd RW, et al. In-stent restenosis after carotid angioplasty-stenting: incidence and management. J Vasc Surg. 2001;33(2):220–5; discussion 225–6.
10. Lal BK, Hobson 2nd RW, et al. In-stent recurrent stenosis after carotid artery stenting: life table analysis and clinical relevance. J Vasc Surg. 2003;38(6):1162–8; discussion 1169.
11. Bosiers M, Peeters P, et al. Does carotid artery stenting work on the long run: 5-year results in high-volume centers (ELOCAS registry). J Cardiovasc Surg (Torino). 2005;46(3):241–7.
12. Beebe HG. Scientific evidence demonstrating the safety of carotid angioplasty and stenting: do we have enough to draw conclusions yet? J Vasc Surg. 1998;27(4):788–90.
13. O'Hara PJ, Hertzer NR, et al. Reoperation for recurrent carotid stenosis: early results and late outcome in 199 patients. J Vasc Surg. 2001;34(1):5–12.
14. Mansour MA, Kang SS, et al. Carotid endarterectomy for recurrent stenosis. J Vasc Surg. 1997;25(5):877–83.
15. Hobson 2nd RW, Goldstein JE, et al. Carotid restenosis: operative and endovascular management. J Vasc Surg. 1999;29(2):228–35; discussion 235–8.
16. Lal BK, Kaperonis EA, Cuadra S, Kapadia I, Hobson 2nd RW. Patterns of in-stent restenosis after carotid artery stenting: classification and implications for long-term outcome. J Vasc Surg. 2007;46:833–40.
17. Faught WE, Mattos MA, et al. Color-flow duplex scanning of carotid arteries: new velocity criteria based on receiver operator characteristic analysis for threshold stenoses used in the symptomatic and asymptomatic carotid trials. J Vasc Surg. 1994;19(5):818–27; discussion 827–8.
18. Lal BK, Hobson IR. Carotid artery occlusive disease. Curr Treat Options Cardiovasc Med. 2000;2(3):243–54.
19. Mintz BL, Hobson 2nd RW. Diagnosis and treatment of carotid artery stenosis. J Am Osteopath Assoc. 2000;100(11 Suppl):S22–6.
20. Ringer AJ, German JW, et al. Follow-up of stented carotid arteries by Doppler ultrasound. Neurosurgery. 2002;51(3):639–43; discussion 643.
21. Robbin ML, Lockhart ME, et al. Carotid artery stents: early and intermediate follow-up with Doppler US. Radiology. 1997;205(3): 749–56.
22. Lal BK, Hobson 2nd RW, et al. Carotid artery stenting: is there a need to revise ultrasound velocity criteria? J Vasc Surg. 2004;39(1): 58–66.
23. Green JF. Mechanical concepts in cardiovascular and pulmonary physiology. Philadelphia: Lea & Febiger Publishers; 1977. p. 47–53.
24. Peterson BG, Longo GM, et al. Duplex ultrasound remains a reliable test even after carotid stenting. Ann Vasc Surg. 2005;19(6):793–7.
25. Stanziale SF, Wholey MH, et al. Determining in-stent stenosis of carotid arteries by duplex ultrasound criteria. J Endovasc Ther. 2005;12(3):346–53.
26. Chi YW, White CJ, et al. Ultrasound velocity criteria for carotid in-stent restenosis. Catheter Cardiovasc Interv. 2007;69(3):349–54.
27. Chahwan S, Miller MT, et al. Carotid artery velocity characteristics after carotid artery angioplasty and stenting. J Vasc Surg. 2007;45(3): 523–6.
28. Lal BK, Hobson RW, Tofighi B, Kapadia I, Cuadra S, Jamil Z. Duplex ultrasound velocity criteria for the stented carotid artery. J Vasc Surg. 2008;47:63–73.
29. Frericks H, Kievit J, et al. Carotid recurrent stenosis and risk of ipsilateral stroke: a systematic review of the literature. Stroke. 1998;29(1):244–50.

# Use of TCD in Monitoring Patients During Carotid Artery Stenting

14

Mark C. Bates

**Abstract**

Transcranial Doppler (TCD) provides visible and audible real-time feedback during carotid stent procedures as otherwise clinically silent small embolic particles reflect microembolic signals (MESs) during their egress from the extracranial carotid artery lesion through the middle cerebral artery en route to the ipsilateral hemisphere. During the formative years of carotid stenting, TCD was an important tool for many pioneers in the field as high-risk anatomic carotid access and lesion characteristics were being defined. In addition, TCD helped us understand the flow dynamics related to distal and proximal occlusive embolic protection platforms. Also, the disturbing storm of microembolic signals (MESs) at different stages during distal filter protection led to optimization of these system designs and procedural technique. One cannot argue the contribution TCD made to the art and science of carotid stenting through amplifying the embolization signal from the devastating clinical event of stroke seen in less than 10% of patients to the silent smaller microembolic signals ubiquitous to every procedure. While the MES data seems to have more of an academic value, the contemporary CAS program should have access to TCD and consider following peri-procedural MCA flow patterns during stenting with proximal flow reversal or flow arrest protection systems. In addition, TCD provides significant insight into the physiology of reperfusion syndrome, and changes in MCA flow velocities in patients at high risk for reperfusion syndrome in the early postprocedure time period may be helpful. The objective of this monograph is to expose the reader to some of the lessons learned from adjuvant transcranial Doppler during carotid stent-supported angioplasty while also providing insight into current clinically relevant applications.

**Keywords**

Carotid stent • Transcranial Doppler • TCD • Microembolic signals • Reperfusion syndrome

## Introduction

It has been over two decades since Aaslid first described the technique of middle cerebral artery range-gated Doppler interrogation via a low-frequency ultrasound transducer stationed just above the zygomatic arch [1]. Since that time, insonation techniques with probe fixation headgear have made continuous real-time imaging much easier, and advances in Doppler technology including "power Doppler" have improved signal clarity [2]. A detailed review of the physics

M.C. Bates, M.D., FACC, FSCAI
Department of Surgery,
Robert C. Byrd Health Sciences Center, West Virginia University,
Charleston Area Medical Center,
Charleston, WV, USA
e-mail: mbates@nexeonmed.com

A.F. AbuRahma, D.F. Bandyk (eds.), *Noninvasive Vascular Diagnosis*,
DOI 10.1007/978-1-4471-4005-4_14, 

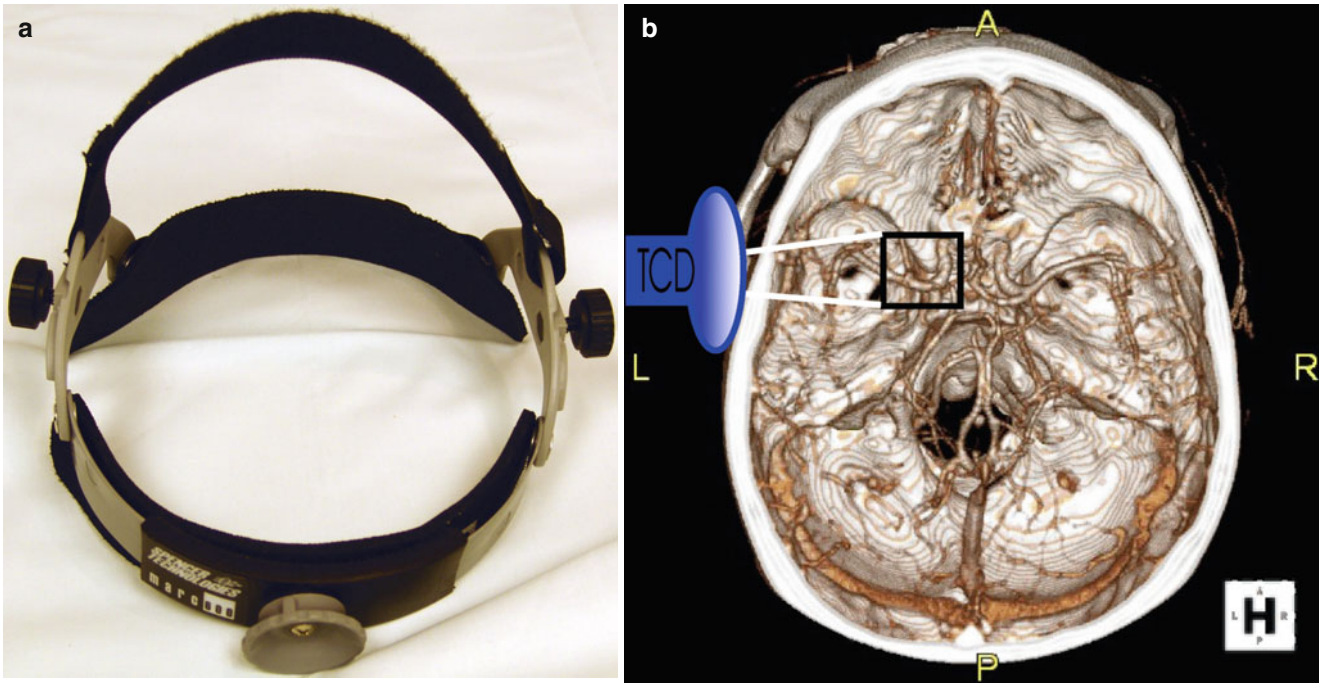


**Fig. 14.1** (**a**) This is a picture of the Spencer technologies headgear that is utilized for securing the transcranial Doppler probe for peri-procedural imaging. The torque device in the front is for tightening the harness depending on the patient's cranial circumference. The lateral devices allow for positioning of the transcranial Doppler in a position appropriate for ideal insonation of the middle cerebral system. (**b**) This is a CT angiogram of a patient who subsequently underwent carotid artery stenting. The "TCD" represents the positioning of the probe, and the square is the insonation window or area being monitored during carotid stenting

and utility of transcranial Doppler (TCD) is eloquently presented by Dr. Alexandrov in the antecedent Chap. 10. The objective of this monograph is to expose the reader to some of the lessons learned from adjuvant transcranial Doppler during carotid stent-supported angioplasty while also providing insight into current clinically relevant applications.

## Background

Carotid endarterectomy (CEA) has been proven in large randomized trials to reduce the risk of stroke or future neurologic events in patients with symptomatic and asymptomatic extracranial cerebrovascular disease [3, 4]. The CEA techniques have matured, and, currently, the risk of a peri-procedural neurologic event is very low when the procedure is performed by experienced surgeons [5, 6]. The inherent risk of transcatheter interaction with the typical friable internal carotid artery lesion and resultant embolization of material to the brain was recognized as a limitation to carotid artery stenting early in the procedure maturation [7–10]. The development of cerebral protection devices including distal occlusive balloons, distal filter systems, and proximal occlusive systems rekindled enthusiasm about carotid artery stenting as an alternative to endarterectomy over the last decade [11–20]. The culmination of all these developments led to a large NIH-funded and corporate-sponsored randomized trial comparing CEA to CAS (CREST – Carotid Revascularization Endarterectomy Versus Stenting Trial). The CREST trial findings suggested the risk of stroke was higher with stenting, but this risk was counterbalanced by increased risk of myocardial infarction noted in the traditional surgical arm [21]. Our center has continued to follow the initial tenants that CAS should be reserved for the high-risk patients as defined in previous randomized studies and series [22–27]. Irrespective of how individual physicians interpret the CREST results, an increase in CAS procedures has followed and underscores the importance of better understanding the embolic risk of this procedure. Transcranial Doppler has given considerable insight to investigators, and early carotid stent pioneers used lessons from procedural TCD feedback to define embolic risks during different stages of the procedure, optimize protection systems, and provide significant insight into the physiology of reperfusion syndrome.

## Transcranial Doppler and Peri-procedural Setup

The patient is placed in the normal supine position on the angiographic table. The TCD headgear (Fig. 14.1a) is placed in a position such that the lateral Doppler transducer fixation gaits can be aligned just above the zygomatic arch along the temporal window. This allows for the continuous sampling of

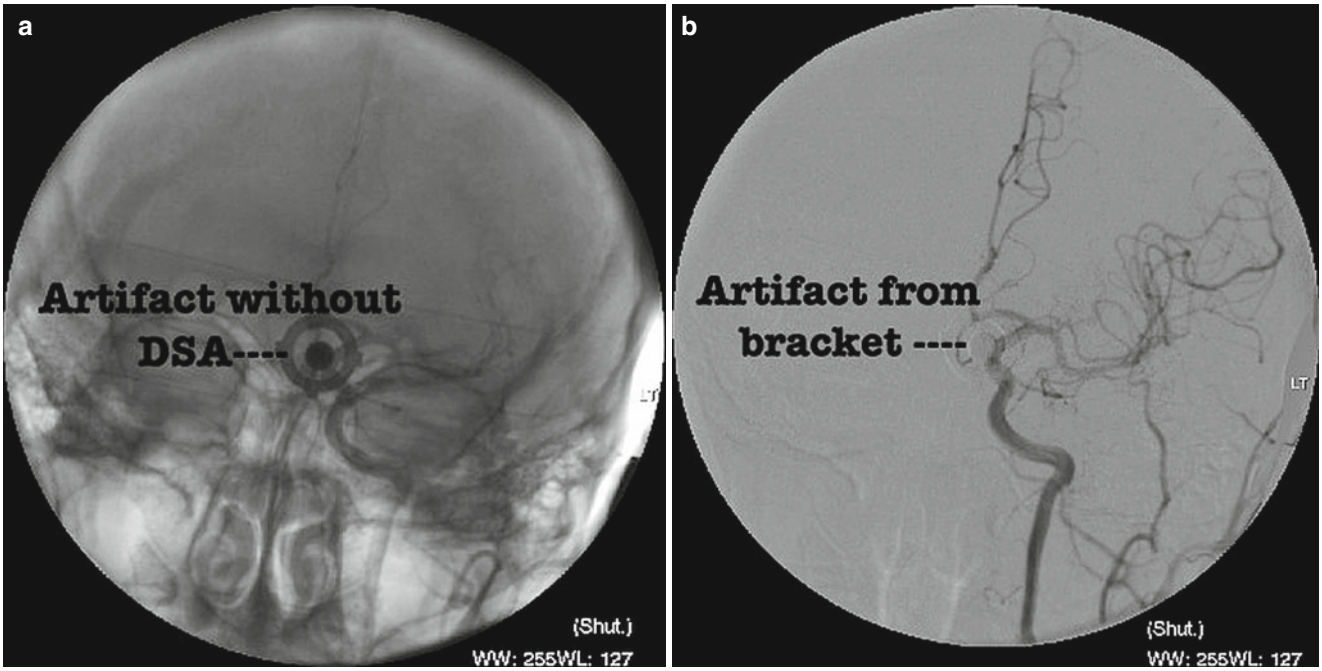


**Fig. 14.2** (**a**) A non-subtracted image illustrating an artifact in the midline related to the ratchet device used to harness the transcranial Doppler. (**b**) During digital subtraction angiography, the artifact silhouette persists, but one can still define the intracranial cerebral anatomy in the AP view without removing the transcranial Doppler harness

pulse wave Doppler signals from the middle cerebral distribution, as detailed in Fig. 14.1b. Fortunately, the headgear is radiolucent, except for the lateral brackets and tightening apparatus, as shown in Fig. 14.2a, b. Thus, digital subtraction intracerebral angiography can be performed without removal of the headgear. The patient is then prepped and draped in standard sterile fashion, and baseline TCD interrogation is performed (Fig. 14.3). Ideally, bilateral continuous pulse flow Doppler insonation of the middle cerebral arteries is monitored and digitally recorded throughout the procedure. It should be noted that anywhere from 9% to 16% of patients might not have an ideal window for accurate insonation of the middle cerebral artery [28, 29]. In the case of inadequate image of window, hand positioning of the probe and continuous monitoring are utilized versus continued attempts at repositioning the probe at different stages in the procedure [28].

## Pre-procedural "Baseline" TCD Observations

The baseline TCD pattern may show blunting of the peak systolic wave in patients with severe extracranial disease [29]. More importantly, the TCD may give some insight into the collateral support via the circle of Willis [30–32]. This information will help the operator better understand the patient's ability to tolerate cerebral protection systems that may arrest or even reverse ipsilateral internal carotid artery flow. Niesen et al. reported the utilization of baseline ratio between the peak systolic velocities in the ipsilateral middle cerebral vessel compared to the contralateral middle cerebral system as a reference for collateral support [33]. Also, the baseline intracranial flow characteristics could be important in predicting patients who are at risk for post-procedural reperfusion syndrome and even intracranial hemorrhage. Mori et al. suggested the possibility of utilizing further hemodynamic testing in patients who are at increased risk for intracranial hemorrhage prior to placing them on the table [34]. This may include utilization of carbon dioxide reactivity or VMR testing with Diamox prior to interaction with the lesion. More recently, a group out of Greece showed that pre-procedure exhausted cerebrovascular reactivity on ipsilateral TCD was an excellent predictor of reperfusion syndrome [35].

## Peri-procedural TCD Observations

Transcranial Doppler allows us to continuously monitor two important parameters during carotid artery stenting. The first is related to insuring preserved middle cerebral flow velocity and pulse volume. The utilization of a proximal or distal occlusive device for cerebral protection does result in interruption or reversal of flow in the ipsilateral internal carotid artery [36]. During internal carotid artery flow arrest or reversal, a dramatic drop in middle cerebral flow velocity on TCD may precede the clinical hemispheric symptoms in patients with severe contralateral disease or inadequate collateral support due to incomplete

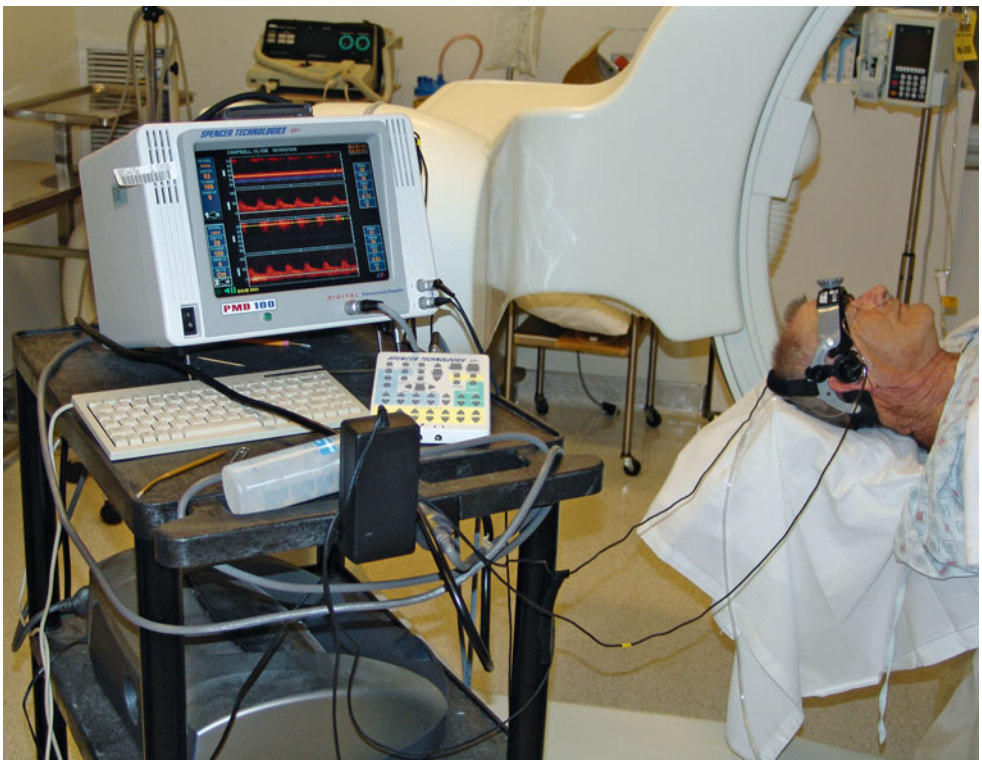


**Fig. 14.3** This illustrates the typical setup during transcranial Doppler monitoring in the angiographic suite. The patient is placed in a supine position, and the transcranial Doppler bracket is fixed to the head prior to baseline angiography

circle of Willis. This provides the operator with additional insight as to how balloon occlusion will be tolerated and whether the procedure will need to be staged. Currently, the most widely tested distal occlusion balloon protection system is the GuardWire (previously known as PercuSurge). This device is a low-pressure balloon and on a .014″ wire that can be navigated across the lesion and then inflated to occlude the internal carotid artery during transcatheter intervention [20]. Utilization of this type of distal balloon occlusion system has proven to be effective in reducing the risk of embolization. However, Nadim Al-Mubarak et al. have shown with TCD the release of particles during balloon deflation that is likely related to inadequate particle retrieval from the cul-de-sac around the balloon [37].

Parodi has shown with TCD the ability to completely reverse flow in the middle cerebral artery by transcatheter occlusion of the ipsilateral common and external carotid artery while at the same time creating negative pressure at the tip of the guiding sheath, as noted in Fig. 14.4 [38]. This may have significant implications for optimizing cerebral protection during carotid stenting and ultimately could facilitate clot retrieval during transcatheter treatment of acute stroke.

It should be noted that TCD suggests that middle cerebral artery flow is reduced by 10–30% when a distal filter is opened due to filter-induced flow resistance [39]. In patients with an intact circle of Willis undergoing carotid stenting with a protection system that preserves flow (i.e., filter), the sudden interruption of flow to the ipsilateral middle cerebral artery could be an ominous finding suggesting a large embolic event or spasm in the internal carotid artery proper. Also, filter systems do have a threshold of particulate debris based on the filtered design and size [40]. If the volume of embolic debris exceeds the filter threshold, then occlusion can occur, and this may be heralded by changes on TCD. Similar changes can occur if there is spasm in the ipsilateral internal carotid artery system related to the distal protection filter [27].

The second variable that is monitored by TCD during carotid artery stenting is the occurrence of microemboli signals (MESs). The reflective properties of microembolic material as it passes through the middle cerebral artery are translated into sudden signal shifts that are depicted as high-velocity transient spikes on the continuous Doppler recording [41–43]. These high-intensity signals may represent the egress of small particles or microembolic debris into the ipsilateral hemisphere [44]. It is difficult to differentiate artifact from small air bubbles versus true embolic debris, and that is one of the limitations of this technology [45–47]. Ex vitro studies by Coggia et al. and Ohki et al. have provided significant insight into when particles are released during different stages of the procedure [48, 49]. The peak embolic risk during angioplasty in the ex vitro model appears to be during balloon deflation [48]. Similar findings are seen in vivo with continuous TCD during carotid stenting at the time of balloon deflation [50, 51]. In our experience, MESs are seen during all stages of carotid stenting with or without protection even with navigation of a .014″ wire across the lesion (Fig. 14.5). Paradoxically, in a study of over 500 patients who underwent CAS with TCD, there was actually a higher number

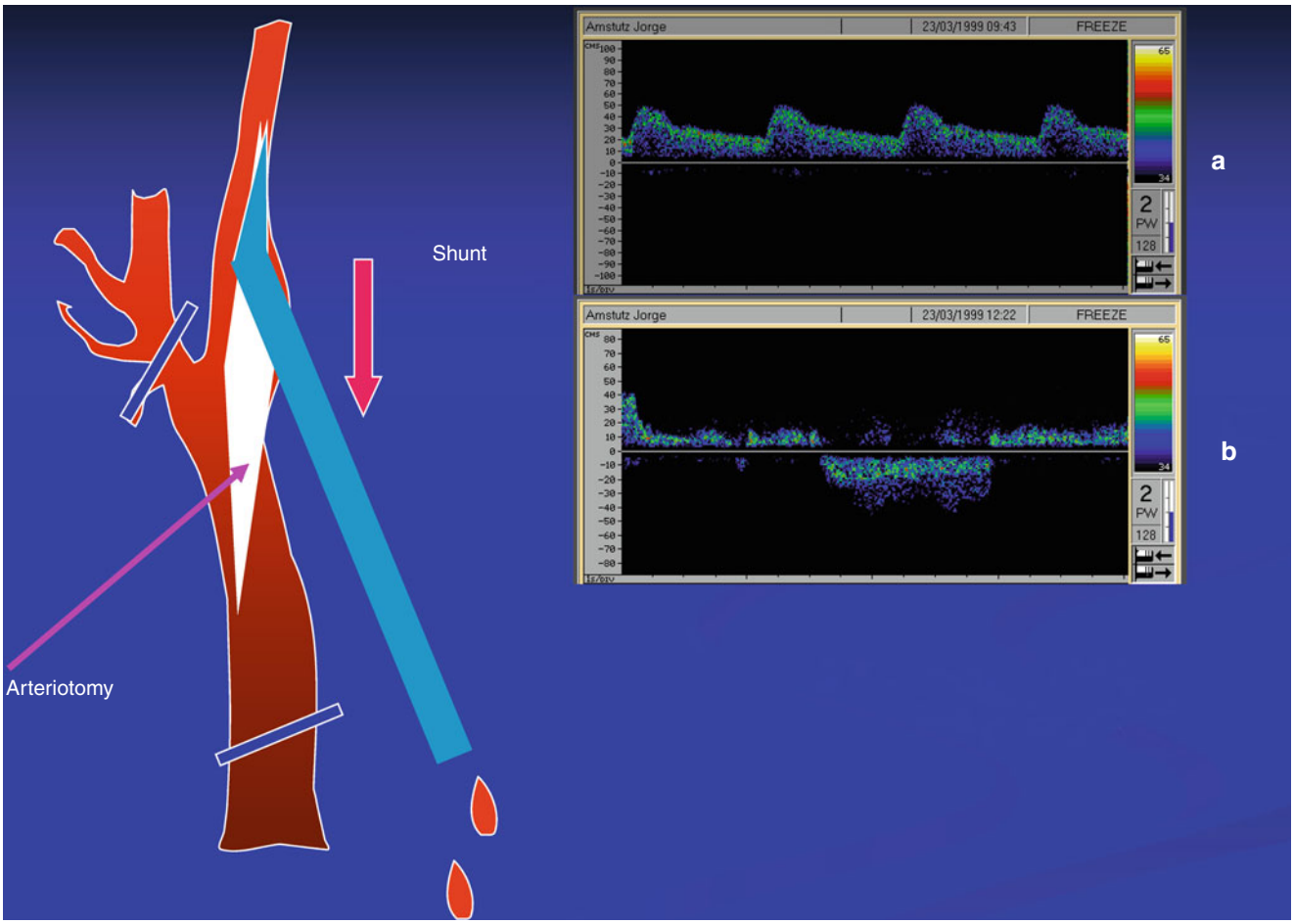


**Fig. 14.4** This was provided compliments of Dr. Juan Parodi from his original work evaluating transcranial Doppler evidence of intentional middle cerebral artery flow reversal during carotid endarterectomy. TCD before (**a**) and after (**b**) arteriotomy and shunt insertion (Courtesy of Dr. Juan Parodi)

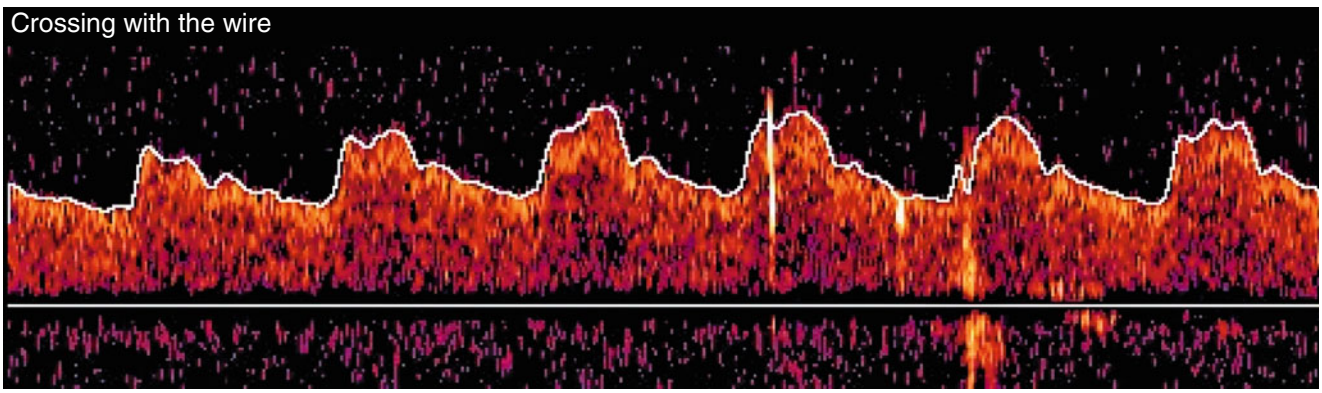


**Fig. 14.5** This shows small subtle microembolic signals (*MESs*) coincident with advancing the wire through the lesion. These MESs are shown as bright signals, the most prominent seen in the fourth complete Doppler pulse sequence

of MESs in the patients with filters in comparison to those without protection, and the clinical significance of these findings have not been clearly defined [52].

In the context of academic applications, a new approach to TCD has been advocated by Garami et al. whereby dual measurements are recorded simultaneously during CAS to evaluate proximal versus distal protection devices [53]. One transducer is positioned in the traditional transcranial window, while another is used to sample flow in the internal carotid via a submandibular window.

## Post-procedural TCD Observations

Some authors have followed TCD with serial interval studies during the first 12 h following carotid stenting [54, 55]. Our center feels that this may be particularly important in patients who are at increased risk for intracranial hemorrhage. The pre-procedural risk factors for reperfusion syndrome and/or intracranial hemorrhage include contralateral severe carotid disease or occlusion, baseline high-grade stenosis or "string sign" with slow-flow, hypertension during the carotid stenting procedure, and baseline decrease of vasoreactivity [56]. Figure 14.6 details the TCD hemodynamic sequence of a

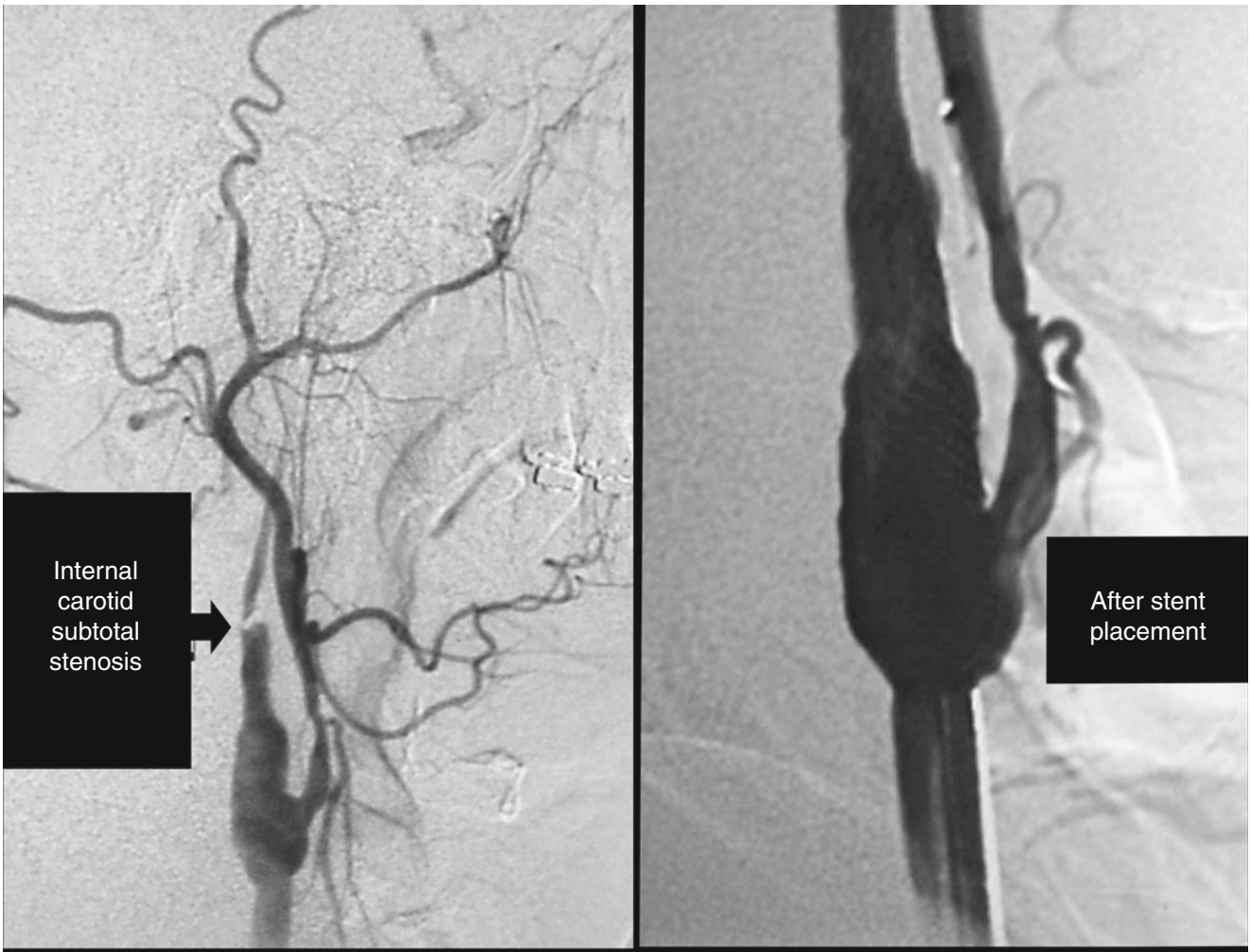

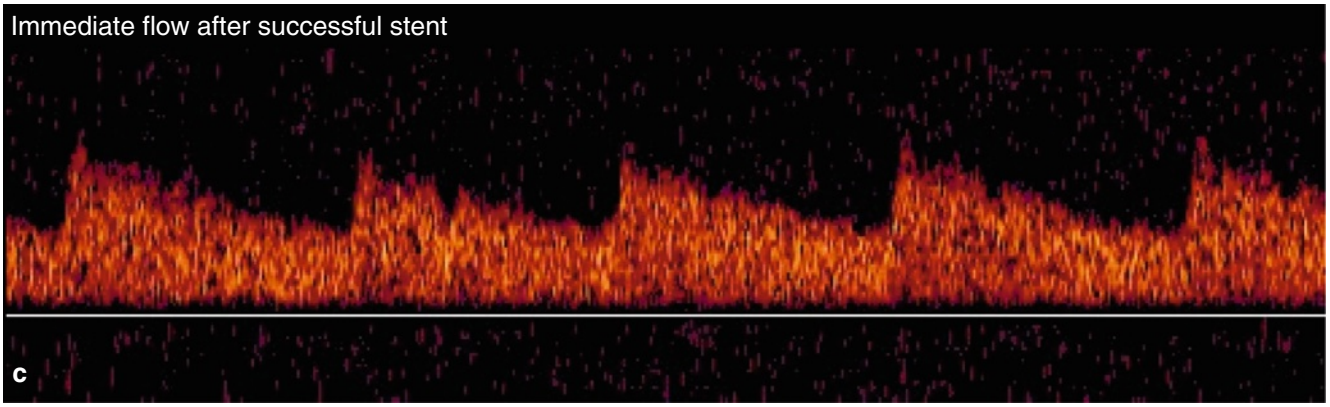


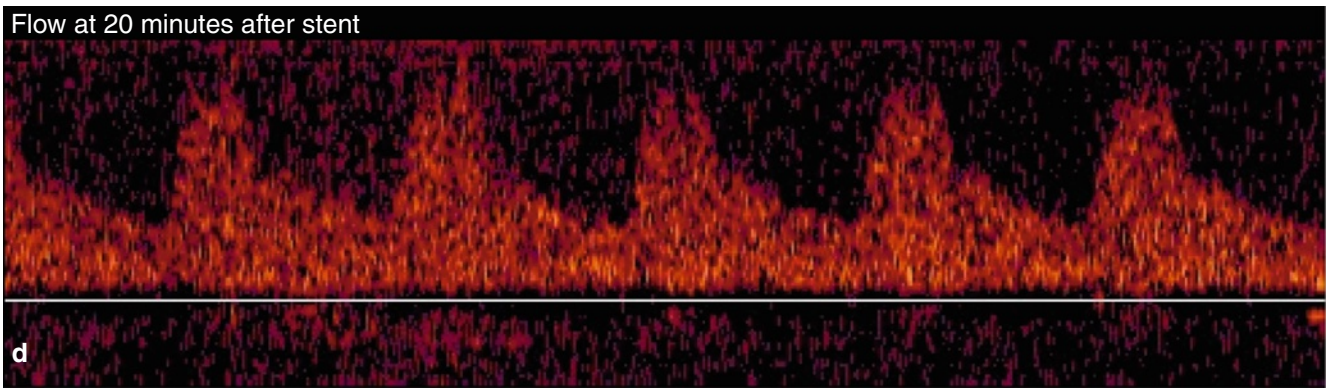


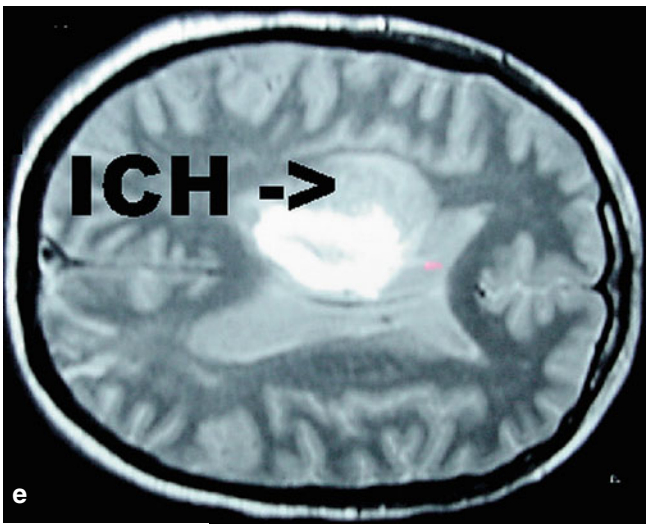


**Fig. 14.6** (continued)

**Fig. 14.6** (**a**) Baseline angiography and follow-up angiography after carotid stenting in a patient with multiple risk factors for postprocedural intracranial hemorrhage. (**b**) Baseline low pulse volume middle cerebral artery Doppler on the patient illustrated in (**a**). (**c**) Immediate flow after carotid stent placement in the patient presented by (**a**). Note that the flow velocity has increased by approximately 30%. (**d**) This shows the flow pattern in the same patient depicted in (**a**). This is 20 min following stent placement, and note that the flow velocity is now three times greater than the baseline velocity. (**e**) This illustrates the CT scan confirming a large intracranial hemorrhage depicted as ICH 12 h after stent placement

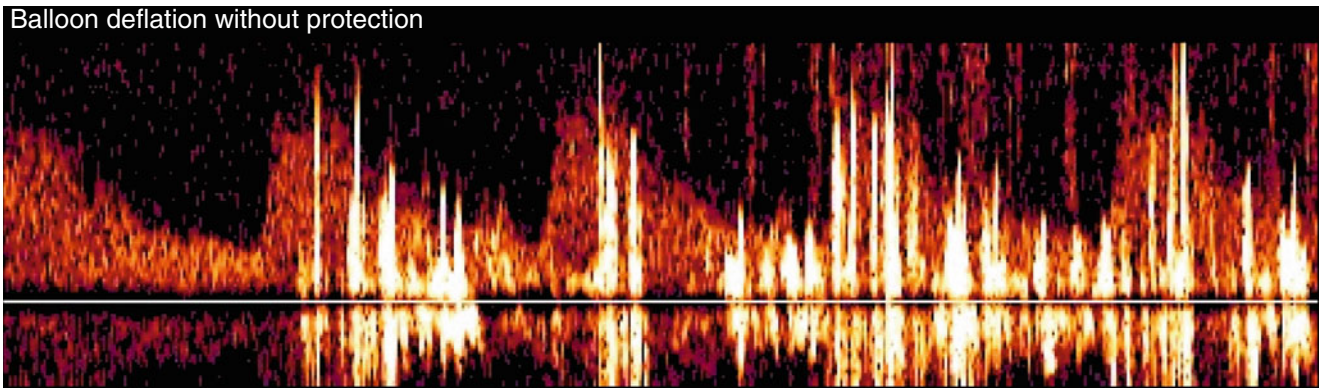


**Fig. 14.7** Multiple MESs in a patient after balloon deflation in our early experience before cerebral protection was available

patient who developed typical reperfusion syndrome complicated by intracranial hemorrhage during our early experience with unprotected carotid stenting 15 years ago.

Few studies have actually performed continuous TCD in the early postoperative after carotid stenting. However, it seems that MESs are common during the recovery period after carotid stenting as well [57].

## Significance of Microemboli During Carotid Artery Stenting

Microembolic signals detected during carotid endarterectomy have been associated with decrease in cognitive function [58]. Similarly, MESs with so-called embolic storms during different stages of carotid stent procedures are associated with ipsilateral defects on early follow-up diffusion-weighted MRI scan [59–63]. Currently, there is very little data with regard to cognitive function in patients following protected carotid artery stenting, but this is a concern. Interestingly, in a small subgroup analysis of patients during the carotid and vertebral artery transluminal angioplasty study (CAVATAS), there were similar outcomes on neurologic testing in both the carotid endarterectomy and carotid stenting groups in spite of a higher number of MESs in the latter [64].

The threshold or "safe" size for microemboli has not been clearly defined. Early work suggests that any particles more than 50 μm in size will not circulate to the venous cerebral system and thus by definition will cause some arteriolar occlusions [65]. Significant work on this front has been done to better understand the decrease in cognitive function that one sees after coronary artery bypass surgery. It appears that based on a postmortem study by Moody et al., the particles causing decreased cognitive function after a coronary artery bypass surgery are less than 70 μm in size [66]. This is particularly important to understand since most distal protection filters have a pore size of 100–120 μm.

## Differentiating Microemboli from Air Bubbles

The differentiation of air bubbles from true atheroemboli has been very difficult. Several techniques have been described, including a defined threshold of greater than 10 hits in a sequence [28]. Different mathematical sequences have also been defined through the years; however, there currently is no ideal way to differentiate these in vivo [46–49].

There are certain stages of the procedure where contamination from air artifact would be less likely. For example, crossing the lesion with the wire as noted in Fig. 14.5 should not be associated with air embolization and is likely true microemboli. Also, many centers have reported the highest numbers of emboli occur with pre-dilatation or post-dilatation as the balloon is deflated, and it is also unlikely there is significant trapped air or artifact during this time, as depicted in Fig. 14.7. On the other hand, one typically sees scattered MESs during contrast injections, which is related to microbubbles in the contrast (Fig. 14.8).

Most of the carotid stents used today are self-expanding stents made of nickel titanium with an outer constraining sheath. There is always a high volume of MES involved with retracting the sheath housing of the self-expanding stent, and some authors have suggested that this is related to the shear force of a stent against the plaque [28]. However, we feel this is related to trapped air within the fabric of the stent and thus less likely of pathologic concern (Fig. 14.9).

### Conclusions

Currently, TCD has not been declared mandatory for peri-procedural adjuvant monitoring in patients undergoing carotid artery stenting based on consensus documents [67]. Many centers subscribe to the bias that the TCD is more of an academic tool best used to help understand the benefits and failure modes of current protection systems. Peri-procedural TCD may be beneficial in patients who are at high risk for reperfusion syndrome as aggressive

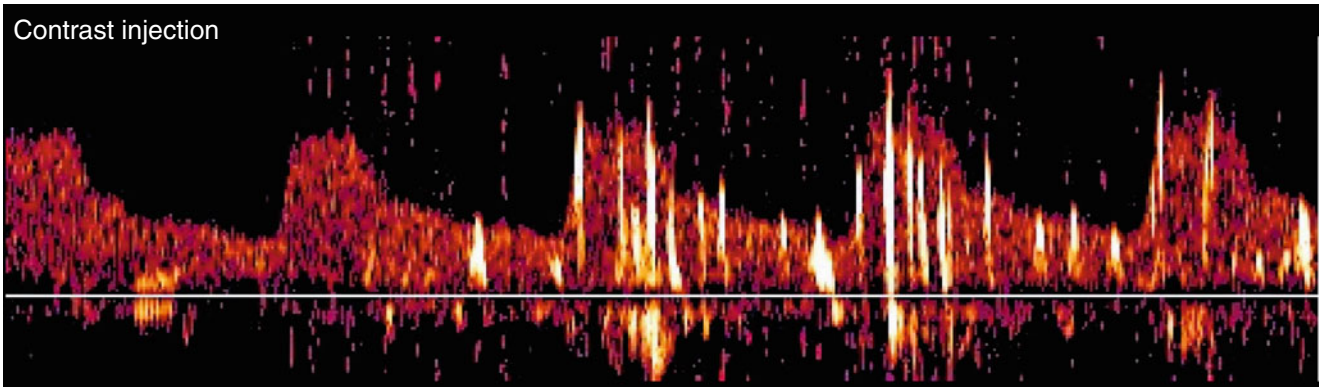


**Fig. 14.8** Multiple air bubble MESs during contrast injection

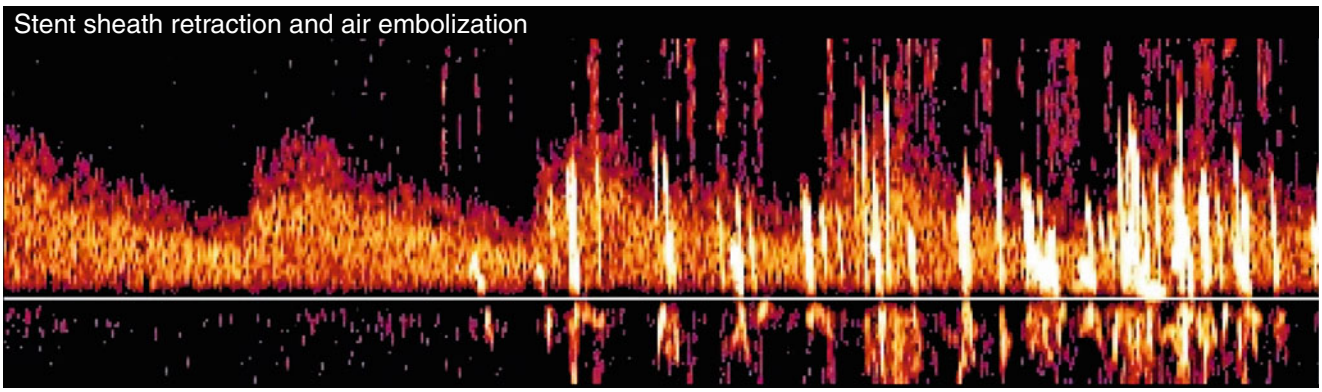


**Fig. 14.9** This shows fairly impressive air bubble microemboli during sheath retraction at the time of stent deployment

hemodynamic monitoring would follow concerning post-procedure middle cerebral flow pattern changes. However, the number of patients experiencing reperfusion syndrome is small, and, thus, level 1 data confirming benefit of TCD will likely never be available.

The burden of embolic load estimated by MESs may give additional insight into the long-term issues of decreased cerebral flow reserve and/or worsening cognitive function after carotid stenting, but linear relationships between embolic load and outcomes have not been confirmed. In our center, TCD has significantly contributed to our understanding of carotid stent procedures, and this feedback has allowed us to improve techniques and participate in the development of newer-generation protection systems. However, the addition of TCD to a carotid stent procedure adds significant time to the case and requires significant consumption of lab technician resources.

In summary, it seems today that TCD should be considered in patients at high risk for reperfusion syndrome or those undergoing carotid stenting with internal carotid artery flow arrest or flow reversal. Only future studies will help us understand the importance of MESs in predicting future issues related to cognitive function. From an academic perspective, ongoing studies evaluating MES frequency with different stent designs and antiplatelet regimens will also advance the art and optimize patient outcomes.

## References

1. Aaslid R, Markwalder TM, Nornes H. Noninvasive transcranial Doppler ultrasound recording of flow velocity in basal cerebral arteries. J Neurosurg. 1982;57(6):769–74.
2. Bogdahn U, Becker G, Winkler J, et al. Transcranial color-coded real-time sonography in adults. Stroke. 1990;21:1680–8.
3. North American Symptomatic Carotid Endarterectomy Trial Collaborators. Beneficial effect of carotid endarterectomy in symptomatic patients with high-grade carotid stenosis. N Engl J Med. 1991;325:445–53.
4. European Carotid Surgery Trialists' Group. MRC European carotid surgery trial: interim results for symptomatic patients with severe or with mild carotid stenosis. Lancet. 1991;337:1235–43.
5. AbuRahma AF, Hannay RS. A study of 510 carotid endarterectomies and a review of the recent carotid endarterectomy trials. W V Med J. 2001;97(4):197–200.
6. Bond R, Rerkasem K, AbuRahma AF, Naylor AR, Rothwell PM. Patch angioplasty versus primary closure for carotid endarterectomy. Cochrane Database Syst Rev. 2004;(2):CD000160.
7. Diethrich EB. Indications for carotid artery stenting: a preview of the potential derived from early clinical experience. J Endovasc Surg. 1996;3:132–9.

8. Naylor AR, Bolia A, Abbott RJ, Pye IF, Smith J, Lennard N, Lloyd AJ, London NJ, Bell PR. Randomized study of carotid angioplasty and stenting versus carotid endarterectomy: a stopped trial. J Vasc Surg. 1998;28(2):326.
9. Leisch F, Kerschner K, Hofman R, Bibl D, Engleder C, Bergmann H. Carotid stenting: acute results and complications. Z Kardiol. 1999;88:661–8.
10. Bettman MA, Katzen BT, Whisnant J, Brant-Zawadski MB, Broderick JP, Furlan AJ, Hershey LA, Howard V, Kuntz R, Loftus CM, Pearce W, Roberts A, Roubin G. Carotid stenting and angioplasty. A statement for healthcare professionals from the councils on cardiovascular radiology, stroke, cardio-thoracic and vascular surgery, epidemiology and prevention, and clinical cardiology, American Heart Association. Stroke. 1998;29:336–48.
11. Theron JG, Peyelle GG, Coskun O, et al. Carotid artery stenosis: treatment with protected balloon angioplasty and stent placement. Radiology. 1996;201:627–36.
12. Wholey MH, Al-Mubarak N, Wholey MH. Updated review of the global carotid artery stent registry. Catheter Cardiovasc Interv. 2003;60:259–66.
13. Ohki T, Veith FJ. Carotid artery stenting: utility of cerebral protection devices. J Invasive Cardiol. 2001;13:47–55.
14. Henry M, Amor M, Klonaris C, et al. Angioplasty and stenting of the extracranial carotid arteries. Tex Heart Inst J. 2000;27:150–8.
15. Reimers B, Corvaja N, Moshiri S, et al. Cerebral protection with filter devices during carotid artery stenting. Circulation. 2001;104:12–5.
16. Parodi JC, Mura RL, Ferreira LM, et al. Initial evaluation of carotid angioplasty and stenting with three different cerebral protection devices. J Vasc Surg. 2000;32:1127–36.
17. Al-Mubarak N, Colombo A, Gaines PA, et al. Multicenter evaluation of carotid artery stenting with a filter protection system. J Am Coll Cardiol. 2002;39:841–6.
18. Mathur A, Roubin GS, Iyer SS, et al. Predictors of stroke complicating carotid artery stenting. Circulation. 1998;97:1239–45.
19. Yadav JS, Roubin GS, Iyer S, et al. Elective stenting of the extracranial carotid arteries. Circulation. 1997;95:376–81.
20. Al-Moubarak N, Roubin GS, Vitek JJ, et al. Effect of the distal-balloon protection system on microembolization during carotid stenting. Circulation. 2001;104:199–2002.
21. Mantese VA, Timaran CH, Chiu D, Begg RJ, Brott TG, CREST Investigators. The carotid revascularization endarterectomy versus stenting trial (CREST): stenting versus carotid endarterectomy for carotid disease. Stroke. 2010;41(10 Suppl):S31–4.
22. Zarins CK. Carotid endarterectomy: the gold standard. J Endovasc Surg. 1996;3:10–5.
23. Yadav JS, Wholey MH, Kuntz RE, Fayed P, Katzen BT, Mishkel GJ, Bajwa TK, Whitlow P, Strickman NE, Jaff MR, Popma JJ, Snead DB, Cutlilp DE, Firth BG, Ouriel K. Stenting and angioplasty with protection in patients at high risk for Endarterectomy Investigators. N Engl J Med. 2004;351(15):1493–501.
24. Ireland JK, Chaloupka JC, Weigele JB, et al. Potential utility of carotid stent assisted percutaneous transluminal angioplasty in the treatment of symptomatic carotid occlusive disease in patients with high neurological risk. Stroke. 2003;34:308.
25. Qureshi AI, Boulos AS, Kim SH, et al. Carotid angioplasty and stent placement using the FilterWire for distal protection: an international multicenter study. Stroke. 2003;34:307.
26. Roubin GS, New G, Iyer SS, et al. Immediate and late clinical outcomes of carotid artery stenting in patients with symptomatic and asymptomatic carotid artery stenosis: a 5-year prospective analysis. Circulation. 2001;103:532–7.
27. MacDonald S, Venables GS, Cleveland TJ, et al. Protected carotid stenting: safety and efficacy of the MedNova NeuroShield filter. J Vasc Surg. 2002;35:966–72.
28. Benichou H, Bergeron P. Carotid angioplasty and stenting: will periprocedural transcranial Doppler monitoring be important? J Endovasc Surg. 1996;3:217–23.
29. Hartmann A, Mast H, Thompson JL, Sia RM, Mohr JP. Transcranial Doppler waveform blunting in severe extracranial carotid artery stenosis. Cerebrovasc Dis. 2000;10(1):33–8.
30. Gomez CR, Brass LM, Tegeler CH, et al. The transcranial Doppler standardization project. J Neuroimaging. 1993;3:190–2.
31. Visser GH, Wieneke GH, van Huffelen AC, Eikelboom BC. The use of preoperative transcranial Doppler variables to predict which patients do not need a shunt during carotid endarterectomy. Stroke. 2003;34:813–9.
32. Reinhard M, Muller T, Roth M, Guschlbauer B, Timmer J, Hetzel A. Bilateral severe carotid artery stenosis or occlusion – cerebral autoregulation dynamics and collateral flow patterns. Acta Neurochir (Wien). 2003;145(12):1053–9.
33. Niesen WD, Rosenkranz M, Eckert B, Meissner M, Weiller C, Sliwka U. Hemodynamic changes of the cerebral circulation after stent-protected carotid angioplasty. AJNR Am J Neuroradiol. 2004;25(7):1162–7.
34. Mori T, Fukuoka M, Kazita K, Mima T, Mori K. Intraventricular hemorrhage after carotid stenting. J Endovasc Surg. 1999;6(4):337–41.
35. Sfyroeras GS, Karkos CD, Arsos G, Liasidis C, Dimitriadis AS, Papazoglou KO, Gerassimidis TS. Cerebral hyperperfusion after carotid stenting: a transcranial Doppler and SPECT study. Vasc Endovascular Surg. 2009;43(2):150–6. Epub 2008 Sep 30.
36. Tan W, Bates MC, Wholey M. Cerebral protection systems for distal emboli during carotid artery interventions. J Interv Cardiol. 2001;14(4):465–74.
37. Al-Mubarak N, Roubin GS, Vitek JJ, Iyer SS. Microembolization during carotid artery stenting with the distal-balloon antiemboli system. Int Angiol. 2002;21(4):344–8.
38. Parodi JC, Bates MC. Angioplasty and stent with reversal of internal carotid flow as a cerebral protection device. In: Greenhalgh RM, editor. ATLAS: vascular and endovascular surgical techniques. 4th ed. London: W.B. Saunders; 2001. p. 198–213.
39. Gossetti B, Gattuso R, Irace L, Faccenna F, Venosi S, Bozzao L, Fiorelli M, Andreoli R, Gossetti C. Embolism to the brain during carotid stenting and surgery. Acta Chir Belg. 2007;107(2):151–4.
40. Kindel M, Spiller P. Transient occlusion of an angioguard protection system by massive embolization during angioplasty of a degenerated coronary saphenous vein graft. Catheter Cardiovasc Interv. 2002;55:2501–4.
41. Moehring MA, Ritcey JA. Microembolus sizing in a blood mimicking fluid using a novel dual-frequency pulsed Doppler. Echocardiography. 1996;13(5):567–71.
42. Moehring MA, Ritcey JA. Sizing emboli in blood using pulse Doppler ultrasound – II: effects of beam refraction. IEEE Trans Biomed Eng. 1996;43(6):581–8.
43. Moehring MA, Klepper JR. Pulse Doppler ultrasound detection, characterization and size estimation of emboli in flowing blood. IEEE Trans Biomed Eng. 1994;41(1):35–44.
44. Crawley F, et al. Comparison of hemodynamic cerebral ischemia and microembolic signals detected during carotid endarterectomy and carotid angioplasty. Stroke. 1997;28(12):2460–4.
45. Devuyst G, Darbellay GA, Vesin JM, Kemeny V, Ritter M, Droste DW, Molina C, Serena J, Sztajzel R, Ruchat P, Lucchesi C, Dietler G, Ringelstein EB, Despland PA, Bogousslavsky J. Automatic classification of HITS into artifacts or solid or gaseous emboli by a wavelet representation combined with dual-gate TCD. Stroke. 2001;32(12):2803–9.
46. Georgiadis D, Uhlmann F, Lindner A, Zierz S. Differentiation between true microembolic signals and artifacts using an arbitrary sample volume. Ultrasound Med Biol. 2000;26(3):493–6.

47. Rodriguez RA, Giachino A, Hosking M, Nathan HJ. Transcranial Doppler characteristics of different embolic materials during in vivo testing. J Neuroimaging. 2002;12(3):259–66.
48. Ohki T, Roubin GS, Veith FJm, et al. The efficacy of a filter in preventing embolic events during carotid artery stenting. An ex-vivo analysis. J Vasc Surg. 1999;30:1034–44.
49. Coggia M, Goeau-Brissonniere O, Duval JL, et al. Embolic risk of the different stages of carotid bifurcation balloon angioplasty: an experimental study. J Vasc Surg. 2000;31:550–7.
50. Antonius Carotid Endarterectomy, Angioplasty, and Stenting Study Group. Transcranial Doppler monitoring in angioplasty and stenting of the carotid bifurcation. J Endovasc Ther. 2003;10(4):702–10.
51. Orlandi G, Fanucchi S, Fioretti C, Acerbi G, Puglioli M, Padolecchia R, Sartucci F, Murri L. Characteristics of cerebral microembolism during carotid stenting and angioplasty alone. Arch Neurol. 2001; 58(9):1410–3.
52. Ackerstaff RG, Suttorp MJ, van den Berg JC, Overtoom TT, Vos JA, Bal ET, Zanen P, Antonius Carotid Endarterectomy, Angioplasty, and Stenting Study Group. Prediction of early cerebral outcome by transcranial Doppler monitoring in carotid bifurcation angioplasty and stenting. J Vasc Surg. 2005;41(4):618–24.
53. Garami ZF, Bismuth J, Charlton-Ouw KM, Davies MG, Peden EK, Lumsden AB. Feasibility of simultaneous pre- and postfilter transcranial Doppler monitoring during carotid artery stenting. J Vasc Surg. 2009;49(2):340–4, 345.e1–2; discussion 345.
54. Abou-Chebl A, Yadav JS, Reginelli JP, Bajzer C, Bhatt D, Krieger DW. Intracranial hemorrhage and hyperperfusion syndrome following carotid artery stenting: risk factors, prevention, and treatment. J Am Coll Cardiol. 2004;43(9):1596–601.
55. Dalman JE, Beenakkers IC, Moll FL, Leusink JA, Ackerstaff RG. Transcranial Doppler monitoring during carotid endarterectomy helps to identify patients at risk of postoperative hyperperfusion. Eur J Vasc Endovasc Surg. 1999;18(3):222–7.
56. Morrish W, Grahovac S, Douen A. Intracranial hemorrhage after stenting and angioplasty of extracranial carotid stenosis. AJNR Am J Neuroradiol. 2000;21:1911–6.
57. Censori B, Camerlingo M, Casto L, Partziguian T, Caverni L, Bonaldi G, Mamoli A. Carotid stents are not a source of microemboli late after deployment. Acta Neurol Scand. 2000;102(1):27–30.
58. Gaunt ME, Martin PJ, Smith JL, Bell PR, Naylor AR. Clinical relevance of intraoperative embolization detected by transcranial Doppler ultrasonography during carotid endarterectomy: a prospective study of 100 patients. Br J Surg. 1994;81:1435–9.
59. van Heesewijk HP, Vos JA, Louwerse ES, Van Den Berg JC, Overtoom TT, Ernst SM, Mauser HW, Moll FL, Ackerstaff RG, Carotid PTA and Stenting Collaborative Research Group. New brain lesions at MR imaging after carotid angioplasty and stent placement. Radiology. 2002;224(2):361–5.
60. Jaeger H, Mathias K, Drescher R, Hauth E, Bockisch G, Demirel E, Gissler HM. Clinical results of cerebral protection with a filter device during stent implantation of the carotid artery. Cardiovasc Intervent Radiol. 2001;24(4):249–56.
61. Wilkinson ID, Griffiths PD, Hoggard N, Cleveland TJ, Gaines PA, Macdonald S, McKevitt F, Venables GS. Short-term changes in cerebral microhemodynamics after carotid stenting. AJNR Am J Neuroradiol. 2003;24(8):1497–9.
62. Jaeger HJ, Mathias KD, Drescher R, Hauth E, Bockish G, Demirel E, Gissler HM. Diffusion-weighted MR imaging after angioplasty or angioplasty plus stenting of arteries supplying the brain. AJNR Am J Neuroradiol. 2001;22(7):1234–5.
63. Schluter M, Tubler T, Steffens JC, Mathey DG, Schofer J. Focal ischemia of the brain after neuroprotected carotid artery stenting. J Am Coll Cardiol. 2003;42(6):1014–6.
64. Crawley F, Stygall J, Lunn S, et al. Comparison of microembolism detected by transcranial Doppler and neuropsychological sequelae of carotid surgery and percutaneous transluminal angioplasty. Stroke. 2000;31:1329–34.
65. Sadoshima S, Heistad DD. Regional cerebral blood flow during hypotension in normotensive and stroke-prone spontaneously hypertensive rats: effect of sympathetic denervation. Stroke. 1983;14(4):575–9.
66. Moody DM, Brown WR, Challa VR, Stump DA, Reboussin DM, Legault C. Brain microemboli associated with cardiopulmonary bypass: a histologic and magnetic resonance imaging study. Ann Thorac Surg. 1995;59(5):1304–7.
67. Bettman MA, Katzen BT, Whisnant J, Brant-Zawadzki M, Broderick JP. Carotid stenting and angioplasty: a statement for healthcare professionals from the Councils on Cardiovascular Radiology, Stroke, Cardio-Thoracic and Vascular Surgery, Epidemiology, and Prevention, and Clinical Cardiology, American Heart Association. Circulation. 1998;97(1):121–3.

# Computed Tomography Angiography and Magnetic Resonance Angiography of the Carotids

15

Ali F. AbuRahma and Hisham Bassiouny

**Abstract**

The imaging modalities most often used to evaluate patients for cervical carotid stenosis are carotid duplex ultrasound, computed tomography angiography (CTA), magnetic resonance angiography (MRA), and digital subtraction angiography (DSA).

Duplex ultrasonography provides an accurate noninvasive tool to determine the degree of carotid stenosis and plaque morphology in most patients. It is usually the initial study in patients who present with a carotid bruit or carotid symptoms. This study is highly dependent on technique.

Meanwhile, CTA has recently been regarded as a valuable test for carotid artery stenosis. It is possible to obtain three-dimensional images of the carotid arteries by CTA, although this requires a specialized workstation and dedicated personnel for data processing. CTA cannot be used to evaluate flow dynamics and as such cannot be used for the diagnosis of subclavian steal or other flow-based lesions. The test is easy to perform and associated with few risks. Arterial access is not required, and there is no associated risk of stroke. The image quality rivals that of DSA when the examination is performed on a high-quality helical scanner and reformatted to three-dimensional images by well-trained personnel. CTA can provide additional information about the conformation and composition of the plaque.

CTA is less susceptible than MRA to overestimating the severity of carotid stenosis. It is extremely fast and offers submillimeter spatial resolution, is less expensive than contrast-enhanced MRA, and has the ability to visualize soft tissue, bone, and blood vessels at the same time. CTA can interrogate the arterial tree from the aortic arch to the circle of Willis.

MRA has the advantage of being noninvasive, does not require iodinated contrast or ionizing radiation, and provides unlimited number of projections of the carotid lumen from a single acquisition.

A.F. AbuRahma, M.D., RVT, RPVI (✉)
Department of Surgery, Robert C. Byrd Health Sciences Center,
West Virginia University,
3110 MacCorkle Ave SE, Charleston, WV 25304, USA

Charleston Area Medical Center,
Charleston, WV, USA

H. Bassiouny, M.D., FACS
Section of Vascular Surgery and Endovascular Therapy,
The University of Chicago,
5841 S. Maryland Ave., MC 5028 Chicago, IL 60637, USA
e-mail: hbassiou@surgery.bsd.uchicago.edu

A.F. AbuRahma, D.F. Bandyk (eds.), *Noninvasive Vascular Diagnosis*,
DOI 10.1007/978-1-4471-4005-4_15, 

Contrast-enhanced MRA used MR technique to provide flow-independent anatomic information. The technique is somewhat similar to CTA with first-pass MRA. Because these images are not dependent on flow, they provide a more accurate assessment of stenosis and visualization of ulcerated plaques.

Additionally, information about the cerebral circulation can be obtained simultaneously, including patency of the carotid siphon and middle cerebral artery. MRA can also assess intrathoracic and intracranial lesions that are not amenable to duplex interrogation. Using dedicated protocols, MRA can also demonstrate specific plaque components, e.g., calcium, lipid, fibrocellular element, or thrombus within the plaques. The ability to use MRA as a diagnostic tool for carotid stenosis is sadly often dependent on local expertise and familiarity with the test.

This chapter summarizes the role of each imaging modality in the diagnosis of carotid artery disease.

**Keywords**
CTA • MRA • Carotid disease • Diagnosis

## Introduction

The two most important features of carotid bifurcation atheroma are the degree of diameter stenosis and the character of the carotid bifurcation plaque. There are clinical scenarios where the clinician requires information on the status of the vessels proximal or distal to the cervical carotid artery, in addition to information about the carotid bifurcation. These factors should be considered when choosing between various carotid imaging studies. Some physicians may use multiple modalities when evaluating a patient with suspected cervical carotid stenosis.

In both the North American Symptomatic Carotid Endarterectomy Trial (NASCET) [1, 2] and the European Carotid Surgery Trial (ECST) [3], a higher degree of stenosis in symptomatic patients was associated with a higher stroke risk. In the Asymptomatic Carotid Atherosclerosis Study (ACAS) [4], there was no correlation between the severity of carotid stenosis and the incidence of stroke; however, there were too few strokes in this study to permit a subgroup analysis of the effect of the degree of stenosis on the ability to benefit from carotid endarterectomy. Angiographic data from the ECST study [5], on contralateral asymptomatic carotid arteries, demonstrated a <2% annual stroke risk in patients with less than 70% asymptomatic stenosis. Asymptomatic lesions with greater degrees of stenosis had a greater risk of stroke: 9.8% for patients with 70–79% stenosis and 14.4% for those with 80–99% stenosis. These data suggest that the degree of stenosis is a marker of stroke risk in both symptomatic and asymptomatic lesions. Pathological studies have demonstrated that more stenotic carotid plaques are more likely to have ulceration, intraplaque hemorrhage, and intraluminal thrombus formation, all of which are clearly related to cerebral embolization and stroke [6].

Plaque morphology is an important feature in assessing future risk of neurologic events. This will be discussed in a separate chapter.

## Selecting Imaging Modalities for Carotid Evaluation

The imaging modalities most often used to evaluate patients for cervical carotid stenosis are carotid duplex ultrasound, computed tomography angiography (CTA), magnetic resonance angiography (MRA), and digital subtraction angiography.

## Carotid Duplex Ultrasound

Duplex ultrasonography provides an accurate noninvasive tool to determine the degree of carotid stenosis and plaque morphology in most patients. It is usually the initial study in patients who present with a carotid bruit or carotid symptoms. The study is highly dependent on technique and should be done in an accredited vascular laboratory (e.g., Intersocietal Commission for the Accreditation of Vascular Laboratories [ICAVL]), and the images should be reviewed by an experienced physician.

Determining the degree of carotid artery stenosis is largely based on an analysis of the peak systolic velocity (PSV) and/or the end-diastolic velocity (EDV) of the carotid artery. A panel of experts from several medical specialties met in October 2002 in San Francisco, California, under the auspices of the Society of Radiologists in Ultrasound to reach a consensus regarding the use of Doppler ultrasound in the diagnosis of internal carotid artery (ICA) stenosis [7]. This

panel of experts recommended a cutoff PSV of the ICA of ≥125 and ≥230 cm/s for predicting angiographic >50% and >70% ICA stenoses, respectively. These recommended criteria are based on an analysis of several published studies and the experience of the panelists rather than values validated against other imaging modalities.

AbuRahma et al. [8] recently analyzed the carotid duplex ultrasound and angiography results of 376 carotid arteries in their institution. Using the consensus criteria, they demonstrated a sensitivity of 93%, a specificity of 68%, and an overall accuracy of 85% for stenosis between 50% and 69%. A PSV of ≥230 cm/s for ≥70% stenosis had a sensitivity of 99%, a specificity of 86%, and an overall accuracy of 95%. Receiver operator curves showed that the ICA PSV was significantly better than EDV or ICA/CCA ratio ($p=0.036$) in detecting ≥70% stenosis and ≥50% stenosis. There was no improvement in accuracy by adding the EDV values and/or the ratios to the PSV values.

Velocity-based estimation of carotid artery stenosis may need to be adjusted in certain circumstances, e.g., higher velocities in the presence of contralateral carotid artery occlusion and higher velocities in women than in men [9, 10]. Extensive vascular calcification, high carotid bifurcation, severe arterial tortuosity, and obesity may also reduce the accuracy of duplex ultrasound. Carotid stents will decrease compliance of the vessel wall and may increase velocity [11]. Duplex ultrasound may also fail to differentiate between subtotal and total carotid occlusion. Intravenous administration of sonographic contrast agents may improve diagnostic accuracy [12, 13], but the safety of these agents has been questioned.

Contrast ultrasound and power Doppler imaging can be used to differentiate between pre-occlusive stenosis and complete occlusion [14]. Duplex imaging of the carotid artery has two major limitations. These include quality dependence on the technician's examination and limitations of visualization of the proximal carotid artery and intracranial portions. Although the intracranial cerebral arteries can be assessed with transcranial Doppler, this technique is not as widely available at most institutions as other imaging modalities. Overall, each vascular laboratory should have in place an internal validation process of their own criteria for their internal use.

## Computed Tomographic Angiography

Computed tomography angiography, CTA, has only recently been regarded as a valuable test for carotid artery stenosis. While use of CTA for carotid disease is not widespread, CTA is a powerful tool with broad applications.

Most CTA is performed via timing bolus technique. This requires approximately 120 cc of intravenous contrast via a 20-gauge intravenous catheter. Motion and interference artifacts from dental amalgam are the primary source of error in data acquisition. Patient positioning with elevation of the jaw, a shoulder harness, and instructions to avoid swallowing can all be used to eliminate this source of error [15].

While early studies show impressive results regarding CT imaging, analysis of the data is somewhat problematic. Carotid stenosis as evaluated by CTA is described as *area* reduction of the carotid lumen. This is calculated digitally from images of the entire artery obtained from the scan. This is in distinction from the "gold standard," digital subtraction angiography, in which *diameter* reduction is calculated from an estimate of true lumen size [16]. Given that NASCET and ACAS data are based on diameter reduction criteria, it is difficult to interpret CTA data in this regard.

It is possible to obtain three-dimensional images of the carotid arteries by CTA though this requires a specialized workstation and dedicated personnel for data processing. Reformatting of the carotid bifurcation images requires specialized training, a difficult resource to provide for a test that has yet to be widely used by vascular surgeons.

Other disadvantages of CTA include the inability to image the vascular structures of the brain simultaneously. Also, CTA cannot be used to evaluate flow dynamics and as such cannot be used for diagnosis of subclavian steal or other flow-based lesions. Other limitations of this technique include cost (compared to duplex ultrasound), contrast exposure, as well as the added concern of radiation exposure. Additionally, a large calcium burden can limit the ability to distinguish contrast from calcium during post-processing imaging.

While there are several drawbacks to CTA, the advantages are many. The test is easy to perform and associated with few risks. Unlike DSA, arterial access is not required, and there is no associated risk of stroke. The image quality rivals that of DSA when the examination is performed on a high-quality helical scanner with fine cuts and reformatted to three-dimensional images by well-trained personnel (Figs. 15.1 and 15.2).

More importantly, CTA can provide additional information about the conformation and composition of the plaque, information that may, in the future, be able to distinguish active, dangerous plaque from stable and more benign plaque. Certainly, CTA can "depict plaque morphology, with calcified plaque easily distinguished from soft or lipid laden plaque" [15]. Whether these factors can predict plaque activity and be used to stratify those patients who are at increased risk for stroke is under investigation. Future research focusing on this issue holds many promises and may direct operative therapy more precisely.

CTA is less susceptible than MRA to overestimating the severity of carotid stenosis. The rapid acquisition of spiral CT images allows excellent timing with contrast administration and provides quality images that can be viewed in

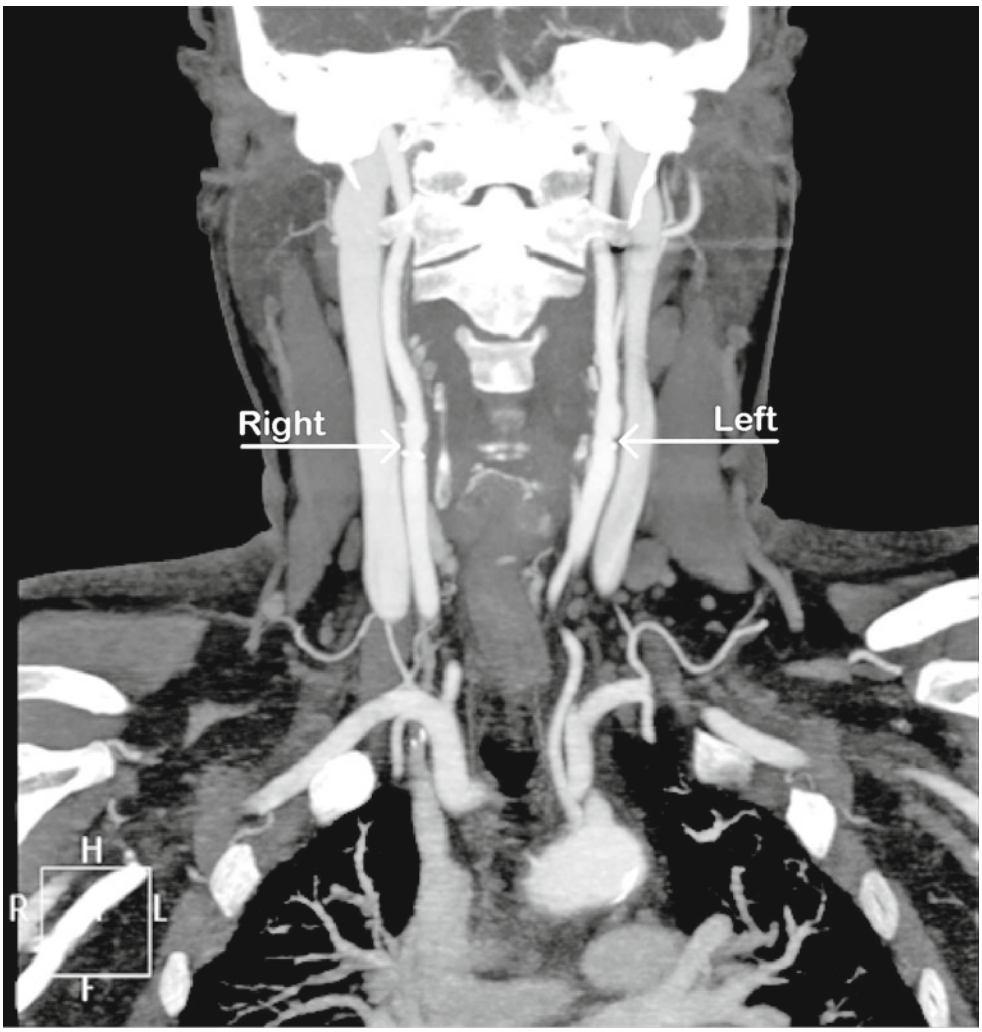


**Fig. 15.1** CTA showing minimal carotid disease at right and left bifurcation (*arrow*)

multiple planes. CTA is extremely fast and offers submillimeter spatial resolution (0.3 vs. 0.8 mm for contrast-enhanced MRA), is less expensive than contrast-enhanced MRA, provides a faster processing time, and has the ability to visualize soft tissue, bone, and blood vessels at the same time. CTA can also demonstrate vascular anomalies, has the ability to quantify the extent of calcification, and can interrogate the arterial tree from the aortic arch to the circle of Willis. Stenoses can be measured with electronic microcalipers based on NASCET or ECST methods [17].

A meta-analysis of 28 studies analyzing the diagnostic accuracy of CTA in comparison to digital subtraction angiography showed a pooled sensitivity of 85% and specificity of 93% for CTA in detecting 70–99% carotid stenosis and a sensitivity and specificity for occlusion of 97% and 99% [18]. CTA was also highly accurate in identifying calcification, but less reliable in describing carotid plaque morphology, specifically the lipid component, or ulceration. CTA appears less reliable than carotid duplex ultrasound or MRA for assessing plaque morphology [19].

## Magnetic Resonance Imaging (MRA/MRI)

MRA has the advantage of being noninvasive, does not require iodinated contrast or ionizing radiation, and provides unlimited number of projections of the carotid lumen from a single acquisition. Two techniques are used: time-of-flight imaging (TOF), a flow-dependent technique; and contrast-enhanced MRA (CE MRA), a filling dependent technique, comparable to the technique of CTA. TOF is a widely used technique to establish the diagnosis of carotid stenosis. "This technique is optimized to minimize the signal from stationary tissue, thereby increasing relative signal from the fresh spins delivered to the volume by blood flow from outside the imaging volume" [15]. There are two modes of TOF: two-dimensional and three-dimensional. Two-dimensional time of flight is more sensitive to slower flow, while 3D TOF depicts a wide range of flow velocities and as such has greater accuracy than 2D for defining internal and external carotid artery morphology [15]. Because this imaging is flow dependent, there is some distortion of

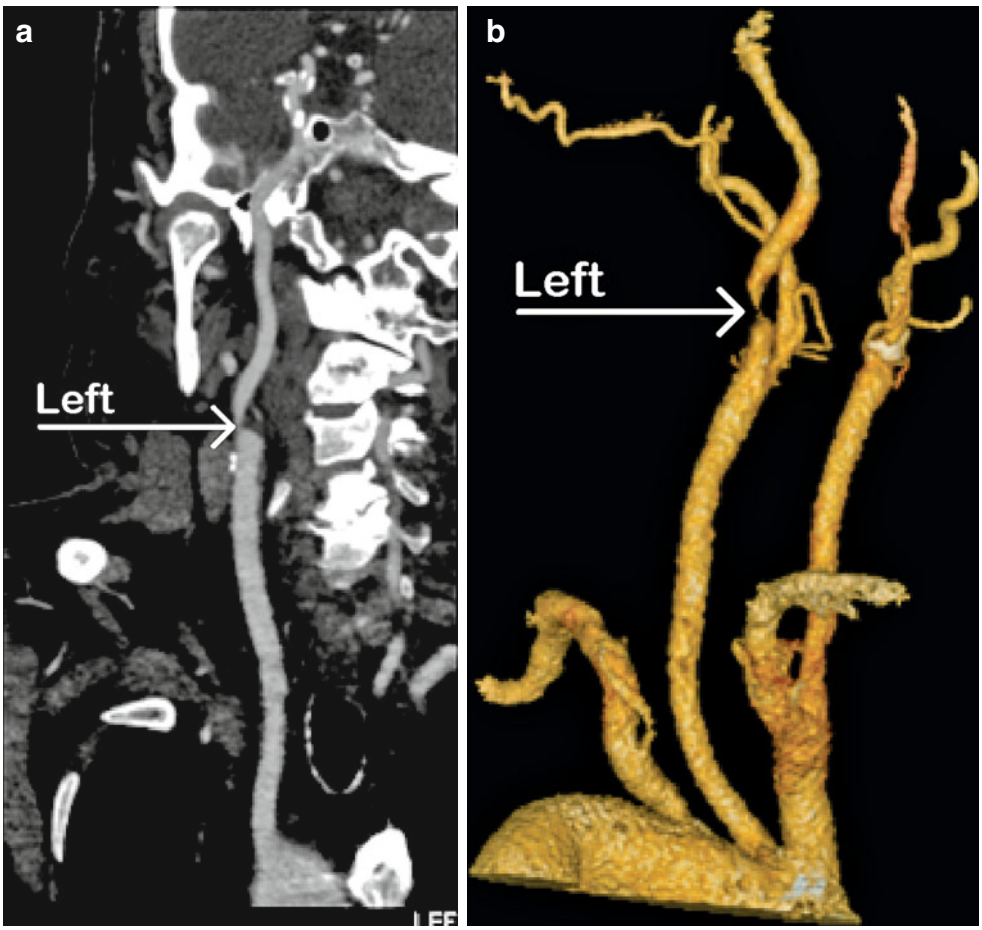


**Fig. 15.2** CTA showing (**a**) severe left proximal internal carotid artery stenosis (*arrow*); (**b**) same patient showing aortic arch vessels (*arrow*)

the carotid anatomy with high-grade lesions or in lesions with turbulent flow. "TOF spins may remain in imaging volume long enough to see numerous pulses and become saturated, thereby causing loss of signal within vessel lumen and inability to depict the vessel contiguous with the lesion" [15]. While this can lead to overestimation of the degree of stenosis and a high false-positive rate, in contrast, the false-negative rate is quite low. Demonstration of minimal disease at the carotid bifurcation on MRA is a highly accurate diagnosis [20].

Contrast-enhanced MRA (CE MRA) uses MR technique to provide flow-independent anatomic information [15]. The technique is somewhat similar to CTA with first-pass MRA. Because these images are not dependent on flow, they provide a more accurate assessment of stenosis and visualization of ulcerated plaques. There may be some technical difficulty capturing the timing bolus; however, once this is overcome, the shorter imaging time increases accuracy secondary to a decreased risk of motion artifact.

The ability to use MRA as a diagnostic tool for carotid stenosis is sadly often dependent on local expertise and familiarity with the test. In centers where the test is widely used, it can provide valuable additional data from that obtained at carotid duplex. MRA has no ionizing radiation or ionic contrast and as such is quite safe for most patients. Additionally, information about the cerebral circulation can be obtained simultaneously including patency of the carotid siphon and MCA.

MRA can also assess intrathoracic and intracranial lesions that are not amenable to duplex interrogation. MRA does not visualize the surrounding soft tissue structures, unless additional magnetic resonance imaging (MRI) is performed and calcium within the plaque is not defined. It cannot be used in patients with implanted ferromagnetic devices (e.g., implantable defibrillators, pacemakers) and is of limited use in uncooperative patients and those with claustrophobia. Gadolinium-based compounds used as a contrast agent for MRA have been associated with nephrogenic systemic fibrosis in patients with preexisting renal disorders [21]. Additionally, small carotid lumens and tortuous vessels can be seen as occlusion or severe stenosis. Finally, the test is quite costly and as such is a less desirable test for screening.

MRA can display vessel anatomy as a rotating three-dimensional angiogram that can be readily interpreted by those

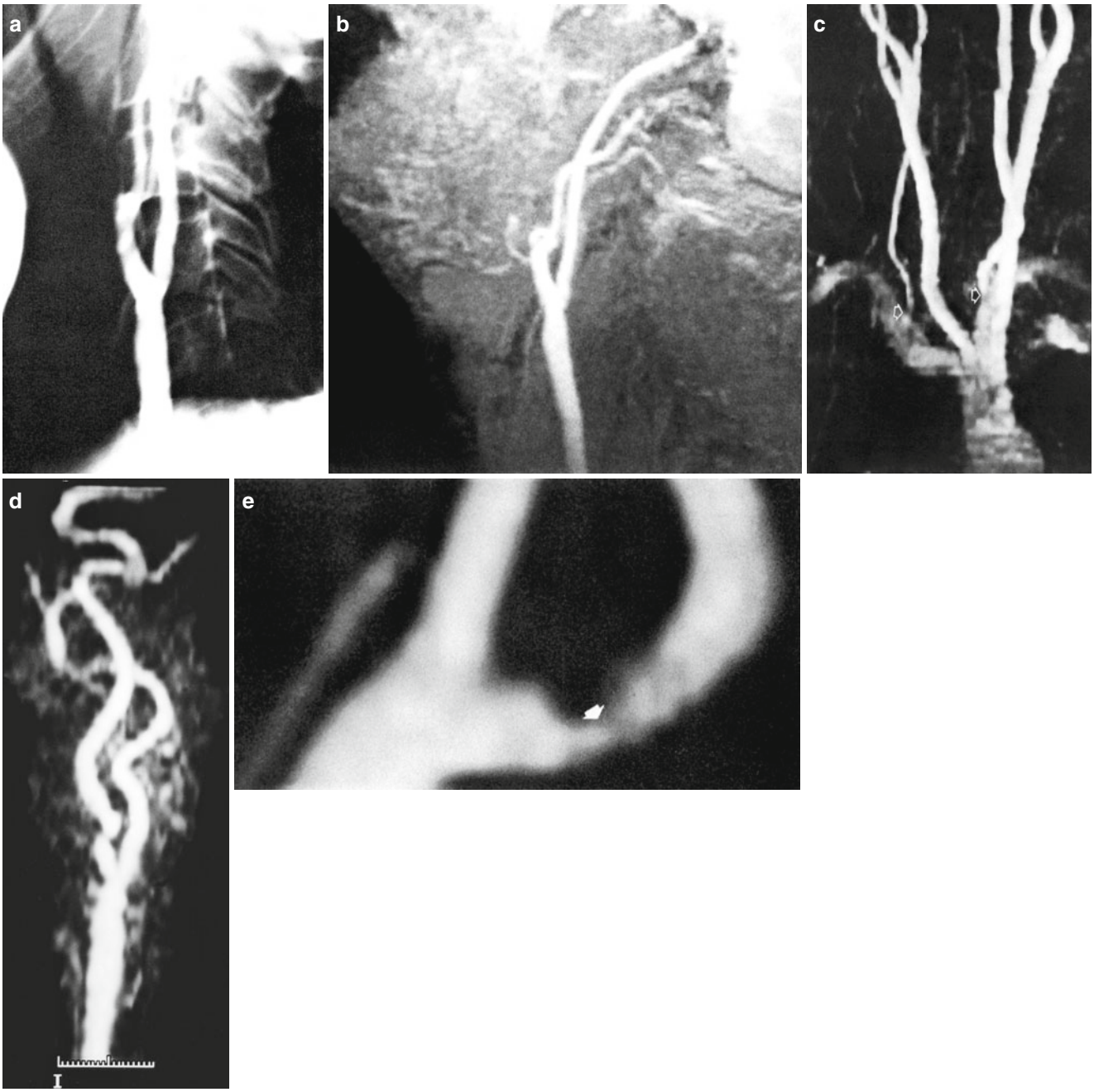


**Fig. 15.3** (**a**) Conventional arteriogram of the carotid bifurcation. (**b**) Magnetic resonance angiogram of the carotid bifurcation [same patient as in (**a**)]. As noted, the quality of this magnetic resonance angiogram is similar to the conventional angiogram seen in (**a**). (**c**) Magnetic resonance angiogram showing the origin of both vertebral arteries (as indicated by the *arrows*). (**d**) Magnetic resonance angiogram of the carotid bifurcation showing a mild to moderate degree of stenosis of the proximal internal carotid artery. (**e**) Magnetic resonance angiogram of the carotid artery bifurcation showing moderate to severe stenosis of the internal carotid artery (*white arrow*)

who did not perform the study (Fig. 15.3). Severe or tight stenoses (≥70%) are usually seen as a flow gap (Fig. 15.4).

More advanced techniques are now being evaluated for visualization of the atherosclerotic plaque and vessel wall. These methods include standard CE MRA and TOF obtained with specialized surface carotid coils to increase the signal-to-noise ratio. Additional techniques include 3D bright-blood MRA and 2D spin-echo and fast spin-echo methods. Data obtained from these techniques demonstrates good correlation with ex vivo plaque morphology. However, the tests are time consuming and technology laden and, as yet, merely experimental [22, 23].

The sensitivity and specificity for diagnosing 70–99% stenosis with time-of-flight (TOF) MRA are identical to

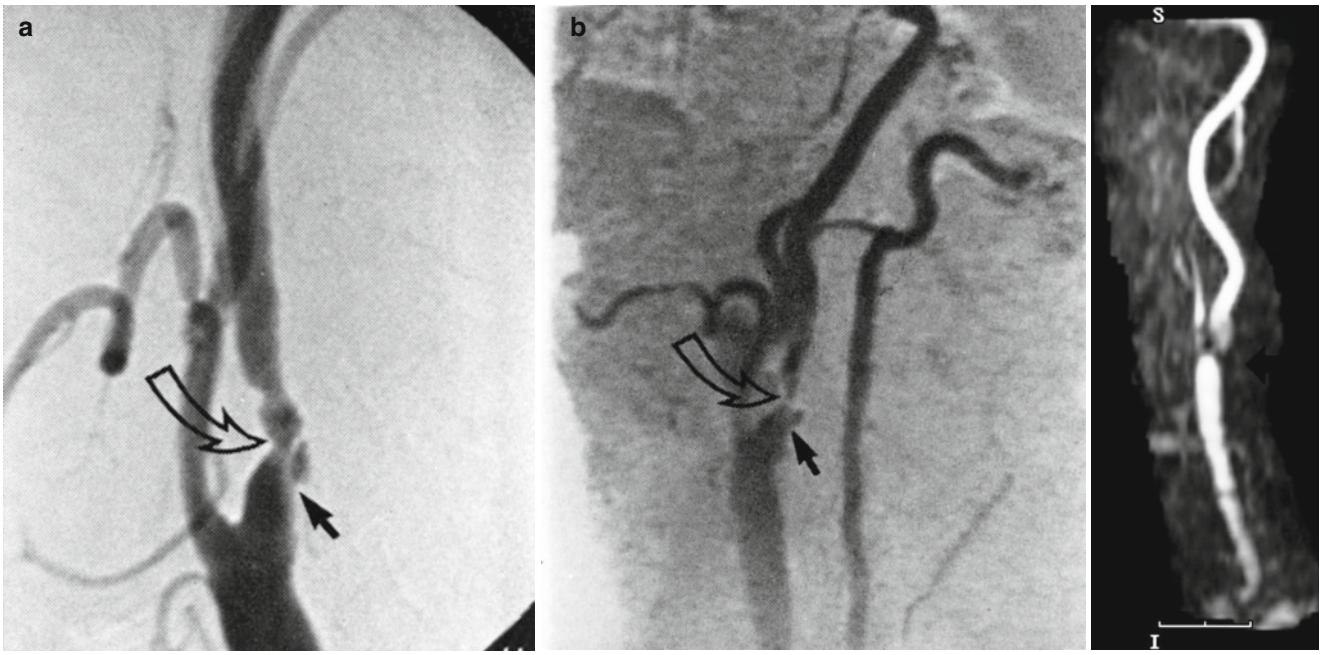


**Fig. 15.4** (**a**) Conventional arteriogram showing severe to tight stenosis of the proximal internal carotid artery (*curved white arrow*) with associated ulceration (*black arrow*). (**b**) Three-dimensional TOF magnetic resonance angiogram of the same patient showing the same tight stenosis with ulceration (*arrow*). (**c**) Carotid magnetic resonance angiogram showing severe to tight stenosis of the internal carotid artery without ulceration as indicated by flow gap

duplex ultrasound (88% and 84%, respectively); however, MRA is less accurate in diagnosing 50–69% stenosis but is quite accurate in diagnosing carotid occlusion [21, 24]. MRI can be used to analyze plaque morphology, specifically the structure of the atherosclerotic plaque. It can identify the lipid-rich necrotic core and the fibrous capsule with high sensitivity and specificity [25] and can distinguish between intact thick, thin, or ruptured fibrous cap [26]. Using dedicated protocols, MR also can demonstrate specific plaque components, e.g., calcium, lipid, fibrocellular element, or thrombus within the plaques.

## Catheter-Based Digital Subtraction Arteriography

Many authorities still consider carotid conventional digital angiography to be the gold standard against all other imaging modalities in patients with extracranial cerebrovascular disease. In one test, evaluation of the aortic arch and extracranial and intracranial cerebrovascular system can be performed. Additionally, DSA is the only test that can definitively diagnose lesions of flow dynamics, such as subclavian steal with clear demonstration of delayed and collateral filling. Flow-dependent lesions are not well demonstrated by CTA or MRA.

Measurement of carotid stenosis using this method is generally done using the NASCET method [1]. Conventional angiography is generally reserved for patients with conflicting imaging studies prior to carotid endarterectomy or in patients considered for carotid stenting. DSA provides high-quality imaging, which is accurate, objective, and easy to interpret. It can identify lesions from the aortic arch to the intracranial vessels. Major limitations of angiography that make it inappropriate as a screening modality include its cost and associated risks, specifically of stroke [27–29]. Although the stroke risk has been quoted as high as 1% in the NASCET trial, in practice, the stroke/TIA risk from carotid angiography is closer to 0.5% [30]. Additionally, the risk of femoral sheath hematoma, while low with a 5-French sheath required for diagnostic angiography, is still 0.1–0.5% [31]. Additionally, in comparison to MRA where there is no ionic contrast or ionizing radiation, DSA holds some risk of renal insufficiency and ionizing radiation.

Finally, DSA provides accurate information regarding the lumen of the carotid artery but fails to provide any information about plaque composition, the vessel wall, or surrounding cervical structures.

Overall, DSA is most useful in patients when less invasive imaging studies produce conflicting results. When duplex is equivocal, DSA is preferred over CT and MR in evaluating patients with renal dysfunction (by minimizing contrast load), obesity, or indwelling ferromagnetic material, which render CTA or MRA technically inadequate or difficult.

## Comparison of CDUS/MRA/CTA/DSA

The UK Health Technology Assessment (HTA) concluded that although contrast-enhanced MRA was the most accurate imaging modality overall, it was limited by inaccessibility, unavailability, and delays. They concluded that color duplex ultrasound remained the preferred imaging modality for identifying patients with 70–99% stenosis [32]. As such, CDUS is the preferred imaging modality for identification of asymptomatic stenosis.

This recommendation was based on several factors, including low cost, a much higher number of strokes likely to be prevented in the long term by the rapid availability of carotid duplex ultrasound in contrast to other imaging, and good sensitivity of imaging in detecting significant stenosis. However, the HTA highlighted the concern of the accuracy of duplex ultrasound in diagnosing 50–69%, which carries a sensitivity of only 36%, with a specificity of 91% [32]. The utility of CDUS will depend on the clinical presentation of the patient. In neurologically symptomatic patients, a diagnosis of stenosis between 50% and 69% by CDUS is sufficient to proceed with surgery based on its specificity. However, the low sensitivity of CDUS in this setting would mandate another imaging study if the CDUS was negative. In neurologically asymptomatic patients, a moderate stenosis (50–69%) diagnosed by CDUS should be confirmed by another imaging study before intervention is undertaken.

## Recommendations for Selection of Carotid Imaging Modalities

1. Color carotid duplex ultrasound in an accredited vascular laboratory is the initial diagnostic testing of choice for evaluating the severity of stenosis in both symptomatic and asymptomatic patients. Under these conditions, unequivocal identification of stenosis of 50–99% in neurologically symptomatic patients or 70–99% in asymptomatic patients is sufficient to make a decision regarding intervention.
2. Color CDUS in an accredited vascular laboratory is the imaging modality of choice to screen asymptomatic populations at high risk.
3. When CDUS is nondiagnostic, or suggests stenosis of intermediate severity (50–69%) in an asymptomatic patient, additional imaging with MRA, CTA, or DSA is required prior to embarking on any intervention.
4. When evaluation of the vessels proximal or distal to the cervical carotid arteries is needed for diagnosis or to plan therapy, imaging in addition to CDUS (either CTA, MRA, or catheter angiography) is indicated. CTA is preferable to MRI/MRA for delineating calcium. When there is discordance between two minimally invasive imaging studies (CDUS, MRA, CTA), DSA is indicated to resolve conflicting results. DSA is generally reserved for situations where there is inconclusive evidence of stenosis on less invasive studies or when carotid artery stenting (CAS) is planned.
5. A postoperative duplex ultrasound, within 30 days, is recommended to assess the status of the endarterectomized vessel. In patients with 50% or greater stenosis on this study, further follow-up imaging to assess progression or resolution is indicated. In patients with a normal duplex and primary closure of the endarterectomy site, ongoing imaging is recommended to identify recurrent stenosis. In patients with a normal duplex ultrasound after patch or eversion endarterectomy, further imaging of the endarterectomized vessel may be indicated if the patient has multiple risk factors for progression of atherosclerosis.
6. Imaging after CAS or CEA is indicated to follow contralateral disease progression in patients with contralateral stenosis greater than or equal to 50%. In patients with multiple risk factors for vascular disease, follow-up duplex may be indicated with lesser degrees of stenosis. The likelihood of disease progression is related to the initial severity of stenosis.

Other indications for alternate carotid imaging are as follows:

1. *Internal carotid pseudo-occlusion*: A staccato Doppler flow signal with a minimal or absent diastolic flow component by duplex ultrasound evaluation is highly suggestive of near or total occlusion of the internal carotid artery in its extracranial course or distally in the siphon region. This should be further confirmed with conventional or magnetic resonance arteriography in patients who are being considered for intervention. In this instance, additional imaging is necessary to determine if a patent ICA string lumen is present with antegrade flow into the distal extracranial and intracranial internal carotid artery or if significant siphon disease is present. Establishing distal internal carotid patency is essential for successful intervention on the stenotic plaque.
2. *Unstable carotid plaque*: Although velocity criteria for high-grade stenosis form a reliable basis for operative intervention, plaque structural morphology remains an important consideration in patients presenting with retinal or hemispheric events. The presence of plaque echolucency by Duplex ultrasound as determined quantitatively by Gray Scale Median score analysis appears to correlate with structural features which connote plaque instability and predisposition to ischemic events [33]. Hence, a moderate non-hemodynamically significant highly echolucent internal carotid plaque should be considered a culprit lesion in the absence of other sources of thromboembolism (cardiac, arch, or intracranial disease). Additional imaging is advised to confirm surface irregularity or ulceration. Selective multiplanar arteriographic views of the suspicious lesion provide optimum image resolution for such determinations.

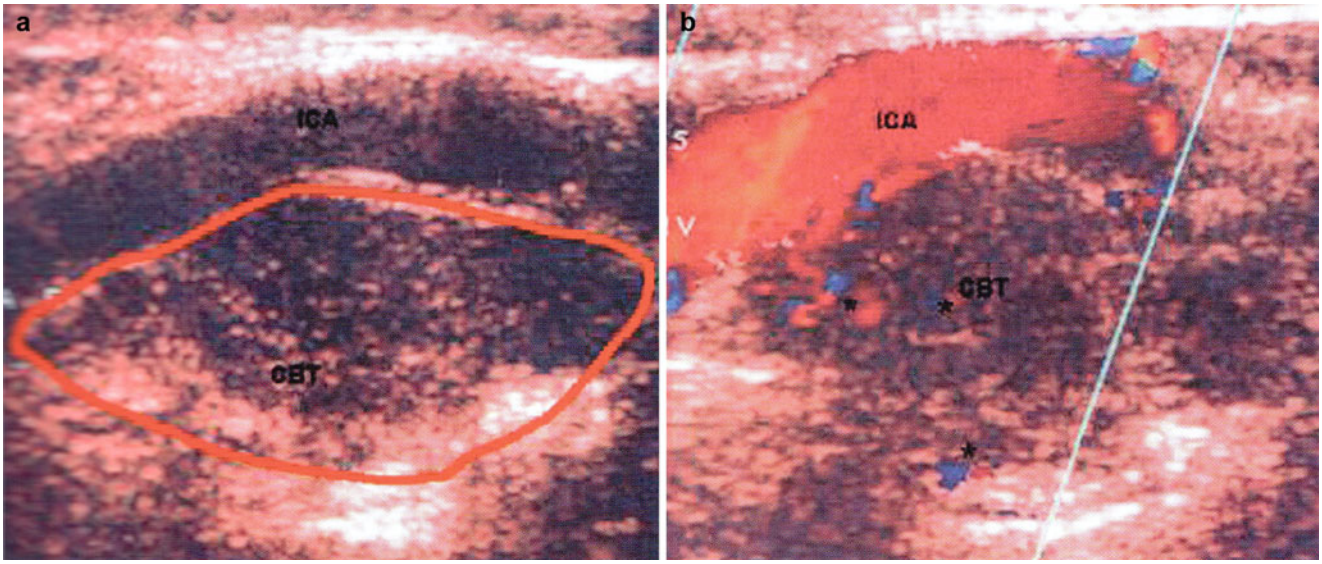


**Fig. 15.5** CDU of a carotid body tumor. B-mode ultrasound demonstrating the tumor outlined in *red*. (**a**) CDU demonstrating color speckling, indicated by the *asterisks* (**b**) (ICA) internal carotid artery. (CBT) carotid body tumor (Reprinted from Schwarze et al. [34]. With permission from Elsevier)

Other imaging techniques continue to evolve for the assessment of plaque structural components that underlie plaque instability. These include spiral CT and MRI for the delineation of such features as calcification, necrosis, intraplaque hemorrhage, and fibrous cap integrity.

3. *Carotid bifurcation thrombus*: Free-floating thrombus involving the carotid bifurcation visualized by duplex ultrasound in a patient with a referable acute ischemic event is an alarming finding. Characteristically, this unusual event is encountered in relatively younger individuals with no apparent evidence of atherosclerotic plaque formation at the carotid bifurcation. Concurrent with a thorough investigation of the embolic source, the presence of carotid thrombus should be confirmed prior to intervention by either serial duplex evaluation or arteriography as some thrombi will lyse or fragment with anticoagulation.
4. *Vertebrobasilar insufficiency*: Patients with symptomatic posterior fossa ischemia who have demonstrable flow reversal in the vertebral artery or evidence of vertebral stenosis and occlusion by duplex should undergo a comprehensive assessment of the vertebrobasilar anatomy and the integrity of the circle of Willis.
5. *Recurrent carotid stenosis*: In most instances, early recurrent carotid stenosis is asymptomatic by virtue of the benign natural history of the underlying intimal hyperplastic response. Recurrent stenosis discovered after many years of carotid intervention is typically related to de novo atherogenesis. Additionally, with the advent of carotid stent/angioplasty for primary treatment of ICA stenoses, the accurate classification of the degree of in-stent restenosis by duplex ultrasound is not yet fully validated. Arteriographic evaluation of the carotid bifurcation is essential to define precisely the nature of the recurrent stenosis and to identify those patients at risk from the presence of a recurrent lesion.
6. *Intracranial pathology*: Patients with history or symptoms, which indicate intracranial cerebral pathology such as aneurysms and arteriovenous malformations, are best investigated with CT, MR, or arteriography.
7. *Fibromuscular dysplasia and associated arteridities*: Atypical diffuse or tandem stenoses involving the common and internal carotid arteries may represent non-atherosclerotic occlusive disease. These conditions typically involve longer segments of the carotid and other arterial beds such as the renal arteries and aortic arch branches. Precise delineation of the extent of disease via additional imaging techniques is critical if intervention is contemplated.
8. *Carotid body tumors*: While carotid ultrasound is an excellent diagnostic test for the presence of carotid body tumors (Fig. 15.5), additional diagnostic studies are helpful to guide operative strategy and may be used for preoperative intervention. CT angiography is a useful adjunct to carotid duplex for defining, preoperatively, the Shamblin classification of the tumor, a useful tool for risk stratification. MRA can also depict tumor vascularization though not as accurately as digital subtraction angiography [35], which, while not essential for preoperative planning, can be helpful to delineate feeding arteries accurately for large tumors. Additionally, for very large tumors, some surgeons may prefer preoperative embolization performed at the time of angiography, though the clinical benefits of this are not definitively confirmed in the literature.

Extracranial cerebrovascular duplex ultrasonography is an excellent diagnostic modality when performed and interpreted in a skilled vascular laboratory. The use of alternative imaging modalities in these specific clinical scenarios provides hemodynamic and morphologic information that compliments the duplex findings for optimal surgical decision making.

## References


1. North American Symptomatic Carotid Endarterectomy Trial Collaborators (NASCET). Beneficial effect of carotid endarterectomy in symptomatic patients with high-grade carotid stenosis. N Engl J Med. 1991;325:445.
2. Barnett HJ, Taylor DW, et al. Benefit of carotid endarterectomy in patients with symptomatic moderate or severe stenosis. North American Symptomatic Carotid Endarterectomy Trial Collaborators. N Engl J Med. 1998;339(20):1415–25.
3. Randomized trial of endarterectomy for recently symptomatic carotid stenosis: final results of the MRC European Carotid Surgery Trial (ECST). Lancet. 1998;351(9113):1379–87.
4. Executive Committee for the Asymptomatic Carotid Atherosclerosis Study. Endarterectomy for asymptomatic carotid artery stenosis. JAMA. 1995;273:1421–8.
5. European Carotid Surgery Trialists' Collaborative Group. Risk of stroke in the distribution of an asymptomatic carotid artery. Lancet. 1995;345:209.
6. Ricotta JJ, Schenck EA, Hassett JM, Deweese JA. Lesion width as a discriminator of plaque characteristics. J Cardiovasc Surg. 1996;4(2):124–9.
7. Grant EG, Benson CB, Moneta GL, Alexandrov AV, Baker JD, Bluth EI, Carroll BA, Eliasziw M, Gocke J, Hertzberg BS, Katarick S, Needleman L, Pellerito J, Polak JF, Rholl KS, Wooster DL, Zierler E. Carotid artery stenosis: grayscale and Doppler ultrasound diagnosis – society of radiologists in ultrasound consensus conference. Ultrasound Q. 2003;19:190–8.
8. AbuRahma AF, Srivastava M, Stone PA, Mousa AY, Jain A, Dean LS, Keiffer T, Emmett M. Critical appraisal of the carotid duplex consensus criteria in the diagnosis of carotid artery stenosis. J Vasc Surg. 2011;53:53–60.
9. Busuttil SJ, Franklin DP, Youkey JR, Elmore JR. Carotid duplex overestimation of stenosis due to severe contralateral disease. Am J Surg. 1996;172:144–7.
10. Comerota AJ, Sales-Cunha SX, Daoud Y, Jones L, Beebe HG. Gender differences in blood velocities across carotid stenoses. J Vasc Surg. 2004;40:939–44.
11. Lal BK, Hobson RW, Tofghi B, Kapadia I, Cuadra S, Jamil Z. Duplex ultrasound velocity criteria for the stented carotid artery. J Vasc Surg. 2008;47:63–73.
12. Sitzer M, Rose G, Furst G, Siebler M, Steinmetz H. Characteristics and clinical value of an intravenous echo-enhancement agent in evaluation of high-grade internal carotid stenosis. J Neuroimaging. 1997;7:S22–5.
13. Ferrer JM, Samso JJ, Serrando JR, Valenzuela VF, Montoya SB, Docampo MM. Use of ultrasound contrast in the diagnosis of carotid artery occlusion. J Vasc Surg. 2000;31:736–41.
14. Bude RO, Rubin JM, Adler RS. Power vs. conventional color Doppler sonography: comparison in the depiction of normal intrarenal vasculature. Radiology. 1994;192:777–80.
15. Phillips CD, Bubash LA. CT angiography and MR angiography in the evaluation of extracranial carotid vascular disease. Radiol Clin North Am. 2002;40:783–98.
16. Cinat M, Lane C, Pham H, Lee A, Wilson S, Gordon I. Helical CT angiography in the preoperative evaluation of carotid artery stenosis. J Vasc Surg. 1998;28:290–300.
17. Bartlet ES, Walters TD, Symons SP. Quantification of carotid stenosis on CT angiography. AJNR Am J Neuroradiol. 2006;27:13.
18. Koelemay MJ, Nederkoom PJ, Reitsma JB, Majoie CB. Systematic review of computed tomographic angiography for assessment of carotid artery disease. Stroke. 2004;35:2306–12.
19. Gronholdt ML. B-mode ultrasound and spiral CT for the assessment of carotid atherosclerosis. Neuroimaging Clin N Am. 2002;12:421–35.
20. Nederkoorn PJ, Elgersma OE, Mali WP, Eikelboom BC, Kappelle LJ, van der Graaf Y. Overestimation of carotid artery stenosis with magnetic resonance angiography compared with digital subtraction angiography. J Vasc Surg. 2002;36:806–13.
21. Nederkoom PJ, van der Graaf Y, Hunink MG. Duplex ultrasound and magnetic resonance angiography compared with digital subtraction angiography in carotid artery stenosis: a systematic review. Stroke. 2003;34:1324–32.
22. Yuan C, Lin E, Millard J, Hwang J. Closed contour edge detection of blood vessel lumen and outer wall boundaries in black-blood MR images. Magn Reson Imaging. 1999;17:257–66.
23. Zhang S, Hatsukami T, Polissar N, Han C, Yuan C. Comparison of carotid vessel wall area measurements using three different contrast-weighted black blood MR imaging techniques. Magn Reson Imaging. 2001;19:795–802.
24. Remonda L, Senn P, Barth A, Arnold M, Lovblad KO, Schroth G. Contrast-enhanced 3D MR angiography of the carotid artery: comparison with conventional digital subtraction angiography. AJNR Am J Neuroradiol. 2002;23:213–9.
25. Yuan C, Mitsumori LM, Ferguson MS, et al. In vivo accuracy of multispectral magnetic resonance imaging for identifying lipid-rick necrotic cores and intraplaque hemorrhage in advanced human carotid plaques. Circulation. 2001;104:2051–6.
26. Hatsukami TS, Ross R, Polissar NL, Yuan C. Visualization of fibrous cap thickness and rupture in human atherosclerotic carotid plaque in vivo with high-resolution magnetic resonance imaging. Circulation. 2000;102:959–64.
27. Hankey GJ, Warlow CP, Molyneux AJ. Complications of cerebral angiography for patients with mild carotid territory ischaemia being considered for carotid endarterectomy. J Neurol Neurosurg Psychiatry. 1990;53:542–8.
28. Davies KN, Humphrey PR. Complications of cerebral angiography in patients with symptomatic carotid territory ischaemia screened by carotid ultrasound. J Neurol Neurosurg Psychiatry. 1993;56:967–72.
29. Leonardi M, Cenni P, Simonetti L, Raffi L, Battaglia S. Retrospective study of complications arising during cerebral and spinal diagnostic angiography from 1998 to 2003. Interv Neuroradiol. 2005;11:213–21.
30. Johnston DC, Chapman KM, Goldstein LB. Low rate of complications of cerebral angiography in routine clinical practice. Neurology. 2001;57(11):2012–4.
31. Lilly MP, Reichman W, Sarazen AA, Carney WI. Anatomic and clinical factors associated with complications of transfemoral arteriography. Ann Vasc Surg. 1990;4:264–9.
32. Wardlaw JM, Chappell FM, Stevenson M, et al. Accurate, practical and cost-effective assessment of carotid stenosis in the UK. Health Technol Assess. 2006;10:iii–iv. ix-x, 1–182.
33. Sabeti M, Tegos T, Nicolaides A, El-Atrozy T, Dhanjil S, Griffin M, Belcaro G, Geroulakos G. Hemispheric symptoms and carotid plaque echomorphology. J Vasc Surg. 2000;31:39–49.
34. Schwarze G, Grogan JK, Bassiouny H. Alternative imaging techniques for extracanial carotid occlusive disease. In: Mansour MA, Labropoulos N, editors. Vascular diagnosis. Philadelphia: Saunders; 2005.
35. Van den Berg R, Wasser MN, van Gils AP, van der Mey AG, Hermans J, van Buchem MA. Vascularization of head and neck paragangliomas: comparison of three MR angiographic techniques with digital subtraction angiography. AJNR Am J Neuroradiol. 2000;21(1):162–70.

# Intraoperative Ultrasound Assessment of Carotid Endarterectomy and Stent-Angioplasty

16

Paul A. Armstrong, Alexis Powell, and Dennis F. Bandyk

**Abstract**

The outcome of carotid interventions depends on technical precision of the arterial repair which can be assessed accurately using ultrasound imaging. Following carotid endarterectomy, duplex ultrasound provides both anatomic (real-time B-mode imaging) and hemodynamic (pulsed Doppler spectral analysis) assessment of the repair, allowing detection of residual stenosis, lumen debris, plaque dissection, and verification of normal low resistance flow in the distal internal carotid artery. Intravascular ultrasound is suited for monitoring carotid stent-angioplasty as the over-the-wire catheter provides high-resolution real-time imaging of the extracranial carotid artery for vessel diameter measurements, selection of stent landing zones, and alerting the interventionist to incomplete stent expansion (residual stenosis) or other abnormalities such as lumen thrombus or vessel dissection proximal or distal to the stent. Intraprocedural ultrasound imaging will identify abnormalities that should be corrected in approximately 5–10% of cases. Detection and immediate repair of detected abnormalities is associated with clinical outcomes similar to reconstructions judged "normal" on initial ultrasound assessment, including perioperative neurologic events and reintervention for restenosis.

**Keywords**

Carotid endarterectomy • Stent-angioplasty • Intraoperative assessment • Intravascular ultrasound • Duplex ultrasound

## Introduction

It is incumbent on the vascular specialist to verify technical adequacy following carotid intervention by open endarterectomy or endovascular stent-angioplasty procedure. Despite careful technique, disease extent and plaque morphology can lead to residual repair site abnormalities which often cannot be recognized by visual inspection and pulse palpation [1–4]. Even when angiographic monitoring is utilized, minor anatomic defects can be dismissed as "not significant." A repair site defect can result in perioperative stroke by particle embolization or repair site thrombosis, but it also can reduce procedure durability by producing a hemodynamic state conducive to development of initial hyperplasia, i.e., recurrent stenosis [5–7]. Since the efficacy of carotid interventions is dependent on a low (3%) neurologic event rate, assessment

P.A. Armstrong, DO (✉)
Division of Vascular and Endovascular Surgery,
University of South Florida, College of Medicine,
4202 East Fowler Avenue, Tampa General Circle
USF Health Building 7th Floor,
Tampa, FL 33606, USA
e-mail: parmstro@health.usf.edu

A. Powell, M.D.
Department of Surgery, University of South Florida,
School of Medicine,
Tampa, FL, USA

D.F. Bandyk, M.D.
Vascular and Endovascular Surgery,
University of California, San Diego,
La Jolla, CA, USA

A.F. AbuRahma, D.F. Bandyk (eds.), *Noninvasive Vascular Diagnosis*,
DOI 10.1007/978-1-4471-4005-4_16, 

**Table 16.1** Clinical reports recommending routine intraoperative duplex ultrasound evaluation of carotid endarterectomy repairs based on number of unsuspected lesions identified, low (<1%) operative stroke rate, and excellent procedure durability (ICA occlusion, restenosis)

| Investigator | No. of CEAs | % Revised | No. of ICA occlusions | Restenosis at 2–3 year |
|---|---|---|---|---|
| Baker et al. [3] | 316 | 3 | 3 (1%) | 3% |
| Papanicolaou et al. [4] | 86 | 11 | 2 (2%) | 0 |
| Panneton et al. [5] | 155 | 9 | 0 | 2% |
| Bandyk et al. [2] | 390 | 8 | 1 (0.3%) | 2% |
| Ascher et al. [6] | 650 | 3 | 0 | 2% |
| Schanzer et al. [10] | 407 | 8 | 0 | 2% |

of all carotid reconstructions is essential as a quality assurance measure [2, 4–6].

Arteriography is the accepted technique for assessment of carotid repairs especially stent-angioplasty. Documentation of <30% residual stenosis and no visualized lumen defect are accepted criteria for technical adequacy. Digital subtraction angiography provides accurate anatomic confirmation of repair site patency and intracranial artery perfusion, but the technique is invasive, requires contrast injection, and may not detect subtle abnormalities such as focal platelet aggregation within the repair site which can produce stroke and internal carotid artery (ICA) thrombosis. The application of duplex ultrasound for carotid endarterectomy assessment and intravascular ultrasound (IVUS) monitoring during carotid stent-angioplasty may be superior to angiographic assessment because these diagnostic techniques provide a higher resolution of vessel imaging, and with duplex ultrasound, hemodynamic assessment of imaged abnormalities is provided which aids in the decision for immediate repair or observation [4–11]. Intraoperative duplex scanning also provides a baseline study for subsequent surveillance testing for the detection of recurrent carotid stenosis. The intraoperative documentation of a "normal" carotid endarterectomy repair by duplex scanning is associated with a low (<1%) perioperative stroke rate and low (<5%) incidence of recurrent stenosis (Table 16.1) [2–6, 8]. The application of IVUS monitoring has been adopted by several vascular groups including ours because ultrasound imaging provides useful information on plaque morphology, for stent sizing, and after stent deployment and balloon dilation verification of adequate stent expansion. A normal stent-angioplasty site based on IVUS imaging predicts absence of residual stenosis by duplex ultrasound and is associated with a 1-year restenosis rate of <10% [2, 4, 6].

While the goal of intraoperative assessment is the detection of repair site lesions, a secondary benefit is recognition of abnormal repair site hemodynamics with the potential to cause recurrent stenosis. Outcome analysis of carotid endarterectomy sites with altered blood flow characteristics such as moderate elevation (150–200 cm/s) in peak systolic velocity (PSV) or residual plague producing <30% lumen stenosis has been shown to reduce the functional patency by development of intimal hyperplasia. The natural history of recurrent stenosis is more benign than an atherosclerotic plaque, but progressive intimal hyperplasia can lead to internal carotid occlusion. Most vascular surgeons recommend repair of asymptomatic recurrent stenosis with duplex findings of a >80% diameter reduction (DR) stenosis [2–4]. Treatment is typically by stent-angioplasty. Similarly, the development of in-stent stenosis is most commonly the result of intimal hyperplasia and, if progressive to a high-grade stenosis, can cause stent occlusion. Following both endarterectomy and stent-angioplasty, the likelihood of recurrent stenosis has been shown to be associated with the presence of residual stenosis [1, 2, 4].

## Carotid Endarterectomy Duplex Scan Protocol and Test Interpretation

Intraoperative duplex scanning of carotid repairs is performed after restoration of ICA blood flow using a "hockey stick" linear array 10–15-MHz ultrasound transducer enclosed in a sterile plastic sheath (Fig. 16.1). Acoustic coupling for vessel imaging is achieved by ultrasound gel in the sheath and saline in the incision. Imaging is accomplished by placing the transducer over the artery and then slowly moving it along the repair beginning in the common carotid artery and proceeding distally to the ICA. If a prosthetic (bovine, polyester) patch was used for vessel closure, lumen imaging is still possible, but use of a polytetrafluoroethylene (PTFE) patch hampers imaging due to air trapped in the PTFE material. Vessel imaging and velocity spectra recordings can be carried by orienting the transducer foot pad along the non-patched vessel circumference. With the assistance of a vascular technologist to optimize instrument setting for imaging and pulsed Doppler spectral analysis, the exam time is less than 10 min including archiving images for the patient medical record.

Duplex scanning should begin at the proximal common carotid artery (CCA) to verify normal proximal endarterectomy end point. The site of proximal clamp occlusion should be imaged since traumatic wall dissection could have occurred. Scanning then proceeds from proximal to distal to confirm a widely patent lumen and normal velocity spectra (Fig. 16.2). Special attention should be paid to endarterectomy end points where residual plaque >2 mm in thickness is

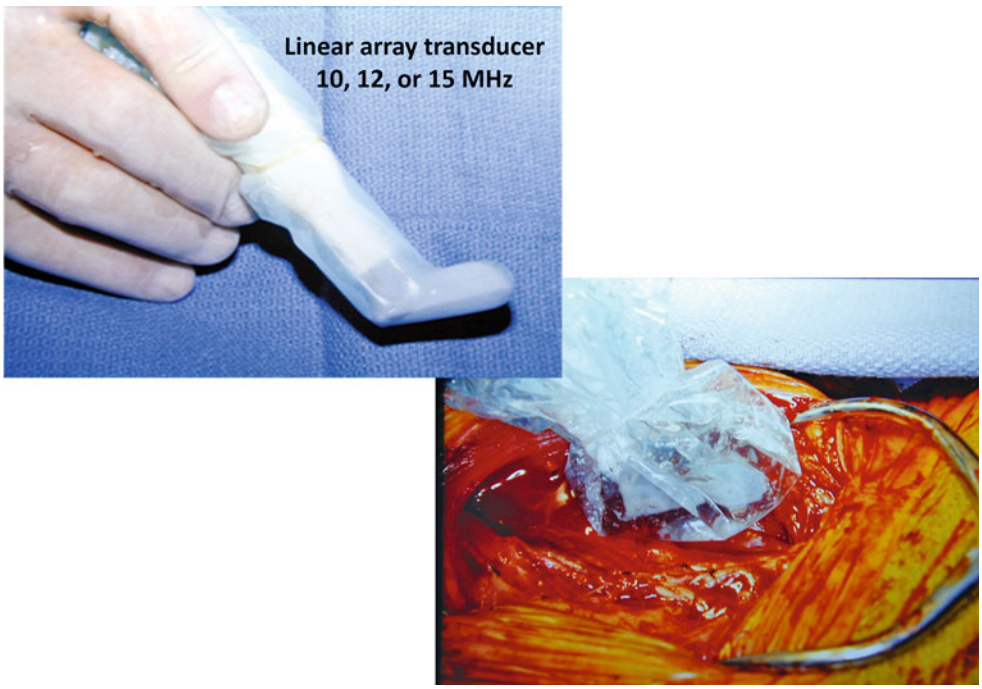


**Fig. 16.1** A "hockey stick" linear array (10–15-MHz) transducer suitable for intraoperative carotid repair site imaging. The small footprint transducer is enclosed in a sterile plastic sheath for scanning within the neck incision directly on the carotid endarterectomy site

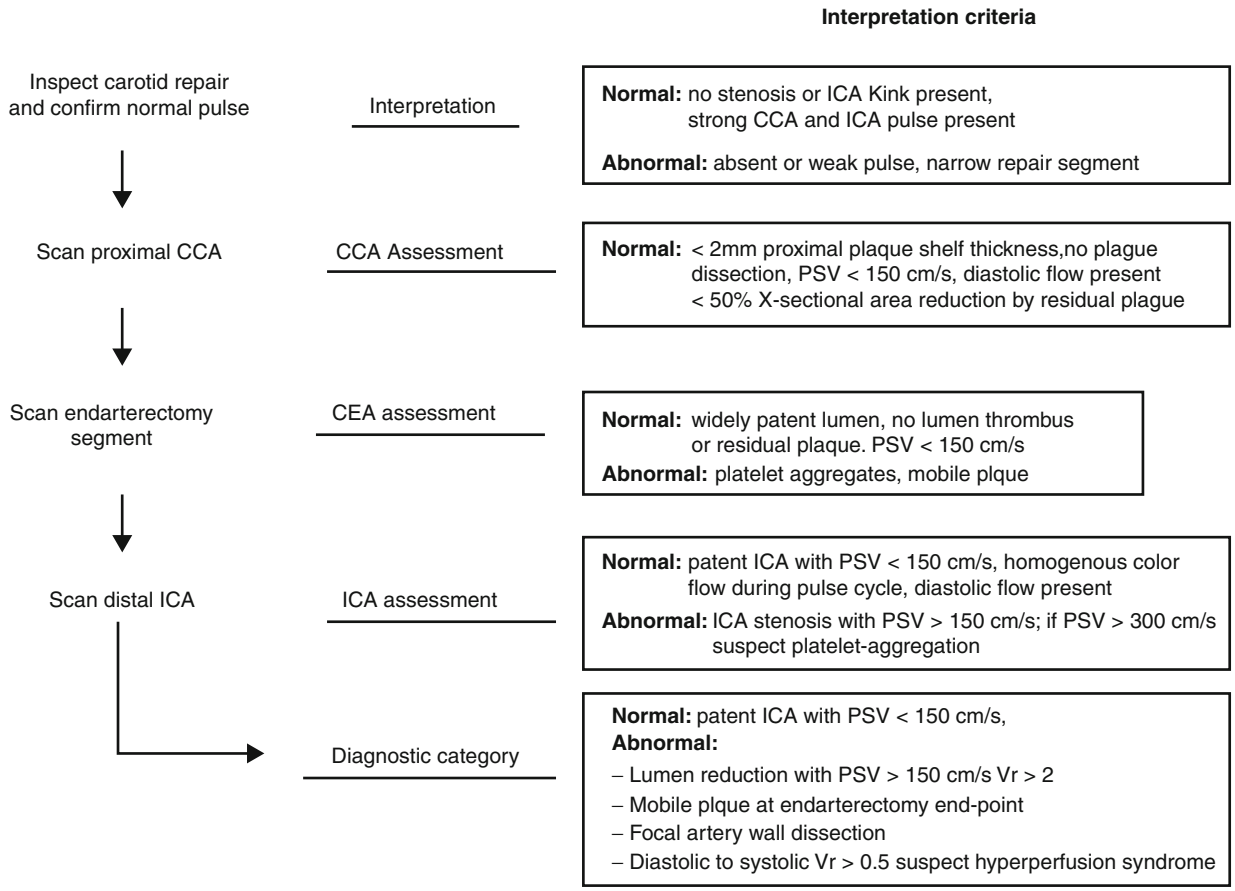


**Fig. 16.2** The duplex ultrasound imaging protocol and interpretation criteria after carotid endarterectomy

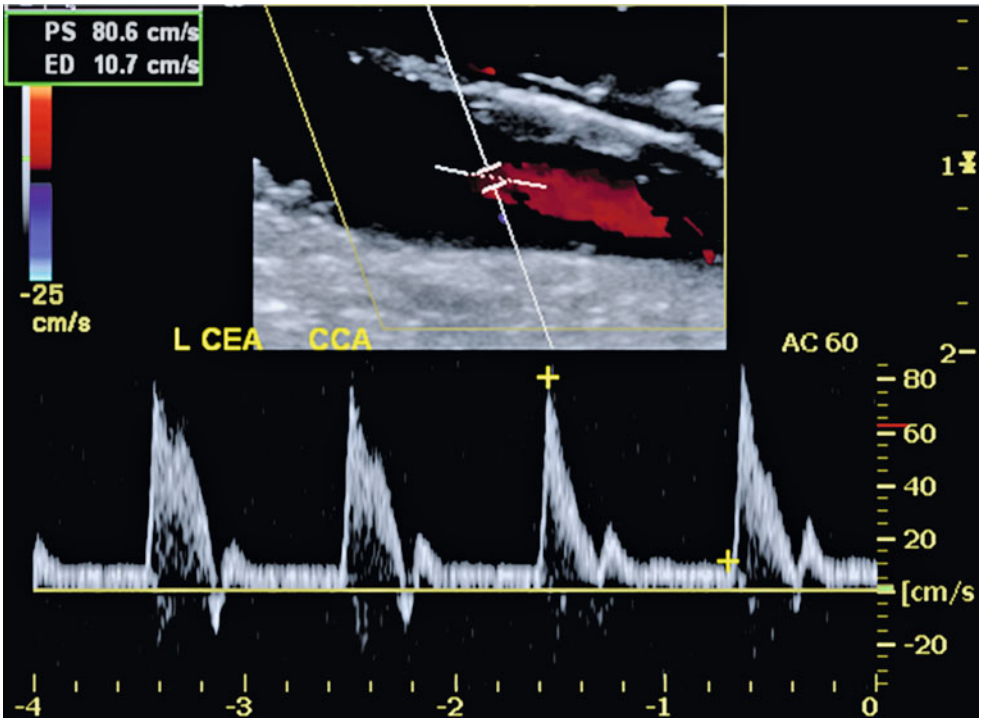


**Fig. 16.3** Duplex ultrasound image of common carotid artery endarterectomy end point showing mild residual plaque but normal velocity spectra (minimal spectral broadening, peak systolic velocity <150 cm/s)

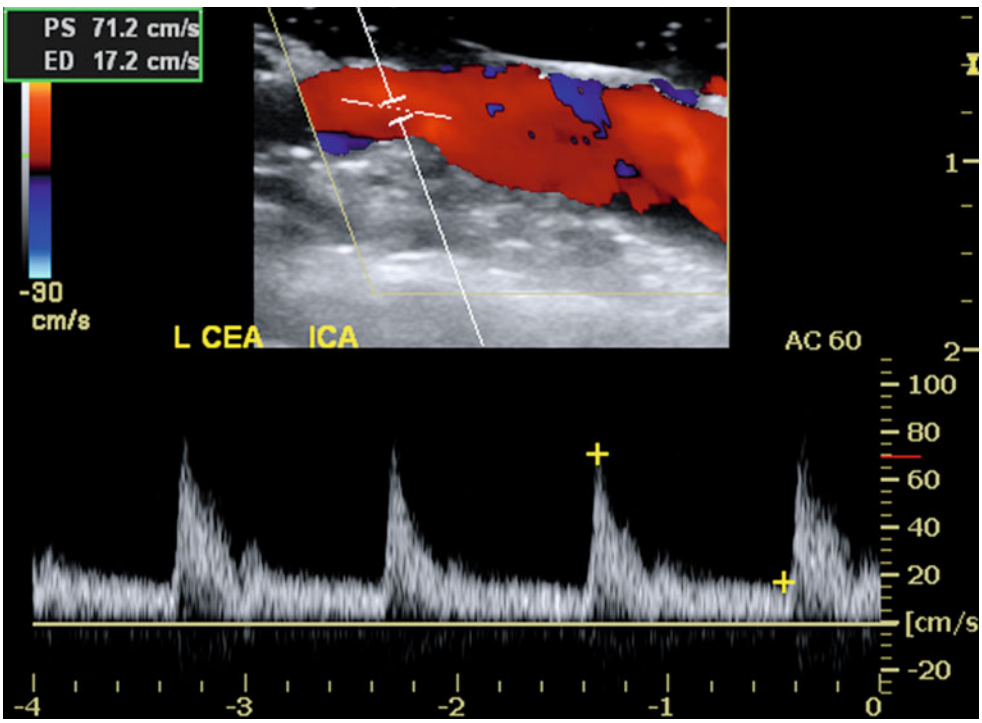


**Fig. 16.4** Duplex ultrasound image of vein patch endarterectomy site with normal color Doppler imaging and velocity spectra (mild spectral broadening, peak systolic velocity <150 cm/s)

abnormal and should be repaired. The normal endarterectomy site should be free of lumen defects, no suture stricture, and PSV should be <150 cm/s (Figs. 16.3 and 16.4). The criteria for an "abnormal" duplex scan depend on the site (CCA, ICA) imaged and the severity of the anatomic defect and associated hemodynamic changes indicating stenosis. Using transverse imaging, the diameter of the proximal ICA (bulb segment) should demonstrate homogenous color flow, and the diameter can be measured which should be <1 cm as larger diameter patched segments are prone to aneurysmal dilation and mural thrombus formation (Fig. 16.5). The external carotid artery (ECA) is imaged to verify patency and

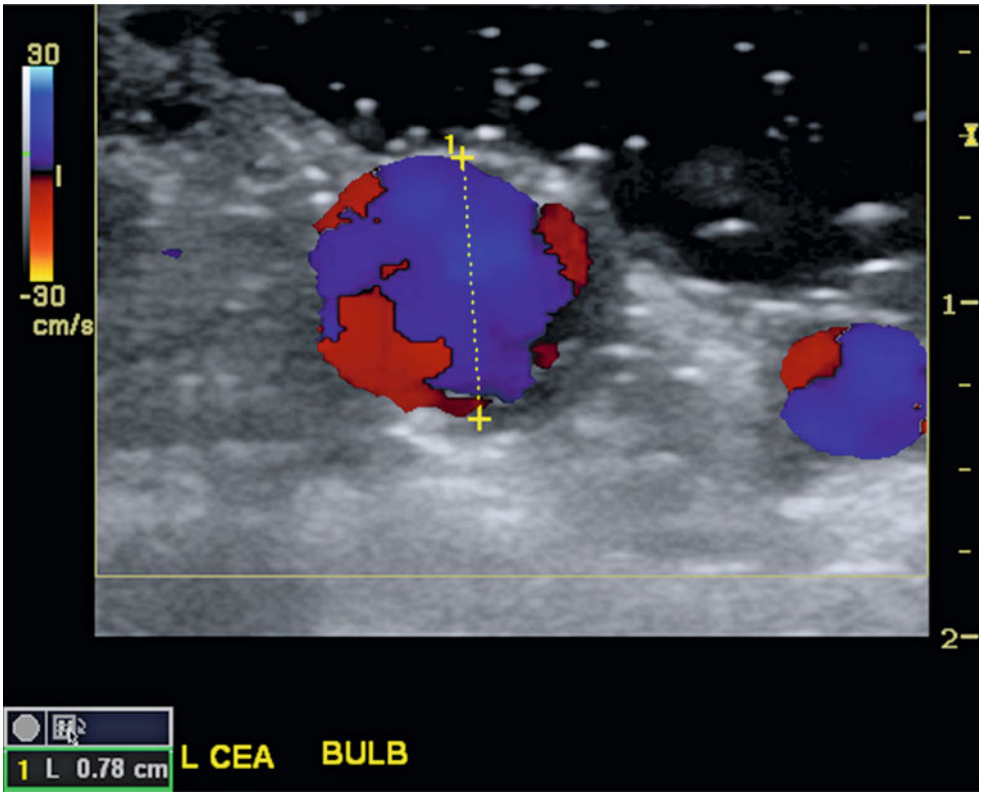


**Fig. 16.5** Transverse duplex scan image of reconstructed carotid bulb showing homogenous color flow, widely patent lumen, and a measured diameter of 0.78 cm

presence of distal plaque dissection since the endarterectomy of this vessel is accomplished using an eversion technique for plaque removal. Most surgeons will reexplore the ECA if occlusion or a focal high-grade stenosis is identified. The ICA should be scanned as far distal as possible especially if a shunt was inserted. When an anatomic defect (plaque edge, ICA suture narrowing, artery kink) is imaged, walking the sample volume through the region allows assessment of changes in PSV. Decision for repair is based on the altered hemodynamics produced by the imaged abnormality with lesions producing focal elevations of PSV > 150 cm/s considered for repair (Fig. 16.6). Spasm of the ICA is identified by a narrow lumen on color or power Doppler and moderate elevations of PSV in the range of 150–200 cm/s. The finding of lumen thrombus and PSV > 300 cm/s usually indicates platelet aggregation has developed, and reexploration is mandatory. Many vascular surgeons will perform angiography when the duplex imaging is abnormal to confirm an anatomic defect prior to proceeding with endarterectomy site reexploration.

On occasion, increased PSV ≥125–150 cm/s with minimal spectral broadening and normal artery imaging can be the result of vasospasm or compensatory collateral flow due to contralateral ICA occlusion. The presence of high diastolic flow in the ICA, i.e., more than 50% of the PSV, may indicate hyperperfusion syndrome with loss of normal intracranial arterial autoregulation. Appropriate therapy for this condition may include meticulous blood pressure control, steroids, and antiseizure drug administration.

The prevalence of endarterectomy site repair based on duplex testing is approximately 5% for CCA and ICA defects (Table 16.1), and additional 3–5% if correction of ECA stenosis/occlusion is included. If the endarterectomy site has normal duplex imaging and velocity spectra findings, the likelihood repair site thrombosis is extremely low (<1%), as is the detection of >50% DR stenosis within 3 months of the procedure. A 2011 report from the Vascular Study Group of New England indicated only one-half of vascular surgeons routinely image carotid repairs with duplex ultrasound being the preferred technique [7]. Routine imaging was not associated with a reduction in operative strokes, but the incidence of restenosis was significantly less.

## Carotid Stent-Angioplasty IVUS Scanning Protocol and Test Interpretation

The high-resolution (0.1 mm) vessel imaging achieved by the 20-MHz IVUS catheter imaging system has been shown to improve clinical outcomes when used to assess the technical result of peripheral angioplasty procedures [12]. IVUS imaging is used in combination with digital fluoroscopy to monitor the carotid artery stent-angioplasty procedure, specifically to select the diameter stent/balloon to deploy, and to interrogate the

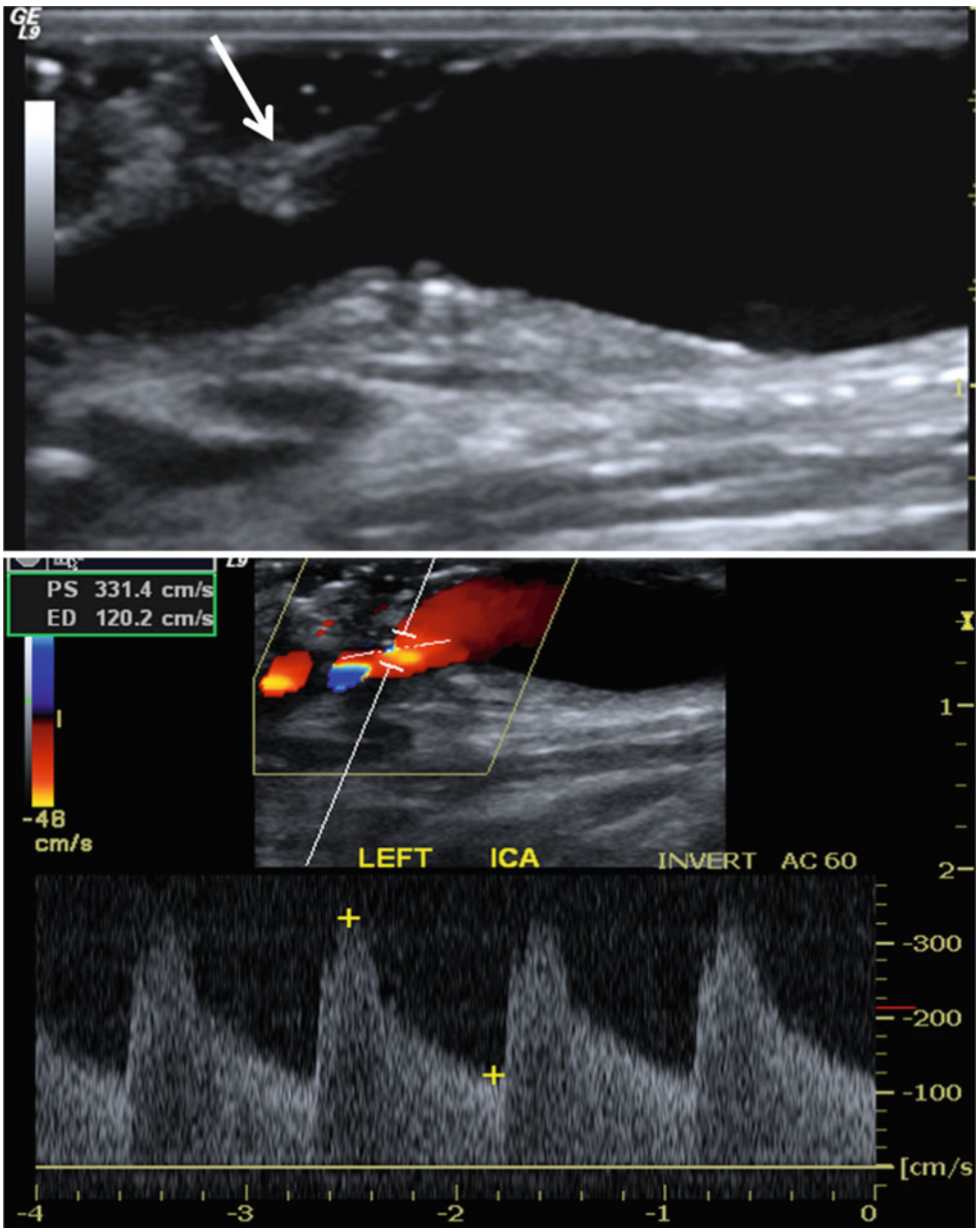


**Fig. 16.6** Abnormal duplex scan of carotid endarterectomy site after polyester patch angioplasty. Residual plaque (*arrow*) is present on anterior wall which narrows the ICA lumen producing elevated peak systolic velocity >300 cm/s with severe spectral broadening. Meets criteria for immediate reexploration

region of stent-angioplasty for residual stenosis. The goal of IVUS imaging is to confirm vessel patency, full stent deployment with an expanded lumen in the region of the atherosclerotic plaque, and no lumen anatomic abnormality [11–13].

The IVUS catheter is delivered to the extracranial carotid bifurcation over a 0.014″ Guidewire platform after a cerebral protection device is deployed in the distal ICA. The IVUS Eagle Eye® Platinum catheter (Volcano Corporation, San Diego, CA) provides both B-mode real-time imaging and a 360° color map imaging for confirmation of blood flow. These features allow confirmation of lumen patency and anatomic imaging to the stent and artery wall (Fig. 16.7). During a carotid stent-angioplasty procedure, IVUS imaging is used to aid the interventionist in estimating disease extent (stenosis length), selecting appropriate proximal and distal stent landing zones in normal or minimally diseased artery, and providing accurate vessel diameter measurements of the ICA and CCA for appropriate stent selection (Fig. 16.8). Following stent-angioplasty, reinsertion of the IVUS catheter pullback imaging alerts the interventionist to abnormalities of stent expansion, which if judged to be inadequate allows immediate endovascular treatment. The application of IVUS imaging during the stent-angioplasty procedure provides unique anatomic information for arterial repair using less contrast administration and angiogram runs without increasing morbidity or sacrificing technical accuracy.

The technical success of carotid stent-angioplasty is generally determined by multiplanar digital subtraction angiography with the goal to achieve <30% residual stenosis relative to the normal distal ICA diameter. Our vascular group

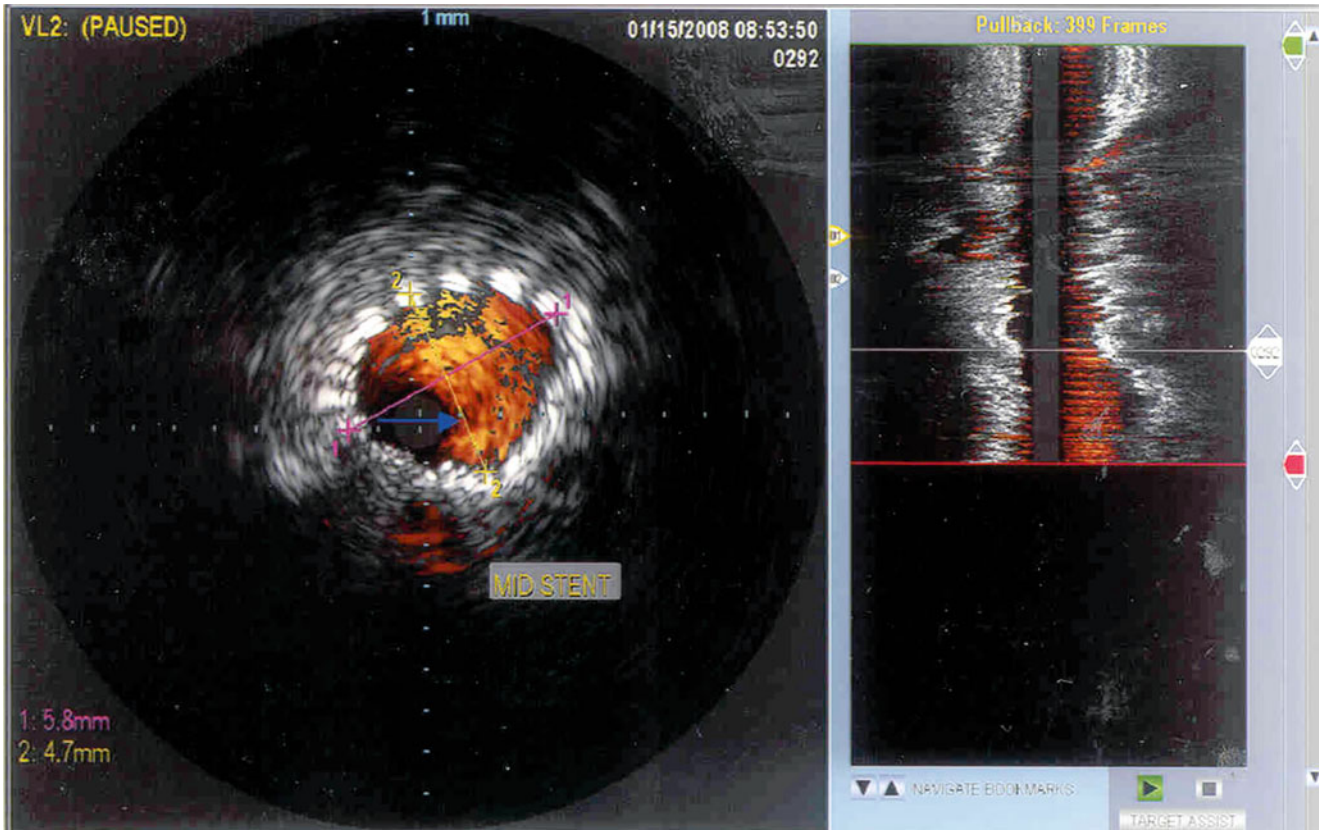


**Fig. 16.7** Intravascular ultrasound (IVUS) image of a stent deployed in the internal carotid artery. Pullback of IVUS catheter identified mild stent deformation compared to distal and proximal stented segments. Color flow indicates widely patent stent without lumen debris

adopted IVUS as a quality control assessment of "adequate" stent deployment and balloon angioplasty in treatment of internal carotid artery atherosclerotic occlusive disease, analogous to the use of intraoperative duplex testing during carotid endarterectomy [2, 10]. Following stent-angioplasty, real-time B-mode IVUS imaging is performed by positioning the IVUS catheter distal to stent in the normal ICA and slowly withdrawing the catheter through the stent visualizing changes in lumen diameter. This maneuver allows identification of regions of poor stent expansion with associated reduction in X-sectional area (Fig. 16.9). The degree of stent deformation may not be readily apparent by angiography. When IVUS confirms improper stent expansion, defined by an irregular or elliptical stent shape with a residual X-sectional area reduction of >30% compared to the distal stent, additional balloon angioplasty is performed typically upsizing the angioplasty balloon 0.5–1.0 mm from the previous size or performing a more prolonged (10 s) balloon angioplasty to expand the carotid bifurcation. Incomplete circular stent expansion after balloon angioplasty is typically caused by calcified carotid bifurcation plaque.

Our vascular group analyzed the anatomic and clinical outcomes of carotid stent-angioplasty with and without IVUS monitoring [11]. Retrospective review of a carotid stent registry data identified 220 consecutive CAS procedures (215 patients) performed with either digital C-arm fluoroscopy alone ($n=110$) or in conjunction with IVUS system ($n=110$). All carotid interventions were conducted with a cerebral protection device. The two groups were comparable for CAS indication, ICA stenosis severity, and atherosclerotic risk factors. All patients were enrolled in an outpatient surveillance program, which included clinical assessment for neurologic events, verification of antiplatelet therapy, and bilateral carotid duplex testing with interpretation according to previously published velocity spectra criteria for CAS procedures [14]. Duplex ultrasound testing was performed in the PACU, at approximately 1 month, every 6 months for 2 years, and then annually if <50% DR stenosis was present. An abnormal duplex finding of in-stent stenosis in the 50–75% DR category was based on color flow imaging of a stenosis, a peak systolic velocity (PSV) > 150 cm/s, and in-stent stenosis velocity ratio >2. The finding of a >75% DR in-stent stenosis (PSV > 300 cm/s in conjunction with EDV > 125 cm/s) prompted cerebral angiography and reintervention, if a >75% DR lesion, was confirmed.

No safety issues were encountered using IVUS catheter imaging prior to and following stent-angioplasty, and mean procedure times were similar with angio-alone CAS procedures. IVUS imaging altered procedural conduct by a lower ($p<0.05$) volume contrast agent injected due to fewer angiogram

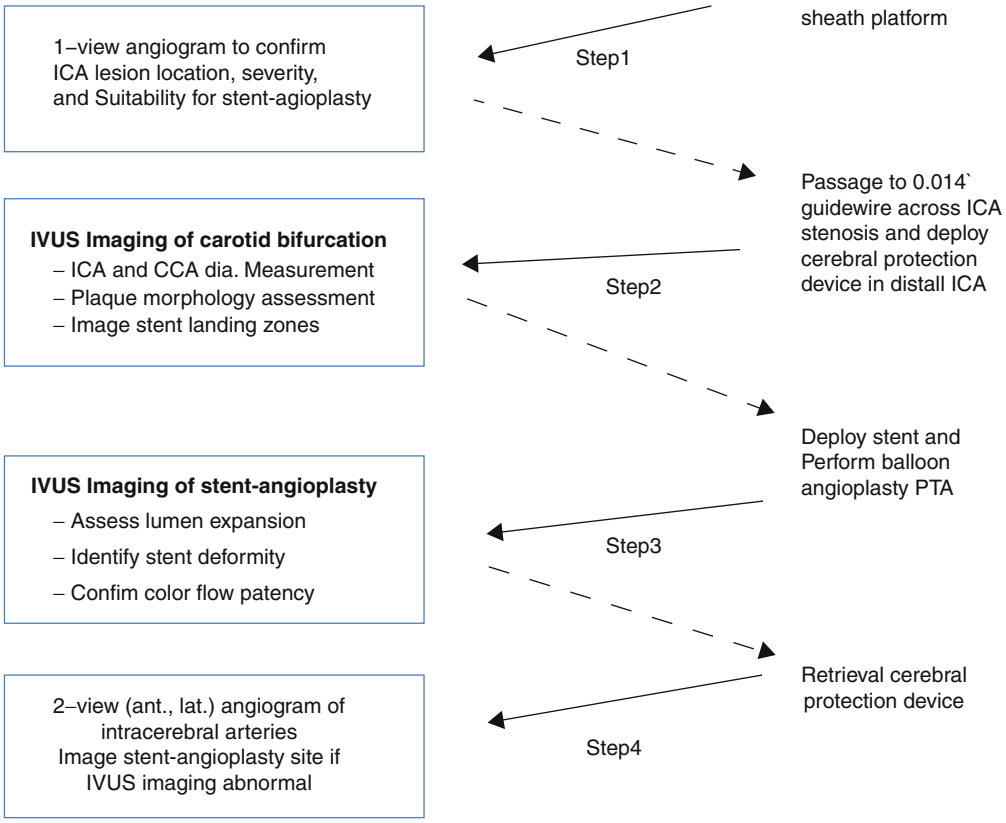


**Fig. 16.8** University of South Florida carotid stent-angioplasty procedure steps using angiography and IVUS imaging to assess technical success

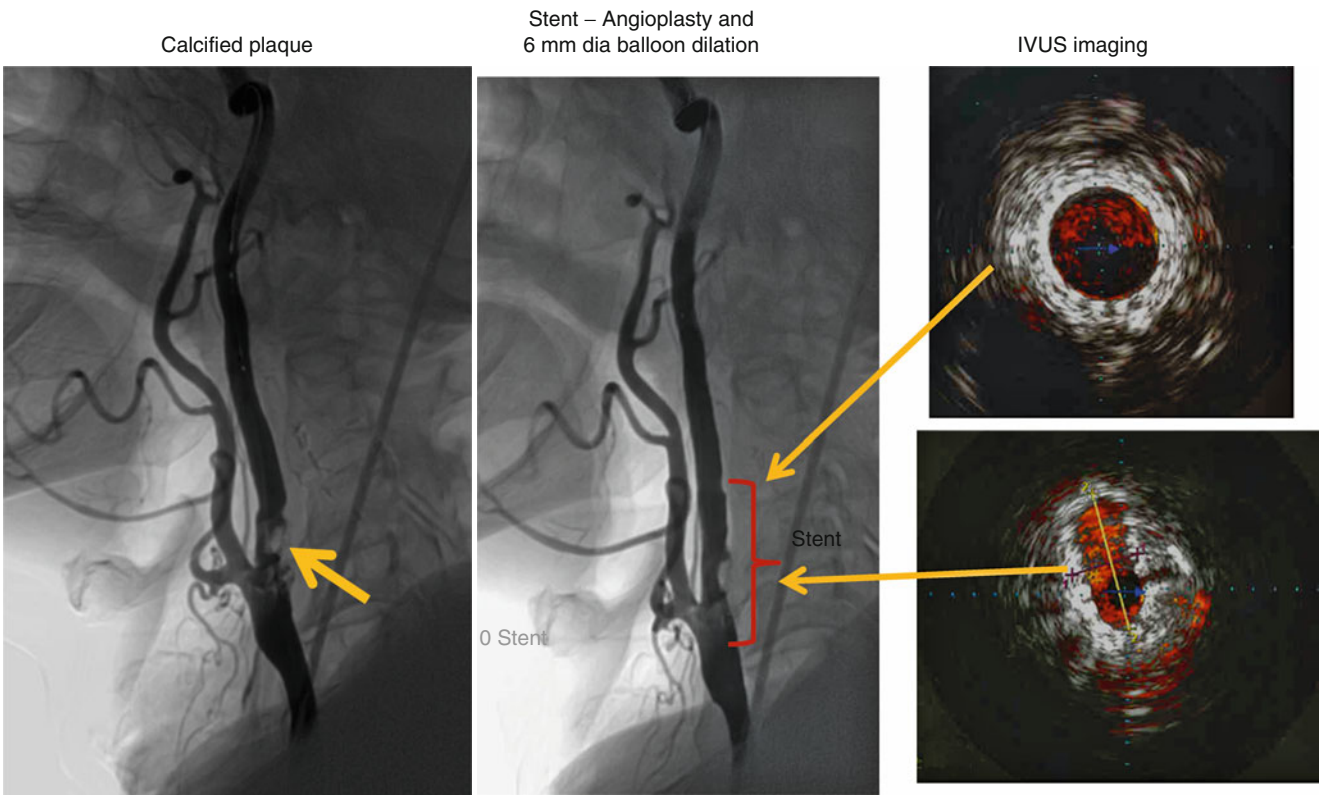


**Fig. 16.9** Angiographic images of a calcified ICA plaque (*arrow*) prior to and following stent-angioplasty. IVUS imaging shows circular stent deployment in distal ICA, but elliptical stent deformation at the plaque (*arrows*) with X-sectional area reduction. Additional 6-mm diameter balloon angioplasty was performed with improvement in lumen diameter

runs for stent sizing and verification of adequate stent deployment and the use of larger diameter angioplasty balloons (typically 6-mm diameter) for final stent-angioplasty based on assessment of residual in-stent lumen diameter and stent deformation by the atherosclerotic plaque. IVUS assessment identified more residual stent abnormalities requiring additional endovascular treatment ($n=12$, 11%) versus performing CAS using angiogram assessment alone ($n=2$, 1.8%). Duplex testing after carotid stenting demonstrated a low incidence of >50% residual (PSV > 150 cm/s) in IVUS monitored groups (7% vs. 18%; $p<0.01$). This difference persisted during patient surveillance with a higher lower freedom from >50% DR in-stent stenosis at 36 months in the angio+IVUS group (94%) than in angio-alone group (78%) indicating a more durable carotid intervention. Four (3.6%) angio-alone CAS sites developed >75% asymptomatic restenosis and underwent repeat balloon angioplasty with one later developing an asymptomatic thrombosis. In the angio+IVUS group, two neurologic events (1 stroke, 1 reperfusion injury) occurred within 30 days, while in the angio-alone treatment group, two patients who underwent CAS of symptomatic ICA stenosis developed a new neurologic event >30 days after the procedure (1 stroke, 1 TIA).

This experience using IVUS to assess the technical adequacy of CAS indicates the diseased carotid artery bifurcation can be safely imaged, and the detailed anatomic information afforded by this diagnostic technique is useful for the evaluation of suitable stent landing zones, selection of an appropriate stent size and angioplasty balloon, and confirmation that appropriate artery wall dilation with stent-wall apposition has been achieved and a severe residual stent deformity is not present. The addition of IVUS imaging to CAS procedure did not increase procedure time or produce an adverse event. We believe the information provided by IVUS resulted in more frequent intraprocedural reinterventions and the use of larger diameter angioplasty balloons and contributed to improved long-term outcomes documented by duplex surveillance with less severe in-stent stenosis (based on maximum PSV values) and reinterventions in the angio+IVUS treatment group. This experience supports our previous recommendation regarding duplex interpretation criteria for grading carotid stent stenosis in that a PSV > 150 cm/s is an abnormal threshold value and correlates with a functional residual stenosis associated with an increased likelihood of progressive in-stent stenosis [14, 15].

## Summary

The application of intraprocedural ultrasound to confirm technical adequacy of open and endovascular interventions is an appropriate quality measure associated with excellent patient and procedure outcomes. The time and expense associated with routine assessment is rewarded by improvement in technical precision of the carotid repair and does not add to procedure morbidity. Ultrasound assessment does require skills in duplex scanning and ultrasound image interpretation, but vascular surgeons treating carotid occlusive disease have the necessary expertise interpretation but need to acquire hands-on training in intraoperative duplex scanning to have confidence in the testing accuracy. Data indicate that vascular surgeons who routinely perform completion imaging studies have lower procedure morbidity and restenosis rates.

## References


1. Kinney EV, Seabrook GR, Kinney LY, Bandyk DF, Towne JB. The importance of intraoperative detection of residual flow abnormalities after carotid artery endarterectomy. J Vasc Surg. 1993;17:912–23.
2. Bandyk DF, Mills JL, Gahtan V, Esses GE. Intraoperative duplex scanning of arterial reconstructions: fate of repaired and unrepaired defects. J Vasc Surg. 1994;20:426–33.
3. Baker WH, Koustas G, Burke K, Littooy FN, Greisler HP. Intraoperative duplex scanning and late carotid artery stenosis. J Vasc Surg. 1994;19:829–33.
4. Papanicolaou G, Toms C, Yellin AE, Weaver FA. Relationship between intraoperative color-flow duplex findings and early restenosis after carotid endarterectomy: a preliminary report. J Vasc Surg. 1996;24:588–96.
5. Panneton JM, Berger MW, Lewis BD, Hallett Jr JW, Bower TC, Gloviczki P, et al. Intraoperative duplex ultrasound during carotid endarterectomy. Vasc Surg. 2001;35:1–9.
6. Ascher E, Marfkevich N, Kallakuri S, et al. Intraoperative carotid artery duplex scanning in a modern series of 650 consecutive primary endarterectomy procedure. J Vasc Surg. 2004;39:416–20.
7. Wallaert JB, Goodney PP, Vignati JJ, et al. Completion imaging after carotid endarterectomy in the Vascular Study Group of New England. J Vasc Surg. 2011;54(2):376–85.
8. Padayachee TS, Arnold JA, Thomas N, Aukett M, Colchester AC, Taylor PR. Correlation of intraoperative duplex findings during carotid endarterectomy with neurological events and recurrent stenosis at one year. Eur J Vasc Endovasc Surg. 2002;24:435–9.
9. Roth SM, Back MR, Bandyk DF, Avino AJ, Riley V, Johnson BL. A rational algorithm for duplex surveillance following carotid endarterectomy. J Vasc Surg. 1999;30:453–60.
10. Schanzer A, Hoel A, Owens CD, Wake N, Nguyen LL, Conte MS, et al. Restenosis after carotid endarterectomy performed with routine intraoperative duplex ultrasonography and arterial patch closure: a contemporary series. Vasc Endovascular Surg. 2007;41:200–5.
11. Bandyk DF, Armstrong PA. Use of intravascular ultrasound as a "quality control" technique during carotid stent angioplasty: are there risks to its use? J Cardiovasc Surg. 2009;50:727–33.
12. Timaran CH, Rosero EB, Martinez AE, et al. Atherosclerotic plaque composition assessed by virtual histology intravascular ultrasound and cerebral embolization after carotid stenting. J Vasc Surg. 2010;52:1188–95.
13. Joan MM, Moya BG, Austi FP, Vidal RG, Arjona YA, Alija MP, et al. Utility of intravascular ultrasound examination during carotid stenting. Ann Vasc Surg. 2009;23:606–11.
14. Armstrong PA, Bandyk DF, Johnson BL, Shames ML, Zwiebel BR, Back MR. Duplex scan surveillance after carotid angioplasty and stenting: a rational definition of stent stenosis. J Vasc Surg. 2007;46:460–6.
15. Aburahma AF, Abu-Halimah S, Bensenhaver J, Dean LS, Keiffer T, Emmett M, et al. Optimal carotid duplex velocity criteria for defining the severity of carotid in-stent restenosis. J Vasc Surg. 2008;48:589–94.

# Intima Media Thickness Measurement: Definition, Predictive Value on Cardiovascular Events, and Contribution to Cardiovascular Risk Evaluation

17

Pierre-Jean Touboul

**Abstract**

Atherosclerosis prevention and its progression has become an important goal in medicine. Atherosclerotic disease is a long and silently evolving disease and hardly reversible when clinical events occur. New biomarkers are useful if they can help in the early characterization of a population that is at intermediate risk in order to detect vascular risk phenotypes and improve their management. Ultrasonography of the carotid arteries is safe, inexpensive, and easy to perform, and it is a reliable and accurate method to detect early signs of increased thickness of the arterial wall or plaque occurrence. Intima media thickness of the carotid artery (CIMT) and plaque are recognized biomarkers which can improve our knowledge and practice in the field of cardiovascular disease evaluation and prevention.

From 1986 to nowadays, thousands of publications have demonstrated the potential of CIMT to anticipate coronary and stroke disease and to provide signals on cardiovascular risk factors by their significant association to hypertension, cholesterol, diabetes, and smoking.

If some recommendations are now published by American and European societies, and standardization of the method is ready for use in clinical practice, we need more data on reference values in different countries to address for clinical use the best accuracy for cardiovascular risk evaluation in individuals. Framingham score may be poor for a large group of patients at intermediate risk and some at low risk. The combination of Framingham score and IMT and/or plaque evaluation may increase the power to prevent myocardial infarction and stroke as demonstrated by recent studies; however, Framingham score only provides the cardiovascular risk at 10 years. This limit makes more difficult the comparison between a score and a biomarker.

**Keywords**

Carotid • Intima media thickness • Stroke • Myocardial infarction • Primary prevention

## Introduction

Atherosclerosis disease starts 20–30 years before the occurrence of clinical events. This vascular disease is a long and silently evolving disease, hardly reversible when clinical events occur. New imaging biomarkers are very useful, helping to early characterize the population at intermediate risk

P.-J. Touboul, M.D.
Department of Neurology and Stroke Center,
Bichat University Hospital and Medical School,
48 rue R Huchard, Paris 75018, France
e-mail: pjtw@noos.fr

A.F. AbuRahma, D.F. Bandyk (eds.), *Noninvasive Vascular Diagnosis*,
DOI 10.1007/978-1-4471-4005-4_17, 

and refine vascular risk phenotypes to improve management. Among x-ray, magnetic resonance, and ultrasound methods, intima media thickness (IMT) is indicated as one of the first modalities, as it is ethically acceptable, safe, reliable, and relatively inexpensive. These requirements are met by high-resolution B-mode imaging, which allow accurate measurements of this structure, with respect of the recommendations on image acquisition and appropriate methodology of the measurement. IMT is made of the two internal layers of the arterial wall: intima and media. The validation between the IMT measured on histologic specimens and ultrasound pattern was first described and validated in 1986 by Paolo Pignoli [1] and confirmed by later studies.

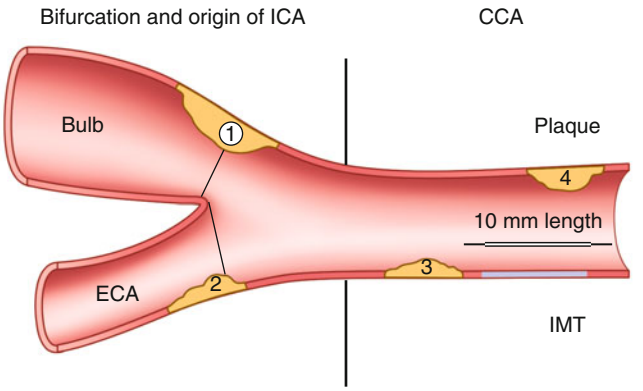


**Fig. 17.1** IMT measurement methodology. *CCA*, *ICA*, *ECA* common, internal, and external carotid artery

## Definition

One of the first main advances in IMT methodology was provided by the first international consensus organized during the 13th and 15th European Stroke Conferences, Mannheim, Germany, Carotid Intima Media Consensus (2004–2006) [2], followed in 2008 by the Consensus Statement of the American Society of Echocardiography [3], which strengthened the recommendations provided on IMT definition and measure.

*Intima media thickness* is defined as "a double-line pattern visualized by echotomography on both walls of the CCAs in a longitudinal image." It is formed by two parallel lines, which consist of the leading edges of two anatomical boundaries: the lumen-intima and media-adventitia interfaces. *Plaque* is a focal structure encroaching into the arterial lumen of at least 0.5 mm or 50% of the surrounding IMT value or demonstrates a thickness >1.5 mm as measured from the media-adventitia interface to the intima-lumen interface [2].

IMT measurement should be performed preferably on the far wall of the common carotid artery, 5–10 mm below the carotid bifurcation in a region free of plaque (Fig. 17.1). Near wall can also be measured; however, its correlation to anatomy was poor due to artifacts coming from the first wall-lumen interface.

## Criteria to Evaluate a New Risk Marker

The AHA published the principles to specifically address criteria for evaluation of new risk markers [4]. To be considered as useful for risk prediction, it should:

- Have an independent statistical association with risk after accounting for readily available and inexpensive risk markers. This association should be based on studies including large numbers of outcome events.
- Include calibration, discrimination, and reclassification index of the predictive model. Calibration addresses the prediction of the proportion of cases that will experience disease. It should display observed versus expected event rates across quartiles of predicted risk for models that do and do not include the new risk marker.

Discrimination addresses the ability to discriminate between the patients who are at higher risk compared with lower risk. The calculation of this parameter is performed by the C index, which is comparable to the area under the ROC curve.

Reclassification index evaluates the number of subjects reclassified into other risk categories based on models that include the new risk marker.

These principles allow a better understanding of the ability of a new biomarker to be included as a potential diagnostic test for clinical evaluation.

## IMT and Atherosclerosis

Baseline IMT is significantly correlated to plaque occurrence at the bifurcation. The prospective studies conducted in general populations [5], aiming at evaluating the plaque occurrence according to the baseline tertile of IMT, have shown that the rate of occurrence of new plaques was greater when the baseline IMT was in a higher tertile [6]. This is true in both sexes and shows that high IMT may predict evolving atherosclerosis. The correlation between IMT and asymptomatic coronary disease has also been demonstrated in coronary angiographic studies.

## Predictive Value on Cardiovascular Events

All studies evaluating the predictive value of IMT on myocardial infarction and stroke occurrence have shown that IMT was an independent and significant factor for myocardial infarction and stroke prediction. In the meta-analysis gathering 37,197 subjects, Lorenz et al. [7] found an overall estimate of the relative risk of myocardial infarction of 1.26

(95% CI, 1.21–1.30) per one standard deviation of common carotid artery IMT difference and 1.15 (95% CI, 1.12–1.17) per 0.10-mm common carotid artery IMT difference (CIMT). For stroke, the relative risks of stroke were 1.32 (95% CI, 1.27–1.38) per one standard deviation common carotid artery IMT difference and 1.18 (95% CI, 1.16–1.21) per 0.10-mm common carotid artery IMT difference. However, age distribution, site, and type of measurement were quite heterogeneous in these studies. The Cardiovascular Health Study has shown comparable results on an asymptomatic population of 65-year-old individuals with a mean follow-up of 6.2 years by comparing the rate of cardiovascular events between the fifth and the first quintile of IMT measured at baseline.

They concluded that carotid IMT was a strong predictor of future vascular events. The relative risk per IMT difference is slightly higher for the end point stroke than for myocardial infarction. In future IMT studies, ultrasound protocols should be aligned with published studies. Data for younger individuals are limited and more studies are required.

### IMT and Cardiovascular Risk Assessment

Age is the major component of Framingham Risk Score (FRS) and CIMT, but CIMT may add information on genetics; protective factors; time exposure to risk factors such as blood pressure, lipids, and smoking; and unknown risk factors. It finally provides individual vascular phenotype.

## ACC/AHA Recommendations Provided in 2010 Guidelines for Cardiovascular Risk Assessment

Coronary calcium scoring was evaluated as class IIa for intermediate risk (10–20% – 10-year risk) and class IIb for low to intermediate (6–20% – 10-year risk). Measurement of IMT class IIa for intermediate risk (10–20% – 10-year risk) (level B), flow mediated dilatation on brachial artery and arterial stiffness as class III (no benefit) [8].

Current risk evaluation is based on risk factors in NCEP-ATP III [9], including hypertension, low HDL, age (men > 45 years; women > 55 years), and family history of premature coronary health disease (first degree: <55 years male; <65 years female). Population having less than two risk factors is considered at low risk and over two risk factors as intermediate to high risk.

Khot et al. [10] published the prevalence of conventional risk factors in a population of 87,869 patients with coronary heart disease. They found a cumulated prevalence of 62.4% for the subjects with 0 or 1 risk factor, confirming that conventional score evaluation needed to be improved by complementary and independent markers of cardiovascular risk in asymptomatic populations. Some studies failed to demonstrate the added value of IMT on top of the Framingham or European score; however, they may have had a too low power explained by the low occurrence of clinical events in the general population and, hence, the noise created by "normal" population and by long-term design necessary for atherosclerosis studies.

In a recent study reported by Nambi et al. [11], the population of ARIC study, including 13,145 individuals followed for approximately 15 years, for incident hard coronary events and revascularization was analyzed. CIMT measurements, which included both IMT and carotid plaque, were incremental to traditional risk factors for prediction of incident cardiovascular events. In particular, among intermediate-risk patients (10–20%, 10-year estimated risk group), the addition of carotid IMT and plaque information led to clinical net reclassification improvement of approximately 9.9%.

Another study investigated the impact of subclinical cardiovascular disease derived from echocardiography and carotid ultrasonography on traditional coronary risk stratification using the FRS in a community-based, multiethnic population [12]. Ultrasonography was performed on 1,445 subjects (aged > 39 years; 40% men; 53% Hispanic, 20% white, 24% black) from the Northern Manhattan Study. Subclinical cardiovascular disease was defined as the presence of left ventricular hypertrophy and/or carotid plaque greater than the gender-specific 75th percentile of the left ventricular mass index and maximal carotid plaque thickness distribution. The prevalence of subclinical cardiovascular disease was examined in each FRS category (low, intermediate, and high risk). In subjects with low or intermediate FRSs, 35% had subclinical cardiovascular disease (low FRS 29%, intermediate FRS 42%). In the intermediate FRS category, subclinical cardiovascular disease was significantly more prevalent in women than in men (53% vs. 32%, $p<0.0001$) and in black and white subjects than in Hispanics (59% and 46% vs. 33%, $p<0.0001$ and $p=0.040$, respectively). In that study, the ultrasound assessment of subclinical cardiovascular disease may have helped to reclassify one-third of subjects with low or intermediate FRS into higher risk groups. In the intermediate FRS category, FRS appears to underestimate the coronary risk more in women than in men and more in whites, and especially in blacks, than in Hispanics.

Plaque is an obvious stage of established atherosclerosis, and all the studies which addressed concomitantly IMT and plaque have shown that having a plaque was more powerful for cardiovascular prediction than IMT alone.

For that reason, there is no need to measure IMT if a plaque is present on the carotid tree.

Having the methodology for CIMT measuring is not sufficient as far as we cannot provide to an individual his own cardiovascular risk profile. This requires reference values that depend on the age, ethnicity, sex, and country. These tables are already published with recent methodology in

some countries [13–16] but are lacking in a large number of developed countries. These data are needed to provide the 75th or 80th percentile in a "normal" population without any risk factors. Some authors propose to derive vascular age from tables of chronological age in the same population [17] and to recalculate the Framingham score with the vascular age; however, even though this seems an attractive process, data are lacking on prospective studies aimed at demonstrating its value with clinical outcomes.

### Conclusion

We are certainly entering into a new era where physicians will combine traditional risk factors with biological or structural biomarkers to improve cardiovascular risk assessment in individuals. More prospective studies are needed to refine this approach and to improve our efforts on targeting individuals with silent atherosclerosis disease to provide them with the most accurate medical care.

## References


1. Pignoli P, Tremoli E, Poli A, et al. Intimal plus medial thickness of the arterial wall: a direct measurement with ultrasound imaging. Circulation. 1986;74:1399–406.
2. Touboul PJ, Hennerici MG, Meairs S, et al. Mannheim carotid intima-media thickness consensus (2004–2006): an update on behalf of the advisory board of the 3rd and 4th watching the risk symposium, 13th and15th European stroke conferences, Mannheim, Germany, 2004, and Brussels, Belgium, 2006. Cerebrovasc Dis. 2007;23:75–80.
3. Stein JH, Korcarz CE, Hurst RT, Lonn E, Kendall CB, American Society of Echocardiography Carotid Intima-Media Thickness Task Force, et al. Use of carotid ultrasound to identify subclinical vascular disease and evaluate cardiovascular disease risk: a consensus statement from the American society of echocardiography carotid intima-media thickness task force. Endorsed by the Society for Vascular Medicine. J Am Soc Echocardiogr. 2008;21(2):93–111.
4. Hlatky MA, Greenland P, Arnett DK, et al. Criteria for evaluation of novel markers of cardiovascular risk: a scientific statement from the American Heart Association. Circulation. 2009;119:2408–16.
5. Zureik M, Ducimetiere P, Touboul PJ, et al. Common carotid intima-media thickness predicts occurrence of carotid atherosclerotic plaques: longitudinal results from the aging vascular study (EVA) study. Arterioscler Thromb Vasc Biol. 2000;20:1622–9.
6. von Sarnowski B, Lüdemann J, Völzke H, et al. Common carotid intima-media thickness and Framingham risk score predict incident carotid atherosclerotic plaque formation longitudinal results from the study of health in Pomerania. Stroke. 2010;41:2375–7.
7. Lorenz MW, Markus HS, Bots ML, et al. Prediction of clinical cardiovascular events with carotid intima-media thickness: a systematic review and meta-analysis. Circulation. 2007;115:459–67.
8. Greenland P, American College of Cardiology Foundation, American Heart Association, et al. 2010 ACCF/AHA guideline for assessment of cardiovascular risk in asymptomatic adults. J Am Coll Cardiol. 2010;56(25):e50–103.
9. National Cholesterol Education Program (NCEP) Expert Panel on Detection, Evaluation and Treatment of High Blood Cholesterol in Adults (Adult Treatment Panel III). Third report of the national cholesterol education program (NCEP) expert panel on detection, evaluation, and treatment of high blood cholesterol in adults (adult treatment panel III) final report. Circulation. 2002;106:3143–421. 22, 2007.
10. Khot UN, Khot MB, Bajzer CT, et al. Prevalence of conventional risk factors in patients with coronary heart disease. JAMA. 2003;290(7):898–904.
11. Nambi V, Chambless L, Folsom A, et al. Carotid intima-media thickness and the presence or absence of plaque improves prediction of coronary heart disease risk in the atherosclerosis risk in communities (ARIC) study. J Am Coll Cardiol. 2010;55:1600–7.
12. Abe Y, Rundek T, Sciacca RR, Jin Z, Sacco RL, Homma S, Di Tullio MR. Ultrasound assessment of subclinical cardiovascular disease in a community-based multiethnic population and comparison to the Framingham score. Am J Cardiol. 2006;98(10):1374–8. Epub 2006 Oct 5.
13. Touboul PJ, Labreuche J, Vicaut E, Belliard JP, Cohen S, Kownator S, Pithois-Merli I, Amarenco P, PARC Study Investigators. Country-based reference values and impact of cardiovascular risk factors on carotid intima-media thickness in a French population: the 'Paroi Artérielle et Risque Cardio-Vasculaire' (PARC) study. Cerebrovasc Dis. 2009;27(4):361–7.
14. Tosetto A, Prati P, Baracchini C, Manara R, Rodeghiero F. Age-adjusted reference limits for carotid intima-media thickness as better indicator of vascular risk: population-based estimates from the VITA project. J Thromb Haemost. 2005;3(6):1224–30.
15. Touboul PJ, Vicaut E, Labreuche J, Acevedo M, Torres V, Ramirez-Martinez J, Vinueza R, Silva H, Champagne B, Hernandez-Hernandez R, Wilson E, Schargrodsky H, CARMELA Study Investigators. Common carotid artery intima-media thickness: the cardiovascular risk factor multiple evaluation in Latin America (CARMELA) study results. Cerebrovasc Dis. 2009;27(4):361–7.
16. Howard G, Sharrett AR, Heiss G, et al. Carotid artery intimal-medial thickness distribution in general populations as evaluated by B-mode ultrasound. ARIC Investigators. Stroke (North Carolina). 1993;24(9):1297–304.
17. Stein J, et al. Vascular age integrating carotid intima media thickness measurement with global coronary risk assessment. Clin Cardiol. 2004;27:388–92.

# Errors and Artifacts of Carotid Ultrasound Evaluation

18

K. Wayne Johnston

**Abstract**

This chapter covers the errors than can be made in the ultrasound evaluation of carotid artery disease and suggests approaches to minimize them. The following are discussed: inter-technologist variability, inconsistent definition of percent stenosis or application of diagnostic criteria, incorrect angle of insonation, clinical situations affecting peak systolic velocity (PSV) measurements, sample volume not positioned at site of maximum stenosis to record PSV, confusing internal and external carotid arteries, lesion obscured by acoustic shadowing, patient factors, and other artifacts.

**Keywords**

Carotid • Errors • Doppler ultrasound

## Abbreviations

| | |
|---|---|
| CI | Confidence intervals |
| ECST | European carotid surgery trial |
| ECT | External carotid artery |
| EDV | End diastolic velocity |
| ICA | Internal carotid artery |
| NASCET | North american symptomatic carotid Endarterectomy Trial |
| PSV | Peak systolic velocity |

This chapter discusses some of the errors that can occur in performing a Doppler ultrasound study to evaluate the severity of extracranial carotid artery disease. Most of the errors seem to be attributable to the technologist. However, it is important to note that errors may be due to the inherent variability of the measurements; patient factors such as movement, obesity, or abnormal arteries (e.g., tortuous vessels); administrative factors such as inadequate training and education of the technologists or reading physicians; and inferior ultrasound equipment or machines that have not been configured appropriately for the examination.

## Variability of Measurements by Technologists and Between Technologists

Trained vascular laboratory technologists are required to make several subjective decisions when performing a carotid ultrasound study and consequently errors may occur, and there may be variability in measurements between technologists. Using a flow model, we observed that adjustment of Doppler angle, sample volume placement, and Doppler gain were the most significant sources of error and variability in the measurement of peak systolic velocity (PSV) [1]. Figure 18.1 illustrates the variability of PSV measurements

K.W. Johnston, M.D., FRCS(C)
Department of Vascular Surgery,
University of Toronto,
Toronto General Hospital,
200 Elizabeth Street, 6EN-210 Toronto, ON M5G 2C4, Canada
e-mail: wayne.johnston@utoronto.ca

A.F. AbuRahma, D.F. Bandyk (eds.), *Noninvasive Vascular Diagnosis*,
DOI 10.1007/978-1-4471-4005-4_18, 

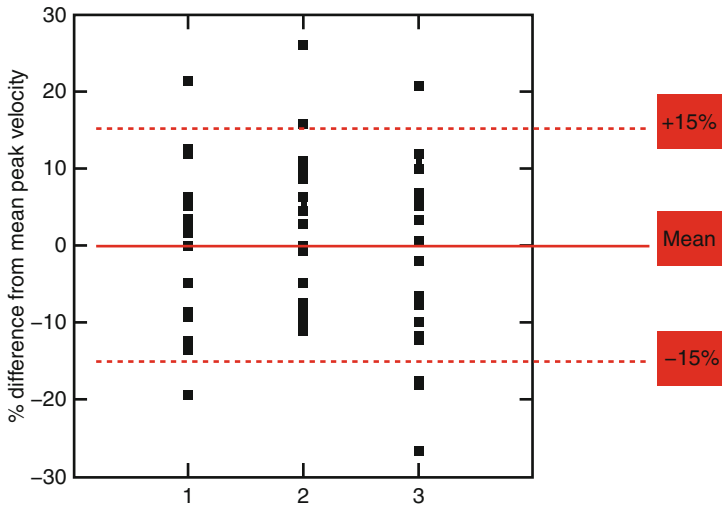


**Fig. 18.1** Variability of measurements of PSV by three ICAVL-accredited technologists from an in vitro flow model

by three trained ICAVL technologists in this controlled situation. Measurements vary from ±15% from the mean value.

In a clinical study, the interobserver variability of measurements of PSV from the internal carotid artery (ICA) by three experienced ICAVL-accredited vascular laboratory technologists was quite large [2]. For individual patients, variability of PSV measurements ranged from −25% to +35% of the average value. When we compared the three technologists, no systematic overestimation or underestimation of the ICA PSV was found. Although individual PSV measurements varied significantly, nonetheless, we noted that the severity of carotid stenosis can be reproducibly categorized into ranges (i.e., <50%, 50–70%, >70%).

## Variability of Diagnostic Velocity Criteria

Numerous studies have evaluated the ultrasound criteria for diagnosing the severity of carotid stenosis. There is variability between laboratories related to the method for defining the percentage stenosis, different machines, and differences in technique. The following is not meant to be a comprehensive review but rather a summary of a few key articles that address the variability in diagnostic criteria. They all defined percentage angiographic diameter stenosis using the NASCET criteria.

A consensus group was organized by the Society of Radiologists in Ultrasound and made the following recommendations[1] for the ultrasound diagnosis of carotid artery disease [3]. They determined that a PSV of ≥125–230 cm/s was consistent with ≥50–69% stenosis, and that a PSV > 230 cm/s was consistent with the diagnosis of ≥70–99% stenosis. Other parameters were considered to be helpful in certain situations where PSV may be inaccurate (e.g., the presence of contralateral high-grade stenosis or occlusion, discrepancy between visual assessment of the carotid plaque and the ICA PSV, low cardiac output, or hyperdynamic cardiac state). An EDV of ≥40 cm/s and an ICA/CCA PSV ratio of ≥2 were consistent with 50–69% stenosis, and an EDV of ≥100 cm/s and a ratio of ≥4 were consistent with 70–99% stenosis.

AbuRahma et al. [4] evaluated the accuracy of the consensus criteria and noted that an angiographic stenosis of 50–69% was detected with a sensitivity of 93%, specificity of 68%, and overall accuracy of 85% for a PSV of 125–230 cm/s. For

[1] First, all internal carotid artery (ICA) examinations should be performed with grayscale, color Doppler, and spectral Doppler US. Second, the degree of stenosis determined at grayscale and Doppler US should be stratified into the categories of normal (no stenosis), less than 50% stenosis, 50 to 69% stenosis, ≥70% stenosis to near occlusion, near occlusion, and total occlusion. Third, ICA peak systolic velocity (PSV) and the presence of plaque on grayscale and/or color Doppler images are primarily used in the diagnosis and grading of ICA stenosis. Two additional parameters (the ICA-to-common carotid artery PSV ratio and ICA end diastolic velocity) may also be used when clinical or technical factors raise concern that ICA PSV may not be representative of the extent of disease. Fourth, ICA should be diagnosed as normal when ICA PSV is less than 125 cm/second and no plaque or intimal thickening is visible, less than 50% stenosis when ICA PSV is less than 125 cm/second and plaque or intimal thickening is visible, 50 to 69% stenosis when ICA PSV is 125 to 230 cm/second and plaque is visible, ≥70% stenosis to near occlusion when ICA PSV is more than 230 cm/second and visible plaque and lumen narrowing are seen, near occlusion when there is a markedly narrowed lumen on color Doppler US, and total occlusion when there is no detectable patent lumen on grayscale US and no flow on spectral, power, and color Doppler US. Fifth, the final report should discuss velocity measurements and grayscale and color Doppler findings. Study limitations should be noted when they exist. The conclusion should state an estimated degree of ICA stenosis as reflected in these categories [3].

detecting a ≥70% stenosis, a PSV of >230 cm/s had a sensitivity of 99%, specificity of 86%, and overall accuracy of 95%. For detecting any grade of stenosis, ICA PSV was significantly better than end diastolic velocity (EDV) or ICA/CCA ratio. Adding the EDV values or the ratios to the PSV values did not improve accuracy. The accuracy of detecting a 50–69% stenosis was improved by using an ICA PSV of 140–230 cm/s rather than 125–230 cm/s.

Braun et al. also noted that when the consensus criteria were used in their patient population, the accuracy was similar to the consensus panel report. A cutoff of 230 cm/s was very accurate; however, a PSV ≥ 240 cm/s was slightly more accurate in their laboratory [5]. They agreed that other parameters (EDV, ICA/CCA PSV ratio, and ICA/CCA EDV ratio) only needed to be used in borderline situations.

Shaalan et al. concluded that a >50% stenosis was optimally detected with a PSV ≥ 155 cm/s and an ICA/CCA ratio of ≥2.0. For ≥80% stenosis, a PSV of ≥370 cm/s, an EDV of ≥140 cm/s, and an ICA/CCA ratio of ≥6 were equally reliable in the diagnosis [5, 6].

In a meta-analysis [7], an angiographic stenosis of ≥50% was identified with a peak systolic velocity ≥130 cm/s [sensitivity of 98% (95% confidence intervals [CI] of 97–100%) and specificity of 88% (95% CI, 76–100%)]. For the diagnosis of angiographic stenosis of ≥70%, a peak systolic velocity ≥200 cm/s has a sensitivity of 90% (95% CI, 84–94%) and a specificity of 94% (95% CI, 88–97%).

These diagnostic criteria provide an excellent guide to individual laboratories; however, in general, it is best practice to have an ongoing quality assurance program to verify the accuracy of the velocity criteria in your patient population and with your machines and ultrasound techniques.

## Clinical Situations Affecting PSV Measurements

### Contralateral Stenosis

Flow velocity can be increased because of a contralateral carotid stenosis; hence, velocity criteria may overestimate the severity of stenosis. This is particularly problematic when the contralateral artery is severely stenosed or occluded. Heijenbrok-Kal et al. normally use a PSV threshold of 230 cm/s for the diagnosis of 70–99% [8]. However, they found that accuracy was improved by using separate PSV velocities for ipsilateral and contralateral carotid arteries. Specifically, for diagnosing a 70–99% stenosis, the optimal PSV threshold for the ipsilateral artery was 280 cm/s, and for the contralateral artery, 370 cm/s. Severe contralateral carotid stenosis is a common cause of a false-positive test, i.e., reporting an ipsilateral carotid stenosis as severe when it is in fact less severe.

### Error After Previous Endarterectomy, Patch, or Stent

Patients who have previously had a carotid endarterectomy with or without patch angioplasty or a carotid stent may develop a recurrent stenosis. Current velocity criteria overestimate the severity of these stenoses after carotid endarterectomy with patch closure [9] or after carotid stenting [10, 11]. Higher velocity criteria need to be adopted.

### Very Severe Carotid Stenosis Versus Complete Occlusion

Peak systolic velocity increases as the severity of the stenosis increases. However, when the stenosis severity is very severe (95–99%), the velocity begins to fall. Preocclusive lesions are associated with only "trickle flow," and the velocity may be <40 cm/s [12].

A total occlusion is diagnosed when there is no detectable patent lumen on gray scale US and no flow on spectral, power, and color Doppler US [3]. Note that it can be very difficult to be certain if an artery is occluded or very severely stenosed with trickle flow even if all ultrasound modalities are used. Since the distinction can have major therapeutic implications, if the results of the ultrasound are uncertain, it is best to report that the artery is either very severely stenosed (trickle flow) or completely occluded.

### Gender

PSV velocity in women averages 10% higher than in men [13]. They showed that the optimal PSV for ≥60% stenosis was 160 cm/s for men and 180 cm/s for women, and for ≥70% stenosis was 185 cm/s for men and 202 cm/s for women. Although gender is not often considered in interpreting a carotid Doppler examination, this study indicates that gender potentially has important implications for patient care.

### Cardiac Output

PSV may be lower if the cardiac output is low or higher in hyperdynamic situations.

## Failure to Define Percentage Severity of Stenosis

There is disagreement on the definition of a percentage stenosis. Grading of the severity of a carotid stenosis is complex for several reasons. Although most express the severity

**Table 18.1** Comparison of NASCET and ECST measurements of percentage diameter stenosis

| NASCET (%) | ECST (%) |
|---|---|
| 30 | 65 |
| 40 | 70 |
| 50 | 75 |
| 60 | 80 |
| 70 | 85 |
| 80 | 91 |
| 90 | 97 |

Based on data from Donnan et al. [26]

of a stenosis as a percentage diameter reduction, some still consider the percentage area stenosis as most appropriate because the change in cross-sectional area in fact determines the increase in velocity.

In defining a stenosis based on diameter reduction, the numerator is the diameter at the site of the maximum carotid stenosis. The denominator has been defined differently in the two major randomized carotid surgery studies. The North American Symptomatic Carotid Endarterectomy Trial (NASCET) definition uses the diameter of the normal distal internal carotid artery as the denominator, whereas the European Carotid Surgery Trial (ECST) uses the estimated diameter of the bulb. Table 18.1 shows a comparison of percentage diameter stenosis calculated by the NASCET and ECST definitions.

In an audit of vascular laboratories in the United Kingdom, Walker and Naylor noted that 26% used the NASCET measurement method, 31% used the ECST method, and 43% did not know [14]. To overcome confusion caused by two grading systems, the NASCET definition is suggested.

## Angle of Insonation Incorrect

One drawback of Doppler-based blood velocity measurements is that the operator must manually specify the angle between the Doppler ultrasound beam and the artery. Using Doppler ultrasound, velocity is calculated from the following: (1) the frequency shift (i.e., the difference between the frequency transmitted by the ultrasound machine and the returned frequency which may be higher or lower if it is reflected by moving red blood cells), (2) the speed of the ultrasound in tissue, and (3) the angle between the ultrasound beam and the path of the red blood cells.

The technologist subjectively aligns the cursor of the sample volume in the center of the artery and parallel to the walls of the artery and at an angle of 60°. Although angles between 45 and 60° are considered satisfactory, the most consistent results are obtained with an angle of 60° – see below. In measuring the velocity, the largest source of error results from errors in accurately aligning the cursor of the sample volume.

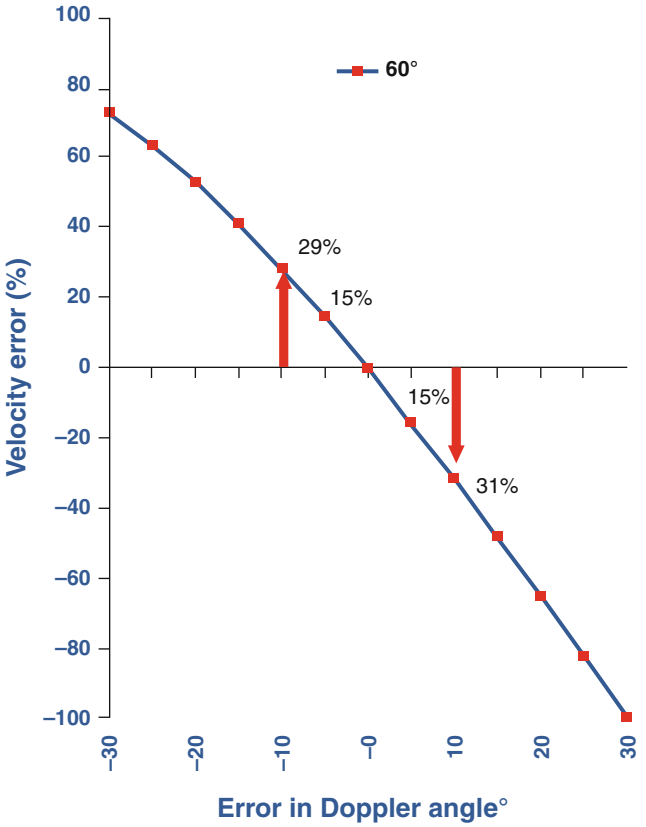


**Fig. 18.2** If the probe/vessel angle is assumed to be correctly positioned at 60°, this figure shows the percentage error in the measurement of the PSV if there is actually an error in setting the probe/vessel angle. If the angle is in fact 29°, the velocity will be 29% less than expected

## Technologist Incorrectly Aligns Cursor

It is quite easy to make a small error in aligning the cursor to be parallel to the artery walls and hence make an error in the measurement of the Doppler angle. Figure 18.2 shows the errors in the measurement of velocity based on errors in the beam/artery angle. Clearly, even quite small errors in angle measurement can result in significant errors in velocity measurement and consequently on evaluation of the severity of a stenosis. Figure 18.3 shows the PSV measurements that would be recorded if the probe/vessel angle is in error. Note that relatively small errors in the angle result in significant PSV measurements and errors in the interpretation of the severity of stenosis.

## Error from Different Angles 45–60

Beach et al. noted that angle-corrected Doppler velocity measurements were higher when higher Doppler examination angles were used [15]. Tola and Yurdakul compared the velocity measurement obtained at 60° and 45° insonation angles [16]. Even though the measurements were corrected

| | Probe/artery angle ERROR in degrees. Technologists thought angle was 60°. | Velocity measurements (cm/s) if correct velocity at 60° is ... | | | | | |
|---|---|---|---|---|---|---|---|
| | | 100 cm/s | 125 cm/s | 150 cm/s | 175 cm/s | 200 cm/s | 250 cm/s |
| | + 15° | 52 | 65 | 78 | 91 | 104 | 129 |
| | + 10° | 68 | 86 | 103 | 120 | 137 | 171 |
| | + 5° | 85 | 106 | 127 | 148 | 169 | 211 |
| Correct angle and correct velocity measurements | 0° | 100 | 125 | 150 | 170 | 200 | 250 |
| | –5° | 115 | 143 | 172 | 201 | 229 | 287 |
| | –10° | 129 | 161 | 193 | 225 | 257 | 321 |
| | –15° | 141 | 177 | 212 | 247 | 283 | 354 |
| | –20° | 153 | 192 | 230 | 268 | 306 | 386 |

**Fig. 18.3** PSV measurements may be in error if the probe/vessel angle is incorrectly evaluated. This figure shows the magnitude of the error for errors from +15° to −20° and for different velocity measurements. These errors may result in different interpretations of the severity of a stenosis

for the probe/vessel angle, measurements at 45° were about 24% lower than at 60°.

Transducers use multiple elements to form the beam, and consequently there are multiple angles to the flow axis. The angle of the middle part of the beam is used to calculate velocity. However, because of the multiple angles, there are a range of velocities (some lower and some higher than the calculated velocity). This geometric spectral broadening may result in an overestimation of the velocity.

To minimize this error, most recommend using a consistent angle of insonation, usually 60°. Although a smaller angle, for example, 45°, will result in smaller errors in velocity estimation, most use 60°. Most critically, it is important to use a consistent angle and validate the results in each vascular laboratory.

### Actual Flow Vector Is Not Parallel to Walls

In calculating velocity, the angle is that between the ultrasound beam and the axis of flow. However, this cannot be determined in a clinical situation, and consequently the sample volume is positioned so that it is parallel to the side walls of the artery on the assumption that the flow direction is parallel to the walls. However, it is important to note that the flow may not be parallel to the walls in certain circumstances, for example, in a tortuous, kinked, or coiled artery or beyond an asymmetrical stenosis. In these cases, it may be impossible to measure an accurate PSV.

### Beam and Sample Volume Positioned Close to the Ends of the Transducer

The most consistent measurements of PSV will be obtained with the beam and sample volume positioned in the center of the transducer rather than at the ends of the transducer. Multiple elements from the transducer are used to produce the beam, and the angle of insonation is calculated from the center of the beam. When the beam is positioned near the end of the transducer, fewer elements may be used to produce the beam than when the beam is positioned in the center of the image. With more active elements, the angle of some of the elements will be significantly greater than the mean angle used to calculate the PSV, and the measured velocity will be higher than obtained when fewer elements are used near the edge of the transducer. Using a consistent beam position along the transducer minimizes these errors.

## Sample Volume Is Positioned Incorrectly

### Peak Velocity Not at Stenosis

Positioning the Doppler sample volume in the throat of a stenosis is important in order to obtain accurate and reproducible measurements of PSV that can quantify the severity of the stenosis. We showed that the flow field is complex at and beyond a stenosis [17]. The peak frequency is maximum within the throat of the stenosis and returns to the prestenotic value within five tube diameters distal to the stenosis. Hence, reproducible peak velocity measurements are obtained only if the Doppler sample volume is positioned at or very near the throat of the stenosis. Figure 18.4 shows that the PSV is maximum in the throat of the stenosis and quickly falls distal to the stenosis. Figure 18.5 illustrates these observations in a clinical example.

The most reproducible recordings are made with the sample volume in the center of the vessel; however, if the stenosis is asymmetrical, the sample volume may need to be positioned off the center axis where the flow velocity is maximum.

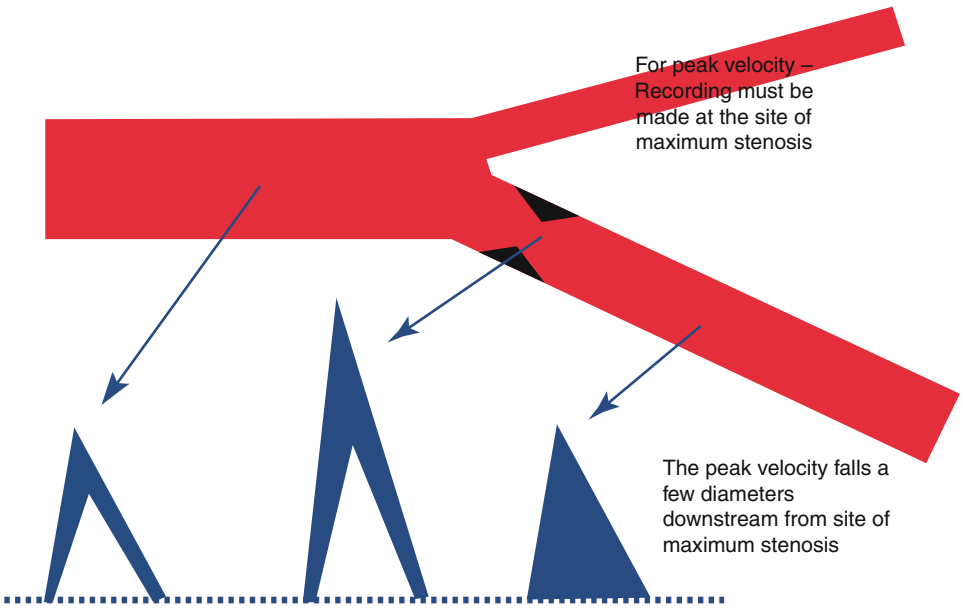


**Fig. 18.4** Diagram illustrating that the maximum PSV is measured in the throat of the stenosis, and distal to the stenosis, the PSV returns to normal within about five vessel diameters

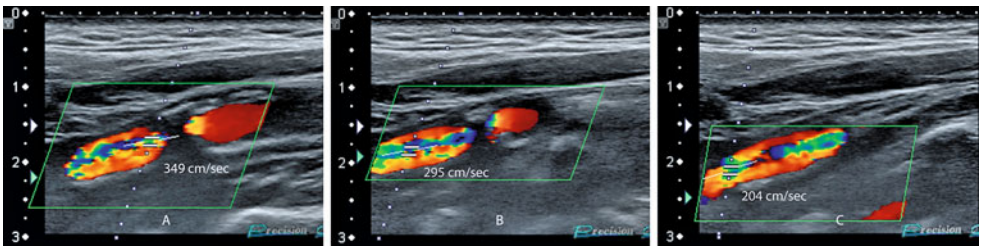


**Fig. 18.5** Clinical example illustrating that (**a**) the PSV is maximum at the stenosis and is lower beyond the stenosis (**b** and **c**)

## Confusing ICA and ECA

The ICA and the external carotid artery (ECA) are distinguished based on the following factors.

## Anatomical Location

The common carotid artery normally divides at the level of the hyoid bone, but the bifurcation may be higher or lower. The ICA is somewhat dilated at its origin (i.e., carotid bulb or sinus). It lies posterior to and lateral to the ECA. It does not have branches except in very rare cases. The ECA takes a more superficial and slightly curved course, passes upward and forward, and then inclines backward into the space behind the neck of the mandible.

On ultrasound, if the transducer is directed medially, the internal carotid artery is identified deep to the sternomastoid muscle, the jugular vein, and the external carotid artery.

## Branches

The ECA has branches, whereas the ICA does not have branches except in very rare cases (see below).

## Temporal Artery Tap

Although it is not a perfectly reliable test, if the temporal artery (a branch of the ECA) is tapped at the level of the zygomatic arch just anterior to the external ear and Doppler recordings are made from the ICA and ECA arteries, fluctuating signals corresponding to the taps are seen in the ECA Doppler recordings (Fig. 18.6), whereas the taps are less prominent or absent in the ICA [18]. When the oscillations are recorded only in one of the branches, it clearly identifies the ECA.

## Doppler Recordings

In normal cases, the ICA Doppler recordings show significant flow during diastole by comparison to the ECA which has higher resistance and has low flow velocity during diastole. When the ICA is stenosed or occluded, the ECA can provide collateral flow to the brain, and the morphology of the ECA recording can reflect low resistance flow and be confused with the morphology of the ICA waveform. Because the ECA has low flow during diastole, color Doppler recordings show a flicker or no flow in the ECA during diastole.

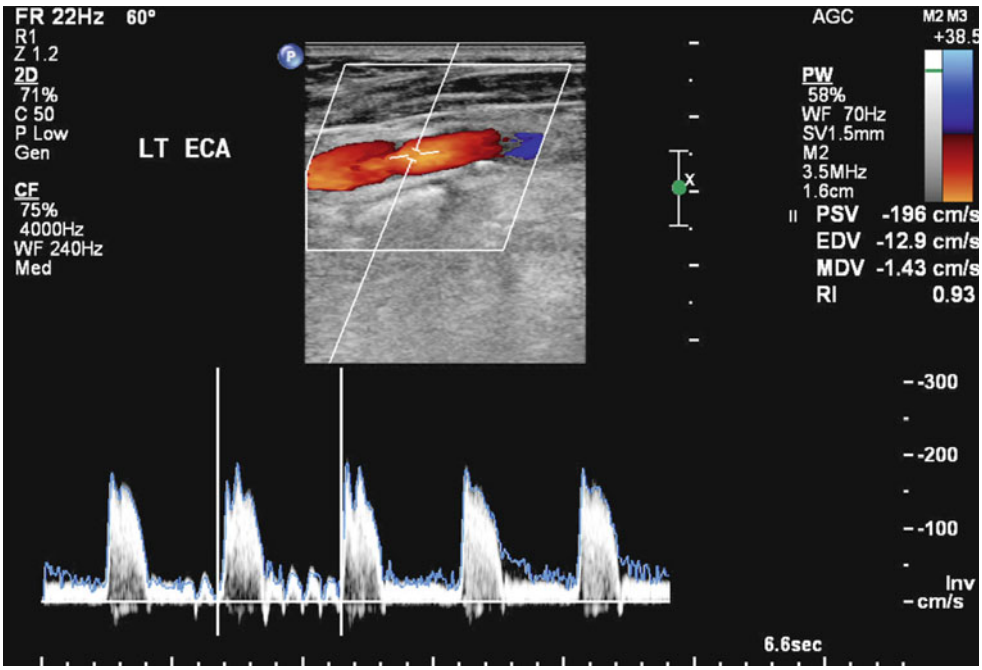


**Fig. 18.6** Temporal artery tap. Fluctuating signals are recorded from the ECA when the temporal artery is tapped

## Congenital Abnormalities

Carotid ultrasound studies may be difficult to interpret if there are abnormalities of the ICA including tortuosity, kinking, coiling, hypoplasia, aplasia, aberrant location, and anomalous branches that originate from the ICA such as the ascending pharyngeal or occipital arteries [19–21]. Very rarely, the common carotid artery may continue as the internal or external carotid without dividing, or the common carotid may be absent and the internal and/or external carotid arteries may originate from the aortic arch.

## Vessel Calcification and Shadowing Obscures Lesions

Acoustic shadowing causes diagnostic problems because it may be impossible to obtain an appropriate Doppler signal and record the maximum PSV from the site of the maximum stenosis (Fig. 18.7). Furthermore, shadowing prevents accurate qualitative evaluation of the morphology of a stenosis from the B-scan.

## Mirror Image Artifacts

Artifacts have been described that lead to diagnostic problems in evaluating the morphology of stenoses and plaques from the B-scan image. Mirror image artifacts are present when a tissue structure is reproduced at an incorrect location in the B-scan image. See Fig. 18.8.

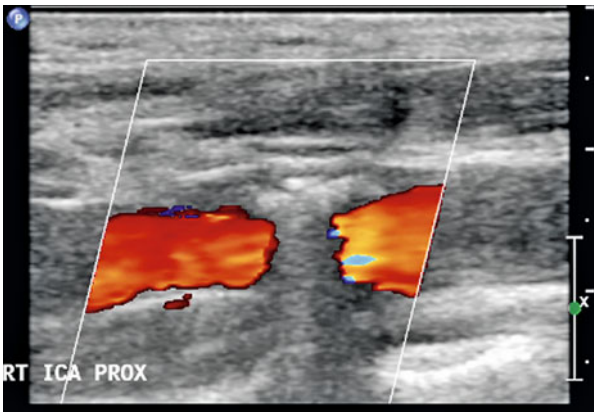


**Fig. 18.7** Acoustic shadowing obscures the severe stenosis and prevents recording of the PSV at the site of the maximum stenosis

The mechanism results when a structure has a strongly reflective interface. The ultrasound signal is reflected back toward the transducer from a tissue interface when there is a difference in the acoustic impedance between the two tissues. In the B-scan image or color flow image, an artifact can occur when the strongly reflecting surface is further reflected by other strongly reflecting surfaces (e.g., at the skin/gel interface or another strongly reflective tissue interface) and is then reproduced at an incorrect location in the B-scan image. The repeated image is always deeper than the real image and is less distinct.

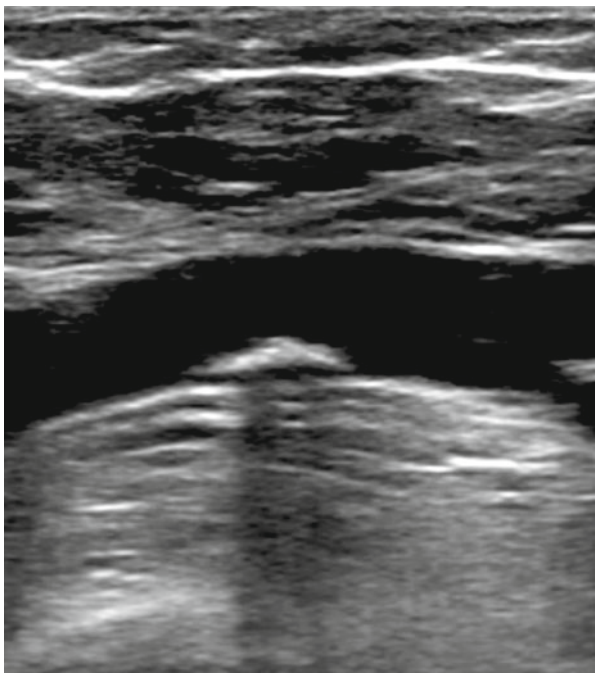

**Fig. 18.8** Mirror image artifacts. A strongly reflective layer in the back wall is reproduced several times deep to the original layer

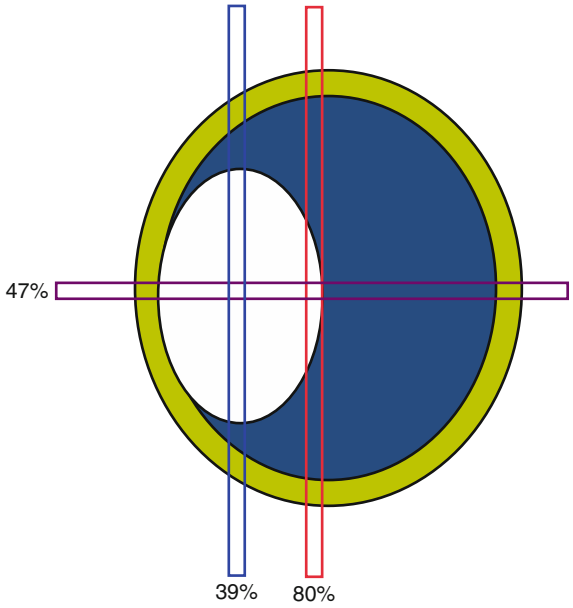


**Fig. 18.9** For this 75% area stenosis, the three lines indicate the percentage diameter stenosis that would be measured from different longitudinal views: 39%, 47%, and 80%

During carotid ultrasound evaluation, Arning et al. noted that mirror image artifacts were detectable in 2.5% of stenosed vessels and could result in misinterpretation of the plaque morphology [22]. Mirror image artifacts were detectable in stenosed vessels when there were strongly reflecting plaques on the vessel wall distant to the transducer head that were insonated obliquely. The artifacts were noted in regions that were hypoechoic or anechoic on B-mode scans. The artifact appeared in both the longitudinal and the transverse projections and also occurred in the power Doppler and in pulsed Doppler modes.

Mirror image artifacts can mimic ulceration in plaques or simulate flow when the artery is actually occluded. However, with experience, most of these artifacts can be recognized and should not affect diagnostic accuracy.

## Refraction

Refraction occurs when an ultrasound beam passes through a boundary between two tissues that have different propagation speeds. This may result in misregistration of both the image and the Doppler sample volume.

## Errors Due to Automated Measurement

It is usually convenient to use automated measurements to record PSV and other velocities. Although manual measurement may be more time-consuming, nonetheless, to prevent errors, manual measurement is important if the Doppler signal is weak or background noise is high (i.e., a poor signal to noise ratio) or if Doppler signals from other vessels overlap the carotid signal.

## Failure to Obtain Two Views of Stenosis

Carotid stenoses are often asymmetrical. Consequently, to evaluate the severity of a stenosis from the B-scan image, it is important to evaluate the stenoses with both longitudinal and transverse images. Figure 18.9 illustrates the diameter of a stenosis that can be measured from different longitudinal views of a stenosis. It stresses the importance of obtaining transverse views as well to confirm the severity of stenosis as assessed on the B-scan image.

## Patient Factors

In some patients, it is extremely difficult to obtain satisfactory recordings. If the patient is uncooperative and moves about during the study, satisfactory recordings may be impossible to obtain. The carotid arteries may be tortuous (Fig. 18.10), calcified, or congenitally abnormal. In an obese patient, resolution can be improved with a lower probe frequency.

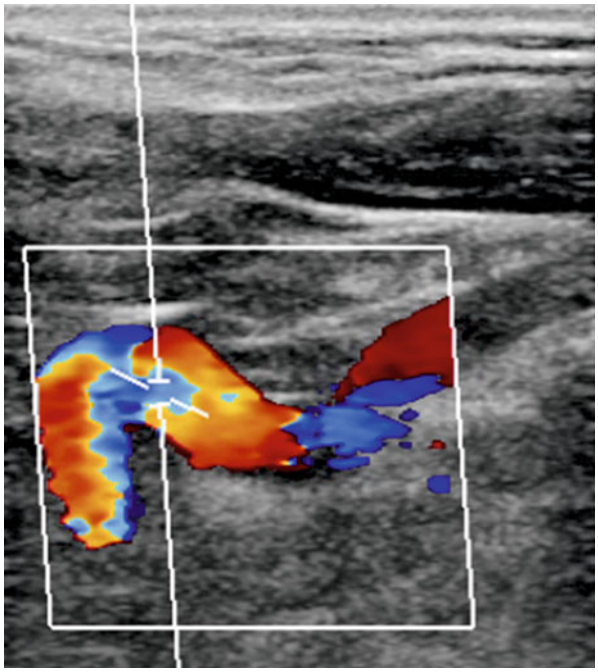

**Fig. 18.10** Tortuous ICA. Measurement of the correction probe/vessel angle may be problematic or impossible

## Other Diseases That May Be Confused with Atherosclerosis

Non-atherosclerotic acquired carotid artery lesions include trauma, false aneurysm, embolism, carotid body tumors, aneurysm, fibromuscular dysplasia, Takayasu's arteritis, and arteriovenous fistula. The following sections discuss some of these pathologies that may cause confusion with the more common carotid atherosclerotic occlusive disease.

### Dissection

Internal carotid artery dissection is an increasingly recognized cause of cerebrovascular events. The diagnosis is usually established based on characteristic clinical symptoms (e.g., pain, focal cerebral symptoms, and Horner's syndrome) and angiographic findings. However, in patients with ischemic cerebral symptoms, ultrasound is quite accurate in the hands of experienced laboratories [23]. The image may show a diffusely narrowed lumen, tapering of the artery, thickened wall perhaps with evidence of flow in the dissection channel or a flap, and absence of atherosclerosis. If the lesion cannot be visualized in the neck, Doppler recordings showing low-frequency alternating flow direction recordings may indicate that there is severe distal disease in the distal ICA [24].

### Fibromuscular Dysplasia

Fibromuscular dysplasia typically affects the medium and larger arteries including the renal and internal carotid arteries of young and middle-aged women. Patients may present with a transient ischemic attack or stroke. Fibromuscular dysplasia may be the basis for stenosis (including a string sign) or dissection and may result in aneurysmal dilatation.

### Takayasu's Disease

Takayasu's arteritis is an inflammation of the aorta and its major branches that may result in arterial narrowing or rarely aneurysm formation. MR angiography or CT angiography is required to evaluate the intrathoracic arteries. Ultrasound can detect arterial wall thickening, stenosis, or aneurysm formation in the carotid and subclavian arteries and may be helpful in detecting minor arterial wall thickening at an early stage (Fig. 18.11). It is useful for distinguishing Takayasu's disease from atherosclerotic disease [25].

**Conclusion**

This chapter reviewed the causes of errors in the ultrasound evaluation of the severity of carotid artery

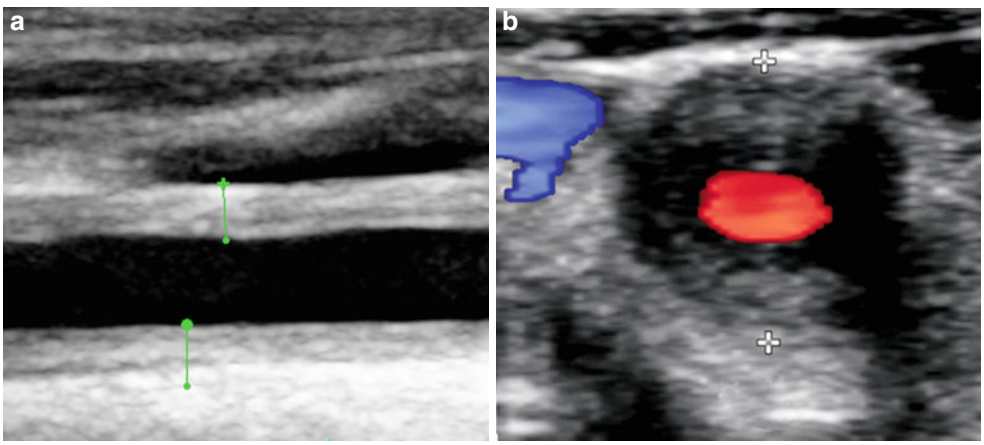


**Fig. 18.11** Takayasu's arteritis showing thickening of the wall and narrowing of the lumen. (**a**) Longitudinal view. (**b**) Transverse view

disease. Errors may be related to the technologist's technique, patient factors, equipment problems, and/or failure to follow appropriate administrative protocols. In minimizing errors in interpretation, it is important to remember that the certainty of the ultrasound diagnosis is increased if data from all modalities is included (i.e., velocity measurements, color Doppler, and B-scan). If all measurements from all three modalities agree, then the likelihood of a correct diagnosis increases. If there is no agreement between the different ultrasound methods, then the accuracy of diagnosis is low and the report should reflect this uncertainty.

## References


1. Lui EY, Steinman AH, Cobbold RS, Johnston KW. Human factors as a source of error in peak Doppler velocity measurement. J Vasc Surg. 2005;42:972–9.
2. Corriveau MM, Johnston KW. Interobserver variability of carotid Doppler peak velocity measurements among technologists in an ICAVL-accredited vascular laboratory. J Vasc Surg. 2004;39:735–41.
3. Grant EG, Benson CB, Moneta GL, et al. Carotid artery stenosis: grayscale and Doppler ultrasound diagnosis–society of radiologists in ultrasound consensus conference. Ultrasound Q. 2003;19: 190–8.
4. AbuRahma AF, Srivastava M, Stone PA, et al. Critical appraisal of the carotid duplex consensus criteria in the diagnosis of carotid artery stenosis. J Vasc Surg. 2011;53:53–9.
5. Braun RM, Bertino RE, Milbrandt J, Bray M. Ultrasound imaging of carotid artery stenosis: application of the society of radiologists in ultrasound consensus criteria to a single institution clinical practice. Ultrasound Q. 2008;24:161–6.
6. Shaalan WE, Wahlgren CM, Desai T, Piano G, Skelly C, Bassiouny HS. Reappraisal of velocity criteria for carotid bulb/internal carotid artery stenosis utilizing high-resolution B-mode ultrasound validated with computed tomography angiography. J Vasc Surg. 2008; 48:104–12.
7. Jahromi AS, Cina CS, Liu Y, Clase CM. Sensitivity and specificity of color duplex ultrasound measurement in the estimation of internal carotid artery stenosis: a systematic review and meta-analysis. J Vasc Surg. 2005;41:962–72.
8. Heijenbrok-Kal MH, Nederkoorn PJ, Buskens E, van der Graaf Y, Hunink MG. Diagnostic performance of duplex ultrasound in patients suspected of carotid artery disease: the ipsilateral versus contralateral artery. Stroke. 2005;36:2105–9.
9. AbuRahma AF, Stone P, Deem S, Dean LS, Keiffer T, Deem E. Proposed duplex velocity criteria for carotid restenosis following carotid endarterectomy with patch closure. J Vasc Surg. 2009;50: 286–91.
10. AbuRahma AF, Abu-Halimah S, Bensenhaver J, et al. Optimal carotid duplex velocity criteria for defining the severity of carotid in-stent restenosis. J Vasc Surg. 2008;48:589–94.
11. Lal BK, Hobson RW, Tofighi B, Kapadia I, Cuadra S, Jamil Z. Duplex ultrasound velocity criteria for the stented carotid artery. J Vasc Surg. 2008;47:63–73.
12. Hood DB, Mattos MA, Mansour A, et al. Prospective evaluation of new duplex criteria to identify 70% internal carotid artery stenosis. J Vasc Surg. 1996;23:254–61.
13. Comerota AJ, Salles-Cunha SX, Daoud Y, Jones L, Beebe HG. Gender differences in blood velocities across carotid stenoses. J Vasc Surg. 2004;40:939–44.
14. Walker J, Naylor AR. Ultrasound based measurement of 'carotid stenosis >70 %': an audit of UK practice. Eur J Vasc Endovasc Surg. 2006;31:487–90.
15. Beach KW, Bergelin RO, Leotta DF, et al. Standardized ultrasound evaluation of carotid stenosis for clinical trials: university of Washington ultrasound reading center. Cardiovasc Ultrasound. 2010;8:39.
16. Tola M, Yurdakul M. Effect of Doppler angle in diagnosis of internal carotid artery stenosis. J Ultrasound Med. 2006;25: 1187–92.
17. Bascom PA, Johnston KW, Cobbold RS, Ojha M. Defining the limitations of measurements from Doppler spectral recordings. J Vasc Surg. 1996;24:34–44.
18. Kliewer MA, Freed KS, Hertzberg BS, et al. Temporal artery tap: usefulness and limitations in carotid sonography. Radiology. 1996; 201:481–4.
19. Luk YS, Man EM, Sy AN. Bilateral hypoplasia of the internal carotid arteries. Singapore Med J. 2010;51:e163–5.
20. Patel SB, Hashmi ZA, Smaroff GG, Cardone JC, Yoon PD. Congenital absence of the left internal carotid artery. Ann Vasc Surg. 2010;24:415.e9–11.
21. Pfeiffer J, Ridder GJ. A clinical classification system for aberrant internal carotid arteries. Laryngoscope. 2008;118:1931–6.
22. Arning C. Mirror image artifacts of color Doppler images causing misinterpretation in carotid artery stenoses. J Ultrasound Med. 1998;17:683–6.
23. Benninger DH, Georgiadis D, Gandjour J, Baumgartner RW. Accuracy of color duplex ultrasound diagnosis of spontaneous carotid dissection causing ischemia. Stroke. 2006;37:377–81.
24. Hennerici M, Steinke W, Rautenberg W. High-resistance Doppler flow pattern in extracranial carotid dissection. Arch Neurol. 1989; 46:670–2.
25. Kissin EY, Merkel PA. Diagnostic imaging in takayasu arteritis. Curr Opin Rheumatol. 2004;16:31–7.
26. Donnan GA, Davis SM, Chambers BR, Gates PC. Surgery for prevention of stroke. Lancet. 1998;351:1372–3.

# Clinical Implications of the Vascular Laboratory in the Diagnosis of Cerebrovascular Insufficiency

19

Ali F. AbuRahma

**Abstract**

Various noninvasive tests for the evaluation of cerebrovascular insufficiency have been described in previous chapters. Most forms of noninvasive testing pose less stress and less expense to the patient than angiography. While early forms of noninvasive testing depended on the presence of severe disease, the current techniques, especially carotid artery imaging, demonstrate the opposite characteristic. Carotid imaging is able to detect minimal disease that is not hemodynamically significant; in fact, overestimation of the degree of stenosis in these cases has been a consistent problem. Nevertheless, any test intended for screening must have a high degree of sensitivity to be used appropriately in the initial assessment of disease. Noninvasive assessment, therefore, combines low risk, low cost, and high sensitivity.

Although we agree that patients should be evaluated by careful history and physical examination, our policy tends to rely on noninvasive vascular testing as an initial step in the diagnosis of carotid artery disease. The results of noninvasive tests may also help in obtaining optimal angiograms. An example is the patient with noninvasive evidence of severe stenosis who has no significant stenosis demonstrated in standard views of the carotid artery bifurcation. The results of the noninvasive tests indicate the need for additional projections, and if the bifurcation region does not show the expected lesion, there is a strong indication for obtaining adequate siphon views. This chapter will summarize the clinical implications of the vascular laboratory in the diagnosis of cerebrovascular insufficiency including the role of magnetic resonance angiography, computed tomography angiography, color duplex ultrasound, and catheter-based digital subtraction arteriography, in single or combination, asymptomatic carotid bruit, management of patients with TIA, intraoperative duplex ultrasound assessment of carotid endarterectomy, and post-CEA stroke. It will also cover the value of duplex ultrasound after carotid endarterectomy, post-carotid artery stenting, diagnosis of temporal arteritis.

**Keywords**

Cerebrovascular insufficiency • Diagnosis • Noninvasive vascular testing

A.F. AbuRahma, M.D., RVT, RPVI
Department of Surgery, Robert C. Byrd Health Sciences Center,
West Virginia University,
3110 MacCorkle Ave SE, Charleston, WV 25304, USA

Charleston Area Medical Center,
Charleston, WV, USA
e-mail: ali.aburahma@camc.org

Various noninvasive tests for the evaluation of cerebrovascular insufficiency have been described in previous chapters. Most forms of noninvasive testing pose less stress and less expense to the patient than angiography. While early forms of noninvasive testing depended on the presence of severe disease, the current techniques, especially carotid artery imaging, demonstrate the opposite characteristic. Carotid imaging is able to detect minimal disease that is not hemodynamically

A.F. AbuRahma, D.F. Bandyk (eds.), *Noninvasive Vascular Diagnosis*,
DOI 10.1007/978-1-4471-4005-4_19, © Springer-Verlag London 2013

significant; in fact, overestimation of the degree of stenosis in these cases has been a consistent problem. Nevertheless, any test intended for screening must have a high degree of sensitivity to be used appropriately in the initial assessment of disease. Noninvasive assessment, therefore, combines low risk, low cost, and high sensitivity.

Although we agree that patients should be evaluated by careful history and physical examination, our policy tends to rely on noninvasive vascular testing as an initial step in the diagnosis of carotid artery disease. The results of noninvasive tests may also help in obtaining optimal angiograms. An example is the patient with noninvasive evidence of severe stenosis who has no significant stenosis demonstrated in standard views of the carotid artery bifurcation. The results of the noninvasive tests indicate the need for additional projections, and if the bifurcation region does not show the expected lesion, there is a strong indication for obtaining adequate siphon views.

Prior to the advent of digital techniques, standard angiograms were routinely used in the evaluation of patients with cerebral ischemic attacks in order to determine whether vascular reconstructive surgery was indicated. Standard angiography was of limited clinical value, particularly as a means of diagnostic screening in asymptomatic patients, because of prohibitive costs, poor patient acceptance, and the risk of arterial catheterization. As a result, noninvasive vascular tests became established as the preferred means of diagnostic screening in asymptomatic patients because they provided an objective method of determining the hemodynamic significance of carotid disease in a safe and relatively cost-efficient manner.

Recent studies have questioned the role of arteriography as the "gold standard" in the evaluation of carotid artery occlusive disease [1–5]. Contrast arteriography has also been noted to have a 1–4% incidence of neurologic complications with about a 1% incidence of stroke reported in the Asymptomatic Carotid Atherosclerosis Study (ACAS) [6]. Other complications of arteriography that were reported include complications at the arterial puncture site (5%) and contrast-induced renal dysfunctions in 1–5%. With this in mind, it would be beneficial and cost-effective if these patients could be safely evaluated without invasive arteriography. Color duplex ultrasonography of the carotid arteries, computed tomography angiography, and magnetic resonance angiography are noninvasive/minimally invasive modalities that can detect and grade carotid artery stenosis. The role of each modality in the diagnosis of carotid artery disease is discussed in detail in Chap. 15.

## Asymptomatic Carotid Bruit

Carotid bruits may be helpful in detecting carotid artery stenosis. Carotid bruits must be differentiated from venous hums which are found in one-fourth of young adults or cardiac murmurs [7]. The venous hum typically increases in quality with the neck turned away from the auscultated side and often disappears with Valsalva maneuver or when patient lies down. Meanwhile, there is no definitive way to differentiate a radiated cardiac murmur or bruit originating from intrathoracic vessels from a cervical carotid bruit; however, cardiac murmurs are more frequently bilateral and more audible in the chest and lower neck than in the mid to upper neck [8, 9]. Patients on dialysis can also have cervical bruits that radiate into the neck secondary to arteriovenous fistula placement [10].

Fell et al. [11] reported on 100 patients with 165 asymptomatic carotid bruits. Duplex scanning showed a normal internal carotid artery in 12 cases (7%), <50% stenosis in 83 (50%), ≥50% stenosis in 61 (37%), and occlusion in 9 (6%). Thus, although the majority of neck bruits were associated with some degree of carotid stenosis, only 43% had ≥50% stenosis, which may justify further workup in selected patients.

Once a neck bruit is determined to be carotid in origin, the next stage is to determine whether this bruit is asymptomatic or symptomatic. This can be determined by the presence or absence of TIA symptoms or stroke as indicated earlier. It should be noted that symptoms referable to the contralateral carotid artery, even in the absence of bruit on that side, may prompt evaluation of patient for symptomatic carotid stenosis on the contralateral side. Carotid bruit may also be absent in patients with severe carotid stenosis in 20–35% of patients [12]. To be noted, a previously audible bruit may disappear if carotid stenosis progresses to severe/tight stenosis or occlusion. Carotid bruits can also originate from the external carotid artery or in patients with an occluded internal carotid artery because of increased blood flow in the external carotid artery.

Several studies have analyzed the significance of carotid bruits. In a subset analysis of the NASCET trial in which the presence of carotid bruits was compared with angiographic imaging of the carotid system, the presence of focal ipsilateral carotid bruits had a sensitivity of 63% and a specificity of 61% for high-grade carotid stenosis (70–99%), and the absence of a bruit did not significantly change the probability of significant stenosis in this group of patients (pretest 52%, posttest 40%) [13]. Ratchford et al. found in a diverse group of patients that the sensitivity of bruit auscultation was low at 56% with a specificity of 98% and a PPV of 25% and a NPV of 99% [14]. They concluded that prevalence of carotid bruits is low in the general population. Also, if bruit is heard in an asymptomatic patient, 25% will have a >60% stenosis; however, the ability to predict plaque by ultrasound was 89%.

The absolute risk of stroke is generally increased in the presence of carotid bruit. In population-based studies, the annual risk of stroke was 2.1% (95% confidence interval [CI], 0.6–8.5) for persons who had a carotid bruit versus

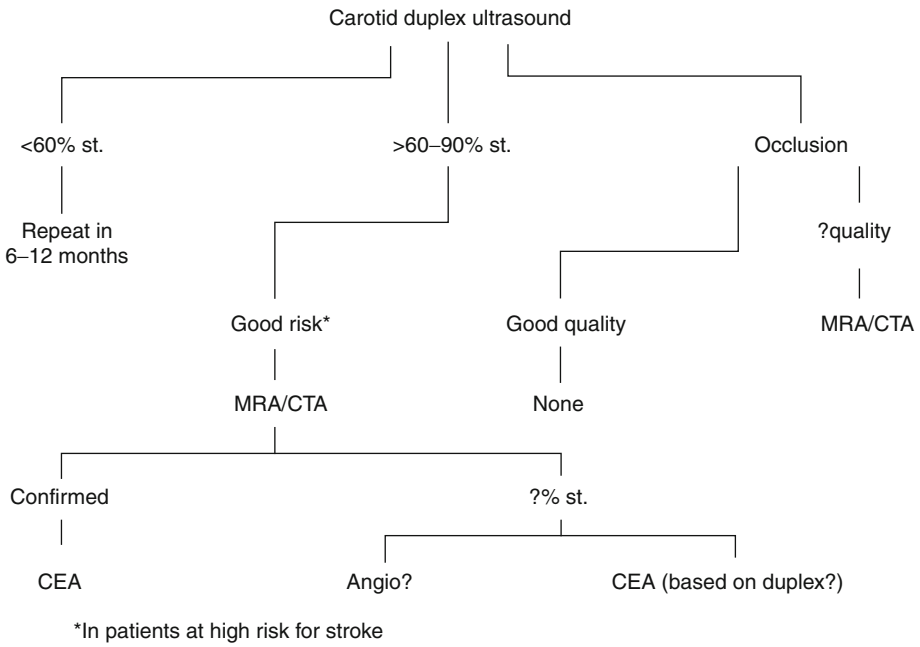


**Fig. 19.1** Management protocol for patients with asymptomatic carotid bruit or nonhemispheric symptoms. *MRA* magnetic resonance angiography, *CEA* carotid endarterectomy, *st*. stenosis

0.86% (95% CI, 0.8–0.9) for those who did not [15–17]. This represents an absolute risk increase for stroke of 1.24% a year and a relative risk for stroke of 2.4. The presence of a carotid bruit remained an independently significant variable, with a relative risk of 2.0, even after adjustment for various risk factors, including hypertension, age, and sex [15].

Carotid bruits have also been shown in meta-analysis to be a useful indicator of systemic atherosclerosis and a prognostic indicator of myocardial infarction and death [18]. MI and death occurred twice as often in patients with versus patients without carotid bruits [18].

With these facts in mind, and given the low absolute risk of stroke in patients with asymptomatic carotid bruits, and the low prevalence of surgically relevant significant carotid stenosis in these patients with a relatively small absolute benefit of CEA, most clinicians pursue further investigations only in patients who carry a high risk of carotid stenosis and stroke and who also carry a low operative risk for CEA [19, 20]. Further evaluation in these patients should only be done if the patients prefer to undergo carotid intervention, whether CEA or stenting, otherwise no further evaluation is indicated.

As indicated earlier, the ACAS study concluded that patients with ≥60% stenoses who were treated medically had a higher stroke rate over a 5-year period in comparison to patients who underwent a CEA. Figure 19.1 summarizes a practical approach in patients with asymptomatic carotid bruits or nonhemispheric symptoms. After the initial step of carotid DUS, if <60% stenosis was detected, it is recommended that the test be repeated in 6–12 months.

If stenosis of ≥60–99% was detected and the patient is a good risk, a magnetic resonance angiogram/CTA can be done to complement the findings of the ultrasound, and if confirmed, a CEA is recommended for patients at high risk for stroke. If the magnetic resonance angiogram/CTA was not conclusive or contradicted the ultrasound findings, then angiography may be considered in centers with a minimal stroke risk rate from angiography. However, in patients with a good quality carotid DUS, an endarterectomy may be considered based on ultrasound findings only. Several authorities would not recommend CEA in asymptomatic patients unless carotid stenosis exceeds 70–80%. In patients who had a good quality ultrasound showing total occlusion, no further follow-up is needed. However, if the quality of the ultrasound was limited, a magnetic resonance image/CTA is recommended to confirm occlusion.

Another indication for studying asymptomatic patients is to screen patients with advanced coronary artery disease or peripheral vascular diseases. Due to the diffuse nature of atherosclerosis, many of these patients have occult carotid bifurcation lesions with a resulting increased risk of stroke. This type of screening is carried out most often in patients who are being considered for cardiac or major peripheral arterial operations in order to detect carotid stenoses that may substantially increase the risk of intraoperative and postoperative stroke. Carotid screening is covered in depth in Chap. 12.

## Patients with Atypical or Nonhemispheric Symptoms

Patients with atypical or nonhemispheric symptoms often do not have a clear indication for angiography. Some of these patients' symptoms include dizziness, blackouts, bilateral visual disturbances, or bilateral motor or sensory

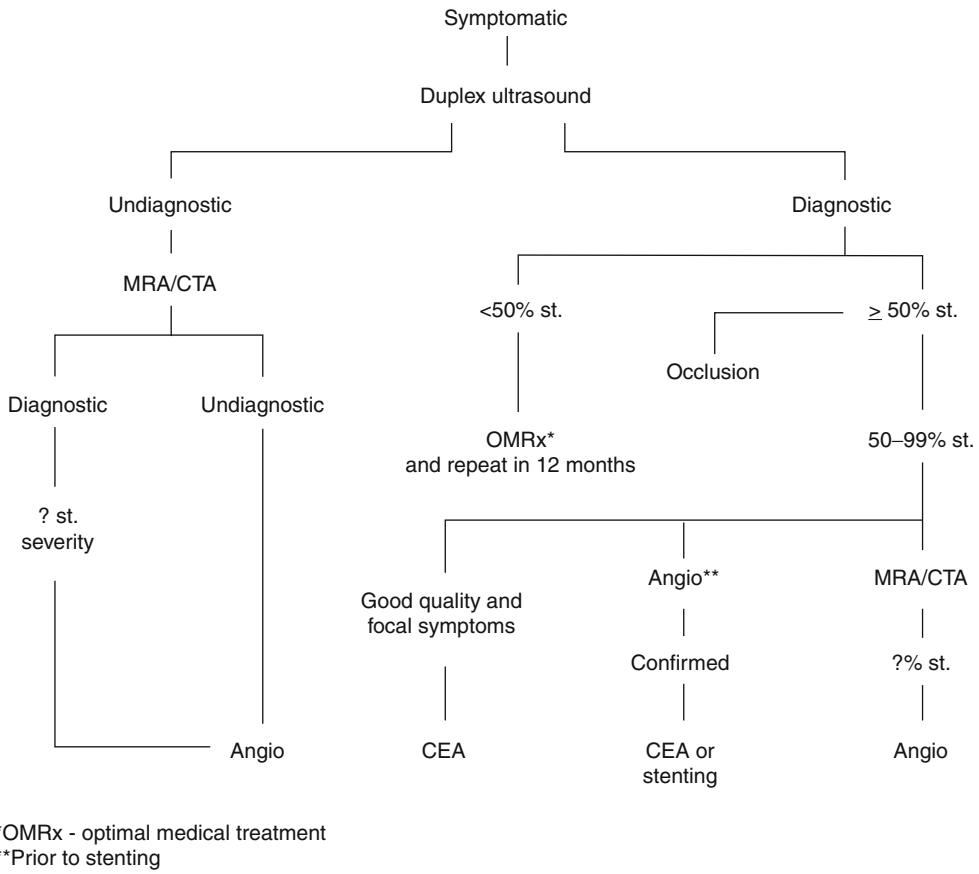


**Fig. 19.2** Management protocol for patients with suspected hemispheric symptoms (cerebrovascular disease). For <50% stenosis, repeat ultrasound in 12 months. *MRA* magnetic resonance angiography, *CEA* carotid endarterectomy, *OMRx* optimal medical treatment, *st*. stenosis

deficits. Since a variety of nonvascular causes, such as orthostatic hypotension, cardiac arrhythmias, and medications, may be responsible for these symptoms, noninvasive carotid testing is important in identifying these patients with hemodynamically significant carotid stenosis. Our management protocol for this group of patients is outlined in Fig. 19.1.

## Patients with Focal Neurologic Deficits (Transient Ischemic Attacks or Strokes)

A major proportion of transient ischemic attacks (TIAs) or permanent focal neurologic deficits in hemispheric distribution or with amaurosis fugax is caused by embolization from ulcerations and atheromatous plaques. Therefore, the purpose of carotid screening in patients with hemispheric neurologic symptoms is to identify lesions that could be the source of cerebral emboli or could reduce cerebral hemispheric blood flow. In the North American Symptomatic Carotid Endarterectomy Trial (NASCET) study [21], carotid endarterectomy was highly beneficial for patients with recent hemispheric TIAs or mild strokes and >70–99% and 50–69% stenoses of the ipsilateral internal carotid artery. Based on these results, patients with symptoms of severe stenoses of the carotid artery should be treated by CEA unless their medical condition makes the risk of surgery prohibitive. Our management protocol for this group of patients is outlined in Fig. 19.2. As noted in Fig. 19.2, the initial step is to obtain a color DUS, and if the study is diagnostic and shows <50% stenosis, the patient is treated medically (e.g., antiplatelet therapy, statins, and risk modifications and repeat color DUS in 12 months). If the stenosis is ≥50%, the ultrasound is of good quality, and the patient has classical focal hemispheric symptoms, a CEA can be done based on the carotid DUS findings alone; or MRA/CTA can be done to complement the ultrasound findings, and if the diagnosis is confirmed, surgery may be considered without angiography. Angiography is reserved for patients with a marginal quality DUS or magnetic resonance angiogram or in patients with contradictory magnetic resonance angiogram and DUS results. If the DUS shows total occlusion and the ultrasound was of good quality, no further workup is usually necessary. For patients with a DUS that is not diagnostic, magnetic resonance angiogram/CTA is done, and if it is diagnostic and the severity of stenosis is established, surgery can be done accordingly. If the MRA/CTA is not diagnostic, angiography is recommended.

**Table 19.1** Selected optimal criteria with best PPV (≥95%) and overall accuracy in detecting ≥60–99% and 70–99% ICA stenosis

| | PPV (%) | Overall accuracy (%) | Sensitivity (%) | Specificity (%) | NPV (%) |
|---|---|---|---|---|---|
| *Best PPV for ≥ 60% ICA stenosis* | | | | | |
| ICA PSV ≥ 220 cm/s | 96 | 82 | 64 | 98 | 76 |
| ICA EDV ≥ 80 cm/s | 96 | 87 | 79 | 97 | 84 |
| ICA/CCA PSV ratio ≥ 4.25 | 96 | 71 | 41 | 99 | 65 |
| ICA PSV and EDV 150 and 65* | 96 | 90 | 82 | 97 | 86 |
| *Best PPV for ≥ 70% ICA stenosis* | | | | | |
| ICA PSV ≥ 300 cm/s | 97 | 80 | 48 | 99 | 76 |
| ICA EDV ≥ 110 cm/s* | 100 | 91 | 75 | 100 | 87 |
| ICA/CCA PSV ≥ none | – | – | – | – | – |
| ICA PSV and EDV 150, 110* | 100 | 91 | 75 | 100 | 87 |

*These values have the best PPV and overall accuracy

**Table 19.2** Selected optimal criteria with best NPV (≥95%) and overall accuracy in detecting ≥60–99% and 70–99% ICA stenosis

| | NPV (%) | Overall accuracy (%) | Sensitivity (%) | Specificity (%) | PPV (%) |
|---|---|---|---|---|---|
| *Best NPV for ≥ 60% ICA stenosis* | | | | | |
| ICA PSV ≥ 135 cm/s[a] | 99 | 80 | 99 | 64 | 71 |
| ICA EDV – none | – | – | – | – | – |
| ICA/CCA PSV ratio ≥ 1.62 | 95 | 71 | 97 | 47 | 62 |
| ICA PSV and EDV – none | – | – | – | – | – |
| *Best NPV for ≥ 70% ICA stenosis* | | | | | |
| ICA PSV >150 cm/s[a] | 99 | 80 | 99 | 69 | 65 |
| ICA EDV ≥ 60 cm/s | 96 | 83 | 94 | 77 | 71 |
| ICA/CCA PSV ≥ none | – | – | – | – | – |
| ICA PSV and EDV – none | – | – | – | – | – |

[a]These values have the best NPV and overall accuracy

## Specific Duplex Criteria for Specific Clinical Situations

In choosing our criteria for peak systolic velocity and end diastolic velocity, we chose the values that gave the highest overall accuracy. However, which criteria to use should depend on the "outcome" desired by the clinician. Although some surgeons have advocated CEA based on duplex criteria alone [5, 22, 23], the decision to proceed with an arteriogram is based on the duplex findings in the majority of patients. The mortality and morbidity of arteriography vary from institution to institution, but can be significant [6, 24]. We propose that vascular laboratories at institutions with significant mortality and morbidity in relation to carotid arteriography use duplex criteria with 95% or greater PPV and the best overall accuracy in order to minimize the number of patients undergoing unnecessary arteriography (Table 19.1). These criteria can also be utilized when CEA is performed without preoperative arteriography. In those institutions where arteriography does not significantly add to the mortality and morbidity of the overall treatment of carotid disease, we suggest using the criteria described in Table 19.2. These criteria have the highest negative predictive value to ensure that only a minimum number of patients with equal to or greater than 60% or 70% stenoses are missed.

A duplex classification was proposed by us which would consist of lesions <30% stenosis, ≥30–49% stenosis, ≥50–59% stenosis, ≥60–69% stenosis, and ≥70% stenosis. This new duplex classification would fit into the existing trials [NASCET, ACAS, and Veteran's Administration Cooperative Study (VA)], and may be of benefit as new conclusions are released [25]. By reporting results using these criteria, the clinician will be better able to make decisions regarding the need for CEA or arteriogram based on the risks and benefits for individual patients. With the added risks of arteriography, decisions to operate would be better based on duplex findings alone. Having PPVs of 90–97% and accuracies of 87–93% can eliminate many unnecessary arteriograms. For those vascular laboratories who may be using the consensus duplex criteria, specific velocities can be used accordingly, as indicated in Chap. 7.

It is important to note that the data obtained by individual vascular laboratories will vary as a result of differences in equipment, abilities, and consistencies of vascular technicians and reader interpretations [25]. Therefore, each laboratory must adapt a method that employs the equipment they use and validate their method when using proposed new duplex criteria.

## Intraoperative Duplex Ultrasound Assessment of Carotid Endarterectomy

Intraoperative use of the B-mode ultrasound imaging system for completion evaluation of the CEA has been advocated by Sigel et al. [26] The development of smaller scanning heads and probes together with techniques of sterilization has made this application feasible. The ultrasound examination can be performed quickly and, unlike angiography, requires no delay for film processing. Nor is it necessary to inject contrast material. Angiography is also associated with the risks of subintimal injections, thromboembolic complications, and allergic reactions.

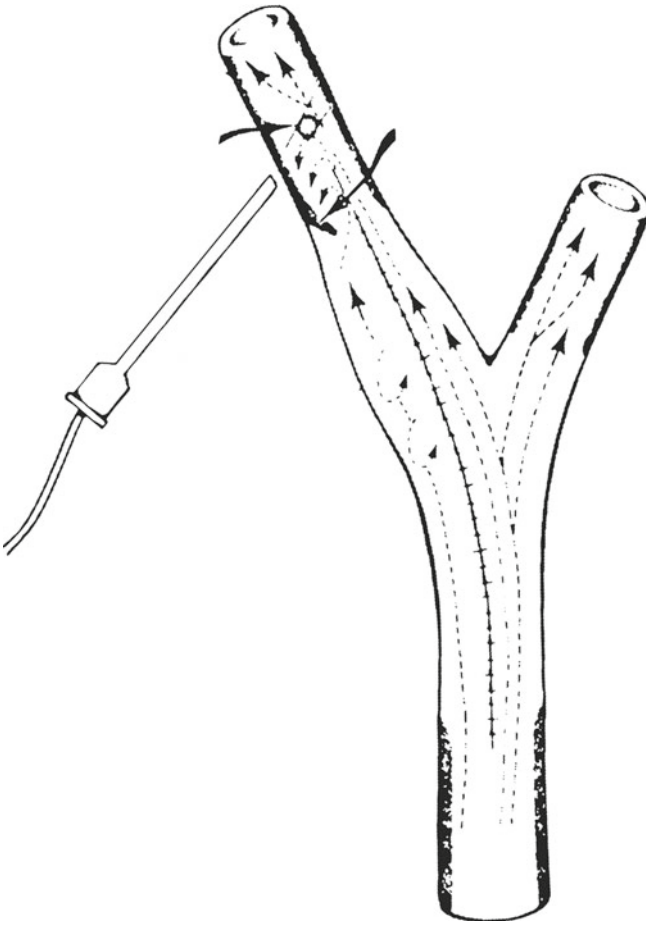

**Fig. 19.3** The application of Doppler probe to detect defects of a repaired internal carotid artery (intimal flap)

Despite careful operative techniques, certain vascular defects can be missed, for example, intimal flaps, luminal thrombus/platelet aggregation, and stricture, that occur in the course of carotid repair (Fig. 19.3). These defects can escape visual inspection and palpation of the repair. If these defects are left undetected, they can result in stroke secondary to thrombus formation, platelet aggregation, or arterial thrombosis, or they may result in postoperative recurrent carotid stenoses. Blaisdell et al. reported the fallibility of clinical assessment by routine completion angiography, which revealed unsuspected defects in 25% of cases [27]. A number of investigators have subsequently confirmed the observations of Blaisdell et al. by using angiography, alone or in combination with various ultrasound techniques, such as continuous-wave Doppler examination, pulse Doppler spectral analysis, or duplex ultrasonography. Intraoperative monitoring has consistently documented severe defects in the internal carotid artery (ICA) or the common carotid artery (CCA) that warranted immediate correction in approximately 2–10% of all repairs [28–34]. Although the percentage of patients with residual repair defects in whom a postoperative stroke would develop if the defects were left untreated is not known, prudent surgical practice dictates that detection and revision of these defects should be done at the primary operation, since the sequelae of an ICA thrombosis are frequently catastrophic.

Baker et al. [30] reported that recurrent stenoses (>75%) developed in 17% of patients with abnormal unrepaired CEAs by intraoperative imaging compared with 4.3% in normal CEAs ($p<0.001$). This suggests that abnormalities detected by intraoperative DUS, if not corrected, may contribute to recurrent carotid stenosis after CEA. Kinney et al. [31] showed the importance of intraoperative scanning in a prospective study of 461 CEAs. They correlated the results of intraoperative assessment by clinical inspection, ultrasound, or arteriography with an end point of stroke. The CEA site was assessed by ultrasound and arteriography in 268 cases, by ultrasound and Doppler spectral analysis alone in 142 cases, and with clinical inspection in only 51 cases. Based on intraoperative assessment, 26 endarterectomies (6%) were revised at the time of the surgery. Perioperative morbidity was similar in cases with normal, mildly abnormal, or no ultrasound. There were 12 temporary (3%) and six permanent (1%) neurologic deficits and six deaths (four strokes and two cardiac events). Based on life-table analysis, the incidence of >50% ICA stenosis or occlusions was increased ($p<0.007$) in patients with residual flow abnormality or no study. However, patients with normal intraoperative studies had a significantly lower rate of late ipsilateral stroke compared with the other patients ($p=0.04$). The incidence of stroke was increased ($p=0.00016$) in patients with ICA restenosis or occlusion (3 of 35) compared with patients without recurrent stenosis (3 of 426) during a mean follow-up of 30 months. It was concluded that a normal intraoperative duplex scan may prevent recurrent stenosis as well as stroke after CEA in the long term.

Most authorities rely on imaging or Doppler flow detection technique to exclude technical defects. The diagnostic signal analysis is highly sensitive and specific (>90%), particularly if pulse Doppler analysis is performed. This technique is simple, widely available, and relatively inexpensive. Although abnormalities of the Doppler flow signal are readily apparent by audible interpretation, quantitative spectral analysis is preferable. With flow- and pressure-reducing lesions, a spectral broadening is present throughout the pulse cycle, and a peak systolic velocity (PSV) exceeding 150 cm/s is noted. Visual inspection of velocity spectra and calculation of PSV can be obtained by a high-frequency pulse Doppler probe or duplex scanning, which permits classification of flow patterns into three categories: normal flow, mild to moderate flow disturbance, and severe flow disturbance [28]. When a significant residual flow abnormality is identified, angiography is usually recommended to delineate the abnormality before reexploration of the repair.

Recently, intraoperative duplex ultrasonography has been advocated because of its ability to provide both anatomic and hemodynamic information [32–35]. Improvements in linear ray scan head design and electronic signal processing, including color-coded velocity display, have made duplex scanning feasible in the operating room and an ideal modality for intraoperative assessment of CEA. Duplex scanning has an advantage over Doppler flow analysis alone, in that the structure of the anatomic defects associated with severe flow disturbance can usually be determined. B-mode imaging is sensitive in detecting small intimal defects in flaps; however, most authorities have not repaired these minor lesions, and the outcome of the procedure has not been adversely influenced [34].

A comparison of intraoperative and early postoperative duplex findings after CEA indicated that a majority of these abnormalities identified by duplex scanning within 3–6 months of CEA represent residual rather than recurrent stenoses [33].

Recently, Ascher et al. [36] reported on the value of intraoperative carotid artery duplex scanning in a modern series of 650 consecutive primary endarterectomy procedures (April 2000–April 2003). Major technical defects at intraoperative duplex scanning (>30% luminal ICA stenosis, free-floating clot, dissection, arterial disruption with pseudoaneurysm) were repaired. CCA residual disease was reported as wall thickness and percent stenosis (16–67%; mean 32% ± 8%) in all cases. Postoperative 30-day TIA, stroke, and death rates were analyzed. There were no clinically detectable postoperative thromboembolic events in this series. All 15 major defects (2.3%) identified with duplex scanning were successfully revised. These included seven intimal flaps, four free-floating clots, two ICA stenoses, one ICA pseudoaneurysm, and one retrograde CCA dissection. Diameter reduction ranged from 40% to 90% (mean, 67 ± 16%), and peak systolic velocity ranged from 69 to 497 cm/s (mean, 250 ± 121 cm/s). Thirty-one patients (5%) with the highest residual wall thickness (>3 mm) in the CCA and 19 (3%) with the highest CCA residual diameter reduction (>50%) did not have postoperative stroke or TIA. Overall postoperative stroke and mortality rates were 0.3% and 0.5%, respectively; combined stroke and mortality rate was 0.8%. One stroke was caused by hyperperfusion, and the other occurred as an extension of a previous cerebral infarct. It was concluded that intraoperative duplex scanning had a major role in these improved results because it enabled detection of clinically unsuspected significant lesions. Residual disease in the CCA does not seem to be a harbinger of stroke or TIA.

Color duplex scanning with a 7.5- to 10-MHz linear ray transducer has been used for intraoperative studies.

These studies are conducted with the transducer covered by a sterile disposable plastic sleeve that contains acoustic gel (Fig. 19.4). The probe is generally positioned in the cervical incision directly over the exposed carotid repair. A sterile solution is instilled into the incision for acoustic coupling. As the surgeon scans the arterial repair, the technologist adjusts the instrument to optimize the Doppler angle, sample volume, color-coded image, and recorded velocity spectra. Vessel walls are imaged at 90°, but blood flow patterns should be evaluated at Doppler angles of <60°.

**Fig. 19.4** Transducer covered by sterile disposal plastic sleeve that contains acoustic gel

For CEAs with primary closure, the entire CEA segment should be examined with duplex ultrasound. The point in the CCA at which the lesion is transected should be examined. Normally, this should leave a distinct shelf, which can be appreciated on B-mode imaging. This can be easily visualized in both transverse and longitudinal views. The velocity data proximal to, in, and distal to the endarterectomy site should also be done in longitudinal view, and sampling of the PSVs in the endarterectomy site should be obtained. Similarly, scanning of the proximal ICA in the bulb and beyond it should be done, and attention should be called to the point of the transaction of the plaque or the end of the plaque distally. The external carotid artery should also be examined for the first few centimeters, looking for residual plaques or areas of thrombus. In patients who have CEAs closed with a patch, either polytetrafluoroethylene (PTFE) or

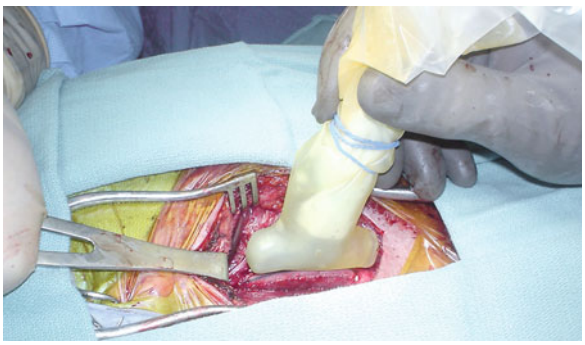

**Fig. 19.5** Probe scanning position for carotid endarterectomy closed with a patch. It is impossible to scan through PTFE patch, but operator can scan along the side of artery, either posterior or anterior to the patch

Dacron, it is impossible to scan through the patch itself because of the air within the wall of the patch. However, it is possible to scan along the side of the artery, either posterior or anterior to the patch, which may yield the necessary information (Figs. 19.5 and 19.6).

The limitations of this technique are largely related to lack of experience, correct measurement of duplex derived flow velocities, recognition of abnormal flow patterns, and transducer size. Intraoperative duplex imaging has the following advantages over angiography: comparable or higher accuracy, safety, ease of repeated use after reexploration, and low cost. Color duplex scanning is also sensitive to variations in anatomy and minor vascular defects that may alter blood flow streamlines. Certain flow patterns produced by carotid patch angioplasty should be noted and should not be regarded as abnormal. Some authorities have reported vascular defects in as many as one-third of their repairs, but only one-third of these appear to justify reexploration. Further details can be seen in Chap. 16.

## Intraoperative Monitoring of Carotid Endarterectomy with Transcranial Doppler Sonography

Transcranial Doppler (TCD) sonography has the advantage of allowing monitoring of both hemodynamic and embolic events, primarily in the middle cerebral artery distribution during CEA. One of the common uses of TCD is intraoperative monitoring to determine whether shunting is necessary and whether the shunt is malfunctioning [37]. TCD can be a useful indicator that early carotid clamping is necessary if multiple emboli were detected [37]. TCD can also be helpful in patients where shunts are not being used since a TCD signal will give an idea of the flow through the middle cerebral artery. The middle cerebral artery cannot be insonated in 5–15% of patients, most commonly because of the lack of a window for Doppler signal penetration of the skull. Severe cerebral ischemia is considered present in the first minute after carotid occlusion if the middle cerebral artery velocity decreases to 15% of the baseline or lower and mild ischemia if it drops to 15–40% of the baseline. An adequate perfusion is present if the velocity is >40% of the baseline [38]. Following insertion of the shunt or upon declamping, a brisk recovery in middle cerebral artery velocity should be seen, usually >80%. Absolute mean velocities of 15 cm/s or even 30 cm/s have been alternatively suggested. A middle cerebral artery velocity of 30 cm/s has correlated roughly with a carotid artery stump blood pressure of 50 mmHg. Some authorities reported that TCD detects critically low flow that results in neurologic deficits, even in the absence of electroencephalographic changes. The converse is also true: a pronounced drop in mean velocity has been observed in conjunction with a normal EEG and no resultant cerebral infarction, the cortex surviving from the other cerebral and leptomeningeal vessels.

In a recent study, Ackerstaff et al. [39] concluded that in CEA, TCD-detected microemboli during dissection and wound closure, ≥90% middle cerebral artery velocity decrease at cross clamping, and ≥100% pulsatility index increase at clamp release are associated with operative stroke. In combination with the presence of preoperative cerebral symptoms and ≥70% ipsilateral ICA stenosis, these four TCD monitoring variables can reasonably discriminate between patients with and without operative stroke. This supports the use of TCD as a potential intraoperative monitoring modality to alter the surgical technique by enhancing a decrease of the risk of stroke during or immediately after the operation.

TCD can also be used in the postoperative period to detect early thrombosis of the carotid artery, continued embolization, or the hyperperfusion syndrome. Another useful indication for TCD monitoring is in the early postoperative period since more than one-half of patients develop emboli in the first 3 h after carotid endarterectomy [40], and a majority of these will stop without further treatment; however, if the TCD indicates an increasing number of these emboli, treatment may be necessary (e.g., dextran infusion). TCD can also be useful in postoperative monitoring by measuring the middle cerebral artery velocities. If these velocities decrease, it may indicate compromising of the carotid endarterectomy site, meanwhile increasing velocities may be indicative of hyperperfusion syndrome. Presently, there is no level 1 evidence that TCD is essential in the routine practice of carotid artery surgery.

It has been reported that markedly increased mean velocity (150% of the baseline) may herald an intracranial hemorrhage. The use of TCD monitoring during CEA has led some surgeons to modify their operative techniques based on hearing a distressing frequency of emboli while operating with

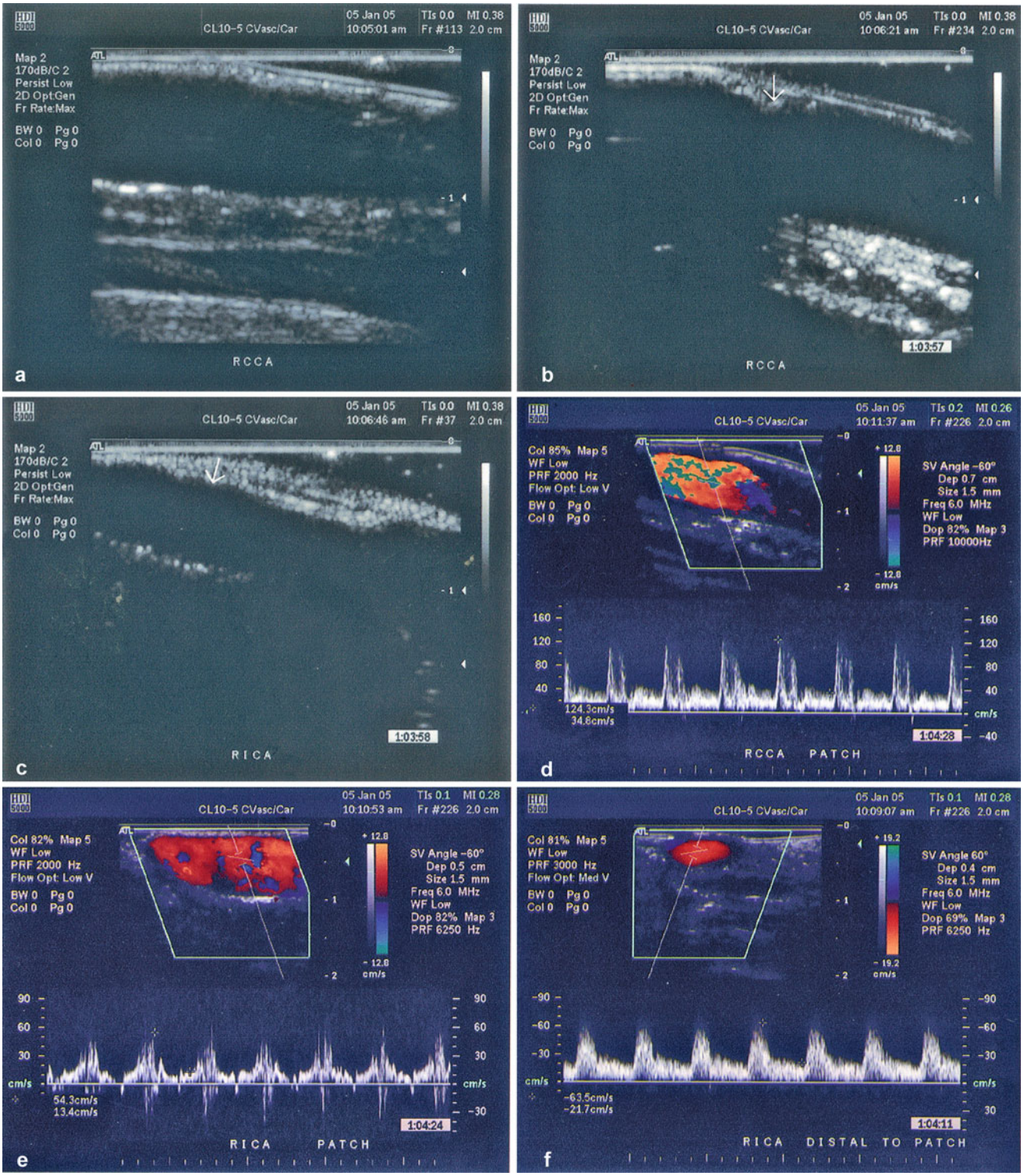


**Fig. 19.6** Intraoperative duplex ultrasound of carotid endarterectomy: (**a**) common carotid artery in gray scale. Note the shelf of the proximal end of carotid endarterectomy, (**b**) common carotid artery bifurcation in *gray scale*, (**c**) internal carotid artery in *gray scale*, (**d**) common carotid artery with color flow, (**e**) internal carotid artery with patch with color flow, (**f**) distal internal carotid artery with color flow

the continuously audible TCD. Further details on TCD are discussed in Chap. 10.

## Patients Who Develop a Neurologic Deficit After Leaving the Operating Room

If patients wake up well after CEA and then develop a neurologic deficit, emergent reexploration is indicated. If the deficit proves to be a TIA as symptoms resolve prior to the return to the operating room, heparin anticoagulation followed by duplex scan is preferred. A thrombosed ICA may be treated operatively or medically (anticoagulation), particularly in patients with dense deficits. A patent carotid without apparent pathology is immediately followed by brain CT/CTA to identify intracranial hemorrhage or other pathology and assess the intracranial vasculature. If negative, oral anticoagulation is started. Thromboembolism of inaccessible intracranial vasculature has been treated with selective catheterization and lytic therapy, although this is still considered investigational. Blood clots found at the endarterectomy site are treated by emergency reexploration.

## Post-carotid Endarterectomy Surveillance

Restenosis is a known entity that occurs after CEA and may vary between 12% and 36%, but the frequency of restenosis varies depending on the diagnostic method used and the frequency of follow-up examinations [41–52]. Several studies have reported on the value of postoperative carotid duplex surveillance, but no consensus has been reached [41–51]. The advantages that have been cited are detection of significant restenosis prior to the onset of neurologic events, which aids in the prevention of potential strokes, and follow-up on the contralateral carotid artery to document the development of surgically correctable stenosis. Opponents of routine postoperative carotid duplex surveillance claim that restenosis is benign in nature; therefore, a large number of strokes may not be prevented by surveillance [44, 45, 47, 48, 51].

Despite the high rate of restenosis, symptoms attributed to restenoses are rare; therefore, several authorities have suggested that routine surveillance of patients after CEA is not efficacious [43, 45, 48].

Several factors were associated with restenosis: continued smoking, small internal carotid artery diameter, operative defect detected at intraoperative assessment, and primary closure after CEA. Moore et al. [53] prospectively determined the incidence of restenosis using Doppler ultrasound follow-up to 5 years in ACAS patients who underwent CEA. The aggregate incidence of residual and recurrent carotid stenosis for all time intervals was 13%. Early restenosis (<2 years) in this group of patients was found in 8% and late restenosis in 2%. Of the 136 patients who were felt to have restenosis, only 8 (5.9%) underwent reoperation, only one of whom was for symptoms. There was also no correlation between late stroke and recurrent stenosis. Similarly, Cao et al. [54] randomized 1,353 who underwent CEA using the eversion technique (678) or standard CEA (primary closure in 419 and patch closure in 256). The life-table estimate of the cumulative risk of restenosis at 4 years was 4% in the eversion CEA group and 9% in the standard CEA group. Almost all of these patients (98%) were asymptomatic.

Mattos et al. [45] described their experience with postoperative carotid duplex surveillance and found an equal stroke-free survival at 5 years between patients with and without >50% restenosis. In addition, only one of 380 patients suffered a stroke in their study, suggesting a benign clinical significance of recurrent carotid artery stenosis. Mackey et al. claim a low rate of clinically significant restenosis [44]. Their retrospective series of 258 patients (348 arteries) show a potential 4% incidence of late strokes, but this included all patients who underwent repeat CEA for asymptomatic restenosis. They also noted that the majority of restenoses (53%) remained asymptomatic and did not progress to occlusion throughout follow-up. Of 10 documented late occlusions, eight did not result in stroke. Eight patients with operable restenosis had TIAs and underwent reoperation. They found that even patients with 75–99% restenosis most often remained asymptomatic (37%) or had TIAs (32%). Only two (11%) of 19 patients with 75–99% restenosis had an unheralded stroke. They felt that postoperative carotid duplex surveillance was not justified due to the low incidence of symptomatic restenosis.

In spite of these findings, investigators have been reluctant to advise that postoperative carotid duplex surveillance be abandoned because the cost-effectiveness of this surveillance has not been formally investigated. Others have reported that high-grade stenosis (>75%), whether caused by myointimal hyperplasia of the CEA site or progressive atherosclerosis of the contralateral carotid artery, is associated with an increased risk of late stroke [31, 51].

Ouriel et al. reported an 11% incidence of restenotic lesions greater than 80%. Although the incidence of symptoms with restenotic lesions was low (12%), the onset of symptoms at the time of occlusion was significant [46]. Forty-two percent of patients became symptomatic at the time of occlusion, with 33% resulting in a stroke. This led to the observation that critical restenoses are precursors to stroke, even if asymptomatic, and, therefore, the detection of >80% restenosis allows future stroke prevention if operative intervention is undertaken [46]. Mattos et al. also described the outcome for >80% restenosis. In their group, one of three patients with >80% restenosis suffered a stroke, one had a TIA, and one remained asymptomatic. This suggests a more serious course once restenosis reaches >80% [45].

So far, a consensus has not yet been reached in the surgical literature regarding the usefulness, cost-effectiveness, or timing of postoperative carotid duplex surveillance.

## Timing of Postoperative Carotid Duplex Surveillance

Several authors have recommended an initial surveillance duplex on the operative carotid system within the first 6 months [42, 45–47, 51] to detect residual stenosis from the operative procedure or early restenosis [46]. For example, Roth et al. [51] recently recommended an initial DUS to ensure a technically successful CEA, with subsequent postoperative carotid duplex surveillance at 1–2 years, as long as restenosis and contralateral stenoses remain <50%. More frequent follow-up (every 6 months) is warranted if >50% stenosis is noted, or with the onset of symptomatic disease [51].

Several studies have reported that the majority of restenoses occurs during the first 1–2 years after CEA. Mattos et al. [42] noted that 70% of restenoses were detected within 1 year after the CEA, and 96% developed within 15 months. Thomas et al. [41] reported that 70% of restenoses in their study occurred within 1 year of the CEA. Similar observations were noted by us previously [49].

Ricco et al. [55] reported on the need for follow-up duplex scan 1 year after CEA was performed with prosthetic patching and intraoperative completion arteriography. A total of 605 CEA procedures with prosthetic patch closure and intraoperative completion arteriography were performed in 540 patients. All patients underwent duplex scan at 4 days and then yearly after the procedure. Intraoperative completion arteriography showed abnormalities in 114 cases, including 17 involving the ICA and 73 involving the external carotid artery. Successful revision was achieved in all cases and confirmed by repeat arteriography. Postoperative duplex scans at 4 days detected three abnormalities involving the ICA (0.5%), including asymptomatic occlusion in one case and residual stenosis >50% in two cases. Ninety-eight percent of patients were stenosis-free at 1 year. Actuarial stroke-free survival was 98.3% at 3 years. Diameter reduction of the contralateral carotid artery progressed over 70% within 1 year after CEA in 22.9% of patients with contralateral carotid stenosis over 50% at the time of the initial intervention. The findings of this study indicate that duplex scan follow-up 1 year after CEA with intraoperative completion arteriography is unnecessary unless postoperative duplex scan demonstrates residual stenosis of the ICA. However, duplex scan at 1 year is beneficial for patients presenting with contralateral carotid artery disease with diameter reduction >50% at the time of CEA.

Lovelace et al. [56] conducted a study on optimizing duplex follow-up in patients with an asymptomatic ICA stenosis of <60%. All patients who underwent initial carotid duplex examination for any indication since January 1, 1995, with at least one patent, asymptomatic, previously nonoperated ICA with <60% stenosis; with 6 months or greater follow-up; and with one or more repeat duplex examinations were entered into the study. On the basis of the initial duplex examination, ICAs were classified into two groups: those with a PSV <175 cm/s and those with a PSV of 175 cm/s or more. Follow-up duplex examinations were performed at varying intervals to detect progression from <60% to 60–99%. A total of 407 patients (640 asymptomatic ICAs with <60% stenosis) underwent serial duplex scans (mean follow-up, 22 months). Three ICAs (0.5%) became symptomatic and progressed to 60–99% ICA stenosis at a mean of 21 months, whereas four other ICAs occluded without stroke during follow-up. Progression to 60–99% stenosis without symptoms was detected in 46 ICAs (7%) (mean, 18 months). Of the 633 patent asymptomatic arteries, 548 ICAs (87%) had initial PSVs <175 cm/s and 85 ICAs (13%) had initial PSVs of 175 cm/s or more. Asymptomatic progression to 60–99% ICA stenosis occurred in 22 (26%) of 85 ICAs with initial PSVs of 175 cm/s or more, whereas 24 (4%) of 548 ICAs with initial PSVs <175 cm/s progressed ($p<0.0001$). The Kaplan–Meier method showed freedom from progression at 6 months, 12 months, and 24 months was 95%, 83%, and 70%, respectively, for ICAs with initial PSVs of 175 cm/s or more versus 100%, 99%, and 95%, respectively, for ICAs with initial PSVs <175 cm/s ($p<0.0001$).

They concluded that patients with <60% ICA stenosis and PSVs of 175 cm/s or more on initial duplex examination are significantly more likely to progress asymptomatically to 60–99% ICA stenosis, and progression is sufficiently frequent to warrant follow-up duplex studies at 6-month intervals. Patients with <60% ICA stenosis and initial PSVs <175 cm/s may have follow-up duplex examinations safely deferred for 2 years.

## Cost-Effectiveness of Postoperative Carotid Duplex Surveillance

There have been reports that postoperative carotid duplex surveillance is not cost-effective since there is such a low incidence of symptomatic restenosis. Patel et al. evaluated the cost-effectiveness of postoperative carotid duplex surveillance [50]. They concluded that postoperative carotid duplex surveillance after CEA has an unfavorable cost-effectiveness ratio. In the process of their analysis, they identified a subset of patients in which postoperative carotid duplex surveillance may be cost-effective. These included patients in whom the rate of progression to >80% stenosis exceeded 6% per year. In their analysis, they felt that some groups of patients could potentially have a rate of disease progression that approaches

or exceeds the level at which postoperative carotid duplex surveillance becomes cost-effective. Some of these include patients with multiple risk factors, for example, smoking, hypertension, hyperlipidemia, diabetes mellitus, coronary artery disease, female gender, and young age. In addition, they concluded that with postoperative carotid duplex surveillance, the rate of carotid artery occlusion could be reduced by 15% per year. Our evaluation of the cost of postoperative carotid duplex surveillance agrees with these conclusions. Three hundred and ninety-nine CEAs were randomized into 135 with primary closure, 134 with PTFE patch closures, and 130 with vein patch closures and followed for a mean of 47 months. Postoperative carotid duplex surveillance was done at 1, 6, and 12 months and every year thereafter (a mean of 4.0 studies/artery). A Kaplan–Meier analysis was used to estimate the rate of ≥80% restenosis over time and the time frame of progression from <50% to 50–79% and ≥80% stenosis.

Greater than or equal to 80% restenosis developed in 24 (21%) with primary closure and 9 (4%) with patching. A Kaplan–Meier estimate of freedom from 50% to 79% restenosis at 1, 2, 3, 4, and 5 years was 92%, 83%, 72%, 72%, and 63% for primary closure and 99%, 98%, 97%, 97%, and 95% for patching. A Kaplan–Meier estimate of freedom from ≥80% restenosis at 1, 2, 3, 4, and 5 years was 92%, 83%, 80%, 76%, and 68% for primary closure and 100%, 99%, 98%, 98%, and 91% for patching ($p < 0.01$).

Out of 56 arteries with 20–50% restenosis, 2/28 patch closures and 10/28 primary closures progressed to 50–<80% restenosis ($p = 0.02$) and 0/28 patch closures and 6/28 primary closures progressed to ≥80% ($p = 0.03$). In primary closures, the median time to progression from <50% to 50–79%, <50% to ≥80%, and 50–79% to ≥80% was 42, 46, and 7 months, respectively. Of the 24 arteries with ≥80% restenosis in primary closures, 10 were symptomatic. Thus, assuming that symptomatic restenosis would have undergone duplex examinations anyway, there were 14 asymptomatic arteries (12%) that could have been detected only by postoperative carotid duplex surveillance (estimated cost of $139,200) and would have been candidates for redo CEA. Of the nine arteries with patch closures (three PTFE and six vein patch closures) with ≥80% restenosis, six asymptomatic arteries (four vein patch closure and two PTFE, 3%) could have been detected by postoperative carotid duplex surveillance. In patients with a normal duplex at the first 6 months, only 4/222 (2%) patched arteries (two asymptomatic) developed ≥80% restenosis versus 5/13 (38%) in patients with abnormal duplex examinations ($p < 0.001$).

Assuming a 5% stroke rate for the 14 repeat CEAs for asymptomatic ≥80% restenosis in the primary closure group in our series [57], 0.7 strokes would be associated with the 14 repeat CEAs and approximately 4.7 strokes would have been prevented through surgical intervention prior to occlusion (assuming a similar outcome of ≥80% restenosis as described by Mattos et al. [45]). There was a net reduction of four strokes in patients with primary closure and an approximate cost of $56,150 per stroke prevented.

Also, assuming a similar outcome of >80% restenosis as described by Ouriel et al. [46] and if one-half of these >80% restenosis would progress to total occlusion (seven patients), and assuming one-third of patients with total occlusion would suffer a stroke, then approximately 2.3 strokes would be prevented by doing the 14 redo CEAs. Since 0.7 strokes would result from repeating 14 CEAs [57], the net effect would be prevention of 1.6 strokes at a cost of $224,600, i.e., $140,250 per stroke prevented. This analysis does not take into consideration the value of duplex screening of the contralateral nonoperated side.

The justification for this cost is unclear without a definite estimate of the economic burden for caring for these stroke victims. Considering the low incidence of >80% restenosis in patients with patch angioplasty closure, the cost-effectiveness of postoperative carotid duplex surveillance appears to be unfavorable and, therefore, should be limited to a single DUS to detect residual stenosis. Subsequent follow-up should be dictated by the results found on the initial scan and the onset of neurologic symptoms.

Our randomized prospective studies confirm that carotid restenosis is a known entity that follows a percentage of patients who undergo carotid surgery. In the past, the clinical significance of carotid restenosis has led some investigators to conclude that postoperative carotid duplex surveillance is not warranted. We showed that based on the incidence of >80% restenosis, postoperative carotid duplex surveillance may be beneficial in patients with primary closure with examinations at 6 months and at 1–2-year intervals for several years. For patients with patching, a 6-month postoperative duplex examination, if normal, is adequate.

## Duplex Ultrasound Surveillance of Carotid Stents

Kupinski et al. [58] conducted a study to evaluate the DUS characteristics of carotid stents including comparing hemodynamic to B-mode and color-flow imaging data in 40 carotid stents placed in the common or internal carotid arteries of 37 patients. DUS examinations included PSV and end diastolic velocity (EDV) taken proximal to the stent (prestent), at the proximal, mid, and distal regions of the stent, and distal to the stent (poststent). The stents were evaluated at 1 day and 3, 6, and 12 months post procedure and yearly thereafter. The average follow-up interval was 6 ± 1 month. In 31 patent ICA stents, the PSV proximally within the stent was 92 ± 6 cm/s with an EDV of 24 ± 2 cm/s. The mid stent PSV was 86 ± 5 cm/s with an EDV of 24 ± 2 cm/s. The distal stent PSV was 90 ± 4 with an EDV of 26 ± 2 cm/s. Proximal to the

stent, the PSV was 70 ± 3 cm/s with an EDV of 17 ± 1 cm/s. Distal to the stent, the PSV was 77 ± 4 cm/s with an EDV of 25 ± 2 cm/s. There were no defects observed on B-mode image and no areas of color turbulence. Three stents developed stenotic areas with PSVs of 251, 383, and 512 cm/s. The EDV was 50, 131, and 365 cm/s, respectively. Poststenotic turbulence was present in each of these stents. An elevated PSV of >125 cm/s was found in 32% of the stents (9 of 28) without evidence of stenosis on B-mode image of poststenotic turbulence. These data demonstrate that velocities within stented carotid arteries can be elevated above established ranges for normal. They concluded that velocity criteria may need to be adjusted when applied to stented carotid arteries. It has been suggested that focal velocity increase at the point of maximal narrowing >150 cm/s and a prestenotic (or prestent) to stenotic segment PSV ratio of l: ≥2 are suggestive of significant in-stent restenosis [59].

## Determination of Progression of Carotid Stenosis

It has now become clear that it is possible to determine major progression of disease in two different categories with duplex scanning technology. Progression of disease from a mild form (20–50% diameter reduction) to a severe form (50–99% diameter reduction) can be accurately detected based on significant changes in peak frequency [60]. In addition, in severe stenosis, it is possible to identify the development of extreme degrees of stenosis (>80% diameter reduction) by the changes in the ratio between peak systolic and end diastolic velocities. The ability to identify such disease progression without invasive arteriographic studies will contribute to our understanding of the natural history of the disease process.

Carotid screening after CEA for the sake of detecting contralateral disease progression has been of much more value. Several studies have reported on the progression of contralateral stenosis after CEA [61–65]. Contralateral carotid stenosis progression was more frequent than ipsilateral recurrent stenosis during the long-term follow-up in these studies. Several studies have also identified that the risk of contralateral carotid artery stenosis progression is dependent on the existing disease at the time of the initial CEA [63–65]. The risk of progression for moderate stenosis at the initial surveillance to severe stenosis can be as high as five times [64].

## Natural History of Carotid Artery Stenosis, Contralateral to Carotid Endarterectomy

A few nonrandomized studies have reported on the natural history of carotid artery stenosis contralateral to CEA. We analyzed the natural history of carotid artery stenosis contralateral to CEA from two randomized prospective trials [49, 66].

The contralateral carotid arteries of 534 patients who participated in two randomized trials comparing CEA with primary closure versus patching were followed clinically and had DUSs at 1 month and every 6 months. Carotid artery stenoses were classified into <50%, ≥50–<80%, ≥80–99%, and occlusion. Late contralateral CEAs were done for significant carotid artery stenoses. Progression of carotid artery stenosis was defined as progress to a higher category of stenosis.

Out of 534 patients, 61 had initial contralateral CEAs, within 30 days of the ipsilateral CEA, and 53 had contralateral occlusions. Overall, 109/420 (26%) progressed at a mean follow-up of 41 months (range: 1–116 months). Progression of contralateral carotid artery stenosis was noted in 5/162 (3%) patients who had baseline normal carotids; 56/157 (36%) patients with <50% carotid artery stenosis progressed versus 45/95 (47%) patients with 50–<80% carotid artery stenosis ($p = 0.003$). The median time for progression was 24 months for <50% carotid artery stenosis and 12 months for ≥50–<80% carotid artery stenosis ($p = 0.035$). Freedom from progression for patients with baseline <50% and ≥50–<80% carotid artery stenosis at 1, 2, 3, 4, and 5 years was 95%, 78%, 69%, 61%, and 48% and 75%, 61%, 51%, 43%, and 33%, respectively ($p = 0.003$). Freedom from progression in patients with baseline normal carotid arteries at 1, 2, 3, 4, and 5 years was 99%, 98%, 96%, 96%, and 94%. Late neurologic events referable to the contralateral carotid artery were infrequent in the whole series (28/420, 6.7%) and included 10 strokes (2.4%) and 18 TIAs (4.3%) (28/258, 10.9% in patients with contralateral carotid artery stenosis); however, late contralateral CEAs were done in 62 patients (62/420, 15%, in the whole series, 62/258, 24%, in patients with contralateral carotid artery stenosis). The survival rates were 96%, 92%, 90%, 87%, and 82% at 1, 2, 3, 4, and 5 years.

We concluded that progression of contralateral carotid artery stenosis was noted in a significant number of patients with baseline contralateral carotid artery stenosis. Serial carotid DUSs every 6–12 months for patients with ≥50–<80% carotid artery stenosis and every 12–24 months for ≤50% carotid artery stenosis are adequate.

## Carotid Endarterectomy Based on Carotid Duplex Ultrasonography Without Angiography

In many centers, carotid evaluation by angiography is no longer done routinely, even when planning for surgery, to eliminate the risk of neurologic events during angiography. The risk of stroke from angiography is around 1% [6].

Although standard conventional angiography is still generally considered to be the definitive diagnostic test for carotid artery stenosis, there has been an increasing interest in performing CEA based on clinical evaluation and duplex scanning only [22, 67–75]. It has been estimated that up to 95% of CEA procedures are currently undertaken on the basis of carotid duplex ultrasound alone [76], again, with no evidence that reliance on this policy compromised patient safety or operability. This is generally done to minimize cost and to expedite surgery on these patients, therefore optimizing the long-term benefit conferred by CEA, specifically for symptomatic patients. However, for clinicians who advocate this policy or who follow this policy, they must keep in mind the following considerations: carotid duplex must be done in an accredited vascular laboratory and interpreted by highly qualified physicians in this field; the method of estimating carotid stenosis must also be defined, for example, the NASCET method, and clinicians must also be aware of duplex ultrasound findings that may suggest an inflow or outflow disease, which if present, other imaging must be added prior to intervention. This has been stimulated by improvement in the accuracy and reliability of color carotid duplex scanning, along with the increasing demands to minimize both the risk of carotid angiography and the cost of medical care. CEAs are generally indicated for high-grade stenoses of asymptomatic patients and in moderate to severe stenoses in patients with hemispheric neurologic events. These stenoses can usually be accurately detected by duplex scanning.

Dawson et al. [72] reviewed arteriograms and duplex scans in 83 patients and found that in 87% the clinical presentation and duplex findings were adequate for patient management. They concluded that arteriography was necessary in 13% that (1) showed an unusual or atypical pattern of disease, (2) had technically inadequate duplex scans, or (3) had an internal carotid artery stenosis of <50%. This group [67] completed a subsequent prospective evaluation of 94 cases that showed that arteriography affected clinical management in only one case (1%). Dawson et al. [67] indicated that while specific indications for CEA without angiography remain controversial, the results of angiography rarely alter the clinical treatment plan when a technically adequate duplex scan shows an 80–99% stenosis in asymptomatic patients or an ipsilateral 50–99% stenosis in patients with hemispheric neurologic symptoms [67].

The duplex and arteriogram results of 85 patients were prospectively evaluated by Moore et al. with a panel of neurologists, neurosurgeons, and vascular surgeons [3]. The duplex scan results were prospectively compared with arteriography. One hundred and fifty-nine of 170 carotid arteries were correctly characterized (94%); hemodynamically significant stenoses were correctly characterized in 100%. Thirty-two CEAs were performed by these authors in 29 patients without angiography. All duplex-predicted lesions were confirmed at surgery, and there were no perioperative strokes.

If arteriography is not done, there is a potential to miss significant lesions in the carotid siphon or an intracranial aneurysm or tumor as the cause of TIAs. However, it is unlikely that carotid siphon disease will produce significant symptoms [77, 78] and, therefore, does not impact the decision to perform CEA. Intracranial aneurysms occur in approximately 1–2% of patients undergoing arteriography [79], but most are small and unlikely to be affected by CEA [79]. With the advances in imaging techniques, the concern for occult brain tumors has become less relevant. These limitations can be overcome by using carotid MRA/CTA.

In addition, associated costs are significant, with some institutions reporting charges for cerebrovascular arteriography as high as $5,000–$6,000. Strandness [80] has suggested that wider use of duplex scanning as the sole preoperative test could result in substantial savings. For instance, if 150,000 CEAs are done annually, with an average cost of angiography of $3,000, the total cost of angiography alone would be $750 million dollars (not counting the costs of an estimated 7,500 TIAs, 1,500 strokes, and 100 deaths). If these same patients had duplex scanning alone, the total costs would be approximately $37 million; this represents a savings annually in the United States alone of $712 million [80]. We have already begun to see a shift in the testing that is done for a preoperative diagnosis. A report from the University of Vermont stated that 87% of their last 130 CEAs were performed without arteriography, with acceptable rates of stroke and death [81].

CEA should not be attempted without MRA/CTA arteriography unless the following criteria are met: [67]

1. The distal ICA is free of significant disease (disease is localized to the carotid bifurcation).
2. The CCA is free of significant disease.
3. Vascular anomalies, kinks, or loops are not present.
4. The duplex scan is technically adequate.
5. Vascular laboratory duplex accuracy is known.

Some potential pitfalls include patients with nonhemispheric symptoms, recurrent stenosis, or ICA stenosis of <50% [67, 72, 81].

However, as experience grows, indications may be expanded.

Therefore, MRA/CTA/conventional angiography are most likely to be useful when the duplex scan is not diagnostic, in patients with atypical lesions that appear to extend beyond the carotid bifurcation, and for stenoses of <50% in patients with classical hemispheric neurologic symptoms.

## Ultrasonic Carotid Plaque Morphology and Carotid Plaque Hemorrhage: Clinical Implications

The lack of neurologic symptoms in many patients with significant carotid stenosis has perplexed many scientists. It has been proposed that the character of the plaque may be as important as or more important than significant stenosis in producing neurologic events.

We [82] examined the importance of ultrasonic plaque morphology and its correlation to the presence of intraplaque hemorrhage and its clinical implications. We studied 152 carotid plaques associated with ≥50% ICA stenoses in 135 patients who had CEAs and characterized them ultrasonographically into irregular/ulcerative, smooth, heterogeneous, homogeneous, or not defined. Heterogeneous plaques were defined as a mixture of hyperechoic, isoechoic, and hypoechoic plaques. In contrast, homogeneous plaques were defined as consisting of only one of the three types of echogenic plaques. An isoechoic plaque was defined as having the echogenicity of a normal intima-media complex. A hyperechoic plaque was brighter than an isoechoic plaque, and a hypoechoic plaque was not as bright as an isoechoic plaque. An irregular plaque was defined as a plaque that lacks a smooth surface with or without an intimal layer. A smooth plaque was defined as a plaque without surface irregularities or ulcerations. All plaques were examined pathologically for the presence of intraplaque hemorrhage. The ultrasonic morphology of the plaques included 63 with surface irregularity (41%), 48 smooth (32%), 59 heterogeneous (39%), 52 homogeneous (34%), and 41 (27%) not defined. Intraplaque hemorrhage was present in 57 out of 63 (90%) irregular plaques and 53 out of 59 (90%) heterogeneous plaques, in contrast to 13 out of 48 (27%) smooth plaques and 17 out of 52 (33%) homogeneous plaques ($p<0.001$). Fifty-three out of 63 (84%) irregular plaques and 47 out of 59 (80%) heterogeneous plaques had TIAs/stroke symptoms, in contrast to 9 out of 48 (19%) for smooth plaques and 15 out of 52 (29%) for homogeneous plaques ($p<0.001$). Fifty-four percent of the irregular plaques and 57% of the heterogeneous plaques had ipsilateral cerebral infarcts, in contrast to 12% of the smooth plaques ($p<0.001$) and 14% of the homogeneous plaques ($p<0.001$). We concluded that irregular and/or heterogeneous carotid plaques are more often associated with intraplaque hemorrhage, neurologic events, and cerebral infarcts. Therefore, ultrasonic plaque morphology may be helpful in selecting patients for CEA.

In another study, we [83] analyzed the natural history of 60–<70% asymptomatic carotid stenosis according to ultrasonic plaque morphology and its implication on treatment.

Patients with 60–<70% asymptomatic carotid stenosis during a 2-year period entered into a protocol of carotid duplex surveillance/clinical examination every 6 months. Their ultrasonic plaque morphology was classified as heterogeneous (Group A, 162) or homogeneous (Group B, 229). CEA was done if the lesion progressed to ≥70% stenosis or became symptomatic.

Three hundred and eighty-two patients (391 arteries) were followed at a mean follow-up of 37 months. The clinical/demographic characteristics were similar for both groups. The incidence of future ipsilateral strokes was significantly higher in Group A than in Group B: 13.6% versus 3.1% ($p=0.0001$, odds ratio 5). Similarly, the incidence of all neurologic events (stroke/TIAs) was higher in Group A than in Group B: 27.8% versus 6.6% ($p=0.0001$, odds ratio of 5.5). Progression to ≥70% stenosis was also higher in Group A than in Group B: 25.3% versus 6.1% ($p=0.0001$, odds ratio 5.2). Forty-four (27.2%) late CEAs were done in Group A (16 for stroke, 21 for TIAs, and seven for ≥70% asymptomatic carotid stenosis) versus 13 (5.7%) for Group B (five for stroke, seven for TIAs, and one for ≥70% asymptomatic carotid stenosis $p=0.0001$, odds ratio 6.2).

We concluded that patients with 60–<70% asymptomatic carotid stenosis with heterogeneous plaquing were associated with a higher incidence of late stroke, TIAs, and progression to ≥70% stenosis than patients with homogeneous plaquing. Prophylactic CEA for 60–<70% asymptomatic carotid stenosis may be justified if associated with heterogeneous plaquing.

In another study [84] of the correlation of ultrasonic carotid plaque morphology and the degree of carotid stenosis, 2460 carotid arteries were examined using color DUS during a 1-year period. Carotid stenoses were classified into <50%, 50–<60%, 60–<70%, and >70–99%.

Heterogeneous plaques were noted in 138 of 794 arteries with <50% stenosis, 191/564 with 50–<60% stenosis, 301/487 with 60–<70% stenosis, and 496/615 with 70–99% stenosis. The higher the degree of stenosis, the more likely it is to be associated with heterogeneous plaques. Heterogeneous plaques were present in 59% of ≥50% stenoses versus 17% for <50% stenoses, 72% of ≥60% stenoses versus 24% for <60% stenoses, and 80% of ≥70% stenoses versus 34% for <70% stenoses ($p < 0.0001$ and odds ratios of 6.9, 8.1, and 8.0, respectively). Heterogeneous plaques were associated with a higher incidence of symptoms than homogeneous plaques in all grades of stenoses: 68% versus 16% for <50% stenosis, 76% versus 21% for 50–<60%, 79% versus 23% for 60–<70%, and 86% versus 31% for ≥70–99% ($p<0.0001$ and odds ratios of 8.9, 11.9, 12.6, and 13.7, respectively). Heterogenosity of plaques was more positively correlated to symptoms than any degree of stenosis (regardless of plaque structure). Eighty percent of all heterogeneous plaques were symptomatic versus 58% for all ≥50% stenoses,68% for all ≥60% stenoses, and 75% for all ≥70% stenoses ($p<0.0001$, $p<0.0001$, and $p=0.02$, respectively).

We concluded that the higher the degree of carotid stenosis, the more likely it is to be associated with ultrasonic heterogeneous plaquing and cerebrovascular symptoms. Heterogenosity of the plaque was more positively correlated to symptoms than to any degree of stenosis. These findings suggest that plaque heterogenosity should be considered in selecting patients for CEA [84].

Differentiating unstable from stable plaques by ultrasound has been hampered by the subjectiveness of interpreting such images [85–88].

Biasi et al. [87] conducted a study to confirm that plaque echogenicity evaluated by computer analysis, as suggested by preliminary studies, can identify plaques associated with a high incidence of strokes. A series of 96 patients with carotid stenosis in the range of 50–99% were studied retrospectively (41 with

TIAs and 55 asymptomatic). Carotid plaque echogenicity was evaluated using a computerized measurement of the median grayscale value (GSM). All patients had a CT brain scan to determine the presence of infarction in the carotid territory.

The incidence of ipsilateral brain CT infarctions was 32% for symptomatic plaques and 16% for asymptomatic plaques ($p=0.076$). It was 25% for >70% stenosis and 20% for <70% stenosis ($p=0.52$). It was 40% in those with a GSM of <50 and 9% for plaques with a GSM of >50 ($p<0.001$) with a relative risk of 4.6 (95% CI, 1.8–11.6).

It was concluded that a computer analysis of plaque echogenicity was better than the degree of stenosis in identifying plaques associated with an increased incidence of CT brain scan infarction and consequently useful for identifying individuals at high risk of stroke.

Kern et al. [86] investigated the value of real-time compound ultrasound imaging for the characterization of atherosclerotic plaques in the ICA. Thirty-two patients (22 men, 10 women; mean age, 75 years) with plaques of the ICA as identified by high-resolution B-mode scanning were investigated with real-time compound ultrasound imaging with the use of a 5- to 12-MHz dynamic range linear transducer on a duplex scanner. Two independent observers rated plaque morphology according to a standardized protocol. The majority of plaques were classified as predominantly echogenic and as plaques of irregular surface, whereas ulcerated plaques were rarely observed. The interobserver agreement for plaque surface characterization was good for both compound ultrasound (kappa=0.72) and conventional B-mode ultrasound (kappa=0.65). For the determination of plaque echogenicity, the reproducibility of compound ultrasound [kappa(w)=0.83] was even higher than that of conventional B-mode ultrasound [kappa(w)=0.74]. According to a semiquantitative analysis, real-time compound ultrasound was rated superior in the categories plaque texture resolution, plaque surface definition, and vessel wall demarcation. Furthermore, there was a significant reduction of acoustic shadowing and reverberations.

They concluded that real-time compound ultrasound was a suitable technique for the characterization of atherosclerotic plaques, showing good general agreement with high-resolution B-mode imaging. This advanced technique allows reduction of ultrasound artifacts and improves the assessment of plaque texture and surface for enhanced evaluation of carotid plaque morphology. This subject will be covered in depth elsewhere in this volume (Chap. 11).

## Carotid Duplex Ultrasound for Intima-Media Thickness

Poli et al. [88] reported on a study of ultrasonographic measurement of the CCA wall thickness in hypercholesterolemic patients, and they concluded that there was a correlation between the thickness of the carotid artery and the presence of cardiovascular risk factors. The measurement consists of determining the distance between the leading edge of the lumen-to-wall interface of the artery and the interface between the media and the adventitia on the artery wall. The combined width of this region is defined as intima-media thickness (IMT). It is believed that patients with larger IMTs had a greater number of cardiovascular risk factors than patients with thinner IMTs. O'Leary et al. [89] reported for the Cardiovascular Health Study Collaborative Research Group that thickening of the carotid wall was a marker for atherosclerosis in the elderly. This study clearly shows the strong cross-sectional relationships between risk factors and the thickness of the wall of both the ICA and the CCA. CCA wall thickening is a diffuse process, whereas ICA wall thickness is a sonographic measurement of carotid plaque thickness and cholesterol deposition. Therefore, an increased internal carotid IMT corresponds to an increased degree of carotid artery stenosis, and the measurement of the ICA wall thickness correlates with the extent of subjectively graded percentage of stenosis [90].

O'Leary et al. [91] showed a clear-cut scaling effect as well as excess risk with increasing thickening of the ICA and the CCA, as well as for a combined score adding measurement from the common and ICAs. IMT is felt to be a marker for future myocardial infarction as well as for stroke. Further details and more updates on this subject are discussed in Chap. 17.

## Carotid Duplex Ultrasound After Neck Trauma

DUS can be used in evaluating vascular injuries of the neck. Although carotid trauma is not strictly a disease of the carotid bifurcation, developments in this area parallel the changes seen in surgery for atherosclerotic disease. Carotid duplex following cervical trauma was prospectively evaluated by Fry et al. [92] Fifteen patients had duplex scan and arteriography, and 11 of these had a region of interest in zone II and four in zone III. One injury was diagnosed by duplex scan in this group and this was confirmed by arteriography; both studies were normal in the remaining 14 patients. On the next 85 patients, Fry et al. then performed duplex scan only, with arteriography reserved only for an abnormal duplex result. In this group, 62 patients had potential injuries in zone II and the remainder in zone III. Seven arterial injuries were identified by duplex scan and confirmed by arteriography. The remaining 76 patients had normal duplex scans and no sequelae up to 3 weeks post discharge. It was concluded that DUS is a valuable tool in evaluating carotid injury.

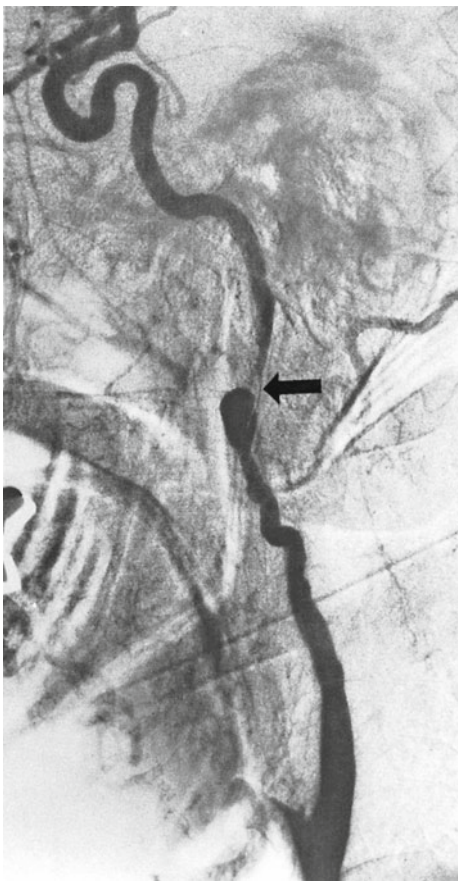

**Fig. 19.7** Carotid arteriogram showing internal carotid artery dissection of the higher cervical portion, as indicated by the (*black arrow*)

## Carotid Duplex Ultrasound for Internal Carotid Artery Dissection

ICA dissection has been reported more often recently than was previously suspected. This disease can appear spontaneously or may follow traumatic events accompanied by the fully developed picture of focal ischemia with facial and neck pain and Horner's syndrome (ptosis, miosis, and anhydrosis). It can also appear with very few symptoms or may even be completely asymptomatic. Using a color flow DUS, the diagnosis can be made when the flow signal is carefully followed over the entire neck region. In the longitudinal section, forward and backward signal components in blue/red color coding are generally seen next to one another in the proximal ICA. Distally, an area free of flow signals marks the proximal end of the dissection. Corresponding Doppler signals characterize partial recanalization with systolic forward and backward signal components, but with diastolic forward flow preservation [93–95]. On angiography, proximally there is a threadlike occlusion/subtotal stenosis of the ICA without a connection to the intracranial vasculature (Fig. 19.7). Monthly follow-up assessments are important, since the majority of the cases spontaneously recanalize.

## Role of Duplex Ultrasound in Vertebrobasilar Insufficiency

During the 1970s and 1980s, there was limited clinical experience in regard to vertebrobasilar insufficiency, due in part to the difficulty in noninvasive study of vertebral artery flow. Furthermore, documented alterations in the vertebral flow may have little bearing on the clinical situation. Keller et al. studied vertebral artery flow using directional Doppler ultrasound in 90 patients, 40 of whom underwent subsequent arteriography [96]. The probe was positioned in the dorsal oropharynx after appropriate topical anesthesia, and the following four determinations were made: (1) the flow direction in each vertebral artery, (2) the related amplitude of both signals, (3) cessation of the flow in either vertebral artery during any part of the cardiac cycle, and (4) response of the vertebral flow to ipsilateral CCA compression. Under normal circumstances, the vertebral flow was always craniad and of equal amplitude in both vessels. It never reached zero during any phase diastole, and it did not change with CCA compression. Alteration of any of these normal observations was diagnostic of vertebral artery occlusive disease with a specificity of 82%. Kaneda et al. [97] simplified the previous technique by positioning the probe just below the mastoid process directed toward the contralateral eye. He reported a diagnostic accuracy of 92%. Others have found the mastoid approach unreliable, since spatial relationships between the probe and the vessel axis were poorly defined and more intervening structures were present.

Recent studies have shown that with adequate skill and patience on the operator's part, the innominate, subclavian, cervical, and prevertebral segment of the vertebral artery can be displayed with real-time duplex ultrasound. Duplex scanning appears to be the most successful and accurate technique to diagnose atherosclerotic lesions of the vertebral arteries in the neck region. With this technique, the cervical segment of the vertebral artery can be visualized and the direction of the flow can be determined, whether antegrade or retrograde, which may be suggestive of subclavian steal. It has been reported that a reliable investigation of the prevertebral segment and the orifice of the vertebral artery is possible in more than 80% of cases. Some studies [97–99] claim more rapid identification and a higher success rate if color flow imaging is used. For detecting stenoses of ≥50% of the arch branches and at the site of the origin of the vertebral artery, duplex scanning has a high sensitivity, specificity, and overall accuracy. However, this technique still has several disadvantages, including the fact that satisfactory displays of the origin of the vertebral artery cannot be achieved in all patients. In addition, it is obvious that in those arteries in which the examination is successfully completed, only a limited spectrum of disease involvement can be identified. Accuracy of ultrasonic examination of the intradural segment

of the vertebral artery can be improved by the use of simultaneous B-mode and color flow imaging. Further details on this subject are covered in Chap. 9.

## Color Duplex Ultrasound in the Diagnosis of Temporal Arteritis

Temporal arteritis is sometimes diagnosed clinically, but a temporal artery biopsy is usually recommended to confirm the diagnosis [100]. The American College of Rheumatology requires three of the following five criteria to be met to establish the diagnosis: age ≥50 years, new onset of localized headache, temporal artery tenderness or decreased pulse, erythrocyte sedimentation rate ≥50 mm/h, and histologic findings. Schmidt et al. [100] examined the usefulness of color duplex ultrasonography in patients suspected of having temporal arteritis. In their prospective study, all patients seen in the departments of rheumatology and ophthalmology from January 1994 to October 1996 who had clinically suspected active temporal arteritis or polymyalgia rheumatica were examined by duplex ultrasonography. They examined both common superficial temporal arteries and the frontal and parietal rami as completely as possible in longitudinal and transverse planes to see if they were perfused, if there was a halo around the lumen, and (using simultaneous pulsed-wave Doppler ultrasonography) if there was a stenosis. Stenosis was considered to be present if blood flow velocity was more than twice the rate recorded in the area before the stenosis, perhaps with waveforms demonstrating turbulence and reduced velocity behind the area of stenosis. Two ultrasound studies were performed and read before the biopsies. Based on standard criteria, the final diagnoses were temporal arteritis in 30 patients, 21 with biopsy-confirmed disease, polymyalgia rheumatica in 37, and negative histologic findings and a diagnosis other than temporal arteritis or polymyalgia rheumatica in 15. They also studied 30 control patients matched for age and sex to the patients with arteritis.

Schmidt et al. [100] found that in 22 (73%) of the 30 patients with temporal arteritis, ultrasonography showed a dark halo around the lumen of the temporal arteries. The halos disappeared after a mean of 16 days (range: 7–56) of treatment with corticosteroids. Twenty-four patients (80%) had stenoses or occlusions of temporal artery segments, and 28 patients (93%) had stenoses, occlusions, or a halo. No halos were identified in the 82 patients without temporal arteritis; 6 (7%) had stenoses or occlusions. For each of the three types of abnormalities identified by ultrasonography, the interrater agreement was ≥95%.

They concluded that there are characteristic signs of temporal arteritis that can be visualized by color duplex ultrasonography. The most specific sign is a dark halo, which may be due to edema of the artery wall. In patients with typical clinical signs and a halo on ultrasonography, it may be possible to make a diagnosis of temporal arteritis and begin treatment without performing a temporal artery biopsy. This subject will be covered in depth in another chapter in this volume.

## Overall Accuracy of Noninvasive Vascular Testing

As noted, various noninvasive vascular tests have been utilized for the diagnosis of extracranial carotid artery disease with varying degrees of overall accuracy. A review of these conflicting results reveals problems in study design and analysis: for example, lack of a prospective blinded approach, differences in criteria or standards indicative of carotid stenosis, failure to compare carotid noninvasive tests against standards, an assumption that the percentage of carotid stenosis on angiography correlates with hemodynamic alterations produced by the lesion, differences in the prevalence of carotid stenosis in the particular population examined, incomplete angiography, and lack of criteria for abnormal test results, skill of technicians, and the inherent accuracy of the test. Although angiography has been the standard against which most noninvasive tests have been measured, it is far from ideal for comparison with physiologic tests designed to detect altered hemodynamics. Furthermore, any significant stenosis in the carotid artery from its origin at the aorta up to and including the ophthalmic artery can result in abnormal test results in the indirect methods of testing. In addition, long-standing collateral pathways that compensate effectively for the hemodynamic effects of the stenotic lesion can produce a normal result in an indirect carotid test. Direct methods do not detect lesions in the upper part of the internal carotid artery, where such lesions can also produce an abnormal result with an indirect test. In an unbranched artery, blood flow is determined by the cross-sectional area of its narrowest portion and by the pressure gradient across it. Accordingly, the extent of stenosis caused by a carotid bifurcation plaque should be calculated by comparing the narrowest diameter of its diseased lumen with the diameter of the undiseased distal internal carotid artery. Although the term "critical stenosis" is generally used to compare the results of noninvasive testing, the exact value necessary to cause a measurable decrease in pressure or alteration in arterial blood flow remains controversial. DeWeese et al. [101] reported that lesions that narrowed the lumen less than 47% and left a residual lumen larger than 3 mm in diameter never caused measurable pressure drops, whereas stenoses greater than 63% of the luminal diameter with residual lumens smaller than 1 mm in diameter always did. Therefore, if systolic pressure distal to an arterial stenosis is measured, lesions that reduce the diameter 50% or more, thus reducing the cross-sectional area by 75% or more, are generally detected. However, if alterations in blood flow are measured, diameter reductions in excess of 67% (more than 90% of the cross-sectional area) are necessary for abnormal test results [102].

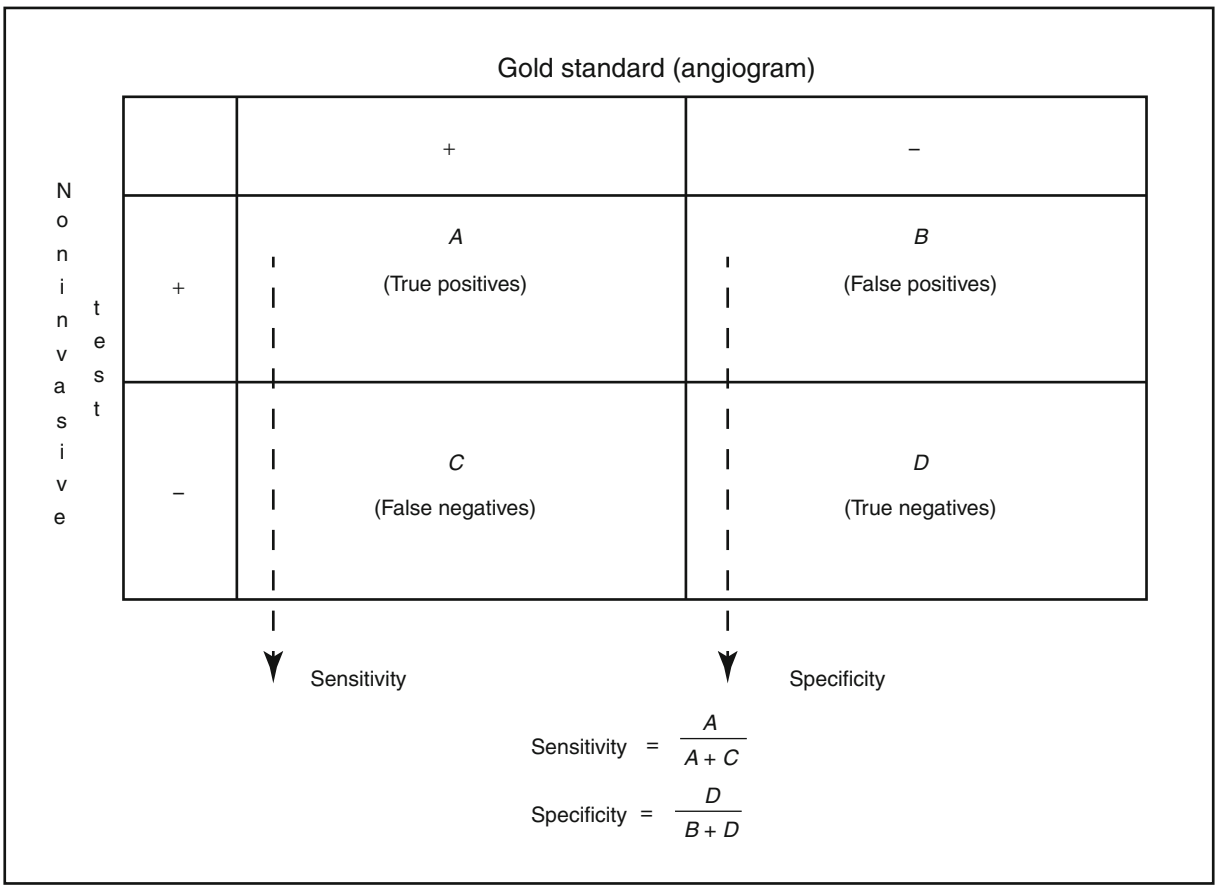


**Fig. 19.8** Method for calculating sensitivity and specificity

Clinically, a stenosis greater than 75% of the diameter or 94% of the area is necessary to cause symptomatic reduction of cerebral blood flow [103]. Since various reports have used diameter reductions from 40% to 75% as their standard of comparison, some variations in the reported results can be explained on this basis.

In addition to problems in study design, many of the carotid noninvasive studies report their results in terms of diagnostic accuracy. Since diagnostic accuracy may vary with the prevalence of disease in the population, it is impossible to compare different series if this term is used. By contrast, if results of carotid noninvasive studies are expressed in terms of sensitivity, i.e., the ability to detect the presence of the disease (true-positive rate) and specificity, i.e., the ability to detect the absence of disease (true-negative rate), these terms should be independent of disease prevalence and allow comparison of one series with another. The following terms are generally used in comparing the accuracy of various noninvasive vascular tests. (1) Sensitivity is calculated by dividing the number of true-positive tests detected noninvasively by the total number of true-positive tests detected by angiography. (2) Specificity is calculated by dividing the true-negative tests detected noninvasively by the total true-negative tests detected by angiography. (3) The false-positive rate is calculated by dividing the number of false-positive tests detected noninvasively by the total number of noninvasive positive tests. (4) The false-negative rate is calculated by dividing the number of false-negative tests detected noninvasively by the total number of negative noninvasive tests. (5) The positive predictive value is the percentage of noninvasive test results that accurately predicts abnormality, in other words, the percentage of positive noninvasive tests that correctly predicted disease as supported by "gold standard" arteriography. It is calculated by the number of true-positive noninvasive testing divided by the number of all positive noninvasive studies (i.e., true plus false-positives). (6) Negative predictive value is defined as the percentage of noninvasive test results that accurately predicts normality, in other words, the percentage of negative noninvasive studies that correctly predicted the absence of disease as supported by "gold standard" arteriography. It is calculated by dividing the number of true-negative noninvasive tests by the number of all negative noninvasive studies (i.e., true plus false-negatives). (7) The overall accuracy is defined as the sum of the true-positive and the true-negative values compared with the total number of tests performed. Figures 19.8, 19.9, and 19.10 are simplified methods of calculating sensitivity, specificity, positive predictive values, negative predictive values, and overall

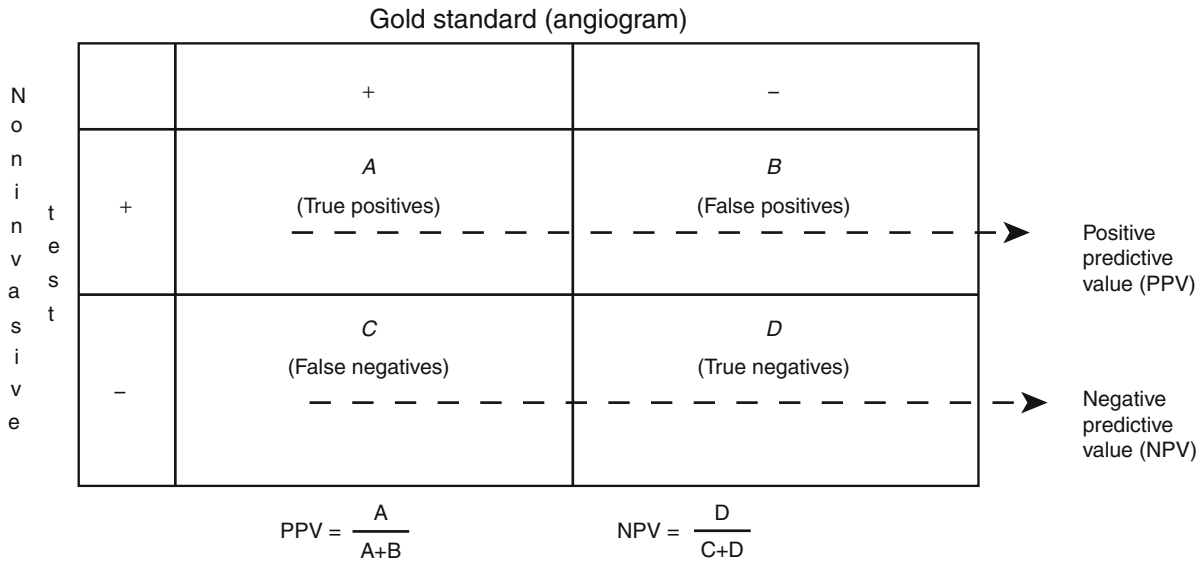


**Fig. 19.9** Method for calculating positive predictive values and negative predictive values

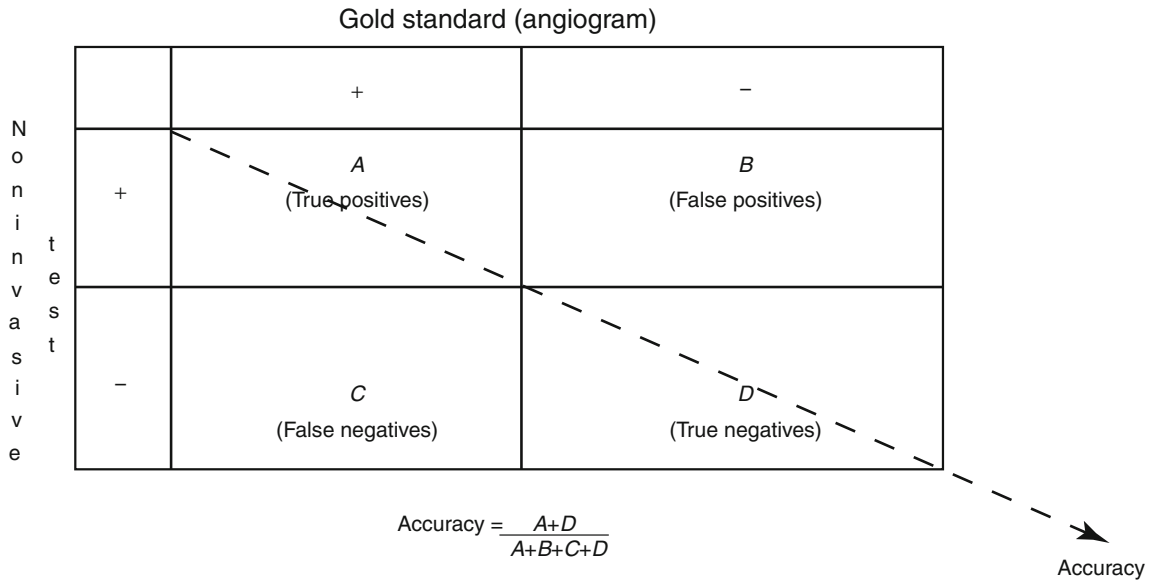


**Fig. 19.10** Method for calculating overall accuracy

accuracy. Although specificity and sensitivity possess certain advantages, they are limited to fixed threshold criteria that are taken as positive for the noninvasive carotid screening test. Expressing the result of a screening test as a receiver operator-characteristic curve avoids the limitations of fixed threshold criteria [103]. This curve plots the dynamic relationship between sensitivity and specificity and allows the examiner to increase or decrease the sensitivity of the tests by varying the threshold criterion for a positive result of that particular test.

## References

1. Cartier R, Cartier P, Fontaine A. Carotid endarterectomy without angiography: the reliability of Doppler ultrasonography and duplex scanning in preoperative assessment. Can J Surg. 1993;36:411–21.
2. Polak JF. Noninvasive carotid evaluation: carpe diem. Radiology. 1993;186:329–31.
3. Moore WS, Ziomek S, Quinones-Baldrich WJ, et al. Can clinical evaluation and noninvasive testing substitute for arteriography in the evaluation of carotid artery disease? Ann Surg. 1988;208:91–4.
4. Norris JW, Halliday A. Is ultrasound sufficient for vascular imaging prior to carotid endarterectomy? Stroke. 2004;35:370–1.

5. Moore WS. For severe carotid stenosis found on ultrasound, further arterial evaluation is unnecessary. Stroke. 2003;34:1816–7.
6. Executive Committee for the Asymptomatic Carotid Atherosclerosis Study. Endarterectomy for asymptomatic carotid artery stenosis. JAMA. 1995;273:1421–8.
7. Jones FL. Frequency, characteristics and importance of the cervical venous hum in adults. N Engl J Med. 1962;267:658.
8. Sauve JS, Laupacis A, Ostbye T, et al. Does this patient have a clinically important carotid bruit? JAMA. 1993;270:2843.
9. Caplan LR. Carotid artery disease. N Engl J Med. 1986;315:886.
10. Messert B, Marra TR, Zerofsky RA. Supraclavicular and carotid bruits in hemodialysis patients. Ann Neurol. 1977;2:535.
11. Fell G, Breslau P, Know RA, et al. Importance of noninvasive ultrasonic Doppler testing in the evaluation of patients with asymptomatic carotid bruits. Am Heart J. 1981;102:221–6.
12. Davies KN, Humphrey PRD. Do carotid bruits predict disease of the internal carotid arteries? Postgrad Med J. 1994;70:433.
13. Sauve JS, Thorpe KE, Sackett DL, et al. Can bruits distinguish high-grade from moderate symptomatic carotid stenosis? The North American symptomatic carotid endarterectomy trial. Ann Intern Med. 1994;120:633.
14. Ratchford EV, Zhezhen J, Di Tullio MR, Salameh MJ, Homma S, Gan R, Boden-Albala B, Sacco RL, Rundek T. Carotid bruit for the detection of hemodynamically significant carotid stenosis: the Northern Manhattan study. Neurol Res. 2009;31:748–52.
15. Heyman A, Wilkinson WE, Heyden S, et al. Risk of stroke in asymptomatic person with cervical arterial bruits: a population study in Evans County, Georgia. N Engl J Med. 1980;302:383.
16. Wiebers DO, Whisnant JP, Sandok BA, O'Fallen WM. Prospective comparison of a cohort with asymptomatic carotid bruit and a population-based cohort without carotid bruit. Stroke. 1990; 21:984–8.
17. Shorr RI, Johnson KC, Wan JY, et al. The prognostic significance of asymptomatic carotid bruits in the elderly. J Gen Intern Med. 1998;13:86.
18. Pickett CI, Jackson JL, Hemann BA, Atwood E. Carotid bruits as a prognostic indicator of cardiovascular death and myocardial infarction: a meta-analysis. Lancet. 2008;371:1587–94.
19. Benavente OR, Moher D, Pham B. Carotid endarterectomy for asymptomatic carotid stenosis: a meta-analysis. BMJ. 1998; 317:1477.
20. Chambers BR, You RX, Donnan GA. Carotid endarterectomy for asymptomatic carotid stenosis. Cochrane Databse Syst Rev 2000; (2):CD001923.
21. North American Symptomatic Carotid Endarterectomy Trial (NASCET) Investigators. Clinical alert: benefit of carotid endarterectomy for patients with high-grade stenosis of the internal carotid artery. National Institute of Neurological Disorders and Stroke, Stroke and Trauma Division. Stroke. 1991;22:816–7.
22. Marshall Jr WG, Kouchoukos NT, Murphy SF, et al. Carotid endarterectomy based on duplex scanning without preoperative arteriography. Circulation. 1988;78(Suppl I):I-1–5.
23. Jackson MR, Chang AS, Robles HA, et al. Determination of 60% or greater carotid stenosis: a prospective comparison of magnetic resonance angiography and duplex ultrasound with conventional angiography. Ann Vasc Surg. 1998;12:236–43.
24. AbuRahma AF, Robinson PA, Boland JP, et al. Complications of arteriography in a recent series of 707 cases: factors affecting outcome. Ann Vasc Surg. 1993;7:122–9.
25. AbuRahma AF, Robinson PA, Stickler DL, et al. Proposed new duplex classification for threshold stenoses used in various symptomatic and asymptomatic carotid endarterectomy trials. Ann Vasc Surg. 1998;12:349–58.
26. Sigel B, Coelho JC, Flanigan DP, et al. Detection of vascular defects during operation by imaging ultrasound. Ann Surg. 1982;196: 473–80.
27. Blaisdell FW, Lin R, Hall AD. Technical result of carotid endarterectomy – arteriographic assessment. Am J Surg. 1967; 114:239–46.
28. Bandyk DF, Govostis DM. Intraoperative color flow imaging of "difficult" arterial reconstructions. Video J Color Flow Imaging. 1991;1:13–20.
29. Hallett Jr JW, Berger MW, Lewis BD. Intraoperative color-flow duplex ultrasonography following carotid endarterectomy. Neurosurg Clin N Am. 1996;7:733–40.
30. Baker WH, Koustas G, Burke K, et al. Intraoperative duplex scanning and late carotid artery stenosis. J Vasc Surg. 1994;19:829–33.
31. Kinney EV, Seabrook GR, Kinney LY, et al. The importance of intraoperative detection of residual flow abnormalities after carotid artery endarterectomy. J Vasc Surg. 1993;17:912–22.
32. Coe DA, Towne JB, Seabrook GR, et al. Duplex morphologic features of the reconstructed carotid artery: changes occurring more than five year after endarterectomy. J Vasc Surg. 1997;25:850–7.
33. Cato R, Bandyk D, Karp D, et al. Duplex scanning after carotid reconstruction: a comparison of intraoperative and postoperative results. J Vasc Tech. 1991;15:61–5.
34. Lane RJ, Ackroyd N, Appleberg M, et al. The application of operative ultrasound immediately following carotid endarterectomy. World J Surg. 1987;11:593–7.
35. Sawchuk AP, Flanigan DP, Machi J, et al. The fate of unrepaired minor technical defects detected by intraoperative ultrasound during carotid endarterectomy. J Vasc Surg. 1989;9:671–6.
36. Ascher E, Markevich N, Kallakuri S, Schutzer RW, Hingorani AP. Intraoperative carotid artery duplex scanning in a modern series of 650 consecutive primary endarterectomy procedures. J Vasc Surg. 2004;39:416–20.
37. Lennard N, Smith JL, Gaunt ME, et al. A policy of quality control assessment reduces the risk of intraoperative stroke during carotid endarterectomy. Eur J Vasc Endovasc Surg. 1999;17:234–40.
38. Halsey Jr JH. Risks and benefits of shunting in carotid endarterectomy. Stroke. 1992;23:1583–7.
39. Ackerstaff RGA, Moons KGM, van de Vlasakker CJW, Moll FL, Vermeulen FEE, Algra A, Spencer MP. Association of intraoperative transcranial Doppler monitoring variables with stroke from carotid endarterectomy. Stroke. 2000;31:1817–23.
40. Gaunt ME, Ratliff DA, Martin PJ, Smith JL, Bell PR, Naylor AR. On-table diagnosis of incipient carotid artery thrombosis during carotid endarterectomy using transcranial Doppler sonography. J Vasc Surg. 1994;20:104–7.
41. Thomas M, Otis S, Rush M, et al. Recurrent carotid artery stenosis following endarterectomy. Ann Surg. 1984;200:74–9.
42. Mattos MA, Shamma AR, Rossi N, et al. Is duplex follow-up cost-effective in the first year after carotid endarterectomy? Am J Surg. 1988;156:91–5.
43. Cook JM, Thompson BW, Barnes RW. Is routine duplex examination after carotid endarterectomy justified? J Vasc Surg. 1990; 12:334–40.
44. Mackey WC, Belkin M, Sindhi R, et al. Routine postendarterectomy duplex surveillance: does it prevent late stroke? J Vasc Surg. 1992;16:934–40.
45. Mattos MA, van Bemmelen PS, Barkmeier LD, et al. Routine surveillance after carotid endarterectomy: does it affect clinical management? J Vasc Surg. 1993;17:819–31.
46. Ouriel K, Green RM. Appropriate frequency of carotid duplex testing following carotid endarterectomy. Am J Surg. 1995;170: 144–7.
47. Ricotta JJ, DeWeese JA. Is route carotid ultrasound surveillance after carotid endarterectomy worthwhile? Am J Surg. 1996;172: 140–3.
48. Golledge J, Cuming R, Ellis M, et al. Clinical follow-up rather than duplex surveillance after carotid endarterectomy. J Vasc Surg. 1997;25:55–63.

49. AbuRahma AF, Robinson PA, Saiedy S, et al. Prospective randomized trial of carotid endarterectomy with primary closure and patch angioplasty with saphenous vein, jugular vein, and polytetrafluoroethylene: long-term follow-up. J Vasc Surg. 1998; 27:222–34.
50. Patel ST, Kuntz KM, Kent KG. Is routine duplex ultrasound surveillance after carotid endarterectomy cost-effective? Surgery. 1998;124:343–53.
51. Roth SM, Back MR, Bandyk DF, et al. A rational algorithm for duplex scan surveillance after carotid endarterectomy. J Vasc Surg. 1999;30:453–60.
52. Qureshi AI, Alexandrov AV, Gegeler CH, Hobson II RW, Baker JD, Hopkins LN. Guidelines for screening of extracranial carotid artery disease: a statement for healthcare professionals from the multidisciplinary practice guidelines committee of the American Society of Neuroimaging: Co-sponsored by the Society of Vascular and Interventional Neurology. J Neuroimaging. 2007;17:19–47.
53. Moore WS, Kempczinski RF, Nelson JJ, Toole JF. Recurrent carotid stenosis: results of the asymptomatic carotid atherosclerosis study. Stroke. 1998;29:2018–25.
54. Cao P, Giordano G, DeRango P, Zannetti S, et al. Eversion versus conventional carotid endarterectomy: late results of a prospective multicenter randomized trial. J Vasc Surg. 2000;31:19–30.
55. Ricco JB, Camiade C, Roumy J, Neau JP. Modalities of surveillance after carotid endarterectomy: impact of surgical technique. Ann Vasc Surg. 2003;17:386–92.
56. Lovelace TD, Moneta GL, Abou-Zamzam AH, Edwards JM, Yeager RA, Landry GJ, Taylor LM, Porter JM. Optimizing duplex follow-up in patients with an asymptomatic internal carotid artery stenosis of less than 60%. J Vasc Surg. 2001;33:56–61.
57. AbuRahma AF, Snodgrass KR, Robinson PA, et al. Safety and durability of redo carotid endarterectomy for recurrent carotid artery stenosis. Am J Surg. 1994;168:175–8.
58. Kupinski AM, Khan AM, Stanton JE, Relyea W, Ford T, Mackey V, Khurana Y, Darling RC, Shah DM. Duplex ultrasound follow-up of carotid stents. J Vasc Ultrasound. 2004;28:71–5.
59. Robbin ML, Lockhart ME, Weber TM, et al. Carotid artery stent: early and intermediate follow-up with Doppler ultrasound. Radiology. 1997;205:749–56.
60. Roederer GO, Langlois YE, Jager KA, et al. The natural history of carotid artery disease in asymptomatic patients with cervical bruits. Stroke. 1984;15:605–13.
61. Sundt Jr TM, Whisnant JP, Houser OW, Fode NC. Prospective study of the effectiveness and durability of carotid endarterectomy. Mayo Clin Proc. 1990;65:625–35.
62. Ricotta JJ, Char DJ, Cuadra SA, et al. Modeling stroke risk after coronary artery bypass and combined coronary artery bypass and carotid endarterectomy. Stroke. 2003;34:1212–7.
63. Raman KG, Layne S, Makaroun MS, et al. Disease progression in contralateral carotid artery is common after endarterectomy. J Vasc Surg. 2004;39:52–7.
64. Martin-Conejero A, Reina-Gutierrez T, Serrano-Hernando FJ, et al. Disease progression in the contralateral carotid artery after endarterectomy. Ann Vasc Surg. 2005;19:662–8.
65. AbuRahma AF, Robinson PA, Mullins DA, Holt SM, Herzog TA, Mowery NT. Frequency of postoperative carotid duplex surveillance and type of closure: results from randomized trial. J Vasc Surg. 2000;32:1043–51.
66. AbuRahma AF, Hannay RS, Khan JH, et al. Prospective randomized study of carotid endarterectomy with polytetrafluoroethylene versus collagen impregnated Dacron (hemashield) patching: perioperative (30-day) results. J Vasc Surg. 2002;35:125–30.
67. Dawson DL, Zierler RE, Strandness Jr DE, et al. The role of duplex scanning and arteriography before carotid endarterectomy: a prospective study. J Vasc Surg. 1993;18:673–83.
68. Horn M, Michelini M, Greisler HP, et al. Carotid endarterectomy without arteriography: the preeminent role of the vascular laboratory. Ann Vasc Surg. 1994;8:221–4.
69. Chervu A, Moore WS. Carotid endarterectomy without arteriography. Ann Vasc Surg. 1994;8:296–302.
70. Mattos MA, Hodgson KJ, Faught WE, et al. Carotid endarterectomy without angiography: is color-flow duplex scanning sufficient? Surgery. 1994;116:776–83.
71. Walsh J, Markowitz I, Kerstein MD. Carotid endarterectomy for amaurosis fugax without angiography. Am J Surg. 1986;152: 172–4.
72. Dawson DL, Zierler RE, Kohler TR. Role of arteriography in the preoperative evaluation of carotid artery disease. Am J Surg. 1991;161:619–24.
73. Kuntz KM, Skillman JJ, Whittemore AD, et al. Carotid endarterectomy in asymptomatic patients: is contrast angiography necessary? A morbidity analysis. J Vasc Surg. 1995;22:706–16.
74. Kent KC, Kuntz KM, Patel MR. Perioperative imaging strategies for carotid endarterectomy: an analysis of morbidity and cost-effectiveness in symptomatic patients. JAMA. 1995;274:888–93.
75. Campron H, Cartier R, Fontaine AR. Prophylactic carotid endarterectomy without arteriography in patients without hemispheric symptoms: surgical morbidity and mortality and long-term follow-up. Ann Vasc Surg. 1998;12:10–6.
76. Loftus IM, McCarthy MJ, Pau H, et al. Carotid endarterectomy without angiography does not compromise operative outcome. Eur J Vasc Endovasc Surg. 1998;16:489.
77. Roederer GO, Langlois YE, Chan ARW, et al. Is siphon disease important in predicting outcome of carotid endarterectomy? Arch Surg. 1983;118:1177–81.
78. Mattos MA, van Bemmelen PS, Hodgson KJ, et al. The influence of carotid siphon stenosis on short and long-term outcome after carotid endarterectomy. J Vasc Surg. 1993;17:902–11.
79. Lord RSA. Relevance of siphon stenosis and intracranial aneurysm to results of carotid endarterectomy. In: Ernst CB, Stanley JC, editors. Current therapy in vascular surgery. 2nd ed. Philadelphia: BC Decker; 1991. p. 94–101.
80. Strandness Jr DE. Extracranial arterial disease. In: Strandness Jr DR, editor. Duplex scanning in vascular disorders. 2nd ed. New York: Raven; 1993. p. 113–58.
81. Pilcher DB, Ricci MA. Vascular ultrasound. Surg Clin North Am. 1998;78:273–93.
82. AbuRahma AF, Kyer III PD, Robinson PA, et al. The correlation of ultrasonic carotid plaque morphology and carotid plaque hemorrhage: clinical implications. Surgery. 1998;124:721–8.
83. AbuRahma AF, Thiele SP, Wulu JT. Prospective controlled study of the natural history of asymptomatic 60% to 69% carotid stenosis according to ultrasonic plaque morphology. J Vasc Surg. 2002;36:437–42.
84. AbuRahma AF, Wulu JT, Crotty B. Carotid plaque ultrasonic heterogeneity and severity of stenosis. Stroke. 2002;33:1772–5.
85. Choo V. New imaging technology might help prevent stroke. Lancet. 1998;351:809.
86. Kern R, Szabo K, Hennerici M, Meairs S. Characterization of carotid artery plaques using real-time compound B-mode ultrasound. Stroke. 2004;35:870–5.
87. Biasi GM, Sampaolo A, Mingazzini P, De Amicis P, El-Barghouty N, Nicolaides AN. Computer analysis of ultrasonic plaque echolucency in identifying high-risk carotid bifurcation lesions. Eur J Vasc Endovasc Surg. 1999;17:476–9.
88. Poli A, Tremoli E, Colombo A, Sirtori M, Pignoli P, Paoletti R. Ultrasonographic measurement of the common carotid artery wall thickness in hypercholesterolemic patients. A new model for the quantitation and follow-up of preclinical atherosclerosis in living human subjects. Atherosclerosis. 1988;70:253–61.

89. O'Leary DH, Polak JF, Kronmal RA, et al. Thickening of the carotid wall. A marker for atherosclerosis in the elderly? Cardiovascular Health Study Collaborative research Group. Stroke. 1996;27:224–31.
90. Polak JF, O'Leary DH, Kronmal RA, et al. Sonographic evaluation of carotid artery atherosclerosis in the elderly: relationship of disease severity to stroke and transient ischemic attack. Radiology. 1993;188:363–70.
91. O'Leary DH, Polak JF, Kronmal RA, Manolio TA, Burke GL, Wolfson Jr SK. Carotid-artery intima and media thickness as a risk factor for myocardial infarction and stroke in older adults. Cardiovascular Health Study Collaborative Research Group. N Engl J Med. 1999;340:14–22.
92. Fry WR, Dort JA, Smith RS, et al. Duplex scanning replaces arteriography and operative exploration in the diagnosis of potential cervical vascular injury. Am J Surg. 1994;168:693–6.
93. Steinke W, Schwartz A, Hennerici M. Doppler color flow imaging of common carotid artery dissection. Neuroradiology. 1990; 32(6):502–5.
94. Sturzenegger M. Ultrasound findings in spontaneous carotid artery dissection. The value of duplex sonography. Arch Neurol. 1991;48(10):1057–63.
95. Cals N, Devuyst G, Jung DK, Afsar N, de Freitas G, Despland PA, Bogousslavsky J. Uncommon ultrasound findings in traumatic extracranial dissection. Eur J Ultrasound. 2001;12:227–31.
96. Keller HM, Meier WE, Kumpe DA. Noninvasive angiography for the diagnosis of vertebral artery disease using Doppler ultrasound (vertebral artery Doppler). Stroke. 1976;7:364–9.
97. Kaneda H, Irino T, Minami T, et al. Diagnostic reliability of the percutaneous ultrasonic Doppler technique for vertebral arterial occlusive diseases. Stroke. 1977;8:571–9.
98. Bartels E, Fuchs HH, Flugel KA. Color Doppler imaging of vertebral arteries: a comparative study with duplex ultrasonography. In: Oka M et al., editors. Recent advantages in neurosonology. Amsterdam: Elsevier Science Publishers; 1992.
99. De Bray JM. Le duplex des axes verebro-sous-claviers. J Echographie Med Ultrasonsound. 1991;12:141–51.
100. Schmidt WA, Kraft HE, Vorpahl K, et al. Color duplex ultrasonography in the diagnosis of temporal arteritis. N Engl J Med. 1997;337:1336–42.
101. DeWeese JA, May AG, Lipchik EO, et al. Anatomic and hemodynamic correlations in carotid artery stenosis. Stroke. 1970;1: 149–57.
102. Gee W. Discussion following: Archie JP, Feldtman RW. Critical stenosis of the internal carotid artery. Surgery. 1981;89:67–72.
103. O'Donnell TF, Pauker SG, Callow AD, et al. The relative value of carotid noninvasive testing as determined by receiver operator characteristic curves. Surgery. 1980;87:9–19.

# Part IV

# Noninvasive Diagnosis of Peripheral Arterial Disease of the Extremities

Dennis F. Bandyk

# Overview of Peripheral Arterial Disease of the Lower Extremity

20

Ali F. AbuRahma and John E. Campbell

**Abstract**

The overall prevalence of peripheral arterial disease (PAD) based on objective data has been evaluated in several epidemiological studies and is in the range of 3–10%, which increases to 15–20% in people over the age of 70 years. The prevalence of asymptomatic PAD of the lower extremity can only be estimated using noninvasive vascular testing in the general population with the ankle-brachial index (ABI) being the most widely used testing.

A number of risk factors for the development of atherosclerosis have been reasonably well established. These factors include hypertension, hypercholesterolemia, cigarette smoking, obesity, diabetes mellitus, stress, sedentary lifestyle, and family history.

Intermittent claudication as a symptom of peripheral arterial disease can be caused by flow-limiting stenosis, which is almost secondary to atherosclerosis.

After the initial diagnosis of chronic lower extremity ischemia is made, it is important to stage the severity of the process accurately. This is crucial because it is the stage of the disease and the natural history of each stage that ultimately determine which therapy is most appropriate.

A variety of noninvasive tests are available for assessment of the lower extremity vascular system.

Perhaps the most useful bedside noninvasive test available to the clinician is the ABI. The most commonly used noninvasive testing used to confirm the disease, assess severity, and to help its localization are segmental Doppler pressure, pulse volume recordings, and duplex ultrasound.

Other important imaging modalities for determining the management strategies include MRA, CTA, and catheter-based angiography.

This chapter will review the basic anatomy, pathophysiology, clinical presentations, various noninvasive tests, and imaging for the diagnosis of peripheral arterial disease (PAD) of the lower extremities. It will also highlight the management outlines.

**Keywords**

Disease • Peripheral arterial disease • Lower extremity

A.F. AbuRahma, M.D., RVT, RPVI (✉)
Department of Surgery, Robert C. Byrd Health Sciences Center, West Virginia University, 3110 MacCorkle Ave SE, Charleston, WV 25304, USA

Charleston Area Medical Center, Charleston, WV, USA
e-mail: ali.aburahma@camc.org

J.E. Campbell, M.D.
Department of Surgery, Robert C. Byrd Health Sciences Center, West Virginia University, Charleston Area Medical Center, Charleston, WV, USA

## Vascular Anatomy of the Lower Extremity

At its most distal aspect, the aorta branches to form paired common iliac arteries. These continue retroperitoneally to the pelvic brim, at which the common iliac vessels branch to form paired internal and external iliac arteries. The internal iliac (or hypogastric) arteries provide blood supply to the pelvic structures, while the external iliac courses inferior to the inguinal ligament to become the common femoral artery.

A.F. AbuRahma, D.F. Bandyk (eds.), *Noninvasive Vascular Diagnosis*,
DOI 10.1007/978-1-4471-4005-4_20, © Springer-Verlag London 2013

The common femoral artery then bifurcates early in its course to form the profunda femoris artery, which supplies the thigh musculature, and the superficial femoral artery, which continues inferiorly to become the popliteal artery at its point of entry into the adductor canal.

The popliteal artery then continues below the knee, where the anterior tibial artery branches, piercing the interosseous membrane to supply the anterior compartment of the lower leg. The tibioperoneal trunk then continues briefly, where the posterior tibial artery branches to course in a plane deep to the soleus muscle. The vessel then continues inferiorly as the peroneal artery. The posterior tibial artery is divided into lateral and medial plantar arteries below the medial malleolus to supply the sole of the foot.

Ultimately, the anterior tibial artery continues onto the dorsum of the foot, where it becomes the dorsalis pedis artery. Here, it anastomoses with branches of the posterior tibial and peroneal arteries to form the plantar arch [1]. On the dorsum of the foot, the dorsalis pedis artery forms two branches: the dorsal metatarsal and the deep plantar arteries. The deep plantar artery penetrates into the sole of the foot and joins the lateral plantar artery (branch of the posterior tibial artery) to form the plantar arch.

The arterial anatomy relevant to the lower extremity circulation is demonstrated in Fig. 20.1.

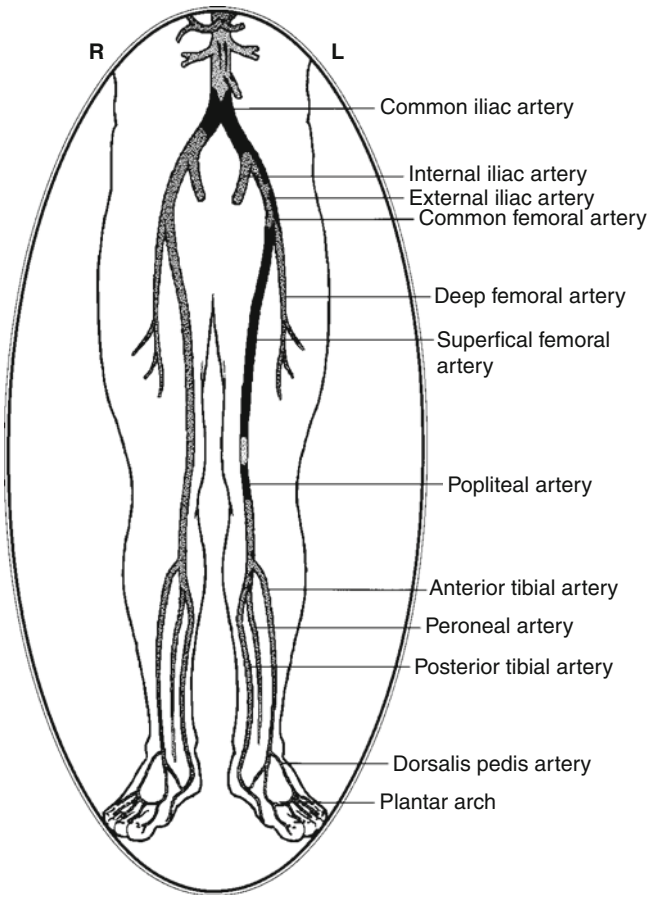


**Fig. 20.1** A normal right arterial tree (except for occlusion of the right common iliac artery) beginning with the common iliac artery down to the pedal branches. The *left side* shows occlusion of the left common iliac artery, stenosis of the left external iliac artery, and occlusion of the left superficial femoral artery, popliteal artery, and diseased tibioperoneal trunk

## Collateral Circulation of the Lower Extremity

In the event of chronic obstruction of major arterial vessels, collateral pathways exist that allow preservation of sufficient distal blood flow to maintain viability of the tissues distally. The degree of adequacy of these pathways determines what degree of functional disability results.

With obstruction at the level of the distal aorta and common iliac arteries, a variety of pathways for collateral circulation exist (Fig. 20.2). Communications may exist between the lumbar and circumflex iliac or hypogastric arteries. Other communications may exist between the gluteal branches of the hypogastric arteries and recurrent branches of the common femoral or profunda femoris arteries. Visceral–parietal communications may also exist at this level between the inferior mesenteric and internal iliac vessels via hemorrhoidal branches at the level of the rectum.

More distally, with obstruction of the common femoral artery, collateral circulation around the hip is provided via communication of the inferior epigastric and deep circumflex branches of the external iliac arteries with the internal pudendal and obturator branches of the internal iliac arteries (Fig. 20.2b).

With chronic obstruction of the superficial femoral artery, collateral circulation to the popliteal artery is provided by communications with the profunda femoris artery via the geniculate arteries as well as descending branches of the lateral femoral circumflex arteries. With popliteal occlusion, it is these geniculate arteries that are responsible for the filling of the more distal tibial vessels as well (Fig. 20.2b). More distally, branches of the peroneal, anterior tibial, and posterior tibial arteries all provide collateral supply to the plantar arch vessels [1, 2].

## Normal Structure of the Arterial Wall

The intima, the innermost layer, consists of a layer of endothelium that lines the luminal surface and overlies one or more layers of smooth muscle. These are then covered by a layer of connective tissue known as the internal elastic lamina.

Just beyond the internal elastic lamina begins the media, which is bounded by the internal and external elastic lamina. The media is composed of smooth muscle cells arranged in layers and lying in a matrix of proteoglycan substance. Collagen and elastin fibers are also present within this layer.

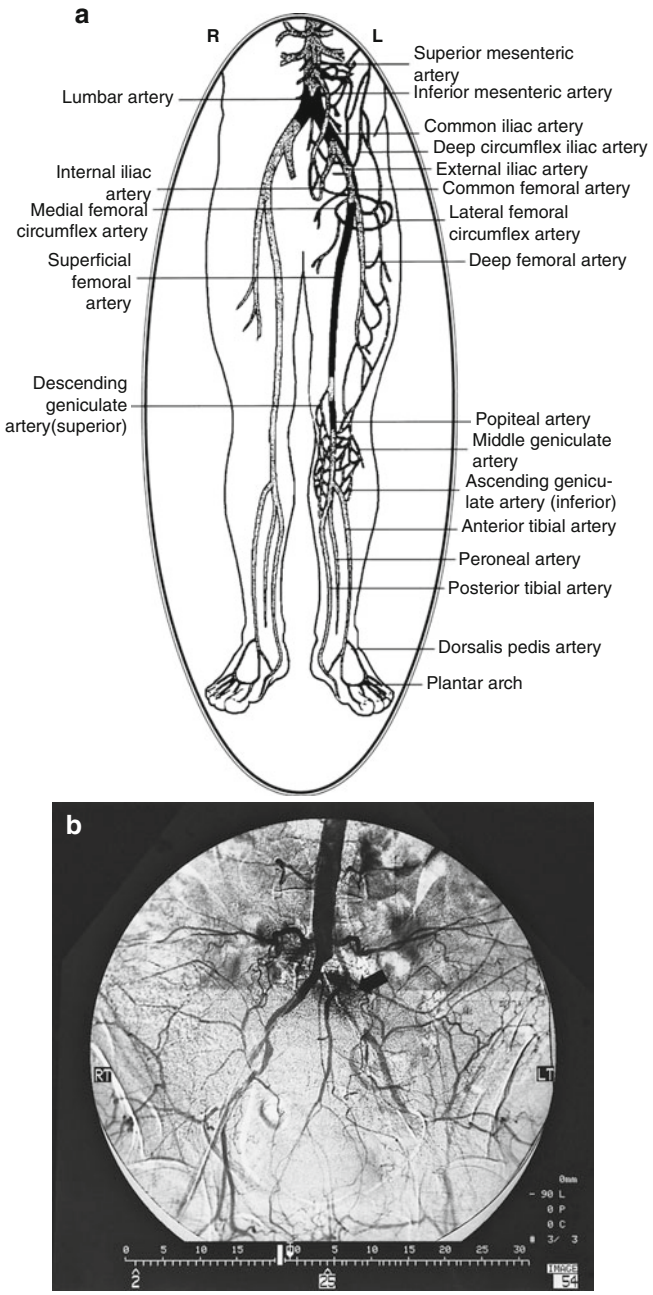


**Fig. 20.2** (**a**) Collateral circulation of the left lower extremity secondary to occlusion of the major arterial segments as noted in Fig. 20.1. (**b**) Arteriogram showing complete occlusion of the left common iliac artery (*arrow*). Note the collateral circulation around the obstruction. This also shows extensive disease of both right and left external iliac arteries

The adventitia is the outermost layer of the arterial wall and the layer responsible for the majority of the vessel's strength. It is composed of connective tissue, fibroblasts, capillaries, neural fibers, and occasional leukocytes. In large vessels, a microvasculature known as the vasa vasorum is present within the adventitial layer, serving to nourish the adventitia and outermost layers of the media [3].

## Incidence/Prevalence of Peripheral Arterial Disease

The overall prevalence of peripheral arterial disease (PAD) based on objective data has been evaluated in several epidemiological studies and is in the range of 3–10%, which increases to 15–20% in people over the age of 70 years [4]. The prevalence of asymptomatic PAD of the lower extremity can only be estimated using noninvasive vascular testing in the general population with the ankle-brachial index (ABI) being the most widely used testing. A resting ABI of ≤0.9 is generally caused by hemodynamically significant arterial stenosis and most often is used as a hemodynamic definition of PAD. This definition in symptomatic individuals (ABI ≤ 0.9) is 95% sensitive in detecting PAD confirmed by angiography and 100% specific in identifying healthy individuals [4]. The PARTNERS (PAD Awareness, Risk, and Treatment: New Resources for Survival) study, which screened 6,979 patients for PAD using an ABI of ≤0.9 or a prior history of lower extremity revascularization, reported the presence of 29% of PAD in the total population [5]. Classic vascular claudication was present in 5.5% of the newly diagnosed patients with PAD, and 12.6% of patients with a prior diagnosis of PAD had claudication. The National Health and Nutritional Examination Survey recently reported on an unselected population of 2,174 individuals aged ≥40 years [6]. The prevalence of PAD ranged from 2.5% in the age group of 50–59 years to 14.5% in individuals >70 years.

The prevalence of symptomatic PAD, i.e., intermittent claudication, would appear to increase from about 3% in patients aged 40 to 6% in patients aged 60 years. Several large population studies have analyzed the prevalence of intermittent claudication as noted in Fig. 20.3. As noted in this figure, the prevalence in patients between 30 and 34 years is less than 1%, which increases to approximately 7% for patients between 70 and 74 years. It has also been reported that in relatively younger age groups, claudication is more common in men, but at an older age, there is little difference between men and women. It has also been reported that black ethnicity increases the risk of PAD by over twofold, which cannot be explained by a higher level of other risk factors for PAD [4].

## Risk Factors

Through epidemiologic data, a number of risk factors for the development of atherosclerosis have been reasonably well established. These factors include hypertension, hypercholesterolemia, cigarette smoking, obesity, diabetes mellitus, stress, sedentary lifestyle, and family history.

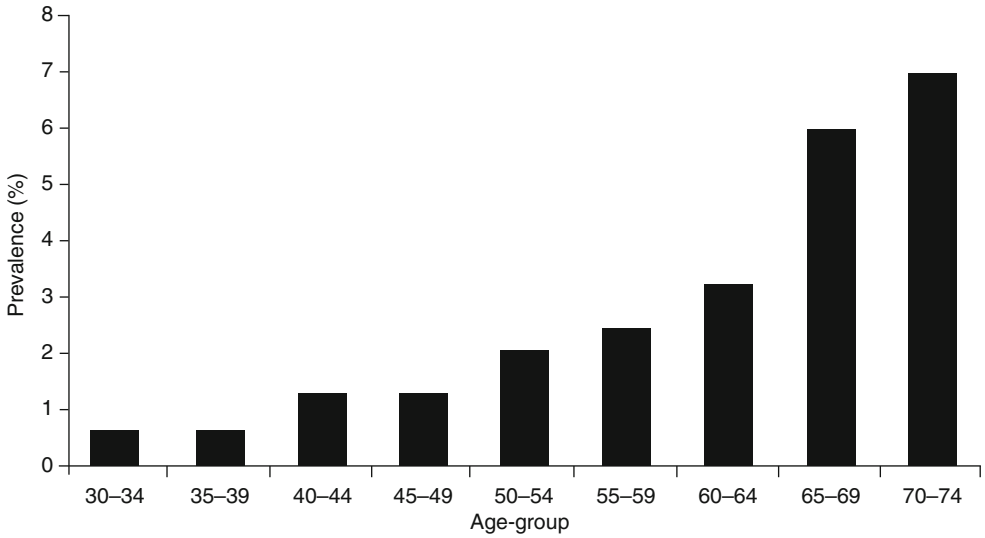


**Fig. 20.3** Weighted mean prevalence of intermittent claudication (symptomatic PAD) in large population-based studies (Reprinted from Norgren et al. [4]. With permission from Elsevier)

## Age

As noted in Fig. 20.3, there is a striking increase in both the incidence and prevalence of PAD with increasing age [4].

Merino et al. analyzed the incidence and risk factors of PAD in a prospective cohort of 700 adult elderly men followed for 5 years and concluded that 12% of adult men aged between 55 and 74 years developed PAD. Besides subjects with a history of cardiovascular disease, men older than aged 70 years and heavy smoker constituted a high-risk group for PAD and, therefore, the object of directed efforts of primary prevention [7].

## Gender

The prevalence of PAD is slightly higher in men than in women, particularly in the younger age group. The ratio of men to women in patients with intermittent claudication ranges between 1:1 and 2:1. This ratio increases in some studies to at least 3:1 in individuals with a severe stage of PAD [4].

## Smoking

Intermittent claudication is three times more common among smokers than nonsmokers. It has also been suggested that the association between PAD and smoking is even stronger than between coronary artery disease and smoking. A diagnosis of PAD is made approximately a decade earlier in smokers than in nonsmokers, and the severity of PAD tended to increase with the number of cigarettes smoked. Smoking cessation is also associated with a decline in the incidence of intermittent claudication, as reported by the Edinburgh Artery Study [8], which concluded that the relative risk of intermittent claudication was 3.7 in smokers compared with 3.0 in previous smokers (who quit smoking for less than 5 years).

## Diabetes Mellitus

Intermittent claudication is twice as common among diabetic patients as among nondiabetics. It has also been estimated that for every 1% increase in hemoglobin A1c, there is a corresponding 26% increased risk of PAD [9]. Insulin resistance plays a major role in clustering of cardiometabolic risk factors, which include hypertension, dyslipidemia, hyperglycemia, and obesity. Insulin resistance is also a risk factor for PAD in patients without diabetes, raising the risk 40–50% [10]. PAD in patients with diabetes mellitus is also more aggressive, compared to nondiabetics with early large vessel involvement combined with distal small vessel disease and neuropathy. Major amputation is also 5–10 times higher in diabetics than in nondiabetics. Based on these findings, a consensus statement from the American Diabetes Association recommended PAD screening with an ABI every 5 years in diabetic patients [11]. There is strong evidence that better control of blood sugar delays the onset of microvascular diabetic retinopathy and nephropathy; however, the effect of such control in progression of macrovascular disease remains controversial [12].

## Dyslipidemia

A fasting cholesterol level greater than 270 mg/dL was associated with a doubling of the incidence of intermittent claudication, based on the Framingham study. However, the ratio of total to high-density lipoprotein cholesterol was the best predictor of occurrence of PAD. Although some studies have shown that total cholesterol is a powerful independent risk factor for PAD, others have failed to confirm this association [4]. An association between hypertriglyceridemia and PAD has also been noted and has been shown to be associated with progression/complications of PAD. Lipoprotein (a) is also a significant independent risk factor for PAD.

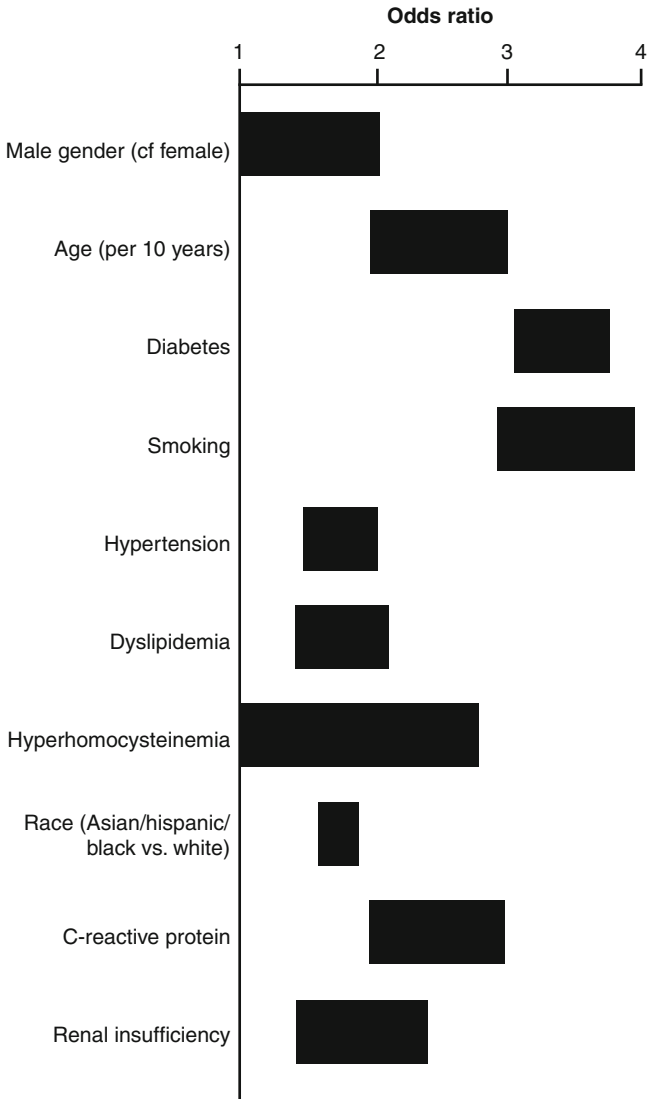


**Fig. 20.4** Approximate range of odds ratios for risk factors for symptomatic peripheral arterial disease (Reprinted from Norgren et al. [4]. With permission from Elsevier)

## Hypertension

Hypertension is associated with all forms of cardiovascular disorders, e.g., PAD. However, it should be noted that the relative risk of developing PAD is less for hypertension than for diabetes or smoking (Fig. 20.4). The role of hypertension in the development of peripheral arterial disease has been controversial, with the Framingham and the Finnish studies arriving at opposite conclusions. Hypertension may have both a cause and effect relation to peripheral arterial disease. Aggressive blood pressure control in newly diagnosed hypertensive patients occasionally decreases perfusion sufficiently to unmask and recognize hemodynamically significant stenotic lesions.

## Hyperhomocysteinemia

The prevalence of hyperhomocysteinemia is higher in patients with PAD, compared with 1% in the general population. Hyperhomocysteinemia is detected in about 30% of young patients with PAD, and it is believed to be an independent risk factor for atherosclerosis. It has also been felt to be a stronger risk factor for PAD than for CAD [4].

## Inflammatory Markers/C-reactive Protein

Recent studies have shown that C-reactive protein (CRP) is higher in asymptomatic subjects who developed PAD in the subsequent 5 years, compared to an age-matched control group who remained asymptomatic. The risk of developing PAD in the highest quartile of baseline CRP was more than twice that in the lower quartile [13].

## Chronic Renal Insufficiency

PAD has been associated with chronic renal insufficiency. In the Heart and Estrogen/Progestin Replacement Study (HERS), chronic renal insufficiency was independently associated with future PAD events in postmenopausal women [14].

## Hypercoagulable States

Hyperviscosity and raised hematocrit have been noticed in patients with PAD, which may be a consequence of smoking. Increased plasma fibrinogen levels have also been associated with PAD in some studies [4].

## Race

PAD, as defined as an ABI of ≤0.9, was more common in non-Hispanic blacks (7.8%) than in whites (4.4%), based on the National Health and Nutrition Examination Survey in the United States. This was also confirmed by the GENOA (Genetic Epidemiology Network of Arteriopathy) study [15].

Finally, a family history has not been found to be a significant independent risk factor in the development of peripheral arterial disease, in contrast to patients with coronary artery disease. Figure 20.4 demonstrates the approximate range of odds ratio for risk factors for symptomatic PAD.

Alzamora et al. reported on the PAD study (PERART/ARTPER) and the prevalence and risk factors in the general population. They performed a cross-sectional, multicenter, population-based study in 3,786 individuals aged over 49 years, randomly selected in 28 primary care centers in Barcelona, Spain. Patients were diagnosed as having PAD if their ABI was <0.9. The prevalence of PAD was 7.6% (10.2% for males and 5.3% for females). A multivariate analysis showed the following risk factors: male sex (odds ratio [OR] 1.62), age (OR 2.00 per 10 years), inability to perform physical activity (OR 1.77 for mild limitation to OR 7.08 for breathless performing any activity), smoking (OR 2.19) for former smokers and (OR 3.83) for current smokers, hypertension (OR 1.85), diabetes (OR 2.01), previous cardiovascular disease

(OR 2.19), hypercholesterolemia (OR 1.55), and hypertriglyceridemia (OR 1.55). Body mass index ≥25 kg/m$^2$ (OR 0.57) and walking more than 7 h/week (OR 0.67) were found as protector factors. They concluded that the prevalence of PAD is low, higher in males, and increases with age in both sexes. In addition to previously described risk factors, they found a protector effect in physical exercise and overweight [16].

### Association of Peripheral Arterial Disease, Coronary Artery Disease, and Cerebrovascular Disease

Pooling evidence from available studies such as the TransAtlantic Intersociety Consensus (TASC) concluded that approximately 60% of patients with peripheral arterial disease have significant coronary artery disease, cerebrovascular disease, or both, whereas about 40% of those with coronary artery or cerebrovascular disease also have peripheral arterial disease [17]. Murabito et al. [18] reported that the diagnosis of concomitant coronary artery disease can be established with a clinical history, physical examination, and EKG in 40–60% of all patients with intermittent claudication.

## Atherosclerosis

### Pathophysiology

Intermittent claudication as a symptom of peripheral arterial disease can be caused by flow-limiting stenosis, which is almost secondary to atherosclerosis. Whether or not a stenotic lesion is flow limiting depends on both flow velocities and the degree of stenosis [19]. Flow velocity at rest has been estimated to be as low as 20 cm/s in the femoral artery. A diameter reduction of >90% would be required for a stenotic lesion at these rates to be considered hemodynamically significant. However, the metabolic requirements in the distal tissue of an exercising or active individual are higher, and the femoral artery velocities may increase up to 150 cm/s, and at this velocity level, a stenosis of 50% can cause significant pressure and flow gradient, leading to inadequate oxygen delivery. In general, patients with mild intermittent claudication typically have a single segment disease, which is often associated with well-developed collateral circulation, in contrast to patients with severe claudication or critical limb ischemia, which is associated with multilevel disease.

The hemodynamic abnormalities of peripheral arterial occlusive disease reflected in ankle-brachial index (ABI) measurements or direct measurement of calf blood flow do not necessarily correlate with walking performance or severity of the claudication symptoms [20]. Biochemical changes and microcirculatory changes induced by the cycle of ischemia and reperfusion have been suggested as evidence of this observation. This may lead to skeletal muscle injury due to distal axonal degeneration, which, in turn, may cause muscle atrophy, further compromising exercise tolerance. This injury may be mediated at the cellular level through increased oxidative stress, generation of oxygen-free radicals, and lipid peroxidation that occurs during reperfusion of ischemic tissue. Several studies have demonstrated the accumulation of several metabolic intermediates, such as acylcarnitines, impaired synthesis of phosphocreatinine, and supranormal levels of adenosine diphosphates [21]. Patients with advanced chronic peripheral arterial disease have an abundance of these antimetabolic compounds, which signify well-established metabolic myopathy. Increased acylcarnitine accumulation has been noted to correlate well with decreased treadmill exercise performance [22].

The basic underlying disease process affecting the arterial wall, and the one responsible for the clinical manifestations of lower extremity peripheral arterial disease, is atherosclerosis. Simply put, atherosclerosis is a disease of medium to large arterial vessels that causes luminal narrowing, thrombosis, and occlusion resulting in ischemia of the end organ involved. The process of atherosclerosis is extremely complex and is the subject of continuous investigation within the medical and surgical community. In addition to lower extremity vascular disease, atherosclerosis is known to produce many other clinical events of importance including, but not limited to, myocardial infarction, stroke, mesenteric vascular insufficiency, and aortic aneurysm formation [23].

Atherosclerosis is primarily a disease of the intima characterized by the proliferation of smooth muscle cells and the accumulation of lipid material. The earliest lesion appears to be that of the fatty streak. In this lesion, lipid accumulates within the vessel wall, either extracellularly or intracellularly, within macrophages known as foam cells. This lesion often forms quite early in the course of the disease and may even be found in the arterial system of young children [24].

The fibrous plaque, the next phase of atherogenesis, is characterized histologically by a thick fibrous luminal cap composed of smooth muscle cells and connective tissue. This plaque typically overlies a core composed of necrotic debris and lipid material (the atheroma). Continued proliferation of smooth muscle cells and accumulation of lipid material result in the luminal narrowing characteristic of the disease [25].

In some cases, although it is unclear why, the plaque may develop features of luminal ulceration and wall calcification or hemorrhage. These changes result in what is known as the complicated lesion of atherosclerosis. The nature of this lesion is far more unstable and is the source for the arterioarterial thromboembolic events observed in these patients [26].

## Theories of Atherosclerosis

The extreme complexity of the atherosclerotic process has resulted in the formulation of several theories to explain its pathogenesis. These theories are based on attempts to account for one or more aspects of the disease and are therefore not mutually exclusive. In general, three theories have emerged as the most reasonable: the response to injury hypothesis, the lipid hypothesis, and the monoclonal (or mutagenic cellular transformation) hypothesis.

### The Response to Injury Hypothesis

The response to injury hypothesis is based on the marked similarity of atherosclerotic lesions to those occurring after experimental injury. The hypothesis states that some form of arterial injury (via the aforementioned risk factors) results in focal disruption of the endothelium, thus allowing interaction between the blood elements and the arterial walls. This then allows interaction of leukocytes and platelets with the disrupted surface. Platelet degranulation results, as does migration of macrophages into the injured intimal layer. One substance released from the platelet—platelet-derived growth factor (PDGF)—is thought to induce the smooth muscle proliferation characteristic of the process [27, 28]. This hypothesis may explain the marked tendency for atherosclerosis to develop in regions of increased turbulence such as that observed at major arterial bifurcations.

### The Monoclonal Hypothesis: Smooth Muscle Proliferation

The monoclonal hypothesis states that the smooth muscle proliferation characteristic of the plaque is similar to a benign neoplasm arising from a single progenitor cell from the monocyte–macrophage lineage. Evidence for this is provided by the observance of a monotypic enzyme pattern in the plaques of heterozygotic individuals, as opposed to the bimorphic pattern seen in the undiseased arterial wall [29]. The aforementioned risk factors function as theoretical mutagens.

This hypothesis considers events that cause smooth muscle proliferation as critical in atherogenesis. Actions of other growth factors may either stimulate or inhibit cell proliferation, depending on the circumstances, as well as on macrophage-derived cytokine activity, such as the finding of transforming growth factor-β receptors in human atherosclerosis [30] provides evidence for an acquired resistance to apoptosis. Resistance to apoptosis may lead to proliferation of a resistant cell subset associated with progression of stenotic lesions.

This theory once again focuses on the smooth muscle proliferation but fails to account for the other features of the lesion. In summary, obviously no one theory provides an adequate explanation for all the pathologic changes observed in atherogenesis. This subject remains a focus of continual investigation worldwide, and it is hoped that with improved understanding of the atherogenic process, better preventive strategies might be developed.

### Lipid Hypothesis

The relatively simple lipid hypothesis states that the lipids within the atherosclerotic lesion are derived from circulating lipoproteins in the bloodstream. Support for this theory has been provided by the Association of Atherosclerosis with elevated levels of LDL [31]. This hypothesis, however, fails to account for other features of the lesion, including smooth muscle proliferation and thrombotic events.

### Vascular Hemodynamic/Atherosclerosis

Vascular hemodynamics are described in Chap. 5. Atherosclerotic occlusive disease primarily affects circulatory flow through energy losses at fixed arterial stenoses. The reasons for this arise from knowledge of the physical properties of blood as a fluid. As blood flow enters an area of stenosis, its velocity increases across the stenosis to maintain constant flow. Energy is then lost with the change in velocity at both the entry to and exit from the stenotic area. The greater the degree of stenosis, the more severe the change in velocity and thus the greater the energy loss. In general, flow studies have demonstrated that significant changes in flow and velocity do not occur until the degree of stenosis approaches 50%, which in turn corresponds to an area reduction of approximately 75%. This is termed critical stenosis.

It is important to remember, however, that resistances in series are additive; thus, multiple subcritical stenoses in series can produce significant hemodynamic changes and result in marked impairment of distal flow [32, 33].

## Clinical Manifestations of PAD

The clinical manifestations of lower extremity atherosclerotic occlusive disease occur along a well-defined spectrum of severity, ranging from intermittent claudication to the observation of trophic changes suggesting impending limb loss.

Claudication is defined as pain (or discomfort) produced with brisk use of an extremity and relieved with rest. We have also observed that the location of the discomfort is typically experienced one joint distal to the stenotic area. For example, disease involving the superficial femoral artery manifests itself via calf claudication. Blood flow is adequate in the resting state; thus, pain occurs only when the increased metabolic demand created by exercising muscle exceeds the supply available due to the degree of fixed arterial obstruction [34]. Aside from diminished distal pulses, significant physical findings are usually absent at this stage.

The differential diagnosis of intermittent claudication should include other conditions, which may be neurologic or musculoskeletal in origin. Calf claudication can be caused by venous claudication, chronic compartment syndrome, Baker's cyst, and nerve root compression. The tight bursting pain of compartment syndrome is generally typical, and venous claudication is relieved by leg elevation. Hip or buttock claudication should be differentiated from pain related to hip arthritis and spinal cord compression. The persistent aching pain caused by variable amounts of exercise and associated symptoms in other joints may distinguish arthritis from claudication. Patients with spinal cord compression frequently present with a history of back pain and have symptoms on standing but require a change in position as well as rest to obtain relief. Foot claudication should be distinguished from other causes related to arthritis or inflammatory processes.

Ischemic rest pain develops when the degree of circulatory impairment progresses to the point at which the blood supply is inadequate to meet the metabolic demand of the muscle even in the resting state. Frequently, the pain increases during periods of lower extremity elevation (lying in a bed) and is relieved with dependency. Physical findings at this stage typically include decreased skin temperature and delayed capillary refill, as well as Buerger's signs (dependent rubor and pallor on elevation).

Trophic changes represent the most severe manifestations of chronically impaired lower extremity circulation. In this stage of the disease, the lower extremity displays actual changes related to ischemia that are visible to the naked eye. These changes range from subtle signs such as dependent rubor, atrophy of skin and muscle, and loss of hair or nail substance to frank ulceration, cyanosis, and gangrene. The presence of trophic changes is suggestive of impending limb loss and necessitates urgent intervention for limb salvage to be possible [35].

## Natural History and Staging

Several studies over the past 40 years have concluded that approximately 75% of all patients with claudication experience symptom stabilization or improvement over their lifetime without the need for any intervention [36, 37]. This clinical improvement or stabilization holds true, despite arteriographic evidence for disease progression in most of these patients. In 25% of claudicant patients, symptoms worsened, particularly during the first year, in approximately 8%, and subsequently at the rate of 2–3% per year. It has been estimated that around 5% of these patients will undergo an intervention within 5 years of their initial diagnosis. Several large studies estimate that 2–4% of these patients will require a major amputation [38, 39]. Diabetes and smoking are the most significant primary risk factors for disease progression and higher intervention and amputation rates. Dormandy and Murray [39] concluded that an ABI of 0.5 on initial diagnosis was the most significant predictor for peripheral arterial disease deterioration requiring intervention. They also observed that men were at higher risk for disease progression than women. Other studies have confirmed that the presence of peripheral arterial disease significantly increased the risk of myocardial infarction, stroke, ischemia of splanchnic organs, and the risk of cardiovascular death. Criqui et al. [40] noted a relative risk of 3.3 for total mortality and a relative risk of 5.8 for coronary artery disease mortality in men with peripheral arterial disease over a 10-year study. They also noted a twofold higher relative risk of a total, coronary, and cardiovascular mortality in symptomatic versus asymptomatic peripheral artery disease patients. It has been estimated that the average life expectancy of patients with intermittent claudication was decreased by about 10 years [36]. A review of over 20 studies by TASC places the 5-, 10-, and 15-year mortality rates for patients with intermittent claudication at 30%, 50%, and 70%, respectively [17].

Determination of the ABI has proven to be a powerful clinical tool. An ABI of <0.5 has been associated with more severe coronary artery disease and increased mortality [41]. It has been demonstrated that patients with an ABI of <0.3 had a significantly lower survival rate than those with a range of 0.31–0.9 [41].

Sheikh et al. reported on the usefulness of postexercise ABI to predict all-cause mortality. They conducted an observational study of consecutive patients referred for ABI measurement before and after fixed-grade treadmill or symptom-limited exercise component to a noninvasive vascular laboratory during a 10-year period. The patients were classified into two groups: Group 1 included patients with an ABI of ≥0.85 before and after exercise, and group 2 included patients with a normal ABI at rest but <0.85 after exercise. A total of 6,292 patients were analyzed. The 10-year mortality rate for groups 1 and 2 was 33% and 41%, respectively. An abnormal postexercise ABI result independently predicted mortality (a hazard ratio of 1.3, $p=0.008$). Additional independent predictors of mortality were age, male gender, hypertension, and diabetes. After the exclusion of patients with a history of cardiovascular events, the predictive value of an abnormal postexercise ABI remained statistically significant (a hazard ratio of 1.67, $p<0.0001$). They concluded that the postexercise ABI was a powerful independent predictor of all-cause mortality and provides additional risk certification beyond resting ABI [42].

Aboyans et al. assessed the general prognosis of patients with PAD according to the disease location in 400 patients. Aortoiliac disease (proximal PAD) and infrailiac disease (distal PAD) were noted in 211 (53%) and 344 (86%) cases, respectively. Male sex and smoking were prevalent in

**Table 20.1** Classification of peripheral arterial disease: Rutherford categories

| Grade | Category | Clinical description |
|---|---|---|
| 0 | 0 | Asymptomatic |
| I | 1 | Mild claudication |
| I | 2 | Moderate claudication |
| I | 3 | Severe claudication |
| II | 4 | Ischemic rest pain |
| III | 5 | Minor tissue loss |
| III | 6 | Major tissue loss |

proximal PAD, whereas an older age, hypertension, diabetes, and renal failure were more prevalent in distal PAD ($p<0.05$). At a mean follow-up of 32 months, the event-free survival curves differed according to the PAD localization ($p<0.03$). Adjusted for sex, age, cardiovascular disease history, cardiovascular disease risk factors, critical leg ischemia status, and treatment, proximal PAD was significantly associated with a worse prognosis (primary outcome hazard 3.28; death hazard ratio 3.18; $p<0.002$) versus distal PAD. This was the first study to report a poorer general prognosis for patients with proximal aortoiliac disease compared to those with more distal disease [43].

After the initial diagnosis of chronic lower extremity ischemia is made, it is important to stage the severity of the process accurately. This is crucial because it is the stage of the disease and the natural history of each stage that ultimately determine which therapy is most appropriate.

The most common staging system used by vascular surgeons today is that devised by the Society of Vascular Surgery and the International Society of Cardiovascular Surgery (SVS/ISCVS). Rutherford et al. [44] defined claudication categories 0–3 as asymptomatic, mild, moderate, and severe (Table 20.1). Categories 4–6 encompass ischemic rest pain and minor and major tissue loss of patients with critical limb ischemia. Rutherford's classification is presently the recommended standard when describing clinical assessment and progress [17]. The other classification that is used by our medical colleagues is the Fontaine classification. In this classification, the stages of the disease are categorized into class I–IV (I corresponds to 0 in Rutherford's classification and IV corresponds to stage III in Rutherford's classification).

### Stage 0 (Asymptomatic)

In stage 0, the patient is symptom-free. The natural history of stage 0 disease is such that few patients will progress to limb loss over a period of 5 years. For this reason, the only treatment recommended for this stage involves risk factor modification such as cessation of smoking, reduction of serum lipids, and improved control of diabetes mellitus. Close observation is also important since any progression to a more advanced stage necessitates a change in the treatment strategy.

### Stage I (Claudication)

Stage I has been further subdivided into two groups based on the claudication distance. Stage IA disease is defined as claudication occurring at a distance of greater than half a block, whereas stage IB disease is defined as claudication occurring at a distance of less than half a block.

The natural history of patients with claudication is such that very few patients will progress to limb loss. The actual percentages in the literature vary somewhat, but the 5-year limb loss rate seems to average approximately 5% [34, 45].

Because of the relatively benign natural history of stage I disease (grade I category), the cornerstone of therapy remains aggressive medical management, particularly for patients with stage IA disease. Stage IB (categories 2 and 3) disease may be considered a relative indication for invasive intervention if medical therapy fails or if the degree of disability is intolerable for the patient. Once again, progression to a more advanced stage necessitates a change in the treatment plan.

### Stage II (Ischemic Rest Pain)

Stage II is generally viewed as the earliest phase of limb-threatening ischemia. The natural history at this stage carries a far worse prognosis. Patients with stage II disease are far more likely to have progression of their disease process and ultimately to suffer limb loss [46]. For this reason, invasive intervention is indicated at this stage.

### Stage III (Trophic Changes)

The presence of trophic changes indicates the most severe underlying circulatory impairment, as evidenced by actual tissue loss or gangrenous changes. Untreated, most patients will progress to gangrene and limb loss. For this reason, an aggressive interventional approach is indicated to limit additional tissue loss and allow limb salvage [46].

It should be noted that progression of patients with PAD from asymptomatic to claudication to rest pain to gangrene or limb loss is generally unpredictable. It has been shown that more than one-half of patients having a below-knee major amputation for ischemic disease had no prior symptoms of leg ischemia as recent as 6 months previously [47]. The incidence of major amputations, according to large population studies, varies from 120 to 500 per million per year, and the ratio of below-knee to above-knee amputation in large surveys is around 1:1. It has also been reported that approximately 60% of below-knee amputations heal by primary intention, while 15% heal after secondary procedures, and 15% will need above knee amputation, while 10% die in the perioperative period.

## Diagnostic Investigation

### History and Physical Examination

As with any condition, evaluation begins with a comprehensive history and physical examination prior to any objective testing.

The initial history should be directed toward the occurrence of pain in the lower extremities. As defined previously, claudication typically manifests itself as pain that occurs with brisk use of an extremity (via walking) and is relieved consistently by several minutes of rest. The location and character of the pain should be reproducible, as should be the claudication distance. Rest pain should also be inquired about and, once again, may be most prominent at night when the legs are elevated. Any history of ulceration, loss of hair, nail substance, or skin/muscle atrophy should be sought. The presence of impotence, frequently present in aortoiliac disease, should be carefully documented.

Because of the systemic nature of atherosclerosis, the possibility of multivessel involvement exists and should be considered in all patients. A careful history should be elicited regarding symptoms of coronary disease (angina or myocardial infarction), cerebrovascular disease (transient ischemic attacks or prior strokes), or previous vascular procedures.

Physical examination begins with a comprehensive head-to-toe assessment. When attention is directed toward the lower extremities, thorough visual inspection should reveal evidence of any trophic changes. It is important to look between the toes as well to avoid missing subtle areas of skin loss. Skin temperature and capillary refill should be assessed and may be diminished with more advanced disease. Pulses should be palpated at all levels and their strength documented as follows: +2 (normal), +1 (diminished), 0 (no palpable pulse). Others classify pulses as 3+, 2+, 1+, and 0.

If the pulse is nonpalpable, a Doppler probe should be used to determine the presence or absence of flow in the vessel and its flow characteristics (monophasic versus biphasic).

### Noninvasive Tests

A variety of noninvasive tests are available for assessment of the lower extremity vascular system. These are discussed in detail in subsequent chapters.

Perhaps the most useful bedside noninvasive test available to the clinician is the ABI. This test may be performed with only a sphygmomanometer and a Doppler probe. To perform the test, Doppler systolic pressure measurements are taken at the level of the ankle (use the higher of posterior tibial or dorsalis pedis artery pressure) and compared with those in the brachial artery as follows:

$$\text{ABI} = \frac{\text{Ankle pressure (mmHg)}}{\text{Brachial pressure (mmHg)}}$$

A ratio of less than 0.9–1 is abnormal. Generally, patients with claudication have indices of 0.5–0.8, whereas those with rest pain have indices of 0.5 or less. When trophic changes are present, the ABI is frequently less than 0.3 [48].

In general, noninvasive testing should precede the ordering of any more invasive evaluations.

### Overview of Noninvasive Testing in PAD

Noninvasive vascular tests help the physician to evaluate the presence or absence of significant arterial occlusive disease, severity of disease, location of disease, and, in the presence of multisegmental disease, which arterial segment is mostly affected.

General indications for obtaining noninvasive assessment of the peripheral arterial system include absence of normal pulses, suboptimal examiner reliability or experience, a clinical history or examination potentially consistent with peripheral arterial occlusive disease, and a planned vascular procedure.

Several noninvasive diagnostic techniques have been used in the diagnosis of peripheral arterial disease: continuous-wave (CW) Doppler ultrasound, pulsed Doppler ultrasound, B-mode ultrasound, and various plethysmographic techniques, including pulse volume recording, thermography, electromagnetic flowmeter, radionuclide angiography, and the use of radioisotopes. The most commonly used methods for diagnosis of peripheral vascular disease of the lower extremity at present are segmental Doppler pressures (with or without Doppler wave analysis) using CW Doppler, pulse volume recording, and Duplex ultrasonography [49–53]. These three commonly used methods will be described in detail in the next chapters.

#### Doppler Ultrasound

The use of ultrasound in the range of 1–10 MHz for medical diagnosis has become widespread since its introduction by Satomura in 1959 [54]. Current instruments either use the Doppler effect to detect flow velocity or rely on tissue reflectance of transmitted sound waves (B-mode ultrasound) to produce acoustic images of blood vessels or a combination of both Doppler and B-mode imaging (duplex ultrasound).

Although Satomura[54] was credited for developing the first Doppler flow detector in 1959, its clinical application was pioneered by Strandness et al. in 1966 [55]. Since then, the instrumentation has been further improved and refined. The principle of this device depends on the observation made by the Austrian physicist, Christian Doppler (1803–1853), who demonstrated that the frequency of light or sound emitted by a source moving toward the observer is higher


**Fig. 20.5** Handheld Doppler ultrasound unit

(shorter wavelength) than the transmitted frequency and lower (longer wave length) when the source is moving away from the observer, e.g., the pitch of the train whistle sounds higher as the train approaches and lower as the train moves away. The Doppler effect can be stated as

$$\bar{V} = \frac{C\Delta f}{2 f_o \cos\theta}$$

where $\bar{V}$ = average flow velocity, $C$ = velocity of sound in tissue, $\Delta f$ = Doppler frequency shift, $f_o$ = transmitting frequency of ultrasound beam, and $\theta$ = angle of the incident sound beam to the blood vessel being examined. Since transmitting frequency, angle of incidence, and sound velocity in tissue can be kept constant, frequency shift ($\Delta f$) becomes proportional to the velocity of blood flow.

There are two types of Doppler ultrasound detectors: CW Doppler ultrasound and pulsed Doppler ultrasound. Both instruments work on the principle of the Doppler effect. This is described in detail in Chap. 4.

*Instrumentation*: Many types of Doppler instruments are commercially available, varying from small, portable, pocket-sized models to more sophisticated instruments. The CW detectors emit an ultrasound beam without interruption. Such devices are not range specific, i.e., they will detect blood flow at any depth within the range of the instrument up to several centimeters, depending upon the frequency of the instrumentation. The pulsed Doppler detectors transmit intermittent bursts of ultrasound that can be sampled for retained signals at various times after transmission, permitting range resolution of detected flow at a given point from the transducer. As mentioned earlier, CW Doppler units can be directional or nondirectional. Figure 20.5 shows a commonly used pocket Doppler unit (Dopplex D900, Huntleigh Diagnostics, Eatontown, NJ); Fig. 20.6 shows a commonly used directional Doppler unit (VasoGuard, Viasys Healthcare, Madison, WI).

## Duplex Ultrasound and Color Flow Imaging

When pulsed ultrasound Dopplers and B-mode scanners are combined, the resulting duplex scan is capable of not only imaging the vessel under study but also detecting blood flow velocity at multiple points within its lumen. Presently, color duplex ultrasonography is the most common instrumentation used in modern vascular laboratories.

Color flow imaging provides the duplex information described above, i.e., combined real-time B-mode imaging (grayscale evaluation) and Doppler spectral analysis. In addition, it evaluates the Doppler flow information for its phase (direction toward or away from the transducer, and color is assigned on this basis) and its frequency content (which determines the hue or shade of the assigned color).

## Plethysmography

*Principle*: The principle of plethysmography is based on graphic recordings of a change in dimension of a portion of the body in response to each heartbeat or in response to temporary obstruction of the venous system (venous occlusion plethysmography) [56]. Most plethysmographs directly or indirectly record the change in column of a digit, limb, or other part of the body. An exception to this is the photoplethysmograph (PPG) that records the change in reflection of light from the change in number of red blood cells in the cutaneous microcirculation.

*Instrumentation*: Various types of plethysmographs have been used in the past. Each type employs a different transducer principle for recording the changes in body dimension:

1. The photoelectric or PPG [57] has been used for many years as a pulse sensor. This technique includes an infrared light-emitting diode [58] to transmit light into skin. Light reflected from blood cells is received by either a photocell or a phototransistor, which permits recording of the pulsatile cutaneous microcirculation. This technique was used in screening for peripheral arterial disease [59], cerebrovascular disease [60], and venous diseases [61]. Recently, Bortolotto et al. [62] in a study assessing vascular aging and atherosclerosis in hypertensive subjects using pulse-wave velocity versus a second derivative of a photoplethysmogram, concluded that an index of the second derivative of photoplethysmography correlated with age and was useful in the evaluation of vascular aging in hypertensive patients [62].
2. The strain-gauge plethysmograph (SGP), originally described by Whitney [63], uses the principle of the change in the resistance of a column of mercury in an elastic gauge as a sensor of digit or limb volume. This technique is simple and versatile in screening for peripheral arterial and venous disease. Modifications of this instrument have permitted electrical calibration of the gauge in situ on the limb [64] and automatic calculation


**Fig. 20.6** VasoGuard, Viasys Healthcare system, a commonly used directional Doppler unit

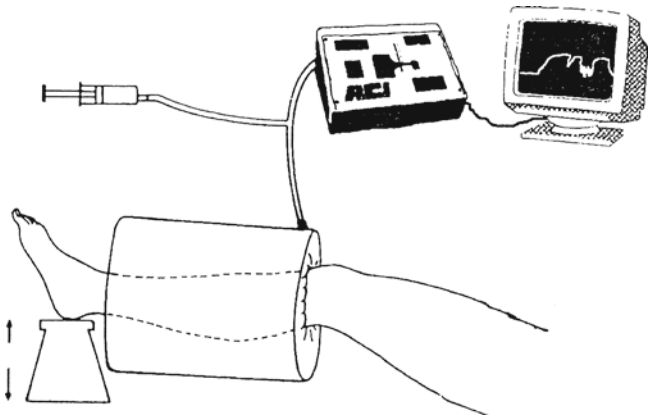


**Fig. 20.7** This is an air plethysmography (APG, [ACI Medical, San Marcos, California])

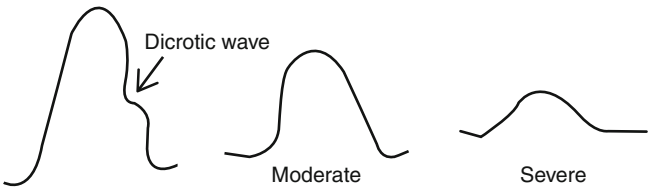


**Fig. 20.8** Pulse-wave tracing. Normal pulse wave has a steep upslope, a relatively narrow peak, and a dicrotic wave on the downslope, which is concave toward the baseline. Note the contour and amplitude in the presence of moderate and severe arterial occlusion

of the limb flow from the excursion of a panel meter needle [65]. This technique is less cumbersome than standard volume plethysmography and has been accepted for measuring limb blood flow [66]. It can also be used to obtain pulse volume waveforms, which have been proven to be valuable in the diagnosis of arterial occlusive disease.

3. The air plethysmograph has been used in a variety of instruments, including the oscillometer, Winsor plethysmograph [67], and pulse volume recorder (PVR) [68], all of which have been used extensively in the evaluation of peripheral arterial occlusive disease and venous diseases. This technique is described in detail in Chap. 22. Volume or air plethysmography utilizes pneumatic cuffs placed at multiple levels around the extremity. By standardizing the injected volume of air and the pressure within the cuff, momentary volume changes of the limb result in pulsatile pressure changes within the air-filled bladder. These changes can be displayed as segmental pressure pulse contours, which correspond closely to a direct intra-arterial recording at that level. By adding venous occlusion to plethysmography, indirect measurements of arterial flow are possible. This can be done by placing a pneumatic cuff on the proximal extremity, which is then inflated to a pressure that temporarily arrests venous outflow without impairing arterial inflow. Under these circumstances, the initial rate of volume change in the distal extremity, as measured by any of the plethysmographic techniques, is equal to the rate of arterial inflow. This is usually expressed as cubic centimeters flow per 100 mL tissue/min. Since resting arterial flow is not reduced until an advanced degree of ischemia is present [68], this technique has not found wide clinical application.
4. Quantitative air plethysmography measures volume changes of the entire lower leg by calibration with pressure changes and expresses these volume changes in absolute units. As shown in Fig. 20.7, an air chamber that surrounds the lower leg is inflated to 6 mmHg, the lowest level at which good chamber/limb contact occurs with minimal venous compression. The leg blood flow is measured during venous occlusion. Calibration is performed by injecting 100 $cm^3$ of air into the chamber and observing the pressure changes. A pneumatic occlusion tourniquet with an attached manometer is applied just proximal to the knee. After equilibration, the tourniquet is rapidly deflated to 50 mmHg to occlude the venous outflow. The increasing leg volume is recorded for 20 s and represents the arterial inflow to the leg during that period. The arterial inflow in cubic centimeters/mL can be calculated from the slope of the volume/time curve during the 20 s. This technology has been reported to be reproducible; however, because it is cumbersome, it is not presently widely used [69].

*Clinical Applications*: Plethysmographic techniques permit evaluation of peripheral vascular disease by one of the following three techniques: pulse-wave analysis, determination of digit or limb blood pressure, and determination of arterial or venous blood flow. Pulse-wave analysis is particularly useful in peripheral arterial and carotid occlusive diseases. Assessment of digit or limb blood pressure permits semiquantitation of peripheral arterial occlusive disease, and the assessment of limb blood flow permits quantitation of peripheral arterial and venous diseases.

*Pulse-Wave Analysis*: The contour and amplitude of the plethysmographic pulsation with each heartbeat is a qualitative guide to the presence and degree of peripheral arterial occlusive disease [70]. Normally, the pulse wave has a steep upslope, a relatively narrow peak, and a dicrotic wave on the downslope, which is concave toward the baseline. In the presence of arterial occlusive disease, the pulse-wave contour is damped with a more gradual upslope, a broad rounded peak, and loss of the dicrotic wave on the downslope, which becomes convex away from the baseline. The amplitude or height of the pulse wave diminishes progressively with increasing arterial obstruction (Fig. 20.8). The amplitude of the pulse wave will also decrease in response to sympathetic stimulation, such as that induced by a deep inspiration.

Recently, Kuvin et al. [71] concluded that finger arterial pulse-wave amplitude was helpful in the assessment of peripheral vascular endothelial function.

The digit and segmental limb systolic blood pressures can be determined by plethysmography. However, such determinations are more simply done by Doppler ultrasound. The measurement of systolic blood pressure usually requires a plethysmography transducer on the distal phalanx [72]. Photo pulse, strain gauge, or air transducers are suitable for detecting the return of pulsations following deflation of a specially designed blood pressure cuff. Such digit pressure measurements are particularly useful in patients with diabetes mellitus, Raynaud's syndrome, and advanced peripheral arterial occlusive disease.

### Transcutaneous $PO_2$

This technology allows quantitative estimation of cutaneous oxygen delivery that is independent of arterial wall mechanical properties (e.g., medial calcinosis) [73]. This monitoring device is a modification of the Clark polarographic oxygen electrode coupled to a servo/controlling heating coil and thermistor. It operates on the principle that vasodilation occurs when the skin heats. At skin temperatures higher than 43°C, the ratio of transcutaneous $PO_2$ ($TCPO_2$) to arterial $PO_2$ is constant and approximates 1. Conventional probes are, therefore, set between 43°C and 45°C.The relationship is complex and affected by several factors, although the $TCPO_2$ is directly related to skin blood flow. Several attempts have been made to increase the accuracy of predictions based on $TCPO_2$ measurements, e.g., response to maneuvers including oxygen inhalation, postocclusion reactive hyperemia, exercise, and leg dependency. None of these maneuvers was found to significantly increase the overall accuracy. Other factors that may limit the accuracy and overall usefulness of this methodology include changes in skin temperature, sympathetic tone, age, edema, hyperkeratosis, and cellulitis. The clinical application of absolute $TCPO_2$ measurement using this technology is limited by the broad overlap of values correlating with the clinical classification of arterial disease. Mild to moderate arterial occlusive disease is generally not detected by reduced $TCPO_2$ levels. The normal range in these patients is ≥40 mmHg. $TCPO_2$ measurements have maximal sensitivity at critically low levels of tissue perfusion; therefore, it is useful in predicting amputation or wound healing in an extremity with severe peripheral vascular occlusive disease. Generally speaking, most wounds or amputations will heal if the $TCPO_2$ is greater than 30 mmHg at that level. For $TCPO_2$ values between 20 and 30 mmHg, the likelihood of healing is unpredictable. For $TCPO_2$ levels of <20 mmHg, most amputations or wounds will not heal [74]. This methodology will be described in detail in a later chapter.

### Laser Doppler Measurements

This method uses a narrow monochromatic incident light source (laser) to interrogate particles [blood cells, red blood cells (RBCs)] moving in the dermal microcirculation. A pickup system records the reflected light, and the Doppler-shifted signal corresponds to the average velocity of the particles. These measurements can vary based on several factors, including significant scattering on both the incident and reflected light beams, and anatomic variables including skin pigmentation, topography, epidermis thickness, random complexity of the microcirculation, and the number of RBCs in the sample volume. The term RBC flux has been used to describe the measurement, as it represents neither velocity nor flow. The signal is a product of the number of moving RBCs in the sample volume and their mean velocity (flux = RBC volume fraction × mean velocity). This noninvasive technology provides continuous readout and it is easy to operate; however, it cannot be calibrated, its reproducibility is frequently problematic, and the data are not expressed in familiar or absolute units (velocity or flow rate) [75]. Systolic skin pressure (SSP) can be measured using a blood pressure cuff applied directly over the sensor. This technique involves inflation of a cuff placed over the sensor until RBC flux stops. The cuff is then deflated, and the SSP is the point at which the recorded signal returns. Laser Doppler fluxometry has been used in association with various maneuvers to detect microangiopathy and predict clinical outcome. Loss of reactive hyperemia response following temporary arterial occlusion and failure to increase RBC flux with skin healing are signs of microangiopathy in diabetic patients with compromised wound healing. In addition, loss of venoarteriolar response, a sympathetic axonal reflex of vasoconstriction when the foot is lowered below the heart level, occurs in the presence of advanced peripheral neuropathy in diabetic patients and may predict wound-healing difficulties.

Eicke et al. [76] conducted a study comparing CW Doppler ultrasound of the radial artery and laser Doppler flowmetry of the fingertips with sympathetic stimulation and concluded that both methods were feasible to monitor flow changes due to sympathetic stimulation.

Kubli et al. [77] in a study of the reproducibility of laser Doppler imaging of the skin blood flow as a tool to assess endothelial function, concluded that endothelium-dependent and -independent responses of dermal blood flow evaluated with laser Doppler imaging are highly reproducible from day to day, at least in healthy nonsmoking young male subjects. These observations have implications for testing for endothelial function in clinical studies.

Correa et al. conducted a comparison of laser Doppler imaging, fingertip lacticemy test, and nailfold capillaroscopy for assessment of digital microcirculation in 44 patients with systemic sclerosis and 40 healthy controls. After acclimatization, all subjects underwent nailfold capillaroscopy (NFC) followed by laser Doppler imaging (LDI) and fingertip lacticemy measurement. NFC was performed with a stereomicroscope

under 10–20× magnification in the ten digits of the hands. Skin blood flow of the dorsum of four fingertips (excluding the thumb) of the left hand was measured using LDI at baseline and for 30 min after cold stimulus. The mean finger blood flow of the four fingertips was expressed as arbitrary perfusion units. Fingertip lacticemy was determined on the fourth left finger before (pre-cold stimulus-fingertip lacticemy) and 10 min after cold stimulus. They concluded that laser Doppler imaging showed a lower digital blood flow in systemic sclerosis patients when compared with healthy controls and correlated well with fingertip lacticemy, both at baseline and after cold stimulus, allowing objective measurement of blood perfusion in systemic sclerosis patients. The lack or correlation between functional and morphological microvascular abnormalities, measured by LDI and NFC, suggests they are complementary tools for evaluation of independent microangiopathy aspects in systemic sclerosis patients [78].

Others used laser Doppler to predict burn wound healing [79].

### Electromagnetic Flowmeter

The electromagnetic flowmeter aids in measuring flow rates and is reasonably accurate in real time without interrupting or restricting the flow stream. When a fluid conductor moves at right angles through a magnetic field, an electrical potential is induced in the fluid perpendicular to both the magnetic field and the direction of the flow. The magnitude of the voltage depends on the spatially averaged velocity flow, the strength of the magnetic field, and the diameter of the blood vessel. The standard noncannulating electromagnetic flow probe consists of an electromagnet and two electrodes embedded in a C-shaped plastic device for easy application to the vessel. The electrodes are located opposite each other and at right angles to the poles of the electromagnets. A voltage proportional to the velocity of flow appears at the interface between the fluid and the vessel wall. In turn, this voltage is conducted across the vessel wall, where it is picked up by the electrodes and is amplified to drive a recording system. The volume flow (in cubic centimeters per second) is measured by a special formula. A supply of calibrated probes of varying diameters are gas-sterilized and made available in the operating room. It is important that the electrodes be kept clean and free of deposits of blood or other protein material since such deposits can alter the electrical resistance and distort the flow recordings. A length of vessel about three times the width of the probe is dissected out to allow easy application and to prevent angulation of the probe. All electrical equipment, particularly the electrocautery, is disconnected prior to using the electromagnetic flowmeter. This is to prevent stray currents from passing through the ground electrodes of the flowmeter, where they could produce an electrical burn or shock. Also, it helps to eliminate troublesome electrical interference. After the probe has been positioned on the vessel, the distal vessel is momentarily occluded in order to adjust the zero. The resulting reactive hyperemia is allowed to subside for a few seconds to several minutes before pulsatile and mean flows are recorded. It is important to ensure that the vessel probe is surrounded by tissue fluids or by saline in order to duplicate the conditions of in vitro calibration. For a branched vessel, or in the case of an end-to-side graft where there are two or more outflow tracts, it is helpful to occlude each of the outflow tracts or branches in turn to obtain some idea of flow distribution.

The flow value (mL/min) is recorded at rest and often following intra-arterial injection of a vasodilating agent (papaverine hydrochloride). A flow value recorded after administration of a vasodilator is termed a stimulated or augmented flow. The electromagnetic flowmeter has been useful in detecting technical errors, such as intimal flaps, kinked or faulty anastomosis and twisted grafts, the presence of emboli or thrombi, and construction of a graft of inadequate size. These problems are detected during operation and are immediately corrected, and reoperation can be avoided [80].

### Magnetic Resonance Angiography

Magnetic resonance angiography (MRA) is a technique used to study blood vessels using magnetic imaging technology. This technique is useful in the assessment of the peripheral vasculature including the aorta, upper and lower extremities, and carotid arterial systems.

Advantages include the lack of need for conventional contrast administration and the noninvasive nature of the test. These factors help to make MRA attractive; however, there are several disadvantages that must be considered. First, the patient is required to remain completely still within a confined space for several minutes, which may be intolerable for some people. The presence of any previously placed aneurysm clips within the brain or the presence of a pacemaker precludes the use of MRA due to the powerful magnetic forces generated. Finally, the presence of turbulent flow can result in signal loss, which may result in an overestimation of the degree of stenosis [81].

Menke and Larsen [82] reported a meta-analysis of accuracy of contrast-enhanced MRA for assessing steno-occlusions in PAD. This included 32 prospective studies that compared MRA with intra-arterial DSA. The overall pooled sensitivity of MRA was 95%, and the specificity was 96% for diagnosing segmental steno-occlusions. The pooled positive and negative likelihood ratios were 21.56 (confidence interval [CI] 15.7–29.69) and 0.056 (CI 0.037–0.083), respectively. MRA correctly classified 95.3%, understaged 1.6%, and overstaged 3.1% of arterial segments. The authors concluded that based on this meta-analysis, that contrast-enhanced MRA has a high accuracy for identifying or excluding clinically relevant arterial stenosis or occlusion in patients with PAD symptoms [82].

## Computed Tomographic Angiography

Until recently, noninvasive imaging options included arterial duplex ultrasound and MRA [83]. Although widely available, arterial duplex ultrasound can be very operator dependent, and significant limitations occur with obese patients and in heavily calcified arterial segments [84, 85]. Magnetic resonance angiography has a high diagnostic accuracy but is costly and not widely available [86, 87]. While conventional digital subtraction angiography (DSA) is considered the gold standard for imaging of peripheral vessels, its invasive nature and inherent risks of vascular complications limit its use.

Meanwhile, computed tomography is increasingly being used as a surrogate for invasive angiography, given the lower costs and less invasive nature [88]. Previous studies with 4 and 16 multidetector computed tomographic (MDCT) angiography in the peripheral vasculature found adequate diagnostic accuracy in comparison with digital subtraction angiography (DSA) [89, 90]. Shareghi et al. evaluated the diagnostic accuracy of 64 multidetector CTA in PAD in 28 consecutive patients with symptomatic lower extremity intermittent claudication and an abnormal ABI. Patients were evaluated by both 64 MDCT and DSA. The aortoiliac and lower extremity arteries were divided into 15 segments per limb (30 segments per patient). Eight hundred forty segments were analyzed in a blinded fashion by physicians with level III CT certification. Segments were classified as grade I (<10% stenosis), grade II (10–49%), grade III (50–99%), and grade IV (occlusion). For all segments evaluated, the overall diagnostic accuracy for detecting grade III and IV lesions was 98% with a sensitivity of 99% and a specificity of 98%. For the aortoiliac segments, the diagnostic accuracy was 98% with a sensitivity of 100% and a specificity of 99%. For the femoropopliteal segments, the overall accuracy was 98% with a sensitivity of 100% and a specificity of 99%. For the infra-popliteal segments, the overall accuracy was 98% with a sensitivity of 97% and a specificity of 99%. One segment could not be visualized by MDCT compared to 49 segments that could not be visualized by DSA. This study demonstrates excellent diagnostic accuracy of 64 MDCT in the detection of hemodynamically significant disease of the lower extremities. More segments are visualized using 64 MDCT than DSA, allowing more complete visualization of the vascular tree. The authors concluded that CTA should be considered in the diagnostic evaluation of symptomatic patients with PAD (Fig. 20.9).

Meanwhile, Brenner and Hall [91], in a review article, reported on the increasing source of radiation exposure after the wide use of CT. CT involves larger radiation doses than the more common conventional X-ray imaging procedure. With the increasing number of CT scans being obtained, the associated radiation dose and the consequent cancer risk in adults, and particularly in children, must be remembered. They concluded that although the risks for any one person are not large, increasing exposure to radiation in the population may be a public health issue in the future [91]. A similar observation was noted by Zhou [92], who reviewed the radiation exposure associated with CT angiograms and coronary intervention in patients with vascular disease and concluded that vascular surgeons must remain vigilant in monitoring radiation exposure for their patients who have a potential for coronary and vascular imaging with radiation. They emphasized the judicious use of alternative imaging modalities when possible, and maintaining the dose as low as reasonably achievable (ALARA) is the responsibility of vascular surgeons and the vascular interventionalist [92].

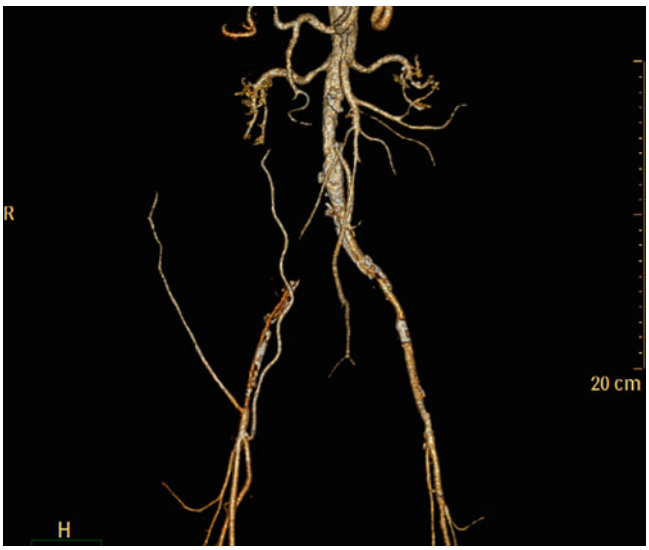


**Fig. 20.9** CTA showing complete occlusion of common iliac artery

## Contrast Angiography (DSA)

DSA has long been the gold standard for the assessment of the aorta and lower extremity vascular tree. The procedure involves arterial puncture, with subsequent passage of a catheter system to the area targeted for imaging. Contrast medium is then injected and radiographs are taken, preferably in more than one plane.

The resolution of angiography may be enhanced via the use of digital subtraction technology. This electronic technique permits digital processing of the video signal from a conventional signal image intensifier fluoroscopic system. In digital subtraction angiography (DSA), a time subtraction technique known as mask-mode radiography is utilized. With this technique, an initial fluoroscopic image is recorded and digitally processed. Contrast is then administered and additional images recorded. Finally, the images are digitally "subtracted" from each other, resulting in radiographs of higher resolution than those obtained with conventional angiography, with smaller amounts of contrast media [93].

Risks of angiography include the risks of arterial puncture, which may result in compromise of the distal circulation due

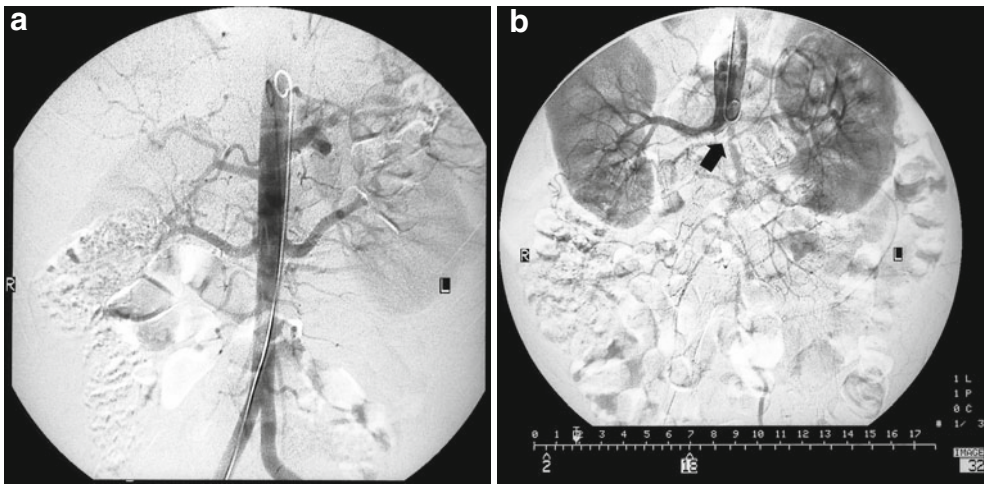


**Fig. 20.10** (**a**) Arteriogram of a normal aorta and right and left common iliac arteries. (**b**) Arteriogram showing complete occlusion of the infrarenal abdominal aorta (*arrow*) at the level of the renal artery

to induction of thrombosis, embolism, or dissection, or in pseudoaneurysm formation, as well as the risks associated with contrast administration. Risks associated with contrast administration include allergic reactions, hypotension, systemic vasodilatation, stroke, and convulsions. Renal insufficiency may also be precipitated via contrast administration. This risk may be minimized via adequate hydration and the use of nonionic low-osmolarity contrast agents [94]. Overall, the morbidity related to angiography may be as high as 7% [95]. Recent studies have reported lower major complication rates for peripheral arteriography (2.1%) [96].

AbuRahma et al. analyzed the complications of diagnostic arteriography performed by a vascular surgeon in a recent series of 558 patients [97]. They reported an overall complication rate of 3.8% (1.3% major) which was comparable to what was published previously (1.9% and 2.9%) but superior to what they published previously as performed by their radiologists (7%, $p < 0.001$). A logistic regression could not find any variables that were significant for the prediction of a major complication. They determined that diagnostic arteriography can be done safely by experienced vascular surgeons with low complication rates that compare favorably with what was published by interventional radiologists.

Therefore, it is generally believed that arteriography should be performed only on those patients in whom invasive intervention is considered. Figures 20.10 and 20.11 illustrate some normal and abnormal findings.

## Treatment Options

Treatment of lower extremity PAD is not the focus of this text. However, a brief review of the various treatment strategies is provided for completeness. Basically, the treatments may be classified into three major categories: (1) medical therapy, (2) surgical therapy, and (3) endovascular therapy.

## Medical Therapy

Medical therapy is the treatment of choice for patients with SVS/ISCVS stage 0 (asymptomatic) and the initial treatment for stage I (claudication) disease. This begins with identification and aggressive modification of risk factors. This includes improving control of hypertension and diabetes mellitus, reduction of serum lipids, dietary modification, and—most importantly—cessation of smoking.

### Smoking Cessation

According to TASC II recommendations [4], the role of smoking cessation in treating the symptoms of claudication is not as clear; studies have shown that smoking cessation is associated with improved walking distance in some but not all patients. Therefore, patients should be encouraged to stop smoking primarily to reduce their risk of cardiovascular events, as well as their risk of progression to amputation and progression of disease, but should not be promised improved symptoms immediately upon cessation.

TASC II has the following recommendations: Patients who smoke should be strongly and repeatedly encouraged to stop smoking [B Recommendation]; they should receive a program of physician advice, group counseling sessions, and nicotine replacement [A Recommendation]; and the addition of antidepressant drug therapy (bupropion) and nicotine replacement greatly enhances cessation rates [A].

### Weight Reduction

Patients with PAD who are overweight (a body mass index [BMI] of 25–30) or who are obese (BMI >30) should receive counseling for weight loss by reduction of calorie intake, carbohydrate restriction, and increased exercise [4].

### Treatment of Hyperlipidemia

The following are the general recommendations for patients with PAD in regard to lipid control [4]:

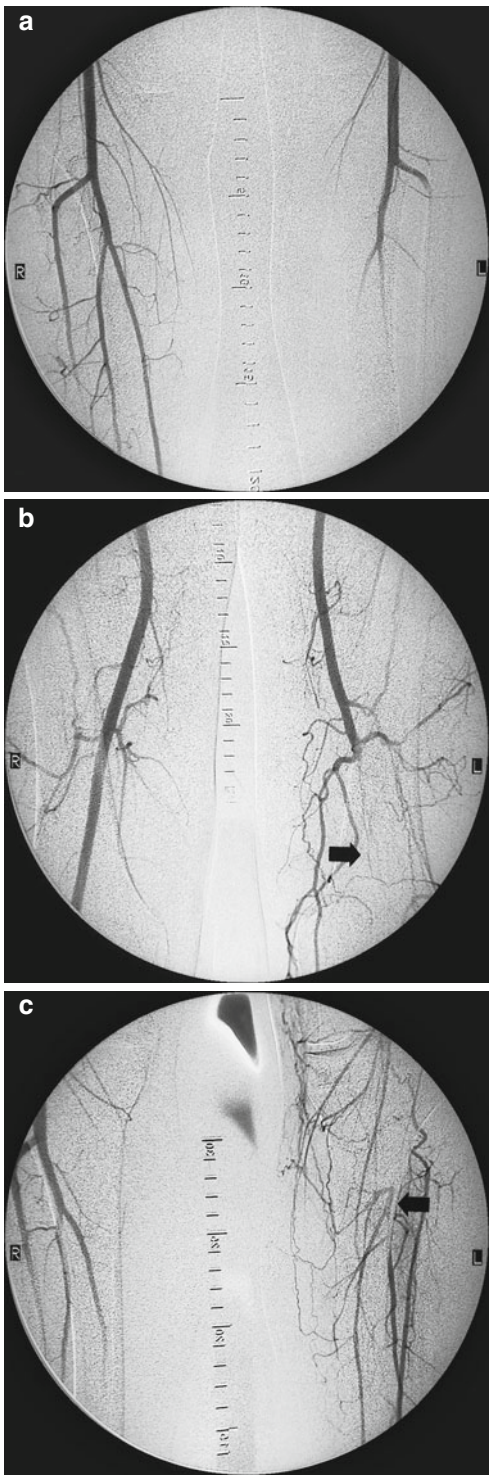


**Fig. 20.11** (**a**) Arteriogram of the right distal popliteal artery and its trifurcation vessel (anterior tibial, tibioperoneal trunk: peroneal artery and posterior tibial artery). (**b**) Arteriogram showing occlusion of the left popliteal artery (*arrow*). (**c**) Arteriogram of the same patient in **b**, showing reconstitution of the distal portion of the tibioperoneal trunk with posterior tibial and peroneal runoff (*arrow*)

All symptomatic and asymptomatic patients with PAD, and no other clinical evidence of cardiovascular disease, should have their low-density lipoprotein (LDL) cholesterol level lowered to below 100 mg/dL. Patients with PAD and a history of vascular disease in other beds, e.g., coronary artery disease, the LDL cholesterol level should be <70 mg/dL. Dietary modification should be the initial intervention to control abnormal lipid levels. It is also believed that statins should be the primary agent to lower LDL cholesterol levels in symptomatic PAD patients to reduce the risk of cardiovascular events [4].

Some studies have suggested that the risk of developing new or worsening claudication can be reduced significantly by lipid-lowering agents [98, 99]. The mechanism of action of these drugs can include plaque stabilization, preventing rupture, and favorable vasomotor effects. A low-density lipoprotein, cholesterol level of <70–100 mg/dL, may be achieved through diet control or lipid-lowering agents if necessary.

Recently, the Cochrane review reported a meta-analysis of 18 trials, including a total of 10,049 participants of lipid-lowering agents for PAD of the lower extremity. The pooled results from all eligible trials indicated that lipid-lowering therapy had no statistically significant effect on overall mortality (O.R. of 0.86, 95% confidence interval [CI] 0.49–1.5) or in total cardiovascular events (O.R. of 0.8, CI 0.59–1.09). However, a subgroup analysis showed that lipid-lowering therapy significantly reduced the risk of total cardiovascular events (O.R. of 0.74). This was primarily due to a positive effect on total coronary events (O.R. of 0.76).

They also showed that pooling of the results from several small trials on the range of different lipid-lowering agents indicated an improvement in total walking distance and pain-free walking distance but with no significant effect on ABI. The author concluded that lipid-lowering therapy was effective in reducing cardiovascular mortality and morbidity in people with PAD. It may also improve local symptoms. They also felt that until further evidence on the relative effectiveness of different lipid-lowering agents is available, the use of statins in people with PAD and a blood cholesterol level ≥3.5 mmoL are indicated [100].

### Treatment of Hypertension

All patients with hypertension should have their blood pressure controlled to below 140/90 mmHg or below 130/80 mmHg if they also have diabetes or renal insufficiency. Thiazides and ACE inhibitors should be considered as the initial blood pressure-lowering drugs in patients with PAD to reduce the risk of cardiovascular events. Beta-blockers are not contraindicated in patients with PAD [4].

### Treatment of Diabetes Mellitus

Patients with diabetes and PAD should have aggressive control of their blood glucose level with a hemoglobin A1c goal of <7% or as close to 6% as possible [4].

### Exercise Therapy

The next essential facet of medical therapy should be institution of an exercise program. Although the mechanism is not

completely understood, exercise does result in improvement in the majority of claudicators willing to comply with the program. It was once thought that the exercise helped to facilitate development of collateral circulation, but this has not been supported by available data. Rather, it is more likely that exercise induces adaptive changes in the muscle, which result in more efficient extraction of oxygen from the blood [101].

Overall, exercise commonly leads to increased claudication-free walking distance, the ability to better perform activities of higher intensity, and improved quality of life [102, 103]. Other benefits of exercise include improved glucose utilization, a reduction in cholesterol and triglyceride levels, and a higher rate of smoking cessation [17].

Sakamoto et al. [104] analyzed patients with PAD who completed a 12-week supervised exercise program in 118 patients and showed that supervised exercise training improved cardiovascular morbidity and mortality in patients with PAD, which suggested that exercise training should be considered as a secondary prevention strategy for these patients [104]. McDermott et al. conducted a randomized controlled study on 156 patients analyzing treadmill exercise and resistive training in patients with and without intermittent claudication and concluded that supervised treadmill training improved 6-min walk performance, treadmill walking performance, brachial artery flow-mediated dilation, and quality of life, but did not improve the short physical performance battery scores of PAD participants with and without intermittent claudication. However, lower extremity resistance training improved functional performance measured by treadmill walking, quality of life, and stair climbing ability [105].

The TASC II recommendation on exercise therapy in patients with intermittent claudication includes the following: Supervised exercise should be made available as a part of the initial treatment for patients with PAD. They also felt that the most effective program employed treadmill or track walking that is of sufficient intensity to bring on claudication, followed by rest over the course of a 30–60-min session. Exercise sessions are typically conducted three times a week for 3 months [4].

## Pharmacologic Therapy

Pharmacologic therapy is available for the treatment of claudication. Pentoxifylline (Trental) was approved by the US Food and Drug Administration for the treatment of peripheral vascular disease. This drug, classified as a hemorrheologic agent, is believed to improve microcirculatory blood flow by enhancing the flexibility of the erythrocyte membrane, thus decreasing blood viscosity [106]. In initial double-masked trials, pentoxifylline treatment yielded a 45% response rate, compared with 23% for placebo [107]. Although this was encouraging, it was obvious that not all patients will respond [108]. Trental is not commonly used nowadays.

Cilostazol (Pletal) has been introduced over the past decade as a new treatment for patients with claudication. It appears to modestly benefit walking ability, and it has other potential useful effects, including inhibition of platelet aggregation and beneficial effect on serum lipids. In a randomized, prospective, double-blind study examining walking ability in patients with peripheral arterial disease with moderate to severe claudication, cilostazol was superior to both placebo and pentoxifylline (Trental) [109].

Double-blind, randomized controlled trials of cilostazol versus placebo or versus other antiplatelet agents in patients with stable intermittent claudication or patients undergoing vascular surgical intervention for PAD were analyzed by a Cochrane Review in 2008. Seven randomized controlled trials comparing cilostazol with placebo were included. They reported that the weighted mean difference (WMD) for the initial claudication distance was improved following treatment with cilostazol (100 mg twice daily). Participants receiving cilostazol (150 mg twice daily) had an increased initial claudication distance, compared with those receiving placebo. There was no increase in major adverse events including cardiovascular events or mortality in patients receiving cilostazol compared with placebo. They concluded that patients with intermittent claudication should receive secondary prevention for cardiovascular disease, and that cilostazol has been to be of benefit in improving walking distance in people with intermittent claudication. There are no data on whether it results in a reduction of adverse cardiovascular events [110]. Haitt et al. [111], in a review of the results of four randomized placebo-controlled trials of cilostazol for the treatment of claudication, showed a clear benefit of cilostazol in patients with PAD.

The TASC II recommendation in regard to pharmacotherapy for symptoms of intermittent claudication include a 3- to 6-month course of cilostazol as the first line of pharmacotherapy for the relief of claudication symptoms, as evidence shows both an improvement in treadmill exercise performance and the quality of life [4].

## Antiplatelet Drug Therapy

Aspirin is a well-recognized antiplatelet agent for secondary prevention, with a clear benefit in patients with cardiovascular disease. Numerous studies from the antithrombotic trialists' collaboration have concluded that patients with cardiovascular disease will realize a 25% odds reduction in subsequent cardiovascular events with the use of aspirin therapy [112]. The most recent meta-analysis has also clearly demonstrated that low-dose aspirin (75–160 mg) is protective and probably safer than a higher dose of aspirin. A recent meta-analysis also showed that when PAD data were combined from trials using not only aspirin but also clopidogrel, ticlopidine, dipyridamole, and picotamide, there was a significant 23% odds reduction in ischemic events in all subgroups of patients with PAD [113]. Antiplatelet drugs are clearly indicated in the management of PAD, although the efficacy of aspirin is uniformly shown only when PAD and cardiovascular disease coexist. The recent TASC II recommendation in regard to

antiplatelet therapy in patients with PAD is summarized here: All symptomatic patients with or without a history of other cardiovascular disease should be given long-term antiplatelet therapy to reduce the risk of cardiovascular morbidity and mortality. Aspirin is effective in patients with PAD who also have clinical evidence of another form of cardiovascular disease, and the use of aspirin in patients with PAD who do not have clinical evidence of other forms of cardiovascular disease can also be considered. They also felt that clopidogrel is effective in reducing cardiovascular events in a subgroup of patients with symptomatic PAD, with or without other clinical evidence of cardiovascular disease [4].

## Surgical Therapy

Surgical therapy remains the gold standard for treatment of limb-threatening ischemia and, in select cases, disabling claudication. Overall, two techniques predominate in the surgical treatment of peripheral vascular disease: endarterectomy and bypass.

Endarterectomy involves removal of the diseased intima and innermost media, leaving behind a smooth arterial surface. It is especially well suited to the treatment of short segmental or ostial lesions such as those seen at the carotid or aortic bifurcations.

Bypass, as the name implies, involves the routing of blood flow around a stenotic or occluded arterial segment using a conduit, typically either autogenous vein or prosthesis [polytetrafluoroethylene (PTFE) or Dacron]. This extremely versatile technique remains the most commonly utilized method in treating arterial occlusive disease of the lower extremity.

Operative therapy is recommended for patients with long segment and multisegmental disease, especially if total occlusion is present. Aortofemoral bypass is associated with a low operative mortality (2–3%) and an 80–85% 5-year patency rate. Iliac reconstruction is generally recommended for isolated unilateral iliac arterial disease, which can also be treated by a femoral artery to femoral artery crossover bypass graft. Infrainguinal arterial reconstruction is associated with a 60–80% 5-year patency rate, with better outcome noted for autogenous vein conduit than for prosthetic bypasses [114].

## Endovascular Therapy

Endovascular therapy is an evolving modality in which devices are introduced directly into the vascular lumen via an open or percutaneous approach. The stenotic areas are then addressed via several techniques:

1. Balloon angioplasty, in which a balloon is expanded across a stenotic area, thus fracturing the plaque and expanding the arterial lumen via a "controlled dissection"
2. Atherectomy, in which a specially designed catheter is used to shave a portion of the plaque from inside the vessel lumen
3. Stenting or stented endovascular grafting, which is an evolving technique involving the placement of an expandable metal stent across the stenotic area

The application of percutaneous endovascular therapy for arterial occlusive disease of the lower extremities continues to increase. The long-term results of endovascular therapy are expected to improve with the progression of the technology supporting these therapeutic interventions. Overall, the initial technical success rates for open surgical procedures and percutaneous endovascular therapy are somewhat similar; however, surgery frequently provides greater long-term patency. On the other hand, angioplasty is often associated with lower morbidity and mortality rates, and late failure of percutaneous endovascular therapies can often be treated successfully with percutaneous reinterventions [115].

## Endovascular Therapy Versus Surgical Therapy

TASC II recommends [4] the following for selecting endovascular therapy versus surgical therapy:

Treatment for aortoiliac lesions: Endovascular therapy is the treatment of choice for type A lesions, and surgical therapy is the treatment of choice for type D lesions. Meanwhile, endovascular therapy is the preferred treatment for type B lesions, and surgical therapy is the preferred treatment for good risk patients with type C lesions; however, in situations where endovascular therapy and open surgical therapy give equivalent short-term and long-term results, endovascular therapy should be used first, and surgical therapy would be considered for failure. The patients' comorbidity, fully informed patient preference, and the local operator experience must be considered when making these recommendations for type B and C lesions.

Treatment of femoral popliteal lesions: A similar recommendation is made for femoral popliteal lesions, i.e., endovascular therapy is the treatment of choice for type A lesions and surgical therapy is the treatment of choice for type D lesions, while endotherapy is the preferred treatment for type B lesions and surgical therapy is the preferred treatment for good risk patients with type C lesions. Figures 20.12 and 20.13 summarize the type of lesions for aortoiliac and femoral popliteal disease.

Type A lesions

- Unilateral or bilateral stenoses of CIA
- Unilateral or bilateral single short ( ≤3 cm) stenosis of EIA

Type B lesions

- Short ( ≤ 3 cm) stenosis of intrarenal aorta
- Unilateral CIA occlusion
- Single or multiple stenosis totaling 3–10 cm involving the EIA not extending into the CFA
- Unilateral EIA occlusion not involving the origins of internal iliac or CFA

Type C lesions

- Bilateral CIA occlusions
- Bilateral EIA stenoses 3–10 cm long not extending into the CFA
- Unilateral EIA stenosis extending into the CFA
- Unilateral EIA occlusion that involves the origins of internal iliac and/or CFA
- Heavily calcified unilateral EIA occlusion with or without involvement of origins of internal iliac and/or CFA

Type D lesions

- Infra-renal aortoiliac occlusion
- Diffuse disease involving the aorta and both iliac arteries requiring treatment
- Diffuse multiple stenoses involving the unilateral CIA, EIA, and CFA
- Unilateral occlusions of both CIA and EIA
- Bilateral occlusions of EIA
- Iliac stenoses in patients with AAA requiring treatment and not amenable to endograft placement or other lesions requiring open aortic or iliac surgery

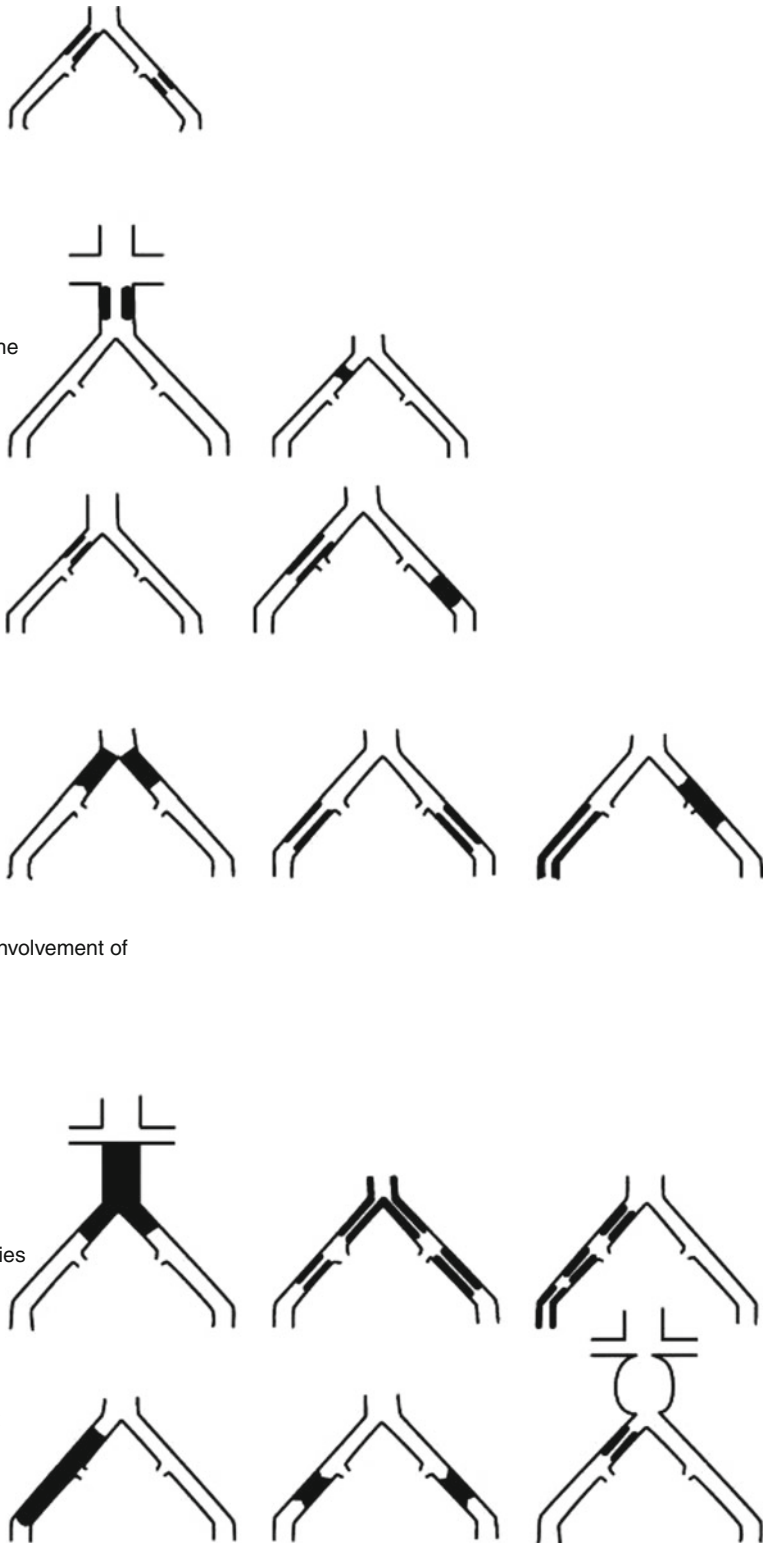

**Fig. 20.12** TASC classification of aortoiliac lesions. *CIA* common iliac artery, *EIA* external iliac artery, *CFA* common femoral artery, *AAA* abdominal aortic aneurysm (Reprinted from Norgren et al. [4]. With permission from Elsevier)

Type A lesions

- Single stenosis ≤ 10 cm in length
- Single occlusion ≤ 5 cm in length

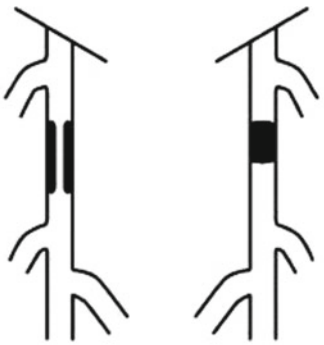

Type B lesions

- Multiple lesions (stenoses or occlusions), each ≤ 5 cm
- Single stenosis or occlusion ≤ 15 cm not involving the infrageniculate popliteal artery
- Single or multiple lesions in the absence of continuous tibial vessels to improve inflow for a distal bypass
- Heavily calcified occlusion ≤5 cm in length
- Single popliteal stenosis

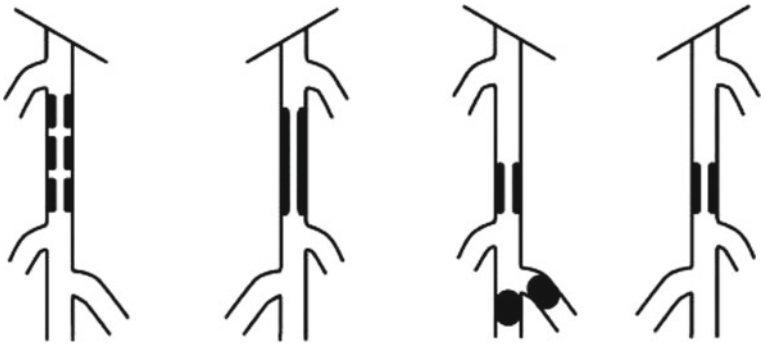

Type C lesions

- Multiple stenoses or occlusions totaling >15 cm with or without heavy calcification
- Recurrent stenoses or occlusions that need treatment after two endovascular interventions

Type D lesions

- Chronic total occlusions of CFA or SFA (> 20 Cm, involving the popliteal artery)
- Chronic total occlusions of popliteal artery amd proximal trifurcation vessels

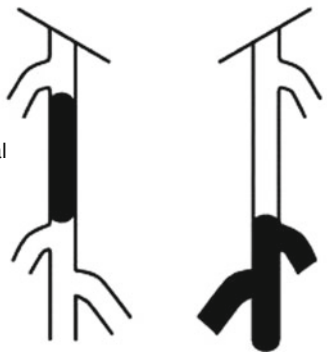

**Fig. 20.13** TASC classification of femoral popliteal lesions. *CFA* common femoral artery, *SFA* superficial femoral artery (Reprinted from Norgren et al. [4]. With permission from Elsevier)

## References


1. Crafts RC. Lower limb. In: Crafts RC, editor. A textbook of human anatomy. New York: Wiley; 1985. p. 397–517.
2. Taylor LM, Porter JM, Winck T. Femoropopliteal occlusive disease. In: Greenfield LJ, editor. Surgery: scientific principles and practice. 2nd ed. Philadelphia: JB Lippincott; 1997. p. 1810–23.
3. Zarins CK, Glagov S. Artery wall pathology in atherosclerosis. In: Rutherford RB, editor. Vascular surgery. 4th ed. Philadelphia: WB Saunders; 1995. p. 203–21.
4. Norgren L, Hiatt WR, Dormandy JA, Nehler MR, Harris KA, Fowkes FGR, on behalf of the TASC II Working Group. Intersociety consensus for the management of peripheral arterial disease (TASC II). J Vasc Surg. 2007;45(Suppl S):S 5–67.
5. Hirsch A, Criqui M, Treat-Jacobson D, Regensteiner J, Creager M, Olin J, et al. Peripheral arterial disease detection, awareness, and treatment in primary care. JAMA. 2001;286(11):1317–24.
6. Selvin E, Erlinger TP. Prevalence of and risk factors for peripheral arterial disease in the United States: results from the National Health and Nutrition Examination Survey, 1999–2000. Circulation. 2004;110(6):738–43.
7. Merino J, Planas A, Elosua R, de Moner A, Gasol A, Contreras C, Vidal-Barraquer F, Clara A. Incidence and risk factors of peripheral arterial occlusive disease in a prospective cohort of 700 adult elderly men followed for 5 years. World J Surg. 2010;34:1975–9.
8. Fowkes FG, Housley E, Cawood EH, Macintyre CC, Ruckley CV, Prescott RJ. Edinburgh artery study: prevalence of asymptomatic and symptomatic peripheral arterial disease in the general population. Int J Epidemiol. 1991;20:384–92.
9. Selvin E, Marinopoulos S, Berkenblit G, Rami T, Brancati FI, Powe NR, et al. Meta-analysis: glycosylated hemoglobin and cardiovascular disease in diabetes mellitus. Ann Intern Med. 2004; 141(6):421–31.
10. Muntner P, Wildman RP, Reynolds K, Desalvo KB, Chen J, Fonseca V. Relationship between HbAIc level and peripheral arterial disease. Diabetes Care. 2005;28(8):1981–7.
11. ADA. Peripheral arterial disease in people with diabetes. Diabetes Care. 2003;26(12):3333–41.
12. Dormandy J, Heeck L, Vig S. Predictors of early disease in the lower limbs. Semin Vasc Surg. 1999;12:109–17.
13. Ridker PM, Stampfer MJ, Rifai N. Novel risk factors for systemic atherosclerosis: a comparison of C-reactive protein, fibrinogen, homocysteine, lipoprotein (a), and standard cholesterol screening as predictors of peripheral arterial disease. JAMA. 2001;285(19): 2481–5.
14. O'Hare AM, Vittinghoff E, Hsia J, Shlipak MG. Renal insufficiency and the risk of lower extremity peripheral arterial disease: results from the Heart and Estrogen/Progestin Replacement Study (HERS). J Am Soc Nephrol. 2004;15(4):1046–51.
15. Kullo IJ, Bailey KR, Kardia SL, Mosley Jr TH, Boerwinkle E, Turner ST. Ethnic differences in peripheral arterial disease in the NHLBI Genetic Epidemiology Network of Arteriopathy (GENOA) study. Vasc Med. 2003;8(4):237–42.
16. Alzamora MT, Fores R, Baena-Diez JM, Pera G, Torar P, Sorribes M, Bicheto M, Reina MD, Sancho A, Albaladejo C, Llussa J, the PERART/ARTPER study group. The peripheral arterial disease study (PERART/ARTPER) prevalence and risk factors in the general population. BMC Public Health. 2010;10:38.
17. TransAtlantic Inter-Society Consensus (TASC) Working Group. Management of peripheral arterial disease (PAD). J Vasc Surg. 2000;31:S5–44, S54–74.
18. Murabito JM, D'Agostino RG, Silbershatz H, Wilson WF. Intermittent claudication: a risk profile from the Framing-ham heart study. Circulation. 1997;96:44–9.
19. Young DF, Cholvin NR, Kirkeeide RL, Roth AC. Hemodynamics of arterial stenosis at elevated flow rates. Circ Res. 1977;41:99–107.
20. Arfvidsson B, Wennmalm A, Gelin J, Dahllof AG, Hallgren B, Lundholm K. Covariation between walking ability and circulatory alterations in patients with intermittent claudication. Eur J Vasc Surg. 1992;6:642–6.
21. Hiatt WR. Nonoperative, nonpharmacologic management of lower extremity occlusive disease. In: Ernst CB, Stanley JC, editors. Current therapy in vascular surgery. Philadelphia: Mosby; 2000. p. 530–3.
22. Hiatt WR, Wolfel EE, Regensteiner JG, Brass EP. Skeletal muscle carnitine metabolism in patients with unilateral peripheral arterial disease. J Appl Physiol. 1992;73:346–53.
23. Ross R, Glomset JA. The pathogenesis of atherosclerosis. N Engl J Med. 1976;295:369–77.
24. Taylor KE, Glagov S, Zarins CK. Preservation and structural adaptation of endothelium over experimental foam cell lesions. Arteriosclerosis. 1989;9:881–94.
25. Faggiotto A, Ross R. Studies of hypercholesterolemia in the nonhuman primate. II. Fatty streak conversion to fibrous plaque. Arteriosclerosis. 1984;4:341–56.
26. Glagov S, Zarins CK, Giddens DP, et al. Atherosclerosis: what is the nature of the plaque? In: Strandness Jr DE, Didishiem P, Clowes AW, et al., editors. Vascular diseases: current research and clinical application. Orlando: Grune & Stratton; 1987. p. 15–33.
27. A Coordination Group in China. A pathological survey of atherosclerotic lesions of coronary artery and aorta in China. Pathol Res Pract. 1985;180:457–62.
28. Stevens SL, Hilgarth K, Ryan VS, et al. The synergistic effect of hypercholesterolemia and mechanical injury on intimal hyperplasia. Ann Vasc Surg. 1992;6:55.
29. Benditt EP. Implications of the monoclonal character of human atherosclerotic plaques. Am J Pathol. 1977;86:693–702.
30. McCaffrey TA, Du B, Fu C, et al. The expressions of TGF-beta receptors in human atherosclerosis: evidence of acquired resistance to apoptosis due to receptor imbalance. J Mol Cell Cardiol. 1999;31:162T.
31. Steinberg D, Parthasarathy S, Carew T, et al. Modifications of low density lipoprotein that increase its atherogenicity. N Engl J Med. 1989;320:915–24.
32. Karayannacos PE, Talukder N, Nerem R, et al. The rule of multiple noncritical arterial stenoses in the pathogenesis of ischemia. J Thorac Cardiovasc Surg. 1977;73:458–69.
33. Cronenwett JL. Arterial hemodynamics. In: Greenfield LJ, editor. Surgery: scientific principles and practice. 2nd ed. Philadelphia: JB Lippincott; 1997. p. 1656–67.
34. Imparato AM, Kim GE, Davidson T, et al. Intermittent claudication: its natural course. Surgery. 1975;78:795–9.
35. Boyd AM. The natural course of arteriosclerosis of lower extremities. Proc R Soc Med. 1962;55:591–3.
36. Bloor K. Natural history of atherosclerosis of the lower extremities. Ann R Coll Surg Engl. 1961;28:36–51.
37. Dormandy JA, Heeck L, Vig S. The natural history of claudication: risk to life and limb. Semin Vasc Surg. 1999;12:123–37.
38. Weitz JI, Byrne J, Clagett GP, Farkouh ME, Porter JM, Sackett DL, Strandness Jr DE, Taylor LM. Diagnosis and treatment of chronic arterial insufficiency of the lower extremities: a critical review. Circulation. 1996;94:3026–49.
39. Dormandy JA, Murray GD. The fate of the claudicant: a prospective study of 1969 claudicants. Eur J Vasc Surg. 1991;5:131–3.
40. Criqui MH, Langer Rd, Fronek A, Feigelson HS, Klauber MR, McCann TJ, Browner D. Mortality over a period of ten years in patients with peripheral arterial disease. N Engl J Med. 1992;326: 381–6.
41. McDermott MM, Feinglass J, Slavensky R, Pierce WH. The ankle-brachial index as predictor of survival in patients with peripheral vascular disease. J Gen Intern Med. 1994;9:445–9.
42. Sheikh MA, Bhatt DL, Li J, Lin S, Bartholomew JR. Usefulness of postexercise ankle-brachial index to predict all-cause mortality. Am J Cardiol. 2011;107:778–82.

43. Aboyans V, Desormais I, Lacroix P, Salazar J, Criqui MH, Laskar M. The general prognosis of patients with peripheral arterial disease differs according to the disease localization. J Am Coll Cardiol. 2010;55:898–903.
44. Rutherford RB, Baker JD, Ernst C, Johnston KW, Porter JM, Ahn S, Jones DN. Recommended standards for reports dealing with lower extremity ischemia: revised version. J Vasc Surg. 1997;26: 517–38.
45. Peabody CN, Kannel WB, McNamara PM. Intermittent claudication: surgical significance. Arch Surg. 1974;109:693–7.
46. Veith FJ, Gupta SK, Wengerter KR, et al. Changing arteriosclerotic disease patterns and management strategies in lower-limb-threatening ischemia. Ann Surg. 1990;212:402–14.
47. Dormandy J, Belcher G, Broos P, Eikelboom B, Laszlo G, Konrad P, et al. Prospective study of 713 below-knee amputations for ischaemia and the effect of a prostacyclin analogue on healing. Hawaii Study Group. Br J Surg. 1994;81(1):33–7.
48. Yao JST. New techniques in objective arterial evaluation. Arch Surg. 1973;106:600–4.
49. AbuRahma AF, Khan S, Robinson PA. Selective use of segmental Doppler pressures and color duplex imaging in the localization of arterial occlusive disease of the lower extremity. Surgery. 1995;118:496–503.
50. Toursarkissian B, Mejia A, Smilanich RP, Schoolfield J, Shireman PK, Sykes MT. Noninvasive localization of infrainguinal arterial occlusive disease in diabetics. Ann Vasc Surg. 2001;15:73–8.
51. Holland T. Utilizing the ankle brachial index in clinical practice. Ostomy Wound Manage. 2002;48:38–40.
52. Adam DJ, Naik J, Hartshorne T, Bello M, London NJ. The diagnosis and management of 689 chronic leg ulcers in a single-visit assessment clinic. Eur J Vasc Endovasc Surg. 2003;25:462–8.
53. Carser DG. Do we need to reappraise our method of interpreting the ankle brachial pressure index? J Wound Care. 2001;10:59–62.
54. Satomura S, Kaneko Z. Ultrasonic blood rheograph. In: Proceedings of the third international conference on medical electronics. London; 1960. p. 254.
55. Strandness Jr DE, McCutcheon EP, Rushmer RF. Application of transcutaneous Doppler flow meter in evaluation of occlusive arterial disease. Surg Gynecol Obstet. 1966;122:1039–45.
56. Landowne M, Katz LN. A critique of the plethysmographic method of measuring blood flow in the extremities of man. Am Heart J. 1942;23:644–75.
57. Hertzman AP. The blood supply of various skin area as estimated by the photoelectric plethysmograph. Am J Physiol. 1938;124: 328–40.
58. Barnes RW, Clayton JM, Bone GE, et al. Supraorbital photo-pulse plethysmography: simple accurate screening from carotid occlusive disease. J Surg Res. 1977;22:319–27.
59. Eldrup-Jorgensen SV, Schwartz SI, Wallace JD. A method of clinical evaluation of peripheral circulation: photoelectric hemodensitometry. Surgery. 1966;59:505–13.
60. Barnes RW, Garrett WV, Slaymaker EE, et al. Doppler ultrasound and supraorbital photoplethysmography for noninvasive screening of carotid occlusive disease. Am J Surg. 1977;134:183–6.
61. Barnes RW, Garrett WV, Hommel BA, et al. Photoplethysmography assessment of altered cutaneous circulation in the post-phlebitic syndrome. Proc Assoc Adv Med Instrum. 1978;13:25–9.
62. Bortolotto LA, Blacher J, Kondo T, Takazawa K, Safar ME. Assessment of vascular aging and atherosclerosis in hypertensive subjects: second derivative of photoplethysmogram versus pulse wave velocity. Am J Hypertens. 2000;13:165–71.
63. Whitney RJ. The measurement of changes in human limb volume by means of mercury-n-rubber strain gauge. J Physiol. 1949;109:5P.
64. Hokanson DE, Sumner DS, Strandness Jr DE. An electrically calibrated plethysmography for direct measurement of limb blood flow. IEEE Trans Biomed Eng. 1975;22:25–9.
65. Barnes RW, Hokanson DE, Wu KK, et al. Detection of deep vein thrombosis with an automatic electrically calibrated strain gauge plethysmograph. Surgery. 1977;82:219–23.
66. Yao JST, Needham TN, Gourmoos C, Irvine WT. A comparative study of strain-gauge plethysmography and Doppler ultrasound in the assessment of occlusive arterial disease of the lower extremities. Surgery. 1972;71:4–9.
67. Winsor T. The segmental plethysmograph: description of the instrument. Angiology. 1957;8:87–101.
68. Darling RC, Raines VK, Brenner V, et al. Quantitative segmental pulse volume recorder. A clinical tool. Surgery. 1972;72:873–7.
69. Nicholaides A. Quantitative air-plethysmography in management of arterial ischemia. In: Bernstein EF, editor. Vascular diagnosis. 4th ed. St. Louis: Mosby; 1993. p. 544–6.
70. Strandness Jr DE. Wave form analysis in the diagnosis of arteriosclerosis obliterans and peripheral arterial disease, a physiologic approach. Boston: Little Brown & Co; 1969. p. 92–113.
71. Kuvin JT, Patel AR, Sliney KA, Pandian NG, Sheffy J, Schnall RP, Karas RH, Udelson JE. Assessment of peripheral vascular endothelial function with finger arterial pulse wave amplitude. Am Heart J. 2003;146:168–74.
72. Gundersen J. Segmental measurement of systolic blood pressure in the extremities including the thumb and the great toe. Acta Chir Scand. 1972;426:1–90.
73. Rich K. Transcutaneous oxygen measurements: implications for nursing. J Vasc Nurs. 2001;19:55–9.
74. Kram HB, Appel PL, Shoemaker WC. Multisensor transcutaneous oximetric mapping to predict below-knee amputation wound healing: use of a critical PO2. J Vasc Surg. 1989;9:796–800.
75. Belcaro G, et al. Evaluation of skin blood flow and venoarteriolar response in patients with diabetes and peripheral vascular disease by laser Doppler flowmetry. Angiology. 1989;40:953–7.
76. Eicke BM, Milke K, Schlereth T, Birklein F. Comparison of continuous wave Doppler ultrasound of the radial artery and laser Doppler flowmetry of the fingertips with sympathetic stimulation. J Neurol. 2004;251:958–62.
77. Kubli S, Waeber B, Dalle-Ave A, Feihl F. Reproducibility of laser Doppler imaging of skin blood flow as a tool to assess endothelial function. J Cardiovasc Pharmacol. 2000;36:640–8.
78. Correa MJU, Andrade LEC, Kayser C. Comparison of laser Doppler imaging, fingertip lacticemy test, and nailfold capillaroscopy for assessment of digital microcirculation in systemic sclerosis. Arthritis Res Ther. 2010;12:R157.
79. Monstrey SM, Hoeksema H, Baker RD, Jeng J, Spence RS, Wilson D, Pape SA. Burn wound healing time assessed by laser Doppler imaging. Part 2: validation of a dedicated colour code for image interpretation. Burns. 2011;37:249–56.
80. Terry HJ. The electromagnetic measurement of blood flow during arterial surgery. Biomed Eng. 1972;7:466–74.
81. Masaryk TJ, Modic MT, Ruggieri PM, et al. Three dimensional (volume) gradient-echo imaging of the carotid bifurcation: preliminary clinical experience. Radiology. 1989;171:801–6.
82. Menke J, Larsen J. Meta-analysis: accuracy of contrast-enhanced magnetic resonance angiography for assessing steno-occlusions in peripheral arterial disease. Ann Intern Med. 2010;153: 325–34.
83. Collins R, Cranny G, Burch J, et al. A systematic review of duplex ultrasound, magnetic resonance angiography and computed tomography angiography for the diagnosis and assessment of symptomatic, lower limb peripheral arterial disease. Health Technol Assess. 2007;11:iii–xiii, 1.
84. Sacks D. Peripheral arterial duplex ultrasonography. Semin Roentgenol. 1992;27:28–38.
85. London NJ, Sensier Y, Hartsborne T. Can lower limb ultrasonography replace arteriography? Vasc Med. 1996;1:115–9.

86. Borrello JA. MR angiography versus conventional x-ray angiography in the lower extremities: everyone wins. Radiology. 1993;187:615–7.
87. Goyen M, Ruehm SG, Debatin JF. MR angiography for assessment of peripheral vascular disease. Radiol Clin North Am. 2002;40:835–46.
88. Lee SI, Miller JC, Abbara S, et al. Coronary CT angiography. J Am Coll Radiol. 2006;3:560–4.
89. Willmann JK, Baumert B, Schertler T, et al. Aortoiliac and lower extremity arteries assessed with 16-detector row CT angiography: prospective comparison with digital subtraction angiography. Radiology. 2005;236:1083–93.
90. Catalano C, Fraioli F, Laghi A, et al. Infrarenal aortic and lower extremity arterial disease: diagnostic performance of multi-detector row CT angiography. Radiology. 2004;231:555–63.
91. Brenner DJ, Hall EJ. Computed tomography – an increasing source of radiation exposure. N Engl J Med. 2007;357:2277–84.
92. Zhou W. Radiation exposure of vascular surgery patients beyond endovascular procedures. J Vasc Surg. 2011;53:39S–43.
93. Turnipseed WD. Diagnosis of carotid artery disease by digital subtraction angiography. In: AbuRahma AF, Diet-rich EB, editors. Current noninvasive vascular diagnosis. Littleton: PSG Publishing; 1988. p. 337–55.
94. Katayama H, Yamaguchi K, Kozuka T, et al. Adverse reactions to ionic and nonionic contrast media: a report from the Japanese Committee on the safety of contrast media. Radiology. 1990;175:621–8.
95. AbuRahma AF, Robinson PA, Boland JP, et al. Complications of arteriography in a recent series of 707 cases: factors affecting outcome. Ann Vasc Surg. 1993;7:122–9.
96. Balduf LM, Langsfeld M, Marek JM, et al. Complication rates of diagnostic angiography performed by vascular surgeons. Vasc Endovasc Surg. 2002;36:439–45.
97. AbuRahma AF, Elmore M, Deel J, Mullins B, Hayes J. Complications of diagnostic arteriography performed by a vascular surgeon in a recent series of 558 patients. Vascular. 2007;15:92–7.
98. Pedersen TR, Kjekshus J, Pyorala K, Olsson AG, Cook TJ, Musliner TA, Robert JA, Haghfelt T. Effect of simvastatin on ischemic signs and symptoms in the Scandinavian Simvastatin Survival Study (4S). Am J Cardiol. 1998;81:333–8.
99. Gould AL, Rossouw JE, Santanello NC, Heyse JF, Furberg CD. Cholesterol reduction yields clinical benefit: Impact of statin trials. Circulation. 1998;97:946–52.
100. Aung PP, Maxwell H, Jepson RG, Price J, Leng GC. Lipid-lowering for peripheral arterial disease of the lower limb (review). Cochrane Libr. 2009;1:1–61.
101. Bylund AC, Hammarsten J, Holm J, et al. Enzyme activities in skeletal muscles from patients with peripheral arterial insufficiency. Eur J Clin Invest. 1976;6:425–9.
102. Gardner AW, Poehlman ET. Exercise rehabilitation programs for the treatment of claudication pain: a meta-analysis. JAMA. 1995;274:975–80.
103. Regensteiner JG, Steiner JF, Hiatt WR. Exercise training improves functional status in patients with peripheral arterial disease. J Vasc Surg. 1996;23:104–15.
104. Sakamoto S, Yokoyama N, Tamori Y, Akutsu K, Hashimoto H, Takeshita S. Patients with peripheral artery disease who completed 12-week supervised exercise training program show reduced cardiovascular mortality and morbidity. Circ J. 2009;73:167–73.
105. McDermott MM, Ades P, Guralnik JM, Dyer A, Ferrucci L, Liu K, Nelson M, Lloyd-Jones D, van Horn L, Garside D, Kibbe M, et al. Treadmill exercise and resistance training in patients with peripheral arterial disease with and without intermittent claudication: a randomized controlled trial. JAMA. 2009;301(2):165–74.
106. Muller R. Hemorrheology and peripheral vascular disease. A new therapeutic approach. J Med. 1981;12:209–35.
107. Porter JM, Cutler BS, Lee BY, et al. Pentoxifylline efficacy in the treatment of intermittent claudication. Am Heart J. 1982;104:66–72.
108. AbuRahma AF, Woodruff BA. Effects and limitations of pentoxifylline therapy in various stages of peripheral vascular disease of the lower extremity. Am J Surg. 1990;160:266–70.
109. Dawson DL. Comparative effects of cilostazol and other therapies for intermittent claudication. Am J Cardiol. 2001;87:19D–27.
110. Robless P, Mikhailidis DP, Stansby GP. Cilostazol for peripheral arterial disease (review). The Cochrane Libr. 2008;3:1–27.
111. Hiatt WR. Medical treatment of peripheral arterial disease and claudication. N Engl J Med. 2001;344:1608–21.
112. ATC. Collaborative meta-analysis of randomized trials of antiplatelet therapy for prevention of death, myocardial infarction, and stroke in high risk patients. Br Med J. 2002;324:71–86.
113. Clagett P, Sobel M, Jackson M, Lip G, Tangelder M, Verhaeghe R. Antithrombotic therapy in peripheral arterial disease: the seventh ACCP conference on antithrombotic and thrombolytic therapy. Chest. 2004;126:S609–26.
114. Comerota AJ. Endovascular and surgical revascularization for patients with intermittent claudication. Am J Cardiol. 2001;87:34D–43.
115. Bates MC, AbuRahma AF. An update on endovascular therapy of the lower extremities. J Endovasc Ther. 2004;11:II-107–27.

# Segmental Doppler Pressures and Doppler Waveform Analysis in Peripheral Vascular Disease of the Lower Extremities

21

Stephen M. Hass and Ali F. AbuRahma

**Abstract**

Segmental Doppler pressures and Doppler waveform analysis are important tools in the diagnosis of patients with peripheral vascular disease of the lower extremities. A complete arterial lower extremity Doppler examination consists of three components: (1) analysis of the arterial analog wave tracing, (2) measurement of the segmental systolic limb pressures, and (3) calculation of the ankle-brachial index (ABI).

Doppler segmental pressures have the same capabilities of analog wave tracing, i.e., to help in identifying the presence and severity of arterial occlusive disease, to provide an objective baseline to follow the progression of peripheral vascular disease of the lower extremity and/or the postoperative course, and to somewhat evaluate the treatment plan.

Four 12×40 pneumatic cuffs are applied at various levels on each leg: as high on the thigh as possible, just above the knee, just below the knee, and above the ankle. The examiner then listens to the posterior tibial and the dorsalis pedis arterial signals. Of these vessels, the one with the strongest Doppler signal is chosen for the ankle pressure. High-thigh, above-knee, below-knee, and ankle pressure readings are taken.

Another component of the arterial lower extremity Doppler examination is the calculation of the ABI. It is generally agreed upon that an ABI of 0.9–1.0 signifies normalcy or minimal arterial occlusive disease, an ABI of 0.5–0.9 signifies a claudication level, less than 0.5 signifies the presence of ischemic rest pain or severe arterial occlusive disease, and less than 0.3 is compatible with trophic changes of the lower extremities.

**Keywords**

Noninvasive vascular testing • Doppler • Peripheral vascular disease • Lower extremities

S.M. Hass, M.D.
Department of Surgery, Robert C. Byrd Health Sciences Center, West Virginia University, Charleston Area Medical Center, Charleston, WV, USA

A.F. AbuRahma, M.D., RVT, RPVI (✉)
Department of Surgery, Robert C. Byrd Health Sciences Center, West Virginia University, 3110 MacCorkle Ave SE, Charleston, WV 25304, USA

Charleston Area Medical Center, Charleston, WV, USA
e-mail: ali.aburahma@camc.org

The credit for first developing Doppler flow detectors belongs to Satomura, whose clinical report appeared in 1959 [1]. However, until Strandness et al. [2] popularized the use of transcutaneous flow detection to study peripheral vascular occlusive disease, the diagnosis or objective assessment of limb ischemia was dependent upon clinical examination, arteriography, or plethysmography. The development of the continuous-wave or pulsed Doppler techniques opened a new field for the diagnosis of peripheral vascular occlusive disease.

A.F. AbuRahma, D.F. Bandyk (eds.), *Noninvasive Vascular Diagnosis*,
DOI 10.1007/978-1-4471-4005-4_21, © Springer-Verlag London 2013

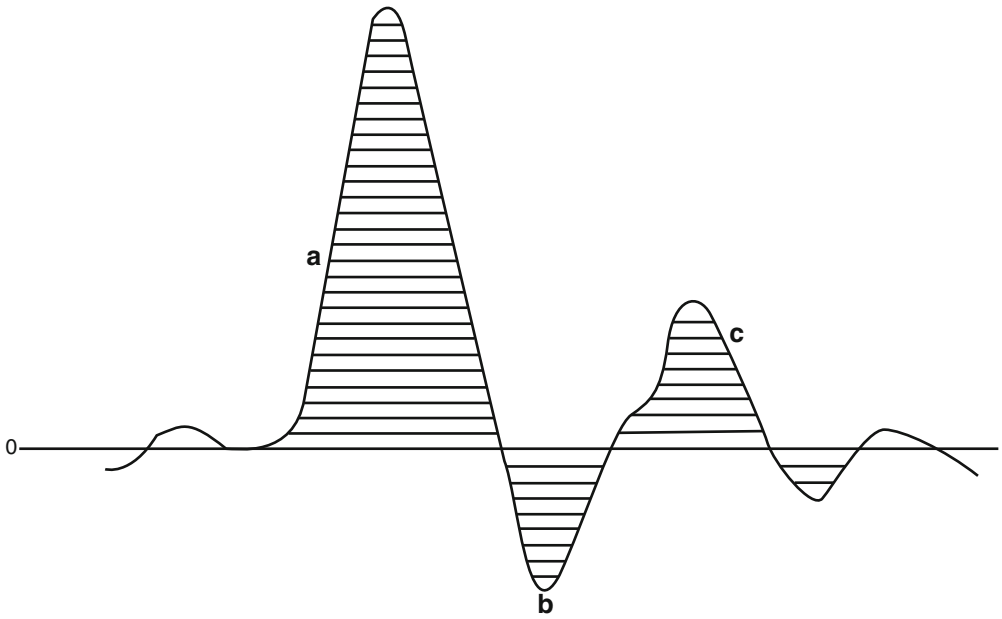


**Fig. 21.1** Normal arterial velocity tracing (multiphasic) ((**a**) systolic component, (**b**) early diastolic component, (**c**) late diastolic component)

## Instrumentation and Physical Principles

A continuous-wave (CW) Doppler velocity detector is used to sense apparent changes in the reflected sound wave frequency produced by the movement of red blood cells relative to an ultrasound probe. An electric oscillator vibrates a piezoelectric crystal (ceramic) at 5–10 MHz.

This produces an ultrasound wave that is transmitted via an acoustic coupling gel into the body. The ultrasonic beam is reflected back to a receiver in the probe by all the structures in its path, including the moving red blood cells. The movement of the blood cells causes a frequency shift (Doppler shift) in the reflected sound wave. The Doppler shift is proportional to the blood flow velocity. There is a Doppler effect whenever there is relative motion between the source and the receiver of the sound. Blood is the moving target and the transducer is the stationary source. Depending on the direction of the flow relative to the Doppler beam, the reflected frequency is higher or lower than the transmitted frequency (Doppler shift). The signal is electrically mixed with the transmitting frequency and processed to produce a frequency in the audible range. A received ultrasonic beam can be amplified and projected audibly through either a loudspeaker or earphones. A second method of displaying the Doppler velocity signal is by converting it to a visible analog waveform. With the analog waveform, the amplified signal is electronically converted and displayed on a channel recorder similar to an ECG (Fig. 21.1).

Therefore, there are several types of Doppler velocimetry: (1) auditory: this processes the Doppler signal as sound. It has the advantage of containing all Doppler frequencies with the exception of those extreme frequencies removed by filtering. A trained technician or physician can easily distinguish normal signals from those received proximal to, within, or distal to a stenosis or occlusion. A higher pitched signal can mean that the probe angle is very acute to the vessel angle or it can indicate a significant arterial occlusion. (2) Analog wave tracing: this method employs a zero-crossing frequency meter to display the signals graphically on a strip chart recorder. It has an acceptable overall accuracy, but it is not as sensitive as the spectral analysis, and it also has the following drawbacks: noise and under- or overestimation of high and low velocities, respectively. (3) Spectral analysis: this method displays frequency on the vertical axis, time on the horizontal axis, and the amplitude of backscattered signals at any frequency and time (Fig. 21.2). It has the advantage of displaying the amplitudes at all frequencies, but it is free of many of the disadvantages that were previously described for the analog wave tracing.

## Indications for Testing

The arterial lower extremity Doppler examination is a useful tool in many aspects of peripheral vascular medicine. It validates the diagnosis of the presence, location, and severity of arterial occlusive disease, helping to differentiate true vascular claudication from pseudoclaudication that arises from neurologic or musculoskeletal disorders. Therefore, this test is indicated for patients with symptoms and signs of arterial occlusive disease, which vary from claudication and rest pain to skin changes suggestive of arterial insufficiency, e.g., nonhealing ulcers [3–7].

The arterial lower extremity Doppler study is also helpful in determining the level of leg amputation and the benefit

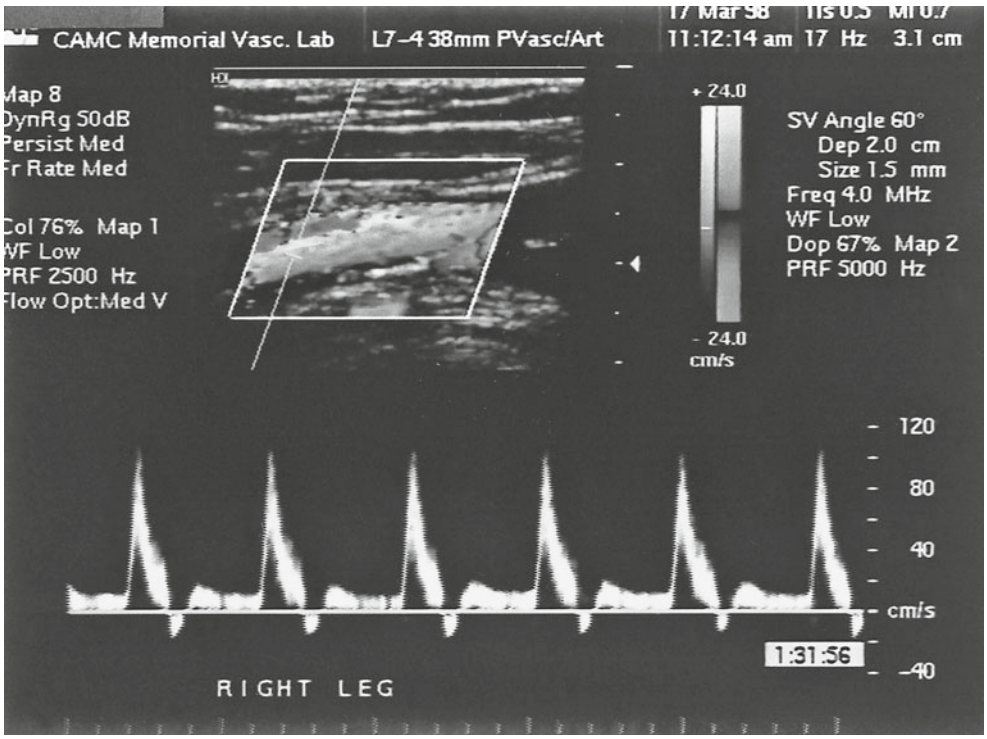


**Fig. 21.2** A spectral analysis of the right common femoral artery. This method displays frequency on the vertical axis, time on the horizontal axis, and the amplitude of backscattered signals at any frequency and time (This picture was taken by a color duplex ultrasound machine)

from lumbar sympathectomy [8–10]. In addition, the Doppler examination is useful in screening patients with Reynaud's disease or syndrome [11], or arteriovenous (AV) fistula [12], and to rapidly assess patients who have suffered possible arterial trauma.

In the case of iatrogenic arterial injury, Doppler ultrasound is suitable for assessing postcatheterization arterial obstruction following femoral or brachial cardiac catheterization or peripheral arteriography. Similarly, any complication following insertion of indwelling arterial monitoring catheters can be readily screened with the Doppler detector. It is also helpful in patients with shock.

Intraoperative measurement of ankle pressures after completion of aortofemoral bypass or aortoiliac endarterectomy can be used to predict the results of the procedure. The determination of segmental pressure measurements in the postoperative period aids in quantitatively assessing the results of aortofemoral bypass (Table 21.1). Ankle to brachial indices can be used to detect progression of lower extremity arterial disease after surgical intervention, which can present as worsening native arterial disease or a failing bypass conduit. These studies can be conducted formally in the vascular lab or rapidly at bedside or the postoperative recovery area using a continuous-wave Doppler and a handheld sphygmomanometer. A drop of the ankle to brachial index of more than 0.15 carries a sensitivity of 41% and a specificity of 84% in detecting the progression of lower extremity arterial disease [13].

**Table 21.1** Indications for arterial Doppler examination

| |
|---|
| 1. Calf pain while walking (claudication) |
| 2. Leg pain at rest, suggestive of ischemia |
| 3. Skin changes suggestive of arterial insufficiency |
| 4. Nonhealing ulcers |
| 5. Previous vascular reconstructive procedures—follow-up |
| 6. Intraoperative application |
| 7. Determination of the level of amputation and the response after lumbar sympathectomy |
| 8. Assistance in the diagnosis of Raynaud's disease or phenomenon and arteriovenous fistula |
| 9. Detection of pulses in shock states or in trauma |

## Methods and Interpretations

The complete arterial lower extremity Doppler examination consists of three components: (1) analysis of the arterial analog wave tracing, (2) measurement of the segmental systolic limb pressures, and (3) calculation of the ankle-brachial index (ABI).

After the history is taken, the patient is allowed to rest in the supine position on the examining table for 10–15 min to ensure the measurement of pressures in the resting state. The patient is placed in the supine position with the extremities at the level of the heart. The head of the bed can be elevated slightly, and the patient's head can rest on a pillow. The patient's hip is generally externally rotated with the knee slightly bent to facilitate the lower extremity evaluation.

Alternative positions for the Doppler lower extremity examination include right or left lateral decubitus (patient on his or her side) or the prone position for access to the popliteal artery.

Gornik et al. recently validated a method of determining the ankle to brachial index in the seated position [14]. This could broaden the availability of peripheral arterial disease testing in patients compromised by musculoskeletal or cardiopulmonary conditions that limit their ability to tolerate the supine position.

The Doppler probe (transducer) must be positioned on the long axis of the vessel. An angle of insonation of approximately 45–60° is usually used for this study. The leg pulses (femoral, popliteal, dorsalis pedis, and posterior tibial) are evaluated by palpation and by audible Doppler signals. The pulses are graded as II, I, or 0, and the Doppler signals are graded as normal (biphasic), abnormal (monophasic), or absent.

## Qualitative Doppler Waveform Analysis

For the lower extremities, Doppler velocity waveforms are recorded from the following arteries bilaterally: (1) common femoral artery at the groin level, (2) superficial femoral artery, (3) popliteal artery, (4) posterior tibial artery (at the level of the medial malleolus), (5) dorsalis pedis artery (at the dorsum of the foot), and (6) occasionally the peroneal artery (at the level of the lateral malleolus). Auditory signals are obtained. If the examiner is using a headset, the right earphone provides forward (antegrade) flow signals, while the left earphone provides reverse (retrograde) flow signals. The qualities of the auditory signals and the waveforms are observed and analyzed.

The normal arterial velocity signal is multiphasic. That is, it is characterized by one systolic and one or more diastolic components (Fig. 21.1). In the major peripheral arteries, the systolic component is a large positive deflection indicative of a high net forward flow velocity. This is followed by a brief period of net flow reversal. This flow reversal is then followed immediately by another positive deflection, the diastolic forward flow component. The brief period of flow reversal characteristic of the major peripheral arterial velocity signal is a function of the generally high resistance of the extremity vascular bed. Lowering resistance, via vasodilation, can eliminate the net flow reversal. The normal arterial velocity signal is also pulsatile, i.e., it cycles with each heartbeat. Thus, the normal nonpulsatile, phasic, low-pitch venous signal is easily differentiated from the pulsatile, multiphasic arterial signal.

Abnormal signals are generally monophasic (Fig. 21.3), nonpulsatile, or absent. Biphasic signals can also be considered abnormal (Fig. 21.3). It is imperative to observe for deterioration of the waveform, e.g., triphasic to biphasic or triphasic to monophasic of the Doppler signal quality from one level to the next level. A monophasic and dampened signal can be obtained proximal to an obstruction as well as distal to it. In the absence of additional obstructions, the distal signal can normalize.

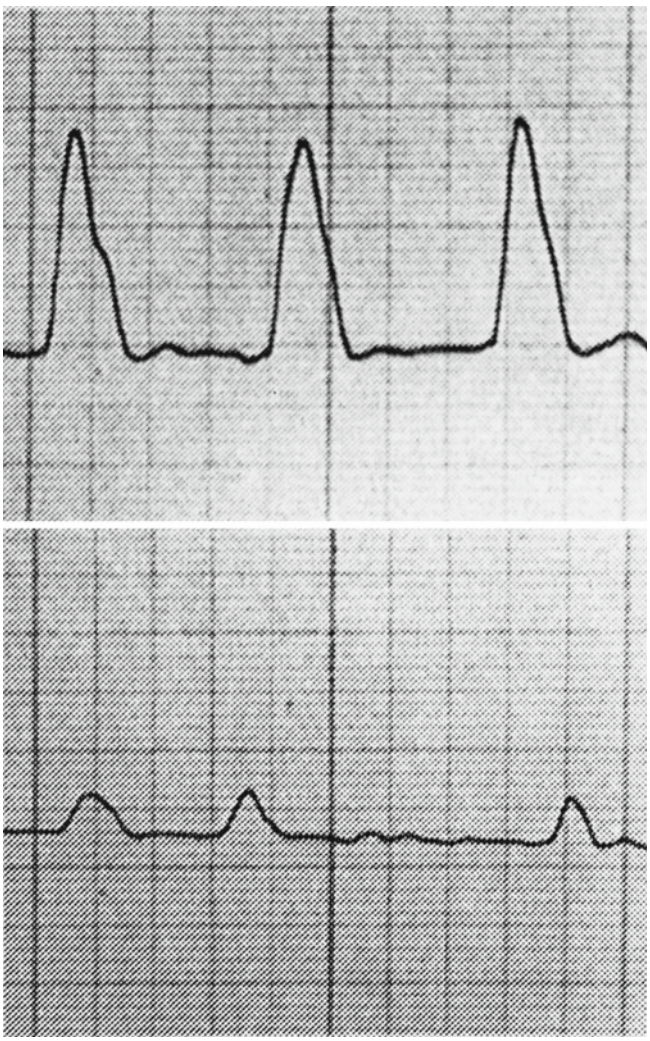

**Fig. 21.3** An abnormal arterial tracing of the lower extremity in a patient with stenosis of the common femoral artery. The upper tracing was recorded from the popliteal artery distal to the obstruction, and the lower tracing was taken at the level of the posterior tibial artery. These signals are monophasic

The arterial velocity signal produced just before an occlusion is characteristically of short duration, i.e., a slapping signal of low amplitude. However, the arterial signal produced over a stenotic segment is a high-pitched signal with less prominent diastolic components. The signal from just beyond the stenotic segment is also characterized by dampened systolic and absent diastolic components, but it is not as high pitched as the stenotic signal. The signal beyond an occluded arterial segment is like a post-stenotic

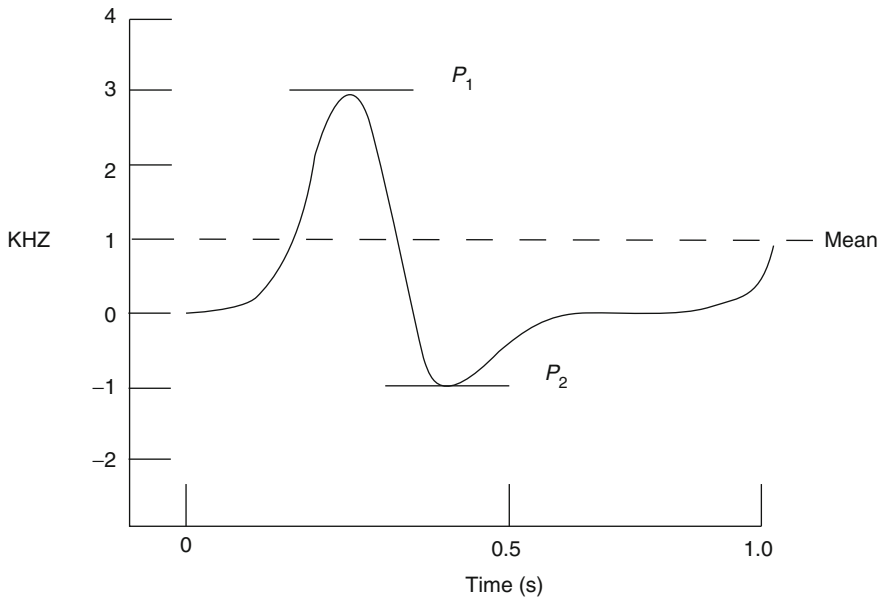


**Fig. 21.4** The method for calculating the pulsatility index

signal, although the systolic component may be of even lower amplitude. The signal produced by the prominent collateral arterial signal is high pitched and almost continuous. These similarities among the abnormal arterial velocity signals make the differentiation difficult. Therefore, if there is difficulty in interpreting these signals, they can be called either normal or abnormal for practical purposes (Fig. 21.3).

As noted in the abnormal wave tracing, a Doppler signal obtained from a common femoral artery that is diseased shows the poor quality of the signal (poor upslope and downslope, with a somewhat rounded peak) (Fig. 21.3). A similar waveform can be obtained from the common femoral artery distal to a proximal iliac artery obstruction. Similarly, the Doppler signals obtained from the posterior tibial artery at the level of the ankle distal to that occlusion is somewhat continuous with low pressure resistance secondary to a vasodilated arterial bed in the presence of proximal arterial obstruction.

## Quantitative Interpretation Criteria of Doppler Waveform

1. *Pulsatility index* (*PI*): This is calculated by dividing the peak-to-peak frequency by the mean (average) frequency [15] signal as seen in Fig. 21.4. This ratio is independent of the beam-to-vessel Doppler angle when using handheld Doppler equipment. As seen in Fig. 21.4, the pulsatility index equals P1–P2 divided by the mean frequency. Normally, the values of the PI increase from the central to peripheral arteries. A PI of >5.5 is normal for the common femoral artery, while a normal PI for the popliteal artery is approximately 8.0. These values decrease in the presence of proximal occlusive disease, e.g., a PI of <4 or 5 in the common femoral artery with a patent superficial femoral artery (SFA) indicates proximal aortoiliac occlusive disease. However, the same reduced PI is not diagnostic if the SFA is occluded.
2. *Inverse damping factor*: This is calculated by dividing the distal PI by the proximal PI of an arterial segment. It indicates the degree to which the wave is dampened as it moves through an arterial segment [15], e.g., severe stenosis or occlusion of the SFA is usually present when the inverse femoral-popliteal dampening factor is less than 0.9 (a normal value = 0.9–1.1).
3. *Transient time*: Systole should be simultaneously evident at a specific site bilaterally. Delay on one side may indicate a more proximal occlusive disease. You must compare the signals bilaterally at the same site.
4. *Acceleration time or index*: This differentiates inflow from outflow disease. It is based on the principle that arterial obstruction proximal to the site of the Doppler probe prolongs the time between the onset of systolic flow to the point of maximum peak in waveforms at the probe site (Fig. 21.5). Figure 21.5a shows a normal common femoral artery tracing. There is a quick systolic upslope representing a normal acceleration time, in contrast to Fig. 21.5b, which shows a slower upslope from the onset of systole to maximum peak from an abnormal common femoral artery tracing. Acceleration time is not prolonged when there is disease distal to the probe. It is applied to those signals evaluated by spectral analysis because it is necessary to maximize sensitivity and minimize artifacts.

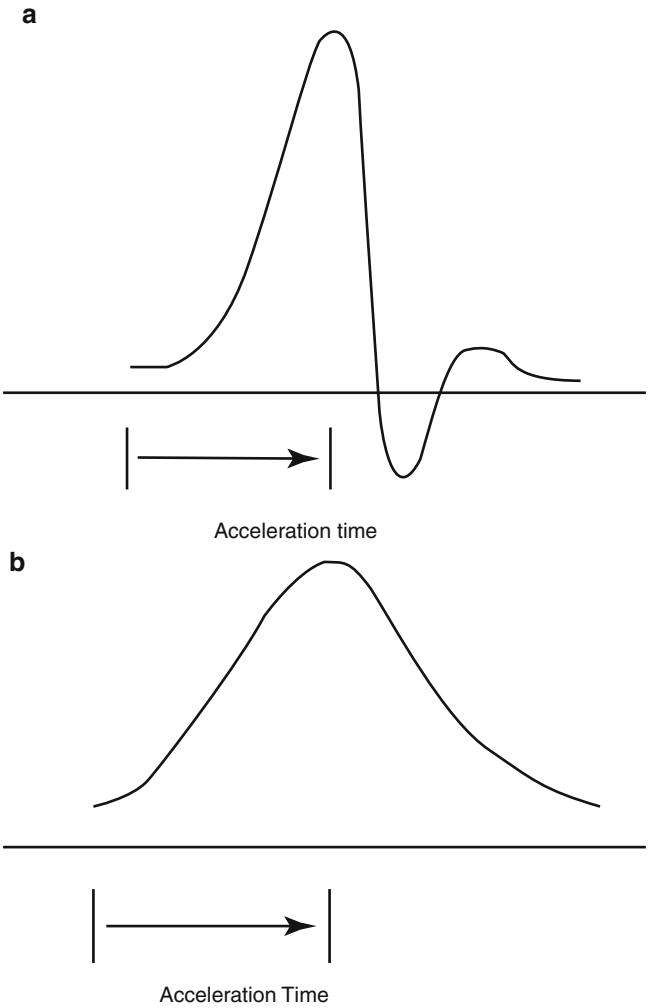


**Fig. 21.5** A normal common femoral artery tracing with a normal acceleration time (**a**) and an abnormal common femoral artery tracing with an abnormal acceleration time (**b**)

Generally, an acceleration time of equal to or less than 133 ms suggests the absence of significant aortoiliac disease. False-positive results can occur with technical errors, e.g., a Doppler angle = 70°, which may dampen the Doppler signal qualities, and in the presence of poor cardiac output since the Doppler flow signal will be attenuated with the waveform detecting slow upstroke, rounded peak, and slow downslope.

5. *Doppler-derived maximal systolic acceleration*: Van Tongeren et al. recently evaluated the Doppler-derived maximal systolic acceleration in determining peripheral arterial occlusive disease in patients with diabetes mellitus [16]. These patients are subject to falsely elevated ankle to brachial indices secondary to medial calcification. They found that a maximal systolic acceleration of >10 m/s$^2$ was highly predictive for the exclusion of peripheral arterial occlusive disease (negative predictive value 95%), whereas a maximal systolic acceleration of <65 m/s$^2$ was highly predictive for the detection of peripheral arterial occlusive disease (positive predictive value 99%).

## Limitations of the Analog Wave Tracing Analysis

The Doppler waveforms may be affected by (1) ambient temperature, (2) uncompensated congestive heart failure resulting in dampened waveforms following exercise, (3) an inability to distinguish stenosis from occlusion, (4) an inability to precisely localize the occlusion, (5) and an inability to be applied on patients with casts or extensive bandages that cannot be removed. It is technologist dependent, and the result can vary with the Doppler angle used.

## Segmental Doppler Pressures

After completion of the examination and analysis of the arterial analog tracings, the second component of the Doppler examination is started, i.e., determinations of the segmental systolic limb pressures. Doppler segmental pressures have the same capabilities of analog wave tracing, i.e., to help in identifying the presence and severity of arterial occlusive disease, to provide an objective baseline to follow the progression of peripheral vascular disease of the lower extremity and/or the postoperative course, and to somewhat evaluate the treatment plan. The results of this testing are usually combined with the Doppler velocity waveform analysis. The patient preparation and positioning are similar to those of the Doppler velocity waveform analysis.

## Technique for Segmental Doppler Pressures

The brachial artery Doppler systolic pressures are measured in each arm. Cuffs of appropriate size (bladder dimension 12 × 40 cm) are placed on each arm. The brachial artery is palpated in the antecubital fossa, and a small amount of acoustic gel is applied to the skin over the artery. The arterial signal is found using the Doppler probe, and then the cuff is inflated until the signal disappears (20–30 mmHg beyond the last audible Doppler signal). The cuff is slowly deflated until the arterial signal is again audible, at which time the pressure is recorded.

Unlike the standard stethoscope, as the cuff is further deflated, the velocity signal will not disappear, so the diastolic pressure cannot be determined.

Four 12 × 40 cm pneumatic cuffs are applied at various levels on each leg: as high on the thigh as possible, just above the knee, just below the knee, and above the ankle (Fig. 21.6a). The examiner then listens to the posterior tibial and the

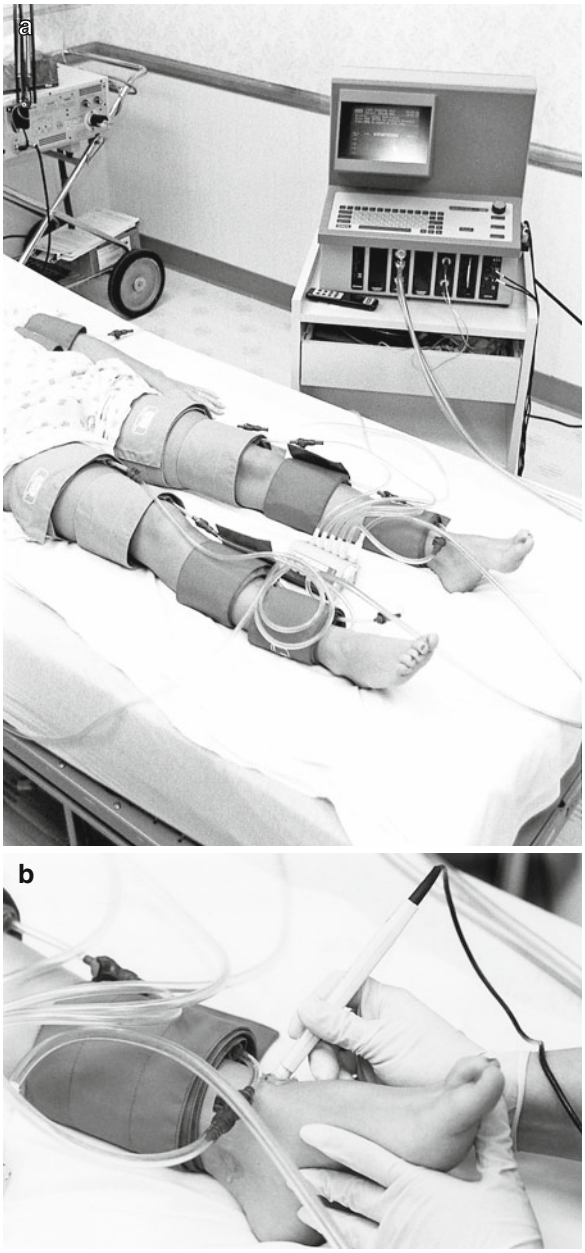


**Fig. 21.6** (**a**) Technique for measuring the segmental Doppler pressures using the four cuff method. (**b**) The application of the Doppler probe on the dorsalis pedis artery

dorsalis pedis arterial signals (Fig. 21.6b). The posterior tibial artery is found just posterior to the medial malleolus, and the dorsalis pedis artery is found on the dorsum of the foot. Occasionally, the peroneal (lateral tarsal) artery is examined (found just anterior to the lateral malleolus). Of these vessels, the one with the strongest Doppler signal is chosen for the ankle pressure. If none of the vessels can be located with the ultrasound probe, the popliteal artery signal is identified in the popliteal fossa. High-thigh, above-knee, below-knee, and ankle pressure readings are taken. An automatic cuff inflator may be used to save time. An alternative method involves using only three cuffs with a single, relatively wide cuff at the mid-thigh.

Several important facts concerning cuff characteristics should be noted. It is most important that the pneumatic bladder of the cuff completely encircle the limb. The bladder of the cuff should be placed over the artery. This is especially important when the bladder does not encircle the limb. Just as bladder length affects the pressure determination, bladder width must also be related to the limb diameter. For the most accurate measurement of blood pressure, the width of the pneumatic cuff should be 20% greater than the diameter of the limb [3]. For all practical purposes, this means that larger arms require wider cuffs. When a cuff is too narrow relative to the limb diameter, an erroneously high pressure (30–90 mmHg greater than arm pressure) results.

The four cuffs used in this test to determine the segmental pressures at different levels of the lower limb are all the same width (12×40 cm), making the pressures at the widest part of the limb (high thigh) erroneously high. Some laboratories use a large (19×40 cm) thigh cuff to satisfy the recommended width/girth relationship and thereby give a more accurate thigh pressure. However, the cuff is so wide that only one can be placed on the thigh. The three-cuff technique utilizes one large cuff placed as high as possible on the thigh. With this technique, a more accurate thigh pressure is obtained (a thigh pressure that is very similar to the higher brachial pressure).

Segmental Doppler pressures of the lower extremity are obtained bilaterally at the following sites and in this order using a handheld or machine sphygmomanometer with automatic display: ankle pressure (using the posterior tibial artery and dorsalis pedis artery); below-knee pressure (calf pressure), using the best signal of the posterior tibial artery or the dorsalis pedis artery; above-knee pressure (same as below-knee pressure, although the popliteal artery can be used if the ankle Doppler signals are difficult to obtain); and high-thigh pressure (the same as above-knee pressure). If a pressure measurement needs to be repeated, the cuff should be fully deflated for about 1 min prior to repeat inflation.

Barnes [4] used a narrower cuff (12×40 cm) for measuring the proximal and distal thigh pressures and accepted the artificially high values obtained. This technique allows an approximation of the common femoral (inflow) artery pressure by the proximal cuff and the superficial femoral artery pressure by the above-knee cuff. When only one large cuff is used on the thigh, the single thigh pressure measured does not differentiate aortoiliac from superficial femoral artery occlusive disease. For convenience, the aneroid manometer is used rather than the mercury manometer. The aneroid manometer has the advantage of being portable, inexpensive, easily exchanged from cuff to cuff, and an accurate pressure registering system.

For the analog wave recording technique, diastolic pressure is taken as the pressure at which there is continuous forward flow during diastole. But this point of return of continuous forward flow in diastole would be difficult to determine in the vasoconstricted or high-resistant limb, because the tracing would be constantly crossing to zero during the period of net flow reversal. The problem is overcome by purposely inducing a state of reactive hyperemia in the vasoconstricted limb. This hyperemia is a state of vasodilation.

## Interpretations

After determination of the segmental systolic limb pressures, analysis of the various segment pressures is done. Normally, the proximal thigh pressure should be 20–30 mmHg higher than that of the arm, and the pressure gradient between adjacent levels of measurement in the leg should be no greater than 20–30 mmHg. A low proximal thigh pressure signifies aortoiliac or common femoral occlusive disease. An abnormal gradient between the proximal thigh and the above- or below-knee cuff is indicative of superficial femoral or popliteal artery occlusive disease. An abnormal gradient between the below-knee and ankle cuffs indicates tibioperoneal disease. Figure 21.7 shows a patient with occlusion of the left superficial femoral artery as indicated by the pressure differential between the high-thigh and above-knee readings (160–116 mmHg, respectively). A horizontal difference of 20–30 mmHg or more suggests significant disease at or above the level of the leg with the lower pressure. Figure 21.8 shows a patient with significant stenosis or occlusion at the aortoiliac level as indicated by low high-thigh pressures bilaterally.

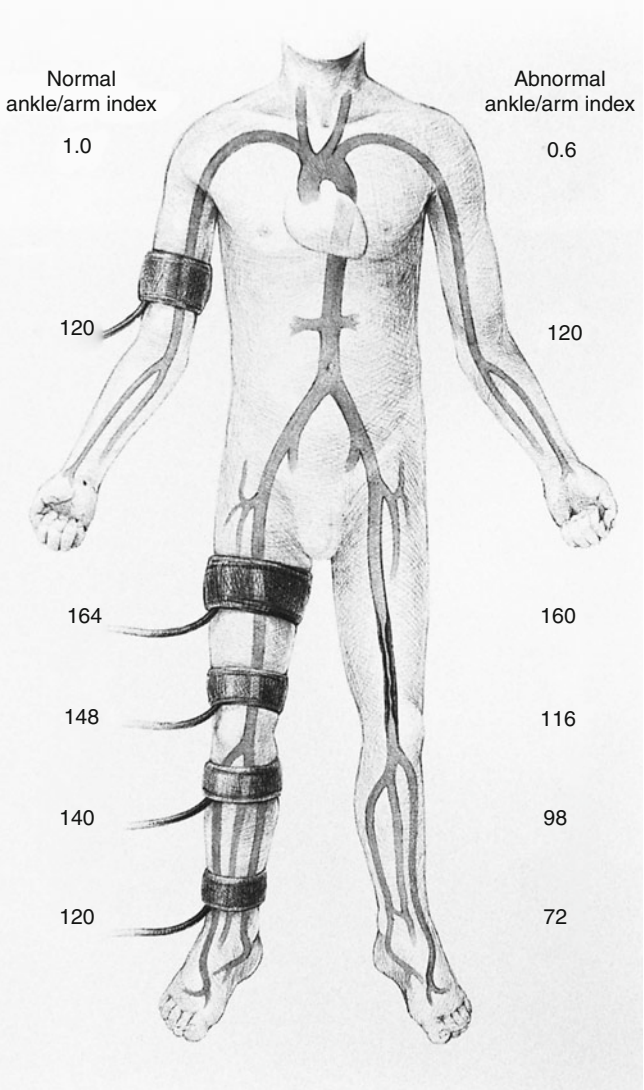


**Fig. 21.7** Segmental systolic limb pressures of a patient with severe stenosis of the left superficial femoral artery

## Thigh Pressure Indices

Thigh pressure/higher brachial pressures are normally greater than 1.2, while 0.8–1.2 suggests aortoiliac occlusive disease, and less than 0.8 indicates that proximal occlusion is likely. When the high-thigh pressure is low compared with the brachial artery pressure, the level of obstruction could be beneath the cuff as well [17]. Thus, the site of obstruction could be the aorta, iliac artery, common femoral artery, or even the proximal superficial femoral artery. With the three-cuff technique, the large, single thigh cuff segmental pressure is normally similar to the brachial pressure.

## Ankle-Brachial Index

Another component of the arterial lower extremity Doppler examination is the calculation of the ankle-brachial index (ABI). From the ankle and brachial systolic pressures, a ratio is obtained that is helpful in determining the presence and magnitude of occlusive disease.

Since normal lower limbs have ankle pressures equal to or greater than their ipsilateral arm pressures (recorded in a supine position), a ratio of 1.0 or greater is taken as normal. However, mild to moderate atherosclerotic disease may not affect resting ankle pressures significantly, so all persons having an ABI of 1.0 or greater will probably benefit from stress testing, e.g., treadmill exercise as described in detail later.

Numerous methods of calculating the ankle to brachial index have been described based on variances in the numerator taken in the ABI equation [18]. The current method recommended by the American College of Cardiology/American Heart Association uses the higher of the two ankle systolic arterial pressures, termed the high ankle pressure (HAP), as the numerator in the ABI equation [19]. A second method

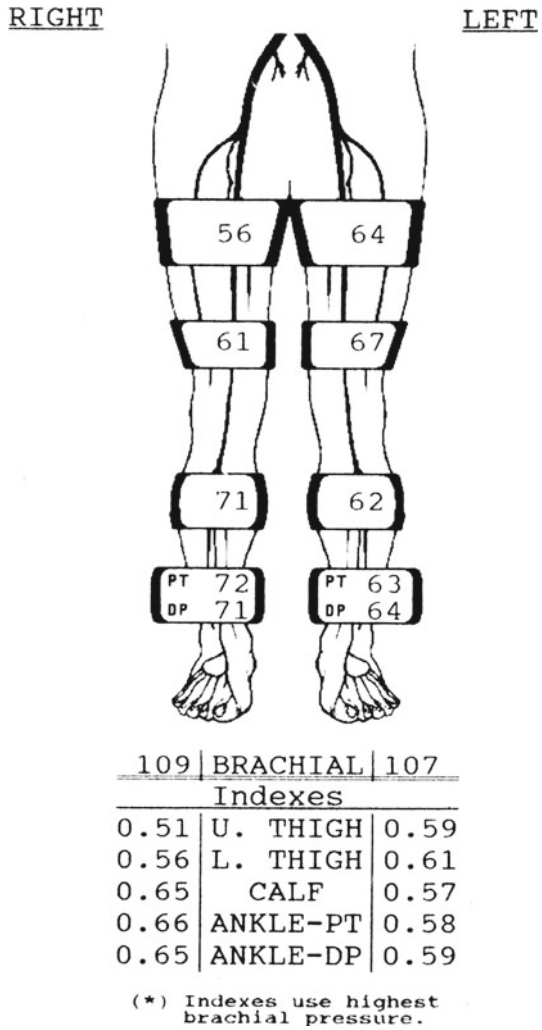


**Fig. 21.8** A patient with significant stenosis or occlusion at the aortoiliac level as indicated by low high-thigh pressures bilaterally

uses the lower of the two ankle systolic arterial pressures, termed the low ankle pressure (LAP) as the numerator when calculating the ABI [20]. Some studies use the average of the two ankle systolic pressures as the numerator [21]. Some studies have used the posterior tibial systolic pressure to calculate the ABI [22].

It is generally agreed upon that an ABI of 0.9–1.0 signifies normalcy or minimal arterial occlusive disease, an ABI of 0.5–0.9 signifies a claudication level, less than 0.5 signifies the presence of ischemic rest pain or severe arterial occlusive disease, and less than 0.3 is compatible with trophic changes of the lower extremity. Some believe that an absolute ankle pressure of less than 50 mmHg, rather than an ABI of 0.5, is better at predicting symptoms at rest. It has also been suggested that an ABI of equal to or more than 0.5 represents single segment involvement and that lower values are more indicative of multilevel disease [5].

## Technique for Toe Doppler Systolic Pressure

The digital study is often done in combination with a physiological lower extremity arterial test, usually a segmental Doppler pressure with or without Doppler waveform analysis. An appropriately sized cuff, the width of which should be at least 1.2 times that of the toe, is applied to the base of the toe(s). Two 2.5-cm cuffs are usually used for fingers and a 2.5–3-cm cuff for the great toe. The digital pulse can be examined using the usual Doppler probe, and a similar technique is applied to measure the Doppler toe pressure.

Normal toe pressures vary from 60% to 80% of the ankle pressures. Values significantly less than this signify digital arterial occlusive disease. The exception to this criteria is when the ankle pressure is artificially high (arterial calcinosis), in which case the toe pressure may be much lower than 80% of the ankle pressure in the absence of digital artery disease. It is generally believed that there is little difference between the toe pressures in diabetics and nondiabetics, which makes toe pressure determination very helpful in patients with very artificially high segmental Doppler pressures at the ankle level [23].

Since toe systolic pressures and/or TBIs are likely to be less affected by medial calcification, false-positive results are rare [24, 25]. While authorities define critical forefoot ischemia as an absolute toe pressure <30 mmHg [26], measurements can be inaccurate in the presence of vasoconstriction due to a cold environment [27]. Thus, a diminished toe pressure can be due to either peripheral arterial disease or vasoconstriction. A toe-to-brachial index (TBI) >0.75 is generally considered as normal, whereas a TBI <0.25 is indicative of significant peripheral arterial disease [28]. A toe pressure of >55 mmHg has been correlated with the ability to heal a foot ulcer in diabetic patients [29].

## Limitations and Sources of Error in Doppler Segmental Pressure Determination

1. *Media sclerosis*: This may cause falsely elevated Doppler pressures in those patients with calcified vessels, e.g., patients with diabetes or end-stage renal disease. Toursarkissian et al. [23] reported the results of a retrospective review of 101 diabetic patients without aortoiliac disease to analyze the ability of various noninvasive tests to predict the level of >50% significant stenosis of infrainguinal arterial disease. Patients were studied with ABI, toe brachial indices (TBI), segmental pulse volume recording (pulse volume recording), segmental pressures, segmental Doppler waveforms, and arteriography. Their findings showed that as a single test, the Doppler waveform appears to have the best angiographic correlation, although the summed diagnosis of combined

Doppler waveform and pulse volume recording data was superior in distinguishing multilevel disease from isolated tibial disease. It was also concluded that segmental Doppler pressures were of limited value in patients with diabetes mellitus, even in multimodality testing.

2. *Hypertension*: When the systemic pressure is elevated, the absolute post-stenotic values are also erroneously high. Since there is no linear relationship between the change in the systemic pressure and the peripheral pressure, the measurement should always be repeated after the systemic pressure has normalized.
3. In patients with multilevel occlusive disease, it is difficult to interpret segmental pressures.
4. *Measurement of pressure postexercise*: Two examiners should carry out the examination simultaneously after physical exertion to evaluate both extremities; otherwise, an adequate rest period between the measurement of the right and left sides is needed. The lower extremity that has the lower resting pressure should be measured first, because the recovery time, postexercise, is otherwise too long in pathological cases.
5. *Edema*: In solid edema, especially lipedema, adequate arterial compression may fail, causing erroneously high pressure values.
6. Patients with uncompensated congestive heart failure may show decreased ankle-brachial indices after exercise.
7. This test cannot distinguish between stenosis and occlusion and cannot precisely localize the area of occlusion, although it can identify a general location. Similarly, it cannot distinguish between common femoral artery disease and proximal external iliac artery disease.
8. *Resting period*: An adequate resting period of 10–20 min before measurements are taken must be observed. Where there are poorly compensated flow obstructions, the resting period should be longer, in order to avoid measuring erroneously low pressure values.
9. *Deflation errors*: Releasing the cuff pressure too quickly (above 5 mmHg/s) causes erroneously low values. Therefore, a deflation velocity of around 2 mmHg/s should be maintained.
10. *Arm-leg measurement intervals*: The time difference between Doppler pressure measurements should not be too long. Intraindividual systemic blood pressure fluctuations can occur and affect the results.
11. *Subclavian stenosis or occlusion*: The systolic blood pressure values measured in this situation are erroneously low; this may give a false impression of normal circulation of the lower extremities.
12. *Flow velocity in the arteries measured*: If the flow velocity in the arteries that are being measured is too low (less than 6 cm/s), it is not possible to receive a Doppler signal. This phenomenon usually occurs at pressures below 30 mmHg.
13. *Effect of the girth of the limb*: When the girth of the limb is large in relation to the width of the cuff, the pressure in the cuff may not be transmitted completely to the vessels in the central part of the limb, and the measured pressures may be erroneously exaggerated. Such high false pressures are commonly encountered in the measurement at the level of the thigh.
14. *Effect of vasomotor tone changes*: Changes in the vasomotor tone may affect the arterial pressures. When the blood flow is increased during peripheral vasodilation induced by exercise, heat, or reactive hyperemia, more pressure energy is used in causing flow through stenotic lesions, small distal vessels, and collaterals; therefore distal pressure is reduced. Conversely, when the patient is cool, or when the flow is lower at rest, the pressure tends to be higher. These considerations will explain the normal pressures measured at rest in limbs with mild stenotic lesions and why ankle and digital pressures may be altered significantly by changes in the vasomotor tone. The high tone of the smooth muscle in the wall of the smaller distal vessels of the limbs may result in an artificial reduction of the measured systolic pressure [30, 31].
15. *Stenosis or occlusion in parallel vessels*: When several parallel vessels of comparable size are under the cuff, the measurement will usually reflect the pressure in the artery with the highest pressure and will not detect stenotic or occlusive lesions in the other vessel. Therefore, these measurements will not detect isolated disease in the internal iliac, profunda femoris, tibial, peroneal, ulnar, or individual digital arteries or interruption of one of the palmer or plantar arches.

## Clinical Studies and Results

An analysis of 150 patients (300 limbs) who had both arterial lower extremity Doppler studies (segmental Doppler pressures and analog wave analysis) and arteriograms was done. Each limb was studied in four arterial segments: 300 iliofemoral, 300 femoral, 282 popliteal, and 275 trifurcation segments. Eighteen popliteal and 25 trifurcation segments were excluded for lack of angiographic visualization (not enough dye).

In the 1,157 segments studied, 793 were found to be normal, of which 758 were confirmed by the arteriogram (96% true-negative and 4% false-negative results). The other 35 segments, which were normal by arterial lower extremity Doppler, were found to have mild to moderate atherosclerotic disease. Of the 364 segments interpreted as abnormal by arterial lower extremity Doppler, 328 were confirmed by the arteriogram (90% true-positive and 10% false-positive results). In the other 36 segments, the arteriogram was normal or showed mild disease. Thus, in a total of 1,157 segments studied, the findings in 1,086 were confirmed by the arteriogram (94% correlation) [32, 33].

## Sensitivity and Specificity of the ABI in Diagnosing Peripheral Arterial Disease

The ABI has a sensitivity of more than 90% and a specificity of more than 95% in diagnosing a 50% stenosis of the lower extremity arteries when compared to standard angiography [34–36]. Schroder et al. found that the high ankle pressure ABI had a sensitivity of 68% and a specificity of 99%, whereas the low ankle pressure ABI sensitivity was 89% and the specificity 93% [37]. According to Niazi et al., the high ankle pressure sensitivity was 69% and specificity 83%, with sensitivity and specificity of the low ankle pressure being 84% and 64% [38]. Thus, one could argue that the low ankle pressure may be a more sensitive measure of peripheral arterial disease and allow improved identification of patients at risk for disease [39]. However, Lange et al. evaluated almost 7,000 patients using five different methods of ABI calculation and found that the high ankle pressure ABI provided the most accurate estimation of peripheral arterial disease in the general population [40].

## Selective Use of Segmental Doppler Pressures and Color Duplex Imaging in the Localization of Arterial Occlusive Disease of the Lower Extremity

With the recent advances in noninvasive vascular technology, color duplex imaging (CDI) has become popular in the diagnosis and localization of aortoiliac and femoropopliteal occlusive disease with a very good correlation to angiography [41–44]. However, because of the cost and time involved in performing a CDI of the lower extremity, many vascular laboratories still rely on segmental Doppler pressures to localize arterial occlusive disease, while others still combine both modalities.

In a previously published study [45], we compared the abilities of segmental Doppler pressures and CDI to accurately categorize the severity of disease. We analyzed 134 patients (268 limbs) who underwent all three tests: segmental Doppler pressures, CDI, and arteriograms.

Segmental Doppler pressures and CDI results were examined to determine their accuracy in localizing high-grade (>50%) stenosis at three levels: aortoiliac-common femoral artery (Level I), superficial femoral artery (Level II), and popliteal artery (Level III).

The sensitivity, specificity, positive and negative predictive values, and overall accuracy for segmental Doppler pressures and CDI were as follows: Level I—63%, 88%, 81%, 75%, and 77%; 93% 99%, 98%, 95%, and 96%, respectively ($p<0.01$); Level II—51%, 99%, 99%, 57%, and 70%; 94%, 98%, 99%, 92%, and 96%, respectively ($p<0.01$); and Level III—55%, 92%, 60%, 90%, and 85%; 78%, 100%, 97%, 95%, and 95%, respectively ($p<0.01$). There was exact agreement between the CDI and arteriogram in regard to the severity of disease in 88% of the limbs (1,170 segments). The presence of superficial femoral artery disease in patients with Level I disease or aortoiliac-common femoral artery disease in patients with Level II disease did not significantly alter the ability of segmental Doppler pressures to localize the disease. The presence of diabetes significantly affected the accuracy of segmental Doppler pressures in localizing superficial femoral and popliteal artery stenosis. An analysis of the ability of segmental Doppler pressure to detect any segment as abnormal, as confirmed by arteriogram, revealed a sensitivity of 88%, specificity of 82%, positive predictive value of 96%, negative predictive value of 60%, and overall accuracy of 87%. We concluded that CDI was superior to segmental Doppler pressures in localizing arterial stenosis at all levels. However, since segmental Doppler pressure is cheaper, it can be used initially if no surgical or endovascular intervention is planned.

## Summary

Doppler ultrasound has the advantage of being inexpensive, noninvasive, and easy to perform. Moreover, it can provide valuable information on the functional impairment caused by vascular lesions, a parameter that its invasive cohort, arteriography, cannot do. These characteristics make the ultrasonic technique an ideal test for the serial evaluation of disease progression and for postoperative follow-up study of reconstructive procedures.

Feigelson et al. [46] used the segmental Doppler pressure ratios and flow velocities by Doppler ultrasound to define cases of large-vessel peripheral arterial disease. They noted that overall measurement of the posterior tibial flow showed the highest sensitivity, specificity, positive predictive value, negative predictive value, and overall accuracy. In addition, an absent or non-recordable posterior tibial peak forward flow occurred in 96% of all limbs with isolated posterior tibial disease, or an ankle ratio of equal to or less than 0.8 considered in parallel yielded a test with a sensitivity of 89%, specificity of 99%, positive predictive value of 90%, negative predictive value of 99%, and overall accuracy of 98%. They concluded that the majority of large-vessel peripheral arterial disease cases can be detected with a single measurement using a handheld Doppler flow meter employed at the ankle.

Like most noninvasive vascular tests, the arterial leg Doppler examination has certain limitations. These include falsely high segmental pressure readings in areas with calcified arteries, artificially elevated high-thigh pressure in very large or obese patients, difficulty in interpretation of segmental pressures in patients with multilevel occlusive disease, difficulty in distinguishing occlusive disease in the aortoiliac segment and common femoral artery, interpretive

problems for high-thigh pressures in patients with isolated hemodynamically significant superficial femoral and deep femoral occlusive disease, and false-negative results in patients with mild vascular occlusive disease who have normal resting segmental systolic pressures.

In patients with diabetes mellitus or chronic renal failure, the vessels may be heavily calcified, leading to factiously high segmental limb pressures. Since the digital arteries are seldom calcified, an accurate toe pressure can usually be measured in spite of an artificially high pressure proximally. Also, the analog wave tracing might be abnormal and, thus, helpful in these patients.

Another difficulty in interpreting segmental pressures occurs in patients with multilevel occlusive disease. In these patients, the proximal lesion might mask distal disease, e.g., if both severe aortoiliac occlusive disease and femoral popliteal stenosis are present, the high-thigh pressure is low. The gradient between the high-thigh and the above-knee cuffs might be quite small, thus masking the disease present between these levels. Also giving a low high-thigh pressure is the combination of isolated, hemodynamically significant, superficial femoral and profunda femoris occlusive lesions.

These problems in the interpretation of high-thigh pressure may be solved in one of several ways. A normal femoral pulse and the absence of an iliac bruit suggest a more distal arterial disease as the cause of the low high-thigh pressure. The common femoral artery pressure may also be obtained noninvasively using an inguinal compression device. This pneumatic device presses the artery against the superior pubic ramus, thus allowing the pressure to be measured as the compression is slowly released. The return of the arterial Doppler signal distal to the groin establishes the endpoint. Despite the presence of a normal iliac segment, monophasic waveforms may occasionally be seen in the common femoral artery when there is a combination of superficial femoral artery occlusion and severe deep femoral artery stenosis.

Other methods, which may help in differentiating aortoiliac occlusive disease from disease of the common femoral artery and/or disease of the superficial femoral artery and deep femoral artery, are the determination of the pulsatility index and the inverse damping factor. The amplitude of the Doppler waveform depends on the angle between the ultrasound probe and the axis of blood flow. As the angle of the probe is changed toward zero degrees, the amplitude of the wave increases, although the shape remains unchanged. Velocity can be calculated only if the probe vessel angle can be measured accurately. Unfortunately, this is usually not possible in humans with any reasonable degree of accuracy. Gosling and King [47] have suggested that the pulsatility index is useful and independent of the probe vessel angle in this regard. Several other researchers have found that it is useful for quantifying the Doppler waveform [48, 49].

As previously discussed, the segmental systolic limb pressure alone is somewhat limited in certain patients in localizing vascular occlusive disease. A combination of segmental limb pressure and analog tracing or color duplex imaging is helpful in determining the level of the vascular occlusion. Recently, Gale et al. [50] quantified improvements in accuracy compared with arteriography when ankle pressures alone (ABI) or segmental blood pressures were added to velocity waveforms obtained by Doppler ultrasound. They concluded that ABIs significantly improved Doppler waveform accuracy at all levels. Compared with ABI, the addition of segmental pressure to waveform data failed to improve accuracy.

## The Value of Stress Testing in the Diagnosis of Peripheral Arterial Disease

A majority of lower limb arterial studies use Doppler ultrasound to measure the resting ankle pressure. While indicative of the presence and relative magnitude of peripheral arterial occlusive disease, the resting ankle pressure does not always correlate well with the degree of exercise limitation.

The most common complaint of patients with chronic arterial occlusion is intermittent claudication, yet functional disability among patients varies. One patient with a resting ankle pressure of 90 mmHg may be able to walk two or three blocks before claudicating, while another with a similar ankle pressure may be forced to stop after walking only a block or less. The best functional test of the physiologic impairment associated with arterial occlusive disease is the measurement of the magnitude and duration of fall in ankle pressure following a constant load of exercise. Various methods of producing this constant stress have been used to evaluate the functional disability of patients with claudication, e.g., treadmill exercise, reactive hyperemia, and isolated leg exercises [47–56]. The two most commonly used methods are treadmill exercise and reactive hyperemia.

## Treadmill Exercise

Patients with advanced arterial ischemia can be adequately evaluated by simply measuring the resting ankle pressure. However, an early lesion might not lower the resting ankle pressure enough to be detected by the usual methods. For example, a patient with typical claudication has normal or borderline resting ankle pressure. More accurate evaluation can be obtained by increasing the flow through exercise and exertion, thereby accentuating the hemodynamic affect of the stenosis.

Exercise testing can also isolate a patient's primary limitation when the patient complains of a combination of

symptoms such as claudication and shortness of breath. If the symptoms are due to pulmonary disability, arterial reconstruction will not be of benefit. Further, exercise testing is useful in distinguishing true claudication from pseudoclaudication caused by neurologic or musculoskeletal conditions or venous insufficiency. It can also weed out suspected malingerers.

Treadmill exercise is preferred over reactive hyperemia because it produces physiological stress that reproduces the patient's ischemic symptoms. However, treadmill testing has the following limitations and/or contraindications: hypertension, shortness of breath, cardiac problems, stroke, or difficulty in walking.

*Indications for stress testing include*:

1. Normal resting lower extremity arterial segmental pressures and pulse volume recordings at rest, with symptoms suggestive of intermittent claudication
2. Mildly normal resting lower extremity segmental pressures and pulse volume recordings (ABI >0.80 but <0.96) with symptoms suggestive of intermittent claudication

## Technique

The resting arm and ankle Doppler pressure are initially recorded with the patient in the supine position. The posterior tibial and dorsalis pedis systolic pressures are taken, and the highest reading is used as the ankle pressure. The ABI is then calculated. The treadmill exercise is done at 2 mph on a 12% grade for 5 min or less, if not tolerated by the patient because of claudication. The ankle and arm pressures are recorded immediately following the test and every minute thereafter for up to 20 min until the pressure returns to the pre-exercise level.

Interobserver validation can play an important role in developing a reliable and objective diagnosis of intermittent claudication using post-exercise ABI testing. Van Langen et al. found an interobserver variability of 10% with ABI measurement at rest versus a 21% interobserver variability of the ABI measurement post exercise [57]. Thus, it may be beneficial to strike a balance between additional confirmatory measurements and belaboring an already time-consuming examination. Indeed, Espeland et al. demonstrated reduction in standard errors and bias by 30–40% in ABI measurements simply by taking two systolic blood pressure measurements at each site rather than the standard single measurement [58].

Electrocardiographic monitoring during the treadmill test is controversial. However, the majority of researchers agree that ECG monitoring is essential for patients who are more than 50 years of age or who have symptoms of heart disease, e.g., angina, myocardial infarction, congestive heart failure, and cardiac arrhythmias. Carroll et al. found that 11% of their patients had to stop the exercise because of ECG changes—5% excessive heart rate, 5% premature ventricular contractions, and 1% ST segment depression [54].

Normally, an increase in the pressure is noted after exercise in healthy individuals, and a drop in the pressure is noted in patients with peripheral vascular disease.

## Interpretation

The time it takes for recovery, the symptoms that are experienced during exercise, and the pressure changes, if any, from pre- to post-exercise status form the basis for interpretation of this test. Doppler ankle pressures that drop to low or unrecordable levels immediately following treadmill exercise and increase to resting level in 2–5 min suggest occlusion at a single level. Meanwhile, when ankle pressures remain reduced or unrecordable for up to 12 min, multilevel occlusions are usually present. Patients with severe or advanced peripheral vascular disease, e.g., with ischemic rest pain, may have unrecordable post-exercise Doppler ankle pressure for 15–20 min.

## Clinical Studies

From a cohort of 1,000 arterial Doppler studies performed on 1,000 patients (2,000 limbs) at the Charleston Division of West Virginia University Medical Center, Charleston, West Virginia, 280 patients (560 limbs) who had resting arterial lower extremity Doppler (ALD) studies and arteriograms were selected. One hundred and twenty-four of these limbs had resting and exercise lower extremity Doppler studies and arteriograms. The Doppler technique described previously was used to measure the resting ankle pressure and the exercise ankle pressure and to calculate the ABI.

To facilitate the correlation, the findings on the arteriograms were classified as normal, mild (<30% stenosis), moderate (30–60% stenosis), severe (>60% stenosis), or occluded. The 124 limbs studied included 46 limbs with occluded arteries, 23 limbs with severe stenoses, 10 limbs with moderate disease, 11 limbs with mild disease, and 34 normal limbs.

The majority of normal limbs or limbs with mild disease had a resting ABI of 0.90 or greater. However, a significant number of patients with severe disease (11 out of 23) or with occluded arteries (8 out of 46) also had a resting index of 0.90 or above. After the treadmill test, most of the severely diseased limbs had a significant drop in the ABI.

After treadmill exercise, all patients with normal limbs had an exercise index above 0.90, signifying excellent correlation between the tests. In comparing patient symptoms to the exercise index, none of the patients with rest pain had an index greater than 0.59. However, 80 limbs out of 101 with claudication had an index greater than 0.59. Ninety-one percent of

**Table 21.2** Segmental pressure readings (mmHg) and ankle-brachial index after exercise in a patient with severe peripheral vascular occlusive disease of the left leg

| Post-exercise (min) | Right ankle (normal) | Left ankle (abnormal) | Arm |
|---|---|---|---|
| 1 | 186 | 50 | 180 |
| 2 | 186 | 58 | 180 |
| 4 | 180 | 60 | 176 |
| 6 | 180 | 70 | 170 |
| 10 | 166 | 78 | 160 |
| 15 | 170 | 90 | 162 |
| 20 | 170 | 130 | 162 |
| Ankle-brachial index | (186/180)1.03 | (50/180)0.27 | |

patients with resting pain had an exercise index less than 0.50 (21 out of 23), and 92% of patients with claudication had an exercise index greater than 0.50% (93 out of 101).

## Test of Functional Capacity

The best functional evaluation of physiologic impairment associated with arterial occlusive disease is the measurement of the magnitude and duration of fall in the ankle pressure following the constant load treadmill exercise test. Table 21.2 presents the readings in a patient with resting right ankle pressure of 180 mmHg and left ankle pressure of 130 mmHg. After exercising on the treadmill for 5 min, the right ankle pressure remained above 180 mmHg, while the left ankle pressure dropped to 50 mmHg. It took 20 min for the left pressure to return to 130 mmHg, indicating severely compromising arterial disease.

Although the ankle pressure response provides physiologic information about the severity of peripheral arterial occlusive disease, it does not pinpoint the location of the arterial obstruction. Strandness and Bell noted that the location of disease had an effect on the magnitude of the pressure drop and the time required for the pressure to return to baseline [52]. Pressure drops following exercise indicate that the obstruction involves the arteries supplying the gastrocnemius and soleus muscles. A large portion of the blood supply to these muscles is derived from the sural arteries, which originate from the popliteal artery; hence, a drop in the ankle pressure following exercise signifies an obstruction of the upper popliteal or superficial femoral arteries or a more proximal vessel. When the obstruction is confined to vessels below the knee, exercise seldom causes claudication or a significant drop in ankle pressure; in fact, the pressure may even rise.

In general, the more proximal the occlusive disease, the more effect it has on the ankle pressure response to exercise. For example, an isolated aortoiliac lesion usually has more functional significance than a lesion confined to the superficial femoral artery. This phenomenon occurs because the more proximal arteries supply a greater muscle mass than do the distal arteries. Consequently, there is more severe and prolonged deviation of blood away from the ankle to the proximal muscle mass.

In patients who have aortoiliac obstruction combined with more distal limb arterial disease, a question of the severity of the aortoiliac disease is frequently raised. If the amplitude of the femoral pulses either at rest or following exercise is reduced, the disease may contribute significantly to the leg symptoms and require correction. However, moderate aortoiliac disease may not significantly affect pulses or high-thigh pressures. Such patients may be candidates for the segmental, reactive hyperemia test.

However, if a low high-thigh pressure is noted on the pre-exercise examination, the contribution by aortoiliac disease to the total limb ischemia may be evaluated by determining the high-thigh and ankle pressure responses following exercise. Normally, the high-thigh pressure will increase after exertion, but aortoiliac disease may diminish it. The relative drop in high-thigh and ankle pressures provides indices by which the contributions of aortoiliac and more distal arterial obstruction may be assessed.

The capacity for walking itself is not a particularly important indicator, mainly because it is not reproducible [53]. Motivation, pain tolerance, and accompanying symptoms may all affect its duration. It correlates poorly with estimated walk intolerance and with objective hemodynamic measurements. Of more importance is the observation of other symptoms that precede claudication. If a patient stops exercising due to shortness of breath, angina, or hip pain before claudication develops, the ankle pressure response may be small and of little help in isolating lower limb arterial insufficiency.

In conclusion, the three factors evaluated during treadmill exercise testing have to be taken into consideration in determining the severity of the vascular occlusive disease, i.e., the duration of exercise, the maximum drop in the ankle index, and the recovery time (the time required for return to baseline pressures).

## Reactive Hyperemia

For some patients, treadmill exercise is not applicable (amputees or persons with musculoskeletal problems) or practical (patients with cardiopulmonary disease or severe claudication), because they cannot perform for a sufficient length of time. In such cases, reactive hyperemia may be used to increase blood flow in the extremities.

To increase blood flow, a thigh cuff is inflated above the systolic pressure (20–30 mmHg above the brachial pressure) for 3–7 min to produce local circulatory arrest, resulting in hypoxia and local vasodilation. After release of the compression, ankle pressures are taken at 15-, 20-, or 30-s

intervals for 3–6 min or until the measurements return to reocclusion level. In normal limbs, the ankle pressures immediately decrease to about 80% of the preocclusion levels but readily rise, reaching 90% levels within 30–60 s. It should be noted that ankle systolic pressures in a normal limb do not decrease after treadmill exercise, whereas a transient pressure decrease in the range of 15–35% does occur at the ankle of normal limbs after reactive hyperemia. In limbs with obstructive arterial occlusive disease, the decrease in pressure coincides well with that seen following exercise, but recovery to resting levels is much faster [55]. The magnitude of the pressure drop depends upon the anatomical extent of the disease process and the degree of functional impairment. Although recovery times are also correlated with the severity of the disease (from less than 1 min to more than 3 min), the correlation is not as good as that given by the maximal depression of the ankle pressure induced by exercise. Patients who have single-level disease generally experience less than a 50% drop in the Doppler ankle pressure, whereas patients with multilevel arterial occlusive disease experience a pressure drop of greater than 50%.

To its benefit, the hyperemic stress test is less time-consuming than the treadmill exercise test, and it can be done in the patient's room, using simple inexpensive equipment. Since the duration of calf occlusion can be prescribed and walking time cannot, the stress may be more centralized than that of exercise testing. It is also less dependent upon patient motivation. The major disadvantage of the test is that it cannot duplicate the maximum exercise load of the treadmill, which is the most effective method in detecting small changes. It fails to elicit the patient's symptoms, and it does not identify any cardiopulmonary disability that might actually be more limiting than the arterial insufficiency. The test is also uncomfortable and thigh compression may be hazardous in limbs with femoral popliteal grafts. Finally, rapid pressure measurements are required to get reproducible results.

Other methods of stress testing have been described in the literature. Isolated leg exercises provide a simple form of stress testing for patients who cannot walk satisfactorily on the treadmill because of cardiac, pulmonary, or orthopedic reasons. In the test's simplest form, the patient flexes and extends the ankles repeatedly. Some investigators have used ankle exercise performed against a fixed load, accomplished by having the patient repeatedly rise up and down on the toes.

## References


1. Satomura S. Study of flow patterns in peripheral arteries by ultrasonics. J Acoust Soc Jpn. 1959;15:151–3.
2. Strandness Jr DE, McCutcheon EP, Rushmer RF. Application of transcutaneous Doppler flow meter in evaluation of occlusive arterial disease. Surg Gynecol Obstet. 1966;122:1039–45.
3. Kirkendall WM, Burton AC, Epstein FH, et al. Recommendation for human blood pressure determinations by sphygmomanometers: report of sub-committee of the postgraduate education committee, American Heart Association. Circulation. 1967;36:980–8.
4. Barnes RW. Noninvasive diagnostic techniques and peripheral vascular disease. Am Heart J. 1979;97:241–58.
5. Holland T. Utilizing the ankle brachial index in clinical practice. Ostomy Wound Manage. 2002;48:38–40.
6. Adam DJ, Naik J, Hartshorne T, Bello M, London NJ. The diagnosis and management of 689 chronic leg ulcers in a single-visit assessment clinic. Eur J Vasc Endovasc Surg. 2003;25:462–8.
7. Carser DG. Do we need to reappraise our method of interpreting the ankle brachial pressure index? J Wound Care. 2001;10:59–62.
8. Yao JST, Bergan JJ. Predictability of vascular reactivity to sympathetic ablation. Arch Surg. 1973;106:676–80.
9. AbuRahma AF, Robinson PA. Clinical parameters for predicting response to lumbar sympathectomy with severe lower limb ischemia. J Cardiovasc Surg. 1990;31:101–6.
10. Barnes RW, Shanik GD, Slaymaker EE. An index of healing of below knee amputation: leg blood pressure by Doppler ultrasound. Surgery. 1976;79:13–20.
11. Sumner DS, Strandness Jr DE. An abnormal finger pulse associated with cold sensitivity. Ann Surg. 1972;175:294–8.
12. Barnes RW. Noninvasive assessment of arteriovenous fistula. Angiology. 1978;29:691–704.
13. McLafferty RB, Moneta GL, Taylor Jr LM, Porter JM. Ability of ankle-brachial index to detect lower extremity atherosclerotic disease progression. Arch Surg. 1997;132:836–40.
14. Gornik HL, Garcia B, Wolski K, Jones DC, MacDonald KA, Fronek A. Validation of a method for determination of the ankle-brachial index in the seated position. J Vasc Surg. 2008;48(5):1204–10.
15. Johnson KW, Maruzzo BC, Kassam M, et al. Methods for obtaining processing and quantifying Doppler blood flow velocity waveforms. In: Yao JST, Nicolaides AN, editors. Basic investigation in vascular disease. London: Churchill Livingstone, Inc.; 1981.
16. Van Tongeren RB, Bastiaansen AJ, Van Wissen RC, Le Cessie S, Hamming JF, Van Bockel JH. A comparison of the Doppler-derived maximal systolic acceleration versus the ankle pressure index or detecting and quantifying peripheral arterial occlusive disease in diabetic patients. J Cardiovasc Surg (Torino). 2010;51(3):391–8.
17. Gerhard-Herman M, Gardin JM, Jaff M, Mohler E, Roman M, Naqvi TZ. Guidelines for noninvasive vascular laboratory testing: a report from the American Society of Echocardiography and the Society for Vascular Medicine and Biology. Vasc Med. 2006;11(3):183–200.
18. Khan TH, Farooqui FA, Niazik K. Critical review of the ankle brachial index. Curr Cardiol Rev. 2008;4(2):101–6.
19. Hirsch AT, Haskal ZT, Hertzer NR, et al. ACC/AHA 2005 guidelines for the management of patients with peripheral arterial disease (lower extremity, renal, mesenteric, and abdominal aortic): a collaborative report from the American Association for Vascular Surgery/Society for Vascular Surgery, Society for Cardiovascular Angiography and Interventions, Society for Vascular Medicine and Biology, Society of Interventional Radiology, and the ACC/AHA ask Force on Practice Guidelines (Writing Committee to Develop Guidelines for the Management of Patients with Peripheral Arterial Disease). J Am Coll Cardiol. 2006;47:e1–192.
20. Diehm C, Kareem S, Diehm N, Jansen T, Lawall H. Does calculation of ankle brachial pressure index need revision? Vasa. 2005; 34:123–6.
21. Murabito JM, Evans JC, Larson MG, Nieto K, Levy D, Wilson PW, Framingham Study. The ankle-brachial index in the elderly and risk of stroke, coronary disease and death. Arch Intern Med. 2003;63:1939–42.
22. Newmann AB, Shemanski L, Manolio TA, et al. Ankle-arm index as a predictor of cardiovascular disease and mortality in the cardiovascular health study. Arterioscler Thromb Vasc Biol. 1999;19: 538–45.

23. Toursarkissian B, Mejia A, Smilanich RP, Schoolfield J, Shireman PK, Sykes MT. Noninvasive localization of infrainguinal arterial occlusive disease in diabetics. Ann Vasc Surg. 2001;15:73–8.
24. Brooks B, Dean R, Patel S, Wu B, Molyneaux L, Yue DK. TBI or not TBI: that is the question. Is it better to measure toe pressure than ankle pressure in diabetic patients? Diabet Med. 2001; 18(12):528–32.
25. Orchard TJ, Strandness DE. Assessment of peripheral vascular disease in diabetes: report and recommendations of an international workshop sponsored by the American Diabetes Association. Circulation. 1992;88(2):819–28.
26. TASC. Management of peripheral arterial disease: transatlantic intersociety consensus. Eur J Vasc Endovasc Surg. 2000;19(SupplA): S1–250.
27. Bonham PA, Cappuccio M, Hulsey T, Michel Y, Kelechi T, Jenkins C, Robison J. Are ankle and toe brachial indices (ABI-TBI) obtained by a pocket Doppler interchangeable with those obtained by standard laboratory equipment? J Wound Ostomy Continence Nurs Soc. 2007;34(1):35–44.
28. Williams DT, Price P, Harding KG. The influence of diabetes and lower limb arterial disease on cutaneous foot perfusion. J Vasc Surg. 2006;44:770–5.
29. Cutajar CL, Marston A, Newcoumbe JF. Value of cuff occlusion pressures in assessment of peripheral vascular disease. BMJ. 1973; 2:392–5.
30. Sawka AM, Carter SA. The effect of temperature on digital systolic pressures in the lower limb in arterial disease. Circulation. 1992;85:1097–101.
31. Carter SA, Tate RB. The effect of body heating and cooling on the ankle and toe systolic pressures in arterial disease. J Vasc Surg. 1992;16:148–53.
32. AbuRahma AF, Diethrich EB, Reiling M. Doppler testing in peripheral vascular occlusive disease. Surg Gynecol Obstet. 1980;150:26–8.
33. AbuRahma AF, Diethrich EB. Doppler ultrasound in evaluating the localization and severity of peripheral vascular occlusive disease. South Med J. 1979;72:1425–8.
34. McDermott MM, Liu K, Criqui MH, et al. Ankle-brachial index and subclinical cardiac and carotid disease. The multi-ethnic study of atherosclerosis. Am J Epidemiol. 2005;162:33–41.
35. Diehm C, Schuster A, Allenberg JR, et al. High prevalence of peripheral arterial disease and co-morbidity in 6880 primary care patients: cross-sectional study. Atherosclerosis. 2004;172:95–105.
36. Dormundy JA, Rutherford RB. Management of peripheral arterial disease (PAD). TASC working group. Trans Atlantic Inter Society Consensus (TASC). J Vasc Surg. 2000;31(1pt2):S1–296.
37. Schroder F, Diehm N, Kareem S, et al. A modified method of ankle-brachial pressure index is far more sensitive in the detection of peripheral arterial disease. J Vasc Surg. 2006;44(3):532–6.
38. Niazi K, Khan TH, Easley KA. Diagnostic utility of the two methods of ankle brachial index in the detection of the peripheral arterial disease of lower extremities. Catheter Cardiovasc Interv. 2006; 68(5):788–92.
39. Espinola-Klein C, Rupprecht HJ, Bickel C, Lackner K, Savvidis S, Messow CM, Munzel T, Blankenberg S. AtheroGene investigators. Circulation. 2008;118(9):961–7.
40. Lange SF, Trampisch HJ, Pittrow D, Darius H, Mahn M, Allenberg JR, Tepohl G, Haberl RL, Diehm C, getABI Study Group. Profound influence of different methods for determination of the ankle brachial index on the prevalence estimate of peripheral arterial disease. BMC Public Health. 2007;7:147.
41. Hatsukami TS, Primozich JF, Zierler RE. Color Doppler imaging of infrainguinal arterial occlusive disease. J Vasc Surg. 1992;16: 527–33.
42. Moneta GL, Yeager RA, Lee RW. Noninvasive localization of arterial occlusive disease: a comparison of segmental Doppler pressures and arterial duplex mapping. J Vasc Surg. 1993;17:578–82.
43. Collier P, Wilcox G, Brooks D. Improved patient selection for angioplasty utilizing color Doppler imaging. Am J Surg. 1990; 160:171–3.
44. Cossman DV, Ellison JE, Wagner WH, et al. Comparison of contrast arteriography to arterial mapping with color-flow duplex imaging in the lower extremities. J Vasc Surg. 1989;10:522–9.
45. AbuRahma AF, Khan S, Robinson PA. Selective use of segmental Doppler pressures and color duplex imaging in the localization of arterial occlusive disease of the lower extremity. Surgery. 1995;118:496–503.
46. Feigelson HS, Criqui MH, Fronek A. Screening for peripheral arterial disease: the sensitivity, specificity, and predictive value of noninvasive tests in a defined population. Am J Epidemiol. 1994;140:526–34.
47. Gosling RG, King DH. Continuous wave ultrasound as an alternative and compliment to x-rays in vascular examination. In: Rebeman RS, editor. Cardiovascular applications of ultrasound. Amsterdam: North Holland Publishers; 1974.
48. Harris PL, Taylor LA, Cave FD, et al. The relationship between Doppler ultrasound assessment and angiography in occlusive arterial disease of the lower limbs. Surg Gynecol Obstet. 1974;138: 911–4.
49. Johnson KW, Cobbold RSC, Kassam M, et al. Real time frequency analysis of peripheral arterial Doppler signals. In: Diethrich EB, editor. Noninvasive cardiovascular diagnosis. Littleton: PSG Publishing; 1980.
50. Gale SS, Scissons RP, Salles-Cunha SX, et al. Lower extremity arterial evaluation: are segmental arterial blood pressures worthwhile? J Vasc Surg. 1998;27:831–9.
51. AbuRahma AF. Correlation of the resting and exercise Doppler ankle arm index to the symptomatology and to the angiographic findings. In: Diethrich EB, editor. Noninvasive assessment of the cardiovascular system. Littleton: John Wright-PSG, Inc.; 1982. p. 287–90.
52. Strandness Jr DE, Bell JW. An evaluation of the hemodynamic response of the claudicating extremity to exercise. Surg Gynecol Obstet. 1964;119:1237–42.
53. Quriel K, McDowell AE, Metz CE, et al. Critical evaluation of stress testing in the diagnosis of peripheral vascular disease. Surgery. 1982;91:686–93.
54. Carroll RM, Rose HB, Vyden J, et al. Cardiac arrhythmias associated with treadmill claudication testing. Surgery. 1978;83:284–7.
55. Baker JD, Daix D. Variability of Doppler ankle pressures with arterial occlusive disease: an evaluation of ankle index and brachial ankle gradient. Surgery. 1981;89:134–7.
56. Halperin JI. Evaluation of patients with peripheral vascular disease. Thromb Res. 2002;106:V303–11.
57. Van Langen H, Van Gurp J, Rubbens L. Interobserver variability of ankle-brachial index measurements at rest and post exercise in patients with intermittent claudication. Vasc Med. 2009;14(3):221–6.
58. Espeland MA, Regensteiner JG, Javamillo SA, Gregg E, Knowler WC, Wagenknecht LE, Bahnson J, Haffner S, Hill J, Hiatt WR, LookAHEAD Study Group. Measurement characteristics of the ankle-brachial index: results from the action for health in diabetes study. Vasc Med. 2008;13(3):225–33.

# Pulse Volume Recording in the Diagnosis of Peripheral Vascular Disease

22

Jeffrey K. Raines and Jose I. Almeida

**Abstract**

The early PVR was available in either a box or cart model. The first units also included a built-in continuous-wave Doppler in two frequencies (9 and 5 MHz). Within 5 years of its introduction, the PVR became an extremely popular device and in wide-scale use throughout the world. In vascular laboratories, its frequency of use was second only to the continuous-wave Doppler systems.

This chapter summarizes the principles of PVR and its various clinical applications in patients with peripheral vascular disease.

**Keywords**

Pulse volume recording • Peripheral vascular disease • Diagnosis

## Introduction

The pulse volume recorder (PVR) was introduced by Raines almost 40 years ago in a thesis based on graduate work conducted at the Massachusetts Institute of Technology (MIT), Harvard Medical School, and Massachusetts General Hospital [1]. The work was sponsored by the National Institute of Health. The work was built on earlier pioneering efforts by investigators such as Winsor [2] and Strandness [3]. The research took advantage of major recent advances in electronics, specifically in the area of pressure transducer design. However, the driving force was the increasing ability of the vascular surgeon to reconstruct peripheral arteries and the associated need to perform accurate diagnostic studies preoperatively and in follow-up.

In 1972, Raines, along with R. Darling, B. Brener, and W. Austen, presented the first clinical paper on the PVR at the Annual Meeting of the Society of Vascular Surgery; this was later published in *Surgery* [4]. Earlier that year (in April 1972), this same group of investigators established the first clinically oriented vascular laboratory at the Massachusetts General Hospital. A similar laboratory was established at about the same time at Northwestern's Medical School by Yao and Bergan. Founding these laboratories included obtaining codes for reimbursement from Medicare and other third party insurance carriers. Three years later, the early experience of this laboratory was presented at the 1975 Annual Meeting of the Society for Vascular Surgery and again published in *Surgery* [5]. At that time, studies within the vascular laboratory were expanding to include functional evaluation of venous disorders and extracranial arterial occlusive disease. At this point, many other centers had developed vascular laboratories and began publishing their results.

J.K. Raines, MME, Ph.D. (✉)
Department of Surgery,
University of Miami Hospital and Clinics,
2101 SE 14 Circle, Homestead, FL 33035, USA
e-mail: drjraines@yahoo.com

J.I. Almeida, M.D., FACS, RPVI, RVT
Department of Vascular Surgery, Miami Vein Center,
Miami, FL, USA

A.F. AbuRahma, D.F. Bandyk (eds.), *Noninvasive Vascular Diagnosis*,
DOI 10.1007/978-1-4471-4005-4_22, 

The early PVR was available in either a box or cart model. The first units also included a built-in continuous-wave Doppler in two frequencies (9 and 5 MHz). Within 5 years of its introduction, the PVR became an extremely popular device and in wide-scale use throughout the world. In vascular laboratories, its frequency of use was second only to the continuous-wave Doppler systems.

Guidelines for establishing vascular laboratories were published along with accuracy studies comparing noninvasive functional studies with angiography and clinical outcome in the areas of peripheral arterial occlusion [6–8], deep venous thrombosis [9–11], and extracranial arterial occlusive disease [12–14].

In 1978, W. Glenn introduced B-mode ultrasound. The first clinical studies using this technique were performed in the Vascular Laboratory of the Miami Heart Institute, which was directed at that time by J. Raines, who a number of years earlier introduced the PVR [15]. Within several years, B-mode ultrasound was producing images of peripheral arterial and venous vessels that were very useful clinically and augmented information obtained from functional studies. With B-mode ultrasound as a basis, ultrasound engineers developed duplex scanning, color duplex scanning, power duplex imaging, and more recently improved imaging with internal computer enhancement, storage, and image transfer.

Clearly technology in the field of noninvasive medical imaging as applied to peripheral vascular disease has been explosive and has made significant clinical contributions. Despite this, functional studies remain an integral component in the investigation of most forms of peripheral vascular disorders, and functional technology has also kept pace. In the remainder of this chapter, a description of how the PVR has been improved over nearly 40 years will be given. This will be followed by descriptions of how the PVR may be used most effectively in today's modern vascular laboratory.

Before closing the introduction, it is instructive to note two important items. First, peripheral vascular disease is a disease of the elderly, and the elderly in the USA, is now the fastest growing segment of the population. The Census Bureau estimates this tread is expected to the year 2030 [16]. This is compounded by the fact that in the USA over the last 20 years mortality from coronary artery disease has been decreasing. This means that more survivors who would have died of coronary artery disease live to present to the vascular laboratory with peripheral vascular disease. Second, while there will be increasing pressure to provide services for peripheral vascular disease, medical providers will be asked to do so at less cost. This means more accurate, less costly outpatient diagnostic studies coupled with effective, less costly therapy. This is both a challenge and an opportunity for manufacturers of equipment and providers of care in peripheral vascular disease.

## Pulse Volume Recorder: 2011

As described in the original PVR development work at MIT [1], in order to maintain proper system calibration when a PVR cuff is placed on an extremity, the system and operator must inflate the cuff to a known cuff pressure (i.e., 65 mmHg thigh, calf, ankle) and also know the amount of injected atmospheric air necessary to produce the cuff pressure. If the volume of injected air does not meet an established criterion (i.e., 75 ± 10 ml, calf/ankle; 400 ± 75 ml, thigh), the operator must reapply the cuff. Whereas a number of manufacturers market PVR-like devices, most do not include this important calibration. These manufacturers have suggested to operators that after cuff application it is *only* necessary to inflate the cuff to the recommended pressure. This assumes each cuff is applied to the same tension despite variation in limb size; we have found results will vary significantly based on operator application and technique. There are manufacturers who provide a good *external* calibration as described above. These systems provide reproducible PVR data that virtually eliminate operator application and technique errors. In our laboratory, working with industry, we have developed a computer-controlled *internal* calibration system that is very accurate and completely eliminates cuff reapplication at any level (Fig. 22.1).

The ability to record and store data is most important to document testing for both reimbursement and certification purposes. The new PVR systems include patient interface ports (i.e., for PVR cuffs and Doppler probes), color monitor, touch screen, and color printer. Studies may be performed in a dedicated laboratory or at the patient's bedside. It should be acknowledged that when earlier systems were making the transition from non-PC-based to PC-based units, the PC units were slow, difficult even for experienced operators to use, and inflexible. With time, technician input, and fast processors, this has changed, and the new systems are both rapid and flexible.

In our view, the major advantages of current systems over earlier PVR systems are accuracy of calibration, clarity and rapid development of data reporting, and rapid storage and transmission.

The primary purpose of performing any level of vascular laboratory testing is to provide the referring physician with information that will improve patient management. If a rapid, accurate, complete, and understandable report is not generated, this is not possible. New PVR systems provide a protocol-like format for general testing, compile the data in a logical sequence and provide guidelines for interpretation.

We compared the time taken to perform a lower extremity arterial study using a standard PVR with that using a PC-based PVR. Evaluation time was divided into three components: (1) time to obtain and record demographics, clinical history, and pulse and bruit grading; (2) time to perform ten PVR arterial tracings and six segmental limb pressures; and (3) time to prepare a final report excluding interpretation. In

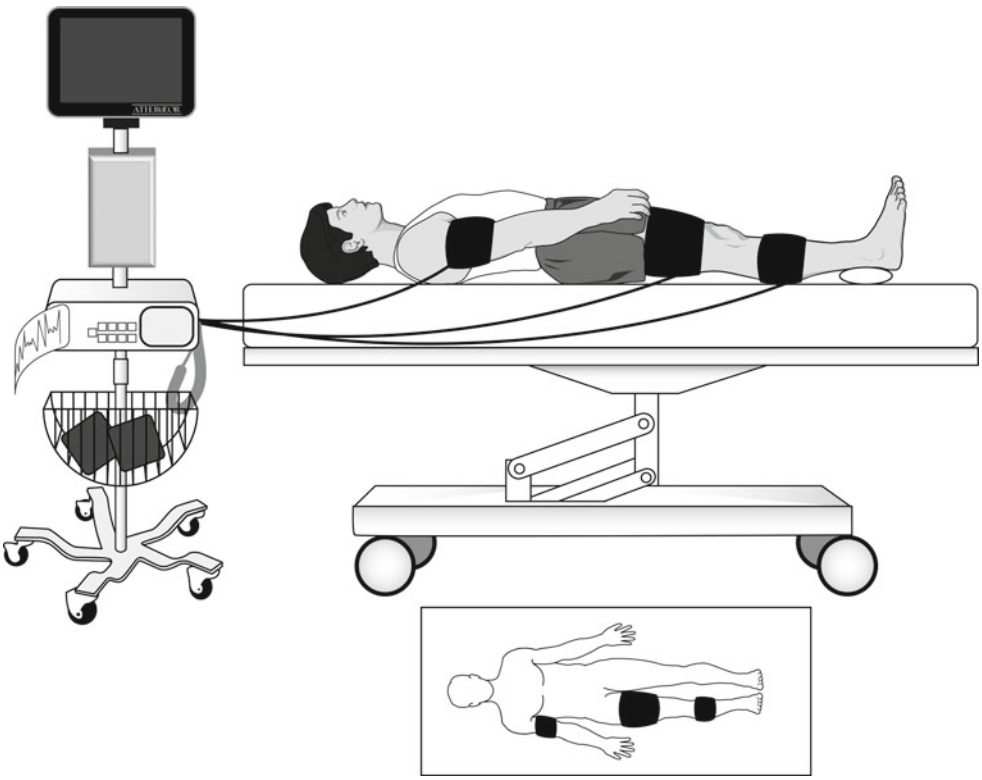

**Fig. 22.1** Picture of a prototype *internally* calibrated pulse volume recorder (PVR). This system is controlled by a computer. The operator interfaces with the unit via a touch screen. The system also has a dedicated printer and modem for report generation

obtaining background information for the standard PVR, the technician recorded the data on a preprinted form that became part of the final report. The technician entered background information for the PC-based PVR directly into the system via a touch screen. Testing was performed using standard protocols for each system and included PVR tracings at the thigh, calf, ankle, metatarsal (TM), and first digital levels bilaterally and limb systolic pressures bilaterally by Doppler technique at the thigh, calf, and ankle levels. Using the standard PVR, the technician had to cut three cardiac cycles from the PVR strip charts, and using tape affix them to the final report. For the PC-based system, the technician electronically selects cycles for reporting and printing. This latter area is where the PC-based system is clearly faster (Table 22.1).

PVR vascular technicians not familiar with the PC-based systems require approximately 3 h of formal training to perform the testing and an additional 10 h of use to obtain the skills to perform the testing to the same degree of speed and confidence obtained by experienced workers.

**Table 22.1** Time taken to perform lower extremity arterial study using a standard PVR and a PC-based PVR

| Component | Standard PVR (min) | PC-based PVR (min) |
|---|---|---|
| Background | 11 | 11 |
| Testing | 18 | 20 |
| Report | 10 | 4 |
| Total ($n=10$) | 39 | 35 |

## Indications and Guidelines for Functional Lower Extremity Arterial Studies

Diagnostic technique and therapeutic methods for peripheral vascular disease have changed significantly since the development of the PVR. However, the questions posed to the vascular laboratory by referring physicians have not changed. These include the following:

1. Is resting ischemia present?
2. Is current perfusion adequate for lesion healing?
3. Will a particular amputation site heal properly?
4. Is vascular claudication present?

Further, for all of the above questions, there is an associated interest in describing as accurately as possible the anatomic location of hemodynamically significant lesions. However, it should be carefully noted that while these are the important questions in over 90% of patients referred to a vascular laboratory for lower extremity occlusion, these questions *cannot* be answered by knowing the anatomy.

These are purely questions of function. Later, we will discuss questions primarily of anatomy.

Before proceeding, it is helpful to describe the patient population presenting to our vascular laboratory. We have carefully reviewed our patient demographics and, when possible, have compared our figures with those of other vascular laboratories; in most cases, the numbers have been very similar. The average age of our patients is 67 years. Two-thirds are

male. Over 75% are current or past cigarette smokers. Approximately 40% have a history of hypertension, and 25% are diabetic. Approximately 20% have elevated blood lipids, and 20–25% are obese by routing criteria. In our series, one-third have had a previous myocardial infarction, and one-tenth (9%) have a history of previous cerebrovascular accident.

## Is Resting Ischemia Present?

Patients with rest pain as their *initial* presentation maybe either diabetic or nondiabetic; however, nondiabetics are more frequent in this category as will be described. Excluding patients presenting with an acute history, the majority of the remaining patients will have a history of vascular claudication. Their description of pain will also almost exclusively be limited to the forefoot. The pain will develop at rest and will transiently be relieved by dangling the foot. This temporarily decreases the local peripheral resistance, increasing local blood flow. Although ischemic pain may present more proximally, more proximal resting pain in the absence of forefoot pain is often not of vascular origin. Since ischemia is a clear indication for surgical reconstruction, its diagnosis must be made with accuracy.

In making this judgment, the following four parameters, in the limb of interest, must be obtained carefully with a PVR at the correct pneumatic gain settings:

PVR amplitude and contour at the ankle level
PVR amplitude and contour at the transmetatarsal level
PVR amplitude and contour at the first digit or most symptomatic digit

### Ankle Pressure

If the ankle pressure is <40 mmHg in the nondiabetic patient and <60 mmHg in the diabetic patient, *resting ischemia may be present*. The difference in criteria is based on the fact that diabetics often have medial calcinosis which artificially elevates distal pressures. It should also be stated that in 10–15% of diabetic cases, distal pressures cannot be measured at all due to medial calcinosis; in these cases, PVR recordings are the only measurements available.

The diagnosis is secured on the basis of the amplitude of the PVR tracings. If a digit of interest has a flatline PVR amplitude, ischemia is very probable. The probability is further increased if the TM and ankle PVR tracings are also flatline or near flatline. It is not hemodynamically possible to have a flatline tracing proximal to a nonflatline tracing. If this occurs, the operator should look for a technical error in the testing. In the ischemic setting, all tracings should be markedly blunted with no reflected wave present in diastole.

**Table 22.2** Guidelines for determining whether current perfusion is adequate for healing

| | Nondiabetic | Diabetic |
|---|---|---|
| Ankle pressure (mmHg) | ≥60 | ≥70 |
| PVR amplitude in digit of interest (mm) | ≥1 | ≥2 |

It is possible to have transient borderline ischemia with digital amplitudes as high as 2 mm; however, this is rare.

## Is Current Perfusion Adequate for Lesion Healing?

Ischemic arterial lesions are almost always present at the digit or near digit levels. More proximal foot lesions (i.e., TM level or heel) are most often secondary to a degree of ischemia *and* chronic trauma (pressure ulceration). In this class of patients, the initial presenters include a higher percentage of diabetics than in the rest pain group. This is due to the clinically recognized fact that diabetic patients are more prone to develop traumatic lesions due to neuropathic loss of sensation and combined large and small vessel involvement [5].

As in the rest pain case, in making this judgment, the following four parameters in the limb of interest must be obtained carefully with a PVR at the correct pneumatic gain settings:

PVR amplitude and contour at the ankle level
PVR amplitude and contour at the TM level
PVR amplitude and contour at the first digit or most symptomatic digit

### Ankle Pressure

Hemodynamics tells us that local perfusion is a function of mean arterial pressure (MAP), mean venous pressure (MVP), and size and number of perfusion vessels. We use systolic pressure as a surrogate for MAP, MVP in a supine subject is near 0 mmHg, and PVR amplitude can be shown to be an adequate surrogate for size and number of perfusing vessels. Table 22.2 is a helpful guideline in determining whether a lesion will heal with the current level of perfusion in the absence of infection, chronic trauma, and microvessel diabetic disease. These stipulations are significant and require a degree of clinical judgment.

## Will a Particular Amputation Site Heal Primarily?

There is a sizable group of patients with advanced arteriosclerotic peripheral vascular disease in whom arterial reconstruction is not possible and who come to amputation.

**Table 22.3** Guidelines for amputation site healing (applicable to diabetic and nondiabetic patients)

| Site | Thigh | Calf | Ankle | TM | Digital |
|---|---|---|---|---|---|
| Above-knee (AK) | ≥2 mm<br>≥0 mmHg | NA | NA | NA | NA |
| Below-knee (BK) | NA | ≥1 mm<br>≥50 mmHg | NA | NA | NA |
| TM | NA | NA | ≥0 mmHg | ≥1 mm | NA |
| Digital | NA | NA | ≥50 mmHg | ≥1 mm | ≥1 mm |

Significant morbidity and mortality rates are present in these patients, particularly in those in whom a more distal amputation fails and who require a second procedure. Measurements in a vascular laboratory with a PVR are helpful in reducing this complication by predicting which amputation site is most likely to heal primarily.

There are four major lower extremity amputations that can be addressed by these measurements. The functional noninvasive measurements necessary for determining amputation site healing potential are a function of the site. Table 22.3 gives guidelines for amputation site healing that are applicable to the diabetic and nondiabetic patient.

## Is Vascular Claudication Present?

Patients in the age range associated with peripheral vascular disease often present with lower extremity pain on exertion. It is important to distinguish symptoms due to neurologic or orthopedic processes from those produced by vascular insufficiency. In fact, both entities may coexist. With vascular insufficiency, it is also important to determine accurately the patient's degree of disability and to establish a quantitative baseline with which the results of medical or surgical treatment can be compared.

In our experience, the presence of vascular claudication and its associated degree of disability cannot accurately be determined from history/physical examination *or hemodynamic measurements taken at rest*. We have therefore evaluated various methods of stressing vascular patients and have determined a small treadmill operating at a fixed grade of 10% at either 1.5 mph (2.4 km/h) or 2.25 mph (3.6 km/h) – choice of speed being a function of the subject's ability – to be the most physiologic and tolerated by the largest percentage of vascular patients. Following resting studies, we determine on the treadmill what we can call maximum walking time (MWT). MWT is the point at which the patient experiences a rapid increase in symptoms. This develops between the initial onset of pain and the point at which the patient can no longer continue. This point has consistently been reproducible. We have *not* found that following PVR amplitudes and/or limb pressures beyond the immediate postexercise measurement are helpful in making the diagnosis more secure.

The guideline we use to establish vascular claudication is a postexercise ankle pressure of <70 mmHg and an ankle PVR amplitude of <5 mm. Note that this criterion represents significant hemodynamic alteration and that it is therefore possible to have significant anatomic disease that does not produce symptoms even with exertion.

Due to the fact that many investigators use the ankle/arm (ankle/brachial) index as a guideline, it deserves mention [17]. We have found the ankle/arm index is helpful in determining the degree of arterial occlusion from the aortic root to the ankle, but it is of far less value than absolute values in criteria associated with resting and exertional vascular insufficiency.

## Location of Arterial Obstruction in the Lower Extremities

As mentioned in the beginning of this section, the major questions requested to be addressed in the vascular laboratory are functional. However, with attention to detail, hemodynamic studies can also localize the major levels of arterial obstruction. The following guidelines are helpful in the anatomical localization of arterial lesions in the lower extremity.

### PVR Reflected Wave

The contour of a PVR tracing is closely associated with the intra-arterial pressure contour. If at rest the reflected wave is absent, this implies the peripheral resistance distal to the point at which the tracing was taken has been reduced. Reduction in peripheral resistance is most often caused by proximal arterial obstruction.

Of course, reduced peripheral resistance and loss of PVR reflected wave are expected following exercise (Fig. 22.2).

### PVR Amplitude

The greater the PVR amplitude, the greater the local pulsatile component of total flow rate (Qp). Generally, the Qp tracks total flow. Further, PVR amplitude is a function of local pulse pressure, and pulse pressure is reduced with arterial occlusion

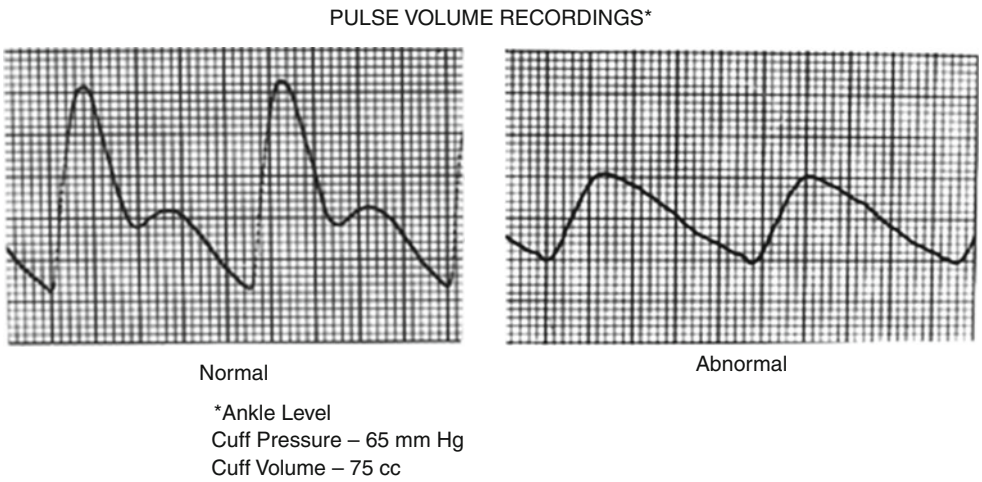


**Fig. 22.2** Normal PVR tracings illustrate rapid rise and fall during systole and the presence of a clear reflected wave in early diastole. When proximal arterial obstruction is present, PVR amplitude (foot to peak) is reduced and the reflected wave is absent

proximal to the point at which the tracing is taken. Therefore, the more reduced the PVR amplitude, the greater the proximal obstruction and the poorer the local perfusion.

## PVR Amplitude Relationships

When PVR tracings are properly calibrated, with an open superficial femoral artery, the PVR calf amplitude is always increased when compared with the thigh and ankle amplitudes. If this is not the case, a superficial femoral artery occlusion should be expected. If the PVR tracing at the thigh level is normal with an open aortoiliac system and the calf PVR tracing amplitude does not augment, an occlusion at the level of Hunter's canal should be suspected.

If the contours of the thigh, calf, and ankle tracings are abnormal (i.e., loss of reflected wave, amplitude reduction) but the calf amplitude is augmented compared with the thigh, this suggests aortoiliac disease with an open superficial femoral/popliteal system.

Whenever there is an abrupt change in PVR amplitude and contour from a proximal measurement to the next segment (i.e., calf to ankle, ankle to TM, TM to digit), occlusion between the two levels should be suspected.

## Post-exercise Measurements

Exercise testing is very helpful in both localizing arterial lesions and determining exercise-related symptoms such as claudication. This has been mentioned previously. Aortoiliac disease produces symptoms in the calf, thigh, and finally in the buttock if exercise is continued. Superficial femoral artery occlusions produce symptoms at the calf level and do not rise to the buttock level. Further, significant aortoiliac disease always produces flatline ankle PVR amplitudes after exercise.

Superficial femoral artery occlusions reduce post-exercise ankle PVR amplitude, but a flatline tracing is rarely seen without proximal involvement.

## Segmental Systolic Limb Pressures

Segmental systolic limb pressures should always be taken bilaterally at the thigh, calf, and ankle levels and compared with the highest brachial pressure. In a normal arterial system, the distal systolic pressures should be slightly higher than the brachial value. When there is a reduction of >20 mmHg between segments, arterial obstruction between segments should be suspected.

It is important to note that often PVR results and systolic limb pressures are supportive. However, since they are derived from different hemodynamic principles, they may differ. It is a good rule of thumb to consider PVR findings more representative of local perfusion and systolic limb pressures more representative of the degree of native vessel occlusion.

## Role of Lower Extremity Arterial Imaging

Clearly over the last 40 years, the ability to accurately image vessels in the lower extremities and measure local velocities with ultrasound has improved dramatically. What has not changed is the *inability* of ultrasound to address the functional questions of ischemia, perfusion, amputation site healing, and the presence of vascular claudication. For this reason, the importance of functional hemodynamic measures should not be lost as our abilities to image continue to improve. Having said that, there are several areas in which lower extremity arterial ultrasound is crucial.

## Imaging Improves Anatomic Localization

In the best of hands, the localization criteria described above have an overall accuracy in multilevel disease of 90%. By definition, the ability to directly image obstruction at the aortoiliac and superficial femoral/popliteal systems can improve this accuracy and should be used in cases of multilevel disease and/or where anatomic considerations are of major importance.

### Graft Surveillance

Vascular grafts placed in lower extremities may occlude acutely or fail over an extended period of time. It is known that grafts in which corrections are made before total occlusions develop have a greater secondary patency.

Minor changes in graft diameter (area) secondary to an obstructive process may not produce significant hemodynamic changes, but may be identified by abnormalities in graft appearance. This is most often true at anastomotic sites.

### Aneurysmal Disease

Functional studies in only selected situations are helpful in identifying femoral or popliteal aneurysms and are never able to measure the size of an aneurysm. In contrast, ultrasound can be used very effectively to identify, measure, and follow femoral and popliteal aneurysms.

## Indications and Guidelines for Functional Lower Extremity Venous Studies

In the previous section, we stated that the average age of patients presenting to a vascular laboratory for lower extremity arterial disease is 67 years, with 75% being male. For venous disease, the age is more than two decades younger, and the majority of patients are female.

In the era of the modern vascular laboratory, lower extremity hemodynamic measurements were first made in the arterial system and expanded to the venous system. For many years, the major question posed to vascular laboratories in the area of venous disease by referring physicians has been: Is deep venous thrombosis (DVT) present? The second most frequently asked question has been: Is venous vascular insufficiency present? It should be acknowledged that duplex ultrasound has replaced other hemodynamic measurements in most modern vascular laboratories. Ultrasound has become the "gold standard" in the diagnosis of extremity deep venous thrombosis and in determining superficial venous system incompetence. The role of the PVR in these settings has been reduced to situations in which detailed knowledge of deep venous resistance is required. This use is described below.

## Is Deep Venous Thrombosis Present?

In 1975, Raines produced a monograph entitled *Application of the Pulse Volume Recorder for Noninvasive Diagnosis of Deep Vein Thrombosis* [18]. This work suggested the measurement of two parameters described as maximum venous outflow (MVO) and segmental venous capacitance (SVC). This investigation was performed at the Massachusetts General Hospital and involved developing a scoring system for DVT using MVO, SVC, venous respiratory waves, and Doppler ultrasound at the femoral and popliteal venous levels. The noninvasive measurements were compared with venography. The details of this work have been published many times and will not be repeated here. The work was also duplicated by many investigators and published extensively [9–11]. Some published studies using this technique have reported a sensitivity as high as 96% with a specificity of 90% [11]. In the author's hands for DVT excluding minor nonextending calf thrombi, the sensitivity has been 95% with an 85% specificity when compared with venography [19].

The modern PVR completely automates the measures of MVO and SVC. Further, the system allows the determination of venous respiratory waves and venous velocity measurements. These data are input to the system and a color report is generated; this report includes the scoring system described above. This information is obtained in less than 30 min with the patient supine on an examining table. This functional method is extremely useful in making a rapid and safe assessment of DVT and is also helpful in determining the degree of hemodynamic venous obstruction present, which correlates with degree of expected valvular damage.

DVT can lead to acute death. For that reason alone, the diagnosis cannot be taken lightly. We have described accurate functional diagnostic studies. However, today, all subjects suspected of having DVT should undergo a vascular laboratory examination that includes venous imaging. The vascular technologist should look for deep venous obstruction in the veins of the lower extremities. In the early stages of DVT, this is often characterized by noncompressibility of the venous structures.

## Is Venous Valvular Insufficiency Present?

The major hemodynamic culprit in venous valvular insufficiency is venous ambulatory hypertension. In the author's laboratory, before the development of photoplethysmography, measurements of venous ambulatory hypertension were taken using a needle in a subject's foot connected to a fluid column. Many PVR systems now include an easy-to-use photoplethysmograph that quickly allows the determination of venous valvular insufficiency at the deep and superficial levels. Details have been published and will not be repeated here [19].

## Functional Studies of the Upper Extremities

### Upper Extremity Arterial Studies

Assessment of the upper extremity arterial system can be performed with the PVR. PVR and limb pressures may be obtained in the upper arm, forearm, and digital levels. These measurements give a clear indication as to the location and

degree of compromise associated with the upper extremity. Atherosclerosis in the upper extremities in comparison with the lower extremities is relatively rare. However, obstruction due to catheter injury and trauma are common. Vasospastic disease also generates patients for this investigation.

## Miscellaneous Studies

The PVR can perform abbreviated protocols for a number of miscellaneous studies. These include upper extremity measurements for thoracic outlet syndrome and vasospastic studies for Raynaud's disease or scleroderma. In the lower extremity, miscellaneous studies may be performed for popliteal entrapment syndrome and arteriovenous and venovenous malformations. PVR and Doppler measurements are also used in male impotence evaluation.

## References

1. Raines JK. Diagnosis and analysis of arteriosclerosis in the lower limbs from the arterial pressure pulse. PhD thesis, Massachusetts Institute of Technology, Cambridge, 1972.
2. Winsor T, Hyman C. A primer of peripheral vascular disease. Philadelphia: Lea and Febiger; 1965.
3. Strandness Jr DE. Peripheral arterial disease. Boston: Little Brown; 1969.
4. Darling RC, Raines JK, Brener BJ, Austen WG. Quantitative segmental pulse volume recorder: a clinical tool. Surgery. 1972;72:873–87.
5. Raines JR, Darling RC, Buth J, Brewster DC, Austen WG. Vascular laboratory criteria for the management of peripheral vascular disease of the lower extremities. Surgery. 1976;79:21–9.
6. Rutherford RB, Lowenstein DH, Klein MF. Combining segmental systolic pressures and plethysmography to diagnose arterial occlusive disease of the legs. Am J Surg. 1979;138:211–8.
7. Raines J, Larsen PB. Practical guidelines for establishing a clinical vascular laboratory. Cardiovasc Dis Bull Texas Heart Inst. 1979; 6:93–123.
8. Barringer M, Poole GV, Shircliffe AC, Meredith JW, Hightower F, Plonk GW. The diagnosis of aortoiliac disease. Ann Surg. 1983; 197:204–9.
9. Sufian S. Noninvasive vascular laboratory diagnosis of deep venous thrombosis. Am Surg. 1981;47:254–8.
10. van Rijn ABB, Heller I, Van Zijl J. Segmental air plethysmography in the diagnosis of deep vein thrombosis. Surgery. 1987;165: 488–90.
11. Naidich JB, Feinberg AW, Karp-Harman H, Karmel MI, Tyma CG, Stein HL. Contrast venography: reassessment of its role. Radiology. 1988;168:97–100.
12. Raines J, Schlaen H, Brewster DC, Abbott WM, Darling RC. Experience with a non-invasive evaluation for cerebral vascular disease. Angiology. 1979;30:600–9.
13. Kempczinski RF. A combined approach to the non-invasive diagnosis of carotid artery occlusive disease. Surgery. 1979;85:689–94.
14. Berkowitz HD. Diagnostic accuracy of ocular pneumoplethysmography attachment for pulse volume recorder. Arch Surg. 1980;115: 190–3.
15. Hashway T, Raines JK. Real-time ultrasonic imaging of the peripheral arteries: technique, normal anatomy and pathology. Cardiovasc Dis. 1980;7:257–64.
16. United States Population Projections. Bureau of the Census, 1993. p. 23–178.
17. Yao ST, Hobbs JT, Irvine WT. Ankle systolic pressure measurements in arterial disease affecting the extremities. Br J Surg. 1969;56:677.
18. Raines JK. Application of the pulse volume recorder for non-invasive diagnosis of deep venous thrombosis [monograph]. Life Sciences, 1975.
19. Abramowitz HB, Queral LA, Finn WR, et al. The use of photoplethysmography in the assessment of venous insufficiency: a comparison to venous pressure measurements. Surgery. 1979;86:434.

# Duplex Scanning for Lower Extremity Arterial Disease

# 23

Paul A. Armstrong, Federico E. Parodi
and Dennis F. Bandyk

**Abstract**

Over the last three decades, duplex ultrasonography has established itself as a fundamental component of diagnostic evaluation and management of arterial disease. The maturation of duplex technology now includes instrumentation which provides comprehensive anatomic and hemodynamic information capable of defining both normal and critical arterial conditions. By combining high-resolution gray-scale imaging with real-time pulsed Doppler spectral analysis, color Doppler, power Doppler, or B-flow imaging, the vascular laboratory can provide critical information relevant to blood flow characteristics, plaque morphology, and vascular anatomy.

The examination is adaptable for use in both the outpatient and inpatient setting including use inside the operating and endovascular suites. Duplex technology is equally suitable for directing both endovascular interventions and open surgical revascularization, permitting not only the identification of disease but also its response to intervention. The reliability of arterial duplex testing depends on the expertise of the vascular technologist and the interpreting physician. Focused peripheral vascular examinations completed in accredited vascular laboratories present quality imaging information capable of providing information analogous to other more expensive contrast imaging modalities. Testing performed and interpreted in an accredited laboratory has sufficient individual diagnostic accuracy to provide information on the character of disease including progression or regression during intervention and surveillance.

**Keywords**

Duplex ultrasound • Diagnosis peripheral arterial disease (PAD) • Intraoperative assessment Duplex surveillance

P.A. Armstrong, D.O. (✉)
Division of Vascular and Endovascular Surgery,
University of South Florida, College of Medicine,
4202 East Fowler Avenue,
Tampa General Circle USF Health Building 7th Floor,
Tampa, FL 33606, USA
e-mail: parmstro@health.usf.edu

F.E. Parodi, M.D.
Division of Chief Vascular and Endovascular Surgery,
UC San Diego, La Jolla, CA, USA

D.F. Bandyk, M.D.
Vascular and Endovascular Surgery, University of California,
San Diego, La Jolla, CA, USA

## Introduction

While the diagnosis of peripheral artery disease (PAD) can be readily established by a focused clinical history and extremity vascular examination, the severity of PAD is best quantified by combining basic examination findings with peripheral arterial testing in the vascular laboratory. Thus, the noninvasive vascular laboratory has evolved as a strategic part of PAD management including defining the distribution of disease and optimizing the treatment of specific vascular conditions such as ischemic rest pain, tissue loss, disabling claudication, or peripheral aneurysmal disease. The adjunct of the noninvasive

A.F. AbuRahma, D.F. Bandyk (eds.), *Noninvasive Vascular Diagnosis*,
DOI 10.1007/978-1-4471-4005-4_23, 

vascular studies have become an essential tool to the vascular clinician by which extended graft patency and improved limb salvage rates can be achieved. Duplex ultrasonography provides detailed anatomic and hemodynamic information on the location, extent, morphology, and severity of vascular disease [1–5]. Scanning is capable of identifying atherosclerotic disease progression, stenosis, or occlusion. Lesion morphology, length, and associated collateral flow can also be confirmed [6–8]. Duplex studies are likewise capable of providing valuable hemodynamic information absent in other noninvasive contrast imaging techniques such as computed tomography (CT) or magnetic resonance (MR) angiography. Information derived from vascular lab arterial testing can then be used to correlate results of physical exam and other diagnostic testing thereby facilitating the development of individualized PAD treatment plan for patients. With the ever-increasing focus on minimally invasive surgical and endovascular options for the treatment of vascular disease, clinicians can now employ portable duplex imaging technologies in all phases of disease treatment. Duplex imaging and Doppler-derived pressure measurements are capable of accurately directing the conduct of endovascular and surgical treatments obviating the routine use of other surveillance diagnostic studies such as contrast angiography [9–13].

Based on the frequently favorable risk–benefit ratio and expanded technologic advances that accompany endovascular therapies, the role of the vascular laboratory and duplex-directed treatment and surveillance can be expected to continue to develop proportionally. By utilizing quality noninvasive vascular testing, the majority of patients with PAD can be classified into an appropriate endovascular, surgical, or surveillance treatment arms obviating the need for routine contrast imaging (Table 23.1).

Certification of the vascular laboratory serves to communicate the laboratory's commitment to delivering valued studies at the highest quality and provides a measurable standardization that can be reproduced regionally. The vascular lab should involve physicians and technologists credentialed and experienced with all facets of scanning and interpretation of vascular testing. Contemporary vascular disease evaluation and management mandates duplex scanning be an integral part of diagnostic and therapeutic algorithms for screening, intervention, and surveillance of PAD. Agency accreditation provides the vascular laboratory with a voice to secure fair reimbursement and guidelines for conducting laboratory services.

**Table 23.1** Percutaneous and open procedural options based on color duplex scan findings

| Duplex diagnosis | Endovascular | Surgery |
|---|---|---|
| *Aortoiliac lesions* | | |
| Focal stenosis | Stent | Endarterectomy/ reconstruction |
| Diffuse disease | Balloon angioplasty<br>Stent | Aortofemoral bypass<br>Femorofemoral bypass |
| Aortic or iliac aneurysm | Stent graft | Surgical reconstruction |
| *Infrainguinal lesions* | | |
| Femoropopliteal segment | | |
| Common femoral | Balloon angioplasty | Endarterectomy/ reconstruction |
| Profunda femoris | Balloon angioplasty | Endarterectomy/ reconstruction |
| Superficial femoral | Balloon angioplasty<br>Atherectomy<br>Stent | Bypass reconstruction |
| Popliteal-tibial segment | Balloon angioplasty<br>Atherectomy | Bypass reconstruction |
| Popliteal aneurysm | Stent graft | Exclusion with bypass |
| Pseudoaneurysm | | |
| Iatrogenic | USGTI[a] | Surgical repair |
| Graft | Stent graft | Surgical reconstruction |
| Arteriovenous fistula | Embolization | Surgical repair |
| Vein graft stenosis | Balloon angioplasty | Surgical revision |

[a]Ultrasound guided thrombin injection

## Preintervention Arterial Testing

Arterial testing should be individualized taking into account current clinical signs and symptoms (e.g., dependent rubor, ulceration, gangrene) and any recent PAD surveillance scans. Symptomatic lower extremity occlusive disease should have limb pressures measured at one or more levels in combination with Doppler or plethysmographic (pulse volume) waveform analysis. Measurements of ankle-brachial systolic pressure index (ABI) and digit systolic pressures can adequately characterize the severity of PAD (Fig. 23.1). Toe systolic pressures are especially helpful in diabetics in whom calcified, incompressible tibial vessels produce erroneously high ABIs (>1.3). Atypical presentations of exertional leg pain, especially in patients with an abnormal ABI (<0.9), should be considered for exercise treadmill testing in order to exclude nonvascular conditions that may be responsible for lower extremity claudication-like pain. Other indications for peripheral arterial testing include absent pulses, disabling claudication, ulceration, gangrene, or rest pain. Any of these findings should prompt a color duplex examination to characterize disease location, extent, severity, and morphology (atherosclerosis, aneurysm). Duplex testing can also identify other relevant concomitant vascular conditions such as renal artery stenosis, aneurysm development, or venous thrombosis.

Duplex scanning is particularly helpful in stratifying the level of occlusive disease (e.g., aortoiliac, femoropopliteal,

popliteal-tibial, or multilevel disease segments). Additional clinical applications for duplex scanning include:

- Evaluation of asymptomatic patients with abnormal (<0.9) ABIs to ascertain intervention by endovascular (e.g., percutaneous angioplasty or stenting) or surgical bypass
- Exclusion of occult inflow (aortoiliac) disease in patients requiring femoral-distal bypass grafting
- Evaluation of specific diseased arterial segments (outflow atherosclerosis or isolated stenoses) visualized on diagnostic arteriography whose hemodynamic significance is not clear
- Alternative imaging to reduce angiographic contrast exposure in patients with renal insufficiency
- Identification of atheroembolism or acute arterial thrombosis (i.e., blue toe syndrome)
- Assessment of percutaneous catheterization sites for pseudoaneurysm or arteriovenous fistula
- Evaluation of vascular injury associated with blunt and penetrating trauma

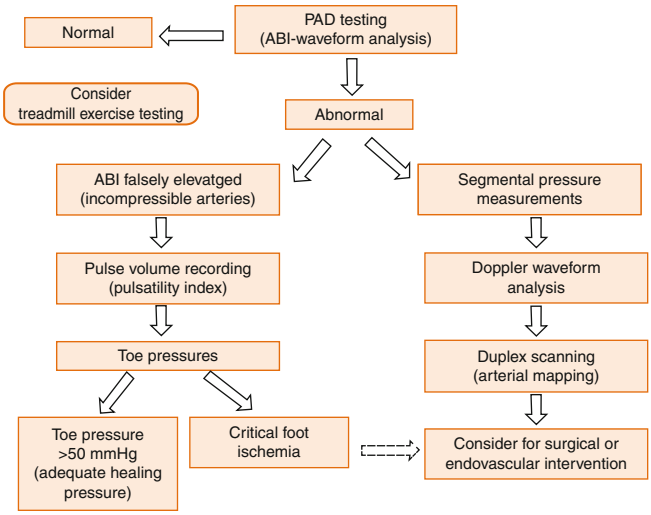


**Fig. 23.1** Vascular laboratory evaluation of peripheral artery disease (*PAD*) by ankle-brachial index (*ABI*), Doppler waveform analysis, pulse volume recordings (*PVR*), digit pressures, exercise testing, and duplex arterial mapping to develop treatment plan

- Surveillance of surgical bypass grafts or reconstructions, endovascular interventions, or dialysis access for stenosis caused by myointimal hyperplasia, fibrosis, or atherosclerosis

The accuracy of duplex scanning is sufficient to permit arterial mapping analogous to contrast arteriography in body regions accessible to diagnostic ultrasound imaging. Classification of lesion severity is based on the same physical principles that apply to the duplex evaluation of the cerebrovascular, renal, and mesenteric circulations. Compared to arteriography, the "gold standard" for peripheral arterial imaging, duplex scanning has a diagnostic accuracy of >80% for the detection of a >50% diameter reducing stenosis or occlusion (Table 23.2) [1, 2, 4, 7–9]. Diagnostic accuracy decreases when multilevel disease is present. However, in the absence of multilevel disease, diagnostic accuracy exceeds 90% for the detection of high-grade stenosis or occlusion involving iliac, femoral, popliteal, or tibial arterial segments. Additionally, several centers have conducted small prospective blind trials comparing duplex imaging to contrast arteriography for planning infrainguinal reconstructions for occlusive disease. These studies indicated that duplex imaging was equal to angiography in predicting suitable distal bypass with confidence intervals in the range of 95% [10, 11]. In more than 50% of patients with symptomatic PAD, duplex scanning will identify disease amenable to endovascular therapy [9, 13]. Duplex imaging to plan infrainguinal bypass procedures for occlusive disease has also been studied in prospective trials with results compared to contrast angiography. Patient outcomes (limb salvage, graft patency) were similar indicating that the clinical accuracy of duplex testing to select appropriate inflow-outflow anastomotic sites for lower limb arterial bypass was equivalent to angiography [10, 11]. Whether an arterial lesion is suitable for endovascular repair generally depends on specific anatomic characteristics. Duplex findings of Trans-Atlantic Inter-Society Consensus (TASC) category A or B lesions indicate endovascular intervention is the preferred treatment (Table 23.3). Technical success rates in excess of 95% can be achieved with clinical results similar to surgical reconstruction. Category C lesions (>4-cm-long calcified stenosis, multilevel disease, 5–10-cm-long chronic occlusions) may also be

**Table 23.2** Diagnostic accuracy (sensitivity/specificity) of color duplex ultrasonography compared with diagnostic contrast angiography for hemodynamically significant lesions

| Author | Iliac artery | Common femoral artery | Deep femoral artery | Superficial femoral artery | Popliteal artery | Tibial artery |
|---|---|---|---|---|---|---|
| Crossman et al.[a] | 81/98 | 70/97 | 71/95 | 97/92 | 78/97 | 50/8 |
| Moneta et al.[a] | 89/99 | 76/99 | 83/97 | 87/98 | 67/99 | 90/2 |
| Allard et al.[a] | 89/99 | 36/98 | 44/97 | 92/96 | 37/92 | – |
| Kohler et al.[a] | 89/90 | 67/98 | 67/81 | 84/93 | 73/97 | – |
| | *Aortoiliac* | | *Femoropopliteal* | | *Tibial* | |
| Hingorani et al.[b] | 81/84 | | 75/90 | | 43/65 | |

[a]Duplex compared to digital subtraction contrast angiography (DSA)
[b]Duplex compared to DSA and magnetic resonance angiography (MRA)

**Table 23.3** TASC (Trans-Atlantic Inter-Society Consensus) classification of lower limb arterial occlusive lesions suitable for percutaneous transluminal angioplasty (PTA)

| | Site of arterial lesion[a] | |
|---|---|---|
| Category | Aortoiliac | Femoropopliteal |
| A | <3 cm focal stenosis | <3 cm focal stenosis or occlusion |
| B | Single stenosis 3–10 cm | 3–5 cm single stenosis or occlusion |
| | Unilateral CIA occlusion | Heavily calcified lesions ≤3 cm |
| | Two stenosis <5 cm | Lesions with tibial occlusion |
| | | Multiple lesions <3 cm |
| C | Unilateral EIA occlusion not involving CFA | Single stenosis or occlusion >5 cm |
| | Unilateral EIA stenosis extending into CFA | Multiple lesions 3–5 cm |
| | Bilateral stenosis 5–10 stenosis | Multiple lesions >5 cm |
| | Bilateral CIA occlusion | |
| D | Iliac stenosis with aortic or iliac aneurysm | Complete CFA or SFA and popliteal or proximal tibial vessel occlusion |
| | Diffuse stenosis >10 cm of CIA, EIA, CFA | |
| | Unilateral occlusion CIA and EIA | |
| | Bilateral EIA occlusion | |

Adapted from [19, 20]
[a]*CIA* common iliac artery, *EIA* external iliac artery, *CFA* common femoral artery, *SFA* superficial femoral artery

**Table 23.4** Most common patterns of lower limb atherosclerosis or location of stenosis after infrainguinal endovascular or surgical intervention

| Arterial segment | Site of occlusive disease or restenosis after intervention |
|---|---|
| Aortoiliac | Distal aorta, proximal and mid-common iliac artery, proximal external iliac artery |
| Femoropopliteal | Common femoral artery, origin of superficial and deep femoral arteries |
| | Distal superficial femoral artery (Hunter's canal) |
| Tibial | Tibial peroneal trunk, origins of the tibial arteries |
| Angioplasty site | Restenosis in region of angioplasty |
| Peripheral stent | Intimal hyperplasia at proximal or distal stent, restenosis in region of most severe lesion |
| Vein bypass | Reversed saphenous vein: proximal graft segment, nonreversed or in situ saphenous vein: distal graft segment |
| Prosthetic bypass | Distal anastomotic region |

amenable to endovascular repair depending on the experience of the vascular surgeon. Endovascular treatment of category D (diffuse stenosis, >10-cm occlusions) lesions is not associated with outcomes comparable to "open" surgical repair or bypass grafting [11, 12, 14]. In applying duplex scanning to patient evaluation, the intent is to characterize the extent and severity of occlusive disease to permit a clinical decision regarding intervention options.

Continued technological advances have improved the imaging quality of color flow Doppler in a manner analogous to arteriography. The classification of occlusive lesions is based on the same general principles that apply to the duplex evaluation of other arterial circulatory systems (e.g., cerebrovascular, mesenteric, renal). When duplex scanning has been used in the evaluation of symptomatic lower limb atherosclerotic disease, approximately 45% of patients have lesions suitable for treatment with endovascular techniques [9, 13]. Whether a diseased arterial segment is suitable for endovascular intervention depends on the specific characteristics of the lesion. In the lower limb, duplex findings of category one or two lesions based on the Society of Cardiovascular and Interventional Radiology guidelines indicate endovascular intervention is a treatment option (Table 23.3) [12]. Technical success rates in excess of 95% can be achieved with clinical results similar to surgical reconstruction. Category three lesions (>4-cm-long calcified stenosis, multilevel disease, 5–10-cm-long chronic occlusions) are also amendable to endovascular procedures. While short-term primary patency rates are comparable to surgical bypass grafting, mid- and long-term patency rates remain below that of surgical reconstruction.

## Color Duplex Peripheral Arterial Examination

For most examinations, 30–45 min should be allotted. The vascular examination room should be kept warm (75–77°F) to avoid vasoconstriction. The patient should be instructed not to eat within 6 hours of the examination in order to reduce abdominal gas in the event that aortoiliac imaging is required. Abdominal imaging begins with a 3–5-MHz phased array transducer with the evaluation of the infrarenal aorta at the level of the renal artery origins and moves caudally toward the iliac arteries. As the exam is continued to the inguinal ligament at the level of the femoral artery, the transducer frequency is increased to a 5–7-MHz probe. Multiple scanning windows may be required for complete insonation/imaging of the pelvic and infrainguinal circulation due to imaging limitations such as obesity (vessels >15 cm deep), bowel gas, large limbs, edema, surgical wounds, ulcers, joint contractures, small vessels, and vessel calcification. Aortic diameter is documented as the technologist moves distally evaluating the iliac circulation, followed by the common femoral, deep femoral, superficial femoral, popliteal, and mid to distal tibial vessels. B-mode imaging can be used to measure diameter

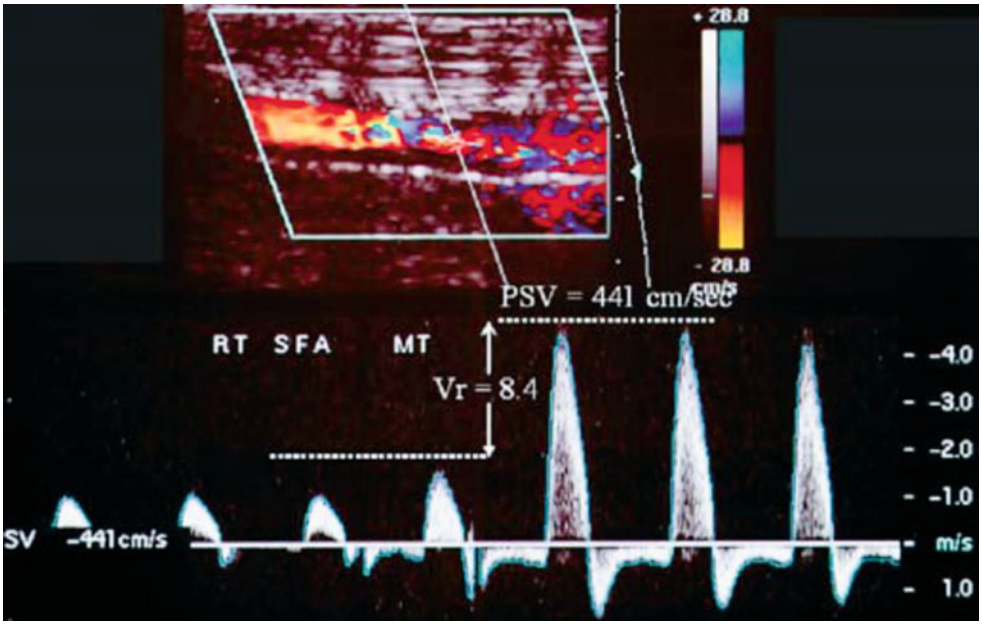


**Fig. 23.2** Duplex scan of superficial femoral artery (*SFA*) with mid-thigh TASC A lesion and symptoms of claudication. At rest, the ABI was 0.78 with a triphasic waveform and was recorded proximally in the SFA. Treadmill exercise testing 12% grade at 1.5 mph for 2 min resulted in decrease in ankle pressure from 132 mmHg at rest to 50 mmHg with exercise. The patient completed PTA with stenting with restoration of normal limb hemodynamics (ABI > 0.9)

and document plaque character or stenosis. Color Doppler permits rapid location of sites of turbulence by lumen narrowing, color map aliasing, color flow jets, and occasionally a tissue bruit. Identification of vessel branching, collateral circulation, aneurysmal change, and occlusive disease as well as sampling blood flow patterns are important components of duplex imaging. Because occlusive lesions have a tendency to develop at specific sites, scanning should particularly be focused on these areas especially when proximal-to-distal changes in velocity waveform configuration are recorded (Table 23.4) [6, 7]. In order to adequately grade the severity of stenosis, a center-stream Doppler angle corrected to 60° with pulsed Doppler spectral analysis is carried out proximal to, at the site of maximum flow disturbance, and distal to the site of stenosis. Attention to changes in velocity waveform (pulsatility) and measurement of peak systolic and end-diastolic blood flow velocities are recorded. Identification of luminal narrowing, plaque character, color map aliasing (turbulent flow), color flow jets, and tissue bruits should be documented if present (Fig. 23.2). Doppler velocity spectra from the distal tibial and pedal arteries are assessed and should aid in correlating waveform pulsatility and peak systolic velocity with measured ABI (Fig. 23.3). Again, this correlation is especially important if heavily calcified or incompressible vessels are present. An ABI value of >1.3 suggests the presence of noncompliant or calcified vessels. Assessment of pulsed Doppler spectra at all stations of the extremity – common femoral, superficial femoral, popliteal, and tibial vessels – allows for comparison of pulsatility index and acceleration time between arterial segments.

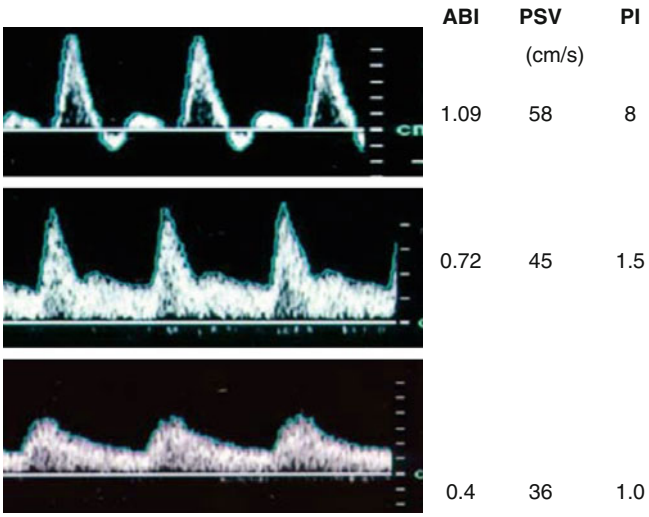


**Fig. 23.3** Pulsed Doppler velocity spectra recorded from the posterior tibial artery at the ankle. Note the changes in the velocity spectral waveform (triphasic to monophasic), accompanied by a decrease in peak systolic velocity (*PSV*) and in pulsatility index (normal: >4), resulting in an overall decrease in ankle-brachial index (*ABI*) from normal (>0.95) to a level of moderate disease (i.e., claudication) (ABI 0.5–0.9) to critical limb ischemia (ABI ≤0.4)

Duplex testing is the recommended diagnostic modality used to evaluate arterial vascular access sites. Ultrasound provides both anatomic and hemodynamic information of the access site allowing for accurate diagnosis of pseudoaneurysm versus hematoma (Fig. 23.4). Duplex imaging then provides imaging detail capable of directing percutaneous thrombin injection in the setting of pseudoaneurysm.

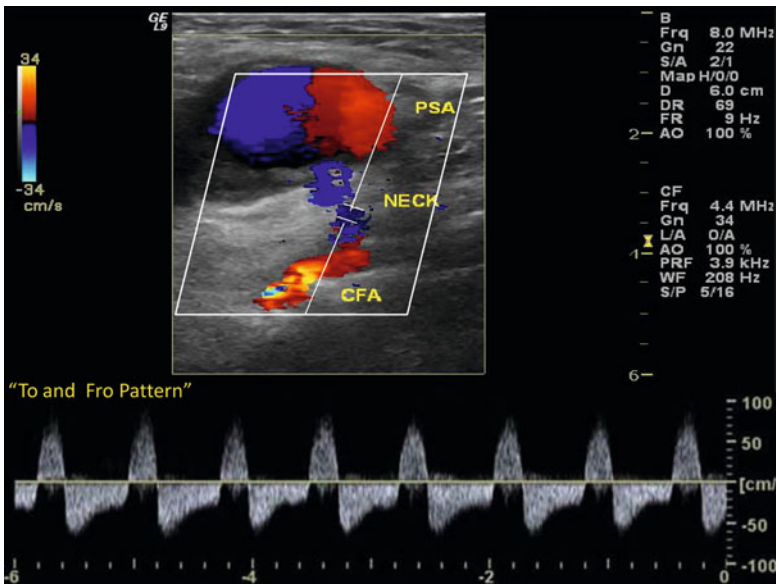


**Fig. 23.4** Iatrogenic common femoral artery pseudoaneurysm with long neck amenable to duplex-guided thrombin injection. Velocity spectra recording from the stalk demonstrate to-and-fro pattern in the neck

## Duplex Criteria for Grading Occlusive Disease

A number of duplex-derived velocity criteria have been validated by comparison with contrast arteriography [1–3, 6]. Utilization of a maximum peak systolic velocity (PSV), end-diastolic velocity (EDV), and velocity ratios (Vr) of PSV proximal to and at the site of maximum stenosis in conjunction with the velocity spectral waveform distal to the stenosis is recommended to categorize first- and second-order (tandem) stenoses. Standardized values for arterial diameter and PSV in the lower extremities have been determined for normal individuals at rest (Table 23.5) [6, 7]. Duplex assessment of the common femoral artery waveform is an accurate predictor of normal or impaired inflow disease from the aortoiliac segment. A monophasic common femoral artery waveform can be associated with an occluded superficial femoral artery, but the acceleration time is typically <130 ms when no pressure-reducing lesion is present. Symptoms of mild claudication (ABI > 0.8) may be associated with a triphasic tibial artery Doppler waveform at rest, but with treadmill exercise testing, the ankle pressure decreases and a more monophasic dampened waveform develops downstream of the obstructive lesion.

Stenosis severity based on PSV and Vr values recorded at the lesion is useful in grading mild (<50%), moderate (50–75%), and severe (>75% or occlusion) peripheral stenosis (Fig. 23.5 and Table 23.6) [6, 7, 13]. Lesions with a velocity spectra indicating a >75% stenosis are typically associated with a >20-mmHg reduction in systolic pressure (Fig. 23.6). Duplex criteria that reliably predict a hemodynamically significant stenosis, i.e., associated with resting peripheral pressure and flow reduction include the following:

- Loss of triphasic waveform configuration at the stenosis
- Damping and reduction in pulsatility in the distal arterial velocity waveform

**Table 23.5** Mean arterial diameter and peak systolic flow velocity (PSV) measured by duplex scanning in patients with normal ankle-brachial indices (ABI)

| Artery | Diameter ± SD[a] (cm) | Velocity ± SD[a] (cm/s) |
|---|---|---|
| Infrarenal aorta | 2.0 ± 3 | 65 ± 15 |
| Common iliac | 1.6 ± 2 | 95 ± 20 |
| External iliac | 0.79 ± 0.13 | 119 ± 22 |
| Common femoral | 0.82 ± 0.14 | 11.4 ± 25 |
| Proximal superficial femoral | 0.60 ± 0.12 | 91 ± 14 |
| Distal superficial femoral | 0.60 ± 0.12 | 94 ± 14 |
| Popliteal | 0.52 ± 0.11 | 69 ± 14 |
| Tibial | – | 55 ± 10 |

[a]*SD* standard deviation

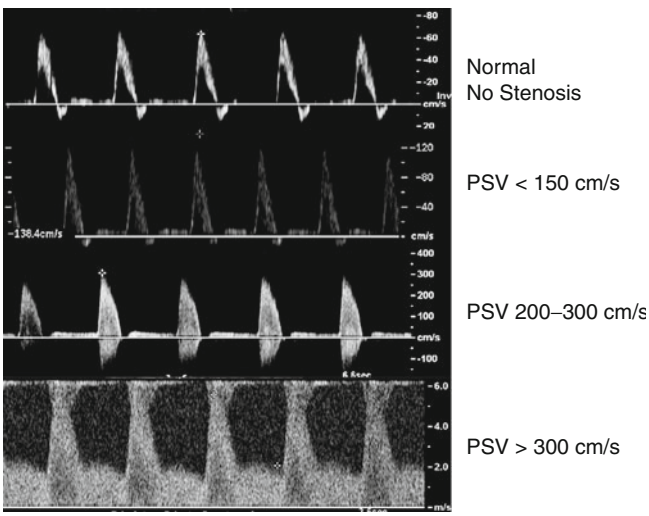


**Fig. 23.5** Lower extremity duplex spectral waveforms typical of normal (**a**) 1–19% diameter reduction, (**b**) 20–49% diameter reduction, (**c**) 50–75% diameter reduction, and (**d**) >75% diameter reduction stenosis as classified in Table 23.6

**Table 23.6** University of South Florida duplex criteria for lower limb arterial occlusive disease

| Percent stenosis (%) | Peak systolic velocity (cm/s) | End-diastolic velocity (cm/s) | Velocity ratio (Vr) | Distal arterial waveform |
|---|---|---|---|---|
| Normal (1–19%) | <150 | <40 | <1.5 | Triphasic |
| 20–49% | 150–200 | <40 | 1.5–2.0 | Triphasic |
| 50–75% | 200–300 | <90 | 2.0–3.9 | Poststenotic turbulence distal to stenosis, monophasic distal waveform |
| >75% | >300 | <90 | >4.0 | Dampened distal waveform and low PSV/EDV[a] in the stenosis |
| Occlusion | Absent flow by color Doppler/pulsed Doppler spectral analysis; length of occlusion estimated from distance between exit and reentry collateral arteries | | | |

[a]*PSV* peak systolic velocity, *EDV* end-diastolic velocity

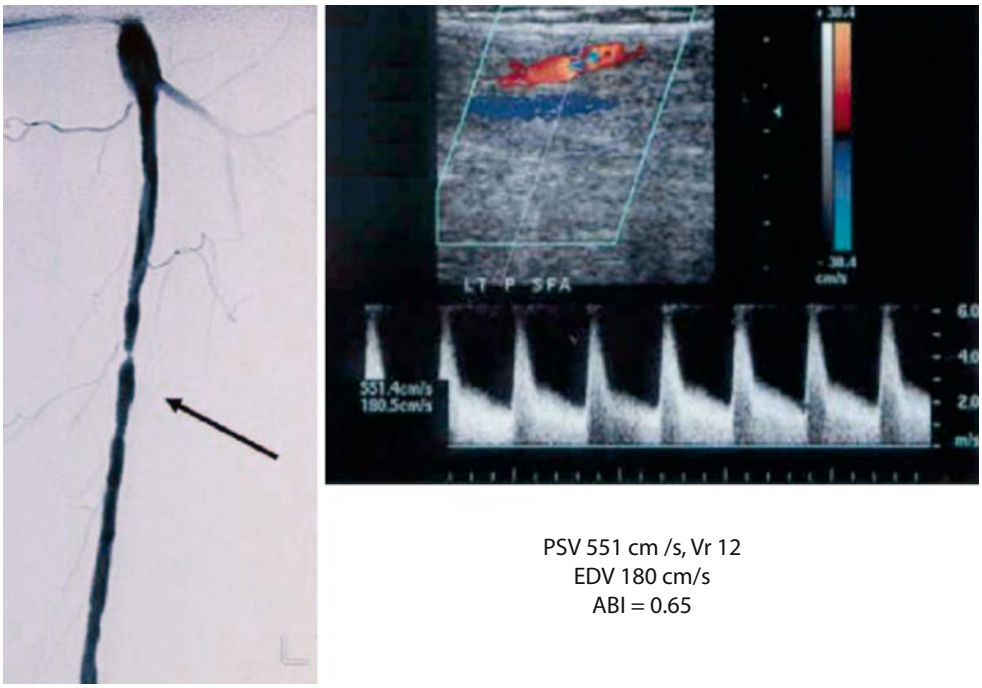


PSV 551 cm /s, Vr 12
EDV 180 cm/s
ABI = 0.65

**Fig. 23.6** Duplex scan corresponding arteriogram of a >75% superficial femoral artery stenosis (*arrow*) with increased peak systolic velocity (*PSV*), velocity ratio (*Vr*), and end-diastolic velocity (*EDV*) with turbulent spectra characteristic of a pressure-reducing lesion accounting for the abnormal ankle-brachial index (*ABI*) of 0.68 measured at rest

- PSV > 250–300 cm/s
- EDV > 0
- Vr > 3 across the stenosis

By using a modified Bernoulli equation, an estimation of systolic pressure gradients across a stenosis can be obtained.

$$\text{Systolic pressure gradient (mmHg)} = (4)\times(\text{PSV}_{\text{at the stenosis}} - \text{PSV}_{\text{proximal to the stenosis}})^2$$

Example:

$$\text{Superficial femoral artery stenosis}: \ \text{PSV}_{\text{stenosis}} = 3.5 \text{ m/s}$$
$$\text{PSV}_{\text{proximal}} = 0.5 \text{ m/s}$$
$$\Delta P = 4\times(3.5-0.5)^2$$
$$\Delta P = 36 \text{ mmHg}$$

As stenosis severity increases, distal arterial pulsatility, velocity and flow decrease. A high resistance pattern develops as the EDV in the stenosis increases, while flow velocity in the inflow vessel decreases. Table 23.7 highlights a set of velocity criteria for grading >50% and >70% diameter reducing stenosis with the diagnostic accuracy of duplex scanning compared to biplanar contrast arteriography [8, 9, 12, 13]. High-grade (>70%) diameter reduction is associated with an EDV > 40 cm/s and a Vr > 5 across the stenosis.

**Table 23.7** Diagnostic accuracy of color duplex ultrasonography criteria in detection of the occlusive disease involving aortoiliac segment compared with arteriography

| Duplex criteria predictive[a] | Positive predictive value (%) | Negative predictive value (%) |
|---|---|---|
| 50–75% DR stenosis | | |
| Vr > 2.8 | 86 | 84 |
| PSV > 200 cm/s | 68 | 91 |
| >70% DR stenosis | | |
| Vr > 5.0 | 65 | 91 |
| EDV > 40 cm/s | 64 | 92 |

[a]*DR* diameter reduction, *Vr* peak systolic velocity ratio across the stenosis, *PSV* peak systolic velocity, *EDV* end-diastolic velocity

Occlusion of an isolated arterial segment is identified by absence of color Doppler flow in the lumen, a preocclusive thump (staccato waveform), marked dampening of distal waveforms, and the presence of exit collateral vessels. Real-time Doppler imaging can be used to estimate (±4 cm) the length of vessel occlusion based on flow in the lumen and the presence of exit/reentry collaterals of distal [1]. The diagnostic accuracy of duplex scanning decreases in the setting of multilevel occlusive disease especially in lesions distal to a proximal high-grade or occlusive lesion. The presence of adjacent high-grade (>75%) stenosis or occlusion reduces diagnostic accuracy of duplex scanning in the distal diseased segment by approximately 10%. The grading of second-order stenosis relies on both high-resolution imaging and modification of velocity criteria for stenosis ranking. These multilevel lesions are characterized by reduced blood flow velocities and a loss of a triphasic waveform. A velocity ratio >2.5 combined with significant lumen narrowing demonstrated with B-mode imaging indicates a >50% diameter reduction stenosis [4]. The reduced sensitivity of color Doppler mapping to accurately grade moderate (>50%) diameter reducing stenosis in low-flow conditions as often seen with critical limb ischemia associated with multilevel tibial occlusive disease deserves consideration for additional contrast angiography imaging to define the extent of multilevel occlusive disease.

## Duplex-Directed Endovascular and Surgical Intervention

Over the past decade, enhanced resolution with new imaging features (i.e., power Doppler, B-flow) has promoted duplex scanning from a simple screening modality to a principal adjunct for directing diagnostic and interventional treatment of PAD. Contemporary vascular clinicians have evolved the utility of duplex arterial mapping to identify segmental and multilevel occlusive disease. Presently, vascular specialists have acquired confidence in performing percutaneous duplex-guided therapeutic interventions including treatment of femoral pseudoaneurysms, saphenous vein ablation, vena cava filters, and atherectomy/stent/angioplasty. In general, PAD can be classified as single-segment (e.g., aortoiliac, femoropopliteal, or tibial) or multilevel disease. Most often, single-segment disease is characterized by short-segment (<5 cm) stenosis or occlusion and is manifested by claudicant-type symptoms that are activity limiting to a variable degree. In this group, the cornerstone of therapy is directed at risk factor modification, development of a walking exercise program, and use of drug therapy (i.e., cilostazol). Serial arterial duplex with or without stress testing can be used to monitor treatment response and progression of symptoms. For those individuals who develop a diminutive clinical course with conservative therapy, duplex scanning can be used to guide recommendations for interventional treatment. Duplex-detected atherosclerotic lesions of iliac or superficial femoral arteries have been successfully treated by percutaneous atherectomy, angioplasty, or stenting. General indications for duplex-guided endovascular intervention include focal or short-segment (<5 cm) occlusions of recent illness (<3 months). TASC A and B lesions, based on the Trans-Atlantic Inter-Society Consensus classification scheme, are readily treated with high success rates and yield enduring clinical results in most patients as compared to open surgical therapy. However, lesions with characteristics of long-segment chronic occlusion (>5 cm), multilevel disease, or heavily calcified stenosis >4 cm (TASC C and D lesions) although amendable to a variety of endovascular treatments have primary patency rates and midterm durability that are inferior to that of surgical intervention [14–17]. While the initial technical success rates of the newer endovascular therapies seem appealing, the endovascular treatment of TASC C and D lesions should be considered for high-risk individuals with critical ischemia who have limited surgical targets or conduit.

Duplex arterial mapping can be used to plan "hybrid" or combined open and endovascular procedures. The increased utilization of covered stent grafts to treat primary atherosclerosis and aneurysmal disease has further expanded the application of procedural duplex scanning. Duplex-guided surgical bypass or peripheral aneurysm repair is associated with similar outcomes to those guided by digital subtraction contrast angiography [18]. Duplex arterial mapping offers an improved safety profile compared to other contrast imaging modalities at a reduced health care cost [19].

## Duplex Surveillance Following Endovascular or Surgical Reconstruction

Early (≤30 days) endovascular failure rates are associated with factors such as elastic recoil, plaque dissection, arterial spasm, stent deformity, or stent fracture. Even in instances of improved ABI after endovascular intervention, abnormal duplex-detected hemodynamics has a negative impact on durability. Other reports have confirmed similar results for endovascular procedures monitored by arteriography or intravascular ultrasound. Given its versatility and accuracy, duplex ultrasonography offers an expanded role for confirmation of technical and hemodynamic success after endovascular intervention. Periprocedural duplex imaging can be used not only to evaluate the technical success of a procedure but can document improvement or correction of the stenosis or occlusion being treated. The additional anatomic and flow-related information supplied by duplex scanning remains an important concept considering that

completion arteriography has been shown to mask significant areas of stenosis especially since residual stenosis noted even 24 h after intervention has been shown to be predictive of bypass deterioration and eventual endovascular treatment failure [20, 21]. Mewissen and colleagues have reported an 84% stenosis-free patency rate in a series of endovascular-treated bypass grafts whose completion duplex scans documented less than a 50% residual stenosis (PSV > 180 cm/s; Vr > 2.5). This compares to only a 15% 1-year clinical success rate for similarly endovascular-treated lesions that demonstrated velocity spectra greater than 50% diameter reduction [20].

The evaluation algorithm for duplex-monitored peripheral endovascular intervention is shown in Fig. 23.7. After successful intervention, the procedural angiogram should demonstrate <20% residual stenosis at the treatment site. Duplex ultrasound should then be employed to confirm normal anatomic definition across the treated region and demonstrate normal treatment site hemodynamics. Since clinically important high-grade occlusive lesions are typically defined by PSV > 300 cm/s and end-diastolic velocities of >40 cm/s, a technically satisfactory endovascular intervention can be defined by a PSV < 180 cm/s with a Vr across the treated segment of less than 2. If residual stenosis is detected by duplex scanning, reintervention by repeat percutaneous balloon angioplasty (PTA), atherectomy, or stent placement should be considered. Should a lesion not respond to these measures and duplex identifies a persistent area of abnormality (i.e., PSV > 250 cm/s), consideration should be given for operative reconstruction or modified short interval surveillance scanning. In an audit of 353 consecutive infrainguinal bypasses, our duplex surveillance program reported that up to 40% of bypass grafts have an abnormality (elevated PSV or lumen reduction) demonstrated on early scanning with approximately 70% of these grafts failing by 3 years if not intervened on. During surveillance moderate stenosis (PSV:180-300 cm/s, Vr 2-3.5) was predictive of grafts at high risk for failure (Fig. 23.8) [22]. Although duplex surveillance will be accompanied by a decrease in primary patency due in large part to "at risk" receiving early secondary interventions, long-term improvements in graft patency and limb salvage can be expected.

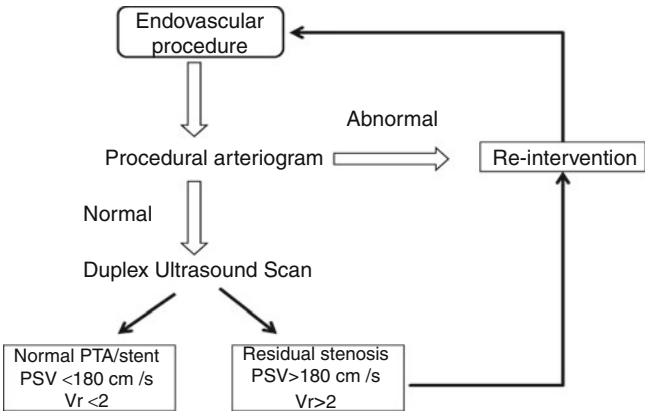


**Fig. 23.7** Evaluation algorithm of infrainguinal endovascular procedures using arteriography and duplex ultrasound

While myointimal hyperplasia continues to be the most common cause identified with late (>30 days) endovascular or

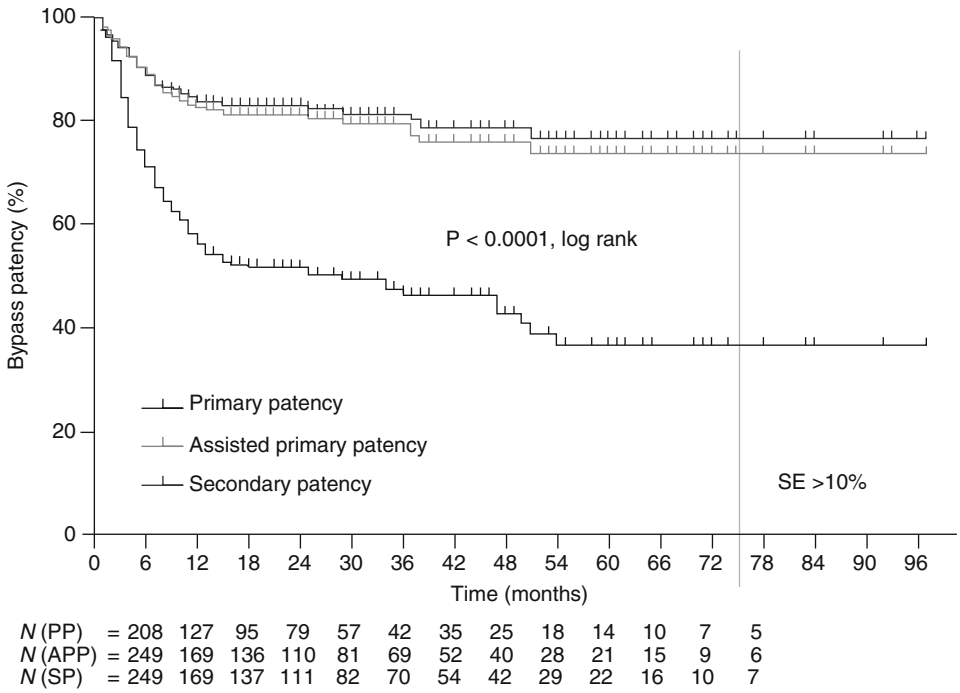


**Fig. 23.8** Kaplan-Meier estimates of patency rates for the University of South Florida experience with duplex-monitored surveillance of 353 lower extremity bypasses

surgical intervention failure, the vascular surgeon must remain mindful that progression of atherosclerosis can also occur. Identification of either new distal occlusive disease or a "failing" vascular reconstruction can be accomplished with routine duplex surveillance lending the high-risk lesion for intervention prior to thrombosis, thus extending functional patency. Lower extremity endovascular or surgical reconstructions are recommended regular duplex assessment with measurement of ABI within 1–3 weeks of the procedure. If normal repair site hemodynamics (i.e., <50% diameter reduction residual stenosis and ABI > 0.2 of pretreatment values) are recorded, surveillance is repeated in 3–4 months, and if again favorable, duplex surveillance is extended to 6-month intervals. Should a moderate stenosis (50–75% diameter reduction) be identified with a normal ABI, a repeat scan is scheduled in 3–4 weeks to determine if further deterioration in repair site hemodynamics is present which would necessitate endovascular or surgical reintervention. A progressive stenosis with a PSV > 300 cm/s and a Vr > 3.5 should prompt contrast digital subtraction angiography to assess lesion character and determine the need for revision by endovascular or surgical means. When employed routinely, a graft surveillance program can afford a low (<3%) primary graft failure rate annually [23].

### Conclusion

Duplex scanning has demonstrated that it has an established and continually expanding role in the management of PAD. While duplex scanning may never completely replace other forms of contrast angiography, it continues to provide a fundamental service for vascular surgeons and their patients. As clinicians intensify a focus on the endovascular treatment of PAD, duplex scanning will continue to accompany their successes. Duplex scanning grants a safe means of attaining a high affinity for effectively diagnosing vascular disease, confirming successful endovascular or surgical intervention, and detecting developing problems in the peripheral circulation of patients with PAD.

## References


1. Crossman DV, Ellison JE, Wagner WH, et al. Comparison of contrast arteriography to arterial mapping with color-flow duplex imaging in the lower extremities. J Vasc Surg. 1989;10:522–9.
2. Moneta GL, Yeager RA, Antonovic R, et al. Accuracy of lower extremity arterial duplex mapping. J Vasc Surg. 1992;15:275–84.
3. Kerr TM, Bandyk DF. Color duplex imaging or peripheral arterial disease before angioplasty or surgical intervention. In: Bernstien EF, editor. Vascular diagnosis. 4th ed. St. Louis: CV Mosby; 1993. p. 527–33.
4. Allard L, Cloutier G, Durand LG, et al. Limitations of ultrasonic duplex scanning for diagnosing lower limb arterial stenosis in the presence of adjacent segment disease. J Vasc Surg. 1994;19:650–7.
5. de Smet AA, Ermers EJ, Kitslaar PJ. Duplex velocity characteristics of aortoiliac stenoses. J Vasc Surg. 1996;23:628–36.
6. Kohler TR, Zierler G, Strandness DE, et al. Can duplex scanning for diagnosis of aortoiliac and femoropopliteal disease: a prospective study. Circulation. 1987;76:1074–80.
7. Jager KA, Risketts HJ, Strandness Jr DE. Duplex scanning for the evaluation of lower limb arterial disease. In: Bernstien EF, editor. Noninvasive diagnostic techniques in vascular disease. St. Louis: CV Mosby; 1985. p. 619–31.
8. Whelan JF, et al. Color flow Doppler ultrasound comparison with peripheral arteriography for the investigation of peripheral arterial disease. J Clin Ultrasound. 1992;20:369–74.
9. van der Heijden FH, et al. Value of duplex scanning in the selection of patients for percutaneous transluminal angioplasty. Eur J Vasc Surg. 1993;7:71–6.
10. Ligush Jr J, Reavis SW, Preisser JS, et al. Duplex ultrasound scanning defines operative strategies for patients with limb threatening ischemia. J Vasc Surg. 1998;28:482–91.
11. Grassbaugh JA, Nelson PR, Ruicidlo EM, et al. Blinded comparison of preoperative duplex ultrasound scanning and contrast arteriography for planning revascularization at the level of the tibia. J Vasc Surg. 2003;37:1186–90.
12. Standards of Practice Committee of the Society of Cardiovascular and Interventional Radiology. Guidelines for percutaneous angioplasty. Radiology. 1990;177:619.
13. Edwards JM, Coldwell DM, Goldman ML, et al. The role of duplex scanning in the selection of patients for transluminal angioplasty. J Vasc Surg. 1991;13:69–74.
14. Langsfeld M, et al. The use of deep duplex scanning to predict significant aortoiliac stenosis. J Vasc Surg. 1988;7:395–9.
15. Hingorani A, Markevich N, Sreedhar K, et al. Magnetic resonance angiography versus duplex arteriography in which patients undergoing lower extremity revascularization: which is the best replacement for contrast arteriography? J Vasc Surg. 2004;39:717–22.
16. Surowiec SM, Davies MG, Shirley WE, et al. Percutaneous angioplasty and stenting of the superficial femoral artery. J Vasc Surg. 2005;41:269–78.
17. Timaran CH, Prault TL, Stevens SL, et al. Iliac artery stenting versus surgical reconstruction for TASC (Trans-Atlantic Inter-Society Consensus) type B and type C iliac lesions. J Vasc Surg. 2003;38:272–8.
18. Bodily K, Buttorff J, Nordesgaard A, Bodily K, Buttorff J, Nordesgaard A. Aortoiliac reconstruction without arteriography. Am J Surg. 1996;171:505–7.
19. Schwarcz TH, Gatz VL, Little S. Arterial duplex ultrasound is the most cost-effective, noninvasive diagnostic imaging modality before treatment of lower-extremity arterial occlusive disease. J Vasc Ultrasound. 2009;33:75–9.
20. Merwissen MW, Kenney EV, Bandyk DF, et al. The role of duplex scanning versus angioplasty in predicting outcome after balloon angioplasty in the femoropopliteal artery. J Vasc Surg. 1992;15:960–6.
21. Spijkrboer AM, Nass PC, de Valois JC. Evaluation of femoropopliteal arteries with duplex ultrasound after angioplasty. Can we predict results at one year? Eur J Vasc Endovasc Surg. 1996;12:418–23.
22. Tinder CN, Chavanpun JP, Bandyk DF. Efficacy of duplex ultrasound surveillance after infrainguinal vein bypass may be enhanced by identification of characteristics predictive of graft stenosis development. J Vasc Surg. 2008;48(3):613–8. Epub 2008 Jul 17.
23. Tinder CN, Bandyk DF. Detection of imminent vein graft occlusion: what is the optimal surveillance program. Semin Vasc Surg. 2009;22:252–60.

# Duplex Surveillance of Infrainguinal Bypass Grafts

# 24

Patrick A. Stone, Dennis F. Bandyk, and Akhilesh K. Jain

**Abstract**

Infrainguinal bypass using greater saphenous vein is a well-established treatment for lower extremity critical limb ischemia. Alternative conduits for revascularization (arm vein, spliced vein, or prosthetic graft) may be used in the absence of a greater saphenous vein. Myointimal hyperplasia resulting in stenosis of the conduit remains the most common etiology of graft failure beyond the perioperative period. Clinical assessment for signs and symptoms of limb ischemia lacks the diagnostic sensitivity to detect developing graft stenosis. Consequently, duplex surveillance is recommended after infrainguinal bypass grafting to identify abnormalities in graft flow characteristics while the bypass graft is still patent. Since the goal of infrainguinal bypass surveillance is to prolong patency and avoid thrombotic occlusion, the measure of its success is the "assisted-primary patency rate." Optimum results can be obtained when duplex surveillance is initiated in the operating room or prior to hospital discharge. The likelihood of graft revision varies with the vein bypass type and is increased when a graft defect is identified on a "predischarge" or early (<6 week) duplex scan. Duplex findings can also be used to select endovascular or surgical treatment options for identified abnormalities. The efficacy of duplex surveillance may be enhanced by modifying testing protocols, e.g., rigorous surveillance for "higher risk" bypasses based on initial duplex scan results and other characteristics.

**Keywords**

Infrainguinal bypass • Duplex surveillance • Critical limb ischemia • High-risk bypass

## Introduction

Vascular laboratory surveillance using duplex ultrasound is recommended after infrainguinal bypass grafting as it benefits patient outcome by improving graft patency [1, 2]. Ideally, duplex testing should begin in the operating room to survey the graft and anastomotic sites for stenosis and to document augmented flow in the runoff arteries and foot. Color duplex imaging is more sensitive than arteriography for intraoperative assessment and detects unrecognized graft abnormalities in 5–10% of reconstructions, permitting immediate correction [3]. The application of duplex graft surveillance has been shown to reduce the incidence of both early (<30 days) and late bypass failure [1, 2, 4]. Infrainguinal

P.A. Stone, M.D., RVT, RPVI
Department of Surgery, Robert C. Byrd Health Sciences Center, West Virginia University, Charleston Area Medical Center, Charleston, WV, USA

D.F. Bandyk, M.D. (✉)
Vascular and Endovascular Surgery, University of California, San Diego, La Jolla, CA, USA
e-mail: dbandyk@health.usf.edu

A.K. Jain, M.D.
Section of Vascular Surgery, Yale University, New Haven, CT, USA

A.F. AbuRahma, D.F. Bandyk (eds.), *Noninvasive Vascular Diagnosis*,
DOI 10.1007/978-1-4471-4005-4_24, 

arterial bypasses, constructed of either autologous vein or a prosthetic graft, are prone to develop intrinsic stenotic lesions, which when progressive cause thrombosis if graft flow is reduced below the "thrombotic threshold velocity." [5–9] Myointimal hyperplasia producing lumen reduction is the most common etiology for graft stenosis, but its temporal occurrence and site(s) of development differ between vein and prosthetic grafts. The occurrence of vein graft stenosis is highest in the 6 months following the procedure and decreases thereafter. Myointimal stenosis is most common at vein valve and anastomotic sites and has anatomic features of a smooth, typically focal (<2 cm) stricture. This acquired lesion has been implicated in nearly 80% of vein bypass failures, with other graft failures caused by technical errors, intrinsic graft lesions, or hypercoagulable states [1, 2, 6, 10]. Following prosthetic grafting, intragraft abnormalities are rare (<10% of all stenoses) with graft stenosis developing most commonly at the distal anastomosis and the adjacent runoff artery. The failure rate of prosthetic grafts (10–15%/year) is higher than autologous vein grafts (2–5%/year) and has been attributed to differences in "thrombotic threshold velocity," myointimal hyperplasia development, and atherosclerotic disease progression [8, 9].

The patterns of infrainguinal graft failure mandate using a direct imaging method, color duplex ultrasound, and hemodynamic assessment (limb pressures, velocity spectra analysis) for effective surveillance. Clinical assessment for symptoms or signs of limb ischemia, even when combined with measurement of ankle-brachial systolic pressure index (ABI), has inferior diagnostic sensitivity for graft stenosis detection. Less than 50% of patients found to have a >70% diameter reducing (DR) graft stenosis admit to claudication symptoms or recognize a change in limb perfusion. Duplex surveillance is used to detect changes in graft flow, identify sites of intrinsic graft lesions or developing stenosis, and grade lesion severity. Serial testing allows timely revision of hemodynamically significant lesions that, if unrepaired, would result in graft thrombosis. The criteria for intervention of an identified "failing graft" are based on reduction of duplex-measured graft peak systolic flow velocity and/or ABI compared to initial postoperative levels. The efficacy of surveillance has been demonstrated in prospective clinical trials with a 15–30% improvement in long-term (>5 year) graft patency rates: higher for autologous vein conduits (>70–80%) than for prosthetic bypass grafts (50–70%) [2, 7, 11–13]. Multiple investigators have observed high graft failure rates in stenotic bypass grafts with a policy of no intervention. Idu et al. reported a 10% graft occlusion rate when a duplex-detected stenosis of >70% was repaired, compared to a 100% graft failure rate when the lesions were untreated [13]. Infrainguinal prosthetic graft patency is also improved by duplex surveillance. Calligaro et al. demonstrated duplex scanning was more sensitive (81%) than ABI with clinical evaluation (24%) with 50% of correctable stenosis found at anastomotic sites [9]. The finding of a low (<45 cm/s) peak systolic graft velocity is a more common finding than duplex-detected stenosis in graft at increased risk for failure.

The goal of graft surveillance is to avert failure by the detection and elective correction of graft abnormalities (technical errors, intrinsic graft lesions, myointimal hyperplasia, and graft aneurysm). Surveillance should be initiated prior to discharge from the hospital and continue indefinitely, with the majority of patients requiring 6-month or yearly evaluation after the 1st year. It has been estimated that a duplex surveillance program is cost-effective if limb loss can be prevented in only 2% of enrolled patients.

## Mechanisms and Hemodynamics of Graft Failure

The interpretation of duplex surveillance studies requires an understanding of the mechanisms of graft failure, arterial bypass graft hemodynamics, and the physiology of graft stenosis. Graft failure occurs by one of three mechanisms: occlusion by thrombosis, hemodynamic failure, or structural failure (aneurysmal degeneration or infection) [1, 6, 13–16]. Graft thrombosis is most frequent during the perioperative (operating room to hospital discharge) period, with a reported incidence of 3–8%. Thereafter, the rate of graft failure is approximately 1%/month during the 1st year and then decreases to <5%/year. The attrition of patency is highly dependent on application of graft surveillance, patient compliance, and the success of graft revision procedures.

Early (<30 days) graft failure is the result of technical errors in bypass construction (anastomotic stricture, retained vein valves, unrecognized intrinsic graft lesions, tunneling errors, graft kinking), a hypercoagulable condition, or inadequate runoff to maintain graft flow above the "thrombotic threshold velocity." [12] Recognition of technical errors and abnormal graft hemodynamics caused by poor runoff is best accomplished by duplex assessment at operation [17]. The key characteristic is a low-velocity or high-resistance graft spectral waveform. Graft thrombosis despite a "normal" intraoperative duplex scan as a rule indicates the presence of a hypercoagulable state.

Graft failure beyond 30 days can result from infection, structural degeneration of the conduit, or graft stenosis caused by intrinsic vein disease or myointimal hyperplasia.

The incidence of graft stenosis varies with graft type ranging from 12% following in situ saphenous vein bypass grafting to 44% for arm vein bypasses [1, 10, 18]. The temporal occurrence of graft stenosis follows a "bell-shaped" curve with the highest prevalence at 6 months following the procedure. Infection producing graft failure is rare (<1%) with autologous venous conduits, but 3–5% with prosthetic graft usage.

Beyond 2 years, atherosclerotic disease progression in the inflow/outflow arteries and venous aneurysm development account for the majority of late graft failures [18]. Atherosclerotic disease progression is related to effective control of the patient's risk factors, i.e., tobacco use, diabetes, hypertension, and hyperlipidemia. Inflow and outflow occlusive diseases are suspected when duplex testing indicates reduction in graft blood flow velocity but no graft abnormality is identified. Aneurysm-related or thromboembolic graft failure should be suspected with graft thrombosis despite a prior duplex showing no stenotic lesions and normal graft flow. Aneurysmal degeneration is infrequent and tends to occur in arm vein conduits and in patients with aortic/popliteal aneurysmal disease. The finding of mural thrombus within a vein or prosthetic conduit is abnormal and indicates the graft is at increased risk for thrombosis.

## Arterial Bypass Hemodynamics

Factors that influence duplex-measured flow velocity and spectral waveforms of graft blood flow include conduit diameter, status of inflow/outflow arteries, severity of preoperative ischemia, and cardiac hemodynamics. The range of peak systolic velocities (PSV) recorded from infrainguinal vein bypasses vary, but the mean graft flow velocity (GFV), i.e., an average of PSV recorded from three or four normal, nonstenotic graft segment along the bypass length, ranges from 50 to 80 cm/s (Table 24.1 and Fig. 24.1) [19–21]. The PSV in a nonstenotic vein conduit <6 mm diameter should be over 40 cm/s, and the graft spectral waveform should demonstrate low outflow resistance, i.e., antegrade flow throughout the pulse wave cycle, in the distal graft segment at operation and in the early postoperative period. Thereafter, if limb pressure is normal (ABI > 0.9), the graft flow resistance increases with time, and graft velocity flow pattern becomes multiphasic with a triphasic arterial flow. Graft flow velocity varies with conduit diameter and bypass type (Fig. 24.2). Belkin et al. reported graft PSV was lower in inframalleolar (pedal) grafts (59 ± 4 cm/s) compared to tibial (77 ± 6 cm/s) and popliteal (71 ± 8 cm/s) vein bypasses [21]. A low graft PSV can be measured in large (>6 mm) diameter vein conduits, i.e., basilic arm vein, and in grafts with disadvantaged runoff (pedal bypass, isolated popliteal/tibial artery segments). If the graft PSV is <40 cm/s in a conduit <6 mm in diameter, a careful search for inflow or outflow arterial lesions should be conducted. The combination of low PSV and absent diastolic flow indicates high outflow resistance and a bypass at increased risk for thrombosis. A low PSV is abnormal but does not predict graft failure in all cases. When identified at operation, it provides the rationale for the perioperative administration of anticoagulation (heparin, warfarin) regimens, or altering the primary procedure by adding a sequential bypass to a second outflow artery or construction of a distal arteriovenous fistula, procedures intended to increase graft flow velocity.

A graft flow pattern of low outflow resistance is prognostic of successful bypass grafting. A bypass graft performed

**Table 24.1** Peak systolic velocity measured by duplex ultrasound from mid- or distal segments of femoropopliteal and femorotibial saphenous vein and PTFE[a] bypass grafts

| Graft type | Number | Peak systolic velocity (cm/s)(mean ± SD) |
|---|---|---|
| In situ saphenous vein | | |
| Femoropopliteal | 65 | 76 ± 12 |
| Femorotibial | 95 | 72 ± 16 |
| Femoral-pedal | 25 | 52 ± 12 |
| Reversed saphenous vein | | |
| Femoropopliteal | 20 | 80 ± 16 |
| Femorotibial | 12 | 69 ± 14 |
| Cephalic/basilic arm vein | | |
| Femoropopliteal/tibial | 68 | 63 ± 12 |
| PTFE, 6 mm diameter | | |
| Femoropopliteal | 20 | 80 ± 16 |
| Femorotibial | 12 | 69 ± 14 |
| PTFE, 5 mm diameter | | |
| Femorotibial | 5 | 77 ± 11 |

Adapted from Refs. [19–21]
[a]*PTFE* polytetrafluoroethylene

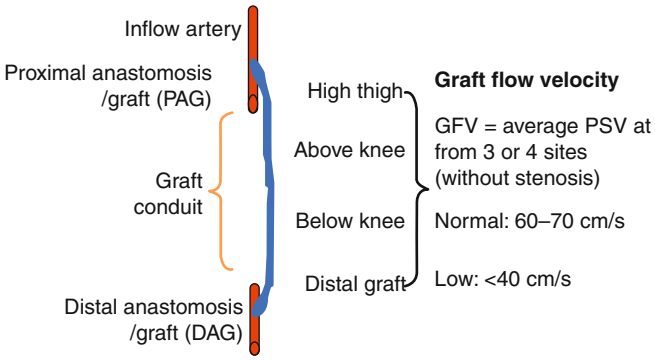


**Fig. 24.1** Schematic depicting the recording sites used for the calculation of mean graft flow velocity

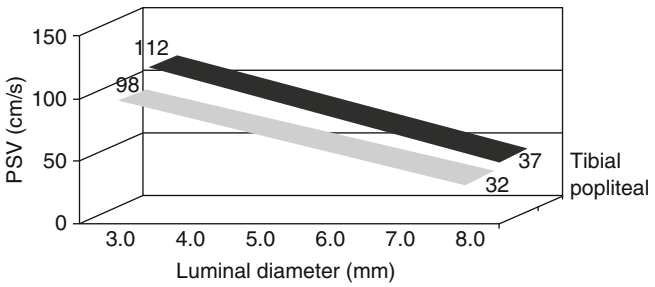


**Fig. 24.2** Duplex-ultrasound-measured peak systolic flow velocity (*PSV*) for tibial and popliteal grafts showing relationship with lumen diameter

for critical limb ischemia should demonstrate this "hyperemic" flow pattern in the distal graft segment and runoff artery, while a bypass performed for claudication may demonstrate triphasic flow immediately. The hyperemia of limb revascularization abates within weeks with the distal graft spectral waveform developing to a triphasic flow pattern if ABI has normalized (Fig. 24.2). Bypasses to the peroneal artery often retain monophasic flow due to collateral flow to the leg and foot. Failure of the graft flow to convert from a biphasic to triphasic spectral waveform has been associated with reduced graft patency. Taylor et al. reported that 54 (86%) of 63 grafts with persistent monophasic waveforms beyond 3 months were frequently found to have developed a graft stenosis or subsequently occluded [5]. In patients with dialysis-dependent end-stage renal disease and severely calcified tibial arteries, a low-flow (PSV in the range of 30–45 cm/s) bypass with minimal or no diastolic flow can occur due to diseased runoff, its associated high outflow resistance, and reduced artery wall compliance.

The identification of changes in graft PSV is important diagnostic criteria for detection of the "failing" bypass graft. Development of a low (<40–45 cm/s) PSV or a decrease in PSV of >30 cm/s in mean graft velocity compared to a prior study indicates a significant change in bypass flow, and a careful search for a graft stenosis should be initiated (Fig. 24.3). The duplex features of a >70%, pressure-reducing stenosis included lumen reduction with color Doppler aliasing, PSV increase to >300 cm/s with spectral broadening, and a PSV ratio (at stenosis compared to proximal to stenosis) >3.5 (Figs. 24.4 and 24.5). The increase in diastole flow velocity is due to flow limitation during systole requiring flow throughout the pulse cycle to supply adequate volume flow to the distal limb. If duplex scanning of the bypass does not identify a stenosis, graft imaging by contrast arteriography or computed tomography (CT) angiography is recommended. Elevated PSV (>150 cm/s) in the graft conduit or anastomosis is abnormal and may be caused by small graft caliber or a stenosis. Graft PSV in the range of 120–160 cm/s can be measured along the entire course of small (3 mm diameter or less) vein conduits. More frequent (every 4–6 weeks) surveillance of these "high"-velocity grafts is recommended because of their propensity to develop long segment strictures. When a progressive increase in PSV to >300 cm/s is identified, replacement of the stricture with an interposition vein bypass should be performed as balloon angioplasty has been found to be a less durable repair.

The development of graft stenosis and impending graft occlusion can be recognized from the graft spectral waveform. A low-velocity, biphasic waveform is the most common configuration associated with an acquired graft stenosis (Fig. 24.3). An abnormal graft waveform of this type is recorded from 50% of grafts with stenosis; the ABI had decreased to 0.4–0.7, and mean graft velocity (MGV) has decreased by 20–30 cm/s. The reduction in waveform pulsatility and return of diastolic flow indicate arteriolar dilation in response to a pressure-reducing lesion. Other types of abnormal graft waveforms include a monophasic waveform with low (<45 cm/s) PSV seen in one-third of graft stenosis with an ABI in the range of 0.7–0.9, and a staccato graft waveform seen in approximately 6% of abnormal grafts and always associated with a high-grade outflow stenosis. This staccato flow pattern indicates a to-and-fro blood flow within a compliant venous conduit, extremely low graft flow, and impending graft thrombosis. Grafts with this flow feature are difficult to evaluate using contrast arteriography, and the condition has been referred to as a graft "pseudoocclusion." The combination of graft PSV measurements, color duplex imaging for anatomic lesions, and ABIs analyzed sequentially during the postoperative period provides a comprehensive characterization of graft and limb hemodynamics. The objective data provided by duplex testing allows detection of graft stenosis, the progression of lesions, and identification of grafts at increased risk for thrombosis.

## Intraoperative Duplex Scanning

Assessment of infrainguinal bypass grafts at operation for technical adequacy can be performed using continuous-wave (CW) Doppler flow analysis, arteriography, angioscopy, and CW Doppler after flow is restored, or color duplex ultrasonography [22–24]. Color duplex ultrasound is the preferred method because it provides both anatomic and hemodynamic assessment of graft function and limb perfusion. When used at operation, approximately 15% of procedures have an unrecognized abnormality with velocity spectra of a stenosis identified. Repair of these problems and documentation of normal graft hemodynamics are associated with a low (<1%) incidence of graft thrombosis. In a series of 626 consecutive infrainguinal vein bypasses, duplex scanning prompted revision of 104 lesions in 96 bypass grafts, which included 82 vein/anastomotic stenoses, 17 vein segments with platelet thrombus, and 5 low-flow grafts. The revision rate was highest ($p < 0.01$) for alternative vein bypass grafts (27%) compared with the other grafting methods (reversed vein bypass grafts, 10%; nonreversed translocated, 13%; in situ, 16%). A normal intraoperative scan on initial imaging ($n = 464$ scans) or after revision ($n = 67$ scans) is associated with a 30-day thrombosis rate of 0.2% and a revision rate of 0.8% for duplex-detected stenosis (PSV > 300 cm/s). By comparison, 20 (21%) of 95 bypass grafts with a residual ($n = 29$ grafts) or unrepaired duplex stenosis ($n = 53$ grafts) or low flow ($n = 13$ grafts) had a corrective procedure for graft thrombosis

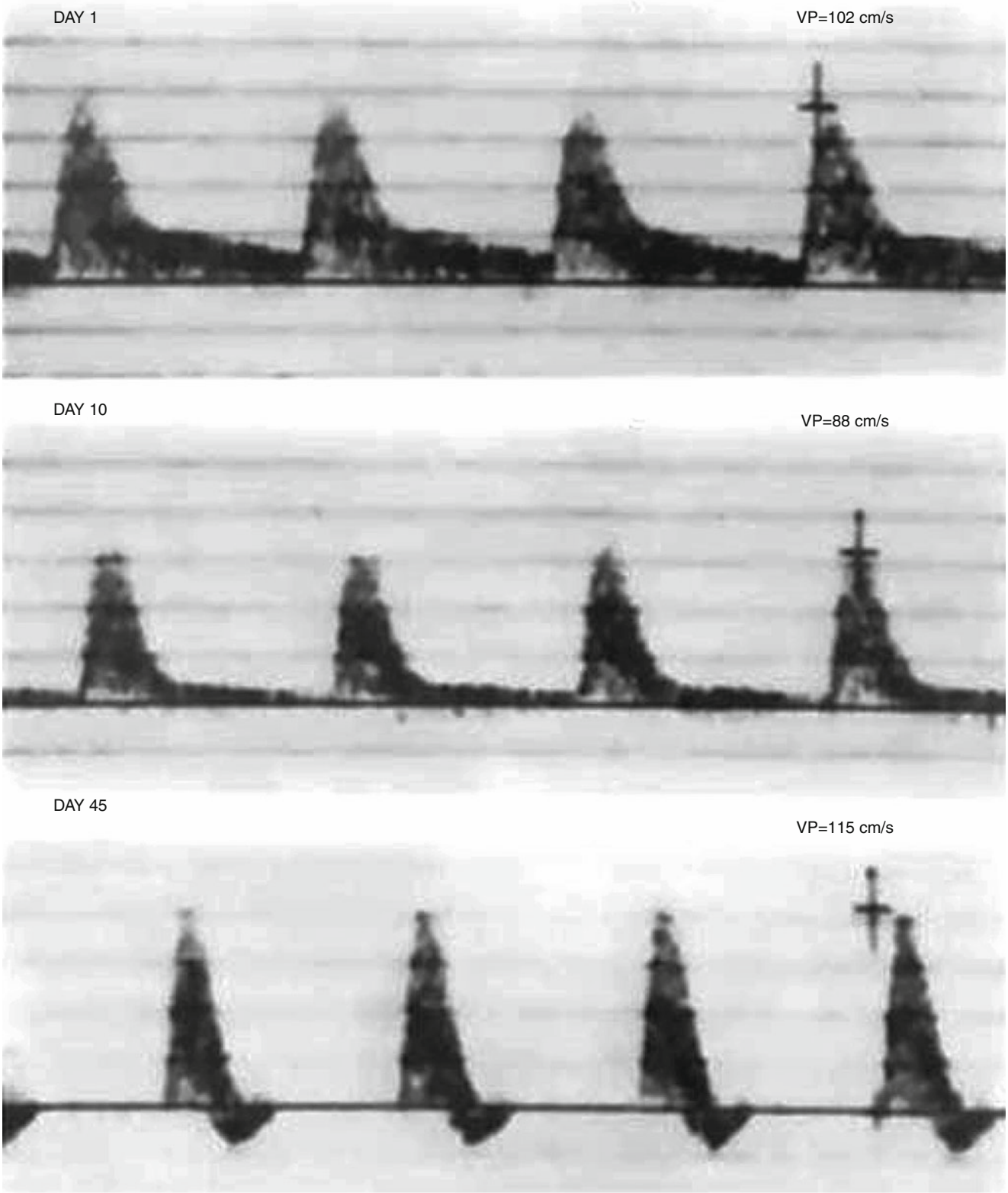


**Fig. 24.3** Velocity spectra recorded from the distal segment of a femoral-peroneal in situ saphenous vein bypass at 1, 10, and 45 days. A low-resistance spectral waveform (flow throughout the pulse cycle) is normal and expected after bypass grafting for critical ischemia. Flow resistance increased with time as evidenced by the decrease in diastolic flow. No significant change in peak systolic velocity (*Vp*) occurred, and the development of a triphasic spectral waveform at day 45 indicates normal bypass graft hemodynamics and distal limb perfusion (ABI > 0.9)

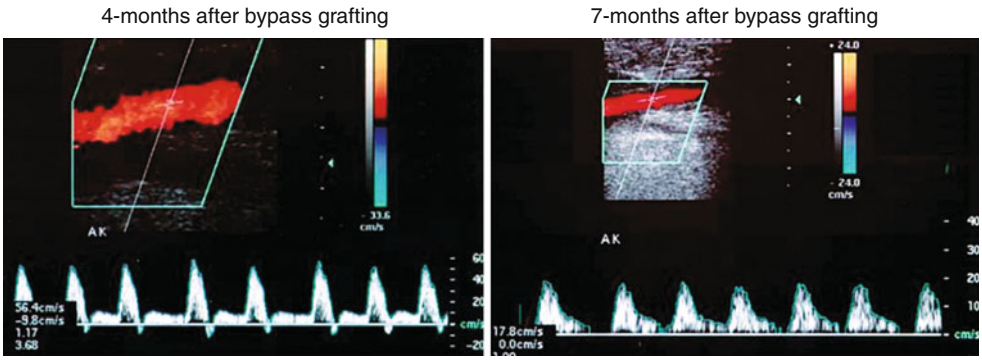


**Fig. 24.4** Duplex-recorded velocity spectra recorded from the above-knee segment of a femoropopliteal vein bypass, demonstrating change in waveform configuration (triphasic to biphasic) and reduction in peak systolic velocity (PSV) from 56 to 18 cm/s caused by the development of a distal anastomotic graft stenosis

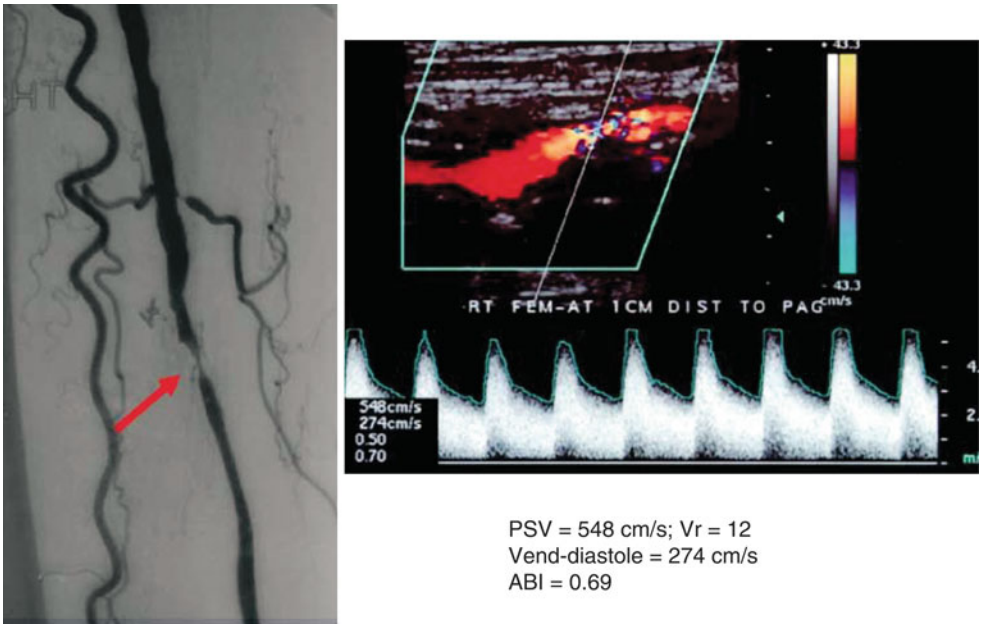


**Fig. 24.5** Angiogram and duplex ultrasound scan of a >75% diameter reducing stenosis of the proximal segment of a superficial femoral artery to anterior tibial artery vein bypass. Peak systolic velocity (*PSV*) is 548 cm/s, velocity ratio is 12, end-diastolic velocity is 274 cm/s, and *ABI* is 0.69 decreased from the initial postoperative value of 0.95 Critical stenosis of femoral artery (*arrow*)

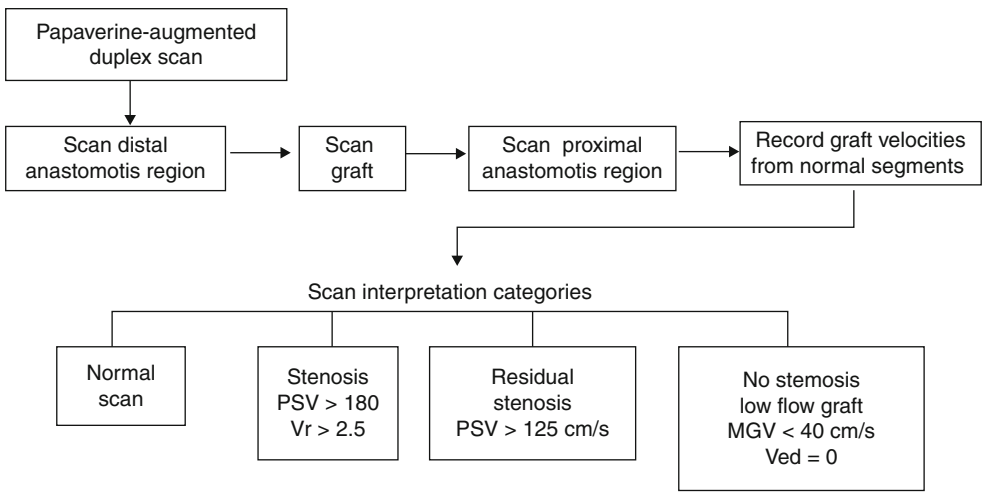


**Fig. 24.6** Algorithm for intraoperative duplex scanning of an infrainguinal vein bypass. Following duplex assessment, the study is classified into one of four categories: normal, stenosis identified, residual stenosis identified, or no stenosis identified, but hemodynamic assessment of graft flow demonstrates low (*PSV* < 40 cm/s) velocity and high resistance (no flow in diastole, Ved = 0)

($n = 8$) or stenosis ($n = 12$); $p < 0.001$. Correction of residual graft defects and rescanning to document absence of residual stenosis reduced the incidence of graft problems identified on postoperative duplex surveillance [25].

The algorithm for intraoperative duplex ultrasound assessment of an infrainguinal vein bypass involves imaging the entire arterial reconstruction and classification of findings into one of four categories (Fig. 24.6 and Table 24.2).

**Table 24.2** Interpretation of intraoperative duplex ultrasound studies of infrainguinal vein bypasses and suggested perioperative management

| Duplex scan category | Graft flow velocity(cm/s) | Peripheral vascular resistance | Interpretation and perioperative management |
|---|---|---|---|
| Normal | >40 | Low | No stenosis identified and graft PSV[a] is normal; administer dextran-40 (25 ml/h, 500 ml) and oral aspirin (325 mg/day) |
| Stenosis<br>PSV > 180 cm/s<br>Vr > 2.5 | <40 | Low | Correct lesion and rescan graft if no residual stenosis is identified but graft PSV is low (<40 cm/s); administer heparin anticoagulation (weight based) or low molecular weight heparin (1 mg/kg sc bid), dextran-40 (25 ml/h), and oral aspirin (325 mg/day) |
| Residual stenosis<br>PSV < 180 cm/s<br>Vr < 2.5 | >40 | Low | Rescan after 10 min to confirm no progression; administer low molecular weight heparin (1 mg/kg sc bid), dextran-40 (25 ml/h), and oral aspirin (325 mg/day) |
| Low flow, no graft stenosis | <40 | High | Consider an adjunctive procedure to increase graft flow (distal arteriovenous fistula, jump/sequential graft to another outflow artery); if not possible treat as low-flow graft with an antithrombotic regimen of heparin anticoagulation, dextran-40, and aspirin (325 mg/day) |

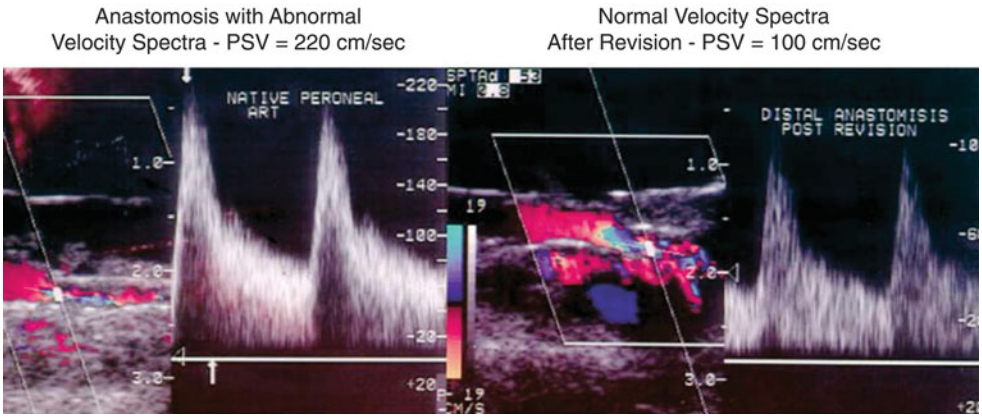


**Fig. 24.7** Intraoperative color duplex scan of a residual stenosis at the distal anastomosis of a femoral-peroneal saphenous vein bypass (*left*). Following revision by vein patch angioplasty, repeat scanning shows normal velocity spectra (*PSV* < 150 cm/s)

Scanning is performed after completion of the bypass graft, and patency is verified by clinical inspection and pulse palpation [26]. A 10–15-MHz linear array transducer, placed in a sterile plastic sleeve containing acoustic gel, is used to scan exposed vessels and graft segments beneath the skin. Imaging of the vein graft, anastomoses, and adjacent native arteries is performed in a longitudinal plane along the vessels, beginning at the distal graft-anastomotic segment and then proceeding proximally to include the entire venous conduit and the inflow artery-proximal anastomosis graft segment. Papaverine HCl (30–60 mg) is injected into the distal vein bypass via a 27-gauge needle to augment flow, thereby increasing the diagnostic sensitivity for stenosis detection. Graft PSV is measured (60° or less Doppler angle) at the proximal and distal anastomosis, at selected sites along the graft length (high-thigh, HT; above-knee, AK; below-knee, BK; and distal graft), and from inflow and outflow arteries. Following in situ saphenous bypass, imaging for patent side branches is performed, and the absence of a side-branch flow is confirmed by the presence of a staccato waveform with distal graft occlusion.

Vein conduit stenosis is the most frequent abnormality found with intraoperative duplex scanning. Other abnormalities, in decreasing frequency, include anastomotic stenosis, platelet thrombus, and low graft flow as a result of outflow disease. Immediate repair is indicated for vein valve/anastomotic sites with PSV > 180 cm/s and a velocity ratio (Vr = PSV at lesion/PSV proximal) of >2.5 (Fig. 24.7). Velocity spectra of a high-grade stenosis (PSV > 300 cm/s) at the site of the imaging graft abnormality may represent formation of platelet thrombus. This graft segment should be replaced and a thrombolytic agent infused downstream to lyse thrombus embolized to the distal graft and runoff arteries. In vein grafts of normal (3–5 mm) caliber, a low PSV was measured in only 13 of the 626 grafts, of which 6 were to blind segments. Five of the 13 grafts failed within 90 days. Rzucidlo et al. [24] also reported a high rate of early graft thrombosis when duplex scanning demonstrated no or low (<8 cm/s) flow in diastole in the distal graft. When a high-resistance, low graft flow is identified, a careful search for a technical error should be performed, and if none is identified, perioperative heparinization or a procedure to increase graft

**Table 24.3** Risk stratification for graft thrombosis based on surveillance data[a]

| Category[b] | High-velocity criteria | | Low-velocity criteria | | Δ ABI |
|---|---|---|---|---|---|
| I (Highest risk) | PSV > 300 cm/s or Vr > 3.5 | and | GFV < 45 cm/s | or | >0.15 |
| II (High risk) | PSV > 300 cm/s or Vr > 3.5 | and | GFV > 45 cm/s | and | <0.15 |
| III (Intermediate risk) | PSV 180–300 cm/s or Vr > 2.0 | and | GFV > 45 cm/s | and | <0.15 |
| IV (Low risk) | PSV < 180 cm/s and Vr < 2.0 | and | GFV>45 cm/s | and | <0.15 |

[a]*PSV* duplex-derived peak systolic velocity at site of flow disturbance, *GFV* graft flow velocity (global or distal), *Vr* PSV ratio at maximum stenosis compared to proximal graft segment without disease, *ABI* Doppler-derived ankle-brachial systolic pressure index
[b]*Category I*: Prompt repair of lesion is recommended – patients are hospitalized and anticoagulated prior to repair. *Category II*: Lesion is repaired electively (within 2 weeks). *Category III*: Lesions are observed with serial duplex examination at 4–6-week intervals and repaired if they progress. *Category IV*: Lesions are at low risk for producing graft thrombosis – follow-up every 6 months; few (<3%/year) failures observed in this group

flow (sequential bypass, distal arteriovenous fistula) should be considered.

## Postoperative Graft Surveillance

Duplex ultrasound is used to confirm graft patency, identify stenotic lesions, assess their risk for producing graft thrombosis, and, if not repaired, monitor stenosis progression.

Testing should include a clinical evaluation for symptoms or signs of limb ischemia, measurement of ABI, and color duplex imaging of the entire bypass graft including anastomosis and inflow/outflow arteries. A "predischarge" scan is recommended to confirm normal functional patency, identify the presence of technical problems and the progression of a residual stenosis detected at operation, and provide baseline graft flow velocities. Upon discharge, patients should be counseled and their primary care physician notified regarding the importance and necessity of graft surveillance. Graft failure has been associated with lack of a surveillance examination within 3 months of the procedure [27]. At each graft surveillance study, patients should also be queried regarding current use of tobacco products and whether they are taking antiplatelet medications. Modifying these two factors associated with graft failure can improve long-term patency.

## Testing Intervals

Factors affecting the frequency of surveillance include the type of bypass and results of the predischarge duplex scan (Table 24.3). Grafts at higher risk include those with residual stenosis, those modified during surgery, and those with low graft velocities. If the predischarge scan is normal, the first outpatient graft surveillance is performed 1 month after discharge. At this time, complete graft imaging should be possible, and if no abnormalities are identified, the next surveillance study is scheduled for 3 months later, and every 6 months thereafter if normal surveillance studies are obtained. Bypasses with low-flow, residual graft lesions or constructed of arm veins should be evaluated every 3 months for the first year.

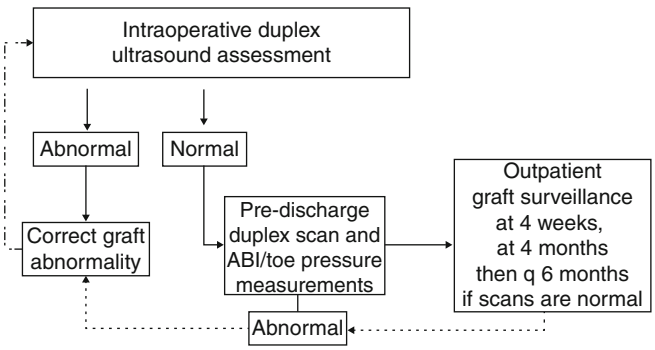


**Fig. 24.8** Duplex surveillance protocol beginning at operation, with rescanning prior to discharge and in the outpatient clinic at regular intervals

## Threshold Velocity Criteria for Graft Revision

Repair of duplex-detected graft stenosis with a PSV > 300 cm/s and Vr > 3.5 is recommended, especially if the lesion has demonstrated progression on serial examinations and MGV has decreased to <45 cm/s [28]. Duplex imaging should demonstrate an anatomic stenosis on power Doppler, and other features of lesion should be characterized including stenosis length, site (graft vs. anastomosis vs. native artery), and the diameter of the graft proximal to the lesion (Fig. 24.8). Other vascular groups also have published similar threshold velocity criteria:

- PSV > 300 cm/s, Vr > 4.0: Mills et al. [29]
- PSV > 300 cm/s, Vr > 3.0: Sladen et al. [30]
- PSV > 250 cm/s, Vr > 3.4: Papanicolaou et al. [31]
- PEDV > 20 cm/s: Buth et al. [32]
- Vr > 3.0: Bell et al. [33]

The risk of graft thrombosis is predicted by using the combination of high- and low-velocity duplex criteria discussed above and the ABI values (Tables 24.3 and 24.4).

In the highest-risk group (Category I), the development of a pressure-reducing stenosis (PSV > 300 cm/s) has produced low flow velocity (GFV < 45 cm/s) in the graft, which, if it decreases below the "thrombotic threshold velocity," will result in graft thrombosis. Prompt repair of Category I lesions

is recommended, while Category II lesions (PSV > 300 cm/s, GFV > 45 cm/s) can be scheduled for elective repair within 1–2 weeks. Category III stenosis (PSV of 150–300 cm/s, Vr < 3.5) is not pressure or flow reducing in the resting limb. Serial scans at 4–6-week intervals are recommended to determine hemodynamic (Figs. 24.9 and 24.10) progression or regression of these lesions. Among graft stenosis detected within the first 3 months of surgery, regression of the lesion occurs in 30–35% of cases, while 40–45% remain stable. Approximately 50% of these "index" graft lesions progress to high-grade (PSV > 300 cm/s, Vr > 3.5) stenosis. In general, serial (4–6-week intervals) duplex scans will determine if a lesion will progress and become "graft threatening" within 4–6 months of identification [8, 9]. In a natural history study of intermediate graft stenosis, Mills et al. [22] found that 63% of lesions progressed, 22% resolved, 10% remained unchanged, and one graft (2%) thrombosed despite more frequent surveillance.

No stenosis is identified in the majority (approximately 80%) of bypass grafts studied with ultrasound, i.e., Category IV scans. For these patients, surveillance at 6-month intervals is generally recommended. For Category IV grafts with a GFV < 45 cm/s, a diligent search should be conducted for additional inflow or outflow occlusive lesions. If none is detected, oral anticoagulation (sodium warfarin) is prescribed to maintain the prothrombin time at an INR of 1.6–2.2, as well as aspirin (81 mg/day). This anticoagulation regimen is also prescribed following femorodistal prosthetic bypass grafting when a GFV of <60 cm/s is measured in the graft by duplex scanning prior to discharge. The rationale for oral anticoagulation is based on the concept of the "thrombotic threshold velocity," which is higher in prosthetic than in vein arterial bypass grafts.

Infrainguinal bypasses constructed with arm (basilic, cephalic) veins require vigilant surveillance because of an observed 42% revision rate for stenosis. Of note, 82% of all spliced arm vein grafts required revision within 1 year of operation compared to 28% of basilic vein grafts ($p < 0.01$). With duplex surveillance and repair of duplex-detected stenosis, a graft patency of 91% at 3 years was achieved. A surveillance program is extremely important in this patient group since failure of the alternative vein bypass would require either a redo prosthetic revascularization, a procedure with poor long-term success, or an amputation [31].

**Table 24.4** Potential of a graft lesion to cause graft thrombosis

| | |
|---|---|
| High-grade stenosis producing low graft flow | High |
| Graft entrapment | High |
| Flow-limiting graft stenosis | Moderate |
| Graft-anastomotic site aneurysm with mural thrombus | Moderate |
| Non-flow-limiting graft stenosis (PSV < 300 cm/s)[a] | Low |
| Residual arteriovenous fistula after in situ vein bypass | Low |

[a]*PSV* peak systolic velocity

## Duplex Criteria for Endovascular Repair of Graft Stenosis

Methods for repair of graft stenosis include open surgical revision (patch angioplasty, interposition grafting, or jump) and endovascular repair using balloon angioplasty. Duplex

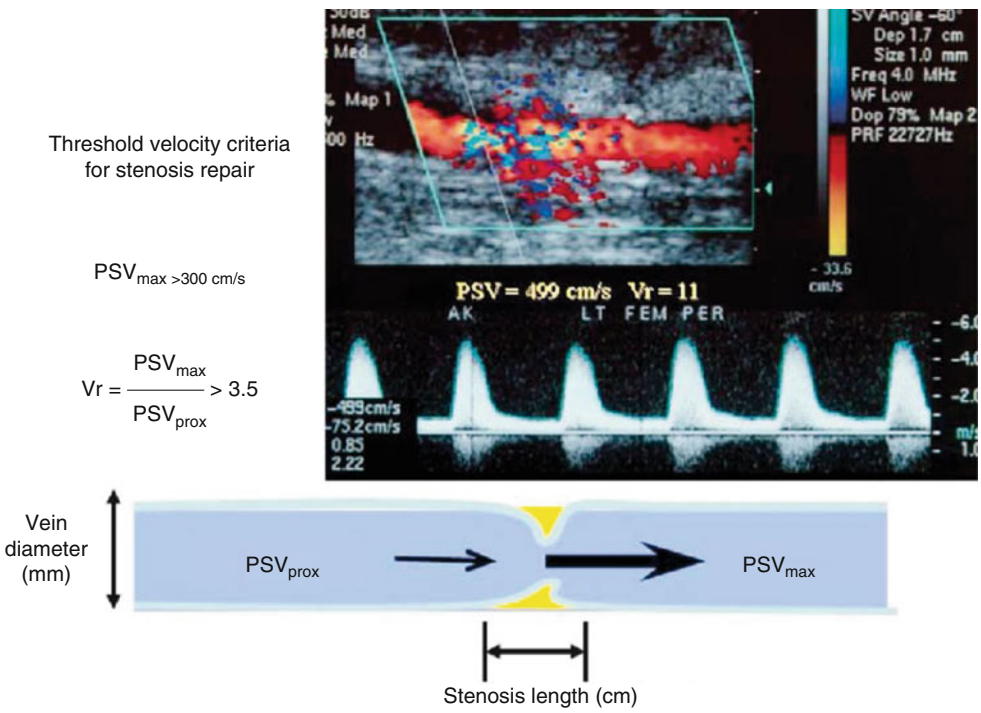


**Fig. 24.9** Duplex characterization of a graft stenosis, including velocity criteria for stenosis repair, vein diameter, and stenosis length

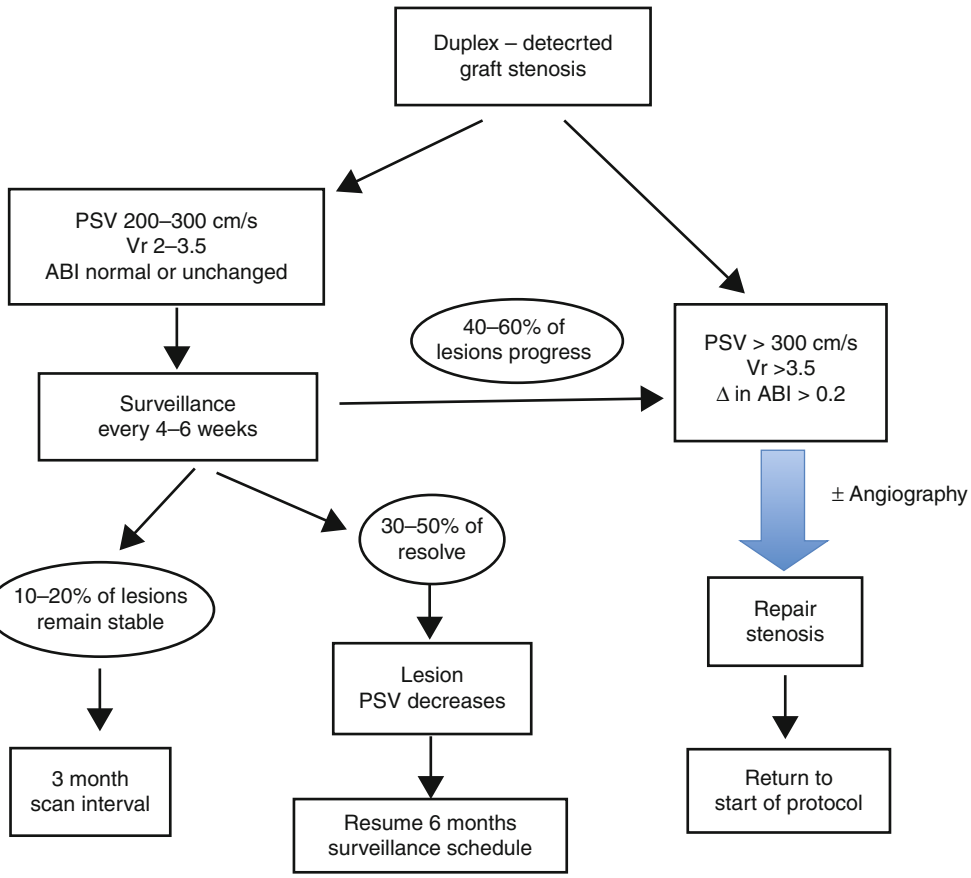


**Fig. 24.10** Algorithm for the surveillance and management of duplex-detected graft stenosis based on peak systolic velocity (*PSV*), velocity ratio (*Vr*), and ankle-brachial index (*ABI*) measurements

testing can be used to select lesions appropriate for balloon angioplasty based on criteria that include severity of stenosis, lesion length, conduit diameter, and appearance time from bypass procedure:

Stenosis severity: PSV > 300 cm/s, Vr > 3.5

Stenosis length: ≤2 cm

Conduit diameter: ≥3.5 cm

Appearance time: >3 months from bypass grafting

Over a 6-year period, 118 (22%) of 525 infrainguinal vein bypasses monitored by duplex ultrasound underwent revision for stenosis. One-half of the lesions met the criteria for endovascular intervention. Stenosis-free patency at 2 years was identical for surgical (63%) and endovascular (63%) interventions. However, the stenosis-free patency varied with timing and type of procedure. The endovascular treatment of a focal (<2 cm) vein graft stenosis >3 months from the initial procedure was associated with an 89% 1-year stenosis-free patency [34]. Following either surgical or endovascular repair, surveillance is similar to that performed after the primary procedures with an initial scan within 1 week to verify absence of residual stenosis at the repair site. Outcome of balloon angioplasty for graft stenosis is varied in the literature (Fig. 24.11). Alexander et al. [35] used balloon angioplasty to treat 101 cases of vein graft stenosis with failure rates of 35% at 6 months and 54% at 1 year. Graft angioplasty was associated with an 8% complication rate. Kasirajan et al. [36] evaluated angioplasty using a "cutting" balloon in 19 patients. During a mean follow-up of 11 months, one (5%) angioplasty site developed stenosis, and no surgical conversions were required.

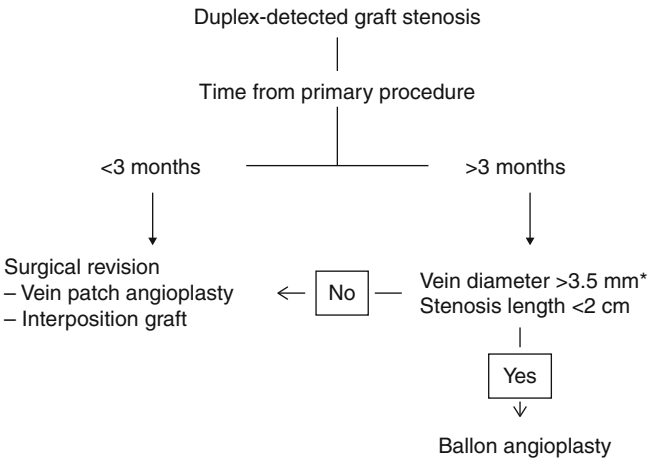


**Fig. 24.11** Treatment algorithm for duplex-detected stenosis based on appearance time (less than or more than 3 months) from operation and anatomic characteristics (vessel diameter, stenosis length). *Stenosis in a graft outflow artery >2 mm in diameter can be considered for endovascular intervention

While the majority of graft stenosis develop during the first postoperative year, Erickson et al. [37] emphasized the

need for indefinite bypass surveillance in a study of 556 bypasses followed up to 13 years. Approximately 20% of the graft abnormalities developed after 2 years. The majority (63%) of the graft defects involved the conduit or the anastomoses. These findings support the continued annual evaluation of infrainguinal bypass for the development of stenosis and for disease progression or aneurysmal changes in the venous conduit.

## Predictors of Graft Stenosis Development

Since the goal of infrainguinal bypass surveillance is to prolong patency and avoid thrombotic events, the measure of its success is the "assisted-primary patency rate." However some surgeons have felt a surveillance program is not cost effective. Duplex ultrasound imaging after infrainguinal bypass was not recommended in the 2007 Inter-Society Consensus for the Management of Peripheral Arterial Disease (TASC II) document based primarily on the results of a European multicenter randomized clinical trial [38]. However, once graft thrombosis occurs, secondary intervention to restore patency is generally not successful or durable. The graft surveillance program, when successful, leads to an increased assisted-primary patency rate, a decreased need for redo bypass grafting, and a prolonged limb salvage in the critical limb ischemia population.

A correlation of early graft flow abnormalities identified by duplex scanning with subsequent development of graft stenosis requiring repair has been reported [11, 39]. In a review of 364 infrainguinal vein bypasses under surveillance starting at 6 weeks, Mofidi et al. [39] reported that 65% bypasses had no significant stenosis at 6 weeks and ran a benign course with a 40-month cumulative patency of 82% and a limb salvage rate of 93%. Of the 29 grafts with a critical stenosis, 15 (52%) were repaired. Furthermore, 11 (38%) grafts were not repaired and occluded during subsequent follow-up. A final three (10%) with critical stenoses were not repaired but did not change during follow-up. Similar results were seen in patients with a 6-week scan demonstrating mild or intermediate flow abnormalities. Over the whole study period, 92 (25%) of the 364 grafts developed a critical or intermediate stenosis. Only 11 of the 92 limbs had any recurrence of symptoms, but 26 had a reduction in ankle-brachial pressure index. No statistically significant difference was observed in graft patency ($p=0.19$) or amputation rates ($p=0.62$) between grafts with repaired stenosis and grafts without stenosis. Untreated grafts with critical or intermediate stenosis had significantly lower patency ($p<0.001$) and higher amputation rates ($p<0.001$). The authors concluded that the flow abnormalities detected at 6 weeks after operation can predict the natural history of a vein graft, and such abnormalities can be used to select grafts for continued duplex surveillance.

In a similar study, Ferris et al. [40] detected graft flow abnormalities in 26% of the 224 infrainguinal vein bypasses of which 52% necessitated revision. They concluded that early duplex scan surveillance singularly detects a clinically significant subgroup of grafts that need revision.

In a recent study by Tinder et al. with the University of South Florida group [41], they identified several characteristics predictive for development of graft stenosis and subsequent secondary intervention. Out of 353 clinically successful infrainguinal vein bypasses performed in 329 patients, 126 bypasses (36%) had 174 secondary interventions based on surveillance duplex testing resulting in a 3-year Kaplan-Meier primary (46%), assisted-primary (80%), and secondary (81%) patency rates. Characteristics predictive of duplex-detected stenosis leading to intervention were "abnormal" initial duplex testing indicating moderate (PSV: 180–300 cm/s, Vr: 2–3.5) stenosis ($p<0.0001$), nonsingle segment saphenous vein conduit ($p<0.01$), warfarin drug therapy ($p<0.01$), and redo bypass grafting ($p<0.001$). Procedure indication, postoperative ABI level, statin drug therapy, and vein conduit orientation were not predictive of graft revision. The natural history of bypasses with abnormal first duplex scan differed from "normal" grafts by more frequent and earlier graft revision for severe stenosis and a lower 3-year assisted-primary patency.

### Conclusion

Routine duplex ultrasound surveillance of lower limb vein and prosthetic bypass grafts is recommended. Optimum results are obtained when duplex surveillance is initiated in the operating room or prior to discharge. Since the majority of graft abnormalities identified occur in asymptomatic patients, criteria for intervention should be based on duplex-measured velocity spectra. High-grade lesions that produce low graft flow have the greatest potential to produce graft thrombosis and should be repaired promptly. Duplex findings can also be used to select either percutaneous balloon angioplasty or open surgical repair. The likelihood of graft revision varies with the vein bypass type and is increased when a graft defect is identified on a "predischarge" or early (<6 week) duplex scan. With time, the incidence of vein graft stenosis decreases; however, secondary to atherosclerotic disease progression in native arteries and aneurysm formation in the vein conduit, lifelong surveillance (yearly after 3 years) is recommended.

## References

1. Bandyk DF, Schmitt DD, Seabrook GR, et al. Monitoring functional patency of in situ saphenous vein bypasses: the impact of a surveillance protocol and elective revision. J Vasc Surg. 1989;11:280–94.

2. Moody AP, Gould DA, Harris PL. Vein graft surveillance improves patency in femoropopliteal bypass. Eur J Vasc Surg. 1990;4:117–20.
3. Bandyk DF, Mills JL, Gahtan V, et al. Intraoperative duplex scanning of arterial reconstructions: fate of repaired and unrepaired defects. J Vasc Surg. 1994;20:426–33.
4. Bandyk DF, Johnson BL, Gupta AK, Esses GE. Nature and management of duplex abnormalities encountered during infrainguinal vein bypass grafting. J Vasc Surg. 1996;24:430–6.
5. Taylor PR, Wolfe HN, Yyrrell MR, et al. Graft stenosis: justification for 1-year surveillance. Br J Surg. 1990;77:1125–8.
6. Mills JL, Harris EJ, Taylor LM, et al. The importance of routine surveillance of distal bypass grafts with duplex scanning: a study of 379 reversed vein grafts. J Vasc Surg. 1990;12:379–89.
7. Lundell A, Linblad B, Bergqvist D, Hansen F. Femoropopliteal graft patency is improved by an intensive surveillance program: a prospective randomized study. J Vasc Surg. 1995;21:26–34.
8. Lawlike NJ, Hanel KC, Hunt J, et al. Duplex scan surveillance of infrainguinal prosthetic bypass grafts. J Vasc Surg. 1994;20:637–41.
9. Calligaro KD, Musser DJ, Chen AY, et al. Duplex ultrasonography to diagnose failing arterial prosthetic grafts. Surgery. 1996;120: 455–9.
10. Gupta AK, Bandyk DF, Cheanvechai D, Johnson BL. Natural history of infrainguinal vein graft stenosis relative to bypass grafting technique. J Vasc Surg. 1997;25:211–25.
11. Mills JL, Bandyk DF, Gahtan V, Esses GE. The origin of infrainguinal vein graft stenosis: a prospective study based on duplex surveillance. J Vasc Surg. 1995;21:16–25.
12. Giannoukas AD, Adrouulakis AE, Labropoulos N, Wolfe JHN. The role of surveillance after infrainguinal bypass grafting. Eur J Vasc Endovasc Surg. 1996;11:279–89.
13. Idu MM, Blankenstein JD, de Gier P, Truyen E, Buth J. Impact of a color-flow duplex surveillance program on infrainguinal vein graft patency: a five-year experience. J Vasc Surg. 1993;17:42–53.
14. Bandyk DF, Bergamini TM, Towne JB, et al. Durability of vein graft revision: the outcome of secondary procedures. J Vasc Surg. 1991;13:200–10.
15. Donaldson MC, Mannick JA, Whittemore AD. Causes of primary graft failure after in situ saphenous vein bypass grafting. J Vasc Surg. 1991;13:137–49.
16. Bergamini TM, Towne JB, Bandyk DF, et al. Experience with in situ saphenous vein bypass during 1981 to 1989: determinant factors of long-term patency. J Vasc Surg. 1991;13:97–106.
17. Johnson BL, Bandyk DF, Back MR, Avino AJ, Roth SM. Intraoperative duplex monitoring of infrainguinal vein bypass procedures. J Vasc Surg. 2000;31:678–90.
18. Armstrong PA, Bandyk DF, Wilson JS, Shames ML, Johnson BL, Back MR. Optimizing infrainguinal arm vein bypass patency with duplex ultrasound surveillance and endovascular therapy. J Vasc Surg. 2004;40:724–31.
19. Bandyk DF, Kaebnick HW, Bergamini TM, et al. Hemodynamics of in situ saphenous vein arterial bypass. Arch Surg. 1988;123: 477–82.
20. Bandyk DF, Seabrook GR, Moldenhaurer P, et al. Hemodynamics of vein graft stenosis. J Vasc Surg. 1988;8:688–95.
21. Belkin M, Mackey WC, Maclaughlin R, et al. The variation in vein graft flow velocity with luminal diameter and outflow level. J Vasc Surg. 1992;15:991–9.
22. Mills JL, Fujitani RM, Taylor SM. The contribution of routine intraoperative completion arteriography to early graft patency. Am J Surg. 1992;164:506–11.
23. Miller Maracaccio EJ, Tannerbaum GE, et al. Comparison of angioscopy and angiography for monitoring infrainguinal bypass grafts: result of a prospective randomized trial. J Vasc Surg. 1993;17:382–98.
24. Rzucidlo EM, Walsh DB, Powell RJ, Zwolak RM, Fillinger MF, Schermerhorn ML, Cronenwett JL. Prediction of early graft failure with intraoperative completion duplex ultrasound scan. J Vasc Surg. 2002;36:975–81.
25. Giswold ME, Landry GJ, Sexton GJ, Yeager RA, Edwards JM, Taylor LM, Moneta GL. Modifiable patient factors associated with reverse vein graft occlusion in the era of duplex scan surveillance. J Vasc Surg. 2003;37:47–53.
26. Gahtan V, Payne LP, Roper LD, et al. Duplex criteria for predicting progression of vein graft lesions. J Vasc Tech. 1995;19:211–5.
27. Westerband A, Mills JL, Kistler S, et al. Prospective validation of threshold criteria for intervention in infrainguinal vein grafts undergoing duplex surveillance. Ann Vasc Surg. 1997;11:44–8.
28. Caps T, Cantwell-Gab K, Bergelin RO, Strandness DE. Vein graft lesions: time of onset and rate of progression. J Vasc Surg. 1995;22:466–75.
29. Mills JL, Wixon CL, James DC, Devine J, Westerband A, Hughes JU. The natural history of intermediate and critical vein graft stenosis: recommendations for continued surveillance or repair. J Vasc Surg. 2001;33:273–80.
30. Sladen JG, Reid JDS, Cooperberg PL, et al. Color flow duplex screening of infrainguinal grafts combining low and high-velocity criteria. Am J Surg. 1989;158:107–12.
31. Papanicolaou G, Zierler RE, Beach RW, et al. Hemodynamic parameters of failing infrainguinal bypass grafts. Am J Surg. 1995;169:238–44.
32. Buth J, Disselhoff B, Sommeling C, et al. Color flow duplex criteria for grading stenosis in infrainguinal vein grafts. J Vasc Surg. 1991;14:729–38.
33. Bell P, et al. At what PSV ratio value should grafts be revised. Eur J Vasc Endovasc Surg. 1998;15:258–61.
34. Avino AJ, Bandyk DF, Gonsalves AJ, Johnson BL, Black TJ, Zwiebel BR, Rahaim MJ, Cantor A. Surgical and endovascular intervention for infrainguinal vein graft stenosis. J Vasc Surg. 1999;29:60–71.
35. Alexander JQ, Katz SG. The efficacy of percutaneous transluminal angioplasty in the treatment of infrainguinal vein bypass graft stenosis. Arch Surg. 2003;138:510–3.
36. Kasirajan K, Schneider PA. Early outcome of “cutting” balloon angioplasty for infrainguinal vein graft stenosis. J Vasc Surg. 2004;39:702–8.
37. Erickson CA, Towne JB, Seabrook GR, et al. Ongoing vascular laboratory surveillance is essential to maximize long term in situ saphenous vein bypass patency. J Vasc Surg. 1996;23:18–27.
38. Davies AJ, Hawdon MR, Thompson SG, VGST participants. Is duplex surveillance of value after leg vein bypass grafting? Principle results of the vein graft surveillance randomized trial (VGST). Circulation. 2005;112:1985–91.
39. Mofidi R, Kelman J, Bennett S, Murie JA, Dawson ARW. Significance of the early postoperative duplex result in infrainguinal vein bypass surveillance. Eur J Vasc Endovasc Surg. 2007;34:327–32.
40. Ferris BL, Mills JL, Hughes JD, Durrani T, Knox R. Is early postoperative duplex scan surveillance of leg bypass grafts clinically important? J Vasc Surg. 2003;37:495–500.
41. Tinder CN, Chavanpun JP, Bandyk DF, Armstrong PA, Back MR, Johnson BL, Shames ML. Efficacy of duplex ultrasound surveillance after infrainguinal vein bypass may be enhanced by identification of characteristics predictive of graft stenosis development. J Vasc Surg. 2008;48:613–8.

# Rationale and Benefits of Surveillance After Prosthetic Infrainguinal Bypass Grafts

25

Keith D. Calligaro, Sandra C. McAffe-Benett, Kevin J. Doerr, Kathryn Mueller, Stephen Kolakowski, and Matthew J. Dougherty

**Abstract**

Infrainguinal revascularization with autogenous conduit remains the gold standard of care for the treatment of critical lower extremity ischemia when bypass is required. One of the major factors diminishing long-term patency of these grafts is the development of stenosis of the graft or inflow and outflow arteries. It is critical to identify these lesions while grafts are patent, as treatment with minor procedures will maintain patency, while treatment after thrombosis is significantly more morbid and less successful. There is widespread evidence to support postoperative duplex ultrasound (DU) surveillance of infrainguinal vein grafts, but there has been surprisingly little investigation for DU surveillance of prosthetic bypass grafts, other than our group.

Clearly intervening for a failing graft is more beneficial than for failed grafts. In several studies, patency rates of failing grafts are significantly better than patency rates of grafts revised after thrombosis. Prior to the routine use of DU, clinical parameters, such as return of ischemic symptoms, and reduction in ankle-brachial indices and pulse volume recordings were used to detect failing grafts.

These modalities lack sufficient sensitivity to detect some stenoses and some become abnormal only after graft occlusion. In our noninvasive laboratory, velocities are measured every 10 cm along the graft, along with measurements at both anastomosis, and proximal and distal to the anatomy. It appears that the benefit of DU surveillance is most apparent in the highest risk autogenous grafts. However, the surveillance of infrainguinal prosthetic grafts has received mixed reviews.

Prosthetic grafts are much more sensitive to low-flow states and resulting thrombosis than autologous vein grafts. When reviewing DU surveillance data on 89 infrainguinal prosthetic bypass grafts at our institution, we found that the sensitivity of abnormal DU findings that correctly diagnosed a failing graft was 88% for femorotibial bypasses but only 57% for femoropopliteal bypasses. The positive predictive value (correct abnormal studies/total abnormal studies) was 95% for femorotibial grafts and 65% for femoropopliteal grafts. Therefore, we concluded that DU surveillance is indicated and worthwhile for prosthetic

K.D. Calligaro, M.D. (✉) • S. Kolakowski, M.D. • M.J. Dougherty, M.D.
Section of Vascular Surgery,
Pennsylvania Hospital,
700 Spruce St., Suite 101,
Philadelphia, PA 19106, USA
e-mail: kcalligaro@aol.com

S.C. McAffe-Benett, BS, RVT • K.J. Doerr, BS, RVT
K. Mueller, BS, RVT
Department of Vascular Surgery, Pennsylvania Hospital,
Philadelphia, PA, USA

A.F. AbuRahma, D.F. Bandyk (eds.), *Noninvasive Vascular Diagnosis*,
DOI 10.1007/978-1-4471-4005-4_25, 

femorotibial grafts, while its utility for prosthetic femoropopliteal grafts remains unproven. Criteria that we use to identify failing arterial bypass grafts at Pennsylvania Hospital include monophasic signal throughout the graft, uniform peak systolic velocities <45 cm/s, any focal peak systolic velocity >300 cm/s, and peak systolic velocity ratio between two adjacent segments >3.5.

Duplex ultrasonography is the method of choice for the surveillance of infrainguinal bypass grafts. Every noninvasive vascular laboratory should continuously correlate its interpretations with arteriographic findings and clinical outcomes. We believe this strategy is useful for prosthetic grafts also.

**Keywords**
Failing graft • Duplex ultrasound • Prosthetic arterial bypass

## Introduction

Infrainguinal revascularization with autogenous conduit remains the gold standard of care for the treatment of critical lower extremity ischemia when bypass is required. One of the major factors diminishing long-term patency of these grafts is the development of stenosis of the graft or inflow and outflow arteries. Twenty to forty percent of all infrainguinal bypass grafts will develop stenosis due to different factors [1]. It is critical to identify these lesions while grafts are patent, as treatment with minor procedures will maintain patency, and while treatment after thrombosis is significantly more morbid and less successful. Clinical examination looking for signs and symptoms of limb ischemia, including pulse evaluation and measurement of ankle systolic pressure, can usually identify only the very high-grade stenoses or occlusions. There is widespread evidence to support postoperative duplex ultrasound (DU) surveillance of infrainguinal vein grafts [2]. There has been surprisingly little investigation for DU surveillance of prosthetic bypass grafts, other than our group [3].

## Natural History

Primary patency of a graft is defined as uninterrupted patency without need for further procedures to maintain patency. Any surgical or percutaneous procedure performed on a patent graft, its anastomosis, or inflow and outflow vessels serves as an endpoint to primary patency but maintains "assisted primary patency." When a graft thromboses, "secondary" patency can be achieved by restoring patency to the graft [4]. As noted, the outcome of procedures performed to prevent graft thrombosis is better than that of procedures to restore patency of an occluded graft [5].

In a large prospective randomized multicenter study, Veith and coworkers compared patency rates of infrainguinal bypasses using autologous vein grafts with those of prosthetic [polytetrafluoroethylene (PTFE)] grafts [6]. For infrainguinal bypasses to the above-knee popliteal artery, primary patency at 48 months was 76% for vein grafts and 54% for PTFE grafts, a difference that was not statistically different. For bypasses to the infrapopliteal arteries, primary patency rates at 48 months were 49% for vein grafts and 12% for PTFE grafts, respectively. This study performed prior to routine duplex surveillance gives a picture of the natural history of these revascularization efforts since graft failure was recorded when graft thrombosis occurred or when any secondary intervention became necessary to treat graft thrombosis.

Prospective observational studies with the use of DU have demonstrated that 20–30% of infrainguinal vein bypasses develop discrete stenoses during the first postoperative year [7]. These lesions are usually the result of myointimal hyperplasia. If these lesions are not corrected, they have been associated with 80% of all graft failures within 3–5 years of the original procedure.

The natural history of bypass grafts with documented DU abnormalities when left untreated is unclear. Approximately 100 total grafts with varying DU abnormalities in one series were followed without revision [8]. Idu and coworkers reported high occlusion rates in a small group of bypass grafts both autogenous and prosthetic with 50% diameter-reducing stenoses on arteriography if left unrevised. In a subsequent prospective randomized study, superior patency rates were found in grafts that were revised based on DU abnormalities [8, 9]. However, only 18 grafts were treated in this series. Mattos and coworkers followed 38 grafts with DU abnormalities and found similarly inferior patency rates in failing grafts that were left unrevised when compared with failing grafts that were revised [10]. We followed 46 failing arterial bypass grafts over a median of 10 months that were not treated for a variety of reasons (difficult anatomy, patient reluctance, etc.) [11]. Only five (10.9%) showed progression of abnormal findings. Only 3 of the 46 failing grafts (6.5%) occluded during the follow-up period.

Clearly intervening for a failing graft is more beneficial than for failed grafts. In a retrospective series of 213 patients from the Mayo Clinic who underwent graft revision of pedal bypasses, 2-year patency rates in failing vs. failed grafts were reported to be 58% and 36%, respectively [12]. These data are supported by Wixon and coworkers who demonstrated that revision of a duplex-identified stenosis was significantly less costly over a 1-year period than revision after graft thrombosis ($17,688 vs. $45,252, respectively) [13].

## Duplex Ultrasonography

Prior to the routine use of DU, clinical parameters, such as return of ischemic symptoms, and reduction in ankle-brachial indices and pulse volume recordings were used to detect failing grafts. These modalities lack sufficient sensitivity to detect some stenoses and some become abnormal only after graft occlusion. Two European studies relying on clinical symptoms to diagnose greater than 50% reduction in graft diameter missed 62–89% of duplex-defined lesions [14, 15]. Even by adding the measurement of ankle-brachial indices, only 46% of grafts with greater than 50% stenoses were diagnosed [16]. In contrast, duplex ultrasonography detected 100% of grafts with the same diameter reduction [15]. Contrary to prior thought, the value of ankle-brachial index appears to be limited in predicting graft failure [16, 17].

In 1985, Bandyk and coworkers published one of the earliest reports about the use of DU-derived blood flow velocity measurements to define graft stenosis that might predict graft failure [18]. The two most important predictors in this series were low peak systolic velocities (<45 cm/s) throughout the graft and the absence of diastolic forward flow, indicating high outflow resistance. The authors also noted that all grafts experienced some degree of increased outflow resistance in the early postoperative period, as evidenced by a generalized drop in peak systolic velocities during follow-up studies. These results were later confirmed by Mills and coworkers on a much larger patient cohort [19]. Once again, a peak systolic velocity of 45 cm/s throughout the graft was suggested as the threshold to predict early graft failure. If the peak systolic velocity was higher than 45 cm/s in this series, the chance for graft failure was 2.1% compared with a 12.6% graft failure rate if the peak systolic velocities were routinely less than 45 cm/s. Only 29% of failing grafts, as diagnosed by DU, showed a reduction in ankle-brachial index measurement greater than 0.15, clearly indicating the higher sensitivity of DU surveillance.

These studies were performed using DU sampling at three positions: proximal anastomosis, mid-graft, and distal anastomosis. This method may miss focal stenoses within the body of the graft or in inflow and outflow vessels. The current technique in most reliable noninvasive vascular laboratories includes sampling the graft with segmental peak systolic velocity measurements along its entire length. In our noninvasive laboratory, velocities are measured every 10 cm along the graft, along with measurements at both anastomosis, and proximal and distal to the anatomy. It appears that the benefit of DU surveillance is most apparent in the highest risk autogenous grafts.

A recent retrospective review by Armstrong and coworkers found a statistically significant benefit of DU surveillance in optimizing the patency of infrainguinal grafts constructed with an arm vein [20]. They found the combination of DU and endovascular therapy achieved an excellent assisted graft patency rate (91%) and limb salvage rate (97%) at 3 years. These statistics are impressive considering half of the bypass required a graft intervention and one-third required surgical revision.

Surveillance programs for infrainguinal vein grafts have been well supported [21]. It would follow that given that prosthetic grafts do have a higher propensity to fail, DU surveillance might be correspondingly more valuable. However, the surveillance of infrainguinal prosthetic grafts has received mixed reviews [8, 22–27]. A prospective randomized study by Lundell and coworkers demonstrated a 25% improvement in infrainguinal vein bypass patency at 3 years (78% vs. 53%) with DU surveillance, but no significant benefit was appreciated with PTFE or PTFE-vein composite graft patency [2]. However, the number of prosthetic infrapopliteal arterial grafts was very small, which may limit the statistical value of the analysis.

We and others have observed significant benefits for surveillance programs for prosthetic grafts [3, 5, 28, 29]. Many feel that prosthetic graft failure often occurs without the harbinger of a discrete stenosis developing. The nature of the lesions that can cause prosthetic graft failure is similar to that of autologous vein grafts. They tend to be located primarily at an anastomosis, in adjacent inflow or outflow arteries, or much less commonly within the body of the graft.

As has been demonstrated for vein grafts, patency rates of thrombosed prosthetic grafts undergoing revision are inferior to assisted primary patency rates for failing prosthetic grafts [5] Sullivan and coworkers demonstrated that thrombolysis for occluded vein grafts had significantly better long-term patency than for prosthetic grafts (69.3% vs. 28.6% at 30 months), which supports aggressive surveillance of prosthetic grafts [30].

## Rationale and Benefits of Surveillance After Prosthetic Infrainguinal Bypass Grafts

Prosthetic grafts are much more sensitive to low-flow states and resulting thrombosis than autologous vein grafts. When reviewing DU surveillance data on 89 infrainguinal prosthetic

bypass grafts at our institution, we found that the sensitivity of abnormal DU findings that correctly diagnosed a failing graft was 88% for femorotibial bypasses but only 57% for femoropopliteal bypasses [3]. The positive predictive value (correct abnormal studies/total abnormal studies) was 95% for femorotibial grafts and 65% for femoropopliteal grafts. Therefore, we concluded that DU surveillance is indicated and worthwhile for prosthetic femorotibial grafts, while its utility for prosthetic femoropopliteal grafts remains unproven.

Several studies have shown that DU surveillance is cost effective when compared with performing graft revisions based on clinical indications alone [13, 31]. Wixon and coworkers concluded that 1-year and 5-year costs of DU surveillance ($7,742 vs. $12,194, respectively) were markedly less than performing graft revisions based on clinical indications alone ($10,842 vs. $16,352, respectively) [13]. They also found that patent grafts revised after DU-detected stenoses had an improved 1-year patency (93% vs. 57%), were associated with fewer amputations (2% vs. 33%) and less frequent multiple graft revisions, and generated fewer expenses 1 year after revision compared to grafts revised after they occluded.

In our protocol, both vein and prosthetic bypass grafts are routinely evaluated by duplex sonography in the early postdischarge period [11]. Thereafter, the graft is followed every 3 months for the first year after bypass operation, every 6 months for the second year, and annually thereafter if no problems are found. A 4.0- to 7.5-MHz probe is utilized with color map imaging. It is essential that the examiner is aware of the origin of the graft and its course. Due to their more superficial location, in situ vein grafts are much easier to follow than anatomically tunneled grafts. The entire graft is scanned beginning at the inflow artery, crossing the proximal anastomosis, moving along the body of the graft every 10 cm, and beyond the distal anastomosis. Peak systolic and diastolic velocities are recorded at these sites. Color flow is used to identify areas of turbulence, which are also sampled. Significant focal increase in flow velocities is more precisely investigated with measurements performed proximal and distal to the focus. At the distal anastomosis, the Doppler angle must be carefully adjusted due to the relatively steep angle of the graft. If consistently low peak systolic velocities are detected throughout the graft, a more detailed examination of the inflow and outflow vessels is necessary. These findings, however, could be consistent with normal flow through a relatively large diameter graft.

## Abnormal Findings

There is no firm consensus on strict criteria for defining stenosis with duplex ultrasonography or on what degree of abnormality mandates revision [10, 32–34]. The published literature has focused on low peak systolic flow velocities (PSFV) [17, 18, 21] and focal increases in peak systolic flow velocities with reference to adjacent areas [8, 9, 28, 35–37]. A combination of these two parameters has also been recommended [38]. A consensus appears to be evolving away from low-flow velocity criteria toward use of a PSV ratio of 3–4. The criteria used at our institution to determine failing grafts are illustrated in Table 25.1.

**Table 25.1** Criteria to identify failing arterial bypass grafts at Pennsylvania Hospital

| |
|---|
| Monophasic signal throughout the graft |
| Uniform peak systolic velocities <45 cm/s |
| Any focal peak systolic velocity >300 cm/s |
| Peak systolic velocity ratio between two adjacent segments >3.5 |

## Indications for Interventions

The optimal threshold of intervention for arterial bypass grafts is still controversial. Most authorities would agree that impending failure of a graft is suggested by the following:

1. Lack of diastolic forward flow throughout the graft as evidenced by monophasic Doppler signals
2. Decreased peak systolic velocities less than 45 cm/s throughout the graft
3. Focal elevations of peak systolic velocities greater than 250–350 cm/s
4. Elevated peak systolic velocity ratios between two adjacent segments, suggested by abnormal elevated ratios, range between 3.5 and 4.0 [8, 10, 39–44]

Gupta and coworkers recommended peak systolic velocity ratios greater than 3.4 and focal peak systolic velocities greater than 300 cm/s [42]. Similar values were also suggested by Mills et al. [19].

Bandyk created a graft surveillance risk stratification model to predict graft thrombosis as illustrated in Table 25.2 [31]. Patients with Category I lesions were hospitalized, anticoagulated, and promptly treated. Patients with Category II lesions were repaired electively within 2 weeks. Category III lesions were closely observed with serial duplex examinations and repaired if the lesions progressed in severity. Category IV lesions at the lowest risk were safely observed. Westerband and coworkers were able to support these criteria with a prospective study and demonstrate all grafts at risk for thrombosis [43].

An interesting finding in Bandyk's series was that of lesion regression when a Category III (intermediate graft stenosis, PSV 150–300 cm/s, Vr < 3.5) lesion is discovered in the first 3 months after surgery; it may regress (30–35%), remain stable, or progress to a high-grade stenosis (40–50%) [31]. Given the variable biological behavior, it is critical to perform serial duplex studies at 4- to 6-week intervals for Category III abnormalities. These lesions will usually stabilize or progress within 4–6 months [10, 42].

**Table 25.2** Risk stratification for graft thrombosis based on surveillance data

| Category | High-velocity criteria | Low-velocity criteria | Drop in ABI |
|---|---|---|---|
| I (highest risk) | PSV > 300 cm/s or Vr > 3.5 | GFV < 45 cm/s | >0.15 |
| II (high risk) | PSV > 300 cm/s or Vr > 3.5 | GFV > 45 cm/s | <0.15 |
| III (intermediate risk) | PSV< 180, >300 cm/s or Vr > 2.0 | GFV > 45 cm/s | <0.15 |
| IV (low risk) | PSV < 180 cm/s or Vr < 2.0 | GFV > 45 cm/s | <0.15 |

*PSV* duplex-derived peak systolic velocity, *Vr* velocity ratio of stenosis to more proximal graft segment of same caliber, *GFV* graft flow velocity, *ABI* Doppler-derived ankle-brachial index

As suggested by the previous study from our group, abnormal duplex findings do not always mandate further therapy [1, 45]. This is especially true if the abnormal finding is moderate PSV ratio elevation near the proximal anastomosis. We speculate that the hemodynamics at vessel bifurcations, which occurs at the typical end-to-side proximal anastomosis, is not strictly comparable to flow dynamics within the graft because of size discrepancies between the graft and native artery. Possibly, this turbulence and the resulting abnormalities in peak systolic velocity ratios at the proximal anastomosis are less predictive of graft thrombosis than the same abnormalities at other locations.

## Recommendation of Lifelong Surveillance

Clearly, duplex surveillance of infrainguinal bypass grafts is beneficial, but how long does the surveillance program need to continue? Most reviews have shown a definite benefit up to 2 years based on the fact that 70–80% of all graft abnormalities develop and require revision during this time period. Erickson and coworkers recommend that surveillance continue indefinitely for autogenous bypass grafts [46]. They reported that 18% of the initial interventions for a duplex-detected lesion occurred after the initial 24-month period. Sixty-three percent of theses defects occurred at an anastomosis. Although the incidence of vein graft stenosis developing decreases over time, atherosclerotic changes continue in native arteries. Another important finding to look for in older vein grafts is aneurysmal degeneration of the vein. Vein dilation is usually focal and can be associated with mural thrombus, which may warrant segmental graft revision. We support the concept of lifelong vein graft surveillance, which also gives the vascular surgeon the opportunity to monitor development of atherosclerosis in other vascular beds.

## Summary

Duplex ultrasonography is the method of choice for the surveillance of infrainguinal bypass grafts. Every noninvasive vascular laboratory should continuously correlate its interpretations with arteriographic findings and clinical outcomes. Any focal peak systolic velocity >300 cm/s or a peak systolic velocity ratio >3.5 between two adjacent segments is generally accepted as a strong indicator for a focal stenosis that may threaten graft patency. Low peak systolic velocities throughout the graft (<45 cm/s), as well as lack of diastolic forward flow as evidenced by loss of biphasic Doppler signals throughout the graft, may also indicate inflow or outflow problems and warrant further investigation. Arteriography and appropriate endovascular or open surgical revision of failing grafts should be judiciously implemented by the vascular surgeon to improve long-term patency and limb salvage rates.

## References

1. Ryan SV, Dougherty MJ, Chang M, Lombardi J, Raviola C, Calligaro K. Abnormal duplex findings at the proximal anastomosis of infrainguinal bypass grafts: does revision enhance patency? Ann Vasc Surg. 2001;15:98–103.
2. Lundell A, Lindblad B, Bergqvist D, Hansen F. Femoropopliteal-crural graft patency is improved by an intensive surveillance program: a prospective randomized study. J Vasc Surg. 1995;21:26–33.
3. Calligaro KD, Doerr K, McAffee-Bennett S, Krug R, Raviola CA, Dougherty MJ. Should duplex ultrasonography be performed for surveillance of femoropopliteal and femorotibial arterial prosthetic bypasses? Ann Vasc Surg. 2001;15:520–4.
4. Rutherford RB, Baker JD, Ernst C, Johnston KW, Porter JM, Ahn S, Jones DN. Recommended standards for reports 23. Rationale and benefits of surveillance after prosthetic infrainguinal bypass grafts dealing with lower extremity ischemia: revised version. J Vasc Surg. 1997;26:517.
5. Sanchez LA, Suggs WD, Veith FJ, et al. Is surveillance to detect failing polytetrafluoroethylene bypasses worthwhile? Am J Surg. 1993;18:981–90.
6. Veith FJ, Gupta SK, Ascer E, et al. Six-year prospective multicenter randomized comparison of autologous saphenous vein and expanded polytetrafluoroethylene grafts in infrainguinal arterial reconstructions. J Vasc Surg. 1986;3:104–14.
7. Mills JL, Harris EJ, Taylor LM, Beckett WC. The origin of infrainguinal vein graft stenosis: a prospective study based duplex surveillance. J Vasc Surg. 1995;21:16–25.
8. Idu MM, Blankenstein JD, de Gier P, et al. Impact of color-flow duplex surveillance program on infrainguinal vein graft patency: a five-year experience. J Vasc Surg. 1993;17:42–53.
9. Lundell A, Linblad B, Bergqvist D, et al. Femoropoplite-alcrural graft patency is improved by an intensive surveillance program: a prospective randomized study. J Vasc Surg. 1995;21:26–34.
10. Mattos MA, van Bemmelen PS, Hodgson KJ, et al. Does correction of stenoses identified with color duplex scanning improve infrainguinal graft patency? J Vasc Surg. 1993;17:54–66.

11. Dougherty MJ, Calligaro KD, Delaurentis DA. The natural history of "failing" arterial bypass grafts in a duplex surveillance protocol. Ann Vasc Surg. 1998;12:255–9.
12. Rhodes JM, Gloviczki P, Bower TC, Panneton JM, Canton LG, Toomey BJ. The benefits of secondary interventions in patients with failing or failed pedal bypass grafts. Am J Surg. 1999;178: 151–5.
13. Wixon CL, Mills JL, Westerband A, Hughes JD, Ihnat DM. An economic appraisal of lower extremity bypass graft maintenance. J Vasc Surg. 2000;32:1–12.
14. Moody P, Gould DA, Harris PL. Vein graft surveillance improves patency in femoropopliteal bypass. Eur J Vasc Surg. 1990;4: 117–21.
15. Disselhoff B, Bluth J, Jakimowicz J. Early detection of stenosis of femoral-distal grafts: a surveillance study using color-duplex scanning. Eur J Vasc Surg. 1989;3:43–8.
16. Barnes RW, Thompson BW, MacDonald CM, et al. Serial noninvasive studies do not herald postoperative failure of femoropopliteal or femorotibial bypass grafts. Ann Surg. 1989;210:486–92.
17. Berkowitz J, Hobbs C, Roberts B, et al. Value of routine vascular laboratory studies to identify vein graft stenoses. Surgery. 1981; 90:971–9.
18. Bandyk DF, Cato RF, Towne JB. A low flow velocity predicts failure of femoropopliteal and femorotibial bypass grafts. Surgery. 1985;98:799–809.
19. Mills JL, Harris EJ, Taylor Jr LM, et al. The importance of routine surveillance of distal bypass grafts with duplex scanning: a study of 379 reversed vein grafts. J Vasc Surg. 1990;12:379–86; discussion 387–389.
20. Armstrong PA, Bandyk DF, Wilson JS, Shames ML, Johnson BL, Back MR. Optimizing infrainguinal arm vein bypass patency with duplex ultrasound surveillance and endovascular therapy. J Vasc Surg. 2004;40:724–30; discussion 730–1.
21. Bandyk DF, Schmitt DD, Seabrook GR, et al. Monitoring functional patency of in situ saphenous vein bypasses: the impact of a surveillance protocol and elective revision. J Vasc Surg. 1989;9: 284–96.
22. Strandness DE, Andros G, Bake D, et al. Vascular laboratory utilization and payment report of the Ad Hoc Committee of the Western Vascular Society. J Vasc Surg. 1992;16:163–8.
23. Lalak NJ, Hanel KC, Junt J, et al. Duplex scan surveillance of infrainguinal prosthetic bypass grafts. J Vasc Surg. 1994;20: 637–41.
24. Baker JD. The vascular laboratory: regulations and other challenges. J Vasc Surg. 1994;19:901–4.
25. TASC Working Group. Management of peripheral arterial disease. J Vasc Surg. 2000;31:S1–296.
26. Hobollah JJ, Nassal MM, Ryan SM, et al. Is color duplex surveillance of infrainguinal polytetrafluoroethylene grafts worthwhile? Am J Surg. 1997;174:131–5.
27. Fasih T, Rudol G, Ashour H, Mudawi A, Bhattacharya V. Surveillance versus nonsurveillance for femoro-popliteal bypass grafts. Angiology. 2004;55(3):251–6.
28. Calligaro KD, Musser DJ, Chen AY, et al. Duplex ultrasonography to diagnose arterial prosthetic grafts. Surgery. 1996;120:455–9.
29. Sanchez LA, Gupta SK, Veith FJ, et al. A ten-year experience with one hundred fifty failing or threatened vein polytetrafluoroethylene arterial bypass grafts. J Vasc Surg. 1991;14:729–38.
30. Sullivan KL, Gardiner Jr GA, Kandarpa K, Bonn J, Shapiro MJ, Carabasi RA, Smullens S, Levin DC. Efficacy of thrombolysis in infrainguinal bypass grafts. Circulation. 1991;83(2 Suppl):I99–105.
31. Bandyk DF. Infrainguinal vein bypass graft surveillance: how to do it, when to intervene, and is it cost-effective? J Am Coll Surg. 2002;194(1 Suppl):S40–52.
32. Nyamekye I, Sommerville K, Raphael M, Adiseshiah M, Bishop C. Non-invasive assessment of arterial stenoses in angioplasty surveillance: a comparison with angiography. Eur J Vasc Endovasc Surg. 1996;12:471–81.
33. Buth J, Disselhoff B, Sommeling C, et al. Color-flow duplex criteria for grading stenosis in infrainguinal vein grafts. J Vasc Surg. 1991;14:716–28.
34. Grigg MJ, Nicolaides AN, Wolfe JHN. Detection and grading of femorodistal vein graft stenoses: duplex velocity measurements compared with angiography. J Vasc Surg. 1988;8:661–6.
35. Bergamini TM, George SM, Massey HT, et al. Intensive surveillance of femoropopliteal-tibial autogenous vein bypasses improves long-term graft patency and limb salvage. Ann Surg. 1995;221: 507–16.
36. Gahtan V, Payne LP, Roper LD, et al. Duplex criteria for predicting progression of vein graft lesions: which stenoses can be followed? J Vasc Tech. 1995;19:211–5.
37. Belkin M, Schwartz LB, Donaldson MC, et al. Hemodynamic impact of vein graft stenoses and their prediction in the vascular laboratory. J Vasc Surg. 1997;25:1016–22.
38. Sladen JG, Reid JDS, Cooperberg PL, et al. Color-flow duplex screening of infrainguinal grafts combining low and high velocity criteria. Am J Surg. 1989;158:107–12.
39. Bandyk DF, Johnson BL, Gupta AK, et al. Nature and management of duplex abnormalities encountered during infrainguinal vein bypass grafting. J Vasc Surg. 1996;24:430–8.
40. Caps MT, Cantwell-Gab K, Bergelin RO, et al. Vein graft lesions: time of onset and rate of progression. J Vasc Surg. 1995;22:466–74.
41. Chalmers RT, Hoballah JJ, Kresowik TF, et al. The impact of color duplex surveillance on the outcome of lower limb bypass with segments of arm veins. J Vasc Surg. 1994;19:279–86.
42. Gupta AK, Bandyk DF, Cheanvechai D, et al. Natural history of infrainguinal vein graft stenosis relative to bypass grafting technique. J Vasc Surg. 1997;25:211–20.
43. Westerband A, Mills JL, Kistler S, et al. Prospective validation of threshold criteria for intervention in infrainguinal vein grafts undergoing duplex surveillance. Ann Vasc Surg. 1997;11:44–8.
44. Idu MM, Buth J, Hop WC, et al. Vein graft surveillance: is graft revision without angiography justified and what criteria should be used? J Vasc Surg. 1998;27:399–411.
45. Dougherty MJ, Calligaro KD, DeLaurentis DA. Revision of failing lower extremity bypass grafts. Am J Surg. 1998;178:126–30.
46. Erickson CA, Towne JB, Seabrook GR, Freischlag JA, Cambria RA. Ongoing vascular laboratory surveillance is essential to maximize long-term in situ saphenous vein bypass patency. J Vasc Surg. 1996;23:18–26.

# Rationale and Benefits of Surveillance After Percutaneous Transluminal Angioplasty and Stenting of Iliac and Femoral Arteries

26

Donald T. Baril and Luke K. Marone

**Abstract**

Surveillance following lower extremity bypass, carotid endarterectomy, and endovascular aortic aneurysm repair has become the standard of care. Conversely, surveillance following lower extremity endovascular interventions is performed somewhat sporadically, in part because the duplex criteria for recurrent stenoses have been ill-defined. Duplex surveillance provides objective, hemodynamic, and anatomic data both pre and post intervention. It appears that duplex surveillance after peripheral endovascular interventions, as with conventional bypass, is beneficial in identifying recurrent lesions which when accompanied by reintervention may preclude failure and occlusion. Although not yet well-studied, it appears that applying routine surveillance following lower extremity endovascular interventions may assist in preventing failure of endovascular interventions.

**Keywords**

Endovascular • Angioplasty • Stenting • Iliac • Femoral • Duplex • Surveillance

## Introduction

Duplex surveillance following infrainguinal autogenous vein bypass has become a mainstay of therapy in the postoperative care of patients with peripheral arterial disease (PAD). Although there has been some debate regarding the utility of rigorous surveillance programs, most favor this approach as it has been demonstrated to assist in avoiding graft failure [1–4]. Conventional surgical revascularization remains a key component of the treatment of patients with PAD; however, there has been a shift over the past decade toward the utilization of endovascular techniques for the treatment of PAD. In particular, the current Trans-Atlantic Inter-Society Consensus Document on Management of Peripheral Arterial Disease (TASC II) recommendations are angioplasty and/or stenting as first-line therapy in the treatment of the majority of aortoiliac and femoropopliteal occlusive lesions [5]. Furthermore, numerous reports have been published regarding the clinical success of endovascular therapies in the treatment of aortoiliac and superficial femoral artery (SFA) lesions [6–15]. Despite these results, failure following endovascular interventions is not uncommon and is most frequently related to the development of progressive disease in the aortoiliac segment and in-stent stenosis in the femoropopliteal segment. This latter failure in the SFA may occur in up to 40% of patients at 1 year [12, 13, 16]. Given this unfortunately common failure mode and the increasing utilization of these techniques, the role of noninvasive testing modalities designed to assist in the maintenance of patency of such interventions appears to be growing. However, unlike conventional lower extremity bypass for which there are well-established reporting standards, presently, the standards for surveillance following endovascular lower extremity interventions are less well-defined.

D.T. Baril, M.D. (✉)
Division of Vascular and Endovascular Surgery,
Department of Surgery, University of Massachusetts Medical School,
55 Lake Avenue North, Worcester, MA 01655, USA
e-mail: Donald.Baril@umassmemorial.org

L.K. Marone, M.D.
Division of Vascular Surgery, Department of Surgery,
University of Pittsburgh Medical Center,
Pittsburgh, PA, USA

A.F. AbuRahma, D.F. Bandyk (eds.), *Noninvasive Vascular Diagnosis,*
DOI 10.1007/978-1-4471-4005-4_26, 

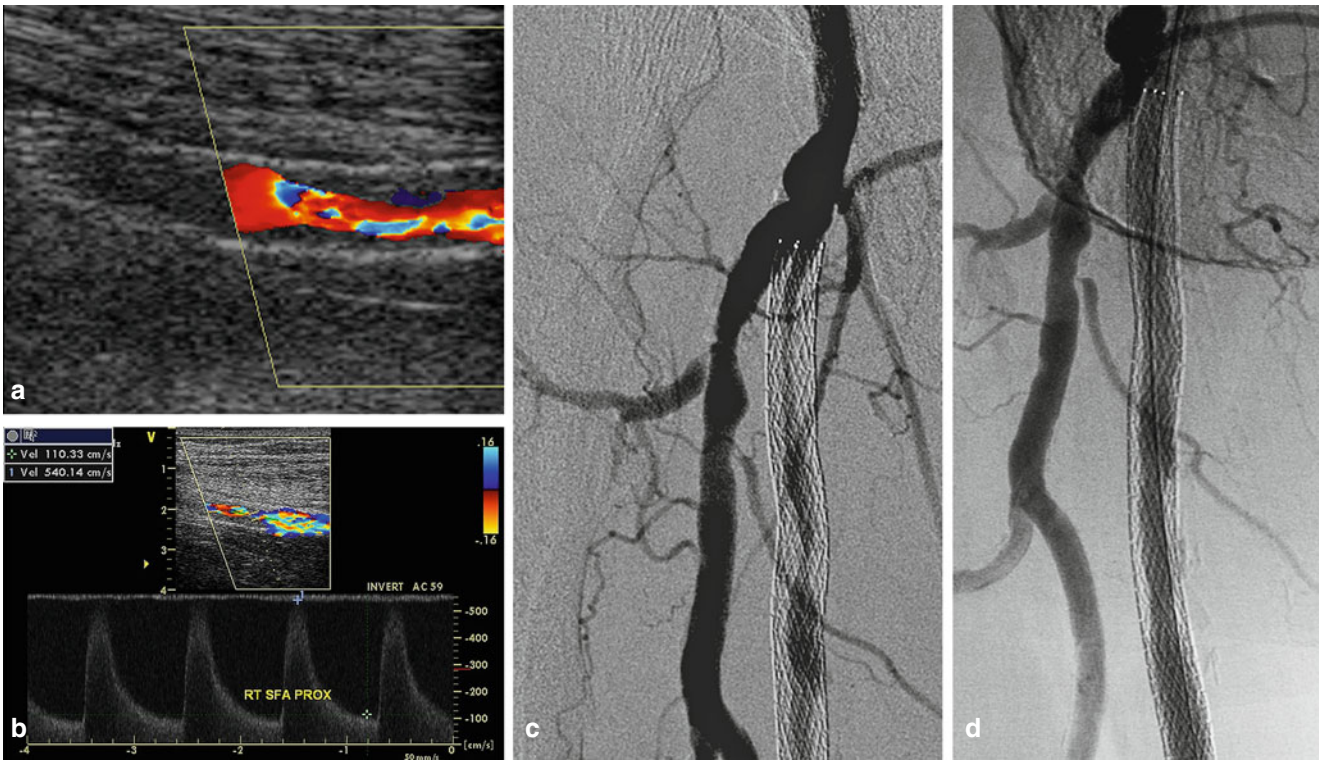


**Fig. 26.1** (**a**) Duplex ultrasound demonstrating moderate stenosis with an elevated peak systolic velocity of 200 cm/s in midportion of SFA stent. (**b**) Duplex ultrasound demonstrating high-grade stenosis with an elevated peak systolic velocity of 540 cm/s in proximal portion of SFA stent. (**c**) Angiogram demonstrating high-grade stenosis in proximal SFA stent. (**d**) Angiogram following atherectomy and re-angioplasty with resolution of in-stent stenosis

## Rationale

The goals of a surveillance program following any form of arterial intervention should help to improve long-term patency, detect impending occlusion, minimize the number and extent of secondary interventions, and hopefully, minimize cost of care. Additionally, the instruments for surveillance should be accurate, accessible, noninvasive, and cost-effective. Presently, there are no standards by which lower extremity endovascular interventions are followed post-procedure. As with surgical bypass, these interventions are unfortunately at risk of failure, the primary mode of which is in-stent stenosis secondary to neointimal hyperplasia. Unfortunately, determinants of endovascular intervention failure are numerous. It appears that different vascular beds suffer from different rates of restenosis following angioplasty and stenting. Furthermore, restenosis rates are typically higher for successfully recanalized occluded arterial segments when compared to simple stenotic lesions. Additional factors which may contribute to restenosis and failure include the clinical indication (critical limb ischemia vs. claudication), lesion length, anatomic lesion location, the presence of concomitant inflow and outflow disease, calcification, and various patient comorbidities.

The timing of failures following endovascular interventions, as with conventional bypass, is quite variable and may occur at any time following intervention, which necessitates the need for long-term surveillance. These patterns of failure tend to mimic the failures after surgical intervention. Early failures (<30 days) are typically technical in origin. Such failures are most commonly related to residual stenoses or iatrogenic dissections. Midterm failures (30 days to 2 years) result from the development of intimal hyperplasia and late failures (>2 years) are due to the progression of atherosclerotic disease.

Although physical exam and symptomatology will help diagnose patients with failed lower extremity endovascular interventions, they have limited value in the prediction of patients who are developing significant restenotic lesions. In our experience, the majority of these patients have mild or no symptoms prior to progressing to high-grade lesions or total occlusion. While ABI measurements certainly add significant information to the clinical picture, the correlation of ABI with angiographic stenosis is not strong and our data suggest that a significant decrease in ABI (>0.15) may not be present until a >60% stenosis exists [17]. Additionally, ABIs are affected by proximal and distal disease and are less useful to localize disease or determine if a failing intervention is the

source of a decrease in ABI. Furthermore, accurate ABIs may be unobtainable in patients with heavily calcified vessels, particularly diabetic patients and those with end-stage renal disease.

Duplex surveillance after endovascular intervention provides much more valuable anatomic and hemodynamic data which enables recognition of restenoses or progression of proximal and/or distal disease in a noninvasive manner (Fig. 26.1).

Failure of lower extremity endovascular interventions presents in a similar fashion to failed surgical bypasses. Claudicants will return to their pre-procedure walking tolerance, while patients with critical limb ischemia (CLI) and rest pain will likely return to rest pain. Certainly, claudicants may complain of decreasing walking tolerance as they develop significant stenoses prior to occlusion, but this is not always the case. However, duplex surveillance will allow for detection of patients progressing to failure and capture them prior to complete occlusion. Furthermore, the restoration of secondary patency (after occlusion of a previously stented SFA) is associated with a lower rate of technical success, and patients are at an increased risk for distal embolization when mechanical thrombectomy techniques are utilized [18, 19]. Conversely, endovascular treatment of patients with in-stent stenosis or new stenotic lesions proximal or distal to a previously treated lesion is relatively low-risk with a high rate of technical success. By combining PSV and velocity ratio data, criteria that are very specific and predictive for both 50% and 80% in-stent stenoses within the superficial femoral artery have been developed. Additionally, the set point which discriminates between these degrees of stenosis is very distinct. Thus, by applying these criteria at appropriate follow-up intervals, in-stent restenosis should be recognized prior to occlusion for the majority of patients.

Unfortunately, the natural history of in-stent restenosis lesions are not clearly defined in either the aortoiliac or femoropopliteal segments. Although it seems appropriate to offer patients secondary or tertiary endovascular procedures to avoid recurrent lifestyle-limiting claudication or severe rest pain, there are other scenarios which are less clear. For patients with CLI and tissue loss, who have had a successful intervention and appropriately healed a wound, is it necessary to reintervene to treat a >80% in-stent stenosis? The answer is unclear. As has been described in the surgical literature [20], additional studies will have to be performed to determine patient and pre-intervention lesion characteristics along with procedural characteristics that may help the efficacy of duplex surveillance in predicting failure of endovascular therapies in the lower extremities. Additionally, the duplex characteristics of these stented lesions will need to be studied further to determine if there are factors predictive of failure which can be evaluated on surveillance imaging.

## Outcome Measures

As with other arterial beds which are followed using duplex surveillance, the utility of protocols to follow lower extremity endovascular interventions is dependent on standardized definitions and criteria. Unlike surgical bypass, whereby the diseased vessel is excluded from the circulation, with endovascular interventions, the diseased vessel remains the primary channel through which blood flows. Therefore, the definition of initial technical success of endovascular interventions varies from conventional surgical technical success and is reported as a residual luminal stenosis less than 30% compared to normal artery proximally by angiography or other imaging [21]. Furthermore, anatomic failure is reported as a restenosis of 50% or greater compared to normal diameter.

In addition to initial technical success, patency over time is also standardized in its definition. Primary patency is defined as uninterrupted patency of the treated vessel without any endovascular to open procedures to maintain or restore patency. Assisted primary patency is uninterrupted patency of the treated vessel with a secondary intervention (e.g., secondary angioplasty). Endovascular interventions performed proximally and distally to the initially treated lesion are included in these secondary interventions. Secondary patency is defined as patency of a vessel after an intervention was undertaken to restore patency following occlusion of a vessel. As alluded to previously, assisted primary patency and secondary patency rates are higher than primary patency rates following endovascular interventions [6–15], and one primary aim of surveillance is to optimize these higher rates with early recognition of failing interventions.

## Technical Considerations of Surveillance Following Endovascular Interventions

When compared to surgical bypass, endovascular interventions differ in numerous ways which are of great importance when considering a surveillance protocol. Additionally, within the realm of lower extremity endovascular interventions, there are a plethora of different techniques and technologies which are used to restore normal arterial flow, all of which may lead to subtle differences that need to be taken into account in duplex surveillance.

Unlike surgical bypass, arterial flow is intentionally maintained through the normal anatomic course with endovascular interventions. As such, there are no proximal and distal anastomoses which need to specifically be surveyed for the development of intimal hyperplasia. However, just with surgical bypass, an important component of surveillance following endovascular interventions is assessment of the inflow and outflow vessels along with the proximal and distal segments of the treated artery itself. This may prove somewhat difficult

when compared to surgical bypass as, often, only the most diseased portion of a vessel is selected to undergo intervention while the vessel proximally and distally may demonstrate some degree of disease, albeit not deemed hemodynamically significant at the time of the initial intervention and therefore left untreated. Additionally, endovascular interventions typically involve controlled trauma to the target lesion, whether via angioplasty or some other mechanism. With angioplasty specifically, the plaque is split and the media is stretched in an effort to increase the lumen size of the vessel. Along with this, there is a risk of embolization and creation of intimal flaps. Furthermore, these plaque fractures and dissection planes may extend proximally and distally to the lesion and create an environment susceptible to intimal hyperplasia.

Given the common anatomic presentation of peripheral arterial disease and its subsequent treatment using endovascular techniques, two specific factors regarding surveillance must be considered. First, as the proximal vessel may not be disease-free, velocities through these segments may be elevated. As such, in addition to evaluating peak systolic velocities (PSV), evaluating the ratios of PSVs at the site of intervention versus the PSVs proximally along with evaluation of the waveforms is of great importance. Second, the entire vessel must be surveyed as there is potential for progression of lesions proximally and distally and not just at the site of interventions.

Although the mainstay of endovascular treatment remains angioplasty with or without stenting, endovascular techniques for the treatment of lower extremity arterial occlusive disease are continuing to evolve with newer technologies. In particular, there are a variety of different atherectomy devices, which utilize rotating blades, laser-generated heat, or ultrasonographic energy to mechanically debulk plaque and restore arterial flow through the true lumen of the vessel. Additionally, conventional angioplasty may also maintain flow through the true lumen. However, often the technique of subintimal angioplasty is used whereby a new lumen is created and plaque is pushed away from this channel. An understanding of these differences in techniques is useful for post-intervention surveillance for both the surgeon/interventionalist and the vascular technologist, as specific anatomic factors related to the procedure may lead to higher rate of restenosis (e.g., reentry point of a subintimal angioplasty) and, subsequently, specific anatomic sites may warrant careful evaluation.

## Surveillance Protocols

Our duplex surveillance protocol consists of the following: Patients are seen in follow-up at 1, 3, and 6 months after their procedure. After this initial 6-month period, patients are then evaluated at 6-month intervals indefinitely. Follow-up consists of an office visit with the treating physician and noninvasive studies including ankle-brachial indices, pulse volume recordings, and complete arterial duplex ultrasound examinations of the treated limb. If a patient undergoes a reintervention, then the protocol is reset from the time of the most recent intervention. For asymptomatic patients who are found to have mild stenoses either in the immediate post-procedure time or at some point during their follow-up, surveillance is transitioned to 3-month intervals. If these patients progress on to high-grade stenoses, as defined by our data, or become symptomatic, they will be offered reintervention. For patients who remain with stable mild asymptomatic lesions after 1 year, they are then transitioned to 6-month follow-up intervals. The importance of follow-up and the rationale behind surveillance is explained in detail to patients prior to their initial intervention and is reiterated at each visit. Certainly, noncompliance may be an issue, particularly for asymptomatic patients.

A standardized scanning protocol is used for patients who have undergone endovascular interventions. All duplex ultrasonography is performed by registered vascular technologists at laboratories approved by the Intersocietal Commission on Accreditation of Vascular Laboratories using either a LOGIQ 9 (General Electric Healthcare, Piscataway, NJ) or a LOGIQ e (General Electric Healthcare, Piscataway, NJ) system. A 7-MHz linear probe is most commonly used at an angle of insonation of 60°, or when not possible, angle correction is used. For evaluation of deeper structures in the abdomen, a low-frequency (2.5–4 MHz) or curved array transducer may be used. The entire treated vessel is examined along with one complete vessel above and one complete vessel below. The PSV is calculated at standardized points within the vessel examined in addition to areas of suspected stenosis. Furthermore, the PSV ratio is calculated at areas of stenosis from the PSV within the stenosis to the PSV within a minimum of at least 3 cm proximal to the stent in the native artery. Additionally, gray-scale imaging and visualization of the vessel and any indwelling stents is reviewed along with evaluation of spectral waveforms.

For aortoiliac interventions, color-flow Doppler imaging is obtained from the distal aorta along the iliac arteries and through the common femoral arteries, the profunda femoris arteries, and the superficial femoral arteries. Spectral velocity waveforms are measured, and waveforms and PSVs within treated segments are compared to velocities proximally in the native vessel. For femoropopliteal interventions, the common femoral artery, the femoral bifurcation, and the length of the superficial femoral artery, as well as the popliteal artery and proximal tibial vessels are imaged. As with iliac interventions, spectral waveforms and PSVs within treated femoropopliteal arterial segments are compared to those in the segments proximally.

## Surveillance Criteria of Lower Extremity Endovascular Interventions

Previously, duplex and noninvasive criteria for the diagnosis of in-stent stenosis had been generalized from data concerning the detection of de novo lesions in previously untreated femoropopliteal vessels or in the detection of vein bypass graft stenosis. However, it has been shown that stent placement

within an arterial segment results in a change in vessel compliance which may alter velocities as measured by duplex [22]. It has also been demonstrated that stent placement in the carotid circulation alters the velocity thresholds for the detection of significant recurrent internal carotid artery stenosis [23]. We have described criteria for the determination of in-stent stenosis after angioplasty and stenting of the superficial femoral artery and used these criteria for the follow-up of patients who have undergone endovascular lower extremity interventions [17]. At present time, there are no specific criteria for the determination of in-stent restenosis after iliac interventions, and, by convention, data from studies of untreated vessels and native stenoses have been applied.

To determine criteria of in-stent stenosis after angioplasty and stenting of the superficial femoral arteries, we reviewed all endovascular interventions for femoropopliteal occlusive disease between May 2003 and May 2008, during which time 330 limbs underwent femoropopliteal angioplasty and stenting. Data pairs of duplex and angiographically measured stenoses within 30 days of each other were analyzed. Angiograms were obtained in anteroposterior and oblique views at the time of initial and secondary or tertiary imaging. The view demonstrating the greatest degree of stenosis was used to determine the percentage of in-stent stenosis.

Linear regression analyses were performed, and receiver operator characteristic (ROC) curves were used to compare angiographic stenosis with PSV and stented SFA velocity/proximal SFA velocity ratio to determine optimal criteria equating to ≥50% and ≥80% stenosis. A linear regression model of PSV versus degree of angiographic stenosis showed a strong adjusted correlation coefficient ($R^2 = 0.60, p < 0.001$). Additionally, there was a strong adjusted correlation coefficient ($R^2 = 0.55$, $p < 0.001$) for velocity ratio versus degree of angiographic stenosis, but only a moderate adjusted correlation coefficient ($R^2 = 0.31$, $p = 0.02$) for decrease in ABI versus degree of angiographic stenosis (Fig. 26.2).

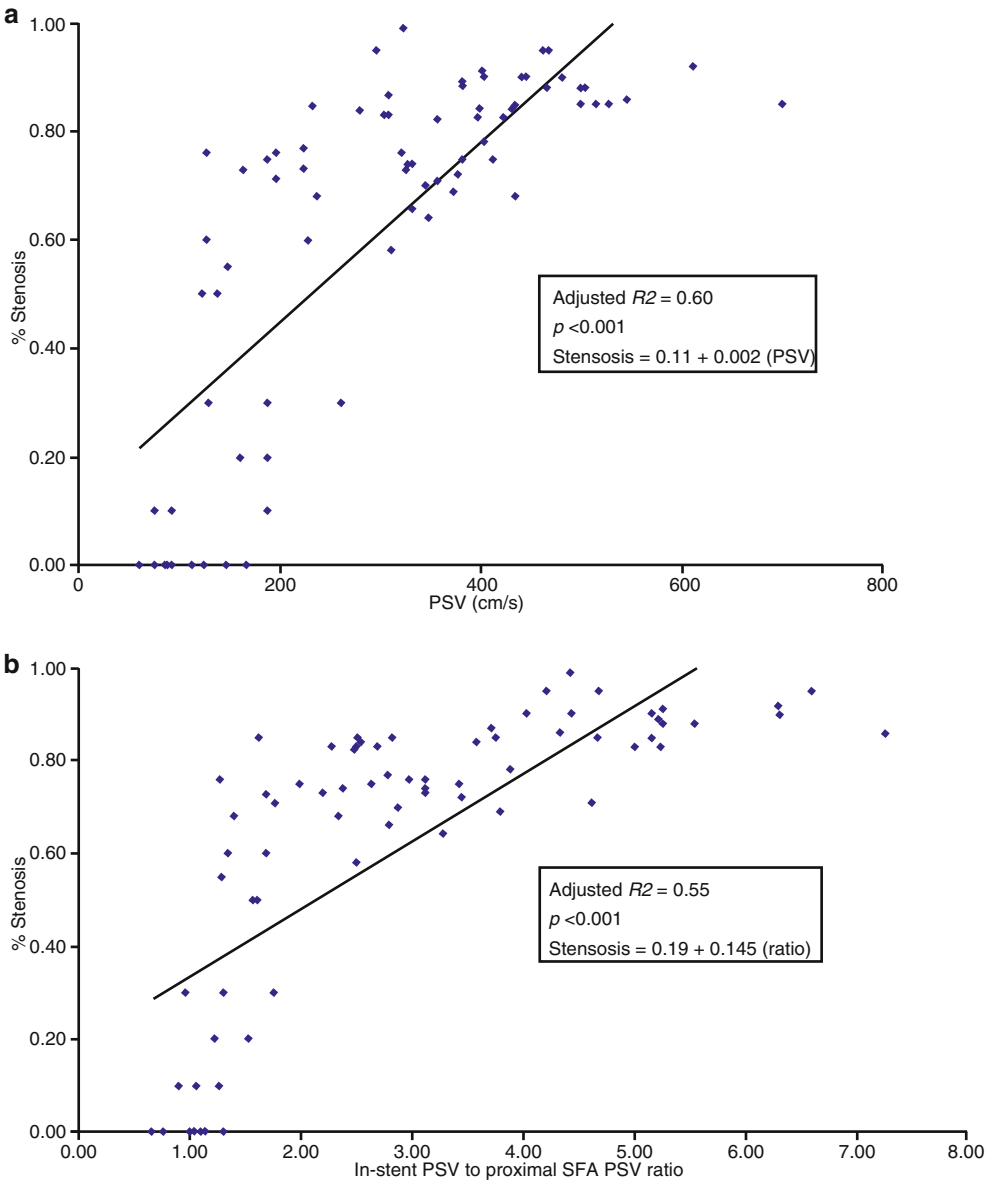


**Fig. 26.2** Scatter plots of the peak systolic velocities (*PSV*) (**a**) and in-stent PSV to proximal superficial femoral artery PSV ratio (**b**)

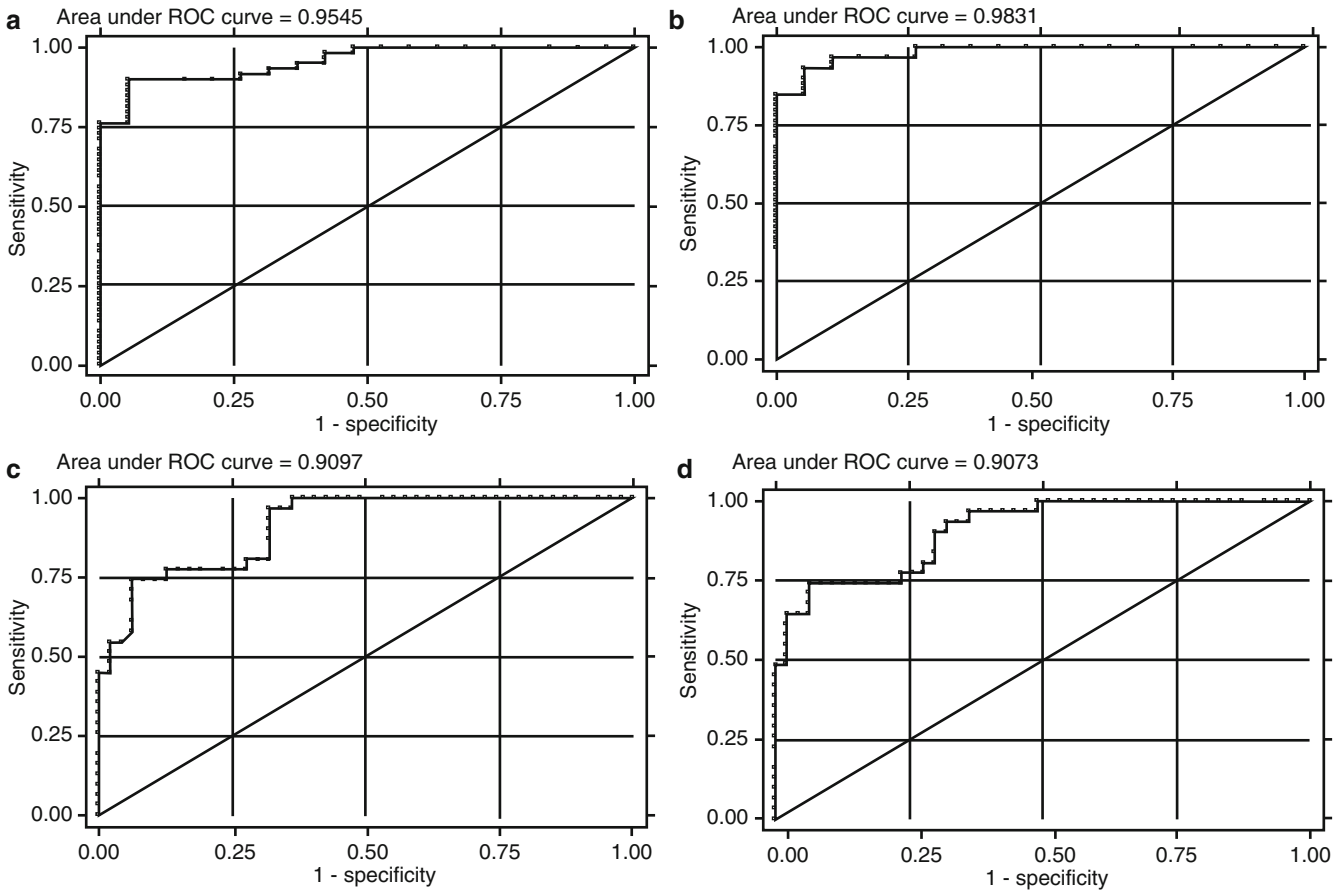


**Fig. 26.3** Receiver operator characteristic curves to differentiate between ≥50% and <50% stenosis in stented arteries by (**a**) PSV and (**b**) velocity ratio. Differentiation between ≥80% and <80% stenosis in stented arteries by (**c**) PSV and (**d**) velocity ratio

To distinguish <50% stenosis from ≥50% stenosis, the cut point on the PSV ROC curve was 189 cm/s. Rounding this value to 190 cm/s was associated with a sensitivity of 88%, a specificity of 95%, a positive predictive value (PPV) of 98%, and a negative predictive value (NPV) of 72%. To distinguish a <50% stenosis from ≥50% stenosis, the cut point on the PSV ratio ROC curve was 1.55. Rounding this value to 1.50 was associated with a sensitivity of 93%, a specificity of 89%, a PPV of 96%, and a NPV of 81%. Combining a PSV ≥ 190 and a ratio ≥1.50 to determine a ≥50% stenosis was associated with a sensitivity of 85%, a specificity of 95%, a PPV of 98%, and a NPV of 67%. Additionally, the odds ratio (OR) for determining a ≥50% stenosis based on a PSV ≥ 190 and a velocity ratio ≥1.50 was 99.99 (95% CI 11.82–845.55, $p<0.001$).

To distinguish <80% stenosis from ≥80% stenosis, the cut point on the PSV ROC curve was 265 cm/s. Rounding this value to 275 cm/s was associated with a sensitivity of 97%, a specificity of 68%, a PPV of 67%, and a NPV of 97%. To distinguish a <80% stenosis from ≥80% stenosis, the cut point on the PSV ratio ROC curve was 3.50. This value corresponded to a sensitivity of 74%, a specificity of 94%, a PPV of 77%, and a NPV 88%. Combining a PSV ≥ 275 and a ratio ≥3.50 to determine a ≥80% stenosis was associated with a sensitivity of 74%, a specificity of 94%, a PPV of 88%, and a NPV of 85%. Additionally, the odds ratio for determining a ≥80% stenosis based on a PSV ≥ 275 and a velocity ratio ≥3.50 was 42.17 (95% CI 10.20–174.36, $p<0.001$) (Fig. 26.3).

## Clinical Benefits of Duplex Surveillance

From the detailed hemodynamic and anatomic data provided by duplex examination, there are multiple clinical benefits obtained from duplex surveillance of lower extremity interventions. As with surveillance following surgical bypass, benefits may be seen over the course of the surveillance period. Early technical issues may be recognized on immediate post-procedure duplex studies, and later, progression of disease of the treated segment and failing interventions may be identified. Additionally, progression of proximal and distal disease may be detected via surveillance.

In the immediate post-procedure period (<1 month), duplex has been demonstrated to detect abnormalities more

frequently than completion angiography [24]. Following intervention, intimal flaps, dissections, fractured plaques, and residual stenoses may be missed on angiography, particularly if multiplanar imaging has not been judiciously used. Given this, reports have even advocated for performing endovascular interventions using primarily duplex imaging at the time of the procedure rather than angiography [25]. Furthermore, abnormal duplex findings on post-procedure imaging have been associated with increased rates of adverse outcomes. Specifically, patients with abnormalities on post-procedure duplex imaging when compared to patients with normal post-procedure studies have been shown to have lower primary patency rates and higher rates of amputation [24, 26, 27].

In addition to surveillance of the treated segment, duplex imaging after endovascular interventions is beneficial in recognizing lesions proximally and distally. This has been shown particularly in the iliac arteries, where up to 44% restenoses occur above or below a treated segment and can be recognized by duplex surveillance [28]. Additionally, duplex surveillance of iliac lesions has demonstrated even greater utility in patients with concomitant outflow reconstructions, a population who is at greater risk for intervention failure [26]. With regard to femoropopliteal lesions, the natural history of stenoses treated using endovascular means and the progression of disease in untreated segments proximally and distally remains poorly elucidated, again, emphasizing the need for surveillance of the entire artery and the neighboring arterial segments.

## Future Directions

Long-term durability of lower extremity endovascular interventions remains an issue which has plagued the advancing technology. Predictors of restenosis and failure of endovascular interventions include anatomic factors such as occlusions, long lesions, and multilevel disease along with patient factors including hypercholesterolemia, hypertension, diabetes mellitus, and renal failure [15, 29–31]. Additional factors that are likely to contribute to decreased long-term patency of endovascular interventions include the degree of calcification, plaque ulceration, and other morphologic characteristics. These morphologic factors have not been fully studied and are not routinely incorporated into pre- or post-procedure studies; however, further investigation may lead to identifying plaque characteristics on pre- and post-procedure duplex imaging which may portend poorer longer-term outcomes and failure [32].

With regard to treated lesions, their long-term natural history also remains unclear. Although restenosis is a well-known complication of endovascular interventions, there are various patterns of restenosis in both the aortoiliac and femoropopliteal segments. With this in mind, particular questions remain unanswered. In particular, do mid-stent restenotic lesions have a different natural history than stent margin lesions, and does anatomic location of a stent influence the surveillance data?

Although we have described criteria of restenosis after angioplasty and stenting of the femoropopliteal segment, this data has not yet been fully validated against a known reference standard. Moreover, surveillance criteria for endovascular interventions of aortoiliac disease are nonexistent, and criteria used for native vessels have been applied. It is evident that additional studies will need to be performed to further develop and solidify these criteria such that they may then be broadly applied.

### Conclusion

At present, there are no accepted standards for surveillance following aortoiliac and femoropopliteal endovascular interventions; however, it appears that surveillance, as for conventional bypass, is beneficial in identifying recurrent lesions which may preclude failure and occlusion. In-stent stenosis following angioplasty and stenting can be predicted by both PSV and velocity ratio data as measured by duplex ultrasound. Although it has not been well-studied as of yet, it appears that applying these criteria during routine surveillance will assist in preventing failure of endovascular interventions and concomitantly be associated with improved long-term functional capacity and limb salvage.

## References

1. Idu MM, Blankenstein JD, de Gier P, Truyen E, Buth J. Impact of a color-flow duplex surveillance program on infrainguinal vein graft patency: a five-year experience. J Vasc Surg. 1993;17(1):42–52.
2. Bandyk DF. Infrainguinal vein bypass graft surveillance: how to do it, when to intervene, and is it cost-effective? J Am Coll Surg. 2002;194(1 Suppl):S40–52.
3. Lundell A, Lindblad B, Bergqvist D, Hansen F. Femoropopliteal-crural graft patency is improved by an intensive surveillance program: a prospective randomized study. J Vasc Surg. 1995;21(1):26–33; discussion 33–4.
4. Mills Sr JL, Wixon CL, James DC, Devine J, Westerband A, Hughes JD. The natural history of intermediate and critical vein graft stenosis: recommendations for continued surveillance or repair. J Vasc Surg. 2001;33(2):273–8; discussion 278–80.
5. Norgren L, Hiatt WR, Dormandy JA, Nehler MR, Harris KA, Fowkes FG, TASC II Working Group. Inter-society consensus for the management of peripheral arterial disease (TASC II). J Vasc Surg. 2007;45(Suppl S):S5–67.
6. Henry M, Amor M, Ethevenot G, Henry I, Mentre B, Tzvetanov K. Percutaneous endoluminal treatment of iliac occlusions: long-term follow-up in 105 patients. J Endovasc Surg. 1998;5(3):228–35.
7. Indes JE, Mandawat A, Tuggle CT, Muhs B, Sosa JA. Endovascular procedures for aortoiliac occlusive disease are associated with superior short-term clinical and economic outcomes compared with open surgery in the inpatient population. J Vasc Surg. 2010;52(5):1173–9.

8. Leville CD, Kashyap VS, Clair DG, Bena JF, Lyden SP, Greenberg RK, O'Hara PJ, Sarac TP, Ouriel K. Endovascular management of iliac artery occlusions: extending treatment to TransAtlantic Inter-Society Consensus class C and D patients. J Vasc Surg. 2006;43(1):32–9.
9. Ferreira M, Lanziotti L, Monteiro M, Abuhadba G, Capotorto LF, Nolte L, Fearnot N. Superficial femoral artery recanalization with self-expanding nitinol stents: long-term follow-up results. Eur J Vasc Endovasc Surg. 2007;34(6):702–8.
10. Krankenberg H, Schlüter M, Steinkamp HJ, Bürgelin K, Scheinert D, Schulte KL, Minar E, Peeters P, Bosiers M, Tepe G, Reimers B, Mahler F, Tübler T, Zeller T. Nitinol stent implantation versus percutaneous transluminal angioplasty in superficial femoral artery lesions up to 10 cm in length: the femoral artery stenting trial (FAST). Circulation. 2007;116(3):285–92.
11. Schillinger M, Sabeti S, Loewe C, Dick P, Amighi J, Mlekusch W, Schlager O, Cejna M, Lammer J, Minar E. Balloon angioplasty versus implantation of nitinol stents in the superficial femoral artery. N Engl J Med. 2006;354(18):1879–88.
12. Surowiec SM, Davies MG, Eberly SW, Rhodes JM, Illig KA, Shortell CK, Lee DE, Waldman DL, Green RM. Percutaneous angioplasty and stenting of the superficial femoral artery. J Vasc Surg. 2005;41(2):269–78.
13. Schillinger M, Sabeti S, Dick P, Amighi J, Mlekusch W, Schlager O, et al. Sustained benefit at 2 years of primary femoropopliteal stenting compared with balloon angioplasty with optional stenting. Circulation. 2007;115(21):2745–9. Epub 2007 May 14.
14. Conrad MF, Cambria RP, Stone DH, Brewster DC, Kwolek CJ, Watkins MT, Chung TK, LaMuraglia GM. Intermediate results of percutaneous endovascular therapy of femoropopliteal occlusive disease: a contemporary series. J Vasc Surg. 2006;44(4):762–9.
15. Baril DT, Marone LK, Kim J, Go MR, Chaer RA, Rhee RY. Outcomes of endovascular interventions for TASC II B and C femoropopliteal lesions. J Vasc Surg. 2008;48(3):627–33.
16. Duda SH, Hosiers M, Lammer J, Scheinert D, Zeller T, Tielbeek A. Sirolimus-eluting versus bare nitinol stent for obstructive superficial femoral artery disease: the SIROCCO II trial. J Vasc Interv Radiol. 2005;16:331–8.
17. Baril DT, Rhee RY, Kim J, Makaroun MS, Chaer RA, Marone LK. Duplex criteria for determination of in-stent stenosis after angioplasty and stenting of the superficial femoral artery. J Vasc Surg. 2009;49(1):133–8; discussion 139.
18. Kasirajan K, Gray B, Beavers FP, Clair DG, Greenberg R, Mascha E, et al. Rheolytic thrombectomy in the management of acute and subacute limb-threatening ischemia. J Vasc Interv Radiol. 2001;12(4):413–21.
19. Sarac TP, Hilleman D, Arko FR, Zarins CK, Ouriel K. Clinical and economic evaluation of the trellis thrombectomy device for arterial occlusions: preliminary analysis. J Vasc Surg. 2004;39(3):556–9.
20. Tinder CN, Chavanpun JP, Bandyk DF, Armstrong PA, Back MR, Johnson BL, Shames ML. Efficacy of duplex ultrasound surveillance after infrainguinal vein bypass may be enhanced by identification of characteristics predictive of graft stenosis development. J Vasc Surg. 2008;48(3):613–8.
21. Ahn SS, Rutherford RB, Becker GJ, Comerota AJ, Johnston KW, McClean GK, Seeger JM, String ST, White RA, Whittemore AD, et al. Reporting standards for lower extremity arterial endovascular procedures. Society for Vascular Surgery/International Society for Cardiovascular Surgery. J Vasc Surg. 1993;17(6):1103–7.
22. Ringer AJ, German JW, Guterman LR, Hopkins LN. Follow-up of stented carotid arteries by Doppler ultrasound. Neurosurgery. 2002;51(3):639–43; discussion 643.
23. Stanziale SF, Wholey MH, Boules TN, Selzer F, Makaroun MS. Determining in-stent stenosis of carotid arteries by duplex ultrasound criteria. J Endovasc Ther. 2005;12(3):346–53.
24. Humphries MD, Pevec WC, Laird JR, Yeo KK, Hedayati N, Dawson DL. Early duplex scanning after infrainguinal endovascular therapy. J Vasc Surg. 2011;53(2):353–8.
25. Ascher E, Marks NA, Hingorani AP, Schutzer RW, Mutyala M. Duplex-guided endovascular treatment for occlusive and stenotic lesions of the femoral-popliteal arterial segment: a comparative study in the first 253 cases. J Vasc Surg. 2006;44(6):1230–7.
26. Back MR, Novotney M, Roth SM, Elkins D, Farber S, Cuthbertson D, Johnson BL, Bandyk DF. Utility of duplex surveillance following iliac artery angioplasty and primary stenting. J Endovasc Ther. 2001;8(6):629–37.
27. Kinney EV, Bandyk DF, Mewissen MW, Lanza D, Bergamini TM, Lipchik EO, Seabrook GR, Towne JB. Monitoring functional patency of percutaneous transluminal angioplasty. Arch Surg. 1991;126(6):743–7.
28. Myers KA, Wood SR, Lee V. Vascular ultrasound surveillance after endovascular intervention for occlusive iliac artery disease. Cardiovasc Surg. 2001;9(5):448–54.
29. Bakken AM, Palchik E, Hart JP, Rhodes JM, Saad WE, Davies MG. Impact of diabetes mellitus on outcomes of superficial femoral artery endoluminal interventions. J Vasc Surg. 2007;46(5):946–58; discussion 958.
30. DeRubertis BG, Pierce M, Ryer EJ, Trocciola S, Kent KC, Faries PL. Reduced primary patency rate in diabetic patients after percutaneous intervention results from more frequent presentation with limb-threatening ischemia. J Vasc Surg. 2008;47(1):101–8.
31. Jämsén TS, Manninen HI, Tulla HE, Jaakkola PA, Matsi PJ. Infrainguinal revascularization because of claudication: total long-term outcome of endovascular and surgical treatment. J Vasc Surg. 2003;37(4):808–15.
32. Ramaswami G, Tegos T, Nicolaides AN, Dhanjil S, Griffin M, Al-Kutoubi A, Belcaro G, Lewis J, Wilkins R, Davies MJ. Ultrasonic plaque character and outcome after lower limb angioplasty. J Vasc Surg. 1999;29(1):110–9. discussion 119–21.

# Duplex Ultrasound in the Evaluation and Management of Post-Catheterization Femoral Pseudoaneurysms

27

Patrick A. Stone and James R. Campbell II

**Abstract**

Ultrasound provides an important role in vessel access by providing direct visualization of the arterial system aiding vessel cannulation. Additionally, ultrasound is used as the primary diagnostic tool for groin access complications and assists treatment strategies, i.e., ultrasound-guided compression and duplex-guided thrombin injection. This chapter covers a review of evaluation and management of post-catheterization femoral artery pseudoaneurysms.

**Keywords**

Femoral pseudoaneurysms • Duplex-guided thrombin injection • Ultrasound-guided compression

The use of percutaneous methods for access during coronary interventions continues to increase with more than 500,000 coronary interventions performed annually in the United States [1]. In concert, the frequency of post-catheterization pseudoaneurysms continues to rise. Larger sheath sizes as well as more advanced anticoagulation regimens during and following percutaneous procedures have resulted in larger arterial defects with decreased ability to obtain hemostasis at the puncture site. Attempts at addressing this problem with closure devices and/or mechanical compression devices have failed to show clinical superiority to standard manual pressure [1]. Percutaneous-based cardiac and peripheral vascular interventions have become first line in the management of most vascular pathology. The vascular surgeon is often requested to evaluate and manage groin related complications following femoral artery access. Duplex ultrasound imaging in patients with symptomatic groin hematomas can identify complications related to the femoral artery puncture site. Hematomas, arteriovenous fistulas, and pseudoaneurysms can all be diagnosed with acceptable accuracy by experienced technicians. Iatrogenic pseudoaneurysms (IPA) following percutaneous access of the femoral artery accounts for the majority of complications requiring further evaluation in clinical practice. Diagnosis as well as treatment of IPA in the twenty-first century is managed almost exclusively by duplex technology. Therefore, the focus of this chapter is directed at evaluation and management of post-catheterization femoral pseudoaneurysms.

## Definition and Incidence

Pseudoaneurysms occur when a disruption in one or more layers of the arterial wall occurs. Arterial puncture sites that do not seal by the intrinsic physiologic hemostatic mechanisms result in arterial bleeding into the soft tissue with subsequent hematoma formation. Occasionally, the hematoma maintains a soft liquid central region while developing a firm outer pseudocapsule. Blood is then permitted to freely circulate from the injured vessel outside into the soft tissue without uncontrolled extravasation. The femoral artery is the

P.A. Stone, M.D., RVT, RPVI (✉)
Department of Surgery, Robert C. Byrd Health Sciences Center, West Virginia University, Charleston Area Medical Center, Charleston, WV, USA
e-mail: pstone0627@yahoo.com

J.R. Campbell II, M.D.
Department of Surgery and Medicine, Robert C. Byrd Health Sciences Center, West Virginia University, Charleston Area Medical Center, Charleston, WV, USA

A.F. AbuRahma, D.F. Bandyk (eds.), *Noninvasive Vascular Diagnosis*,
DOI 10.1007/978-1-4471-4005-4_27, 

**Table 27.1** Risk factors for iatrogenic pseudoaneurysms

| |
|---|
| Increasing sheath size |
| Cannulation of artery other than common femoral artery |
| Calcified artery |
| Increased body mass index |
| Concurrent anticoagulation |
| Combined arterial and venous puncture |
| Failure to provide appropriate postoperative compression |

most common vessel for both cardiac and peripheral vascular interventions and therefore the most common site for pseudoaneurysm development. Risk factors for development of pseudoaneurysms include the use of anticoagulation either at the time of arterial cannulation or in the immediate postprocedure period, increasing age, female gender, concomitant venous puncture, and increasing sheath/catheter size [2] (Table 27.1). Location of arterial cannulation also affects the frequency of this complication. Examples of arterial cannulation error include front and back wall arterial puncture. Puncture of the superficial or deep femoral arteries instead of the common femoral artery often leads to complications. The common femoral artery is anterior to the femoral head of the femur, and success of manual compression relies on a firm structure posterior to the femoral artery to obtain hemostasis. Cannulation of the external iliac artery, above the inguinal ligament, does not allow adequate compression above the puncture site and frequently results in retroperitoneal bleeding.

The reported incidence of IPA ranges widely from 0.05% up to 9%. This wide incidence range is the result of variations in protocols used to assess IPAs. In a prospective study of over 500 patients with routine evaluations with duplex, an incidence of 7.7% was reported [3]. This figure is substantially larger than that seen in clinical practice, since only symptomatic patients are typically assessed. According to the Society of Cardiovascular and Interventional Radiology, an acceptable rate of IPA and/or arteriovenous fistula should be ≤0.2% [4].

## Diagnosis

Clinical suspicion for IPA should follow any percutaneous intervention resulting in a swollen groin or soft tissue hematoma. Hard signs of persistent bleeding include pulsatile bleeding at the access site or expanding hematoma. The presence of a femoral bruit or thrill may also indicate an IPA; however, their absence does not exclude it. Most commonly, IPA is associated with a painful access site with associated hematoma and ecchymosis of varying size. Unfortunately, physical examination alone is notoriously

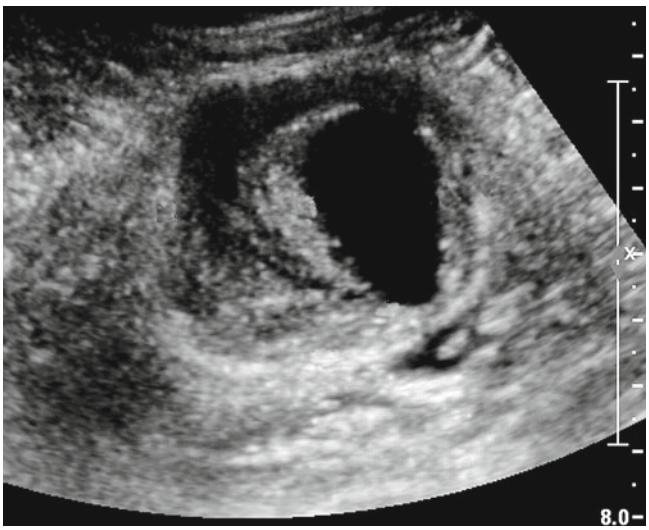


**Fig. 27.1** B-mode image of preinjection partially thrombosed pseudoaneurysm

inaccurate in identifying IPA. Angiography was historically the gold standard for diagnosis of IPA, until Mitchell et al. reported successful diagnosis by color duplex ultrasound in 1987 [5]. Since that time, arterial duplex evaluation has emerged as the gold standard and initial modality for diagnosing an IPA, with nearly 100% diagnostic accuracy. We typically use a 5- to 7-mHz probe in longitudinal orientation with vessel sampling and velocity measurements of the femoral artery and its branches. Changing orientation to the transverse plane allows diagnostic confirmation, sac size measurement, and evaluation for presence of thrombus within the pseudoaneurysm (Fig. 27.1). Duplex evaluation should include views of the inflow, distal external iliac, common femoral, deep femoral, and proximal superficial femoral arteries. Visualization of the common femoral vein is particularly important to exclude the presence of an associated arteriovenous fistula. IPA anatomic features to be reported should include maximum sac size, diameter of sac with flow, sac shape, neck diameter, and length. The sac size of the pseudoaneurysm should be measured in maximum squared centimeters, which is the most important parameter for determining treatment options. However, the length and width of the neck are also important to record. Larger neck widths often directly correlate with larger arterial defects that are generally more refractory to treatment with minimally invasive techniques. Multilobed IPA(s) likewise may be more difficult to treat. In our previous series, up to 20% of IPA(s) were multilobed. Typical characteristics noted on duplex imaging include a swirling of color flow within a hematoma outside of the underlying artery, color flow signal in a tract leading to a sac, and classic to-and-fro color flow in the pseudoaneurysm sac (Fig. 27.2).

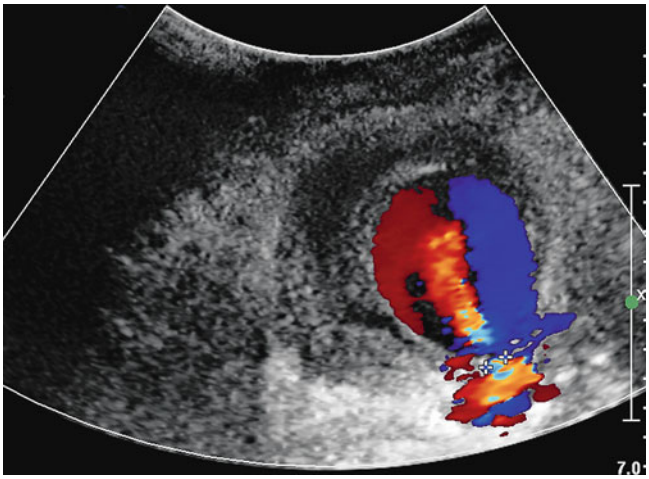

**Fig. 27.2** Duplex imaging with to and fro flow. Pseudoaneurysm neck marked

## Treatment Options

### Observation

Several small studies have reported successful closure in more than 50% of pseudoaneurysms by observation alone; however, these studies were not able to identify variables that could accurately predict which IPA(s) could be safely observed. In a prospective study evaluating the natural history of femoral vascular complications following coronary catheterization, all puncture sites were evaluated with physical examination prior to patient discharge. This series reported observation of seven femoral pseudoaneurysms with maximum sac diameter ≤3.5 cm with no complications and 100% thromboses at 4 weeks [2]. In a series of similar size, 9 of 16 IPA(s) thrombosed with observation. Larger IPA(s) and those associated with anticoagulation were associated with more frequent failures in the patients observed [6]. The largest series of conservative management of patients with femoral pseudoaneurysms is reported by Toursarkissian et al. [7]. Eighty-two patients with IPA(s) were followed at 2, 4, 8, and 12 weeks with duplex imaging of the femoral artery. A spontaneous thrombosis rate was observed in 89% of patients with no adverse events noted during observation. The mean time for spontaneous closure was 23 days, with mean 2.6 duplex examinations per patient performed [7]. Exclusion criteria for observation included IPA(s), >3 cm, concurrent anticoagulation, severe pain, or inability to comply with recommended follow-up examinations. Unfortunately, adoption of an observation policy for small IPA(s) (1–3 cm) does raise some concerns. These concerns included compliance with follow-up, patient fears of aneurysmal rupture (especially those with previous diagnosis of aneurysm), and finally costs to the health care system. These concerns have modified our management strategy in select patients with pseudoaneurysms in this size range.

### Ultrasound-Guided Compression

Until the early 1990s, femoral cutdown with suture repair of the femoral defect was the standard treatment for those not managed conservatively. In 1991, Fellmeth et al. described a nonoperative technique for thromboses of IPAs and arteriovenous fistulas. With an overall success rate of 93%, this noninvasive alternative to surgical repair was welcomed [8]. Following this initial report, the use of ultrasound-guided compression (UGC) became the first-line treatment for those who were hemodynamically stable and without associated infection or skin necrosis. This technique includes a linear or curvilinear probe (5 or 7 MHz) to compress the IPA and arrest IPA blood flow. Real time, duplex, and color Doppler are used to identify the neck of the pseudoaneurysm. Manual compression is subsequently applied by the technologist to the neck of the aneurysm with the transducer, permitting flow through the native artery while preventing flow into the pseudoaneurysm sac. Continuous evaluation during compression is essential to arrest flow in the pseudoaneurysm sac and ensure flow in the native artery. Pressure is maintained for 10-min intervals, at the end of which pressure is slowly released and flow into the pseudoaneurysm reassessed. This is continued until thrombosis, operator fatigue, or patient discomfort occurs. Success with this treatment modality generally ranges from 60% to 90% [9–11]. Despite this acceptable success rate, compression times in excess of 1 h can be required and multiple compression sessions may be required to induce thrombosis of >10% of IPA(s). Factors associated with failed compression have been evaluated in previous publications. Ongoing anticoagulation has been shown in several series to significantly reduce successful compression, as reported by Coley et al. [10] and Eisenburg et al. [12]. They describe failure rates of 38% and 70%, respectively, in anticoagulated patients, whereas failure rates in the groups without concurrent anticoagulation were 5% and 26%. In addition, 75% of those in Coley's series ultimately had their anticoagulation stopped and underwent repeat UGC with successful thrombosis. Also a series by Dean et al. reported a 73% success rate of UGC in 77 patients with uninterrupted anticoagulation, with seven patients requiring multiple sessions (12.5%) to obtain sustained thrombosis. Maximum aneurysm diameter appeared to be the best predictor of successful treatment with UGC [13]. With increasing pseudoaneurysm sac size, the technical success of ultrasound-guided compression decreases. Coley et al. achieved a 100% success rate in pseudoaneurysms <2 cm but only a 67% success with

UGC in those 4–6 cm. Although it seems intuitive that a shorter tract length and larger neck diameter would have less success with compression, this has not been widely reported. Limited data is available on neck length or diameter on success of ultrasound-guided compression. A small series reported a short tract length (<5 mm) had unfavorable compression outcomes; however, this study was limited by a small sample size of only 12 patients [14].

Complications following UGC include arterial or venous thrombosis. Also, several cases of pseudoaneurysm rupture have also been reported. Successful thrombosis occurs at an acceptable rate, but there are several limitations to this technique. These include the requirement at some facilities for a physician to be present during the entire procedure, potential long procedures times, local patient discomfort that often requires conscious sedation, and newer techniques with higher success rates now being available.

## Ultrasound-Guided Thrombin Injection

In 1986, Cope and Zeit described a technique of ultrasound-guided percutaneous injection of bovine thrombin into a pseudoaneurysm sac with successful thrombosis [15]. This technique was actually described prior to the adoption of ultrasound-guided compression. Although an appealing method for handling IPA, this technique took over a decade to widely replace ultrasound-guided compression. During that time interval, several authorities have compared their experience of ultrasound-guided compression to that of ultrasound-guided thrombin injection (UGTI) [16–22] (Table 27.2). UGTI has greater technical success in all series included in this review. All series however are retrospective series except a small prospective randomized trial by Lonn et al. with 15 patients in each group [22]. In addition to great immediate technical success, the subsequent recurrence rate is also low [23–36].

UGTI can be performed at bedside or in the vascular laboratory. Some clinicians use local anesthetic; however, with experience single punctures can be achieved and conscious sedation has never been required in our experience. A 1-ml syringe and spinal needle (20–22 gauge) is used to administer the bovine thrombin (100–1,000 units/ml). Using B-mode imaging, the needle tip is visualized and directed into the IPA sac (Fig. 27.3). The interventionalist should ensure the needle tip is just inside the sac and as far from the IPA neck as technically possible. This minimizes the chance of forcing thrombus or thrombin into the neck and the native circulation. Injection is performed into the sac under duplex visualization at 0.1-ml increments until successful obliteration of flow into the aneurysm sac is achieved (Fig. 27.4). Thrombin is an active form of factor II (prothrombin). It transforms inactive fibrinogen to fibrin, its active form.

**Table 27.2** Ultrasound-guided compression (UGC) versus ultrasound-guided thrombin injection (UGTI)

| Reference | *N* (UGC)/(UGTI) | Success (%) (UGC)/(UGTI) |
|---|---|---|
| Weinmann et al. [16] | 30/33 | 87/100 |
| Gorge et al. [17][a] | 36/30 | 17/93 |
| Taylor et al. [18] | 40/29 | 63/93 |
| Stone et al. [19] | 47/27 | 57/96 |
| Paulson et al. [20] | 281/26 | 74/96 |
| Khoury et al. [21] | 189/131 | 75/96 |
| Lonn et al. [22][b] | 15/15 | 40/100 |

[a]Prospective, all patients initially UGC, UGTI if failed compression
[b]Prospective randomized trial

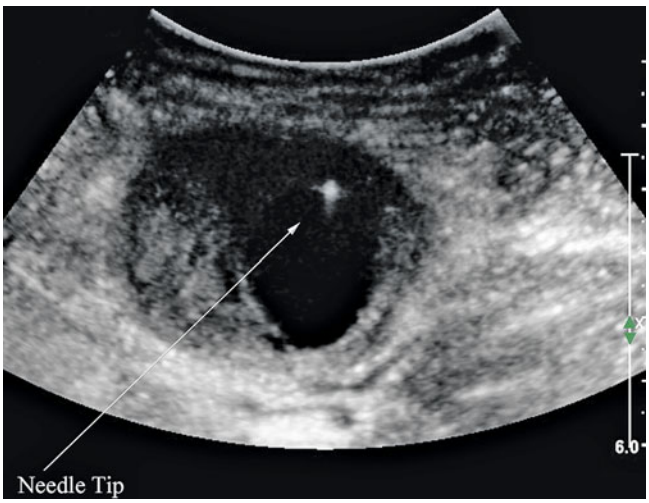


**Fig. 27.3** Needle tip located away from pseudoaneurysm neck

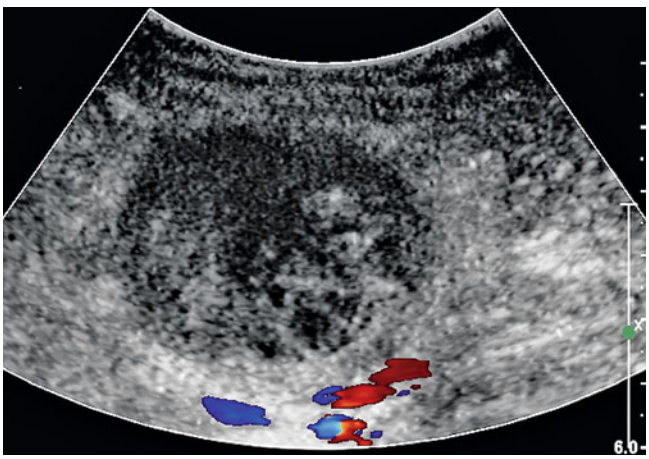


**Fig. 27.4** Duplex imaging successful of thrombosis pseudoaneurysm. Absent color flow visualized

Fibrin subsequently contributes to thrombus formation. As a result of limited blood flow in the pseudoaneurysm sac, thrombin can propagate thrombus that would often be cleared in sites of normal blood flow. After successful

thrombosis, the native circulation is assessed for changes compared to the preprocedural status. Following successful thrombosis, bed rest is recommended for a period of 4–8 h.

Complications following thrombin injection are reported infrequently. The most feared complications are arterial thrombosis and distal embolization. Distal embolization has occurred in less than 1% of the reviewed literature, with some authors noting improved circulation spontaneously. Others have been successfully treated by intra-arterial thrombolytic therapy or surgical thrombectomy. Limited evidence suggests that distal embolization is associated with short and wide pseudoaneurysm necks. Also, most cases reported in the literature have occurred in aneurysms with maximum sac diameter <3 cm. Other complications seen only in case reports include allergic reactions to bovine thrombin with severity ranging from generalized urticaria to anaphylaxis. Infection after injection has also been reported occasionally, and one case of rupture was identified in a comprehensive literature review.

**Table 27.3** Literature review of PSA recurrences

| Author | Number of successful initial DGTI | Number of recurrence at follow-up |
|---|---|---|
| Liau et al. [23] | 5 | 0 (24 h) |
| Kang et al. [24] | 20 | 0 (1–4 days) |
| Lennox et al. [25] | 30 | 0 (1 day and 3 weeks) |
| Brophy et al. [26] | 15 | 0 (1 week) |
| Sackett et al. [27] | 29 | 0 (24 h) |
| Pezzullo et al. [28] | 23 | 1 (24 h) |
| Paulson et al. [20] | 23 | 0 (24 h) |
| Tamim et al. [29] | 10 | 0 (1 and 3 weeks) |
| La Perna et al. [30] | 66 | 3 (24 h) |
| Calton et al. [31] | 52 | 2 (24 h) |
| Sheiman et al. [32] | 50 | 0 (within 10 days) |
| Olson et al. [33] | 17/15 | 1 (24 h)/1 (1 week) |
| Friedman et al. [34] | 40 | 0 (24 h)/1 (1 week) |
| Khoury et al. [21] | 126 | 9 (1–30 days) |
| Chattar-Cora et al. [35] | 39 | 0 (24 h) |
| Krueger et al. [36] | 110 | 6 (24 h)/4 (1 week) |
| Paulson et al. [37] | 103 | 0 (24 h) |
| Stone et al. [38] | 103 | 2 (1 week) |

*PSA* pseudoaneurysms, *DGTI* duplex-guided thrombin injection

## Experience from Our Institution

As a high volume cardiac and vascular intervention center with over 10,000 femoral artery access procedures annually, we have had extensive experience with post-catheterization pseudoaneurysms. We first reported our early results of duplex-guided thrombin injection versus ultrasound-guided compression in 2003 [19]. With successful thrombosis in only 57% of those with compression therapy as opposed to 97% with duplex-guided thrombin injection, the use of compression therapy has been abandoned at our facility. Further experience of 82 patients with iatrogenic pseudoaneurysms, including 12 complexes, demonstrated successful thrombosis in 97% of patients treated with UGTI. We also reviewed the number of duplex studies in these patients which often included diagnostic, treatment, and follow-up examination. Since we determined only 5% of the follow-up ultrasounds were clinically significant, we have adopted a policy of clinical follow-up after successful thrombosis. We also compared our recurrence rate with that of over 600 iatrogenic pseudoaneurysms in the available literature and found <3% recurrence rate after successful duplex-guided thrombin injection (Table 27.3). As a result of these excellent technical success rates, low recurrence rates, and overall patient acceptance and applicability, our group and most vascular specialists now consider duplex-guided thrombin injection as the initial treatment of choice. Further experience at our institution has adopted a fast track approach to pseudoaneurysms which include treatment at the time of diagnosis and limiting duplex examinations as a cost-effective method [38]. Additionally, with the success and safety of this treatment strategy, we also perform UGTI in an outpatient setting for those requiring treatment after discharge or in patients who fail observation. This includes treatment in our vascular laboratory with the patient returning to our preadmission area for discharge after bed rest of 4–6 h.

Currently, we are reviewing our results of managing patients with IPA that underwent coronary artery bypass grafting within 30 days of diagnosis. Previously, we recommended routine surgical repair at the time of CABG in those patients diagnosed with IPA. This is based on the concern of aggressive anticoagulation at the time of surgery and bleeding from the IPA. Upon review we have managed over 20 patients similar to patients not scheduled for CABG. This has included observation of those with sac size <3 cm and UGTI for those >3 cm. We have found no cases that have required emergent repair during the hospitalization and no recurrences in those successfully treated with UGTI.

## Future Trends

Recently, a series has evaluated patients with suspected pseudoaneurysms with both laboratory and noninvasive imaging [39]. Platelet counts and D-dimer levels were analyzed in relation to presence or absence of femoral pseudoaneurysm, as well as maximum aneurysm size. D-dimer (ug/ml) levels were significantly higher in patients with pseudoaneurysms compared to those without ($p < .001$). Also the serum platelet count was significantly lower in patients with pseudoaneurysm, 172 × 1000/μL versus 274 × 1000/μL in patients without IPA. The potential of these findings is

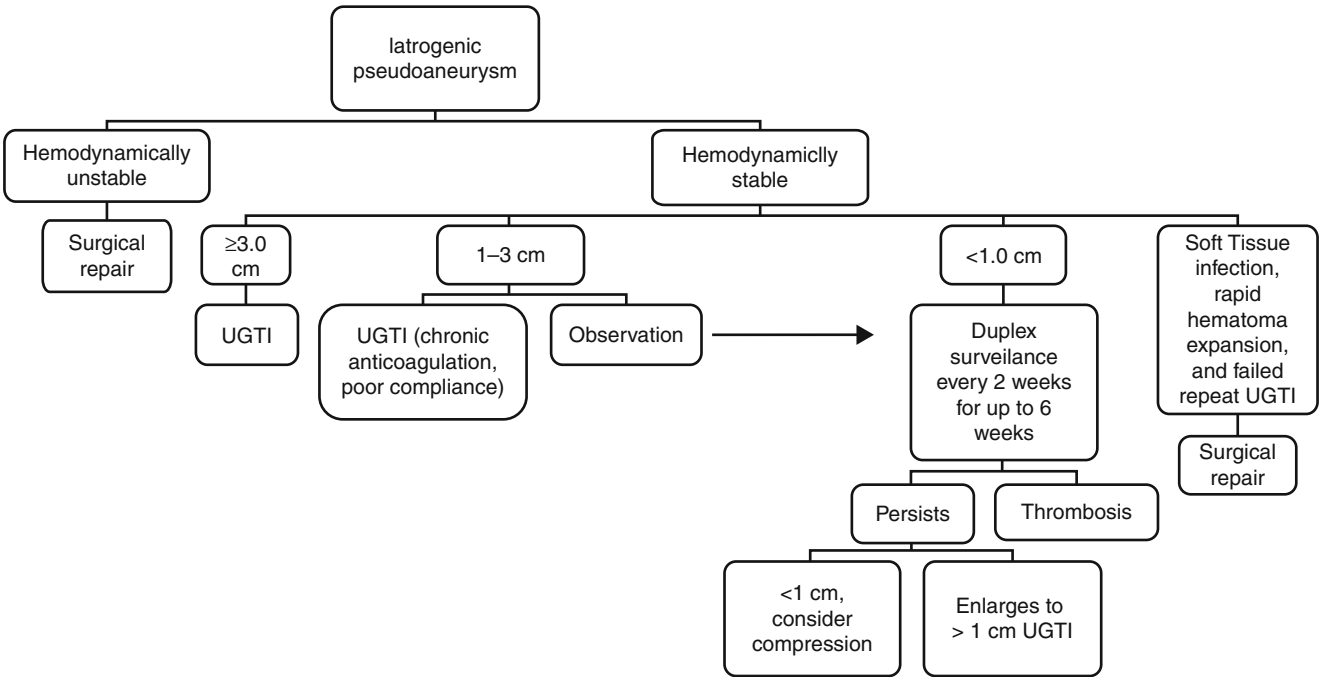


**Fig. 27.5** Treatment algorithm

important to clinical practice. If future larger studies support these results then D-dimer might be used to determine which patients with groin hematomas should undergo ultrasound imaging to rule out IPA. A high negative predictive value of a low serum D-dimer could reduce the number of negative ultrasound exams in patients with groin hematomas.

## Surgical Intervention

Under some circumstances, surgical repair remains the best treatment strategy to address IPA. Patients presenting with hemodynamic instability and soft tissue infection should have surgical repair. In addition, those patients with failed minimally invasive techniques should be considered for surgical repair (Fig. 27.5).

### Conclusion

With increasing numbers of percutaneous-based procedures for both cardiac and peripheral vascular pathology and the use of more advanced anticoagulation regimens, iatrogenic pseudoaneurysms will continue to occur despite our best efforts. An ultrasound-guided diagnosis and treatment paradigm is available with nearly 100% accuracy for both diagnosis and treatment. Duplex image-guided therapy is now considered the first-line management of iatrogenic pseudoaneurysms replacing ultrasound-guided compression or surgical repair in most instances. Vascular specialist should be familiar with how to evaluate and manage this complication of arterial cannulation.

## References

1. Koreny M, Riedmuller E, Nikfardjam M, Siostrzonek P, Mullner M. Arterial puncture closing devices compared with standard manual compression after cardiac catheterization: systemic review and meta-analysis. JAMA. 2004;291(3):3507.
2. Kresowik TF, Khoury MD, Miller BV, et al. A prospective study of the incidence and natural history of femoral vascular complications after percutaneous transluminal coronary angioplasty. J Vasc Surg. 1991;13:328–36.
3. Katzenschlager R, Ugurluoglu A, Ahmade A, et al. Incidence of pseudoaneurysm after diagnostic and therapeutic angiography. Radiology. 1995;195:463–6.
4. Standards of Practice Committee of the Society of Cardiovascular and Interventional Radiology. Standard for diagnostic arteriography in adults. J Vasc Interv Radiol. 1993; 4:385.
5. Mitchell DG, Needleman L, Bezzi M, Goldberg B, Kurtz AB, Penneli RG, Rifkin MD, Vialaro M, Balatrowich OH. Femoral artery pseudoaneurysm: diagnosis with conventional duplex and color Doppler US. Radiology. 1987;165:687–90.
6. Kent KC, McArdle CR, Kennedy B, Baim DS, Anninos E, Skillman JJ. A prospective study of the clinical outcome of femoral pseudoaneurysms and arteriovenous fistulas induced by arterial puncture. J Vasc Surg. 1993;17:125–33.
7. Toursarkissian B, Allen BT, Petrinec D, Thompson RW, Rubin BG, Reilly JM, Anderson CB, Flye MW, Sicard GA. Spontaneous closure of selected iatrogenic pseudoaneurysms and arteriovenous fistulae. J Vasc Surg. 1997;25:803–9.

8. Fellmeth BD, Roberts AC, Bookstein JJ, Freishlag JA, Forsythe JR, Buckner NK. Postangiographic femoral artery injuries: nonsurgical repair with ultrasound guided compression. Radiology. 1991;178: 671–5.
9. Cox GS, Young JR, Gray BR, Grubb MW, Hertzer NR. Ultrasound-guided compression repair of postcatheterization pseudoaneurysms: results of treatment in one hundred cases. J Vasc Surg. 1994;19(4): 683–6.
10. Coley BD, Roberts AC, Fellmeth BD, Valji K, Bookstein JJ, Hye RJ. Postangiographic femoral artery pseudoaneurysms: further experience with ultrasound guided repair. Radiology. 1995;194(2):307–11.
11. Hood DB, Mattos MA, Douglass MG, Barkmeirer LD, Hodgson KJ, Ramsey DE, et al. Determinants of success of color-flow duplex guided compression of repair of femoral pseudoaneurysms. Surgery. 1996;120(4):585–8.
12. Eisenburg L, Paulson EK, Kliewer MA, et al. Sonographically guided compression repair of pseudoaneurysms: further experience from a single institution. AJR Am J Roentgenol. 1999;173:1567–73.
13. Dean SM, Olin JW, Piedmonte M, Grubb M, Young JR. Ultrasound-guided compression closure of postcatheterization pseudoaneurysms during concurrent anticoagulation: a review of seventy-seven patients. J Vasc Surg. 1996;23:28–35.
14. Diprete DA, Cronan JJ. Compression ultrasonography: treatment for acute femoral artery pseudoaneurysms in selected cases. J Ultrasound Med. 1992;11:489–92.
15. Cope C, Zeit R. Coagulation of aneurysms by direct percutaneous thrombin injection. AJR Am J Roentgenol. 1986;147:383–7.
16. Weinmann EE, Chayen D, Kobzantzev ZV, Zaretsky M, Bass A. Treatment of postcatheterization false aneurysms: ultrasound-guided compression vs. Ultrasound-guided thrombin injection. Eur J Vasc Endovasc Surg. 2002;23:68–72.
17. Gorge G, Kunz T, Kirstein M. A prospective study on ultrasound-guided compression therapy of thrombin injection for treatment of iatrogenic false aneurysms in patients receiving full-dose antiplatelet therapy. Z Kardiol. 2003;92(7):564–70.
18. Taylor BS, Rhee RY, Muluk S, Trachtenberg J, Walters D, Steed DL, Makaroun MS. Thrombin injection versus compression of femoral artery pseudoaneurysms. J Vasc Surg. 1999;30:1052–9.
19. Stone P, Lohan J, Copeland SE, Hamrick Jr RE, Tiley EH, Flaherty SK. Iatrogenic pseudoaneurysms: comparison of treatment modalities, including duplex-guided thrombin injection. W V Med J. 2003;99(6):230–2.
20. Paulson EK, Sheafor DH, Kliewer MA, Nelson RC, Eisenberg LB, Sebastin MW, Sketch Jr MH. Treatment of iatrogenic femoral arterial pseudoaneurysms: comparison of US-guided thrombin injection with compression therapy. Radiology. 2000;215(2):403–8.
21. Khoury M, Rebecca A, Greene K, Rama K, Colaiuta E, Flynn L, Berg R. Duplex scanning-guided thrombin injection for the treatment of iatrogenic pseudoaneurysms. J Vasc Surg. 2002;35:517–21.
22. Lonn L, Olmarker A, Geterud K, Risberg B. Prospective randomized study comparing ultrasound-guided thrombin injection to compression in the treatment of femoral pseudoaneurysms. J Endovasc Ther. 2004;11(5):570–6.
23. Liau CS, Ho FM, Chen MF, Lee YT. Treatment of iatrogenic femoral artery pseudoaneurysm with percutaneous thrombin injection. J Vasc Surg. 1997;26(1):18.
24. Kang SS, Labropoulos N, Mansour MA, Baker WH. Percutaneous ultrasound guided thrombin injection: a new method for treating postcatheterization femoral pseudoaneurysms. J Vasc Surg. 1998;27(6):1032–8.
25. Lennox AF, Delis KT, Szendro G, et al. Duplex-guided thrombin injection for iatrogenic femoral artery pseudoaneurysm is effective even in anticoagulated patients. Br J Surg. 2000;87(6):796–801.
26. Brophy DP, Sheiman RG, Amatulle P, Akbari CM. Iatrogenic femoral pseudoaneurysms: thrombin injection after failed US-guided compression. Radiology. 2000;214(1):278–82.
27. Sackett WR, Taylor SM, Coffey CB, et al. Ultrasound guided thrombin injection of iatrogenic femoral pseudoaneurysms: a prospective analysis. Am Surg. 2000;66(10):937–42.
28. Pezzullo JA, Dupuy DE, Cronan JJ. Percutaneous injection of thrombin for the treatment of pseudoaneurysms after catheterization: an alternative to sonographically guided compression. AJR Am J Roentgenol. 2000;175(4):1035–40.
29. Tamim WZ, Arbid EJ, Andrews LS, Arous EJ. Percutaneous induced thrombosis of iatrogenic femoral pseudoaneurysms following catheterization. Ann Vasc Surg. 2000;14(3):254–9.
30. La Perna L, Olin JW, Goines D, et al. Ultrasound-guided thrombin injection for the treatment of postcatheterization pseudoaneurysms. Circulation. 2000;102(19):2391–5.
31. Calton Jr WC, Franklin DP, Elmore JR, Han DC. Ultrasound-guided thrombin injection is a safe and durable treatment for femoral pseudoaneurysms. Vasc Surg. 2001;35(5):379–83.
32. Sheiman RG, Brophy DP. Treatment of iatrogenic femoral pseudoaneurysms with percutaneous thrombin injection: experience in 54 patients. Radiology. 2001;219(1):123–7.
33. Olsen DM, Rodriguez JA, Vranic M, et al. A prospective study of ultrasound-guided thrombin injection of femoral pseudoaneurysm: a trend toward minimal medication. J Vasc Surg. 2002;36(4): 779–82.
34. Friedman SG, Pellerito JS, Scher L, et al. Ultrasound-guided thrombin injection is the treatment of choice for femoral pseudoaneurysms. Arch Surg. 2002;137(4):462–4.
35. Chattar-Cora D, Pucci E, Tulsyan N, et al. Ultrasound guided thrombin injection of iatrogenic pseudoaneurysm at a community hospital. Ann Vasc Surg. 2002;16(3):294–6.
36. Krueger K, Zaehringer M, Strohe D, Stuetzer H, Boecker J, Lackner K. Postcatheterization pseudoaneurysm: result of US-guided percutaneous thrombin injection in 240 patients. Radiology. 2005;236: 1104–10.
37. Paulson EK, Nelson RC, Mayes CE, Sheafor DH, Sketch Jr MH, Kliewer MA. Sonographically guided thrombin injection of iatrogenic femoral pseudoaneurysms. Further experience of a single institution. AJR Am J Roentgenol. 2001;177:309–16.
38. Stone PA, AbuRahma AF, Flaherty SK. Reducing duplex examinations in patients with iatrogenic pseudoaneurysms. J Vasc Surg. 2006;43:1211–5.
39. Hoke M, Koppensteiner R, Schillinger M, Haumer M, Minar E, Wiesbauer F, Huber CD. D-dimer testing in the diagnosis of transfemoral pseudoaneurysm after percutaneous transluminal procedures. J Vasc Surg. 2010;52:383–7.

# 28 Lower Extremity Arterial Mapping: Duplex Ultrasound as an Alternative to Arteriography Prior to Femoral and Popliteal Reconstruction

Enrico Ascher, Anil P. Hingorani, Natalie Marks, and Sergio X. Salles-Cunha

**Abstract**

The clinical experience with periprocedural duplex ultrasound detailed in this chapter is based on over 2,000 lower extremity open and endovascular arterial revascularization procedures. The topics discussed include goals of testing, detailed protocols of duplex ultrasound arterial mapping (DUAM), rationale of preoperative DUAM for revascularization decision making, and comparison of DUAM with other imaging modalities such as contrast arteriography (XRA), magnetic resonance angiography (MRA), and computed tomography arteriography (CTA). The limitations and pitfalls of duplex arterial testing are discussed as well as the learning curve for this diagnostic technique including necessary components to be followed during the training phase for replacing other imaging modalities with DUAM.

**Keywords**

Preoperative arterial duplex ultrasound • Arterial mapping • Duplex arteriogram • Lower extremity revascularization

## Introduction

The goal of this chapter is to discuss the following topics: (1) distinct goals of specific vascular laboratory arterial examinations, (2) detailed protocols for duplex ultrasound arterial mapping (DUAM), (3) various philosophies for implementation of a preoperative arterial ultrasound mapping, and (4) advantages of DUAM over contrast arteriography (XRA), magnetic resonance angiography (MRA), and computed tomography arteriography (CTA). This discussion represents a summary of the experience acquired with over 2,000 lower extremity arterial revascularization procedures performed based on preoperative and perioperative ultrasound imaging [1–13].

The distinct goals of specific arterial examinations include (1) screening, (2) definitive diagnosis, (3) preoperative or preprocedural mapping, (4) intraoperative assessment either during open or endovascular surgery, and (5) postoperative follow-up evaluation. The various protocols for arterial imaging can be detailed and time consuming or short and very targeted. Advanced communication between sonographer and surgeon planning the procedure for every particular patient is necessary to save time by creating imaging shortcuts.

The philosophies or steps for implementation of a peripheral arterial mapping protocol include (1) identification of the primary objective for every particular assessment,

E. Ascher, M.D. (✉)
Division of Vascular and Endovascular Surgery,
Lutheran Medical Center, Brooklyn, NY, USA

Department of Surgery, Mount Sinai School of Medicine,
960 - 50th Street, 1st Floor, Brooklyn, NY 11291, USA
e-mail: easchermd@gmail.com

A.P. Hingorani, M.D., FACS
Attending Surgeon, Lutheran Medical Center,
Brooklyn, NY, USA

Department of Surgery, Mount Sinai School of Medicine,
Brooklyn, NY, USA

N. Marks, M.D., RVT
Vascular Laboratory, Total Vascular Care, Inc
Brooklyn, New York, NY, USA

S.X. Salles-Cunha, Ph.D., RVT
Department of Imagenology,
Vascular Ultrasound Consultant, Itanhaém, São Paulo, SP, Brazil

A.F. AbuRahma, D.F. Bandyk (eds.), *Noninvasive Vascular Diagnosis,*
DOI 10.1007/978-1-4471-4005-4_28, 

(2) comparison of ultrasonographic and arteriographic findings for specific segments of the peripheral arterial tree, (3) evaluation of virtual decision making based on ultrasound examinations, (4) appraisal of actual decision making, and (5) assessment of procedures based entirely on preoperative and perioperative ultrasound imaging.

Advantages of DUAM are primarily based on imaging of the arterial wall and hemodynamic data availability in addition to lower cost, portability, noninvasiveness, freedom of malignancy risk, and concomitant mapping of veins to be used as arterial conduit.

## Arterial Examinations

This section summarizes details of specific arterial examinations according to their goals and objectives [1–16]. It fulfills the first two objectives of this chapter.

### Screening

Peripheral arterial screening is commonly consists of the measurement of ankle pressures. Systolic ankle pressures are compared to brachial pressures, and the ankle-brachial systolic blood pressure ratio, or ankle-brachial index (ABI), is calculated. An ABI below 1 is abnormal and warrants further investigation of the peripheral vascular system. An ABI below 0.5 suggests severe peripheral arterial disease and evaluation by a vascular surgeon or interventionist. Contrary to the popular belief, we feel that the lowest ABI should be employed as a screening criterion [17]. Relation of calf arterial perfusion rate is stronger to the lowest than highest ABI.

Flow waveform analysis of the anterior and posterior tibial arteries at the ankle may replace ABI as a screening method, particularly in the diabetic and renal insufficiency patients with incompressible arteries. Arterial incompressibility may be total or partial, resulting in nonmeasurable or falsely elevated ABI [18]. The toe-brachial index could also be used as a screening method in patients with incompressible tibial arteries [19–21]. Triphasic flow waveforms are normal. Monophasic waveforms suggest severe peripheral arterial occlusive disease.

### Definitive Diagnosis

Although pulse volume recording (PVR) and segmental pressure measurements have been used in the vascular laboratory, a protocol based on ABI and flow waveforms obtained at the common femoral, midsuperficial femoral, popliteal, and distal tibial arteries is recommended from the perspective of arterial mapping. With this protocol, an expert interpreter can predict the levels of significant arterial obstruction with accuracy greater than 80% when compared to X-ray arteriography [22, 23]. Upper calf and thigh pressures may not present additional information once the ABI and waveforms are analyzed. From the arterial mapping learning point of view, the early experience can be acquired with a continuous-wave Doppler. The sooner the sonographer starts using a duplex scanner to obtain the waveforms, the better. The next training step would be to scan the femoropopliteal arteries while looking for the sites to collect the waveforms. With this approach, the sonographer is acquainted with arterial mapping of the ankle and from below the knee to the groin. Proper imaging at the adductor canal level requires specific training. Additional experience is needed for upper calf and aortoiliac arterial mapping.

### Preoperative Mapping

DUAM of the lower extremities requires information about the procedure being considered based on clinical findings and definitive diagnosis. Clinical findings may dictate if treatment is limited to the aortoiliac segment or the femoropopliteal segment or if a distal bypass is being considered. The aortoiliac or femoropopliteal treatment may be a bypass or an endovascular procedure. The protocols for arterial mapping described below are subdivided into three segments: (1) aortoiliac, (2) femoropopliteal, and (3) infrapopliteal. They are complemented by venous mapping if an autogenous conduit is considered.

#### Aortoiliac Segment

A long protocol demands an attempt at a complete aortoiliac mapping from the renal arteries down to the groin. Imaging of the aortoiliac segment may be suspended (1) if the primary objective is infrainguinal revascularization, (2) if the waveform of the common femoral artery is clearly triphasic, and (3) if intraoperative pressure measurements are scheduled following the infrainguinal procedure.

The patients receive instructions to get ready for an abdominal ultrasound scan. They should not eat, chew gum, or smoke for about 10 h prior to the examination, usually scheduled in the morning. Antigas medication is recommended if not contraindicated.

A low-frequency abdominal transducer is commonly used to image the aorta and its bifurcation. Imaging is performed in transverse, longitudinal, and oblique planes, pending aortic elongation and tortuosities. Aortic flow waveforms are obtained above and below the level of the renal arteries and proximal to the aortic bifurcation. Occlusion, aneurysms, conditions of the arterial wall, and degree of stenosis are assessed based on B-mode, color flow, or power Doppler imaging. Local increase in velocity may be employed to

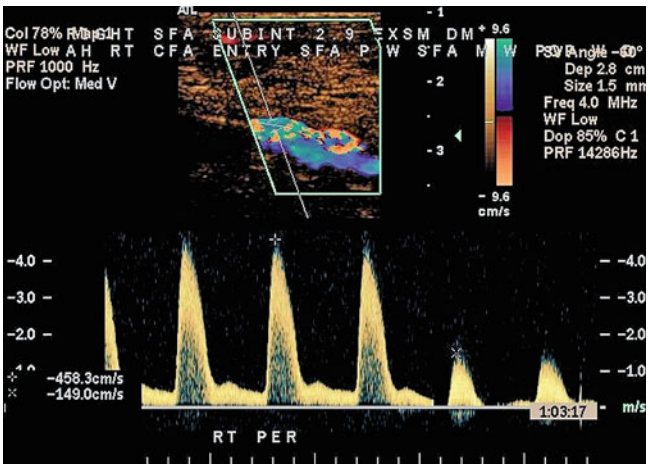


**Fig. 28.1** Significant increase in local velocity, confirmed by aliasing in color and PSV ratio. Severe peroneal artery stenosis suggested based on PSV ratio >3 (458.3/149 = 3.07)

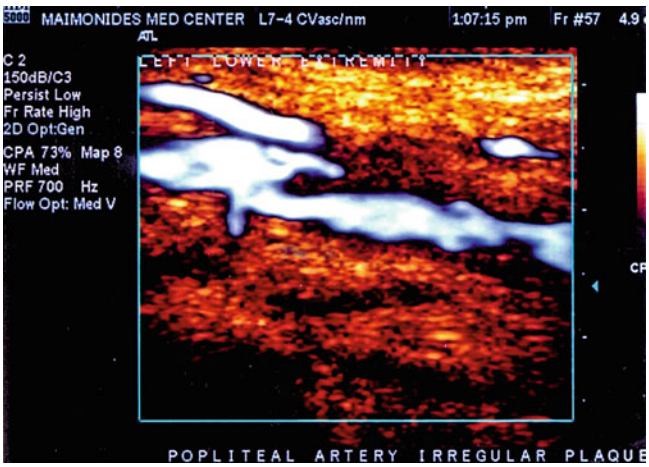


**Fig. 28.2** Longitudinal image of the popliteal artery showing irregular plaque. Imaging must continue distally in search of a distal anastomotic site

grade severe stenosis. If dilatation of a stenosis is considered, the test may be repeated after treadmill exercise.

The iliac arteries are also commonly imaged with a low-frequency abdominal transducer. Patient size may allow the use of a linear transducer, particularly during imaging of the external iliac artery. Images are obtained in transverse, longitudinal, and several oblique positions. Patient and transducer positioning are constantly changed to obtain appropriate images. Forceful pressure to bring the transducer closer to the iliac artery segment under scrutiny is common. Flow waveforms are obtained at the proximal and distal common iliac arteries and at various segments of the external iliac artery. Occlusion, aneurysms, stenosis, and conditions of the arterial wall are observed with B-mode, color flow, and power Doppler imaging. Aliasing and increased velocities are scrutinized at stenotic sites. Usually, a local doubling in peak systolic velocity represents a hemodynamic significant stenosis corresponding to a 50% diameter reduction. A local tripling in peak systolic velocity corresponds to a severe stenosis greater than 75% diameter reduction (Fig. 28.1). A significant stenosis should result in a monophasic flow waveform distal to the stenotic site. Plaques in large iliac arteries, however, may not alter the triphasic characteristic of the common femoral waveform. Examination after treadmill exercise is recommended to evaluate such cases [24].

Patency or obstruction of the iliac arteries and aorta is reevaluated during the treatment procedure. Intra-arterial pressure measurements are performed from the groin and compared to brachial pressures. A decrease greater than 20 mmHg indicates the presence of a hemodynamically significant stenosis. Pressure measurements are more sensitive to detection of a stenosis once iliac flow is increased after an infrainguinal procedure. The drop in pressure across a stenosis is proportional to the flow rate through the lesion. Pending intra-arterial pressure evaluation, dilatation, and perhaps stenting of the iliac artery may be considered in addition to infrainguinal reconstruction.

In summary, the long protocol requires imaging from the perirenal aorta to the groin in both extremities. The short protocol does not include aortoiliac mapping if the common femoral waveforms are clearly triphasic and intra-arterial pressures are going to be measured during the treatment procedure.

## Femoropopliteal Segment

DUAM is commonly performed with a high-frequency linear transducer. Imaging of the adductor canal may have to be performed with a low-frequency sector probe in the patient with a large thigh. A monophasic flow waveform in the popliteal artery is indicative of severe stenosis or segmental occlusion of the femoropopliteal segment. The scan of these arteries is performed in transverse and/or longitudinal sections to obtain B-mode, color flow, and/or power Doppler images. High persistence and low velocity scale improve detection of low flow in obstructed arteries. Many patients requiring treatment have segmental occlusion(s) of the femoropopliteal arteries.

Endovascular treatment of this segment requires complete mapping. Serial significant stenoses or occlusions can be present.

A short protocol can be established if the patient is a candidate for a distal bypass or even a femoropopliteal bypass. The arterial mapping continues from the common femoral to the site of most proximal occlusion or severe stenosis. The site of a proximal anastomosis is then selected within this patent segment. The scan is then restarted at the popliteal artery. This artery is scanned in its entirety to determine if it is a candidate for the site of the distal anastomosis (Fig. 28.2).

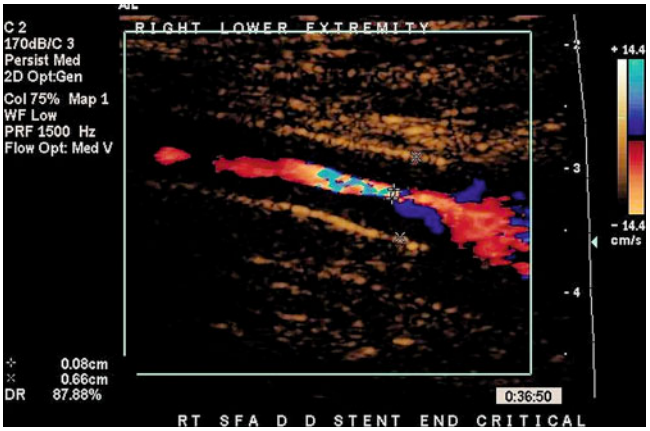


**Fig. 28.3** Critical (87.88%) restenosis in the previously stented superficial femoral artery

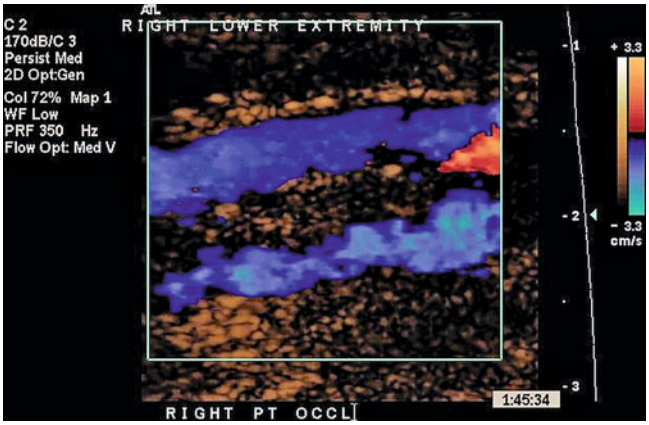


**Fig. 28.4** Imaging of the posterior tibial veins identifies the occluded artery as the posterior tibial artery

Occlusions are confirmed by lack of color flow or Doppler waveforms performed in very low, high sensitive velocity scales. The first stenosis may be graded based on velocity measurements. Doubling or tripling at the stenotic locale indicates a hemodynamic significant or severe stenosis, usually equated to a 50% or 75% diameter reduction. The hemodynamic energy lost in the first stenosis precludes velocity grading of additional, distal, sequential stenoses. It may be possible to locate such stenoses based on aliasing at low, high sensitive color flow velocity scales. An apparent aliasing signal may be obtained. Otherwise, stenoses are perceived based on narrowing of the color flow channel (Fig. 28.3). Branch analysis clarifies sites of collateral flow takeoff prior to severe obstructions and/or collateral flow reentry distal to such obstructions.

In summary, a long femoropopliteal imaging protocol is required prior to an endovascular procedure. A short protocol from the common femoral down to the first occlusion/severe stenosis site is acceptable to select the location of the proximal anastomosis of a bypass graft. Imaging of the entire popliteal artery is recommended in both instances. Imaging must continue distally in search of a distal anastomotic site. Color flow bleeding beyond stenotic lumen or noncircular lumen requires additional imaging for a complete evaluation.

## Infrapopliteal Arteries

Imaging of diseased infrapopliteal arteries demands appropriate patient preparation. The room and the patient must be warm. Creating conditions for vasodilation of the peripheral arteries helps detection of patent segments. Mapping may actually be easier in patients with inflammatory or infectious conditions due to the degree of vasodilation already present. Detection of patent, small segments is most difficult in extremities with severe rest pain and cold feet. Manual compression maneuvers may elicit blood movement in apparently occluded segments. Performing the scan with the leg dependent may actually help visualization of small arteries dilated by the hydrostatic pressure. Contrast ultrasound mapping is recommended prior to amputation based on lack of a distal target for a bypass graft.

DUAM is performed with high-frequency linear transducers. The posterior artery at the ankle is an easy start. Occlusion or patency is determined. If patent, the scan continues until the tibioperoneal trunk, if anatomically or ultrasonographically possible, or until a reentry branch distal to an occlusion. Edema, large legs, and occlusions make imaging difficult. Occlusions are documented by association with the posterior tibial veins (Fig. 28.4). Large legs and edema may have to be scanned with a low-frequency sector probe.

On occasion, color flow imaging of a patent distal posterior tibial artery is followed toward the posterior terminal branch of the peroneal artery into the peroneal artery. Once the proximal scan of the posterior tibial artery is completed, the scan continues distally through the common plantar artery and its bifurcation. The objectives of the distal scan are to find a potential plantar target for a distal anastomosis or to evaluate the posterior tibial artery runoff in case the distal anastomosis is to be placed at the calf or ankle level. A short protocol may start at the ankle and stop at the most distal location of a stenosis or occlusion that needs to be bypassed. Wasting time imaging occluded or diseased arteries that are going to be bypassed is avoided.

The mapping of the anterior tibial artery follows a similar routine in the anterior compartment. First, the segment at the ankle is evaluated. The relation to the tibia and fibula is essential for identification of the anterior tibial artery. The learning of cross-sectional anatomy is extremely valuable. A monophasic waveform indicates proximal severe stenosis or occlusion. The scan toward the popliteal artery can be performed in transverse or longitudinal sections. Although a B-mode scan is potentially feasible, longitudinal color flow or power

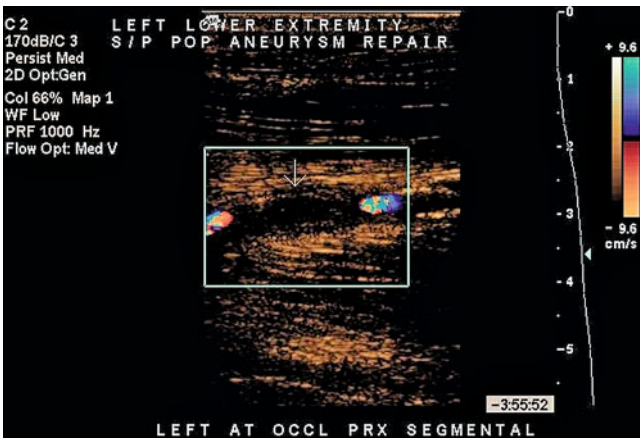


**Fig. 28.5** Short focal occlusion of proximal anterior tibial artery (*arrow*)

Doppler imaging is most common and practical. A patent distal anterior tibial may be fed via the anterior terminal branch of the peroneal artery. The anterior tibial veins are smaller than the posterior tibial veins. Therefore, identification of potentially occluded segments must rely on other secondary information. For example, the arterial channel may appear irregular in sites where the flow is diverged via short collaterals. Long collaterals may also take over the task to deliver blood to patent distal segments. A sector probe may be needed to image the proximal part of the anterior tibial artery. From a posterior approach, the anterior tibial artery branches deeply from the popliteal artery. A common beginner's error is to identify a superficial, posterior branch of the popliteal artery as the anterior tibial artery instead of a geniculate branch or an artery toward the gastrocnemius muscle.

Once the proximal scan of the anterior tibial artery is completed, the scan continues distally through the dorsal pedal artery. It is necessary to pay attention to anatomic variants that include tarsal arteries or unusual endings of the anterior terminal branch of the peroneal artery. The dorsal pedal divides into a deep plantar branch that communicates with the posterior circulation and a more superficial transmetatarsal artery that eventually feeds the digits. The objectives of the distal scan are to find a potential pedal target for a distal anastomosis at the dorsal pedal artery or to evaluate the anterior tibial artery runoff in case the distal anastomosis is to be placed at the calf or ankle level. A short protocol may start at the ankle and stop at the most distal location of a stenosis or occlusion that needs to be bypassed (Fig. 28.5). Wasting time imaging occluded or diseased arteries that are going to be bypassed is avoided.

The peroneal artery is approached with a high-frequency probe at a posterolateral position. Learning cross-sectional anatomy to identify the peroneal vessels in relation to the fibula is recommended. Longitudinal color flow or power Doppler scanning is preferred to transverse or B-mode imaging for practical reasons. If possible, a transverse scan is highly informative about other arteries, veins, and anatomic references. Completion of a peroneal artery scan is less likely than completion of a posterior tibial or anterior tibial artery scan. The problems are encountered in a large, edematous calf. The proximal peroneal artery and the tibioperoneal trunk are often difficult, and they may have to be studied with a low-frequency sector probe. Branching and collateral networks may create difficulties in identifying a patent peroneal artery. Bypasses have been extended to a branch of the peroneal artery initially identified as the peroneal artery on arteriography. Ultrasound has the advantage of identifying the peroneal veins adjacent to the peroneal artery. The anterior and posterior terminal branches of the peroneal artery may feed the distal posterior tibial and anterior tibial arteries. Therefore, posterior or anterior tibial ABIs may actually represent peroneal pressures. A short protocol may start at the ankle and stop at the most distal location of a stenosis or occlusion that needs to be bypassed. Wasting time imaging occluded or diseased arteries that are going to be bypassed is avoided.

## The Anastomotic Site

Ultrasound B-mode imaging allows for detailed examination of the arterial walls. A thin, flexible, compressible arterial segment can be selected. A rigid, calcified wall can be avoided. Although calcification may be a hindrance for ultrasonic evaluation of some stenoses, a great advantage of ultrasound is to identify all calcified segments and redirect the anastomotic site to a soft arterial segment. The surgeon may opt for a local endarterectomy and patch over a stenotic site to provide blood flow not only distally but proximally also. Often the bypass graft provides enough pressure to dilate small arteries and collaterals that feed the muscles upstream. A decision has to be made if the arterial wall is thickened. Initially, the tendency is to avoid a thickened wall as a site for a distal anastomosis. Close examination, however, has shown that vascular surgeons have approached thickened arteries and have performed anastomoses in arteries apparently normal by arteriography. Indeed, if needed, an anastomosis may even be performed over a calcified segment [25]. Nevertheless, ultrasound imaging can classify the segments into soft, thickened, or calcified.

## Vein Mapping

Arterial mapping should either start or end with vein mapping, particularly if a distal bypass graft is being considered as treatment [13]. Anastomotic sites may be altered based on length of vein available for the bypass. Saphenous or arm vein mapping is performed with high-frequency transducers. Venous patency and conditions of the vein wall are evaluated. Diameters and length of vein available are measured. Location of the vein may be marked on the skin to facilitate the surgical procedure. Tributaries may be marked if an in situ bypass is being considered. A cephalic vein 2 mm in

diameter often dilates to become a 4-mm bypass graft [26]. The arm veins dilate with placement of a tourniquet in the upper arm. Saphenous veins do not dilate as much. A dilation maneuver to determine if vein diameter can increase with temperature or hydrostatic pressure is recommended if the saphenous vein diameter is less than 4 mm. The vein wall must be thin. Thickened walls suggest a previous event of venous thrombosis. Usually these vein segments are avoided. Valve sinuses can be disrupted. The ultrasound imaging shows various structures apparently floating in the vein valve sinus region. The potential for causing graft stenosis or occlusion exists if these segments are implanted.

In summary, veins are mapped in conjunction with the arteries to plan for arterial revascularization. The conditions of the venous wall, vein diameters, and length available are recorded.

### Posttreatment Follow-Up

Ultrasound or physiologic testing is recommended to follow patients (1) with mild peripheral arterial disease, (2) treated medically, (3) who had an endovascular procedure, or (4) who had open surgery, particularly a bypass graft.

### Procedure Follow-Up

Follow-up of bypass grafts in the postoperative period and at 3, 6, 9, 12, 18, and 24 months and yearly thereafter is recommended. Long protocols include evaluation of the bypass graft and proximal and distal arteries, particularly the bypass runoff arteries. A stenosis can be graded based on the B-mode/color flow imaging or on increased velocities. The scan must continue after one defect is found. The graft or arteries may have additional stenoses. A short protocol can be performed based on the measurements of volumetric blood flow rate in milliliters/minute. If a first ultrasound scan is normal, then flow rate can become a parameter to indicate the need for another complete scan. If flow rate decreases by 20–30% between tests, then a complete scan is indicated. Several details, however, must be followed during flow rate measurement. Only pulsatile flow must be considered. Diastolic flow is variable and adaptable to numerous conditions of vasodilation. It is recommended that measurements be performed in similar conditions of vasodilation as indicated by toe temperatures. Recommended toe temperature for such measurements is 28°C (26–30°C). Another indication for a full duplex ultrasound evaluation is if pulsatile flow rate falls below a minimum flow threshold value indicating poor perfusion: <50, 40, 30 ml/min of pulsatile flow for bypass grafts to the popliteal, tibial, or paramalleolar level, respectively. Low flow states are not caused only by graft or peripheral arterial obstruction. A failing heart is often the cause of a low flow state. A low flow state with unobstructed peripheral conduits is an indicator of a poor heart condition with a high mortality rate within 1 year. The natural history of endovascular procedures has yet to be determined for most of the procedures now performed. Follow-up, therefore, should be more stringent than that for bypass grafts. A full duplex ultrasound evaluation is recommended. Sites of wall thickening, neointimal proliferation, and stenoses are documented with imaging and velocity measurements. Stents have different compliance than arteries, apparently causing increases in velocity. Criteria used to classify arteries as normal or stenosed still need to be adapted to stented conduits. In summary, peripheral arterial procedures must be followed routinely and constantly at least for the first 12 months. Detection and treatment of stenoses provide better long-term patency rates than thrombectomy of an occluded bypass or than a secondary vascular reconstruction [27].

### Patient Follow-Up

Patient follow-up includes testing the contralateral limb besides evaluation of an extremity treated with open or endovascular surgery. Eventually, the contralateral limb will demand similar treatment. Patients treated medically are often tested annually in the vascular laboratory. Patients at risk of developing significant peripheral arterial occlusive disease should also be tested routinely. All these patients benefit from a vascular rehabilitation program designed to educate patients on risk factors, peripheral arterial disease, dieting, and exercise habits. Indeed, patient conditioning is suggested prior to surgical treatment to potentially minimize the operative morbidity.

## Implementation

This section deals with the third objective of this chapter. It discusses several philosophies to prepare a team for DUAM as the sole preoperative imaging modality prior to open or endovascular surgery to treat the ischemic leg.

### Fundamental Objective

Many have the misconception that the fundamental objective of DUAM is to replace X-ray contrast arteriography. Such a concept is fundamentally wrong. As an analogy, one of the problems with a nuclear power plant that had to be closed was that they were not monitoring the fundamental variable.

A valve was being monitored as closed or opened. That is an indirect variable. The fundamental information needed was if there was flow or not through the valve. The valve could be closed and defective, allowing flow of unwanted material through the conduit.

The fundamental objective of DUAM is to permit safe and effective treatment. For a bypass, for example, if DUAM permits appropriate selection of the locations for the proximal and distal anastomoses, then agreement with arteriography becomes secondary.

An important point to consider is that several alternatives of treatment exist. A patient may go to different doctors and receive different proposals of treatment. Indeed, a study demonstrated that the same surgeon, receiving the same clinical and imaging information, may opt for different forms of treatment in almost one-third of the cases [28]. More specifically, one service may have preference to perform a bypass to the peroneal artery, while another service may use the anterior tibial artery as the preferred target. The fundamental concept is that DUAM becomes very effective if it is the target for the particular surgeon or team that is actually treating the patient. Constant and specific communications between the ultrasonographer and the surgical team are a major prerequisite for successful preoperative arterial mapping. This principle is also applicable to arteriography. If a clinical decision has been made to treat the aortoiliac segment, an infrainguinal arteriogram is unnecessary. In contrast, a beautiful arteriogram of the proximal arteries is unnecessary if the surgeon needs a detailed evaluation of the arteries of the leg and foot [29].

In summary, the fundamental objective of DUAM is to provide information for effective treatment, not to mimic arteriography. The needs of the treatment team must be met. Continuous interaction between the vascular laboratory and the surgical team creates the basis to accomplish the fundamental objective of DUAM.

## Learning Phase

The learning phase includes a gradual evolution from detection of flow waveforms with a continuous-wave Doppler to complete or limited imaging protocols to define the operative procedure. Progressively, this phase includes detection of flow waveforms at the common femoral, superficial femoral, and distal infrapopliteal arteries with a duplex ultrasound scanner. Segmental imaging and flow evaluation are accomplished. The next step is to image the entire femoropopliteal segment as waveforms are recorded during a segmental physiologic evaluation. Imaging of the aortoiliac segment and of infrapopliteal arteries then becomes the hardest step. As the training, skills, and confidence improve, then the steps described below represent alternatives to document the qualifications of the team.

## Comparison with Arteriography

The initial training most likely includes comparison between DUAM and arteriography or, now, MRA [6, 9, 10, 13, 15]. Several studies have compared accuracy, sensitivity, specificity, and predictive values of ultrasound mapping to arteriographic findings. Some have had better success in detecting obstructions in the aortoiliac segment and others in the femoropopliteal segment. Agreement in the comparison of infrapopliteal findings has been inferior to agreement in the comparison of findings in the most proximal segments. One error is to consider arteriography or MRA as reference standards. These techniques often fail to demonstrate arteries distal to occlusions or do not have enough anatomical landmarks for the necessary identification of the vessels visualized. Ultrasound is often incomplete in large, edematous segments with calcified arteries. Another drawback noted in several studies was the strict dependence on velocity measurements only. Increased velocities are inadequate for analysis of secondary, distal stenoses. All color flow duplex Doppler information must be considered. Apparently, documentation of a patent segment by any technique should be the standard. Nevertheless, segmental comparison with arteriography or MRA helps training of the ultrasonographer and improves confidence to determine if the ultrasound is informative, in agreement or not with other techniques.

## Virtual Decision Making

Studies have compared surgical decisions based on ultrasound mapping with decisions based on arteriographic imaging [13, 30, 31]. Usually, such decisions were from different interpreters. Although this process is effective for training, it fails to consider that multiple alternatives for treatment are possible in many patients. Furthermore, interpersonal variability in surgical decision making must be taken into consideration.

A variant of virtual decision making that was successful at the Maimonides Medical Center was to analyze the decision made by one vascular surgeon based on the surgeon's own ultrasound scanning. A senior vascular surgeon accepted or rejected the surgical decision based on ultrasound while observing the corresponding arteriogram. This learning phase demonstrated that 15 cases were needed to educate the ultrasonographer and to perceive the preferences of the vascular surgeon. Another lesson was to recognize when the ultrasound examination was incomplete either due to ana-

tomic or pathologic constraints or to lack of patient cooperation with the study. Patients in contracted positions, or constantly moving, for example, are not ideal for ultrasound mapping.

## Actual Decision Making

Several variants at various levels are available for actual decision making:

1. The patient may be scheduled for surgery based on the ultrasound mapping with the plan to perform an intraoperative, pretreatment, or prebypass arteriogram.
2. The treatment plan or the bypass may be actually carried out based on the preoperative ultrasound mapping, and completion X-ray arteriography is performed at the end of the procedure.
3. The treatment plan is carried out based on ultrasound, and a completion ultrasound arteriogram is performed at the end of the procedure.

Conditions to perform X-ray arteriography and to measure intra-arterial pressures are highly desirable, even if the entire treatment is planned based on preoperative and perioperative ultrasound imaging. Such techniques become prominent if treatment of an iliac artery follows infrainguinal revascularization.

## Disadvantages of Ultrasonography

Ultrasound (US) has several limitations as mentioned below. Some frequently mentioned disadvantages, however, may be dogmatic, while others can be reinterpreted as potential advantages:

1. US requires contact with the skin. Certain patients have profound wounds that preclude appropriate placement of the US probe to conduct a high-quality examination.
2. US often requires patient collaboration. Although possible to perform an US examination in a sedated patient, a preoperative examination is most commonly performed with the patient awake. High-quality US is almost impossible in patients with major contractures.
3. US is "operator dependent." This is a common saying that should be considered extremely dogmatic. It is true that US is operator dependent. As if the other technologies were not operator dependent! Skill is required not only to perform an arteriogram, for example, but detailed knowledge is essential for the selection of the proper arteriographic, MR, and CT sequences. Tridimensional reconstruction also requires special training and specific knowledge. In conclusion, all technologies employed for peripheral arterial imaging are "operator dependent."

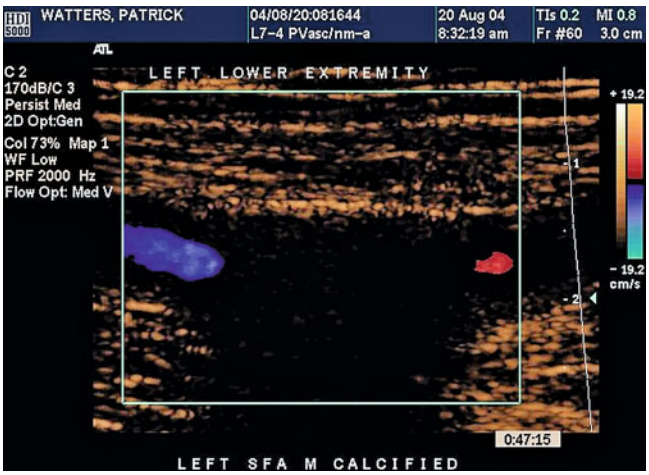


**Fig. 28.6** The lumen of this calcified segment of the superficial femoral artery cannot be assessed by ultrasound due to dense shadow obscuring the color flow signal

4. US is inadequate in large patients and in edematous segments. The list of conditions that preclude a high-quality US examination may be comparable or even smaller than the lists that preclude a high-quality arteriogram, MR, or CT.
5. US fails to categorize stenosis in the presence of calcified walls or plaques (Fig. 28.6). This disadvantage of US can be used advantageously during DUAM. A significant stenosis or even occlusion may not be properly diagnosed in calcified arterial segments. However, this information is valuable in the selection of an anastomotic site, the primary goal of DUAM.
6. US has a small field of view. The other techniques can be presented as images that are readily understood and quickly assimilated. In contrast, many small US images need to be interpreted. This problem may be circumvented with drawings that describe the US findings. Extended or panoramic images address this issue to a certain extent. Computer reconstruction of a large image using cropping, rotation, and collage of small pictures is not too different than selecting two-dimensional MR images of a tridimensional data set.

## Advantages of Ultrasound Mapping

DUAM has multiple advantages over arteriography, MRA, and CTA:

1. DUAM is a noninvasive technique. Not even MRA can claim the degree of noninvasiveness associated with US. MRA requires injection of a contrast agent via a venous catheter. The magnetic field can dislodge body implants and affect the behavior of cardiac pacemakers. Indeed, at

the Maimonides Medical Center, the contraindications to the performance of MRA reach double digits. The morbidity associated with X-ray contrast arteriography is well known. Hematomas, pseudoaneurysms, and even fistulas have been created by needle puncture and catheter placement. Allergic reaction to contrast and renal morbidity are serious contraindications to arteriography, especially if the patient is a diabetic in renal failure. The latest claim against X-ray technology is that it is carcinogenic. In particular, the use of CT must be restricted significantly.

2. DUAM is portable. Arterial mapping can be performed in the vascular laboratory, in the emergency room, in the patient's room, in the operating room, in the recovery room, or almost everywhere. Access to the other technologies is limited.
3. DUAM shows the arterial wall and the obstructive plaque. Arteriography is strictly a luminogram, showing only flow. MRI and CT could, theoretically, show the arterial wall and the obstructive material. Their resolution at present, however, is inferior to that of US B-mode characterization.
4. DUAM provides hemodynamic data. Although theoretically possible with MRA, none of the other techniques presently available provides velocity and volumetric flow rate data. Hemodynamic data detected with US improves evaluation of the cardiovascular conditions including the peripheral runoff.
5. DUAM detects low flow in any direction. Arteriography often fails to detect flow distal to an obstruction [31, 32]. MRA often fails to detect flow in directions not predicted by the algorithm employed. CTA often fails to demonstrate flow in small arteries. In contrast, US is capable not only of detecting low flow but also of demonstrating blood movement in arteries without apparent flow.
6. DUAM provides information in all three dimensions. X-ray arteriography fails to describe properly stenoses that cause noncircular lumens. One single projection is inadequate in many applications. Two, even three projections or rotational arteriography cause an overload of contrast and radiation. MRA can be tridimensional, but in practice, only the longitudinal lumen is described in multiple projections. The contrast and radiation doses to obtain images of small infrapopliteal vessels with CTA are large and often fail to provide needed information. US allows for examination in all directions, creating images in transverse, longitudinal, and oblique planes.
7. DUAM provides anatomic information. US can identify the major arteries in the leg and even foot by observation of concomitant veins and other adjacent anatomical structures. CT and MRI could perform the same task if algorithms to detect both arteries and veins are developed. MRA and X-ray arteriography may provide misleading information related to the actual vessel being visualized. The interpretation of collaterals, for example, can be erroneous with luminograms.
8. DUAM is "fast." Depending on how time is measured, a 1-h DUAM procedure can be considered fast compared to the other techniques. MRA can be time-consuming. CTA and even MR need expert reconstruction that may not be available until the data are analyzed overseas, for example. If the time spent by the patient in the recovery room after X-ray arteriography is included, then this technique must be considered slower than ultrasonography.
9. DUAM is inexpensive. However, reimbursement for preoperative arterial mapping that replaces other, more expensive technologies must increase to make the US testing viable. Hospitals and physicians will continue to use X-ray arteriography, MRA, and even CTA if reimbursement for DUAM is not competitive and if they have to continue subsidizing the DUAM procedure.

**Conclusions**

Duplex ultrasound arterial mapping provides information leading to effective treatment of the lower extremity. Personnel training, open mindedness, and increased reimbursement could make DUAM a preferred option for most cases in a service geared toward patient and personnel safety and simplicity of diagnosis, perioperative imaging, and follow-up.

## References

1. Ascher E, Mazzariol F, Hingorani A, Salles-Cunha SX, Gade P. The use of duplex ultrasound arterial mapping as an alternative to conventional arteriography for primary and secondary infrapopliteal bypasses. Am J Surg. 1999;178:162–5.
2. Mazzarriol F, Ascher E, Salles-Cunha SX, Gade P, Hingorani A. Values and limitations of duplex ultrasonography as the sole imaging method of preoperative evaluation for popliteal and infrapopliteal bypasses. Ann Vasc Surg. 1999;13:1–10.
3. Mazzariol F, Ascher E, Hingorani A, Gunduz Y, Yorkovich W, Salles-Cunha SX. Lower-extremity revascularization without preoperative contrast arteriography in 185 cases: lessons learned with duplex ultrasound arterial mapping. Eur J Vasc Endovasc Surg. 2000;19:509–15.
4. Ascher E, Hingorani A, Markevich N, Costa T, Kallakuri S, Khanimoy Y. Lower extremity revascularization without preoperative contrast arteriography: experience with duplex ultrasound arterial mapping in 485 cases. Ann Vasc Surg. 2002;16:108–14.
5. Hingorani A, Ascher E. Dyeless vascular surgery. Cardiovasc Surg. 2003;11:12–8.
6. Soule N, Hingorani A, Ascher E, Kallakuri S, Yorkovich W, Markevich N, et al. Comparison of magnetic resonance angiography (MRA) and duplex ultrasound arterial mapping (DUAM) prior to infrainguinal arterial reconstruction. Eur J Vasc Endovasc Surg. 2003;25:139–46.

7. Ascher E, Markevich N, Schutzer RW, Kallakuri S, Jacob T, Hingorani A. Small popliteal artery aneurysms: are they clinically significant? J Vasc Surg. 2003;37:755–60.
8. Ascher E, Hingorani A, Markevich N, Schutzer RW, Kallakuri S. Acute lower limb ischemia: the value of duplex ultrasound arterial mapping (DUAM) as the sole preoperative imaging technique. Ann Vasc Surg. 2003;17:284–9.
9. Hingorani A, Ascher E, Markevich N, Kallakuri S, Hou A, Schutzer RW, Yorkovich W. Magnetic resonance angiography versus duplex arteriography in patients undergoing lower extremity revascularization: which is the best replacement for contrast arteriography? J Vasc Surg. 2004;39:717–22.
10. Hingorani A, Ascher E, Markevich N, Kallakuri S, Schutzer RW, Yorkovich W, Jacob T. A comparison of magnetic resonance angiography, contrast arteriography and duplex arteriography for patients undergoing lower extremity revascularization. Ann Vasc Surg. 2004;18:294–301.
11. Ascher E, Hingorani A, Markevich N, Yorkovich W, Schutzer RW, How A, et al. Role of duplex arteriography as the sole preoperative imaging modality prior to lower extremity revascularization surgery in diabetic and renal patients. Ann Vasc Surg. 2004;18:433–9.
12. Ascher E, Markevich N, Schutzer RW, Kallakuri S, How A, Nahata S, et al. Duplex arteriography prior to femoral-popliteal reconstruction in claudicants: a proposal for a new shortened protocol. Ann Vasc Surg. 2004;18:544–51.
13. Ascher E, Salles-Cunha SX, Hingorani A, Markevich N. Duplex ultrasound arterial mapping before infrainguinal revascularization. In: Mansour MA, Labropoulos N, editors. Vascular diagnosis. Philadelphia: Elsevier Saunders; 2005.
14. Beebe HG, Salles-Cunha SX. Rational use of the vascular diagnostic laboratory. In: Zelenock GB, editor. Problems in general surgery. Philadelphia: J.B. Lippincott Company; 1994. p. 527–41.
15. Beebe HG, Salles-Cunha SX. Vascular laboratory testing for arterial disease. In: Greenfield LJ, Mulholland MW, Oldham KT, Zelenock GB, Lillimoe KD, editors. Surgery: scientific principles and practice. 3rd ed. Philadelphia: Lippincott Williams & Wilkins; 2001. p. 1604–13.
16. Salles-Cunha SX, Wakefield TW. Vascular diagnostics with special emphasis on ultrasound. In: Mulholland MW, Lillemoe KD, Doherty G, et al., editors. Greenfield's surgery: scientific principles and practice. 4th ed. Philadelphia: Lippincott Williams & Wilkins; 2006.
17. Salles-Cunha S, Andros G, Harris R, Dulawa L, Oblath R, Schneider P. Poster. Infrapopliteal hemodynamics in patients with different anterior and posterior tibial artery pressures. In: Program of the 6th San Diego symposium on vascular diagnosis, San Diego; 15–21 Feb 1992. p. 31.
18. Salles-Cunha SX, Vincent DG, Towne JB, Bernhard VM. Noninvasive ankle blood pressure measurements by oscillometry. Tex Heart Inst J. 1982;9:349–57.
19. Vincent DG, Salles-Cunha SX, Bernhard VM, Towne JB. Noninvasive assessment of toe systolic pressures with special reference to diabetes mellitus. J Cardiovasc Surg. 1983;24:22–8.
20. Vollrath KD, Salles-Cunha SX, Vincent DG, Towne JB, Bernhard VM. Noninvasive measurement of toe systolic pressures. Bruit. 1980;4:27–30.
21. Sondgeroth TR, Salles-Cunha SX, Vollrath KD, Towne JB. Variability of toe pressure measurements. Bruit. 1982;6:14–6.
22. Gale SS, Scissons RP, Salles-Cunha SX, Dosick SM, Whalen RC, Pigott JP, Beebe HG. Lower extremity arterial evaluation: are segmental arterial blood pressures worthwhile? J Vasc Surg. 1998; 27:831–9.
23. AbuRahma AF, Khan S, Robinson PA. Selective use of segmental Doppler pressures and color duplex imaging in the localization of arterial occlusive disease of the lower extremity. Surgery. 1995; 118:496–503.
24. Coffi SB, Ubbink DT, Zwiers I, van Gurp JA, Legemate DA. Improved assessment of the hemodynamic significance of borderline iliac stenosis with use of hyperemic duplex scanning. J Vasc Surg. 2002;36:575–80.
25. Ascer E, Veith FJ, Flores SA. Infrapopliteal bypasses to heavily calcified rock-like arteries. Management and results. Am J Surg. 1986;152:220–3.
26. Salles-Cunha SX, Andros G, Harris RW, Dulawa LB, Oblath RW. Preoperative, noninvasive assessment of arm veins to be used as bypass grafts in the lower extremities. J Vasc Surg. 1986;3: 813–6.
27. Bandyk D, Bergamini TM, Towne JB, Schmitt DD, Seabrook GR. Durability of vein graft revision: the outcome of secondary procedures. J Vasc Surg. 1991;13:200–8.
28. Kohler TR, Andros G, Porter JM, Clowes A, Goldstone J, Johansen K, et al. Can duplex scanning replace arteriography of lower extremity arterial disease? Ann Vasc Surg. 1990;4:280–7.
29. Schneider PA, Ogawa DY. Is routine preoperative aorto-iliac arteriography necessary in the treatment of lower extremity ischemia? J Vasc Surg. 1998;28:28–34.
30. Wain RA, Berdejo GL, Delvalle WN. Can duplex scan arterial mapping replace contrast arteriography as the test of choice before infrainguinal revascularization? J Vasc Surg. 1999;29:100–7.
31. Lowery AJ, Hynes N, Manning BJ, Mahendran M, Tawfik S, Sultan S. A prospective feasibility of duplex ultrasound arterial mapping, digital-subtraction angiography, and magnetic resonance angiography in management of critical lower limb ischemia by endovascular examination. Ann Vasc Surg. 2007;21(4): 443–51.
32. Salles-Cunha SX, Engelhorn C, Miranda Jr F, Burihan E, Lourenco MA, Engelhorn AL, Cassou MF. Distal revascularization: comparison of incomplete images of infrapopliteal arteries in severely ischemic lower extremities. J Vasc Bras. 2003;2 Suppl 1:S34.

# Noninvasive Diagnosis of Upper Extremity Arterial Disease

29

Gregory L. Moneta

**Abstract**

Diagnosis of upper extremity arterial disease is complex as ischemia of the upper extremity may be caused by systemic disease as well as localized manifestations of atherosclerosis. For chronic disorders of upper extremity ischemia, Raynaud's syndrome is often the initial presenting symptom. Noninvasive testing for upper extremity arterial disease includes digital pressures, segmental arm pressures, arterial waveforms using photoplethysmography and/or continuous wave Doppler, and testing for cold-induced vasospasm as well as evaluation with duplex ultrasound for evidence of arterial stenosis or aneurysm. Noninvasive studies facilitate the diagnosis of vasospasm when bilateral abnormalities of digit circulation are induced by cold or emotional stimuli with normal findings at rest. Systemic disorders of digital circulation are characterized by bilateral abnormalities of digital circulation at rest with normal findings proximal to the wrist. More proximal lesions are diagnosed by abnormalities of segmental pressures or duplex findings suggestive of aneurysm or stenosis. Applied properly, with background knowledge of the conditions resulting in upper extremity ischemia, the combination of the history and physical examination, plain x-rays of the shoulder and neck, blood tests, and noninvasive and possibly invasive examinations of the arteries of the upper extremity arteries can in the large majority cases determine the etiology of upper extremity ischemia and guide treatment.

**Keywords**

Upper extremity ischemia • Raynaud's syndrome • Vasospasm • Digital artery • Segmental pressures • Duplex ultrasound • Plethysmography • Cold testing • Connective tissue disease Embolization

## Introduction

Symptomatic arterial disease of the upper extremity accounts for approximately 5% of cases of extremity ischemia. Atherosclerosis is by far the most common disorder affecting lower extremity arteries. However, ischemia in the upper extremity may be caused by a variety of systemic diseases as well as atherosclerosis. Diagnosis of upper extremity arterial disease is therefore complex. History and physical examination, plain x-rays of the neck and shoulder regions, blood tests, and noninvasive and possibly invasive examinations of the arteries of the upper extremity arteries may all be needed.

The information required for the diagnosis of upper extremity ischemia can often be accomplished using only noninvasive testing. Noninvasive testing in combination with the history and physical exam will generally provide the information required to diagnose and guide treatment for upper extremity ischemia. Noninvasive testing for upper

G.L. Moneta, M.D.
Department of Vascular Surgery,
Oregon Health and Science University,
3181 SW Sam Jackson Park Road, Portland, OR 97239, USA
e-mail: monetag@ohsu.edu

A.F. AbuRahma, D.F. Bandyk (eds.), *Noninvasive Vascular Diagnosis*,
DOI 10.1007/978-1-4471-4005-4_29, 

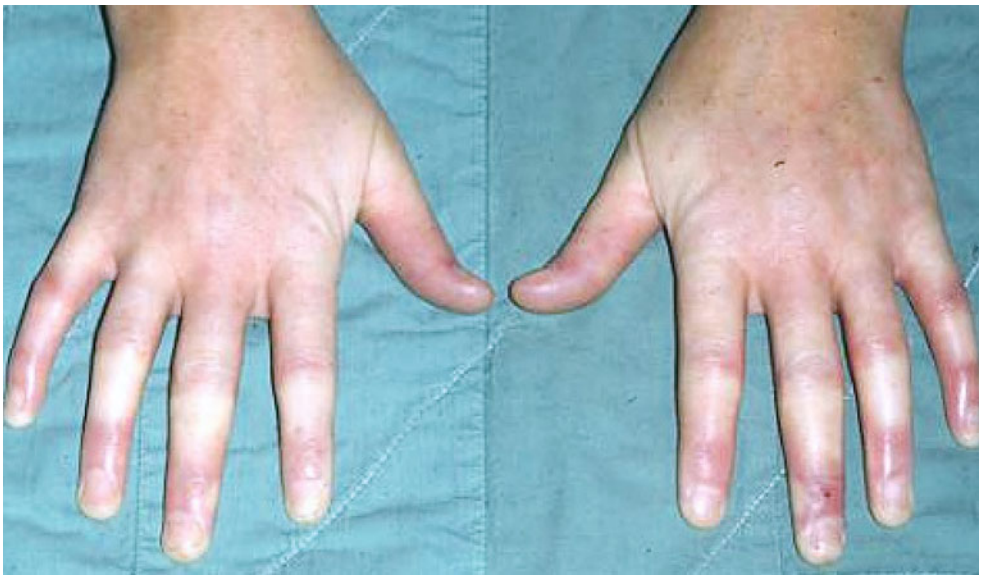

**Fig. 29.1** Raynaud's attack in a 46-year-old female

extremity arterial disease includes segmental arm pressures, digital pressures and arterial waveforms using photoplethysmography, and testing for cold-induced vasospasm. Duplex evaluation can also be important but often has a more limited role than in evaluation of lower extremity disease.

## Presentation

Most clinical conditions producing upper extremity ischemia will include Raynaud's syndrome as a manifestation. Classic Raynaud's attacks consist of intense pallor of the fingers in response to cold or emotional stimuli followed by cyanosis and rubor with rewarming (Fig. 29.1). Full recovery occurs 15–45 min after the inciting stimulus is removed. Classic tricolor attacks do not occur in all patients. Some patients develop only pallor or cyanosis during attacks. Patients may even complain of cold hands without color changes but will have abnormal findings on noninvasive examinations identical to classic Raynaud's patients.

Patients with Raynaud's syndrome are divided into two groups. Raynaud's disease is a term used to describe an idiopathic benign form of intermittent digital ischemia. "Raynaud's phenomenon" describes a similar symptom complex in association with an underlying disease. An underlying condition will be discovered in association with Raynaud's syndrome in only 5% of cases [1]. However, it is well recognized associated diseases may not be diagnosed when a patient presents with Raynaud's attacks [2]. Distinction between Raynaud's disease and Raynaud's phenomenon is therefore artificial. Raynaud's attacks should be considered a symptom that requires a diagnosis rather than a diagnosis in itself. That diagnosis in most cases will be idiopathic episodic vasospasm. In cool, damp climates, 6–20% of the population, particularly young females, report Raynaud's symptoms [3]. Vasospasm, outside that induced by vasoactive medications or ergot, rarely results in ulceration or gangrene (Fig. 29.2). Digital ulceration or gangrene in association with Raynaud's attacks should trigger a work-up to evaluate for digital artery occlusions and an underlying condition that leads to digital artery occlusion.

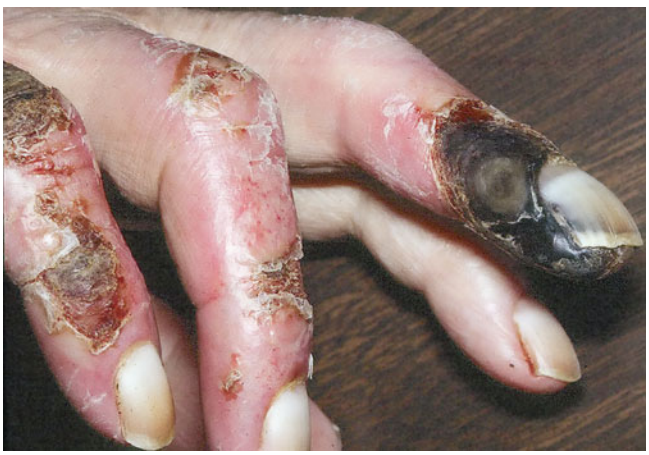

**Fig. 29.2** Digital gangrene in a patient with long-standing diabetes and renal failure. Digital gangrene is almost associated with digital artery obstruction

## Pathophysiology

A useful classification scheme for diagnosis of upper extremity ischemia based on vascular laboratory and physical examination findings is to divide patients into those with large artery disease and those with small artery disease. Serologic testing further facilitates determination of prognosis [4].

**Table 29.1** Diseases associated with intrinsic digital artery occlusions

| Disease type | Example |
|---|---|
| Connective tissue disease | Scleroderma, CREST syndrome, systemic lupus erythematosus, rheumatoid arthritis, Sjøgren's syndrome, mixed connective tissue disease, dermatomyositis, small and medium vessel vasculitis |
| Atherosclerosis and occlusive arterial disease | Atherosclerosis obliterans, atheroembolism, diabetic distal arterial disease, thromboangiitis obliterans (Buerger's disease) |
| Thromboembolism | Cardiac embolism, arterial embolism, paradoxical embolism |
| Large vessel vasculitis | Takayasu's arteritis, extracranial temporal arteritis |
| Dynamic entrapment | Arterial thoracic outlet syndrome |
| Occupational arterial trauma | Hypothenar hammer syndrome, vibration-induced Raynaud's syndrome |
| Drug-induced vasospasm | β-blockers, vasopressors, epinephrine, ergot, cocaine, amphetamines, vinblastine/bleomycin |
| Infections | Parvovirus, hepatitis B and C, antigenemia, sepsis/disseminated intravascular coagulation |
| Malignancy | Multiple myeloma, leukemia, adenocarcinoma, astrocytoma |
| Hematologic | Polycythemia vera, thrombocytosis, cold agglutinins, cryoglobulinemia |

**Table 29.2** Conditions resulting in embolization to upper extremity digital arteries

| Source | Example |
|---|---|
| Cardiac | Atrial fibrillation, atrial thrombus, valvular disease, myxoma |
| Trauma | Blunt and penetrating trauma, occupational/ hypothenar hammer syndrome |
| Aneurysm | Subclavian artery or more peripheral artery aneurysm (ulnar artery aneurysm) |
| Fibromuscular disease | |

Small artery occlusive disease accounts for the very large majority of patients presenting with upper extremity ulceration or gangrene (Table 29.1). Large artery diseases generally produce serious upper extremity symptoms by embolization to the digital arteries (Table 29.2). Proximal occlusive disease of the subclavian artery rarely causes limb-threatening ischemia unless complicated by distal embolization to forearm or digital arteries.

Patients with vasospastic Raynaud's syndrome do not have arterial obstruction at any level and have normal digital artery pressures at room temperature. An increased force of cold-induced arterial spasm causes arterial closure in such patients. Patients with obstructive Raynaud's syndrome have obstruction of arteries between the heart and the distal phalanx. These patients must have sufficiently severe arterial obstruction to cause a significant reduction in resting digital artery pressure to produce a Raynaud's attack. Obstruction of both arteries of a single digit is generally needed. A normal vasoconstrictive response to cold is sufficient to overcome diminished intraluminal distending pressure and cause arterial closure, thereby mimicking a vasospastic Raynaud's attack. Figure 29.3 schematically demonstrates the relationship between finger pressure and finger temperature for normals and patients with vasospastic or obstructive Raynaud's syndrome.

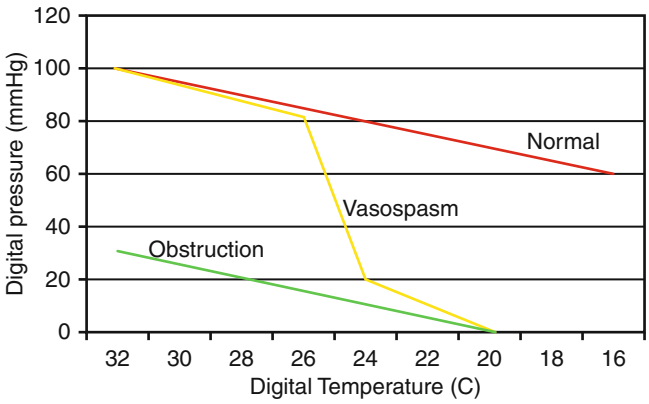


**Fig. 29.3** The normal response to cold is a linear decline in digital artery pressure. The vasospastic Raynaud's patients have a steeper decline in pressure until a threshold temperature is reached, then near instantaneous occlusion. The obstructive Raynaud's patients have lower normothermic digital artery pressures and a near normal vasoconstrictive response to cold

## Noninvasive Diagnostic Techniques

Although the physical examination is frequently completely normal in patients with Raynaud's syndrome, all noninvasive vascular laboratory testing of the upper extremities should be preceded by a physical examination. Obviously, a complete pulse examination should be performed with attention to the strength and quality of pulses as well as the presence of aneurysms or bruits. In addition, the fingers should be carefully inspected for ulcers. Hyperkeratotic areas may suggest healed ulcers. Hands and fingers should be examined for telangiectasias, skin thinning, tightening, or sclerodactyly, findings suggesting autoimmune disease. Signs and symptoms of nerve compression syndromes should also be sought. Carpal tunnel syndrome is seen in about 15% of Raynaud's patients [5].

## Segmental Arm Pressures

Upper extremity segmental pressures are obtained by measuring blood pressure with pneumatic cuffs above the elbow, below the elbow, and above the wrist while insonating the

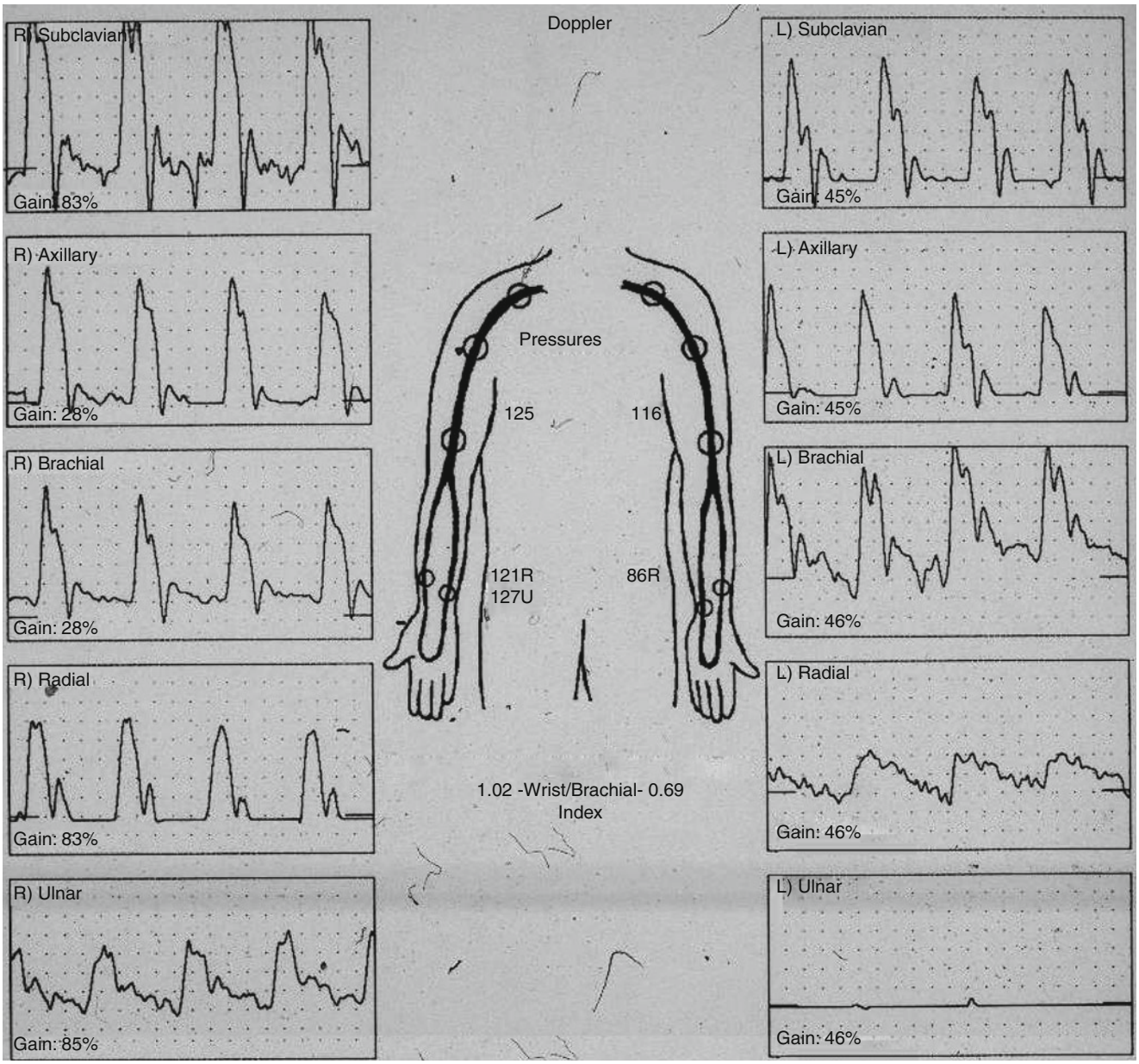


**Fig. 29.4** Segmental arm pressures and waveforms demonstrating abnormal pressures and waveforms at the radial and ulnar arteries in the left upper extremity. The study indicates arterial occlusive disease distal to the brachial artery in the left upper extremity

radial or ulnar artery at the wrist using a continuous wave Doppler. Doppler-derived or plethysmographic waveforms are also recorded at the different levels. Abnormal waveforms or pressures indicate arterial disease proximal to the site where the waveform or pressure was obtained.

A systolic pressure measurement is taken from the upper arm (brachial artery) and at the wrist (radial and ulnar arteries). A 12-cm blood pressure cuff is usually sufficient for measuring the brachial artery pressure. A 10-cm blood pressure cuff just above the wrist is used to measure radial and ulnar artery systolic pressures. Normally, there is no significant systolic pressure gradient between the brachial and wrist levels. A normal wrist/brachial blood pressure ratio is therefore 1.0. A blood pressure difference between the two arms of more than 15 mmHg is indicative of a stenosis or occlusion on the side of the lower pressure. Decreased pressures and/or abnormal waveforms at the above-elbow cuff site indicate occlusive disease at or proximal to the elbow. Normal above-elbow pressures with abnormalities at the above-wrist sites indicate brachial and/or proximal ulnar/radial arterial occlusive disease, respectively (Fig. 29.4). A blood pressure difference between levels or between the radial and ulnar arteries of more than 15 mmHg also indicates an occlusive lesion.

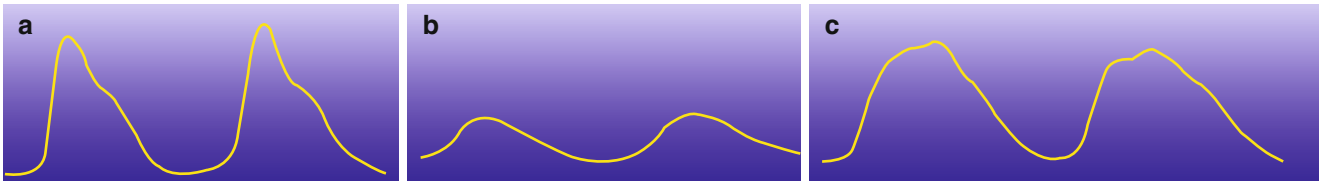


**Fig. 29.5** (**a**) Schematic of a normal PPG waveform with rapid upstroke and typical dicrotic notch. (**b**) Schematic of an obstructive PPG waveform with prolonged upstroke and rounded peak. (**c**) Peaked pulse PPG waveform. The dicrotic notch is shifted up on the waveform

## Digital Pressures and Plethysmography

Digital pressure measurements and digital plethysmography are extremely useful in the evaluation of upper extremity ischemia [6]. Photoplethysmography (PPG) or strain gauge plethysmography are both used to measure digital blood pressure and to obtain pulse waveforms. PPG is preferred by most vascular laboratories because the equipment is easier to use and more durable. PPG also allows recording of volume pulses from the tips of the fingers. This can help to document obstruction within digital arteries themselves.

To measure digital pressures, the PPG photo cell is attached to the fingertip pulp with double-sided tape or small strain gauges are placed around the fingertip. One-inch (2.5 cm) blood pressure cuffs are placed around the proximal phalanx. Waveforms are recorded using pulse tracings obtained at high speed to facilitate evaluation of the shape of the waveform. Upstroke time of the waveform should be <0.2 s. Normal waveforms may or may not have a dicrotic notch (Fig. 29.5a). An obstructive waveform has a rounded peak with an upstroke time that is prolonged (Fig. 29.5b). Finger PPG waveforms are not quantitative. Waveform amplitude is therefore not important with amplitude dependent on the gain setting, not blood flow.

Patients with vasospasm will often have an abnormally shaped waveform termed a "peaked pulse." This is thought to represent abnormal elasticity and rebound of palm and digital arteries (Fig. 29.5c).

Finger blood pressures are measured by inflating cuffs placed at the base of the fingers. Pulsations are recorded at reduced chart recorder speeds as the cuffs are inflated. After digital pulsations are obliterated, the cuff is slowly deflated until the pulsation returns. This pressure is the digital artery pressure.

Finger temperature should be measured before performing digital plethysmography and/or obtaining finger blood pressures. If the finger temperature is less than 28–30°C, false-positive results may be obtained because of cold-induced vasospasm. Hand and/or whole body warming should first be performed in patients with low finger temperatures. Finger temperatures should be recorded, so interpreting physician do not attribute abnormal findings to obstruction when the underlying problem is actually vasospasm.

Digital blood pressure is normally within 20–30 mmHg of brachial pressure. A ratio of finger systolic pressure to brachial systolic pressure >0.80 is normal. Normal values, however, do not necessarily rule out digital artery occlusive disease. Patients with very distal digital artery occlusive disease can have normal finger pressures since the digital cuff is around the proximal phalanx. Occlusive disease in a single digital artery can also be missed if the other digital artery in that finger is normal. Patients with bilateral digital PPG abnormalities generally have a small vessel systemic disorder, such as scleroderma or mixed connective tissue disease (Fig. 29.6). Those with unilateral abnormalities should be strongly considered for an ipsilateral source of embolism such as a subclavian or ulnar artery aneurysm (Fig. 29.7).

## Cold Challenge Testing

Digital temperature recovery time after immersion of the hand in ice water for a short period is the simplest cold intolerance test. Hand and body warming may be required prior to immersion. Pre-immersion digital temperatures must be above 30°C. The patient's hand is immersed in a container of ice water for 30–60 s. The test should be used with caution in patients with classic Raynaud's attacks. In such cases, cold testing adds little to the clinical management of Raynaud's syndrome. Cold immersion testing is uncomfortable and poorly tolerated by patients with significant Raynaud's syndrome symptoms, and pressures can fall to unrecordable levels in such patients.

After the hand is dried, fingertip temperatures are measured every 5 min for 45 min, or until the temperature returns to pre-immersion levels. Normal individuals have a digital temperature recovery time to pre-immersion levels of <10 min. This test is very sensitive for detecting cold-induced vasospasm but is nonspecific. Half of patients with a positive test have no clinical manifestations of cold sensitivity [7].

A better test for cold sensitivity is the digital hypothermic challenge test described by Nielsen and Lassen [8]. In the so-called Nielsen examination, a specially designed finger cuff is placed around the proximal phalanx on the test finger and

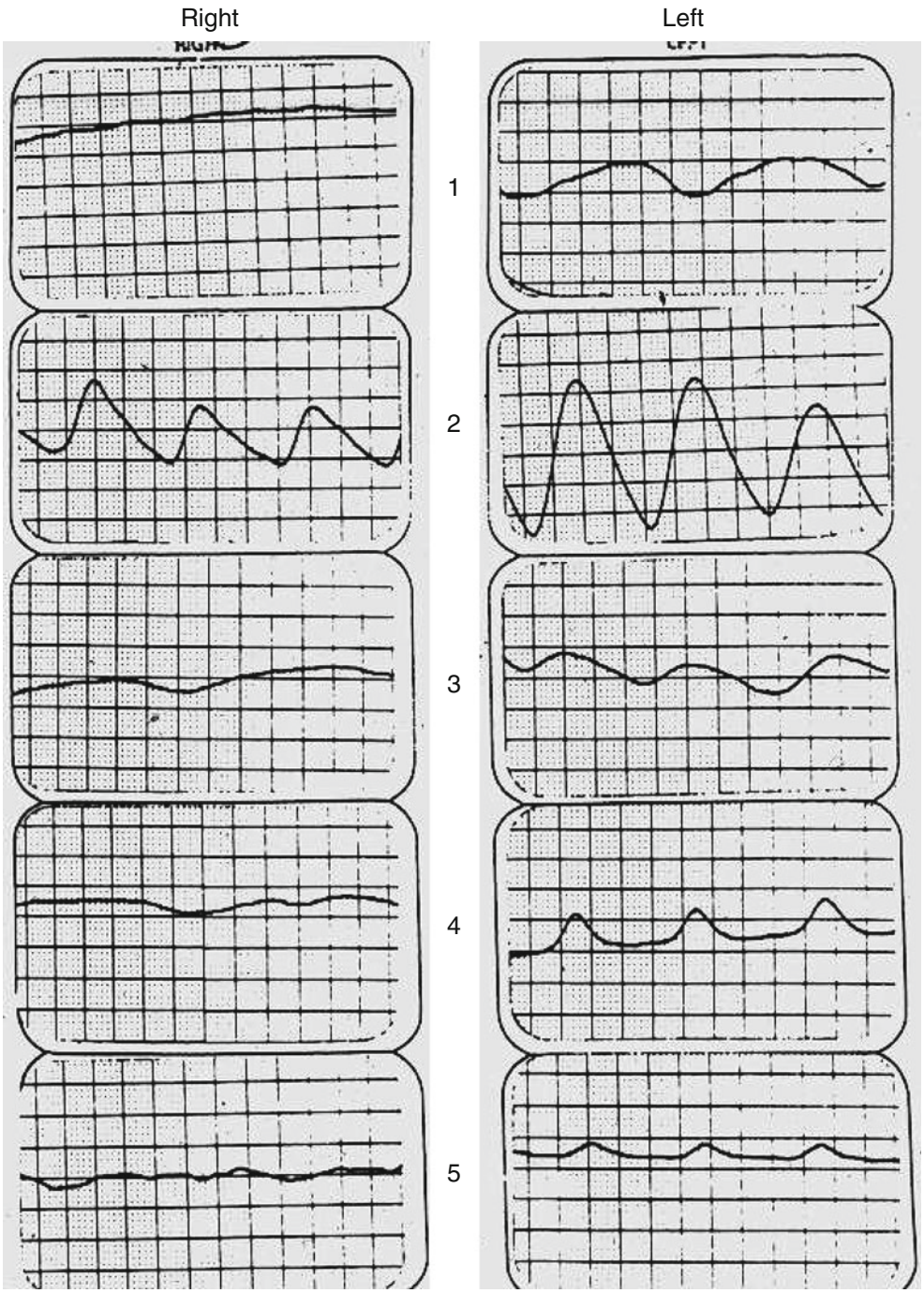


**Fig. 29.6** Bilateral abnormal digital artery waveforms in a patient with scleroderma

perfused with progressively cooler fluid. Test finger pressure is compared with the pressure from an uncooled "reference" finger (Fig. 29.8). The test is considered positive for cold-induced vasospasm if the test finger pressure is reduced by more than 17% compared to the reference finger [8].

Other tests for cold-induced vasospasm include thermal entrainment, digital laser Doppler response to cold, thermography, venous occlusion plethysmography, and digital artery caliber measurement. None are widely accepted or employed [9–11].

## Duplex Ultrasound Examination of Upper Extremity Arteries

Duplex can be used in the assessment and diagnosis of both aneurysm and occlusive disease of the upper extremity arteries. Doppler-derived waveforms from upper extremity arteries reflect high resting resistance and are similar to those from lower extremity arteries in a resting subject. Upper extremity artery waveforms are normally triphasic. There is a sharp systolic peak followed by brief diastolic

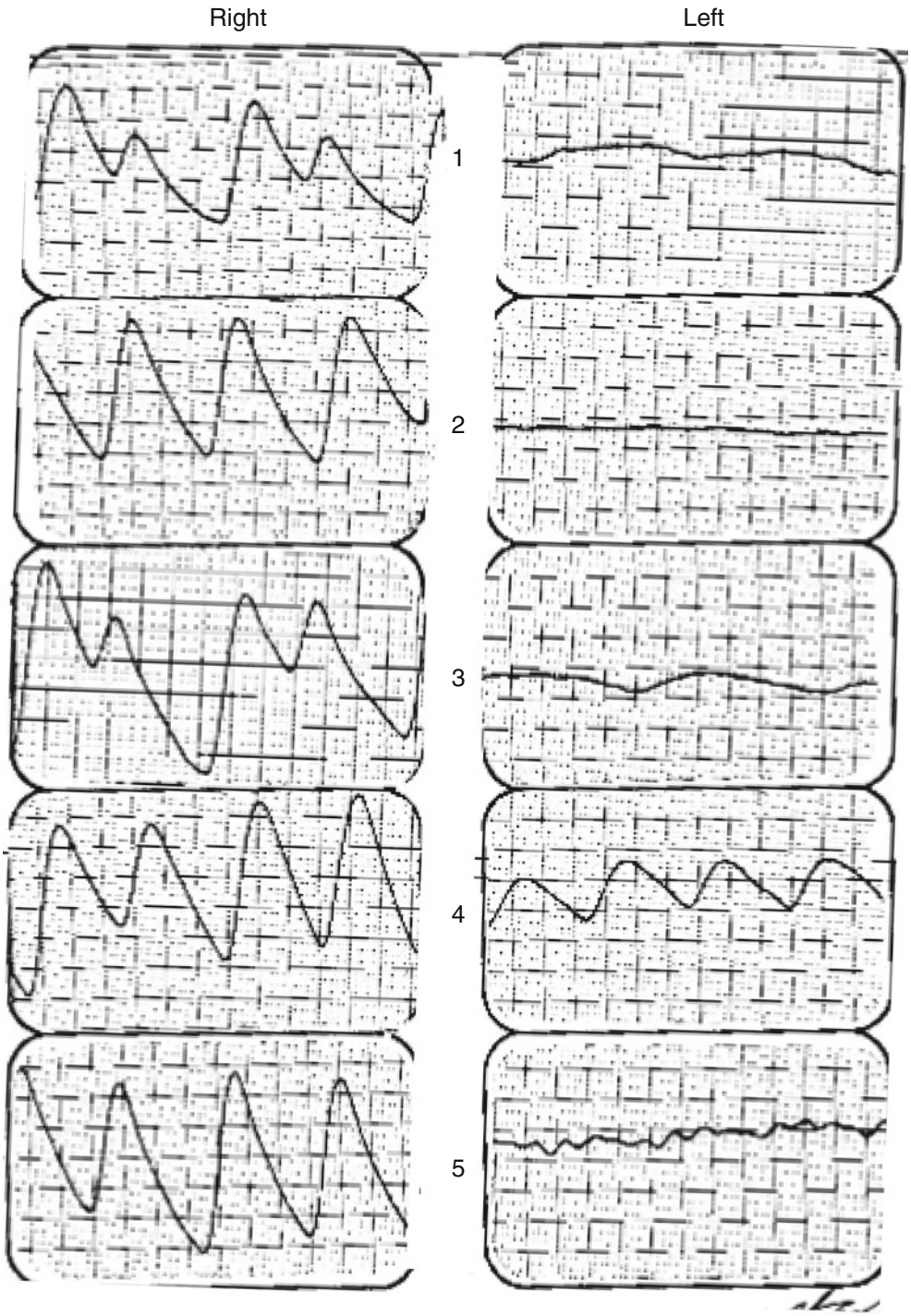


**Fig. 29.7** Unilateral abnormal digital artery waveforms in a patient with a subclavian artery aneurysm secondary to a cervical rib

flow reversal and minimal forward flow at end diastole (Fig. 29.9).

Peak systolic velocities normally range from 80 to 120 cm/s in the subclavian artery and from 40 to 60 cm/s in the forearm arteries. Radial and ulnar artery velocities should be similar. Elevated peak systolic velocities (jets), poststenotic turbulence, and dampened distal waveforms with loss of end-systolic flow reversal are characteristic findings associated with high-grade stenosis (Fig. 29.10). There are no validated velocity criteria to classify stenosis in upper extremity arteries. General guidelines are listed in Table 29.3.

Investigators evaluated 578 arterial segments in 66 upper extremities from 57 patients. The goal was to validate velocity criteria to detect a >50% stenosis as determined by digital subtraction angiography. The criteria utilized for >50% stenosis was a peak systolic velocity (PSV) ratio >2, relating the PSV of the narrowed segment to that of the artery

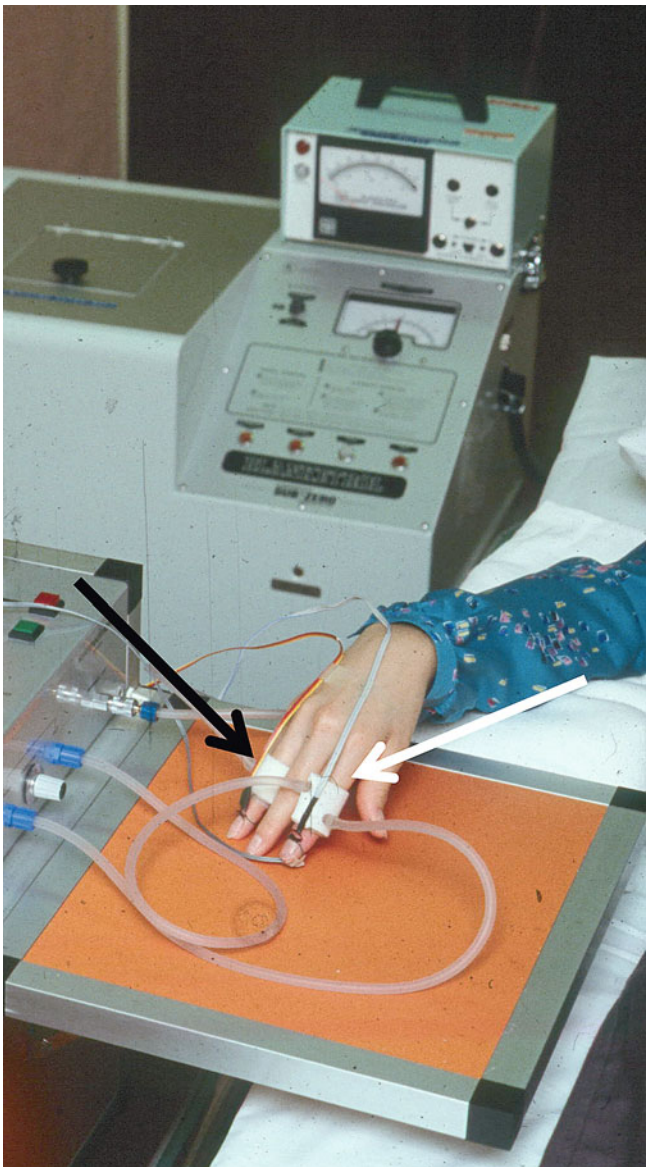

**Fig. 29.8** Device for performance of digital hypothermic challenge or Nielsen's test. The *white arrow* indicates the digital cuff that is used to cool the test finger. This allows controlled application of cold to induce a vasospastic response. The *black arrow* indicates the reference finger. Strain gauges on the finger tips are used to measure the digital pressures. See text

immediately proximal to the lesion. Using a PSV ratio of >2 as criteria for >50% stenosis, duplex correctly identified 15 of 19 high-grade stenoses in upper extremity arteries (sensitivity 79%, specificity 100%) [12].

The angle of insonation can be difficult to determine, examining proximal brachiocephalic arteries leading to potentially false elevations of peak systolic velocities. The true significance of the stenosis may, however, be inferred through interpretation of more distal waveforms. A triphasic waveform distal to a high peak systolic velocity suggests a falsely elevated proximal peak systolic velocity. Comparison of bilateral brachial artery pressures is also useful to help determine the hemodynamic significance of an elevated proximal peak systolic velocity.

Upper extremity arterial occlusion documented by duplex ultrasound is inferred from absence of flow within the lumen of the artery (Fig. 29.11). Multiple structures in the forearm (tendons, nerves, and muscle fascicles) can be mistaken for occluded arteries. Fortunately, the arterial anatomy of the forearm is mostly constant, and the superficial location of the arteries in the arm below the elbow facilitates a sonographer's ability to correctly insonate the forearm arteries. When necessary, the examination can be facilitated by exercise or warming the extremity.

Duplex can be used to evaluate for the monitoring of upper extremity bypass grafts (Fig. 29.12a, b) and the infrequent upper extremity aneurysm. When an aneurysm is encountered, measurements are obtained in the transverse view of the proximal, mid, and distal site in both the A/P and lateral orientations. An attempt is made to visualize intraluminal thrombosis. It is important to visualize the vessel in a true axial plane so as to not falsely overestimate aneurysm diameter with an oblique view. Atherosclerosis and trauma are well-known risk factors for aneurysms of the upper extremity arteries. When encountered, they may present with a pulsatile mass, thrombosis, or embolization of the axillary, brachial, radial, ulnar, and digital arteries. In particular, duplex evaluation of subclavian artery "aneurysms" can be challenging due to their often subtle fusiform nature and location in proximity to the bony landmarks of the thoracic outlet.

The ulnar artery passes deep to the hook of the hamate bone in the hand. This is a site of arterial degeneration that can result from repeated use of the hand as a hammer, the so-called hypothenar hammer syndrome with ulnar artery aneurysm. Patients generally present with symptoms of finger ischemia from embolization to digital and palmar arteries.

## Technique and Interpretation

Potential impediments to an upper extremity arterial duplex examination include the presence of wounds/dressings, IV access, and orthopedic fixation devices. The patient is positioned supine with head elevated. Brachial blood pressures are recorded. Each arm is sequentially examined. The subclavian, axillary, brachial, radial, and ulnar arteries are all examined. Peak systolic velocities are documented point to point in each vessel. A 45–60-degree angle of insonation in the longitudinal plane is optimal, and a "stenosis profile" consisting of a pre-stenosis Doppler PSV, stenosis PSV, and post-stenotic turbulence is documented for stenotic sites.

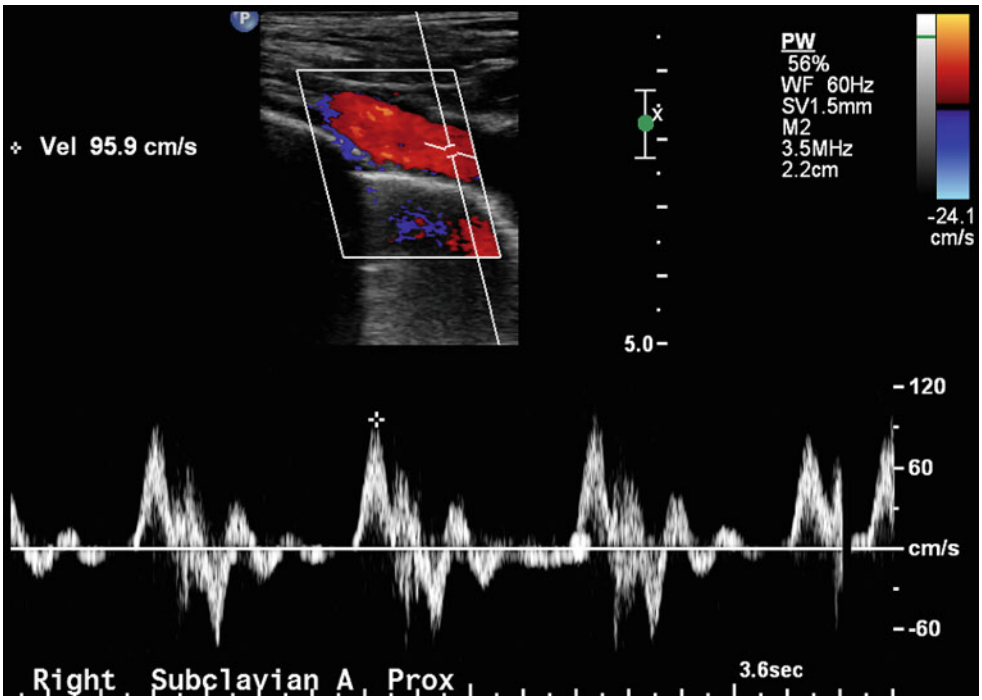


**Fig. 29.9** Normal triphasic subclavian artery duplex-derived waveforms

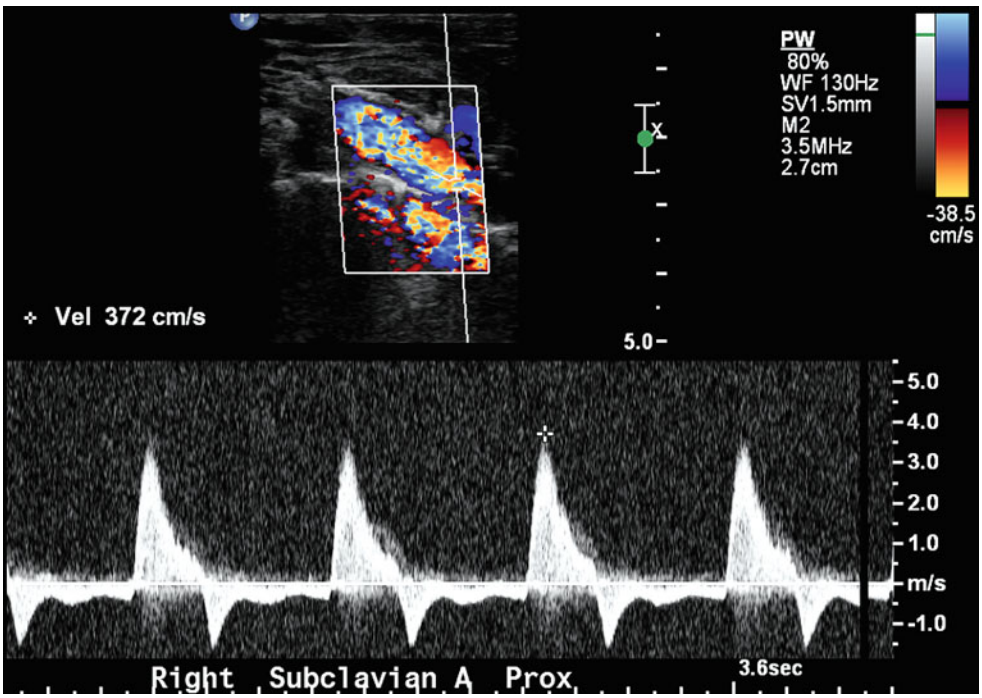


**Fig. 29.10** Markedly elevated peak systolic velocity in a patient with proximal subclavian artery stenosis

Examination of the subclavian artery can generally be accomplished with a 5-MHz transducer. The windows for insonation of the origin of the subclavian artery include the sternal notch (Fig. 29.13) and supraclavicular or infraclavicular approaches. Obese patients may require lower MHz transducers. A small footprint 3–5-MHz transducer is used for the sternal notch window. The artery is identified in the transverse view, and the transducer is rotated 90° to obtain a longitudinal view for obtaining waveforms. Using the sternal notch window, a recent study found 48 out of 50 right and 25 of 50 left subclavian artery origins [12].

The subclavian artery is followed as it crosses under the clavicle and over the first rib. The proximal axillary artery is identified deep to the pectoralis muscles with an anterior approach. More distally, the axillary artery is examined with the arm externally rotated and positioned 45° from the body

**Table 29.3** Duplex ultrasound criteria for evaluation of upper extremity arterial stenosis

| Condition | Characteristics |
|---|---|
| Normal | Uniform waveforms, biphasic or triphasic waveforms, clear window beneath systolic peak |
| <50% diameter reduction | Focal velocity increase, spectral broadening, possibly triphasic or biphasic flow |
| >50% diameter reduction | Focal velocity increase, loss of triphasic or biphasic velocity waveform, post-stenotic flow (color bruit) |
| Occlusion | No flow detected |

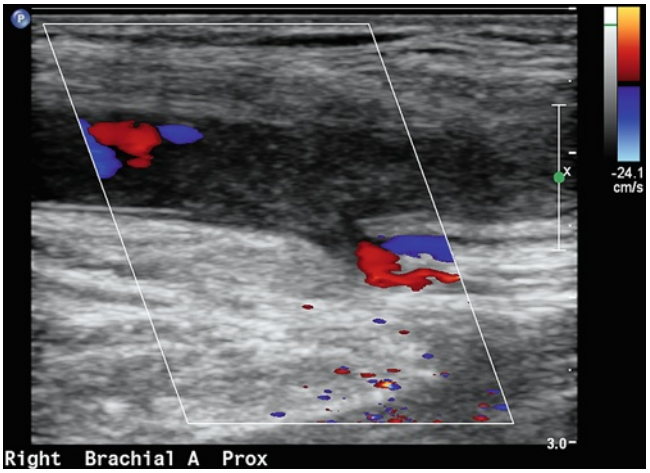


**Fig. 29.11** Color flow image of a brachial artery occlusion secondary to embolism

(pledge position). There is normally no difference noted in the artery caliber as the subclavian artery becomes the axillary artery. The brachial artery assumes a more superficial course in the medial arm between the biceps muscles anteriorly and the triceps muscles posteriorly. Waveforms from the proximal, mid, and distal brachial, radial, and ulnar arteries are obtained. Any areas of stenosis, occlusion, or aneurysmal enlargement are documented as previously described.

Provocative maneuvers in an attempt to elicit compression of the subclavian artery as supportive evidence for possible neurogenic TOS are, unfortunately, widely practiced. Patients are examined with a series of positional changes of the upper extremity in an attempt to provoke compression of the subclavian artery with the unproven implication that this is indicative of compression of the brachial plexus (Fig. 29.14). Other noninvasive vascular lab techniques including segmental pressures with pulse volume recordings (PVR) and/or digital photoplethysmography (PPG) may also be used with these maneuvers. Patients are examined at baseline with the arms adducted and then with a series of positional maneuvers of the upper extremity to elicit and document compression of the subclavian artery. To prevent any missed occlusions or false-negative exams, the exam can be conducted with the segmental cuffs using PPG waveforms as a guide. Significant changes in subclavian artery velocities and waveforms are recorded for evaluation by the interpreting physician.

## Hemodialysis Access Evaluation

Duplex scanning for pre- and postoperative evaluations of hemodialysis access is increasing. A duplex examination of the upper extremity arteries in conjunction with venous duplex evaluation and mapping is useful in evaluating the quality of vessels and hence the likelihood of successful creation of autogenous access. Implementing a comprehensive duplex evaluation prior to fistula placement enabled one group to increase their rates of construction of autogenous AV fistulas from 14% to 63% and with an increase in cumulative patency at 1 year from 48% to 83% [13]. Common guidelines for the upper extremity arteries are arteries free of significant calcification and an arterial diameter of >2 mm with an arterial velocity >40 cm/s [14]. One hundred percent early failure has been reported with arterial diameters <1.5 mm [15].

Duplex is used to evaluate the maturation of an AV fistula and assess for stenotic lesions or other lesions associated with well-developed access sites. The overall diameter and wall thickness of the arterialized vessel can be assessed (Fig. 29.15). Potentially critical stenoses can also be identified. The hypothesis is that early correction of these stenoses can improve rates of maturation and fistula use, as well as increase primary assisted patency. This has yet to be conclusively proven.

### Conclusions

A wide range of upper extremity arterial conditions can be evaluated reliably and effectively in the vascular laboratory. Combined with the history and physical examination, the vascular laboratory plays a key role in the diagnosis and management of patients with upper extremity arterial disease.

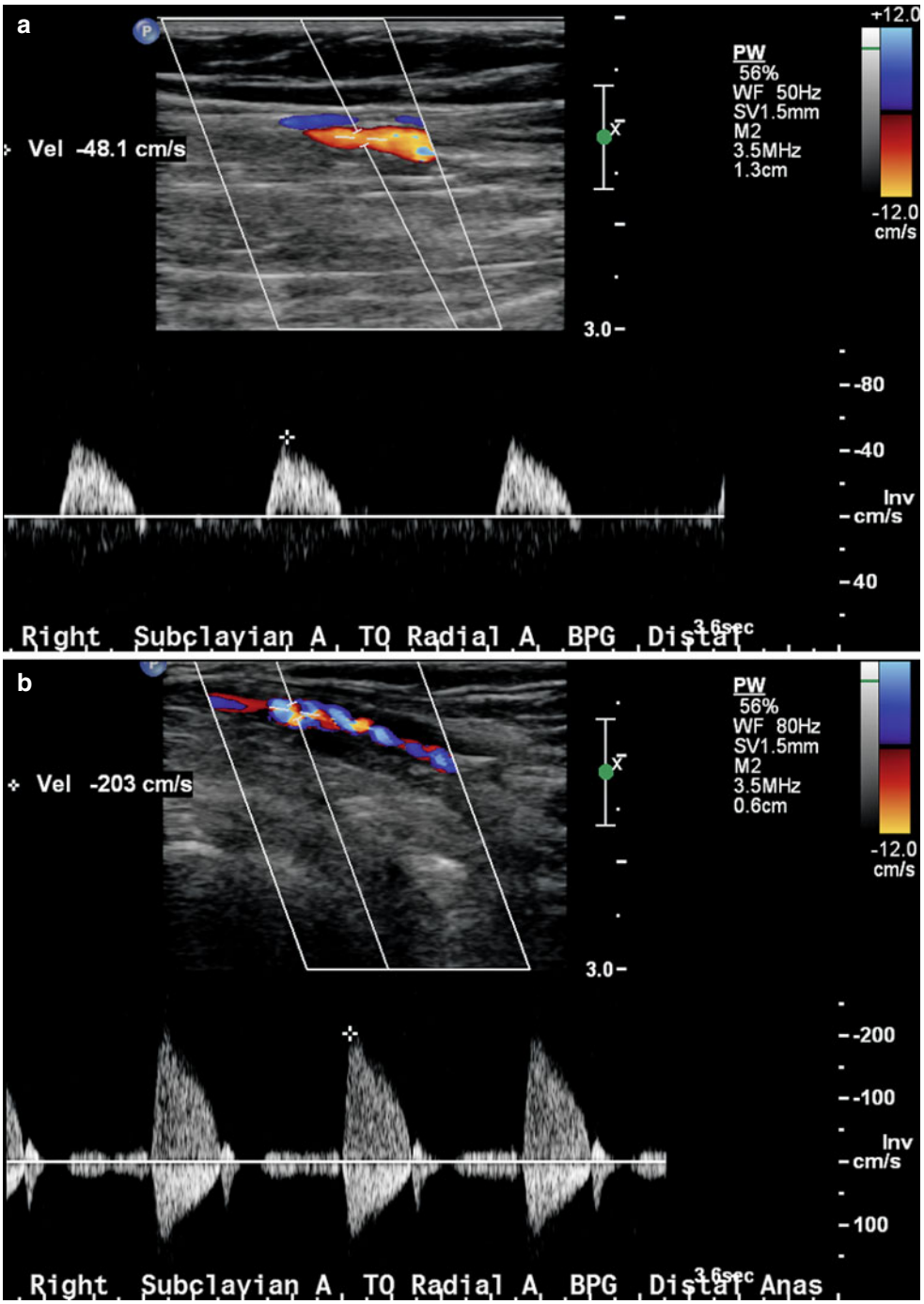


**Fig. 29.12** (**a**, **b**) Duplex waveform obtained from the distal aspect of a 10-year-old subclavian to proximal radial artery reverse vein bypass graft. The waveform in (**a**) is monophasic as it was obtained immediately prior to a severe stenosis at the distal anastomosis (**b**)

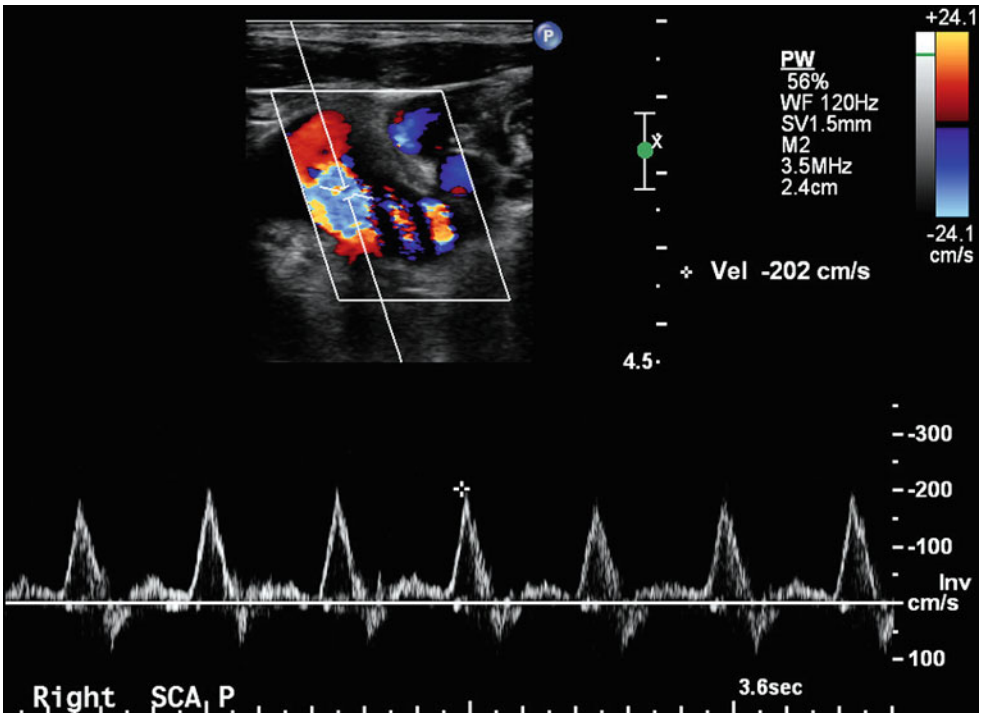


**Fig. 29.13** A small footprint transducer is used to obtain color flow images and duplex-derived arterial waveforms of the right proximal subclavian artery via the sterna notch

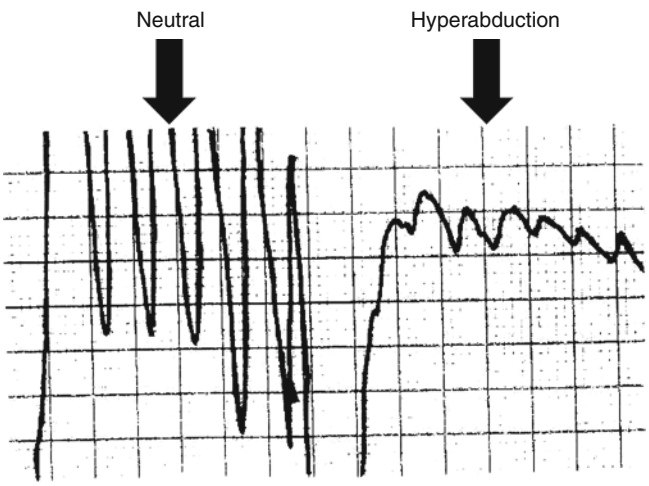


**Fig. 29.14** Digital PPG recordings indicating positional compression of the subclavian artery. The study was performed in a subject without symptoms of thoracic outlet syndrome

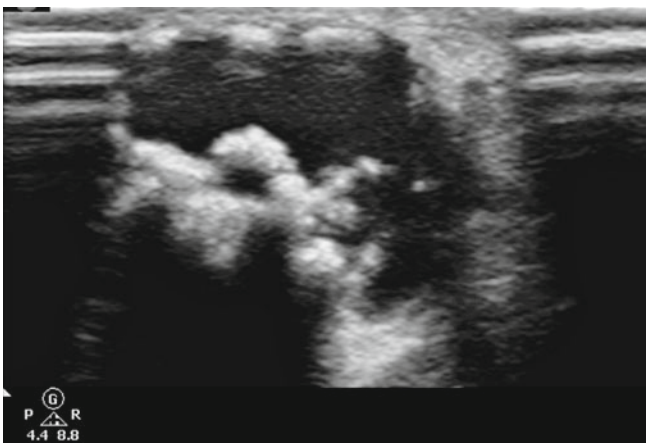

**Fig. 29.15** Gray scale image of calcified chronic thrombus in a 10-year-old radial cephalic fistula

## References

1. Allen E, Brown G. Raynaud's disease: a critical review of minimal requisites for diagnosis. Am J Med Sci. 1932;83:187–200.
2. Hirschl M, Hirschl K, Lenz M, et al. Transition from primary Raynaud's phenomenon to secondary Raynaud's phenomenon identified by diagnosis of an associated disease: results of ten years of prospective surveillance. Arthritis Rheum. 2006;54:1974–81.
3. Edwards JM. Basic data concerning Raynaud's syndrome. Ann Vasc Surg. 1994;8:509–13.
4. Landry GJ, Edwards JM, McLafferty RB, et al. Long-term outcome of Raynaud's syndrome in a prospectively analyzed patient cohort. J Vasc Surg. 1996;23:76–85.
5. Waller DG, Dathan JR. Raynaud's syndrome and carpal tunnel syndrome. Postgrad Med. 1985;61:161–9.
6. McLafferty RB, Edwards JM, Taylor Jr LM, et al. Diagnosis and long-term clinical outcome in patients presenting with hand ischemia. J Vasc Surg. 1995;22:361–9.
7. Porter JM, Snider RL, Bardana EJ, et al. The diagnosis and treatment of Raynaud's phenomenon. Surgery. 1975;77:11–23.
8. Nielsen SL, Lassen NA. Measurement of digital blood pressure after local cooling. J App Phys Resp Environ Exerc Phys. 1977;43:907–10.
9. Lutolf O, Chen D, Zehnder T, Mahler F. Influence of local finger cooling on laser Doppler flux and nailfold capillary blood flow velocity in normal subjects and in patients with Raynaud's phenomenon. Microvasc Res. 1993;46:374–82.

10. Lafferty K, de Trafford JC, Roberts VC, et al. Raynaud's phenomenon and thermal entrainment: an objective test. BMJ Clin Res. 1983;286:90–2.
11. Singh S, de Trafford JC, Baskerville PA, et al. Digital artery caliber measurement: a new technique of assessing Raynaud's phenomenon. Eur J Vasc Surg. 1991;5:199–205.
12. Yurdakul M, Tola M, Uslu OS. Color Doppler ultrasonography in occlusive diseases of the brachiocephalic and proximal subclavian arteries. J Ultrasound Med. 2008;27:1065–70.
13. Silva M, Hobson II RW, Pappas PJ, et al. A strategy for increasing use of autogenous hemodialysis access procedures: impact of preoperative noninvasive evaluation. J Vasc Surg. 1998;27:302–8.
14. Ferring M, Henderson J, Wilmink A, et al. Vascular ultrasound for the pre-operative evaluation prior to arteriovenous fistula formation for haemodialysis: review of the evidence. Nephrol Dial Transplant. 2008;23:1809–15.
15. Wong V, Ward R, Taylor J, et al. Factors associated with early failure of arteriovenous fistulae for haemodialysis access. Eur J Vasc Endovasc Surg. 1996;12:207–13.

# Duplex Utilization of Radial Artery Imaging

30

Leon Salem, Jorge Rey, Sean P. Roddy,
and R. Clement Darling III

**Abstract**

Radial artery duplex ultrasound is used in different clinical situations. It has been used to document changes in the radial artery in a variety of systemic diseases, such as hypertension, end-stage renal disease, and coronary artery disease. Radial artery duplex is used for mapping of the radial artery prior to harvesting for coronary artery bypass grafting and in conjunction with forearm muscle flaps. This is important in order to assess suitability as a conduit, as well as to minimize the risk of hand ischemia after harvesting. Radial artery duplex has been used to assess suitability for transradial coronary interventions and to evaluate the impact of cannulation of the radial artery. Arterial mapping prior to construction of a radiocephalic arteriovenous fistula has been used in order to identify factors associated with failure. The protocol for radial artery duplex is described.

**Keywords**

Radial artery • Coronary artery bypass grafting • Transradial coronary interventions Arteriovenous fistula

## Introduction

In this chapter, we will review the applications and protocols for duplex ultrasound arterial mapping of the radial artery. Duplex ultrasound has been used in different clinical situations. These include use of duplex ultrasound as a guide to performing radial arterial punctures as well as assessing the suitability of the radial artery as conduit for either coronary artery bypass grafting (CABG) or the creation of an arteriovenous fistula.

## Anatomy of the Radial artery

The brachial artery terminates as the radial and ulnar arteries in the proximal forearm within the antecubital fossa (Fig. 30.1). The radial artery passes along the radial side of the forearm to the wrist. It then winds backward, around the lateral side of the hand, beneath the tendons of the abductor pollicis longus and extensor pollicis longus and brevis to the upper end of the space between the metacarpal bones of the thumb and index finger. Finally, it passes forward between the two heads of the first interosseous dorsalis, into the palm of the hand, where it crosses the metacarpal bones and at the ulnar side of the hand unites with the deep volar branch of the ulnar artery to form the deep volar arch. In one out of every eight, the radial artery originates more proximally, either from the axillary artery or uppermost brachial artery

L. Salem, M.D. • J. Rey, M.D. • S.P. Roddy, M.D.
Department of Vascular Surgery, Albany Medical Center Hospital,
43 New Scotland Avenue MC157, Albany, NY 12208, USA

R.C. Darling III, M.D. (✉)
Department of Vascular Surgery, Albany Medical Center Hospital,
43 New Scotland Avenue MC157, Albany, NY 12208, USA

The Vascular Group, Albany Medical College,
Albany, NY, USA
e-mail: darlingc@albanyvascular.com

A.F. AbuRahma, D.F. Bandyk (eds.), *Noninvasive Vascular Diagnosis*,
DOI 10.1007/978-1-4471-4005-4_30, 

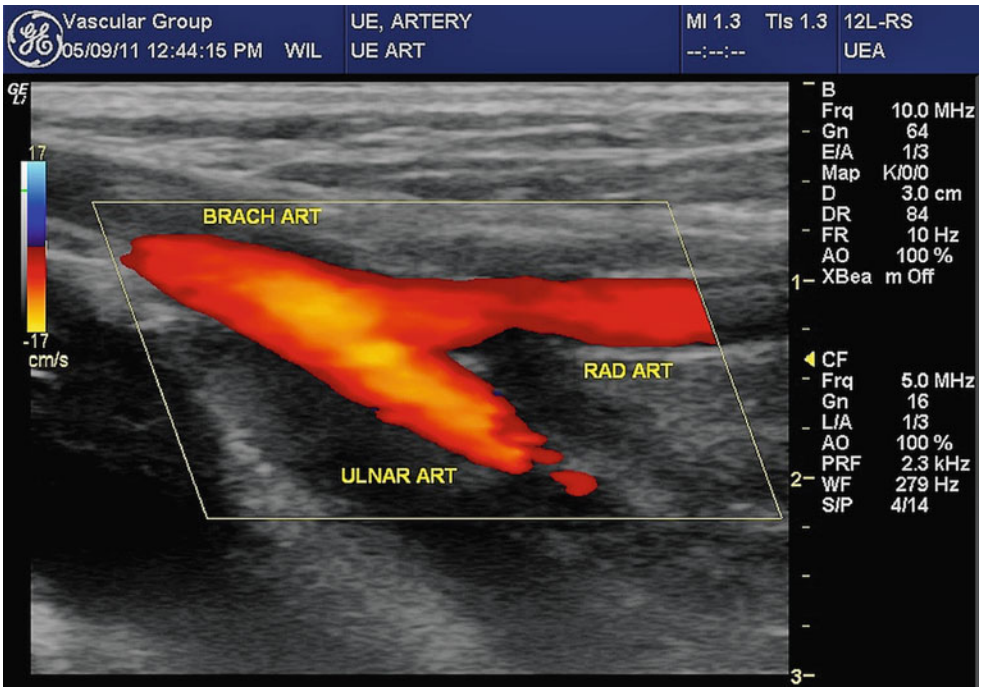


**Fig. 30.1** Brachial artery bifurcation

rather than the latter vessel at the elbow. In the forearm, it deviates less frequently from its normal position than the ulnar artery. In some instances, the radial artery lies on the deep fascia instead of beneath it. Alternatively, it has been observed on the surface of the brachioradialis, instead of under its medial border. Similarly at the wrist, it has been identified superficial to, instead of beneath, the extensor tendons of the thumb [1].

## Protocol

The examination is usually performed with the patient supine and the arm alongside the body where the radial artery can be easily assessed. A linear transducer in the 5–10-MHz range is often employed given that this probe is the same transducer used to examine the brachial artery. Otherwise, a transducer with higher frequencies above 10 MHz can improve resolution and visualization of this vessel, which is smaller and more superficial than the brachial artery. An expanded field of view along the radial artery facilitates transfer of information. It requires training and may take time if the artery is diseased or has an irregular course.

Some examinations should be performed in worst-case conditions. For example, if the radial artery is to be excised, the remaining collateral flow must be enough to feed the hand comfortably in conditions of severe vasoconstriction. The patient should be tested in a cold environment and perhaps a colder than usual central body temperature. This philosophy can be extended to other situations such as creation of an arteriovenous fistula or graft for dialysis. Potential for success or failure can be demonstrated. Testing in worst-case conditions does not preclude examination in normal conditions.

Alternatively, some examinations should be performed in best-case conditions. Arterial imaging improves if physiological and technical parameters are optimized. Arteries dilate and blood flow rates increase with heat. The patient then should be mapped while warm, in a warm environment, and after maneuvers to promote vasodilation such as exercise and immersing the hand in warm water.

Several technical factors facilitate imaging of small or diseased arteries:

- High-frequency transducers improve resolution.
- Low scale applied to color flow and duplex Doppler increases sensitivity.
- Some instruments have special algorithms for detection of low velocity or low volume.
- Proper steering improves color flow and duplex Doppler signals.
- Increased persistence augments perception of color flow.

## Ultrasonographic Changes in the Radial Artery in Systemic Disease

Duplex has been used to define anatomic changes in the radial artery in a wide array of systemic diseases. Thickness of the intima-media layer of the carotid artery has been recognized as a marker for atherosclerosis and a predictor of death and cardiovascular events in patients with coronary

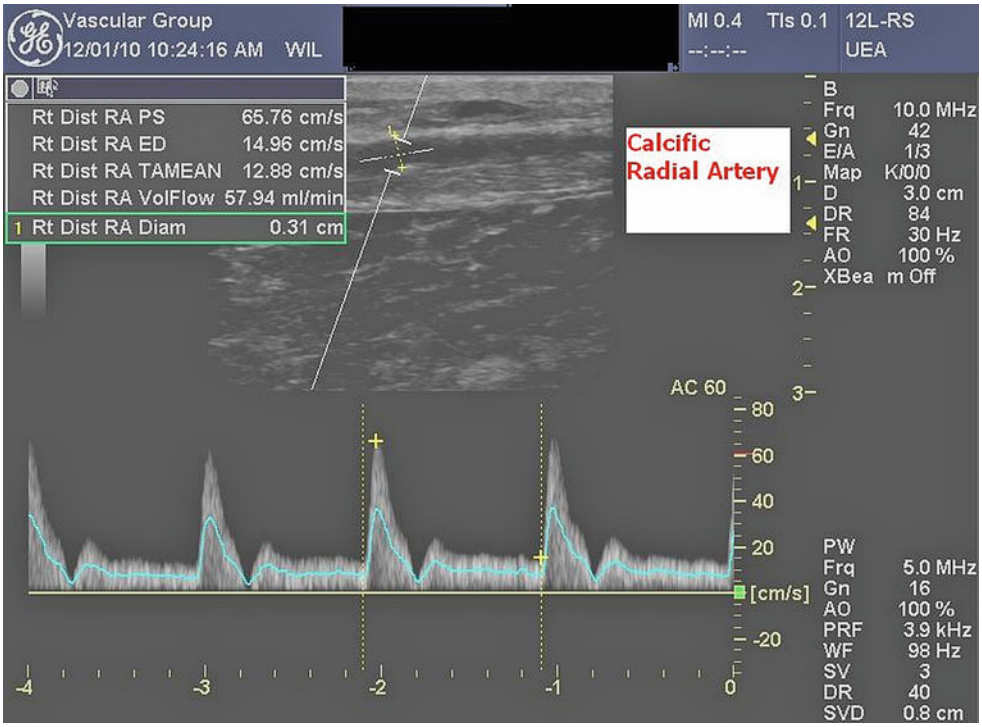


**Fig. 30.2** Calcified radial artery

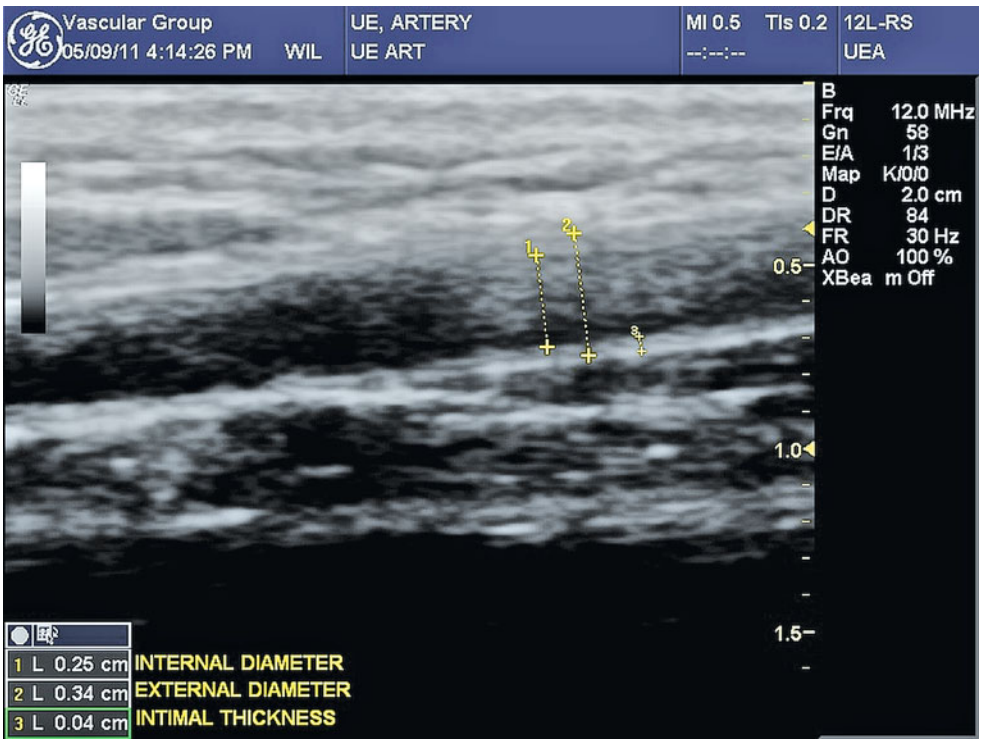


**Fig. 30.3** Radial artery diameter and intimal thickness

artery disease [2]. Although clinically relevant, upper extremity atherosclerosis is infrequent; intimal hyperplasia of the upper extremity arteries is thought to reflect global atherosclerosis (Figs. 30.2 and 30.3) [3, 4]. Ultrahigh-resolution ultrasound, also referred to as ultrasound biomicroscopy, using a 55-MHZ probe is a novel technique that enables the operator to define changes to the individual layers of smaller arteries such as the radial artery [5]. A study that compared prehypertensive and hypertensive patients with healthy subjects showed an increase of 12–14% in the thickness of the intimal layer of the radial artery, while there was no significant difference in the thickness of the medial layer [6]. Similar

changes were documented in the radial artery in patients with coronary heart disease, with increase in the thickness of the intima of 19% compared to healthy subjects, with no significant changes to the thickness of the media [7]. Another study evaluated the changes in subjects with end-stage renal disease (ESRD) [8]. Compared with healthy subjects, nonhypertensive patients with ESRD had 39% thicker intima and 18% greater media in the radial artery.

The effect of iron overload on radial artery structure was also studied. In normotensive patients with genetic hemochromatosis, there was found an increase in radial artery wall thickness and decrease in distensibility. After iron depletion therapy, there was a decrease in wall thickness and increase in distensibility similar to the radial arteries of healthy subjects [9].

The clinical value of these assessments still needs to be evaluated, but the thickness of the intima may serve as a noninvasive tool for early detection of atherosclerosis.

## Radial Artery Mapping for Coronary Bypass

Arterial mapping has been increasingly accepted prior to harvesting the radial artery for coronary bypass. Radial artery diameter and reactivity can be assessed (Fig. 30.4). The radial artery has several favorable features as a coronary graft, including a caliber similar to that of the coronary arteries, appropriate length for complete coronary revascularization, and adequate wall thickness and resistance. Presently, several cardiovascular surgeons request that vascular laboratories perform preoperative noninvasive mapping of the forearm vessels prior to radial artery harvesting to assess the suitability of the radial artery for graft replacement and to avoid ischemic complications to the hand.

Harvesting of the radial artery may occasionally lead to ischemic complications of the hand (particularly the thumb and index finger), which could be deprived of blood flow in patients with anatomical variations that do not allow adequate collateral flow across the palm. The incidence of this complication is generally low [10, 11]. There are several contraindications to using the radial artery as a graft conduit, including ischemic symptoms in the upper extremity, history of arterial trauma, and Raynaud's syndrome. The use of the radial artery in the dominant arm is generally avoided, but this contraindication seems to be less important when adequate noninvasive evaluation conveys minimal risk. The two major objectives of this evaluation are (1) to ensure that the radial artery is free of disease and is of appropriate size and (2) to eliminate the possibility of postharvest ischemia of the hand.

The contribution of increased ulnar flow in the absence of radial artery flow has been assessed by digital pressures and other signs of increased collateral circulation. The value of increased ulnar velocities during radial artery compression remains a controversial issue [12].

The anatomic feature that permits radial artery harvesting without ischemic complications is the presence of collateral anastomosis across the palm between the radial and ulnar arteries, in the form of several arches. The most significant collateral pathway is the superficial palmar arch, which typically originates from the ulnar artery and provides the majority of arterial supply to the digits. The dorsal and deep palmar

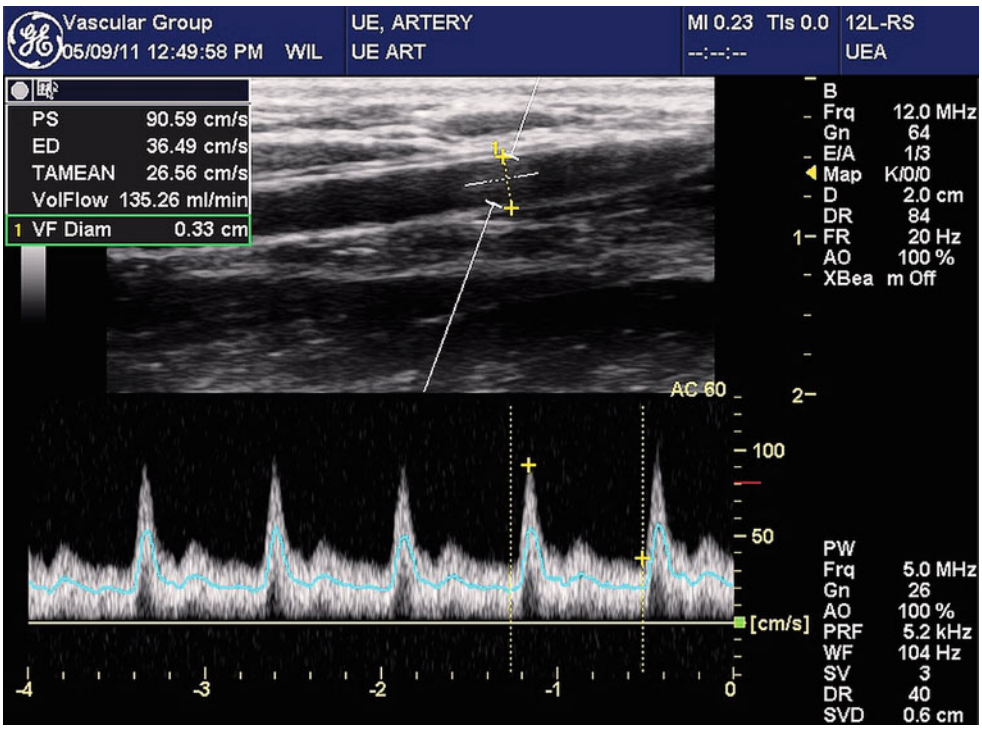


**Fig. 30.4** Radial artery diameter and flow rate

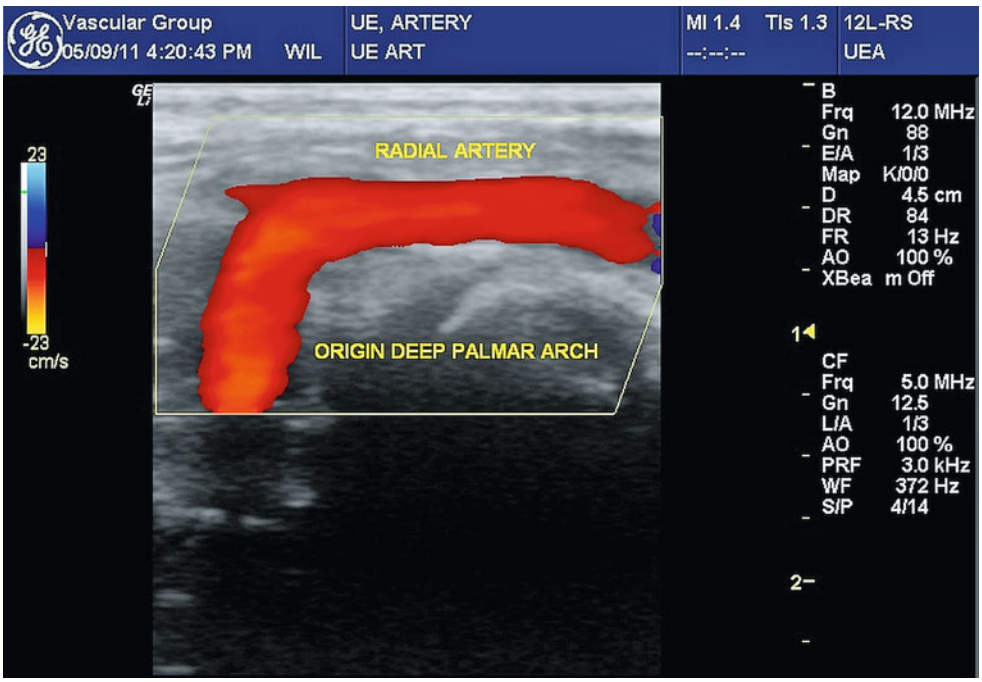


**Fig. 30.5** Deep palmar arch

arches usually originate from the radial artery and are generally smaller than the superficial palmar arch and its branches (Fig. 30.5). Overall, if the superficial palmar arch is intact, collateral flow to the radial aspect of the hand should be adequate if the radial artery is excised. However, there are several anatomic variations that may lead to hand ischemia with radial artery harvesting, for example, incomplete superficial palmar arch, radial artery dominance of the superficial palmar arch, and absence or malformation of the ulnar artery. These variations have been reported to vary from 6% to 34% [13]. Several methods were advocated to evaluate the capability of the ulnar artery to provide adequate perfusion to the hand in the event of radial artery harvesting. These include the clinically modified Allen test, digital blood pressure measurement [14], segmental pressure measurement [15], laser Doppler flowmetry [14], pulse oximetry [16], flow measurement with photoplethysmography [16], and modified Allen test with Doppler ultrasound [10, 13, 17]. In the clinically modified Allen test, the hand is deprived of perfusion by clinching the fist and compressing the ulnar and radial arteries until the hand is exsanguinated and is then observed for return of color upon release of the ulnar artery. This test is believed to be subjective and unreliable with a significant number of false-negative and false-positive results [18]. The measurement of digital systolic blood pressure is objective, and although a pressure drop of more than 40 mmHg has been proposed as an indicator of hand ischemia, the choice of this value is somewhat arbitrary and needs validation. The measurement of oxygen saturation in the digits with radial artery compression is also objective, but substantial variations in perfusion do not always result in changes in saturation [11, 16].

A Doppler ultrasound version of the clinical Allen test has been used in several studies, mostly using continuous wave Doppler ultrasound and some with color Doppler ultrasound [10, 13, 17]. This examination involves Doppler interrogation of the radial portion of the superficial palmar arch before and after radial artery compression and assessment for the presence and/or reversal of flow as an indicator of an intact arch providing adequate collateral flow [10, 13, 17]. In three previously reported studies [10, 13, 17], using the modified ultrasound Allen test with continuous-wave Doppler, in the follow-up of patients who underwent radial artery harvesting, none of the 113 patients who had negative studies (i.e., intact palmar arches) had signs of hand ischemia. Zimmerman et al. [19] examined 358 patients who underwent coronary artery bypass graft replacement, who were evaluated using modified ultrasound Allen test, and reported 53 radial arteries were harvested with no single case of hand ischemia. They began their examination with a modified ultrasound Allen test. If this test indicated that the arch was not intact, the examination was ended. If collateral flow through the ulnar artery was demonstrated, they proceeded to evaluate the radial and ulnar arteries for any evidence of obstructive disease or atherosclerosis.

The ultrasound Allen test utilizes a 7- to 10-MHz linear transducer that is placed in the crease of the proximal palm at the base of the thumb. The superficial palmar arch of the radial artery can be identified coursing anteriorly at this location. The approximate location of this vessel can generally be found by drawing a line along the longitudinal axis of the center of the index finger to the point of its intersection with the crease at the base of the thumb or the thenar eminence.

Flow in this artery is normally directed toward the transducer and into the superficial palmar arch. The direction of flow in this artery can be easily determined by using color Doppler ultrasound. Color Doppler ultrasound is generally employed to locate the artery and spectral imaging to evaluate and document the change in flow direction. While the superficial palmar arch is insonated, the radial artery is compressed at the wrist, and the ultrasonographer watches for a reversal of flow, implying that the arch is complete, or lack of flow, implying that the arch is incomplete. Reversal of flow implies that the radial artery may be harvested with safety. Complete lack of flow in this artery with compression essentially precludes the use of the ipsilateral radial artery.

Although there are no specific velocity criteria to grade stenoses in the upper extremity arteries, the application of velocity criteria on other vessels may apply. These include a focal increase in peak systolic velocity, poststenotic turbulence, and dampening of the waveform distal to the lesion.

## Radial Forearm Flap

Mapping of the upper extremity arteries is recommended for appropriate decision making in selecting a radial flap for plastic surgery [20]. Preexisting vascular disease as detected by ultrasonography eliminates donor vessels, reduces the risk of hand ischemia, and reduces failure of free flaps. In a study that included 121 patients planned to have free radial forearm flaps, all were evaluated with both duplex ultrasound as well as the Allen test [21]. Five of the 121 patients had an alternative flap selected as a consequence of the duplex ultrasound evaluation. Only a single flap failed, and there were no ischemic complications of the hand.

Excision of the radial artery during harvesting of the forearm flap significantly alters the flow patterns of the distal upper extremity [22]. Compensatory increased flow rates were noted in the anterior and posterior interosseous and ulnar arteries. Mapping the ulnar artery alone is, therefore, an insufficient evaluation if the radial artery is being harvested. The contributions of the interosseous arteries must be taken into consideration.

## Evaluation of the Radial Artery with Transradial Coronary Interventions

The radial artery is becoming a more common site for coronary interventions due to its superficial location that allows easy access and control of hemostasis, as well as increased patient satisfaction due to immediate ambulation postprocedure and shortened length of stay. New low-profile systems are introduced which allow for coronary interventions using a 4 Fr sheath.

The anatomic variations of the radial artery and their impact on transradial coronary catheterizations were evaluated in a study that included 1,191 patients [23]. The mean radial artery luminal diameter was 2.6 ± 0.41 mm (range 1.15–3.95 mm). The radial artery diameter was larger than the outer diameter of 5 Fr sheath in 82.7% of patients. Radial artery occlusion was associated with coronary interventions when a sheath larger than 5 Fr was used. Thrombosis of the radial artery near the puncture site occurred in nine cases (0.8%), but there were no cases of hand ischemia. Tortuosity of the radial artery was found in 4.2% of the patients, more commonly in older patients, and was associated with prolonged procedure times, but not with thrombosis of the radial artery. Anatomic variations of the radial artery were not associated with either prolonged procedure times or thrombosis of the radial artery.

Another study found that a small diameter of the radial artery was associated with radial artery occlusion, and a small difference between the radial artery diameter and the sheath was associated with development of stenosis in the radial artery [24]. Complications involving the radial artery were reported to be as high as 9% for developing occlusion and 22% for developing stenosis in patients undergoing transradial coronary catheterization [24]. Therefore, ultrasonographic assessment of the radial artery may be useful for determining the suitability of the patients for transradial coronary angiography and intervention as well as the size of the sheath used.

Repeated transradial interventions were shown to be technically feasible with no statistical difference in access times but were associated with increased incidence of thrombosis (2.6%) and, on long-term ultrasonographic follow-up, were associated with radial artery stenosis [25]. A study that used intravascular ultrasound confirmed that narrowing of the radial artery lumen after repeat transradial interventions was secondary to intima-media thickening [26]. Physiological studies showed that several months after transradial interventions, the vasodilatory properties of the radial artery were preserved, but the lumen remained smaller [27, 28]. These findings raise concerns about the use of the previously accessed radial artery as a conduit for coronary artery bypass grafting.

## Evaluation of the Radial Artery Prior to Creation of Arteriovenous Fistula (AVF) for Hemodialysis

Radiocephalic AVF have been recommended as the first option for patients under 65 and nondiabetics but are associated with higher failure rates due to failure to mature, low flow rates, or early thrombosis. Although venous mapping to evaluate the size and quality of veins is routinely performed,

the role of arterial ultrasound is less clear. Radial artery size on preoperative evaluation has been correlated with patency of radiocephalic AVFs [29–34]. AVF using a radial artery measuring between 1.5 and 2 mm is likely to fail and may indicate creation of a more proximal access site. A prospective randomized study is required to better define the ultrasonographic criteria for the success of AVF.

## References


1. Gray H. Anatomy of the human body. 20th ed. New York: Bartelby.com; 2000.
2. Zielinski T, Dzielinska Z, Januszewicz A, et al. Carotid intima-media thickness as a marker of cardiovascular risk in hypertensive patients with coronary artery disease. Am J Hypertens. 2007;20(10):1058–64.
3. Chowdhury UK, Airan B, Mishra PK, et al. Histopathology and morphometry of radial artery conduits: basic study and clinical application. Ann Thorac Surg. 2004;78(5):1614–21.
4. Ruengsakulrach P, Brooks M, Sinclair R, Hare D, Gordon I, Buxton B. Prevalence and prediction of calcification and plaques in radial artery grafts by ultrasound. J Thorac Cardiovasc Surg. 2001;122(2):398–9.
5. Razuvaev A, Lund K, Roy J, Hedin U, Caidahl K. Noninvasive real-time imaging of intima thickness after rat carotid artery balloon injury using ultrasound biomicroscopy. Atherosclerosis. 2008;199(2):310–6.
6. Myredal A, Gan LM, Osika W, Friberg P, Johansson M. Increased intima thickness of the radial artery in individuals with prehypertension and hypertension. Atherosclerosis. 2010;209(1):147–51.
7. Myredal A, Osika W, Li Ming G, Friberg P, Johansson M. Increased intima thickness of the radial artery in patients with coronary heart disease. Vasc Med. 2010;15(1):33–7.
8. Johansson M, Myredal A, Friberg P, Gan LM. High-resolution ultrasound showing increased intima and media thickness of the radial artery in patients with end-stage renal disease. Atherosclerosis. 2010;211(1):159–63.
9. Failla M, Giannattasio C, Piperno A, et al. Radial artery wall alterations in genetic hemochromatosis before and after iron depletion therapy. Hepatology. 2000;32(3):569–73.
10. Serricchio M, Gaudino M, Tondi P. Hemodynamic and functional consequences of radial artery removal for coronary artery bypass grafting. Am J Cardiol. 1999;84(11):1353–6, A1358.
11. Nunoo-Mensah J. An unexpected complication after harvesting of the radial artery for coronary artery bypass grafting. Ann Thorac Surg. 1998;66(3):929–31.
12. Sullivan VV, Higgenbotham C, Shanley CJ, et al. Can ulnar artery velocity changes be used as a preoperative screening tool for radial artery grafting in coronary artery bypass? Ann Vasc Surg. 2003;17(3):253–9.
13. Starnes SL, Wolk SW, Lampman RM, et al. Noninvasive evaluation of hand circulation before radial artery harvest for coronary artery bypass grafting. J Thorac Cardiovasc Surg. 1999;117(2):261–6.
14. Levinsohn DG, Gordon L, Sessler DI. The Allen's test: analysis of four methods. J Hand Surg Am. 1991;16(2):279–82.
15. Winkler J, Lohr J, Rizwan H. Evaluation of the radial artery for use in coronary artery bypass grafting. J Vasc Technol. 1998;22(1):23–9.
16. Fuhrman TM, Pippin WD, Talmage LA, Reilley TE. Evaluation of collateral circulation of the hand. J Clin Monit. 1992;8(1):28–32.
17. Pola P, Serricchio M, Flore R, Manasse E, Favuzzi A, Possati GF. Safe removal of the radial artery for myocardial revascularization: a Doppler study to prevent ischemic complications to the hand. J Thorac Cardiovasc Surg. 1996;112(3):737–44.
18. Greenhow DE. Incorrect performance of Allen's test – ulnar-artery flow erroneously presumed inadequate. Anesthesiology. 1972;37(3):356–7.
19. Zimmerman P, Chin E, Laifer-Narin S, Ragavendra N, Grant EG. Radial artery mapping for coronary artery bypass graft placement. Radiology. 2001;220(2):299–302.
20. Thomson PJ, Musgrove BT. Preoperative vascular assessment: an aid to radial forearm surgery. Br J Oral Maxillofac Surg. 1997;35(6):419–23.
21. Ganesan K, Stead L, Smith AB, Ong TK, Mitchell DA, Kanatas AN. Duplex in the assessment of the free radial forearm flaps: is it time to change practice? Br J Oral Maxillofac Surg. 2010;48(6):423–6.
22. Ciria-Llorens G, Gomez-Cia T, Talegon-Melendez A. Analysis of flow changes in forearm arteries after raising the radial forearm flap: a prospective study using colour duplex imaging. Br J Plast Surg. 1999;52(6):440–4.
23. Yoo BS, Yoon J, Ko JY, et al. Anatomical consideration of the radial artery for transradial coronary procedures: arterial diameter, branching anomaly and vessel tortuosity. Int J Cardiol. 2005;101(3):421–7.
24. Nagai S, Abe S, Sato T, et al. Ultrasonic assessment of vascular complications in coronary angiography and angioplasty after transradial approach. Am J Cardiol. 1999;83(2):180–6.
25. Yoo BS, Lee SH, Ko JY, et al. Procedural outcomes of repeated transradial coronary procedure. Catheter Cardiovasc Interv. 2003;58(3):301–4.
26. Wakeyama T, Ogawa H, Iida H, et al. Intima-media thickening of the radial artery after transradial intervention. An intravascular ultrasound study. J Am Coll Cardiol. 2003;41(7):1109–14.
27. Sanmartin M, Goicolea J, Ocaranza R, Cuevas D, Calvo F. Vasoreactivity of the radial artery after transradial catheterization. J Invasive Cardiol. 2004;16(11):635–8.
28. Madssen E, Haere P, Wiseth R. Radial artery diameter and vasodilatory properties after transradial coronary angiography. Ann Thorac Surg. 2006;82(5):1698–702.
29. Lemson MS, Leunissen KM, Tordoir JH. Does pre-operative duplex examination improve patency rates of Brescia-Cimino fistulas? Nephrol Dial Transplant. 1998;13(6):1360–1.
30. Parmar J, Aslam M, Standfield N. Pre-operative radial arterial diameter predicts early failure of arteriovenous fistula (AVF) for haemodialysis. Eur J Vasc Endovasc Surg. 2007;33(1):113–5.
31. Hamish M, Geddoa E, Reda A, et al. Relationship between vessel size and vascular access patency based on preoperatively ultrasound Doppler. Int Surg. 2008;93(1):6–14.
32. Brimble KS, Rabbat CG, Schiff D, Ingram AJ. The clinical utility of Doppler ultrasound prior to arteriovenous fistula creation. Semin Dial. 2001;14(5):314–7.
33. Malovrh M. Non-invasive evaluation of vessels by duplex sonography prior to construction of arteriovenous fistulas for haemodialysis. Nephrol Dial Transplant. 1998;13(1):125–9.
34. Wong V, Ward R, Taylor J, Selvakumar S, How TV, Bakran A. Factors associated with early failure of arteriovenous fistulae for haemodialysis access. Eur J Vasc Endovasc Surg. 1996;12(2):207–13.

# Protocol and Mapping Techniques Prior to Hemodialysis Access Planning

# 31

Jennifer A. Sexton, Robyn A. Macsata, and Anton N. Sidawy

**Abstract**

Successful hemodialysis access placement is of utmost importance for patients with chronic kidney disease and end-stage renal disease, and it is optimized by preoperative evaluation and planning. This evaluation includes history and physical examination by the surgeon as well as noninvasive imaging. In this chapter, we discuss the preoperative workup for hemodialysis access including vein mapping of the superficial and deep venous systems of the upper extremity as well as segmental pressures, pulse-volume recording, and arterial duplex imaging. Each test is used preoperatively with the goal of improving outcomes for hemodialysis access placement.

**Keywords**

Upper extremity • Vein mapping • Segmental pressures • Pulse-volume recording • Arterial duplex ultrasound

## Introduction

Chronic kidney disease (CKD) and end-stage renal disease (ESRD) are serious medical conditions that continue to affect thousands of patients each year in the United States. According to the Center for Disease Control (CDC), in 2007, renal disease resulted in 46,448 deaths, the ninth leading cause of death, accounting for 1.9% of total deaths. The total number of new ESRD patients was 112,476 in 2008, with a prevalence of 547,982 [1].

J.A. Sexton, M.D.
Department of Surgery, Georgetown University Hospital, Washington Hospital Center, Washington, DC, USA

R.A. Macsata, M.D.
Department of Surgery, Washington DC VA Medical Center, Washington, DC, USA

A.N. Sidawy, M.D., MPH (✉)
Department of Surgery, George Washington University Hospital, 2150 Pennsylvania Avenue, NW, Washington, DC 20037, USA
e-mail: ansidawy@aol.com

Medicare costs for ESRD rose 13.2% to $26.8 billion in 2008 and accounted for 5.9% of the Medicare budget [2]. During that same year, a patient with a patent and functioning autogenous arteriovenous (AV) access had a total cost of $64,701, which was 28% and 18% lower, respectively, than total yearly costs for patients with hemodialysis access catheters ($90,110) and patients with prosthetic AV grafts ($79,337) [2]. Total yearly costs for vascular access events are also 60% less costly in patients with autogenous AV access as compared to patients with a hemodialysis catheter or a prosthetic AV access [2]. Therefore, it is imperative that autogenous AV access be created correctly and successfully on the first attempt to maximize the long-term health of the patient as well as to decrease the overall cost [3].

Surgery for hemodialysis access placement is one of the most commonly performed vascular surgical procedures in the United States. With over 354,000 ESRD patients depending on hemodialysis for treatment [4], it is of utmost importance to have patent hemodialysis access. Creating successful autogenous arteriovenous access is based on a thorough and adequate preoperative workup.

A.F. AbuRahma, D.F. Bandyk (eds.), *Noninvasive Vascular Diagnosis*,
DOI 10.1007/978-1-4471-4005-4_31, 

## History and Physical Examination

Placing a successful AV access does not begin in the operating room, but it begins many months before, initially with careful evaluation by primary care providers that identify patients with CKD early, prior to the point in time that they need to start hemodialysis. Patients should be referred to the vascular access surgeon for permanent access when their creatinine clearance is less than 25 mL/min. Once the patient is in the surgeon's office, a careful preoperative history and physical should be taken.

A thorough history includes documentations of the patient's dominant upper extremity, history of all previous hemodialysis access sites, recent history of peripheral indwelling intravenous catheters, peripherally inserted central catheters (PICC) lines, and other sites of previous central venous access (including pacemakers and defibrillators). Additional information necessary for complete evaluation includes a detailed list of comorbidities, especially diabetes mellitus, peripheral vascular disease, congestive heart failure, advanced age, and female gender, as there have been reports that these factors may be associated with increased difficulty in establishing patent autogenous AV access [5–7]. History of thrombotic events and history of trauma to the upper extremities are important to recognize; consideration of further workup for a hypercoagulable disorder or radiographic imaging is appropriate in these cases, respectively.

A physical examination is systematically completed for every patient, evaluating both the arterial and venous anatomy. Therefore, the physical examination is focused on the upper extremities but also includes a brief systemic examination, especially of the heart and lungs.

## Arterial Examination

The arterial inflow is assessed first, keeping in mind the two important issues for a successful AV access: adequate blood flow to the AV access to support hemodialysis and maintenance of blood flow to the extremity distal to the AV access [8]. The brachial, radial, and ulnar arteries are examined on both extremities and are evaluated for compressibility and pulse and pressure equality. An experienced clinician will be able to identify healthy pulses as well as those that are abnormal. An Allen test is performed to evaluate the patency of the palmar arch. Bilateral upper extremity blood pressure is measured and documented and should be equal. A significant difference suggests the presence of an arterial stenosis or obstruction [8]. If there are any abnormalities in the arterial examination, including weak or unequal pulses and blood pressure, further investigation is performed with segmental pressures, pulse-volume recording (PVR), or duplex ultrasound (DU), as discussed in detail later in this chapter.

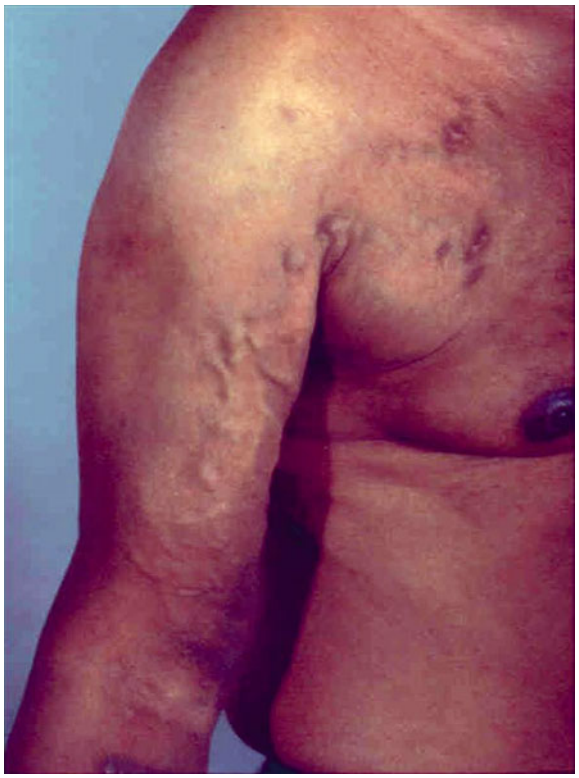

**Fig. 31.1** Bulging upper extremity collateral veins as a result of central stenosis

## Venous Examination

Next, the venous outflow is evaluated with and without the presence of a tourniquet in place. Normal outflow veins are continuous and distensible. Many ESRD patients, by the time they are sent for AV access placement, have had numerous peripheral intravenous cannulations or attempts, which may damage the veins to the point that successful AV access placement is compromised [8]. Veins that can neither be seen on physical examination nor distended with a tourniquet may be sclerosed, and further investigation is performed with upper extremity vein mapping by DU, as discussed in detail later in this chapter.

The patient is then examined for evidence of central venous stenosis. All patients who have had subclavian vein access, central venous ports, or PICC line placements are at risk for developing central vein stenosis. Gonsalves et al. reported a 7% incidence of new central vein stenosis or occlusion in patients who had prior central venous access [9], though reported incidence has ranged from 3% to 38% in prior studies [10–12]. Any note of edema or prominent venous collaterals in the proximal extremity and chest areas suggests a possible central venous stenosis (Fig. 31.1). If any venous abnormalities are noted on physical examination or surgical access is planned for the same side as a prior central access site, further evaluation of the central venous system is performed with ultrasound [13], followed by venogram if

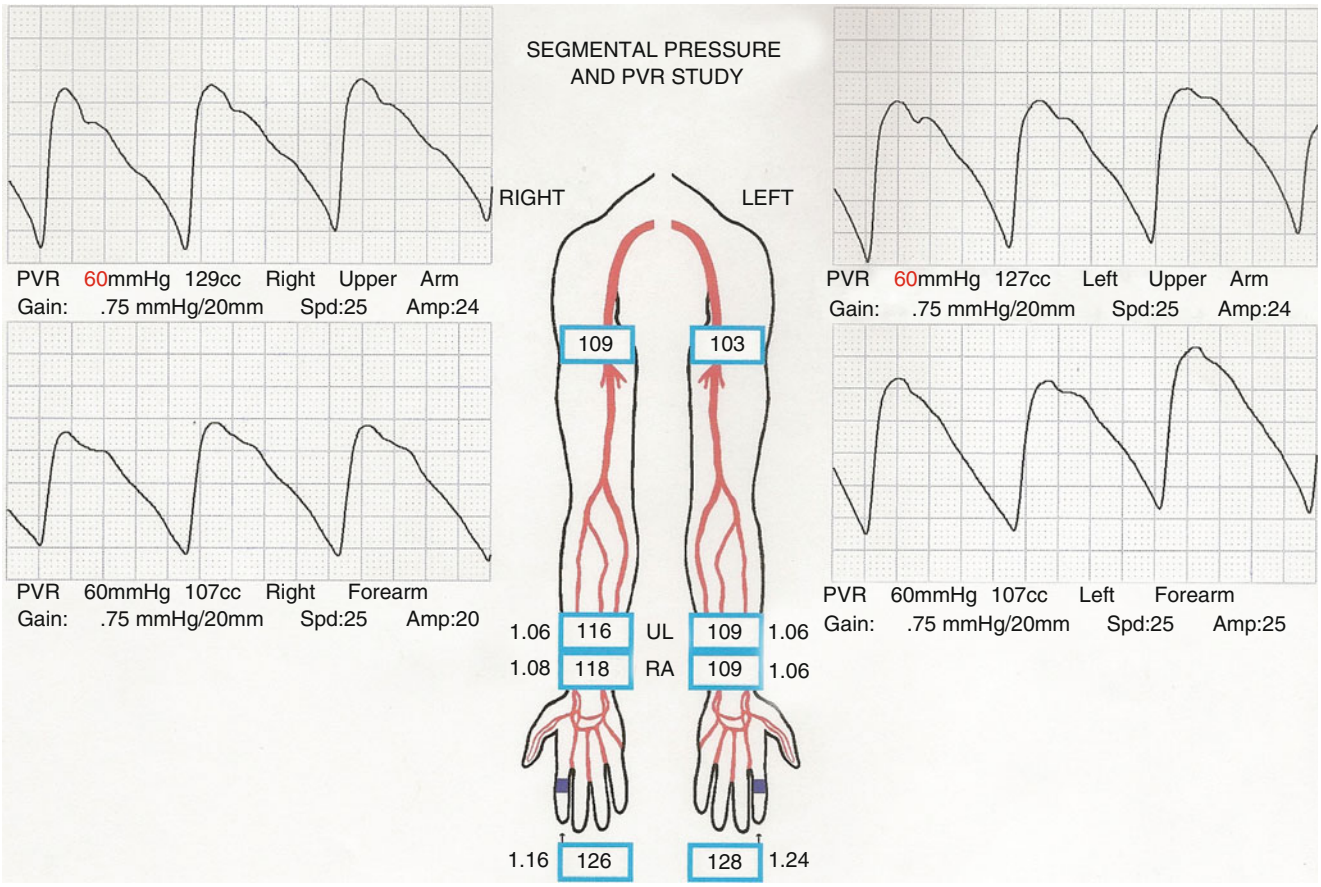


**Fig. 31.2** Normal upper extremity segmental pressures and PVR. Pressures are equal bilaterally and the triphasic waveform has a strong upslope, a dicrotic notch, and a steep downslope

any suggestion of stenosis or occlusion is noted on noninvasive imaging, as discussed in detail later in this chapter.

### Additional Examination

Further upper extremity examination includes a neurologic examination in order to document the presence of neuropathy or motor and sensory dysfunction. A skin examination should document scars from prior access procedures, other operations, and trauma. The chest should also be examined for presence of scars from possible prior central venous access sites. Indications of congestive heart failure, such as jugular venous distention, result in a cardiology consultation preoperatively to maximize cardiac function prior to surgery [14].

## Diagnostic Imaging

### Noninvasive Arterial Imaging

If any abnormality is detected during the physical examination of the arterial inflow, subsequent evaluation starts with noninvasive imaging, beginning with segmental arterial pressures and either pulse volume recording (PVR) or duplex ultrasound. Arteriography is the gold standard for diagnosis of arterial stenosis; however, there are several limitations to consider, especially in patients with CKD. For all patients, arteriography is invasive, with risk of puncture site complications, including hematoma, pseudoaneurysm, dissection, or thrombosis. CKD patients have an added risk of contrast-induced nephropathy (CIN), which may result in the patient requiring hemodialysis at a sooner date. Preexisting renal dysfunction is the most important risk factor for the development of CIN, and the incidence increases with the degree of preprocedure renal dysfunction [15]. Therefore, arteriogram should be reserved for patients with abnormal noninvasive imaging as discussed below.

#### Segmental Arterial Pressure

Segmental pressures are obtained initially after an abnormal upper extremity arterial examination and are performed in a similar manner to segmental pressures in the legs. Blood pressure cuffs are placed on the upper arm, forearm, and finger to give an estimate of the level of disease in the upper extremity, and the brachial, radial, and ulnar arteries are assessed with Doppler ultrasound, while digital arteries are assessed using photo-plethysmography (PPG).

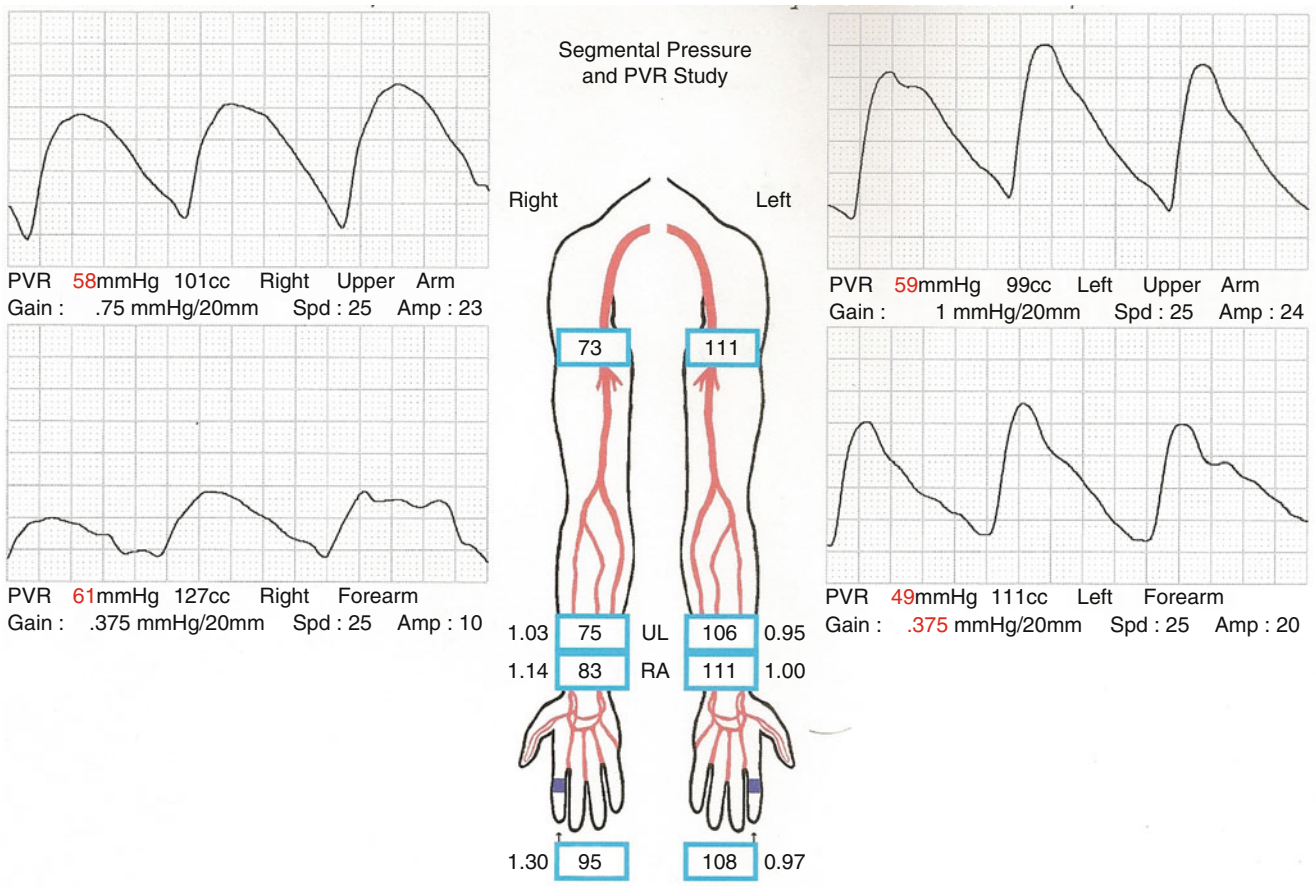


**Fig. 31.3** An abnormal upper extremity segmental pressure and PVR. The pressure in the right upper arm is significantly lower than that on the left. The PVR on the right also has lost the dicrotic notch and shows evidence of dampening

Pressures should be equal, without pressure gradient, in both extremities, as in Fig. 31.2. If the arm pressures at the same cuff level on opposite arms differ by more than 20 mmHg or the pressure measurements between adjacent cuff sites on the same arm differ by more than 10 mmHg [16], this is indicative of occlusive disease with a significant stenosis, as indicated in the right arm of Fig. 31.3. The main drawback of segmental pressures is the abnormally high values seen due to calcified vessels, which is commonly seen in diabetic patients. In this group of patients, a finger brachial index may be obtained. A normal finger/brachial index should be greater than 0.7; when the index is below 0.7, it suggests obstruction to flow and should prompt further evaluation of the upper extremity arterial system with PVRs and/or DU [17].

## Pulse-Volume Recording

Like segmental pressure measurements, PVR, using volume plethysmography, also uses interval blood pressure cuffs that detect the arterial pulsations and gives the sum of the blood flow in the arteries of that segment of the upper extremity [18]. This is displayed as a triphasic arterial waveform, as seen in Fig. 31.2. The normal waveform has a sharp upslope, a dicrotic notch, and a downslope. There should be no evidence of dampening, which indicates a stenosis proximal to the respective cuff [19]. When a significant stenosis is detected, the dicrotic notch is typically lost first, followed by a more shallow upstroke and, finally, an overall decreased amplitude of the arterial waveform (see Fig. 31.3). This test does not require compression of the vessels, and, therefore, these waveforms should be unaffected by arterial calcification. Any abnormality seen on the PVRs should be further evaluated by arteriography.

## Duplex Ultrasonography

Color flow DU is used to assess the arterial inflow when abnormalities are detected during segmental pressures or PVRs. Using DU, the entire arterial anatomy of the upper extremity, including the subclavian artery, may be visualized and allows for evaluation of arterial diameter as well as presence of arterial stenosis or calcification, and abnormal arterial wall thickening [19] (Fig. 31.4).

Multiple studies have evaluated minimum diameter necessary for successful AV access, and both 1.5 and 2.0 mm

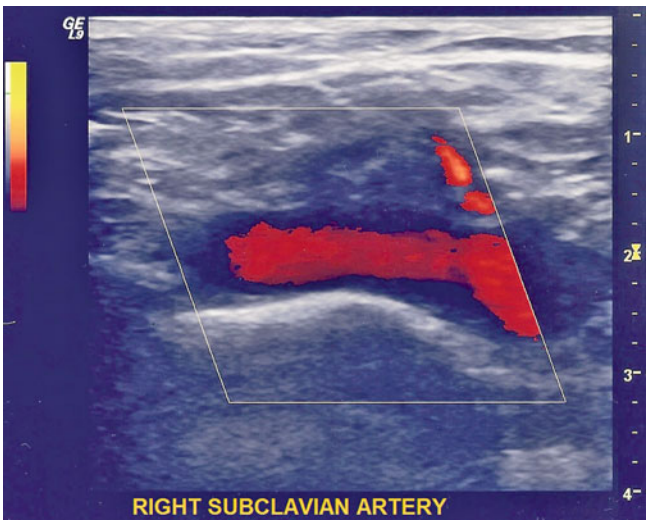


**Fig. 31.4** Duplex ultrasound of a normal right subclavian artery

have been used as the minimally accepted internal arterial diameters; however, unobstructed inflow artery diameter of 2.0 mm has more often been used as a predictor of success [20, 21]. Lemson et al. reported that patients with failed forearm fistulas had significantly smaller mean preoperative radial artery diameters compared to patients with matured fistulas (1.9 vs. 2.8 mm) [22].

An additional benefit to DU diagnostic capabilities is its possible use for therapeutic procedures such as DU-guided angioplasty. This has been described for treatment of lower extremity occlusive disease, carotid disease, and non-maturing AV access as an alternative to standard angiography with angioplasty in an effort to avoid radiation exposure and contrast material, especially in patients with renal insufficiency [23].

## Noninvasive Venous Imaging

### Superificial Venous System

DU is critical to the complete evaluation of the venous outflow. All patients who have an abnormal venous examination or do not have adequately visualized superficial veins on physical examination should undergo superficial vein mapping with DU prior to any attempt at creating AV access. Many times, the veins are simply too deep to be palpated or visualized, even with a tourniquet in place. In one study, 53.5% had poor or absent veins on physical examination; however, with duplex ultrasound, adequate veins were found in 77% of this group of patients [24]. The forearm venous network is superficial and easily imaged with duplex ultrasound (see Figs. 31.5a–d). The preoperative vein mapping should visualize the entire length of the cephalic and basilic veins, evaluating diameter, continuity, distensibility, and presence of large branches.

Preoperative vein mapping has been shown in numerous studies to increase the rate of autogenous AV access construction. Robbin et al. noted an increase in autogenous AV access placement from 32% to 58% after a preoperative DU program was started [25]. They also noted that preoperative vein mapping resulted in a change in the type and/or location of access surgery planned just after physical examination alone for 31% of their patients, including eight patients who received an autogenous rather than a prosthetic AV access [25].

Multiple studies have shown preoperative DU to predict successful AV access placement [26]. With preoperative DU, Silva et al. were able to demonstrate an increase in autogenous access placement from 14% to 63%, a decrease in early failure rate of the autogenous access from 38% to 8.3%, and a 1-year patency rate of 83% [21] when a venous luminal diameter of 2.5 mm or greater was used. Ascher also reported an increase of placement of autogenous AV access as well as an increase in the overall 1-year primary patency rate from 45% to 72% after implementation of a DU program [27]. Despite these promising results, there are additional studies that show that an increase in placement of autogenous AV access resulted in an increase of primary failure. A study by Miller et al. reported an early patency rate of only 47% and an 81% patency rate at 1 year [5]; this is likely due to the increased use of smaller caliber veins.

Multiple studies have looked at the minimal acceptable diameter for veins. Mendes et al. noted that patients with a cephalic vein size of 2.0 mm or less were less likely to have a successful wrist autogenous access than if the cephalic vein was greater than 2.0 mm. This study reported that primary patency at 3 months increased from 16% for veins less than 2.0 mm to 76% for greater than 2.0 mm diameter. These veins were measured without using a tourniquet, but with the patient reclined and the arm dependent [28]. Silva et al. required veins greater than 2.5 mm for autogenous access and greater than 4 mm for nonautogenous access [21], while Ascher et al. used the criteria of a 2-mm vein at the wrist and greater than 3 mm in the upper arm [27]. Both of these studies measured veins using a tourniquet in place.

### Central Venous System

If any abnormality is detected on history or physical examination, including prior central venous catheters, PICC lines, or multiple previous failed attempts at AV access in the same arm, a deep venous DU should be performed. Upper extremity contrast venography has remained the gold standard for diagnosis of proximal venous obstruction; however, the risk of the invasive procedure with administration of contrast to a patient with CKD is undesirable. DU has been found to have a specificity of 97% and a sensitivity of 81% for detecting central venous outflow obstruction [29]; therefore, DU is extremely useful for CKD patients. In this study, color flow DU was most accurate in detecting outflow obstruction in the

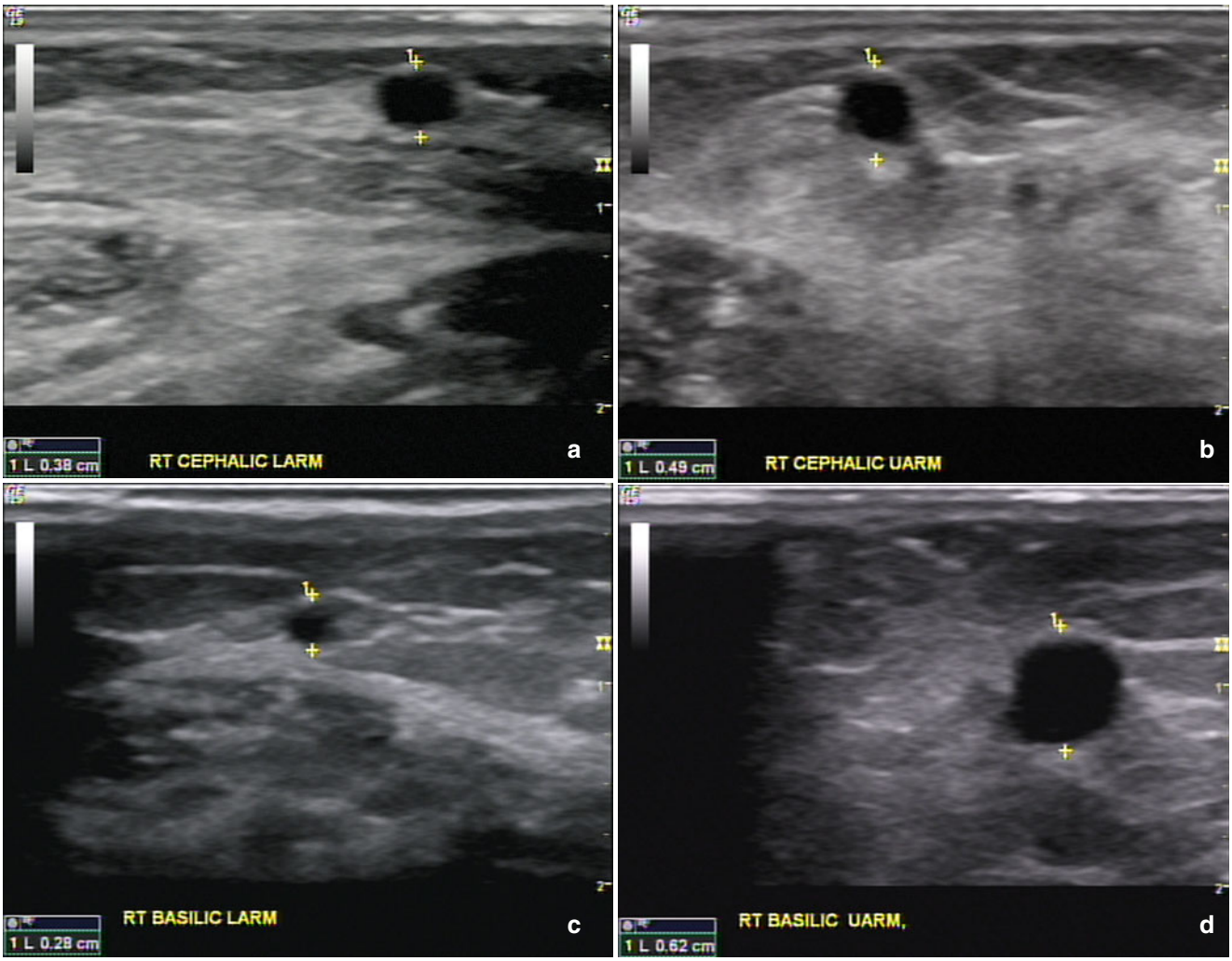


**Fig. 31.5** (**a**–**d**) Preoperative ultrasound images of the right cephalic and basilic vein in the upper and lower arm

subclavian vein (sensitivity of 94%) and least accurate for lesions in the axillary vein (sensitivity of 67%) [29].

DU criteria for proximal venous outflow obstruction include the absence of spontaneous phasic flow, vein incompressibility, or absence of flow augmentation with distal venous compression [29]. The subclavian vein can be directly visualized (see Fig. 31.6). The superior vena cava and innominate vein can be measured indirectly by observance of decreased respiratory phasicity and transmitted cardiac pulsatility in the subclavian and jugular veins [25].

As in the case of ultrasound-guided arterial treatments, the DU examination can also guide the treatment of venous stenosis. It avoids the use of contrast material, therefore eliminating the risk of contrast-induced nephropathy in these high-risk patients. Several studies have shown excellent results with this method for venous stenosis as well as for non-maturing autogenous AV [27, 30, 31]. If DU is nondiagnostic, venography should be performed.

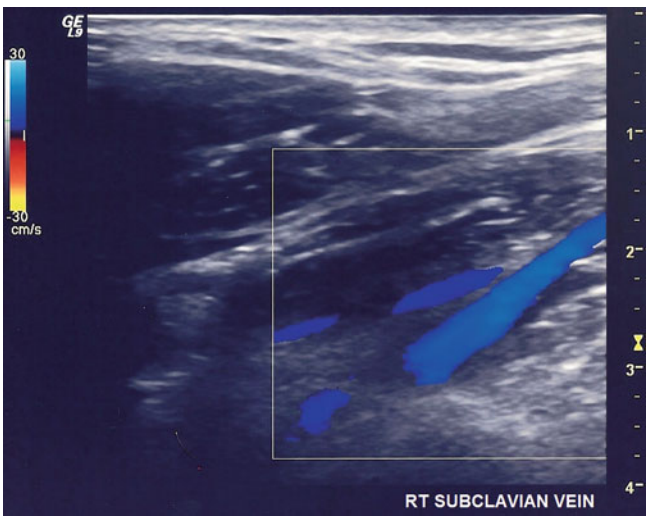


**Fig. 31.6** Color flow duplex ultrasound of a normal right subclavian vein

## Conclusion

In summary, preoperative planning is imperative for creating autogenous AV access. The National Kidney Foundation-Kidney Dialysis Outcomes Quality Initiative (NKF-DOQI) guidelines as well as the clinical practice guidelines for the surgical placement and maintenance of arteriovenous hemodialysis access of The Society for Vascular Surgery have given clear recommendations aimed at creating autogenous AV access [14, 32], in particular, the use of noninvasive imaging to augment the placement of autogenous AV access. By using the noninvasive tools and guidelines that are available, the goal of increasing the number of functional autogenous arteriovenous access may be achieved.

## References


1. Incidence & prevalence of ESRD. In: U.S. renal data system, USRDS 2010 annual data report: atlas of chronic kidney disease and end-stage renal disease in the United States. National Institutes of Health, National Institute of Diabetes and Digestive and Kidney Diseases, Bethesda; 2010. http://www.usrds.org/2010/pdf/v2_02.pdf. Accessed 15 Feb 2011.
2. Costs of ESRD. In: U.S. renal data system, USRDS 2010 annual data report: atlas of chronic kidney disease and end-stage renal disease in the United States. National Institutes of Health, National Institute of Diabetes and Digestive and Kidney Diseases, Bethesda; 2010. http://www.usrds.org/2010/pdf/v2?11.pdf. Accessed 15 Feb 2011.
3. Schon D, Blume SW, Niebauer K, et al. Increasing the use of arteriovenous fistula in hemodialysis: economic benefits and economic barriers. CJASN. 2007;2:268–76.
4. Treatment modalities. In: U.S. renal data system, USRDS 2010 annual data report: atlas of chronic kidney disease and end-stage renal disease in the United States. National Institutes of Health, National Institute of Diabetes and Digestive and Kidney Diseases, Bethesda; 2010. http://www.usrds.org/referencef.htm. Accessed 19 Feb 2011.
5. Miller PE, Tolwani A, Luscy CP, et al. Predictors of adequacy of arteriovenous fistulas in hemodialysis patients. Kidney Int. 1999;56:275–80.
6. Astor BC, Coresh J, Powe NR. Relation between gender and vascular access complications in hemodialysis patients. Am J Kidney Dis. 2000;36:1126–34.
7. Hakaim AG, Nalhandian M, Scott T. Superior maturation and patency of primary brachiocephalic and transposed basilica vein arteriovenous fistulae in patients with diabetes. J Vasc Surg. 1998;27:154–7.
8. Beathard GA. Physical examination of the dialysis vascular access. Semin Dialysis. 1998;11:231–6.
9. Gonsalves CF, Eschelman DJ, Sullivan KL, et al. Incidence of central vein stenosis and occlusion following upper extremity PICC and port placement. Cardiovasc Interv Radiol. 2003;26:123–7.
10. Foley MJ. Radiologic placement of long-term central venous peripheral access system ports (PAS port): results in 150 patients. JVIR. 1995;6:255–62.
11. Cardella JF, Cardella K, Bacci N, et al. Cumulative experience with 1273 peripherally inserted central catheters at a single institution. JVIR. 1996;7:5–13.
12. Allen AW, Megargell JL, Brown DB, et al. Venous thrombosis associated with the placement of peripherally inserted central catheters. JVIR. 2000;10:1309–14.
13. Currier CB, Widder S, Ali A, Kuusisto E, Sidawy AN. Surgical management of subclavian and axillary vein thrombosis in patients with a functioning arteriovenous fistula. Surgery. 1986;100:25.
14. Sidawy AN, Spergel LM, Desarab A, et al. Society for Vascular Surgery. The Society for Vascular Surgery: clinical practice guidelines for the surgical placement and maintenance of arteriovenous hemodialysis access. J Vasc Surg. 2008;48(5 Suppl):S20–5.
15. Parfrey PS, Griffiths SM, Barrett BJ. Contrast material-induced renal failure in patients with diabetes mellitus, renal insufficiency, or both. A prospective controlled study. N Engl J Med. 1989;320:143–9.
16. Hennerici MG, Neuerburg-Heusler D. Vascular diagnosis with ultrasound. 2nd ed. New York: Thieme; 2005. p. 150–80.
17. Vascular medicine, evidence based vascular medicine reviews. http://www.angiologist.com/2010/11/28/upper-extremity-artery-disease. Accessed 16 Mar 2011.
18. Vascular medicine, evidence based vascular medicine reviews. http://www.angiologist.com/2010/09/24/pulse-volume-recording. Accessed 03 Jan 2011.
19. Brown PW. Preoperative radiological assessment for vascular access. Eur J Vasc Endovasc Surg. 2006;31:64–9.
20. Malovrh M. The role of sonography in the planning or arteriovenous fistulas for hemodialysis. Semin Dialysis. 2003;16:299–303.
21. Silva MB, Hobson RW, Pappas PJ, et al. A strategy for increasing use of autogenous hemodialysis access procedures: impact of preoperative noninvasive evaluation. J Vasc Surg. 1998;27:302–8.
22. Lemson MS, Leunissen KM, Tordoir JH. Does preoperative duplex examination improve patency rates of Brescio-Cimino fistulas? Nephrol Dial Transplant. 1998;13:1360–1.
23. Ascher E, Hingorani A, Marks N. Duplex-guided balloon angioplasty of failing or nonmaturing arterio-venous fistulae for hemodialysis: a new office-based procedure. J Vasc Surg. 2009;50:594–9.
24. Malovrh M. Native arteriovenous fistula: preoperative evaluation. Am J Kidney Dis. 2002;39:1218–25.
25. Robbin ML, Gallichio ML, Deierhoi MH, et al. US vascular mapping before hemodialysis access placement. Radiology. 2000;217:83–8.
26. Koskoy C, Kuzu A, Erden I. Predictive value of color Doppler ultrasonography in detecting failure of vascular access grafts. Br J Surg. 1995;82:50–2.
27. Ascher E, Gade P, Hingorani A, et al. Changes in the practice of angioaccess surgery: impact of the dialysis outcome and quality initiative recommendations. J Vasc Surg. 2000;31:84–92.
28. Mendes RR, Farber MA, Marston WA, et al. Prediction of wrist arteriovenous fistula maturation with preoperative vein mapping with ultrasonography. J Vasc Surg. 2002;36:460–3.
29. Passman MA, Criado E, Farber MA, et al. Efficacy of color flow duplex imagining for proximal upper extremity venous outflow obstruction in hemodialysis patients. J Vasc Surg. 1998;28:869–75.
30. Bacchini G, Cappello A, La Milia V, et al. Color Doppler ultrasonography imaging to guide transluminal angioplasty of venous stenosis. Kidney Int. 2000;58:1810–3.
31. Marks N, Acher E, Hingorani Ap. Duplex-guided repair of failing or nonmaturing arterio-venous access for hemodialysis. Perspect Vasc Surg Endovasc Ther. 2007;19:50–5.
32. National Kidney Foundation. KDOQI clinical practice guidelines and clinical practice recommendations for 2006 updates: hemodialysis adequacy, peritoneal dialysis adequacy and vascular access. Am J Kidney Dis. 2006;48 suppl 1:S1–322.

# Role of Duplex Ultrasound in Dialysis Access Surveillance

32

Martin R. Back and Dennis F. Bandyk

**Abstract**

Dialysis access dysfunction and failure is common in the end-stage renal disease patients requiring hemodialysis. Problems include failure of access maturation, conduit injury caused by cannulation, thrombosis, inadequate volume flow, and aneurysmal degeneration. Duplex ultrasound is an accurate and useful diagnostic technique to assess dialysis access function. The detection of conduit and anastomotic stenosis, measurement of volume flow, and assessment of hand perfusion for steal syndrome is possible. Duplex scanning can provide the necessary anatomic and hemodynamic information to identify clinically important abnormalities as well as plan a remedial endovascular or "open surgical" interventional procedure. Measurement of access volume flow is prognostic for effective dialysis and access patency, including determining if access maturation has occurred and when to intervene for a duplex-identified access stenosis. A duplex-measured volume flow of >800 mL/min predicts a clinically successful dialysis access. The application of duplex surveillance after autogenous vein or prosthetic bridge graft access construction has the potential to improve patency and function in the renal failure patient whose life is dependent on hemodialysis.

**Keywords**

Duplex ultrasound surveillance • Hemodialysis access dysfunction • Arteriovenous fistulae Arteriovenous prosthetic bridge graft • Volume flow rate • Access stenosis

Maintenance of a functional dialysis access requires vigilance in caring for patients with end-stage renal disease (ESRD) receiving hemodialysis. Both autogenous fistulas (AVF) and prosthetic bridge grafts are associated with a spectrum of anatomic and hemodynamic abnormalities that interfere with dialysis access function. The failure rate of dialysis access procedures, that is, primary patency rate based upon "intention to treat" reporting standards, has been reported as high as 40% at 1 year for both autogenous and prosthetic conduits [1, 2]. The most common problems are failure of autogenous vein accesses to mature, access thrombosis, false aneurysm formation, venous hypertension producing limb edema, and arterial steal syndrome producing hand ischemia. In the majority of patients, salvage of dialysis access conduit is possible but the subsequent assisted primary patency and secondary patency rates at 1 year are 60–80% for AVFs and 50–70% for polytetrafluoroethylene (PTFE) bridge grafts [1, 2]. The rationale for dialysis access surveillance is based on the principle that surgical or endovascular intervention to maintain or improve functional patency is more successful when performed on a patent but "failing" dialysis access than on one that has thrombosed. Duplex ultrasound is ideally suited for the detection of access

M.R. Back, M.D., RPVI, RVT (✉)
Division of Vascular and Endovascular Surgery,
University of South Florida, College of Medicine,
2 Tampa General Circle, Suite 7001, Tampa, FL 33606, USA
e-mail: mback@health.usf.edu

D.F. Bandyk, M.D.
Vascular and Endovascular Surgery,
University of California, San Diego,
La Jolla, CA, USA

A.F. AbuRahma, D.F. Bandyk (eds.), *Noninvasive Vascular Diagnosis*,
DOI 10.1007/978-1-4471-4005-4_32, 

stenosis, which reduces volume flow to levels that result in ineffective or difficult hemodialysis. Monitoring of dialysis access function is a recommended "quality assurance" guideline, but the efficacy of duplex ultrasound surveillance to improve patency and function is an unverified application, primarily because a prospective, randomized clinical trial has not been conducted.

Surveillance of dialysis access function requires use of accurate diagnostics and successful reparative interventions to verify access to both anatomy and hemodynamics is suitable for conduit cannulation and hemodialysis. The goal is to preserve a high-flow, subcutaneous conduit that can have a two-needle cannulation to deliver blood to and from a dialysis filter circuit. In general, three times weekly hemodialysis requires at least a 10-cm length of subcutaneous (<1 cm depth) conduit for cannulation with a volume flow rate of >600–800 mL/min [3, 4]. The National Kidney Foundation (www.kidney.org) in their Dialysis Outcome Quality Initiative (DOQI) guidelines 9–11 recommends "prospective surveillance of dialysis access grafts for hemodynamically significant stenosis" [3]. Evidence-based data indicate that surveillance combined with lesion repair "improves patency and decreases the incidence of thrombosis." The surveillance protocol should include weekly physical examination in the dialysis unit, and the use of anatomic and physiologic techniques to detect access stenosis or flow reduction [5–8]. Diagnostic methods available to clinicians include access recirculation calculations, venous line pressures, ultrasonic dilution techniques, duplex ultrasound testing for stenosis detection and volume flow measurement, and contrast fistulography. The best surveillance method is one that is accurate, safe, practical regarding patient care, and ideally reimbursed by Center for Medicare Services (CMS) or other healthcare providers. Although duplex ultrasound is well suited for dialysis access surveillance, the current CMS payment guidelines for CPT 93900 (duplex scan of hemodialysis access) will not pay for routine surveillance testing. Payment is provided if any sign or symptom of access dysfunction exists, such as decreased thrill on physical examination, difficulty in needle cannulation, clot formation during hemodialysis, an elevated venous line dynamic pressure (>200 mmHg) during dialysis at a flow of 200 mL/min, access recirculation of 12% or greater, or an otherwise unexplained urea reduction ratio of <60%. Documentation of medical necessity is required for CMS reimbursement if both a duplex scan and a diagnostic fistulogram is performed to assess dialysis access dysfunction.

The development of a focal stenosis in the venous conduit or prosthetic bridge graft venous outflow is the prevalent mode of dialysis access failure, including the failure of a newly constructed access to mature. Stenotic lesions can develop at the arterial anastomosis, within the vein or prosthetic conduit, and in the central veins of the thorax. Significant stenosis, i.e., >50% diameter-reducing (DR) are found in 80–90% of thrombosed access grafts [6, 7]. In some instances, restoration of access patency by endovascular or surgical thrombectomy will not identify a causative anatomic lesion, suggesting there is another etiology for thrombosis, such as transient hypotension, hypovolemia, a hypercoagulable condition, prolonged access compression after cannulation, or improper access cannulation. Duplex ultrasound mapping allows for both the detection of access stenosis as well as the measurement of volume flow, a characteristic critically important for a successful hemodialysis session. These data are useful for patient management, including decisions regarding when a newly constructed dialysis access can be used, is there an abnormality present interfering with access maturation, and is low access flow caused by a "correctable" lesion(s). By using appropriate interpretation criteria, duplex testing allows the clinician to determine the significance of detected stenosis relative to the level of access volume flow that would compromise hemodialysis. Other anatomic lesions that may interfere with access function or longevity can also be identified, such as pseudoaneurysm formation, conduit mural thrombus, cannulation site hematoma, or perigraft seroma. Repair of duplex- or fistulogram-detected stenosis by open surgical revision or percutaneous transluminal angioplasty (PTA) can restore functional patency and extend access survival [2, 8–12]. Prospective clinical studies comparing results of surgical versus endovascular intervention have reported equivalent success in the management of the "thrombosed" or "stenotic" access conduit. Intervention decisions are typically based on lesion morphology and site, age of the dialysis access, conduit type, and operator experience or preference. Since most access lesions develop within the first year, duplex testing is of most value early after access construction and during this time period. Since the efficacy of access surveillance may differ between prosthetic bridge grafts and autologous AVFs, the interpretation criteria regarding access maturation and appropriate volume flow differ and testing should be tailored to the access type and individual patient.

## Dialysis Access Diagnostics

Historically, dialysis access surveillance relied primarily on anatomic assessment using contrast digital subtraction arteriography to identify correctable lesions producing dysfunction or thrombosis. A "clinically significant" stenosis reduces lumen diameter >50%, e.g., >75% cross-sectional area reduction, and is associated with a resting pressure gradient and therefore a reduction in volume flow. Current DOQI recommendations support the application of physiologic testing methods for surveillance including duplex ultrasound, assess recirculation, venous line pressure measurements, and

Doppler volume flow measurements. These direct and indirect diagnostic methods can identify the "low" volume flow or "failing" dialysis access, whose threshold values are predictive of conduit thrombosis or difficult hemodialysis. The minimum volume flow threshold for satisfactory hemodialysis is reported to be 500 mL/min; but for effective dialysis in 2–3-h session with a circuit flow of 300–450 mL/min, a higher access flow is required – ideally in the range of 800–1,200 mL/min. After dialysis access construction, volume flow increases during the subsequent weeks and months due to venous outflow and inflow artery dilation. This "maturation" process is more rapid within the first month, which allows bridge graft accesses to be used earlier that an autogenous vein access. Overall, the autogenous forearm AVF and bridge graft has a lower flow rate than an arm AVF or prosthetic bridge graft due to smaller diameter inflow radial/ulnar arteries and outflow vein conduit. Since volume flow is an important criterion of dialysis access maturation, duplex testing prior to cannulation is an important and recommended evaluation. When a contrast fistulogram or duplex scan identifies a >50% diameter-reducing (DR) stenosis, intervention should be based on the measured level of access volume flow. Stenosis can be detected in one-quarter of patients with clinically functioning dialysis accesses. The goal of surveillance is to use sequential testing to monitor access function and identify hemodynamic changes prior to access thrombosis, which typically occurs when volume flow falls below a level of 500–600 mL/min.

## Contrast Fistulography

Access imaging by catheter injection of iodinated contrast agents is considered the "gold standard" for assessment of arterial inflow, anastomotic sites, venous/prosthetic conduit, and the central veins of the thorax. Using digital subtraction techniques and multiplanar imaging, the entire upper extremity arterial and venous anatomy can be evaluated. Grading of stenosis severity is accurate including the assessment of multilevel occlusive lesions. The fistulogram can also detect aneurysms (true and false) and conduit mural thrombus, conditions that increase thrombotic risk and require repair. Fistulography is invasive, expensive, and has associated risks, and it should not be used as a primary method for evaluating dialysis access for anatomic lesions, but is better used to evaluate the "failing" access or perform endovascular therapy on a known abnormality. Administration of iodinated contrast in ESRD patients not yet receiving hemodialysis with recently constructed but dysfunctional access conduits should be avoided to prevent acceleration of renal failure. In such cases, duplex ultrasonography can be used to identify stenoses for intervention. A contrast study is always used in conjunction with a planned or anticipated endovascular procedure. Duplex monitoring of a dialysis access angioplasty can be used to confirm improvement in volume flow and absence of residual stenosis. A catheter-directed venogram is the preferred technique to evaluate the central (axillary, subclavian, brachiocephalic, superior vena cava) venous system for obstruction or stenotic lesions produced by prior venous dialysis catheters or cardiac pacemaker leads.

## Access Recirculation

Recirculation within a hemodialysis access conduit is defined as dialyzed blood returning through the venous needle that reenters the extracorporeal circuit through the arterial needle. If measured accurately, *access recirculation* does not occur unless the blood flow rate through the access conduit is generally less than that prescribed through the dialyzer circuit [13]. Measurement of recirculation percentage of 12% or greater correlates with low volume flow and is an indicator of inefficient hemodialysis. Access recirculation is calculated using the measured concentration of blood urea nitrogen (BUN) according to the formula

$$U_s - U_a / U_s - U_v \times 100\%$$

where $U_s$ is the systemic [BUN], $U_a$ is arterial line [BUN], and $U_v$ is the venous line [BUN]. Existing methods (three-needle, peripheral vein techniques) of measurement of systemic [BUN] are prone to error and overestimation of recirculation because of arteriovenous and venovenous equilibrium. Alternatively, a two-needle, slow/stop flow method for urea recirculation may decrease these errors [14]. Recirculation measurements are made during hemodialysis and can be repeated serially over time, but have not generally been predictive of dialysis access thrombosis. Urea recirculation values of greater than 15% at a dialyzer flow rate of 400 mL/min have had an acceptable accuracy for identifying access conduits with stenosis but not found to be useful in prospective studies in predicting access thrombosis [15–18]. Measurement of access recirculation is not considered a preferred method for identification of a failing access and is not suited for surveillance. If an abnormal access recirculation value is measured, duplex testing should be performed to measure volume flow.

## Venous Line Pressure Measurement

Elevation of pressure measured in the drip chamber of the venous cannula downstream of the dialysis pump and membrane unit can occur with venous outflow obstruction. Since venous stenosis is a common cause of access failure, serial measurement of venous line pressures is an accepted

surveillance technique. Accuracy of the pressure measurement is highly dependent on proper matching of the dynamic response of the catheter – transducer system, transducer zeroing relative to height differences in the system, and elimination of air bubbles or blood clots. Both static (measured under no dialyzer flow condition) and dynamic (with dialyzer flow) venous line pressures have been utilized. Measurement of line pressure with the dialysis flow rate held constant at 200–250 mL/min for several minutes is the preferred technique. Testing is performed prior to proceeding with hemodialysis at a flow rate of 300–400 mL/min with a line pressure <150 mmHg considered normal.

The diagnostic accuracy of venous line pressures in detection of >50% DR stenoses is sufficient for surveillance testing. A dynamic venous pressures >150 mmHg during three consecutive dialysis sessions had an 86% sensitivity and 93% specificity for detection of >50% venous outflow stenosis by confirmed fistulography [10]. Mean dynamic venous line pressure was significantly higher in patients with >50% DR angiographic-confirmed stenosis (126 ± 35 mmHg) than in accesses without stenosis (95 ± 22 mmHg) [19]. When used alone, venous line pressure measurements have not been predictive of access thrombosis [5, 18, 19]. Testing is most sensitive to the development of venous anastomotic or outflow stenosis since lesions proximal to venous cannula will not be detected. Serial venous line pressure measurements can recognize the "failing" access, and a threshold value in the 150–200 mmHg is an appropriate indication to proceed with additional diagnostic testing such as duplex ultrasound.

## Volume Flow Measurement

Serial volume flow measurement of the patent dialysis access holds promise as the most accurate method for access surveillance. The relationship between low-volume flow rate and thrombosis risk has been clearly demonstrated. By comparison, the relationship between presence of stenosis and conduit flow rates remains to be fully defined. A duplex-detected stenosis with a <2 mm residual lumen diameter, peak systolic velocity > 400 cm/s, and peak systolic velocity ratio > 2 across the stenosis indicates >50% DR but is not always associated with low (<500 mL/min) access volume flow. Duplex-derived volume flow calculations and Doppler ultrasonic techniques have been used to estimate time-averaged blood flow rates. Since the diameter of the vessel and time-averaged velocity can be measured by ultrasound methods, volume flow can be calculated using the formula

$$Q = vA = v(\pi d^2)/4$$

where $v$ is the time- and spatially averaged velocity over the lumen cross-section and $d$ and $A$ are the lumen diameter and cross-sectional area at the site of velocity measurement. Assumptions made in this calculation are that blood flow is minimally disturbed and axial-symmetric at the recording site, and the lumen cross-section is circular. Testing should not be performed during or immediately after dialysis, since reduction in blood pressure caused by hypovolemia is a potential source of error by providing low volume flow estimates. Duplex ultrasound volume flow should be measured on a nondialysis day in a normotensive patient. The software package for this calculation is available on essentially all contemporary duplex ultrasound units. For upper extremity autogenous accesses with variable vein diameters and branching patterns, volume flow measurement from the inflow artery is an appropriate option. Sites of flow measurement should be carefully selected – no stenosis or lumen narrowing should be imaged and pulsed Doppler velocity spectra should demonstrate only mild-to-moderate spectral broadening (Fig. 32.1). Vessel diameter (anterior-posterior dimension) is measured with transducer scanlines perpendicular to the long axis of the conduit in a longitudinal/sagittal view. The pulsed Doppler sample volume is sized to encompass the entire lumen, and the velocity spectra recorded at a Doppler angle of 60°. The time-averaged velocity is calculated over two to three pulse cycles. Measurements are obtained in the inflow artery and at two to three locations along the access conduit, typically several (3–4) vessel diameters downstream of the arterial anastomosis, at mid-graft, and proximal to any venous anastomosis (Fig. 32.2). Experimental validation of duplex-derived volume flow measurements have been performed in baboons with an average error of 13% and good correlation ($r = 0.9$) with timed blood collection at flow rates in the range of 300 mL/min [20]. Similar validation data does not exist for the high volume and disturbed flow conditions present in arteriovenous access conduits but it is estimated that the reproducibility error is approximately 20–25%.

Access flow can also be measured during hemodialysis sessions using the transit-time, ultrasonic dilution method. Separate ultrasound transducers are placed on the arterial and venous dialysis tubing and the lines are reversed so that the arterial line is downstream of the venous line within the access conduit. The dialysis circuit flow is fixed at 200–300 mL/min and ultrafiltration turned off. Rapid injection of 5–10 mL of normal saline at body temperature into the venous line dilutes the red cell mass in blood flowing through the access and results in alteration of the Doppler-derived velocity waveform recorded by the arterial line transducer. The measured areas under the perturbed velocity versus time curve at the venous ($S_v$) and arterial ($S_a$) lines and the known dialyzer flow rate ($Q_b$) allows calculation of the access flow rate by the relation:

$$Q = Q_b \left( S_v / S_a - 1 \right)$$

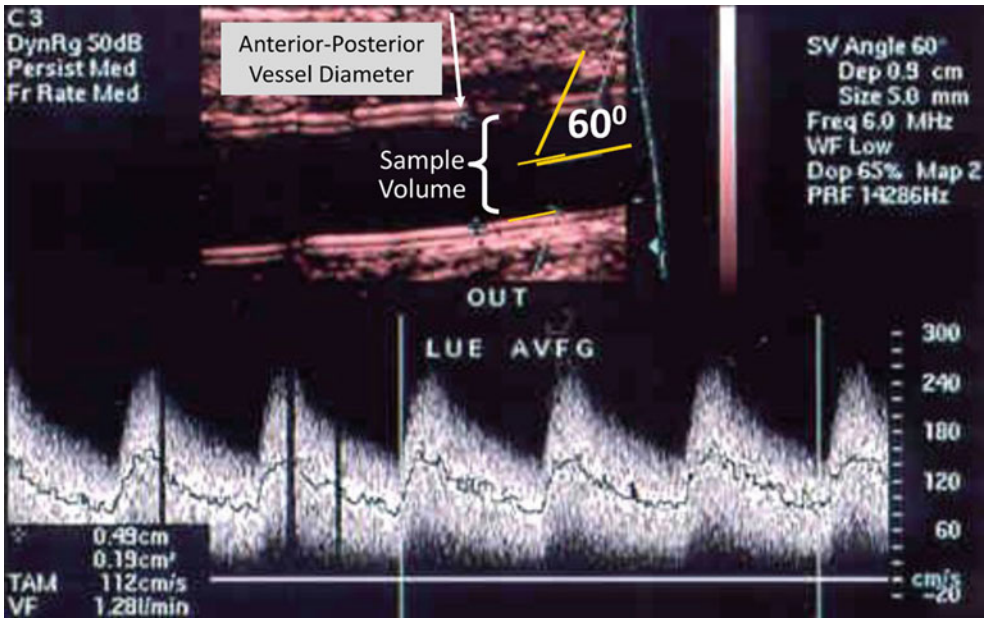


**Fig. 32.1** Duplex ultrasound image of a 6 mm diameter dialysis bridge graft with a calculated volume flow of 1,280 mL/min. Note velocity spectra were recorded at a 60° Doppler angle, the pulsed-Doppler sample volume encompasses the entire lumen, and time-averaged, mean velocity measured over three pulse cycles

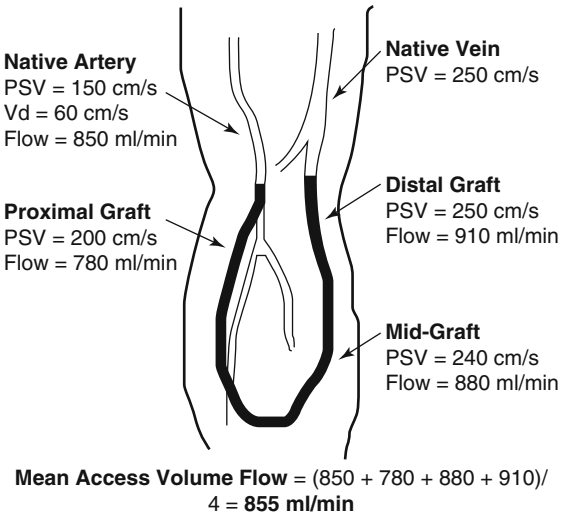


**Fig. 32.2** Schematic of forearm loop prosthetic bridge graft for dialysis showing typical duplex scan recording sites of peak systolic velocity (PSV, cm/s) and volume flow (mL/min) measurements. Mean graft flow calculated as the average of measurements recorded from inflow brachial artery and three graft sites

Accuracy of the access flow calculation appears independent of dialyzer flow rates between 177 and 350 mL/min but requires careful positioning of the arterial needle within the center stream of the access flow [21]. Two or three access flow measurements should be made for reproducibility as the error between consecutive measurements averages 5% [20]. Clinical comparison of ultrasound dilution and Doppler-derived flow rate measurements have yielded acceptable agreement (correlation coefficients 0.79–0.83) over a wide range of access flows [17, 22, 23]. The ultrasound dilution technique does not have a tendency to over- or underestimate flow rates except in accesses with conduit stenosis where dilution measurements were lower than obtained by duplex ultrasound [22].

Low-volume flow rates (<300–500 mL/min) have been shown to be predictive of PTFE bridge graft failure (Table 32.1) [5, 17–19, 24–28]. The thrombotic risk increases whether measured by Doppler-derived or ultrasound dilution techniques. The association between low-volume flow and AVF patency is not as strong as for prosthetic bridge grafts, felt due to lower thrombotic potential of the venous conduit. The combination of access stenosis with low-volume flow is also predictive of access failure [5, 19]. Flow rates were significantly less in conduits with stenosis than in functioning conduits with a maintained stenosis-free patency. In fact, the flow rate values in stenotic conduits were similar to those measured in accesses with subsequent thrombotic events [5]. These observations confirm access conduit stenosis associated with a low or reduction in volume flow increases thrombotic risk. It should be noted that in some access conduits with low volume flow rates, a stenosis may not be detected. In these instances, a careful search for inflow or central vein occlusive disease should be conducted. Mechanisms of thrombosis in low flow, nonstenotic access includes interval development of heart failure, hypovolemia, hypotension, hypercoagulability, or extrinsic pressure on the graft (e.g., during access decannulation).

Controversy exists regarding the threshold access volume flow that should prompt intervention or additional imaging studies such as contrast fistulography. Based on current retrospective and uncontrolled prospective data, PTFE bridge grafts with access flow rates below 700–800 mL/min and reduced peak systolic velocities in the inflow brachial or radial artery <90 cm/s should be imaged with duplex

**Table 32.1** Correlation of hemodialysis access blood flow rate measurements with arteriography and graft failure measures

| Author | Access type | Technique | Threshold value (mL/min) | Validation angio? | Findings |
|---|---|---|---|---|---|
| Rittgers et al. [24] | PTFE | Doppler | <450 | No | 100% Failure 2 weeks |
| Shackleton et al. [25] | PTFE | Doppler | <450 | No | 83% Sensitivity,75% specificity failure 2–6 weeks |
| Sands et al. [23] | PTFE | Doppler | < 800 | No | 93% Failure 6 months* |
| Johnson et al. [28] | PTFE | Doppler | <400 | No | 64% Failure 3 months* |
| | AVF | Doppler | <320 | No | Lower 1° and 2° patency rates* |
| May et al. [17] | PTFE | Dilution | 1,150 | No | Relative risk failure 3 months = I |
| | | | 750 | | 1.5* |
| | | | 300 | | 2.4* |
| Bay et al. [18] | PTFE | Doppler | 700–1,000 | no | Relative risk intervention/failure 6 months = 1 |
| | | | 300–500 | | 1.4* |
| | | | <300 | | 2.0* |
| Bosman et al. [19] | Graft | Filution | 1,061 | Yes | Nonstenotic |
| | | | 664 | | >50% Stenosis* |
| Besarab et al. [22] | PTFE | Dilution | 1,121 | Yes | No event |
| | | | 605 | | Stenosis/intervention* |
| | | | 540 | | Failure* |
| | AVF | Dilution | 1,057 | Yes | No event |
| | | | 313 | | Stenosis/intervention* |
| | | | 475 | | Failure* |
| Back et al. [27] | AVF | Doppler | <800 | No | 77% Accuracy failure (thrombosis/reintervention 6 months)* |
| | PTFE | | <800 | No | 63% Accuracy failure |
| | AVF | | <500 | No | 67% Accuracy failure |
| | PTFE | | <500 | No | 63% Accuracy failure |

*$p < 0.05$, statistically different group

scanning. Strauch et al. [7]. used a lower volume flow cutoff (350 cm/s) to identify grafts that will likely fail without intervention. Similarly, measured flow rates less than 400 mL/min in AVFs should prompt angiographic assessment.

Back et al. [27] found a threshold volume flow rate of 800 mL/min was a better discriminate of failing and functional AVFs and bridge grafts (with accuracy of 77%) than a flow rate greater than or less than 500 mL/min (accuracy of 67%). Regardless of the threshold levels chosen, grafts demonstrated to have flow-reducing stenosis should be monitored for concomitant reduction in volume flow. Optimal intervals for surveillance measurement of access flow rates have not been specified and may differ with access type and graft diameters. Since access failure is most common during the first postoperative year, surveillance at 3-month intervals may be appropriate.

## Duplex Ultrasound

Duplex scanning of a dialysis access provides both imaging and hemodynamic assessment of the arterial inflow, conduit, and venous outflow with precision comparable to contrast fistulography. The subcutaneous location of the access conduits allows the use of high-frequency (7.5–10 MHz) linear array transducers to obtain high-resolution vessel imaging. Both transverse and longitudinal/sagittal B-mode, color Doppler, and power Doppler imaging can be used to image the access, anastomotic regions, and venous outflow including the central veins to the extent possible. The technique of duplex mapping is identical to peripheral artery scanning with color/power Doppler imaging for stenosis and pulsed-wave Doppler velocity spectra recording for stenosis classification in DR categories of <50% and >50% based on peak systolic (PSV), end-diastolic (EDV) velocity. The velocity spectra of dialysis access hemodynamics are one of high-flow and low resistance with "normal" dialysis conduit PSV > 150 cm/s (Fig. 32.1). The resistive index should be 0.7 or less. Spectral broadening is typically present especially within the arterial anastomotic regions due to PSV > 200 cm/s and vessel tortousity, producing highly disturbed flow conditions. Proper selection of the color bar and velocity scale helps to minimize aliasing artifacts associated with color Doppler imaging. Access graft stenosis is identified by color flow imaging of a narrowed lumen and at least doubling of peak systolic velocities compared with adjacent graft segments (Fig. 32.3). A perivascular color artifact may be present and represents a tissue bruit caused by turbulent

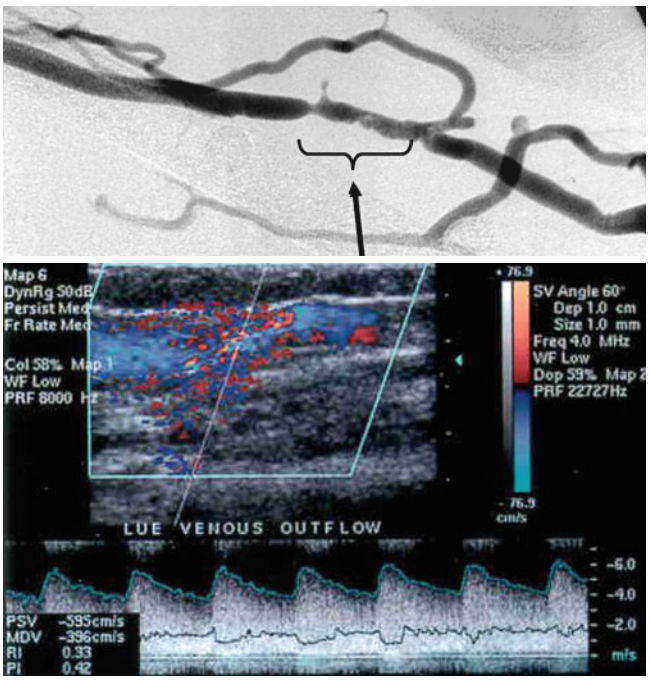


**Fig. 32.3** Contrast fistulogram and duplex scan of a >50% DR segmental venous stenosis. Peak systolic velocity (PSV) of 600 cm/s, EDV of 400 cm/s, and velocity ratio of 4 across stenosis predictive of >50% stenosis. Volume flow (VF) was measured at 700 mL/min; VF/$PSV_{stenosis}$ < 1.5. Note red/blue color pixels outside the vessel in the duplex scan image caused by a tissue bruit

**Table 32.2** Duplex classification of dialysis access stenosis

| Scan interpretation | Recorded velocity spectra | Color Doppler imaging |
|---|---|---|
| Normal | Arterial anastomosis >200 cm/s<br>Mid-graft PSV > 150 cm/s | No graft stenosis imaged, patent venous outflow |
| <50% DR stenosis | PSV anastomosis 200–400 cm/s<br>PSV conduit lesion <400 cm/s<br>Local PSV ratio < 2<br>Mid-graft PSV 100–150 cm/s | Decrease in lumen diameter |
| >50% DR stenosis | PSV anastomosis >400 cm/s<br>PSV conduit lesion >400 cm/s<br>Local PSV ratio > 2<br>Mid-graft PSV < 100 cm/s<br>If volume flow/$PSV_{stenosis}$ < 2; repair lesion | Focal lumen reduction, diameter <2–3 mm |
| Occlusion | No Doppler signal in conduit | Conduit occluded |

flow and vessel wall/tissue vibration. The duplex criteria for classification criteria dialysis access stenosis severity is based on PSV in the stenosis and reduction of conduit flow velocity in a nonstenotic segment (Table 32.2). In general, a >50% DR, flow-reducing stenosis is associated with PSV > 400 cm/s and a conduit and inflow artery PSV < 150 cm/s. When the access is thrombosed, the inflow artery will demonstrate multiphasic, high-resistance velocity spectra and no Doppler signal will be recorded within the occluded access conduit. In general, a hemodynamically significant (>50% DR) stenosis that impairs volume flow and should be repaired has the duplex features of a PSV > 400 cm/s, EDV > 250 cm/s, a local PSV ratio > 2, and a residual color or power Doppler flow lumen than 2–3 mm in diameter.

The diagnostic accuracy (sensitivity, specificity, positive predictive value) of duplex testing compared to contrast fistulogram for the detection of >50% DR stenosis is approximately 80% (Table 32.3) [17, 29–34]. Several reports used direct measurement of DR by B-mode and color flow imaging for identification of >50% stenoses. Tordoir et al. [33] used duplex-measured velocity criteria for >50% DR stenosis within bridge grafts, AVFs, and venous outflow. In a smaller clinical series, Older et al. [34] showed that 83% of duplex-detected lesions with >50% DR stenosis confirmed by fistulography had a threshold peak systolic velocity greater than 400 cm/s or peak systolic velocity ratio greater than 3. Diagnostic errors are primarily due to the limited ability of duplex testing to identify central vein obstruction or stenosis with reported a diagnostic sensitivity of 81% for >50% DR axillary, subclavian, or brachiocephalic venous stenosis or occlusion [31–35].

Routine surveillance of dialysis access has demonstrated the prevalence of >50% DR stenosis (based on PSV and PSV ratio values, fistulogram confirmation) in the range of 30–48% [18, 31–33]. Indicating access stenosis is a common duplex finding, especially for PTFE bridge grafts, despite the access exhibiting sufficient functional patency such that hemodialysis and continued conduit cannulation is not compromised. The mean number of stenoses identified in the bridge graft conduit or outflow veins ranged from 1.4 to 1.8. Correlation studies of duplex-detected stenosis with subsequent access thrombosis have yielded mixed results. Although duplex-detected stenosis within a dialysis access has been associated with reduced primary patency compared to "normal" scans, prospective clinical trials and prophylactic endovascular treatment of detected lesions did not demonstrate significant improvement in assisted primary patency for prosthetic bridge grafts [17, 18, 32]. These results suggest the presence of an access stenosis alone should not be the sole criteria for intervention. Since dialysis access failure is related to volume flow, duplex surveillance should include both imaging for stenosis and measurement of volume flow with repair of lesions associated with low (500–800 mL/min) volume flow. The ratio of volume flow (VF) to PSV at a duplex-identified stenosis ($PSV_{stenosis}$) may be a useful parameter to aid in decision making or predict access patency. A VF/$PSV_{stenosis}$ value <2 indicates a stenosis with a PSV of 400 cm/s should be repaired; but if the value is >2, VF of the access is adequate, i.e., >800 mL/min, and the access can be used for hemodialysis. Site of stenosis should be monitored

**Table 32.3** Results of duplex surveillance of dialysis access grafts for detection of conduit stenoses

| Author | Access type | Threshold value | Validation fistulogram | Diagnostic accuracy |
|---|---|---|---|---|
| Middleton et al. [29] | PTFE+ AVF | >50% DR | Yes | 87% Sensitivity |
| Dousset et al. [30] | Graft | >50% DR | Yes | 86% Sensitivity, 60% specificity |
| MacDonald et al. [31] | PTFE | >50% DR | Yes | 84% Sensitivity |
| Lumsden et al. [32] | PTFE | >50% DR | Yes | 76% Sensitivity |
| Tordoir et al. [33] | Graft | >50% DR | Yes | |
| | | PSV > 300 | | 92% Sensitivity, 84% specificity |
| | | PSV ratio > 3 | | 75% Sensitivity, 96% specificity |
| | AVF | PSV > 375 | Yes | 79% Sensitivity, 84% specificity |
| | Venous outflow | PSV > 250 | Yes | 95% Sensitivity, 97% specificity |
| Older et al. [34] | PTFE+ AVF | PSV > 400 cm/s PSV ratio > 3 | Yes | 83% Positive predictive value |

for progression with serial duplex testing at 1–2 month intervals.

Duplex testing can also detect other access abnormalities that interfere with hemodialysis or threaten patency. Aneurysms or pseudoaneurysm are readily detected by color flow imaging and are easily distinguished from hematoma by the presence of flow. Small pseudoaneurysm (5 mm diameter) caused by repetitive cannulation tend to remain stable while large pseudoaneurysm (>1 cm diameter) typically enlarge and should ideally be repaired. Lumen thrombus can also be detected by duplex scanning and is a sign of access dysfunction and associated with eventual access thrombosis.

## Application of Duplex Surveillance

In our vascular group, duplex ultrasound is the preferred method for dialysis access surveillance (Table 32.4). Whether the testing is performed beyond the early postoperative period depends in part on the patient's nephrologist's willingness to participate in the surveillance program. Following dialysis access construction, duplex testing is performed prior to initiation of hemodialysis. Thereafter, there should be a medical indication for testing. Since a minimum access volume flow rate is necessary for hemodialysis, testing prior to initial access cannulation is perform to verify a suitable (>10 cm) length of normal conduit for needle access, confirm a volume flow level indicative of "maturation" as well as assess whether any stenotic or other anatomic abnormality (patent vein side-branch) is present. Subsequent testing is performed to detect and manage "developing" stenotic segments based on both stenosis severity and level of access volume flow. Clinical studies have showed volume flow rates in PTFE bridge grafts to be the only reliable predictor of access thrombosis [17, 18]. Weekly measurement of dynamic venous line pressures has acceptable sensitivity for detection of venous outflow obstruction, and when a high (>200 mmHg) dynamic pressure is recorded, duplex testing that includes volume flow measurement is appropriate [5, 15, 16, 19, 22].

**Table 32.4** Guidelines for dialysis access testing using duplex ultrasound

| |
|---|
| *Dialysis access imaging* |
| Scanning performed in both longitudinal/sagittal and transverse planes |
| Document location and extent of perigraft fluid collections and masses |
| Mapping should proceed from artery inflow, through the arterial anastomosis, the entire length of the dialysis conduit, through the venous anastomosis if present, and into outflow central veins |
| Native artery is imaged proximal to the arterial anastomosis and volume flow measured |
| Volume flow measurements calculated at several locations along the access conduit at sites of normal lumen caliber and minimally disturbed flow conditions |
| Sites of lumen abnormality (stenosis, thrombus, aneurysm) and large branches for nontransposed AVF are documented in a schematic of the dialysis access |
| Sites of lumen stenosis are classified based on velocity spectra recorded proximal to, at the site of stenosis, and distal to stenosis |
| *Documentation* |
| Peak systolic velocity (PSV) within native inflow artery (radial, brachial) |
| PSV in dialysis graft or along autologous venous conduit |
| PSV in arterial and venous anastomotic regions |
| Peak systolic and end-diastolic velocities at site of stenosis, including calculation of PSV ratio |
| Volume flow measured and calculated at three to four sites – averaged to determine a mean volume flow rate for the access conduit |
| Images of all pathology (thrombus, hematoma, seroma, abscess), measurement of aneurysm or pseudoaneurysm size and document presence of thrombus |
| *Diagnostic criteria* |
| Normal artery inflow velocities: PSV 100–400 cm/s, EDV 0–200 cm/s |
| Normal venous velocities: PSV 50–200 cm/s, central veins lower PSV with phasic velocity spectra |
| Conduit or anastomotic stenosis: PSV > 400 cm/s, PSV ratio > 2, luminal diameter <2–3 mm |
| High-resistance flow pattern suggests low volume flow and impending graft occlusion |
| Retrograde flow in the native artery beyond conduit inflow anastomosis indicates arterial steal |
| Severe arterial steal and hand/digit ischemia: digit pressures <60 mmHg |
| Perigraft fluid collections indicate absence of graft healing and may be sign of infection when found along entire prosthetic graft length |

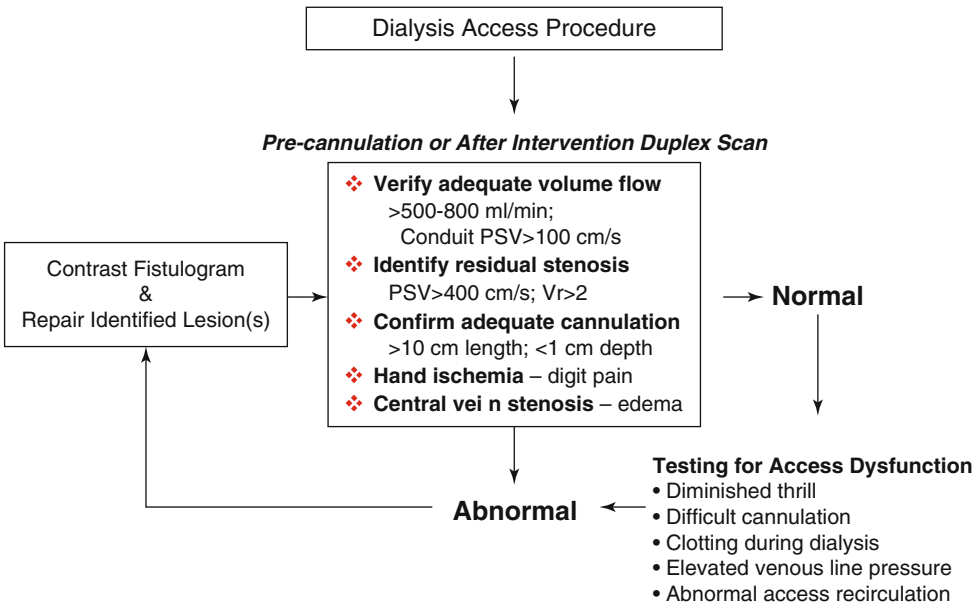


**Fig. 32.4** Recommended duplex ultrasound surveillance algorithm

The surveillance protocol begins with a precannulation duplex scan performed within 2 weeks after prosthetic bridge graft and 3–4 weeks after AVF constructions (Fig. 32.4). Testing includes both imaging and hemodynamic assessment to verify healing of the subcutaneous perigraft region and absence of residual hematoma or seroma that could preclude successful needle cannulation and sufficient volume flow for hemodialysis. In patients with symptoms of hand ischemia (numbness, grip weakness, pain), testing should include recording velocity spectra from the distal forearm radial and ulnar arteries, and digit pressure measurements with and without access compression. A digit pressure <60 mmHg indicates clinically significant hand ischemia. Arterial duplex "mapping" and serial waveform comparisons along the limb may allow localization of arterial occlusive lesions responsible for ischemic steal and help plan intervention (inflow subclavian/axillary endovascular intervention, distal revascularization/interval ligation (DRIL)) procedures and relocation of the access inflow anastomosis to a more distal artery or duplex-guided conduit plication. Patients developing significant limb edema early after access construction should have a detailed assessment of venous outflow and central vein system to detect an occlusive lesion causing venous hypertension and to facilitate endovascular therapy. In the absence of distal arterial ischemic or venous hypertensive symptoms after access construction, if conduits are found to have a lower than expected volume flow (<800 mL/min) with a detected stenosis or long length (>2 cm), small caliber (<4 mm) vein segment of an AVF, then repair is done to assure successful dialysis can be performed. Repeat duplex testing is performed after endovascular or open surgical intervention to confirm improvement in access hemodynamics (volume flow >800 mL/min and normalization of velocities across the repair site; Fig. 32.5). In access conduits possessing a poor thrill after initial construction and accompanied by extremely low volume flow rates <500 mL/min without ultrasound-detectable stenotic segments, then contrast fistulography should be performed that includes arterial inflow and central venous outflow imaging to further identify flow limiting lesions for repair. For access conduits having an acceptable thrill but possessing marginal (500–800 mL/min) volume flow with no identified stenosis, access cannulation should be withheld and duplex scanning repeated in 1 month to reassess volume flow and to detect any evolving stenosis, usually resulting from early myointimal hyperplasia. Thereafter, dialysis access surveillance is applied selectively for documented medical indications based on signs or symptoms of access dysfunction, inadequate hemodialysis, cannulation difficulties, or conduit false aneurysm (Fig. 32.6). Data regarding "expected" volume flow rate based on dialysis access type is limited as evidenced by Table 32.1 data. It is known that the initial volume flow of forearm autogenous AVFs is less than prosthetic bridge grafts constructed either in the forearm or arm. Basilic vein transposition accesses exhibit volume flow and other duplex ultrasound characteristics similar to 6- or 7-mm diameter prosthetic bridge grafts. Duplex surveillance of 125 consecutive dialysis access procedures (34 forearm fistulae, 53 arm fistulae, 38 prosthetic bridge grafts) performed in 108 patients demonstrated that precannulation mean volume flow rates differed based on access configuration; radiocephalic AVF:771 ± 435 mL/min; brachiocephalic AVF:1,616 ± 790 mL/min; brachiobasilic transposition AVF: 185 ± 585 mL/min; and prosthetic bridge grafts: 1,270 ± 604 mL/min. Peak systolic velocity at the arterial anastomosis was approximately 400 cm/s and mid-conduit PSV was approximately 250 cm/s, and similar in the various access types and configurations [27].

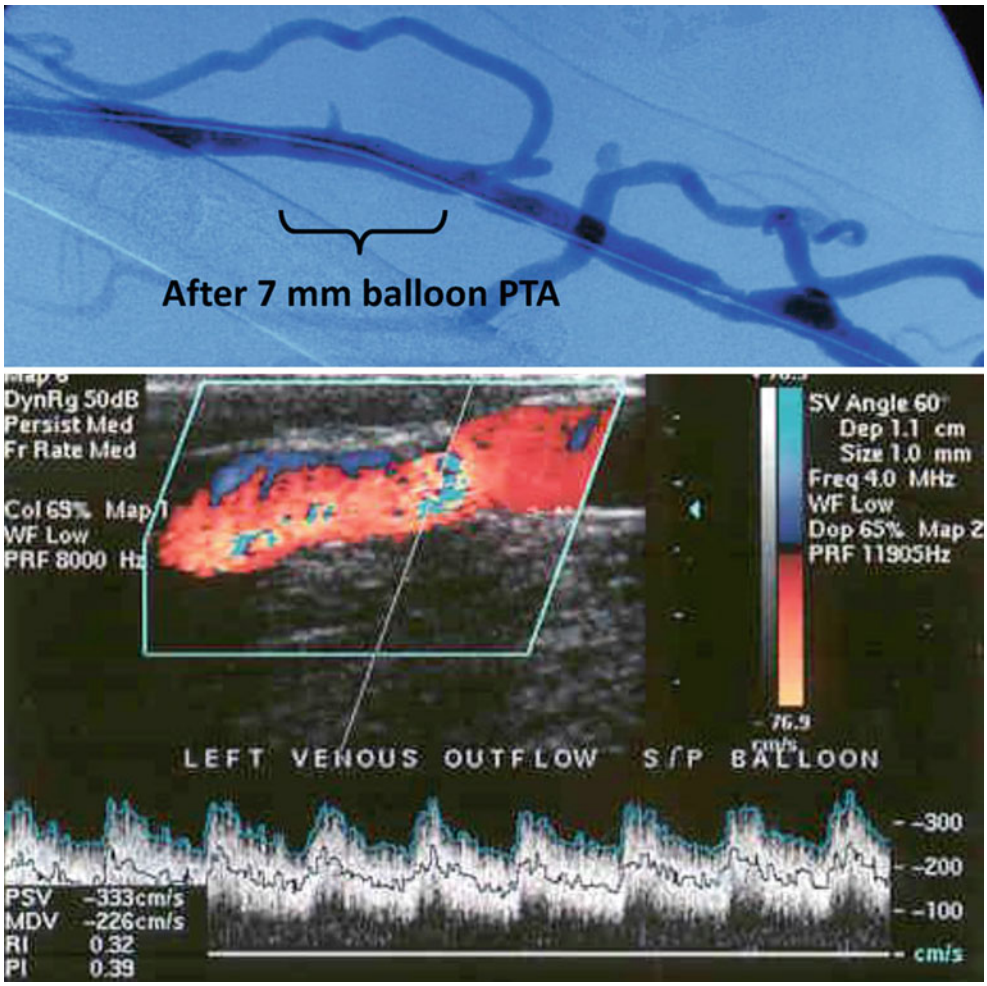


**Fig. 32.5** Contrast fistulogram and intraprocedural duplex scan of vein segment shown in Fig. 32.3 after 7 mm diameter transluminal balloon angioplasty. Volume flow increased to 1,400 mL/min ($VF/PSV_{stenosis}=6$) with reduction in PSV (330 cm/s), EDV (226 cm/s), and PSV ratio (1.8) indicating a <50% DR residual stenosis which corresponds to fistulogram findings

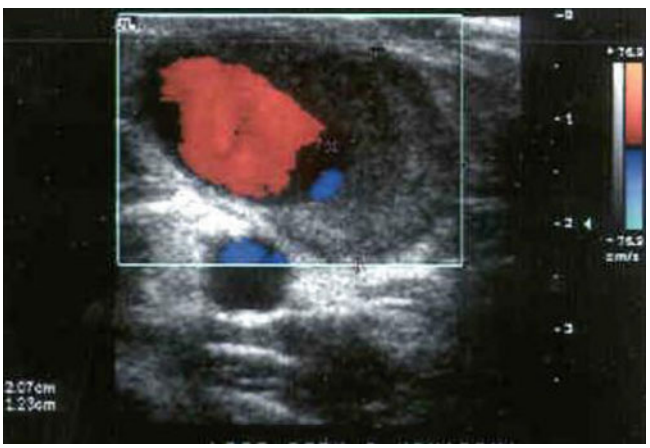

**Fig. 32.6** Color Doppler image of dialysis access false aneurysm with patent lumen and thrombus

Based on initial duplex testing performed within 2–4 weeks of the procedure, the access sites were deemed "adequate" for dialysis or "nonmaturing" by the presence of detected high-grade stenoses (peak systolic velocity >400 cm/s, velocity ratio >2, and minimal diameter <2–3 mm) and subjected to remedial interventions (endovascular or open). Remedial interventions were needed in 10 (26%) bridge grafts and 18 (21%) fistulae "nonmaturing" due to occlusive lesions. Conduit flow rates differentiated "nonmaturing" (606 ± 769 mL/min) from "maturing" (1,140 ± 857 mL/min) fistulae ($p=0.01$). After remedial procedures to improve function in "nonmaturing" conduits, volume flow increased to 1,159 ± 502 mL/min and at a level similar to access conduits not requiring a remedial procedure (1,374 ± 805 mL/min). Analysis of subsequent patient outcomes over a 2- to 3-year period demonstrated a threshold conduit flow rate of 800 mL/min was a better discriminator of "failing" versus and functional fistulae and bridge grafts (accuracy 77%) than flow rate greater or less than 500 mL/min (accuracy 67%). Overall, remedial procedures were required in 42% of accesses with initial flow <800 mL/min compared to 12% of accesses with initial flow >800 mL/min ($p<0.05$). The average mean duration of primary (no subsequent intervention performed) patency was similar in access requiring (11.5 months) or not requiring (12.9 months) a remedial procedure.

Routine duplex surveillance after dialysis access does not yield comparable assisted primary patency rates to those

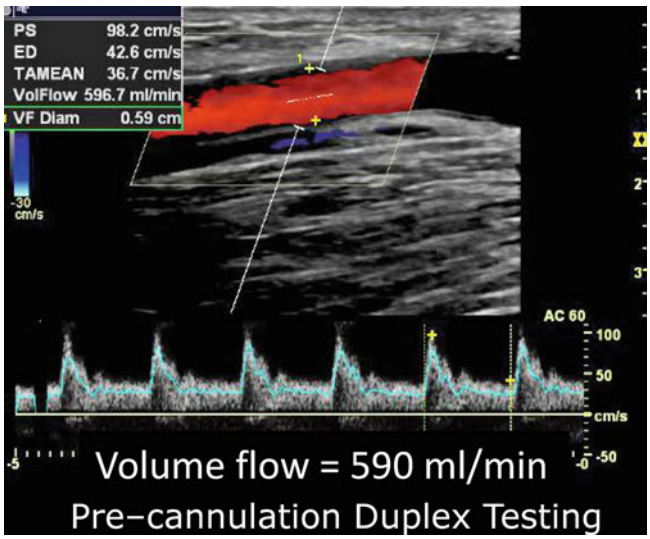


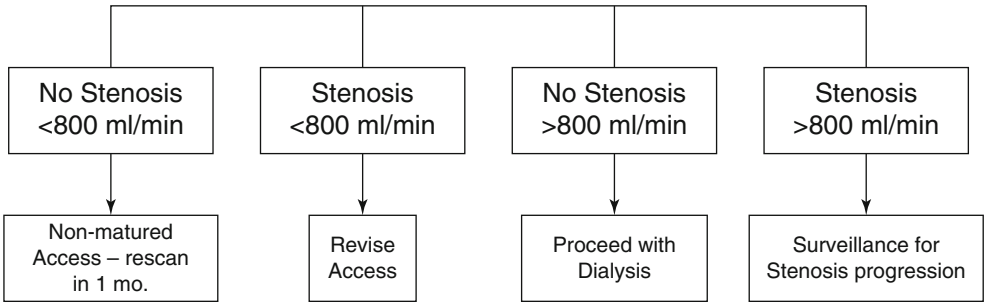


**Fig. 32.7** Precannulation duplex scan study demonstrating volume flow <800 mL/min. Management based on presence or absence of duplex-identified stenosis. For nonmaturing autogenous vein access, fistulogram and balloon angioplasty of small caliber vein segments may be performed

obtained following lower extremity vein bypass grafting. Assisted patency rates are in the range of 50% compared to 80–90%, respectively. Several prospective but uncontrolled studies documented a significant decrease in number of thrombotic events and increased conduit patency following elective surgical or endovascular intervention for duplex- or fistulogram-identified dialysis access stenosis [8–10]. Benefit is most likely to occur when the surveillance technique is conducted by experienced clinicians and the lesion(s) treated are truly "hemodynamically" important based on both anatomic and physiologic criteria. Since access stenosis is a relatively common finding on imaging studies and is not independently predictive of thrombotic failure, duplex testing with volume flow measurement has the potential to improve the efficacy of surveillance.

Based on the DOQI guidelines and available clinical reports, selected duplex surveillance of dialysis access procedures is recommended. Refinements of the surveillance algorithm including testing intervals, test interpretation criteria, and identification of "high-risk" access conduits and patients for ongoing evaluation require further development. At present, a baseline duplex evaluation is recommended at the time of "anticipated" graft maturation followed by "expectant" subsequent evaluations based on development of access dysfunction (Fig. 32.7). Access imaging combined with the calculation of volume flow by Doppler-derived techniques should be the primary surveillance methods for both autogenous and prosthetic dialysis accesses. The "low-flow" (<800 mL/min) conduits typically harbor a stenotic lesion and should be considered for remedial intervention to improve access hemodynamics and functional patency. When flow rates fall below 500–800 mL/min for either PTFE bridge grafts or AVFs, contrast fistulography should be considered unless duplex imaging clearly identifies a significant graft or anastomotic stenosis for directed intervention. Access flow in this range is associated with an increased thrombotic risk and additional diagnostic testing is appropriate. If measurement of volume flow is not possible or deemed unreliable, intervention for a progressive duplex-identified stenosis with velocity spectra consistent with a critical stenosis (PSV > 400 cm/s, EDV > 250 cm/s, velocity ratio > 2, mid-graft velocity <150 cm/s, residual lumen <2–3 mm diameter) is recommended. Elective surgical or endovascular treatment of fistulogram-confirmed >50% DR stenosis should be pursued. An important feature of a duplex surveillance program is confirmation of improved access flow rate and hemodynamic correction of access stenosis after intervention. Validation of a broader, routine duplex surveillance program after access construction (beyond the selected algorithm detailed herein and supported by current DOQI recommendations) would

require a well-designed, large, prospective, randomized clinical trial. This may prove a difficult task given the variable expertise in duplex ultrasound testing, and follow-up compliance of the infirmed, renal failure patient population.

## References


1. Hodges TC, Fillinger MF, Zwolak RM, Walsh DB, Bech F, Cronenwett JL. Longitudinal comparisons of dialysis access methods: risk factors for failure. J Vasc Surg. 1997;26:1009–19.
2. Cinat ME, Hopkins J, Wilson SE. A prospective evaluation of PTFE graft patency and surveillance techniques in hemodialysis access. Ann Vasc Surg. 1999;13:191–8.
3. NKF-KDOQI. Clinical practice guidelines. www.kidney.org/professionals/kdoqi/guidelines. accessed 2006.
4. Bowser A, Bandyk D. Surveillance program for hemodialysis access. In: Yao JST, Pearce WH, editors. Trends in vascular surgery. Chicago: Precept Press; 2002.
5. Besarab A, Lubkowski T, Frinak S, Ramanathan S, Escobar F. Detecting vascular access dysfunction. ASAIO J. 1997;43: M539–43.
6. Palder SB, Kirkman RL, Wittemore AD, et al. Vascular access for hemodialysis: patency rates and results of revision. Ann Surg. 1985;202:235–9.
7. Strauch BS, O'Connell RS, Geoly KL, et al. Forecasting thrombosis of vascular access with Doppler color flow imaging. Am J Kidney Dis. 1992;19:554–7.
8. Sands JJ, Miranda CL. Prolongation of hemodialysis access survival with elective revision. Clin Nephrol. 1995;44:329–33.
9. Beathard GA. Percutaneous transvenous angioplasty in the treatment of vascular access stenosis. Kidney Int. 1992;42:1390–7.
10. Schwab SJ, Raymond JR, Saeed M, Newman GE, Dennis PA, Bollinger RR. Prevention of hemodialysis fistula thrombosis: early detection of venous stenoses. Kidney Int. 1989;36:707–11.
11. Brooks JL, Sigley RD, May Jr RJ, Mack MR. Transluminal angioplasty versus surgical repair for stenosis of hemodialysis grafts: a randomized study. Am J Surg. 1987;153:530–1.
12. Dapunt O, Feurstein M, Rendl KH, Prenner K. Transluminal angioplasty versus conventional operation in the treatment of hemodialysis fistula stenosis: results from a 5 year study. Br J Surg. 1987;74: 1004–5.
13. Besarab A, Sherman R. The relationship of recirculation to access blood flow. Am J Kidney Dis. 1997;29:223–9.
14. National Kidney Foundation. Dialysis outcome quality initiative clinical practice guidelines for vascular access. Am J Kidney Dis. 1997;30(Suppl J):SIS0–91.
15. Windus DW, Audrain J, Vanderson R, et al. Optimization of high-efficiency hemodialysis by detection and correction of fistula dysfunction. Kidney Int. 1990;38:337–41.
16. Daniels ID, Berlyne OM, Barth RH. Blood flow rates and accesses recirculation in hemodialysis. Int J Artif Organs. 1992;15:470–4.
17. May RE, Himmelfarb J, Yenicesu M, et al. Predictive measures of vascular access thrombosis: a prospective study. Kidney Int. 1997;52:1656–62.
18. Bay WH, Henry ML, Lazarus JM, et al. Predicting hemodialysis access failures with color flow Doppler ultrasound. Am J Nephrol. 1998;18:296–304.
19. Bosman PJ, Boereboom FTJ, Smits HFM, et al. Pressure or flow recordings for the surveillance of hemodialysis grafts. Kidney Int. 1997;52:1084–8.
20. Zierler BK, Kirkman TR, Kraiss LW, et al. Accuracy of duplex scanning for measurement of arterial volume flow. J Vasc Surg. 1992;16:520–6.
21. Depner TA, Krivitski NM. Clinical measurement of blood flow in hemodialysis access fistulae and graft by ultrasound dilution. ASAIO J. 1995;41:M745–9.
22. Besarab A, Lubkowski T, Frinak S, Ramanathan S, Escobar F. Detection of access strictures and outlet stenoses in vascular accesses: which test is best? ASAIO J. 1997;43:M543–7.
23. Sands J, Glidden D, Miranda C. Hemodialysis access flow measurement: comparison of ultrasound dilution and duplex ultrasonography. ASAIO J. 1996;42:M899–901.
24. Rittgers SE, Garcia-Valdez C, McCormick JT, Posner MP. Noninvasive blood flow measurement in expanded PTFE grafts for hemodialysis access. J Vasc Surg. 1986;3:635–42.
25. Shackleton CR, Taylor DC, Buckley AR, et al. Predicting failure in PTFE vascular access grafts for hemodialysis: a pilot study. Can J Surg. 1987;30:442–4.
26. Sands J, Young S, Miranda C. The effect of Doppler flow screening studies and elective revisions on dialysis access failure. ASAIO J. 1992;38:M524–7.
27. Back MR, Maynard M, Winkler A, Bandyk DF. Expected flow parameters within hemodialysis access and selection for remedial intervention of nonmaturing conduits. Vasc Endovascular Surg. 2008;42(2):150–8.
28. Johnson CP, Zhu Y, Matt C, et al. Prognostic value of intraoperative blood flow measurements in vascular access surgery. Surgery. 1998;124:729–38.
29. Middleton WD, Picus DD, Marx MV, Melson GL. Color Doppler sonography of hemodialysis vascular access: comparison with angiography. AJR. 1989;152:633–9.
30. Dousset V, Grenier N, Douws C, et al. Hemodialysis grafts: color Doppler flow imaging correlated with digital subtraction angiography and functional status. Radiology. 1991;181:89–94.
31. MacDonald MJ, Martin LG, Hughes JD, et al. Distribution and severity of stenoses in functioning arteriovenous grafts: a duplex and angiographic study. J Vasc Technol. 1996;20:131–6.
32. Lumsden AB, MacDonald MJ, Kikeri D, et al. Prophylactic balloon angioplasty fails to prolong the patency of PTFE arteriovenous grafts: results of a prospective randomized study. J Vasc Surg. 1997;24:382–92.
33. Tordoir JHM, deBruin HG, Hoeneveld H, Eikelboom BC, Kitslaar PJ. Duplex ultrasound scanning in the assessment of arteriovenous fistulas created for hemodialysis access: comparison with digital subtraction angiography. J Vasc Surg. 1989;10:122–8.
34. Older RA, Gizienski TA, Wilkowski MJ, Angle JF, Cote DA. Hemodialysis access stenosis: early detection with color Doppler ultrasound. Radiology. 1998;207:161–4.
35. Passman MA, Criado E, Farber MA, et al. Efficiency of color flow duplex imaging for proximal upper extremity venous outflow obstruction in hemodialysis patients. J Vasc Surg. 1998;28:869–75.

# Noninvasive Evaluation for Congenital Arteriovenous Fistulas and Malformations

33

Robert B. Rutherford

**Abstract**

The main focus of this chapter will be on diagnostic approaches that are available in most vascular diagnostic laboratories (VDLs). The application of noninvasive VDL tests in diagnosing vascular anomalies containing arteriovenous fistulas (AVFs) use basically the same methods and instrumentation used for assessing peripheral arterial occlusive disease, most of which are qualitative, not quantitative. They gauge the pressure, volume, or velocity changes associated with the contained AVFs but do not visualize the AVFs themselves, as magnetic resonance imaging can do. The latter applications are therefore also mentioned. These diagnostic methods are covered elsewhere in this book and are not described at length here. Rather, the utility of these diagnostic tests in this setting is discussed, in terms of the instrumentation used, the interpretation or analysis of the test results, and appropriate clinical applications, as well as diagnostic limitations. These "physiologic" VDL tests can provide much useful clinical decision-making information regarding AVFs occurring in peripheral congenital vascular anomalies. Their different application in diagnosing AVFs is described along with a brief description of the hemodynamic characteristics of arteriovenous fistulas, as needed to perform and properly interpret these tests. Their main limitations are that most can be applied only to peripheral or extremity AVFs and arteriovenous malformations (AVMs). But when the diagnostic goals are simply to determine the presence or absence of AVFs in an extremity with congenital vascular anomalies and the relative magnitude of their peripheral hemodynamic effects, these methods serve well.

**Keywords**

Congenital vascular malformations • Noninvasive diagnosis • Segmental limb pressure measurements • Segmental plethysmography • Velocity waveform analysis • Magnetic resonance imaging

## Introduction

This chapter addresses the application of noninvasive vascular diagnostic laboratory (VDL) testing and comments on complementary imaging techniques, in the evaluation of vascular anomalies containing arteriovenous fistulas (AVFs). In applying the methods described, it helps to have a concept of the hemodynamic or physiologic changes that characterize vascular anomalies (VA) (*Note*: the commonly used term congenital vascular malformations (CVMs) is no longer in use, being redundant, and has been replaced by vascular anomalies). This chapter will focus on VAs containing arteriovenous fistulas (AVFs). Vascular anomalies can take several forms: ranging from diffuse micro fistulas to macro fistulas that involve major artery distributions, and more mature maturational defects, which tend to involve a single artery. The anatomy of the VA are characterized in two

R.B. Rutherford, M.D.
Department of Surgery, University of Colorado Medical Center, 14337 Dorsal Street, Corpus Christi, TX 78418, USA
e-mail: rbruth@aol.com

A.F. AbuRahma, D.F. Bandyk (eds.), *Noninvasive Vascular Diagnosis*,
DOI 10.1007/978-1-4471-4005-4_33, 

categories using the Hamburg classification [1]: (1) predominantly AVFs (estimated to constitute just over one-third of all VAs) and (2) AVFs constituting part of more complex *mixed* anomalies, e.g., those present in VAs that may *even* be predominantly venous [2]. The latter are the most difficult to identify with noninvasive test and imaging studies. Nevertheless, noninvasive methods available in the vascular laboratory can provide useful clinical decision-making information regarding such AVFs, with one important proviso; they must be located in the extremities – an important qualification. Fortunately the majority of these vascular conditions are.

Clinicians using vascular testing methods described in this chapter should have knowledge about clinical diagnosis, obtained by history and physical examination in addition to testing modalities available in the noninvasive vascular laboratory. In general, vascular testing should be considered an adjunct to clinical findings and the anatomy depicted by magnetic or computed tomography imaging. Clinically significant AVMs will typically present well before adult life because a vascular "birthmark," localized skin color change, overlying varicose veins, or other prominent blood vessels, or occasionally, a distinct vascular mass or tumor or enlargement of the limb (increase in the length or girth) has gained the attention of parent or child. Changes in limb dimension are unusual in very early childhood and in the absence of significant AVFs, but minor differences may be overlooked early on. Characteristically, these occur as the result of long-standing AVFs present during the growth period, but it should also be noted such changes in girth or length also have been observed with pure venous anomalies, in the absence of AVFs, as in the von Klippel-Trenaunay syndrome. Whether or not the reported absence of AVFs relates to failure to detect micro fistulous AVFs in predominantly venous anomalies, described in an earlier era before noninvasive tests (NITs) were employed, is debatable, for it is true that such small AV fistulas are often missed by angiography, the imaging technique most commonly applied in the past [3].

One other sometimes confusing aspect should be mentioned here. The majority of "birthmarks" – often the signal to parents that something is "wrong" with their child – may indeed be a signal of a vascular anomaly, and some "birthmarks that appear in childhood may indeed be sentinel lesions." However, birthmarks in childhood can also represent true hemangiomatous lesions and others can be superficial VAs, i.e., cutaneous capillary or superficial venous malformations, which are still commonly referred to as "cavernous malformations." Differentiating between these two entities and true sentinel lesions is extremely important in early childhood and usually can be done on clinical grounds alone, based upon their time of appearance and their growth rate, or lack of growth with time. Importantly, juvenile hemangiomas are true tumors, with a rapid endothelial turnover, which characteristically are discovered shortly after birth, undergo rapid early growth then spontaneously involute, usually between 2 and 8 years of age, whereas true vascular malformations, including cavernous malformations, and sentinel lesions overlying an arteriovenous malformation (AVM) are present at birth and characteristically maintain the same size relative to the growing child. Juvenile hemangiomas may leave an inelastic scar after involuting, but this can be dealt with later, as necessary. The point here is that intervention is unnecessary with the former lesions, although a number of treatment claim success (dry ice applications or superficial salves). Significantly, juvenile hemangiomas may be found to have high flow characteristics on ultrasound study.

The diagnostic methods described here are all aimed at detecting AVFs in VAs and can even be used, albeit with some differences, in diagnosing acquired AVFs, i.e., those due to iatrogenic and other penetrating trauma in an extremity.

The instrumentation employed is basically the same as used in diagnosing peripheral arterial occlusive disease: segmental limb pressures and plethysmography, velocity waveform analysis, and duplex scanning [4]. The former three have been called "physiologic testing" by those who stress imaging methods, e.g., radiology-run vascular laboratories, but it is the hemodynamic or physiologic attributes of AVFs that distinguish them, so these methods will be described here.

A number of considerations govern how these diagnostic methods can be applied in diagnosing AVFs. First, a basic understanding of the hemodynamic characteristics of arteriovenous fistulas is needed in order to perform and properly interpret these tests. (This has already been discussed above.) Second, the diagnostic capabilities and limitations of the different tests to be described must be understood in applying them. "Physiologic" VDL tests simply gauge the pressure, volume, or velocity changes associated with peripherally located AVFs but do not visualize the AVFs, as duplex ultrasound imaging can do. Third, most of these tests have limitations, e.g., (a) they are primarily qualitative and not quantitative, and (b) they can only be applied to peripheral or extremity AVFs and AVMs. Fourth, congenital and acquired AVFs differ from each other significantly in terms of their anatomic localization. Congenital AVFs are rarely isolated lesions; they more commonly occur in clusters within major arterial distributions, but may be even more diffuse in location, involving an entire limb segment. As a result, they can only be localized to a particular limb segment by these so-called physiologic tests. They may be visualized, and their characteristics identified, by Doppler ultrasonography, but even this modality usually will usually not completely encompass them. Finally, the diagnostic goals may vary considerably in different clinical settings and this significantly

affects the application of the tests. In this regard, appropriately sized smaller cuffs will be needed for the very young who are brought in by their parents for evaluation.

The simplest diagnostic goal may be to determine the presence or absence of an AVF or AVFs, but beyond their presence, which may be clinically obvious, the relative magnitude of the AVF's peripheral hemodynamic effects should be gauged, or the lesion(s) overall effect on the peripheral circulation determined. For example, the presence or magnitude of a distal "steal" or, in other words, the severity of the associated distal ischemia can be determined.

An additional word of caution is appropriate at the outset. The AGA (Always Get an Angiogram) approach, commonly applied by practicing physicians faced with these problems must be actively resisted. Very few of these conditions constitute true emergencies and the "urge" to obtain an angiogram prior to referral unfortunately opens the door to those who can't seem to resist intervening, with embolo- or sclerotherapy, which may be ill-advised and untimely in the very young patient. Pointedly, even in young children, any intervention for AVFs is not only not an emergency, but is better done when the patients is old enough to be "cooperative."

The main focus of this chapter will be on diagnostic approaches that should be available in most VDLs. The basic diagnostic methods and the instrumentation behind each of these diagnostic methods will be covered elsewhere in this book, and will not be described at length here. Rather their utility in this setting will be discussed, in terms of the instrumentation used, the interpretation or analysis of the test results, and appropriate clinical applications as well as diagnostic limitations.

## Clinical Evaluation

Localized warmth and vascular-based color changes (birthmarks), prominent veins, compressibility of vascular masses, the presence of a thrill or bruit, and inequalities in the dimensions of the limb (as measured from the anterior iliac spines) all should be noted. However, while the triad of birthmark, varicose veins, and limb enlargement is well known, and usually sought, a limb presenting with these may or may not harbor major AVFs. In fact, the presence of AVFs in such limbs has been the basis for the traditional distinction between the Parkes Weber and von Klippel-Trenaunay syndromes, the former being associated with AVFs and the latter not. (This might reflect the diagnostic limitations of the day, it being claimed that the latter are associated with micro AVFs.) The point is that these are not of clinical significance. The limbs harboring these anomalies may appear quite similar, i.e., their outward physical findings are similar, regardless of the presence of AVFs. In addition, this triad is not consistently found in congenital AVMs. In Sziylagyi's classic study of 82 cases of angiographically proven congenital AVFs, this classic triad was present in only 57% [3].

## Diagnostic Studies for Congenital AVFs or AVMs

The vascular diagnostic techniques described below, if used knowingly, can be valuable in ruling in or out the presence of AVFs in this setting, in patients presenting with atypical (location, age of onset) varicose veins and/or a birthmark, with or without limb enlargement [5]. Depending on the location and relative magnitude of the component AVFs, the same simple "physiologic tests" used in diagnosing peripheral arterial occlusive disease can also be employed in diagnosing AVFs or AVMs, and they can do it relatively inexpensively, avoiding the need for angiography, which is particularly important since many of the presenting patients are young children. Although qualitative in nature, the degree of abnormality observed in these tests in association with congenital AVFs should also give the clinician a rough impression of their relative magnitude, and thus be sufficient for clinical decision making and parental counseling. Increasingly, the current workhorse of the VDL, the duplex scan, has found useful application in evaluating AVFs. It adds important additional perspective; therefore its use will also be described here.

## Characteristic Hemodynamic Changes Associated with AVFs: Diagnostic Implications

Arteriovenous fistulas can be considered a "short-circuit" between the high-pressure arterial and the low-pressure venous systems. If the AVFs present in vascular anomalies are hemodynamically significant enough, they will result in (1) an arterial pressure drop/decrease ("steal") distally, due to a significant diversion of flow into the venous system rather than through the peripheral microcirculation, (2) increased pulsatility (which can be measured as volume change), and (3) an increase in velocity, often with turbulence (seen best with a duplex ultrasound probe).

The mean arterial blood pressure distal to an arteriovenous fistula is nearly always reduced to some degree, although minor degrees of change may be within the accuracy range of these methods. This lower distal pressure is the result of blood being shunted away from the distal arterial tree into proximal low-resistance pathways offered by the arteriovenous communication(s). The reduction in mean pressure is greatest when the fistula is large and the arterial collaterals are small or poorly developed. On the other hand, when the fistula is small and the collaterals are well developed, there may be little or no perceptible pressure effects away from the

fistula itself. AV malformations (AVMs), usually containing a number of AVFs may, in combination, have the same hemodynamic effects of a single large AVF. Thus, the magnitude of the pressure drop across an AVM, or the limb segment containing congenital AVFs, can provide a fair assessment of their hemodynamic significance. If the pressure drop and flow diversion are significant enough, there may even be a measurable degree of distal ischemia, one that can be detected by standard VDL tests. If overall fistula flow is great enough, there will also be associated venous hypertension. The latter is not readily measured noninvasively but increased flow velocity in the major vein draining the affected limb, when compared to its normal contralateral counterpart, can and should be assessed, as it will add to the diagnostic impression. A large AVF or AVM can produce significant pressure swings, locally perceived as increased pulsatility, which are reflected in associated volume changes in the involved limb segment, and these can be detected plethysmographically. Finally, AVFs are associated with significant velocity changes that are greatest closest to the AVF. To appreciate the basic nature of these velocity changes, and how best to detect them, one must first appreciate that a pattern of low flow and high resistance characterizes the normal resting extremity circulation. This is in contrast to the high-flow and low-resistance pattern associated with exercise. The velocity patterns associated with peripherally located AVFs are similar to those associated with exercise, and readily distinguished from than those observed in the normal resting limb by studying arterial velocity in the VDL. Thus, by understanding the characteristic underlying hemodynamic changes associated with AVFs, and thus knowing what to look for, congenital lesions containing AVFs can be detected and their relative severity assessed by studying the arterial pressure, volume, and velocity changes they produce, using VDL tests designed to gauge these same hemodynamic parameters.

## Diagnostic Tests: Descriptions and Applications

The focus of this section will be on diagnostic approaches still available in most VDLs, which can be applied to the diagnosis of peripheral AVFs, whether they be single, or multiple, as characteristic of AVMs. The same noninvasive "physiologic" tests used for many decades in the diagnosis of peripheral arterial occlusive disease can be applied here. More recently, duplex scanning has greatly augmented these noninvasive tests. The basic diagnostic methods and the instrumentation behind these tests have been covered earlier in this book (Chaps. 21 and 22), and will not be described at length here, but their utility in this setting will be discussed, as will their interpretation, appropriate clinical applications as well as their limitations. It should be emphasized at the outset that while the pressure, flow volume, and velocity changes associated with AVFs located in an extremity can be readily assessed in the VDL that, particularly with the noninvasive physiologic tests, this application assumes that the findings in the abnormal extremity can be compared to those of the normal contralateral extremity.

Segmental limb pressure measurements are a standard technique described in detail in Chap. 21. Noninvasive methods of measuring segmental systolic blood pressures are reasonably accurate and reproducible and are painless and simple in application. Briefly, a pneumatic cuff is placed around the limb segment at the chosen level and inflated to above systolic pressure. As the cuff is deflated, the systolic pressure at which blood flow returns distal to the cuff is noted by some distally placed flow sensor (e.g., Doppler probe, mercury-in-silastic strain-gauge, photoplethysmograph, pulse volume recorder, or any other sensor capable of detecting flow distal to the cuff). This is analogous to taking a patient's pressure in the arm using an aneroid or mercury manometer. In the upper extremity, pressure measurements can be made using cuffs placed at the upper arm, forearm, wrist, or finger levels; in the lower extremity, segmental pressure measurements are usually made at the high or low thigh, and the calf, ankle, foot, or toe. Although ankle pressures are primarily used in screening for occlusive disease (as in the ankle-brachial index [ABI]), multiple segmental cuffs can be used to detect and localize AVFs, particularly AVMs. Importantly, cuffs should be applied bilaterally to allow comparison with the normal contralateral limb.

## Interpretation of Findings

A hemodynamically significant arteriovenous fistula will reduce mean arterial pressure in the limb near and distal to the fistula. But these cuffs measure systolic pressure, and even though mean pressure is reduced in the arterial tree as one approaches an AVM, the pressure swings between systolic and diastolic (i.e., the pulse pressure) are increased, so that systolic pressure may well be measured as being elevated proximal to, or at the level of a fistula or group of AVFs (e.g., an AVM). Again, the systolic pressure can be detected as being elevated only by comparison with that of the opposite limb at the same level [5]. It will also be elevated if the pressure cuff has been placed directly over an AVM or its afferent branches. Compared to the contralateral extremity, cuffs at or above a hemodynamically significant fistula or group of fistulas (AVM) will usually record a higher systolic pressure, and those below the fistula will record a normal or lower systolic pressure, with major fistulas being associated with a detectable degree of distal steal or pressure decrease. Such pressure differences between equivalent limb segments

or levels, greater than measurement variability, indicate a significant AVM or group of AVFs.

## Segmental Plethysmography

Segmental plethysmography is also as standard technology described in Chap. 22, which uses cuffs of precise dimensions applied at various levels/locations along an extremity, much as for measuring segmental limb pressures. In this diagnostic setting, plethysmographic recordings are extremely helpful. Air-filled cuffs are normally used, but in some VDLs mercury-in-silastic "cuffs" are employed. The contour of the resulting tracing is generally assessed in terms of magnitude and shape. When the pulse-sensing cuff is placed over the fistula(s) or just proximal to an AVM, the pulse volume may be observed to be increased, reflecting increased pulsitility [5, 6]. In a limb with significant congenital AVFs, the increased pulsations observed plethysmographically are diagnostic in themselves (Fig. 33.1). Although the pulse contour (PVR) may be normal (or nearly so) in a limb distal to an AVF or AVM, it is frequently reduced, particularly in the presence of a "steal" (reduced pressure distal to an AVF) (Fig. 33.2) [7]. As in the case of segmental limb pressure measurements, the reduction in pulse-volume recordings (PVRs) distally depends on the magnitude of the fistula(s) and the adequacy of the collateral development. Therefore, very much as described for segmental limb pressures above, plethysmography tracings are increased in magnitude above or at the level of an AV fistula, or group of AV fistulas (AVM) and, depending on the degree of fistula flow and therefore the degree of distal "steal," the tracings below the fistula will be reduced or, at best, normal in magnitude. A study of the tracings compared with the contralateral extremity will not only allow detection of AVFs in an extremity but allow their segmental location or level to be identified. The degree of change in these cuff tracings reflects the underlying lesion's hemodynamic significance and may help with counseling regarding prognosis and timing of intervention.

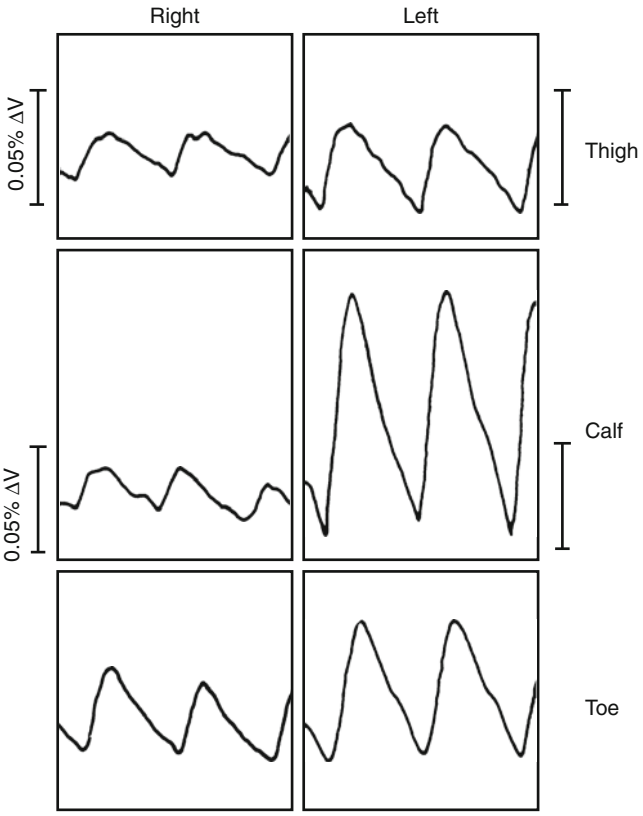


**Fig. 33.1** Plethysmographic (PVR) tracings at thigh, calf, and toe levels in a 4-year-old girl with multiple congenital AV fistulas involving the entire left leg (Reprinted from Rutherford [5]. With permission from Elsevier)

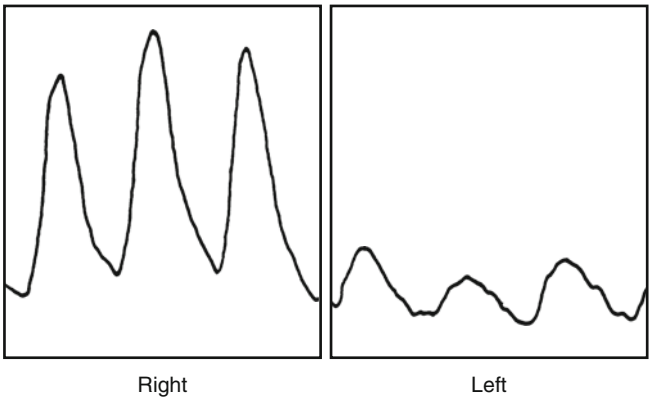


**Fig. 33.2** Toe plethysmographic tracings from a patient with a congenital AVM involving the left calf. The reduced PVRs reflect a distal steal from this, but not to critical ischemic levels for some pulsitility remains. The left ankle pressures was 55 mmHg (Reprinted from Rutherford [5]. With permission from Elsevier)

## Velocity Waveform Analysis

Velocity tracings can be recorded over any extremity artery by a Doppler probe connected to the DC recorder and strip chart, or more commonly nowadays, by the velocity readout of a duplex scanner. This is increasingly being done by the latter technique nowadays, not only because the duplex scan has become the "workhouse" of most VDLs but also because it offers other valuable information in this setting (see below). The strip chart recording of velocity waveforms generated by a Doppler probe is uncommonly performed today as a separate test. Nevertheless, the characteristic findings are the same with either instrument and will be described here. In evaluating for AVFs, the velocity is recorded over the major proximal inflow artery, e.g., femoral or axillary. The reason for selecting this location, rather than directly over the suspected fistula(s) will become apparent later, in describing

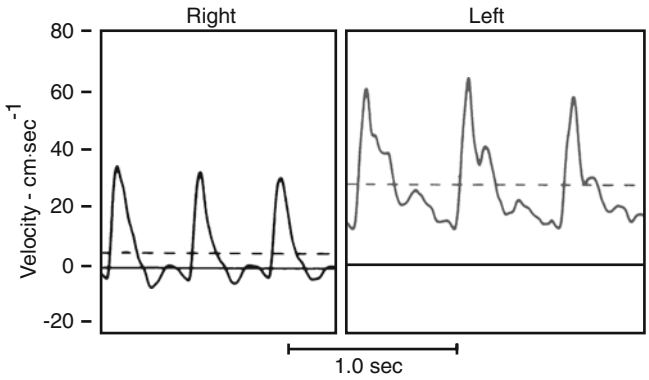


**Fig. 33.3** Velocity tracing from the femoral arteries in a 4-year-old girl with a large AVM involving the left thigh. Note that the tracing on the left, compared to the normal right tracing, has higher peak and mean (*dashed line*) systolic velocity, and there is no end systolic reversal. Rather, there is high flow continuing throughout diastole, as a result of which the tracing does not drop back to the zero baseline at the end of diastole, but is elevated well above the zero baseline (Reprinted from Rutherford [5]. With permission from Elsevier)

duplex scan findings. A high-velocity flow pattern in an artery leading to the area of suspicion is good evidence that the artery is serving as the inflow for AVFs [7, 8]. For many if not most clinical purposes, a qualitative estimate of flow velocity and the contour of the analog velocity tracings or "waveforms" obtained in this manner with a directional Doppler velocity detector, or duplex scanner, provides sufficient information for diagnosing the presence of AVF(s), and the magnitude of the changes provides some indication of the magnitude of fistulous flow.

To recognize a tracing diagnostic of AVFs, one must realize that, in contrast, the velocity tracings of a resting normal extremity is characterized by end-systolic reversal following peak systolic flow, followed by low flow in early diastole and negligible flow in late diastole. Such a low-flow, high-resistance pattern is most pronounced in the lower extremity. In the upper extremity, there may be little end-systolic reversal. However, high-flow low-resistance arterial velocity pattern, while seen in a number of high flow visceral arteries (e.g., the renal, carotid, celiac arteries), in the extremities, such a high-flow pattern is seen after exercise, and after sympathetic blockade, but, importantly, also in association with AVFs. In these settings, peak systolic velocity may be quite high but, of more diagnostic significance, there is continuous flow throughout diastole and a the "dip" in the tracing between systole and diastole does not approach the zero velocity baseline, let alone show the typical end-systolic reversal of the normal resting extremity. The characteristic arterial pattern associated with arteriovenous fistulas, as shown in Fig. 33.3, thus consists of (1) an elimination of end-systolic reversal and (2) a marked increase in diastolic velocity, which appears to "elevate" the entire tracing above the zero-velocity baseline. The degree of elevation in end-diastolic velocity correlates directly with the flow increase caused by the arteriovenous fistula [5, 6]. By using these characteristic Doppler velocity signals as a guide, one can detect and localize congenital arteriovenous communications that otherwise might escape detection [9, 10]. Peripheral AVFs constituting 5% of extremity flow or more can be readily detected by this means alone. This test is more sensitive than segmental pressures and plethysmography, and can be detected by a duplex scan.

Although these changes are diagnostic enough that comparison with the other extremity would not seem necessary, this comparison still holds value, to rule out hyperemia and similar velocity signals there. Hyperdynamic flow is associated with conditions such as beriberi or thyrotoxicosis but since, in these conditions, the effect is generalized, it would affect all extremities, emphasizing the importance of comparing with the contralateral normal extremity. False-positives can occur in other hyperemic settings, e.g., inflammation associated with superficial thrombophlebitis, lymphangitis, bacterial infection, and thermal or mechanical trauma. Other causes of hyperemia isolated to an individual vessel or limb (e.g., exercise or reactive hyperemia following a period of ischemia) are transient. Externally applied heat, local infection (e.g., cellulitis or abscess), or sympathetic blockade (permanent or transient, as in epidural anesthesia) can also increase flow velocity and give this pattern, but none of these should create any significant confusion in the usual patient referred to the VDL for evaluation of congenital AVFs, and some (e.g., throtoxicosis, beri-beri, high fever) should produce bilaterally equal changes.

## Evaluation for Congenital Arteriovenous Fistulas Using These Three Physiologic Tests in Combination

These three tests are preferably done in combination for their findings and reinforce each other, and they share the advantages that they are inexpensive, easily applied, and require only basic operator or interpretive skill. The instrumentation is simple and used on an everyday basis in most VDLs. Some limitations to the above tests must be noted, however. They include the following: (1) These tests give qualitative rather than quantitative information. (2) They can be applied only to arteriovenous fistulas located in the extremity proper (i.e., at or below the highest cuff or point of Doppler probe interrogation). Thus, pelvic AVMs could not be studied by these methods. (3) It should again be noted that in children appropriately smaller cuffs are required. (4) These tests may not detect diffuse congenital micro fistulas or overall fistula flow constituting less than 5% of total extremity flow. (5) Single limb studies may not be diagnostic unless compared with a normal contralateral extremity. Nevertheless, in combination, these tests can be very useful for screening for congenital AVFs in the extremities of patients presenting with suggestive signs (e.g., a vascular "birthmark," atypical (early

onset/unusual location) varicose veins, or limb enlargement), and for detecting, roughly localizing, and assessing the relative magnitude of such congenital lesions. With anatomically localized lesions, these tests, with or without duplex scanning (see below) suffice for most clinical decision-making.

## Duplex Scanning

It is recognized that duplex ultrasound scanning plays an increasing role in today's VDL. The basic duplex scanner combines an ultrasound image with a focused directional Doppler probe. In modern instruments, the velocity signal is color-coded so that red represents arterial flow and blue represents venous flow (going in opposite directions). The velocities are also displayed on the screen, as needed, for specific applications (e.g., bypass graft surveillance, carotid artery interrogation).

Because the duplex scanner provides velocity information, it can serve as a practical means of performing velocity waveform analysis, the observed patterns serving as a simple yet sensitive means of diagnosing an AVF. Because of the other additional information obtainable from duplex scanning, it has mostly replaced using a simple Doppler probe connected to a DC recorder and strip chart for this purpose. High-peak mean velocity readings recorded over the main inflow artery of the involved extremity, compared with those at the same location of the contralateral normal extremity, will often confirm the presence of an arteriovenous fistula in that limb. As pointed out above, the characteristic pattern of the velocity tracing, with its elevated end-diastolic flow, and its extended persistence over the inflow artery should distinguish this high-velocity reading from the more focused high-velocity reading observed in association with a arterial or bypass graft stenosis.

The software of some of today's duplex scanners also allows a rough estimation of volume flow, with diameter measurements being used to estimate cross-sectional area and the velocity signals and the angle of incidence of the probe allowing the Doppler equation to be applied (flow = velocity (frequency shift) × cosine theta (angle of incidence of the ultrasound beam) × cross-sectional area, divided by $C$ (velocity of sound in tissue, a constant)). However, a problem in using the duplex scan to obtain accurate velocity or flow measurements directly over an AVF is the presence of turbulence and multidirectional flows associated with aliasing. On the other hand, the flashes of yellow representing turbulent fistula flow will be seen, and these along with higher than normal arterial velocities upstream are, in themselves, diagnostic of AV shunt flow. So the diagnosis is readily made by this approach, but quantification is not possible at the fistula site. Congenital arteriovenous fistulas are more complex, especially when part of an AVM, but their high-flow patterns are readily recognized and, by moving the scan head, the nature and extent of the more localized superficial lesions can sometimes be delineated. This in itself can be diagnostic, and is particularly useful when applied to mass lesions, which often present with a network of varicosities near the surface of the skin. Higher than normal flows in these veins will also betray an underlying AVM. The diagnostic dilemma here is that these varicosities may either be part of a venous malformation or be associated with an underlying arteriovenous malformation, but this be resolved by their flow characteristics.

The problem not being able to directly measure fistula flow can be accomplished indirectly by comparing velocity readings obtained proximally over the major inflow artery of the involved limb with those from the contralateral normal extremity recorded at the same level. The latter approach is recommended when quantitative measurements of fistula flow are desired for decision-making purposes. Subtracting the contralateral normal limb flow from that of the involved limb will provide a fair estimate of AV shunt flow in the involved limb as long as the interrogation sites and monitoring techniques are the same for both limbs.

Duplex scanners offer the advantage that they are in everyday use in today's VDLs for many other applications, so the necessary instrumentation and the operator skills are available. The duplex scan is rather versatile in evaluating AVFs, used either to interrogate a penetrating wound or groin hematoma following a catheterization procedure, or the limb of a young patient suspected of harboring congenital AVFs. It may directly visualize and interrogate AVFs as well as provide velocity evidence of their existence, e.g., high flow in the artery leading to suspected AVFs. On the other hand, in some congenital anomalies, where multiple AVFs may be spread out over a larger area, the duplex scanner may still be useful, even though not being able to directly visualize all the fistulous mass, and in larger mass lesions, it may not be able to delineate the full anatomic extent of an AVM. Like the previously described "physiologic" tests, it can be applied to extremity lesions but not to central lesions, e.g., in the trunk or pelvis. Much of its application is qualitative not quantitative, although rough flow estimates are possible using the technique described. So, it can detect and generally localize AVMs and guide or monitor thrombotic or embolic therapy in those congenital lesions that are relatively superficially located and reasonably well localized.

## Competing and Complementary Diagnostic Studies

### Arteriography

Arteriography was the gold standard in the past, before noninvasive tests and imaging became available. Unfortunately, many if not most primary care physicians presented with such

patients today perpetuate this primary reliance on angiography due to lack of awareness of the value of noninvasive tests and imaging. This misguided "AGA" approach is particularly unfortunate because angiography is only required if the need for therapeutic intervention for congenital arteriovenous fistulas has been determined and will be undertaken soon, in which case it can be obtained at the same time as embolotherapy. The presence or absence of congenital arteriovenous fistulas, and their relative severity (the latter determining prognosis), can be determined by noninvasive methods in most cases, assuming comparison with normal limb and the additional use of duplex scanning as described. This overall approach allows management decisions to be made, and the parents advised, without the use of arteriography as a diagnostic tool. Furthermore, arteriography may fail to demonstrate the fistula or fistulas either because they are too small or because the flow is too rapid. Furthermore, arteriography is invasive, associated with certain risks (contrast allergy, idiosyncratic reaction, renal toxicity), expensive, and uncomfortable and a major consideration in infants and young children is that it risks injury to their smaller arteries such that it usually requires either general anesthesia or heavy sedation and analgesia, and therefore hospital admission.

However, while this addiction to contrast angiography deserves opposition, there are a number of noninvasive or mini-invasive imaging approaches that have emerged in recent years that deserve mention here in that they offer significant additional perspectives over that which can be achieved by the "physiologic" VDL diagnostic methods described above, particularly in the evaluation of congenital AVFs. These diagnostic modalities include: (1) radionuclide quantification of AV shunting, (2) computed tomography (CT), and (3) magnetic resonance imaging (MRI). Additional discussion of these is included here to provide the reader with sufficient knowledge of their capabilities and clinical applications, as additional diagnostic options that must be considered in this setting. On the other hand, it must be realized that these new imaging methods are considerably more *expensive* and time-consuming than VDL testing, and require a considerable degree of patient cooperation (difficult in the very young or the claustrophobic) so that if the additional perspective they offer is not required for decision-making, their immediate use may be inappropriate or at least may be delayed until later, a particular advantage in dealing with very young children.

## Radionuclide AV Shunt Quantification

Radionuclide-labeled albumen microspheres can be used to diagnose and more or less quantitative arteriovenous shunting. Unfortunately, this method, one that is within the capabilities of any modern hospital's nuclear medicine laboratory, has been largely overlooked. The basic principle behind the study is simple: radionuclide-labeled albumen microspheres too large to pass through capillaries are injected into the inflow artery proximal to the suspected AVM. Those passing through arteriovenous communications are trapped in the next vascular bed, in the lung, and may be quantified by counting the increased radioactivity in the lungs, with a gamma camera, or a discrete sample of it, by maintaining a rectilinear scintillation scanner in a fixed position over a limited pulmonary field [6, 11]. The fraction of microspheres reaching the lungs is determined by comparing these counts with the lung counts following another injection of microspheres introduced into any peripheral vein, 100% of which should lodge in the lungs. (This latter injection is usually reduced to one-fourth, or less, than the arterial injectate to allow relatively equal counting efficiencies.) The agent commonly used consists of a suspension of 35-μm human albumin microspheres labeled with technetium-99 m (similar to that commonly used in lung scans) but other radionuclide labels have been used.

The basic formula is: % AV shunt = the ratio of the lung counts after the arterial injection (lung counts A) to the amount of radioactivity injected (injectate A) divided by the ratio of the counts over fixed lung field after venous injection (lung counts V) to the amount of radioactivity injected (injectate V). (*Note*: "Injectate" in this formula is determined by counting of the injecting syringes before and after the injection.)

The study is minimally invasive, relatively simple to perform, causes little discomfort, and carries a negligible risk. It roughly quantifies the degree of AV shunting, something none of the other tests do. Because shunt flow can be quantified, the results have prognostic value [5, 6]. One can, in this way, better estimate the hemodynamic significance of an AVF(s) or AVM and thus be better able to predict the need for and timing of intervention. Serial measurements can also be used to gauge the success of interventions designed to eliminate or control AVMs. The radionuclide-labeled albumen microspheres commonly used in lung scans can be used here, and so this approach is both practical and useful for studying patients with suspected congenital arteriovenous fistulae [2, 6]. In patients with diffuse or extensive congenital vascular malformations presenting with a vascular "birthmark," varicose veins, and/or limb overgrowth, it may be difficult to distinguish clinically between patients with multiple AVFs (so-called Parkes Weber syndrome), some so small they cannot be visualized arteriographically, and those with the same triad but with predominantly venous malformations (e.g., von Klippel-Trenaunay syndrome). The labeled microsphere study solves this dilemma. Importantly, the success of surgical or endovascular interventions in

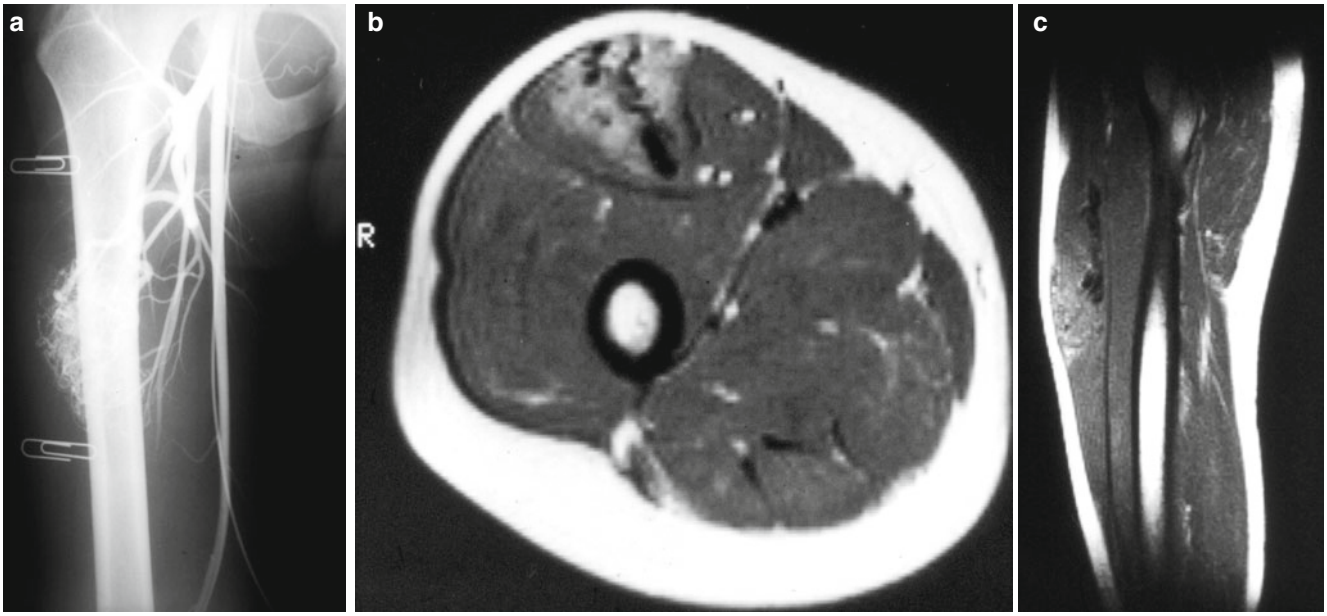


**Fig. 33.4** (**a**) Arteriogram prior to referral of a 23-year-old male with a "localized" AVM, "suitable for surgical excision," (**b**) MRI (cross-sectional view) of AVM lesion, showing involvement of entire anterior muscle compartment, and (**c**) MRI (longitudinal view) of the same AVM. MRI views indicate resection not possible without including nerves that would leave patient unable to raise leg. He was therefore treated with embolotherapy (Reprinted from Pearce et al. [14]. With permission from Elsevier)

eliminating or controlling AVMs can be adequately gauged by pre- and post-intervention studies. Finally, serial measurements will indicate whether the fistula is following a stable or a progressive course and whether previously dormant arteriovenous communications have begun to open up or "grow," as has been claimed to occur with the approach of puberty. In short, while it has a number of values, unfortunately, it is currently underutilized.

Although naturally occurring "physiologic" arteriovenous shunts are present in normal human extremities, less than 3% of the total blood flow (and usually much less) is diverted through these communications, so they normally do not produce an interpretive error [11]. However, measurements made during anesthesia are not accurate because anesthesia, both general and regional, significantly increases shunting through these naturally occurring arteriovenous communications. The examiner must be also be aware that the percentage of blood shunted through arteriovenous communications can be quite significant, in the range of 20–40%, in the limbs of patients soon after sympathetic denervation, and in patients with cirrhosis, or those with hypertrophic pulmonary osteopathy [12]. Finally, this study shares the limitation of the physiologic studies previously described in that it does not readily localize the lesion. However, several injections can be made at key locations in the arterial tree at the time of arteriography, if a gamma camera is present, and these can quantified against a later venous injection, to give localizing information.

## Magnetic Resonance Imaging and CT Scan

The previously described VDL studies cannot properly assess the anatomic extent of large or deep vascular malformations, and even angiographic studies tend to underestimate their full anatomic extent. Computed tomography (CT) will usually demonstrate the location and extent of the lesion and even the involvement of specific muscle groups and bone [13, 14]. Offsetting these desirable features of CT are the need for contrast, the lack of an optimum protocol for its administration, and the practical limitation of having to use multiple transverse images to reconstruct the anatomy of the lesion. A 3D reconstruction of CT angiography data overcomes some of these limitations, but subtracting away muscle, skin, and bone, as performed in most vascular applications, prevents the true anatomic extent of AVMs from being accurately determined.

Magnetic resonance imaging (MRI) possesses a number of distinct advantages over CT in evaluating vascular malformations. There is no need for contrast (gadolinium, but not contrast in the usual sense), the anatomic extent is more clearly demonstrated, longitudinal as well as transverse sections may be obtained, and the flow patterns in the congenital malformation can be characterized. An example is shown in Fig. 33.4a–c. As a result, MRI has become the pivotal diagnostic study in the evaluation of most vascular malformations presenting with mass lesions.

## Overall Diagnostic Strategy and Clinical Correlation

Although predominantly venous malformations are more common than arteriovenous malformations (roughly half vs. one-third of all vascular anomalies), determining whether or not a vascular anomaly or malformation contains AVFs is the usual starting point, even in presumed venous lesions, and particularly in presumed von Klippel-Trenaunay syndrome. The VDL can provide much useful information in this regard, using segmental limb pressures and plethysmography, velocity wave form analysis, and duplex scanning, and most vascular malformations containing AVFs can be evaluated adequately enough with these basic VDL tests for clinical decision-making. A radionuclide-labeled microsphere shunt study can added if it is important to quantify the AV shunting, and magnetic resonance imaging (MRI) is used in mass lesions to determine their anatomic extent, particularly the involvement of adjacent muscle, bone and nerves, which in turn determines respectability of mass lesions. It also demonstrates the lesion's flow characteristics (e.g., distinguishing venous from arteriovenous malformations).

After utilizing the above diagnostic tests, without the use of contrast angiography, one should be able to categorize the lesion as either one of the following: a localized AVF, an extensive malformation with macrofistulous AVFs (an AVM) fed by specific named vessels, diffusely scattered microfistulous AVFs (which may or not be associated with venous malformations), venous angiomas (an extratruncular venous malformation consisting of multiple venous lakes located to the side of major veins), a congenital defect of the deep veins, or an arterial anomaly. In most cases, duplex scanning will aid in sorting these out if the noninvasive "physiologic" tests are not definitive. Angiography should be rarely used initially, being saved to guide interventions once they have deemed necessary. The need for surgical intervention is limited to the more localized AV malformations that may be resectable (less than 10%). Larger AVMs, composed of macro AVFs can be "controlled" but rarely cured by modern embolotherapy, which is more effective for venous or lymphatic mass lesions. Diffuse micro AVFs and extensive or diffuse venous malformations usually require no treatment other than conservative management of the associated venous hypertension (e.g., by elastic stockings and intermittent elevation). Thus, the noninvasive studies featured in the today's VDL, and described above, can and should play a pivotal role in the diagnosis of AVMs, and in ruling in or out AVFs as significant components of other congenital vascular anomalies.

## References


1. Belov S. Anatomopathological classification of congenital vascular defects. Semin Vasc Surg. 1993;6:219–24.
2. Tasnadi G. Epidemiology and etiology of congenital vascular malformations. Semin Vasc Surg. 1993;6:200–3.
3. Szilagyi DE, Smith RF, Elliott JP, et al. Congenital arteriovenous anomalies of the limbs. Arch Surg. 1976;111:423.
4. Rutherford RB, Fleming PW, Mcleod FD. Vascular diagnostic methods for evaluating patients with arteriovenous fistulas. In: Diethrich EB, editor. Noninvasive cardiovascular diagnosis: current concepts. Baltimore: University Park Press; 1978. p. 189–203.
5. Rutherford RB. Congenital vascular malformations of the extremities. In: Moore WS, editor. Vascular surgery: a comprehensive review. 5th ed. Philadelphia: WB Saunders; 2000.
6. Rutherford RB. Noninvasive testing in the diagnosis and assessment of arteriovenous fistula. In: Bernstein EF, editor. Noninvasive diagnostic techniques in vascular disease. St. Louis: CV Mosby; 1982. p. 430–42.
7. Brener BJ, Brief DK, Alpert J, et al. The effect of vascular access procedures on digital hemodynamics. In: Diethrich EB, editor. Noninvasive cardiovascular diagnosis: current concepts. Baltimore: University Park Press; 1978. p. 189–203.
8. Barnes RW. Noninvasive assessment of arteriovenous fistula. Angiology. 1978;29:691.
9. Bingham HG, Lichti EL. The Doppler as an aid in predicting the behavior of congenital cutaneous hemangioma. Plast Reconstr Surg. 1971;47:580.
10. Pisko-Dubienski ZA, Baird RJ, Bayliss CE, et al. Identification and successful treatment of congenital microfistulas with the aid of directional Doppler. Surgery. 1975;78:564.
11. Rhodes BA, Rutherford RB, Lopez-Majano V, et al. Arteriovenous shunt measurement in extremities. J Nucl Med. 1972;13:357.
12. Rutherford RB. Clinical applications of a method of quantitating arteriovenous shunting in extremities. In: Vascular surgery. 1st ed. Philadelphia: WB Saunders; 1977. p. 781–3.
13. Rauch RF, Silverman PM, Korobkin M, et al. Computed tomography of benign angiomatous lesions of the extremities. J Comput Assist Tomogr. 1984;8:1143.
14. Pearce WH, Rutherford RB, Whitehill TA, Davis K. Nuclear magnetic resonance imaging: its diagnostic value in patients with congenital vascular malformations of the limbs. J Vasc Surg. 1988;8:64.

# Noninvasive Vascular Testing for the Trauma Patient

34

Vincent L. Rowe, John Moos, and Fred A. Weaver

**Abstract**

For decades, the management of traumatic vascular injuries to the extremity has challenged surgeons. However, even during the dark times of conflict in the United States, where surgeon faced an inordinate amount of mangled extremities, surgical technique was advanced and not only benefited military personnel but eventually civilian victims. Parallel to the course of surgery with movement toward minimally invasive techniques, the diagnosis of vascular trauma has progressed from an invasive, often low-yielding surgical exploration to a selective, noninvasive paradigm. Outside of overt signs of vascular injury (e.g., pulsatile bleeding), reliance solely on physical examination lacked the sensitivity to support an adoption of a less invasive diagnostic approach. Ankle-brachial index (ABI) was paramount in guiding clinicians to proper selection of injured patients who benefited from further diagnostic investigations or observation. Color-flow duplex scanning also contributed to a noninvasive diagnostic testing for vascular injuries in the extremity. However, due to variability in results based on technician expertise, off-hour unavailability, and stagnant technological movement the role of color-flow duplex remained limited. Conversely, computed tomography is emerging as the diagnostic modality of choice for vascular trauma. Current multidetector units allow accurate acquisition of long body segment in minutes. Due to the increasing application of computed tomography (CT) angiography, digital subtraction angiography has been relegated from the "gold standard" diagnostic modality to a treatment modality. This chapter discusses the progression of this overall change in the diagnostic management of patients with traumatic vascular injuries.

**Keywords**

Trauma • Lower extremity • Arterial injury • Diagnosis • Noninvasive • Vascular

## Introduction

Over the past century, the surgical management of extremity vascular injuries has undergone dramatic changes. During the era of World War I and II, repair of vascular injuries was rarely performed and ligation of injured vessels was the standard practice. Unfortunately, this practice resulted in an unacceptably high amputation rate in excess of 70% [1]. The poor results from arterial ligation prompted surgeons Hughes and Spencer to reconsider the proper management of traumatic vascular injuries [2, 3]. As such, during the Korean War, vascular surgical techniques had advanced to allow

V.L. Rowe, M.D., FACS (✉)
Division of Vascular Surgery, Department of Surgery, Keck School of Medicine at the University of Southern California, Los Angeles, CA, USA

Healthcare Consultation Center II, 1520 San Pablo Street, Suite 4300, Los Angeles, CA 90033, USA
e-mail: vincent.rowe@med.usc.edu

J. Moos, M.D. • F.A. Weaver, M.D., FACS, MMM
Division of Vascular Surgery, Department of Surgery, Keck Medical Center of USC, Los Angeles, CA, USA

A.F. AbuRahma, D.F. Bandyk (eds.), *Noninvasive Vascular Diagnosis*,
DOI 10.1007/978-1-4471-4005-4_34, 

implementation of formal repair for peripheral vascular arterial injuries. In the Vietnam War, further surgical refinements led to the repair of both arterial and venous injuries becoming the standard of care in the majority of clinical situations [4, 5]. Continuing refinements in arterial surgery over the ensuing three decades have reduced limb loss in most civilian series to less than 10–15% [6–8]; however, long-term disability, predominantly resulting from associated skeletal and nerve injuries, remains a persistent problem for 20–50% of patients [9]. To date, approximately 90% of all peripheral arterial injuries occur in an extremity. Civilian studies report the majority of arterial injuries to be in the upper extremity, while the past military experiences defines lower extremity injuries to be more common [3].

## Mechanism of Injury

The initial and ultimate outcome of vascular injury depends, in large part, on the wounding agent or mechanism of injury. Determining the mechanism of injury, whether it be blunt, high velocity, or low velocity penetrating trauma, is of utmost importance if the surgeon is to utilize available diagnostic and treatment options appropriately. Peripheral vascular injuries in an urban environment most often result from penetrating trauma from knives or bullets. In a series of penetrating injuries, arterial injuries were due to gunshot wounds in 64%, knife wounds in 24%, and shotgun blasts in 12% [10].

Traditionally, high-velocity firearm injuries are thought to occur in the battlefield, but with increasing frequency, they are the causative agent in civilian vascular trauma. In addition to the vascular injury, extensive associated musculoskeletal injury is commonplace. Vascular injuries in this setting result from the dissipation of energy into the surrounding tissues, fragmentation of the projectile or of bone, or transmission of the blast effect [11]. Experimental studies have demonstrated a positive correlation between muzzle velocity and the microscopic extent and "length" of damage to the vessel wall [12]. In many ways, these wounds mimic lower-velocity shotgun injuries in their devastating combination of penetrating and blunt tissue injury [13].

Falls and motor vehicle accidents are the most common causes of blunt injury and are becoming more frequent, owing to the ever-increasing mobility of modern society [12, 14]. The morbidity of blunt vascular injuries can be magnified by associated fractures, dislocations, and crush injuries to muscles and nerves.

## Diagnostic Evaluation

Due to the fact that the majority of significant vascular injuries present with signs of either loss of extremity pulses, overt bleeding or shock, diagnosis is usually not a challenge. However, in some situations, the initial vascular injury may remain undiagnosed until life threatening hemorrhage or end organ ischemia becomes evident.

### History

Paramount to the initial assessment for a vascular injury is a proper history. First responders should be questioned for the following findings at the scene of injury: presence or absence of shock, the amount and character of bleeding (bright-red pulsatile bleeding suggesting an arterial origin or dark blood suggesting a venous origin), or the use or application of a tourniquet. Upon arrival to the hospital, it is possible for the bleeding to have abated, falsely lowering the suspicion of a significant vascular injury. However, the clinician must remain aware of the remote possibility of a secondary hemorrhagic event at anytime. Determination of the mechanism of injury is paramount in the history evaluation. Additional questioning is obtained concerning underlying comorbidities, such as, long-standing diabetes mellitus, underlying peripheral arterial disease, or established peripheral neuropathies that may confound the evaluation of vascular system.

### Physical Examination

Similar for all trauma patients, the initial physical assessment must be performed after the patient is completely disrobed. In any penetrating trauma, evaluation of the location of possible entry and exit wounds in relation to anatomic structures should be sought. After completion of the primary and secondary survey of the trauma patient, attention should be focused on the exclusion of a vascular injury. Comprehensive pulse examination still remains one of the most important assessment measures and should be performed on all patients with suspected vascular injury. Presence and strength of a pulse should be documented from the groin to the foot on both extremities. The clinician must be aware of the trauma patient who possesses underlying peripheral arterial disease (PAD). In this case, because of the bilateral distribution of chronic lower extremity PAD, the absence of pulses in the contralateral leg will serve as a vital comparison of the baseline circulatory status.

Clinical suspicion for a vascular injury should not be lowered based on the presence of a normal pulse palpated distal to the area of injury. As many as 50% of patients can harbor an occult vascular injury with a reported "normal" pulse examination. In addition to a thorough pulse examination, capillary refill and temperature should be documented. Because of the close proximity of major nerves to the extremity vessels, a thorough neurologic examination is critical to assess the functional potential of the extremity. Interestingly, the incidence of nerve injury in the lower extremity is

**Table 34.1** Traumatic vascular injury

| Hard signs | Soft signs |
|---|---|
| Observed pulsatile bleeding | Significant hemorrhage by history |
| Arterial thrill by manual palpation | Neurological abnormality |
| Bruit auscultated over or near area of arterial injury | Diminished pulse compared to contralateral extremity |
| Absent distal pulse | Proximity bony injury or penetrating wound |
| Visible expanding hematoma | |

reported to be one-third that of trauma to the upper extremity [15–17]. In the infrageniculate region, the close proximity of major nerves has led to an incidence of associated nerve injuries between 8% and 58%. [15, 16, 18, 19]. Therefore, it is extremely important to document a thorough neurological examination. Nerve injuries have been reported to result in long-term severe neurological deficit in up to 20% of patients and is a key determinant in the decision for limb salvage or primary amputation, confirming the need for a thorough initial evaluation [20, 21].

Associated bony injuries are reported to occur in approximately 35% of lower extremity penetrating and blunt trauma [15, 22]. In patients who present with obvious deformities, bony injuries are easily appreciated. However, even the most minor appearing injured extremity may harbor an occult bony disruption. Christian et al. identified unrecognized arterial injuries in 50% of patients presenting with severe tibial fractures [23]. Therefore, a series of plain radiographs to assure the absence of a fracture is obligatory in the evaluation of lower extremity trauma.

Extremity arterial injuries have varied clinical presentations. A minority of patients present with obvious clinical evidence, or "hard signs," of an arterial disruption such as pulsatile external bleeding, an enlarging hematoma, absent distal pulses, or an ischemic limb (Table 34.1). For patients with overt signs of arterial injury, immediate surgical exploration in the operating room, without further diagnostic testing, is preferred. In most instances, when arteriography is required, an intraoperative arteriogram is sufficient to identify the location and extent of injury and to guide the surgical repair. These signs aid clinicians by stratifying patients into those with or without severe ischemia.

A complete vascular examination should include an ankle-brachial index (ABI). Pressure readings from the lower of the two pedal vessels are compared to the arm blood pressure. Doppler arterial pressure measurements and calculation of pressure indices was first introduced in the 1970s for the assessment of chronic PAD limbs. However, it was not until the early 1990s when ABI became an effective diagnostic modality in the workup of a patient with a possible traumatic vascular injury. In a study of 100 consecutive injured limbs, Lynch and Johanason showed arterial injuries that required intervention were discovered in 14 cases, and an ABI less than 0.90 predicted the injury with 87% sensitivity and 97% specificity [24]. Because two of the arteriograms were falsely positive, sensitivity and specificity of ABI less than 0.90 were even higher—95% and 97%—when clinical outcome was the standard. As such, ABI became a routine part of the vascular assessment of the injured extremity.

## Imaging Studies

### Ankle-Brachial Indices and Selective Angiography

The diagnostic approach to extremity trauma has changed dramatically over the last few decades. Initially, the influences from combat experience lead to the aggressive approach of mandatory exploration for all penetrating trauma to an extremity. However, application of this policy to civilian injuries resulted in negative exploration rate as high as 84% in penetrating trauma patients [25]. These patients had undergone expensive, nontherapeutic operations, which occasionally resulted in additional morbidity.

With the availability of arteriography in most trauma centers, this diagnostic modality supplanted wound exploration for penetrating extremity trauma. As was the case with wound exploration, mandatory or routine screening arteriography for proximity wounds, in the absence of other suspicious clinical findings, resulted in a large proportion of normal arteriograms (90%), at significant cost [1]. In addition, arteriograms were found to be less than perfect, having a low, but real, incidence of false-negative and false-positive findings. Because of its invasive nature and the potential nephrotoxicity of contrast media, arteriography also occasionally results in serious complications, thus increasing patient morbidity and further increasing the cost of care.

It became apparent that many unnecessary angiograms were performed in the trauma setting. Intense evaluation of the role of proximity in predicting a vascular injury leads to a significant change in the management of penetrating extremity trauma. Weaver et al. examined the yield of a vascular injury when proximity alone was the sole indicator for angiography in extremity trauma [26]. Over an 18-month period, 373 patients with penetrating trauma distal to the deltopectoral groove in the upper extremity and distal to the inguinal ligament in the lower extremity were evaluated. Arteriograms were obtained for patients with "hard or soft signs" of vascular trauma (Table 34.1) or in the absence of these findings, when the path of the penetrating object was judged to be in close proximity to a major vascular structure. In the 216 patients with one or more abnormal physical findings, an arterial injury was identified by arteriography in 65 (30%), whereas in the absence of physical findings (157 patients) only minor injuries were identified in 17 (11%). Only a pulse deficit, neurologic deficit, or shotgun injury

correlated ($p < 0.05$) with arteriographic evidence of a major arterial injury.

Later, authors from the same institution sought to validate the utility of ABI in assessing patients with penetrating vascular trauma of the extremity. A follow-up study investigated the ability of Doppler indices to detect occult arterial injuries in a consecutive cohort of 514 patients with unilateral, isolated penetrating extremity injuries [27]. Arteriography was limited to patients with a pulse deficit, neurologic deficit, shotgun injury, or one or more "soft" signs or a Doppler ankle/brachial index (ABI) of less than 1.00. All patients with arteriographic evidence of a major arterial injury had either a pulse deficit or ABI below 1.00.

A selective use of angiography in evaluation of patients with penetrating extremity trauma was recently confirmed by Conrad [28]. Five hundred and thirty-eight patients were reviewed retrospectively. Similar to previous studies, angiography was limited to patients presenting with an abnormal pulse examination or Doppler indices less than 1.0. Patients with a normal physical examination and Doppler indices of 1.0 or greater were discharged home without further workup. Three hundred patients with asymptomatic proximity wounds and normal physical examination were discharged home. Fifty-one percent of these discharged patients were available for an average follow-up of 9.8 months. There were no missed injuries or late complications identified in the group.

For blunt extremity trauma, the indications for arteriography parallel what has been established for penetrating injuries. A prospective study analyzed the results of arteriography in 53 patients with unilateral blunt lower extremity trauma [29]. Thirty-one patients had physical findings suggestive of an arterial injury, and an arterial injury was demonstrated in 15. A pulse deficit or decrease capillary refill correlated significantly ($p < .05$) with arteriographic evidence of injury. Of the 15 arterial injuries, 12 were found in patients who had one or both of these findings and four of those injuries required repair. In the remaining 22 patients with neither a pulse deficit nor decreased capillary refill, three minor injuries were found, none of which required repair.

Another series of blunt injuries focused specifically on 115 patients with knee dislocations [30]. Popliteal artery injury was demonstrated arteriographically in 27 of 115 (23%) patients. An abnormal pedal pulse identified popliteal artery injuries with sensitivity of 85% and specificity of 93%. All injuries that required intervention were associated with a diminished pulse. Dennis reported an identical experience in 37 patients with knee dislocations [31]. In all patients who required popliteal repair, pedal pulses were absent. More recently, Abou-Sayed and Berger confirmed the sensitivity of physical examination in 52 patients with blunt popliteal artery injuries [32]. Twenty-three patients, with a normal pulse examination, did not undergo angiography and required no vascular interventions. Angiography was performed in 13 patients with normal pulse examinations (at the discretion of the attending surgeon); similarly, no clinically significant lesions were identified that required intervention. Again, the assertion that the clinical examination can define a subset of high-risk patients who need an arteriogram, and possibly surgical repair, was validated.

Based on these published reports, a consensus has developed that for penetrating or blunt extremity trauma, arteriography is indicated only for patients with either an abnormal extremity pulse examination or Doppler index less than 1. Careful physical examination and pressure measurements appropriately select the vast majority of patients (>95%) who have significant arterial injury and require arteriography.

## Plain Radiographs

Plain films are part of a standard diagnostic evaluation for a trauma patient. In patients with blunt trauma, fractures or dislocations in key anatomical areas may alert the clinician to the possibility of a vascular injury (i.e., posterior knee dislocation). Radio-opaque markers placed at the point of entry and exit of penetrating trauma wounds may be helpful in determining the trajectory of the penetrating object. Attention to all foreign bodies should be given. In the special situation of a repeat trauma patient, the clinician must be aware of possible retained foreign bodies from prior trauma.

## Color Flow Duplex Ultrasonography

Duplex ultrasonography is the melding of pulse-wave Doppler and high resolution B-mode ultrasound. Because of continued improvements in noninvasive vascular imaging, color flow duplex ultrasonography (CFD) has been suggested as a substitute for or complement to arteriography [33]. CFD has several obvious advantages: it is noninvasive, painless, portable, and can easily be brought to the patient's bedside, emergency room, or operating room. Repeated and follow-up examinations are easily performed without morbidity and are relatively inexpensive. The duplex is also able to detect vascular injuries to non-conduit vessels such as the profunda femoris artery, where ABI measurements would be registered as normal.

Bynoe and colleagues reported sensitivity of 95%, specificity of 99%, and accuracy of 98% when CFD was used to evaluate blunt and penetrating injuries of the neck or extremities, and Fry and coworkers [34, 35] documented 100% sensitivity and 97.3% specificity in a similar series. In these two studies, however, a comparison arteriogram was available for only a minority of patients. Bergstein and associates reported on 67 patients who had 75 penetrating extremity injuries, all of whom underwent both CFD and

arteriography [36]. Using arteriography as the gold standard, CFD had two false-negative results and one false-positive (sensitivity 50%, specificity 99%). Gagne and coworkers published a series of 37 patients with proximity injuries in 43 extremities [37]. Arteriography identified three injuries to the deep femoral, superficial femoral, and posterior tibial arteries that were not identified by CFD. However, CFD did detect a superficial femoral artery intimal flap that arteriography missed.

Despite some uncertainty about the ability of CFD to detect all arterial injuries, these reports suggest that nearly all major injuries that require therapeutic intervention can be identified, potentially at considerable costs savings as compared with arteriography [33]. Ordog has estimated a multimillion dollar cost savings if CFD and outpatient follow-up, rather than arteriography and inpatient observation, were used to exclude extremity arterial injuries [38].

Contrary to the success of these reports, use of CFD in the workup of trauma patients presents some challenges. Technician dependence, limited availability during off hours, and limited visualization of chest and in some cases, the abdomen are possible pitfalls of CFD. Our institutional experience with CFD in the evaluation of extremity trauma confirmed the operator dependence of CFD and, we felt for CFD to be used effectively, an institutional investment in experienced vascular technologists and interpreting physicians would be required [39]. This expense could be lessened over the long term if the current effort to train surgeons in the use of diagnostic ultrasound for intracavitary trauma were extended to include extremity vessels.

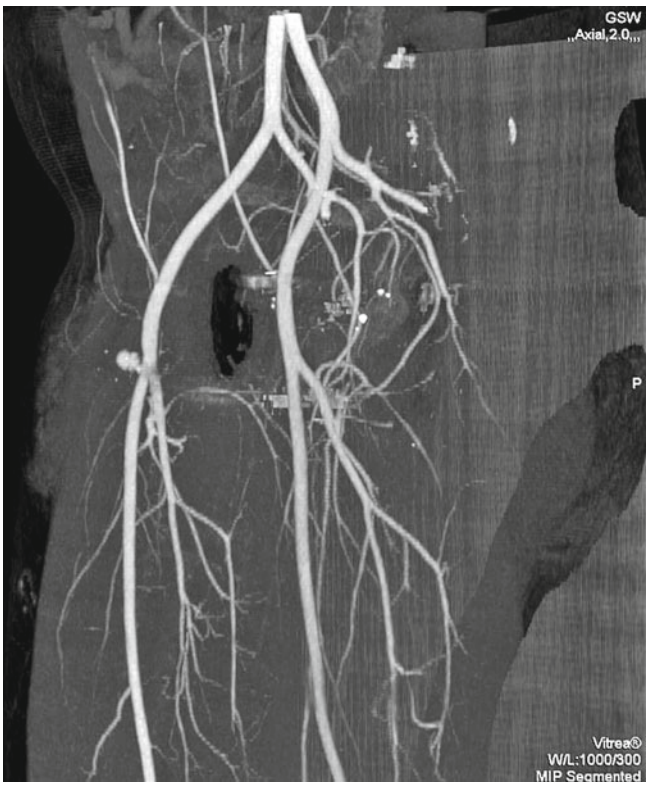


**Fig. 34.1** CFA injury + pseudoaneurysm. Right common femoral artery injury with pseudoaneurysm adjacent to the bifurcation. Small filling defects seen within the right deep and superficial femoral arteries at the bifurcation, which may represent blood clot versus intimal injury

## Computed Tomography Angiography

Years ago, computed tomography angiography (CTA) began challenging the need for digital angiography in the evaluation of trauma patients with suspected vascular injuries. However, now with advances in technology to newer 64-row multi-detector CT scanning, digital angiography is being supplanted by CTA in many trauma centers [40–43]. Current scanners with multi-detector scanning and three-dimensional reformation capabilities provide rapid acquisition of isotropic data sets of long vascular territories within seconds. Therefore, CT scanning can now integrate extremity images in the routine thoraco-abdominal trauma imaging without a significant increase in scanning time. When compared to digital angiography for trauma patients, CTA has the distinct advantage of being equivalent in accuracy, more time efficient, less invasive, and less expensive in the diagnosis of traumatic vascular injuries. Current CT scanning is also readily available and provides simultaneous imaging of surrounding body structures and adjacent anatomical locations in a single examination. Through remote computer access, set injection protocols and lack of arterial puncture complications, staff radiologists can provide diagnostic reading offsite.

CT scan evidence of a vascular injury includes the following findings: contrast extravasation, extravasated contrast material collections (Fig. 34.1), loss of opacification or occlusion of arterial segment (Fig. 34.2), abrupt vessel narrowing (signifying either spasm, dissection or external compression), early venous opacification (signifying an arteriovenous fistula), and an abnormal vessel caliber or course [43].

Soto and colleagues performed one of the early comparisons between CTA and digital angiography for evaluation of suspected vascular injuries in extremity trauma patients [44]. In this study, all extremity trauma patients referred for digital angiography underwent CTA. Two independent observers documented sensitivity and specificity levels greater than 90% respectively for diagnosis of vascular injuries, with and interobserver agreement of 0.9 (kappa statistics). More recently, studies from institutions with more advanced CT scan technology confirmed the diagnostic utility and accuracy in the evaluation of trauma patients [41, 42]. Inaba and associates utilized multi-detector CT scan angiography for

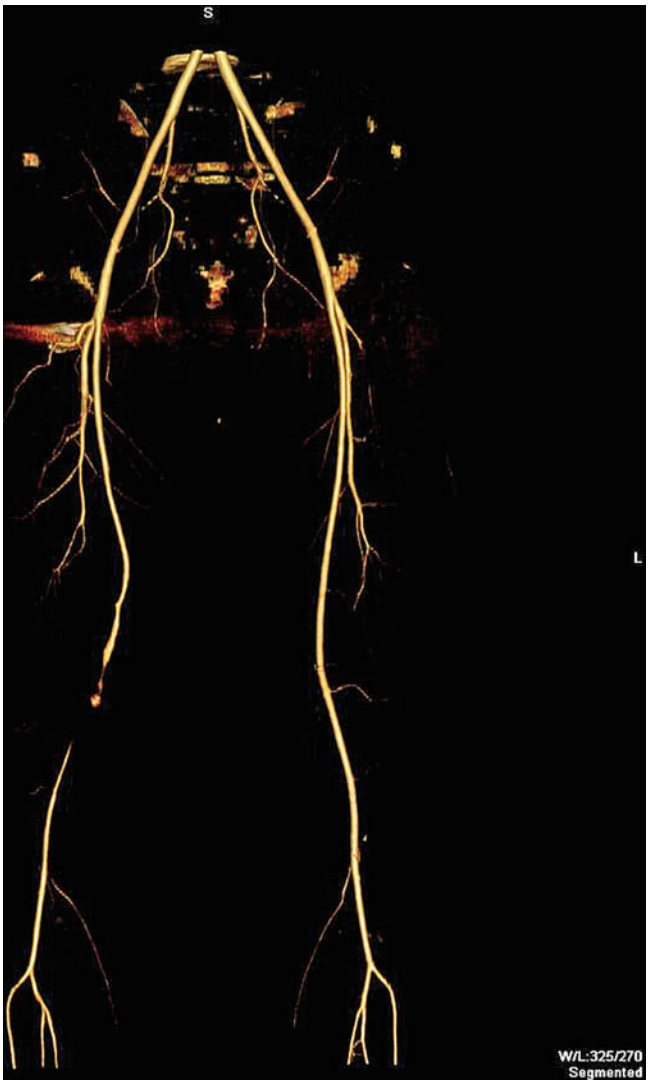


**Fig. 34.2** Right popliteal artery injury. Pseudoaneurysm of the proximal right popliteal artery in the adductor canal with a short segment of occlusion just distal to the pseudoaneurysm. There is distal reconstitution of the popliteal artery

59 trauma patients with lower extremity injuries and documented 100% sensitivity and specificity in the diagnosis of a clinically significant vascular injury [45]. The one missed injury in their patient cohort was secondary to artifact from a retained missile fragment. Most recently, Inaba and colleagues followed up their earlier study and reported similar findings [46]. Sensitivity and specificity both reached 100% in detecting clinically significant traumatic vascular injuries of the lower extremity. The shortcoming of computed tomography continued to appear in artifact formation from retained missile fragments. Other recognized disadvantages of CT angiography include artifact formation due to motion or calcified plaques and high volume of iodinated contrast usage. If an endovascular treatment option is contemplated, deleterious effects of sequential intravenous contrast boluses must be considered in the patient management.

## Magnetic Resonance Arteriography

Magnetic resonance arteriography (MRA) has increased in popularity for the diagnosis of vascular disorders; however, its application to trauma patients is not widely accepted. Compared with other modalities, MRA has the advantage of imaging multiple anatomical areas simultaneously and being noninvasive, preventing the need for contrast agents. Unfortunately, MRA is not easily accessible in the majority of hospitals, and the presence of metallic orthopedic instrumentation limits widespread usage for trauma patients [47].

## References

1. Patel K, Rowe VL. Vascular trauma to the extremities, chapter 155. In: Rutherford R, editor. Vascular surgery, vol. 2. 7th ed. Philadelphia: W.B. Saunders Publishers; 2010. p. 2361–73.
2. Hughes CH. Arterial repair during the Korean war. Ann Surg. 1958;147:555.
3. Rich NM. Surgeon's response to battlefield vascular trauma. Am J Surg. 1993;166:91.
4. Rich NA, Baugh JH, Hughes CW. Acute arterial injuries in Vietnam: 1,000 cases. J Trauma. 1970;10:359.
5. Martin LC, McKenney MG, Sosa JL, et al. Management of lower extremity arterial trauma. J Trauma. 1994;37(4):591–9.
6. Melton SM, Croce MA, Patton JH, et al. Popliteal artery trauma. Ann Surg. 1997;225:518.
7. Wagner WH, Caulkins E, Weaver FA, et al. Blunt popliteal artery trauma: 100 consecutive cases. J Vasc Surg. 1988;7:736.
8. Wagner WH, Yellin AE, Weaver FA, et al. Acute treatment of popliteal artery trauma: the importance of soft tissue injury. Ann Vasc Surg. 1994;8:557.
9. Weaver FA, Papanicolaou G, Yellin AE. Difficult peripheral vascular injuries. Surg Clin North Am. 1996;76:843.
10. Pasch AR, Bishara RA, Lim LT, et al. Optimal limb salvage in penetrating civilian vascular trauma. J Vasc Surg. 1986;3:189.
11. Fackler ML. Wound ballistics: a review of common misconceptions. JAMA. 1988;259:2730.
12. Amato JJ, Billy LJ, Gruber RP, et al. Vascular injuries: an experimental study of high and low velocity missile wounds. Arch Surg. 1970;101:167.
13. Mayer JP, Lim LT, Schuler JJ, et al. Peripheral vascular trauma from close-range shotgun injuries. Arch Surg. 1985;120:1126.
14. White RA, Scher LA, Samson RH, et al. Peripheral vascular injuries associated with falls from heights. J Trauma. 1987;27:411.
15. Ballard JL, Bunt TJ, Malone JM. Management of small artery vascular trauma. Am J Surg. 1992;164:316–9.
16. Rich NM, Spencer FC. Concomitant fractures and nerve trauma. In: Rich NM, Spencer FL, editors. Vascular trauma. Philadelphia: WB Saunders Co; 1978. p. 125–56, 380–1.
17. Rowe VL, Salim A, Lipham J, Asensio J. Shank arterial injuries. Vascular trauma: complex and challenging injuries, part II. Surg Clin N Am. 2002;82(1):91–104.
18. Bole PV, Purdy RT, Munda RT, Moallem S, DeVanesan J, Clauss RH. Civilian arterial injuries. Ann Surg. 1976;183:13–23.
19. Smith RF, Elliott JP, Hageman JH, Szilagyi DE, Xavier AO. Acute penetrating arterial injuries of the neck and limbs. Arch Surg. 1974;109:198–205.
20. Sitzmann JV, Ernst CB. Management of arm arterial injuries. Surgery. 1984;96:895–901.
21. Weaver FA, Rosenthal RE, Waterhouse G, et al. Combined skeletal and vascular injuries of the lower extremities. Am Surg. 1984;50(4):189–97.

22. Grossman MD, Reilly P, McMahan D, et al. Gunshot wounds below the popliteal fossa: a contemporary review. Am Surg. 1999;65(4): 360–5.
23. Christian EP, Bosse MJ, Robb G. Reconstruction of large diaphyseal defects without free fibular transfer, in grade III-B tibial fractures. J Bone Joint Surg Am. 1989;71A:994–1004.
24. Lynch K, Johansen K. Can Doppler pressure measurement replace "exclusion" arteriography in the diagnosis of occult extremity arterial trauma? Ann Surg. 1991;214:737.
25. Guede JW, Hobson RW, Padberg FT, et al. The role of contrast arteriography in suspected arterial injuries of the extremities. Am Surg. 1985;51:89.
26. Weaver FA, Yellin AE, Bauer M, et al. Is arterial proximity a valid indication for arteriography in penetrating extremity trauma? A prospective analysis. Arch Surg. 1990;125:1256.
27. Schwartz MR, Weaver FA, Yellin AE, et al. Refining the indications for arteriography in penetrating extremity trauma: a prospective analysis. J Vasc Surg. 1993;17:166.
28. Conrad MF, Patton Jr JH, Parikshak M, et al. Evaluation of vascular injury in penetrating extremity trauma: angiographers stay home. Am Surg. 2002;68:269.
29. Applebaum R, Yellin AE, Weaver FA, et al. The role of routine arteriography in blunt lower extremity trauma. Am J Surg. 1990;160:221.
30. Fayiga YJ, Valentine RJ, Myers SI, et al. Blunt pediatric vascular trauma: analysis of forty-one consecutive patients undergoing operative intervention. J Vasc Surg. 1994;20:419.
31. Dennis JW, Frykberg ER, Veldenz HC, et al. Validation of nonoperative management of occult vascular injuries and accuracy of physical examination alone in penetrating extremity trauma: 5- to 10-year follow up. J Trauma. 1998;44:24.
32. Abou-Sayed H, Berger DL. Blunt lower-extremity trauma and popliteal artery injuries. Revisiting the case for selective arteriography. Arch Surg. 2002;137:585.
33. Meissner M, Paun M, Johansen K. Duplex scanning for arterial trauma. Am J Surg. 1991;161:552.
34. Fry WR, Smith RS, Sayers DV, et al. The success of duplex ultrasonographic scanning in diagnosis of extremity vascular proximity trauma. Arch Surg. 1993;128:1368.
35. Bynoe RP, Miles WS, Bell RM, et al. Noninvasive diagnosis of vascular trauma by duplex ultrasonography. J Vasc Surg. 1991; 14:346.
36. Bergstein JM, Blair JF, Edwards J, Towne JB, Wittmann DH, Aprahamian C, Quebbeman EJ. Pitfalls in the use of color-flow duplex ultrasound for screening of suspected arterial injuries in penetrated extremities. J Trauma. 1992;33:395–402.
37. Gagne PJ, Cone JB, McFarland D, et al. Proximity penetrating extremity trauma: the role of duplex ultrasound in the detection of occult venous injuries. J Trauma. 1995;39:1157.
38. Ordog GJ, Balasubramanium S, Wasserber J, et al. Extremity gunshot wounds: I. Identification and treatment of patients at high risk of vascular injury. J Trauma. 1994;36:358.
39. Schwartz M, Weaver F, Yellin A, Ralls P. The utility of color flow Doppler examination in penetrating extremity arterial trauma. Am Surg. 1993;59:375.
40. Fleiter TR, Mervis S. The role of 3D-CTA in the assessment of peripheral vascular lesions in trauma patients. Eur J Radiol. 2007;64:92.
41. Busquéts AR, Acosta JA, Colón E, et al. Helical computed tomographic angiography for the diagnosis of traumatic arterial injuries of the extremities. J Trauma. 2004;56:625.
42. Peng PD, Spain DA, Tataria M, et al. CT angiography effectively evaluates extremity vascular trauma. Am Surg. 2008;74:103.
43. Gakhal MS, Sartip KA. CT Angiography signs of lower extremity vascular trauma. Am J Roentgenol. 2009;193:W49.
44. Soto JA, Múnera F, Cardoso N, et al. Diagnostic performance of helical CT angiography in trauma to large arteries of the extremities. J Comput Assist Tomogr. 1999;23(2):188.
45. Inaba K, Potzman J, Munera F, et al. Multi-slice CT angiography for arterial evaluation in the injured lower extremity. J Trauma. 2006;60:502.
46. Inaba K, Branco BC, Reddy S, et al. Prospective evaluation of multidetector computed tomography for extremity vascular trauma. J Trauma. 2011;70:808.
47. Rubel IF, Potter H, Barie P, et al. Magnetic resonance venography to evaluate deep venous thrombosis in patients with pelvic and acetabular trauma. J Trauma. 2001;51:622.

# Clinical Implications of the Vascular Laboratory in the Diagnosis of Peripheral Arterial Disease

35

Ali F. AbuRahma

**Abstract**

Our understanding of the pathophysiology, clinical manifestations, and natural history of peripheral vascular disorders must constantly be coupled with an appreciation of current diagnostic and therapeutic tools (noninvasive vascular testing, CTA, magnetic resonance angiography, conventional angiography, and angioplasty/stenting). This chapter will provide an entry point into clinical problem solving by considering the areas of screening, assessment prior to and immediately after intervention, surveillance (long-term, usually after intervention), and certain special areas of the peripheral arterial system. These include: selection of arterial reconstruction, healing response, amputation sites, compression syndromes, penile circulation, upper extremity ischemia, arteriovenous malformation, hemodialysis access graft, and arterial aneurysms.

**Keywords**

Noninvasive vascular testing • Vascular • Diagnosis • Artery disease

Our understanding of the pathophysiology, clinical manifestations, and natural history of peripheral vascular disorders [1, 2] must constantly be coupled with an appreciation of current diagnostic and therapeutic tools (computed tomographic angiography [CTA], magnetic resonance angiography, conventional angiography, and angioplasty/stenting). This chapter will provide an entry point into clinical problem solving by considering the areas of screening, assessment prior to and immediately after intervention, surveillance (long-term, usually after intervention), and certain special areas of the peripheral arterial system.

A.F. AbuRahma, M.D., RVT, RPVI
Department of Surgery, Robert C. Byrd Health Sciences Center, West Virginia University, 3110 MacCorkle Ave SE, Charleston, WV 25304, USA

Charleston Area Medical Center, Charleston, WV 25304, USA
e-mail: ali.aburahma@camc.org

## Screening: "Does Peripheral Arterial Disease Exist?"

The most practical, well-studied method is resting ankle-brachial index (ABI) [3]. Values in the range of 0.85–0.90 are usually chosen to signify a positive result. Attention to operator training is important for valid results [4]. Postexercise or reactive hyperemia studies are not usually performed for screening purposes. An individual with a positive test is at increased risk for all cardiovascular events (cardiac, cerebral, or extremity).

Kravos and Bubnic-Sotosek [5] reported on the role of ankle-brachial index screening for peripheral artery disease (PAD) in asymptomatic patients between 50 and 70 years of age. They selected 107 patients and collected data on gender, age, risk factors, and laboratory tests and measured the ABI. Twenty (19%) patients were found to have PAD. Smoking, high total cholesterol, high triglycerides, and diabetes mellitus were associated with a low ABI and the presence of PAD. Smoking, diabetes, and age were identified as the strongest

A.F. AbuRahma, D.F. Bandyk (eds.), *Noninvasive Vascular Diagnosis*,
DOI 10.1007/978-1-4471-4005-4_35, 

predictors of PAD and having more risk factors was associated with a lower ABI. They felt that it is not necessary to measure the ABI in patients aged 50–70 years if they only have one risk factor, except for patients with diabetes and those who smoke. In contrast, it seems to be useful to measure the ABI in patients with multiple risk factors for PAD.

Mourad et al. [6] conducted a prospective, observational, real-life, epidemiologic study (ELLIPSE) of screening unrecognized PAD using ABI in high cardiovascular risk patients free from symptomatic PAD. The prevalence of PAD (ABI < 0.9) was calculated in 2,146 asymptomatic patients ≥55 years of age who were at high cardiovascular risk and who were hospitalized in the departments of cardiology, diabetology, geriatrics, internal medicine, or neurology in metropolitan France. The discriminatory power of the model was evaluated by calculating the area under the curve (AUC) of the receiver operating characteristic curve. The ABI was <0.9 in 41% of patients. In the multivariate analysis, arterial bruit (odds ratio [OR] 1.92, $p<0.0004$), absence of ≥1 pulse (OR 2.18), regular smoking (OR 1.49, $p<0.0001$), previous non-Q-wave myocardial infarction (OR 1.50, $p=0.02$), creatinine clearance <60 mL/min (OR 1.33, $p=0.008$), and treated hypertension (OR 1.28, $p=0.03$) were significantly associated with PAD. Although risk increased with the number of variables, the model, based on clinical symptoms and on medical history parameters, was not discriminatory (AUC = 0.66). They concluded that the high prevalence of asymptomatic PAD in this patient population suggests that ABIs should be systematically performed in high-risk hospitalized patients to ensure that appropriate secondary prevention programs are initiated.

McDermott et al. [7] also found that among 156 participants with PAD with and without intermittent claudication, lower ABI values were significantly associated with a poorer walking endurance.

## Assessment of Location and Severity of Peripheral Vascular Disease

The primary use of noninvasive tests in patients with lower extremity vascular problems is to obtain objective, quantitative determinations instead of the subjective categories resulting from physical examination. Both Doppler ultrasound (continuous-wave) and the pulse volume recorder (PVR) have proved useful in defining the severity and the location of arterial occlusive disease [8–12]. However, the application of duplex ultrasonography over the past 25 years has been more helpful in localizing and grading the severity of peripheral vascular disease [13].

In patients presenting with lower extremity pain on exercise, it is most important to distinguish symptoms due to neurologic or orthopedic diseases from those produced by vascular insufficiency. In fact, both entities may coexist. If a true claudication is present, it is also important to accurately determine the patient's degree of disability and to establish a quantitative baseline with which the effect of medical or surgical therapy can be compared.

In the initial evaluation for the presence or absence of true claudication, the arterial leg Doppler study, using the segmental pressure determination with the analog wave tracing or PVRs, should be used, preferably measured after treadmill exercise. The simplest, most reliable means of confirming peripheral vascular occlusive disease of the lower extremity is measurement of the ankle systolic pressure and the calculation of the ABI. As described in Chap. 21, the normal resting ABI is generally around 1.0. In patients whose resting values are borderline, stress testing should be induced by treadmill exercise or reactive hyperemia. Although normal patients may transiently lower their ankle systolic pressure 15–20 mmHg, those with even mild occlusive disease usually show a prolonged pressure decrease in excess of 50 mmHg. In persons who become symptomatic during treadmill exercise, but whose ankle pressure remains normal, a nonvascular cause for their pain should be evaluated. Although an abnormal response to exercise confirms the presence of hemodynamically significant arterial disease, it does not exclude the possibility of coexistent neurospinal compression. The magnitude of the pressure drop should parallel the severity and location of the patient's symptoms. The ABI has also been helpful in determining the severity of vascular occlusive disease as described in previous chapters. Raines et al. [9] classified the PVRs into five categories, which, when combined with pressure data, were helpful in defining various clinical states of ischemia, e.g., claudication, rest pain, or foot necrotic lesions.

Anatomic localization of hemodynamically significant peripheral vascular lesions by noninvasive testing is another important contribution to patient management. It is important to note that laboratory findings and physical findings must be combined to localize a lesion accurately. One parameter (physiologic testing) is generally not sufficient. The case of combined disease (aortoiliac and femoropopliteal-tibial) is, by far, the most challenging. In 5–10% of patients with combined disease, noninvasive analysis, while defining the hemodynamics, cannot accurately localize the main contributing lesion. In these cases, an invasive femoral artery pressure study may be indicated. Localization of the disease is of critical importance; e.g., in the patient who has thigh and buttock pain secondary to a neurospinal compression and a well-collateralized, asymptomatic superficial femoral artery occlusion, both resting and postexercise ABIs may be appropriately abnormal. Yet, if the postexercise thigh pressure and the PVRs are normal, a nonvascular cause for the patient's symptoms is suggested. Furthermore, since angiography is notoriously inaccurate in assessing the

functional significance of iliac artery stenosis, some physiologic measurement of arterial inflow is essential before a distal bypass is constructed.

As described previously, the combination of the segmental Doppler pressures and the analog wave tracings could be helpful in the localization of peripheral vascular occlusive disease. However, determination of segmental pressure has certain limitations in patients with multilevel occlusive disease. In these patients, the proximal lesion might mask the distal disease; e.g., if both severe aortoiliac occlusive disease and femoral popliteal stenosis are present, the high-thigh pressure is low. The gradient between the high-thigh and the above-knee cuffs might be quite small, thus masking the disease present between these levels. Also giving a low high-thigh pressure is the combination of isolated, hemodynamically significant, superficial femoral and profunda femoral occlusive lesions. These problems in the interpretation of the pressure may be solved in one of several ways. A normal femoral pulse and the absence of an iliac bruit suggest a more distal arterial disease as the cause of the low high-thigh pressure. The common femoral artery pressure may also be obtained noninvasively using an inguinal compression device. This pneumatic device presses the artery against the superior pubic ramus, thus allowing the pressure to be measured as the compression is slowly released. The return of the arterial Doppler signal distal to the groin establishes the endpoint. Despite the presence of a normal iliac segment, monophasic waveforms may occasionally be seen in the common femoral artery when there is a combination of superficial femoral artery occlusion and severe deep femoral artery stenosis.

Other physiologic methods, which might help in differentiating aortoiliac occlusive disease from disease of the common femoral artery and/or disease of the superficial femoral artery and deep femoral artery, are the determination of the pulsatility index (PI) and the inverse damping factor. These were described in Chap. 21. Hemodynamically significant aortoiliac stenosis is unlikely if the femoral artery PI is greater than 6.0 at rest, whereas significant disease is probable if the PI is less than 5.0. When the value is between 5.0 and 6.0, the aortoiliac segment may be normal or abnormal, and further assessment is required by Doppler recording or direct pressure measurement after exercise or reactive hyperemia. Superficial femoral artery occlusion or severe stenosis is usually present if the inverse femoral popliteal damping factor is less than 0.9. A value between 0.9 and 1.1 may be normal or abnormal. When the inverse tibial damping factor is less than 1.0, significant tibial arterial occlusive disease is present.

Another hemodynamic method of determining the location of peripheral vascular occlusive disease relies on the amplitude of the calf pulse volume recording. With the use of a single large thigh cuff for lower extremity PVRs, the amplitude of the calf PVR is constantly increased relative to that of the thigh when the superficial femoral artery is patent. This finding is an artifact due to the relative volumes of the thigh and calf cuffs. Since the thigh cuff contains five to seven times more air than the calf cuff, segmental pulse volume changes that occur with each cardiac cycle result in relatively smaller pressure changes within the thigh cuff and, hence, relatively smaller thigh PVRs. Despite its basis in cuff artifact, calf augmentation is a reliable indicator of superficial femoral artery patency. If the amplitude of the calf PVR is equal to or only slightly greater than that of the thigh (less than 25%), and if there is an obvious deterioration in the contour of the waveform, superficial femoral artery stenosis or a short, well-collateralized occlusion should be suspected. For augmentation to occur, the superficial femoral artery must be patent to the origin of the sural artery in the midpopliteal region. When augmentation is noticed, but there is a 20 mmHg or greater decrease in the segmental pressure from the thigh to the calf, distal popliteal or proximal tibial artery occlusions are usually found [14].

Over the past two decades, duplex ultrasonography has been used more frequently for localizing and grading the severity of peripheral vascular disease with accuracies of greater than 90% [13, 15]. The first step prior to vascular intervention is segmental pressure determination, which is often followed by duplex mapping of the involved arteries.

If intervention is deferred, identified lesions can be followed to detect changes. If surgical intervention is chosen, a CTA or operating room angiogram with or without magnetic resonance angiography may provide a cost-effective solution, bypassing the need for formal preoperation angiography. If angioplastic intervention appears to be warranted, it is prudent to do it concurrently with the diagnostic study. A reasonable idea of lesion location and severity will help to make these practical decisions, along with the availability of ever improving operating room radiology apparatus.

Koelemay et al. [15] evaluated the value of duplex scanning in allowing selective use of arteriography in the management of patients with severe lower leg arterial disease. Management was based on duplex scanning and intraarterial subtraction angiography was performed only when indicated. A total of 125 limbs in 114 patients were evaluated (74% of which was for rest pain or tissue loss). In 97 (78%) of limbs, management was based on duplex scanning only. It compromised conservative treatment [number = 33, 0% after intraarterial digital subtraction angiography (DSA)], PTA (number = 25, 16% intraarterial DSA), femoropopliteal bypass graft (number = 29, 17% intraarterial DSA), femorotibial bypass graft (number = 29, 62% intraarterial DSA), and other surgical procedures (number = 8, 4% intraarterial DSA). Overall, the 30-day mortality rate was 4%, and the 2-year survival rate was 83%. The 2-year primary and secondary patency and limb salvage rates were 75%, 93%, and 93% after femoropopliteal bypass operations, respectively.

The 1-year primary and secondary patency and limb salvage rates were 35%, 73%, and 74%, respectively, after a femorocrural bypass operation. There was no difference in patient characteristics, indications for a specific treatment, and immediate and intermediate term outcome between the study and reference population. They concluded that management of patients with severe lower leg ischemia could be based on duplex scanning in most patients without a negative effect on clinical outcome, whether early or at 2-year follow-up.

## Prognosis and Medical Therapeutic Implications

Several noninvasive vascular tests, particularly the Doppler ankle pressures, have been applied to the study of the progression of peripheral vascular occlusive disease [16–20].

Wilson et al. in a study of nondiabetic patients with claudication who were followed for 5 years, reported that symptomatic improvement was likely without surgery when the ABI exceeded 0.60, but was unlikely when the ABI was less than 0.50 [17]. In patients with severe ischemia, Paaske and Tonnesen found that 82% of those with a toe pressure index (toe pressure divided by brachial pressure) of less than 0.07 underwent a major amputation within 2 years and 27% died [18]. These results indicate that toe pressures provide important information that can be helpful in making clinical decisions about the management of individual patients on a more rational basis.

Development of peripheral vascular occlusive disease in the second limb in patients with unilateral occlusive disease process is frequent [16]. The American Heart Association recognized that Doppler pressure measurements provide a sensitive index of arterial obstruction and can be performed repeatedly [20]. The brachial-ankle pressure difference was noted to correlate significantly with various risk factors of atherosclerosis, e.g., smoking, hyperlipidemia, and hypertension [21]. Several researchers noted that such measurements could also be used to quantitate the severity of the arterial sclerotic process and to evaluate the relationship to the factors that influence its progression. Ankle pressure measurements were used to estimate prevalence of peripheral arteriosclerotic disease and were applied to the study of the prevalence of atherosclerosis in patients with diabetes mellitus [22–24].

McLafferty et al. [25] reported that the ABI is relatively insensitive in identifying the progression of lower extremity arterial occlusive disease as demonstrated by the use of imaging studies. They studied patients with prior suprainguinal or infrainguinal lower extremity revascularization. Progression of lower extremity arterial occlusive disease in native arteries was determined by comparing a preoperative (baseline) arteriogram with late follow-up arteriography or duplex scanning. Progression of lower extremity arterial occlusive disease was defined as a decrease in the ABI of 0.15 or greater, and progression by imaging studies was defined as an increase in one category of stenosis. They concluded that in studies of natural history or therapy for atherosclerosis, imaging studies should be used in preference to the ABI to evaluate progression of lower extremity arterial occlusive disease more accurately [25].

Measurement of Doppler pressures can also be used to guide and evaluate medical therapy. Vasodilators have been noted to decrease digital blood pressure distal to occlusion and are probably not indicated, particularly in the presence of severe ischemia [26]. Meanwhile, clofibrate resulted in a significant improvement in the response of ankle pressure to exercise in patients with intermittent claudication and a high plasma fibrinogen level [27]. Quick and Cotton [28], in a study of patients with intermittent claudication, noted that cessation of smoking was followed by significant improvement in the walking distance, resting Doppler ankle pressure, and ankle pressures after exercise, whereas patients who continued to smoke showed no significant changes. Segmental pressure measurements have also been helpful in the management of patients with arterial obstruction secondary to ergotism that may regress spontaneously [29], and to assist in the treatment of severe ischemia with drug-induced systemic hypertension by monitoring distal systolic pressure [26].

## Correlation of ABI and General Atherosclerosis

Several studies have analyzed the correlation of ABI, general atherosclerosis, and cardiovascular and overall mortality. Reich et al. [30] conducted a study to determine whether elevated levels of inflammatory and hemostatic markers (von Willebrand factor [vWF], Fibrinogen, D-dimer, factor VII, factor VIII, PAI-1, tPA, beta-thromboglobulin [β-TG], C-reactive protein, and white blood count) are associated with an increased prevalence of PAD, as measured by a low ABI. They studied 13,778 participants from the Atherosclerosis Risk in Communities (ARIC) study in a cross-sectional analysis after adjustment for major cardiovascular risk factors. PAD was positively associated with fibrinogen, vWF, factor VIII, white blood count, D-dimer, β-TG, and C-reactive protein ($p$ for trend <0.05) but not with the other markers. They concluded that plasma levels of inflammatory and hemostatic markers are elevated in PAD, suggesting that these processes are involved in the pathophysiology of PAD.

Li et al. [31] analyzed the relationship of ABI with all causes of mortality and cardiovascular mortality in Chinese inpatients after 3 years of follow-up. A total of 3,210 patients were followed until an end point was reached. The mean

follow-up time was 38 months. Patients with an ABI of ≤0.4 were significantly older than other ABI categories ($p<0.001$) at baseline. The cardiovascular disease and all-cause mortality were highest (27.5% and 37.7%, respectively) after a 3-year follow-up in patients with an ABI ≤ 0.4. There was a significant increasing tendency in mortality with decreasing ABI levels ($p<0.001$). The Kaplan–Meier curves of survival showed a decreasing survival rate with the ABI decreasing, not only for all-cause mortality, but also for cardiovascular disease mortality ($p<0.001$). After an adjustment for other risk factors, patients with an ABI ≤ 0.4 were 3.1 times as likely to die as those with an ABI in the range of 1.00–1.4; patients with an ABI ≤0.4 were about five times as likely to die of cardiovascular disease as those with an ABI in the range of 1.00–1.4. Even patients with an ABI in the range of 0.41–0.90 were more than 1.5 times as likely to die, or die of cardiovascular disease (relative risk = 2.1) as those with an ABI in the range of 1.00–1.4. They concluded that a low ABI is related to a higher cardiovascular disease and all-cause mortality, compared with a normal ABI. ABI should be routinely evaluated as a marker of atherosclerosis to assess the risk of cardiovascular disease mortality.

A low ABI is associated with atherosclerosis and an increased risk of cardiovascular and cerebrovascular events. Screening for a low ABI can identify asymptomatic higher risk group potentially amenable to preventive treatments. Fowkes et al. [32] conducted a study to determine the effectiveness of aspirin in preventing events in people with a low ABI identified by screening the general population. The Aspirin for Asymptomatic Atherosclerosis trial was an intention-to-treat double-blind randomized controlled trial conducted from April 1998 to October 2008, involving 28,980 men and women aged 50–75 years living in central Scotland, free of clinical cardiovascular disease, recruited from a community health registry, and had an ABI screening test. Of those, 3,350 with a low ABI (≤0.95) were entered into the trial, which was powered to detect a 25% proportional risk reduction in events. A once daily dose of 100 mg of aspirin or placebo was given. The primary end point was a composite of initial nonfatal or fatal stroke, coronary event, or revascularization. There were two secondary end points: (1) all initial vascular events defined as a composite of a primary end point event or angina, intermittent claudication, or transient ischemic attack; and (2) all-cause mortality. After a mean follow-up of 8.2 years, 357 participants had a primary end point event (13.5 per 1,000 person-years). No significant difference was found between groups (13.7 events per 1,000 person-years in the aspirin group versus 13.3 in the placebo group; hazard ratio [HR], 1.03). A vascular event comprising the secondary end point occurred in 578 participants (22.8 per 1,000 person-years) and no significant difference between groups (22.8 events per 1,000 person-years in the aspirin group versus 22.9 in the placebo group; HR 1.00). There was no significant difference in all-cause mortality between groups (176 versus 186 deaths, respectively; HR 0.95). They concluded that among participants without clinical cardiovascular disease, identified with a low ABI based on screening of the general population, the administration of aspirin compared with placebo did not result in a significant reduction in vascular events.

Meves et al. [33] conducted a study of an open, prospective, cohort study in the primary care setting. A total of 6,880 unselected patients who were older than 65 years were categorized according to the absence or presence of PAD and followed up for vascular events or deaths over 5 years. PAD was defined as an ABI of <0.9 or history of previous peripheral revascularization and/or limb amputation and/or intermittent claudication. During the 5-year follow-up (29,915 patient-years), 183 patients had a stroke (incidence per 1,000 patient-years: 6.1 cases). In patients with PAD ($n=1,429$) compared to those without PAD ($n=5,392$), the incidence of all stroke types standardized per 1,000 patient-years with the exception of hemorrhagic stroke was about doubled (for fatal stroke tripled). The corresponding adjusted hazard ratios were 1.6 for total stroke, 1.7 ischemic stroke, 0.7 for hemorrhagic stroke, 2.5 for fatal stroke, and 1.4 for nonfatal stroke. They found that lower ABI categories were associated with higher stroke rates. Other than an advanced age, previous stroke, and diabetes mellitus, PAD was a significant independent predictor for ischemic stroke. They concluded that the risk of stroke is substantially increased in patients with PAD, and PAD is a strong predictor for stroke.

El-Manyar et al. [34] also reported on the relation of ABI and the extent of atherosclerosis in patients from the Middle East (the AGATHA-ME study) in a cross-sectional multicenter study. They concluded that the ABI is related to the risk factor profile and to the site and extent of atherosclerosis. Gender and diabetes mellitus were associated with the worst parameters.

## Perioperative Evaluation

Direct examination with the Doppler detector or duplex imaging has been applied preoperatively to determine whether there is a flow in the distal vessels, which may help to plan distal bypass operations in the calf.

Ascher et al. reported previously on the efficacy of duplex arteriography as the sole imaging technique (without contrast angiography) in the management of patients with chronic and acute lower limb ischemia [35, 36]. A reliable assessment of inflow and outflow arteries could be made with duplex ultrasonography, even in very low-flow situations [36]. Duplex arteriography is also an effective method for preoperative diagnosis of a thrombosed popliteal artery aneurysm and for identifying the available outflow vessels

for urgent revascularization. Duplex arteriography identifies the inflow, patent distal runoff vessels, and the presence of a suitable saphenous vein for revascularization.

Canciglia and Mandolfino [37] reported on the role of infrainguinal endovascular procedures based upon the results of duplex scanning. Their study included 120 arterial hemodynamic relevant lesions that were treated with endovascular therapy, 47 were localized in the aortoiliac segment, 55 in the femoro-popliteal segment, and 18 were infrapopliteal. A total of 107 out of 120 lesions (89%) were successfully dilated, 105 lesions (88%) predicted by preoperative duplex scanning were confirmed by contrast arteriography at the time of surgery. Intraoperative arteriography revealed an additional 15 lesions (12%). Duplex scanning had an accuracy and sensitivity of 86% in the selection of aortoiliac lesions for endovascular procedures, 91% for femoropopliteal lesions, and 78% for infrapopliteal lesions. They concluded that duplex scanning may be a safe alternative to contrast arteriography for patients with chronic limb ischemia. However, adequate training and experience is necessary to utilize this technique for the selection of patients for infrainguinal endovascular procedures.

Hingorani et al. [38] conducted a study of 906 patients who had 1,020 duplex arteriograms. Overall, 207 duplex arteriographies were done intraoperatively and the remainder were done preoperatively. The procedure that were done based on duplex arteriography included: endovascular procedures (363), bypass to an infrapopliteal artery (325), bypass to the popliteal artery (262), no intervention (75), inflow bypass procedures to the femoral arteries (46), thrombectomy (11), embolectomy (9), amputation (8), and debridement (4). The areas that were not well-visualized included: infrapopliteal (221), iliac (73) femoral (26), and popliteal (17). Additional imaging after duplex arteriography was necessary in 102 cases to obtain enough information to plan lower extremity revascularization. They concluded that in 90% of patients that were reviewed, duplex arteriography was able to obtain the necessary information for a lower extremity revascularization. Severe tibial vessel calcification is the most common cause of an incomplete duplex arteriogram and determines when alternative imaging modalities are needed.

Although routine intraoperative arteriography might detect intraoperative accident or inadequate vascular reconstruction, it is cumbersome and occasionally may be misleading since it provides visualization in only one plane. Noninvasive intraoperative physiologic monitoring provides an immediate, quantitative assessment of the success or failure of arterial surgery. Doppler ankle systolic pressures can be measured intraoperatively or immediately after surgery. Depending on the nature of the arterial reconstruction and extent of uncorrected distal disease, the postoperative change in the ABI will vary. However, if the ABI has not risen to 50% of preoperative levels within 1 h after declamping, the graft should be systematically checked for technical problems, and an intraoperative or immediate postoperative angiogram should be considered [39].

Segmental plethysmography or duplex imaging for intraoperative monitoring might be more practical than Doppler ultrasound because of the difficulty in preventing movement of the Doppler probe during operation. Also, some patients with multilevel disease arrive in the recovery room after successful aortofemoral bypass so vasoconstricted that no Doppler signal can be detected in the lower legs. In the recovery room, serial determination of the ABI or the PVRs provide objective evidence of the graft function. Since pulses are palpable in only 25% of patients, and their feet frequently remain cold and pale for several hours following surgery [40], such objective measurements provide nursing personnel with valuable parameters to monitor continued function of the vascular reconstruction.

Rzucidlo et al. [41] found that intraoperative completion duplex ultrasound may also predict early graft failure. They reviewed the results of intraoperative duplex scans that were selectively performed after completion of 45 tibial/pedal vein bypass grafts at high risk for failure. A 10-MHz low-profile transducer was used to scan the entire graft at bypass completion, and all grafts were determined to be technically adequate (absence of retained valves, arteriovenous fistulas, or localized velocity increases, and the presence of bypass-dependent distal pulses). Peak systolic and end diastolic velocities were measured at each anastomosis, in the outflow artery, and in the proximal and distal portions of each graft. Resistive indices were calculated at each measurement point (peak systolic velocity – end diastolic velocity/peak systolic velocity). Twenty infragenicular vein bypass grafts (44%) thrombosed within 12 months. Intraoperative hemodynamic parameters were significantly different between grafts that remained patent or thrombosed. The end diastolic velocity was lower ($5 \pm 1$ cm/s versus $13 \pm 3$ cm/s, $p = 0.02$) and the resistive index was higher (0.90 versus 0.81, $p < 0.01$) in the proximal portions of grafts that thrombosed within 12 months. The distal end diastolic velocity was also lower ($6 \pm 1$ cm/s versus $15 \pm 2$ cm/s, $p < 0.01$) and the distal resistive index was higher (0.89 versus 0.78, $p < 0.01$) in grafts that thrombosed. A multivariate analysis revealed that only a low distal end diastolic velocity was predictive of early graft failure ($p < 0.05$). A distal bypass end diastolic velocity of <8 cm/s was a predictor of early graft thrombosis with a sensitivity of 76% and a specificity of 75%. An absence of diastolic flow predicted early graft failure with a 100% specificity and 100% positive predictive value. They concluded that a low end diastolic velocity on the intraoperative duplex scan was associated with early thrombosis of tibial level vein grafts. When these values are observed, measures should be taken to improve graft hemodynamic parameters.

## Selection of the Arterial Reconstructive Procedure

### Choice of Treatment Based on Duplex Scanning

Based on duplex findings, patients found to have unilateral focal stenosis or short (<5 cm) occlusions of recent onset (less than 3 months) involving the common iliac or superficial femoral arteries should be considered for PTA (balloon angioplasty/stent with or without catheter-directed thrombolysis). Such treatment results in high (>95%) technical success and can yield clinical results similar to those following surgical intervention. When duplex scanning indicates features of more extensive disease, the use of PTA is possible, but to date endovascular treatment does not yield long-term patency comparable to bypass grafting, especially in treatment of long arterial occlusions. PTA of these lesions should be considered only for patients with critical ischemia who are deemed a surgical risk, or patients with unfavorable anatomy for bypass grafts, or in the absence of a suitable autologous vein for use as a bypass conduit.

Most patients with critical limb ischemia have multilevel occlusive disease and require additional vascular imaging studies (contrast arteriography, magnetic resonance angiography) beyond that afforded by duplex scanning. Duplex scanning can be used to determine whether iliac angioplasty is feasible for patients with combined aortoiliac and infrainguinal disease [42, 43]. The surgeon can then decide whether to proceed with a staged iliac PTA followed by distal bypass or perform a simultaneous inflow/outflow revascularization. For patients with unilateral or contralateral absence of femoral pulses and long-segment arterial occlusion by duplex imaging, proceeding with aortofemoral, femorofemoral, or axillofemoral bypass grafting without arteriography is appropriate. In treatment of infrainguinal disease, surgical intervention (endarterectomy, bypass grafting) without arteriography is possible in selected patients with single segment occlusive or aneurysmal disease. Femoral endarterectomy with or without profundaplasty, femoropopliteal bypass grafting, and repair of femoral or popliteal aneurysms can be performed based on duplex scan findings. If imaging of the distal vessels is not optimal, intraoperative arteriography can be performed to exclude downstream lesions. Patients with arteriomegaly and diffuse atherosclerosis with multiple tibial artery involvement should undergo preoperative CTA or arteriography prior to bypass grafting.

### Aortofemoral Popliteal Reconstruction

Garrett et al. suggested that if the ABI does not increase by 0.1 or more immediately following aortofemoral bypass, concomitant distal bypass should be considered [44]. However, other authors have noted that the immediate index was the same or actually lower than the preoperative value in some of their patients with multilevel disease who subsequently improved significantly over the next 4–6 h [45], thus seriously challenging the validity of this observation. Studies by Dean et al. indicate that 90% of femoral popliteal grafts inserted in limbs with an ABI of less than 0.20 failed in the early postoperative period [46]. This merely reflects the adverse effect of high runoff resistance of graft patency. Nevertheless, a few patients with an ABI less than 0.20 will obtain satisfactory results. A successful outcome can be expected in limbs with a preoperative ABI of greater than 0.50 [47].

Others reported the importance of the pressure measurements in the assessment of patients prior to vascular surgery or angioplasty, in the immediate and long-term follow-up after the procedures, and in the objective evaluation of the results [48, 49].

### Profundaplasty

The segmental systolic pressure determination can also be helpful in determining whether profundaplasty is successful or not. When performed for limb salvage, profundaplasty as an isolated procedure is effective in 33–86% of cases [50]. For a profundaplasty to be successful, the profunda femoris artery must be severely stenotic, and the profunda-popliteal collateral bed must be well developed. If the collateral resistance is too high, profundaplasty will reduce the total limb resistance by an insufficient amount, and the distal portions of the limb will remain ischemic. To predict the outcome of profundaplasty, Boren et al. developed an index of collateral arterial resistance across the popliteal segment [50]. This index is calculated by dividing the gradient across the knee (above-knee pressure minus below-knee pressure) by the above-knee pressure. When the index was less than 0.25, successful results were obtained in 67% of cases; but when the index was greater than 0.50, there were no successful results.

### Lumbar Sympathectomy

With the advances in endovascular therapy, lumbar sympathectomy is rarely done nowadays for critical limb ischemia. Sympathectomy does not relieve claudication and is performed only as a means of improving the skin blood flow in ischemic areas. Although pressure measurement does not directly indicate the magnitude of the local blood flow, the level is correlated with the ability of the peripheral arteries to dilate. The arterioles tend to be maximally dilated in ischemic tissues. When the perfusion pressure is quite low, this

dilatation is necessary to maintain adequate tissue nutrition. Sympathectomy might also be questionable in patients with diabetes mellitus in which a significant number of patients had autosympathectomy; hence, the objective evidence of sympathetic activity in the terminal vascular bed is important.

During deep inspiration, an individual with normal sympathetic activity has a prompt decrease in digital pulse volume [51]. This can be documented using a mercury-in-silastic strain gauge or the PVR. Another important point is whether the resistance vessels in the affected extremity are capable of further vasodilation. This can be answered by demonstrating a doubling of the resting digital pulse volume following the reactive hyperemia test (a 5-min period of ischemia induced by inflating a proximal pneumatic cuff above the systolic pressure) or by direct warming of the extremity. In normal extremities, the pulse volume after induced reactive hyperemia is several times that of the resting pulse, thus reflecting the ability of the peripheral arterioles to dilate further. This effect can be demonstrated even in the presence of proximal arterial occlusive disease.

Yao and Bergan [52], in a study of patients with ischemic rest pain and pregangrenous changes of the foot who were not candidates for reconstructive surgery and who underwent lumbar sympathectomy, reported that 96% of limbs with an ABI below 0.21 failed to benefit from lumbar sympathectomy and required amputation. All limbs with an ABI greater than 0.35 had a satisfactory response. Walker and Johnston [53] observed that sympathectomy was unlikely to be successful in an ischemic limb with associated neuropathy, regardless of the level of the ankle pressure. In the absence of neuropathy, a successful outcome was likely in limbs with rest pain or digital gangrene, provided that the ankle pressure exceeded 30 mmHg. Their analysis suggested that a favorable response might be expected in about 50% of limbs with more severe ischemia (forefoot or heel gangrene) when the ankle pressure was greater than 60 mmHg. Using these criteria, their accuracy in predicting failure was 78%, and in predicting success was 93%.

In a prospective study of 85 lumbar sympathectomies for inoperable peripheral vascular disease, we analyzed the correlation between lumbar sympathectomy, ABI, popliteal-brachial index, and the clinical presentation. These patients were also studied to determine if predicted clinical criteria, single or combined, could be defined for selection of patients who might benefit from lumbar sympathectomy. Good results were obtained if at 6 months after surgery pain at rest was absent, ischemic ulcers had healed, and there were no major amputations. In this study, 77% of all limbs with a preoperative ABI ≥ 0.3 had a good outcome in contrast to a 94% failure for an index of <0.3 ($p < 0.001$). Sixty-nine percent of all limbs with a popliteal-brachial index ≥0.7 had a good outcome versus 52% if the index was <0.7 ($p = 0.199$). Patients with rest pain, simple leg ulcers, and toe gangrene had a good outcome if the ABI was ≥0.3 and if the postoperative ABI increased by ≥0.1. The popliteal-brachial index and diabetic status had no prognostic value [54].

Tiutiunnik [55] studied the microcirculation state in lower extremities using laser Doppler flowmetry in 37 patients with obliterating atherosclerosis before and after lumbar sympathectomy performance. It was established that laser Doppler flowmetry may be applied for estimation of the microcirculation bed function state and prognosis of the lumbar sympathectomy results [55].

In general, patients with an ABI of greater than 0.25% have a favorable response to lumbar sympathectomy. However, patients with indices even higher than that might fail to respond and eventually might require amputation, thus demonstrating that other factors such as infection, neuropathy, and patency of the pedal vessels might adversely affect the outcome.

## Postoperative Follow-Up

The vascular laboratory has also been helpful in detecting impending graft failure [56, 57]. Stenoses may develop in the femoropopliteal or femorotibial graft without producing any symptoms or alteration in the pulses of the graft or at the periphery. These silent stenoses, which often evolve into total occlusion, can be detected if the ankle pressure is followed closely in the months and years after operation. Close observation is particularly important during the first year, since about 75% of such events occur within this period. A previously stable ABI that drops by 0.20 or more suggests the need for arteriographic investigation [39]. As a rule, operative correction is easy and the ankle pressure often returns to normal levels.

Over the past decade, duplex ultrasound has been frequently used for postoperative graft surveillance, described in detail in Chaps. 24 and 25. If one waits for a significant change in ABI or segmental pressures, the golden opportunity to correct a stent or graft while still patent may be lost. Waiting for thrombosis and then doing a secondary procedure carries a reduced chance for long-term success.

Duplex ultrasound can also be used to guide PTA of failing infrainguinal bypass grafts. Marks et al. [58] reported their experience in duplex guided balloon angioplasty of failing infrainguinal bypass grafts in 25 patients. The site of the most significant stenotic lesion was in the conduit in 18 cases, at the outflow in 11 cases, and at the inflow in four cases. All arterial (20) or graft (13) entry site cannulations were performed under direct duplex visualization. Duplex scanning was used to manipulate the guide wire and directional catheters from the ipsilateral common femoral artery to a site beyond the most distal stenotic lesion. Selection and

placement of balloons and stents were also guided by duplex. In 11 cases (33%), the contralateral common femoral artery was used as the entry site and a standard approach (fluoroscopy and contrast material) was employed. Completion duplex exams were obtained in all cases. The overall technical success rate was 97% (32/33 cases). In only one case, the outflow stenotic lesion in the plantar artery could not be traversed with the guidewire due to extreme tortuosity. The overall local complication rate was 6% (two cases), and the overall 30-day survival rate was 100%. The overall 6-month limb salvage and primary patency rates were 100% and 69%, respectively. They concluded that the duplex-guided endovascular therapy is an effective modality for the treatment of failing infrainguinal arterial bypasses.

## Healing Response

### Ischemic Skin Lesions

Skin ulcers of the lower extremities may be arterial, venous stasis, neuropathic (e.g., diabetic), or occasionally related to other systemic causes. Raines et al. [9] suggested that healing of ischemic ulcers was likely in nondiabetic patients at an ankle pressure >65 mmHg, and in diabetic patients if the ankle pressure was >90 mmHg. Healing was unlikely if the ankle pressure was <55 mmHg in nondiabetic patients and <80 mmHg in diabetic patients. They also emphasized the importance of the forefoot or digital plethysmography, stating that if a pulsatile, metatarsal PVR was present, the probability of healing was 90%. Carter reported that all limbs with ischemic ulcers required amputation when the ankle pressure was <55 mmHg [59]. With pressures >55 mmHg, 92% of the lesions in nondiabetics healed. In diabetics, 33% healed with an ankle pressure in the 55–70 mmHg range. He also found that foot lesions usually healed if the toe pressure was >30 mmHg in nondiabetics or 55 mmHg in diabetics. Ramsey et al. [60] reported that toe pressures had more prognostic value than ankle pressures. Lesions failed to heal in 92% of limbs with an ankle pressure <80 mmHg, but they also failed to heal in 45% of limbs with higher ankle pressures. When the toe pressure was <30 mmHg, the failure rate was 95%; but when the toe pressure was >30 mmHg, only 14% did not heal.

These figures can help the vascular surgeon decide what therapy to use in patients with ulceration, e.g., revascularization, amputation, or conservative therapy. For example, continuing to dress and debride an ulcer on the foot of a patient with diabetes and a toe pressure of 20 mmHg or an ankle pressure of 45 mmHg is probably a futile exercise; but this same regimen is likely to be valuable when the toe pressure is >30 mmHg. These figures also serve to point out the beneficial effects that a relatively small increase in ankle pressure can have in regard to skin healing. If, for example, an iliac reconstruction or profundaplasty raises the ankle pressure only 20 mmHg, from 50 to 70 mmHg, or the toe pressure from 20 to 35 mmHg, the chance of healing an ischemic lesion may be greatly enhanced, despite the persistence of severe femoropopliteal or below-knee lesions.

Measurement of transcutaneous oxygen tension can be used to predict wound healing. Ruangsetakit et al. [61] in a prospective study, investigated the threshold of transcutaneous oxygen tension (TcPO(2)) values in predicting ulcer healing in patients with critical limb ischemia. The study included 50 patients who had critical limb ischemia with chronic ischemic ulcers or gangrenous toes. Baseline ulcers were measured using a wound measurement system (Visitrak, Smith & Nephew). TcPO(2) was measured at rest in the supine position and with a 30° leg elevation. Infective and ischemic ulcers were debrided and gangrenous toes were amputated. Ulcer outcome was classified as: (1) a healing ulcer showing good epithelialization or granulation at both base and edges, or a decrease in ulcer area during the study; or (2) a nonhealing ulcer showing poor granulation tissue formation or a pale base and necrotic edges, or deterioration in an ischemic ulcer. The mean ABI was $0.75 \pm 0.39$. Thirteen patients (26%) had a TcPO(2) of <20 mmHg, of which none showed any improvement in ulcer healing ($p < 0.001$). Fifteen patients (30%) had a TcPO(2) of >40 mmHg, of which all progressed to complete ulcer healing ($p < 0.001$). In the 20–40 mmHg group (22 patients, 44%), ten patients (45%) had a TcPO(2) drop of <10 mmHg with leg elevation of 30°, of which eight achieved complete ulcer healing ($p < 0.001$). Twelve patients (55%) had a TcPO(2) drop of >10 mmHg with leg elevation of 30°, of which 11 showed no ulcer healing ($p < 0.001$). They concluded that a TcPO(2) measurement is noninvasive, accurate, and a good predictor of ischemic ulcer healing for cutoff TcPO(2) values of <20 mmHg and more than 40 mmHg. In addition, the leg elevation method for TcPO(2) might provide an important adjunct in the assessment of patients with borderline values.

Open venous ulcers in patients with combined arterial and venous insufficiency are difficult to treat. Adequate compression therapy is contraindicated in patients with an ABI of <0.7, and patients with an ABI of 0.5–0.8 have been shown to heal poorly. Lantis et al. [62] decided to undertake an aggressive approach of percutaneous revascularization for these patients. Twenty-seven patients with clinical and duplex scan evidence of chronic venous insufficiency, active leg ulcers, and impaired arterial perfusion (ABI of <0.7) were treated using a protocol that required performing percutaneous revascularization before ambulatory compression therapy. Patients were followed at 2-week intervals before and after revascularization. Wound measurements and time to complete closure were also recorded. The patients' healing rates were compared to previously published rates of

impaired arterial perfusionvenous wound closure; 25% closure at 10 weeks and 50% at 19 weeks. At the time of enrollment, the average ABI and wound sizes were 0.56 and 12 $cm^2$, respectively. On average, the wounds had remained open for 17 weeks. After the intervention, the average ABI was 0.97, average time taken to complete closure was 10 weeks, closure rate at 10 weeks was 75%, and absolute closure rate was 100%. They concluded that although previous studies have shown that closure of mixed arterial venous ulcers occur without arterial intervention, attaining a near normal ABI allows for a timelier wound closure. Therefore, they advocate an aggressive approach of percutaneous revascularization in this population.

## Amputation Sites

The selection of amputation site can make the difference between a bed or wheelchair existence versus successful prosthetic rehabilitation. A successful amputation must remove all necrotic or infected tissue, and it must be possible to fit the amputation stump with a functional and easily applied prosthesis with a good blood supply at the level of the proposed amputation to allow primary healing. This, particularly, is very critical when it comes to a mid-thigh amputation versus a below knee amputation, which deprives the patient of the opportunity for subsequent ambulation under most circumstances, even though the amputation might heal without difficulty if an above knee amputation is done. On the other hand, if a distal amputation site, e.g., a below knee, is selected and the blood supply is inadequate, this will necessitate further surgery with higher morbidity and mortality. A below-knee amputation as opposed to above-knee amputation has several advantages including making it easier to ambulate, a consideration that is extremely important in older patients. In most series, older patients who undergo unilateral below knee amputation show a >90% success rate of rehabilitation to ambulation in contrast to only 30% for patients with above knee amputations.

The presence of pulses in the affected lower extremity, or nonobjective assessment of skin temperature based on clinical judgment, or clinical judgment alone, does not yield information with consistent enough correlation to amputation healing to serve as a sound basis for clinical decision making. Robbs and Ray [63] retrospectively analyzed the results of healing in 214 patients who underwent lower limb amputation in which the amputation level was determined by such objective criteria. They reported a failure rate of 9% for above-knee amputation in contrast to 25% for below-knee amputation. They concluded that skin flap viability could not be predicted by the extent of the ischemic lesion in relation to the ankle joint, the popliteal pulse status, or angiographic findings. van Den Broek et al. [64] challenged these findings in recent reports in which 53 patients undergoing amputations of the lower limb were evaluated in terms of clinical criteria, PVR, Doppler pressures, photoplethysmographic skin perfusion pressures, and angiography. They reported that although not as reliable as photoplethysmographic skin perfusion pressures, angiographic findings correlated significantly with the success of healing.

Various noninvasive methods were described to assess the level of amputation sites. These included Doppler ankle and calf systolic blood pressure measurements with or without PVR [65–67], xenon-133 skin blood flow studies [68, 69], digital or transmetatarsal photoplethysmographic pressures [70], transcutaneous oxygen determination [71–73], skin fluorescence after the intravenous infusion of fluorescent dye [74–76], laser Doppler skin blood flow [77], skin temperature evaluation [78], pertechnetate skin blood pressure studies [79, 80], and photoelectrically measured skin color changes [81]. Transcutaneous oxygen pressure will be described in detail in a later chapter.

### Skin Fluorescence

Skin fluorescence holds significant promise as a minimally invasive test. Initial studies measured skin fluorescence with a Wood's ultraviolet light after the intravenous injection of fluorescence. This technique is somewhat more invasive than the Doppler ankle systolic pressure measurement or PVR, however, it is less complicated and less invasive than xenon-133 skin blood flow or pertechnetate skin perfusion measurement. New fluorometers that can provide objective numerical readings quickly without the need for a Wood lamp have enhanced the value of this technique. Silverman et al. [82] reported on the use of fiber-optic fluorometry for selecting digital, transmetatarsal, below-knee, and above-knee amputation levels. In 86 cases with cellulitis at the site of amputation, preoperative fluorometry clearly distinguished between healing and nonhealing sites. The amputation healed in all but one patient whose dye fluorescence index was >42. This technique maintained its high accuracy even in patients with diabetes mellitus. These authors pointed out that dye fluorescence index values between 38 and 42 constitute a transitional zone in which the precision of fluorometric determination is unclear. Fluorometry has an advantage over other techniques such as laser Doppler perfusion and transcutaneous oximetry in assessment of patients with multiple sites on the same limb.

### Doppler Systolic Pressure Determinations in Amputation Sites

Raines et al. [9] reported that primary healing of below-knee amputation was likely if the calf pressure was above 65 mmHg or the ankle pressure was above 30 mmHg. Healing was unlikely if the calf pressure was <65 mmHg or the ankle pressure was <30 mmHg. Transmetatarsal amputation will generally heal primarily if any detectable amplitude is present at the transmetatarsal level. Toe amputation has a very good

prognosis for healing if an amplitude is measurable at the digit base. Others reported that in patients with a calf systolic pressure of 50–75 mmHg, primary healing of below-knee amputations can be expected in 88–100% [83]. However, in another study Barnes et al. concluded that there was no significant difference in the mean blood pressure between the groups with healed and failed amputations, regardless of the level of pressure measurement, and observed healing in 90% of below-knee amputations in extremities with unobtainable pressure at the below-knee or ankle levels [66].

Verta et al. [84] reported that there was little chance that toe amputations would heal if the ankle pressure was <35 mmHg. However, Nicholas et al. [67] noted failure of 60% of forefoot amputations when the ankle pressure was <75 mmHg. Thus, a low-ankle pressure appears to be an ominous sign. High-ankle pressure, on the other hand, does not signify a favorable prognosis, since this high pressure could be secondary to arterial calcification and might not reflect the presence of pedal or digital arterial obstruction. Consequently, failure of toe amputations or transmetatarsal amputation is not unusual, even when the ankle pressure exceeds 100 mmHg [66, 85].

In general, a calf pressure >40 mmHg or an ankle pressure above 30 mmHg provides reasonable assurance that the below-knee amputation will heal, but lower values should not deter the surgeon from attempting an amputation at this level if other signs are favorable.

Apelquist et al. [65] reported on the value of systolic ankle and toe pressure measurements in predicting healing in patients with diabetic foot ulcers and presented data for both patients who underwent amputation and those who did not. Primary healing was achieved in 85% of patients with a toe pressure of >44 mmHg, whereas 63% of patients with toe pressures of <45 mmHg experienced healing without amputation. In contrast, below-knee amputations with ankle pressures in excess of 80 mmHg were associated with healing, and 20 of 21 of these patients who underwent amputation had toe pressures in excess of 50 mmHg. They concluded that different Doppler pressure levels have to be used to predict primary healing for diabetic ulcers compared to healing after minor amputation.

## Compression Syndromes

Vascular laboratory testing can be helpful in thoracic outlet syndrome [86–88] and popliteal artery entrapment [89, 90].

## Thoracic Outlet Syndrome

Thoracic outlet syndrome occurs when there is a compression of the neurovascular bundle by shoulder structures that may include the cervical rib, costoclavicular space, or scalene muscle. The symptoms of this syndrome generally include numbness or tingling of the arm and pain or aching of the shoulder and forearm. Exercise and upward arm positions can increase the symptoms [86]. It should be noted that around 25% of the population have asymptomatic compression.

Most authorities believe that the pain associated with thoracic outlet syndrome is neurogenic, secondary to nerve compression at the lowest trunk of the brachial plexus by the first rib or occasionally a cervical rib. The subclavian artery or vein is occasionally compressed, and this might be associated with arterial ischemia of the upper extremity or symptoms and signs of axillary subclavian vein thrombosis.

Various noninvasive techniques can be used in the diagnosis of thoracic outlet syndrome, which may include plethysmographic techniques and/or Doppler waveform analyses to detect vascular changes. The photoplethysmograph (PPG) is attached to the index finger, or the continuous wave Doppler is used to monitor the radial artery, or a brachial cuff is applied to monitor plethymographic pulse volume waveforms. Resting waveforms are obtained, and then the patient's arm is placed in various positions as the pulsations are monitored at each position. The following technique is applied for the application of PVR in patients with thoracic outlet syndrome.

The patient is first asked to sit erect on the side of an examining table. A PVR monitoring cuff is placed on the upper arm and is inflated to 65 mmHg. Recordings are taken in the following positions: (1) erect, with hands in lap; (2) erect, with arm at a 90° angle in the same plane as the torso; (3) erect, with arm at a 120° angle in the same plane as the torso; (4) erect, with arm at a 90° angle in the same plane as the torso, with the shoulders in extended military-type brace; (5) the same position as in (4), but with head turned sharply toward the monitored arm; and (6) the same position as in (4), but with the head turned sharply away from the monitored arm.

In general, PVR amplitude increases as the arm is elevated. Arterial compression is present if the PVR amplitude goes flat in any of the above positions. However, many asymptomatic patients (around 25%) may have a positive test in some of the positions outlined. Since the syndrome is often bilateral, the other arm should always be studied.

Duplex imaging with or without color can also be used to aid in the diagnosis of thoracic outlet syndrome where both axillary subclavian arteries or veins can be imaged at resting and at various maneuvers as described above.

Wadhwani et al. [88] studied color Doppler sonographic findings in five clinically suspected cases of thoracic outlet syndrome. The subclavian artery and vein were studied in varying degrees of abduction to assess the severity of the syndrome. Significant changes, including increased velocities, preocclusion, and occlusion in the subclavian artery in varying degrees of abduction, were noted in four of five

cases. Blunted flow in the axillary artery (four patients) and a rebound increase in velocities on release of abduction were noted in three patients. These changes suggested that significant narrowing was causing symptoms. They concluded that color Doppler sonography is a noninvasive, effective method compared with digital subtraction angiography in the diagnosis of thoracic outlet syndrome.

Gillard et al. [87] evaluated the diagnostic usefulness of provocative tests, Doppler ultrasonography, electrophysiological investigations, and helical computed tomography (CT) angiography in thoracic outlet syndrome. They prospectively evaluated 48 patients with clinical suspicion of thoracic outlet syndrome. Standardized provocative tests such as an electromyogram and somatosensory evoked responses, a Doppler ultrasonogram, and a helical CT arterial and/or venous angiogram with dynamic maneuvers were done on each patient. The final diagnosis was established by excluding all other causes based on all available data. The agreement between the results of each investigation and the final diagnosis was evaluated. Provocative tests had mean sensitivity and specificity values of 72% and 53%, respectively, with better values for the Adson test [positive predictive value (PPV), 85%], the hyperabduction test (PPV, 92%), and the Wright test. Using several tests in combination improved specificity. Doppler ultrasonography visualized vascular parietal abnormalities and confirmed the diagnosis in patients with at least five positive provocative tests. Electrophysiologic studies were useful mainly for the differential diagnosis in detecting concomitant abnormalities. It was concluded that although helical CT angiography provided accurate information on the locations and mechanism of vascular compression, the usefulness of this investigation for establishing the diagnosis of thoracic outlet syndrome and for obtaining pre-therapeutic information remains unclear.

## Popliteal Artery Entrapment Syndrome

Ischemic pain with exercise (running, not walking) may occur because of intermittent compression of the popliteal artery by the medial head of the gastrocnemius muscle [89]. In such cases, the popliteal artery passes medial to or through the fibers of the medial head of the gastrocnemius muscle, which may have an anomalous origin on the femur either cephalad or lateral to its normal position on the posterior surface of the medial femoral condyle. This will cause episodic and functional occlusion of the popliteal artery that occurs with each active plantar flexion. The syndrome may be characterized by a history of unilateral intermittent claudication in young men and the laboratory findings of diminution of ankle PVRs with sustained plantar flexion and/or passive dorsiflexion of the foot or abnormal Doppler pulse waves with decreased ankle systolic pressure [89]. The demonstration of the medial deviation of the popliteal artery on arteriogram will confirm it. Popliteal artery entrapment syndrome can also be induced during reconstruction of femoral popliteal bypass, and this can also be detected by using PVR. Duplex ultrasound can also be helpful in the diagnosis of this syndrome [90].

## Penile Circulation

Impotence can be psychogenic, neuorogenic, hormonal, vascular, or drug-related. Diabetes mellitus is often a factor in both neurogenic and vasculogenic impotence. Doppler evaluation in erectile dysfunction has a significant role in determining the cause of erectile dysfunction. The advantages of penile Doppler and pharmacologic duplex ultrasonography include objective, minimally invasive evaluation of penile hemodynamics at a relatively low cost. Various parameters, such as diameter of the cavernosal artery, peak systolic flow velocity, degree of arterial dilatation and acceleration time, have been suggested for the diagnosis of arteriogenic erectile dysfunction, but peak systolic flow velocity is the most accurate indicator of arterial disease [91]. Doppler penile pressure studies are helpful in identifying a possible vascular cause [92]. Similarly, plethysmography has been used effectively to quantitate penile blood flow [93].

A pneumatic cuff measuring 2.5 cm in width (2.5 × 12.5 cm or 2.5 × 9 cm) is applied to the base of the penis. A return of blood flow when the cuff is deflated can be detected by a mercury strain-gauge plethysmograph, a photoplethysmograph applied to the anterolateral aspect of the shaft, or a Doppler flow probe (Fig. 35.1). Although some investigators have positioned the probe over the dorsal penile arteries, others have emphasized the importance of detecting flow in the cavernosal artery. Because the penile blood supply is paired, an obstruction may occasionally be limited to only one side. It has been recommended that the pressures be measured on both sides of the penis [94]. In normal individuals under 40 years of age, the penile-brachial index (penile pressure divided by the brachial systolic pressure) was found to be 0.99 ± 1.15 [92].

Patients over the age of 40 years without symptoms of impotence tend to have lower indices. Penile-brachial indices >0.75–0.8 are considered compatible with normal erectile function; an index of <0.60 is diagnostic of vasculogenic impotence [92, 95].

Knowledge of the penile pressure can be used to guide the surgeon in planning the operative approach to aneurysmal or obstructive occlusive disease of the aortoiliac segment. Maintenance of blood flow to the internal iliac artery will preserve potency and restoration of flow to this artery and will often improve penile pressure and erectile function.

**Fig. 35.1** Method for measuring the penile Doppler pressures using a Doppler flow probe on the dorsal penile artery

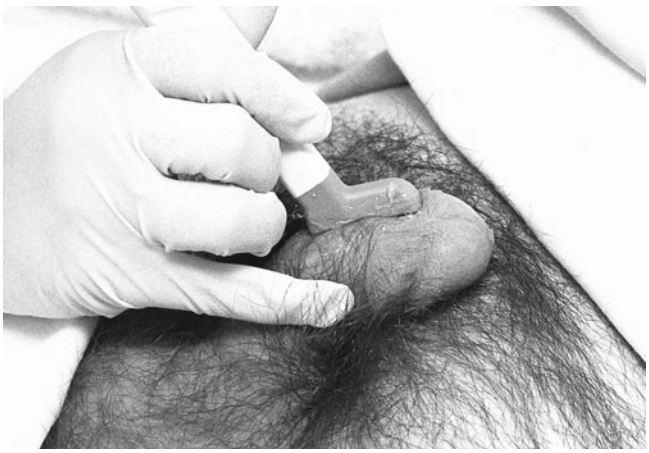

**Fig. 35.2** Position of the scan head (duplex ultrasound) for examination of the cavernous artery. Notice the scan head is positioned on the ventral aspect of the penis

However, Mahe et al. [96] found that a normal penile pressure cannot rule out the presence of lesions on the arteries supplying the hypogastric circulation in patients with arterial claudication. They evaluated the diagnostic accuracy of the penile brachial index (PBI) <0.60 to investigate arteriographic lesions on arteries supplying the hypogastric circulation in 88 male patients referred for Fontaine stage II. A ROC curve was used to define the diagnostic performance of the PBI and search for a specific cutoff point in this population. The accuracy for detecting an arterial stenosis or occlusion on at least one side was 69%. A PBI of ≤0.45 had a sensitivity of 74% and a specificity of 68% in discriminating the 19 patients with bilateral arterial occlusion from the other 66 patients. They concluded that the PBI is relatively insensitive for the detection of proximal abnormal blood flow impairment, except in cases of bilateral occlusion of the arteries supplying the hypogastric circulation in patients with claudication.

Inuzuka et al. [97] conducted a study to assess the pelvic circulation during endovascular abdominal aortic aneurysm repair (EVAR) with a new monitoring system measuring penile and buttock blood flow. They measured the PBI during EVAR by pulse-volume-plethysmography. They also measured bilateral gluteal tissue oxygen metabolism with near-infrared spectroscopy to provide a gluteal tissue oxygenation index. They studied 22 men who underwent aorto-uni-iliac stent graft with crossover bypass for exclusion of abdominal aortic aneurysms. Twelve patients underwent aorto-uni-common iliac artery stent graft and ten underwent aorto-uni-external iliac artery stent graft. They reported an immediate reduction in the PBI during the EVAR procedure in all patients. After revascularization of the ipsilateral limb of the stent graft, the recovery of the PBI was significantly less in the aorto-uni-external iliac artery stent graft group. After completion of the crossover bypass, the PBI returned to baseline values. There was a bilateral reduction in gluteal tissue oxygenation index during malperfusion of the internal iliac artery in both groups. After revascularization of the ipsilateral limb of the stent graft, the ipsilateral tissue oxygenation index returned to the baseline level in the aorto-uni-common iliac artery stent graft patients, but recovery was incomplete in the aorto-uni-external iliac artery stent graft patients. In contrast, the contralateral tissue oxygenation index remained low in both groups after revascularization of the ipsilateral limb of the stent graft. Only after completion of crossover bypass did the contralateral tissue oxygenation index recover to the baseline level in both groups. They concluded that both the tissue oxygenation index at the buttocks and the PBI are a sensitive reflection of pelvic hemodynamics. Penile blood flow and bilateral gluteal blood flow are supplied via different circulations and both should be monitored for full assessment of the pelvic circulation.

## Duplex Imaging Techniques for Penile Circulation

Duplex imagings can be used to assess penile circulation as follows. The cavernous arteries are measured bilaterally in an A/P transverse orientation. Color Doppler imaging is also a sensitive means of detecting cavernous artery blood flow, thus permitting more rapid identification of these vessels (Figs. 35.2 and 35.3) [98]. The examiner measures the PSVs in the dorsal and cavernous arteries bilaterally (Figs. 35.4 and 35.5). This is followed by injections of specific medications, e.g., papaverine and/or prostaglandin by the urologist utilizing the lateral aspect of the proximal shaft of the penis (Fig. 35.6). Repeat velocity measurements are obtained postinjection. These can be measured at 1 or 2 min after injection; multiple measurements may be obtained at various increments for up to 6 min after the injection. PSV and end-diastolic velocity measurements are obtained from the proximal cavernous arteries before full erection is achieved. This

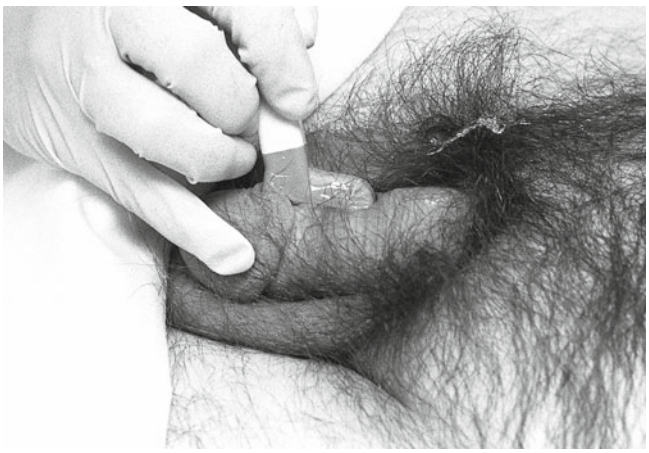

**Fig. 35.3** Position of the scan head to show the dorsal penile artery. Notice the position of the scan head on the dorsal aspect of the penis

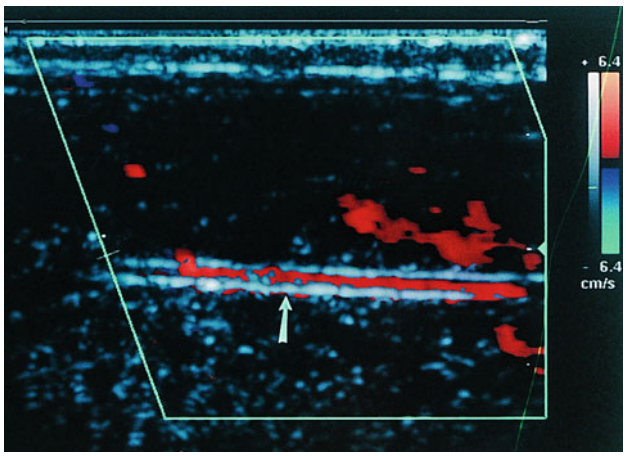


**Fig. 35.4** A color duplex image of the cavernous artery. Please note the color flow as indicated by the *arrow*

may require taking several measurements to obtain the highest velocity recording. The deep dorsal vein flow velocity is also measured from a dorsal approach, with light probe pressure. The dimensions of the cavernous arteries are also measured in the A/P and transverse views during systole. The examiner should observe the time elapsed since injection and document when velocities are recorded.

It has been noted that PSVs generally increase after injection: a normal velocity is equal to or greater than 30 cm/s, 25–29 cm/s is a marginal value, and <25 cm/s is considered an abnormal velocity. To be noted, since the time when the highest PSV is reached after injection varies among individuals, it is imperative to obtain serial measurements. These velocities may occur 5, 10, 15, or 20 min after injection, with a nearly equal distribution. Postinjection, the deep dorsal venous flow velocity should not increase with the following criteria to be followed: normal, <3 cm/s; moderate increase, 10–20 cm/s; and markedly increased, >20 cm/s. It has been suggested that an increase to >4 cm/s may indicate a venous leak, which could contribute to the erectile dysfunction. The diameter of the cavernous arteries normally increases (dilates) after injection.

Measurement of PSVs in the cavernousal arteries after intracavernousal injection currently appears to be the best ultrasound approach for evaluating patients with suspected arteriogenic impotence [98–100].

Several other studies recently reported on the value of color duplex ultrasonography in the diagnosis of vasculogenic erectile dysfunction [101–105].

Roy et al. [103] conducted a study to evaluate the role of duplex sonography for flaccid penis and the potential role in the evaluation of impotence. Their goal was to assess the potential value of PSV measurements on the flaccid penis in the diagnosis of arteriogenic impotence. Forty-four men underwent duplex Doppler sonography with peak systolic measurements before and after intracavernous injection of prostaglandin E(1). Three different cutoff values for lowest normal PSV before injection—5, 10, and 15 cm/s—were tested. Thirteen patients had arteriogenic insufficiency based on post intracavernous injection duplex sonography and clinical response. Results for different cutoff PSV values of 5, 10, and 15 cm/s in diagnosing arteriogenic impotence were: sensitivity 29%, 96%, and 100%; specificity 100%, 92%, and 23%; negative predictive value 80%, 92%, and 100%; positive predictive value 100%, 81%, and 41%; and overall accuracy 79%, 93%, and 44%, respectively. In the flaccid state, there was a significant difference in mean PSV between the "normal" group (12.6 ± 0.9 cm/s) and the arteriogenic impotence group (7.7 ± 1.1 cm/s). Twenty-nine patients with a bilateral PSV of 10 cm/s or less before intracavernous injection had a normal clinical response. They concluded that a cutoff PSV value of 10 cm/s in the flaccid state had the best accuracy in predicting arterial insufficiency. Duplex Doppler sonography is proposed as the initial test to evaluate the penile arterial supply and to determine whether patients are good candidates for therapy with intracavernous injection.

Gontero et al. [106] conducted a study regarding the fact that an increased sympathetic tone may cause an equivocal response to a prostaglandin E1(PGE1) penile Doppler ultrasound examination interpreted as a venous leak. They evaluated the ultrasound parameters and erectile response to the addition of phentolamine to a PGE1 penile Doppler ultrasound examination to ascertain whether the addition of phentolamine would abolish a suboptimal response. This study included 32 patients who had either a clinical suspicion of venogenic impotence or a previous Doppler ultrasound pattern of venous leakage. These patients underwent a Doppler ultrasound after a total dose of 20 μg of PGE1. The peak systolic velocity (PSV), end diastolic velocity (EDV), and grade of erection were documented. If erectile response was

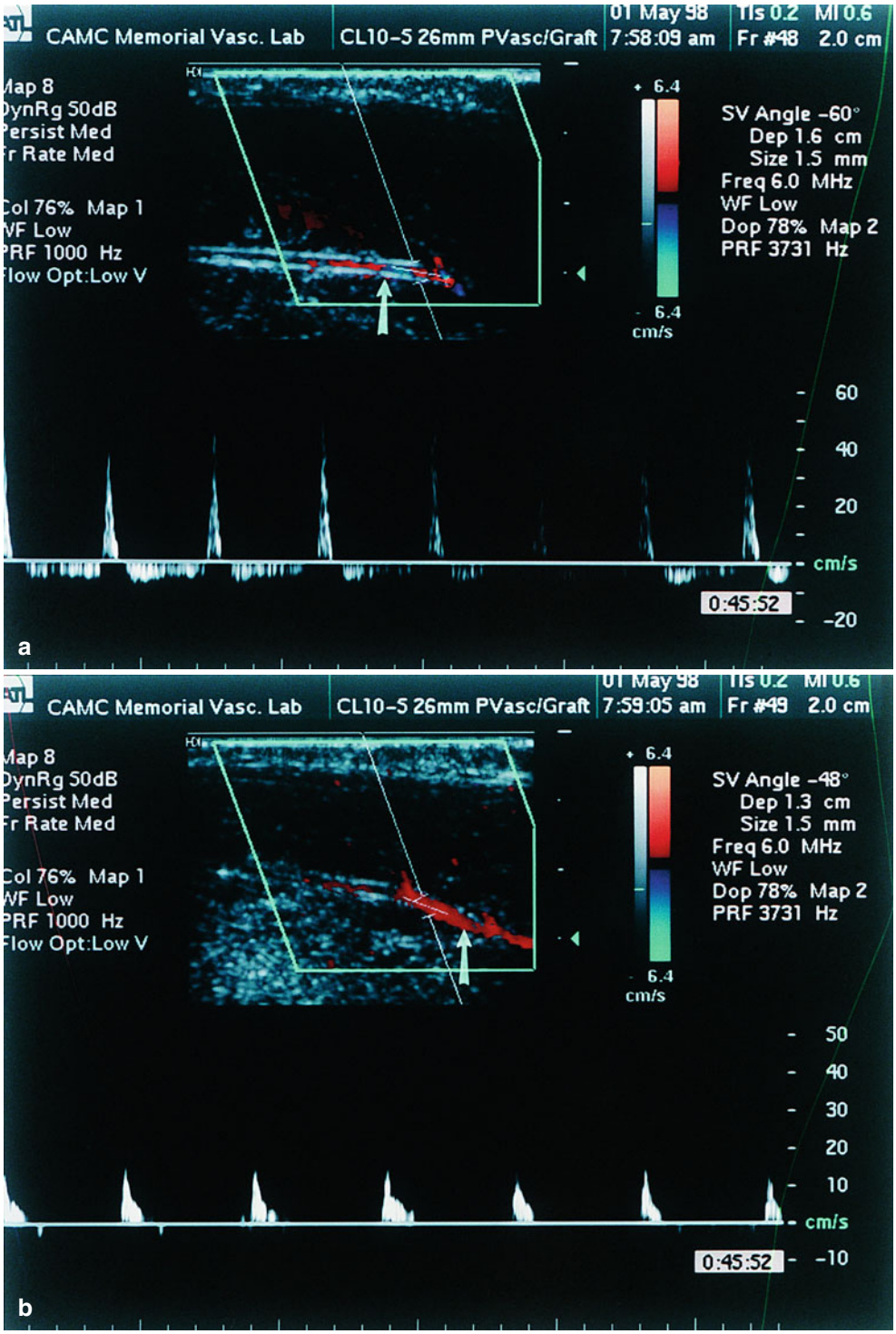


**Fig. 35.5** (**a**) A color duplex image of the cavernous artery (see *arrow*). The Doppler flow velocity spectrum with a peak systolic velocity of approximately 40 cm/s is shown at the bottom of the figure. (**b**) A color duplex image of the cavernous artery (see *arrow*). The Doppler flow velocity spectrum with a peak systolic velocity of approximately 15 cm/s is shown at the bottom of the figure

suboptimal, regardless of the EDV measurement, 2 mg of intracavernosal phentolamine was administered and measurements were repeated. Six patients had a normal erectile response, and the remaining 26 received phetolamine. A significant increase in PSV between baseline and 20 μg PGE1 ($p<0.001$) was observed in all cases. There was a significant increase in the grade of erection ($p=0.0001$) and a significant reduction in the EDV ($p=0.0001$) after phentolamine. They observed a reduction in the EDV to below 0.0 cm/s (−1) in 16 patients. Four patients with an EDV < 5.0 cm/s (−1) but >0.0 cm/s (−1) had an improved erectile response following phentolamine, while six showed persistent EDV elevation >5 cm/s (−1). No priapism was documented. They felt that it is essential to ensure cavernosal

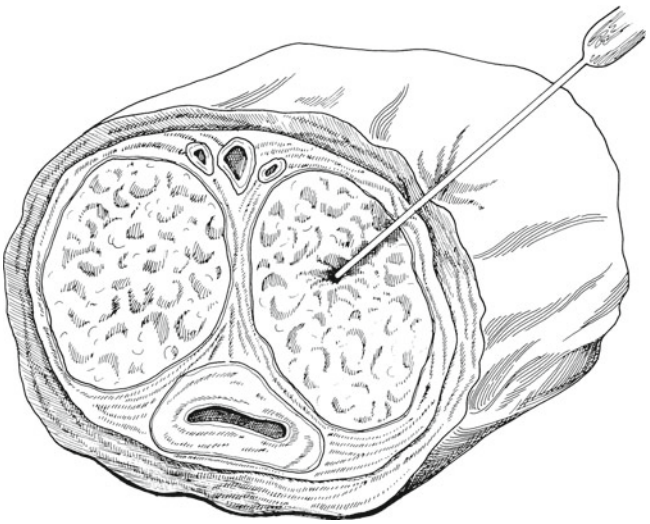

**Fig. 35.6** An illustration of the structure of the penis with the position of the needle used for injection of vasodilators

relaxation using phentolamine before a Doppler ultrasound diagnosis of venous leak is made. This two-stage assessment will allow this to be done efficiently and with a low risk of priapism.

## Upper Extremity Ischemia and Vasospastic Diseases

Upper extremity ischemia is relatively infrequent and can be caused by atherosclerosis, vasospasm, emboli, and trauma, which might be caused by diagnostic arterial catheterization. The segmental pressures and Doppler flow or PVRs can be measured at the level of the upper arm, forearm, and wrist, as well as in one or more digits to aid in diagnosing and localizing the obstructing lesion. Doppler ultrasound can accurately assess the patency of the palmar arch, which should be considered in all patients suspected of having intrinsic small vessel disease of the hand, or prior to cannulation of either the radial or the ulnar arteries. After catheterization, pressure data can be used to determine whether an accident has occurred. With spasm, the blood pressure drops only moderately and recovers rapidly.

Sumner and Strandness [107] described the characteristic peaked pulse seen in the digit volume pulse contours of patients with cold sensitivity secondary to collagen vascular disease or other forms of intrinsic digital artery disease. This is in contrast to patients with pure vasospasm where the contour is normal in configuration, but of decreased amplitude. Figure 35.7 shows three typical digit pulse contours obtained with a mercury-in-silastic plethysmograph. The normal pulse contour has a sharp systolic upswing that rises rapidly to a peak, and then drops off rapidly toward the baseline. The downslope of this curve is bowed toward the baseline and usually contains a prominent dicrotic notch midway between the peak and baseline. In contrast, the pulse found distal to an arterial obstruction is considerably more rounded as seen in the obstructive contour. The upswing is delayed, the downslope is bowed away from the baseline, and there is no dicrotic notch. In several cases of arterial obstruction, no pulse is perceptible. The peaked pulse has a somewhat more delayed upswing than the normal pulse. Near the peak there is an anacrotic notch. On the downslope, a dicrotic notch is present that is less prominent and located closer to the peak than normally seen.

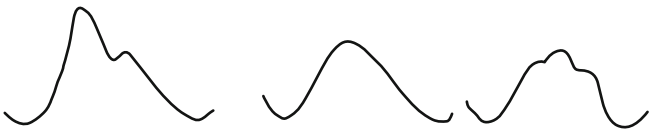

**Fig. 35.7** Digit pulse contours. From *left to right*: normal contour, obstructive contour, peaked contour

At room temperature, digital perfusion may be normal in persons with early vasospastic disease. To examine these patients, baseline PVRs of all digits are obtained. The hands are then immersed in iced water for 3 min, or as long as tolerated. Serial digital PVRs are measured as rewarming occurs. If they fail to return to baseline levels within 5 min, a pathologic degree of vasospasm is likely. Measuring digit or toe pressure might also be helpful in distinguishing between primary vasospastic Raynaud's disease and obstructive organic disease or Raynaud's syndrome. In the primary disease, the digital pressure is almost normal, but in the obstructive disease, the digital pressure is markedly decreased. It should be noted that the toe pressure is normally a few millimeters of mercury less than the arm pressure and the finger pressure is a few millimeters higher than the arm pressure in young adults, but almost equal to the arm pressure in old patients. After the hands are immersed in iced water, the digital pressure in a normal individual will drop very slightly, but will return to normal very rapidly. In patients with primary vasospastic disease, the digital pressure will drop more significantly and might take a few minutes or more to come back. The digital pressure in organic obstructive disease will drop very dramatically (from 60 to 0 mmHg) and will take longer to return to normal. Further details of upper extremity vascular evaluation will be described in another chapter.

## Arteriovenous Malformations

Arteriovenous malformations (AVMs) or fistulas can be congenital or acquired (e.g., traumatic). They consist of an

abnormal connection between a high-pressure arterial system and a low-pressure venous system, causing marked hemodynamic and anatomic changes. AVMs may involve proximal and distal arteries and veins as well as collateral arteries and veins. Its diameter and length predict the resistance it offers. If the fistula is proximal in its location (close to the heart), the potential for cardiac complications, primarily cardiac failure, increases. This is in contrast to peripheral fistulas, which are less likely to cause congestive heart failure, but more likely to cause limb ischemia. Generally, flow in the artery proximal to the fistula is greatly increased, especially during diastole, because the fistula markedly reduces resistance, and this is in contrast to what is seen in a normal artery. The proximal venous flow is also increased and becomes more pulsatile in character. The blood pressure distal to the fistula is somewhat reduced. The direction of the blood flow, on the other hand, is normal if the fistula resistance exceeds that of the distal vascular bed. If the fistula is chronic and large, arterial blood flow may be retrograde. A long-standing chronic fistula tends to elevate venous pressure, and blood flow is retrograde in the distal vein, which is associated with an incompetent valve.

Diagnosis of AVM may be evident on physical examination by (1) the presence of a characteristic bruit, (2) the presence of secondary varicosities and cutaneous changes of chronic venous insufficiency, (3) the obliteration of the thrill producing bradycardiac response, or (4) the association of a birthmark and limb overgrowth in patients with congenital AVM. However, such combinations are often lacking. Szilagyi et al. [108] reported in one of the largest series of AVMs that the classic triad of birthmark, varicosities, and limb enlargement was present in only 30% of patients, with various other combinations of signs present in 38% and 32% of those presenting with only a single physical finding. Various noninvasive diagnostic tests have been used for the diagnosis of extremity AV fistula including (1) Doppler segmental limb systolic pressure determination, (2) segmental limb plethysmography or PVRs, and (3) analysis of arterial velocity waveforms.

The reduced peripheral resistance associated with AVM decreases the mean arterial pressure proximally, but increases the pulse pressure [109]. Accordingly, proximal to the malformation, segmental systolic pressures are usually increased compared with the contralateral normal extremity. Beyond the malformation, they are normal, except in the case of stealing from distal arterial flow, when they may be decreased. The decreased peripheral resistance eliminates the reverse flow, which is seen in the normal Doppler analog wave tracing and increases the forward flow, particularly during diastole. Consequently, the end-diastolic velocity waveforms are elevated above the zero baseline in direct proportion to the decrease in peripheral resistance. However, this pattern can be seen in cases of reactive hyperemia, after vasodilator drugs, in warming of the extremity, in inflammation, and after sympathectomy. In the absence of these conditions, it is diagnostic of AVM.

The PVR can also be helpful in the diagnosis of these malformations. The AVM increases the segmental limb volume changes normally produced by pulsatile arterial flow and can be detected with the PVR. The PVRs proximal to the fistula are uniformly increased. The anacrotic slope and peak are sharper with loss of the dicrotic wave. Distal to the fistula, the PVRs are often entirely normal. The same principles can be applied in evaluating patients with angioaccess for kidney failure, premature atypical varicose veins, unequal limb growth, or hemangiomas of the extremity.

Labeled microsphere methods can be used to estimate the AV shunt flow of an extremity. The percentage of total extremity flow that passes through AVMs may be measured by comparing the relative levels of pulmonary radioactivity following an arterial, and then a peripheral venous injection of a radionuclide-labeled human albumin microsphere [109]. These methods may be used to confirm or exclude the diagnosis of AVM, particularly if the results of the noninvasive vascular tests are equivocal. They also provide a quantitative estimate of the AV shunt flow, which may be helpful in determining its prognosis and the need for any therapeutic interventions. Patients with congenital AVM may also present primarily as venous pathology, e.g., varicose veins. Some of these may harbor AVM and have secondary venous insufficiency, whereas others may have a venous anomaly, but no AVM (e.g., Klippel–Trenaunay or Parks–Weber syndrome). These can be investigated by various venous noninvasive studies that will be described later. Various venous abnormalities can be detected, including deep venous valvular insufficiency, which can be diagnosed by simple Doppler ultrasound or venous duplex imaging or PPG.

In spite of the role of various noninvasive vascular tests described earlier, other testing may be necessary in many patients with AVM of the extremities to achieve sufficient information on which to base major clinical decisions. Magnetic resonance imaging, which is preferable to contrasted enhanced CT, might be necessary in evaluating congenital vascular malformation [110]. Magnetic resonance imaging gives a better definition of the anatomic extent and the feasibility of surgical resection than CT and allows multiplanar views (Fig. 35.8). This topic is described in more detail in Chap. 33.

## Hemodialysis Access Graft Imaging

Duplex scanning of hemodialysis access grafts documents abnormalities and abnormal velocity or volume flow

measurements commonly associated with a graft malfunction. Imaging of these grafts is indicated in the following circumstances: elevated venous pressure, difficult needle placement, loss of graft thrill, swelling around the graft site, perigraft mass, recirculation, abnormal laboratory values, and underdeveloped Cimino fistula.

## Technique

No specific preparation is required prior to the examination. The patient may sit or lie in the supine position and clothing may need to be removed, depending on the location of the access graft. The extremity is inspected for raised or flattened areas of edema, or discoloration of the hand or digits. The presence of a pulse is abnormal and the presence of a palpable thrill is a normal finding. Brachial pressures should be obtained and should be equal bilaterally. A 5–10 MHz linear transducer can be used and the graft should be examined in both transverse and longitudinal scan planes. Both the inflow artery, the entire length of the graft, and the outflow veins should be imaged. Velocities or volume flow measurements must be done at the anastomotic sites, mid-graft, puncture sites, and sites of obvious lumen reduction. If color flow imaging is available, observe the image for frequency increases, turbulence, and flow channel changes. The following can be some of the limitations of this technique: excessive swelling, infection, anatomic variations, uncooperative patients, and visualization of the graft less than 48 h after placement. The technician or examiner should be familiar with the type of hemodialysis access graft to facilitate mapping. Figure 35.9 is an example of these grafts.

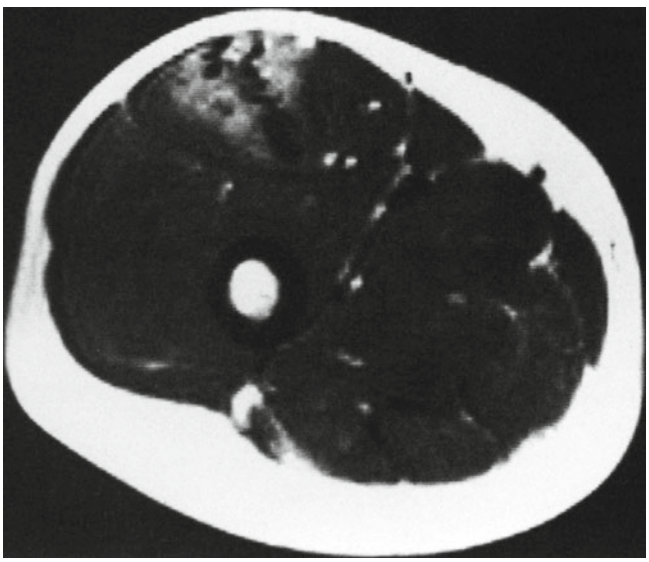

**Fig. 35.8** Magnetic resonance imaging of the lower extremity showing a vascular mass with high flow changes in the anterior medial compartment of the thigh region (involving the vastus medialis muscle) as noted in the upper portion of this transverse view

## Interpretations

As indicated earlier, the following should be identified and documented as to location, extent, and type: aneurysmal changes (including pseudoaneurysms), puncture sites for hematomas or leaks, thrombus, and perigraft fluid collection.

PSVs vary according to the graft type and normally can be quite elevated. Presently, there are no standardized velocity criteria for hemodialysis access grafts. It is generally recommended to have follow-up studies, which will provide specific comparisons to previous studies. A low PSV obtained throughout the graft could suggest an arterial inflow dysfunction. It is generally believed that the venous anastomosis and outflow veins are the most common sites of stenosis in these grafts, which can be caused by an increased arterial pressure introduced through the vein and/or intima hyperplasia. Occasionally, steal syndrome can be observed whereby the distal arterial blood flow is reversed into the venous circulation of the lower systems. This can be manifested by pain on exertion of the affected extremity as well as pallor and coolness of the skin distal to the shunt.

Table 35.1 summarizes a generally agreed upon interpretation criteria that is adapted from an Advanced Technology Laboratory manual.

## Volume Flow Criteria

Low blood flow volume through a hemodialysis graft can be predictive of graft failure. A noninvasively derived value of <450 mL/min has been associated with graft stenosis or

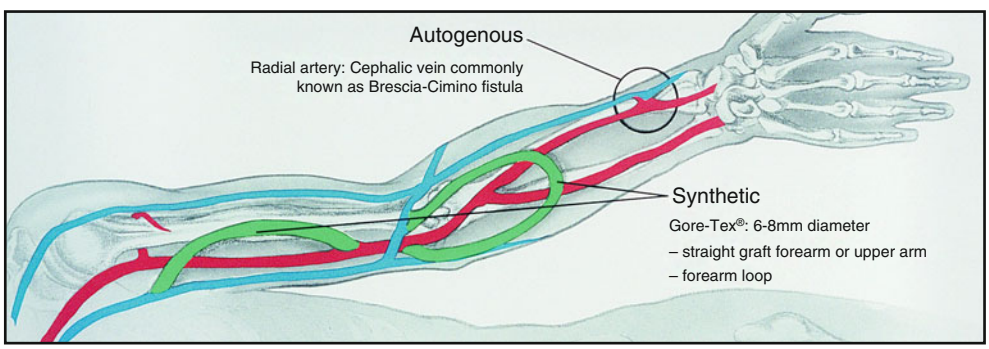


**Fig. 35.9** Illustration showing various AV grafts. As noticed in this figure, these grafts can be autogenous (radial artery to cephalic vein) or synthetic (Gore-Tex graft between the brachial artery and the antecubital vein or between the brachial artery and the distal axillary or proximal brachial veins)

**Table 35.1** Dialysis access graft imaging: interpretation criteria

| Classification | Velocity (cm/s)* | | Image characteristics |
|---|---|---|---|
| Normal | Mid-graft | Anastomotic sites | No visible narrowing |
| | >150 cm/s | >300 cm/s | Distended outflow veins |
| | | | Aneurysms, puncture sites, perigraft fluid may be visible |
| Moderate stenosis | Mid-graft | Anastomotic sites | Decrease in lumen diameter |
| | 100–150 cm/s | >300 cm/s at stenosis | Echogenic narrowing |
| | | | Wall abnormalities |
| Severe stenosis | Mid-graft | | Intraluminal echogenicity |
| | <100 cm/s | | <2 mm lumen |
| | | | >50% diameter reduction |
| | | | Marked velocity acceleration |
| | | | Marked reduction in lumen diameter with color Doppler |
| Inflow stenosis | Inflow anastomosis site | Mid-graft | Intraluminal echogenicity |
| | >300 cm/s with turbulence | <100 cm/s | <2 mm lumen at velocity acceleration |
| | Monophasic spectra with graft compression | No velocity acceleration at outflow anastomosis | |
| Outflow stenosis | Inflow anatomosis site | Focal velocity acceleration (could be mild, outflow, or distal vein) | Intraluminal echogenicity |
| | <300 cm/s (decreases as distal stenosis progresses) | >300 cm/s | <2 mm lumen velocity acceleration |
| | Mid-graft | | Prominent collateral veins around outflow |
| | <100 cm/s | | |
| Occlusion | No Doppler signal | | Intraluminal echogenicity |
| | | | Graft walls appear collapsed |
| | | | Occluded vein may not be visible |

*Denotes measurement of velocity in cm/s

dysfunction and impending failure, and some investigators use this finding as additional diagnostic criteria. However, it is to be noted that determination of the flow volume through a graft can produce variable results due to variations in technique and instrumentation as well as fundamental limitations of Doppler for this procedure.

### Interpretation Pitfalls

This includes the following: low systemic pressure, poor Doppler angle, central venous stenosis or occlusion, well-collateralized occlusion, velocity acceleration without lumen reduction, and degree of stenosis is not absolute in predicting access failure [111, 112]. This subject will be covered in more depth in a later chapter.

## Arterial Aneurysms

An arterial aneurysm is generally defined as an abnormal dilatation of an artery of equal to or more than one and a half of the normal adjacent arterial segments. These aneurysms can be true aneurysms, which are defined as a dilatation of all layers of the arterial wall, differentiating it from a pseudoaneurysm, which does not contain arterial wall layers, but rather is a pulsating hematoma completely separate from the artery except for the communicating neck or channel through which the blood travels to reach it. The false or pseudoaneurysm is usually secondary to an injury that produces a hole in the arterial wall that permits the blood to escape under pressure, generating a false aneurysm. Once the hematoma is formed, and if confined by the surrounding structures and if there is continuous blood flowing from the artery to this region, a false aneurysm is created that is covered by a fibrous capsule. These are usually secondary to arterial catheterization as seen after a cardiac catheterization or peripheral arterial interventions, particularly if a larger sheath is used.

A dissecting aneurysm occurs when a small tear of the intima allows the blood to form a cavity between the two walls, a new lumen (false lumen) is formed, and blood may flow through this lumen as well as through the original true lumen to supply branch arteries. This condition is usually secondary to weakening of the media of the artery and the development of an intimal tear through which the blood then leaks into the media. Arterial dissection is most often seen or noted in the thoracic aorta, which may not be secondary to atherosclerosis.

The most common location of arterial aneurysms is the infrarenal abdominal aorta (Fig. 35.10), but they can occur in nearly any artery of the body. Peripheral arterial aneurysms are commonly seen in the femoral and popliteal artery

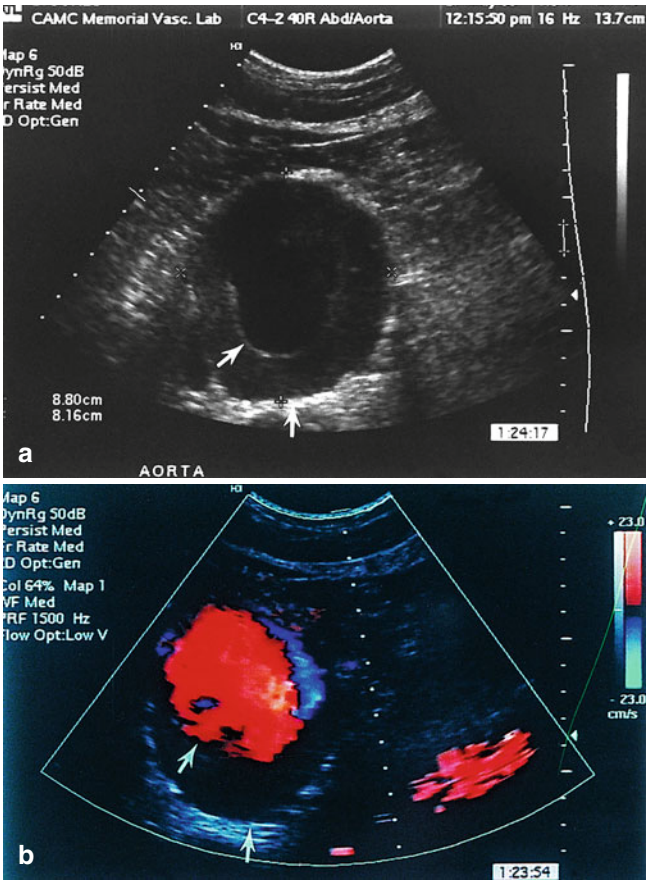


**Fig. 35.10** (**a**) A duplex ultrasound image of an abdominal aortic aneurysm measuring 8.8 cm in AP diameter and 8.16 cm in transverse diameter. Please notice the presence of thrombus between the inside and outside *arrows*. (**b**) A color duplex ultrasound image of the same abdominal aortic aneurysm showing the lumen as noted in *color* and the thrombus as indicated by *arrows*

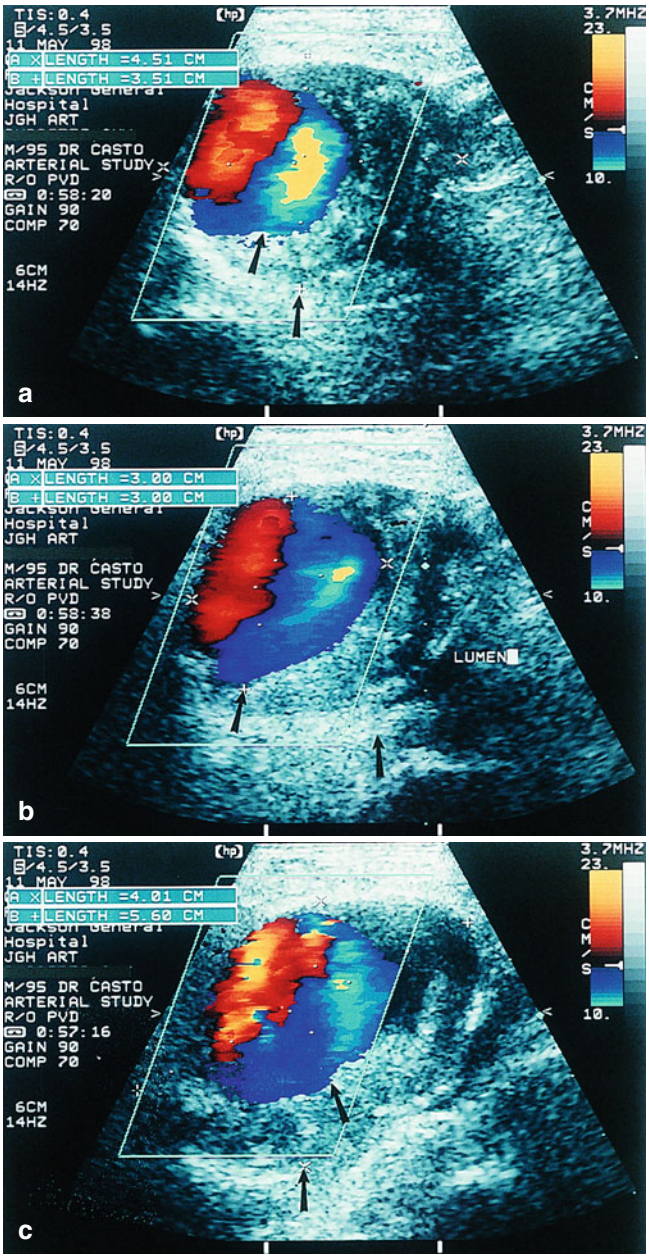


**Fig. 35.11** (**a**) A color duplex ultrasound image showing a right common femoral artery aneurysm in transverse view that measures around 4.51 cm in transverse diameter, and 3.51 cm in AP diameter. Please notice the presence of thrombus between the outside wall as indicated by the outside *arrow*, and the inside lumen as indicated by the inside *arrow*. (**b**) A color duplex ultrasound image showing the same patient as in (**a**) with measurement of the inside lumen (3 cm in transverse diameter and 3 cm in AP diameter). Notice the thrombus between the inside lumen and the outside wall (*arrows*). (**c**) A color duplex ultrasound image showing the same patient as in (**a**) with an aneurysm measuring 5.6 cm in length and 4.01 cm in AP diameter (*longitudinal view*)

regions. These peripheral aneurysms can be bilateral (over 50%), as seen in Figs. 35.11 and 35.12.

The causes of aneurysms are unknown, but may include atherosclerosis, poor arterial nutrition, congenital defects, infection, and iatrogenic injury. Aneurysms are usually fusiform, i.e., diffuse circumferential dilatation of the arterial segment, but can be sacular. The major complications of arterial aneurysms include rupture and distal embolizations. As noted in Figs. 35.10, 35.11, and 35.12, these aneurysms have the propensity to form thrombotic material at the walls.

Abdominal aortic aneurysms are usually discovered incidentally in about 50% of patients, i.e., asymptomatic patients, 25% of patients present with symptoms that may vary from abdominal and/or back pain, and the remaining 25% of patients present with rupture with the classical triad of abdominal or back pain, pulsating mass, and hypotension. Peripheral arterial aneurysms can also be discovered incidentally as a pulsating mass, or can present with distal arterial embolization. The diagnosis is usually confirmed by B-mode ultrasonography or duplex ultrasound (Figs. 35.10, 35.11, and 35.12). Other modalities used to confirm aneurysms include CT scanning and magnetic resonance imaging. This subject will be covered in more depth in a later chapter.

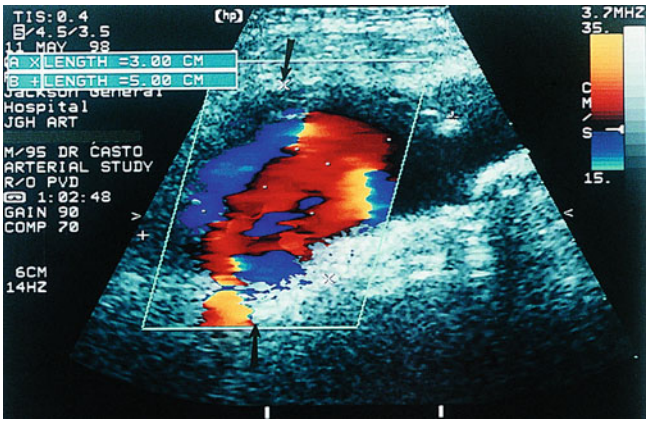


**Fig. 35.12** A color duplex ultrasound image of the same patient as in Fig. 35.11a showing another aneurysm of the left common femoral artery that measures 5 cm in length and 3 cm in AP view (*arrows*)

## Endothelial Dysfunction

Long before atherosclerosis becomes clinically manifest, endothelial dysfunction is evident and can be demonstrated by changes in brachial artery size during reactive hyperemia. The fact that brachial artery dysfunction correlates with coronary artery dysfunction is an important discovery [113].

Vinet et al. [114] reported on vascular reactivity at rest and during exercise in middle-aged obese men and the effects of short-term, low-intensity, exercise training. They concluded that that in obese men, conduit (brachial artery) and resistance vessel reactivity is depressed, but a short-term low-intensity exercise training improves distensibility and endothelium dependent vasodilation in the large conduit artery, but not post ischemic or exercise muscle blood flow.

## References

1. Weitz JI, Byrne J, Clagett GP, et al. Diagnosis and treatment of chronic arterial insufficiency of the lower extremities: a critical review. Circulation. 1996;94:3026–49.
2. AbuRahma AF. Noninvasive assessment of critical leg ischemia. In: Bartolucci R, Battaglia L, D'Andrea V, De Antoni E, editors. Critical lower limb ischemia – principles and practice. Rome: Nuova Editrice Grafica; 2002. p. 99–114.
3. Feigelson HS, Criqui MH, Fronek A, et al. Screening for peripheral arterial disease: the sensitivity, specificity, and predictive value of noninvasive tests in a defined population. Am J Epidemiol. 1994;140:526–34.
4. Ray SA, Srodon PD, Taylor RS, et al. Reliability of ankle: brachial pressure index measurement by junior doctors. Br J Surg. 1994;81:188–90.
5. Kravos A, Bubnic-Sotosek K. Ankle-brachial index screening for peripheral artery disease in asymptomatic patients between 50 and 70 years of age. J Int Med Res. 2009;37:1611–9.
6. Mourad JJ, Cacoub P, Collet JP, Becker F, Pinel JF, Huet D, Sevestre-Pietri MA, Priollet P, on behalf of the ELLIPSE Scientific Committee and Study Investigators. Screening of unrecognized peripheral arterial disease (PAD) using ankle-brachial index in high cardiovascular risk patients free from symptomatic PAD. J Vasc Surg. 2009;50:572–80.
7. McDermott MM, Ferrucci L, Guralnik JM, Dyer AR, Liu K, Pearce WH, Clark E, Liao Y, Criqui MH. The ankle-brachial index is associated with the magnitude of impaired walking endurance among men and women with peripheral arterial disease. Vasc Med. 2010;15:251–7.
8. AbuRahma AF, Diethrich EB. The Doppler testing in peripheral vascular occlusive disease. Surg Gynecol Obstet. 1980;150:26–8.
9. Raines JK, Darling RC, Buth J, et al. Vascular laboratory criteria for the management of peripheral vascular disease of the lower extremities. Surgery. 1976;79:21–9.
10. Toursarkissian B, Mejia A, Smilanich RP, Schoolfield J, Shireman PK, Sykes MT. Noninvasive localization of infrainguinal arterial occlusive disease in diabetics. Ann Vasc Surg. 2001;15:73–8.
11. Holland T. Utilizing the ankle brachial index in clinical practice. Ostomy Wound Manage. 2002;48:38–40.
12. Adam DJ, Naik J, Hartshorne T, Bello M, London NJ. The diagnosis and management of 689 chronic leg ulcers in a single-visit assessment clinic. Eur J Vasc Endovasc Surg. 2003;25:462–8.
13. AbuRahma AF, Khan S, Robinson PA. Selective use of segmental Doppler pressures and color duplex imaging in the localization of arterial occlusive disease of the lower extremity. Surgery. 1995;118:496–503.
14. Kempczinski RF. Segmental volume plethysmography: the pulse volume recorder. In: Kempczinski RF, Yao JST, editors. Practical noninvasive vascular diagnosis. Chicago: Year Book Medical Publishers; 1982. p. 105–17.
15. Koelemay MJ, Legemate DA, de Vos H, van Gurp AJ, Balm R, Reekers JA, Jacobs MJ. Duplex scanning allows selective use of arteriography in the management of patients with severe lower leg arterial disease. J Vasc Surg. 2001;34:661–7.
16. Strandness Jr DE, Stahler C. Arteriosclerosis obliterans. Manner and rate of progression. JAMA. 1966;196:1–4.
17. Wilson SE, Schwartz I, Williams RA, et al. Occlusion of the superficial femoral artery: what happens without operation. Am J Surg. 1980;140:112–8.
18. Paaske WP, Tonnesen KH. Prognostic significance of distal blood pressure measurements in patients with severe ischemia. Scand J Thorac Cardiovasc Surg. 1980;14:105–8.
19. Nicoloff AD, Taylor Jr LM, Sexton GJ, Schuff RA, Edwards JM, Yeager RA, Landry GJ, Moneta GL, Porter JM, Hemocysteine and Progression of Atherosclerosis Study Investigators. Relationship between site of initial symptoms and subsequent progression of disease in a prospective study of atherosclerosis progression in patients receiving long-term treatment for symptomatic peripheral arterial disease. J Vasc Surg. 2002;35:38–46.
20. Prineas RJ, Harland WR, Janzon L, et al. Recommendations for use of noninvasive methods to detect atherosclerotic peripheral arterial disease – in population studies. Circulation. 1982;65:1561A–6.
21. Janzon L, Bergentz SE, Ericsson BF, et al. The arm-ankle pressure gradient in relation to cardiovascular risk factors in intermittent claudication. Circulation. 1981;63:1339–41.
22. Beach KW, Brunzell JD, Strandness Jr DE. Prevalence of severe arteriosclerosis obliterans in patients with diabetes mellitus. Arteriosclerosis. 1982;2:275–80.
23. Criqui MH, Fronek A, Barrett-Connor E, et al. The prevalence of peripheral arterial disease in a defined population. Circulation. 1985;71:510–5.
24. Hiatt WR, Marshall JA, Baxter J, et al. Diagnostic methods for peripheral arterial disease in the San Luis Valley diabetes study. J Clin Epidemiol. 1990;43:597–606.
25. McLafferty RB, Moneta GL, Taylor LM, et al. Ability of ankle-brachial index to detect lower extremity atherosclerotic disease progression. Arch Surg. 1997;132:836–41.

26. Gundersen J. Segmental measurements of systolic blood pressure in the extremities including the thumb and the great toe. Acta Chir Scand. 1972;426:1–9.
27. Postlethwaite JC, Dormandy JA. Results of ankle systolic pressure measurements in patients with intermittent claudication being treated with clofibrate. Ann Surg. 1975;181:799–802.
28. Quick CR, Cotton LT. The measured effect of stopping smoking on intermittent claudication. Br J Surg. 1982;69:S24–6.
29. Kempczinski RF, Buckley CJ, Darling RC. Vascular insufficiency secondary to ergotism. Surgery. 1976;79:597–600.
30. Reich LM, Heiss G, Boland LL, Hirsch AT, Wu K, Folsom AR. Ankle-brachial index and hemostatic markers in the atherosclerosis risk in communities (ARIC) study cohort. Vasc Med. 2007;12:267–73.
31. Li X, Luo Y, Xu Y, Li J, Hu D. Relationship of ankle-brachial index with all-cause mortality and cardiovascular mortality after a 3-year follow-up: the China ankle-brachial index cohort study. J Hum Hyperts. 2010;24:111–6.
32. Fowkes FGR, Price JF, Stewart MCW, Butcher I, Leng GC, Pell AC, Sandercock PAD, Fox KAA, Lowe GDO, Murray GD, for the Aspirin for Asymptomatic Atherosclerosis Trialists. Aspirin for prevention of cardiovascular events in a general population screened for a low ankle brachial index: a randomized controlled trial. JAMA. 2010;303(9):841–8.
33. Meves SH, Diehm C, Berger K, Pittrow D, Trampisch HG, Burghaus I, Tepohl G, Allenberg JR, Endres HG, Schwertfeger M, Darius H, Haberl RL, getABI Study Group. Peripheral arterial disease as an independent predictor for excess stroke morbidity and mortality in primary-care patients: 5-year results of the getABI study. Cerebrovasc Dis. 2010;29:555–6.
34. El-Menyar A, Amin H, Rashdan I, Souliman K, Deleu D, Saadat K, Al Mahmeed W, Bakir S, Wasif A, Ben Brek A, Bazargani N, Aziz AA, Sigh R, Hatou I, Mahmoud H, Al Suwaidi J. Ankle-brachial index and extent of atherosclerosis in patients from the Middle East (the AGATHA-ME study): a cross-sectional multicenter study. Angiology. 2009;60:329–34.
35. Ascher E, Hingorani A, Markevich N, Costa T, Kallakuri S, Khanimoy Y. Lower extremity revascularization without preoperative contrast arteriography: experience with duplex ultrasound arterial mapping in 485 cases. Ann Vasc Surg. 2002;16:108–14.
36. Ascher E, Hingorani A, Markevich N, Schutzer R, Kallakuri S. Acute lower limb ischemia: the value of duplex ultrasound arterial mapping (DUAM) as the sole preoperative imaging technique. Ann Vasc Surg. 2003;17:284–9.
37. Canciglia A, Mandolfino T. Infrainguinal endovascular procedures based upon the results of duplex scanning. Int Angiol. 2008;27:291–5.
38. Hingorani AP, Ascher E, Marks N, Puggioni A, Shiferson A, Tran V, Jacob T. Limitations of and lessons learned from clinical experience in 1,020 duplex arteriography. Vascular. 2008;16:147–53.
39. O'Donnell TF, Cossman D, Callow AD. Noninvasive intraoperative monitoring: a prospective study comparing Doppler systolic occlusion pressure and segmental plethysmography. Am J Surg. 1978;135:539–46.
40. Baird RN, Davies PW, Bird DR. Segmental air plethysmography during arterial reconstruction. Br J Surg. 1979;66:718–22.
41. Rzucidlo EM, Walsh DB, Powell RJ, Zwolak RM, Fillinger MF, Schermerhorn ML, Cronenwett JL. Prediction of early graft failure with intraoperative completion duplex ultrasound scan. J Vasc Surg. 2002;36:975–81.
42. van der Heijden FH, Legemate DA, van Leeuwen MS, Mali WP, Eikelboom BC. Value of duplex scanning in the selection of patients for percutaneous transluminal angioplasty. Eur J Vasc Surg. 1993;7:71–6.
43. Whelan JF, Barry MH, Moir JD. Color flow Doppler ultrasonography: comparison with peripheral arteriography for the investigation of peripheral vascular disease. J Clin Ultrasound. 1992;20:369–74.
44. Garrett WV, Slaymaker EE, Heintz SE. Intraoperative prediction of symptomatic result of aortofemoral bypass from changes in ankle pressure index. Surgery. 1977;82:504–9.
45. Brener BJ, Brief DK, Alpert J. Clinical usefulness of noninvasive arterial studies. Contemp Surg. 1980;16:41–55.
46. Dean RH, Yao JST, Stanton PE, et al. Prognostic indicators in femoropopliteal reconstructions. Arch Surg. 1975;110:1287–93.
47. Corson JD, Johnson WC, LoGerfo FW, et al. Doppler ankle systolic blood pressure. Prognostic value in vein bypass grafts of the lower extremity. Arch Surg. 1978;113:932–5.
48. Rutherford RB. Standards for evaluating results of interventional therapy for peripheral vascular disease. Circulation. 1991;83:I-6–11.
49. Tooke JE. European consensus document on critical limb ischaemia. Vasc Med Rev. 1990;1:85–9.
50. Boren CH, Towne JB, Bernhard VM, et al. Profundapopliteal collateral index. A guide to successful profundaplasty. Arch Surg. 1980;115:1366–72.
51. Strandness Jr DE, Sumner DS. Hemodynamics for surgeons. New York: Grune & Stratton, Inc.; 1975. p. 573–82.
52. Yao JST, Bergan JJ. Predictability of vascular reactivity to sympathetic ablation. Arch Surg. 1973;107:676–80.
53. Walker PM, Johnston KW. Predicting the success of a sympathectomy: a prospective study using discriminant function and multiple regression analysis. Surgery. 1980;87:216–21.
54. AbuRahma AF, Robinson P. Clinical parameters for predicting response to lumbar sympathectomy with severe lower limb ischemia. J Cardiovasc Surg. 1990;31:101–6.
55. Tiutiunnik AA. The significance of laser Doppler flowmetry for the prognosis and outcome evaluation of lumbar sympathectomy in patients with obliterating vascular arteriosclerosis of lower extremities. Klin Khir. 2003;3:49–51.
56. Bandyk DF, Schmitt DD, Seabrook GR, et al. Monitoring functional patency of in situ saphenous vein bypasses: the impact of a surveillance protocol and elective revision. J Vasc Surg. 1989;9:286–96.
57. Calligaro K, Doerr K, McAffee-Bennett S, Krug R, Raviola CA, Dougherty MJ. Should duplex ultrasonography be performed for surveillance of femoropopliteal and femorotibial arterial prosthetic bypasses? Ann Vasc Surg. 2001;15:520–4.
58. Marks NA, Hingorani AP, Ascher E. Duplex guided balloon angioplasty of failing infrainguinal bypass grafts. Eur J Vasc Endovasc Surg. 2006;32:176–81.
59. Carter SA. The relationship of distal systolic pressures to healing of skin lesions in the limbs with arterial occlusive disease with special reference to diabetes mellitus. Scand J Clin Lab Invest. 1973;128 suppl 31:239–43.
60. Ramsey DE, Manke DA, Sumner DS. Toe blood pressure – valuable adjunct to ankle pressure measurement for assessing peripheral arterial disease. J Cardiovasc Surg. 1983;24:43–8.
61. Ruangstetakit C, Chinsakchai K, Mahawongkajit P, Wongwanit C, Mutirangura P. Transcutaneous oxygen tension: a useful predictor of ulcer healing in critical limb ischaemia. J Wound Care. 2010;19:202–6.
62. Lantis II JC, Boone D, Lee L, Mends D, Benvenisty A, Todd G. The effect of percutaneous intervention on wound healing in patients with mixed arterial venous disease. Ann Vasc Surg. 2011;25:79–86.
63. Robbs JV, Ray R. Clinical predictors of below-knee stump healing following amputation for ischemia. S Afr J Surg. 1982;20:305–10.
64. van den Broek TA, Dwars BJ, Rauwerda JA, et al. A multivariate analysis of determinants of wound healing in patient after amputation for peripheral vascular disease. Eur J Vasc Surg. 1990;4:291–5.
65. Apelqvist J, Castenfors J, Larsson J, et al. Prognostic value of systolic ankle and toe blood pressure levels in outcome of diabetic foot ulcer. Diabetes Care. 1989;12:373–8.

66. Barnes RW, Thornhill B, Nix L. Prediction of amputation wound healing roles of Doppler ultrasound and digit photoplethysmography. Arch Surg. 1981;116:80–3.
67. Nicholas GG, Myers JL, DeMuth Jr WE. The role of vascular laboratory criteria in the selection of patients for lower extremity amputation. Ann Surg. 1982;195:469–73.
68. Holloway Jr GA. Cutaneous blood flow responses to infection trauma measured by laser Doppler velocimetry. J Invest Dermatol. 1980;74:1–4.
69. Malone JM, Anderson GG, Lalka SG, et al. Prospective comparison of noninvasive techniques for amputation level selection. Am J Surg. 1987;154:179–84.
70. Schwartz JA, Schuler JJ, O'Conner RJ, et al. Predictive value of distal perfusion pressure in the healing of amputation of the digits and the forefoot. Surg Gynecol Obstet. 1982;154:865–9.
71. Christensen KS, Klarke M. Transcutaneous oxygen measurement in peripheral occlusive disease: an indicator of wound healing in leg amputation. J Bone Joint Surg Br. 1986;68:423–6.
72. Lee TQ, Barnett SL, Shanfield SL, et al. Potential application of photoplethysmography technique in evaluating microcirculatory status of STAMP patients: preliminary report. J Rehabil Res Dev. 1990;27:363–8.
73. Wyss CR, Harrington RM, Burgess EM, et al. Transcutaneous oxygen tension as a predictor of success after an amputation. J 85. Bone Joint Surg (Am). 1988;70:203–7.
74. Graham BH, Walton RL, Elings VB, et al. Surface quantification of injection fluorescein as a predictor of flap viability. Plast Reconstr Surg. 1983;71:826–33.
75. McFarland DC, Lawrence FF. Skin fluorescence: a method to predict amputation site healing. J Surg Res. 1982;32:410–5.
76. Silverman DG, Roberts A, Reilly CA, et al. Fluorometric quantification of low-dose fluorescein delivery to predict amputation site healing. Surgery. 1987;101:335–41.
77. Holloway Jr GA, Burgess EM. Preliminary experiences with laser Doppler velocimetry for the determination of amputation levels. Prosthet Orthot Int. 1983;7:63–6.
78. Golbranson FL, Yu EC, Gelberman HH. The use of skin temperature determination in lower extremity amputation level selection. Foot Ankle. 1982;3:170–2.
79. Dwars BJ, Rauwerda JA, van den Broek TA, et al. A modified scintigraphic technique for amputation level selection in diabetics. Eur J Nucl Med. 1989;15:38–41.
80. Holstein P, Trep-Jensen J, Bagger H, et al. Skin perfusion pressure measured by isotope wash out in legs with arterial occlusive disease. Clin Physiol. 1983;3:313–24.
81. Stockel M, Ovesen J, Brochner-Mortensen J, et al. Standardized photoelectric techniques as routine method for selection of amputation level. Acta Orthop Scand. 1982;53:875–8.
82. Silverman DG, Rubin SM, Reilly CA, et al. Fluorometric prediction of successful amputation level in the ischemic limb. J Rehabil Res Dev. 1985;22:23–8.
83. Barnes RW, Chanik GD, Slaymaker EE. An index of healing in below-knee amputation: leg blood pressure by Doppler ultrasound. Surgery. 1976;79:13–20.
84. Verta Jr MJ, Gross WS, VanBellen B, et al. Forefoot per-fusion pressure and minor amputation for gangrene. Surgery. 1976;80:729–34.
85. Bone GE, Pomajzl MJ. Toe blood pressure by photoplethysmography: an index of healing in forefront amputation. Surgery. 1981;89:569–74.
86. Dale WA, Lewis MR. Management of thoracic outlet syndrome. Ann Surg. 1975;181:575–85.
87. Gillard J, Perez-Cousin M, Hachulla E, Remy J, Hurtevent JF, Vinckier L, Thevenon A, Duquesnoy B. Diagnosing thoracic outlet syndrome: contribution of provocative tests, ultrasonography, electrophysiology, and helical computed tomography in 48 patients. Joint Bone Spine. 2001;68:416–24.
88. Wadhwani R, Chaubal N, Sukthankar R, Shroff M, Agarwala S. Color Doppler and duplex sonography in 5 patients with thoracic outlet syndrome. J Ultrasound Med. 2001;20:795–801.
89. Darling RC, Buckley CJ, Abbott WM, et al. Intermittent claudication in young athletes: popliteal artery entrapment syndrome. J Trauma. 1974;14:543–52.
90. Abbas M, Calydon M, Ponosh S, Theophilus M, Angel D, Tripathi R, Prendergast F, Sieunarine K. Sonographic diagnosis in iatrogenic entrapment of a femoropopliteal bypass graft. J Ultrasound Med. 2004;23:859–63.
91. Golijanin D, Singer E, Davis R, Bhatt S, Seftel A, Dogra V. Doppler evaluation of erectile dysfunction – part 2. Int J Impot Res. 2007;19:43–8.
92. Kempczinski RF. Role of the vascular diagnostic laboratory in the evaluation of male impotence. Am J Surg. 1979;138:278–82.
93. Britt DB, Kemmerer WT, Robison JR. Penile blood flow determination by mercury strain gauge plethysmography. Invest Urol. 1971;8:673–8.
94. Ramirez C, Box M, Gottesman L. Noninvasive vascular evaluation in male impotence. Technique. Bruit. 1980;4:14–9.
95. Nath RL, Menzoian JD, Kaplan KH, et al. The multidisciplinary approach to vasculogenic impotence. Surgery. 1981;89:124–33.
96. Mahe G, Leftheriotis G, Picquet J, Jaquinandi V, Saumet JL, Abraham P. A normal penile pressure cannot rule out the presence of lesions on the arteries supplying the hypogastric circulation in patients with arterial claudication. Vasc Med. 2009;14:331–8.
97. Inuzuka K, Unno N, Mitsuoka H, Yamamoto N, Ishimaru K, Sagara D, Suzuki M, Konno H. Intraoperative monitoring of penile and buttock blood flow during endovascular abdominal aortic aneurysm repair. Eur J Vasc Endovasc Surg. 2006;31:359–65.
98. Quam JP, King BF, James EM, et al. Duplex and color Doppler sonographic evaluation of vasculogenic impotence. AJR. 1989;153:1141–7.
99. Benson CB, Vickers MA. Sexual impotence caused by vascular disease: diagnosis with duplex sonography. AJR. 1989;153:1149–53.
100. Paushter DM. Role of duplex sonography in the evaluation of sexual impotence. AJR. 1989;153:1161–3.
101. Aversa A, Caprio M, Spera G, Fabbri A. Non-invasive vascular imaging for erectile dysfunction. J Endocrinol Invest. 2003;26:122–4.
102. Mancini M, Negri L, Maggi M, Nerva F, Forti G, Colpi GM. Doppler color ultrasonography in the diagnosis of erectile dysfunction of vascular origin. Arch Ital Urol Androl. 2000;72:361–5.
103. Roy C, Saussine C, Tuchmann C, Castel E, Lang H, Jacqmin D. Duplex Doppler sonography of the flaccid penis: potential role in the evaluation of impotence. J Clin Ultrasound. 2000;28:290–4.
104. Altinkilic B, Hauck EW, Weidner W. Evaluation of penile perfusion by color-coded duplex sonography in the management of erectile dysfunction. World J Urol. 2004;22:361–4.
105. Aversa A, Sarteschi LM. The role of penile color-duplex ultrasound for the evaluation or erectile dysfunction. J Sex Med. 2007;4:1437–47.
106. Gontero P, Sriprasad S, Wilkins CJ, Donaldson N, Muir GH, Sidhu PS. Phentolamine re-dosing during penile dynamic colour Doppler ultrasound: a practical method to abolish a false diagnosis of venous leakage in patients with erectile dysfunction. Br J Radiol. 2004;77:922–6.
107. Sumner DS, Strandness Jr DE. An abnormal finger pulse associated with cold sensitivity. Ann Surg. 1972;175:294–8.
108. Szilagyi DE, Smith RF, Elliott JP, et al. Congenital arteriovenous anomalies of the limbs. Arch Surg. 1976;111:423–9.
109. Rutherford E, Fleming PW, McLeod FD. Vascular diagnostic methods for evaluating patients with arteriovenous fistulas. In: Diethrich EB, editor. Noninvasive cardiovascular diagnosis. Baltimore: University Park Press; 1978. p. 217–30.

110. Pearce WH, Rutherford RB, Whitehill TA, et al. Nuclear magnetic resonance imaging: its diagnostic value in patients with congenital vascular malformations of the limbs. J Vasc Surg. 1988;8:64–70.
111. Rittgers SE, Garcia-Valdez C, McCormick JT, et al. Noninvasive blood flow measurement in expanded polytetrafluoroethylene grafts for hemodialysis access. J Vasc Surg. 1986;3:635–42.
112. Tordoir JH, Hoeneveld H, Eikelboom BC, et al. The correlation between clinical and duplex ultrasound parameters and the development of complications in arteriovenous fistulas for hemodialysis. Eur J Vasc Surg. 1990;4:179–84.
113. Anderson TJ, Uehata A, Gerhard MD, et al. Close relation of endothelial function in the human coronary and peripheral circulations. J Am Coll Cardiol. 1995;26:1235–41.
114. Vinet A, Karpoff L, Walther G, Startun A, Obert P, Goret L, Dauzat M, Perez-Martin A. Vascular reactivity at rest and during exercise in middle-aged obese men: effects of short-term, low-intensity, exercise training. Int J Obes. 2010;35:1–9.

# Part V

# Noninvasive Diagnosis of Venous Disorders of the Extremities

Patrick A. Stone

# Overview of Venous Disorders

# 36

Albeir Y. Mousa

**Abstract**

There is growing recognition of the importance of venous pathology in our daily practice. With a better understanding of venous insufficiency distribution and its consequences, it is being proved that the main pathology of venous disease is not an obstructive process as previously thought. There are several methods to classify venous diseases, such as distribution and severity; however, the most effective way is to assess the severity based on clinical, etiological, anatomical, and pathophysiological aspects. This international classification is not only an efficient description, but is imperative in determining appropriate management. It is crucial to understand the new terminology, not only to keep up with the American Venous Forum updates, but also to serve as a common language among venous specialists. This chapter is an overview of venous disorders, both from anatomical and pathophysiological aspects, with a brief update on the new horizons in the management of venous disease.

**Keywords**

Venous • Superficial • Deep • Reflux • CEAP • Deep venous thrombosis • Perforator Phlegmasia • Incompetence

## Anatomy and Pathophysiology

The main function of the venous system is to act as a reservoir and conduit to return blood to the heart. Unlike the well-defined layered structure of the arterial wall, the majority of veins only have a single layer, and some of the large veins possess an internal elastic lamina, therefore veins can be distended significantly, which can contribute to venous disorders.

As the blood is filtered at the capillary level, the entire cardiac output volume (an average of 5 L/min) will be received into the peripheral venous system. Since a well-developed muscular layer is lacking, blood return to the heart depends on a complex series of extrinsic (muscle pump) and intrinsic factors (one way valves) to achieve antegrade venous flow to the heart. The main and simple classifications of the venous system are superficial, perforating, and deep, depending on the relationship to the deep fascia.

In 2001, an International Interdisciplinary Committee was designated by the presidents of the International Union of Phlebology (IUP) and the International Federation of Anatomical Associations to update the official *Terminologia Anatomica* [1]. The committee with the participation of members of the Federative International Committee for Anatomical Nomenclature (FICAT) outlined a Consensus Document at a meeting held in Rome on the occasion of the 14th World Congress of the IUP. Terminological recommendations of the committee were published [2] and these new, possibly unfamiliar terms are used throughout this chapter (Table 36.1).

A.Y. Mousa, M.D.
Department of Surgery, Robert C. Byrd Health Sciences Center, West Virginia University, 3110 MacCorkle Ave. SE, Charleston Area Medical Center, Charleston, WV 25304, USA
e-mail: amousa@hsc.wvu.edu

A.F. AbuRahma, D.F. Bandyk (eds.), *Noninvasive Vascular Diagnosis*, DOI 10.1007/978-1-4471-4005-4_36, 

**Table 36.1** Important changes in the nomenclature of lower extremity veins

| Old nomenclature | New nomenclature |
|---|---|
| Femoral vein | Common femoral vein |
| Superficial femoral vein | Femoral vein |
| Sural veins | Sural veins; soleal veins; gastrocnemius veins (medial and lateral) |
| Huntarian perforator | Mid-thigh perforator |
| Cockett's perforators | Paratibial perforator |
| | Posterior tibial perforators |
| May's perforator | Intergemellar perforator |
| Gastrocnemius point | |

**Table 36.2** Perforating veins (PV) of the leg

| | |
|---|---|
| Gluteal perforators | Superior gluteal, midgluteal, lower gluteal PV |
| Thigh perforators | Medial thigh PV (formerly Hunter's perforator) |
| | (PV of the femoral canal or Inguinal PV) |
| | Anterior thigh, lateral thigh PV, Posterior thigh PV (posteromedial, sciatic, posterolateral PV) Pudendal PV |
| Knee perforators | Medial knee PV (formerly Boyd's perforator) Suprapatellar, lateral knee, infrapatellar, popliteal fossa PV |
| Leg (calf) perforators | Paratibial, posterior tibial PV (formerly Cockett's perforators) Anterior leg, lateral leg PV |
| | Posterior leg PV (medial and lateral gastrocnemius, Intergemellar, para-achillean PV) |
| Ankle perforators | Medial ankle, lateral ankle, anterior ankle PV |
| Foot perforators | Dorsal foot or intercapitular PV |
| | Medial, lateral, plantar foot PV |

The superficial venous system consists of a variable web-like plexus of veins, which are located superficial to the deep fascia and serve as a conduit to allow blood to pass centrally to the deep system, and eventually to the right atrium. The main superficial veins of the lower extremity are the great and short saphenous veins. The great saphenous vein (GSV) originates in the medial aspect of the dorsum of the foot and ascends anteriorly to the medial malleolus and becomes more posteromedially at the knee level and more medially at the thigh, where it ends by piercing the deep fascia at the cribriform fascia to join the common femoral vein at the saphenous-femoral junction (SFJ). The majority of patients have at least two major tributaries above the knee, the anterior and posterior circumflex. Three important pelvic tributaries join the GSV at the SFJ: the superficial inferior epigastric, the superficial external pudendal, and the superficial circumflex iliac veins. The clinical relevance of some of these veins will be discussed later. A duplicated main GSV is not uncommon, and many patients will have anterior or posterior accessory veins that run parallel to the main GSV.

The short saphenous vein (SSV) originates in the lateral aspect of the dorsum of the foot, passes posterolaterally to the Achilles tendon and runs posteriorly at midline superficial to the deep fascia, where it enters the popliteal fossa between the two heads of gastrocnemius. Most commonly, it joins the popliteal vein above the knee, but in some cases, it may join the GSV or deep muscular veins of the thigh.

The principal return of blood flow from the lower extremities is through the deep veins. In the calf, the deep veins are paired and named for the accompanying arteries. Therefore, the anterior tibial, posterior tibial, and peroneal artery are accompanied by their paired veins, which are interconnected. These join to form the popliteal vein, which may also be paired. As the popliteal vein ascends, it becomes the femoral vein [3]. Near the groin, this is joined by the deep femoral vein, which becomes the common femoral vein and then the external iliac vein proximal to the inguinal ligament.

The perforating veins are a communicating plexus of veins between the superficial and deep systems. They are named according to their location (Table 36.2). Understanding the anatomy of these veins will not only aid in determining the location of certain venous ulcers, but also in planning for therapy.

These veins penetrate anatomic layers, which gives them the name perforating veins. Veins that interconnect on the same anatomic layer are called communicating veins. In the leg, and using the now disfavored eponyms, the principal perforating veins have been named after an English surgeon, Frank Cockett. The Cockett I perforating vein is approximately 6 cm, measured from the floor in the standing patient. The Cockett II perforating vein clusters at about 12 cm, and the Cockett III is at 18 cm. These, and the 24 cm perforating vein, may need to be identified as tibial perforating veins in limbs with severe chronic venous insufficiency as they become targets for the surgeon. These perforating veins connect the posterior arch circulation to the posterior tibial veins.

In the upper anteromedial calf, a perforating vein is found and in the distal thigh, there are perforating veins. Above these in the mid-thigh, the perforating veins are named after John Hunter (Fig. 36.1).

## Normal Physiology of Venous Flow

Under normal conditions, about 90% of the venous return in the lower extremities is via deep veins, mainly facilitated through compartmental muscular contraction of the foot, calf, and thigh against tight fascia. The highest pressure is generated by the calf muscle and is estimated to be about 65%, in comparison to 15% generated by the thigh muscles [4]. As the muscle contracts, the pressure raises within the

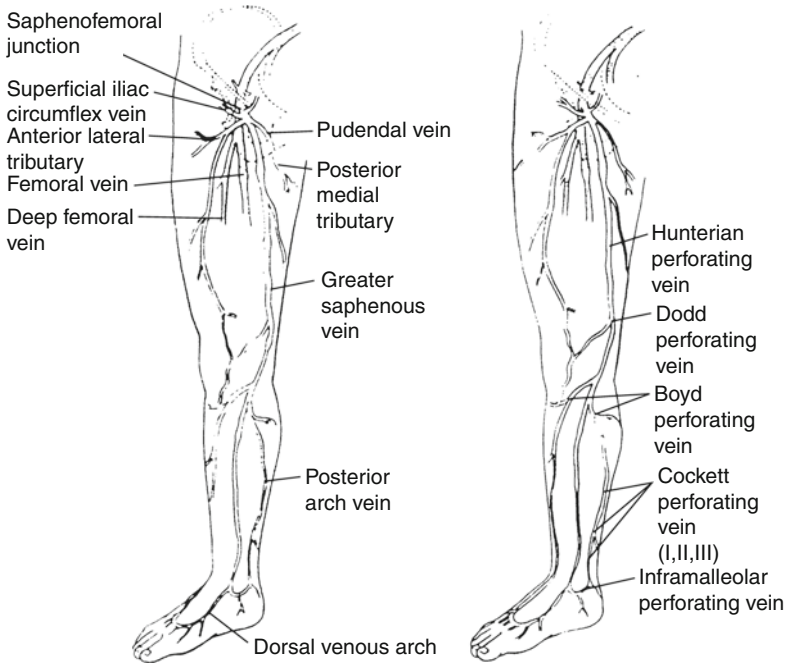


**Fig. 36.1** The main superficial veins and perforating veins. Note that the Cockett perforating veins are part of the posterior arch circulation and that important tributaries to the saphenous vein at the groin include the anterolateral and posteromedial tributaries, either of which may simulate a duplication of the saphenous circulation

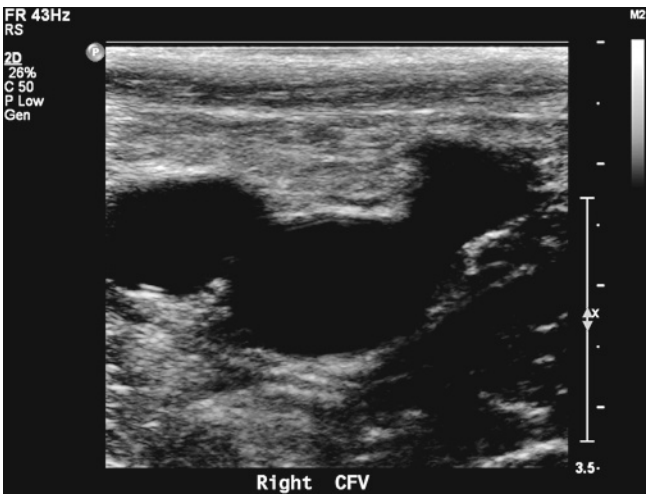


**Fig. 36.2** B-mode duplex ultrasound for normal saphenofemoral junction showing the Mickey Mouse duplex sign, GSV, CFV, and CFA

compartment which allows antegrade flow to the heart. In the meantime, valve closure prevents reverse venous flow or refluxing to the superficial system. As the muscle relaxes, the pressure within the compartment decreases and allows antegrade flow of venous blood from the superficial to the deep system (Figs. 36.2 and 36.3).

There are many methods to classify venous diseases, depending on factors such as distribution and severity; however, the most effective method is to assess severity based on clinical, etiological, anatomical, and pathophysiological aspects. This international classification is not only an efficient description, but useful in determining appropriate management. Understanding the new terminology is crucial, not only to keep up with the American venous forum update, but also to serve as a common language among venous specialists.

## Revised CEAP Classification of Venous Disorders

### C: Clinical Findings

The letter "C" is based on clinical findings, usually seen on physical examination [5, 6]:

$C_0$ = no visible venous disease
$C_1$ = telangiectatic or reticular veins
$C_2$ = varicose veins
$C_3$ = edema
$C_4$ = skin changes without ulceration
$C_5$ = skin changes with healed ulceration
$C_6$ = skin changes with active ulceration

More than one number may be assigned if the patient has several findings on clinical examination. After the numeric subscript, the letter "a" is assigned if the patient is asymptomatic or "s" if the patient experiences symptoms. Lastly, an additional number may follow the "s" to denote the severity of the symptom. The clinical disability scores for chronic venous insufficiency are:

0 = a patient who is asymptomatic, and thus has no disability
1 = a patient who is symptomatic, but can function without a support device
2 = a patient who can work an 8-h day with a support device
3 = a patient who is unable to work, even with a support device

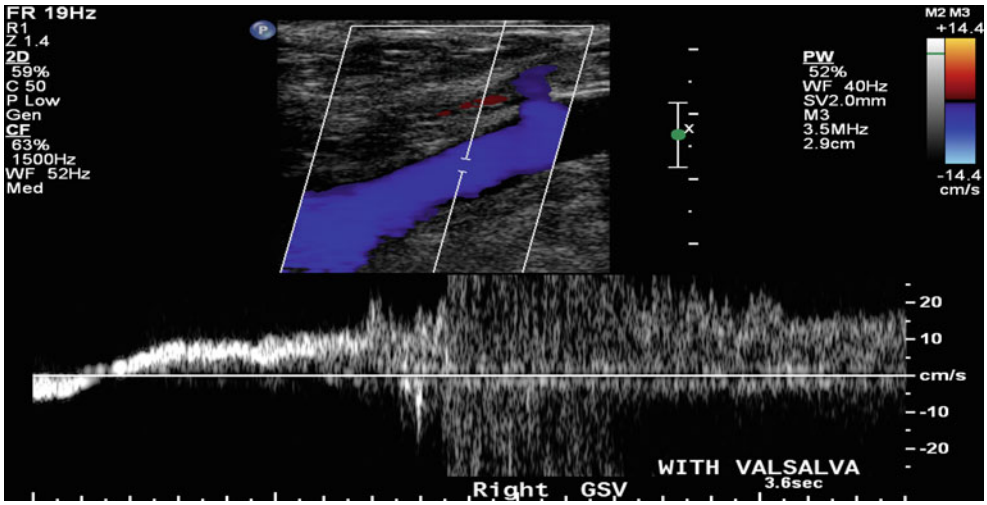


**Fig. 36.3** B-mode duplex ultrasound for significant reflux at the saphenofemoral junction elicited with Valsalva maneuver (>0.5 s)

### E: Etiology

The "E" stands for etiology, with subscript "c" for congenital disease, "p" for primary disease (not due to another cause), or "s" for secondary venous disease, usually due to prior deep vein thrombosis.

### A: Anatomic Findings

The "A" refers to the anatomic findings, usually based on duplex ultrasound examination. The options are as follows:

*Superficial veins* ($A_s$)

1. Telangiectasias or reticular veins
2. Great saphenous vein—above the knee
3. Great saphenous vein—below the knee
4. Small saphenous vein
5. Nonsaphenous

*Deep veins* ($A_d$)

6. Inferior vena cava
7. Common iliac
8. Internal iliac
9. External iliac
10. Pelvic: gonadal, broad ligament
11. Common femoral
12. Deep femoral
13. Femoral (between the groin and the knee)
14. Popliteal
15. Crural: anterior tibial, posterior tibial, peroneal
16. Muscular: gastrocnemius, soleus

*Perforating veins* ($A_p$)

17. Thigh
18. Calf

### P: Pathophysiologic Component

The "P" refers to the pathophysiologic component, with subscript "r" for reflux, "o" for obstruction, or "r, o" for both reflux and obstruction.

There are multiple ways to understand venous disorders:

1. Obstructive
   (a) Acute
   Superficial
   Deep
   (b) Chronic
   Superficial
   Deep
2. Valvular dysfunction (Incompetence)
   (a) Superficial
   (b) Deep
   (c) Perforators
3. Inflammatory
   (a) Superficial thrombophlebitis
4. Congenital
   (a) May–Turner syndrome
   (b) Paget–Schrotter syndrome
   (c) Klippel–Trenaunay syndrome

## Superficial Thrombophlebitis

Superficial thrombophlebitis (STP) is an inflammatory condition associated with thrombus formation within the superficial veins. It commonly occurs in the lower extremity; however, the incidence in the upper extremity is increasing, secondary to intravenous instrumentation. It usually has a benign and self-limited course. Clinical presentations include pain, redness, and swelling along the course of the affected vein. Fever and malaise are not uncommon. The pathophysiology can be explained in light of Virchows's triad consisting of blood stasis, endothelial injury, and hypercoagulability. Therefore, a history of minor trauma or long travel may be the initial nidus for STP. Proper diagnosis and appropriate treatment is crucial to alleviate the pain

**Table 36.3** Hypercoagulability factors

| Thrombophilia | Normal | Incident VTE | Recurrent VTE | Incidence (95% CI) |
|---|---|---|---|---|
| Factor V Leiden | 3–7 | 12–20 | 30–50 | 150 (80–260) |
| Antithrombin III deficiency | 0.02–0.04 | 1–2 | 2–5 | 500 (320–730) |
| Protein C deficiency | 0.02–0.05 | 2–5 | 5–10 | 310 (530–930) |
| Protein S deficiency | 0.01–1 | 1–3 | 5–10 | 710 (530–930) |
| Hyperhomocysteinemia | N/A | N/A | N/A | N/A |
| Antiphospholipid Ab | N/A | N/A | N/A | N/A |
| Prothrombin G20210A | 1–3 | 3–8 | 15–20 | 350 |
| Combined thrombophilias | N/A | N/A | N/A | 840 (560–1,220) |
| Factor VIII (>200 IU/dL) | N/A | N/A | N/A | N/A |

and discomfort. A venous duplex scan will delineate the distribution of the STP and rule out the presence of DVT [7, 8]. The incidence of DVT is estimated to be as high as 40% in patients with STP. Migratory STP should raise the suspicion for underlying malignancy or other thrombophilias. Some diseases, such as Buerger's disease, may be associated with migratory STP. Treatment is usually conservative and includes graduated compression stockings (30–40 mmHg), ambulation, and nonsteroidal antiinflammatory medications (Ibuprofen). Antibiotics are not recommended unless there is surrounding cellulitis. Special attention should be paid to a free-floating GSV thrombus at the SFJ, which should be treated with anticoagulation, or an IVC filter in those who have a contraindication to anticoagulation. Patients with iliofemoral DVT that meet the free-floating criteria are at significant risk for a pulmonary embolism, despite the administration of heparin [9].

## Deep Venous Thrombosis (DVT)

Venous thromboembolism (VTE) is the fourth leading cause of death in Western countries. It is a common cause of morbidity and mortality. Although it is a preventable disease, the incidence of VTE exceeds 1/1,000 persons, with almost 400,000 new cases annually in the United States. Of patients who survive the initial event of VTE, 30% will have some kind of recurrence and 30% will develop postphlebitic syndrome within 10 years. Despite overwhelming evidence for the effectiveness of regimens [10–13], the concern over bedside prophylaxis and management often dissuades physicians from complying with guidelines.

The Virchow triad is often used to explain the development of perioperative DVT. Vascular stasis occurs primarily in the great veins of the body, which act as a reservoir system for circulation. At any given moment, approximately 70% of the total blood is contained in the venous system. Stagnation of venous blood is more likely when the patient is lying flat under the effect of anesthesia, particularly during laparoscopic surgery. The second component, hypercoagulability, occurs as a consequence of decreased clearance of the procoagulant factors (as seen in Table 36.3), or depletion of the lytic system (with or without underlying coagulopathies). The third component, endothelial damage, results from direct trauma to the vessel or by placement of a prosthetic graft. The combined influence of these factors promotes the development of venous thrombi in low-flow areas (e.g., subadjacent to the venous valves or adjacent to foci of intimal disruption). The propagation of thrombus leads to the development of overt DVT [14–20].

Leg swelling causes passive muscle engorgement and dilation of the muscle fibrils. These, in turn, activate pain receptors located in the muscle spindle and account for muscle discomfort. Stretching of the muscle aggravates the discomfort; this is the physiologic basis for the Homan's sign (calf tenderness on dorsiflexion of the foot).

Additional factors that contribute to the pain are the inflammatory mediators released from stable clots that can contribute to the redness and leg swelling. DVT can be caused by numerous etiologies, including traumatic, vasculitic, hematologic, and drug-induced (Figs. 36.4 and 36.5).

### Causes of DVT

  - *General*Age, immobilization longer than 3 days, pregnancy and the postpartum period, major surgery in previous 4 weeks, long plane or car trips (>4 h) in previous 4 weeks
- *Medical*
  - Cancer, previous DVT, stroke, acute myocardial infarction (AMI), congestive heart failure (CHF), sepsis, nephrotic syndrome, ulcerative colitis, multiple trauma, CNS/spinal cord injury, burns, lower extremity fractures, vasculitis, systemic lupus erythematosus (SLE) and the lupus anticoagulant, Behçet syndrome, homocystinuria
- *Hematologic*
  - Polycythemia rubra vera, thrombocytosis, inherited disorders of coagulation/fibrinolysis, antithrombin III

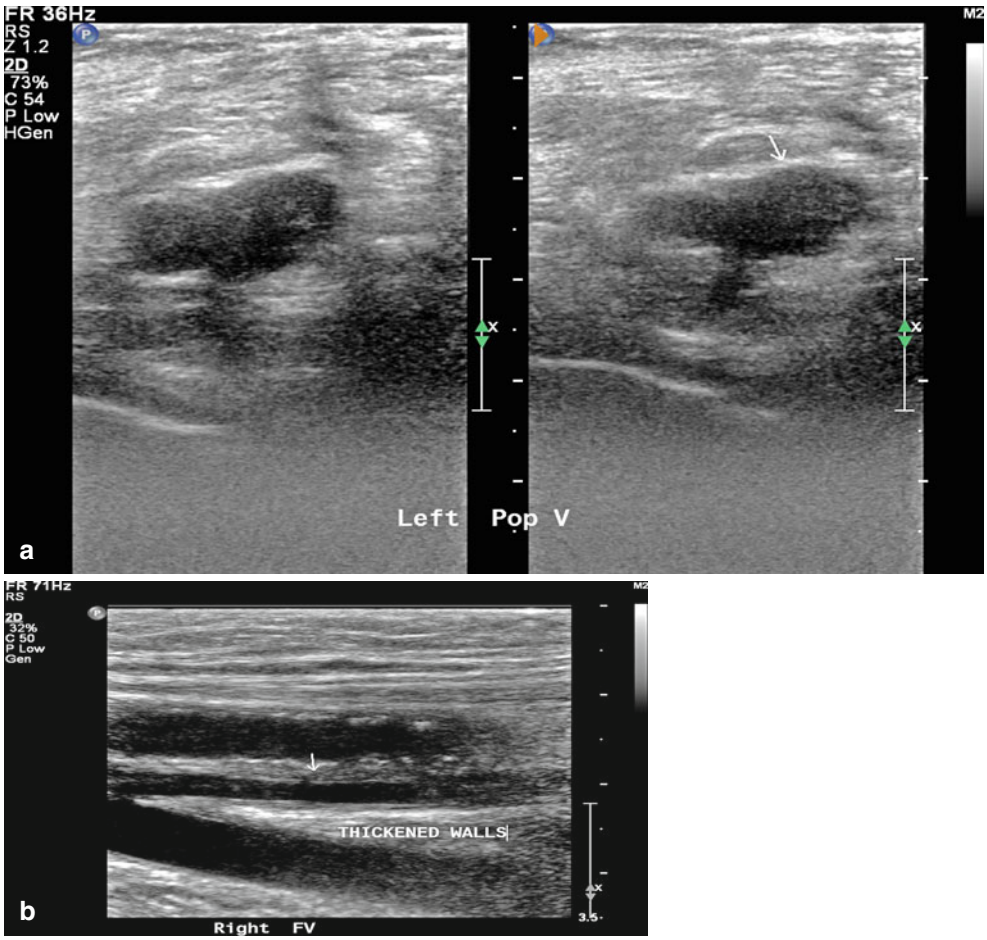


**Fig. 36.4** Duplex ultrasound showing acute DVT of popliteal vein with both B-mode (*arrow*) (**a**) and colored duplex (*arrow*) (**b**)

deficiency, protein C deficiency, protein S deficiency, Factor V Leiden, dysfibrinogenemias, and disorders of plasminogen activation

- *Drugs/medications*
  - IV drug abuse, oral contraceptives, estrogens, heparin-induced thrombocytopenia

## Pulmonary Embolism (PE)

Pulmonary embolism (PE) is one of the most dreaded complications of DVT. The true prevalence of perioperative PE is unknown; it varies according to the type of surgery, the use and type of prophylaxis, and the mode of diagnosis. Estimates indicate that without prophylaxis, fatal PE occurs in 0.1–0.8% of patients undergoing elective general surgery, 2–3% of those undergoing elective hip replacement, and up to 4–7% of those undergoing surgery for a fractured hip. The incidence of VTE increases after the age of 60 [10, 11].

Secondary to a potential lethal outcome of PE, early diagnosis is imperative for prompt therapy. Clinical presentation (shortness of breath, chest pain, and hemoptysis) and certain clinical criteria have been validated in the literature. The most commonly used validated criteria are the Wells score, which has been modified from year 1995 to 2001.

(a) Previous history of PE or DVT—1.5 points
(b) Clinical suspicion of DVT—3 points
(c) Tachycardia—3 points
(d) Alternative diagnosis is less likely than PE—3 points
(e) Active or previous diagnosis of cancer within 6 months—1 point
(f) Recent surgery ± immobilization within 4 weeks—1.5 points
(g) Recent history of hemoptysis—1.0 points

Score:

(a) <2 points—low probability
(b) 2–6 points—moderate probability
(c) >6 points—high probability

## Testing for Pulmonary Embolism

D-*Dimer Testing*: It is very sensitive but less specific for PE; therefore negative D-Dimer may exclude the presence of PE with great certainty.

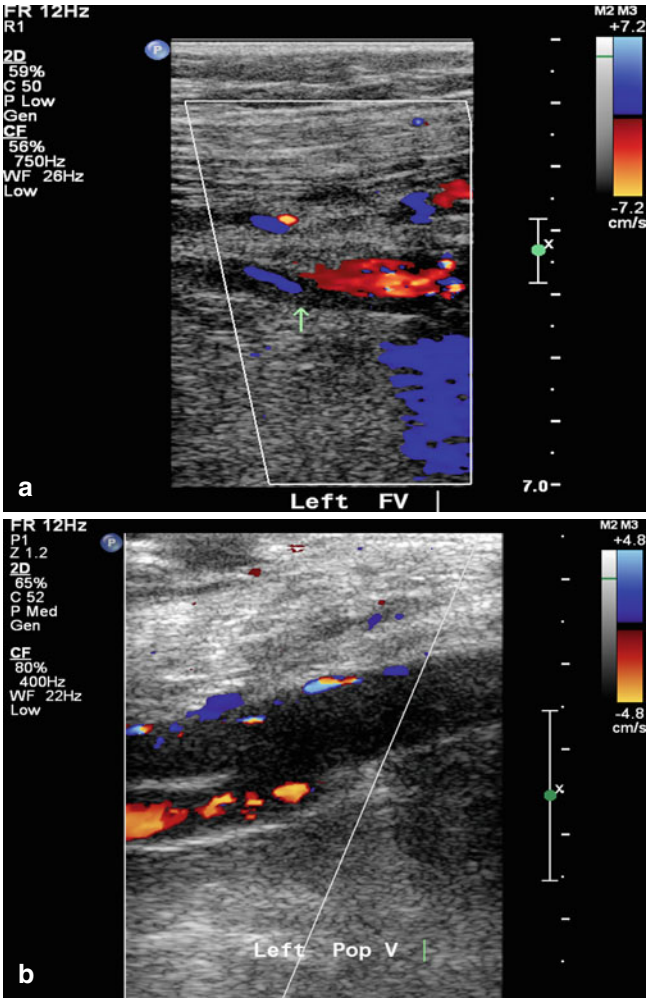


**Fig. 36.5** Duplex ultrasound showing chronic DVT of femoral vein with both B-mode (*arrow*) (**a**) and colored duplex (**b**)

*CT Pulmonary Angiography* (*CTPA*): Pulmonary angiogram was used to be the standard diagnostic tool to confirm a diagnosis of PE; however, advances in the multidetector CT machines with thinner slices have surpassed conventional pulmonary angiography as the diagnostic golden test for diagnosis of PE.

*Ventilation/Perfusion Scan* (*V/Q Scan*): It detects areas of the lung that are still ventilated but not perfused secondary to an occluded main pulmonary artery or its segmental branches. This test can be utilized in certain patients with an iodine allergy or in pregnant women, as radiation exposure for this test is significantly less than conventional pulmonary angiography. A positive V/Q scan is strengthened by a positive duplex ultrasound for DVT of an extremity.

*Pulmonary Embolism Rule-Out Criteria* (*PERC*) *Rule*: This is sensitive for ruling out PE: it includes age >50, heart rate >100, RA SAO2 94, prior DVT, or PE. If all are negative, the risk of PE is less than 2% [21].

## Isolated Soleal and Gastrocnemius Vein Thrombosis (ISGVT)

At the time of writing this chapter, there is no consensus regarding ISGVT and the ideal treatment for this condition remains undefined. Also, the recent guidelines (8th edition) on the *Antithrombotic and Thrombolytic Therapy* by the American College of Chest Physicians [22] did not arrive at a consensus regarding this issue. A recent study has shown that in patients with ISGVT, there was no difference whether anticoagulation therapy was used or not [23].

Another study demonstrated a 16% extension of ISGVT to deep veins, mainly the tibial veins. The presence of malignancy in this study was the only predictor of extension without the use of anticoagulation. Therefore, we think that the ideal management for ISGVT is to recommend early ambulation, compression stockings (30–40 mmHg), and repeating the venous duplex in 72 h, preferably by the same technologist. Any sign of thrombus extension to deep veins will warrant use of full anticoagulation, if there are no contraindications. The subset of patients who are at higher risk for thrombus extension, such as cancer and hemodialysis patients, may warrant more surveillance or treatment with anticoagulation.

## Venous Thrombosis in Unusual Sites

In the modern era of increasing rates of cardiac and infusion device implantations, the incidence of upper extremity DVT is increasing. VTE can occur in different venous territories, such as cerebral venous sinuses, renal, and visceral veins. Generally there is no consensus for treating these VTEs, therefore treatment should be individualized according to the presenting symptoms for each patient.

## Upper Extremity Venous Thrombosis

With the expanding and increasing indications for the use of defibrillators, pace makers, infusaports, and temporary dialysis accesses, the prevalence of asymptomatic UEVT is almost 50% in hospitalized patients. Other causes should be evaluated in patients with a sudden onset of UEVT, such as thoracic outlet syndrome (TOS) and neoplasms [20, 24, 25]. Fortunately, the risk of PE from UEVT is lower than for iliofemoral DVT: the rate of PE in patients with DVT involving the axillosubclavian system is 10–20% in comparison to 30–50% from the iliofemoral system. Until now, there has not been a validated consensus for treating these patients; however, UEVT with TOS should be treated with catheter-directed thrombolysis in conjunction with anticoagulation, followed by decompression surgery [26–30]. The current consensus for central line catheters (CLC) is removal of the

catheter and full anticoagulation. Secondary to a significant high risk of line-induced DVT, catheter placement in the subclavian vein is not recommended.

### Renal Vein Thrombosis (RVT)

The epidemiology of RVT is not well characterized; however, nephritic syndrome has been shown to be a high risk factor for developing RVT. Other conditions, such as renal cell carcinoma, have the propensity to invade renal veins in 25% of patients, and are usually a sign of a worse prognosis. Full anticoagulation is advisable if there are no contraindications, however its duration is not well established.

### Mesenteric Vein Thrombosis (MVT)

This was first described in 1935, and many factors can contribute to MVT, such as inherited thrombophilias, malignancies, liver diseases, and even pregnancy. Treatment with full anticoagulation is warranted; however, surgical exploration with bowel resection may be needed in severe cases.

### Ovarian Vein Thrombosis (OVT)

OVT is a rare, but serious complication in the postpartum phase. It is more common on the left side and can be associated with thrombus extension to the left renal vein or even PE. The current treatment is a 7-day course of heparin and antibiotics. In the absence of neoplasm, the outcome of OVT is quite benign with a durable long-term outcome [31, 32].

## Advanced Venous Thrombosis

(a) *Phlegmasia alba dolens* (PAD): This is indicated by significant swelling without cyanosis.

*Plegmasia cerula dolens* (PCD): This is indicated by significant swelling and cyanosis. It is the intermediate phase between PAD and venous gangrene. Expeditious intervention can salvage the limb [33].

(b) *Venous gangrene* (VG): This is indicated by full thickness skin necrosis, resulting in advanced cases of iliofemoral DVT. Partial thickness skin necrosis, e.g., blebs or blisters, can be noted in the early phase of VG.

*Phlegmasia cerula dolens* (PCD): This is characterized by massive limb swelling with cyanosis. It is caused by massive thrombosis and occlusion of the major venous system with significantly compromised venous outflow [34]. Multiple triggering factors can be involved including hypercoagulable syndrome, trauma, surgery, and even malignancy, which is the most common triggering factor and is present in approximately 20–40% of patients [35–38]. PCD has been reported with external compressive conditions such as May–Thurner syndrome and during the third trimester of pregnancy.

PCD was described by Gregoire in 1938, who made a clear distinction between PCD and plegmasia alba dolens (PAD). The first treatment for this condition is credited to Leriche and Geissendorfer, who performed the first thrombectomy in 1939 for cases of PCD. Historically, surgical thrombectomy has been the procedure of choice for PCD, after failure of anticoagulation and in pending venous gangrene cases.

Venous thrombosis is very extensive and patients present with significant pain and swelling of the extremity. Extension of the thrombosis to small venous capillaries will result in massive sequestration of fluid within tight facial compartments, which can compromise arterial inflow to the extremity. Salvage of the limb can be achieved if intervention is pursued before venous gangrene occurs.

PCD is more common in the lower extremities, especially on the left side, and involvement of the upper extremity can occur in up to 5% of cases. Up to 50% of cases will be preceded by PAD and characterized by pain with blanching edema (alba). In untreated cases, more venous thrombosis will contribute to cyanosis, which is pathognomonic to PCD and arterial ischemia. When venous gangrene develops, it echoes the distribution of the cyanosis. Arterial pulses can still be present in the early phase when the venous gangrene is superficial; however, in advanced scenarios, gangrene can involve muscular compartments with a subsequent increase in compartment pressures. At this phase, pulse deficit and arterial ischemia are inevitable.

## Superficial Venous Incompetence (SVI)

SVI is the most common form of venous disease that can occur secondary to valve dysfunction. Valve dysfunction can occur as a result of direct injury, phlebitis, DVT, or from a hormonal effect on the venous wall. Also, congenital weakness of the venous wall may allow venous dilation under normal pressure with subsequent valve failure (Fig. 36.3) [39].

Valvular dysfunction will allow retrograde flow through the affected segment, which will initiate a vicious circle of venous dilation, more valvular dysfunction, and venous hypertension. Over time, these incompetent veins become visibly dilated, elongated, tortuous, and at this stage they are recognized as varicose veins (CEAP 2).

There are two clinical syndromes of venous hypertension in the superficial venous system:

1. *Junctional*: usually occurs at the junctions between GSV and CFV at the SFJ, or between the SSV and popliteal

vein. As its name indicates, disease starts proximal and proceeds distally.
2. *Perforator*: usually occurs when the primary perforator valve fails, and is common at the mid-proximal thigh and proximal calf. Patients usually present with a cluster of veins distally and disease starts to proceed proximally [40, 41].

## Incidence

Among the different types of chronic venous disorders (CVD), chronic venous insufficiency (CVI) is considered the most common. CVI is the seventh leading cause of debilitating disease in the United States. It is estimated that up to 35% of the adult population has some form of CVD [41].

SVI is a significant morbid condition, and the risk of DVT is three times higher in patients with SVI. Approximately 500,000 Americans have ulceration due to superficial venous disease, and approximately 100,000 are disabled because of their condition. Also, the population-based cost in the United States [42–44] for the treatment of CVI and venous ulceration has been estimated to be over $1 billion/year. As many as 50% of patients with untreated varicose veins will develop superficial thrombophlebitis (STP) at some time, and unrecognized DVT is present in as many as 45% of patients with STP.

## Pathophysiology

Under normal conditions with efficient valves and muscle pumps, pressure is almost zero in the lower extremity during ambulation. During standing, pressure may rise, but it is relatively low. However, with dysfunctional valves, venous pressure is high during ambulation and standing and this contributes to venous hypertension. High venous pressure contributes to edema, impaired arterial inflow, protein deposition, perivascular fibrin cuffing, and red cell extravasation [45–49].

Both red cell extravasation and perivascular fibrin cuffing are the main theories to explain venous ulcers in the lower extremity. Red cell extravasation allows disposition of hemosidrin, which is remarkably irritant to skin with subsequent itching and skin breakdown. Fibrin cuffing is another valid theory, which outlines poor tissue oxygenation to be the inciting factor for developing venous ulcers [50].

Among chronic nonhealing ulcers of the lower extremity, the most common type is venous ulcers. Because most venous ulcers are mainly caused by venous reflux that is confined to the superficial venous system [51], we can conclude that the majority of lower extremity ulcers are secondary to SVI, and only a minority are caused by chronic DVT or valvular insufficiency in the deep veins.

## Congenital Venous Disorders

*Paget Schroetter Syndrome PSS* (*Effort Thrombosis*): This was initially described in relation to thoracic outlet syndrome (TOS), secondary to compression of the subclavian-axillary system between the scalene muscles and the first rib. This syndrome is considered to have lower incidence than the neurogenic TOS, however, it is more frequently secondary to catheterization of the subclavian vein. It is estimated that up to two-thirds of patients with subclavian lines will develop some sort of central venous stenosis. The clinical presentation includes severe, painful, upper extremity swelling with significant superficial venous engorgement. Treatment should include thrombolysis followed by TOS decompression. Iatrogenic PSS should be treated with thrombolysis followed by angioplasty in a select group of patients.

*May–Thurner Syndrome* (*MTS*; *Iliac Vein Compression Syndrome*): This syndrome was first described in 1957. After evaluation of 430 cadavers, May and Thurner hypothesized that extensive DVT is common in the left lower extremity secondary to external compression of the left iliac vein by the right iliac artery. Patients usually present with acute extensive DVT of the left lower extremity [52]. The true prevalence of this syndrome is still unknown, but it has been estimated to occur in 2–5% of patients who undergo evaluation for lower extremity venous disorders. The pathology of this condition is secondary to partial obstruction of the vein by the overlying artery, which contributes to subsequent physical entrapment of the left common iliac vein and may contribute to intimal hypertrophy of the vein. Regardless of the mechanism, this will cause iliac vein outflow obstruction with subsequent extensive ipsilateral DVT. Treatment of MTS includes staged therapy of thrombolysis with prophylactic retrievable IVC filter placement, followed by angioplasty/stenting of the left iliac vein. IVUS is an excellent tool to calibrate the diameter of the iliac vein, and a self-expanding stent is appropriate in this setting [49].

*Klippel–Trenaunay Syndrome* (KTS): This includes port-wine stains, varicose veins, and bony or soft-tissue hypertrophy. These patients are likely to have an anomalous superficial venous system with significant reflux. Due to atresia of the deep venous system, careful diagnostic evaluation is required. Treating the superficial venous reflux may require conservative measures since any surgical intervention may cause a loss of venous outflow in the affected limb. As in other conditions of venous insufficiency, capillary hemangiomas

(port-wine stains) of KTS can lead to local skin ulceration, bleeding, and possible infection.

## Diagnostic Evaluation of Chronic Venous Disease

Diagnosis is based on a thorough physical exam in conjunction with a duplex ultrasound [53]. The clinical evaluation will determine the severity and distribution of the CVI. Symptoms and signs should be evaluated in light of CEAP classifications, including telangiectasias, varicose veins, venous edema, skin discoloration, and venous ulceration.

*Duplex Ultrasonography* (*DU*): Using standing venous reflux protocol, DU for CVD is substantially different from that used for DVT. The study for reflux is tedious and requires more time to evaluate the level and severity of reflux and to include the assessment of both reflux and obstruction in the deep, superficial, and perforating veins from iliac to calf veins [54]. DU can be tailored according to the degree of clinical exam, for example in telangiectasias (clinical class 1), examination of the superficial veins is sufficient. For varicose veins, edema, skin discoloration, and ulcerations (clinical class 2–6), full examination of the entire three components (superficial, deep, perforator) are essential, especially if intervention is planned. With DU, it is feasible to distinguish between primary and secondary CVI, as the former has valvular reflux and varicose changes while the latter has luminal scarring and recanalization in postphlebitic syndrome. The main limitation of the DU is that it is operator and equipment dependent, and also appreciating reflux in early post-phlebitic syndrome may be difficult.

*Physiologic Noninvasive Tests* (*PT*): These are volumetric studies that quantify the reflux and can be helpful in establishing a baseline before therapy and a comparison scale afterward. Among many PT, air plethysmography (APG) is of clinical significance and can be used to give a quantitative estimate of venous reflux [55]. However with the advent and advances in DU, the clinical applicabilities of all PT tests are decreasing [56].

*Venography*: This was the gold standard test, however its role is decreasing with the advances in DU. Descending venography can be used in obstructive conditions to estimate the severity of reflux and to provide additional information regarding the patent venous channels. Ascending venography can be used to provide a road map for venous return and characterize the anatomy of the patent collaterals.

## Management of Varicose Veins

The initial treatment is multidisciplinary and includes exercise [57] and compression stockings [58–60]. When conservative therapy fails, surgical intervention should be offered. The main components of therapy are to defunctionalize GSV from the circulation and to minimize the effect of venous hypertension on varicose veins. With the advent of minimally invasive procedures, vein stripping is now considered a part of history. Laser or radiofrequency ablation of the affected vein is replacing standard vein stripping [61–67]. Details of this therapy are beyond the scope of this chapter; however, ablation is associated with less pain, a shorter stay, more patient satisfaction, and a faster recovery.

**Acknowledgment** The author records his special thanks to Dr. Mary Emmett for reviewing the content of this chapter.

## References

1. Federative International Committee for Anatomical Terminology. Terminologia anatomica. Stuttgart: George Thieme Verlag; 1998.
2. Caggiati A, Bergan JJ, Gloviczki P, Jantet G, Wendell-Smith CP, Partsch H, International Interdisciplinary Consensus Committee on Venous Anatomical Terminology. Nomenclature of the veins of the lower limbs: an international interdisciplinary consensus statement. J Vasc Surg. 2002;36:416–22.
3. Bundens WP, Bergan JJ, Halasz NA, Murrary J, Drehobl M. The superficial femoral vein: a potentially lethal misnomer. JAMA. 1995;274:1296–8.
4. Ludbrook J. The musculovenous pumps of the human lower limb. Am Heart J. 1966;71:635–41.
5. Eklof B, Rutherford RB, Bergan JJ, Carpentier PH, Gloviczki P, Kistner RL, et al. Revision of the CEAP classification for chronic venous disorders: consensus statement. J Vasc Surg. 2004;40(6):1248–52.
6. Allegra C, Antignani PL, Bergan JJ, Carpentier PH, Coleridge-Smith P, Cornu-Thenard A, et al. The "C" of CEAP: suggested definitions and refinements: an International Union of Phlebology conference of experts. J Vasc Surg. 2003;37(1):129–31.
7. Moneta GL. Regarding "the 'C' of CEAP: suggested definitions and refinements: an International Union of Phlebology conference of experts". J Vasc Surg. 2003;37(1):224–5.
8. Gillespie D, Glass C. Importance of ultrasound evaluation in the diagnosis of venous insufficiency: guidelines and techniques. Semin Vasc Surg. 2010;23(2):85–9.
9. Labropoulos N, Leon Jr LR. Duplex evaluation of venous insufficiency. Semin Vasc Surg. 2005;18(1):5–9.
10. Norris CS, Greenfield LJ, Herrmann JB. Free-floating iliofemoral thrombus. A risk of pulmonary embolism. Arch Surg. 1985;120(7):806–8.
11. Kosir MA, Kozol RA, Perales A, McGee K, Beleski K, Lange P, et al. Is DVT prophylaxis overemphasized? A randomized prospective study. J Surg Res. 1996;60(2):289–92.
12. McLeod RS, Geerts WH, Sniderman KW, Greenwood C, Gregoire RC, Taylor BM, et al. Subcutaneous heparin versus low-molecular-weight heparin as thromboprophylaxis in patients undergoing colorectal surgery: results of the Canadian colorectal DVT prophylaxis trial: a randomized, double-blind trial. Ann Surg. 2001;233(3):438–44.
13. Clarke JL. DVT prophylaxis: confronting a public health menace. Am J Med Qual. 2010;25(1 Suppl):4S–15.
14. Schumann SA, Ewigman B. Is it DVT? Wells score and D-dimer may avert costly workup. J Fam Pract. 2007;56(12):1010–2.
15. Villemur B, Bosson JL, Diamand JM. Deep venous thrombosis (DVT) after hip or knee prosthesis. Evaluation of practices for prevention and prevalence of DVT on Doppler ultrasonography. J Mal Vasc. 1998;23(4):257–62.

16. Guptan RC. Regarding "is there an increased risk for DVT with VNUS closure procedure?". J Vasc Surg. 2003;38(5):1140.
17. Komenaka IK, Nguyen ET. Is there an increased risk for DVT with the VNUS closure procedure? J Vasc Surg. 2002;36(6):1311.
18. Lindholm C. DVT: the forgotten factor in leg ulcer prevention. J Wound Care. 2002;11(1):5.
19. Neumann V, O'Connor RJ, Bhakta BB, Tennant A. DVT and pulmonary embolism after acute infection. Lancet. 2006;368(9531):201; author reply 201.
20. Hingorani AP, Ascher E, Markevich N, Schutzer RW, Kallakuri S, Mutyala M, et al. Prospective evaluation of combined upper and lower extremity DVT. Vasc Endovascular Surg. 2006;40(2):131–4.
21. Kline JA, Courtney DM, Kabrhel C, Moore CL, Smithline HA, Plewa MC, et al. Prospective multicenter evaluation of the pulmonary embolism rule-out criteria. J Thromb Haemost. 2008;6(5):772–80.
22. Hirsh J, Guyatt G, Albers GW, Harrington R, Schunemann HJ, American College of Chest Physician. Antithrombotic and thrombolytic therapy: American College of Chest Physicians Evidence-Based Clinical Practice Guidelines (8th edition). Chest. 2008;133(6 Suppl):110S–2.
23. Sales CM, Haq F, Bustami R, Sun F. Management of isolated soleal and gastrocnemius vein thrombosis. J Vasc Surg. 2010;52(5):1251–4.
24. Ault M, Artal R. Upper extremity DVT: what is the risk? Arch Intern Med. 1998;158(17):1950–2.
25. Monreal M, Raventos A, Lerma R, Ruiz J, Lafoz E, Alastrue A, et al. Pulmonary embolism in patients with upper extremity DVT associated to venous central lines–a prospective study. Thromb Haemost. 1994;72(4):548–50.
26. O'Brien PJ, Ramasunder S, Cox MW. Venous thoracic outlet syndrome secondary to first rib osteochondroma in a pediatric patient. J Vasc Surg. 2011;53(3):811–3.
27. Molina JE. Regarding "combination treatment of venous thoracic outlet syndrome: open surgical decompression and intraoperative angioplasty". J Vasc Surg. 2005;42(3):593; author reply 593.
28. Schneider DB, Dimuzio PJ, Martin ND, Gordon RL, Wilson MW, Laberge JM, et al. Combination treatment of venous thoracic outlet syndrome: open surgical decompression and intraoperative angioplasty. J Vasc Surg. 2004;40(4):599–603.
29. Lozano P, Doaz M, Riera R, Gomez FT. Venous thoracic outlet syndrome secondary to congenital pseudoarthrosis of the clavicle. Presentation in the fourth decade of life. Eur J Vasc Endovasc Surg. 2003;25(6):592–3.
30. Glass BA. The relationship of axillary venous thrombosis to the thoracic outlet compression syndrome. Ann Thorac Surg. 1975; 19(6):613–21.
31. Marsh P, Price BA, Whiteley MS. Prevalence and management of ovarian venous insufficiency in the presence of leg venous insufficiency. Phlebology. 2007;22(4):192.
32. Sutaria R, Subramanian A, Burns B, Hafez H. Prevalence and management of ovarian venous insufficiency in the presence of leg venous insufficiency. Phlebology. 2007;22(1):29–33.
33. Mahorner H. Diagnosis and treatment of phlegmasia alba dolens and phlegmasia cerulea dolens. Am Surg. 1968;34(3):210–2.
34. Mousa A, Henderson P, Dayal R, Bernheim J, Kent KC, Faries PL. Endoluminal recanalization in a patient with phlegmasia cerulea dolens using a multimodality approach. Vascular. 2005;13(5): 313–7.
35. Bird RL, Hamilton G. Treatment options for phlegmasia cerulea dolens. J Vasc Surg. 1995;21(6):998–9.
36. Harris Jr EJ, Kinney EV, Harris Sr EJ, Olcott CT, Zarins CK. Phlegmasia complicating prophylactic percutaneous inferior vena caval interruption: a word of caution. J Vasc Surg. 1995;22(5):606–11.
37. Jazayeri S, Tatou E, Cheynel N, Becker F, Brenot R, David M. A spontaneous rupture of the external iliac vein revealed as a phlegmasia cerulea dolens with acute lower limb ischemia: case report and review of the literature. J Vasc Surg. 2002;35(5):999–1002.
38. Kuo I, Smith J, Abou-Zamzam Jr AM. A multimodal therapeutic approach to phlegmasia cerulea dolens in a pediatric patient. J Vasc Surg. 2011;53(1):212–5.
39. Allegra C, Bergan J. Update on fundamental causes and management of chronic venous insufficiency. Executive summary. Angiology. 2003;54 Suppl 1:S1–3.
40. Bergan JJ. Venous insufficiency and perforating veins. Br J Surg. 1998;85(6):721–2.
41. Delis KT, Ibegbuna V, Nicolaides AN, Lauro A, Hafez H. Prevalence and distribution of incompetent perforating veins in chronic venous insufficiency. J Vasc Surg. 1998;28(5):815–25.
42. Aita DJ, Kvamme P, Rice JC, Kerstein MD. Venous insufficiency: a late sequelae of four-compartment fasciotomy in the lower extremity? Am Surg. 1993;59(9):574–7.
43. Thurston OG, Williams HT. Chronic venous insufficiency of the lower extremity. Pathogenesis and surgical treatment. Arch Surg. 1973;106(4):537–9.
44. Cranley JJ, Krause RJ, Strasser ES. Chronic venous insufficiency of the lower extremity. Surgery. 1961;49:48–58.
45. Manfredini R, Zamboni P. Regarding "chronic venous insufficiency is associated with increased platelet and monocyte activation and aggregation". J Vasc Surg. 2000;32(3):622.
46. Pappas PJ, You R, Rameshwar P, Gorti R, DeFouw DO, Phillips CK, et al. Dermal tissue fibrosis in patients with chronic venous insufficiency is associated with increased transforming growth factor-beta1 gene expression and protein production. J Vasc Surg. 1999;30(6):1129–45.
47. Powell CC, Rohrer MJ, Barnard MR, Peyton BD, Furman MI, Michelson AD. Chronic venous insufficiency is associated with increased platelet and monocyte activation and aggregation. J Vasc Surg. 1999;30(5):844–51.
48. Raffetto JD, Mendez MV, Marien BJ, Byers HR, Phillips TJ, Park HY, et al. Changes in cellular motility and cytoskeletal actin in fibroblasts from patients with chronic venous insufficiency and in neonatal fibroblasts in the presence of chronic wound fluid. J Vasc Surg. 2001;33(6):1233–41.
49. Raju S, Owen Jr S, Neglen P. The clinical impact of iliac venous stents in the management of chronic venous insufficiency. J Vasc Surg. 2002;35(1):8–15.
50. Fukuoka M, Okada M, Sugimoto T. Foot venous pressure measurement for evaluation of lower limb venous insufficiency. J Vasc Surg. 1998;27(4):671–6.
51. Treiman GS, Copland S, McNamara RM, Yellin AE, Schneider PA, Treiman RL. Factors influencing ulcer healing in patients with combined arterial and venous insufficiency. J Vasc Surg. 2001;33(6):1158–64.
52. Taheri SA, Williams J, Powell S, Cullen J, Peer R, Nowakowski P, et al. Iliocaval compression syndrome. Am J Surg. 1987;154(2): 169–72.
53. Asbeutah AM, Riha AZ, Cameron JD, McGrath BP. Reproducibility of duplex ultrasonography and air plethysmography used for the evaluation of chronic venous insufficiency. J Ultrasound Med. 2005;24(4):475–82.
54. Ruckley CV, Evans CJ, Allan PL, Lee AJ, Fowkes FG. Chronic venous insufficiency: clinical and duplex correlations. The Edinburgh vein study of venous disorders in the general population. J Vasc Surg. 2002;36(3):520–5.
55. Criado E, Farber MA, Marston WA, Daniel PF, Burnham CB, Keagy BA. The role of air plethysmography in the diagnosis of chronic venous insufficiency. J Vasc Surg. 1998;27(4):660–70.
56. Fukuoka M, Sugimoto T, Okita Y. Prospective evaluation of chronic venous insufficiency based on foot venous pressure measurements and air plethysmography findings. J Vasc Surg. 2003;38(4): 804–11.
57. Padberg Jr FT, Johnston MV, Sisto SA. Structured exercise improves calf muscle pump function in chronic venous insufficiency: a randomized trial. J Vasc Surg. 2004;39(1):79–87.

58. Partsch H, Menzinger G, Borst-Krafek B, Groiss E. Does thigh compression improve venous hemodynamics in chronic venous insufficiency? J Vasc Surg. 2002;36(5):948–52.
59. Felty CL, Rooke TW. Compression therapy for chronic venous insufficiency. Semin Vasc Surg. 2005;18(1):36–40.
60. Agu O, Baker D, Seifalian AM. Effect of graduated compression stockings on limb oxygenation and venous function during exercise in patients with venous insufficiency. Vascular. 2004;12(1):69–76.
61. Gloviczki P, Bergan JJ, Rhodes JM, Canton LG, Harmsen S, Ilstrup DM. Mid-term results of endoscopic perforator vein interruption for chronic venous insufficiency: lessons learned from the North American subfascial endoscopic perforator surgery registry. The North American Study Group. J Vasc Surg. 1999;29(3):489–502.
62. Huang Y, Jiang M, Li W, Lu X, Huang X, Lu M. Endovenous laser treatment combined with a surgical strategy for treatment of venous insufficiency in lower extremity: a report of 208 cases. J Vasc Surg. 2005;42(3):494–501; discussion 501.
63. Kundu S, Lurie F, Millward SF, Padberg Jr F, Vedantham S, Elias S, et al. Recommended reporting standards for endovenous ablation for the treatment of venous insufficiency: joint statement of the American Venous Forum and the Society of Interventional Radiology. J Vasc Surg. 2007;46(3):582–9.
64. Mendes RR, Marston WA, Farber MA, Keagy BA. Treatment of superficial and perforator venous incompetence without deep venous insufficiency: is routine perforator ligation necessary? J Vasc Surg. 2003;38(5):891–5.
65. Merchant RF, Pichot O. Long-term outcomes of endovenous radiofrequency obliteration of saphenous reflux as a treatment for superficial venous insufficiency. J Vasc Surg. 2005;42(3):502–9; discussion 509.
66. Neglen P, Eklof B, Kulwicki A, Davies A, Deschamps T, Garcia M, et al. Prevention and treatment of venous ulcers in primary chronic venous insufficiency. J Vasc Surg. 2010;52(5 Suppl):15S–20.
67. Tawes RL, Barron ML, Coello AA, Joyce DH, Kolvenbach R. Optimal therapy for advanced chronic venous insufficiency. J Vasc Surg. 2003;37(3):545–51.

# Plethysmographic Techniques in the Diagnosis of Venous Disease

37

Shadi Abu-Halimah and William A. Marston

**Abstract**

Various techniques of plethysmography have been developed to evaluate venous function in the lower extremity. They have been extensively investigated, but have been replaced with color duplex scanning for the anatomic examination of the deep and superficial venous systems. In the current management of venous disease, plethysmography is useful to assist in the management of complex venous disease when multiple anatomic abnormalities are identified and to document improvement in venous function after interventions are performed. In this way, it functions similarly to an ankle-brachial index to document improvement after arterial revascularization is performed.

Several plethysmographic techniques have been developed employing different sensors to measure changes in blood volume in a limb including strain-gauge plethysmography (SGP), impedance plethysmography (IPG), photoplethysmography (PPG), and air plethysmography (APG). These will be described in detail after the general concepts of plethysmographic evaluation for reflux and obstruction are reviewed.

**Keywords**

Venous disease • Plethysmography • Diagnosis

The term "plethysmography" is derived from the Greek words *plethynein* (to increase) and *graphein* (to record), yielding a definition of to record changes in volume. In venous disease, plethysmography is a noninvasive way to record the changes in limb volume with various maneuvers to diagnose venous disease. In limbs, tissues like bone, adipose tissue, muscle and skin have a relatively constant volume and changes in volume are attributable to changes in blood volume.

Various techniques of plethysmography have been developed to evaluate venous function in the lower extremity. They have been extensively investigated, but have been replaced with color duplex scanning for the anatomic examination of the deep and superficial venous systems. While duplex ultrasonography has become the noninvasive test of choice to diagnose obstruction and reflux in the lower extremity, this modality cannot determine the hemodynamic significance of the anatomic abnormalities identified. In the current management of venous disease, plethysmography is useful to assist in the management of complex venous disease when multiple anatomic abnormalities are identified and to document improvement in venous function after interventions are performed. In this way, it functions similarly to an ankle-brachial index to document improvement after arterial revascularization is performed.

Several plethysmographic techniques have been developed employing different sensors to measure changes in blood volume in a limb including strain-gauge plethysmography (SGP), impedance plethysmography (IPG), photoplethysmography (PPG), and air plethysmography (APG).

S. Abu-Halimah, M.D.
Department of Vascular Surgery, UNC Hospitals, Chapel Hill, NC, USA

W.A. Marston, M.D. (✉)
Vascular Surgery Division, Department of Surgery, UNC Hospitals, 3024 Burnett Womack Bldg. CB #7212, Chapel Hill, NC 27599, USA
e-mail: sky@med.unc.edu

A.F. AbuRahma, D.F. Bandyk (eds.), *Noninvasive Vascular Diagnosis*,
DOI 10.1007/978-1-4471-4005-4_37, 

These will be described in detail after the general concepts of plethysmographic evaluation for reflux and obstruction are reviewed.

## Plethysmographic Measurement of Venous Obstruction

Thrombi in the deep venous system increase venous outflow resistance and decrease venous compliance. These are the parameters that plethysmography measures as a means of detecting DVT. The increase in outflow resistance depends on whether the thrombi are totally or only partially occlusive, their length, the number of venous segments involved, and the location and extent of collateral development [1]. Venous pressure distal to the site of thrombosis is elevated depending on the increase in outflow resistance. Since the volume of blood leaving the leg is ordinarily unchanged in the presence of a thrombus, the same volume of blood traversing an elevated resistance will result in an increase in venous pressure. If, however, clots are very extensive, involving both the deep and superficial systems, there may be a decrease in blood flow. This occurs in the condition known as phlegmasia cerulea dolens.

Thrombi may reduce apparent venous compliance in several ways. First, when venous pressure is already elevated, the volume of blood in veins peripheral to an obstruction is already increased, and further rise in venous pressure will result in less additional filling. Second, venous walls become stiffer as they are distended by increased pressure. The third way is actually a reflection of the method used for measuring venous compliance. Compliance is usually measured as the volume change that occurs with a given rise in pressure divided by the baseline limb volume. If the veins are partially filled with thrombus, the degree to which they can expand by increasing their volume is limited since the residual capacity is limited. Finally, thrombi actually alter the elastic properties of venous walls, making them stiffer (Fig. 37.1) [2].

To diagnose chronic venous insufficiency, these tests rely on the fact that the lower extremity veins are not filled to maximum capacity when the patient is in the supine position. With positional changes or when outflow is occluded by a pressure cuff, the venous system can accommodate increased volume before reaching maximal venous capacitance. With subsequent rapid positional changes or release of an externally inflated pressure cuff, patients with normal outflow exhibit rapid emptying of their lower extremity veins. These tests now routinely use an occlusion cuff, which has increased standardization by avoiding active patient movement and positional changes.

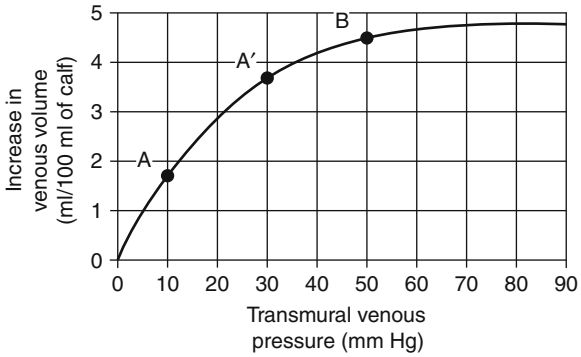


**Fig. 37.1** Calf venous pressure–volume curve. Pressure in the normal limb is low (*A*), but is elevated in the limb with acute deep venous thrombosis (*A'*). Inflating the thigh cuff to 50 mmHg increases the volume of the normal limb by almost 3% (*A* to *B*); however, in the abnormal limb, the volume increase is less than 1% (*A'* to *B*) (Reprinted from Sumner [2]. With permission from Elsevier)

Positioning of the patient is critical in these tests. The patient is placed supine with the leg elevated 20–30° on a soft heel support to enable venous drainage. The knee is flexed 10–20° to prevent obstruction of popliteal vein outflow. The volume sensor (air cuff, mercury strain gauge, or impedance electrodes) is placed around the calf or leg. An "occluding cuff" consisting of an air-filled bladder is wrapped around the thigh. When this cuff is suddenly inflated to a pressure exceeding that in the underlying veins (usually 50–60 mmHg), venous outflow is prevented by the collapse of the veins [3]. Pressures of this level, which are well below diastolic arterial pressure, have little effect on the diameter of the underlying arteries. Since arterial inflow is not affected by cuff inflation, blood is trapped in the leg distal to the cuff until the venous pressure rises to equal that in the cuff. At this point, venous outflow resumes.

When the veins are first occluded, the volume of blood in the calf rises in proportion to the rate of arterial inflow, gradually decreasing as the calf veins fill and their intraluminal pressure rises. Once venous pressure becomes equivalent to the cuff pressure, the calf volume ceases to increase and the recorded curve reaches a plateau. The volume increase that occurs from baseline to the plateau is a measure of venous compliance. Once a stable plateau is reached, the cuff is suddenly deflated, allowing the underlying thigh veins to expand. The blood trapped in the calf then rushes out, initially propelled by a pressure gradient equivalent to the 50 mmHg developed during the time of occlusion. The initial rate of outflow, as reflected by the initial slope of the outflow curve, is inversely proportional to venous resistance. As blood leaves the calf, distal venous pressure falls, thus decreasing the pressure gradient and the rate of outflow. The outflow curve is, therefore, curvilinear, with the convexity facing the baseline. When the venous pressure again returns to the

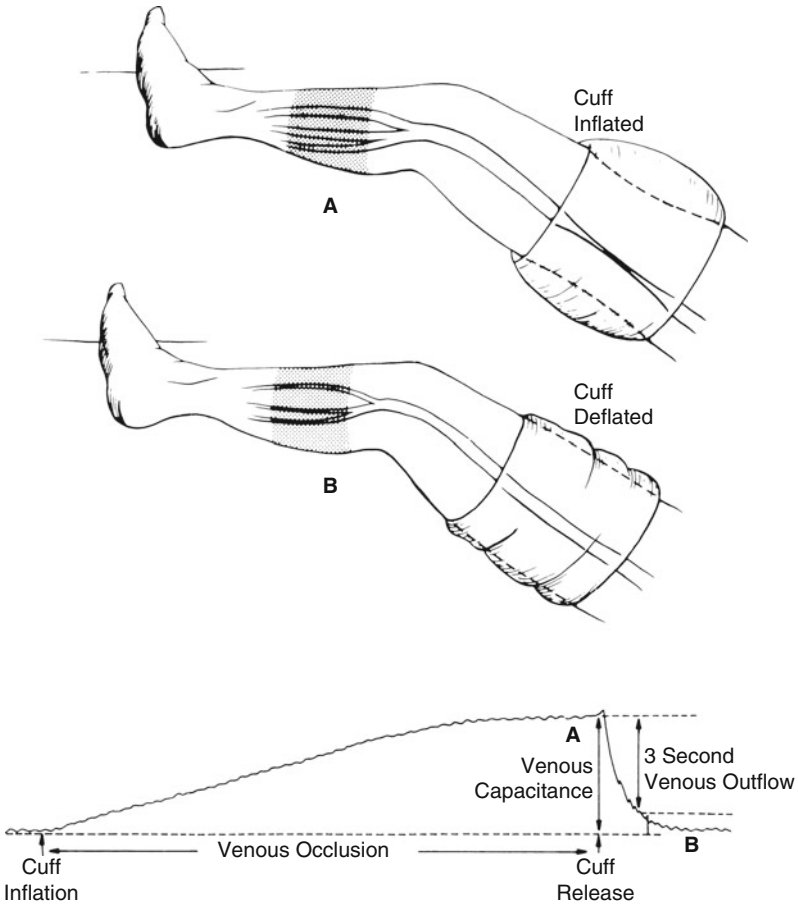


**Fig. 37.2** Venous outflow plethysmography. *Above*: correct positioning of the leg, cuff, and electrodes. *Below*: Typical normal tracing (Reprinted from Wheeler and Anderson [4]. With permission from Elsevier)

baseline level, the volume curve also returns to baseline (Figs. 37.2 and 37.3) [5].

Plethysmography suffers from poor sensitivity in the diagnosis of acute venous thrombosis as nonocclusive or minor thrombi in areas with well-developed collateral flow may result in little change in the measurement of volume changes. However, plethysmography may be useful in the evaluation of outflow obstruction to determine the hemodynamic importance of an anatomic abnormality or to document improvement following venous stenting [6].

## Plethysmographic Measurement of Venous Reflux

Plethysmography can be used to identify abnormal reflux in the lower extremity by examining volume changes when moving the limb from the supine to standing position. The test exploits the concept that the volume of the leg increases when placed in a dependant position. If venous valve function is good, this increase in volume occurs slowly compared to the rapid increase in volume that occurs with poor valve function. Again, plethsymography cannot identify the specific area of valve dysfunction, but the overall sequelae of venous reflux. Protocols using calf muscle contraction can also be performed with plethysmography to examine calf muscle pump function as a further measure of venous hemodynamics. These measures can be useful in the separation of venous reflux from other potential causes of limb pain. A patient may have reflux in a venous segment, but if their plethysmographic test measures are normal, the refluxing vein may not be causing symptoms and a search for other causes is warranted.

## Strain-Gauge Plethysmography (SGP)

The technique of SGP employs a silastic conductor tube connected to a plethysmograph via electrical contacts. As the gauge is stretched by a change in calf circumference the resistance increases in the conductor and a voltage change is recorded. The strain gauge is calibrated such that a 1% increase in voltage corresponds to a 1% change in limb volume. The venous volume (VV) is defined as the difference between baseline volume and the volume at peak venous capacitance, while the maximal venous outflow (MVO) is measured from the steepest portion of the outflow curve [7].

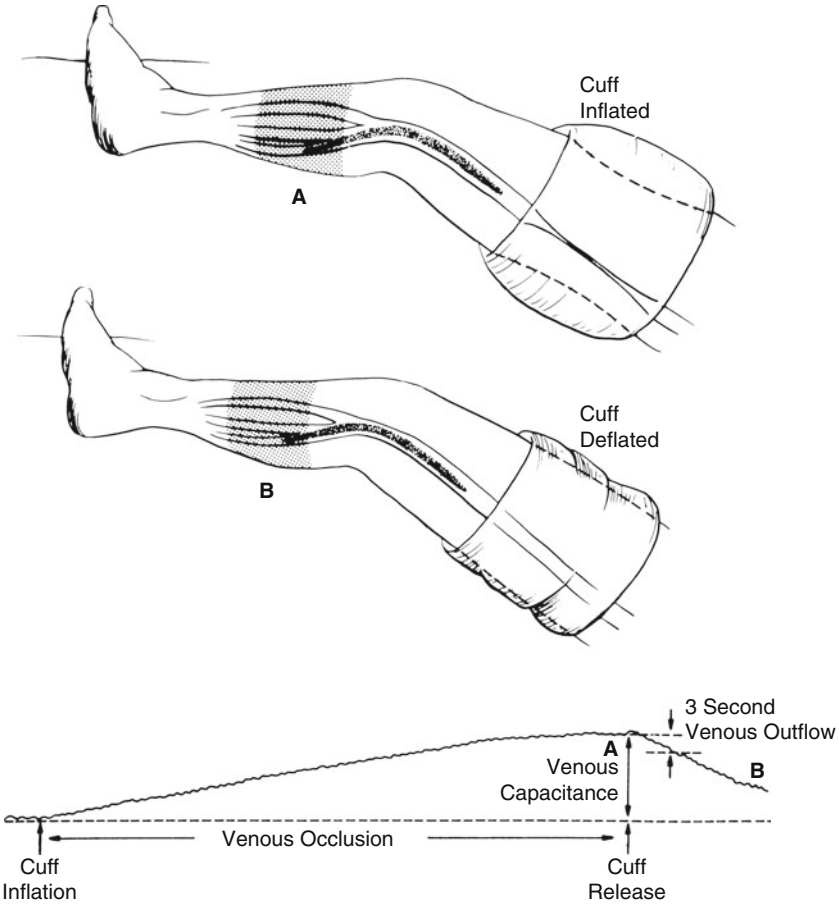


**Fig. 37.3** Venous outflow plethysmography. Typical abnormal tracings. The 3-s outflow is markedly reduced with recent deep venous thrombosis (Reprinted from Wheeler and Anderson [5]. With permission from Elsevier)

SGP has primarily been utilized in the diagnosis of DVT, based on evaluation of the MVO. Normal values for venous volumes average 2–3% above baseline, while limbs with venous outflow pathology would record a VV of less than 2%. This however is an unreliable diagnostic criterion, with MVO being a more reliable diagnostic tool [8]. Barnes and associates [9] reported the MVO to have a sensitivity of 90% for above the knee DVT, but only 66% for below the knee DVT, while the overall specificity was 81%. Rooke et al. [10] evaluated patients during exercise using strain-gauge plethysmography by plotting volume against time for each limb, calculating the volume of blood expelled and the time required for veins to refill following exercise. They observed that a shortened postexercise refilling time accurately identified limbs with incompetence, the clinical severity of incompetence was inversely related to refilling time, and the type of exercise performed had little effect on the study results.

Prolonged recumbency, postural changes, muscle wasting, arterial insufficiency, and cardiac failure may alter venous filling and lead to measurement errors with this technique. Thrombosis in tributary veins, partially occlusive clots; clots in one of a paired vein; or the presence of significant collaterals from previous episodes of thrombosis may not affect capacitance or outflow significantly and could result in normal or nearly normal VV and VO recordings. For these reasons, SGP is rarely used for the measurement of venous obstruction or reflux at the current time.

## Impedance Plethysmography (IPG)

Changes in limb circumference produce a comparable change in the electrical resistance, which is proportional to relative volume change. Impedance plethysmographs consist of electrodes wrapped around the leg. An increase in blood volume decreases impedance and is amplified to reflect volume change.

Increased limb volume results in decreased resistance. Two electrodes are placed 10 cm apart on the calf muscle to be evaluated. The voltage output is used to derive the resistance based on Ohm's law (voltage = current × resistance) and is then displayed as a continuous tracing. A thigh occlusion cuff is inflated and the tracing change across the electrodes is measured as it rises. After rapid cuff deflation, the tracing falls to baseline levels in 3–4 s.

The "rise" of the tracing from the baseline to the plateau measures venous capacitance, and the "fall" of the tracing

from the peak value over a 3 s period measures venous outflow. These measurements are plotted on a graph with the vertical axis representing the "fall" and the horizontal axis representing the "rise" [11].

In general, high capacitance and outflow indicate normal venous function and a low probability of DVT; conversely, low capacitance and outflow are highly suggestive of abnormal venous function with a high probability of DVT. The sensitivity of IPG in diagnosing DVT ranges from 33% to 96%, with accuracy improving when a five-test sequence is used. The test is more sensitive in patients with symptomatic and proximal DVT. Asymptomatic patients or those with DVT below the knee have significantly lower test sensitivity. The difference can be attributed to nonocclusive thrombi and well-developed collaterals [12–15].

The inaccuracies of this technique are due to the same issues that affect SGP; specifically, any condition that prevents patient cooperation obstructs access to the limb, elevates venous pressure, or reduces blood supply will produce false-positive or false-negative results. For these reasons, given the reliability of duplex ultrasound techniques, SGP and IPG are now rarely used to diagnose DVT. Neither modality has been well characterized as a diagnostic technique in the hemodynamic evaluation of chronic venous insufficiency (CVI).

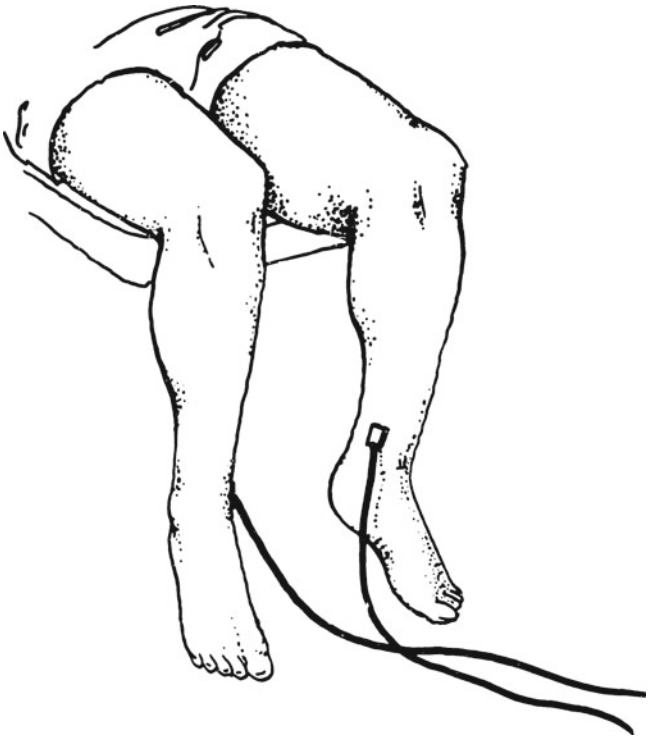

**Fig. 37.4** Photoplethysmography (PPG): patient positioning

## Photoplethysmography (PPG)

PPG uses light absorbance by hemoglobin as a reflection of blood volume in the venous and capillary networks in the skin to estimate the degree of venous stasis.

PPG uses a transducer that emits infrared light from a light-emitting diode into the dermis. The amount of light absorbed from the transducer is a good estimation of blood volume in the venous and capillary networks of the skin. The backscattered light is measured by an adjacent photo detector, and net absorption is displayed as a line tracing. Absorption of light is high when skin venous and capillary blood is increased during sitting or standing; conversely, it is decreased during exertion when venous blood is expelled from the limb by the action of the calf muscles.

The patient is asked to sit comfortably with the legs hanging freely. The transducer is applied to the leg and a baseline recording is obtained. The patient is then asked to perform five consecutive ankle flexion/extension maneuvers. The tracing drops as the calf muscles empty the veins. The time taken to recover to 90% of the original baseline tracing after the exertion is completed is recorded as the venous refill time (VRT, Fig. 37.4) [16, 17].

In normal individuals, VRT tends be longer than 20 s and can extend to as long as 60 s. Significant venous reflux results in a VRT of less than 20 s, and reducing times generally

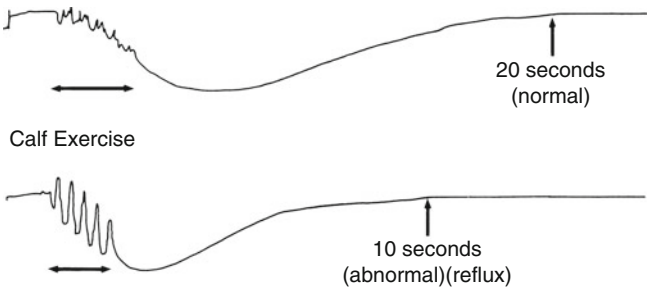


**Fig. 37.5** Venous reflux measured by photoplethysmography (PPG). Incompetent valves result in venous refilling time of less than 20 s

reflect increasing severity of reflux. In the presence of abnormal findings, the test can be repeated with a tourniquet inflated (50 mmHg) eliminating reflux in the superficial system to identify the source of reflux (Fig. 37.5).

Although PPG can provide an assessment of the overall physiologic function of the venous system, it is most useful as a relatively simple measure to detect the presence of venous reflux. Quantitative measurements are not obtained. PPG measurements have not been proved to be a strong discriminator of the severity of CVI.

In addition to being inversely proportional to the degree of reflux, refill time is also affected by arterial inflow. In the presence of occlusive arterial disease, VRT may be reduced despite an absence of venous reflux. This test also requires

full patient cooperation, and inability to perform the contraction maneuvers or inability to access the calf for proper placement of the transducer will preclude accurate results. VRT can vary depending on the site of photosensor placement, the small sample area obtained, and the type and amount of exercise performed during the recording. Placement near the site of a varicose or perforating vein may also affect the results. The test has limited reliability in differentiating deep from superficial reflux despite the addition of tourniquet testing. Because of its inability to reliably grade the severity of CVI, PPG has limited utility for assessing the results of corrective venous surgical procedures. Therefore, PPG is a reasonable measure of the presence or absence of CVI that is best used when no further information concerning the venous hemodynamic situation is desired. If information on the severity of CVI or evaluation of improvement after venous surgery is required, a quantitative test will be more useful [18].

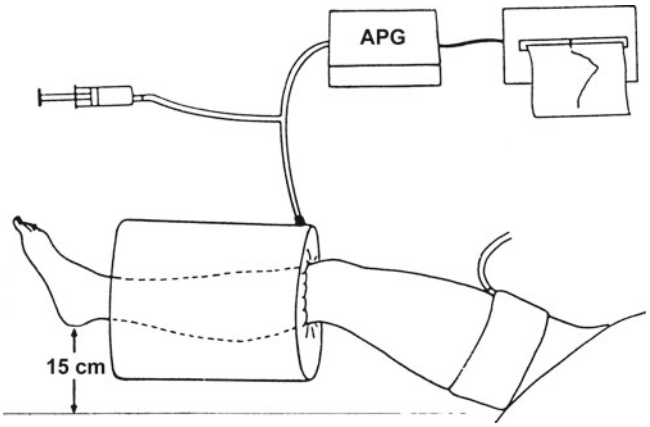


**Fig. 37.6** Air plethysmography (*APG*)

## Air Plethysmography (APG)

Air plethysmography utilizes a technique to improve on the shortcomings of PPG and other types of plethysmography that have limited sampling areas. It employs a low pressure air-filled cuff measuring 30–40 cm in length that is applied to the lower leg from knee to ankle. The cuff is connected to a plethysmograph that is very sensitive to volume changes in the cuff allowing precise quantitative evaluation of volume changes of the entire lower leg from knee to ankle. The patient lies supine initially with the leg elevated and supported at the heel, allowing the cuff to be applied to the lower leg. The cuff is inflated to a pressure of 6 mmHg to provide snug apposition to the limb without compressing the superficial veins. A baseline volume in the supine position is obtained with the patient resting. The patient then moves to a standing position supported by a walker to remove weight from the tested limb. The volume tracing gradually increases until a plateau is reached. The patient then performs one calf contraction/tiptoe maneuver followed by rest. A subsequent series of ten tiptoe maneuvers completes the test procedure. The test protocol may be repeated with the use of a thigh tourniquet to isolate the deep venous system from the superficial system (Fig. 37.6).

The data calculated from the tracings obtained are illustrated in Fig. 37.7. The venous volume (VV) is the difference in limb volumes obtained in the resting and standing positions. The venous filling index (VFI) is calculated by measuring 90% of the VV and dividing this volume by the time the limb requires to refill to 90% of the VV after moving to the standing position. Expressed in cc per second, VFI measures the average filling rate of the dependant leg and is slow in normal limbs. The volume of blood ejected with one tiptoe movement divided by the VV gives the ejection fraction (EF), and the limb volume remaining after ten tiptoe movements divided by the VV gives the residual volume fraction (RVF).

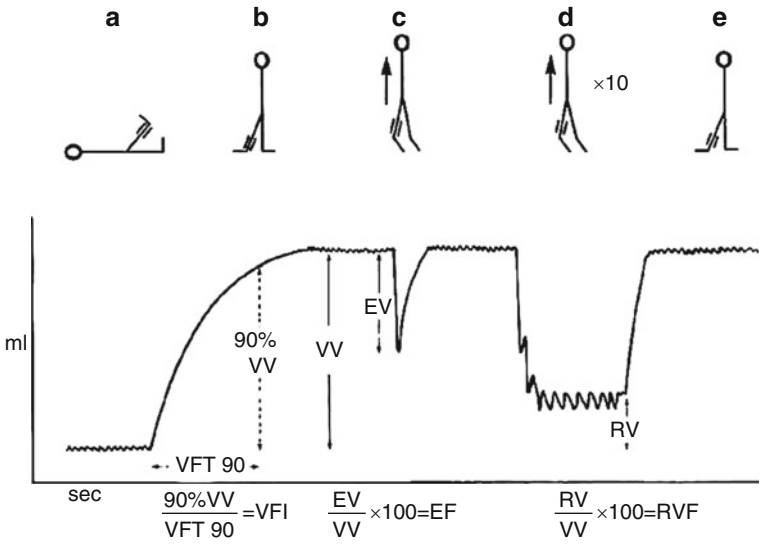


**Fig. 37.7** Diagrammatic representation of typical recording of volume changes during standard sequence of postural changes and exercise. The patient is in a supine position with the leg elevated 45° (**a**); patient standing with weight on the nonexamined leg (**b**); single tiptoe movement (**c**); ten tiptoe movements (**d**); same as in (**b**)/(**e**). *VV* functional venous volume, *VFT* venous filling time, *VFI* venous filling index, *EV* ejected volume, *RV* residual volume, *EF* ejection fraction, *RVF* residual volume fraction (Reprinted from Marston et al. [19]. Copyright © 1987 with permission from The Society of Vascular Surgery)

**Table 37.1** Prevalence of the sequelae of venous disease in relation to VFI in 134 limbs with venous disease studied with air plethysmography

| | Sequelae of venous disease | | |
|---|---|---|---|
| VFI (mL/s) | Swelling (%) | Skin changes (%) | Ulceration (%) |
| <3 | 0 | 0 | 0 |
| 3–5 | 12 | 19 | 0 |
| 5–10 | 46 | 61 | 46 |
| >10 | 76 | 76 | 58 |

Reprinted from Christopoulos et al. [21]. With permission from John Wiley & Sons

Limitations of both PPG and APG methodology are seen in patients with limited ability to stand unassisted or perform vigorous tiptoe maneuvers. Also, in patients with advanced CVI, particularly in classes 5 and 6, the ankle joint range of motion is frequently limited, as reported by Back et al. [20]. It is unclear whether some of the changes in EF and RVF seen in these groups are related to intrinsic dysfunction of the calf muscle pump, or an inability of the patient to activate the pump due to reduced ankle range of motion. APG is also limited in patients with obesity due to a maximum cuff size at the ankle. PPG therefore may be the only option in patients with larger limbs.

A VFI < 2 mL/s was associated with clinically normal limbs, and increasing levels of VFI were associated with more severe symptoms (Table 37.1) [21]. The VFI is believed to provide a reasonable approximation of the global function of the lower extremity venous system in resisting reflux in the standing position. The EF and RVF are measures of the efficacy of the calf muscle to pump blood out of the leg. The RVF was found to correlate closely with ambulatory venous pressure (AVP) throughout the range of AVP measurements, with lower RVF values representing better calf pump function (normal RVF defined as <35%) [22].

In an evaluation of 186 limbs, Criado et al. assessed the ability of APG parameters to predict the clinical severity of CVI. This is important primarily in the objective use of these tests for selection of patients for venous surgery and the monitoring of results and prediction of improvement after surgery. They reported that, of the APG parameters measured, VFI was the best predictor of the clinical severity of CVI. Ninety-three percent of limbs with a VFI < 2 mL/s were clinically Class 0 and only 9% of patients with a VFI > 5 were Class 0. VFI was found to have 80% sensitivity and 99% positive predictive value for detecting abnormal reflux. A successful surgical intervention in patients with CVI lowered the VFI to a normal level [23].

APG can be utilized as other techniques to evaluate venous outflow and diagnosis of DVT utilizing same method of the "pulse volume recorder". It is used in much the same way as the strain-gauge plethysmograph. A single pneumatic cuff placed around the calf and inflated with 10 $cm^3$ of air serves as the volume sensor. An occlusion cuff is placed around the thigh and inflated to 50–80 mmHg; then venous capacitance and MVO are measured. A venous score is calculated based on the 1 s outflow, the venous capacitance, a ratio of the venous capacitances of the two legs, the presence or absence of respiratory variations in limb volume, and Doppler ultrasonographic findings. A venous score of 4 or less excludes DVT, 5–7 is uncertain, and a score greater than eight implies venous obstruction [24, 25]. Nicolaides and Sumner have calculated the outflow fraction by dividing the 1-s VO by VV. Nicolaides has reported that the outflow fraction is higher than 38% in limbs with normal VO, 30–38% in patients with partial VO obstruction, and less than 30% in limbs with severe obstruction [22].

The VFI is useful for monitoring improvement in venous function and in predicting long-term outcome after venous surgical procedures. In a review of 71 patients undergoing venous surgery, Owens and associates reported that 94% of patients in whom the VFI corrected to less than 2 mL/s after venous surgery were asymptomatic after a mean follow-up of 44 months [6].

The VFI predicts recurrence of venous ulcers. In patients with healed leg ulcers, a VFI higher than 4 mL/s was associated with an increased risk for recurrence when compared with those with a VFI lower than 4 mL/s. For each 1 mL/s greater than 4 mL/s, the risk of ulcer recurrence increased 17%. Based on this information, APG parameters can be used to assist in the selection of patients at higher risk for recurrent ulceration who may wish to consider corrective venous procedures [26].

## Comparison of APG to PPG

APG, by sampling a large portion of the calf area, provides a better measure than PPG of the global venous function of the limb. APG accurately separates normal limbs from those with CVI, and the parameters that significantly ($p<0.05$) differentiated the two groups were VFI, VV, EF, and RVF. The PPG refill time has a sensitivity of 100% to identify reflux; however, the specificity is only 60%. Furthermore, the kappa coefficient between duplex and APG is 0.83, whereas between duplex and PPG it was only 0.47, concluding that APG is a better method of evaluating venous reflux than PPG. APG provides a quantitative analysis that appears to be useful in the selection and follow-up of patients undergoing venous reconstructive or ablative surgery [27].

## Selective Use of Noninvasive Venous Studies

When considering the need for venous noninvasive testing, several factors must be considered, including the clinical status of the patient, the question(s) being asked in each individual

patient, and the ability of the patient to comply with the requested study. Also, for routine clinical use, the technician time required and use of vascular lab resources are important issues. Less experienced technicians, or those in low volume labs would likely require longer examination times. The frequent use of multiple tests results in a large use of vascular technician time, a resource that may be in short supply in some situations. Therefore, studies should be ordered only when the information generated is important to the clinical management of the patient, unless involved in a research protocol. Some patients are technically poor candidates for study. Morbidly obese patients with suspected venous disease are poor candidates for APG due to cuff size limitations. These patients can generally be studied by PPG but the results may be less reliable. Duplex examination is more difficult in patients with obesity, but some reflux information can usually be generated, particularly in the lower leg. Patients who have difficulty standing without assistance are occasionally unable to perform proper tiptoe movements, rendering some APG and PPG measurements unreliable. These patients can often have a VFI performed with APG if they can move from a lying to standing position with assistance. In our clinic population, we estimate that 25–35% of patients with venous leg ulcers are unable to comply with the requirements for a full venous duplex and APG evaluation including calf muscle exercises.

If the only question asked is whether or not venous disease is present, and no details concerning anatomy or severity of CVI are necessary, PPG is a reasonable choice. It can determine the presence or absence of venous disease and is relatively rapid to perform. But if the primary question concerns the anatomic site of reflux in order to plan intervention, a supine and standing duplex evaluation should be performed. If the primary question concerns the severity of CVI, or whether improvement has occurred after intervention, APG measurements should be performed.

Specific situations in which hemodynamic measurement of venous function are important in clinical management:

1. Differentiation of venous symptoms from other causes of lower extremity pain
2. Evaluation of the hemodynamic significance of incompetent perforator veins
3. Evaluation of the improvement in venous hemodynamics in a patient with multisystem valvular incompetence after intervention to correct one area of incompetence.
4. Prediction of long-term outcome after surgical or endoluminal venous procedures.

## References


1. Sumner DS. Diagnosis of deep venous thrombosis. In: Rutherford RB, editor. Vascular surgery. Philadelphia: W.B. Saunders Company; 1995. p. 1698–743.
2. Sumner DS. Diagnosis of deep vein thrombosis by straingauge plethysmography. In: Bernstein EF, editor. Vascular diagnosis. St. Louis: C.V. Mosby; 1993. p. 811–9.
3. Barnes RW, Collicott PE, Sumner DS, et al. Noninvasive quantitation of venous hemodynamics in postphlebitic syndrome. Arch Surg. 1973;107:807.
4. Wheeler HB, Anderson Jr FA. Impedance plethysmography. In: Kempczinski RF, Yao JST, editors. Practical noninvasive vascular diagnosis. Chicago: Mosby; 1987.
5. Wheeler HB, Anderson Jr FA. Diagnosis of deep vein thrombosis by impedance plethysmography. In: Bernstein EF, editor. Vascular diagnosis. St. Louis: C.V. Mosby; 1993. p. 820–9.
6. Owens LV, Farber MA, Young ML. The value of air plethysmography in predicting clinical outcome after surgical treatment of chronic venous insufficiency. J Vasc Surg. 2000;32:961–8.
7. AbuRahma AF. Strain-gauge plethysmography in diagnosis of deep vein thrombosis. In: AbuRahma AF, Diethrich EB, editors. Current noninvasive vascular diagnosis. Littleton: PSG Publishing Company, Inc.; 1988. p. 271–81.
8. Hallbook T, Gothlin J. Strain-gauge plethysmography and phlebography in diagnosis of deep venous thrombosis. Acta Chir Scand. 1971;137:37.
9. Barnes RW, Collicott PE, Mozersky DJ, et al. Noninvasive quantitation of maximum venous outflow in acute thrombophlebitis. Surgery. 1972;72:971.
10. Rooke TW, Heser JL, Osmundson PJ. Exercise strain-gauge venous plethysmography: evaluation of a “new” device for assessing lower limb venous incompetence. Angiology. 1992;43:219.
11. Hull R, van Aken WG, Hirsch J, et al. Impedance plethysmography: using the occlusive cuff technique in the diagnosis of venous thrombosis. Circulation. 1976;53:696.
12. Hall R, Hirsch J, Sackett DL. Impedance plethysmography: the relationship between venous filling and sensitivity and specificity for proximal vein thrombosis. Circulation. 1978;53:696.
13. Wheeler HB. Diagnosis of deep vein thrombosis: review of clinical evaluation and impedance plethysmography. Am J Surg. 1985;150:7.
14. Comerata AJ, Katz ML, Grossi RJ, et al. The comparative value of noninvasive testing for diagnosis and surveillance of deep venous thrombosis. J Vasc Surg. 1988;7:40.
15. Agnelli G, Cosmi B, Radicchia S, et al. Features of thrombi and diagnostic accuracy of impedance plethysmography in symptomatic and asymptomatic deep vein thrombosis. Thromb Haemost. 1993;70(2):266.
16. Abramowitz HB, Queral LA, Flinn WR, et al. The use of photoplethysmography in the assessment of venous insufficiency: a comparison to venous pressure measurements. Surgery. 1979;86:434–40.
17. Nicolaides AN, Miles C. Photoplethysmography in the assessment of venous insufficiency. J Vasc Surg. 1987;5:405.
18. Criado E. Laboratory evaluation of the patient with chronic venous insufficiency. In: Rutherford RB, editor. Vascular surgery. Philadelphia: W.B. Saunders Company; 1995. p. 1771–85.
19. Marston WA, Christopoulos DG, et al. Air plethysmography and the effect of elastic compression on venous hemodynamics of the leg. J Vasc Surg. 1987;5:148–59.
20. Back TL, et al. Limited range of motion is a significant factor in venous ulceration. J Vasc Surg. 1995;22(5):519–23.
21. Christopoulos D, Nicolaides AN, Szendro G. Venous reflux: quantitation and correlation with the clinical severity of chronic venous disease. Br J Surg. 1988;75:352–6.
22. Nicolaides AN, Sumner DS, editors. Investigation of patients with deep vein thrombosis and chronic venous insufficiency. London: Med-Orion; 1991. p. 39–43.
23. Criado E, Farber MA, Marston WA, Danniel PF, Burnham CB, Keagy BA. The role of air plethysmography in the diagnosis of chronic venous insufficiency. J Vasc Surg. 1998;27:660–70.

24. Howe Jr HR, Hansen KJ, Plonk Jr GW. Expanded criteria for the diagnosis of deep venous thrombosis: use of the pulse volume recorder and Doppler ultrasonography. Arch Surg. 1984;119: 1167.
25. Schroeder PJ, Dunn E. Mechanical plethysmography and Doppler ultrasound: diagnosis of deep vein thrombosis. Arch Surg. 1982;117:300.
26. McDaniel HB, Marston WA, Farber MA, et al. Recurrence of chronic venous ulcers on the basis of clinical, etiologic, anatomic, and pathophysiologic criteria and air plethysmography. J Vasc Surg. 2002;35(4):723.
27. Bays RA, Healy DA, Atnip RG, et al. Validation of air plethysmography, photoplethysmography, and duplex ultrasonography in the evaluation of severe venous stasis. J Vasc Surg. 1994;20(5):721.

# Venous Duplex Ultrasound of the Lower Extremity in the Diagnosis of Deep Venous Thrombosis

38

M. Ashraf Mansour

**Abstract**

Acute lower extremity deep venous thrombosis (DVT) is a common clinical problem in both in-patients and outpatients. The clinical symptoms and signs are often vague and nonspecific, therefore an accurate diagnostic test is needed to help guide management. Venous color-flow duplex scanning has been refined over the last two decades and now become the "gold standard" test for acute DVT. The technique of scanning and findings of acute DVT are described.

**Keywords**

Acute deep venous thrombosis • Duplex scan • Noninvasive diagnosis

## Introduction

Venous thromboembolism (VTE) has been recognized as an important health problem for decades, and yet, decreasing its incidence has been elusive. Recently, the Surgeon General of the United States has issued a document widely distributed to healthcare workers highlighting the importance of this disease [1]. The exact incidence of deep venous thrombosis (DVT) is not known since up to half of the cases confirmed at autopsy went unrecognized antemortem [2]. In the United States, it is estimated that nearly 900,000 cases of DVT are identified annually and 300,000 deaths occur due to pulmonary embolism (PE) [3]. The incidence of DVT in hospitalized patients is variable. Without prophylaxis, the lowest incidence is found in medical patients, 10–20%, while the highest incidence is 40–60% in patients undergoing major orthopedic procedures [4, 5]. The long-term morbidity in patients suffering from an acute episode of DVT is also considerable [6–9]. The development of chronic venous insufficiency with its dreaded sequelae of chronic swelling, pain, and ulceration leads to increased costs in healthcare in addition to the loss of work productivity for patients. The objective of this chapter is to describe the role of venous duplex ultrasonography in the diagnosis of lower extremity DVT.

## Pathophysiology of Acute DVT

Historically, venous disease has been recognized since 1550 BC in the Ebers papyrus. However, in 1856, it was the German physician Rudolf Virchow (1821–1902) who postulated that thrombosis in a blood vessel occurs due to abnormalities in flow, viscosity, or vessel wall injury [10]. Subsequently, this has been referred to as "Virchow's triad." In clinical practice, patients on prolonged bed rest develop stasis due to inactivity and the loss of the foot and calf muscle pumps, normally activated by walking. Abnormal blood viscosity is recognized in patients suffering from thrombophilia (e.g., antithrombin III, protein C & S deficiency, factor V gene mutations, etc.) or other blood dyscrasias (e.g., polycythemia, multiple myeloma, etc.). Finally, vessel wall injury can occur due to extrinsic (trauma) or intrinsic (atherosclerosis) causes [2]. Thus it is evident that there are many risk

M.A. Mansour, M.D., RVT, FACS
Spectrum Health,
Grand Rapids, MI, USA

Department of Cardiovascular Surgery,
Spectrum Health Medical Group, Michigan State University,
4100 Lake Drive SE, Suite 300, Grand Rapids, MI 49546-8816, USA
e-mail: ashmans2@aol.com, ashraf.mansour@spectrum-health.org

A.F. AbuRahma, D.F. Bandyk (eds.), *Noninvasive Vascular Diagnosis*,
DOI 10.1007/978-1-4471-4005-4_38, 

**Table 38.1** Risk factors for VTE

| |
|---|
| Increasing age |
| Immobility, paralysis |
| Previous DVT |
| Malignant disease |
| Surgery |
| Trauma |
| Obesity |
| Pregnancy |
| Estrogen therapy |
| Nephrotic syndrome |
| Heart failure |
| Indwelling venous catheters |

Modified from Caprini [3]

**Table 38.2** Comparison of diagnostic modalities for lower extremity DVT

| Test | Accuracy | Limitations |
|---|---|---|
| Venous duplex | Sens: 93–100%<br>Spec: 97–100% | Operator-dependent, experience |
| Contrast venography | Sens: 100%<br>Spec: 100% | Up to 15% indeterminate, invasive |
| IPG | Sens: 73–96%<br>Spec: 83–95% | Inaccurate if nonocclusive thombus |
| CT venography | Sens: 93–100% | Invasive |
| MR venography | Sens: 87–100%<br>Spec: 95–100% | Cost |
| Nuclear scintigraphy ($I^{125}$-Fibrinogen) | Sens: 21–83%<br>Spec: 54–97% | Invasive<br>Not available in U.S. |

factors that have been recognized to predispose a patient to VTE [2–9]. The initiation of thromboprophylaxis in hospitalized patients should be based on risk assessment at the time of admission [3–5] (Table 38.1).

## Venous Duplex Scanning

Prior to the development of ultrasound scanners, contrast venography was considered the "gold standard" for the diagnosis of lower extremity DVT. Currently, venous duplex scanning is considered the gold standard, and contrast venography is reserved for special circumstances such as when an endovascular intervention is planned [2, 11–14]. Other invasive techniques include CT and MR venography, which are indicated in the evaluation of abdominal and pelvic veins or lower extremity vascular malformations. The other noninvasive techniques are described in Chaps. 36 and 37 (Table 38.2).

### Indications

The symptoms and signs of acute lower extremity DVT are nonspecific. The most common indications to test for a lower extremity DVT include localized pain, swelling, or redness in the calf or thigh, and calf pain with passive dorsiflexion (Homan's sign) [2, 13, 14]. In order to decrease the probability of a negative test, many physicians obtain a D-dimer level [15]. D-dimer is a fibrin degradation product released in the circulation when fibrinolysis starts on a formed blood clot. The value of D-dimer testing is when it is negative, meaning that it is unlikely that a blood clot is present. A positive D-dimer is present in many conditions, including trauma, pregnancy, inflammatory conditions, and recent surgery [15–18]. The Wells clinical score uses a point system to assess the probability of a DVT (Table 38.3).

**Table 38.3** Wells scoring

| Clinical characteristic | Point |
|---|---|
| Malignancy | 1 |
| Paralysis, paresis, cast | 1 |
| Recently bedridden for 3 days or more | 1 |
| Localized tenderness along course of a deep vein | 1 |
| Entire leg swollen | 1 |
| Calf swelling, 3 cm or increased circumference | 1 |
| Pitting edema in the symptomatic leg | 1 |
| Collateral superficial veins on symptomatic leg | 1 |
| Alternative diagnosis at least as likely as DVT | –2 |

Modified from Wells et al. [15]
*Probability*:
High >3 points
Intermediate 1–2 points
Low 0 points

### Instrumentation

Venous duplex scanning of the lower extremity can be performed with several transducers. In a normal adult of average body weight, a 5–10 MHz linear transducer is selected. In a larger or morbidly obese individual, a 3–5 MHz curved transducer will be required to image a deeper plane [9, 11]. In some patients, it may be necessary to use more than one transducer, a lower frequency for the abdomen and groin, and a higher frequency in the calf. In a complete lower extremity venous duplex examination, all three functions are utilized: B-mode, Doppler flow, and color flow.

### Technique

Since most ultrasound equipment is portable, venous duplex scanning can be performed in the vascular lab or at the bedside in the Emergency Department or Intensive Care Unit. The patient is positioned supine, and ideally the bed can be tilted for a reverse Trendelenberg or modified Fowler position. When possible, the thigh and calf are slightly externally rotated. To image the abdominal veins, patients should be fasting for 6 h prior to the exam.

The exam starts by placing the probe in the groin area. Examination of the deep veins, the femoral and common

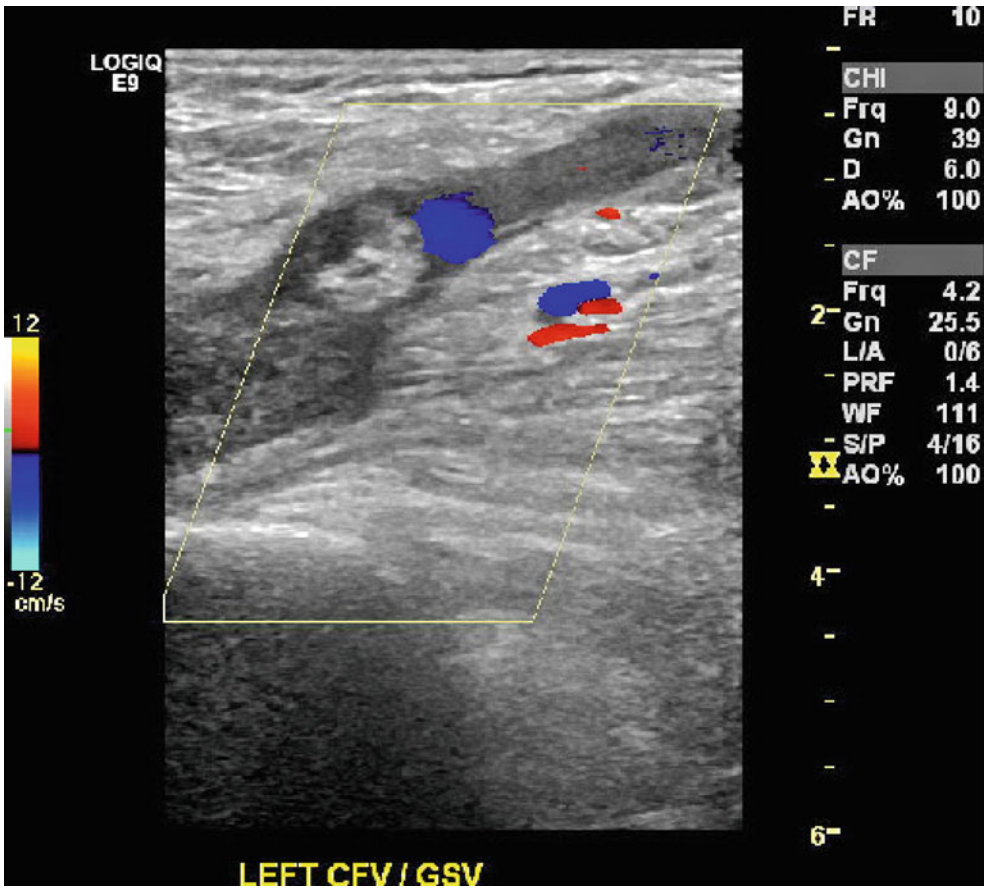


**Fig. 38.1** Saphenofemoral junction showing thrombus by B-mode, and near absence of color flow

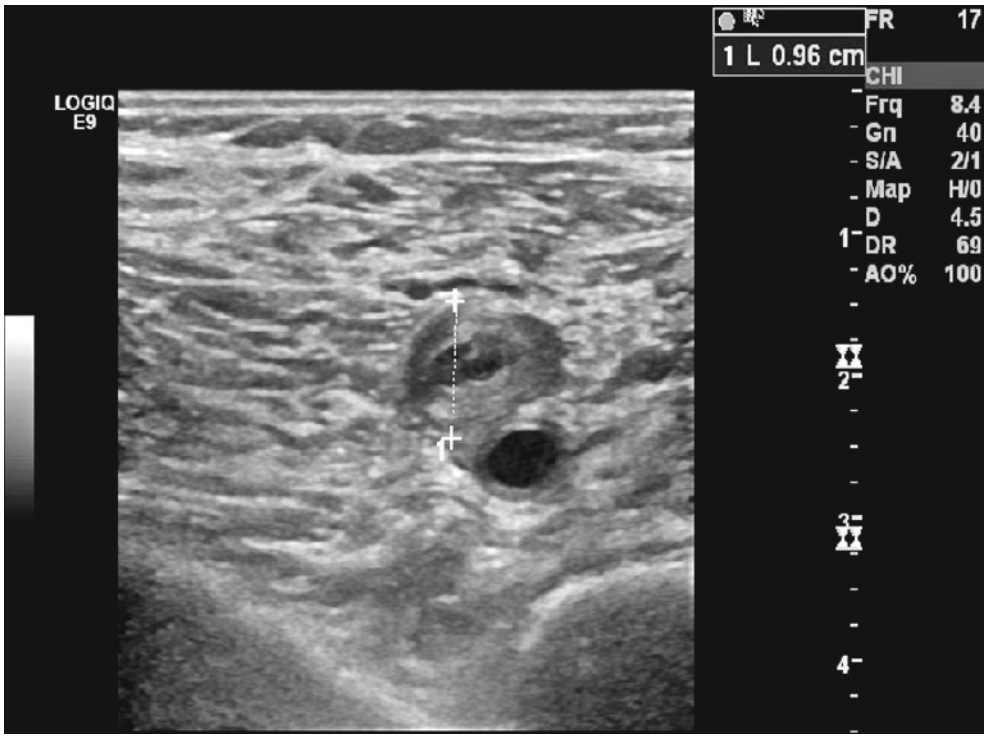


**Fig. 38.2** Acute DVT of the popliteal vein with hyperechoic material filling and distending the vein. The popliteal artery is adjacent showing normal echodensity of flowing blood

femoral veins, is performed in both the transverse and longitudinal views [9, 11, 14]. The great saphenous vein is imaged as it enters the saphenofemoral junction (Fig. 38.1). With each venous segment identified, gentle compression is exerted to see if the vein walls collapse (Fig. 38.2). This maneuver should be done every 3–5 cm along the length of the medial thigh and popliteal fossa. In addition to compression, Doppler flow is documented by placing the cursor in

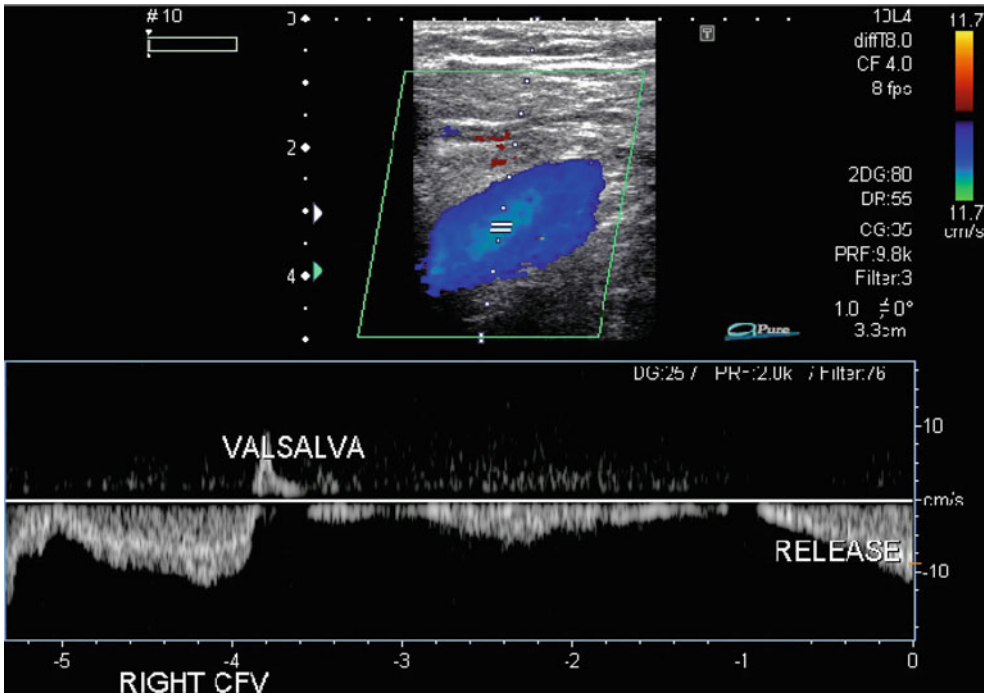


**Fig. 38.3** Normal color-flow and biphasic Doppler flow in a patent right common femoral vein

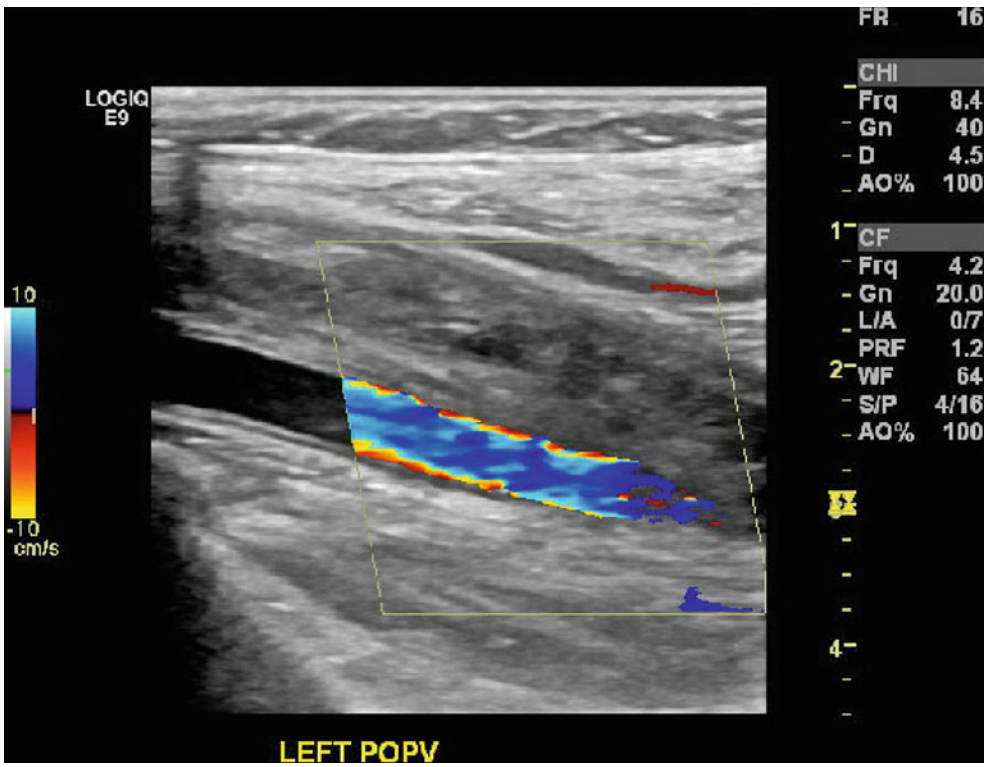


**Fig. 38.4** Acute DVT in the popliteal vein, normal arterial flow in the popliteal artery

the middle of the flow channel in longitudinal view. Here, the examiner is observing for spontaneous and phasic flow, as well as the presence of distal augmentation that normally occurs when the calf is gently squeezed (Fig. 38.3). Color-flow is also documented in each segment. For the popliteal vein, the probe is positioned behind the knee and requires that the patient cooperate (Fig. 38.4). All segments of this vein should be thoroughly examined, above, at, and below the knee, with compression, Doppler, and color flow as previously described.

Next, the tibioperoneal trunk, posterior tibial and peroneal veins are examined (Fig. 38.5). Imaging starts at the ankle and proceeds cephalad. The probe is aimed in a posteromedial plane. It is most helpful, but not necessary, if the patient is able to sit

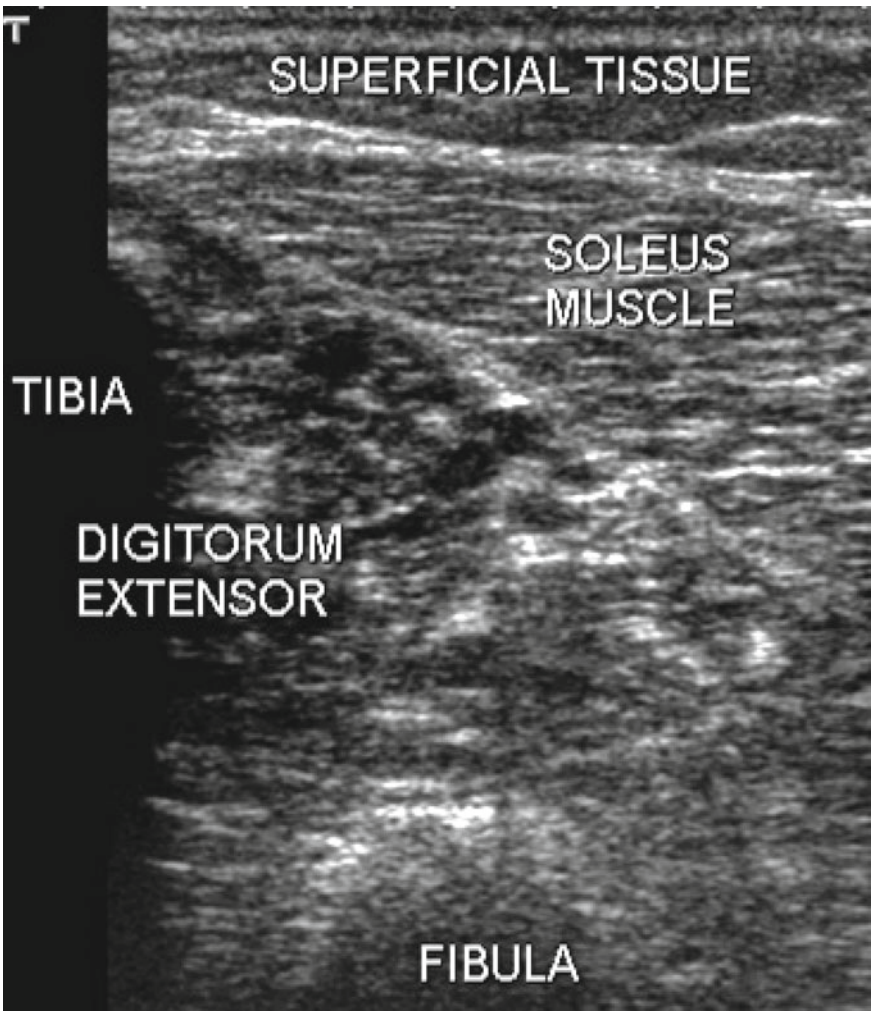


**Fig. 38.5** Anatomy of the popliteal fossa

dangling the legs. After compression is demonstrated, Doppler and color flow are documented in the often paired posterior and peroneal veins. The anterior tibial veins can be imaged from an anterolateral plane. In the absence of trauma or fractures, the likelihood of an anterior tibial DVT is less than 1%, and therefore, it is not included in the routine lower extremity exam.

After the tibial veins, the soleal and gastrocnemial veins are imaged near their confluence with the popliteal vein at the popliteal skin crease. The soleal veins are found just below the sural triangle as the soleus muscle is the first structure under the fascia (Fig. 38.5). The veins are traced in both directions toward the posterior tibial or peroneal veins, and compressed against the posterior surface of the tibia and fibula. The medial and lateral gastrocnemius veins are identified at the confluence with the popliteal vein, and traced to their respective muscle belly, with compression and flow demonstrated along the course. If compression is not possible, the examiner will have to rely on color flow imaging at a low-flow setting (PRF less than 1500 Hz).

To complete the lower extremity venous duplex exam, the small and great saphenous veins should be imaged. The small saphenous vein courses posterior in the calf until it joins the popliteal vein around the knee level (Fig. 38.6). The great saphenous vein courses medially from just anterior to medial malleolus to the saphenofemoral junction in the groin (Fig. 38.7). Of course, the examiner should be aware, from a careful history, if the saphenous veins have been either partially or totally harvested for a previous bypass procedure, or if the veins were ablated or stripped to treat superficial venous insufficiency.

In order to have a complete evaluation, the pelvic and abdominal veins should be ideally imaged (Fig. 38.8). However, this is quite a challenging task and usually requires an experienced sonographer. The inferior vena cava may be obscured by bowel gas. Similarly, the common and external iliac veins may be difficult to visualize. Obtaining information on the outflow vein is especially important in cases when there is continuous flow in the femoral vein (Fig. 38.9). For pelvic veins, the usual compression maneuvers are obviously not possible, so the examiner has to rely on Doppler and color-flow. In experienced hands, occlusive and partially occlusive iliac vein thrombi can be detected as well as left iliac vein stenosis, such as in the May–Thurner Syndrome. Venous duplex can also be used to follow-up on patients who had endovascular recanalization of occluded iliac veins and venous stents.

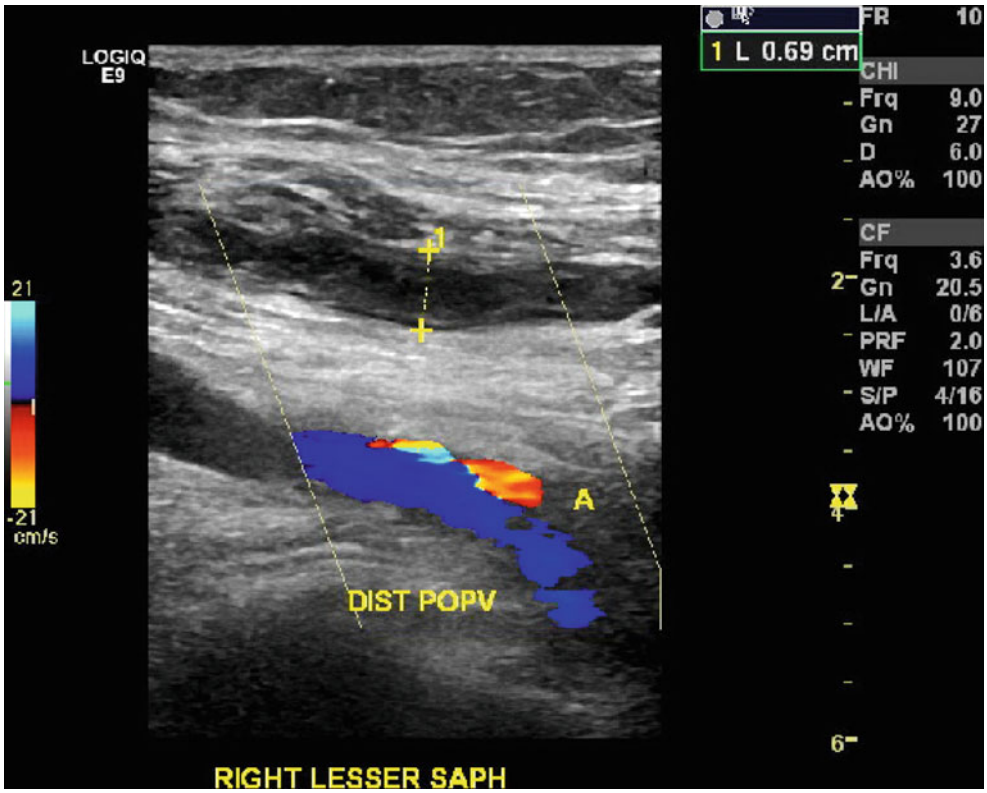


**Fig. 38.6** Acute thrombus in small saphenous vein

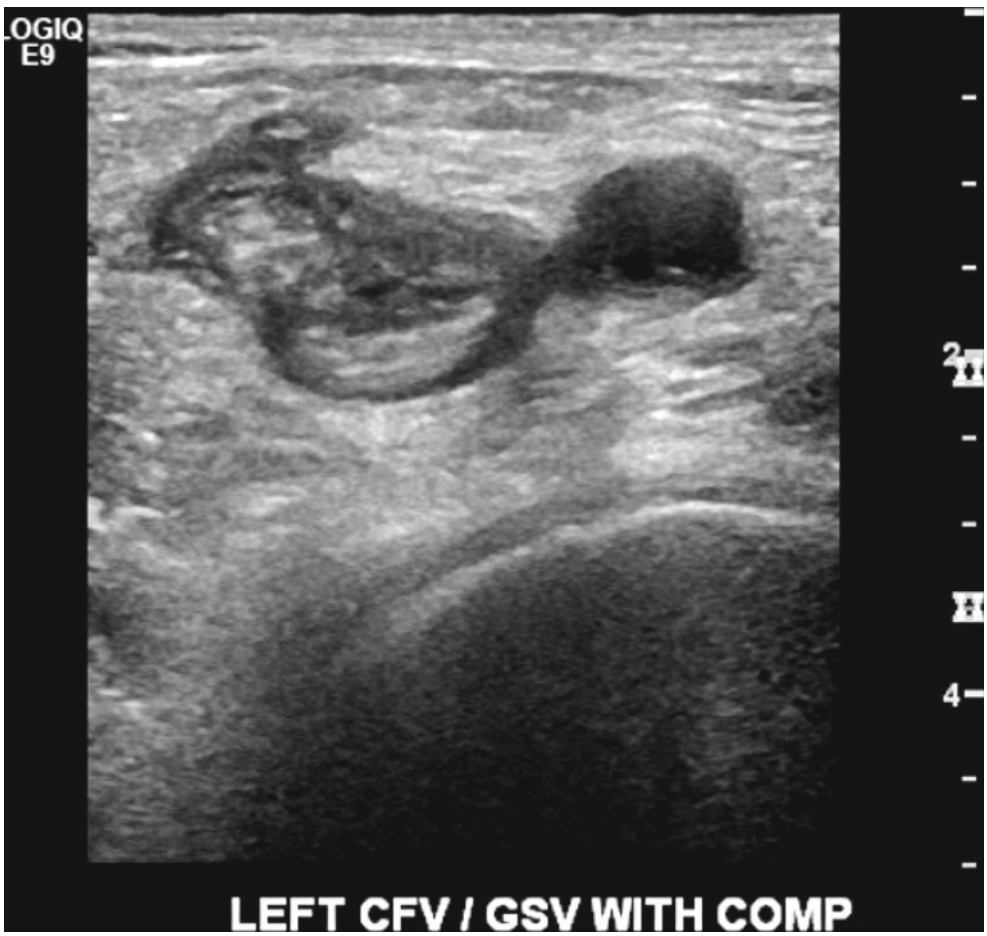


**Fig. 38.7** Thrombus filling the saphenofemoral junction, with failure to compress the vein due to thrombus (this picture is sometimes called "Mickey Mouse ears" view)

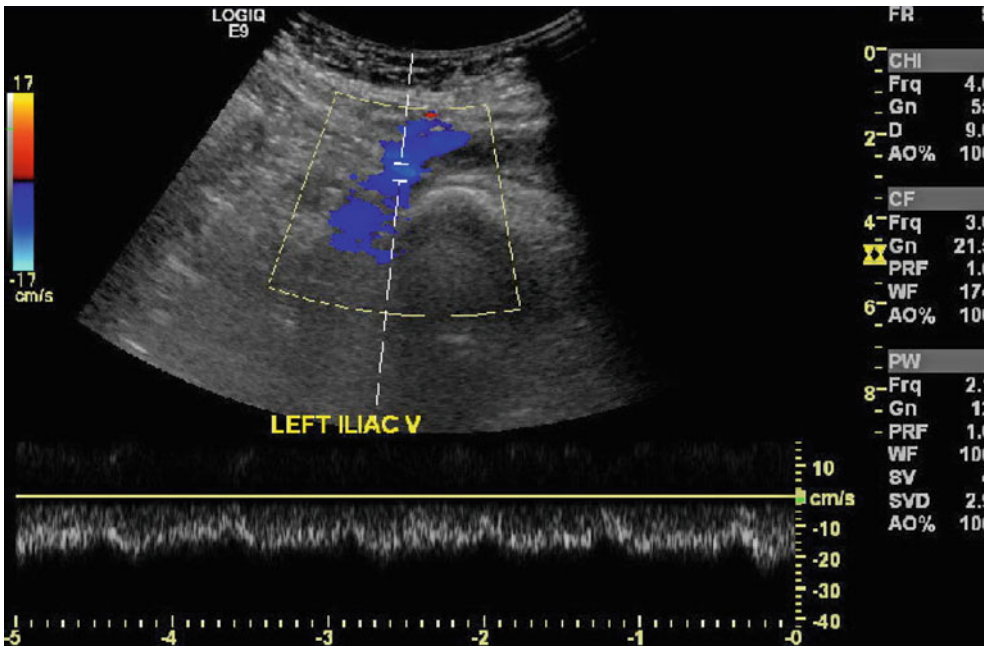


**Fig. 38.8** Iliac vein with absence of phasic flow, suspected thrombus in inferior vena cava

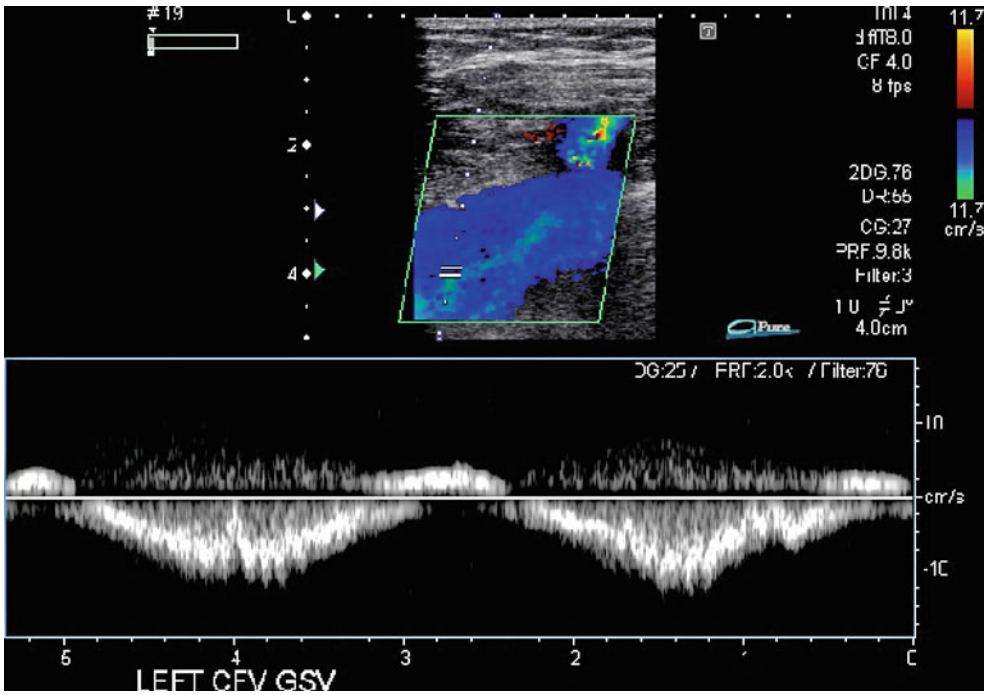


**Fig. 38.9** Patent femoral vein and saphenofemoral junction. Continuous flow seen in patients with congestive heart failure or fluid overload

## Diagnosis of DVT

In order to make the diagnosis of DVT, several criteria have to be present on B-mode imaging, Doppler, and color-flow. The classic completely occlusive thrombus distending the vein is not always present. On B-mode, failure to oppose the vein walls, or compression, is pathognomonic (Fig. 38.10). Finding echogenic material in the vein lumen, a filling defect on color flow imaging and absence of Doppler signal in the affected segment will confirm the diagnosis. On the other hand, complete vein compression, detection of phasic Doppler venous flow, and normal wall-to-wall color filling indicate a normal vein without evidence of DVT. As the acute deep venous thrombosis ages, the sonographic characteristics change. The clot becomes more echogenic with brighter echoes, and partial recanalization is detected by improved color flow and

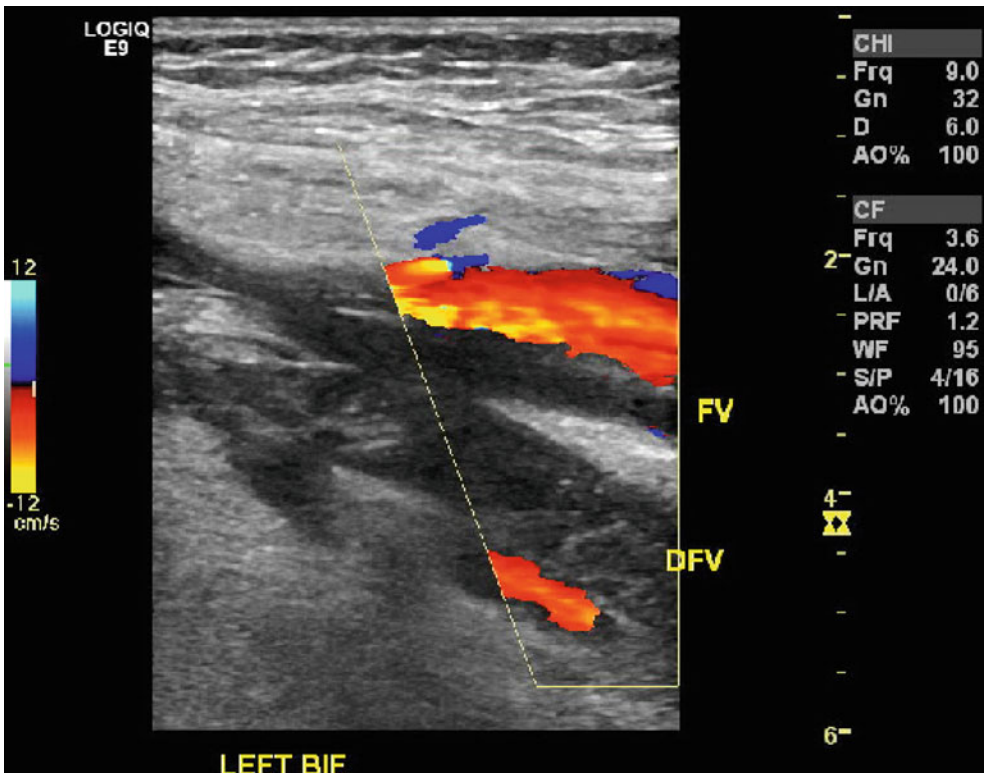


**Fig. 38.10** Complete obstruction of common femoral and deep femoral with acute deep venous thrombosis. Normal flow in arteries

**Table 38.4** Acute versus chronic DVT on duplex scan

| Diagnostic criterion | Acute DVT | Chronic DVT |
|---|---|---|
| Compressibility | Spongy | Firm |
| Vein diameter | Dilated | Decreased |
| Echogenicity | Echolucent | Echogenic |
| Composition | Homogenous | Heterogenous |
| Lining | Smooth | Irregular, rough |
| Collaterals | Absent | Present |
| Flow channel | Confluent | Multiple |
| Free-floating tail | May be present | Absent |

Modified from Meissner et al. [2]

formation of collateral veins around the obstructed segment. As the clot organizes and scars down, permanent changes occur including a stiffer vein wall, irregular lining or synechia and brighter echoes [2] (Table 38.4).

In some instances, the venous duplex scan may be negative or inconclusive. It is advisable in these cases to perform a follow-up duplex scan in 5–7 days. It is even more important to do a repeat scan if the patient is not receiving anticoagulation. The treating clinician has to decide whether or not treatment is indicated based on a negative or inconclusive scan.

## Reporting

The interpretation of the venous duplex scan should include all the findings and a summary of the diagnosis. The final report should state: (1) acute or chronic DVT, (2) segment or segments involved, (3) involvement of the superficial venous structures, if present, (4) the status of the contralateral femoral vein, even in cases when a unilateral study is ordered, and finally (5) any observed incidental findings that could explain or obscure the diagnosis, e.g., the presence of a Baker's cyst in the popliteal fossa. A preliminary report is most often required to determine the treatment course (admission, anticoagulation). Critical findings on the test, such as acute arterial occlusion, the presence of a popliteal aneurysm or free-floating thrombus, should be communicated person to person immediately to the ordering physician.

## Special Considerations

The hallmark findings of acute DVT previously described are not always present. The accuracy of duplex scans for acute DVT should be greater than 90% [2, 11, 14]. However, the exam may be technically difficult to perform in obese patients, or in the presence of edema. In some trauma cases, proper imaging may be difficult because of injured structures or the presence of hardware, such as external fixators. The sonographer should be aware that imaging the iliac, deep femoral, and peroneal veins are technically the most challenging. The diagnosis of acute on chronic DVT also requires some experience.

Despite the existence of a plethora of clinical studies on DVT, there is still controversy on whether bilateral scans should be performed on all patients or if patients with isolated calf DVT should be treated. ICAVL recommendations are in favor of scanning the contralateral femoral vein even in asymptomatic patients. The University of Washington group has proposed the initiation of a prospective randomized controlled study for patients with isolated calf DVT comparing anticoagulation to no treatment. Until further evidence is reported, it is probably prudent to obtain a follow-up duplex scan in a week if the patient is not receiving treatment.

## References


1. U.S. Department of Health and Human Services. The surgeon general's call to action to prevent deep vein thrombosis and pulmonary embolism; 2008. Available at: http://www.surgeongeneral.gov/topics/deepvein. Accessed 1 May 2011.
2. Meissner MH, Wakefield TW, Ascher E, Caprini JA, Comerota AJ, et al. Acute venous disease: venous thrombosis and venous trauma. J Vasc Surg. 2007;46:25S–53.
3. Caprini JA. Risk assessment as a guide for the prevention of the many faces of venous thromboembolism. Am J Surg. 2010;199:S3–10.
4. Geerts WH, Pineo GF, Heit JA, Berqvist D, et al. Prevention of venous thromboembolism. Chest. 2004;126:338S–400.
5. Geerts WH, Bergqvist D, Pineo GF, Heit JA, et al. Prevention of venous thromboembolism. American College of Chest Physicians evidence-based clinical practice guidelines (8th edition). Chest. 2008;133:381S–453.
6. Heit JA, Silverstein MD, Mohr DN, et al. The epidemiology of venous thromboembolism in the community. Thromb Haemost. 2001;86:452–63.
7. Fowkes FJ, Price JF, Fowkes FG. Incidence of diagnosed deep vein thrombosis in the general population: systematic review. Eur J Vasc Endovasc Surg. 2003;25:1–5.
8. Meissner MH, Moneta G, Burnand K, Gloviczki P, et al. The hemodynamics and diagnosis of venous disease. J Vasc Surg. 2007;46:4S–24.
9. Labropoulos N, Tassiopoulos AK. Chapter 41: Vascular diagnosis of venous thormbosis. In: Mansour MA, Labropoulos N, editors. Vascular diagnosis. 1st ed. Philadelphia: Elsevier Saunders; 2005. p. 429–38.
10. Illig KA, Deweese JA. Venous and lymphatic disease: an historical review. In: Gloviczki P, Yao JST, editors. Handbook of venous disorders. 2nd ed. London: Arnold; 2001. Chap. 1, p. 3–10.
11. Mattos MA, Sumner DS. Direct noninvasive tests (duplex scan) for the evaluation of chronic venous obstruction and valvular incompetence. In: Gloviczki P, Yao JST, editors. Handbook of venous disorders. 2nd ed. London: Arnold; 2001. Chap. 12, p. 120–31.
12. Hirsch J, Lee AY. How we diagnose and treat deep vein thrombosis. Blood. 2002;99:3102–10.
13. Goodacre S, Stevenson M, Wailoo A, Sampson F, et al. How should we diagnose suspected deep-vein thrombosis? Q J Med. 2006;99:377–88.
14. Mintz BL, Araki CY, Krithatis A, Hobson RW. Venous duplex ultrasound of the lower extremity in the diagnosis of deep venous thrombosis. In: Abu Rahma AF, editor. Noninvasive vascular diagnosis. 2nd ed. London: Springer; 2007. Chap. 35, p. 385–93.
15. Wells PS, Anderson DR, Rodger M, et al. Evaluation of D-dimer in the diagnosis of suspected deep-vein thrombosis. N Engl J Med. 2003;349:1227–35.
16. Bernardi E, Camporese G, Buller HR, Siragusa S, et al. Serial 2-point ultrasonography plus D-dimer vs. leg color-coded Doppler ultrasonography for diagnosing suspected symptomatic deep vein thrombosis. JAMA. 2008;300:1653.
17. Johnson SA, Stevens SM, Woller SC, Lake E, et al. Risk of deep vein thrombosis following asingle negative whole-leg compression ultrasound. JAMA. 2010;303:438–45.
18. Palareti G, Cosmi B, Legnani C, Tosseto A, et al. D-dimer testing to determine the duration of anticoagulation therapy. N Engl J Med. 2006;355:1780–9.

# Venous Duplex Ultrasound of the Upper Extremities

39

Joann M. Lohr

**Abstract**

Upper extremity deep vein thrombosis (UEDVT) accounts for 10% of all DVT cases. Upper extremity DVT may be primary (30%) or secondary (70%). Upper extremity DVT has been inaccurately regarded as a rare and benign disease and is an understudied condition with severe consequences. Most primary cases have associated underlying anatomic anomalies; however 20% of episodes are idiopathic. Indwelling catheters are the most common risk factor for secondary UEDVT. Pulmonary embolism (PE) is the most devastating complication reported in up to 36% of cases. Pulmonary embolism is twice as common with secondary UEDVT than with primary UEDVT. Venous anatomy, including zones of the upper extremity and a venous duplex scanning protocol for the upper extremity, is described. Indications for duplex imaging, thrombus characteristics and locations, and soft tissue abnormalities including abscesses, cysts, aneurysms, and pseudoaneurysms are all presented. Limitations and potential pitfalls are defined for duplex imaging of the upper extremity. Requirements for the Intersocietal Commission for the Accreditation of Vascular Laboratories (ICAVL) certification for upper extremity duplex imaging are presented. A comparison of upper extremity and lower extremity DVT is given. Duplex ultrasonography is the method of choice for the initial diagnosis of patients suspected with thrombosis of the upper extremities. However, in patients with isolated flow abnormalities, contrast venography should be performed. The use of CT scanning and MRV are also discussed. In children, more than 50% of the UEDVT events are due to the presence of central venous lines. Treatment options are briefly reviewed for UEDVT. The concept of venous patency restoration followed by relief of extrinsic compression is the accepted therapeutic approach for the treatment of primary UEDVT. Three different types of thrombi can occur in association with central venous catheters. The catheter adherent fibrin sleeve is the most common. The likelihood of developing catheter-related UEDVT is related to the number of punctures during catheter insertion, the number of catheters inserted, the location of the catheter tip, the duration of catheterization, the type of catheter used, the type of fluid administered, catheter-related infection, hypercoagulable states, and the presence of congestive heart failure. The incidence of UEDVT is increasing perhaps due to the increased use of central lines or due to increased awareness of the disease process. The first step in treatment is to evaluate the need for continued catheter use and to establish vessel patency.

J.M. Lohr, M.D., FACS, RVT
Department of Vascular Surgery, Good Samaritan Outpatient Center,
6350 Glenway Avenue, Suite 208, Cincinnati, OH 45211, USA

Good Samaritan Hospital, Cincinnati, OH, USA
e-mail: jlohr@lohrss.com, geri_meister@trihealth.com

A.F. AbuRahma, D.F. Bandyk (eds.), *Noninvasive Vascular Diagnosis*,
DOI 10.1007/978-1-4471-4005-4_39, 

**Keywords**

Duplex characteristics of acute and chronic thrombi • Upper extremity DVT • Primary upper extremity DVT • Secondary upper extremity DVT • Diagnosis options in adults with upper extremity DVT • Diagnosis options in children with upper extremity DVT • Evaluation of upper extremity pain and swelling • Diagnosis of upper extremity pain and swelling Duplex anatomy of the upper extremity including zones and veins visualized • Soft tissue abnormalities of the upper extremity • ICAVL requirements for duplex imaging of the upper extremity

## Introduction

The number of patients who come into the vascular laboratory for evaluation of upper extremity problems is far smaller than the number who come for lower extremity testing. However, this number has recently grown, accompanied by the increase in radial artery harvesting for coronary bypass grafting and the Dialysis Outcomes Quality Initiatives (DOQI) recommendations for increased establishment of arteriovenous fistula (AVF) [1]. Preoperative vein mapping for dialysis access has had a significant impact on the use of the vascular laboratory. Unfortunately, the ability of the vascular laboratory to provide information is limited by reimbursement issues, scheduling problems, and technologist availability.

The age-adjusted incidence and total rates of upper extremity deep vein thrombosis (UEDVT) are 15 (95% confidence interval [CI], 12–19) and 16 (95% CI, 13–20), respectively, as compared with 74 and 91 per 100,000 population for lower extremity deep vein thrombosis. The incidence per 100,000 in total rates of UEDVT is not significantly different by sex [2].

About 10% of all episodes of deep venous thrombosis occur in the upper extremity [3]. Venous thrombosis of the upper extremity may be divided into primary or secondary. Associated risk factors for primary UEDVT include thoracic outlet, anatomic anomalies, and coagulation defects. However, 20% of episodes are unexplained [3]. Risk factors for secondary UEDVT include a central indwelling catheter, nonmalignancy-related coagulopathies, malignancy, infection, previous surgery, renal failure, immobility, history of lower extremity DVT, concurrent lower extremity DVT, cardiomyopathy, sarcoidosis, trauma, pacemaker, stroke, vasculitis, and medications.

Upper extremity DVT had previously been regarded as a benign and rare disease. This should no longer be the case. Patients may present with swelling and pain but they may also be completely asymptomatic and objective confirmation is mandatory prior to determining a treatment path. Upper extremity DVT is an understudied condition with serious consequences [4].

Risk level is assessed in the article by Shah et al. It ranges from a high of 72% for a central indwelling catheter to as low as 4% for medication [4]. The most devastating complication of UEDVT is the potential for progression to pulmonary embolism (PE). In the past, this has been thought to be a rare complication; however, recent data suggest that it may be present in as many as 36% of cases [5]. Pulmonary embolism is found more often in catheter-related upper extremity DVT and is twice as likely to be seen in connection with secondary DVT as with primary [6, 7]. One recent study reported a higher mortality rate and greater incidence of PE when UEDVT cases were compared with the lower extremity deep vein cases [8].

Most cases of UEDVT are thought to be asymptomatic. Among patients who do have symptoms pain is the most common, occurring in 63% of cases. Edema is the most common physical finding, occurring in 98% of cases [9]. Signs and symptoms of UEDVT are nonspecific. The differential diagnosis includes superficial venous thrombophlebitis, lymphedema, neoplastic compression leading to outlet obstruction, hematoma, contusion, muscle tears, occult fractures, hypertrophic ossification, and chronic regional pain syndrome [4]. Clinical examination findings are extremely unreliable for making the diagnosis. Prevalence of the disease is greater than 50% in symptomatic patients [5]. Objective testing is needed for confirmation of the diagnosis before beginning treatment. The incidence of DVT in the upper extremities appears to be increasing. This may be real or due to the great incidence of use of indwelling catheters.

Primary UEDVT is also known as Paget–Schroetter syndrome or effort vein thrombosis. It is most common in young male athletes or laborers who repeatedly abduct and extend their arm. It most commonly occurs in the dominant arm and is often related to obstruction of the thoracic outlet and the underlying venous stricture. The obstruction may be due to compression from the first rib or an anomalous cervical rib, congenital fibrous bands, or compression from the anterior scalene muscle [10]. Extrinsic compression causes repetitive trauma that leads to venous stenosis. This will be completely discussed in Chap. 40 by Dr. Julie Ann Freishlag.

The prevalence of complications of UEDVT has been reported in several observational studies [3]. Mortality ranges from 0% to 50%. Pulmonary embolism ranges from 2% to 36%. Fatal PE is reported 0% of the time or as often as 20% of the time. The occurrence of UEDVT has been reported to

**Table 39.1** Indications for upper extremity scans

| Indications | Number |
|---|---|
| Upper extremity venous duplex to rule out thrombosis | 191 |
| Upper extremity dialysis evaluations | 142 |
| Upper extremity radial artery bypass harvest | 16 |
| Upper extremity graft surveillance | 35 |
| Evaluation for line placement | 9 |
| Upper extremity arterial duplex | 8 |
| Upper extremity symptoms with/without cold challenge | 35 |
| Thoracic outlet evaluation | 6 |
| Total | 442 |

Adapted from Lohr [14]. With permission from Elsevier

**Table 39.2** Veins involved in thrombosis[a]

| Veins involved | Total |
|---|---|
| Subclavian | 103 |
| Cephalic | 99 |
| Internal jugular | 78 |
| Axillary | 59 |
| Brachial | 56 |
| Basilic | 61 |
| External jugular | 19 |
| Radial | 6 |
| Antecubital | 8 |
| Ulnar | 3 |
| Total | 492 |

Adapted from Lohr [14]. With permission from Elsevier
[a]Several patients had multiple vein segments involved

range from 4% to 11% and post-thrombotic syndrome has been reported to occur 4–35% of the time [3]. Upper extremity phlegmasia cerulea dolens constitutes 2–5% of all phlegmasia cases [11]. These cases are all secondary to either an underlying hypercoagulable state or malignancy. The consensus is that early diagnosis followed by intervention provides the most favorable results [12, 13].

## Imaging

Upper extremity evaluations have increased to 13.9% of all studies performed annually in this vascular laboratory, up from 4.8% only 5 years ago. Table 39.1 lists the indications for upper extremity scans conducted over a 12-month interval. Only 43% (191/442) of the upper extremity evaluations were done to rule out thrombosis.

A total of 701 upper extremity venous duplex scans to rule out thrombosis were analyzed. Some 38% were positive for thrombosis and isolated superficial venous thrombosis was identified in 85 patients. Distribution and sites of veins are presented in Table 39.2. When considering the anatomic distribution of acute UEDVT, the subclavian and internal jugular veins were the most commonly involved sites. Multiple patients have been reported to have concomitant deep and superficial system involvement [15]. The rate of asymptomatic catheter-related DVT is high and may be lowered by correct initial positioning of the central venous catheter tip either positioned in the superior vena cava or at the junction between the right atrium and the superior vena cava [16].

Patients with suspected UEDVT should undergo duplex scanning. Diagnostic accuracy of upper extremity duplex scanning is very good with sensitivity and specificity of 78–100% and 82–100% [10]. Accuracy can be improved by having the patient perform Valsalva maneuvers, the sniff test, or by utilizing further tests. Duplex ultrasound may also detect axillary and cervical lymphadenopathy possibly secondary to malignancy. Compression is limited with poor visualization of the proximal subclavian vein. The brachiocephalic vein and the superior vena cava are beyond the clavicle and sternum [10]. CT scanning may detect a central thrombus as well as extrinsic compression of the vessel. However, it has the disadvantage of requiring a contrast load and has not been fully validated. Magnetic resonance studies accurately detect central thrombus and provide a detailed evaluation of collaterals and blood flow; however, it has limited availability, the patient may be claustrophobic and it may be not be suitable in some patients with implants (see Table 39.3) [17].

## Anatomy

Veins of the arm drain via the brachial or cephalic system. The brachial vein flows into the axillary vein, which is then joined by the cephalic vein to form the subclavian vein. The axillary vein is contiguous to the brachial vein traveling in the tunnel formed by the clavicle and subclavius muscle, anterior on the scalene muscle laterally, the first rib posterior-inferiorly, and the costo-clavicular ligament medially. In the subscapular region, the axillary vein receives both the subscapular and suprascapular veins. There are many anastomotic collateral pathways that can potentially bypass the axillary subclavian venous system. They may be divided into the shoulder to chest wall, the shoulder to ipsilateral anterior neck, the shoulder to ipsilateral posterior neck, and the shoulder to contralateral neck. In the event of axillary vein thrombosis, collaterals will usually develop from the shoulder to the chest wall. If the thrombosis extends to the subclavian vein, the collaterals generally develop to the posterior ipsilateral neck or from the shoulder to the contralateral neck [18] (see Fig. 39.1).

Thoracic outlet syndrome (TOS) refers to compression of the neurovascular bundle including the brachial plexus, subclavian artery, and subclavian vein as it exits the thoracic inlet delimited by the scalene muscles, the clavicle, and the

**Table 39.3** Advantages and disadvantages of imaging modalities used to diagnose upper extremity deep vein thrombosis

| | Advantages | Disadvantages |
|---|---|---|
| Ultrasound | Inexpensive<br>Noninvasive<br>Reproducible | May fail to detect central thrombus that is directly below the clavicle |
| CT scan | May detect central thrombus<br>May detect the presence of extrinsic vessel compression | Contrast dye<br>Not fully validated |
| Magnetic resonance | Accurately detects central thrombus<br>Provides detailed evaluation of collaterals and blood flow | Limited availability<br>Claustrophobia<br>Not suitable for some patients with implanted metal |

Adapted from Joffe and Goldhaber [17]. With permission from Lippincott Williams and Wilkins

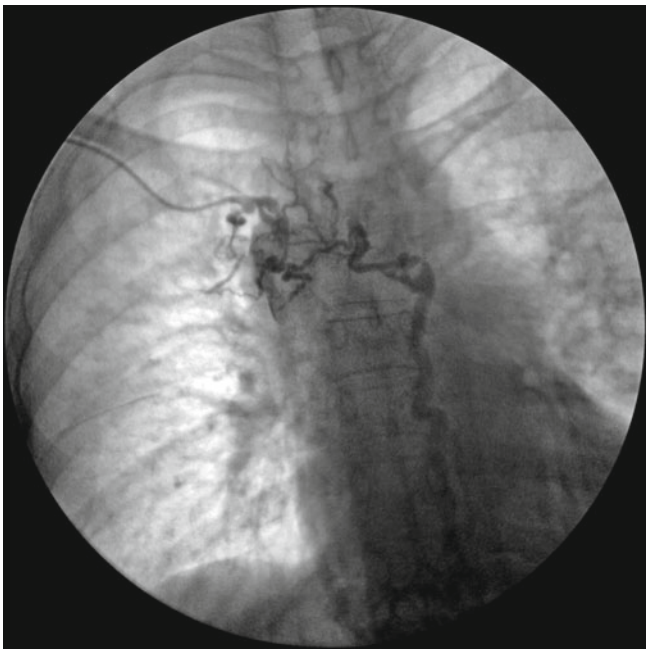

**Fig. 39.1** Chronic subclavian occlusion with well-developed collaterals

first rib. Cervical ribs, musculofascial bands, and clavicular first rib anomalies have also been described as other causes. Symptoms include a combination of vascular and neurologic findings [19].

## Duplex Imaging Technique

The upper extremity examination begins with a detailed assessment of signs, symptoms, past medical history, and risk factor analysis. The patient is then placed in a supine position and the radial vein is visualized from the wrist to the brachial vein. Next, the ulnar vein is followed from the wrist to the antecubital fossa; where the ulnar and radial veins form the brachial vein; the brachial vein is followed into the upper arm. At the junction of the basilic and brachial veins, the axillary vein is formed. The axillary vein is followed under the shoulder in the direction of the clavicle. The junction of the cephalic and axillary veins forms the subclavian vein. The junction of the subclavian and jugular veins originating at the innominate vein is not visualized routinely because of its depth; however, Doppler signals analyzed in this area provide indirect information about the patency of the central veins and newer color scanners have increased the ability to image them. Doppler signals of the subclavian vein are assessed. Normally, the flow is spontaneous and phasic with augmentation, and no reflux is identified. The internal jugular vein is examined from the clavicle cephalad until it dives under the mandible. Doppler signals of the internal jugular vein also are obtained to assess spontaneous and phasic flow. Finally, the superficial veins are assessed by following the basilic vein along the ulna until it joins the brachial vein. The largest-diameter antecubital vein connects the basilic and cephalic systems at the antecubital fossa. The antecubital perforator also is seen connecting the cephalic and brachial veins. The cephalic vein is traced along the radius and up the arm, where it joins with the axillary vein. The antecubital, cephalic, and basilic veins are the superficial veins of the upper extremity.

For reporting convenience and ease of communication, the upper extremity is divided into zones (see Fig. 39.2). In each examination, the position of the probe and localizing abnormal findings are reported. Each zone covers approximately 10 cm in length. Zone 1 is located at the suprasternal notch, Zone 3 at the acromial clavicular process, Zone 5 at the anticubital fossa, and Zone 8 at the wrist. Zones are used to report thrombus location allowing accurate comparison between studies and technologists.

When a visible intraluminal thrombus is identified, several of its characteristics are assessed to determine its relative age. These characteristics include clot occlusiveness, clot retraction, clot distention, vein compressions, echogenicity and homogeneity, the development of collateral venous channels, and recanalization. The clot may be partially or totally occluding. A totally occluding clot indicates an acute process. Free-floating thrombi actually are tethered distally but extend cephalad in the vein without a more proximal attachment to the vessel wall. These

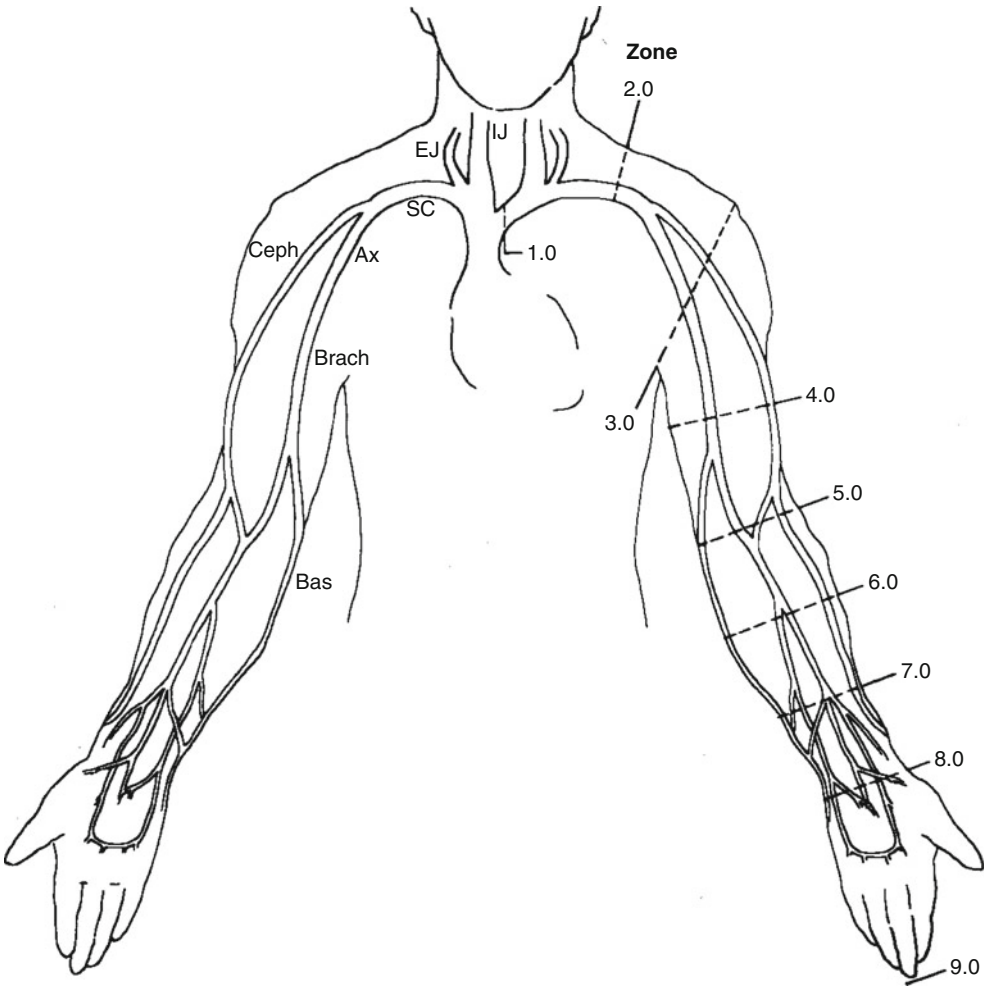


**Fig. 39.2** Zones of reference for upper extremity venous scanning: midline = 1.0, acromion = 3.0, elbow = 5.0, wrist = 8.0, and fingertips = 9.0 (Adapted from Lohr [14]. With permission from Elsevier)

**Table 39.4** Clot characteristics: relative value in clot aging

| Characteristic | Acute value | | Chronic value | |
|---|---|---|---|---|
| Degree of occlusion | Total | *** | Partial | *** |
| Free-floating | Free | **** | Stationary | ** |
| Clot retraction | Retracted | *** | Adherent | *** |
| Clot distention | Distended | *** | Contracted | ** |
| Clot compressibility | Soft | **** | Firm | * |
| Surface character | Smooth | ** | Irregular | * |
| Echogenicity | Faint | * | Bright | * |
| Homogeneity | Homogeneous | ** | Heterogeneous | ** |
| Collaterals | Absent | * | Present | **** |
| Recanalization | Absent | * | Present | **** |

Adapted from Lohr [14]. With permission from Elsevier
*Four asterisks* (****) indicate a diagnostic level, *three asterisks* (***) good, *two asterisks* (**) fair, and *one asterisk* (*) poor (nondiagnostic). Each asterisk indicates the relative value to be given to each criterion in interpretation of clot age. Many criteria are valuable only when present, and the overall decision represents a weighted average

free-floating thrombus tails exhibit a side-to-side waving in the venous lumen that can be induced by gently bouncing the probe on the skin or with respiration. Free-floating tails usually become attached to the venous wall within 1–2 weeks. Characteristics of thrombi help age the thrombus (see Table 39.4).

Because of the limited ability to compress the deep venous system, especially in the area where the subclavian passes beneath the clavicle, technical modifications such as the use of adjunctive procedures and color flow duplex analysis are critical for correct assessment. In the areas where the vein may not be accessible to compression color Doppler, it is

important to pay close attention to color flow gain settings to avoid oversaturation, which may obscure small intraluminal clots or areas of incomplete thrombosis [20].

It is important to document the full extent of the disease including the contralateral neck and proximal arm. Radionuclide venography may be of further benefit to diagnose Port-A-Cath thrombosis in clinical practice [21]. Duplex ultrasonography is the method of choice for the initial diagnosis of patients suspected with thrombosis of the upper extremities. However, in patients with isolated flow abnormalities, contrast venography should be performed [22]. Imaging pitfalls to avoid include the cephalic vein being diagnosed as the axillary vein. Probable occlusion of the internal jugular vein may also occur and mirror image artifact may result in the appearance of two subclavian veins in the supraclavicular region [23].

The use of duplex imaging of the upper extremity has increased dramatically. In the instance of dialysis access, upper extremity evaluations increasingly are being requested before placement. Preoperative evaluation of dysfunctional dialysis grafts allows operative planning [24]. Vein mapping improves graft durability in patients with disadvantaged outflow and vein size, and continuity can be established. The protocol implemented in the author's vascular laboratory evaluates both veins and arteries (see Fig. 39.3). Blood flow in the superficial palmar arch is assessed at baseline with radial and ulnar comparison. In addition, calcifications and aberrant arterial anatomy are identified. Veins are evaluated using tourniquet distention if less than 3 mm at rest.

## Venous Abnormalities on Duplex Exam

Clot retraction is defined as the concentric separation of the thrombus from the vein walls; there appears to be a very thin gap between the thrombus and the circumference of the venous wall. Retraction is thought to occur within a few hours of thrombus formation through clot contraction of the platelet fibrin mesh formation and extrusion of serum. Clot retraction usually lasts only 1–2 weeks, and then the clot becomes adherent to the vein wall.

Clot distention occurs when the vein is dilated to a larger-than-normal diameter by a thrombus in a cross-sectional area. In this context, clot distention differs from venous distention caused by obstruction or by venous hypertension in the absence of an intraluminal thrombus. In the latter, it is possible to completely collapse the wall of the vein with the pressure of the probe and receive a Doppler signal. Veins exhibiting clot distention gradually shrink over several weeks to months.

An acutely thrombosed vein may be partially compressible. Unlike a chronically thrombosed vein, acute thrombi can be deformed by only light probe pressure. When viewed transversely, the round vein appears oblong. A thrombus remains soft for approximately 24 h after formation. The clot surface may be smooth or irregular; this usually is best assessed by a longitudinal view of the thrombus tip. Acute thrombi tend to have smooth, rounded tips because of continued surrounding flow (Fig. 39.4a, b).

Echogenicity is defined as the overall brightness of the clot compared with the surrounding tissues. Brightly echogenic thrombi tend to be chronic because serum reabsorption makes them denser. Apparent changes in echogenicity may be influenced by electrical gains of the instruments, depth of the structure being assessed, and acoustic shadow of the overlying tissues, making echogenicity a somewhat subjective finding. Homogeneity is also assessed. Acute thrombi tend to be homogeneous, whereas chronic thrombi tend to be heterogeneous.

Development of collateral venous channels is an absolute sign of chronic thrombosis. These channels are very small, lie parallel to the main vein trunk, and do not contain valves. Normal venous tributaries are larger, enter the main venous channel at an acute angle, and contain valves. Collateral venous channels are best visualized in a transverse field and may be seen as early as 1–2 weeks after initial thrombosis; however, they usually are not visible for a month or more after venous occlusion.

Recanalization is evidenced by an open, collapsible channel that runs through a thrombus. The recanalized channel, which is surrounded entirely by a clot, tends to occur rather late.

Using the aforementioned characteristics, thrombi are classified as acute, chronic, or indeterminate. Classification must be based on the characteristics of the entire thrombus rather than on an isolated segment because the deep venous thrombosis is a continuing process. For this reason, a single thrombus may manifest various aging characteristics in different regions. Repeat duplex scans are often necessary and commonly show the evolution of characteristics that are equivocal with the initial scans.

## Upper Extremity DVT in Children

Venous thrombolic events are recognized as a growing clinical problem in children. The incidence of these events in prospective population based studies reported by International Registries (Canadian, German, and Dutch) revealed the presence of at least one associated underlying medical condition in most cases. Among all of the registries, the presence of a central venous line was the most common etiologic factor. In children more than 50% of the upper extremity venous thromboembolic events are due to the presence of central venous lines. Spontaneous venous thromboemboli are rare in children and usually involve the renal veins in the neonatal

**TRIHEALTH – GOOD SAMARITAN HOSPITAL**
**JOHN J. CRANLEY VASCULAR LABORATORY**

**DIALYSIS ACCESS, DUPLEX ARTERIAL AND VENOUS MAPPING**
**TECHNICAL WORKSHEET**

Patient Name: Date:

Tech: Tape: Meter:

Planned Procedure:

| Brachial Blood Pressure | Right | Left |
|---|---|---|

DOMINANT HAND: RIGHT ☐ Left ☐

| ARM STUDIED R L | VEIN | | VEIN | |
|---|---|---|---|---|
| LOCATION | Pre | Post | Pre | Post |
| 1 | | | | |
| 1.5 | | | | |
| 2 | | | | |
| 2.5 | | | | |
| 3 | | | | |
| 3.5 | | | | |
| 4 | | | | |
| 4.5 | | | | |
| 5 | | | | |
| 5.5 | | | | |
| 6 | | | | |
| 6.5 | | | | |
| 7 | | | | |
| 7.5 | | | | |
| 8 | | | | |

| | Velocity | Diameter |
|---|---|---|
| Brachial Artery | | |
| Proximal | | |
| Mid | | |
| Distal | | |
| Radial Artery | | |
| Proximal | | |
| Mid | | |
| Distal | | |

| BRV | NV | N | TA | PA | TI | PI | TX | PC |
|---|---|---|---|---|---|---|---|---|
| CEPH | | | | | | | | |
| BAS | | | | | | | | |
| IJ | | | | | | | | |
| SCV | | | | | | | | |

| SPA | Velocities | |
|---|---|---|
| Baseline | | Radial Dom ☐ |
| Radial Comp | | Ulnar Dom ☐ |
| Ulnar Comp | | Mixed ☐ |

COMMENTS:

**Fig. 39.3** Evaluation of the arteries and veins protocol

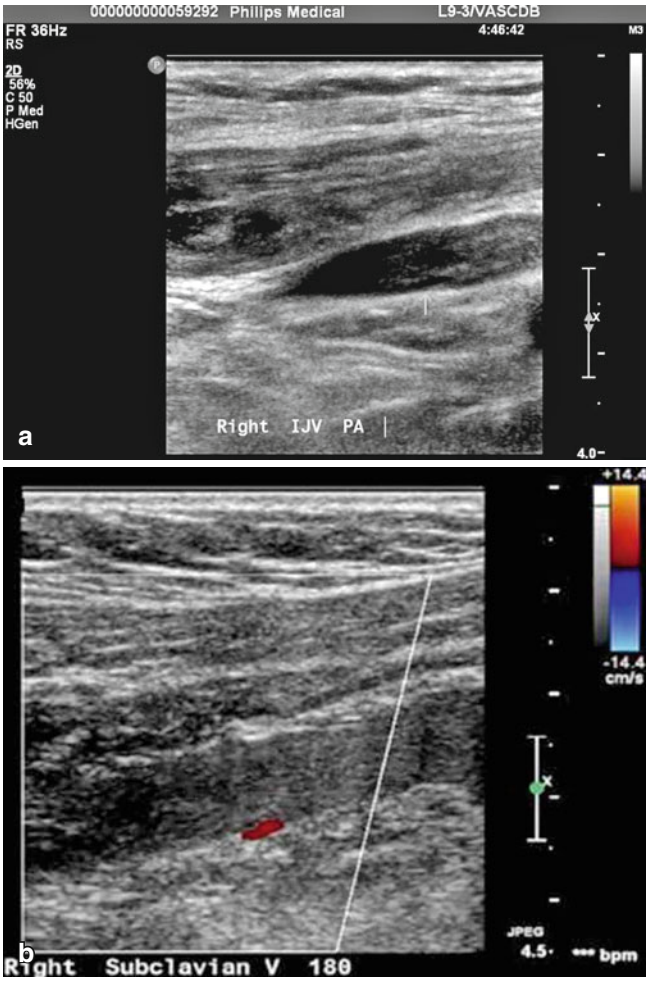


**Fig. 39.4** (**a**) Acute internal jugular vein partially occlusive DVT. (**b**) Subclavian vein occlusion

period or the lower extremity venous system in the older age groups [25–28].

## Soft-Tissue Abnormalities on Duplex Examination

Some scans are performed to evaluate soft-tissue abnormalities, which can be differentiated by their characteristics. The features of a pseudoaneurysm include visible intraluminal swirling and turbulent Doppler spectra. Further, common associated findings include a centrifugal thrombus with a superimposed arterial spectrum and a visible arterial laceration or communication.

Abscesses, on the other hand, have hyperechoic contents, give off no Doppler signal, have inducible eddy motions and often have an echo-dense capsule. Commonly associated findings include regional solidification.

Hematomas exhibit a variable echo density, are non-compressible, have no fluid movements, or clear margins and give off no Doppler signal. If hematomas are less than 12 h old, they may be hypoechoic with focal liquefaction. If they are more than 2 weeks old, dissection through the soft tissues is commonly seen.

Edema fluid is radiolucent, follows tissue planes, and is not compressible. Lymph nodes are spherical and encapsulated with a mixed internal echogenicity, and are noncompressible. Small lymph nodes may be invisible or difficult to see. Large lymph nodes are seen in the presence of infection, cellulitis, or tumors. In fact, the duplex scan image of large, swollen lymph nodes shows architecture strikingly similar to the cross-section of a lymph node that is depicted in pathology textbooks.

Cysts are slightly echogenic and are best seen in a transverse view, where they can be distinguished from the surrounding tissue structures. Cysts may be partially compressible and at times, may compress an artery or vein, causing an increase in peak velocity signals.

Duplex scanning holds special value for the evaluation of aneurysms, pseudoaneurysms and for the surveillance of grafts. In the past 5 years, there has been rapid expansion in the use of duplex imaging for the diagnosis and evaluation of upper extremity venous thrombosis, arterial suitability, and soft-tissue abnormalities and for the evaluation of grafts. Requests for examination of the upper extremity have increased and this area of clinical interest likely will continue to expand (Fig. 39.5).

A multicenter collaborative study that assessed the accuracy of lower extremity duplex scanning reported that the procedure was 97% sensitive in extremities with positive phlebograms [29]. However, the phlebogram was negative in 191 extremities and was considered to be incorrect in 6 instances. Thus the phlebogram was not a perfect standard when negative, and the duplex scan was slightly more accurate [30, 31].

It has not been possible to generate similar data for the upper extremity because there is a blind area behind the clavicle. Thus a negative duplex scan does not absolutely rule out thrombosis of the subclavian vein. In the author's study, a phlebogram was requested when there was doubt; unfortunately, only 10 were obtained. Although all were confirmatory, it is possible that some subclavian vein thromboses were missed. In most cases, however, a negative duplex scan and normal Doppler signals in the subclavian vein were accepted as evidence of normal venous flow. Rapid-sequence spiral CT scanning offers another modality to evaluate this area.

In the author's vascular laboratory, all scans are performed with commercially available high-resolution duplex instrumentation. Both black-and-white and color scanners are used. The interpreting physician grades all scans for quality using a three-part system:

- *Poor* indicates that a portion of the scan was not interpretable or a segment of the extremity was not visualized.

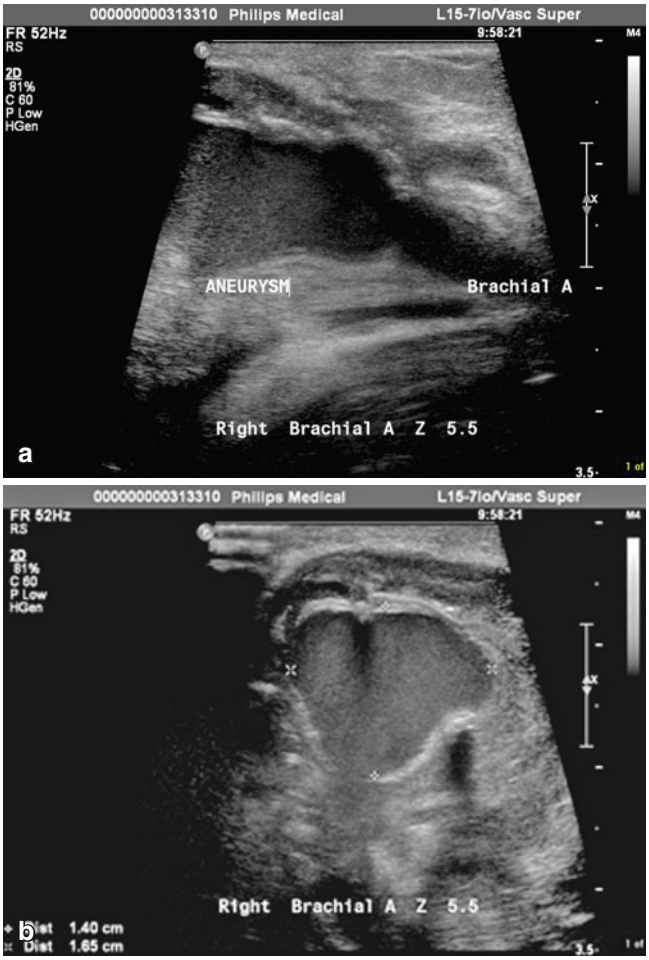


**Fig. 39.5** (**a**) Transverse and longitudinal view of brachial artery aneurysm, zone 5.5. (**b**) Aneurysmal segment measures 1.40 × 1.65 cm. Note the normal diameter vessel to the right of the image

- *Fair* indicates that diagnosis could be made but the entire extremity was not well visualized.
- *Good* indicates that all structures were well visualized.

Because duplex scanning has become the standard of practice to evaluate extremity veins, grading and assessment are an important means to ensuring the accuracy and reliability of a vascular laboratory.

To perform at the level required for ICAVL certification, a vascular laboratory must conduct phlebography in less than 10% of patients. Because duplex scanning is significantly dependent on the technologist's skill, quality control issues are central to continuing validation of this test. Formal comparison with phlebography is no longer available in this laboratory. When possible, blinded duplicate scanning programs by different technologists are used as a method to document quality control and improve test reliability. Further, physicians who are responsible for interpreting findings and overseeing the vascular laboratory must be personally skilled in the techniques of venous duplex imaging and the use of equipment. Finally, better scanner resolution also has improved the results of venous duplex imaging [32–37].

Catheter-induced thrombosis is an increasingly common event because the central veins are used more often for access, nutrition, chemotherapy, and monitoring. In the author's study, the most common associated risk factor for upper extremity thrombosis was a central or peripheral venous catheter. Indwelling catheters and malignancy were the most commonly combined risk factors; however, no identifiable risk factors were present in 10% (11/107) of patients with thrombosis. Hyperalimentation (TPN) was infused in 27% of patients with thrombosis. Further, screening and venography demonstrate that 30–60% of patients with central venous catheters will have a thrombus in the axillary subclavian venous segment, and 3% of these patients will develop clinically symptomatic subclavian vein thrombosis. Pulmonary emboli have been reported in 5–12% of a series of upper extremity thrombosis and it is estimated that 1% of these patients will die. Major vein thrombosis in the upper extremities, much like that in the lower extremities, may spread from a superficial vein into the deep system; therefore, upper extremity surveillance of isolated superficial vein thrombosis (SVT) is recommended [38, 39].

## Comparison of Upper and Lower Extremity DVT

Thrombosis of the upper extremity has distinct characteristics when compared to the venous thromboembolism of the lower extremity. The American DVT Registry Database enrolled over 5,000 consecutive adult patients with acute DVT between October 2001 and October 2010, which reported approximately 11% of patients with UEDVT. The database included catheter-related venous thromboembolic disease of the upper extremity (6% of total cases), noncatheter-related venous UEDVT (5% of total cases), and lower extremity DVT (89% of total cases) [40].

When compared with lower extremity DVT, UEDVT patients were younger, less often white, leaner, had a lower body mass index, and most frequently presented with edema and less commonly with extremity discomfort, dyspnea, or chest pain [41]. Patients with UEDVT also had symptomatic PE less frequently (3% vs. 16%, $P < 0.001$) [40]. The differences reported in comparison of lower extremity DVT in the upper extremity includes patients less frequently had a family history of venous thromboembolism (18% vs. 31%, $P = 0.06$) or concomitant PE (8% vs. 31%, $P = 0.001$). Additionally, they were less frequently carriers of Factor V Leiden (12% vs. 30%, $P = 0.009$) and had lower thrombin generation marker levels [41].

Recurrence occurred in 2 of 50 patients (4%) with UEDVT versus 15% of those with lower extremity DVT. After 5 years,

the likelihood of recurrence was 2% in the UEDVT patients versus 19% among those with lower extremity DVT [41]. Clinical presentation complications of UEDVT including embolism recurrence appear to be different from lower extremity DVT. A lower rate of symptomatic PE was reported in previous studies [2, 40, 41]. Recurrence of DVT is far more likely in patients who have an unprovoked or idiopathic DVT [2]. There are few data to identify individuals with idiopathic UEDVT who are at highest risk of recurrence. The optimal duration of anticoagulation is not clear. Recurrence rates for UEDVT over a period of 3–6 months are very low. It is likely that prolonged anticoagulation is not required for most patients. It is not possible, however, to identify those who are at highest risk of recurrence and who therefore might benefit from long-term anticoagulation [42].

Cancer patients who have a central venous catheter have an increased incidence of thromboembolism of the arm [43]. The risk in the presence of injury and during the puerperium was twofold or more increased although not significantly. In contrast, hormone replacement therapy, unusual exercise, travel, and obesity do not increase the risk of UEDVT. Hormone users had an increased risk in the presence of prothrombotic mutations or surgery. Obese persons (BMI greater than 30 kg/m$^2$) undergoing surgery had a 23-fold increased risk of arm thrombosis compared to nonobese persons undergoing surgery. Most risk factors for thrombosis in the leg are also risk factors for arm thrombosis [43].

Unexplained or recurrent UEDVT should prompt a search for an inherited hypercoagulable state or underlying malignancy. Upper extremity DVT is frequently asymptomatic until complications ensue; a high index of suspicion is required for patients with one or more risk factors for thrombosis [43, 44].

Pulmonary embolism and postthrombotic syndrome are the most common sequelae of UEDVT. Traditionally, anticoagulant therapy is giving way to a multimodal approach involving transcatheter thrombolytic therapy followed by a minimum 3 months of warfarin sodium anticoagulation, venous decompression as needed, and balloon angioplasty with stenting for the residual stricture. Low-dose anticoagulant therapy can safely and effectively mitigate the increased risk of UEDVT associated with central venous catheters [44].

Gene mutations associated with UEDVT include Factor V, prothrombin 20210A, methylenetetrahydrofolate reductase MTHFR (C677T1), protein C deficiency, protein S deficiency, fibrinogen, and antithrombin III deficiency. Acquired thrombophilias include malignancy, congestive heart failure, pregnancy, antiphospholipid syndrome, nephrotic syndrome, liver disease, disseminated intravascular coagulation, sepsis, heparin-induced thrombocytopenia, vasculitic disorders, and inflammatory bowel disease. Other risk factors include implanted pacemakers, trauma, previous thrombosis, antineoplastic agents, oral contraceptives, thoracic outlet syndrome, strenuous exercise, and central venous catheter use (both percutaneous and subcutaneous) [44].

## Secondary Upper Extremity Thrombi

Three different types of thrombi can occur in association with central venous catheters. The most common is a "catheter adherent fibrin sleeve," which starts at the point of entry of the catheter into the vein and extends toward the catheter tip, with the length proportional to the duration of the catheterization. Catheter adherent fibrin sleeves are asymptomatic but fragments can detach when the catheter is removed and embolize to the lungs. Additional types of thrombi include the nonocclusive mural thrombus and thrombus causing complete occlusion of the vein [44] (Fig. 39.6a, b).

The likelihood of developing catheter related UEDVT is also affected by additional mechanical factors including the number of punctures during catheter insertion, the number inserted and the changing of catheters, the location of the catheter tip, the duration of catheterization, the type of catheters used, the type of fluid administered, catheter-related

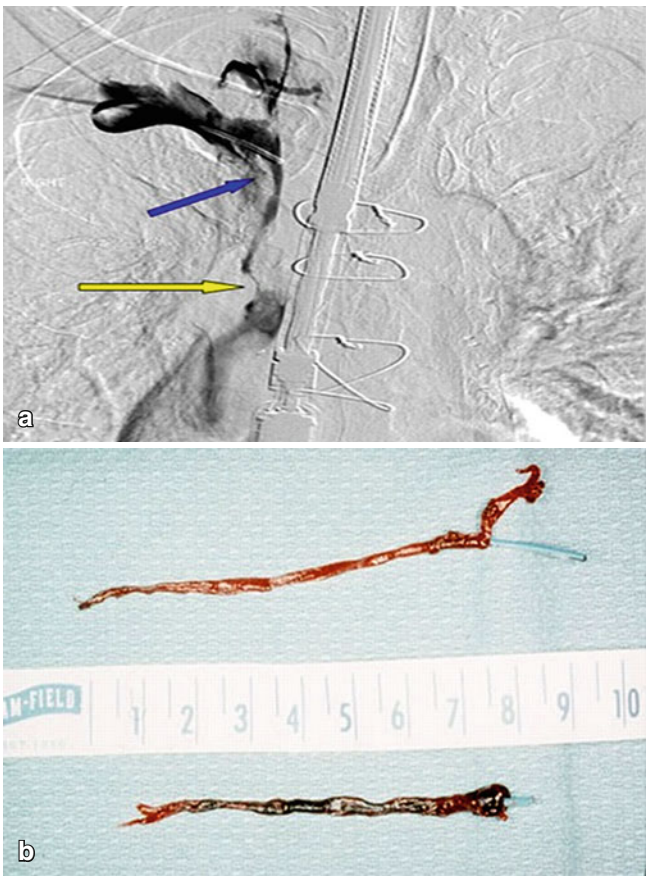


**Fig. 39.6** (**a**) Occluded subclavian vein related to catheter (*blue arrow*) with collateral flow (*yellow arrow*). (**b**) Catheter adherent thrombus

infection, hypercoagulable states, and the presence of congestive heart failure [44]. Kearns and colleagues found that UEDVT occurred in 60% of patients with catheter tips placed in the axillosubclavicular and innominate veins compared to 21% of patients with the tips in the superior vena cava at the caval atrial junction [45]. Koksoy and associates found that two factors correlated significantly with the development of central venous catheter related thrombosis. First, the number of vein punctures (1 vs. 2, $P<0.01$) and second the composition of the infusion solution (crystalloid versus parenteral nutrition, $P=0.01$) [46].

The incidence of UEDVT with implanted pacemakers has been reported to be less than 5%; however, since a large number of these are asymptomatic the incidence may actually be higher [44]. Upper extremity DVT may also complicate the use of peripheral venous catheters and peripherally inserted central venous catheters. Intravenous drug abusers also have an increased risk of UEDVT, resulting in the spread of superficial phlebitis to the deep venous system. Occasionally drugs may be injected directly into the subclavian vein and thrombosis may result from repeated trauma or infection. Other reported causes of UEDVT include intravenous immune globulin infusion and seat belt injuries [44]. Another study by Bauersachs et al. suggests that ovarian stimulation and development of ovarian hyperstimulation syndrome (OHSS) are significant risk factors for the appearance of UEDVT. Hemo concentration, increased activation of coagulation, possibly in addition to thrombophilia, and the underlying hematologic changes during pregnancy were suggested as potential pathophysiologic factors triggering the UEDVT during OHSS [47]. UEDVT has also been reported to complicate coronary artery bypass, whole blood donation and ambulatory blood pressure monitoring [48–50].

Girolami et al. reported that lung cancer and lymphomas represented a majority of cancers found in patients presenting with UEDVT [51]. Ulnar vein thrombosis as a manifestation of Loa loa filariasis has also been reported [52]. Kuriakose et al. recently reported chest ports and peripheral ports have a significantly associated high incidence of UEDVT [53]. Sarcoidosis may also result in lymphadenopathy, which can cause venous compression.

Patients who developed new or worsening central vein stenosis or occlusion have significantly ($P=0.03$) longer catheter dwell times than patients without central vein abnormalities. New central vein stenosis or occlusion occurred in 7% of patients following upper extremity placement of venous access devices. Patients with longer catheter dwell time as were more likely to develop central vein abnormalities. In order to preserve vascular access for dialysis fistulae and grafts and adhere to the Dialysis Outcomes Quality Initiative guidelines, alternative venous access sites should be considered for patients with chronic renal insufficiency and end-stage renal disease. This group of authors also suggest a 7% risk of developing central vein stenosis or occlusion occurs in patients who undergo placement of a peripherally inserted central catheter (PICC) or venous infusion port in the upper arm [54]. In a review of pediatric patients, the incidence of DVT related to PICCs 11–50% was lower than the incidence related to central venous catheters as described in the pediatric literature, [55].

In patients receiving chemotherapy the cytotoxic effects of 5-fluorouracil on the vascular endothelium are the likely link to thrombotic complications. Alternative methods for administering chemotherapy should be considered, namely continuous infusion versus bolus dose administration [56]. Thrombosis rates associated with PICC may be as low as 3.9%. The smallest acceptable catheter diameter should be used to decrease the incidence of thrombosis [57]. Thrombosis may be a complication of central venous catheter-associated *Staphylococcus aureus* bacteremia. In 2008, Crowley et al. suggested that patients with central venous catheter-associated with *S. aureus* bacteremia should undergo ultrasound to detect thrombosis even if physical examination is normal [58]. Hemostasis at the puncture site for transradial cardiac catheterization using an Elastoplast compression bandage supported by a tourniquet has also been reported to cause UEDVT [59]. Circumferential taping should be avoided.

## Treatment

The treatment of primary and secondary UEDVT is undergoing evolution but upper extremity DVT should not be considered a benign event. Risks factors for UEDVT associated with the use of central venous catheters in cancer patients were identified by Verso et al. Using logistic regression, they found that 50 of 310 (16.1%) had either the catheter tip misplaced in the upper half of the superior vena cava, left-sided central venous catheter insertion, or chest radiotherapy as independent risk factors for thrombosis. In addition to these risk factors, the presence of distant metastatic disease increased the risk of thrombosis in patients compared to those receiving placebo [60].

In cancer patients treated with chemotherapy, 7.3% had VTE during or within 3 months of chemotherapy treatment. The annual incidence was 10.9%. The incidence of VTE was specifically high in patients treated with a combination of fluorouracil and leucovorin because of colorectal cancer. Trials are underway to evaluate the use of prophylactic anticoagulant treatment in this study group [61].

Approximately 30% of all primary UEDVTs are associated with exercise induced venous compression, 20% with thrombophilic defects and 26% with oral contraceptives. Obesity and hyperlipidemia do not appear to be associated with primary UEDVT [62]. The debate exists over UEDVT as a manifestation of a hypercoagulable state. In a patient with

primary UEDVT, screening for deficiencies in antithrombin III, protein C, protein S, and APC resistance would not be justified although it might be reasonable to determine if the carrier state of prothrombin G20210A mutation is present for oral contraceptive users as this has been shown to increase the risk [63].

In a meta-analysis of the impact of inherited thrombophilia on venous thromboembolism in children, it was found that 11.4% of children with nonidiopathic thrombosis, overall regardless of their thrombophilic status developed a second VTE. Secondary events were mainly in adolescents and occurred in approximately 80% of affected children after withdrawal of anticoagulant therapy. In the present meta-analysis, a significant association with recurrent VTE in children was found for protein C, protein S, and antithrombin deficiency, the Factor II variant; and two or more genetic traits. Pediatric carriers of the Factor V mutation or elevated lipoproteins (a) did not show an increased risk for recurrent VTE in this present analysis [64].

D-dimer may have very limited usefulness in clinical management of the patient with suspected UEDVT. There is limited specificity in patients with UEDVT. There is a high prevalence of cancer, permanent catheter, and inpatients in this population with significant concomitant disease, all of which can contribute to elevated D-dimer levels [65].

## Conclusions

Upper extremity DVT should no longer be regarded as an uncommon or benign disease. It is usually associated with risk factors including central line, malignancy, coagulation defects; however, up to 20% of UEDVTs are apparently spontaneous. The clinical picture is characterized by swelling, pain, and functional impairment, although UEDVT may be completely asymptomatic. Up to 36% of patients develop PE, which may be fatal. Postthrombotic sequelae and recurrent thromboembolism are frequent complications. Unfractionated or low-molecular-weight heparin followed by anticoagulation should be regarded as the treatment of choice. Thrombolysis and surgery may be indicated in select cases. Prophylaxis with low-dose heparin or low-dose warfarin therapy is necessary whenever central venous catheters are positioned [66].

Despite active treatment PE and postthrombotic syndrome may arise during follow-up with patients. Pulmonary embolism may develop in up to 36% of cases and appears to be more frequent in patients with central venous catheters. Mortality rate in patients with UEDVT range from 10% to 50% and are mainly related to underlying conditions such as end-stage cancer and age. Fatal PE may occasionally contribute to the overall mortality rate [66].

In the most recent CHEST guidelines looking at clinical outcomes of patients with UEDVT and results from the computerized Registry of patients with Venous Thromboembolism (RIETE) it was concluded that patients at presentation with UEDVT have less often clinically overt PE than those with lower limb DVT but their 3-month outcome is similar. Among patients with UEDVT, those with cancer have a far worse outcome [67].

Dr. Hingorani and colleagues recently tried to predict morbidity and mortality associated with UEDVT based on thrombus location and treatment. They concluded that contrary to the initial hypothesis of a relationship between the site of the thrombosis and incidence of PE and mortality, their data demonstrated no statistical differences in mortality or incidence of PE among the groups studied. Additional data suggested that both isolated internal jugular and isolated brachial DVT needs to be treated with equal consideration compared to other sites of UEDVT. Since many of these patients with UEDVT did not die of clinically apparent PE but rather multiorgan system failure, UEDVT may be thought of as a marker for the severity of systemic illness of the patient rather than just as a cause of venous thromboembolism [68].

Outpatient low-molecular-weight heparin may be safely used for treatment of UEDVT [69, 70]. In looking at the hemodynamic and morphologic evaluation and sequelae of primary UEDVT treated with anticoagulant therapy, patients who were treated conservatively had significantly reduced venous outflow capacity and a residual thrombus was common. Swelling of the arm was the most common symptom and one-third had a moderate grade of postthrombotic syndrome. However, there was no clear relation between hemodynamic and morphologic factors and the development of postthrombotic syndrome in this study, which was limited to 31 patients with a mean follow-up of 5 years after the acute DVT episode [71]. Symptomatic UEDVT carries a low risk of recurrent thromboembolism. The rates of recurrent thromboembolism and postthrombotic syndrome are lower than those observed in cohorts of patients with thrombosis of the lower extremities [72]. The first step in treatment is to establish vessel patency. Evaluation of the need for continued catheter use is critical (see Fig. 39.7). The treatment for primary proximal UEDVT is presented in Chap. 40.

Postthrombotic syndrome of the upper extremity is associated with significant functional disability and reduced quality of life. Patients in whom the dominant arm is involved appear to fare much worse than those who have involvement of the nondominant arm. This study used the Villalta postthrombotic scale modified for the upper extremity to diagnose the postthrombotic syndrome. Patients also completed questions on degree of functional disability (DASH questionnaire) and generic (SF-36) and disease-specific (VEINES-QOL) quality of life surveys. Larger prospective studies to identify prognostic factors that lead to postthrombotic syndrome after UEDVT are needed [74].

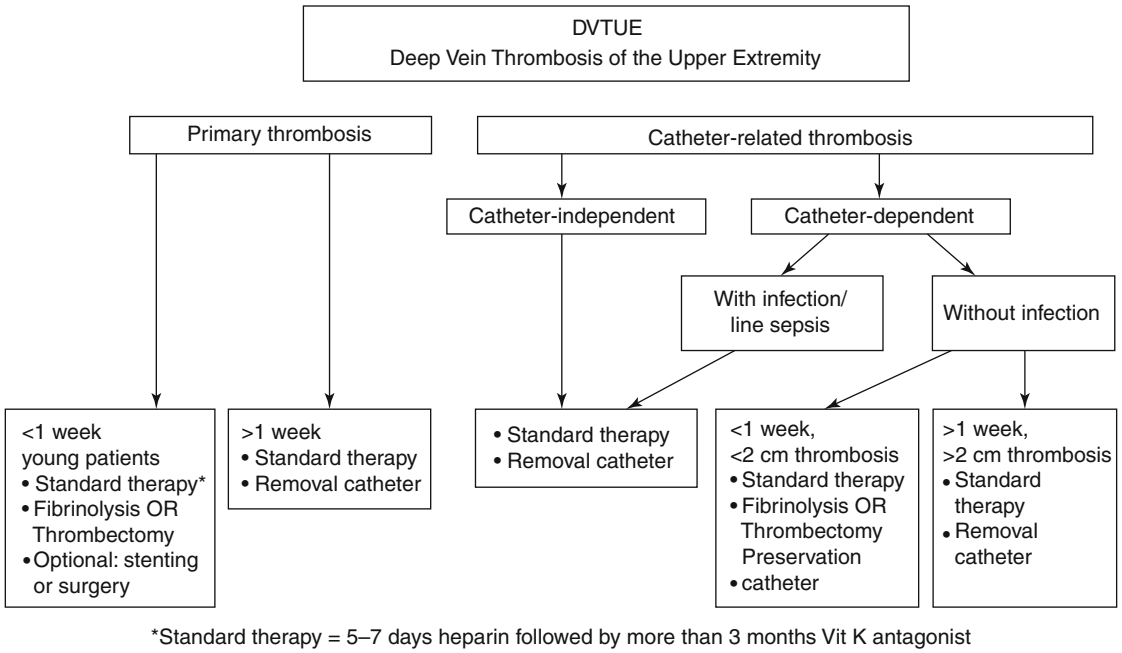


**Fig. 39.7** Algorithm for therapy of deep vein thrombosis of the upper extremities (Modified from Baarslag et al. [73]. With permission from Springer-Verlag)

## Summary

The growing number of uses for duplex imaging for upper extremity veins and arteries has expanded the indications and frequency of the application [75]. Currently, upper extremity venous imaging and duplex scans are used to assist peripherally inserted central catheter (PICC) line and central line insertion. Duplex imaging can also facilitate access to central veins for lytic treatment. Increasingly, upper extremity venous imaging is moving not only from the diagnostic realm but also into that of therapeutics and treatment.

Duplex imaging is a practical method of diagnosis for upper extremity venous thrombosis. The small mass of the upper extremity, as compared to the lower extremity, makes scanning easier and more likely to be accurate. Upper extremity venous imaging can effectively assist in the diagnosis of a spectrum of conditions including aneurysms, cysts, hemorrhages, and thrombosis of grafts. Although the blind area behind the clavicle requires careful insonation, the area may be decreased by recent color-flow imaging. Still, thorough evaluation of the Doppler signal in this area is important in preventing false-negative interpretations of central vein thrombosis. The use of duplex scanning is growing to include the evaluation of upper extremity abnormalities and arterial anomalies. This growth is expected to increase as venous imaging proves useful in diagnostic, as well as therapeutic and treatment situations.

Upper extremity DVT is an increasing clinical problem which requires immediate and accurate diagnostic techniques. Optimal treatment for upper extremity thrombosis is not known with certainty. Two general goals of therapy are to alter propagation of thrombi and reduce the risk of secondary events. Secondary treatment aims to allow recanalization of thrombus, which should ideally preserve normal anatomy. Patients with secondary thrombosis rapidly become asymptomatic with use of anticoagulant therapy and removal of the thrombogenic stimulus, for instance the catheter.

Superior vena caval filter placement should be considered if the patient cannot tolerate even a small PE, anticoagulation is contraindicated, anticoagulation therapy fails to prevent embolization, or the patient suffers a major bleeding episode while undergoing anticoagulation therapy. The Greenfield filter is the best filter for this location.

In general, therapy for primary thrombosis is directed at minimizing long-term sequelae of venous insufficiency, often requiring a multimodal approach. There is a spectrum of four different treatment options available for UEDVT, including anticoagulant therapy, fibrinolytic therapy, surgery, or interventional radiology techniques.

Evidence from large clinical trials is lacking. Anticoagulant therapy is however considered to be the cornerstone of therapy for thrombosis of the upper extremities. There are a few studies that have prospectively compared the safety and efficacy of anticoagulant therapy and thrombolytic therapy. The advantages of thrombolytic therapy are more complete resolution to thrombi and better restoration of patency of the veins. It is assumed and has been shown in small studies that patent veins will result in fewer postthrombotic complications. The great disadvantage of fibrinolytic therapy is the

greater risk of bleeding. Catheter-directed thrombolysis may decrease the risk of bleeding; however, there are no controlled trials or more recent data looking at either systemic thrombolysis or catheter directed thrombolysis in patients with UEDVT. Data on mechanical thrombolytic therapy is also severely lacking.

In patients with secondary thrombosis, maintenance of venous patency is mandatory for indwelling lines and life support, for each restoration of flow is vital. In addition, preservation of the functional line can be achieved. Venous mechanical thrombectomy does appear to be safe and is easy to perform with good immediate results. Multimodality therapy including surgical intervention may be needed in effort vein thrombosis or to reestablish venous patency [73]. The treatment of UEDVT is continuing to evolve.

**Acknowledgments** I would like to acknowledge Geri Meister, Angela N. Fellner, Ph.D., and the Good Samaritan Hospital Library staff for their assistance in preparation of this chapter.

## References

1. Kidney Disease Outcomes Quality Initiative (K/DOQI) guidelines. 2004. Available at: www.kidney.org/professionals/kdoqi/guidelines_bp/index.htm. Accessed 23 May 2012.
2. Spencer FA, Emery C, Lessard D, et al. Upper extremity deep vein thrombosis: a community-based perspective. Am J Med. 2007;120:678–84.
3. Bernardi E, Pesavento R, Prandoni P. Upper extremity deep vein thrombosis. Semin Thromb Hemost. 2006;32:729–36.
4. Shah MK, Burke DT, Shah SH. Upper extremity deep vein thrombosis. South Med J. 2003;96:669–72.
5. Prandoni P, Polistena P, Bernardi E, et al. Upper-extremity deep vein thrombosis. Risk factors, diagnosis, and complications. Arch Intern Med. 1997;157:57–62.
6. Prandoni P, Bernardi E. Upper extremity deep vein thrombosis. Curr Opin Pulm Med. 1999;5:222–6.
7. Kooij JD, van der Zant FM, van Beck EJ, et al. Pulmonary embolism in deep venous thrombosis of the upper extremity: more often in catheter-related thrombosis. Neth J Med. 1997;50:238–42.
8. Hingorani A, Ascher E, Hanson J, et al. Upper extremity versus lower extremity deep venous thrombosis. Am J Surg. 1997;174:214–7.
9. Burihan E, de Figueiredo LF, Francisco Jr J, et al. Upper extremity deep venous thrombosis: analysis of 52 cases. Cardiovasc Surg. 1993;1:19–22.
10. Sajid MS, Ahmed N, Desai M, et al. Upper limb deep vein thrombosis: a literature review to streamline the protocol for management. Acta Heamatol. 2007;118:10–8.
11. Kammen BF, Soulen MC. Phlegmasia cerulea dolens of the upper extremity. J Vasc Interv Radiol. 1995;6:283–6.
12. Rutherford RB, Hurlbert SN. Primary subclavian-axillary vein thrombosis: consensus and commentary. Cardiovasc Surg. 1996;4:420–3.
13. Khan SN, Stansby G. Current management of Paget-Schroetter syndrome in the UK. Ann R Coll Surg Engl. 2004;86:29–34.
14. Lohr JM. Upper extremity venous duplex imaging. In: Ashraf Mansour M, Labropoulos N, editors. Vascular diagnosis. 1st ed. Philadelphia: Elsevier Saunders; 2005. p. 469–77.
15. Schmittling ZC, McLaffety RB, Bohannon WT, et al. Characterization and probability of upper extremity deep venous thrombosis. Ann Vasc Surg. 2004;18:552–7.
16. Luciani A, Clement O, Halimi P, et al. Catheter-related upper extremity deep venous thrombosis in cancer patients: a prospective study based on Doppler US. Radiology. 2001;220:655–60.
17. Joffe HV, Goldhaber SZ. Upper extremity deep vein thrombosis. Circulation. 2002;106:1874–80.
18. Richard 3rd HM, Selby Jr JB, Gay SB, et al. Normal venous anatomy and collateral pathways in upper extremity venous thrombosis. Radiographics. 1992;12:527–34.
19. Makhoul RG, Machleder HI. Developmental anomalies at the thoracic outlet: an analysis of 200 consecutive cases. J Vasc Surg. 1992;16:534–42.
20. Fraser JD, Anderson DR. Venous protocols, techniques, and interpretations of the upper and lower extremities. Radiol Clin North Am. 2004;42:279–96.
21. Wang YF, Cherng SC, Chiu JS, et al. Application of upper extremity radionuclide venography as a diagnostic approach for Port-A catheter thrombosis. J Chin Med Assoc. 2006;69:358–63.
22. Baarslag HJ, van Beek EJ, Koopman MM, et al. Prospective study of color duplex ultrasonography compared with contrast venography in patients suspected of having deep venous thrombosis of the upper extremities. Ann Intern Med. 2002;136:865–72.
23. Weber TM, Lockhart ME, Robbin ML. Upper extremity venous Doppler ultrasound. Radiol Clin North Am. 2007;45:513–24.
24. Wladis AR, Mesh CL, White J, et al. Improving longevity of prosthetic dialysis grafts in patients with disadvantaged venous outflow. J Vasc Surg. 2000;32:997–1005.
25. Andrew M, David M, Adams M, et al. Venous thromboembolic complications (VTE) in children: first analyses of the Canadian registry of VTE. Blood. 1994;83:1251–7.
26. Nowak-Göttl U, von Kries R, Göbel U. Neonatal symptomatic thromboembolism in Germany: two year survey. Arch Dis Child Fetal Neonatal Ed. 1997;75:F163–7.
27. van Ommen CH, Heijboer H, Büller HR, et al. Venous thromboembolism in childhood: a prospective two-year registry in the Netherlands. J Pediatr. 2001;139:676–81.
28. Schmidt B, Andrew M. Neonatal thrombosis: report of a prospective Canadian and international registry. Pediatrics. 1995;96:939–43.
29. Cranley JJ, Higgins RF, Berry RE, et al. Near parity in the final diagnosis of deep venous thrombosis by duplex scan and phlebography. Phlebology. 1989;4:71–4.
30. Cranley JJ. Seeing is believing: a clot is a clot, on a duplex scan or phlebogram. Echocardiography. 1987;4:423.
31. Cranley JJ. Diagnosis of deep venous thrombosis. In: Bernstein EF, editor. Recent advances in noninvasive diagnostic techniques in vascular disease. St. Louis: Mosby; 1990.
32. Flannagan LD, Sullivan ED, Cranley JJ. Venous imaging of the extremities using real-time B-mode ultrasound. In: Bergan JJ, Yao JST, editors. Surgery of the veins. Orlando: Grune & Stratton; 1984.
33. Karkow WS, Ruoff BA, Cranley JJ. B-mode venous imaging. In: Kempezinski RF, Yao JST, editors. Practical noninvasive vascular diagnosis. Chicago: Mosby; 1987.
34. Kerr TM, Cranley JJ, Johnson JR, et al. Analysis of 1084 consecutive lower extremities involved with acute venous thrombosis diagnosed by duplex scanning. Surgery. 1990;108:520–7.
35. Kerr TM, Lutter KS, Moeller DM, et al. Upper extremity venous thromboses diagnosed by duplex scanning. Am J Surg. 1990;160:202–6.
36. Sullivan ED, Peter DJ, Cranley JJ. Real-time B-mode venous ultrasound. J Vasc Surg. 1984;1:465–71.
37. Talbot SR. Use of real-time imaging in identifying deep venous obstruction: a preliminary report. Bruit. 1982;6:41–2.
38. Lutter KS, Kerr TM, Roedersheimer LR, et al. Superficial thrombophlebitis diagnosed by duplex scanning. Surgery. 1991;110:42–6.

39. Gloviczki P, Kazmier FJ, Hollier LH. Axillary-subclavian venous occlusion: the morbidity of a nonlethal disease. J Vasc Surg. 1986;4:333–7.
40. Joffe HV, Kucher N, Tapson VF, et al. Upper-extremity deep vein thrombosis. A prospective registry of 592 patients. Circulation. 2004;110:1605–11.
41. Lechner D, Wiener C, Weltermann A, et al. Comparison between idiopathic deep vein thrombosis of the upper and lower extremity regarding risk factors and recurrence. J Thromb Haemost. 2008;6:1269–74.
42. Baglin T, Luddington R, Brown K, et al. Incidence of recurrent venous thromboembolism in relation to clinical and thrombophilic risk factors: prospective cohort study. Lancet. 2003;362:523–6.
43. Blom JW, Doggen JM, Osanto S, et al. Old and new risk factors for upper extremity deep venous thrombosis. J Thromb Haemost. 2005;3:2471–8.
44. Kommareddy A, Zaroukian MH, Hassuna HI. Upper extremity deep venous thrombosis. Semin Thromb Hemost. 2002;28:89–99.
45. Kearns PJ, Coleman S, Wehner JH. Complications of long arm catheters: a randomized trial of central vs peripheral tip location. J Parenter Enteral Nutr. 1996;20:20–4.
46. Koksoy C, Kuzu A, Erden I, et al. The risk factors in central venous catheter-related thrombosis. Aust N Z J Surg. 1995;65:796–8.
47. Bauersachs RM, Manolopoulos K, Hoppe I, et al. More on: the 'ART' behind the clot: solving the mystery. J Thromb Haemost. 2007;5:438–9.
48. Ambrosetti M, Salerno M, Dentali F, et al. Upper extremity deep vein thrombosis and pulmonary embolism after coronary bypass surgery: a case report and preliminary results from a prospective study evaluating patients during cardiac rehabilitation. Ital Heart J. 2004;5:241–4.
49. Covin RB, Rich NL, Aysola A. Upper-extremity deep venous thrombosis complicating whole blood donation. Transfusion. 2004;44:586–90.
50. Marschang P, Niederwanger A, Gasser RW, et al. Symptomatic upper extremity deep vein thrombosis as a complication of ambulatory blood pressure monitoring. Thromb Haemost. 2008;100:711–2.
51. Girolami A, Prandoni P, Zanon E, et al. Venous thromboses of upper limbs are frequently associated with occult cancer as compared with those of lower limbs. Blood Coagul Fibrinolysis. 1999;10:455–7.
52. Petersen S, Rønne-Rasmussen J, Basse P. Thrombosis of the ulnar veins – an unusual manifestation of Loa loa filariasis. Scand J Infect Dis. 1998;30:204–5.
53. Kuriakose P, Colon-Otero G, Paz-Fumagalli P. Risk of deep venous thrombosis associated with chest versus arm central venous subcutaneous port catheters: a 5-year single-institution retrospective study. J Vasc Interv Radiol. 2002;13:179–84.
54. Gonsalves CF, Eschelman DJ, Sullivan KL, et al. Incidence of central vein stenosis and occlusion following upper extremity PICC and port placement. Cardiovasc Intervent Radiol. 2003;26:123–7.
55. Dubois J, Rypens F, Garel L, et al. Incidence of deep vein thrombosis related to peripherally inserted central catheters in children and adolescents. CMAJ. 2007;177:1185–90.
56. Tham J, Albertsson M. Upper extremity deep venous thrombosis in patients with 5-fluorouracil-containing adjuvant chemotherapy – three case reports and a review. Acta Oncol. 2004;43:108–12.
57. Grove JR, Pevac WC. Venous thrombosis related to peripherally inserted central catheters. JVIR. 2000;11:837–40.
58. Crowley AL, Peterson GE, Benjamin Jr DJ, et al. Venous thrombosis in patients with short- and long-term central venous catheter-associated *Staphylococcus aureus* bacteremia. Crit Care Med. 2008;36:385–90.
59. Hall IR, Lo TS, Nolan J. Deep vein thrombosis in the arm following transradial cardiac catheterization: an unusual complication related to hemostatic technique. Catheter Cardiovasc Interv. 2004;62:346–8.
60. Verso M, Agnelli G, Kamphuisen PW, et al. Risk factors for upper limb deep vein thrombosis associated with the use of central vein catheter in cancer patients. Int Emerg Med. 2008;3:117–22.
61. Otten HM, Mathijssen J, ten Cate H, et al. Symptomatic venous thromboembolism in cancer patients treated with chemotherapy: an underestimated phenomenon. Arch Intern Med. 2004;164:190–4.
62. Vaya A, Martinez-Triguero M, Romagnoli M, et al. Lack of association between hemorheological alterations and upper-extremity deep vein thrombosis. Clin Hemorheol Microcirc. 2009;41:279–85.
63. Vaya A, Mira Y, Mateo J, et al. Prothrombin G20210A mutation and oral contraceptive use increase upper-extremity deep vein thrombotic risk. Thromb Haemost. 2003;89:452–7.
64. Young G, Albisetti M, Bonduel M, et al. Impact of inherited thrombophilia on venous thromboembolism in children: a systematic review and meta-analysis of observational studies. Circulation. 2008;118:1373–82.
65. Merminod T, Pellicciotta S, Bounameaux H. Limited usefulness of D-dimer in suspected deep vein thrombosis of the upper extremities. Blood Coagul Fibrinolysis. 2006;17:225–7.
66. Bernardi E, Piccioli A, Marchiori A, et al. Upper extremity deep vein thrombosis: risk factors, diagnosis, and management. Semin Vasc Med. 2001;1:105–10.
67. Muñoz FJ, Mismetti P, Poggio R, et al. Clinical outcome of patients with upper-extremity deep vein thrombosis: results from the RIETE registry. Chest. 2008;133:143–8.
68. Hingorani A, Ascher E, Marks N, et al. Morbidity and mortality associated with brachial vein thrombosis. Ann Vasc Surg. 2006;20:297–300.
69. Savage KJ, Wells PS, Schulz V, et al. Outpatient use of low molecular weight heparin (Dalteparin) for the treatment of deep vein thrombosis of the upper extremity. Thromb Haemost. 1999;82:1008–10.
70. Shah MK, Black-Schaffer RM. Treatment of upper limb deep vein thrombosis with low molecular weight heparin. Am J Phys Med Rehabil. 2003;82:415–7.
71. Persson LM, Arnhjort T, Lärfars G, et al. Hemodynamic and morphologic evaluation of sequelae of primary upper extremity deep venous thromboses treated with anticoagulation. J Vasc Surg. 2006;43:1230–5.
72. Prandoni P, Bernardi E, Marchiori A, et al. The long term clinical course of acute deep vein thrombosis of the arm: prospective cohort study. BMJ. 2004;329:484–5.
73. Baarslag HJ, Koopman MM, Reekers JA, et al. Diagnosis and management of deep vein thrombosis of the upper extremity: a review. Eur Radiol. 2004;14:1263–74.
74. Kahn SR, Elman EA, Bornais C, et al. Post-thrombotic syndrome, functional disability and quality of life after upper extremity deep venous thrombosis in adults. Thromb Haemost. 2005;93:499–502.
75. Lohr JM, Paget DS, Smith JM, et al. Upper extremity hemodynamic changes after radial artery harvest for coronary artery bypass grafting. Ann Vasc Surg. 2000;14:56–62.

# Role of the Noninvasive Vascular Laboratory in Thoracic Outlet Syndrome

40

Diana Call, Holly L. Grunebach, and Julie Ann Freischlag

**Abstract**

The thoracic outlet is an area encompassing the structures above and below the first rib, which provides passage of the axillary and subclavian artery, vein, and brachial plexus as they travel from the neck and chest down the upper arm. An abnormality anywhere along this pathway results in an impingement of blood flow or neurologic transmission, which results in a condition known as thoracic outlet syndrome (TOS). Clinical symptoms of TOS can vary depending on the type of structure compressed and therefore is subdivided into two categories: neurogenic and vascular. Vascular TOS can be further divided into venous and arterial disease. In the nonacute stage, the majority of the vascular TOS patients present clinically with the same vague symptoms as the neurogenic TOS group, making diagnosis and delineation of subsequent treatment challenging. With vast improvements in ultrasound equipment, there is considerable emphasis placed on the utility of duplex imaging in the upper extremity. A TOS duplex ultrasound protocol and diagnostic interpretation, with a focus on the anatomic relationship of the upper extremity vessels, normal and abnormal color filling, and velocities with and without maneuvers, is described within this chapter. This ever expanding role of the noninvasive vascular examination, in the confirmation, treatment, and follow-up of the TOS patients has proven to have diagnostic usefulness.

**Keywords**

Thoracic outlet syndrome (TOS) • Paget-von Schroetter • Vascular ultrasound • Subclavian vein and artery

## Introduction

The thoracic outlet is an area encompassing the structures above and below the first rib. It provides passage for the axillary and subclavian artery, subclavian vein, and brachial plexus as they travel from the neck and chest down the upper arm [1]. An abnormality anywhere along this pathway can result in impinged blood flow, impaired neurologic transmission, or combination of both, which ultimately results in a condition known as thoracic outlet syndrome (TOS). The term TOS was first used in 1956 by Peete, and remains in use today for a complex array of signs and symptoms [2]. Two of the most common culprits in aggravating this syndrome are enlargement of the muscles within the scalene triangle, specifically the scalene anticus, and abnormalities of the first or cervical ribs, which is seen in about 10% of the population [3].

The clinical symptoms of TOS can vary depending on the type of structure compressed and therefore is divided into two subgroups: neurologic TOS and vascular TOS. The symptoms in both groups are primarily brought on by changes in arm position, which compress blood vessels and/or nerves

D. Call, BS, RVT
Division of Vascular Surgery and Endovascular Therapy,
Johns Hopkins Hospital,
Baltimore, MD, USA

H.L. Grunebach, MMS, MSPH • J.A. Freischlag, M.D. (✉)
Department of Surgery, Johns Hopkins Hospital,
720 Rutland Avenue 759 Ross, Baltimore, MD 21205, USA
e-mail: jfreisc1@jhmi.edu

A.F. AbuRahma, D.F. Bandyk (eds.), *Noninvasive Vascular Diagnosis*,
DOI 10.1007/978-1-4471-4005-4_40, © Springer-Verlag London 2013

in the thoracic outlet [4]. Neurogenic TOS is the most common, seen in 95% of cases, and results when there is compression of the brachial plexus with positional changes of the arm. Clinically in this group of patients, the presentation of neurogenic TOS can be vague. Symptoms can range in severity from parethesias and intermittent aches of the arm and hand to severe weakness, fatigue, and wasting of the hand or forearm muscles. An initial conservative approach to treatment is taken in this patient population. The focus is primarily on physical therapy and scalene block with possible consideration for an operation based on the outcome of nonsurgical management. Conversely, vascular TOS, although less common, results in the compression, irritation, or direct injury of the subclavian vein or artery and the symptoms are well established [5]. In the acute stage, symptoms of venous TOS include pain, swelling, and cyanosis. Subclavian vein compression in TOS is the potential cause of axillosubclavian thrombosis, also known as Paget–von Schroetter syndrome or "effort thrombosis."[4] Effort thrombosis is an uncommon, but not rare entity. The annual incidence reported is estimated at about 2 per 100,000 people [6]. The incidence of venous TOS is 3%. Arterial TOS is even rarer and the least frequently encountered form of TOS at 1% incidence. Clinically, acute arterial TOS presents differently from venous TOS with common symptoms of ischemic fingers and severe arm claudication. Both the venous and arterial groups of patients are managed aggressively with a surgical approach compared to the neurogenic TOS group.

In the nonacute stage, the majority of the vascular TOS patients present clinically with the same vague symptoms as the neurogenic TOS patients, making diagnosis and subsequent treatment difficult. Noninvasive testing combined with a detailed history and thorough physical examination are the initial steps in differentiating and diagnosing when patients present with clinical symptoms of TOS without a clear etiology established.

Useful physical examination tools to determine the possible extent of compression within the thoracic outlet include the Elevated Arm Stress Test (EAST), Adson's test, assessing for scalene tenderness, upper extremity strength, and range of motion. Initially plain X-ray studies of the chest and cervical spine should be obtained. These X-rays provide important information regarding the evidence of cervical ribs, rudimentary ribs, and abnormal transverse processes [7].

The EAST involves the patient elevating their arms overhead at 90° while moving each finger tip to the thumb as rapidly as possible until stopping by command, reproduction of symptoms, or fatigue. TOS patients will often complain during the EAST examination of some combination of pain, parethesias, and pallor of the affected hand [1]. Normally, patients without TOS can perform the EAST for 3 min. This test replicates in most TOS patients the same symptoms they have been experiencing in their daily lives and is highly valued in the initial assessment process. The Adson's maneuver is also used as a means of evaluating for TOS. This test is performed with patient sitting upright while the clinician palpates the radial pulse. The patient is then asked to turn their head toward the symptomatic side while inhaling. If the radial pulse on the affected side decreases significantly or disappears, the test is considered positive. However, a positive Adson's test can occur in the asymptomatic patient and so this finding alone can be used to support but not confirm arterial TOS [8].

For many years, the physical examination and indirect physiological examination were the only noninvasive ways to evaluate these clinically suspicious TOS patients. However, with rapidly changing advancements in ultrasound technology, a greater emphasis is being placed on this modality in establishing a TOS diagnosis. Direct imaging and flow analysis of the upper extremity vasculature is growing in favor as a reliable diagnostic tool in the clinically suspicious TOS patient.

## Indirect Physiological Testing

Historically the role of the noninvasive laboratory in a patient with a clinical suspicion of TOS has been limited to physiological nonimaging tests specific to the arterial compression component of this syndrome. Plethysmographic techniques and Doppler waveform analysis with arm maneuvers have been utilized to detect arterial changes with this testing modality. To detect changes in blood flow in the subclavian artery, three techniques have been heavily utilized including: a photoplethysmograph sensor (PPG) placed on the patient's index finger, continuous wave Doppler is used to monitor the radial artery, and brachial cuff is applied to monitor plethysmographic pulse volume waveforms [9]. Waveforms are obtained at rest and then the patient's arm is moved into various positions while the pulsations are documented at each position.

Standard positioning to examine plethysmographic pulses in the radial artery requires the patient to sit erect on the examination table with their legs dangling off. The patient is asked to remain relaxed with hands in their lap for resting waveforms. The patient is then asked to place their arms at a 90° angle in the same plane as the torso, 180° angle in the same plane as torso, and in an exaggerated military stance. In addition, the Adson maneuver positioning is included in the TOS protocol of many vascular labs. Adson maneuver positioning is described as exaggerated military stance with head turned sharply toward the arm being tested initially and then with the head turned sharply away from the arm being tested. During all of these maneuvers, the arterial waveforms are obtained for interpretation and analysis. Additionally, since

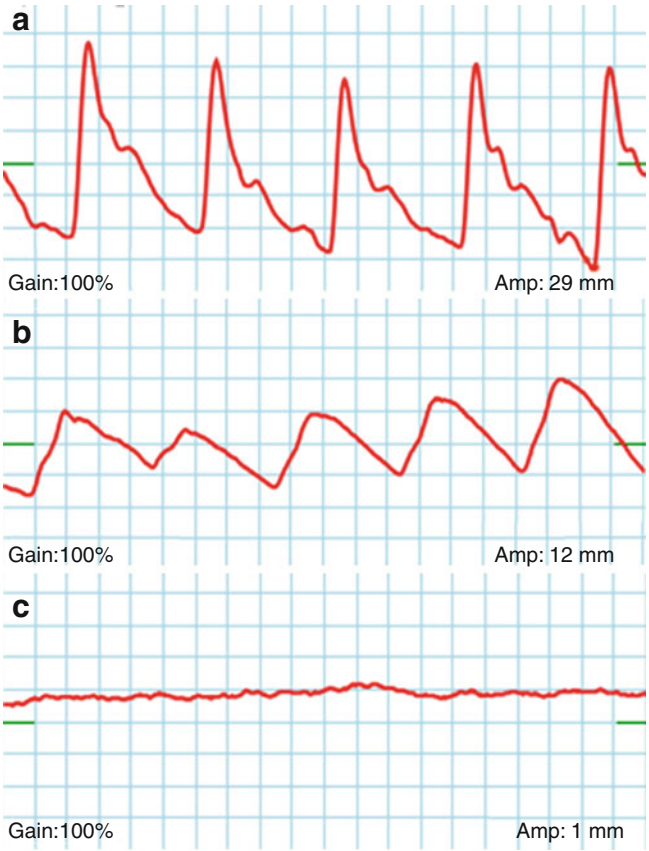


**Fig. 40.1** Photoplethysmographic waveforms (PPG). (**a**) Normal waveforms. (**b**) Borderline abnormal with partial attenuation of waveforms. (**c**) Abnormal with complete flattening of the waveforms

TOS is often bilateral, the patient's noninvasive testing should include examination of both arms.

In the normal patient, the initial resting waveform is maintained throughout the various arm positions; however, if the initial resting waveform changes with any of the patient's arm positions this is considered abnormal. The change in the waveform can be as subtle as a partially reduced waveform and as obvious as a completely obliterated waveform (see Fig. 40.1). It has been estimated that as high as 25% of asymptomatic patients have an abnormal test in some of the positions outlined [10]. This fact, in addition to the disagreement among vascular clinicians regarding how to treat the symptomatic patient with abnormal waveforms during noninvasive physiological test, additional testing modalities are sought by many to confirm the diagnosis of TOS.

## Direct Testing with Duplex Ultrasound

Duplex ultrasound has become increasingly accepted as a diagnostic tool in the evaluation of patients suspected of upper extremity arterial disease and venous thrombosis in the vascular community for well over 10 years. With the recent vast improvements in ultrasound equipment, there has been considerable emphasis placed on the expanded role of duplex imaging in the upper extremity. Advances in gray-scale resolution and color Doppler technology permit direct visualization of thrombus, stenosis, collateral vessels, as well as sensitive spectral waveform analysis [11]. These recent advances have greatly reduced, if not eliminated, in most patients, the previous upper extremity ultrasound challenges of insonating the area under the clavicle. With these advancements in duplex imaging, the noninvasive vascular lab has the potential to help aid in the confirmation, treatment, and follow-up care of patients who present with the clinical suspicion of TOS.

Recent studies have been directed toward defining the role of duplex imaging and color Doppler ultrasound with and without maneuvers in diagnosing patients suspected of vascular TOS. In 2001, Wadhwani et al. [15] reported on the effectiveness of duplex imaging with color Doppler ultrasound with maneuvers in five patients clinically suspected of arterial TOS. In 2009, Pacheco et al. published a case study that demonstrated comparable results of duplex ultrasound examination with abduction maneuvers to diagnose venous TOS [5]. Ultimately, both studies found the changes in Doppler waveforms and velocities with and without maneuvers to be an effective method in confirming vascular TOS.

## Our Clinical Experience or Experience from Our Institution

As a referral center for TOS at a university medical center, we have seen and evaluated well over 1,000 patients for TOS in the past 6 years. Working closely with the vascular surgery clinical team, our Intersocietal Commission for the Accreditation of Vascular Laboratories (ICAVL) accredited Non-Invasive Vascular Lab has gained extensive experience in the evaluation, diagnosis, treatment and follow-up of this large volume of TOS patients. A total of 312 patients have undergone thoracic outlet syndrome surgical intervention between January 2004 and June 2010. Noninvasive vascular lab studies were performed on these patients as part of the initial evaluation process based on an established algorithm (see Fig. 40.2).

### TOS Ultrasound Evaluation

All venous and arterial TOS ultrasound examinations were performed by the use of a Phillips iU22 or Phillips 5000 (Bothell, WA) with an 8–4 MHz linear array and 8–5 MHz curved array transducer by a registered vascular sonographer in an ICAVL accredited lab.

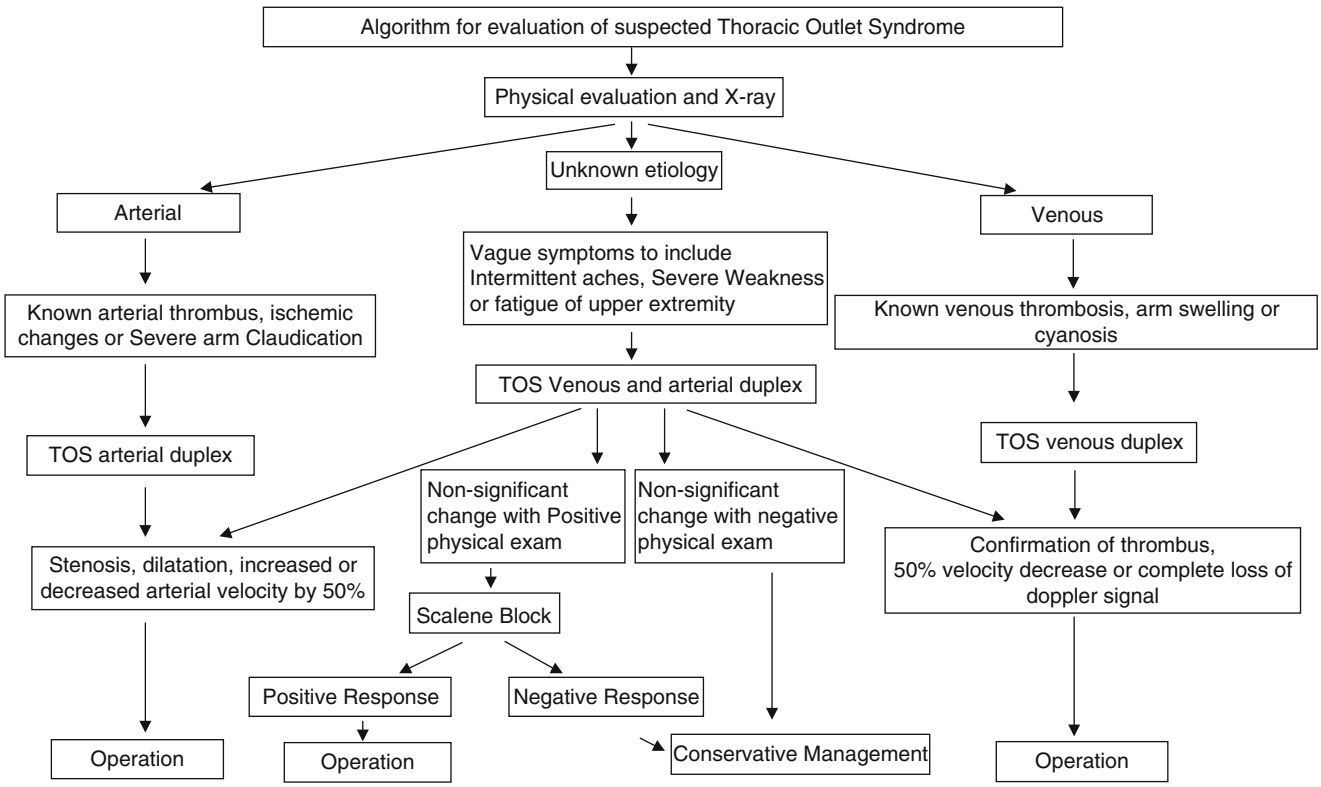


**Fig. 40.2** Algorithm for evaluation of suspected thoracic outlet syndrome

## TOS Protocol

The examination begins with the patient supine, arms relaxed in the neutral resting position, and without any elevation of the head. Evaluation of the patient's symptomatic side is performed first with head turned slightly to the contralateral side. The transducer is placed in the transverse plane on the patient's neck and the internal jugular vein (IJV) is identified. The IJV is examined with gray scale imaging with and without compression cephalad to caudad to evaluate for the presence of occlusive or nonocclusive thrombosis. The IJV is then examined with color Doppler imaging in the longitudinal plane, taking care not to induce manual compression on the vein. Doppler waveform tracings are obtained during quiet respiration. The transducer is then moved back into the transverse plane in the mid-neck region and the IJV is followed inferiorly to the junction of the proximal subclavian vein. The ultrasound probe is placed transversely and slightly medially just superior to the proximal part of the clavicle for the complete evaluation of the proximal subclavian vein. In gray scale, the proximal subclavian vein is examined with and without compression to assess for the presence of occlusive or nonocclusive thrombosis. Doppler angle correction is then utilized in order to obtain waveform and velocity measurements during quite respiration in this proximal region of the subclavian vein. The transducer is then repositioned beneath the clavicle and directed medially to identify and evaluate the mid to distal portion of the subclavian vein as it travels beneath the clavicle in the costoclavicular space [12]. Attention is directed to the location of the subclavian vein as it relates to the subclavian artery. Anatomically, the subclavian vein normally lies superficial and caudal to the subclavian artery and courses with the artery when imaged in the transverse plane [13]. Any deviation in expected anatomic location or inability to identify the subclavian vein should be documented. Identifying the location of subclavian vein to its adjacent subclavian artery is important in differentiating the main vein from enlarged venous collaterals in the subclavicular area (see Fig. 40.3). Gray-scale imaging with and without compression is performed to assess for the presence of occlusive or nonocclusive thrombus in the mid-distal subclavian vein. Color Doppler imaging is then utilized with the probe in the longitudinal plane to evaluate for color filling in the mid through distal subclavian vein. Any reduction or absence of color filling in the vein in this region is documented. Doppler angle correction

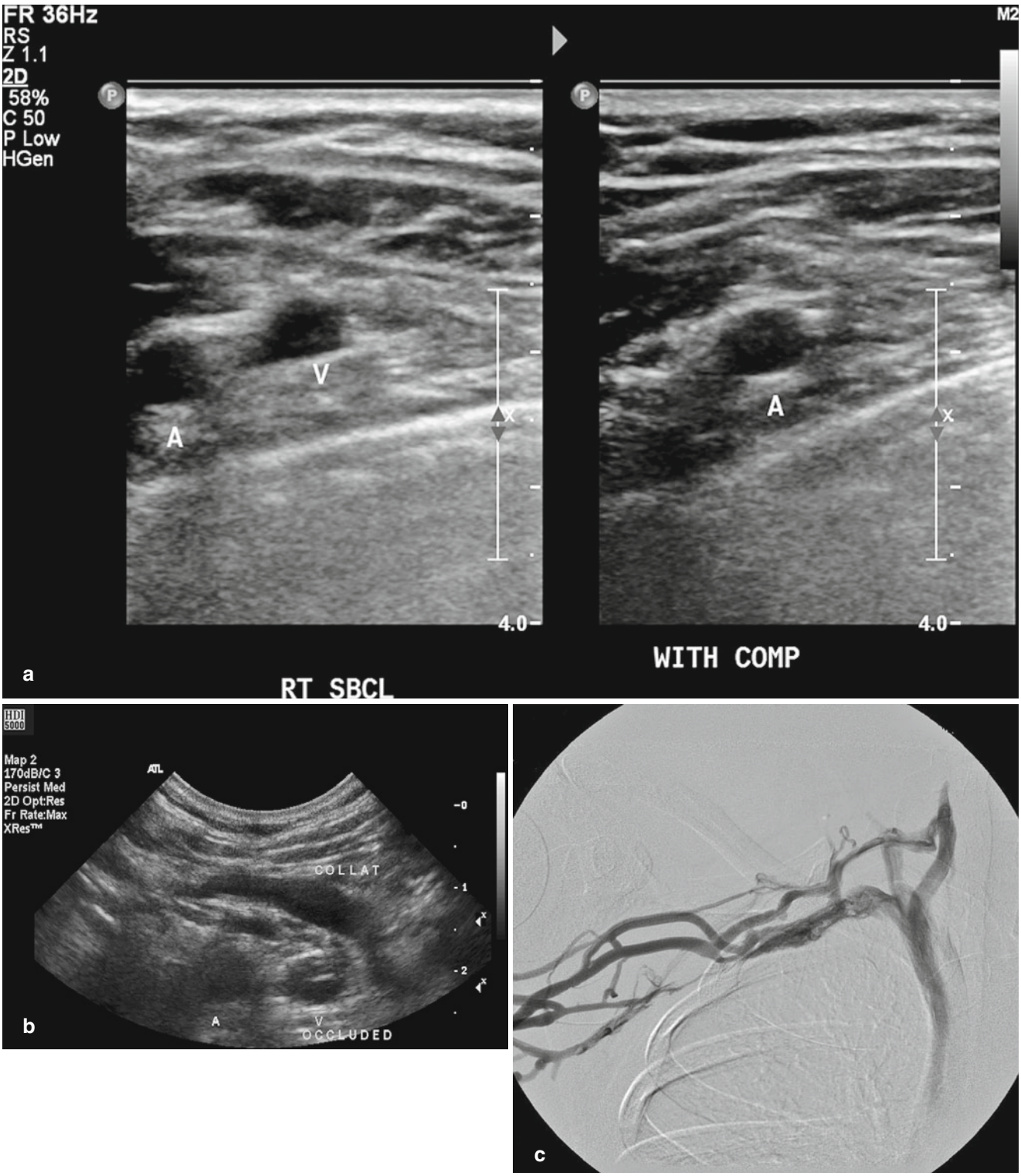


**Fig. 40.3** (**a**) Duplex image of normal anatomic position of subclavian vein and artery. (**b**) Duplex scan demonstrating abnormal occluded subclavian vein with large collateral vein. (**c**) Corresponding venogram confirming occluded subclavian vein with large collateral

is then utilized in order to obtain waveform and velocity measurements during quiet respiration in the distal region of the subclavian vein just proximal to the confluence with the cephalic vein.

Next, duplex ultrasound imaging is performed to evaluate the axillary vein. For consistency purposes within a lab, the axillary vein is defined as the vein just distal to the confluence of the cephalic and subclavian vein. The axillary vein continues to the armpit or axilla. The axillary vein lies medial and inferior to the axillary artery in its normal anatomic position. It is important to identify the location of the axillary vein in relationship to the axillary artery in transverse. This view is necessary in order to differentiate the axillary vein from the presence of any possible enlarged venous collaterals. The cephalic vein can be confused with the axillary vein in the clinical setting of axillary vein thrombosis [11]. Both gray scale and color Doppler imaging are performed with and without compression to asses for occlusive or nonocclusive thrombus of the axillary vein. Doppler analysis with angle correction is then utilized in order to obtain waveform and velocity measurements during quite respiration in the axillary vein.

All studies are bilateral using the same TOS venous protocol described previously. We have noted from our experience, similar to the Rochester, NY group, that a significant number of patients experience venous compression of the contralateral side warranting a bilateral examination [14].

For patients who are suspected to have an arterial component of TOS by means of physical and clinical examinations, a scanning technique similar to the venous TOS protocol is employed. As with venous TOS examination, the anatomic location and course of the upper extremity vessels should be carefully noted and documented. Examination in gray scale and color flow imaging of the subclavain artery and axillary artery is done to assess for nonocclusive or occlusive thrombus and evidence of stenosis or vessel dilatation. Angle-corrected Doppler analysis and velocity measurements are documented in the subclavian and axillary artery.

Duplex imaging first must assess for acute and/or occlusive thrombus in the subclavian and axillary vein or artery with patient's arm in the neutral position. Once this has been established, attention is directed toward assessing for any changes of velocities in these vessels with patient's arm in full abduction. The transducer is positioned once again beneath the clavicle and directed medially to visualize the distal subclavain and proximal axillary vein, or artery if clinically indicated, in the resting position. Next the patient is asked to slowly abduct their arm while visualization of the vessel is maintained during the maneuvering. Once the patient has fully abducted their arm, an angle-corrected Doppler waveform and velocity is obtained in these locations in both the veins and/or arteries (see Figs. 40.4 and 40.5). Gray-scale and color Doppler imaging are performed as well to access for any stricture of these vessels.

## Diagnostic Interpretation of TOS Duplex Examination

Venous compression is diagnosed when a 50% or greater reduction in velocities is demonstrated or when there is a complete loss of Doppler signal in subclavain and/or axillary vein upon arm abduction maneuvers (see Table 40.1). An increase in velocities in the subclavian and axillary vein from resting position to abduction is not considered to be significant evidence for venous narrowing.

Normal velocities in the subclavian and axillary artery are in the range of 50–110 cm/s [15]. Aneurysmal dilatation or stenosis in the subclavian or axillary artery are measured and documented. The diagnostic criterion for significant arterial compression is based on a 50% or greater increase or decrease in these normal velocities or complete cessation of flow in the subclavain and/or axillary artery during arm abduction maneuvers (see Table 40.2).

## TOS Postoperative Protocol

Noninvasive testing is also useful in assessing a patient's progress after surgical intervention, particularly in the vascular TOS group. Patients with TOS complicated by a venous thrombosis undergo a venogram 2 weeks after the operation to determine vessel patency and venoplasty is done as indicated to dilate the vein. If dilation occurs, the patient remains on warfarin bridged to subcutaneous heparin [16, 17]. A follow-up upper extremity venous duplex with maneuvers is done 1 month after the venogram to reevaluate vessel patency. If there is no flow within the vein with abduction maneuvers, the patient remains on this medication and follows up in vascular lab for duplex imaging reassessment. We feel this residual compression, seen on duplex, is due to postoperative inflammation, which subsides practically in all patients by 8–12 weeks after surgery. Once flow within the vessel is confirmed, the patient will undergo vascular lab studies at 6 and 12 month intervals. This vascular lab noninvasive duplex imaging study with maneuvers and velocity measurements is instrumental in guiding the surgical team when making recommendations for the duration of anticoagulation medication. Patients who have hypercoagulable disorders, such as Factor V Leiden, may need lifelong anticoagulation and their needs are addressed on an individual basis.

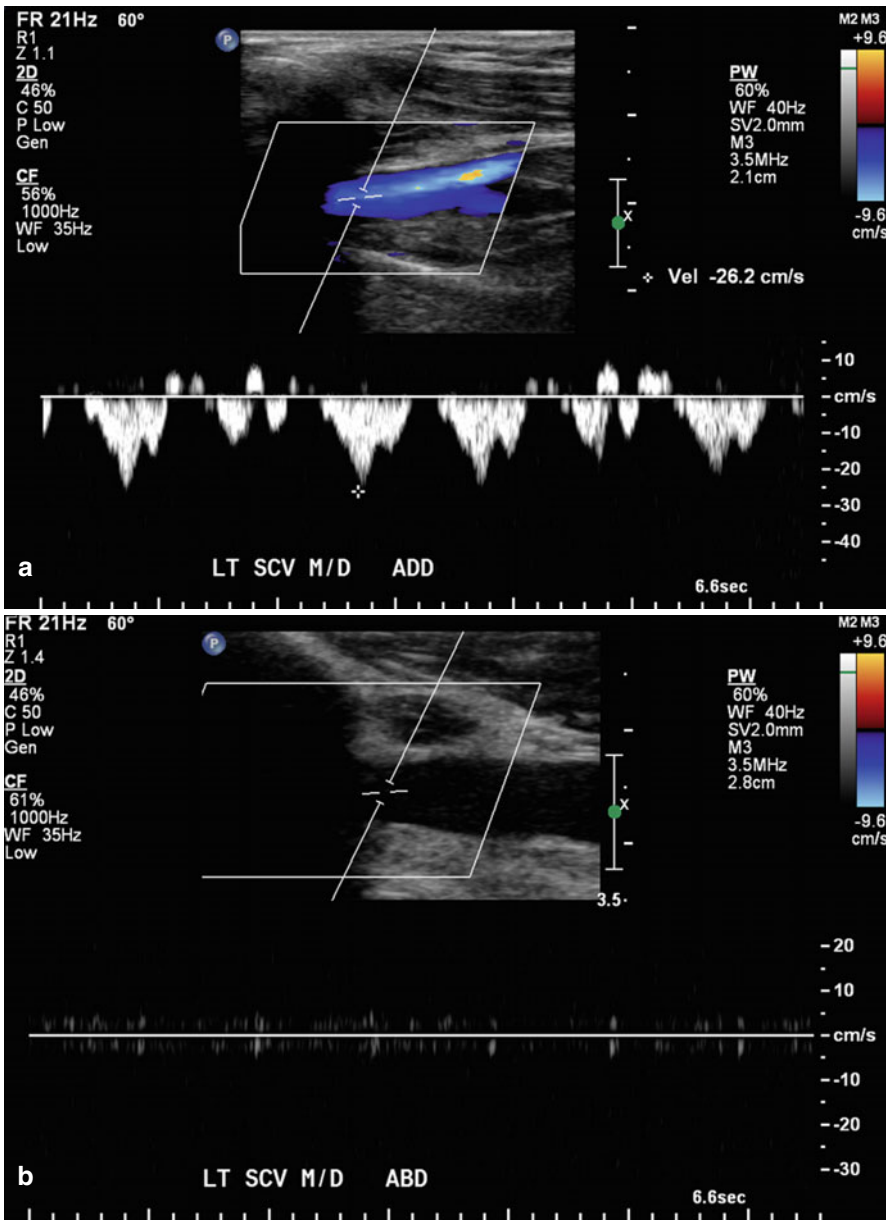


**Fig. 40.4** (**a**) Normal venous flow velocities at rest. (**b**) Abnormal (complete cessation of flow) venous flow velocities with maneuvers

Noninvasive testing is also useful in monitoring the progress of a patient postoperatively with arterial TOS. Patients have their first follow-up study 1 month after surgery. For the arterial TOS patients who required an upper extremity bypass graft duplex scanning, established protocol and frequency of studies are followed thereafter. The arterial patients who presented with embolization of the upper extremity will remain on anticoagulation for 6 months with follow-ups including vascular lab evaluations at 6 and 12 month intervals after embolization.

The results of these noninvasive vascular imaging evaluations are useful in determining how the vessel is recovering from vascular compression associated with TOS. During the recovery period, if the patient complains of persistent pain, currently prescribed refractory pain management is done or begins to experience vascular changes in the upper extremity, aggressive management is undertaken with an appointment made as quickly as possible with the vascular lab. Obtaining either an upper extremity venous or arterial duplex with maneuvers, depending on the diagnosis, is essential to determine vessel health. The data received from this test gives the surgical clinician accurate information in order to plan the next step of the treatment plan in the TOS vascular group.

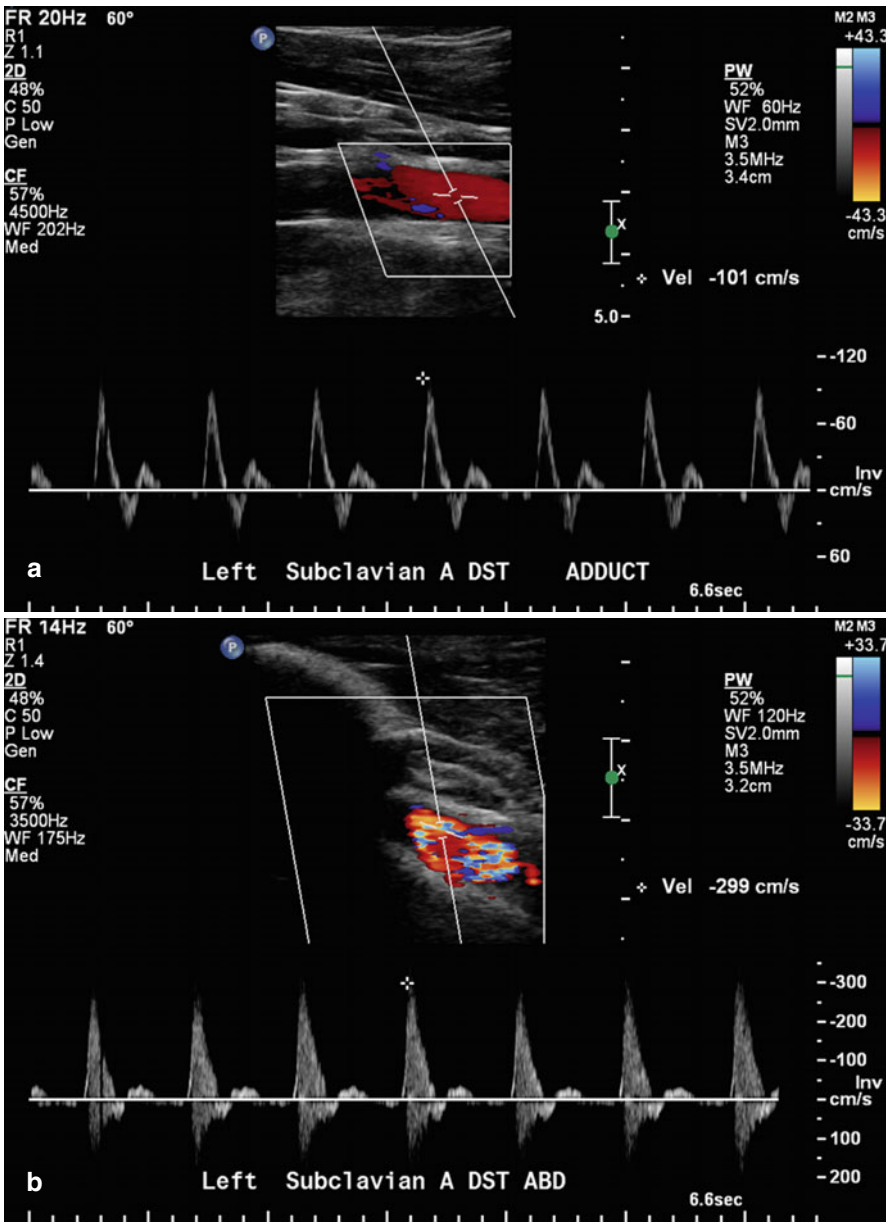


**Fig. 40.5** (**a**) Normal arterial flow velocities at rest. (**b**) Abnormal (>50% increase) arterial flow velocities with maneuvers

**Table 40.1** Venous TOS diagnostic interpretation

| Normal | Abnormal |
|---|---|
| Veins are free of echoes | Veins have echogenic or echolucent material (nonocclusive or occlusive) |
| Color flow fills lumen | Absent or reduced color filling |
| Vein walls collapse where anatomically appropriate with slight probe pressure | Noncompressible or spongy compression of the vein walls where anatomically appropriate |
| Normal spontaneous and phasic Doppler signal at rest and with abduction | Vein maybe dilated |
| No significant change or loss in velocities from resting position to abduction | Possible collaterals veins demonstrated<br>Absent, continuous or nonphasic Doppler flow signal at rest<br>Significant change in velocities from resting position to abduction<br>50% Decrease in velocities from resting<br>Complete loss of Doppler signal or a velocity of 0 |

**Table 40.2** Arterial TOS diagnostic interpretation

| Normal | Abnormal |
|---|---|
| No evidence of homogenous or heterogeneous material | Arteries have homogenous or heterogeneous material (nonocclusive or occlusive) |
| No evidence by B-mode imaging of narrowing or dilatation | Absent or reduced color filling of lumen |
| Color flow fills lumen | Aneurysmal dilatation or narrowing of artery |
| Normal triphasic Doppler signal at rest and with abduction | Absent or monophasic Doppler flow signal at rest |
| No significant change or loss in velocities from resting position to abduction | Significant change in velocities from resting position to abduction<br>50% Decrease or increase in velocities from resting<br>Complete loss of Doppler signal or a velocity of 0 |

**Conclusion**

The role of the noninvasive vascular laboratory in the evaluation of patients with thoracic outlet syndrome has been expanded and perfected over the years. The use of color duplex imaging is confirmatory in identifying subclavian as well as axillary vein thrombosis avoiding more expensive computed tomography scans and magnetic resonance imaging. In cases where there is significant arterial compression, demonstrated by color duplex imaging with abduction maneuvers, the patient can be operated on in a timely manner to prevent thrombosis or embolization. Subclavian artery aneurysms can also be easily visualized which avoids other expensive scans with radiation exposure. Postoperatively, color duplex imaging can evaluate patency of vessels and help determine the length of time anticoagulation should be employed. The mastery of TOS duplex imaging does require dedication and experience. Attention to the anatomic relationship of upper extremity vessels and close evaluation of velocity measurements with abduction maneuvers are key diagnostic tools obtained in the noninvasive vascular laboratory for the confirmation, treatment, and follow-up of TOS.

## References


1. Machleder H. Neurogenic thoracic outlet compression syndrome. In: Machleder H, editor. Vascular disorders of the upper extremity. 3rd ed. Armonk: Futura Publishing Co. Inc; 1998. p. 131–5.
2. Roos DB. Historical perspectives and anatomic considerations. Thoracic outlet syndrome. Semin Thorac Cardiovasc Surg. 1996;8:183–9.
3. Machleder H. Introduction to neurovascular compression syndromes at the thoracic outlet. In: Machleder H, editor. Vascular disorders of the upper extremity. 3rd ed. Armonk: Futura Publishing Co. Inc; 1998. p. 109–30.
4. Dale WA, Lewis MR. Management of TOS. Ann Surg. 1975;181:575–85.
5. Pacheco H, Yesenko S, Gornik H, et al. Venous thoracic outlet syndrome diagnosed using duplex ultrasound. J Vasc Ultrasound. 2009;33(4):184–7.
6. Lindblad B, Tengborn L, Bergqvist D. Deep vein thrombosis of the axillary-subclavain veins: epidemiologic data, effects of different types of treatment and late sequel. Eur J Vasc Surg. 1988;2:161–5.
7. Kreienberg P, Shah D, Darling III RC, et al. Thoracic outlet syndrome. In: Mansour MA, Labropoulos N, editors. Vascular diagnosis. 1st ed. Philadelphia: Elsevier Saunders; 1994. p. 517–22.
8. Thompson R, Bartoli M. Neurogenic thoracic outlet syndrome. In: Cronenwett JL, Gloviczki P, Johnston KW, et al., editors. Rutherford vascular surgery. 6th ed. Philadelphia: Elsevier Saunders; 2005. p. 1347–64.
9. Rumwell C, McPharlin M. Vascular technology. 4th ed. Pasadena: Davies Publishing; 2009. p. 170–1.
10. AbuRahma A, Bergan J. Noninvasive vascular diagnosis. 2nd ed. London: Springer; 2007. p. 356–7.
11. Nazarian G, Foshager M. Color Doppler sonography of the thoracic inlet veins. Radiographics. 1995;15(6):1357–71.
12. Longley D, Yedicka J, et al. Thoracic outlet syndrome: evaluation of the subclavian vessels by color duplex sonography. AJR Am J Roentgenol. 1992;158:623–30.
13. Chin E, Zimmerman P, Grant E. Sonographic evaluation of upper extremity deep venous thrombosis. J Ultrasound Med. 2005;24:829–38.
14. Doyle A, Wolford H, Davies M, et al. Management of effort thrombosis of the subclavain vein: today's treatment. Ann Vasc Surg. 2007;21:723–9.
15. Wadhwani R, Chaubal N, Sukthankar R, et al. Color Doppler and duplex sonography in 5 patients with thoracic outlet syndrome. J Ultrasound Med. 2001;20:795–801.
16. DeLeon R, Chang D, Hassoun H, et al. Multiple treatment algorithms for successful outcomes in venous thoracic outlet syndrome. Surgery. 2009;145:500–7.
17. Guzzo J, Chang K, Demos J, et al. Preoperative thrombolysis and venoplasty affords no benefit in patency following first rib resection and scalenectomy for subacute and chronic subclavian vein thrombosis. J Vasc Surg. 2010;52:662–3.

# Venous Imaging for Reflux Using Duplex Ultrasonography

41

Dimitrios Karakitsos and Nicos Labropoulos

**Abstract**

Chronic venous disease is very prevalent and has significant socioeconomic impact in the society. After physical examination is performed duplex ultrasound (DU) has become the method of choice for evaluating venous disease. This is because it is noninvasive, portable, easily repeatable, has great resolution, evaluates anatomy and function, offers very good differential diagnosis, and has relatively low cost. DU examination should be performed with the patient in the standing position to increase its diagnostic yield. Cutoff values for venous reflux have been established and generally accepted with a retrograde flow of >500 ms for superficial, deep calf veins, deep femoral, and perforator veins and >1,000 ms for common femoral, femoral, and popliteal veins. Anatomic variations in both the superficial and deep venous systems are very common (i.e., duplication of the popliteal or femoral vein, hypoplasia of the great saphenous vein); hence, careful examination is mandatory. Segmental reflux has a mild to moderate clinical presentation, while extensive involvement is associated with skin changes. Around 80% of patients with chronic venous disease have reflux alone, 17% have reflux and obstruction, while obstruction alone is uncommon. The combination of reflux and obstruction has usually the worst prognosis. Site-specific DU examination is important in tailoring therapeutic interventions according to pertinent findings. DU is important for obtaining venous access, performing endovenous ablation, foam sclerotherapy, while it can also be useful for vein angioplasty and stenting, insertion of inferior vena cava filters, and guide thrombolysis. The introduction of intravascular ultrasound has facilitated the development of strategies to overcome limitations of ultrasound technology. Examination of lower extremities can be challenging especially in obese patients, in the presence of edema, while inability of the patient to cooperate during the examination can impact the quality of testing. Despite these limitations, DU remains the standard of care in detecting vein disease.

**Keywords**

Chronic venous disease • Venous reflux • Obstruction • Duplex ultrasonography

D. Karakitsos, M.D., Ph.D., MRCP
Intensive Care Unit, General State Hospital of Athens, Athens, Greece

N. Labropoulos, B.Sc. (Med), DIC, RVT, Ph.D. (✉)
Department of Surgery, Division of Vascular Surgery, Stony Brook University Medical Center, HSC T19 Rm 90, Stony Brook, NY 11794-8191, USA
e-mail: nlabrop@yahoo.com

## Introduction

Venous reflux is defined as retrograde blood flow which is in the opposite direction from physiological centripetal flow [1]. Retrograde flow occurs physiologically just before valve closure and pathologically due to valve absence or incompetence.

A.F. AbuRahma, D.F. Bandyk (eds.), *Noninvasive Vascular Diagnosis*,
DOI 10.1007/978-1-4471-4005-4_41, © Springer-Verlag London 2013

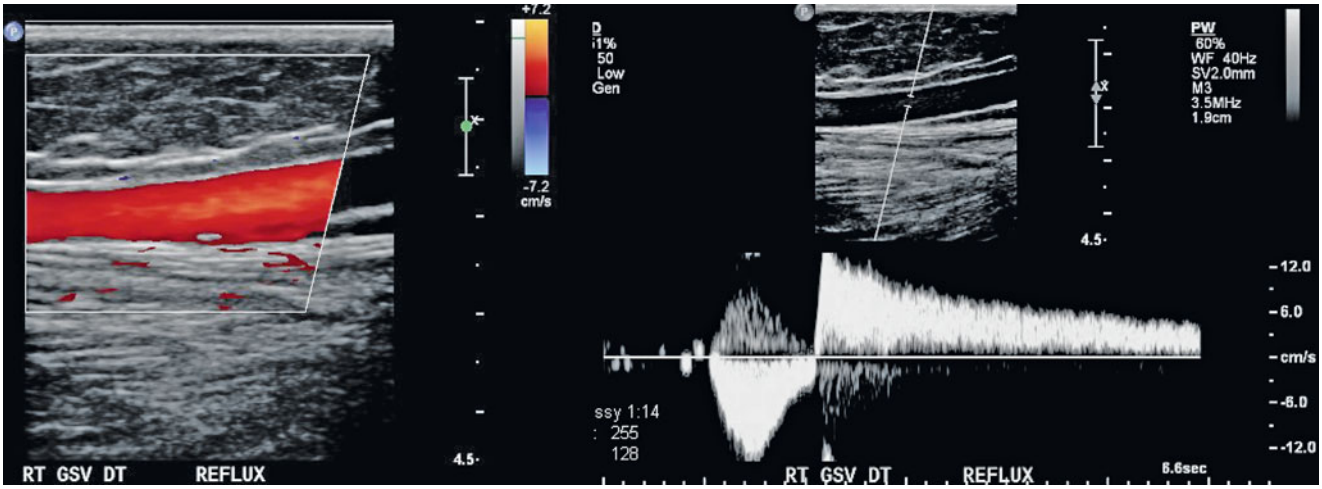


**Fig. 41.1** Reflux in the GSV in the lower thigh is demonstrated with color flow (*left panel*) and with Doppler waveform (*right panel*). *Red flow* (positive signal) going toward the transducer in the GSV is retrograde flow indicating reflux. The duration of the retrograde flow is >4 s as seen by the Doppler waveform

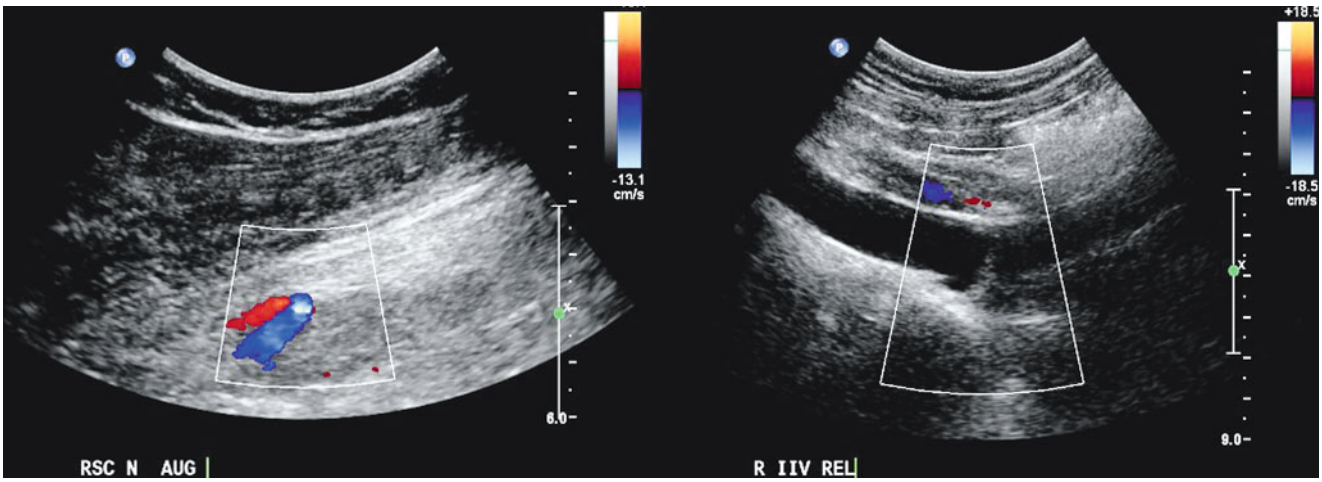


**Fig. 41.2** Use of lower frequency transducer to examine deeper veins in thigh and pelvis. Examination of the sciatic nerve veins in the posterolateral thigh is seen on the (*left panel*). Two veins are seen below the sciatic nerve. The right internal iliac vein is normal during the Valsalva maneuver on the (*right panel*)

Pathologic etiologies include vein dilatation, post-thrombotic recanalization, or local inflammation and remodeling [2, 3]. Physiologic venous flow reversal accounts for the fraction of the second that it takes for the valve leaflet apposition [2]. However, acceptable physiologic flow reversal is diverse for different veins. This may be due to the fact that larger veins have a larger diameter and fewer valves compared to smaller ones; hence, the expected time for their valve leaflets to come together is longer. Venous valves are typically bicuspid and they are implemented to direct the flow from the superficial to the deep system and from proximal to distal. These valves along with the venous "pump" are major determinants of venous flow [4].

Currently, the best way to evaluate venous reflux is by Duplex ultrasound (DU). Its superiority over contrast-enhanced venography has been demonstrated in several studies [5–11]. During the ultrasound examination, color-flow imaging is used to detect the artery (red) and then the adjacent veins (blue). Absence of retrograde color flow on release of the compression indicates competent valves, while the appearance of red color in the vein indicates the presence of reflux (Fig. 41.1). The latter is documented by recording the Doppler waveform. Multi-frequency linear array transducers are typically used for assessment of superficial and deep reflux. For veins located within 1 cm of the skin, high-frequency transducers are used with ample gel to facilitate imaging. For veins located >6 cm from the skin, a 3-MHz transducer is preferred. This is necessary for the deep veins in obese patients and in the scanning of the abdominal and pelvic veins (Fig. 41.2).

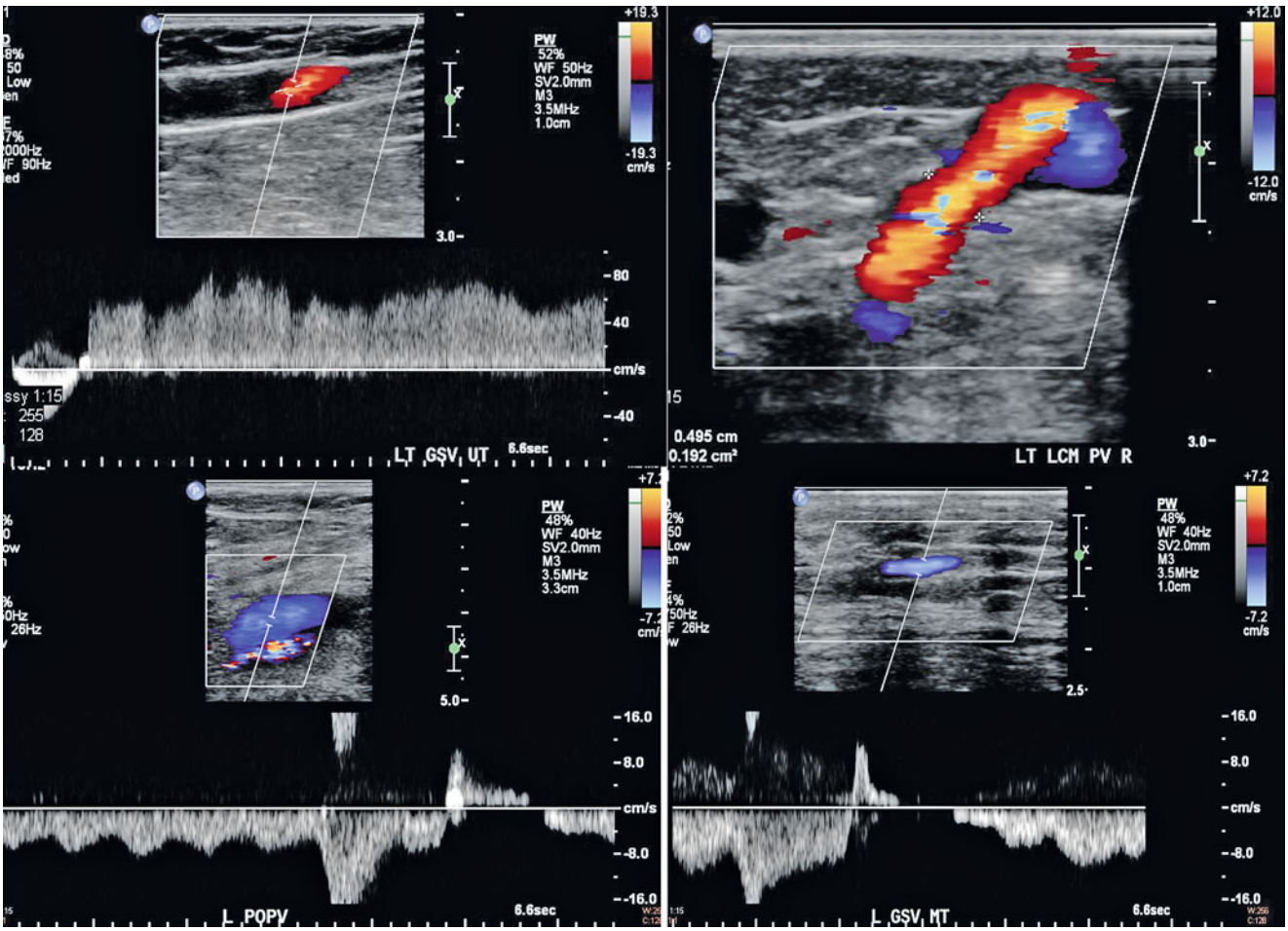


**Fig. 41.3** High velocity prolonged reflux is seen in the thigh segment of GSV (*upper left panel*). A dilated incompetent lower calf perforator measuring 4.9 mm from the same patient is shown on the (*right upper panel*). Physiologic flow reversal is seen in both the popliteal vein (*left lower panel*) and the GSV (*right lower panel*). The duration of retrograde flow was <1 s in the popliteal vein and <0.5 s in the GSV as shown by the timescale (distance between two large divisions is 1 s)

Previous studies utilized diverse methodologies for defining cutoff values regarding Doppler velocities and physiologic reflux time. The vast majority of these studies utilized either the cuff deflation and/or the Valsalva maneuver to establish cutoff values for reflux >500 ms [5–11]. The only study that evaluated most of the lower extremity veins (16 vein sites examined on each limb), with the largest sample size ($n=80$ healthy limbs and $n=60$ CVD limbs), provided the following cutoff values for venous reflux: reverse flow >500 ms for superficial, deep calf veins, and deep femoral vein >1,000 ms for common femoral, femoral, and popliteal veins (PVs), and >350 ms for perforating veins (Fig. 41.3) [1]. This study demonstrated that patients should be examined in the erect position in order to increase the yield of the DUS examination for the detection of reflux [1].

DUS may further contribute in the classification of chronic venous disease into primary, secondary, or congenital based upon the pathophysiology of the detected reflux. Primary chronic venous disease, without a demonstrable cause, is by far the most common type (64–79%) compared to the secondary (18–28%) that is frequently the sequelae of deep venous thrombosis (DVT). Congenital reflux (<5%) is rarely recognizable early on, although it exists since birth, due to an insulate in early symptoms and signs [2, 12].

## General Ultrasound Examination and Clinical Considerations

Evaluation of venous reflux should start with the patient in the standing position, facing toward the examiner, and with the examined limb being in slight flexion and external rotation. If the patient is unable to stand, the veins from the midthigh and below can be assessed in the sitting position. If the test is performed on a bed, the torso should be elevated >45°. The supine position is inappropriate for detection of

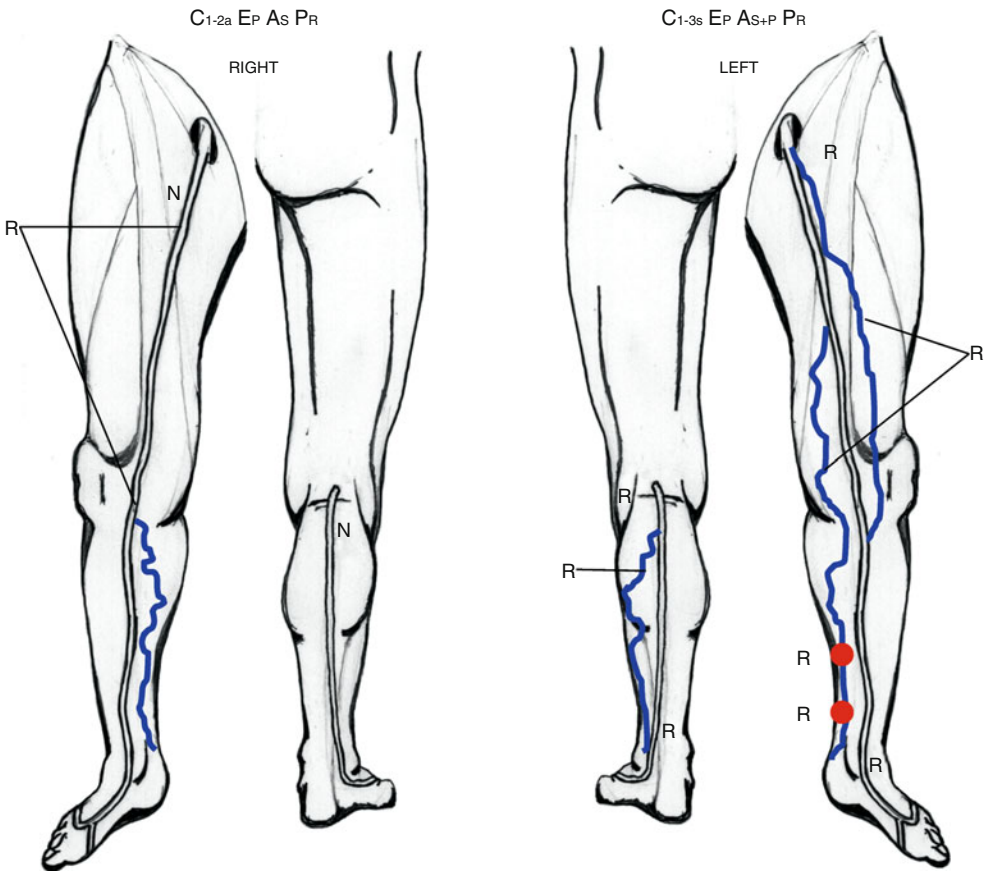


**Fig. 41.4** Duplex ultrasound report showing the distribution and extent of reflux. The patient presented with varicose veins in both extremities but she was symptomatic only in the left side. She had burning sensation, itching, and pain on prolong standing that was relieved with limb elevation. On the *right side*, reflux was found in the GSV from the upper thigh to the knee and at a medial calf tributary of the GSV. SSV and deep veins were normal. On the *left side*, there was reflux throughout the extent of GSV, in the anterior accessory saphenous vein, a medial calf tributary, two medial calf perforator veins, SSV throughout its length, and a lateral calf tributary. The deep veins were normal

reflux and measurement of vein diameters [1, 12]. Compression with release distal to the point of examination is referred to as augmentation. The former may be applied with several methods: release after a calf squeeze for proximal veins or a foot squeeze for calf veins, manual compression of vein clusters, pneumatic cuff deflation, active foot dorsiflexion and relaxation, and Valsalva maneuver. The vein behaves as a low pressure, collapsible conduit: with compression, its flow is increased in a distal-to-proximal direction and upon release, the blood flow reverses instantaneously [2]. Hence, if valves are competent no retrograde flow is documented. In contrast, if valves are incompetent blood continues to flow in the opposite direction. In an effort to standardize procedures, automated pneumatic cuffs with rapid inflation and subsequent rapid deflation are used [12]. However, in patients with increased BMI or significant edema, the compression technique is difficult to apply, therefore dorsiflexion/plantar flexion or the Valsalva maneuver can be used. The latter is commonly used to evaluate the groin veins especially if the initial compression technique applied provides negative results.

DUS examination protocol starts with the CFV, femoral with deep femoral veins, and continues with the saphenofemoral junction (SFJ) at the terminal and preterminal valves and the associated tributaries, followed by the popliteal vein (PV) and deep calf veins. Thereafter, the superficial veins examined include: great saphenous vein (GSV), small saphenous vein (SSV), their tributaries, and the nonsaphenous veins (Fig. 41.4). Two layers of fascia surround the GSV and with ultrasound imaging (transverse) is referred to as the saphenous eye. SSV is located in the triangular fascia, surrounded by the crural fascia and the gastrocnemius muscle heads. Perforator veins of the lower extremity are usually the last to be evaluated by DUS. They connect the superficial and deep veins traversing the deep fascia, which is visualized easily on B-mode due to its echogenic, collagen-derived structure. Outward flow in perforator veins is seen only in conjunction with superficial and deep vein reflux.

Anatomic variations in both the superficial and deep veins are common. Careful examination and identification of these variations is necessary. Duplication of the PV and femoral vein is common and rare in GSV and SSV. Triple systems may be seen (popliteal, and femoral), and some veins may be hypoplastic or aplastic (e.g., posterior tibial, GSV, and SSV) [13, 14].

Reflux confined to the superficial veins often has a mild to moderate clinical presentation (C1–C3), while involvement of the deep and perforator veins is more often associated with skin damage (C4–C6) [15]. Patients with chronic venous disease exhibit 80% reflux, 17% reflux and obstruction, and

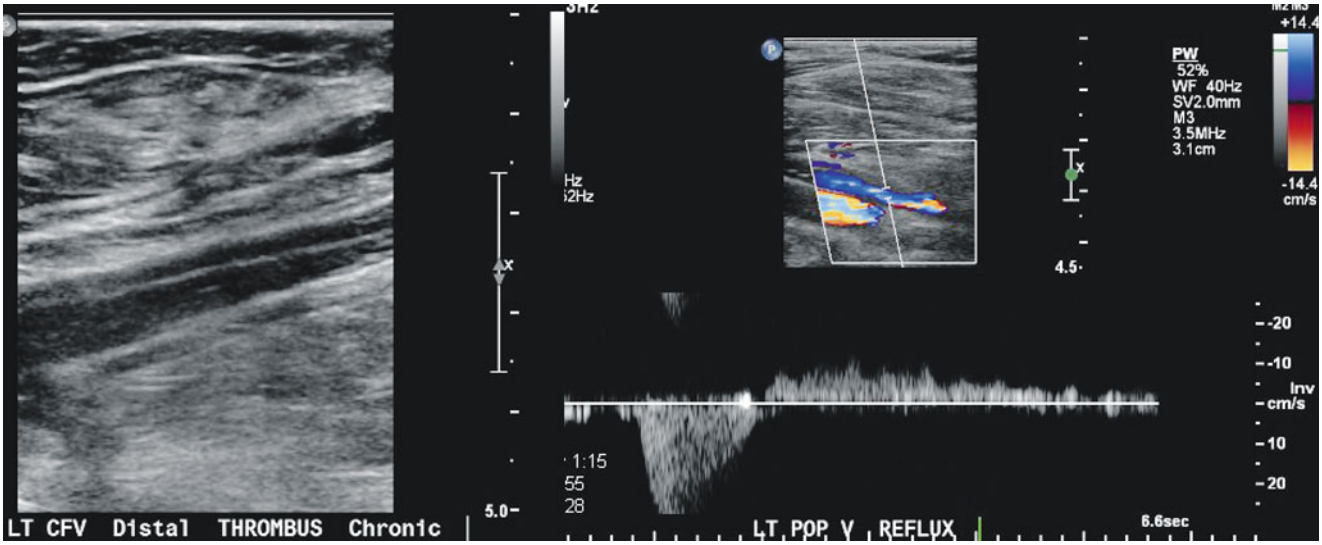


**Fig. 41.5** Post-thrombotic changes in the left common femoral vein (*left panel*). Intraluminal echoes are seen demonstrating partial recanalization. Popliteal vein reflux on the same patient (*right panel*). The vein is partially recanalized and has prolonged reflux

only 2% obstruction alone [16]. Old thrombus and/or scar tissue often produces bright echoes within the lumen of the vein of similar brightness to surrounding tissues. In cases of partial recanalization, flow channels are seen and are often incompetent. The vein lumen may be reduced in size and is sometimes not well seen by DUS throughout its length. The vein walls may be thickened and collateral veins are often seen around the area of obstruction (Fig. 41.5) [2].

The combination of obstruction and reflux has a worse prognosis for the development of skin lesions, also known as lipodermatosclerosis [17–20].

Recently, ultrasound-guided-catheter-directed thrombolysis, which involves administration of thrombolytics directly through the side ports of a catheter traversing the thrombus, has been employed in the treatment of venous thrombosis. This technique has been shown to reduce the incidence of post-thrombotic syndrome. A randomized trial has compared catheter-directed thrombolysis followed by 6 months of warfarin with medical treatment alone (intravenous heparin followed by warfarin). This study enrolled 35 of 207 screened patients with acute iliofemoral DVT. Six months after treatment, the patency rate was significantly higher in the group that received catheter-directed thrombolysis (72% vs. 12%), and the prevalence of venous reflux was significantly lower (11% vs. 41%) [21]. Furthermore, the largest observational series from the National Deep Venous Thrombosis Registry demonstrated that patients with iliofemoral DVT had significantly greater 1-year patency rates than patients with femoropopliteal DVT (64% vs. 47%) [22]. The above data demonstrate the multifactorial role of DUS in the diagnosis and monitoring of venous disease.

## Site-Specific Ultrasound Examination

### Great Saphenous and Accessory Saphenous Veins

The standard ultrasound examination in the groin should begin by identifying the saphenofemoral junction (SFJ), which is located medially to the common femoral artery. Adjacent to the SFJ, various tributaries can be visualized along with the terminal and preterminal valves of the GSV [23, 24]. Reflux is generated by various sources such as SFJ incompetence or lower extremity and pelvic vein insufficiency. The latter is suspected whenever there is a sudden increase in GSV diameter and represents one of the signs of pelvic congestion syndrome along with reflux, which is defined as chronic pelvic pain caused by incompetent ovarian veins. Approximately 10% of women have incompetent ovarian vein valves and of them around 40% experience chronic pelvic signs and symptoms directly as a result of venous congestion (Fig. 41.6) [25–27]. Also, imaging should include the inguinal lymph node area, as well as the full length of the GSV and associated tributaries should be followed up to the ankle. Documentation of the GSV diameter and its distance from the skin is essential since these are used to guide endovenous treatment options [28].

### Small Saphenous Vein and Its Thigh Extension

Examination starts in the popliteal fossa with the patient standing. Transverse views to visualize the veins within the popliteal fossa and longitudinal views to identify the presence

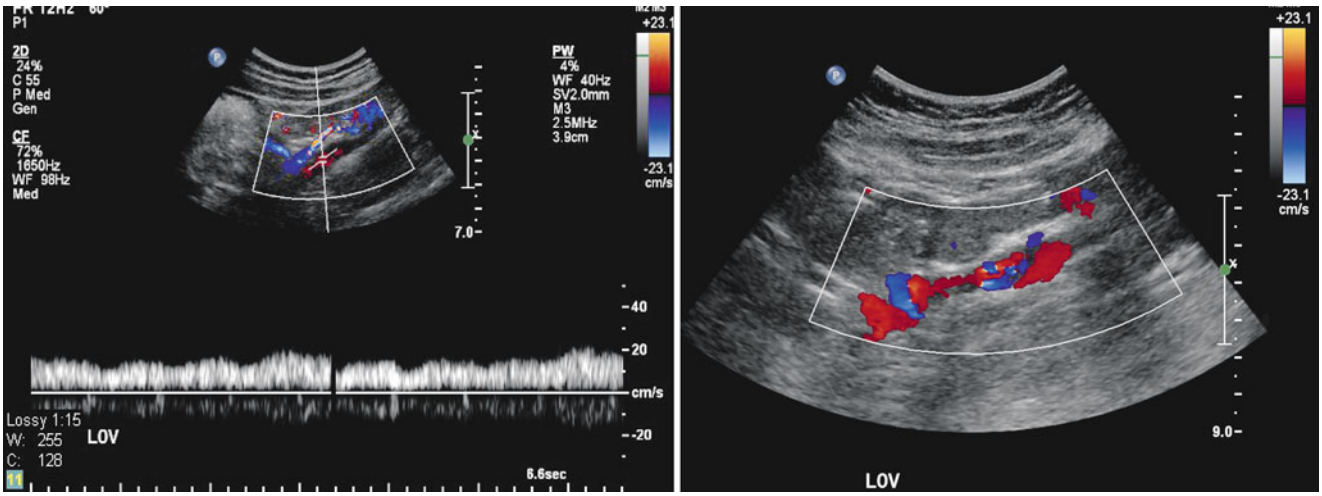


**Fig. 41.6** Reflux in the left ovarian vein in a female patient who had two pregnancies and presented with pelvic pain (*left panel*). Multiple incompetent ovarian veins are seen in the (*right panel*) in a female patient who presented with pelvic pain and dysuria

of the saphenopopliteal junction (SPJ) are applied. It is important to rule out SPJ incompetence with SSV reflux [28]. The latter may occur during calf muscle contraction or compression (systolic phase) and suggests possible PV and/or FV obstruction; however, reflux is typically more obvious during calf release (diastolic phase) [29]. The SSV may join the PV medially, posteriorly, or laterally, hence it is advisable to document its location in relation to the PV circumference [30]. A central interconnection element of the local venous circuit is the SSV thigh extension that most often unites GSV near the groin [29]. Documentation of the reflux direction from SFJ to SSV or from saphenopopliteal joint (SPJ)/SSV to GSV should be recorded [31].

## Perforator Veins

Veins are identified as perforators only if they pierce through the deep fascia. Their locations are recorded as above or below the knee. The above-knee perforators are further divided as upper, middle, and lower thigh. Those in the below-knee segment are divided as upper, middle, and lower thirds of the calf [32]. Both transverse and oblique scanning are used to evaluate these veins because their long axis is visualized in these planes. Reflux or outward flow in perforator veins is observed in combination with the superficial and deep veins. Bidirectional flow may be seen in some perforator veins, however, only the net outward flow (from deep to superficial) is being evaluated to determine reflux [33]. The examination starts from the medial malleolus, following the cross-sectional image of the posterior arch and GSV upward to the knee region. The anterior arch, the anterior and posteromedial accessory veins, and other thigh tributaries are scanned only if they are varicose [34]. The SSV is imaged from the lateral malleolus until its insertion in the PV. Medial and lateral varicose tributaries of this vein are also scanned. Finally, any area with varicose veins or a vein cluster is scanned for detecting perforators.

## Deep Veins: Deep Thigh Veins – Popliteal Vein – Deep Crural Veins

The CFV is examined in the longitudinal view for phasic flow with respiration, cessation of flow with deep inspiration, possible reflux with the Valsalva maneuver, and flow during the compression of the thigh or the calf. Whenever continuous flow is detected in the CFV, the scanning protocol is extended to the inferior vena cava and to the iliac vessels in search of a possible obstruction [35]. Presence of retrograde flow distal to the SFJ corresponds to true deep venous reflux.

PV is examined in its full length, above and below the SPJ, while its anatomic and hemodynamic relationship with the gastrocnemius vein should be clarified. The last part of the examination of the deep veins of the leg involves the depiction of the deep crural veins with the patient usually in the standing or sitting position. Posterior tibial and peroneal veins should be examined in all patients with past and/or present DVT, as especially the latter are the most commonly affected veins of the calf [36]. These veins are imaged well from the medial aspect of the calf. If the peroneal veins are not seen from this window, then imaging is performed from the posterolateral aspect of the calf.

### Nonsaphenous Veins

Nonsaphenous veins are superficial venous segments that are not part of the GSV or SSV system. Nonsaphenous venous reflux occurs more commonly in females with previous pregnancies [37]. Nonsaphenous segments that are usually involved are the gluteal, posterolateral thigh perforator, vulvar, lower posterior thigh, popliteal fossa tributaries, knee perforator, and sciatic nerve veins. Patients are examined in the erect position and DUS evaluation is also directed in identifying possible connections with the saphenous and deep veins [38]. The presence of gluteal and/or vulvar varices directs the DUS examination to the pelvic veins [25]. Adjunctive imaging modalities are magnetic resonance venography, CTV or contrast-enhanced venography with selective views of the left renal vein, ovarian, and iliac veins to increase the diagnostic yield and guide therapeutic interventions in cases of pelvic reflux [25–27].

## DUS-Guided Management for Combined Deep and Superficial Reflux

Presence of combined superficial and deep venous reflux is common (~25%) [38]. Patients with combined deep and superficial reflux might improve clinically when the saphenous system is treated [39]. The ESCHAR randomized study showed that in patients with active ulceration, saphenous treatment combined with compression versus compression alone reduced ulcer recurrence risk at 4 years by 25%; however, it did not increase the wound healing rate [40]. The results of saphenous treatment in patients with combined superficial and deep venous reflux are still vague. Despite the fact that CFV reflux can be corrected in most cases, combined femoropopliteal or popliteal vein reflux corrects less often [40]. Deep venous reflux may arise by both primary valve failure and post-thrombotic valve damage, while venous overload is considered another important factor [38].

Finally, there may be patients who exhibit remaining deep venous reflux despite treatment of the superficial reflux. In these patients, specialized treatment options such as valvuloplasty or axillary vein transfer can be applied [32–34]. However, patients with post-thrombotic valves are difficult to treat [32–35].

## DUS-Guided Interventions

DUS provides vital information before the ablation of superficial and perforator veins such as the vein diameter, anatomic topography of the area, and possible variations. During ablation, DUS is used to guide vascular access and wire or catheter placement [41]. DUS-guided foam sclerotherapy has been used to treat varicose veins of all sizes; however, the procedure may need to be repeated to achieve secondary success [42]. For foam sclerotherapy, DUS is important in pretreatment diagnosis, treatment monitoring/guidance, post-treatment efficacy evaluation, and surveillance [43].

In a recent British study, it was demonstrated that DUS-guided foam sclerotherapy had the lowest initial cost, but a higher requirement for further interventions [44].

Vein angioplasty plus stenting has replaced surgery in several clinical cases such as the iliofemoral and caval outflow obstruction. Hence, DUS can be used preoperatively to establish the diagnosis, intraoperatively to guide vascular access, and postoperatively to assess the patency of the stent [45]. DUS-guided placement of IVC filters may be considered in cases of critical care patients as the method can be easily applied at the bedside and offers the advantage of decreased irradiation [46]. The introduction of intravascular ultrasound (IVUS) facilitated the development of strategies to overcome the limitations of standard ultrasound technology. IVUS is a promising new technique that is superior to single-plane venography in the investigation of patients with venous obstruction [47]. IVUS shows intraluminal details, trabeculations, and webs that may be hidden by the contrast dye. Other advantages of IVUS are its ability to demonstrate external compression directly, wall thickness, and neointimal hyperplasia. Recently, it has been suggested that successful placement of IVC filters using IVUS-guided imaging at the bedside in critically ill patients can be established through an evidence-based prospectively implemented algorithm [48].

## Recurrent Varices After Surgery (REVAS)

Following surgery to correct reflux, the occurrence of recurrent varices (REVAS) is frequently seen [49]. Hence, a consensus was developed to classify patients with REVAS and incorporate this classification as a complement into the advanced CEAP classification [50]. REVAS is a clinical definition that includes true recurrences, residual refluxing veins, and varicose veins caused by the progression of the disease, and its frequency ranges from 20% to 80% depending upon the definition of the condition and the duration of follow-up [48]. DUS has been used to monitor these patients following therapeutic interventions. The sources of reflux in patients with REVAS were of multiple origins and occurred in almost 50% of them at the SFJ [51, 52]. The below-knee saphenous trunks exhibit higher prevalence of reflux compared to the above-knee trunks because the GSV

is oftentimes stripped to the knee level and the SSV is ligated without stripping. Finally, no apparent source of reflux is documented in approximately 10% of the patients and in 17% of them is of pelvic or abdominal origin [52]. Patients with REVAS especially at the SFJ are treated with DUS guided foam sclerotherapy.

## Limitations of Ultrasound

DUS exhibits inherent technical limitations and is an operator dependent imaging modality [1, 2]. Examination of the lower extremities can be challenging especially regarding small calf veins which may be hard to visualize clearly [2]. Detection of partial thrombotic obstruction within the lumen of the vein may be difficult to interpret [49]. However, complete DUS examination (proximal and distal) has become the standard of care in detecting DVT and venous reflux in recent years [1–12]. Several anatomic limitations exist that may influence the examination of different venous segments such as the presence of bowel gas in the detection of abdominal or pelvic veins. Presence of diffuse or localized edema in patients with heart and renal failure or following surgery, respectively, may cause difficulties in the DUS examination of the venous system of the lower extremities [15, 38]. Also, anatomic variations, morbid obesity, inability of the patient to cooperate during the examination, and inability of the operator to perform a full scanning due to wounds and bandages has lead to the utilization of other noninvasive as well as invasive imaging modalities in routine practice such as catheter-based contrast-enhanced venography, magnetic resonance venography, and computed tomography [2, 14, 38, 49]. Despite the above mentioned limitations, DUS remains a simple, noninvasive, and yet dynamic method with low relative cost for the detection of venous pathology.

## References


1. Labropoulos N, Tiongson J, Pryor L, Tassiopoulos AK, Kang SS, Ashraf Mansour M, Baker WH. Definition of venous reflux in lower-extremity veins. J Vasc Surg. 2003;38:793–8.
2. Labropoulos N, Leon Jr LR. Duplex evaluation of venous insufficiency. Semin Vasc Surg. 2005;18:5–9.
3. Bergan JJ, Schmid-Schönbein GW, Smith PD, Nicolaides AN, Boisseau MR, Eklof B. Chronic venous disease. N Engl J Med. 2006;355:488–98.
4. Ibegbuna V, Delis KT, Nicolaides AN. Haemodynamic and clinical impact of superficial, deep and perforator vein incompetence. Eur J Vasc Endovasc Surg. 2006;31:535–41.
5. Van Bemmelen PS, Bedford G, Beach K, Strandness DE. Quantitative segmental evaluation of venous valvular reflux with duplex ultrasound scanning. J Vasc Surg. 1989;10:425–31.
6. Van Bemmelen PS, Beach K, Bedford G, Strandness Jr DE. The mechanism of venous valve closure. Its relationship to the velocity of reverse flow. Arch Surg. 1990;125:617–9.
7. Araki CT, Back TL, Padberg Jr FT, Thompson PN, Duran WN, Hobson 2nd RW. Refinements in the ultrasonic detection of popliteal vein reflux. J Vasc Surg. 1993;18:742–8.
8. Masuda EM, Kistner RL, Eklof B. Prospective study of duplex scanning for venous reflux: comparison of valsalva and pneumatic cuff techniques in the reverse Trendelenburg and standing positions. J Vasc Surg. 1994;20:711–20.
9. Lagattolla NR, Donald A, Lockhart S, Burnand KG. Retrograde flow in the deep veins of subjects with normal venous function. Br J Surg. 1997;84:36–9.
10. Jeanneret C, Labs KH, Aschwanden M, Bollinger A, Hoffmann U, Jäger K. Physiological reflux and venous diameter change in the proximal lower limb veins during a standardised valsalva manoeuvre. Eur J Vasc Endovasc Surg. 1999;17:398–403.
11. Jeanneret C, Jäger KA, Zaugg CE, Hoffmann U. Venous reflux and venous distensibility in varicose and healthy veins. Eur J Vasc Endovasc Surg. 2007;34:236–42.
12. Coleridge-Smith P, Labropoulos N, Partsch H, Myers K, Nicolaides A, Cavezzi A, UIP. Duplex ultrasound investigation of the veins in chronic venous disease of the lower limbs--UIP consensus document. Part I. Basic principles. Eur J Vasc Endovasc Surg. 2006;31:83–92.
13. Caggiati A, Ricci S. The caliber of the human long saphenous vein and its congenital variations. Anat Anz. 2000;182:195–201.
14. Cavezzi A, Labropoulos N, Partsch H, Ricci S, Caggiati A, Myers K, Nicolaides A, Smith PC UIP. Duplex ultrasound investigation of the veins in chronic venous disease of the lower limbs--UIP consensus document. Part II. Anatomy. Eur J Vasc Endovasc Surg. 2006;31:288–99.
15. Beebe HG, Bergan JJ, Bergqvist D, et al. Classification and grading of chronic venous disease in the lower limbs. A consensus statement. Eur J Vasc Endovasc Surg. 1996;12:487–91.
16. Labropoulos N, Gasparis AP, Pefanis D, Leon Jr LR, Tassiopoulos AK. Secondary chronic venous disease progresses faster than primary. J Vasc Surg. 2009;49:704–10.
17. Labropoulos N, Patel PJ, Tiongson JE, Pryor L, Leon Jr LR, Tassiopoulos AK. Patterns of venous reflux and obstruction in patients with skin damage due to chronic venous disease. Vasc Endovascular Surg. 2007;41:33–40.
18. Labropoulos N, Tassiopoulos AK. Chronic venous ulcers. Hawaii Med J. 2000;59:246–7.
19. Coleridge Smith PD, Thomas P, Scurr JH, Dormandy JA. Causes of venous ulceration: a new hypothesis. Br Med J. 1988;296:1726.
20. Kahn SR, Shrier I, Julian JA, Ducruet T, Arsenault L, Miron MJ, Roussin A, Desmarais S, Joyal F, Kassis J, Solymoss S, Desjardins L, Lamping DL, Johri M, Ginsberg JS. Determinants and time course of the post-thrombotic syndrome after acute deep venous thrombosis. Ann Intern Med. 2008;149:698–707.
21. Elsharawy M, Elzayat E. Early results of thrombolysis vs. anticoagulation in iliofemoral venous thrombosis. A randomised clinical trial. Eur J Vasc Endovasc Surg. 2002;24:209–14.
22. Mewissen MW, Seabrook GR, Meissner MH, Cynamon J, Labropoulos N, Haughton SH. Catheter-directed thrombolysis for lower extremity deep venous thrombosis: report of a national multicenter registry. Radiology. 1999;211:39–49.
23. Labropoulos N, Leon L, Engelhorn CA, Amaral SI, Rodriguez H, Kang SS, Mansour AM, Littooy FN. Sapheno-femoral junction reflux in patients with a normal saphenous trunk. Eur J Vasc Endovasc Surg. 2004;28:595–9.
24. Labropoulos N, Kang SS, Mansour MA, Giannoukas AD, Buckman J, Baker WH. Primary superficial vein reflux with competent saphenous trunk. Eur J Vasc Endovasc Surg. 1999;18:201–6.
25. Venbrux AC, Chang AH, Kim HS, et al. Pelvic congestion syndrome (pelvic venous incompetence): impact of ovarian and internal iliac vein embolotherapy on menstrual cycle and chronic pelvic pain. J Vasc Interv Radiol. 2002;13:171–8.

26. Kim HS, Malhotra AD, Rowe PC, Lee JM, Venbrux AC. Embolotherapy for pelvic congestion syndrome: long-term results. J Vasc Interv Radiol. 2006;17:289–97.
27. Belenky A, Bartal G, Atar E, Cohen M, Bachar GN. Ovarian varices in healthy female kidney donors: incidence, morbidity, and clinical outcome. AJR Am J Roentgenol. 2002;179:625–7.
28. Labropoulos N, Kokkosis AA, Spentzouris G, Gasparis AP, Tassiopoulos AK. The distribution and significance of varicosities in the saphenous trunks. J Vasc Surg. 2010;51:96–103.
29. Kurt A, Unlü UL, Ipek A, Tosun O, Gümüs M, Zan E, Dilmen G, Tas I. Short saphenous vein incompetence and chronic lower extremity venous disease. J Ultrasound Med. 2007;26:163–7.
30. Daher A, Jones V, da Silva AF. The role of popliteal vein incompetence in the diagnosis of saphenous-popliteal reflux using continuous wave Doppler. Eur J Vasc Endovasc Surg. 2001;21:350–2.
31. Labropoulos N, Leon M, Nicolaides AN, Giannoukas AD, Volteas N, Chan P. Superficial venous insufficiency: correlation of anatomic extent of reflux with clinical symptoms and signs. J Vasc Surg. 1994;20:953–8.
32. Labropoulos N, Tassiopoulos AK, Bhatti AF, Leon L. Development of reflux in the perforator veins in limbs with primary venous disease. J Vasc Surg. 2006;43:558–62.
33. Labropoulos N, Mansour MA, Kang SS, Gloviczki P, Baker WH. New insights into perforator vein incompetence. Eur J Vasc Endovasc Surg. 1999;18:228–34.
34. Labropoulos N, Delis K, Mansour MA, Kang SS, Buckman J, Nicolaides AN, Baker WH. Prevalence and clinical significance of posterolateral thigh perforator vein incompetence. J Vasc Surg. 1997;26:743–8.
35. Labropoulos N, Delis K, Nicolaides AN, Leon M, Ramaswami G. The role of the distribution and anatomic extent of reflux in the development of signs and symptoms in chronic venous insufficiency. J Vasc Surg. 1996;23:504–10.
36. Labropoulos N, Tassiopoulos AK, Kang SS, Mansour MA, Littooy FN, Baker WH. Prevalence of deep venous reflux in patients with primary superficial vein incompetence. J Vasc Surg. 2000;32:663–8.
37. Labropoulos N, Tiongson J, Pryor L, Tassiopoulos AK, Kang SS, Mansour MA, Baker WH. Nonsaphenous superficial vein reflux. J Vasc Surg. 2001;34:872–7.
38. Labropoulos N, Giannoukas AD, Delis K, Mansour MA, Kang SS, Nicolaides AN, Lumley J, Baker WH. Where does venous reflux start? J Vasc Surg. 1997;26:736–42.
39. Knipp BS, Blackburn SA, Bloom JR, Fellows E, Laforge W, Pfeifer JR, Williams DM, Wakefield TW, Michigan Venous Study Group. Endovenous laser ablation: venous outcomes and thrombotic complications are independent of the presence of deep venous insufficiency. J Vasc Surg. 2008;48:1538–45.
40. Gohel MS, Barwell JR, Taylor M, Chant T, Foy C, Earnshaw JJ, Heather BP, Mitchell DC, Whyman MR, Poskitt KR. Long term results of compression therapy alone versus compression plus surgery in chronic venous ulceration (ESCHAR): randomised controlled trial. BMJ. 2007;335:83.
41. Hissink RJ, Bruins RM, Erkens R, Castellanos Nuijts ML, van den Berg M. Innovative treatments in chronic venous insufficiency: endovenous laser ablation of perforating veins: a prospective short-term analysis of 58 cases. Eur J Vasc Endovasc Surg. 2010;40:403–6.
42. Ceulen RP, Jagtman EA, Sommer A, Teule GJ, Schurink GW, Kemerink GJ. Blocking the saphenofemoral junction during ultrasound-guided foam sclerotherapy – assessment of a presumed safety-measure procedure. Eur J Vasc Endovasc Surg. 2010;40:772–6.
43. Breu FX, Guggenbichler S, Wollmann JC. Duplex ultrasound and efficacy criteria in foam sclerotherapy from the 2nd European consensus meeting on foam sclerotherapy, Tegernsee, Germany. Vasa. 2008;37:90–5.
44. Gohel MS, Epstein DM, Davies AH. Cost-effectiveness of traditional and endovenous treatments for varicose veins. Br J Surg. 2010;97:1815–23.
45. Wahlgren CM, Wahlberg E, Olofsson P. Endovascular treatment in postthrombotic syndrome. Vasc Endovascular Surg. 2010;44:356–60.
46. Uppal B, Flinn WR, Benjamin ME. The bedside insertion of inferior vena cava filters using ultrasound guidance. Perspect Vasc Surg Endovasc Ther. 2007;19:78–84.
47. Neglen P, Thrasher TL, Raju S. Venous outflow obstruction: an underestimated contributor to chronic venous disease. J Vasc Surg. 2003;38:879–85.
48. Killingsworth CD, Taylor SM, Patterson MA, Weinberg JA, McGwin Jr G, Melton SM, Reiff DA, Kerby JD, Rue LW, Jordan Jr WD, Passman MA. Prospective implementation of an algorithm for bedside intravascular ultrasound-guided filter placement in critically ill patients. J Vasc Surg. 2010;51:1215–21.
49. Labropoulos N, Leon L, Kwon S, Tassiopoulos A, Gonzalez-Fajardo JA, Kang SS, Mansour MA, Littooy FN. Study of the venous reflux progression. J Vasc Surg. 2005;41:291–5.
50. Perrin MR, Guex JJ, Ruckley CV, de Palma RG, Royle JP, Eklof B, Nicolini P, Jantet G. Recurrent varices after surgery (REVAS), a consensus document. REVAS group. Cardiovasc Surg. 2000;8:233–45.
51. Perrin M, Allaert FA. Intra- and inter-observer reproducibility of the recurrent varicose veins after surgery (REVAS) classification. Eur J Vasc Endovasc Surg. 2006;32:326–32.
52. Perrin MR, Labropoulos N, Leon Jr LR. Presentation of the patient with recurrent varices after surgery (REVAS). J Vasc Surg. 2006;43:327–34.

# Ultrasound-Guided Cava Filter Placement

42

Bryan T. Fisher Sr and Thomas C. Naslund

**Abstract**

Pulmonary embolism from deep venous thrombosis reduces the cross-sectional area of the pulmonary vascular bed, resulting in an incremental increase in pulmonary vascular resistance and subsequent increased right ventricular afterload. Thus, large or recurrent pulmonary emboli can be fatal. Anticoagulation alone can decrease the mortality rate to less than 5%, but cannot be used universally in all patient populations. The advent of the inferior vena cava filter has drastically changed the management of patients with lower extremity deep venous thrombosis and a contraindication to anticoagulation. Developed in the 1940s, this device has evolved into a modality that has proven effective at preventing life-threatening pulmonary emboli. Mechanical caval interruption devices have since improved as well, including a significant decrease in delivery sheath size, which aids in achieving post-procedural hemostasis. Because of these improvements, IVC filter placement has changed from a procedure performed exclusively in the operating room with venotomy to a bedside percutaneous procedure using ultrasound guidance. Successful use of transabdominal duplex ultrasound and IVUS eliminate the need for radiocontrast dye administration thus avoiding the known risk of renal failure and anaphylaxis. Other advantages include decreased radiation exposure to the patient and hospital personnel, reduced need for patient transport, and decreased cost compared to traditional placement in the operating room suite. In a cost containment era, it is feasible to think that future mechanical caval interruption will occur more commonly at the bedside than in the traditional operating theater.

**Keywords**

Bedside • Ultrasound-guided • IVC filter placement • Intravascular ultrasound

Forty-three years ago, Lazar Greenfield reasoned that there had to be a better way to prevent pulmonary emboli [1]. His inspiration for development of a vena cava filter occurred after a 23-year-old multi-trauma patient died secondary to complications of an open pulmonary embolectomy. Two years later, the IVC filter was introduced as a safe and reliable means of preventing fatal pulmonary emboli. Mechanical caval interruption has since evolved with technological advances with decreasing introducer sizes from a procedure performed exclusively in the operating room with venotomy to bedside percutaneous procedure [2–23]. The latter has become a convenient, reliable, and safe alternative for critically ill patients (Figs. 42.1, 42.2, 42.3, and 42.4).

Transabdominal duplex ultrasound (DUS) and intravascular ultrasound (IVUS) have emerged as familiar and adaptable techniques for vena cava filter insertion (Table 42.1). Accordingly, our rapid advances in diagnostic

B.T. Fisher Sr, M.D.
Department of Vascular Surgery, Vanderbilt University Medical Center, Nashville, TN, USA

T.C. Naslund, M.D. (✉)
Department of Vascular Surgery, Vanderbilt University Medical Center, D-5237 Medical Center North, Nashville, TN 37232-2735, USA
e-mail: bryan.fisher@vanderbilt.edu

A.F. AbuRahma, D.F. Bandyk (eds.), *Noninvasive Vascular Diagnosis*,
DOI 10.1007/978-1-4471-4005-4_42, © Springer-Verlag London 2013

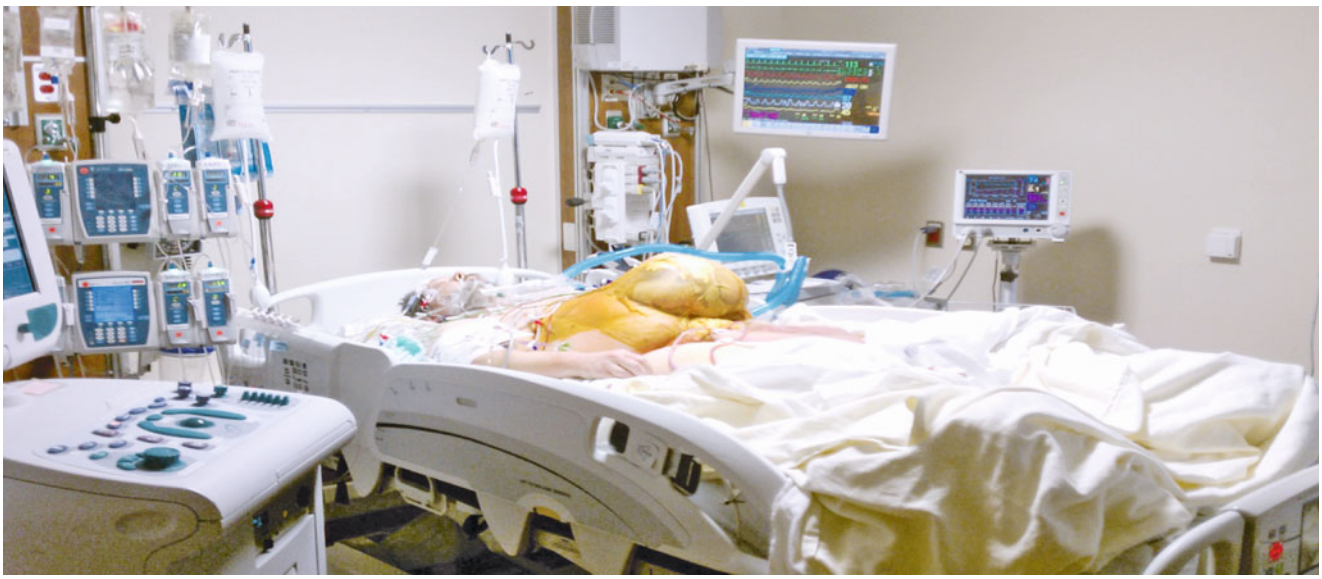

**Fig. 42.1** Global- and close-up view of modern intensive care unit suite. Note space limitations at the head of the bed in the first image

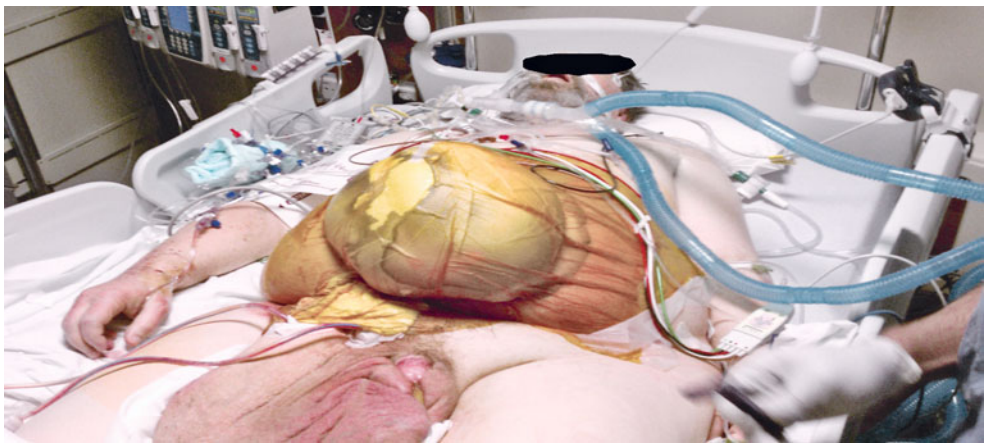

**Fig. 42.2** Same obese male s/p incarcerated inguinal hernia repair requiring paralysis for open abdominal decompression postoperatively. Pt is high risk for DVT due to immobility and anticoagulation is contraindicated given his recent operation

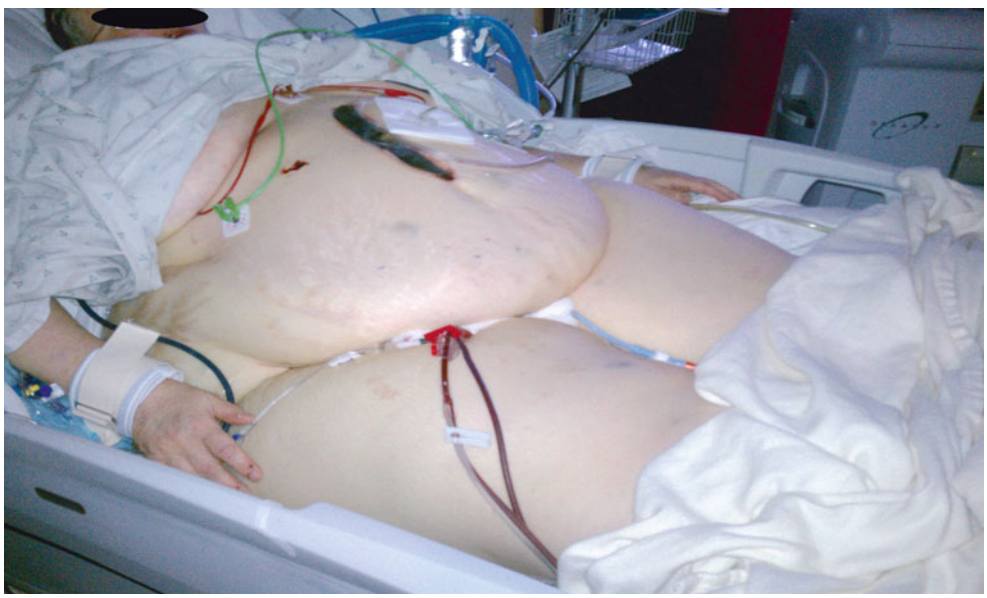

**Fig. 42.3** A morbidly obese patient at high risk for DVT prior to bedside filter placement

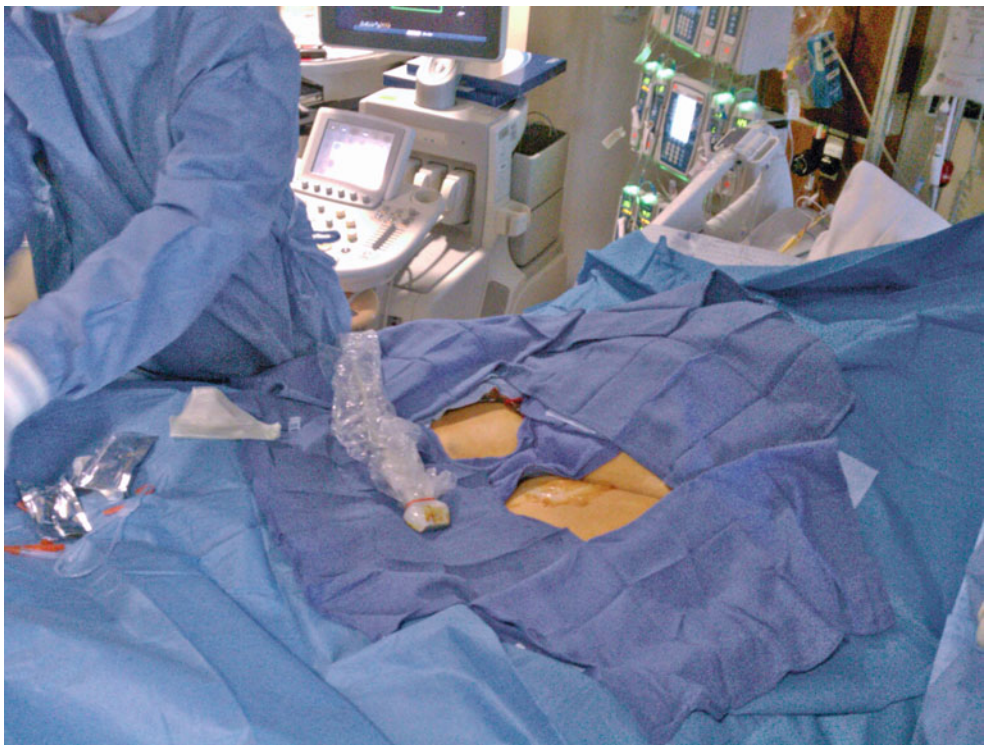

**Fig. 42.4** Same patient as in Fig. 42.3 after sterile preparation of the groin. Note that an assistant may be needed to retract excess skin and fat in morbidly obese patients

**Table 42.1** Series of ultrasound-guided vena cava filter placement

| Author | Year | *N* | Modality | Location | Technical success (in %) | Misplacement (in %) | Overall complication rate (in %) |
|---|---|---|---|---|---|---|---|
| Killingsworth [2] | 2010 | 109 | IVUS | Bedside | 97 | 6 | 5 |
| Aidinian [4] | 2009 | 14 | IVUS | Bedside | 100 | 0 | 0 |
| Spaniolas [3] | 2008 | 47 | IVUS | IR/Angio/OR | 100 | 2 | 15 |
| Kardys [5] | 2008 | 31 | IVUS | OR | 97 | 3 | 3 |
| Corriere [9] | 2005 | 382 | DUS | Bedside | 97 | 5 | 2 |
| Rosenthal [10] | 2004 | 94 | IVUS | Bedside | 97 | 3 | 6 |
| Garrett [11] | 2004 | 28 | IVUS | Bedside | 93 | 8 | 15 |
| Gamblin [12] | 2003 | 36 | IVUS | OR | 94 | 0 | 0 |
| Wellons [13] | 2003 | 45 | IVUS | IR/bedside | 94 | 3 | 6 |
| Conners [14] | 2002 | 284 | DUS | Bedside | 98 | 2 | 4 |
| Ashley [15] | 2001 | 21 | IVUS | OR | 100 | 0 | 0 |
| Ebaugh [16] | 2001 | 26 | IVUS | Bedside | 92 | 4 | 12 |
| Bonn [17] | 1999 | 30 | IVUS | IR Suite | 100 | 0 | 0 |
| Sato [18] | 1999 | 53 | DUS | Bedside | 98 | 0 | 2 |

*DUS* duplex ultrasound, *IVUS* intravascular ultrasound, *OR* operating room, *IR* interventional radiology

imaging quality have allowed us to push the envelope of making filter placement less invasive to the patient. It is natural to think that this technology will eventually be so robust that it makes bedside placement the new norm in IVC filter placement.

Pulmonary embolism reduces the cross-sectional area of the pulmonary vascular bed, resulting in an incremental increase in pulmonary vascular resistance and subsequent increased right ventricular afterload [24]. In its most severe form, cardiopulmonary collapse ensues leading to death. Ten percent of patients who develop pulmonary embolism die within the first hour, and 30% die subsequently from recurrent embolism, making prevention and prompt recognition, when prevention fails, a priority [25]. Anticoagulation alone can decrease the mortality rate to less than 5%, but cannot be used universally in all patient populations. Thus, absolute and relative indications for IVC filter placement include, and are largely unchanged (Table 42.2).

**Table 42.2** Indications for IVC filter placement

| | |
|---|---|
| Absolute indications | Documented VTE w/contraindications to anticoagulation* |
| | Documented VTE despite adequate anticoagulation |
| | Complications arising from anticoagulation |
| | Concurrent pulmonary embolectomy |
| | Failure of alternate caval interruption methods |
| Relative indications | Proximal free-floating iliofemoral thrombus (>5-cm-free-floating tail) |
| | Propagation of an iliofemoral thrombus despite therapeutic anticoagulation |
| | VTE in certain high-risk populations including those with severely compromised cardiopulmonary function (e.g., severe pulmonary hypertension) undergoing high-risk operations (e.g., spine or bariatric operations) |

## Absolute Indications

Generally accepted absolute indications for IVC filter insertion include:

1. Contraindications to anticoagulation*
2. Documented VTE while in the therapeutic anticoagulation range
3. Complications arising from anticoagulation
4. Concurrent pulmonary embolectomy
5. Failure of alternate caval interruption methods

*Examples of contraindications to anticoagulation include clinical evidence of active or recent hemorrhage (i.e., intracranial, gastrointestinal) recent or planned major operation, or severe traumatic injuries.

## Relative Indications

Traditional relative indications for IVC filter placement include:

1. Detection of a proximal free-floating iliofemoral thrombus (>5 cm free-floating tail)
2. Propagation of an iliofemoral thrombus despite therapeutic anticoagulation
3. VTE in certain high-risk populations including those with severely compromised cardiopulmonary function (e.g., severe pulmonary hypertension) undergoing high-risk operations (e.g., spine or bariatric operations) [22, 26]

## Prophylactic Indications

Prophylaxis against VTE remains the most common indication for IVC filter insertion in most modern series [22]. While not supported by randomized trials, a growing clinical experience drives prophylactic filter placement following trauma in patients at highest risk for PE including severe head injury and coma, spinal cord injuries with neurological deficit, spine fractures with immobility, pelvic and multiple long bone fractures, and perhaps, direct venous trauma. Other recommended prophylactic indications include malignancy, hemorrhagic stroke, recent neurological surgery, or concurrent open bariatric surgery [15–18].

## Technique

### Equipment

The bedside filter insertion techniques that are described below have been developed through extensive clinical experience and have been optimized with the following equipment: Stainless Steel Over-the-Wire Greenfield Vena Cava Filter (Boston Scientific, Natick, MA), Gunther Tulip Vena Cava Filter (Cook Medical, Bloomington, IN), a portable duplex ultrasound system (Philips Medical Systems, Andover, MA), and a portable IVUS imaging system (Galaxy IVUS imaging system with an Atlantis PV Peripheral Imaging Catheter, 15 MHz, SF profile, Boston Scientific, Natick, MA). Although our experience with ultrasound-guided cava filter insertion has been dominantly accomplished with the retrievable Gunther Tulip filter and to a lesser extent the stainless steel Greenfield filter, the described techniques can be readily applied to placement of other commercially available IVC filters.

## Technique for Transabdominal Duplex Ultrasound

### Preprocedural Imaging

Our preferred technique for both transabdominal duplex and intravascular ultrasound guided filter placement has been previously described [23]. Though not always available, any CT images of the abdomen are reviewed to allow preprocedural determination of the IVC filter diameter. Initial transabdominal duplex ultrasound is performed to define the suitability of bedside filter placement under ultrasound guidance. The inferior vena cava is interrogated transversely and longitudinally at the renal vein confluence. Adequate visualization of a renal vein (or right renal artery) is mandatory to guide accurate filter insertion. Before proceeding, it is important to confirm an IVC diameter <28 mm, and patency of the iliocaval and femoral venous systems, respectively. Visualization of intraluminal thrombus should steer the clinician toward conversion to conventional cavography under fluoroscopic guidance. Alternate central venous access, such as the internal jugular or brachial, in the setting of bilateral

common femoral or iliac venous thromboses is possible, but routine use of the internal jugular vein is discouraged due to the space limitations inherent to critical care rooms and achieving wire access to the inferior vena cava without fluoroscopic guidance can be challenging (Fig. 42.1).

### Filter Placement Technique

After the administration of a local anesthetic, ultrasound-guided seldinger technique is used to cannulate the common femoral vein and place a 0.035-in. guide-wire into the IVC. The device delivery sheath is inserted to the level of the renal vein-IVC confluence. The delivery catheter containing the preloaded IVC filter (whether permanent or temporary) is placed into the sheath and advanced to the tip of the sheath. When implanting a Greenfield filter, the wire should be removed to precisely identify the tip of the filter. Once the renal vein-IVC confluence is clearly recognized in the transverse orientation, the sheath and filter are positioned caudal to the renal vein ostium. At this stage, the ideal deployment position is reached. When visualized longitudinally, the filter should be easily recognized and its tip should approach the right renal artery, a reliable landmark for the renal vein-IVC confluence. The filter is then deployed under continuous ultrasound guided visualization.

### Completion Imaging

After deployment, correct filter position, complete leg expansion, and presence/lack of tilt are confirmed via immediate transabdominal ultrasound and subsequent abdominal plain film. Gentle manual compression to the site where the device entered the vein (as opposed to the needle mark in the skin) provides rapid and lasting hemostasis.

## Technique for Intravascular Ultrasound

### Preprocedural Imaging

The location and patency of the common femoral veins at the intended venous puncture sites are confirmed with duplex ultrasonography, similar to the transabdominal approach. Then, the puncture site and surrounding 1 cm of the tissue is infiltrated with local anesthesia. The common femoral vein is cannulated and a guidewire is inserted into the IVC percutaneously. An 8-Fr sheath is then inserted into the common femoral vein through which the IVUS probe is advanced into the IVC to the level of the right atrium. Venous anatomy is sequentially identified during a "pull-back" technique including the right atrium, hepatic veins, renal veins, infrarenal IVC, and iliac venous confluence (Figs. 42.5, 42.6, 42.7, 42.8, and 42.9). The IVUS catheter is withdrawn to a site immediately caudad to the lowest renal vein and the IVC diameter is determined.

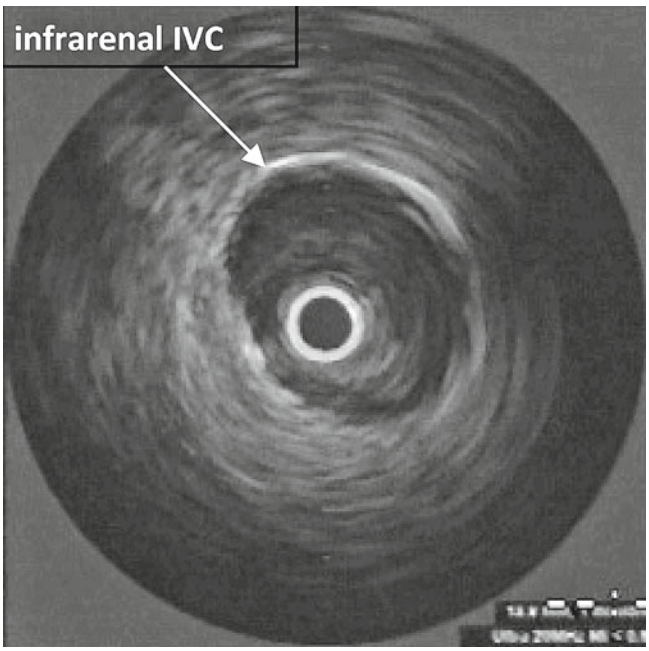


**Fig. 42.5** IVUS view of the IVC

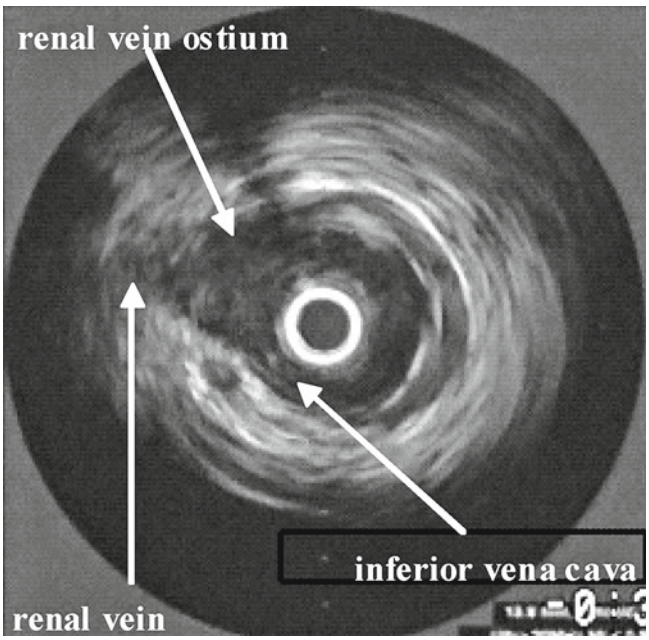


**Fig. 42.6** Renal vein ostium

### Dual Venous Access

We recommend a dual venous access technique for IVC filter placement. This technique employs contralateral venous

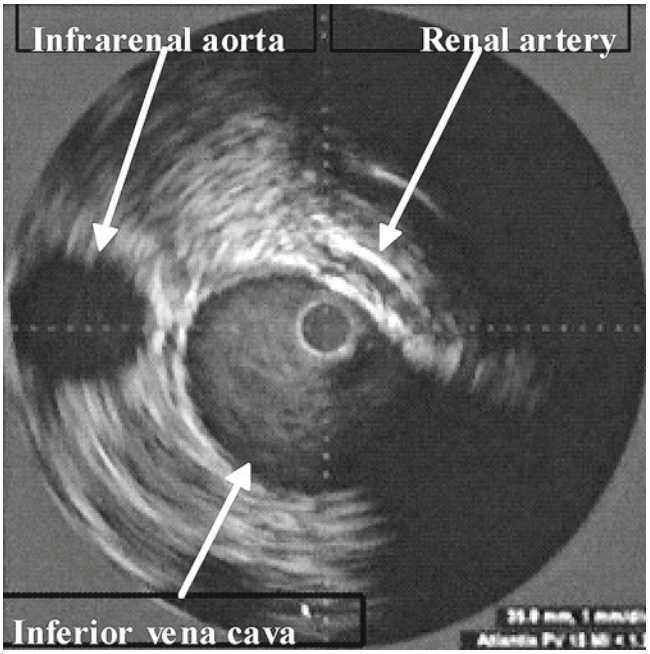


**Fig. 42.7** Infrarenal aorta, IVC, and right renal artery

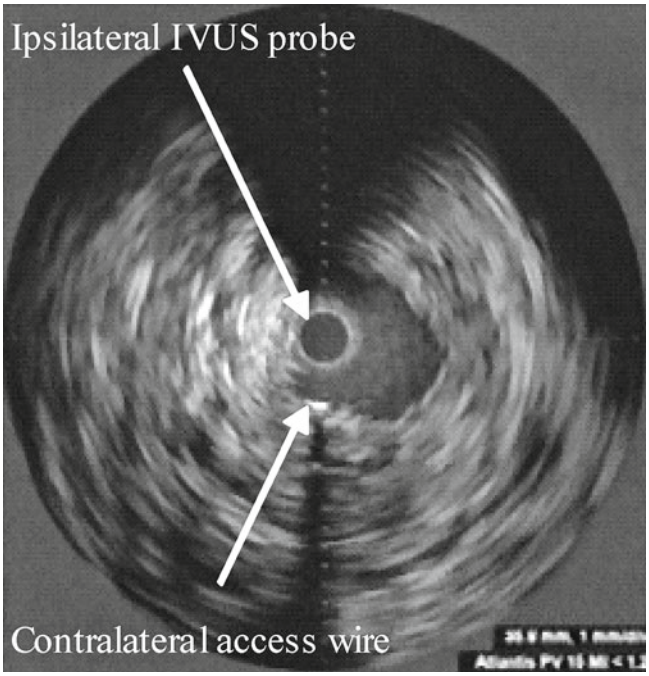


**Fig. 42.9** Wire visualized from contralateral access

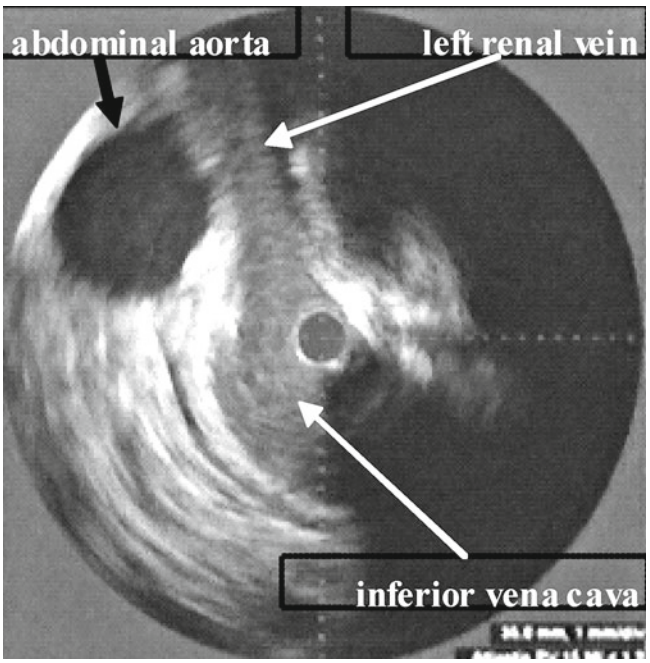


**Fig. 42.8** IVC, left renal vein, and aorta

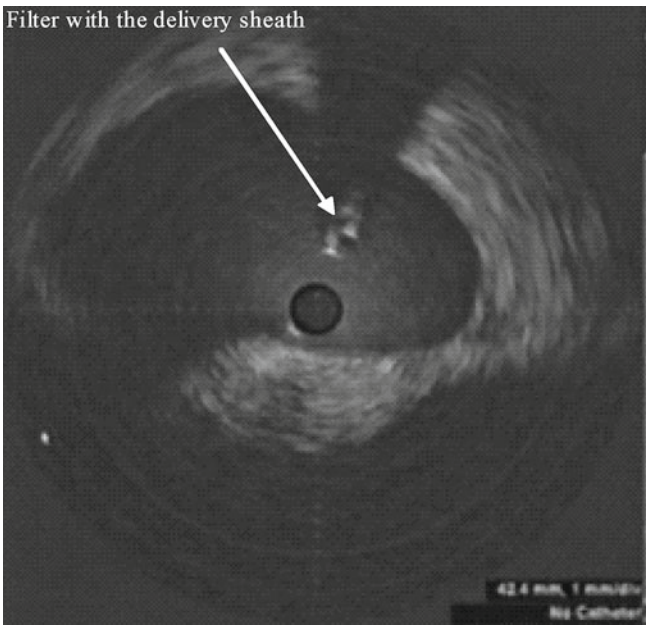


**Fig. 42.10** Undeployed filter still within delivery sheath

cannulation to assist with filter insertion. Occasionally, contralateral femoral venous thrombosis necessitates dual ipsilateral venous cannulation through dual ipsilateral sheath insertion. A 0.035-in. guidewire is advanced through the contralateral venous access site and advanced to the renal vein confluence as confirmed with IVUS imaging. The device delivery sheath is then inserted above the renal vein-IVC confluence. The IVC filter (whether permanent or temporary) is placed into the sheath and advanced to the tip of the sheath. Then as a unit and under IVUS guidance, the sheath and filter delivery catheter are withdrawn to a level immediately caudad to the renal vein confluence (Fig. 42.10). Once an appropriate filter position is verified, the IVUS probe and wire are withdrawn and the filter is deployed (Fig. 42.11).

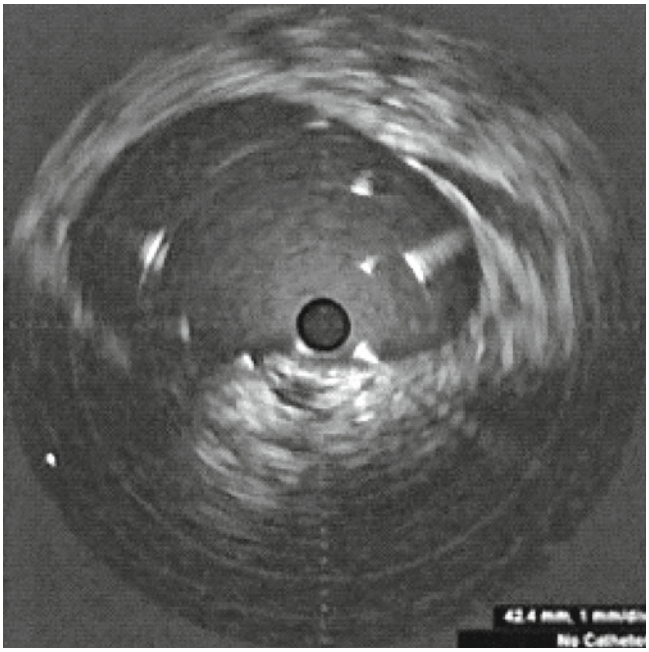

**Fig. 42.11** Deployment of filter confirmed by visualization of filter prongs

## Single Venous Access

Venous anatomy is similarly defined with IVUS as in the dual venous access technique. Once "pull-back" venous surveillance is accomplished, the IVUS probe is removed. The IVUS catheter is then premeasured against the filter delivery catheter in order to determine the length from the hub of the sheath to the tip of the filter. The premeasured length is then noted on the IVUS probe by calibration markings or a securely placed tie. The IVUS probe is inserted via the device delivery sheath and advanced to a position corresponding to the length of the filter delivery catheter. The sheath and IVUS probe are withdrawn until a position immediately below the lowest renal vein is reached. After removal of the IVUS probe, the filter delivery catheter is fully inserted and deployed. Thus, in the single venous access technique, IVUS guides sheath positioning and subsequently, filter positioning is assumed relative to the sheath.

## Completion Imaging

To confirm complete leg expansion and appropriate position, the IVUS probe may be carefully inserted until the filter legs are visualized confirming apposition to the caval wall (Fig. 42.11). Further, cephalad advancement of the IVUS catheter is strongly discouraged to avoid entrapment in the filter and/or filter movement. A standard radiograph of the abdomen is obtained to evaluate filter position, tilt, and leg expansion. Gentle manual compression at the venous access site achieves hemostasis.

## Advantages

Successful use of transabdominal duplex ultrasound and IVUS eliminate the need for radiocontrast dye administration. Although the risk of contrast-induced nephropathy is low in the general medical population, critically ill patients not uncommonly experience renal dysfunction from associated hypotension, volume depletion, and acute critical illness. Moreover, ultrasound guidance avoids the risk of adverse contrast-related reactions, which affect 4–8% of the US population [27]. Utilization of ultrasound imaging eliminates radiation exposure to the patient and patient care area including attendant care personnel and neighboring patients. Importantly, ultrasound-guided filter placement facilitates bedside insertion and circumvents the effort and risk of transporting critically ill or injured patients [4]. Multiple case series report that complications during patient transport occur up to 70% of the time [28–30]. Whether related to equipment failure or lack of experience in transport personnel, patient safety is compromised by transport from the controlled environment of the critical care unit. Finally, bedside filter insertion also eliminates interventional suite or operating room charges, anesthesia, and the need for additional support for the surgical team. In an era of medical cost containment, the reduced expense of bedside filter insertion is quickly realized and yields significant cost savings.

## Disadvantages

The principle disadvantage of transabdominal duplex ultrasound is occasional inadequate preprocedural IVC visualization. Obesity, pregnancy, bowel distention, abdominal wounds, and anasarca from large volume resuscitation or acute illness may impair IVC imaging and thereby interfere with filter insertion using transabdominal ultrasonography [31]. Furthermore, immobilization from orthopedic fixation or spine fracture precautions impedes maneuvers to improve visualization. Nonetheless, adequate IVC visualization is achievable in 85–92% of the trauma patients [4, 14, 18, 19]. Intravascular ultrasound, an imaging modality not impaired by body habitus or bowel gas, can often overcome the limitations of transabdominal duplex ultrasound and retain the advantages of bedside filter insertion. Although operator expertise is a perceived limitation of ultrasound-guided filter placement, clinical experience is rapidly acquired, and it is unusual that proficiency is a limiting factor of the technique [14]. Another potential disadvantage of ultrasound is its inability to reliably detect venous anomalies. The clinical

significance of this shortcoming should be considered, but careful review of available CT images (which are usually available) can help.

## Complications

The overall complication rate associated with ultrasound-guided IVC filter placement is consistently low. Series employing transabdominal duplex ultrasound report an overall complication rate of 1.8–8.2%; a similar complication rate is reported with IVUS (Table 42.1).

### Misplacement/Malpositioning

The most commonly reported complication of IVC filter insertion under ultrasound guidance is misplacement, occurring in 0–8% of the insertions in various series (Table 42.1). Image misinterpretation can lead to misplacement in the common iliac vein and suprarenal vena cava, respectively. Filter retrieval and repositioning, or secondary deployment of a correctly positioned filter are methods of managing common iliac vein deployment.

### Insertion Site Thrombosis (IST)

Deep venous thrombosis at the venous access site occurs in up to 16.7% of the patients, and appears to be related to post-procedural compression of the access site. Although not consistently associated with sheath size, the double venous puncture technique may be associated with a higher incidence of IST [23]. The reported incidence of IST is a function of the intensity of duplex ultrasound surveillance of the venous access site. With routine surveillance, IST may occur in up to one-third of the patients following IVC filter insertion [22].

### Filter Migration

Filter migration, defined as movement >1 cm from the implantation site, is an often dramatic, although usually insignificant observation [32, 33]. Migration occurs in approximately 5% of Greenfield filters and is similar among contemporary devices. Rarely has migration to the heart and pulmonary arteries been described.

### Tilting/Incomplete Deployment

Filter tilting or asymmetric position is frequently described in conical-shaped models, but is rarely associated with inadequate embolic protection [34, 35]. Partial or complete deployment failure is an uncommon event with modern IVC filter designs.

### Device Failure/Pulmonary Embolism (PE)

Device failure, or failure of the filter to provide adequate embolic protection, is fortunately uncommon but consistent among available devices (2.6–3.8%) [22]. The incidence of fatal pulmonary embolism is typically <1%. No particular factors have been attributed to device failure other than filter misplacement and malpositioning.

### IVC Thrombosis

IVC thrombosis is an uncommon clinical event following filter insertion but may occur in up to 3.6% of the filter insertions [21, 34–39]. Notably, IVC thrombosis may predispose to recurrent deep venous thrombosis and the post-thrombotic syndrome. The rate of IVC thrombosis is similar among currently available filters, and is independent of infrarenal or suprarenal position.

### Fracture

With long-term follow-up, filter fracture is unusual. The Simon nitinol filter, however, is associated with a disproportionate rate of limb fracture (14.1%) [22]. Nonetheless, no adverse events, including device failure, have been associated with its presence.

### Caval Penetration

Caval penetration by filter prongs, strut fracture, or from device migration or tilting is an infrequent (4.4%) and overwhelmingly asymptomatic (0.4%) event. However, penetration of the vena cava with perforation of adjacent retroperitoneal viscera (i.e., duodenum) has been reported. Although not uncommon, IVC penetration is rarely associated with adverse clinical consequences [7].

## Long-Term Outcomes

The Greenfield filter is the most studied vena caval filter, and offers excellent long-term patency and protection from recurrent embolism. Prevention of recurrent embolism is approximately 96% at 20 years while patency consistently exceeds 95% despite discontinuation of systemic

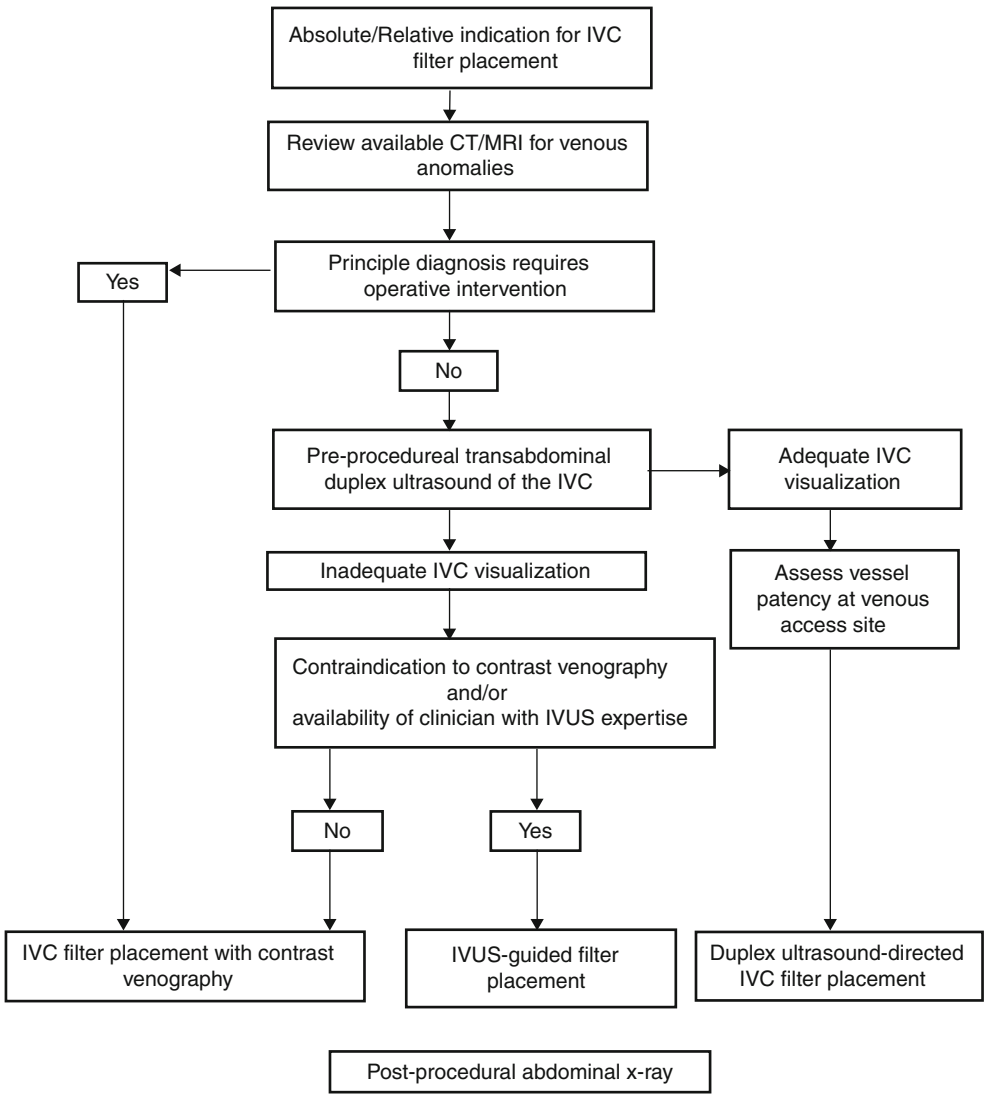


**Fig. 42.12** Suggested algorithm for ultrasound-guided cava filter placement. *IVC* inferior vena cava, *IVUS* intravascular ultrasound, *DUS* duplex ultrasound

anticoagulation [37]. Equivalent patency and protection is observed in the suprarenal position and though studied less frequently, in the superior vena cava [38]. Shorter, yet reasonable, follow-up from more modern filters suggests similar trends in success.

## Financial Considerations

Ultrasound guidance for IVC filter insertion is cost-effective. Eliminating patient transportation, attendance of ancillary personnel, professional fees, and the use of an operating room or interventional suite reduce expense associated with filter insertion.

According to Conners and associates [14], bedside filter placement with duplex ultrasonography yielded overall single institution annual savings of $124,000 ($2,388 per inserted filter) when compared to filter placement by fluoroscopy. Other investigators have reported similar economic advantages in addition to reduced OR utilization [16, 18, 19, 21].

## Suggested Algorithm for IVC Filter Placement

A suggested algorithm is provided to guide clinical decision-making and to maximize utilization of ultrasound imaging for filter placement (Fig. 42.12). When IVC anatomy cannot be visualized by surface ultrasound or IVUS, transport to the angiography suite for contrast venography is indicated. Though a rare event, when the IVC diameter exceeds 28 mm, options for caval interruption include placement of a Bird's Nest filter (Cook Medical, Bloomington, IN) or bilateral common iliac vein filters.

## References


1. Garber K. The clot stopper. Am Herit Invent Technol. 2006;22(1):34–9.
2. Killingsworth CD, Taylor SM, Patterson MA, Weinberg JA, McGwin Jr G, Melton SM, Reiff DA, Kerby JD, Rue LW, Jordan Jr WD, Passman MA. Prospective implementation of an algorithm for bedside intravascular ultrasound-guided filter placement in critically ill patients. J Vasc Surg. 2010;51(5):1215–21.
3. Spaniolas K, Velmahos GC, Kwolek C, Gervasini A, De Moya M, Alam HB. Bedsideplacement of removable vena cava filters guided by intravascular ultrasound in the critically injured. World J Surg. 2008;32(7):1438–43.
4. Aidinian G, Fox CJ, White PW, Cox MW, Adams ED, Gillespie DL. Intravascular ultrasound – guided inferior vena cava filter placement in the military multi-trauma patients: a single-center experience. Vasc Endovascular Surg. 2009;43(5):497–501.
5. Kardys CM, Stoner MC, Manwaring ML, Barker M, Macdonald KG, Pender JR, Chapman 3rd WH. Safety and efficacy of intravascular ultrasound-guided inferior vena cava filter in super obese bariatric patients. Surg Obes Relat Dis. 2008;4(1):50–4. Epub 2007 Dec 11.
6. Nicolaou S, Talsky A, Khashoggi K, Venu V. Ultrasound-guided interventional radiology in critical care. Crit Care Med. 2007;35(5 Suppl):S186–97. Review.
7. Chiou AC. Intravascular ultrasound-guided bedside placement of inferior vena cava filters. Semin Vasc Surg. 2006;19(3):150–4. Review.
8. Uppal B, Flinn WR, Benjamin ME. The bedside insertion of inferior vena cava filters using ultrasound guidance. Perspect Vasc Surg Endovasc Ther. 2007;19(1):78–84.
9. Corriere MA, Passman MA, Guzman RJ, et al. Comparison of bedside transabdominal duplex ultrasotmd versus contrast venography for inferior vena cava filter placement: what is the best imaging modality? Ann Vasc Surg. 2005;19:229–34.
10. Rosenthal D, Wellons ED, Levitt AB, et al. Role of prophylactic temporary inferior vena cava filters placed at the bedside under intravascular ultrasOlmd guidance in patients with multiple trauma. J Vasc Surg. 2004;40:958–64.
11. Garrett IV, Passman MA, Guzman RJ, et al. Expanding options for bedside placement of inferior vena cava filters with intravascular ultrasound when transabdominal duplex ultrasound imaging is inadequate. Ann Vasc Surg. 2004;18:329–34.
12. Gamblin TC, Ashley DW, Burch S, et al. A prospective evaluation of a bedside tedmique for placement of inferior vena cava filters: accuracy and limitations of intravascular ultrasound. Am Surg. 2003;69:382–6.
13. Wellons ED, Matsuura JH, Shuler BW, et al. Bedside intravascular ultrasound-guided vena cava filter placement. J Vasc Surg. 2003;38:455–8.
14. Conners MS, Becker S, Guzman RJ, et al. Duplex scan-directed placement of inferior vena cava filters: a five-year institutional experience. J Vasc Surg. 2002;35:286–91.
15. Ashley DW, Gamblin TC, Burch ST, et al. Accurate deployment of vena cava filters: comparison of intravascular ultrasound and contrast venography. J Trauma. 2001;50:975–81.
16. Ebaugh JL, Chiou AC, Morasch MD, et al. Bedside vena cava filter placement guided with intravascular ultrasound. J Vasc Surg. 2001;34:21–6.
17. Bonn J, Liu JB, Eschelman DJ, et al. Intravascular ultrasound as an alternative to positive-contrast vena cavography prior to filter placement. J Vasc Interv Radiol. 1999;10:843–9.
18. Sato DT, Robinson KD, Gregory RT, et al. Duplex directed caval filter insertion in multi-trauma and critically ill patients. Ann Vasc Surg. 1999;13:365–71.
19. Benjamin ME, Sandager GP, Cohn EL, et al. Duplex ultrasound insertion of inferior vena cava filters in multitrauma patients. Am J Surg. 1999;178:92–7.
20. Neuzil DF, Garrard CL, Berkman RA, et al. Duplex-directed vena caval filter placement: report of initial experience. Surgery. 1998;123:470–4.
21. Neuzil DF, Naslund TC, Bass JG, et al. Cost-effective method for bedside insertion of vena caval filters in trauma patients. J Trauma. 1997;43:752–8.
22. Streiff MB. Vena caval filters: a comprehensive·review. Blood. 2000;195:3669–77.
23. Passman MA, Dattilo JB, Guzman RJ, et al. Bedside placement of inferior vena cava filters by using transabdominal duplex ultrasonography and intravascular ultrasound imaging. J Vasc Surg. 2005;42:1027–32.
24. Goldhaber SZ, Elliott CG. Gregory Elliott acute pulmonary embolism: part I: epidemiology, pathophysiology, and diagnosis. Circulation. 2003;108:2726–9.
25. Desciak MC, Martin DE. Perioperative pulmonary embolism: diagnosis and anesthetic management. J Clin Anesth. 2011;23(2):153–65.
26. Kaufman JA, Kinney TB, Streiff MB, et al. Guidelines for the use of retrievable and convertible vena cava filters: report from the society of interventional radiology multidisciplinary consensus conference. J Vasc Interv Radiol. 2006;17:449–59.
27. Dillman JR, Strouse PJ, Ellis JH, Cohan RH, Jan SC. Incidence and severity of acute allergic-like reactions to i.v. nonionic iodinated contrast material in children. AJR Am J Roentgenol. 2007;188(6):1643–7.
28. Fanara B, Manzon C, Barbot O, Desmettre T, Capellier G. Recommendations for intra-hospital transport of critically ill patients. Crit Care. 2010;14(3):R87.
29. Szem JW, Hydo LJ, Fischer E, et al. High-risk intrahospital transport of critically ill patients: safety and outcome of the necessary "road trip". Crit Care Med. 1995;23:1660–6.
30. Steady HE. Patient's outcome: intrahospital transportation and monitoring of critically ill patients by a specially trained ICU nursing staff. Am J Crit Care. 1998;7:282–7.
31. Chiou AC. Intravascular ultrasound-guided bedside placement of inferior vena cava filters. Semin Vasc Surg. 2006;19:150–4.
32. Rectenwald JE, Greenfield LJ, Henke PK, et al. Vena caval interruption procedures. In: Rutherford RB, editor. Vascular surgery. 6th ed. Philadelphia: Elsevier Saunders; 2005. p. 1086–94.
33. Janjua M, Omran FM, Kastoon T, et al. Inferior vena cava filter migration: updated review and case presentation. J Invasive Cardiol. 2009;21:606–10.
34. Wu GS, Gilet A, Kirshbaum M, et al. Inferior vena cava filter migration with severe deformity of filter. J Vasc Interv Radiol. 2009;20:1257–9.
35. Kinney TB. Update on inferior vena cava filters. J Vasc Interv Radiol. 2003;14:425–40.
36. Kinney TB, Rose SC, Weingarten KE, et al. IVC filter tilt and asymmetry: comparison of the over-the-wire stainless-steel and titanium Greenfield IVC filters. J Vasc Interv Radiol. 1997;8:1029–37.
37. Ganguli S, Tham JC, Komlos F, et al. Fracture and migration of a suprarenal inferior vena cava filter in a pregnant patient. J Vasc Interv Radiol. 2006;17:1707–11.
38. Greenfield LJ, Proctor MC. Twenty-year clinical experience with the Greenfield filter. Cardiovasc Surg. 1995;3:199–205.
39. Turba UC, Glaiberman C, Picus D, et al. Management of severe vena cava filter tilting: experience with bard G2 filters. J Vasc Interv Radiol. 2008;19:449–53.

# Intravascular Ultrasound for Venous Stenting and Inferior Vena Cava Filter Insertion

43

Peter Neglén

**Abstract**

Presently venous intravascular ultrasound (IVUS) is mainly used to diagnose venous stenosis, to guide stenting of venous obstruction, and to assist in placement of IVC filters. IVUS visualizes the vessel from inside the lumen outward and penetrates the adjacent structures. It gives the full 360° view of the crosscut vessel lumen, the character of the luminal wall, and possible external compression. For appropriate coverage of the entire lumen in the iliocaval system, an ultrasound frequency of ~12.5 MHz or lower is necessary. The disposable IVUS catheter rides usually coaxially on a guidewire placed in the vein percutaneously. After advancing the IVUS catheter to a level above the area of interest, images are obtained during catheter withdrawal through the lumen and digitally stored.

The diagnosis of ilio-caval outflow obstruction must ultimately be made by morphological investigations, preferably IVUS. The use of IVUS in these patients has the dual purpose of accurately diagnosing the degree, extent, and nature of obstruction and aiding in appropriate placement of the stent. Stenting can be performed without venography, using only IVUS in combination with fluoroscopy.

There has also been a transition from placement of IVC filters in the interventional suite under fluoroscopy with venography to an IVUS-guided bedside deployment. The use of IVUS is obviously beneficial in patients with contraindications to iodinated contrast dye or limitations of radiation exposure. It also decreases the radiation exposure for the interventionalist. Morbidly obese patients may exceed the weight limits of the angiographic table. Prophylactic IVC filters are increasingly placed in critically ill and multiple trauma patients. To transport these ICU patients to an interventional suite is cumbersome.

The cost of the technology has hampered widespread use, but it can be expected that the costs for the equipment will decrease with increased utilization.

**Keywords**

IVUS • Venous imaging • Adjuncts to IVC filter placement

Intravascular ultrasound (IVUS) was introduced in the late 1990s. It was initially used to aid arterial endovascular interventions and was shown to be beneficial for complex procedures and diagnostic dilemmas [1]. Later, IVUS was introduced to assist venous endovascular procedures. Phlebography with the contrast dye injection delineates the lumen of the vessel but does not give any information of the wall or surrounding tissue. Indirect signs may suggest impingement of the vessel wall or luminal irregularities in the presence of post-thrombotic disease. To delineate the lumen adequately, several oblique images have to be acquired. Contrarily, the intravascular ultrasound (IVUS) visualizes the vessel from inside the lumen outward and penetrates the

P. Neglén, M.D., Ph.D.
Department of Vascular Surgery, SP Vascular Center,
3 Parthenonos Street, 4730 Trimiklini, Limassol, Cyprus
e-mail: pneglenmd@gmail.com

A.F. AbuRahma, D.F. Bandyk (eds.), *Noninvasive Vascular Diagnosis*,
DOI 10.1007/978-1-4471-4005-4_43, 

adjacent structures. It gives the full 360° view of the crosscut vessel lumen, the character of the luminal wall, and possible external compression. Although the benefits are obvious, the cost of the technology has hampered its widespread use. Presently venous IVUS is mainly used to diagnose venous stenosis, to guide stenting of venous obstruction, and to assist in placement of IVC filters.

## The IVUS Catheter Technique

The IVUS catheters are disposable and designed in two configurations: rotating mirror catheter and multiple array transducers catheter. The rotating design type consists of an acoustic mirror and transducer assembly at the tip of the catheter. The mirror is rotated by a wire inside the catheter attached to a motor drive. The chamber in which the mirror rotates is filled with saline, taking care to avoid introduction of air bubbles. The signal travels from the rotating mirror through the fluid-filled chamber to the transducer, producing a 360° cross-sectional image. An example of this design is the Atlantis® SR Proimaging catheter used with the iLAB® imaging system (Boston Scientific Corporation, Natick, MA, USA). The multi-array IVUS design incorporates multiple crystals surrounding the tip of the catheter (360°), has no movable parts, and no chamber, and thus does not require any fluid injection. The multiple signals from each crystal are integrated into a cross-sectional image. An example of this configuration is the Visions® PV8.2F imaging catheter connected to the s5 imaging system either based in a separate movable tower or integrated into the interventional laboratory setup (Volcano™ Therapeutics Inc., Rancho Cordova, CA, USA).

Each individual catheter comes with a preset frequency. The depth of penetration is greater with lower frequency, while the resolution improves with higher frequencies. For appropriate coverage of the entire lumen in the ilio-caval system, a catheter of ~12.5 MHz or lower is usually utilized. This frequency will penetrate to a depth of at least 30 mm. Optimal visualization is obtained when the catheter runs in the center of the vessel with the crosscut area perpendicular to the wall. Owing to the curvature of the vessel, the catheter is, however, not always tracking in the center but runs along the wall in an eccentric position. The resulting crosscut lumen area is, therefore, not necessarily perpendicular to the longitudinal axis of the vessel (Fig. 43.1). The oblique crosscut area may be oblong and may not represent the true lumen area. With the off-center position, the ultrasound must commonly penetrate the entire diameter of the large venous capacitance vessels. With outside compression and oblique projection, the longest diameter may even exceed 30 mm.

The IVUS catheter is placed in the vein percutaneously. Following an ultrasound-guided cannulation, a guidewire (usually 0.035 in.) is inserted and manipulated into the intended position depending on the type of intervention. A sheath (usually 8–9F) is placed percutaneously to facilitate repeated access. The IVUS catheter is threaded over the guidewire to assist the passage of the catheter within the venous lumen. The catheter rides either coaxially over the guidewire, which is placed in a central lumen along the catheter, or in a monorail fashion, where the catheter is attached only at the distal 1–2 cm of the tip. The coaxial placement of the guidewire improves tracking and prevents kinking, and thus has an advantage in that aspect. A monorail-style catheter may be problematic when a tight stenosis or severe tortuosity of the vein is encountered. Advancing the catheter and the guidewire as one unit may sometimes facilitate passage. After advancing the IVUS catheter to a level above the area of interest, images are obtained during catheter withdrawal through the lumen. This is performed slowly manually or by a mechanical pullback device. This allows a smooth and continuous image acquisition, which is not always possible during insertion of the catheter. The images are seen in real time and may be stored digitally for later analysis by the built-in software of the ultrasound imaging system.

Bright echoes are produced close to the high frequency ultrasound tip, which is more noticeable with the multi-array IVUS catheter (Fig. 43.1). This catheter allows digital subtraction of the artifact, the so-called ring down, but in so doing limits the visualization close to the catheter. This maneuver is not necessary with the rotating mirror catheter. The guidewire in the monorail system often creates an acoustic shadow, hiding a wedge of the crosscut area. This error is not seen with coaxial guidewires. By rotating the IVUS catheter, the "shadowed" areas can be visualized (Fig. 43.1).

The anatomic orientation of the visualized structures is often not accurate. The image is variably rotated. The only way to correctly orientate the field during ilio-caval imaging is to relate the image to the position of constant anatomic landmarks. The right renal artery most commonly crosses posterior to the IVC; the right common iliac artery crosses above the left common iliac vein, which is anterior to the dense bone; and the iliac artery is usually lateral and anterior to the iliac vein (Fig. 43.2). The anatomic orientation, however, is not a major issue in diagnosis of venous obstruction or venous stenting or placement of IVC filters.

**Fig. 43.1** The bright echoes close to a multi-array catheter may be "ringed down" (*top*). The guidewire of a monorail type of catheter may create a wedge-formed acoustic shadow. By rotating the catheter, the hidden areas can be visualized (*middle*). Rarely is the IVUS catheter tracking in the center of the vessel to register a true crosscut area. An eccentric position of the IVUS may exaggerate the lumen (*bottom*)

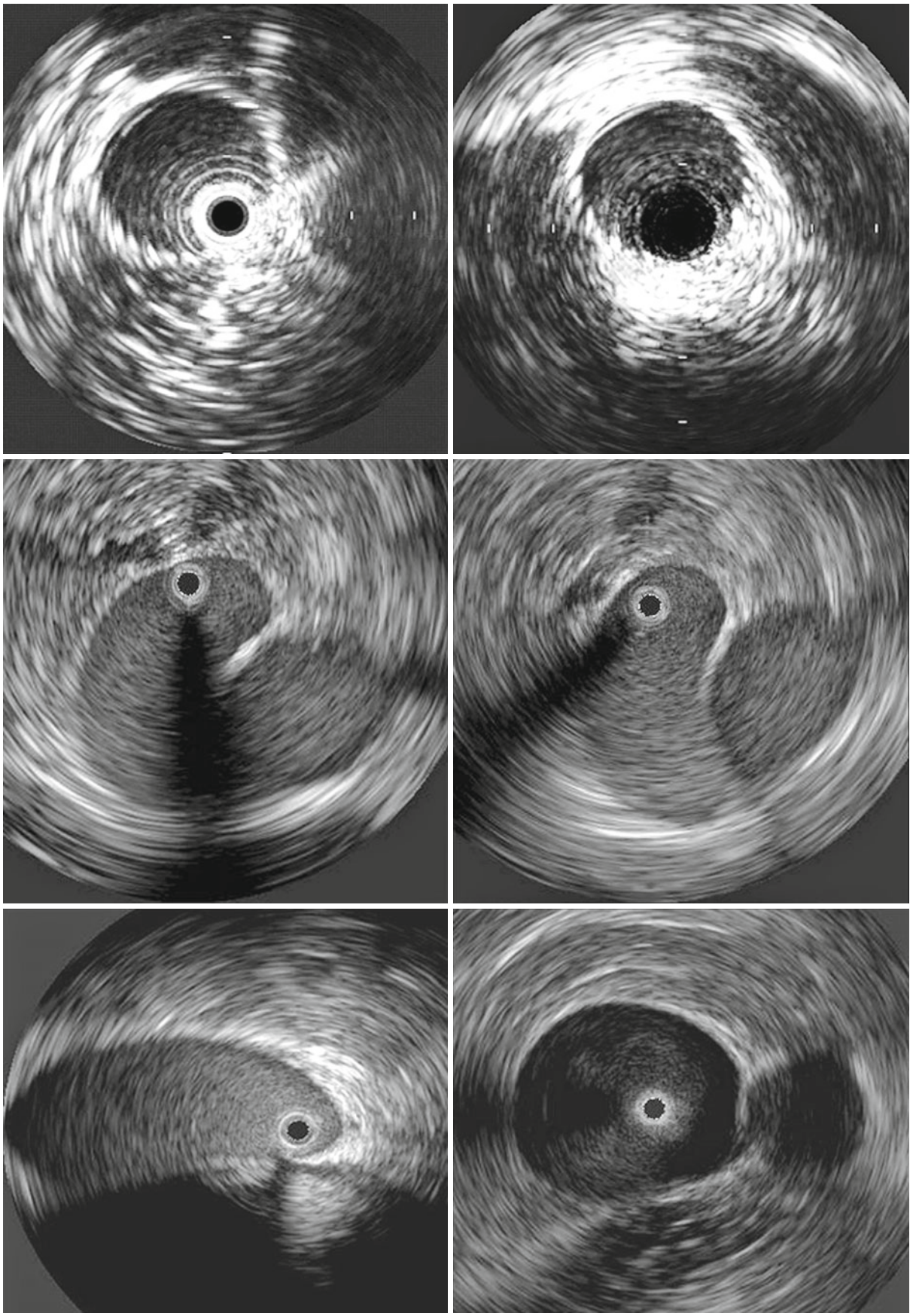

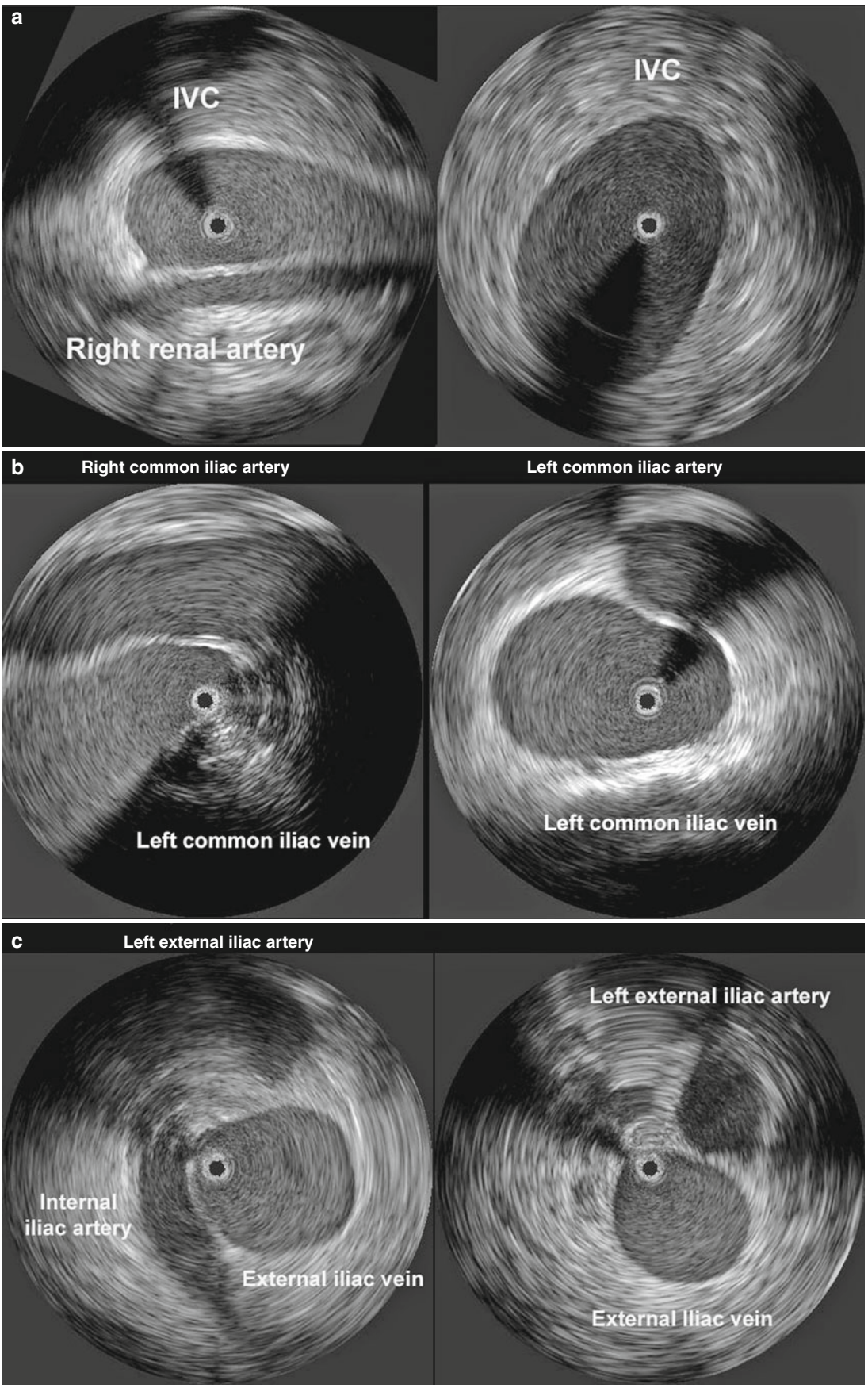
a
IVC
Right renal artery
IVC
b
Right common iliac artery
Left common iliac artery
Left common iliac vein
Left common iliac vein
c
Left external iliac artery
Internal iliac artery
External iliac vein
Left external iliac artery
External Iliac vein

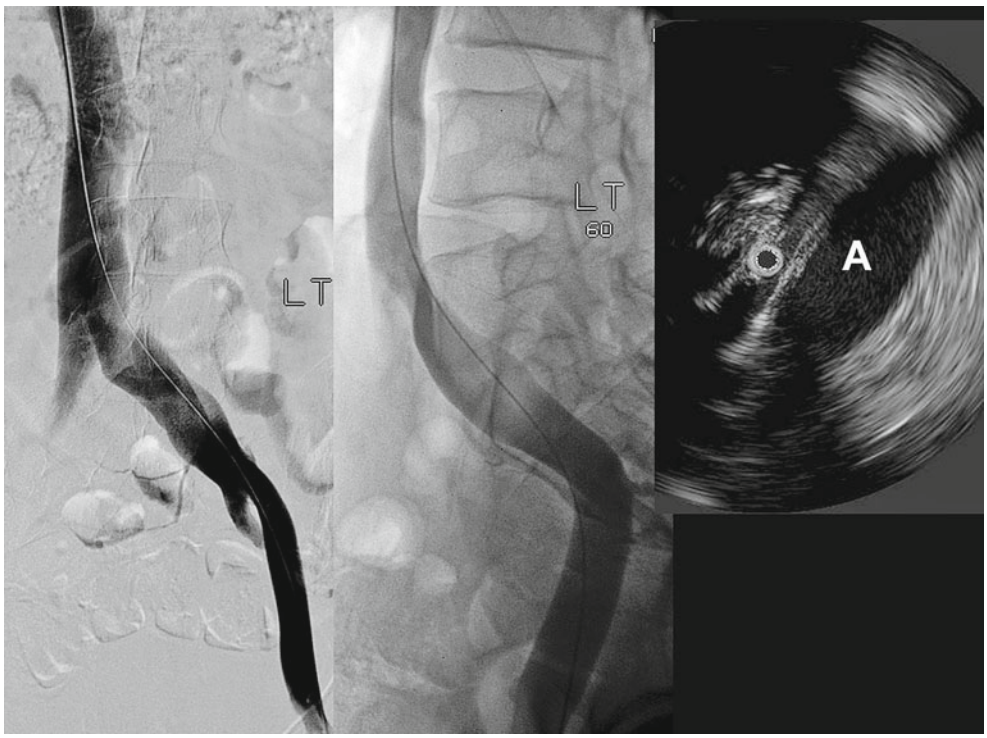


**Fig. 43.3** Transfemoral venogram in AP view (*left*) and with 60° rotation (*middle*). The right common iliac artery (*A*) makes a distinct corkscrew-like impression on the vein in the oblique projection, while only a slight translucency is seen on the AP view. The severity of the stenosis at the vessel crossing is better appreciated on IVUS. The *black circle* within the vein is the IVUS catheter (*right*)

## Diagnostic Venous IVUS

Venoplasty and stenting of the iliac vein is presently the "method of choice" in the treatment of ilio-caval chronic venous obstruction [2–9]. The importance of venous outflow obstruction in the pathophysiology of chronic venous disorder has been increasingly recognized, and it is apparent that reflux alone cannot explain the symptoms and signs of many patients. Although it is previously well known that the combination of reflux and obstruction creates the worst scenario, iliofemoral outflow obstruction may play a larger role in the pathophysiology of chronic venous disorders than previously thought. The iliac vein is the common outflow tract of the lower extremity and chronic obstruction of this segment appears to result in more severe symptoms than does lower segmental blockage. Distal obstructions appear to be better compensated by collateral formation than are proximal lesions. Therefore, the ilio-caval venous segment has been the target area for balloon dilation and stenting.

Since it is not known at what degree of obstruction the venous flow is restricted, no tests are presently available for the accurate diagnosis of hemodynamically significant venous outflow obstruction [10]. Commonly used routine non-invasive tests such as outflow air or strain-gauge plethysmographic tests and duplex Doppler ultrasound may indicate an outflow obstruction, but a normal test does not exclude significant ilio-caval blockage. Even invasive pressure tests, e.g., femoral exercise pressures, arm-foot venous pressure differential and hyperemia-induced pressure increase, are not sufficiently accurate. Presently, the diagnosis of outflow obstruction must ultimately be made by morphological investigations.

A single-plane transfemoral antegrade venogram is the routine morphologic investigation of the ilio-caval outflow. This type of venogram in the anterior-posterior plane is inferior to multiple oblique imaging, especially in the presence of iliac compression from external structures. These lesions compress the vein in different body planes and may therefore be visualized only in certain projections. Using angiographic techniques including subtraction and power injection of contrast dye further increases the sensitivity (Fig. 43.3). Even multi-plane venogram, however, may underestimate the

**Fig. 43.2** (**a**) Constant anatomic landmarks allow a correct rotation of the IVUS catheter. The right renal artery usually traverses posterior to the IVC (*left*). The aorta along the normal below-renal IVC is not seen with this magnification (*right*). The *black circle* within the vein is the IVUS catheter. (**b**) The right iliac artery crosses anterior to the left iliac vein, sometimes creating varying degrees of compression (*left*). The left- and right common iliac artery follow the vein in an anterolateral position (*right*). The *black circle* within the vein is the IVUS catheter. (**c**) The internal iliac artery crosses over the iliac vein medially as it leaves the common iliac artery and dives down into the pelvis following the internal iliac vein (*left*). The external iliac artery continues distally in the anterolateral position to the vein (*right*). The *black circle* within the vein is the IVUS catheter

severity and extent of the obstructive lesion as compared to direct imaging by IVUS, which is currently superior to any other imaging technique of venous ilio-caval outflow. Development of new MR-venography and spiral CT techniques may in the future replace invasive morphologic studies, but needs validation by IVUS. Although definition of a hemodynamically significant venous stenosis is lacking, a morphological obstruction of >50% stenosis has arbitrarily been chosen to be significant because of favorable clinical response when stented [11]. The treatment of choice of venous outflow obstruction is balloon venoplasty and stenting.

Venous outflow blockage will presently only be found in patients with chronic venous disorders if the treating physician is aware of its potential importance and suspect its presence. It is common to restrict venous workup with duplex Doppler ultrasound of the lower extremity to below the inguinal ligament, and then mainly for detection of reflux. This is insufficient to detect ilio-caval outflow obstruction. A more aggressive approach toward diagnosis is warranted in some patients. Ultrasound investigation should routinely be extended to involve the ilio-caval venous outflow, and in select cases with pertinent symptoms, be complemented by morphological studies such as multi-plane transfemoral venogram or, preferably, IVUS. In our practice, IVUS is used generously in symptomatic patients with venographic findings of stenosis or visualization of collaterals, which can be considered an indicator of obstruction, or when plethysmographic or pressure tests are positive for obstruction. Symptoms may range from painful swelling to severe stages with lipodermatosclerosis or ulcer. Patients of special interest are those with symptoms (especially pain) out of proportion to detectable pathology or those with typical symptoms but no detectable lesions on standard tests, those with no improvement of symptoms after standard treatment, and those with previous deep vein thrombosis. The use of IVUS in these patients has the dual purpose of accurately diagnosing the degree and nature of obstruction and aiding in appropriate placement of the stent.

Using the built-in software program, the actual crosscut lumen area can be calculated by planimetry and the length of different diameters measured (Fig. 43.4). Regardless of its shape and varying diameters in different projections, the true stenosis can be delineated and compared to the non-obstructed proximal or distal vein lumen. Several studies have shown that IVUS is superior in detection of the extent and morphologic degree of stenosis as compared to single-plane venography [2, 12–14]. On average, the transfemoral venogram significantly underestimated the degree of stenosis by 30%. The venogram was actually considered "normal" in at least one-fourth of limbs despite the fact that IVUS showed >50% stenosis [3]. In a similar population of 304 limbs, the stenosis was <50% in 42% of venograms but in only 10% of the IVUS. On the other hand, the venous stenosis was >70% in 32% of venograms, but twice as often with IVUS. Using the IVUS findings as the standard, the venogram had a poor sensitivity (45%) and a negative predictive value of 49% in detecting an obstruction >70% [12]. Another study of 104 limbs has shown similar result for diagnosis of >50% stenosis. Slightly more than half the patients (58%) had significant stenosis by IVUS although 10 limbs had normal venogram and 24 limbs had inaccurate location or extent on venogram. The sensitivity to detect >50% stenosis was 43% and the negative predictive value 56% [15].

The lack of correlation of the extent of venous lesion on venography and findings on IVUS is striking. More often than not, the extent of stenosis in limbs with thrombotic and non-thrombotic obstruction is greater on IVUS. This is of great importance for placement of stents. The true extent and severity of recurrent in-stent stenosis is probably best assessed by IVUS.

Finer intraluminal lesions are difficult to visualize with venography. The injected contrast dye may hide such lesions. Delicate intraluminal details, such as webs, frozen valves, and trabeculations, can be detected by ultrasound, but they are rarely seen on venography (Fig. 43.5) [16]. Despite the high resolution of IVUS, it is inferior to angioscopy in identifying the thin valve leaflets. IVUS failed to detect 76% of valve stations identified by angioscopy [14].

The IVUS can detect varying degrees of echogenicity in intraluminal masses, the vessel wall, and the surrounding tissue. Increased echogenicity of the vessel wall may indicate increased fibrosis and wall thickness often seen in post-thrombotic veins. Varying echogenicity of intraluminal thrombi may correlate with the age of the thrombus. Fresh thrombus appears more hypoechoic than older thrombus and is surrounded by inflammatory edema (Fig. 43.6). This may allow age determination of different parts of an extensive deep vein thrombus. Compliance of the venous wall is reflected by phasic movement during respiration. Lack of respiratory variations of the vein wall indicates less compliance with a stiffer wall. None of these observations are possible with venography. Contrarily, collateral formation is poorly shown by IVUS. Only axial collateral formation in close proximity to the native vein can be detected by IVUS. Venogram may occasionally fail to distinguish these from the main vein [16].

Arterial obstruction is usually due to thickening of the wall with plaque formation. Only rarely does outside compression play a major role. In the venous system, outside compression mainly by arterial structures appears to play a major role even in limbs with ilio-caval post-thrombotic obstruction. The relationship between the left iliac vein compression by the right iliac artery and DVT of the left lower extremity is well known [17]. Typically, a stenosis of the left proximal common iliac vein is caused by compression by the right common iliac artery with secondary band or web

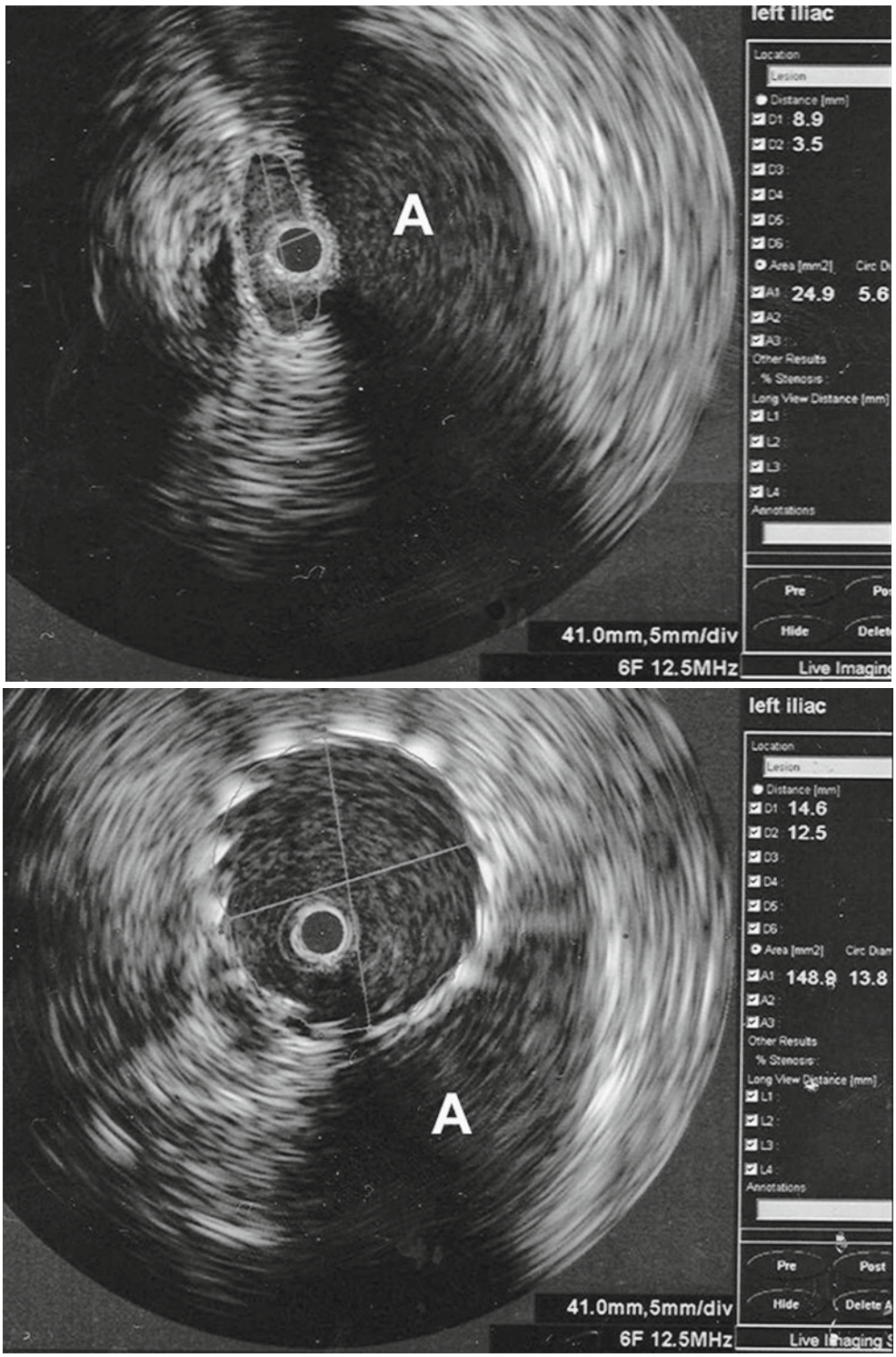


**Fig. 43.4** Measurement of the crosscut area before (*top*) and after venous stenting (*below*). The measurements are displayed at the right aspect of the screen. The area increased from 24.9 to 148.9 mm$^2$ with the dilation. The longest and shortest diameters are given in addition to the calculated diameter as if the measured area represented a circle. The adjacent artery is marked with an *A*. The *black circle* within the vein is the IVUS catheter

formation (Fig. 43.7) [18]. The stenosis is rarely focal when imaged by IVUS. The artery has an oblique course causing a narrowing, although less, along the major length of the common iliac vein. In addition, approximately 30% of the limbs with compression disease have been shown by IVUS to have stenosis beyond the common iliac vein [3]. Although this lesion is classically described to occur in the left iliac vein in younger females, it is not an uncommon finding in males, in elderly patients and in the outflow of the right limb [19]. On venogram such a compression may be indirectly suggested by showing a widening of the iliac vein, a "thinning" of the contrast dye resulting in a translucence of the area, and the presence of transpelvic collaterals, sometimes despite a normal appearance of the iliofemoral vein (Fig. 43.8). With

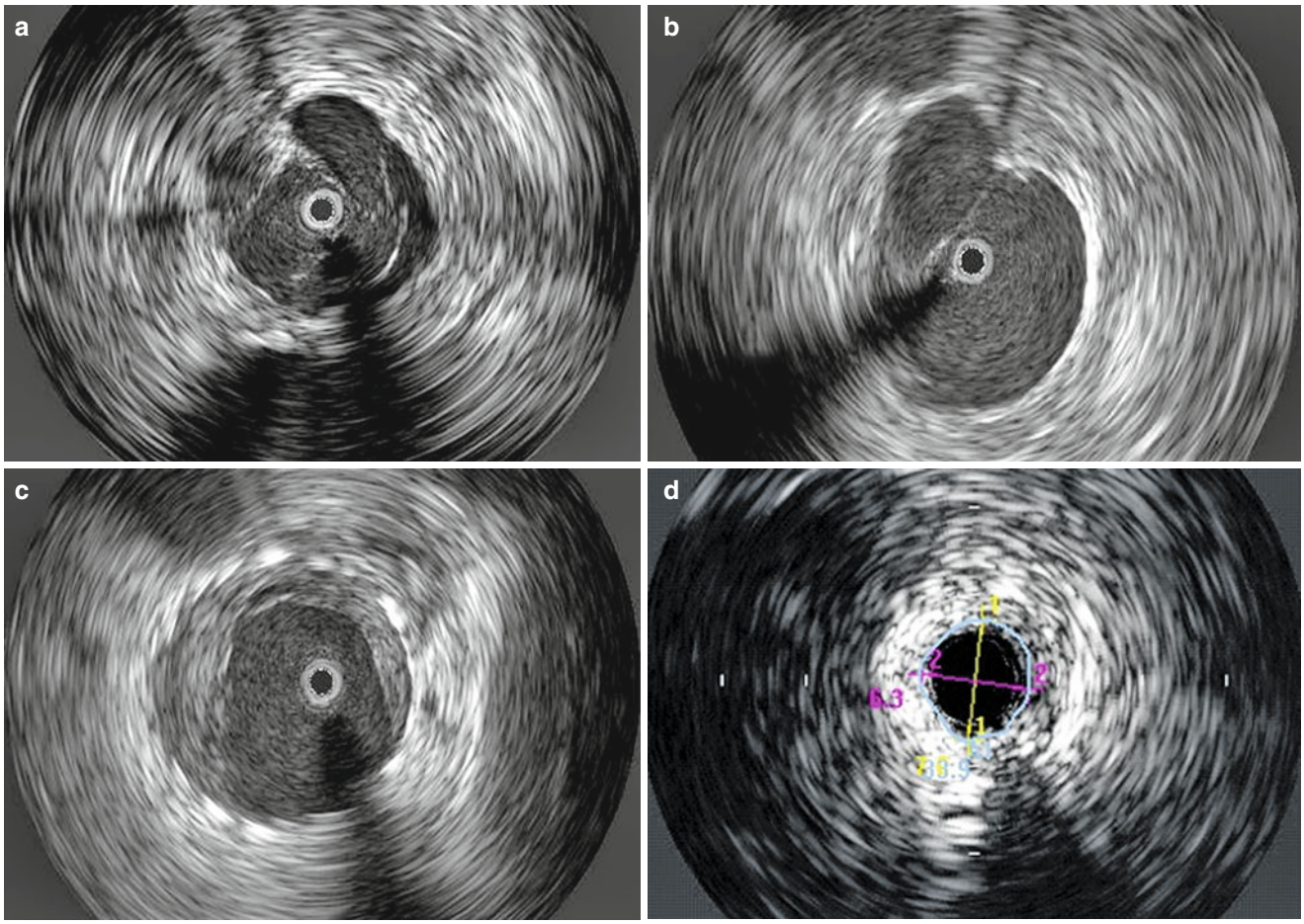


**Fig. 43.5** Images obtained by venous intravascular ultrasound (IVUS): (**a**) Trabeculation with multiple lumina; (**b**) Intraluminal septa; (**c**) In-stent restenosis precisely identifying the stent, neointimal hyperplasia and remaining lumen; (**d**) Compression of the IVC by a circumferentially growing liver cancer. The *black circle* inside the vein represents the inserted IVUS catheter

IVUS, the compressed vein can be clearly delineated between the overriding artery and the posterior bone structure [9, 20]. This compression results in an hourglass deformity of the vein of varying degrees with frequently observed secondary intraluminal lesions such as web formation. The compression visualized by IVUS is more extensive than that shown by venogram. IVUS investigation in 16 limbs with iliac compression syndrome showed that the iliac vein compression extended distally, involving the external iliac or common femoral veins in 68% (11/16). A filling defect representing thrombi was identified in 25% (4/16) and synechia in the compressed vein lumen was seen in 44% (7/16). These additional findings on IVUS led to modification of the intervention in 50% of limbs [13].

## IVUS Assistance During Stenting

As pointed out above, the IVUS is an invaluable diagnostic tool, but it is also vital for correct placement of stents [12, 13, 21]. Ultrasound-guided cannulation of the femoral or popliteal vein caudal to the obstruction is performed, a guide wire is inserted over which an appropriately sized sheath is placed. The guide wire is advanced through the non-occlusive or occlusive obstruction. The IVUS catheter is inserted over the wire and placed cephaled to the obstruction. The images are collected during withdrawal of the catheter. Venoplasty and stent placement are performed after the diagnosis of a >50% obstruction is made. First, the appropriate diameter of the stent is determined by using the IVUS. The lumen dimensions below and above an obstruction can be used for this purpose. In stenosis close to the IVC, the preobstructive dimensions of the vein are usually used. The intrinsic software of the ultrasound machines calculates the greatest and least diameters and the absolute value for the crosscut area. It also calculates a diameter corresponding to the same crosscut area presuming that the area is a perfect circle. This is very helpful in assessing the stent diameter. It is important to oversize the average stent diameter by at least 2–3 mm. Excessive oversizing is rarely a problem in the venous obstruction as compared to the arterial. The risk of rupture with hemorrhage is minimal in the low-pressure venous system. In our experience of more than 1,500

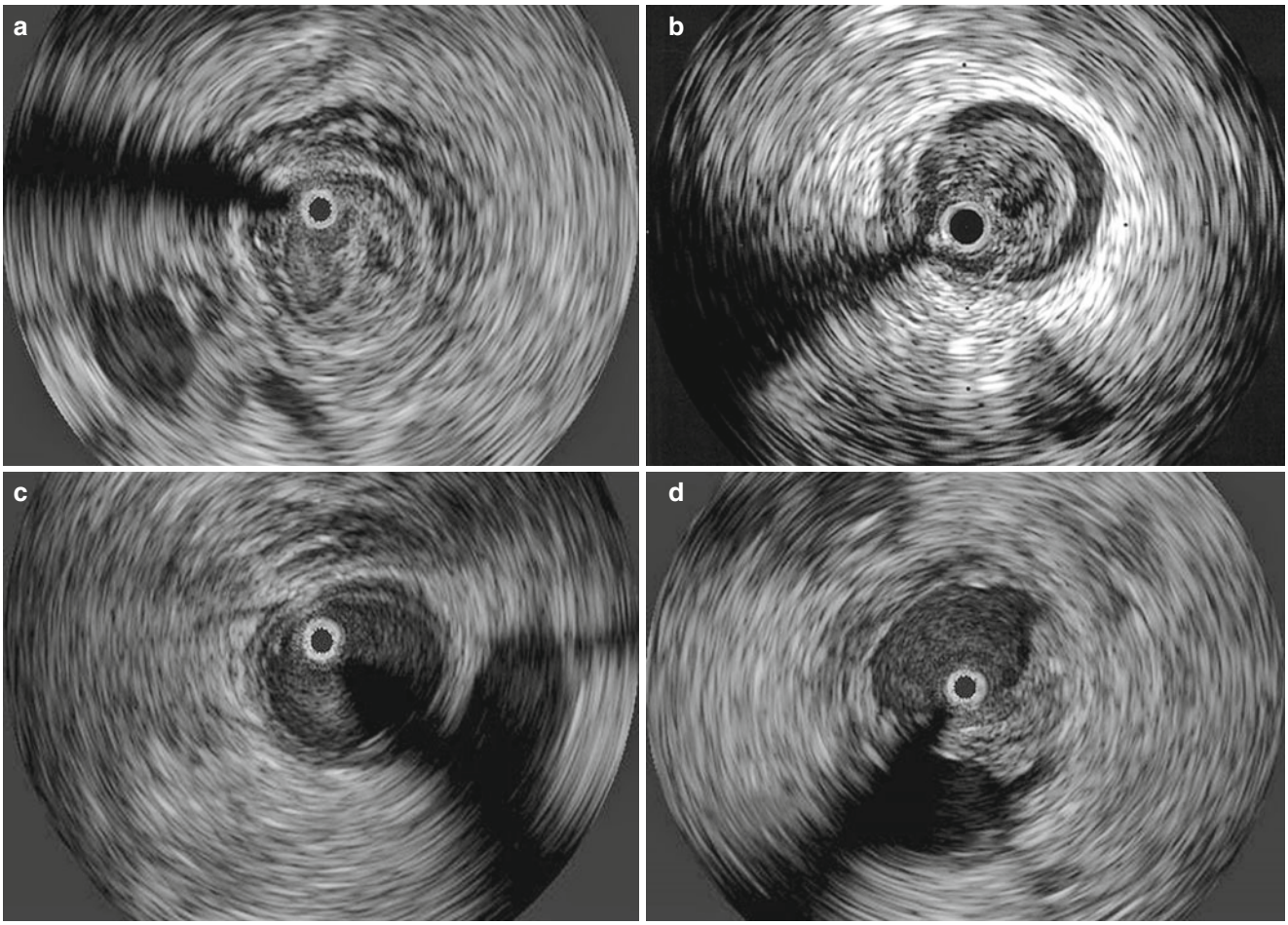


**Fig. 43.6** (**a**) Relatively acute DVT with partial obstruction of the lumen and surrounding inflammatory edema; (**b**) An older, well defined thrombus adherent to the vessel wall, which is fibrosed with increased echogenicity; (**c**) Complete clearance of a thrombus after lysis, but edema of the vessel wall (double-contour) remains; (**d**) Partial lysis of a thrombus after lysis, but the vessel is more than 50% patent. The *black circle* inside the vein represents the inserted IVUS catheter

venous stent procedures, no clinical rupture has occurred although completely occluded veins have been dilated to 12–16 mm width. Dissection of the vascular wall does not develop in the vein owing to a different wall structure and disease process than found in the artery. The venous wall is more homogenous with post-inflammatory fibrosis as compared to the arteriosclerotic wall with heterogeneous plaque formation with varying calcifications. On the other hand, undersizing a venous stent is often problematic. Insertion of a stent with too small a diameter will not allow a satisfactory fixation to the venous wall and may result in an immediate proximal migration. This will necessitate percutaneous stent recovery from the IVC or right atrium, which may be a laborious undertaking.

After determining the stent diameter, it is vital to identify by IVUS the proximal and distal disease-free endpoints of the area to be stented. When treating a stenosis close to the confluence of the iliac veins and the IVC with a Wallstent,™ it is important to place the top of the stent well into the IVC. The braided nature of that stent may otherwise result in retrograde migration (squeezing) of the stent when the proximal end is placed too near the stenosis [2]. Nitinol stents are supposed to be placed just at the confluence, which is difficult without the assistance of IVUS. As described above, the diseased vein segment is frequently more extensive in reality than appreciated by venography. Therefore, the accurate extent of the diseased venous segment is determined by measuring the length of withdrawal of the IVUS catheter from proximal to distal landing points. IVUS is essential in recanalization of occluded iliofemoral veins. The recoil is frequently complete and, short of performing a contralateral transfemoral venogram, IVUS is the only way to determine the stenting endpoints adequately. It is vital to cover the entire obstruction as outlined by the IVUS to avoid early restenosis and occlusion and ensure a sufficient venous inflow to maintain patency.

The guidewire is kept in place throughout the stenting procedure. The IVUS is repeated after stent placement and dilation of the stent (Fig. 43.8). The degree of recoil and the apposition to the venous wall can be visualized and repeat dilation or additional stenting can performed as necessary.

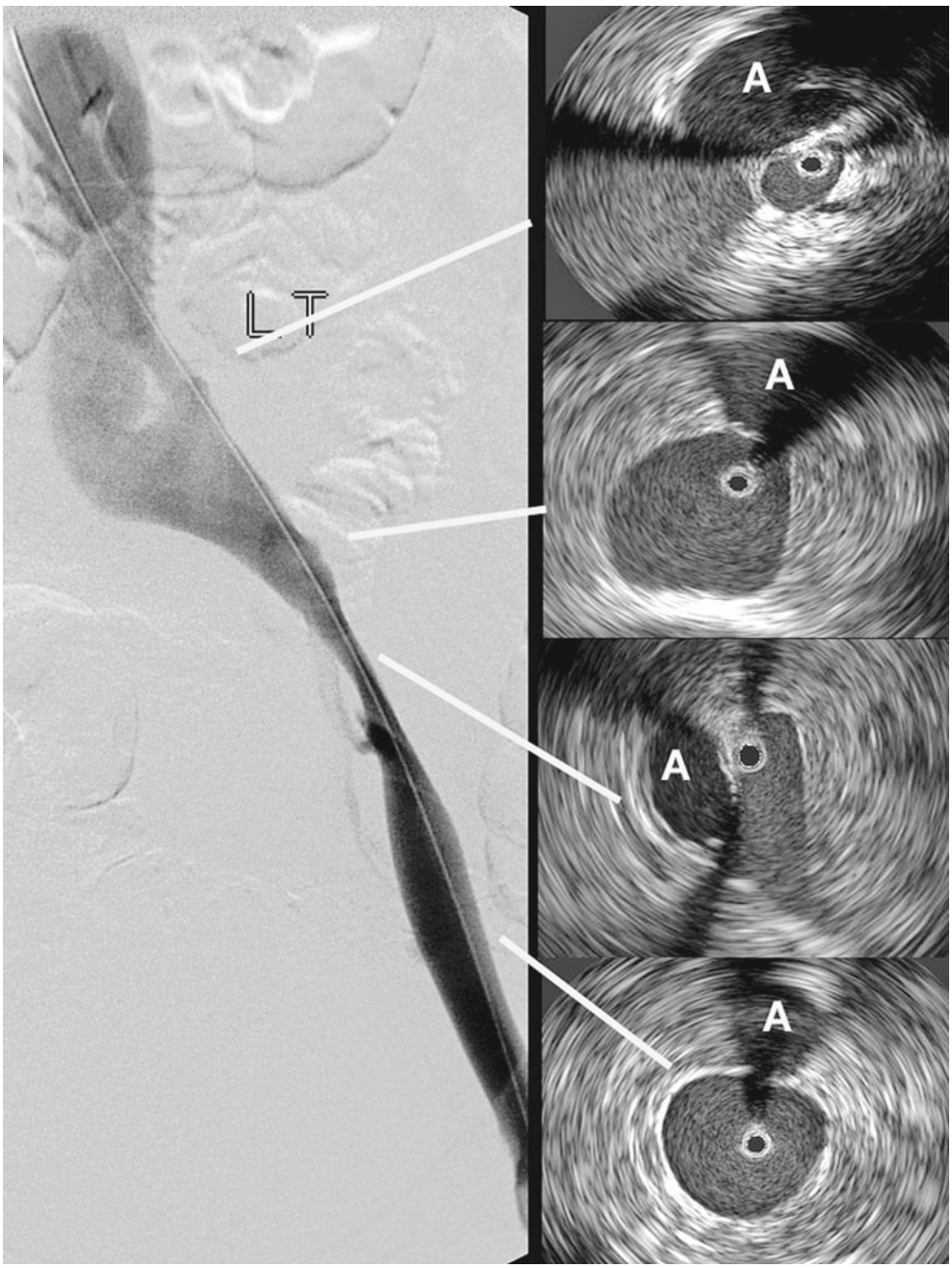


**Fig. 43.7** IVUS images and corresponding transfemoral venogram show a complex non-thrombotic obstruction due to an iliac compression syndrome. The common iliac vein is compressed in the frontal plane with a formation of septum clearly shown by IVUS. The external iliac vein is compressed in the saggital plane by the internal iliac artery. The adjacent artery is marked with an *A*. The *black circle* within the vein is the IVUS catheter

The use of IVUS decreases considerably the use of contrast during the stenting procedure. If there are absolute or relative contraindications to the use of contrast dye, the procedure can be performed completely without venography, using only IVUS in combination with fluoroscopy.

The role of IVUS in diagnosis of morphologic venous outflow obstruction may in the future be replaced by non-invasive studies or MR-venography or spiral CT of later generations. However, the additional information obtained by using IVUS as an adjuvant tool at the stenting procedure (accurate degree and extent of obstruction and finding of previously non-revealed lesions) is most valuable and will be difficult to replace. Presently, I consider the use of IVUS vital for adequate stenting of venous obstructions.

## IVUS and Placement of IVC Filters

The use of IVC filters has increased exponentially the last few years, especially for temporary prophylaxis for potential pulmonary embolism. During the last decade, there has been a transition from placement of IVC filters in the interventional suite under fluoroscopy and determination of filter site by transfemoral venography to a safe and relatively simple

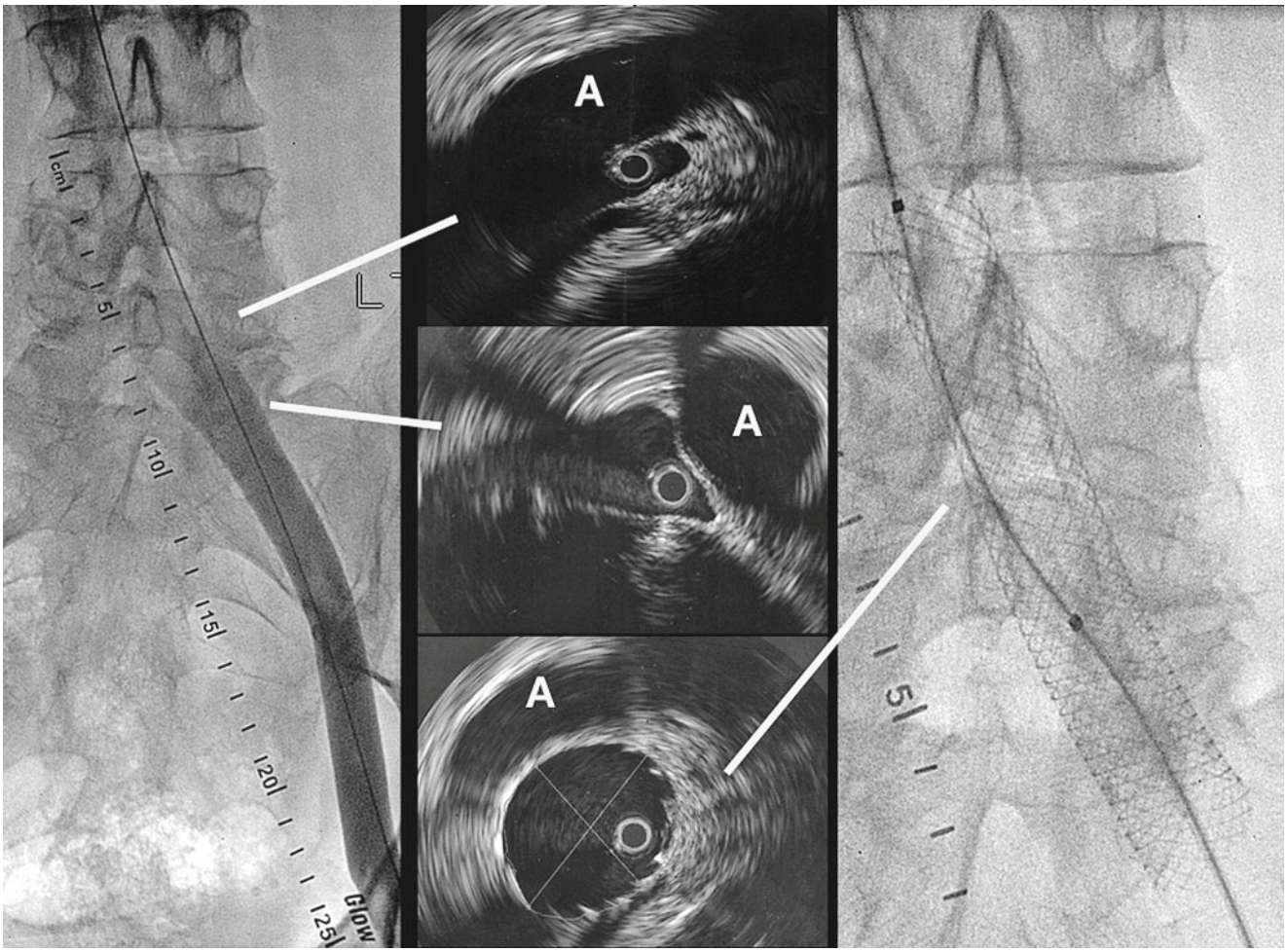


**Fig. 43.8** AP view of transfemoral antegrade venogram, which appears normal with no obvious stenosis or collateral formation (*left*). IVUS of the same vein at different levels shows severe proximal common iliac vein (CIV) stenosis due to compression by the crossing iliac artery and partial obstruction of the mid-CIV (*top and middle, center*). A stent was inserted (*right*) and the final result shown by IVUS (*bottom, center*). The adjacent artery is marked with an *A*. The *black circle* within the vein is the IVUS catheter

IVUS-guided bedside deployment. The use of IVUS is obviously beneficial in patients with contraindications to iodinated contrast dye or limitations of radiation exposure, e.g., in patients with renal insufficiency, severe allergy to iodine, or during pregnancy. It also decreases the radiation exposure for the interventionalist. Morbidly obese patients may exceed the weight limits of the angiographic table. Prophylactic IVC filters are increasingly placed in critically ill patients and in cases with multiple traumas. To transport these ICU patients to the interventional suite is cumbersome. Bedside external ultrasound has previously been used to guide placement in these patients. This can, however, be difficult in obese patients, patients with abdominal injuries or wounds, and during pregnancy. The difficulty to visualize the IVC and the renal veins in these patients lead to a higher failure rate of 10.8–15% (failure of proper deployment in the infrarenal IVC) [22]. IVUS is a better alternative for placement guidance in those patients. When patients performed in the interventional suite, the rate misplacement of IVC filters are rare (0.7–2.0%) when placed under imaging [23]. In recent reports, the use of IVUS alone for deployment has shown a failure rate of ~3% [24–26]. IVUS does not add to the risk of venous access thrombosis. The rate of thrombosis at the femoral insertion site of all techniques varies between 3% and 12% [27]. Rosenthal et al. reported, however, only one access site thrombosis in 94 cases (1%) following bedside IVUS-guided filter insertion [25].

## Techniques of IVUS-Guided Filter Placement

There are several techniques described. They have several basic steps in common. Before the vein is accessed, bilateral femoral ultrasound is performed to ensure that there is no obstruction at the intended access site. If available, a previous CT scan can give additional information in this regard

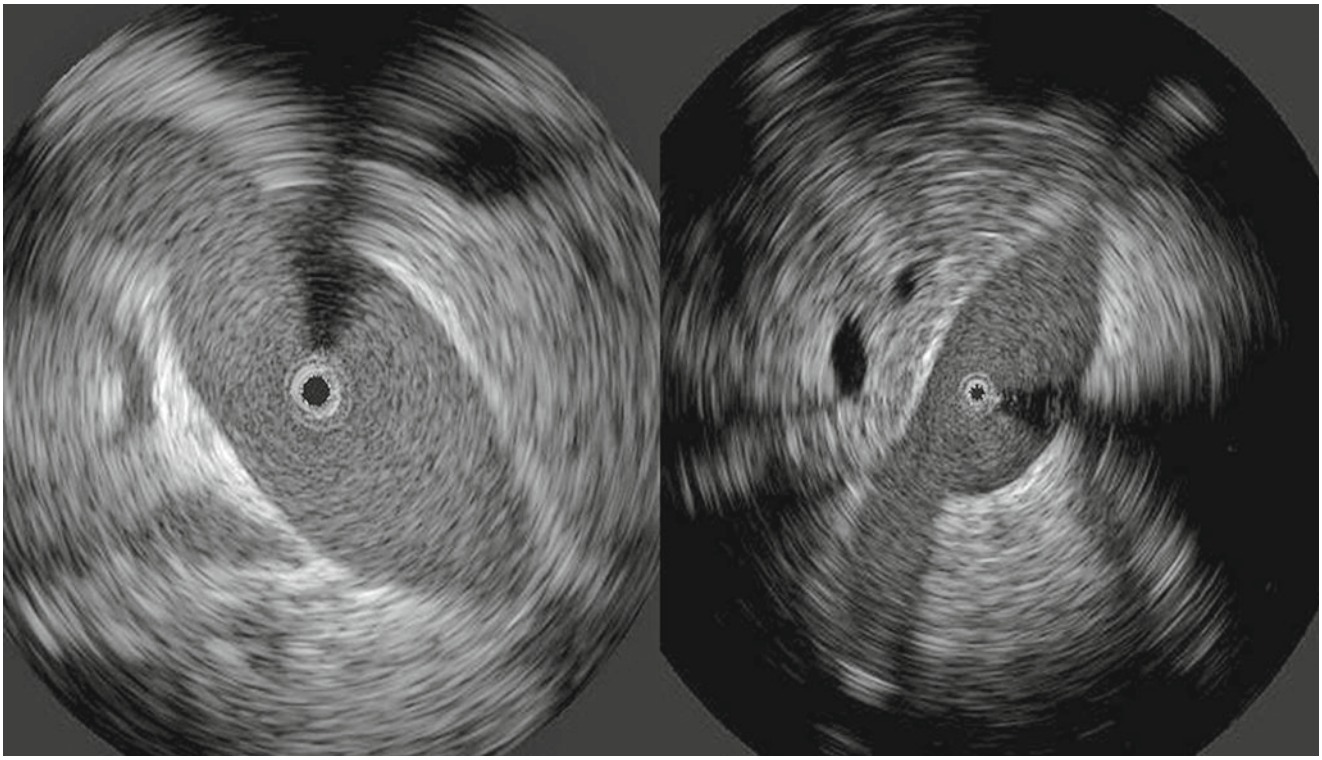

**Fig. 43.9** The tip of the IVUS catheter (the *black circle*) is placed at the level of the lowest renal vein. The contralateral, slightly more cephaled vein is also vaguely visualized. This is the intended level of the tip of the IVC filter. These structures in addition to the right renal artery crossing should always be visualized before filter placement

and also elucidate the presence of any venous anomaly. Most often, the right common femoral vein is used because of the less acute angle at the ilio-caval confluence, but the left common femoral or the jugular veins are alternative access points. After ultrasound-guided access, placement of a 0.035-in. guidewire into the IVC and sheath placement, the IVUS is inserted and pushed cephaled to the atrium. During pullback of the catheter, images are acquired and the hepatic and renal veins are identified (Fig. 43.9), the traversing of IVC by the right renal artery is visualized (Fig. 43.2a), absence of a caval thrombosis is verified, and the ilio-caval confluence located. The infrarenal IVC diameter is measured in two planes to ensure that the appropriate filter is used. The cephaled level of the filter is located by the IVUS probe to be just below the level of the most caudal renal vein or at the renal artery crossing. From this level, the IVC filter will be deployed caudally ensuring a placement in the infrarenal IVC with the tip at or just below the level of the renal veins. A bedside anterio-posterior abdominal plain X-ray is usually performed postintervention to record the location of the IVC filter, its proper opening, and presence of any significant tilt.

The described basic goals can be achieved by a single-puncture technique with external reference; double-puncture, unilateral or bilateral techniques with deployment under direct vision; or single-puncture technique with sheath reference. Matsumura's group initially reported the bedside IVUS technique to place IVC filters in 1999 [28]. After single access, the site of the IVC filter was determined as described above. The inserted length of the IVUS catheter was marked externally on a measuring tape on the drape. This length was then referenced to the length of the deployment device. After removal of the IVUS catheter, the IVC filter device was inserted to the same length and deployed blindly. The external reference was felt to be imprecise. Although the results were good, other techniques were developed.

Using the double-puncture technique, two different accesses are obtained, one for the IVUS catheter and one for the filter device [29, 30]. The two punctures are either made in the unilateral femoral vein, 1 cm apart or bilaterally in the common femoral veins. After deciding the level of deployment by the IVUS images, the top of the filter is placed adjacent to the IVUS head under direct vision by the IVUS. The IVUS is withdrawn to below the filter to prevent entanglement with the release of the filter, the device sheath withdrawn to this lower level, and the filter released precisely. The IVUS probe may be carefully advanced through the filter after the deployment if no resistance is encountered. Repeat imaging can confirm that the tip of the filter is positioned at the level of the renal veins and that the filter legs are engaging the IVC wall. Although never proven, it is felt that two femoral puncture sites increase the risk of access site

thrombosis and a more precise single stick procedure would have less complication and be simpler.

If the size of the sheath for the IVUS catheter and the sheath for the selected IVC filter deployment device is the same or larger, a modified precise single-access technique can be used [31]. The IVUS probe is placed through the IVC filter introducer sheath and the filter landing site is located below the renal veins as described above. The long sheath is pushed over the IVUS catheter until it is shown on the IVUS image. While keeping the IVUS catheter in a fixed position, the sheath can be moved back and forth over the IVUS catheter head until precise placement of the top of the sheath is ensured. The IVUS catheter is removed and the device, e.g., a Celect™ or Günther-Tulip™ filter (Cook Medical, Bloomington IN, USA), is advanced into the sheath and deployed identical to the deployment under fluoroscopic guidance. This method is certainly the most elegant of all the methods. A modified technique can be used for the Greenfield filter. The initial 8F IVUS sheath has to be exchanged for the 15F introducer sheath over a wire and the IVUS catheter reloaded. It is pushed to the top of the sheath, which is placed precisely below the renal veins. The sheath has to be withdrawn the length of the unreleased Greenfield filter (~7 cm) and the device inserted and released in a routine manner [32].

All these blind bedside techniques require practice and there is a learning curve. It is recommended that fluoroscopic imaging with venography be initially combined with the IVUS-guided placement. This gives the operator the opportunity to correlate the IVUS images with venographic findings and actually observe the deployment, which otherwise is blind. It has been suggested that 20 cases should be performed in the interventional suite before one embark on the bedside techniques solely guided by IVUS. The future may see IVUS incorporated into guidewires or deployment devices.

Although intuitively one would think that the simpler bedside IVUS-guided IVC filter technique should be less costly, this has not been proven. This may be due to the capital investment of the ultrasound machine and the high cost of the individual disposable IVUS probes. However, the potential savings by less use of staff and general resources, the avoidance of transportation of critically ill or injured patients to the interventional suite, the decreased radiation exposure to patient and interventionalist, and the absence of contrast dye complications are difficult to assess. It can be expected that the costs for the equipment will decrease with increased use of IVUS and this will make it more readily available.

## Other Potential Applications

The IVUS is a valuable adjuvant to surgical thrombectomy or thrombolysis of iliofemoral DVT. Remaining thrombus attached to the wall, the age of the thrombus, post-lytic edema of the venous wall, and possible external compression may be identified (Fig. 43.6). This may assist in determination of the duration of lytic treatment and any adjuvant stent placement.

## References


1. Nishanian G, Kopchok GE, Donayre CE, White RA. The impact of intravascular ultrasound (IVUS) on endovascular interventions. Semin Vasc Surg. 1999;12:285–99.
2. Neglén P, Raju S. Balloon dilation and stenting of chronic iliac vein obstruction: technical aspects and early clinical outcome. J Endovasc Ther. 2000;7:79–91.
3. Neglén P, Berry MA, Raju S. Endovascular surgery in the treatment of chronic primary and post-thrombotic iliac vein obstruction. Eur J Vasc Endovasc Surg. 2000;20:560–71.
4. Raju S, Owen Jr S, Neglén P. The clinical impact of iliac venous stents in the management of chronic venous insufficiency. J Vasc Surg. 2002;35:8–15.
5. Raju S, McAllister S, Neglén P. Recanalization of totally occluded iliac and adjacent venous segments. J Vasc Surg. 2002;36:903–11.
6. Juhan C, Hartung O, Alimi Y, Barthelemy P, Valerio N, Portier F. Treatment of nonmalignant obstructive iliocaval lesions by stent placement: mid-term results. Ann Vasc Surg. 2001;15:227–32.
7. Nazarian GK, Austin WR, Wegryn SA, et al. Venous recanalization by metallic stents after failure of balloon angioplasty or surgery: four-year experience. Cardiovasc Intervent Radiol. 1996;19:227–33.
8. Blattler W, Blattler IK. Relief of obstructive pelvic venous symptoms with endoluminal stenting. J Vasc Surg. 1999;29:484–8.
9. Hurst DR, Forauer AR, Bloom JR, Greenfield LJ, Wakefield TW, Williams DM. Diagnosis and endovascular treatment of iliocaval compression syndrome. J Vasc Surg. 2001;34:106–13.
10. Neglén P, Raju S. Proximal lower extremity chronic venous outflow obstruction: recognition and treatment. Semin Vasc Surg. 2002;15:57–64.
11. Neglén P, Hollis KC, Olivier J, Raju S. Stenting of the venous outflow in chronic venous disease: long-term stent-related outcome, clinical, and hemodynamic result. J Vasc Surg. 2007;46:979–90.
12. Neglén P, Raju S. Intravascular ultrasound scan evaluation of the obstructed vein. J Vasc Surg. 2002;35:694–700.
13. Forauer AR, Gemmete JJ, Dasika NL, Cho KJ, Williams DM. Intravascular ultrasound in the diagnosis and treatment of iliac vein compression (May-Thurner) syndrome. J Vasc Interv Radiol. 2002;13:523–7.
14. Satokawa H, Hoshino S, Iwaya F, Igari T, Midorikawa H, Ogawa T. Intravascular imaging methods for venous disorders. Int J Angiol. 2000;9:117–21.
15. Hingorani A, Alhabouni S, Ascher E, et al. Role of IVUS versus venograms in assessment of iliac-femoral vein stenosis. J Vasc Surg. 2011;52:804.
16. Neglén P, Raju S. In-stent recurrent stenosis in stents placed in the lower extremity venous outflow tract. J Vasc Surg. 2004;39:181–7.
17. Cockett FB, Thomas ML, Negus D. Iliac vein compression. Its relation to iliofemoral thrombosis and the post-thrombotic syndrome. Br Med J. 1967;2:14–9.
18. Negus D, Fletcher EW, Cockett FB, Thomas ML. Compression and band formation at the mouth of the left common iliac vein. Br J Surg. 1968;55:369–74.
19. Raju S, Neglén P. High prevalence of nonthrombotic iliac vein lesions in chronic venous disease: a permissive role in pathogenicity. J Vasc Surg. 2006;44:136–43.
20. Ahmed HK, Hagspiel KD. Intravascular ultrasonographic findings in May-Thurner syndrome (iliac vein compression syndrome). J Ultrasound Med. 2001;20:251–6.

21. Neglén P, Tackett Jr TP, Raju S. Venous stenting across the inguinal ligament. J Vasc Surg. 2008;48:1255–61.
22. Sato DT, Robinson KD, Gregory RT, et al. Duplex directed caval filter insertion in multi-trauma and critically ill patients. Ann Vasc Surg. 1999;13:365–71.
23. Aidinian G, Fox CJ, White PW, Cox MW, Adams ED, Gillespie DL. Intravascular ultrasound – guided inferior vena cava filter placement in the military multitrauma patients: a single-center experience. Vasc Endovascular Surg. 2009;43:497–501.
24. Killingsworth CD, Taylor SM, Patterson MA, et al. Prospective implementation of an algorithm for bedside intravascular ultrasound-guided filter placement in critically ill patients. J Vasc Surg. 2010;51:1215–21.
25. Rosenthal D, Wellons ED, Levitt AB, Shuler FW, O'Conner RE, Henderson VJ. Role of prophylactic temporary inferior vena cava filters placed at the ICU bedside under intravascular ultrasound guidance in patients with multiple trauma. J Vasc Surg. 2004;40:958–64.
26. Kassavin DS, Constantinopoulos G. The transition to IVUS-guided IVC filter deployment in the nontrauma patient. Vasc Endovascular Surg. 2011;45:142–5.
27. Joels CS, Sing RF, Heniford BT. Complications of inferior vena cava filters. Am Surg. 2003;69:654–9.
28. Oppar WP, Chiou AC, Matsumura JS. Intravascular ultrasound-guided vena cava filter placement. J Endovasc Ther. 1999;6:285–7.
29. Matsuura JH, White RA, Kopchok G, et al. Vena caval filter placement by intravascular ultrasound. Cardiovasc Surg. 2001;9:571–4.
30. Passman MA, Dattilo JB, Guzman RJ, Naslund TC. Bedside placement of inferior vena cava filters by using transabdominal duplex ultrasonography and intravascular ultrasound imaging. J Vasc Surg. 2005;42:1027–32.
31. Jacobs DL, Motaganahalli RL, Peterson BG. Bedside vena cava filter placement with intravascular ultrasound: a simple, accurate, single venous access method. J Vasc Surg. 2007;46:1284–6.
32. Passman MA. Regarding "bedside vena cava filter placement with intravascular ultrasound: a simple, accurate, single venous access method". J Vasc Surg. 2008;48:257.

# The Role of Duplex Ultrasound Before, During, and After Endovenous Procedures

44

Peter F. Lawrence

**Abstract**

Duplex ultrasound is a critical component of the evaluation of patients with venous insufficiency, as well as being of great value during endovenous procedures and also postprocedure to assess results. Although history and physical exam may identify some venous abnormalities and physicians-in-training are still taught to assess the venous system by physical exam, physical exam is limited in assessing the full range of potential venous abnormalities, particularly those below the skin surface that cannot be easily visualized. Obvious venous diseases such as ulcers, lipodermatosclerosis, visible varicosities, and superficial thrombophlebitis can be identified by physical exam; however, duplex ultrasound is required to determine the anatomy and the location, etiology, and severity of most cases of chronic venous insufficiency. The duplex ultrasound findings of venous thrombosis or occlusion, venous valvular reflux and dilatation, and agenesis or hypoplasia of the superficial and/or deep venous system at various locations in the lower extremity are the key to determining treatment options.

**Keywords**

Assessment of endovenous ablation • Assessment of venous reflux • Duplex scan assessment of venous incompetence • Duplex ultrasound • Endovenous procedures • Saphenous ablation • Ultrasound assessment of venous incompetence • Ultrasound assessment post endovenous ablation • Ultrasound techniques

Duplex ultrasound is a critical component of the evaluation of patients with venous insufficiency, as well as being of great value during endovenous procedures and also postprocedure to assess results. Although history and physical exam may identify some venous abnormalities and physicians-in-training are still taught to assess the venous system by physical exam, physical exam is limited in assessing the full range of potential venous abnormalities, particularly those below the skin surface that cannot be easily visualized. Obvious venous diseases such as ulcers, lipodermatosclerosis, visible varicosities, and superficial thrombophlebitis can be identified by physical exam; however, duplex ultrasound is required to determine the anatomy [1] and the location, etiology, and severity of most cases of chronic venous insufficiency. The duplex ultrasound findings of venous thrombosis or occlusion, venous valvular reflux and dilatation, and agenesis or hypoplasia of the superficial and/or deep venous system at various locations in the lower extremity are the key to determining treatment options [2].

P.F. Lawrence, M.D.
Department of Surgery, Ronald Reagan UCLA Medical Center, 200 Medical Plaza, Suite 510-6, Los Angeles, CA 90095, USA
e-mail: pflawrence@mednet.ucla.edu

## Ultrasound Diagnosis of Venous Disease Preprocedure

### Technique

### Equipment

The venous system can be best evaluated with a 10–12 MHz transducer that images the superficial veins immediately

A.F. AbuRahma, D.F. Bandyk (eds.), *Noninvasive Vascular Diagnosis*,
DOI 10.1007/978-1-4471-4005-4_44, © Springer-Verlag London 2013

under the skin, as well as the deep venous system in normal-sized adults, which may be up to 30 cm deep in an obese patient. Occasionally, a lower 5–10 MHz transducer is needed for very large patients to image the deep veins in the leg. Although portable ultrasound equipment can detect gross changes in the superficial and deep systems, the resolution necessary in some patients to evaluate for chronic changes in the vein wall, reflux in deep veins, etc., makes a high resolution ultrasound system with B mode, color flow, and bidirectional velocity waveforms the optimal system. Since some patients will need to be assessed for venous thrombosis in the calf veins, deep thigh veins, and superficial veins postprocedure, a system with high resolution is also necessary in some of these situations. Our approach is to use a high-resolution scanner for the pre- and post-procedure evaluation and to use a portable scanner for the procedure, when less resolution is required. In addition, some insurance companies require evidence of vein diameter, reflux, and location images that can be viewed prior to authorization. Reports, without images, of findings are often considered inadequate for authorization. A report accompanied by electronically saved images and physiological printouts with vein diameter measurement is frequently required before the procedure is authorized.

## Patient Position

Patients must be examined in both the supine (occasionally prone) and standing positions to evaluate all aspects of venous disease. DVT and venous anatomy are best assessed in the supine position. Valve incompetence, venous reflux, and the maximum diameter of the vein are best measured in the standing position. Most insurance companies will only authorize a venous procedure when it has been performed in the patient in standing position.

## Assessment of the Deep System

The deep venous system must be evaluated for patency or occlusion, valvular reflux, and chronic changes in the wall, which could be indicative of a prior episode of deep venous thrombosis. The initial duplex exam should begin in the supine position. Once the common femoral vein has been identified, it should be assessed for size, reflux with and without a Valsalva maneuver and distal compression, and for chronic wall changes. Common femoral reflux is very common with concomitant saphenous reflux and often is corrected when the saphenous vein reflux is corrected, so common femoral reflux should not be considered as a sign of deep venous insufficiency unless the superficial veins are normal or after they have been ablated. A similar evaluation of the femoral vein (formerly called the superficial femoral vein [3]) and popliteal veins is routinely performed in most vascular labs. The presence of a deep venous occlusion or chronic changes in the vein wall, indicative of a prior episode of deep venous thrombosis, increases the risk of a subsequent DVT, when an endovenous procedure is performed, and so should be noted.

## Assessment of Superficial (Axial) Veins

The most common complaint of patients with varicose veins is the presence of visible varicose veins in the legs, often initially occurring in the medial calf, but also occurring at many other sites in the leg. These varicose veins may be primary (due to superficial venous disease alone), or they may be a reflection of deep venous insufficiency. Assessment of the superficial axial veins, such as the great and small saphenous vein, should be performed by duplex ultrasound, because the proximal portion of these veins is too deep to assess by physical exam alone. Incompetence of the valves at the junction of these veins with the deep system is too deep to be assessed by any technique other than duplex ultrasound exam. Incompetence of the most proximal portion of an axial vein is also often the initial indication of venous insufficiency. Consequently, the size of the axial veins at the junction with the deep system, as well as the degree of reflux, measured in seconds, in the standing position, is the best indicator of superficial venous insufficiency. The great and small saphenous vein can also develop insufficiency without proximal reflux when a perforating vein in the thigh or calf connects to the axial system, and becomes incompetent, with reflux into the superficial system, causing axial vein dilatation and insufficiency. To identify problems all along the axial venous system, duplex ultrasound of the entire great saphenous and small saphenous system should be performed in the standing position.

## Assessment of Perforator Veins

When perforator veins become incompetent, they create ambulatory superficial venous hypertension and ultimately leg swelling, lipodermatosclerosis, and venous ulceration. Perforator incompetence often occurs after an episode of deep vein thrombosis, but may also occur when primary deep valvular incompetence creates venous hypertension, which is then transmitted into the perforator veins. As with superficial and deep veins, perforator incompetence should be assessed in the standing position, and both the length of time in reflux, measured in seconds, as well as the maximum diameter of the vein, is critical in assessing the contribution of the perforator veins to chronic venous insufficiency.

## Assessment of Tributary Veins

Although axial and perforator veins are responsible for the most severe superficial venous disease, tributary vein incompetence, which is frequently the cause of visible varicose veins, is one of the most important venous problems for patients, since they are both symptomatic and the most cosmetically displeasing. These veins should also be assessed in

the standing position by duplex ultrasound and their connection to axial veins, perforators, and the deep system helps to determine the optimal treatment. If these veins directly connect to incompetent superficial axial or perforator veins, then eradication of both the axial or perforator vein and the tributary vein is needed to not only remove the vein but also prevent future recurrence.

## Accredited Vascular Lab Criteria for Venous Insufficiency

There are SVS published vascular lab criteria for venous disease [2], and each insurance company publishes its own criteria.

### Present of Reflux

Most vascular labs consider reflux of >0.5 s in the standing position to indicate venous incompetence, although the longer the reflux, the more severe the venous disease.

### Size of Veins

Currently, most vascular labs consider axial and perforator veins that are >3 mm in diameter and have associated reflux to be abnormal.

### Location of Reflux

Most reflux originates at the junction of the superficial vein with the deep vein, although more distal reflux may occur when incompetent perforators connect the superficial and deep systems.

## Insurance Company Ultrasound Criteria for Authorization of Treatment of Venous Disease

Patients with venous insufficiency who seek treatment usually have medical insurance, and most insurance plans require detailed documentation of the venous system by duplex ultrasound for authorization of procedures (Table 44.1). Although venous disease is unlikely to improve without treatment, most insurance companies require that the duplex ultrasound have been performed within the past 6 months, assuming that an old study may not accurately reflect the location, pathogenesis, and degree of venous insufficiency.

**Table 44.1** Ultrasound criteria used by insurance companies for authorization (endovenous ablation of axial and perforator veins)

| |
|---|
| 1. Vascular lab (accredited) standards |
| (a) Written report that can be reviewed by an insurance company |
| (b) Images recorded and available for review, including anatomy, reflux, and measurements of size |
| (c) Cursor used for electronic measurements and recorded on the image |
| 2. Patient examined in the standing position |
| 3. Reflux, if in great saphenous or small saphenous, present at the junction of the superficial and deep venous system |
| 4. Vein diameter >3 mm (some use >5 mm) |
| 5. Reflux in vein is >0.5 s (some use >1.0 s) |

### Presence of Superficial Reflux

Previously, the simple presence of reflux was all that was required for authorization of an endovenous procedure, but many insurance companies now require that the length of time of the reflux be documented. Although >0.5 s is the SVS vascular lab standard for venous reflux, some health plans now require >1 s of reflux to authorize a venous procedure, based on the rationale that longer reflux time is indicative of more severe venous disease.

### Location of Reflux

Although any refluxing vein can cause symptoms, most insurance authorizations require that the reflux occur at the proximal junction of the superficial vein with the deep venous system. Consequently, duplex scan reports that state that the reflux is at the saphenous-femoral junction or saphenopopliteal junction are less likely to be denied or require a peer-to-peer review. Astute clinicians know that a refluxing distal saphenous vein can be as symptomatic as a refluxing proximal saphenous vein, but there is still a higher likelihood of insurance denial when the reflux occurs distally.

### Size of the Refluxing Vein

Although any refluxing vein can cause symptoms, there are general size criteria, which vary from one insurance company to another. In the western United States, most companies require a vein to be >3 mm to justify insurance coverage and some require a vein to be >5 mm. To achieve this threshold, all patients must be evaluated in the standing position. Since veins dilate during the day and after prolonged standing, we often ask patients with marginal-sized veins to undergo their duplex ultrasound at the end of the day, and after a period of prolonged standing. Since venous symptoms occur at the end of the day, when the veins are most dilated, it seems logical to test patients when they are most symptomatic.

## Role of Ultrasound During Venous Procedures

### Technique

The proper use of duplex ultrasound during an endovenous ablation procedure, whether using a laser or a radiofrequency catheter, is a key to successful ablation. Duplex ultrasound competency by the vascular surgeon is critical for these procedures. An ultrasound transducer should be used to initially

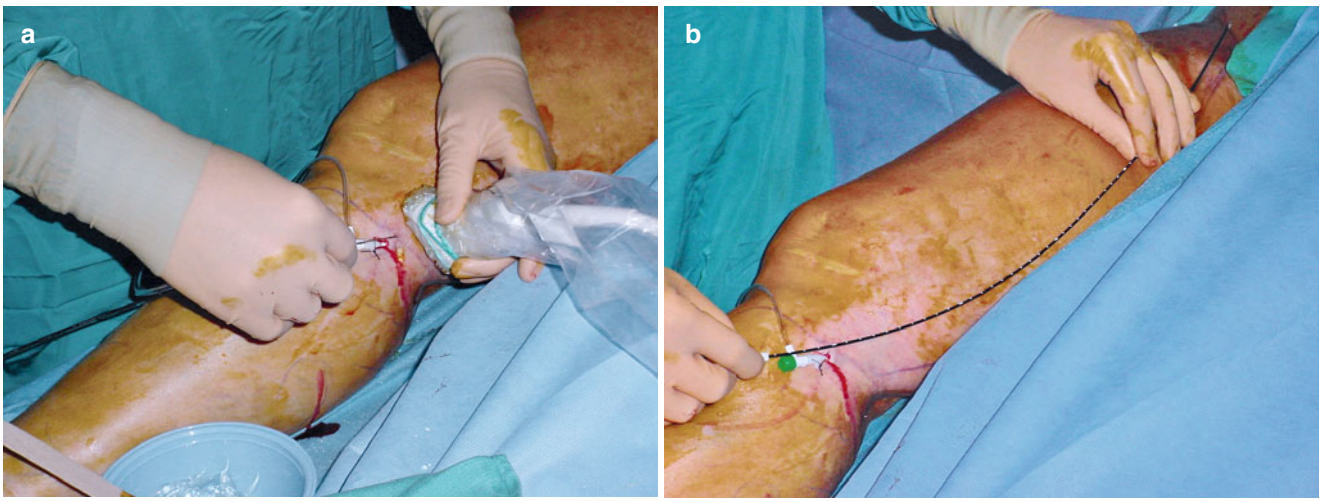


**Fig. 44.1** (**a**) Ultrasound guidance is used to identify the saphenous vein below the knee and for micropuncture technique to enter the vein and place the sheath. (**b**) As the catheter is passed up the saphenous vein, it can be visualized by duplex ultrasound

identify the path of the incompetent vein, for micropuncture access to the vein, during positioning of the catheter at the junction between the superficial and deep system, during infiltration of tumescence solution, and to visualize and compress the vein during the ablation procedure.

## Duplex Venous Evaluations Immediately Prior to the Procedure

Some patients arrive for the ablation procedure with a duplex scan having only been performed at another facility or with incomplete information from a unaccredited vascular lab. Consequently, a duplex scan can be used by the vascular surgeon performing the ablation procedure to confirm the findings from another vascular lab and to prepare for the procedure, before opening the disposable supplies, which are expensive and would be wasted if the procedure did not need to be performed. Prior to the ablation procedure, duplex ultrasound should be used to confirm the location of the reflux, diameter of the vein(s), and then to mark the path of the vein or site of ablation. This usually requires the patient to be in a sitting or standing position, particularly if confirmation of valve reflux is needed. If the access vein for ablation procedure is small on this initial evaluation, nitroglycerine can be placed over the site of access to dilate the vein and make access easier. If a patient is fearful of needle sticks, then the entire path of the vein can be marked with duplex scan imaging and topical xylocaine placed on the skin along the path of the incompetent vein to reduce the discomfort from the needle sticks that are used for local anesthesia and tumescence.

## Duplex Scan During the Procedure

Endovenous ablation procedures should be performed using a tilt table and portable or fixed duplex ultrasound.

## Saphenous Ablation

Percutaneous placement of the catheter in the below knee saphenous vein is the access site of choice (Fig. 44.1). The vein can be identified by finding the saphenous vein in the thigh, which is under the fascia in the medial thigh. If this vein is followed from the thigh to the calf, it usually is of adequate caliber for access. Once access is obtained under ultrasound guidance and the sheath has been placed, the catheter is then passed up the saphenous vein and parked 2 cm from the saphenous femoral junction and below the epigastric vein. This position is best determined using B-mode ultrasound guidance in both the transverse and saggital planes. The distance between the tip of the catheter and the junction of the superficial and deep vein should be measured with the ultrasound cursor. The relationship of the catheter to the epigastric vein is variable, so distance from the saphenofemoral junction is the most critical measurement. Liberal injection of tumescent solution, consisting of saline, xylocaine, and epinephrine, is placed around the saphenous vein from the catheter insertion site to the saphenofemoral junction, under ultrasound guidance. Although different techniques may be used to deliver tumescence, we place the transducer in a transverse position and observe the infusion ultrasonically as a spinal needle infuses the tumescent solution into the perivenous space. The vein should be moved to at least 2 cm below the skin to avoid skin burn, and the tumescence should surround the entire vein to eliminate pain when the vein is being ablated. When the patient is placed in the Trendelenberg position to minimize vein diameter during ablation, the catheter position should be rechecked by duplex scan with respect to the junction. During ablation, the vein can be visualized under ultrasound guidance, to assure that compression over the vein is directly transmitted to it.

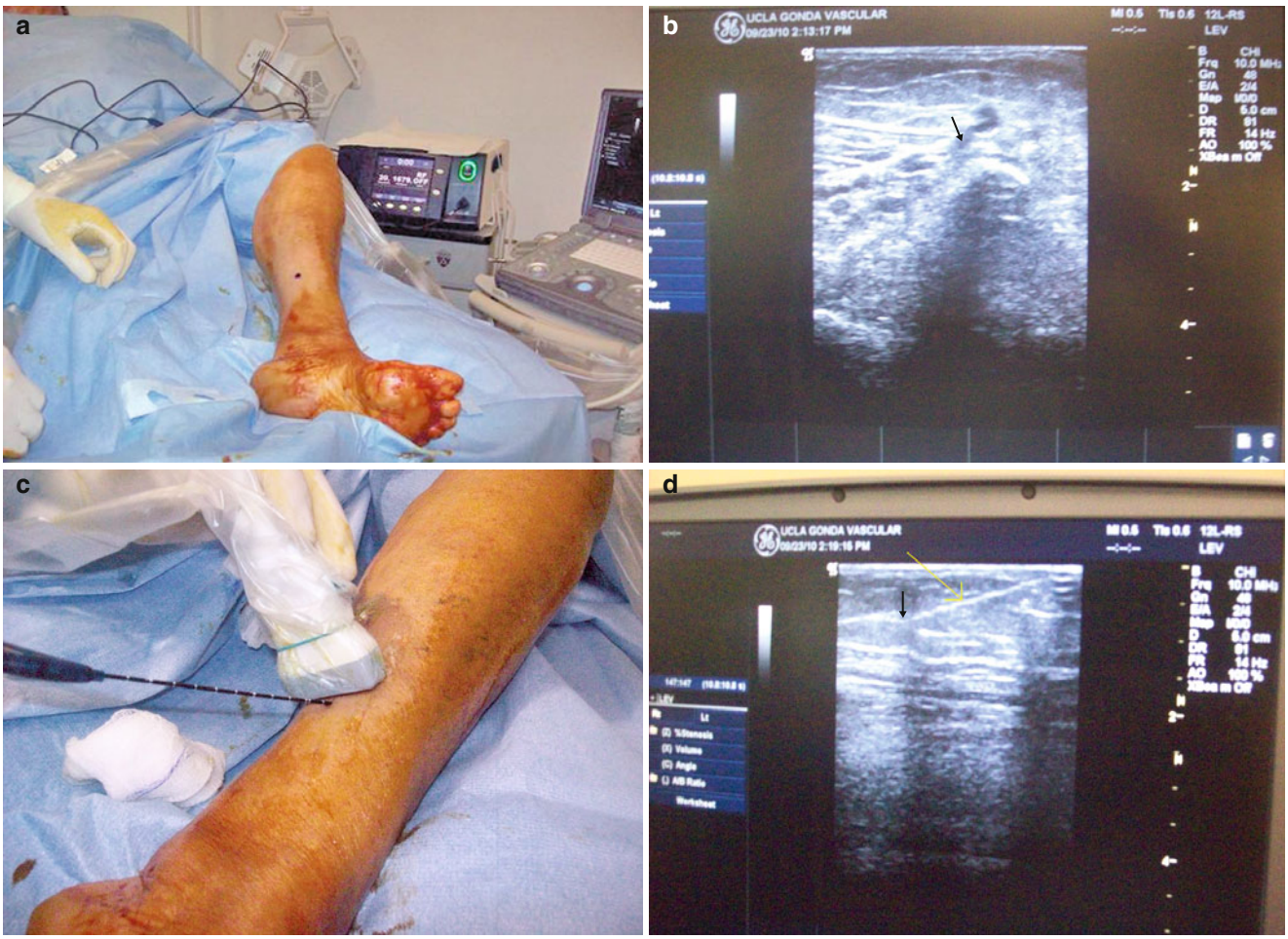


**Fig. 44.2** (**a**) The site of the perforator incompetence is marked on the skin with the patient in reversed Trendelenberg position. (**b**) The duplex ultrasound (*arrow*) show the incompetent vein and the fascial defect, best seen by B-mode scan. (**c**) The transducer is held in one hand while the perforator vein is accessed by placing the catheter at a 45° angle and penetrating the skin. (**d**) Once the catheter is below the skin, it should be advanced under ultrasound guidance until it enters the perforator vein at the level of the fascia (*arrows*). Blood can usually be aspirated when the vein is entered

### Small Saphenous Ablation

The principles of small saphenous vein ablation are similar to great saphenous ablation, but the procedure is most easily performed with the patient in the prone position. With the small saphenous vein, there is no epigastric vein equivalent to identify the sapheno-popliteal junction. In addition, the risk of sensory sural nerve injury is high, so tumescence must be used liberally to separate the vein from the nerve.

### Perforator Vein Ablation

Accomplishing successful perforator ablation requires even more skill than saphenous ablation [4] (Fig. 44.2). Ultrasound guidance in both a transverse and axial plane is used as the catheter is placed in the perforating vein at the level of the fascia. It is then used to visualize the catheter as a local anesthetic is placed around the catheter/vein junction, to control pain during ablation, during ablation to observe the process and compress the vein, during repositioning of the catheter, and following ablation to determine successful closure of the incompetent perforator vein. The technique for ablation should be based on the IFU for the device, as well as reports from the literature of techniques specifically designed for ablation of perforating veins [5].

The patient is initially placed in reversed Trendelenberg position on an electronic tilt table and a portable duplex scanner used for duplex imaging by the operating surgeon. The incompetent veins that have been previously identified in a vascular lab must be confirmed by the surgeon prior to the procedure [6]. Once the incompetent veins are marked, the ultrasound transducer, covered with a sterile sheath, should be used to identify the incompetent perforating vein immediately above the ulcer. The stylet is placed into the skin at a 45° angle and the ultrasound transducer is rotated 90° to confirm the position in each plane as the stylet is advanced to the junction of the perforator vein and the fascia. An attempt is made to puncture the wall of the vein at the

level of, or immediately below, the fascia, and ultrasound guidance is the key to successful penetration of the perforator vein. Once the location of the catheter in the vein is confirmed, the stylet is removed, the catheter position again confirmed, and the catheter is then surrounded with 1% lidocaine, injected along the catheter to the level of the fascia, while being visualized ultrasonically. The patient is then placed in Trendelenberg position, the position of the catheter again confirmed, and the vein is treated while observing the boiling of the blood at the tip of the catheter. Although an attempt should be made to confirm successful ablation postprocedure using color flow scanning, the lidocaine in the region of the perforator vein frequently causes an appearance of occlusion, even when the compression from fluid is extrinsic to the vein.

## Role of Ultrasound Postprocedure

### Assessment of Ablation Success

#### Saphenous Ablation

We routinely obtain a duplex ultrasound 24–72 h following the ablation procedure to determine if the vein has been successfully closed and to classify the site or level of closure, since there is a risk of extension of thrombus from the superficial incompetent vein into the deep venous system. In our experience, virtually 100% of patients have successful ablation of the great saphenous vein. A classification system guides the management of a patient postprocedure—if the vein is closed well away from the junction with the deep system, no further management is needed. If the vein is closed right up to the deep system, then further observation is usually recommended, while those patients whose ablation is associated with thrombus extending into the deep system are treated with anticoagulation until the thrombus retracts back into the superficial vein.

#### Perforator Ablation

Confirmation of closure of the perforating vein is obtained at the next office visit by a vascular lab technician. Perforator closure is defined as no blood flow in a previously incompetent perforator vein, demonstrated in a sitting or standing position, by duplex ultrasound.

### Assessment of Level of Closure

We uniformly obtain duplex ultrasound within 4 days of the procedure to determine the level of closure for all saphenous veins, due to concerns about the risk of developing proximal thrombus that may extend into the deep vein from the site of endovenous ablation (Fig. 44.3). We have developed a classification system for levels of endovenous closure of the saphenous vein, created a treatment algorithm for saphenous thrombosis which occurs in or immediately adjacent to the common femoral vein, and determined risk factors for post-RFA thrombosis that is immediately adjacent to or into the femoral vein.

#### Levels of Closure

In patients who have successful ablation of the saphenous vein, there are six potential levels of closure, from below the epigastric vein to DVT [7]. We use an ablation classification system of level of vein closure, as well as an algorithm for management of patients, based on level of vein closure, to manage patients postablation. We have used this classification system to guide management, and using this approach, have not had a single patient progress from saphenous closure to common femoral vein thrombosis or pulmonary embolism. Patients with level 1 or 2 closure do not need further follow-up; level 3 needs close observation, while those with level 4 or 5 are treated with low molecular weight heparin until the thrombus retracts. We have not had a patient present postprocedure with DVT in the common femoral vein, in spite of performing the procedure on >1,500 patients and doing routine duplex scan surveillance on every patient.

### Assessment of Leg Pain

Patients may complain of many sources of pain following either endovenous ablation or microphlebectomy, even after successful ablation of the vein has been confirmed. In this situation, duplex ultrasound is used to image the area of pain and determine the etiology of pain, which is frequently from hematoma or superficial thrombophlebitis in a residual varicose vein, which may not have been fully removed.

### Assessment of Remaining Venous Incompetence

Once a limb has been treated for venous incompetence, patients may still have residual symptoms or varicose veins, which were not fully treated during the endovenous ablation. Further treatment should be dependent on the location, size, and extent of reflux in the residual vein. Many patients receive authorization only for an ablation procedure, in anticipation that the tributary veins will be reduced in diameter to a minimal size and become pain-free. However, patients with initial large tributaries often have residual pain and tributaries of a visual appearance and size that is unacceptable to the patient. Consequently, repeat duplex scanning is needed to document the size, location, and extent of reflux following ablation, and to obtain insurance authorization for another procedure.

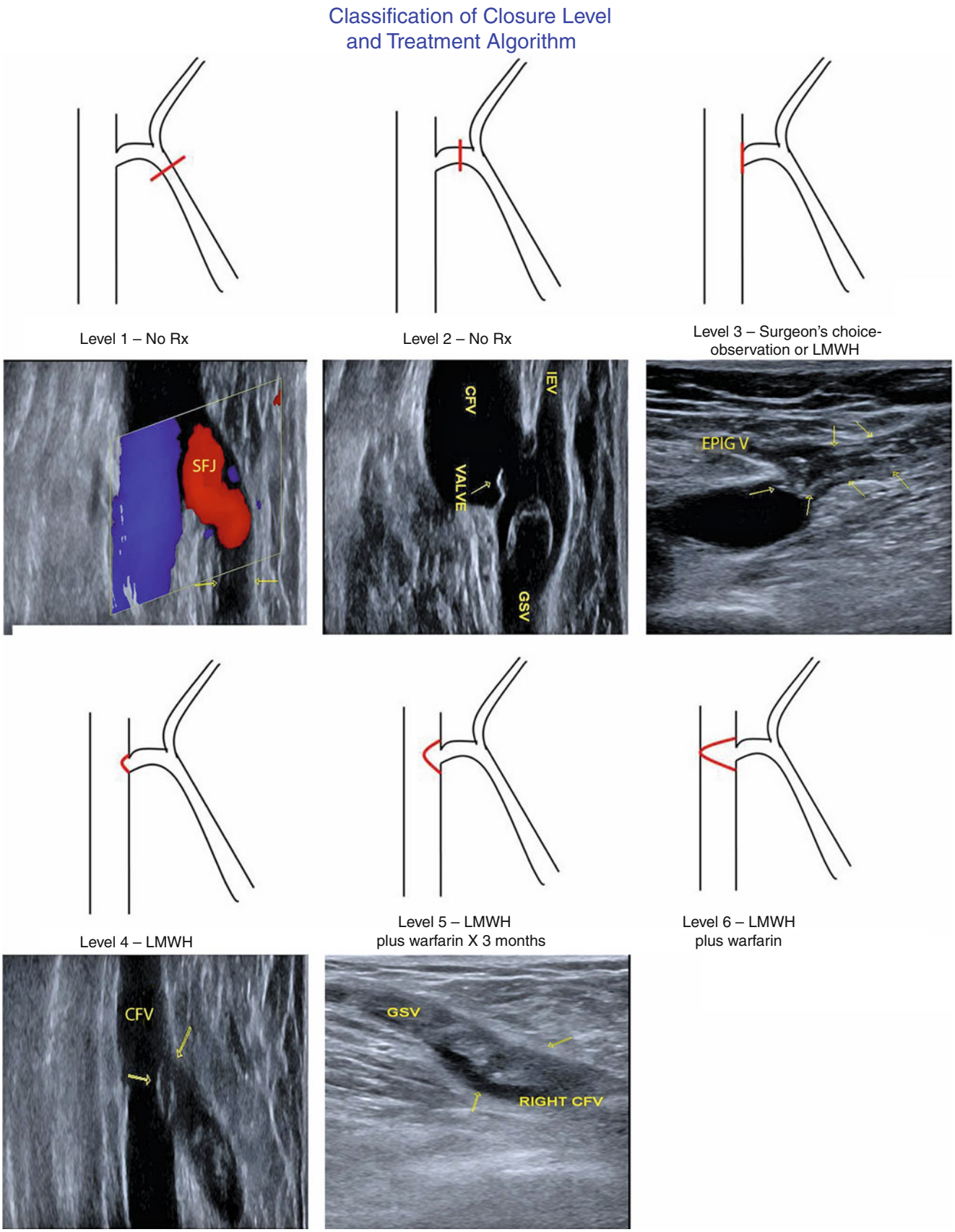


**Fig. 44.3** Levels 1, 2, and 3 ablations are at or below the saphenofemoral junction and require no further treatment, while levels 4 and 5 bulge into the common femoral vein (*arrows*) and usually require short-term anticoagulation, until the thrombus retracts back into the saphenous vein. We have not encountered a level 6 thrombosis, but would fully anticoagulate the patient and treat for DVT

## Conclusion

Duplex ultrasound has a fundamental role in managing patients who undergo endovenous ablation of superficial axial veins and perforator veins. Ultrasound is used pre-procedure to document the anatomy, level, and degree of venous insufficiency, and to obtain insurance authorization for the procedure. During the procedure, duplex ultrasound guidance is used to identify the veins requiring treatment, facilitate percutaneous access to the veins being treated, to guide tumescent placement around the vein being treated, and to observe the vein while it is being treated. Following the procedure, the duplex ultrasound confirms the successful closure of the vein, determines the level of closure, and determines whether there is a risk of thrombus extending into the vein.

## References

1. Caggiati A, Rosi C, Heyn R, Franceschini M, Acconcia M. Age-related variations of varicose veins anatomy. J Vasc Surg. 2006;44:1291–5.
2. Gloviczki P, Comerota AJ, Dalsing MC, et al. The care of patients with varicose veins and associated chronic venous diseases: clinical practice guidelines of the society for vascular surgery and the American venous forum. J Vasc Surg. 2011;53:2S–48.
3. Caggiati A, Bergan J, Gloviczki P, Jantet G, Wendell-Smith J, Partsch H. Nomenclature of the veins of the lower limb: extensions, refine nomenclature of the veins of the lower limbs: an international interdisciplinary consensus statement. J Vasc Surg. 2005;41:719–24.
4. Lawrence PF, Alktaifi A, Rigberg D, et al. Endovenous ablation of incompetent perforator veins is effective treatment for recalcitrant venous ulcers. J Vasc Surg. 2010;52:525.
5. Elias S, Peden E. Ultrasound-guided percutaneous ablation for the treatment of perforating vein incompetence. Vascular. 2007;15:281–9.
6. Lawrence PF, Harlander-Locke M, Alktaifi A, Farley S, et al. The impact of ablation of incompetent veins on ulcer healing. J Vasc Surg. 2011;53:109S–10.
7. Lawrence PF, Chandra A, Wu M, Rigberg DA, Gelabert HG, Jimenez JC, DeRubertis BG. Classification of endovenous closure and treatment algorithm. J Vasc Surg. 2010;52:388–93.

# Preoperative Saphenous Vein Mapping

# 45

Melissa D. Shah, R. Clement Darling III, Benjamin B. Chang, Philip S.K. Paty, Paul B. Kreienberg, Sean P. Roddy, Kathleen J. Ozsvath, Manish Mehta, Abdul Khan, and Dhiraj M. Shah

**Abstract**

Saphenous vein mapping is an integral portion of planning an infrainguinal arterial reconstruction. Only 60% of the greater saphenous veins are one continuous tube from the groin to the ankle. There are significant variances to be known preoperatively in order to minimize incisional complications and also allow the surgeon to perform the optimal arterial reconstruction. Additionally, a great amount of information can be gleaned from the quality of the saphenous vein and in the era of endovascular treatment, this may be a factor in influencing the type of intervention or reconstruction that the surgeon performs. The surgeon and patient will benefit from the maximum amount of information not only about the anatomic location for inflow and outflow but also most importantly for the adequacy and availability of autogenous venous conduit.

**Keywords**

Saphenous vein mapping • Distal bypass

## Overview

The successful performance of any arterial bypass procedure ideally starts with the surgeon being armed with the maximal amount of information about the patient. This is commonly thought of as a history, physical examination, arteriography, and any preoperative testing for medical clearance. This should also include noninvasive testing in the evaluation of vein conduit to improve the surgeon's revascularization options. Historically, the saphenous vein was most frequently encountered by surgeons during a vein stripping, and certainly preoperative anatomic definition of the saphenous vein was not performed. In addition, it has taken the surgical community time to regard veins as more than passive tubes awaiting use as an arterial bypass. As knowledge of the physiologic importance of the in vivo autogenous vein became available to the surgical community, such as the passive and active roles of the venous endothelium, methods were progressively developed to preserve the function and structure of the vein. In this context, it became increasingly apparent that minimizing intraoperative injury to the vein conduit was desirable. In addition, because of the frequent anatomic variations seen in any of the superficial veins used for arterial bypass, improved preoperative knowledge of the vein allowed surgeons to select the most satisfactory veins available while avoiding those that were too small or otherwise diseased while minimizing the dissections required to make this choice. In our experience, this has led to lower wound complications and long-term morbidity [1, 2]. This last point cannot be overemphasized as wound complications from vein harvest sites are a frequent and troublesome post-operative sequelae of arterial bypass surgery.

M.D. Shah, M.D. • B.B. Chang, M.D. • P.S.K. Paty, M.D.
P.B. Kreienberg, M.D. • S.P. Roddy, M.D. • K.J. Ozsvath, M.D.
M. Mehta, M.D., MPH • A. Khan, RDMS, RVT • D.M. Shah, M.D.
Department of Vascular Surgery, Albany Medical Center Hospital,
43 New Scotland Avenue MC157, Albany, NY 12208, USA

R.C. Darling III, M.D. (✉)
Department of Vascular Surgery, Albany Medical Center Hospital,
43 New Scotland Avenue MC157, Albany, NY 12208, USA

The Vascular Group, Albany Medical College,
Albany, NY, USA
e-mail: darlingc@albanyvascular.com

A.F. AbuRahma, D.F. Bandyk (eds.), *Noninvasive Vascular Diagnosis*,
DOI 10.1007/978-1-4471-4005-4_45, 

The overall goal of this chapter is to supply the clinician and technologist with the necessary knowledge for performing preoperative vein mapping while, hopefully, convincing him or her of its utility and the rationale for its use. Like many technologic advances, the need for vein mapping may seem unjustified, especially to surgeons who have performed these operations for decades without this knowledge. But like automobiles, microwaves, and smart phones, vein mapping eases the life of the surgeon as well as the patient's operation that it soon becomes indispensable.

## Preoperative Imaging with Venography

At Albany Medical Center, preoperative vein imaging evolved hand-in-hand with the reintroduction of the in situ bypass technique [3]. While initial cases were performed by incising the skin and saphenous (or superficial) fascia overlying the saphenous vein followed by incising the valves with the modified Mills valvulotome ("open" technique), further evolution of the instrumentation led to the development of the Leather and other commercially available valvulotomes, which are passed blindly up the vein from a below-knee incision to the groin incision ("closed" technique). The use of a closed technique, although attractive in terms of decreasing operative dissection and operative time, is sensitive to variations in vein anatomy as the surgeon does not directly expose and thereby examine the entire vein or veins available, making the evaluation and selection of the best available vein more difficult. In addition, certain branching patterns, when unrecognized, are frequently points of injury to the bypass when a closed technique is used.

For these reasons, the saphenous vein was for several years imaged with ascending contrast venography. The results of these studies were summarized in part by Shah et al. [4]. The methods reported in that paper are still effective and useful in some selected cases. The distal branch of the saphenous vein is punctured with a small gauge angiocatheter in the foot, ideally in one of the many prominent side branches covering the medial aspect of the foot as part of the dorsal venous arch. The use of a tourniquet is helpful for the puncture, but should be removed subsequently. Iodinated contrast medium is injected via the angiocatheter into the saphenous vein and fluoroscopy is used to define venous anatomy. The vein is then flushed with heparinized saline after the venogram is completed to minimize the chance of contrast-induced thrombosis.

Alternatively, the same information may be gained intraoperatively at the beginning of the bypass procedure. An incision is made over the saphenous vein, usually just below the knee. Once the vein is identified, the vein is cannulated through an opened side branch with a small gauge angiocatheter (sheath only) and a single X-ray is taken of the thigh after 10–12 ml of contrast is injected. Digital subtraction venography can also be used if readily available such as in "hybrid" operating rooms. On-table venography has the advantage of eliminating a separate preoperative invasive test, but is less likely to give the surgeon the complete picture of the vein.

Although these venographic techniques were used in several hundred bypass procedures, as aforementioned, they are both invasive and require radiation exposure. Importantly, venography gives relatively little information regarding vein quality in terms of wall thickness, calcification, and other aspects of morphology that are more apparent with ultrasonographic techniques. Venography is also not a practical method of imaging multiple extremities in the same patient at the same time.

There are some circumstances in which these methods are still of use. First, when one is first starting to perform duplex vein mapping, accuracy may be verified by performing venograms. This is especially important when the imager encounters variations that he or she has not seen previously and helps shorten the learning period for the ultrasonographer. Second, there are individuals in whom the vein anatomy is sufficiently complicated and/or difficult to image with duplex due to patient habitus (extreme obesity) or uncooperativity for whom an intraoperative venographic study could be useful. Third, emergency cases, especially when done late at night, when duplex is less likely to be available may benefit from on-table venography instead. Mostly, this technique is of historic interest only.

## Ultrasound Imaging of the Saphenous Vein

After duplex ultrasound became available at our institution, its advantages over contrast venography were readily apparent. After a period of time trying to develop a technique and method of duplex imaging, this now widely accepted technology became the method of choice for venous imaging in 1985 and has continued with a few minor modifications until the present day [5, 6].

The noninvasive nature of ultrasound is one of its most attractive features. This is most significant in patients who have contrast sensitivity who may require imaging of more than one vein at a time. This is most common in redo cases where imaging of contralateral great saphenous vein, bilateral small (lesser) saphenous veins, residual ipsilateral great saphenous vein and arm veins is necessary. This allows the surgeon to pick and choose among several conduit options in order to complete the reconstruction in the most efficient manner possible with the fewest incisions.

There is a wealth of other information that ultrasound can deliver that has proven to be of use for the surgeon. The "quality" of the vein affects vein performance as an arterial conduit. While this has been long understood to include vein diameter, quality also reflects other aspects of vein morphology such as

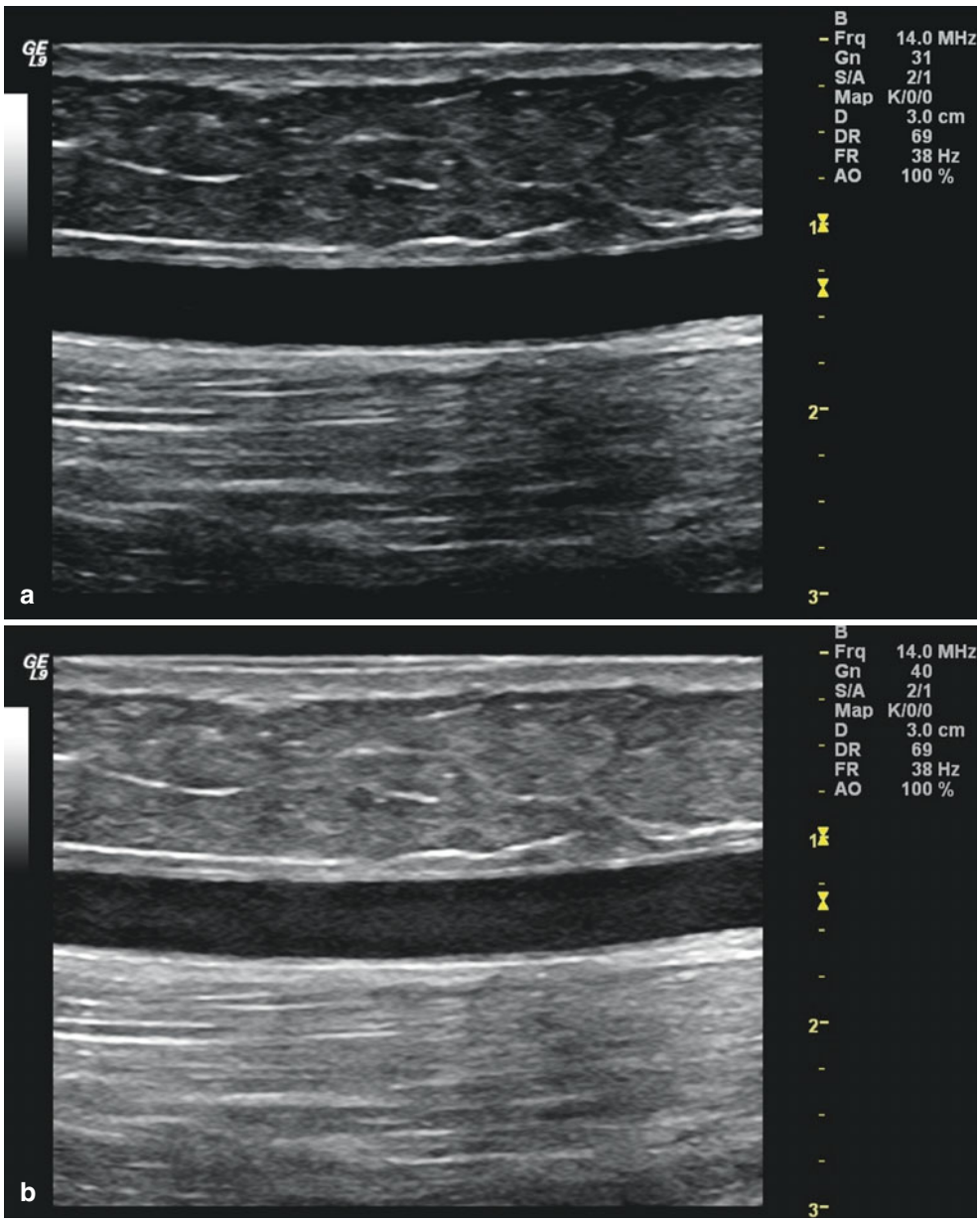


**Fig. 45.1** (**a**) Ultrasound power low. (**b**) Ultrasound power high

the presence of recanalization, sclerotic areas, and thick vein walls [7, 8]. This information allows the operator to avoid the use of suboptimal veins whenever possible and to thereby help maximize bypass patency.

## Method of Imaging

The equipment necessary for adequate saphenous and other superficial vein mapping is the same that is commonly employed in vascular imaging studies of most kinds. A 10–12 MHz transducer is generally employed. Lower frequency ultrasound probes are occasionally useful to image deeper veins in extremely obese individuals, but do not transduce with the resolution necessary for delineating the important details seen with the higher megahertz probes. A 4.5 MHz pulsed Doppler is also occasionally employed to primarily check for vein patency. Color is rarely, if ever, necessary and may in some circumstances obfuscate important details. The reason that color flow is usually not helpful is that the unaugmented flow rates in these superficial veins provides only sporadic color filling of the vessel which is of little use in outlining their course. The transmit power (in decibels) of the transducer probe is generally turned down as this delivers a cleaner, clearer image by minimizing scatter. Focal zones should be adjusted to maximize the near-field resolution (Fig. 45.1).

Because the course of the vein is drawn upon the skin with indelible marker and then stain, the unprotected probe

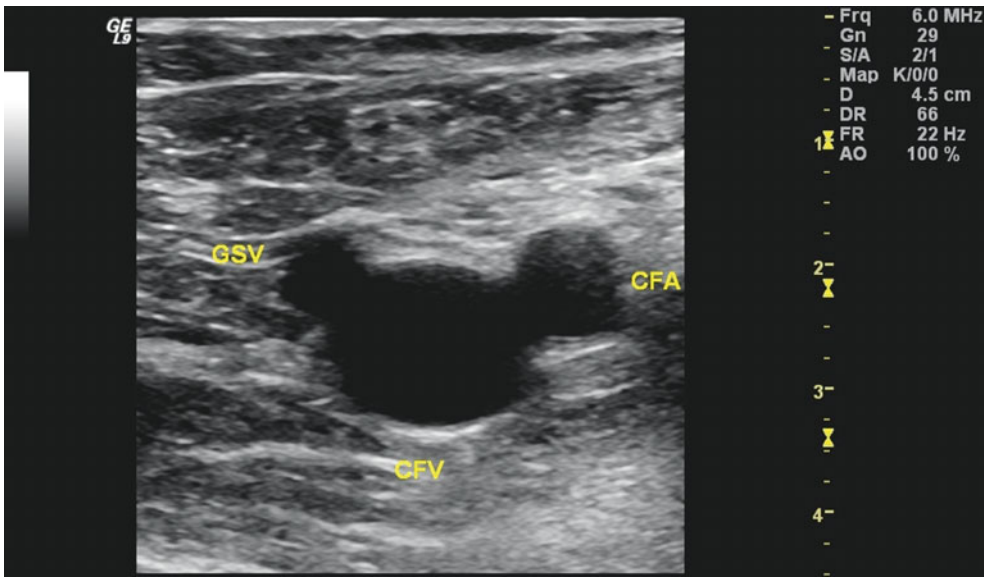


**Fig. 45.2** Mickey mouse

head may become permanently stained, especially through the relatively porous probe membrane. In order to avoid this, the probe is covered with a plastic probe cover containing ultrasound gel. The medium between probe and skin must be aqueous and not air for adequate ultrasound transmission. Preparation of the examination area or room is of vital importance for successful mapping. The room should be well heated in order to minimize peripheral venoconstriction. For the same reason, the patient should remain clothed and/or covered, exposing only the necessary limb. Sometimes, keeping the exposed foot covered is also useful. Finally, the room is generally kept dark in order to assist with visualization of the ultrasound image on the display.

Positioning for imaging of the great saphenous vein usually requires the stretcher to be placed in reverse Trendelenburg with the knee slightly flexed and the hip externally rotated. Standing the patient is usually not necessary for the majority of cases and is certainly not well tolerated by many in this patient group. Occasionally, the patient may be kept in a standing position at the end of the procedure to check the vein size under maximal pressure. In the past, tourniquets were employed in an effort to maximally dilate these veins but this has proven to be poorly tolerated by the patients and has therefore been abandoned.

Imaging of the saphenous vein can be started at either one of three logical sites: the ankle, the knee, or the groin. Generally, the groin is favored as the saphenofemoral junction can usually be positively identified with its characteristic relationship to the common femoral vein and artery ("Mickey Mouse," Fig. 45.2). In very obese patients, however, this may be difficult to image even with the lower-frequency transducers. Beginning imaging at the knee may avoid some of the above problems, but it is much easier to follow the wrong vein or to miss double systems.

These superficial veins have very little internal pressure, and are exquisitely sensitive to external pressure such as from the probe itself. Therefore, the weight of the probe and the examiner's hand should be supported by the fourth and fifth fingers offset from the course of the vein. The examiner can check his or her technique by examining the vein in cross section: it should be round, not elliptical (Fig. 45.3).

Held in this way, the probe is applied at or near the groin in a transverse plane. Held in this plane, the probe may be moved in a medial-lateral direction until the vein is visualized. Generally, the vein runs slightly medial to the midline of the thigh at this point. The vein may be followed into the saphenofemoral junction to confirm its identity. The vein may be compressed to confirm patency. If this is in doubt, pulsed Doppler may be used in conjunction with manual compression of the distal leg.

Care should be taken to keep the probe as perpendicular to the skin as possible in order to help the surgeon make his or her incisions directly over the vein. This is entirely possible in most cases where the leg is tant, but can be unavoidably inaccurate if the tissue of the skin is sagging or otherwise very redundant. Correct marking of the course of the vein on the skin requires some experience and constant feedback from operating room findings.

Once the vein is identified in the transverse plane, the probe is slowly rotated 90° to insonate the vein in a longitudinal plane. The position of the vein may then be marked at either end of the probe. We use a Sharpie King Size Permanent Marker with a chisel tip because it will mark through gel (and it will stay wet when left uncapped). As the probe is moved distally, a new dot is made every inch or so. After the remainder of the scan is completed, the dots are painted over with a continuous line. We use carbol fuchsin stain (originally

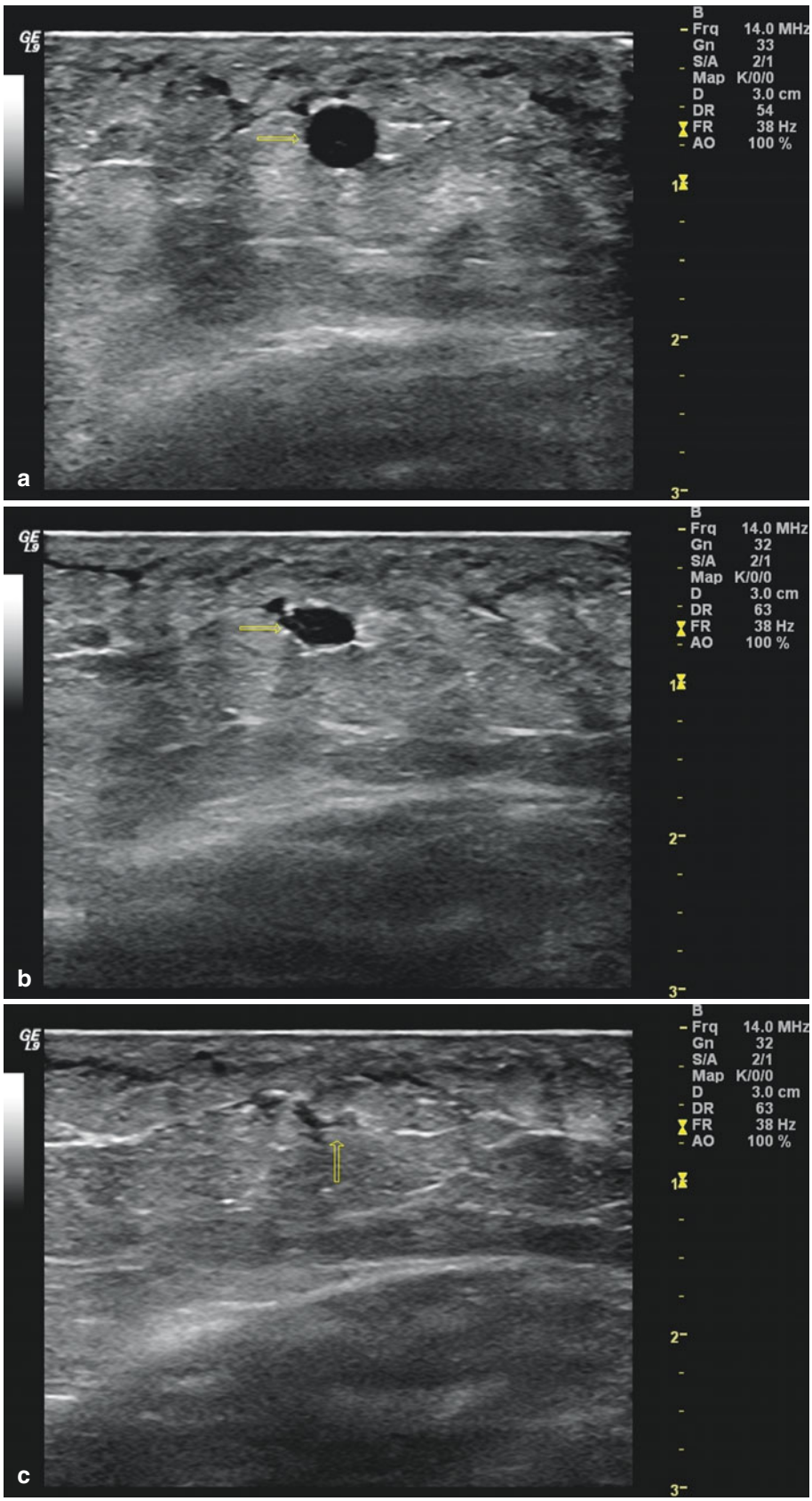


**Fig. 45.3** (**a**) Transverse vein image, no pressure—vein round. (**b**) Transverse vein image, mild pressure—vein elliptical. (**c**) Transverse vein image excess pressure, vein not visualized (*arrow*–greater saphenous vein)

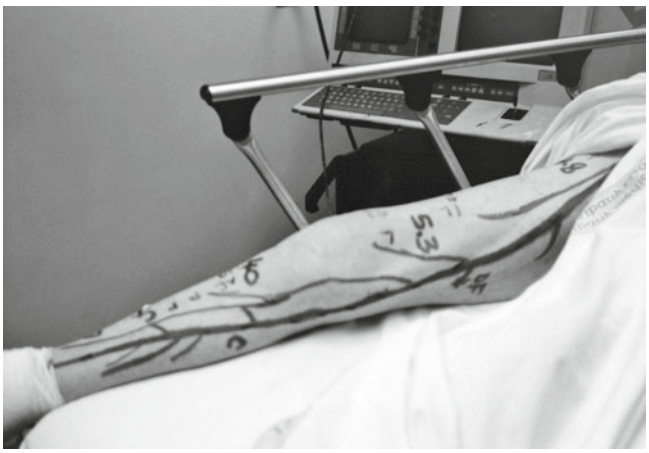

**Fig. 45.4** Vein map

obtained from the radiation oncology department) applied with a cotton-tip applicator. This provides the operator with a map of the underlying vein (Fig. 45.4). This map should provide the surgeon with a detailed picture of the vein but it does not necessarily precisely indicate the best place for the surgeon to place the incisions; this requires some judgment from the surgeon in addition to the external map.

The size of the vein can also be measured. This is best done with the vein imaged in the transverse plane. Usually the vein size is determined in the groin, the distal thigh, and three equidistant points along the lower leg. Any marked changes in vein diameter along the course of the vein should also be marked. The limitations of these measurements should be stressed. Because they are obtained with the vein under venous pressure, they generally underestimate the diameter of the vein when the vein is connected to arterial pressure. In addition, these measurements are taken of the inside diameter of the vein, not the outside diameter. The surgeon should regard these measurements as the minimum size of the available vein. It is very important that the surgeon does not abandon the thought of using the vein without visually inspecting the vein at the time of operation. The vein by ultrasound may appear quite small and actually be quite acceptable upon arterialization. The vein size is roughly underestimated by a millimeter or more by ultrasonography under venous pressure.

As the probe is moved from the groin to the ankle, the vein is held in a longitudinal plane. As marks are made on the skin, the probe is rotated to a transverse plane every 3–4 in. at which time the vein may be compressed to confirm patency and its diameter measured and recorded. Other data that should be generally noted include the relationship of the vein to the superficial and deep fascia and the relative depth of the vein in regards to the skin. It does help if the ultrasonographer has some direct experience with the relationship of the saphenous vein to the fascia. Knowing that the main vein usually runs deep to the saphenous fascia, for instance, allows for the ultrasonographer to avoid tracking more superficial subcutaneous veins which may be as large or larger [9]. This is especially the case when the patient has large varicosities of the thigh where selecting the proper vein to track and follow is largely a matter of identifying the vein with the proper relationship to the saphenous compartment.

Other more subtle but no less important data that may be obtained include information about the vein wall. Normally, the intimal-medial complex appears as a thin, single, well delineated reflection. With the probe in the longitudinal plane, an abnormal appearance of the vein wall should be noted (Fig. 45.5). This may be expressed in the report by describing the vein wall as being thickened (worrisome), calcified (worrisome but often usable), irregular (very worrisome, with possible recanalization), or sclerotic (almost certainly not usable). These notations are somewhat subjective and really describe a whole class of vein wall abnormalities but are of paramount importance to the surgeon as it allows for some preoperative planning to avoid using these diseased veins whenever possible.

Patients in this group may have variable amounts of peripheral edema. This complicates imaging considerably as the layers of edematous tissue may appear similar to a vein by ultrasound. This is the one condition in which use of color flow imaging is useful; distal compression will help define the vein from the surrounding fluid-filled tissue planes especially with color flow imaging.

At this point, the entire vein should have been completed in the first pass from the groin to the ankle. There should be a line of black dots along the course of the vein. The vein is rescanned from top to down but with the probe held in the transverse plane. During this pass, major branches are noted and marked. This includes known named tributaries such as the posterior (medial) and anterior (lateral) accessory saphenous veins in the upper thigh as well as major perforators, which are seen as posterior or posteriolateral branches that dive through the deep fascia to communicate with the deep venous system (Fig. 45.6). Preoperative identification of these points will allow the surgeon to gain access to the vein with a minimum amount of dissection and to ligate these perforators efficiently.

After the main branches are marked, the scan may be completed by connecting the dots with the carbol fuchsin stain, leaving the surgeon a cutaneous map upon which the operation may be planned. In addition, a form depicting the leg (or arm) being mapped is filled out. This form has a diagram of the mapped vein and notation for abnormalities, configuration, vein size, depth and any other data felt to be useful to the operator. This entire procedure may take as little as 15 min with a single simple system, although longer periods of time are required for more complicated cases [10].

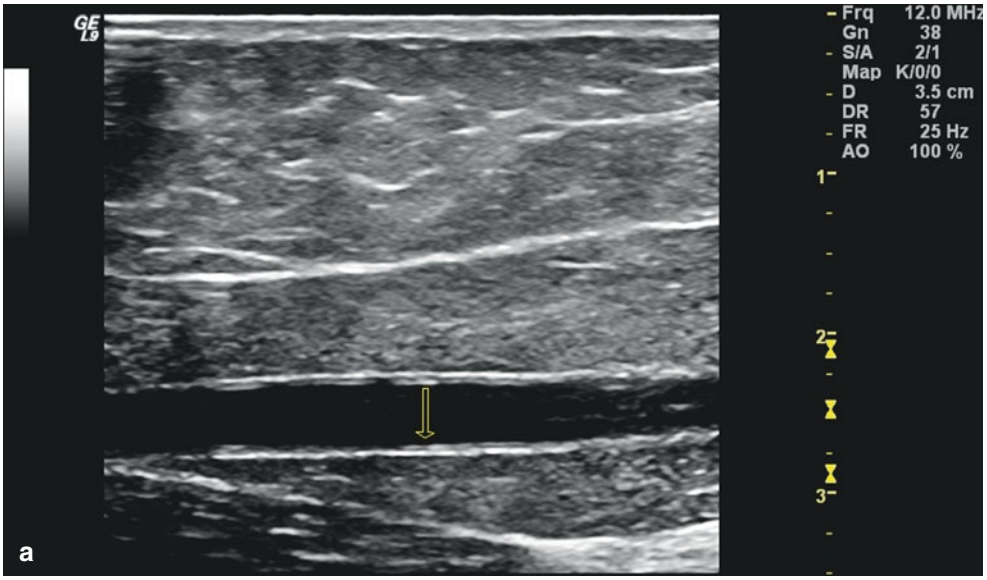


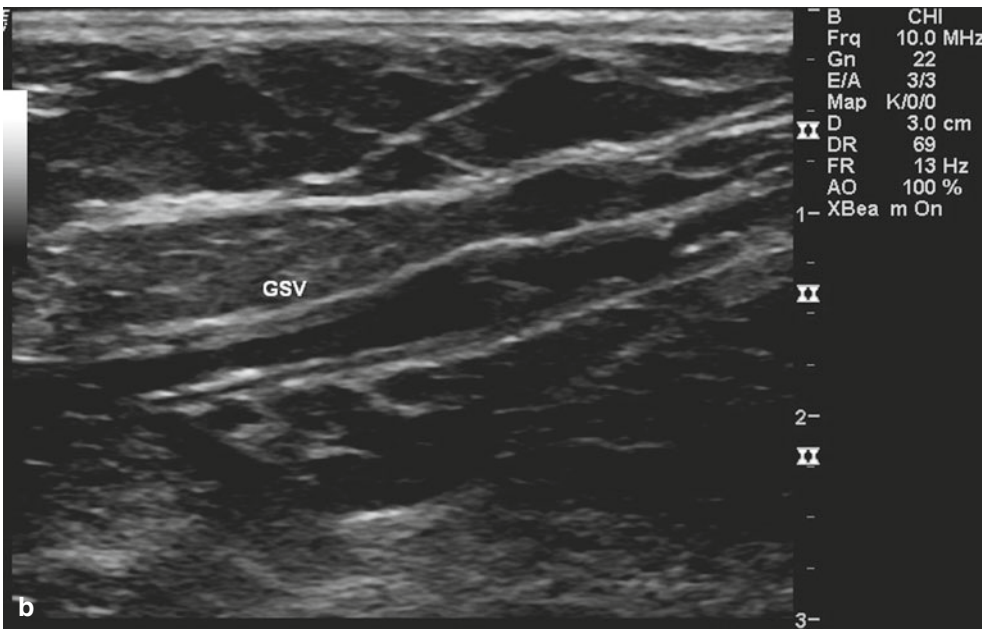


**Fig. 45.5** (**a**) Normal vein wall (*arrow*). (**b**) Thickened (post phlebitic) vein wall

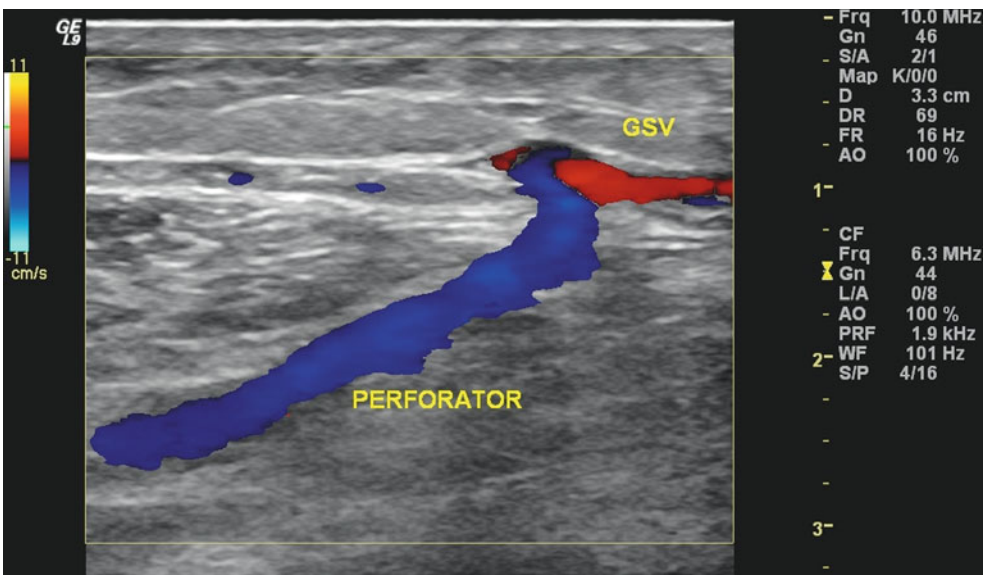


**Fig. 45.6** Perforator to deep system from saphenous vein

## Saphenous Vein Variants

During imaging, many branches of the vein may be encountered. Some of these branches will prove, upon imaging, to be long parallel venous systems [11]. While most surgeons regard the great saphenous vein as a single tube running up the medial aspect of the leg, this has proven to be the case in only 55% of the several thousand limbs now scanned. Familiarity with these variations is important for both the ultrasonographer and the surgeon.

For most purposes, the variations in saphenous vein anatomy may be classified into two groups: above the knee and below the knee. The most common single configuration of the thigh saphenous vein is what is termed a single medial dominant vein, seen in about 60% of cases. This is the "typical" configuration in which the vein is a single trunk running medially along the thigh and within the saphenous compartment. In addition, it curves away from the patient's midline (concave outward).

In the other 40% of cases, important variations exist in the thigh. The thigh saphenous vein may have a single anterior or lateral dominant system in 8% of cases (Fig. 45.7). In this setting, the thigh vein runs more anterolaterally than the main GSV and is superficial to the saphenous fascia. It tends to have many more, smaller branches, is thinner-walled, and curves toward the patient's midline (concave inward). The lateral system arises as the anterior accessory saphenous vein, usually the first and largest lateral branch just distal to the saphenofemoral junction. Although a single lateral dominant system can be used for bypass, closed *in situ* techniques should be employed more cautiously due to its thin wall and profusion of branches.

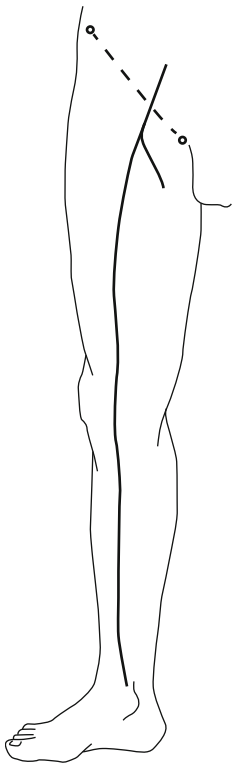

**Fig. 45.7** Single lateral dominant system, 8%

The saphenous vein may have both posterior (medial) and anterior (lateral) systems running along the entire thigh that remain relatively separate from each other even below the knee [12]. These double systems may have a larger posterior (medial dominant double system) or anterior (lateral dominant double system) branch, or both systems may be equal in caliber (Fig. 45.8). This pattern occurs in about 8% of cases. It is vitally important for the ultrasonographer to pick up this variant and to give the surgeon some idea which vein is better, if any, in order for the surgeon to place the incisions over the appropriate place. In addition, the surgeon can use the ultrasound information to avoid wasting time chasing the less satisfactory vein.

The saphenous vein may have a closed loop in the thigh portion in about 7% of cases (Fig. 45.9). This type of vein tends to be a poor candidate for closed in situ bypass valvular disruption as the surgeon cannot ensure instrumenting the larger of the branches of the loop, and the start and finish of the loop are points especially prone to injury from intraluminal instrumentation.

In about 16% of cases, the saphenous vein divides in the distal two-thirds of the thigh (Fig. 45.10). Both branches run parallel into the lower leg. If not identified by mapping, the surgeon can easily isolate the wrong (smaller) system at the knee, usually the posterior arch vein. Furthermore, the point of division of the vein is likewise prone to injury from blind intraluminal instrumentation.

In 1–2% of cases, the saphenous vein anatomy is sufficiently complicated, usually reflecting multiple loops and parallel systems as to be difficult to characterize ultrasonographically. The surgeon should be notified of this, and careful exploration and/or the use of intraoperative venography are possible adjunctive methods for these cases. These are rarely pleasurable and often tedious experiences.

## Calf Saphenous Vein Anatomy

The saphenous vein commonly divides at or just below the knee joint into an anterior and posterior system. The common situation, seen in 58% of cases, has the anterior branch being the dominant system and the posterior arch vein being a tributary (Fig. 45.11). The anterior system is generally deeper, thicker-walled, and has fewer branches than the posterior system. It lies between the deep and superficial fascia and travels with the saphenous nerve.

The posterior system is the single dominant system in about 7% of cases (Fig. 45.12). This vein runs in a subcutaneous plane, is thinner-walled, has many small branches, and is

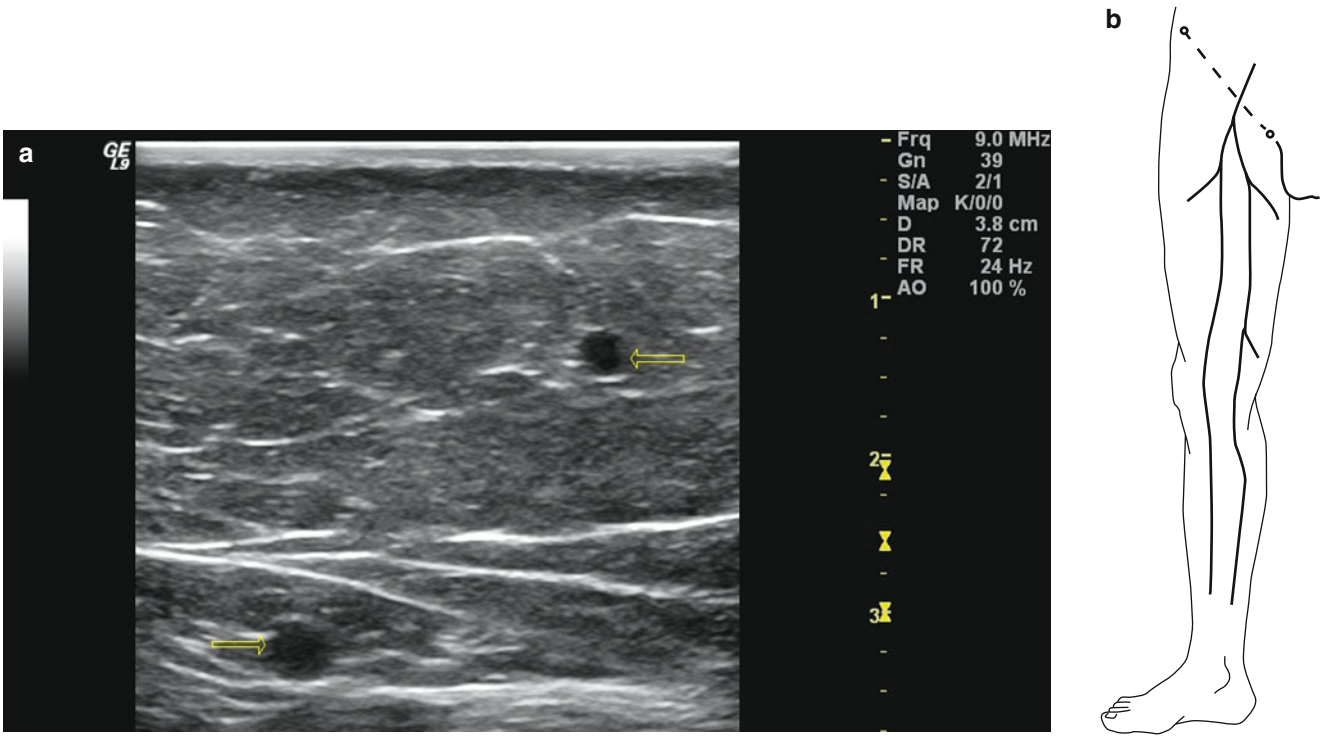


**Fig. 45.8** (**a**) Superficial lateral and deeper medial systems. (**b**) Components of a double system, 8%

**Fig. 45.9** Closed loop in thigh, 7%

**Fig. 45.10** Branching of saphenous vein in distal thigh, 16%

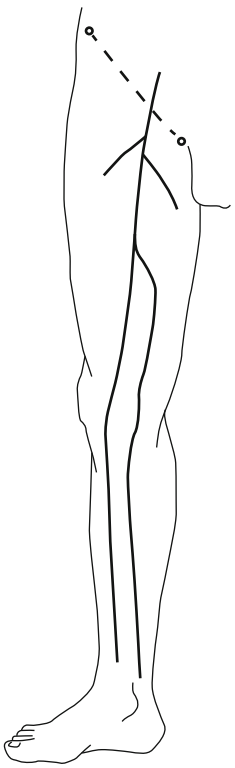

sometimes a continuation of the posterior accessory saphenous vein which may communicate with the great saphenous vein via intersaphenous veins [13, 14]. This vein is generally more difficult to prepare surgically for bypass but may be adequate when the dominant system. Incisions for this variant tend to be more posterior in the calf and less deep.

The saphenous vein has both complete anterior and posterior systems in about 35% of cases. The systems divide at the

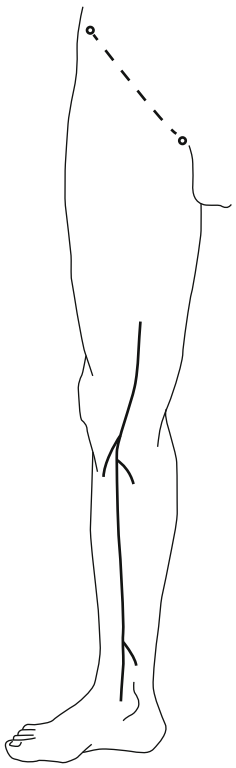

**Fig. 45.11** Typical calf saphenous vein anatomy, 58%

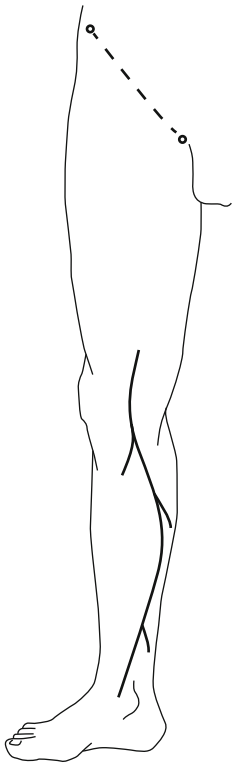

**Fig. 45.12** Single posterior dominant, 7%

knee, and rejoin at the junction of the middle and lower one-third of the leg. In this situation, the anterior system is dominant in most (85%) of cases and posterior dominant in 15% of this subgroup (Fig. 45.13).

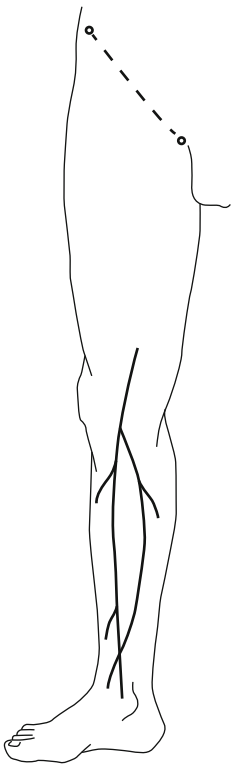

**Fig. 45.13** Double calf system, 35% (anterior dominant 85%)

In less than 1% of vein maps, the saphenous systems of veins are tripled or otherwise too complex for accurate imaging by ultrasound.

## Small Saphenous Vein

The small, but not often lesser, saphenous vein travels in the posterior calf and ankle subcutaneously with the sural nerve starting at the saphenopopliteal junction and proceeding distal to the plantar arch. It lies superficial to the deep fascia and overlays the gastrocnemius muscle. The small saphenous vein is mapped in a similar fashion as the great saphenous vein, with the hip externally rotated and the knee slightly flexed. The cranial extension of the small saphenous vein runs between the biceps femoris and semimembranosis muscles and may communicate with the great saphenous vein via the posterior thigh circumflex vein (the vein of Giacomini) [14]. When present, the vein of Giacomini can increase the usable length of the small saphenous vein and can also be accessible from a supine and medial surgical approach.

## Proper Use of Mapping Data

Like any test, there are limitations in data that any study purports to deliver. First and foremost, like any ultrasound data, mapping is highly dependent on a close working relationship

between the technologist and surgeon. The technologist needs to become familiar with the anatomic variants of the saphenous vein and the details of vein anatomy that affect the bypass procedure. The surgeon, in turn, must close the loop by informing the ultrasonographer if the map was accurate or if the data provided was inaccurate or not usable.

Mapping is appropriate to define the presence or absence of vein and the minimum size of the vein. Conversely, it does not accurately define the size of the vein under arterial pressure. Thus, in good hands, if the surgeon is told that there is no vein, then this is probably true. If the surgeon is told that the vein is present but small, then the vein should be examined in the operating room to decide if it is usable.

The map drawn upon the skin can be fairly accurate, but less so in obese patients. It can serve as a guide in the placement of the first two (proximal and distal) incisions over the vein, but the vein should be then identified before the incisions are connected. The map does not obviate the need for surgical judgment in regards to this point. With a vein mapping report of length, diameter, and quality of the vein, but in the absence of the cutaneous map, the vein can still be identified at the groin or the ankle without unnecessary exploratory incisions.

Venous anatomic variants are very well delineated with good mapping. This requires considerable training for both parties and mistakes will be made early on. Branches and perforators are moderately well identified, helping the surgeon make decisions such as open versus closed technique. Valves, however, are not well imaged sonographically.

Irregularities of the vein wall, when present, are very accurately identified with ultrasonography. Many of these findings are somewhat subtle at first and require experience to accurately describe. Failing to identify irregularities during vein mapping, however, is no guarantee that the vein quality is good. A proper map and good clinical judgment together can ease many steps in the process of limb revascularization.

## References


1. Shah DM, Darling III RC, Chang BB, Fitzgerald KM, Paty PSK, Leather RP. Long term results of in situ saphenous vein bypass: analysis of 2058 cases. Ann Surg. 1995;222:438–48.
2. Shah DM, Paty PSK, Leather RP, Chang BB, Darling III RC, Feustel PJ. Optimal outcome following tibial artery bypass: analysis of 1300 cases. Surg Gynecol Obstet. 1993;177:283–7.
3. Leather RP, Shah MD, Karmody AM. Infrapopliteal arterial bypass for limb salvage: increased patency and utilization of the saphenous vein used in-situ. Surgery. 1981;90:1000–8.
4. Shah DM, Chang BB, Leopold PW, Corson JD, Leather RP, Karmody AM. The anatomy of the greater saphenous venous system. J Vasc Surg. 1986;3:273–83.
5. Leopold PW, Shandall AA, Kupinski AM, Chang BB, et al. The role of B-mode venous mapping in infrainguinal arterial bypasses. Br J Surg. 1989;76:305–7.
6. Darling III RC, Kupinski AM. Preoperative evaluation of veins. In: Leather RP, editor. Seminars in vascular surgery, vol. 6. Philadelphia: Saunders; 1993. p. 155–8.
7. Marin ML, Veith FJ, Panetta TF, et al. Saphenous vein biopsy: a predictor of vein graft failure. J Vasc Surg. 1993;18:407–14.
8. Marin ML, Gordon RE, Veith FJ, et al. Human greater saphenous vein: histologic and ultrastructural variation. Cardiovasc Surg. 1994;2(1):56–62.
9. Ricci S, Georgiev M. Ultrasound anatomy of the superficial veins of the lower limb. J Vasc Technol. 2002;26:183–99.
10. Kupinski AM. Ultrasound mapping of the superficial venous system. Vasc US Today. 2002;7:25–44.
11. Kupinski AM, Evans SM, Khan AM, et al. Ultrasonic characterization of the saphenous vein. Cardiovasc Surg. 1993;1:513–7.
12. Caggiati A, Bergan JJ, Gloviczki P, Janter G, Wendell-Smith CP, Partsch H. Nomenclature of the veins of the lower limb: an international interdisciplinary consensus statement. J Vasc Surg. 2002;36:416–22.
13. Haeger K. The surgical anatomy of the sapheno-femoral and sapheno-popliteal junctions. Anat Rec. 1942;82:93–102.
14. Caggiati A, Bergan J, Gloviczki P, Eklof B, Allegra C, Partsch H. Nomenclature of the veins of the lower limb: extensions, refinements, and clinical applications. J Vasc Surg. 2005;41:719–24.

# Part VI

# Deep Abdominal Doppler

Dennis F. Bandyk

# Ultrasound of the Hepatoportal Circulation

46

Carol B. Benson and Mary C. Frates

**Abstract**

Doppler assessment of blood flow through the liver has become an important clinical tool for evaluating abnormalities of the liver. Alterations in flow patterns in the portal and hepatic vessels can provide important information about the anatomy, physiology, and pathology of the liver and cardiovascular system. As a result, liver Doppler has become part of the evaluation of any patient with known or suspected liver disease. Proper equipment and techniques are required for adequate evaluation of hepatic blood vessels.

The hepatic artery supplies 25–30% of the blood flow to the liver; however, this amount may be diminished in patients with celiac artery disease, or increased in the setting of diminished portal venous flow.

The portal vein carries 70–75% of the blood flow to the liver. Flow patterns in the portal vein may be altered with liver disease or cardiac disease. Portal hypertension is the most common abnormality of the portal vein and can lead to diminished, absent, or reversed portal flow. The portal vein may also become thrombosed with portal hypertension or other disease states such as hypercoagulability.

The hepatic venous waveform is typically multiphasic. Altered liver parenchyma can cause a dampened or monophasic waveform, while cardiac disease can cause exaggeration of the retrograde components of the cycle. Occlusion or thrombosis of hepatic veins can lead to parenchymal changes in the liver and, ultimately, to portal hypertension.

The Doppler findings in the hepatic arteries, portal veins, and hepatic veins of the liver provide important clues to pathology in the liver. In addition, Doppler interrogation of these vessels can be used to monitor patients with known liver pathology to assess progression of disease and determine when interventions may be required.

**Keywords**

Liver Doppler • Portal vein • Portal hypertension • Hepatic vein • Cirrhosis

## Introduction

Doppler assessment of blood flow through the liver has become an important clinical tool for evaluating abnormalities of the liver. Examination of inflow patterns in the complex parallel circulations of arterial and portal inflow and in the hepatic venous outflow can provide important information about the anatomy, physiology, and pathology of the liver and cardiovascular system. In addition, Doppler can be used to monitor patients with known liver pathology to assess

C.B. Benson, M.D. (✉) • M.C. Frates, M.D.
Department of Radiology, Harvard Medical School,
Boston, MA, USA

Department of Radiology, Brigham and Women's Hospital,
75 Francis St., Boston, MA 02115, USA
e-mail: cbenson@partners.org; mfrates@partners.org

A.F. AbuRahma, D.F. Bandyk (eds.), *Noninvasive Vascular Diagnosis*,
DOI 10.1007/978-1-4471-4005-4_46, 

progression of disease and determine when interventions may be required.

This chapter provides an overview of Doppler evaluation of the hepatic arterial blood supply, the portal venous system, and the draining hepatic veins. First, the discussion will focus on the instrumentation and techniques required for obtaining color Doppler images and spectral waveforms from hepatic and portal vessels. This will be followed by a description of the normal anatomy and normal Doppler waveforms for the hepatic vessels. Next will be a description of the use of Doppler in the clinical setting, followed by the Doppler findings seen in various types of liver pathology affecting the hepatic arteries, portal veins, and hepatic veins. While this is not intended to be an exhaustive review of all liver pathology, this chapter should offer an in-depth explanation of the value of Doppler ultrasound in hepatoportal vessels for diagnosing abnormalities of the liver and its circulation.

## Instrumentation and Technique

Modern ultrasound systems designed for imaging the adult abdomen support broad bandwidth transducers, which can perform multiple functions, including real-time grayscale sonographic imaging, color and power Doppler imaging, and spectral Doppler waveform acquisition. In general, the liver is evaluated with transducer frequency settings between 3 and 5 MHz, often with harmonic imaging. Color and spectral Doppler of hepatic vessels, however, may require lower frequencies, in the range from 2 to 4 MHz, for optimal assessment. Most broad bandwidth transducers and ultrasound systems allow for imaging and Doppler to be used at different frequencies, independent of the frequency of the other. Thus, while imaging the liver with color Doppler, the grayscale setting could be at 5 MHz with harmonics, while the color Doppler could be optimized at 3 MHz [1].

Grayscale imaging is essential not just for imaging the liver, but also for locating hepatic vessels and for differentiating one from another. Color and power Doppler can each be used to locate and identify vessels. Color Doppler provides information about presence of flow and flow direction. Power Doppler, more sensitive than color Doppler, provides information about presence and location of flow. Some ultrasound systems have the capability of displaying directional power Doppler, a color mapping of blood flow with the sensitivity of power Doppler, and the ability to show direction of flow like color Doppler [2]. Spectral Doppler is used to acquire waveforms from various vessels to provide information about velocities of blood flow in the vessels as well as the characteristics of the flow.

The vessels of the liver are more difficult to evaluate with Doppler than are vessels in the neck or extremities for several reasons. The arteries and veins in the liver are deep in the abdomen in the right upper quadrant. Finding a sonographic window to visualize the liver may be challenging because intervening bowel gas may obscure the liver when scanning anteriorly, and the ribs may block the ultrasound beam when scanning from the right side. Bowel gas can be minimized by requiring patients to fast for at least 8 h prior to their scheduled examination. Scanning from the right often requires careful placement of the transducer in an intercostal space to avoid shadowing from the ribs. Different intercostal spaces provide windows at different levels of the liver. During scanning, one maneuver that can help with visualization of the liver and its vessels is to ask the patient to take a deep breath and hold it. With deep inspiration, some of the liver may move to a position inferior to the costal margin, providing a window through which much of the liver may be visualized by angling the transducer superiorly. The liver also moves inferiorly when the patient is turned into a left lateral decubitus position, another maneuver that could yield a good window into the right upper quadrant.

For Doppler assessment of hepatic vessels, the same maneuvers that are used for grayscale imaging can be employed. Low-frequency transducers are needed to penetrate to the depth of the vessels and to interrogate vessels for blood flow. These lower-frequency transducers may be less sensitive to slow flow than are higher-frequency transducers. As a general rule, the Doppler setting should be set at the highest frequency possible to obtain a good Doppler waveform without giving up sensitivity to flow due to attenuation of the beam.

The hepatic artery and portal veins radiate from the porta hepatis at the inferomedial center of the liver toward the periphery of the liver, and the hepatic veins course from the periphery of the liver toward the inferior vena cava located posterior and superior. For adequate spectral waveform analysis, the angle of the Doppler signal should be no greater than 60°. Finding a good Doppler angle for interrogation of these vessels adds an additional challenge to the sonographic examination. The evaluation of various vessels and their branches may require the examiner to scan the patient from multiple sites in the anterior and right upper abdomen. In particular, the main portal vein and its right branches are best assessed from the right side through an intercostal space, while the left portal branches are best assessed from an anterior approach below the ribs. The hepatic veins are usually better imaged with an anterior subcostal approach, although scanning from the right may also be successful.

Good Doppler technique includes optimal setting of the scale and baseline. With both color and spectral Doppler, the scale should be set as low as possible without causing

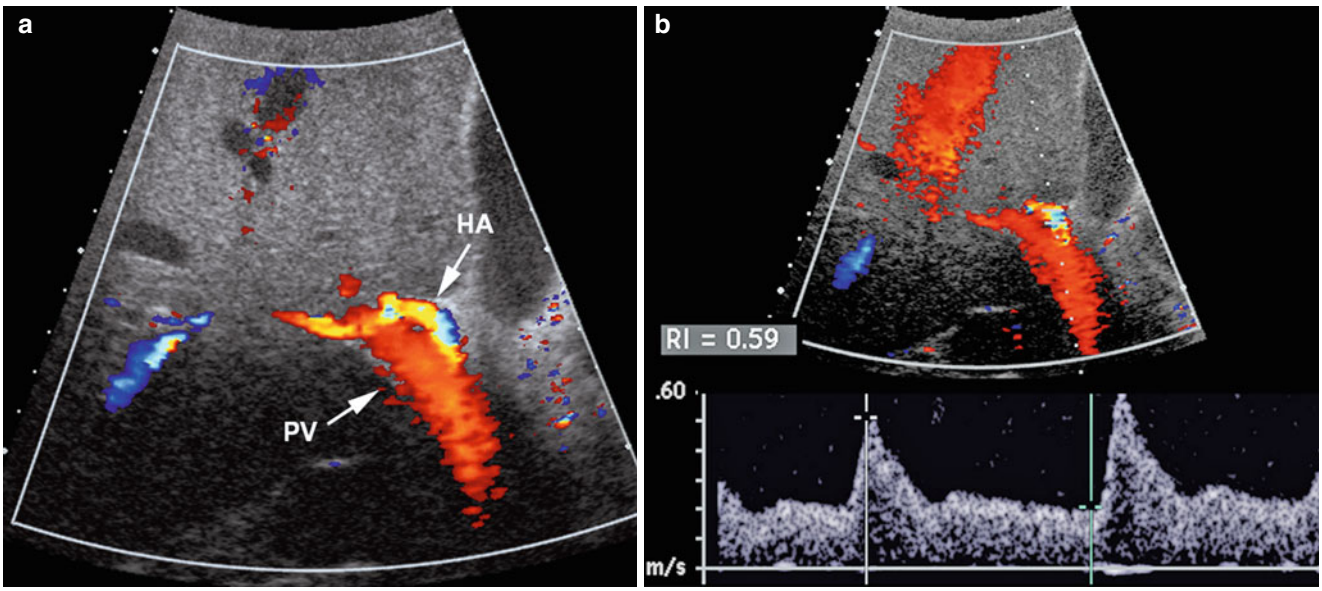


**Fig. 46.1** Hepatic artery waveform. (**a**) Color Doppler image of porta hepatis demonstrating high flow in the hepatic artery (*arrow*, *HA*) adjacent to the portal vein (*arrow*, *PV*), which has slower flow. (**b**) Spectral waveform from the hepatic artery showing low resistance arterial flow with a resistive index of 0.59

aliasing of the signal in the vessel being interrogated. If the flow is unidirectional, the baseline can be moved to allow for further decrease in the scale before aliasing will occur [1, 3].

## Anatomy and Normal Doppler

### Hepatic Artery

In normal patients, the hepatic artery or arteries supply the liver with 25–30% of its blood flow [4, 5]. The main hepatic artery is one of the major branches of the celiac artery, arising from the celiac axis shortly after its origin from the upper abdominal aorta. The artery courses into the liver at the porta hepatis, then branches into right and left branches. Variations in hepatic artery anatomy are common, with approximately 25% of patients having more than one hepatic artery [6]. The most common variants are a replaced right hepatic artery and a replaced left hepatic artery. With a replaced right hepatic artery, a second hepatic artery arises from the superior mesenteric artery and enters the liver to become the artery to the right lobe of the liver. When the left hepatic artery is replaced, it usually arises from the left gastric artery, a branch of the celiac artery. Within the liver, the hepatic arterial branches travel in parallel with the portal vein and its branches. The hepatic artery is small. The main hepatic artery can be seen with grayscale imaging in the portal hepatis, but its individual branches are typically not visible.

The Doppler waveform of the hepatic artery is characterized by unidirectional, pulsatile, low resistance, arterial flow. That is, the waveform has a sharp systolic peak and continued antegrade flow throughout the cardiac cycle. The resistive index (RI), calculated as:

$$\mathrm{RI} = \frac{(\text{Peak systolic velocity}) - (\text{End diastolic velocity})}{(\text{Peak systolic velocity})}$$

is normally 0.55–0.70 (Fig. 46.1) [7].

### Portal Veins

In normal patients, the portal veins provide 70–75% of the hepatic blood supply. The main portal vein is formed by the confluence of the splenic vein and the superior mesenteric vein in the mid epigastrium, posterior to the pancreas. It travels into the liver at the porta hepatis, and then branches into the right and left portal veins. The right portal vein branches further into anterior and posterior branches shortly after the main portal vein bifurcation. (Fig. 46.2). Variations of this anatomy are common, seen in about 35% of patients. The most common variant is trifurcation of the main portal vein into the right posterior, right anterior, and left portal veins, with other variants including bifurcation of the main portal vein into the right posterior branch and a common trunk for the right anterior branch and the left portal vein. The portal vein and its branches are considerably larger than the hepatic arteries. As a result, the main portal vein

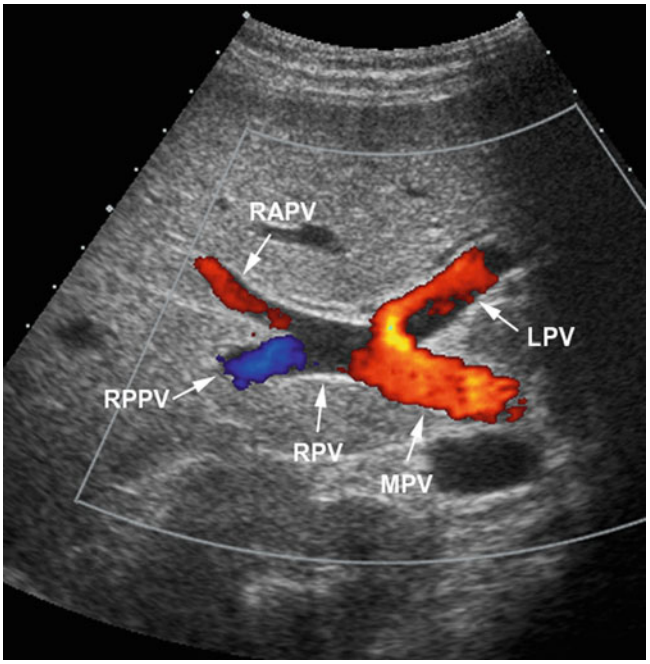


**Fig. 46.2** Main portal vein and its branches. Color Doppler sonogram of the porta hepatis showing the main portal vein (*arrow*, *MPV*), branching into the left portal vein (*arrow*, *LPV*) and right portal vein (*arrow*, *RPV*), as well as bifurcation of the right portal vein into anterior (*arrow*, *RAPV*) and posterior (*arrow*, *RPPV*) branches

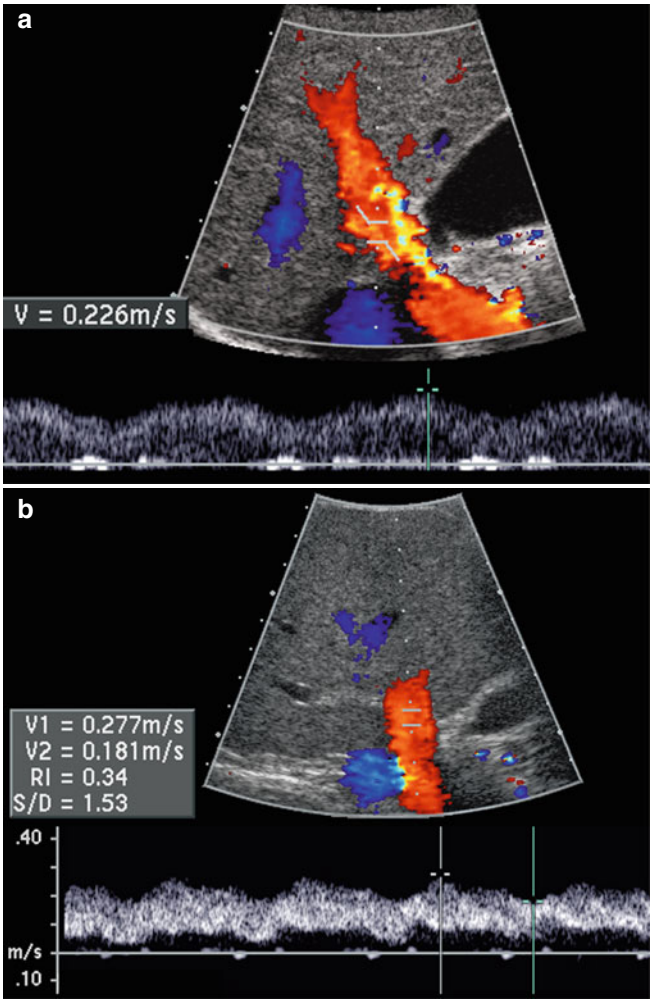


**Fig. 46.3** Portal vein waveform. (**a**) Color and spectral Doppler sonogram of the main portal vein, demonstrating continuous, antegrade, mildly undulating flow into the liver with a peak velocity of 22.6 cm/s. (**b**) Portal Doppler waveform showing mild pulsatility with the lowest velocity (18.1 cm/s) measuring >0.5 times the peak velocity (27.7 cm/s)

and its branches can be seen farther out into the liver parenchyma with grayscale imaging than the hepatic arteries [8].

Normal Doppler waveform of the portal veins demonstrates continuous antegrade flow toward the liver with a mildly undulating pattern. Flow is affected by respiration and cardiac pulsatility, although the effect is normally mild. The mean velocity in the portal vein is typically 15–30 cm/s, while the peak velocity has a broad range of normal from 15 to 40 cm/s. In general, variations in velocities in the main portal vein are small, with the lowest velocity measuring more than half the highest velocity. That is,

$$\frac{\text{Lowest velocity}}{\text{Highest velocity}} < 0.5$$

(Fig. 46.3) [7, 9, 10].

## Hepatic Veins

The hepatic veins drain all the blood from the liver into the inferior vena cava. That is, all the blood entering the liver through the portal vein and hepatic arteries is drained through the hepatic veins directly into the inferior vena cava. Three main hepatic veins are typically present: the left, middle, and right. The left hepatic vein travels between the medial and lateral segments of the left lobe of the liver. The middle hepatic vein courses between the right and left lobes of the liver, and the right hepatic vein courses between the anterior and posterior segments of the right lobe (Fig. 46.4). Variations of hepatic venous anatomy are common, with an additional right inferior hepatic vein in some patients and merging of the middle and left hepatic veins into a single vessel in others [11].

Normal hepatic veins have a multiphasic pattern during the cardiac cycle, with flow predominantly away from the liver and toward the heart except during short segments of the cycle. Starting with atrial systole, the first part of the hepatic vein waveform is typically retrograde, or back into the liver, as a result of increased pressure in the right atrium

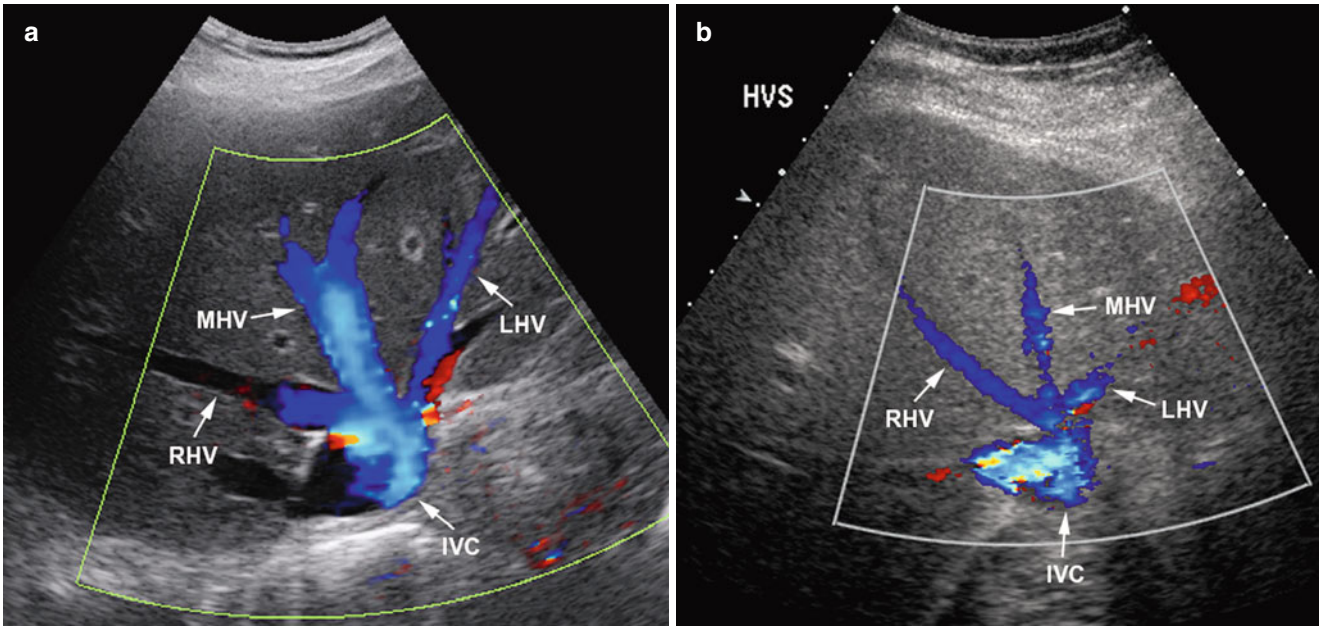


**Fig. 46.4** Hepatic veins. (**a**) and (**b**) Color Doppler sonograms of liver demonstrating flow in left (*arrow*, *LHV*), middle (*arrow*, *MHV*), and right (*arrow*, *RHV*) hepatic veins as they converge into the inferior vena cava (*arrow*, *IVC*)

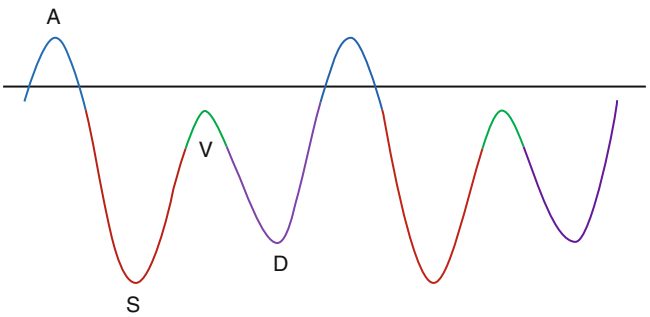


**Fig. 46.5** Hepatic venous waveform. Diagram demonstrating the components of the multiphasic hepatic venous waveform. Flow below the baseline is toward the heart away from the liver. Flow above the baseline is away from the heart back toward the liver. The *blue* A-wave is seen during atrial systole, the *red* S-wave during ventricular systole, and the *purple* D-wave during diastole. The *green* V-wave is a transitional wave between ventricular systole and diastole, when flow decreases and the tricuspid valve shifts into the right atrium

as the atrium contracts. This is termed the A-wave. In some patients, the A-wave is not retrograde, but rather has markedly diminished antegrade flow compared to the rest of the waveform. After atrial systole is ventricular systole, during which blood is propelled out of the heart into the great arteries. In addition, the tricuspid valve is drawn into the right ventricle, increasing negative pressure in the atrium, drawing blood back to the heart. During ventricular systole, the hepatic vein waveform demonstrates flow toward the inferior vena cava and is called the S-wave. Flow is maximal toward the heart during this portion of the cardiac cycle. Toward the end of systole, the tricuspid valve shifts away from the right ventricle. During this period, the hepatic waveform usually demonstrates a decrease in flow velocity toward the heart, or even a bit of reversed flow away from the heart, making the V-wave. Lastly, during diastole, the tricuspid valve is open, and the atria and ventricles fill with blood. The hepatic waveform during this part of the cycle is called the D-wave and characteristically demonstrates antegrade flow with velocities almost as great as during cardiac systole (Fig. 46.5) [11].

The multiphasic pattern of hepatic venous flow is sometimes considered to have four components, the A-wave, V-wave, S-wave, and D-wave, and is sometimes called triphasic. The latter term is used by those who consider the V-wave to be a transitional period and not its own wave. No matter which term is used to characterize the waveform, it is important to recognize the normal appearance of the hepatic venous waveform in order to identify abnormalities of flow in these vessels (Fig. 46.6) [11].

The hepatic venous waveform is affected by respiration. In particular, during inspiration and Valsalva, the multiphasic waveform may become monophasic, or flattened, with diminished flow toward the heart. Thus, it is best to assess the hepatic veins at end expiration or during quiet respiration. Because of this, imaging and Doppler acquisition may be difficult because the scan should not be performed with the patient in suspended respiration after taking a deep breath. Intercostal views may be necessary, as the subcostal approach may not be adequate [11].

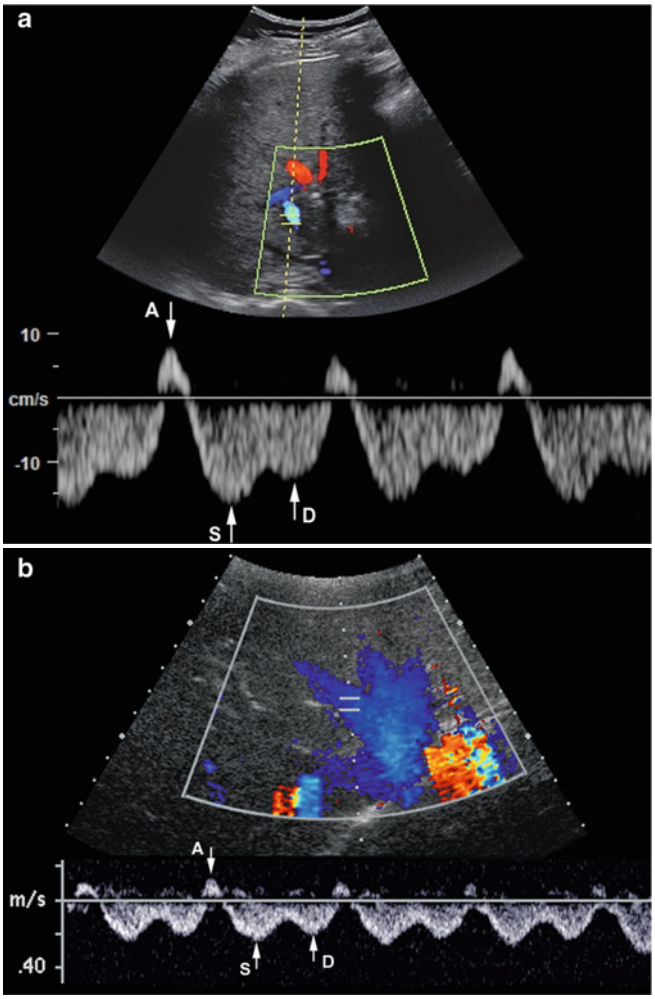


**Fig. 46.6** Hepatic vein waveforms. (**a**) and (**b**) Color and spectral Doppler of the hepatic vein, demonstrating normal multiphasic flow with the A-wave (*arrow*, *A*), S-wave (*arrow*, *S*), and D-wave (*arrow*, *D*). The V-wave, defined by some as a separate wave, is the depression between the S- and D-waves

## Role of Doppler in Assessment of the Liver

Color and spectral Doppler are used in conjunction with grayscale imaging of the liver to identify blood vessels in the liver and assess the vessels for presence and direction of flow. In addition, Doppler is used to evaluate the dynamics of flow within the vessel [11]. Diseases of the liver alter the parenchyma, which in turn, alters blood flow in the arteries and veins leading into the liver, within the liver, and exiting the liver [7]. Thus, Doppler studies should be performed to help determine if the liver parenchyma is abnormal. Once the presence of liver disease has been established, Doppler is used to help determine the severity of disease and to monitor progression [12].

Common indications for liver Doppler are listed in Table 46.1. The most common indication is suspected or known portal hypertension. These patients are monitored closely to detect changes in portal venous flow and to look for the development of collateral vessels. Patients with known or suspected liver disease, such as cirrhosis or hepatitis B or C, may benefit from Doppler studies, because the Doppler assessment may provide information about the severity of disease. Doppler is also an important tool for monitoring the progression of these diseases to determine when intervention is necessary. In addition to the indications above, patients with systemic diseases, such as hypercoagulability and atherosclerosis, may develop abnormalities of the vessels entering or exiting the liver, leading to damage to the liver.

**Table 46.1** Indications for performing liver Doppler

| |
|---|
| Portal hypertension |
| Abnormal liver function tests |
| Hepatitis B |
| Hepatitis C |
| Cirrhosis |
| Metastatic disease in the liver |
| Suspected veno-occlusive disease after hematopoietic stem cell transplantation |
| Trauma |
| Hypercoagulable state |
| Gastrointestinal bleed |

## Abnormalities of the Hepatic Artery

Altered blood flow in the hepatic artery typically results from one of two pathologic processes, arterial stenosis, or hepatic parenchymal disease. The most common site of atherosclerotic disease affecting blood flow in the hepatic artery is in the celiac artery near its origin from the aorta. A stenosis of 70% or greater in the celiac axis is considered hemodynamically significant and can lead to diminished blood flow to the liver through the hepatic artery. The diagnosis of celiac stenosis is made with spectral Doppler when the peak systolic velocity measures greater than 200 cm/s in the celiac artery (Fig. 46.7). Additional findings with celiac stenosis may include an abnormal tardus-pardus waveform in the main hepatic artery [13, 14].

Liver parenchymal disease and liver congestion may cause increased vascular resistance in the liver. The increased resistance is reflected in the hepatic artery waveform as diminished diastolic flow and an elevated Doppler resistive index measuring >0.70 (Fig. 46.8). Common pathologies associated with an elevated resistive index in the hepatic artery include cirrhosis, acute hepatitis, metastatic disease, congestive heart failure, and hepatic vein obstruction.

A few rare entities may lead to an abnormally low resistive index in the hepatic artery that measures <0.55. Such entities include vascular malformations with arteriovenous

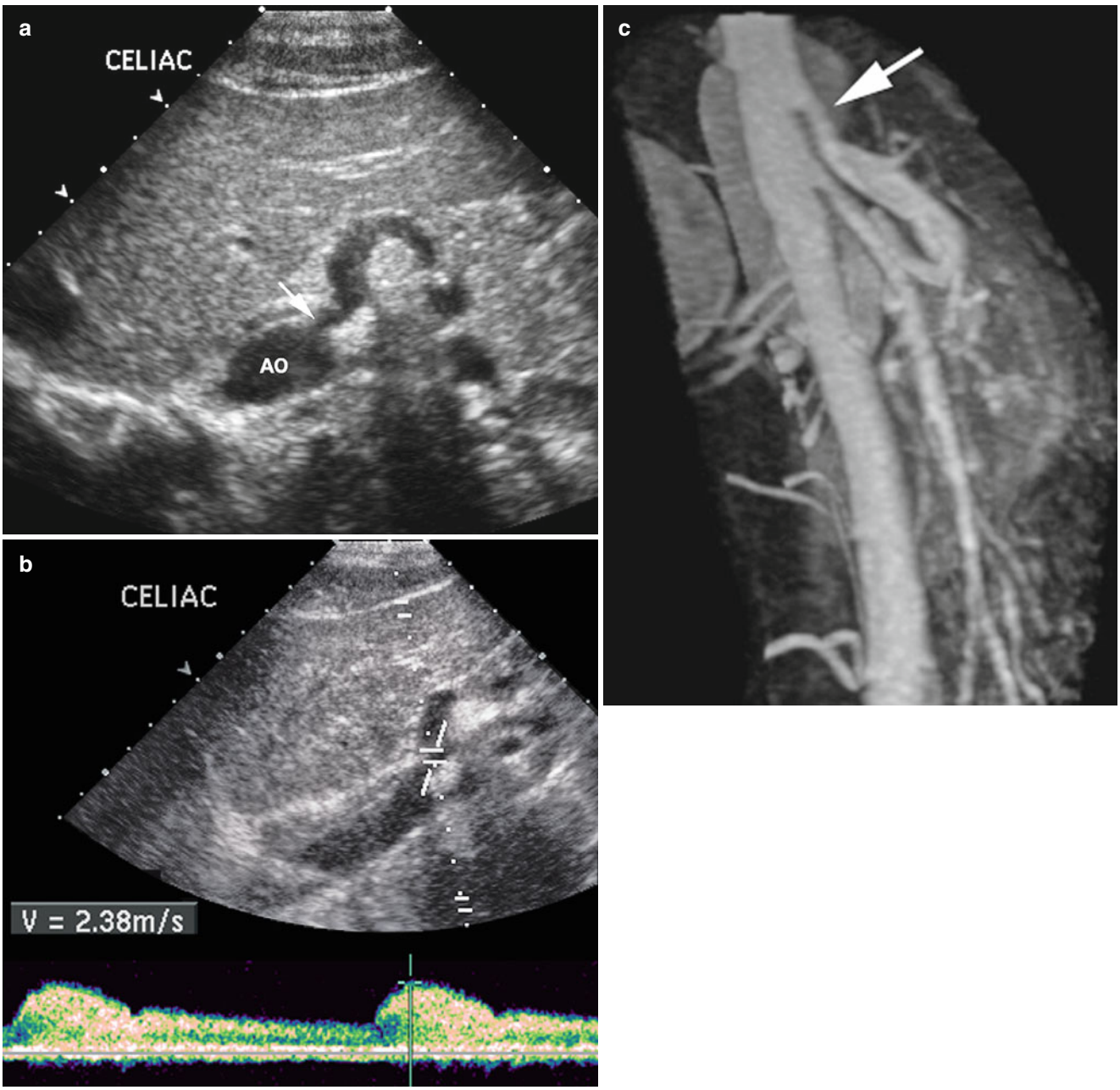


**Fig. 46.7** Celiac artery stenosis. (**a**) Transverse sonogram demonstrating stenosis (*arrow*) at the origin of celiac artery from the aorta. (**b**) Sagittal midline image of celiac origin from aorta with spectral Doppler showing elevated velocity of 238 cm/s, indicative of stenosis. (**c**) Sagittal midline magnetic resonance angiogram of abdominal aorta and its branches showing celiac stenosis at its origin (*arrow*)

shunting, arteriovenous or arterioportal shunt, and significant stenosis of the celiac artery or the hepatic artery.

## Abnormalities of the Portal Venous System

### Altered Portal Venous Hemodynamics

The normal portal venous waveform demonstrates continuous antegrade flow toward the liver with mild respiratory variation and mild cardiac pulsatility. Abnormalities of flow in the main portal vein include increased flow, diminished flow, to-and-fro flow, reversed flow, absent flow, and exaggerated cardiac pulsatility (Fig. 46.9). Each of these abnormalities may indicate one of several pathologic states (Table 46.2) [1, 7]. When abnormal blood flow is detected in the main portal vein, assessment of the portal vein branches is important to determine the distribution or extent of the abnormality. Flow direction and waveform characteristics should be assessed in the three main branches of the main portal vein, the right posterior, right anterior, and left portal veins.

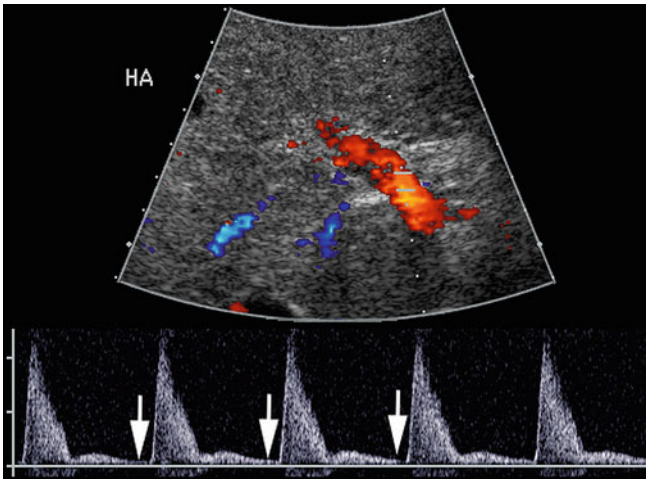


**Fig. 46.8** High resistance hepatic artery flow. Color Doppler sonogram with spectral waveform below of the hepatic artery in a patient with cirrhosis, demonstrating almost no end diastolic flow (*arrows*), indicative of high resistance to arterial inflow

Because each type of altered blood flow pattern may be seen with several different pathologic processes, and because some pathologic processes may manifest one of several patterns of altered portal venous flow, we discuss various disease entities and describe how Doppler is used to diagnose and monitor these diseases.

## Portal Hypertension

Portal hypertension is defined as increased pressure in the portal vein such that the pressure gradient between the portal vein and the inferior vena cava is 12 mmHg or greater [5]. Portal hypertension can develop from presinusoidal pathologies, such as sarcoidosis, lymphoma, or schistosomiasis, or from postsinusoidal pathologies, such as cirrhosis, hepatic vein thrombosis (Budd-Chiari syndrome), or veno-occlusive disease after bone marrow transplantation. Rarely, portal hypertension develops from extrahepatic diseases, such as prehepatic portal vein compression or posthepatic hepatic vein or inferior vena cava obstruction [4, 5, 15].

The most common cause of portal hypertension is liver cirrhosis. Cirrhosis may result from a number pathologies affecting the liver (Table 46.3), the most common being alcoholism and chronic active hepatitis B [16]. Cirrhosis is liver parenchymal fibrosis that results from a chronic insult to the liver that causes cell damage and death, and the damaged cells are then replaced by fibrosis. The fibrotic liver parenchyma causes increased vascular resistance, which leads to elevated pressure in the portal veins and, thus, portal hypertension.

The sonographic evaluation for portal hypertension starts with grayscale imaging of the liver to locate and assess the diameter of the main portal vein in the porta hepatis and the parenchyma of the liver. Signs of cirrhosis in the liver include coarse hepatic parenchyma, nodular liver contour, enlargement of the left and caudate lobes and a small right lobe, and focal masses. Extrahepatic signs include ascites and splenomegaly. Doppler assessment begins with the portal confluence to document presence and direction of flow in the splenic vein (Fig. 46.10). Next, flow should be assessed in the main portal vein with color and spectral Doppler, to determine flow direction and mean and peak velocities. Flow direction should be assessed in the anterior and posterior branches of the right portal vein and in the left portal vein. Lastly, a careful search for collateral vessels should be performed, using grayscale and color Doppler, to look for a recanalized umbilical vein, coronary vein collaterals, and varices around the gallbladder or in the region of the gastroesophageal junction [4, 7].

The development and progression of portal hypertension is associated with changes in the portal vein and its flow. Early stages of portal hypertension are characterized by diminished portal flow to the liver. This is manifested by dilation of the main portal vein diameter to more than 1.3 cm and mean flow velocities of less than 15 cm/s (Fig. 46.11). In response to the diminished portal venous inflow, flow will compensatorily increase in the hepatic arteries. As the disease progresses and vascular resistance in the liver parenchyma increases, intrahepatic arterial flow is shunted to the intrahepatic portal veins, rather than through its normal pathways to the hepatic veins. Continued increased vascular resistance causes increased arterioportal shunting, and flow in the portal vein will become less and less, until it stops and the portal vein thromboses, or until flow in the portal vein reverses direction and flows away from the liver. The diversion of portal venous flow away from the liver leads to the development of portosystemic collateral vessels outside the liver [4, 5].

**Fig. 46.9** Abnormal portal vein waveforms. (**a**) To-and-fro flow in the main portal vein in a patient with tricuspid regurgitation is seen in the spectral waveform below the color Doppler sonogram. The waveform shows antegrade flow toward the liver (*arrowheads*) and retrograde flow away from the liver (*arrows*) during each cardiac cycle. (**b**, **c**) Color Doppler sonogram of portal vein showing (**b**) antegrade flow toward the liver in *red* and (**c**) retrograde flow away from the liver in *blue*, during the cardiac cycle. (**d**) Reversed flow in the portal vein in another patient shown in the color Doppler sonogram as *blue* in the portal vein and on the spectral waveform as flow below the baseline. (**e**) Exaggerated cardiac pulsatility in another patient with congestive heart failure, demonstrating markedly diminished portal vein flow (*arrow*) during part of each cardiac cycle

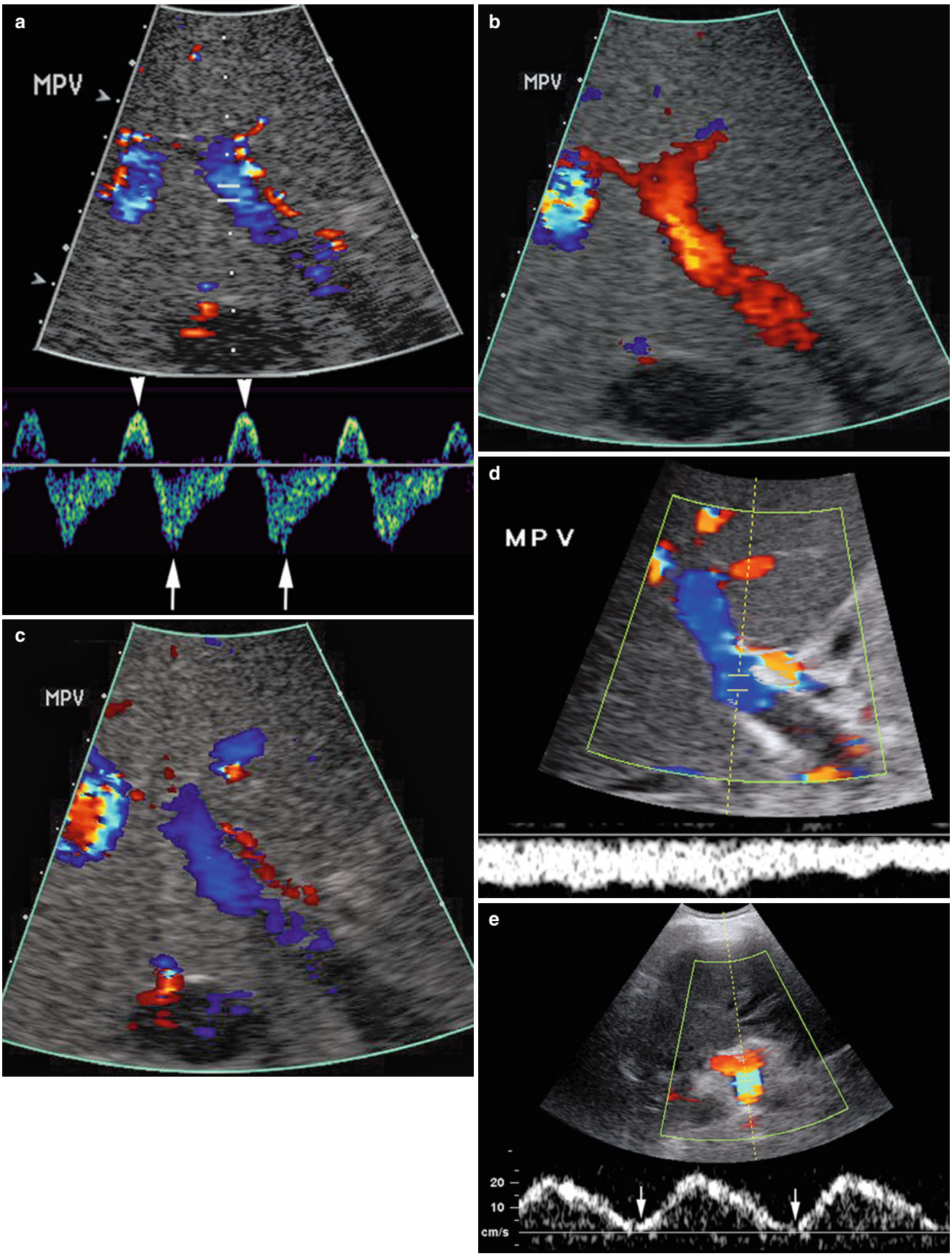
a
MPV
b
MPV
c
MPV
d
MPV
e
20
10
cm/s

**Table 46.2** Causes of altered blood flow in the main portal vein

| Abnormal flow pattern | Pathology |
|---|---|
| Increased portal venous flow | Intrahepatic portosystemic shunt |
| | Portal-to-hepatic vein shunt |
| | TIPS |
| | Recanalized umbilical vein |
| | Portosystemic shunt to coronary vein |
| Diminished portal venous flow | Portal hypertension |
| | Hepatic congestion |
| | Metastatic disease |
| | Hepatic vein thrombosis |
| To-and-fro portal venous flow | Portal hypertension |
| | Arterioportal shunting with cirrhosis |
| | Hepatic congestion |
| | Metastatic disease |
| Reversed portal venous flow | Portal hypertension |
| | Arterioportal shunting with cirrhosis |
| | Hepatic congestion |
| | Metastatic disease |
| Absent portal venous flow | Portal hypertension |
| | Hepatic congestion |
| | Metastatic disease |
| | Hypercoagulable state |
| | Splenic vein thrombosis |
| | Tumor in the portal vein |
| Exaggerated cardiac pulsatility | Congestive heart failure |
| | Tricuspid regurgitation |
| | Arterioportal shunting with cirrhosis |

**Table 46.3** Causes of cirrhosis and portal hypertension

| |
|---|
| Alcohol consumption |
| Hepatitis B infection |
| Hepatitis C infection |
| Steatohepatitis |
| Chronic congestive heart failure |
| Cystic fibrosis |
| Bile duct destruction or primary biliary cirrhosis |
| Sclerosing cholangitis |
| Congenital biliary atresia |
| Hemochromatosis |
| Wilson's disease (copper storage disease) |
| Glycogen storage disease |
| Autoimmune hepatitis |

A number of sonographic and Doppler criteria have been proposed for the diagnosis of portal hypertension (Table 46.4). The long list of criteria exists because no single criterion has a good sensitivity or specificity for portal hypertension. This is because variations in the progression of portal hypertension are common and changes in the portal vein are highly dependent on the development and location of portosystemic shunts [4, 5, 17]. For example, in some cases, instead of developing portosystemic collaterals outside the liver, portosystemic shunts develop within the liver via a recanalized umbilical vein or through a spontaneous shunt between the portal vein and one of the hepatic veins. In these two situations, flow in the portal vein will likely be normal or increased and the portal vein diameter will remain normal size. It is important to remember that, because of the various types of changes in portal venous flow, the presence of normal flow in the portal vein does not exclude portal hypertension. Identifying

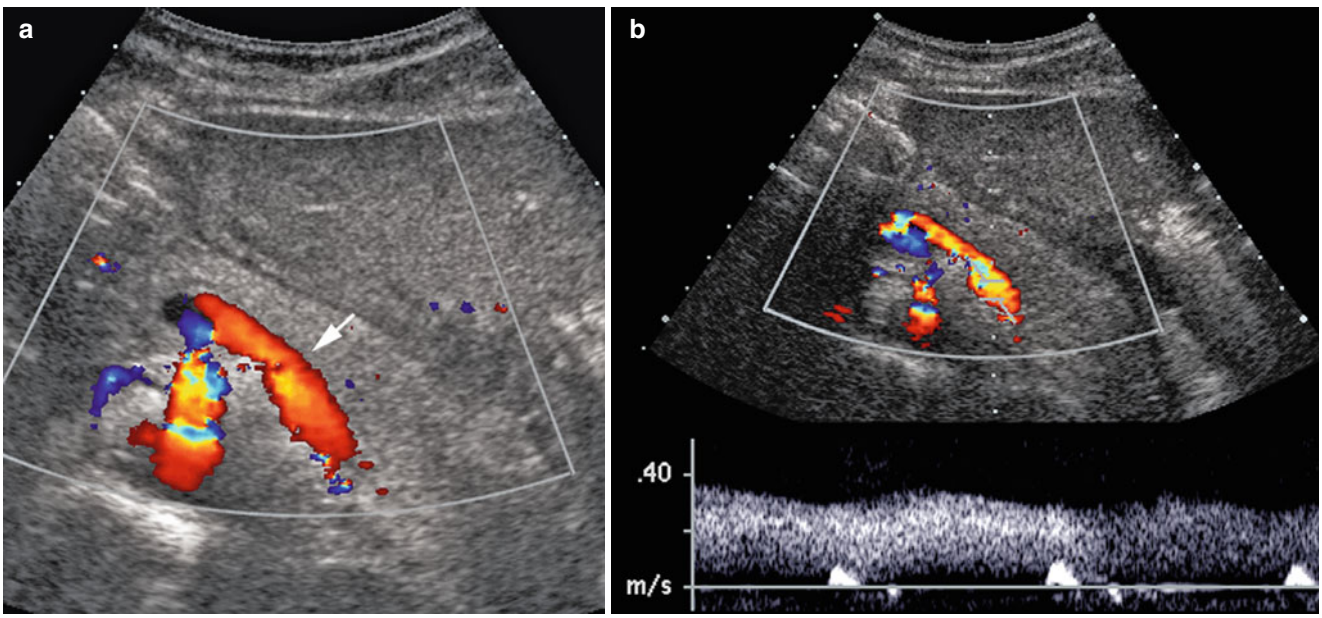


**Fig. 46.10** Splenic vein flow. (**a**) Color Doppler sonogram demonstrating normal flow in the splenic vein (*arrow*), toward its confluence with the superior mesenteric vein to form the portal vein. (**b**) Spectral waveform from splenic vein showing continues antegrade flow toward the portal confluence

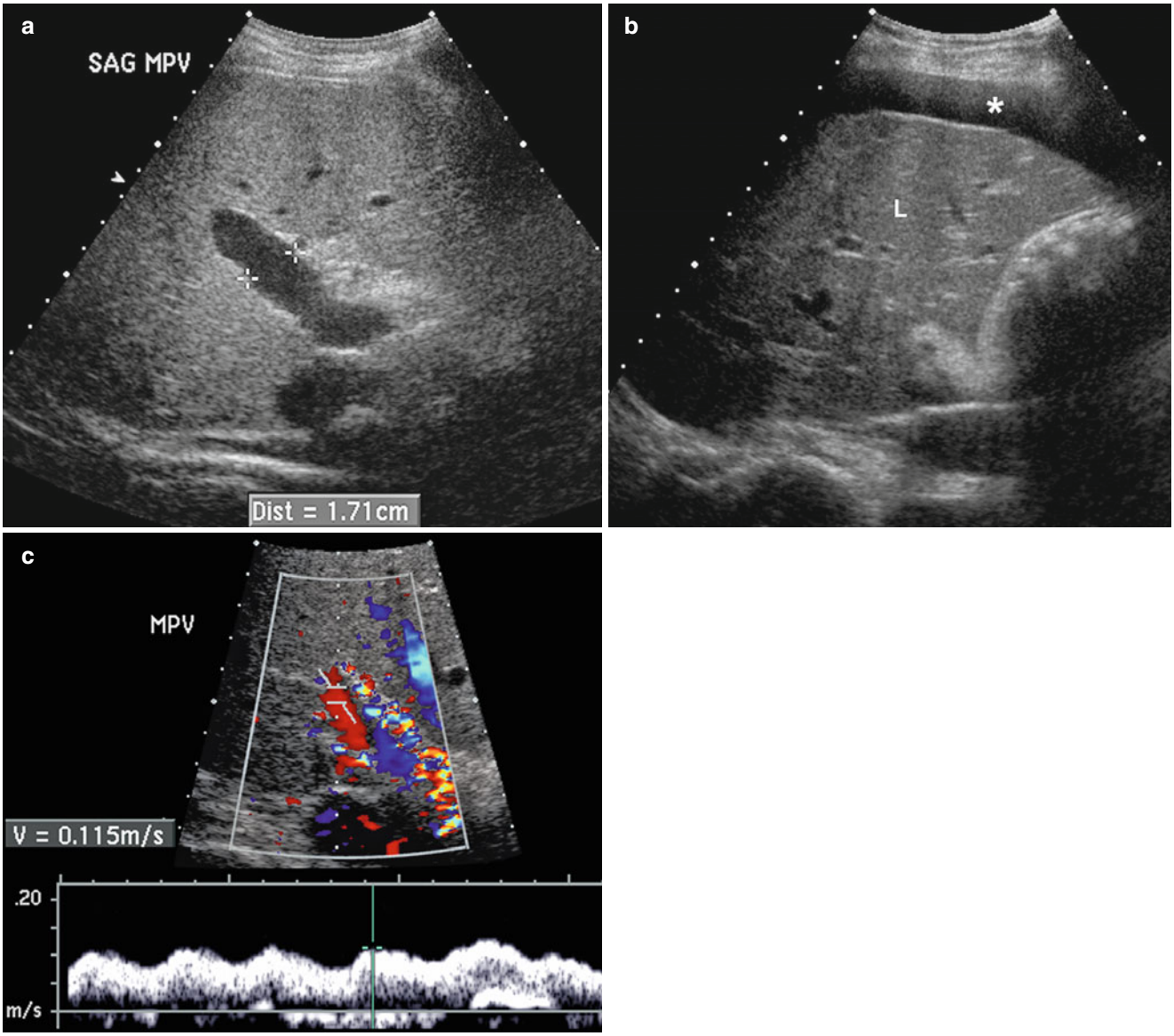


**Fig. 46.11** Portal hypertension. (**a**) Grayscale sonogram in a patient with portal hypertension demonstrating dilatation of the main portal vein to >1.7 cm (calipers). (**b**) Grayscale image from another patient with portal hypertension demonstrating ascites (*) around the liver (*L*). (**c**) Spectral waveform from the portal vein in the same patient showing abnormally slow flow in the portal vein with peak velocity of 11.5 cm/s

**Table 46.4** Sonographic and Doppler criteria for diagnosing portal hypertension

| |
|---|
| Portal vein mean velocity < 15 cm/s |
| Portal vein peak velocity < 20 cm/s |
| To-and-fro flow in the portal veins |
| Absent portal vein flow |
| Reversed portal vein flow |
| Portal vein thrombosis |
| Diminished portal vein fluctuations |
| Portal vein diameter > 1.3 cm |
| Portosystemic collaterals[a] |

[a]Most accurate means of diagnosing portal hypertension

collateral vessels or intrahepatic portosystemic shunts is the most accurate means of diagnosing portal hypertension, e.g., whether the shunts are within the liver or extrahepatic [4, 5].

## Portosystemic Shunts with Portal Hypertension

Portosystemic shunts may occur spontaneously within the liver or outside the liver. These shunts divert blood away from the portal vein branches and sinusoids within the liver into veins draining directly into the inferior vena cava. Portosystemic shunts may also be created surgically outside the liver, or placed within the liver from the portal to the hepatic veins with nonsurgical interventional techniques [18, 19].

The most common path of collateral flow that may develop with portal hypertension is through the coronary vein (also called the gastric vein), which carries blood from the main portal vein away from the liver. This type of collateral circulation often results in esophageal varices and, thus, carries risk of upper gastrointestinal hemorrhage. Coronary vein

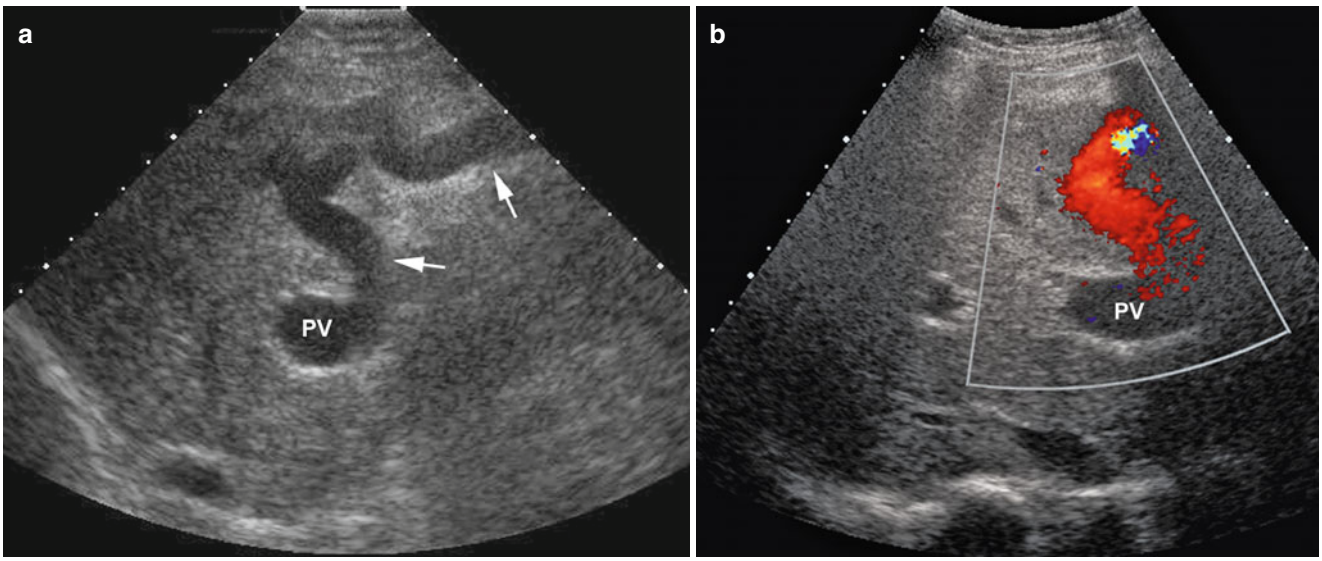


**Fig. 46.12** Dilated coronary vein collateral. (**a**) Transverse sonogram of liver demonstrating dilated coronary vein (*arrows*) coursing from the portal vein (*PV*) along the posterior medial border of the liver. (**b**) Color Doppler sonogram showing in red that the dilated coronary vein is carrying blood away from the portal vein (*PV*)

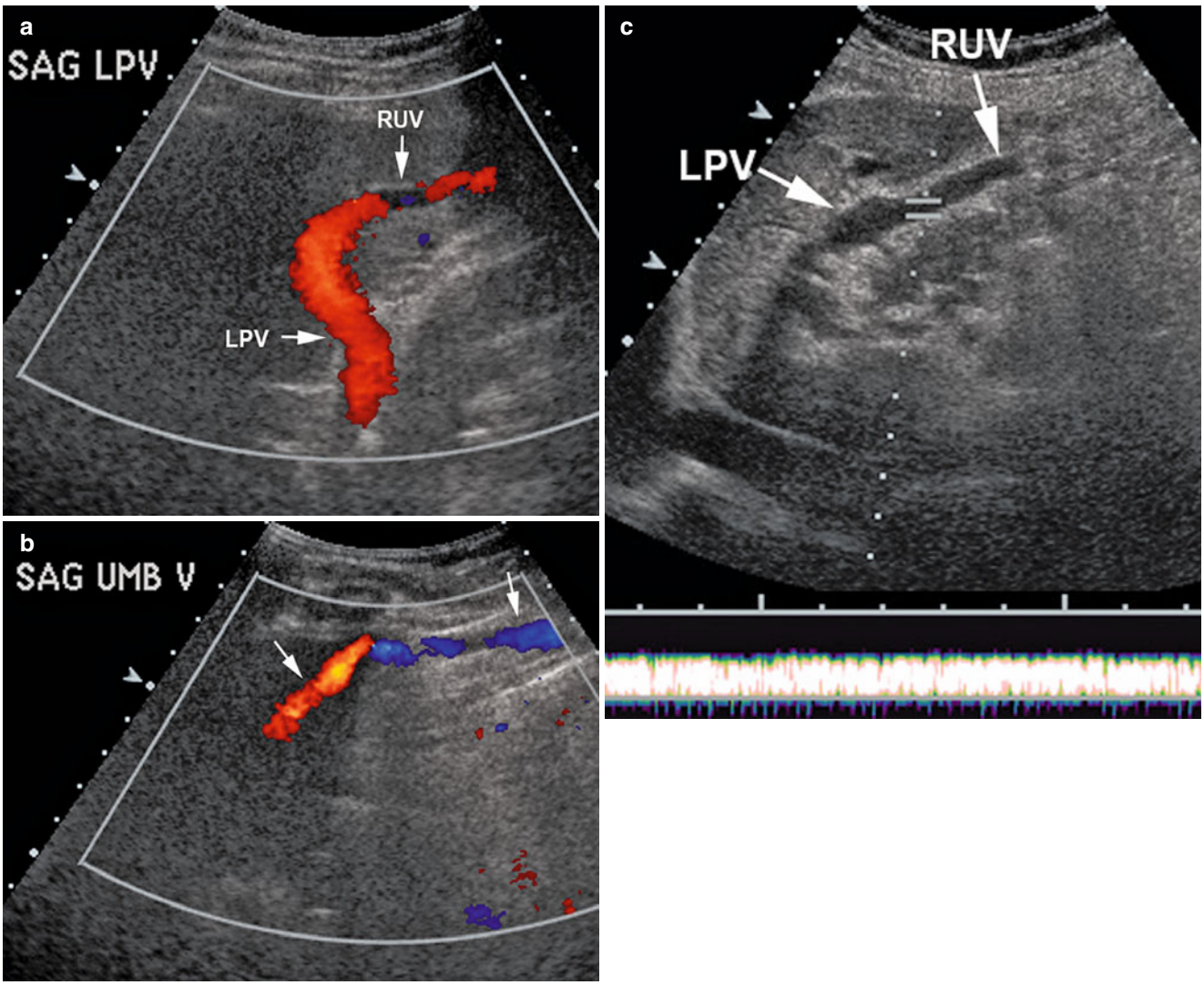

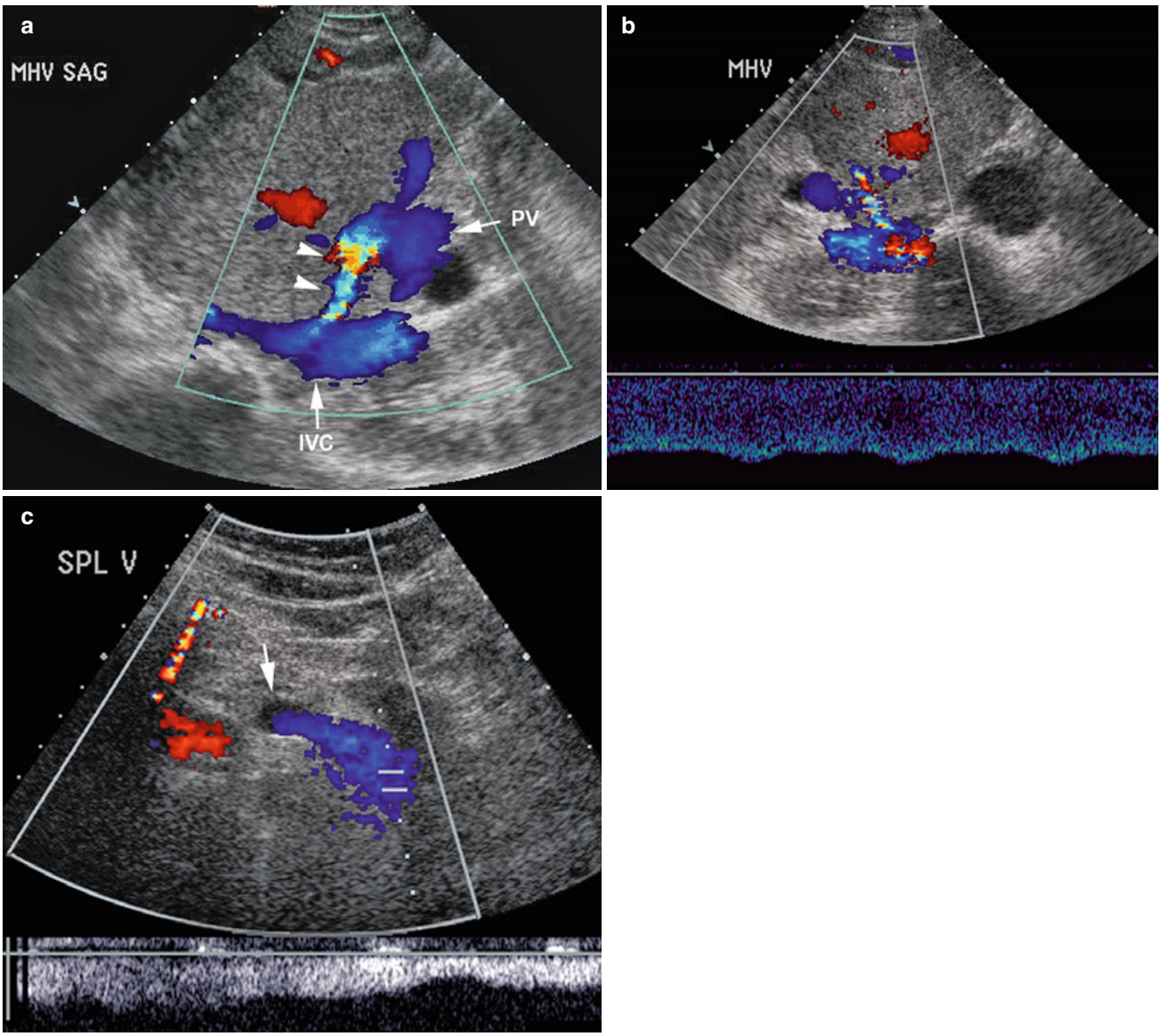


**Fig. 46.14** Portosystemic shunts. (**a**) Color Doppler sagittal sonogram of the liver demonstrating a vessel with high flow (*arrowheads*) carrying blood from the portal vein (*arrow*, *PV*) to the inferior vena cava (*arrow*, *IVC*), representing a shunt from the portal vein to the middle hepatic vein. (**b**) Color and spectral Doppler of the portal-hepatic shunt showing steady flow from the portal vein directly to the inferior vena cava. (**c**) In a different patient with a splenorenal shunt, the sagittal color and spectral Doppler sonogram demonstrates a vessel carrying blood from the splenic vein (*arrow*) inferiorly toward the renal vein through the splenorenal shunt

collaterals are visible with ultrasound and color Doppler as tortuous dilated vessels in the porta hepatis, around the pancreas, and around the gastroesophageal junction (Fig. 46.12) [20].

Another common collateral pathway is through a recanalized umbilical vein or paraumbilical vein, which carries blood from the left portal vein away from the liver to the anterior abdomen through the superficial epigastric veins [18]. The umbilical vein is seen as a dilated patent vessel coursing through the falciform ligament, carrying blood away from the liver (Fig. 46.13).

Other forms of portosystemic shunting can occur spontaneously either inside the liver, via a spontaneous portal hepatic vein shunt, or outside the liver (Fig. 46.14). The most common spontaneous extrahepatic shunt is a splenorenal shunt [21].

**Fig. 46.13** Recanalized umbilical vein. (**a**) Color Doppler sonogram of left lobe of liver showing flow from the porta hepatis through the left portal vein (*arrow*, *LPV*) to a recanalized umbilical vein (*arrow*, *RUV*). (**b**) The recanalized umbilical vein (*arrows*) carries the blood from the left portal vein away from the liver. (**c**) Recanalized umbilical vein (*arrow*, *RUV*) in another patient carrying blood from the left portal vein (*arrow*, *LPV*) away from the liver

Surgical shunts, most often connecting the splenic vein to the left renal vein, were previously used to treat severe portal hypertension and recurrent gastrointestinal hemorrhage. Since the development of the transjugular intrahepatic portosystemic shunt (TIPS), surgical shunts are now rarely performed [19]. Evaluation of extrahepatic surgical portosystemic shunts is often difficult with ultrasound and Doppler because of their deep location in the abdomen. However, shunt patency can be assessed by confirming reversed flow in the splenic vein from the portal confluence toward the spleen. Flow in the main portal vein is also frequently reversed.

## Transjugular Intrahepatic Portosystemic Shunts (TIPS)

Transjugular intrahepatic portosystemic shunts (TIPS) are placed with nonsurgical interventional techniques such

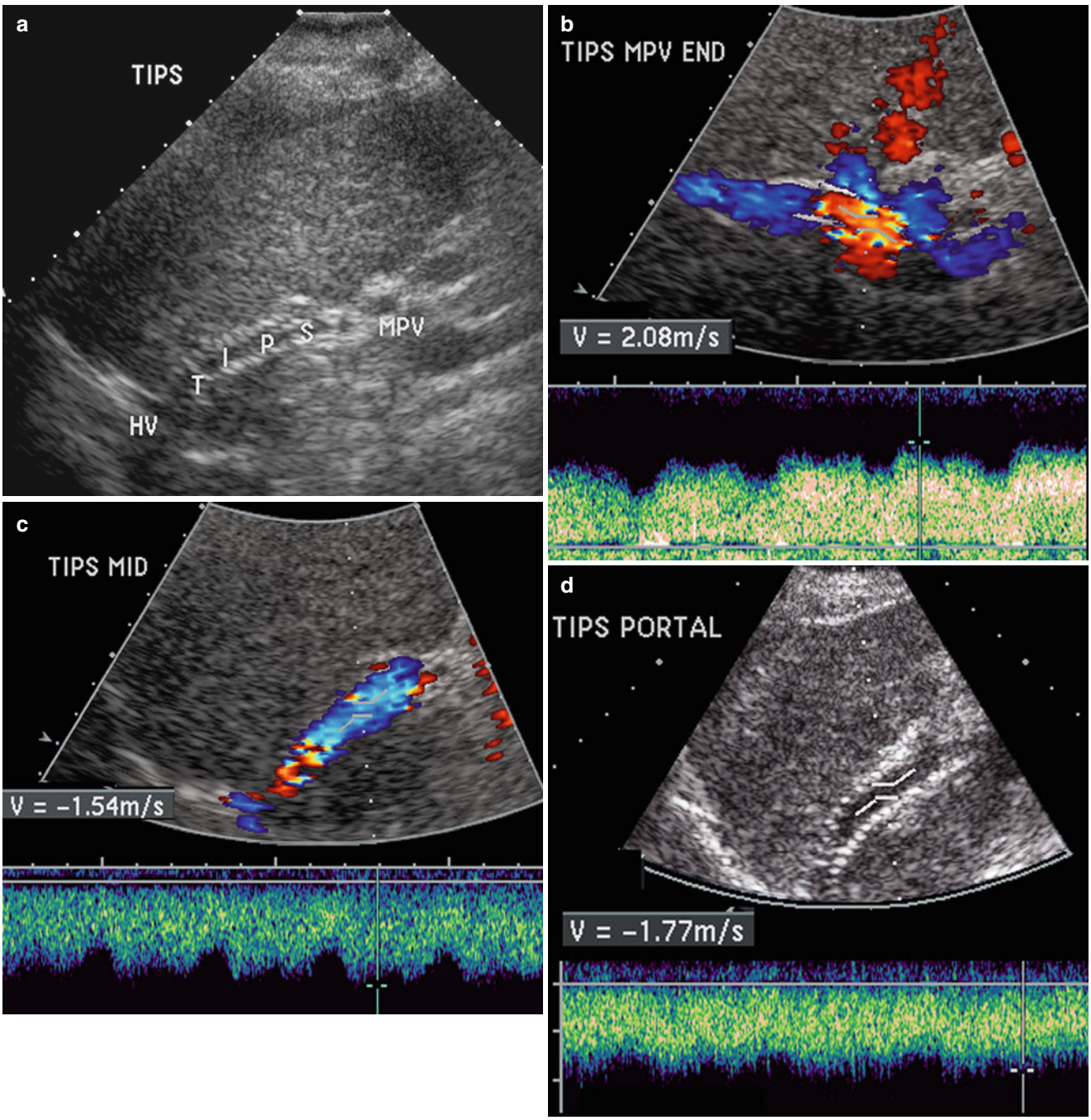


**Fig. 46.15** Transjugular intrahepatic portosystemic shunt (*TIPS*). (**a**) Sonogram demonstrating TIPS with echogenic wall, connecting the main portal vein (*MPV*) to a hepatic vein (*HV*). (**b**, **c**) Color and spectral Dopplers from same TIPS as (**a**) demonstrating peak flow velocity of 208 cm/s at the portal end of the TIPS (**b**) and 154 cm/s in mid-TIPS (**c**). (**d**–**f**) Spectral waveforms from another TIPS demonstrating normal flow velocities at the portal end (**d**), mid (**e**), and hepatic end (**f**)

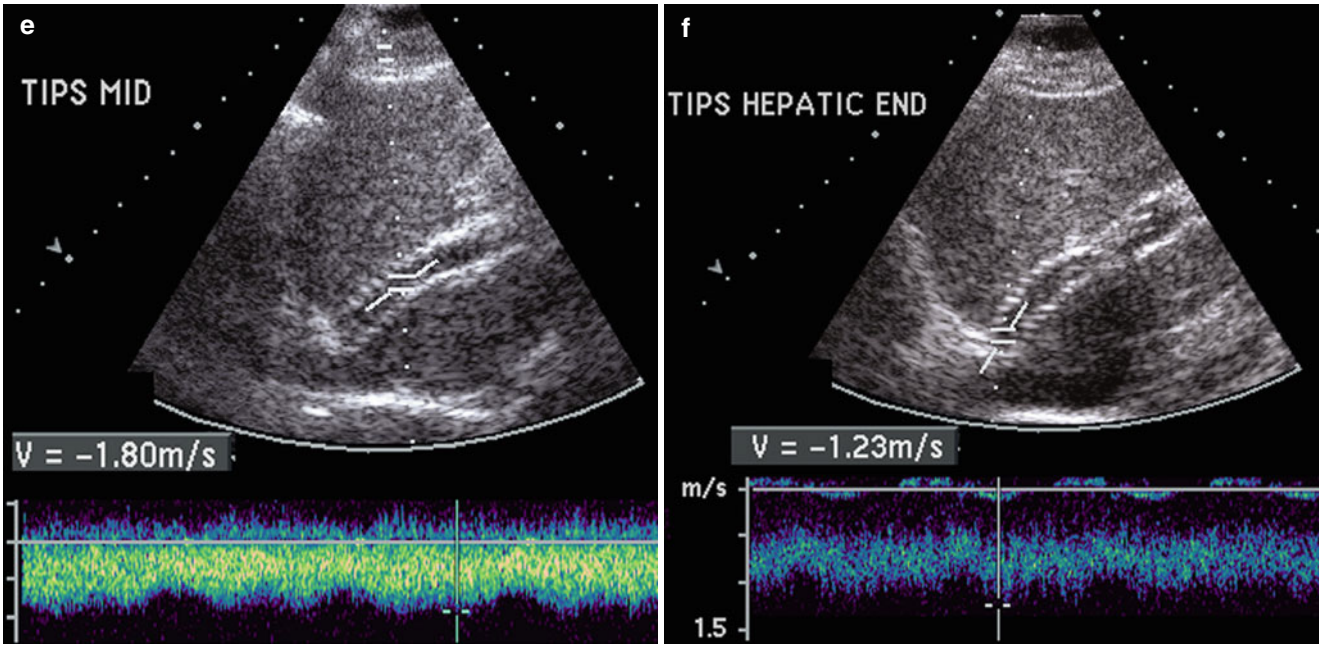


**Fig. 46.15** (continued)

**Table 46.5** Sonographic and Doppler criteria for diagnosing TIPS malfunction

| |
|---|
| Portal vein mean velocity < 20 cm/s |
| >30–50% decrease in portal vein mean velocity over time |
| TIPS velocity < 90 cm/s |
| TIPS velocity > 190 cm/s |
| Decrease in TIPS velocity of > 40 cm/s |
| Increase in TIPS velocity of > 60 cm/s |
| No flow in TIPS |
| Diminished portal vein fluctuations |
| Antegrade flow in left or right portal veins |
| Velocity change along TIPS of > 100 cm/s |

that the shunt connects the portal venous system through the hepatic venous system to the intrahepatic portion of the inferior vena cava. Most often, the shunt is placed between the main portal vein or the right portal vein and the right or middle hepatic vein. The TIPS provides a large conduit to carry blood from all the portal veins directly into the inferior vena cava. The primary function of the TIPS is to alleviate portal hypertension, particularly in patients with refractory ascites or recurrent upper gastrointestinal bleeding [22].

With functioning TIPS, blood in the main portal vein flows antegrade toward the liver and normally from the portal confluence to the TIPS. Intrahepatic portal vein branches typically have reversed flow, from the periphery of the liver back toward the main portal vein, where blood can then be shunted through the TIPS to the inferior vena cava. Sonographic and Doppler assessment of the TIPS requires evaluating flow direction and velocity throughout the TIPS, from its origin at the portal end to its end in the hepatic vein, as well as flow in the main portal vein and its primary branches. Flow within the TIPS should be continuous in a portal-to-hepatic direction with a velocity of 90–190 cm/s (Fig. 46.15). Flow in the main portal vein should be continuous and antegrade with mean velocities of at least 30 cm/s. Flow in the portal vein branches is usually continuous and retrograde [23–27]. Assessment of the right posterior portal vein branch is often not possible, due to occlusion of this vein by the TIPS, or due to obstructed visualization by the shunt. It is important to assess flow in the portal veins and TIPS using proper technique, with angle of Doppler insonation <60° and careful angle correction for velocity measurements, since velocity measurements play a key role in assessing the continued function of the TIPS.

Multiple diagnostic criteria have been proposed for identifying a malfunctioning stent (Table 46.5) [23–28]. If any of these criteria is present, stent malfunction is likely. The most common cause of malfunction is stenosis of the TIPS, which causes various abnormalities in the TIPS' velocities including increased flow to >190 cm/s (Fig. 46.16), decreased flow to <60 cm/s, or a flow gradient across the stent of >100 cm/s. Changes in the portal venous Doppler, including decrease in portal vein velocities over time, mean portal vein velocity of <15 cm/s, or antegrade flow in the left and right portal vein branches, are secondary signs of impending TIPS failure. Stent occlusion is diagnosed when there is no flow in the TIPS (Fig. 46.17).

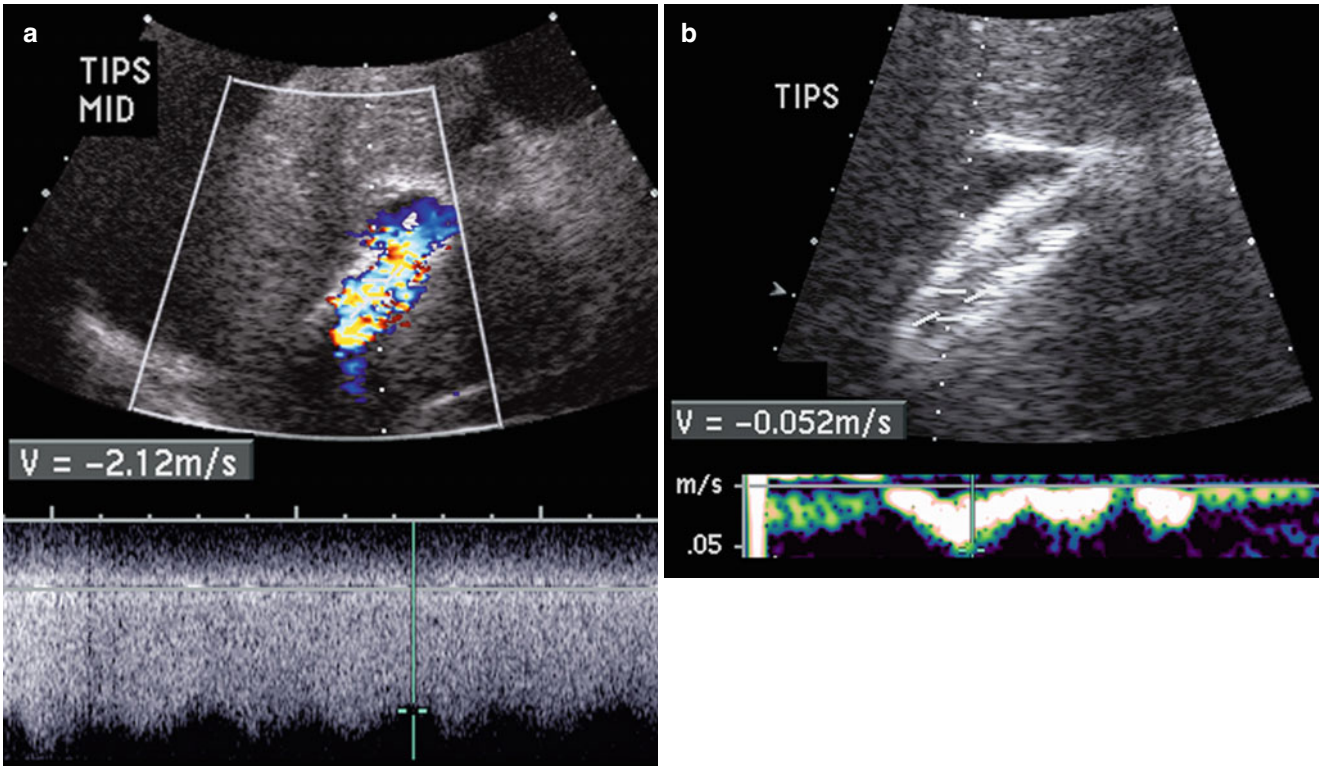


**Fig. 46.16** TIPS malfunction. (**a**) Color and spectral Doppler sonogram of TIPS demonstrating mildly elevated velocities of 212 cm/s, raising concern for malfunction. (**b**) Three months later, there is almost no flow in the TIPS with a peak velocity of only 5 cm/s

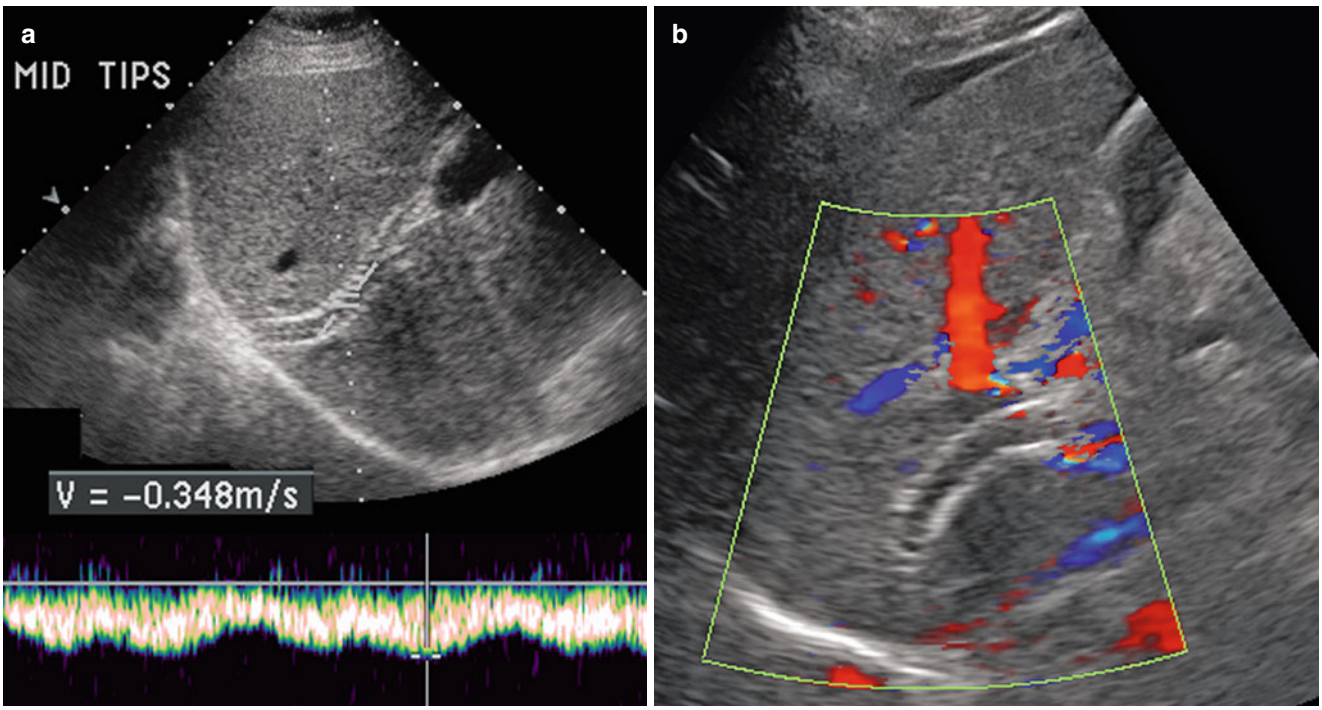


**Fig. 46.17** TIPS malfunction and occlusion. (**a**) Spectral Doppler from mid-TIPS demonstrating slow flow at 35 cm/s. (**b**) Follow-up color Doppler sonogram demonstrates no flow in the TIPS due to occlusion

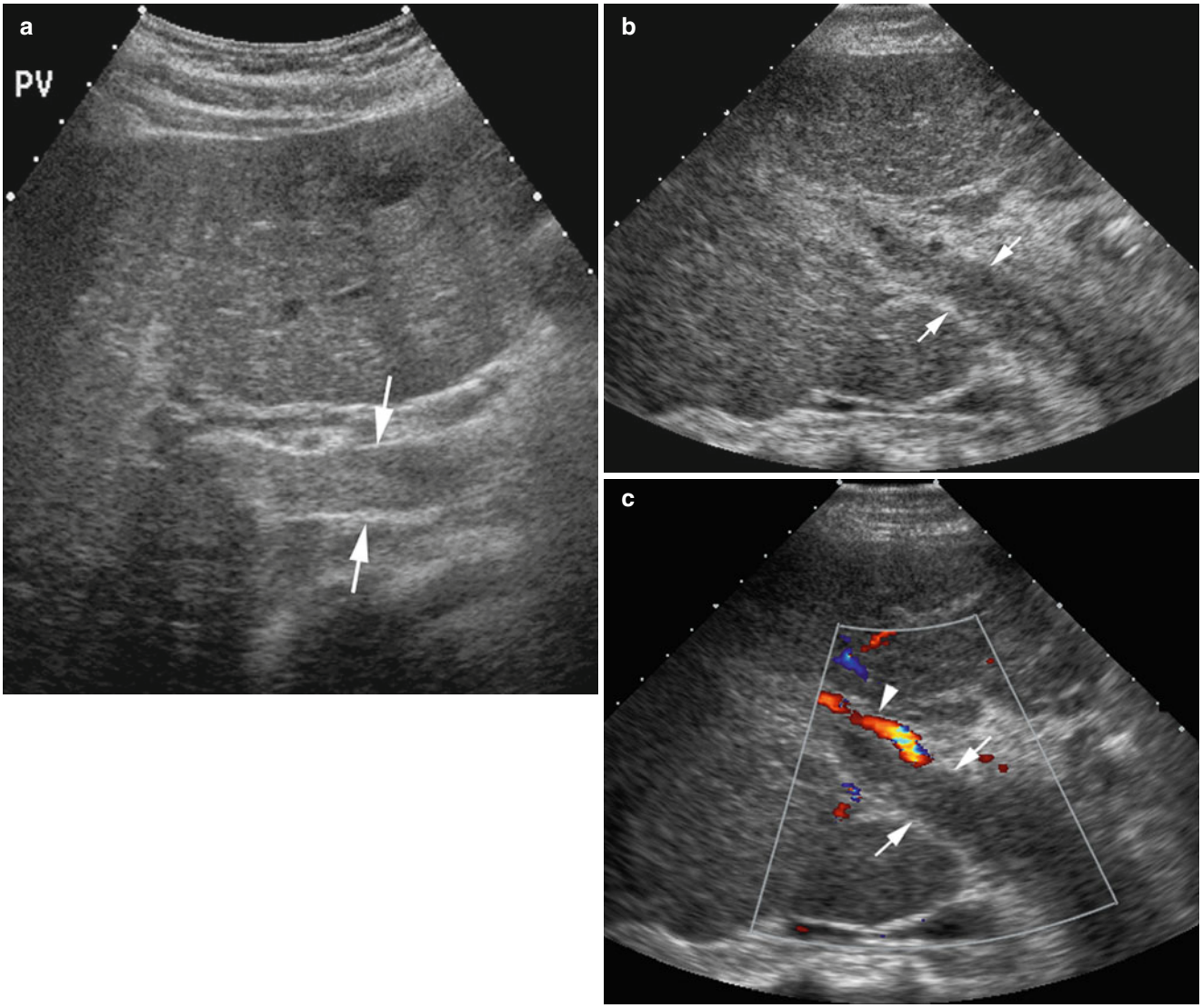


**Fig. 46.18** Portal vein thrombosis. (**a**, **b**) Sonograms of porta hepatis in two different patients showing the main portal vein (*arrows*) expanded and filled with echoes due to thrombosis. The echo texture of the liver in (**b**) is coarse and heterogeneous due to advanced cirrhosis. (**c**) Color Doppler image of same patient as (**b**) showing no flow in the portal vein (*arrows*), adjacent to the patent hepatic artery (*arrowhead*)

## Portal Vein Thrombosis

Portal vein thrombosis can occur as a complication of cirrhosis with portal hypertension, hypercoagulable states, pancreatitis, veno-occlusive disease after bone marrow transplantation, malignancy, and after splenectomy [4, 7, 29, 30]. Often patients have two or more risk factors, such as cirrhosis and malignancy together. With complete portal vein thrombosis, no flow will be identified in the portal vein with Doppler and echoes fill the vein lumen (Fig. 46.18). With partial portal vein thrombosis, the lumen will be partially filled with echoes and flow can be identified around the thrombus (Fig. 46.19).

In some cases, thrombosis of the portal vein is due to tumor growing in the vein, a finding that is important to distinguish from bland thrombus in the vein. The most common malignancies associated with tumor thrombus in the portal vein are hepatocellular carcinoma, pancreatic cancer, and cholangiocarcinoma [7, 31]. When tumor thrombus is present in the portal vein, the sonographic

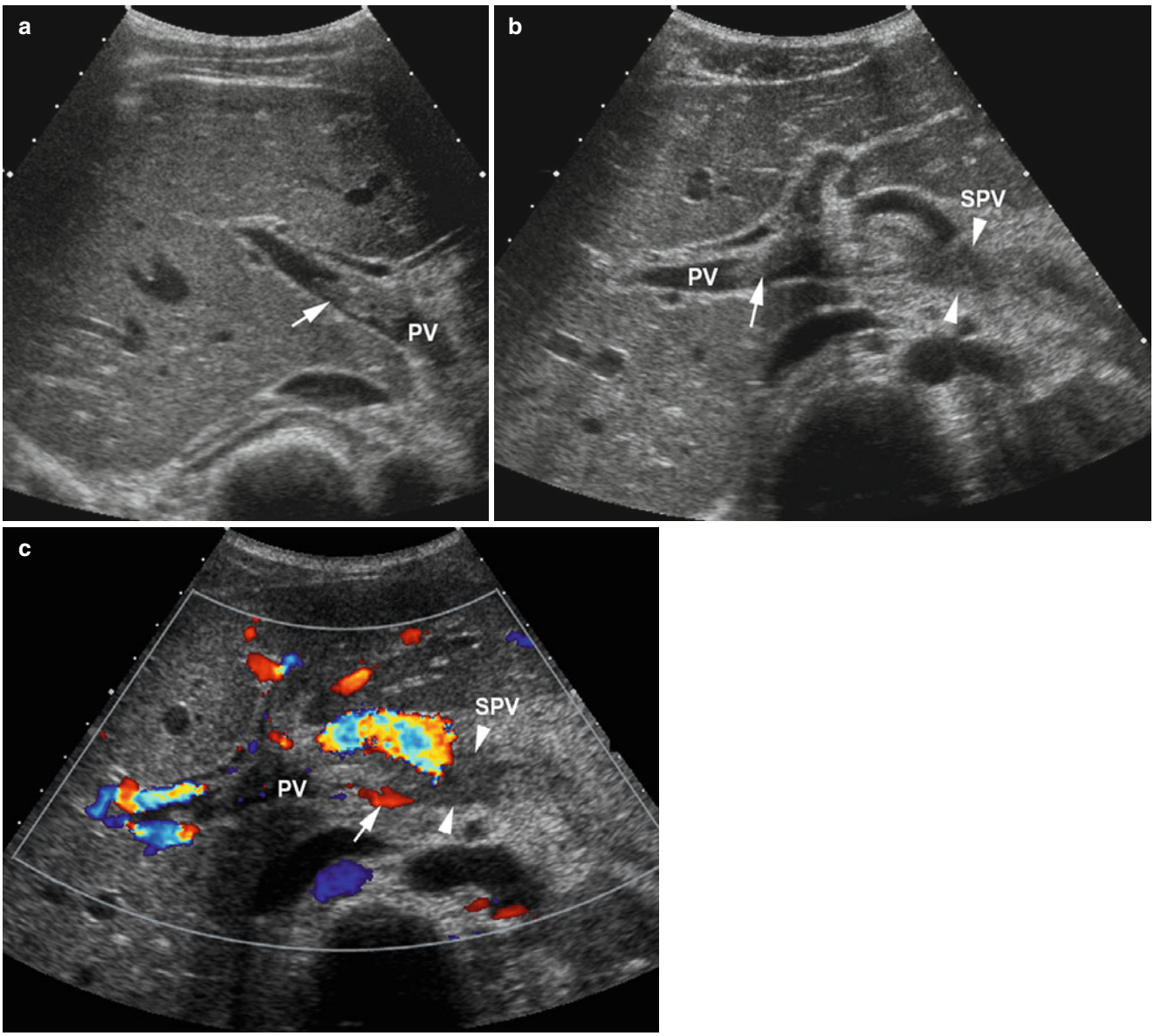


**Fig. 46.19** Portal vein partial thrombosis. (**a**) Sonogram of porta hepatis demonstrating thrombus (*arrow*) partially obstructing the portal vein (*PV*). (**b**) Sonogram of same patient showing thrombus filling the splenic vein (*SPV*, *arrowheads*) and partially filling the portal vein (*PV*) (*arrow*). (**c**) Color Doppler of same area as (**b**) showing no flow in splenic vein (*SPV*, *arrowheads*) and a small amount of flow in the portal vein (*PV*) around the thrombus (*arrow*)

appearance of the thrombus tends to be more heterogeneous than bland thrombus. In addition, tumor thrombus often expands the portal vein (Fig. 46.20). With color Doppler, small blood vessels may be seen within the tumor thrombus, confirming that the intraluminal material is solid tissue and not bland thrombus [31].

Longstanding portal vein thrombosis often leads to the formation of collateral vessels in the porta hepatis and around the thrombosed portal vein, a change termed cavernous transformation of the portal vein. Collateral vessels may shunt blood from the portal to the systemic veins, or they may be portal-to-portal shunts, carrying blood around the thrombosed portions of the main portal vein to intrahepatic portal veins. With color Doppler imaging, serpiginous vessels with blood flow are seen in and around the porta hepatis (Fig. 46.21) [7, 32].

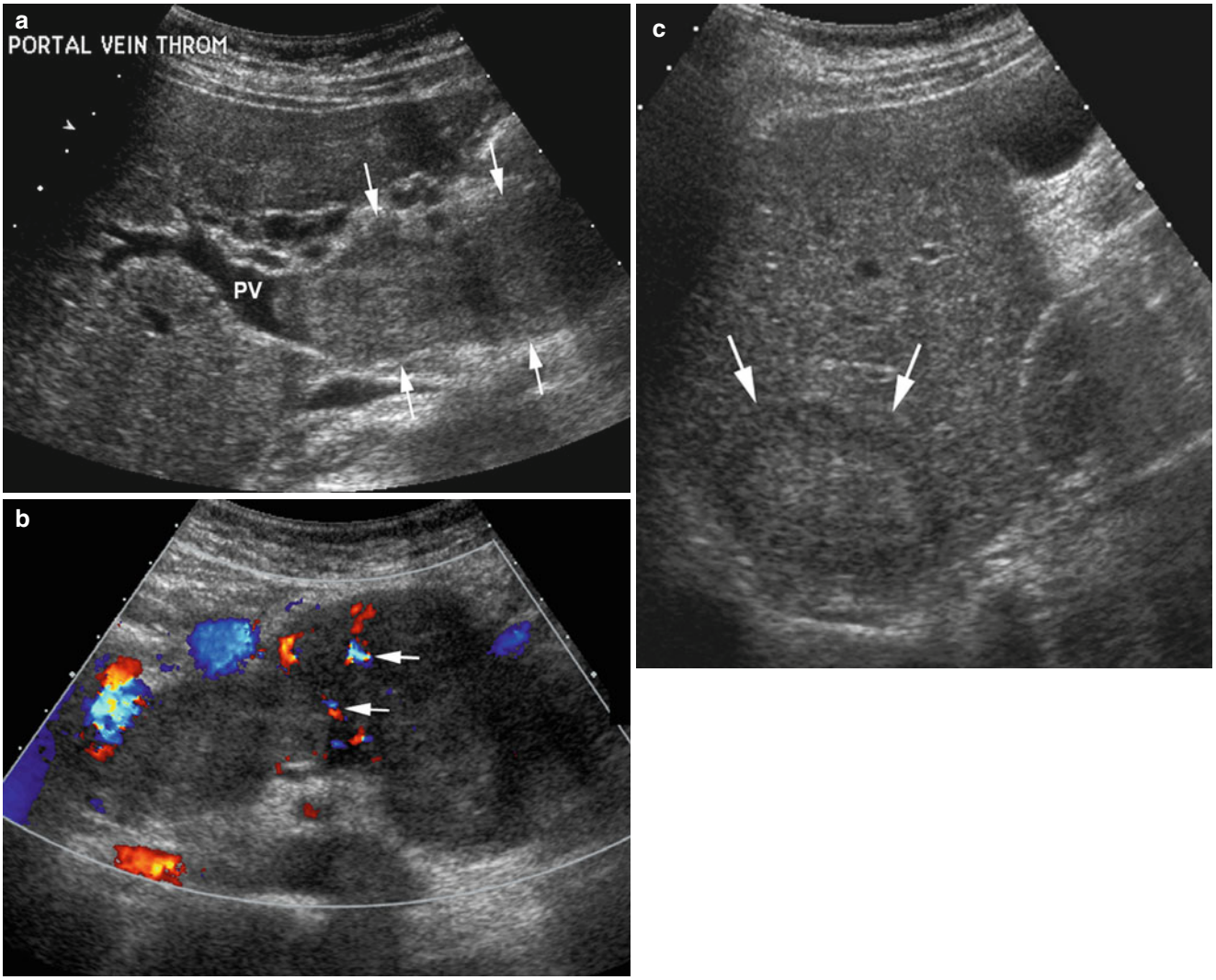


**Fig. 46.20** Tumor thrombus in portal vein. (**a**) Transverse view showing large tumor (*arrows*) expanding portal vein (*PV*). (**b**) Color Doppler of tumor in portal vein showing scattered blood flow (*arrows*) confirming that this is tumor. (**c**) Transverse sonogram of liver showing metastatic lesion in posterior right lobe (*arrows*) representing a metastasis

## Portal Vein Air

Air in the portal veins is an ominous finding, often indicating serious medical problems including bowel ischemia and intra-abdominal infection, such as diverticulitis and acute appendicitis. In premature infants, portal vein air may be seen with necrotizing enterocolitis. In adults, bowel ischemia typically results from mesenteric stenosis or occlusion from atherosclerotic disease or emboli, and is occasionally accompanied by air in the intrahepatic portal veins. On ultrasound, air in the portal vein is typically found in the anterior left lobe of the liver, the nondependent portion of the liver, and appears as scattered bright echoes in the region of the peripheral portal triads or throughout the liver parenchyma (Fig. 46.22) [33].

# Abnormalities of the Hepatic Veins

## Abnormal Hepatic Venous Waveforms

Absence of the normal multiphasic or triphasic hepatic venous waveform may be indicative of intrahepatic or extrahepatic disease. A monophasic waveform, character-

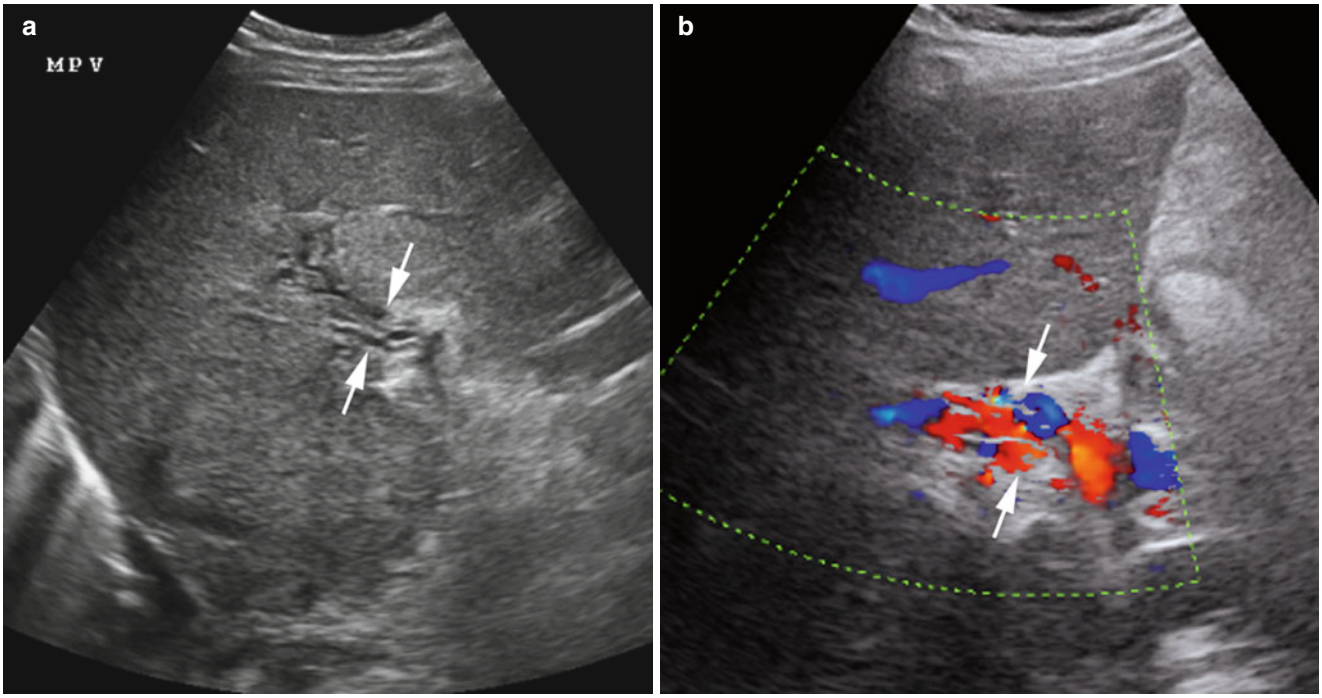


**Fig. 46.21** Cavernous transformation of thrombosed portal vein. (**a**) Sonogram through liver and porta hepatis showing several small vessels (*arrows*) where the portal vein should be visible. (**b**) Color Doppler of same region showing flow in the multiple vessels replacing the thrombosed portal vein (*arrows*)

ized by reversed flow or no A-wave, may be indicative of diffuse liver parenchymal disease, particularly if the disease causes increased stiffness of the liver. When a monophasic waveform is obtained with spectral Doppler, it is important to make sure the patient was not holding his/her breath and not performing a Valsalva maneuver, because either of these physiologic states can temporarily produce a monophasic waveform [34]. A true monophasic waveform in the hepatic vein has continuous antegrade flow throughout the cardiac cycle with dampened or absent undulation. Cirrhosis is the most common cause of a monophasic waveform [35]. The waveform is flattened and lacks retrograde flow because the liver is stiff and the hepatic veins are compressed (Fig. 46.23). Pathologies that will cause a similar pattern include liver steatosis, chronic hepatitis, extensive metastatic disease, and veno-occlusive disease [7, 11].

The hepatic vein waveform is also abnormal if the A-wave is exaggerated (Fig. 46.24). This finding is seen with congestive heart failure or with tricuspid regurgitation.

## Budd-Chiari Syndrome

Occlusion of the hepatic veins and the accompanying signs and symptoms are known as Budd-Chiari syndrome. Hepatic vein thrombosis can occur in patients with abnormal hypercoagulability and in patients with myeloproliferative disorders. Extension of hepatic tumor into the hepatic veins can also lead to occlusion of the veins. Other causes include thrombosis of the inferior vena cava from hypercoagulability or tumor and severe congestive heart failure [4, 7, 36, 37]. Hepatic vein thrombosis occurs much less frequently than does portal vein thrombosis.

With Budd-Chiari syndrome, sonography and Doppler will reveal minimal or no flow in the hepatic veins (Fig. 46.25). Sometimes, echoes will be seen filling the lumens of the hepatic veins. Careful assessment of the inferior vena cava should be performed when hepatic venous thrombosis is diagnosed, to help determine the etiology of the hepatic vein occlusion. Other sonographic findings that typically accompany Budd-Chiari syndrome include ascites, enlarged caudate lobe, gallbladder wall edema, portal hypertension, and splenomegaly [4, 37].

## Veno-Occlusive Disease

Veno-occlusive disease is a complication of hematopoietic stem cell transplantation that causes clot and fibrin deposition in the liver sinusoids, obstructing venous flow through the hepatic parenchyma. Patients with preexisting liver disease prior to stem cell transplantation are more likely to develop this complication than others. The clinical signs and symptoms are similar to Budd-Chiari and include ascites

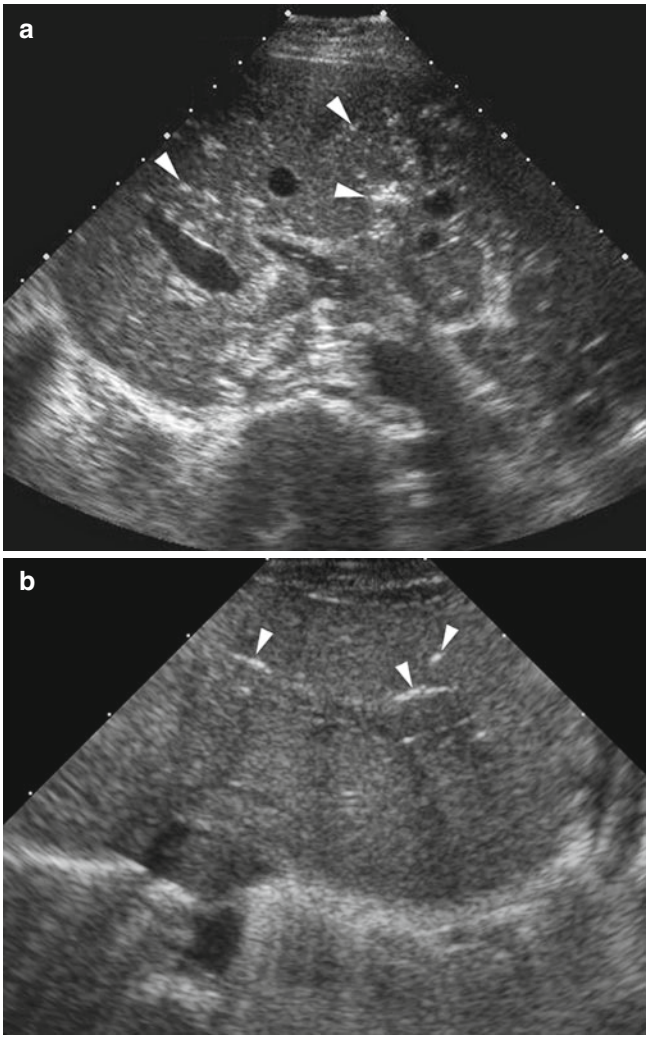


**Fig. 46.22** Air in portal veins. (**a**) Transverse image of an adult liver showing multiple scattered bright punctate and linear echoes (*arrowheads*) representing air in portal veins. (**b**) Image of left lobe of liver in a neonate with necrotizing enterocolitis, showing bright linear and punctate echoes (*arrowheads*) in the nondependent part of the liver, representing portal venous air

and portal hypertension. In addition, patients may have hepatomegaly and jaundice. Ultrasound and Doppler findings are nonspecific and include increased resistive indices in the hepatic artery and diminished or reversed flow in the portal veins [38, 39]. The hepatic venous waveforms obtained from the main hepatic veins may appear dampened or monophasic [7, 38].

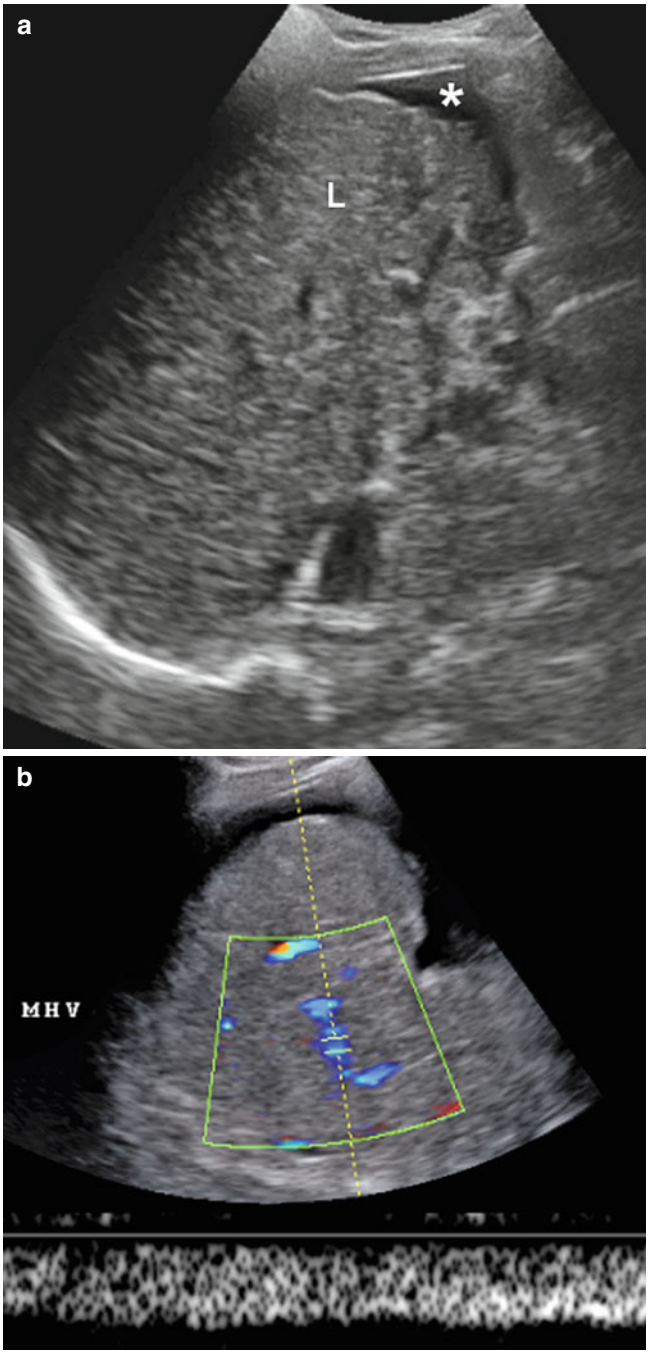


**Fig. 46.23** Monophasic hepatic vein waveform with cirrhosis. (**a**) Sonogram of right upper abdomen demonstrating lobular contour of liver (*L*) and ascites (*). (**b**) Color and spectral Doppler of middle hepatic vein in same patient showing monophasic flow away from the liver toward the heart

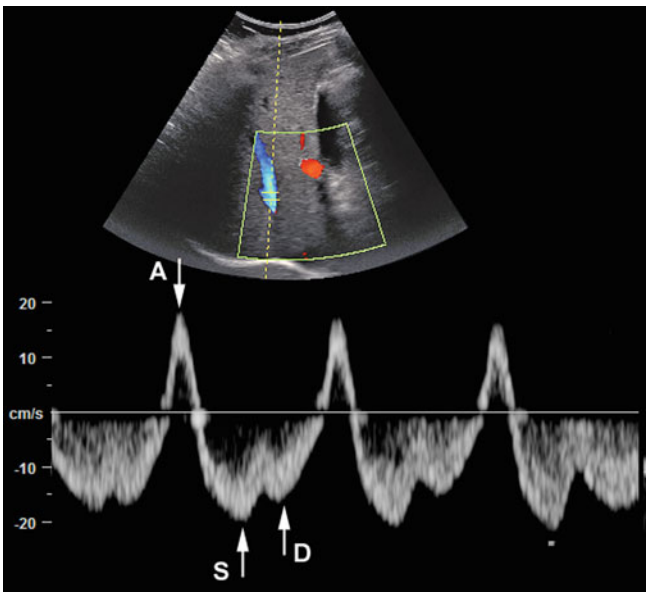


**Fig. 46.24** Exaggerated hepatic venous A-waves. Color and spectral Doppler of hepatic vein showing large A-wave (*arrow*, *A*) of retrograde flow during atrial contraction, with normal appearing S- (*arrow*, *S*) and D (*arrow*, *D*) waves

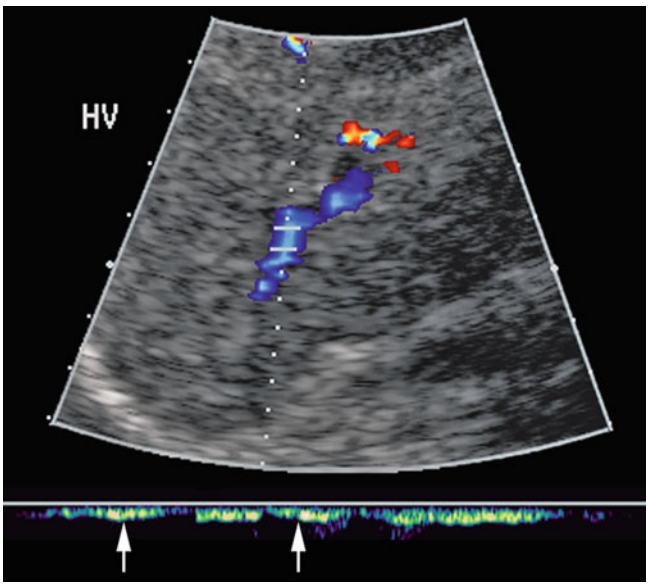


**Fig. 46.25** Budd-Chiari syndrome. Color and spectral Doppler of liver and hepatic vein showing small intrahepatic vein with minimal blood flow (*arrows*) due to occlusion of the veins distally

## References


1. Burns PN, Patriquin H, Lafortune M. Deep Doppler in the liver vasculature. In: AbuRahma AF, Bergan J, editors. Noninvasive vascular diagnosis: a practical guide to therapy. 2nd ed. London: Springer; 2007. p. 431–49.
2. Kim SH, Lee JM, Kim YJ, Lee JY, Han JK, Choi BI. High-definition flow Doppler ultrasonographic technique to assess hepatic vasculature compared with color or power Doppler ultrasonography. J Ultrasound Med. 2008;27:1491–501.
3. Kruskal JB, Newman PA, Sammons LG, Kane RA. Optimizing Doppler and color flow US: application to hepatic sonography. Radiographics. 2004;24:657–75.
4. Zweibel WJ. Ultrasound assessment of the hepatic vasculature. In: Zweibel WJ, Pellerito J, editors. Introduction to vascular ultrasonography. 5th ed. Philadelphia: Elsevier Saunders; 2005. p. 585–609.
5. Robinson KA, Middleton WD, Al-Sukaiti R, Teefey SA, Dahiya N. Doppler sonography of portal hypertension. Ultrasound Q. 2009; 25:3–13.
6. Egorov VI, Yashina NI, Fedorov AV, Karmazanovsky GG, Vishnevsky VA, Shevchenko TV. Celiaco-mesenterial arterial aberrations in patients undergoing extended pancreatic resections: correlation of CT angiography with findings at surgery. J Pancreas. 2010;11:348–57.
7. McNaughton DA, Abu-Yousef MM. Doppler US of the liver made simple. Radiographics. 2011;31:161–88.
8. Covey AM, Brody LA, Getrajdman GI, Sofocleous CT, Brown KT. Incidence, patterns, and clinical relevance of variant portal vein anatomy. Am J Roentgenol. 2004;183:1055–64.
9. Chuo LS, Mahmud R, Salih QA. Color Doppler ultrasound examination of the main portal vein and inferior vena cava in normal Malaysian adult population: a fasting and post prandial evaluation. Internet J Cardiovasc Res. 2005;2:1–9.
10. Yardi HR, Sotoudeh H. Assessment of normal Doppler parameters of portal vein and hepatic artery in 37 healthy Iranian volunteers. Iran J Radiol. 2006;3:213–6.
11. Sheinfield MH, Bilali A, Koenigsberg M. Understanding the spectral Doppler waveform of the hepatic veins in health and disease. Radiographics. 2009;29:2081–98.
12. Su ZZ, Shan H, Ke WM, He BJ, Zheng RQ. Portalsystemic hymodynamic changes in chronic severe hepatitis B: an ultrasonographic study. World J Gastroenterol. 2008;14:795–9.
13. Lim HK, Lee WJ, Kim SH, Lee SJ, Choi SH, Park HS, Do YS, Choo SW, Choo IW. Splanchnic arteral stenosis or occlusion: diagnosis at Doppler US. Radiology. 1999;211:405–10.
14. Moneta GL, Lee RW, Yeager RA, Taylor LM, Porter JM. Mesenteric duplex scanning: a blinded prospective study. J Vasc Surg. 1993; 17:79–84.
15. Franchis R. Revising consensus in portal hypertension: report of the Baveno V consensus workshop on methodology of diagnosis and therapy in portal hypertension. J Hepatol. 2010;53:762–8.
16. Severi T, van Malenstein H, Verslype C, van Pelt JF. Tumor initiation and progression in hepatocellular carcinoma: risk factors, classification, and therapeutic targets. Acta Pharmacol Sin. 2010;31:1409–20.
17. Liu CH, Hsu SJ, Liang CC, Tsai FC, Lin JW, Liu CJ, Yang PM, Lai MY, Chen PJ, Chen JH, Kao JH, Chen DS. Esophageal varices: noninvasive diagnosis with duplex Doppler US in patients with compensated cirrhosis. Radiology. 2008;248:132–9.
18. Ahn J, Cooper JM, Silberzweig JE, Mitty HA. Venographic appearance of portosystemic collateral pathways. Br J Radiol. 1997;70: 1302–6.
19. Henderson JM, Boyer TD, Kutner MH, Galloway JR, Rikkers LF, Jeffers LJ, Abu-Elmagd K, Connor J. Distal splenorenal shunt versus transjugular intrahepatic portal systematic shunt for variceal bleeding: a randomized trial. Gastroenterology. 2006;130:1643–51.
20. Drose JA. Abnormal liver function tests. In: Sanders RC, Winter TC, editors. Clinical sonography: a practical guide. 4th ed. Philadephia: Lippincott Williams and Wilkins; 2007. p. 94–106.
21. Tarantino G, Citro V, Conca P, Riccio A, Tarantino M, Capone D, Cirillo M, Lobello R, Iaccarino V. What are the implications of the spontaneous spleno-renal shunts in liver cirrhosis? BMC Gastroenterol. 2009;9:89.
22. Goykhman Y, Ben-Haim M, Rosen G, Carmiel-Haggai M, Oren R, Nakache R, Szold O, Klausner J, Kori I. Transjugular intrahepatic portosystemic shunt: current indications, patient selection and results. Isr Med Assoc J. 2010;12:687–91.

23. Pan JJ, Chen C, Caridi JG, Geller B, Firpi R, Machicao VI, Hawkins IF, Soldevila-Pico C, Nelson DR, Morelli G. Factors predicting survival after transjugular intrahepatic portosystemic shunt creation: 15 years' experience from a single tertiary medical center. J Vasc Interv Radiol. 2008;19:1576–81.
24. Zizka J, Elias P, Krajina A, Michl A, Lojik M, Ryska P, Maskova J, Hulek P, Safka V, Vanasek T, Bukac J. Value of Doppler sonography in revealing transjugular intrahepatic portosystemic shunt malfunction. Am J Roentgenol. 2000;175:141–8.
25. Wachsberg RH. Doppler ultrasound evaluation of transjugular intrahepatic protosystemic shunt function: pitfalls and artifacts. Ultrasound Q. 2003;19:139–48.
26. Bilbao JI, Quiroga J, Herrero JI, Benito A. Transjugular intrahepatic portosystemic shunt (TIPS): current status and future possibilities. Cardiovasc Intervent Radiol. 2002;25:251–69.
27. Abraldes JG, Villanueva C, Banares R, Aracil C, Catalina MV, Garci A-Pagan JC, Bosch J. Hepatic venous pressure gradient and prognosis in patients with acute variceal bleeding treated with pharmacologic and endoscopic therapy. J Hepatol. 2008;48:229–36.
28. Kurmis TP. Transjugular intrahepatic portosystemic shunt: an analysis of outcomes. ANZ J Surg. 2009;79:745–9.
29. Rajani R, Björnsson E, Bergquist A, Danielsson A, Gustavsson A, Grip O, Melin T, Sangfelt P, Wallerstedt S, Almer S. The epidemiology and clinical features of portal vein thrombosis: a multicentre study. Aliment Pharmacol Ther. 2010;32:1154–62.
30. Seeger M, Günther R, Hinrichsen H, Both M, Helwig U, Arlt A, Stelck B, Bräsen JH, Sipos B, Schafmayer C, Braun F, Bröring DC, Schreiber S, Hampe J. Chronic portal vein thrombosis: transcapsular hepatic collateral vessels and communicating ectopic varices. Radiology. 2010;257:568–78.
31. Rossi S, Rosa L, Ravetta V, Cascina A, Quaretti P, Azzaretti A, Scagnelli P, Tinelli C, Dionigi P, Calliada F. Contrast-enhanced versus conventional and color Doppler sonography for detection of thrombosis of the portal and hepatic venous systems. Am J Roentgenol. 2006;186:763–73.
32. De Gaetano AM, Lafortune M, Patriquin H, DeFranco A, Aubin B, Paradis K. Cavernous transformation of the portal vein: patterns of intrahepatic and splanchnic collateral circulation detected with Doppler sonography. Am J Roentgenol. 1995;165:1151–5.
33. Abboud B, Hachem JE, Yazbeck T, Doumit C. Hepatic portal venous gas: physiopathology, etiology, prognosis and treatment. World J Gastroenterol. 2009;15:3585–90.
34. Petersen JF, Dakhil AZ, Jensen DB, Sondergaard B, Bytzer P. Abnormal hepatic vein Doppler waveform in patients without liver disease. Brit J Radiol. 2005;78:242–4.
35. Sudhamshu KD, Matsutani S, Maruyama H, Aklike T, Saisho H. Doppler study of hepatic vein in cirrhotic patients: correlation with liver dysfunction and hepatic hemodynamics. World J Gastroenterol. 2006;12:5853–8.
36. Bargallo X, Gilabert R, Nicolau C, Garcia-Pagan JC, Ayuso JR, Bru C. Sonography of Budd-Chiari syndrome. Am J Roentgenol. 2006;187:W33–42.
37. Boozari B, Bahr MJ, Kubicka S, Klempnauer J, Manns MP, Gebel M. Ultrasonography in patients with Budd-Chiari syndrome – diagnostic signs and prognostic implications. J Hepatol. 2008;49:572–80.
38. Senzolo M, Germani G, Cholongitas E, Burra P, Burroughs AK. Veno occlusive disease: update on clinical management. World J Gastroenterol. 2007;13:3918–24.
39. Matsumoto Y, Horiike S, Sakagami J, Fujimoto Y, Taniguchi K, Shimizu D, Shimura K, Uchiyama H, Kuroda J, Nomura K, Shimazaki C, Taniwaki M. Early ultrasonographic diagnosis and clinical follow-up of hepatic veno-occlusive disease after allogeneic bone marrow transplantation in a patient with acute lymphoblastic leukemia. Intern Med. 2009;48:831–5.

# Duplex Evaluation of the Renal Arteries

47

Marsha M. Neumyer and John Blebea

**Abstract**

The application of duplex ultrasound for the evaluation of patients with renal artery disease provides the clinician with detailed information on location, extent, and severity of vascular disorders. Validated protocols have been developed for evaluation and classification of normal and pathologic renal artery and renal parenchymal flow. Using a combination of B-Mode, color and/or power Doppler imaging, and Doppler velocity spectral waveforms it is possible to define renal artery anatomy and the blood flow patterns associated with stenosis, occlusion, fibromuscular dysplasia, elevated renovascular resistance, and renal vein thrombosis. Determination of flow-limiting stenoses in the adult and pediatric main or accessory renal arteries is based primarily on the peak systolic velocity measurement and the presence of post-stenotic turbulence. B-Mode imaging enables the characterization of arterial and parenchymal pathology and perivascular tumors or masses that may cause extrinsic compression of the renal artery, renal vein, and the kidney. While sonographic evaluation of the renal arteries and kidneys can be technically challenging, the study has been shown to have value when used both prior to and following intervention. While not routinely required, contrast-enhanced imaging may facilitate visualization of greater lengths of the renal artery, the renal ostium, and accessory renal arteries in some patients.

**Keywords**

Renal duplex ultrasound • Renovascular hypertension • Doppler • Medial fibromuscular dysplasia • Intrinsic renal parenchymal disease • Contrast-enhanced imaging

## Introduction

Hypertension afflicts almost one-third of all adult Americans, thereby affecting 74 million individuals, and its incidence is increasing [1]. "Renovascular hypertension" is classically defined as systemic hypertension resulting from renal arterial compromise, most frequently due to atherosclerotic disease in adults [2]. The conclusion, however, that hypertension is related directly to an arterial lesion would require complete reversal of the hypertension after relief of the stenosis or obstruction, which is something that is infrequently seen. Therefore, although it has been estimated that 2–6% of patients have underlying renal disease as the cause of their elevated blood pressure, the true prevalence of renovascular hypertension is unknown and varies with the population studied [3]. In selected patient groups, such as children or young adults, or those with severe diastolic hypertension, the prevalence of renal artery stenosis is up to 38% and progression of stenosis occurs in more than 10% of patients depending on the severity of their initial artery stenosis [4–6]. Renal artery stenosis is more likely to be found in adults with abrupt

M.M. Neumyer, B.S., RVT (✉)
Vascular Diagnostic Educational Services,
Vascular Resource Associates,
4832 Springtop Drive, Harrisburg, PA 17111-3609, USA
e-mail: mnvdes@aol.com

J. Blebea, M.D.
Department of Surgery, University Hospitals of Cleveland,
Case Western Reserve University School of Medicine,
Cleveland, OH, USA

A.F. AbuRahma, D.F. Bandyk (eds.), *Noninvasive Vascular Diagnosis*,
DOI 10.1007/978-1-4471-4005-4_47, 

onset or exacerbation of chronic hypertension, angiotensin-converting-enzyme-inhibitor-induced azotemia, otherwise unexplained renal insufficiency or flash pulmonary edema out of proportion to left ventricular dysfunction, and in hypertensive children [7]. Although the long-term prognosis for patients with renovascular hypertension is worse than that of patients who do not have identifiable lesions, successful treatment of such lesions is possible and can be associated with improvement of the hypertension and associated cardiac and renal insufficiency in some patients [8]. Identification of renal artery stenosis is important because treatment may control or cure renovascular hypertension, prevent loss of renal mass, or stabilize renal function in chronic renal failure [9]. Efficacy of revascularization procedures for the treatment of renal artery stenosis, in association with clinical hypertension, has recently been questioned by the results of recent large-center prospective studies, underlining the continuing need to better identify which patients would benefit from such interventions [10, 11].

Since renal artery disease, due to either arterial stenosis or fibromuscular dysplasia, is correctable, identification of affected patients is clinically important. Historically, contrast arteriography has been the diagnostic test of choice for renovascular disease. This procedure, however, offers mostly anatomic information without correlative hemodynamic data or a causal linkage between identified disease and hypertension or renal dysfunction. In addition, its invasive nature and associated 3–5% complication rates, especially in the setting of associated renal functional impairment, effectively precludes its use as a screening test for renal artery stenosis and, in the majority of cases, even as a confirmatory diagnostic procedure. For most clinicians, arteriography is performed in association with planned therapeutic intervention. Other less invasive diagnostic procedures include magnetic resonance angiography (MRA) and computed tomographic angiography (CTA). Both of these modalities, however, are relatively expensive and include the need for intravenous contrast which can be nephrotoxic and contraindicated. The published sensitivity and specificity of MRA in the diagnosis of renal artery stenosis is greater than 90%, although it has a tendency to overestimate the degree of stenosis, and its accuracy in real-life situations is less than that reported from academic centers of excellence [12]. In addition, the use of gadolinium as a contrast agent, particularly in patients with diminished renal function, has been associated with development of nephrogenic systemic fibrosis [13]. MRA also should not be used in patients with certain implanted devices (i.e., pacemakers, defibrillators, cochlear implants, and spinal cord stimulators) or in claustrophobic patients. In a similar manner, three-dimensional volume CTA has a reported sensitivity and specificity of 94% and 93%, respectively, in the diagnosis of renal artery stenosis [12, 14]. Its accuracy is comparable with MRA but it has the added risks of ionizing radiation and nephrotoxicity from iodinated and larger volume of contrast agents. Furthermore, severe renal artery calcification may obscure luminal narrowing [15]. Because the cost of both MRA and CTA further precludes their use as the initial diagnostic modality, they are most useful as secondary confirmatory studies. Duplex sonography offers the benefits of low cost and absence of ionizing radiation or routine need for intravenous contrast. It is a noninvasive and painless procedure. Technological advances in the past decade with improved low frequency transducers, Doppler resolution, and digital imaging have made vascular ultrasound the technique of choice in the initial evaluation of the renal arteries. Renal duplex scanning can detect renal artery stenosis, determine its anatomic location, and help define its hemodynamic significance with sensitivity and specificity of 85% and 92%, respectively [16].

## Etiology of Renal Artery Disease

Atherosclerosis is the cause of 90% of cases of renal artery stenosis [17, 18]. It most frequently involves the ostium and proximal third of the renal artery while more distal lesions are seen in 15–20% of patients [19]. Hemodynamically significant lesions may be accompanied by post-stenotic dilatation. Risk factors for the development of atherosclerotic renal artery stenosis include increasing age, hypertension, tobacco use, coronary artery disease, peripheral vascular disease, hyperlipidemia, and diabetes mellitus. Men are affected twice as frequently as women and bilateral lesions occur in 30% of patients [20]. In contrast, although medial fibromuscular dysplasia is the second most common curable cause of renal artery stenosis, it occurs far less frequently. It overwhelmingly affects females in a 9:1 ratio with patients usually in their 30s and involves the middle and distal portion of the main renal artery with extension into the first-order branches in 25% of patients. It occurs bilaterally more than 35% of the time although, when involving just one side, the right side is most frequently affected [21]. Angiographically, the renal arteries have a beaded appearance with alternating stenoses and aneurysmal dilatations [22]. The etiology of fibromuscular dysplasia is unknown although there may be, at least in part, a genetic component. Other less common causes of renal dysfunction include aortic dissections involving the renal vessels, spontaneous or traumatic isolated renal artery dissections or disruptions, renal artery aneurysms, atheroembolization to the renal arteries, progressive atherosclerotic stenosis leading to complete occlusion, arteriovenous fistulas, mid-abdominal aortic coarctation, developmental congenital stenoses, arteritis, and extrinsic compression by tumors or other masses [2].

## Renal Duplex Ultrasonography

Greene et al. were the first to use renal duplex sonography to characterize blood flow patterns in the normal and diseased renal artery [23]. Using B-Mode imaging and Doppler velocity waveforms, they described renal artery anatomy, blood flow rates, and velocity patterns. Rittgers et al. demonstrated that disturbances in the Doppler velocity waveform occur before significant reductions in blood flow [24]. Significant stenoses were associated with marked flow disturbance exemplified by blunting of the systolic peak and loss of the systolic spectral window. There was also a decrease in the velocity distal to severe lesions along with associated post-stenotic turbulence.

Other investigators subsequently developed and validated protocols for the evaluation and classification of normal and pathologic renal artery flow [16, 25, 26]. Studies by Avasthi et al. proposed criteria for the identification of renal artery lesions in humans: a peak systolic renal artery velocity greater than 100 cm/s, spectral broadening due to turbulence, and loss of the diastolic flow component for hemodynamically significant stenoses while the absence of any detectable flow identified an occlusion of the renal artery [27]. Subsequent studies found that a peak systolic renal artery velocity of 100 cm/s is too low to yield acceptable sensitivities for detection of flow-reducing stenoses and that the loss of the diastolic flow component will often be reflective of intrinsic parenchymal dysfunction rather than arterial stenosis [25, 26]. Additionally, flow is commonly detected within the kidney even when the renal artery is occluded because of flow through ureteral and adrenal collateral branches.

The most widely used classification of renal artery stenosis relies on the Doppler-derived systolic velocity, a comparison with the systolic velocity recorded in the proximal abdominal aorta, and flow patterns along the length of the renal artery. Duplex diagnosis of a flow-limiting lesion is dependent on demonstration of a focal increase in systolic velocity. Hoffman et al. demonstrated a sensitivity of 95% and a specificity of 91% for identification of a significant flow-reducing stenosis, defined as a >60% diameter reduction, using a peak systolic (PSV) renal artery velocity of >180 cm/s [28]. Similar excellent results with a sensitivity and specificity of 98% was attained with a PSV of >200 cm/s [29]. Absolute velocity measurements may potentially be affected by systemic factors, such as blood pressure and cardiac output, and thus a comparison with aortic peak systolic velocity is routinely used. Kohler and others have shown that a ratio of the peak systolic velocities of the renal artery to that of the abdominal aorta of >3.5 is predictive of renal artery stenosis of >60% diameter reduction [29, 30]. The usefulness of this ratio has been validated in multiple centers [25, 26, 31]. Although the velocity in the abdominal aorta, as well as renal artery velocity, decreases with age, flow velocities have fortunately been shown to be independent of body surface area [23]. Examination of the spectral flow patterns within the renal artery is also helpful in diagnosing stenoses. The presence of post-stenotic turbulence is confirmatory of a hemodynamically significant lesion. Doppler spectral broadening has not been useful as a diagnostic parameter because the Doppler sample volume size is large in relation to the diameter of the small-caliber renal artery.

**Table 47.1** Duplex criteria for classification of renal artery stenosis

| Classification | RAR | PSV | PST |
|---|---|---|---|
| Normal | <3.5 | <120 cm/s | Absent |
| <60% stenosis | ≤3.5 | >180 cm/s | Absent |
| >60% stenosis | >3.5 | >180 cm/s | Present |
| Occlusion | N/A | N/A | N/A |
| | | Low velocity, low amplitude parenchymal signals | |

*RAR* renal-aortic velocity ratio, *PSV* peak systolic velocity, *PST* post-stenotic signal, *N/A* not applicable

Renal artery stenosis is classified into four diagnostic categories based on duplex ultrasound criteria: normal, less than 60% stenosis, greater than 60% stenosis, and occlusion (Table 47.1). Lesions that represent less than 60% diameter-reducing stenosis are distinguished by an elevated systolic velocity of greater than 180 cm/s but a renal-to-aortic ratio of less than 3.5 and no post-stenotic turbulence. Clinically, it is still important to diagnose these lesions in order to identify patients who may benefit from continued monitoring for progression of disease. Confirmation of renal artery occlusion is dependent on the B-Mode image of the renal artery to confirm proper location for Doppler insonation and demonstration of absence of flow in the renal artery. False-negative studies may result from insonation of nearby collateral or polar branches in cases of multiple renal arteries.

Renal size, as reflected by the ultrasound-measured length of the kidney, is useful in ascertaining potential intervention for renal artery stenosis. It has been shown that renal length decreases significantly in the presence of severe renal artery stenosis [32, 33]. Caps and his colleagues reported that kidneys with a renal artery peak systolic velocity greater than 400 cm/s, and cortical end-diastolic velocities less than or equal to 5 cm/s, were at high risk for progression to renal atrophy (Fig. 47.1) [34]. An atrophic kidney, usually defined as less than 8 cm in length, is unlikely to benefit from revascularization procedures. Although some clinicians have been aggressive in such circumstances, the results with either surgical or endovascular revascularization have been disappointing as reperfusion of the ischemic kidney is not likely to reverse parenchymal changes [35–37]. On the other hand, studies suggest that improved renal function may be expected when intervention is performed prior to progression of the lesion to critical levels of renal impairment [36] or in cases where renal function has acutely deteriorated [38, 39].

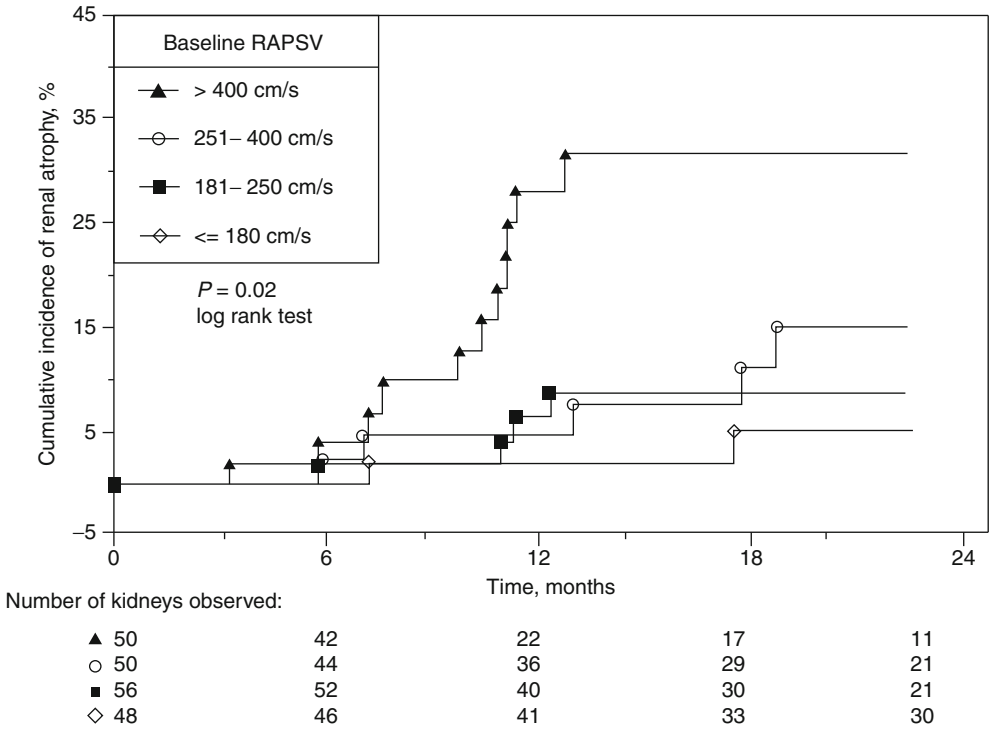


**Fig. 47.1** Cumulative index of renal atrophy stratified according to baseline renal artery peak systolic velocity (*RAPSV*, in cm/s). Standard error is <10% through 24 months for all plots (Reprinted from Caps et al. [34]. With permission from Nature Publishing Group)

However, measurement of renal length alone is not a sensitive enough indicator to detect significant renal artery stenosis and progression to arterial occlusion [34]. Therefore, measurement of kidney length is useful to assist in the proper selection of patients for revascularization but inadequate by itself in defining the presence of a hemodynamically significant renal artery stenosis.

## Duplex Ultrasound Evaluation of the Renal Arteries

### Anatomy of the Renal Arterial System

The kidneys are located between the 12th thoracic and 3rd lumbar vertebrae lying retroperitoneally in the dorsal abdominal cavity. The right kidney usually lies slightly more inferior to the left. While the kidneys decrease in size with increasing age, the normal organ length is 8–13 cm with a width of 5–7 cm. In less than 1% of the population, the kidneys may be joined at their lower poles by an isthmus of tissue which lies anterior to the aorta at the level of the fourth or fifth lumbar vertebrae, forming a horseshoe-shaped organ [40].

For the purpose of sonographic interrogation, the kidneys are segmented into four main areas. The renal artery, vein, and ureter enter the kidney through the *renal hilum* that forms the *renal sinus.* The sinus, which in large part is comprised of fat and some fibrous tissue, contains the renal artery and vein, and the collecting and lymphatic systems. For this reason, it is normally brightly echogenic on sonographic imaging (Fig. 47.2). The parenchymal tissue of the kidney is divided into two parts: *the medulla* and *cortex*. The cortex constitutes the outermost area of the kidney lying just beneath the renal capsule. Cortical tissue (columns of Bertin) lies between the triangular-shaped medullary pyramids which carry urine from the cortex to the renal pelvis. The 12–18 pyramids generally have lower echogenicity than the cortex and are usually seen well in the normal adult patient.

Attention to both surface and internal anatomic landmarks facilitates sonographic localization of the renal arteries. Using a surface landmark, the renal arteries are located approximately 2 cm below a transverse plane (the transpyloric plane) located midway between the suprasternal notch and the symphysis pubis. This plane cuts through the lower border of the first lumbar vertebrae, the ninth costal cartilages and the pylorus. The renal arteries can be visualized arising from the lateral or postero-lateral wall of the abdominal aorta. Soon after its origin, the right renal artery will arch inferiorly and then slightly posteriorly to go behind the inferior vena cava (IVC) and the right renal vein. The left renal artery usually originates from the aortic wall slightly more cephalad than the right and courses superiorly and then posterior to the splenic artery, left renal vein and is crossed by the inferior mesenteric vein.

Between 12% and 22% of patients have variant anatomy which includes duplication of the main renal arteries or accessory polar arteries, a feature found more often on the left than on the right [41, 42]. In the majority of patients, the accessory renal arteries arise from the aortic wall below

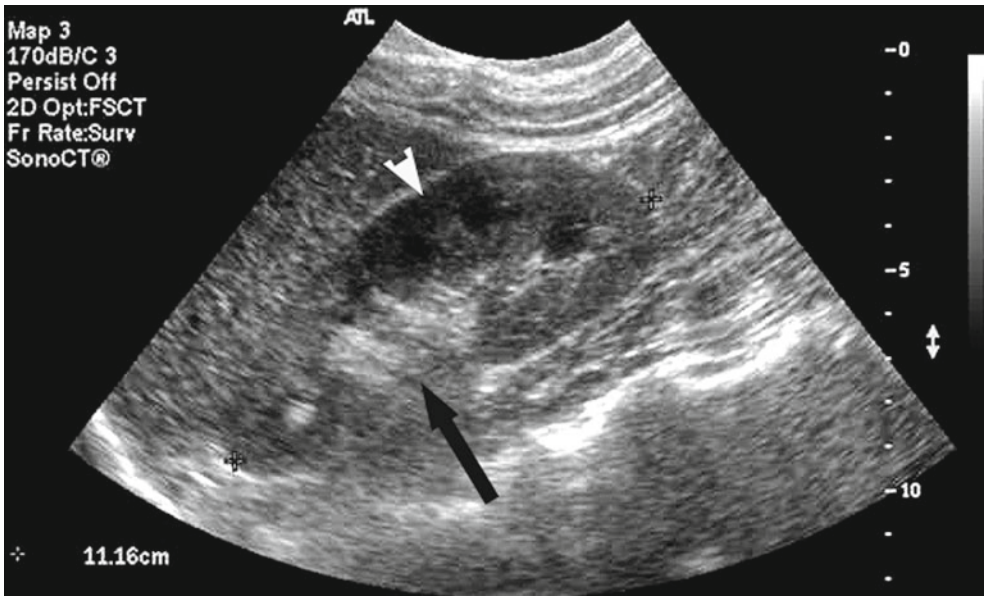


**Fig. 47.2** Longitudinal B-Mode image of a normal adult kidney demonstrates echogenicity of the renal sinus (*black arrow*) and definition of the renal cortex and pyramids (*white arrowhead*)

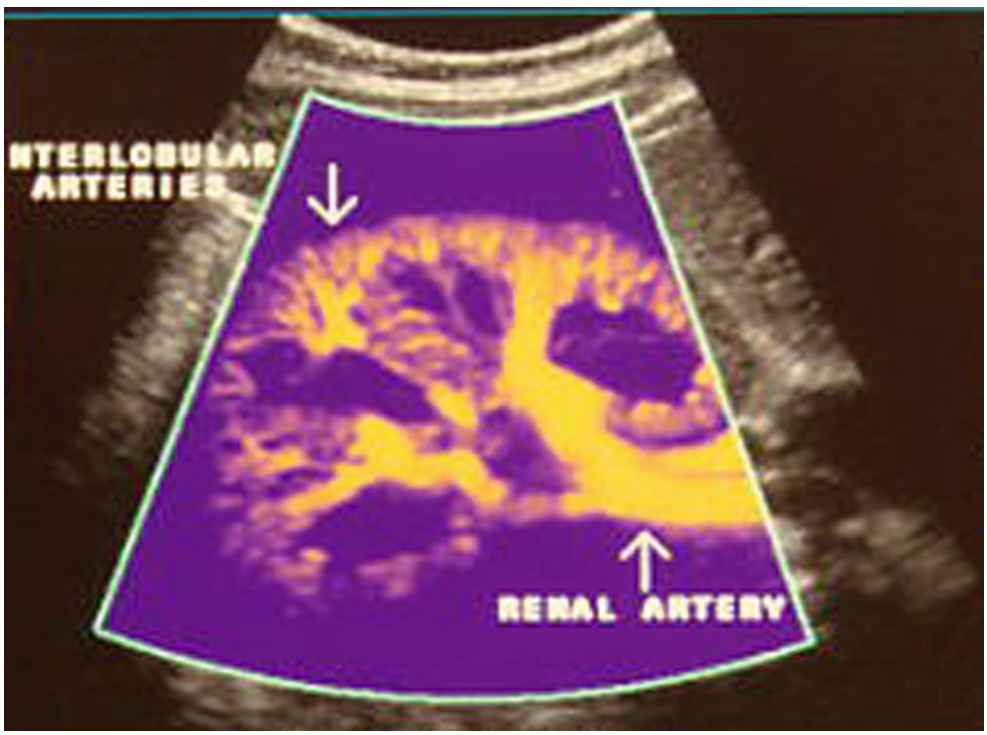


**Fig. 47.3** Transverse color flow image of the vasculature of a normal kidney demonstrating anterior and posterior segmental branches of the main renal artery. Courtesy of Philips Ultrasound

the main renal artery and course to the polar surfaces of the kidney while the main renal arteries enter the kidney through the renal hilum. Occasionally, accessory renal arteries originate from the common or internal iliac, superior or inferior mesenteric, adrenal, or right hepatic arteries.

The renal artery normally gives rise to two to five anterior and posterior segmental branches, which supply blood to upper-, mid-, and lower poles of the kidney (Fig. 47.3). The segmental arteries give rise to interlobar arteries which course along the sides of the renal pyramids. At the level of the corticomedullary junction, the interlobar arteries branch into the arcuate arteries, which travel across the superior border of the pyramids and give rise to the interlobular arteries. The interlobular arteries course toward the surface of the kidney forming the afferent glomerular arterioles.

On each side, the renal vein courses anteriorly from the renal hilum with the ureter arising posteriorly. The renal artery normally lies between the vein and the ureter. On the

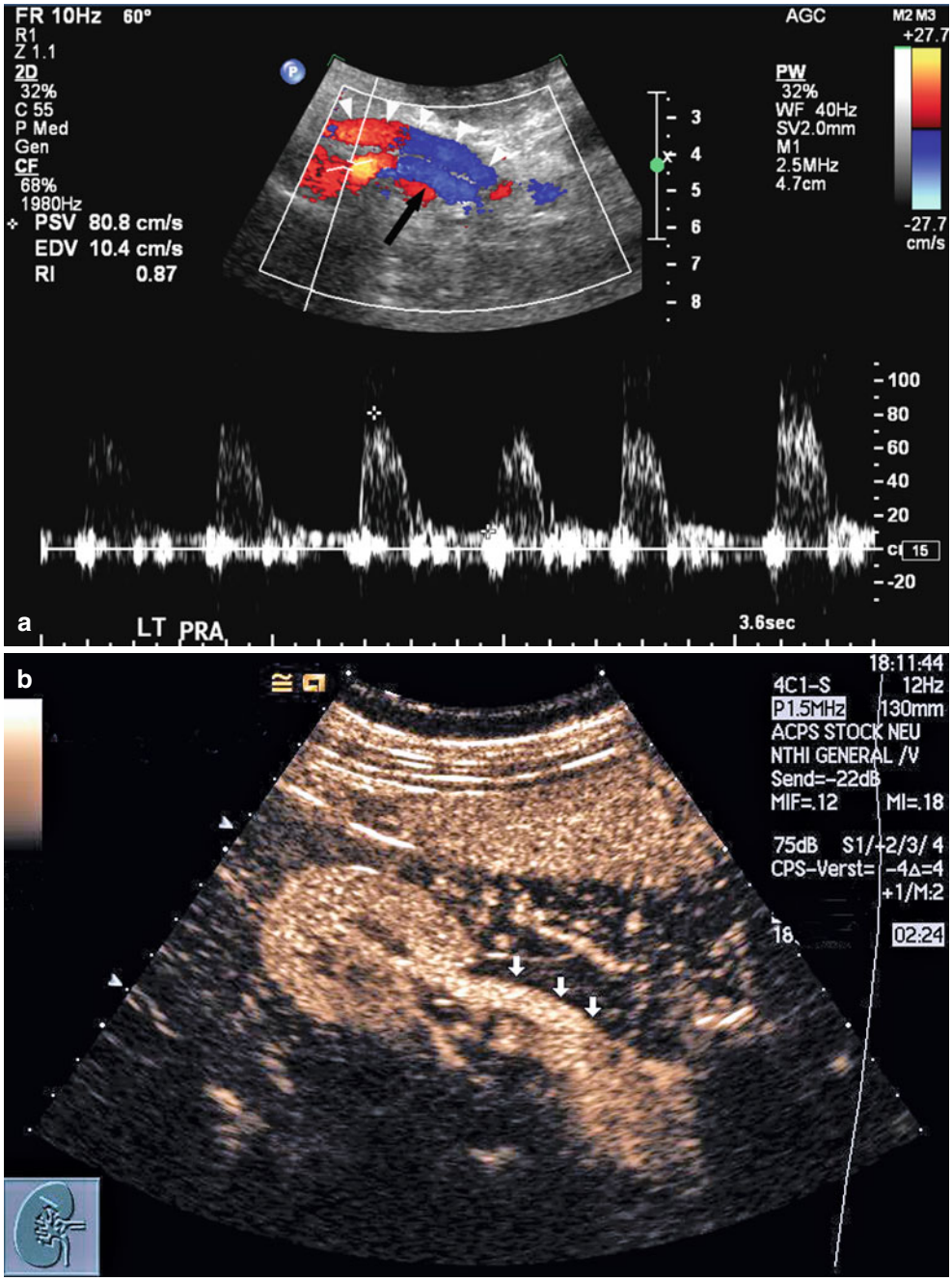


**Fig. 47.4** (**a**) Transverse color flow image of the abdominal aorta, superior mesenteric artery, portal vein confluence, IVC, and left renal vein. Note the left renal vein (*white arrowheads*) crossing over the renal artery (*black arrow*) and anterior aortic wall. (**b**) A longitudinal view of the right renal vein (*arrows*) following intravenous contrast (Image courtesy of Konrad Stock, M.D.)

right, the renal vein has a short course from the hilum of the kidney to the IVC. While venous anatomy may be anomalous in many patients (primarily due to multiple veins), the left renal vein normally courses anterior to the aorta and posterior to the superior mesenteric artery (Fig. 47.4). In 3% of patients, the left renal vein may take a completely retroaortic path while up to 18% of patients will demonstrate a bifid (circumaortic) left renal vein with both a retroaortic branch and another branch coursing anterior to the aorta [43, 44]. It is important to be aware of these anatomic anomalies because the left renal vein is used as a major anatomic landmark for locating the renal arteries during the sonographic examination.

## Technique

### Patient Preparation and Positioning

Although patients are required to fast for 6–8 h prior to the sonographic examination to reduce excessive abdominal gas that would make visualization of the renal arteries and veins

more difficult, we have not found it necessary to use cathartics. Patients are allowed to take their usual medications with small sips of water. Diabetic patients are permitted to have dry toast and clear liquids in the morning of the study in order to prevent development of hypoglycemia while awaiting their sonogram. Because of this concern, diabetic patients are also the first ones scheduled in the morning. It is recommended that all patients refrain from smoking or chewing gum because these activities increase the amount of swallowed air in the stomach.

Once in the vascular laboratory, the patient is placed on the examination table in the supine position with the head slightly elevated and the feet lower than the heart. This allows the viscera to descend into the lower abdomen and pelvis, increasing the likelihood of finding acceptable acoustic windows. With the patient in this position, the aorta, mesenteric, and proximal-to-mid segments of the renal arteries are visualized. For examination of the distal renal arteries, renal veins, and the kidneys themselves, the patient is moved to the right or left lateral decubitus position with the arm raised over their ear and their legs extended to elongate the body. A prone position, using intercostal scan planes, may occasionally be required for a thorough examination of the kidneys and distal renal arteries. In patients with a low rib cage, it may also be helpful to have them raise their arms over their head to elevate the ribs and allow improved access to the proximal renal arteries.

## Equipment

A high-resolution ultrasound system with pulsed Doppler transducers ranging in frequency from 2.25 to 5.0 MHz is required to allow adequate penetration to the depths of the aorta and distal renal arteries. Although color flow and power Doppler imaging are not absolutely required for successful renal vascular examination, these technologies will greatly facilitate visualizing the vessels, identification of regions of flow disturbance, and confirmation of arterial and/or venous occlusion. The sonographer must optimize the B-Mode, color, and spectral Doppler information throughout the examination because velocities may vary over small regions of the renal arterial and venous systems due to tortuosity and short-segment lesions, dissections, or webs.

## Examination of the Aorta, Mesenteric, and Renal Arteries

The examination is initiated with evaluation of the aorta beginning at the level of the diaphragm and continuing to its bifurcation. B-Mode imaging is used to determine the presence of atherosclerotic plaque, aneurysmal dilation, or dissection. The evaluation is complemented with color flow imaging to highlight any regions of disturbed flow. Selective Doppler spectral waveforms are recorded at the level of the celiac and superior mesenteric artery origins. The aortic peak systolic velocity is documented and retained for later utilization in calculation of the renal to aortic velocity ratios.

Branches of the celiac and superior mesenteric arteries may course in close proximity and may be mistaken for accessory or main renal arteries. To help prevent such confusion, Doppler spectral waveforms may be recorded from both the celiac and superior mesenteric arteries with the primary purpose being recognition of the mesenteric flow patterns. A secondary benefit would be detection of unsuspected mesenteric occlusive disease.

The aorta is thereafter imaged in the cross-sectional plane at the level of the superior mesenteric artery. Just inferior to this level, the left renal vein can be identified as it crosses anterior to the aorta (Fig. 47.4). Although this vein serves as a useful landmark for locating the renal arteries, care must be taken to identify anomalous venous anatomy. The vein diameter and flow patterns should be assessed to rule out thrombosis or extrinsic compression due to overlying small bowel or superior mesenteric artery compression syndrome.

Although the renal arteries usually arise from the midlateral or posterolateral wall of the aorta at the level of the second lumbar vertebrae, just posterior to the left renal vein, there can be much anatomic variability in their location (Fig. 47.5a). The location of accessory renal arteries is even more unpredictable and therefore easy to miss. Color flow imaging facilitates the identification of the arteries and makes it easier to follow their course from the origin to the midsegment of the vessel. When neither color flow nor power Doppler allows satisfactory vessel identification, the use of intravenous ultrasound contrast can be helpful.

To rule out orificial stenotic disease commonly associated with plaque on the aortic wall, the Doppler sample volume is swept slowly from within the lumen of the aorta and through the renal artery ostium. In making the transition from the aorta into the renal artery, the high-resistance aortic flow pattern changes to a low-resistance configuration in the renal artery. Dependent on the angulation of the renal ostium, it may be difficult to maintain appropriate angle correction during the transition maneuver. Regardless of this technical limitation, high velocity, turbulent signals reliably indicate stenotic ostial disease.

Using the smallest sample volume, Doppler spectral waveforms are recorded continuously throughout the visualized length of the renal arteries. The highest peak systolic velocity in the vessel is documented being careful to utilize an angle of insonation less than 60° (Fig. 47.5a). If needed, the patient is moved to the right or left lateral decubitus, lateral oblique, or prone position for interrogation of the mid-to-distal renal artery and renal parenchymal vessels. Color

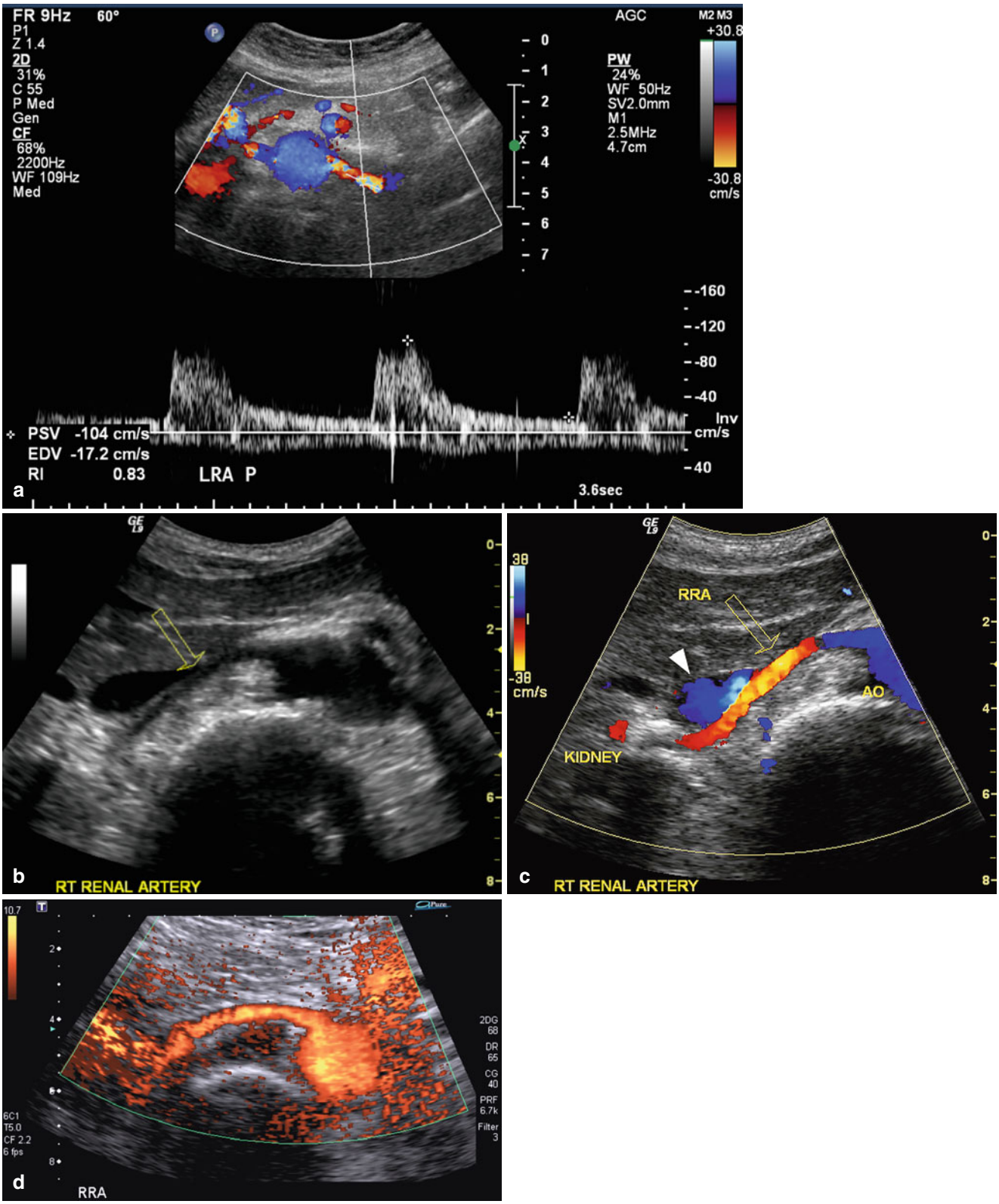


**Fig. 47.5** (**a**) Color flow image of the abdominal aorta and left renal artery demonstrating appropriate angle correction for demonstration of Doppler spectral waveforms within the renal artery. A low resistance spectral pattern is evident which is characteristic of normal renal arterial blood flow. (**b**) Particularly on the right side, it may be more difficult to identify the full length of the renal artery (*open arrow*). (**c**) The use of color Doppler greatly improves visualization of the right renal artery (*open arrow*), particularly as it goes posterior to the vena cava (*white arrowhead*). (**d**) In difficult circumstances, power Doppler can even more effectively display the entire renal artery

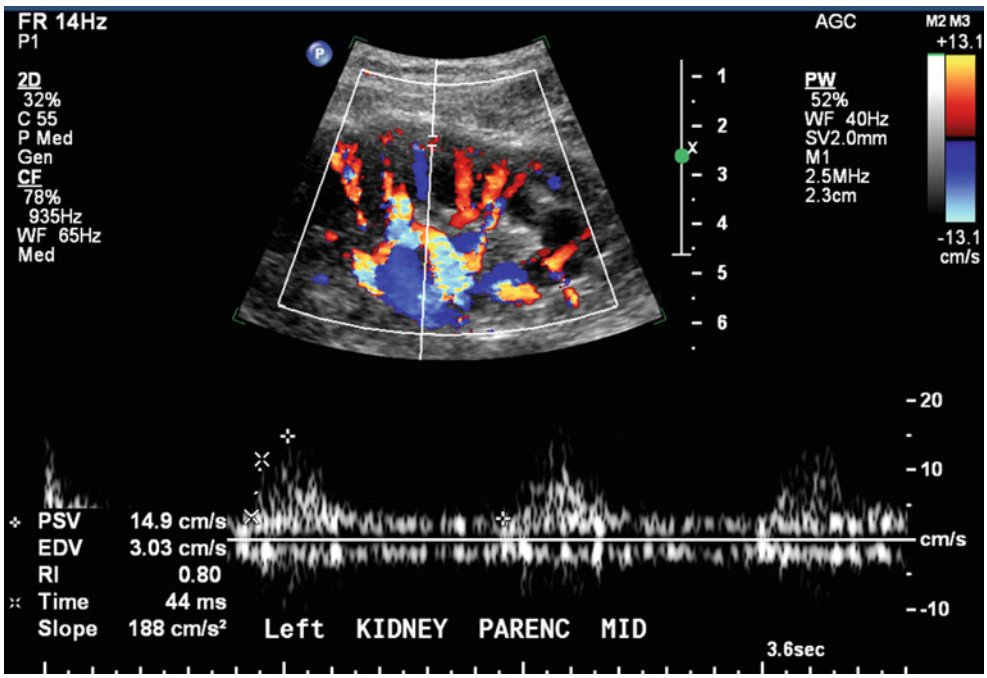


**Fig. 47.6** Color flow image and Doppler spectral waveforms from the arcuate arteries within the renal cortex. Normal renal parenchymal flow is characterized by constant forward diastolic flow

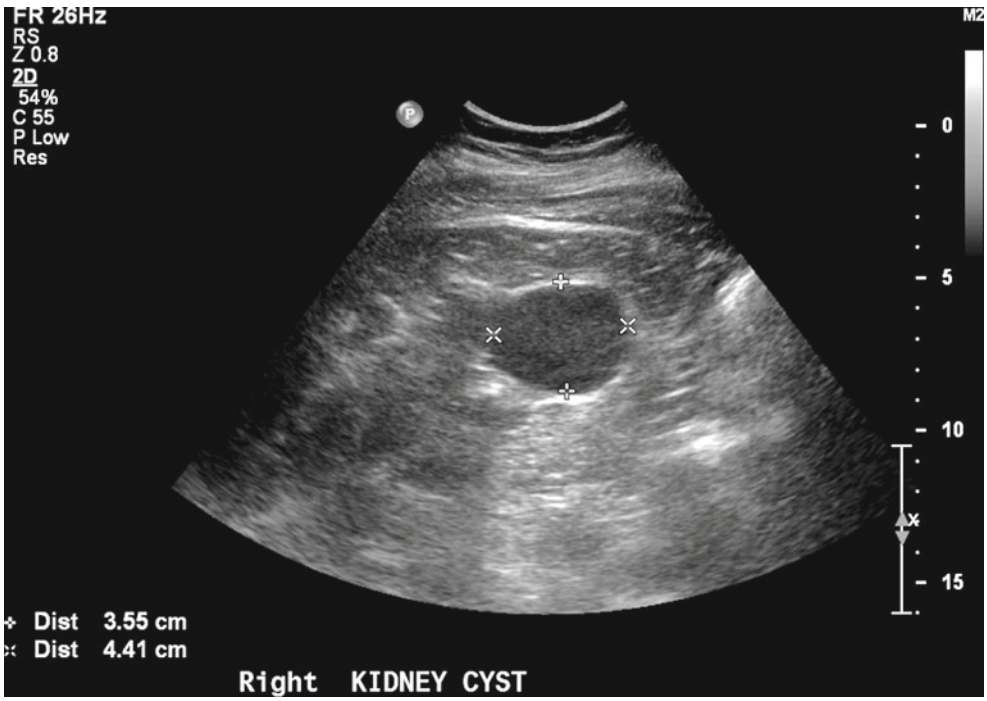


**Fig. 47.7** Benign echolucent renal cysts are commonly found in the body of the kidney

and/or power Doppler imaging may facilitate appropriate angle correction and identification in cases of vessel tortuosity (Fig. 47.5b–d).

## Evaluation of Renal Parenchymal Blood Flow

Blood flow patterns are documented throughout the distal renal artery and the interlobar and arcuate arteries of the renal medulla and cortex (Fig. 47.6). Using a 0° angle of insonation, spectral waveforms are recorded throughout the kidney, noting regions of increased signal amplitude and disordered or absent flow. The signals with the highest peak and end-diastolic velocities are documented from the vessels within the medulla and cortex of the upper-, mid-, and lower poles of the kidney. The presence of cortical thinning, cysts, masses, renal calculi, hydronephrosis, and/or perinephric fluid collections is noted (Fig. 47.7).

## Measurement of Renal Size

Because renal atrophy would be a contraindication to revascularization, the pole-to-pole length of each kidney is documented during each study (Fig. 47.8). Normal renal length is between 9 and 13 cm in the greatest longitudinal plane and there is usually less than 1 cm difference in renal lengths between the two kidneys. The length of the organ is measured during maximum inspiration using a flank approach to optimize visualization of the renal margins on both poles.

## Evaluation for Renal Vein Thrombosis

Although most renal studies are performed for examination of the arterial circulation, renal vein thrombosis can lead to acute renal failure and referral to the vascular laboratory. Confirmation of renal vein thrombosis can be technically challenging. The vein may be dilated with acute thrombus or contracted when it has been chronically thrombosed. Optimization of the grayscale image is needed to demonstrate intraluminal echoes that indicate thrombosis (Fig. 47.9). Doppler spectral examination will document the absence of blood flow within the vein and a retrograde, blunted diastolic flow component in the renal arterial signals (Fig. 47.10). In the case of renal cell carcinoma, extensive tumor involvement in the renal vein is common with extrusion and propagation into the IVC. In patients with a thrombosed IVC, possibly associated with prior placement of a vena caval filter, retrograde thrombosis may extend into the renal veins.

## Contrast Enhanced Imaging

Duplex imaging of renal artery stenosis can be technically challenging and is influenced by both operator expertise and patient factors, such as overlying bowel gas, obesity, and inability to optimally position the patient due to lack of patient cooperation [31]. Contrast enhancement to improve imaging and increase diagnostic accuracy is prevalent in radiologic techniques such as angiography, computed tomography (CT), and MRI. Ultrasound contrast agents are stabilized gas microbubbles that enhance ultrasound signals due to the difference between them and the surrounding blood in terms of compressibility and density. They reflect transmitted ultrasound waves strongly, enhancing echogenicity at both fundamental and harmonic frequencies, which provides improved vascular imaging and tissue differentiation [45, 46]. Intravenous ultrasound contrast agents have been found to improve ultrasound diagnostic accuracy and are approved for use in the heart with utility also reported in the liver, mesenteric, and peripheral vasculature [47–49] (Fig. 47.11).

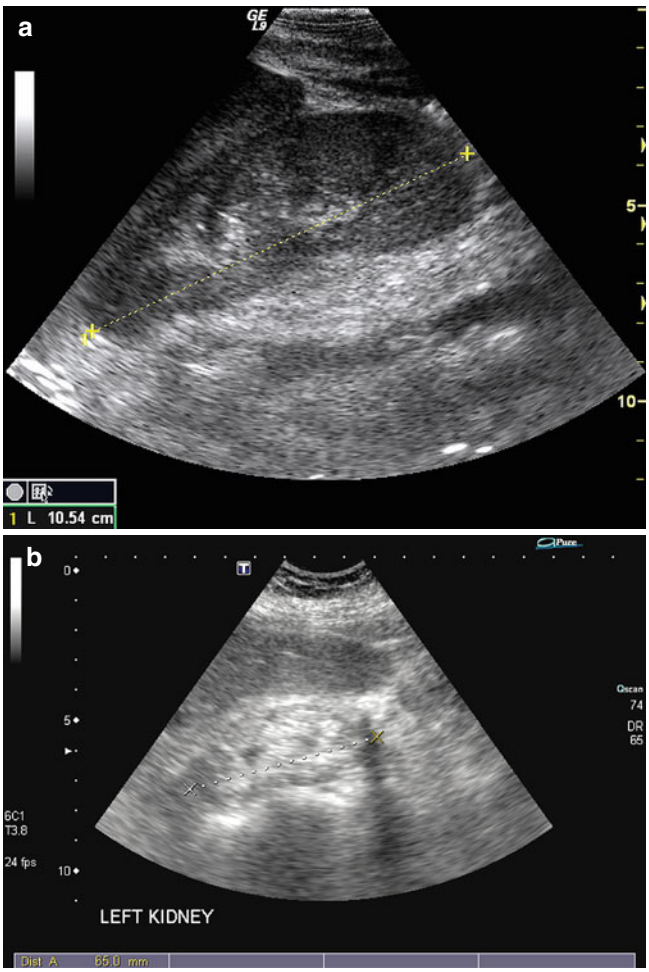


**Fig. 47.8** The pole-to-pole length of the kidney is measured to evaluate suitability for revascularization of stenotic lesions. Normal adult kidney length is greater than 9 cm (**a**) while atrophic organs are significantly shorter and more echogenic in character (**b**)

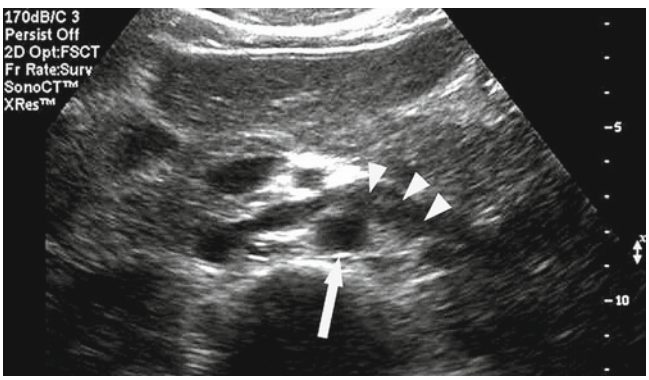


**Fig. 47.9** Transverse abdominal B-Mode image of the aorta (*arrow*) and the crossing left renal vein demonstrating dilation of the vein and intraluminal echoes (*arrowheads*) consistent with thrombus

A prospective study examined the use of perflutren contrast agent (Definity, DuPont) to improve imaging of the renal arteries [50]. This agent is composed of three phos-

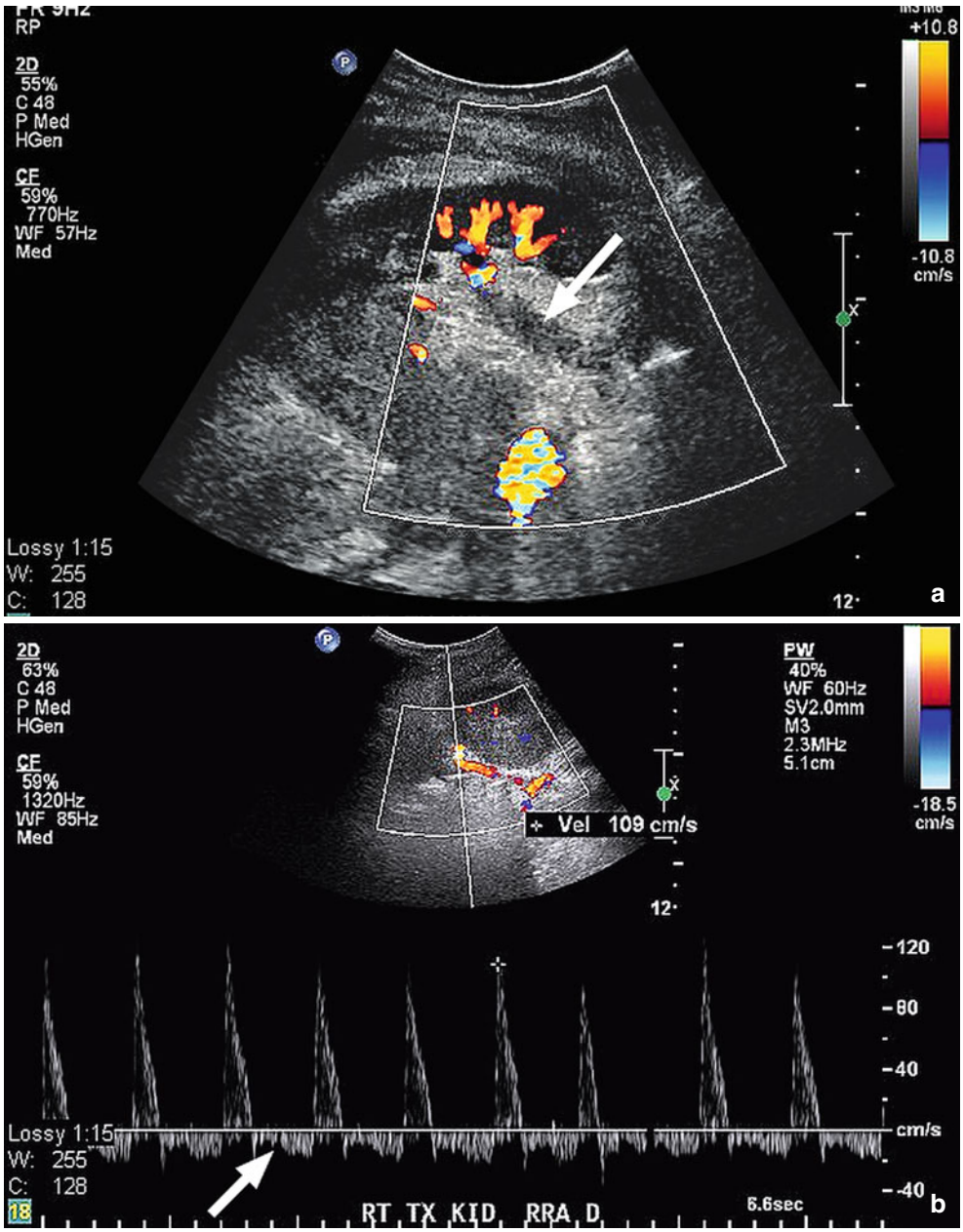


**Fig. 47.10** (**a**) Longitudinal color duplex image of a transplanted kidney showing lack of color flow and echogenic thrombus in the dilated renal vein (*arrow*). (**b**) Doppler spectral waveforms recorded from the inflow renal artery. Note the retrograde diastolic flow (*arrow*) suggestive of obstruction to venous outflow from the kidney (Images courtesy of Nicos Labropoulos, Ph.D.)

pholipids and a perfluoropropane gas that, when mixed together, form lipid-encapsulated-gas-filled microbubbles [48]. Because the microbubbles are less than 5 μm in diameter, and thus smaller than red blood cells, they pass easily through the pulmonary microcirculation and are rapidly cleared by respiration from the systemic circulation within 5 min of their infusion. This particular agent requires mixing for 45 s at 4,500 oscillations/min in a specific vial shaker. For this study, a volume of 1.3 ml of agitated contrast solution was injected into a 50 ml bag of 0.9% sterile saline solution, which was subsequently infused intravenously at a rate of 2 ml/min via an 18-guage needle throughout the duration of the duplex examination. The results of the ultrasound examination, with and without contrast enhancement, were compared with intra-arterial angiography. Both duplex alone and duplex with contrast demonstrated excellent identification of the renal arteries (Table 47.2). Overall visualization of the renal arteries was 85% for standard duplex and 94% following contrast. Contrast infusion was particularly helpful in identifying additional accessory arteries and visualization of hemodynamically significant stenotic vessels. A total of five of seven arteries not visualized by color flow duplex was detected following the infusion of contrast, resulting in an additional 10% (5/48) of vessels visualized. In addition, significantly longer lengths of the renal arteries were visualized in continuity when contrast was infused (3.9 cm as compared to 3.3 cm [$P = 0.001$]).

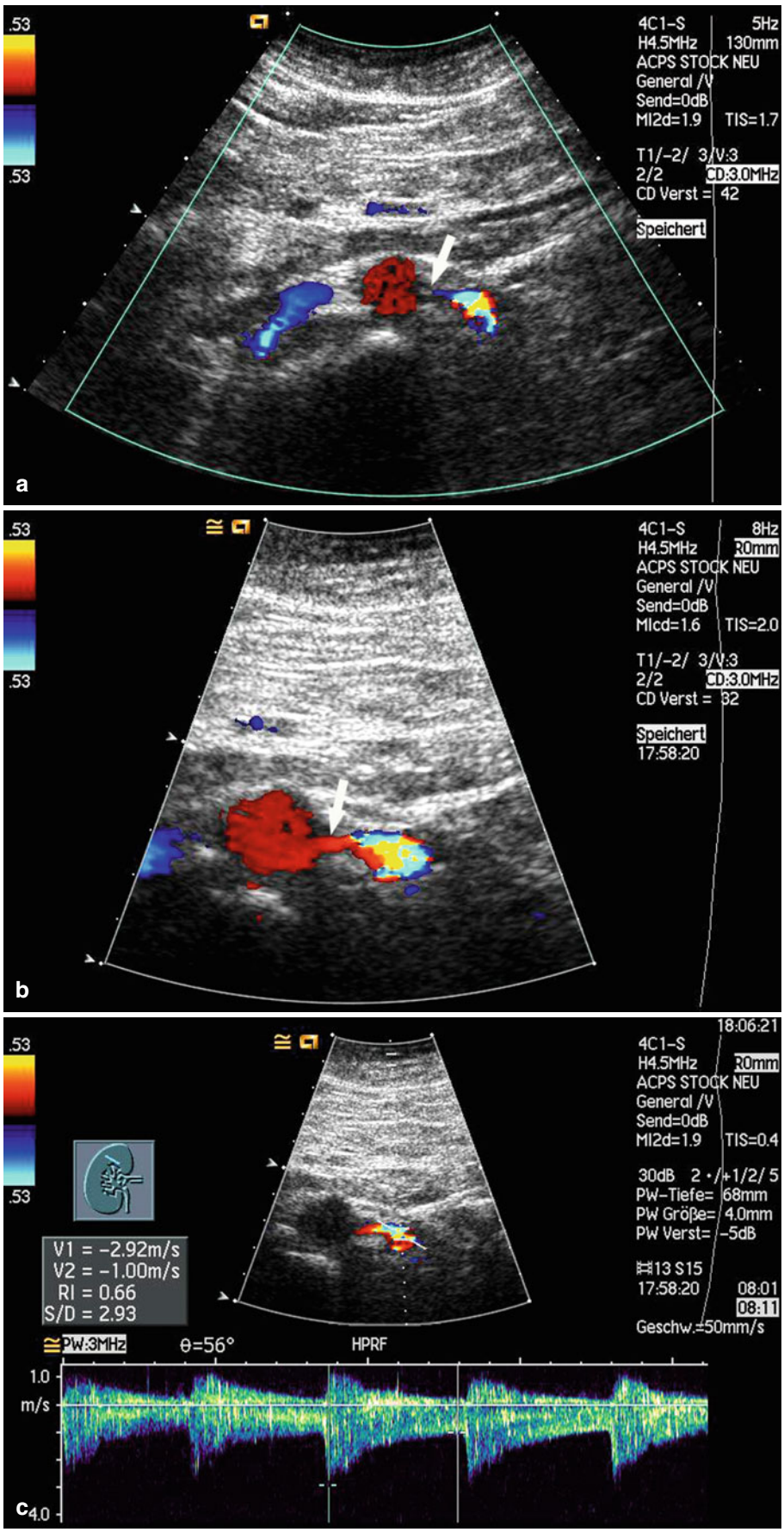


**Fig. 47.11** (**a**) Transverse color flow image of an atherosclerotic abdominal aorta without contrast is unable to demonstrate the origin (*arrow*) of the left renal artery. (**b**) With the addition of contrast, the proximal portion of the renal artery (*arrow*) is well visualized. (**c**) This allows accurate placement of the sample volume to identify the presence of a high-grade stenosis (Images courtesy of Konrad Stock, M.D.)

**Table 47.2** Visualization of renal arteries with intravenous contrast

| Renal arteries | Duplex alone | Duplex + contrast |
|---|---|---|
| All renal arteries (48) | 41 (85%) | 45 (94%) |
| Main (43) | 40 (93%) | 42 (98%) |
| Accessory (5) | 1 (20%) | 3 (60%) |
| Normal/minimal disease (32) | 30 (94%) | 31 (97%) |
| Stenosis > 60% (12) | 9 (75%) | 12 (100%) |
| Occlusion (4) | 3 (75%) | 3 (75%) |
| Visualized length of artery | 3.3 ± 0.3 cm | 3.9 ± 0.3 cm |

Modified from Blebea et al. [49]. With permission from Elsevier

**Table 47.3** Doppler velocities following contrast administration

| Renal arteries | Duplex alone | Duplex + contrast |
|---|---|---|
| Normal/minimal disease (cm/s) | 112 ± 6 | 123 ± 7[b] |
| Stenosis > 60% (cm/s) | 173 ± 20[a] | 194 ± 18[a,b] |
| All (cm/s) | 127 ± 7[a] | 144 ± 8[a,b] |

Modified from Blebea et al. [49]. With permission from Elsevier
[a]$P < 0.001$ versus normal
[b]$P < 0.001$ versus duplex alone

There were no complications associated with the use of the intravenous contrast. The patients experienced no changes in blood pressure or heart rates during the contrast infusion and no deterioration of renal function as measured by blood urea nitrogen or serum creatinine levels, consistent with the experience of other investigators [48, 51]. Insonated Doppler velocities, however, were increased following contrast administration by an average of 10% in normal or minimally diseased vessels and 12% in stenotic vessels (Table 47.3). Although these differences were statistically significant, they did not lead to a change in the category of stenosis. This artifactual increase in measured Doppler velocities has been noted in both human and in vitro studies [49, 52]. As contrast agents become more extensively used, separate velocity criteria may need to be established. Currently, however, the 10–12% increase in peak systolic velocities does not represent a large enough difference to require immediate attention but should be kept in mind for borderline results.

House et al. used contrast enhancement (Levovist, Schering, Berlin, Germany) for technically unsuccessful studies or to improve diagnostic confidence in sonographic detection of recurrent stenosis in stented renal arteries [53]. Use of contrast enhancement improved the technical success rate from 89% to 95% and also increased diagnostic confidence in a significant number of examinations.

The results from these studies indicate that contrast-enhanced duplex imaging of the renal arteries is safe but not routinely required when an experienced sonographer performs the study. However, it can increase vessel visualization and thus allow more specific placement of the pulsed Doppler sample volume. This may increase overall accuracy of the study in patients with stenoses and accessory renal arteries or in approximately 10% of patients whose vessels are not initially successfully visualized. No comparative studies have been done among different contrast agents. Another perflutren-based contrast agent (Optison, Amersham Health) is FDA approved for echocardiography and has the potential benefit of not requiring a specific vial mixer before infusion. A recent controversy about a potential increased mortality risk of intravenous contrast agents in patients undergoing echocardiography has not been substantiated [54]. It is hoped that the FDA will approve noncardiac indications for ultrasound contrast agents in the near future.

## Special Considerations

### Accessory and Multiple Renal Arteries

Approximately 30% of the population has multiple renal arteries on one side and another 10% have bilateral multiple vessels [41, 43]. Duplicate renal arteries usually arise from the lateral aortic wall and are directed toward the central hilum of the kidney while accessory polar renal arteries course toward the upper or lower poles of the kidney. For an unknown reason, more accessory renal arteries are seen on the left as compared to the right side. When only a single accessory artery is present, it is usually supplying the lower pole of the kidney. In the presence of an accessory vessel, the main renal artery is usually of near-normal caliber while the accessory vessels have a smaller diameter. When multiple renal arteries occur, none of the vessels may be dominant and it is quite difficult to be certain that velocity measurements have been acquired from all vessels.

Positive identification of all accessory polar renal arteries by B-Mode imaging is not generally possible because of the small diameter of these vessels and lack of clinical suspicion for their presence. While color flow imaging may facilitate recognition of accessory renal arteries, it is important to remember that color encodement of Doppler-shifted frequencies from blood flow is angle dependent and accessory renal arteries may arise from the aortic wall at angles between 70° and 90° (Fig. 47.12). To overcome this problem, power Doppler imaging, which relies on the amplitude of the returned Doppler signal and is not as angle dependent as color Doppler imaging, may prove beneficial for detection of these small vessels.

There are several scanning maneuvers that can be used to detect the presence of supernumery renal arteries. It is helpful to increase the size of the Doppler sample volume and scan in the para-aortic region, moving from the level of the main renal artery origin to the aortic bifurcation to detect any additional low resistance signals that could imply renal arterial flow. Lumbar arteries can be confused with accessory

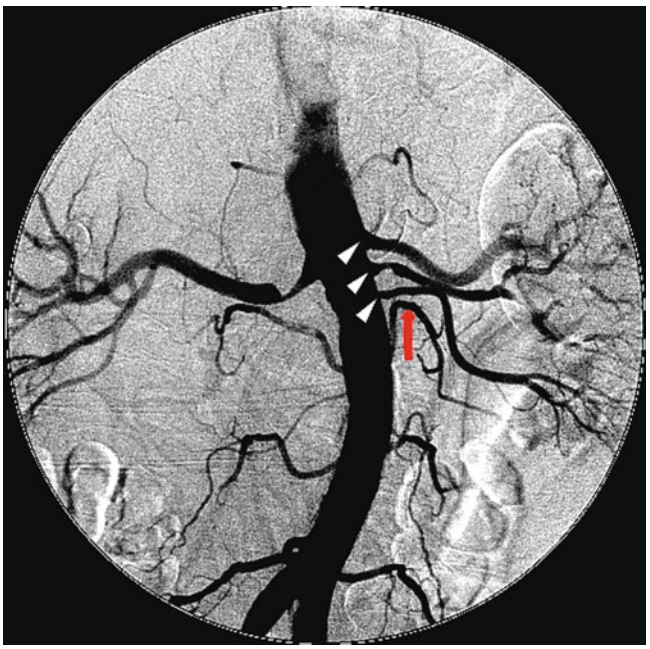

**Fig. 47.12** Digital subtraction angiogram illustrating three renal arteries on the left (*white arrowheads*) with the mid-renal demonstrating a 50% stenosis. An adjacent lumbar artery (*red arrow*) can be misconstrued as another accessory artery if it is not followed distally to confirm that it does not lead to the kidney

renal arteries but these have a more posterior origin from the aorta. A sagittal image of the IVC may reveal multiple right renal arteries beneath this vessel. Using color and/or power Doppler, the origins of the renal arteries can quite often be visualized from a coronal view of the aorta (the "banana peel" approach). This is not only an excellent imaging approach in adult patients but this view also facilitates identification of fetal supernumery renal arteries during second or third trimester in utero evaluations. Accessory polar renal arteries can often be identified on a long axis or transverse color/power Doppler image of the kidney but their identity must be confirmed by tracing the vessel back to its origin. It should also be noted that the use of an intravenous contrast agent has improved the detection of accessory renal arteries [49].

## Occlusion of the Main Renal Artery

Diagnosis of an occluded main renal artery can be difficult because the sonographer is appropriately concerned that it has not been possible to adequately visualize flow within the vessel rather than prematurely concluding that the vessel is thrombosed. Excessive overlying abdominal gas that may compromise visualization compounds this hesitation. After optimizing Doppler spectral and color flow parameters for detection of very slow flow, and possibly the use of intravenous contrast, it is possible to look for secondary indications of renal artery occlusion. With chronic occlusion and atrophy, kidney length is less than 8 cm and there can be a significant >3 cm difference in length as compared with the contralateral kidney. Intraparenchymal insonation demonstrates low cortical velocity of <10 cm/s with low amplitude and a delayed systolic upstroke. The presence of cortical blood flow is a result of collateral flow to the kidney through adrenal and ureteral vessels.

## Horseshoe Kidney

Horseshoe kidneys are not common, occurring in less than 1% of autopsies. Most often, the organs are fused at the lower pole, with approximately 10% of kidneys joined at the upper pole. This large unified kidney, connected by an isthmus of renal parenchyma of variable size, will lie anterior to the aorta usually at the level of the fourth or fifth lumbar vertebrae. Horseshoe kidneys are usually found in patients who present for investigation of a pulsatile abdominal mass or they may be discovered incidentally during an abdominal ultrasound examination.

Anatomically, the kidney is supplied by multiple renal arteries and drained by multiple renal veins at unpredictable locations [40, 43]. Multiple arteries may arise from the iliac arteries or the distal aorta. Their location, posterior to the body of the kidney, makes it difficult to identify these arteries and even more challenging to diagnose the presence of stenoses. In patients with an underlying abdominal aortic aneurysm, diagnosing renal artery stenosis is best accomplished with contrast angiography.

## Renal Aneurysms

Aneurysmal dilatation of the renal artery usually involves the main segment of the renal artery or its first-order branches [55]. Although aneurysms may also occur intraparenchymally, this location is seen in only approximately 10% of cases. Renal aneurysms are most easily identified with color flow imaging (Fig. 47.13). Their large size, compared to the native vessel, makes identification relatively easy. Intervention is generally recommended for aneurysms of 2 cm or greater in diameter. Therefore, it is important to measure the maximal diameter of the aneurysm, either in preparation for surgical repair or as a baseline for monitoring future growth. The specific location is less important although differentiation between an aneurysm involving the renal artery and an intraparenchymal position is helpful in selecting proper therapy. Rarely, there is an associated arteriovenous fistula that makes the initial diagnosis more challenging.

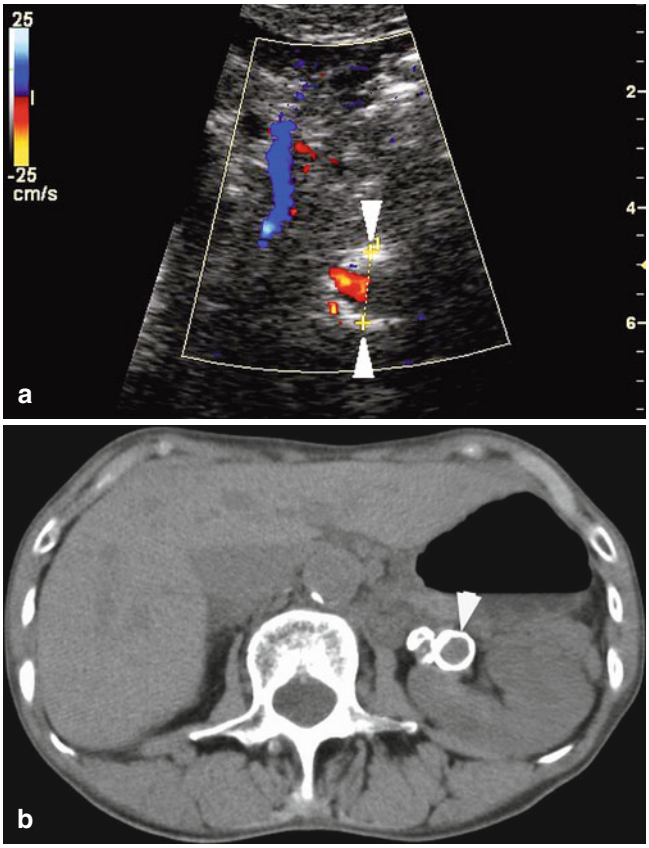


**Fig. 47.13** (**a**) A left renal artery aneurysm is measured transversely on a sonographic image. Color flow evaluation is difficult due to circumferential calcification in the wall of the aneurysm. (**b**) The calcified aneurysm, located just beyond the bifurcation of the renal artery, is seen on CT scan without intravenous contrast

## Fibromuscular Dysplasia

Fibromuscular dysplasia (FMD) is a term encompassing several histologic forms of arterial wall changes of which medial fibroplasia is the most common [2, 22]. As a group, FMD is the second most common cause of renal artery stenosis and accounts for up to one-third of cases of renovascular hypertension in adults. This nonatherosclerotic disease process is seen almost exclusively in females and presents as a "string of beads" angiographic appearance with web-like stenotic segments alternating with post-stenotic dilations. It involves the mid-to-distal segments of the renal artery and will frequently extend into branch vessels with characteristic superimposed high- and low-velocity signals (Fig. 47.14). Awareness that this disease affects primarily young women, in the third or fourth decade of life, an age group not usually affected by renal atherosclerosis, may aid in identification of this disorder. The less common variants of FMD, perimedial dysplasia and intimal fibroplasia, are not associated with post-stenotic dilations. Intimal fibroplasias, in particular, produce a smooth concentric stenosis. Differentiation between the types of FMD is neither practical nor necessary during sonographic examination. Because fibromuscular dysplasia is often found bilaterally, it is important to search for similar flow patterns in the contralateral renal artery.

## Renal Artery Bypass Grafts

Similar to peripheral bypasses, renal artery bypass procedures are followed postoperatively for the development of stenosis to allow intervention before graft occlusion occurs. When evaluating renal artery bypass grafts, it is helpful to know specific details of the surgical procedure including the origin of the graft, conduit used (prosthetic or autologous saphenous vein), and location and type of distal anastomosis. An operative drawing indicating the donor artery, graft course, and recipient vessel is very useful. Renal artery bypass grafts commonly originate from a prosthetic aortic graft, the native aorta, or the iliac arteries. Other less common inflow sources include the hepatic or gastroduodenal arteries on the right side and the superior mesenteric or splenic arteries on the left side.

As with extremity bypass grafts, the anastomotic regions must be carefully interrogated with spectral and color Doppler because intimal hyperplasia and stenosis most commonly occurs at the anastomotic sites. If the conduit is a saphenous vein, attention is given to the possibility of retained valves or stenosis developing at the site of valve leaflets. The donor and recipient vessels are also examined for progression of atherosclerotic disease. If graft occlusion is suspected, dampening of the velocity spectral waveform is expected within the renal parenchyma.

## Renal Artery Stents

The sonographic technique for evaluation of the renal artery following balloon angioplasty and stenting is identical to that used for evaluation of the native renal artery prior to intervention [56]. In the majority of patients, the metallic stents are well visualized and their location within the renal artery easily determined because the metal stents are brightly echogenic (Fig. 47.15a). The aortic wall adjacent to the renal artery orifice should be carefully evaluated with high resolution B-Mode, real-time compound, or harmonic imaging, to determine how far the stent protrudes into the lumen of the aorta. Similarly, the length of the stented segment should be examined to confirm complete deployment and uniform apposition to the wall of the renal artery without echogenic thrombus (Fig. 47.15b) or distal dissection. Color flow and power Doppler can be helpful to localize the lumen, or thrombosis (Fig. 47.15c, d).

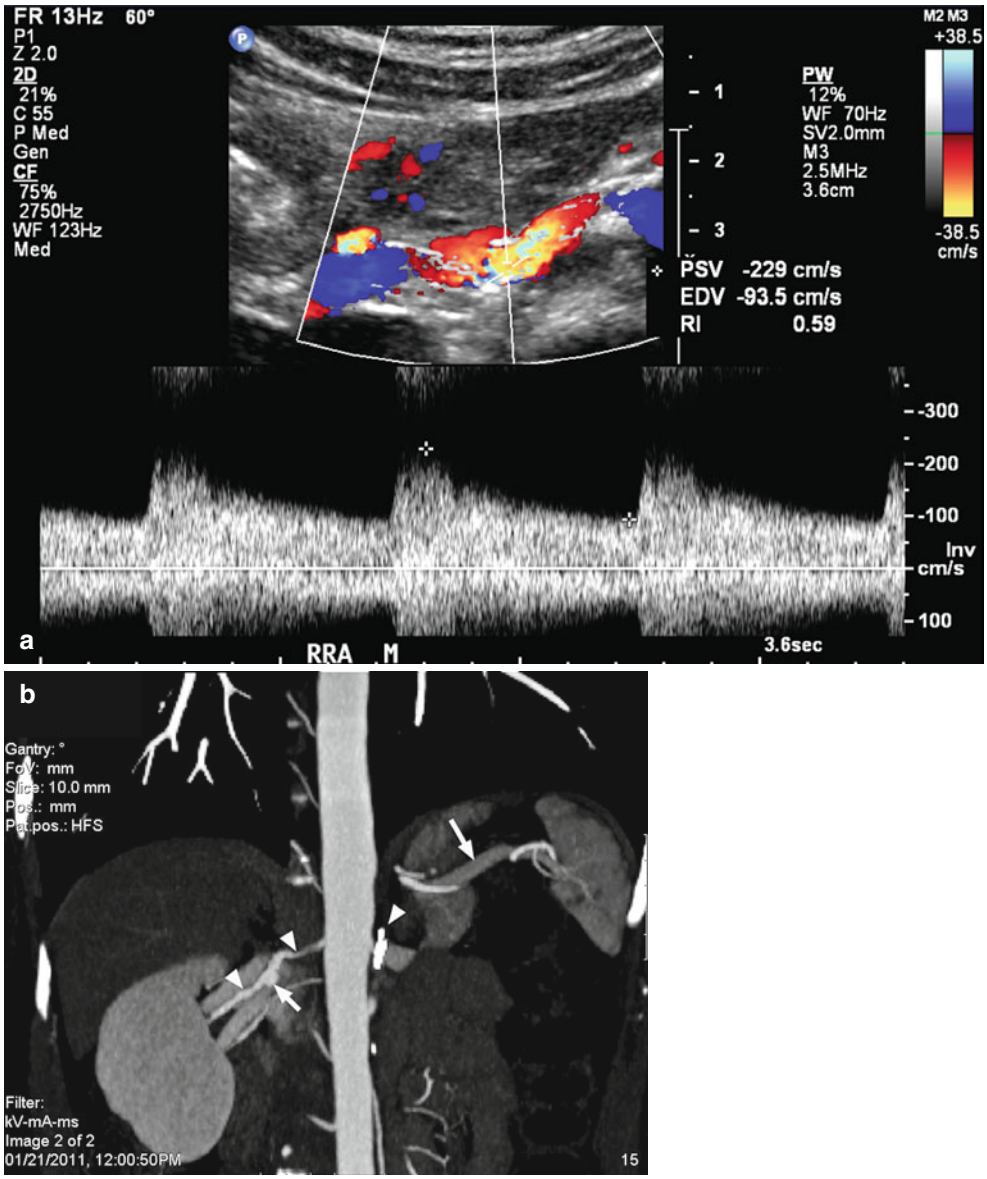


**Fig. 47.14** (**a**) Color duplex and Doppler spectral waveforms from a patient with medial fibromuscular dysplasia. There is turbulent flow with color variegation and high-velocity bidirectional signals. (**b**) The associated computed tomography angiogram illustrating on the right side the irregular arterial wall (*arrowheads*) with an intervening segment of dilatation (*arrow*). On the left side, the artery had previously been resected and a proximal metallic clip placed upon the origin (*arrowhead*). The distal portion of an aorta-to-renal autologous vein bypass graft is also seen (*arrow*)

Using color or power Doppler imaging and Doppler spectral evaluation (Fig. 47.15e, f), the stent is examined throughout its origin, proximal-, mid-, and distal segments with the study extended into the distal native renal artery and the vessels within the kidney. Marked flow disturbances at the renal artery orifice may indicate that the stent is protruding too far into the aortic lumen. High-velocity signals at this location suggest that aortic flow patterns are severely disrupted and pressure-flow gradients have developed. Minimal flow disturbance is usually noted in the proximal stented segment of the artery. A slight elevation in the systolic velocity may be found due to the rigidity of the stent and consequent decreased vessel wall compliance. In the absence of flow-limiting stenosis in the proximal stent, the peak systolic velocity range should approximate that seen in normal, unstented renal arteries.

The native renal artery normally tapers as it courses distally. Placement of a renal stent results in slight dilation of the stented segment of the vessel compared to the diameter of the native artery distal to the stent. Given this, a flow gradient may be present at the distal end of the stent because the blood is flowing from a large diameter vessel to a smaller diameter segment. Even though the diameter mismatch across the distal end of the stent is quite small, slightly elevated Doppler velocity signals and disordered color flow patterns may be encountered. Careful attention must be given to the flow patterns at the distal end of the stent to ensure that they are the result of a stent-diameter to vessel-diameter mismatch and not due to flow-reducing stenosis distal to or within the stent. Increased peak and end diastolic velocities with post-stenotic turbulence suggest flow-reducing stenosis.

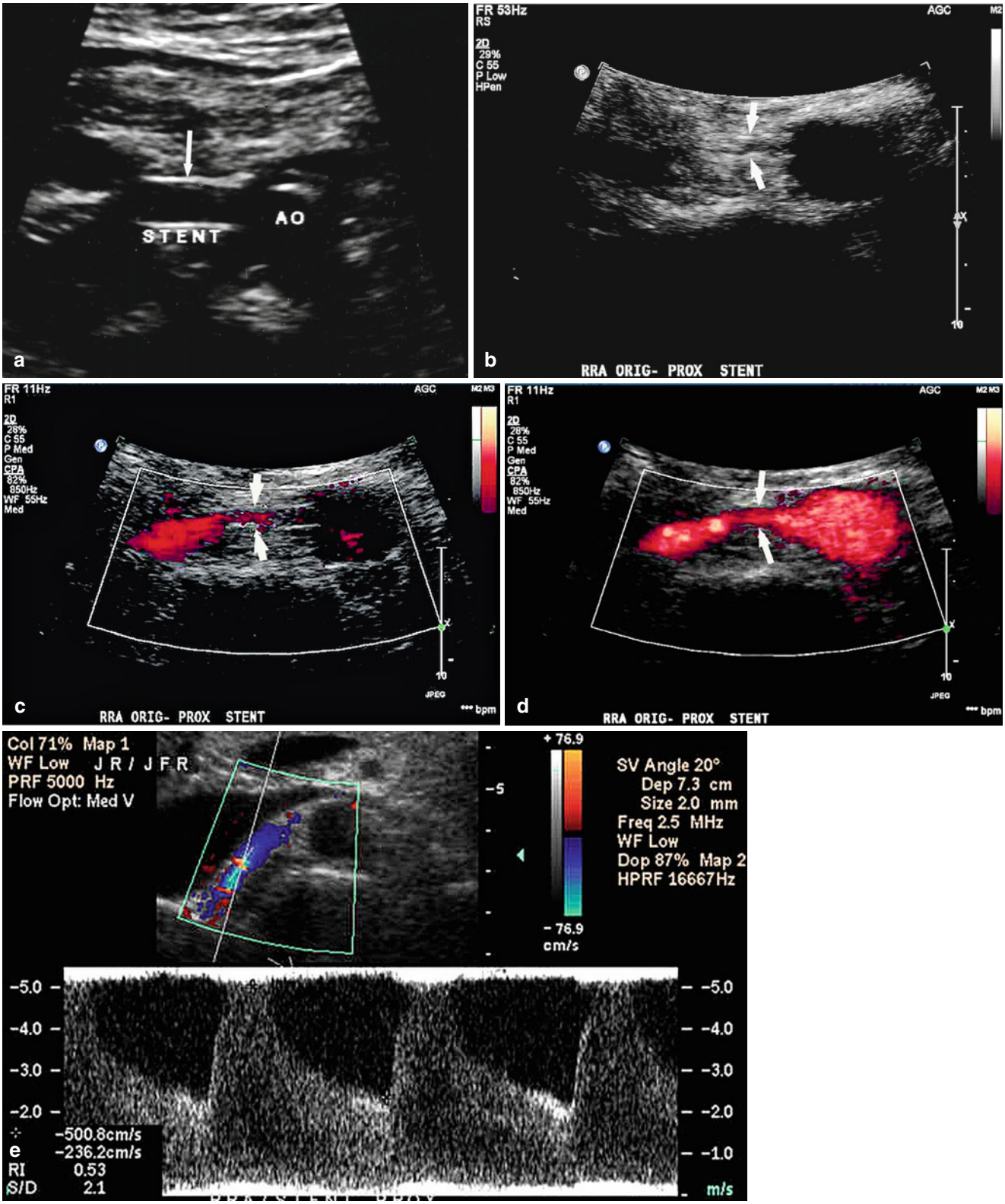


**Fig. 47.15** (**a**) Cross-sectional abdominal B-Mode image of the aorta and the proximal right renal artery demonstrates the echogenic walls of a renal stent (*arrow*). High-resolution imaging confirms uniform apposition of the stent to the walls of the artery. (**b**) In a different patient, B mode imaging suggests intrastent echogenic thrombus with poorly defined edges (*arrow*). (**c**) Color Doppler defines flow within the stent (*arrow*). (**d**) Power Doppler more clearly defines flow and location of the artery (*arrow*). (**e**) The very high velocities noted at peak systole and end diastole suggest flow-reducing stenosis. (**f**) In a different patient, the stent has thrombosed with visible echogenic intrastent thrombus (*small arrow*). The Large *white arrow* points to the long axis view of the aorta.

**Fig. 47.15** (continued)

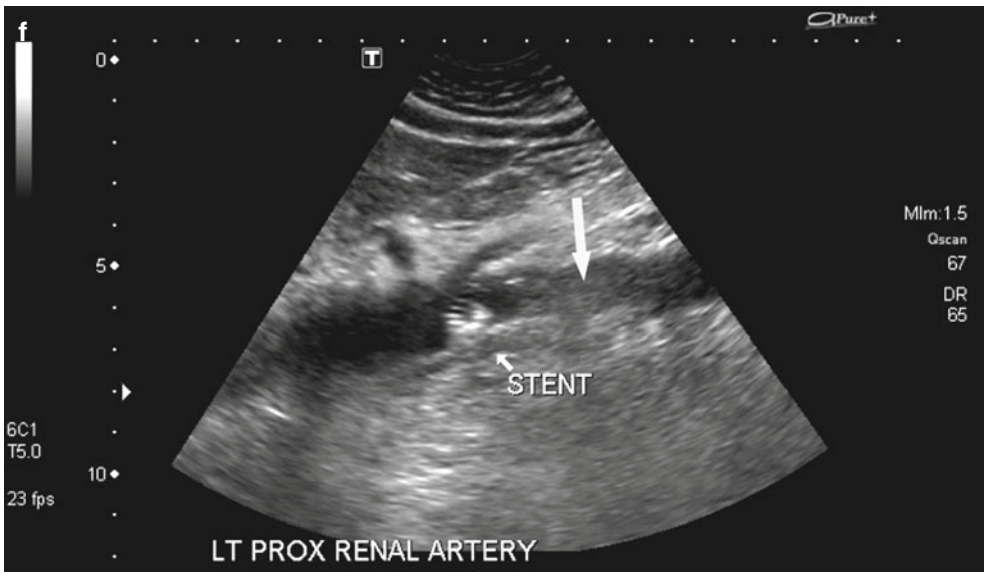


**Fig. 47.16** Color flow image and Doppler insonation of the aorta just proximal to the renal artery origins showing a sharp systolic upstroke and peak

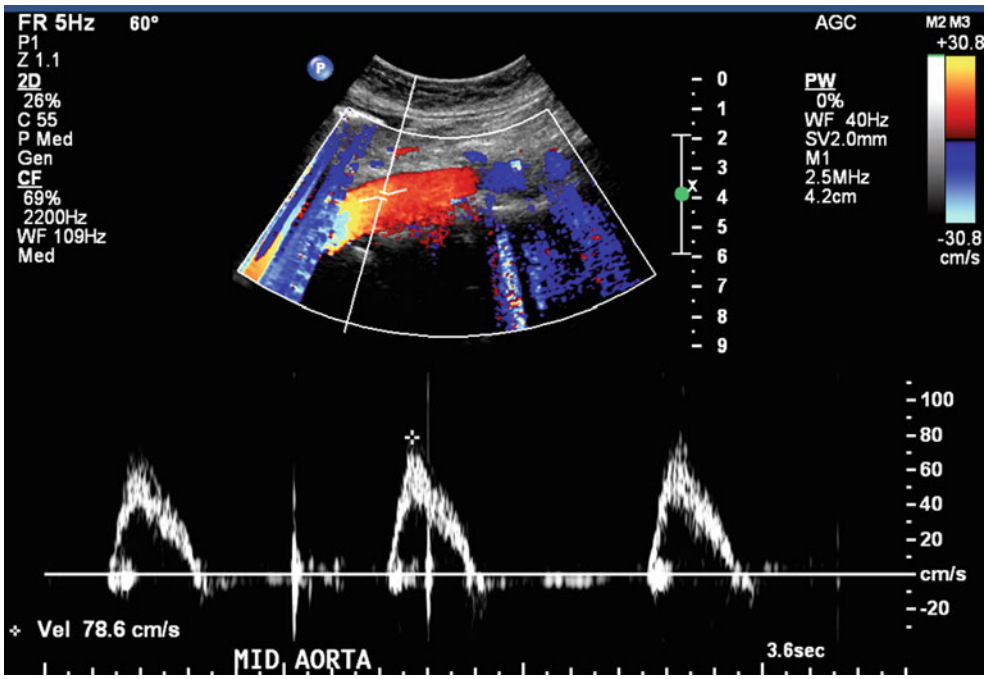


## Interpretation of Doppler Spectral Waveforms and Images

### The Abdominal Aorta

A rapid systolic upstroke and a sharp systolic peak characterize Doppler spectral waveforms recorded from the abdominal aorta proximal to the renal artery origins (Fig. 47.16). Because this segment of the aorta carries flow to the low-resistance vascular beds of the liver, spleen, and kidneys, the flow pattern is most commonly biphasic with a peak systolic velocity range of 60–100 cm/s. Distal to the renal arteries, the velocity may decrease slightly and the waveform morphology becomes triphasic, consistent with flow to the high-resistance lower extremity peripheral arterial bed.

Flow disturbances may be noted at the renal artery orifices, but high-velocity turbulent signals should not be found in the absence of aortic wall plaque or orificial renal artery lesions. Kohler and others [16, 29, 30] demonstrated that a ratio of the peak systolic renal artery velocity and the peak systolic aortic velocity that is equal to or less than 3.5 offers excellent sensitivity for confirming the absence of flow-reducing (>60% diameter reduction) renal artery stenosis. Narrowing of the renal artery will result in elevation of velocity while

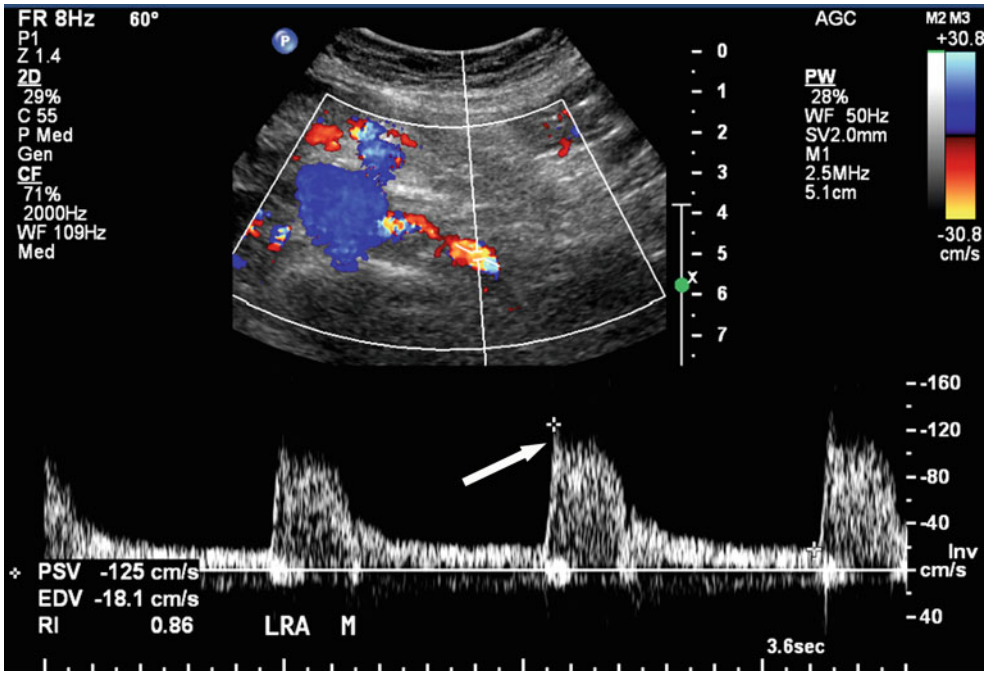


**Fig. 47.17** The flow pattern in normal renal arteries is characterized by rapid systolic upstroke, an occasional early systolic peak (*arrow*), and constant forward diastolic flow

the aortic velocity remains relatively stable. In cases where the aortic velocity exceeds 100 cm/s due to stenotic disease, coarctation, or increased cardiac output, the renal-aortic velocity ratio will be too low and will, therefore, underestimate the severity of renal artery stenosis. For example, if the aortic velocity is 120 cm/s and the renal artery velocity is 240 cm/s, the renal aortic ratio will be 2.0, incorrectly suggesting the absence of any renal artery stenosis. Similarly, in patients with an aortic aneurysm, increased distal impedance due to aortic stenosis or occlusion, or a low cardiac output, lower than normal peak systolic aortic velocities (<40 cm/s) will result in overestimation of the severity of renal disease based on the renal-aortic peak systolic velocity ratio. However, requiring both a renal artery peak systolic velocity >180 cm/s and a post-stenotic turbulence will obviate such potential pitfalls in identifying a hemodynamically significant renal artery stenosis (Table 47.1).

## Normal Renal Artery

A rapid systolic upstroke and peak systolic velocities ranging from 90 to 120 cm/s characterize the normal renal arterial waveform with the renal-aortic peak systolic velocity ratio being less than or equal to 3.5 (Table 47.1). Systole is followed by rapid deceleration to forward diastolic flow with a velocity at least one-third of the systolic value. Quite often an early systolic, or compliance, peak may be found on the systolic upstroke (Fig. 47.17). This is thought to be a reflection of the expansion and recoil of the artery that occurs with each systolic pulse and, indirectly, may reflect the degree of renovascular resistance in the distal parenchymal vessels. The compliance peak may be found either higher or lower than the actual systolic peak. As an indicator of proximal renal artery stenosis, a delay in the systolic acceleration time (AT) of more than 100 ms from the onset of systole is abnormal.

Flow patterns throughout the normal renal artery are characterized by constant forward diastolic flow due to the low resistance of the renal arterial system. Decreased diastolic flow to zero, or actual flow reversal, should not normally be seen because such findings would be characteristic of impedance to arterial inflow or obstruction to venous outflow from the organ. The ratio of end-diastolic to systolic flow remains fairly constant throughout the normal renal arterial tree although the peak systolic velocity will decrease proportionately from the main renal artery to the level of the renal cortex. Distal renal artery peak systolic velocity is normally 70–90 cm/s. Systolic velocity in the renal medullary arteries averages 30–50 cm/s, assuming a 0° angle of insonation, while more distal cortical velocity averages 10–20 cm/s.

## Less Than 60% Renal Artery Stenosis

As the severity of renal artery stenosis increases, the peak systolic velocity will increase to meet downstream flow demands. Stenotic lesions that reduce the diameter of the renal artery 30–60% will cause color flow disturbances and the peak systolic renal artery velocity to exceed 180 cm/s. However, the degree of arterial narrowing is not yet severe enough to cause post-stenotic turbulence and the renal-aortic peak systolic velocity ratio will remain less than 3.5.

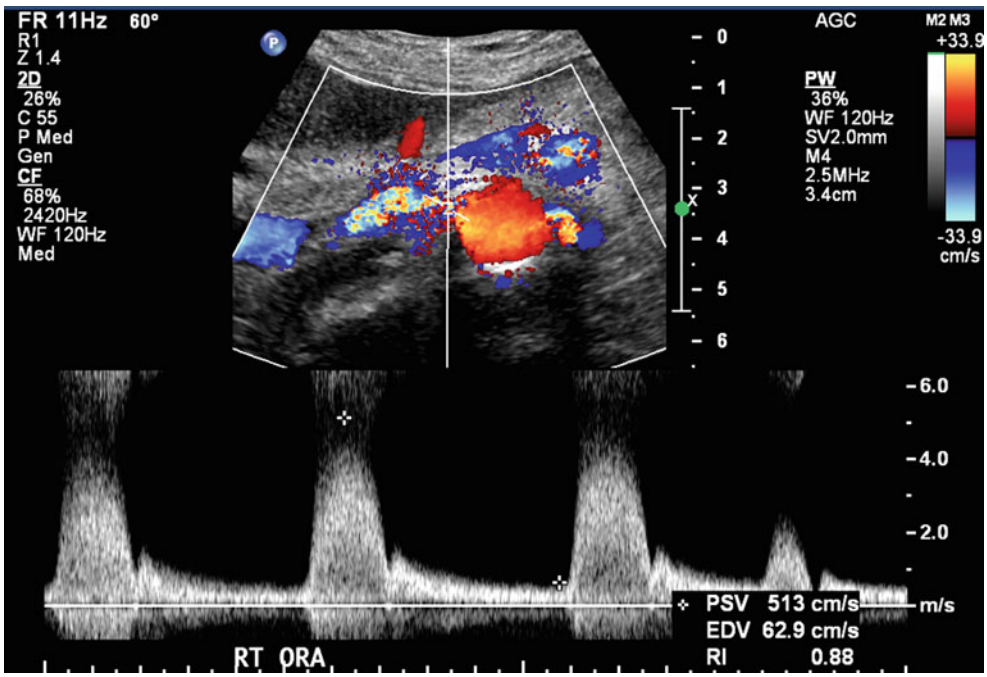


**Fig. 47.18** Flow-reducing renal artery stenosis (>60% diameter reduction) is associated with peak systolic velocities that exceed 180 cm/s and post-stenotic turbulence

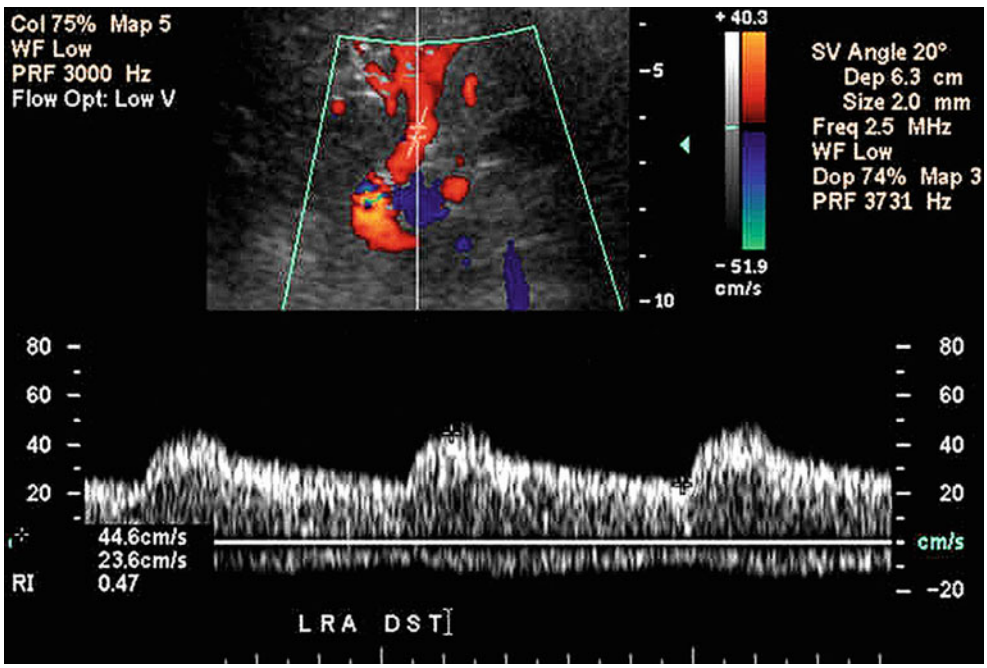


**Fig. 47.19** Distal to critical renal artery lesions (>80% diameter reduction), the systolic upstroke of the Doppler spectral waveform will be delayed, the compliance peak will disappear, and the peak systolic velocity will be decreased

## Hemodynamically Significant Renal Artery Stenosis

When reduction of the renal artery diameter exceeds 60%, post-stenotic turbulence will become apparent and the peak systolic renal artery velocity will significantly exceed 180 cm/s (Fig. 47.18). It is important in cases where the aorta is diseased, thus preventing the use of the renal-aortic ratio, to confirm the presence of a post-stenotic signal, as this signifies a pressure-flow gradient and differentiates a hemodynamically significant lesion from a less severe stenosis. Doppler spectral and color flow parameters must be adjusted throughout the interrogation of the lesion to reveal the decrease in velocity that occurs immediately proximal to a stenosis, the high-velocity signals within the lesion, and the decrease in velocity distally that is associated with the post-stenotic turbulence that develops downstream. Distal to critical lesions, >80% diameter reduction, systolic upstroke will be delayed, the compliance peak may disappear, and the peak systolic velocity will decrease (Fig. 47.19).

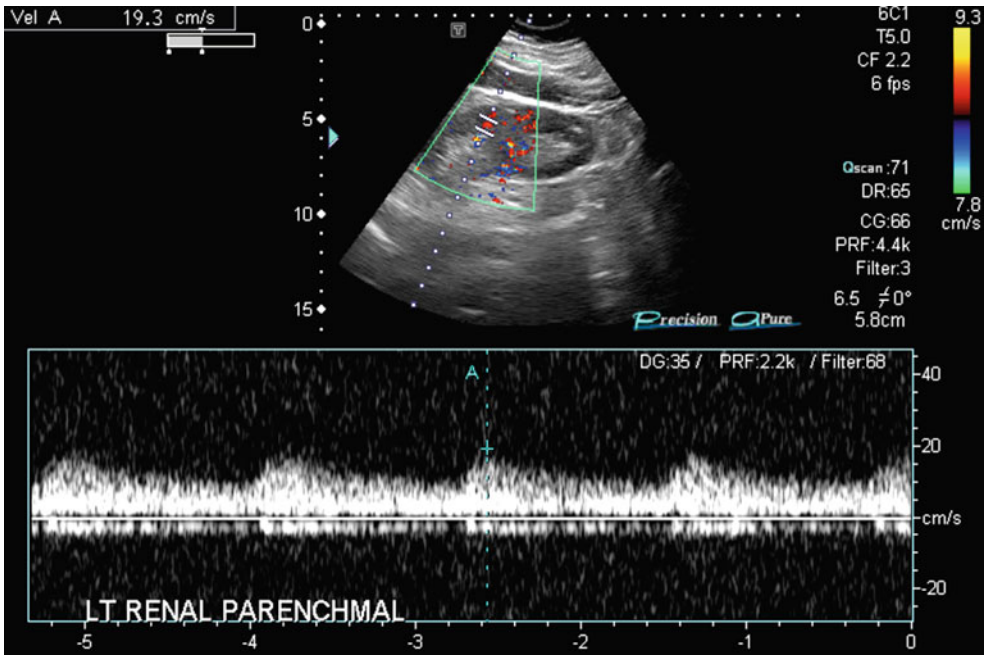


**Fig. 47.20** Blood flow to the kidney may continue via ureteral and adrenal collaterals when the renal artery is chronically occluded. Low amplitude blunted Doppler spectral waveforms with diminished velocities will be seen throughout the parenchyma of the kidney

## Renal Artery Occlusion

Renal artery occlusion is diagnosed by definitively identifying the main renal artery and documenting lack of flow in its lumen. Multiple image planes may be required to ensure the absence of flow in all segments of the renal artery. If the entire length of the renal artery is not well visualized with the patient placed in the supine position, it may be useful to move the patient to the lateral decubitus, oblique, or prone position. From a near decubitus position, the kidney can be imaged through an intercostal or subcostal approach using a coronal scan plane from the flank. With the patient lying prone and flexed in the mid-section over a pillow or foam wedge, an intercostal acoustic window and optimal acute angle of insonation can be obtained for evaluation of the renal hilum and distal renal artery. The lack of arterial flow in a chronically occluded main renal artery produces distal artery and cortical flow of <10 cm/s with a low amplitude waveform configuration throughout the renal parenchyma as a result of collateral flow to the kidney (Fig. 47.20). After optimizing color, power, and spectral Doppler sensitivity to exclude the very low flow of a pre-occlusive lesion, it is also useful to compare parenchymal velocity and signals with those in the contralateral kidney.

## Renal Parenchymal Dysfunction (Medical Renal Disease)

Doppler spectral waveforms recorded throughout the renal parenchyma help differentiate normal renovascular resistance from patterns associated with intrinsic parenchymal disorders. Normally, the diastolic velocity in the interlobar and arcuate arteries of the renal parenchyma is more than 30% of the systolic velocity and resistance remains low even in kidneys with flow-reducing renal artery stenosis. It is thought that the kidney compensates for the reduction in pressure and flow through vasodilation, which in turn lowers vascular resistance.

When renal function becomes impaired, diastolic flow decreases, suggesting impedance to arterial inflow to the microvasculature of the kidney and increased vascular resistance (Fig. 47.21). Although renovascular resistance tends to increase slightly with aging, marked decrease in diastolic flow can be associated with a wide variety of etiologies including acute tubular necrosis, glomerulonephritis, polycystic disease, diabetic nephropathy, or severe obstructive hydronephrosis. A diastolic-to-systolic velocity ratio less than 0.30 is consistent with parenchymal dysfunction with more diminished values often associated with elevated blood urea nitrogen and serum creatinine levels. Others have utilized the resistive index (RI), the ratio of the difference between peak and minimum velocity divided by peak velocity, and the pulsatility index (PI), the ratio of the difference between peak and minimum velocity divided by mean velocity, in an analogous manner for both intrinsic renal disease and as an indication of renal transplant rejection [57, 58].

Although it is not uncommon to find low-resistance waveforms in a kidney with a severe proximal renal artery stenosis, the same should not be true for the contralateral nondiseased organ if such waveform abnormalities are due to a proximal stenosis rather than a systemic intrinsic parenchymal disease. Therefore, both sequential monitoring of flow patterns and comparison with the contralateral organ are recommended.

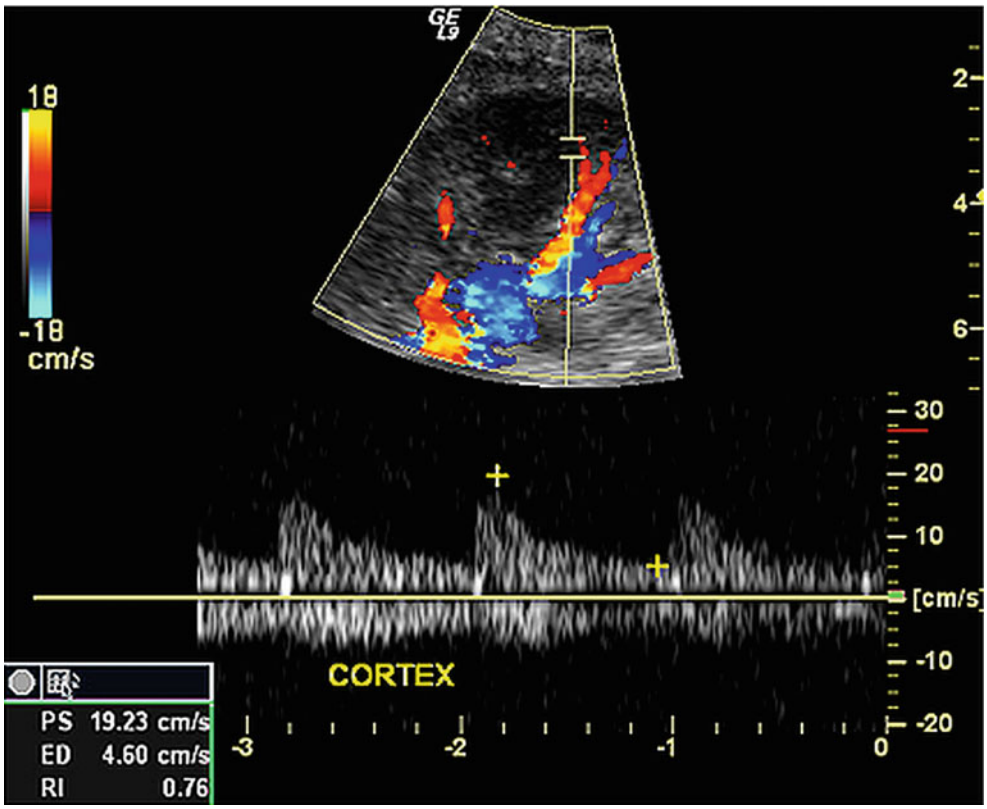


**Fig. 47.21** Doppler spectral waveforms from the interlobar arteries of a kidney with parenchymal dysfunction (medical renal disease). As renovascular resistance increases, diastolic flow decreases

## Renal Hilar Evaluations

With earlier technology, or for those who have limited experience with direct evaluation of the renal artery and its parenchymal branches, some have advocated a limited examination of the renal arteries within the renal hilum. Such proposed techniques depend on recognizing the distal hemodynamic consequences of more proximal significant stenosis. A limited evaluation offers the attractiveness of lessening the technical challenge and decreasing the duration of the examination with possibly a lower incidence of inadequate studies compared with direct evaluation of the entire renal arterial system. Several investigators have reported excellent sensitivities and specificities for detection of significant renal artery stenosis using parameters calculated from the hilar Doppler spectral waveforms (Fig. 47.22) [59–61]. An *acceleration index* (AI), defined as the slope of the systolic upstroke (kHz/s) divided by the transmitted frequency, of less than 3.78 (kHz/s/MHz) has been shown by Handa et al. to have an accuracy of 95%, sensitivity of 100%, and specificity of 93% [59]. Martin et al. calculated the AT, defined as the time interval between the onset of systole and the initial compliance peak, to predict flow-reducing proximal renal artery disease [60]. In their study, an AT greater than 0.10 s was superior to use of an AI and yielded a sensitivity of 87% and a specificity of 98%. Stavros and his colleagues have additionally used the absence of the compliance peak to suggest significant renal artery stenosis [61].

The indirect examination of the renal hilar arteries is performed with the patient in a lateral decubitus or prone position using an intercostal scan plane. From a transverse image of the kidney, the distal renal artery is interrogated along its axis using a 0° angle of insonation. It is important to record Doppler velocity waveforms using the highest transducer frequency possible to obtain adequate signals, a large sample volume, and a sweep speed of 100 ms.

Although the potential for limited, but accurate, diagnostic evaluations is suggested by these initial investigations, sufficient prospective studies have not been done to validate these criteria. Indeed, in studies from other institutions, AT, AI, and absence of a compliance peak have been shown to be unsatisfactory predictors of 60–79% diameter-reducing renal artery stenosis. Acceptable sensitivity and specificity have been associated only with lesions that exceed 80% diameter reduction by arteriography. Although the limited hilar examination provides complementary information, especially in cases where the entire length of the renal artery cannot be visualized, a complete evaluation of the renal arterial system is much preferred. We do not recommend using hilar evaluations as an alternative to a complete and

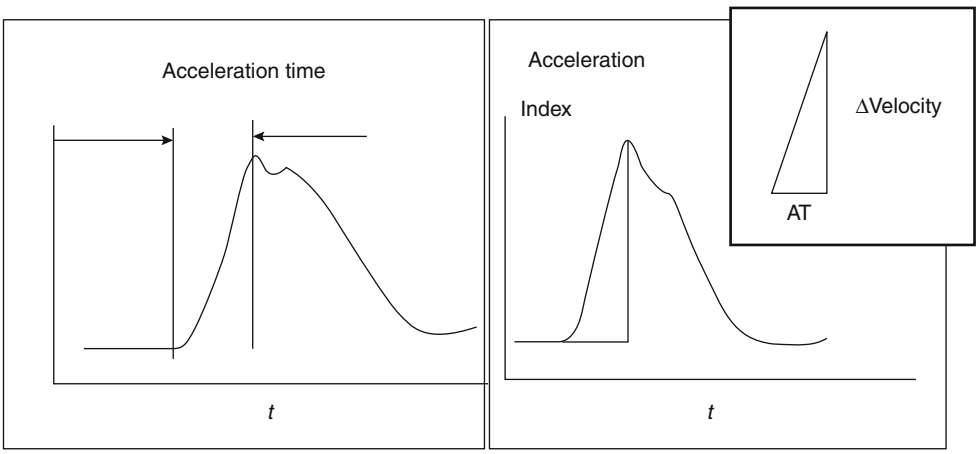


**Fig. 47.22** Diagram illustrating method of calculation of acceleration time (*AT*) and acceleration index (*AI*). AT is the time interval from the onset of flow to the initial (compliance) peak. AI is the slope of the systolic upstroke divided by the transmitted frequency

direct examination of the main renal artery because it yields no information regarding the anatomic location of a proximal lesion. A direct comparison on the accuracy of hilar analysis as opposed to Doppler scanning of the main renal artery found that hilar AT is significantly less sensitive and less accurate in diagnosing hemodynamically significant renal artery stenosis [62]. In addition, a well-collateralized kidney with a proximal renal artery occlusion cannot be differentiated from a high-grade stenosis [60]. In patients with concomitant renal parenchymal disease, the AT and index may be normalized and the AT can be influenced by the peak systolic renal artery velocity [59–61]. The effect of blood flow from multiple renal arteries on hilar Doppler evaluations has also yet to be adequately determined. With present high-quality ultrasound systems, and experienced technologists with certification and adequate training, a complete examination of the renal artery is possible in more than 90% of patients [50].

## Renal Vein Evaluation

When the renal vein is thrombosed or filled with tumor, intraluminal echoes should be demonstrated within the lumen. Care must be taken to optimize the B-Mode image because fresh thrombus may have the same acoustic properties as flowing blood. If the patient is thin, the renal vein will be noncompressible and may be dilated if the thrombotic process is acute or contracted with chronic thrombosis. Doppler spectral waveforms should demonstrate absence of flow in the main trunk of the vein. There will be a lack of phasic flow proximal to the obstructed segment and minimal phasicity in the distal venous segments if the thrombosed segment is recanalized or if venous collaterals have developed. If there is extrinsic compression of the vein, disturbed color flow and high-velocity Doppler signals will be found in the region of venous narrowing.

## Evaluation of Renal Artery Stents

Although there remains controversy in terms of appropriate patient selection and indications for renal revascularization [63], renal angioplasty and stenting is in wide clinical use and is associated with in-stent re-stenosis requiring regular surveillance and noninvasive follow-up [64]. There are a number of factors that need to be considered in the interpretation of Doppler velocity waveforms and images in vessels with renal artery stents. The number and the location of renal stents will influence velocity patterns. If stents are placed in sequence in the renal artery, arterial compliance will be decreased along the length of the stented segment and slight elevation of velocities may be noted throughout the vessel. A diameter mismatch between the stented segment and the native renal artery will more likely be noted in stents that are placed in the smaller diameter distal renal artery.

A distal focal increase in velocity in the stent-native vessel transition site is more likely to be associated with a diameter mismatch while high-velocity flow disturbance that is propagated over a longer distance and throughout the length of the stent is more commonly found with flow-reducing stenosis. If a significant lesion is suspected, it is helpful to confirm the presence of a post-stenotic signal and dampening of the velocity signal downstream. Comparing velocity data to that obtained during previous duplex examinations can yield valuable clues that may help to confirm progressive stenotic disease. Elevated velocities due to vessel diameter mismatch should remain stable while increased velocity due to stenosis may demonstrate a temporal change.

In a prospective observational study, Thalhammer and his colleagues evaluated the renal RI and peak systolic stent velocity at baseline, 1 day, and 6 months following the intervention as predictors for in-stent restenosis [65]. At 6 months postprocedure, 16.8% of patients had developed in-stent restenosis. While the RI increased significantly in this group of patients, it was not predictive of restenosis. Peak systolic

velocity and age of the patient were independent predictors for elevated RI at 6 months. Elevated in-stent peak systolic velocity was higher (1.4 ± 0.4 m/s vs. 1.0 ± 0.3 m/s) 1 day following the procedure in patients with subsequent restenosis and was noted to be an independent predictor for restenosis.

As in the evaluation of native vessels, however, main renal artery and in-stent peak systolic velocity are the mainstay of stent surveillance. Chi et al. identified in-stent restenosis exceeding 70% diameter reduction based on a renal-aortic velocity ratio >5.1, a peak systolic velocity >395 cm/s, and the presence of a post-stenotic signal [66]. A lower peak systolic velocity (>280 cm/s) and renal-aortic velocity ratio (>4.5) were used by Mohabbat and colleagues for identification of flow-reducing (>60% diameter reduction) renal stent stenosis [67]. Similar velocities were associated with angiographically confirmed in-stent restenosis in a study by Fleming et al. [68]. While a renal artery peak systolic velocity of 250 cm/s resulted in a low sensitivity (59%), these investigators documented an excellent specificity (95%), accuracy (83%), and positive predictive value (87%). Although ideally each laboratory should establish and validate its own criteria for stent stenosis, there are relatively few institutions with sufficient numbers of angiographically correlated results with long-term follow-up to successfully accomplish this goal. At present, recognizing that the reduced arterial compliance in the stented vessel segment is associated with increased velocities, criteria for hemodynamically significant in-stent stenosis will necessarily be higher than those applied to native vessels. It is therefore reasonable to utilize Mohabbat et al's [67] criteria of a peak systolic velocity of >280 cm/s and a RAR ratio of >4.5 to define a hemodynamically significant stenosis because theirs is the largest clinical series yet reported and it defines a stenosis of greater than 60%, analogous to the threshold with native vessels. The decision for further investigation and intervention will be a clinical one but will most likely require more stringent criteria, as per Chi et al. [66]. Of use in such clinical decision making will be the comparison with data obtained for each patient soon after stent placement, as a baseline, and changes in the obtained values as a function of time. The PSV and RAR will also be evaluated in light of distal artery spectral waveform configuration, parenchymal waveforms and velocities, along with B mode imaging to suggest any stent kinking or intimal hyperplasia ingrowth.

## Prediction of Outcome of Interventions for Renal Artery Stenosis

While success has been attained with both noninvasive and invasive techniques for identification of renal artery stenosis, relatively little success has been achieved with prospective selection of patients whose renal function or blood pressure will improve following correction of the renal stenosis. Multiple factors affect the outcome of surgical or percutaneous intervention including severity of the renal artery stenosis, the procedure used to treat the lesion, nephrotoxicity to the angiographic contrast agents, atheroembolism, and the presence of pre-existing intrinsic renal parenchymal disease. Several investigators have evaluated the use of quantitative measurements of Doppler spectral waveform parameters to determine the level of resistance to flow in the segmental arteries of the kidney as predictors of favorable outcome to intervention. Radermacher and his colleagues [69], in a retrospective study, calculated a RI [(1 − end diastolic velocity divided by maximal systolic velocity) × 100] in 138 patients who had either unilateral or bilateral renal artery stenosis of at least 50% diameter reduction and underwent renal angioplasty or surgical bypass. Creatinine clearance and ambulatory blood pressures were documented prior to intervention and at 3, 6, and 12 months and then yearly following the procedure. The mean follow-up was 32 months. Based on this study, they concluded that patients with a renal RI value of at least 0.8 were unlikely to experience significant improvement in blood pressure, renal function, or organ survival following correction of renal artery stenosis. Similarly, Tullis et al. recommended a renal artery end diastolic ratio from the contralateral kidney in patients with unilateral atherosclerotic renal artery stenosis to predict response to renal revascularization [70]. However, two prospective studies were unable to confirm these results [71, 72]. While some institutions continue to measure these indexes, the clinical use of such a RI does not appear to be widespread.

## Pediatric Renal Duplex Evaluations

Renovascular disease is an uncommon but important cause of hypertension in children because it is potentially amenable to curative treatment [73]. The true prevalence of renovascular hypertension in children is difficult to quantify because early cases are mild and usually unsuspected but it has been estimated to be the cause of elevated blood pressure in 5–10% of cases [73]. There are a number of etiologic causes, including fibromuscular dysplasia, neurofibromatosis, vasculitis, and extrinsic compression from tumors, such as neuroblastoma and Wilm's tumors. The majority of reversible cases, however, involves fibromuscular dysplasia. Beyond the already mentioned causes of renovascular hypertension, children are also prone to catheter-associated thromboembolic disease, mid-aortic coarctation, renal vein thrombosis, idiopathic arterial calcification, congenital renal artery stenosis, and congenital rubella syndrome. Catheter-associated thromboembolism in infants has a reported incidence ranging from 3.5% to 23% in autopsy series to 95% in prospective ultrasound studies [74].

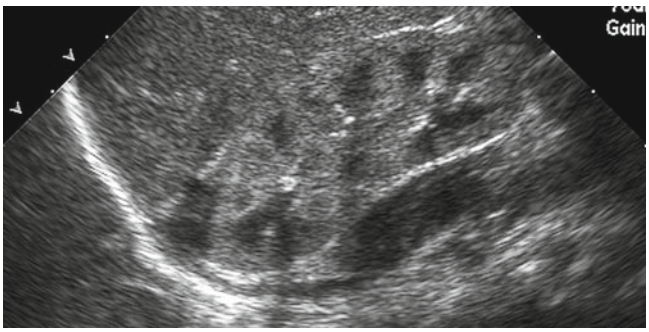

**Fig. 47.23** Longitudinal B-Mode image of an infant kidney illustrating the overall increased parenchymal echogenicity, prominent renal pyramids, and absence of a distinct renal sinus

The sonographic examination of the renal vasculature and kidneys in children parallels the study performed in an adult but special considerations must be given to renal anatomy, pathology, and the diagnostic criteria used to define flow-limiting disease in the pediatric patient.

## Pediatric Renal Anatomy

The kidney is positioned lower in the abdomen in infants than the adult kidney and, most commonly, is fully ascended when the child is around 6 years of age. For the first 3 months, the renal parenchyma is more echogenic than the parenchyma of an adult kidney and the renal pyramids are more prominent (Fig. 47.23). Because the renal sinus in an infant is not infiltrated with fat, it is less echogenic than that of an adult kidney. Fetal lobulations are apparent in the cortex for the first several years and, when persistent, may suggest hypertensive insult. In the infant with renal artery thrombosis, the renal parenchyma initially demonstrates little alteration in echogenicity, but with time there is loss of corticomedullary differentiation, diffusely increased parenchymal echogenicity, and decreased renal size consistent with chronic ischemia. In contrast, when the renal vein is thrombosed the affected kidney is enlarged. Absence of flow distal to the thrombosed vessel segment and, in the case of chronic thrombosis, the presence of collaterals, may be demonstrated with optimized color flow imaging.

## Diagnostic Criteria

Unlike renal duplex evaluations in adult patients, well-validated criteria based on peak systolic renal artery velocity and a renal-aortic ratio has not been established for pediatric studies but the PSV criteria and Doppler waveform analysis used for adult studies are generally applied [75]. In addition, the majority of investigators employ RIs and ATs to confirm >60% flow-reducing stenosis in infants [76, 77] even though others have indicated that the RI is neither sensitive nor specific as an indicator of increased resistance to renal flow [78]. In a normal adult, the RI in the segmental or interlobar arteries of the kidney does not exceed 0.7. In infants, the RI is normally higher than in an adult but is commonly less than 0.85 and most often exceeds this value when flow-limiting renal artery stenosis (>60% diameter reduction) is present. The exception to this is in infants and children who have recently undergone cardiac bypass. In such cases, the RI is most often elevated to greater than 1.0 for the first 3 days. Sigirci et al. demonstrated that the RI correlates linearly with plasma renin and aldosterone levels and correlates inversely with AT [76]. Their studies also indicated that RI decreases with age while AT increases with age.

Segmental renal artery systolic ATs vary widely with age from 71 ± 21.5 ms in infants to 103 ± 26.5 ms in children 6–12 years of age. In infants with renal artery stenosis of at least 60% diameter reduction, the AT generally exceeds 0.1 s. Patriquin and her colleagues studied the segmental and interlobar arteries in 20 children in whom renal artery stenosis was suspected [79]. They noted that the AI and RI were significantly lower in renal arteries with stenosis exceeding 75% diameter reduction than in normal renal arteries. In the absence of renal artery disease, the AI was 4–7. The AI ranged from 0.7 to 2.6 in renal arteries with at least 75% stenosis. A RI of 0.56 or less predicted stenosis with 95% probability.

Renal atrophy is associated with progression of flow-compromising renal artery disorders. In neonates, the kidney is usually <4 cm in pole-to-pole length when the renal artery is occluded and <6 cm in children 1 year of age. As in adult studies, low-amplitude, low-velocity flow signals can be detected throughout the renal parenchyma with spectral Doppler when the renal artery is occluded.

While measurement of flow parameters such as the RI, AI, and AT have shown value for identification of renal vascular disorders in the pediatric patient, these studies quite often must be performed in the neonatal intensive care unit. As such, they are limited by portability of the ultrasound equipment; less than ideal acoustic windows for insonation of the renal arteries, renal veins, and kidneys; life support lines and tubing; and mechanical ventilation.

### Conclusion

Duplex sonography of the renal arteries and kidneys is the diagnostic test of choice in the initial evaluation of renovascular hypertension or suspected renal artery pathology. Beginning with the evaluation of the aorta and the entire length of the main renal artery, color flow sonography is helpful in localizing the vessel, giving a preliminary assessment of disturbed flow and possible underlying stenosis, and allowing accurate placement of the Doppler sample volume for documenting the velocity measurement

and spectral waveform analysis. Peak Doppler systolic velocity measurements in the main renal artery provide the basis for the determination of hemodynamically significant stenoses. In combination with color and/or power Doppler imaging, B-Mode visualization is helpful in diagnosing and localizing other arterial and parenchymal pathology, such as fibromuscular dysplasia, aneurysms, dissections, parenchymal masses and cysts, and extra-renal tumors or masses that may induce extrinsic compression. Measurement of kidney length is important in determining usefulness of therapeutic interventions and sequential monitoring of renal function. Parenchymal assessment, with both Doppler velocity measurements and color and power Doppler flow imaging, provides an indication of intrinsic renal disease and the likelihood of improvement in renal function following revascularization of the kidney. The role of limited, indirect renal hilar scanning is best used as a complement to the complete interrogation of the renal vascular system. Duplex ultrasound is an ideal technology for natural history studies on renal arterial dysfunction and follow-up after endovascular or surgical revascularization. It can be a technically demanding study dependent on the experience and capability of the sonographer. Intravenous contrast agents may be helpful in challenging cases where the vessels are difficult to image.

## References


1. Cutler JA, Sortie PD, Wolz M, Thom T, Fields LE, Roccella EJ. Trends in hypertension prevalence, awareness, treatment, and control rates in united states adults between 1988–1994 and 1999–2004. Hypertension. 2008;52:818–27.
2. Textor SC. Current approaches to renovascular hypertension. Med Clin North Am. 2009;3(3):717–32.
3. Dunnick NR, Sfakianakis GN. Screening for renovascular hypertension. Radiol Clin North Am. 1991;29:497–510.
4. Little MA, O'Brien E, Owens P, et al. A longitudinal study of the yield and clinical utility of a specifically designed secondary hypertension investigation protocol. Ren Fail. 2003;25:709–17.
5. Buller CE, Nogareda JG, Ramanathan K, Ricci DR, et al. The profile of cardiac patients with renal artery stenosis. J Am Coll Cardiol. 2004;43:1606–13.
6. Davis RP, Pearce JD, Craven TE, Moore PS, et al. Atherosclerotic renovascular disease among hypertensive adults. J Vasc Surg. 2009;50(3):564–71.
7. Chobanian AV, Bakris GL, Black HR, et al. The seventh report of the joint national committee on prevention, detection, evaluation, and treatment of high blood pressure: The JNC7 report. JAMA. 2003;289:2560–72.
8. Kane GC, Xu N, Mistrik E, Roubicek T, Stanson AW, Garovic VD. Renal artery revascularization improves heart failure control in patients with atherosclerotic renal artery stenosis. Nephrol Dial Transplant. 2010;25:813–20.
9. Cherr GS, Hansen KJ, Craven TE, Edwards MS. Surgical management of atherosclerotic renovascular disease. J Vasc Surg. 2002;35(2):236–45.
10. ASTRAL Investigators, Wheatley K, Ives N, Gray R. Revascularization versus medical therapy for renal-artery stenosis. N Engl J Med. 2009;361:1953–62.
11. Bax L, Woittiez AJJ, Kouwenberg AJ, Mall W, et al. Stent placement in patients with atherosclerotic renal artery stenosis and impaired renal function a randomized trial. Ann Intern Med. 2009;150:840–8.
12. Rountas C, Vlychou M, Vassiou K, et al. Imaging modalities for renal artery stenosis in suspected renovascular hypertension: prospective intraindividual comparison of color Doppler US, CT angiography, GD-enhanced MR angiography, and digital subtraction angiography. Ren Fail. 2007;29(3):295–302.
13. Hoppe H, Spagnuolo S, Froehlich JM, Nievergelt H, et al. Retrospective analysis of patients for development of nephrogenic systemic fibrosis following conventional angiography using gadolinium-based contrast agents. Eur Radiol. 2010;20(3):595–603.
14. Zhang HL, Sos TA, Winchester PA, Gao J, Prince MR. Renal artery stenosis: imaging options, pitfalls, and concerns. Prog Cardiovasc Dis. 2009;52:209–19.
15. Baumgartner I, Lerman LO. Renovascular hypertension: screening and modern management. Eur Heart J. 2011;32:1590–8.
16. Williams GJ, Macaskill P, Chan SF, et al. Comparative accuracy of renal duplex sonographic parameters in the diagnosis of renal artery stenosis: paired and unpaired analysis. Am J Roentgenol. 2007;188(3):798–811.
17. Safian RD, Textor SC. Renal artery stenosis. N Engl J Med. 2001;344(6):431–42.
18. Stanley JC. Natural history of renal artery stenoses and aneurysms. In: Calligaro KD, Dougherty MJ, Dean RH, editors. Modern management of renovascular hypertension and renal salvage. Baltimore: William & Wilkins; 1996. p. 15–45.
19. Working Group on Renovascular Hypertension. Detection, evaluation, and treatment of renovascular hypertension. Arch Intern Med. 1987;147:820–9.
20. Garovic VD, Textor SC. Renovascular hypertension and ischemic nephropathy. Circulation. 2005;112:1362–74.
21. Stanley JC, Gewertz BL, Bove BL, et al. Arterial fibrodysplasia: histopathologic character and current etiologic concepts. Arch Surg. 1975;110:561–6.
22. Olin JW, Sealove BA. Diagnosis, management, and future developments of fibromuscular dysplasia. J Vasc Surg. 2011;53(3):826–36.
23. Greene ER, et al. Noninvasive characterization of renal artery blood flow. Kidney Int. 1981;20:523–9.
24. Rittgers SE, Norris CS, Barnes RW. Detection of renal artery stenosis: experimental and clinical analysis of velocity waveforms. Ultrasound Med Biol. 1985;11:523–31.
25. Taylor DC, Kettler MD, Moneta GL, et al. Duplex ultrasound scanning in the diagnosis of renal artery stenosis: a prospective evaluation. J Vasc Surg. 1988;7:363–9.
26. Neumyer MM, Wengrovitz M, Ward T, Thiele BL. The differentiation of renal artery stenosis from renal parenchymal disease by duplex ultrasonography. J Vasc Technol. 1989;13:205–16.
27. Avasthi PS, Voyles WF, Greene ER. Noninvasive diagnosis of renal artery stenosis by echo-Doppler velocimetry. Kidney Int. 1984;25:824–9.
28. Hoffman U, Edwards JM, Carter S, et al. Role of duplex scanning for the detection of atherosclerotic renal artery disease. Kidney Int. 1991;39:1232–9.
29. Olin JW, Piedmonte MR, Young JR, DeAnna S, Grubb M, Childs MB. The utility of duplex ultrasound scanning of the renal arteries for diagnosing significant renal artery stenosis. Ann Intern Med. 1995;122:833–8.
30. Kohler TR, Zierler RE, Martin RL, et al. Noninvasive diagnosis of renal artery stenosis by ultrasonic duplex scanning. J Vasc Surg. 1986;4:450–6.
31. Hansen KJ, Tribble RW, Reavis SW, et al. Renal duplex sonography: evaluation of clinical utility. J Vasc Surg. 1990;12:227–36.

32. Moran K, Muihall J, Kelly D, et al. Morphological changes and alterations in regional intrarenal blood flow induced by graded renal ischemia. J Urol. 1992;148:1463–6.
33. Shanley PF. The pathology of chronic renal ischemia. Semin Nephrol. 1996;16:21–32.
34. Caps MT, Zierler RE, Polissar NL, et al. The risk of atrophy in kidneys with atherosclerotic renal artery stenosis. Kidney Int. 1998;53:735–42.
35. Hallett Jr JW, Fowl R, O'Brien PC, et al. Renovascular operations in patients with chronic renal insufficiency: do the benefits justify the risks? J Vasc Surg. 1987;5:622–7.
36. Cambria RP, Brewster DC, L'Italien GJ, et al. Renal artery reconstruction for the preservation of renal function. J Vasc Surg. 1996;24:371–80.
37. Erdoes LS, Berman SS, Hunter GC, Mills JL. Comparative analysis of percutaneous transluminal angioplasty and operation for renal revascularization. Am J Kidney Dis. 1996;27:496–503.
38. Hansen KJ, Thomason RB, Craven TE, et al. Surgical management of dialysis-dependent ischemic nephropathy. J Vasc Surg. 1995;21:197–209.
39. Guzman RP, Zierler RE, Isaacson JA, et al. Renal atrophy and renal arterial stenosis: a prospective study with duplex ultrasound. Hypertension. 1994;23:346–50.
40. Glodny B, Petersen J, Hofmann KJ. Kidney fusion anomalies revisited: clinical and radiological analysis of 209 cases of crossed fused ectopia and horseshoe kidney. BJU Int. 2009;103(2):224–35.
41. Spring DB, Salvatierra Jr O, Palubinskas AJ, et al. Results and significance of angiography in potential kidney donors. Radiology. 1979;133:45–7.
42. Kliewer MA, Tupler RH, Hertzberg BS, et al. Doppler evaluation of renal artery stenosis: interobserver agreement in the interpretation of waveform morphology. Am J Roentgenol. 1994;162:1371–6.
43. Urban BA, Ratner LE, Fishman EK. Three-dimensional volume-rendered CT angiography of the renal arteries and veins: normal anatomy, variants, and clinical applications. Radiographics. 2001;21:373–86.
44. Kadir S. Kidneys. In: Kadir S, editor. Atlas of normal and variant angiographic anatomy. Philadelphia: Saunders; 1991. p. 387–428.
45. Shalhoub J, Owen DRJ, Gauthier T, Monaco C, Leen ELS, Davies AH. The use of contrast enhanced ultrasound in carotid arterial disease. Eur J Vasc Endovasc Surg. 2010;39:381–7.
46. Cotter B, Mahmud E, Kwan OL, DeMaria AN. New ultrasound agents: expanding upon existing clinical applications. In: Goldberg BB, editor. Ultrasound contrast agents. Mosby: St. Louis; 1997. p. 31–42.
47. Robbin ML, Eisenfeld AJ, et al. Perflenapent emulsion: an US contrast agent for diagnostic radiology-multicenter double-blind comparison with a placebo. Radiology. 1998;207:717–22.
48. Kitzman DW, Goldman ME, Gillam LD, Cohen JL, Aurigemma GP, Gottdiener JS. Efficacy and safety of the novel ultrasound contrast agent perflutren (Definity) in patients with suboptimal baseline left ventricular echocardiographic images. Am J Cardiol. 2000;86:669–74.
49. Blebea J, Volteas N, Neumyer M, Dawson K, Ingraham J, Assadnia S, et al. Contrast-enhanced duplex ultrasound imaging of the mesenteric arteries. Ann Vasc Surg. 2002;16:77–83.
50. Blebea J, Zickler R, Volteas N, Neumyer M, Assadnia S, Anderson K, Atnip R. Duplex imaging of the renal arteries with contrast enhancement. Vasc Endovasc Surg. 2003;37:429–36.
51. Weissman NJ, Cohen MC, Hack TC, Gillam LD, Cohen JL, Kitzman DW. Infusion versus bolus contrast echocardiography: a multicenter, open-label, crossover trial. Am Heart J. 2000;139:399–404.
52. Forsberg F, Liu JB, Burns PN, et al. Artifacts in ultrasonic contrast agent studies. J Ultrasound Med. 1994;13:357–65.
53. House MK, Dowling RJ, King P, et al. Doppler ultrasound (pre-and post-contrast enhancement) for detection of recurrent stenosis in stented renal arteries: preliminary results. Australas Radiol. 2000;44(1):36–40.
54. Geleijnse ML, Krenning BJ, Nemes A, van Dalen BM, et al. Incidence, pathophysiology, and treatment of complications during dobutamine-atropine stress echocardiography. Circulation. 2010;121:1756–67.
55. Chandra A, O'Connell JB, Quinones-Baldrich WJ, Lawrence P. Aneurysmectomy with arterial reconstruction of renal artery aneurysms in the endovascular era: a safe, effective treatment for both aneurysm and associated hypertension. Ann Vasc Surg. 2010;24(4):503–10.
56. Neumyer MM. Duplex scanning after renal artery stenting. J Vasc Technol. 2003;27(3):177–83.
57. Sharma AK, Rustom R, Evans A, Donnolly D, et al. Utility of serial Doppler ultrasound scans for the diagnosis of acute rejection in renal allografts. Transpl Int. 2004;17:138–44.
58. Platt JF, Ellis JH, Rubin JM, et al. Intrarenal arterial Doppler sonography in patients with nonobstructive renal disease: correlation of resistive index with biopsy findings. Am J Roentgenol. 1990;154:1223–7.
59. Handa N, Fukunaga R, Etani H, et al. Efficacy of echo-Doppler examination for the evaluation of renovascular disease. Ultrasound Med Biol. 1988;14:1–5.
60. Martin RL, Nanra RS, Wlodarczyk J. Renal hilar Doppler analysis in the detection of renal artery stenosis. J Vasc Technol. 1991;15(4):173–80.
61. Stavros TA, Parker SH, Yakes YF, et al. Segmental stenosis of the renal artery: pattern recognition of the tardus and parvus abnormalities with duplex sonography. Radiology. 1992;184:487–92.
62. Motew SJ, Cherr GS, Craven TE, et al. Renal duplex sonography: main renal artery versus hilar analysis. J Vasc Surg. 2000;32(3):462–9.
63. Edwards MS, Corriere MA. Contemporary management of atherosclerotic renovascular disease. J Vasc Surg. 2009;50:1197–210.
64. Stone PA, Campbell JE, AbuRahma AF, Hamdan M, et al. Ten-year experience with renal artery in-stent stenosis. J Vasc Surg. 2011;53:1026–31.
65. Thalhammer C, Ferriani V, Husmann M, et al. Predictive value of duplex ultrasound for restenosis after renal artery stenting. Clin Hemorheol Microcirc. 2010;45(2–4):217–24.
66. Chi YW, White CJ, Thornton S, Milani RV. Ultrasound velocity criteria for renal in-stent restenosis. J Vasc Surg. 2009;50(1):119–23.
67. Mohabbat W, Greenberg RK, Mastracci TM, et al. Revised duplex criteria and outcomes for renal stents and stent grafts following endovascular repair of juxtarenal and thoracoabdominal aneurysms. J Vasc Surg. 2009;49(4):827–37.
68. Fleming SH, Davis RP, Craven TE, et al. Accuracy of duplex sonography scans after renal artery stenting. J Vasc Surg. 2010;52(4):953–7.
69. Radermacher J, Chavan A, Bleck J, Vitzhum A, Stoess B, et al. Use of Doppler ultrasonography to predict the outcome of therapy for renal-artery stenosis. N Engl J Med. 2001;344(6):410–7.
70. Tullis MJ, Zierler RE, Caps MT, Bergelin RO, Cantwell-Gab K, Strandness Jr DE. Clinical evidence of contralateral renal parenchymal injury in patients with unilateral atherosclerotic renal artery stenosis. Ann Vasc Surg. 1998;12(2):122–7.
71. Zeller T, Müller C, Frank U, et al. Stent-angioplasty of severe atherosclerotic ostial renal artery stenosis in patients with diabetes mellitus and nephrosclerosis. Catheter Cardiovasc Interv. 2003;58:510–5.
72. Voiculescu A, Schmitz M, Plum J, et al. Duplex ultrasound and renin ratio predict treatment failure after revascularization for renal artery stenosis. Am J Hypertens. 2006;19:756–63.
73. Tullus K, Brennan E, Hamilton G, Lord R. Renovascular hypertension in children. Lancet. 2008;371(9622):1453–63.
74. Ford KT, Teplick SK, Clark RE. Renal artery embolism causing neonatal hypertension. Radiology. 1974;113:169–70.
75. Brun P, Kchouk H, Mouchet B, Baudouin V, et al. Value of Doppler ultrasound for the diagnosis of renal artery stenosis in children. Pediatr Nephrol. 1997;11:27–30.

76. Sigirci A, Hallac T, Akyncy A, et al. Renal interlobar artery parameters with duplex Doppler sonography and correlations with age, plasma rennin, and aldosterone levels in healthy children. AJR Am J Roentgenol. 2006;186:828–32.
77. Wong SN, Lo RN, Yu EC. Renal blood flow pattern by noninvasive Doppler ultrasound in normal children and acute renal failure patients. J Ultrasound Med. 1989;8:135–41.
78. Dillon MJ. The diagnosis of renovascular disease. Pediatr Nephrol. 1997;11(3):366–72.
79. Patriquin HB, Lafortune M, Jequier J-C, et al. Stenosis of the renal artery: assessment of slowed systole in the downstream circulation with Doppler sonography. Radiology. 1992;184:479–85.

# Duplex Evaluation After Renal Intervention

48

Shawn H. Fleming and Kimberley J. Hansen

**Abstract**

Duplex sonography to detect hemodynamically significant renal artery stenosis and renal artery occlusion has evolved as the screening test of choice for main renal artery disease. In addition, renal duplex sonography is a valuable intraoperative study to confirm the technical success of open renal artery repair and useful to establish the hemodynamic result after percutaneous intervention. Finally, renal duplex is a valuable follow-up surveillance technique to evaluate both open operative repair and percutaneous intervention, with or without stenting. This chapter summarizes these applications and the anticipated results of each technique.

**Keywords**

Renal duplex sonography • Renal artery repair • Percutaneous intervention • Open operative repair • Surveillance duplex sonography

## Introduction

Duplex sonography to detect hemodynamically significant renal artery stenosis and renal artery occlusion has evolved as the screening test of choice for main renal artery disease. In addition, renal duplex sonography is a valuable intraoperative study to confirm the technical success of open renal artery repair and useful to establish the hemodynamic result after percutaneous intervention. Finally, renal duplex is a valuable follow-up surveillance technique to evaluate both open operative repair and percutaneous intervention, with or without stenting. This chapter will summarize these applications and the anticipated results of each.

S.H. Fleming, M.D. • K.J. Hansen, M.D. (✉)
Department of Vascular and Endovascular Surgery,
Wake Forest Baptist Medical Center, Medical Center Boulevard,
Winston-Salem, NC 27157, USA
e-mail: kjhansen@wakehealth.edu

## Renal Duplex Sonography Before Renal Artery Repair and Intervention

Over the past 20 years, more than 30,000 percutaneous duplex sonography examinations have been performed at Wake Forest. Renal duplex sonography is our screening study of choice for main renal artery disease. In adults evaluated for renovascular insufficiency (i.e., ischemic nephropathy), a negative renal duplex effectively excludes a renovascular cause for renal failure [1]. In this instance, the study is used to search for renal artery disease to both kidneys or critical stenosis to a solitary kidney. In children and young adults, a negative renal duplex does not exclude significant renovascular disease contributing to hypertension. Despite significant improvements in probe design and the addition of color flow technology, only half of supranumary renal arteries are identified and branch renal artery disease is often not detected.

In addition to anatomic information regarding the hemodynamic significance of main renal artery lesions, recent studies of renal duplex in select patient populations have demonstrated strong associations between Doppler derived measures from the renal parenchyma and the severity of

A.F. AbuRahma, D.F. Bandyk (eds.), *Noninvasive Vascular Diagnosis*,
DOI 10.1007/978-1-4471-4005-4_48, 

hypertension, the risk of progressive renal failure, and the risk of death [2]. Features of the Doppler spectrum analysis taken from both segmental hilar renal arteries and from intraparenchymal interlobular and arcuate arteries have been suggested to reflect the severity of parenchymal fibrosis as well as glomerular arteriolosclerosis [3]. The resistive index (RI) (i.e., the proportion of diastolic relative to systolic Doppler shift) has been presumed to be a surrogate marker for renal damage and studies have correlated RI with histopathologic findings [3, 4]. Collectively considered, these data support the notion that extra- and intrarenal Doppler methods may correlate with intrarenal arteriolosclerosis and that these measures may predict renal function and hypertension response after renal artery repair and catheter-based intervention.

Rodemacher et al. proposed a predictive role for RI in a prospective cohort study of 131 patients [5]. After renal revascularization, 73% of patients with RI less than 0.8 had a decrease in mean arterial blood pressure ≥10%. When patients demonstrated RI ≥ 0.8 before revascularization, only 3% had a decrease in blood pressure and 80% experienced a decline in creatinine clearance. After 32 months, 46% of all patients with RI > 0.8 became dialysis dependent. These findings have been supported by Cone et al., who examined the end diastolic ratio measured from the renal parenchyma and response to revascularization [6]. These authors demonstrated a significant and independent association with improved blood pressure and improved renal function when end diastolic ratio exceeded 0.3.

Our experience with RI and diastolic ratios in over 1,000 patients receiving both open operative repair and catheter-based intervention has suggested a relationship between RI and renal function response but not blood pressure response. Most importantly, a strong and independent relationship with RI and follow-up mortality has been demonstrated for patients after both open repair and catheter-based intervention [7]. Consequently, we do not make treatment decisions for intervention based on this single measure alone but consider RI in the context of other parameters associated with response to intervention and dialysis-free survival.

## Intraoperative Duplex Sonography

Compared with open operative repair at other locations, intraoperative assessment of open renovascular repair has proved difficult by angiographic methods. Intraoperative angiography requires multiple contrast boluses for complete anatomic evaluation in multiple planes. Following warm renal ischemia, branch renal artery and parenchymal arteriolar vasospasm occur frequently in response to contrast injection and may provide inaccurate impression of the intrarenal vascular architecture. Finally, more than half of hypertensive patients subjected to renovascular repair have associated excretory renal insufficiency (i.e., ischemic nephropathy), increasing the risk of contrast nephropathy [8].

By comparison, intraoperative renal duplex sonography is free of limitations and potential complications associated with intraoperative angiography. Duplex images provide excellent anatomic detail sensitive to less than 1 mm. Imaged defects can be viewed in a multitude of sagittal and transverse projections with uninterrupted blood flow. Moreover, spectral analysis proximal and distal to an image defect provides hemodynamic information regarding associated flow disturbance (Fig. 48.1). The absence of renal toxicity, limitless anatomic projection, and the addition of hemodynamic data make intraoperative duplex the method of choice to assess technical aspects of open operative renal artery repair.

Intraoperative studies are performed with a 5 MHz linear array probe with Doppler color flow. The probe head is

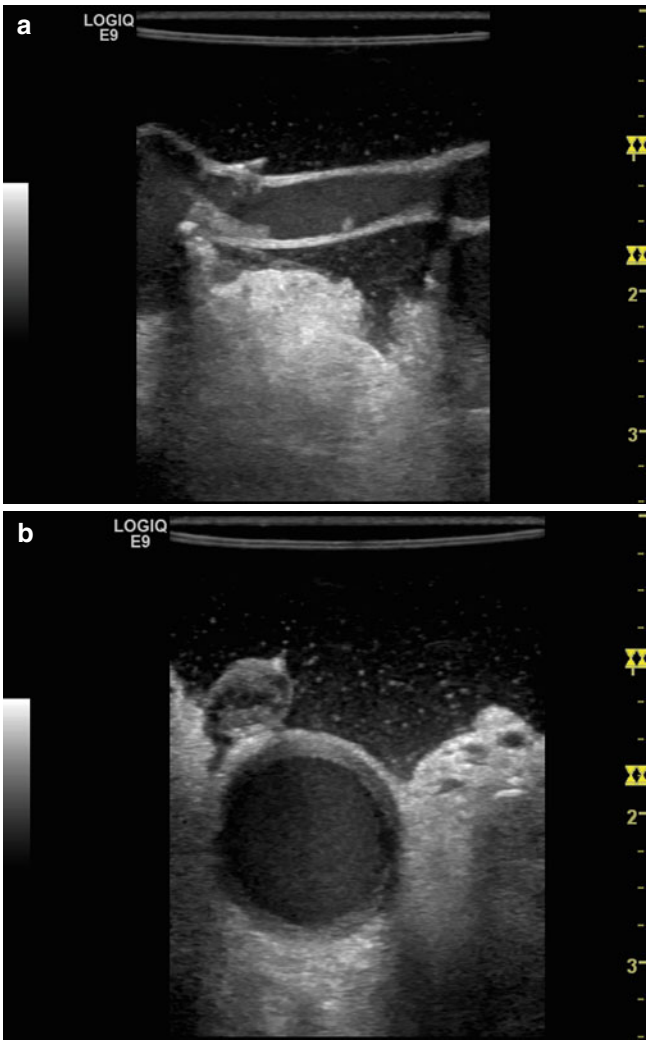


**Fig. 48.1** Intraoperative duplex sonography of main renal artery prior to repair in longitudinal (**a**) and transverse view (**b**). Post-repair duplex (**c**) with corresponding spectral waveform analysis and renal parenchymal signals (**d**)

**Fig. 48.1** (continued)

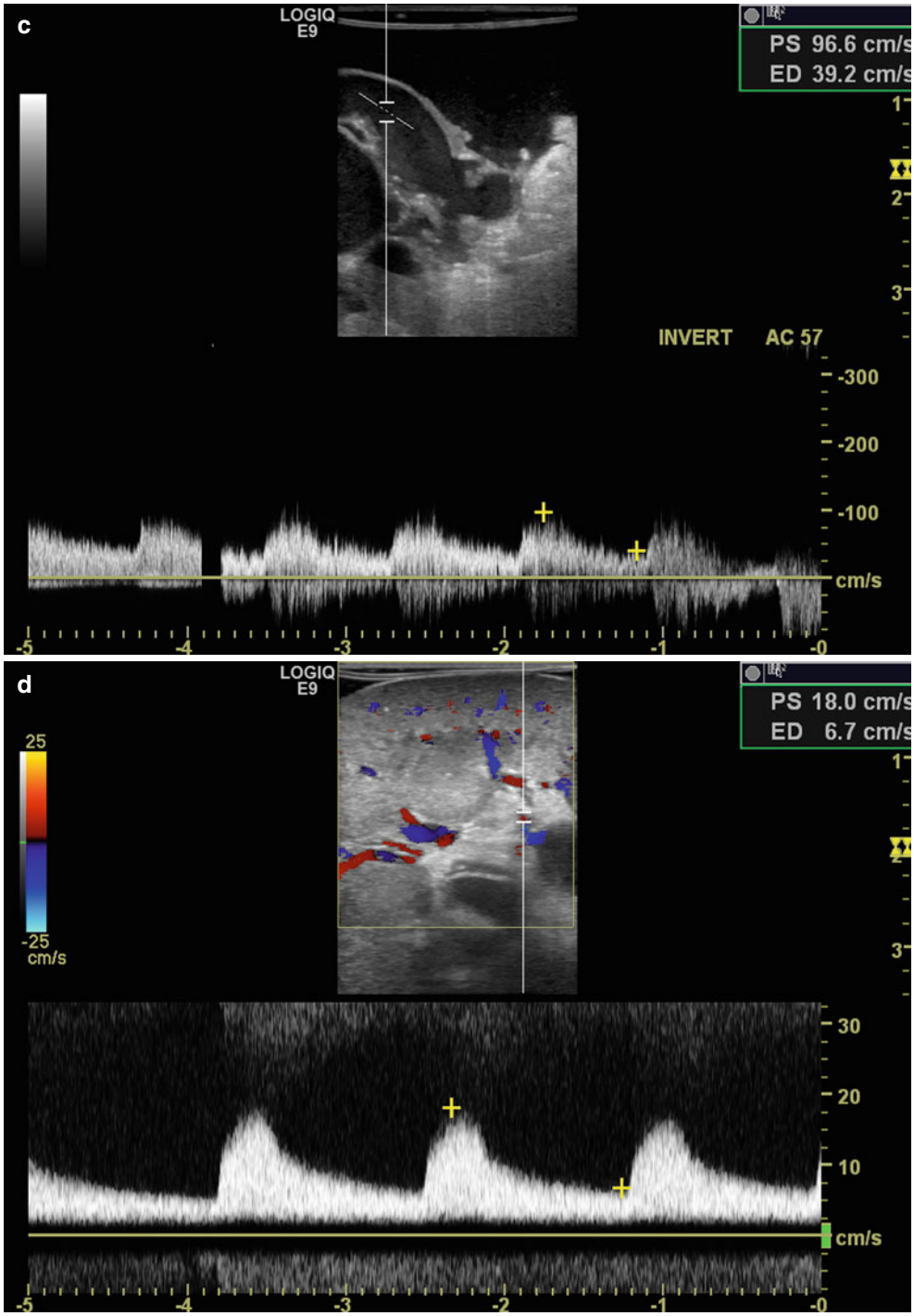


placed in a sterile plastic sheath containing acoustic gel. The operative field is flooded with warm saline and scanned images are first obtained in the longitudinal projection. Care is taken to image the aorta, the renal artery origin and the entire renal artery from origin to hilum. All defects seen in longitudinal projection are imaged in transverse fashion to confirm their anatomic presence and estimate the contribution to luminal narrowing. Doppler samples are then obtained proximal and distal to the imaged defects in longitudinal projection to determine their potential contribution to flow disturbance. Finally, intrarenal Doppler signals from the interlobar and arcuate branches are obtained in the upper, mid portion, and lower pole of the kidney.

The criteria for intraoperative defects creating ≥60% diameter reduction are similar to surface renal duplex sonography studies (Table 48.1). These criteria have been validated in an animal model of graded renal artery stenosis and compared with pre- and post-operative angiography in more than

**Table 48.1** Intraoperative Doppler velocity criteria for B-scan defects

| Defect | Criteria |
|---|---|
| <60% of diameter-reducing RA defect | RA-PSV from entire RA < 1.8 m/s |
| >60% diameter-reducing RA defect | Focal RA-PSV > 1.8 m/s and *distal* turbulent velocity waveform |
| Occlusion | No Doppler-shifted signal from renal artery B-scan image |
| Inadequate study for interpretation | Failure to obtain Doppler samples from entire main renal artery |

Modified from Hansen et al. [9]. With permission from Springer Science+Business Media

100 patients. Unlike surface duplex sonography in which the Doppler sample is large relative to the renal artery diameter, the Doppler sample can be accurately positioned within the mid-center of arterial flow. However, at this mid-center location at least moderate spectral broadening is inherent to the Doppler spectrum after open repair in the absence of anatomic defect.

During intraoperative renal duplex sonography, the interaction between surgeon and vascular technologist is important. Both B-scan images and velocity estimates from spectral data are enhanced by the participation of a vascular technologist. Although the surgeon is responsible for manipulation of the probe head to ensure optimal B-mode images at likely sites of technical error, the power and time adjustments to minimize artifact are best made by an experienced technologist. Close cooperation is required to obtain complete pulse Doppler sampling and estimate velocities associated with B-scan defects. Although often overlooked, the participation in intraoperative studies enhances the technologist's subsequent ability to obtain satisfactory surface renal duplex images during follow-up surveillance.

In over 500 intraoperative renal duplex sonographies after renal artery reconstruction, the average time for intraoperative scan was less than 5 min [10]. Complete B-scan and Doppler derived velocity data were obtained in over 98% of cases. Renal duplex sonography was considered normal, free of any B-scan defect in 77% of cases while B-scan defects were present in 23%. Eleven percent of defects had Doppler velocity estimates exceeding 1.8 m/s with post-stenotic turbulence and these were defined as major. These major defects underwent immediate operative revision and in each case a significant defect was discovered and corrected. Successful revision was verified by a second intraoperative duplex study. In follow up, 97% of these open operative repairs have maintained primary patency without recurrent stenosis at a 5-year follow up. Neither uncorrected minor B-scan defects nor corrected major B-scan defects have correlated with subsequent failure of open repair.

B-scan defects designated as major or minor by Doppler velocity criteria provide accurate information to guide intraoperative revision. There are, however, special circumstances that deserve comment. Intraoperative duplex study after renal repair may occasionally demonstrate peak systolic velocity that exceeds criteria for critical stenosis in the absence of anatomic defect. In these circumstances, peak systolic velocity is elevated uniformly throughout the repair with no focal velocity change and no distal turbulent waveform. Intraoperative studies of this type are most commonly encountered after renal artery repair in children and young adults for non-atherosclerotic disease. Increased peak systolic velocity can also be observed in transition from main renal artery to segmental renal vessels after branch renal artery repair. In the absence of the defect, no distal turbulent waveform will be observed. Finally a renovascular repair to a solitary kidney frequently has elevated velocities throughout without evidence of turbulence.

Other special considerations concern diastolic features of the Doppler spectrum in the absence of technical error. An abnormal diastolic spectrum may be observed after revascularization of chronic renal ischemia reflecting an increased vascular resistance in response to reperfusion. The spectrum may demonstrate brief acceleration times and virtually no diastolic flow. These changes reflect a reactive vasospasm, which can be defined by interarterial administration of 30 mg papavarine. The Doppler spectral signature characteristic for renal artery flow will normalize within 2–3 min (Fig. 48.2).

The rates of primary patency of open renal artery repair without recurrent stenosis are estimated in Fig. 48.3. This patency rate was achieved after revision of major B-scan defects in 12% of repair [11]. Although a disproportionate number of major defects were observed after transaortic endarterectomy, when revision was directed by intraoperative completion duplex, equivalent patency was observed among different reconstructive techniques. The significance of primary patency after open operative repair is profound. Whether by restenosis or occlusion treated by either reconstruction or nephrectomy, failed open operative renovascular repair is associated with an increased risk of eventual dialysis dependence, which is significant and independent of other risk factors [11].

## Renal Duplex Sonography After Open Operative Repair of Renovascular Disease

Anatomic success of open operative renovascular repair is often assumed on the basis of a favorable blood pressure response. However, a favorable blood pressure response can occur after graft thrombosis and renal infarction, the equivalent of nephrectomy. Alternatively, a favorable blood pressure response can occur when renal perfusion is altered sufficiently to impair the renin-angiotensin system yet leaves residual lesions that may represent technical failure. For these reasons, follow-up renal angiography was for many years the method

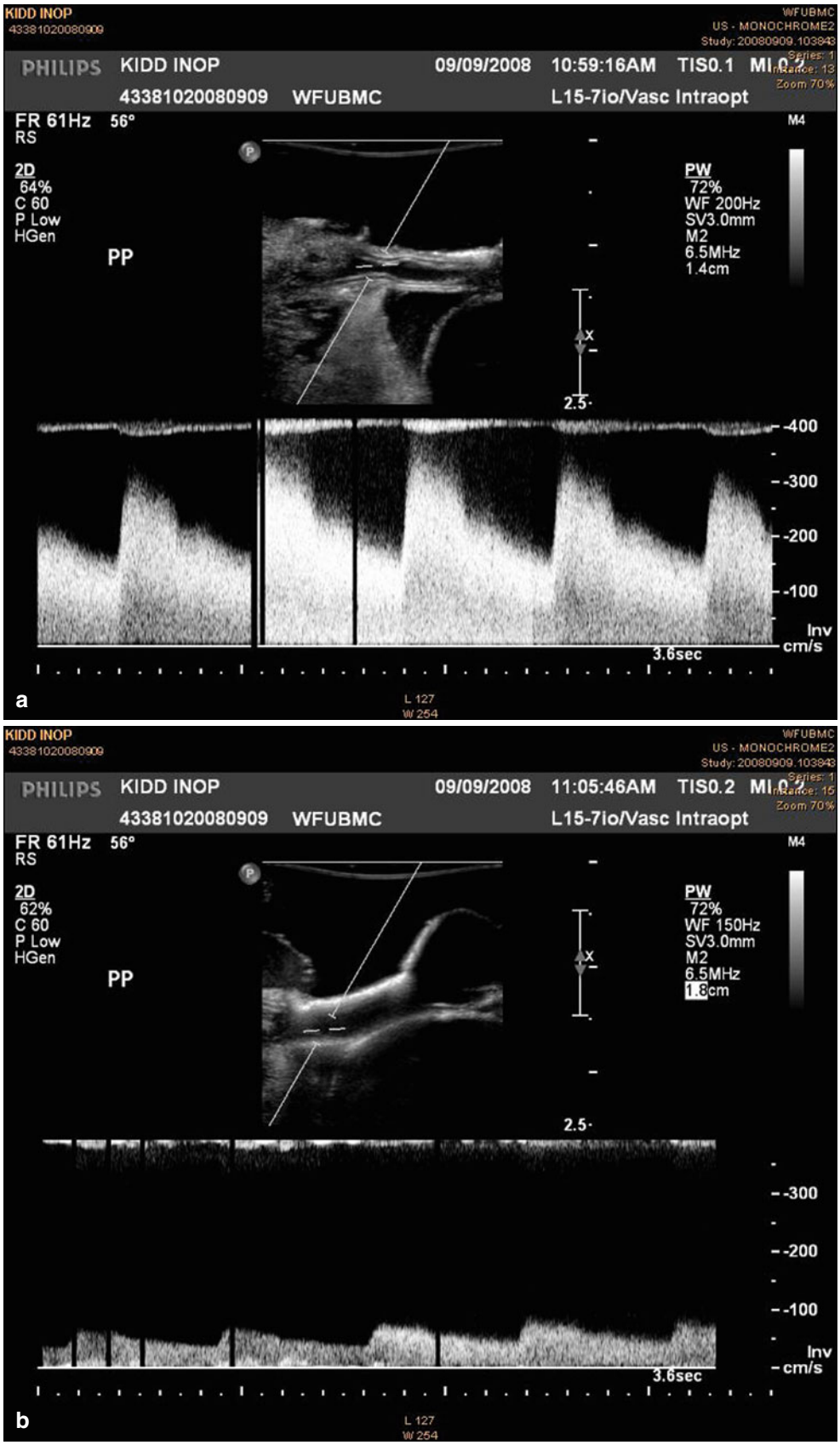


**Fig. 48.2** Intraoperative duplex sonography depicting B-mode and spectral waveform analysis of main renal artery spasm pre (**a**) and post (**b**) papaverine injection

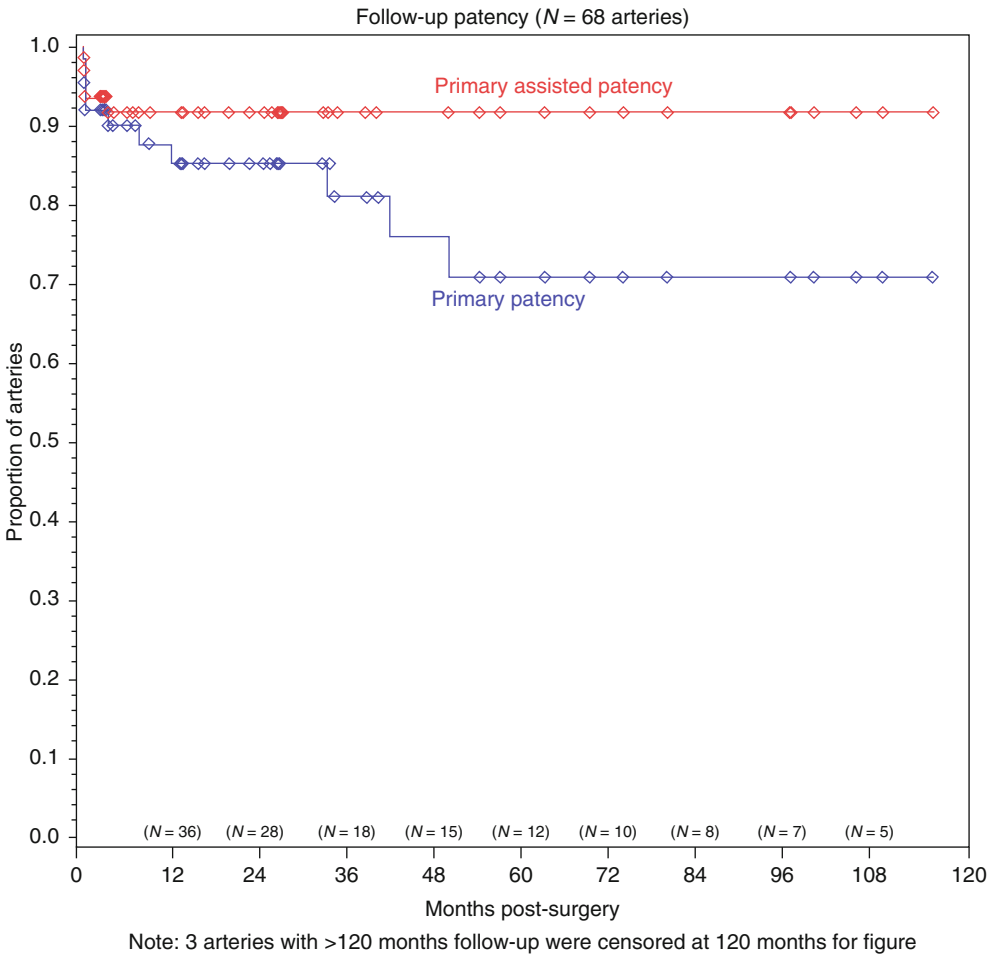


**Fig. 48.3** Product-limit estimates of primary patency (*blue*) and primary-assisted patency (*red*) in 68 arteries. The standard error of the estimate does not exceed 10% (Modified from Crutchley et al. [11]. With permission from Elsevier)

of choice for follow-up surveillance. Fortunately, our experience with percutaneous renal duplex after both open operative repair and percutaneous intervention has proved a valid substitute to assess the technical success or failure of intervention.

For post-operative surveillance, patients are fasted overnight to minimize the bowel gas interference. B-scan images and Doppler shifted signals are first obtained in a supine position with either a 2.25 MHz phased ray probe or 4/2.25 MHz curved ray probe each with Doppler color flow capability. Positioned in the abdominal midline just below the xiphoid process, the sagittal B-scan image of the upper aorta defines the origin of the visceral vessels. At this level, a center stream aortic velocity may be estimated. Using the origin of the superior mesenteric artery and the left renal vein as references, the native origin of each main renal artery can usually be defined in transverse projection during peak inspiration. Knowledge of the operation type is valuable to define suprarenal or infrarenal origins of bypass grafts.

For complete post-operative study, sequential renal artery Doppler shifted signals and estimated peak systolic velocities are obtained throughout the renal artery and continuity from aorta to renal hilum. In kidneys with normal parenchymal renovascular resistance, demonstration of forward flow throughout diastole is consistent but not uniquely characteristic of the renal artery spectrum—the celiac axis and its branches also demonstrate forward flow during diastole and may be confused with the renal artery signal.

B-scan imaging and Doppler interrogations are repeated using a flank approach with the patient in the decubitus position. The flank approach improves B-scan image quality and Doppler signal strength. From the flank, the liver (right) and the kidney (left) provide solid organ acoustic windows free of bowel gas interference. In this position, the surface transducer can be placed closer to the areas of renal artery repair improving image quality. Improper selection of insonation angle and its impact on estimated peak systolic velocity are reduced. After renal artery interrogation is complete, the kidney length, width, and thickness are determined. Doppler signals are obtained from the region of the hilar vessels and the arcuate and interlobar arteries.

The criteria for ≥60% diameter reducing stenosis and renal artery occlusion are identical to criteria for native renal arteries [12]. However, other authors have suggested other criteria to reduce the technical demands of post-operative evaluation. Acceleration time obtained from spectral analysis

renal hilar vessels has been advocated. Proponents have suggested hilar spectral analysis obtained by flank approach minimizes technical demand compared to main renal artery interrogation reducing scanning time. However, our evaluation of acceleration time as a criterion for renovascular disease after open operative renovascular repair has demonstrated high specificity but low sensitivity. When a prolonged acceleration time exceeding 55 ms exists, a proximal renal artery restenosis can reliably be assumed. However, a normal acceleration time does not exclude disease and is observed in the majority of patients with native or recurrent stenosis after repair. For these reasons, we continue to rely upon complete interrogation of the renal artery repair from the aortic origin to renal hilum with critical stenosis defined by focal increase in peak systolic velocity ≥1.8 m/s combined with distal turbulent waveform. These latter criteria provide a sensitivity/specificity greater than 90% with greater than 90% positive and negative predicted value.

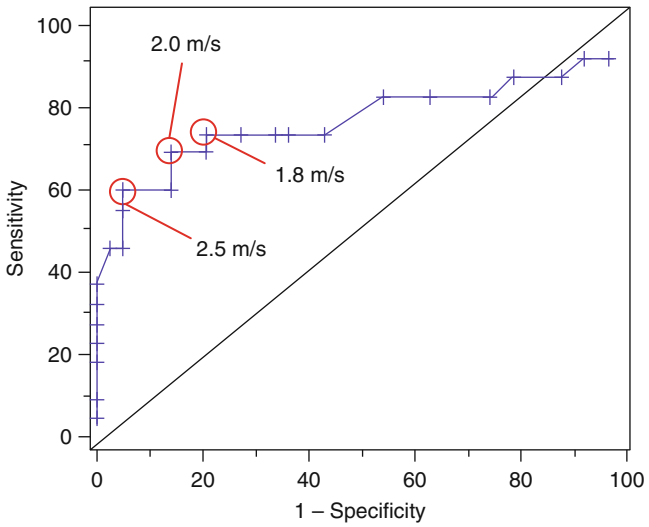


**Fig. 48.4** Receiver operating characteristic curve for renal artery peak systolic velocity to predict >60% diameter reducing restenosis (Modified from Fleming et al. [17]. With permission from Elsevier)

## Renal Duplex Sonography After Renal Artery Angioplasty and Stenting

Despite the value of renal duplex sonography in screening, intraoperative assessment and post-operative surveillance after open operative repair, authors have recently questioned the utility of renal duplex after percutaneous angioplasty and endoluminal stenting (PTAS) for renovascular disease [13, 14]. Most commonly, these authors have suggested that velocity criteria accurate for native renovascular disease are associated with unacceptable rates of false positive studies when applied after PTAS. Changes in compliance of the renal artery after placement of an endoluminal stent, is most frequently cited for false positive studies after PTAS. Contrary do this presumed increase in blood flow velocity, decrease vessel wall compliance would be expected to increase the propagation speed of the ultrasound sound within the stent. However, this increase in propagation speed should not affect the blood flow velocity or its measurement because the latter is based on the Doppler shifted signal from the moving blood elements. This latter view is supported by Doppler flow wire measurements with and without endoluminal stents [15, 16]. Furthermore, despite the compliance changes associated with operative renal artery repair (i.e., renal artery bypass and endarterectomy) we have observed a high correlation between native duplex criteria for intraoperative assessment and post-operative surveillance compared with angiography.

The receiver operating characteristic curve for renal artery peak systolic velocity to predict a ≥60% diameter reducing restenosis and associated scatter plot for renal artery peak systolic velocity are provided in Figs. 48.4 and 48.5 [17]. This analysis summarizes data from 49 patients who had angiographic imaging after PTAS. These data suggest that renal duplex criteria for recurrent stenosis after PTAS are similar to those for native renal artery renovascular disease. This view is shared by other authors but certainly not all. Based on comparative digital subtraction and angiography from 24 subjects, other investigators have suggested a PSV of >2.3 m/s to detect hemodynamic restenosis [18]. Chi et al. reporting on 67 consecutive patients after PTAS with suspected renal restenosis selected for repeat angiography based on PSV > 2 m/s suggested a PSV criteria 3.95 m/s to define >70% diameter reducing renal artery stenosis [14].

Many reports for renal duplex sonography to define both native renovascular disease and restenosis after PTAS cite renal aortic ratio (RAR) as a discriminating criteria for significant renal artery narrowing. The rationale first proposed for RAR was that renal artery velocity reflected aortic velocity in combination with increased velocity associated with the renal artery lesion. However, data from both population-based studies and patient management have demonstrated no correlation between aortic peak velocity and renal artery peak velocity [1, 19]. Rather, the association between renal artery stenosis and renal duplex sonography resides entirely with renal artery peak systolic velocity. Consequently, the RAR term can be viewed as a spurious correlation rather than discriminating criteria for both native stenosis and restenosis after PTAS.

### Conclusion

Renal duplex sonography has proved clinically useful in the management of atherosclerotic renovascular disease. Renal duplex is the screening method of choice for renal

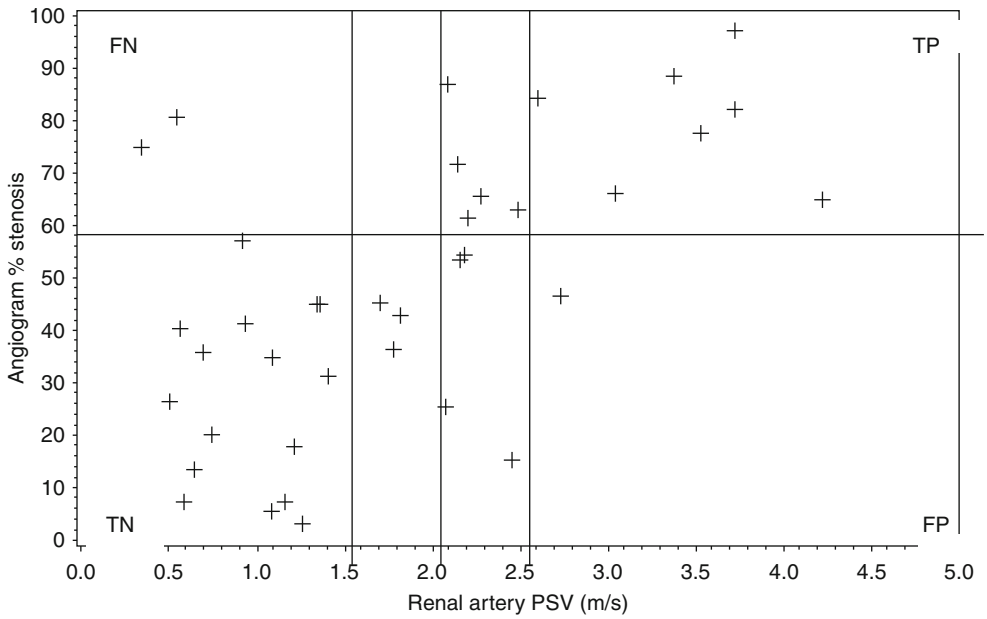


**Fig. 48.5** Scatter plot for renal artery peak systolic velocity (PSV; meters/second) versus percent diameter reducing stenosis by angiography (Modified from Fleming et al. [17]. With permission from Elsevier)

artery lesions contributing to hypertension and/or excretory renal insufficiency (i.e., ischemic nephropathy). Renal duplex sonography has also proven useful as an intraoperative completion study after open operative repair. Renal duplex accurately defines patency, restenosis, and occlusion after operative repair of renovascular disease. Finally, we have found renal duplex useful after percutaneous angioplasty and endoluminal stenting.

## References


1. Hansen KJ, Tribble RW, Reavis SW, Canzanello VJ, Craven TE, Plonk Jr GW, Dean RH. Renal duplex sonography: evaluation of clinical utility. J Vasc Surg. 1990;12(3):227–36.
2. Pearce JD, Edwards MS, Craven TE, English WP, Mondi MM, Reavis SW, Hansen KJ. Renal duplex parameters, blood pressure, and renal function in elderly people. Am J Kidney Dis. 2005;45(5):842–50.
3. Mostbeck GH, Kain R, Mallek R, Derfler K, Walter R, Havelec L, Tscholakoff D. Duplex Doppler sonography in renal parenchymal disease. Histopathologic correlation. J Ultrasound Med. 1991;10(4):189–94.
4. Ikee R, Kobayashi S, Hemmi N, Imakiire T, Kikuchi Y, Moriya H, Suzuki S, Miura S. Correlation between the resistive index by Doppler ultrasound and kidney function and histology. Am J Kidney Dis. 2005;46(4):603–9.
5. Radermacher J, Ellis S, Haller H. Renal resistance index and progression of renal disease. Hypertension. 2002;39(2 Pt 2):699–703.
6. Cohn Jr EJ, Benjamin ME, Sandager GP, Lilly MP, Killewich LA, Flinn WR. Can intrarenal duplex waveform analysis predict successful renal artery revascularization? J Vasc Surg. 1998;28(3):471–80; discussion 480–1.
7. Pearce JD, Craven TE, Edwards MS, Corriere MA, Crutchley TA, Fleming SH, Hansen KJ. Associations between renal duplex parameters and adverse cardiovascular events in the elderly: a prospective cohort study. Am J Kidney Dis. 2010;55(2):281–90.
8. Hansen KJ. Prevalence of ischemic nephropathy in the atherosclerotic population. Am J Kidney Dis. 1994;24(4):615–21.
9. Hansen KJ, Reavis SW, Dean RH. Duplex scanning in renovascular disease. Geriatr Nephrol Urol. 1996;6:89–97.
10. Hansen KJ, O'Neil EA, Reavis SW, Craven TE, Plonk Jr GW, Dean RH. Intraoperative duplex sonography during renal artery reconstruction. J Vasc Surg. 1991;14(3):364–74.
11. Crutchley TA, Pearce JD, Craven TE, Edwards MS, Dean RH, Hansen KJ. Branch renal artery repair with cold perfusion protection. J Vasc Surg. 2007;46(3):405–12.
12. Hudspeth DA, Hansen KJ, Reavis SW, Starr SM, Appel RG, Dean RH. Renal duplex sonography after treatment of renovascular disease. J Vasc Surg. 1993;18(3):381–8.
13. Mohabbat W, Greenberg RK, Mastracci TM, Cury M, Morales JP, Hernandez AV. Revised duplex criteria and outcomes for renal stents and stent grafts following endovascular repair of juxtarenal and thoracoabdominal aneurysms. J Vasc Surg. 2009;49:827–37.
14. Chi YW, White CJ, Thornton S, Milani RV. Ultrasound velocity criteria for renal in-stent Restenosis. J Vasc Surg. 2009;50:119–23.
15. Duong MH, Mackenzie TA, Zwolak RM, Kaplan AV, Robb JF, Thompson CA. Correlation of invasive Doppler flow wire with renal duplex ultrasonography in the evaluation of renal artery stenosis: the Renal Artery Stenosis Invasive Doppler (RAIDER) study. J Vasc Surg. 2007;45:284–8.
16. Savader SJ, Lund GB, Venbrux AC. Doppler flow wire evaluation of renal artery blood flow before and after PTA: initial results. J Vasc Interv Radiol. 1998;9(3):451–60.
17. Fleming SH, Davis RP, Craven TE, Deonanan JK, Godshall CJ, Hansen KJ. Accuracy of duplex sonography scans after renal artery stenting. J Vasc Surg. 2010;52(4):953–7; discussion 958.
18. Bakker J, Beutler JJ, Elgersma OEH, de Lange EE, de Kort GAP, Beek FJA. Duplex ultrasonography in assessing restenosis of renal artery stents. Cardiovasc Intervent Radiol. 1999;22:475–80.
19. Kohler TR, Zierler RE, Martin RL, Nicholls SC, Bergelin RO, Kazmers A, et al. Noninvasive diagnosis of renal artery stenosis by ultrasonic duplex scanning. J Vasc Surg. 1986;4:450–6.

# Duplex Ultrasonography of the Mesenteric Circulation

49

David G. Neschis and William R. Flinn

**Abstract**

Arterial occlusive disease of the celiac and superior mesenteric arteries is rare and patients with symptomatic mesenteric ischemia are encountered infrequently. However, the clinical manifestations of mesenteric arterial occlusive lesions remain enigmatic and range from asymptomatic to catastrophic. Acute occlusions of the celiac artery (CA) and the superior mesenteric artery (SMA) due to thrombosis or embolism can produce extensive, irreversible gut ischemia requiring emergency treatment, and the mortality from these events remains among the highest of all vascular emergencies.

In this chapter, we review duplex scanning technique and findings in both normal and diseased states. Clinical applications including visceral artery aneurysms, celiac artery compression syndrome, and visceral ischemic syndromes are discussed. In this chapter, we have also incorporated more recent data related to post-procedure surveillance of both open surgical reconstruction and endovascular intervention.

Mesenteric duplex scanning can become a routine noninvasive diagnostic testing modality for the evaluation of patients with suspected visceral ischemia since earlier diagnosis and treatment will significantly reduce the risk of catastrophic gut infarction in these patients. Like all deep abdominal duplex scanning, mesenteric scanning is more technologically demanding than scanning vessels of the neck or extremities. However, continued refinement of the duplex instrumentation make these examinations exciting areas of clinical advancement.

**Keywords**

Duplex ultrasound • Celiac artery • Superior mesenteric artery • Mesenteric ischemia Mesenteric bypass • Mesenteric artery stenting

Arterial occlusive disease of the celiac and superior mesenteric arteries is rare and patients with symptomatic mesenteric ischemia are encountered infrequently. However, the clinical manifestations of mesenteric arterial occlusive lesions remain enigmatic and range from asymptomatic to catastrophic. Acute occlusions of the celiac artery (CA) and the superior mesenteric artery (SMA) due to thrombosis or embolism can produce extensive, irreversible gut ischemia requiring emergency treatment, and the mortality from these events remains among the highest of all vascular emergencies. The true incidence of chronic atherosclerotic occlusive disease of the main mesenteric vessels is not well established, the precise relationship to symptoms is poorly understood, and the rate of disease progression is undocumented. It is well accepted that severe, multi-vessel disease may initially

D.G. Neschis, M.D. (✉)
Department of Surgery, The Maryland Vascular Center, Baltimore Washington Medical Center, University of Maryland School of Medicine, 301 Hospital Drive, Baltimore, MD 21061, USA
e-mail: dneschis@bwmc.umms.org

W.R. Flinn, M.D.
Division of Vascular Surgery, University of Maryland School of Medicine, Baltimore, MD, USA

A.F. AbuRahma, D.F. Bandyk (eds.), *Noninvasive Vascular Diagnosis*,
DOI 10.1007/978-1-4471-4005-4_49, 

produce nonspecific symptoms such as pain after eating ("abdominal angina") and weight loss—symptoms that are often mistaken for more common gastrointestinal disorders such as peptic ulcer, gallstone disease, or an occult malignancy. Early diagnosis and treatment of chronic mesenteric ischemia may be of critical importance since progression to thrombosis with gut infarction is fatal in over half the cases when it occurs. However, the nonspecific clinical manifestations of chronic mesenteric ischemia have led to a delay in diagnosis in most patients since arteriography was required in the past for detection of occlusions of the mesenteric vessels. As duplex ultrasound scanning was applied to an increasing number of peripheral and visceral arterial disorders, it was evident that this technique could be adapted to examine the main mesenteric vessels. In this way, mesenteric duplex scanning might serve as an "entry level" noninvasive diagnostic test for the very small number of patients actually suspected of having mesenteric ischemia. In others, it might be used to investigate more thoroughly the significance of mesenteric occlusive lesions found by arteriography performed for unrelated reasons. Finally, it could be useful for follow-up of those patients who have undergone visceral revascularization procedures.

Some deep abdominal duplex scanning, including renal and mesenteric arteries [1, 2], the vena cava [3], and the portal venous system [4–6] is now performed in most vascular laboratories or ultrasound departments. However, the low prevalence of mesenteric arterial occlusive disease has resulted in fewer patients to examine routinely compared with other disorders such as carotid artery disease or even renovascular disease. Deep abdominal ultrasonography remains one of the most challenging applications of noninvasive testing due to variations in body habitus and fat distribution, the presence of respiratory motion, and the depth and the variable anatomy of the major abdominal vessels. Even normal mesenteric anatomy is complex with the major vessels and their branches running in a spatially unpredictable fashion. The mesenteric arterial anatomy may become even more variable when large collateral vessels have developed in the presence of occlusive lesions. Duplex scan evaluation of visceral vessels may also be obscured by bowel gas found in normal patients or those with gastrointestinal disorders.

Atherosclerotic lesions of the visceral vessels usually occur at or near the origins of the CA and SMA ("ostial lesions") from the abdominal aorta (Fig 49.1), which is the most predictable part of the mesenteric anatomy even when more distal branchings are complex. Most clinically important lesions will be identified by examination of the origins of the CA and SMA, and scanning of the proximal 2–4 cm of these vessels. It is generally felt that significant clinical symptoms, and/or the risk of gut infarction exist only when there is severe stenosis or occlusion of at least two main mesenteric vessels. Arteriography is still required to determine the need for treatment and the best therapeutic options, but mesenteric duplex scanning may be useful to select those patients who would benefit most from arteriographic study. Thus, one clinical use of mesenteric duplex scanning would be the identification of normal vessels or those with mild to moderate atherosclerosis where arteriography could be avoided, and another would be to identify accurately severe occlusive disease of the CA and SMA where mesenteric arteriography would determine the subsequent clinical management of the patient.

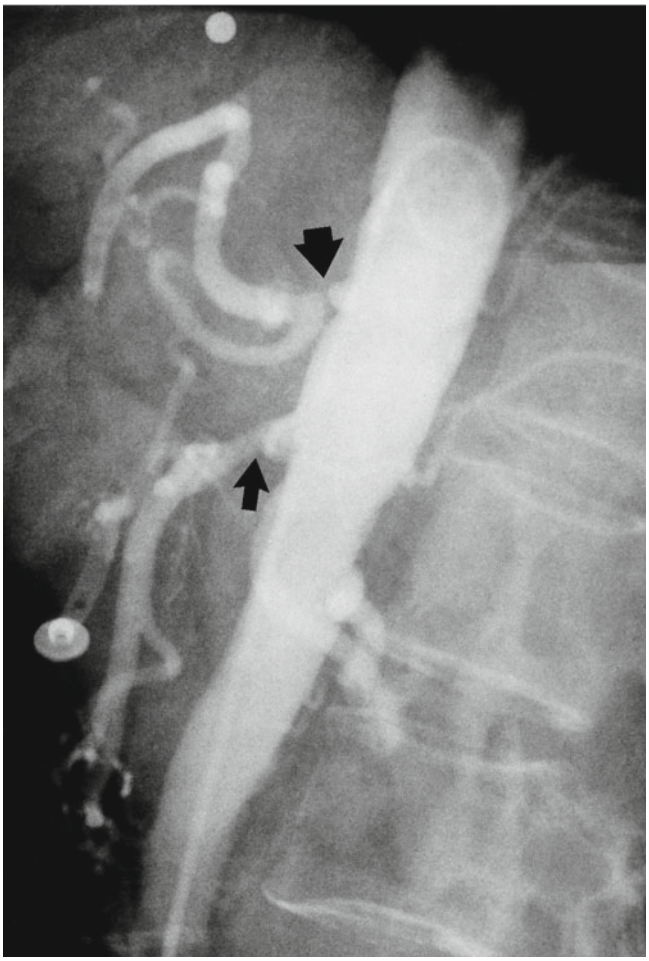

**Fig. 49.1** Lateral view demonstrating the typical ostial location of most atherosclerotic lesions in the main mesenteric vessels. There is a severe stenosis of both the celiac (*larger arrow*) and superior mesenteric arteries (*smaller arrow*) near their origins from the aorta

## Mesenteric Duplex Scanning: Technique

As with all deep abdominal duplex scans, intestinal gas will compromise the technical success of mesenteric examination. An overnight fast is adequate preparation for most elective cases, but simethicone-containing compounds may be useful in cases where bowel gas remains a problem.

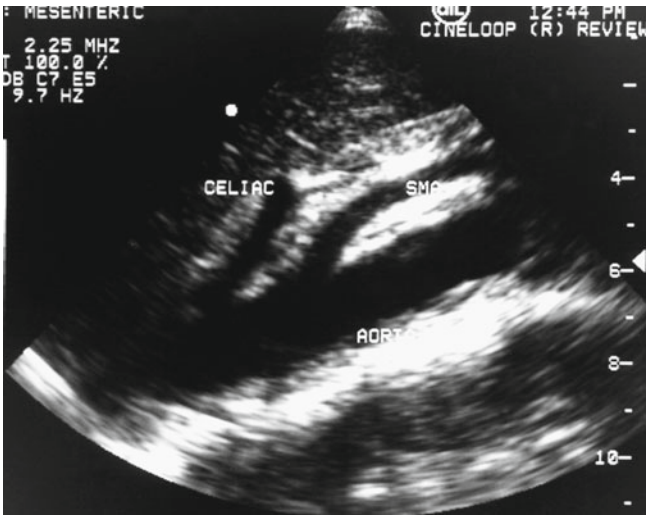


**Fig. 49.2** Sagittal scan of the aorta in a normal patient is similar to the lateral aortogram and demonstrates the origins and proximal portions of the celiac trunk and the superior mesenteric artery. Pulsed Doppler sampling is performed in the proximal portions of these vessels where most occlusive disease occurs. *SMA* superior mesenteric artery

In patients with a more acute problem, the ileus produced by any intra-abdominal inflammatory processes (e.g., acute mesenteric ischemia, cholecystitis, pancreatitis, diverticulitis) greatly limits the usefulness of mesenteric scanning. When a technically adequate examination can be performed it may be useful in directing further diagnostic evaluation, but in emergent cases where mesenteric ischemia is suspected, arteriography should be performed without delay.

Mesenteric duplex scanning is performed with the patient supine and the head slightly elevated. Low frequency, dedicated abdominal probes are used for mesenteric, renal, hepato-portal, and vena caval scanning. An anterior-posterior midline approach is used to obtain a sagittal scan of the aorta. The origins of the CA and SMA are usually visualized as they course ventrally from the aorta (Fig. 49.2) above the level where the left renal vein crosses the aorta. Most atherosclerotic occlusive lesions in the CA and SMA are at or near the origins of the vessels from the aorta, so insonation of the first few centimeters of each vessel is usually adequate for diagnosis. The inferior mesenteric artery (IMA) originates from the left side of the infrarenal aorta a few centimeters above the aortic bifurcation.

Pulsed Doppler examination is performed using a 1.5–2.0-mm-sample volume. Peak systolic velocity (PSV), end diastolic velocity (EDV), waveform configuration, and direction of flow are recorded. Doppler angles of insonation = 60° must be employed when sweeping through the vessels. Rizzo et al. [7] observed that pulsed-Doppler arterial flow velocities from the mesenteric vessels should be measured at angles of insonation less than 60° or falsely elevated peak systolic velocities will be recorded even in normal vessels. The anatomy of the vessels often produces sudden changes in vessel direction and it is incumbent upon the technologists to be as certain as possible about the location and angle of the sample.

Accurate examination of the celiac trunk may be challenging. The celiac trunk is rarely longer than 1–2 cm and the anatomy of its branches (common hepatic, splenic, and left gastric) may be extremely variable. The left gastric artery is rarely identified by duplex scan and routine examination includes the celiac, hepatic, and splenic arteries. While flow in the origin of the CA roughly parallels that in the SMA ventral from the aorta, the branching of the celiac trunk results in rapid changes in the direction of arterial flow at almost 90° to the right (hepatic) and left (splenic) of the main celiac trunk. These anatomic relationships can be appreciated with a transverse B-mode scan of the CA, which has been termed the "rabbit-ear" or "seagull" appearance (Fig. 49.3).

Identification and pulsed-Doppler spectral analysis is easier in the SMA than in the celiac trunk. There are generally no major branches of the SMA visualized on routine examination. However, a "replaced right hepatic artery" may originate from the SMA in up to 20% of normal cases. Some patients may even have a common trunk origin of both the CA and SMA. The variable collateral patterns that are present in cases of occlusion of a single main mesenteric artery may be even more confusing. Large gastroduodenal or pancreaticoduodenal branches may serve as collateral communication between the CA and SMA and these may be difficult to interpret by an inexperienced examiner.

The IMA has not been routinely studied but may be identified by scanning down the infrarenal aorta toward the bifurcation where it is generally the only vessel originating from the left side of the aorta. Isolated stenosis or occlusion of the IMA is rare but it may play a major role in the visceral collateral circulation. The presence of a markedly enlarged and thereby, easily identifiable IMA may suggest significant occlusive disease of the SMA with the IMA serving as the collateral (Fig. 49.4). However, many patients with mesenteric arterial disease have associated aortoiliac occlusions. Here, the IMA may be occluded, but large lumbar collaterals may be mistaken for the IMA on duplex scanning. Another potential source of error in attempt to scan the IMA is the presence of an accessory lower pole left renal artery, which would also originate from the left side of the infrarenal aorta. Overall, in most cases it is sufficient to focus the examination on occlusive lesions at the origins of the CA and SMA, since this is the area of involvement in most clinically relevant disease.

Color Doppler scanning allows more rapid identification of the origins of the CA and SMA from the abdominal aorta and will reduce the time required for an examination. Color-flow scanning may help visually identify focal areas of flow disturbance that require further interrogation, or help one

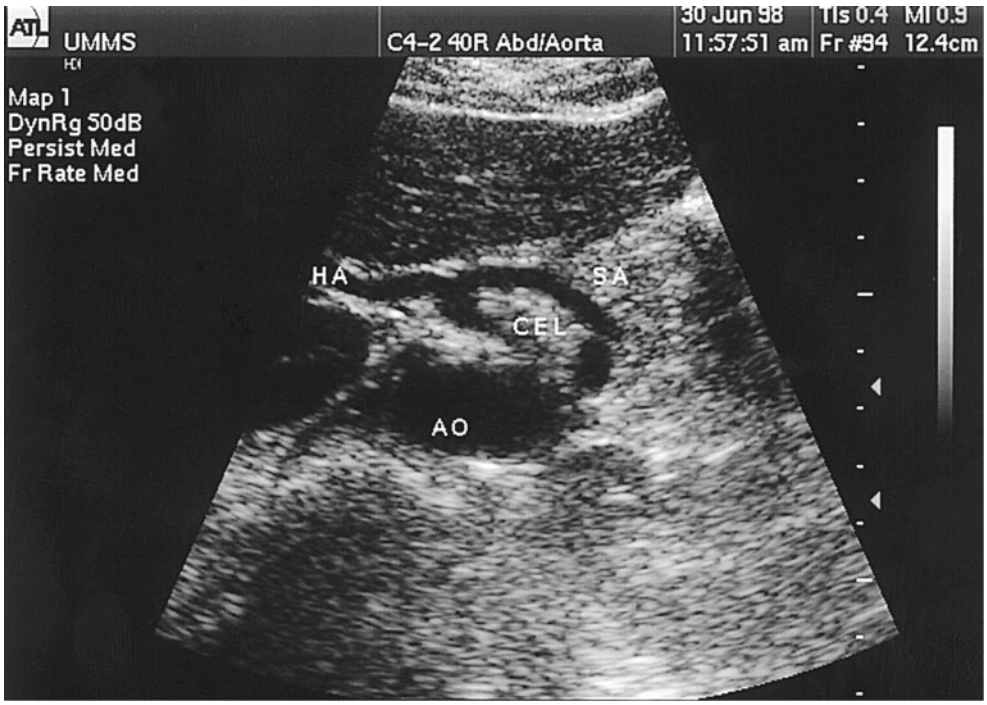


**Fig. 49.3** Doppler spectral analysis in the celiac trunk (*CEL*) may be challenging due to changes in the angle of insonation produced by its branching into the splenic artery (*SA*) and the common hepatic artery (*HA*). These sudden changes in the direction of flow in the celiac branches can produce falsely elevated flow velocities unless the angle of insonation is carefully controlled at = 60°. *Ao* aorta

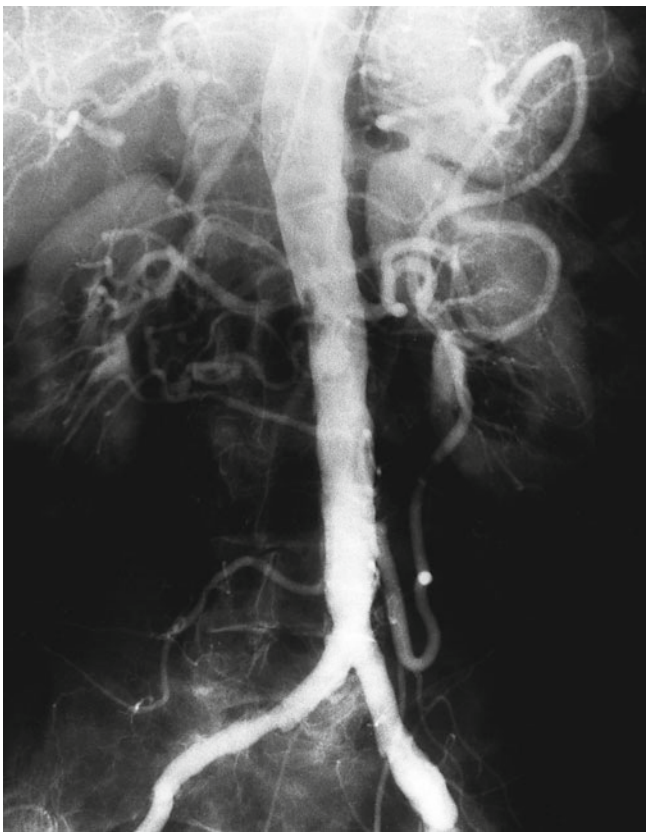

**Fig. 49.4** Aortogram demonstrating a dramatically enlarged inferior mesenteric artery (*IMA*) originating from the left side of the infrarenal aorta several centimeters above the aortic bifurcation. Retrograde flow through the "meandering mesenteric" collateral is demonstrated in this patient with an SMA occlusion

detect the absence of flow in one or both of the major mesenteric vessels suggesting occlusion. It is important to remember, however, that color assignment is based almost entirely upon direction of flow. The anatomic variations discussed above make it evident that beyond the origins of these vessels, sudden changes in flow direction can produce confusing color-flow patterns even in normal subjects.

Reliable, broadly accepted diagnostic Doppler frequency, or flow velocity parameters have not been developed for the mesenteric circulation as they have been in most other systems (carotid, renal, bypass grafts, etc.). Most reports of visceral arterial duplex scanning emphasize the determination of PSV, EDV, and the presence or absence of early diastolic reversal of flow. Similar to carotid scanning, significant stenoses are most often identified by a focal increase in systolic and diastolic velocities, and occlusions are identified by the absence of flow, or flow reversal. Unlike renal artery duplex scanning, no improvement in diagnostic accuracy has been observed by normalizing visceral arterial velocity measurements to those in the aorta through the calculation of flow velocity ratios [8, 9]. Some investigators have reported quantitative blood flow (ml/min) measurements using Doppler derived velocity information in either the portal venous system [10, 11], or in the mesenteric arterial circulation [12–15]. Although there is considerable research interest in volumetric flow data, this estimation is subject to significant error [16–18], and most diagnostic laboratories do not perform such measurements. The presence of elevated PSV and localized turbulence appears to correlate better with angiographically demonstrated arterial lesions in both the peripheral and the central circulation.

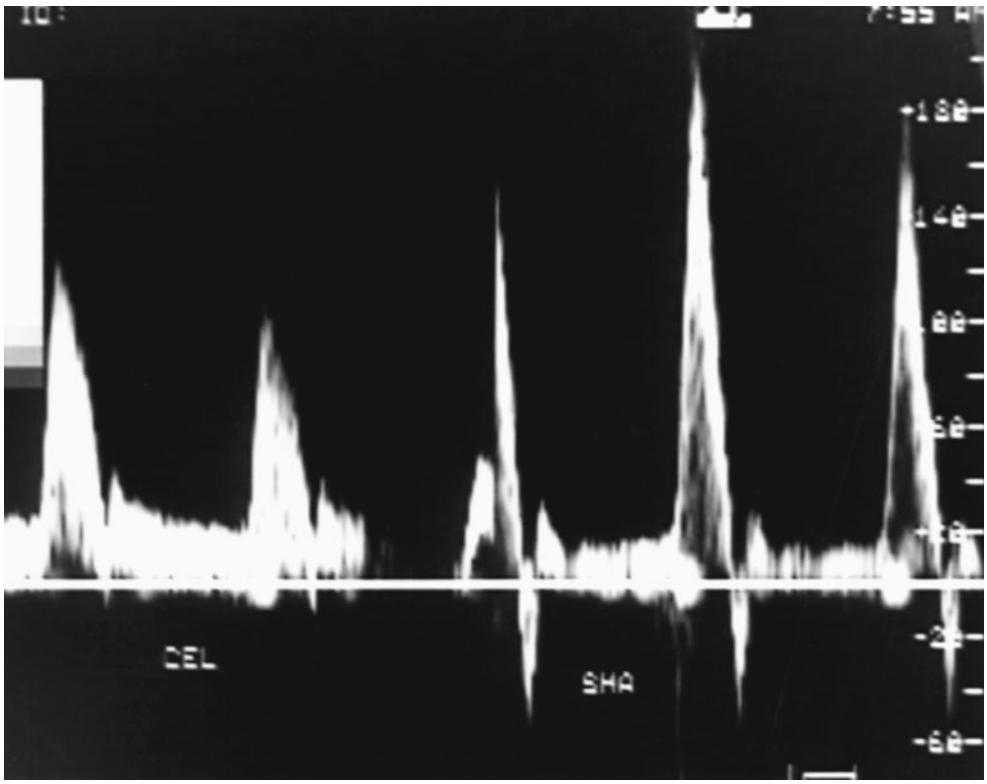


**Fig. 49.5** The normal fasting SMA waveform (*right spectra*) is recognizably different from the celiac artery (*CEL*, *left*). The triphasic pattern of the normal SMA is reminiscent of that found in higher resistance peripheral arteries

## Normal Findings

Mesenteric arterial velocity waveforms have certain specific characteristics. At rest, blood flow in a normal SMA has a higher resistance Doppler velocity pattern with early diastolic flow reversal in most cases, and late diastolic forward flow (triphasic waveform; Fig. 49.5). Blood flow in the CA as in the renal arteries, has a low resistance Doppler velocity pattern with continuous forward flow during the entire cardiac cycle (Fig. 49.6). Spectral waveforms recorded from normal IMA are similar to those from the SMA with a higher resistance pattern with early diastolic flow reversal.

## Clinical Applications

### Physiologic Measurements

Duplex scanning of the mesenteric vessels in normal individuals has been used successfully to characterize the physiological changes that occur in the visceral circulation after eating. The most reproducible changes occur in the SMA, where significant increases in PSV are seen up to an hour after eating [19]. Also, the SMA flow waveform shifts to a low resistance pattern characterized by forward flow throughout the cardiac cycle with loss of the early diastolic flow reversal. The composition of the meal, including volume, energy content, and the nutritional composition, may influence the observed changes in mesenteric flow velocities after a meal [1, 4, 15, 20]. Fat and carbohydrates appear to be the nutritional components of the meal that produce the most significant postprandial increases in measured PSV [15].

Duplex scanning has also been used to demonstrate the effects of drugs on intestinal blood flow. Several investigators have demonstrated changes in mesenteric arterial flow following the infusion of splanchnic vasodilators such as glucagon and secretin, and vasoconstrictors such as vasopressin [19, 21]. Lilly et al. [19] observed that the changes in superior mesenteric arterial flow following glucagon infusion closely paralleled those observed after a meal.

### Visceral Aneurysms

Aneurysms of the mesenteric vessels are extremely rare and the clinical usefulness of duplex scanning for the detection of mesenteric aneurysms remains anecdotal. Ultrasonographic diagnosis of aneurysms of the superior mesenteric [22–24], hepatic [25, 26], splenic [27, 28], gastroduodenal [29], middle colic [30], and pancreaticoduodenal [31] arteries has been reported, but in these cases scanning was often performed due to uncertain gastrointestinal or abdominal complaints. However, duplex scanning may be useful in such cases to select patients for more thorough, focused vascular exam with CT, MRI, or arteriography. Color-flow duplex ultrasonography may be useful for differentiating saccular false aneurysms of the superior mesenteric and splenic artery

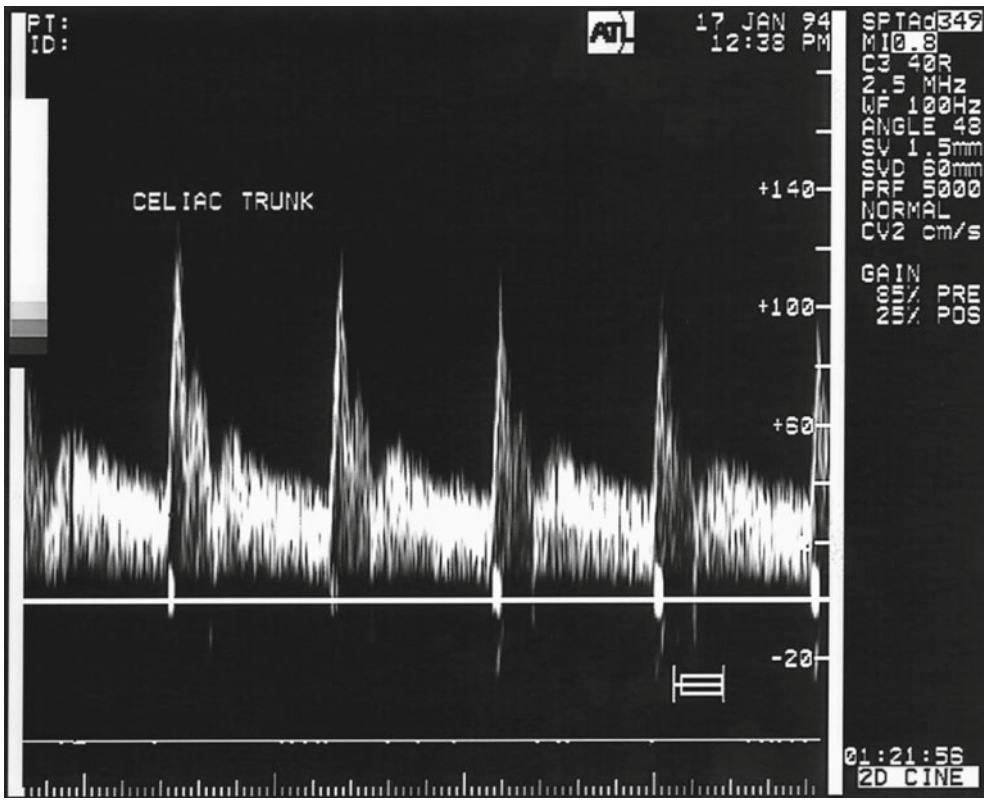


**Fig. 49.6** Velocity spectrum from a normal celiac artery demonstrating continuous forward flow throughout systole and diastole

from other more benign, nonvascular fluid collections in the setting of pancreatitis or other retroperitoneal inflammatory conditions. However, as noted above, an associated ileus with excessive bowel gas may preclude a diagnostic study.

### Celiac Artery Compression Syndrome (Median Arcuate Ligament Syndrome)

A focal increase in flow velocities identified at the origin of the CA may be due to extrinsic compression of the CA by the median arcuate ligament of the diaphragm, particularly when this finding is detected in a younger individual. Celiac artery compression syndrome has been reported to produce gastrointestinal symptoms in some patients, but most clinicians regard this as a benign condition with little or no risk of intestinal infarction. In fact, duplex scanning of these lesions is more likely to be performed to evaluate the finding of the celiac stenosis on an arteriogram performed for other reasons (Fig. 49.7). This "lesion" is usually associated with a normal arterial wall and normal aorta with no evidence of atherosclerotic plaque. Scanning during deep inspiration with breath holding produces a relaxation of the diaphragmatic crus and often results in a return of normal celiac velocities, which confirms the diagnosis.

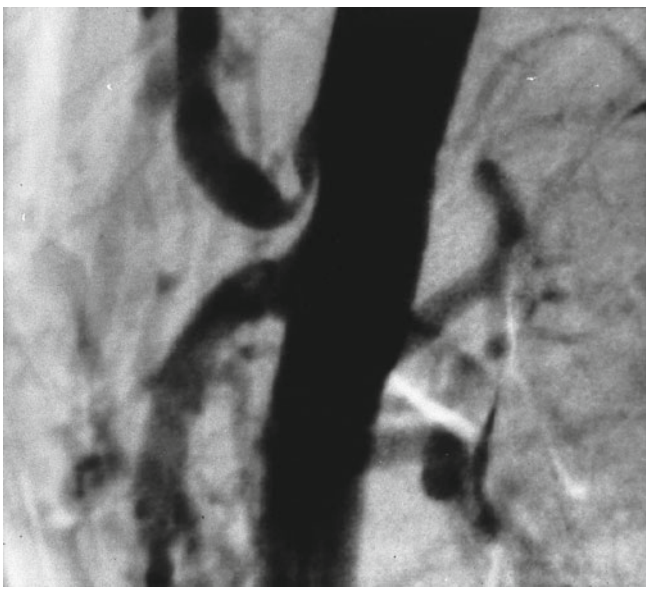

**Fig. 49.7** Characteristic arteriographic appearance of proximal celiac artery stenosis due to compression by the median arcuate ligament of the diaphragm. Note there is no evidence of atherosclerosis in the aorta or the SMA. Deep inspiration in this case produced a normalization of both duplex scan findings and the arteriogram

### Visceral Ischemic Syndromes

The use of duplex ultrasonography as a screening test to detect major mesenteric arterial occlusive disease in patients suspected of having chronic intestinal ischemia has attracted interest among clinicians, since the diagnosis of mesenteric occlusive disease in the past required arteriography. Jäger

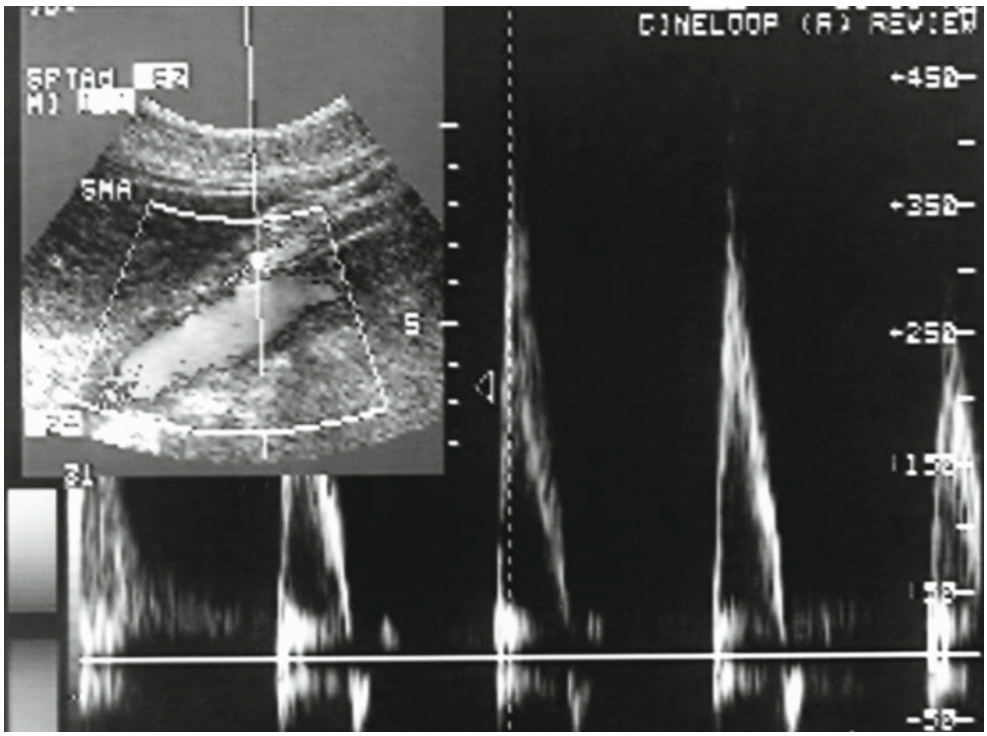


**Fig. 49.8** Duplex scan of the proximal SMA reveals a markedly elevated peak systolic velocity >350 cm/s. This suggests the presence of a >70% SMA stenosis

et al. [32] first reported abnormal pulsed Doppler waveforms with increased PSVs and marked spectral broadening and in both the CA and SMA of a patient with severe atherosclerotic stenosis in both vessels and symptoms of chronic visceral ischemia. Other authors [33, 34] have used similar criteria of distorted Doppler flow patterns or absence of detectable flow to document high-grade stenosis or occlusion of the intestinal arteries. Moneta et al. [35] reported ultrasound visualization of an enlarged IMA in several patients with high-grade stenosis or occlusion of the celiac and superior mesenteric vessels where that vessel had become the major collateral supply to the bowel.

Standardized velocity criteria for duplex scan diagnosis of hemodynamically significant lesions of the mesenteric arteries (similar to those used in the diagnosis of extracranial carotid artery disease) have not been thoroughly refined. Considering the low prevalence of mesenteric disease compared to carotid disease and the small number of arteriograms available for comparison, it would appear unlikely that such discrete diagnostic criteria would be forthcoming soon. Nevertheless, several studies can provide general ranges for diagnosis which will be clinically useful for the practitioner. Moneta et al. [9] compared the results of mesenteric duplex scanning to arteriography in 34 patients with known atherosclerosis. This group included patients with suspected visceral ischemia as well as others requiring routine arteriography for lower extremity ischemic symptoms. An analysis of their accumulated data revealed that PSVs above 275 cm/s in the SMA (normal = 125–163 cm/s) could predict a severe SMA stenosis (>70%) with a sensitivity and specificity of 89% and 92%, respectively. A similar diagnostic accuracy was observed by these investigators when PSVs exceeded 200 cm/s in the CA. Total occlusions of the CA and SMA were also accurately diagnosed by duplex scan in this report. This initial retrospective study failed to demonstrate the usefulness of a "mesenteric:aortic" systolic velocity ratio to predict the presence of a severe stenosis in the CA or SMA as has been observed in duplex scanning of the renal arteries. In a subsequent report [36] these investigators prospectively evaluated these diagnostic criteria in 100 patients having arteriograms and demonstrated that mesenteric duplex scanning was indeed sufficiently accurate to be clinically useful as a screening examination in cases with suspected CA or SMA occlusive disease (Fig. 49.8).

The usefulness of mesenteric duplex scanning for the diagnosis of significant CA and SMA lesions was confirmed in the report of Bowersox et al. [37] that compared mesenteric duplex scanning with arteriograms in 25 patients, most of whom were suspected of having visceral ischemia. These investigators observed that a >50% stenosis of the SMA could be best predicted by duplex scan measurement of a fasting PSV > 300 cm/s or an EDV of >45 cm/s. These authors were unable to establish reliable duplex scan velocity criteria for CA stenosis. They observed that the anatomy of the CA compromised precise insonation as noted previously in this chapter. Considering the small sample size and the fact that most patients were symptomatic, it is possible that anatomic and collateral variants would account for the

observed compromise. Further emphasizing the difficulties encountered in an attempt to define precise duplex ultrasound diagnostic criteria for mesenteric occlusive lesions, Healy et al. [38] were unable to identify any definitive velocity criteria for detection of CA or SMA stenoses.

These observations generally serve to reinforce the continued need for prospective studies with arteriographic correlation. However, as noted above, cases available for study are seen infrequently. Nevertheless, the general principles of duplex scan detection of a "critical" stenosis or occlusion in any arterial system apply in the mesenteric vessels: (1) a focal marked elevation in PSV, particularly associated with elevated EDV, (2) poststenotic turbulence with reduced flow velocities beyond the stenosis, and (3) absence of flow in an anatomically well defined arterial segment, particularly with flow reversal beyond the lesion (suggestive of occlusion). The key to success in the mesenteric circulation relies not so much upon precise velocity criteria, but in accurate anatomic identification of the vessels and control of the technologic variables for Doppler examination.

## Perioperative Applications

### Intraoperative Applications

As with all vascular reconstructions, early technical success is essential in the outcome of mesenteric revascularization. Due to the intra-abdominal location of the bypass, early graft failure may not be readily apparent. Abdominal pain is an unreliable symptom following laparotomy and if the patient goes on to gut infarction, the outcome is almost uniformly fatal. It is clear then that intraoperative assessment of the technical conduct of mesenteric revascularization procedures is an important clinical component of these procedures. The portability of modern ultrasound equipment and increasing surgeon familiarity with these techniques has led to an increase use of duplex ultrasound scanning to assess technical success following renal and mesenteric revascularization procedures. Oderich and colleagues evaluated the use of intraoperative duplex scanning in 68 patients undergoing operative visceral revascularization [39]. Patients who were identified to have an abnormal intraoperative mesenteric duplex examination had a higher incidence of early graft thrombosis, reintervention, and higher perioperative mortality. The authors concluded that the duplex scan evaluation helped optimize early technical success of mesenteric revascularization procedures.

### Post-operative Applications

Revascularization of symptomatic mesenteric arterial occlusions is optimal management, but in the past the patency of these reconstructions, like initial diagnosis, could only be determined by arteriography. Sandager et al. [40] first reported the use of duplex ultrasonography to evaluate the patency of visceral arterial reconstructions. Duplex scanning successfully documented graft function in six of the seven visceral bypass grafts and findings were correlated with standard arteriography. McMillan et al. [41] reported successful duplex scan follow-up of mesenteric bypass procedures in 30 cases. This study also demonstrated that reliance on recurrence of abdominal symptoms alone has sensitivity as low as 33% in the detection of mesenteric graft occlusion. Duplex scanning can provide accurate noninvasive documentation of the patency of visceral revascularization procedures without requiring contrast-based imaging (Fig. 49.9).

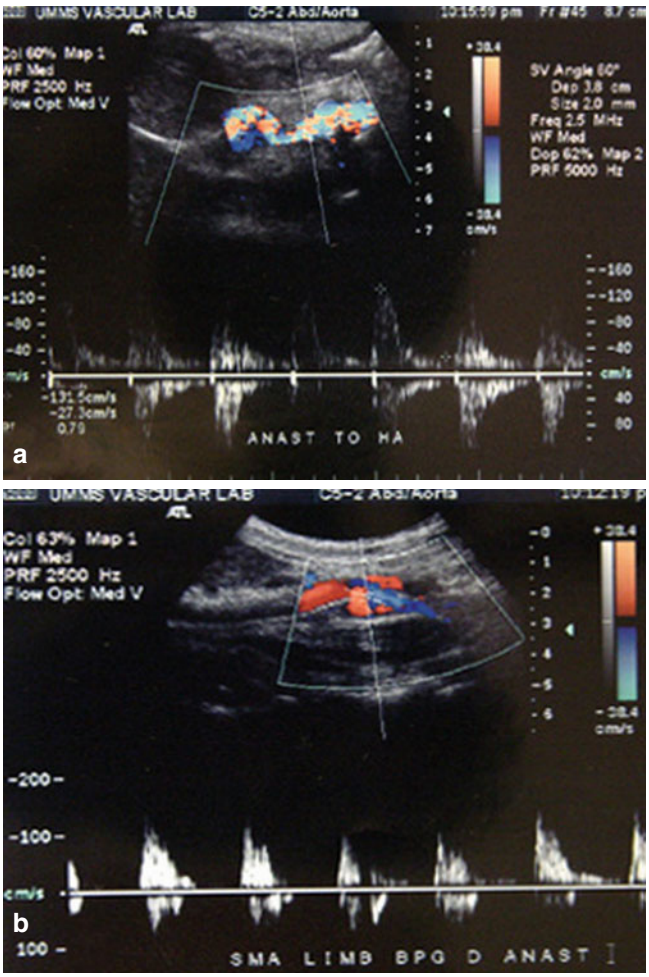


**Fig. 49.9** Duplex scan demonstrating patency of a bifurcated arterial bypass graft with one limb to the hepatic artery (**a**) and one limb to the SMA (**b**)

Liem and colleagues evaluated the duplex characteristics of 43 mesenteric bypass grafts in 38 patients [42]. Mid-graft velocities were not significantly impacted by graft material, inflow artery, target artery, or graft configuration (antegrade vs retrograde). Although there were also no characteristics that predicted future graft thrombosis, velocities in patent grafts

remained stable from study to study with mid-graft PSVs generally between 100 and 200 cm/s. The authors recommended secondary imaging (computed tomography angiography or conventional angiography) if the PSV ≥ 300 or <50 cm/s. There is also a suggestion that a significant change in velocity from one study to the next may be indicative of a stenosis. Limitations of this study include a small sample number and the absence of angiographic correlation. The role of prospective surveillance of these grafts is unknown at present. However, increased experience with post-operative duplex scanning of mesenteric bypass grafts will allow a more accurate documentation of late patency for these procedures, an aspect that has been incompletely studied in the past due to the requirement for repeated invasive contrast studies. Overall, it has become evident that duplex ultrasonography can be used successfully to document the post-operative patency of surgical procedures performed for revascularization of the mesenteric vessels, eliminating the need in most cases for the use of more invasive contrast studies. However, it should be remembered that the anatomic construct of these revascularization procedures may be quite complex and often not anatomically intuitive, to even an experienced ultrasonographer. Antegrade bypass from the supraceliac aorta, retrograde bypass from the infrarenal aorta (Fig. 49.10), or iliac arteries; with prosthetic or vein grafts may be performed. Thus, optimal performance of post-procedural scanning in these cases will be greatly facilitated by provision of the details of the surgical procedure to the ultrasonographer performing the exam.

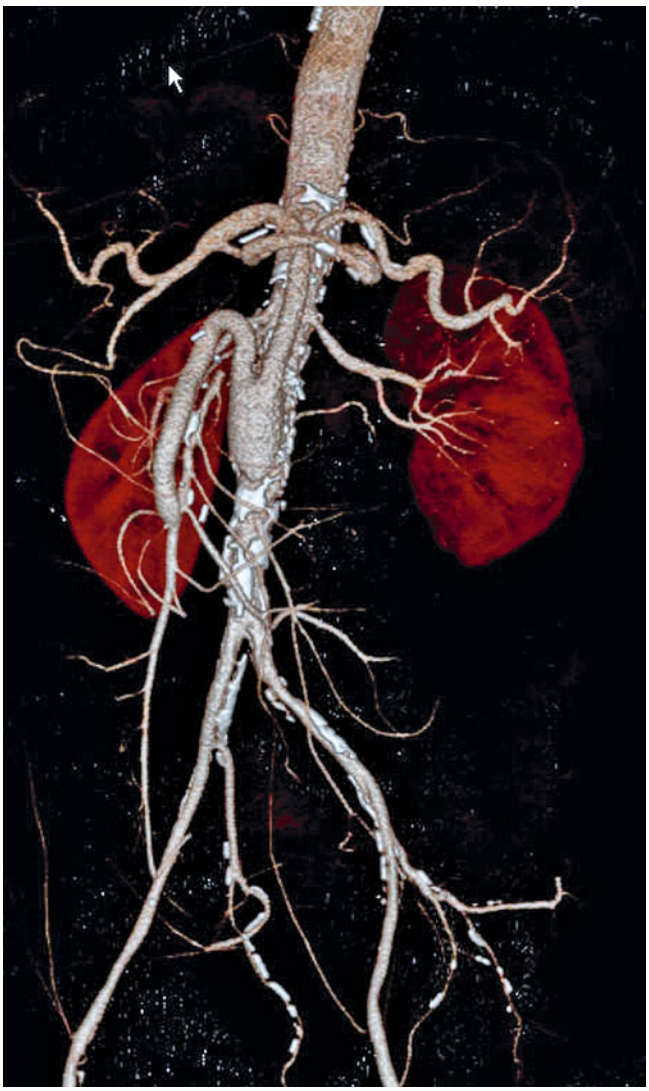

**Fig. 49.10** Aortoceliac and mesenteric bypass with a Dacron bifurcation graft using a retrograde technique from the infrarenal aorta. Surgeons wishing to perform post-operative mesenteric duplex scanning must inform the ultrasonographer about the precise surgical details of these reconstructions that are often anatomically complex

## Endovascular Intervention

Endovascular interventions including balloon angioplasty and stenting have been performed routinely in the renal arteries, and these techniques have also proven to be effective for treatment of mesenteric arterial occlusive lesions. (Fig. 49.11). Steinmetz and colleagues reported their experience in 19 patients with chronic mesenteric ischemia treated by balloon angioplasty or stenting [43]. The authors reported a 100% technical success rate although in 7 of the 19 cases only one of the two vessels intended for treatment was successfully treated. In seven cases, stenting was required due to recoil or residual stenosis. Patients having angioplasty and/or stenting in this series were followed up with duplex ultrasound for a mean of 31 months. The primary patency was 75% and long-term pain relief noted in 85% of patients for whom follow-up was available. Three patients developed symptomatic restenosis and were treated with redo angioplasty with resolution of pain. Two other patients were found to have asymptomatic restenosis and were followed conservatively [43]. AbuRahma and colleagues report on 22 patients with 24 symptomatic mesenteric arterial lesions treated with balloon angioplasty/stenting over a 4.5-year period [44]. In this series, the initial technical success as defined, per vessel, as residual stenosis <30% and pressure gradient <10 mmHg was 96%. Over a mean follow-up period of 26 months, the primary late clinical success rate was 61% with a freedom from restenosis (=70%), as documented by objective duplex examination, of 30%. Freedom from recurrent symptoms was 67%. Four-year survival rate in these patients was 53% [44].

Duplex ultrasound has been used to evaluate patency following endovascular revascularization of mesenteric arteries (Fig. 49.11). Excellent correlation has been found between a significant decrease in PSV following angioplasty/stenting and a favorable clinical response [45]. PSV following these endovascular treatments may occasionally remain in the abnormal range (>275 cm/s) [45]. Although the PSV will be

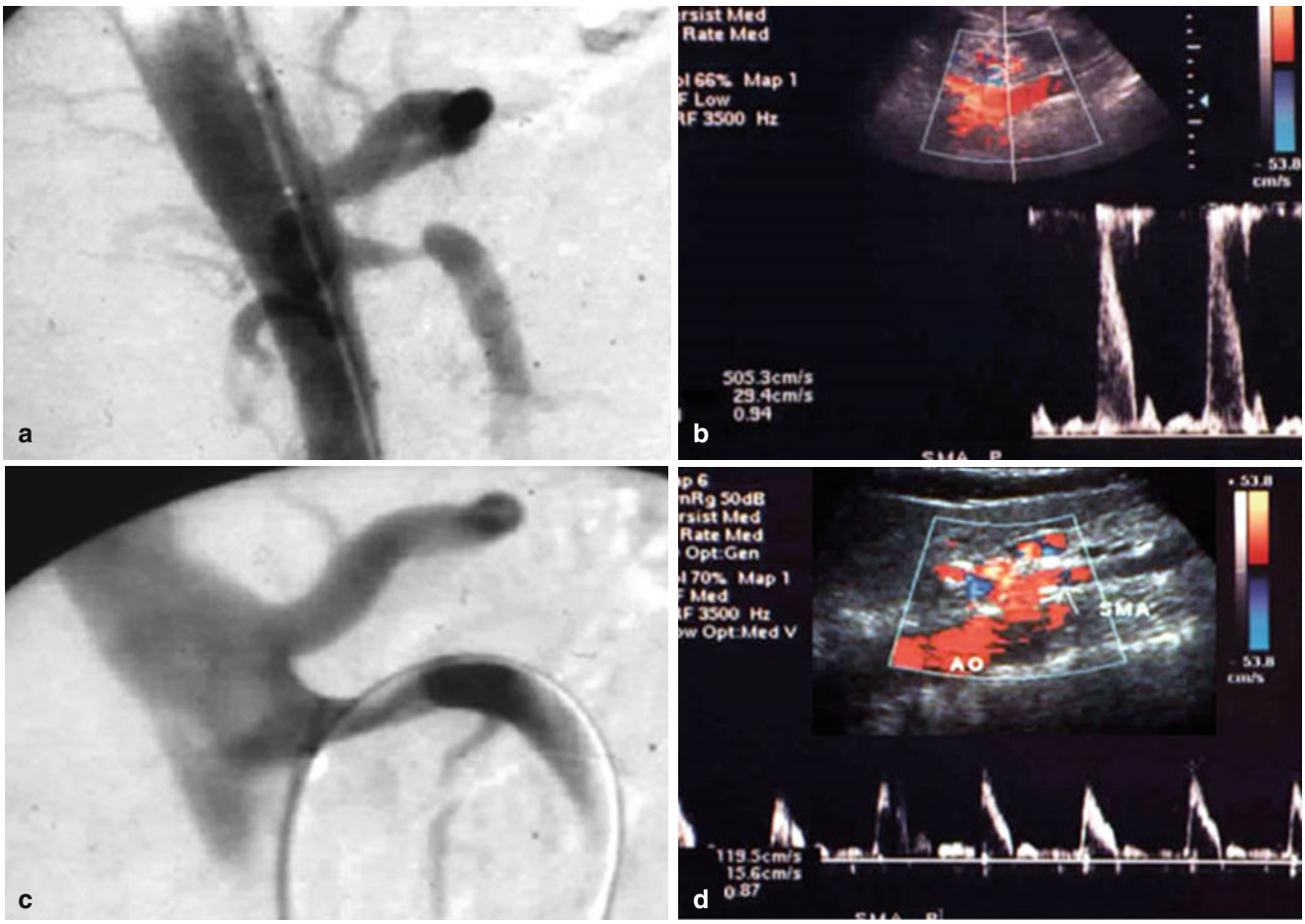


**Fig. 49.11** (**a**) Aortogram depicting high-grade stenosis in the proximal SMA, (**b**) corresponding duplex image demonstrating significantly elevated peak systolic velocities of 505 cm/s at the level of the stenosis, (**c**) angiogram post-percutaneous angioplasty and stenting demonstrating resolution of the SMA stenosis, (**d**) corresponding duplex image demonstrating a patent stent (*arrow*) and reduction of peak systolic velocities to normal (120 cm/s)

significantly lower than pre-procedure levels. Sharafuddin and colleagues suggest scanning the SMA beyond the stent, and performing the study in a strictly fasting state to reduce artifactual increases in PSV observed in the SMA [45].

In one more recent study, PSV in successfully stented SMAs remained above 275 cm/s in all cases [46]. Mitchell et al. report on 13 patients with early post-stent duplex information [46]. While mean PSV pre- and poststent dropped from 450 to 336 cm/s respectively, no stented patient had SMA PSV under the cutoff for >70% native artery stenosis. Similarly, albeit in a smaller series, Fenwick et al. note velocities consistent with >70% stenosis in three out of four successful SMA stent procedures without recurrence of symptoms or weight loss [47].

Based on the experience to date, it does not appear that criteria for native SMA stenosis can be reliably applied to post-stent Duplex evaluation. Until new, stent specific, criteria are established and validated, we would recommend an early post-stent duplex be obtained and serve as a baseline, reserving intervention for either return of symptoms or for significant elevation of PSV over the new baseline measurement.

## Acute Mesenteric Ischemia

Acute mesenteric ischemia is usually produced by mesenteric embolism or mesenteric thrombosis. It would be ideal to provide direct duplex scan identification of discrete mesenteric arterial occlusions in these cases particularly since the approach to treatment may be different. If patients with acute major mesenteric arterial occlusions were examined very early in the clinical course of these problems, duplex scanning might provide an accurate assessment. However, diagnosis is often delayed in these patients and the associated ileus that rapidly develops renders the scan virtually useless. Takahashi et al. [48] reported dramatically reduced portal venous flow by duplex ultrasonography in one patient with acute mesenteric infarction. Reduced portal vein flow is

an indirect reflection of severely reduced mesenteric arterial blood flow and its lack of specificity would be of limited clinical usefulness in the majority of cases. Prompt arteriography or CT angiography is the diagnostic examination of choice in such cases since excessive delay in the diagnosis can lead to irreversible intestinal infarction.

## Image Enhancement

Unlike vessels in the neck or extremities, the ability to image the mesenteric vessels can often be difficult due to patient body habitus or bowel gas. The low-frequency transducer needed to image at the appropriate depth is hampered by poorer B-mode image resolution. This leads to less accurate placement of the Doppler sample volume. Investigational substances are being developed and studied to assist in enhancing ultrasound imaging of blood vessels. The ideal ultrasound contrast agent would have the appropriate density and acoustic properties to strongly reflect transmitted ultrasound waves. Additionally the contrast agent would be physiologically inert, small enough to easily pass through capillaries, and persist in the vasculature long enough to complete the study. Perflutren (Definity, Dupont Pharmaceuticals Co.) is one such agent. It can be agitated, injected into a bag of sterile saline solution, and infused intravenously. Blebea et al. studied perflutren in 17 patients to examine its potential usefulness in evaluating the mesenteric arteries [49]. The authors concluded that the contrast material appeared to be safe, but that it is not routinely required and did not significantly improve the accuracy of standard duplex imaging. However, the use of contrast material may be helpful when visualization is difficult with standard techniques due to patient obesity or excessive abdominal gas.

## Population Screening

Although duplex ultrasonography has gained acceptance as a first line screening test for patients with suspected chronic intestinal ischemia [50], the incidence of mesenteric arterial stenosis in the general population has not been well studied. Hansen and colleagues studied over 550 elderly volunteers in an effort to estimate the population-based prevalence of mesenteric artery stenosis in elderly Americans [51]. Using criteria of celiac PSV > 200 cm/s and SMA PSV > 270 cm/s, or occlusion of either vessel, the authors determined 17.5% of the individuals studied had either a significant celiac or SMA stenosis or occlusion. The majority (10.5%) has isolated celiac stenosis. 1.3% had combined SMA and celiac stenosis. However, 0.9% had isolated SMA stenosis, whereas 0.4% had celiac occlusion. When all patients with mesenteric arterial stenosis were considered, there was no association with symptoms of weight loss. The authors did note, however, that the combination of celiac occlusion and SMA stenosis was significantly associated with weight loss and concurrent renal artery disease.

### Conclusion

Mesenteric duplex scanning can become a routine noninvasive diagnostic testing modality for the evaluation of patients with suspected visceral ischemia since earlier diagnosis and treatment will significantly reduce the risk of catastrophic gut infarction in these patients. Like all deep abdominal duplex scanning, mesenteric scanning is more technologically demanding than scanning vessels of the neck or extremities. However, continued refinement of the duplex instrumentation makes these examinations exciting areas of clinical advancement since there have previously been no other reliable noninvasive techniques for assessment of major intra-abdominal vessels. Like other duplex scan applications, mesenteric duplex scanning can be used to ensure the technical efficacy of mesenteric revascularization procedures, whether surgical or endovascular. Mesenteric duplex scanning can then provide a means of late follow-up assessment of these procedures to document their durability, or prevent late procedural failure.

## References

1. Flinn WR, Sandager GP, Lilly MP, et al. Duplex scan of mesenteric and celiac arteries. In: Bergan JJ, Yao JST, editors. Arterial surgery: new diagnostic and operative techniques. Orlando: Grune and Stratton; 1988. p. 367.
2. Blackburn DR. Color duplex imaging of the mesenteric and renal arteries. J Vasc Technol. 1991;15:139.
3. Sandager GP, Zimmer S, Silva MB, Flinn WR. Ultrasonographic characteristics of transvenous vena caval interruption devices. J Vasc Technol. 1992;16:17–21.
4. Ackroyd N, Gill R, Griffiths K, et al. Duplex scanning of the portal vein and portasystemic shunts. Surgery. 1986;90:591.
5. Ralls PW. Color Doppler sonography of the hepatic artery and portal venous system. AJR Am J Roentgenol. 1990;155:517.
6. Grant EG, Tessler FN, Gomes AS, et al. Color Doppler imaging of portosystemic shunts. AJR Am J Roentgenol. 1990;154:393.
7. Rizzo RJ, Sandager G, Astleford P, et al. Mesenteric flow velocity variations as a function of angle of insonation. J Vasc Surg. 1990;11:688.
8. Healy DA, Neumeyer MM, Atnip RG, Thiele BL. Evaluation of mesenteric vascular disease with duplex ultrasound. Circulation. 1990;82(Suppl III):III-460.
9. Moneta GL, Yeager RA, Dalman R, et al. Duplex ultrasound criteria for diagnosis of splanchnic artery stenosis or occlusion. J Vasc Surg. 1991;14:511–20.
10. Moriyasu F, Ban N, Nishida O, et al. Clinical application of an ultrasonic duplex system in the quantitative measurement of portal blood flow. J Clin Ultrasound. 1986;14:579.
11. Sato S, Ohnishi K, Sugita S, Okuda K. Splenic artery and superior mesenteric artery blood flow: nonsurgical Doppler US measurement

in healthy subjects and patients with chronic liver disease. Radiology. 1987;164:347.
12. Qamar MI, Read AE, Skidmore R, et al. Transcutaneous Doppler ultrasound measurement of coeliac axis blood flow in man. Br J Surg. 1985;72:391.
13. Qamar MI, Read AE, Mountford R. Increased superior mesenteric artery blood flow after glucose but not lactulose ingestion. Q J Med. 1986;233:893.
14. Jäger K, Bollinger A, Vallie C, Ammann R. Measurement of mesenteric blood flow by duplex scanning. J Vasc Surg. 1986;3:462.
15. Moneta GL, Taylor DC, Helton WS, et al. Duplex ultrasound measurement of postprandial intestinal blood flow: effect of meal composition. Gastroenterology. 1988;95:1294.
16. Gill RW. Measurement of blood flow by ultrasound: accuracy and sources of error. Ultrasound Med Biol. 1985;11:625.
17. Hoskins PR. Measurement of arterial blood flow by Doppler ultrasound. Clin Phys Physiol Meas. 1990;11:1.
18. Taylor GA. Blood flow in the superior mesenteric artery: estimation with Doppler US. Radiology. 1990;174:15.
19. Lilly MP, Harward TRS, Flinn WR, et al. Duplex ultrasound measurement of changes in mesenteric flow velocity with pharmacologic and physiologic alteration of intestinal blood flow in man. J Vasc Surg. 1989;9:18.
20. Flinn WR, Rizzo RJ, Park JS, Sandager GP. Duplex scanning for assessment of mesenteric ischemia. Surg Clin North Am. 1990; 70:99.
21. Nishida O, Moriyasu F, Nakamura T, et al. Relationship between splenic and superior mesenteric venous circulation. Gastroenterology. 1990;98:721.
22. Gooding GAW. Ultrasound of a superior mesenteric artery aneurysm secondary to pancreatitis: a plea for real-time ultrasound of sonolucent masses in pancreatitis. J Clin Ultrasound. 1981;9:255.
23. Bret PM, Bretagnolle M, Enoch G, et al. Ultrasonic features of aneurysms of splanchnic arteries. J Can Assoc Radiol. 1985; 36:226.
24. Mourad K, Guggiana P, Minasian H. Superior mesenteric artery aneurysm diagnosed by ultrasound. Br J Radiol. 1987;60:287.
25. Paolella L, Scola FH, Cronan JJ. Hepatic artery aneurysm: an ultrasound diagnosis. J Clin Ultrasound. 1985;13:360.
26. Stokland E, Wihed A, Ceder S, et al. Ultrasonic diagnosis of an aneurysm of the common hepatic artery. J Clin Ultrasound. 1985;13:369.
27. Bolondi L, Casanova P, Arienti V, et al. A case of aneurysm of the splenic artery visualized by dynamic ultrasonography. Br J Radiol. 1981;54:1109.
28. Derchi LE, Biggi E, Cicio GR. Aneurysms of the splenic artery: noninvasive diagnosis by pulsed Doppler sonography. J Ultrasound Med. 1984;3:41.
29. Green D, Carroll BA. Aneurysm of the gastroduodenal artery causing biliary obstruction: real-time ultrasound diagnosis. J Ultrasound Med. 1984;3:375.
30. Verma BS, Bose AK, Bhatia HC, Katoch R. Superior mesenteric artery branch aneurysm diagnosed by ultrasound. Br J Radiol. 1991;64:169.
31. Grech P, Rowlands P, Crofton M. Aneurysm of the inferior pancreaticoduodenal artery diagnosed by real-time ultrasound and pulsed Doppler. Br J Radiol. 1989;62:753.
32. Jäger KA, Fortner GS, Thiele BL, Strandness DE. Noninvasive diagnosis of intestinal angina. J Clin Ultrasound. 1984;12:588–91.
33. Nicholls SC, Kohler TR, Martin RL, Strandness Jr ED. Use of hemodynamic parameters in the diagnosis of mesenteric insufficiency. J Vasc Surg. 1986;3:507.
34. Hartnell GG, Gibson RN. Doppler ultrasound in the diagnosis of intestinal ischemia. Gastrointest Radiol. 1987;12:285.
35. Moneta GL, Cummings C, Caston J, Porter JM. Duplex ultrasound demonstration of postprandial mesenteric hyperemia in splanchnic circulation collateral vessels. J Vasc Technol. 1991;15:37.
36. Moneta GL, Lee RW, Yeager RA, et al. Mesenteric duplex scanning: a blinded prospective study. J Vasc Surg. 1993;17:79–86.
37. Bowersox JC, Zwolak RM, Walsh DB, et al. Duplex ultrasonography in the diagnosis of celiac and mesenteric artery occlusive disease. J Vasc Surg. 1991;14:780–8.
38. Healy DA, Neumyer MM, Atnip RG, Thiele BL. Evaluation of celiac and mesenteric vascular disease with duplex ultrasonography. J Ultrasound Med. 1992;11:481–5.
39. Oderich GS, Panneton JM, Macedo TA, et al. Intraoperative duplex ultrasound of visceral revascularizations: optimizing technical success and outcome. J Vasc Surg. 2003;38:684–91.
40. Sandager G, Flinn WR, McCarthy WJ, et al. Assessment of visceral arterial reconstruction using duplex scan. J Vasc Technol. 1987; 11:13.
41. McMillan WD, McCarthy WJ, Bresticker MR, et al. Mesenteric artery bypass: objective patency determination. J Vasc Surg. 1995;21:729–41.
42. Liem TK, Segall JA, Wei W, et al. Duplex scan characteristics of bypass grafts to mesenteric arteries. J Vasc Surg. 2007;45:922–8.
43. Steinmetz E, Tatou E, Favier-Blavoux C, et al. Endovascular treatment as first choice in chronic intestinal ischemia. Ann Vasc Surg. 2002;16:693–9.
44. AbuRahma AF, Stone PA, Bates MC, et al. Angioplasty/stenting of the superior mesenteric artery and celiac trunk: early and late outcomes. J Endovasc Ther. 2003;10:1046–53.
45. Sharafuddin MJ, Olson CH, Sun S, et al. Endovascular treatment of celiac and mesenteric arteries stenosis: applications and results. J Vasc Surg. 2003;38:692–8.
46. Mitchell EL, Chang EY, Landry GJ, et al. Duplex criteria for native superior mesenteric artery stenosis overestimates stenosis in stented superior mesenteric arteries. J Vasc Surg. 2009;50:335–40.
47. Fenwich JL, Wright IA, Buckenham TM, et al. Endovascular repair of chronic mesenteric occlusive disease: the role of duplex surveillance. ANZ J Surg. 2007;77:60–3.
48. Takahashi H, Takezawa J, Okada T, et al. Portal blood flow measured by duplex scanning during mesenteric infarction. Crit Care Med. 1986;14:253.
49. Blebea J, Volteas N, Neumyer M, et al. Contrast enhanced duplex ultrasound imaging of the mesenteric arteries. Ann Vasc Surg. 2002;16:77–83.
50. Moneta GL. Screening for mesenteric vascular insufficiency and follow-up of mesenteric artery bypass procedures. Semin Vasc Surg. 2001;14:186–92.
51. Hansen KJ, Wilson DB, Craven TE. Mesenteric disease in the elderly. J Vasc Surg. 2004;40:45–52.

# The Role of Color Duplex Ultrasound in Patients with Abdominal Aortic Aneurysms and Peripheral Aneurysms

50

Shaun M. Stickley and George H. Meier III

**Abstract**

Ultrasound diagnosis has been used for abdominal aortic aneurysms (AAAs) and peripheral aneurysms for many years; yet, the nuances required for proper interrogation and interpretation can be quite difficult. While CT and ultrasound have been used interchangeably, it has become clear that the measurements derived are not necessarily equivalent. Newer ultrasound technology allows CT and ultrasound images to be fused for correlation of differences between these modalities. This fusion technology may allow differences between the imaging techniques to be resolved during the real-time ultrasound evaluation.

Major trials such as the UK Small Aneurysm Trial utilized ultrasound as the primary modality for imaging AAAs that did not yet require intervention. Once an aneurysm reaches the size appropriate for intervention, then CT scans provide an objective data set that can be used in a number of ways for procedural planning. The complementary use of CT and ultrasound for the management of AAAs is critical to the proper management of these patients. By using ultrasound, radiation and intravenous contrast can be avoided until intervention planning becomes necessary.

In the periphery, ultrasound has always had a pre-eminent role in the diagnosis and management of extremity aneurysms in particular. Both femoral and popliteal aneurysms can be followed and management planned based on ultrasound alone. While ultrasound in the abdomen may be limited by bowel gas and patient body habitus, in the periphery these issues are rarely a concern. Overall, ultrasound and CT imaging are complementary modalities that allow both deep imaging and noninvasive surveillance depending on the clinical scenario.

**Keywords**

Ultrasound diagnosis of aneurysms • Abdominal aortic aneurysm • Popliteal aneurysms • CT scans for AAA diagnosis • Femoral aneurysms • CT versus ultrasound for AAA diagnosis

## Introduction

The diagnosis and management of abdominal and peripheral aneurysms is a challenging area for vascular surgery, with continuous advances in the areas of aneurysm screening, treatment, and long-term follow up. The role of ultrasound in aneurysm management is changing as treatment strategies advance for vascular disease [1]. During the early years of abdominal aortic aneurysm (AAA) management, ultrasound became a tool for both screening and long-term surveillance of AAA progression prior to treatment. With the traditional open AAA treatment by aortic graft replacement, long-term post-treatment surveillance was generally not necessary. Nonetheless, in 1991 a major advancement in AAA treatment occurred with the introduction of endovascular aortic replacement (EVAR) using covered stent grafts [2]. This new

S.M. Stickley, M.D. • G.H. Meier III, M.D., RVT, FACS (✉)
Department of Surgery, Division of Vascular Surgery,
University Hospital, Medical Science Building,
231 Albert Sabin Way ML0558, Cincinnati, OH 45267, USA
e-mail: george.meier@uc.edu

A.F. AbuRahma, D.F. Bandyk (eds.), *Noninvasive Vascular Diagnosis*,
DOI 10.1007/978-1-4471-4005-4_50, 

less invasive option brought with it the new problem of "endoleak" and the possibility that the stent graft might fail to control AAA expansion, exposing the patient to a continued risk of rupture [3–5]. Additional new issues such as stent graft migration within the aneurysm sac and complications associated with femoral vessel access also challenged the success of EVAR [6]. Ultrasound surveillance for AAA was further supported by the publication of the UK Small Aneurysm Trial in 1999. This landmark trial was the first to use ultrasound as the standard surveillance method for detecting AAAs appropriate for intervention [7]. For these reasons, routine surveillance after EVAR became the standard for stent graft treated patients.

Unfortunately, ultrasound has traditionally been viewed as a subjective technology, with significant variability in technical expertise among technologists and centers. Many centers have yet to adopt routine protocols that use ultrasound for AAA surveillance. Recent studies have attempted to address concerns of ultrasound use in aneurysm management, but significant controversy still exists in the use of this technology [1, 8–12]. As of yet, no clear ultrasound surveillance protocol has be defined among centers that treat aortic disease.

## Imaging for AAA

### History of AAA Imaging

The natural history of AAA has been well known for years, with progressive aneurysm expansion leading to eventual rupture over time. The timely diagnosis and appropriate treatment of aortic aneurysms can have a significant impact on overall patient life expectance. Based on epidemiology data from the 1990s, it has been estimated that aortic aneurysms account for about 17,000 deaths/year, with just over half of the related deaths caused by AAAs [13]. Until the first successful AAA repair by Dubost in 1951, the ability to correctly diagnose an AAA was not a significant benefit to the patient [14]. Szilagyi published the first series on the natural history of aortic aneurysms in 1947. Using the plain film X-ray technology available at that time, he concluded that aneurysms 6 cm in AP diameter had a 50% risk of rupture [15]. During that same time period, Estes further demonstrated that AAAs greater than 5 cm in diameter had a 20% risk of rupture at 5 years [16]. Once an aneurysm reached the 5 cm threshold, the risk of surgical aneurysm repair was viewed as less than that for continued observation.

The use of physical exam in the diagnosis of AAA is both of historical interest and practical use in modern AAA diagnosis. The classic presentation of a hypotensive patient with a large pulsatile abdominal mass is still today a vital initial screening tool for the diagnosis of a ruptured AAA presenting for care. The accuracy of physical exam to detect AAAs is highly dependent on aneurysm size, but is also significantly influenced by the body habitus of the patient and the depth of the aorta within the abdominal cavity [17]. Physical exam may be up to 82% accurate in the diagnosis of AAA larger than 5.0 cm, but in modern practice the use of advanced imagining techniques, usually the CT scan, has become the standard [18].

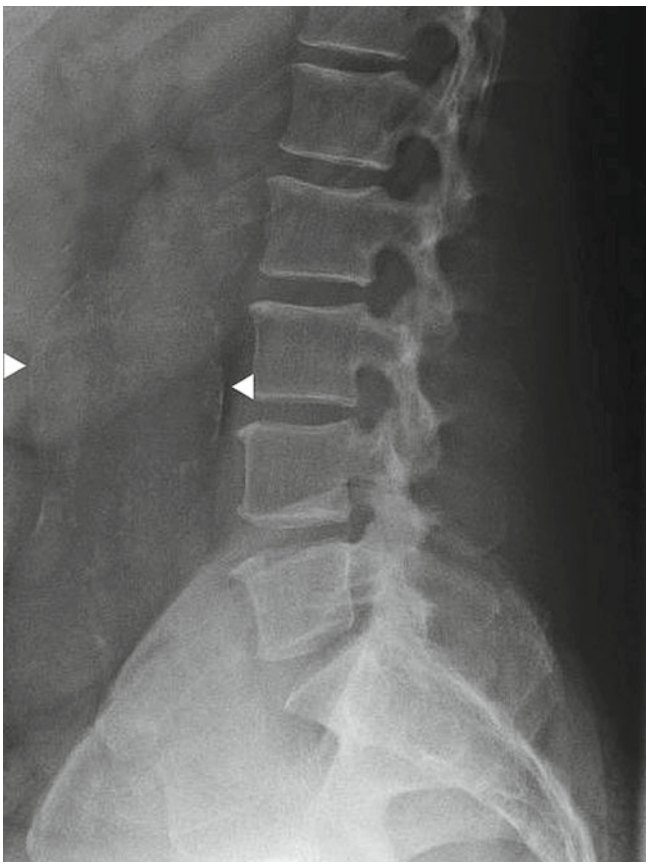

**Fig. 50.1** Lateral lumbosacral X-ray film, demonstrating calcifications (*arrowheads*) indicative of AAA

The first imaging modality routinely used for AAA diagnosis and long-term surveillance was the abdominal X-ray. X-ray diagnosis relied on calcification of the aneurysm wall for visualization of the sac, with a lateral lumbosacral X-ray film used to measure aortic diameter (Fig. 50.1). These early attempts to define AAA size were complicated by the magnification seen on lateral X-ray imaging. Early research into the relationship of AAA size and the risk of rupture showed that AAAs larger than 5 cm on plain films had a 20% risk of rupture at 5 years [16]. Until the UK Small Aneurysm Trial was published in 1999, surgical intervention was traditionally reserved for asymptomatic aneurysms over 5 cm in diameter [7]. This landmark study set a new benchmark diameter of 5.5 cm by ultrasound for the treatment of asymptomatic AAAs, which remains the standard today. As newer, more accurate methods of diagnosing and following AAAs were developed, plain film X-rays became less common for

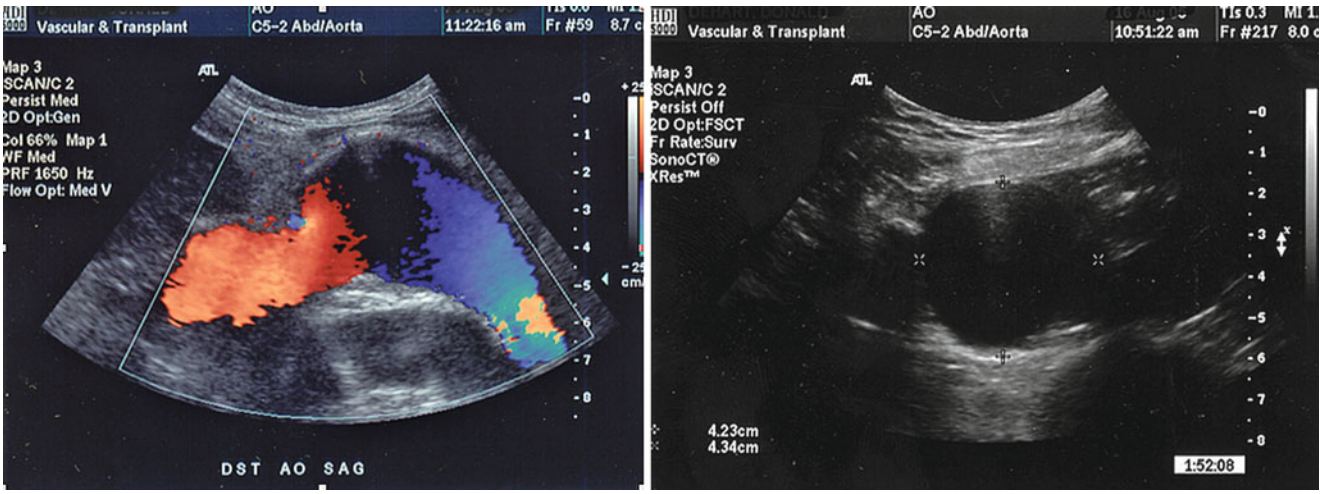


**Fig. 50.2** US of native aorta, sagittal and transverse

AAA assessment. Nonetheless, with the development of endovascular aortic stent grafts, X-rays once again play an important role in evaluating endograft migration or stent fracture, by defining the position of the metal components of the stent graft relative to fixed bony landmarks [19, 20].

## Ultrasound for AAA Imaging

With the development of effective treatment options for AAA, accurate diagnostic methods became more important. The first reported ultrasound visualization of the abdominal aorta in the 1960s introduced ultrasound as a potential method of AAA detection [21]. Continued advancement in ultrasound technology during that time period, with the introduction of B-mode imaging, allowed for two-dimensional (2D) visualization of the aorta and assessment of aortic cross sectional diameter. A comparison between AAA diameter measurements made by lateral plain X-ray, B-mode ultrasound, and intraoperative direct aortic measurement demonstrated ultrasound to be a more accurate method of AAA size determination [22]. At about the same time, lateral plain film X-ray was shown to overestimate AAA size by 1 cm on average, while B-mode ultrasound was within 0.5 cm of true aortic diameter in 75% of the patients [23]. These early findings led to ultrasound being the dominant test for AAA screening and long-term pre-intervention surveillance (Fig. 50.2). Ultimately, this led to the use of ultrasound as the standard for the UK Small Aneurysm Trial.

## CT Scanning for AAA Imaging

The use of computed tomography for axial cross sectional imaging of the body was a significant advancement in diagnostic imaging in many clinical areas including AAA. Initially, CT scanning was used for the diagnosis of intracranial pathology, but quickly advanced as a method to image other areas of the body [24]. Today advanced cardiac gated CT scanning produces remarkable high-quality images (Fig. 50.3), but there are increasing concerns related to overall radiation exposure to the patient [25].

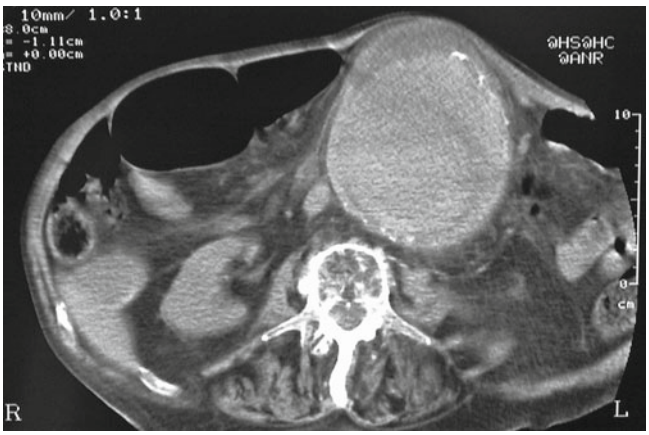


**Fig. 50.3** Large abdominal aortic aneurysm by CT. In this case, palpation easily confirms diagnosis and size. CT scan was performed for evaluation for rupture

In addition to radiation exposure, CT scanning for aortic evaluation requires the use of intravenous contrast [26]. While noncontrast CT can be used to assess aortic size or potential AAA rupture, more complex issues such as visceral vessel placement and aortic suitability for EVAR may require the use of intravenous contrast [27]. In an increasingly older patient population with many comorbid medical issues, patients with chronic renal insufficiency are frequently being evaluated for aortic intervention. As a result, repeated contrast CT scanning as a surveillance method for their AAA

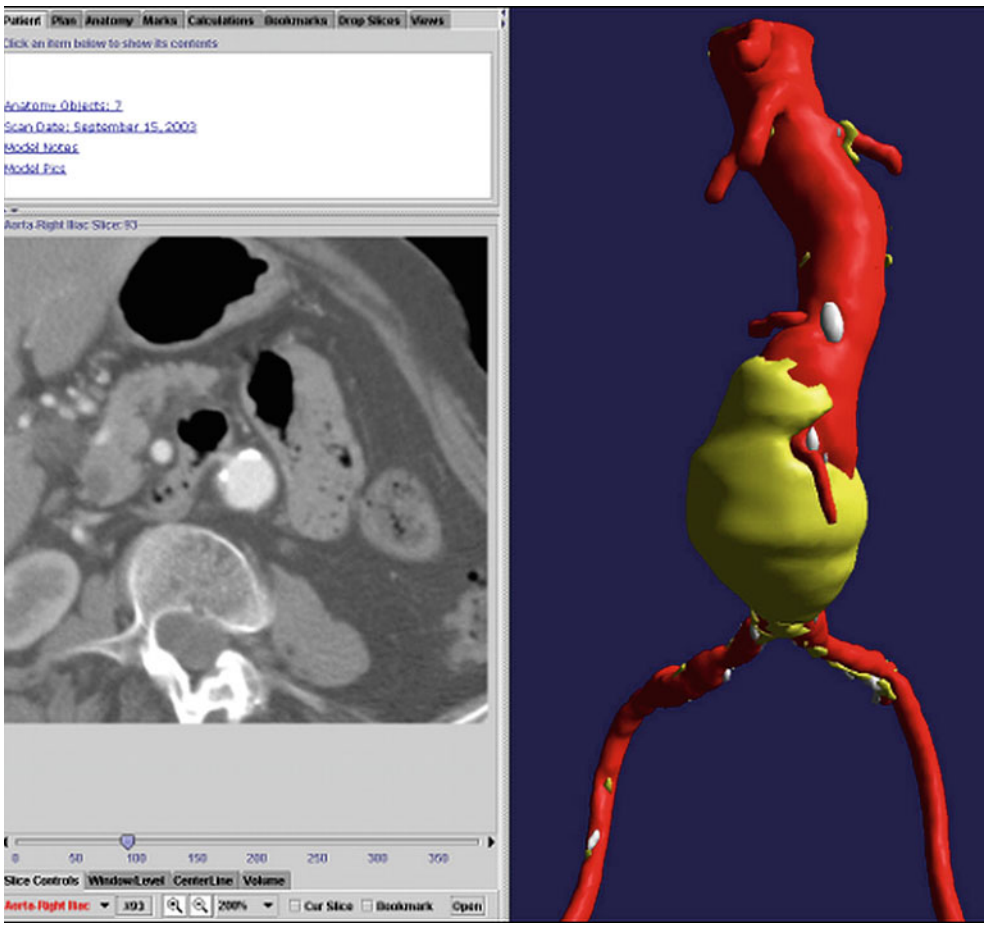


**Fig. 50.4** 3D reconstruction of CT data

pretreatment or following EVAR may expose the patient to prohibitive renal toxicity.

As CT technology continued to improve, the data generated became a continuous data set with the advent of "spiral" CT. This continuous data set allowed for images to be reformatted in any plane and allowed 3D reconstructions. These 3D images allow for a more accurate assessment of aortic diameter, neck angulation, location of renal and visceral vessels, and tortuosity of iliac vessels [28]. The ability to manipulate the 3D images to correct for aortic angulation allows the true aortic diameter perpendicular to the aortic center line to be determined. This measurement has become critical to assessing the aortic neck, particularly with severe degrees of neck angulation (Fig. 50.4). Currently, 3D reconstruction programs such as M2S (New Lebanon, NH) or TeraRecon (Foster City, CA) allow for more accurate EVAR planning. Furthermore, virtual aortic endograft placement can be performed on these CT reconstructions allowing assessment preoperatively for potential endograft options and issues of iliac artery access.

With the current resolution of aortic CT angiography, many centers have eliminated catheter-based angiography prior to aortic surgery. Several studies have confirmed that a high-quality CT scan is all that is needed for endograft sizing prior to EVAR [9, 27]. Patients with favorable anatomy and a suitable aneurysm for EVAR may not require advanced image reconstruction. In patients with complex aneurysm issues, 3D imaging has become a valuable tool for operative planning (Fig. 50.4). These high-resolution images now allow AAAs originally felt to be a poor candidate for EVAR to benefit from endovascular repair.

## Ultrasound Versus CT Scanning for AAA

In the United States, asymptomatic AAAs are frequently first diagnosed from a CT scan obtained in evaluation of unrelated issues [29]. In addition, CT scanning is the primary operative planning method used for endograft sizing and determination of suitable aortic anatomy using endovascular aortic reconstruction. Due to this common association of AAA diagnosis and EVAR evaluation, patients are frequently evaluated by serial CT scanning until the 5.5 cm threshold is reached, justifying repair. In the UK Small Aneurysm Trial, ultrasound was used as the standard imaging modality to determine AAA diameter. In 2009, the OVER trial looked at the US VA population and randomized patients to open versus endovascular aortic repair once the AAA reached 5.0 cm in diameter. This study protocol allowed for the use of aortic measures from ultrasound, CT scans or MRI [30]. All modalities were viewed as equivalent for entry into this trial.

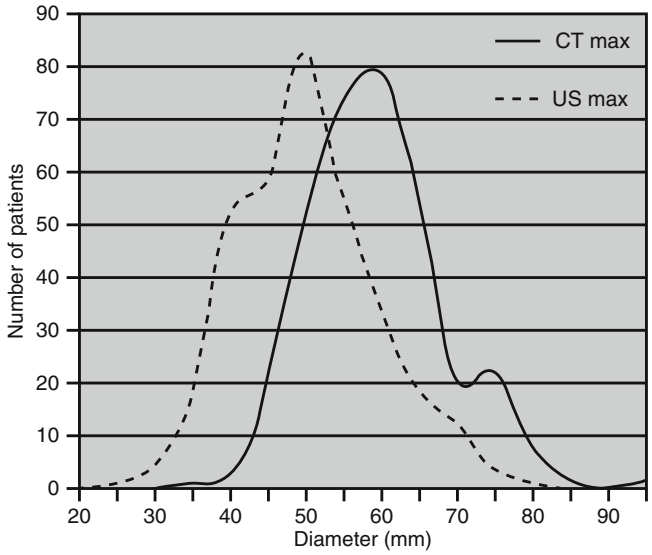


**Fig. 50.5** CT diameter (*black line*) versus ultrasound diameter (*dotted line*) in the same patients (Adapted from Sprouse et al. [31]. With permission from Elsevier)

In the United States, CT has been considered by some to be the "gold standard" in aortic diameter measurement. Recent studies have suggested that CT tends to significantly overestimate true aortic size, especially in severely angulated aortas. In 2001, a direct comparison of core lab ultrasound and CT data from the original Ancure endograft trial was performed [31]. In that study, 334 paired scans were evaluated and 95% of CT scan measurements were larger than the paired ultrasound images (Fig. 50.5). The average difference was 9.5 mm ($P<0.01$). From this original study, it was unclear why there was such a significant difference between imaging modalities. Subsequently, further study evaluated 3D CT reconstruction (M2S, Lebanon, NH) to measure maximal aortic diameter perpendicular to center line flow, and compared this diameter to matched ultrasound maximal diameter measurements. When CT diameter was corrected for a diameter perpendicular to center line flow, the difference between ultrasound and CT decreased to 0.9 mm, which was not statistically significant. Further subgroup analysis showed that an aortic angulation of less than 25° resulted in good correlation between ultrasound and axial CT scan, but once the angulation was greater than 25° CT significantly overestimated aortic diameter (Fig. 50.6) [9]. Ultrasound

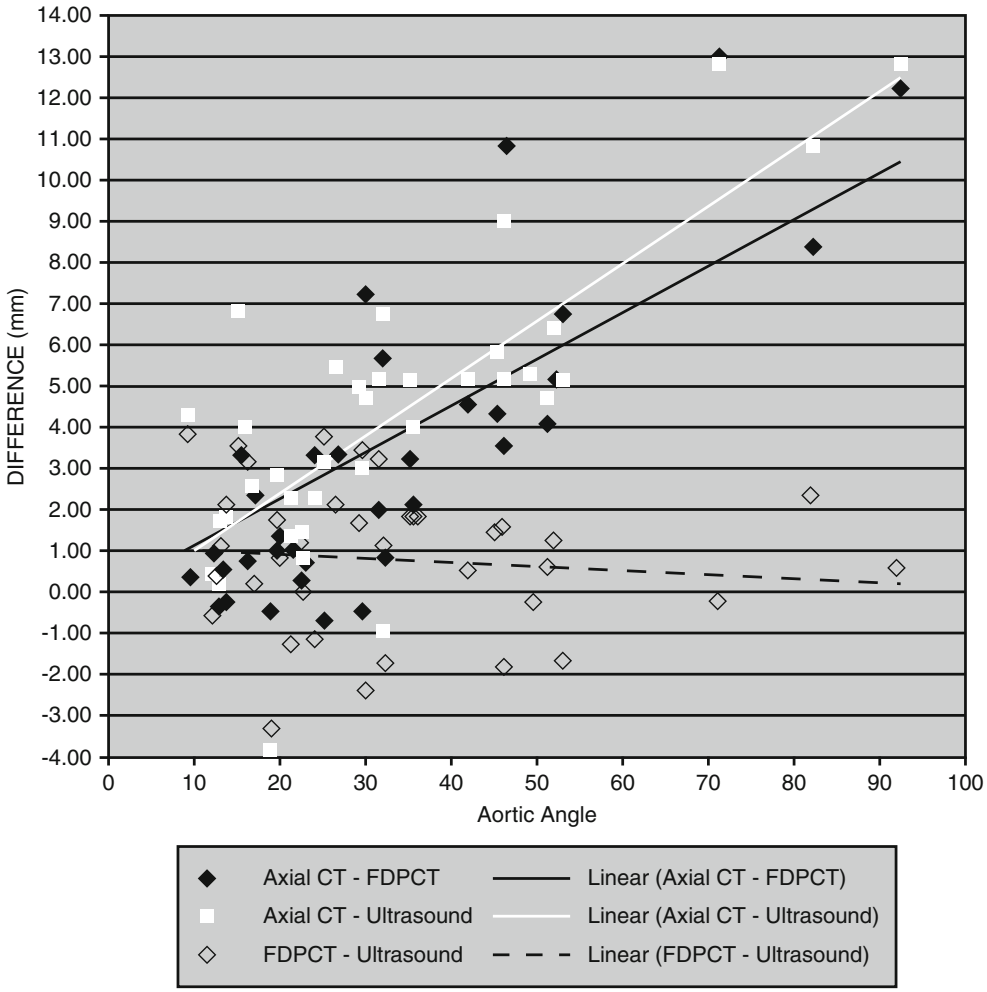


**Fig. 50.6** The effect of aortic angulation on differences between axial CT, flow directed perpendicular (*FDP*) CT, and ultrasound (Adapted from Sprouse et al. [9]. With permission from Elsevier)

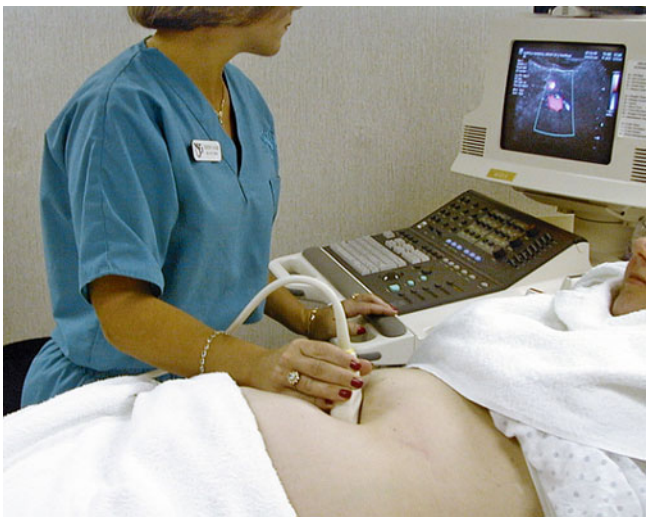

**Fig. 50.7** Positioning for ultrasound scanning of abdominal aorta or aortic endograft

aortic diameter measurement is more likely to measure the true aortic diameter since technologists are routinely taught to adjust the imaging plane in real time to produce an image perpendicular to the aortic center line axis, resulting in a round cross section rather than an oval (Fig. 50.7). As a result, in patients with extremely angulated aortas, CT may significantly overestimate the true aortic diameter.

Ultrasound is not without potential drawbacks. Ultrasound is frequently criticized for being an operator dependent imaging modality, while CT scanning is commonly perceived as more objective. Vascular laboratories undertaking aortic studies should be equipped with the most up to date instrumentation and standardized scanning protocols should be used to produce the highest quality aortic examination. The important issues of patient preparation and scanning technique will be discussed further below.

## Aortic Ultrasound Technique

### Indications for Aortic Ultrasound

Since the introduction of ultrasound, the application of advanced ultrasound imaging has proven to be a powerful tool for AAA screening and post-intervention surveillance of aortic stent grafts. The results of the UK Small Aneurysm Trial and other studies have advanced ultrasound as the primary screening, diagnostic, and surveillance method used in most institutions that have modern vascular laboratories.

The ultrasound evaluation of patients with known AAA disease is more than simply a diagnostic study. Careful ultrasound examination can be used in surgical planning and assessment of patients with appropriate anatomy for endograft treatment [32]. Pre-operative ultrasound examinations can evaluate the location of renal arteries in relation to the aneurysm neck, the tortuosity and luminal diameter of access iliac vessels, and amount of aneurysm thrombus and diameter of the residual aortic lumen.

**Table 50.1** Indications for aortoiliac ultrasound

| |
|---|
| Aortic aneurysm disease screening |
| Lifestyle limiting hip or buttock claudication |
| Absent or decreased femoral pulses |
| Ischemic lower extremity digits |
| Post-intervention aortoiliac evaluation |
| Abdominal bruit |
| Evaluation of abdominal aortic dissection |

The new capabilities of ultrasound machines to combine imaging data from other scanning modalities such as MRI or CT, with live ultrasound images, is termed image "fusion" technology. In image fusion, a known structure such as the portal vein bifurcation is registered on the 3D data set to be fused and coregistered with the live ultrasound image. As the ultrasound provides live images, the fused comparison image is viewed simultaneously. The images can be overlaid or viewed side by side in real time. Color flow from the ultrasound can be overlaid onto the CT or MR image. In the future, ultrasound data can be fused from prior ultrasound examinations to allow precise measurement of diameters or assessment for migration. Unfortunately, there is currently no standard for 3D ultrasound data in DICOM, limiting the use of this modality between different manufacturers.

Additionally, the same technology allows a "GPS" function for precise localization of anatomic structures during an ultrasound examination. If the ultrasound probe needs to be moved to a different plane, a marker can be placed in the region of interest and relocated from the alternative approach. As long as the patient does not change positions, the data will remain coregistered and the ultrasonographer can return to the same location repetitively.

The current indications for aortoiliac ultrasound, including aortic aneurysm disease screening, are listed in Table 50.1. In addition, ultrasound can be used in the evaluation of the abdominal component resulting from aortic dissection. The benefit of ultrasound in aortic dissection is in assessing the visceral and renal arteries, as well as the addition of physiologic data and flow characteristics to the gray scale imaging of the dissection.

Ultrasound is limited by many technical factors. Ultrasound is highly dependent on the skill of the technologist performing the study and the real time assessment of imaging and physiologic data by the person performing the examination. The final interpretation of the study by a physician is heavily influenced by the quality and accuracy of the information provided to the physician by the technologist. Abdominal vascular studies can be very demanding in time

**Table 50.2** Technical limitations for a successful aortoiliac ultrasound study

| |
|---|
| Technologist technical skill level and interpretation |
| Obesity |
| Recent abdominal surgery |
| Excessive bowel gas |
| Poor patient compliance during study |

and technique. Obese patients, recent abdominal surgery, excessive bowel gas, and poor patient compliance are all limiting factors to aortic ultrasound studies (Table 50.2).

## Equipment

As ultrasound technology continues to advance, the importance of using high quality, modern equipment is vital to vascular laboratories that evaluate aortic pathology. To perform an adequate assessment of the aorta, a high resolution ultrasound instrument should be capable of enhanced B-mode imaging, pulsed Doppler, color flow imaging, and harmonic imaging. Commonly, the 2–5 MHz low frequency pulse Doppler transducer is used, but it may be necessary to use a combination of many different transducers to produce the best study possible. A curved array, phased array, or mechanical sector transducer may all be needed throughout the study. As newer instruments become available and enhanced imaging modalities are developed they should be used as necessary to assist in these studies The development of imagine fusion technology and precise GPS localization of anatomic structures from one ultrasound scan to the next will only enhance the ability of ultrasound as a method of endograft surveillance. As of yet, neither image fusion nor GPS navigation from prior ultrasound scans has been evaluated in a clinical study.

## Patient Preparation

The importance of patient preparation for scanning cannot be overstated. Patients should fast overnight in an effort to reduce the amount of bowel gas present at the time of imaging. Some centers have gone even further and recommend that patients avoid foods that are known to increase bowel gas for several days prior to the scheduled study. Patients should also avoid smoking or chewing gum the day of the ultrasound study. Patients are usually permitted to take all their regular medications with a sip of water the morning of the examination.

At the start of the study, patients should be informed that at times it may be necessary to apply a considerable amount of pressure to the transducer to obtain the appropriate image. At any time the patient should be encouraged to report to the technologist any discomfort so corrective measures can be taken. The patient may have to move several times during the study, from supine to either right or left lateral decubitus, or potentially to almost prone. Due to body habitus or comorbid medical conditions, some patients may not tolerate the different positions needed, emphasizing the importance of good communication between the technologist and patient throughout the study.

## Study Protocol

The ultrasound evaluation of the aorta requires a systematic approach. Prior to performing the study, it is important to have a thorough understanding of any prior aortic studies.

## B-mode Imaging

Once familiar with the aneurysm the technologist begins the study with a B-mode examination of the entire abdominal aorta. Start the examination with an anterior approach imaging in B-mode. The aorta is evaluated in both transverse and longitudinal planes from the celiac artery to past the iliac arteries. B-mode imaging allows for an assessment of both aortic diameter and the basic configuration of the aorta. The aortic diameter should be recorded superiorly, at the infrarenal neck of the aneurysm, and at the bifurcation. It is important to evaluate the maximal residual aortic diameter in a plane perpendicular to the long axis of the aorta, and record the diameters of the common, internal, and external iliac arteries.

## Pulsed Doppler

After completing the B-mode assessment, Doppler should be used throughout the entire native aorta to evaluate for areas of increased velocity representing stenosis. Doppler is also a good method to evaluate the renal arteries, the external iliac arteries, and femoral vessels for areas of stenosis. Doppler can be used to evaluate for renal stenosis as indicated by an increase in flow velocity.

## Color Doppler

Color Doppler is used within the aneurysm sac to evaluate for branches and thrombus. The entire aneurysm sac is systematically scanned in an effort to identify the location and type of any branches. These may be important during and after aortic aneurysm treatment as they may remain a source

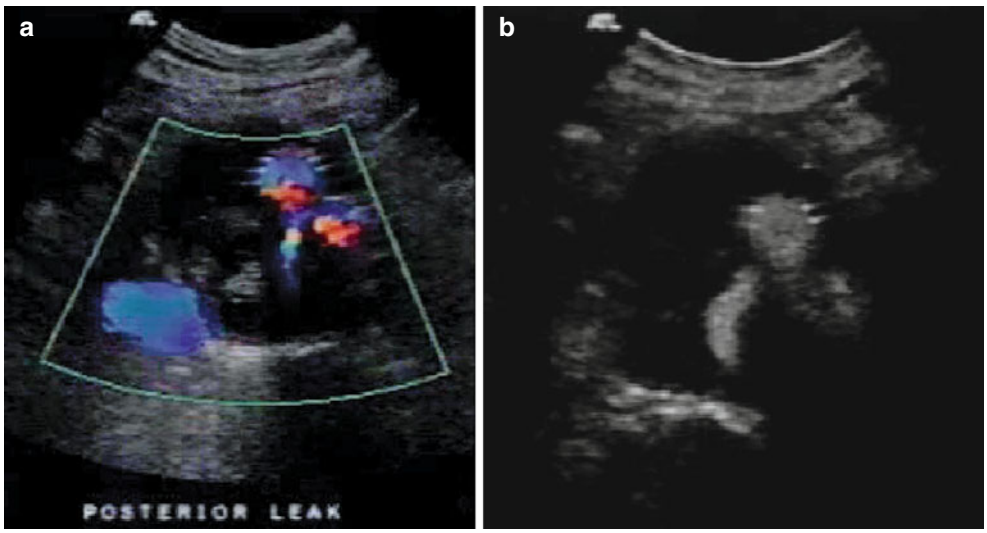


**Fig. 50.8** Color flow duplex showing endoleak (**a**) and corresponding endoleak demonstrated with intravenous ultrasound contrast (**b**)

of flow into the aneurysm sac after endovascular repair. The amount of laminar thrombus, particularly when it extends close to the renal arteries, should be noted as well. Care should be taken to lower the wall filters on the ultrasound machine so that an accurate assessment of the interface between the wall and the blood flow can be undertaken.

## Aneurysm Sac Size

Ultrasound is an accurate method for following aortic diameter. Current literature suggests a high correlation between ultrasound and CT scanning for maximum aortic diameter [1, 8, 10, 33, 34]. Most studies now show less than a 5 mm difference in measured aortic sac diameter between CT and ultrasound [35]. As has been showed in AAA screening, CT scanning tends to overestimate AAA size relative to ultrasound [9]. The key to successful endograft surveillance is in the trend in aortic diameter, followed by the same imaging modality over time.

One potential downfall of ultrasound is the ability to measure asymmetric aneurysms as the same location at each scan. CT scan has the ability to measure aortic diameter at a given distance from a fixed branch vessel. New 3D ultrasound methods may help with this issue, but have yet to be fully evaluated. The use of the GPS navigation function may provide a method of precise localization of the same point along the aneurysm between two ultrasound scans.

## Ultrasound Contrast

Recent advancement in ultrasound technology has further increased the potential role of ultrasound in AAA treatment. Ultrasound contrast has been used to enhance blood flow imaging for the past 30 years in many clinical areas. While the use of ultrasound contrast has been most common for cardiac imaging, any clinical setting where blood flow is important becomes a potential use for ultrasound contrast imaging. Obviously, aortic and branch vessel ultrasound, a technically demanding area of ultrasound, is an important area where blood flow imaging is critical. While contrast enhanced ultrasound (CEUS) can be used to better define the visualization of small blood vessels with slow flow, the greatest benefit to using ultrasound contrast enhanced imaging is in the post-endovascular treatment patient. With the introduction of CEUS in post-EVAR scanning, the potential for detection of endoleaks appears to have increased significantly (Fig. 50.8) [36, 37]. In addition, high-quality ultrasound has been evaluated as a potential option of intraoperative visualization for endograft placement [38].

The use of CEUS has been investigated as a possible solution to the reported low sensitivity of duplex ultrasound for endoleak detection [36, 37, 39–42]. The principles of CEUS are based in the use of harmonic imaging with microspheres that resonate at that harmonic frequency. The microsphere resonance improves blood flow detection and therefore the potential to detect slow or limited blood flow.

## Imaging for Peripheral Aneurysms

While imaging for AAAs is focused on overall aneurysm size as a predictor of the risk of rupture, peripheral aneurysm imaging must measure aneurysm size as a predictor of overall complications from the aneurysm, including rupture, thrombosis, and embolization. While rupture can rarely occur in lower extremity peripheral aneurysms, it is the embolization of laminar thrombus from within the lumen that leads to most of the complications [43]. Destruction of

runoff vessels or thrombosis of the aneurysm and the runoff together are significant clinical issues that remain unsolved today. In fact, the majority of popliteal aneurysm patients will have disadvantaged runoff at the time of diagnosis, implying an embolic etiology from the laminar thrombus within the aneurysm [44].

Lower extremity peripheral aneurysms can occur anywhere from the groin to the knee. Often degeneration of one segment of the artery represents a systemic defect where multiple other segments may be ultimately affected [45] (Fig. 50.9). In some cases, diffuse arteriomegaly may be present. Therefore, surveillance ultrasound after treatment of a peripheral aneurysm is critical to long-term success. Not only is surveillance of the graft used to treat the aneurysm necessary but also surveillance of the remaining untreated arterial segments should be performed at least yearly [46]. Similarly, patients with peripheral aneurysms are significantly more likely to have an associated AAA.

## Femoral Aneurysms

The most common aneurysm of the femoral artery is a femoral pseudoaneurysm, discussed elsewhere in a separate chapter. Pseudoaneurysms are a common problem in the femoral artery due to the use of this vessel for access to the arterial tree for angiography and interventions. Direct arterial trauma from needle puncture or sheath placement leads to the classic pseudoaneurysm of the femoral artery.

True aneurysms of the femoral artery (Fig. 50.10) contain all layers of the arterial wall and represent a degenerative process of the arterial wall, similar to that seen in AAAs. True aneurysms of the femoral artery are relatively uncommon, certainly less likely to occur than pseudoaneursyms. As noted above, aneurysmal disease is often a diffuse issue with contralateral aneurysms being common and further degeneration in different areas of the ipsilateral extremity being possible as well. Therefore, the presence of an aneurysm in either lower extremity necessitates a scan of the entire lower extremity arterial tree to rule out other areas of aneurysmal degeneration (Fig. 50.9). While in many centers this is performed using CT angiography, the necessity for repetitive surveillance would favor ultrasound as the primary surveillance modality. Once a decision is made for intervention on one of the aneurysmal segments, then CT angiography or conventional angiography is appropriate in most situations.

**Fig. 50.9** Surface mapping of a CT angiogram, demonstrating areas of arterial degeneration in addition to the right popliteal aneurysm. These areas would warrant surveillance for further aneurysmal degeneration in the future

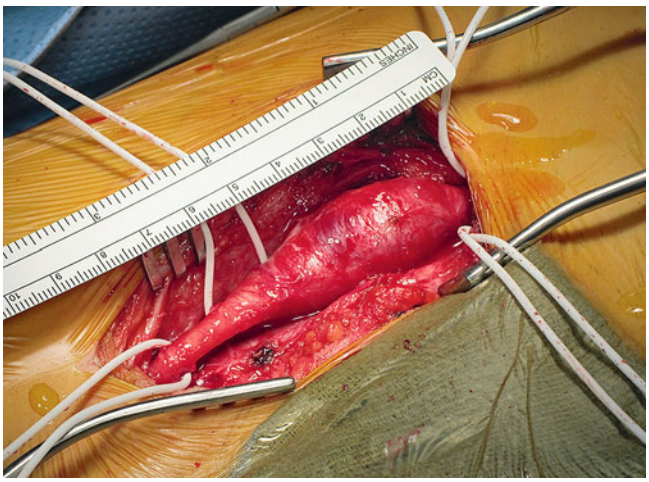

**Fig. 50.10** True aneurysm of the femoral artery at the time of operative exclusion

## Popliteal Aneurysms

The most common peripheral aneurysm typically arises in the popliteal artery. These aneurysms tend to be fusiform, with some saccular components. As enlargement continues, the slow flow along the arterial wall typically leads to laminar thrombus deposition (Fig. 50.11). While this can occur at any diameter, the amount of thrombus increases over diameters of 2 cm [47]. The presence of any laminar thrombus suggests a risk of distal embolization, necessitating close surveillance or repair. In some cases, laminar thrombus may be seen in arteries smaller than 2 cm, and risk of aneurysm thrombosis does not appear to be predicted by aneurysm size [48]. In these situations, close follow up or repair may be warranted due to this risk, but exact data is not available. Traditionally the recommended diameter for aneurysm repair has been 2 cm [49], without prospective data to validate this threshold.

Physical exam for popliteal aneurysm may be misleading, but the key is to have a low threshold for ultrasound assessment since tortuosity and aneurysms are often indistinguishable on physical exam. As a baseline for any patient, ultrasound assessment provides diameter data; if popliteal arterial diameter exceeds 10 mm or if laminar thrombus is present, then lower extremity physiologic testing to measure baseline ABI is also appropriate. Enlargement of the artery on subsequent exam or decrease in ABI may both be significant factors in determining the timing of popliteal aneurysm repair. Surveillance should generally be performed at least yearly for patients with popliteal arteries greater than 10 mm.

Given the variability of popliteal aneurysms, repair is dependent on many factors. First and foremost is overall aneurysm size. Larger aneurysms not only have the higher risk of laminar thrombus and distal embolization noted above [50], but also are associated with a higher risk of other

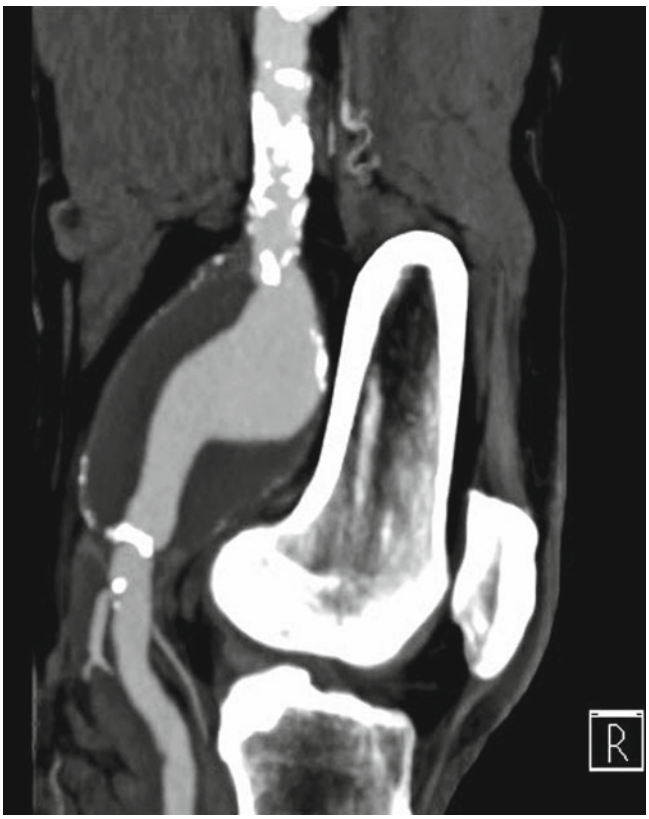


**Fig. 50.11** Sagittal CTA of a popliteal aneurysm demonstrating extensive laminar thrombus

complications such as local venous compression (Fig. 50.12) or even rupture. Again the 20 mm threshold has been traditionally used, although little hard data exists to support this value. Prior to elective lower extremity aneurysm repair, a general bilateral ultrasound survey is warranted to rule out the presence of other potentially synchronous aneurysms.

Surveillance after popliteal aneurysm repair should be routine, since the development of other aneurysms is common [51]. Typically, yearly duplex ultrasound surveillance should be performed in most cases, with contralateral duplex screening done at least every 3 years.

## Summary

Additional research will likely further support the use of ultrasound as the primary post-EVAR surveillance modality in stable aneurysms. To date, numerous studies have evaluated the role of ultrasound in post-endograft surveillance. Clearly, ultrasound is an easy and accurate method of determining aortic aneurysm sac diameter. Many vascular labs have become very adept at using ultrasound to look for endograft complications such as endoleaks or graft migration. Nonetheless, the real issue with endograft surveillance is residual aneurysm sac diameter. In patients who have a

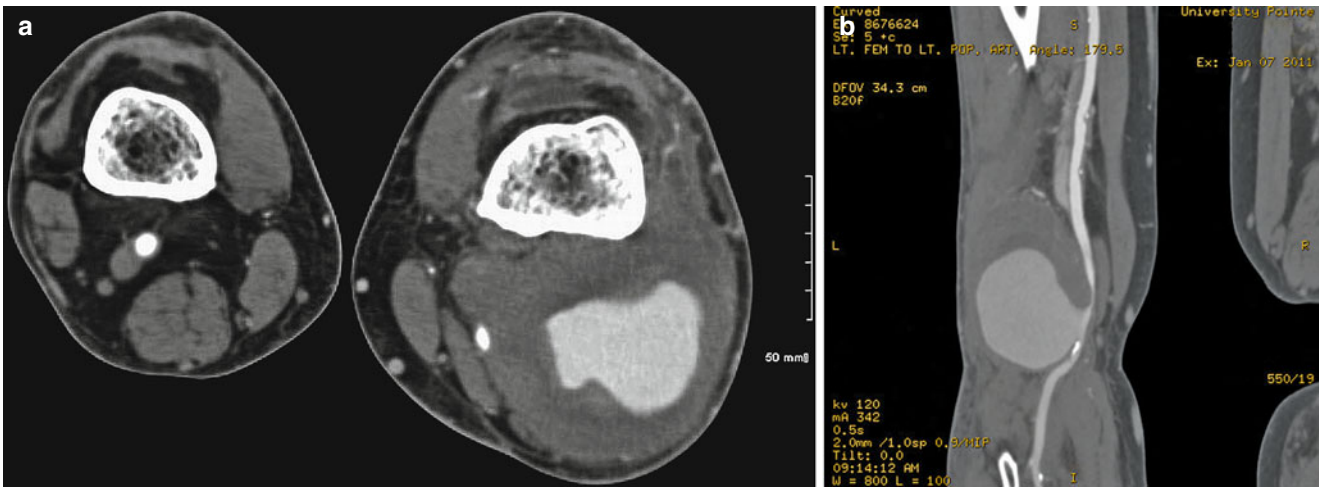


**Fig. 50.12** Axial (**a**) and sagittal (**b**) CTA of popliteal aneurysm presenting with venous compression with venous congestion and unilateral limb swelling. The aneurysm measured over 9 cm in greatest diameter

shrinking or stable aneurysm after endograft placement, it appears safe and cost effective to follow these patients long term with ultrasound alone. As new technology such as ultrasound contrast, image fusion, and GPS navigation become mainstream and are evaluated they will only enhance and expand the utility of ultrasound in AAA management.

## References


1. Raman KG, et al. Color-flow duplex ultrasound scan versus computed tomographic scan in the surveillance of endovascular aneurysm repair. J Vasc Surg. 2003;38(4):645–51.
2. Parodi JC, Palmaz JC, Barone HD. Transfemoral intraluminal graft implantation for abdominal aortic aneurysms. Ann Vasc Surg. 1991;5(6):491–9.
3. Sato DT, et al. Endoleak after aortic stent graft repair: diagnosis by color duplex ultrasound scan versus computed tomography scan. J Vasc Surg. 1998;28(4):657–63.
4. Heilberger P, et al. Postoperative color flow duplex scanning in aortic endografting. J Endovasc Surg. 1997;4(3):262–71.
5. Parent FN, et al. The incidence and natural history of type I and II endoleak: a 5-year follow-up assessment with color duplex ultrasound scan. J Vasc Surg. 2002;35(3):474–81.
6. Fillinger MF. Postoperative imaging after endovascular AAA repair. Semin Vasc Surg. 1999;12(4):327–38.
7. Brown LC, Powell JT. Risk factors for aneurysm rupture in patients kept under ultrasound surveillance. UK small aneurysm trial participants. Ann Surg. 1999;230(3):289–96; discussion 296–7.
8. Teodorescu VJ, Morrissey NJ, Olin JW. Duplex ultrasonography and its impact on providing endograft surveillance. Mt Sinai J Med. 2003;70(6):364–6.
9. Sprouse 2nd LR, et al. Is ultrasound more accurate than axial computed tomography for determination of maximal abdominal aortic aneurysm diameter? Eur J Vasc Endovasc Surg. 2004;28(1):28–35.
10. Collins JT, Boros MJ, Combs K. Ultrasound surveillance of endovascular aneurysm repair: a safe modality versus computed tomography. Ann Vasc Surg. 2007;21(6):671–5.
11. Chaer RA, et al. Duplex ultrasound as the sole long-term surveillance method post-endovascular aneurysm repair: a safe alternative for stable aneurysms. J Vasc Surg. 2009;49(4):845–9; discussion 849–50.
12. Beeman BR, et al. Duplex ultrasound factors predicting persistent type II endoleak and increasing AAA sac diameter after EVAR. J Vasc Surg. 2010;52(5):1147–52.
13. Gillum RF. Epidemiology of aortic aneurysm in the United States. J Clin Epidemiol. 1995;48(11):1289–98.
14. Dubost C, Allary M, Oeconomos N. Resection of an aneurysm of the abdominal aorta: reestablishment of the continuity by a preserved human arterial graft, with result after five months. AMA Arch Surg. 1952;64(3):405–8.
15. Szilagyi DE, et al. Contribution of abdominal aortic aneurysmectomy to prolongation of life. Ann Surg. 1966;164(4):678–99.
16. Estes Jr JE. Abdominal aortic aneurysm; a study of one hundred and two cases. Circulation. 1950;2(2):258–64.
17. Fink HA, et al. The accuracy of physical examination to detect abdominal aortic aneurysm. Arch Intern Med. 2000;160(6):833–6.
18. Demos NJ. Severe vascular impairment of the left half of the colon. Int Abstr Surg. 1963;117:205–12.
19. Palombo D, et al. Changes in the proximal neck of abdominal aortic aneurysms early after endovascular treatment. Ann Vasc Surg. 2003;17(4):408–10.
20. Thurnher S, Cejna M. Imaging of aortic stent-grafts and endoleaks. Radiol Clin North Am. 2002;40(4):799–833.
21. Donald I, Brown TG. Demonstration of tissue interfaces within the body by ultrasonic echo sounding. Br J Radiol. 1961;34:539–46.
22. Maloney JD, et al. Ultrasound evaluation of abdominal aortic aneurysms. Circulation. 1977;56(3 Suppl):II80–5.
23. Hertzer NR, Beven EG. Ultrasound aortic measurement and elective aneurysmectomy. JAMA. 1978;240(18):1966–8.
24. Ommaya AK. Computerized axial tomography of the head: the EMI-scanner, a new device for direct examination of the brain "in vivo". Special article Surg Neurol. 1973;1(4):217–22.
25. Paul JF, Abada HT. Strategies for reduction of radiation dose in cardiac multislice CT. Eur Radiol. 2007;17(8):2028–37.
26. Simoni G, et al. Helical CT for the study of abdominal aortic aneurysms in patients undergoing conventional surgical repair. Eur J Vasc Endovasc Surg. 1996;12(3):354–8.
27. Aziz I, et al. Accuracy of three-dimensional simulation in the sizing of aortic endoluminal devices. Ann Vasc Surg. 2003;17(2):129–36.

28. Sprouse 2nd LR, et al. Is three-dimensional computed tomography reconstruction justified before endovascular aortic aneurysm repair? J Vasc Surg. 2004;40(3):443–7.
29. Gouliamos AD, et al. Screening for abdominal aortic aneurysms during routine lumbar CT scan: modification of the standard technique. Clin Imaging. 2004;28(5):353–5.
30. Lederle FA, et al. Outcomes following endovascular vs open repair of abdominal aortic aneurysm: a randomized trial. JAMA. 2009;302(14):1535–42.
31. Sprouse 2nd LR, et al. Comparison of abdominal aortic aneurysm diameter measurements obtained with ultrasound and computed tomography: is there a difference? J Vasc Surg. 2003;38(3):466–71; discussion 471–2.
32. Truijers M, et al. Endovascular aneurysm repair: state-of-art imaging techniques for preoperative planning and surveillance. J Cardiovasc Surg (Torino). 2009;50(4):423–38.
33. Pages S, et al. Comparison of color duplex ultrasound and computed tomography scan for surveillance after aortic endografting. Ann Vasc Surg. 2001;15(2):155–62.
34. Nagre SB, et al. Evaluating outcomes of endoleak discrepancies between computed tomography scan and ultrasound imaging after endovascular abdominal aneurysm repair. Ann Vasc Surg. 2011;25(1):94–100.
35. Singh K, et al. The difference between ultrasound and computed tomography (CT) measurements of aortic diameter increases with aortic diameter: analysis of axial images of abdominal aortic and common iliac artery diameter in normal and aneurysmal aortas. The tromso study, 1994–1995. Eur J Vasc Endovasc Surg. 2004;28(2):158–67.
36. Henao EA, et al. Contrast-enhanced duplex surveillance after endovascular abdominal aortic aneurysm repair: improved efficacy using a continuous infusion technique. J Vasc Surg. 2006;43(2):259–64; discussion 264.
37. Cantisani V, et al. Prospective comparative analysis of colour-Doppler ultrasound, contrast-enhanced ultrasound, computed tomography and magnetic resonance in detecting endoleak after endovascular abdominal aortic aneurysm repair. Eur J Vasc Endovasc Surg. 2011;41(2):186–92.
38. White RA, et al. Intravascular ultrasound: the ultimate tool for abdominal aortic aneurysm assessment and endovascular graft delivery. J Endovasc Surg. 1997;4(1):45–55.
39. Ten Bosch JA, et al. Contrast-enhanced ultrasound versus computed tomographic angiography for surveillance of endovascular abdominal aortic aneurysm repair. J Vasc Interv Radiol. 2010;21(5):638–43.
40. Sommer WH, et al. Comparison of time-resolved CT-angiography, contrast-enhanced ultrasound and digital subtraction angiography in a patient with a small type II endoleak after endovascular aneurysm repair. Clin Hemorheol Microcirc. 2010;45(1):19–25.
41. Mirza TA, et al. Duplex ultrasound and contrast-enhanced ultrasound versus computed tomography for the detection of endoleak after EVAR: systematic review and bivariate meta-analysis. Eur J Vasc Endovasc Surg. 2010;39(4):418–28.
42. Clevert DA, et al. Imaging of aortic lesions with color coded duplex sonography and contrast-enhanced ultrasound versus multislice computed tomography (MS-CT) angiography. Clin Hemorheol Microcirc. 2008;40(4):267–79.
43. Anton GE, et al. Surgical management of popliteal aneurysms. Trends in presentation, treatment, and results from 1952 to 1984. J Vasc Surg. 1986;3(1):125–34.
44. Lilly MP, et al. The effect of distal arterial anatomy on the success of popliteal aneurysm repair. J Vasc Surg. 1988;7(5):653–60.
45. Whitehouse Jr WM, et al. Limb-threatening potential of arteriosclerotic popliteal artery aneurysms. Surgery. 1983;93(5):694–9.
46. Dawson I, Sie RB, van Bockel JH. Atherosclerotic popliteal aneurysm. Br J Surg. 1997;84(3):293–9.
47. Szilagyi DE, Schwartz RL, Reddy DJ. Popliteal arterial aneurysms. Their natural history and management. Arch Surg. 1981;116(5):724–8.
48. Inahara T, Toledo AC. Complications and treatment of popliteal aneurysms. Surgery. 1978;84(6):775–83.
49. Lowell RC, et al. Popliteal artery aneurysms: the risk of nonoperative management. Ann Vasc Surg. 1994;8(1):14–23.
50. Silver TM, et al. Gray scale ultrasound evaluation of popliteal artery aneurysms. AJR Am J Roentgenol. 1977;129(6):1003–6.
51. Ravn H, Bjorck M. Popliteal artery aneurysm: epidemiology and modern management. Acta Chir Belg. 2009;109(1):13–9.

# Role of Color Duplex Ultrasound for Aortic Endografts

# 51

Rabih Chaer, Tracey A. Richardson, and Michel S. Makaroun

**Abstract**

Endovascular aneurysm repair (EVAR) requires lifelong surveillance for potential complications, including endoleak, change in aneurysm size, graft migration, structural graft failure, and limb outflow impairment. Duplex ultrasound is noninvasive, safe, and cheap, and has been shown to be a valuable tool for EVAR surveillance. The purpose of this chapter is to examine the use of color flow ultrasound in aortic endografts and present the evidence supporting EVAR follow up with duplex scanning.

**Keywords**

Endovascular • Aneurysm • Ultrasound

## Introduction

Endovascular aneurysm repair (EVAR) has seen rapid diffusion as a minimally invasive alternative to open repair and is currently widely accepted for the treatment of abdominal aortic aneurysms. Although EVAR offers immediate advantage over open aneurysm repair with lower perioperative mortality and morbidity [1–3], it carries the need for lifelong surveillance for potential complications, including endoleak, change in aneurysm size, graft migration, structural graft failure, and limb outflow impairment caused by limb stenosis or occlusion. The ideal surveillance modality should be noninvasive, cheap, and reproducible, with high sensitivity and specificity for the detection of endograft-related adverse events. Computed tomography with intravenous contrast injection (CT) is currently the standard for long-term EVAR surveillance, but is associated with increased cost [4] and radiation exposure [5]. It could also contribute to the decline in renal function seen after EVAR as a result of contrast nephropathy [6]. Color-flow duplex ultrasound (DUS) scanning can also detect endoleaks as well as size changes over time but is more operator dependent [7]. It has, however, the distinct advantage of being noninvasive, safer, and cheaper than CT scans. Several studies have established the ability of duplex scanning to detect endoleaks and demonstrated a good correlation with CT for the measurement of the sac diameter of abdominal aortic aneurysms [7–12]. More recently, duplex scanning as the only follow up modality, has been reported to provide a safe follow-up modality for EVAR [13]. The purpose of this chapter is to examine the use of color flow ultrasound in aortic endografts and present the evidence supporting a selective policy of EVAR follow up with duplex scanning.

R. Chaer, M.D. (✉)
Division of Vascular Surgery, PUH,
200 Lothrop Street Suite A-1011, Pittsburgh, PA 15213, USA
e-mail: chaerra@upmc.edu

T.A. Richardson, AS, RDMS, RVT • M.S. Makaroun, M.D.
Department of Vascular Surgery, University of Pittsburgh Medical Center, Pittsburgh, PA, USA

## Published Literature

### US for AAA Diameter Measurement

DUS imaging is a noninvasive alternative to CT scans for post-EVAR surveillance, and is thought to be equivalent in monitoring diameter size changes. It has the theoretical advantage of allowing the ultrasound technologists to correct for the angulation error seen in CT scan measurements

A.F. AbuRahma, D.F. Bandyk (eds.), *Noninvasive Vascular Diagnosis*,
DOI 10.1007/978-1-4471-4005-4_51, 

by placing the US transducer perpendicular to the course of the aorta [14, 15]. DUS imaging has a high degree of correlation with CT scans and a similar degree of variability in AAA diameter measurements. It has comparable accuracy for aortic aneurysm US diameter measurements in post-EVAR surveillance, when performed by certified vascular technologists in an accredited vascular laboratory and according to a carefully devised and standardized protocol [10, 12, 15].

### US for Endoleak Detection

Studies comparing CDU with CT scan for endoleak detection have produced mixed results. Sato et al. [7] and d'Audiffret et al. [16] both showed that CDU is an excellent screening test for endoleaks, with sensitivities of 97% and 96%, respectively. Elkouri et al. [12], on the other hand, found poor results for CDU endoleak detection, with a sensitivity of 25% and specificity of 89%. Most older studies comparing CDU with CT for endoleak detection, however, show modest sensitivities of 52–81% and good negative predictive value (NPV) of 86–95% [10, 16–20].

Recent EVAR surveillance data, using modern ultrasound equipment has documented a high sensitivity and negative predictive value with duplex US in detecting endoleaks requiring intervention, allowing a better identification of the type of endoleak when compared to CT scan [21]. CDU imaging detected endoleaks requiring intervention in 89% of cases, whereas CT detected endoleak in 58% ($P < .05$). The ability to correctly identify the type of endoleak as confirmed at time of intervention was 74% with CDU imaging vs. 42% with CT ($P < .05$). CDU, for the detection of endoleak requiring intervention, had a sensitivity of 90%, specificity of 81%, (NPV) of 99%, and positive predictive value (PPV) of 16%, while CT had a sensitivity of 58%, specificity of 87%, NPV of 98%, and PPV of 15%.

Therefore, DUS should be able to detect most endoleaks, and in some studies even more endoleaks than CT [21], especially slow endoleaks such as type II where delayed CT imaging may be required. In addition, positional endoleaks can only be recognized with DUS imaging, suggesting that DUS can better appreciate those patients who may require intervention.

Nevertheless, several limitations of US surveillance need to be recognized as they might limit the general applicability of these results, including operator dependence, suboptimal examinations due to bowel gas or body habitus, and availability as well as time commitment, limiting broader application. In addition, US cannot identify all endograft related adverse events that may require a reintervention, such as graft migration or kinking.

### US for Iliac Limb Follow Up

EVAR is often performed in patients with significant iliac tortuosity or patients with atherosclerotic occlusive disease, resulting at times in iliac limb kinking, stenosis or occlusion. Duplex US surveillance can be helpful not only for the evaluation of distal Type I endoleaks from iliac attachment sites, but also for assessment of iliac limb hemodynamics, permitting the possible early detection of flow abnormalities that might compromise patency. Although there are no standard duplex velocity criteria for iliac limb stenosis, color flow duplex is well established for the evaluation of native iliac disease and can identify limb kinks or adjacent stenoses that may allow early treatment and prevent adverse clinical events such as ischemia or thrombosis. Hemodynamic data obtained from DUS iliac limb imaging therefore provides more physiologic information and may allow more accurate identification of patients requiring reintervention than CT scan.

## Contrast Enhanced Ultrasound

Ultrasound contrast agents are characterized by microbubbles of gas encapsulated within a lipid shell that, and can significantly increase the ultrasound signal strength. The use of CEUS for EVAR surveillance has been widely reported, with high sensitivity and specificity for the diagnosis of endoleaks [22–24]. This imaging modality, however, is not widely available and increases the study time and cost of EVAR surveillance. It is also not approved in the United States for that purpose and requires vascular lab personnel that can start intravenous access and monitor the patient's clinical status and hemodynamics. Nevertheless, CEUS offers promise as a safe and sensitive modality for endoleak detection, and may be particularly attractive for patients with renal dysfunction, obviating the need for CT scanning and the associated exposure to radiation and nephrotoxic agents.

## Cost Considerations

The need for lifelong surveillance has called into question the cost-effectiveness of EVAR. This is affected by direct as well as indirect costs, many of which can be attributed to the expense of imaging, but also the management of related complications [25–30]. A recent study reported that >65% of postoperative EVAR costs are due to CT scanning alone [4]. In addition, contrast nephropathy affects 7–12% of patients after CT angiography [3, 31], adding to the cost of surveillance. A cost analysis study in patients following post-EVAR showed that cost savings of $1595 per patient per year can be realized by eliminating CT scan surveillance, with no aneurysm related adverse events in patients switched to

ultrasound follow up [32]. This study confirmed that surveillance of EVAR patients can be performed accurately, safely, and cost-effectively with DUS as the sole imaging study, and is likely to underestimate the magnitude of cost effectiveness since it does not take into account the direct and indirect costs related to the complications of contrast nephropathy and radiation exposure.

## Imaging Technique

The purpose of ultrasound imaging post-EVAR is to evaluate endovascular aortic stent grafts for patency, as well as aneurysm sac enlargement and the presence of endoleak or other complications. DU imaging can also identify hemodynamic or anatomical abnormalities that may impair graft function.

### Patient Preparation and Positioning

The examiner should instruct the patient to fast 6–8 h before the exam to minimize the amount of bowel gas present at the time of the study. Smoking or gum chewing should be discouraged the morning of the exam due to the fact that it may increase the amount of air swallowed, therefore increasing the occurrence of bowel gas. However, if needed, the patient may take morning medications with water. A bowel cathartic preparation is usually not necessary.

A full EVAR surveillance study can take up to 30–45 min, but this can be significantly shorter in busy centers with experienced ultrasonographers. The exam is performed with the patient lying supine with the head slightly elevated to a level of comfort. The lateral decubitus position may be useful when supine acoustic windows prove to be inadequate or with individuals who have a large abdominal girth.

Imaging in different positions can actually be useful in the detection of suspected endoleaks that are difficult to image. If an endoleak is suspected but cannot be clearly defined, turning the patient to a left and/or right decubitus position and rescanning the area in question can prove to be helpful. Intermittent endoleaks can result in an unstable aneurysm sac that should be suspected on ultrasound imaging in the setting of graft migration, graft and aneurysm sac pulsatility, echolucent regions in the sac thrombus, and sac growth. Such signs should prompt special positioning of the patient to search for positional endoleaks. Intermittent endoleaks have been described in a series of 13 patients, all of whom had sac enlargement [33]. There was evidence of positional dependence in 11 of the 13 cases. This represents an incidence of less than 1% in a series of more than 1,200 endovascular repairs. These endoleaks were not seen on CT scans in 80% of studies, and 11 of 13 were not seen on supine angiography.

## Examination Guidelines

### Required Equipment and Settings

- Appropriate duplex instrumentation, which includes B-mode imaging and Doppler spectral analysis of flow dynamics. Color and power Doppler imaging is strongly desirable in complimenting the examination.
- Imaging transducer frequency should be set between 2.0 and 4.0 MHz (curved linear probe) for adequate penetration.
- Doppler transducer frequency must be set between 2.0 and 4.0 MHz for adequate penetration.
- Hardcopy capabilities should include color static images or electronic color storage. In addition, electronic video clip storage should be available.

### Stent Graft Evaluation Post-EVAR

A standard exam protocol for EVAR surveillance should be predetermined and validated in each vascular laboratory. The following steps are typically required for optimal imaging that includes the following expectations:

- *B-mode gray scale* imaging is used to evaluate and document the location and position of the stent fixation sites (proximal aortic and distal iliac neck) to evaluate stent-to-wall apposition.
- The region of maximal aneurysm size should be identified in both transverse (transaxial) and sagittal/longitudinal planes. Transverse measurements are compiled for the maximum diameter of the aneurysm sac. Diameter measurements are taken in anterior/posterior and transverse orientations at peak systole from outer wall to outer wall (Fig. 51.1).

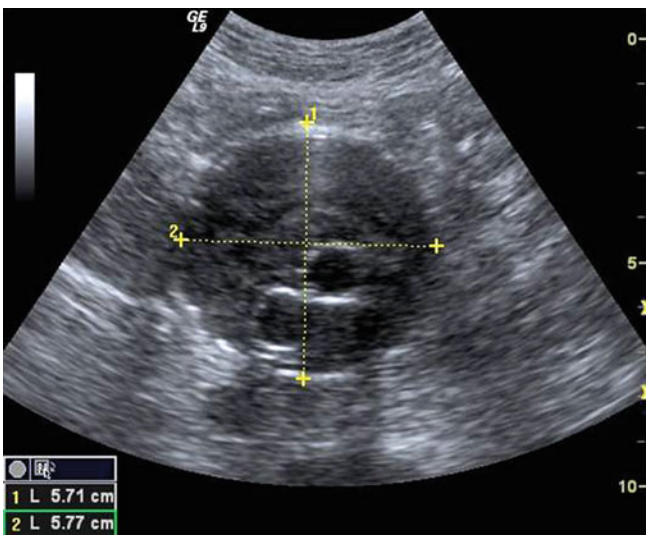


**Fig. 51.1** Cross sectional B-mode image showing the widest diameter of the residual aneurysm sac, outer wall to outer wall measurement. (*1*) anterior/posterior and (*2*) longitudinal measurement

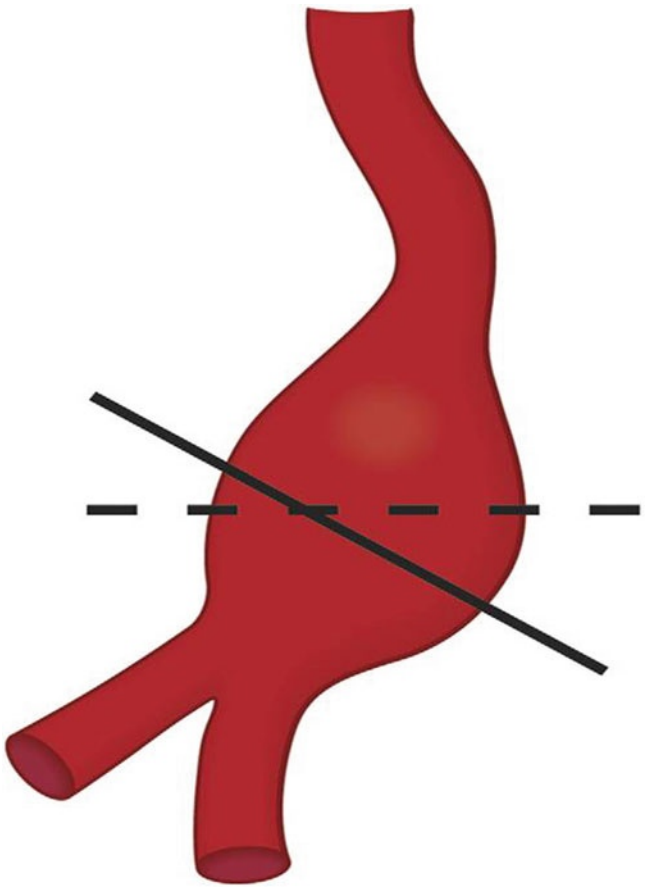

**Fig. 51.2** Transducer placement must be perpendicular to the aorta

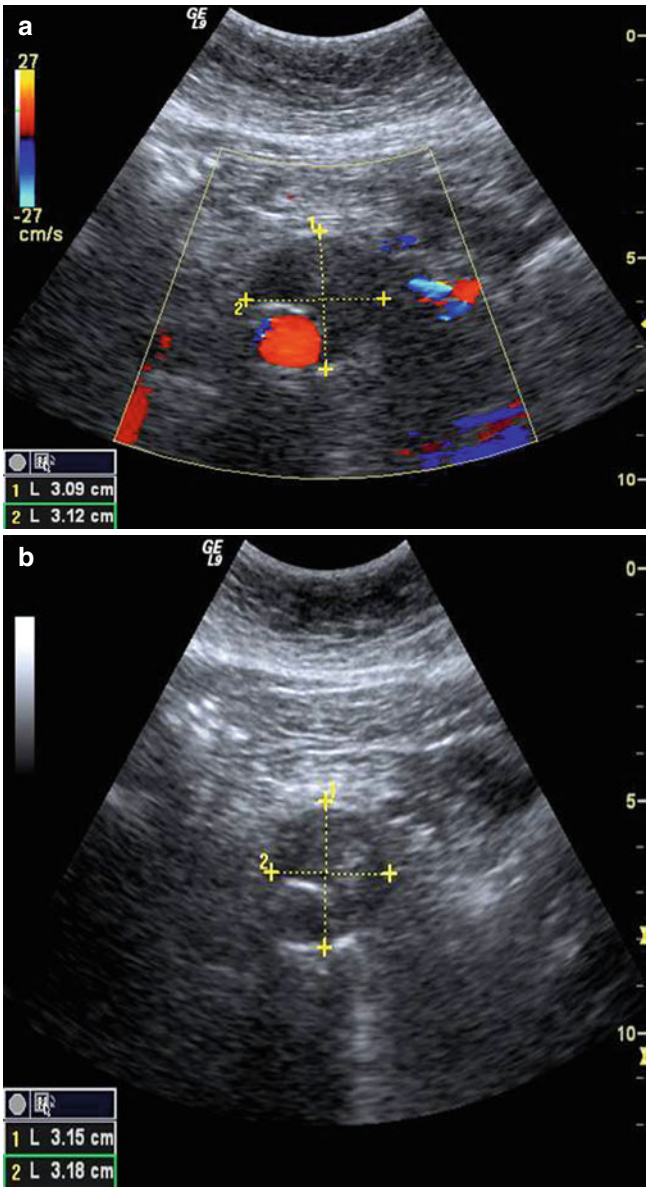


**Fig. 51.3** (**a**) Color Doppler, (**b**) B-mode; Cross-sectional view of residual aneurysm sac showing that the aneurysm has collapsed down around the stent

- It is imperative that the measurements be made perpendicular to the aorta, not transverse to the body. Patients often have a severely angulated aorta, and adjusting the transducer to be perpendicular or orthogonal to the aorta is crucial in order to obtain accurate measurements, even if this requires imaging in an oblique plane to the body (Fig. 51.2).
- The residual aneurysm sac should also be examined for areas of echolucency or motion/pulsation in the excluded lumen as that may represent an endoleak (Figs. 51.3 and 51.4).

*Color and pulsed wave Doppler* is next used to obtain a cross sectional color image of the aneurysm sac demonstrating color filling of the stent graft to demonstrate patency (Fig. 51.5).

- PW spectral waveforms from the body of the graft should be recorded through each limb of the stent graft to show patency (Fig. 51.6). This is then followed by assessment for any twisting, kinking, or deformity of the graft (Figs. 51.7 and 51.8).
- Color and spectral Doppler is also used to assess the attachment/fixation sites with special attention to the detection of any flow outside the lumen of the graft (Fig. 51.9), which would indicate an endoleak.
- The aneurysm sac should be examined throughout in both sagittal and transverse planes to detect flow outside the endografts that may represent an endoleak (Fig. 51.10). Special attention should be directed to hypoechoic areas and the absence of flow confirmed by Doppler.
- The Doppler image of patent aneurysm sac branches (i.e., lumbar, inferior mesenteric artery, internal iliac artery) should be particularly noted, and flow direction should be documented.

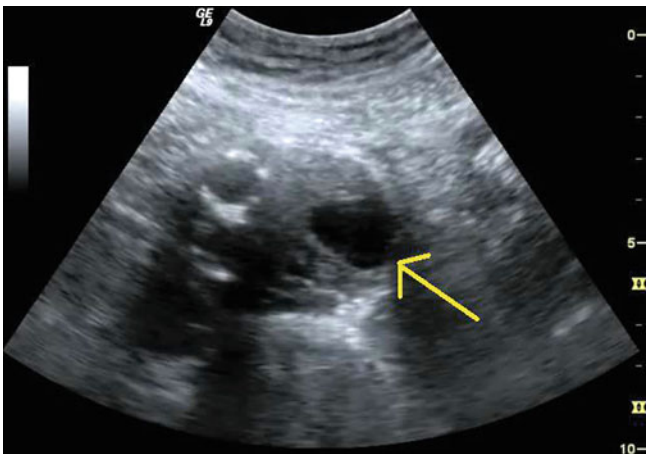

**Fig. 51.4** Cross sectional B-mode image of the residual aneurysm sac showing areas of echolucency (*arrow*)

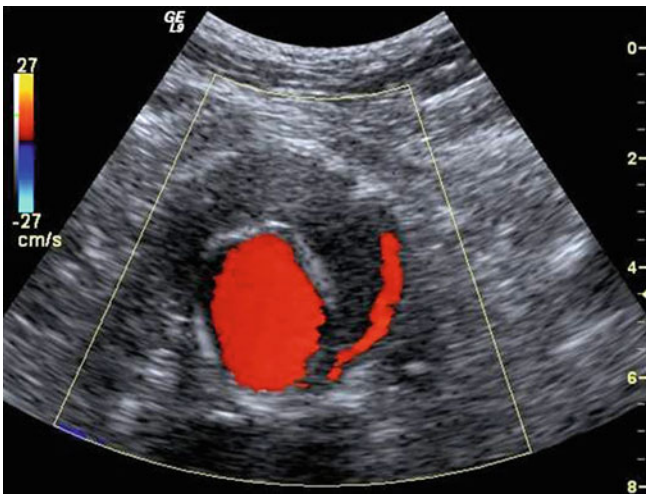


**Fig. 51.5** Cross sectional color image of the aneurysm sac demonstrating color filling of the stent graft to demonstrate patency

- PW spectral waveforms should be recorded from any region of extra graft flow detected within the aneurysm sac and from aortic side branches (document direction and source of flow.) To and fro Doppler signals typically identify the origin of the branch flow in type II endoleaks. (Figs. 51.11, 51.12 and 51.13). That characteristic may not be present, however, in cases when leaks enter and exit the sac through different branches.

Artifactual pulsatile color may be present if the color sensitivity settings are high. With a low color setting, the scanner will prioritize the movement as blood flow versus pulsatile movement of the adjacent graft. Other imaging artifact can occur with abdominal bowel gas or atherosclerotic calcification of the aortal wall.

Nevertheless, a Doppler waveform will differentiate true perigraft flow from color artifact. A true endoleak will be identified in both longitudinal and transverse views, which may help differentiate it from an artifact.

## Surveillance Policy Changes

The following is a summary of the evolution of our surveillance policy over the years. In 2003, a new follow-up schedule for EVAR surveillance was initiated for selected patients treated at the University of Pittsburgh Medical Center (UPMC). Annual duplex scanning as the sole imaging modality was offered as early as 1 year post-EVAR for those patients with a collapsed aneurysm sac <4 cm in diameter. This policy was expanded 1 year later to include patients with significant shrinkage of the aneurysm sac to any size, or a stable aneurysm without enlargement for 2 years whether a Type II endoleak was present or not. Patients with contrast allergy or significant renal insufficiency (serum creatinine >2) were switched at earlier intervals depending on aneurysm size and presence or absence of endoleaks. Diameter measurements were defined as the minor axis of the largest axial slice on CT. A significant shrinkage was considered to be a minimum of 5 mm from the baseline 1-month CT. A stable aneurysm was defined as an aneurysm with <3 mm increase in diameter from baseline. Patients with enlargement of the sac by ≥3 mm from the baseline CT were not considered for switching. Most patients underwent duplex scanning to complement the CT scan when the decision to switch the patient was made. All patients with suboptimal studies secondary to anatomy or body habitus were not switched to duplex scanning surveillance.

By the time of our last review, 184 patients (159 males) were switched to duplex scanning surveillance between 2003 and 2006 [13]. All duplex scanning examinations were technically satisfactory for determination of aneurysm size and presence of an endoleak. The mean follow up on duplex scanning was only 24 ± 13 months (range 1–4 years). Initial follow up of these patients included X-rays and CT 1 month after EVAR, 6 months (for patients on investigational protocols), 12 months, and yearly thereafter 13. Following commercial release of each graft, the 6-month follow up was discontinued because of the low incidence of adverse events detected [34].

Following our timeline changes in policy, the duplex scanning follow-up schedule was initiated 34 ± 24 months after EVAR (range 1–112 months). The mean aneurysm diameter at baseline was 54 ± 8 mm and had decreased to 40 ± 11 mm before the decision to implement duplex-scanning-only surveillance. Three new endoleaks were diagnosed during the duplex-only surveillance, only one presenting with sac enlargement. All prompted CT evaluation: one Type II endoleak with stable sac size that could not be identified

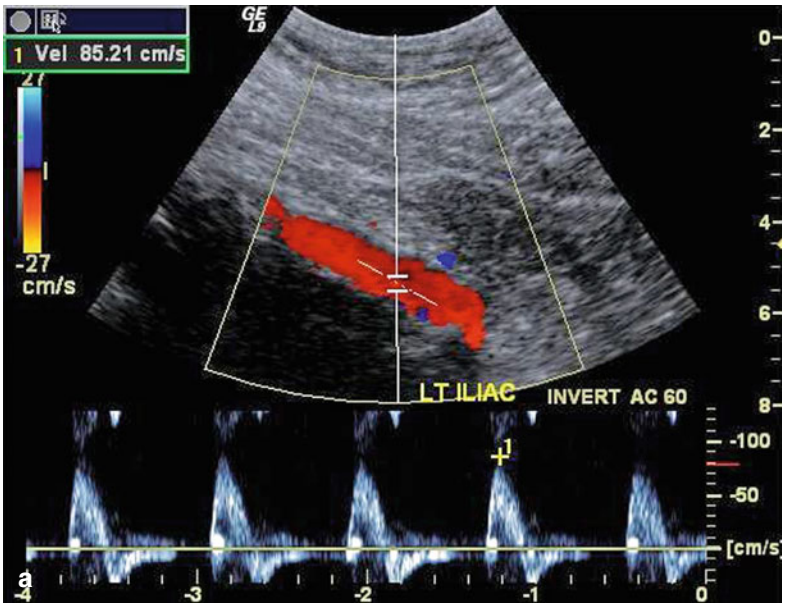
1 Vel 85.21 cm/s
27
-27
cm/s
LT ILIAC
INVERT AC 60
-100
-50
[cm/s]
a

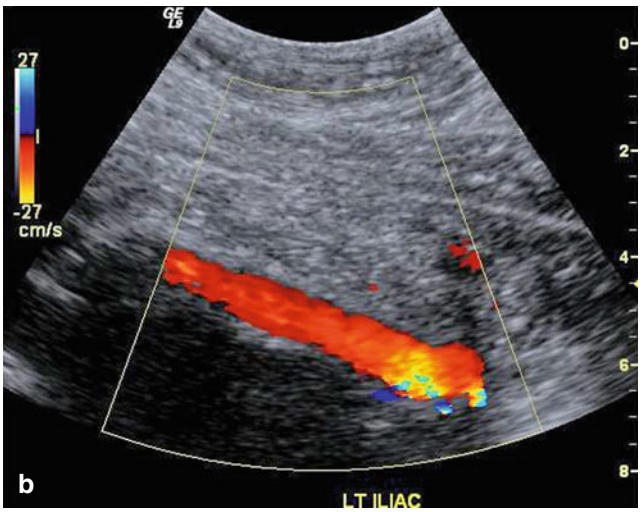
27
-27
cm/s
b
LT ILIAC

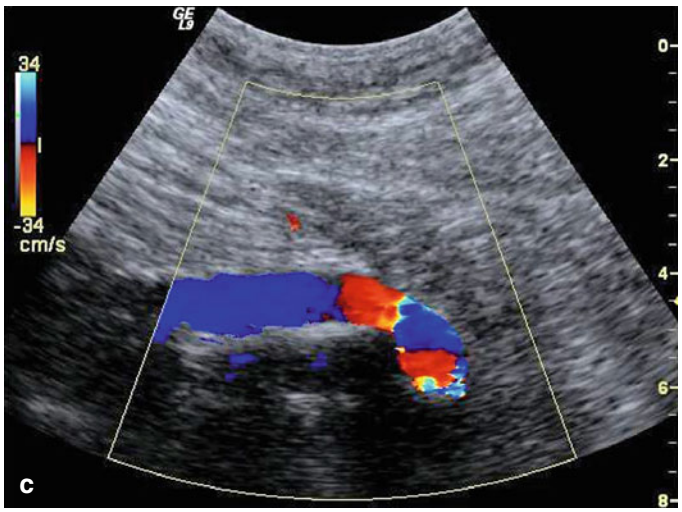
34
-34
cm/s
c

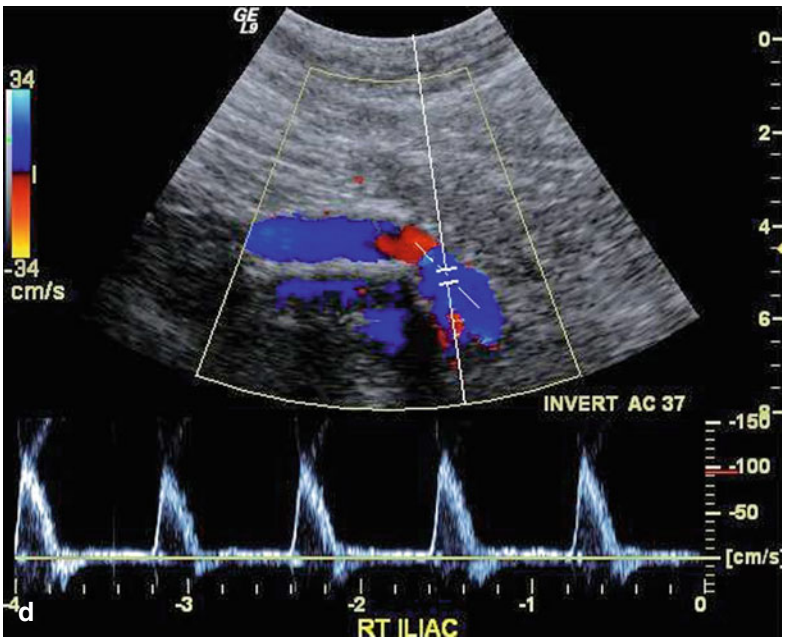
34
-34
cm/s
INVERT AC 37
-150
-100
-50
[cm/s]
d
RT ILIAC

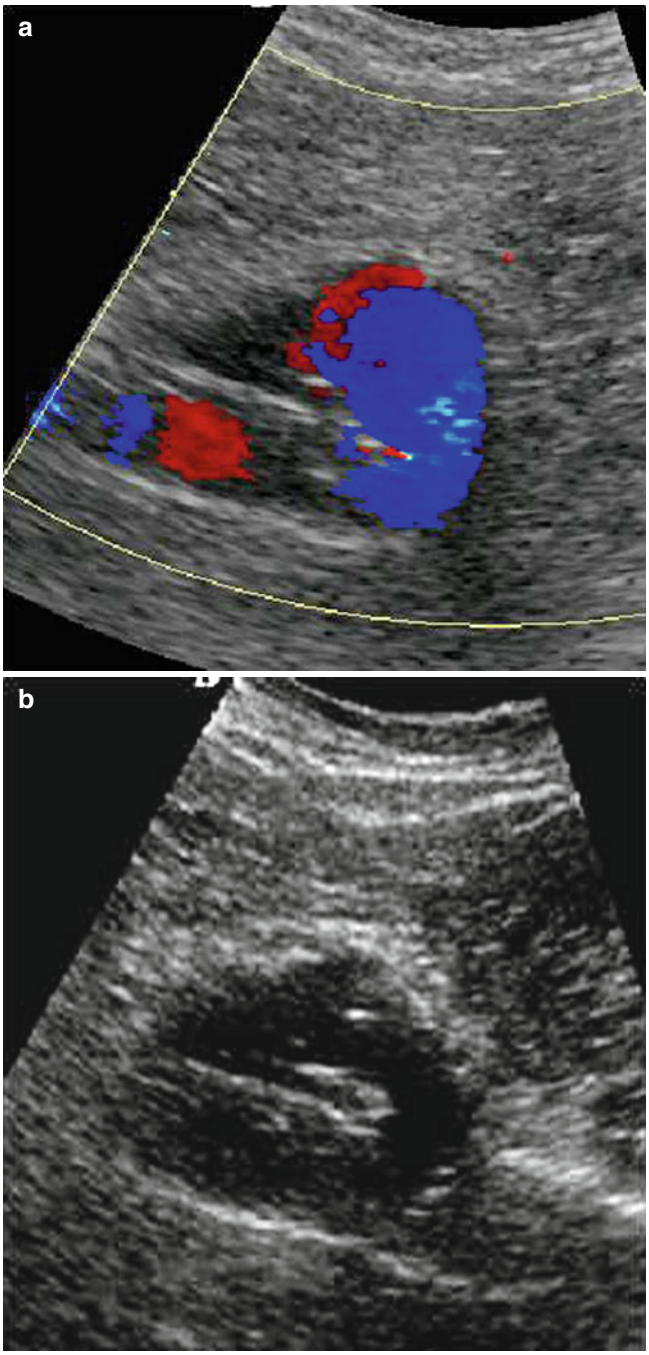


**Fig. 51.7** (**a**, **b**) Both color Doppler and B-mode images shows a detachment and kinking of left limb of the stent graft (Type I endoleak)

on the CT obtained 3 months later, and two distal Type I endoleaks that required limb extension. No patient had a clinical adverse event during the period of observation No

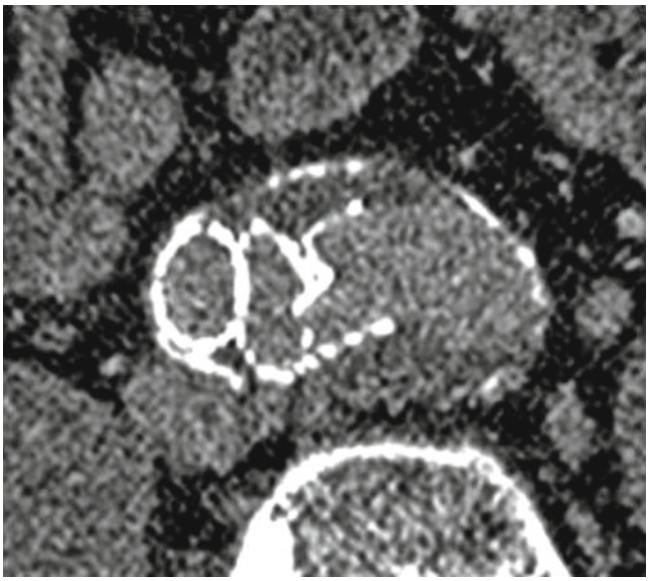

**Fig. 51.8** Corresponding CT images of the detached left iliac limb

ruptures or graft occlusions were noted [13]. These findings demonstrated to us the safety of using Duplex scanning as a replacement modality for CT in the FU of EVAR.

Since these changes were adopted slowly over time, we evaluated how many patients would be suited for the switch and how early after EVAR it could be implemented, based on our current criteria. The clinical and follow-up imaging records of 200 consecutive patients with available imaging, treated in 2004 and 2005 were reviewed, demonstrating that 97% of patients are eligible for duplex-scanning-only surveillance by 3 years after EVAR. This finding is quite encouraging as it suggests that the majority of patients can be followed with US only surveillance post-EVAR.

These results and others confirm the safety and efficacy of US surveillance post-EVAR, which can be applied to most patients, potentially as early as 30 days postprocedure after the first CT scan follow up. Candidate patients include:

1. All patients with baseline renal insufficiency
2. Patients with no endoleak after 1 year on CT scan
3. Patients with endoleak but no size increase after 2 years
4. All patients with collapsed or shrinking sac

However, it is to be noted that patients with initial suboptimal anatomy for EVAR may be at a higher risk for future complications and be better followed by CT at least intermittently alternating CDU with CT to detect early changes in aortic neck anatomy and morphology. Other patients who may not benefit from strict US follow up include those being

**Fig. 51.6** (**a**) left iliac limb color and spectral Doppler signal, (**b**) Color Doppler image left iliac limb, (**c**) Color Doppler image right iliac limb, (**d**) Color and spectral Doppler image right iliac limb; Color Doppler and PW Doppler waveforms through each limb of the stent graft to show patency

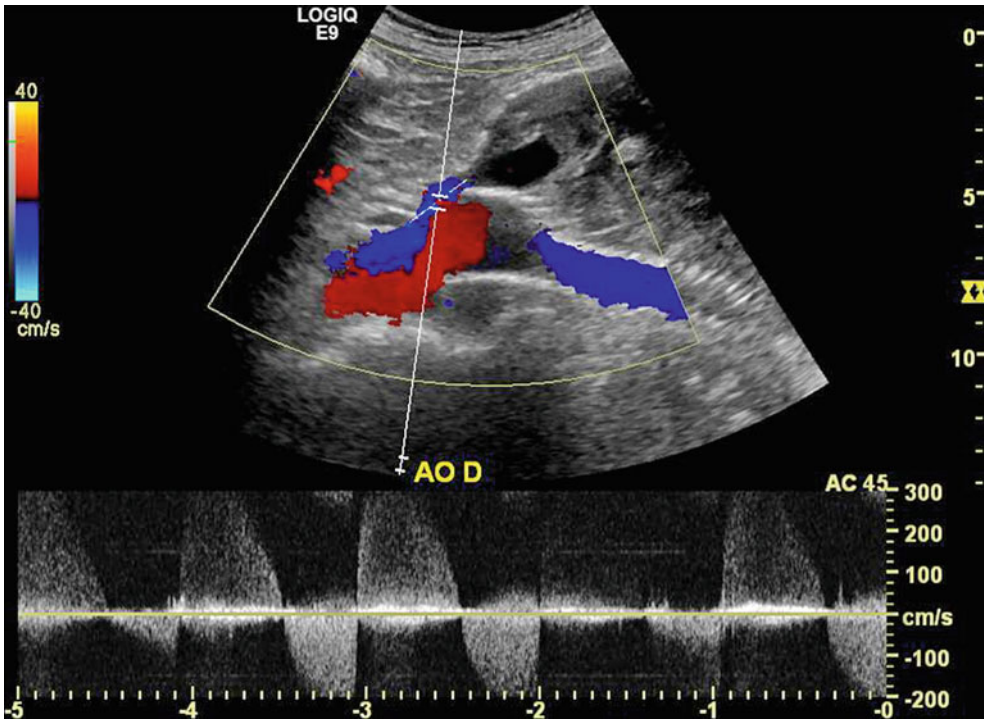


**Fig. 51.9** Color and PW spectral Doppler image showing a Type 1 endoleak at the proximal fixation sites

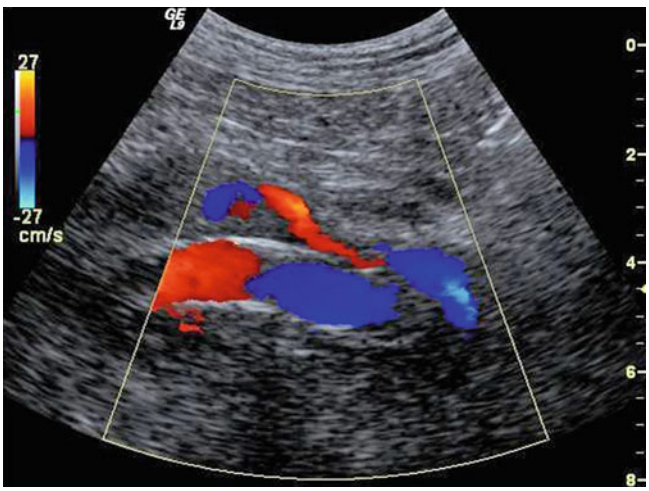


**Fig. 51.10** Color Doppler image showing a Type 1 endoleak at the left iliac limb distal fixation sites

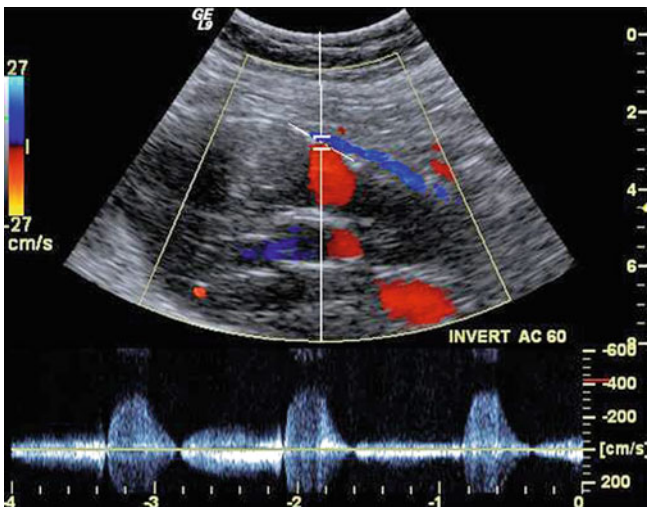


**Fig. 51.11** Color and PW spectral Doppler image showing a Type II endoleak with reversed flow through the IMA

concomitantly followed for a thoracic aortic aneurysm, and patients with excessive bowel gas, ascites, or a challenging body habitus. A CT may still be indicated every 5 years to detect remote aneurysmal changes or other structural defects.

It should be noted that our recommendations may not be universally accepted, but are similar to the recent guidelines issued by the Society for Vascular for post-EVAR surveillance [35]. The guidelines recommend contrast enhanced CT imaging at 1 and 12 months during the first year after EVAR, and also at 6 months in patients with endoleak or other abnormality of concern. If neither an endoleak nor aneurysm enlargement is documented during the first year after EVAR, the guidelines suggest CDU as a reasonable alternative to CT imaging for post-operative surveillance, with the recommendation that these studies be performed by a skilled technician in an accredited noninvasive vascular laboratory.

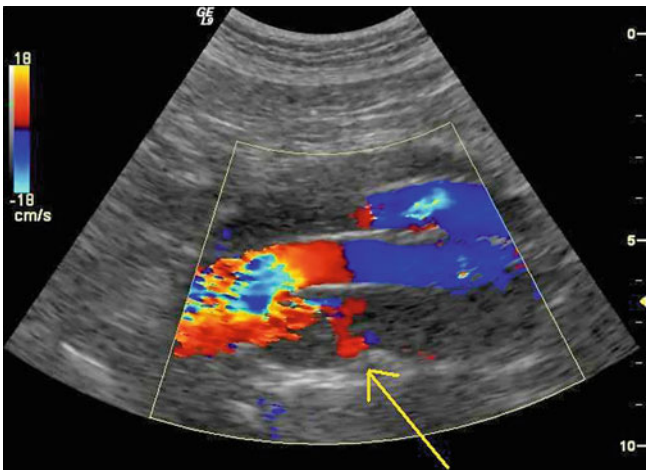


**Fig. 51.12** Color Doppler image showing a Type II endoleak with reversed flow through a posterior lumbar branch (*arrow*)

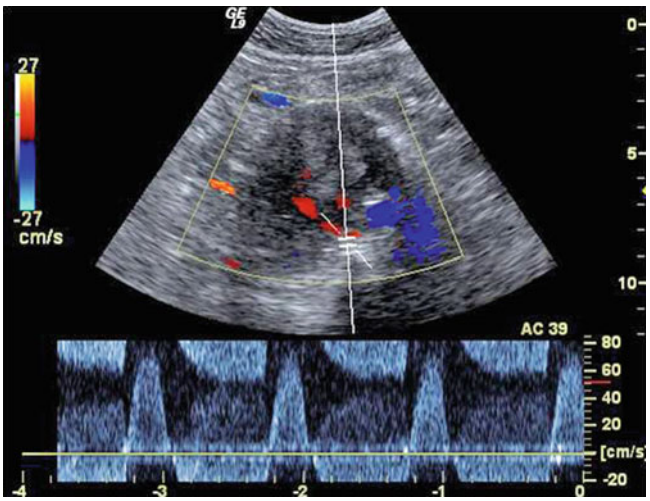


**Fig. 51.13** To and Fro Doppler signal at the origin of a posterior lumbar leak, systole (inflow) and diastole (outflow)

## Conclusion

Although several other follow-up modalities have been proposed for EVAR follow up, duplex scanning remains the simplest, cheapest, and most expeditious, especially in an office-based setting. With longer follow up and accrual of more experience with this regimen, earlier switch to duplex scanning surveillance should have an even more significant socioeconomic impact. It is also conceivable that this follow-up policy, which is applicable to most patients, could significantly expand the justified use of EVAR for aneurysm treatment since it eliminates the costs and complications associated with CT scan protocols. Follow-up regimens post-EVAR continue to be refined, with a clear trend toward readily available office-based surveillance. However, even in the setting of collapsed nonpressurized excluded aneurysm sacs, it may be prudent to continue obtaining a CT scan every 5 years to detect new remote aneurysms.

## References

1. Prinssen M, Verhoeven EL, Buth J, Dutch Randomized Endovascular Aneurysm Management (DREAM) Trial Group, et al. A randomized trial comparing conventional and endovascular repair of abdominal aortic aneurysms. N Engl J Med. 2004;351:1607–18.
2. Blankensteijn JD, de Jong SE, Prinssen M, Dutch Randomized Endovascular Aneurysm Management (DREAM) Trial Group, et al. Two-year outcomes after conventional or endovascular repair of abdominal aortic aneurysms. N Engl J Med. 2005;352:2398–405.
3. EVAR trial participants. Endovascular aneurysm repair versus open repair in patients with abdominal aortic aneurysm (EVAR trial 1): randomised controlled trial. Lancet. 2005;365:2179–86.
4. Prinssen M, Wixon CL, Buskens E, Blankensteijn JD. Surveillance after endovascular aneurysm repair: diagnostics, complications, and associated costs. Ann Vasc Surg. 2004;18:421–7.
5. Brenner DJ, Hall EJ. Computed tomography – an increasing source of radiation exposure. N Engl J Med. 2007;357:227722–84.
6. Walsh SR, Tang TY, Boyle JR. Renal consequences of endovascular abdominal aortic aneurysm repair. J Endovasc Ther. 2008;15:73–82.
7. Sato DT, Goff CD, Gregory RT, et al. Endoleak after aortic stent graft repair: diagnosis by color duplex ultrasound scan versus computed tomography scan. J Vasc Surg. 1998;28:657–63.
8. Tomlinson J, McNamara J, Matloubieh J, et al. Intermediate follow-up after endovascular aneurysm repair: can we forgo CT scanning in certain patients? Ann Vasc Surg. 2007;21:663–70.
9. AbuRahma AF. Fate of endoleaks detected by CT angiography and missed by color duplex ultrasound in endovascular grafts for abdominal aortic aneurysms. J Endovasc Ther. 2006;13:490–5.
10. AbuRahma AF, Welch CA, Mullins BB, Dyer BJ. Computed tomography versus color duplex ultrasound for surveillance of abdominal aortic stent-grafts. J Endovasc Ther. 2005;12:568–73.
11. Sandford RM, Bown MJ, Fishwick G, et al. Duplex ultrasound scanning is reliable in the detection of endoleak following endovascular aneurysm repair. Eur J Vasc Endovasc Surg. 2006;32:537–41.
12. Elkouri S, Panneton JM, Andrews JC, et al. Computed tomography and ultrasound in follow-up of patients after endovascular repair of abdominal aortic aneurysm. Ann Vasc Surg. 2004;18:271–9.
13. Chaer RA, Gushchin A, Rhee R, Marone L, Cho JS, Leers S, Makaroun MS. Duplex ultrasound as the sole long-term surveillance method post-endovascular aneurysm repair: a safe alternative for stable aneurysms. J Vasc Surg. 2009;49(4):845–9; discussion 849–50.
14. Lederle FA, Wilson SE, Johnson GR, Reinke DB, Littooy FN, Acher CW, et al. Variability in measurements of abdominal aortic aneurysms. J Vasc Surg. 1995;21:945–52.
15. Han SM, Patel K, Rowe VL, Perese S, Bond A, Weaver FA. Ultrasound-determined diameter measurements are more accurate than axial computed tomography after endovascular aortic aneurysm repair. J Vasc Surg. 2010;51(6):1381–7; discussion 1387–9.

16. d'Audiffret A, Desgranges P, Kobeiter DH, Becquemin JP. Follow-up evaluation of endoluminally treated abdominal aortic aneurysms with duplex ultrasonography: validation with computed tomography. J Vasc Surg. 2001;33:42–50.
17. Wolf YG, Johnson BI, Hill BB, Rubin GD, Fogarty TJ, Zarins CK. Duplex ultrasound scanning versus computed tomographic angiography for postoperative evaluation of endovascular abdominal aortic aneurysm repair. J Vasc Surg. 2000;32:1142–8.
18. Collins JT, Boros MJ, Combs K. Ultrasound surveillance of endovascular aneurysm repair: a safe modality versus computed tomography. Ann Vasc Surg. 2007;21:671–5.
19. Golzarian J, Murgo S, Dussaussois L. Evaluation of abdominal aortic aneurysm after endoluminal treatment: comparison of color duplex sonography with biphasic helical CT. Am J Roentgenol. 2002;178:623–8.
20. Raman KG, Missig-Carol N, Richardson T. Color-flow duplex ultrasound scan versus computed tomographic scan in the surveillance of endovascular aneurysm repair. J Vasc Surg. 2003;38:645–51.
21. Schmieder GC, Stout CL, Stokes GK, Parent FN, Panneton JM. Endoleak after endovascular aneurysm repair: duplex ultrasound imaging is better than computed tomography at determining the need for intervention. J Vasc Surg. 2009;50(5):1012–7; discussion 1017–8.
22. Cantisani V, Ricci P, Grazhdani H, Napoli A, Fanelli F, Catalano C, Galati G, D'Andrea V, Biancari F, Passariello R. Prospective comparative analysis of colour-Doppler ultrasound, contrast-enhanced ultrasound, computed tomography and magnetic resonance in detecting endoleak after endovascular abdominal aortic aneurysm repair. Eur J Vasc Endovasc Surg. 2011;41(2):186–92.
23. Ten Bosch JA, Rouwet EV, Peters CT, Jansen L, Verhagen HJ, Prins MH, Teijink JA. Contrast-enhanced ultrasound versus computed tomographic angiography for surveillance of endovascular abdominal aortic aneurysm repair. J Vasc Interv Radiol. 2010;21(5):638–43.
24. Mirza TA, Karthikesalingam A, Jackson D, Walsh SR, Holt PJ, Hayes PD, Boyle JR. Duplex ultrasound and contrast-enhanced ultrasound versus computed tomography for the detection of endoleak after EVAR: systematic review and bivariate meta-analysis. Eur J Vasc Endovasc Surg. 2010;39(4):418–28.
25. Noll RE, Tonnessen BH, Mannava K, Money SR, Sternbergh CW. Long-term postplacement cost after endovascular aneurysm repair. J Vasc Surg. 2007;46:9–15.
26. Sternberg CW, Money SR. Hospital cost of endovascular versus open repair of abdominal aortic aneurysms: a multicenter study. J Vasc Surg. 2000;31:237–44.
27. Bosch JL, Kaufman JA, Beinfeld MT, Miraude EA, Brewster DC, Gazelle GS. Abdominal aortic aneurysms: cost-effectiveness of elective endovascular and open surgical repair. Radiology. 2002;225:337–44.
28. Bosch JL, Lester JS, McMahon PM, Beinfeld MT, Halpern EF, Kaufman JA, et al. Hospital costs for elective endovascular and surgical repairs of infrarenal abdominal aortic aneurysms. Radiology. 2001;220:492–7.
29. Patel ST, Haser PB, Bush Jr HL, Kent CK. The cost-effectiveness of endovascular repair versus open surgical repair of abdominal aortic aneurysms: a decision analysis model. J Vasc Surg. 1999;29:958–72.
30. Clair DG, Gray B, O'Hara PJ, Ouriel K. An evaluation of the costs to health care institutions of endovascular aortic aneurysm repair. J Vasc Surg. 2000;32:148–52.
31. Parfrey PS, Griffiths SM, Barrett BJ, Paul MD, Genge M, Withers J, et al. Contrast material-induced renal failure in patients with diabetes mellitus, renal insufficiency, or both. A prospective controlled study. N Engl J Med. 1989;320:143–9.
32. Beeman BR, Doctor LM, Doerr K, McAfee-Bennett S, Dougherty MJ, Calligaro KD. Duplex ultrasound imaging alone is sufficient for midterm endovascular aneurysm repair surveillance: a cost analysis study and prospective comparison with computed tomography scan. J Vasc Surg. 2009;50(5):1019–24.
33. Busch K, White G, May J, Harris J, Doyle J, Forbes M, Makeham V, Burnett A. Ultrasound detection of intermittent and positional dependent endoleaks; evidence for a novel mechanism of AAA Sac growth after endovascular repair. In: 12th world congress of the world federation for ultrasound in medicine and biology, Sydney; 30 Aug–3 Sep 2009.
34. Go MR, Barbato JE, Rhee RY, Makaroun MS. What is the clinical utility of a 6-month computed tomography in the follow-up of endovascular aneurysm repair patients? J Vasc Surg. 2008;47:1181–6.
35. Chaikof EL, Brewster DC, Dalman RL, Makaroun MS, Illig KA, Sicard GA, Timaran CH, Upchurch Jr GR, Veith FJ, Society for Vascular Surgery. The care of patients with an abdominal aortic aneurysm: the society for vascular surgery practice guidelines. J Vasc Surg. 2009;50(4 Suppl):S2–49.

# Part VII

# Miscellaneous

Ali F. AbuRahma

# Transcutaneous Oxygen Tension: Principles and Applications

52

Jeffrey L. Ballard

**Abstract**

Empiric means of assessing limb perfusion are not adequate due to lack of sensitivity and specificity. However, transcutaneous oxygen tension has proven to be a useful tool in the evaluation of chronic lower extremity ischemia (CLI). The unique design of the transcutaneous sensor makes it possible to obtain accurate measurements of oxygen ($pO_2$) tension on the surface of the skin. Transcutaneous oxygen ($tcpO_2$) measurements can be used for minor and major lower extremity amputation level determination. In addition, $tcpO_2$ measurements facilitate prospective management of diabetic as well as non-diabetic patients with CLI.

**Keywords**

Transcutaneous oxygen measurement • Transcutaneous oxygen monitoring • Skin surface oxygen tension • Prospective management of diabetic foot problems • Chronic limb ischemia • Peripheral arterial disease

Empiric means of assessing limb perfusion are not adequate due to lack of sensitivity and specificity. However, there are a number of objective tools that can be used to accurately assess the degree of limb ischemia. Among the validated modalities, transcutaneous oxygen tension has proven to be quite useful in the evaluation of chronic lower extremity ischemia (CLI). The unique design of the transcutaneous sensor makes it possible to obtain accurate measurements of oxygen ($pO_2$) and carbon dioxide ($pCO_2$) tension on the surface of the skin. This chapter will discuss the physiology of transcutaneous oxygen ($tcpO_2$) measurements and demonstrate how these measurements can be used for minor and major lower extremity amputation level determination. In addition, $tcpO_2$ measurements will be shown to be essential for the prospective management of diabetic as well as non-diabetic patients with CLI.

J.L. Ballard, M.D.
Department of Vascular Surgery, St. Joseph Hospital,
1140 W. La Veta Avenue, Suite 850, Orange, CA 92868, USA
e-mail: jeffreyballard@visoc.org

## Physiology of the Measurement

Modern transcutaneous instrumentation has improved considerably from the viewpoint of maintenance, application, and routine use. A small sensor is applied to the skin with an airtight self-adhesive fixation ring. The heating element of the transcutaneous sensor increases the temperature beneath the sensor to 44°C. Heating the sensor creates local skin hyperemia, a decrease in blood flow resistance and compensatory arteriolarization of capillary blood. This effectively raises the $pO_2$ and decreases the $pCO_2$ values toward arterial levels [1, 2]. Contact liquid between the skin and sensor allows the underlying dermal tissue $pO_2$ to be in equilibrium with the sensor after 15–20 min. In practice, stable $tcpO_2$ readings are generally achieved in 20–30 min.

$TcpO_2$ monitoring is completely noninvasive and atraumatic if sensor placement at one skin site is limited to a maximum of 4 h. The test can be accomplished with the patient comfortably supine at ambient room temperature in an outpatient setting. Oxygen inhalation, change in limb position, and chest wall normalized $tcpO_2$ values can also be used to increase the specificity and sensitivity of the test [3–5]. Current monitors such as the TCM400 from Radiometer

A.F. AbuRahma, D.F. Bandyk (eds.), *Noninvasive Vascular Diagnosis*,
DOI 10.1007/978-1-4471-4005-4_52, © Springer-Verlag London 2013

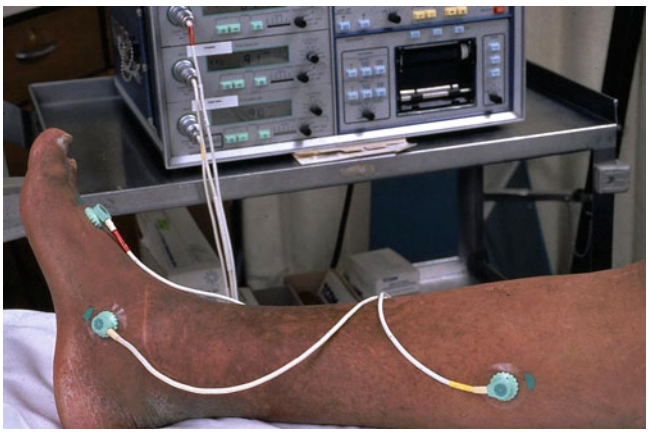

**Fig. 52.1** *Right leg* with sensors in place. Paper tape, placed over the sensor cup, can assist in keeping electrode stable and in constant contact with skin

(Radiometer, Copenhagen, Denmark) are not only portable but also provide up to six simultaneous measurements of transcutaneous oxygen tension. As demonstrated in Fig. 52.1, the modified Clark sensors are usually placed on the dorsal aspect of the forefoot between the great and second toe roughly 5 cm proximal to the second toe tip (forefoot measurement), on the medial aspect of the hind foot in front of or behind the malleolus (hind foot measurement) and 10 cm below the patella on the medial aspect of the calf (below-knee measurement) for basic lower extremity $tcpO_2$ mapping. The sensor can also be placed 10 cm above the patella on the medial aspect of the thigh for an above-knee measurement. Inaccurate readings may occur if the sensor is placed over a tendon or exposed bone. For optimal results, the sensor should be placed on skin that is free of edema, ulceration, hyperkeratosis, or cellulitis.

Tissue ischemia or inadequate perfusion to support major wound healing is presumed when the absolute $tcpO_2$ value is less than 30 mmHg. For practical purposes, a low $tcpO_2$ value can be interpreted as either reduced generalized arterial $pO_2$, as in the case of patients suffering from cardiopulmonary diseases or reduced regional blood flow due to impaired arterial $pO_2$ supply from atherosclerosis. Many investigators have reported that wound healing can occur in some patients with a low $tcpO_2$ value [6–16]. This can be partially explained by the non-linear relationship between $tcpO_2$ and cutaneous blood flow. Matsen et al. [12] reported that $tcpO_2$ measurements are mostly dependent on arterial-venous gradients and cutaneous vascular resistance. In essence, there can be nutritive blood flow to the skin even with a $tcpO_2$ level of 0 mmHg.

One of the techniques used to improve the accuracy of $tcpO_2$ measurements is sensor probe heating (44°C), which minimizes local vascular resistance. This makes transcutaneous oxygen tension more linear with respect to cutaneous blood flow. Additional techniques used to improve $tcpO_2$ accuracy include measurements performed before and after oxygen inhalation or change in limb position, oxygen isobar extremity mapping, and transcutaneous oxygen recovery half-time.

Wyss et al. [13] evaluated the results of $tcpO_2$ measurements used as a predictor of successful wound healing following amputation. The study analyzed 162 patients who had 206 lower extremity amputations. The authors concluded that transcutaneous oxygen is a reliable indicator of local tissue ischemia and that it can be used to predict failure of amputation healing due to tissue ischemia. However, there are two theoretical inadequacies that must be considered when using $tcpO_2$ measurements. First, the measurement is quite localized and one value may not represent of the overall degree of limb ischemia. Second, as previously mentioned, there may still be some nutritive flow to the skin despite a $tcpO_2$ level of 0 mmHg.

Despite the fact that in theory a $tcpO_2$ value of 0 mmHg at a proposed site of amputation does not always indicate ischemia that precludes healing, a $tcpO_2$ level of 20 mmHg or less clearly indicates severe limb ischemia. In the Wyss study [13], a $tcpO_2$ measurement of 20 mmHg or less was associated with a rate of failure for amputations distal to the knee that was more than ten times the 4% rate of failure in patients that had a $tcpO_2$ level of more than 20 mmHg.

## Clinical Applications in Peripheral Vascular Disease

### Selecting the Appropriate Amputation Level

Many authors have reported on the successful use of transcutaneous oxygen measurements to determine the appropriate lower extremity amputation level [6–16]. One of the initial reports on this topic was by Franzeck et al. [7]. Mean $tcpO_2$ levels in patients who experienced primary healing of a lower extremity amputation were compared to those of patients who failed to heal their amputation. The respective values for healing and nonhealing were $36.5 \pm 17.5$ and less than 30 mmHg. However, three of nine patients whose $tcpO_2$ level was less than 10 mmHg healed primarily.

In a study of below-knee amputations, Burgess et al. [6] noted that all 15 amputations that were associated with a $tcpO_2$ level greater than 40 mmHg healed. Primary wound healing was noted in 17 of 19 below-knee amputations with a $tcpO_2$ measurement between 1 and 40 mmHg, but none of the three patients with a below-knee level of 0 mmHg healed their amputation. Katsamouris et al. [9] reported that lower extremity amputations healed in all 17 patients with a $tcpO_2$ level greater than 38 mmHg or a $pO_2$ index (chest wall control site) greater than 0.59. Ratliff et al. [11] reported that below-knee amputations healed in 18 patients with a $tcpO_2$ measurement greater than 35 mmHg, whereas healing failed

in 10 of 15 with a $tcpO_2$ value less than 35 mmHg. In a study of 42 lower extremity amputations (28 below-knee and 14 above-knee), Christiansen and Klarke [14] found that 27 of 31 patients with a $tcpO_2$ level greater than 30 mmHg healed primarily. Seven patients with values between 20 and 30 mmHg healed although four patients had delayed healing. The amputation stumps of all four patients with a value below 20 mmHg failed to heal because of skin necrosis.

Data from Wyss et al. [13] are comparable to those yielded by a prospective study evaluating multiple tests used for amputation level selection. In this study, $tcpO_2$ measurements were prospectively compared to transcutaneous carbon dioxide tension, transcutaneous oxygen-to-carbon dioxide tension, foot-to-chest transcutaneous oxygen tension, intradermal xenon-133 clearance level, ankle brachial index, and the absolute popliteal artery pressure for accuracy in amputation level selection. All metabolic variables exhibited a high degree of statistical accuracy in predicting amputation healing, but none of the other tests showed statistical reliability. All amputations in this study (transmetatarsal, below-knee, and above-knee) healed primarily when the $tcpO_2$ measurement was greater than 20 mmHg and there were no false-positive or false-negative results [10]. It was also noted that successful prediction of amputation healing for any of the metabolic parameters was not affected by the presence of diabetes mellitus. This finding is similar to the observation of Wyss et al. [13].

In contrast to lower extremity amputations in nondiabetics, which usually result peripheral vascular disease primarily, most amputations in diabetic patients result from various combinations of contributing causes including neuropathy, ischemia, alterations of white cell function, infection or gangrene, faulty wound healing, cutaneous ulceration, and minor trauma [15]. Malone et al. [10] and Christensen and Klarke [14] concluded that a transcutaneous oxygen tension of 20 mmHg or more accurately predicted amputation site healing and found no difference in the healing rate between diabetics and nondiabetics. Computerized analysis of various transcutaneous metabolic parameters by Malone et al. [10] demonstrated a high association with primary amputation site healing with the following values: transcutaneous oxygen tension greater than 20 mmHg, transcutaneous carbon dioxide value less than 40.5 mmHg, transcutaneous oxygen-to-transcutaneous carbon dioxide index greater than 0.472 and foot-to-chest transcutaneous oxygen index greater than 0.442.

The above data reinforce the fact that elective lower extremity amputation should not be performed without objective testing to ensure selection of the most distal amputation site that will heal primarily yet allow removal of infected, painful, or ischemic tissue [15, 16]. A variety of techniques are available to achieve this, depending on available equipment, the amputation level under consideration, and the accuracy of the chosen modality [16]. $TcpO_2$ measurements continue to be a reliable technique; however, it is not suitable for whole limb mapping.

The ultimate role of any method used for amputation level determination is to inform the surgeon of the quantitative risk of nonhealing at the proposed site of surgery. The level of amputation can then be decided on the basis of this objective finding in conjunction with surgeon's clinical judgment and patient's physical findings. For example, a surgeon might perform an amputation distal to the knee through a site with a very low $tcpO_2$ level in a patient who is well motivated, relatively young, and otherwise healthy. Such an amputation would almost certainly be ruled out in a fragile elderly person who faces a limited prospect for successful rehabilitation.

## Prospective Treatment of Diabetic Foot Problems

Successful treatment of the patient with diabetes and limb-threatening ischemia requires an accurate assessment of limb perfusion. Presenting clinical symptoms may be misleading. Physical examination of pedal pulses or ankle/brachial index (ABI) may not be accurate due to the non-compressible nature of a diabetic patient's peripheral arteries. Often, the cause of the presenting foot problem is multifactorial and commonly used non-invasive lower extremity hemodynamic studies lack discriminative accuracy. On the other hand, arteriography is ultimately accurate. However, it is invasive, expensive, and carries a small but well-defined set of associated complications [17, 18]. In this setting, $tcpO_2$ measurements can be extremely useful as they are noninvasive, inexpensive, and reproducible [19–24].

In a clinical experience reported by Ballard et al. [25], $tcpO_2$ measurements were prospectively demonstrated to accurately predict severity of foot ischemia in patients with diabetes. Based on clinical experience and previously published amputation level determination data, an absolute transmetatarsal $tcpO_2$ measurement of 30 mmHg was used as the threshold value for selection of a treatment option. If the level was 30 mmHg or greater, the patient's foot problem was managed conservatively with local wound care, wound debridement, or minor foot amputation. If the level was less than 30 mmHg, arteriography of the involved limb was performed to plan arterial reconstruction or to perform percutaneous intervention to improve foot perfusion.

Thirty-one of 36 (86%) limbs in the conservatively managed group were treated successfully including 73% (11/15 ft) of limbs without a palpable pedal pulse. The mean time to wound healing was 6.85 weeks and there were five treatment failures. In the operative/endovascular group, 83.3% of limbs achieved a TM $tcpO_2$ level ≥30 mmHg after treatment. Twenty-two of 26 (85%) limbs in this group had complete resolution of their presenting foot problem. The mean time to wound healing was 9.52 weeks. Treatment failures

eventually led to 3 BKAs (1 failed necessitating revision to the AK level) and 1 above-knee amputation.

The pre-treatment pedal pulse examination was more accurate than an ABI in predicting forefoot $tcpO_2$ values above or below 30 mmHg. Further, an abnormal arteriogram was predicted by both a low TM $tcpO_2$ level and the absence of a palpable pedal pulse, but not by an ABI <60. The presence of a pedal pulse was 100% accurate for identifying limbs with a TM $tcpO_2 \geq 30$ mmHg, but there were an additional 17 limbs with a measurement ≥30 mmHg and no palpable pedal pulse. Following arterial bypass or angioplasty, a TM $tcpO_2$ level ≥30 mmHg was highly accurate in predicting a successful outcome. Ultimately, an initial or post-intervention TM $tcpO_2$ level ≥30 mmHg was more accurate than a palpable pulse in predicting either wound healing or resolution of rest pain. An ABI ≥ 0.60 was also associated with a successful outcome, but due to non-compressible vessels, this was only able to be calculated in 41/62 (66%) limbs.

Certainly diabetic patients without pedal pulses do have arteriosclerotic lesions, some of which can be reconstructed. However, this prospective study demonstrated that such surgical revascularization is not obligatory. In fact, well-performed $tcpO_2$ measurements predicted distal ischemic wound healing in 90% of cases. Furthermore, conservative management was not only cost effective when compared to surgical or endovascular revascularization, but time to wound healing was not statistically significantly different between the two groups (6.84 weeks versus 9.52 weeks, $P = 0.169$).

As demonstrated in the study outlined above, an absolute TM $tcpO_2$ level ≥30 mmHg appears to be an accurate cutoff point for the selection of treatment for almost all diabetic foot problems. The conservative management scheme, however, requires diligent patient follow-up. There must be a commitment by the surgeon to perform wound debridements and staged procedures (i.e., minor foot amputations or split-thickness skin grafts). Proper outpatient wound care is essential. Finally, a higher TM $tcpO_2$ threshold (40 mmHg) should be used to select management of calcaneal gangrene or extensive non-healing ulcerations. Table 52.1 demonstrates an algorithm for the elective management of diabetic patients with limb-threatening ischemia based on $tcpO_2$ level.

Padberg et al. [26] confirmed our previous findings and demonstrated that $tcpO_2$ measurements alone are sufficient to objectively stratify the degree of lower extremity arterial ischemia. They compared $tcpO_2$ measurements to arterial segmental pressures (ASPs) and arterial segmental indices (ASI) in 204 ischemic lower extremity sites in patients with either diabetes, chronic renal failure or neither disease process. Stepwise multiple regression analysis demonstrated $tcpO_2$ mapping to be superior to ASP and ASI for all endpoints. As demonstrated by others, predictive accuracy of $tcpO_2$ measurements was unaffected by the presence of diabetes and ASP and ASI were misleading and inaccurate. Interestingly, because of reduced accuracy of ASP and ASI, $tcpO_2$ remained the diagnostic modality of choice even for the non-diabetic patient with arterial ischemia of the lower extremity.

**Table 52.1** Algorithm for elective management of the diabetic patient with limb-threatening foot ischemia

| |
|---|
| A. If forefoot/hind foot $tcpO_2$ level is ≥30 mmHg (with or without a palpable pedal pulse): |
| Outpatient wound care, wound debridement, or minor foot amputation. |
| B. If forefoot/hind foot $tcpO_2$ level is <30 mmHg or conservative treatment is unsuccessful after 4–6 weeks: |
| Arteriography, with revascularization as needed. |
| C. If forefoot/hind foot $tcpO_2 < 30$ mmHg and there is pedal edema or cellulitis: |
| Repeat test after resolution, before proceeding with arteriography. |
| D. If there is calcaneal gangrene/non-healing ulcer: |
| Use higher hind foot $tcpO_2$ threshold of 40 mmHg and obtain arteriogram after 2–4 weeks of unsuccessful conservative treatment. |

Finally, Petrakis and Sciacca [27] use distal limb $tcpO_2$ measurements as a prognostic parameter in the selection of diabetic patients for placement of a permanent spinal cord stimulation device. Sixty diabetic patients had implantation of a spinal cord electrical generator after failed conservative or surgical treatment of severe peripheral vascular disease. The clinical peripheral vascular disease status of each patient was either Fontaine's stage III or IV. Forefoot and hind foot $tcpO_2$ measurements were compared to toe pressure Doppler measurements before device implantation as well as 2 and 4 weeks postoperative. Pain relief of over 75% and foot salvage was achieved in 35 patients, while partial success with pain relief greater than 50% and foot salvage for at least 6 months was obtained in 12 other patients. Amputation for persistent gangrene, non-healing ulceration, or unrelenting rest pain was performed in the remaining 13 patients.

Interestingly, clinical improvement and foot salvage were both associated with a significant increase in the 2 week post-operative $tcpO_2$ measurement while the ankle brachial index and toe pressure did not change under spinal cord stimulation. These data suggest that a 2 week testing period before permanent spinal cord stimulation is not only useful regarding prognosis but also cost saving. Only patients who experience a significant increase in distal limb $tcpO_2$ in addition to pain relief should be considered for permanent implantation of a spinal cord stimulator.

## Prospective Treatment of Chronic Lower Extremity Ischemia

Much the same as described above for the treatment of diabetic patients, $tcpO_2$ measurements can be useful for selecting management of ill-defined leg/ft complaints particularly

in elderly patients with multiple medical problems. For instance, an adequate $tcpO_2$ level (≥30 mmHg) at the forefoot and hind foot may obviate the need for an arteriogram and support non-operative management. On the other hand, a low $tcpO_2$ level likely indicates a situation that will require a higher level of care. The potential need for arteriography and arterial revascularization can be thoroughly discussed with the patient and family prior to treatment. This ensures reasonable expectations. Finally, a dramatic improvement in $tcpO_2$ measurement following treatment is not only gratifying, but at least 90% of patients will experience a successful outcome.

$TcpO_2$ measurements can also be used to determine whether endovascular treatment has been successful at the skin level of nondiabetic as well as diabetic patients with peripheral arterial occlusive disease (PAD). Wagner et al. [28] previously demonstrated that percutaneous transluminal angioplasty (PTA) has a positive effect on oxygen supply to the skin in patients with PAD. In this study, 34 patients with PAD had $tcpO_2$ measurements obtained at the dorsum of the foot 1 day before PTA, during PTA, 1 day after PTA, and 6 weeks after PTA. A significant increase in $tcpO_2$ was noted immediately following PTA as well as 1 day and 6 weeks later.

Pardo et al. [29] evaluated the efficacy of endovascular revascularization in diabetic patients with critical limb ischemia after treatment with PTA by comparing $tcpO_2$ measurements with the ankle-brachial index (ABI) post-PTA. They prospectively studied 151 consecutive diabetic patients with posterior tibial and dorsalis pedis Doppler, ABI, $tcpO_2$, and duplex scan results. If two of the four mentioned examinations were abnormal, arteriography was performed and, if appropriate, PTA was performed concomitantly. At least 64 patients were considered suitable candidates for PTA. After PTA, ABI increased from $0.67 \pm 0.25$–$0.84 \pm 0.25$ ($P < 0.001$) and $TcpO_2$ increased from $27.20 \pm 11.10$–$40 \pm 12.10$ mmHg ($P < 0.001$). While the $TcpO_2$ could be measured in all patients, the ABI was not measurable in up to 25% of patients due to non-compressible vessels. Statistical analysis revealed a meager correlation between the techniques used: $TcpO_2$ and ABI ($P = 0.20$). Their study suggests that an increase in $TcpO_2$ values in diabetic patients following PTA is a marker of improved microvascular revascularization and that simply obtaining a post-treatment ABI may not be as informative.

Arroyo and colleagues [30] used $tcpO_2$ measurements to determine when previously ischemic tissue had adequate perfusion to support major wound healing. Eleven patients with severe chronic limb ischemia defined as a forefoot $tcpO_2 \leq 30$ mmHg were entered into this prospective study. $TcpO_2$ measurements were recorded prior to lower extremity bypass and on post-operative days one, two, and three. A statistically significant increase in mean transcutaneous oxygen pressure was observed between the pre-operative and the day 3 post-operative measurements. Despite this finding, some bypass patients still had low $tcpO_2$ values (<30 mmHg) even on post-operative day 3. Nevertheless, this small clinical series suggests that unless urgent, adjunctive minor foot amputation or major débridement should wait until at least 3 days after successful lower extremity bypass. This will ensure that there is now adequate perfusion at the foot level to support major wound healing. This clinical recommendation could also be used to select appropriate timing of minor foot amputations or major débridements that are performed after endovascular procedures.

Finally, $tcpO_2$ measurements have even been used to noninvasively detect lesions in the arterial network supplying blood flow to the hypogastric circulation. A study was performed a few years ago by Abraham et al. [31] in which they selected 43 patients suspected of proximal aortoiliac occlusive disease and 34 without suspected proximal ischemia. $TcpO_2$ measurements were obtained from the buttock region bilaterally in addition to a chest reference value. Arteriography was compared to normalized $tcpO_2$ measurements during and after treadmill exercise in addition to other comparisons. A mean drop in the $tcpO_2$ measurement of at least 15 mmHg in either group was both sensitive (range 79–83%) and specific (range 82–86%) for the diagnosis of a positive arteriogram. The arteriogram was defined as positive when there was at least a 75% stenosis noted on the same side as the $tcpO_2$ drop in one or more of the following arteries: aorta, common iliac, or internal iliac. Thus, it appears that an exercise-induced drop in buttock $tcpO_2$ pressure is a sensitive and specific indicator of either a hemodynamically significant lesion proximal to or within the hypogastric artery. These measurements could be used to noninvasively and objectively assess the skin level response to endovascular or surgical treatment of infrarenal aortic or proximal iliac artery lesions.

## References


1. Baumbach P. Understanding transcutaneous $PO_2$ and $PCO_2$ measurements. Copenhagen: Radiometer A/S; 1986. p. 1–54.
2. Steenfos HH, Baumbach P. Transcutaneous $PO_2$ in peripheral vascular disease. Copenhagen: Radiometer A/S; 1986. p. 1–18.
3. Moosa HH, Peitzman AB, Makaroun MS, Webster MW, Steed DL. Transcutaneous oxygen measurements in lower extremity ischemia: effects of position, oxygen inhalation, and arterial reconstruction. Surgery. 1988;103(2):193–8.
4. Andrews KL, Boon AJ, Dib M, Liedl DA, Yacyshyn A, Yacyshyn V. The use of elevation and dependency to enhance the predictive value of transcutaneous oxygen pressure measurements in the assessment of foot amputation healing. PM R. 2010;2(9):829–34.
5. Larsen JF, Jensen BV, Christensen KS, Egeblad K. Forefoot transcutaneous oxygen tension at different leg positions in patients with peripheral vascular disease. Eur J Vasc Surg. 1990;4:185–9.
6. Burgess EM, et al. Segmental transcutaneous measurements of $PO_2$ in patients requiring below the knee amputations for peripheral vascular insufficiency. J Bone Joint Surg Am. 1982;64:378–92.

7. Franzeck UK, et al. Transcutaneous $PO_2$ measurement in health on peripheral arterial occlusive disease. Surgery. 1982;91:156–63.
8. Friedmann LW. The prosthesis – immediate or delayed fitting? Angiology. 1972;23:513–24.
9. Katsamouris A, et al. Transcutaneous oxygen tension in selection of amputation level. Am J Surg. 1984;147:510–6.
10. Malone JM, et al. Prospective comparison of noninvasive techniques for amputation level selection. Am J Surg. 1987;154:179–84.
11. Ratliff DA, et al. Prediction of amputation healing: the role of transcutaneous $PO_2$ assessment. Br J Surg. 1984;71:219–22.
12. Matsen FA, et al. The relationship of transcutaneous $PO_2$ and laser Doppler measurements in human model of local arterial insufficiency. Surg Gynecol Obstet. 1984;159:418–22.
13. Wyss CR, et al. Transcutaneous oxygen tension as a predictor of success after an amputation. J Bone Joint Surg Am. 1988;70:203–7.
14. Christensen KS, Klarke M. Transcutaneous oxygen measurement in peripheral occlusive disease: an indicator of wound healing in leg amputation. J Bone Joint Surg Br. 1986;68:423–6.
15. Ballard JL, Malone JM. Amputation in the diabetic. In: Rutherford RB, editor. Seminars in vascular surgery. Philadelphia: W.B. Saunders Co.; 1992. p. 257–63.
16. Malone JM, Ballard JL. Amputation level determination techniques. In: Bernstein EF, editor. Vascular diagnosis. St. Louis: Mosby-Year Book, Inc.; 1993. p. 568–74.
17. Kim D, Orron DE. Techniques and complications of angiography. In: Kim D, Orron DE, editors. Peripheral vascular imaging and intervention. St. Louis: Mosby-Year Book, Inc.; 1992. p. 83–109.
18. Weisberg LS, Kurnik PB, Kurnik BRC. Risk of radiocontrast neuropathy in patients with and without diabetes mellitus. Kidney Int. 1994;45:259–65.
19. Hauser CJ, Klein SR, Mehringer CM, Appel P, Shoemaker WC. Superiority of transcutaneous oximetry in noninvasive vascular diagnosis in patients with diabetes. Arch Surg. 1984;119:690–4.
20. Hauser CJ, Klein SR, Mehringer CM, et al. Assessment of perfusion in the diabetic foot by regional transcutaneous oximetry. Diabetes. 1984;33:527–31.
21. Modesti PA, Boddi M, Poggesi L, et al. Transcutaneous oximetry in evaluation of the initial peripheral artery disease in diabetics. Angiology. 1987;38(6):457–61.
22. Hauser CJ. Tissue salvage by mapping of skin surface transcutaneous oxygen tension index. Arch Surg. 1987;122:1128–30.
23. Fronek A. Clinical experience with transcutaneous $pO_2$ and $pCO_2$ measurements. In: Bernstein EF, editor. Vascular diagnosis. St. Louis: Mosby-Year Book, Inc.; 1993. p. 620–5.
24. Lalka SG, Malone JM, Anderson GG, Hagaman RM, McIntyre KE, Bernhard VM. Transcutaneous oxygen and carbon dioxide pressure monitoring to determine severity of limb ischemia and to predict surgical outcome. J Vasc Surg. 1988;7(4):507–14.
25. Ballard JL, Eke CC, Bunt TJ, Killeen JD. A prospective evaluation of transcutaneous oxygen ($TcPO_2$) measurements in the management of diabetic foot problems. J Vasc Surg. 1995;22:485–92.
26. Padberg FT, Back TL, Thompson PN, Hobson RW. Transcutaneous oxygen ($TcPO_2$) estimates probability of healing in the ischemic extremity. J Surg Res. 1996;60:365–9.
27. Petrakis E, Sciacca V. Prospective study of transcutaneous oxygen tension ($TcpO_2$) measurements in the testing period of spinal cord stimulation in diabetic patients with critical lower extremity ischaemia. Int Angiol. 2000;19:18–25.
28. Wagner HJ, Schmitz R, Alfke H, Klose KJ. Influence of percutaneous transluminal angioplasty on transcutaneous oxygen pressure in patients with peripheral arterial occlusive disease. Radiology. 2003;226:791–7.
29. Pardo M, Alcaraz M, Ramón Breijo F, et al. Increased transcutaneous oxygen pressure is an indicator of revascularization after peripheral transluminal angioplasty. Acta Radiol. 2010;51:990–3.
30. Arroyo CI, Tritto VG, Buchbinder D, et al. Optimal waiting period for foot salvage surgery following limb revascularization. J Foot Ankle Surg. 2002;41:228–32.
31. Abraham P, Picquet J, Vielle B, et al. Transcutaneous oxygen pressure measurements on the buttocks during exercise to detect proximal arterial ischemia: comparison with arteriography. Circulation. 2003;107:1896–900.

# Arterial and Venous Intravascular Ultrasound Applications

53

Edward B. Diethrich and Donald B. Reid

**Abstract**

Intravascular ultrasound (IVUS) is a catheter based endovascular guidance system which was developed initially in interventional cardiology but has been very successfully translated to peripheral interventions. The catheters are small with tiny transducers which can be easily introduced over a guidewire percutaneously. Because the ultrasound probe is introduced at such close proximity to the vessel, great detail and therefore important information of the disease can be obtained. IVUS is an expensive imaging modality and its use has tended to be for the more complex cases such as endoluminal grafting, carotid stenting, or cases of critical limb ischemia. However, the ability for the operating room to successfully use IVUS in such situations depends on a regular ability to use and understand its clinical value. Fortunately IVUS has become much more readily understandable and user friendly in the operating room not only with technical improvements in catheters but also within the IVUS machine operator interface as well as with advances such as three-dimensional reconstruction, color flow, and virtual histology (VH). This latest development of VH IVUS has led to a greater appreciation of plaque type and how the disease in the wall of the vessel will behave at the moment of endoluminal treatment. The role of IVUS is expanding to assist with endovenous interventions. Further advances in IVUS are likely to come from forward looking IVUS, which may help negotiate chronic total occlusions. There is no doubt that the role and use of IVUS in peripheral interventions are increasing and the cost effectiveness and clinical value are becoming more practical and established.

**Keywords**

Intravascular ultrasound • Virtual histology

## Introduction

Intravascular ultrasound (IVUS) is a catheter-based guidance system that facilitates accurate placement during endovascular procedures and while it was originally developed in cardiology, IVUS is now used in a wide variety of peripheral interventions—both arterial and venous [1–4]. Accurate imaging before and after balloon angioplasty as well as following stenting is crucially important in achieving a successful clinical outcome. The IVUS probe is passed into the vessel lumen, and because the ultrasound probe is in such close proximity, great detail is possible with significant magnification of the images compared with conventional extracorporeal ultrasound. IVUS provides histologic detail of the vessel wall and also demonstrates blood flow within the lumen [5, 6].

The early IVUS probes rotated mechanically inside a catheter, sweeping an ultrasound signal around 360° similar to a radar sweeping around a ship at sea. But the disadvantage of

E.B. Diethrich, M.D. (✉)
Arizona Heart Foundation,
Phoenix, AZ, USA
e-mail: ediethrich@azheart.com

D.B. Reid, M.D., FRCS
Department of Vascular and Endovascular Surgery,
Wishaw Hospital, Scotland, UK

A.F. AbuRahma, D.F. Bandyk (eds.), *Noninvasive Vascular Diagnosis*,
DOI 10.1007/978-1-4471-4005-4_53, 

such early rotating catheters was that the probe did not configure coaxially with the guidewire. This meant that it did not track smoothly through the artery and could damage it. Furthermore, the images were two-dimensional axial cuts, which being only "black and white" were difficult to interpret. Fortunately many advances have now made IVUS much more easily understandable in the operating room environment [7].

IVUS has two main clinical roles. It provides a diagnostic ability to assess and measure the severity of disease before treatment and also evaluates the completeness of treatment following intervention [8–10]. Arteriography provides the endovascular surgeon with details of the collateral circulation, vessel contour, quality of flow, and inflow and outflow. IVUS, however, allows greater appreciation of the vessel wall than the lumen and can distinguish between soft plaque and calcification. Intimal flaps, thrombus formation, and ulceration are also visible with IVUS and the luminal diameter and cross-sectional areas can also be measured. IVUS can also detect lesions missed on conventional arteriography [4]. IVUS can be used following percutaneous transluminal angioplasty, atherectomy, laser, thrombolysis, and endoluminal grafting. It has also been used recently to visualize venous abnormalities and guide treatment in patients with multiple sclerosis being treated for venous insufficiency of the jugular and azygous veins.

This very practical assistance within the operating room environment has become much easier to use with the developments of three-dimensional reconstruction, color flow, and virtual histology IVUS. Its use is described in detail in this chapter together with the latest technical advances of IVUS and its application in many different peripheral situations.

## Technical Aspects of IVUS Applications and Peripheral Interventions

There are two main IVUS systems currently commercially available. The Galaxy system (Boston Scientific, Natick, MA) uses mechanically rotating probes, which provide grayscale IVUS imaging with two- and three-dimensional reconstructions. The second system is the Volcano system (Volcano Corporation, Rancho Cordova, CA), which uses phased array imaging with probes that are coaxial (with fast exchange versions). The main advantage of the Volcano Therapeutics system is that it also provides colored blood flow imaging. This has significant diagnostic advantages over "grayscale" IVUS [5].

Probe size varies depending on the situation. In general, high-frequency, low-profile probes are used in the smaller arteries to obtain high-quality resolution, for example, using 20 MHz transducers. To achieve a greater penetration of ultrasound distance for larger vessels, 10-MHz catheters are required [5]. We use 2.9F, 20-MHz catheters that configure with 0.014-in. guide-wires for the smaller arteries such as the carotid, renal, superficial femoral, popliteal, and tibial

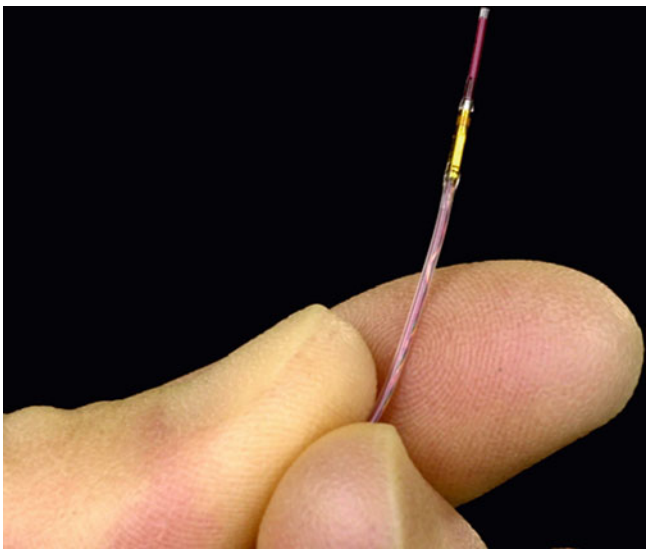

**Fig. 53.1** A 2.9F Eagle Eye IVUS probe compatible with a 0.014-in. guidewire


**Fig. 53.2** A motorized pullback sled device

arteries (Fig. 53.1). A 3.5F, 135-cm-long, fast-exchange catheter that is coaxial for 30 cm of its length and configures with a 0.018 in. wire has an ultrasound diameter range of 24 mm. We find this suitable for larger arteries such as the iliac. An 8.2F probe with a maximum diameter of 60 mm that is compatible with a 0.035-in. guidewire is used for the great vessels: the abdominal and thoracic aortas. Motorized pullback sled devices are available for peripheral interventions from both Boston Scientific and Volcano Corporation

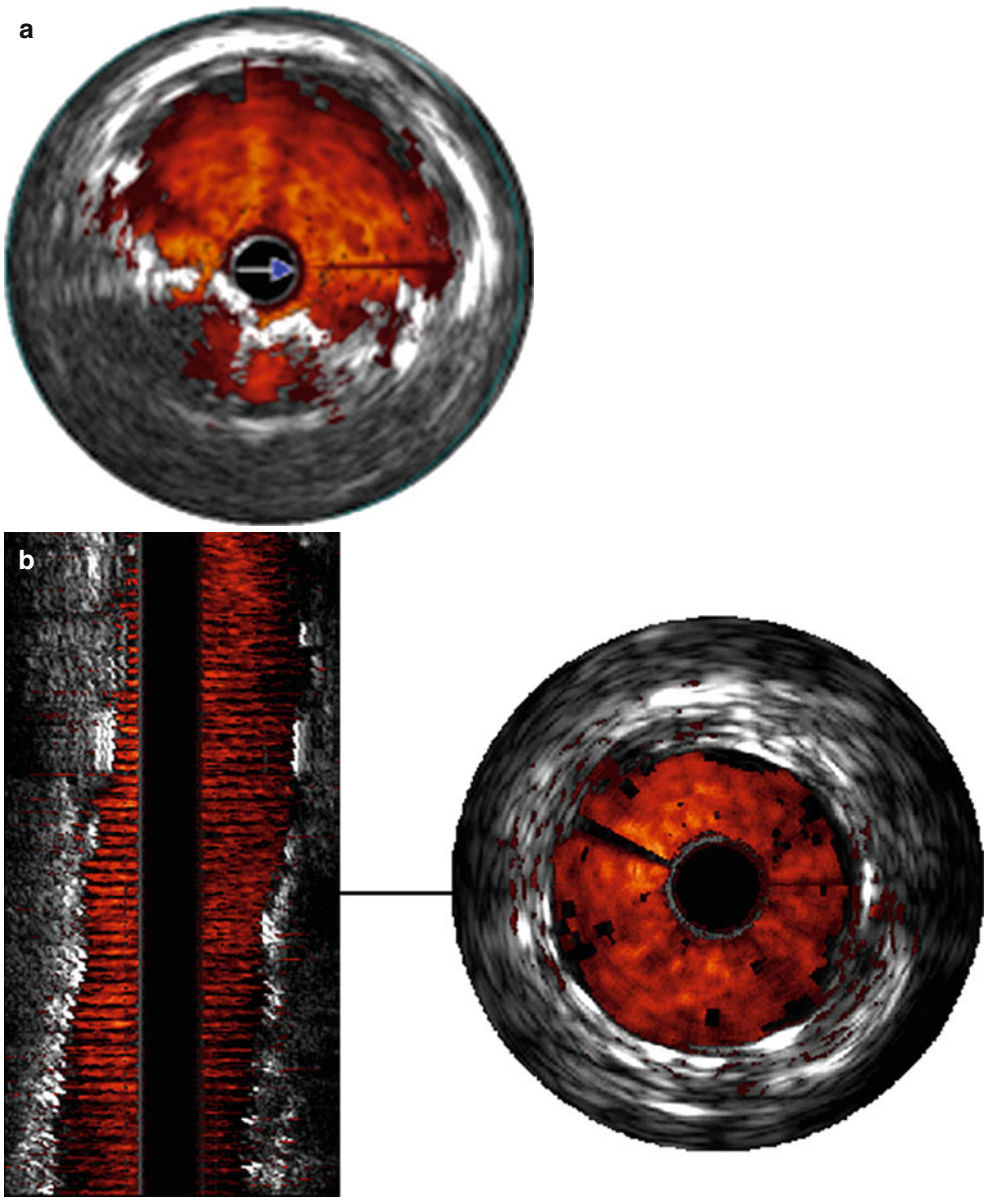


**Fig. 53.3** (**a**) Two-dimensional color IVUS showing an incompletely deployed stent. (**b**) Two- and three-dimensional color IVUS showing improved stent deployment following reballooning

(Fig. 53.2). However, they are rarely used in peripheral interventions because long-distance pullbacks are necessary compared to coronary artery evaluation and the pullback devices are slow and time consuming. Most have a maximum speed of just 1 mm/s.

The IVUS image created is a circular axial cut with a central disk artifact caused by the catheter. Real-time imaging displays the vessel wall and lumen at 30 frames/s allowing pulsatility of the artery wall to be seen. The ultrasound images display the vessel wall in histologic detail: the thin inner intima reflects the signal brightly while the media is a dark circumferential ring. Outside, the adventitia is also bright and reflective. Calcification typically reflects the ultrasound signal completely causing dark shadowing behind it (Fig. 53.3).

Three-dimensional reconstruction of the two-dimensional axial images produces a picture similar in appearance to an angiogram allowing the whole length of the vessel under examination to be viewed at the one time without the need for repeated pullbacks (Fig. 53.3). Consecutive axial images are stacked by powerful computing during a pullback of the ultrasound catheter through the vessel. A computerized edge tracking formula (algorithm) then aligns the consecutive frames [6]. The three-dimensional reconstruction can be viewed as either "longitudinal" or "volume" views. The longitudinal reconstruction is immediately available in the operating room and can be rotated around the longitudinal axis of the catheter to provide oblique and lateral perspectives. The volume view takes 2–3 min longer to create and has some artifact, since the raw data are altered.

A smooth and steady pullback is necessary to acquire high-quality reconstructions.

Color flow IVUS was developed by EndoSonics (Rancho Cordova, CA, now Volcano Corporation). ChromaFlo is the computer software that detects blood flow and colors it red. The software detects the differences between adjacent IVUS frames. As the blood cells move through the artery, they move through the IVUS image frames. The software detects differences between adjacent frames and colors the image red. ChromaFlo detects faster flowing blood and colors it yellow. However, at present, flow velocities cannot be measured using this technique. ChromaFlo does not utilize the Doppler effect [5]. Color flow IVUS has been a very helpful addition because it shows clearly where the lumen meets the vessel wall. This was not always apparent in "black and white" IVUS, especially if the vessel wall contained dark echolucent plaque or soft thrombus. There are many clinical situations that color IVUS assists in but none more so than arterial dissection. A specific catheter, the Pioneer (Medtronic, MN), has been developed to identify true from false lumen and steer the guidewire (and treatment) accordingly.

Virtual histology IVUS (VH IVUS) is a new advance [11–14]. Where color IVUS has highlighted the blood flow in the lumen, VH IVUS aims to identify and color code plaque type in the artery wall. Conventional IVUS uses the amplitude of reflected ultrasound from the different components of the vessel and converts it into an image with a grayscale. VH IVUS analyzes the spectrum of reflected radiofrequency (RF) ultrasound signals and then classifies the spectral type into four categories of plaque:

1. Fibrous tissue—densely packed collagen fibers with no evidence of lipid accumulation.
2. Fibrofatty—loosely packed collagen fibers with regions of fatty deposit.
3. Necrotic core—localized areas of loss of matrix containing lipid, typically with microcalcifications.
4. Dense calcium—focal areas of dense calcium.

Each category is color coded (dark green—fibrous, light green—fibrofatty, red—necrotic core, white—calcification) and this is superimposed over the conventional grayscale IVUS image (Fig. 53.4). Comparison with coronary artery histologic examination has produced 80–93% accuracy rates [11].

The clinical value of VH IVUS has yet to be defined, however, soft lipidic, necrotic core plaques have been implicated in acute ischemic syndromes such as plaque rupture. Detection of such "vulnerable" plaques using VH IVUS could have major treatment implications [10, 15]. While to date most work on VH IVUS has been in the coronary arteries, the peripheral arteries merit similar investigation, particularly the carotid arteries, since plaque rupture there can cause stroke. Treating such vulnerable plaque by stenting may 1 day become routine practice despite there being no hemodynamic stenosis if such vulnerable plaque is shown to be a high risk of stroke.

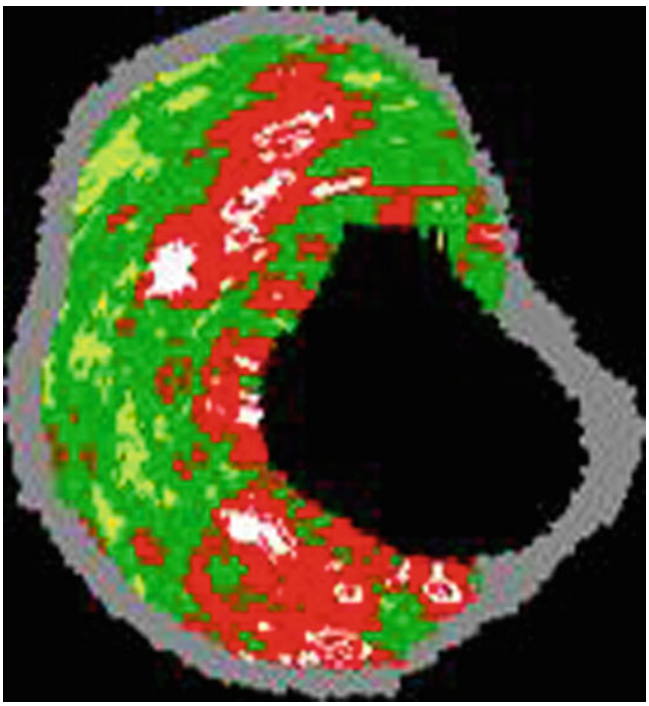

**Fig. 53.4** Color-coded virtual histology IVUS of a calcified thin cap fibroatheromatous "vulnerable" plaque containing calcification (*white*), fibrous plaque (*dark green*), fibrofatty plaque (*light green*), and necrotic core plaque (*red*) (Courtesy of Volcano Corporation)

We have used VH IVUS most often in carotid artery stenting. We have found that such evaluation of carotid artery disease helps to anticipate how the plaque will behave at the moment of treatment. Will it resist complete stent expansion or break up and embolise to the brain? VH IVUS can only be performed in small caliber vessels using the Eagle Eye Catheter that has a range of 20 mm diameter.

## Performing a Pullback

When the IVUS catheter has been chosen for the artery being treated (based on the size of the artery and the range of ultrasound that the catheter images), the probe is then flushed with heparinized saline and gently introduced over the wire. To obtain color flow, a "reference" function needs to be performed on the IVUS machine when the probe is in the arterial lumen. This removes near-field vision artifact, a characteristic of phased array IVUS imaging. The probe is passed into the artery beyond the disease and a slow and steady pullback is begun through the area in order to interrogate the lesion. Two- and three-dimensional views are then assessed.

## Operative and Anatomic Situations

### Carotid Angioplasty and Stenting

There are special features to bear in mind when stenting the carotid artery. It is particularly susceptible to incomplete stent deployment since heavy calcification resists complete stent expansion [16]. Furthermore, the internal carotid artery is not always uniform in diameter but is narrower distally and wider near its origin [17]. Stenting can also compromise the origin of the external carotid artery by compression, and recurrent stenosis following carotid endarterectomy may respond differently during stenting compared with a primary atherosclerotic lesion [18, 19]. The IVUS operator must appreciate these aspects and avoid dislodging embolic material or causing intimal dissection to the artery through overzealous instrumentation.

IVUS is a powerful tool in carotid stenting; however, the penalties are high if the disease is underestimated or the stent is badly deployed. We use IVUS more frequently now in carotid stenting since the introduction of cerebral protection devices. Immediately after deploying the protection device, IVUS can assess the lesion and take measurements to help stent and balloon sizing. We currently use the Eagle Eye Platinum catheter (Volcano Corporation, Rancho Cordova, CA), which is a low-profile 2.9F 20-MHz probe that configures with the 0.014-in. wire of most cerebral protection devices (Fig. 53.5).The IVUS probe is advanced into the distal internal carotid artery, and the pullback is begun. The distal internal carotid artery has a characteristic appearance on IVUS because it is so thin and usually spared of disease. The histologic layers are elegantly seen. Measurements can be taken just above the lesion to help size balloon and stent diameters, and the degree of stenosis can also be assessed to decide whether predilation is required or whether primary stent deployment can be performed [20]. While currently plaque morphology can be subjectively assessed by IVUS, the new advance of VH IVUS (Volcano Corporation, Rancho Cordova, CA) is promising since it will provide classified histologic plaque types.

Following stenting, the IVUS probe is introduced again and a pullback assesses the completeness of stent deployment. IVUS measurements of the minimum stent diameter can be made to decide whether further ballooning is required. Mid-stent waisting is a common finding. In general, a minimum stent diameter of more than 4 mm is recommended in the internal carotid artery to avoid residual hemodynamically significant stenosis [7]. The stent should be uniformly well expanded

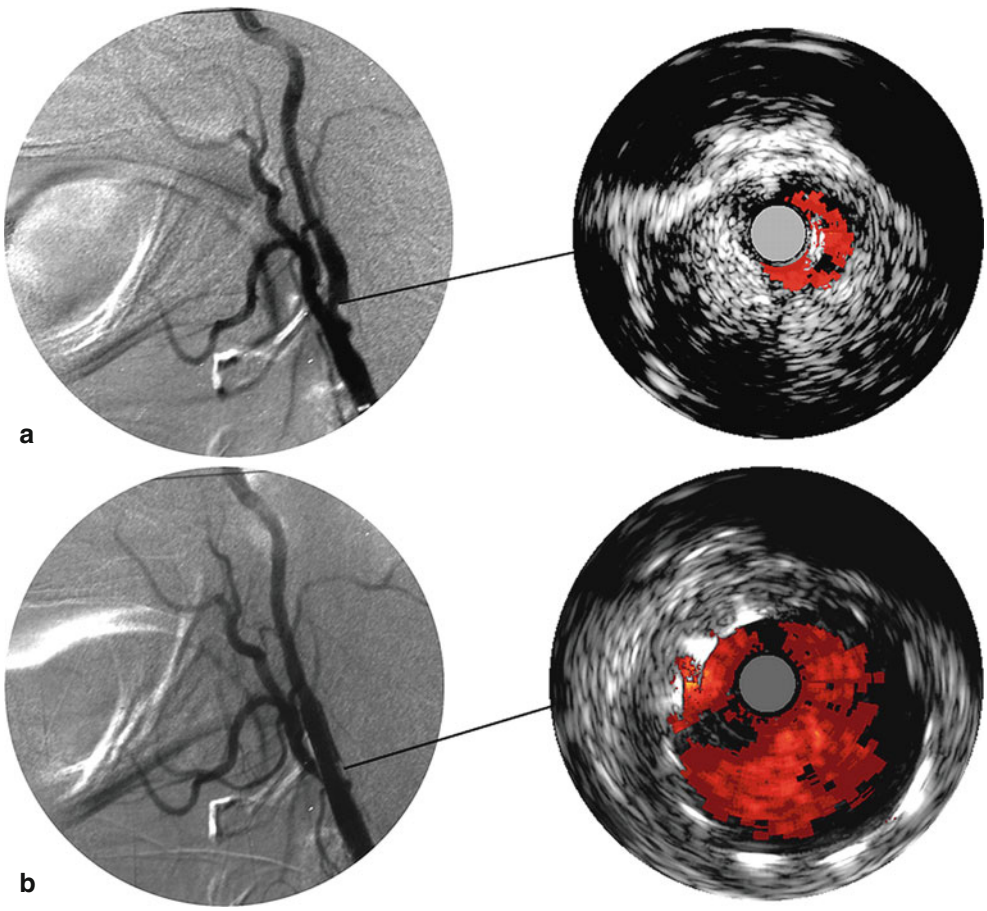


**Fig. 53.5** (**a**) Intraoperative carotid angiogram and IVUS showing a stenosis of the internal carotid artery. (**b**) There is resolution of the stenosis poststenting. IVUS confirms excellent stent deployment

throughout its length following deployment. It should also appose completely to the artery wall with no space apparent between the stent and the vessel. It is important to make sure that the length of the lesion is covered by the expanded stent such that no proximal or distal disease is left untreated. A careful inspection for intimal dissection is also important.

Despite our enthusiasm for carotid IVUS, passing balloon catheters and the IVUS probes up and down the internal carotid artery is not without hazard even with protection devices. The decision to reballoon or deploy another stent needs to be made cautiously. The advantages must be weighed against the risks of possible complication for the patient. Sometimes it is best to accept a reasonable deployment rather than overpursue it.

Stenting the origin of the common carotid artery from a retrograde carotid approach poses a challenge to all endovascular specialists. The common carotid artery comes off the aortic arch or the innominate artery, and accurate stent location at the origin is difficult using aortography alone because of the natural curvature of the arch [20] (Fig. 53.6). Accurate placement is possible using IVUS by passing the IVUS probe down the common carotid artery from above. Fluoroscopy visualizes the radiopaque transducer as it passes down the vessel. Blood flow is displayed in color pulsing red with each cardiac cycle. When the probe passes from the stenosis into the aorta, there is a sudden change in the size of the luminal color. Together with fluoroscopy, this technique pinpoints the origin of the vessel exactly for accurate device deployment. The same technique can also be used to stent the origin of all the supraaortic vessels.

## Thoracic Aorta

In the thoracic aorta, a larger probe is required (8.2F) with more penetration (10 MHz), a larger diameter of 60 mm, and compatibility with a larger guidewire (0.035 in.). IVUS is useful in assessing and measuring the neck of a thoracic aneurysm being treated by endoluminal grafting. The exact origin of the subclavian artery can also be identified (Fig. 53.7). IVUS also defines the extent of thoracic dissection and greatly assists treatment of coarctation of the aorta [21].

## Abdominal Aorta

Similarly in endoluminal grafting for abdominal aortic aneurysm, IVUS provides accurate measurements of neck

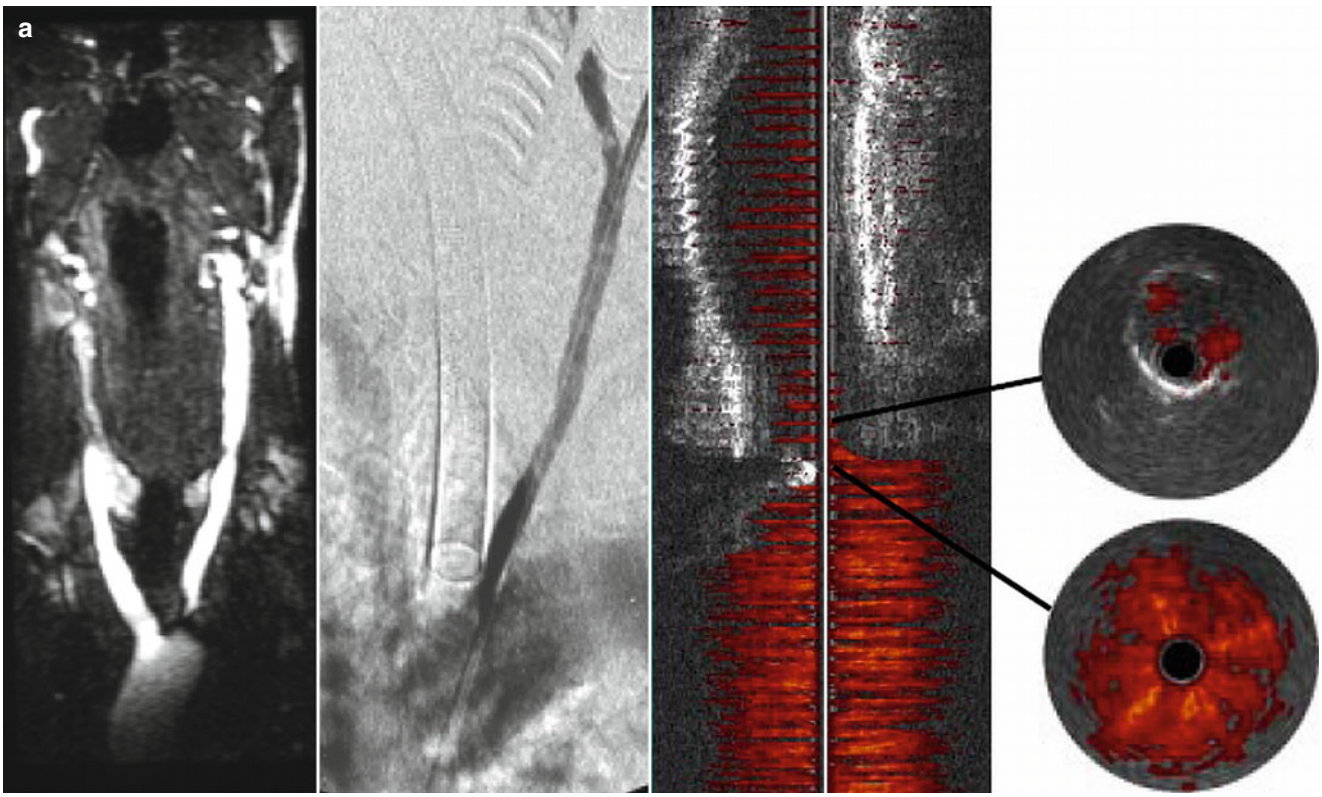


**Fig. 53.6** (**a**) Magnetic resonance angiography showing a tight stenosis at the origin of the left common carotid artery. At operation, the IVUS probe is passed down from a cervical access assisting road mapping. Two- and three-dimensional color IVUS locates the origin of the carotid artery. (**b**) Two- and three-dimensional color IVUS showing accurate stenting at the origin of the common carotid artery together with the completion angiogram (Reprinted from Irshad et al. [20]. With permission from Informa Healthcare)

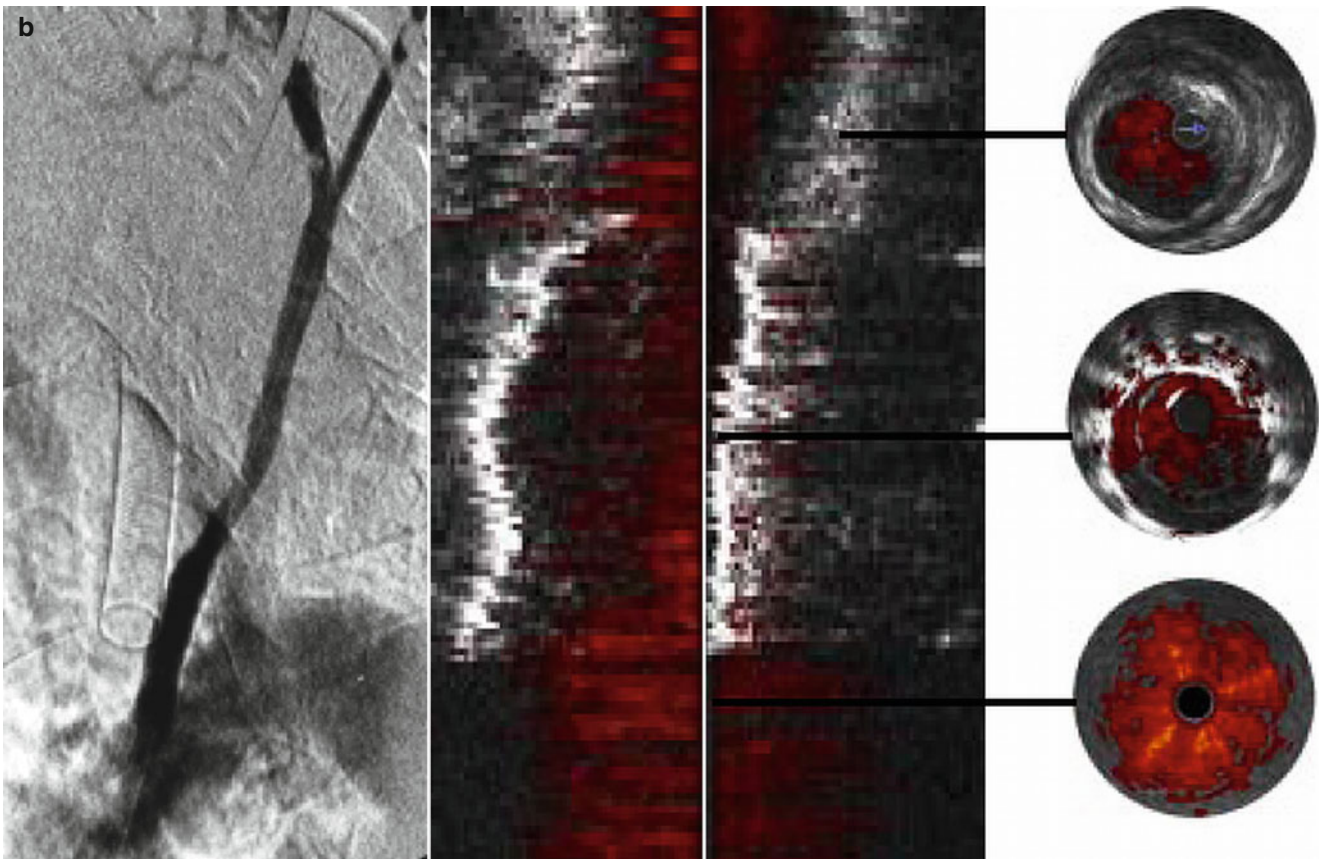


**Fig. 53.6** (continued)

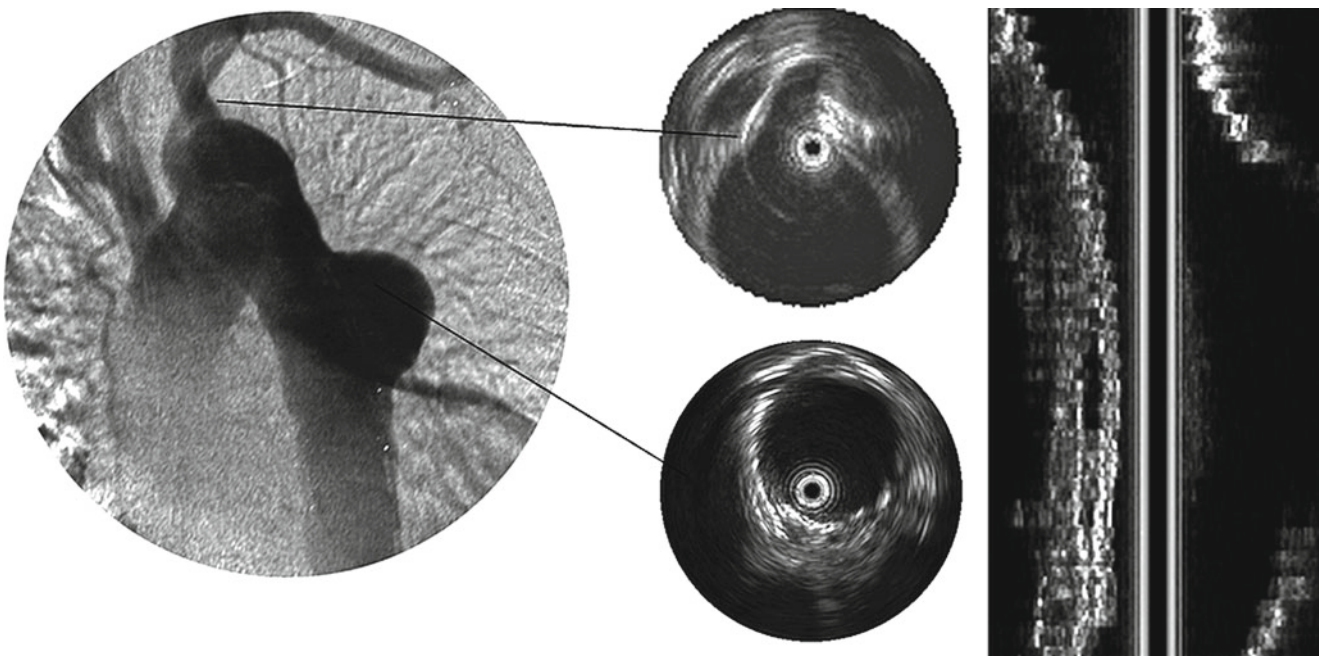

**Fig. 53.7** A thoracic aortic aneurysm. IVUS demonstrates the origin of the left subclavian artery, the neck, and the aneurysm

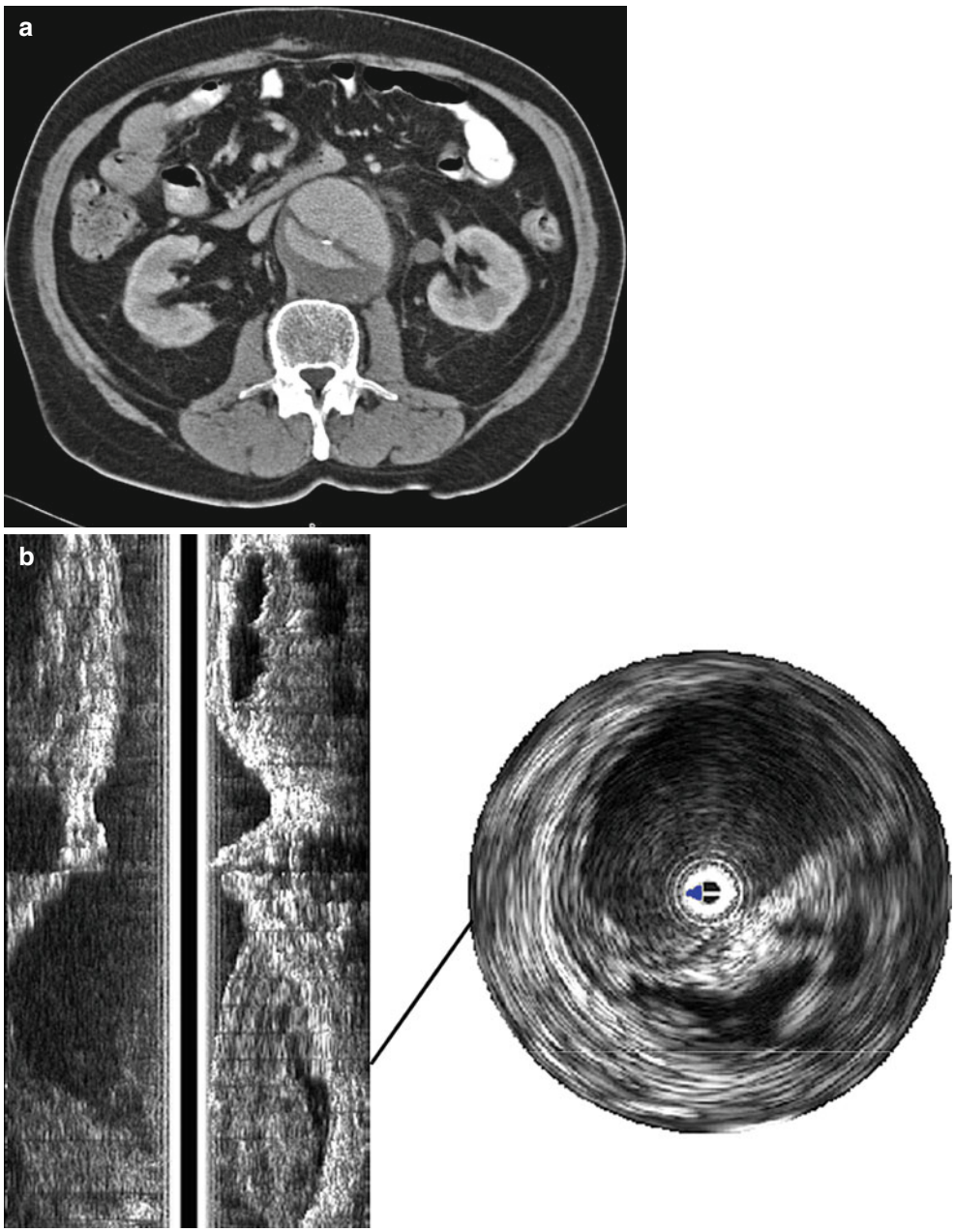


**Fig. 53.8** (**a**) CT scan of an aortic aneurysm showing dissection. (**b**) Two- and three-dimensional IVUS of the abdominal aortic aneurysm demonstrating thrombus with a flapping dissection

diameters and assessment of the iliac arteries [3]. The IVUS catheter is advanced from the groin to a level just above the renal arteries. The proximal and then the distal necks of the aneurysm are measured together with the luminal length requiring grafting. The amount of calcification and mural thrombus is noted, and assessment of the shape of the proximal and distal necks can indicate how well the endoluminal graft will exclude the aneurysm. IVUS provides a greater understanding of the case than computed tomography (CT) alone (Fig. 53.8). Immediately following endoluminal graft deployment it is difficult to obtain good IVUS images because of tiny pockets of air trapped in the endomaterial and because of the metal endoskeleton. These both cause bright reflection of ultrasound. Further technological advances with IVUS or the endoluminal grafts in this situation are necessary since color IVUS could potentially detect endoleak and its source in the operating room at the time of device implantation [4].

In occlusive disease of the aorta, IVUS provides accurate diameters to judge balloon and stent sizing [1]. This is important since ballooning the aorta with too large a balloon to only a few atmospheres can cause aortic rupture.

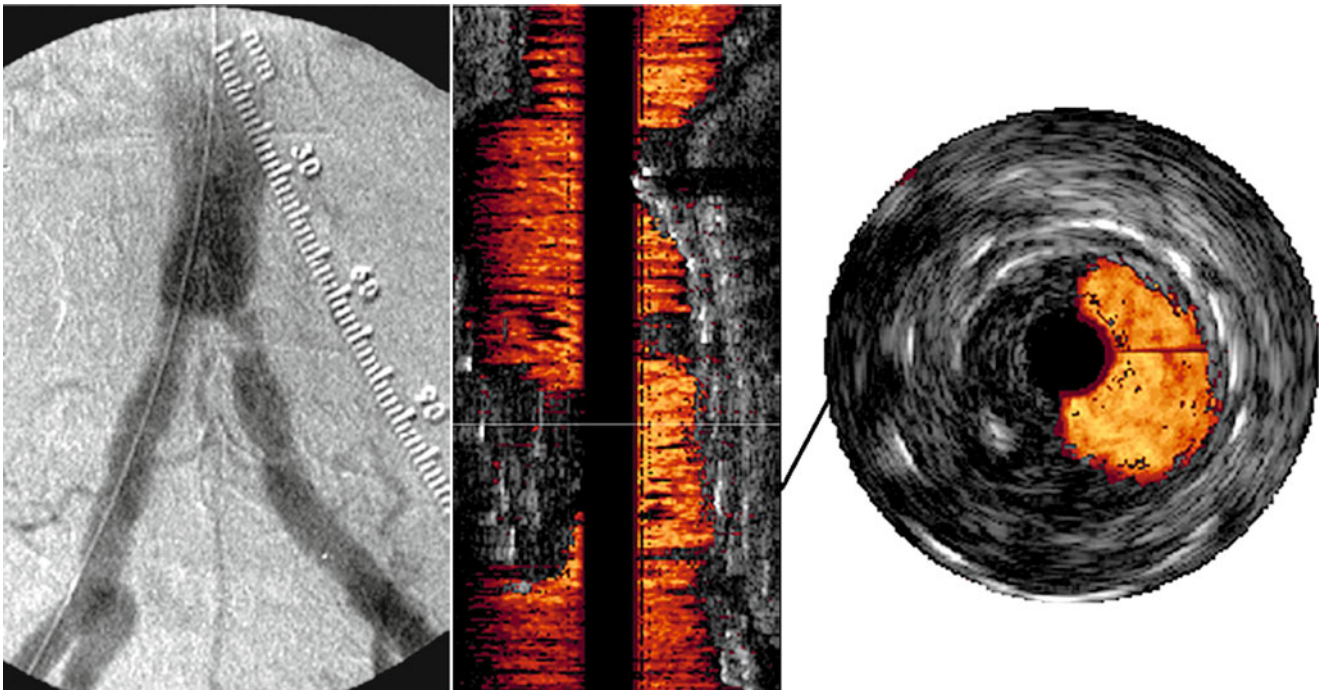

**Fig. 53.9** Angiogram and color IVUS demonstrating restenosis of the left common iliac stent. Neointimal hyperplasia can be seen inside the stent struts

## Iliac Arteries

The iliac arteries are tortuous and deeply placed in the abdomen and pelvis. It is, therefore, not surprising that IVUS can occasionally detect disease not apparent on arteriography. However, the main use of IVUS in the iliac arteries is to check stent deployment. We use IVUS routinely in this situation together with arteriography and measurements of arterial pressure gradients before and after stenting. This "triple assessment" thoroughly examines the completeness of treatment (Fig. 53.9), particularly for patients with critical limb ischemia [4].

## Infrainguinal Arteries

We have used IVUS in the infrainguinal arteries to assist the placement of endoluminal grafts in unfit patients with occlusive disease who might otherwise have undergone distal bypass surgery for critical limb ischemia [4] (Fig. 53.10). We routinely balloon and stent on the 0.018-in. guidewires to avoid time-consuming wire exchanges for IVUS examination. A combination balloon/IVUS catheter originally developed for coronary angioplasty is commercially available. We have found them extremely useful at swiftly checking the results of tibial angioplasty [4].

## Venous IVUS

IVUS can also be used to assist endovascular assessment and treatment in the venous circulation. It can be used at the patient's bedside to accurately place caval filters, especially when intravenous X-ray contrast is contraindicated. Most recently, we have used IVUS to understand venous abnormalities in patients with multiple sclerosis with chronic cerebrospinal venous insufficiency [22]. These patients have venous narrowing or abnormal valves in the internal jugular and azygous veins. We have found IVUS extremely helpful in identifying lesions in a very new field. Not only are we able to appreciate the pathology better but also our completeness of treatment (Fig. 53.11).

## Discussion

IVUS is probably more helpful in peripheral interventions than in the coronary situation, assessing the completeness of treatment and providing detailed and accurate luminal measurements. However, it is perceived by many as an expensive guidance system with little support from clinical data and studies. While there are no cost-effective studies of IVUS in the periphery, there are some studies of its clinical value. Arko et al. reported in a retrospective study an improved clinical outcome in patients undergoing iliac stenting

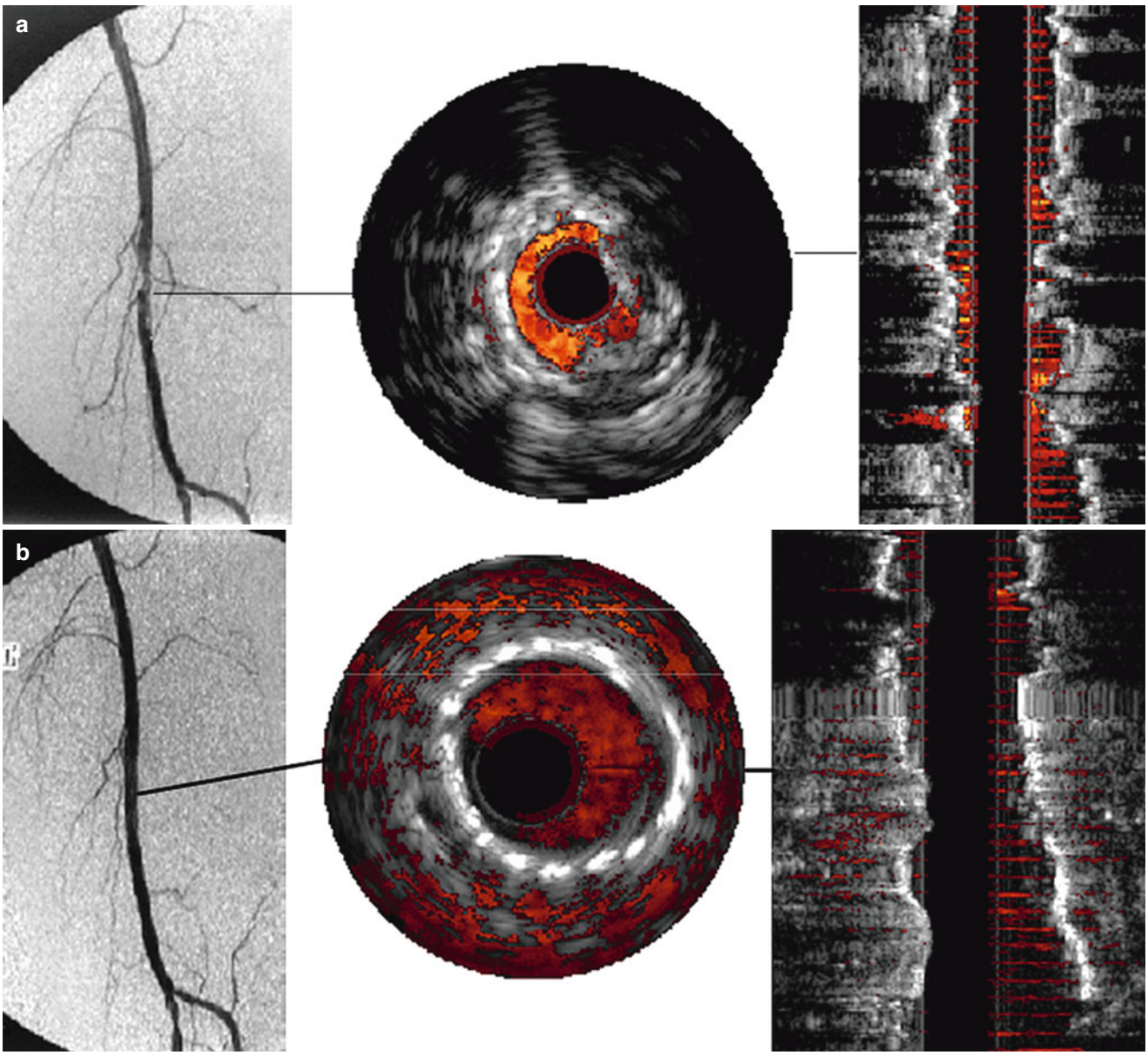


**Fig. 53.10** (**a**) A critical stenosis of the popliteal artery in a patient with critical limb ischemia. IVUS demonstrates a tight and calcified stenosis. (**b**) Angiography and IVUS show resolution of the stenosis following deployment of a balloon-mounted endoluminal graft

compared to those who had no IVUS assistance [23]. Another study of 100 consecutive peripheral interventions reported that IVUS detected that 34% of the patients had unsatisfactory stent deployment despite a satisfactory completion angiogram. Following retreatment, the cross-sectional area through the stent was increased by 42% (52 of these patients were undergoing carotid stenting) [7].

In another study, 131 patients underwent renal artery stenting with IVUS evaluation. IVUS detected unsuspected maldeployment of the stent in 23.5% of cases. The IVUS findings included 22 (14.4%) instances of incomplete stent apposition/expansion, 8 (5.2%) dissections, and 6 (3.9%) incompletely covered ostia [24].

A favorable limb salvage rate in 50 consecutive patients undergoing IVUS-guided treatment for critical limb ischemia also reported the beneficial use of IVUS [4]. IVUS was crucial in 32% of cases, discovering unsuspected disease and inaccurately deployed stents. Limb salvage rate was 79% at 3 years despite the fact that nearly 25% of the patients were diabetic [4]. Such studies lend support to IVUS having clinical outcome benefit, but no randomized controlled peripheral trial has yet been undertaken.

We have become sufficiently familiar with IVUS to use it in patients with renal failure and contrast allergy to treat them without angiography. Together with fluoroscopy, the IVUS probe can be used to road map the intervention. This

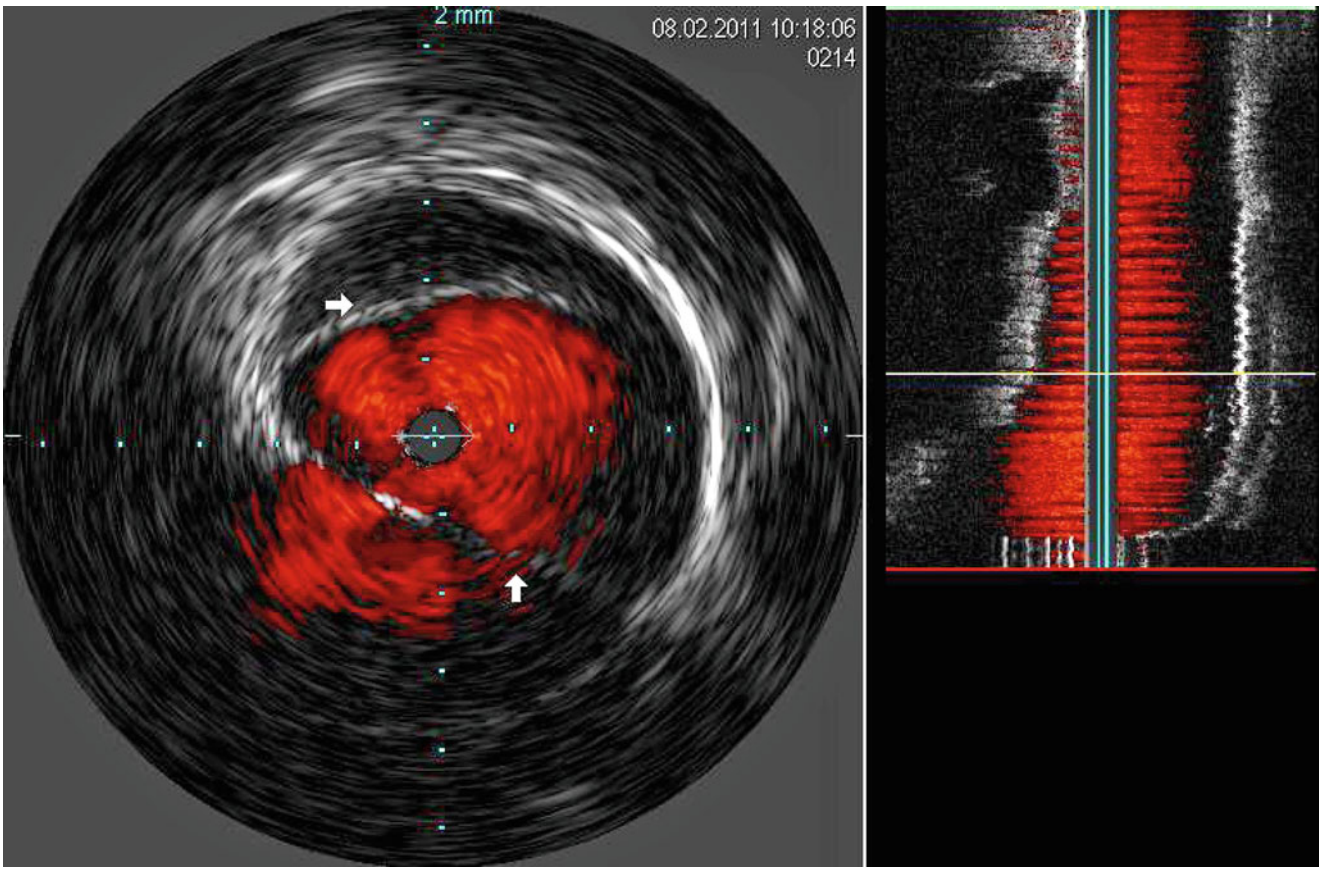


**Fig. 53.11** Color flow IVUS of an abnormal valve at the lower end of the internal jugular vein in a patient with multiple sclerosis and chronic cerebrospinal venous insufficiency. The valve leaflets (*arrows*) did not open and close normally and were seen on IVUS to be like an obstructing web preventing normal venous flow

technique of IVUS-guided treatment is very gratifying for the operator and is greatly assisted by the preoperative evaluation of the patient with magnetic resonance angiography [25].

We have found IVUS especially helpful in complex cases. However, the operating room team needs to frequently use IVUS so that when it is needed (e.g., an emergency case) it is quickly available and used with experience. Technology has advanced IVUS with great benefit, especially the additions of color flow and three-dimensional reconstruction which make it much more user friendly in the operating room. However, industry could perhaps do more to manufacture probes specifically for peripheral interventions that have a low profile and are compatible with 0.035-in. guidewires.

VH-IVUS allows the operator to identify the type of plaque in the artery being treated. The CAPITAL Study compared "virtual" with true histology in 153 sections of carotid plaque. VH IVUS was performed immediately prior to carotid endarterectomy in order to obtain VH images and these were then compared in a blinded study with true histological sections. The predictive diagnostic accuracy of VH IVUS to agree with true histology in different carotid plaque types was, in thin cap fibroatheroma 99.4%, calcified thin cap fibroatheroma 96.1%, fibroatheroma 85.9%, fibrocalcific 85.5%, pathological intimal thickening 83.4%, and calcified fibroatheroma 72.4%. This study validated the accuracy of VH IVUS in identifying plaque types. "Vulnerable" plaque types were the most accurately identified. [26–28]

## Conclusions

Peripheral endovascular procedures have advanced and replaced many open vascular surgical operations at an astonishing rate in the past decade. There is now an overwhelming variety of devices, and technology being used to treat arterial and venous disease from inside the vessel lumen. The successful use of these new endovascular techniques heavily relies on good imaging. A strong knowledge and understanding of IVUS is important because it is able to guide and assess the completeness of endovascular treatment. Its perceived expense has resulted in its underuse in peripheral interventions despite advances of color flow IVUS and three-dimensional reconstruction, which have made it much more readily understandable within the operating room environment.

While IVUS is still driven by interventional cardiologists, industry has an opportunity to translate much of the technology to the peripheral setting. The latest advance in IVUS is virtual histology, which is potentially promising in improving our understanding of how plaque will behave when treated. If the complexity of endovascular procedures continues to increase and the limitations of conventional imaging continue to be appreciated, it is likely that IVUS will increasingly find a larger role in peripheral inventions.

## References


1. Diethrich EB. Endovascular treatment of abdominal occlusive disease; the impact of stents and intravascular ultrasound imaging. Eur J Surg. 1993;7:228–36.
2. Laskey WK, Brady ST, Kussmaul WG. Intravascular ultrasonographic assessment of the results of coronary artery stenting. Am Heart J. 1993;125(6):1576–83.
3. White RA, Scoccianti M, Back M, et al. Innovations in vascular imaging; arteriography, three-dimensional CT scans, and two and three dimensional intravascular ultrasound evaluation of an abdominal aortic aneurysm. Ann Vasc Surg. 1994;8(3):285–9.
4. Irshad K, Rahman N, Bain D. The role of intravascular ultrasound and peripheral endovascular interventions. In: Heuser RR, Henry M, editors. Textbook of peripheral vascular interventions. London: Martin Dunitz; 2004. p. 25–34.
5. Irshad K, Reid DB, Miller PH, et al. Early clinical experience with color three-dimentional intravascular ultrasound in peripheral interventions. J Endovasc Ther. 2001;8:329–38.
6. Reid DB, Douglas M, Diethrich EB. The clinical value of three-dimentional intravascular ultrasound imaging. J Endovasc Surg. 1995;2:356–64.
7. Reid DB, Diethrich EB, Marx P, Wrasper R. Clinical application of intravascular ultrasound in peripheral vascular disease. In: Seigel RJ, editor. Intravascular ultrasound imaging in coronary artery disease. New York: Marcel Dekker; 1998. p. 309–41.
8. Gussenhoven EJ, van der lugt A, Pasterkamp G. Intravascular ultrasound predictors of outcome after peripheral balloon angioplasty. Eur J Vasc Endovasc Surg. 1995;10:279–88.
9. Cavaye DM, Diethrich EB, Santiago OJM, et al. Intravascular ultrasound imaging: an essential component of angioplasty assessment and vascular stent deployment. Int Angiol. 1993;12:212–20.
10. Katzen BT, Benenati JF, Becker GJ, et al. Role of intravascular ultrasound in peripheral atherectomy and stent deployment. Circulation. 1991;84:2152. Abstract.
11. Vince DG, Davies SC. Peripheral application of intravascular ultrasound virtual histology. Semin Vasc Surg. 2004;17:119–25.
12. Kuchalakanti P, Rha SW, Cheneau E. Identification of "vulnerable plaque" using virtual histology in angiographically benign looking lesion of proximal left anterior descending artery. Cardiovasc Radiat Med. 2003;4(4):225–7.
13. Nair A, Kuben BD, Obuchowski N, Vince DG. Assessing spectral algorithms to predict atherosclerotic plaque composition with normalized and raw intravascular ultrasound data. Ultrasound Med Biol. 2001;27(10):1319–31.
14. Nair A, Kuban BD, Tuzcu EM, et al. Coronary plaque classification with intravascular ultrasound radiofrequency data analysis. Circulation. 2002;106:2200–6.
15. Schartl M, Bocksch W, Koschyk DH, et al. Use of intravascular ultrasound to compare effects of different strategies of lipid-lowering therapy on plaque volume and composition in patients with coronary artery disease. Circulation. 2001;104:387–92.
16. Diethrich EB, Ndiaye M, Reid DB. Stenting in the carotid artery: initial experience in 110 patients. J Endovasc Surg. 1996;3:42–62.
17. Reid DB, Diethrich EB, Marx P, et al. Intravascular ultrasound assessment in carotid interventions. J Endovasc Surg. 1996;3:203–10.
18. Diethrich EB, Marx P, Wrasper R, et al. Percutaneous techniques for endoluminal carotid interventions. J Endovasc Surg. 1996;3:182–201.
19. Reid DB, Irshad K, Miller S, et al. Endovascular significance of the external carotid artery in the treatment of cerebrovascular insufficiency. J Endovasc Ther. 2004;11:727–33.
20. Irshad K, Bain D, Miller PH. The role of intravascular ultrasound in carotid angioplasty and stenting. In: Henry M, editor. Angioplasty and stenting of the carotid and supra-aortic trunks. London: Martin Dunitz; 2004. p. 127–33.
21. Irshad K, Miller PH, McKendrick M, et al. The role of IVUS for stentgraft repair in TAA and TAD. In: Amor M, Bergeron P, editors. Thoracic aorta endografting. Marseille: Com & Co; 2004. p. 73–7.
22. Zamboni E, Galeotti R, Menegatti E, et al. A prospective open – label study of endovascular treatment of chronic cerebrospinal venous insufficiency. J Vasc Surg. 2009;50:1348–58.
23. Arko F, Mattauer M, McCullugh R, et al. Use of intravascular ultrasound improves long-term clinical outcome in the endovascular management of atherosclerotic aorto iliac occlusive disease. J Vasc Surg. 1998;27:614–23.
24. Dangas G, Laird JR, Mehran R. Intravascular ultrasound guided renal artery stenting. J Endovasc Ther. 2001;8:238–47.
25. Reid AW, Reid DB, Roditi GH. Vascular imaging: an unparalleled decade. J Endovasc Ther. 2004;II(Suppl II):II163–79.
26. Diethrich EB, Irshad K, Reid DB. Virtual histology intravascular ultrasound in peripheral interventions. Semin Vasc Surg. 2006;19:155–62.
27. Irshad K, Millar S, Velu R, et al. Virtual histology intravascular ultrasound in carotid interventions. J Endovasc Ther. 2007;14:198–207.
28. Diethrich EB, Pauliina Margolis M, Reid DB. Virtual histology intravascular ultrasound assessment of carotid artery disease: the Carotid Artery Plaque Virtual Histology Evaluation (CAPITAL) study. J Endovasc Ther. 2007;14:676–86.

# Three-Dimensional Vascular Imaging and Power Doppler Angiographic Imaging

54

Ali F. AbuRahma and Phillip J. Bendick

**Abstract**

Current ultrasound technology allows non-invasive flow imaging techniques to generate images similar in nature to conventional angiography as well as the efficient rendering of volumetric data into three-dimensional (3D) images. Power Doppler particularly has been useful in this regard to more thoroughly evaluate the extracranial carotid artery system and the peripheral arterial system. Enhanced diagnostic data has been seen in 76% of carotid studies and in 71% of studies of the peripheral arteries, including the aorto-iliac system and renal arteries. Differentiation of total versus near total carotid artery occlusion was improved using power Doppler angiography compared to conventional duplex ultrasound with color Doppler imaging. 3D image reconstruction allows more precise lumen measurements, with 87% agreement with conventional angiography. The sensitivity of 3D imaging to a >50% diameter stenosis was 100%; the positive predictive value for >50% diameter stenosis was 81%. 3D imaging was also able to detect all plaque surface ulcerations seen on conventional angiography. Additional vascular applications for 3D imaging and power Doppler angiography include transcranial evaluation of the circle of Willis and its major branches, evaluation of overall perfusion of organs such as the kidney or liver, tumor vascularity and differentiation of benign versus malignant masses, and, in conjunction with an ultrasound contrast agent, better characterization of solid masses and atherosclerotic plaque.

**Keywords**

Three-dimensional imaging • Power Doppler • Doppler angiography

## Introduction

From the very early days of bistable ultrasound imaging, it has been the goal of clinicians and engineers to develop techniques for the three-dimensional (3D) imaging of structures and systems within the body. As early as 1956, Howry et al. [1] proposed "stereoscopic" viewing of body structures. Since that time a number of schemes to accomplish 3D imaging have been attempted to realize the potential value of rendering volumetric data [2–4], but until very recently these have met with limited success in their clinical application [5–9]. These early efforts all required extensive off-line, non-real time processing of image data, often with significant operator interaction, and provided reconstructions with reduced resolution and/or inadequate image registration. Despite these constraints, 3D imaging with off-line processing of grayscale image data has been applied for a number of years in a wide variety of clinical situations, including fetal imaging, breast ultrasound, urology, ophthalmology, hepatobiliary ultrasound, and echocardiography [10–17]. More

A.F. AbuRahma, M.D., RVT, RPVI
Department of Surgery, Robert C. Byrd Health Sciences Center, West Virginia University, 3110 MacCorkle Ave SE, Charleston, WV 25304, USA

Charleston Area Medical Center, Charleston, WV, USA

P.J. Bendick, Ph.D. (✉)
Division of Vascular Surgery, William Beaumont Hospital, 3601 W. Thirteen Mile Road, Royal Oak, MI 48073, USA
e-mail: pbendick@beaumont.edu

A.F. AbuRahma, D.F. Bandyk (eds.), *Noninvasive Vascular Diagnosis*, DOI 10.1007/978-1-4471-4005-4_54, © Springer-Verlag London 2013

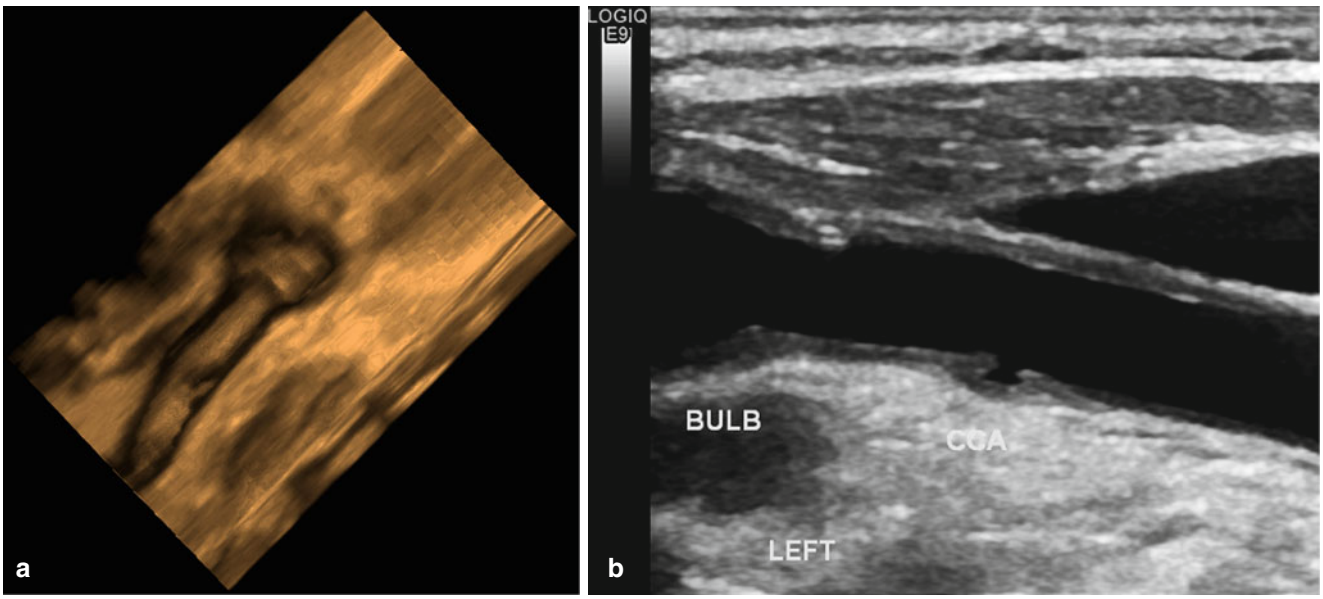


**Fig. 54.1** (**a**) 3D gray scale (*colorized*) image of carotid artery atherosclerotic disease in the distal CCA with a small surface ulceration. (**b**) Corresponding B-mode (2D) image showing small plaque ulceration initially seen in 3D reconstruction

recently freehand scanning techniques have been combined with the necessary computational power and high-speed data processing capabilities to produce more timely and accurate 3D images within a more acceptable time frame close to "real time." [18, 19] These same limitations for general ultrasound imaging have applied as well to vascular imaging, with the additional constraint that the target organs, in this case the blood vessels of the peripheral vascular system, are anatomically small structures with increased requirements for high-resolution imaging [20–22].

For 3D vascular imaging, there are two alternatives to visualization: the first is imaging of the arterial wall and related echogenic tissue using conventional B-mode echoes for reconstruction; the second is to visualize the blood flow within the lumen using either color Doppler or power Doppler, providing an indirect image of luminal narrowing and the luminal surface, which are often the areas of interest.

An advantage of vascular imaging is that the region of interest is often somewhat limited so that a fixed probe orientation can be used over short segments of the vascular anatomy, allowing the use of freehand scanning. Higher frequency ultrasound probes, with center frequencies beyond 12 MHz and improved electronic focusing in 1- or 2D, are now widely available to give very high-resolution grayscale data (Fig. 54.1). Recent improvements in power Doppler imaging have provided a signal related to blood flow volume with good sensitivity to very low flow velocities characteristic of those seen near the vessel wall, with improved resolution of the lumen-vessel wall interface (Fig. 54.2).

## 3D Power Doppler Angiography

Bendick et al. [23] evaluated the accuracy of 3D power Doppler angiography in the carotid artery bifurcation compared with digital subtraction contrast angiography and surgical findings at carotid endarterectomy. Thirty-two patients were studied, with 64 vessels available for correlation. Luminal narrowing was categorized according to standard gradations of percent stenosis or total occlusion, using direct measurements from the 3D images without knowledge of the angiographic results and applying the methodology of stenosis measurement of the NASCET study (Fig. 54.3). In addition, surface morphology of the 3D images was evaluated to determine the extent of luminal narrowing, defined as focal, moderate (<1 cm), or lengthy (>1 cm), as well as the presence of plaque ulceration. Three carotid bifurcations had atherosclerotic lesions that were too heavily calcified for adequate power Doppler angiography and could not be classified by 3D imaging. Of the remaining 61 bifurcations, 53 were accurately classified as to percent stenosis, giving an overall accuracy of 87%, similar to results obtained when Doppler velocity criteria are used to categorize lesion severity. The sensitivity of 3D imaging to a >50% diameter stenosis was 100%; the positive predictive value for >50% diameter stenosis was 81% (21 of 26 bifurcations) (Fig. 54.4). All four total occlusions were correctly identified by 3D imaging.

In the evaluation of the extent of lesions, 11 of 13 (85%) were correctly classified as focal, 24 of 29 (83%) as being of moderate extent of <1 cm, and 14 of 14 (100%) as extended

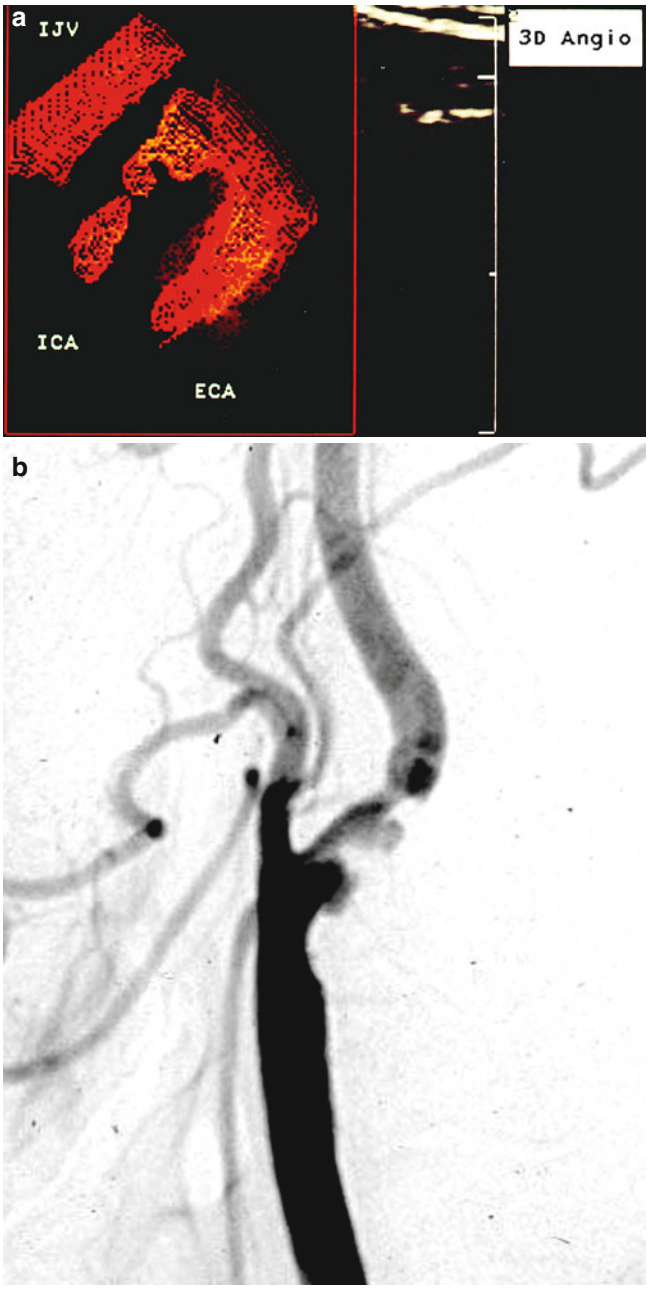


**Fig. 54.2** (**a**) 3D power Doppler reconstruction of a carotid artery bifurcation showing an ulceration in the lesion just past the origin of the internal carotid artery (*ICA*). *IJV* internal jugular vein, *ECA* external carotid artery. (**b**) Corresponding arteriogram showing ulcerated plaque in proximal ICA

lesions of >1 cm. Five lesions were considered to be ulcerated by 3D angiography (Fig. 54.2) with four of these ulcerations shown by subtraction angiography. 3D power Doppler angiography was believed to provide an accurate noninvasive technique comparable to subtraction angiography for the anatomic evaluation of carotid bifurcation atherosclerotic disease, with selectable viewing projections that helped eliminate vessel overlap and other artifacts. The technique complemented the hemodynamic data already available from conventional 2D

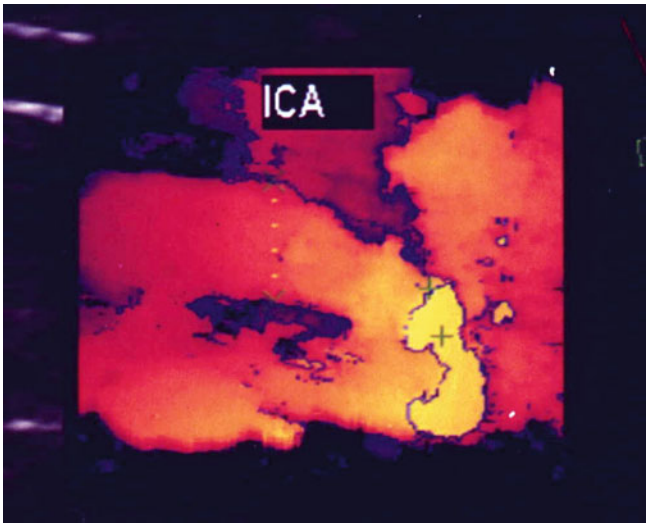


**Fig. 54.3** 3D reconstruction of a carotid bifurcation region applying the NASCET methodology for stenosis measurement, with ultrasonic calipers on the internal carotid artery showing the minimal lumen diameter (X) and the distal ICA lumen diameter (+). Also note the small ulcerative crater at midlesion

duplex ultrasound, but at this time could not replace it; instead, it allowed a more thorough evaluation of any obstructive disease present without significant additional testing.

Delcker et al. [24] investigated 3D power Doppler angiography for transcranial imaging of the major intracranial vessels. Previous studies have shown improved ability for transcranial duplex ultrasound to detect and image the intracranial vessels using power Doppler compared with color Doppler imaging [25, 26]. Delcker et al. also studied the use of a transpulmonary-stable ultrasound contrast agent. When their 3D studies were compared with diagnostic cerebral angiography, they had imaging success rates of 100% for the ipsilateral anterior cerebral artery, middle cerebral artery (with three or more branches), posterior cerebral artery, and posterior communicating artery, and 90% for the anterior communicating artery. On the side contralateral to the transducer, imaging success rates were 90% for the anterior cerebral artery, 80% for the middle cerebral artery (again with three or more branches), and 100% for the posterior cerebral artery. They concluded that 3D transcranial power Doppler angiography with contrast agent enhancement provided significant improvements in the visualization and evaluation of the major intracranial arteries.

## Recent Clinical Experience Using Power Doppler Angiography

A number of other reports have been published on the clinical utility of power Doppler ultrasound in vascular patients [27–30]. The most recent report evaluated 53 patients referred

to the vascular laboratory who had conventional color duplex ultrasound followed by power Doppler imaging [31]. All 53 patients had conventional arteriography to verify the duplex ultrasound results. Patients were seen for the following indications: Carotid/Vertebral Artery – (1) subtotal versus total carotid occlusion; (2) tortuosity of the artery with limited imaging; (3) the presence of significant disease by spectral Doppler velocity measurements with limited imaging on conventional duplex examination; (4) patients with heavy calcification and limited imaging; and (5) high and/or deep internal carotid arteries. Deep Lying Arteries – Renal/Aorta: (1) limited imaging secondary to obesity or bowel gas and (2) nonvisualization of the renal origin. Peripheral Arteries – (1) subtotal versus total occlusion and (2) anatomy with limited imaging on conventional color duplex ultrasound. The color duplex imaging and the power Doppler examinations were performed by experienced registered vascular technologists in an accredited vascular laboratory using an HDI 5000 Phillips, ATL system (Bothell, WA). Sequential parallel longitudinal views and perpendicular cross-sectional views were obtained on both color duplex and power Doppler imaging. The display quality of both sonographic examinations was classified as satisfactory or unsatisfactory by both the technologist and the interpreting physician. A satisfactory image was defined as one with clearly seen anatomy and well-visualized pathology of the examined vessel. Power Doppler imaging was considered to be of positive diagnostic value if the results of that examination were helpful in differentiating subtotal from total occlusion, optimizing image quality, or visualizing deep-lying vessels (e.g., renal artery) that were not seen on conventional duplex examination. If the two portions of the duplex examination were inconsistent, the final conclusion was decided based on the results obtained by conventional arteriography.

A positive diagnostic value was achieved using power Doppler imaging in 22 out of 29 (76%) carotid artery examinations. Similarly, 10 out of 14 (71%) peripheral artery examinations had a positive diagnostic value. Four out of five (80%) renal artery examinations had a positive diagnostic value, while three out of five (60%) aortoiliac examinations had a positive diagnostic value. Overall, a positive diagnostic value was achieved by adding power Doppler imaging in 39 out of 53 arteries (74%, Table 54.1). The overall sensitivity of power Doppler imaging in patients with a positive diagnostic value was 95% and the positive predictive value was 97%.

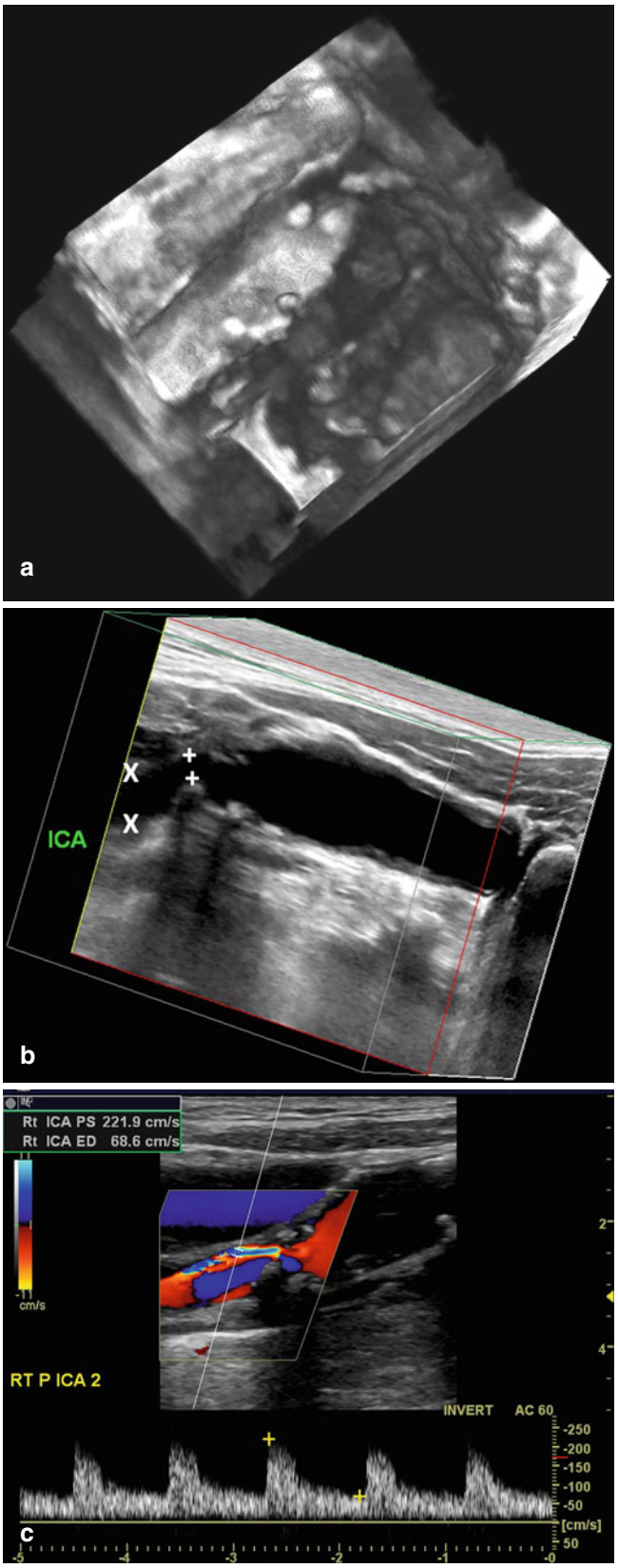


**Fig. 54.4** (**a**) 3D reconstruction of a carotid bifurcation region showing the coronal view (not obtainable with 2D imaging) of a complex, irregular atherosclerotic lesion at the origin of the ICA. (**b**) 3D reconstruction of a carotid bifurcation region showing a 50–70% diameter reduction in the proximal internal carotid artery (*ICA*); the minimum lumen diameter was 2.5 mm (+) and the distal ICA lumen measured 5.8 mm (×), a 58% diameter reduction. (**c**) Spectral Doppler data for the lesion shown in (**b**) with a peak systolic velocity of 221 cm/s and an end-diastolic velocity of 68 cm/s, corresponding to a 50–70% diameter reduction

**Table 54.1** Positive diagnostic value of power Doppler arteriography[a]

| Arteries | Positive Dx value | No change | Total |
|---|---|---|---|
| Carotid/vertebral | 22 (76%) | 7 (24%) | 29 |
| Peripheral | 10 (71%) | 4 (29%) | 14 |
| Renal | 4 (80%) | 1 (20%) | 5 |
| Aorta/iliacs | 3 (60%) | 2 (40%) | 5 |
| Total | 39 (74%) | 14 (26%) | 53 |

[a]Overall sensitivity of power Doppler imaging in patients with positive diagnostic value = 95% and positive predictive value = 97%

**Table 54.2** Carotid indications for power Doppler imaging

| | Positive Dx value | No change | Total |
|---|---|---|---|
| Subtotal/total occlusion | 5 (83%) | 1 (17%) | 6 |
| Suboptimal image | 10 (71%) | 4 (29%) | 14 |
| High/deep internal carotid artery | 4 (80%) | 1 (20%) | 5 |
| Tortuous artery | 3 (75%) | 1 (25%) | 4 |
| Total | 22 (76%) | 7 (24%) | 29 |

**Table 54.3** Peripheral and renal indications for power Doppler imaging

| | Positive Dx value | No change | Total |
|---|---|---|---|
| *Peripheral* | | | |
| Subtotal/total occlusion | 6 (75%) | 2 (25%) | 8 |
| Suboptimal image | 4 (67%) | 2 (33%) | 6 |
| Total | 10 (71%) | 4 (29%) | 14 |
| *Renal* | | | |
| Obscure origin | 3 (100%) | 0 | 3 |
| Suboptimal image | 1 (50%) | 1 (50%) | 2 |
| Total | 4 (80%) | 1 (20%) | 5 |
| *Aorta/iliacs* | | | |
| Suboptimal image | 3 (60%) | 2 (40%) | 5 |

Table 54.2 summarizes the indications of power Doppler imaging and the positive diagnostic value in carotid artery applications. As noted, five out of six patients (83%) who were believed to have total carotid occlusion by conventional color duplex were confirmed to have subtotal occlusion by adding power Doppler imaging. However, 10 out of 14 (71%) carotid artery patients who were believed to have suboptimal images had an improved image on power Doppler imaging. Table 54.3 summarizes the findings in patients for whom the indications included peripheral arteries, renal arteries, and aortoiliac arteries. Six out of eight (75%) patients with a questionable subtotal versus total occlusion by conventional duplex examination were confirmed to have subtotal occlusion by power Doppler imaging. Overall, 10 out of 14 (71%) patients with peripheral arterial examinations had a positive diagnostic value. Four out of five (80%) renal examinations resulted in a positive diagnostic value, which included three patients in whom the origin of the renal arteries was not seen by conventional duplex examinations. Three out of five (60%) aortoiliac examinations resulted in a positive diagnostic value. Figures 54.5, 54.6, 54.7, 54.8, 54.9, 54.10, 54.11, 54.12, and 54.13 illustrate various clinical scenarios where a positive diagnostic value was achieved by adding power Doppler imaging.

## Limitations of Power Doppler Angiography

The limitations of power Doppler angiography are those that have long been recognized for all applications of ultrasound. Present techniques remain strongly operator dependent. All probe maneuvers must be carefully controlled and done in a smooth, constant speed motion as power Doppler is very susceptible to transient or erratic motion artifacts. Patient cooperation is also essential during the ultrasound scanning procedure. Specific to vascular imaging and the detection of obstructive disease are the limitations imposed by the lesion itself. Very complex heterogeneous lesions are less a limitation for power Doppler angiography than gray scale imaging since it is based on a less "noisy" signal for its image. However, the presence of atherosclerotic lesion or vessel wall calcification that prevents the transmission of any ultrasound signals remains a significant limitation to data acquisition and display.

## Additional Clinical Applications of 3D Vascular Ultrasound

A number of investigators have used 3D ultrasound to evaluate atherosclerotic lesions in the carotid artery to assess plaque characteristics, plaque volume, and the effects of medical treatment [32–35]. Seabra et al. [34] have demonstrated the utility of freehand 3D reconstructions of carotid artery plaque in obtaining non-standard views not available in conventional 2D scanning to better evaluate plaque echogenicity characteristics. 3D ultrasound measurements of combined vessel wall/plaque volume have been able reliable in detecting very small changes representing either an increase or a decrease in volume associated with medical therapy over time intervals as short as 3 months [33, 35].

An increasing amount of research is being done using 3D imaging to characterize the vascularity of solid organs and lesions, such as the kidney or tumors. 3D gray scale reconstructions have been used to evaluate lesions in their entirety as well as calculate solid organ or lesion volume as an indicator of tumor resolution or growth. Because of the increased sensitivity of power Doppler to low flow velocities, not only can the major conduit arteries be imaged but the much smaller interlobular and arcuate arteries in the renal cortex can also be displayed, very nearly to the capsule itself. Rubin et al. [36] showed that a 2D power Doppler

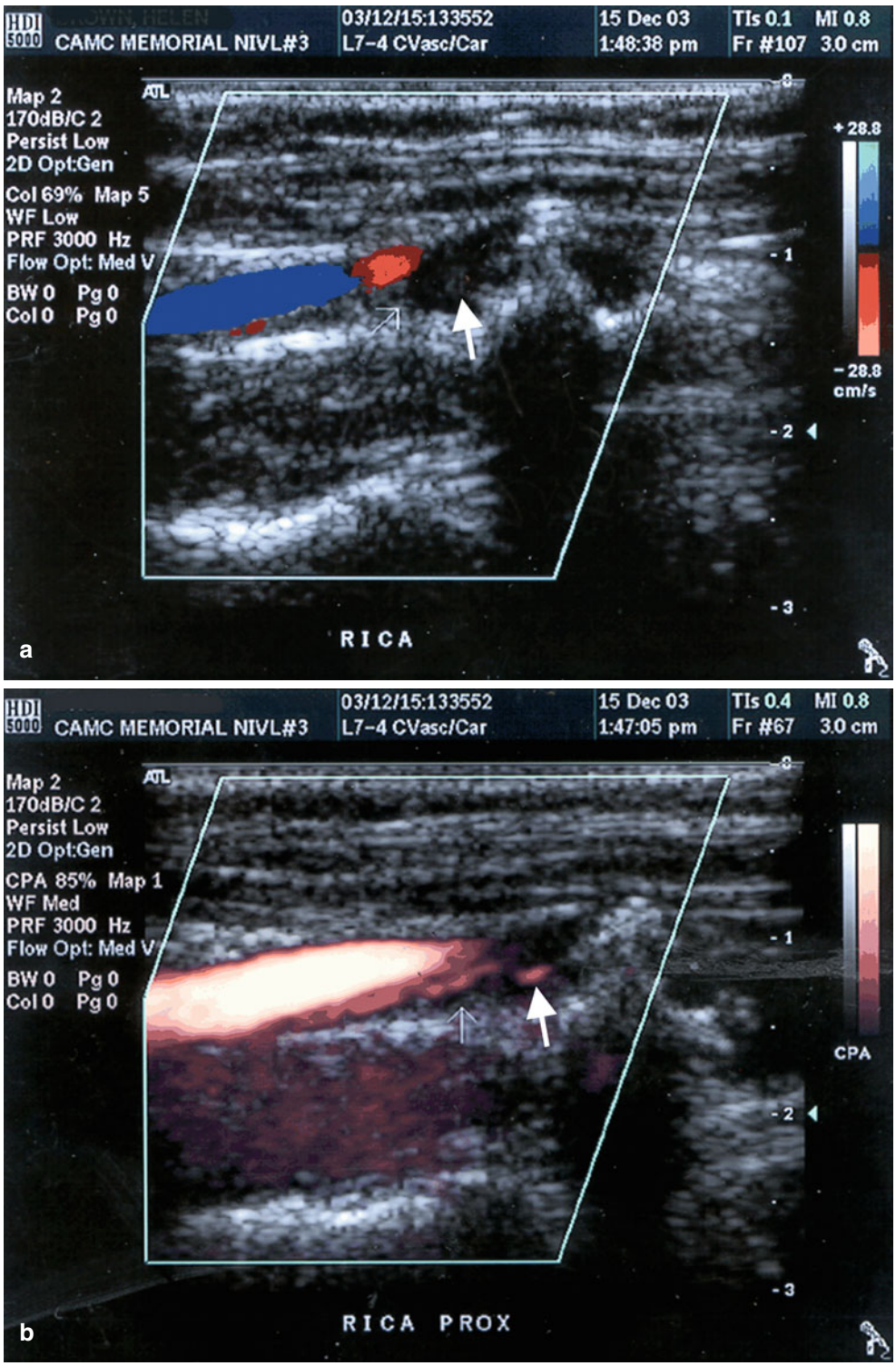


**Fig. 54.5** (**a**) Color duplex imaging of a right ICA suggesting total occlusion (*arrows*), (**b**) power Doppler image of same artery showing string sign (*arrow*), i.e. subtotal occlusion (Reproduced from AbuRahma et al. [31]. With permission from BC Decker, Inc.)

image of the renal vasculature can be used to estimate the fractional moving blood volume within a specific region of the kidney, demonstrating significant changes in this parameter as a function of hydration status as well as the effects of an arterio-venous fistula in a transplant kidney. A cross-sectional scan that sweeps through the kidney will store these consecutive power Doppler image frames to make possible a reconstruction that shows the anatomic extent of perfusion throughout a 3D tissue region of interest (Fig. 54.14). Similar displays can be generated for other tissues within the body such as liver, thyroid, breast, and the ophthalmic vasculature. 3D power Doppler angiography

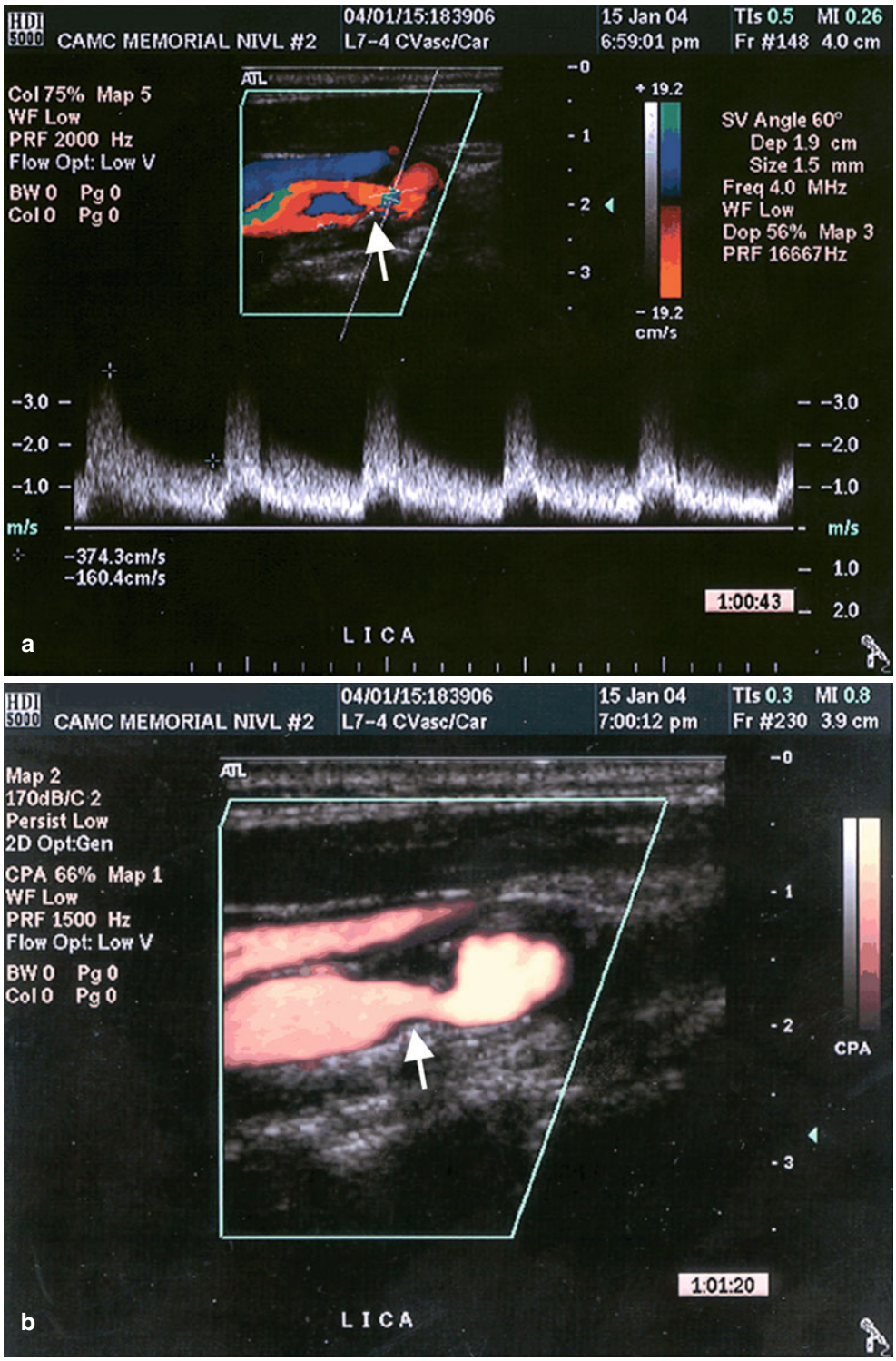


**Fig. 54.6** (**a**) Suboptimal image of left ICA by conventional duplex ultrasound (*arrow*), (**b**) better image is obtained by adding power Doppler ultrasound (*arrow*) (Reproduced from AbuRahma et al. [31]. With permission from BC Decker, Inc.)

has been implemented in a number of these vascular beds to investigate specific clinical problems. In a prospective study of 24 patients Carson et al. [37] examined the vascularity of breast masses seen on mammography and correlated their findings with the pathology noted in biopsy specimens. In addition to conventional grayscale image criteria, vascular criteria were identified for grading the 3D angiographic images and a numeric score between 1 (benign extreme) and 5 (malignant extreme) was assigned. These parameters included inner and outside (to 1 cm) vascularity, the presence and number of visible shunt vessels, vessel wrapping around the mass and vessel tortuosity, vessel enlargement, and related (beyond 1 cm) or unusual vascularity indicated by the presence of multiple large vessels

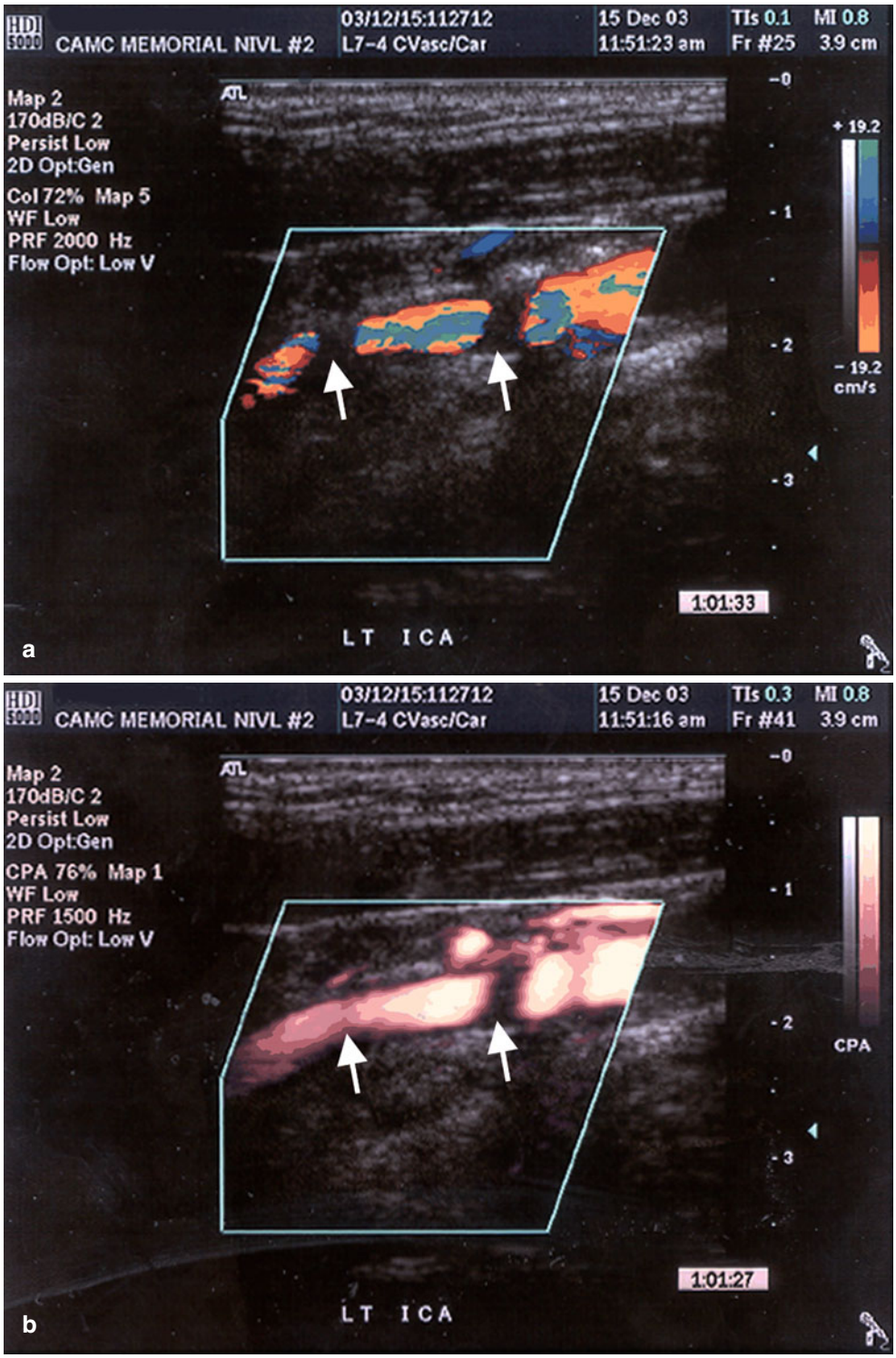


**Fig. 54.7** (**a**) Left ICA with multiple defects of color flow (secondary to shadowing, *arrows*), (**b**) color flow is seen in one area and somewhat seen in the other area (*arrows*) when power Doppler was added (Reproduced from AbuRahma et al. [31]. With permission from BC Decker, Inc.)

with elevated flows. Most helpful in the discrimination of malignant versus benign lesions were extensive inner vascularity, with a mean score of 3.3 versus 2.2 for malignant versus benign; extensive outside vascularity, 3.7 versus 2.4; the presence of clearly identified, multiple shunt vessels, 2.7 versus 2.1; and significant vessel wrapping around the mass, 3.5 versus 1.9. For a fixed sensitivity of 90%, 3D power Doppler angiography improved lesion specificity to 85% compared with 79% for 2D conventional color or power Doppler images (which could include the individual frames used to reconstruct the eventual 3D image). Only for the 3D reconstruction data did lesion vascularity display a trend toward statistical significance, which was somewhat limited by the small sample size. In a recent

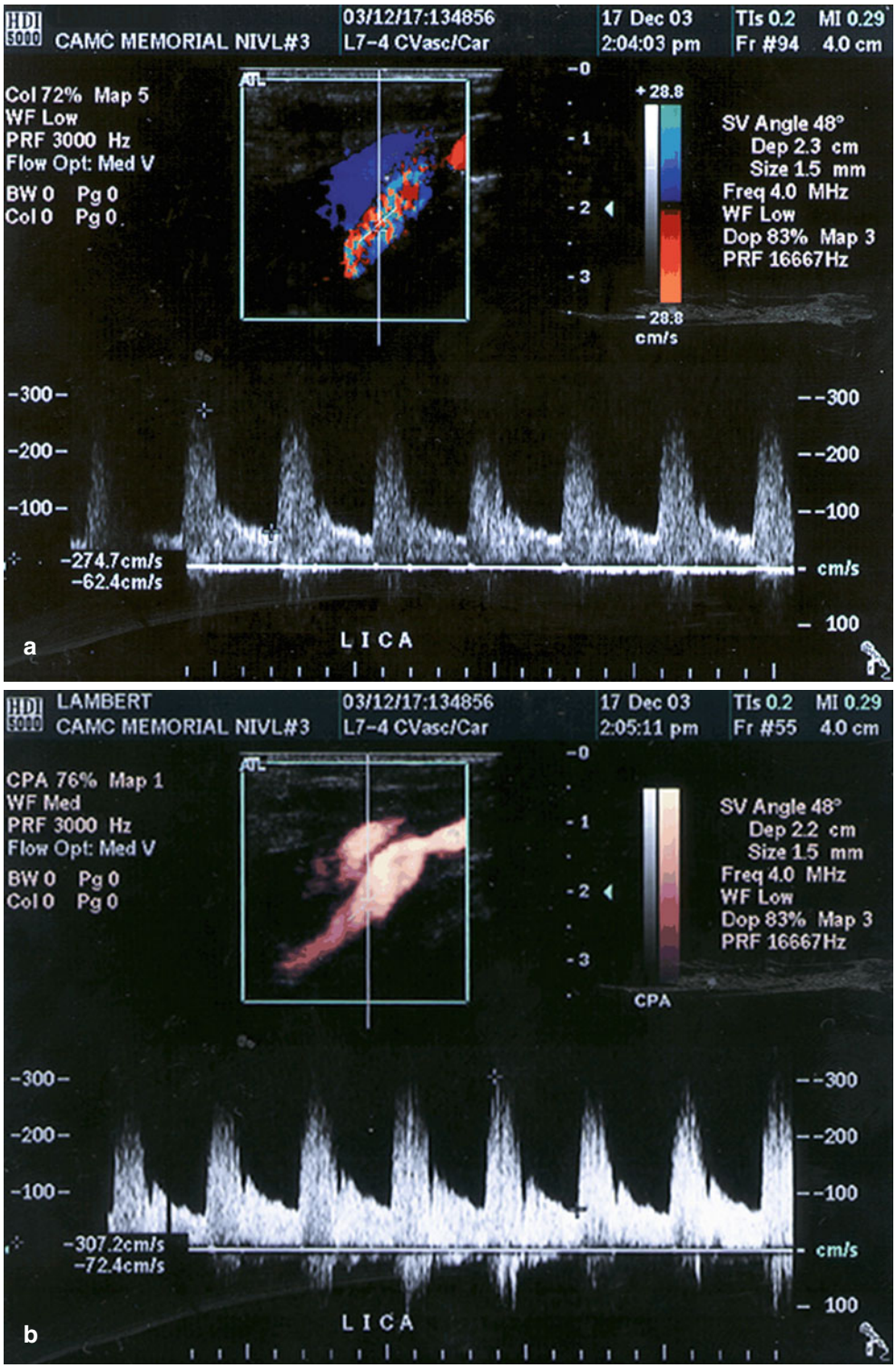


**Fig. 54.8** (**a**) A deep-lying left ICA with suboptimal imaging on color duplex ultrasound, (**b**) shows a well-defined stenosis using power Doppler ultrasound (Reproduced from AbuRahma et al. [31]. With permission from BC Decker, Inc.)

similar study, Huang et al. used 3D power Doppler imaging to differentiate benign from malignant breast masses with a sensitivity of 94%, a positive predictive value of 73%, and an overall accuracy of 81% [38].

More recent research studies have combined 3D imaging with enhancement by an ultrasound contrast agent (not FDA approved in the USA at this time for applications other than left ventricular opacification) to evaluate tumor vascularity, particularly lesions of the liver [39–42]. The addition of an ultrasound contrast agent allows better definition of solid organ and lesion vascularity, particularly in hyperenhanced or hypoenhanced lesions, as well as improved detection and

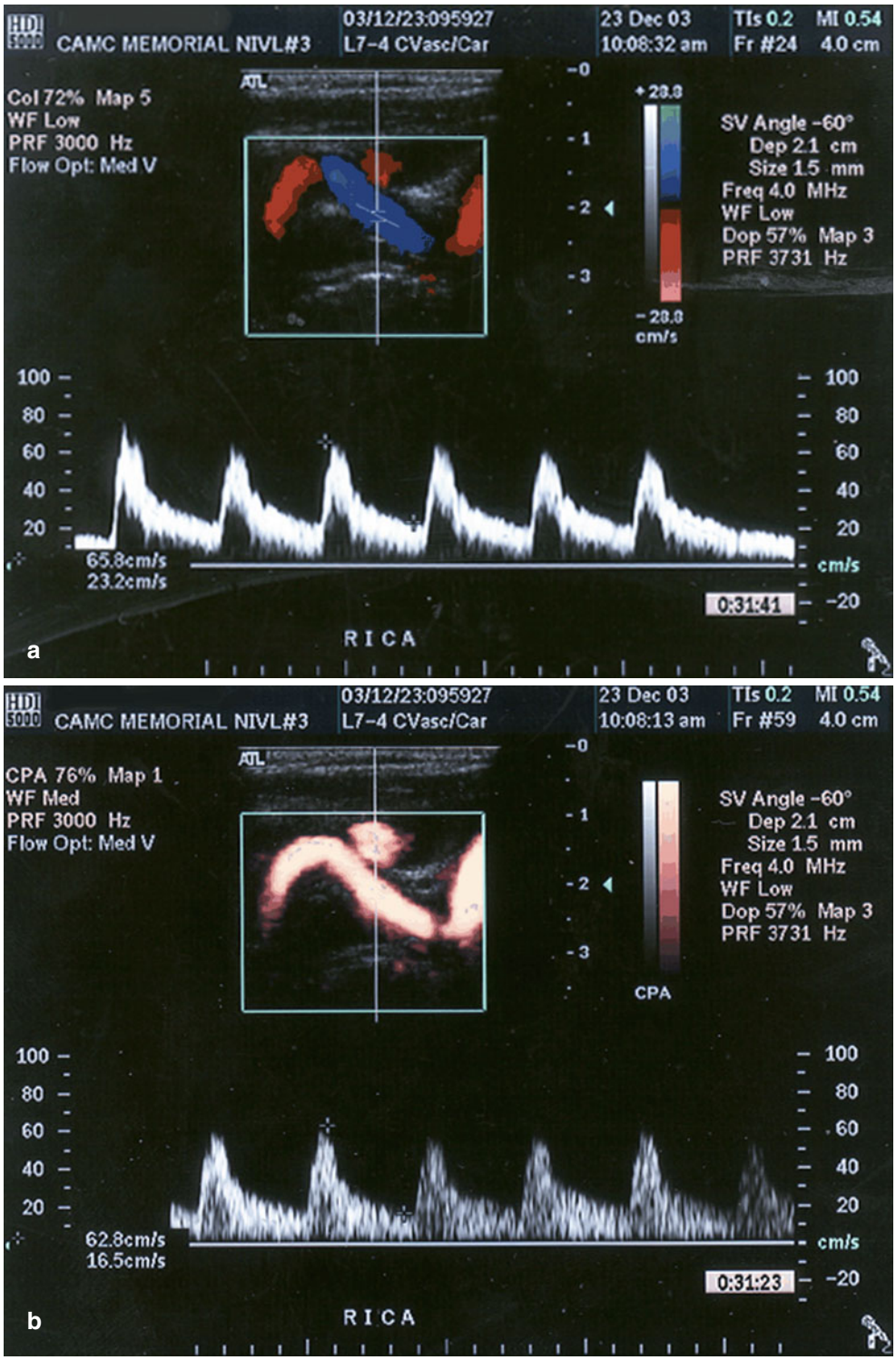


**Fig. 54.9** (**a**) A tortuous ICA with poor image of the tortuous segment, (**b**) clearly shown tortuosity using power Doppler imaging (Reproduced from AbuRahma et al. [31]. With permission from BC Decker, Inc.)

display of smaller occult lesions [39, 40]. Luo et al. [41] used a series of 282 patients with known liver lesions (60% hepatocellular carcinoma) to develop a grading system for vascular and enhancement patterns during the arterial and early and late venous stages of perfusion. They then applied this system prospectively to differentiate lesions in 160 patients with sensitivity and specificity over 90%. Similar systems have been used to differentiate lesions for the staging, targeting, and follow up of liver tumors subjected to radiofrequency ablation [39, 42]. With contrast enhanced 3D ultrasound they found improved image quality in 94% of patients during treatment response evaluation and increased diagnostic confidence postablation in 41 of 51 patients (80%).

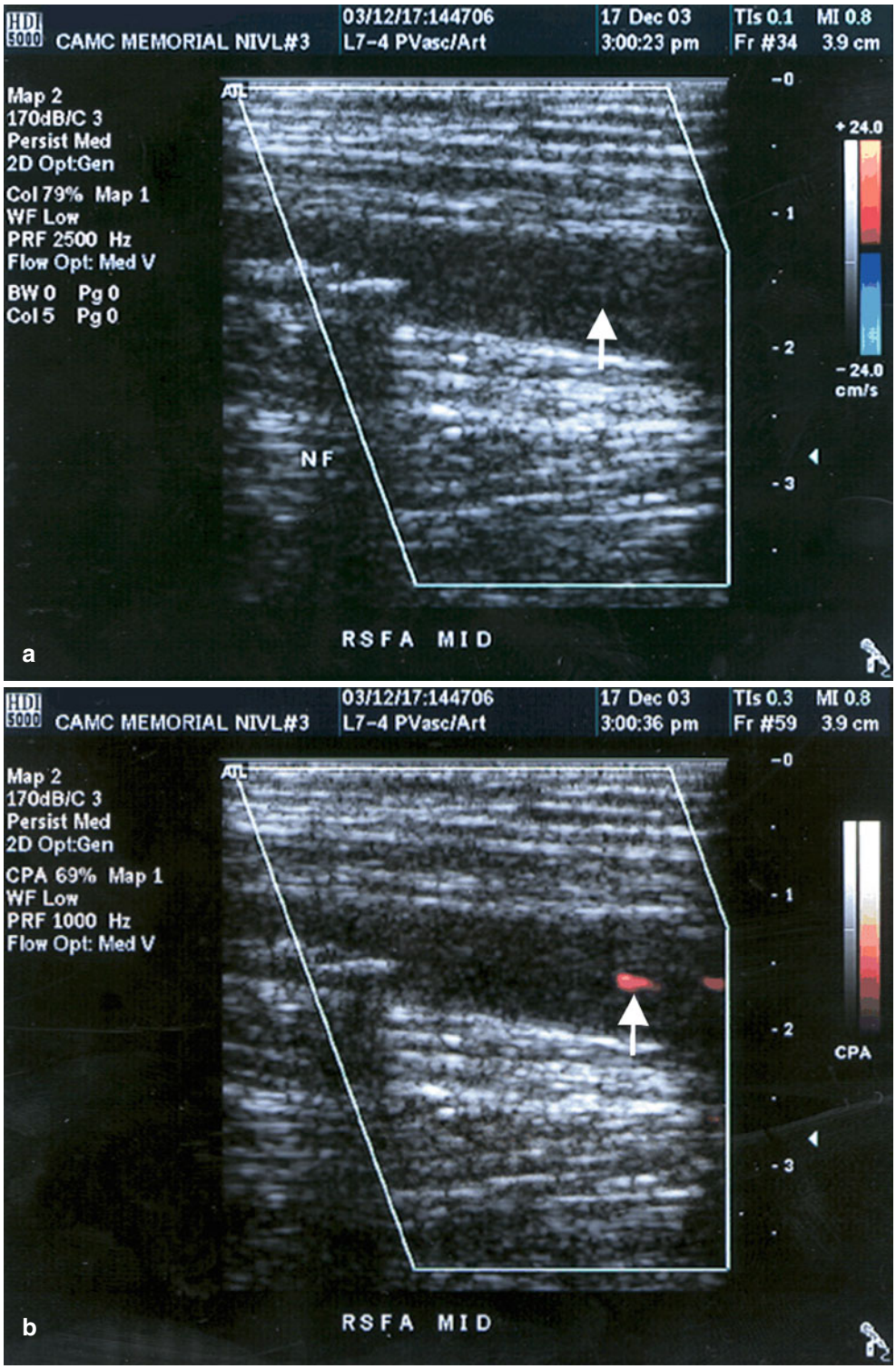


**Fig. 54.10** (**a**) Color duplex imaging showing a right mid-superficial femoral artery occlusion (*arrow*), (**b**) a string sign was seen (*arrow*) when power Doppler imaging was added (Reproduced from AbuRahma et al. [31]. With permission from BC Decker, Inc.)

## 3D Intravascular Ultrasound

Additional reports of 3D vascular imaging have used intravascular ultrasound (IVUS) with high-frequency transmit/receive crystals placed at the tip of a catheter, primarily in the coronary arteries [7, 43]. Investigators have been able to identify segments of angiographically "silent" atherosclerosis and quantify the degree of narrowing caused by either atherosclerotic lesions or post-angioplasty intimal hyperplasia. IVUS has also proved helpful in the placement of coronary stents and investigators have found good

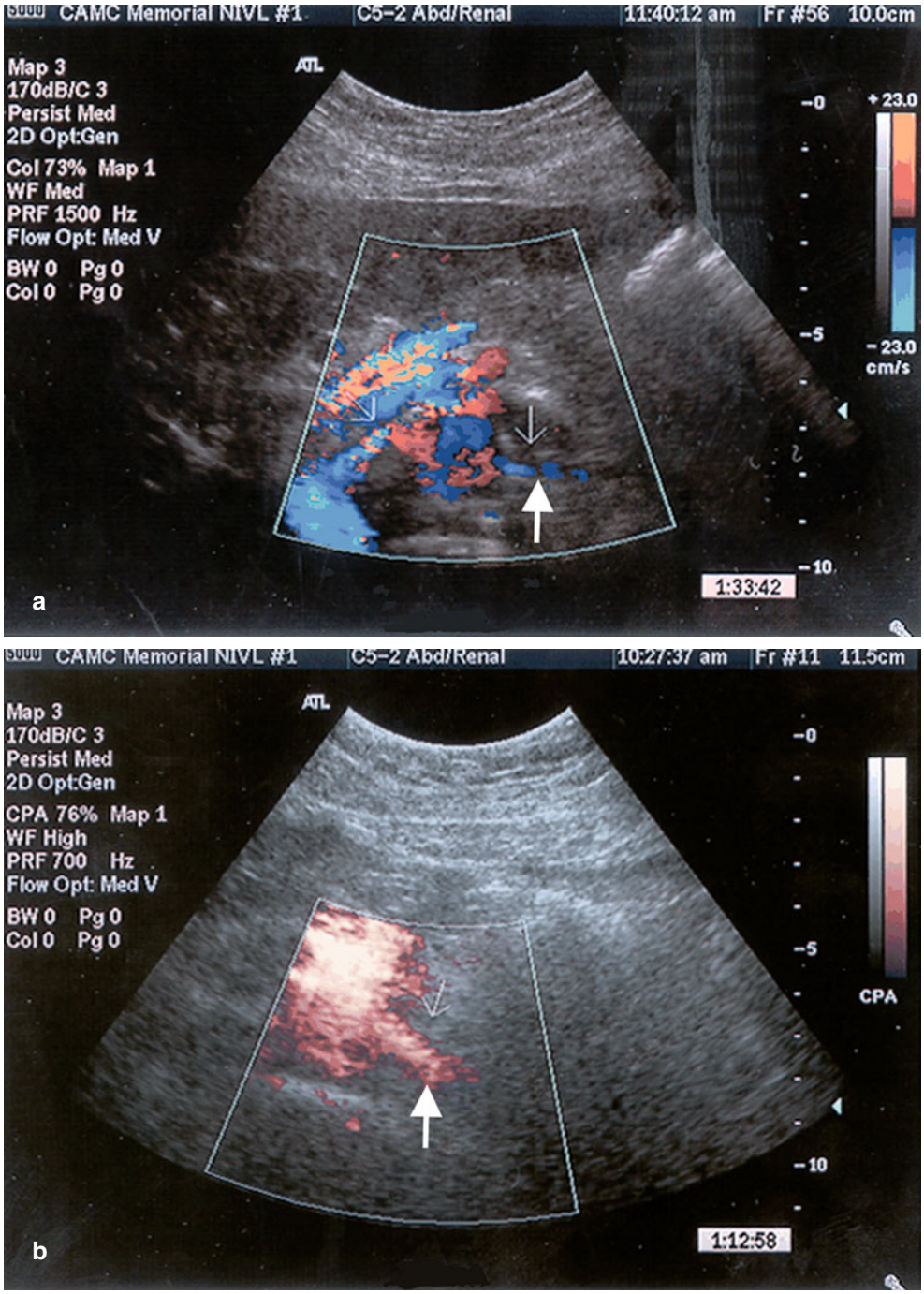


**Fig. 54.11** (**a**) A color duplex image of the renal artery which does not clearly show the orifice of the renal artery (*arrows*), (**b**) the origin of the renal artery is well seen using power Doppler imaging (*arrows*) (Reproduced from AbuRahma et al. [31]. With permission from BC Decker, Inc.)

correlation between IVUS and conventional angiographic video densitometry in post-angioplasty measurements of vessel cross-sectional lumen area [7, 44]. The potential exists for increased peripheral vascular utilization of 3D vascular imaging as endovascular stent grafting becomes more widespread; 3D IVUS has been shown to provide a nearly real-time perspective of the morphologic features of the vascular anatomy and of the stent graft placement during the procedure [45].

## Future of 3D Vascular Imaging and Power Doppler Angiography

The future of 3D imaging for vascular applications appears promising. 3D imaging of the vessel wall remains primarily a research tool, with a variety of imaging and data processing techniques in development. Multiplanar 3D imaging of atherosclerotic lesions allows selection of the optimal image for identifying plaque ulceration, gray scale median values to

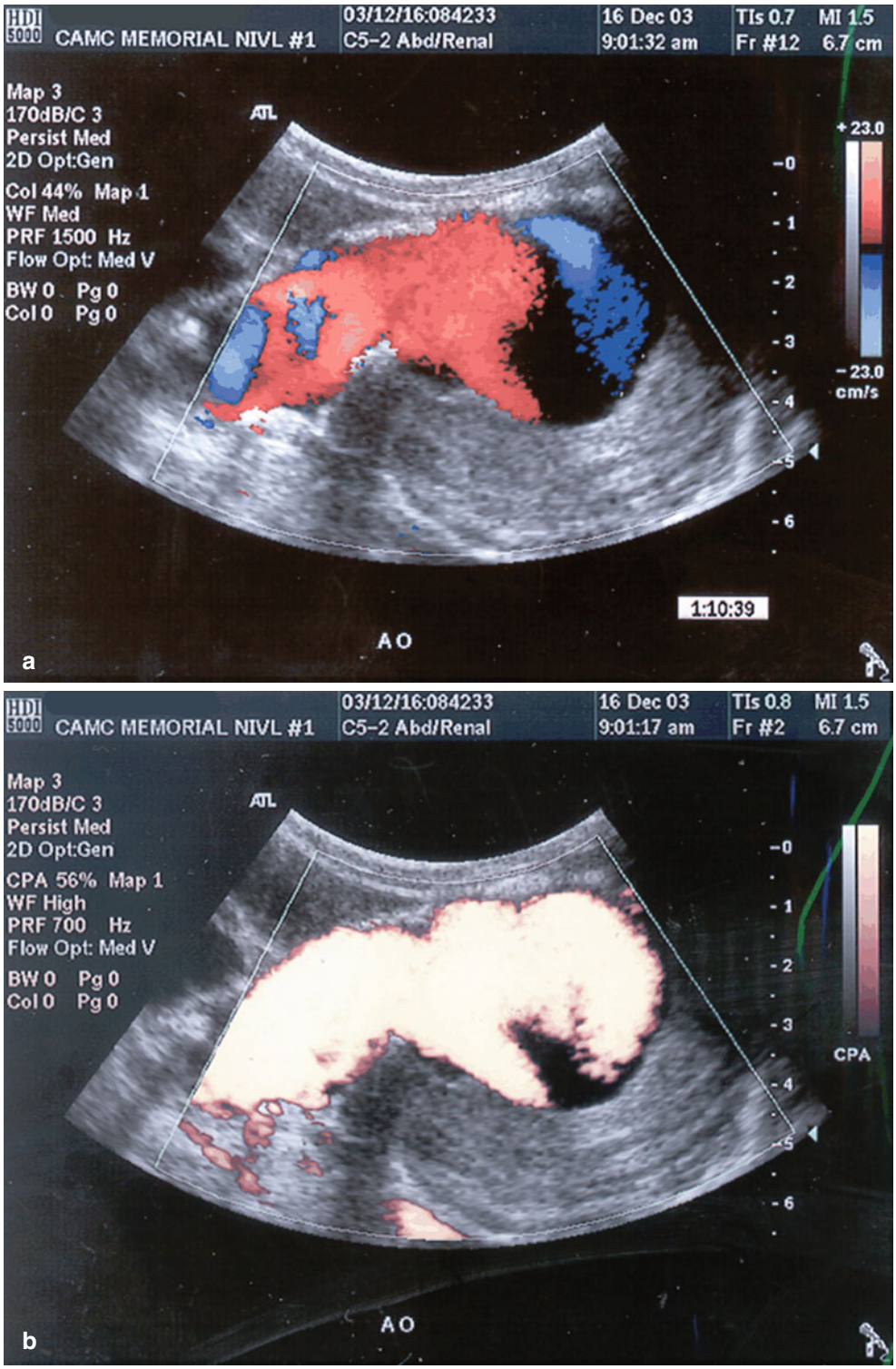


**Fig. 54.12** (**a**) A color duplex image of an abdominal aortic aneurysm, (**b**) a better definition of the color flow and morphology using power Doppler ultrasound (Reproduced from AbuRahma et al. [31]. With permission from BC Decker, Inc.)

evaluate plaque core content, and plaque neovascularity. Patients with minimal atherosclerotic disease derive a secondary benefit from acquiring 3D data sets by reconstructing them into standard 2D images, shortening the overall examination time. 3D ultrasound also provides an opportunity to directly compare sequential screening examinations for changes in plaque surface morphology and total plaque area/volume as a means of evaluating response to medical therapies.

The best results to date have relied on invasive IVUS using very high-frequency transducers for maximal image resolution. Reported results have been good for 3D

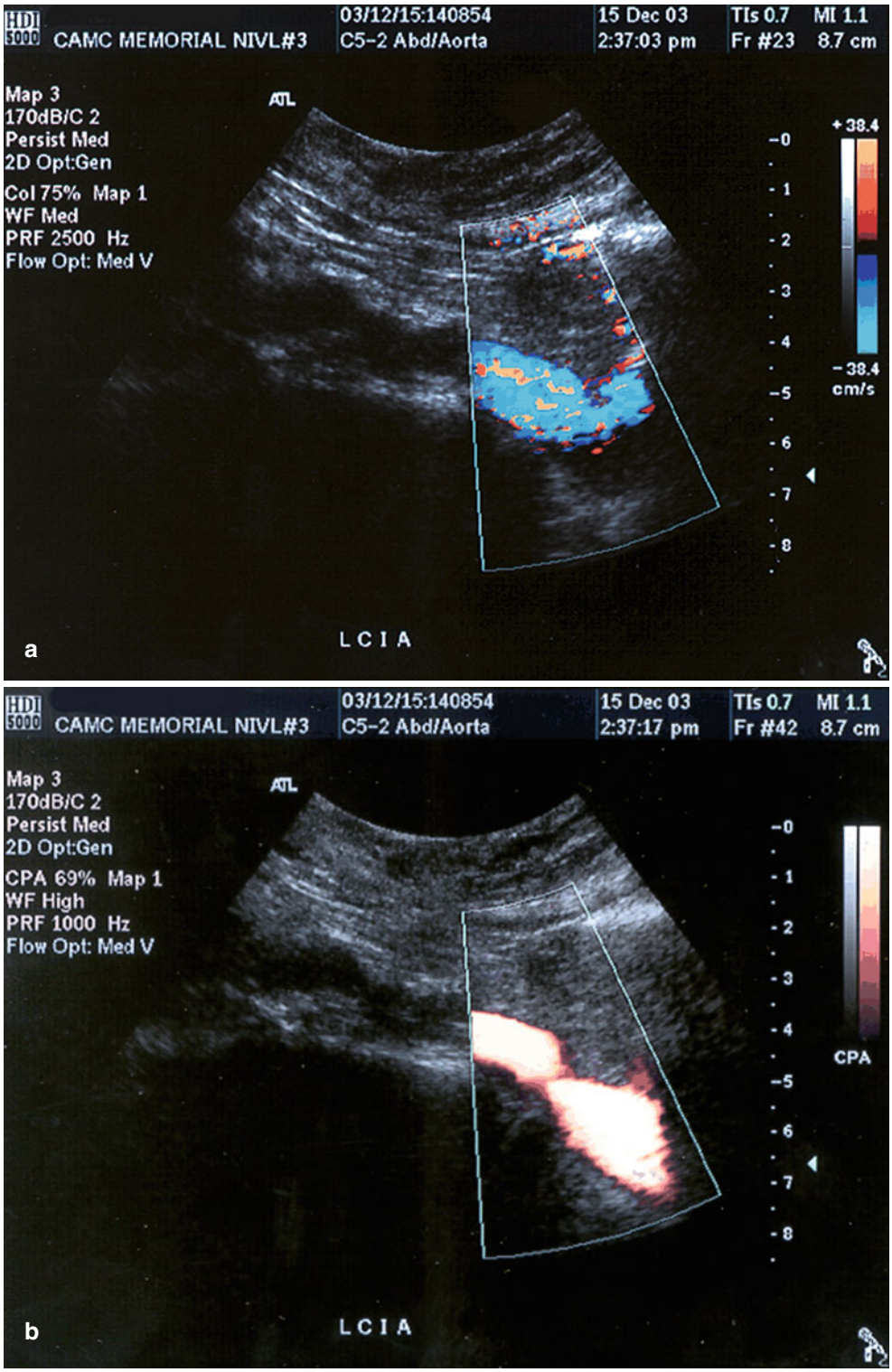


**Fig. 54.13** (**a**) A limited color duplex image of a deep-lying left common iliac artery, (**b**) a clearer image using power Doppler imaging (Reproduced from AbuRahma et al. [31]. With permission from BC Decker, Inc.)

visualization of atherosclerotic lesions, both in peripheral arteries and in the coronary arteries. These images have provided valuable feedback, for example, in the placement of stents and in the assessment following their deployment. The techniques being developed should provide the capability to extend other current 2D applications, making it possible to investigate preoperatively the extent of any tumor invasion of adjacent vascular structures. In addition, 3D imaging will allow more thorough evaluation of extrinsic vascular compression syndromes, guiding the management of cases of May-Thurner syndrome or thoracic outlet compression causing Paget-von Schroetter syndrome [46].

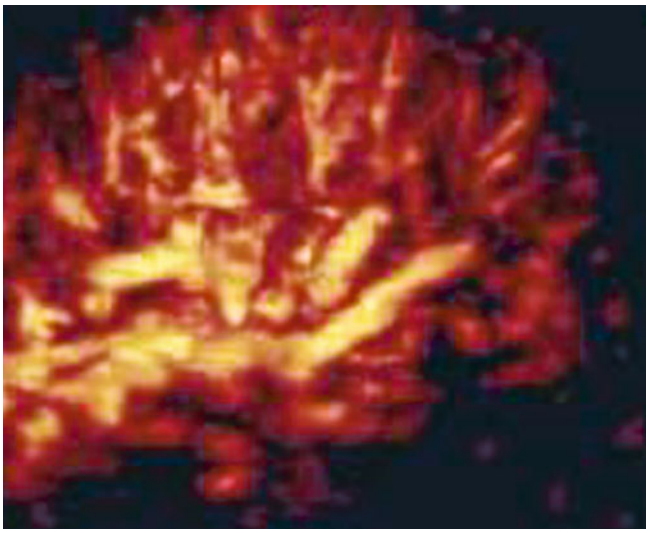

**Fig. 54.14** Three-dimensional vascular reconstruction of a kidney using power Doppler imaging, which demonstrates the major branch arteries and the vascularity of the cortical regions

3D power Doppler angiography has been more readily applied to clinical problems. This is in part because of its ease of use, the ability to use freehand scanning, a good signal-to-noise ratio giving a well-defined blood–tissue interface, and the speed with which these 3D images can be reconstructed and displayed. 3D power Doppler angiography has been shown to be capable of defining the severity and extent of atherosclerotic obstructive lesions, characterizing the vascularity of other lesions, and extending the use of 2D power Doppler imaging to further define parameters related to solid organ perfusion in, for example, the kidneys. The vascular supply and distribution in other organ systems, such as the orbit of the eye, have not been well studied yet, but the technological capability is present, with adequate resolution, to make such studies possible.

## References


1. Howry DH, Posakony G, Cushman R. Three dimensional and stereoscopic observation of body structures by ultrasound. J Appl Physiol. 1956;9:304–6.
2. Moritz WE, Medema DK, Ainsworth M, et al. Three-dimensional reconstruction and volume calculation from a series of nonparallel, real-time, ultrasonic images. Circulation. 1980;62(Suppl):111–43.
3. Steen E, Olstad B. Volume rendering of 3D medical ultrasound data using direct feature mapping. IEEE Trans Med Imaging. 1994;13:517–25.
4. Detmer PR, Bashein G, Hodges T, et al. 3D Ultrasonic image feature location based on magnetic scan head tracking: in vitro calibration and validation. Ultrasound Med Biol. 1994;20:923–36.
5. Rankin RN, Fenster A, Downey DB, et al. Three-dimensional sonographic reconstruction: techniques and diagnostic applications. AJR Am J Roentgenol. 1993;161:695–702.
6. Roelandt JR, DiMario C, Pandian NG, et al. Three-dimensional reconstruction of intracoronary ultrasound images: rationale, approaches, problems and directions. Circulation. 1994;90:1044–55.
7. von Birgelen C, Kutryk MJB, Gil R. Quantification of the minimal luminal cross-sectional area after coronary stenting by two- and three-dimensional intravascular ultra-sound versus edge detection and videodensitometry. Am J Cardiol. 1996;78:520–5.
8. Di Mario C, von Birgelen C, Prati F, et al. Three-dimensional reconstruction of two-dimensional intravascular ultrasound: clinical or research tool? Br Heart J. 1995;73 Suppl 2:26–32.
9. Franceschi D, Bondi JA, Rubin JR. A new approach for three-dimensional reconstruction of arterial ultrasonography. J Vasc Surg. 1992;15:800–5.
10. Kelly IM, Gardener JE, Brett AD, et al. Three-dimensional US of the fetus: work in progress. Radiology. 1994;192:253–9.
11. Levine RA, Weyman AE, Handschumacher MD. Three-dimensional echocardiography: techniques and applications. Am J Cardiol. 1992;69:121H–30.
12. Moskalik A, Carson PL, Meyer CR, et al. Registration of three-dimensional compound ultrasound scans of the breast for refraction and motion corrections. Ultrasound Med Biol. 1995;21:769–78.
13. Nelson TR, Pretorius DH, Slansky M, et al. Three-dimensional echocardiographic evaluation of fetal heart anatomy and function. J Ultrasound Med. 1996;15:1–9.
14. Lee W, Comstock CH, Kirk JS, et al. Birthweight prediction by three-dimensional ultrasound volumes of the fetal thigh and abdomen. J Ultrasound Med. 1997;16:799–805.
15. Cusumano A, Coleman DJ, Silverman RH, et al. Three-dimensional ultrasound imaging: clinical applications. Ophthalmology. 1998;105:300–6.
16. Marks LS, Dorey FJ, Macairan ML, et al. Three-dimensional ultrasound device for rapid determination of bladder volume. Urology. 1997;50:341–8.
17. Fine D. Three-dimensional ultrasound imaging of the gall-bladder and dilated biliary tree: Reconstruction from real-time B-scans. Br J Radiol. 1991;64:1056–7.
18. Barry CD, Allott CP, John NW, et al. Three-dimensional freehand ultrasound: image reconstruction and volume analysis. Ultrasound Med Biol. 1997;23:1209–24.
19. von Ramm OT, Smith SW, Carroll BA. Real-time volumetric US imaging. Radiology. 1994;193(P):308.
20. Rosenfield K, Kaufman J, Pieczek A, et al. Real-time three dimensional reconstruction of intravascular images of iliac arteries. Am J Cardiol. 1992;70:412–5.
21. Riccabona M, Nelson TR, Pretorius DH, et al. Distance and volume measurement using three-dimensional ultrasonography. J Ultrasound Med. 1995;14:881–6.
22. King DL, King Jr DL, Shao MY. Evaluation of in vitro measurement accuracy of a three-dimensional ultrasound scanner. J Ultrasound Med. 1991;10:77–82.
23. Bendick PJ, Brown OW, Hernandez D, et al. Three-dimensional vascular imaging using Doppler ultrasound. Am J Surg. 1998;176:183–7.
24. Delcker A, Turowski B. Diagnostic value of three-dimensional transcranial contrast duplex sonography. J Neuroimaging. 1997;7:139–44.
25. Kenton AR, Martin PJ, Evans DH. Power Doppler: an advance over colour Doppler for transcranial imaging? Ultrasound Med Biol. 1996;22:313–7.
26. Postert T, Federlein J, Przuntek H, et al. Insufficient and absent acoustic temporal bone window: potential and limitations of transcranial contrast-enhanced color-coded sonography and contrast-enhanced power-based sonography. Ultrasound Med Biol. 1997;23:857–62.
27. Steinke W, Ries S, Artemis N, Schwartz A, Hennerici M. Power Doppler imaging of carotid artery stenosis. Stroke. 1997;28:1981–7.
28. Griewing B, Morgenstern C, Driesner F, Kallwellis G, Walker ML, Kessler C. Cerebrovascular disease assessed by color-flow and

power Doppler ultrasonography: comparison with digital subtraction angiography in internal carotid artery stenosis. Stroke. 1996;27:95–100.
29. Keberle M, Jenett M, Beissert M, Jahns R, Haerten R, Hahn D. Three-dimensional power Doppler sonography in screening for carotid artery disease. J Clin Ultrasound. 2000;28:441–51.
30. Bucek RA, Reiter M, Dirisamer A, Haumer M, Fritz A, Minar E, Lammer J. Three-dimensional color Doppler sonography in carotid artery stenosis. AJNR Am J Neuroradiol. 2003;24:1294–9.
31. AbuRahma AF, Jarrett K, Hayes JD. Clinical implications of power Doppler three-dimensional ultrasonography. Vascular. 2004;12:293–300.
32. Chiu B, Egger M, Spence JD, et al. Quantification of carotid vessel wall and plaque thickness change using 3D ultrasound images. Med Phys. 2008;35:3691–710.
33. Mallett C, House AA, Spence JD, et al. Longitudinal ultrasound evaluation of carotid atherosclerosis in one, two and three dimensions. Ultrasound Med Biol. 2009;35:367–75.
34. Seabra JC, Pedro LM, e Fernandes JF. A 3-D ultrasound-based framework to characterize the echo morphology of carotid plaques. IEEE Trans Biomed Eng. 2009;56:1442–53.
35. Krasinski A, Chiu B, Spence JD, et al. Three-dimensional ultrasound quantification of intensive statin treatment of carotid atherosclerosis. Ultrasound Med Biol. 2009;35:1763–72.
36. Rubin JM, Adler RS, Fowlkes JB, et al. Fractional moving blood volume: estimation with power Doppler US. Radiology. 1995;197:183–90.
37. Carson PL, Moskalik AP, Govil A, et al. The 3D and 2D color flow display of breast masses. Ultrasound Med Biol. 1997;23:837–49.
38. Huang YL, Kuo SJ, Hsu CC, et al. Computer-aided diagnosis for breast tumors by using vascularization of 3-D power Doppler ultrasound. Ultrasound Med Biol. 2009;35:1607–14.
39. Xu HX, Lu MD, Xie XH, et al. Three-dimensional contrast-enhanced ultrasound of the liver: experience of 92 cases. Ultrasonics. 2009;49:377–85.
40. Leen E, Kumar S, Khan SA, et al. Contrast-enhanced 3D ultrasound in the radiofrequency ablation of liver tumors. World J Gastroenterol. 2009;15:289–99.
41. Luo W, Numata K, Morimoto M, et al. Differentiation of focal liver lesions using three-dimensional ultrasonography: retrospective and prospective studies. World J Gastroenerol. 2010;16:2109–19.
42. Numata K, Luo W, Morimoto M, et al. Contrast enhanced ultrasound of hepatocellular carcinoma. World J Radiol. 2010;2:68–82.
43. von Birgelen C, DiMario C, Reimers B, et al. Three-dimensional intracoronary ultrasound imaging: methodology and clinical relevance for the assessment of coronary arteries and bypass grafts. J Cardiovasc Surg. 1996;37:129–39.
44. Goldberg SL, Colombo A, Nakamura S, et al. Benefit of intravascular ultrasound in the deployment of Palmaz–Schatz stents. J Am Coll Cardiol. 1994;24:996–1003.
45. White RA, Donayre CE, Walot I, et al. Preliminary clinical outcome and imaging criterion for endovascular prosthesis development in high-risk patients who have aortoiliac and traumatic arterial lesions. J Vasc Surg. 1996;24:556–71.
46. Chengelis DL, Glover JL, Bendick P, et al. The use of intravascular ultrasound in the management of thoracic outlet syndrome. Am Surg. 1994;60:592–6.

# Contrast-Enhanced Ultrasound

# 55

Daynene Vykoukal, Javier E. Anaya-Ayala,
Alan B. Lumsden, and Mark G. Davies

**Abstract**

The clinical application of contrast-enhanced two-dimensional echocardiography was initially introduced in 1968 and demonstrated significant improvement in visualization compared to noncontrast-enhanced ultrasound. Its use has expanded to multiple vascular territories including the thoracic and abdominal aorta, carotid artery, lower extremity arteries, and venous circulation. Current contrast agents consist of stabilized gas-filled microbubbles (1–7 μm in diameter) that offer adequate safety profiles and improved efficacy. Microbubbles do not diffuse out of the circulation and thus behave as blood-pool marker are able to pass through the capillary pulmonary bed, and are stable enough to achieve enhancement for the duration of the examination. Although detectable with Doppler systems, special multipulse insonating sequences have been developed that selectively display their presence, whether in large vessels or in the microvasculature; this latter vascular beds can now be interrogated for the first time with ultrasound. The effect of microbubbles depends on the fact that gases are compressible, whereas tissue is relatively incompressible. This chapter focuses on the biology, clinical applications, and future advancements in contrast enhanced ultrasound. Developments in material engineering and biotechnology will continue to improve the current standards and expectations; a better understanding of the dynamic flow of microvascular beds and focused delivery of biological compounds should enhance end organ imaging and therapeutic strategies.

**Keywords**

Contrast-enhanced Ultrasonography • Contrast agent • Microbubbles • Endovascular procedures • Vascular imaging

D. Vykoukal, Ph.D. • J.E. Anaya-Ayala, M.D.
Department of Cardiovascular Surgery,
Methodist DeBakey Heart & Vascular Center,
6550 Fannin, Smith Tower, Suite 1401,
Houston, TX 77030, USA

A.B. Lumsden, M.D. (✉)
Department of Cardiovascular Surgery,
Methodist DeBakey Heart & Vascular Center,
6550 Fannin, Smith Tower, Suite 1401, Houston, TX 77030, USA

Department of Surgery, Weill Medical College at Cornell University,
Houston, TX, USA
e-mail: ablumsden@tmhs.org

M.G. Davies, M.D., Ph.D., MBA
Department of Surgery, Weill Medical College at
Cornell University, New York, NY, USA

Department of Cardiovascular Surgery, Methodist DeBakey
Heart & Vascular Center, Houston, TX, USA

Department of Research and Education, Methodist DeBakey
Heart & Vascular Center, Houston, TX, USA

A.F. AbuRahma, D.F. Bandyk (eds.), *Noninvasive Vascular Diagnosis*,
DOI 10.1007/978-1-4471-4005-4_55, © Springer-Verlag London 2013

## Introduction

The clinical application of contrast-enhanced two-dimensional echocardiography was originally introduced by Gramiak and Shah in 1968 [1, 2], and its use has demonstrated significant benefit [3]. The first agents used were "free" microbubbles that had several limitations due to low persistence and efficacy. The development of newer contrast materials has explored several approaches [2, 4]. Aqueous solutions, colloidal suspensions, and emulsions were initially studied as potential contrast agents; however, their safety and efficacy were not compatible with ultrasound. Current contrast agents consist of stabilized gas-filled microbubbles (1–7 μm in diameter) that offer adequate safety profiles and improved efficacy. Their properties approach that of the ideal contrast agent, which should be nontoxic and injectable intravenously. Microbubbles do not diffuse out of the circulation and thus behave as blood-pool markers [5], are able to pass through the capillary pulmonary bed, and are stable enough to achieve enhancement for the duration of the examination. Although detectable with Doppler systems, special multipulse insonating sequences have been developed that selectively display their presence, whether in large vessels or in the microvasculature, which can thus be interrogated for the first time with ultrasound. Their effect depends on the fact that gases are compressible, whereas tissue is relatively incompressible [5].

## Basic Principles of Contrast-Enhanced Ultrasound Agents

Current contrast agents are composed of stabilized microbubbles made with sugar matrices, albumin, lipids, or polymer shells with or without surfactants; these elastic shells enhance microbubble stability by adding physical support and reducing surface tension at the gas–liquid interface. The choice of size for clinical microbubbles is determined by the diameter of the pulmonary capillaries (the narrowest in the body), since they must be able to cross the lung bed to produce systemic enhancement after intravenous injection [3]. In practice, this means that they must be smaller than 7 μm in diameter [6]. Simple air-filled microbubbles have evolved to incorporate gases with low diffusion coefficients, such as perfluorocarbons. Their low solubility in blood and increased persistence permit longer examination times [7, 8]. Manipulation of the type of gas used and the structure of the encapsulating shell is currently used to prolong contrast enhancement. The classification of contrast agents is dependent on pharmacokinetics (Table 55.1). The different contrast agents are basically distinguished by their ability to cross the pulmonary circulation and have tissue- or organ-specific phases in addition to their vascular phase [9]; for example, Levovist (SHU 508A, Schering, Berlin, Germany) localizes to the liver and spleen once eliminated from the blood pool, approximately 20 min after the intravenous injection [10]. The mechanism of this phenomenon is not fully understood at this time, but it is believed that the microbubbles adhere to the sinusoids. Other examples include Sonazoid (Nycomed Amersham, Oslo, Norway) and Sonovist (SHU 563A Schering, Berlin, Germany), which are phagocytosed by hepatic Kupffer cells [11]. It is worth noting that Kupffer cells are not found in metastases or hepatic carcinomas, and therefore these agents accumulate only in normal liver (Fig. 55.1). Contrast agents increase the backscatter of the ultrasound signal intensity, thus improving Doppler analysis as well as enhancing the grayscale echostructure on specific imaging sequences by up to 25 dB (a greater than 300-fold increase) [12]. The image quality that contrast agents provide is dependent on the properties of the agent as well as the imaging sequence and signal processing method. Each agent behaves uniquely within a certain ultrasound field, allowing signal processing manipulation to optimize microbubble detection [13]. Specific contrast-imaging sequences have been developed by tailoring the acoustic power, the transmit and receive frequencies, the pulse frequency, and the pulse phase and amplitude to each contrast agent for maximal efficacy. Adverse effects are a possible outcome of administration of any drug or contrast agent, including ultrasound contrast agents. Most adverse events with ultrasound contrast agents, though, are rare and of mild intensity [14]. Most commonly, patients experience a temporary alteration in their sense of taste, pain at the injection site, a warm facial sensation, or a generalized flush [15]. Other previously reported adverse events include dyspnea, chest pain, headache, and nausea [16–18]. Studies have reported that the incidence of adverse events with ultrasound contrast agents is similar to that in a control group [19]. Nevertheless, ultrasound contrast agents have a superb safety profile with no specific renal, liver, or cerebral toxicities.

## Mechanics of Ultrasonographic Contrast

Microbubble behavior is influenced by the local acoustic power [20], which depends on the output power of the ultrasound system, the transmit frequency, and the attenuation of the ultrasound beam with depth. The mechanical index (MI) reflects output power, and therefore correlates with the local acoustic power. As mentioned previously, each contrast agent behaves uniquely at a given MI, and consequently each agent will have its own optimal imaging sequence.

**Table 55.1** Ultrasound contrast agents

| Agent | Company | Gas | Shell | Approval |
|---|---|---|---|---|
| *First generation, nontranspulmonary vascular* | | | | |
| Free microbubbles | Schering | Air | None | |
| Echovist (SHU 454) | | Air | Galactose | Europe |
| *Second-generation, transpulmonary vascular, short half-life (<5 min)* | | | | |
| Albunex | Molecular biosystems | Air | Albumin | United States |
| Levovist (SHU 508 A) | Schering | Air | Palmitic acid | Europe, Japan |
| *Third-generation transpulmonary vascular longer half life (>5 min)* | | | | |
| Aerosomes (definity MRX115, DMP115) | Bristol-Meyers-Squibb | Perfluoropropane | Phospholipid | United States |
| Echogen (QW3600) | SonoGen | Dodecafluoropentane | Surfactant | [a] |
| Optison (FSO 69) | Amersham | Octafluoropropane | Albumin | United States |
| Sono Vue (BR1) | Bracco | Sulfur hexafluoride | Phospholipid | Europe |
| Imaivst (AF0150) | Alliance | Perfluorohexane | Surfactant | United States |
| *Transpulmonary with organ-specific phase* | | | | |
| Levovist (SHU 508A) | Schering | Air | Palmitic acid | Europe, Japan |
| Sonavist (SHU 563A) | Schering | Air | Cyanoacrylate | [b] |
| Sonazoid (NC100100) | Amersham | Perfluorocarbon | Surfactant | [a] |

[a]Currently in clinical trials
[b]Clinical development stopped

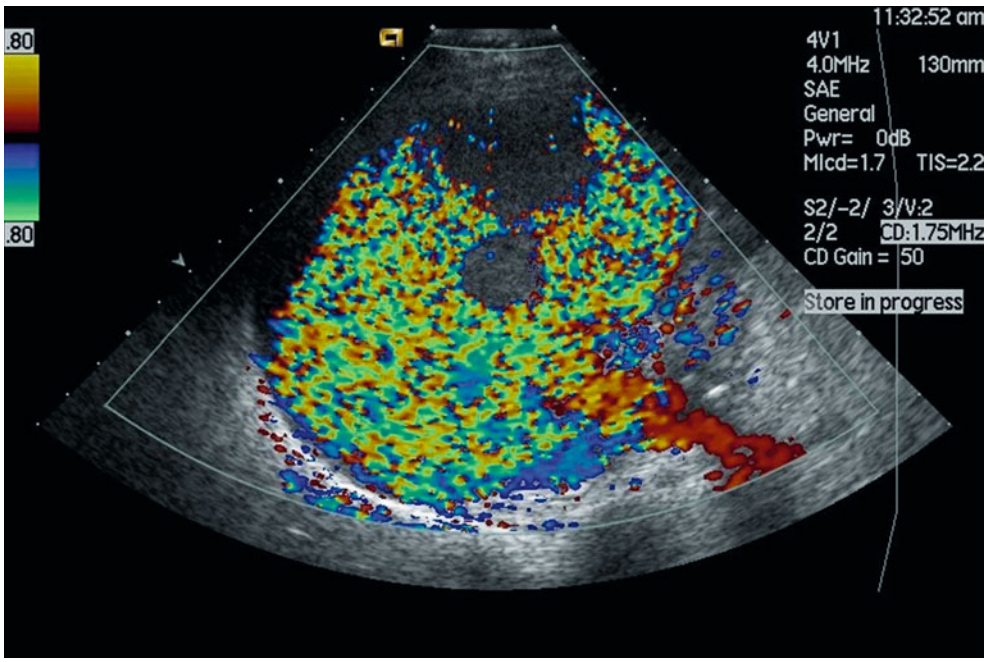


**Fig. 55.1** Imaging 3 min after Levovist injection improves the delineation of tumor metastases (Reprinted from Harvey et al. [12]. With permission from Elsevier)

## Low Acoustic Power (MI < 0.1)

At low MI, symmetrical oscillations occur and the frequency of the scattered signals is the same as the transmitted pulse. Microbubbles resonate equally and symmetrically (linear response) with the high and low pressures generated by the incident ultrasound wave with minimal destruction. They act as very efficient signal scatterers, which is attributed to the difference in their compressibility and density compared to the surrounding tissues (Fig. 55.2). Scattering efficiency increases as a function of microbubble radius to the sixth power, and therefore larger bubbles display higher backscatter coefficients [8]. Furthermore, increasing shell stiffness or gas density in turn decreases the microbubble response. Under low MI imaging, the intensity of the scattered signal is linearly related to that of the incident ultrasound beam [12]. Low MI is useful in conventional Doppler applications and real-time contrast imaging.

## Intermediate Acoustic Power (0.1 < MI < 0.5)

The amplitude of the microbubble oscillations in an ultrasound field increases as the MI is increased. As the amplitude increases, the microbubble oscillations become asynchronous with the ultrasound wave (Fig. 55.3). By manipulating the local acoustic power, the microbubbles begin to echo a harmonic response at frequencies that differ from that of the incident wave (fundamental frequency).

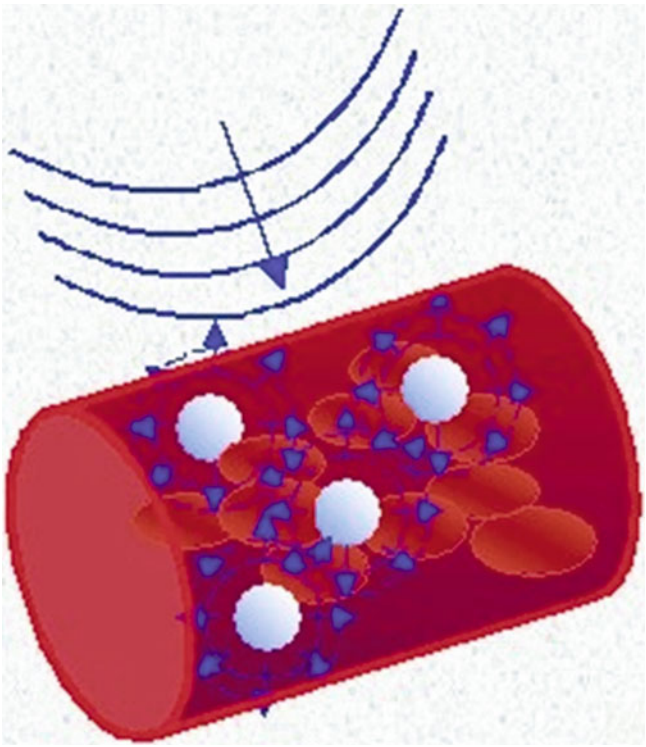

**Fig. 55.2** Resonance of microbubbles (Image courtesy of Dr. E. Stride, University College London, UK)

The highest intensity response is that of the second harmonic response, which is found at twice the fundamental frequency. Those responses found at higher frequencies are called higher harmonics. Specific types of harmonics called ultraharmonics can be obtained at specific frequencies such as those at 1.5 or 3.5 times the fundamental frequency [8]. Intermediate MI imaging possesses two main advantages. First, the technique enables avoidance of microbubble destruction while eliciting a good harmonic contrast signal. Second, the harmonics elicited from the surrounding tissues are reduced. As the advantage of contrast agents is their harmonic echo, any tissue harmonics become the background "noise." Tissue is less compressible and denser than the microbubbles, therefore requiring a higher MI for a harmonic response. Intermediate MI scanning allows for a higher contrast-to-tissue ratio compared to a high MI by limiting the tissue harmonic response, and thus eases the removal of the background "noise" from the contrast signal [20].

## High Acoustic Power (MI > 0.5)

The destruction of microbubbles occurs at higher acoustic powers. The encapsulating shell is broken and the gas diffuses into the surrounding fluid. The rupture of the microbubble causes an intense echo, very rich in nonlinear (harmonic) components (Figs. 55.4 and 55.5). Although the destruction of contrast agents is often viewed as a limitation, it allows for improved sensitivity in microbubble detection. When color and power Doppler are used, the change in the echo of two consecutive pulses is seen as a particular color pixel. These color signals thus correlate with the distribution of the microbubbles with little affect from blood flow characteristics [8].

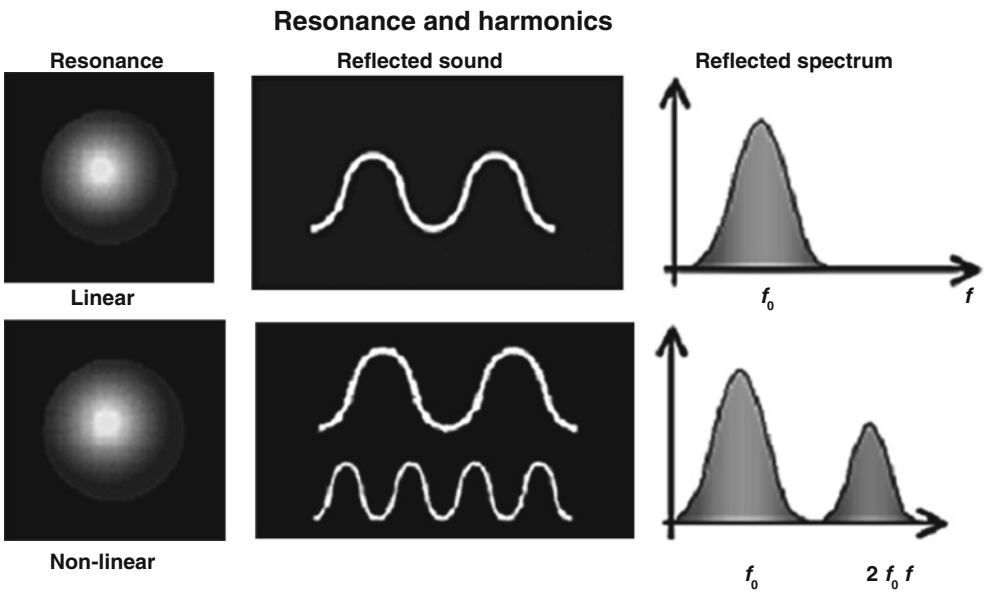


**Fig. 55.3** Nonlinear microbubbles return not only the fundamental (transmitted frequency) but also a second harmonic frequency that is at twice the transmitted frequency (Image courtesy of Dr. David Adams)

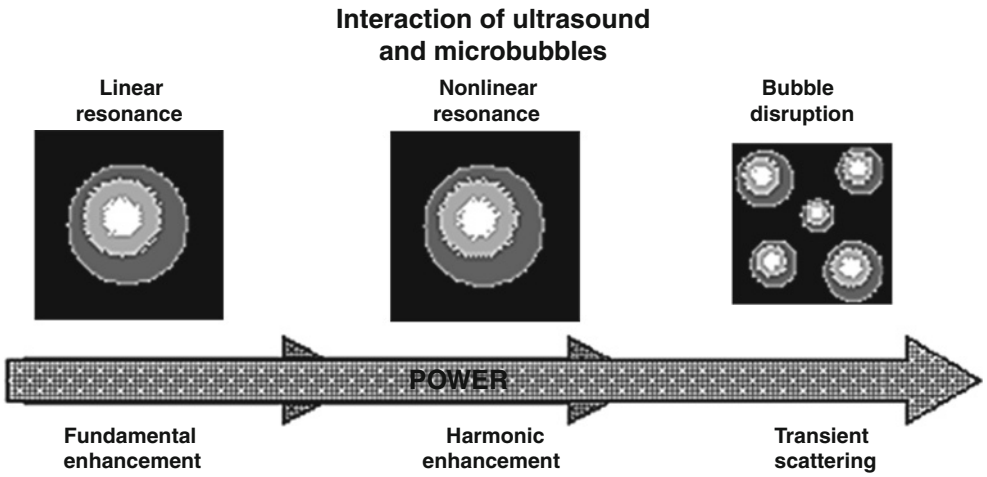


**Fig. 55.4** As acoustic power is increased, microbubbles move from a linear response to a nonlinear, harmonics-producing response. At maximum power, destruction of the microbubbles occurs (Image courtesy of Dr. David Adams)

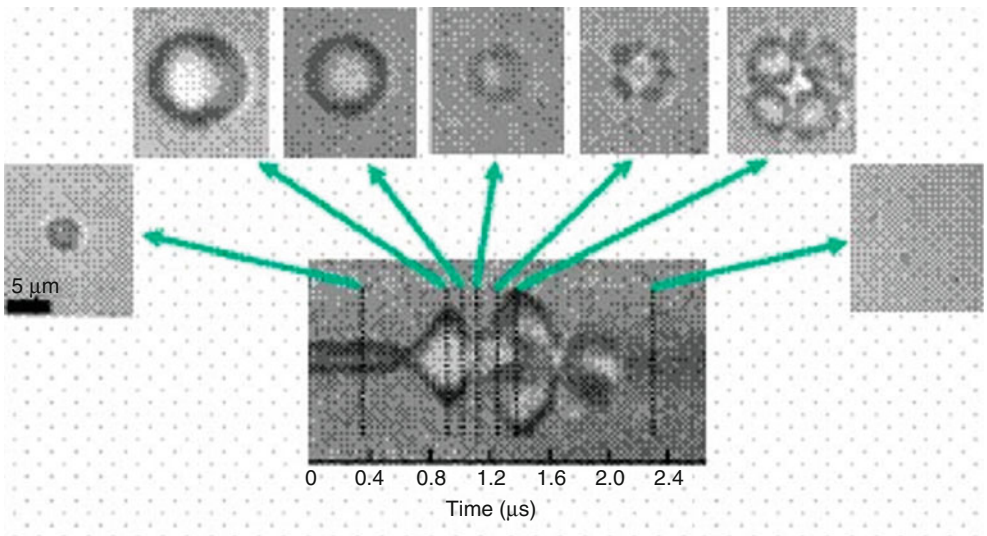


**Fig. 55.5** Electron microscopy image of a microbubble responding to increasing ultrasound MIs

## Microbubble Technology

Technological advances in microbubble engineering have focused on the optimization of tissue-specific binding of microbubbles by manipulation of the components of the encapsulating shell. One such strategy exploits the disease-related upregulation of surface receptors in activated leukocytes that bind nonspecifically to either albumin or lipid in the microbubble shell [21]. Linder et al. studied the binding of albumin and lipid shells to activated leukocytes after reperfusion injury and exposure to proinflammatory cytokines. Albumin binds to the β2-integrin Mac-1 on the activated leukocytes, which in turn binds to intercellular adhesion molecule (ICAM)-1 expressed on endothelial cells in areas of inflammation. Lipids are found to undergo opsonization by the complement system and bind via a complement receptor to activated leukocytes. By adding phosphatidylserine to the lipid shell, there is a sixfold increase in the affinity of the microbubble to the activated leukocytes due to increased complement attachment to the lipid shell [21, 22]. Inflammation-specific binding of microbubbles can augment the visualization of inflammatory atherosclerotic plaques. Since the amount of microbubbles bound correlates with the amount of inflammation, contrast-enhanced ultrasound (CEUS) will be able to determine the inflammatory phenotype of plaques, thus identifying those plaques with increased vulnerability to thrombosis. Another strategy to enhance the tissue-specific retention of microbubbles is the conjugation of ligands or antibodies that recognize specific antigens or receptors on a specific tissue type (Fig. 55.6). One example is the attachment of an oligopeptide to the shell surface that recognizes the glycoprotein IIb/IIIa integrin receptor on activated platelets [24, 25]. This allows the visualization of thrombus by the binding of microbubbles to platelets, as well as a means for clot lysis when the microbubbles are ruptured using an ultrasound beam [26]. A modification of this strategy achieved by adding the attachment of a chemical spacer, such as polyethylene glycol, allows the ligand to be projected further away from the shell surface, thus increasing its affinity for tissue-specific antigens or receptors [27]. In addition to tissue-specific binding, new microbubbles are now being

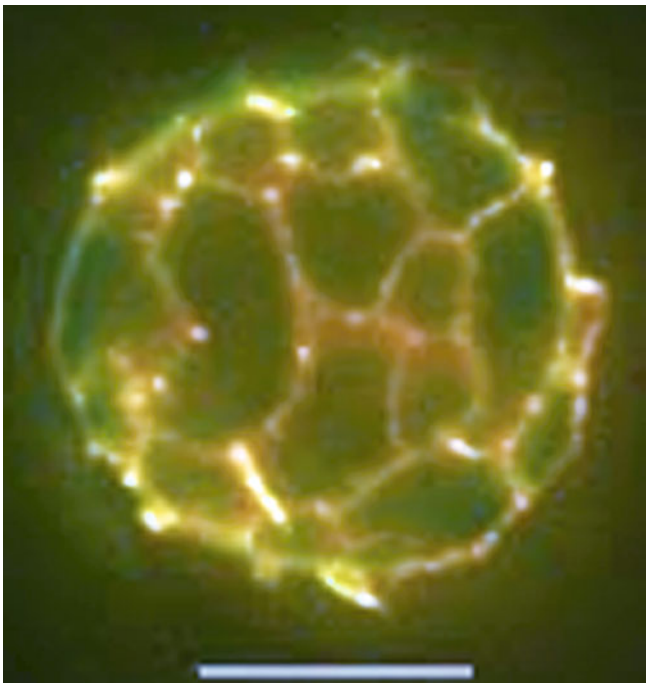

**Fig. 55.6** Fluorescent targeted microbubble (Reprinted from Borden et al. [23]. With permission from American Chemical Society)

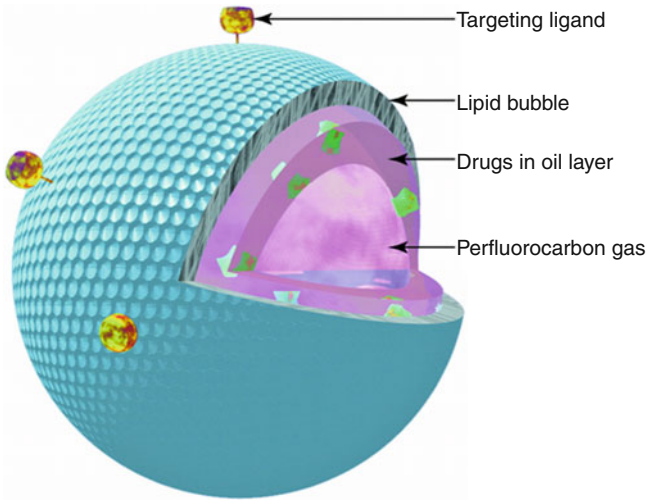


**Fig. 55.7** Schematic of a microbubble with ligands conjugated to its outer shell and encapsulating drugs (Image courtesy of Dr. Evan Unger, University of Arizona. Tucson, AZ)

used as a vehicle for drug and gene delivery (Fig. 55.7). Chemotherapeutic and thrombolytic agents and plasmid DNA are encapsulated in an oil emulsion within the microbubble. Once the microbubbles have reached their target tissue, an ultrasound beam with a high MI is used to rupture the bubbles and release the agent. This focal destruction of microbubbles decreases the systemic concentration of an agent, thus improving its therapeutic index and limiting systemic toxicities [28]. Encapsulation of genes also protects naked DNA and vectors from plasma endonucleases and hepatic clearance, which limits their stability [28] (Fig. 55.8). Engineering microbubbles as target-specific therapeutic delivery vehicles will have a wide range of applications in the diagnosis and therapy of numerous medical conditions. Stabilized gas microbubbles can be functionalized with antibodies or peptides to specifically bind receptors overexpressed on vascular endothelial cells, thereby generating sensitive intravascular molecular imaging probes. Moreover, they can also be loaded with drugs and genes and release these payloads upon exposure to destructive ultrasound pulses [29, 30].

## Ultrasound Imaging Techniques

### B-Mode and Color Imaging

Contrast agents can be employed when using conventional B-mode imaging and Doppler imaging modalities, including color, power, and spectral imaging. They can be used to opacify fluid-containing cavities such as the bladder, uterus, cardiac chambers (Fig. 55.9), and some large venous structures. Echovist (Schering AG, Berlin, Germany) has been used for sonosalpingography [32] and Levovist (Schering) has been used to detect vesicoureteric reflux [33]. This allows equally sensitive and specific imaging alternatives to conventional radiographs while avoiding ionizing radiation exposure. The limitation of contrast agents with B-mode imaging is that there is no added enhancement in solid structures. Doppler imaging provides excellent detection of microbubbles, but it is limited by color blooming and oversaturation artifacts [8].

### Stimulated Acoustic Emission

This microbubble destructive modality involves an initial wave of ultrasound at a high MI, which ruptures the microbubbles. Signal responses are recorded before and after this destruction, and the loss of correlation between the two signals maps the distribution of the contrast agent [10]. As mentioned above, some organ-specific contrast agents accumulate only in normal liver tissue. This characteristic has been utilized to detect liver metastases using Levovist. Metastases appear as signal defects [34] (Figs. 55.10 and 55.11).

### Contrast-Enhanced Dynamic Flow

Conventional Doppler imaging can be used with multiple pulse techniques. After the ideal bandwidth is determined, consecutive pulses are emitted. The flow signals are isolated from static tissue signals by amplifying their intercorrelation at different times, and the static tissue signals are removed. This technique, called advanced dynamic flow, allows better

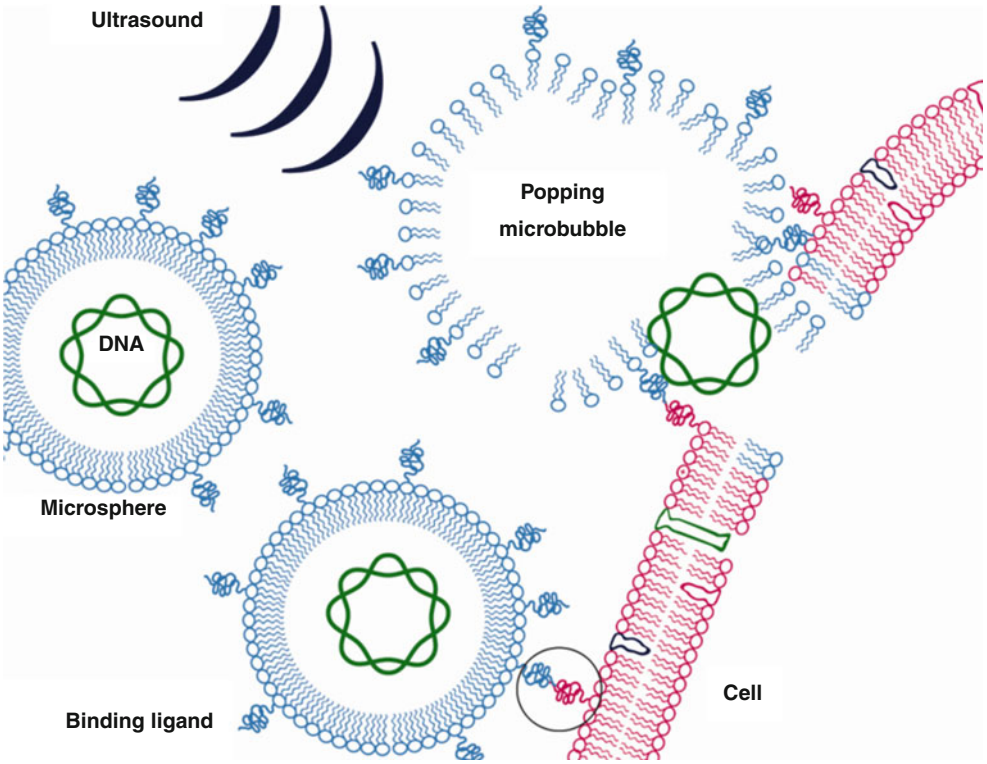


**Fig. 55.8** Schematic of microbubble gene delivery (Image courtesy of Dr. Evan Unger, University of Arizona. Tucson, AZ)

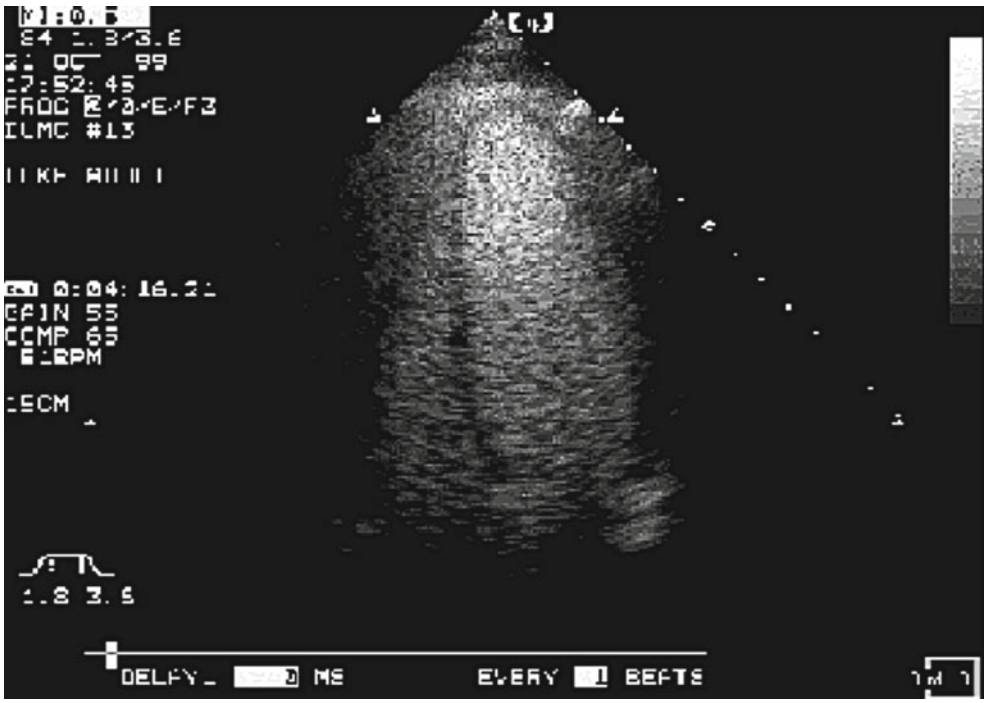

**Fig. 55.9** An apical four-chamber view demonstrating optimal left ventricular opacification with microbubbles (Reprinted from McCulloch et al. [31]. With permission from Elsevier)

spatial delineation of the microvasculature of superficial structures compared to conventional Doppler modes (Fig. 55.12). However, its sensitivity is limited by the depth of the structure of interest. The utilization of contrast agents with this technique expands its uses to the visualization of deep structures, hypoperfused structures, and even real-time perfusion imaging using lower MIs to preserve microbubbles [8].

## Harmonic Imaging

This is a nonlinear imaging modality that can detect microbubble harmonic responses at a higher sensitivity than the response from the surrounding tissues. The weaker non-harmonic echos from the multiple responses from the body wall (as with obese patients) are filtered from the final image

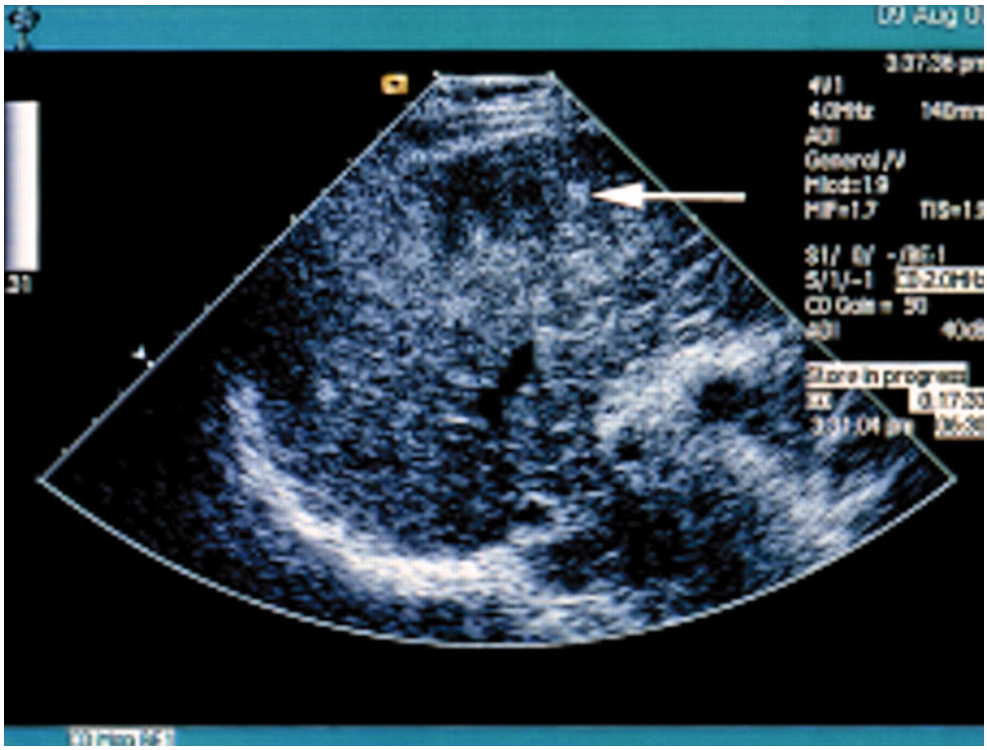

**Fig. 55.10** B-mode imaging shows the liver is heterogeneous with an ill-defined lesion (*arrow*) (Image courtesy of Dr. Evan Unger, University of Arizona. Tucson, AZ)

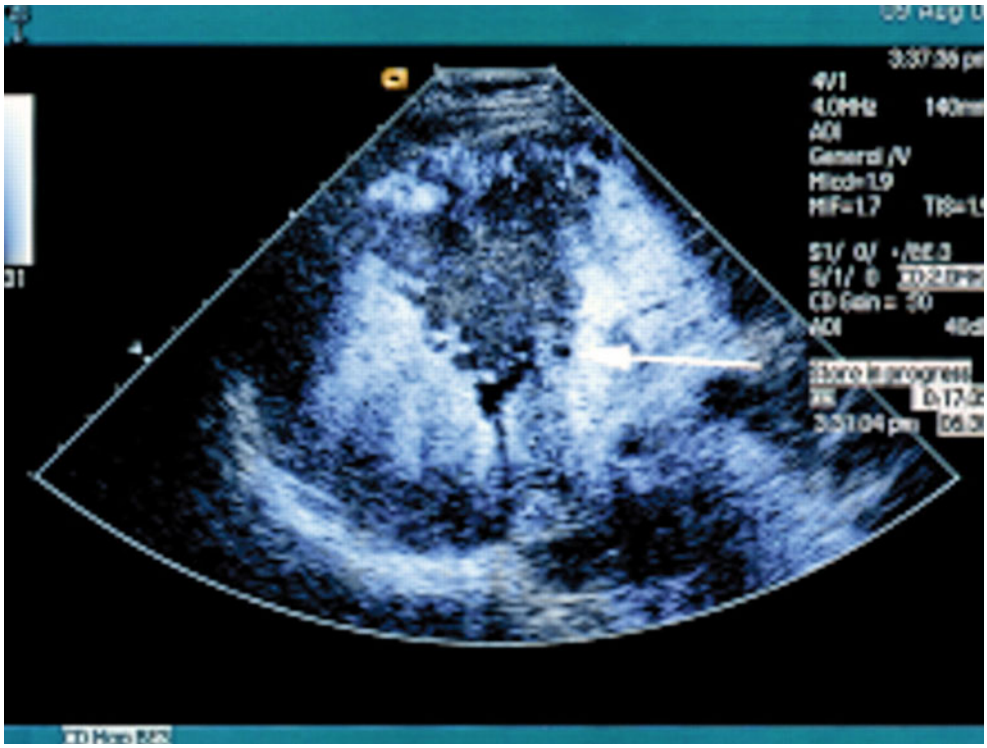

**Fig. 55.11** The presence of liver-specific microbubbles (Levovist) administered 5 min earlier. A defect is clearly seen in the central right lobe of the liver, with several additional defects thought to represent additional satellite foci of hepatocellular carcinoma (arrow) (Image courtesy of Dr. Evan Unger, University of Arizona. Tucson, AZ)

as well, improving the signal-to-noise ratio [12]. This sensitivity is derived from the fact that the microbubbles produce a unique nonlinear, harmonic response that can be separated from the tissue echos and large vessel blood flow. Currently, there are commercially available transducers that can both emit ultrasound energy and detect the microbubble harmonic response. These transducers are tuned in to detect the resonant frequency of microbubbles, which range in diameter from 1 to 9 μm, in the 1–9 MHz range [35, 36]. Several techniques can be used with harmonic imaging to refine the

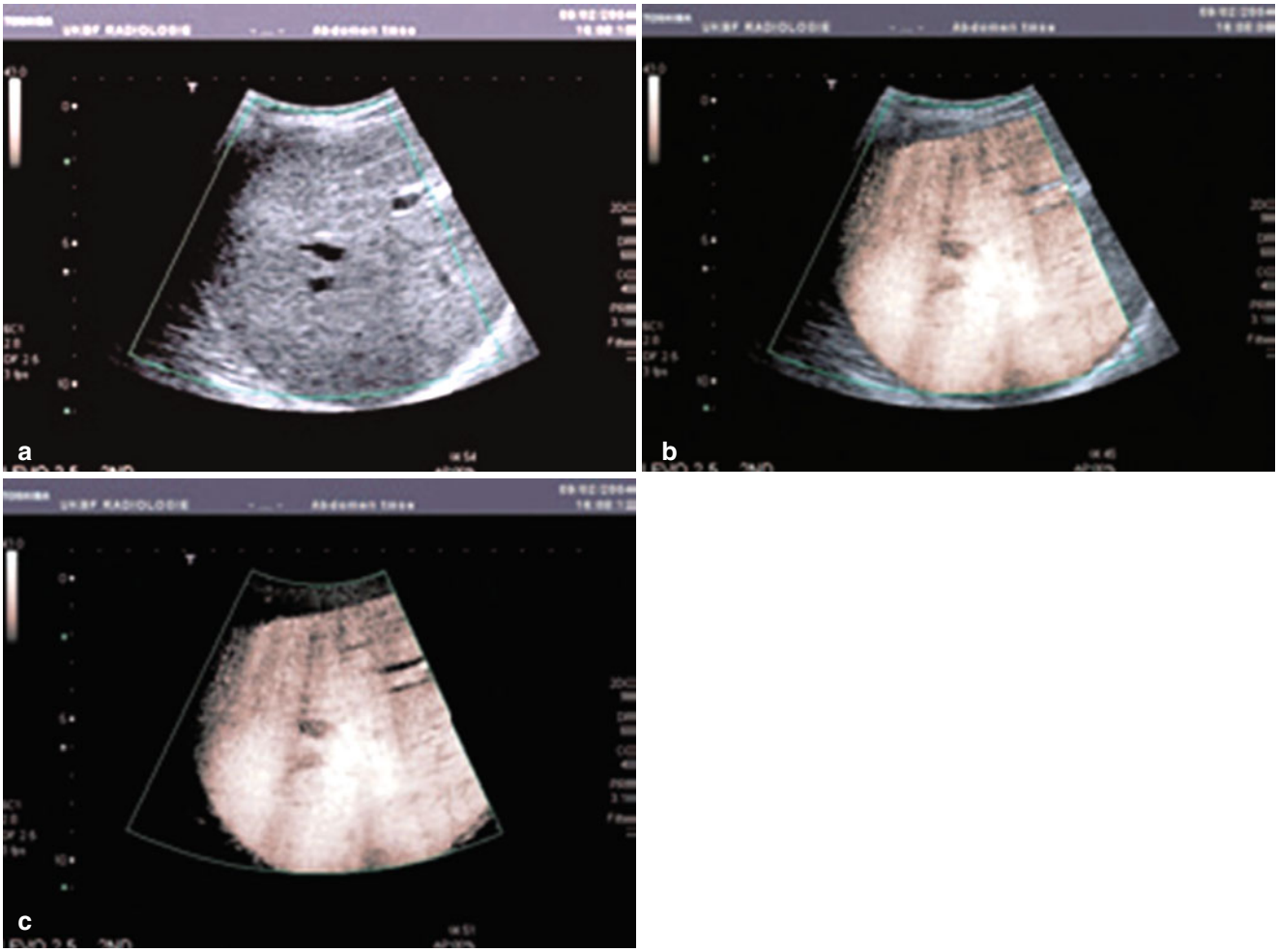


**Fig. 55.12** Normal liver scanned at high MI using advanced dynamic flow in the liver-specific late phase 4:50 min post-Levovist. Advanced dynamic flow can be displayed (**a**) as conventional B-mode only, (**b**) as a combination of B-mode and colorized contrast information, or (**c**) as a contrast only image (Images courtesy of Dr. Thomas Albrecht, Vivantes Hospital. Berlin, Germany)

detection of the nonlinear, harmonic response of the contrast agents including conventional imaging, subtraction techniques using single (coherent imaging mode) or multiple pulses (pulse or phase inversion), and a combination of the latter for multiframe subtraction techniques. Conventional imaging uses a monopulse technique in which a single pulse of ultrasound is emitted and the second harmonic of the microbubble echo is isolated using filters. The microbubble signal returns at 10–15 dB higher than the signal from the surrounding clutter. Harmonic imaging can provide gray scale and Doppler information; however, it does have its limitations. First, the filtering process to isolate the second harmonic from the fundamental frequency affects the image quality. Also, the increased attenuation of the harmonic frequency compared to the fundamental frequency limits the depth of the imaging capabilities [8].

Pulse or phase inversion involves the emission of two consecutive pulses in inverted phases and the detection of the difference of the unique resonance of microbubbles in each phase [36]. Since microbubbles have a unique harmonic response to the consecutive pulses, the difference in the echo signals in the two phases results in an increased sensitivity in the detection of the microbubbles (Fig. 55.13). Power pulse inversion utilizes these same principles using a multipulse technique. The multipulse technique adds to the sensitivity of the modality and improves the differentiation between liquids and solids, as well as limiting motion artifacts [14]. Intermittent imaging and scanning are employed when using a high MI imaging modality for microbubble destruction [8]. This approach allows for replenishment of the contrast agent between images. The frame rate is reduced to about 1 frame/s compared to the conventional 30 frames/s. The frame rate can also be synchronized with the cardiac cycle so that the microbubble can be carried into the area of interest where the microbubbles have been destroyed. Depending on the imaging delay time after the microbubbles have been destroyed, regions with either increased or decreased blood volumes can be determined. Intermittent

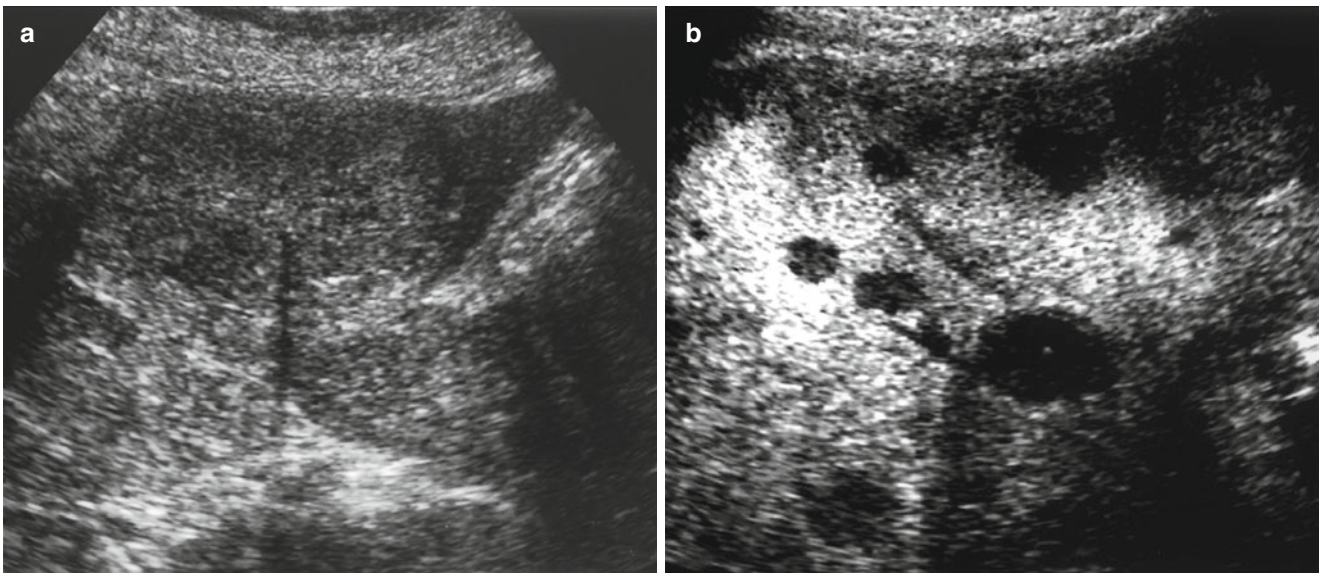


**Fig. 55.13** A 78-year-old man with metastatic liver disease. (**a**) Native B-mode sonogram shows inhomogeneous parenchyma of the liver, suggestive of focal liver lesions. (**b**) Contrast-enhanced late-phase pulse-inversion sonogram shows clear demarcation of multiple focal lesions without enhancement surrounded by enhanced liver parenchyma. Liver biopsy revealed metastatic liver disease by adenocarcinoma. Diffuse infiltration of the liver was confirmed on CT (Reprinted from von Herbay et al. [37]. With permission from American Roentgen Ray Society)

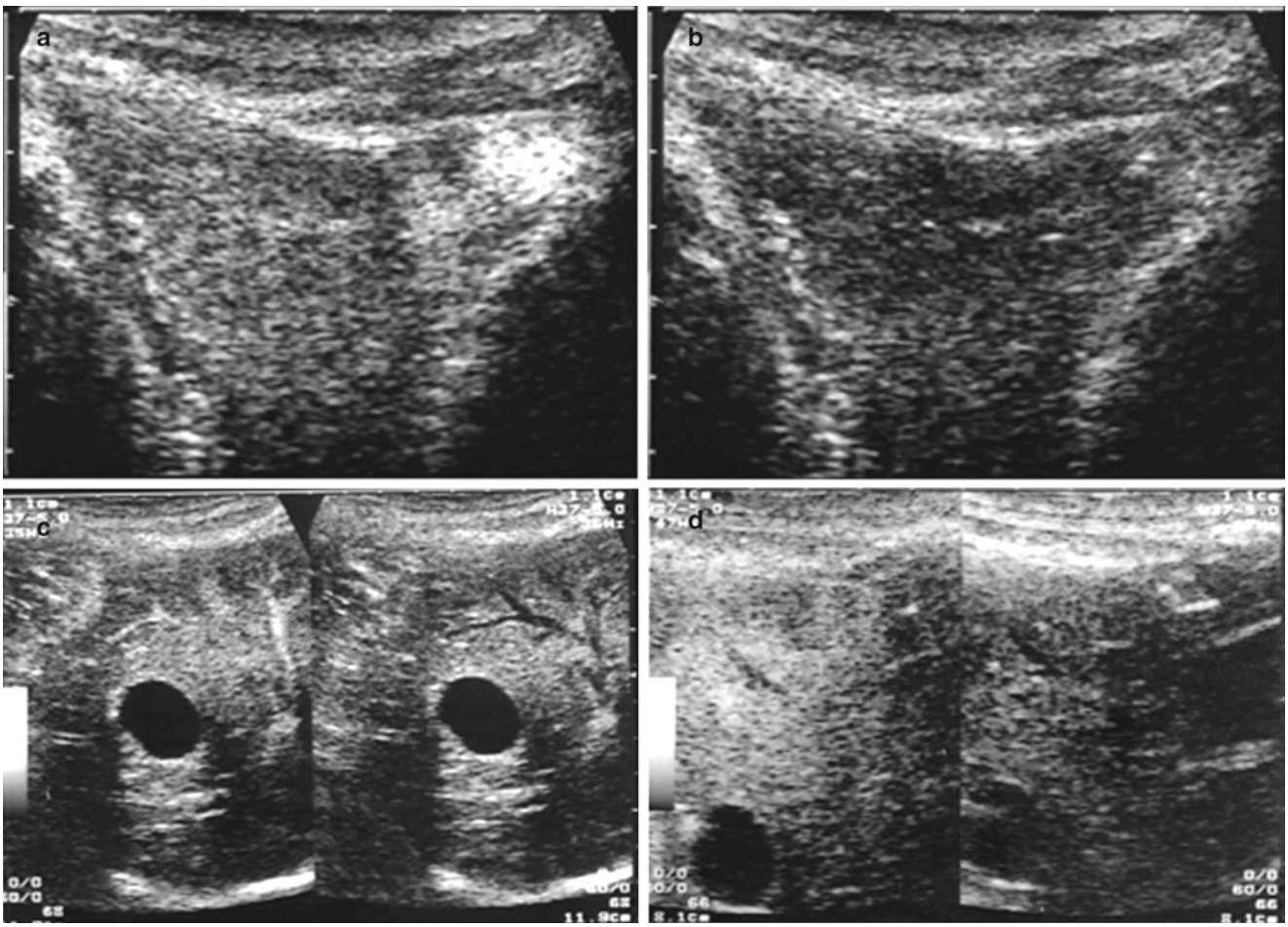


**Fig. 55.14** Contrast echography images obtained using the flash echo imaging system (harmonic imaging). (**a**, **b**) First and second frames of intermittent scanning (interval: 4 s, multiple frame scanning: three frames); (**c**) dual window method (interval: 1 s, multiple-frame scanning: two frames); and (**d**) intermittent scanning (*left*) with monitoring (Reprinted from Kamiyama et al. [38]. With permission from Elsevier)

imaging is thus limited by its inability to provide real-time imaging. Another limitation is motion artifact between image acquisitions.

## Flash Echo Imaging

Flash echo imaging is a technique that involves using a low MI between intermittent high MI destructive phases and following the target to be imaged during the entire study. A real-time anatomic image and a contrast-enhanced image during bubble destruction can be viewed simultaneously on the image screen [8] (Toshiba Medical Systems, Tokyo, Japan) (Fig. 55.14).

## Real-Time Digital Subtraction

Another imaging sequence involves real-time digital subtraction of a bubble-destruction phase image from a consecutively acquired background image taken milliseconds apart. This technique limits motion artifact and improves the visibility of the microbubbles in the resulting image [8] (Fig. 55.15).

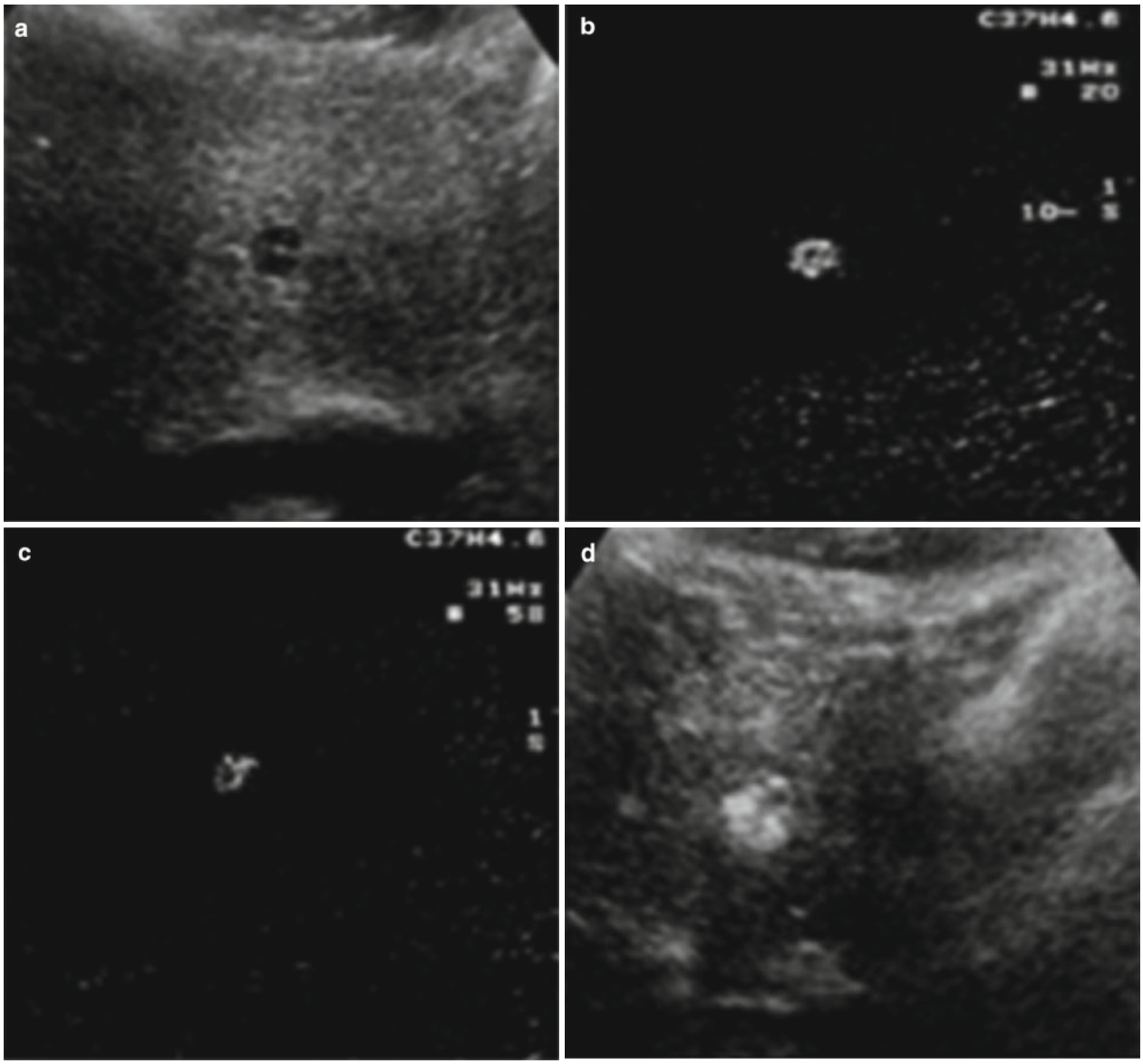


**Fig. 55.15** A 72-year-old woman with a hemangioma (diameter, 12.7 mm) on the left liver. (**a**) Subcostal plain ultrasound (US) scan shows a hypoechoic nodule in the left lobe. (**b**) Digital subtraction image (DSI) of the same tumor, at 50 s after the injection, shows hyperenhancement. (**c**) DSI of the same tumor, at 5 min after the injection, shows hyperenhancement. (**d**) US angiography of the same tumor, at 5 min after the injection, shows hyperenhancement. (**e**) Hepatic angiogram obtained during the arterial phase shows a hypervascular tumor. (**f**) Hepatic angiogram obtained during the late phase shows a hypervascular tumor (Reprinted from Yamamoto et al. [39]. With permission from Demetrios Spandidos, Spandidos Publications)

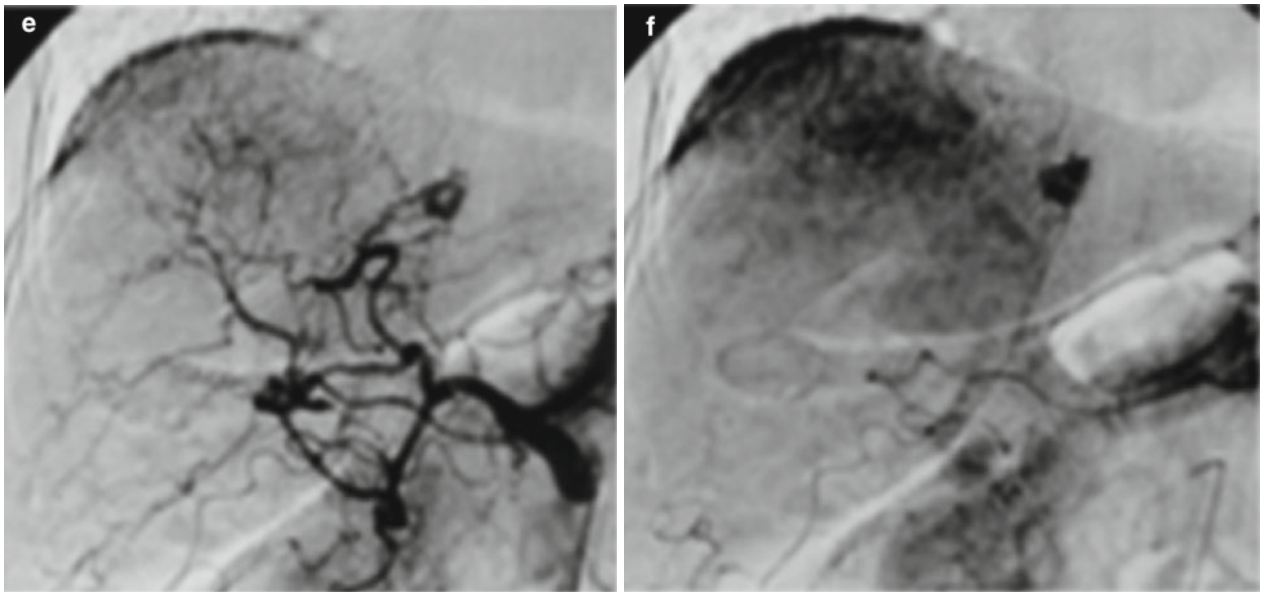


**Fig. 55.15** (continued)

## Clinical Applications of Ultrasound Contrast Agents

### Assessment of Vascular Abnormalities

Imaging of vascular structures using CEUS allows simultaneous assessment of the vascular lumen (using the CEUS signal) and the vascular wall (using the classical B-Mode signal). Thus, vascular anatomy and vessel patency can be evaluated, allowing reliable detection of several vascular abnormalities [40]. Since CEUS can easily be used at the bedside and during interventions, it is also suitable for guiding and monitoring vascular interventions and following them up [41]. CEUS can also be used to image vascular plaques. Location and extension as well as ulcerations can be visualized.

### Renovascular Assessment

Diagnosis of renal artery stenosis, determination of microperfusion, and extent of infarcts, as well as delineation of solid or cystic masses are all applications of CEUS that are being studied. It has been shown that using contrast agents with ultrasound evaluation improved the efficacy of the scan by enhancing the operator's ability to visualize the renal arteries and by increasing the number of definitive examinations. Although angiography has been considered the "gold standard" in the evaluation of renal artery stenosis, its invasiveness and patient exposure to radiation and nephrotoxic contrast agents restrict its use as a screening modality. Conventional Doppler ultrasound is routinely used for renal artery stenosis evaluation; however, studies have shown that there is great variability from center to center in its correlation to angiographic findings. In addition, the ability to obtain technically successful examinations was also shown to vary among the studies. Avasthi et al. reported good correlation between the studies when evaluating 52 renal arteries with both Doppler ultrasound and angiogram [42]. They reported 89% sensitivity and 73% specificity for Doppler ultrasound in detecting lesions with a greater than 50% lumen reduction. Technically adequate examinations were performed in approximately 84% of the patients. Similarly, Norris et al. performed successful examinations in 90% of the patients studied, with Doppler ultrasound having 73% sensitivity and 97% specificity when compared to angiography [43]. In contrast, Berland et al. obtained adequate examinations in only 58% of their patients, while being unable to identify any of the seven patients who had renal artery stenosis on angiogram. They reported only 37% specificity, as patients without renal artery stenosis were detected on only 7 out of 19 ultrasound examinations [44]. Desberg et al. reported success in only 51% of ultrasound examinations [45]. Such variability in the success of Doppler ultrasound in the evaluation of renal artery stenosis is reflective of the technical difficulty of performing an adequate examination in a wide variety of patients. Patient body habitus and variable renal artery anatomy also complicate examinations. CEUS is proving to be the imaging modality that can overcome these limitations. Claudon et al. reported the results of a randomized crossover study of 198 patients from 14 European centers who were referred for renal arterial angiography because they were suspected of having renal arterial stenosis [15]. They reported a 63.9–83.8% increase in successful examinations when adding contrast to the ultrasound scan, including in obese patients and those with renal dysfunction. When comparing Doppler

ultrasound to angiography, CEUS results correlated with angiographic results in the diagnosis or exclusion of renal artery stenosis more often than conventional Doppler ultrasound ($p=0.001$). In addition, Lacourciere et al. reported results from 78 patients involved in a Canadian multicenter controlled pilot study who were undergoing evaluation for renal artery stenosis comparing captopril-enhanced scintigraphy and unenhanced and enhanced ultrasound [46]. Results revealed that CEUS examination yielded a diagnosis in more patients than unenhanced ultrasound or scintigraphy—99%, 82%, and 81%, respectively ($p=0.002$). The proportion of technically successful ultrasound examinations increased significantly with the addition of contrast. CEUS has also been used to evaluate the microperfusion of the kidney and to define areas of ischemia or infarct. Renal perfusion has been quantified by using a high MI to destroy microbubbles, then using low MI intermittent harmonic imaging at various pulse intervals to plot pulse interval versus video intensity to derive microbubble velocity (MV) and renal blood volume fraction (BVF) [47] (Fig. 55.16). Wei et al. showed that measuring the rate of microbubble replenishment after destruction reflected MV. When the tissue is completely replenished with contrast, the signal reflects the tissue BVF. The product of MV and BVF correlates with tissue nutrient blood flow (NBF) [48]. Total renal blood flow (RBF) is estimated by cortical MV since >90% of total RBF supplies the renal cortex. Wei et al. showed that CEUS provides an assessment of RBF and tissue NBF that correlates with blood flow measurements obtained with a conventional Doppler flow probe [47]. The added assessment of NBF with CEUS allows the evaluation of renal pathologies that affect NBF with little affect on RBF and vice versa. Thus, CEUS provides improved information on the perfusion pattern of the kidneys in conditions such as pyelonephritis, embolism to the kidney, and post-transplant assessment of a transplanted kidney [49]. In addition to the imaging capabilities of CEUS, recent reports have demonstrated nonvector gene transfer into the kidney using microbubbles and ultrasound as a delivery vehicle. For example, Lan et al. studied the use of ultrasound and microbubbles to transfer a doxycycline-regulated Smad7 gene into the kidney as a potential therapy for renal fibrosis. They found that compared with nonultrasound treatment, the combination of ultrasound microbubble-mediated delivery largely increased Smad7 transgene expression up to a 1,000-fold in all kidney tissues [50]. CEUS is an imaging and therapeutic modality that will hopefully provide a safe, noninvasive, and easily applicable alternative in the management of renal disease.

## Echocardiography

Left ventricular cavity opacification (LVO) is clinically important in the evaluation of cardiac structure and ventricular function in resting and stress echocardiography. In the United States, contrast agents are FDA approved for ventricular opacification and enhancement of endocardial border

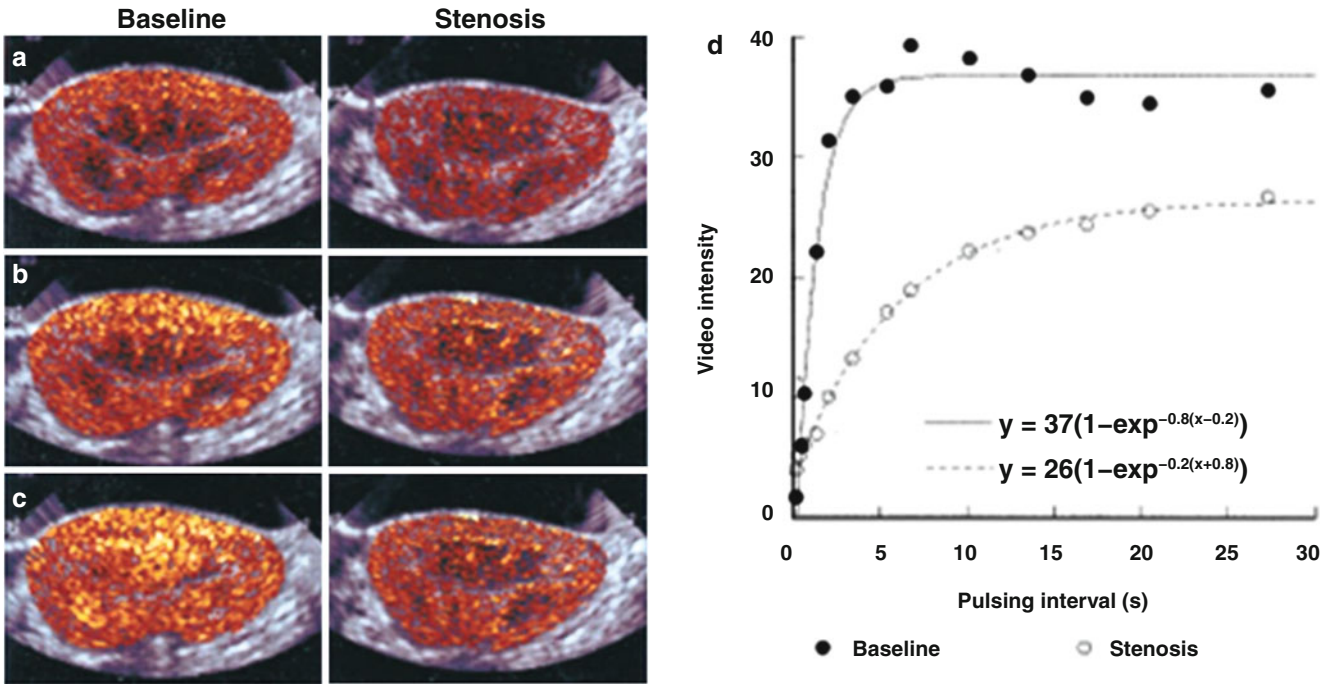


**Fig. 55.16** Background-subtracted color-coded images obtained from an animal at progressively longer pulsing intervals (**a**–**c**), at baseline and in the presence of a flow-limiting renal artery stenosis. The pulsing interval versus video intensity curves obtained from the cortex during both stages are shown in (**d**). The lower rate of rise of video intensity (*open* versus *closed circles*) was reflected by a significant decrease in cortical microbubble velocity from 0.8 to 0.2 $s^{-1}$ (Image courtesy of Dr. Kevin Wei, Oregon Health & Science University, Portland, OR)

definition. CEUS is used in those patients with a technically suboptimal echocardiogram. Contrast has been shown to increase the diagnostic capability of echocardiograms in numerous studies. In one study with 200 patients, the patient cohort was selected on the basis of suboptimal baseline echocardiograms with nonvisualization of at least 2 of 6 segments in the apical four-chamber view. CEUS in these patients converted a nondiagnostic study to a diagnostic echocardiogram in 75% of those patients examined. This added improvement in image quality resulted in a greater ability to answer the primary referral question in as many as 50% of patients [51]. Similar findings have been observed after left ventricular (LV) opacification produced by intravenous injections of investigational contrast agents [19, 52].

Administration of an intravenous contrast agent has also been shown to enable more accurate measurement of LV volume and ejection fraction in humans [53]. It has also been demonstrated clinically that with the use of contrast agents, harmonic imaging produces improvements over fundamental imaging in LVO, endocardial border definition, and reviewer confidence in the assessment of systolic function [14, 15, 20, 21, 36, 43, 49, 54]. The use of contrast agents has been demonstrated in other cardiac pathologies. The diagnosis of complications of myocardial infarction, such as wall rupture and left ventricle pseudoaneurysm formation, has been facilitated by the use of contrast agents. CEUS has also been used to improve the accuracy of transesophageal echocardiography in ascending aortic dissection by discriminating the true and false lumen. Intracardiac masses, such as tumors or thrombi, have been easier to identify with the use of ultrasonic contrast.

## Other Applications

### Plaque Assessment

The significance of inflammation in relation to plaque stability has been well established in animal models of disease. The inflammatory response includes the recruitment of monocyte-derived macrophages and leukocytes to atherosclerotic endothelium leading to plaque propagation, increased susceptibility of rupture, and vascular remodeling [55]. Identifying these inflamed, vulnerable plaques would be valuable in determining which patients would require an immediate intervention to prevent ischemic complications from a ruptured plaque. Those microbubbles with shells composed of albumin or lipids bind to activated leukocytes in response to ischemic injury or exposure to proinflammatory mediators. The extent of leukocyte binding by these microbubbles correlates with the amount of inflammation, allowing for quantification of the extent of the inflammatory process [19, 56]. The albumin and lipid shells of microbubbles bind to these activated leukocytes via different mechanisms, although they both require the upregulated expression of adhesion molecules stimulated by activated leukocytes in response to inflammation. Albumin is bound via the leukocyte β2-integrin Mac-1 to endothelial ICAM-1, while lipid shells become coated with complement proteins that are recognized by complement receptors on the leukocyte surface [21, 22, 28, 56]. Once the microbubble is bound to the leukocyte, it is phagocytosed completely by neutrophils and monocytes. Within these cells the microbubble remains capable of oscillating enough to create an echo response [24, 56]. Another strategy for the targeting of inflamed plaques involves engineering the microbubbles to incorporate ligands to extracellular adhesion molecules (ECAMs) into the encapsulating shell. Targeting of ECAMs allows for tissue-specific binding since they are expressed on the surfaces of plaques, in neovessels of plaques, and in adventitial vessels, and are absent in normal vessels [56, 57] (Fig. 55.17). ECAMs known to be associated with atherosclerosis include ICAM-1, vascular cell adhesion molecule (VCAM)-1, selectins, and the integrin αvβ3 [56, 57]. Several investigators have exploited the expression of ECAMs to target regions of inflammation. Villaneueva et al. targeted activated endothelial cells in a flow chamber system by conjugating a monoclonal antibody to ICAM-1 on the surface of a microbubble encapsulated in a lipid shell [58]. Demos et al. employed this same strategy using acoustically active liposomes instead of microbubbles. They demonstrated in vivo targeting of these antibody-carrying liposomes to inflamed atherosclerotic plaques within the carotid arteries of pigs [59]. Linder et al. also used antibodies to P-selectin to target inflamed venules as a means of identifying ischemia-reperfusion injury [21].

Yet another strategy for identifying inflamed plaques acts by targeting the neovessels within their core. Angiogenesis-targeted microbubbles have been created by attaching antibodies to αv integrin. Leong-Poi et al. demonstrated the adherence of these microbubbles to arterioles, capillaries, and venules in areas of angiogenesis [60]. Currently, the feasibility of creating microbubbles to αvβ3 integrin found within the neovessels of the plaque core is being studied as a means of localizing plaque inflammation.

### Mesenteric Evaluation

Bowel ischemia is a surgical condition that is often difficult to diagnose. Nonspecific symptoms and laboratory results, along with the limitations of diagnostic imaging, make the evaluation for bowel ischemia challenging. The gold standard, angiography, is an invasive imaging modality that is not easily performed and provides limited information on the microperfusion of the bowel wall. Its invasiveness limits its use as a screening test for bowel ischemia. Conventional

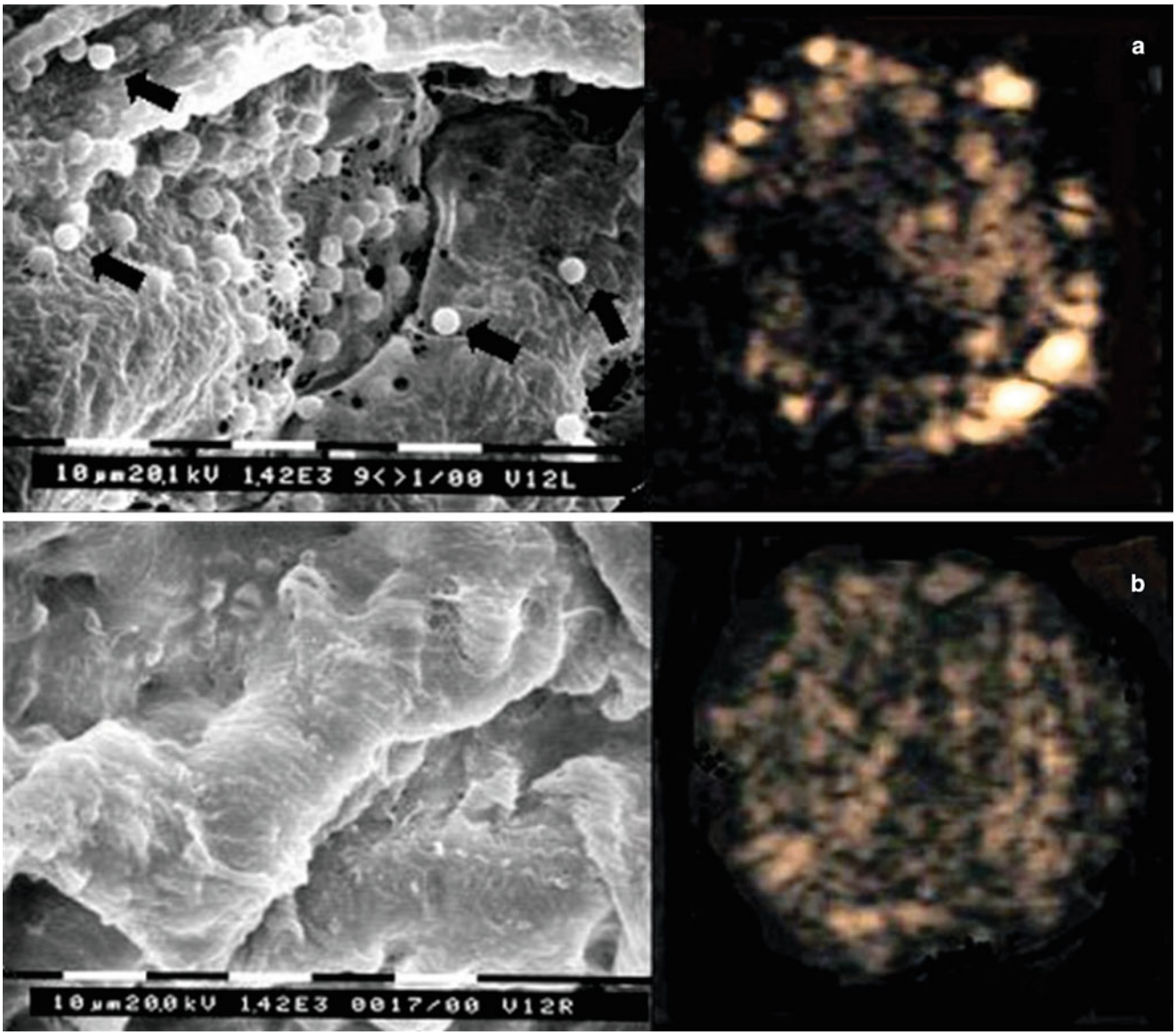


**Fig. 55.17** Ultrasound images with low mechanical index pulse sequence scheme showing the presence of microbubbles binding to the arterial endothelium in a balloon-injured carotid artery (**a**, *right*) and the absence of microbubbles in the control noninjured carotid artery (**b**, *right*). Scanning electron microscopy revealed sites of injury with endothelial denudation and attachment of microbubbles (*black arrows*) to the denuded endothelium only in the injured vessel (**a**) and normal appearing endothelium in the control vessel (**b**) (Image courtesy of Dr. Thomas R. Porter, The University of Nebraska Medical Center. Omaha, NE)

Doppler ultrasound is noninvasive; however, it is limited in its ability to evaluate transmural bowel wall perfusion. Using CEUS in the evaluation of bowel ischemia is a relatively new application being studied by investigators in Japan [54, 61] (Fig. 55.18). Early results, which included a study of 51 patients who had evidence of small bowel dilation on plain abdominal radiographs, were reported. All patients underwent conventional color power Doppler initially to identify the most dilated or nonperistaltic loop of bowel, and then CEUS was performed to evaluate that loop for 2 min at 4-s intervals. Twenty of the 51 patients had bowel ischemia, 5 due to thromboembolism of the superior mesenteric artery and 15 due to strangulation of the small bowel. CEUS signals were classified as normal, diminished, or absent. All five patients with thromboembolism were found to have absent signals. Seven of the 15 with strangulation had absent signals, 5 had diminished signals, and 3 had normal signals. All the patients without bowel ischemia had normal CEUS examinations. The sensitivity and specificity of CEUS in identifying bowel ischemia was 85% (95% CI: 62.1%, 96.8%) and 100% (95% CI: 90.8%, 100%), respectively. The positive predictive value was 100% (95% CI: 83.8%, 100%) and negative predictive value was 91.2% (95% CI: 76.3%, 98.1%) [61].

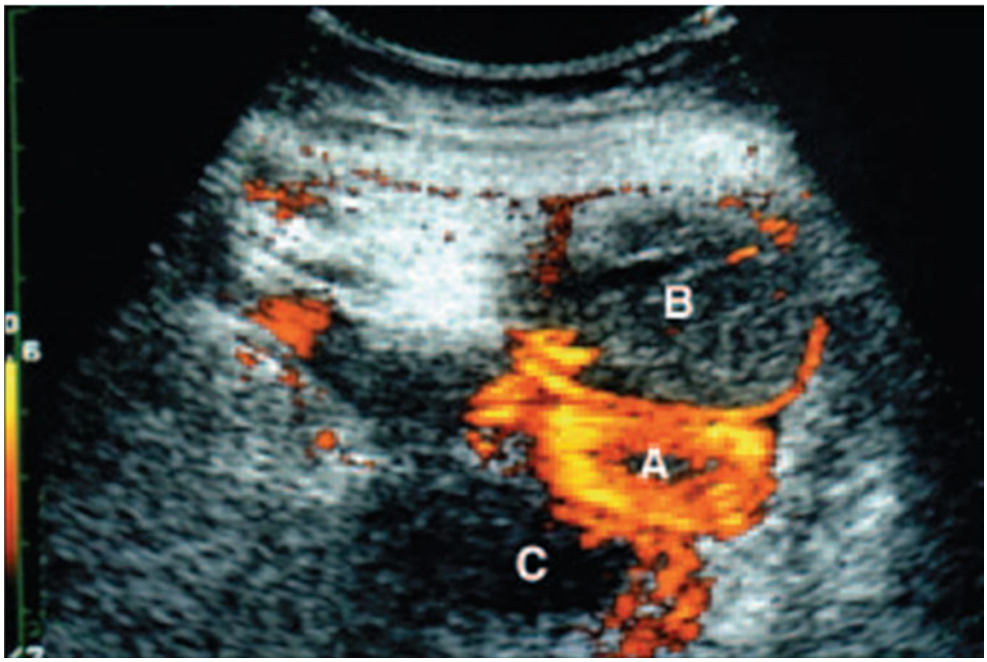


**Fig. 55.18** US scan obtained in a 68-year-old man with bowel strangulation. Bowel segments show normal (*A*), diminished (*B*), and absent (*C*) color signals (Reprinted from Hata et al. [61]. With permission from Radiology Society of North America)

## Carotid Assessment

Cerebrovascular accident continues to be a major source of morbidity and mortality in the United States, and duplex ultrasonography is considered the primary modality for screening. However, while it is inexpensive and readily accessible, its ability to discriminate the echogenicity of ulcerations and plaques and the precise degree of stenosis and to differentiate occlusion from "string sign" stenoses is not optimal. Again, angiography is the gold standard examination, but is limited to outlining the luminal profile in finite angular projections while not truly depicting the plaque or ulceration [62]. CEUS was used to evaluate carotid artery disease and was compared with traditional duplex and angiography [63]. Kono et al. evaluated 19 internal carotid arteries in ten subjects. This study found a strong correlation between CEUS and conventional angiography in determining the degree of stenosis ($r=0.988$). Contrast ultrasound also depicted ulceration in more patients than angiography. A strong correlation was also found between CEUS and ex vivo magnetic resonance (MR) imaging of the carotid plaque ($r=0.979$). These results demonstrate the potential utility of ultrasonographic agents in the screening and potential follow up of carotid disease. Contrast avoids much of the artifact generated by color studies, and does not necessarily suffer from the angular variability found with Doppler evaluations of velocity measurement (Fig. 55.19). The use of sonographic contrast agent tends to increase the sensitivity of the ultrasound examination in carotid artery diseases, overcoming some of its limitations and improving the detectability of blood flow within the vessels, with no need for complex maneuvers and discomfort for the patient [64].

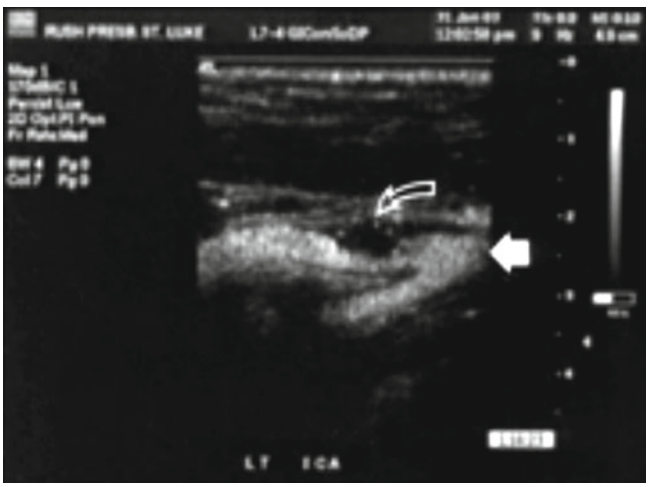

**Fig. 55.19** Contrast-enhanced carotid artery of a patient with a moderate atherosclerotic plaque in the internal carotid artery (arrow) (Image courtesy of Dr. Steven B. Feinstein, Rush University Medical Center, Chicago, IL)

## Aortic Evaluation: Abdominal Aortic Aneurysm

In the past decade, endovascular aneurysm repair (EVAR) has become the preferred method for infrarenal abdominal aortic aneurysm (AAA) repair in patients with suitable anatomy. While the benefits of the minimally invasive approach are obvious, continued surveillance for possible complications is required in these patients, including continued aneurysm growth, endoleaks, and device migration. The gold standard is computed tomography (CT), which is associated with increased cost, exposure to nephrotoxic agents, and exposure to ionizing radiation. Several recent reports have shown that CEUS is a possible alternative as a surveillance

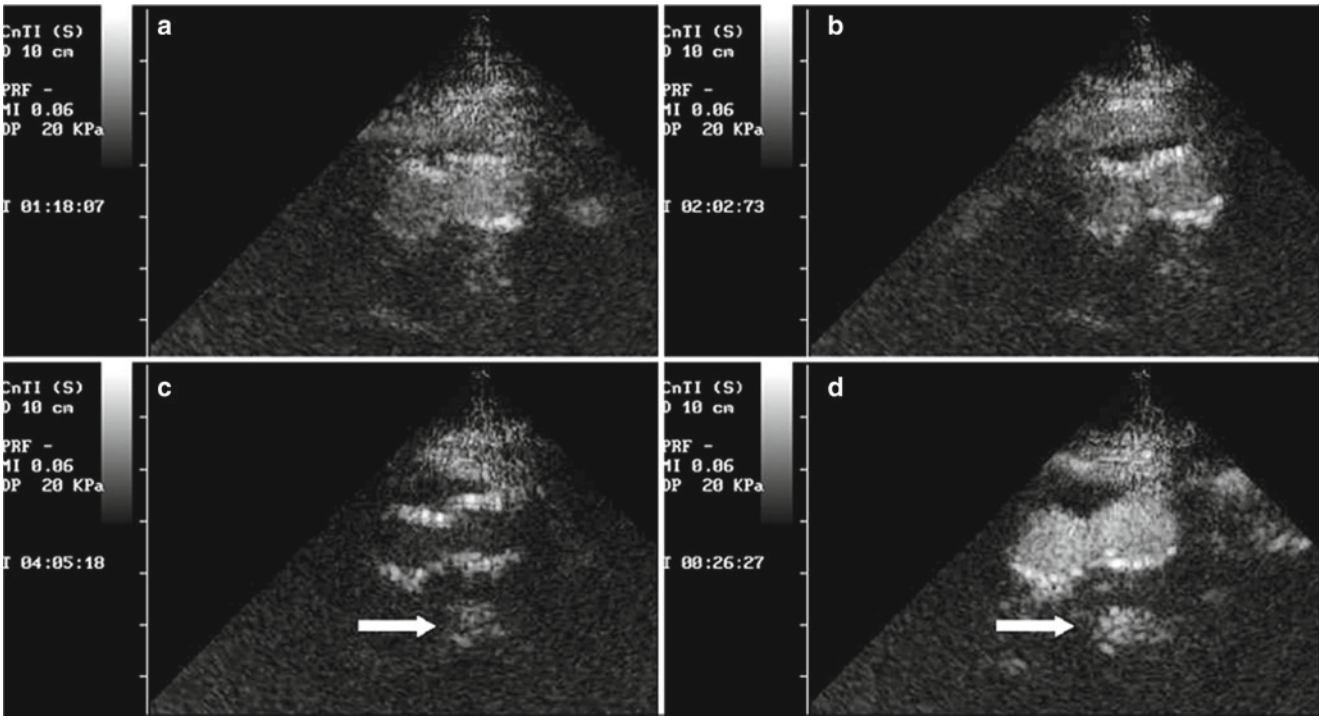


**Fig. 55.20** Transverse contrast-enhanced US scans with an anterior approach of a patient with an enlarging abdominal aortic aneurysm. Endoleak or other complications were not visualized at duplex US and CT angiography. (**a**–**c**) Images obtained after administration of an initial bolus of 2.4 ml of second-generation contrast agent show enhancement and slight contrast agent uptake 4 min after contrast agent administration. (**a**) Image obtained in arterial phase. (**b**) Image obtained in venous phase. (**c**) Image shows contrast agent uptake posterior to iliac branches (*arrow*). (**d**) Image obtained after administration of a second bolus of 2.4 ml of contrast agent better depicts endoleak (*arrow*) (Reprinted from Napoli et al. [65]. With permission from Radiology Society of North America)

modality. Recently, Bendick et al. found eight endoleaks after endovascular repair, two of which were missed on CT. Napoli et al. found 1 type I, 6 type II, 1 type III, and 2 undefined leaks that were all missed by CT. Bargellini et al. found 8 type II endoleaks on CEUS that were missed on CT (Fig. 55.20). Our own experience with CEUS after endovascular AAA showed nine endoleaks found with contrast ultrasound, three of which were not demonstrated on CT. Ultrasonographic contrast was shown to be safe and reliable in all of these studies, and is a promising adjunct in the surveillance of AAA after endovascular repair [65–67]. A study by Henao et al. published in 2006 confirmed previous observations that suggested the efficacy of CEUS versus computed tomography angiography (CTA). Using a continuous infusion technique, the authors visualized 8 type II endoleaks and 1 type I after EVAR, whereas CTA identified 5 type II and 1 type I [68]. Interestingly, the amount of time available to search for endoleaks was substantially greater with a continuous infusion. Their continuous infusion modality may have contributed to improved detection compared with previous reports of bolus contrast. On the other hand, CEUS imaging also has limitations. Patient's habitus (obesity) and bowel gas can interfere with imaging, and the patient must cooperate. The results of US are operator-dependent, and obtaining quality images requires training and specific skills. Furthermore, CTA provides superior information related to graft anchoring and integrity, aneurysm morphologic changes or visceral vessels patency [69].

Early and sensitive detection of endoleaks, which is indeed highly desirable during the initial intervention when endovascular treatment can be administered immediately, might therefore improve long-term outcomes. Recently Kopp et al. [70] evaluated the use of CEUS for visualization of the proximal aortic and distal iliac landing zones and for exclusion or detection of relevant endoleaks. This study suggested that the application of intraoperative CEUS might become an additional imaging modality, especially for patients with impaired renal function, allergy to iodine-based contrast fluids or possibly risk for iodine-induced hyperthyroidism. This application was accomplished in 14 out of 17 patients as verified by intraoperative angiography and postoperative CEUS, CT, or MR angiographies.

## Lower Limb Evaluation

Duplex ultrasonography in the evaluation of infrainguinal arterial disease is important in the evaluation, planning, and follow-up of reconstructive efforts. However, little has been published describing the use of contrast agents as an adjunct.

A 2002 European study demonstrated the use of CEUS in 14 patients and found that all vessels that appeared occluded by the use of contrast-enhanced duplex were also occluded on angiogram. However, the ultrasound study found four cases of patent vessels that were not visualized on conventional angiography. These visualized arteries were thought to be collaterals, rather than the named vessels in question, which was a limitation in the application of CEUS in this study [71].

### Molecular Imaging Using CEUS: Evaluation of Angiogenesis and Cell Therapy

The use of CEUS molecular imaging techniques has also been extended to the evaluation of angiogenesis and cell therapy [72]. Angiogenesis is a complex, multistep process regulated by the interplay of several pro- and antiangiogenic factors [73]. Since microbubble contrast agents are purely intravascular, the specific target for molecular imaging of angiogenesis must be present within the vascular space, and ideally expressed on the luminal surface of the angiogenic vessel. There are several molecules expressed on the vessel endothelium that serve as suitable molecular targets for imaging of angiogenesis; although numerous studies have investigated CEUS molecular imaging of angiogenesis in tumor models, fewer experimental studies have examined the potential of CEUS to evaluate angiogenesis and neovasculagenesis in models of cardiovascular disease [72]. Of the potential targets, the majority of experience to date has been with microbubbles targeted to alpha-integrins [74]. These agents have been developed by conjugation of either monoclonal antibodies (mAbs) targeted against alpha v integrins or arginine-glycine-aspartate (RGD)-containing peptides that have strong affinity for select integrins. This application was subsequently extended to image revascularization in a clinically relevant rat model of chronic hind limb ischemia, using echistatin-bearing microbubbles [75]. In this model, after unilateral iliac artery ligation, blood flow to the ischemic limb immediately decreases to 25% of normal resting values and over the next 2 weeks increases to 40% due to angiogenesis. In this study, CEUS molecular imaging of Alpha V Beta 3 expression using an RGB peptide-conjugated microbubble agent was able to assess both the endogenous arteriogenic response to chronic occlusion peripheral arterial disease (PAD) as well as the therapeutic neovascularization response to prolonged growth factor administration (FGF-2). With accelerated growth in research into stem cell therapy to treat cardiovascular diseases, there is a need to develop imaging modalities to track progenitor cells in vivo. CEUS techniques have now been developed that would potentially allow the tracking of delivered progenitor cells in vivo. Preliminary experiments that at the very least provide proof of concept have been reported [76, 77].

## Applications in Venous System

### Assessment of Portal Vein Thrombosis

Based upon the reported preliminary clinical experience [78, 79], CEUS appears to be a reliable technique for evaluating the patency of the veins of the portal systems. CEUS was significantly more sensitive than color Doppler sonography for both the detection and characterization of thrombi, and it was also more sensitive than conventional sonography for thrombus characterization. Portal vein thrombosis (PVT) is an important complication that occurs in 0.6–16% of patients with compensated liver cirrhosis and in 35% in patients with decompensated liver cirrhosis and hepatocellular carcinoma [80]. Patients with cirrhosis and early hepatocellular carcinoma may have either malignant or benign thromboses. The assessment of the malignant or benign character of PVT is very important with regard to the available therapeutic options. CEUS has demonstrated an important role for assessment. “Benign” thrombi are usually avascular and do not enhance in the arterial phase. When the portal venous thrombus contains malignant vascularity, it enhances in the arterial phase and wash out occurs in the portal and late phases [81].

### Venous Vascularization and Inflammation on CEUS in Deep Venous Thrombosis: Ongoing Clinical Trial

A search of the clinicaltrials.gov website revealed a recently approved observational prospective study. The aim of this clinical trial is to determine the presence and degree of venous perivascular revascularization and inflammation as assessed by CEUS in patients with acute deep venous thrombosis (DVT) and superficial vein thrombophlebitis (SVT). The investigators hypothesized that venous perivascular revascularization and inflammation assessed by CEUS can be quantified, will be significantly more pronounced in perivascular tissue of the thrombosed vessel compared to a nonaffected vein and control group, and that these findings will directly correlate with levels of inflammatory markers. This clinical trial is expected to provide novel data on the pathophysiological concept of thrombosis and thrombus resolution [82].

## Future Directions

Ongoing advances in ultrasound technology and microbubble engineering will expand applications of CEUS as a diagnostic tool as well as a therapeutic modality. As science continues to provide new insight into the body’s molecular

processes and into disease pathology, these new discoveries will translate into potential targets for microbubbles and improved utility of CEUS. As mentioned above, microbubbles have the ability to target areas of early inflammation. Albumin- and lipid-encapsulated microbubbles bind to activated leukocytes in a nonspecific manner. Additional studies have shown the feasibility of targeting-specific imaging via attachment of antibody-coated microbubbles to endothelial adhesion molecules expressed during inflammation [21, 56–59]. Recently, Weller et al. proposed a means of translating the basic science of target-specific microbubbles and ultrasound to the clinical setting. Their previous studies have shown the importance of microbubble antibody density in the binding of microbubbles to their intended target [83]. Therefore, in search of a means of improving microbubble adhesion to improve the signal-to-noise ratio of the ultrasound images, Weller et al. attempted to detect inflammation via a multitargeted approach. They compared microbubbles with antibodies to both ICAM-1 and the selectin family of leukocyte adhesion molecules to those with only a single inflammatory target to show that multitargeting inflammation would increase overall microbubble adhesion strength. Since microbubble binding is linearly related to the degree of inflammation, they proposed that CEUS with multitargeted microbubbles will allow clinical evaluation of early inflammation before it is evident, as well as provide a means to monitor the progression of inflammatory plaques or peripheral vascular disease. Microbubbles with equal amounts of anti-ICAM-1 antibody and sialyl Lewis X (binds to selectin) were prepared and compared to those with each moiety alone [84]. These microbubbles were perfused across endothelial cells activated by interleukin-1β at four different concentration levels, demonstrating four different severities of inflammation, which was assessed by the quantitative determination of ICAM-1 expression. Weller et al. found that ICAM-1-targeted microbubbles had an adhesion strength that was linearly related to the degree of inflammation. Additionally, microbubble adhesion strength was improved with multitargeted microbubbles when compared to single-targeted microbubbles, allowing for improved sensitivity in detecting inflammation. Weller et al. concluded that ultrasound evaluation with multitargeted microbubbles to various ECAMs may be a sensitive, noninvasive means of detecting not only the presence of inflammation, but the severity as well.

Targeting of early, middle, and late inflammatory endothelial surface antigens has the potential to delineate the molecular processes involved in inflammation and determine the "stage" of the inflammatory process. CEUS has the potential to decrease the requirements for more costly imaging studies, decrease the rate of equivocal, conventional examinations, and increase the diagnostic accuracy and confidence of ultrasound studies in general. More studies are required to fully delineate the indications for its use as a broadly applicable adjunct. Cost analysis studies are needed to justify the potentially sweeping changes this modality may bring to its many diagnostic, and potentially, therapeutic applications.

Recently, nanoparticle-containing composites have attracted attention for functional and molecular imaging investigations [85]. It has been reported that some solid nanoparticles, such as silica, polystyrene, and superparamagnetic iron oxide (SPIO) nanoparticles are able to boost the acoustic impedance, increase backscattered signals, and consequently contribute to contrast enhancement for US [86, 87].

## Conclusion

The risk of the development of malignancies due to radiation exposure and nephrotoxicity secondary to iodinated contrast agents has lead to the search for better noninvasive studies and surveillance modalities after endovascular procedures, particularly after aortic endografting. Newer technologies are continuously evolving, and the "perfect" surveillance tool still does not exist. Developments in material engineering and biotechnology will continue to improve the current standards and expectations; a better understanding of the dynamic flow of microvascular beds and focused delivery of biological compounds should enhance end organ imaging and therapeutic strategies.

## References

1. Gramiak R, Shah P, Kramer DH. Ultrasound cardiography: contrast studies in anatomy and function. Radiology. 1969;92:939.
2. Gramiak R, Shah P. Echocardiography of the aortic root. Invest Radiol. 1968;3:356–66.
3. Mulvagh SL, et al. Second harmonic imaging of an intravenously administered echocardiographic contrast agent: visualization of coronary arteries and measurements of coronary blood flow. J Am Coll Cardiol. 1996;27:1519–25.
4. Ophir J, Parker KJ. Contrast agents in diagnostic ultrasound. Ultrasound Med Biol. 1989;15(4):319–33.
5. Section 6 – mechanical bioeffects in the presence of gas-carrier ultrasound contrast agents. American Institute of Ultrasound in Medicine. J Ultrasound Med. 2000;19(2):120–42, 154–68.
6. Cosgrove D. Ultrasound contrast agents: an overview. Eur J Radiol. 2006;60(3):324–30.
7. Calliada F, et al. Ultrasound contrast agents: basic principles. Eur J Radiol. 1998;27(Suppl2):S157.
8. Correas JM, et al. Ultrasound contrast agents: properties, principles of action, tolerance, and artifacts. Eur Radiol. 2001;11(8):1316–28.
9. Correas JM, et al. Ultrasound contrast agents. Examples of blood pool agents. Acta Radiol Suppl. 1997;412:101–12.
10. Blomley MJ, et al. Stimulated acoustic emission to image a late liver and spleen-specific phase of Levovist in normal volunteers and patients with and without liver disease. Ultrasound Med Biol. 1999;25(9):1341–52.

11. Marelli C. Preliminary experience with NC100100, a new ultrasound contrast agent for intravenous injection. Eur Radiol. 1999;9 Suppl 3:S343–6.
12. Harvey CJ, et al. Advances in ultrasound. Clin Radiol. 2002;57(3):157–77.
13. Burns PN. Harmonic imaging with ultrasound contrast agents. Clin Radiol. 1996;51 Suppl 1:50–5.
14. Tiemann K, et al. Real-time contrast echo assessment of myocardial perfusion at low emission power: first experimental and clinical results using power pulse inversion imaging. Echocardiography. 1999;16(8):799–809.
15. Claudon M, et al. Renal arteries in patients at risk of renal arterial stenosis: multicenter evaluation of the echoenhancer SH U 508A at color and spectral Doppler US. Levovist Renal Artery Stenosis Study Group. Radiology. 2000;214(3):739–46.
16. Cohen JL, et al. Improved left ventricular endocardial border delineation and opacification with OPTISON (FS069), a new echocardiographic contrast agent. Results of a phase III multicenter trial. J Am Coll Cardiol. 1998;32(3):746–52.
17. Myreng Y, et al. Safety of the transpulmonary ultrasound contrast agent NC100100: a clinical and haemodynamic evaluation in patients with suspected or proved coronary artery disease. Heart. 1999;82(3):333–5.
18. Kaps M, et al. Safety and ultrasound-enhancing potentials of a new sulfur hexafluoride-containing agent in the cerebral circulation. J Neuroimaging. 1999;3:150–4.
19. Grayburn PA, et al. Phase III multicenter trial comparing the efficacy of 2% dodecafluoropentane emulsion (EchoGen) and sonicated 5% human albumin (Albunex) as ultrasound contrast agents in patients with suboptimal echocardiograms. J Am Coll Cardiol. 1998;32(1):230–6.
20. Averkiou M, et al. Ultrasound contrast imaging research. Ultrasound Q. 2003;19(1):27–37.
21. Lindner JR, et al. Microbubble persistence in the microcirculation during ischemia/reperfusion and inflammation is caused by integrin- and complement-mediated adherence to activated leukocytes. Circulation. 2000;101(6):668–75.
22. Lindner JR, et al. Noninvasive imaging of inflammation by ultrasound detection of phagocytosed microbubbles. Circulation. 2000;102(5):531–8.
23. Borden MA, Martinez GV, Ricker J, et al. Lateral phase separation in lipid-coated microbubbles. Langmuir. 2006;22(9):4291–7.
24. Unger EC, et al. In vitro studies of a new thrombus-specific ultrasound contrast agent. Am J Cardiol. 1998;81(12A):58G–61.
25. Schumann PA, et al. Targeted-microbubble binding selectively to GPIIb IIIa receptors of platelet thrombi. Invest Radiol. 2002;37(11):587–93.
26. Tachibana K, Tachibana S. Albumin microbubble echocontrast material as an enhancer for ultrasound accelerated thrombolysis. Circulation. 1995;92(5):1148–50.
27. Klibanov AL. Targeted delivery of gas-filled microspheres, contrast agents for ultrasound imaging. Adv Drug Deliv Rev. 1999;37(1–3):139–57.
28. Lidner JR. Evolving applications for contrast ultrasound. Am J Cardiol. 2002;90(10A):72J–80.
29. Klibanov AL. Ligand-carrying gas filed microbubbles: ultrasound contrast agents for targeted molecular imaging. Bioconjug Chem. 2005;16:9–17.
30. Ferrara KW, Borden MA, Zhang H. Lipid shelled vehicles: engineering for ultrasound molecular imaging and drug delivery. Acc Chem Res. 2009;42:881–92.
31. McCulloch M, Gresser C, Moos S, et al. Ultrasound contrast physics: a series on contrast echocardiography. J Am Soc Echocardiogr. 2000;13(1):962.
32. Ayida G, et al. Hysterosalpingo-contrast sonography (HyCoSy) using Echovist-200 in the outpatient investigation of infertility patients. Br J Radiol. 1996;69(826):910–3.
33. Darge K, et al. Reflux in young patients: comparison of voiding US of the bladder and retrovesical space with echo enhancement versus voiding cystourethrography for diagnosis. Radiology. 1999;210(1):201–7.
34. Blomley MJ, et al. Improved imaging of liver metastases with stimulated acoustic emission in the late phase of enhancement with the US contrast agent SH U 508A: early experience. Radiology. 1999;210(2):409–16.
35. Burns PN, Hope Simpson D, Averkiou MA. Nonlinear imaging. Ultrasound Med Biol. 2000;26 Suppl 1:S19–22.
36. Simpson DH, Burns PN, Averkiou MA. Techniques for perfusion imaging with microbubble contrast agents. IEEE Trans Ultrason Ferroelectr Freq Control. 2001;48(6):1483–94.
37. von Herbay A, Vogt C, Haussinger D, et al. Late phase pulse-inversion sonography using the contrast agent Levovist: differentiation between benign and malignant focal lesions of the liver. AJR Am J Roentgenol. 2002;179:1273–9.
38. Kamiyama N, Moriyasu F, Mine Y, et al. Analysis of flash echo from contrast agent for designing optimal ultrasound diagnostic systems. Ultrasound Med Biol. 1999;25:411–20.
39. Yamamoto K, Shiraki K, Nakanishi S, et al. The usefulness of digital subtraction imaging with Levovist in the diagnosis of focal hepatic tumors. Int J Oncol. 2003;2(2):353–8.
40. Clevert DA, et al. Imaging of aortic abnormalities with contrast-enhanced ultrasound. A pictoral comparison with CT. Eur Radiol. 2007;17:2991–3000.
41. Clevert DA, Kopp R. Contrast enhanced ultrasound for endovascular grafting in infrarenal abdominal aortic aneurysm in a single patient with risk factors for the use of iodinated contrast. J Vasc Interv Radiol. 2008;19:1241–5.
42. Avasthi PS, Voyles WF, Greene ER. Noninvasive diagnosis of renal artery stenosis by echo-Doppler velocimetry. Kidney Int. 1984;25(5):824–9.
43. Norris CS, et al. Noninvasive evaluation of renal artery stenosis and renovascular resistance. Experimental and clinical studies. J Vasc Surg. 1984;1(1):192–201.
44. Berland LL, et al. Renal artery stenosis: prospective evaluation of diagnosis with color duplex US compared with angiography. Work in progress. Radiology. 1990;174(2):421–3.
45. Desberg AL, et al. Renal artery stenosis: evaluation with color Doppler flow imaging. Radiology. 1990;177(3):749–53.
46. Lacourciere Y, et al. Impact of Levovist ultrasonographic contrast agent on the diagnosis and management of hypertensive patients with suspected renal artery stenosis: a Canadian multicentre pilot study. Can Assoc Radiol J. 2002;53(4):219–27.
47. Wei K, et al. Quantification of renal blood flow with contrast-enhanced ultrasound. J Am Coll Cardiol. 2001;37(4):1135–40.
48. Wei K, et al. Quantification of myocardial blood flow with ultrasound-induced destruction of microbubbles administered as a constant venous infusion. Circulation. 1998;97(5):473–83.
49. Correas JM, et al. Contrast-enhanced ultrasonography: renal applications. J Radiol. 2003;84(12 Pt 2):2041–54.
50. Lan HY, et al. Inhibition of renal fibrosis by gene transfer of inducible Smad7 using ultrasound-microbubble system in rat UUO model. J Am Soc Nephrol. 2003;14(6):1535–48.
51. Shaw LJ, et al. Use of an intravenous contrast agent (Optison) to enhance echocardiography: efficacy and cost implications. Optison Multicenter Study Group. Am J Manag Care. 1998;4(Spec No):SP169–76.
52. Kitzman DW, et al. Efficacy and safety of the novel ultrasound contrast agent perflutren (definity) in patients with suboptimal baseline

left ventricular echocardiographic images. Am J Cardiol. 2000; 86(6):669–74.
53. Hundley WG, et al. Administration of an intravenous perfluorocarbon contrast agent improves echocardiographic determination of left ventricular volumes and ejection fraction: comparison with cine magnetic resonance imaging. J Am Coll Cardiol. 1998;32(5): 1426–32.
54. Yoshida S, et al. Evaluation of flash echo imaging of the canine gastrointestinal tract. J Ultrasound Med. 2000;19(11):751–5.
55. Ross R. Atherosclerosis – an inflammatory disease. N Engl J Med. 1999;340(2):115–26.
56. Lindner JR. Detection of inflamed plaques with contrast ultrasound. Am J Cardiol. 2002;90(10C):32L–5.
57. Blankenberg S, Barbaux S, Tiret L. Adhesion molecules and atherosclerosis. Atherosclerosis. 2003;170(2):191–203.
58. Villanueva FS, et al. Microbubbles targeted to intercellular adhesion molecule-1 bind to activated coronary artery endothelial cells. Circulation. 1998;98(1):1–5.
59. Demos SM, et al. In vivo targeting of acoustically reflective liposomes for intravascular and transvascular ultrasonic enhancement. J Am Coll Cardiol. 1999;33(3):867–75.
60. Leong-Poi H, et al. Noninvasive assessment of angiogenesis by ultrasound and microbubbles targeted to alpha(v)-integrins. Circulation. 2003;107(3):455–60.
61. Hata J, et al. Evaluation of bowel ischemia with contrast enhanced US: initial experience. Radiology. 2005;236(2):712–5.
62. Van Damme H, Vivario M. Pathologic aspects of carotid plaques: surgical and clinical significance. Int Angiol. 1993;12(4):299–311.
63. Kono Y, et al. Carotid arteries: contrast-enhanced US angiography – preliminary clinical experience. Radiology. 2004;230(2):561–8.
64. Clevert DA, et al. Imaging of carotid arterial diseases with contrast-enhanced ultrasound (CEUS). Eur J Radiol. 2011;80(1):68–76. Epub 2011 Feb 26.
65. Napoli V, et al. Abdominal aortic aneurysm: contrast enhanced US for missed endoleaks after endoluminal repair. Radiology. 2004;233(1):217–25.
66. Bendick PJ, et al. Efficacy of ultrasound scan contrast agents in the noninvasive follow-up of aortic stent grafts. J Vasc Surg. 2003;37(2):381–5.
67. Bargellini I, et al. Type II lumbar endoleaks: hemodynamic differentiation by contrast-enhanced ultrasound scanning and influence on aneurysm enlargement after endovascular aneurysm repair. J Vasc Surg. 2005;41(1):10–8.
68. Henao EA, et al. Contrast-enhanced duplex surveillance after endovascular abdominal aortic aneurysm repair: improved efficacy using a continuous infusion technique. J Vasc Surg. 2006;43(2):259–64; discussion 264.
69. Thompson MM, et al. Comparison of computed tomography and duplex imaging in assessing aortic morphology following endovascular aneurysm repair. Br J Surg. 1998;85:346–50.
70. Kopp R, et al. First experience using intraoperative contrast-enhanced ultrasound during endovascular aneurysm repair for infrarenal aortic aneurysms. J Vasc Surg. 2010;51(5):1103–10.
71. Ubbink DT, Legemate DA, Llull JB. Color-flow duplex scanning of the leg arteries by use of a new echo enhancing agent. J Vasc Surg. 2002;35(2):392–6.
72. Leong-Poi H. Molecular imaging using contrast-enhanced ultrasound: evaluation of angiogenesis and cell therapy. Cardiovasc Res. 2009;84(2):190–200.
73. Buysschaert I, Carmeliet P, Dewerchin M. Clinical and fundamental aspects of angiogenesis and anti-angiogenesis. Acta Clin Belg. 2007;62:162–9.
74. Eliceri BP, Cheresh DA. Role of alpha v integrins during angiogenesis. Cancer J. 2000;6 Suppl 3:S245–9.
75. Leong-Poi H, et al. Assessment of endogenous and therapeutic arteriogenesis by contrast ultrasound molecular imaging of integrin expression. Circulation. 2005;111:32.
76. Kuliszewski MA, et al. Molecular imaging of endothelial progenitor cell engraftment using contrast-enhanced ultrasound and targeted microbubbles. Cardiovasc Res. 2009;83:817–23.
77. Cui W, et al. A new method for stem cell imaging using contrast ultrasound. Circulation. 2008;118:S642.
78. Tarantino L, et al. Diagnosis of benign and malignant portal vein thrombosis in cirrhotic patients with hepatocellular carcinoma: color Doppler US, contrast-enhanced US, and fine-needle biopsy. Abdom Imaging. 2006;31(5):537–44.
79. Janssen HLA, et al. Extrahepatic portal vein thrombosis: aetiology and determinants of survival. Gut. 2001;49:720–4.
80. Amitrano L, et al. Risk factors and clinical presentation of portal vein thrombosis in patients with liver cirrhosis. J Hepatol. 2004;40: 736–41.
81. Claudon M, et al. Guidelines and good clinical practice recommendations for contras enhanced ultrasound (CEUS) update 2008. Ultraschall Med. 2008;29:28–44.
82. Venous vascularization and inflammation on contrast-enhanced ultrasound (CEUS) in patients with thrombosis. 2011. http://clinicaltrials.gov/ct2/show/NCT01367769?term=Venous+vascularization+and+inflammation+on+contrast+enhanced+ultrasound&rank=1. Accessed 20 July 2011.
83. Weller GE, et al. Modulating targeted adhesion of an ultrasound contrast agent to dysfunctional endothelium. Ann Biomed Eng. 2002;30(8):1012–9.
84. Weller GE, et al. Targeted ultrasound contrast agents: in vitro assessment of endothelial dysfunction and multitargeting to ICAM-1 and sialyl Lewis(x). Biotechnol Bioeng. 2005;92(6): 780–8.
85. Galperin A, Margel S. Synthesis and characterization of radiopaque magnetic core-shell nanoparticles for X-ray imaging applications. J Biomed Mater Res B Appl Biomater. 2007;83(2):490–8.
86. Norton SJ, Vo Dinh T. Imaging the distribution of magnetic nanoparticles with ultrasound. IEEE Trans Med Imaging. 2007;26: 660–6.
87. Oh J, et al. Detection of magnetic nanoparticles in tissue using magneto-motive ultrasound. Nanotechnology. 2006;17:4183–90.

# Coding and Reimbursement for Vascular Lab Testing

56

Robert M. Zwolak

**Abstract**

Noninvasive vascular lab studies constitute an integral portion of the vascular surgeon's diagnostic armamentarium. Studies are safe, inexpensive compared to advanced diagnostic imaging, and when performed by qualified individuals, highly accurate and reproducible. In order to maintain a viable noninvasive lab, a manager must understand the nuances of coding, insurance carrier coverage policies, and many details regarding reimbursement.

**Keywords**

Advance Beneficiary Notice • Ambulatory Payment Category • APC • CPT Code • Diagnosis Related Group • DRG • Doppler • Duplex ultrasound • Physiologic examination

A family of just over 20 CPT codes is used to report ultrasound-based diagnostic noninvasive vascular laboratory studies. This renders the infrastructure of vascular lab coding relatively straightforward, but the application of these codes in the everyday business of running a lab becomes substantially more complex. Several aspects of reporting vascular lab studies differ from those of traditional surgical or evaluation and management (E&M) coding. Perhaps, the most important issue is that reporting the diagnostic vascular exams depends on the physical setting where the study takes place. For example, reporting studies performed in a physician's office is completely different from reporting the same exams when performed in a hospital, moreover, in the hospital there is an important difference depending on whether the individual undergoing the test is an inpatient or an outpatient.

Next, it is crucial to understand that a diagnostic study is composed of two distinct components, technical and professional. The technical component focuses on collection of information and is usually performed by a specially trained technologist. The professional component includes review of the physiologic, imaging, and Doppler data along with the written preliminary information provided by the technologist. A final interpretation is compiled and printed. The basic data and the final report must be archived and available for review. Coding shorthand for the technical component is "TC," while the professional interpretation modifier is "PC" or "-26" in coding parlance. Of these latter two, the abbreviation –26 will be used throughout this chapter.

## Reporting Based on Site of Service—Physician's Office

There are actually four distinct sites of service from which the technical portion of vascular lab studies may be reported. These are (1) the physician's office; (2) the independent diagnostic testing facility (IDTF); (3) the hospital outpatient department; and (4) the hospital inpatient area. The most straightforward setting from a coding perspective is the physician's office where the typical study is likely to include both technical and professional components. When performed simultaneously, the combination of technical and professional components is reported by use of the five-digit CPT code without any trailing modifiers such as TC or –26.

R.M. Zwolak, M.D., Ph.D.
Section of Vascular Surgery,
Dartmouth-Hitchcock Medical Center,
One Medical Center Drive,
Lebanon, NH 03756, USA
e-mail: robert.m.zwolak@hitchcock.org

A.F. AbuRahma, D.F. Bandyk (eds.), *Noninvasive Vascular Diagnosis*,
DOI 10.1007/978-1-4471-4005-4_56, 

An example would be the patient who undergoes a complete (technical plus professional) bilateral extracranial cerebrovascular duplex exam in a physician's office. The appropriate CPT code is 93880, and no trailing modifier would be added. Provided in this manner, the complete service is commonly described by the word "global," but this application of "global" should not be confused with surgical services in which global implies inclusion of a certain number of postoperative days.

If only the technical portion of an extracranial cerebrovascular study were performed in the physician's office it would be reported as 93880-TC. If only the professional interpretation were done in the office, it would be a 93880-26. It is important to realize that in almost all circumstances, payment for the global service represents the sum of payments for the technical component plus the professional component.

## Site of Service—IDTF

An IDTF is a diagnostic testing facility not associated with a physician's office or hospital. The regulations defining this entity were published originally in the October 31, 1997, issue of the *Federal Register*, and a multitude of revisions and refinements have followed. The purpose of an IDTF is to provide diagnostic tests but not to treat patients, and the Centers for Medicare and Medicaid Services (CMS) regularly updates the complex set of requirements. The most recent regulatory event involving IDTFs is a provision in Section 135(a) of the Medicare Improvements for Patients and Providers Act of 2008 (MIPPA) that requires accreditation of IDTFs that provide "advanced diagnostic imaging." MIPPA defines advanced diagnostic imaging as including magnetic resonance imaging, computed tomography, nuclear medicine imaging, and positron emission tomography. MIPPA expressly excludes X-ray, ultrasound, and fluoroscopy procedures from their definition of advanced imaging, and IDTFs are not required to undertake accreditation for these latter three modalities. Further details about IDTFs are beyond the scope of this chapter, but suffice to conclude that any physician involved or potentially involved in an IDTF needs a much more detailed and focused document than I could provide.

## Site of Service—Hospital Outpatient and Inpatient

When a hospital employs the technologists and owns or leases the relevant equipment, the technical portion of outpatient noninvasive vascular studies is reported by a completely different set of codes titled the "Ambulatory Payment Category," or "APC" system. These are published as part of the Medicare Hospital Outpatient Prospective Payment System (HOPPS). The HOPPS APC system is a provision of the Balanced Budget Act of 1997, created to provide a prospective payment system for diagnostic studies, surgical procedures, and E&M services performed on outpatients at a hospital facility. One of the goals of the HOPPS system was to collapse the number of individual payments to a level far less than the approximately 8,000 CPT codes. Thus, for all but the most common procedures, multiple CPT codes are bundled into each APC. In fact, for the first 6 years of the APC system, all vascular lab studies were reportable through use of only two APC codes, APC 96 for all vascular physiologic studies and APC 267 for all vascular duplex exams. The Society for Vascular Surgery and the Society for Vascular Ultrasound complained vociferously to the Heath Care Financing Administration (now CMS) that this two-bucket plan lacked sufficient granularity to represent the actual work performed in vascular labs. The Agency responded, albeit slowly. In 2004, APC 266 was added to represent two duplex exams of lesser complexity, and now in 2012 we have a family of five APCs that corresponds to the vascular lab studies. APCs 96 and 97 represent two complexity levels of physiologic studies, and APCs 265, 266, and 267 are used to report duplex exams of low, medium and high complexity [1, 2]. Table 56.1 provides the proposed 2012 crosswalk between CPT codes and APC codes. These crosswalks can change annually, so it behooves the manager of a hospital-based lab to check the Medicare website or reliable private sources each year.

It should be remembered that this APC discussion relates only to the technical portion of vascular lab studies performed in hospitals on outpatients. The professional interpretation of these exams is reported by traditional CPT codes with addition of the −26 modifier to identify the studies as being professional component only. A coding example reflecting this segment would be performance of a complete bilateral lower extremity venous duplex exam on an outpatient Medicare beneficiary for the indication of sudden onset lower extremity swelling. The hospital-based vascular lab would report APC 0267, and the interpreting physician would submit 93970-26.

Finally, if a vascular lab study is performed on a hospital inpatient, it would be most common for the technical component to be bundled in the prospective payment for the hospitalization. Medicare uses "Diagnosis Related Groups" or "DRGs" for this purpose, and many private carriers also utilize the DRG approach. The vascular lab would identify performance of the exam, typically by CPT code or APC, but this would be used exclusively for internal hospital accounting purposes. The overall hospital payment would be based on the DRG, and frequently the DRG will not be impacted by the vascular lab results. In this setting, the interpreting physician would report a −26 modified CPT code. A typical example is the hospital ICU inpatient requiring a bilateral lower extremity venous duplex exam. Technical billing rolls into the DRG, and the interpreting physician reports 93970-26.

**Table 56.1** 2012 CPT APC Vascular Lab technical component crosswalks

| CPT | CPT descriptor | APC |
|---|---|---|
| 93880 | Duplex extracranial arteries, complete bilateral | 0267 |
| 93882 | Duplex extracranial arteries, unilateral or limited | 0267 |
| 93886 | Transcranial Doppler intracranial arteries; complete | 0267 |
| 93888 | Transcranial Doppler intracranial arteries; limited | 0265 |
| 93890 | Transcranial Doppler; vasoreactivity study | 0266 |
| 93892 | Transcranial Doppler; emboli detection, no bubble injection | 0266 |
| 93893 | Transcranial Doppler; emboli detection with bubble injection | 0266 |
| 93922 | Limited bilateral extremity artery physiologic study 1–2 levels | 0097 |
| 93923 | Complete bilateral extremity arterial physiologic study ≥3 levels | 0096 |
| 93924 | Treadmill lower extremity physiologic exam | 0096 |
| 93925 | Duplex lower extremity arteries or bypass grafts; complete bilateral | 0267 |
| 93926 | Duplex lower extremity arteries or bypass grafts; unilateral or limited | 0266 |
| 93930 | Duplex upper extremity arteries or bypass grafts; complete bilateral | 0267 |
| 93931 | Duplex upper extremity arteries or bypass grafts; unilateral or limited | 0266 |
| 93965 | Physiologic study of extremity veins, complete bilateral | 0096 |
| 93970 | Duplex extremity veins including compression; complete bilateral | 0267 |
| 93971 | Duplex extremity veins including compression; unilateral or limited | 0266 |
| 93975 | Duplex arterial inflow and venous outflow of abdominal, pelvic, scrotal or retroperitoneal organs, complete study | 0267 |
| 93976 | Duplex arterial inflow and venous outflow of abdominal, pelvic, scrotal or retroperitoneal organs, limited study | 0267 |
| 93978 | Duplex aorta, IVC, iliac vasculature, or bypass grafts; complete | 0267 |
| 93979 | Duplex aorta, IVC, iliac vasculature, or bypass grafts; unilateral or limited | 0266 |
| 93980 | Duplex arterial inflow and venous outflow, penile vessels; complete | 0267 |
| 93981 | Duplex arterial inflow and venous outflow, penile vessels; follow-up or limited | 0267 |
| 93982 | Physiologic study implanted wireless pressure sensor aneurysm sac | 0097 |
| 93990 | Duplex hemodialysis access including arterial inflow, body of access and venous outflow | 0266 |

Reprinted from CMS 2012 HOPPS NPRM Median Cost File
CPT descriptors are abbreviated. See CPT Manual for complete descriptors and associated introductory material

## Vascular Lab Coverage Requirements and Advanced Beneficiary Notice

In order to meet Medicare coverage requirements, all vascular laboratory studies must (1) have a valid, recorded medical indication; (2) be ordered by a licensed independent provider; (3) have archived retrievable test data; and (4) include a physician's professional interpretation. Each of these will be examined in more detail.

What constitutes a valid medical indication can be a frustrating issue for vascular lab managers because the clinical indications as listed on the requisition or physician's order determine whether or not a service is covered, meaning paid, by the insurance carrier. A clinical indication that the ordering provider believes is totally appropriate, may not be considered valid by the carrier. For instance, a 60-year-old-lifelong smoker and his primary care provider may believe that a first-time carotid duplex exam is entirely appropriate especially if two of the patient's brothers and three of his sisters have all suffered strokes. However, the patient's insurance carrier may consider this a noncovered "screening" exam if the patient has no lateralizing neurologic symptoms. The lab manager is then faced with a dilemma. Refusing to do the exam antagonizes the patient and the ordering provider. On the other hand, performing the exam with no expectation of payment can only be done a limited number of times if the lab is to remain fiscally viable.

From the Medicare perspective, the correct approach in this setting is for the lab to provide the patient with an "Advanced Beneficiary Notice" or "ABN," a document that explains to the patient that he or she is about to undergo a test that the Carrier believes is not medically indicated and will therefore not cover. This ABN approach, while meeting payer requirements, may oftentimes engender ill will. The patient may ask why the doctor is ordering an unindicated test. If not exceptionally clear and tactful, the vascular lab manager's response may confuse the patient even further, potentially delaying the schedule or resulting in patient refusal to undergo the exam. The best way to avoid this annoying and oftentimes costly issue is to educate one's ordering providers regarding the relevant national and local coverage decisions. For the Medicare program, an updated

list of coverage decisions may be found at https://www.cms.gov/medicare-coverage-database/indexes/national-and-local-indexes.aspx.

## Vascular Lab Retrievable Data

The value of archived retrievable vascular lab data is obvious in terms of patient care. As part of the service provided to patients and those who order lab studies, the vascular report should compare current test results to those of prior exams. In order to do so efficiently, the lab must have ready access to archived data. Previous era hard copy image and report storage was labor intensive, but without organized records it was a nightmare trying to find previous exams for comparison. Most laboratories have now eliminated that problem with use of digital Picture Archive and Communication Systems (PACS). While there is no additional reimbursement for implementing a PACS system, the additional retrieval ability will also serve to protect the vascular lab in case of a post-payment audit.

The current Medicare initiative to eliminate overpayment to providers is called the Medicare Recovery Audit Contractor program, or RAC. RAC pilot programs were performed in six states from 2005 to 2008, allowing Medicare to recover nearly $1 billion in supposed overpayments. Congressional Ways and Means Committee extrapolations estimated a nationwide rollout would net a $10 billion recovery. Thus, Medicare started an expanded program in 2009 focusing on hospitals with impacts widely noted during 2010. Currently, the RACs are investigating physicians, laboratories, and other types of providers. A solid set of records demonstrating quality data, appropriate clinical indications, and accurate coding and billing will be of great assistance should Medicare decide your lab merits a RAC evaluation.

## Reimbursement for Physician Interpretation

What constitutes an appropriate physician interpretation, and how does it differ from what the technologist provides? From Medicare's perspective, noninvasive vascular studies have two distinct components, one technical, and the other professional. While approximately 80% of payment for a complete vascular lab diagnostic service (technical plus professional) represents reimbursement for the technical portion of the exam, the final physician's interpretation must be identifiable if the 20% reflecting the professional component is to be earned. The technologist's core role is to collect accurate Doppler and imaging data and to organize it in such a manner that the physician can provide the best possible interpretation. In some cases, this means that the technologist could provide a preliminary data assessment. It is the interpreting physician's core responsibility to review all data for content and accuracy, and to provide a final interpretation of the data based on his or her laboratory and clinical knowledge. The most straightforward way to demonstrate how the interpreting physician adds value to a vascular lab study may be through example. For instance, during an extracranial cerebrovascular study, the technologist collects a series of B-mode ultrasound images, Doppler velocity spectra, and color-flow images. The technologist's responsibility is to record and annotate the data accurately. The lab may use a literature-based interpretation scale to convert Doppler velocities to internal carotid stenosis estimates, and while this conversion may be identified by the technologist, it is the responsibility of the interpreting physician to review all the data, perform an assessment about accuracy such as correct application of Doppler angle adjustment, and to ensure that a final interpretation considers and weighs all information appropriately. As another example, elevated velocities in an internal carotid indicate presence of a stenosis, but standard grading scales may lead to an overestimate of severity if the contralateral internal carotid is completely occluded. This observation should be noted by the interpreting physician in the final report. Likewise, areas of heavy calcification may preclude adequate Doppler velocity analysis because the ultrasound waves are reflected by the dense plaque. If this is a very short segment, and if the waveforms just beyond the blind spot are similar to those on the inflow side, the interpreting physician may conclude that the short calcified area likely does not contain a flow-limiting stenosis. The opposite assessment may be reached by the physician if the outflow waveform demonstrates a blunted systolic upstroke and a low peak velocity. These are just a few examples of how the final interpretation may differ from the preliminary data presentation based on knowledge and clinical correlation provided by the interpreting physician.

## Complete Versus Limited Vascular Studies 93880, 93922, and 93923

CPT descriptors for the vascular lab codes commonly use the terms "complete" or "limited," but there is little or no documentation of the threshold requirements to report the more comprehensive exam. Exactly what does CPT, or for that matter Medicare, require for a study to be considered a complete bilateral exam? Oftentimes we need to look outside the coding world to find reasonable answer. The Intersocietal Commission for Accreditation of Vascular Laboratories (ICAVL) has promulgated detailed recommendations for a thorough examination of most vascular beds, and these serve as excellent proxies for CPT reporting purposes in the absence of actual CPT guidance [3]. For instance, ICAVL standards call for detailed assessment of the carotid bifurcation

as well as Doppler sampling of the cervical vertebral artery as required components of a complete extracranial cerebrovascular duplex examination. In contrast, CPT does not provide any details that I can find of what CPT 93880 *Duplex scan of extracranial arteries*; *complete bilateral* actually entails. In situations where CPT is silent, I recommend the following ICAVL guidelines.

For some vascular lab codes, recent CMS activity has led to more focused definitions. For example, the lower extremity arterial physiologic examination, CPT code 93922, was identified during a CMS screen of services with faster than anticipated volume grown. CMS believes that volume growth unexplained by disease prevalence may be due to overly generous relative value unit (RVU) assignment. A major question then evolved regarding what a provider must do to meet the minimum requirements for this code. The pre-2011 CPT descriptor was vague, and there was no background literature in CPT or at CMS to bolster the descriptor. With no way to answer the question regarding minimum service, it is no surprise that CMS was then poised to attack the physician work RVU. It was impossible to conduct a physician relative work survey without more clearly defining the service, and therefore the stakeholder professional societies, led by SVS, submitted a CPT coding proposal to focus the definition. After considerable debate and many revisions, the 2010 CPT Panel vote favored this very detailed new descriptor for 93922 which first appeared in the 2011 CPT Manual [4]:

> Limited bilateral noninvasive physiologic studies of upper or lower extremity arteries, (e.g., for lower extremity: ankle/brachial indices at distal posterior tibial and anterior tibial/dorsalis pedis arteries plus bidirectional, Doppler waveform recording and analysis at 1–2 levels, or ankle/brachial indices at distal posterior tibial and anterior tibial/dorsalis pedis arteries plus volume plethysmography at 1–2 levels, or ankle/brachial indices at distal posterior tibial and anterior tibial/dorsalis pedis arteries with transcutaneous oxygen tension measurements at 1–2 levels)

For those familiar with the earlier definition of 93922, this long paragraph may seem like overkill, but no longer is there any confusion about what constitutes the service. In addition, this clear detailed descriptor provided a solid platform on which to survey for physician work. That survey was performed in 2010, and recommendations were presented to CMS. The Agency reviewed the survey, felt it valid, and published the physician work RVU for the 2011 calendar year [5]. The previous work RVU was retained because a more clear service definition was created, and while that definition may be wordy, the actual service is essentially what high quality vascular labs have been doing for decades. At first glance, some might conclude that "no change" in work RVU is not a major victory, but an in-depth look at recent diagnostic cardiology and radiology services should lead to the opposite conclusion. In addition, the CPT Editorial Panel definition of this service now closely resembles the clinical requirements set out by ICAVL, a remarkable achievement.

For the vascular lab manager more interested in code application than historical development, this example of what happened to 93922 and its family members 93923 and 93924 should provide convincing evidence that CPT is a living entity with revisions and new codes every year. Annual review of the new and revised codes is essential. The Medicare Fee Schedule can be downloaded at no cost from the CMS website. The AMA CPT manual is updated every year and is the authoritative source for code descriptors. Finally, the Society for Vascular Surgery now has a vascular-specific Coding Manual that is also updated yearly. These are solid investments [6, 7].

## Intraoperative Duplex Examinations

Completion duplex exams following carotid endarterectomy and bypass grafts are routine in some practices. Although there are no published exclusions for reporting a completion duplex exam that I am aware of, the technical portion of the study would not typically be reportable because the study is being done in the hospital on a hospital inpatient; therefore, the entire technical aspect of the patient's hospital stay will be reimbursed by DRG. The small professional fee related to interpretation of the vascular lab study may be reportable if the exam meets all the requirements of archived images and a formal interpretation. An example of reporting an intraoperative carotid duplex would be 93882-26 recognizing that this is a unilateral exam (93882) and only the professional portion is being reported (−26). A completion duplex following lower extremity bypass grafting would be reported as a 93926-26.

## The Deficit Reduction Act Limits Office-Based Technical Reimbursement

Vascular surgeons commonly ask why Medicare payment for vascular lab studies fails to follow the long-established convention that the allowable payment in dollars equals the sum of the relative values units multiplied by the Medicare Conversion Factor. The answer is the Deficit Reduction Act (DRA) of 2005 (although it was signed by the President early in 2006). When searching for funds to enhance the Medicare Advantage HMO plans, an aide of House Ways and Means Committee Chair Bill Thomas noticed that a significant discrepancy exists between technical payments for certain imaging exams depending on whether they are paid in the office setting where the Medicare Physicians Fee Schedule dictates the payments vs. those exams paid under the HOPPS. This discrepancy exists because the two systems have completely different methods by which to set payment. Without regard to which of the methods more accurately reflects the

resources required to complete an imaging exam, the Ways and Means Committee wrote a provision subsequently incorporated in the DRA stating that office based imaging services would receive the lesser of the Hospital Outpatient APC payment or the Medicare Fee Schedule allowable. The DRA was implemented in 2007 and affected CT, MR, PET, ultrasound, and echocardiography. In the first year, CMS spent $1.7 billion less on imaging than during the prior year despite the fact that the number of imaging studies per beneficiary increased by 3.2%. Based on the need to cut Medicare spending, my prediction is that the DRA will never be abolished.

The one notable bit of good news related to the DRA is that SVS convinced CMS that the extremity physiologic codes should be excluded from the DRA because there is no imaging involved. This prevented about $65 million per year from being siphoned from Part B Medicare payments for noninvasive lab studies. Thus, there is no negative impact of the DRA on CPT 93922-93924. However, the DRA penalty on a complete extracranial carotid/vertebral duplex exam is over $50 per study. The technical component of this test was reimbursed $216 in 2006, and for the past 5 years, the Medicare payment has been just over $150 thanks to the DRA.

### Conclusion

The vascular lab provides a hugely important service to our vascular disease patients. Like all other types of imaging, vascular lab study payments are coming down. At this point, if a vascular technologist is not performing studies throughout a full workday, that lab is likely to be running at a deficit.

## References


1. Department of Health and Human Services. Centers for Medicare & Medicaid Services CMS-1525-P Medicare and Medicaid Programs: Hospital Outpatient Prospective Payment; bulatory Surgical Center Payment; Hospital Value-Based Purchasing Program; Physician Self-Referral; and Provider Agreement Regulations on Patient Notification Requirements. Fed Regist. 2011;76(137):42170–393.
2. Department of Health and Human Services. Centers for Medicare & Medicaid Services CMS-1525-P Proposed Median Costs for Hospital Outpatient Services, by HCPCS code for CY2012. www.cms.hhs.gov/apps/ama/license.asp?file=/HospitalOutpatientPPS/Downloads/CMS-1525-P_NRPM_Median_Files.zip. 2011. Accessed 30 Sept 2011.
3. Intersocietal Commission for the Accreditation of Vascular Laboratories. The 2010 ICAVL Standards. www.icavl.org/icavl/_standards.htm. 2010. Accessed 30 Sept 2011.
4. Abraham M, Ahlman JT, Boudreau AJ, et al. American Medical Association. CPT 2011, Professional edition. Chicago: AMA Press; 2010.
5. Department of Health and Human Services. Center for Medicare & Medicaid Services 42 CFR Parts 405, 409, 410 et al. Medicare Program; Payment Policies Under the Physician Fee Schedule and Other Revisions to Part B for CY 2011, Final Rule. Fed Regist. 2010;75(228):73170–860.
6. American Medical Association. CPT 2012, Professional edition. Chicago: AMA Press; 2012.
7. Roddy SP, Zwolak RM. SVS vascular surgery coding guide, 2011 edn. Society for vascular surgery. Chicago: IL; 2012.

# Clinical Application of Ultrasound Guidance in Arterial and Venous Access

57

Patrick A. Stone and Mohit Srivastava

**Abstract**

The use of ultrasound by vascular specialists has continued to increase over the past two decades. Historically, access for venous and arterial cannulation has been guided by landmark techniques. Ultrasound with the availability of portable devices, most operating theaters and interventional suites are equipped with specified units for physician use. This chapter describes common percutaneous cannulation sites and how access can be assisted by ultrasound technology. In addition, available literature comparing this modality to other methods of vascular access is examined.

**Keywords**

Ultrasound guided • Image guided vascular access • Sonographic-based access

## Introduction

Over the last decade, the use of ultrasound-guided imaging to obtain arterial and venous access has exponentially increased in most centers. Traditional techniques to access the vascular tree had relied on either anatomic landmarks or palpation. This can be limited and time consuming in vessels that are deep in location or variable from normal anatomy. It is essential, therefore, for all vascular specialists to become facile with sonographic-guided access.

At our institution, our residents and fellows have experienced a substantial increase in the amount of hands on training with ultrasound guidance. All residents are oriented thoroughly on the appropriate techniques utilized, and each is required to use a portable ultrasound machine during access attempts throughout their training. This has resulted in a decrease of our overall complication rate and led to significantly less patient discomfort.

This chapter is dedicated to providing information for practitioners involved in both simple and complicated vessel cannulation. The most commonly accessed vessels for diagnostic and interventional procedures are covered, with the most essential content directed toward technique and available literature supporting ultrasound-guided intervention. Finally, our philosophy of ultrasound-guided access in specific case scenarios will hopefully provide an easy way to identify those situations in which this method can be used as the only form of entry.

## Central Venous Access

### Internal Jugular Vein

Our group is commonly consulted for the placement of both tunneled and nontunneled central venous catheters. The preferred site in such patients has always been the jugular vein. In predominantly nonemergent situations, it is easily cannulated at the bedside and offers a lower infection rate than

P.A. Stone, M.D., RVT, RPVI (✉)
Department of Surgery, Robert C. Byrd Health Sciences Center, West Virginia University, Charleston Area Medical Center, Charleston, WV, USA
e-mail: pstone0627@yahoo.com

M. Srivastava, M.D.
Department of Surgery, Robert C. Byrd Health Sciences Center, West Virginia University, Charleston Area Medical Center, Charleston, WV, USA

A.F. AbuRahma, D.F. Bandyk (eds.), *Noninvasive Vascular Diagnosis*,
DOI 10.1007/978-1-4471-4005-4_57, 

other locations. The vein is also used as an access site for the placement of inferior vena cava filters and their subsequent retrieval. Although the later is far more common, most filters do have a jugular delivery system for use if needed.

Ultrasound is first used to identify the vessel, with B-mode imaging, in a transverse orientation. In most patients, the vein is located lateral to the carotid artery, within the carotid sheath. In a standard gray scale view, it has a larger diameter and more of an oval shape. Pulsations of the neighboring artery can also be seen, which helps preliminarily identify the correct structure to be targeted.

The vein should be assessed for compressibility and the presence of both acute and chronic thrombosis. Acute clot does not display the thickened vessel wall and hyperechoic thrombus that a chronic one will; however, it does demonstrate a significant lack of compressibility. When this occurs, confirmation with color Doppler is necessary, and a lack of spontaneous, phasic venous flow should lead the operator to choose a different site for access. Chronic deep venous thrombosis does not always mandate a similar approach; however, the vessel is not generally seen as a preferred option.

The vein can be accessed at the junction of the sternal and clavicular heads of the sternocleidomastoid, as in the traditional landmark method, or at the base of the neck via a lateral approach. Although techniques with two operators have been described, we prefer to use the "one-handed" technique in which the operator holds the ultrasound probe with one hand and insert the needle with the other [1].

Here, the ultrasound probe is placed on the patient's neck in a transverse orientation to the jugular vein and a local anesthetic is administered. A 19-gauge needle is used to enter the vessel while in the B-mode function. For standard central non-tunneled catheters, this is accomplished with the needle oriented at a 45° angle, just above the middle of the probe. Once access is attained, a guidewire is passed and the ultrasound probe can be used to follow the single echogenic point it creates for a short distance to the base of the clavicle. A catheter or sheath can then be placed (See Figs. 57.1 and 57.2).

For tunneled catheters, our group has preferred the lateral approach to the jugular vein, which was initially described by Silberzweig and Mitty in 1998 [2]. A standard transverse view is obtained at the base of the neck with the ultrasound probe placed parallel to and just above the clavicle. Both the anesthetic and access needle are inserted into the skin at a similar 45° angle, lateral to the transversely oriented probe. Following the needlepoint is essential to prevent a "through and through" puncture of the carotid artery, which occurs if the needle tip is out of plane with the ultrasound beam. We have found that this approach minimizes the risk of kinking by allowing a gentle curve of the catheter at the base of the neck into the lateral wall of the vein. The probe can also be reoriented to show a longitudinal plane, where insertion of the guidewire into the innominate vein can be followed (See Fig. 57.3).

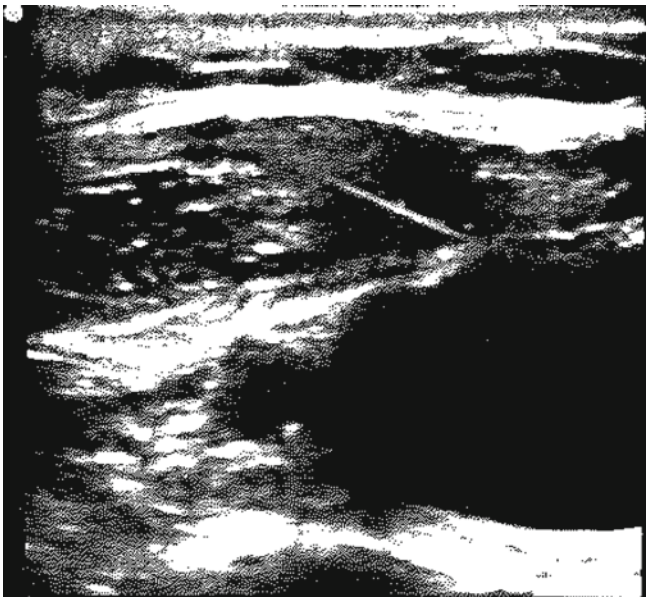

**Fig. 57.1** Percutaneous insertion of needle into the jugular vein

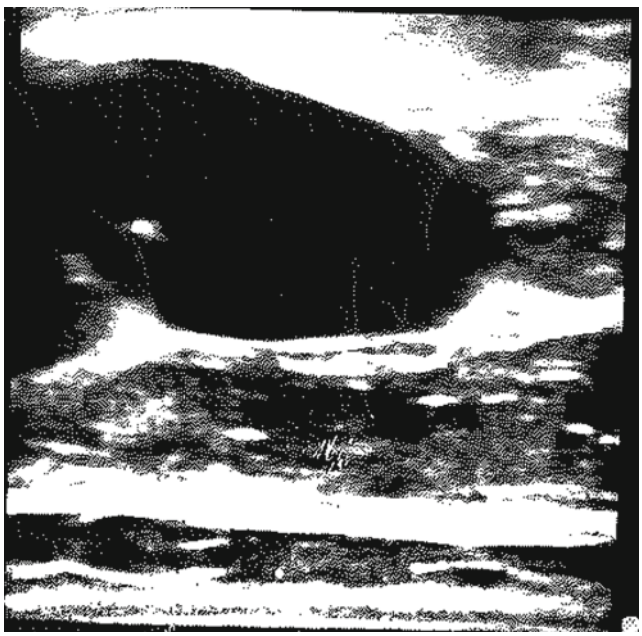

**Fig. 57.2** Echogenic tip of needle in the lumen of the jugular vein, transverse view

One of the most compelling early studies to examine the effectiveness of using ultrasound was performed by Denys et al. in 1993. Their group prospectively analyzed over 300 patients accessed by both traditional landmark techniques as well as ultrasound guidance. A higher technical success rate was seen with ultrasound-guided access (100% vs. 88.1%), with 78% of veins successfully punctured on first pass attempts as opposed to 38% with the traditional landmark based group. The average time to access from skin to vein

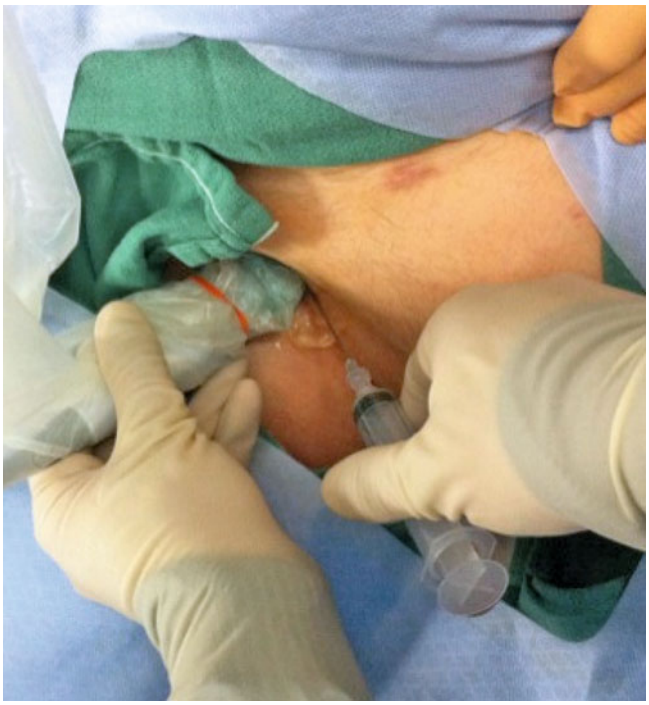

**Fig. 57.3** "Low and lateral" approach to sticking the jugular vein for tunneled catheters

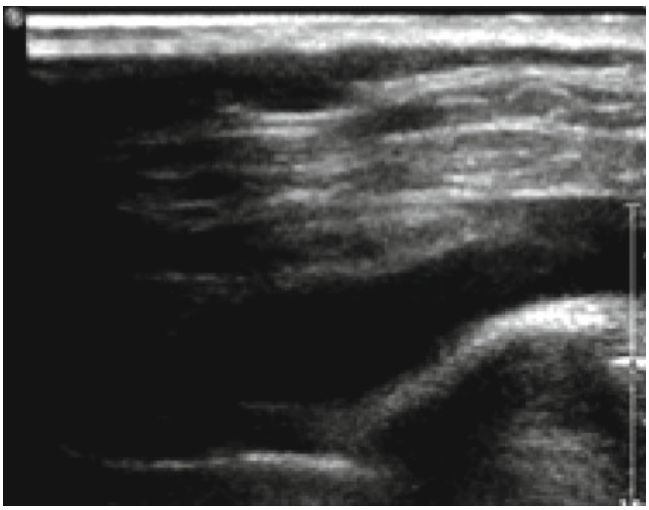

**Fig. 57.4** Subclavian vein, longitudinal plane (B-Mode)

was 9.8 and 44.5 s, respectively, and complication rates were significantly less in the ultrasound group with regards to inadvertent carotid artery puncture, brachial plexus irritation, and access site hematomas [3].

Subsequently, several other prospective trials have compared the ultrasound-guided access with that of landmark techniques, most of which were randomized and controlled. A randomized trial of 450 critical care patients demonstrated a higher technical success rate with an ultrasound-guided access and showed complications with the landmark method were much higher. Carotid artery puncture rates of over 10% and a hematoma rate of 8.4% were seen, as compared to 1.1% and 0.4%, respectively, in patients with ultrasound-guided access. A direct correlation was also observed between blood stream infection and the number of passes, which was substantially reduced by imaging-guided puncture [4]. Three years later, Turker et al. conducted a randomized study involving 380 patients comparing ultrasound guided to that of landmark techniques. This was one of the lowest reported carotid puncture and hematoma rates while using the landmark technique (4.73% and 3.68%); however, there was still a statistically significant increase as compared to ultrasound-guided access [5].

In 2003, a meta-analysis of central venous cannulation was performed, examining studies of the internal jugular, subclavian, and femoral veins. The jugular vein was the most studied access site but all sites were included for analysis. A relative risk reduction of 86% was found for failed catheter placement, 57% for placement complications, and 41% for failure on first attempt when ultrasound-guided access was used. Most series also showed fewer required attempts for successful cannulation and less time to access when ultrasound was used as an adjunct [6].

## Subclavian Vein

The subclavian vein has also been used for both temporary and permanent central catheters, albeit less frequently. It is accessed in the costoclavicular space of the thoracic outlet. The subclavian vein, artery, and brachial plexus all pass through this space, in close proximity to the pleural cavity making a precise puncture is critical. Arterial cannulation is difficult to manage, especially once a sheath has been inserted, and pneumothoraces have been reported much more frequently with subclavian vein access attempts than with the jugular vein.

A standard transverse view is more difficult to obtain, and longitudinal views below and above the clavicle are often employed. In addition, conventional compression is not usually feasible secondary to the bony architecture surrounding the vein, and the presence of intraluminal echoes and respiratory phasicity with Doppler waveform analysis are generally all that is used to assess the vein for clot burden. The skin puncture is at the junction of the medial two-thirds and lateral one-third of the clavicle, and the needle is visualized in the same plane as it enters the lumen of the vessel. A classic Seldinger technique then ensues (See Fig. 57.4).

Series comparing landmark with ultrasound-guided techniques are limited; however, the results have shown ultrasound guidance to be superior in certain outcomes. Between 1994 and 1998, three prospective, randomized trials by Branger et al., Gualtieri et al., and Lefrant et al. showed a

statistically significant relative risk reduction of 86% of failed catheter placement along with a lower complication rate [7–9]. The sample sizes were not as large as those seen in some of the series looking at the internal jugular vein, but ultrasound has shown itself to be of clear benefit in accessing the vein. We feel strongly that in both routine and complex situations ultrasound should be considered for vessel cannulation. The difficulty with visualization around the clavicle can be more technically demanding, but the results with the use of two-dimensional imaging far outweigh the risks associated without it.

### Femoral Vein

The common femoral vein is viewed as the simplest access point to the deep venous circulation. This is predominantly due to its location and the lower risks associated with access compared to others. The vein lies medial to the common femoral artery and travels with the artery proximally under the inguinal ligament. It can be easily cannulated while the patient lies in the supine position, and is currently the site most amenable to emergency access.

The ultrasound probe is oriented transversely over the femoral vessels, parallel to the groin crease. Similar to the jugular vein, the vein is compressed and B-mode assessment of intraluminal thrombus is done. Once patency is confirmed, the needle is positioned inferior to the midportion of the probe and directed at a 45° angle into the plane of the ultrasound beam. The echogenic tip is followed as it advances through the *anterior* wall of the vein.

Success rates have been well established for a number of years. In 1990, Mallory et al. was one of the first to show a significant decrease in the amount of time to cannulation (2.5 vs. 6 min) as well as a higher number of successful cannulations with the first pass [10]. Since then, five different studies—both prospective and retrospective—have confirmed their group's results. For the most part, retrospective series have reported better technical success, including more successful first attempt punctures along with lower hematoma rates and inadvertent femoral artery punctures [11, 12].

A prospective study by Hilty et al. evaluated femoral cannulation in patients undergoing cardiopulmonary resuscitation, showing a relative risk reduction of failed catheter placement by 71% [13]. Another prospectively randomized trial of 110 patients undergoing femoral vein dialysis catheter insertion reported improved technical success (98.2% vs. 80%) and reduced complications (18.2% vs. 5.5%) in patients randomized to ultrasound-guided access [14].

We have previously published our institutional experience with central venous access for inferior vena cava filter placement. The focus of our study was on the safety of using the subclavian vein for access during inferior vena cava filter placement. A striking finding during our review, however, was how fast the procedures were when performed using the femoral vein for access [15]. During filter placement, we also routinely assess the femoral veins with the probe. This helps visualize any clot burden, acute or chronic, in addition to reducing the number of passes for successful cannulation and inadvertent punctures. The later can be devastating in this clinical scenario in that some patients may already be on anticoagulation.

### Popliteal and Tibial Veins

The popliteal vein is rarely accessed and is clearly the least accessed of all deep veins. The most common circumstance that this occurs is in patients with acute deep venous thrombosis undergoing thrombolysis. The popliteal veins lie on either side of the popliteal artery and branch distally into the tibial veins, similar to the corresponding arterial anatomy. Intraluminal thrombus is often present making access to either popliteal vein challenging, and avoidance of inadvertent arterial puncture is paramount in patients undergoing lytic therapy.

The most common technique to access the vein is via prone positioning, and ultrasound insonation should occur by a transverse orientation. A standard angle of 45° is used, however, it is often seen that a steeper angle of approximately 60° can be needed. In the popliteal fossa, the veins are superficial during a prone approach, and we have found that identifying the small saphenous vein can sometimes be helpful. Following its course as it empties into the popliteal vein can make access easier by identifying a more superficial vein to cannulate, especially if there is already a significant thrombus burden in the popliteal veins. Once the needle has entered the lumen, the procedure can be continued (See Fig. 57.5).

The anterior tibial and posterior tibial veins are even less accessed than the popliteal. They may be of some use in ascending venography, when peripheral intravenous catheters in the feet cannot be attained. The patient is usually in a supine position, and the ultrasound image helps identify both tibial veins for each corresponding artery. Accessing one will allow for a suitable catheter injection and ascending venogram. Occasionally, we have even used the posterior tibial vein for lytic access, but this is only done if attempts at cannulating the popliteal vein are unsuccessful.

## Peripheral Venous Access

### Great and Small Saphenous Veins

With the advent of radiofrequency and laser ablation, endovenous procedures for great saphenous (GSV) ablation

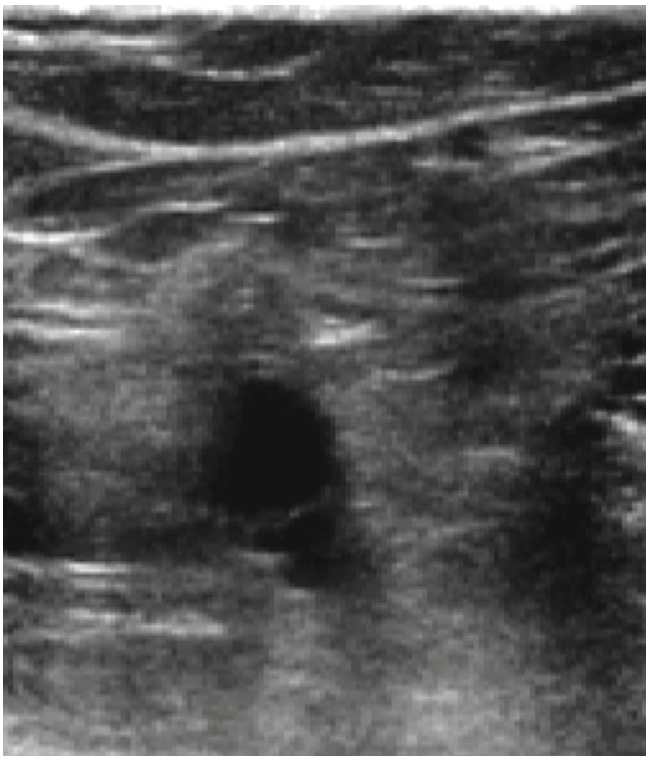

**Fig. 57.5** Popliteal veins (transverse view, B-Mode)

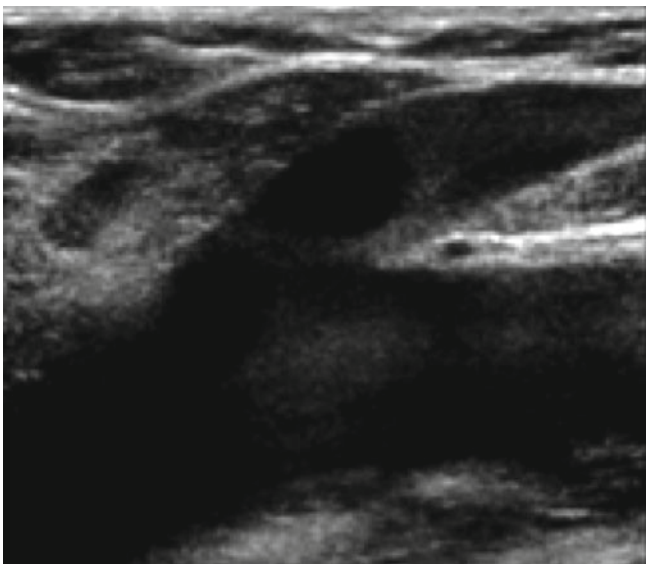

**Fig. 57.6** Sapheno-femoral junction (longitudinal plane, B-mode)

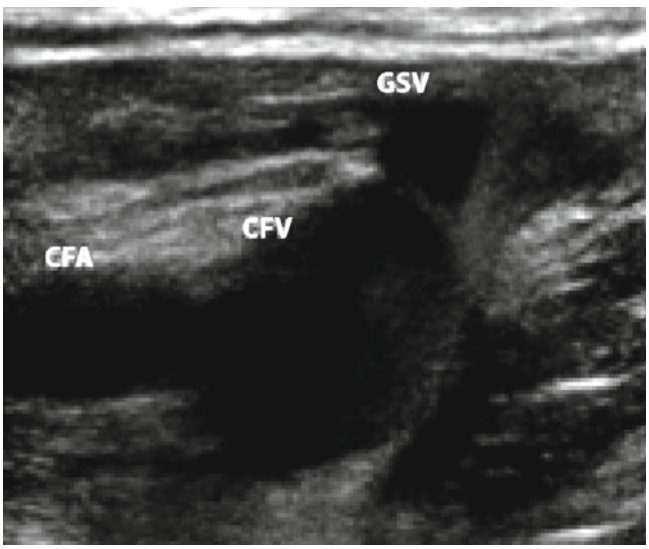


**Fig. 57.7** Transverse view of common femoral artery, common femoral vein, and great saphenous vein (transverse view, B-Mode)

can now be performed without surgical intervention in the majority of patients. It produces similar results, with significantly decreased morbidity. Ultrasound only aids in providing safe access to accomplish these various procedures.

The GSV lies within the saphenous sheath and runs down the medial border of the entire lower extremity. It is a superficial vein, with four or more large sets of perforators throughout its course. Typically, in reflux surgery, the vein is larger than 3 mm in its entirety and is accessed at the level of the medial condyle of the femur. The needle is inserted at a 45° angle to the skin surface, directly beneath the probe. In a transverse view, the needle tip is identified superior to the vein, and puncture can occur in either this view or a longitudinal one, as the needle is advanced. Upon blood return, a standard seldinger technique is used for sheath placement. An ablative catheter is then inserted, and visualization of its tip should always be ensured. Here, a longitudinal view of the sapheno-femoral junction is imperative. In this view, the superficial epigastric vein is visualized, and the catheter should be withdrawn to a point inferior to this branch. Finally, a transverse projection is employed again and tumescence anesthesia is injected within the saphenous sheath along the entire course of the vein (See Figs. 57.6 and 57.7).

The small saphenous vein is cannulated in ablative procedures and lower extremity deep venous thrombosis lytic cases. Ultrasound can be used to identify the small saphenous vein approximately three to four fingerbreadths below the level of the lateral femoral condyle on the lateral aspect of the lower extremity, and a standard image guided technique is utilized. The literature regarding the use of ultrasound to access this vein is limited; however, it is clearly less invasive and is likely associated with a lower complication rate.

## Basilic Vein

The superficial veins of the upper extremity are most often times accessed by nursing or ancillary staff during peripheral intravenous access. At our institution, specialty nurses also

achieve access for peripherally inserted central catheters. Portable ultrasound units are used at the bedside to do so, and they are present in each hospital for use by all staff if needed.

It is only on occasion that our group needs to access the basilic vein in the interventional suite, with the most common case being thrombolysis for upper extremity deep venous thrombosis. The basilic vein is identified in the transverse plane just above the antecubital fossa. It lies on the medial portion of the upper arm over the groove between the biceps and triceps muscles.

## Arterial Access

### Common Femoral Artery

The common femoral artery is the most common artery accessed for percutaneous based arterial procedures. Several techniques have been used, including "the best pulse," fluoroscopic guidance, and ultrasound guidance. Our group routinely utilizes the fluoroscopic-guided principle in patients with palpable femoral pulses. We do, however, recommend ultrasound guided arterial access in several specific case scenarios. These include endovascular aortic aneurysm repair, planned thrombolysis, a nonpalpble pulse, and antegrade access. If access is not achieved in the proper location, devastating complications can be seen. Accessing the superficial or deep femoral arteries may result in either a groin hematoma or pseudoaneurysm upon removing the intra-arterial sheaths. This is secondary to lack of bony surface to compress the artery against posteriorly. Punctures occurring above the common femoral artery can lead to significant retroperitoneal bleeding. Severe pain, extensive transfusion requirements, and operative exploration can all result.

In the majority of patients, the common femoral artery is located anterior to the medial 1/3 portion of the femoral head. Proximally, the transition from the external iliac artery to the common femoral artery is divided anatomically by the inguinal ligament. Distally, it bifurcates into the femoral and profunda femoris arteries at variable levels. Fluoroscopic-guided access is performed by solely identifying the medial border of the femoral head. This method allows for the artery to be punctured in what is most likely the common femoral portion, with only a small percentage of vessels displaying a high bifurcation where the superficial femoral artery may inadvertently be cannulated. In this situation, pressure can often times still be held due to the fact that the femoral head is still present to hold the vessel against. Doppler needles and visualization of calcium in the wall of the vessel can sometimes aid in this type of access, especially with arteries that are not palpable.

Ultrasound offers a unique benefit of identifying atherosclerotic plaque within the evaluated vessel, in addition to accurate placement. It is our practice to identify the bifurcation first and trace up to the common femoral artery in a transverse view. Then, the probe is turned to create a longitudinal projection through which the needle can be advanced into the common femoral artery. The standard 45° angle of needle entry into the skin is employed and the entire body of the needle is seen in the longitudinal view entering at a point just above the bifurcation. In an effort to decrease both periprocedural embolization and thrombosis, any areas of the artery that display severe plaques are avoided.

The literature supporting the use of ultrasound as compared to fluoroscopic-guided technique is limited. A recent prospective trial randomized 1,004 patients to receiving either fluoroscopic-guided puncture or ultrasound-guided puncture of the femoral artery. The overall cannulation rate was similar between the two groups; however, the ultrasound-guided cohort was more successful at first pass access (83% vs. 46%) and median time to puncture (136 vs. 148 s). The study also demonstrated a lower complication rate with ultrasound guided femoral access (1.4% vs. 3.4%), with the major difference in regards to hematomas >5 cm [16].

In the past 2 years, our group has favored ultrasound-guided techniques to obtain access for percutaneous endovascular aneurysm repair. The need for accurate access with >20 french sheaths cannot be underscored, and we have relied on ultrasound-guided punctures of the common femoral artery to allow safe placement of these larger sheaths. Recently, in 2008, Arthurs et al. examined 88 patients who underwent total percutaneous closure for aortic aneurysm repair. Although retrospective, their group identified a significant benefit of ultrasound guided common femoral access. It not only decreased operative time, but they also found a higher technical success rate as well as a lower conversion to open repair with its use [17].

### Popliteal Artery

The popliteal artery is cannulated predominantly for retrograde access, and it can be used for peripheral arterial interventions. Our group has generally not preferred the use of this site due to fear of complications; however, with ultrasonic imaging this can be minimized. The ultrasound probe is placed in a transverse plane similar to the technique for accessing the popliteal vein, but a slight cranial angle is added for better visualization.

In 2005, Yilmaz et al. retrospectively looked at 174 patients who underwent retrograde popliteal artery access for both claudication and critical limb ischemia. In a total of 234 procedures, the overall complication rate was 6.4%, with only 4.3% being related to arterial puncture. It is clearly a safe method with sonographic guidance, and although it is not our preference, it is still a valid option for access [18].

## Brachial Artery

The brachial artery is the second most common arterial site accessed in peripheral intervention. The brachial artery is found in the groove just underneath the bicipital aponeurosis, with the median nerve coursing medial to it. There are typically paired brachial veins on each side, as is seen in the popliteal and tibial arteries of the lower extremity. Higher complication rates, including thrombosis, have been reported here and are primarily related to the small diameter of the vessel.

Many vascular specialist use this site for visceral and renal angiography/and intervention. Percutaneous techniques rely on either palpation of the artery, use of Doppler needle, or ultrasound guidance. It is our preference to use ultrasound guidance by transverse and longitudinal imaging similar to that employed in the common femoral artery. It allows for visual identification of the artery and reduces the number of unsuccessful punctures. Additionally we are able to determine the size of the brachial artery prior to access and can better determine the ability to tolerate larger sheaths for planned interventions.

## Radial Artery

The radial artery was traditionally only used for inpatient arterial access in blood pressure monitoring. Recently, however, it has gained significant interest as a site for percutaneous cannulation. The artery is being used in both diagnostic and therapeutic cardiac catheterization, and cannulation rests mostly on palpable pulsation of the vessel. Ultrasound imaging has proven a useful adjunct, and a recent meta-analysis reported a definite benefit. An improved first pass success rate of 71% was seen, and even though most trials did not use uniform criteria for their outcome measurements, a trend toward reduced number of attempts and a faster time to catheterization was seen [19]. Our group has not utilized the radial artery for any peripheral procedures, but it is a viable option for use and its acceptance is growing.

**Table 57.1** 2010 reimbursement for ultrasound assisted access

| | 2010 Medicare reimbursement ($) |
|---|---|
| Professional fee | 15.87 |
| Technical fee | 20.92 |
| Total cost | 36.79 |

## Reimbursement

Reimbursement is available when ultrasound is used to gain vessel access. It is dependent on three primary components during the dictation of each procedure. The first is that the operator must document the patency of the selected vessel (i.e., widely patent, patent but with area of stenosis, etc…). Second, the operator must document the real-time visualization of needle entry using ultrasound as a guide. Third, the operator must have documentation of permanent recording and reporting. Please see Table 57.1 for the reported physician reimbursement in 2010. CPT + 76937

### Conclusion

In conclusion, ultrasound imaging provides a safe, effective way to visualize a vessel while achieving access. It provides both gray scale imaging and Doppler flow to better assess the vessel for stenosis or thrombosis. It gives

**Table 57.2** Major randomized controlled trials for ultrasound guided arterial and venous access

| Trial | Arterial/venous | No. of patients | First pass success (FP)/overall success rate (OS) ultrasound vs. traditional | Complication rates (%) traditional vs. ultrasound |
|---|---|---|---|---|
| Troianos et al. [20] | Venous | 160 | 73% vs. 54% (FP)<br>100% vs. 96% (OS) | 8.43% vs. 1.39% (Arterial Puncture) |
| Denys et al. [3] | Venous | 928 | 78% vs. 38% (FP)<br>100% vs. 88.1% (OS) | 13.2% vs. 2.9% |
| Branger et al. [7] | Venous | 130 | 96.8% vs. 86.2% (FP) | 3.1% vs. 2.3% |
| Teichgraber et al. [21] | Venous | 100 | 96% vs. 52% (FP) | 12% vs. 0% (Arterial Puncture) |
| Lefrant et al. [9] | Venous | 286 | 64.3% vs. 65.7% (FP)<br>86.7% vs. 90.9% (OS) | 16.8% vs. 5.6% |
| Augoustides et al. [22] | Venous | 429 | 80.9% vs. 68.9% (FP) | 4.2% vs. 4.2% (Arterial Puncture) |
| Karakitsos et al. [4] | Venous | 900 | 100% vs. 94.4% (OS) | 23.3% vs. 1.5% |
| Prabhu et al. [14] | Venous | 110 | 85.5% vs. 54.5% (FP)<br>98.2% vs. 80% (OS) | 18.2% vs. 5.5% |
| Turker et al. [5] | Venous | 380 | 99.47% vs. 97.36% (OS) | 4.4% vs. 0.5% |
| Seto et al. [16] | Arterial (Fluoro-scopic vs. Ultrasound) | 1,004 | 83% vs. 46% (FP) | 3.4% vs. 1.4% |

significantly more information than both anatomic landmarks and fluoroscopy can provide. All clinicians engaging in peripheral percutaneous intervention should have a thorough knowledge of how to image each of the vessels discussed in this chapter, and have the ability to interpret the image seen, using it as a guide to access the vessel lumen effectively with a needle (See Table 57.2).

## References


1. Feller-Kopman D. Ultrasound-guided internal jugular access: a proposed standardized approach and implication for training and practice. Chest. 2007;132:302–9.
2. Silberweig JE, Mitty HA. Central venous approach using image guidance. AJR Am J Roentgenol. 1998;170(6):1617–20.
3. Denys BG, Uretsky BF, Reddy PS. Ultrasound-assisted cannulation of the internal jugular vein: a prospective comparison to the external landmark-guided technique. Circulation. 1993;87(5):1557–62.
4. Karakitsos D, Labroppoulos N, De Groot E. Real-time ultrasound-guided catheterization of the internal jugular vein: a prospective comparison with the landmark technique in critical care patients. Crit Care. 2006;10:R162.
5. Turker G, Nur Kaya F, Gurbert A. Internal jugular vein cannulation: an ultrasound-guided technique versus a landmark-guided technique. Clinics. 2009;64(10):989–92.
6. Hind D, Calvert N, Mcwilliams R. Ultrasonic locating devices for central venous cannulation: meta-analysis. BMJ. 2003;327(7411):361.
7. Branger B, Dauzat M, Zabadani B, et al. Pulsed Doppler sonography for the guidance of vein puncture: a prospective study. Artif Organs. 1995;19(9):933–54.
8. Gualtieri E, Deppe S, Sipperly M. Subclavian vein catheterization: greater success rate for less experienced operators using ultrasound guidance. Crit Care Med. 1995;23(4):692–7.
9. Lefrant J, Cuvillon P, Benezet J, et al. Pulsed Doppler ultrasonography guidance for catheterization of the subclavian vein: a randomized study. Anesthesiology. 1998;88(5):1195–201.
10. Mallory DL, Mcgee WT, Shawker TH, Brenner M, et al. Ultrasound-guidance improved the success rate of internal jugular vein cannulation. Chest. 1990;98:157–60.
11. Farrell J, Gellens M. Ultrasound guided cannulation versus the landmark guided technique for acute hemodialysis access. Nephrol Dial Transplant. 1997;12:1234–7.
12. Zollo A, Cavatorta F, Galli S. Ultrasound-guided cannulation of the femoral vein for acute hemodialysis access with silicone catheters. J Vasc Access. 2001;2:56–9.
13. Hilty WM, Hudson PA, Levitt MA, Hall JB. Real-time ultrasound-guided femoral vein catheterization during cardiopulmonary resuscitation. Ann Emerg Med. 1997;29:331–6; discussion 337.
14. Prabhu Mayoor V, Juneja D, Gopal Palepu B. Ultrasound-guided femoral dialysis access placement: a single-center randomized trial. Clin J Am Soc Nephrol. 2010;5:235–9.
15. Stone P, AbuRahma AF, Hass SM. TrapEase inferior vena cava filter placement: use of subclavian vein. Vasc Endovascular Surg. 2004;38(6):505–9.
16. Seto AH, Abu-Fadel MS, et al. Real time ultrasound guidance facilitates femoral arterial access and reduces vascular complications. JACC Cardiovasc Interv. 2010;3(7):751–8.
17. Arthurs Zachary M, Starnes Benjamin W, Sohn Vance Y. Ultrasound-guided access improves rate of access-related complications for totally percutaneous aortic aneurysm repair. Ann Vasc Surg. 2008;22:736–41.
18. Yilmaz S, Sindel T, Luleci E. Ultrasound-guided retrograde popliteal artery catheterization: experience in 174 consecutive patients. J Endovasc Ther. 2005;12(6):714–22.
19. Shiloh AL, Savel RH, Paulin LM, et al. Ultrasound-guided catheterization of the radial artery: a systematic review and meta-analysis of randomized clinical trials. Chest. 2010. doi:10.1378/chest.10-0919.
20. Troianos C, Jobes D, Ellison N, et al. Ultrasound-guided cannulation of the internal jugular vein: a prospective, randomized study. Anesth Analg. 1991;72:823–6.
21. Teichgraber U, Benter T, Gebel M, et al. A sonographically guided technique for central venous access. AJR Am J Roentgenol. 1997;169:731–3.
22. Augoustides JG, Horak J, Ochroch AE, et al. A randomized controlled clinical trial of real time needle-guided ultrasound for internal jugular venous cannulation in a large university anesthesia department. J Cardiothorac Vasc Anesth. 2005;19(3):310–5.

# Noninvasive Vascular Laboratory Glossary

The following glossary has been collected to help the noninvasive vascular laboratory technician understand the many terms used in the vascular laboratory.

**A-mode** In diagnostic ultrasound, a one-dimensional presentation of a reflected sound wave in which echo amplitude (*A*) is displayed along the vertical axis and time of rebound (depth) along the horizontal axis; the echo information is presented from interfaces along a single line in the direction of the sound beam.

**Absorption** Conversion of sound to heat.

**AC (alternating current) coupled** Output signal to graphic display only responds to changes faster than 0.5 Hz (one complete cycle every 2 s).

**Acceleration** Change in velocity.

**Acoustic** Having to do with sound.

**Acoustic impedance** Property of a medium equal to the product of density and propagation speed.

**Acoustic propagation properties** Characteristics of a medium that affect the propagation of sound through it.

**Acoustic shadow** Loss of acoustic properties of structures lying behind an attenuating structure.

**Acoustic variables** Pressure, density, temperature, and particle motion – functions of space and time in a sound wave.

**Acrocyanosis** Symmetric mottled cyanosis of the hands and feet associated with coldness and sweating. It is a vasospastic disorder accentuated by cold or emotion and relieved by warmth.

**ADC** Analog-to-digital converter.

**Aliasing** Improper Doppler shift information from a pulsed-Doppler or color-flow instrument when true Doppler shift exceeds one half the pulse repetition frequency.

**Allen test** A test performed to check the continuity of the palmer arch normally supplied by both the radial and ulnar arteries. The test may be performed using Doppler ultrasound, photoplethysmography, or strain-gauge plethysmography.

**Amaurosis fugax** Temporary partial or total blindness often resulting from transient occlusion of the retinal arteries. May be a symptom of impending cerebrovascular accident.

**Ampere** The unit of electric current used in Ohm's law, $I = E/R$, where $I$ = intensity, $E$ = electromotive force, and $R$ = resistance. It measures the rate at which electric current is transferred.

**Amplification** The act of enlarging, increasing, or extending.

**Amplitude** The maximal height of a wave form, either from the baseline, or peak to peak.

**Analog** Representing numerical values by physical quantities, so as to allow the manipulation of numerical data over a continuous range of values. A chart recorder is an analog form of data presentation.

**Anastomosis** A natural or surgical communication between blood vessels.

**Anechoic** Echo-free.

**Aneurysm** A bulging of the wall of a vein or artery, due to a thinning or weakening by disease or congenital abnormality.

**Angle of incidence** Angle at which an ultrasound beam strikes an interface (with respect to the normal or perpendicular angle); in Doppler ultrasound, the angle of the beam with respect to the flow axis.

**Ankle/brachial index** A numerical comparison of the systolic blood pressures in the arm and ankle, obtained by dividing the ankle pressure by the arm pressure. Values below 1.0 indicate varying degrees of ischemia.

**Annular** Ring-shaped.

**Annular array** Array made up of ring-shaped elements arranged concentrically.

**Antegrade (anterograde) flow** Blood flowing toward the Doppler probe. By convention, this is heard in the left ear when using a stereo headset.

**Anticoagulant** A substance which prevents or retards blood clotting, such as heparin.

**Aperture** Size of transducer or group of elements.

**Apodization** Nonuniform (involving different voltage amplitudes) driving of elements in an array to reduce grating lobes.

**Array** Transducer array.

A.F. AbuRahma, D.F. Bandyk (eds.), *Noninvasive Vascular Diagnosis*,
DOI 10.1007/978-1-4471-4005-4, © Springer-Verlag London 2013

**Arrhythmia** Abnormal rhythm of the heart beat.

**Arterial compliance** The property of healthy arterial walls to expand and contract with blood flow pulsations.

**Arterial inflow** Pertaining to blood flow into the lower extremities to the level of the common femoral arteries.

**Arterial insufficiency** Inadequate blood supply in the arterial system usually caused by stenosis or occlusion proximal to the inadequately supplied area.

**Arterial occlusive disease** Any disease process which closes the arteries.

**Arterial outflow** Pertaining to blood flow between common femoral artery and trifurcation.

**Arterial runoff** Pertaining to blood flow from trifurcation (branching of popliteal artery into anterior tibial, peroneal, and posterior tibial arteries) to the digital arteries of the foot.

**Arteriography** Invasive radiologic procedure involving injection of a radiopaque substance into the arteries. Long recognized as the "gold standard" for arterial evaluation, the procedure carries definite mortality and morbidity risks and give no functional information. Essentially the same as angiography.

**Arterioles** The smallest arterial vessels (0.2 mm diameter) resulting from repeated branching of the arteries. They are composed of smooth muscle only and conduct blood from the arteries to the capillaries.

**Arteriosclerosis** Generic term which encompasses a variety of conditions causing the artery walls to thicken, harden, and lose elasticity.

**Arteriovenous malformation (AVM)** Abnormal connection between the arterial and venous systems. May be traumatic, congenital, or surgical, as in dialysis.

**Atheroma** A deposit of fatty (or other) substances in the inner lining of the artery wall.

**Atherosclerosis** A form of arteriosclerosis in which the inner layer of the artery wall is made thick and irregular by deposits of atheroma. These deposits result in a decrease in vessel diameter.

**Attenuation** Decrease in amplitude and/or intensity as a wave travels through a medium.

**Attenuation coefficient** Attenuation per unit length of wave travel.

**Augmentation** The normal increase in the Doppler sound of venous flow upon compression distal to the Doppler probe or release of compression proximal to the probe. Augmentation resulting from release of distal compression or application of proximal compression indicates valvular incompetence.

**Autocorrelation** A rapid technique, used in most color-flow instruments, for obtaining mean Doppler shift frequency.

**Axial** In the direction of the transducer axis (sound travel direction).

**Axial resolution** The minimum reflector separation along the sound path that is required to produce separate echoes (i.e., to distinguish between two reflectors).

**B-Scan** A brightness image that represents a cross section of an object through the scanning plane.

**B-Mode** A two-dimensional diagnostic ultrasound presentation of echo-producing interfaces in a single plane; the intensity of the echo is represented by modulation of the brightness (*B*) of the spot; the position of the echo is determined from the position of the transducer and the transit time of the acoustical pulse.

**Back pressure** The pressure increase, engorgement, and dilation proximal to a narrowed blood vessel (such as the internal carotid artery).

**Backscatter** Sound scattered back in the direction from which it originally came.

**Bandwidth** Range of frequencies involved in an ultrasound pulse.

**Baseline shift (Zero-shift)** Movement of the zero Doppler-shift frequency or zero flow speed line up or down on a spectral display.

**Basilar artery** An artery formed by the union of the two vertebral arteries, which partially supply the brain and terminate in the circle of Willis.

**Beam** Region containing continuous-wave sound; region through which a sound pulse propagates.

**Beam area** Cross-sectional area of a sound beam.

**Beam former** The part of an instrument that accomplishes electronic beam scanning, apodization, steering, focusing, and aperture with arrays.

**Bernoulli effect** Pressure reduction in a region of high-flow speed.

**Bidirectional** Indicating Doppler instruments capable of distinguishing between positive and negative Doppler shifts (forward and reverse flow).

**Bidirectional Doppler** A Doppler instrument capable of determining whether the frequency of the Doppler shift is above or below the transmission frequency, permitting determination of blood flow toward or away from the probe.

**Bifurcation** The site of division into two branches, as in an artery. Often the area of atherosclerotic deposits.

**Bistable** Having two possible states (e.g., on or off; white or black).

**Bistable display** Display in which all recorded spots have the same brightness.

**Bit** Binary digit.

**Bradycardia** Abnormally slow heart rate (under 60 beats/min).

**Bruit** An auscultatory sound caused by blood turbulence. The turbulence is caused by deposits in the arterial lumen which alter normal hemodynamics.

**Burst** A cycle or two of voltage variation.

**Burst-excited mode** A mode of operation by which a transducer is driven by a cycle of alternating driving voltage.

**Bypass** A surgically created detour between two points in a physiologic pathway, often to circumvent obstruction. Similar to shunt.

**C-mode** Mode of operation in which the display records a spot brightening for each pulse delivered from the receiver, producing a cross-sectional image parallel to the body surface (C-scan).

**C-Scan** An image that is a cross section of the object parallel to the surface and at a depth selected by gating.

**Carotid arteries** The right and left common carotid arteries are the major arteries supplying blood to the head and neck. The common carotid artery bifurcates into the external (supplies skin and muscle tissue) and the internal (supplies eye and brain tissue) arteries.

**Cathode ray tube** A display device that produces an image by scanning an electron beam over a phosphor-coated screen.

**Cavitation** Production and dynamics of bubbles in sound.

**Cerebral vascular accident (CVA)** Impeded blood supply to a part of the brain generally caused by one of the following: (1) blood clot formation in the vessel (thrombosis); (2) rupture of the vessel wall (hemorrhage); (3) an obstruction in the form of a clot or other material from another part of the vascular system which flows to the brain (embolism); (4) pressure on the vessel, as by a tumor.

**Cerebrovascular** Pertaining to the blood vessels and circulation of the brain.

**Channel** An independent element, delay, and amplifier path.

**Circle of Willis** Arterial circle of the cerebrum composed of the anterior, middle, and posterior communicating arteries. This important anastomosis connects the bilateral carotid circulation with the vertebral circulation and may be a source of collateralization in internal carotid artery occlusive disease.

**Claudication** Pain and dysfunction of the lower extremity due to arterial insufficiency during exercise. Usually intermittent, and relieved with rest.

**Clutter** Noise in the Doppler signal that is generally caused by high-amplitude, Doppler-shifted echoes from the heart or vessel walls.

**Coarctation** Literally, a pressing together. In practice, a narrowing of a vessel, usually congenital in origin.

**Collagen disease** Any of various clinical syndromes characterized by widespread alterations of connective tissue including inflammation and degeneration. Included are polyarteritis and systemic lupus erythematous.

**Collateral circulation** The circulation established through anastomotic communicating channels, when the direct blood supply is compromised or abolished.

**Color-flow display** The presentation of two-dimensional, real-time Doppler shift or time shift information superimposed on a real-time, gray-scale, anatomic cross-sectional image. Flow directions toward and away from the transducer (i.e., positive and negative Doppler or time shifts) are presented as different colors on the display.

**Comet tail** A series of closely spaced reverberation echoes.

**Common femoral artery** A major artery of the thigh at the level of the inguinal ligament, arising from the external iliac artery and terminating in the superficial femoral artery.

**Compensation** Equalization of received echo amplitude differences caused by different attenuations for different reflector depths; also called depth gain compensation (DGC) or time gain compensation (TGC).

**Compliance** Distensibility; nonrigid stretchability of vessels.

**Composite** Combination of a piezoelectric ceramic and a nonpiezoelectric polymer.

**Compressibility** Ability of a material to be reduced to a smaller volume under external pressure.

**Compression** Reduction in differences between small and large amplitudes; region of high density and pressure in a compressional wave.

**Constructive interference** Combination of positive or negative pressures.

**Continuous mode** Continuous-wave mode.

**Continuous-wave** A wave in which cycles repeat indefinitely; not pulsed.

**Continuous-wave (CW) Doppler** A Doppler instrument which emits an ultrasound beam without interruption. It is not range-specific and so will detect flow at any depth of penetration governed by the frequency of the probe.

**Contralateral** Pertaining to the opposite side of the body.

**Contrast resolution** Ability of a gray-scale display to distinguish between echoes of slightly different amplitudes or intensities.

**Convex array** Curved linear array.

**cos** Abbreviation for cosine.

**Coupling medium** A gel used to provide a good sound path between a transducer and the skin by eliminating the air between the two.

**Crescendo TIAs** Transient ischemic attacks (TIAs) increasing in frequency over a given period of time.

**Critical Reynolds number** The Reynolds number above which turbulence occurs.

**Cross-correlation** A rapid technique for determining time shifts in echo arrival; a technique used to determine flow speeds without using the Doppler effect.

**Cross talk** Leakage of strong signals in one direction channel of a Doppler receiver into the other channel; can produce the Doppler mirror-image artifact.

**CRT** Cathode ray tube.

**Crystal** Element.

**Cuff artifact** Consistently high segmental blood pressure in the lower extremity resulting from the use of narrow segmental cuffs which may not completely transmit cuff pressure to the vessels in the central part of the limb (i.e., the femoral artery). This effect is most pronounced in the upper thigh where true normal blood pressure corresponds closely to brachial pressure. Cuff artifact must be considered to avoid false-negative examinations; it can be avoided with the use of wide (17–22 cm) contoured thigh cuffs.

**Curie point** Temperature at which an element material loses its piezoelectric properties.

**cw** Abbreviation for continuous wave.

**Cyanosis** A bluish-purple discoloration of the membranes and skin, due to the presence of excessive amounts of reduced (deoxygenated) hemoglobin in the capillary arteries.

**Cycle** One complete variation of an acoustic variable.

**DAC** Digital-to-analog converter.

**Damping** Material placed behind the rear face of a transducer element to reduce pulse duration; also, the process of pulse duration reduction.

**Damping factor** The ratio of two adjacent pulsatility indexes.

**DC (direct current) coupled** Output signal to graphic display responds to steady-state conditions as slow shifts from baseline. Gives baseline information as well as changes above or below.

**Dead zone** Distance closest to the transducer in which imaging cannot be performed.

**Decibel (dB)** A unit expressing the ratio of two amounts of electrical or acoustical power equal to ten times the logarithm (base 10) of the power ratio. A logarithmic scale compresses large signal amplitudes and expands small ones, allowing both to be displayed at the same time.

**Deep vein thrombosis (DVT)** The presence of a blood clot in the deep venous system of the lower extremity. This condition most often arises in the calf veins and, if untreated, may result in pulmonary embolism.

**Demodulation** Conversion of voltage pulses from radio frequency (RF) to video form.

**Density** Mass divided by volume.

**Depth gain compensation** Compensation.

**Depth of penetration** Depth in tissue at which intensity is reduced to some fraction of what it was at the transducer surface.

**Destructive interference** Combination of positive and negative pressures.

**Detail resolution** Ability to image fine detail and to distinguish closely spaced reflectors. (See axial and lateral resolution.)

**DGC** Depth gain compensation.

**Digital** Related to a procedure or system in which data are represented by discrete units (numerical digits).

**Digital scan converter** Computer memory that stores echo information.

**Digital-to-analog converter (DAC)** A device that converts a (digital) number to a proportional voltage amplitude.

**Disk** A thin, flat, circular object.

**Disturbed flow** Flow that cannot be described by straight, parallel stream lines.

**Doppler** A diagnostic instrument which emits an ultrasonic beam into the body. The ultrasound is reflected back from moving structures within the body at a frequency higher or lower than the transmitted frequency (Doppler shift). The shift is amplified and presented as a sound or graphic (chart) display.

**Doppler angle** The angle between the sound beam and the flow direction.

**Doppler effect** The observed frequency change of reflected sound due to reflector movement relative to the source or the observer.

**Doppler equation** The mathematical description of the relationship between Doppler shift frequency, Doppler angle, propagation speed, and reflector speed.

**Doppler sample volume** See sample volume.

**Doppler shift** Reflected frequency minus incident frequency.

**Doppler shift frequency** Doppler shift.

**Doppler spectrum** The range of frequencies present in Doppler-shifted echoes.

**Dorsalis pedis artery** The main artery in the dorsum of the foot.

**Dorsum** The back or analogous to the back – dorsal, *adj.*

**Duplex instrument** An ultrasound instrument that combines gray-scale sonography with pulsed Doppler and, possibly, continuous-wave Doppler.

**Duty factor** Fraction of time that pulsed ultrasound is actually on.

**Dynamic aperture** Aperture that increases with increasing focal length (to maintain constant focal width).

**Dynamic focusing** A continuously variable reception focus that follows the changing position of the transmitted pulse.

**Dynamic imaging** Rapid-frame-sequence imaging; real-time imaging.

**Dynamic range** Ratio (in dB) of largest power to smallest power that a system can handle.

**Echo** Reflection of acoustic energy.

**Echogenic** A medium that contains structures capable of producing echoes.

**Eddies** Regions of circular flow patterns present in turbulence.

**Edema** Swelling due to increased fluid in the tissues.

**Effective reflecting area** The area of a reflector from which sound is received by a transducer.

**Electric impulse** A brief excursion of electric voltage from its normal value, usually zero.

**Electric voltage** Electric potential or potential difference expressed in volts.

**Electricity** A form of energy associated with the displacement or flow of electrons.

**Element** The piezoelectric component of a transducer assembly.

**Embolus, pl. emboli** An obstruction to circulation composed of blood clot, air, fat, tumor, or other substance.

**Endarterectomy** The surgical removal of endarterium and atheromatous material from an arterial segment that has become stenosed.

**Energy** Capability of doing work.

**Enhancement** Increase in reflection amplitude from reflectors that lie behind a weakly attenuating structure.

**Ensemble length** Number of pulses used to generate one color-flow image scan line.

**Etiology** The study of the cause of disease; pathogenesis.

**External focus** A focus produced by a lens attached to a transducer element.

**Extracranial** Anatomical structures outside the cranial vault (skull).

***f* number** Focal length divided by transducer size (aperture).

**False-negative rate** Statistical research term indicating the rate of negative results on a diagnostic test when disease was actually present.

**False-positive rate** Statistical research term indicating the rate of positive results on a diagnostic test when no disease was actually present.

**Far zone (far field, Fraunhofer zone)** The region of a sound beam in which the beam diameter increases as the distance from the transducer increases.

**Fast Fourier transform (FFT)** Digital computer implementation of the Fourier transform.

**Femoral artery** The chief artery of the thigh, arising from the external iliac artery and terminating in the popliteal artery.

**Femoral vein** A major vein adjacent to the femoral artery in the thigh. It arises from the external iliac vein and continues into the popliteal vein behind the knee.

**Filter** An electric circuit that passes frequencies within a certain range.

**Fistula, arteriovenous (AV)** An abnormal communication between an artery and a vein, often resulting in cavity or aneurysm formation and abnormal Doppler flow dynamics.

**Flow** To move in a stream; volume flow rate.

**Flow speed** Rate of motion of a portion of a flowing fluid.

**Fluid** A material that flows and conforms to the shape of its container; a gas or liquid.

**Focal length** Distance from focused transducer to center of focal region or to the location of the spatial peak intensity.

**Focal region** Region of minimum beam diameter and area.

**Focal zone** Length of the focal region.

**Focus** To concentrate the sound beam into a smaller beam area than would exist without focusing.

**Force** That which changes the state of rest or motion of an object.

**Fourier transform** A mathematical technique for obtaining a Doppler frequency spectrum.

**Fractional bandwidth** Bandwidth divided by operating frequency.

**Frame** Display image produced by one complete scan of the sound beam.

**Frame rate** Number of frames displayed per unit time, usually seconds.

**Fraunhofer zone** Far zone.

**Freeze frame** Constant display of the last frame entered into memory.

**Frequency** Number of regular recurrences in a given time, e.g., heartbeats or sound vibrations.

**Frequency spectrum** The range of frequencies present; in a Doppler instrument, the range of Doppler shift frequencies present in the returning echoes.

**Fresnel zone** Near zone.

**Frontal artery** A terminal branch of the ophthalmic artery often used as the site for indirect internal carotid artery Doppler evaluation.

**Gain** Ratio of output to input electrical power.

**Gating** Electronically controlled transmission or reception of signal.

**Grating lobes** Additional weaker beams of sound traveling out in directions different from the primary beam as a result of the multielement structure of transducer arrays.

**Gray scale** Range of brightness between white and black.

**Gray-scale display** A display in which the intensity (amplitude) information is recorded as changes in brightness.

**Heat** Energy resulting from thermal molecular motion.

**Hemiparesis** A slight paralysis or incomplete loss of muscular power on one side of the body.

**Hemiplegia** Paralysis of one side of the body. May be temporary (TIA) or permanent (stroke).

**Hemodynamics** The study of the interrelationship of blood pressure, blood flow, vascular volumes, physical properties of the blood, heart rate, and ventricular function.

**Hertz (Hz)** Unit of frequency, one cycle/s; unit of pulse repetition frequency, one pulse/s.

**Homans' sign** Pain in the calf and popliteal area on passive dorsiflexion of the foot, which may indicate deep venous thrombosis of the calf.

**Hue** The color perceived due to the frequency of light.

**Hydrophone** A small transducer element mounted on the end of a narrow tube; a piezoelectric membrane with small metallic electrodes.

**Hydrostatic pressure** A pressure created in a fluid system by the weight of the fluid itself.

**Hypercholesteremia** An excess of blood cholesterol.

**Hyperechoic** Having relatively strong echoes.

**Hyperemia** The presence of an increased amount of blood in a body part. See Reactive hyperemia.

**Hypoechoic** Having relatively weak echoes.

**Impedance** Alterations of resistance with application of current Ohm's law applies. Density multiplied by sound propagation speed.

**Impedance plethysmograph (IPG)** An instrument employing measurement electrodes that sense changes in a minute electric current sent through a portion of the body by means of separate electrodes proximal and distal to the sensing electrodes. Changes in electrical impedance of a limb are a reflection of the change in blood content and limb volume.

**Impulse** A brief excursion of electric voltage from its normal value, usually zero.

**Incidence angle** Angle between propagated sound beam direction and line perpendicular to the media boundary.

**Inertia** Resistance to acceleration.

**Infarct** A localized area of ischemic tissue necrosis due to inadequate arterial blood supply.

**Infrasound** Sound below range of human hearing (less than 20 Hz).

**Intensity** Total energy in an acoustic wave as it travels through a space per unit of time. $\text{Intensity} = \frac{\text{Power}}{\text{Area}}$.

**Intensity reflection coefficient** Reflected intensity divided by incident intensity.

**Intensity transmission coefficient** Transmitted intensity divided by incident intensity.

**Interface** Surface between two media.

**Interference** Combination of positive and/or negative pressures.

**Internal focus** A focus produced by a curved transducer element.

**Intima** The innermost lining of the arterial wall; endarterium.

**Intracranial** Refers to structures located within the cranium (skull).

**Invasive procedure** A procedure characterized by instrumental penetration of the tissues; arteriography and venography are invasive procedures.

**Ipsilateral** Pertaining to anatomical structures on the same side of the body.

**Ischemia** Local reduction of blood supply, due to obstruction of inflow or arterial blood, or to vasoconstriction. Symptoms may include pallor, coldness, impairment of function, pain, and gangrene.

**Kilohertz (kHz)** 1,000 cycles/s.

**Kinematic viscosity** Viscosity divided by density.

**Laminar flow** Fluid moving in concentric rings parallel to the axis of a tube. The center stream of fluid has the greatest velocity, with velocities diminishing in successive rings from the axis, and slowest at the tube wall for fully developed steady flow. The velocity profile is parabolic such that $U_{\max} / U_{\text{mean}} \cong 2$.

**Lateral** Perpendicular to the direction of sound travel.

**Lateral resolution** Minimum reflector separation perpendicular to the sound path required for separate reflections to be produced.

**Lead zirconate titanate** A ceramic piezoelectric material.

**Lens** A curved material that focuses a sound or light beam.

**Lesion** A structural or functional alteration due to disease.

**Linear array** An array made up of rectangular elements in a line.

**Linear phased array** A linear array operated by applying voltage pulses to all elements but with small time differences.

**Linear switched array** A linear array operated by applying voltage pulses to groups of elements sequentially.

**Logarithm** The power to which 10 must be raised to equal the original number. Example: the common logarithm of 100 is 2. $10^2 = 100$.

**Longitudinal resolution** Minimum reflector separation along the sound path required for separate reflections to be produced.

**Longitudinal wave** Wave in which the particle motion is parallel to the direction of wave travel.

**Luminance** Brightness of a presented hue and saturation.

**M-Mode (motion made)** Mode of operation in which the display records a spot brightening for each pulse delivered from the receiver, producing a one-dimensional time display of reflector position (motion).

**Mass** Measure of an object's resistance to acceleration.

**Matching layer** Material placed in front of the front face of a transducer element to reduce the reflection at the transducer surface.

**Maximum venous outflow (MVO) examination** A noninvasive plethysmographic procedure performed to determine the presence of deep vein thrombosis.

**Mean frequency** The average frequency in one line of the Doppler spectrum. May be computed with several different algorithms.

**Mechanical index** An indicator of nonthermal mechanism activity; equal to the peak rarefactional pressure divided by the square root of the center frequency of the pulse bandwidth.

**Mechanical transducer** A transducer that scans the beam by moving the element(s) or a beam reflector with a motor drive.

**Medium** Material through which a wave travels.

**Megahertz (MHz)** One million cycles/s. Doppler transducer crystals usually operate at 2–10 MHz.

**Microprocessing** The processing of electronic signals using a small digital computer, normally a single integrated circuit.

**Mirror image** An artifactual gray-scale, color-flow, or Doppler signal appearing on the opposite side (from the real structure or flow) of a strong reflector.

**Mode frequency** The strongest (brightest) frequency in one line of the Doppler spectrum.

**Morbidity** Conditions inducing disease; also, the ratio of unhealthy individuals to the total population of a given group.

**Multipath** Relating to paths to and from a reflector that are not the same.

**Multiple reflection** Several reflections produced by a pulse encountering a pair of reflectors.

**Myocardial infarctions (MI)** Damage or necrosis of an area of heart muscle resulting from reduction of blood supply; heart attack.

**Nasal artery** A small artery arising from the ophthalmic artery and running across the dorsum of the nose. May be a source of collateral circulation from the contralateral side in internal carotid occlusive disease.

**Near zone (near field, Fresnel zone)** The region of a sound beam in which the beam diameter decreases as the distance from the transducer increases.

**Necrosis** The pathologic death of a cell or group of cells in contact with living cells. Similar to gangrene.

**Neurogenic** Caused or affected by a dysfunction of the nervous system, e.g., neurogenic impotence.

**Noise** Thermally generated, random variations in a voltage signal.

**Nondirectional** A Doppler instrument which assesses flow, via frequency shift, without regard for direction of blood flow.

**Noninvasive** A procedure which has no instrumental penetration of the tissues. Ultrasound is noninvasive.

**Normal incidence** Sound direction perpendicular to media boundary.

**Nyquist limit** The Doppler shift frequency above which aliasing occurs; one half the pulse repetition frequency.

**Oblique incidence** Sound direction not perpendicular to media boundary.

**Occlusion** The state of being closed or shut, as a venous or arterial occlusion.

**Oculoplethysmography (OPG)** A procedure by which changes in eye volume as related to arterial blood flow are detected and recorded. These volume changes may be expressed as pulse delays or as variations in ophthalmic artery pressure, indirectly evaluating internal carotid circulation.

**Ohm** The ohm is the unit used to measure electrical resistance. One ohm is the resistance which will permit one ampere of current to flow under an electromotive force of one volt.

**Ohm's law** $I = E/R$, where $I$ = (intensity) current in amperes, $E$ = electromotive force of potential difference in volts, and $R$ = resistance.

**Operating frequency** Preferred (maximum efficiency) frequency of operation of a transducer.

**Ophthalmic artery** The major artery of the eye, arising as a branch of the internal carotid artery and terminating in numerous branches including the frontal and supraorbital arteries.

**Oscillator gate** The electronic portion of a pulsed Doppler system that converts the continuous voltage of the oscillator to a pulsed voltage.

**Pansystolic bruit** A bruit that extends throughout systole from the first to second heart sounds. Usually highly significant for arteriosclerotic disease. May be tapering or crescendo.

**Parabolic flow** Laminar flow with a profile in the shape of a parabola.

**Particle** Small portion of a medium.

**Particle motion** Displacement, speed, velocity, and acceleration of a particle.

**Patency** The condition of blood flow through an open vessel. Opposite of occluded.

**Pathogenesis** The origin and course of disease development.

**Peak frequency** The highest visible frequency in a Doppler spectrum.

**Pedal pulse** Pulses of the foot.

**Penetration** Imaging depth.

**Penile/brachial index** An index obtained by dividing the penile blood pressure by the brachial blood pressure. Values of less than 1.0 may suggest a vasculogenic etiology for urologic symptoms.

**Perforating veins (communicating veins)** Venous channels that link the superficial and deep venous systems. Found predominantly below the knee, containing valves enabling unidirectional flow from superficial to deep veins, they vary in number from 90 to 200 over the entire course of the leg.

**Period** Time/cycle.

**Periorbital** Enclosing or affecting the tissues around the orbit (eye). The periorbital Doppler examination is frequently utilized to assess the internal carotid circulation.

**Peripheral resistance** Impedance to blood flow in the systemic vascular bed. Results in elevated blood pressure.

**Peripheral sympathetic tone** A state of normal tension in the peripheral vasculature caused by the sympathetic nervous system. Under certain conditions this tone may be altered by sympathectomy.

**Perpendicular** Geometrically related by 90°.

**Perpendicular incidence** Sound direction that is perpendicular to a media boundary.

**Phantom** A tissue-equivalent device that has some characteristics that are representative of tissues (e.g., scattering or attenuation properties).

**Phase** A description of progress through a cycle; one full cycle is divided into 360° of phase.

**Phase quadrature** Two signals differing by one fourth of a cycle.

**Phased array** An array that steers and focuses the beam electronically (with short time delays.)

**Phased linear array** Linear array with phased focusing added; linear array with phased steering of pulses to produce a parallelogram-shaped display.

**Phlebitis** Inflammation of a vein, with or without infection and thrombus formation.

**Phlebography** See venography.

**Phleborheograph (PRG)** An instrument which records the moving currents within the venous system to diagnose deep vein thrombosis.

**Phonoangiography (CPA)** The oscillographic recording of the amplitude of an arterial bruit with respect to time, as detected by a sensitive microphone. Hard copy is derived from a chart recording or Polaroid photograph of the image obtained on a storage oscilloscope.

**Photoplethysmograph (PPG)** An instrument which uses light to assess changes in skin blood perfusion; related to blood flow and limb volume change.

**Piezoelectric crystal** A crystal used to transmit and receive ultrasound information. When excited by electrical charge, the crystal vibrates and sends ultrasound waves. When excited by reflected ultrasound waves, the piezoelectric crystal emits an electrical signal which in turn is processed to indicate frequency of ultrasound energy received.

**Piezoelectricity** Conversion of pressure to electrical voltage.

**PIND** Permanent ischemic neurological deficit; synonymous with cerebral vascular accident.

**Pixel** Picture elements (dots) on the video display of an image of spectrum analyzer. The unit into which imaging information is divided for storage and display in a digital instrument.

**Plaque** A patch or small differentiated area on a body surface. In vascular disease this usually refers to vessel disturbances of the intima. Consists of a collection of platelets, fibrin, lipids, calcium salts, and smooth muscle cells.

**Plethysmograph** Any instrument which measures limb volume change through a change in quantity of blood therein. Types: air, water, impedance, strain-gauge, and photoplethysmography.

**Plug flow** Flow with all fluid portions traveling with the same flow speed and direction.

**Poise** Unit of viscosity.

**Poiseuille's law** The mathematical description of the dependence of volume flow rate on pressure, vessel length and radius, and fluid viscosity.

**Polyvinylidene fluoride** A piezoelectric thin-film material.

**Popliteal artery** A major leg artery, located behind the knee, arising from the femoral artery and terminating in the anterior tibial, posterior tibial, and peroneal arteries.

**Popliteal vein** A major leg vein, located behind the knee and adjacent to the popliteal artery. It arises from the femoral vein and continues into the anterior and posterior tibial veins and peroneal veins.

**Postphlebitic syndrome** Chronic venous insufficiency resulting from deep venous thrombosis of the lower extremity. Symptoms may include edema, pain, varicose veins, and leg ulceration.

**Postprocessing** Signal processing done after memory.

**Power** Rate at which work is done; rate at which energy is transferred.

**Power Doppler** Color-flow display in which colors are assigned according to the strength (amplitude, power, intensity, energy) of the Doppler-shifted echoes.

**Preprocessing** Signal processing (gain, compensation, etc.) done before memory.

**Pressure** Force divided by area in a fluid.

**Priority** The gray-scale echo strength below which color-flow information is preferentially shown on a display.

**Probe** Transducer assembly.

**Propagation** Progression or travel.

**Propagation speed** Speed with which a wave moves through a medium.

**Proximal** Nearest the point of origin along the course of any asymmetrical structure; nearer to the attached end.

**Pseudoclaudication** Pain on walking, usually in the thigh and buttocks, caused by herniated disc or spinal cord neoplasm. It is relieved by rest and may be distinguished from intermittent claudication usually by variation in the walk-pain-rest cycle and by the location of the pain.

**Pulmonary embolism (PE)** Any obstruction to circulation lodged in the lung vasculature. Such obstruction often results from deep vein thrombosis of the lower extremity.

**Pulsatile flow** Flow that accelerates and decelerates with each cardiac cycle.

**Pulsatility index (PI)** A Doppler wave form index defined as the peak-to-peak height of the wave divided by the mean height. The PI is a direct measure of severity of wave form damping which is independent of probe angle. This results in more reproducible data.

**Pulse** A brief excursion of a quantity from its normal value; a few cycles.

**Pulse duration** Interval of time from the beginning to the end of a pulse.

**Pulse-echo diagnostic ultrasound** Ultrasound imaging in which pulses are reflected and used to produce a display.

**Pulse reappearance time (PRT)** The time needed for a toe pulse to reappear following 4 min of suprasystolic occlusion. The pulses are recorded on a strain-gauge plethysmograph.

**Pulse repetition frequency (PRF)** Number of pulses per unit time. Sometimes called pulse repetition rate.

**Pulse repetition period** Time from the beginning of one pulse to the beginning of the next.

**Pulse volume recorder (PVR)** Segmental air plethysmograph which employs changes in cuff pressure to indicate changes in limb volume due to blood flow.

**Pulsed mode** Mode of operation in which pulsed ultrasound is used.

**Pulsed ultrasound** Ultrasound produced in pulsed form by applying electric pulses or voltages of a few cycles to the transducer.

**Pulsed wave** A wave consisting of a series of pulses, each containing a few cycles of ultrasound; not continuous.

**Pulsed wave Doppler** Single transducer system in which bursts of ultrasound are transmitted; reception of returning signals is determined by gate which allows flow to be assessed at specific sites and depths.

**PVDF** Polyvinylidene fluoride, a piezoelectric thin-film material.

**PZT** Lead zirconate titanate.

**Quality factor (Q factor)** Operating frequency divided by bandwidth.

**Radial artery** A major artery of the forearm, arising from the brachial artery and terminating in the palmar arch.

**Radio frequency** Voltages representing echoes in cyclic form.

**Range ambiguity** An artifact produced when echoes are placed too close to the transducer because a second pulse was emitted before they were received.

**Range equation** Relationship between round-trip pulse travel time and distance to a reflector.

**Range gating** Selection of the depth from which echoes are accepted based on echo arrival time.

**Rarefaction** Region of low density and pressure in a compressional wave.

**Rayl** Unit of impedance.

**Raynaud's disease** Intermittent pallor, cyanosis, or rubor of the digits, usually induced by cold or emotion, with normal arterial flow and the absence of other primary causal disease.

**Raynaud's phenomenon (syndrome)** Intermittent pallor, cyanosis, or rubor of the digits usually induced by cold or emotion, often secondary to chronic arterial occlusive disease.

**Reactive hyperemia** Increased blood flow resulting from distention of the blood vessels in response to temporary occlusion.

**Real-time display** Display system in which the image is continuously reviewed and updated as the target changes or moves.

**Recanalization** Restoration of a lumen in a blood vessel following thrombotic occlusion.

**Receiver gate** A device that allows only echoes from a selected depth (arrival time) to pass.

**Rectification** Conversion from an alternating (reversing) to a direct (one-way) form of voltage.

**Reflection** Acoustic energy reflected from a structure; intensity of reflection depends upon acoustic impedance ratios at the interface.

**Reflection angle** Angle between reflected sound direction and line perpendicular to media boundary.

**Reflector** Media boundary that produces a reflection; reflecting surface.

**Refraction** Change of sound direction on passing from one medium to another.

**Registration** Positioning of reflectors in the display.

**Rejection** Eliminating smaller-amplitude voltage pulses.

**Resistance** Pressure difference divided by volume flow rates for steady flow.

**Resolution** The ability to separate in space, time, or strength (detail, temporal, and contrast resolutions, respectively).

**Resonance frequency (RF)** Operating frequency.

**Rest pain** Pain in an extremity at rest, due to chronic arterial occlusive disease. Such patients usually have an ankle/brachial index of 0.5 or less.

**Retrograde flow** Blood flowing away from the Doppler probe. By convention, this is heard in the right ear when using a stereo headset.

**Reverberation** Multiple reflections.

**Reynold's number** Abstract dimensionless number used to describe disturbed flow of a fluid in a tube or past an obstruction. A number that depends on flow speed and viscosity to predict the onset of turbulence.

**RIND** Reversible ischemic neurologic deficit.

**Ring-down artifact** An artifact resulting from a continuous stream of sound emanating from an anatomic site.

**Rubor** Redness; a classical sign of inflammation.

**Sample volume** Site of flow detection; size of sample volume determined by beam diameter and length of ultrasound burst.

**Saturation** The amount of hue present in a mix with white.

**Scan converter** A device that stores a gray-scale image and allows it to be displayed on a television monitor.

**Scan line** A line produced on a display by moving a spot (produced by an electron beam) across the face at constant speed.

**Scanhead** Transducer assembly.

**Scanning** Sweeping a sound beam to produce an image.

**Scatterer** An object that scatters sound because of its small size or its surface roughness.

**Scattering** Diffusion or redirection of sound in several directions on encountering a particle suspension or a rough surface.

**Sclerosis** A hardening or thickening of the arteries, produced by proliferation of fibrous connective tissue and deposit of lipids and calcium salts.

**Section thickness** Thickness of the scanned tissue volume perpendicular to the scan plane; also called slice thickness.

**Sector** A geometric figure bounded by two radii and the arc of a circle included between them.

**Segmental blood pressure (SBP)** The blood pressure obtained by placing a series of blood pressure cuffs at regular intervals on an extremity to determine the severity and level of arterial disease.

**Sensitivity** Statistical research term indicating the ability of a diagnostic test to detect disease when disease is actually present. Poor sensitivity is a high false-negative rate. Ability of an imaging system to detect weak echoes.

**Shadowing** Reduction in reflection amplitude from reflectors that lie behind a strongly reflecting or attenuating structure.

**Shock-excited mode** Excitation of a transducer by a brief driving voltage impulse.

**Shunt** A natural or surgically created anastomosis or channel, diverting flow from one pathway to another. Similar to bypass.

**Side lobes** Minor beams of sound traveling out in directions not included in the primary beam.

**Signal** Information-bearing voltages in an electric circuit; and acoustic, visual, electric, or other conveyance of information.

**Snell's law** Relates incidence and transmission angles of refraction with varying propagation speeds from one medium to another medium.

**Sound** Traveling wave of acoustic variables.

**Sound beam** The region of a medium that contains virtually all the sound produced by a transducer.

**Source** An emitter of ultrasound (transducer).

**Spatial pulse length** Length of space over which a burst or pulse occurs.

**Specificity** Statistical research term relating the ability of a diagnostic test to indicate normality when no disease is actually present. Poor specificity is a high false-positive rate.

**Speckle** The granular appearance of images and spectral displays that is caused by the interference of echoes from the distribution of scatterers in tissue.

**Spectral analysis** Separation of frequencies in a Doppler signal for display as a Doppler spectrum.

**Spectral broadening** The widening of the Doppler shift spectrum; that is, the increase of the range of Doppler shift frequencies present that occurs because of a broadened range of flow velocities encountered by the sound beam; this occurs for disturbed and turbulent flow.

**Spectral display** Visual display of a Doppler spectrum

**Spectral width** Range of Doppler shifts or flow speeds present at a given point in time.

**Spectrum** The complete range of Doppler shift frequencies and amplitudes.

**Spectrum analyzer** Using one or two bidirectional Dopplers, a spectrum analyzer employs microprocessing to display and analyze the complete frequency range of the Doppler shift for more complete diagnostic information regarding an arterial stenosis.

**Specular reflection** Reflection from a large (relative to wavelength), flat, smooth boundary.

**Speed** Displacement divided by the time over which displacement occurs.

**Speed error** A propagation speed that is different from the assumed value (1.54 mm/ms).

**Stasis** Cessation of blood flow. In the venous system of the lower extremity, stasis may contribute to deep vein thrombosis.

**Stenosis** Constriction or narrowing of vessel lumen.

**Stiffness** Property of a medium; applied pressure divided by the fractional volume change produced by the pressure.

**Stoke** Unit of kinematic viscosity.

**Stokes-Adams syndrome** Syncope of cardiac origin occurring most often in patients with a pulse rate of less than 40 beats/min and complete atrioventricular block.

**Strain-gauge plethysmograph (SPG)** An instrument which assesses blood flow through detection of limb volume changes as reflected by impedance changes in an elastic tube filled with an electroconductive metal, placed around the limb being examined.

**Stream line** A line representing the path of motion of a particle of fluid.

**Strength** Nonspecific term referring to amplitude or intensity.

**Stroke** Informal term for cerebrovascular accident.

**Supine position** Lying on the back, face upward.

**Supraorbital artery** One of several terminal branches of the ophthalmic artery. The supraorbital artery exits the orbit usually through the supraorbital notch and anastomoses with the superficial temporal artery. The supraorbital artery is often the site of an indirect Doppler internal carotid artery evaluation.

**Sympathectomy** Excision of a portion of the sympathetic (autonomic) nervous system. May be used as surgical therapy for chronic arterial vasoconstriction.

**Syncope** An episodic loss of consciousness of brief duration with complete recovery.

**Syndrome** A group of signs and symptoms, which, when considered together, are presumed to characterize a disease.

**Tachycardia** Excessive rapidity of heart action; elevated heart rate.

**Temperature** Condition of a body that determines transfer of heat to or from other bodies.

**Temporal resolution** Ability to distinguish closely spaced events in time; improves with increased frame rate.

**Test object** A device without tissue-like properties that is designed to measure some characteristic of an imaging system.

**Thermal index** An indicator of thermal mechanism activity (estimated temperature rise); a value equal to transducer acoustic output power divided by the estimated power required to raise tissue temperature by 1°C.

**Thoracic outlet compression syndrome** A condition in which nerves, arteries, and veins serving the upper extremity may be compressed at the outlet from the thoracic cavity. Primarily a mechanical neurologic dysfunction, arteries or veins may be compromised as well, in which case Doppler ultrasound and photoplethysmography may be of value in diagnosis.

**Threshold** Rejection.

**Thrombophlebitis** Inflammation of a vein associated with thrombosis.

**Thrombosis** The formation of a thrombus.

**Thrombus** A blood clot formed within the heart or blood vessels.

**Time gain compensation (TGC)** Selective gain amplification with time to compensate for loss in echo intensity due to attenuation; permits echoes from greater depths to have the same intensity as those from shallow sites.

**Transcutaneous (percutaneous)** Performed through the skin. Doppler ultrasound is a noninvasive transcutaneous examination.

**Transducer** A device that transforms one kind of energy into another. The Doppler probe contains a crystal that changes electrical energy into ultrasound energy, and back again. The speaker is also a transducer.

**Transducer array** A transducer assembly containing several transducer elements.

**Transducer assembly** Transducer element(s) with damping and matching materials assembled in a case.

**Transducer element** A piece of piezoelectric material in a transducer assembly.

**Transient ischemic attack (TIA)** An episode of transient cerebral symptoms, including visual disturbances, memory loss, hemiparesis, numbness, dizziness, and speech difficulties which are of brief duration and resolve with no residual dysfunction. Usually related to atherosclerotic thrombotic disease and often a prelude to cerebrovascular accident.

**Transmetatarsal amputation** Amputation of toes across the metatarsals.

**Transmission angle** Angle between transmitted sound (incident sound beam crossing medium boundary is now transmitted sound beam) direction and line perpendicular to media boundary.

**Transmission gel** A substance specifically formulated to transmit ultrasound from the transducer to the body tissues. Air is a poor transmitter of ultrasound.

**Turbulence** The occurrence of eddies and vortices in blood flow, usually caused by a stenotic process which reduces vessel lumen diameter. A bruit may result from this turbulence.

**Ulnar artery** A major artery of the forearm arising from the brachial artery and terminating in the palmar arch.

**Ultrasound** Very high frequency sound far beyond the range of hearing. Often expressed in megahertz (MHz) or millions of cycles/s.

**Ultrasound transducer** A device that converts electric energy to ultrasound energy and vice versa.

**Unidirectional** A Doppler instrument which assesses flow in one direction only and gives no information as to direction in relation to the probe. This may be satisfactory for peripheral vascular evaluation, but discrimination of direction is needed for the cerebrovascular examination.

**Valsalva maneuver** Forcible exhalation against the closed glottis (vocal folds) which increases intrathoracic pressure and impedes venous return.

**Valvular incompetence (insufficiency)** A condition in which a vascular valve does not completely close, causing blood to leak in an abnormal direction (backflow, reflux).

**Variable focusing** Transmission focus with various focal lengths.

**Variance** Square of standard deviation; one of the outputs of the auto-correlation process; a measure of spectral broadening (i.e., spread around the mean).

**Vasculogenic** Originating from, or relating to, the vascular system.

**Vasoconstriction** Narrowing of the vessel lumen caused by contraction of the muscular vessel walls.

**Vasodilation** Enlargement of the vessel lumen due to relaxing of the muscular vessel walls.

**Vasospasm** A localized, intermittent contraction of a blood vessel.

**Vector array** Linear sequenced array that emits pulses from different starting points and (by phasing) in different directions.

**Velocity** Speed with direction of motion specified.

**Velocity detector** An ultrasound Doppler instrument which detects the velocity of blood flow transcutaneously. This is expressed by the formula: $\Delta^F = \frac{2\mathrm{Fo}V(\cos\theta)}{C}$

where $C$ = velocity of sound in blood
$\Delta^F$ = Doppler frequency shift
Fo = frequency of transmitted ultrasound
$V$ = blood velocity
$\theta$ = probe angle to vessel

**Venography** Radiographic examination of veins following injection of contrast medium. This is an invasive procedure with associated hazards and is not satisfactory for serial studies; phlebography.

**Venous capacitance (VC)** Ability of a vein or system of veins to accommodate a large quantity of blood.

**Venous insufficiency (incompetence, reflux)** Malfunction of the venous valves which allows blood to flow in a retrograde direction. See postphlebitic syndrome.

**Venous outflow (VO)** A noninvasive plethysmographic procedure to determine the presence or absence of a deep vein thrombosis by measuring the emptying rate (milliliters of flow/100 cc tissue/min or percent/min) in the deep veins postrelease of a venocclusive cuff.

**Vertebral artery** One of two bilateral arteries arising from the subclavian artery, coursing through the neck, and terminating in the basilar artery. Along with the internal carotid arteries, the vertebral arteries are the source of blood supply to the midbrain.

**Video** Demodulated amplitude voltages representing echoes.

**Viscosity** Resistance of a fluid to flow.

**Voltage burst** A cycle or two of voltage variation.

**Voltage impulse** Brief excursion of voltage from its normal value.

**Volume flow rate** Volume of fluid passing a point per unit time (s or min).

**Vortices** Regions of circular flow patterns present in turbulence.

**Wall filter** An electric filter that passes frequencies above a set level and eliminates strong, low-frequency Doppler shifts from pulsating heart or vessel walls.

**Wave** Traveling variation of wave variables.

**Wave variables** Quantities that are functions of space and time in a wave.

**Wavelength** Length of space over which a cycle occurs.

**Window** An anechoic region appearing beneath echo frequencies presented on a Doppler spectral display.

**Work** Force multiplied by displacement.

**Wrap around** The shift of Doppler information on a spectral display to the wrong side of the base line (caused by aliasing).

**Zero crossing detector** An electrical circuit which allows chart recording of Doppler signals. This circuit determines when an incoming signal passes through a zero point and produces an output proportional to the average (root mean square) (RMS) frequency at which such crossings occur. An analog detector that yields mean Doppler shift as a function of time.

# Index



A.F. AbuRahma, D.F. Bandyk (eds.), *Noninvasive Vascular Diagnosis*,
DOI 10.1007/978-1-4471-4005-4, © Springer-Verlag London 2013